ASB American Society of Biomechanics

FOUNDED IN 1977

ABSTRACT BOOK

# ASB Annual Meeting

**AUGUST 13 - 16 2025**

David L. Lawrence Convention Center **Pittsburgh, PA**

www.asbweb.org

#ASB2025

# KNEE ADDUCTION MOMENT, NOT MUSCLE COMPOSITION, PREDICTS MEDIAL-TO-LATERAL CARTILAGE THICKNESS RATIO IN INDIVIDUALS WITH KNEE OSTEOARTHRITIS

*Skylar C. Holmes[1], Akshay Chaudhari[1], Garry Gold[1], Anthony Gatti[1], Katherine Boyer[2]
[1]Stanford University
[2]University of Massachusetts Amherst
*Corresponding author's email: scholmes@stanford.edu

**Introduction:** Knee extensor (KE) weakness is a hallmark of knee osteoarthritis (KOA) that reduces the capacity to attenuate load on the knee during walking [1] and can impact the cartilage mechanical environment. However, KE peak torque alone is not a strong predictor of KOA progression [1] perhaps because it does not adequately capture muscle characteristics important for muscle function in locomotion. A recent study reported that muscle absolute and specific power (power per unit muscle area) and intramuscular fat (IMF) content, measures of muscle quality, are associated with radiographic severity of KOA [2,3]. The knee adduction moment (KAM), a surrogate for medial compartment compressive loading during walking, is also a predictor of the presence and severity of radiographic KOA [4]. It is thought that both mechanical (joint loads and muscle power) and systemic factors (adipose tissue via production of cytokines and adipokines) play an important role in cartilage homeostasis [5]. While mechanical and systemic factors have been linked to radiographic KOA severity, it is not clear how they relate, alone or in combination, to more specific measures of cartilage thickness. Thus, the purpose of this study was to determine how gait and muscle characteristics together impact cartilage thickness. We hypothesized that there would be a negative association between KAM, IMF and cartilage thickness and a positive association between specific power and cartilage thickness.

**Methods:** Seventeen adults with symptomatic KOA (9F, age: 70±4y, BMI: 25.9±3, KOOS Pain: 69.3±12) participated in this study. 3-dimensional biomechanics were collected as participants walked across 2 force plates at self-selected speed. Early and late stance peak KAM (KAM1 & 2) were extracted. Peak isokinetic power at 120°/s (Watts) from 3 trials was quantified with dynamometry (Biodex System 4 Pro, Shirley, NY). Axial images of the thigh were obtained in a 3T MRI system using a multi-echo (6-point) Dixon sequence (slice thickness: 8 mm). A region of interest was drawn around the KE muscle group on each slice [6] from which peak fat-free muscle cross-sectional area (CSA, $cm^2$) and fat fraction (%) were quantified (MATLAB). Specific power was calculated as the ratio of peak power and maximum CSA. Images of the affected knee were obtained using a 3-dimensional Double Echo Steady State sequence (slice thickness: 0.67 mm, in-plane resolution: 0.27 mm). Cartilage thickness in each region was calculated using the 3D Euclidean distance from the bone to articular surface [7]. The medial-to-lateral (M/L) cartilage thickness ratio was defined as the mean medial femoral weight-bearing thickness divided by mean lateral femoral weight-bearing thickness. Separate linear regression models were used to assess the relationships between KAM1, KAM2, specific power, IMF and M/L cartilage thickness ratio ($\alpha$= 0.05).

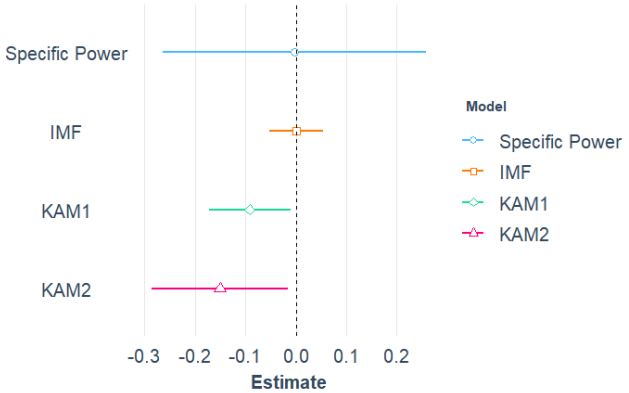


**Figure 1:** Forest plots with beta coefficients with 95% CI for all regression models. If the coefficient does not cross zero there was a significant association with M/L ratio (p <.05).

**Results & Discussion:** In the individual models: specific power and IMF were not associated with M/L ratio (p=0.63 and p=0.95, Figure 1) but KAM1 (p=.009, $\beta$= -0.08) and KAM2 (p=.032, $\beta$= -0.11) were. In agreement with prior work [8], there was a negative association between the KAM and the M/L thickness ratio indicating greater KAM is associated with thinner medial relative to lateral cartilage, consistent with more severe medial KOA. A lack of a relationship between muscle composition (specific power and IMF) and M/L ratio emphasizes the poor understanding of the relationship between KE muscle characteristics and the mechanical environment for joint tissue. Studies that have found KE muscle power is an important predictor of pain and quality of life [9] and thus muscle power may have more relevance to disease progression via a decrease in functional ability rather than severity via cartilage thinning.

**Significance:** Joint loading via the KAM appears to have a stronger impact on cartilage thickness ratio than muscle composition. Specific power and IMF may have more relevance to functional ability and symptomatic severity rather than structural progression of KOA. Thus, interventions focused on improving muscle strength and reducing IMF may improve patient reported outcomes and functional ability but may not impact structural progression. Further research is needed to determine how altered muscle composition and joint loading may interact and impact overall disease status.

**Acknowledgments:** This research was supported by the National Institute of Aging under Award Number F31AG079538, a UMass Dissertation Grant, and an ISB Matching Dissertation Grant.

**References:** [1] Takagi et al. (2018) *Knee Surg Sports Traumatol Arthrosc* 26(9) [2] Culvenor et al. (2018), *Arthritis Care Res* 69(8) [3] Cummings et al. (2023) *J Gerontol A Biol Sci Med Sci.* 78(11 [4] Baliunas et al. (2002) *Osteoarthritis Cartilage* 25(6) [5] Berenbaum et al. (2018) *Nat Rev Rheumatol* 14 [6] Fitzgerald et al. (2021) *J Physiol*. 599(12) [7] Belibi et al., ISMRM 2025 [8] Erhart-Hledik et al. (2015) *J Biomech.* 48(14) [9] Reid et al.(2015), *Arthritis Rheumatol* 67(12)

# OLDER ADULTS ACTIVATE MUSCLES EARLIER IN RESPONSE TO ACTIVITY

*Millissia A. Murro, Fany Alvarado, Grace K. Kellaher, Nancy T. Nguyen, Mayumi Wagatsuma, Jeremy R. Crenshaw, Jocelyn F. Hafer
Kinesiology & Applied Physiology, University of Delaware
*Corresponding author's email: murrom@udel.edu

**Introduction:** In older adults, greater muscle fatigability may result in detrimental changes in function and mobility due to alterations in muscle function in response to bouts of activity [1]. These changes in response to bouts of activity are often assessed by examining changes in gait mechanics, muscle strength, or muscle activation with an assumption that changes in gait may be due to changes in muscle strength or activation [2,3]. Changes in muscle strength cannot be directly assessed during gait, hindering our ability to understand how strength directly influences the changes in gait we see in response to activity. Assessment of muscle activation, where the focus is typically on overall activation magnitude, can be done during gait to allow for a more direct understanding of the influence of muscle function on gait mechanics. However, there are conflicting findings regarding how magnitude changes in response to a bout of activity. These conflicting findings limit our understanding of how muscle activation magnitude may impact the changes in gait mechanics we see following a bout of activity. In addition to activation magnitude, muscle activation can be described by the timing of peak activation. Assessment of muscle activation timing would allow us to test whether changes in muscle activation timing influence changes in gait mechanics. Additionally, understanding the relationship between the timing of peak muscle activation and muscle power, a known measure of fatigue, would allow us to understand if any changes we see are due to reduced muscle capacity in response to activity. Therefore, the purpose of this study is two-fold: 1) to examine changes in the timing of peak muscle activation in response to a bout of activity, and 2) to examine the correlation between the changes in the timing of peak muscle activation and muscle power following a bout of activity. We hypothesized that peak muscle activation would occur later following a bout of activity and that changes in the timing of peak muscle activation would be related to changes in muscle power following a bout of activity.

**Methods:** 13 older adults (6M/7F, 62.7±3.4 years) were included in this analysis. Individuals performed isotonic knee extensor muscle testing at 50% of their maximal isometric torque before and after a 34-minute treadmill walk (34MTW). During the 34MTW, we collected EMG from the rectus femoris, vastus lateralis, vastus medialis, and medial gastrocnemius. Data were collected during the first 4 minutes (pre) and the last 4 minutes (post) of the 34MTW at the same self-selected walking speed. EMG data was high-pass filtered using a second-order Butterworth filter at 30 Hz, rectified, and low-pass filtered at 6 Hz to create a linear envelope. The variables of interest were peak knee extensor power and the timing of peak muscle activation (% gait cycle, HS-HS). The difference in the timing of peak muscle activation pre- to post-activity was examined using a one-tailed paired t-test. The change in each variable pre-to-post 34MTW was determined (Δ=post-pre). A Pearson Correlation Coefficient was used to assess the relationship between changes in the timing of muscle activation and muscle power following a bout of activity ($\alpha$=0.05).

**Results & Discussion:** Peak activation occurred earlier following the bout of activity in the rectus femoris and vastus medialis (p=0.001, Cohen's d=1.04 and p=0.01, Cohen's d=0.74; Fig. 1). No differences were found for the medial gastrocnemius (p=0.10, Cohen's d=0.37) and the vastus lateralis (p=0.15, Cohen's d=0.30) following the bout of activity. The Δ in the timing of peak rectus femoris muscle activation was significantly correlated with the Δ in muscle power (r=0.70, p=0.008). This correlation indicates that a shift toward an earlier peak rectus femoris activation was associated with a larger decrease in muscle power following the bout of activity.

The earlier timing of peak activation of the rectus femoris and vastus medialis muscles indicates a potential preparatory response during gait due to the bout of activity. Although contrary to what we hypothesized, previous studies have also seen an earlier onset of muscle activation following muscle fatigue, particularly during movement initiation tasks [4]. Our findings may indicate that this also occurs during cyclical or continuous movements. We also found that the alterations in the rectus femoris timing of muscle activation correlate with fatigue measured by changes in power. This may indicate that the changes in rectus femoris timing are a response to reduced muscle capacity.

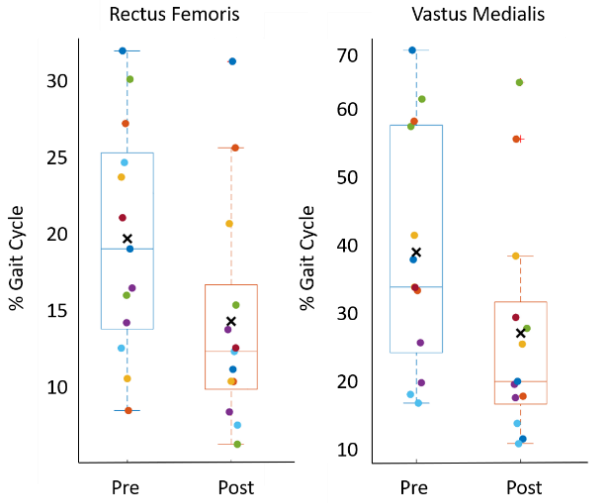


**Figure 1**. The timing of peak muscle activation represented pre- and post-bout of activity. Each colored dot represents an individual subject.

**Significance:** Most muscle activation research focuses on either peak or mean muscle activation during gait, limiting our understanding of how the timing of muscle activation may influence gait mechanics. This work shows that muscles may activate earlier following a bout of activity and that such changes in muscle timing may relate to fatigue. Future research should focus on understanding the timing of peak muscle activation during gait and its relation to the timing of kinematic and kinetic variables.

**Acknowledgments:** Work supported by NIGMS/NIH grant U54-GM104941

**References:** [1] Eldadah, *PMR* 2010, 2(5):406-13, [2] Christie et al., *Med Sci Sports Exerc* 2011, 43(4): 568–577, [3] Zhang et al., *J Engineering in Medicine* 2022, 236(9):1365–1374 [4] Strang et al., *Exp Brain Res* 2009, 197:245–254

# Inequalities in Diabetes-Related Foot Amputations Among U.S. Adults

*Ghazal Mashhadiagha[1,2], Brian L. Davis[2]

[1]Cleveland Clinic Foundation Cleveland, OH
[2]Cleveland State University Cleveland, OH
*Corresponding author's email: g.mashhadiagha@vikes.csuohio.edu

**Introduction:** A comprehensive report on the problem of diabetes prior to 2000 [1] provides data that relate to African American and white diabetic populations that have similar rates of health insurance coverage (93 and 96% respectively). In these groups the annual rates of ulceration and amputation from 1993 through 1996 were 50 and 21 per 100,000 (white patients) and 120 and 78 per 100,000 for the black population. Since that report, the inequality in risks between racial groups has persisted. In a survey covering 2000 – 2020 [2], the highest rates of hospitalization for nontraumatic lower-extremity amputations (NLEA's) during 2012–2019 were among non-Hispanic (NH) Black adults. In terms of gender differences, NLEA hospitalization rates were higher among males during 2000–2020, with increasing rates of NLEA hospitalizations among both sexes during 2009–2020. While the literature has addressed issues related to racial and gender differences, what has not been addressed are the inequalities related to repeated amputations. These were the focus of the current study.

**Methods:** This study utilized the MIMIC-IV clinical database to analyze patterns of amputations among diabetic patients [3]. The dataset included 774 patients, with 564 White, 59 Hispanic Latino, 8 American Indian, 143 Black, 208 female, and 566 male. Data extraction was performed using SQL queries in Google BigQuery, where diabetic patients were identified based on ICD-10 diagnosis codes (E08–E13) and retrieved relevant demographic, hospitalization, and procedural details. Amputation cases were further filtered using ICD-10-PCS codes (0Y6) and categorized by location (e.g., toe, foot, leg) and laterality (left or right). After data were extracted, statistical analyses were performed using Python and Minitab. Descriptive statistics, including age distributions, were computed and visualized. ANOVA models were applied to assess the impact of race, gender in the time intervals of first and second amputations.

**Results & Discussion:** The time between subsequent amputations was significantly ($p<0.05$) affected by both race and gender (Fig 1). Males had longer times between amputations for all races except White, and White females had longer intervals between amputations than any other racial group.

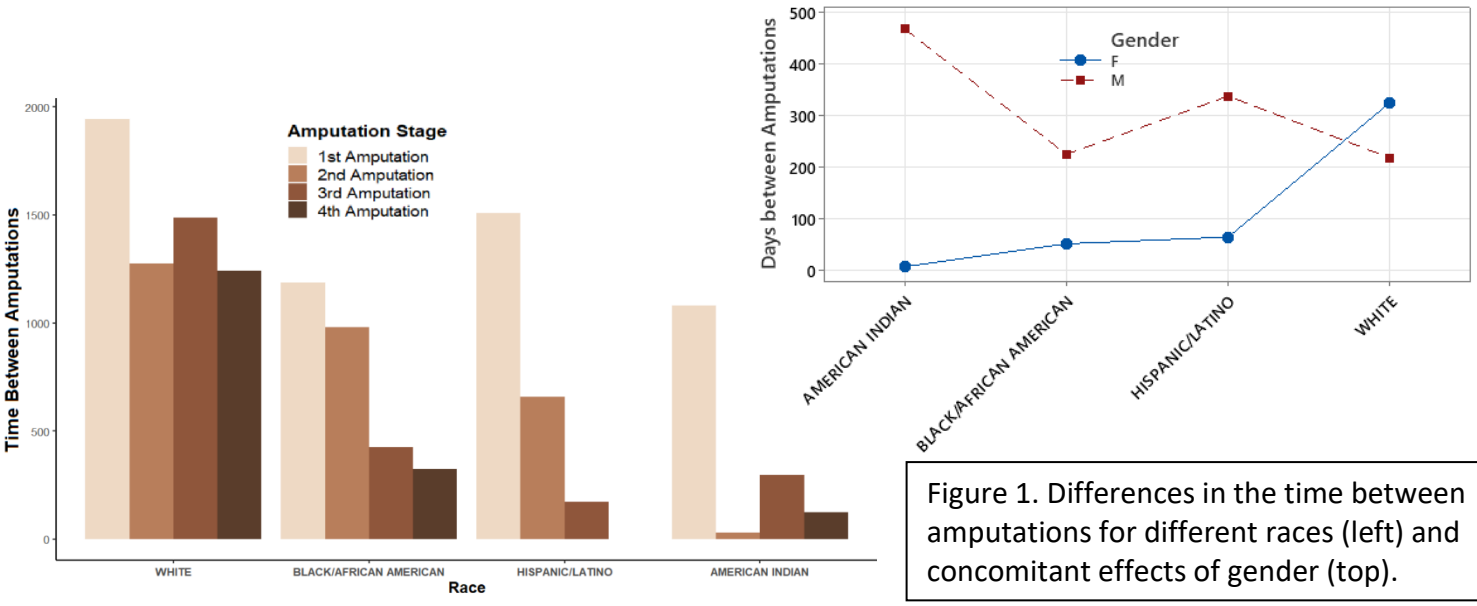


Figure 1. Differences in the time between amputations for different races (left) and concomitant effects of gender (top).

**Significance:** This study demonstrates the effectiveness of integrating BigQuery, Python for large-scale clinical data analysis. The findings provide insights into the progression of diabetes-related amputations and highlights the added risk for higher frequency amputations in American Indian, Black and Hispanic populations, especially amongst female patients.

**References:**

[1] Connecticut Diabetes Surveillance Report: Connecticut Diabetes Control Program (2000).
[2] Saelee et al. Trends and Inequalities in Diabetes-Related Complications Among U.S. Adults, 2000–2020. Diabetes Care 2 January 2025; 48 (1): 18–28.
[3] Goldberger AL, Amaral LAN, Glass L, Hausdorff JM, Ivanov PCh, Mark RG, Mietus JE, Moody GB, Peng C-K, Stanley HE. PhysioBank, PhysioToolkit, and PhysioNet: Components of a New Research Resource for Complex Physiologic Signals. Circulation 101(23):e215-e220 [Circulation Electronic Pages; http://circ.ahajournals.org/content/101/23/e215.full]; 2000 (June 13).

# FEASIBILITY OF COMMUNITY BASED BIOMECHANICS DATA COLLECTION IN INDIVIDUALS WITH KNEE OSTEOARTHRITIS

Ryan C. McCloskey[1*], Alex Gruber[1,2], Sean Leapley[1], Jenna M. Qualter [1], Heather K. Vincent[1], Kerry E. Costello[1]
[1]University of Florida, Gainesville, FL, USA; [2]University of Wisconsin-Madison, Madison, WI, USA
*email: r.mccloskey@ufl.edu

**Introduction:** Marker-based motion capture systems are considered the "gold standard" for assessing joint loading patterns, however, they require specialized equipment, precise placement of markers on anatomical locations, and are typically used in controlled environments. This type of data collection often results in small, homogenous samples of participants who have the means to travel to the site and take the time to participate. In musculoskeletal conditions with multiple risk factors and diverse symptom presentations, such as knee osteoarthritis (OA) [1], these limitations hamper development of personalized biomechanical interventions. Video-based, markerless motion capture (e.g., Theia Markerless) has emerged as a promising alternative and is feasible for gait data collection outside of lab environments [2]. Further, conducting research at community sites may encourage study participation in older adults and result in more representative samples [3-4]. This study aimed to evaluate the feasibility of community based, markerless biomechanics data collections in individuals with knee OA during activities of daily living (ADLs) by evaluating timing of data collection segments at on-campus and community sites.

**Methods:** This interim analysis is part of an ongoing study (Shared Strides) assessing the feasibility of markerless motion capture during ADLs at community sites. Data collections were performed as single-day events at 2 sites over a 6-week period: a laboratory adjacent to a physical therapy clinic on the University of Florida campus (1 date) and a classroom in a day-use, community, senior recreation center (2 dates). Screening was conducted either by phone, with eligible participants (aged ≥ 40 years with knee OA) scheduling a time and location in advance, or on-site for "walk-in" participants using the same criteria. Participants provided informed consent, completed a series of questionnaires (demographics, knee symptoms, research preferences), and performed 3 trials each of 8 ADLs (self-selected and fast-paced walking, double- and single-leg balance, squatting, sit-to-stand, and step-up/step-down from a single step). During ADLs, motion was recorded using Vicon Nexus software and a set of 8 FLIR cameras (100 Hz), with force data recorded concurrently with 2 AMTI ACG-O force platforms (1000 Hz) embedded within a 3.6m Accugait walkway. Start and end times of each segment of the data collection (travel time, equipment set-up/breakdown, informed consent, questionnaires, and individual trials of motion capture) were recorded and descriptive statistics were calculated for each site.

**Results & Discussion:** Although transit to the community site was longer (28.5 min vs. 7 min), equipment set-up and calibration times were comparable. On-campus set-up took 95 min (n=5 study team members), while community set-up took 59-87 min (n=4 each) for the two dates. Differences were mainly driven by calibration time and warrant further investigation into the effects of spatial constraints and lighting. System breakdown was comparable across sites, averaging 29.5 min. Twenty-seven total participants enrolled across the 2 sites (20F; 73.2 ± 6.6 years; 21 community, 6 on campus). Length of data collection segments were comparable between sites (Fig. 1) with total time per person averaging 69.4 min. While a greater potential for walk-ins may have contributed to the larger sample size at the community site (10.5 vs. 6 participants/day), based on the observed length of the motion capture segment of the data collection, adding more pre-scheduled participants could increase these numbers to approximately 25 participants/day (motion capture is currently the rate-limiting step as it only allows for one participant at a time, while the other segments can be completed by multiple participants concurrently). Of the 8 ADLs, walking took the longest at both sites, 7.6 ± 2.2 min, given the need for the participant to land completely on a force plate.

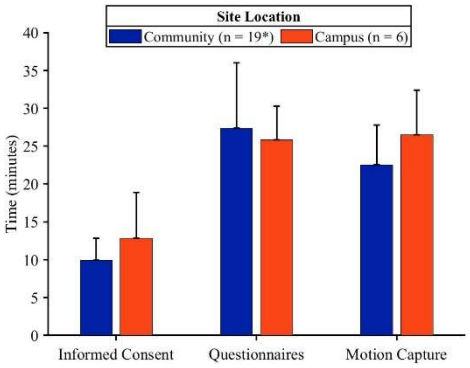


**Figure 1.** Average and standard deviation of the length of each segment of data collection by site (*data loss occurred for 2 of 21 participants at the community site)

**Significance:** These results suggest community-based, markerless motion capture assessment of ADLs in individuals with knee OA is feasible. Collecting data at community sites could improve accessibility and participation in motion analysis measures beyond laboratory settings. Future work could optimize research team size and ADL selection to tailor community biomechanics data collections to various research questions.

**Acknowledgments:** Supported by NIH P30AG028740 and NCATS UL1TR001427.

**References:** [1] Das et al. (2023), *Sci Rep*; [2] McGuirk et al. (2022), *Front Hum Neurosci*; [3] Rigatti et al. (2022), *J Appl Gerontol*; [4] Wieland et al. (2021), *Mayo Clin Proc*

# ACCEPTABILITY OF COMMUNITY BASED, MARKERLESS BIOMECHANICS DATA COLLECTION WITH INDIVIDUALS WITH KNEE OSTEOARTHRITIS

Jenna M. Qualter[1*], Kathryn A. Stofer[1], Ryan C. McCloskey[1], Heather K. Vincent[1], Kerry E. Costello[1]
[1]University of Florida Department of Mechanical and Aerospace Engineering, Gainesville, FL
*email: jqualter@ufl.edu

**Introduction:** Knee osteoarthritis (OA) impacts over 650 million people worldwide with significant variation in symptom severity and progression rates among patients. Biomechanical interventions could improve outcomes by addressing abnormal knee joint loading [1]; however, patient responsiveness has been inconsistent, most likely due to the heterogenous nature of the population [2]. Therefore, advances in OA science will require large samples to account for patient-specific risk factors when investigating biomechanical measures of gait and function. The recent validation of markerless motion capture enables rapid, large-scale biomechanics data collection to be performed effectively outside of a traditional lab setting [3-4]. This may reduce barriers associated with conventional biomechanics research and result in more representative samples [5-6]. This study aimed to assess acceptability of community-based biomechanics data collection using markerless motion capture in individuals with knee OA.

**Methods:** This is an interim analysis of an ongoing study (Shared Strides) examining the feasibility of markerless motion capture at community sites. Individuals aged ≥ 40 years with knee OA were screened via phone and scheduled for a specific site and time or "walked-in" and were screened on site. Eligible participants chose to attend a data collection at either the University of Florida campus (laboratory adjacent to a physical therapy clinic) or a community site (day-use senior recreation center). Data collections were single day events with multiple participants per day. The community site was situated in a publicly accessible classroom, allowing greater possibility of walk-ins. Acceptability was assessed with a custom questionnaire about preferences and reasons for participation. Symptoms were assessed using the Knee Injury and Osteoarthritis Outcome Score (KOOS). Descriptive statistics were calculated for each site.

**Results & Discussion:** Three sessions (2 community, 1 on-campus) were conducted over a 6-week period. Of 55 individuals screened, 27 enrolled (20 F; 73.2 ± 6.6 yrs). An additional 8 were eligible but unable to attend the scheduled dates/locations; 4 of these are scheduled for data collections in the next month. Enrolled participants at both sites were primarily highly educated, retired, non-Hispanic White females with moderate OA. Nine participants (33%) indicated no prior research participation; of these, 8 participated at the community site.

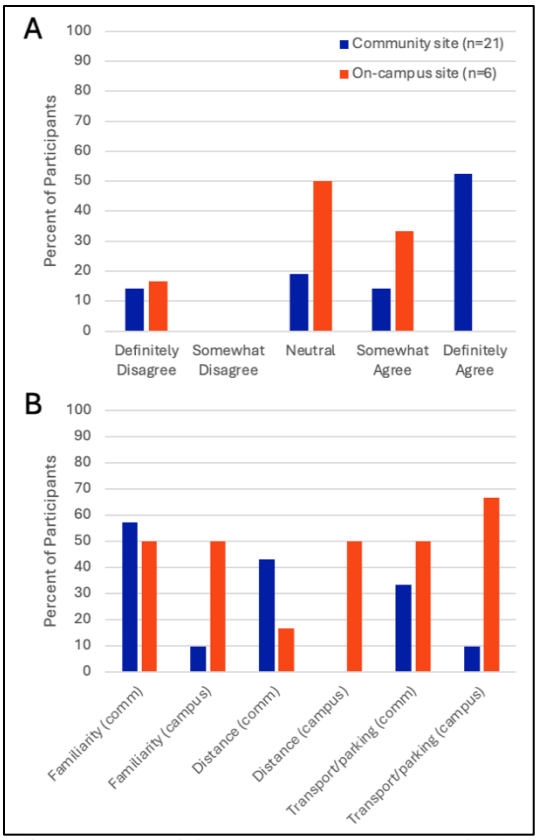


*Figure 1. A: Participant level of agreement with "I am more likely to participate in a data collection like the one I did today if it was at a community location instead of on the UF campus" B: Reasons affecting their response.*

Overall, participants expressed a desire for flexibility and familiarity with data collection locations. Participants at both sites reported they would be more likely to participate in this type of data collection if it occurred at a community location versus on campus (Fig. 1). Although most participants indicated a choice of site did not affect their ability to participate, 17 (63%) reported that it affected their desire to participate. Around 50% reported a choice of date influenced their participation. Anecdotally, some participants reported prior visits to the on-campus clinic while others reported regular visits to the senior center, which may have contributed to their familiarity with and preference for a specific site. Eighteen (69.2%) participants reported a transit time of less than 30 minutes to the collection site, indicating proximity may have influenced site preference; notably, while all participants at the on-campus clinic drove, 3 participants at the community site used alternative forms of transportation (person-powered or public transport). At the community site, "altruism" and "learning more about your own health" were the most reported reasons for study participation, surpassing other motivations such as "financial compensation" and "personal health benefits".

**Significance:** This interim analysis suggests markerless, community-based biomechanics data collection is acceptable for individuals with knee OA, potentially increasing overall engagement. However, these findings will be confirmed in a larger sample. Future biomechanics studies may consider community-based collection to better align with participant preferences.

**Acknowledgments:** Supported by NIH P30AG028740 and NCATS UL1TR001427.

**References:** [1] Reeves et al. Nat Rev Rheumatol 2011; [2] Deveza et al. Rheumatology (Oxford) 2018; [3] Kanko et al. J Biomech 2021; [4] McGuirk et al. Front Hum Neurosci 2022; [5] Rigatti et al. J Appl Gerontol 2022; [6] Wieland et al. Mayo Clin Proc 2021

# DETERMINING THE CHANGES IN GLUTEAL MUSCLE FORCE REQUIREMENTS AFTER GLUTEUS MAXIMUS TENDON TRANSFER FOR HIP ABDUCTOR INSUFFICIENCY

*Madison M. Wissman, Cecilia Pascual-Garrido, Michael D. Harris
Washington University in St. Louis, St. Louis, MO, USA
*Corresponding author's email: m.wissman@wustl.edu

**Introduction:** Hip abductor strength insufficiency causes lateral hip pain and impaired gait in up to 20% of adults 60 years and older [1-3]. Gluteal tendon repair may improve abductor function and pain, but many patients are not repair candidates or have unsuccessful surgeries due to advanced gluteus medius (Gmed) and gluteus minimus (Gmin) tear and degeneration [4]. Thus, transferring the anterior third of the gluteus maximus (Gmax) tendon is emerging as a salvage option to treat severe abductor deficiencies [5]. While this surgery can reduce pain, postoperative outcomes remain inconsistent, and many patients experience persistent Trendelenburg gait and limited abduction strength [4]. There has yet to be an analysis of post-surgical alterations to gluteal forces or their relationship to functional kinematics during daily activities. The objectives of this study were to use musculoskeletal models to quantify gluteal forces during walking pre- and post-Gmax tendon transfer, and to test the predictive ability of the models to simulate kinematic and muscle force changes representative of patients with hip abductor insufficiency. We hypothesized that the Gmax would produce greater forces during gait after Gmax tendon transfer, and that the Gmed and Gmin would produce less force post-transfer.

**Methods:** We updated a musculoskeletal model [6] with pelvis, femur, and muscle geometry of an adult female [7]. Unilateral Gmed and Gmin weakness was simulated by reducing the maximum isometric force of each muscle by 50% [2, 4]. Gmax tendon transfer was then simulated by moving the insertion of the anterior Gmax actuator on the side of the weakened abductors to a point 5mm above the lesser trochanter on the most lateral aspect of the femur [8]. Both the weakened model and the post-surgery model were constrained to walk using normal gait kinematics and ground reaction forces from experimental data of the subject. Muscle activations and forces pre- and post-surgery were estimated using OpenSim Moco [9]. Because many patients with hip abductor insufficiency exhibit Trendelenburg gait [10], we created a second set of models that used an optimal control problem in OpenSim Moco to predict changes to gait kinematics in response to the weak abductors and subsequent Gmax transfer. The cost function minimized sum of squared muscle excitations and deviation from normal gait kinematics. We compared pre- and post-surgery joint angles and gluteal muscle forces both when kinematics were constrained and when allowed to change in response to weakened muscles.

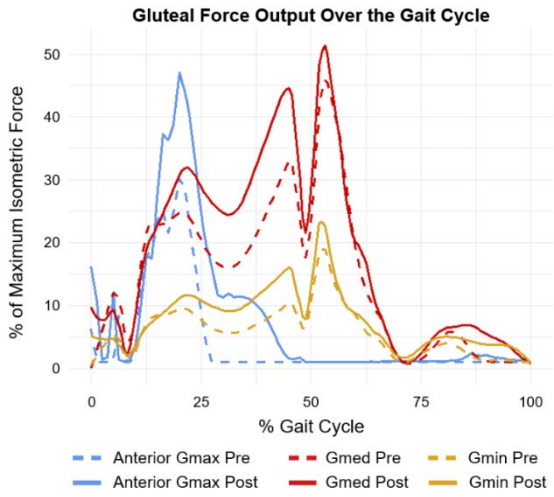


**Figure 1.** Force output from anterior Gmax, Gmed, and Gmin during gait with altered kinematics pre- and post-surgery. Force values scaled to respective maximum isometric force for each muscle or actuator.

**Results & Discussion:** When constrained to normal gait kinematics, the anterior Gmax, Gmed, and Gmin produced 100% of their maximum isometric force during the stance phase pre- and post-transfer; this was not consistent with our hypothesis. The requirement to produce 100% of the muscles' maximum isometric force for unchanged kinematics suggests that achieving normal gait even post-surgery is unrealistic for patients with severe weakness. When allowed to alter kinematics, OpenSim Moco predicted a Trendelenburg gait pattern, with lumbar bending oscillation increasing from 19° to 23° and pelvis obliquity increasing from 8° to 10°. Force output from the relocated anterior Gmax actuator increased post-surgery by almost 20% of its maximum isometric force, and Gmed and Gmin force output also increased by as much as 15% and 5% of their maximum force, respectively (Fig. 1). These results partially support our hypothesis but demonstrate unexpected Gmed and Gmin force increases. If patients respond this way after surgery, partial Gmed restoration, as commonly attempted during surgery [11], may aid in recovery of function. Higher demand on all gluteal muscles post-surgery may also indicate benefits of graduated strengthening of the Gmax, Gmed, and Gmin during rehabilitation. This study was an introductory test of the ability of musculoskeletal simulation to estimate short-term hip force and kinematics changes after Gmax transfer surgery, and it is limited by its use of experimental data from one healthy adult. Future work will focus on model validation and address other factors such as Gmax innervation and kinematic asymmetry.

**Significance:** This study is one of the first to investigate the impact of Gmax tendon transfer surgery on gluteal muscle forces and motion in patients with hip abductor weakness. Understanding muscle force requirements and potential kinematic changes post-surgery may better inform surgical candidate selection as well as rehabilitation targets and strategies to optimize surgical outcomes.

**Acknowledgments:** Funding provided by NIAMS K01AR072072 and R01AR081881.

**References:** [1] Quisquater, L et al, *Orthop,* 43(4), 2020; [2] Nazal, MR et al, *Arthrosc,* 36(8), 2020; [3] Maldonado, DR et al, *JBJS Open Access*, 5(4), 2020; [4] Song, BM et al, *J Arthroplasty,* 39(4), 2024; [5] Whiteside, LA *Clin Orthop Relat Res,* 470, 2012; [6] Lai, AKM et al, *Ann Biomed Eng,* 45:2762-2774, 2017; [7] Song, K et al, *Comput Methods Biomech Biomed Eng*in, 22(3), 2019; [8] Inclan, PM et al, *Arthrosc Tech,* 12(5), 2023; [9] Dembia, CL et al, *PLoS Comput Biol,* 16(12), 2020; [10] Allison, K et al, *Clin Biomech,* 32, 2016; [11] Jimenez-Telleria, I et al, *Orthop Rev,* 14(3), 2022.

# IMPACT OF INCREASED RESPIRATORY LOAD ON PREFRONTAL CORTICAL ACTIVATION UNDER VARYING TASK COMPLEXITIES OF TRAIL-WALKING TASK

Alka Bishnoi[1], * Manuel E. Hernandez[2]
[1]Kean University
[2]University of Illinois Urbana-Champaign
*Corresponding author's email: mhernand@illinois.edu

**Introduction:** Breathing influences brain function and motor coordination by modulating neural oscillations linked to cognitive, sensory, and motor outputs [1]. Excessive breathing effort may disrupt this synchronization, increasing cognitive strain or gait instability during walking. This study examined the effects of breathing rate (BR) on prefrontal cortical (PFC) activation during single-task and trail-walking task (TWT) paradigms [2] in a diverse aging population. We hypothesized that adults with higher BR would exhibit greater PFC activation, particularly during TWT, compared to those with lower BR.

**Methods:** The design of this study was cross-sectional. This study was done as per Institutional review board guidelines at the Mobility and Fall Prevention Laboratory of University of Illinois Urbana-Champaign. Forty-five adults (50±20 years of age, 27 females) walked at a comfortable walking speed on an instrumented treadmill with and without performing a TWT. Continuous breathing rate (BR) was monitored using a Hexoskin smart shirt (Carre Technologies, Montreal, QC, Canada) and analyzed in this study during the resting position. Functional Near-Infrared Spectroscopy using the fNIRS Imager 1200 system (fNIR devices, LLC, Potomac, MD, USA) was used to quantify PFC oxygenated hemoglobin ($HbO_2$) levels during $TWT_A$ (Trail walking task condition A that consisted of numbers only for participants to step on as accurately as possible) and $TWT_B$ (Trail walking task condition B that consisted of numbers and letters for participants to step on as accurately as possible). A linear mixed effects model was conducted to investigate the effects of BR, task, and their interaction on $HbO_2$ levels while controlling for age and fitness level (Vo2 max). Prefrontal cortical activation (Mean $HbO_2$ levels) were primary outcome measures.

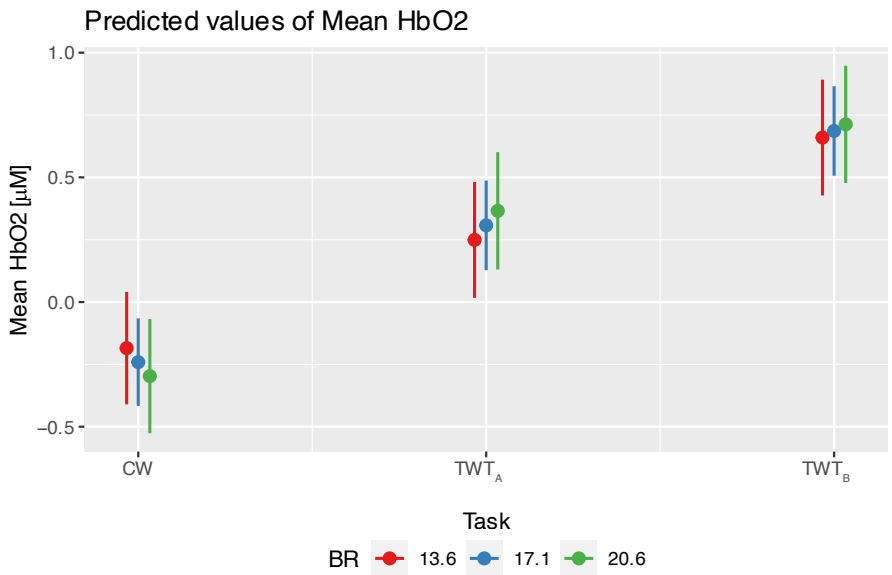


**Figure 1:** Predicted values of mean oxygenated hemoglobin for adults with different breathing rate levels during different walking tasks, including comfortable walking (CW), trail walking

**Results & Discussion:** Mean $HbO_2$ levels differed significantly between single-task and TWT conditions across varying breathing rates. Adults with lower breathing rates showed reduced prefrontal cortex (PFC) activation during TWT compared to single task walking and to adults with higher breathing rates, even after controlling for age and fitness levels. Furthermore, adults with lower breathing rates exhibited decreased $HbO_2$ during the less cognitively demanding $TWT_A$ condition compared to the more demanding $TWT_B$ condition, indicating greater attentional resource allocation as difficulty of task increased. Notably, no association was observed between breathing rate and walking speed, suggesting that walking speed did not influence the relationship between breathing rate and neural activation. No additional statistically significant effects were identified.

**Significance:** The present findings provide evidence of the effects of BR on PFC activation, while dual task walking in diverse aging population. The results showed higher PFC activation during TWT walking was associated with higher BR adults compared single task walking and lower BR. This provides future researchers and clinicians with an incentive to examine causal relationships between exercise interventions, controlled breathing performance and neural activation patterns while dual task walking to potentially decrease the risk of falls.

**Acknowledgments:** We thank participants and members of the Mobility and Fall Prevention Research Lab for making this work possible.

**References:** [1] Heck et al. (2017), *Frontiers in Neural Circuits* 115(10); [2] Bishnoi and Hernandez (2025), *Archives of Gerontology and Geriatrics Plus* 2(1).

# EXECUTIVE FUNCTION PREDICTS AGE-RELATED REDISTRIBUTION OF JOINT POWER FROM ANKLE TO HIP DURING GAIT

Kenneth Harrison*[1], Keven G. Santamaria-Guzman[1], Brandon M. Peoples[1], Jaimie A. Roper[1]
Auburn University[1], Auburn, Alabama
*Corresponding author's email: kdh0077@auburn.edu

**Introduction:** Aging is associated with a redistribution of power generation during walking, typically shifting from ankle plantarflexion to hip flexion power (Boyer et al., 2023; Franz, 2016; Winter et al., 1990). While this biomechanical adaptation is well-documented, the role of cognitive function in this shift remains unclear. The age-related increase in cortical control of locomotion (Seidler et al., 2010) suggests that executive function may play a crucial role in maintaining optimal gait mechanics. Due to the established relationship between executive function and motor control in aging, we hypothesized that better executive function would be associated with preserved ankle-dominant power generation strategies in older adults.

**Methods:** Young (n=17, 20 ± 2) and older adults (n=14, 66 ± 6) walked on an instrumented split-belt treadmill at self-selected speeds. Kinetic data were collected at 1000 Hz and kinematic data at 100 Hz using a 17-camera motion capture system. Peak ankle plantarflexion (A2) and hip flexion (H3) power were calculated using inverse dynamics. Executive function was assessed using Trail Making Test delta scores (TMT-B minus TMT-A), where higher scores indicate reduced cognitive flexibility. The A2/H3 power ratio quantified the distribution of propulsion between joints. Higher values indicate greater reliance on ankle plantarflexion during late-stance (push-off) versus hip flexion during early swing (pull-off) to propel the body forward. Group differences were assessed using Welch's t-test, and the relationship between executive function and joint power strategy was examined using multiple linear regression with age group, TMT delta scores, and their interaction as predictors.

**Results & Discussion:** Older adults demonstrated significantly lower A2/H3 power ratios compared to young adults (1.16 W/kg ± 0.73 vs 1.96 W/kg ± 0.82, $p$ = .018), confirming a redistribution from ankle to hip power generation with age. A significant interaction between age group and executive function ($p$ = .019, $R^2$ = 0.32) revealed divergent relationships between cognitive flexibility and joint power strategy across age groups. In older adults, better executive function was associated with higher A2/H3 ratios, suggesting that preserved cognitive flexibility supports maintenance of ankle-based power generation. The opposing relationship in young adults, where executive function showed minimal influence on joint power distribution, likely reflects the automated nature of locomotor control in healthy young adults who rely predominantly on subcortical and reflexive mechanisms for gait regulation (Dewolf et al., 2021).

**Significance:** This study provides novel evidence for age-dependent relationships between executive function and locomotor control strategies. Our findings suggest that aging increases the reliance on cortical resources for gait control, particularly in maintaining ankle-driven power generation patterns. The relationship between preserved executive function and ankle power generation in older adults is especially meaningful given that ankle power is a primary contributor to forward propulsion and walking speed. Understanding this relationship provides new opportunities for intervention, suggesting that combined cognitive and motor training might better preserve the ankle-dominant power generation strategy that supports efficient, independent mobility in aging populations. Future research should investigate the influence of cognitive function on age-related changes in joint power strategy under ecologically valid conditions, such as dual task walking or under matched speeds, to better understand this relationship during real-world mobility challenges.

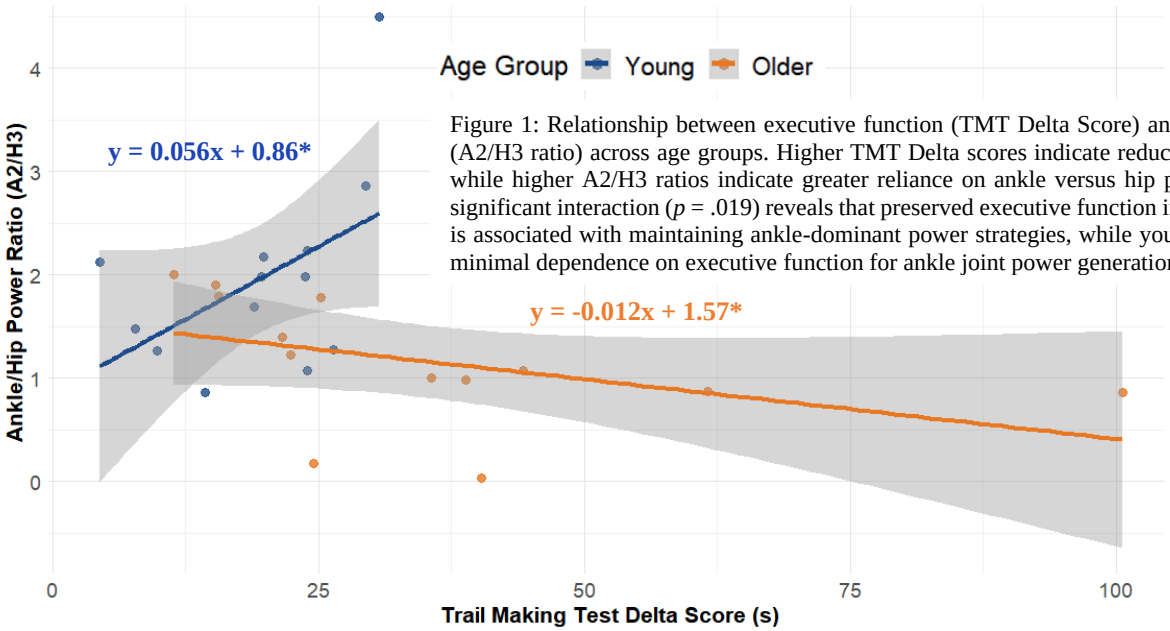


Figure 1: Relationship between executive function (TMT Delta Score) and joint power strategy (A2/H3 ratio) across age groups. Higher TMT Delta scores indicate reduced executive function, while higher A2/H3 ratios indicate greater reliance on ankle versus hip power generation. The significant interaction ($p$ = .019) reveals that preserved executive function in older adults (orange) is associated with maintaining ankle-dominant power strategies, while young adults (blue) show minimal dependence on executive function for ankle joint power generation.

**References:** [1] Boyer et al. (2023), Exp Gerontol 173, [2] Franz (2016), Exerc Sport Sci Rev 44(4), [3] Seidler et al. (2010), Neurosci Biobehav Rev 34(5), [4] Winter et al. (1990), Phys Ther 70(6), [5] Dewolf (2021) Frontiers Neurosci 15

# GAIT VARIABILITY CHANGES IN OLDER ADULTS WITH AND WITHOUT KNEE OSTEOARTHRITIS WITH A PROLONGED WALK

*Skylar C Holmes[1,2], Hunter Brierly[2], Jacob Thomas[2], Jane A Kent[2], Katherine A Boyer[2]
[1.] Stanford University
[2] University of Massachusetts Amherst
*Corresponding author's email: scholmes@stanford.edu

**Introduction:** Knee Osteoarthritis (KOA) is a chronic musculoskeletal disease that results in joint pain, stiffness, and muscle weakness. KOA is a leading cause of mobility disability in adults and is associated with increased fall risk compared with age-matched controls [1]. Older adults (>65 yr) with KOA have greater spatiotemporal gait variability than age-matched controls [2], which may contribute to their greater falls risk [3]. Muscle weakness has been suggested as a contributing factor to increased gait variability in older adults and those with KOA [4]. Further, muscle fatigue induced with a repeated sit-to-stand task increased step width and step length variability [5]. We have reported significant knee extensor (KE) muscle fatigue (decrease in peak power) in both KOA and older healthy (OH) adults in response to a 30-minute treadmill walk (30MTW) [6]. Notably, those with KOA were also weaker than OH. Our aim was to quantify the impact of a 30MTW on spatiotemporal gait variability in these older adults with and without KOA. It was hypothesized that increases in variability with KOA would be greater than for OH due to the combined effects of muscle weakness and muscle fatigue in response to the 30MTW.

**Methods:** We consented and enrolled 15 older adults with KOA (6F, Age:71±4 yr, BMI:27±4 kg/m$^2$, KOOS Pain:69±9) and 15 controls (7F, Age:73±3 yr, BMI: 24±3 kg/m$^2$, KOOS Pain: 98±6), as approved by the University of Massachusetts IRB. Baseline KE muscle power and fatigue following a 30MTW at preferred walking pace were quantified by isokinetic dynamometry (System 4, Biodex, USA) at 120 dps. Motion capture data (Qualisys Inc, Sweden) from markers placed on the feet (heel cluster, 1$^{st}$ and 5$^{th}$ metatarsal heads) were obtained as participants completed the 30MTW. At min 7, 14, and 20 the treadmill was raised to a 3% incline for 1 min to mimic real-world intensity challenges. Data were captured for 10-30 s at 200 Hz at min 2 and 30, resulting in 7-30 strides of data per participant at each timepoint. Heel-strike timepoints were calculated from foot marker velocity and used to identify individual strides. The mean and standard deviation of stride length and step width at min 2 and min 30 of the 30MTW. Effects of group (KOA, OH) and time (start, end) on each participant's stride length and step width means and SD (variability) were tested by 2x2 ANOVA. Unpaired t-tests were used to test for differences between groups in % change in stride length and step width means and variability from start to end of the 30MTW ($p<0.05$).

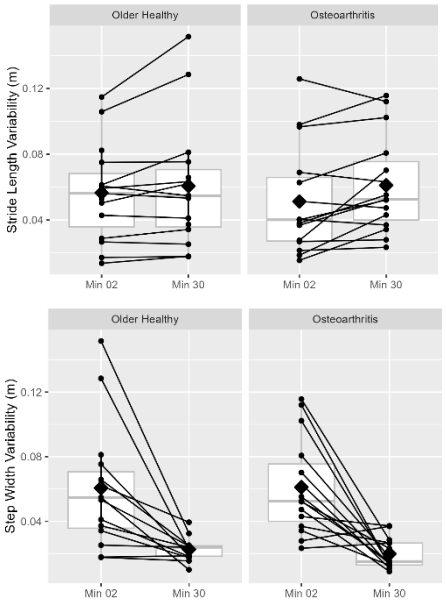


**Fig1: Top.** Stride length variability for OH (left) and KOA (right) at min 2 and 30 of the treadmill walk. **Bottom.** Step width variability for OH (right) and KOA (left) at min 2 and 30 of the treadmill walk.

**Results & Discussion:** KOA were weaker than OH at baseline (p=0.005, KOA: 142±37 W, OH: 193±81 W), and KE peak power decreased post 30MTW in both groups (p=0.002). There were no differences in mean stride length or step width between groups or with time ($p\geq0.1$). There was an effect of time but not group on stride length variability (individual SD), with both groups increasing stride length variability after the 30MTW (Fig 1). The relative change in stride length variability was greater for KOA (+37±54%) compared with OH (+7±18%), p= 0.05. There was also an effect of time but not group for step width variability, with both groups decreasing step width variability during the walk (Fig 1). A decrease in step width variability contrasted with our hypothesis, but both too much and too little variability in stride width has been linked with falls history in older adults [7]. Muscle power has been inversely related to gait variability in frail older adults [4]. The results of this study suggest that although mild muscle weakness in KOA did not alter the gait variability as compared to older healthy adults at baseline, muscle fatigue in response to the 30MTW may compound weakness to result in greater changes in stride length variability for KOA.

**Significance**: Physical activity, including walking, is recommended as a non-pharmacological approach to managing KOA symptoms [9]. The results of this study suggest that prolonged walking that can result in muscle fatigue may increase the risk of falls for those with KOA through its impact on stride length and step width variability. Increased stride length variability has also been shown to increase the metabolic cost of walking [8]. Thus, there may also be consequences of muscle fatigue in KOA for walking energetics and fatiguability.

**Acknowledgments:** NIH R01 AG068102; F31 AG079538; UMass Dissertation Grant; ISB Matching Dissertation Grant

**References:** [1] Dore et al., (2016) Arth Care & Res [2] Tanpure et al. (2023) *J Orthop.* [3] Hausdorff et al. (2001) *Arch Phys Med Rehabil*. [4] Martinikorena et al. (2016) *J Am Med Dir Assoc*. [5] Helbostad et. al (2007) *J Gerontol A* 62(9) [6] Holmes (2024) *UMass ScholarWorks* [7] Brach et al. (2005) *J Neuroeng Rehabil* [8] Grimmitt et al. (2024) *bioRxiv* [9] Kraus et al., (2019) *MSSE*.

# THE INFLUENCE OF GAIT VARIABILITY ON HUMAN ODOMETRY

Tyler M. Wiles[1*], Alli Grunkemeyer[1], Nick Stergiou[1,2], Aaron D. Likens[1]
[1]Department of Biomechanics, University of Nebraska at Omaha
[2]Department of Physical Education & Sports Science, Aristotle University, Thessaloniki
*Corresponding author's email: tylerwiles@unomaha.edu

**Introduction:** Humans have exceptional navigation skills. Those navigational skills are evident in blindfolded distance perception tasks, where participants are guided along a path and then asked to reproduce the distance themselves. Humans are also able to complete the hypotenuse of a triangle after being guided along its two sides. However, the mechanisms for accomplishing these navigational feats have not reached a consensus. Gait kinematics have been suggested to alter distance perception—investigated by changing stride lengths, for example—and we investigated if the temporal structure of gait variability can affect distance perception in three different age groups [1].

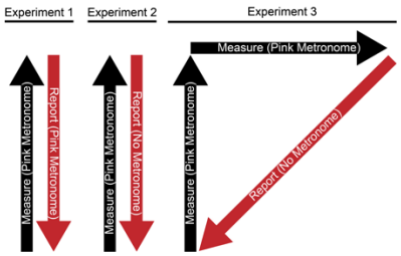


Figure 1: Paths per experiment

**Methods:** Healthy adults were recruited to complete a four-minute walk to calculate their stride interval mean and standard deviation. Using those values, unique pink (correlations between strides), white (no correlations between strides), and isochronous (identical strides) auditory cues were created for each walking bout in the distance perception experiments. Pink and white auditory cues can be used to alter gait variability and are typical of younger and older adults, respectively [2-3]. Participants synchronized their right heel-strike to the auditory metronome's structure while wearing open-back headphones and a blindfold. In experiment 1 (4 young (19-35), 5 middle (36-64), 4 old (65+)), participants were guided along 10 or 30 meters (m) (Measure) and then asked to reproduce that same distance (Report) while synchronizing their footsteps to the auditory cues (Fig. 1). In experiment 2 (5 young, 4 middle, 4 old), participants walked without cues during the Report (Fig. 1). Experiment 3 (4 young, 2 middle, 3 old) was the same as the previous, but participants had to return to their original starting location after completing the triangle's first two sides (Fig. 1). Participants were assigned to one experiment and given three randomized attempts per condition and distance. Experiment-specific Bayesian RMANOVAs determined if metronome condition, distance, or age group, affected error.

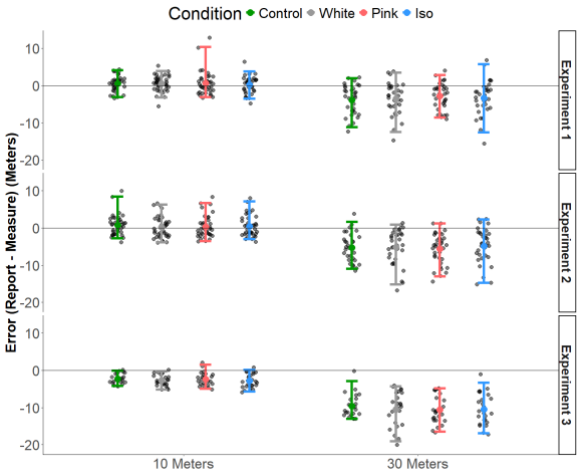


Figure 2: Accuracy for each distance, metronome condition, and experiment. Colored dots represent the mean with 95% credible intervals. Black points are individual results. Horizontal line is perfect accuracy.

**Results & Discussion:** For all experiments, our results did not support a distance, condition, age group interaction (All $BF_{10} < 1$; Fig. 2). All experiments had extreme support of distance playing a role in error, ($BF_{10} > 100$), where 30m was always less accurate than 10m. No experiment supported auditory cues changing distance perception (All $BF_{10} < 0.56$). These findings suggest that temporal structure of variability does not influence one's distance perception. Another question pertains to inconsistent evidence that healthy adults experience age-related deteriorations in distance perception [4-5]. Our results anecdotally support an age group × distance interaction for experiment 2 ($BF_{10} = 2.25$) and especially 3 ($BF_{10} = 789.34$), but no main effect (All $BF_{10} < 1$). Focusing only on experiment 3 due to the extreme support, middle-aged adults (-1.98 ± 1.56m) had lower error compared to older (-2.24 ± 1.88m) and younger adults (-3.05 ± 1.38m) for the 10-meter condition (Fig. 3). At 30m, older adults (-8.94 ± 4.52m) were more accurate than middle-aged (-9.50 ± 3.13m) and young adults (-11.4 ± 3.75m). Although these findings point to minor differences between age groups, it is possible that the source is purely random rather than diminished haptic feedback [5].

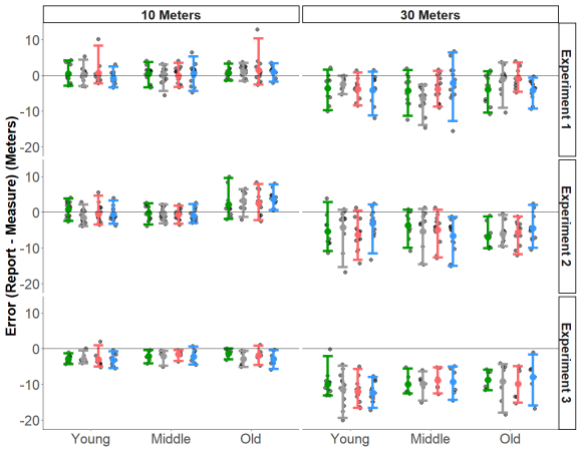


Figure 3: The same results as Figure 2 split by age group.

**Significance:** Temporal gait manipulations did not improve distance perception in healthy groups. However, it is possible that the cognitively impaired and Alzheimer's patients might exhibit distance perception improvements with this method.

**Acknowledgements:** UNO GRACA, Nebraska Research Initiative, NSF 212491, NIH P20GM109090 and P20GM152301.

**References:** [1] Harrison (2020), *Ecol. Psychol.* 32; [2] Kaipust et al. (2013), *Ann. Biomed. Eng.* 41; [3] Goldberger et al. (2002), *Proc. Natl. Acad. Sci.* 99; [4] Wiles et al. (2025), *Psychol. Res.* 89; [5] Yu et al. (2021), *Psychol. Sci.* 32.

# ISCHEMIC PRECONDITIONING ALTERS GAIT MECHANICS IN PATIENTS WITH KNEE OSTEOARTHRITIS

* Shraddha Sudhir[1], Nikou Nikoumanesh[1], Steven A. Garcia[2], Kharma C. Foucher[2], Lindsay S. Hannigan[1]
[1]Department of Physical Therapy, University of Illinois at Chicago, Chicago
[2]Department of Kinesiology and Nutrition, University of Illinois at Chicago, Chicago
*Corresponding author's email: ssudhi5@uic.edu

**Introduction:** Knee osteoarthritis (KOA) is a leading cause of disability and affects over 650 million adults over the age of 40 worldwide [1]. Although altered gait mechanics are a key characteristic of KOA and its progression, few treatments outside of physical activity and gait retraining have shown to change gait mechanics. Therefore, the purpose of this study was to evaluate changes in gait mechanics after a single session of ischemic preconditioning (IC) in older adults with symptomatic KOA. We hypothesized that a single session of IC would reduce knee varus angle and knee adduction moment in the involved limb and reduce trunk lateral flexion.

**Methods:** Thirty-one older adults with symptomatic KOA (13F/18M, 62.97±8.55 years, 94.62±28.57 kg, 170.27±18.47 cm) walked on a split-belt treadmill with 3D motion capture at a self-selected speed before and immediately after a single session of IC (n=15) or sham (n=16) treatment. IC and sham treatment were administered on the involved thigh while the participants lay supine. IC and sham treatments consisted of 5 minutes of inflation (225mmHg for IC and 25mmHg for sham) followed by 5 minutes of reperfusion, for 5 cycles (50 minutes). The involved limb was defined as the knee with greatest KOA symptoms.

Triplanar knee, hip, and trunk kinematics and kinetics were measured on both sides during the 6-minute walk test. Kinematic data were reduced to 101 points from heel strike (>20N) to ipsilateral heel strike to represent 0-100% of the gait cycle and kinetic data were reduced to 101 points from heel strike to ipsilateral toe off (<20N) to represent 0-100% of stance phase and normalized to mass (Nm/kg). Change scores were calculated by subtracting pre-gait from post-gait for each 1% of gait cycle (kinematics) or stance phase (kinetics) with 90% confidence intervals. Differences in change scores between groups were considered significant if the 90% confidence intervals did not overlap for three or more consecutive points and were reported as mean differences (MD) ± standard deviation.

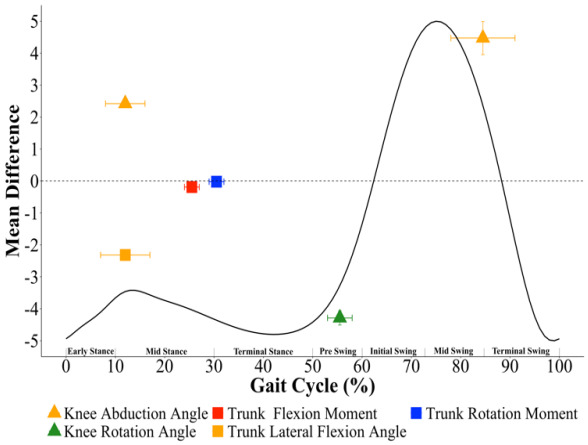


**Figure 1.** Mean differences for significant differences in gait kinematics (°) and kinetics (Nm/kg) change scores between IC and sham groups in the involved limb. Vertical error bars represent pooled standard deviations for mean differences and horizontal error bars represent duration across the gait cycle where 90% confidence intervals did not

**Results & Discussion:** The IC group demonstrated reduced knee valgus during early stance (2.42±0.1°) and swing (4.5±0.5°), and less knee external rotation (4.3±0.2°) during terminal stance in the involved limb. During mid-stance, the IC group demonstrated increased trunk lateral flexion (2.3±0.07°) towards the involved side, increased trunk extension moment (0.19±0.005Nm/kg), and reduced trunk rotation moment (0.02±0.001Nm/kg) towards the involved side compared to sham on the involved side (Figure 1). There were no other changes in gait in the involved side after a single session of IC. In the uninvolved limb, the IC group demonstrated increased hip external rotation moment (0.06±0.01Nm/kg) and trunk rotation moment towards the involved side (0.03±0.002Nm/kg) during early stance compared to the sham group. The IC group also demonstrated reduced vertical ground reaction force (0.25±0.04N/kg) on the uninvolved limb during mid stance compared to the sham group. There were no changes in kinematics in the uninvolved side after a single session of IC. These gait alterations, largely in the frontal and transverse planes, suggest that a single session of IC can improve the screw-home mechanism that is often dysfunctional in older adults with KOA [2]. These gait alterations could be due of improved quadriceps and hip abductor strength after IC [3]. Further, changes in gait mechanics in both the involved and uninvolved limbs, despite administering IC on the involved thigh, suggest a systemic effect of IC [4]. Thus, IC should continue to be investigated as a novel, passive, clinical intervention to improve function and mobility in older adults with symptomatic KOA.

**Significance:** A single session of IC alters gait kinematics and kinetics in both the involved and uninvolved limbs suggesting improvements in the dysfunctional screw home mechanism that is necessary for maintaining knee stability and managing joint loading. IC is a novel, passive treatment that presents a paradigm-shift in the clinical management of symptomatic KOA and can improve function and reduce disability in older adults with symptomatic KOA. In future work, IC could be used as a complementary treatment to physical therapy or strengthening sessions and could be administered over multiple sessions (chronically) to assess lasting effects on gait and function.

**Acknowledgments:** This study was funded by the Provost's Graduate Research Award through the Graduate College at the University of Illinois at Chicago.

**References:** [1] Cui A et al. (2020), *EClinicalMedicine*, 29; [2] Bytyqi D et al. (2014), *Int Orthop* 38; [3] Sudhir S et al. (2024), *J Musculoskelet Neuronal Interact.* 24(4). [4] Hyngstrom AS et al. (2020), *J Appl Physiol* 129(6).

# STIFF-KNEE GAIT IS ASSOCIATED WITH WALKING ENERGETICS AND FORWARD PROPULSION IN PERSONS WITH KNEE OSTEOARTHRITIS

Steven A. Garcia*, Doyin Ogundiran, Joy Itodo, Oiza Peters, Paige Perry, Kharma Foucher
[1] Department of Kinesiology and Nutrition, University of Illinois Chicago; Chicago, IL, USA,
*Corresponding author's email: stevenag@uic.edu

**Introduction:** Individuals with knee osteoarthritis (OA) experience significant disability including altered walking patterns and poor mobility [1]. Compared to age-matched controls, those with knee OA walk slower, walk less efficiently and expend more energy per distance walked [2]. Age-related declines in muscle strength and walking mechanics contribute to poor walking efficiency irrespective of OA [3]. However, OA may worsen these age-related gait and muscular impairments, which may underlie poorer mobility and walking efficiency compared to non-OA counterparts. For instance, those with knee OA walk with increased dynamic knee stiffness in early- and midstance [4]. During these gait phases, the knee supports and redistribute energy across the limb to facilitate push-off. Given that effective push-off is critical for mobility and walking efficiency, it is plausible that poor energy transfer from altered knee mechanics may play a role in reduced walking speeds and high energetic costs with OA. Nonetheless, it remains unclear how poor early stance knee mechanics are linked with impaired push-off mechanics and walking energetics in those with OA. Here, we evaluated associations between dynamic joint stiffness, propulsive mechanics (ankle/hip peak power generation, power redistribution ratios), and walking speed/energetics ($v02_{cost}$) in those with knee OA. We hypothesized 1) greater dynamic joint stiffness in early and midstance would be associated with poor propulsive mechanics (i.e., reduced joint powers and higher redistribution ratios), and 2) dynamic joint stiffness would explain additive variance in walking speed and walking energetics (unique from propulsive mechanics) in those with knee OA .

**Methods:** Twenty-four participants with knee osteoarthritis (Sex: 16F,8M, Age:56±9 yrs., Body Mass Index: 33.2±6.1 kg/m2) from a previous study completed treadmill biomechanical assessments and energetics during steady-state walking [5]. Treadmill biomechanics (marker sampling: 120Hz, force sampling: 2040 Hz) were collected at a preferred speed and $V02_{cost}$ (ml/kg*m) per unit distance was determined during a 2.5min steady state walk. For biomechanical measures, raw marker and force data were imported into Visual3D for standard Inverse Dynamics analyses and filtered at 6Hz using a fourth order lowpass Butterworth digital filter. Dynamic joint stiffness (Nm/kg*m) was calculated as the slope of the line-of-best-fit of the knee flexion angle-knee flexion moment plot during early and midstance (Fig. 1). Propulsive characteristics included the peak ankle and hip joint positive powers (W/kg). Redistribution ratios were quantified as the ratio of total positive hip to ankle work during stance phase (scale 0-2: 2 = propulsive work done by hip). The average of 10 steps for all biomechanical variables during treadmill walking was used for further analyses. Partial correlations controlling for sex were used to evaluate associations between dynamic joint stiffness metrics, $V02_{cost}$ and propulsive characteristics.

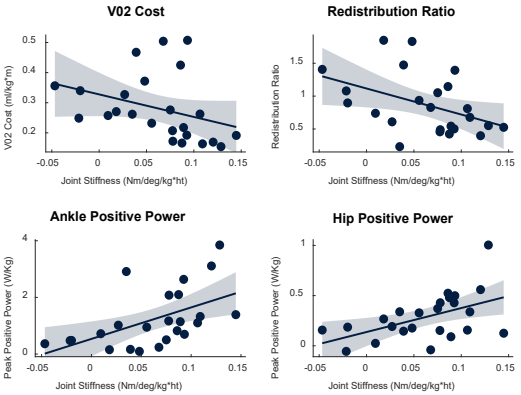


**Figure 1:** Scatter plots depicting associations between Stiffness, $V02_{cost}$ and propulsive characteristics. **Note**: Scatters are of non-transformed data for visualization. Spearman *rho* (covariate: sex) were used in analyses.

**Results & Discussion:** Age was not associated with any variable ($p > 0.05$) and was excluded as a covariate. Data were not normally distributed and thus Spearman's rho was utilized to evaluate associations controlling for sex. In the affected limb, we observed that greater dynamic knee stiffness in early stance was associated with faster walking speeds (*rho* = -0.55, $p<0.01$), lesser $V02_{cost}$ (*rho* = -0.57, $p<0.01$) and lesser redistribution ratio (*rho* = -0.50, $p=0.01$). We also observed that greater knee stiffness in early stance was associated with greater peak ankle (*rho* = 0.703, $p<0.01$) and hip (*rho* = 0.46, $p=0.027$) positive powers. No associations were observed between gait variables, walking speed and $V02_{cost}$ in the non-affected limb. Lastly, redistribution ratio was the primary predictor of walking speed ($\beta = -0.27$, $p < 0.01$) and $V02_{cost}$ ($\beta = 0.53$, $p < 0.01$) while early stance dynamic knee stiffness did not predict additional variance in either walking speed ($\Delta p = 0.11$) or $V02_{cost}$ ($\Delta p = 0.27$). Reduced walking speeds and greater energy expenditure with aging and knee OA are thought to stem from reduced ankle power and overreliance on the hip muscles for propulsion. However, hallmark OA gait features are typically observed in early stance often described as a "stiff-knee" pattern. Contrary to hypotheses, *greater* joint stiffness was linked with faster walking speeds, reduced $V02_{cost}$ and more favorable propulsion mechanics. However, knee stiffness was not uniquely associated with walking speed or $V02_{cost}$ over what was predicted by propulsive metrics. Adequate levels of joint stiffness are necessary for efficient shock absorption and energy transfer during gait while too little stiffness may represent unstable gait. We reason those walking slower with greater $V02_{cost}$ may exhibit a more unstable gait pattern in early stance evidenced by lesser dynamic stiffness.

**Significance:** Stiff-knee gait mechanics were associated with push-off mechanics in those with OA which may suggest that impaired knee function may contribute to mobility decline in those with knee OA. However, future work is needed to verify the relative impact of early stance gait alterations and impaired propulsive mechanics on reduced walk speeds and high energy costs of walking with OA.

**Acknowledgments:** University of Illinois, Chicago Center for Clinical and Translational Science Pilot Grant #UL1TR002003.

**References: [1]** Astephen, J.L., et al. J Orthop Res, 2008. [2] Waters R.L., et al. Clin Orthop Relat Res, 1987. [3] Boyer, K.A., et al., Exp Gerontol, 2023. [4] Zeni, J.A., Jr. and J.S. Higginson. Clin Biomech, 2009. [5] Foucher, K.C., et al. Clin Biomech, 2021.

# DETECTION OF TRANSLATIONAL PERTUBATIONS USING LOWER-LIMB KINEMATICS DURING LOCOMOTION

*Maria T. Tagliaferri[1], Leonardo Campeggi[1], Owen N. Beck[2], Inseung Kang[1]
[1]Department of Mechanical Engineering, Carnegie Mellon University, Pittsburgh, PA, 15213 USA.
[2] Department of Kinesiology and Health Education, The University of Texas at Austin, Austin, TX, 78712 USA.
*email: mtagliaf@cmu.edu

**Introduction:** Maintaining dynamic stability during locomotion requires both anticipatory and reactive neuromuscular control to counteract perturbations, reducing fall risk [1]. Interventions to improve walking balance, such as wearable robotic devices, show promise for fall prevention. However, their effectiveness is limited by the absence of a standardized metric for real-time perturbation detection. [2]. While whole-body angular momentum (WBAM) is commonly used to identify gait disturbances [3], its computational complexity and subject-dependent variability limit its practicality for exoskeleton control. In contrast, tracking deviations in lower-limb kinematic states provides a more efficient and responsive method for detecting walking perturbations. This study proposes a novel ground perturbation detection model that monitors 16 lower-limb kinematic states in a local coordinate system and identifies perturbation onset using a single threshold across subjects and perturbation types. The model's performance is evaluated in trip- and slip-type perturbations, as these are common causes of falls in aging gait. We hypothesize that a ground perturbation detector using lower-limb kinematic states will outperform a WBAM-based model through faster and more accurate detection. Our underlying rationale is that the kinematic states are highly sensitive to gait disturbances, allowing efficient and accurate tracking in real-time with minimal computation [4].

**Methods:** We analyzed an open-source gait biomechanics dataset to examine responses to ground translation perturbations during locomotion. The dataset included motion capture and WBAM data from able-bodied subjects undergoing 96 perturbation trials with varying directions and magnitudes. To track kinematic states, we monitored the relative position and velocity of the center of mass (COM) and feet within a local coordinate system to minimize global drift effects (Fig. 1A).

We quantified the instantaneous kinematic state variance, at time $i$, by computing deviations from steady-state mean ($\bar{x}$) and standard deviation ($\sigma$) using Eq. 1 and illustrated in Fig. 1B. We then introduced a cumulative stability deviation metric of all $n$ states, φ, to detect perturbations (Eq. 2).

$$\alpha_i = \begin{cases} 0, & \text{if } |\bar{x}_i - x_i| \le 2\sigma_i, \\ x_i - (\bar{x}_i \pm 2\sigma_i), & \text{otherwise.} \end{cases} \quad (1)$$

$$\varphi_i = \frac{1}{n}\sum_{j=1}^{n} \frac{\alpha_i}{2\frac{\sigma_i}{\bar{x}_i} + \alpha_i} \quad (2)$$

A parameter sweep using the open-source dataset optimized the detection threshold for φ, balancing accuracy and detection delay. To benchmark performance, we implemented a standard perturbation detection model using WBAM and compared its accuracy to our method. Additionally, a pilot human-subject experiment exposed five participants to controlled trip- and slip-type perturbations on a split-belt treadmill. Motion capture and force plate data were processed to compute φ in pseudo real-time, enabling perturbation detection and response analysis.

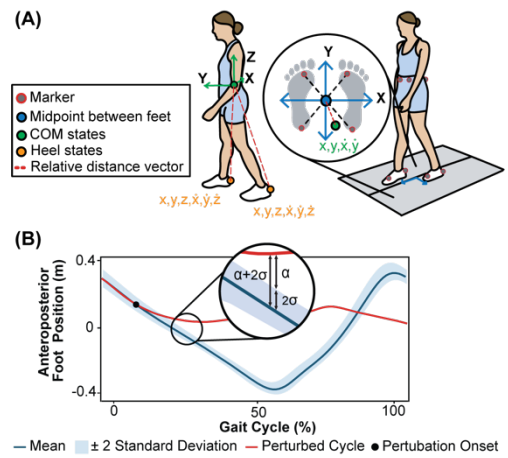


**Figure 1**. (A) Kinematic state-based perturbation detection tracked the relative distance between the COM and each foot. Eight position and eight velocity states were monitored. A local coordinate system was set at the midpoint between the feet in the horizontal plane, projecting the COM position into it. Vectors (red dashed lines) tracked the relative distance over time. (B) Visual representation of state variance calculation. α is the Euclidean distance between the current state value and the edge of 2 standard deviations (σ) from the mean.

**Results & Discussion:** On pilot experimental data, our model classified perturbed and unperturbed gait cycles with 98.8% accuracy and detected perturbations within 23.1% of the gait cycle following perturbation onset. Compared to the WBAM-based baseline, our model exhibited a 46.8% higher accuracy, albeit with an 11.11% longer detection delay (not including computational time). However, given the average stride duration of 1006.9 ms for pilot participants, our model's 231 ms detection time is faster than the average time it takes for an older adult to perform a corrective step in response to perturbations [5].

To improve real-time capabilities, future work will focus on deploying the model with wearable IMU sensors and reducing the required gait cycles for nominal state determination. Expanding evaluations under diverse perturbation conditions and subject demographics will improve model generalizability, particularly for older adults, whose prolonged reaction times may benefit even more from our method compared to healthy young adults.

**Significance:** This study presents a novel kinematic state-based perturbation detection model that outperforms existing WBAM-based methods in accuracy while maintaining real-time feasibility. By leveraging deviations from steady-state gait dynamics, our approach enables fast and reliable detection of gait perturbations, which is critical for applications in fall prevention and balance augmentation. The ability to generalize across datasets without extensive user-specific tuning suggests potential for widespread deployment in clinical rehabilitation settings [3]. Moreover, our findings provide a foundation for future research in adaptive exoskeleton control, ultimately enhancing mobility and safety for individuals at risk of falls, including older adults and individuals with neuromotor impairments.

**References:** [1] Bruijn *et al*., *J R Soc Interface*, 2013; [2] Leestma *et al*., *IEEE Robot Autom Lett*, 2024; [3] Shokouhi *et al*. *Sci Rep*, 2024; [4] Jiang et al., *Hum Mov Sci*, 2014; [5] Lim *et al.,* J Kor Phys Ther, 2021.

# AGE-RELATED DIFFERENCES IN THE STEP-TO-STEP CONTROL OF FOOT PLACEMENT DURING PROLONGED WALKING

Ethan Simaitis[1*], Yujin Kwon[2], and Jason R. Franz[1]
[1] Lampe Joint Department of Biomedical Engineering, UNC Chapel Hill & NC State University, Chapel Hill, NC, USA,
[2] Department of Rehabilitation Medicine, Seoul National University Hospital, Seoul, South Korea
*Corresponding author's email: simaitis@email.unc.edu

**Introduction:** Older adults are more susceptible to muscle fatigue than younger adults, which has the potential not only to reduce walking endurance, but also to compromise muscle force responsiveness and thereby walking stability. Indeed, our research group recently discovered that walking-related fatigue precipitates increased vulnerability to balance perturbations [1]. However, age-related differences in the underlying adaptations that take place during prolonged walking and may predispose to walking instability remain largely unknown. Analytical approaches designed to quantify the control of step-to-step walking dynamics can provide valuable insight into these adaptations, helping to reveal how the nervous and muscular systems interact to regulate locomotor control. The purpose of this study was to quantify the neuromuscular adaptations in foot placement control that occur over time and how these adaptations differ between younger and older adults. We hypothesized that step-to-step changes in step length and step width would become less tightly regulated over time, with more pronounced effects in older than in younger adults.

**Methods:** We recruited 15 younger (YA; age: 24.5±4.6 yrs) and 15 older (OA; age: 73.3±4.9 yrs) adults to participate in this study. Each participant's preferred walking speed was determined by averaging the time taken to traverse a 30-meter walkway across three trials, measured using timing gates (YA: 1.34±0.11 m/s vs. OA: 1.20 ± 0.20 m/s; p=0.105). Participants walked at their preferred walking speed for 5 minutes as a warm-up. Participants then performed a 30-minute walking task at the same speed. Kinematic data of the pelvis and lower extremities collected using 3D motion capture were used to calculate time series of step widths (SW) and step lengths (SL). Step-to-step correlations for both step width and step length were analyzed using a 1$^{st}$-order detrended fluctuation analysis (DFA). A two-way repeated-measures ANOVA evaluated the effects of age (younger, older) and time (six, 5-minute bins) on DFA scaling exponents (α). To further investigate whether the effects of time differed by age group, we performed separate one-way repeated-measures ANOVAs for younger and older adults. Post-hoc pairwise comparisons were conducted to explore trends observed in the main analysis and identify the specific time points in which they occurred.

**Results & Discussion:** Figure 1 A/B summarize DFA α values for SW and SL over time, respectively. Across age groups, we found a significant main effect of time for $\alpha_{SW}$ (p=0.026) but not for $\alpha_{SL}$ (p=0.470). Pairwise comparisons revealed that this was driven by a statistical trend toward decreased $\alpha_{SW}$ from the first to the second time bin (p=0.077). Upon further analysis, age-specific ANOVAs revealed that this pairwise statistical trend was evident only in younger adults (YA: p=0.059, OA: p=0.616). Figure 1 C/D summarize group-average differences in SW and SL across time, respectively. Partially consistent with the timing of differences in DFA α values, pairwise comparisons revealed significant decreases in SW and increases in SL only in younger adults and only across earlier time bins. Taken together, our results suggest that younger but not older adults relaxed their step-to-step regulation (i.e., temporal persistence) of SW while adopting narrower and longer steps as walking duration increases. Conversely, given their relatively invariant step kinematics and step-to-step control across time, older adults appear not to have the same capacity for such adjustments. We posit that such adjustments may depend on having reliable sensory feedback, muscle force responsiveness, and/or balance confidence, all of which may have been diminished for our older adults. As a potentially complimentary explanation, we were surprised to find a significant main effect of age revealing narrower SW across all time bins for older than for younger adults (Fig. 1C). Narrower steps may introduce a biomechanical constraint on the extent to which walking adaptations may be deployed.

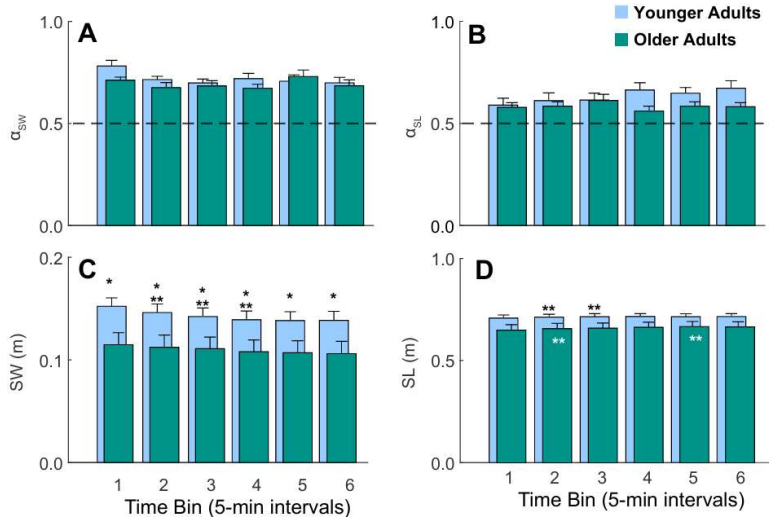


**Figure 1:** (A/B) Detrended fluctuation analysis results. We interpreted these scaling exponents as α > 0.5 indicating that deviations in one direction are likely to be followed by deviations in the same direction (i.e., persistent). (C/D) Step width and step length results. Single asterisk (*) indicates a significant difference between old and young adults, and double asterisks (**) indicates a significant difference from the previous time bin (p < 0.5). Time bins represent successive 5-minute intervals, covering a total of 30 minutes.

**Significance:** Collectively, our findings suggest that older adults may have a limited capacity for adaptive gait adjustments which could increase their vulnerability to instability in the context of walking-related fatigue.

**Acknowledgments:** This work was supported by the Korea Health Technology R&D Project through the Korea Health Industry Development Institute (KHIDI), funded by the Ministry of Health and Welfare, Republic of Korea (grant number: HI19C1095), and by the US National Institutes of Health (R01AG058615).

**References:** [1] Kwon et al. (2023) *J Electromyogr Kinesiol*.

# A CLOSER LOOK AT THUMB FORCE MEASUREMENT: ARE CLINICAL TOOLS OVERLOOKING KEY DETAILS?

*Ryan Harth[1], Adam Chrzan[1], and *Tamara Reid Bush[1]
[1]Department of Mechanical Engineering, Michigan State University, East Lansing MI, USA
*Corresponding authors' emails: harthrya@msu.edu, reidtama@msu.edu

**Introduction:** Roughly 40% of adults over the age of 55 are experiencing thumb osteoarthritis (OA) [1]. For many people, OA can cause joint pain, swelling, thumb weakness, and disability in tasks of daily living [1,2]. In order to reduce these ailments, surgery has been shown to effectively reduce pain [3]. Currently, both pre and post-surgery, therapists use simple tools to assess the strength of the thumb [4], however these methods do not isolate the thumb. The inability to capture forces specific to the thumb has made it difficult to quantify changes in function that result from treatment or therapy. The goal of this study was to compare three currently used clinical tools with 1) a research device and 2) a new tool that has the potential for translation to the clinic. It was hypothesized that the measurements from the clinical tools would differ from both the research device and the new tool, but that the measures between the research device and new tool would be the same.

**Methods:** 6 healthy participants (3 male, 3 female) completed all tests. There were three groups of devices for these experiments; the current clinical tools which include the pinch gauge (used for tip and key postures) and dynamometer (Fig. 1), the research tool (thumb force isolator (TFI)) and the new tool (the simplified thumb force isolator (STFI)). The TFI (Fig. 2a) was developed in the lab to isolate the forces of the thumb from the other fingers. However, this device was large, had an expensive 6-axis force transducer, was difficult to use and required a connection to a computer with specialized software. This led to the development of a simpler tool, much more likely to be translated into the clinic for use (Fig. 2b,c). The STFI also had the ability to isolate thumb forces like the TFI, but was more compact, had a single axis load cell, was inexpensive, simple to use and did not require a computer or specialized software.

Participants were asked to complete three trials of push and three trials of pull with the TFI and the STFI. The maximum force from each set of three trials was recorded. Participants were also asked to complete three trials of each the tip pinch, key pinch, and grip strength, and again, the maximum was selected.

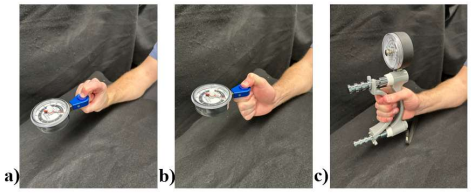


**Figure 1:** Current clinical tools, a) tip pinch, b) key pinch, c) grip strength.

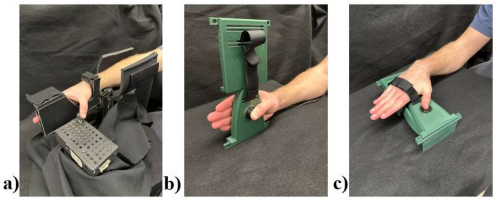


**Figure 2:** Demonstration of the TFI (a) and STFI (b&c) in use for both testing positions. a) TFI in pull position, b) STFI pull position which is similar to grabbing a book off the shelf without the use of other fingers, c) STFI push position which is similar to typing on a keyboard.

**Table 1:** Average force in each of the positions tested across all participants. The current clinical measures are green and the TFI and STFI in blue. *Significantly different from all clinical measurements ($p<0.05$), **significantly different from grip strength and key pinch ($p<0.05$).

| Position | Average Force (Standard Deviation) (Newtons) |
|---|---|
| Grip Strength | 364.75 (52.5) |
| Key Pinch | 88.61 (17.8) |
| Tip Pinch | 37.32 (9.1) |
| STFI Pull** | 40.06 (18.5) |
| TFI Pull** | 37.72 (10.4) |
| STFI Push* | 15.66 (6.0) |
| TFI Push* | 19.34 (4.8) |

**Results & Discussion:** Overall, the STFI was able to replicate the forces of the equivalent thumb tests from the more complex TFI and data were not significantly different between the pull tests or between the push tests ($p>0.05$). In terms of clinical measures, the grip strength values were much higher than all other data sets (Table 1). This was because grip strength utilized all of the other fingers. Additionally, patients can complete the measurement without even using their thumb. The key pinch force measurement was higher than the values for the STFI and TFI as well due to the increased leverage from the rest of the hand. With the tip pinch, while the values were similar to the values of the STFI and TFI, it is difficult to isolate whether the limiting factor in the measurement is the thumb or the index finger. Both the TFI and STFI successfully quantified the force generated by the thumb in the push and pull motions. However, the STFI's compact design coupled with the fact it is simple to use and inexpensive, means it has strong potential to be easily translatable into the clinic and will add to the understanding of thumb function.

**Significance:** The need to quantify thumb function, particularly force abilities, is important to physical therapists, clinicians, and patients; this permits them to track their improvements before and after surgery, therapy or other treatments. There is no clinically available tool that is capable of measuring isolated thumb forces. Isolated force measurements and this new tool have significant potential to help bolster the understanding of the recovery process for people struggling with thumb OA and improve overall care for patients. The STFI was designed to be used in a similar manor to current clinical tools to make the process easy for physical therapists and clinicians to understand and implement into their testing routine. The STFI also has the ability to record a time trace of force allowing the care teams to see how force generation changes with time along with the maximum force throughout treatment. In the future, the device will also be able to interface with the medical records to upload data directly to a patient's folder for easier comparison between visits.

**Acknowledgments:** Corewell Health-Michigan State University Alliance Grant supported portions of this research.

**References:** [1] Teunissen J., et al., Osteo & Cart, 30(4): 578-585, 2022 [2] Anakwe R., et al., BMJ, 343(7834): 1160-1167, 2011 [3] Grobet, C., et al., JHS, 47(5): 445-453, 2022 [4] Villafañe J., et al., J Man and Phys Ther, 35(2): 110-120, 2012.

# CHANGES IN AN IMU-DERIVED METRIC OF JOINT POWER AFTER A BOUT OF ACTIVITY

*Fany Alvarado, Millissia A. Murro, Nancy Nguyen, Mayumi Wagatsuma, Grace Kellaher, Jeremy Crenshaw, Jocelyn F. Hafer
Department of Kinesiology and Applied Physiology and Biomechanics and Movement Science Program, University of Delaware
*Corresponding author's email: fany@udel.edu

**Introduction:** Joint powers provide insight into the biomechanics of the lower extremities, and they can be altered due to changes in gait speed [1], aging [2], pathology [3], or in response to a bout of activity [4]. Typically, joint powers can only be measured in lab settings with motion capture technology and force plates. However, gait differs when measured in a lab vs. in the real-world, so a method to estimate or track changes in joint powers outside the lab is needed. We previously showed that inertial measurement unit (IMU) derived metrics track with joint powers across subjects walking at different speeds [5-6]. IMUs cannot directly measure joint powers, but angular velocity is a component of power that can be directly captured from IMUs. To use this method confidently to track changes in joint powers outside the lab, we must test whether these IMU-derived metrics can detect within-individual changes in joint powers. Previous work demonstrated that joint powers at the hip, knee, and ankle decreased in response to a bout of activity (repeated squats) [4]. Whether an IMU metric of joint power would change similarly in response to activity is unknown. Therefore, the purpose of this study was to investigate whether an IMU-derived metric of joint power changed in response to a 34-minute walk.

**Methods:** Eight healthy older adults (64.6 ±3.8years; 6F/2M) walked on an instrumented treadmill for 34 minutes. Seven IMUs (Opal v2, APDM, Clario) were placed on the sacrum, thigh, shank, and feet. All participants walked for 34 minutes at a self-selected walking speed (1.4±0.1 m/s) with three challenge periods during which the walking speed increased by 50% for one minute. The first and last 4 minutes of the 34-minute walk were selected for analysis. IMU angular velocity data about medial-lateral segment axes were computed using a functional sensor-to-segment orientation method [7]. Gait events were identified using a continuous wavelet transform. Foot trajectories were computed using a zero-velocity update algorithm [8]. Thresholds were used to select single strides by eliminating strides <1m or >2m in length. Peak segment angular velocities about the medial-lateral axis of the thigh, shank, and foot were detected. Outcome variables included peak shank angular velocity during early stance (5-25% stance, to track negative knee joint power), and peak hip and foot angular velocities during the second half of stance (50-100% stance, to track propulsive hip and ankle powers, respectively). A paired samples t-test was used to determine whether each IMU metric changed in response to the 34-minute walk ($p<0.05$).

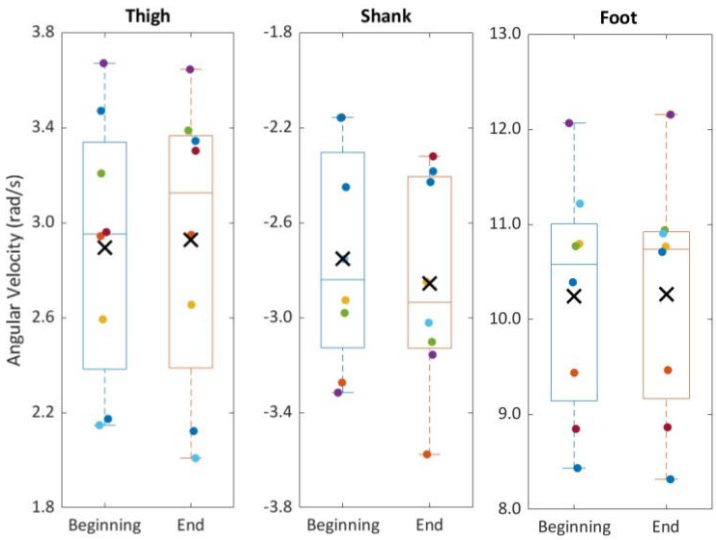


**Figure 1:** Boxplot comparing average angular velocity for each participant from the beginning to the end of the walk. The x represents the group means.

**Results & Discussion:** Thigh, shank, and foot angular velocities did not change in response to a 34-minute walk (thigh: beginning 2.9±0.5 rad/s vs. end 2.9±0.6 rad/s, $p=0.13$; shank: beginning -2.8±0.4 rad/s vs end -2.9±0.4, $p=0.61$; foot: beginning 10.2±1.2 vs. end 10.3±1.2, $p=0.77$; Figure 1). This suggests that hip, knee, and ankle joint powers were similar at the beginning and end of the walk. Our results may indicate that the walking activity was not sufficient to induce changes in joint powers where a previous study's squatting protocol was [4]. Additionally, our healthy older adult population may have been more active than the healthy young adults in Zhang et al. [4], whose exclusion criteria included those who performed regular activity. Other data, such as strength, rate of perceived exertion (RPE), and kinetics that we have yet to analyze could help explain the current results and provide more insight into why angular velocities remained unchanged after a 34-minute walk. Examining whether there were changes in knee extensor strength or gait kinetics from the beginning to the end of the walk will help us determine whether these IMU metrics accurately track joint powers over time.

**Significance:** This study aimed to investigate the ability of an IMU-derived power metric to detect changes in joint power after a bout of activity. Our findings suggest thigh, shank, and foot angular velocities - and thus potentially hip, knee, and ankle joint powers - did not change after a 34-minute walk. Additional studies with procedures that definitively alter gait kinetics will be necessary to better determine whether these IMU metrics are able to detect meaningful changes in joint powers.

**Acknowledgments:** Work supported by NIGMS/NIH grant U54-GM104941.

**References:** [1] Winter (1983), *Clin Orthop Rela Res* 147(175); [2] DeVita & Hortobagyi (2000), *J Appl. Physiol* 1804-1811(88); [3] McGibbon (2002), *J Rheumatol* 2410-2419(29); [4] Zhang et al., (2022), *J EM* 1365-1374(9); [5] Hafer (2020), *J Biomech* 106; [6] Alvarado (2023) *ASB*; [7] Mihy et al., medRxiv 2022.11.29.22282894; [8] Rebula (2013), *Gait Posture* 974-980(38)

# EXPLORING A STICK DROP PARADIGM WITH A SMARTPHONE APP FOR REACTION TME TESTING

*Shores, CMV[1], Redfern, MS[1], McNeish, BL[2]
[1]Department of Bioengineering, University of Pittsburgh
[2]Departement of Physical Medicine and Rehabilitation, University of Pittsburgh
*Corresponding author's email: CMS402@pitt.edu

**Introduction:** Simple reaction time (SRT) is a fundamental measure of cognitive and motor function. Beyond average response time, intra-individual simple reaction time variability (IIRV) has emerged as a biomarker for neurological integrity [1]. IIRV has been linked to sustained attention, impulsivity, and cognitive conditions such as attention deficit hyperactivity disorder, chemotherapy associated cognitive dysfunction, dementia, Parkinson's disease, and motor dysfunctions like falls and sarcopenia [2]. As a result, IIRV is a promising non-invasive measure for monitoring cognitive and motor health. However, accurate SRT measurement typically requires specialized equipment, limiting clinical accessibility.

The ReactStick (RS), a validated drop-and-catch device with millisecond precision using a 1000 Hz accelerometer, addresses this clinical need [3]. The ReacStick's stick drop paradigm offers significant advantages over computer paradigms but, it is costly, fragile, and impractical outside research settings due to its reliance on trained examiners and manual data recording. To overcome these limitations, we developed ComplexCortex (CC), an iPhone app leveraging the phone's built-in 100 Hz accelerometer to measure SRT. While smartphones offer accessibility and computational power for scalable assessments, their lower sampling rate may reduce precision. We hypothesize that CC will produce comparable trial-to-trial variability to RS but with greater mean reaction times due to hardware limitations.

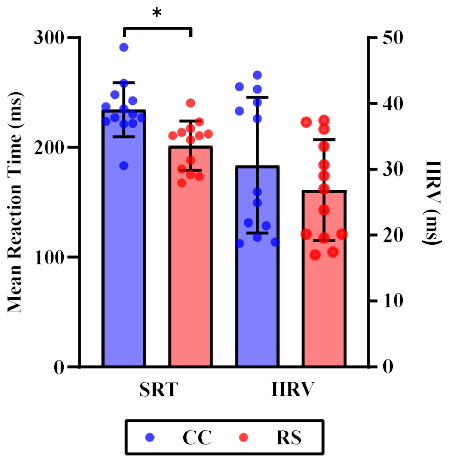


**Figure 1:** The comparison of CC (blue) and RS (red), between SRT and IIRV. Mean SRT is significantly different ($p < 0.05$) for n=6 participants. IIRV has no statistical difference for n = 11 participants

**Methods:** Participants in this ongoing trial include healthy older females (n = 10, Age = 68.7 ± 3.9) and chemotherapy treated breast cancer survivors (n = 3, Age = 75.7 ± 3.68) without reported cognitive dysfunction. This study focuses on simple mode testing, in which participants sit at a desk with their hand positioned in a pinch grip, hanging off the edge. In the RS protocol, an examiner drops the device at randomized 2–5 second intervals across 12 trials (2 practice, 10 data collection). The CC protocol mirrors this procedure but replaces the RS with an extended selfie stick and a smartphone, with detection occurring through the app. To assess normality, a Kolmogorov-Smirnov test was utilized. A paired t-test compared mean reaction times between RS and CC, while Bartlett's test assessed differences in IIRV. Statistical analysis was conducted using MATLAB.

**Results & Discussion:** Paired t-tests revealed significant differences in mean reaction times between the smartphone app and RS for some participants (n = 6, $p < 0.05$) (Fig. 1). However, Bartlett's test indicated no significant differences in IIRV for most participants (n = 11, $p > 0.05$) (Fig. 1). On average, the CC mean time was 32.84ms higher than RS. Similarly, the average CC IIRV time was 3.75ms higher than RS. These differences likely stem from the smartphone's lower accelerometer sampling rate and processing latency, as well as potential variations in device handling, grip force, or drop dynamics, which will be the subject of future studies. This study demonstrates the early feasibility of using mobile applications with a smartphone to measure IIRV but not mean SRT.

**Significance:** These findings are significant as they support further research into the reliability and validation of CC's ability to measure IIRV and mean simple reaction time. Specifically, this work will drive future studies evaluating the psychometric properties of CC in healthy, aging, and clinical populations, allowing for continuous refinement of the mobile application's code. This adaptability is a key advantage over other devices, which may lack the flexibility for customization and improvement. While other mobile applications can assess simple reaction time using screen tapping, the stick-drop paradigm is particularly engaging for older adults, addressing motivation and effort limitations often seen in clinical testing. Given IIRV's potential as a biomarker for cognitive function and motor control, CC could enable large-scale, real-time monitoring in clinical settings without requiring expensive or specialized equipment. Additionally, its capability for at-home testing with results synced to care providers could significantly reduce clinical burden while improving accessibility and continuity of care.

**Acknowledgments:** The work was supported in part by P30AG02482 from University of Pittsburgh Claude D. Pepper Older Americans Independence Center to BLM.

**References:** [1] Jayakody et al. (2021), *Gait Posture* 89; [2] Graveson et al. (2016), *Gerontol Ser B* 71(5). [3] Eckner et al. (2012), *Psychol Assess* 24 (1).

# AGING-RELATED CHANGES IN REGULATION OF BRAIN-HEART COHERENCE DURING DUAL TASKING

Kübra Akbaş[1], Kelsi Petrillo[1], Hossein Ehsani[1], *Nima Toosizadeh[1]
[1]Department of Rehabilitation and Movement Sciences, School of Health Professions, Rutgers University
*Corresponding author's email: nima.toosizadeh@rutgers.edu

**Introduction:** The aging process affects and contributes to the declination of physiological performance in the human body, as well as the regulation and synchronization of these systems, leading to impairments in motor function, cardiac autonomic control, and cognition [1]. While deficits in the motor, cardiac, and brain systems have been studied individually, the effect of aging on their interconnection is not well understood. There has been recent interest in brain-heart interactions [2] and, among brain imaging modalities, functional near-infrared spectroscopy (fNIRS) is novel and feasible for dynamic tasks. Here, we aim to investigate aging-related differences in the coherence between fNIRS and heart rate (HR) response to dual tasking and draw insights on the dysregulation of brain-heart interactions; as an exploratory goal, we will also consider the effect of mild cognitive impairment (MCI) on fNIRS-HR coherence, as compared to cognitively healthy older adults. For the current study we will implement a previously developed upper-extremity function (UEF) test with dual tasking to assess cognitive impairment, where the test involved rapid elbow flexion and backwards counting [3].

**Methods:** Young controls (18-30 years) and older adults (≥60 years) were voluntarily recruited for this study. Participants sat still with no interaction or movement for a baseline rest of 3 minutes, then performed a 3-minute dual task comprising arm flexion and counting backwards by threes. HR was obtained from a wearable two-lead ECG sensor (360° eMotion Faros) attached to the left side of the chest. Brain activity was measured using an fNIRS system (Artinis Brite) with 22 channels on the frontal and parietal lobes. fNIRS data were motion-corrected and low-pass filtered, and HR data were smoothed using a moving average filter; both fNIRS and HR were resampled to 1 Hz. Coherence was determined by calculating the time-varying wavelet coherence [4] between the fNIRS and HR signals, then averaging the values within a 0.05-0.12 Hz frequency band; this frequency band was selected based on the coherence plots of all participants' channels and is a more conservative range of the blood-oxygen-level-dependent (BOLD) signal frequency [5]. Coherence was then averaged across all 22 channels, as well as channels corresponding to six brain regions: primary sensory, visual motor, motor, anterior prefrontal cortex (PFC), front eye fields, and dorsolateral PFC.

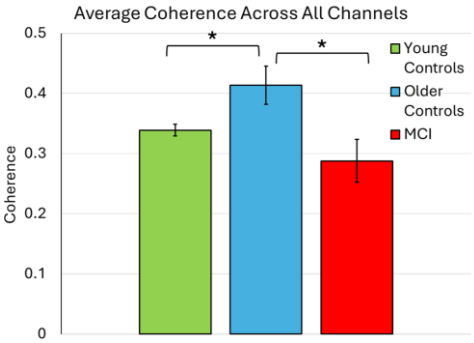


**Figure 1:** Coherence averaged across all 22 channels for young controls, older controls, and older adults with MCI. Error bars represent standard error.

**Results & Discussion:** This study included 22 young controls (age = 25.5 ± 2.6 years) and 11 older adults—8 cognitively healthy older controls (age = 68.3 ± 3.6 years) and 3 older adults with MCI (age = 72 ± 1.5 years). Older adults were separated based on their MoCA assessment, with 24 used as the delineating score. The fNIRS-HR coherence averaged across all 22 fNIRS channels, as well as all six brain regions, presented significant differences between the young and older controls ($p<0.0412$, Fig. 1, Table 1). Interestingly, the young controls presented lower coherence than the older controls, indicating reduced synchronization between the brain and cardiac systems, which could be attributed to the inherent chaos and complexity in healthy physiological signals [1]. Additionally, in agreement with previous research showing increased brain activity with aging in dual tasking [6], increased coherence in the older adult group may be a form of compensatory mechanism, where the body synchronizes the brain and cardiac systems to better allocate resources for the increased demand of the dual task. Lastly, the average across all 22 channels, primary sensory, front eye fields, and dorsolateral PFC brain regions were found to be significantly different between the cognitively healthy older adults and older adults with MCI ($p<0.0135$, Fig. 1). Although there were too few MCI participants, this trend of reduced coherence in older adults with MCI raises an interesting question regarding the effect of cognitive ability on the brain-heart interconnection, which should be investigated in the future research.

**Table 1:** Average ± Standard Deviation Coherence Values for Different Brain Regions Between Participant Groups

| Group | Average Across All Channels | Primary Sensory | Visual Motor | Motor | Anterior Prefrontal Cortex | Front Eye Fields | Dorsolateral Prefrontal Cortex |
|---|---|---|---|---|---|---|---|
| YC | 0.339 ± 0.044 | 0.336 ± 0.040 | 0.345 ± 0.043 | 0.346 ± 0.060 | 0.342 ± 0.073 | 0.335 ± 0.053 | 0.318 ± 0.060 |
| OA | 0.414 ± 0.089 | 0.408 ± 0.084 | 0.419 ± 0.120 | 0.402 ± 0.092 | 0.405 ± 0.101 | 0.426 ± 0.092 | 0.450 ± 0.060 |
| OA with MCI | 0.288 ± 0.062 | 0.286 ± 0.049 | 0.268 ± 0.006 | 0.260 ± 0.068 | 0.326 ± 0.137 | 0.272 ± 0.051 | 0.287 ± 0.055 |
| YC vs. OA *p*-value (Cohen's d) | **0.0045*** (0.381) | **0.0020*** (0.407) | **0.0088*** (0.372) | **0.0331*** (0.208) | **0.0412*** (0.188) | **0.0054*** (0.380) | **0.0002*** (0.504) |

*$p<0.05$; YC: Young Control; OA: Older Adults; MCI: Mild Cognitive Impairment

**Significance:** The results of this study can be used to better understand how the brain-heart interaction is affected by age and provides insight into screening methods for the effects of aging and potential cognitive deficits. Additionally, fNIRS measurements may provide a simpler solution for capturing abnormalities in brain functions and networks, making it widely applicable for future studies.

**Acknowledgments:** This project was supported by one award from the National Institute on Aging (NIA/NIH-1R01AG076774-01A1) and one award from the National Science Foundation (NSF 2236689 - CAREER).

**References:** [1] Lipsitz (2002), *J Gerontol A Biol Sci Med Sci* 57(3): p.B115-B125. [2] Piper et al. (2014), *New J Phys*, *16*(11): p.115012. [3] Ehsani et al. (2019) *Clin Interv Aging* 14: p.659-669. [4] Cui et al. (2012), *Neuroimage* 59(3): p.2430-2437. [5] Zheng et al. (2021), *Sci Rep* 11(1): p.12042. [6] Ohsugi et al. (2013), *BMC neuroscience* 14: p.1-9.

# WHEN GAIT MATTERS: STEP LENGTH VARIABILITY MAY BE A STRONGER PREDICTOR OF COGNITIVE STATUS THAN STEP WIDTH OR WALKING SPEED RESERVE

Breanna R Morales[1], Jack P Manning[1], Jennifer M Yentes[1]
[1] Department of Kinesiology and Sport Management, Texas A&M University, College Station, TX
email: bmorales7@tamu.edu

**Introduction:** Mobility impairments, particularly changes in gait, have been linked to cognitive decline and neurodegenerative diseases [1,2]. While slow walking speed is a well-established predictor of morbidity and mortality [3], less is known about the role of walking speed reserve (WSR). WSR is the difference between maximal and preferred walking speed and may serve as a potential marker of cognitive function. Also, gait variability, particularly in step length and step width, may reflect underlying neural control mechanisms associated with cognitive health. Higher variability in these parameters has been linked to impaired motor control and cognitive decline in aging populations [4]. While cognitive decline is often associated with aging, factors such as higher physical activity levels, better sleep quality, and overall health may help preserve cognitive function and reduce the risk of impairment [5]. This study aimed to determine whether WSR, step length variability, step width variability, age, sleep quality, and physical activity are significant predictors of cognitive status, assessed via the Montreal Cognitive Assessment (MoCA). Identifying such predictors could enhance early detection of cognitive impairment and provide insight into the motor-cognitive relationship.

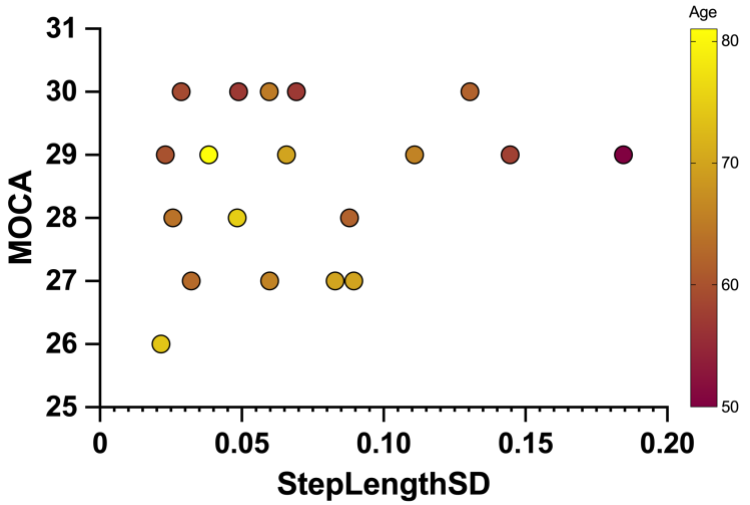


**Figure 1: Figure 1:** Scatterplot depicting the relationship between step length SD and MoCA scores. Higher step length SD is associated with worse cognitive status or lower MoCA scores. Color intensity represents age, with darker colors indicating younger participants.

**Methods:** Nine middle-aged adults (59.2±4.1 years; 3 male) and seven older adults (70.8±5.2 years; 4 male) participated in this study. Cognitive status was assessed using the MoCA. Sleep quality and physical activity were evaluated using the Pittsburgh Sleep Quality Index and the International Physical Activity Questionnaire, respectively. Preferred walking speed was determined on a treadmill. Maximal walking speed was determined by increasing treadmill speed from preferred speed in increments of 0.4 m/s every 30 seconds until participants exhibited a flight phase. WSR was calculated as the difference between maximal and preferred walking speeds. Step length and step width average, standard deviation (SD), and coefficient of variation (CV) were calculated from both right and left steps for the entire walking bout. Two multiple linear regression models were used to predict MoCA scores. Model one used the predictors of average, standard deviation, and coefficient of variation of step length, and the second model used step width. Both models included WSR, age, sleep quality, and physical activity as additional predictors.

**Results & Discussion**: A multiple linear regression assessed predictors of MoCA scores. The step length model explained 56.9% of variance ($R^2 = 0.569$, $F(7, 11) = 2.07$, $p = 0.135$). Step length variability, both SD and CV, were significant predictors, with step length SD ($\beta = -4.19$, $p = 0.025$) and step length CV ($\beta = +3.77$, $p = 0.025$) strongly associated with MoCA. As shown in Figure 1, lower step length SD was associated with better cognitive status (i.e., higher MoCA scores), reinforcing its potential as a marker of cognitive function. The differential relationship of SD and CV with MoCA scores suggests that absolute variability (i.e., SD) may be more strongly linked to cognitive status than relative variability (i.e., CV). Age also significantly predicted MoCA ($\beta = -0.69$, $p = 0.031$), while WSR, step length average, sleep quality, and physical activity were non-significant. The step width model explained 41.0% of MoCA variance ($R^2 = 0.410$, $F(7, 11) = 1.09$, $p = 0.430$), with no significant predictors. These results suggest that variability-based measures may be more sensitive predictors of cognitive status than average measures, with step length variability emerging as a stronger predictor than step width variability. This reinforces its potential as a marker of cognitive decline. Notably, physical activity and sleep quality were not significant predictors, suggesting that gait variability may reflect cognitive status independently of these factors.

**Significance:** Step length variability emerged as a significant predictor of cognitive status, suggesting its potential as a marker for cognitive decline. In contrast, step width variability, WSR, sleep quality, and physical activity did not reach significance, which may be partly due to limited sample size or the possibility that these measures were less sensitive to early cognitive changes in this cohort. These findings support further investigation of step length variability as a non-invasive biomarker for cognitive decline, while highlighting the need for larger studies or different measurement approaches to clarify the roles of step width, WSR, sleep quality, and physical activity.

**Acknowledgments:** Funding for this project was provided by a Texas A&M University College of Education and Human Development R3 award.

**References:** [1] Verghese et al., 2007 *JNNP, 929-935* [2] Muir et.al 2011 *Gait and Posture, 96-100* [3] Studenski et.al 2011 *JAMA* [4] Byun et al., 2023 *Alzheimer's Research & Therapy, 15* [5] Falck et.al 2018 *Journal of Alzheimer's Disease, 63*

# ASSESSING AGE-RELATED ALTERATIONS IN BRAIN CONNECTIVITY USING DUAL TASKING

Kelsi Petrillo[1], Hossein Ehsani[1], Kubra Akbas[1], *Nima Toosizadeh[1,2,3]
[1] Department of Rehabilitation and Movement Sciences, School of Health Professions, Rutgers University
[2] Department of Neurology, Rutgers Health, Rutgers University
3 Brain Health Institute, Rutgers University
*Corresponding author's email: nt496@shp.rutgers.edu

**Introduction:** The global proportion of older adults (age>65) is increasing and expected to reach 16% by 2050 [1]. Aging causes both structural and functional changes in the brain. A robust understanding of changes during healthy aging is critical for improved identification of diseases associated with aging, such as dementia [2]. Functional near-infrared spectroscopy (fNIRS) is a neuroimaging technique that measures changes in brain activity via cerebral blood flow. Functional connectivity measures the correlation of neural activation between structures that are not anatomically connected. Previous fNIRS work identified reduced resting-state cerebral activity and connectivity in the prefrontal cortex due to aging [2]. We previously developed an upper extremity function (UEF) dual task, which may be used for screening diseases such as dementia [3]. Motor outcomes from the UEF dual task, such as variability and complexity, have been shown to be different in groups of older adults with varying cognitive function [3-4]. The current study aimed to identify changes in brain activity and functional connectivity due to healthy aging during the UEF dual task to improve its clinical viability for early screening of diseases.

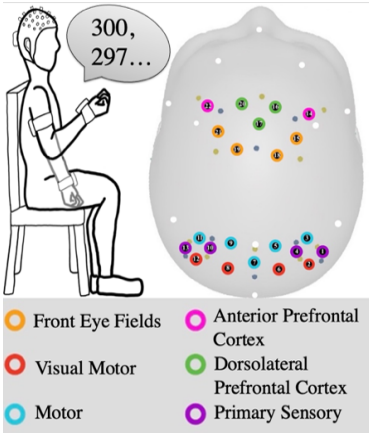


**Figure 1.** Experimental design, including UEF dual task and fNIRS cap layout.

**Methods:** Participants were grouped based on age: young adults (YA; n = 16, age = 21.13±2.45) and older adults (OA; n =17, age = 73.24 ±4.51). fNIRS measurements were taken as participants completed a 3-minute rest period followed by a 3-minute UEF dual-task. The motor component of the dual task was consistent right arm flexion and extension, while the cognitive component was serial subtraction by threes (Fig 1). The fNIRS measurements were focused on the frontal and parietal lobes (Fig 1). Between channel connectivity during each task was calculated for every channel pair using correlation values, which were averaged across all channels.

**Results:** For both the rest and dual-task, Shapiro-Wilk tests indicated average connectivity was not normally distributed ($p<0.05$), so non-parametric tests were used. A pairwise Wilcoxon test revealed no significant effect of age group on average connectivity during rest ($p=0.250$) (Fig 2). However, during the dual task there was a significant effect of group on average connectivity ($p = 0.004$) (Fig 2). During the rest, the average connectivity across all channels was 0.370 for YA and 0.440 for OA. During the dual task, the average connectivity was 0.340 in YA and 0.437 in OA. Further, although the trend was not significant, connectivity generally decreased from the resting state in YA but did not change in OA.

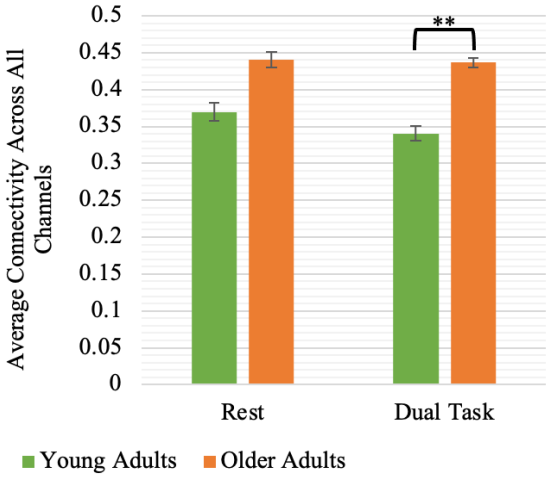


**Figure 2.** Average connectivity across all fNIRS channels during a rest and UEF dual task for young adults and older adults (**$p<0.01$). Error bars represent standard error.

**Discussion:** Differences in connectivity between age groups were significant only during the dual task. Older adults experience greater dual task cost compared to younger adults due to greater competition of limited resources [5]. The average connectivity across all channels during the dual task was lesser compared to the rest in YA, while it was constant in OA. This difference may reflect compensatory mechanisms; OA recruit additional structures during the dual task to overcome limited resources. Previous work found that YA experience increased unilateral activation during a gait dual task compared to rest, whereas OA have increased bilateral activation and higher overall prefrontal cortex activation [6]. It has also been hypothesized that healthy, young brains deactivate networks involved in rest, such as the default mode network, to better attenuate to the task at hand, while older adults do not [7]. These findings support the hypothesis that a lesser dual task cost in YA results in the recruitment of fewer brain structures, compared to OA.

**Significance:** The results of this study give insight as to why cognitive deficits in older adults are related to alterations in motor function during a UEF dual task. These data can be used as a baseline for healthy older adults to use the UEF dual task for screening diseases associated with aging, such as Alzheimer's disease. Additionally, fNIRS measurements in older adults during task activities may be a simple solution for capturing abnormalities in deeper brain structures and brain networks, such as the default mode network.

**Acknowledgments:** This project was supported by one award from the National Institute on Aging (NIA/NIH-1R01AG076774-01A1) and one award from the National Science Foundation (NSF 2236689 - CAREER).

**References:** [1] Gu, et al. (2021), China CDC Weekly 604-613 (28). [2] Yeung, et al. (2019), Neuropsychol Rev 139–166 (31). [3] Toosizadeh, et al. (2019), Sci Rep 10911 (9). [4] Ehsani, et al. (2020), Comp Biol Med 103705 (120) [5] Papegaaij, et al. (2017), PLOS ONE 12 (12). [6] Hassan, et al. (2022), Eur J Appl Physiol 965-974 (122). [7] Crockett, et al. (2017), Front in Aging Neurosci 302547 (9).

# INTRADISCAL PRESSURE DISTRIBUTIONS IN DEGENERATED INTERVERTEBRAL DISCS

* Asghar Rezaei[1], Chih-Hsiu Cheng, Areonna Schreiber, Babak Dashtdar, Maria Astudillo Potes, Xifeng Liu, Kai-Nan An, Kenton Kaufman, Lichun Lu[1*]

[1]Department of Physiology and Biomedical Engineering, Mayo Clinic, Rochester, MN, USA

*Corresponding author's email: lu.lichun@mayo.edu

**Introduction:** Intervertebral discs (IVDs) are located between vertebral bodies, undergo a wide range of spinal column motions, and transfer compressive loads to adjacent vertebral bodies. The centrally-located nucleus pulposus in a healthy disc is a jelly-like substance that transfers spinal loads uniformly across vertebral bodies. IVDs undergo dramatic degenerative changes with age, more than any other musculoskeletal tissue [1]. These age-related declines initially affect the nucleus pulposus and expand outward to the annulus pulposus. These deteriorations in the material properties of the disc components limit its functionality and may cause back pain, especially in the elderly. Various techniques have been used to measure IDP, including needle pressure sensors or tiny pressure transducers surgically implanted in the nucleus pulposus [2]. However, techniques that measure local pressure values inside healthy discs may not provide reliable estimates of spinal loads in degenerated discs.

In the current study, a novel approach was introduced to measure IDP distributions within human cadaveric degenerated discs. Mechanical testing was conducted on all segments, and their pressure distributions were recorded from the initiation of the loading until vertebral fracture. The aim of the study was to measure IDP distributions within the IVD under extreme loading conditions and assess whether pressure distributions changed with the magnitude of loading.

**Methods:** Four fresh frozen cadaveric torsos (two females and two males) with an average age of 73 (±13) years were obtained from the Mayo Clinic Clinical Anatomy Laboratory, following the Institutional Review Board approval (17-009728) [3]. The spines were dissected from torsos, three-level segments were isolated, and posterior elements were removed from the vertebrae, ensuring that the entire load is transferred through the IVD. In total, six segments were prepared with superior and inferior vertebral bodies potted in poly (methyl methacrylate) (PMMA) to facilitate imaging and testing. Quantitative computed tomography (QCT) imaging was performed using a Siemens Somatom Definition Scanner (Siemens Healthcare GmbH, Germany). Images were collected at 120 kVP, 220 mAs, and reconstructed, using a sharp algorithm to evaluate whether the disc could be resected and to determine the resection line. The degree of IVD degeneration was assessed using Adams classifications. High resolution thin-film pressure sensors (Model 5051, Tekscan, Inc., Boston, MA) were used to record IDP distributions during compressive loading. These sensors are square (55.9mm×55.9mm) with a thickness of 0.1 mm. Sensors were calibrated using a custom-made pressure calibration chamber as well as experimental force-displacement data. The IVD of interest was resected entirely using a diamond band saw to divide the segment into two separate parts. Then, the sensors were inserted into the cut area of the disc. The entire disc cross sectional-area was divided into nucleus and annulus to estimate the amount of pressure and force carried by these regions. mechanical testing was conducted by an MTS 858 Mini Bionix II (MTS Systems Corporation, Eden Prairie, MN).

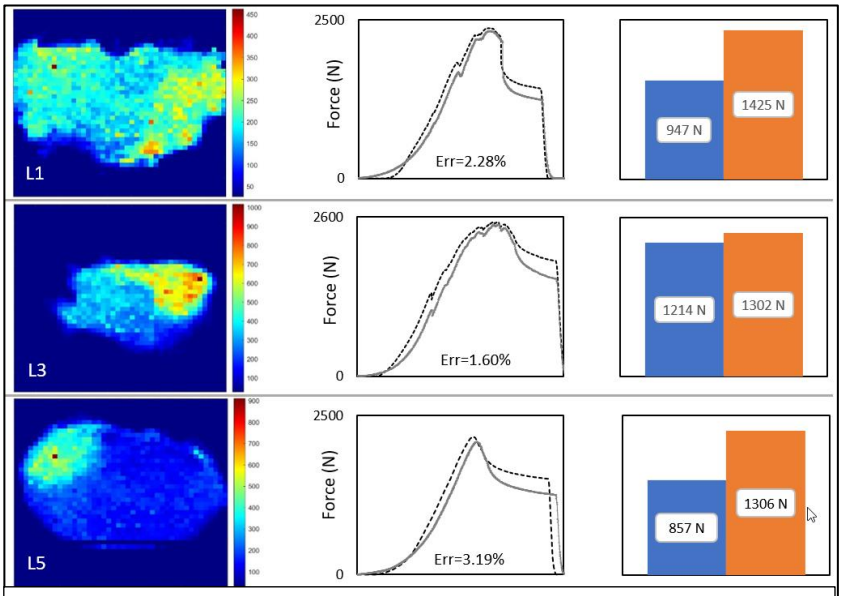


Figure 1. First column illustrates pressure distribution maps in the IVD; Second column shows force data measured from the load cell (solid lines) and estimated from pressure (dashed lines) along with errors for estimated values given at maximum force; and Third column shows the load experienced by the annulus (in blue) and annulus (in orange) [3].

**Results & Discussion:** Pressure recordings were performed successfully during testing for all the specimens. Figure 1 shows pressure distribution maps for three specimens. As illustrated, all the pressure profiles were asymmetrical with larger pressure values experienced by the annulus regions. Pressure values were location dependent throughout the cross-sectional area. Minimum pressure values were found in the nucleus regions. Average pressure across the entire region was 265 (131) kPa with nucleus region experiencing an average of 316 (195) kPa and the annulus region 239 (100) kPa. Next, force data was estimated using pressure measurements and compared with force values measured using the load cell. Average fracture force was measured as 1977 N (757) by the load cell and estimated as 2039 (801) N by pressure data, leading to an error of 2.72%. of total load, with nucleus pulposus experiencing 806 (418) N (or 40% of the entire load) and annulus fibrosis experiencing 1233 (432) N (or 60% of the entire load). Assessment of IDP distributions can provide valuable insight into DD, spinal load assessment, and potentially vertebral fractures.

**Significance:** The current study sheds light on how disc degeneration leads to heterogeneous and asymmetrical patterns of spinal loading transfer. Such patterns may eventually lead to degenerative spinal pathologies such as disc herniation.

**Acknowledgments:** This work was supported by the Eagles 5th District Cancer Telethon Funds and NIH grants K25AG068368 and R01AR56212.

**References:** [1] Miller et al. (1998), *Spine* 13(2); [2] Sato et al. (1999), *Spine* 24(23); [3] Rezaei et al. *JMBE* (2025)

# THE RELATIONSHIP BETWEEN TIBIAL BONE DENSITY AND PEAK KNEE ADDUCTION MOMENT DURING LEVEL WALKING IN OLDER ADULTS

*Shelley Oliveira Barbosa[1], Tom Gale[1], Emelia Krakora[1], Raghav Ramraj[1], Kenneth Urish[1], William Anderst[1]
[1]Department of Orthopaedic Surgery, University of Pittsburgh, Pittsburgh, PA
*Corresponding author's email: shelleyob@pitt.edu

**Introduction:** It is estimated that 10 million people 50 years of age or older in the United States have osteoporosis; additionally, over 43 million people have low bone mineral density (BMD), increasing their risk for osteoporosis [1]. Individuals with low bone density have an increased risk of complications associated with total knee arthroplasties such as revision surgery, periprosthetic fracture, and aseptic loosening [2,3]. The external knee adduction moment (KAM) has been proposed as an easy to acquire surrogate measure of medial and lateral compartment knee loading that is associated with knee pain [4] and knee osteoarthritis [5]. Although previous studies have looked at the relationship between volumetric BMD and gait in young healthy adults using peripheral quantitative computed tomography [6] associations between BMD and peak KAM in older adults are lacking. The objective of this analysis was to investigate the relationship between tibial BMD and peak external KAM during gait in older asymptomatic adults. We hypothesized that BMD in the medial tibia and the ratio of medial to lateral compartment BMD would be correlated with peak KAM.

**Methods:** All participants provided written informed consent to participate in this IRB-approved study. Participants were recreationally active asymptomatic older adults with no history of knee injury nor medical diagnosis of osteoarthritis or osteoporosis. All participants received a bi-lateral computer tomography (CT) of their tibia (0.40x.40x.625mm) and completed six trials of level walking (3 trials of heel-strike to mid-stance and 3 trials of midstance through push-off) while synchronized biplane radiographs were collected at 100 images/s (80 kV, 125 mA, 1 ms exposure per image). Participants walked at a self-selected speed on a dual-belt instrumented treadmill where ground reaction forces were collected at 1000 Hz. CT pixel values were converted from Hounsfield Units into bone mineral density values using a calibration phantom (Mindways Software, Inc). Eight regions of interest located within the central 1/3rd of the middle 50% of the plateau width were identified on the medial and lateral tibial plateaus using an automated computer algorithm (Figure 1). The top region of interest (ROI) was 3 mm thick, and the subsequent ROIs were each 2 mm thick. Average BMD (mg/cm$^3$) within each ROI was calculated. Tibia motion during gait was tracked using a validated model-based tracking technique with an accuracy of 0.7 mm, 0.9° [7]. Coordinate systems were constructed on the right side and were mirrored onto the left side [8]. Tibial position was combined with ground reaction force to calculate external KAM and normalized to height and mass. Impact and push-off phase peak KAMs (Nm/kg·m) were identified. Spearman correlation was used to identify associations between the peak external KAM and BMD density within each subsection and the average of all medial and lateral sections of the tibia. Associations between peak KAM and the medial to lateral BMD were also evaluated with significance set at $p<0.05$.

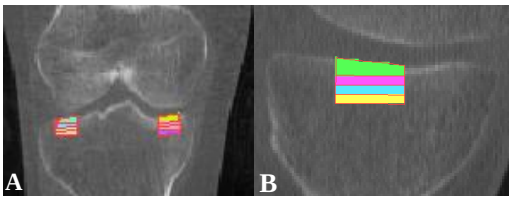


**Figure 1: (A)** Coronal view of a right knee CT with medial and lateral sections of the tibia identified. **(B)** Sagittal view of the right knee with regions of interest identified in color ROI 1 (green), ROI 2 (pink), ROI 3 (teal), and ROI 4 (yellow).

**Results and Discussion:** Data from 20 subjects (39 knees; 10F, age 64.6±9.4 years, BMI 27.21±4.3 kg/cm$^2$) are included in this analysis. Average walking speed was 0.80±0.17m/s. Bone mineral density in ROI 3 of the medial section of the tibia was inversely correlated with the peak external KAM during push-off ($p=0.019$, $\rho=-0.374$). The average BMD of the entire medial section of the tibia was inversely correlated with the peak external KAM during push-off ($p=0.041$, $\rho=-0.329$). No correlations were found with peak external KAM during the impact phase or with any peak KAM and the ratio of medial to lateral BMD. Qualitatively, the medial BMD was higher compared to the lateral compartment, and bone mineral density decreased with each successive distal subsection (Table 1). Contrary to our hypotheses, we found greater BMD in the medial tibia was associated with lower peak external KAM, specifically during the push-off phase of gait. This is believed to be the first report to link tibial BMD and peak external KAM in older asymptomatic adults. Additional analysis is needed to assess the association between femur BMD and KAM during gait, as well as during different loading conditions.

**Table 1.** Average Tibial Bone Mineral Density (±1 SD). All units are mg/cm$^3$.

| Subsections | Lateral | Medial |
|---|---|---|
| ROI 1 | 393.3 ± 71.6 | 467.8 ± 81.6 |
| ROI 2 | 283.9 ± 77.7 | 387.5 ± 107.6 |
| ROI 3 | 200.5 ± 49.7 | 241.4 ± 75.7 |
| ROI 4 | 159.7 ± 37.1 | 182.1 ± 46.1 |

**Significance:** Determining BMD using quantitative CT is time consuming and exposes the patient to radiation. External KAM has been proposed as a non-invasive means to infer the ratio of medial to lateral compartment loading in the knee, which could be a useful surrogate for medial to lateral BMD measured using quantitative CT. This information could be useful for pre-operative planning, osteoporosis treatment prior to surgery, intra-operative decision making (utilization of cement during knee arthroplasty), and understanding post-operative implant micro-motion. However, these results suggest peak external KAM during gait is not associated with medial versus lateral compartment loading in the knee during gait or with tibial BMD.

**Acknowledgments:** This work was supported by a research grant from Smith&Nephew and NIH grant UL1 TR001857.

**References:** [1] U.S. Department of HHS, Osteoporosis Workgroup (2025); [2] Harris et al. (2023), *J Arthroplasty*; [3] Meyer et al. (2024), *J Arthroplasty*; [4] Zongpan et al. (2023), *Eur J Phys Rehabil Med;* [5] Sharma et al. (1998), *Arthritis Rheum*; [6] Thewlis et al. (2021), *Bone*; [7] Tashman and Anderst (2003), *J Biomech Eng*; [8] Gale and Anderst (2019), *J Orthop Res*.

# ASSESSING KNEE JOINT MECHANICS IN KNEE OSTEOARTHRITIS PHENOTYPES IN AGING ADULTS

Mariana V. Jacobs[1*], Sarah Malek[2], Stephen T. Duncan[1], Jeffrey B. Selby[1], Christopher S. Fry[1], Michael A. Samaan[1]
[1]University of Kentucky, Lexington, KY; [2]Purdue University, West Lafayette, IN
*Corresponding author's email: mariana.jacobs@uky.edu

**Introduction:** Approximately 17% of the U.S. population over the age of 45 exhibit symptomatic knee osteoarthritis (OA) consisting of radiographic signs of knee joint degeneration and knee-related pain [1]. Patients with knee OA consist of sub-populations that experienced either knee joint injury resulting in knee post-traumatic OA (PTOA) or age-related (idiopathic; IDIO) knee OA. Prior work has also shown that knee PTOA results in more rapid cartilage degeneration compared to IDIO [2]. There is a lack of information regarding the biomechanical factors that distinguish these OA phenotypes, which in turn may lead to the generalization of rehabilitation protocols for aging individuals with knee OA. Assessment of these phenotype-based differences in gait mechanics will provide clinicians with the knowledge needed to develop scientifically justified, *OA phenotype specific*, interventions to mitigate knee OA disease progression in the aging population. Therefore, the purpose of this study was to assess knee joint kinematics, kinetics, and knee joint muscle strength between healthy asymptomatic aging adults, and individuals with end-stage knee OA (both PTOA and IDIO) prior to a total knee arthroplasty (TKA). We hypothesized that 1) aging individuals with end-stage OA will exhibit declined knee joint strength and ambulate with altered knee joint mechanics when compared to healthy aging adults and 2) aging adults with PTOA would exhibit more detrimental knee mechanics compared to aging adults with IDIO.

**Methods:** We tested four participants (4F; 60.1±11.2 yrs; BMI 32.3±4.4 $kg \cdot m^{-2}$) with PTOA and 5 participants (3F; 66.4±2.3 yrs; BMI 31.4±3.7 $kg \cdot m^{-2}$) with IDIO prior to a TKA. Retrospective data from 8 asymptomatic adults (7F; 56.1±9.1 yrs; BMI 27.0±3.2 $kg \cdot m^{-2}$) were used for control data. KOOS pain scores were obtained for OA participants. Each participant completed a 20-second walking trial at a comfortable, self-selected speed on a dual-belt instrumented treadmill [3]. The surgical limb and dominant limb was selected as the test limb for the OA groups and control groups, respectively. Gait speed and 3D knee joint kinematics and internal joint moments during the stance phase (heel strike–toe off) were compared between the PTOA, IDIO and control groups. Isometric quadriceps and hamstrings peak torque were measured using an isokinetic dynamometer**.** The OA groups had higher BMIs than the control group ($p<0.05$). Between-group differences in demographics and gait parameters were assessed using separate ANCOVAs (covariate of BMI) with a Bonferroni post hoc adjustment. KOOS scores were compared with an independent t-test. Statistical significance was set at 0.05.

**Results & Discussion:** Quadriceps and hamstrings strength as well as KOOS pain scores were similar between groups ($p>0.05$). Despite slower walking speeds and lower internal knee adduction and internal rotation moments, the PTOA group exhibited a higher peak internal knee abduction moment (i.e., external knee adduction moment) compared to controls (Table 1). Compared to controls, the IDIO group walked slower and ambulated with a lower internal knee flexor moment during terminal stance and a lower internal knee adduction moment. These results suggest that when compared to controls, the PTOA and IDIO groups exhibit different gait-related compensations. The PTOA and IDIO groups walk at similar speeds, yet the PTOA group ambulates with a lower peak knee extensor moment during terminal stance, a more valgus knee joint and larger frontal plane ROM. Given that quadriceps strength was similar between PTOA and IDIO ($p>0.05$), these phenotype differences in knee mechanics may suggest worse quadriceps function during walking as well as more pronounced alterations in frontal plane knee mechanics in PTOA compared to IDIO.

| **Table 1. Gait parameters presented as BMI adjusted mean ± standard error** | **Control** | **PTOA** | **IDIO** | **ANCOVA p-value** | **Control vs. PTOA** | **Control vs. IDIO** | **PTOA vs. IDIO** |
|---|---|---|---|---|---|---|---|
| KOOS Pain Score | - | 60.4 ± 4.6 | 52.7 ± 2.8 | - | - | - | 0.18 |
| Gait Speed ($m \cdot s^{-1}$) | 0.90 ± 0.06 | 0.48 ± 0.08 | 0.56 ± 0.07 | 0.003 | 0.004 | 0.008 | 1.00 |
| Peak Knee Ext Moment at TS ($Nm \cdot kg^{-1}$) | 0.11 ± 0.04 | 0.01 ± 0.06 | 0.23 ± 0.05 | 0.019 | 0.621 | 0.264 | 0.019 |
| Peak Knee Flex Moment at TS ($Nm \cdot kg^{-1}$) | -0.47 ± 0.07 | -0.41 ± 0.09 | -0.14 ± 0.08 | 0.018 | 1.00 | 0.028 | 0.083 |
| Peak Knee ABD Angle (deg) | -2.97 ± 0.75 | -3.88 ± 1.00 | 0.02 ± 0.87 | 0.017 | 1.00 | 0.089 | 0.025 |
| Peak Knee ROM Frontal (deg) | 5.71 ± 0.80 | 7.99 ± 1.08 | 3.94 ± 0.94 | 0.032 | 0.423 | 0.604 | 0.03 |
| Peak Knee ADD Moment ($Nm \cdot kg^{-1}$) | 0.31 ± 0.04 | 0.08 ± 0.05 | 0.15 ± 0.04 | 0.006 | 0.007 | 0.037 | 0.724 |
| Peak Knee ABD Moment ($Nm \cdot kg^{-1}$) | -0.11 ± 0.03 | -0.31 ± 0.05 | -0.2 ± 0.04 | 0.026 | 0.025 | 0.433 | 0.262 |
| Peak Knee Int Rot Moment ($Nm \cdot kg^{-1}$) | 0.29 ± 0.03 | 0.12 ± 0.04 | 0.2 ± 0.04 | 0.025 | 0.023 | 0.228 | 0.462 |

*KEM: Knee Extensor Moment; KFM: Knee Flexor Moment; Int Rot: Internal Rotation; TS: Terminal Stance, ADD: Adduction, ABD: Abduction*

**Significance:** Our results support our hypotheses that knee joint mechanics differ between knee OA phenotypes and that aging adults with end-stage knee OA ambulate with altered knee joint mechanics compared to healthy controls. More specifically, our data suggests that alterations in knee joint mechanics are knee OA phenotype specific and may be due to the differing pathomechanism of knee OA development in these OA phenotypes. This information suggests that knee OA gait-related rehabilitation may need to be targeted to specific OA phenotypes in order to improve symptoms and to mitigate knee OA disease progression in the aging population. Future work should include a larger sample size, an assessment of hip and ankle mechanics during a more demanding task (e.g., sit-to-stand), and additional assessments of knee joint muscle rate of torque development.

**Acknowledgements:** NIH (K01-AG073698 and UL-TR001998)

**References:** [1] Lawrence et al. Arthritis Rheum. 2008;58(1):26-35. [2] Wei et al. J Orthop Res. 2017;27(7):900-6. [3] Jacobs et al. J Occup Environ Hyg. 2025;22(1):1-7

# AN EXPLORATORY COMPARISON OF RECOVERY KINEMATICS BETWEEN LAB-INDUCED TRIPS AND NATURALLY-OCCURRING REAL-WORLD TRIPS

Youngjae Lee[1], Neil B. Alexander[2], Christopher T. Franck[1], Michael L. Madigan[1]*
[1]Virginia Tech; [2]University of Michigan
*Corresponding author's email: mlm@vt.edu

**Introduction:** Numerous laboratory studies have induced trips among older adults to explore the biomechanical mechanisms underlying trip-induced falls, to identify factors affecting trip recovery, and to evaluate fall prevention interventions. While these studies have yielded a wealth of knowledge, it is not clear whether trip recovery kinematics differ between the lab and real world. Any such differences may influence how laboratory findings should be generalized to the real world. Therefore, the goal of this exploratory study was to compare sternum drop, a key measure of trip recovery kinematics [1], between lab-induced trips and naturally occurring real-world trips. Three hypotheses were posed: H1-sternum drop would not differ between real-world trips and lab-induced trips; H2-sternum drop would exhibit greater variance after real-world trips than after lab-induced trips; and H3-sternum drop after real-world trips would be associated with sternum drop after lab-induced trips.

**Methods:** Twenty adults (8M and 12F; mean (SD) age 71.8 (4.6) years old) wore inertial measurement units (IMUs) on each foot and sternum, sampled at 128 Hz, and a digital voice recorder on the wrist daily for three weeks to capture real-world losses of balance kinematics and to document related contextual details [2]. Participants then completed a single laboratory session during which they were exposed to two lab-induced trips while wearing the same three IMUs. Tripping kinematics were characterized using sternum drop which was defined to be the decrease in sternum IMU height from trip onset to touchdown of the first recovery step [1]. An increase in sternum drop toward +infinity indicates poorer trip recovery performance.

**Results & Discussion:** A total of 24 real-world trips were reported with all resulting in successful recoveries (i.e., no falls). Among the 14 participants who reported at least one real-world trip, their 28 lab-induced trips resulted in 12 recoveries, 10 falls, and 6 artefactual trips that were excluded from further analysis. Regarding H1 and H2, results differed depending upon whether falls after lab-induced trips were included in the analysis. When including all falls and recoveries after lab-induced trips (Figure 1a and 1b), sternum drop was 8.8 cm smaller in the real world than in the laboratory ($p < 0.001$). The variance of residuals of sternum drop after using a mixed-model ANOVA to account for the effects of setting, training group, and repeated measurements was lower in the real world ($\sigma^2 = 12.6$ cm$^2$) than in the laboratory ($\sigma^2 = 120.2$ cm$^2$; $p < 0.001$). When including only recoveries after lab-induced trips (Figure 1c and 1d), sternum drop did not differ between the real world and laboratory ($p = 0.163$). The variance of residuals of sternum drop after using a mixed-model ANOVA to account for the effects of setting, training group, and repeated measurements was lower in the real world ($\sigma^2 = 13.1$ cm$^2$) than in the laboratory ($\sigma^2 = 74.2$ cm2; $p < 0.001$). Regarding H3, sternum drop in the real world was not associated with the mean of each participant's two lab-induced trips for both cases ($R^2 < 0.01$; $p >= 0.757$). Some of our results can be explained by lab-induced trips requiring greater physical demands for recovery than real-world trips due to participant lab instructions to walk at a slightly hurried speed and using an aggressive obstacle height (8.6 cm) compared to at least some real-world trips that occurred with no obstacle. This resulted in more falls in lab than in the real world, a higher mean sternum drop in the lab, and enabled a wider range of sternum drop values in the lab. The lack of association between lab and real-world sternum drop may be due to inherent variability of trip recovery kinematics [3] and its dependence on complex and wide-ranging factors [4].

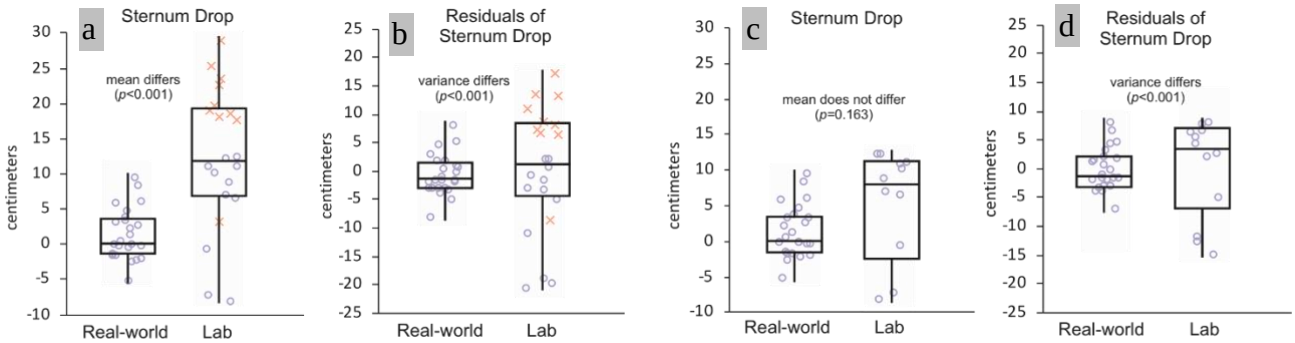


Figure 1. When including lab falls and recoveries (a,b), sternum drop was larger and more variable than in the real world. When only including lab recoveries since all real-world trips were recoveries (c,d), sternum drop did not differ yet variance was larger in the lab than in the real world.

**Significance:** While matching gait speed and obstacle height between the real world and lab may improve agreement in kinematics between the two settings, the resulting reduction of physical demands of trip recovery in the lab may hinder the identification of factors contributing to falls. Nevertheless, additional research appears warranted to clarify the relationship between lab and real-world trips.

**Acknowledgments:** This research was supported by the National Institute on Aging of the NIH (R21AG075430). The authors would also like to thank Michelle Morris for her contributions.

**References:** [1] Lee et al. (2025) *J Biomech*; [2] Lee et al. (2025) *JAGS*; [3] Owings et al. (2000) *JAGS*; [4] Horak et al. (1989) *J Neurophysiol*.

# EYE DROP BOTTLE STABILITY IS RELATED TO SENSORIMOTOR PERFORMANCE IN OLDER ADULTS

*Daniel Duque Urrego[1], Cameron Haire[2], Alanson P. Sample[2], David T. Burke[2], Susan H. Brown[2], Paula Anne Newman-Casey[2], and Stephen M. Cain[1]
[1]West Virginia University, Morgantown, WV and [2]University of Michigan, Ann Arbor, MI
*Corresponding author's email: dd00055@mix.wvu.edu

**Introduction:** Glaucoma is the main cause of irreversible blindness in the United States, and older adults, who often demonstrate worse upper limb motor control [1], represent the primary population affected [2]. In this study, we performed a general upper limb sensorimotor assessment, a balance test, and measured eye drop bottle stability during instillation events. Prior work indicates that bottle stability correlates with successful eye drop instillation [3]. Our goal is to understand how standing balance, dexterity, proprioception, and force generation are related to bottle stability. This understanding will inform strategies for improving medication instillation success in older adults. We hypothesized that (1) the sensorimotor assessment results would be associated with bottle-stability measures and (2) standing balance would be significantly associated with eye drop bottle stability while standing.

**Methods:** In our University of Michigan IRB (HUM00162357) approved study, sixty-eight older adults (28M, 38F, 2 preferred not to answer; age: 73.1 ± 5.5 years) were recruited and provided written informed consent. Inclusion criteria targeted individuals 65–100 years old who were not currently using prescription eye drops and could perform basic physical tasks. We measured forearm and upper arm body segment lengths. We quantified subject balance (standing balance board test) [4], hand and finger grip strength (three-finger pinch force, grip force) [5], tactile sensitivity (monofilament tests for index and ring fingers), dexterity and hand function (timed tasks: grooved pegboard test, fastening and unfastening buttons, shoe-lacing, pinning/unpinning safety pins, manipulating coins, and cutting putty), and proprioception (manipulandum). Participants applied eye drops with their dominant hand into both eyes during three different body postures (standing, sitting, and laying), performing at least three attempts in each eye in each position (18 total instillation attempts). An IMU secured to the bottom of the eye drop bottle measured the bottle's linear acceleration and angular velocity. Stability metrics [6] were calculated during instillation periods (when the bottle is still and a drop is being dispensed) using the free acceleration data (acceleration resolved into the inertial frame with gravity removed). In this study, we focused only on stability measures calculated from linear acceleration and jerk along the bottle's longitudinal axis: mean acceleration, root mean squared acceleration, and mean jerk. Statistical analyses employed an adaptive LASSO approach with a three-degree factorial design on the sensorimotor results. Model selection was guided by AICc. Because residuals were initially non-normal, a Box-Cox transformation was applied to dependent variables. Sensorimotor predictors were normalized before entering the LASSO model.

**Results & Discussion:** Table 1 summarizes significant effects for stability metrics in three positions (laying, sitting, and standing). Wald Chi-Square tests identified key predictors and interactions ($p < 0.05$). Overall, bottle stability during standing stability was most strongly associated with standing balance performance. In sitting, bottle stability was most associated with three-finger pinch force. In the laying conditions, stability metrics were jointly influenced by dexterity (timed tasks) and force production (grip force). Additional analysis not detailed here reveals that other bottle stability metrics (maximum acceleration, total excursions, 95% confidence spheres, and ellipsoids) are also strongly associated with sensorimotor performance.

**Significance:** One key recommendation suggested by our findings is to avoid eye drop instillation while standing due to decreased bottle stability in that posture. While some sensorimotor traits such as dexterity and proprioception are difficult to modify, grip force is more amenable to change, either by strengthening the user's grip or by reducing the force required to dispense a drop. Therefore, adjusting bottle design to lower the necessary squeeze force could significantly improve bottle stability and, therefore, medication-instillation success among older adults.

**Acknowledgments:** Supported by the NIH National Institute of Biomedical Imaging and Bioengineering (R01EB032328).

**References:** [1] Seidler et al. (2006) *Brain Res Bull*. [2] Ehrlich et al. (2024) *JAMA Opht.* [3] Duque Urrego et al. (*In Preparation*) *PLOS One*. [4] Chang et al. (2014) *Clin J Sport Med*. [5] Backman et al. (1997) *The Occup Ther Jour of Rese*. [6] Mancini et al. (2012) *J NeuroEngineering Rehabil*.

**Table 1.** Effects test results by position. Bottle stability in laying is primarily associated with dexterity and hand strength. Bottle stability in sitting is associated most with pinch force. Bottle stability while standing is significantly associated with standing balance.

| Position | Stability Metric | Sensorimotor Assessment | $\chi^2$ | p-value |
|---|---|---|---|---|
| Laying | Mean Acceleration | Shoe-Lacing *Safety Pins*Upper Arm Length | 11.13 | 0.0009 |
| | | Balance Board | 8.03 | 0.0046 |
| | | Grip Force*Ratio(Upper Arm /Forearm Length) | 4.80 | 0.0285 |
| | | Grip Force*Unfastening Buttons | 3.90 | 0.0483 |
| | RMS Acceleration | Balance Board | 5.65 | 0.0175 |
| | | Shoe-Lacing*Safety Pins*Upper Arm Length | 4.61 | 0.0317 |
| | Mean Jerk | Balance Board | 5.37 | 0.0205 |
| Sitting | Mean Acceleration | Pinch Force | 4.96 | 0.0259 |
| | RMS Acceleration | Pinch Force | 4.55 | 0.033 |
| Standing | Mean Acceleration | Balance Board | 15.37 | <.0001 |
| | RMS Acceleration | Balance Board | 13.67 | 0.0002 |
| | Mean Jerk | Balance Board | 17.59 | <.0001 |

# EVALUATING STERNUM DROP AS A NEW TRIP RECOVERY PERFORMANCE MEASURE

Youngjae Lee, Michael L. Madigan*
Grado Department of Industrial and Systems Engineering, Virginia Tech, Blacksburg, VA, United States
*Corresponding author's email: mlm@vt.edu

**Introduction:** Three key requisites for successful trip recovery include limiting trunk flexion, maintaining adequate hip height to enable repeated stepping, and completing recovery steps to extend the base of support [1,2]. The purpose of this study was to evaluate sternum drop as a new measure of trip recovery performance. Sternum drop was defined here as the decrease in sternum height from trip onset to touchdown of the first recovery step over the trip obstacle. It is geometrically dependent on trunk flexion and hip height, which are two of the three trip recovery requisites (Figure 1). We hypothesized that sternum drop would 1) exhibit at least good correlation (> 0.50) with commonly used trip recovery measures, and 2) differ between falls and recoveries.

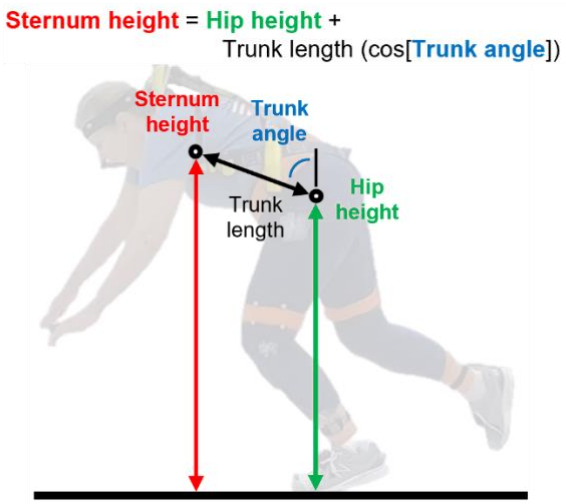


Figure 1. The geometric relationship between sternum height and its dependence on trunk angle and hip height.

**Methods:** Thirty community-dwelling older adults (18F and 12M; mean ± SD age = 71.8 ± 4.4 years; height = 1.68 ± 0.10 m; mass = 77.1 ± 16.8 kg) were exposed to two lab-induced trips while walking on a walkway with optoelectronic motion capture (OMC) markers and inertial measurement units (IMUs) attached to the body. Each trip was classified as either a fall, recovery, harness-assist, or miss based on the force applied to the safety harness and video review. Sternum drop was calculated separately using both OMC markers and IMUs. Other trip recovery measures were determined using only OMC markers and included trunk flexion angle and hip height, both at touchdown of the first recovery step. A repeated-measures correlation coefficient ($r_{rm}$) [3] was used to characterize correlations between outcome measures. A mixed-model analysis of variance (ANOVA) was used to investigate differences between falls and recoveries after tripping.

**Results & Discussion:** Sternum drop from OMC exhibited strong correlation with trunk angle at touchdown ($r_{rm}$ = 0.94, $p$ < 0.001) and hip height at touchdown ($r_{rm}$ = -0.90, $p$ < 0.001; Figure 2) and stenum drop from IMU ($r_{rm}$ = 0.95, $p$ < 0.001). Sternum drop from OMC ($p$ < 0.001) and sternum drop from IMU ($p$ = 0.001) both differed between falls and recoveries (Figure 3). These results supported our hypotheses.

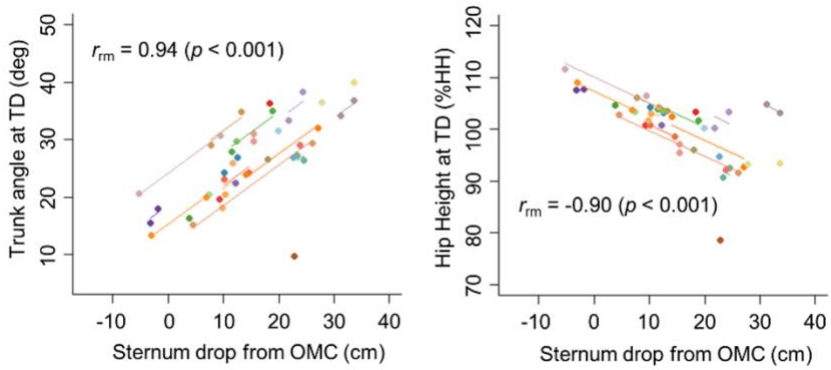


Figure 2. Repeated measures correlation plots. TD = touchdown of the first recovery step over the trip obstacle; %HH = % of hip height while standing.

**Significance:** Our findings support sternum drop as a valid trip recovery measure. It may also be more sensitive to trip recovery performance than other measures that focus on only one trip recovery requisite. Sternum drop can also be captured using a single IMU, thus potentially enabling its use in either clinical or non-research settings.

**Acknowledgments:** This research was supported by the National Institute on Aging of the NIH (R21AG075430). The content is solely the responsibility of the authors and does not necessarily represent the official views of NIH.

**References:** [1] Pavol et al. (2001), *J Geron* 56(7); [2] Pijnappels et al. (2005), *Gait & Posture* 21(4); [3] Bakdash & Marusich (2017), *Front Psychol* 8.

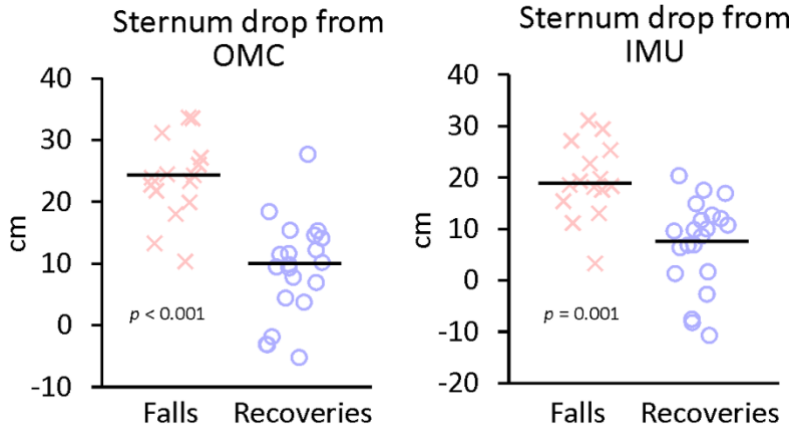


Figure 3. Comparison of sternum drop measures between falls and recoveries. The horizontal bar represents the mean.

# TOWARD BIOMECHANICALLY VALID SYNTHETIC HUMAN MOTION: AN INITIAL ASSESSMENT

*Adrian Krieger[1], Changseob Song[1], Inseung Kang[1]
[1]Department of Mechanical Engineering, Carnegie Mellon University, Pittsburgh, PA 15213, USA
*Corresponding author's email: adriank@andrew.cmu.edu

**Introduction:** Collecting human motion data for exoskeleton applications can be time-intensive and expensive, requiring professional motion capture systems and trained personnel. These challenges become more pronounced when working with clinical populations or high-risk scenarios (e.g., falling, tripping), which demand specialized equipment, clinical oversight, and patient availability. Generative methods like diffusion models could help alleviate the data collection problem through the creation of synthetic data [1]. Although diffusion models have primarily gained traction in the image domain, recent efforts use diffusion to generate joint positions over time for human motion. While variations like the Motion Diffusion Model (MDM) [2], which uses a text-to-motion approach, show promising results, the generated motions are often not biomechanically accurate enough for use in real-world applications like exoskeleton control. Addressing existing research gaps in motion diffusion is essential for generating high-quality, biomechanically accurate synthetic motions suitable for exoskeleton development.

**Methods:** Our approach, illustrated in Fig. 1a, deploys the text-to-motion MDM from [2], varying the text prompts to change the generated motions. The MDM uses the specified prompt to generate three-dimensional joint keypoints over six seconds (120 frames). We then convert these keypoints to joint angles using the methodology from [3], focusing on the hip and knee joints. This method computes hip and knee joint angles by measuring the angles between vectors connecting the pelvis, spine, hip, knee, and ankle keypoints. To compare the MDM-generated joint angles to real, untrained data, we collected both cyclic (forward walking at 1m/s) and non-cyclic data (squat) from 3 subjects using a Vicon motion capture system and converting the marker-less recordings to joint angles using Theia3D (Theia Markerless Inc., CA). We then used two prompts for the MDM: "Person walks forward" (generating 9 samples) and "Training squat and stand back up" (generating 3 samples). For both real and synthetic data, the left and right joint angles were averaged.

**Results & Discussion:** As seen in Fig. 1b and 1c, the MDM-generated joint angles qualitatively resemble those from the 3 human subjects for both forward walking and squatting. For the walking example, the root mean square difference (RMSD) between the MDM and mean real data was 12.87 degrees for the hip, and 18.25 degrees for the knee. These findings highlight the potential for diffusion-generated synthetic data to augment or even replace aspects of real motion data collection. However, we found the MDM to be limited in creating data outside of the level-ground locomotor tasks (e.g. incline walking, stair climbing), and the used HumanML3D dataset [4] limits the accuracy of the generated motions, since the text labels only contain qualitative labels rather than detailed kinematic descriptors. The MDM also fails to generate movements of specific speeds (e.g. 0.5m/s), and only changes the walking gait through coarse language cues such as "quickly" or "fast". As seen in Fig. 1d, the generated movement is sometimes quite different from expected movement patterns, in this case showcasing extreme foot positioning in the squat. Also, when attempting to mimic clinical populations by restricting the range of joint motion in the text prompt, the model typically generated either completely alternate movements or motions that did not adhere to the constraints.

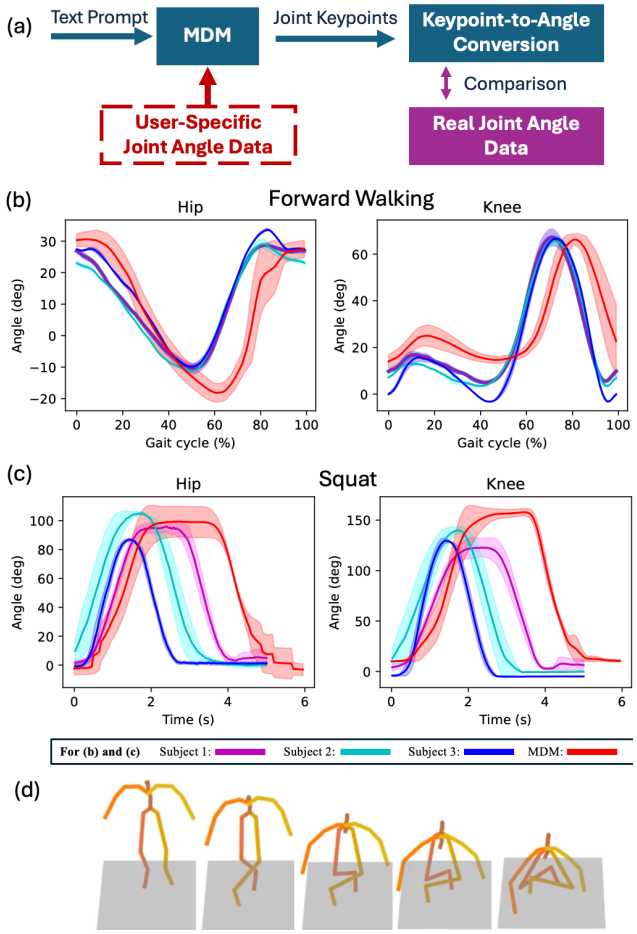


**Figure 1:** (a) Synthetic motion generation pipeline. The first and second blue blocks are deployed from [2] and [3], respectively. The purple block indicates our own collected motion capture data. The red block shows our future work to personalize the synthetic data with user-specific motion data. (b) Joint angles for hip and knee (mean ± SD, 9 gait cycles) across three human subjects and the MDM (Motion Diffusion Model) output for the walking prompt. (c) Joint angles (mean ± SD, 3 trials) across three human subjects and the MDM output for the squatting prompt. (d) Visualized output of MDM-generated keypoints for five squat frames (at 0.7s, 1.2s, 1.5s, and 2.6s out of a total of 6 seconds) for a sample that generated unrealistic posture/motion.

**Significance:** The ability to generate high-quality synthetic data can minimize the demand for specialized laboratory equipment, especially in scenarios involving unsafe movements or pathological gait patterns. While MDM-generated synthetic data is promising, this domain requires more effort to replace real data with synthetic data. We aim to investigate how quantitatively labelled data can improve the accuracy of the MDM approach, with the goal of generating personalized data across a diverse set of locomotor tasks using just a small user-specific dataset of low difficulty tasks (i.e. walking).

**References:** [1] Azizi et al. (2023), TMLR; [2] Tevet et al. (2023), ICLR; [3] Song et al. (2025), ICORR. [4] Guo et al. (2022), CVPR

# PERSONALIZATION OF IMU-BASED JOINT KINEMATIC ESTIMATION USING COMPUTER VISION

*Changseob Song[1], Bogdan Ivanyuk-Skulskyi[2], Adrian Krieger[1], Kaitao Luo[1], Inseung Kang[1]
[1]Department of Mechanical Engineering, Carnegie Mellon University, Pittsburgh, PA 15213, USA
[2]CRIStAL, University of Lille, Lille, 59000, France and Cyclope.ai, Nanterre, 92000, France
*Corresponding author's email: changseob@cmu.edu

**Introduction:** By estimating lower-limb joint kinematics, clinicians and biomechanics researchers can monitor subjects' gait patterns and use this information for rehabilitation and the control of assistive devices, such as exoskeletons [1]. Many studies have utilized deep learning (DL) models to estimate joint kinematics from inertial measurement unit (IMU) signals [2]. However, these DL models require new datasets every time they are adapted to arbitrary users, especially when dealing with abnormal pathological gait patterns. Moreover, motion capture data for DL models can only be collected in specialized laboratory environments equipped with expensive systems. In contrast, rapid advancements in computer vision have enabled the use of artificial intelligence for human pose estimation (HPE) [3]. With just a monocular camera like a smartphone, estimated joint kinematics can be easily obtained. Although vision-based pose estimation cannot operate in real time without a third-perspective camera view, particularly during daily outdoor ambulation, it can still provide new ground-truth data to replace professional motion capture systems. We hypothesize that computer vision-based HPE can personalize IMU-based kinematics estimation by rapidly adapting to unseen gait patterns that existing DL models, trained only on able-bodied (AB) subjects, have not encountered. The newly adapted DL model is expected to exhibit lower kinematics estimation errors for subjects with novel gait patterns compared to the pre-trained model.

**Methods:** We prototyped a wearable sensing suit (Fig. 1a) with a portable computer (Model 4B, Raspberry Pi, UK) capable of running the DL model in real time and three IMUs (ICM-20948, TDK InvenSense, Japan) attached to the pelvis and both thighs. We used an open-source vision transformer model, ViTPose [4], to extract full-body joint kinematics using a monocular camera. Along with ViTPose, we employed YOLOv8 [5] to detect the human subject, and Video-Pose3D [6] to reconstruct three-dimensional keypoints from the two-dimensional outputs of ViTPose (Fig. 1b). We trained a temporal convolutional network (TCN) to estimate joint kinematics from IMU data. As an example of pathological data, we placed a knee brace (Fig. 1c) on subjects to emulate a stiff-knee (SK) gait pattern. After training the TCN model with able-bodied (AB) subject data (three subjects; one minute for four speed conditions: 0.4, 0.7, 1.0, and 1.3 m/s), we investigated the effect of the SK dataset size on transfer learning to train an adapted AB+SK model. As demonstrated in Fig. 1d, 6% of the SK dataset—equivalent to only one to two gait cycles—was sufficient to converge the test error of the adapted model, and we used that portion of the dataset for validation experiments.

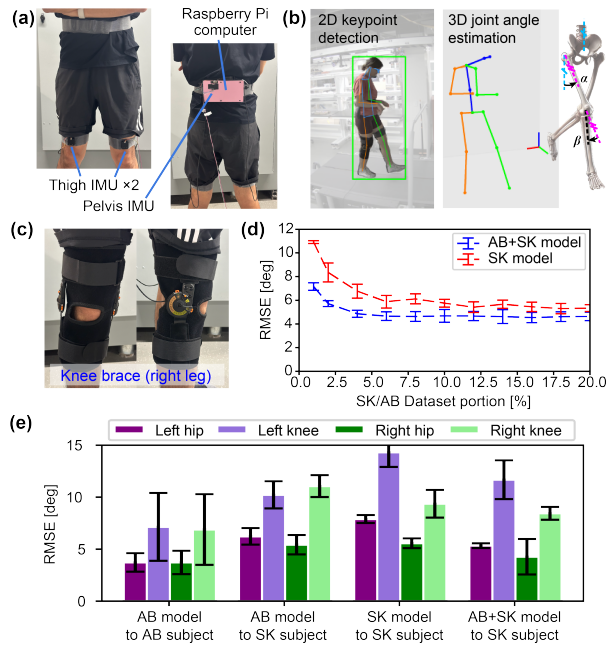


**Figure 1:** (a) Wearable sensing suit for kinematics estimation. (b) Pose estimation pipeline using a monocular video. (c) Knee brace for emulate stiff-knee gait. (d) SK and AB+SK models' estimation errors across varying SK-to-AB dataset ratios (mean ± SD for three subjects). (e) Estimation RMSE for each model across four lower-limb joints (mean ± SD for three subjects).

**Results & Discussion:** As shown in Fig. 1e, the AB model's estimation error on AB subjects was 5.4 degrees root-mean-square-error (RMSE), whereas its estimation on SK subjects was 8.2 degrees RMSE. Since we only used 1 to 2 gait cycles of SK data, the SK model's estimation on SK subjects was the highest—9.3 degrees RMSE. The AB+SK model's estimation on SK subjects was the lowest—7.4 degrees RMSE, which represents improvements of 9.7% compared with the AB model and 19.9% compared with the SK model. This result aligns with our hypothesis that computer vision-extracted kinematics can adapt and personalize the pre-existing model, yielding lower estimation error than both the AB and SK models.

**Significance:** This computer vision-powered adaptation pipeline has the potential to be an effective tool for monitoring joint kinematics in real time, especially in scenarios where professional motion capture facilities are unavailable and only minimal video data can be collected for a new user's gait pattern. Since many patient monitoring systems will continuously deploy wearable sensor-based DL solutions, we expect that this technology will benefit both users and clinical staff in diverse practical scenarios like outdoor ambulations. Furthermore, we anticipate that our system can be integrated into a hip exoskeleton, where DL models can be generalized to both AB and SK users.

**Acknowledgments:** This work was supported in part by the Kwanjeong Educational Foundation.

**References:** [1] P. B. Shull et al., *Gait & Posture*, vol. 40, no. 1, pp. 11–19, 2014; [2] E. Rapp et al., *Journal of Biomechanics*, vol. 116, p. 110229, 2021; [3] C. Zheng et al., *ACM Comput. Surv.*, vol. 56, Aug. 2023. [4] Y. Xu et al., *arXiv*, 2204.12484, 2022. [5] Ultralytics, 2023. [6] D. Pavllo et al., *2019 CVPR*, pp. 7745–7754, 2019.

# UNSUPERVISED DISCOVERY OF HUMAN MOTION PRIMITIVES FROM BIOMECHANICAL DATA

Carlos Carrasquillo[1*], Aakash Bajpai, Lena Ting[1], Anirban Mazumdar[1], Aaron Young[1]
[1]Georgia Institute of Technology, Atlanta, GA
*Corresponding author's email: ccarrasquillo3@gatech.edu

**Introduction:** End-to-end deep learning-based controllers for wearable robotics have emerged as promising solutions to user independence, generalizability, and task agnosticism. These models can map exoskeleton sensor data to human physiological states such as biological joint moments. However, studies have found that directly applying biological joint moments is not metabolically optimal. Researchers believe there exists a transformation from biological joint moments to optimal actuator torques. Recently, Molinaro et al. proposed constant delay and scaling factors to transform end-to-end biological torque estimates into optimal exoskeleton torques [1], but the use of universal constants risks potential metabolic benefits from biomechanically distinct movements. We hypothesize that identifying optimal transformations for distinct movements—termed *motion primitives*—can enable wearable assistance that reduces metabolic cost compared to existing task-independent controllers. First, we must construct a primitive library that represents most of human movement in a small number of learned primitives. The underlying hypothesis is that human motion consists of a finite set of fundamental movement patterns that can be extracted from biomechanical data without injecting domain-specific knowledge.

**Methods:** We trained a variational autoencoder with discrete reparameterization to encode biomechanics data while ensuring only one active motion primitive at a time (Fig. 1A). To learn lower-limb motion primitives grounded in kinematics and kinetics, we extracted joint angles and moments from the hip, knee, and ankle. To examine the effect of temporal context on primitive extraction, we constructed input sequences spanning 200–1000 ms around each timestep. We hypothesized that excessively short or long primitive durations would increase the number of primitives, with an optimal duration existing between these extremes. We trained models with latent spaces spanning 2–50 primitives and fit exponential saturation models to mitigate overfitting. The optimal number of primitives was determined as the smallest value for which the model's performance remained within 25% of its asymptotic limit, and the optimal duration was identified from the model with the fewest primitives. This hyperparameter optimization was conducted separately for both walking-only data only and a large dataset containing cyclic and non-cyclic tasks [2] to analyze trends in primitive representation.

**Results & Discussion:** Both approaches identified 600 ms as the optimal primitive duration (Fig. 1B), with 5 primitives for the walking-only dataset and 12 for the complete dataset. While the learned primitives overlapped significantly, each captured distinct kinematic and kinetic patterns (Fig. 1C). To evaluate model performance, we tested them on 1.25 m/s treadmill walking trials from unseen subjects. Both models identified motion primitives aligned with push-off, swing, weight acceptance, and stance phases. When given complete walking and step-up trials, both models were able accurately construct finite state machines without additional tuning (Fig. 1D). The model trained on the complete dataset was also especially effective at generating state machines for novel (i.e., unseen) tasks.

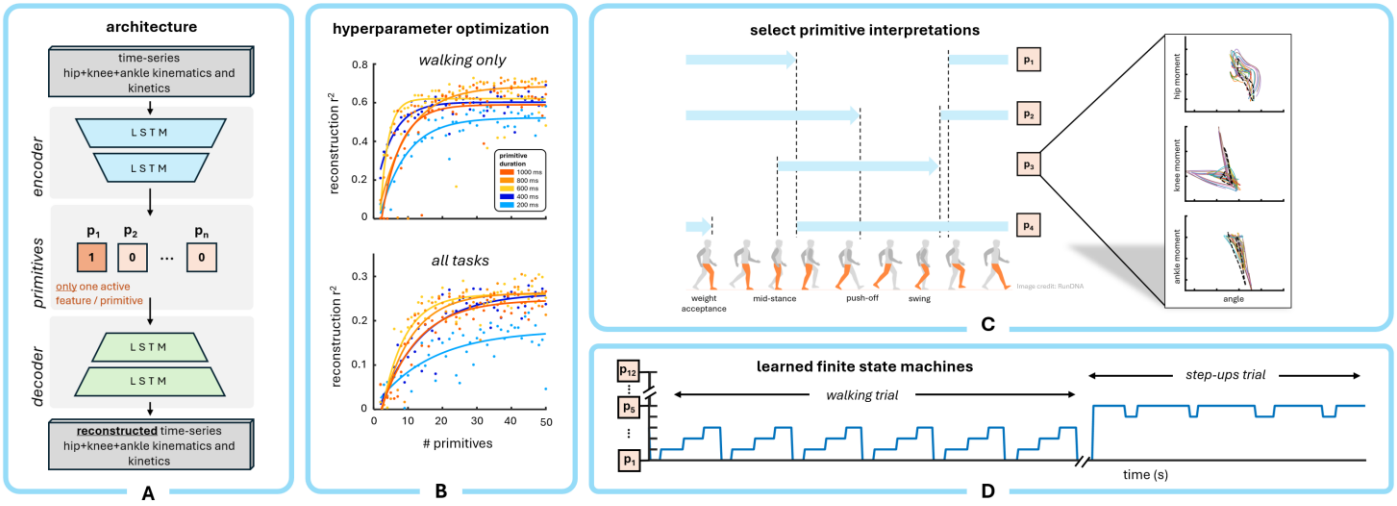


**Figure 1:** (A) The architecture of the variational autoencoder. (B) A comparison of model performance for varying numbers of primitives and input sequence span. The 600 ms model achieved highest reconstruction accuracies at lower primitive counts. (C) An interpretation of the four learned primitives for walking. The torque-angle curves associated with primitive $p_3$ (dashed black curves) are shown along with 20 representative validation datapoints assigned to $p_3$. (D) Primitive assignments of the complete dataset model when subject to a walking trial followed by a step-ups trial.

**Significance:** To our knowledge, this is the first attempt to discretize human movement using kinematics and kinetics without incorporating domain-specific knowledge. Our findings suggest that despite natural variability, human movement can be decomposed into a finite set of fundamental patterns. Future work will focus on optimizing each primitive for a wearable device and determining the optimal biological torque transformations for each, paving the way towards a fully end-to-end wearable robotics control strategy.

**Acknowledgements:** This research is supported in part by an ARO-awarded NDSEG fellowship.

**References:** [1] Molinaro et al., *Science Robotics* 9(88); [3] Keaton et al., Scientific Data 10(924)

# PERSONALIZING GAIT ENTRAINMENT: A REINFORCEMENT LEARNING APPROACH TO OPTIMIZING PERTURBATION MAGNITUDE

Omik Save[†,1], Junmin Zhong[†,2], Suhrud Joglekar[1], Jennie Si*[,2], and Hyunglae Lee*[,1]
[1]School for Engineering of Matter, and Transport, and Energy, Arizona State University, Tempe, AZ, USA
[2]School of Electrical, Computer, and Energy Engineering, Arizona State University, Tempe, AZ, USA
[†]Equal Contributied First Authors, *Corresponding authors' email: {si, hyunglae@asu.edu}

**Introduction:** Entrainment is the synchronization of human walking to external periodic stimuli including mechanical perturbations, which naturally motivates gait adaptations in users [1], [2]. However, the therapeutic potential of entrainment-based rehabilitation is limited due to arbitrary selection of perturbation magnitudes, which lead to sporadic entrainment success [1]. To address this issue, we introduce a novel framework, Offline Learning and In-situ Adaptation for Personalization (OLAP), that uses a reinforcement learning-based (RL) approach to personalize the minimum perturbation magnitude that leads to consistent entrainment in healthy individuals.

**Methods:** We recruited 13 healthy and diverse individuals (7 for offline RL training, and 6 for in-situ validation) to perform 90-second perturbed walking trials using a soft exosuit [2] that generated periodic hip flexion perturbations. The exosuit could simulate periodic perturbation magnitudes corresponding to actuator pressure between 25 and 125 *kPa*, with a resolution of 12.5 *kPa*. The location of perturbation corresponding to each gait cycle (normalized between 0-100%) is defined as a perturbation phase. The treadmill walking speed throughout each experiment was set constant to participants' preferred walking speed and the perturbation frequency matched their natural stride frequency. We performed OLAP in three main stages (Fig. 1A): 1) Training data collection, 2) Offline Deep Q-Network (DQN) learning, and 3) In-situ adaptation for personalization validation. During training data collection, the 7 participants performed perturbed walking trials at 25, 50, 75, 100, and 125 *kPa* magnitudes in randomized order with each condition repeated thrice. From each trial, we obtained a state-vector ($\boldsymbol{s} \in \mathbb{R}^3$) representing phase-variability ($\sigma_\phi$), entrainment success-failure outcome ($\rho \in [0,1]$), and magnitude of perturbation tested ($\tau$). A trial is labelled successfully entrained ($\rho = 1$) if the perturbation phases in the last 30 strides were contained within $\pm 10\%$ gait cycle of the mean perturbation phase [2]. Phase variability refers to the standard deviation of all the perturbation phases in the same stride analysis window. The choice of these state-vector components was justified due to their inherent influence on entrainment consistency. The DQN agent was then trained offline on several sequences of state-vectors from the training data such that each transition would result in only 25 *kPa* magnitude change (step change). Finally, during in-situ adaptations, the pretrained DQN agent informed perturbation magnitude changes ($a \in [ICR, DCR, NC]$), based upon the state-vectors obtained in new participants. The action changes and their corresponding magnitude are, ICR (increase): +12.5 *kPa*, DCR (decrease): -12.5 *kPa*, and NC (no change): 0 *kPa*. Convergence during adaptation trials was achieved when either three consecutive successful trials resulted in 'NC' action from the agent or 5 successive trials where the magnitude alternated between two neighbouring values ($|\Delta\tau_{max}| = 12.5$ *kPa*).

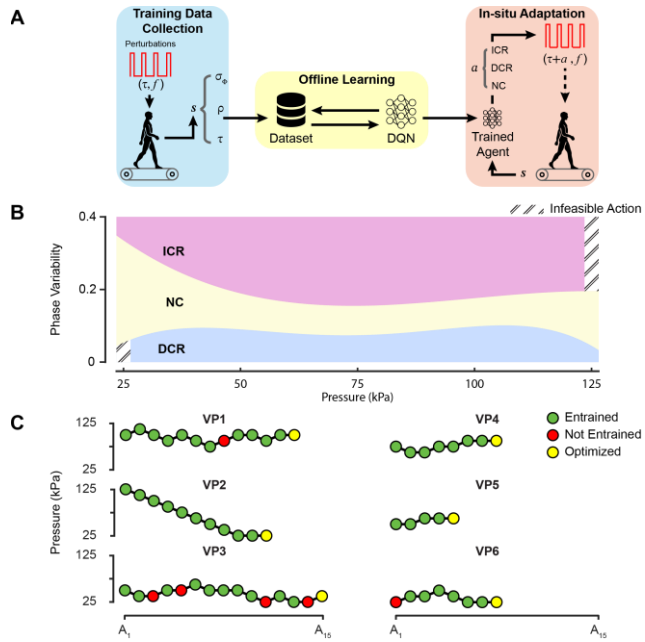


**Fig. 1. A:** Overview of the OLAP framework for entrainment personalization. '$f$' (Hz) represents the participants' natural walking frequency that was also used to set the perturbation frequency. '$\boldsymbol{s}$' is the state-vector in each perturbed trial and '$a$' represents the three-dimensional action space corresponding to perturbation magnitude changes during adaptation trials for magnitude personalization. **B:** Converged policy of the trained DQN agent displaying a nonlinear relationship between perturbation magnitude and phase variability in the offline training population. The boundaries do not explicitly represent relationship with entrainment likelihood. **C:** Optimization summary of in-situ adaptation trials ($A_n, n \in [1, 15]$). 'Yellow' markers represent personalized optimum magnitude in each participant upon meeting the convergence criteria.

**Results & Discussion:** Phase variability and entrainment likelihood are nonlinearly related across perturbation magnitudes (Fig. 1B). The data limitations made it infeasible to build probabilistic models for determining rule sets that would guide perturbation magnitude changes and achieve the objective. Nonetheless, the DQN agent was able to learn these nonlinear relationships between entrainment biomechanics in the offline dataset and successfully personalize the magnitude for 6 new participants, each within 15 perturbed walking trials each (Fig. 1C).

**Significance:** Our framework represents the first systematic method to personalize perturbation magnitude for achieving consistent entrainment in healthy individuals. Our results demonstrate that OLAP is both time- and data-efficient and can learn the complex relationships between different biomechanical components affecting entrainment consistency from a very limited dataset. The benefits of OLAP in this study makes it highly suitable for developing entrainment-based rehabilitation protocols that induce persistent gait adaptation in neurodivergent population groups through consistently successful entrainment.

**References:** [1] Ochoa et al. (2017), *J Neurophysiol* 118(4); [2] Save et al. (2024), *IEEE Trans. Neural Sys. Rehab. Eng.* 32.

# RANDOM FOREST CLASSIFIER OF STAIR ASCENT AND DESCENT EMBBEDED IN A ROBOTIC ANKLE FOOT ORTHOSIS

*Samuel C. Hopkins[1], Zachary F. Lerner[1]
[1] Mechanical Engineering Department, Northern Arizona University, Flagstaff AZ 86001 USA
*Corresponding author's email: ssh252@nau.edu

**Introduction:** Cerebral palsy is the leading childhood disability, affecting 500,000 children in the United States [1]. Solid ankle foot orthoses (SAFOs) are rigid ankle braces that provide stability and gait corrections to address ankle deficiencies common in CP. While effective for flat, level ground walking, SAFOs often fail to provide significant benefits during other activities of daily living that require a greater range of motion, such as getting in and out of a car or navigating stairs [2]. We previously developed a real-time, differential and adjustable stiffness AFO (DAS-AFO) capable of automatically modulating stiffness as a function of walking speed in real-time [3]. Other similar devices have been created within the past few years [4]. New controllers are needed for these systems that sense user intent and modulate stiffness for a wider variety of terrains and tasks.

Machine learning (ML) techniques have made significant progress in the field of activity recognition but have not made the jump to mobile platforms. IMUs, goniometers, and EMG sensors are commonly used to train ML models that predict activities like climbing stairs. However, these models are trained offline and have not been deployed in real-world contexts like an AFO where the prediction power is relevant. Thus, the purpose of this study was to develop and validate an online, personalized machine learning model embedded in our DAS-AFO platform capable of distinguishing level ground walking from stair ascent and descent. We present initial pilot testing in 6 unimpaired individuals (3 male, 3 female, ages =19-24).

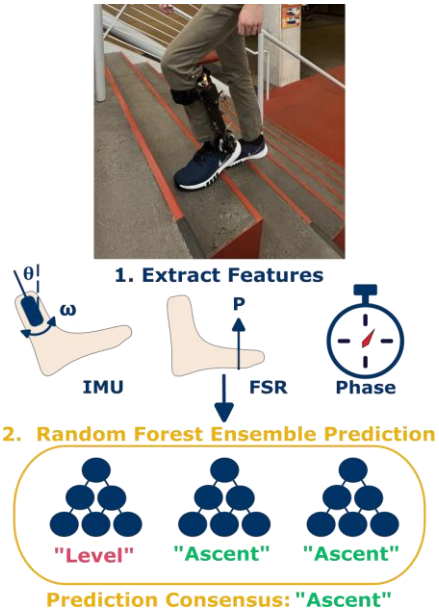


**Figure 1:** While walking with a DAS-AFO, gait kinematics, pressure under the sole, and phase time are input into a Random Forest model, which then predicts the activity of the wearer.

**Methods:** The DAS-AFO used in this study incorporated an IMU mounted at mid-shank and a force sensitive resistor (FSR) under the forefoot. Using these sensors, the device recorded gait phase times, minima and maxima of shank-to-vertical angle, sagittal plane angular velocity, and pressure under the sole. These features were input into a Random Forest ML model, as the user walked for 60 steps over level ground, 60 steps of stair ascent, and 60 steps of stair descent. These steps were split equally between low (120 Nm/rad) and high stiffness (350 Nm/rad) to ensure the model was robust to DAS-AFO parameters. The model was validated for each participant using 10-fold validation while hyperparameters (max tree depth, number of estimators, samples per leaf, and maximum number of leaf nodes) were tuned using a GridSearch method. The model was generated and carried on a laptop normally used to control the DAS-AFO via Bluetooth. The model was tested as participants walked over 30 steps of level ground, 30 steps upstairs, 30 steps downstairs while the model predicted the ambulation condition in real-time. A second set of 30 steps over sloped terrain was included to test generalizability to uneven terrain. The model was evaluated using the harmonic mean of precision and recall, or F1-score, for each class averaged across participants. Precision is a measure of how often positive predictions are correct, while recall is a measure of how often the model predictions are true.

**Results & Discussion:** On level ground, the model achieved an F1 score of 0.991 for low stiffness and 0.986 for high stiffness. For stair ascent, the F1 score was 0.966 and 0.938 for low and high stiffnesses respectively. For stair descent, the F1 score was 0.923 and 0.892 for low and high stiffnesses respectively. Averaging all three classes, the model's F1 score for low stiffness was 0.960 and 0.926 for high stiffnesses. Overall, the model performed best on level ground walking, followed by stair ascent, while descent was the least accurate condition. There was a slight drop in performance of 0.034 percentile points from low to high stiffness.

**Significance:** Our study demonstrates the high predictive ability of a Random Forest machine learning model with minimal model training requirements when embedded in an adaptive AFO in unimpaired users. Additionally, there was minimal impact on performance due to changing device stiffness indicating robust predictions. A limitation of this study is that we did not test model accuracy across multiple days. Additionally, a smaller handheld device would be preferred to the laptop used in this study; future work should aim to replicate the ML functionality in Android and iOS systems. This work, demonstrating the feasibility of this approach in real-world applications, justifies further validation in individuals with CP, who have more heterogenous gait patterns. Training was completed in less than an hour, while a simple toggle was used to label each mode as the user walked; thus, this approach could be feasible for clinical or at-home implementation.

**Acknowledgments:** This work was supported in part by NICHD of the NIH under Award Number R41HD113494.

**References:** [1] Odding et al. (0019), *Gait & Posture* 69; [2] Bayón et al. (2023), *J NeuroEng Rehabil* 20(1).; [3] Hopkins et al. (2024) *IEEE Robotics and Automation Letters.* 9(2); [4] Noort et al. (2024) *J NeuroEng Rehabil* 21(132)

# AI-BASED REFERENCE MODEL FOR PERSONALIZED ROBOT-ASSISTED GAIT TRAINING FOR DEPENDENT AMBULATORY CHRONIC STROKE SURVIVORS

*Derong Yang[1], Wen Liu[1]
[1]Department of Physical Therapy, Rehabilitation Science, and Athletic Training, University of Kansas Medical Center, Kansas City, KS 66160, United States
*Corresponding author's email: dyang2@kumc.edu

**Introduction:** Chronic stroke survivors with wheelchair dependence face significant barriers to gait training and need novel gait rehabilitation programs developed for their special needs.[1] Traditional and currently available gait training methods, such as therapist-assisted treadmill training or robotic training systems, often suffer from high labor-demanding, high cost, or lacking accessibility.[2] To address these limitations, we developed WalkAfresh (Fig. 1), a novel gait training device designed to facilitate hip flexion and ankle dorsiflexion by mechanically pulling the impaired leg using a servomotor and a pulling cord connected to the thigh brace and foot strap on the impaired leg. This device effectively reduces the controlled/constrained movement degrees of freedom in the affected limb, thereby promoting active patient participation and motor learning while minimizing sensory disruptions. During gait training, a therapist can adjust pulling length and pulling speed through the control panel of the device to match the specific treadmill speed for the individual under the gait training. The control software of the device automatically generates an initial guess of values of the two parameters using a formula with only a few anthropometric and geometric parameters. To improve the initial guess, we conducted this study to establish a prediction model between a set of input variables including treadmill speed, participant's anthropometric and demographic characteristics, and the two output variables of pulling length and pulling speed in healthy adults when they walk on a treadmill using the WalkAfresh device. This model will generate a better initial guess to match healthy adults' walking patterns and help us in future studies of gait training in stroke survivors using the WalkAfresh device.

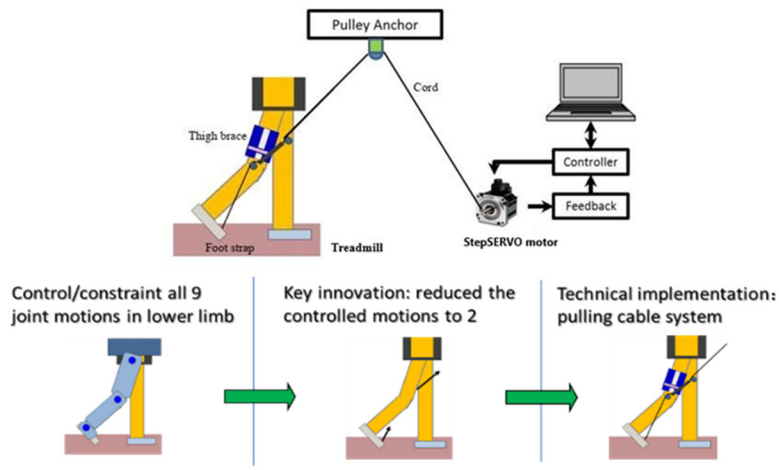


**Figure 1:** Illustration of the training device, WalkAfresh, and its design principles.

**Methods:** Fifteen consented healthy adults participated in this study. Anthropometric and demographic data, along with device encoding data recorded during participants' walk trials at varying treadmill speeds while using the WalkAfresh device, were collected. A multilayer perceptron neural network (MLPNN) was implemented to predict pulling parameter settings (Fig. 2).

**Results & Discussion:** After data preprocessing including outlier detection, missing data imputation, and feature scaling, a total of 94 recorded data sets were included in this machine learning modeling. The trained MLPNN demonstrated robust predictive accuracy with a test loss of 0.0252 and a mean absolute error (MAE) of 0.1292. The 5-fold Cross-validation results (loss: 0.0263, MAE: 0.1271) indicated good generalizability without overfitting. The model effectively captured nonlinear relationships between input variables (the individual anthropometric, demographic, and treadmill speeds) and output variables (pulling length and pulling speed), highlighting the potential for machine learning in personalized rehabilitation. However, limitations such as small sample size necessitate further validation with a more diverse participant pool.

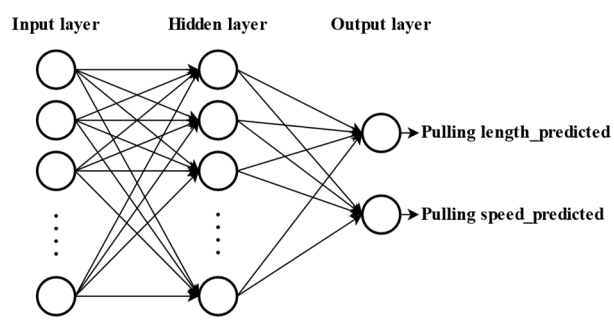


**Figure 2:** The structure of the MLPNN model.

**Significance:** This study provides a fundamental framework for integrating AI-driven personalization into gait training for stroke survivors. By leveraging machine learning to tailor training parameters, WalkAfresh could improve rehabilitation efficiency, enhance patient outcomes, and expand accessibility to long-term gait training.

**Acknowledgments:** This research was supported by the National Institutes of Health (NIH) under grant number 5R01HD108466-02.

**References:** [1] Tavares et al. (2022), *J Funct Morphol Kinesiol* 7(4); [2] Liu et al. (2018), Top Stroke Rehabil 25(5).

# AUTOMATED MACHINE LEARNING TO SIMPLIFY THE APPLICATION OF WEARABLE SENSORS

*Mojtaba Mohasel[1] and Corey Pew[1]
[1]Montana State University, Mechanical and Industrial Engineering, Bozeman, MT, USA
*Corresponding author's email: seyedmojtabamohasel@montana.edu

**Introduction:** Advances in sensor technology have provided biomechanists with a wealth of data for developing health monitoring applications. The creation of efficient tools is essential to convert raw sensor data into usable clinical outcomes (daily activities, falling, mobility, etc.). Automated machine learning (AutoML) is a fast emerging tool designed to facilitate model development for non-experts. However, current AutoML models, such as the Classification Learner app in MATLAB, Alibaba Cloud PAI AutoML [1], and Microsoft Azure ML [2], require paid subscriptions, are typically general-purpose, and function as black boxes, failing to address the specialized needs of biomechanists. Current limitations in AutoML open the field to the development of an open-source AutoML system specifically designed for processing time varying wearable sensor data (inertial measurement unit (IMU), Surface EMG, Load cell) for activity recognition tasks (*Performance*). In addition, since the application of the model is often in research and healthcare, biomechanists need to understand how choices made by AutoML during model development (*Education*). This study aims to address these knowledge gaps by developing a customized AutoML tool capable of generating high *performance* models with a method for user *education*.

**Methods:** The customized tool for IMU data, AutoIMU, was developed using publicly available activity recognition datasets, including AReM [3], PAMAP2 [4], WISDM [5], and Opportunity [6]. These datasets feature multiple IMU configurations and include several types of activities of daily living, such as jogging, sitting, standing, and ascending stairs. Design requirements for AutoIMU included: ability to input raw sensor data, optimizing window and overlap size, developing and optimizing an ML model (1-dimensional convolutional neural network (1D CNN)), extracting time-domain features (1D CNN) and frequency-domain features (Short-Time Fourier Transform + 2D CNN), handling class imbalance (weighted cross-entropy loss), providing a guided user interface for direct use, and delivering descriptive outcomes. AutoIMU employed a genetic algorithm (GA) for neural architecture search and hyperparameter optimization to develop high *Performance* models [7].

AutoIMU pursued the user *Education* aim by tracing the evolution of each hyperparameter and presenting its history through specific plots (called gene domination). These plots utilize the concept of natural selection, illustrating how each hyperparameter evolves in the form of genes that dominate the population over generations.

To demonstrate the efficacy of AutoIMU, we compared its performance to Mcfly [8], an existing open-source AutoML system designed for high *performance* activity recognition and user *education*. A Wilcoxon signed-rank test with p-value < 0.05 indicates a significant difference in model performance.

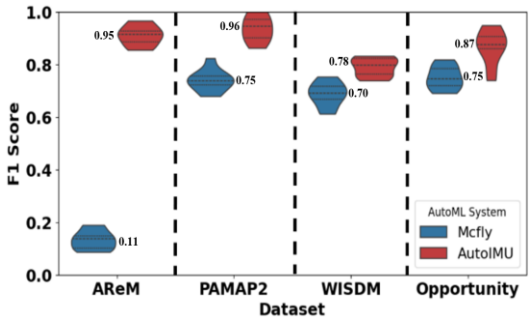


***Figure 1:*** *AutoIMU vs. Mcfly macro average F1-scores compared across four datasets. The mean F1-score numerical values are shown for each method.*

**Results & Discussion:** A comparison of macro-average F1-score *Performance* of ten top performing models from each AutoML system indicates that AutoIMU outperforms Mcfly in all datasets (p-value < 0.05) (Fig. 1). AutoIMU's superior performance can be attributed to its window and overlap optimization, extraction of time- and frequency-domain features, use of a weighting method in the cross-entropy loss function to handle class imbalance, and application of GA for optimization. By comparison, Mcfly uses a fixed window size determined by the user, optimizes four neural network architectures (CNN, DeepConvLSTM, ResNet, and InceptionTime), lacks a specific method for handling class-imbalanced data, and relies on random search for hyperparameter optimization. The architecture that Mcfly employs is designed for relatively large datasets, which explains its poor performance on AReM. In contrast, AutoIMU is robust to dataset size, which is ideal for research and clinical applications where data may be limited.

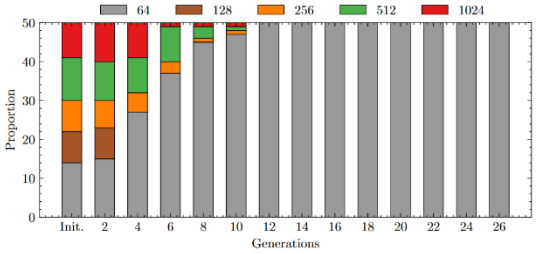


***Figure 2:*** *An example gene domination plot for window size. Different window sizes shown in different colors*

AutoIMU explains the hyperparameter selection process using a gene domination plot for user *Education* (Fig. 2). The x-axis represents generations, while the y-axis shows the proportion of window sizes. The population consists of 50 trained neural networks with different window sizes, with colors representing their proportions in the population. Initially ("Init."), the population is diverse, with window sizes evenly distributed due to random initialization. As generations progress, a window size of 64 (gray) gradually dominates, as this size achieves a higher F1-score *Performance*. AutoIMU illuminates the hyperparameter selection process by providing a historical view of the chosen hyperparameters. In contrast, Mcfly illustrates only the final average performance per network depth without showing the selection process. However, Mcfly has developed some tutorials to educate users and conducted a survey with 30 participants to evaluate its *Educational* effectiveness. A limitation of this study is the lack of a measurement of user *Education* aim to show its success. Future work for AutoIMU will include conducting a user survey to measure the effectiveness of its educational aim and adding a graphical user interface.

**Significance**: Biomechanists can adopt the open-source Python code of AutoIMU to develop high *Performance* models without machine learning expertise, with visualizations explaining hyperparameter significance (*Education*).

**References:** 1) Wang et al, IEEE IISWC, 2019; 2) Barnes J, Microsoft Azure Essentials, 1st ed, Microsoft, 2015; 3) Palumbo et al, Springer, 2013; 4) Reiss et al, IEEE ISWC, 2012; 5) Kwapisz et al, ACM SIGKDD Explor. Newsl., (12) 2011; 6) Roggen et al, IEEE INSS, 2010; 7) Lu et al, GECCO, 2019; 8) Van Kuppevelt et al, SoftwareX, (12) 2020.

# INTEGRATING MULTIPLE BIOSENSORS TO MODEL POSTURAL AGILITY

*Charlize Lowrie[1], Mitchell Wollen[1], William Saunders[1], Nathan Adams[1], Caspian Bell[1], Christoper Aliperti[1], Rebecca Zifchock[1], Josiah Steckenrider[1], Gregory Freisinger[1]
[1]Department of Civil and Mechanical Engineering, United States Military Academy
*Corresponding author's email: charlize.lowrie@gmail.com

**Introduction:** Postural control can be described as a spectrum spanning postural stability, postural agility, and dynamic stability [1]; and is employed to track and treat neurological and musculoskeletal impairments [2]. While most research to date focuses on static or quasi-static balance tasks that describe postural stability [3, 4]. This study focuses specifically on postural agility, defined as the ability to actively and accurately alter the location of the center of mass (COM) in response to visual stimuli [1]. The postural agility protocol employed in this research involves a custom MATLAB-based video game called BlockRunner [1], where a subject controls their position in a simulated environment using a force plate. To gain insight into the neuromuscular basis of movements associated with postural agility during this protocol, this study integrates low-cost surface electromyography (sEMG) sensors in combination with force plate data collected during the game. This novel methodology to model postural agility will enable additional capabilities for active lower limb prostheses and a validated method for obtaining data beyond a laboratory setting.

**Methods:** The BlockRunner game utilizes data from an AMTI AccuGait-Optimized portable force plate to display the subject's position relative to blocks that appear to be moving towards them in a simulated environment (Fig. 1b). The subject attempts to dodge the objects on the screen to find a clear path of travel by shifting their COM in the medial-lateral direction, reflected by changes in the center of pressure (COP) recorded by the force plate. (Fig. 1c). At the same time, surface electrodes (Myoware Muscle Sensor 2.0) are attached to muscles in the lower leg according to SENIAM conventions [5] (reference S1-S6 in Fig. 2) to measure muscle activation corresponding to the changes in COP. The sEMG data is pre-processed and synchronized to the force plate data according to the data synchronization protocol (Fig. 2). Time domain features are extracted from the sEMG and force plate data (Fig. 2). A machine learning classifier is then trained to predict the movement of the subject's COP throughout the postural agility protocol using the sEMG features.

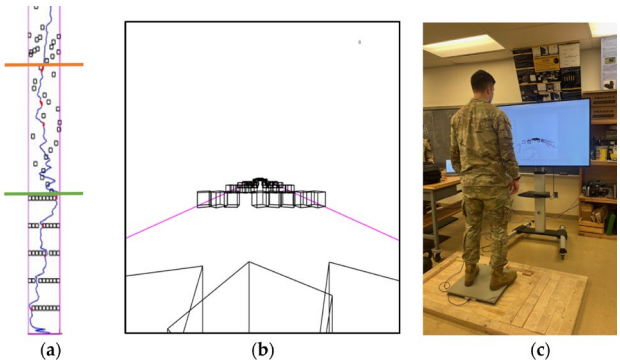


**Figure 1:** (a) Aerial view of the track in the BlockRunner game with the orange and green lines separating the three stages. (b) View from the perspective of a subject during gameplay. (c) Testing setup for collection of force plate data. [1]

**Results & Discussion:** The primary result of this research is the machine learning pipeline described in Figure 2. This pipeline includes the simultaneous data collection from the sEMG and force plate, preprocessing and data synchronization, feature extraction from both data sources, and finally the training of the machine learning model to classify the movement of the subject's COP. Data collection is underway to refine the classification model and validate its accuracy.

**Significance:** The outcome of this research is expected to provide a greater understanding of how muscles in the lower leg contribute to movements of a subject's center of pressure while conducting postural agility tasks. Once deployed, this model can provide novel capabilities to active lower limb prosthetics, providing patients with improved postural agility. Additionally, expected strong correlations between force plate metrics and sEMG will validate that sEMG can serve as a non-invasive, cost-effective method for obtaining data during dynamic postural control tasks. Using sEMG as a validated method for obtaining data outside of the laboratory will increase the breadth of research that can be done to aid in the application of postural control tasks as diagnostic measures for neurological and musculoskeletal impairments.

**References:**
[1] Aliperti et. al. (2024), *Sensors* 24(23), 7420; [2] Caeyenberghs et. al. (2010), *Hum. Brain Mapp.* 31, 992–1002; [3] Lee & Sun (2018). *J. Physiol. Anthr.* 37, 27; [4] Murillo et. al. (2012), *Hum. Mov. Sci.* 31, 1224–1237; [5] Merletti et. al. (1997), http://www.seniam.org/.

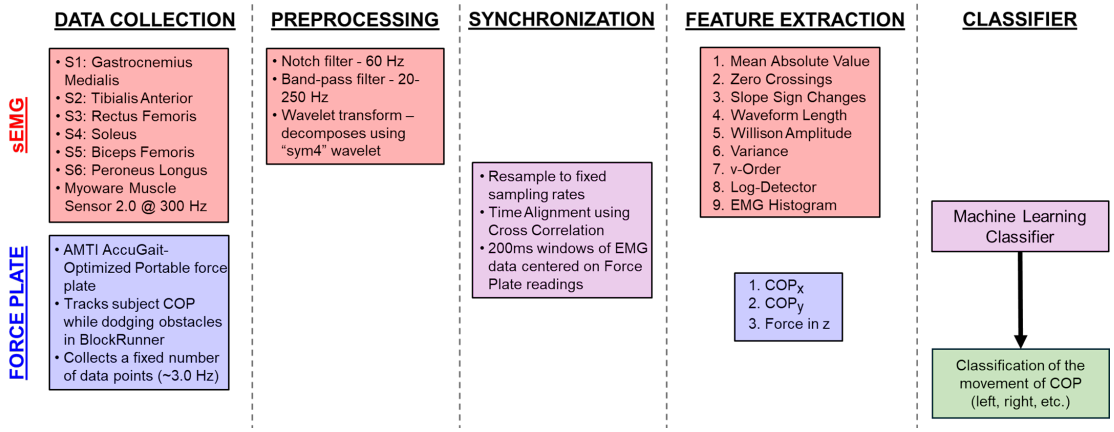


**Figure 2:** Process from data collection to labels assigned by the machine learning classifier.

# DETERMINING OPTIMAL IMU SENSOR PLACEMENT TO PREDICT CENTER OF PRESSURE VELOCITY DURING PERTURBED STANDING IN THE CHRONIC STROKE POPULATION

*Isabelle Museck[1], Jesse Dean[1,2]
[11]Medical University of South Carolina, [2]Ralph H. Johnson VA Health System
*museck@musc.edu

**Introduction**: Neurological damage following a stroke can greatly impact standing balance, creating significant long-term impairments that affect approximately half of post-stroke individuals [1-2]. Balance plays a crucial role in performing daily activities and reducing the risk for falls. Improving balance can significantly increase independence and improve quality of life for stroke survivors [1]. Recent work has suggested that sensory augmentation can improve balance performance by delivering stimulation based on real-time biomechanical measures of the body's dynamic state [2]. Portable inertial measurement units (IMUs) can allow such augmentation to be delivered outside of a laboratory setting. Machine learning models have demonstrated the potential to use real-time wearable sensor data to accurately estimate biomechanical measures linked to balance performance, such as center of mass (CoM) and center of pressure (CoP) motion [3]. Specifically, Temporal Convolutional Networks (TCN) are a promising approach for estimating the state of the body from real-time IMU data during both perturbed and unperturbed conditions [5]. Our aim was to quantify how the predictive performance of an optimized TCN model for perturbed standing CoP is influenced by the quantity and positioning of IMUs.

**Methods:** Optimal sensor location was investigated using data from 15 individuals with chronic stroke and our TCN model with previously optimized hyperparameters. Participants wore 7 IMU sensors (sacrum, bilateral thighs, shanks, and feet) and performed a series of 30-second standing trials on a force plate with their eyes open. The standing surface translated mediolaterally on an unpredictable sum-of-sines (0.1-0.9 Hz) trajectory. Participants were instructed to remain quiet and relaxed, while translation amplitude gradually increased for each trial until CoP rms velocity exceeded 20 mm/s. Models were trained using the leave-one-trial-out validation approach with all three components (magnetometer-accelerometer-gyroscope) and directions (x-y-z) of the IMU sensors as inputs, and the corresponding true CoP velocity measurements from the force plate serving as the targets. CoP velocity was chosen as the target output because it reflects sensitive changes in sway and captures real-time postural stability adjustments [6]. Initially, the models were trained using data from each of the seven IMUs. The average validation RMSE among trials and among each of the 10 participants were recorded for each sensor configuration. The best performing sensor was then combined and trained with each possible combination of the remaining sensors. This process was repeated iteratively until the best performing configurations of 1-6 sensors were identified.

| No IMUs | Sensor Configuration | Avg RMSE [mm/s] |
|---|---|---|
| 1 | R shank | 7.31 (3.05) |
| 2 | R shank/ R foot | 6.80 (2.84) |
| 3 | R shank/L shank/ R foot | 6.63 (3.15) |
| 4 | R shank/L shank/ R foot/L foot | 6.52 (3.17) |
| 5 | R shank/L shank/ R foot/L foot/ R thigh | 6.41 (3.00) |
| 6 | R shank/L shank/ R foot/L foot/ R thigh/ Sacrum | 6.25 (3.00) |
| 7 | All | 6.30 (3.03) |

**Table 1:** Best performing configurations among participants, given the number of IMUs used in the model.

**Results & Discussion:** The sensor combinations yielding the best estimation performance can be seen in **Table 1.** When using a single sensor to estimate center of pressure, the right shank IMU performed the best, with an average validation RMSE value of 7.31 (+/- 3.05 mm/s). Other recent studies have identified the lower back and feet to be the best locations for model predictions during walking [3,7-8]. However, our study focused on CoP estimation during quiet, perturbed standing, which differs from the walking conditions in these studies. During relaxed standing, the shanks undergo mediolateral accelerations and angular velocities as the legs adjust to maintain posture during translation, likely explaining their optimal performance in our application. The varying results, along with differences in tasks, populations, and perturbation conditions across studies, suggests that optimal sensor placement is highly context dependent. **Fig 1** represents the average RMSE for each quantity of sensors. There is a less than 3% decrease in RMSE values when going from 3-4, 4-5, 5-6, and 6-7 sensors to make predictions. These results demonstrate only a small change (<5%) in RSMSE after 3 sensors which is consistent with a similar study investigating the effects of reducing the number of IMUs on walking CoP predictions in healthy individuals from an LSTM model. This study also found insignificant gain in model performance above 3-5 sensors [7].

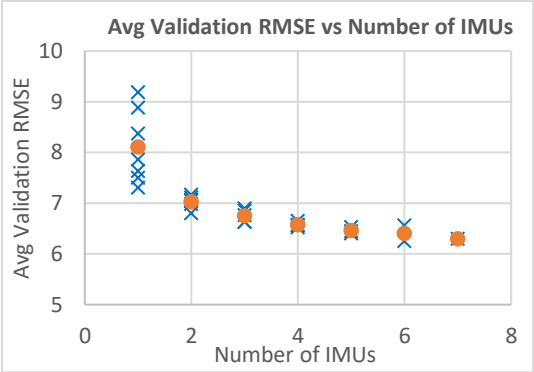


**Fig 1:** Dependence of validation error on the number of IMUs used as input into TCN model (blue x's- average of a different placement configuration; red points- averages for each quantity of IMUs)

**Significance:** Wearable technologies offer a low-cost, portable way to track biomechanical characteristics. Reducing the size of a wearable system by using fewer IMUs contributes to lower costs and increased usability. The results from this study will guide the development of machine learning systems and integrated wearable technologies that provide real-time sensory augmentation for balance rehabilitation.

**Acknowledgments:** This work is supported by NSF award #OIA-2242812.

**References:** [1] Schmid, et al. (2023) *Topics Stroke Rehab*, *20*(4), 340–346; [2] Sienko, et al. (2018) *Front Neuro*, *9*, 944; [3] Museck, et al. (2024) *Sensors*, *24*(22), 7280;[5] Leestma, et al.(2024), *Annals of Biomed. Engr*, 52, 2013–2023;[6] Masani, et al. (2014). *Gait&Posture*, *39*(3), 946–952; [7] Podobnik, et al.(2020), *Sensors*, *20*(21), 6136; [8] Wu, et al. (2020) *Front Bioen Biotech*,8:566474.

# TOWARDS GENERAL MOTION TRACKING IN PHYSICS-BASED SIMULATION

*Hyoungseo Son[1], Seungmoon Song[1]
[1] Department of Mechanical and Industrial Engineering, Northeastern University, Boston, MA
*Corresponding author's email: son.hyo@northeastern.edu

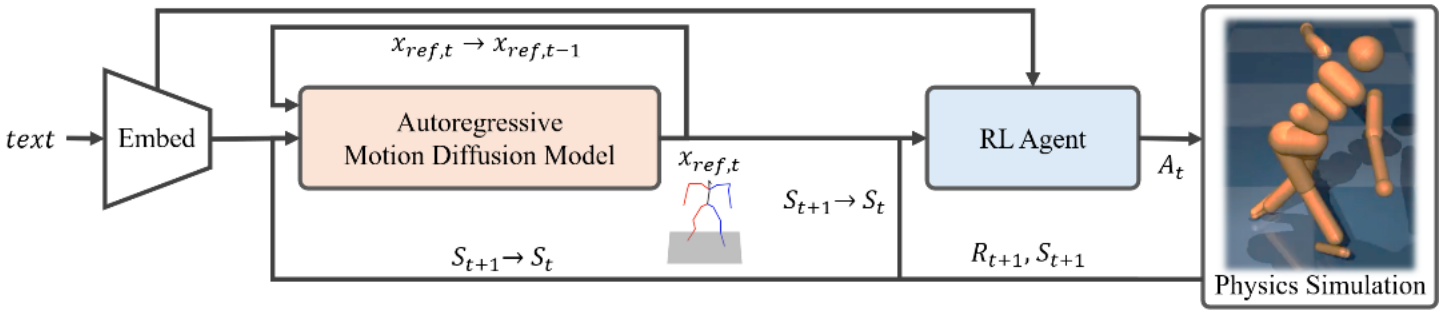


**Figure 1:** Overview of the Framework, $\boldsymbol{x_{ref}}$: target pose, $\boldsymbol{R}$: reward from simulation, $\boldsymbol{A}$: action from RL agent, $\boldsymbol{S}$: state

**Introduction:** Diffusion model–based human motion generation has been actively studied in recent years [5]. Research on physically plausible motion generation has gained traction by incorporating physics-based constraints into diffusion models [8, 9, 3]. In addition, studies have explored trajectory-following motion generation with diffusion models [7]. On the other hand, Reinforcement learning (RL) has been widely used for imitation learning in simulation environments, where agents learn to replicate real-world motion-captured data [6, 2, 10]. We present a framework for performing text-to-motion in physics simulation. To achieve this, we train a autoregressive motion diffusion model [4] and torque-based deep learning policy using reinforcement learning on a motion dataset to output physically feasible actions that follow the target motion.

**Methods:** We plan to train an autoregressive-motion diffusion model (A-MDM) [4] that takes text or other conditions along with the current observation as input and outputs the next target pose. The target pose, together with the text embedding, is then provided as input to the RL agent. The RL agent's actions are joint torques that drive the simulated humanoid. After one control step, the simulation returns the reward and the next state (Fig 1). We use the HumanML3D dataset [1]. For the physics simulation, we used MuJoCo and Gymnasium's humanoid-v5 model. HumanML3D comprises 22 kinematic chain position data points. Since the simulation model and the dataset do not have exactly matching dimensions or kinematic chain characteristics, similarity between them cannot be measured solely by Euclidean distance. Therefore, we compute the reward using the directional error of each segment and the position error for a selected subset of joints.

$$R_{j,t} = \frac{1}{N}\sum_{i}^{N} \exp\left(k\frac{\boldsymbol{j}_{target,i} \cdot \boldsymbol{j}_{sim,i} - 1}{2}\right)$$

$$R_{e,t} = \frac{1}{M}\sum_{i}^{M} \exp\left(-k\frac{\left\|\boldsymbol{e}_{target,i} - \boldsymbol{e}_{sim,i}\right\|}{2}\right)$$

Reward is expressed as $R_t = w_j R_{j,t} + w_e R_{e,t}$ where $R_j$ refers to the reward that minimizes the discrepancy between the directional vector motions of each joint pair in the target motion and the simulation, $R_e$ represents the reward that minimizes the joint position differences for a selected subset of joints, where the total number of joints considered is $M$. Reward is used for updating the RL agent's policy. The RL policy is updated using the Proximal Policy Optimization (PPO) algorithm [11]. The autoregressive part of the diffusion model feeds its output back as input, which can lead to discrepancies between the physics simulation and the dataset. To address this, we replace the autoregressive part with physically feasible motion data generated through reinforcement learning (Fig 1). Since the dimensions of the model and the motion do not exactly match, the initial state is computed by minimizing the error term used in the reward through the least squares method (Fig 2).

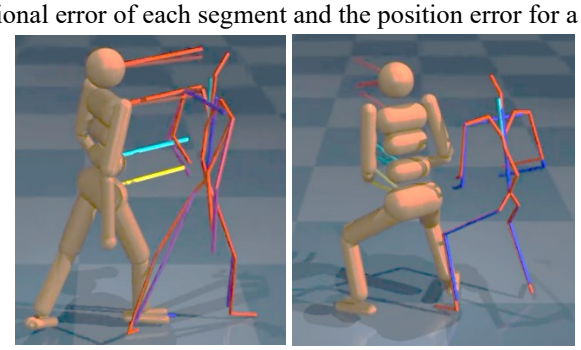

**Figure 2:** Pose following example. The figure consists of two panels, each showing a different motion. In the left half of each panel, the simulation model is shown tracking the target motion. In the right half, both the target and simulation motions are presented with overlaid vector errors using a color map.

**Results & Discussion:** We have implemented the simulation environment, including the process for determining the initial state via the least squares method. By the conference date, the Motion Diffusion Model and the RL agent are expected to be fully trained to generate motion in simulation from text prompts.

**Significance:** This study aims to develop a general controller for human models that can follow a wide range of motions. Although the current work is limited to a torque-driven model, there have been many recent attempts to apply reinforcement learning to neuromechanical simulations [10]. A long-term goal is to extend this approach to musculoskeletal models, enabling text-to-musculoskeletal motion generation.

**Acknowledgments:** This research is partially funded by the National Institutes of Health (R00AG065524).

**References:** [1] Guo et al. (2022), CVPR, pp. 5152–5161;[2] Park et al. (2022), ACM SIGGRAPH '22;[3] Peng et al. (2023), arXiv:2312.06553;[4] Shi et al. (2024), ACM Trans. Graph., 43;[5] Tevet et al. (2023), ICLR;[6] Wang et al. (2023), arXiv:2312.04393;[7] Xie et al. (2024), ICLR;[8] Xu et al. (2023), ICCV;[9] Yuan et al. (2023), ICCV;[10] Song et al. (2021), J Neuroeng Rehabil, 18(1);[11] Schulman et al. (2017), arXiv:1707.06347

**AI-Based Wearable Gait Analysis for Proactive Fall Risk Prediction**

* Patrick Kim[1]
[1]The Governor's Academy
*Corresponding author's email: hjpkim706@gmail.com

**Introduction:** Gait analysis is an essential approach to understanding neuromuscular control and the progression of various chronic conditions, including Parkinson's disease and diabetic neuropathy. Subtle gait alterations can provide early indicators of emerging pathologies. Traditional analytical methods, such as classical statistical modeling or threshold-based outlier detection, sometimes fail to capture these nuanced deviations in high-dimensional signals (e.g., accelerometer and gyroscope data). Recent advances in deep learning techniques, notably autoencoders and Generative Adversarial Networks (GANs), have shown promise in effectively modeling complex time-series data. In this study, we present an AI-based framework for detecting anomalous gait patterns, aiming to identify abrupt changes using publicly available datasets.

**Methods:** We utilized the UCI Human Activity Recognition (HAR) dataset [1], comprising tri-axial accelerometer and gyroscope data collected from smartphones worn by participants during various daily activities. Data preprocessing involved segmenting continuous recordings into fixed-length windows (2 seconds, 50% overlap) and normalizing each dimension. Two distinct anomaly detection models were then developed: (1) an autoencoder trained to reconstruct typical gait patterns by minimizing mean squared error loss, and (2) a GAN, where the generator learned to produce realistic gait sequences while the discriminator classified sequences as normal or abnormal. Both models were trained solely on normal gait segments (80% of normal data) for 100 epochs, with early stopping based on validation loss. Synthetic anomalies (e.g., artificially inserted abrupt stops and shifts in gait rhythm) were introduced in the remaining 20% of the data to evaluate model performance. Classification metrics such as accuracy, sensitivity, and specificity were computed to quantify anomaly detection.

**Results & Discussion:** Our results demonstrated that the autoencoder-based model achieved an overall detection accuracy of 92.5%, with a sensitivity of 0.90 and specificity of 0.94. The average reconstruction error for normal segments remained low (0.08 ± 0.01), whereas artificially perturbed segments exhibited elevated error values (0.20 ± 0.03). Similarly, the GAN-based approach achieved an accuracy of 93.2%, indicating its comparable efficacy in modeling the distribution of normal gait. Notably, the GAN showed marginally higher sensitivity (0.92) for subtle gait perturbations, although its specificity (0.93) was slightly lower. These findings underscore the potential of deep learning–based frameworks to capture high-dimensional gait dynamics and accurately detect atypical patterns. However, variations in participants' gait style and limited data size could influence generalizability, warranting future research with diverse cohorts and real-world perturbations.

**Significance:** By rapidly identifying even minor deviations in gait, these AI-based approaches can facilitate early intervention and continuous monitoring in clinical and everyday settings. Widespread implementation may provide a proactive means to enhance patient outcomes, support rehabilitative strategies, and extend our understanding of how subtle motor changes contribute to the onset and progression of neurological and musculoskeletal conditions.

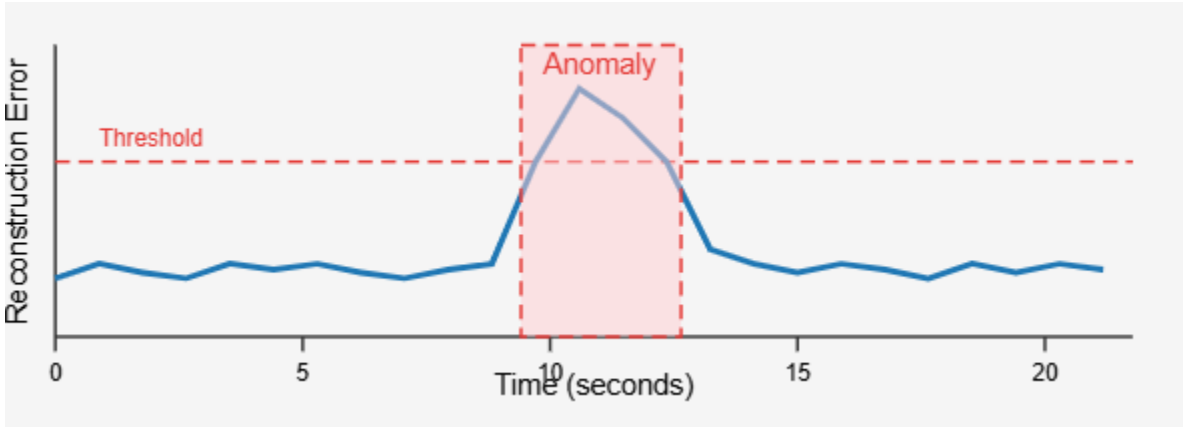


**References:** [1] Anguita, D., Ghio, A., Oneto, L., Parra, X., & Reyes-Ortiz, J. L. (2013). A Public Domain Dataset for Human Activity Recognition Using Smartphones. 21th European Symposium on Artificial Neural Networks, Computational Intelligence and Machine Learning (ESANN). [2] Zeng, W., & Wang, G. (2019). Gait Analysis with Deep Learning for Abnormal Event Detection. Journal of Biomechanics, 56(2), 123–132. [3] Choi, A., Park, S., & Kim, M. (2020). Deep Learning–Based Anomaly Detection in Gait Analysis. Biomechanics and Modeling in Mechanobiology, 19(5), 1033–1045.

# AI-ASSISTED GRADING: EFFECTS ON STUDENT GRADES, FACULTY WORKLOAD, AND FEEDBACK QUALITY

Nikita Kuznetsov, Ph.D.
Department of Rehabilitation, Exercise, & Nutrition Sciences, College of Allied Health Sciences, University of Cincinnati
*Corresponding author's email: kuznetna@ucmail.uc.edu

**Introduction:** While generative artificial intelligence (genAI) discussions in higher education often focus on academic misconduct, its potential for improving grading and student feedback remains underexplored [1]. Grading open-ended written responses in large undergraduate biomechanics and kinesiology courses presents challenges in maintaining grading consistency and providing timely feedback. This study investigates the integration of genAI (ChatGPT-4o) into grading workflows for short-answer exam questions in an upper-division Kinesiology course. The primary objectives were to (1) examine the effects of AI-supported grading on student grades, comparing Faculty-only grading, AI-assisted grading (Faculty+AI), and AI-only grading, (2) evaluate the quantity and quality of feedback provided to students using these grading methods, (3) assess student perceptions of AI-generated feedback, and (4) analyze workload implications, specifically the time required for AI-assisted grading compared to traditional faculty-only grading.

**Methods:** In Fall 2024, I taught a junior-level Kinesiology course (HLSC 3023) at the University of Cincinnati, with 117 students. The course included lectures, hands-on labs, and three exams. During the course, short-answer exam responses were graded using the Faculty+AI approach, which included: (1) rubric development (2-point, 1-point, 0-point criteria), (2) AI evaluation of student responses using ChatGPT-4o based on the rubric, (3) faculty review of AI-generated feedback, and (4) final grading and feedback entry in the course learning management system for student review. After the semester concluded, responses from 20 students on four short answer questions from Exam 2 and Exam 3 (80 responses total) were randomly selected and manually regraded by the instructor without reference to prior AI-assisted grades. The questions were at the level of "Comprehension" in Bloom's taxonomy and asked about Q-angle and its relation to knee valgus/varus, foot pronation during gait, scapulohumeral rhythm, and muscle activity to extend the fingers. Three grading conditions were compared: (1) Faculty-only, (2) Faculty+AI, and (3) AI-only (this was the grade given by AI without faculty corrections). Absolute agreement between the grading methods was assessed using the intraclass correlation coefficient (ICC) [2]. A post-course survey sent to all students in the course collected qualitative and quantitative insights into student experiences with AI-generated feedback (N=51).

**Results & Discussion:** Faculty-only grading resulted in the highest average grades (1.56), followed by Faculty+AI grading (1.46), while AI-only grading was the strictest (1.01), leading to a 35% lower average grade than faculty-only grading (Fig. 1). Reliability analysis indicated excellent-to-good agreement (ICC > 0.70) between Faculty+AI and Faculty-only grading, but lower agreement between Faculty-only and AI-only (ICC = 0.31-0.39), similar to a previous study [3]. One question had poor agreement between Faculty-only vs. Faculty+AI (ICC = 0.37) due to human grading error in two responses in Faculty-only method, where full credit was given despite inaccuracies in responses. These findings suggest that AI-assisted grading leads to slightly lower student grades than Faculty-only grading, likely due to reduced human grading error.

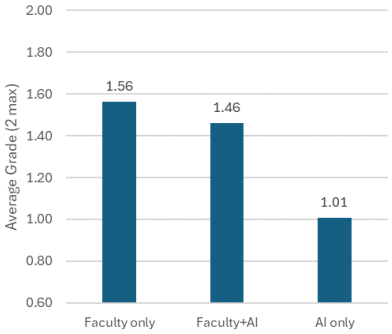


**Figure 1:** Average grades on short answer responses from two exams by grading method. Max score is 2.

Faculty+AI grading significantly increased feedback quantity, averaging 80.4 words per response compared to 17.6 words in Faculty-only grading. However, grading time increased approximately 1.75-2 times, with AI-assisted grading taking 85.5 seconds per response versus 52.5 seconds for Faculty-only grading. Estimated grading time for Exam 2 was 2 hours and 32 minutes (Faculty-only) vs. 4 hours and 26 minutes (Faculty+AI), and for Exam 3, 4 hours and 17 minutes (Faculty-only) vs. 8 hours and 22 minutes (Faculty+AI). Grading time increased due to the need to review both student responses and AI-generated feedback.

Student perceptions of AI-assisted grading were generally positive, with 90% expressing openness to its use. The benefits mentioned by the students included clearer, more detailed feedback, better conceptual breakdowns, and positive reinforcement. However, they also expressed concerns about grading strictness and transparency in AI evaluations. Among students, 45% fully supported AI-assisted grading without reservations, while another 45% preferred AI-generated feedback only when reviewed by faculty. The remaining 10% favored human-only grading, citing concerns about AI misinterpreting complex responses.

**Significance:** This study highlights genAI's potential to enhance grading feedback quantity and quality in large movement science classes but also highlights the need for faculty expertise. Collaborative Faculty+AI grading has the potential to minimize human error and increase the consistency of grading across students. Although AI-assisted grading increases workload in its current form, optimization, and iterative improvements could mitigate this drawback. This study gave insight into student perceptions of faculty's use of generative AI to provide feedback on their work, which is important to consider as AI gets more integrated into biomechanics teaching.

**Acknowledgments:** I thank Danya Ghussin for her help with data preparation.

**References:** [1] Ogunleye et al. (2024), *Educ Sci* 14(6); [2] Hallgren (2012), *Tutorials Quant Meth Psychol* 8(1); [3] Wetzlet et al, (2024), *Teach. Psychol*, https://doi.org/10.1177/00986283241282696

# Automated analysis of the worn condition for shoes: using smartphone pictures, convolutional neural networks, and thin-film modeling to predict loss in traction

*Gerard Aristizábal Pla[1], Matthew Kaboly[1], Sydney Clements[1], William Miller[1], Kurt Beschorner[1]
[1]Department of Bioengineering, University of Pittsburgh, Pittsburgh, PA
*Corresponding author's email: gea62@pitt.edu

**Introduction:** Slips and falls remain a leading cause of workplace injuries. Worn shoe outsoles alter tread geometry, leading to elevated fluid pressures at the shoe-floor interface and an increased likelihood of slipping. Current methods for assessing shoe slip risk are often costly or impractical for routine use. Images captured via smartphones provide a practical and affordable method for evaluating slip risk in worn footwear. This study aimed to advance the use of smartphones for assessing shoe slip risk by: (1) assessing the accuracy of a series of convolutional networks, namely two U-Nets [1] and a Resnet-50 [2], in automatically identifying the largest worn region from phone images, and (2) investigating the association between predicted peak fluid pressures from the largest worn regions and experimentally-measured peak fluid pressures, coefficient of friction, and friction loss (i.e., percent coefficient of friction relative to baseline). Following Sundaram et al. [3] and Beschorner et al. [4], we hypothesized that higher predicted peak fluid pressures would be associated with higher experimental peak fluid pressures and lower coefficient of friction values.

**Methods:** Fifteen participants wore two distinct pairs of shoes with varying tread patterns in their workplaces (IRB PRO15030214) [5]. Each pair was worn for one month at a time. The coefficient of friction was assessed at baseline and after each month of wear using a slip tester. Peak fluid pressures were simultaneously measured with an array of fluid pressure sensors embedded in the floor of the slip tester. Images of shoes (n=902) were taken with a smartphone (iPhone 12, Apple). Ground-truth masks were generated using Fiji's (Fiji, Schindelin et al. [6]) polygon tool and converted into binary masks with the "Create Mask" feature. For aim 1, a U-Net was trained on 449 images to automate the shoe outsole detection from the background. A Resnet-50 was then trained on 700 images (350 worn, 350 new, unmatched pairs) to classify the shoes in being either worn or new. Finally, a U-Net was trained on 202 images from [5] to automate the worn region detection for shoes that were classified as worn using data augmentation techniques (e.g., rotations, horizontal flips). Images were first pre-processed using contrast-limited adaptive histogram equalization technique to enhance outsole details. U-Net and Resnet-50 model performances were assessed using 80% of the data for training, 10% of the data for validating and 10% of the data for testing. For aim 2, 119 images of worn shoes [5] were used to create ground-truth masks of the largest worn regions. These masks of the largest worn regions were input into a numerical solver of Reynolds' Equation to simulate fluid pressure dynamics between contacting surfaces [4].

We visually inspected U-Net performance, evaluated Resnet-50 performance using accuracy, and conducted simple linear regressions to explore relationships between predicted peak fluid pressures and experimental peak fluid pressures (square root transformation), coefficient of friction values and friction loss (log transformation).

**Results & Discussion:** (1) The first U-Net successfully distinguished shoe outsoles from the backgrounds. Representative model predictions for a sample image are shown in Figure 1 (Figure 1B). The Resnet-50 was able to classify shoes in being worn or new with an accuracy of 96%. Finally, the last U-Net was able to successfully distinguish worn regions from the outsoles. Representative model predictions for a sample image are shown in Figure 1 (Figure 1C). The convolutional networks demonstrated their potential in automatically identifying worn regions. The performance of the networks could be enhanced with additional phone images, as we had a limited data set consisting of only 902 images. (2) Higher predicted peak fluid pressures were associated with higher experimental peak fluid pressures ($R^2$=0.052, p=0.0091), lower coefficient of friction values ($R^2$=0.25, p<0.001) and increased friction loss ($R^2$=0.14, p<0.001). The assumption that the entire worn region was in contact with the ground may have contributed to lower predictive ability of the models. Representative fluid pressure predictions are shown in Figure 1 (Figure 1D).

**Significance:** This study demonstrates the feasibility of using smartphones combined with convolutional networks and fluid modeling to automate the worn region analysis and predict fluid pressures in worn shoes. The findings of this study establish a link between predicted fluid pressures and coefficient of friction, offering a novel approach to assessing traction performance and slip risk. Future work should focus on improving the neural networks accuracy, by expanding the data set of images and validating these methods across diverse shoe designs and floor contaminants. These efforts could lead to practical, cost-effective tools for reducing workplace injuries caused by slips and falls.

**Acknowledgments:** The authors thank NIOSH R01 H010940 for funding.

**References:** [1] Ronneberger et al. (2015), *ArXiv* 1505; [2] He et al. (2016), *CVPR* [3] Sundaram et al. (2020), *J Biomech* 105; [4] Beschorner et al. (2009), *Tribol. Trans* 52(4); [5] Hemler et al. (2022), *Footwear Science* 14(1). [6] Schindelin et al. (2012), *Nat. Methods* 9(7).

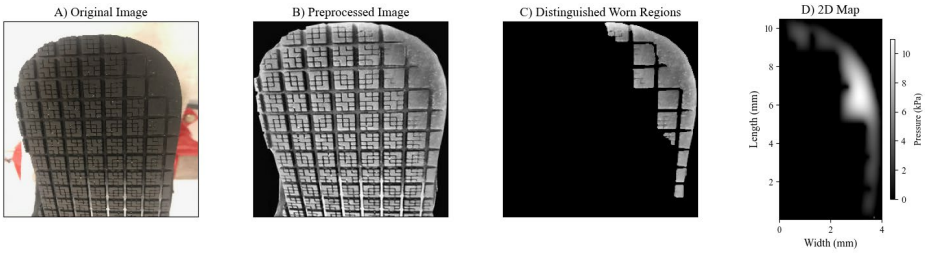


**Figure 1:** A) Raw smartphone image. B) Filtered distinguished outsole image. C) Distinguished worn regions from the outsole. D) Fluid pressure predictions from the largest worn region.

# EVALUATION OF AUTO-SEGMENTATION'S ABILITY TO ACCURATELY DEFINE ANKLE BONE EDGES

*Abdulganeey Olawin [1], Emily C. Gray[1], Tom Gale[1], Hogan MaCalus[1], William Anderst[1]
[1]Department of Orthopaedic Surgery, University of Pittsburgh, Pittsburgh, PA
*Corresponding author's email: aod18@pitt.edu

**Introduction:** Bone models generated from CT scans can improve diagnosis of bone-related diseases, development of personalized treatment plans, and planning of surgical procedures [1]. While manual segmentation of CT scans remains the gold standard, it is labor-intensive and time-consuming [2,3]. Auto-segmentation using artificial intelligence provides a significantly faster alternative and has the potential to eliminate interobserver variability. However, its accuracy across different patient populations, particularly those with various bone pathologies, remains unclear. Several studies have assessed the accuracy of auto-segmentation using the Dice Similarity Coefficient (DSC) and the Average Surface Deviation (ASD), but no studies have specifically evaluated auto-segmentation accuracy at the bone edges using a 1-pixel Dice Similarity Coefficient (1-pxl DSC). This edge-only score is critical in determining whether auto-segmentation can accurately capture the edges of the bones, which is particularly important for conditions such as osteoarthritis, where subtle surface deviations may influence clinical decisions. This study aimed to compare commercially available auto-segmentation software (Simpleware, Synopsys) with manual segmentation of the distal tibia, talus, and calcaneus with a healthy control group and a pathological patient group. We hypothesized that the 1-pixel Dice score would be lower than the full DSC due to inaccuracies in edge segmentation and that auto-segmentation would be more accurate for asymptomatic controls compared to participants with foot and ankle pathology.

**Methods:** Patients post lateral ligament reconstruction (LLR) with the Broström technique (inclusion: age 18-50 years), patients post syndesmosis repair (SR) with either a suture button or a screw fixation (inclusion: age 18-45 years), and a healthy control group (inclusion: age 21-45, BMI 18-30kg/m$^2$) were included in this study. Ankle CT scans including a bone density phantom (Mindways Software, Inc.) were obtained and each CT slice was bone-density corrected prior to segmentation. Each scan was resliced to make isometric voxels (range: 0.50mmx0.50mmx0.50mm to 0.69x0.69x0.69mm). The tibia, talus, and calcaneus were manually segmented using commercial software (Mimics 24, Materialise). Auto-segmentation was performed (Simpleware, Synopsys), and segmentation accuracy was evaluated using DSC, 1-pxl DSC, and ASD with manual segmentation serving as the reference standard. The mean surface deviation was calculated in MATLAB as mesh-to-mesh deviation. Differences in the DSC, 1-pxl DSC and ASD were analyzed using Welch's ANOVA, and Games-Howell post-hoc test was used if significant difference was found ($p < 0.05$)

**Results:** A total of 54 ankle CT scans were analyzed, including 2 scans from 2 LLR patients, 12 scans from 6 SR patients (both injured and contralateral sides) and 40 scans from 20 healthy asymptomatic participants. Auto segmentation of the tibia, calcaneus, and talus took an average of 12 seconds per scan, whereas manual segmentation took approximately 30 minutes per scan. DSC scores showed no significant differences between auto and manual segmentation among the participant groups, indicating that auto-segmentation achieved a high level of agreement with manual segmentation overall (Fig 1A). However, the auto-segmentation 1-pxl DSC was significantly lower, confirming that auto-segmentation struggled with accurately delineating bone edges (Fig 1A). There was no significant difference in the ASD between patient groups and all were negative, indicating that auto-segmentation was not significantly better at the surface for healthy participants than for patients and that auto-segmentation consistently under segmented the CT scans (Fig 1B).

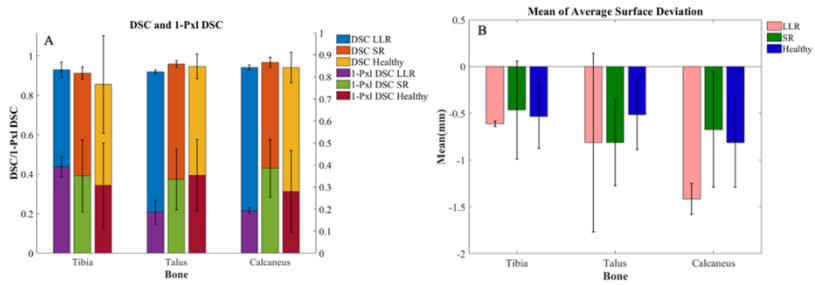


*Figure 1: The average and standard deviation of (A) the DSC and 1-pixel DSC and (B) ASD for the distal tibia, talus and calcaneus for patients who underwent lateral ligament reconstruction, syndesmosis repair and healthy asymptomatic patients. * indicates significant differences with p < 0.05*

**Discussion:** This study confirmed that the 1-pxl DSC was lower than the full DSC, confirming our hypothesis that auto-segmentation has poor accuracy at bone edges. However, contrary to our expectations, auto-segmentation was not significantly more accurate for healthy controls compared to participants with ankle pathology. This may be due to the relatively young age of all participants in our cohort. The ASD and the 1- pixel DSC results suggest that while auto-segmentation can generate sufficiently accurate models for certain applications, its reduced edge accuracy may limit its use in research applications, clinical evaluation, and surgical planning, that require high precision, such as detecting small exostoses or subtle degenerative changes in osteoarthritis.

**Significance:** Auto-segmentation is a promising method for generating 3D bone models quickly. However, due to its limitations in edge accuracy, its clinical utility may be restricted in cases where precise anatomical delineation is critical. Further research is needed to refine segmentation algorithms and improve their accuracy.

**References:** [1] Humayun et al. Quant Imaging Med Surg, 2024, [2] Lalone EA, et al., Medical Engineering and Physics, 2015, [3] Bott KN, et al., Diagnostics, 2023, [4] Pitcairn et al. Journal of Biomechanics, 2020.

# ASSESSING TWO COMPUTED TOMOGRAPHY IMAGE SEGMENTATION METHODS USING MORPHOLOGY FOR APPLICATION IN ABDOMINAL AORTIC ANEURYSM

**Emily G. Stephan[1], Katherine E. Kerr[1], Pete H. Gueldner[1], Indrani Sen[2], Tiziano Tallarita[2], Joseph C. Wildenburg[3], Nathan L. Liang[1,4,5], David A. Vorp[1,4,6-12], Timothy K. Chung[1,10]**

(1) Department of Bioengineering, University of Pittsburgh, Pittsburgh, PA, USA (2) Division of Cardiovascular Surgery, Mayo Clinic Health Systems, Eau Claire, Wisconsin, USA (3) Department of Interventional Radiology, Mayo Clinic Health Systems, Eau Claire, Wisconsin, USA (4) Department of Surgery, University of Pittsburgh, Pittsburgh, PA, USA (5) Division of Vascular Surgery, University of Pittsburgh, Pittsburgh, PA, USA (6) Department of Chemical and Petroleum Engineering, University of Pittsburgh, Pittsburgh, PA, USA (7) McGowan Institute for Regenerative Medicine, University of Pittsburgh, Pittsburgh, PA, USA (8) Department of Cardiothoracic Surgery, University of Pittsburgh, Pittsburgh, PA, USA (9) Clinical and Translational Sciences Institute, University of Pittsburgh, Pittsburgh, PA, USA (10) Department of Mechanical Engineering and Materials Science, University of Pittsburgh, Pittsburgh, PA, USA (11) Center for Vascular Remodelling and Regeneration, University of Pittsburgh, Pittsburgh, PA, USA (12) Magee Women's Research Institute, University of Pittsburgh, Pittsburgh, PA, USA

Corresponding author's email: egs75@pitt.edu

**Introduction:** Abdominal aortic aneurysm (AAA) is a degeneration of the infrarenal segment of the aorta, which leads to its progressive dilatation. AAA has a high incident rate and is highly correlated with age; 66% of all AAA incidents occur in ages 75 or higher [1]. AAA rupture has an extremely high mortality rate, as up to 83% of patients die before they can have emergency surgery on the aorta [2]. If a patient is diagnosed with AAA, a clinician will determine if surgery is necessary based on the maximum transverse diameter of the AAA. There are limitations to this metric, as is a poor prognosticator and has a high rupture rate below the threshold. Currently, biomechanical parameters must be extracted through stress analysis, which requires time-consuming manual segmentation of the aorta from manual images which is the current gold standard. As manual segmentation is time-intensive, clinical adoption of biomechanic has not been widespread. Image segmentation processes can be expedited by introducing automation into this stress analysis, potentially eliminating the need for manual segmentation. In this study, we present two methods for segmenting medical images (automatic and semi-automatic) and compare their results to those of the gold standard method (manual). One current automatic process for image segmentation has been published by the Stanford Machine Intelligence for Medical Imaging group, called Comp2Comp [3]. As for semi-automatic segmentation, our group has developed an in-house segmentation pipeline for AAA segmentation under provisional US patent US63/544,046 [4][5].

**Methods:** This study used CT images from the University of Pittsburgh Medical Center (UPMC) and Mayo Clinic Health System (MCHS). The UPMC dataset was analyzed in accordance with the University of Pittsburgh IRB guidelines, following the Department of Health and Human Services regulations under protocol #STUDY19060084. The MCHS dataset was approved under protocol IRB #23-004028. De-identified CT scans from MCHS were securely transferred to the University of Pittsburgh under data use agreement #DUA00004445. Manual segmentation was performed using the 3D Slicer software. The semi-automatic method was implemented via a custom MATLAB script and required a user to trace the outline of the aorta from a coronal and sagittal plane. For automatic segmentation, Comp2Comp was utilized and implemented in a NVIDIA GPU workstation [3]. Select morphological analysis was conducted to measure the similarity between methods using three metrics: maximum transverse diameter, wall asymmetry, and wall tortuosity. Wall asymmetry is defined as the perpendicular distance between the centerline and a straight line connecting its proximal and distal ends. Wall tortuosity refers to the quantified AAA buckling by measuring the deviation of the aorta from a centroid spanning the renal arteries to the aortic bifurcation to determine statistical significance, a Wilcoxon signed rank test was performed [6]. Additionally, the time required to complete the semi-automatic segmentation was recorded.

**Results & Discussion:** The results of the three selected metrics and segmentation types are shown to the right in **Table 1**. The semi-automatic segmentation metrics were provided three statistically insignificant differences compared to the statistically significantly different when compared to the manual augmentation. The automatic segmentation produced only one statistically significant difference, and two statistically insignificant differences compared to the manual segmentation. Meaning that for the statistically significant differences, the p-value was greater than our alpha value. For a time, the difference between semi-automatic and automatic segmentation, when compared to the manual, is significantly different with a p-value of less than 0.001. The manual segmentation time varies on time but is typically about an hour long. The semi-automatic segmentation time was 129 seconds $\pm$ 53.3 seconds, and the automatic segmentation time was 28.5 seconds $\pm$ 9.4 seconds.

**Table 1: Three methods of segmentation and their morphological indices and significant differences**

| Metrics | Manual | Semi-Automatic | Automatic | Semi-Automatic vs. Manual | Automatic vs. Manual |
|---|---|---|---|---|---|
| Max Diameter (cm) | $6.34 \pm 2.45$ | $6.51 \pm 1.95$ | $5.97 \pm 4.83$ | p=.03 | p=.20 |
| Mean Wall Asymmetry | $4.67 \pm 4.29$ | $0.93 \pm 1.16$ | $5.03 \pm 3.79$ | p=.005 | p=.63 |
| Wall Tortuosity | $1.10 \pm 0.24$ | $0.94 \pm 0.26$ | $0.99 \pm 0.19$ | p=.04 | p=.05 |

**Significance:** This study has significant implications for AAA diagnosis by addressing the inefficiency of manual segmentation, the current clinical use. Semi-automatic segmentation closely aligns with the results of manual segmentation, while significantly reducing the processing time. Automatic segmentation also reduces the segmentation time, but more data is needed to ensure accurate segmentation for clinical adoption. Automating CT image segmentation for AAA enhances diagnostic efficacy and integrates the use of AI-driven tools in clinical applications. This shift could help change AAA assessment for the better by making biomechanical evaluations more practical in clinical settings.

**Acknowledgments:** This work was funded and supported by JHF, PinCH, and the Chancellor's Gap Fund

**References:** [1] Howard, D. P. et al, National Library of Medicine, 4(8), 2015. [2] Haque et al., American Family Physician, 106(2):165-172, 2022. [3] Blankemeier, L. et al., arXiv preprint, arXiv:2302.06568, 2023. [4] Chung, T.K et al., US Provisional Patent US63/544,046, 2023. [5] Raghavan, M. L. et al. Transl. Stroke Res., 5:252-259, 2014. [6] King, A. P. et al, *ScienceDirect*, 3:6-7, 2019.

# THE CONCURRENT EQUIVALENCE AND RELIABILITY OF IN-LAB MARKERLESS MOTION CAPTURE IN ESTIMATING KIMEMATIC WAVEFORMS DURING LOAD CARRIAGE

*Carlie J. Daquino[1], Brent Alvar[1], Arnel Aguinaldo[1]
[1]Point Loma Nazarene University Biomechanics Lab, Dept. of Kinesiology, Point Loma Nazarene University, San Diego, CA
*Corresponding author's email: cdaquino0023@pointloma.edu

**Introduction:** Load carriage requires service members (SM) to carry heavy loads for extended periods of time, altering trunk and lower limb kinematics. The weight requires postural adjustments to maintain balance and stability, resulting in greater trunk flexion, pelvic tilt, hip rotation and abduction, and knee flexion [2,3]. These biomechanical changes can lead to musculoskeletal injuries [1]. Motion capture can evaluate the impact of load carriage on gait aiding in minimizing injury, informing equipment design, and ensuring greater protection of SM. Marker-based motion capture (MB) analyzes movement and identifies body segments using reflective markers placed on bony landmarks. Markerless motion capture (ML) utilizes deep learning networks to track and estimate 3D positioning of an individual. There is limited data on the use of a ML system compared to a MB system in estimating kinematics during load carriage. The purpose of the study was to evaluate *Theia3D* (ML) to a MB system in measuring trunk flexion, pelvic tilt, hip flexion, knee flexion, and ankle dorsiflexion during load carriage. It was hypothesized that across the gait cycle, *Theia3D* measures kinematics similarly to a MB system during load carriage.

**Methods:** Twelve healthy participants completed 10 walking trials while carrying an 18 kg pack. The time series data and ensemble-averaged kinematics for sixty strides were evaluated through statistical parametric mapping (SPM). SPM identifies specific suprathreshold regions throughout the gait cycle (right heel strike (RHS) to RHS) in which ML data is statistically significantly ($p < 0.05$) different from the MB derived data.

**Results & Discussion:** The time series data indicates less agreement between modalities in estimating trunk flexion, pelvic tilt, hip flexion, and ankle dorsiflexion, and higher agreement in measuring knee flexion during load carriage. There was a consistent 18° offset between modalities in measuring trunk flexion. Similarly, hip flexion and ankle dorsiflexion were significantly different throughout the gait cycle, but the kinematic curves were similar in shape with a 10° offset with the ML system underestimating kinematics compared to the MB modality (Figure 1A). These offsets could be a result of a systematic bias due to different modelling definitions. The modalities measured pelvic tilt similarly, but the agreement in the time series data could be a result of the pelvis moving through less range of motion during gait. Knee flexion was measured similarly throughout the entire gait cycle, indicating that joint kinematics with larger ranges of motion are highly comparable among the MB and ML modalities during load carriage (Figure 1B).

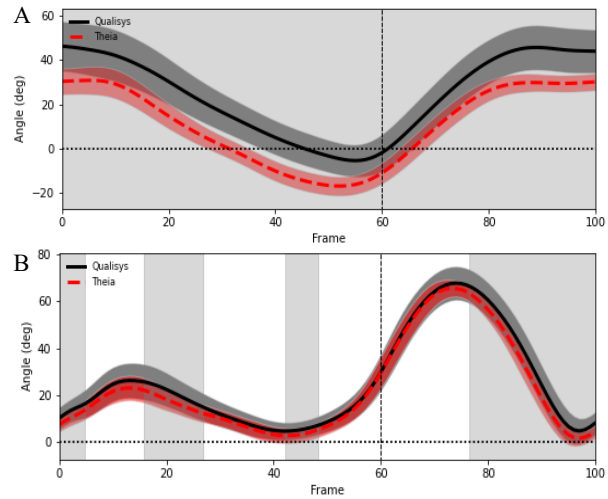


**Figure 1:** Sample SPM plots for (A) Hip Flexion and (B) Knee Flexion from RHS to RHS. The solid line is the MB derived data, and the dashed line is ML derived data. The gray regions are suprathreshold regions.

**Significance:** The results suggest that MB and ML motion capture systems estimate knee flexion similarly, but display significant differences in measuring trunk, pelvis, hip, and ankle sagittal plane kinematics. Researchers and clinicians should consider the differences in modelling methods and systematic biases when utilizing a MB or ML system. Each system may be better suited for specific scenarios. MB systems can be used in more controlled settings, while a ML system may be more appropriate when joint centers are occluded. During load carriage, the pack tends to obstruct joint centers, making it difficult to measure kinematics. Therefore, the ML technology may be an effective alternative for measuring kinematics during load carriage.

**Acknowledgments:** This project was conducted as a thesis at Point Loma Nazarene University.

**References:** [1] Birrell and Haslam. (2009), *Ergonomics* 52(10).
[2] Coll et al., (2024), *Ann Biomed Eng*.
[3] Walsh and Low (2021). *Appl Ergon* 93.

# TOWARDS A FOUNDATIONAL MODEL OF PATHOLOGICAL GAIT KINEMATICS

*Robert D. Magruder[1], Selim Gilon[1], Emily Y. Miller[1], Scott Uhlrich[1]
[1]University of Utah, Department of Mechanical Engineering
*Corresponding author's email: rd.magruder@utah.edu

**Introduction:** Motion capture enables precise quantification of motor function, but distilling this high-dimensional time-series data into actionable insights—such as quantification of impairment [1] or prediction of surgical outcomes [2]—remains challenging. Typically, these tasks require large pathology-specific datasets that are costly to acquire. A foundational model of gait—one that distills salient features of healthy and pathological gait into a low-dimensional space—could enable diverse downstream applications for a variety of pathologies without requiring large training datasets. Variational autoencoders (VAEs) are well-suited for learning latent representations of kinematics data [3]. Here, we trained a VAE to create a latent representation of walking kinematics and evaluated its utility in two downstream tasks: *(1)* surgical effect prediction and *(2)* quantifying walking impairment in individuals with Parkinson's Disease (PD). We hypothesize that a model predicting an individual's kinematics after hip replacement surgery from the latent representation of pre-surgical walking kinematics will be more accurate than applying the average kinematic effect of surgery to each individual. Additionally, we expect that a Gait Impairment Score (GIS)—defined as the distance of an individual's VAE-derived gait representation from a normative reference—will correlate with gait speed, a common indicator of gait performance and health, and clinician-graded walking quality (UPDRS) in individuals with PD.

**Methods:** We computed kinematics from seven whole body motion capture datasets using a 36 degree-of-freedom OpenSim model [4], [5] and AddBiomechanics [6]. The aggregated dataset includes 14,103 strides from 659 individuals, including unimpaired individuals (age 8–86) and those with cerebral palsy, hip osteoarthritis (OA), knee OA, stroke, Parkinson's Disease (PD), and several muscular dystrophies. We trained a VAE to encode a matrix of walking kinematics (40 rotations and translations x 24 time points) into a 20-dimensional latent vector ($z$). Datasets were split by individuals into 70% training, 15% validation, and 15% test, with pre- and post-total hip replacement surgery data from hip OA patients kept together. The PD dataset was withheld from VAE training entirely as an unseen pathology. For our first hypothesis, we trained a single-layer neural network to predict post-surgical $z$ from pre-surgical $z$, then compared (t-test, $\alpha$=0.05) this model's validation set performance to a naïve surgical effect predictor that applies the mean kinematic change from surgery to each individual's pre-surgical kinematics. In our second hypothesis, we defined GIS as the L2 norm of the difference between an individual's $z$ and the mean $z$ of unimpaired individuals; a larger GIS indicates more impaired gait. We then correlated GIS for both off- and on-medication states to clinician-assessed walking quality (UPDRS).

**Results & Discussion:** *(1)* Our VAE-based model predicted kinematics after total hip replacement more accurately (1.4° less error, p=0.007) than assuming all individuals experience the average kinematic improvement (Fig. 1a). Predicting post-surgical gait improvements could inform surgical decisions or be used to guide pre-surgical rehabilitation to improve outcomes. More broadly, the ability to predict an individual's response to different interventions could enable precise treatment of conditions for which there are many interventional options (e.g., cerebral palsy).

*(2)* In the PD dataset that we withheld from VAE training, our GIS moderately correlated with gait speed (r=-0.58, p<0.001), and it correlated with UPDRS III: walking during both on- off- medication states (r=0.63, p<0.001; Fig. 1b). UPDRS scores are discrete clinician-graded measures of walking quality, so GIS could offer a more granular assessment of walking quality. Since GIS represents the deviation in an individual's kinematics from unimpaired kinematics, GIS may be more sensitive to movement abnormalities that are visually apparent to clinicians but not captured in gait speed.

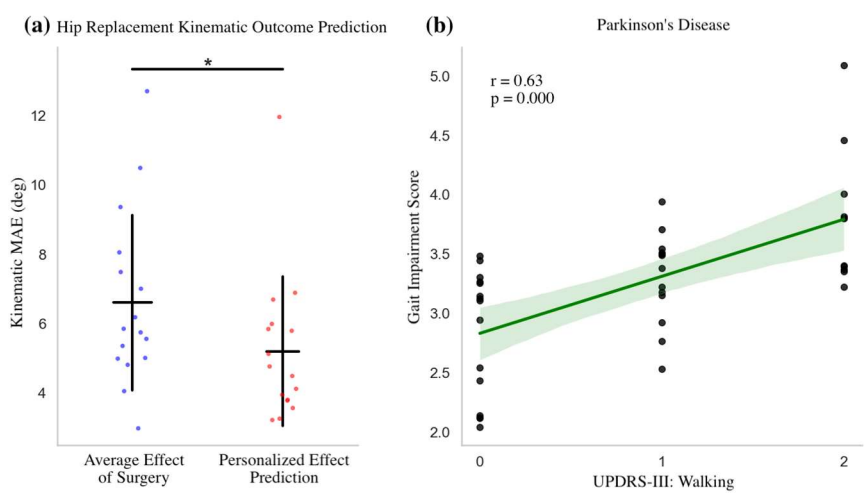


**Figure 1: (a)** The VAE-based model (red) predicts post-surgical kinematics more accurately (lower mean absolute error [MAE]; *p=0.0072) than a model assuming an average effect of surgery (blue). **(b)** Our VAE-based Gait Impairment Score correlates with clinician-rated mobility (UPDRS-III: walking) for individuals with Parkinson's Disease (r=0.63, p<0.001). The linear regression fit is shown with shaded 95% confidence interval.

**Significance:** Our low-dimensional representation of gait kinematics predicted the effect of an orthopaedic surgery, and it enabled the computation of an impairment score that correlated with clinical measures of gait performance on a pathology that was not used in model training. In conjunction with accessible tools for quantifying kinematics, this pathology-independent latent representation of walking could accelerate the development of biomechanics-based functional outcome measures and personalized rehabilitation.

**References:** [1] Schwartz and Rozumalski (2008), *Gait & Posture* 28(3). [2] Rajagopal et al. (2018), *Sci Reports* 8. [3] Chen et al. (2016), *IEEE-RAS*. [4] Rajagopal et al. (2016), *IEEE Trans Biomed Eng* 63(10). [5] Seth et al. (2018), *PLOS Comp Bio* 14(7). [6] Werling et al. (2023), *PLOS One* 18(11).

# DETECTING EMOTIONS FROM GAIT BIOMECHANICS: A MACHINE LEARNING APPROACH

*Angeloh Stout[1], Justin Cadenhead[1], Mrigank Maharana[1], Ashley Guzman[1], Luke Fisanick[1], Katherine Brown[1], **Gu Eon Kang[1]
[1]University of Texas at Dallas, Department of Bioengineering
* Email: Angeloh.Stout@utdallas.edu ** Email: GuEon.Kang2@utdallas.edu

**Introduction:** Recent studies have consistently demonstrated that emotions influence gait through biomechanical changes, such as altered joint motion, upper body posture, smoothness and spatiotemporal parameters [1-3]**.** This indicates that gait biomechanics could serve as a valuable tool for uncovering emotional information. Despite rapid advances in machine learning, its application in detecting emotions through gait biomechanics remains relatively underexplored. This study aimed to explore the application of machine learning techniques to gait biomechanics for detecting emotional states. Our hypothesis was that specific emotional states—such as anger, fear, joy, and sadness—alter gait biomechanics, which can then be used for accurate emotional classification.

**Methods:** We recruited 15 young healthy adults (10 females; mean age = 20.69 ± 2.09 years; mean body mass index = 22.84 ± 2.36 kg/m$^2$). To induce targeted emotions—anger, joy, sadness, fear, and neutral emotion—we employed the autobiographical memories paradigm [1-3]. Participants recalled personal memories associated with each emotion. Prior to walking, participants were asked to evoke these memories and began walking on a 10-meter pathway once the emotion was intensely felt. After each walk, they rated the emotion's intensity using a 5-point Likert scale. Participants completed three gait trials for each emotion in a block, with the order of emotions randomized. During the trials, a 16-camera motion capture system (Vicon, UK) recorded data from 74 markers attached to the whole body. We used Visual3D (HAS Motion, Canada) to compute spatiotemporal gait parameters and joint kinematics variables.

Before applying machine learning techniques, we created a dataset consisting of 155 predictors (i.e., biomechanical variables), and 204 observations (i.e., all emotional walking trials). There were 5 initial classes to represent anger, fear, joy, and sadness, but to account for individual variation in baseline gait, each outcome was normalized to the participant's respective neutral trials, resulting in a four-class prediction model. We then applied machine learning techniques (multilayer perception, random forest, k-nearest neighbours, logistic regression, and XGBoost) to evaluate test accuracy, to measure the overall proportion of correct predictions made by the model. Precision and recall were also assessed to understand the model's ability to correctly identify the different emotional states. Precision refers to how many predicted positive instances are correct, while recall measures how well the model identifies all the actual positive instances. The F1 score was calculated to represent a balance of the combined measure of both precision and recall. Additionally, Gini importance was evaluated to identify the key biomechanical variables contributing most to the model's predictions. This metric is derived from the calculation of Gini impurity, which quantifies the degree of class heterogeneity at each decision node in the tree. Features that result in greater reduction of Gini impurity upon splitting are considered more significant in the predictive process. These metrics, along with leave-one-out cross-validation (LOOCV) method, were used to assess the performance and generalizability of the model.

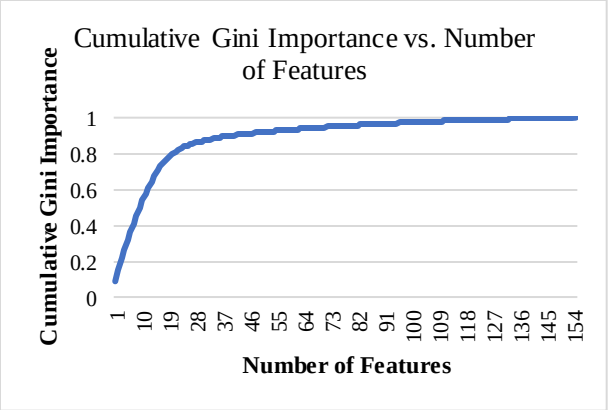


**Figure 1. Gini importance versus number of features plot**

**Results & Discussion:** Preliminary results of the machine learning model with all predictors show that emotional states can improve prediction accuracy (**Table 1**). Although the accuracy was relatively low, the one-in-four random guess baseline suggests the model still effectively predicts emotional states based on gait. These results allow us to reject the null hypothesis, confirming that emotions can be predicted using gait parameters. Gini importance results (**Figure 1**) demonstrate that the model's performance improves as additional predictors are added, peaking at a total of 1 with all predictors. Notably, an elbow point at 23 features indicates that these top 23 predictors contribute significantly to the model's predictive power.

**Table 1.Classification Performance Metrics**

| Model | Accuracy | Precision | Recall | F1 Score |
|---|---|---|---|---|
| **Multilayer Perceptron** | 0.37 | 0.29 | 0.37 | 0.29 |
| **Random Forest** | 0.40 | 0.29 | 0.40 | 0.31 |
| **K-Nearest Neighbour** | 0.36 | 0.28 | 0.35 | `0.27 |
| **Logistic Regression** | 0.39 | 0.34 | 0.39 | 0.31 |
| **XGBoost** | 0.43 | 0.35 | 0.42 | 0.35 |

**Significance:** The results indicate that prediction models based on human movement can be effective. While our pilot study with 15 participants provides valuable insights, increasing the sample size could improve accuracy and reliability. Future research could explore advanced techniques, such as ensemble methods, and refine parameter tuning for optimal performance. Additionally, future testing could assess a one-to-all predictor dataset to further optimize feature engineering.

**References:** [1] Gross et al. (2012), *Hum Mov Sci* 31, 202-221; [2] Kang and Gross. (2015), Hum Mov Sci, 40, 341-351; [3] Kang and Gross. (2016), *J Biomech* 49, 4022-4027

# DEEP LEARNING-BASED FOOT PLACEMENT PREDICTION MODELS REVEAL MULTI-TIMESCALE CONTROL

*Wei-Chen Wang[1], Antoine De Comite[1], Alexandra Voloshina[2], Monica Daley[2], Nidhi Seethapathi[1]
[1]Massachusetts Institute of Technology, Cambridge, MA, USA
[2]University of California, Irvine, Irvine, CA, USA
*Corresponding author's email: wangeric@mit.edu

**Introduction:** Human locomotion in the real world uses multiple input modalities for control – such as body states and visual gaze – and can unfold on multiple timescales to guide dynamic foot placement. Existing data-driven models of locomotion are limited to treadmill walking with fixed-timescale linear assumptions [1] that may not capture multi-modal and context-dependent control inherent in the real world. To address this, we develop a deep learning framework to analyze large-scale locomotion data in uneven terrain walking and running [2, 3]. By comparing the predictive power of different input modalities on future foot placement to a baseline model, our framework eliminates significant inter-trial variability, revealing input modality- and environment-dependent foot placement control timescales.

**Methods**: We hypothesize that foot placement control depends on the history of body and environmental states. To test this, our deep learning framework is trained on input modalities including kinematics of the center of mass (CoM)-relevant states, swing-foot states, full-body states, and gaze fixations (Figure 1A), to predict future foot placement. These inputs are integrated over different windows to identify the amount of history needed for prediction at each gait phase. We incorporate a trial ID embedding in our deep learning framework to separately learn the trial-specific components of the foot placement, reducing inter-trial variability in prediction (Figure 1B). Given the high correlation between modality-based and baseline prediction intercepts across trials (Figure 2B), we analyze the relative predictive power as shown in Figure 2A, further reducing inter-trial variability.

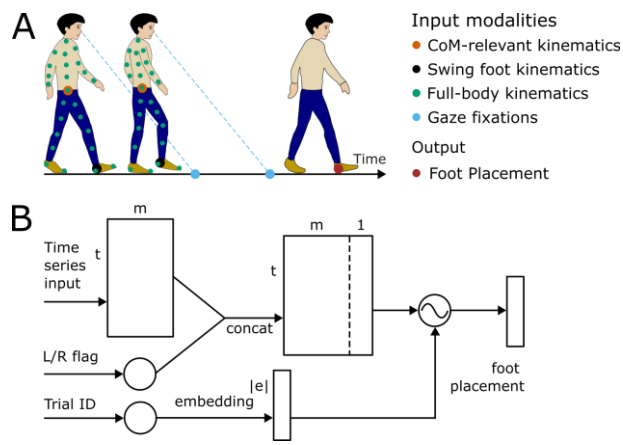


**Figure 1:** Overview of the modeling framework. **A**. Hypothesized input modalities and foot placement output. **B**. Network architecture of the controller.

**Results & Discussion:** The relative predictive power reveals distinct control timescales across modalities. During overground walking on rough terrain, we observe that lateral foot placements are visually guided, with gaze fixations contributing earlier to prediction than both CoM-relevant and full-body kinematics (Figure 2C), possibly to inform path planning to navigate complex terrain. This result quantifies the extent to which, in challenging environments, individuals rely on vision to plan foot placement before relying on postural body state information. In addition, our findings indicate that full-body kinematics are predictive of foot placement earlier than CoM-relevant kinematics, which suggests two potential underlying mechanisms. First, the preparatory movements of the whole body, distributed throughout the gait cycle, may provide early cues that optimize CoM trajectories, thereby improving predictive power [4]. Alternatively, the full-body kinematics could capture the whole-body angular momentum (WBAM), which integrates contributions from all body segments and influences foot placement before CoM kinematics [5]. Future work in analyzing the individual body segments could provide deeper insights into their specific roles in foot placement planning.

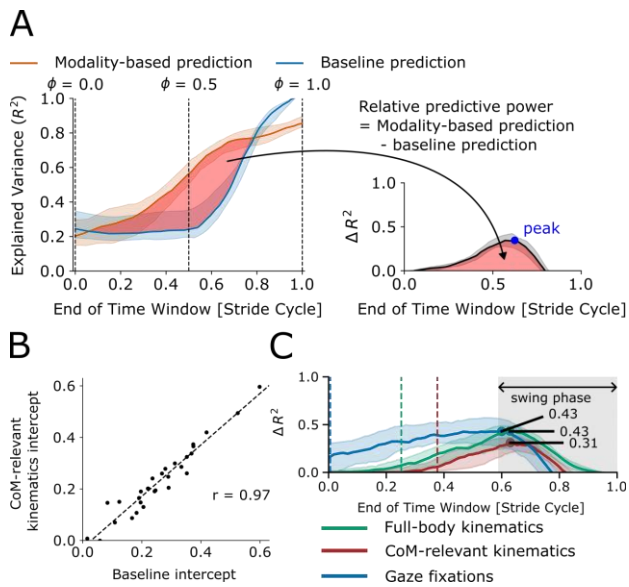


**Figure 2:** Relative predictive power. A. $R^2$ across gait phase for modality-based and baseline predictions. The intercept is the $R^2$ at gait phase 0. The red shaded area represents the relative predictive power ($\Delta R^2$). B. Correlation between baseline and CoM-relevant kinematics intercepts. C. $\Delta R^2$ of CoM-relevant, full-body kinematics and gaze fixations for lateral foot placement prediction during overground rough terrain walking. The vertical lines indicate the control timescale for each input modality when its predictive power outperforms the baseline model by 5%. The gray shaded region represents swing phase.

**Significance:** We introduce a data-driven deep learning framework that reveals multi-timescale control strategies across input modalities, and can be extended to other motor actions. By comparing the predictive power to the baseline model, we reduce inter-subject variability and quantify the additional variance explained by the input modality. Such nonlinear data-driven models of locomotion can inform the development of human movement simulations and assistive robot controllers that are better aligned with human locomotor control in the real world.

**References:** [1] Wang & Srinivasan (2014). *Bio lett* 10(9): 20140405. [2] Voloshina & Ferris (2015). *J exp bio* 218(5): 711-719. [3] Matthis et. al. (2018). *Current bio* 28(8): 1224-1233. [4] Nayeem et. al. (2021). *PLOS Comp Bio* 17(12):e1009597. [5] Leestma et. al. (2023). *J Exp Bio* 226(6):jeb244760.

# VALIDITY OF MARKERLESS MOTION ANALYSIS USING A DYNAMIC TIME WARPING APPROACH

Eleonora Cabai[1], Jorge Chahla[1], Leonardo Metsavaht, Gustavo Leporace, *Jonathan A. Gustafson[1]
[1]Rush University Medical Center, Chicago, IL. USA
*Corresponding author's email: jonathan_a_gustafson@rush.edu

**Introduction:** Motion analysis offers valuable insights into human movement that have aided in the diagnosis and treatment of musculoskeletal conditions to improve patient outcomes. Traditional marker-based motion capture (MoCap) systems require specialized equipment and setup. In contrast, markerless systems offer a more accessible alternative, but their reliability is still a concern [1], with most validation studies to date only evaluating differences in discrete peak values of kinematic trajectories. The objective of this study was to assess the differences in dynamic time series trajectories of marker-based and markerless MoCap systems during a lateral step-down task, a key activity for evaluating several pathologic orthopedic conditions.

**Methods:** Three-dimensional kinematics data were measured from 22 individuals with femoroacetabular impingement (n=7), patellofemoral pain (n=11), and healthy, asymptomatic subjects (n=4) as part of an ongoing, IRB-approved prospective study to develop large-data biomechanical models of various orthopedic conditions. Individuals were outfitted with a marker set combining ISB recommendations [2] with the CAST method [3] and conducted repeated lateral step-down trials (n=3) from a 30 cm box while both a marker-based optoelectronic motion capture system (Qualisys) and markerless system (Theia) collected movements.

A Python script was developed to segment the data into comparable samples by identifying key events (START, MID, END) based on the center of gravity of the pelvis (z-axis) and extracting the relevant kinematics per segment. Data were scaled by min and max values for each variable and time normalized. Kinematics of the trunk, pelvis, hip, knee, and ankle were compared across both systems (Figure 1) using both Dynamic Time Warping (DTW)—a technique for quantifying the similarity between time series [4] (**Figure 1**)—and cross-correlation analysis (*dtw* function from tslearn, *corrcoef* function from numpy, Python 3.13.1).

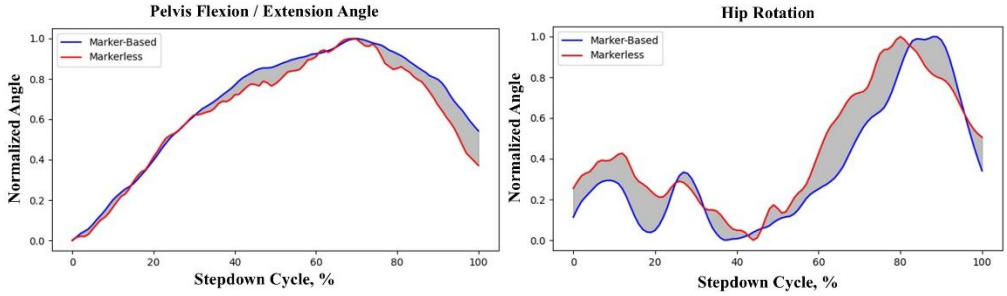


**Figure 1.** Example of Dynamic Time Warping Analysis for pelvis (left) and trunk (right) kinematics

**Results & Discussion:** The cohort comprised 13 females (age: 36.1 ± 11.4 years, BMI: 22.6 ± 2.8 kg/m$^2$) and 9 males (age: 36.8 ± 10.9 years, BMI: 26.7 ± 3.9 kg/m$^2$). We found an average and median DTW distance of 0.88 and 0.81, respectively (**Table 1**). The lowest DTW distances—indicating a high degree of similarity between marker-based and markerless—were found for the sagittal knee angle (mean 0.13, median 0.08). In contrast, the highest DTW distances were found for the transverse knee angle (mean 1.92, median 1.74) and the frontal ankle angle (mean 2.22, median 2.29).

Cross-correlation was strong, with an overall mean of 0.67. High correlation was found for variables exhibiting low DTW distances, including both sagittal and frontal plane hip angles (mean 0.98 and 0.93, median 1.00 and 0.98). Interestingly, frontal plane ankle angle (mean -0.13, median -0.10) had negative correlations, suggesting potential measurement noise in the two systems at specific segments in the time series.

Future work will expand this cohort to 100 subjects and implement a regression model to adjust markerless data and reduce systematic biases, improving data alignment and enhancing the accuracy of markerless motion capture.

**Table 1:** DTW and cross-correlation of kinematic variables (mean±SD)

| Variable | Plane | DTW | Cross-Correlation |
|---|---|---|---|
| Trunk Angle | Flexion/extension | 1.42 ± 1.15 | 0.42 ± 0.61 |
| | Lateral lean | 1.39 ± 0.63 | 0.37 ± 0.40 |
| | Transverse rotation | 1.30 ± 0.71 | 0.50 ± 0.38 |
| Pelvic Angle | Anterior/posterior tilt | 0.63 ± 0.83 | 0.86 ± 0.41 |
| | Pelvic drop | 1.05 ± 0.78 | 0.61 ± 0.34 |
| | Transverse rotation | 1.97 ± 0.51 | 0.74 ± 0.25 |
| Hip Angle | Flexion/extension | 0.16 ± 0.15 | 0.98 ± 0.06 |
| | Abduction/adduction | 0.31 ± 0.33 | 0.93 ± 0.17 |
| | Internal/external rotation | 1.98 ± 0.80 | 0.28 ± 0.40 |
| Knee Angle | Flexion/extension | 0.13 ± 0.10 | 0.98 ± 0.03 |
| | Varus/valgus | 1.57 ± 0.82 | 0.38 ± 0.40 |
| | Internal/external rotation | 1.92 ± 0.69 | 0.02 ± 0.44 |
| Ankle Angle | Dorsiflexion/plantarflexion | 0.22 ± 0.13 | 0.96 ± 0.04 |
| | Inversion/eversion | 2.22 ± 0.73 | -0.13 ± 0.37 |
| Overall | | 0.88 ± 0.91 | 0.67 ± 0.46 |

**Significance:** We compared marker-based and markerless kinematics using Dynamic Time Warping (DTW) to find similarity between the measurement systems, validating kinematic trajectories of the trunk, hip, knee, and ankle. Improved confidence in the use of markerless motion analysis technologies can enhance research via lower operational costs and enhanced efficiency. By understanding and improving these systems, physicians can achieve more accurate results without the need for physical markers.

**Acknowledgments:** The authors would like to thank funding from the Rush-IBTS Research Fellowship Program for this work.

**References:** [1] Mündermann (2006), J NeuorEng & Rehab. [2] Wu et al., (2002), J Biomech. [3]. Thewlis et al., (2008), J App Biomech. [4] Lee (2019), J Exercise Rehab.

# BEYOND 3D KINEMATICS: A MACHINE LEARNING APPROACH TO IDENTIFYING MOVEMENT PHENOTYPES ACROSS MULTIPLE TASKS IN ORTHOPAEDIC PATIENTS

Eleonora Cabai[1], Jorge Chahla[1], Leonardo Metsavaht, Gustavo Leporace, *Jonathan A. Gustafson[1]
[1]Rush University Medical Center, Chicago, IL. USA
*Corresponding author's email: jonathan_a_gustafson@rush.edu

**Introduction:** Healthy, functional movement in humans contains inherent variability due to the complex interactions between biomechanical constraints and neuromotor strategies. Traditional movement analysis often focuses on group averages for single tasks, limiting insights into individualized patterns [1]. This study introduces a novel framework utilizing machine learning to identify interpretable movement phenotypes using multi-joint, multi-task 3D kinematics across subjects with orthopedic pathologies.

**Methods:** Three-dimensional kinematics data were collected from 24 individuals with femoroacetabular impingement (FAI, n=7), patellofemoral pain (PFP, n=13), and healthy, asymptomatic subjects (HNC, n=4) as part of an ongoing, IRB-approved prospective study to develop large-data biomechanical models of various orthopedic conditions. Individuals were outfitted with a marker set combining ISB recommendations [2] with the CAST method [3] and conducted repeated gait, squat, and lateral step-down trials (n=3) while a marker-based optoelectronic motion capture system (Qualisys) collected movements. Strength and Range of Motion (ROM) data were also measured for the knee, hip and ankle.

A Python pipeline was developed to: (1) temporally align movement sequences using pelvis center-of-mass trajectories (z-axis) to identify task phases (START, MID, END); (2) normalize kinematic waveforms (trunk, pelvis, hip, knee, ankle) via min-max scaling; and (3) temporally reshape data to conform to a standardized frame length. Due to incomplete data for one or more tasks, 6 subjects (1 FAI, 5 PFP) were excluded. For each of the remaining subjects, we constructed a matrix where each row represented a specific task (gait, squat, lateral step-down), and each column depicted the mean, standard deviation, median, and maximum of the dynamic time warping (DTW) distance (*dtw* function from tslearn) across repetitions of the same task for that particular subject. The features in the matrix, which reflect the intra-subject variability, were then standardized via Z-scores (*StandardScaler* function from sklearn, Python 3.13.1). The Z-scores served as input for Principal Component Analysis (PCA), retaining enough components to preserve 95% of the total variability. The results from PCA were subsequently fed into a K-Means clustering model (*KMeans* function from sklearn), with a cluster count optimized based on the silhouette score [4] to identify task-specific movement phenotypes.

**Results & Discussion:** The cohort comprised 11 females (age: 37.4 ± 11.5 years, BMI: 22.4 ± 2.9 kg/m$^2$) and 7 males (age: 40.7 ± 9.2 years, BMI: 26.8 ± 4.4 kg/m$^2$). Movement phenotypes were identified using 3D kinematic waveforms of the trunk, pelvis, hip, knee, and ankle during the three functional tasks and four distinct phenotypes emerged from the analysis.

Non-parametric analyses (Kruskal-Wallis with Mann-Whitney U post-hoc tests [5]) were employed to accommodate the small sample size (n=18), and clusters 1 and 3 (n=2 each) were excluded from statistical analysis due to small sizes. Statistically significant differences were revealed in sagittal-plane knee kinematics ($U = 4.0$, $p = 0.007$, effect size = -0.73) between Cluster 2 and Cluster 0, suggesting phenotypes may reflect strategies on sagittal-plane knee mechanics. No significant inter-cluster differences were observed in trunk, pelvic, hip, or coronal-plane knee kinematics ($p > 0.05$). Trends toward significance occurred in ankle dorsiflexion ($p = 0.07$) and hip external rotation ROM ($p = 0.1$).

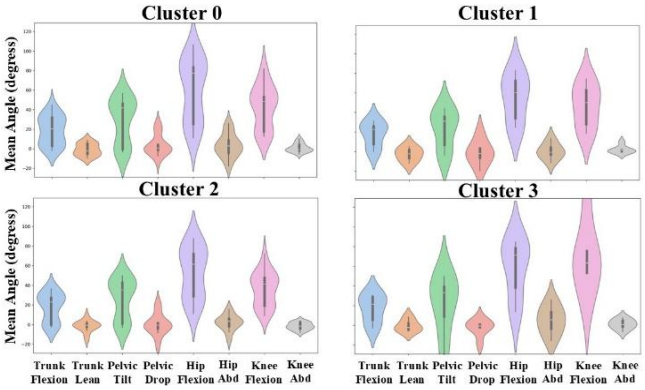


Figure 1. Violin plots of kinematic variables across identified clusters from gait, bilateral squat, and lateral stepdown tasks

Using this novel hierarchical clustering approach, we identified unique movement-based phenotypes that span across pathologies. Our Cluster 2 and Cluster 0 groups comprise of healthy control, FAI, and PFP patients, which aligns with common observations that patients with different pathologies and/or symptoms may exhibit similar movement strategies. A limitation of our analysis is that the small cluster sizes limit generalizability and highlight the need for larger cohorts. Future work will expand the cohort to 100 subjects across several other tasks (e.g., running, jumping, etc.) and validate these phenotypes against clinical outcomes.

**Significance:** We developed a novel framework utilizing machine learning to identify interpretable movement phenotypes using multi-joint, multi-task 3D kinematics across subjects with orthopedic pathologies. This framework overcomes current challenges in the biomechanics field that focus on data analysis of a specific task, commonly reporting statistics on discrete metrics (e.g., range of motion, peak values at specific time points, etc.). We found that individuals can be grouped based on their kinematic data across three (or more) distinct tasks using hierarchical clustering algorithms on the complete time-series kinematic curves. This approach offers more significant insights into movement patterns throughout various tasks, allowing for more precise movement analysis and interpretation.

**Acknowledgments:** The authors would like to thank funding from the Rush-IBTS Research Fellowship Program for this work.

**References:** [1] Phinyomark (2015), J Biomech; [2] Wu et al., (2002), J Biomech. [3]. Thewlis et al., (2008), J App Biomech [4] Rousseeuw (1987), J Comp & App Math; [5] Young-Shand (2023), JOR.

# VALIDITY OF USING SMARTPHONE CAMERA AND HUMAN POSE ESTIMATION ALGORITHM FOR DYNAMIC MOVEMENT ANALYSIS

*Huaqing Liang and Steven Leigh
Marshall University, Huntington, WV
*Corresponding author's email: liangh@marshall.edu

**Introduction:** Quantitative motion analysis is essential in various domains, including performing movement analysis in laboratory settings, designing injury prevention protocols for athletic populations, and making informed decisions about return-to-play in rehabilitation clinics. However, the current gold standard for quantitatively recording and analyzing dynamic movements relies on optical motion capture systems, which utilize reflective markers and expensive cameras to capture marker trajectories. While highly accurate, such systems are primarily set up in lab environments and are more commonly used for research purposes rather than in everyday clinical rehabilitation settings [1]. Consequently, clinicians such as physical therapists and school sport teams' coaches, often resort to qualitative and observational dynamic movement analysis. Such analysis is subjective, is reliant on individual's experience, and often lacks sufficient reliability. Therefore, there is a clear need for a cost-effective and reliable movement analysis system that can be readily applied in clinical or field evaluations.

Recent advancements in deep learning and human pose estimation offer a promising solution [2]. These technologies can detect body landmarks in images or videos captured by commodity cameras, derive trajectories of these landmarks, and provide key joint kinematic outcomes automatically and within a few minutes. The primary objective of this study is to assess the validity of current algorithms for analyzing human motion compared to the gold standard of optical cameras.

**Methods:** This preliminary dataset includes 12 young adults (8M/4F, 25.6±2.89 years) who are physically fit. Participants performed a series of dynamic movements including walk, run, jog backwards, single leg continuous hops, counter-movement vertical jump (CMVJ), rebound jumping (Rebound), side shuffles, and reaction cutting drills. We captured the lower-body movements simultaneously with 2 systems: 1) a 6-camera Vicon Nexus motion capture system with a customized lower body model for collecting marker data; and 2) the OpenCap open-source software and two iPhones (iPhone 15, Apple Inc.) placed on the front and 45 degrees in the front-left direction for recording the movements. We processed the marker data using MS3D (MotionSoft, Durham, NC) software to build skeletal models and obtained joint angle time series data. We obtained the joint angle time series data from the OpenCap software after the data were automatically processed with a trained pose estimation algorithm [3]. Only the walk, CMVJ, and Rebound tasks with 3 repetitions for each task are presented here. Differences between joint angle time histories were evaluated continuously with statistical parametric mapping.

**Results & Discussion:** Hip flexion/extension and ankle dorsiflexion /plantarflexion was similar between motion capture and OpenCap across the entire gait cycle for walking trials (Fig. 1). Knee flexion calculated by OpenCap was significantly greater than knee flexion calculated by motion capture during the stance phase (0-50%) and the end of the swing phase (95-100%) for walking trials ($z^*=4.030$, $p = 0.008$). Hip flexion/extension and knee flexion was similar between motion capture and OpenCap for all CMVJ and rebound trials. Ankle dorsiflexion calculated by OpenCap was significantly greater than ankle dorsiflexion calculated by motion capture at the bottom of the countermovement for CMVJ ($z^* = 4.214$, $p = 0.013$) and at initial landing for the rebound ($z^* = 4.428$, $p = 0.042$).

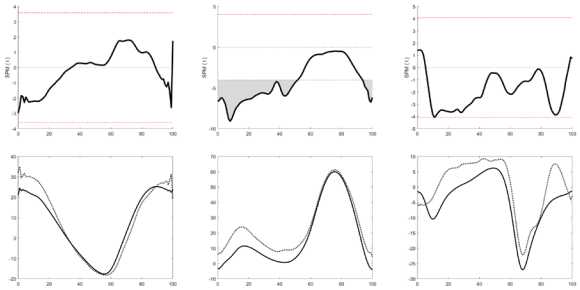

**Figure 1:** Statistical parametric mapping comparison and normalized, averaged joint angle time history for hip flexion /extension, knee flexion/extension, and ankle dorsiflexion/ plantarflexion for all walking trials. The solid lines represent values calculated by an optical motion capture system, and the dotted lines represent values calculated by OpenCap.

In general, OpenCap produces joint angle time histories consistent with a gold standard of optical motion capture. The differences between the systems occurred for knee flexion during the stance phase of walking when the range of motion is relatively small and limb motion is affected by ground reaction force, and for ankle dorsiflexion at the bottom of a landing when limb motion is affected by ground reaction force. For larger ranges of motion, OpenCap appears a viable alternative to optical motion capture.

Additionally, the Vicon system required about half an hour for a participant's marker setup and about 2 hours for data processing for each participant. The OpenCap software required about 5 minutes to setup and the data processing was almost instantaneously.

**Significance:** This preliminary analysis suggests that smartphone-based motion analysis is feasible to use for kinematics analysis of simple dynamic movements, with a high accuracy to generate 3D joint kinematics parameters compared to the optical motion capture system. Additionally, the smartphone-based motion capture system is cheaper, is more convenient to use, requires less training, and demands less human-labour for data processing.

**Acknowledgments:** We would like to thank the team behind the OpenCap to provide this open-source software and make this work possible. The OpenCap software is accessible at www.opencap.ai.

**References:** [1] Klöpfer-Krämer et al. (2020) *Injury*. 51 Suppl 2:S90-S96. [2] Stenum et al. (2024) *PLOS Digit Health*. 3(3):e0000467. [3] Uhlrich et al. (2023), *PLoS Comput Biol.* 19(10):e1011462.

# HUMAN ACTIVITY RECOGNITION USING LARGE LANGUAGE MODELS'S FEW-SHOT LEARNING OF WEARABLE DATA

Mohammed Alnemer[1], Zedong Hao[1], Jay Sunil Goenka[1], Rachneet Kaur[2],* Manuel E. Hernandez[1]
[1]University of Illinois Urbana-Champaign
[2]JP Morgan AI Research
*Corresponding author's email: mhernand@illinois.edu

**Introduction:** The rapid advancement of Large Language Models (LLMs) has introduced new possibilities for analyzing sequential data, including time series, a domain traditionally covered by statistical methods and deep learning architectures such as Recurrent Neural Networks (RNNs) and Long Short-Term Memory (LSTM) networks. These conventional models have been widely used for time series classification and labeling due to their ability to capture temporal dependencies, but they often require extensive feature engineering, large labeled datasets. In contrast, LLMs, originally designed for natural language processing, have demonstrated remarkable adaptability across diverse tasks through in-context learning and prompting techniques. This raises the question of whether LLMs can effectively classify time series data without task-specific fine-tuning, offering a potentially more flexible and accessible alternative to traditional methods. Given their ability to process structured numerical input and infer relationships across sequences, LLMs may offer new advantages in time series analysis. This study explored the potential of LLMs for time series classification, specifically in labeling time series data corresponding to different activities using Zero-Shot Learning (ZSL) and Few-Shot Learning (FSL).

**Methods:** This study used the WISDM Activity Prediction Dataset v1.1, a large-scale publicly sourced dataset designed for human activity recognition (HAR) using smartphone-based accelerometer data [1]. This dataset is widely used for classification tasks. The dataset contains 1,098,207 samples from 36 unique users, each recorded at a sampling rate of 20 Hz. The six activities classified in this dataset included Walking (38.6%), Jogging (31.2%), Walking Upstairs (11.2%), Walking Downstairs (9.1%), Sitting (5.5%), and Standing (4.4%).

| | Gemini ZSL | Gemini FSL (different user) | Gemini FSL (same user) |
|---|---|---|---|
| Image Input | 29.59% | 49.65% | 54.16% |
| Numerical Input | 26.67% | 23.33% | 33.33% |

**Table 1:** Accuracy of LLM activity recognition in different trials.

To ensure the dataset could be precisely read by LLMs, we normalized the data, segmented data in 10-s segments, added activity labels, and converted to an LLM-readable format. After processing the dataset, we inputted the graphics and texts separately to the Application Programming Interface (API) of LLAMA3 and Gemini with ZSL and FSL.

For the ZSL trial, we: (1) Randomly selected 10 Unlabeled subsets for each of 6 activity types from the same user, (2) Inputted the selected Unlabeled subsets into API, asked the LLM to analyze the activity type of each subsets based on the numerical/graphical features respectively, and (3) Based on the outputs from LLM, calculated the accuracy of activity prediction using image or numerical inputs.

For the FSL trial, we followed the following steps for the same and different users: (1) Randomly selected 2 Labeled subsets for each of 6 activity types from the same/different user, (2) Inputted the selected Labeled subsets into LLM, asked LLM to identify the relationship between the numerical/graphical features and the corresponding activity type, and generated the Chain of Thought (CoT) as well, (3) Randomly selected 10 Unlabeled subsets for each of 6 activity types from the same/different user as Labeled subsets, (4) Inputted the selected Unlabeled subsets into API, asked the LLM to analyze the activity type of each subset based on the numerical/graphical features based on the previous study of the Labeled subsets and CoT, (5) Based on the outputs from LLM, calculated the accuracy of activity prediction.

**Results & Discussion:** Comparing the accuracy in different trials (Table 1), we found that the image input of accelerometer data resulted in higher accuracy for LLM prediction than the numerical input. FSL resulted in generally higher accuracy for LLM prediction than ZSL. We also found that applying the data from the same user improved accuracy compared to generalization to a new user. Furthermore, compared to chance (1/6 or 16.7%), even ZSL provided an ability to detect different activities. However, for the LLAMA3 model, we have found low levels of accuracy.

**Significance:** Our study explored the use of LLMs for time series classification in human activity recognition by using accelerometer data. By evaluating the Gemini and LLAMA3 LLMs under different prompting methods, we found the potential of LLM models to analyze the human activity data in different forms. Our study demonstrates that the LLM models could effectively predict human activity using ZSL on both numerical and visual accelerometer data, consistent with recent work [2]. Future work can examine if these findings can be extended to pathological human activity patterns, which may provide a viable method to diagnose diseases.

**Acknowledgments:** We thank members of the Mobility and Fall Prevention Research Lab for their contributions to performance benchmarking and making this work possible.

**References:** [1] Kwapisz et al. (2010), *Proceedings of the Fourth International Workshop on Knowledge Discovery from Sensor Data (at KDD-10),* Washington DC; [2] Ji et al. (2024), *2024 IEEE International Workshop on Foundation Models for Cyber-Physical Systems & Internet of Things (FMSys).*

# TRANSFER LEARNING FOR BIOLOGICAL JOINT MOMENT ESTIMATION IN STROKE POPULATIONS

Vaidehi Wagh[1], Dongho Park[2], Aaron Young[2], Inseung Kang[1,3]
[1]Robotics Institute, Carnegie Mellon University, Pittsburgh PA
[2]Department of Mechanical Engineering, Georgia Institute of Technology, Atlanta GA
[3]Department of Mechanical Engineering, Carnegie Mellon University, Pittsburgh PA
*Corresponding author's email: vwagh@andrew.cmu.edu

**Introduction:** Biological joint moment estimation plays a crucial role in determining control parameters for assistive exoskeletons, which have the potential to enhance mobility in stroke populations. An increasing availability of human biomechanics datasets has enabled the estimation in able-bodied populations using state-of-the-art deep learning models [1,2]. However, there is a lack of well-represented datasets in clinical populations such as stroke due to the heterogenous nature of stroke gait as well as the time, cost, and resource intensive nature of biomechanical data collection. Thus, machine learning based joint moment estimation in stroke populations has not been explored. Transfer learning is a machine learning technique that leverages knowledge from a source task to improve the performance on a target task, especially when the target task lacks high-quality data [3]. In this study, we employed transfer learning to estimate hip joint moments for a stroke subject by fine-tuning a Temporal Convolutional Network (TCN) model trained on an able-bodied biomechanics dataset. We hypothesized that retraining the able-bodied model using minimal stroke data would improve model performance on the stroke dataset.

**Methods:** We used a 5-subject able-bodied (AB) dataset consisting of 21 cyclic and acyclic tasks, with similar task representation as [4] for training. Unilateral data were collected using IMUs placed on the back, pelvis, thigh, shank and foot, as well as pressure insoles corresponding to the paretic side of the stroke (ST) subject. Three-axis accelerometer and gyroscope data from 5 IMUs, along with the vertical ground reaction force at the foot were used as input features and hip joint moment was used as the label for training a model. A TCN model [5] was implemented in accordance with previous literature [1,6] where it was validated for joint moment estimation in able-bodied populations. We used root mean square error (RMSE) as our loss function. The model was trained using leave-one-out cross fold validation, where subjects were 'left-out' for testing and validation each and the rest were used for training. We used a single subject stroke dataset consisting of 4 walking tasks of which 2 were used for testing and retraining. The linear output layer of the best-performing AB model was retrained using ST data (4-5 gait cycles from 1 task, 5 seconds), while the rest of the layers were frozen. Testing was performed in three parts: AB data was tested on the AB model (AB/AB), ST data was tested on the AB model (ST/AB), and ST data was tested on the retrained ST+AB model (ST/ST+AB) using RMSE as the comparison metric.

**Results & Discussion:** As shown in Fig. 1 (a), RMSE increased on testing ST data on the AB model due to differences in stroke gait patterns as compared to able-bodied patterns (0.149 Nm to 0.465 Nm). Supporting our hypothesis, post retraining with a small subset of ST data, the model learned subject-specific stroke gait patterns, reducing RMSE from 0.465 Nm to 0.336 Nm (~27% decrease). Visual comparison of the time-varying plots (b)-(d) in Fig.1 also validates the hypothesis.

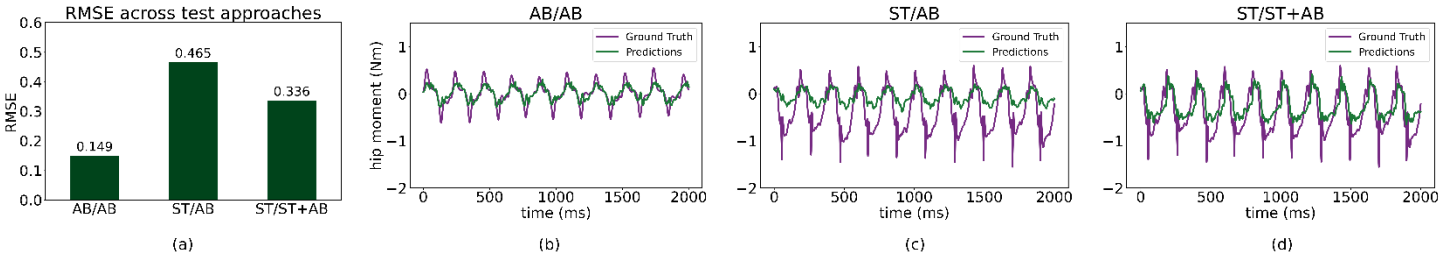


**Figure 1:** (a) RMSE across three test approaches. (b)-(d) Model predictions vs ground truth hip moments across time (ms) for three test approaches

**Significance:** Our study applied transfer learning to enable joint moment estimation in stroke populations where data availability poses a challenge to standard ML approaches. Our approach also allowed for customization of a general model to a patient with minimal data (0.14% of the size of able-bodied training data) causing a 27% decrease in error, eliminating computational costs associated with training custom models. This technique shows promise in facilitating tailored approaches to patient-specific exoskeleton control to aid mobility and rehabilitation. While this pilot study encourages the use of transfer learning for improving model performance on stroke data, further work is necessary to quantify the amount of retraining data, select optimal retraining tasks, and develop robust transfer learning pipelines to ensure satisfactory outcomes in joint moment estimation.

**References:**

[1] Molinaro et al. IEEE Trans. on Med Rob and Bio; 2022;4(1):219-29. [2] Liew et al. J Biomechanics.;129:110820. [3] Weiss et al. J Big data. 2016 Dec;3:1-40. [4] Scherpereel et al. Sci Data 10, 924 (2023) [5] Bai et al.; arXiv:1803.01271. [6] Scherpereel et al.; IEEE Trans. on Biomed Eng. 2024 Apr 15.

# ARTIFICIAL INTELLIGENCE FOR STREAMLINED CAI DIAGNOSIS: SINGLE-MARKER GAIT ANALYSIS USING MACHINE LEARNING

*Jaeyoung Cho[1], Victor M. Bonilla[1], Erik A. Wikstrom[2], Jaeho Jang[3]
[1]Department of Aerospace and Mechanical Engineering, The University of Texas at El Paso
[2]Department of Exercise & Sport Science, The University of North Carolina at Chapel Hill
[3]Department of Kinesiology, The University of Texas at El Paso
*Corresponding author's email: jcho4@utep.edu

**Introduction:** Lateral ankle sprains are highly common, costly (>$1 billion annually), and up to 70% result in chronic ankle instability (CAI). CAI is characterized by recurrent ankle sprains and altered movement patterns during walking. CAI plays a substantial role in the early onset of ankle posttraumatic osteoarthritis [1]. Diagnosing CAI relies on clinical observation and self-reported information from patients. Patient-reported outcomes are commonly used surveys/questionnaires to diagnose if an individual has CAI, as recommended by the International Ankle Consortium statement [2]. However, patient-reported outcomes can be influenced by various factors (e.g., subjectivity, health literacy, cultural or language differences) that may result in biased or inaccurate results.

While biomechanical analysis objectively identifies pathological movement patterns in CAI, traditional methods require extensive data collection from full-body marker sets and force plates, making them time-intensive and computationally expensive. These constraints limit their feasibility for clinical settings, where quick and accessible diagnostic tools are needed. However, advances in artificial intelligence (AI) and machine learning offer a more accessible possible alternative by identifying CAI-related gait alterations using minimal data. Specifically, AI-driven models could effectively distinguish individuals with and without CAI using only the most relevant marker data—such as the lateral malleolus of the affected limb. Therefore, the purpose of this study was to determine whether AI-driven analysis can accurately detect CAI presence using data from a single retroreflective marker during walking.

**Methods:** Data was collected using a 3-D motion capture system to analyze walking biomechanics on a force-measuring treadmill. Each subject walked for two minutes, and 50 steps were analyzed per subject. We analyzed the raw 3D marker trajectory data – *x(t), y(t), and z(t)* – of the involved ankle (i.e., lateral malleolus). The marker data were processed via the fast Fourier transform (FFT) and principal component analysis (PCA), which convert the 3600x1 time series data into 16x1 feature vector (Fig. 1). The achieved feature vector was then fed into the multilayer perception (MLP) model that was trained to provide "0" for the gait pattern from the control group and "1" for those from CAI. The trained MLP model was used to examine the possibility of CAI for each gain pattern in the validation group.

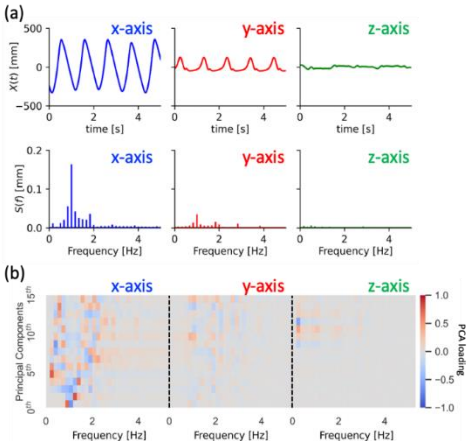


Figure 1. Processing of 3-D trajectory data of the involved ankle using the fast Fourier transform and principal component analysis.

**Results & Discussion:** Our results of CAI prediction based on the trained MLP model with 10-fold cross-validation can be seen in Fig. 2. Briefly, the 10-fold cross-validation divides the database into 10 sets (5-6 subjects each), where one dataset is reserved as a validation set while the remaining nine sets are used for the training process. Upon the end of the training, the prediction model is validated to the reserved validation set, and this training-validation process is repeated until all the sets are used as a validation set at least once. The 10-fold cross-validation minimizes the influence of potential bias between the training and validation set, providing robust validation of the developed model. The 10-fold cross-validation showed that the developed MLP model can diagnose CAI with 81% accuracy – i.e., the area under the receiver-operating-characteristic curve (AUC) was 0.81.

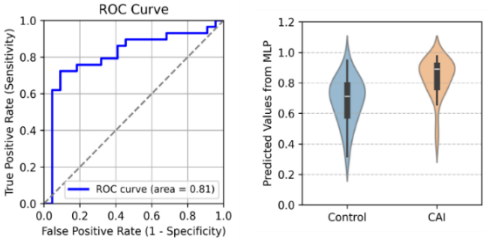


Figure 2. Receiver operating characteristic of AI-based CAI diagnostics with a violin plot showing the distribution of output from MLP model for control and CAI subject, respectively.

This study shows that a single marker can diagnose CAI with 81% accuracy, reducing data demands while maintaining reliability and clinical feasibility. Integrated into clinical workflows, such a model could streamline CAI diagnosis and assist clinicians in early intervention and targeted rehabilitation plans. Smartphone-based motion capture, such as OpenCap [3], could further enhance the practicality and scalability of this approach by enabling markerless data collection in real-world settings. While 81% accuracy is promising, there is room for improvement—potentially by incorporating additional biomechanical variables to refine the model. The study focused on a single marker, which, while efficient, might not fully capture the complexity of CAI biomechanics.

**Significance:** Beyond CAI, this methodology has the potential to be applied to the diagnosis of other musculoskeletal injuries and movement disorders using minimal datasets, making biomechanical assessment more practical for clinicians and researchers.

**Acknowledgments:** This study was funded by NATA Research & Education Foundation (Grant 1516OGP001) and the ACSM Foundation's Carl V. Gisolfi Memorial Fund.

**References:** [1] Hertel & Corbett. (2019), *J Athl Train* 54(6); [2] Gribble et al. (2014), *J Athl Train 49*(1), [3] Uhlrich et al. (2023), PLoS Comput Biol 19(10).

# THE EFFECT OF GROWTH PERIOD TREADMILL TRAINING ON VOLUNTARY PHYSICAL ACTIVITY IN ADULTHOOD

*Jessica Murawski[1], Derek Jurestovsky[1], Stephen J. Piazza[1], and Jonas Rubenson[1]
[1]Dept. of Kinesiology, The Pennsylvania State University, University Park, PA, USA
*Corresponding author's email: jam1798@psu.edu

**Introduction:** A quarter of the global population does not meet the recommended levels of physical activity and around 80% of adolescents are insufficiently physically active [1], a major contributing factor to increased risk of mortality and metabolic and cardiovascular disease [2]. Globally, physical inactivity levels have increased with each generation [3]. Exercise during childhood and adolescence has the potential not only to establish activity as a habit, but also to reduce physical barriers to exercise in adulthood by making it less effortful.

A recent finding in our laboratory was that guinea fowl that underwent extensive treadmill training during growth had larger aerobic capacity than control animals following training. Remarkably, this difference persisted after a 6-month period of no forced exercise in large pens. The elevated exercise capacity results in a relative effort of movement that is lower in adult animals that underwent growth-period exercise. As part of this ongoing study of the effects of growth-period exercise on locomotor function and energetics using a guinea fowl animal model, we examined the voluntary behavior of these same guinea fowl when singly housed in a large pen during the 6-month washout period. We hypothesized that animals that underwent extensive treadmill training during growth exhibit higher levels of movement in their pens compared to untrained control animals, indicating that training leads to higher voluntary levels of adult activity, perhaps elevating aerobic capacity post-washout.

**Methods:** A total of 60 guinea fowl were acquired as two-days old keets. At 2 weeks of age, they were separated into an exercise group (EXE) and a control group (CON). EXE birds were trained on treadmills with a 6° incline for 5 days a week at a speed of 1.33 $ms^{-1}$. The CON group remained in their cages during the training period, with no exercise outside of the cages except for occasional treadmill accommodation runs. After one year of training, both groups were transferred to large pens for 6 months and training ceased.

During this period, activity was recorded three times daily for 10 minutes using an overhead video camera sampling at 20 frames per second. The 6-month period was separated into three 2-month periods. The videos for a subset of these birds (EXE n=9; CON n=11) during the third of these periods were analyzed using DeepLabCut markerless pose estimation software to track individual bird movements in each video. The total distance traveled per unit of time was calculated for each animal.

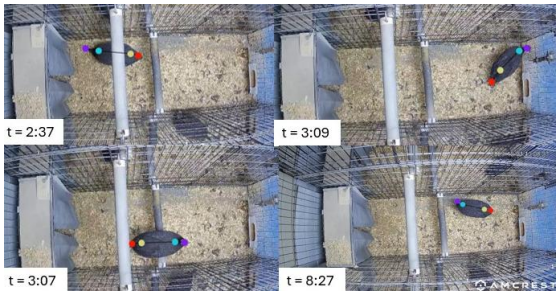


**Figure 1:** The 4 markerless points from DeepLabCut on a guinea fowl at four time points in a single video. The four markers are: head (purple), shoulder (blue), tail base (yellow), and tail end (red).

**Results & Discussion:** The hypothesis that EXE animals would exhibit grater activity was not supported by the results. DeepLabCut successfully tracked four markerless points on each animal as it moved in its pen in three videos per animal (Fig. 1). The average distance traveled per unit time for each group shows no significant differences between groups ($p = 0.577$; 0.098 ± 0.04 m/s for EXE and 0.117 ± 0.08 m/s for CON) (Fig.2).

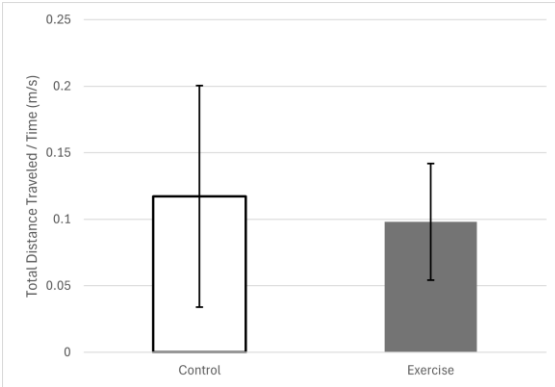


**Figure 2:** The average distance traveled, time normalized for the length of the videos analyzed.

**Significance:** The finding of no significant difference in distance traveled between groups suggests that the post-washout between-group difference in aerobic capacity cannot be attributed to differences in the voluntary activity of the birds during the washout. It may be that the birds developed lasting physiological or structural adaptations that caused their aerobic capacity to remain elevated even without further training. Further analysis of videos from all of the time points is currently underway.

**Acknowledgments:** We would like to thank the Animal Care Staff and lab technicians. Supported by NIH Grant R01AR080711.

**References:** [1] World Health Organization. Physical activity fact sheet. (2021).; [2] Haileamlak A *Ethiop J Health Sci.* 2019.; [3] Ozemek, C., Lavie, C. J., & Rognmo, Ø. Prog *Cardiovasc Dis* (2019).

# NEEDLE AXIAL FORCE AND INSERTION SPEED DURING CADAVERIC CANINE EPIDURAL

Claudia C.V.S. Smith[1], Carolyn L. Kerr[2], Scott Brandon[1]
[1]School of Engineering, University of Guelph
[2]Ontario Veterinary College, University of Guelph
csmith33@uoguelph.ca

**Introduction:** Epidural needle insertion is a complex procedure that is a core skill of anesthesia training in human and veterinary medicine [1]. Incorrect needle placement can cause serious complications including nerve damage, extreme headaches, inadequate anesthesia, paralysis, or death [2]. During insertion, haptic feedback experienced by the veterinarian through the needle is the first indicator that the spinal needle is correctly located in the epidural space; the needle is inserted between the final lumbar vertebrae and sacrum until the veterinarian feels a 'pop' as a sudden drop in resistance [1]. Axial needle insertion forces can vary widely between species [3] and with insertion speed [4]. This study aimed to quantify the insertion forces within the tissue layers and particularly the crucial 'pop' of the ligamentum flavum within the canine species.

The objective of this study was to quantify the maximum insertion forces required to penetrate the skin and ligamentum flavum with a spinal needle in canine specimens. It was hypothesized that distinct local maximum forces would occur during the penetration of skin and ligamentum flavum, due to their greater stiffness versus other intermediate tissues. Since the ligament is stiffer than skin, maximum force was expected to be greater for ligament versus skin. Secondly, it was hypothesized that the insertion speed would be not statistically different from 2 mm/s, which is the commonly assumed average speed in literature [5].

**Methods:** A custom device, consisting of a 5 kg load cell (DYMH-103, CALT, China) and proximity sensor (VL53L1X, Sparkfun, USA), was developed to measure handheld insertion force and speed using a spinal needle (2.5 in, 20 gauge, Quincke, BD, USA). Six ethically sourced 28-32 kg canine cadavers were prepared for needle insertion.

Force and needle insertion distance were recorded during four trials for each specimen, except the final specimen which had two successful trials. For each trial, an epidural needle insertion procedure was performed by an experienced veterinarian; the trial ended when 'loss of resistance' was perceived, indicating that the tip of the needle was in the epidural space. To confirm needle placement, the veterinarian injected contrast into the catheter after the first trial, and fluoroscopic images were recorded after each trial.

Data was analysed using MATLAB and a paired t-test, one sample t-test, and Wilcoxon signed rank were performed with Jasp (Version 0.19.3). Each trial began when more than 0.2 N was recorded and ended at the final local minima. The first and final peaks in the dataset were selected as the skin and ligament respectively. Data from each trial was organized into five sections (Fig 1). Speeds were found for each section and an overall average speed was found in each trial by averaging these values.

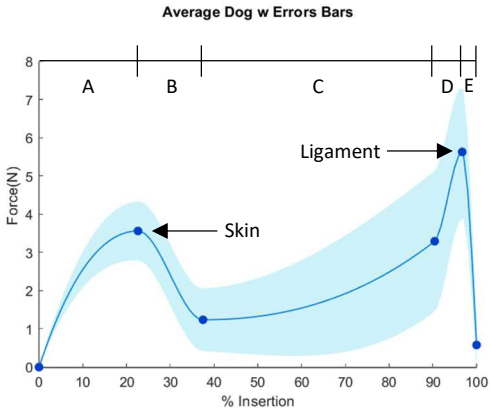


**Figure 1:** Average axial force during handheld epidural needle insertion in canines, from skin contact (0%) to epidural space (100% insertion).

**Results & Discussion:** Average maximum forces required to penetrate the skin and ligament tissues were 3.56 N and 5.63 N respectively (Fig 1). Most similar data in literature are for human or porcine tissues whose forces are considerably higher. One study found that it took 12.9 N to puncture porcine skin and 12.1 N to puncture human ligament, which is 3.6x and 2.2x higher when compared to the respective canine tissues in these findings [3]. These results are meaningful as they contribute to a body of data that has not been explored for canine subjects which can be used to improve study tools such as simulators in curricula.

It was also found that the force required to penetrate the ligament was significantly higher than the force required to penetrate the skin (paired t-test $p<0.001$). This supported our hypothesis that the ligament was the most difficult tissue structure to penetrate. This is likely due to a combination of friction which steadily increases as the needle further descends into the tissue, and the tissue's inherent stiffness. This is important to consider when designing synthetic training models that require accurate haptic feedback for each tissue.

The overall average needle insertion speed was 7.95 mm/s, which was statistically different from the often assumed insertion speed of 2 mm/s (one sample t-test $p<0.001$, Wilcoxon $p<0.001$) [5]. Similar studies have inserted spinal needles at a constant speed, but these results may suggest that their recorded force values will be higher due to setting ~4x lower speeds.

**Significance:** This investigation has characterized the axial needle insertion force during epidural needle insertion in canines and has further contributed to the understanding of the haptic feedback the veterinarian experiences when approaching the epidural space. Future simulators and training procedures need to recognize that insertion speed may be much faster than previously thought, and therefore accurate haptic forces may be much lower than in literature. The act of quantifying relevant species-specific tissue properties prior to designing simulators or curricula may lead to more accurate simulators. This could result in more capable veterinarians and therefore improved patient care.

**References:** [1] Aarnes (2016), *Handbook of Small Animal Regional Anesthesia and Analgesia Techniques*; [2] Mo *et al.* (2021), *Optik* 242; [3] Holton (2001), *Stud. Health Technol. Inform.* 81; [4] Traczynski et al. (2024), *J. of Mech. Behav. Of Biomed. Mat.* 150; [5] Naemura *et al.* (2008), *International Conf of IEEE Eng in Med and Bio Society*.

# EVALUATION OF HEMIARTHROPLASTY BEARING MATERIALS IN ANIMAL MODELS: A SCOPING REVIEW

Landon M. Begin[1,2], Victoria Marino, Francesca De Vecchi, Douglas C. Moore[2], Markus A. Wimmer, Joseph J. Crisco[1,2]
[1]Institute for Biology, Engineering, and Medicine, Brown University, Providence, RI
[2]Department of Orthopaedics, The Warren Alpert Medical School of Brown University, Providence, RI
*Corresponding author's email: landon_begin@brown.edu

**Introduction:** Osteoarthritis (OA) is a leading cause of disability, particularly in older adults, and often results in significant joint pain and loss of function [1]. In advanced cases, where conservative treatments are ineffective, joint replacement surgeries are commonly considered. A less frequently utilized approach is hemiarthroplasty, which involves the partial replacement of an articulating joint. Unlike total joint replacement, hemiarthroplasty replaces only one surface of the joint with a bearing material, preserving healthy bone and cartilage for patients with localized OA [2]. Ongoing bench and translational research are focused on improving hemiarthroplasty bearing material (HBM) performance and improving clinical outcomes for patients. This scoping review was performed to synthesize and summarize the current literature on animal models that have been employed in HBM evaluation.

**Methods:** Using Covidence, a scoping review was performed to compile studies focusing on hemiarthroplasty bearing surfaces and joint health, following the Arksey and O'Malley methodological framework. Databases queried included PubMed, Scopus, Google Scholar, and the Cochrane Library (December 2024). Included studies evaluated live animals implanted with biomaterials that articulated against articular cartilage. The data extracted focused on the materials tested, animal models used, duration of animal survival, gait analysis, image analysis, histological staining, and cartilage scoring systems.

**Results:** Our search returned 1,798 studies, but only 24 *in vivo* studies that evaluated HBMs against articular cartilage (Fig.1). Of the 24 studies, 6 evaluated two or more HBMs. Metals were tested most often (15 studies): 10 studies evaluated Cobalt Chromium alloys, 3 evaluated Titanium alloys, and 2 evaluated Stainless Steel. Hard and soft Polymers were evaluated in 8 studies: 7 studies evaluated Polyvinyl Alcohol hydrogels and 1 study evaluated Polyetheretherketone (PEEK). Ceramics were evaluated in 4 studies, including Partially Stabilized Zirconia (n=1), Alumina Ceramic (n=1), Zirconia (n=1), and 1 evaluated a ceramic material but provided no details as to its composition. Pyrolytic Carbon was evaluated in 4 studies. Six studies compared two or more HBMs, five of which found metals to be inferior to the comparator HBM. Five species of animals were used to evaluate HBMs (Fig. 1): dogs (n=11), rabbits (n=6), sheep (n=5), rats (n=1), and goats (n=1). The animal survival durations varied: 2 to 78 weeks (dogs), 4 to 104 weeks (rabbits), 12 to 52 weeks (sheep), 26 weeks (rats), and 12 weeks (goats). Gait analysis was conducted in 13 studies, though only subjective gait observations were reported for 10 studies, while 3 used force plates to monitor weight bearing. All 24 studies utilized imaging, including *in vivo* radiographs, while micro-radiographs, scanning electron microscopy, computed tomography (CT), and micro-CT were performed post-harvest; however, only 3 studies used these imaging modalities to analyze cartilage degeneration/wear. Histological staining was used in all 24 studies: Safranin-O (14 studies), Hematoxylin and Eosin (13 studies), Toluidine blue (7 studies), Giemsa (3 studies), and several other individual stains. All studies semi-quantitatively evaluated cartilage wear: 9 used Mankin or Modified Mankin scoring, and several studies used their own scales, such as "wear grades" 1 to 5, "gross appearance" 0 to 10, and "histologic scores" 0 to 3. 10 studies did not identify the scoring system they used.

**Discussion:** We identified trends in HBM selection, animal models, study duration, and outcome measures. Metals were the most tested HBMs, with dogs and rabbits as the most used animal models. The proximal (11 studies) and distal femur (9 studies) were the most frequently used anatomic sites, though few incorporated quantitative gait or cartilage wear imaging assessments. Cartilage health was primarily evaluated using the Mankin scoring system. All 24 studies assessed cartilage wear via histology, however the outcome variables reported and scoring systems used varied. In 5 of the 6 comparative studies, inferiority of metals was based upon their association with loss of cartilage thickness, degradation of articular cartilage, quicker onset of cartilage degeneration, and cellular changes (morphology/loss of matrix). There was an apparent shift in animal species used over time: most (8/11) of the studies that used dogs were conducted 20 to 41 years ago, while 11 of the 12 rabbit, sheep, and goat studies were conducted in the last 20 years.

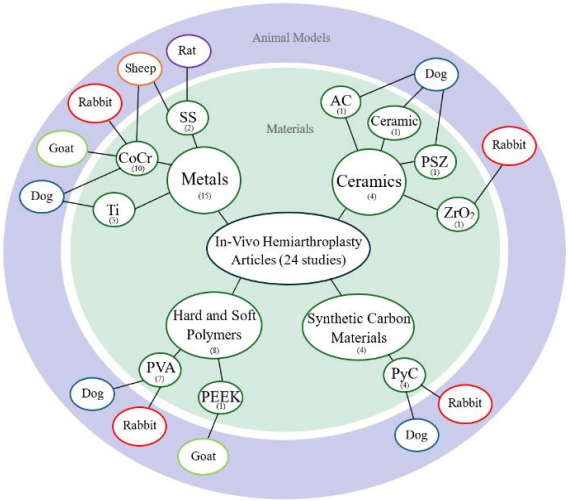


**Figure 1:** Web chart providing a breakdown of materials evaluated, with the number of studies evaluated for each ((#)) and the associated animal models used.

**Significance:** This scoping review was performed to summarize methods and outcome variables used to evaluate HBMs *in vivo*. Within this sector of research studies, there was no standardized animal model used, or outcome variables reported, though all evaluated cartilage damage histologically. The absence of the ability to make material-to-material comparisons and/or aggregate the results in reviews or meta-analyses presents a challenge to translating novel hemiarthroplasty biomaterials to clinical practice.

**Acknowledgments:** Supported in part by NIH/NIAMS under award number R01AR082898. Other contributors: Quianna Vaughan

**References:**
[1] Katz JN et al., 2021. JAMA. [2] Waldorff EI et al., 2013. J. Arthroplasty.

# DEVELOPMENT OF SMALL BONE IMPLANTS IN A PORCINE MODEL FOR CARPAL BONE REPLACEMENT

*Quianna M. Vaughan, Amy M. Morton, Douglas C. Moore, Joseph J. Crisco
[1] Department of Orthopaedics, Warren Alpert Medical School of Brown University, Providence, RI
*Corresponding author's email: quianna_vaughan@brown.edu

**Introduction:** Wrist pathologies, including osteoarthritis, fractures, and ligament injury, can result in instabilities and pain impairing an individual's quality of life [1]. Carpal bone replacements provide a motion-preserving treatment option. However, implant designs are challenging due to the wrist's anatomical complexity [2]. The ability to test novel implant designs and new materials in a preclinical animal model would be a valuable tool for advancing small bone replacement. The YMP carpus has been identified as a potential model for the human carpus because of similarities in size, anatomy, and bone composition. Therefore, we are investigating radial carpal bone (RCB) replacement in the Yucatan minipig (YMP) as a preclinical large animal model to test novel materials and implant designs. The YMP RCB is homologous to the scaphoid in the human wrist. The specific purposes of this study were to: 1) determine the spectrum of sizes and shapes of the YMP RCB; 2) generate a set of implants for YMP RCB replacement; and 3) develop and assess a method to estimate YMP-specific implant size and fit for animals in an *in vivo* pilot study.

**Methods:** 35 YMP forelimbs (6M, 12 F, age: 25.1 ± 9.8 months, weight: 62.6 ± 15.2 kg) were imaged using a clinical CT scanner to establish a database of RCBs. A density-based threshold was used to define the cortical bone surfaces and 3D models of the RCB and exported as closed triangular meshes. Volume and bounding box (BB) dimensions (VD - volar-dorsal, PD - proximal-distal, and RU - radial-ulnar) of the RCB models were calculated using custom-written MATLAB (Mathworks, US) scripts. Multiple linear regression was performed to define the relationship between animal age and weight and RCB volume and separate linear regressions were performed to identify the relationships between RCB volume and the three BB dimensions. A mean-shaped bone (RCB-MS) was generated from the RCB dataset using ShapeWorks Studio v6.2.1. The RCB-MS was anisotropically scaled using the linear regression equations to yield a set of 9 implants, which were fabricated from CoCr. Four YMPs from an *in vivo* pilot study, approved by the institution's IACUC committee, received CoCr replacement RCB implants. RCB implant sizes for these animals were estimated by using the animal's age and weight as inputs to the multiple linear regression equation, though final implant size was selected by the surgeon at the time of surgery. Implant fit was examined by comparing the Predicted and Surgeon-Selected implants to the RCBs of the *in vivo* animals. To do so, distances (mm) were calculated between the surfaces of the implants and RCBs of the *in vivo* animals harvested at 12 weeks. A Two-tailed Wilcoxon matched-pairs signed-rank test assessed differences in distances between the Predicted RCB Implant and Surgeon-Selected Implant.

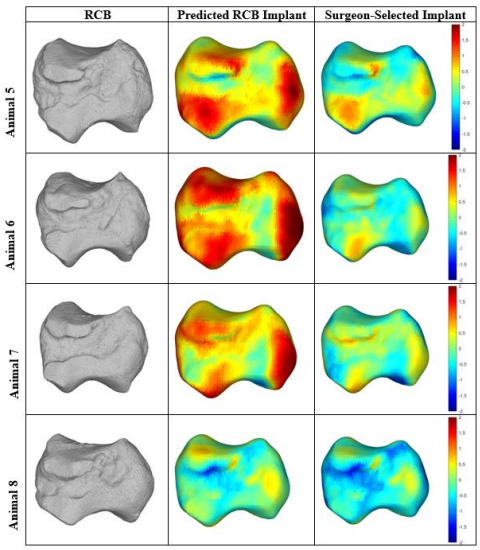


**Figure 1**: Surface distances (mm) between the implants and RCBs visualized across the implant surface of the Predicted and Surgeon-Selected Implants (n=4).

**Results & Discussion:** The bone volumes of the RCB dataset ranged from 1339.7 to 2712.9 $mm^3$ (mean: 1808.1 ± 361.4 $mm^3$). The bounding box dimensions ranged in length from 18.4 to 23.9 mm in the VD dimension (mean: 20.6 ± 1.6 mm), 14.5 to 20.1 mm in the PD dimension (mean: 16.8 ± 1.4 mm), and 10.4 to 14.1 in the RU dimension (mean: 11.9 ± 1.1 mm). The RCB-MS volume was 2171 $mm^3$ with BB dimensions of 21.8 mm in VD, 17.9 mm in PD, and 12.3 mm in RU. The relationship between animal age and weight and RCB volume had an $R^2$ of 0.80. There was a strong correlation between RCB volume and the VD dimension with an $R^2$ of 0.90, and in the RU dimension with an $R^2$ of 0.73 ($p < 0.001$ for both). There was a modest correlation observed between RCB volume and PD dimensions ($R^2 = 0.51$; $p < 0.001$). The set of 9 implant sizes ranged in volume from 986.9 to 4410.0 $mm^3$ with an average volume increment of 427.9 $mm^3$. BB dimensions of the implants ranged from 16.6 to 27.5 mm in VD, 14.0 to 21.6 in PD, and 9.4 to 16.4 in RU with an average increment of 1.4 mm in VD and 0.9 mm in PD and RU. The mean value for the distance from the Predicted RCB Implants to the RCBs was 0.7 ± 0.3 mm (n=4). The mean value for the distance between the Surgeon-Selected Implants to the RCBs was 0.4 ± 0.1 mm (n=4). The distance between surfaces of the implants and RCBs was significantly greater ($p < 0.001$) for the Predicted RCB Implants compared to the Surgeon-Selected Implants in three animals (Animals 5-7), and significantly smaller ($p < 0.0001$) in one animal (Animal 8) (Fig 1). The model overpredicted RCB Implant size using animal age and weight.

**Significance**: Establishing a model that uses age and weight to determine a range of implant sizes available to surgeons in the OR could reduce the cost and time associated with preoperative imaging and planning. We showed the feasibility of a porcine preclinical animal model for carpal bone replacement.

**Acknowledgement:** Supported in part by NIH/NIAMS under award number R21AR082130.

**References:** [1] Geoghegan et al. (2024), *BR J Surg* 111(4). [2] Rainbow et al. (2016), *J Hand Surg Eur Vol.* 41(1).

# MULTIARTICULAR MECHANICAL CONNECTIONS OF THE PLANTARIS TENDON IN KANGAROO RATS

*David Lin[1], Destinee Ditton[2], Nathen Schiele[2], Craig McGowan[3]
[1]School of Chem. Eng. and Bioengineering and Dept. of Integrative Physiol. & Neurosci., Washington State University
[2]Biol. Systems Eng., University of Idaho [3]Dept. of Integrative Anat. Sci., University of Southern California
*Corresponding author's email: davidlin@wsu.edu

**Introduction:** Even though many leg muscles are multiarticular, they usually have a single tendon insertion on a distal limb. Previously, we measured the contribution of the plantaris (PL) muscle to ankle plantarflexion in kangaroo rats, a small bipedal hopper [1]. In this previous study, we assumed that the main function of the PL was ankle plantarflexion, as in many terrestrial vertebrates. However, in further anatomical dissections, we found that the PL tendon also extends to the plantar surface of the foot and inserts on the distal phalanges, in addition to its connection to the calcaneus. The objective of this study was twofold: detail the anatomical connections of the PL tendon in kangaroo rats with a novel imaging technique; and experimentally measure the moment generated at the metatarsal-phalangeal (MTP) joint by electrical stimulation of the PL. We expected that: imaging shows that the PL tendon insertion at the calcaneus to be different than the gastrocnemii (GAS) muscles because the continuation of the PL tendon to the phalanges; and the PL could generate substantial MTP moment relative to another MTP plantarflexor (the Digital Flexor (DF) muscle) because of the relatively large mass of the PL in kangaroo rats. The implication of this dual tendinous connection is the PL has the synergistic mechanical actions of stiffening the MTP joint and of generating ankle plantarflexion moments, both of which are necessary to a enable the generation of ground reaction forces in the propulsive phase of hopping.

**Methods:** Nine wild adult desert kangaroo rats were caught in the Mojave Desert in Nevada (mean body mass:114 g). All animal procedures were approved by the Washington State University Institutional Animal Care and Use Committee. For each animal, in situ mechanical experiments measured the amount of MTP joint moment and stiffness generated by the PL, combined GAS, and DF muscles. Under anesthesia, the femur was mechanically stabilized, we inserted wire electrodes into GAS, DF, and PL muscles, and we placed buckle-type force transducers on the GAS and PL tendons. We then placed the toes into a holder attached to the mechanical testing system (model 1300A, Aurora Scientific, Canada) that measured MTP joint angle and moment. We then stimulated each muscle separately, and when isometric moment was steady, we imposed a 34° dorsiflexion of the MTP joint to measure the joint stiffness generated by each muscle. Simultaneous measurements of PL and GAS force, MTP moment, and MTP angle were made for each trial.

For imaging, we used a contrast-enhanced micro-computed tomography that allows for 3D imaging of tendons together with bone on two of the hindlimbs [2]. The tissues were stained with phosphotungstic acid (PTA), which increased the X-ray absorption of the tendons. High resolution scans were taken by a Bruker SkyScan 1275 micro-CT scanner and used for 3D image reconstruction.

**Results & Discussion:** Stimulation of the three muscles resulted in forces ranging from 11 to 100% of the estimated maximal force. Stimulation of the GAS resulted in no MTP moments, showing that the GAS was a pure ankle plantarflexor (Fig. 1). Stimulation of the PL and DF resulted in MTP moments, with maximal moments estimated to be 1.2 and 0.93 N-cm, respectively. Estimates of maximal MTP stiffness generated by the PL and DF were 0.060 and 0.045 N-cm/deg, respectively.

Images of the ankle joint showed distinct GAS and PL tendons, with the GAS tendon clearly inserting into the posterior portion of the calcaneus in the sagittal cross-section. The PL tendon did not show an insertion into the calcaneus in the sagittal cross-section, instead, wrapping around the GAS tendon and continuing to the plantar surface of the foot. In the posterior-lateral surface view, connective tissue emanating from the PL tendon can be observed attaching to the lateral and medial surfaces of the calcaneus.

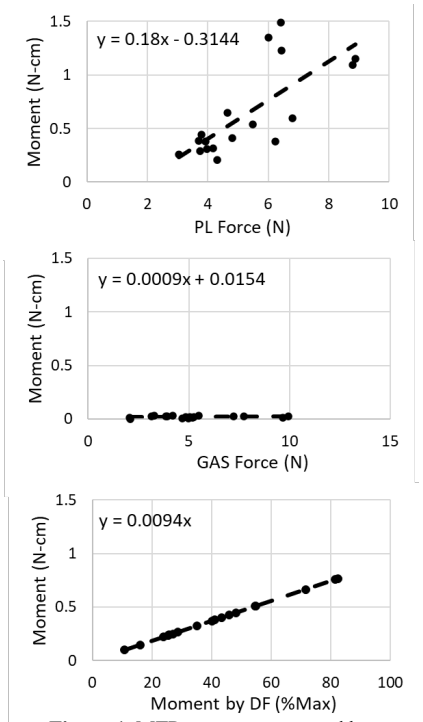


**Figure 1.** MTP moment generated by stimulation of PL, GAS, and DF muscles.

Our results supported the expectation that the PL could generate substantial MTP moments, larger than the DF, which is the largest pure MTP plantarflexor muscle in kangaroo rats. Imaging and stimulation data supported the expectation that GAS and PL tendons were separate and that PL tendon had an atypical connection to the calcaneus.

**Significance:** In this study, we documented by imaging and by mechanical experiments that the PL muscles in kangaroo rats have tendon insertions that are atypical to most multiarticular leg muscles, attaching to two distal bones, the calcaneus and phalanges. Functionally, the PL can generate substantial ankle and MTP plantarflexion moments. Specifically, the PL could be important for maintaining MTP stiffness, which is necessary for transmitting forces from proximal muscles and generating ground reaction forces in the propulsive phase. Moreover, the attachment to the calcaneus simultaneously creates ankle plantarflexion, which is automatically coordinated with the increase in MTP stiffness.

**Acknowledgments:** This work was supported by NSF grants #2128545 (DCL) and #2128546 (CPM) and NIH P20GM103408 (NRS).

**References:** [1] Javidi et al. (2019), *Ann Biomed Eng* 47; [2] Ditton et al. (2024), *MethodsX* 12.

# HOW DO MECHANICAL STIMULI AT THE MUSCLE TISSUE SCALE VARY DURING RESISTANCE EXERCISE?

*Katherine R. Knaus[1], Mark R. Viggars[2], Casey L. Sexton[3], Andrew D. McCulloch[4], Karyn A. Esser[2]
[1]Colorado School of Mines; [2]University of Florida; [3]University of Alabama Birmingham; [4]University of California San Diego
*Corresponding author's email: katherine.knaus@mines.edu

**Introduction:** Muscle plasticity can be stimulated by mechanical loading from increased muscle use. Biomechanical studies that investigate load characteristics in specific use cases are critical to understanding functional muscle changes in response to interventions. Because skeletal muscle mass is inversely related to mortality, aging, and disease [1], there is considerable interest in understanding the mechanisms by which resistance exercise can elicit hypertrophy, i.e., increase muscle mass. While methods to explore molecular mechanisms of hypertrophy in response to overload have grown increasingly sophisticated [1], studies provide limited characterization of mechanical loads in muscle during prescribed resistance training. Muscle tissue loading during a resistance exercise is a function of biomechanics of the body and structural architecture of the muscle. Biomechanical studies, particularly those utilizing simulations, have shown how external loads connect to joint kinetics and muscle forces during motion and have linked muscle structure variability with mechanical function in those motions [2,3], but so far have not been used to characterize muscle loads at the tissue level during exercise.

Mice are used extensively in hypertrophy mechanism studies utilizing advanced molecular-based approaches; however, we have limited information on mouse muscles mechanics in the overload conditions of these studies. Dynamic imaging of muscle contractions reveals regional variations in mechanics [3] and sarcomere measurements in mice demonstrate non-uniformity across active muscle [4], yet molecular studies do not account for regional load variability within a muscle of interest. Further variations in muscle force across repetitions performed during an exercise session could arise from fatigue [5]. *We hypothesize that the tissue loads will vary spatially in mouse dorsiflexor muscles during fixed-end contractions in resistance exercise and that these load gradients will differ with contraction force.* We aim to predict regional differences in mechanical stimuli by quantifying stresses and strains in three regions of the tibialis anterior (TA) and extensor digitorum longus (EDL) muscle during contractions representative of a resistance exercise intervention.

**Methods:** All experiments were performed with the approval of the Animal Care and Use Committee at the University of Florida. Twelve Jackson C57Bl/6 mice (6F/6M, 29±7wks, 30±5g) performed an *in vivo* resistance exercise protocol of high force electrically stimulated tetanic dorsiflexor muscle contractions (Aurora Scientific). Force-frequency tests were performed to establish stimulation frequency to generate 80% max force that was used for the exercise protocol where mice completed 10 sets of 8 repeated 1s contractions (rest: 6s/rep, 120s/set). Peak contraction forces for each exercise rep were normalized by the max force from the force-frequency test and mean normalized peak force for each rep during exercise was found across all mice. An hour post-exercise, mice were anesthetized, and TA and EDL muscles were dissected and measured before freezing for RNA sequencing. Dorsiflexor muscles were also measured in 12 control mice (6F/6M, 26±4wks, 32±6g) before freezing and in 6 additional mice (3F/3M, 12wks, 25±5g) used for more detailed structural analysis. These 6 mice were perfusion fixed for microCT imaging and dissection to measure TA and EDL muscle architecture.

A 3D finite element model (FEM) of mouse dorsiflexors was created to represent experimental muscle measurements. The FEM was meshed as tetrahedral elements with assigned fiber directions in FEBio [3]. Fixed-end contraction simulations were performed by increasing muscle activation to predict musculotendon deformation and force production. Fiber strain and first principal stress were averaged for elements in the distal, middle, and proximal third of the TA and in the EDL.

**Results & Discussion:** The mice produced varied mean peak forces across the 80 contractions performed during the resistance exercise protocol (Fig. 1). FEM simulations were performed at the average exercise contraction force (53% max) and at the greatest exercise contraction force (88% max). With the average force simulation, FEM predicted strains decreased in magnitude (negative strains for muscle shortening) from the proximal to distal TA while stress was similar across regions but increased in variability from proximal to distal (Figure 1). Greatest force simulations demonstrated similar trends in strain a stress, however, stress and strain variability increased. Regional strain gradients suggest that muscle tissue mechanical stimuli are non-uniform and could contribute to region-specific hypertrophy response. Further, varied muscle forces across the exercise session and subsequent effects on regional stress and strain gradients alter mechanical stimuli, such that fatigability may impact muscle mechanics to affect exercise response.

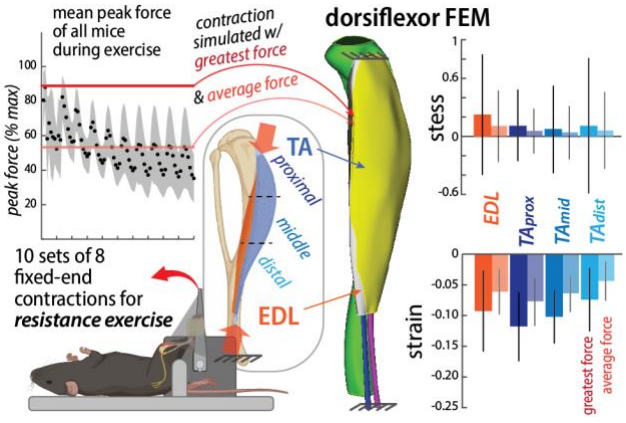


**Figure 1:** *FEM predicted stress and strain in exercise experiment*

**Significance:** Resistance exercise improves human health by mechanically stimulating muscle plasticity to increase mass. Prescribing exercise to elicit these benefits requires identifying a "dose" – a quantifiable prescription metric that can be mapped to specific effects. Study results quantifying tissue mechanics during exercise move us towards better exercise dosing by providing biomechanical insight to the characterization of muscle plasticity mechanisms needed for intervention design to combat loss of function in aging and disease.

**Acknowledgments & References:** This work is supported by the Wu Tsai Human Performance Alliance; [1] Roberts MD et al (2023). *Physiol Rev*, *103*(**4**): 2679-2757; [2] Delp SL et al (2007). *IEEE Tr BME*, *54*(**11**):1940-1950; [3] Knaus KR et al (2022). *J Biomech*, **130**:11087; [4] Moo EK et al (2017). *Front Physiol*, *8*:1015; [5] Enoka RM & J Duchateau (2008). *J Physiol*, *586*(**1**), 11–23.

# THE EFFECT OF CHRONIC LIMB LOADING ON THE TIBIALIS CRANIALIS MOMENT ARM IN GUINEA FOWL

*Roberto Castro Jr.[1], Kavya Katugam-Dechene[1], Talayah A. Johnson[1], Jonas Rubenson[1], Stephen J. Piazza[1]
[1]Dept. of Kinesiology, The Pennsylvania State University, University Park, PA, USA
* Email: Castroroberto@psu.edu

**Introduction:** The muscle moment arm is a parameter important to muscle function: The moment arm determines the joint moment produced for a given muscle force, and it also determines how much muscle shortens for a given joint rotation. Thus, muscle moment arm determines mechanical advantage, but it also influences muscle force as determined by the force-length-velocity relationship [1]. It is well established that muscles adapt to chronic loading stimulus but whether moment arms undergo similar adaptation in response to loading and activity remains unknown. This question is important not only for understanding the plasticity of moment arms but also because of the increase in a sedentary lifestyle, especially among growing children.

We examined this question using an avian model, the guinea fowl (*Numida meleagris*). In a previous study done in our lab we found evidence that the Achilles tendon moment arm of guinea fowl that underwent high acceleration training during the growth period were larger [2]. To examine this question, we subjected animals to a chronic limb loading stimulus that targeted the tibialis cranialis muscle. We hypothesized that the moment arm of the tibialis cranialis muscle would be larger on the loaded side when compared to either the unloaded side or to the limbs of control birds.

**Figure 1**: Measurement of tendon excursion and limb kinematics

**Methods:** Twenty guinea fowl were obtained as day-old keets and were randomly assigned to a CON group (n=10) or a LL group (n=10). From 2 weeks to 16 weeks of age, limb loaded animals were unilaterally loaded with a mass equal to 3.5% of their body weight placed above the right ankle. In addition, all animals underwent twenty minutes of training 3 times per week in which there were herded around a large circular pen. Animals were euthanized at 16 weeks of age.

The tibialis cranialis muscle moment arms on both sides in both the LL and control groups were measured using the tendon excursion method. The limb being tested was secured using bone clamps (Fig.1). Bone pins were drilled into the femur, tibiotarsus and tarsometatarsus segments. Cluster of four retroreflective markers fastened to each bone pin were tracked by a 6-camera motion analysis system Kestrel 300). A cable transducer was connected to the tibialis cranialis tendon via a suture to measure tendon travel. For each limb (loaded and unloaded) the ankle joint was cycled through its range of motion while limb motion and tendon travel data were recorded simultaneously. Linear fits were performed to tendon excursion versus angle. Moment arm was computed as the derivative of tendon excursion versus ankle joint.

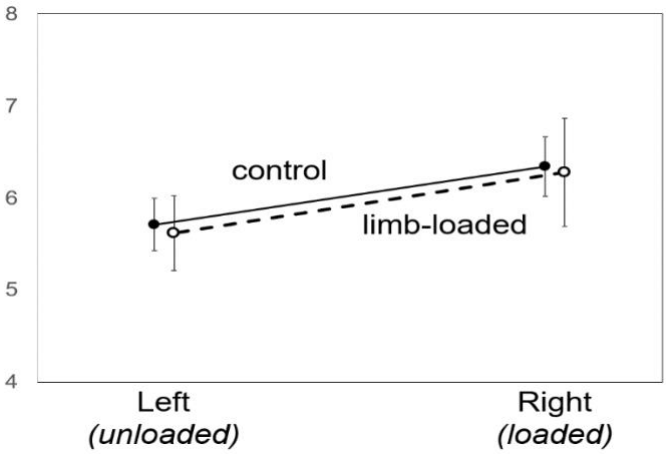


**Figure 2**: Average moment arms for control and limb loaded animals. For the limb loaded group the right side was loaded.

**Results & Discussion:** To date, we have tested and analysed data from 7 limb loaded 8 control birds. A mixed-effects general linear model revealed no significance difference between the moment arms of control and limb loaded birds($p=0.661$). Significant bilateral differences ($p<0.001$) were found for both groups; the moment arm of the right limb was consistently larger (Fig. 2). There was no significant interaction between side and group ($p=0.918$); the right tibialis cranialis moment arm was larger compared to the left. The difference between sides we found for CON birds was unexpected, and we are presently investigating whether this can be attributed to experimental artifact

**Significance:** Our study is among the first to explore plasticity of muscle moment arms during growth. The findings from our work will reveal the extent to which muscle moment arms should be considered when investigating how the structure and function of the musculoskeletal system adapts to variation in load stimulus and physical activity.

**Acknowledgments:** This study was supported by NIH grants R21AR071588 and R01AR080711.

**References:** [1] Lee & Piazza (2009). J.Exp.Biol, 212(22): 3700-3707; [2] Salzano MQ (2020) PhD Dissertation Penn St University.

# MARKERLESS MOTION CAPTURE FOR FULL-BODY ANALYSIS OF HORSES

*Sarah K. Shaffer[1], Omar Medjaouri[1], Brian Swenson[1], Travis Eliason[1], Daniel P. Nicolella[1]
[1] Southwest Research Institute, San Antonio, Texas
*Corresponding author's email: sarah.shaffer@swri.org

**Introduction:** There is a need for methods to track equine gait, both to aid in clinical examinations and to provide performance feedback. The gold-standard available for three-dimensional (3D) kinematic analysis in horses is marker-based motion capture, which requires small markers to be placed on the animal; sensor-based systems are also used. However, current methods are difficult to use outside of a research setting, require expertise during data collection and processing, and can be time-consuming to scale to many animals. To our knowledge, existing equine markerless motion capture methods are limited to planar analysis and have limited output metrics. This work presents a markerless motion capture methodology for horses, where three-dimensional, full-body kinematics are calculated using multi-camera video data, offering a more scalable and labor-efficient approach compared to traditional techniques.

**Methods:** A multi-step pipeline, based on the Engine for Automated Biomechanical Analysis [1], was used to determine three-dimensional (3D) kinematics from multi-camera video data (Fig. 1). In Step 1, the 2D location of 54 anatomic landmarks (markers) are identified in each camera view by a convolutional neural network (CNN). In Step 2, triangulation is performed to reconstruct the 3D location of each marker using the 2D predictions and camera calibration data. In Step 3, a musculoskeletal model is regionally scaled using predicted markers. In Step 4, inverse kinematics (IK) is performed on the musculoskeletal model to produce kinematic trajectories.

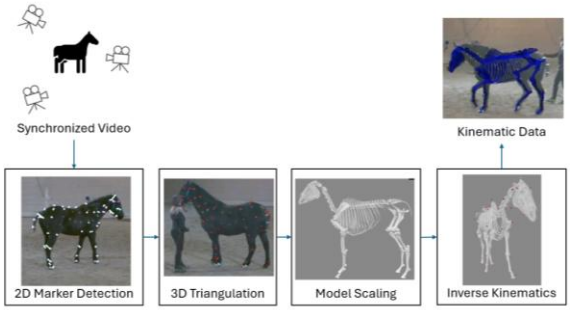


**Figure 1:** Analysis pipeline

A CNN was trained to predict the 54 markers using images of horses with labeled marker locations. Training data consisted of labeled images from the Poses for Equine Research Dataset (PFERD; [2]) and an additional ~69k labeled images from marker-based motion capture studies and open-source datasets [3-8]. Marker-based motion capture data from one horse in the PFERD data (PFERD ID 5) was held as ground-truth data for validation. An equine rigid body biomechanics model (Fig 2) was modified to add degrees-of-freedom and restrict joints to their physiologic ranges [9]; the model had 23 joints and 35 degrees of freedom (DOF). Virtual markers corresponding to the 54 markers predicted by the CNN were added to the model so that 3D kinematics could be calculated via IK in OpenSim during Step 4.

To assess the analysis pipeline (Fig 1), we evaluated 2D performance of the CNNs (Step 2), the 3D error between predicted data and marker-based motion capture data (Step 3), and joint angles calculated using predicted and ground-truth data (Step 4) using validation horse data. 2D performance of the CNNs was evaluated using the percentage correct keypoints (markers) within a threshold distance (radius bone length) for each CNN; reported values indicate the percent of markers correctly predicted within the threshold distance to the ground-truth marker locations. The distance between 3D marker location after triangulation and ground-truth data was determined for 14 strides at the walk, 24 strides at the trot, and 8 strides at the canter. The root-mean-square-error (RMSE) between kinematic trajectories calculated via IK using predicted and ground-truth data was calculated for the same set of strides.

**Results & Discussion:** The 2D network evaluation indicated that the network could place markers close to the correct location, with some noise. 82% of predicted markers were within 25% of the radius bone's length to their correct location. However, only 49% of predictions were within 10% of radius length to their true location. Our 3D error is consistent with observations of noise in the 2D predictions. Median 3D prediction error was between 3.1 – 4.1 cm at the walk, trot, and canter; the average 3D prediction error was slightly higher (3.6 – 6.5 cm). This error is higher than what is acceptable in human markerless motion capture applications; it could be reduced with additional training data allowing for more accurate 2D predictions. Joint angle RMSE was less than 10° for 32, 26, and 30 DOF at the walk, trot, and canter. Angle RMSE increased distally, which is typical in human markerless motion capture systems.

**Significance:** This study demonstrates that three-dimensional markerless motion capture is feasible in horses. The developed methodology represents an advancement in technologies available for equine kinematic analysis. The primary limitation of this work is the small amount of training data and simplifications in the biomechanics model. A future validation against a gold-standard is needed, however, the agreement between angles calculated using ground-truth and network-predicted markers gives initial evidence that this method could be competitive with gold-standard systems in the future.

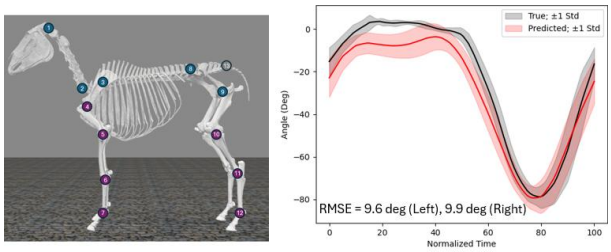


**Figure 2:** Left) Equine biomechanics model; joints have three rotational degrees of freedom (blue), one rotational degree of freedom (purple), or are fused (grey). Right) Carpus angle (#6) calculated using predicted and ground-truth data at the trot.

**Acknowledgments:** This project was funded by Southwest Research Institute's Internal Research and Development Program.

**References:**[1] Templin, Southwest Research Institute, 2020.[2] Li, "PFERD", 2024. [3] Yu, "AP-10K", 2021. [4] Banik, *arXiv*, 2021.[5] Niknejad, *J ASABE*, 2023. [6] Symons, *Equ Vet J*, 2014.[7] Rohlf, *Animals*, 2023.[8] Bonilla Lemos Pizzi, *Animals*, 2024.[9] van Bijlert, *Int Comp Bio*, 2024.

# BUILT FOR BALANCE: UNIQUE KNEE JOINT MORPHOLOGY OF BIRDS ENABLES PASSIVE UNIPEDAL STANCE

*Skylar Taylor[1], Karen Graham[1], Asia Humphrey[1], Young-Hui Chang[1]
[1]Comparative Neuromechanics Lab, School of Biological Sciences, Georgia Tech, Atlanta, Georgia
*Corresponding author's email: staylor314@gatech.edu

**Introduction:** Many different bird species are known to exhibit one legged stance, with flamingos being some of the most recognizable birds to engage in this behavior [1]. A peculiar aspect of this unipedal stance is that it has the potential for high energy expenditure. Birds have a characteristically "crouched" limb posture, where their femur is nearly horizontal, placing the knee extensor muscles at a poor effective mechanical advantage (EMA) [2]. Birds are known for being capable of maintaining this limb posture for long periods of time, even sleeping in unipedal stance. It is suggested that there is a passive stabilization mechanism in the bird knee joint capable of passive weight support [3]. We hypothesized there to be musculoskeletal features of the knee joint unique to birds that passively stabilize the animal in the frontal and sagittal planes, respectively, due to: (1) an asymmetric distal femoral epiphysis; and (2) biomechanical coupling due to bi-articular muscles crossing the knee and ankle joints.

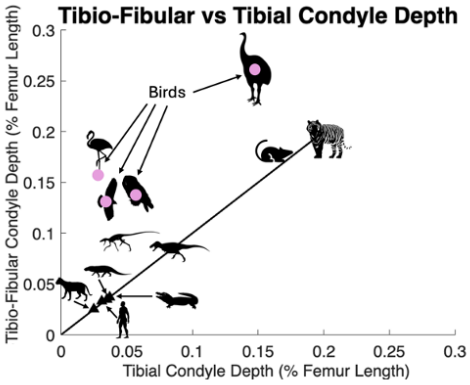


**Figure 1:** Medial vs Lateral Condyle depth. Black line represents 1:1 symmetry. Birds are shown with a pink dot.

**Methods:** We quantified the morphological structure of the knee joints of representative extant and extinct genera of birds (6 *Phoenicopterus*, 6 *Accipiterine*, 2 *Bubo*, 1 *Dinornis*), mammals (1 *Felis*, 1 *Panthera*, 2 *Homo*, 3 *Rattus*), and reptiles (1 *Alligator*, 1 *Prestosuchus*, 1 *Tyrannosaurus*, 1 *Macelognathus*). Data from each taxonomic group are represented by a silhouette in Figure 1. During dissections we manipulated soft tissue and bony structures to identify morphological features and digitized joint movements that may be capable of enabling passive stabilization in the frontal and sagittal planes. Some specimens were analysed using digital images from bone libraries or literature [4,5,6,7]

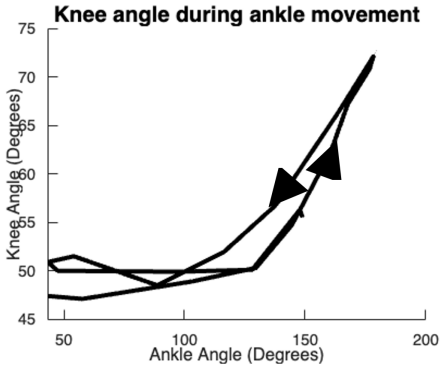


**Figure 2:** Ankle angle vs Knee Angle. Manual extension of the ankle joint results in a corresponding extension of the knee joint.

**Results & Discussion:** We found significant medio-lateral asymmetry in the distal femoral condyles in bird knee joints compared to both mammals and reptiles ($P < 0.05$, t-test). This asymmetry was not seen in any of the mammal and reptile species assessed in this study (Fig 1). We propose that this asymmetry is a unique adaptation for unipedal stance in birds. Bones are known to adapt their shape to the forces acting upon them [8]. The protrusion of the tibiofibular (lateral) condyle creates a frontal plane medio-lateral asymmetry that suggests frontal plane forces only found in the bird knee joint. Manipulation of disarticulated bones showed that the tibiofibular condyle fits into a gap between the tibia and fibula. We propose that this elongated condyle maintains forceful contact with the fibula during unipedal stance. In addition to this contact force, the tension in the lateral collateral ligament, and a medial tibial contact force provide a stabilizing moment triad in the knee frontal plane during unipedal stance.

Furthermore, during manipulation of bird carcasses, we discovered a sagittal plane passive stay mechanism. The biarticular attachments of the tibialis cranialis (TC) and gastrocnemius muscles (GA) biomechanically couple the sagittal plane movements of the ankle and knee joints (**Fig 2**) [10]. This biomechanical coupling increases knee stiffness as the ankle is extended. At full ankle extension, as in unipedal stance, the knee joint stiffens to resist both flexion and extension perturbations. Together, these morphological features appear to enable a passive stabilization of the bird knee joint during unipedal stance.

**Significance:** The asymmetrical shape of bird femurs and the unique biarticular muscle insertion of the TC muscle suggest universal musculoskeletal features for unipedal stance on a class scale. The presence of a passive stay mechanism in the bird knee joint appears to counteract the detrimental biomechanical and energetic effects created by the poor effective mechanical advantage of crouched limb postures present in all birds (*Aves*).

**Acknowledgments:** We thank Zoo Atlanta and the Birmingham Zoo for providing cadaveric materials; Georgia Tech Invention Studio for use of 3D scanners

**References:** [1] Clark, G. A. (1973), *Bird Banding*; [2] Biewener A. A. (1989) *Science*; [3], Chang & Ting (2017) *Biology Letters*; [4] Massonne, et al.(2019) *Paleontology and Evolutionary Science*; [5] Lacerda, et al (2016) *Peer J*; [5] Göhlich, et al (2005) *Canadian Journal of Earth Sciences*; [7] UMORF data is provided courtesy of the University of Michigan Museum of Paleontology;[8] Prendergast & Huiskes (1995) *Springer Nature*; [9] Ward et al (2002) *The Auk*

# KNEE JOINT FORCES DURING UNASSISTED AND EXOSKELETAL-ASSISTED SIT-TO-STAND AND STAND-TO-SIT MANEUVERS

Salma Mohammed[1], Gabriela B. De Carvalho[1], Harish Sekar[1], Vishnu D. Chandran[2], Ann M. Spungen[3], *Saikat Pal[1,3]
[1]New Jersey Institute of Technology, Newark, NJ, USA; [2]Hospital for Special Surgery, New York, NY, USA;
[3]James J. Peters Veterans Affairs Medical Center, Bronx, NY, USA
*Corresponding author's email: pal@njit.edu

**Introduction:** Wearable robotic exoskeletons have the potential to restore upright mobility in persons with neurological disorders, such as spinal cord injury (SCI). The growing demand for these devices emphasizes the need to quantify lower limb joint forces during everyday tasks, such as sit-to-stand and stand-to-sit maneuvers. However, experimental methods to quantify lower limb joint forces during exoskeletal-assisted tasks, such as instrumented implants, are cost-prohibitive and invasive, making computational simulations the only viable alternative. Accordingly, the **goal** of this study was to develop a computational framework to quantify the knee joint forces during unassisted and exoskeletal-assisted sit-to-stand and stand-to-sit maneuvers using a subject-specific virtual simulator.

**Methods:** We recruited an able-bodied man (41 years, 176 cm, 89.4 kg) to train in exoskeletal-assisted sit-to-stand and stand-to-sit in the ReWalk P6.0. We analyzed the participant's 3-D motion data during unassisted and exoskeletal-assisted sit-to-stand and stand-to-sit from a single motion capture session, including simultaneous measurements of 3-D marker trajectories, ground reaction forces, electromyography (EMG), and exoskeleton encoder data. We scaled a generic OpenSim model [1] to match the participant's mass and segment dimensions. A full-scale geometry of the ReWalk P6.0 was integrated with the scaled human model to create a subject-specific human-robot model. The human-robot model consisted of 37 degrees of freedom (DoF) for the human, and 10 DoF for the exoskeleton. We performed inverse kinematics and inverse dynamics analyses in OpenSim to obtain joint angles and moments, respectively.

Next, EMG-tracked muscle-driven simulations were performed using OpenSim Moco's *MocoInverse* tool [2] to compute the knee joint forces during unassisted and exoskeletal-assisted sit-to-stand and stand-to-sit maneuvers. All simulations were performed using a model without the exoskeleton geometry to simplify the models. We replaced the default muscle model with the DeGrooteFregly2016 muscle model to make our virtual simulator well-suited for optimal control problems in OpenSim Moco [3]. In this preliminary study, we excluded exoskeleton interaction forces and motor toques from our EMG-tracked muscle-driven simulations of unassisted and exoskeletal-assisted sit-to-stand and stand-to-sit.

**Results & Discussion:** We quantified knee joint forces during three trials of both unassisted and exoskeletal-assisted sit-to-stand and stand-to-sit maneuvers. Our peak joint forces during unassisted sit-to-stand and stand-to-sit were comparable to published *in vivo* [4] studies, providing confidence in our computational framework (Fig. 1A-B). Differences in timing of peak joint forces during unassisted stand-to-sit are likely due to differences in cycle resampling methods (Fig. 1B). We extended our computational framework to quantify the knee joint forces during exoskeletal-assisted sit-to-stand and stand-to-sit maneuvers, for which *in vivo* data are not available. Peak joint forces ranged from 2.65-3.76 BW and 1.75-2.29 BW during exoskeletal-assisted sit-to stand and stand-to-sit, respectively (Fig. 1C-D). The high knee joint forces during the hold phase of exoskeletal-assisted sit-to-stand (Fig. 1C) were due to the dynamics of maintaining the flexed human-robot pose upright against gravity.

**Significance:** To the best of our knowledge, this is the first study to quantify knee joint forces during exoskeletal-assisted sit-to-stand and stand-to-sit in an FDA-approved exoskeleton. This framework provides a non-invasive and cost-effective method to quantify the forces experienced in the long bones of persons with SCI and assess their risk of fracture during exoskeletal-assisted tasks.

**Acknowledgments:** VA RR&D #1 I01 RX003561; NSF GRFP 1000346414 (De Carvalho, fellow ID: 2022346414).

**References:** [1] Rajagopal et al. (2016), *IEEE Trans Biomed Eng* 63(10); [2] Dembia et al. (2020), *PLoS Comput Biol* 16(12); [3] De Groote et al. (2016), *Ann Biomed Eng* 44(1); [4] Kutzner et al. (2010), *J Biomech* 43(11).

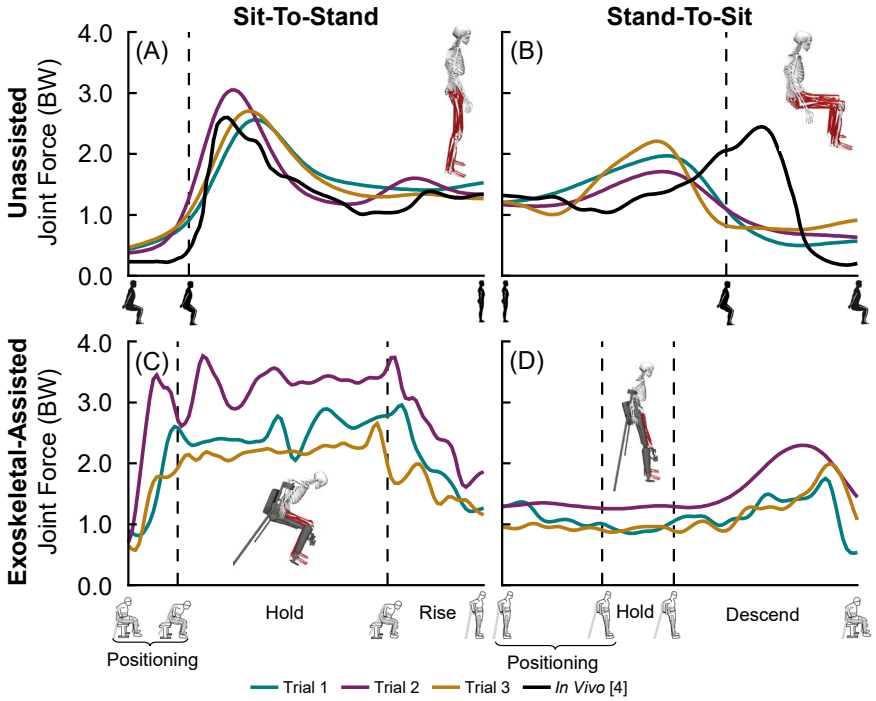


**Figure 1:** Knee joint forces from an able-bodied participant during three trials of unassisted sit-to-stand (A) and three trials of unassisted stand-to-sit (B) compared to published *in vivo* data [4]. Knee joint forces during three trials of exoskeletal-assisted sit-to-stand (C) and three trials of exoskeletal-assisted stand-to-sit (D). The knee joint forces were normalized by the weight of the human. Vertical lines represent the start/end of bench contact during unassisted maneuvers, and the start and end of the hold phase during exoskeletal-assisted maneuvers.

# KNEE JOINT FORCES DURING EXOSKELETAL-ASSISTED WALKING IN AN FDA-APPROVED EXOSKELETON: COMPARSION BETWEEN SPINAL CORD INJURED AND ABLE-BODIED PARTICIPANTS

*Gabriela B. De Carvalho[1], Ann M. Spungen[2], William A. Bauman[3], Saikat Pal[1,2]
[1]New Jersey Institute of Technology, Newark, NJ, USA; [2]James J. Peters Veterans Affairs Medical Center, Bronx, NY, USA;
[3]Icahn School of Medicine at Mount Sinai, New York, NY, USA
*Corresponding author's email: gbd5@njit.edu

**Introduction:** Wearable robotic exoskeletons are currently the only clinical approach to restore upright mobility for persons with spinal cord injury (SCI). Persons with SCI have severely osteoporotic bones and are at high risk of fragility fractures, with the knee being the most common site of fracture [1]. Bone fractures in persons with SCI have been reported during clinical trials of exoskeletal-assisted walking (EAW). The growing demand for wearable robotic exoskeletons emphasizes the need for the quantification of knee joint forces during EAW in FDA-approved devices. FDA approval of these devices is important because patients have access only to FDA-approved devices in clinics and for in-home use. Accordingly, the **goal** of this study was to quantify knee joint forces during EAW in an FDA-approved device, the ReWalk P6.0. First, we tested our computational framework on unassisted walking from an able-bodied (AB) participant and compared these results to *in vivo* data. Next, we built on this verified framework to simulate EAW from an AB participant. Finally, we simulated EAW from a participant with SCI and evaluated the effects of robot motor torques on knee joint forces.

**Methods:** We recruited one AB participant (male, 41 years, 176 cm, 89.4 kg) and one participant with SCI (male, 49 years, 171 cm, 72.5 kg, ASIA impairment scale A, injury level T6, 24 years since injury) to train in EAW in the ReWalk P6.0. We recorded the 3-D motion of the AB participant during unassisted walking and EAW, including simultaneous measurements of marker trajectories, ground reaction forces, electromyography (EMG), and exoskeleton encoder data. Similarly, we recorded the 3-D motion of the participant with SCI during EAW, but without the EMG data. A generic OpenSim musculoskeletal model [2] was scaled to match each participant's anthropometry. A full-scale geometry of the ReWalk P6.0 was added to create subject-specific human-robot models. We performed inverse kinematics and inverse dynamics analyses in OpenSim to estimate joint angles and moments, respectively.

We created a virtual simulator in OpenSim to reproduce unassisted walking and EAW. EMG-tracked muscle-driven simulations were performed using OpenSim Moco [3] to compute the knee joint forces of the AB participant during unassisted walking and EAW. For the EAW trials, human-robot interaction forces were modeled by OpenSim's bushing forces (linear spring-damper systems), and applied to regions of exoskeleton support cuffs/bands. Stiffness parameters of bushing elements were calibrated using experimental data from an instrumented knee bracket. Interaction forces were estimated using OpenSim's force reporter and applied to models without exoskeletal geometries. For the participant with SCI, there were no EMG data because of muscle inactivity below the level of lesion. Knee joint forces were computed using muscle-driven simulations with muscle control signals constrained to a maximum value of zero.

Since the muscles were inactive during EAW in the participant with SCI, OpenSim Moco reproduced the prescribed motion primarily using robot motor torques. The muscles were unable to balance the contributions from these motor torques, and hence, these contributions are not included in joint force analysis in Opensim Moco. To overcome this limitation, we developed custom scripts in Matlab to include the contributions of motor torques on knee joint forces. We computed the moment arm from the exoskeleton knee joint to the human knee joint. Next, we calculated the knee joint forces from the flexion-extension torques applied at the exoskeleton knee joint, and added these forces to the knee joint forces from OpenSim Moco.

**Results & Discussion:** Our knee joint forces during unassisted walking are comparable to published *in vivo* studies [4], providing confidence in our computational framework (Fig. 1A-D). We built on this framework to quantify the knee joint forces during EAW, for which direct comparison to experimental data is not available. Peak knee joint forces during EAW for the AB participant were up to 3.20 BW. From OpenSim Moco, knee joint forces during EAW for the participant with SCI were substantially lower (peak 0.92 BW) than the AB participant because of muscle inactivity. Adding the contributions of motor torques increased knee joint forces during EAW to up to 3.01 BW for the participant with SCI (Fig. 1A-D).

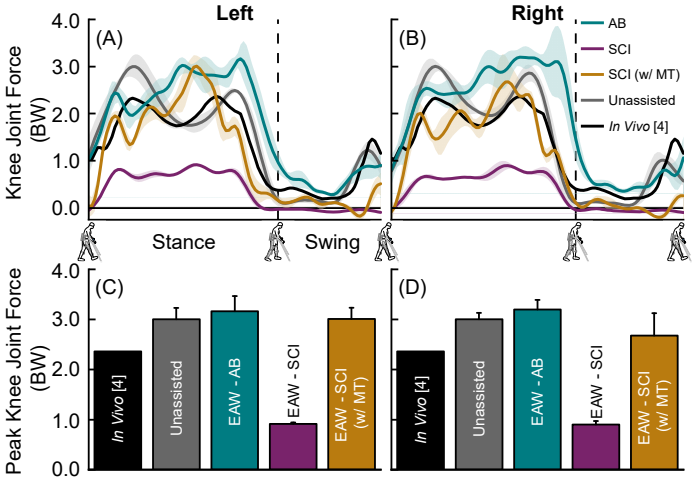


**Figure 1:** Average (±1 SD) knee compressive forces (A-D) from unassisted walking and EAW trials compared to published *in vivo* data from unassisted walking [4]. An AB participant performed unassisted walking and EAW trials. A participant with SCI performed EAW trials. The knee joint forces were normalized by the weight of the human. Vertical lines represent toe-off during EAW. w/ MT: with Motor Torques

**Significance:** Our computational framework provides a non-invasive and cost-effective approach to quantify the forces on the long bones of persons with SCI and assess their risk of fracture during EAW.

**Acknowledgments:** VA RR&D #1 I01 RX003561; NSF GRFP 1000346414 (Fellow ID: 2022346414).

**References:** [1] Grassner et al. (2017), *J Spinal Cord Med* 41(6); [2] Rajagopal et al. (2016), *IEEE Trans Biomed Eng* 63(10); [3] Dembia et al. (2020), *PLoS Comput Biol* 16(12); [4] Fregly et al. (2012), *J Orthop Res* 30(4).

# EFFECT OF PARALLEL ELASTIC ELEMENT STIFFNESS ON UCL STRAIN DURING A BASEBALL PITCH: A BIOMECHANICAL MODEL

*Ben Baker[1], *Kalin Blinstrub[1], Dustin L. Crouch[1] (*co-first authors)
University of Tennessee, Knoxville – [1]Tickle College of Engineering,
bennyb@vols.utk.edu, kblinstr@vols.utk.edu

**Introduction:** As many as 38% of major league baseball pitchers in 2024 [1] and 27% of elite high school baseball pitchers [2] have undergone reconstructive ulnar collateral ligament (UCL) surgery, which requires 12-18 months of recovery. An arm sleeve that offloads the UCL during pitching could potentially reduce the number of UCL injuries and their associated costs. Damage to ligaments such as the UCL depends on strain, which is a function of load magnitude and ligament mechanical properties. At least one sleeve (Kinetic Arm, The Perfect Arm LLC) incorporates passive elastic elements (EEs) that are designed to reduce UCL load and corresponding strain, among other claimed benefits. However, the relationship between UCL strain and the mechanical stiffness of such EEs has not been reported. Therefore, the objective of our preliminary study was to develop a simple biomechanical model to quantify the relationship between UCL strain and the mechanical stiffness of an EE ($k_{EE}$) placed on the medial side of the elbow and in parallel with the UCL.

**Methods:** Multiple soft-tissue structures, including the UCL and muscles, contribute to the elbow varus moment, which is a reaction moment generated in response to the elbow valgus moment imposed by the pitching movement (Fig.1). We assumed that the UCL and EE are linearly elastic and have constant moment arms (ma) with respect to the elbow varus-valgus angle. Ligament damage reportedly occurs at strains as low as about ε = 0.06 [3]. Given the prevalence of UCL injury among baseball pitchers, we assumed that a typical pitch would result in a strain of $\varepsilon_{UCL}$ = 0.1 at which damage to the UCL is expected. We calculated the $k_{EE}$ required to reduce $\varepsilon_{UCL}$ in increments of 0.01 strain, up to 0.1 (i.e., full off-loading of the UCL). Based on a reported length of the UCL, ($l_{UCL}$) of 0.045m [4], a strain of $\varepsilon_{UCL}$ = 0.1 corresponds to $\Delta l_{UCL}$= 0.0045m. The equation used to calculate $k_{EE}$ was:

$$k_{EE} = \frac{M_{EE}}{\Delta\theta * ma_{EE}^2}$$

Where $M_{EE}$ is the elbow varus moment generated by the EE, $\Delta\theta$ is the increase in the elbow valgus angle corresponding to $\Delta l_{UCL}$ and assuming $ma_{UCL}$= 0.03m [5], and $ma_{EE}$ was assumed to be 0.04m. Since it is not clear how $M_{EE}$ off-loading would be shared among the soft-tissue structures, two sets of $k_{EE}$ values were calculated for each of two "extreme" sharing assumptions: (1) the EE reduced the elbow varus moment generated by the UCL only and (2) the EE reduced the elbow varus moment proportionally across all structures. For the first assumption, we computed the reduction in UCL varus moment, $\Delta M_{UCL}$, for each 0.01 increment in strain reduction, and then set $M_{EE} = \Delta M_{UCL}$. For the second assumption, a decrease in $\varepsilon_{UCL}$ of 0.01 represents a 10% reduction relative to $\varepsilon_{UCL}$ during a typical, unsupported pitch; therefore, assuming the same percent reduction across all soft-tissue structures, $M_{EE}$ was set as a percentage (in 10% increments) of the reported total elbow varus moment (115 N-m) during an unsupported pitch [6].

**Results & Discussion:** Our model predicted that, to reduce $\varepsilon_{UCL}$ from 0.10 to 0.06 (the "safe zone" or injury threshold), $k_{EE}$ would need to be somewhere between 40,023 N/m (assuming off-loading of UCL only) and 380,291 N/m (assuming uniform off-loading across all soft-tissues). The assumption of uniform off-loading is more realistic as it would occur naturally in passive soft tissues based on the behavior of parallel elastic elements according to classical mechanics. Active muscle-tendon actuators, which are estimated to contribute at least 35% to the total elbow varus moment, would also likely be off-loaded; exoskeletons with elastic elements placed in parallel with muscle-tendons have been shown reduce muscle activations. There were several major limitations of our simplified lumped-parameter model, including a linear-elastic UCL, planar mechanics, low anatomical resolution, and assumed $\varepsilon_{UCL}$=0.10 during a pitch. In future studies we will adapt our analysis to a more advanced upper extremity musculoskeletal model with real-world pitching biomechanical data. We will also explore designs and materials that can achieve the desired UCL off-loading.

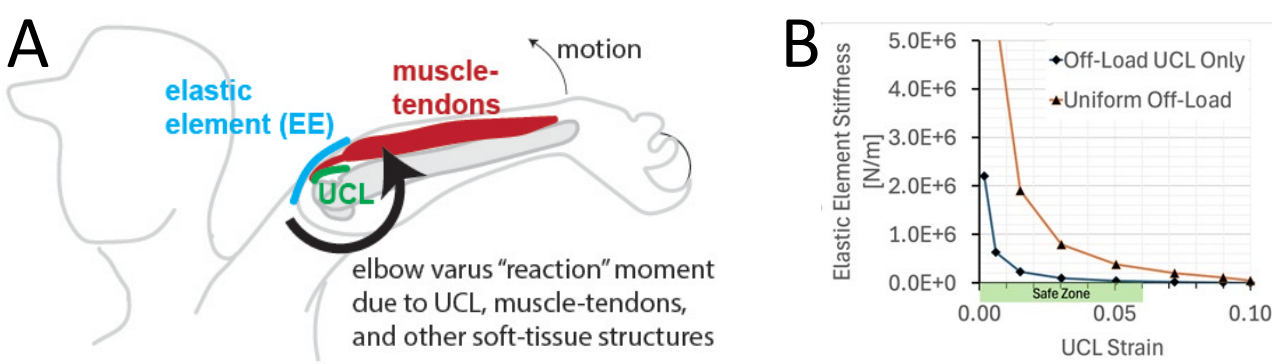


**Fig.1**: (A) Diagram of upper extremity and contributions to the elbow varus moment during a pitch. (B) Relationship between UCL strain and elastic element stiffness ($k_{EE}$); each curve plots the stiffness for one of two assumptions for how off-loading by the elastic element is shared or distributed among the soft tissues that contribute to the elbow varus moment.

**References:** [1] Roegele J, @MLBPlayerAnalys (x.com) [2] Kamei K, Sasaki E, JSES Int, 5(2), 2020; [3] Provenzano PP, J Appl Physiol, 92(1), 2002; [4] Torres SJ, Curr Rev Musculoskel Med, 14(2), 2025; [5] Andrews JR, et al., AJSM, 29(6), 2001; [6] Trigt BV, et al., Int Biomech, 8(1), 2021.

# HUMAN JOINT LEVEL FORCE RESPONSIVENESS AND CONTROL WITH EXOSKELETON ASSISTANCE

*Amro Alshareef[1,3], Gregory S Sawicki[1,2,3]
[1] Woodruff School of Mechanical Engineering [2] Wallace H. Coulter Dept. of Biomedical Engineering
[3] Institute for Robotics and Intelligent Machines, Georgia Institute of Technology, Atlanta GA, USA
*Corresponding author's email: aalshareef6@gatech.edu

**Introduction:** With significant advancements in wearable technologies for assisting locomotion and augmenting balance, there is a growing need to understand how such devices affect sensorimotor control of movement. Exoskeletons act mechanically in parallel to a joint, influencing the existing sensorimotor control loops that govern human movement [1]. As a result, although exoskeletons may be optimized for certain outcome metrics, the way they interact with our governing sensorimotor control system may have unintended impacts on overall agility and stability [2]. Recent work has begun to quantify human force responsiveness [3] and effects of neuromotor regulation on joint impedance [4]. Here we measure human joint level force responsiveness with and without exoskeletal assistance in a dynamometer, allowing for controlled isometric contractions to achieve set torque targets and measure joint-level force responsiveness and control. We hypothesize that the no torque assistance condition will have greater accuracy of force control than the myoelectric controller due to the human's inherent forward model of its sensorimotor control system (which does not include an exoskeleton).

**Methods:** Two young adults wearing an ankle exoskeleton (Dephy EB60 Exoboots) were placed in a dynamometer (Biodex) to measure ankle torque output during isometric contractions. Participants were given an auditory metronome at 15 bpm indicating the start and end of each 4 second step cycle, a visual target line on a screen of the torque target to reach, and visual feedback of their real-time torque. A randomly selected two out of ten cycles per condition were blinded by removing the visual target and torque feedback from the participant's view. Eight randomized trial conditions were conducted, with 4 torque targets at 20%, 40%, 60%, and 80% of maximum voluntary contraction across 2 exoskeleton conditions (No Torque Assistance (NT) and Proportional Myoelectric Control (PMC) with a maximum assistance level of 10 Nm) and 10 step cycles within each trial. There was a 20 second break between every trial, and all 8 trials were repeated after a 60 second break to investigate the effects of motor adaptation. The step responses were quantified using classical controls metrics including rise time, bandwidth, overshoot, steady-state error, steady-state variability, and fall time [3]. Higher bandwidth indicates higher responsiveness, and a lower steady-state error and steady-state variability indicates greater accuracy.

**Results & Discussion:** Increased torque targets correlated with lower responsiveness and lower accuracy for the system. In the first repetition, both the NT condition and the PMC conditions had a similar bandwidth, however in the second repetition the bandwidth of the PMC condition increased for the 20, 40, and 80% conditions, indicating potential adaptation to the exoskeleton assistance and improved responsiveness as opposed to the NT condition (Fig. 1B). Steady-state variability increased for the NT condition in the 20, 40 and 60% conditions between the first and second repetition, while remaining consistent in the PMC condition across both repetitions (Fig. 1B). Furthermore, in the second repetition the participants couldn't reach the 80% MVC target due to fatigue in the NT condition but were able to reach and maintain 80% MVC with PMC assistance (Fig. 1A). Although both exoskeleton conditions performed similarly in the first repetition, the improved performance of PMC in the second repetition suggests a potential benefit of exoskeleton assistance to the inherent sensorimotor control system's accuracy and responsiveness after adaptation and sensory reweighting.

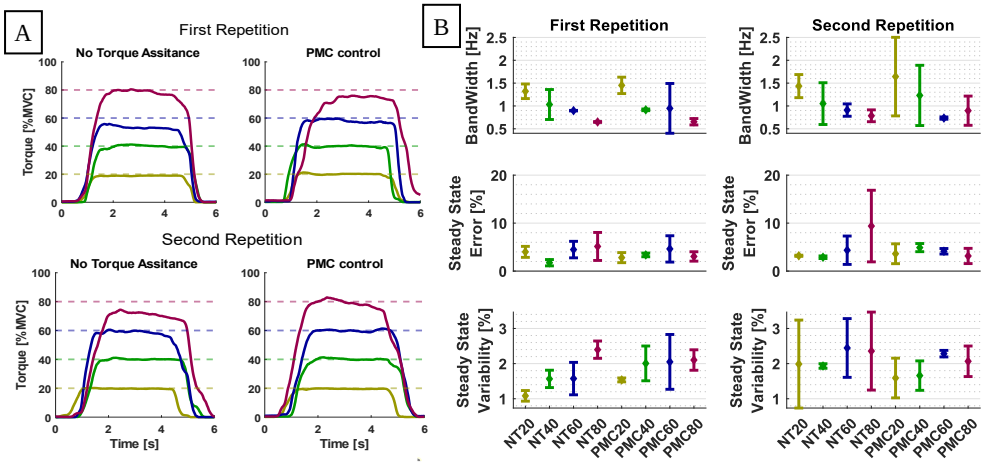


**Figure 1:** A) the average step response for n=2 participants across the four target torque conditions, 2 exoskeleton assistance types (left and right), and two repetitions of the trials (top and bottom). B) The bandwidth (top), steady state error (middle), and steady state variability (bottom) of the system across all conditions in the first (left) and second (right) conditions.

**Significance:** Investigating the effects of exoskeleton assistance on human force responsiveness will provide insights into the human sensorimotor control loop during physiologically relevant excursions. Modeling the human neuromuscular system as a feedback control system and incorporating external exoskeletal influences can offer crucial insights into the effects of exoskeletons the sensorimotor feedback. These insights can help illuminate the sensory weighting that occurs within humans, and further the potential of exoskeleton to counteract the effects of age and disease, such as altered tendon stiffness and increased instability.

**Acknowledgments:** This work was done with support from the NSF GRFP.

**References:** [1] Abram et al. (2022), *Curr Biol* 32; [2] Antonellis et al. (2018), *Plos One* 13; [3] Kudzia et al. (2022), *Sci Rep* 12; [4] Wind et al. (2020) *Sci Rep* 10.

# KICKING IT OFF: DOES TODDLER LEG MUSCLE ACTIVATION WHILE DRIVING CHANGE WITH POSTURE?

*Madeleine E. McCreary[1], Kimberly A. Ingraham[1], Heather A. Feldner[1], Katherine M. Steele[1]
[1]University of Washington, Seattle, WA
*Corresponding author's email: mmccrear@uw.edu

**Introduction:** New powered mobility devices like the Permobil Explorer Mini provide access to self-initiated mobility for young children with disabilities, which is critical for social, communication, cognitive, perceptual, and motor development [1,2]. The unique design of the Explorer Mini allows driving while sitting or standing and free full-body movement. Moving the joystick with a full-body expression has been commonly observed in children with disabilities [3,4]. This study aimed to quantify leg muscle activations and co-contraction patterns while driving the Explorer Mini. Evaluating leg muscle activity is important to understand how children coordinate voluntary movements and the impact of different biomechanical constraints. Since many children with disabilities have reduced selective motor control, we expected elevated leg muscle activity while driving and more leg activation in the standing posture than sitting [5].

**Methods:** We enrolled 9 children with motor disabilities (age: 21.6 ± 6.1 months) to attend four in-lab visits where they engaged with an instrumented Explorer Mini in an enriched play environment (Fig. 1A). Within each visit, participants completed a 15–20-minute session in each posture (order randomized). The seat was adjusted to position participant knees at 90° for seated sessions and maximum extension for standing sessions. Electromyography (EMG) electrodes were placed bilaterally on the quadriceps femoris (QF) and biceps femoris (BF) muscle groups. EMG data were high pass filtered at 20 Hz, demeaned, rectified, lowpass filtered at 10 Hz, and normalized to the maximum value of the visit. We evaluated EMG data for 10-second bouts: 5 seconds before and after joystick initiation (when the joystick was moved away from neutral). To compare EMG activity between postures and across visits, we quantified QF and BF area under the curve (AUC) per bout. We performed linear regression of AUC between bilateral muscle pairs (*e.g.*, left QF vs right QF) and QF/BF muscles and evaluated the variance accounted for ($R^2$) by each model. To identify muscle activation patterns, we performed dimensionality reduction of the combined QF and BF EMG data through principal component analysis. A randomly initialized k-means clustering algorithm sorted all bouts into distinct muscle activation groups using the first three principal components and we calculated the proportion of bouts in each group for both postures.

**Results & Discussion:** For both postures, there was an increase in QF AUC and a decrease in BF AUC from Visit 1 to 4 (Fig. 1B). The QF AUC increased more in the standing posture while BF AUC decreased more in the sitting posture. The QF and BF AUC had a stronger linear relationship in standing ($R^2 = 0.61$) than sitting ($R^2 = 0.45$), indicating more co-contraction of antagonist muscle pairs while standing. Similarly, bilateral muscle pair AUC had a stronger linear relationship for standing ($R^2 = 0.48$) versus sitting ($R^2 = 0.26$), indicating more inter-limb coordination while in the standing posture. Five unique patterns of leg activation were identified around joystick initiation from cluster analysis (Fig. 1C). There was minimal EMG activity with joystick initiation (black)for 50% of sitting (Range: 11-94%) and 40% of standing (Range: 4-95%) bouts. A low peak near the time of joystick initiation (red) encompassed 30% of sitting (Range: 5-60%) and 32% of standing bouts (Range: 4-60%). Three clusters had high peaks that occurred at different times around joystick initiation. A peak before joystick initiation with a sharp decrease (blue), accounted for 6% of sitting (Range: 1-17%) and 9% of standing bouts (Range: 1-18%). Sustained elevated activity peaking around joystick initiation (green) encompassed 4% of sitting (Range: 0-16%) and 6% of standing bouts (Range: 0-17%). A peak after joystick initiation (pink), accounted for 10% of sitting (Range: 0-21%) and 13% of standing bouts (Range: 0-22%).

**Significance:** Children with disabilities commonly activated their leg muscles, with moderate co-contraction between legs and antagonist muscles, when initiating movement with the joystick. The standing posture had a greater proportion of bouts with elevated EMG activity, higher co-contraction, and more inter-limb coordination. The presence of leg muscle activity aligns with hypotheses that Explorer Mini use may support independent standing and balance [4]. While arm muscle activity was not monitored in the study to reduce child distraction, understanding how children with disabilities coordinate upper and lower limb muscle activity during self-initiated mobility is an important area of future research to support development, play, and participation.

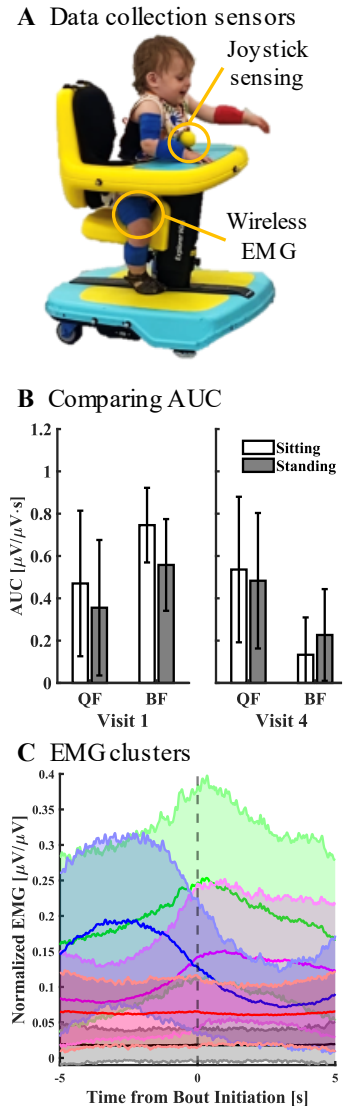


**Figure 1:** A) Explorer Mini with sensors to monitor joystick position & EMG electrodes on leg muscles. B) From Visit 1 to 4, QF AUC increased & BF AUC decreased. C) Five patterns of QF and BF activity identified around joystick initiation (average ± one standard deviation).

**Acknowledgments:** We thank the Center for Research & Education on Accessible Technology and Experiences (CREATE) and the Institute for Learning and Brain Sciences (I-LABS) for their support of this work, and LUCI for instrumenting the Explorer Mini.

**References:** [1] Logan et al. (2023), *Behav. Sci.* 13(5); [2] Campos et al. (2000), *Infancy* 1(2); [3] Ingraham et al. (2025), *TNSRE* 33; [4] Zaino et al. (2024), *Assist. Technol.*; [5] Cahill-Rowley & Rose (2014), *DMCN* 56(6).

# DESIGN AND EVALUATION OF TWO 3D-PRINTED PNEUMATIC SOFT ROBOT PROTOTYPES FOR FINGER EXTENSION REHABILITATION

*Brittany Heintz Walters[1], Maggie Deal[1], Max Anderson[1], Eric Olson[2], Jhet C. Young[2], Yen-Lin Han[2]
[1]Department of Kinesiology, Seattle University, Seattle, WA, USA
[2]Department of Mechanical Engineering, Seattle University, Seattle, WA, USA
*Corresponding author's email: bwalters1@seattleu.edu

**Introduction:** Impaired hand function is one of the most common motor deficits after stroke [1]. Therapist-guided repetitive movements reduce motor impairments but can be labor-intensive and time-consuming [2]. Robotic devices supplement therapist-guided rehabilitation but the actuation mechanisms (e.g., motors, cables) can be costly, complex, and rigid, limiting accessibility [3]. Soft robots have the potential to overcome these limitations due to pliability and lower-cost fabrication, but most facilitate finger flexion [e.g., 4]. Given that stroke commonly affects finger extension [1], we aim to develop a lower-cost, user-friendly device for finger extension. We present the design of two 3D-printed soft robot extensor prototypes and their preliminary evaluation in healthy adults.

**Methods:** Two pneumatic prototypes were designed and tested, Prototype A and Prototype B (Fig. 1). The designs were informed by testing of previous iterations [4,5]. The prototypes rest in a curved shape and extend when air pressurizes internal segments. Prototype A has a single segment for simpler fabrication. Prototype B has multiple segments to focus points of motion around finger joints (Fig. 2). Air passages connecting the segments act as deformation points. Both prototypes were 3D-printed using Fused Deposition Modelling (FDM) with Thermoplastic Polyurethane (TPU). FDM enables rapid prototyping of complex, single-piece designs. TPU is flexible, elastic, and airtight.

To test geometry changes and inform continued device development, the prototypes were tested in 8 healthy adults (19–28 years; 4 f, 4 m). Range of motion (ROM) with soft robot actuation was assessed at the metacarpophalangeal (MCP), proximal interphalangeal (PIP), and distal interphalangeal (DIP) joints using Kinovea motion analysis software. Participants were seated with their hands in a custom-built manipulandum and forearms supported in neutral. The pneumatic soft robot extended the right index finger until full actuation was achieved. Participants were instructed to relax their hands and not assist the device. Electromyography (Delsys Trigno) was used to record extensor digitorum communis muscle activity during device actuation [7]. Muscle activity was also recorded 5 s prior to device actuation while the participant was asked to relax to establish a baseline. Three trials were performed for each prototype. Passive ROM of the MCP, PIP, and DIP joints was also assessed [8].

**Figure 1:** General design of Prototype A (left) and Prototype B (right). The prototype is positioned on the palmar side of the finger.

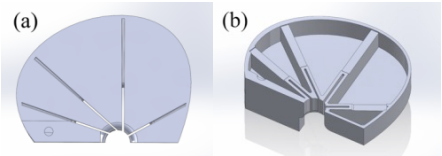


**Figure 2:** External (a) and internal (b) views of Prototype B. Multiple segments acted as deformation points during actuation.

**Results & Discussion:** Actuation of the pneumatic prototypes successfully resulted in finger extension for all participants (Table 1). Prototype A reached full actuation in 56.38 s ± 7.73 s, consistent with that needed for effective hand rehabilitation exercises (i.e., 60 s) [9], while Prototype B reached full actuation in 68.63 ± 5.10 s.

**Table 1:** Finger range of motion (ROM) from soft robot actuation relative to passive finger ROM for Prototype A and Prototype B.

| | **Prototype A (mean ± SD)** | | | **Prototype B (mean ± SD)** | | |
|---|---|---|---|---|---|---|
| **Measure** | MCP | PIP | DIP | MCP | PIP | DIP |
| Device ROM (°) | 5.29 ± 7.25 | 32.00 ± 7.92 | 18.43 ± 5.08 | 3.15 ± 3.67 | 43.93 ± 5.42 | 24.40 ± 3.68 |
| Percent Passive ROM | 94.25 ± 8.13 | 79.75 ± 5.42 | 88.10 ± 3.68 | 95.35 ± 6.87 | 73.32 ± 4.14 | 84.83 ± 2.56 |

There was no difference in extensor digitorum communis muscle activity during actuation compared to baseline, demonstrating that ROM occurred from device actuation rather than voluntary muscle activation. Given the potential for reduced neuromuscular function after stroke [1], the ability of the device to produce motion without voluntary activation is important in demonstrating device efficacy. Greater extension ROM and less time to full actuation for Prototype A versus B supports further development of Prototype A.

**Significance:** Results demonstrate the efficacy of a soft robot with a pneumatic actuator in terms of finger extension range of motion. The current study is a step towards the realization of an accessible, lower-cost device for hand rehabilitation and mitigating impaired hand function in stroke survivors. Future research will seek continued development of Prototype A.

**Acknowledgements:** This research was supported by the American Society of Biomechanics Junior Faculty Research Award and the National Science Foundation 22-603: Mid-Career Advancement Award.

**References:** [1] Raghavan (2015), *Phys Med Rehabil Cli 26*(4); [2] Dobkin & Bruce (2004), *Lancet Neurol 3*(9); [3] Balasubramian et al. (2012), *Am J Phys Med Rehab 91*(11); [4] Yap et al. (2016), *J Med Devices 10*(4); [5] Olson et al. (2025), *IEEE RoboSoft*; [6] Heintz Walters et al. (2024), *DMD2024-1056;* [7] Hermens et al. (2000), *J Electromyogr Kines 10*(5); [8] Lewis et al. (2010), *Am J Occup Ther 64*(4); [9] Danion et al. (2002), *E J Appl Phys 88*.

# CHANGES OF KNEE LAXITY AND STIFFNESS IN TIBIAL ROTATION IN KNEE OSTEOARTHRITIS

Zongpan Li[1], Raziyeh Baghi[1], Giovanni Oppizzi[1,2], Peter Bowman[1], Li-Qun Zhang[1,2,3] *
[1] Department of Physical Therapy & Rehabilitation Science, University of Maryland, Baltimore, Maryland, USA
[2] Fischell Department of Bioengineering, University of Maryland, College Park, Maryland, USA
[3] Department of Orthopaedics, University of Maryland, Baltimore, Maryland, USA
*Corresponding author's email: l-zhang@som.umaryland.edu

**Introduction:** Altered varus-valgus laxity/stiffness have been found in patients with medial tibiofemoral knee osteoarthritis (OA) [1]. These alterations are believed to contribute to clinical symptoms and dysfunctions in knee OA [2]. Patients with knee OA exhibit restricted knee motions in the transverse plan [3], which may relate to altered angular laxity and mechanical stiffness in tibial rotation. However, to our knowledge, the knee laxity and stiffness in tibial rotation have not been studied. This study used a novel robot-controlled device to quantitatively assess knee laxity and stiffness in tibial rotations, and to compare them between patients with medial tibiofemoral OA and age-matched healthy older adults.

**Methods:** Patients with medial tibiofemoral OA and age-matched healthy older adults were recruited. Participants were seated with their knees flexed at 90° on a robot-controlled off-axis training device (**Fig. 1**), with a clamp applied to medial and lateral femoral condyles to immobilize the femur. A custom ankle brace immobilized the ankle, minimizing the ankle movement and rotating the tibia with foot/ankle as a whole during the test. The footplate was rotated horizontally by the motor (SA01-100W/48V, Mecapion, Korea) with a six-axis force/torque sensor (JR3, Woodland, CA), until it reached 5 Nm passive resistance torque limits or 45° terminal angle in tibial internal rotation (IR) or external rotation (ER) [4]. A total of three cycles were conducted for each participant. Joint laxity was recorded as the endpoint angle at which 5 Nm passive resistance torque occurred or the 45° terminal angle reached in either IR/ER. For the joint stiffness calculation, a 4$^{th}$-order polynomial curve between the torque and tibial rotation angle was fitted. The slope of the fitted curve represents joint stiffness at each point, and the stiffness against tibial rotation angle was plotted. The stiffness (IR/ER) was computed as the average of the slopes at all time points during IR/ER. During the test, a handheld switch was provided for emergency stop. Student t-tests were used to compare the joint laxity and stiffness between knee OA and healthy controls. We also used paired t-tests to compare laxity and stiffness between IR and ER.

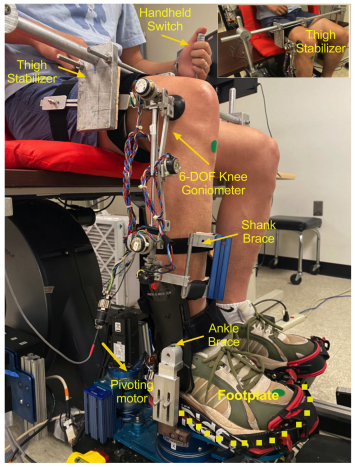


**Figure 1:** Equipment and experimental settings.

**Results & Discussion:** This study involved 8 patients with medial tibiofemoral knee OA (67.9 ± 7.6 years), and 8 age-matched healthy older adults (63.5±9.9 years). **Fig. 2** illustrates typical curves for laxity and stiffness for a patient with medial tibiofemoral OA and a healthy participant. Patients with knee OA exhibited significantly larger joint laxity ($P$=0.041) in IR but lower stiffness in ER ($P$=0.019) than controls. We also observed significantly lower laxity but higher stiffness in IR than that in ER in both groups ($P$=0.007–0.046) (**Fig 3**). This is the first study to quantitatively examine the laxity and stiffness in tibial rotations in knee OA patients. During weight-bearing activities, foot progression angle (toe-in/out) would affect the rotational alignment of the lower-limb kinetic chain, causing re-distribution of the knee impact loading. Hence, gait retraining by modifying foot progression angle has been used as a useful approach to reduce knee joint loading and alleviate symptoms of knee OA [5]. Our work highlights the importance of mechanical joint properties in tibial rotations. Future studies are needed to identify contributing factors of such altered joint mechanical changes, which could be potential targets to improve joint stability in transverse knee motions and promote the treatment of knee OA.

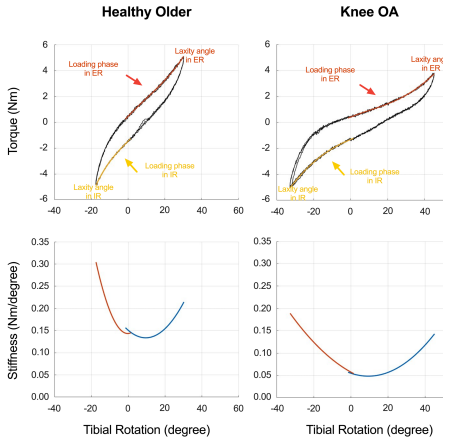


**Figure 2:** Typical curves for laxity and stiffness in OA and controls.

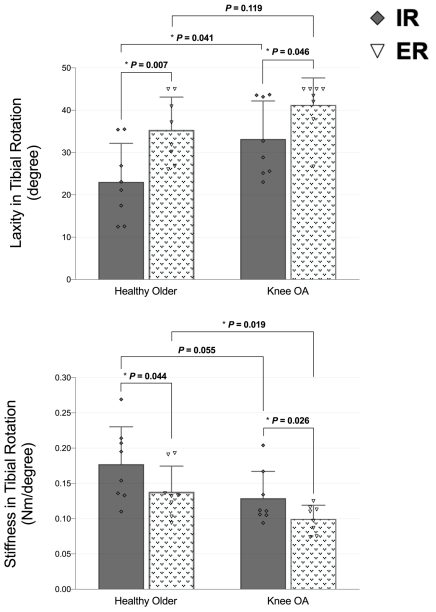


**Figure 3:** Laxity and stiffness between OA and healthy controls; and between IR and ER.

**Significance:** This study introduces a novel method to quantitatively measure laxity and stiffness in tibial rotation for knee OA. Patients with medial tibiofemoral OA may have increased joint laxity and decreased mechanical stiffness in tibial rotation. It may provide a scientific basis for developing individualized assessment and training programs for knee OA rehabilitation.

**References:** [1] Creaby et al. (2010), *Arthritis Care Res* 62(9); [2] Esch et al. (2006), *Arthritis Rheumatol* 55(6); [3] Bytyqi et al. (2014), *Int Orthop* 38(6); [4] Zhang et al. (2008), *J Orthop Res* 26(7); [5] Wang et al. (2021), *Arthritis Care Res* 73(12).

**Muscle activity during walker-based exoskeleton use in children with cerebral palsy**

Katie M. Landwehr-Prakel[1], Anna M. Fragomeni[2], Kristie F. Bjornson[3], Chet T. Moritz[2,4], Heather A. Feldner[2], Katherine M. Steele[1]
[1]Department of Mechanical Engineering, University of Washington, [2]Department of Rehabilitation Medicine, University of Washington [3]Seattle Children's Research Institute, [4]Department of Electrical and Computer Engineering, University of Washington
*Corresponding author's email: klandweh@uw.edu

**Introduction:** Children with cerebral palsy (CP) often exhibit muscle weakness, spasticity, and impaired motor control, which can limit their ability to walk independently [1]. To support walking, children with CP often use mobility aids, such as orthoses, gait trainers, or walkers. One such intervention is the Trexo exoskeleton (Trexo Robotics, Mississauga, ON), which provides hip and knee actuation to generate a walking pattern over ground as the feet push against the ground and propel the device forward. Research has shown that Trexo use can improve sleep and bowel function [2] [3] and has hypothesized that Trexo use may encourage muscle activation similar to walking [4]. However, whether and how children with CP activate their muscles in the Trexo remains an open question. The purpose of this study was to quantify how muscle activity changes during Trexo use in children with CP. We hypothesized that children with CP would exhibit muscle activity during Trexo use that is similar to patterns observed during walking.

**Methods:** Four children with CP (1M/3F, age: 32 ± 8.0 months, GMFCS Levels III-V) participated in this study. This study was approved by the University of Washington Institutional Review Board (STUDY00014877) and registered at ClinicalTrials.gov (#NCT05520359). Each participant completed up to 6 visits, which included multiple sessions of walking using the Trexo. Speed (steps/min), device settings, and the length of each session were determined by the researcher, physical therapist, and caregiver by monitoring the child's comfort and engagement. To assess muscle activity, surface electromyography (EMG) was recorded bilaterally from the biceps femoris (BF), vastus lateralis (VL), and rectus femoris (RF). EMG data were filtered, rectified, and normalized to the 95th percentile of maximum excitation across all sessions in a visit. To measure changes in activation for each muscle, area under the curve (AUC) was averaged across the stance (first 60%) and swing phase (final 40%) of all gait cycles.

**Results & Discussion:** All four participants displayed cyclic muscle activity while using the Trexo (Figure 1). Quadriceps activity was greatest in stance for three of four participants, with an average 7.6% (range -0.2-16.0%) increase in RF activity in stance relative to swing. The RF had greater sustained activity throughout stance than the VL in three of four participants. Hamstring activity peaked in mid or terminal stance, which differs from patterns observed in typical gait. Since knee extension peaks near terminal stance, this may be indicative of activity triggered by stretching the hamstrings. The variability among participants underscores the importance of personalized approaches in optimizing device settings to support muscle function and coordination during robotic-assisted gait training.

**Significance:** This study provides preliminary evidence that muscles are active during Trexo use among young, non-ambulatory children with CP. Understanding how muscles are active during Trexo use can help clinicians and researchers customize treatment protocols with the exoskeleton for children with CP.

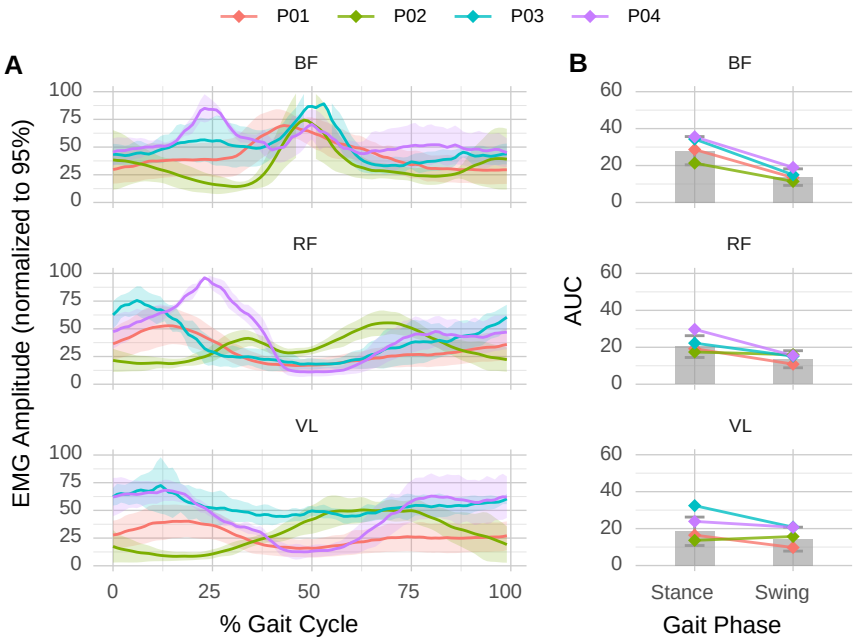


**Figure 1:** Muscle activity outcomes of A) Average BF, RF, and VL EMG Amplitude (normalized to 95%) during the gait cycle. B) Area under the curve (AUC) for each muscle. Gray bars represent the mean across all four participants (±SD). The overlaid points represent average AUC for each participant and lines to highlight individual differences.

**Acknowledgements:** This work was supported by the Seattle Children's Hospital CP Research Fund. We would like to thank the participants and their families for their time and participation, as well as Kevin Doherty-Regalia, Avni Sisodiya, and Grace O'Connor for their assistance with data collection.

**References:** [1] Kerr Graham et al. (2016), Nat Rev Dis Primers 2(1); [2] Diot et al. (2023), Children 10(3); [3] Diot et al. (2021), Disabil Rehabil Assist Technol 18(5); [4] Bradley et al. (2024) Front Neurosci 18.

# MODULAR INSOLE TECHNOLOGY: A NOVEL APPROACH FOR PRESSURE REDISTRIBUTION IN DIABETIC FOOT

*Gurpreet Singh[1], Arnab Chanda[2]
[1]Centre for Biomedical Engineering, Indian Institute of Technology Delhi, India
[2]Department of Biomedical Engineering, All India Institute of Medical Sciences Delhi, India
*Corresponding author's email: singh.gurpreet191@gmail.com

**Introduction:** Diabetic foot ulceration is a common complication of diabetes, and if left untreated, it can lead to infection and, in severe cases, require amputation. Various medical interventions have been employed to redistribute pressure on the plantar fascia, which is a primary factor contributing to ulcer formation [1,2]. However, conventional insole fabrication methods are often time-intensive, requiring several days to adequately isolate and alleviate pressure from high-risk ulceration sites [3].

To overcome these limitations, there is a critical need for an affordable, adaptable, and patient-specific insole capable of effectively offloading pressure from any targeted region of the plantar surface in diabetic patients. The present study focuses on the development and validation of a customized modular insole specifically designed to mitigate plantar pressure. The developed insole has potential applications in post-operative medical care and wound management, offering an effective intervention for ulcer prevention and treatment.

**Methods:** The modular pressure offloading insole was designed to offload pressure from ulcerated areas of the foot by incorporating removable supporting segments. These segments create a void beneath the affected region, facilitating more even weight distribution and reducing localized pressure on the ulcer. Fig. 1 provides a comprehensive overview of the design, fabrication, and testing process of the modular insole.

The fabrication process utilizes high-quality materials and advanced manufacturing techniques to ensure the insole's durability, comfort, and effectiveness. Additionally, an in-house pressure measurement device, integrated with force-sensitive resistor (FSR) sensors, was developed to assess pressure distribution, specifically average zonal pressure (AZP) and the insole's offloading efficiency. To evaluate its performance, the modular insole was tested both quantitatively and qualitatively on two participant groups—fifteen healthy individuals and fifteen diabetic patients—under both standing and walking conditions. The obtained results were systematically compared to validate the insole's efficacy in reducing plantar pressure in diabetic patients while enhancing overall comfort and mobility.

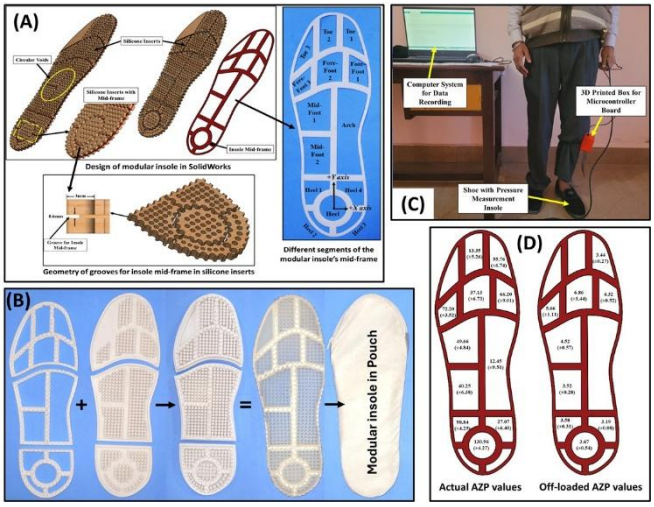


**Figure 1:** (A) SolidWorks design of modular insole and 3D-printed mid-frame for holding the inserts; (B) Fabrication of modular insole; (C) Diabetic volunteer with insole in-shoe for trials; (D) AZP values (in kPa, mean ±S.D.) for diabetic participants.

**Results & Discussion:** The study revealed that diabetic patients exhibited lower average zonal pressure (AZP) values compared to healthy individuals in both standing and walking conditions. In the standing condition, the highest AZP values were recorded at the heel region, with a mean ± standard deviation of 122.39 ± 3.62 kPa for healthy participants and 67.92 ± 12.45 kPa for diabetic participants. A similar trend was observed during walking, where the maximum AZP values were again recorded at the heel region, measuring 195.16 ± 3.19 kPa for healthy individuals and 130.96 ± 4.27 kPa for diabetic patients.

Furthermore, across all nine offloading conditions, the AZP values for both healthy and diabetic participants exhibited consistency in both standing and walking scenarios, confirming the efficacy of the modular insole in redistributing plantar pressure. The findings highlight that the heel region is particularly prone to ulceration, emphasizing the importance of effective pressure offloading. The modular insole demonstrates significant potential as a preventive intervention to reduce plantar pressure in diabetic patients, thereby mitigating the risk of ulcer formation.

**Significance:** This study will benefit diabetic patients by providing an analysis of plantar pressure, which can help prevent ulceration or re-occurrence. Overall, this study emphasizes the importance of accessible and innovative solutions for managing diabetic foot ulcers. This particular insole can effectively intervene for ulceration during post-operative medical care and wound care.

**Acknowledgments:** Gurpreet Singh is grateful to the Ministry of Education, Government of India, for awarding the Prime Minister's Research Fellowship (Ref: IITD/Admission/Ph.D./PMRF/2020–21/4062) for pursuing his doctoral research program at IIT-Delhi, India.

**References:**

[1] Jeffcoate WJ, et al., *Lancet.* **361**:1545-1551, 2003.
[2] Singh N, et al., *JMMA.* **293**:217-228, 2005.
[3] Chhikara K, et al., *Annals of 3D Printed Medicine.* **8**:100085, 2022.

# THE EFFECT OF PASSIVE-MECHANICAL PROSTHETIC KNEE AND ANKLE-FOOT COMPONENTS ON GAIT SAFETY DURING RAMP AMBULATION

Miguel Vaca[1,2,3*], Rebecca Stine[2], Kiley Lynn Armstrong[1], Matthew J. Major[1,2], Steven A. Gard[1,2]
[1]Northwestern University, Chicago, IL; [2]Jesse Brown VAMC, Chicago IL; [3]University of Minnesota, Minneapolis MN
*Corresponding author's email: miguelvm@u.northwestern.edu

**Introduction:** Persons with lower limb loss experience a high prevalence of falls (52-57%) and fall-related injuries (40.4%) [1], and previous studies identified that most falls in transfemoral prosthesis users (TFPUs) occur while walking [2]. Ensuring gait safety on ramps for TFPUs is challenging due to limited motor control of prosthetic knee flexion during stance phase. Unlike level walking, knee flexion range is larger to adapt to inclines and declines. During gait, the main contributing factors for safety are the prosthetic knee, the ankle-foot mechanism and user compensatory strategies. These three elements must interact to achieve four primary objectives during gait: 1) maintain prosthetic limb stability by preventing knee buckling in early stance [3], 2) initiate knee flexion in late stance, 3) avoid prosthetic limb collision with the ground in mid-swing [4] and 4) achieve full knee extension in terminal swing [5]. While some evidence of interaction between prosthetic knee and ankle-foot components exists, uncertainty regarding how they achieve gait safety objectives in the presence of compensatory mechanisms remains. The current study examined the effects of different combinations of commonly prescribed passive-mechanical prosthetic ankle-foot and knee components on gait safety during ramp ambulation in unilateral TFPUs with an additional focus on the influence of gait compensatory strategies.

**Methods:** Ethical approval was granted by the Jesse Brown VA IRB. Ten TFPUs (29-67 years old, 83.72±17.10 kg; 1.70±0.09 m) completed four testing sessions. During each session, the participants were randomly fitted with one of the four different combinations of two ankle-foot components (hydraulic vs non-articulated) and two prosthetic knees (polycentric vs single axis). Following accommodation, participants walked on an instrumented ramp until five clean foot strikes on a force plate were recorded for both limbs and both directions (incline/decline). Four primary outcomes variables were quantified for gait safety: Prosthetic Knee Angular Impulse (PKAI), Pre-swing Knee Moment (PSKM), Timing of Timing of Swing Knee Extension (TSKE) and Toe clearance (TC). Reflective markers were placed on anatomical landmarks of the arms, legs, and pelvis according to a modified Helen Hayes set to define a 12-segment body model. Kinematic data were collected using a 12-camera motion capture system (Motion Analysis Corp., Rohnert Park, CA) and kinetic data were acquired using two force plates (AMTI, Watertown, MA).

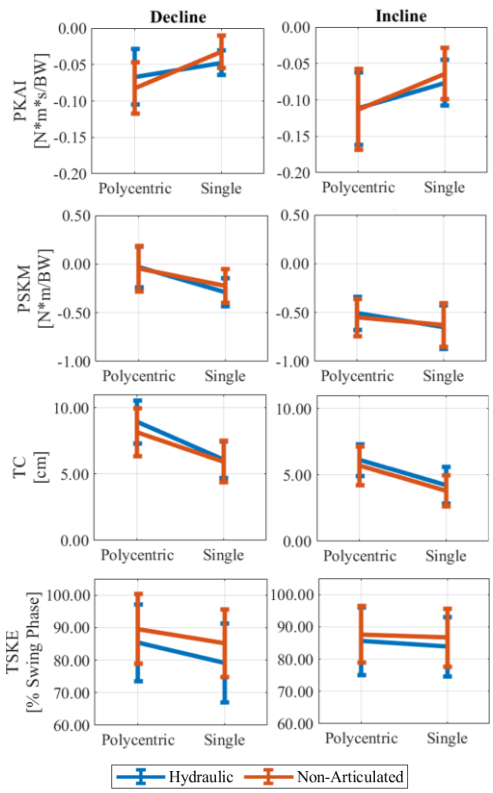


**Figure 1:** Results for decline and incline walking at each prosthetic combination across participants, denoted by separate colors.

**Results & Discussion:** Figure 1 displays the results for incline and decline walking. Table 1 summarize the p-value results for knee, foot, and their interaction. These results suggest that gait safety is improved (i.e., more negative PKAI, smaller PSKM, increased TC and later TKSE) while using the polycentric knee for decline and incline surfaces and during swing phase (i.e., increased TC and later TKSE) while using a hydraulic foot. Contrary to previous results on level walking, there was only an interaction between the prosthetic knee and ankle-foot components for PKAI at incline surfaces. It appears that the prosthetic knee had a larger effect on gait safety during stance phase on ramps, while the prosthetic knee and hydraulic foot were additive during swing phase on ramps. The interaction observed during decline walking for PKAI could be the attributed to the allowed stance flexion (~15º) of the polycentric knee which in addition to the hydraulic foot could create some issues since only one of them could be activated during the loading response.

| Effect Source | PKAI | | PSKM | | TC | | TSKE | |
|---|---|---|---|---|---|---|---|---|
| | Decline | Incline | Decline | Incline | Decline | Incline | Decline | Incline |
| Knee | <.001* | <.001* | <.001* | <.001* | <.001* | <.001* | <.001* | 0.04 |
| Foot | 0.205 | 0.066 | 0.462 | 0.727 | 0.951 | <.001* | <.001* | 0.002* |
| Knee*Foot | <.001* | 0.043 | 0.037 | 0.157 | 0.131 | 0.566 | 0.185 | 0.834 |

**Table 1:** Statistical P-values for Primary Outcomes *The significant effects are highlighted.

**Significance:** This study presented evidence on the interaction of prosthetic knee and ankle-foot components supporting gait safety during ramp ambulation. These results inform our understanding of prosthetic leg design to improve gait safety and minimize falls.

**Acknowledgements:** This study was supported by the Department of Defense (grant no. W81XWH1910447).

**References:** [1] Wong et al. (2016), *J Rehabil Med* 48(1); [2] Kim et al. (2001), *PM&R* 11(4); [3] Hisano et al. (2020), *Gait & Posture* 77; [4] Rosenblatt et al. (2017), *Prosthet Orthot Int* 41(4); [5] Kent et al. (2021), IEEE *Tran on N S and Rehab Eng* 29.

# THE EFFECT OF AXIS OF ROTATION LOCATION ON ANKLE-FOOT ORTHOSIS STIFFNESS

*Katherine Vaiciulis, Rachel Vitali, Deema Totah
Department of Mechanical Engineering, University of Iowa, Iowa City, IA
*Corresponding author's email: katherine-vaiciulis@uiowa.edu

**Introduction:** Ankle-foot orthoses (AFOs) are assistive devices typically used to support the lower limb in individuals with neurological and/or musculoskeletal conditions that affect normative gait (e.g. cerebral palsy, multiple sclerosis). Individuals require different amounts of AFO support, or stiffness. AFO stiffness has been defined as the device's resistance to sagittal plane motion around an axis of rotation, typically the ankle joint. AFOs with experimentally optimized stiffness result in decreased walking energy cost compared to supplier recommended AFOs [1]. Thus, accurate measurement of AFO stiffness is important for optimizing treatment outcomes. While there is no standard for AFO testing and stiffness measurement, research testing apparatuses do exist. One study showed significant differences in measured stiffnesses of the same AFOs between testing apparatuses [2]. One potential reason for these differences could lie in the testing apparatus's surrogate ankle model. Although the physical designs vary, AFO testing apparatuses typically model the ankle as a fixed hinge joint. However, the biological ankle is not fixed and translates during walking in three rotational degrees of freedom [3], resulting in a continuously shifting axis of rotation. Proximal-distal translations in AFO bending axis location have a small but statistically significant effect on user gait parameters [4]. This suggests that modeling the ankle as a fixed, rather than dynamically translating joint might have an impact on measured AFO stiffness. Therefore, AFO stiffnesses measured in fixed-joint apparatuses may not accurately capture the user-experienced stiffness. This work investigated the effect of static translations of the axis of rotation on experimentally measured AFO stiffness.

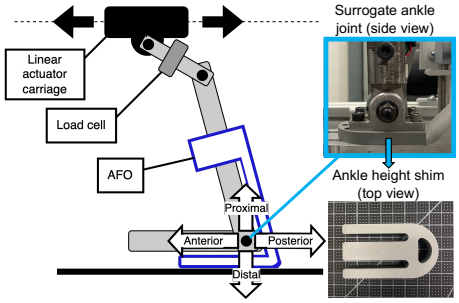


**Figure 1:** AFO in an instrumented stiffness measurement apparatus and surrogate ankle with slotted shims for changing rotation axis location.

**Methods:** This experiment used an existing validated AFO benchtop testing apparatus [5] to flex AFOs between 10° of plantarflexion (PF) and dorsiflexion (DF). Dynamic moment and angle data about the surrogate ankle joint were collected during testing. AFO stiffness was calculated as a piecewise linear regression of the resulting torque-angle curve. For this experiment, the apparatus's clamp that holds the AFO in place was redesigned to include through-slots to accommodate anterior-posterior translations of the surrogate ankle joint. Additively manufactured shims of various thicknesses were placed below the surrogate ankle to implement proximal-distal translations (Fig. 1). The translations applied were multiples of the standard deviation ($\sigma$) of biological ankle joint translation during flexion [6]. AFO stiffness was measured at the original apparatus's surrogate joint location (center) and at translations of $\pm\sigma$ (2 mm proximal-distal, 2.5 mm anterior-posterior) and $\pm 2\sigma$ (4 mm proximal-distal, 5 mm anterior-posterior). Maximum translations of $\pm 9$ mm proximal-distal and $\pm 13$ mm anterior-posterior were also implemented to encompass possible differences in rotation axis location between testing apparatuses or AFO users. One 3D-printed carbon fiber nylon, solid ankle AFO was tested over three runs for each ankle location in a randomized order. Each run cycled the AFO ten times at ~32 deg/s, representative of slow walking speed [7]. The average measured AFO stiffness of each run (10 cycles) was compared across runs and different rotation axis locations using a one-way repeated measures ANOVA (with $\alpha = 0.05$).

**Results & Discussion:** Differences in measured PF stiffnesses across rotation axis locations (Fig. 2) were larger than differences in DF stiffnesses, but neither were statistically significant (p=0.085 for PF stiffness and p=0.378 for DF stiffness). These results conflicted with a similar study for a lower stiffness, thermoplastic, articulating AFO that found minimum stiffness for center alignment and significantly increased stiffness at anterior-posterior alignments [8]. One notable difference between these experiments is that we measured dynamic stiffness, while the other study measured quasi-static stiffness. Furthermore, the material and design of the AFOs differed. Solid ankle AFOs like the one used in our study are typically on the stiffer end of prescribed AFOs. Future work will evaluate the effect of shifting the rotation axis location on measured stiffness for a variety of AFOs of different sizes, stiffnesses, materials, and designs.

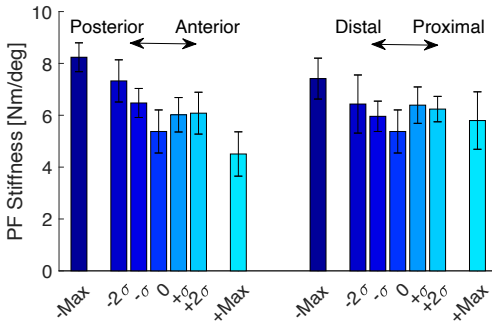


**Figure 2:** Measured plantarflexion (PF) stiffness about varying rotation axis locations. Error bars signify one standard deviation around the mean.

**Significance:** Evaluating the effect of rotation axis location on measured AFO stiffness is necessary for defining rotation axis alignment standards in AFO testing. Standardization of AFO testing methods is necessary for cross-study comparison and accurate stiffness quantification. Accurately quantifying AFO stiffness is a crucial step towards optimized user treatment outcomes and improved mobility.

**Acknowledgments:** Funded by start-up funds from the University of Iowa.

**References:** [1] Waterval et al. (2021), *J Neuroeng Rehabil.* 18(1); [2] Shuman et al. (2023), *J Neuroeng Rehabil.* 20(1); [3] McKeon et al. (2019) *J. Athl. Train.* 54(6); [4] Ranz et al. (2016), *Clinical Biomechanics* 37; [5] Totah et al. (2021), *Mechatronics* 77; [6] de Asla et al. (2006), *J. Orthop. Res.* 24; [7] Mentiplay et al. (2018), *Gait & Posture* 65; [8] Gao et al. (2011), *POI* 35(2).

# ACTIVE PROSTHETIC WRIST CONTROL REDUCES COMPENSATORY MOVEMENTS AND IMPROVES FUNCTIONAL OUTCOMES

*Grace H. Li[1], Mira Mutnick[2], Dylan Wallace[3], Cynthia Chestek[2], Deanna Gates[1]
[1]School of Kinesiology, University of Michigan, Ann Arbor, MI
[2]Department of Biomedical Engineering, University of Michigan, Ann Arbor, MI
[3]Department of Robotics, University of Michigan, Ann Arbor, MI
*Corresponding author's email: gracehyl@umich.edu

**Introduction:** Most commercial, upper limb prostheses either have a locked wrist or passive wrist control where the user must rotate the wrist using their intact limb. Without wrist motion, users must compensate with their upper body (i.e. shoulder and trunk) to properly orient their hand to interact with objects. These trunk compensations can contribute to pain and discomfort over time [1]. Previous studies show that increasing wrist dexterity in upper limb prostheses helps decrease trunk or shoulder compensatory movements when handling objects [2,3]. Prior studies have also compared wrist control when coupled with only opening and closing of the terminal device and found decreased trunk compensations and improved functional outcomes when active wrist rotation was enabled [4]. This preliminary case study aims to compare the biomechanical and functional outcomes of having active wrist control versus no wrist control when coupled with multiple hand grips. We hypothesized that use of an active wrist would decrease compensatory trunk movements and improve functional outcomes relative to no wrist control.

**Methods:** A 58-year-old female with right transradial limb loss participated in this study (Clinical Trial No. NCT03260400). The participant controlled an iLimb Quantum (Ossur, Reykjavik, Iceland) prosthetic hand with a wrist rotation unit. Linear discriminant analysis pattern recognition classifiers were trained on eight pairs of domed surface electrodes to control either multiple hand grips (No Wrist) or multiple hand grips and wrist pronation/supination (Wrist). The participant completed the Coffee Task (CT) [5] and the Clothespin Relocation Task (CRT) [6] with and without wrist control in two experimental sessions. The CT had five main segments that required different grip transitions in sequence: (1) grab a cup and pour the contents into the coffee maker water reservoir (using fist/power), (2) place a coffee pod in the pod holder (pinch), (3) press the start button on the coffee maker (point), (4) grab the cup from underneath the dispenser (fist), and (5) open a sugar packet (pinch). The CRT was performed with two iterations: (1) Up (relocating three clothespins from a horizontal pole to a vertical pole) and (2) Down (from a vertical pole to a horizontal pole) to assess wrist rotation. We measured three-dimensional trunk-room angles during the pour segment of the CT [7] and during full attempted clothespin transfers of the CRT using a 12-camera motion capture system (Motion Analysis, Rohnert Park, CA) with four reflective markers on her trunk (C7, T8, sternum, and xiphoid process). We then compared the trunk range of motion (ROM) to a normative dataset from a participant without upper limb loss. We also assessed the functional outcomes of the CT using completion time (s) and the CRT using failure rate (%), calculated as the percentage of clothespins dropped.

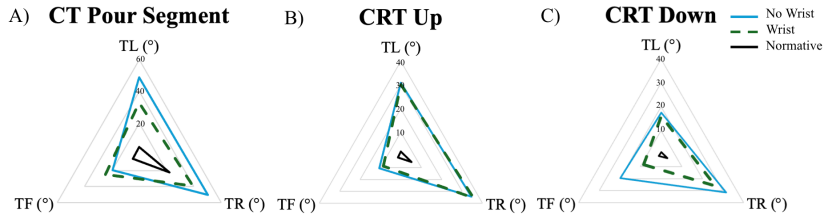


**Figure 1:** Average trunk compensations (TL = lateral lean, TR = axial rotation, TF = flexion/extension) for A) CT Pour Segment, B) CRT Up, and C) CRT Down with and without active wrist control and compared to a normative value.

**Results & Discussion:** The participant made large trunk compensations during the pour segment of the CT with no wrist control. Trunk lateral lean and axial rotation were reduced when active wrist control was added, though not to normative levels (Figure 1A). Wrist control also reduced the average completion time of the full CT from 132.0s to 124.9s. Trunk flexion/extension ROM decreased when active wrist control was used during CRT Down (Figure 1C), but was not affected during CRT Up (Figure 1B). Additionally, wrist control reduced the average failure rate from 88.9% to 55.6% for CRT Up and from 88.9% to 33.3% for CRT Down. Thus, while the strategies employed still relied on trunk compensation, active wrist control led to greater success in task completion, especially for CRT Down. These results agree with [4], which found active wrist control reduced task failure rate and decreased trunk lateral lean and flexion/extension ROM. The tasks in this study required different starting orientations and movements of the prosthetic hand and wrist to complete each task. The pour segment of the CT and CRT Down both require wrist pronation to complete the task, while CRT Up requires wrist supination. Thus, the different orientation requirements for each task highlights when wrist rotation would be beneficial for reducing compensatory movements.

**Significance:** Active wrist control has the potential to reduce compensatory trunk movement during some functional upper limb tasks, especially those requiring wrist pronation.

**Acknowledgments:** This work was supported by the National Institutes of Health under Award R01NS105132. The opinions expressed in this article are the authors' own and do not reflect the view of the National Institutes of Health. We would like to thank Ossur for the use of the prosthetic hand, and Sara Isgro and Ziyad Emara for their assistance with data processing.

**References:** [1] Ostlie et al. (2011), *Arch Phys Med Rehabil*., 92(12); [2] Demofonti et al. (2023) *Anat Rec. (Hoboken)*, 306(4); [3] Choi, S., Cho, W., & Kim, K. (2023), *J Neuroeng Rehabil.,* 20(1); [4] Olsen et al. (2024) *Sci Rep*., 14(1); [5] Lee et al. (2024) *J Neuroeng Rehabil.,* 21(21); [6] Hussaini, A., & Kyberd, P. (2017), *Prosthet Orthot Int*. 41(3); [7] Lee et al., (2022) *J Neuroeng Rehabil.,* 20(6)

# EFFECTS OF A WEARABLE HAMSTRINGS ASSISTIVE DEVICE ON LEG MOTION IN OVERGROUND SPRINTING

Quinn Castner[1*], Divya Srinivasan[1,2], Reed D. Gurchiek[1]
[1]Department of Bioengineering, Clemson University; [2]Department of Industrial Engineering, Clemson University
[*]Corresponding Author's email: qcastne@clemson.edu

**Introduction:** Hamstring strain injuries are among the most common injuries in field-based sports, with high recurrence rates [1,2]. The incidence and playing time lost have increased over the last 20 years [3], and the recovery time is longer in secondary than in index injuries [4]. While existing devices have been shown able to assist in walking, running, and lifting toward improved efficiency or reducing injuries [5,6], few, if any, have been developed to offload the hamstrings during running. We have designed a wearable, passive assistive device for offloading the hamstring muscles during running to improve rehabilitative outcomes. It includes an elastic band with a proximal attachment at the posterior waist and a distal attachment at the ankle and crosses the knee posteriorly. Various components enable adjusting the geometry of the band and thereby modifying the hip and knee moment arms. An optimal design would (1) permit an athlete to run with their natural kinematic pattern while (2) reducing the amount of active force production required of the hamstrings. In this way, the device would not impede running performance while providing assistance toward reducing re-injury risk. In this study, we examined the first of these two design criteria and sought to quantify changes in leg motion due to wearing the device during an overground sprint. The design of the device is such that the elastic band stretches and shortens with the hamstrings during running. Thus, we hypothesized that the device would not significantly alter leg motion.

**Methods:** Nine participants were recruited to run four maximal-effort 40-yard sprints following a warm-up. The first two were performed without wearing the device, and the last two were performed with the device. Participants were given sufficient time to become familiar with the device and rest between trials to avoid fatigue. The band strain in a standing posture was set to 39% for all participants. Previous research shows hamstring strain peaks at approximately 12% during top-speed running [7]. Assuming our band stretches similarly, the tension in the band would peak at approximately 64 N. Running speed was measured using a linear transducer (1080 Sprint 1, 1080 Motion). We focused our initial study on the motion of the shank because the large eccentric loads required of the hamstrings are to arrest the rotation of the shank in preparation for subsequent foot contact. Thus, we quantified leg motion in this study using the sagittal plane angular velocity of the shank measured with a gyroscope (BlueTrident, Vicon) worn just superior to the lateral malleolus. This signal was also used for stride segmentation using an algorithm described previously [8]. We quantified the mean absolute difference (MAD) between the ensemble average angular velocity signal of the two trials in each condition for strides 4 through 9. The first 3 were neglected to avoid biomechanical nuances associated with the start of a sprint and at least 9 were available for every participant. We also compared the with-band vs. average no-band differences with the no-band vs. average no-band differences. Mathematically, this is equivalent to comparing the standard deviation of the leg motion across the two within-condition trials with the average taken from the no-band condition in both cases. This amounts to a difference in standard deviation (DSD). To facilitate interpretation of both outcomes (MAD and DSD), we expressed each as a percentage of the range of the signal during the no-band condition. Finally, we compared the top speed and 40-yard time between conditions.

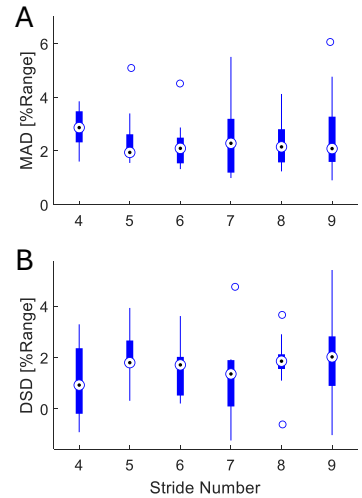


**Fig. 1.** Boxplots of (A) mean absolute difference (MAD) in shank angular velocity and (B) the difference in standard deviation between with-band and no-band conditions. All values are expressed as a percentage of the signal range from the no-band condition.

**Results & Discussion:** Wearing the band slightly decreased top running speed by an average of 0.09 m/s (1.05%) and increased sprint time by an average of 0.06 s (1.14%). On average, the mean absolute difference in the shank motion between conditions was less than 2.5% (Fig. 1A), and the difference in standard deviation was less than 2% (Fig. 1B) across all strides. While these small changes are likely clinically irrelevant, future research should verify the clinical utility of the device to reduce reinjury rates. Moreover, we did not measure the assistance provided by the device. While we could make an estimate based on the material properties of the elastic band and previous work on hamstring kinematics during running, future research is necessary to confirm that the offloading is sufficient to reduce injury risk.

**Significance:** A key design criterion of a device for offloading hamstrings during running is that it does not encourage an unnatural running motion. This study quantified the efficacy of our device in meeting this criterion, and the results are promising. If the offloading assistance is shown to be clinically meaningful in future work, this device could help reduce hamstring re-injury rates and improve rehabilitative outcomes (e.g., faster return-to-play time).

**Acknowledgements:** This work was supported by the Robert H. Brooks Sports Science Institute and the Clemson University Department of Bioengineering.

**References:** [1] Visser et al. (2012), *Br J Sports Med* 46(2); [2] Maniar et al. (2023) *Br J Sports Med* 57(2); [3] Ekstrand et al. (2023) *Br J Sports Med* 57(5); [4] Danielsson et al. (2020), *BMC Musculoskelet Disord.* 21(641); [5] Sawicki et al. (2020) *J Neuroeng Rehabil* 17(1); [6] Alemi et al. (2020) *Human Factors* 62(3); [7] Schache et al. (2012), *Med Sci Sports Exerc* 45(6); [8] Gurchiek et al. (2025) *Med Sci Sports Exerc* 57(3)

# EXEREXO: EXPLORING THE EFFECTS OF ASSISTIVE AND RESISTIVE ANKLE EXOSKELETON TORQUE ON WALKING MECHANICS AND ENERGETICS

*Arshad Mandani[1], Zachary Lerner[2], Zachary Graham[3], Gregory Sawicki[1]
[1]Physiology of Wearable Robotics Lab, School of Mechanical Engineering, Georgia Tech, Atlanta, Georgia
[2]Biomechatronics Lab, School of Mechanical Engineering, Northern Arizona University, Flagstaff, Arizona
[3]Institute for Human and Machine Cognition, Pensacola, Florida
*Corresponding author's email: amandani3@gatech.edu

**Introduction:** Lower-limb exoskeletons have been historically applied to the improvement of human movement, particularly walking, with the goal of reducing metabolic cost [1]. Assistive torque, through powered or unpowered means, complements biological moments to replicate or augment natural human motions in elderly, impaired, or clinical populations. The opposite application of exoskeletons has shown promise in the same populations, seeking to provide resistance to functional tasks with the intention of muscle strengthening, neuromuscular function improvement, and targeted rehabilitation resulting in measurable improvements in walking mechanics and muscle activation [2, 3]. The same robotic devices designed to restore and rehabilitate can be refocused on exercise training, increased metabolic effort, and targeted muscle activation in healthy individuals seeking to capitalize on exercise volume. This study aims to explore the benefits to exercise training with the use of an ankle exoskeleton capable of providing both assistive and resistive ankle torques. Analogous to standard workout practices, equal exercise effort can be achieved through low weight, high repetition conditions (exoskeleton assistance, fast walking speeds) and high weight, low repetition conditions (exoskeleton resistance, slow speeds). We hypothesize that measures of effort and exercise volume increase across walking speeds and resistive exoskeleton intervention can provide improved training benefits at lower speeds, creating instances of equal exercise volume across a landscape of training conditions.

**Methods:** A powered, cable-driven ankle exoskeleton (Biomotum) is used to provide 3 torque conditions (zero-torque, 15 Nm plantarflexion assistance, 15 Nm plantarflexion resistance) at 3 walking speeds (1.00, 1.25, 1.50 m/s) during walking bouts of 5 minutes (with 5 minutes intermittent rest between trials). This study produces heart rate, metabolic energy expenditure [4], unilateral EMG, lower body inverse kinematics and kinetics, ground reaction forces, and self-reported perceived exertion (per the Borg scale [5]) data. The average propulsive ground reaction forces observed in each of the three zero-torque conditions are presented as live biofeedback targets during the speed-matched assist and resist conditions, serving as a proxy for real-time ankle power and encouraging the participant to preserve constant ankle dynamics across all exoskeleton conditions (Figure 1B). Two additional trials are conducted without biofeedback (assist and resist at 1.25 m/s) in a condition-randomized order before the remaining six trials are conducted in a speed and condition-randomized order. Heart rate, gross metabolic power, and perceived exertion are the main metrics of exercise intensity while the applied exoskeleton torque (positive for assistance, negative for resistance), is subtracted from the net ankle moment to isolate the biological contribution to ankle moment and power. The preliminary study was collected with an n=1 population.

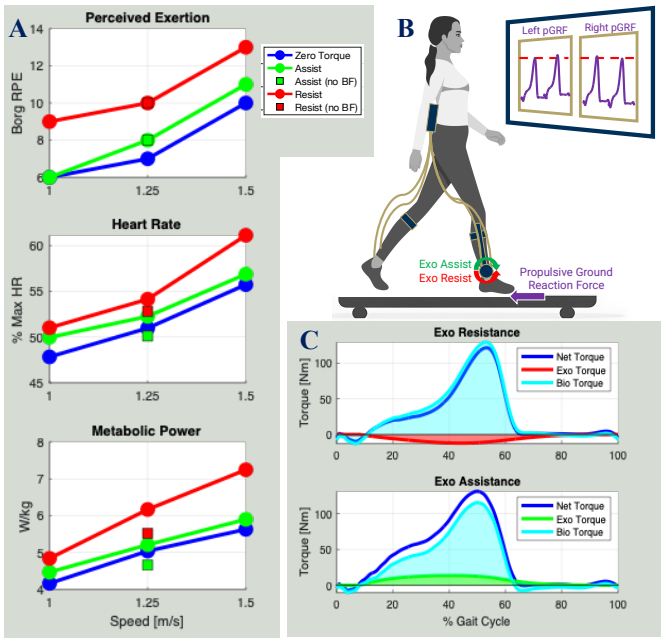


**Figure 1A:** Measures of exercise effort across exo conditions and speeds, including no-biofeedback conditions. **Figure 1B:** Propulsive ground reaction force real-time biofeedback targets during speed-matched trials. **Figure 1C:** Biological and exo contributions to net torque in assist and resist conditions.

**Results & Discussion:** All measures of exercise effort, including self-reported perceived exertion (RPE), heart rate, and gross metabolic power increased across walking speeds with similar patterns represented across all exo conditions (Figure 1A). In each metric, walking at slow speed with resistive intervention equated to assist or zero-torque conditions at higher speeds, showcasing the potential for equal exercise volume at lower physical speeds. Additionally, there is a larger biological contribution to net ankle moment in the resistance condition to overcome negative exo torque compared to the assistance condition, which supplements a reduced biological moment (Figure 1B). Gross metabolic power increased by 12% in both assistance and resistance biofeedback conditions when compared to no-biofeedback conditions. This demonstrates the need for real-time cues to guarantee participants experience the full effects of exoskeleton assisted exercise training.

**Significance:** This preliminary study demonstrates the viability of exoskeletons to be used as exercise training devices, exceeding the historically established use cases of mobility restoration and rehabilitation. This study also demonstrates the need for biofeedback cues to encourage users to engage standard levels of ankle power when exposed to exoskeleton intervention. Increased amounts of exercise volume can be achieved at lower repetitions with higher loads, translating knowledge of exercise training from the gym to the world of wearable robotics.

**References:** [1] Sawicki et al. (2020), *J Neuroeng Rehabil*; [2] Bulea et al. (2022), *Proc IEEE RAS EMBS*; [3] Swaminathan et al. (2023), *J Neuroeng Rehabil;* [4] Brockway (1987), *Hum Nutr Clin Nutr*; [5] Borg (1982), *Med Sci Sports Exer.*

# SELF-ADAPTIVE PASSIVE ELBOW MOVEMENT ASSISTANCE (PEMA-S): A PORTABLE EXOSKELETON FOR ENHANCING ELBOW MOBILITY IN FLEXOR HYPERTONIA THROUGH ANGLE-SPECIFIC ASSISTANCE

Ha T. Ngo[1], Thanh Q. Phan[1,2], and *Sang Wook Lee[1,2,3,4]

[1] Catholic University of America, Washington, DC; [2] National Rehabilitation Hospital, Washington, DC; [3] Korea Advanced Institute of Science and Technology, Daejeon, Korea; [4] Rehabilitation Medicine Department, National Institute of Health, Bethesda, MD.

*Corresponding author's email: leesw@cua.edu

**Introduction:** Chronic upper extremity (UE) impairment affects up to 60% of stroke survivors, significantly limiting their function [1]. One of the primary contributors to this impairment is flexor hypertonia, characterized by motoneuronal hyperexcitability that leads to angle-dependent flexion moments, restricting elbow range of motion (ROM). While robotic rehabilitation devices have been effective in restoring function, most devices are laboratory-bound, limiting therapy frequency and accessibility [2]. Conversely, portable devices can be used outside clinical settings but often lack the adaptability to account for dynamic fluctuations in muscle tone characteristic of post-stroke motor impairments [3][4]. To address this, we developed PEMA-S (Self-Adaptive Passive Elbow Movement Assistant), an enhanced, portable exoskeleton that provides real-time adaptive assistance based on both elbow angle and user effort (Fig. 1A). By integrating force sensors, PEMA-S can detect volitional user input, adjusting assistance levels accordingly to optimize support while promoting active engagement. This improvement enhances assistance performance, particularly for individuals with severe hypertonia, ensuring more effective compensation for angle-dependent resistance. The device's efficacy was validated through a mathematical model and pilot testing, demonstrating its potential to improve functional movement and elbow ROM in stroke rehabilitation.

**Methods:** Three healthy subjects (all males, age: 33 yrs old $\pm$1.5) participated in this research study. Four pairs of surface electrodes were placed on the anterior deltoid (AD), lateral deltoid (LD), short head of biceps brachii (BB), and lateral head of triceps brachii (TB) to measure EMG activity. Participants performed elbow extensions (90° to 0°) under three conditions: no assistance (NA), passive assistance (PA), and self-adaptive force-dependent assistance (LA/HA/FA). Assistance levels were set to 30–50% of the maximum EMG recorded from the TB. Movements were guided by a visual cue (a time bar) and segmented into three phases: waiting ($T_1$ = 3 sec), extending ($T_2$ = 3 sec), and holding ($T_3$ = 2 sec). In the passive assistance condition (PA), the device was worn but deactivated, with participants countering 60–70% of simulated hypertonia resistance. The self-adaptive condition tested three assistance levels: low (LA: actuator engaged at 80% of participant effort), high (HA: engaged at 20% effort), and full assistance (FA: device support combined with external aid).

**Results and Discussion:** The mathematical model (Fig. 1B) indicates that the device provides assistive force decreasing from 0° to 90°, with increased support at lower flexion and reduced assistance near full extension to counteract hypertonia. Triceps activation consistently decreased with higher assistance, reducing antagonist muscle effort, while biceps activation showed only modest changes, particularly at the high assistance levels (Fig. 1C). The Co-Contraction Index (CCI) slightly increased with more assistance, possibly due to the increase in the biceps activation for joint stabilization under assistance, but the relative changes in CCI were smaller than those in triceps activation (Fig. 1D). These results suggest the device reduces agonist muscle activation without significantly affecting antagonist cocontraction, though the small sample size (n=3) limits generalizability. Increasing the sample size and testing with stroke survivors will help validate its effectiveness and rehabilitative efficacy for chronic stroke survivors.

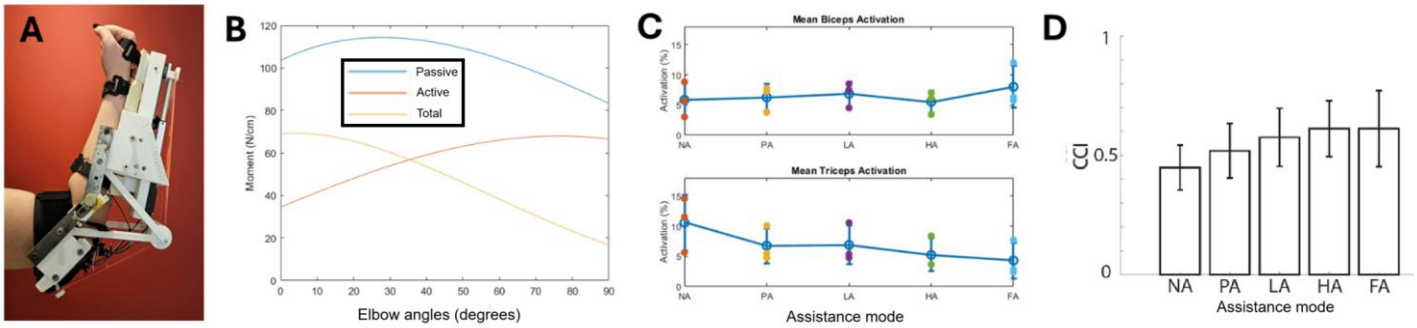


**Figure 1:** (A) PEMA-S (B) Theocratical Results of the Model (C) Biceps and Triceps Activation Across Assistance Levels (D) Co-contraction

**Significance:** PEMA-S was able to provide adaptive assistance to improve the elbow ROM by counteracting angle-dependent flexor hypertonia. By enhancing accessibility through its portable design, the device allows for more frequent rehabilitation beyond clinical settings, potentially improving and expediting functional recovery of elbow flexor hypertonia in stroke survivors.

**Acknowledgement:** This work was supported by NIDILRR (90REMM0001).

**References:**[1] Barry et al. (2020), Arch Phys Med Rehabil 101(7). [2] Lo et al. (2017), JBI Database Syst Rev Implement Rep 15(12). [3] Phan et al. (2019), IEEE Int Conf Rehabil Robot, 2019, 1209–1214. [4] Sanchez et al. (2006), IEEE Trans Neural Syst Rehabil Eng 14(3).

# THE EFFECTS OF DIFFERENT TERRAINS AND INCLINED SURFACES ON FORCE GENERATION IN ASSOCIATION WITH A WHEELCHAIR

*Somlata Dev Sharma[1], *Tamara Reid Bush[1]
[1]Department of Mechanical Engineering, Michigan State University, East Lansing, MI 48823
*Corresponding author's email: sharm242@msu.edu, reidtama@egr.msu.edu

**Introduction:** Manual wheelchair users encounter varying levels of resistance when navigating different surfaces, which can significantly impact their mobility and physical exertion. Understanding the forces required to initiate movement of a wheelchair across different surfaces is crucial for improving the accessibility of individuals who use wheelchairs. Previous studies have explored kinetic and kinematic factors influencing wheelchair propulsion on both level and non-level surfaces, while highlighting the heightened physical effort required when maneuvering across inclines and uneven terrains [1][2]. Additionally, some work has investigated wheelchair propulsion via rolling resistance of some surface types [3]. Determining the minimum force needed to overcome the resistance associated with various surfaces and terrains is key to determining the force a user must generate with their upper extremities [4]. However, there has been limited work in this area, particularly around initiation forces for different terrains and at an inclined angle. Our study addresses this gap by analyzing the initiation force on identical surface materials (carpet and tile) in both flat and 5° inclined conditions, as well as investigating cement, gravel, grass and pea stones. The goal of this study was to determine the effect of surface types including inclination on the initiation forces in association with manual wheelchair usage.

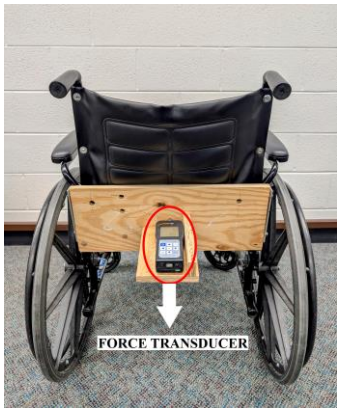


**Figure 1:** Custom built attachment with force transducer mounted on the seat back.

**Methods:** A standard manual wheelchair (Invacare, Elyria, Ohio) was used in this study. An attachment was secured to the frame of the wheelchair to accommodate a single axis force transducer, while permitting measurement of a pushing force parallel to the ground (Fig. 1). 7 participants (5 males, 2 females) were included in this study. Participants sat on the wheelchair, and an external force was applied via the force transducer until the minimum force required to initiate rolling motion was achieved across six distinct flat surfaces (Carpet, Tile, Cement, Gravel, Grass and Pea Stones) and two inclined (5°) surfaces (Tile and Carpet). Each participant underwent five trials per surface and the peak force value to initiate movement per trial was recorded from the force transducer. The data were normalized according to participant weights and the average force of the five trials of each participant was calculated for all the surfaces. A repeated-measures ANOVA was used to identify force differences across surfaces and incline conditions. Pairwise comparisons between surfaces with Bonferroni adjustment was assessed using SAS 9.4 (Cary, North Carolina).

**Results & Discussion:** The results indicated significant differences in forces between surfaces (Fig. 2). Pea stones required the highest force (30.4 ± 3.3 %BW), demonstrating the greatest resistance and was significantly different from all other surfaces ($p < 0.0001$). Forces to initiate motion on grass were significantly larger than carpet, tile, cement and gravel ($p < 0.0001$). Tile required the least force (8.2 ± 0.3 %BW), indicating the least resistance initiating motion. There were no statistically significant differences in initiation force among carpet, tile, cement and gravel ($p \geq 0.05$) which suggests that these surfaces impose comparable resistance on manual wheelchair users, indicating similar biomechanical demands to initiate motion. Both the inclined carpet (65.5% increase) and inclined tile (97.6% increase) required significantly higher initiation forces than their flat counterparts ($p < 0.0001$).

**Significance:** The findings of this study have important implications for both accessibility and urban planning. By quantifying initiation forces across various terrains, this research provides a method by which valuable insights for users, engineers, and policymakers involved in wheelchair mobility can be gleaned. These force data can also be used in conjunction with the torque generated by a wheelchair user. Doing so facilitates the development of direct relationships between individual abilities and the strength needed to traverse a surface and surface types. Thus, users of manual wheelchairs can anticipate if they can safely traverse through a particular surface.

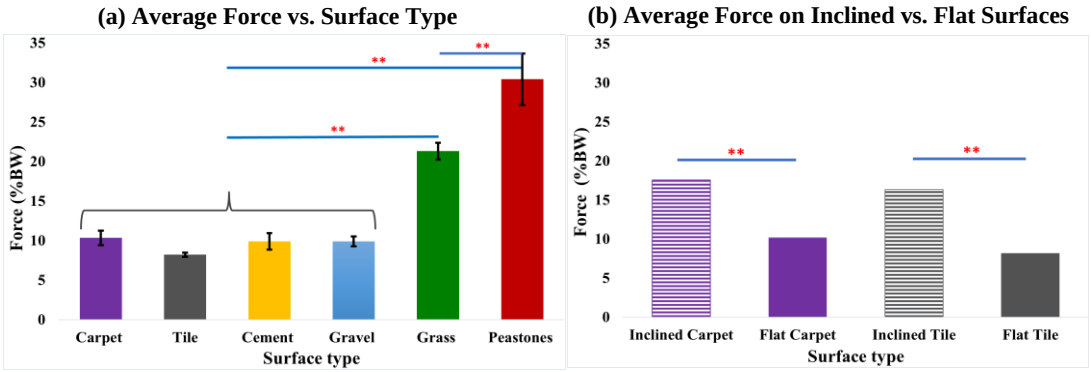


**Figure 2:** (a) Average force required to initiate rolling across six flat surfaces. (b) Average force on flat and inclined surface with both carpet and tile. **Indicated significant differences ($p < 0.05$).

**References:** [1] Koontz et al. (2005), *JRRD* 42(4); [2] Spinal Cord Injury Research Evidence (SCIRE) Project. Kinetics and Kinematics of Wheelchair Propulsion on Non-Level Surfaces.; [3] Hurd et al. (2008), AJPM&R 87(12); [4] Ott et al. (2021), RATE 8.

# COMPARATIVE STUDY OF SHOULDER JOINT STIFFNESS IN DYNAMIC MOVEMENT AND STATIC POSTURE TASKS

Seunghoon Hwang[1], Katia Ponce[2], Suhrud Joglekar[1], and Hyunglae Lee[1,*]
[1]School for Engineering of Matter, Transport and Energy, Arizona State University, Tempe, USA
*Corresponding author's email: hyunglae.lee@asu.edu

**Introduction:** The human shoulder is a highly mobile joint that requires a delicate balance between stability and mobility to enable precise and effective upper limb function across various tasks. Stability is maintained through a complex interplay of bones, ligaments, tendons, and muscles, which collectively provide resistance against external disturbances–often described as stiffness[1]. While some studies have characterized shoulder joint stiffness using system identification techniques and robotic platforms in 3D space, most have focused on static posture tasks[2]. To address this gap, this study aims to characterize shoulder joint stiffness during dynamic movement tasks in 3D space. Furthermore, to deepen our understanding of task-dependent shoulder joint stability, we compare stiffness between dynamic movements and static postures, offering insights into how shoulder joint stability adapts to movement demands.

**Methods:** Twenty healthy young adults (10 males, 10 females; mean age: 23.7 years; mean mass: 65.6 kg) participated in this study, which was approved by the Arizona State University IRB (STUDY 00009059). We employed a custom-designed, parallel-actuated shoulder exoskeleton robot that applied rapid position perturbations directly to the shoulder joint[3] (Fig. 1A). A graphical user interface displayed both the current shoulder position and a target position (45° or 90°), and participants moved between these positions under an admittance controller at three horizontal postures (20°, 45°, and 70°). During movement, the exoskeleton randomly delivered ramp perturbations (6° amplitude, 150 ms rise time) around 67.5° of shoulder flexion. Each posture condition included eight blocks of ten trials–five with perturbations and five without–resulting in a total of 40 perturbed trials. Surface electromyographic signals were recorded from the anterior, medial, and posterior deltoid muscles, while 3D kinematics and shoulder torque data were captured at 250 Hz.

A static posture experiment was conducted for each horizontal arm position, consisting of four blocks of ten perturbed trials (totaling 40 trials per posture). Participants maintained deltoid muscle activation within ±1.5% of target levels (derived from mean activations in the dynamic tasks) for two seconds before perturbations were applied. Prior to estimating shoulder joint impedance, both kinematic and torque data were low-pass filtered at 10 Hz using a fourth-order Butterworth filter. A second-order parametric model was then fitted using the Levenberg–Marquardt nonlinear least squares method[4], with 100 bootstrapped samples (60% of total perturbed trials) used for statistical analysis. Finally, the quality of the stiffness estimation was evaluated by calculating the variance accounted for (%VAF) between the measured torque and the torque estimated by the impedance quantified.

**Results & Discussion:** System identification exhibited high accuracy, as evidenced by the average (SD) %VAF of 95.1 (0.6)% during dynamic movement tasks and 96.4 (1.1)% during static posture tasks. Group results showed that shoulder joint stiffness was significantly lower ($p < 0.001$) during dynamic movements compared to static postures across all three horizontal extension arm postures. Specifically, stiffness during dynamic movement was reduced by 34.9%, 18.5%, and 15.9% at the 20°, 45°, and 70° postures, respectively, compared to static posture (Fig. 1D) However, inertia ($p = 0.153$) and damping ($p = 0.902$) did not exhibit significant differences between dynamic movements and static postures (Fig. 1B-C).

These results suggest that shoulder joint stability may decrease during dynamic movements compared to static postures. This difference may be attributed to the stress relaxation behavior of ligaments and tendons, wherein preconditioning—resulting from repeated elongation during dynamic movement—lowers internal tissue stress and reduces stiffness[5]. This may partly explain why stiffness measured during dynamic movement tends to be lower than that in static postures.

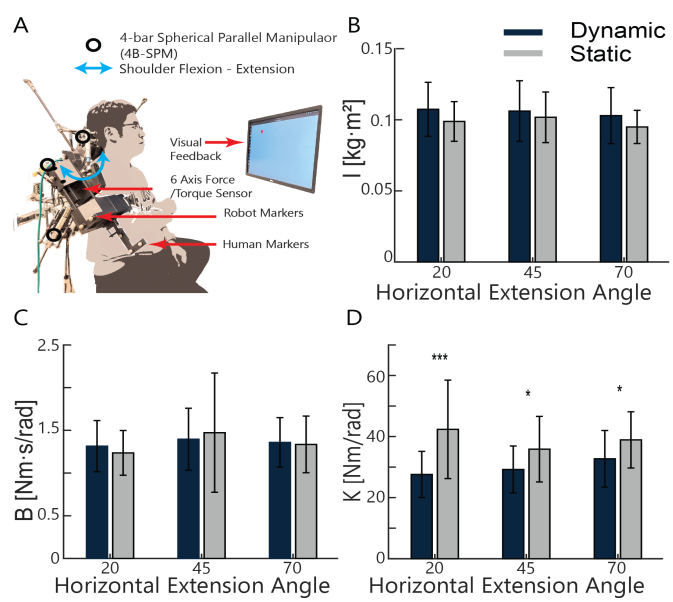


**Figure 1:** A) Experiment setup for characterization of shoulder stiffness. B-D) Comparison of inertia, damping, and stiffness between dynamic motion and static posture.

**Significance:** These findings highlight the significant influence of task-related factors on shoulder joint stiffness, revealing notably lower stiffness during dynamic movements compared to static postures. This study provides a foundational understanding of how the shoulder joint balances stability and mobility across different conditions. It also establishes a basis for investigating changes in shoulder stiffness following neuromuscular injuries, offering insights that could guide the development of targeted rehabilitation strategies.

**References:** 1. Lugo, R et al. (2008), European Journal of Radiology. 2. S. Hwang et al. (2024), *IEEE Transactions on Biomedical Engineering (TBME)*. 3. D. Chang et al. (2021), *IEEE International Conference on Robotics and Automation (ICRA)*. 4. Kearney, R. E et al. (1997), *IEEE Transactions on Biomedical Engineering (TBME)*. 5. Machiraju, C et al. (2006) Computer methods and programs in biomedicine.

# OPENEXO: EXPERIMENTAL VALIDATION OF AN OPEN-SOURCE MODULAR EXOSKELETON

*Jack R. Williams[1], Shanpu Fang[1], Daniel Colley[1], Noah Enlow[1], Zachary F. Lerner[1]
[1]Northern Arizona University
*jack.williams@nau.edu

**Introduction:** The field of wearable robotic exoskeletons is rapidly expanding [1]. Despite this, there are several barriers to entry, such as the lengthy and costly developmental process and the necessity for broad expertise, that discourage many from pursuing research in this area. Additionally, many exoskeletons are designed for a specific utility which limits their flexibility to adapt to answer new questions, further hindering growth. To address these limitations, we have developed an open source, modular, exoskeleton system ("OpenExo") for individuals interested in working in this domain [2]. This system was designed to be adaptable to accommodate different configurations, including single joint assistance of the hips, ankles, and elbows, and multi-joint applications like combined hip-and-ankle assistance. Here we present the initial experimental validation of these configurations to highlight its potential.

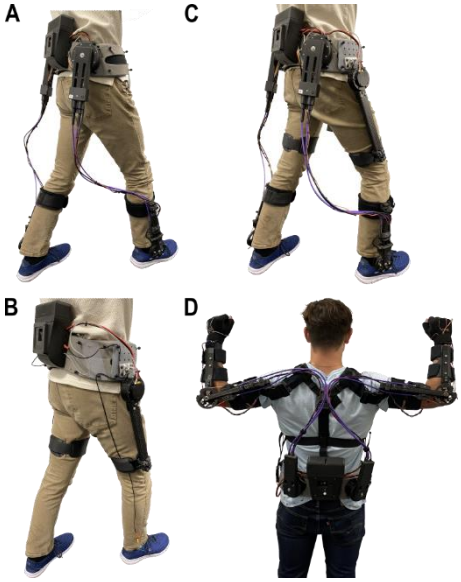


**Figure 1.** OpenExo configurations include the **(A)** ankle, **(B)** hip, **(C)** combined hip-and-ankle, and **(D)** elbow.

**Methods:** This open-source framework provides users access to all aspects of the design process, including the software, electronics, hardware, and control subsystems. The system was experimentally validated under four configurations (**Fig 1**) which include: indoor and outdoor walking with ankle assistance (n = 1; [3]), hip assistance during 7.5° incline walking on a treadmill (n = 2; [4]), hip-and-ankle assistance during level treadmill load carriage (n = 2; 22.5% BW), and weightlifting to fatigue with elbow flexion assistance (n = 2; [5]). For all walking conditions, users performed 60 minutes of exoskeleton acclimation the day prior to testing. Indoor treadmill assessments were evaluated with and without assistance by having the user perform the activity of interest while outfitted with a portable, indirect calorimetry metabolic unit (K5, COSMED). Each indoor walking activity lasted eight minutes from which the average cost of transport (COT) of the last two minutes was calculated by estimating the metabolic power via Brockway's equation and normalizing to the metabolic power of a resting baseline, participant body mass, and walking speed [2]. The outdoor ankle exoskeleton test consisted of one user walking about a 1650 m outdoor trail with and without ankle exoskeleton assistance while time was recorded. The elbow assistance task consisted of users performing weight curls with a 19.5 kg box in sync with a 60-beats-per-minute metronome. This task was performed with and without elbow assistance (order randomized), with the outcome variable of interest being the number of repetitions until fatigue. Given the limited sample size, only percent difference between the assistance and no-assistance conditions was characterized.

**Results & Discussion:** OpenExo was beneficial for a variety of users across multiple configurations. While receiving ankle exoskeleton assistance during level walking indoors, the user observed an 8% reduction in the COT (vs. no exoskeleton; Shod: 2.19 $Jkg^{-1}m^{-1}$; Exo: 2.02 $Jkg^{-1}m^{-1}$), suggesting a potential benefit of assistance. When this same user walked in this configuration while on an outdoor trail, they were able to complete the trail in 13% less time, compared to walking without the device, which could suggest improved walking speed and/or walking duration capacity with assistance. When configured to hip-only assistance for incline treadmill walking, one user experienced an 8% (Shod: 6.72 $Jkg^{-1}m^{-1}$; Exo: 6.17 $Jkg^{-1}m^{-1}$) and another a 14% (Shod: 7.35 $Jkg^{-1}m^{-1}$; Exo: 6.29 $Jkg^{-1}m^{-1}$) reduction in the COT compared to walking without the device; which is consistent with other state-of-the-art devices found in literature [6]. While providing combined hip-and-ankle assistance while carrying 22.5% of their body weight, two users experienced 8% (Shod: 2.68 $Jkg^{-1}m^{-1}$; Exo: 2.46 $Jkg^{-1}m^{-1}$) and 18% (Shod: 2.59 $Jkg^{-1}m^{-1}$; Exo: 2.13 $Jkg^{-1}m^{-1}$) reductions in the COT, compared to walking with no device, suggesting improved movement capacities (such as further walking distances and reduced fatigability) when supporting additional load. Finally, the device was configured for upper extremity elbow assistance to aid users in weightlifting tasks. In both instances of this pilot work, users were able to substantially increase the number of repetitions while receiving elbow flexion assistance, with one user increasing their repetitions from 7 to 14 (+100%) and another increasing their repetitions from 6 to 22 (+267%). This could have significant implications in ergonomic environments, with the potential to reduce workplace fatigue and decrease injury risk [5].

**Significance:** To the best of our knowledge, OpenExo is the world's first fully open source (software, electronics, hardware, and control subsystems with supporting documentation for each) exoskeleton device and thus has immense potential as an accessible tool for established researchers and novices (e.g., biomechanist) who want to contribute to the field. The preliminary experimental validations presented here, while limited to a small sample size, suggest comparable performance to other state-of-the-art research devices. Future work will explore more in-depth validation of these, and other, configurations.

**Acknowledgments:** We thank Drs. Karl Harshe, Pamela Bosch, and Collin Bowersock for their assistance with data collections. This work was supported in part by the NAU foundation, NIH/NICHD R01HD107277, and NSF2045966.

**References:** [1] Sawicki et al. (2020), *J Neuro Rehab* 17(25); [2] Williams et al. (2024), *bioRxiv*; [3] Orekhov et al. (2021), *J Neuro Rehab* 18(163); [4] Bryan et al. (2021), *Int J Rob Res* 40(45); [5] Colley et al. (2024) *IEEE TMRB* 6(4); [6] Seo et al. (2017), *ICORR*.

# EFFECTS OF MUSIC ON POSTURAL CONTROL AMONG BREAST CANCER SURVIVORS WITH CHEMOTHERAPY-INDUCED NEUROPATHY (CIN)

*Lise Worthen-Chaudari[1], Bhillie Luciani[1], Maryam Lustberg[3]
[1]Department of Physical Medicine & Rehabilitation, The Ohio State University, Columbus, OH
[2] Yale Cancer Center, Yale University, New Haven, CT
*Corresponding author's email: liseworthen@gmail.com

**Introduction:** Up to 80% of breast cancer (BC) survivors who undergo chemotherapy develop chemotherapy-induced neuropathy (CIN) [1], which causes pain, numbness, tingling, and/or burning in the extremities [2]. In addition to dysfunctional sensation, CIN causes balance impairments [3] and increases fall risk [4]. These sensorimotor deficits represent an important clinical target for intervention among survivors with CIN. Treatment options are currently lacking, however. Treatment currently tends to focus on masking symptoms, using drugs such as gabapentin or duloxetine, rather than rehabilitating the underlying sensorimotor deficits [1]. Therefore, there is a critical need for novel interventions capable of rehabilitating the sensorimotor deficits associated with CIN.

One potentially novel avenue through which we might be able to rehabilitate these sensorimotor deficits involves active listening to rhythmic music. Current theories of music cognition predict that listening to music might improve both balance and pain for humans through mechanisms such as vestibular system [5–10], dopamine [11], and/or oxytocin [12] stimulation. Indeed, music that scored high in "groove", as measured by Janata's validated musical groove rating method, was found to regulate postural control responses in a healthy population [13]. Listening to music might prove to be a simple treatment for sensorimotor deficits associated with CIN [14].

As an initial step in studying the potential to rehabilitate on CIN-related deficits through rhythmic musical stimuli, we evaluated the within-session effect of music on postural control among BC survivors. We recreated the experiment performed by Ross et al. [13] among young healthy adults in a cohort of BC survivors. We hypothesized that listening to music would modulate postural control while survivors performed a task of quiet standing with eyes closed.

**Methods:** This research protocol was approved by The Ohio State University Institutional Review Board. Participants were recruited from The Ohio State University Medical Oncology Clinic. Criteria for inclusion were: breast cancer diagnosis, more than 3 months post-end of chemotherapy exposure, reported CIN symptoms of any severity, and balance deficits defined as outside of the 60$^{th}$ percentile confidence interval of the norm [15]. Postural control data was collected for 30s per condition on four different days per participant, following a repeated measures design [15].

We consented 52 eligible BCS with CIN. Three were lost to follow up after consenting, but before bas dropping out of the study before we completed baseline data collection. Among 49 BCS (48 female/1 male; age mean (SD) = 61.2(9.65); years since last chemotherapy exposure = 2.94(2.13)), we collected quiet standing with eyes closed (QEC) first and quiet standing with eyes closed and music play (QEC_m) second in all cases. Participants were instructed to close their eyes after the researcher counted down "3-2-1" for both conditions [16]. For QEC_m conditions, we used a classic Tango composition with a cadence of approximately 118 beats per minute entitled *La Cumparsita*. Per Ross et al. (2016), we instructed participants to listen to the beat of the music for approximately 15 seconds in order to acclimatize to the rhythm before commencing the countdown to close their eyes [13]. Per Will and Berg (2007), we used musical stimuli with a cadence of approximately 120 bpm, the periodic acoustic pace found to optimize central auditory motor entrainment [17].

Center of Pressure (COP) data were analyzed as previously reported [15-16]. Briefly, the following variables were calculated: COP area (COPa), COP mean velocity in the frontal plane (COPvelml), COP amplitude in the frontal plane (RMSml) [18] and sample entropy of COP (SEI) [19]. Repeated baseline data were pooled and COP variables collect in silence vs with music were analyzed using a paired t-test with Holms-Bonferroni post hoc correction (QEC v QEC_m).

**Results & Discussion:** Relative to standing quietly in silence (QEC), standing quietly while listening to Tango music of approximately 120 bpm (QEC_m) was associated with increased COP SEI ($p=0.012$) as well as reductions across the following variables of interest: COPvelml ($p=0.005$), COPa ($p=0.0083$), and RMSml ($p=0.009$). Thus, our earlier report, in a rehabilitation journal, indicating music improved postural control for a small cohort of 8 cancer survivors [14] is confirmed in this larger cohort of 49 BC survivors with CIN and quantifiable balance deficits.

**Significance:** The potential to modulate postural control simply by listening to music has exciting implications for treatment of motor control deficits. More research is needed to explore the potential to induce positive training effects through listening to music and/or physical training performed to rhythmic music.

**Acknowledgments:** This research was funded by R21-AG068831 and R01-AG084676.

**References:** [1] Herschman (2011), *Breast Cancer Res Treat* 125(3); [2] Jaggi & Singh (2012), *Toxicology* 291(1-3) ; [3] Monfort (2016), *Gait Posture* 48; [4] Bao (2016), *Br Canc Res Treat* 159; [5] Phillips-Silver & Trainor (2008), *Brain Cognition* 67(1); [6] Phillips-Silver & Trainor (2005), *Science* 308; [7] Todd & Cody (2000), *J Acoust Soc Am* 107(1); [8] Todd & Lee (2015), *Front Hum Neurosci* 9; [9] Todd (2014), *Hearing Res* 309; [10] Todd (2000), *Hearing Res* 141(1-2); [11] Salimpoor (2011), *Nat Neurosci* 14(2); [12] Grape (2002), *Integr Phys Beh Sci* 38; [13] Ross (2016), *J Exp Psychol Learn* 42(3); [14] Worthen-Chaudhari (2023), *Arch Phys Med Rehab* 140; [15] Worthen-Chaudhari (2018), *Gait Posture* 64; [16] Reed (2020), *Plos One* 15(8); [17] Will & Berg (2007), *Neurosci Lett* 424(1); [18] Prieto (1996), *Trans Biomed Eng* 43; [19] Roerdink (2011), *Hum Mov Sci*.

# EFFECTS OF PICKLEBALL ON UNILATERAL STATIC BALANCE AND DYNAMIC BALANCE FOR YOUNG ADULTS WITH INTELLECTUAL DISABILITIES

*Alana J. Turner[1], Emma Wilkinson[1], McKenzie Hardee[1], Riley Hieb[1], Taylor Redensky[1], Kiana Brown[1], Adam C. Knight[2], & Harish Chander[3]
[1]Coastal Carolina University, Conway, SC
[2]Mississippi State University, Mississippi State, MS
[3]University of Mississippi Medical Center, Jackson, MS
*Corresponding author's email: aturner4@coastal.edu

**Introduction:** Nearly 1.3 million adults in the United States (US) have an intellectual disability (ID) [1]. Falls are a prevalent and serious concern among individuals with ID [1]. Research indicates that people with ID are at a higher risk of falls compared to the general population [1]. This increased risk can be attributed to factors such as impaired motor skills, balance impairments, and the side effects of medications [2]. Understanding the prevalence and causes of falls in this population is crucial for developing effective prevention strategies and improving overall quality of life. Pickleball (PB) is a rapidly, growing low-impact paddle sport in the US, combining areas of tennis, badminton, and table tennis [3]. Previous literature reports PB promotes social interactions, enhances life satisfaction, and helps reduce depression for older adults [3]. PB also requires players to move about a court while incorporating a variety of swing variations. The quick pivots, lunges, and lateral movements are similar to those observed in a traditional balance training protocol. However, there is limited research on the effects of PB on balance for young adults with ID. Therefore, the purpose of this research was to investigate the effects of an adapted PB program on static and dynamic balance for young adults with ID. Due to the type of agility movement requirements for PB which are like a balance training protocol, we expected to observe improvements in balance after the PB intervention.

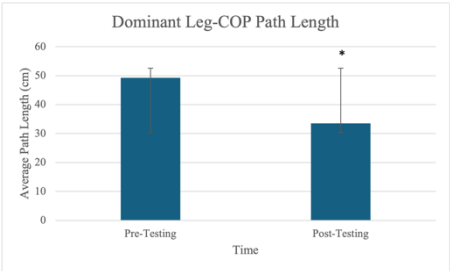


Figure 1: Dominant leg mean difference of COP PL from pre-testing to post-testing. "*" indicates significance. Standard deviation bars displayed.

**Methods:** 12 participants with a mild ID (76.48 ± 19.37 kg, 163.48 ± 9.37 cm, 20 ± 1.61 years of age, 4 females, 8 males) participated in a 14- week adapted PB program. Participants completed two 50-minute sessions twice a week. The study followed a repeated measures design (pre, mid, and post) one week before the intervention, 7 weeks during intervention, and one week after the intervention. Static balance included unilateral stance on the dominant leg (DL) (10s) and non-dominant leg (NDL)(10s) on a BTrackS (San Diego, CA) force platform. Static balance center of pressure (COP) sway measurements included: average displacement (AD) (cm), average 95% ellipsoid area (EA) ($cm^2$), average velocity (AV) (cm/s), and path length (PL) (cm). Dynamic balance included a Timed Up & Go (TUG) and measurements included movement time (s). A paired-samples t-test compared mean differences from pre-post intervention, pre-mid intervention, and mid-post intervention results ($\alpha \leq 0.05$) with IBM SPSS (Version 29.0.0) (Chicago, IL).

**Results & Discussion:** For DL, sway variables significantly decreased from pre-testing to post-testing for AD (0.42 cm, $t(11) = 2.387$, $p = 0.038$), EA (10.19 $cm^2$, $t(11) = 1.906$, $p = 0.047$), AV (1.55 cm/s, $t(11) = 4.457$, $p < 0.001$), and PL (15.73 cm, $t(11) = 4.621$, $p < 0.001$), indicating improvements in balance performance after the PB intervention. For NDL, sway variables significantly decreased from pre-testing to post-testing for AD (0.29 cm, $t(11) = 2.846$, $p = 0.017$), EA (7.85 $cm^2$, $t(11) = 3.280$, $p = 0.008$), AV (2.71 cm/s, $t(11) = 1.844$, $p = 0.047$), and PL (12.91 cm, $t(11) = 2.678$, $p = 0.023$), demonstrating improvements in sway variables after the PB intervention. For dynamic balance, TUG movement times also significantly decreased from pre-testing to post-testing (0.51 s, $t(11) = 2.100$, $p = 0.044$) and mid-testing to post-testing (0.66 s, $t(11) = 2.161$, $p = 0.038$), representing faster movement times and mobility after 7 and 14 weeks of intervention. These results align with the type of movements incorporated in the intervention and the nature of the sport of PB. For example, PB players are constantly shifting their center of gravity (COG) throughout their base of support (BOS) while executing quick, technical paddle skills with asymmetrical upper-limb swing variations. This constant movement of the COG with asymmetrical upper body movements while playing PB over the course of 14-week biweekly classes is challenging and trains the postural control system by integrating and organizing changing sensory information while utilizing a feedforward process for quick response times, especially for those with postural control deficits like ID. PB also requires individuals to move laterally as well as in the anterior and posterior directions while moving about the court, targeting more dynamic and unilateral lower limb movements. Therefore, this type of intervention is training anticipatory postural adjustments, which assists in the displacement of the individual's COP while moving throughout the court while the individual is contacting the wiffleball with rapid change of the three degrees of freedom of the dominant arm's glenohumeral joint. Overall, this agility-type movement across time could result in decreases in sway measurements for those with ID presenting improvements in balance performance (Fig. 1).

**Significance:** These results indicate a need to create and recommend non-traditional fall prevention programs to reduce the prevalence of falls for young adults with ID. By promoting adapted activities, this could motivate those with ID to not only improve balance and mobility but to become physically active. Moving forward, it could be possible to recommend an adapted PB program to improve balance if these individuals do not have access to traditional methods of balance training like physical therapy.

**References:** [1] Haynes & Lockhart (2012), *J Biomech* 45(14); [2] Hale et al. (2007), *JIDR* 51(4); [3] Casper & Jeon (2019), *J Aging Phys Act* 27(1)

# LEVODOPA-INDUCED DYSKINESIA IN PARKINSON'S DISEASE CAUSES INFLEXIBLE MULTISEGMENTAL COORDINATION DURING STANDING

Joseph A. Aderonmu*, Dobromir Dotov, Ph.D., Carolin Curtze, Ph.D.
Department of Biomechanics, University of Nebraska at Omaha, NE, USA
*Corresponding author's email: jaderonmu@unomaha.edu

**Introduction:** People with Parkinson's disease (PD) who exhibit levodopa-induced dyskinesias (LID) have greater postural sway after taking levodopa, the standard and most effective treatment for PD [1]. LID are involuntary hyperkinetic movements that emerge with long-term levodopa use [2] and have been associated with increased instability in superior body segments, that is, the head and trunk during standing [3]. The body achieves postural control by stabilizing its segments relative to gravity, visual and vestibular reference frames, and using sensorimotor strategies for the center of mass stability [4]. Since segmental instability occurs in people with PD who exhibit LID, more work is needed to understand the quality of coordination between body segments while standing.

Our goal is to address how LID in PD affects multisegmental coordination. We quantified coordination between the head and the pelvis during standing. We used Joint Recurrence Quantification Analysis (JRQA) which is suitable for understanding the coupling between interacting systems. Here, we report percent determinism, one of the JRQA outcome measures, as it is sensitive to the presence of coordination between the coupled systems [5]. Due to the instability of superior body segments in people with PD with LID, we hypothesized that people with PD who exhibit LID will have an increase in percent determinism between the head and pelvis in the ON medication state, which will not be observed in the OFF-medication state.

**Methods:** Twenty-five participants with PD (with LID: n=13, age: 69 ± 5.6; without LID: n=12, age: 69 ± 8.2) and 10 healthy controls (age: 72 ± 5.8) completed 30-second postural sway tasks during quiet standing (single task) and while performing serial subtractions by 3's (dual task). PD participants were assessed in the OFF-medication state (at least 12 hours since the last levodopa dose) and the ON state (about 1 hour post-levodopa intake). Healthy controls were assessed without medication. Accelerations from the head and pelvis in anteroposterior (AP) and mediolateral (ML) directions were recorded using Opal IMUs (APDM, Portland, OR) at 128 Hz and filtered with a fourth-order Butterworth filter (20 Hz cutoff frequency). We employed Joint Recurrence Quantification Analysis (JRQA) to investigate head-pelvis coordination. JRQA evaluates the shared recurrence of two or more dynamical systems by preserving each system's phase space, enabling the quantification of coordination when they reapproach their phase states simultaneously [5, 6]. We used percent determinism as a metric to quantify the coupling between the head and the pelvis. Differences between the percent determinism across medication states (OFF, ON), Task (Single, Dual), and Groups (PD with or without LID, healthy controls) were tested statistically with linear mixed-effects models.

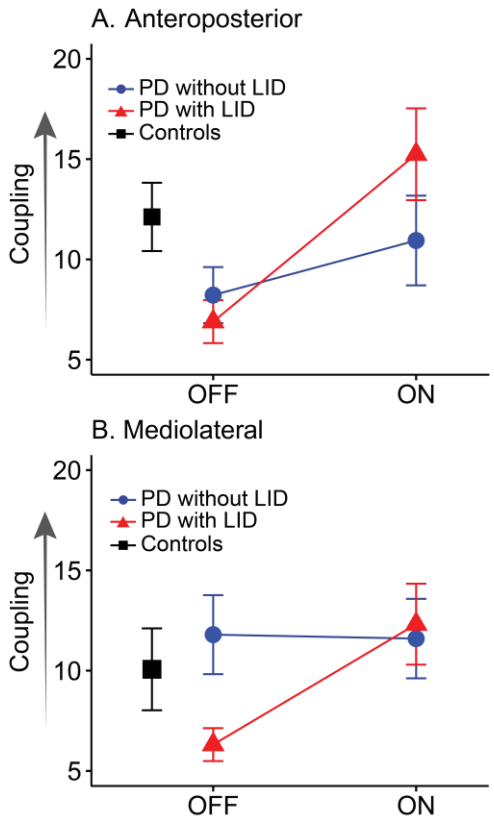


**Figure 1.** During standing, people with PD who exhibit LID showed higher head-pelvis coupling in the ON compared to the OFF state in both AP and ML directions. In the OFF state, they exhibit lower head-pelvis coupling than healthy controls in the AP direction. Coupling is defined in terms of the percent determinism between the head and pelvis obtained from JRQA. Plots display mean ± SE.

**Results & Discussion:** In support of our hypothesis, in the ON-medication state, people with PD who exhibit LID had significantly higher percent determinism in both anteroposterior and mediolateral directions compared to the OFF state (AP: $p < 0.001$, Cohen's $d = -1.07$, Figure 1; ML: $p < 0.001$, Cohen's $d = -1.22$, Figure 1). Also, compared to healthy controls, people with PD who exhibit LID had significantly lower percent determinism in the OFF state in the anteroposterior direction ($p = 0.043$, Cohen's $d = 0.80$).

A lower percent determinism in people with PD who exhibit LID in the OFF state compared to healthy controls represents lower multisegmental coupling during standing. However, when ON medication, the coupling between body segments became higher in people with PD who exhibit LID. These results suggest a potential feature of inflexible coordination that occurs in the ON medication state for people with PD who exhibit LID. This feature is not observed in people with PD without LID when ON medication and thus represents a distinctive medication response in people with PD who exhibit LID.

**Significance:** Until now, postural control has focused on global univariate stability measures. However, our findings suggest that assessing the quality of coordination between body segments may reveal pathological features of postural control and provide novel evidence of inflexible multisegmental coordination while standing in people with PD who exhibit LID.

**References:** [1] Curtze et al. (2015), *Mov. Disord. 30*(10); [2] Manson et al. (2012), *J Parkinsons Dis. 2*(3); [3] Aderonmu and Curtze (2024), *J. Biomech.* 112421; [4] Horak and MacPherson, (1996) *Oxford Univ. Press, pp.* 255-292; [5] Webber and Marwan (2015), *Theor. Best Pract.* 426; [6] Romano et al., (2004), *Phys. Lett.* 330(3-4)

# INFLUENCE OF BRA TYPE, BODY COMPOSITION, AND SEX HORMONE LEVELS ON CENTER OF PRESSURE MEASURES DURING GAIT IN FULL-BUSTED WOMEN

*Stacey L. Gorniak[1], Abigail Clement[2], Saba Yazdekhasti[1], Emily P. LaVoy[1]
[1]Department of Health and Human Performance, University of Houston, Houston, TX
[2]Department of Chemical and Petroleum Engineering, University of Kansas, Lawrence, KS
*Corresponding author's email: sgorniak@uh.edu

**Introduction:** The goal of the current project was to evaluate the change in center of pressure (COP) characteristics as a reflection of foot placement variability in women during dynamic physical activities such as walking, jogging, and while wearing three different bras: a conventional bra and two sports bras designed for full-busted women. COP characteristics have been found to be altered by the presence of back pain, which is common in our population of interest. We chose to assess COP characteristics to provide insight into foot placement variability changes across the time span of performance in each of the physical activities tested, as foot placement variability across tasks in which one or both feet leave the ground provide insight into how whole-body center of mass trajectories may be controlled. The pliable nature of breast tissue induces 3D breast motion during physical activity that may result in reactive COP shifts to control whole-body center of mass trajectory in response to 3D breast motion. These COP shifts may reflect changes in foot placement strategies during dynamic tasks that may co-occur with alterations in 3D joint moments—which in turn may increase biomechanical risk factors for orthopedic injuries. By providing adequate breast support by using bras specifically designed for full-busted women, it may be possible to reduce COP migration by reducing foot placement variability. It is also possible that the amount of COP migration (reflecting variability in foot placement during dynamic tasks) in women may be influenced by body fat and its distribution and sex hormone profiles. Accordingly, we explored the impact of anthropometry and serum-based sex-hormone profiles as covariates on COP measures in this study.

**Methods:** Twenty (20) healthy full-busted women who performed regular physical activity participated in this study. Participants were excluded if their self-declared breast size was smaller than D cup or larger than H cup. Each participant attended two in-person testing sessions on the same day: (1) body composition scanning and blood draw; and (2) postural and biomechanical evaluation of each bra condition. Biomechanical evaluation included 3 bra conditions (conventional bra, sports bra Model S, and sports bra model B). Biomechanical analysis of full-body kinetics during physical activities was measured via FIT5 dual belt incline treadmill with embedded force plates (Bertec Corp, Columbus, OH). This observational cross-sectional study was approved by the University of Houston Institutional Review Board (STUDY00003644).

**Results:** Bra condition differences emerged in some COP characteristics during treadmill testing (COP Area: $p < 0.001$; Major Axis Length: $p < 0.001$; Minor Axis Length: $p < 0.001$) such that the conventional bra condition was associated with larger COP characteristics across all treadmill speeds as compared to the Model S and B bras. No difference was found between the Model S and Model B bras. Treadmill speed influenced variability in some COP measures (COP Area: $p < 0.001$; Major Axis Length: $p < 0.001$; Minor Axis Length: $p < 0.001$). Consistent recurrence of covariates in COP data such as specific hormonal markers (e.g., luteinizing hormone (LH)) and body fat distribution (e.g., percent trunk fat) was found.

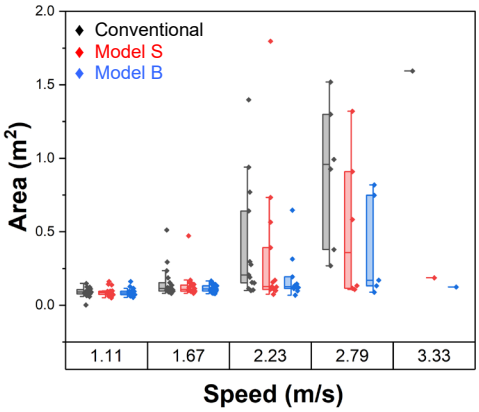


**Figure 1:** COP Area across treadmill speeds in all 3 bra conditions. Participants were permitted to stop at any speed of their choice. Most participants stopped the treadmill trials at 2.23m/s (jogging).

**Discussion:** COP area characteristics were dramatically larger as gait speed increased—particularly in the conventional bra condition—indicating higher variability in COP migration area and thus foot placement when breast support is insufficient. Changes in COP placement is likely reflective of changes in limb positions and foot landing strategies adopted by study participants during running while using a conventional bra. This may occur to counteract excessive 3D breast movement or to explore different limb configurations to reduce commonly reported discomfort in the chest, shoulders, neck, and breasts. Increased anthropometry metrics were found to be negatively associated with COP area, indicating that increased mass and its distribution results in smaller COP area. Evaluated sex-hormones were found to have an impact on statistical models, meaning that their inclusion in the models is important to uncovering other (e.g. main) effects within the dataset. Inclusion of each of these hormones helped clarify the strong effects of LH, such that higher levels of LH (e.g., during ovulation) is associated with reduced COP area.

**Significance:** These data suggesting that bra type may be influential for reduced COP migration and reduced COP variability, leading to more stereotyped behaviors with less limb position deviations and better anticipatory balance control during performance of gait-based activities. Additionally, we suggest that complete hormonal profiles be measured in study participants instead of relying on self-reported menstrual cycle duration to estimate hormonal phase.

**Acknowledgments:** This work was supported by the National Science Foundation (NSF) award #2150415 for summer funding for AC. This work was also supported by summer funding to SY and materials loan by Bounceless (PI: Gorniak).

# REACTIVE ADAPTATION TO REPEATED STANDING TRIPS IN YOUNG ADULTS

Sara Mahmoudzadeh Khalili[1*], Diane' Brown[1], Caroline Simpkins[1], Feng Yang[1]
Department of Kinesiology and Health, Georgia State University, Atlanta, GA, USA
*Corresponding author's email: smahmoudzadehkhalil1@student.gsu.edu

**Introduction:** Falls are a major public health concern, affecting both older and younger adults [1]. Trips account for 29% [2] to 53% [3] of all fall incidents. Training individuals to enhance their responses to postural perturbations, particularly trips, is crucial for reducing fall risk and associated injuries. One effective strategy to prevent perturbation-related falls involves "learning through falling," achieved by safely exposing individuals to repeated perturbations [4]. Perturbation-based training (PBT) focuses on improving balance recovery through intentional, recurrent, and unexpected postural disturbances in a controlled environment [5]. Most of the extant studies focused on trip-based PBT among older adults or during walking [5, 6]. However, how young adults adapt to repeated trips remains understudied. This study investigated whether young adults can quickly adapt to repeated standing-trip trials on a treadmill. We hypothesized that healthy young adults can rapidly adapt to repeated standing trips and demonstrate greater reactive stability against forward balance loss on the last trip than on the first.

**Methods:** Twenty healthy young adults (12 males, 8 females, mean ± standard deviation age: 26.35±5.94 years; mass: 74.24±17.21 kg; height: 1.72±0.09 m) participated in this study. After signing the written consent form, participants' anthropometric measures were recorded, and 26 reflective markers were attached to bony landmarks, with an additional marker placed on the treadmill belt to capture its movement. After a 3-minute overground warm-up walking, participants donned a full-body safety harness. They then moved to the ActiveStep treadmill (Simbex, NH), where the harness was linked to an overhead arc. Participants were informed that they would first stand on the treadmill without perturbation and later experience trip-like belt movement. Following the completion of six standing trials without trips on the treadmill, they experienced the first trip (T1) perturbation without any knowledge about the characteristics of the trip. The trip was generated by quickly moving the stationary belt to 1.2 m/s backward within 300 ms followed by the belt speed returning to 0 m/s in another 300 ms. The total belt displacement during the simulated trip was 0.36 m backward. Then, participants underwent four more identical trips (T2–T5). Full-body kinematics were recorded at 100 Hz using a 9-camera motion capture system (Vicon, UK). The recovery step was the first forward step taken to regain balance after perturbations. The recovery leg liftoff (LO) and the touchdown (TD) were identified using a belt marker and foot kinematics. T1 and T5 were analyzed to investigate participants' reactive adaptive responses. The primary outcome, dynamic gait stability, was defined by the kinematic relationship between the body's center of mass (COM) and the base of support (BOS) per the Feasible Stability Region (FSR) theory [7]. It was calculated at LO and TD. Secondary outcome measures included the step latency (the duration from the mechanical trip onset to LO), step duration (the time from LO to TD), step length (the anteroposterior distance between the heels at TD and normalized to body height (*bh*)), step speed (step length divided by step duration, *bh*/s), and trip distance at LO (the belt displacement from trip onset to LO and expressed in *bh*). The Wilcoxon Signed-Rank test or paired *t*-tests were used for statistical analyses in SPSS 29.0 (IBM, NY) with $\alpha = 0.05$.

**Results & Discussion:** At LO, the COM was more backward relative to the BOS on T5 than on T1, while COM velocity remained unchanged between the two trips (Table 1). This posterior shift of the COM relative to the BOS contributed to better stability on T5 compared to T1. At TD, the COM position showed no significant difference between T1 and T5; however, COM velocity was significantly slower on T5 than on T1. Stability at TD was comparable between T1 and T5. On T5, participants initiated their recovery step sooner and executed the recovery step more quickly compared to T1. Due to the earlier initiation of the recovery step, the trip distance at LO was significantly shorter on T5 compared to T1, lowering the intensity of the perturbation on T5. Our participants showed similar recovery step lengths on both trips. These results indicate that by the last trip, participants were able to execute a more effective recovery step compared to the first trip. These findings also suggest that repeated standing-trips on the treadmill promote reactive adaptive improvements in dynamic stability control and recovery step implementation in young adults. The limitations of our study included the absence of examining proactive adaptive responses, the lack of electromyography measurements, and the use of just standing-trials. Future work is needed to further explore how trip-based PBT can reduce falls in various populations.

**Table 1.** Comparisons of primary and secondary outcome measures in mean ± standard deviation between the first (T1) and last (T5) trips.

| Outcomes | T1 | T5 | *p*-value |
|---|---|---|---|
| COM position at LO | 1.06±0.13 | 0.91±0.09 | **<0.001** |
| COM velocity at LO | 0.27±0.03 | 0.27±0.02 | 0.69 |
| Stability at LO | 0.75±0.04 | 0.69±0.05 | **<0.001** |
| COM position at TD | 0.08±0.36 | -0.04±0.21 | 0.17 |
| COM velocity at TD | 0.04±0.02 | 0.02±0.01 | **<0.05** |
| Stability at TD | 0.06±0.17 | -0.01±0.10 | 0.10 |
| Step latency (s) | 0.27±0.04 | 0.24±0.02 | **<0.01** |
| Step duration (s) | 0.24±0.03 | 0.20±0.02 | **<0.001** |
| Step length (/*bh*) | 0.22±0.07 | 0.22±0.04 | 0.92 |
| Step speed (*bh*/s) | 0.93±0.31 | 1.13±0.23 | **<0.01**[#] |
| Trip distance (/*bh*) | 0.11±0.02 | 0.09±0.01 | **<0.01** |

[#] The Wilcoxon Signed-Rank test was used.

**Significance:** This study provides insights into the ability of young adults quickly adapting to standing-trips. The results also expand our understanding of how young adults adapt to standing-trips from a biomechanical perspective. Given that falls are a serious health concern and PBT is safe and convenient, our findings are clinically meaningful, which can assist us with developing trip-based PBT paradigms for people at a high fall risk.

**References**: [1] James, M.K., et al. (2018), *J. Safety Res.* **64**. [2] Stevens, J.A., et al. (2014), *Inj. Epidemiol.* **1**(1). [3] Blake, A., et al. (1988), *Age Ageing* **17**(6). [4] Pai, Y.-C., et al. (2007), *Phys. Ther.* **87**(11). [5] Grabiner, M.D., et al. (2014), *Exerc. Sport Sci. Rev.* **42**(4). [6] Aviles, J., et al. (2019), *J. Gerontol.* **74**(9). [7] Yang, F., et al. (2007), *J. Biomech.* **40**(4).

# ACUTE AND CHRONIC EFFECTS OF MILD TRAUMATIC BRAIN INJURY ON REACTIVE BALANCE

*Cecilia Monoli[1], Paula K. Johnson[2], Amanda J. Morris[3], Ryan M. Pelo[1], Leland E. Dibble[1], Peter C. Fino[1]
[1]University of Utah, Salt Lake City, UT
[2]Rocky Mountain University of Health Professions, Provo, UT
[3]California State University – Sacramento, Sacramento, CA
*Corresponding author's email: cecilia.monoli@utah.edu

**Introduction:** Postural instability frequently occurs after mild traumatic brain injury (mTBI) [1], with 20-60% of individuals reporting chronic symptoms months later [2], and functional limitations up to one year post-injury [3]. While acute and chronic deficits in static standing, gait, and turning are well-documented after mTBI [4], impairments on reactive balance - the ability to recover stability in response to unexpected disturbances - remain unclear. This cross-sectional study examines the acute and chronic effects of mTBI on reactive balance and their relationship with self-reported symptoms.

**Methods:** A total of 82 participants provided informed written consent to participate in this IRB-approved study. Participants included: acute mTBI (N = 19, 5F/14M; M (SD) age = 31.8 (8.9) years) defined as those reporting symptoms from an injury within 4 to 14 days; chronic mTBI (N = 22, 17F/5M; M (SD) age = 30.6 (9.0) years) defined as those reporting persisting symptoms from an mTBI that occurred between 3 weeks and 3 years prior; and age- and gender- matched healthy controls (N = 41, 23F/18M; M (SD) = 29.3 (8.0) years). Reactive balance was assessed using the Instrumented-modified Push and Release test [5], in which participants were leaned outside their base of support and unpredictably released, requiring steps to regain balance. The test was performed in four directions (forward, backward, right, left) under both single- and dual-task conditions [6]. Participants wore four IMUs (Opal; APDM Inc, Portland, OR) on right and left feet, lumbar spine (L3–L5), and sternum (approximately over the manubrium). Raw linear accelerations and angular velocities were processed through custom MATLAB (r2023b; MathWorks, Natick, MA) algorithms. Primary outcomes were the median *time to stability*, defined as the time (s) from release of support to complete stabilization, across all four directions and the maximum *step latency*, defined as the time (ms) from release of support to the first foot movement, across all four directions [5,7]. Participants with mTBI also completed the Dizziness Handicap Inventory (DHI) and the Neurobehavioral Symptom Inventory (NSI) to assess dizziness handicap and overall symptom severity, respectively. Group differences relative to healthy controls were analysed using linear mixed model, adjusted by age and sex. Pair-wise effect sizes were computed using Hedges' g. The relationship between reactive balance and symptoms was examined using partial correlation coefficients adjusted for age and sex.

**Results & Discussion:** Time to stability (Fig. 1A) progressively increased across groups, with small effects between acute mTBI and healthy control groups (single task $p = 0.152$, $g = 0.468$; dual task $p = 0.190$, $g = 0.351$), and significant differences between chronic mTBI and healthy control groups in both single ($p < 0.001$, $g = 0.978$) and dual task ($p < 0.001$, $g = 1.076$). Step latency (Fig. 1B) was significantly longer for the acute mTBI group compared to controls in both single ($p = 0.004$, $g = 0.954$) and dual task ($p = 0.015$, $g = 0.766$). Step latency did not differ between chronic mTBI and healthy control groups. No significant differences were observed in symptom severity between acute and chronic mTBI groups. There was a moderate positive correlation between time to stability and both DHI (single task $r = 0.549$ $p = 0.028$, dual task $r = 0.458$ $p = 0.075$) and NSI (single task $r = 0.550$ $p = 0.027$, dual task $r = 0.434$ $p = 0.093$) in the acute mTBI group. Step latency in single task condition also correlated with DHI ($r = 0.603$, $p = 0.011$) for the acute mTBI group. No associations were observed between balance metrics and self-reported questionnaires for chronic mTBI. These findings complement with prior work showing reactive balance deficits in acute, symptomatic athletes [6], suggesting a further association between reactive balance deficits and symptoms. Additionally, these results suggest that reactive balance deficits evolve as symptoms persist after mTBI, and people may adopt maladaptive compensatory strategies (e.g., faster latencies) that do not improve overall balance (e.g., time to stability) or associate with self-reported symptoms.

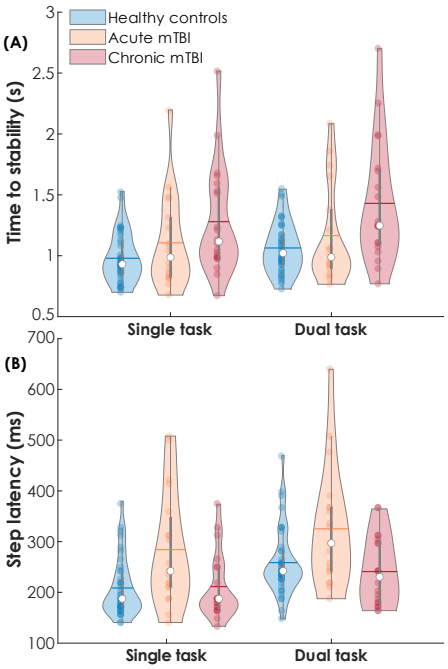


**Figure 1:** Violin plots of time to stability and step latency for single and dual task I-mP&R for the three groups.

**Significance:** The study highlights the potential maladaptive effect of persisting symptoms of mTBI on reactive balance. The moderate correlations between reactive balance deficits and self-reported symptoms in acute mTBI underscore the clinical relevance of assessing balance recovery alongside symptom management. These results highlight the complex nature of persisting symptoms after mTBI and encourage the assessment of reactive balance.

**Acknowledgements:** This project was supported by Pac-12 grants #5-04 Pac-12-Utah-Fino-19-01 and #9-01 Pac-12-Utah-Fino-23-0, and the NIH/NICHD R21HD10089. The authors wish to thank for their help in this project Nick Kreter, Cecilia Martindale, Sarah Hill, Shu Yang, and Ben Cassidy.

**References:** [1] Harmon et al. (2019), *Clin J Sport Med* 29(2); [2] Sweeny et al. (2020), *Brain Inj*. 34(10); [3] Nelson et al. (2019) *JAMA Neurol.* 76(9); [4] Fino et al. (2018), *Gait & Posture* (62); [5] Morris et al. (2022), *J Sport Rehabil*. 31(4); [6] Monoli et al. (2025) *Neurorehab and Neural Repair;* [7] Morris et al. (2020), *Front Sports Act Living* 2.

# RESTRICTED ANTIPHASE TRUNK MOTION INCREASES SWAY VELOCITY AND ANKLE TORQUE DURING QUIET STANCE

*Robert Creath[1], Veronica Venezia[1], Benjamin Hinkley[1], Niclas Sharp[1], Christopher Sciamanna[2]
[1]Lebanon Valley College, Department of Exercise Science
[2]Pennsylvania State University, College of Medicine
*Corresponding author: creath@lvc.edu

**Introduction:** Previous work established that antiphase A-P motion between trunk and leg segments was present during quiet stance with the qualification that the trunk and legs were in-phase (moving together) for postural sway frequencies below ~1 Hz and antiphase (moving in opposition) for higher frequencies [1].

Trunk-leg coordination during quiet stance was investigated by reducing antiphase trunk motion using a hip-knee orthotic (HKO) brace that locked hip and knee positions but allowed free motion at the ankle (Figure 1). The motivation came from a study by Kato et al [2] where they simulated trunk and knee stiffness in older and younger adults using wooden splints affixed to the body, leaving knee and ankle joints to move freely. The authors noted increased sway acceleration and velocity, and reduced antiphase trunk motion, although the increase was attributed to aging effects [2]. The prevailing theme is that antiphase trunk motion is always present and can be perturbed by altering sensory or support surface conditions. Kato's work suggested hip stiffness could alter antiphase trunk sway, although no systematic study had been performed.

The purpose of this study was to simulate hip and knee stiffness using the HKO brace while maintaining consistent sensory and support surface conditions to compare the presence or absence of antiphase trunk motion. Based on previous results [1,2] we predicted that increased trunk and leg sway velocity would result from reduced antiphase trunk motion when hip and knee joints are locked.

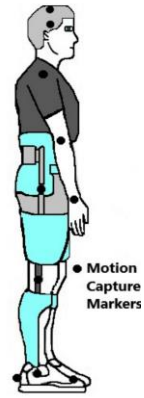


Figure 1: HKO brace and positions of motion capture markers.

**Methods:**

- 18 healthy participants (7 males, 20.5 ± 1.2 y) with no known musculoskeletal or neurological problems
- Three experimental conditions: 1) hip locked (HL, fixed hip with unrestricted ankle flexion [knee locked]), 2) hip unlocked (HU, unrestricted hip and ankle motion [knee locked]), and 3) no brace (NB).
- An HKO supported the participants' trunk, upper, and lower legs (Fig. 1). The brace consisted of a rigid plastic shell fitted to the torso between the sternum and hip with adjustable Velcro straps. The lower and upper legs were similarly restricted by adjustable thigh and shank braces. Hip and knee joint flexions were restricted by rigid locking mechanisms.
- Participants performed two 130-second trials for each condition with eyes open.
- Motion capture (Motion Analysis Corp; 240 Hz) defined head, trunk, legs, and foot segments (Fig. 1).
- Ground reaction forces were measured using an AMTI force plate (Watertown, MA; 240 Hz)
- Measures: Trunk and leg segment amplitude spectral density, coherence, cophase, and ankle torque (AT)
- Data analysis: The natural log of the ASDs was compared using a repeated-measures ANOVA with Tukey HSD. Frequency-by-frequency comparisons were made using the Method of False Discovery.

**Hypothesis Results & Discussion:** Amplitude spectral density calculations showed that trunk and leg sway velocities increased when antiphase trunk sway was restricted (HL condition) compared to the HU and NB conditions. Coherence and cophase estimates identified in-phase trunk-legs sway below 1 Hz and antiphase at higher frequencies for all three experimental conditions similar to previous results [1]. The results demonstrated that the restriction of antiphase trunk movement (HL condition) caused an increase in trunk and leg sway velocities. The implications for patient populations and older adults experiencing hip stiffness are an expected increased risk for loss of balance and disruptions of postural control, possibly leading to falls.

**Exploratory Results & Discussion:** An unexpected result was the change in AT between experimental conditions. Amplitude spectral density calculations showed that AT decreased when hip motion was unrestricted (HU and NB conditions) and increased when hip motion was restricted (HL condition). Legs-AT cophase calculations showed that the legs lagged the application of AT at all frequencies, while trunk-AT cophase estimates showed the trunk lagged AT below 1 Hz (in-phase trunk motion) and led AT at higher frequencies (antiphase trunk motion). While the legs-lagging-AT phase relationship is not surprising, the implications of the trunk-leading-AT for antiphase trunk motion was surprising. When combined with the observed changes in trunk and legs sway velocities for changes in the restriction of hip movement, it appears as though antiphase trunk motion plays a role in regulating sway velocity, and that reduced hip motion leads to increased AT requirements for balance corrections.

**Significance:** Experimental results showed that antiphase trunk sway reduced body sway velocity if trunk motion is unrestricted and increased body sway velocity when trunk motion is restricted. The absence or reduced amplitude of antiphase trunk sway may predict people at high risk for loss of balance and falls due to increased body sway velocity and AT requirements necessary to make postural corrections during quiet upright stance. Furthermore, it suggests that a combination of ankle strength exercises and hip flexibility may improve postural control by reducing body sway velocity thereby reducing the risk for loss of balance and falls.

**References:** [1] Creath et al. (2005), *Neurosci Lett.* 377(2); [2] Kato et al. (2014), *Gait Posture* 40(1).

# EFFECTS OF SOMATOSENSORY AUGMENTATION ON MEDIOLATERAL STANDING BALANCE

Olivia P. Laird[1], Amber V. White[1], *Jesse C. Dean[1,2]
[1]Division of Physical Therapy, Medical University of South Carolina; [2]Ralph H. Johnson VA Health Care System
*Corresponding author's email: deaje@musc.edu

**Introduction:** Investigation of the sensorimotor control of standing balance has primarily focused on anteroposterior sway, despite the prevalence of mediolateral balance deficits in many clinical populations (e.g., stroke) [1]. This gap may be partially addressed through sensory augmentation, in which artificial feedback provides the nervous system with information about the dynamic state of the body [2]. This approach has the potential to both reveal the contributions of sensory feedback to balance control and improve clinical balance performance [2]. In preliminary work, we found that augmenting somatosensory hip abductor feedback reduced mediolateral sway when balance was challenged. Specifically, hip vibration with an intensity proportional to mediolateral center of pressure (CoP) velocity reduced mediolateral CoP displacement. Here, we seek to extend these results to other sources of somatosensory feedback that can influence the control of mediolateral balance. We hypothesized that the delivered vibration would augment the natural somatosensory signal in real-time, allowing participants to respond to perturbations more rapidly and reduce the amplitude of their mediolateral sway.

**Methods:** 12 participants (7F/5M; age=23±1 years) stood with standardized foot position on a force plate undergoing unpredictable, continuous mediolateral translation. Translation trajectories followed a sum-of-sines (frequencies=0.1-0.9 Hz) pattern, increasing sway in the frequency range that dominates typical postural control. For each participant, translation amplitude was set to elicit a mediolateral CoP rms velocity of 20 mm/s, standardizing task difficulty. Participants donned vibrating tactors in locations that can influence mediolateral balance control: lateral trunk [3], hip abductors [4], medial/lateral ankle tendons [5], and foot sole [6]. These tactors were controlled based on real-time mediolateral CoP velocity to augment somatosensory feedback. For example, sway to the right was accompanied by vibration of the right hip abductor tactor, as this muscle would be lengthened during rightward sway. Vibration intensity scaled with CoP velocity magnitude. Participants faced a black screen, were instructed to cross their arms and stand still and relaxed, and completed randomized-order 1-minute experimental trials; five with no vibration, and five with vibration delivered to each of the four targeted locations. Our primary outcome measure was mediolateral CoP displacement standard deviation, with a corresponding secondary outcome of CoP velocity. To provide further insight into the potential cause of any changes in these traditional sway measures, we fit a simple 2-parameter model (delay and damping) able to predict CoP motion in response to mediolateral translations.

**Results & Discussion:** Across the four vibration locations, sensory augmentation did not significantly reduce CoP displacement ($p=0.39$; Fig. 1A), contradicting our hypothesis. However, the sensory augmentation did influence sway behavior, as we observed significant increases in CoP velocity ($p<0.001$; Fig. 1B), damping ($p<0.001$; Fig. 1C), and delay ($p<0.001$; Fig. 1D). While increased damping would intuitively be expected to reduce sway, simple model simulations found that the accompanying increase in delay would produce the type of results observed here. These experimental results are inconsistent with our preliminary work, in which sensory augmentation targeting the hip abductors caused decreases in CoP displacement. The most likely explanation for this inconsistency is that participants in the earlier work stood with their eyes closed, possibly decreasing their baseline balance performance and making them more likely to benefit from augmented somatosensation. Supporting this possibility, the baseline delay values from this prior (eyes closed) work were substantially longer than in the present (eyes open) work, and were reduced by somatosensory augmentation. In combination, these results suggest that a key element of effective sensory augmentation will be reducing rather than lengthening motor control delays. Achieving this goal may require predicting future mechanical state, rather than relying solely on real-time feedback [7].

**Significance:** Somatosensory augmentation can influence how individuals respond to balance challenges. Parallel experiments are investigating the effects of these methods on balance among individuals with chronic stroke, with promising results. In the longer term, this approach has the potential to produce clinically accessible tools in which balance training is supplemented with non-invasive vibration controlled by real-time estimates of the user's mechanical state, such as with portable inertial measurement units.

**Acknowledgments:** This work was partially supported by NSF award #OIA-2242812.

**References:** [1] Gray et al. (2017), *J Neurol Phys Ther* 41(4). [2] Sienko et al. (2018), *Front Neurol* 9. [3] Schonhaut et al. (2024) *J Biomech* 166(112043). [4] Popov et al. (1999) *Eur J Neurosci* 11(3307). [5] Kavounoudias et al. (1999) *J Physiol* 532(869). [6] Kavounoudias et al. (1998) *Neuroreport* 9(3247). [7] Beck et al. (2023) *Sci Robot* 8(75).

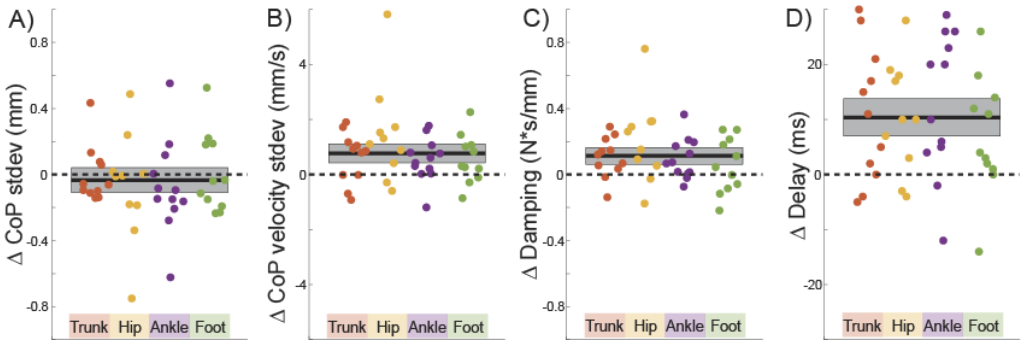


**Figure 1:** Change in outcome measures with respect to the experimental condition without vibration. Each dot represents an individual participant for each vibration location, solid black horizontal lines are the mean change across vibration locations, and shaded areas are the 95% confidence intervals. Dashed horizontal lines indicate no change from the no vibration condition.

# CLINICAL BALANCE AND MOBILITY OUTCOMES FOLLOWING TOTAL HIP ARTHROPLASTY

Katarzyna Puzio[1], Sheryl Bourgaize[1], Alyssa M. Tondat[1], Emiko Arshard[1], Marina Mourtzakis[1], Tina Mah[2], Matthew Snider[3], Paul Grosso[3], Brandon Girardi[3], Oliver Gauthier-Kwan[3], Stephanie Nemirov[3], Carla Girolametto[3], Kailyn Clarke[3], & Andrew C. Laing[1*]
[1]Department of Kinesiology and Health Sciences, University of Waterloo, Waterloo, ON, Canada. [2] Schlegel-UW Research Institute for Aging, Waterloo, ON, Canada. [3]Grand River Hospital, Kitchener, ON, Canada
*Corresponding author's email: actlaing@uwaterloo.ca

**Introduction:** Total hip arthroplasty (THA) is a common orthopedic procedure. Over 140,000 THAs were performed in the United States in 2023 [1] with projections of a further 176% increase by 2040 [2]. While patient-reported outcome measures are widely used to assess surgical outcomes, their inherent subjectivity and focus on pain and stiffness may limit their ability to capture aspects of optimal functional performance. The objectives of this study were to addresses these limitations through assessment of balance and functional mobility following THA, and to characterize the time-course of changes post-surgery. It was hypothesized that functional outcomes would improve progressively at 6-weeks and 6-months post-THA.

**Methods:** The study cohort comprised ten adults (six males, four females) who underwent elective THA with a mean (SD) age of 66.2 (8.7) years. Data collection occurred at three time points: pre-operative (within one-week pre-THA), six weeks post-THA, and six months post-THA. During each assessment session, participants performed the Berg Balance Scale (BBS) protocol which involved 14 functional balance sub-tasks in domains such as stance, reaching, turning, and posture transitions. Following validated approaches [3], patient performance of each task was rated by an investigator (author SB) with scores ranging from 0-4. In addition, sub-task scores were summed to create an overall BBS score ranging from 0-56. Finally, maximum forward reach distance (in cm) was explicitly measured. While a wireless inertial measurement unit system (APDM Opal Mobility Lab System) captured additional spatiotemporal parameters, the focus of this study was on conventional clinical balance and mobility metrics. One-way repeated measures ANOVA with post-hoc pairwise comparisons assessed the effect of time-point on each functional outcome.

**Results & Discussion:** While overall Berg Balance Scale scores improved progressively following THA (with means of 45.0, 47.4, and 50.4 at pre, 6-week post, and 6-month post THA time points, respectively), the differences did not reach statistical significance ($p = 0.233$). In contrast, there were significant effects of time point on specific balance sub-tasks (Figure 1). Specifically, significant improvements post-THA were observed for standing on one leg ($p = 0.006$), reaching forward ($p = 0.0014$), picking up an object ($p = 0.047$), and turning 360 degrees ($p = 0.003$). In addition, forward reach **distance** significantly improved following THA ($p < 0.001$), and was the variable associated with the largest effect size (generalized eta squared = 0.31).

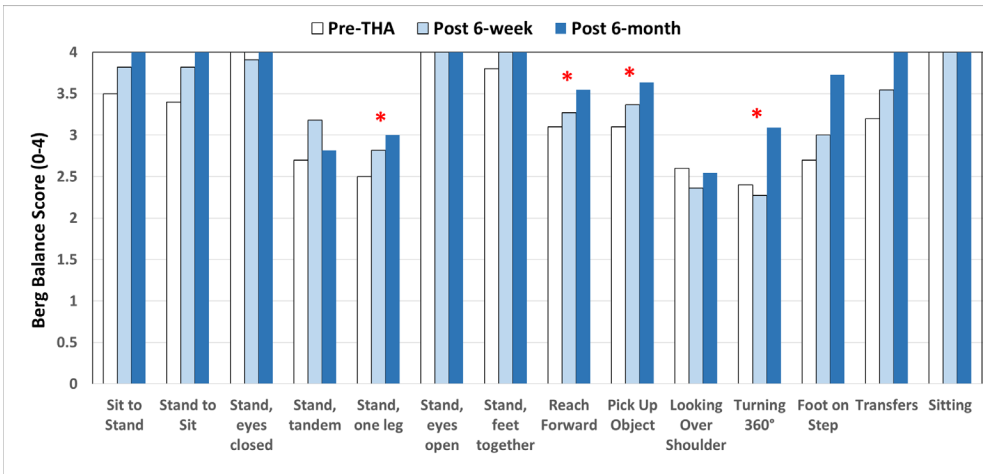


**Figure 1:** Berg Balance test values for each sub-task at baseline (before THA), 6 weeks post-THA and 6 months post-THA.* indicates significant differences across time points

These findings demonstrate progressive functional recovery following THA, with the most substantial improvements manifesting at 6 months post-surgery. The observed enhancement across a range of balance tasks suggests that THA not only addresses pain and joint mobility but also facilitates meaningful improvements in functional performance and dynamic balance.

**Significance:** The findings from this study provide novel evidence of functional recovery and balance improvements following THA. This research may help inform the development of more precise, evidence-based rehabilitation protocols and provide initial benchmarks for post-surgical THA progress. Several domains of impaired balance were observed – these could represent targets for both THA prehabilitation and rehabilitation programs. Finally, this research identified tasks from the Berg Balance Scale that may have ceiling affects for THA patients – this could help inform more efficient research protocols in the future.

**Acknowledgments:** Funded by the Ontario Ministry of Health & the Natural Sciences and Engineering Research Council of Canada.

**References:**[1] American Joint Replacement Registry (AJRR) Annual Report, 2024; [2] Shichman et al., *Journal of Bone and Joint Surgery Open Access*, 2023; 8(1): e22.00112.; [3] Berg et al. Physiotherapy Canada, 1989; 41(6):304-311.

# EFFECT OF BONE-ANCHORED LIMBS ON DYNAMIC BALANCE IN MULTIPLE ACTIVITIES OF DAILY LIVING

Grace Georgiou[1*], Nicholas Vandenberg[1], James Tracy[2], Cory Christiansen[2], Jason Stoneback[2], Brecca Gaffney[1,2]
[1]University of Colorado Denver, [2]University of Colorado Anschutz Medical Campus
*Corresponding author's email: grace.georgiou@ucdenver.edu

**Introduction:** Individuals with transfemoral amputation (TFA) using socket prostheses are at a higher risk of falls, which can lead to reduced mobility and quality of life [1]. This heightened risk is primarily attributed to decreased proprioception from the loss of joint musculature and altered load transmission [2]. Bone-anchored limbs (BAL) are an alternative to socket prostheses that directly attach the prosthesis to the residual limb. Evidence has shown that BAL use improves osseoperception, static balance, and spatiotemporal variability [3,4]. However, these previous investigations were performed during low demand activities, which are not representative activities where falls occur more often and were also longitudinal studies without comparison to successful socket users making them less generalizable. For fall risk, whole body angular momentum (WBAM) is a common measure used to quantify dynamic balance, as larger ranges in WBAM signify worsened dynamic balance and higher fall risk [5,6]. Although it is known that socket prosthesis users have larger ranges of WBAM compared to able-bodied individuals [7] the effect of BAL use on WBAM remains unknown. Thus, the objective of this study was to determine how BAL use effects WBAM during multiple activities of daily living as compared to successful transfemoral socket prosthesis users. We hypothesized that BAL users would have lower ranges of WBAM compared to socket users.

**Methods:** Whole-body motion capture data was collected from 11 participants with TFA, consisting of 7 socket prosthesis users (5M/2F: 58.2(12.4) y/o: BMI: 24.0(5.8) kg/m$^2$) and 4 BAL users (1M/3F: 55.8(12.4) y/o: BMI: 24.0(1.6) kg/m$^2$), during 6 different activities: level walking at self-selected speeds, walking as fast as possible, 90 degree turn around the amputated limb, 90 degree turn around the intact limb, a step-up task with the intact limb, and step down task with the amputated limb. Models were then made in Visual 3D for each participant, including prosthesis inertial property adjustments [8]. WBAM was calculated across all activities in all three planes and scaled by mass, height, and a scalar value to create a unitless metric ($\sqrt{gravity * height}$), as previously described [9]. WBAM for the turn tasks were transformed into a local coordinate system that aligned with the center of mass trajectory. Range of WBAM was then calculated in each plane and compared across groups using Cohen's *d* effect sizes (medium effect: 0.5≤d<0.8; large effect: d≥0.8).

**Results & Discussion:** BAL users had lower ranges of WBAM than socket users in all three planes (Figure 1). Most notably, BAL users demonstrated smaller frontal plane WBAM range in all activities compared to socket users. The regulation of WBAM in the frontal plane has previously been established to be critical for balance, with larger ranges being indicative of reduced dynamic stability and greater fall risk [5]. The lower ranges for BAL users indicate there is better regulation of WBAM possibly due to improvements in movement coordination and increased abductor muscle strength that occur after BAL implantation [10]. In the sagittal plane the BAL users had a lower range of WBAM in the self-selected gait and turn around the intact limb tasks. As the ankle plantarflexors are the primary muscles used in propulsion, it has been shown that people with amputation using socket prostheses have worse regulation and larger WBAM ranges compared to their able-bodied counterparts [7,11]. This reduced regulation has been attributed as a compensatory strategy to aid in propulsion by generating more anteriorly directed momentum, primarily in the trunk [12]. The results suggest that BAL users have a more efficient propulsion technique compared to their socket counterparts. Additionally, WBAM between-group differences were greater as the biomechanical demand of the task increased. Notably, BAL users had smaller ranges of WBAM in the frontal and transverse planes for both turning tasks, suggesting that even during activities where falls occur more, the BAL users are at a reduced risk compared to their socket counterparts due to greater WBAM regulation. These changes in dynamic balance likely come from increases in limb perception from osseoperception and improved force transmission that occurs after BAL implantation [3,10]. Collectively, the present findings indicate BAL users have better dynamic balance, and potentially lower fall risk, than their socket user counterparts.

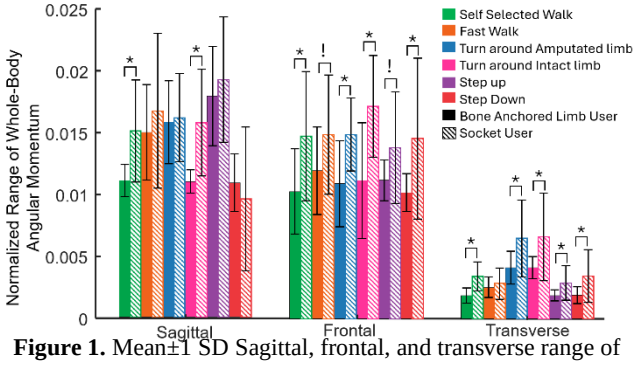


**Figure 1.** Mean±1 SD Sagittal, frontal, and transverse range of WBAM for BAL (solid) and socket prosthesis (hashed) users during each task. * represents Cohen's d≥0.8 and ! represents Cohen's 0.5≤d<0.8

**Significance:** Understanding how BAL use influence dynamic balance in activities of daily living as compared to successful socket users can help improve the understanding of how this novel prosthesis positively influences balance and possible long term fall risk. BAL users had better regulated WBAM, which likely indicates reduced fall risk.

**Acknowledgments:** University of Colorado Bone-Anchored Limb Research Group and the National Institutes of Health (K01AR080776).

**References:** [1] Kim et al. (2019). *PM&R*, *11*(4); [2] Hunter et al. (2017) *PM&R*, *9*(170); [3] Häggström et al. (2013). *JRRD*, *50*(10); [4] Gaffney et al. (2023). *Gait Posture*, *100*(132); [5] Nott et al. (2014). *Gait Posture*, *39*(1); [6] Vistamehr & Neptune. (2021). *J Biomech*, *128*; [7] Silverman & Neptune. (2011) *J Biomech*, *44(3)*; [8] Ferris et al. (2017). *J Biomech*, *54(*44); [9] Gomez et al. (2024). *J Biomech*, *168*; [10] Vandenberg et al. (2023) *J Biomech*, *155*; [11] Neptune et al (2001). *J Biomech*, *34*; [12] Gaffney et al. (2016). *Gait Posture*, *45(151)*

# NEUROMECHANICAL CHARACTERIZATION OF HUMAN TRUNK FUNCTION DURING REAL-WORLD UPPER LIMB TASKS

*Zhiqi Liu[1], Quinn Boser[2], Albert H. Vette[1,3,4]
[1]Dept. of Biomedical Engineering, University of Alberta, Canada; [2]Faculty of Medicine & Rehabilitation, University of Alberta, Canada; [3]Dept. of Mechanical Engineering, University of Alberta, Canada; [4]Glenrose Rehabilitation Hospital, Edmonton, Canada
*Corresponding author's email: zl3@ualberta.ca

**Introduction:** Upper limb function, such as reaching or manipulating and transporting objects, is essential in successfully performing activities of daily living (ADL). However, individuals with neuromuscular impairments (e.g., stroke survivors or individuals with spinal cord injury) often face challenges when performing such activities, significantly impacting their independence and quality of life. Notably, regaining arm and hand function has been ranked as the highest priority among individuals with spinal cord injury [1]. While reduced upper limb function is often attributed to arm and hand impairments, recent research suggests that also trunk stability plays a crucial role in this domain, given the trunk's importance in maintaining dynamic balance [2]. While past studies have primarily focused on the involvement of the trunk in gait and seated posture, our understanding of its role in upper limb function is still limited. Motivated by this limitation, the objective of this study was to comprehensively quantify the neuromechanics of the trunk in upper limb function, focusing on detailed trunk kinematics, the activity of major trunk muscles, and their relation in able-bodied individuals.

**Methods:** Twenty-five able-bodied individuals (12 female; 25 right-handed; age: 24 ± 4 years; body weight: 67.7 ± 9.6 kg; height: 171.4 ± 7.7 cm) participated in this study, which was approved by the university's research ethics board. The previously designed *Pasta Box Task* and *Cup Transfer Task* [3] were chosen as the experimental tasks as they adequately mimic upper limb ADL while providing consistent data for segmentation and analysis. The *Pasta Box Task* required the participant to complete three consecutive movements: (1) transporting a box of pasta from a side-table to a low shelf; (2) transporting the box of pasta from the low shelf to a high shelf; (3) transporting the box of pasta from the high shelf to the original side-table. The *Cup Transfer Task* was composed of four consecutive movements: (1) side-grasping a filled cup and transporting it across a vertical barrier; (2) top-grasping another filled cup and transporting it across the barrier; (3) top-grasping and returning the second cup; and (4) side-grasping and returning the first cup. The weight of the pasta box and cups was manipulated to examine the effect of a typical-weight and a heavy-weight condition on the trunk's neuromechanics. Trunk motion was quantified using a three-segment model (Fig. 1), and a 12-camera Vicon motion capture system recorded the three-dimensional (3D) kinematics of the trunk and upper limb. A wireless Delsys electromyography (EMG) system was used to measure the activity of ten trunk muscles and four shoulder and upper arm muscles.

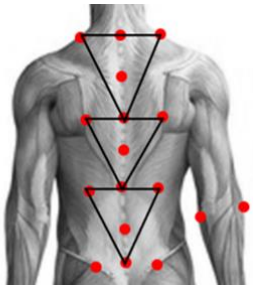

**Figure 1:** Three-segment trunk model used in 3D kinematics analysis (red dots representing marker locations; from top to bottom: upper trunk, mid-trunk and lower trunk segments).

**Results & Discussion:** The lower trunk and mid-trunk segments exhibited greater range of motion (ROM) in lateral bending and axial rotation in comparison to the upper trunk during the *Pasta Box Task*. While ROM varied significantly across participants, within-participant differences in ROM between the typical-weight and the heavy-weight conditions were not statistically significant ($p > 0.05$), except for ROM in flexion-extension. Trunk axial rotation angles correlated with hand position in the transverse plane.

The external obliques (EO) and erector spinae (ES) muscles exhibited distinct activation patterns during the *Pasta Box Task*, which were correlated with changes in axial rotation and flexion-extension angles. Normalized EMG peak values were significantly higher when transporting the heavy-weight pasta box for the left EO and all back muscles, i.e., the thoracic and lumbar ES (Fig. 2; one participant). The left and right rectus abdominis (LRA, RRA) were minimally and consistently active during the *Pasta Box Task*, suggesting their primary role in tonic trunk stabilization, e.g., via co-contraction.

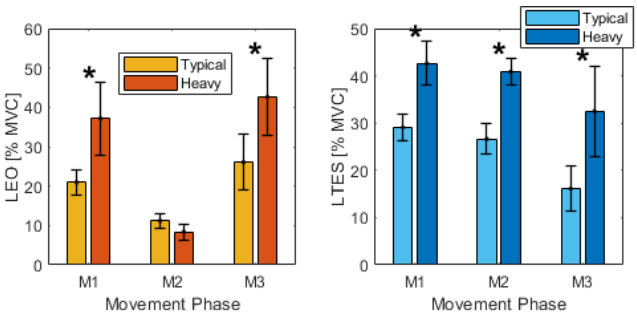


**Figure 2:** Maximum activity of the LEO and LTES muscles in dependence of movement phase (*Pasta Box Task*; 1 participant).

**Significance:** Our results utilizing the trunk's kinematics and the activity of its major muscles demonstrate the significant role of trunk neuromechanics in upper limb ADL. These findings will be highly valuable in the design of advanced assistive technologies, such as active trunk support via transcutaneous spinal stimulation used in closed-loop controlled neuroprostheses and upper body exoskeletons, e.g., for individuals with spinal cord injury and stroke survivors. A deeper understanding of trunk function could also drive the development of novel rehabilitation strategies.

**Acknowledgments:** This research was supported by the SMART Institute at the University of Alberta, and particularly the NSERC SMART CREATE Training Program. The author also acknowledges the *Neuromuscular Control & Biomechanics Lab* and *BLINC Lab* at the University of Alberta for their resources and support, and the undergraduate student interns for their assistance in conducting the experiments.

**References:** [1] Anderson, Kim D, *Journal of Neurotrauma* (2004). [2] Wee, Seng K et al., *Physical Therapy* (2015). [3] Valevicius, Aïda M et al., *PLoS One* (2018).

# EXPLORATION OF A CLINICAL APPLICATION OF LOW-COST INERTIAL MEASUREMENT UNITS AND A CUSTOM-BUILT ANDROID APPLICATION

Joey Wagner[1], Alex Roop[1], Kylie Evoy[2], Morgan Bleicher[2], Megan Gangl[2], Grant Kuhn[2], Daniel Panchik[2], Meghan Chemidlin[3], Alicia Reiser[3], *Kurt M. DeGoede[1]
Schools of [1]Engineering and Computer Science and [2]Sciences and Health, Elizabethtown College
[3]A Rise Above Occupational Therapy Service,
*Corresponding author's email: degoedek@etown.edu

**Introduction:** Head injuries, such as concussions, can have serious and lasting consequences including neurological problems (e.g., headaches, memory loss, and mood swings) and physical symptoms (e.g., dizziness and loss of balance) [1, 2]. With such a common and dangerous injury, treatment needs to be available and effective. Occupational therapists (OTs) play a crucial role in identifying the impacts of such injuries, and finding treatment for their patients, returning them to the life they had before the injury [3]. However, treatment options can be limited. With the wave of widespread, affordable technology, new applications can be designed to aid not just from within the clinical practice but right from the patient's home. We hypothesize that low-cost inertial measurement units (IMUs) integrated into in an Android programming environment can track patient movements, facilitate targeted exercises, and provide OTs with unique evaluation metrics.

**Methods:** The project originated from a collaborative vision between graduate student OTs at Elizabethtown College and local OT clinicians [4]. The proposed exercise involved the alignment of two IMUs: one attached to the patients' wrist and the other on their forehead. The wrist IMU would function as the target for the patient, allowing them to create targets for themselves at home or under the supervision of a professional in a clinic. Once the patient creates the target, they would try to align the sensor on their forehead with the one on their wrist. Alignment would be signalled by a chime from the phone indicating the completion of one repetition. The user can set the number of repetitions for the exercise beforehand. Each exercise would be accompanied by a CSV file displaying the time it took to complete each rep, their angular position over time, and the quaternion values produced by the IMUs. Production of this idea was constructed loosely on an existing project at Elizabethtown College called eTherapy. However, the original app's IMUs were no longer being open sourced bringing on the need for new sensors. WitMotion quickly became a top candidate due to their company size, quality, and affordability (<$50 each) [5]. With the new sensors, development of eTherapy II was completed by two undergraduate students, both new to the Android development cycle, over the course of 8 weeks.

**Results & Discussion:** The resulting study followed an emergent design and involved a small sample of three patients. While the initial exercise was successful, its real-world execution did not align with the anticipated user experience reported by the OTs. Testing revealed key usability challenges, particularly the frequent and time-consuming need for sensor calibration. This is a critical limitation for patients intending to partake in an hour-long session. In addition to this, the OTs reported that the application struggled to conduct accurate measurements when the target was placed below the horizon. OTs' subjective assessments indicated that the exercise might be too challenging for some patients. Caution is advised, as one patient exhibited involuntary movements (dystonia) during the exercises.

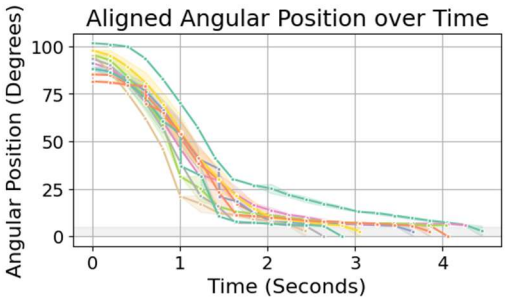


**Figure 1:** Patient data from a midline test. Each color corresponds with a different repetition. Suggests a 5-degree offset from midline.

The OTs continued their exploratory evaluation and pivoted the use of the sensors to something different. Using the exact same code as the original exercise, they repurposed the application to track a patient's degree off midline—previously assessed without direct measurement capabilities. This adaptation involved placing one sensor on a target while the patient was instructed to align their forehead with the target. By leveraging objective sensor data, the OTs were able to quantify deviations more accurately, enabling more precise pre- and post-assessment comparisons (Fig. 1). Unfortunately, user feedback revealed a potential bias in measurement validity, as some patients reported that they felt like they could cheat the measurement by relying on the auditory cues designed for the original exercise. Future improvements to this measurement include removal of auditory cues and the addition of directional data to aid the OTs in their measurements, as the current system does not keep track of the side of the midline the patient favors.

**Significance:** The results of this interdisciplinary research suggest that simple custom applications and low cost IMUs can be effectively utilized to assist recovery for specific patient groups.

**Acknowledgments:** Elizabethtown College Summer Creative Arts and Research Program

**References:** [1] Mayo Clinic (2025), Mayo Clinic: Concussion - Symptoms and Causes; [2] Finley et al. (2017), *J Neurophysiol* 118(2); [3] Vantieghem et al. (2020), *Med Sci Sports Exerc* 52(4); [4] D. Panchik et al. (2025), World Congress on Brain Injury, Montreal. [5] WitMotion (2021), *FCC Report* 2AZAR-BWT901CL.

# EXAMINING THE RELATIONSHIP BETWEEN BALANCE, FEAR OF FALLING, AND FALLS IN OLDER ADULTS

*Amanda Holtzman[1], Jordan Wilson[1], Kimberly Bigelow[1]
[1] Department of Mechanical & Aerospace Engineering, University of Dayton, Dayton, OH USA
*Corresponding author's email: holtzmana1@udayton.edu

**Introduction:** Falls are a serious problem in older adults where roughly 1 in every 3 individuals over the age of 65 fall each year [1]. A fall can be defined as "an unexpected event in which the participant comes to rest on the ground, floor, or lower level" [1].
Having their own personal past experiences or hearing of others' fall experiences can instill fear into the individual that the same will happen to them [2]. Individuals who have a fear of falling tend to limit their activity and mobility to try to avoid the risk of falling all together [2]. By doing so, they are decreasing their muscle mass as well as their ability to balance, leading to a more likelihood of falling [2]. An individual with lower-extremity weakness is four times more likely to fall, while an individual with balance impairments is three times more likely to fall [1]. The objective of this study was to examine differences between fallers and non-fallers for balance and fear of falling, as well as examine the relationship between fear of falling and balance results. We hypothesized that fallers would have significantly higher (worse) balance in all quiet-standing testing conditions, as well as higher scores (greater fear) on the Falls Efficacy Scale-International (FES-I).

**Methods:** 31 individuals over the age of 55 (mean age: 70.55 ± 8.54) gave written informed consent and participated in the study. They were asked to complete a demographics and falls history survey to determine if they were a faller or non-faller. Participants then completed the Falls Efficacy Scale-International (FES-I) assessment [3], reporting their concern about the possibility of falling while completing a variety of daily tasks. The result of the FES-I is a score out 64, with higher scores indicating greater fear (16-19 "low"; 20-27 "moderate", 28-64 "high" [4]).

Participants also completed a quiet standing balance test, standing on a force plate, where they removed their shoes and had their arms crossed for the entirety of the test. They completed two 30 seconds trials for each test condition (Eyes open on flat platform (EOFP), Eyes closed on flat platform (ECFP), Eyes open on foam surface (EOFOAM), and Eyes closed on foam surface (ECFOAM)).

Between the two trials for each condition, the RMS Sway Distances were averaged and then averaged again across all the participants. The total FES-I scores were also averaged across all the participants. This data was imported into SPSS where a Mixed Models Linear Analysis was performed. This was used to determine the level of significance between non-fallers and fallers for each condition as well as for FES-I.

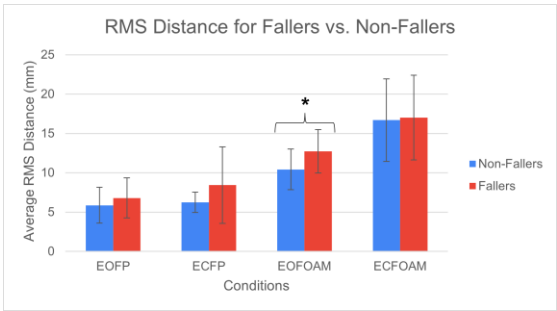


**Figure 1:** The RMS Sway Distance the individual traveled from their center of mass for fallers compared to non-fallers. Significance levels: (* = $p \leq 0.05$, ** = $p \leq 0.01$, *** = $p \leq 0.001$)

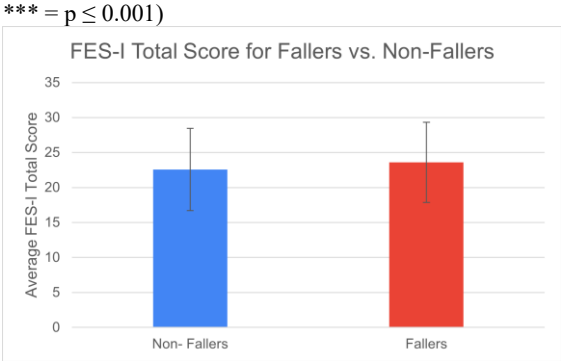


**Figure 2:** The Total FES-I Scores for fallers compared to non-fallers.

**Results & Discussion:** 15 participants self-reported as having fallen in the last 12 months ("fallers"). Fallers had higher RMS (worse balance) than non-fallers in all test conditions, with fallers having significantly higher ($p=0.028$) RMS in the EOFOAM condition (Fig. 1).

Average FES-I scores were not significantly different between fallers and non-fallers (Fig. 2), suggesting that assessing stability may be more insightful than assessing fear of falling.

Examining the relationship between RMS results and FES-I results, correlations were fairly low ($R^2$: 0.0027 – 0.2673), though relationship between RMS and FES-I were consistently stronger (higher $R^2$) in fallers compared to non-fallers.

Taken together, these results suggest that fear of falling does not strongly relate to fall status. This may be because some older adults who are especially fearful restrict their activities so they do not challenge their balance and therefore do not experience a fall, while others who may have lower fear of falling may be especially active and put themselves in situations that increase likelihood of falling. This points to the need to examine activity levels and circumstances of falls when seeking to understand the differences between fallers and non-fallers.

**Significance:** Clinicians around the world are trying to proactively identify older adults who may be at risk of falling so that intervention can be taken. These results indicate that fallers may be more instable, but that both fallers and non-fallers may similarly be affected by fear of falling. This suggests that clinicians may benefit from addressing fear of falling in all patients.

**References:**

[1] Bradley S. M. (2011), *The Mount Sinai journal of medicine* 78(4)
[2] Elwell, Valerie (2022), *UCI Health*
[3] Greenberg, S. A. (n.d.). Assessment of Fear of Falling in Older Adults: The Falls Efficacy Scale-International (FES-I)
[4] Delbaere, K., Close et al. (2010), *Age and ageing* 39(2)

# FACTORS ASSOCIATED WITH FALLS AFTER A STANDING-SLIP IN PEOPLE WITH MULTIPLE SCLEROSIS

Diane′ Brown[1], MS*, Jiyun Ahn[1], MS, Sara Mahmoudzadeh Khalili[1], MS, Feng Yang[1], PhD
Department of Kinesiology and Health, Georgia State University, Atlanta, GA USA
**Corresponding author email*: dbrown201@student.gsu.edu

**Introduction:** Multiple sclerosis (MS) affects 2.8 million people worldwide [1]. People with MS (PwMS) experience a heightened risk of falls [2]. Fall prevention interventions are crucial for this population. To develop effective fall prevention strategies, understanding the risk factors contributing to falls in PwMS is essential. Previous studies have identified multiple fall risk factors such as fall history, walking speed, disability level, cognition, and balance via self-reported real-life fall data. However, recount inaccuracy and uncontrolled fall causes could contaminate the self-reported data. Lab-based treadmill-induced slips or trips have been widely used as a standardized platform to induce falls and assess fall risk in various populations [3,4]. Nonetheless, no study has applied treadmill-based postural perturbations to PwMS to assess their fall risk. This study aimed to identify what physical and cognitive factors could differentiate fallers from non-fallers after a novel simulated standing-slip in PwMS. Considering their potential link with disease progression, age, disability level, gait speed, leg muscle strength, fall history, and cognition level were examined. We hypothesized that the factors of our interest would be significantly worse among fallers than non-fallers following an unexpected standing-slip.

**Methods:** This cross-sectional study enrolled 26 PwMS (23/3 females/males, mean ± standard deviation age: 48.92 ± 14.25 years). All participants were able to walk independently for at least 25 feet, had no musculoskeletal or cardiorespiratory illnesses, had no prior perturbation training experience, and showed a Patient Determined Disability Steps (PDDS) score between 0 and 4. Exclusion criteria included severe cognitive impairment (Blessed Orientation Memory Concentration or BOMC score ≥ 10) and low bone density (*T*-score < -2.5). After written consent was obtained, demographic information was collected. Next, participants completed a fall history questionnaire [5]. Following a 5-min walking warmup, participants walked on a 10-m linear walkway at normal and fast speeds. The time to cover the middle 25-foot portion of the walkway was recorded. They then wore a safety harness, which was connected to a loadcell and then an overhead arc on an ActiveStep treadmill (Simbex, NH). Participants were instructed to stand on the treadmill initially and they would experience a "slip-like" movement later. They were also told to recover their balance in case of a slip. After 5-6 slip-free standing trials, an unexpected standing-slip occurred. The slip was created by accelerating the treadmill belt to 1.2 m/s in 0.3 s and then decelerating it to zero within another 0.3 s, simulating a 0.36-m slip. Next, participants completed isometric strength tests for bilateral knee extensors and flexors on an isokinetic dynamometer (Biodex System 4, NY). Strength data were normalized by body mass. Gait speed was calculated by dividing the 25-foot distance by the time used to complete it. A participant was categorized as a faller if the peak loadcell force after the slip onset was greater than 30% of the body weight [6]. Otherwise, they were deemed as non-faller. Independent *t*-tests compared continuous outcome measures (age, mass, height, PDDS, BOMC, fast and normal gait speeds, knee extensor, and flexor strength) between fallers and non-fallers. Fisher's exact test was used to analyze categorical outcomes (retrospective faller status and sex). The significance level was set at $p \leq 0.05$. All analyses were performed using SPSS 29.0.

| Variable | Faller (17) | Non-faller (9) | *p*-value |
|---|---|---|---|
| Fallers in the past year * | 10 | 5 | 0.598 |
| Age (*year*) | 51.12 (12.77) | 44.78 (16.69) | 0.145 |
| Sex (F/M) * | 15/2 | 8/1 | 0.732 |
| Mass (*kg*) | 79.25 (11.16) | 76.17 (16.83) | 0.290 |
| Height (*cm*) | 165.91 (10.85) | 165.68 (6.05) | 0.477 |
| PDDS (/8) | 2.29 (1.86) | 1.00 (1.00) | **0.033** |
| BOMC (/30) | 0.47 (1.50) | 0.67 (0.87) | 0.361 |
| Fast gait speed (*m/s*) | 1.23 (0.49) | 1.62 (0.24) | **0.017** |
| Normal gait speed (*m/s*) | 0.93 (0.25) | 1.12 (0.16) | **0.027** |
| Knee strength (*Nm/kg*) | | | |
| - Dominant extensor | 1.25 (0.29) | 1.44 (0.22) | **0.048** |
| - Dominant flexor | 0.83 (0.22) | 1.14 (0.29) | **0.002** |
| - Non-dominant extensor | 1.09 (0.38) | 1.53 (0.27) | **0.003** |
| - Non-dominant flexor | 0.70 (0.37) | 1.05 (0.27) | **0.009** |

Table 1: Comparison of demographics, physical function, cognition, and disease information (mean ± SD) between fallers and non-fallers after a standing-slip among 26 PwMS. *: Fisher's exact test was used.

**Results & Discussion:** After the slip, 17 participants fell and nine did not. Among the fall risk factors assessed, PDDS, gait speed, and bilateral knee strength were significantly better in non-fallers than in fallers (Table 1) while other factors were comparable between groups. The results partially support our hypothesis. Our results indicated that the disability level, gait speeds, and knee joint strengths could be related to falls in PwMS after an unexpected slip. This finding aligns with conclusions from the literature that disease progress, mobility declines, and muscle weakness increase fall risk in PwMS [7,8]. This study included a small, sex-unequal, and relapsing-remitting MS-dominant sample size with just the standing-slip as the postural perturbation, which may weaken the generalizability of our findings. More studies with diverse samples and varied perturbations and tasks are warranted.

**Significance:** Our findings showed that disability level, gait speed, and leg strength are linked to falls after a well-controlled slip perturbation. This observation is consistent with the literature. Our study could provide clinically meaningful information for us to accurately assess the fall risk and develop effective fall prevention interventions for PwMS.

**Acknowledgments:** This study was partially supported by the National MS Society via a Pilot Research Grant (1904-PP33855).

**References:** [1] Walton, C et al. (2020), *Mult Scler J 26(14)*; [2] Planche, V et al. (2016), *Eur J Neurol 23(2)*; [3] Li, J et al. (2021*), J Neurophysiol 127 (1)*; [4] Joshi, M et al. (2018), *Int Biomech 5(1)*; [5] Talbot, L et al. (2005*), BMC Public Health 5*; [6] Yang, F et al. (2011), *J Biomech 44(12);* [7] Yang, F et al. (2019), *Mult Scler Relat Disord 27*; [8] Chung, L et al. (2008), *Med Sci Sports Exerc 40(10).*

# QUANTIFYING THE CONNECTION BETWEEN ANKLE PROPRIOCEPTION AND POSTURAL RESPONSE TO MULTI-DIMENSIONAL PSEUDORANDOM PERTURBATIONS

Sophia G. Chirumbole[1], Manami Fujii[1], Daniel M. Merfeld[1], *Ajit MW Chaudhari[1]
[1]The Ohio State University Wexner Medical Center

*Corresponding author's email: chirumbole.5@osu.edu

**Introduction:** Falls are the second leading cause of unintentional injury and deaths worldwide. Each year, a staggering 37.3 million falls are severe enough to require medical attention. Further, falls can cause significant morbidity and mortality and significantly impact quality of life, so balance improvement and fall prevention is critically important [1]. Understanding reactive balance response is key to providing more informed rehabilitation and exercise prescription for those at an increased risk of falling. Balance ability is closely intertwined with proprioception, which we define here as the sensation of joint angle. Proprioception involves the awareness of joint position and movement as well as the integration with other somatosensory, visual, and vestibular information to contribute to the brain's comprehensive picture of body position in space, allowing for smooth and stable postural control and reaction to possible unexpected perturbations [2]. Further, poor proprioceptive information, or decreased accuracy of awareness of joint position and movement, can significantly impact postural control and heighten risk of falling. Understanding the relationship between proprioception and reactive balance performance may provide an opportunity to improve balance, and henceforth, reduce fall risk via specific therapies tailored to improve proprioceptive abilities. Proprioception sensitivity can be measured by active joint position sense (aJPS) testing, which requires participants to remember a joint position angle and then attempt on their own to reproduce the joint angle [3,4]. Recently, we successfully characterized postural responses to 1, 2, and 3 degree of freedom (DoF) pseudorandom perturbations designed to challenge postural control [5,6]. Therefore, the current study tested the hypothesis that reactive balance performance would be associated with ankle joint proprioception.

**Methods:** Ten healthy adults participated after providing IRB-approved informed consent (37 ± 15 years old, 8M 2F). Ankle joint proprioception was quantified using a previously-validated digital inclinometer application [3]. Ten plantar-dorsiflexion aJPS error trials were collected on each participant's dominant ankle. The absolute value of each raw aJPS error value was determined. The trimmed average of the middle eight values was calculated for each participant for subsequent analysis. Reactive balance performance was measured using two embedded force plates within a commercially available perturbation platform (Virtualis VR, Montpellier, France). The platform delivered pseudorandom 3 DoF (tilts in canal coordinates (RALP & LARP) and earth-vertical translation) perturbations over 3 minutes. Participants were instructed to stand as still as possible, with their eyes closed. Anecdotally, participants described these perturbations as similar to standing on a platform floating on moving water. The raw center of pressure (CoP) data in the anteroposterior (AP) direction was 4th order Butterworth low-pass filtered at 20 Hz and used to calculate mean AP CoP velocity. Linear regression was used to examine the association between aJPS error and mean AP CoP velocity.

**Results & Discussion:** We found a negative linear relationship between ankle aJPS error and AP mean velocity during the three-dimensional pseudorandom balance perturbation trial (adjusted $R^2$=0.472, p=0.0169, Fig. 1). This negative linear relationship suggests that individuals with less proprioceptive acuity react with lower velocity to pseudorandom perturbations. This result agrees with a previous study that suggested that proprioceptive inputs trigger the rapid, automatic, and coordinated postural responses to unexpected movement of a support surface, so, with poorer proprioception, the body may not have as much ability to react and ensure coordinated control of the body center of mass and balance to rapid pseudorandom perturbations [7,8].

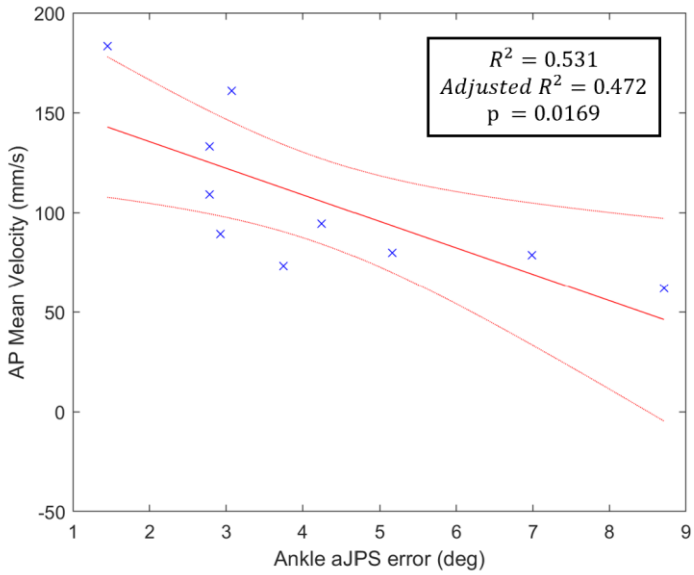


**Figure 1:** Ankle proprioception sensitivity (aJPS error) was significantly associated with reactive balance performance (mean velocity in the AP direction).

**Significance:** Joint proprioception contributes to reactive balance performance when examined in isolation. More comprehensive evaluation is needed to understand the relative contributions of all sensory systems to imbalance and falls.

**Acknowledgments:** This work was supported by the National Institutes of Health [5R01AG073113-02].

**References:** [1] World Health Organization (2021), *WHO Documentation Services*; [2] Han et al. (2016), *J Sport Health Sci.* 5:80–90; [3] Chirumbole et al. (2024), *PLOS One* 19(9):e0308737; [4] Chaudhari (2024), *https://code.osu.edu/chaudhari.2/levelbelt*; [5] Wagner et al. (2024), *Front. Hum. Neurosci.* 18:1471132*;* [6] Fujii et al. (2024), *3DAHM Conference Abstract;* [7] Henry et al. (2019), *J Neurophysiol* 122(2):525–538; [8] Stapley et al. (2002), *J Neurosci* 22:5803–5807.

# TESTING THE FEASIBILITY OF DEPLOYING STANDING AND WALKING BALANCE PERTURBATIONS IN PATIENTS WITH DEMENTIA WITH LEWY BODIES

*Emily Eichenlaub[1], Andrea Bozoki[2], and Jason R. Franz[1]
[1]Lampe Joint Dept. of BME, UNC Chapel Hill and NCSU, USA, [2]Dept. of Neurology, UNC Chapel Hill, USA
*Corresponding author's email: emeich@email.unc.edu

**Introduction:** Falls among older adults pose a significant public health concern, with an estimated 3 million emergency room visits due to fall-related injuries each year [1]. As our aging population continues to grow, the prevalence of Dementia is expected rise. Specifically, Dementia with Lewy Bodies (DLB) affects memory, executive function, and motor planning. Thus, individuals diagnosed with DLB are nearly two-times more likely to fall than age-matched controls, with an annual fall incidence more than three-times that of individuals with Alzheimer's disease [2-3]. Due to this increased risk of falls, many studies have examined the efficacy of interventional cognitive and physical exercise programs to improve balance in populations with Dementia [4-5] or sought to differentiate Dementia subtypes by examining specific characteristics in static postural control [6]. However, to the best of our knowledge, no studies have deployed ecologically relevant lab-based perturbation paradigms to understand the underlying neuromechanical changes in balance control caused by DLB. Thus, our study sought to determine the feasibility of deploying standing and walking balance perturbations in older adults with DLB. Here, we determine the feasibility of deploying a perturbation protocol in patients with DLB using: (1) an objective measure of protocol completion rate and (2) a subjective measure of survey responses to determine whether they would complete this study again.

**Methods:** Thus far, 5 older adults diagnosed with mild-moderate DLB have participated in this study (age: 74.0±5.7 yrs, preferred walking speed: 0.84±0.44 m/s, Montreal Cognitive Assessment score: 21.6±2.8). Participants first completed the Montreal Cognitive Assessment (MoCA) to assess executive function, visuospatial abilities, and memory. Participants then responded to rapid treadmill-belt accelerations and decelerations over 200 ms at 6 m/s$^2$ during both standing and walking. Walking perturbations were delivered at the instant of heel strike. We delivered perturbations either unexpectedly (i.e., unanticipated) or at the end of a 3-s verbal countdown (i.e., anticipated). The full protocol consisted of 12 standing perturbations (3 repetitions of direction × anticipation combinations) and 16 walking perturbations (2 repetitions of direction × anticipation × side combinations). Standing and walking protocol completion rates were calculated on a weighted scale for each perturbation (no use of safety bars = 1, use of safety bars following a perturbation = 0.5, use of safety bars prior to perturbation = 0.25). After completing the protocol to the best of each participant's ability, a 5-point Likert score exit survey was administered. Success metrics: (i) ≥80% of DLB participants will report ≥4/5 on "…would complete a study like this again" and, (ii) ≥80% of DLB participants will successfully complete the perturbation protocol.

**Results & Discussion:** Results thus far show a 98±4% completion rate for standing perturbations and 74±36% completion rate for walking perturbations, suggesting moderate feasibility of deploying perturbations in this population. Despite reducing the treadmill speed by almost 50% from their preferred walking speed, two participants were not able to complete the walking perturbations due to unfamiliarity with treadmill walking and physical limitations unrelated to their DLB diagnosis (i.e., back pain, cardiac fitness) (**Fig. 1A**). Therefore, we note that comorbidities, rather than DLB per se, were significant contributors to <80% completion rates for walking perturbations. Perhaps as a consequence, data thus far suggest that completion rates were relatively unrelated to MoCA scores (**Fig. 1B**). Based on Likert scale exit survey scores, all participants responded that they would be somewhat (4/5) to very likely (5/5) to complete a study like this again (4.6±0.5). We conclude that patients diagnosed with DLB are able to successfully complete standing perturbations, which shows promise as a tool to elucidate the effects of this dementia subtype on postural balance control to aid in earlier diagnostics and perturbation training interventions. However, overground walking perturbations may be a better alternative to treadmill-belt perturbations in patient populations with significant comorbidities. Lastly, the enthusiastic response of all participants to participate in similar studies in the future, regardless of protocol completion, shows promise for successful recruitment and further exploration on the effects of dementia on stability and balance in the future.

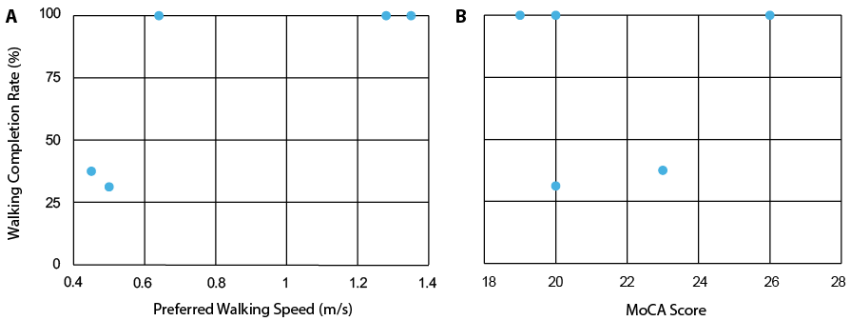


**Figure 1.** The relationship between participants' (A) preferred walking speed and (B) MoCA scores to walking balance perturbation completion rate.

**Significance:** Based on these preliminary results, the use of ecologically relevant balance perturbations in those with dementia shows promise for 1) earlier diagnosis and monitoring of disease progression and 2) evaluating the efficacy of physical, cognitive, and/or pharmacological intervention.

**Acknowledgments:** Supported by the National Institutes of Health (F31AG084241).

**References:** [1] Moreland et al. (2023), *J Aging and Health*; [2] Lach et al. (2017), *Res Gerontol Nurs* 10(3); [3] Tsujimoto et al. (2022), *Internal Medicine* 61(11). [4] Toots et al. (2016), *J Am Geriatr Soc* 64(1); [5] Lamb et al. (2018), *Health Technol Access* 22(28); [6] Fujita et al. (2024), *J Gerontology* 79(4).

# GAIT PERFORAMNCE AT THE CONCLUSION OF A COLLEGIATE ATHLETIC CAREER: ROLE OF REPETITIVE HEAD IMPACTS

*Thomas A. Buckley[1], Barry A. Munkasy[2], Caitlin Gallo[1], Scott Passalugo[1]
[1]Department of Kinesiology and Applied Physiology, University of Delaware, Newark, DE.
[2] Department of Health and Kinesiology, Georgia Southern University, Statesboro, GA.
*Corresponding author's email: TBuckley@udel.edu

**Introduction:** Repetitive head impacts (RHI) are head impacts which commonly occur in collision sports such as football or ice hockey, but do not result in concussions or acute symptoms. The current evidence suggests that accumulated RHI over the course of a collision sport career results in neurological damage in a dose-response manner. However, the current focus of the literature has been on cognitive performance and behavioral assessment and older adults with RHI exposure tend to deficits. Current postural control assessments have generally been limited to simplistic clinical measures (e.g., Romberg stance, Balance Error Scoring System (BESS)) which likely lack sensitivity to identify subtle differences. For example, multiple seasons of collegiate soccer did not adversely affect BESS performance in male or female soccer players. (1) Single task gait performance is well recognized as critical activity of daily living and has been termed a 6$^{th}$ vital sign given strong correlations and associations between gait velocity and many life outcomes. Therefore, the purpose of this study was to assess gait velocity and step length at the conclusion of the athletic careers of RHI exposed and non-RHI exposed student-athletes as this is likely the last exposure to routine RHI. We hypothesized that that the RHI exposed group would have worse gait performance secondary to potential neurological impairments from RHI exposure.

**Methods:** We enrolled 62 National Collegiate Athletic Association student-athletes at the conclusion of their athletic career who participated in either RHI related sports (N=34; Football, Men's Lacrosse, Soccer, Ice Hockey) or non-RHI sports (N=28; Softball, Volleyball, Basketball, Baseball, Track & Field, Field Hockey, and Rifle). All participants were assessed in the same semester their last season (e.g., Fall for Football; Spring for Lacrosse) after the season was over. All participants performed five trials of single task (motor only) gait and were instrumented with five inertial measurement units (APDM Inc, Portland, OR) which are valid and reliable for stepping characteristics. (2) The IMUs were placed bilaterally on the feet and arms as well one on L5 and participants walked down a 10 m walkway. Step Length and Step Velocity were normalized to height and compared between groups with independent samples t-tests and Cohen's d effect sizes, but outcomes are presented raw (not normalized) for ease of interpretation.

**Results & Discussion:** There were no significant differences between groups for Step Velocity (Non-RHI: 1.13 + 0.21 m/s and RHI: 1.15 + 0.16 m/s, t=0.29, p=0.077, *d*=0.11). (Figure 1) There was no difference between groups for Step Length (Non-RHI: 62.5 + 9.4 cm and RHI: 61.2 + 8.3 cm, t=0.54, p=0.59, *d*=0.15).

The lack of differences between groups suggests that at the conclusion of their collegiate careers, RHI did not adversely affect single task gait performance. This finding is consistent with emerging data showing that RHI do not adversely affect gait performance which has been observed in incoming college student-athletes, (3) changes over the course of a collegiate athletic career, (4) or in middle aged RHI exposed rugby players (5). While neurocognitive deficits have been reported in former RHI exposed athletes, the emerging evidence suggests that gait performance remains unaffected in young and into middle aged adults. Moving forward, gait performance, including multiple modalities of dual task (cognitive-motor) challenges across the lifespan with a particular focus on older adults. Important considerations, including lifestyle factors especially physical activity levels, should be considered in these future studies.

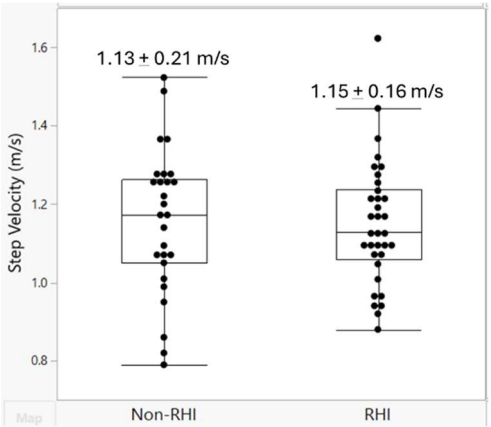


*Figure 1. There was no significant difference between groups for single task gait velocity (t=0.29, p=0.77)*

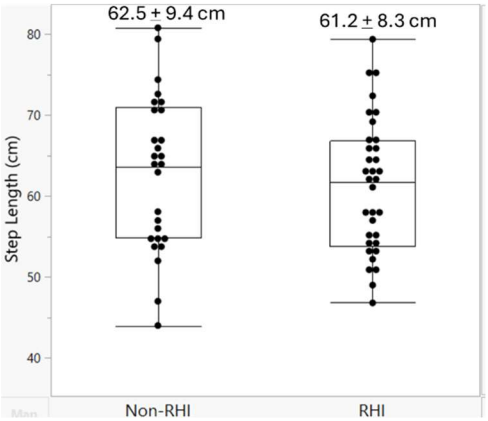


*Figure 22. There was no significant difference between groups for single task Step Length (t=0.54, p=0.59)*

**Significance:** For most collegiate student-athletes, college sports will be their highest level of participant and the end of their exposure to RHI. The results of this study suggest that, at least when still young, there are no apparent deficits associated with RHI exposure and single task gait performance. More challenging postural control tasks (e.g., dual task, virtual reality protocols) can be implemented in the future to identify potential subtle deficits which could drive rehabilitative programs to maintain QoL.

**Acknowledgments:** This study was funded, in part, by grants from NIH/NINDS (1R21NS122033, R03NS104371).

**References:** (1) Caccese, MSSE, 2023, (2) Howell, J Biomech 2015, (3) Oldham, MSSE 2020, (4) Buckley J Head Trauma Rehab, 2025, (5) Hunzinger J Sport Health Sci 2023

# COLLEGIATE FEMALE LACROSSE PLAYERS DEMONSTRATE ASYMMETRY IN TIME TO STABILIZATION FOLLOWING LATERAL HOPS

Gwyneth Laukaitis[1,2], Kevin D. Dames[2*]
[1]NYU, New York, New York
[2]Biomechanics Laboratory, SUNY Cortland, Cortland, New York
*Corresponding author's email: kevin.dames@cortland.edu

**Introduction:** Ball sports, such as lacrosse, involve many change of direction, cutting, or landing skills which challenge the athlete's dynamic stability and contribute to the high prevalence of lower extremity injuries in these sports [1]. Dynamic stability can be quantified via Time to Stabilization (TTS), which is derived from the force profile to characterize the interval between a hop landing and arrest of the participant's momentum in the forward, sideways, or vertical directions. Deficits in TTS are observed with ankle instability [2], anterior-cruciate ligament injury [3], and non-athletes relative to athletes [4]. Despite susceptibility of female lacrosse athletes to non-contact lower extremity injuries [1], this population has not been well represented in the TTS literature. We hypothesized that TTS would differ between limbs and between medial vs. lateral hop directions in NCAA Division III female lacrosse athletes.

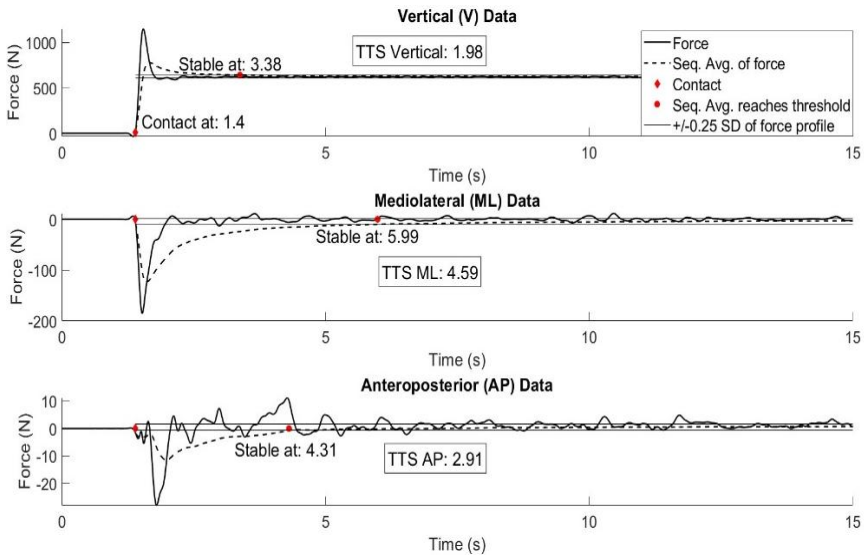


Fig 1. Representative trial

**Methods:** Twenty-eight healthy athletes (average [SD], Age: 19 [1] years, Height: 1.65 [0.06] m, Mass: 66.75 [9.08] kg, BMI: 24.53 [3.20] kg·m$^{-2}$) performed medial and lateral hops onto a force platform using their dominant and non-dominant limbs. Participants hopped from a distance equal to a quarter of their leg length (0.93 [0.04] m) from the platform's edge and remained still on the tested limb for a minimum of 10 seconds after landing. TTS was calculated from the medial lateral (ML), anterior-posterior (AP), and vertical force profiles as the point where the sequential average fell within 0.25 standard deviations of the trial's average force after contact [4] (see Fig. 1).

All outcomes met the assumption of normality (Shapiro-Wilk $p > .05$). A series of Limb (Dominant or Non-Dominant) by Hop Direction (Medial or Lateral) ANOVAs with repeated measures were performed ($\alpha = .05$).

**Results & Discussion:** No limb*direction interactions were observed. Lateral hops presented greater postural challenge (i.e., longer TTS) in ML ($F = 54.522$, $p < .001$), while Vertical ($F = 36.097$, $p < .001$) and AP ($F = 5.226$, $p = .030$) TTS were longer following medial hops. Collectively, this challenges previous conclusions of medial and lateral hop symmetry for TTS observed in a recreationally active sample of mixed female and male participants [5]. The greater susceptibility to ankle injury following a lateral hop [6] coincides with the longer TTS for our sample in that hop direction, suggesting this task is more challenging. Likewise, the dominant limb stabilized faster than non-dominant for ML TTS ($F = 5.541$, $p = .026$). An assumption of medial-lateral hop direction and bilateral limb symmetry ignores range of motion and anatomical disparities at the ankle and potential functional adaptations to sport training.

Table 1. Mean (SD) Time to Stabilization results by limb and direction

| | Lateral Hop | Medial Hop | Limb Effect (partial $\eta^2$) | Direction Effect (partial $\eta^2$) |
|---|---|---|---|---|
| **Medial-Lateral (s)** | | | | |
| Dominant | 4.56 (0.10) | 4.41 (0.13) | $p = .026$ | $p < .001$ |
| Non-dominant | 4.61 (0.08) | 4.42 (0.12) | $_p\eta^2 = 0.170$ | $_p\eta^2 = 0.669$ |
| **Anterior-Posterior (s)** | | | | |
| Dominant | 2.52 (0.65) | 2.71 (0.92) | $p = .992$ | $p = .030$ |
| Non-dominant | 2.45 (0.81) | 2.79 (0.90) | $_p\eta^2 = 0.000$ | $_p\eta^2 = 0.162$ |
| **Vertical (s)** | | | | |
| Dominant | 1.67 (0.27) | 1.86 (0.25) | $p = .233$ | $p < .001$ |
| Non-dominant | 1.66 (0.24) | 1.79 (0.23) | $_p\eta^2 = 0.052$ | $_p\eta^2 = 0.572$ |

**Significance:** Worse balance, indicated by longer TTS, was observed in laterally directed hops and in the non-dominant limb. These deficits can inform strength training programs intended to improve neuromuscular coordination. Athletes' training may promote asymmetry through limb specialization to excel in their sport.

**Acknowledgments:** This work was supported by a Summer Research Fellowship from SUNY Cortland.

**References:** [1] Hasan et al. (2023), *Physician and Sportsmedicine* 51(2); [2] Ross et al. (2005), *J Athl Train* 40(4); [3] Webster & Gribble (2010), *J Athl Train* 45(6); [4] Saunders et al. (2014), *J Sports Sciences* 32(11); [5] Liu & Heise (2013), *J Applied Biomech* 29(5); [6] Hertel (2002), *J Athl Train* 37(4).

# DOES LIMB SPECIALIZATION IN TRACK AND FIELD INTRODUCE ASYMMETRY IN DYNAMIC STABILITY?

Aaron X. Jones, Bryanne Bellovary, Jason Parks, Kevin D. Dames*
SUNY Cortland, Cortland, New York
*Corresponding author's email: kevin.dames@cortland.edu

**Introduction:** Time to Stabilization (TTS) represents the time it takes for a person to become still after a hop landing. Lower times suggest greater dynamic stability [1]. Whereas self-reported leg dominance does not seem to have a significant impact on TTS performance in DIII ball sport athletes [2], functional limb asymmetry may still be present [3]. This is relevant to track and field athletes, who have unique preferences in limb use that may or may not match traditional self-reported limb dominance questions. For example, hurdlers do not prefer to alternate their lead limb over the hurdle, which trains one limb to leap and one to land, and the powerful take-off limb may not be the same which they would use to kick a ball. Neuromuscular changes in the coordination, strength, and stability between limbs may emerge over time. This study compares TTS following forward hops in healthy male controls to varsity DIII Track & Field athletes. We hypothesize differences between limbs, groups, and force component directions (Vertical, V; Anteroposterior, AP; and Mediolateral, ML). Data presented are preliminary and data collections are ongoing.

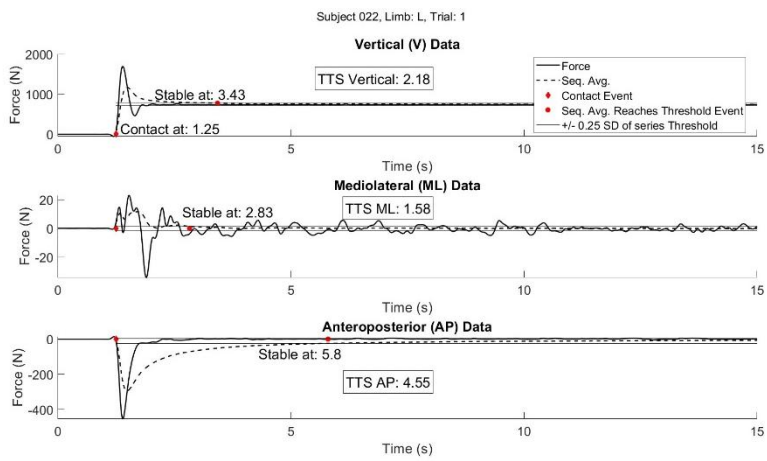


Fig 1. Representative trial

**Methods:** The current sample includes NCAA Division III male Track & Field Athletes (N = 14; average [SD], age: 19 [1] years, height: 1.81 [0.06] m, mass: 75.42 [6.62] kg) that compete in a sprint, hurdle, and/or jump event and male Controls that are not members of a varsity sport (N = 8; average [SD], age: 22 [1] years, height: 1.79 [0.07] m, mass: 82.75 [9.66] kg). The target sample will contain 19 participants in each group. Participants took two forward steps then hopped from one limb onto a force platform where they landed with the opposite limb. Hop distance was at least one leg length's distance from the center of the force plate [4]. TTS was calculated according to Saunders et al. [1] as shown in Fig. 1.

An ANOVA with repeated measures assessed Limb (Preferred Take-off or Lead Limb for Athletes; Dominant or Non-dominant for Controls) by Direction (V, ML, or AP) by Group (Athlete or Control) effects ($\alpha = .05$).

**Results & Discussion:** Existing cohorts are equal for height ($p = 0.438$), but Control participants have shorter lower extremities ($p = 0.037$, Mean Difference = 5.61 cm) and are heavier ($p = 0.047$, Mean Difference = 7.33 kg) than the Athletes. The Limb*Direction*Group interaction was not significant ($F = 0.720$, $p = 0.493$) while the Limb*Direction interaction was significant ($F = 4.126$, $p = 0.023$) (Fig 2). As expected, the AP component of the force stabilizes after ML ($p < .001$) and V ($p < .001$), with no difference evident between ML and V ($p = 0.339$). While the ML and V components are equivalent in the Non-preferred limb ($p = 1.0$), a trend of ML stabilizing faster than V for the Preferred limb emerged (N = 16 of 22 participants; $p = 0.183$).

The current lack of group differences and similarity to existing evidence on forward hop TTS outcome magnitudes [4] suggests track athletes may not have better dynamic stability than typical healthy males. However, preliminary distinctions in the ML direction following a forward hop suggest deficits in the Non-Preferred limb which may contribute to ankle injury [5]. Functional roles of each limb that contribute to asymmetry may persist in athletes and should be considered in return-to-play decisions following injury [6].

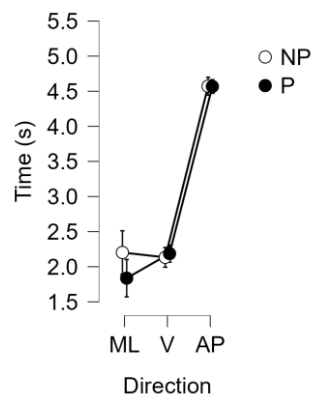


Fig 2. Mean TTS and 95% Confidence Interval for Preferred (P) and Non-Preferred (NP) limbs by force component.

**Significance:** Preliminary results suggest asymmetry in stabilizing in the medial-lateral direction between limbs. Existing findings are primarily driven by the athlete cohort (14 of 22 participants) which may indicate the full anticipated sample could identify the asymmetry is associated with training. The target sample will include 19 Athletes and matched number of Controls to have greater power to detect limb or group functional differences. Regardless, descriptive outcomes for male Track & Field athletes fits a previously unaddressed cohort in TTS literature.

**References:** [1] Saunders et al. (2014), *J Sports Sciences* 32(11); [2] Bartlett & Mazzone (2022), *Adv Ortho Sports Med* (1); [3] Kozinc & Sarabon (2021), *PLoS One* 16; [4] Liu & Heise (2013), *J Applied Biomech* 29(5); [5] Ross et al. (2005), *J Athl Train* 40(4); [6] Simon et al. (2021), *Int J Sports Med* 42(4).

# THE RELATIONSHIP BETWEEN KNEE ISOKINETIC STRENGTH MEASURES AND BILATERAL BALANCE PERFORMANCE IN UNIVERSITY STUDENTS

Ben W. Meyer[1*]
[1]Shippensburg University
*Corresponding author's email: bwmeyer@ship.edu

**Introduction:** The purpose of this project was to compare the relationship of the performance of university students in knee isokinetic (KI) strength tests and bilateral comparison (BC) balance assessments. Recent studies have found a significant relationship between KI strength tests and balance performance in volleyball players [1,2], female gymnasts [3], soccer players [4], and football players [5]. In these studies, the researchers compared KI test measures to balance performance using: level 2 dynamic platform, Y-balance tests, a rocking platform with 15 degree range of motion, level 4 dynamic platform, and center of pressure measurements, respectively.

This project aimed to add to the body of literature in the relationship of strength and balance domain by utilizing three KI testing speeds and a static balance platform with university students. Due to the recent literature indicating that there is a significant relationship between KI strength measures and balance performance, it was hypothesized that participants in the present study would have significant relationships between their KI strength values and BC balance measures for both limbs.

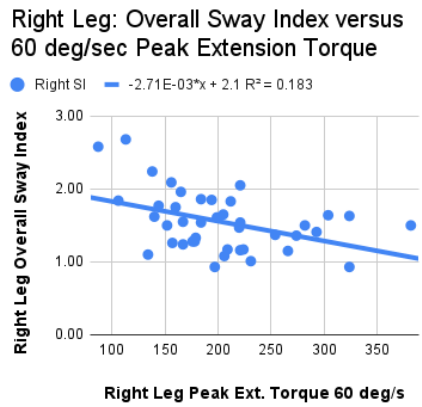


**Figure 1:** Relationship between right limb isokinetic peak torque and overall sway index.

**Methods:** Seventeen males and twenty-three females (age = 22 ± 2 yrs; mass = 79 ± 16 kg; height = 1.72 ± 0.10 m) participated in the study. Participants came from a variety of backgrounds (e.g., softball, football, recreational athlete, etc.). Each participant completed the KI tests using a Biodex Isokinetic Dynamometer. The BC tests were completed using a Biodex Balance System SD. All participants wore athletic footwear, and the test order was randomized. The limb positioning recommendations provided by Biodex were used.

The KI test consisted of five repetitions of maximal exertion knee flexions and extensions at 60, 180, and 300 deg/sec. Peak extension and flexion torque values were recorded for both limbs at each speed. The BC test required participants to stand on a single leg for 30 seconds while maintaining upright balance on a static platform. Sway index (SI) data for the medio-lateral and antero-posterior directions were provided, as well as an overall SI. The overall SI scores for the BC tests were used for data analysis. The relationship between the KI peak torques and BC overall SI values was assessed using correlation coefficients ($r$) and linear regression analyses. Statistical significance was set at $\alpha = 0.05$. Twelve total comparisons were made (strength to balance: right/left limbs x flexion/extension x 60/180/300 deg/s).

**Results & Discussion:** Of the twelve comparisons made, all six of the strength-to-balance relationships involving the right limb were significant. The largest correlation was found in the relationship between the right leg peak extension torque at 60 deg/s and the overall SI ($r = -0.427$, $p = 0.006$, see Figure 1). The $r$ values for the other comparisons involving the right limb ranged from -0.330 to -0.382 ($p < 0.05$ for each). In contrast, only one of the six strength-to-balance relationships involving the left limb was significant (left leg peak extension torque at 180 deg/s and overall SI, $r = -0.333$, $p = 0.036$). The $r$ values for the other five comparisons involving the left limb ranged from -0.126 to -0.285 ($p > 0.05$ for each). No significant trend was found for changes in the strength of correlation across KI testing speeds.

Results of the correlation analyses indicate that there is a significant relationship between strength and balance for right limb measures. The (mostly) lack of significant findings for the left limb points to the need for practitioners to investigate this area in more depth. Asymmetry indices and hamstring-to-quadriceps ratios were also examined in this project, but they lacked any significant relationship to balance performance. Future research should examine other measures that may provide useful insights.

**Significance:** The results of this study add to the literature examining the relationship between strength and balance performance. Assessments such as isokinetic strength and balance are used extensively in clinical, research, and sport settings. Substantial time and attention are given to the improvement of balance. Measures that provide insight into balance performance have practical application for patients, clients, and athletes. The results of this study provide researchers with ideas for future research examining the relationship between strength and balance tests.

**Acknowledgements:** The author would like to thank the College of Education and Human Services at Shippensburg University.

**References:** [1] Aka et al. (2020), *IJAEP* 9; [2] Soylu et al. (2020), *J Hum Sport Ex* 15(3); [3] Kyselovičová et al. (2023), *Front Phys* 13; [4] Sliwowski et al. (2021), *Peer J* 9; [5] Tasmektepligil (2016), *Anthropol,* 23(3)

# INVESTIGATING THE DUAL-TASK EFFECT OF SENSORY INTREGRATION FOR NAVIGATION AND DYNAMIC BALANCE CONTROL FOLLOWING MILD TRAUMATIC BRAIN INJURY

*Sam Beech[1], Maggie K. McCracken[1], Christina Geisler[1], Leland E. Dibble[1], Colby R. Hansen[1], Sarah H. Creem-Regehr[1], Peter C. Fino[1]
[1]University of Utah
*Corresponding author's email: samuel.beech@utah.edu

**Introduction:** Individuals with mild traumatic brain injuries (mTBI) exhibit poorer balance and greater dual-task interference on balance and gait than healthy controls, showing a larger decrease in walking speed from baseline when concurrently performing a cognitive task. This dual-task effect in mTBI populations has been observed across various cognitive tasks, such as the Stroop task, pitch discrimination, and continuous memory recall [1, 2]. However, these tasks do not fully reflect the cognitive demands encountered during daily mobility. Specifically, as we move throughout the world, we maintain a stable representation of our position and orientation within the environment by integrating visual, vestibular, and proprioceptive feedback. When all sensory cues are available, this integration process is efficient and requires minimal attentional resources; however, as the number of available cues declines, sensory integration demands more attentional resources [3]. Consequently, navigation demands more cognitive resources as sensory cues diminish, potentially disrupting balance. Although daily mobility involves both navigation and balance control, this dual-task interaction has not been directly investigated in people with mTBI. In this experiment, we used a virtual reality (VR) homing task (Fig. 1) to determine the effect on mTBI on dual-task interference between navigation and balance as people navigated under conditions with varying sensory feedback.

**Methods:** Preliminary data has been collected for 8 healthy controls (HC) and 12 people with recent mTBI (3–12 weeks post-injury, Neurobehavioral Symptom Inventory score: $M = 28.1$, $SD = 14.9$). The virtual homing task was presented using an HTC Vive Pro Eye, with trackers placed on both ankles and over the L5/S1 junction to record the spatial locations of the base of support and the approximate center of mass, respectively. Participants completed a triangle completion task, beginning at a fixed starting point and walking to three markers in sequence (black-red-blue) while visual landmarks were displayed in the background. Upon arrival at the third (blue) marker, the VR display turned off for ten seconds, and the markers were removed. The headset then illuminated again, and participants walked to their estimated position of the first (black) marker in three sensory feedback conditions: 1) Consistent self-motion and visual cues, where the visual landmarks were not removed during the blackout; 2) Self-Motion Only, where the visual landmarks were removed during the blackout; 3) Vision Only, where the visual landmarks were not removed, but the participants were rotated in chair during the blackout to eliminate vestibular and proprioceptive cues. Navigation performance was assessed using the spatial error between the estimated and actual position of the first marker. To measure balance, we extracted the mean and variability (SD) of step width, step length, and the mediolateral margin of stability (ML MoS) at each contralateral toe-off during the homing phase.

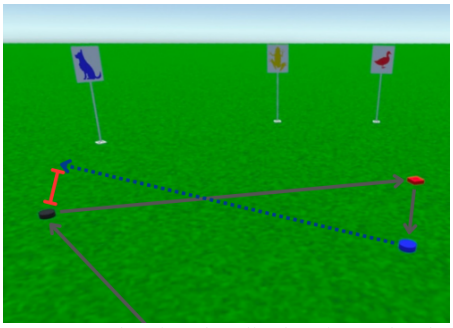

**Figure 1:** The virtual reality homing task. The blue dashed line shows the homing path and the solid red line shows the spatial error.

**Results & Discussion:** Due to the limited sample size, we present only descriptive statistics and effect sizes. Although the overall average step lengths were similar between the two groups (HC = 45.2 cm, mTBI = 45.4 cm; $d = 0.052$), the mTBI group consistently took wider steps across all conditions: Consistent (HC = 24.0cm, mTBI = 25.2cm; $d = 0.297$), Self-Motion Only (HC = 23.9cm, mTBI = 25.5cm; $d = 0.390$), particularly in the Vision Only condition (HC = 23.9cm, mTBI = 26.0cm; $d = 0.559$). When measuring the dual-task interaction for balance control, the change in the ML MoS from the Consistent to the Self-Motion Only condition was minimal for both groups (HC = -0.1cm, d = 0.012; mTBI = 0.2cm, $d = 0.058$), but the mTBI group showed a larger increase than the HCs from the Consistent to the Vision-Only condition (HC = 0.9cm, $d = 0.304$; mTBI = 1.5cm, $d = 0.482$). When measuring the dual-task interaction for navigation, the mTBI group showed larger increases in the spatial error between the estimated and actual marker positions from the Consistent to the Self-Motion Only condition (HC = 5.14cm, $d = 0.181$; mTBI = 11.93cm, $d = 0.421$), and from the Consistent to the Vision Only condition (HC = 10.67cm, $d = 0.377$; mTBI = 15.16cm, $d = 0.535$). These results indicate a balance-first dual-task interaction, where the mTBI participants widened their base of support to maintain balance control when navigating under the cognitively demanding single-cue conditions. Comparison of the step-width variability between the two groups supports this conclusion, as the mTBI group showed lower variability in both single-cue conditions: Self-Motion (HC = 8.0cm, mTBI = 7.3cm; $d = 0.200$) and Vision Only (HC = 8.7cm, mTBI = 7.3cm; $d = 0.427$), indicating greater use of cognitive resources for controlling foot placement [4].

**Significance:** Preliminary results suggest that individuals with mTBI show a larger dual-task interaction between sensory integration for navigation and balance control than healthy controls. The increased cognitive demand of navigating with limited sensory feedback resulted in a balance-first dual-task interaction, where the participants with mTBI used a greater number of cognitive resources to control their foot placement and widen their base of support to maintain stability at the expense of sensory integration for navigation. This demonstrates that the heightened dual-task effect in individuals with mTBI extends to daily mobility, as they may alter their gait and find navigation challenging in environments with limited sensory feedback, such as noisy, visually sparse, or disorienting settings.

**References:** [1] Howell et al. (2014), *Exp. Brain Res*, 232; [2] Yang et al. (2024) *Neurorehab Neural Rep*; [3] Oliveira et al. (2017), *J Neurophys*, 118(4); [4] Grabiner & Troy (2005), *J NeuroEng Rehabil*, 2, 1-6.

# WALK THIS WAY: CROCS® AND THE IMPACT OF HEEL-STRAP UTILIZATION ON OVERGROUND GAIT PERFORMANCE AND LOWER-LIMB KINEMATICS

Fabricio Saucedo[1]*, Venkata Naga Pradeep Ambati[2], Thiago Ribeiro Teles Santos[3]
[1]Department of Kinesiology, Penn State Altoona, Altoona, PA, USA
[2]Department of Kinesiology, California State University at San Bernardino, San Bernardino, CA, USA
[3]Department of Physical Therapy, Universidade Federal de Uberlândia, Uberlândia, MG, BR

*Corresponding author's email: fns5045@psu.edu

**Introduction:** Shoes have considerable impact on overall health and quality of life [1]. Gait kinematics can undergo alterations from the type of shoe being worn that can enhance performance or result in musculoskeletal stress [2-3]. With shoes like the classic clog manufactured by Crocs® being commonplace in the food or medical industry, the shoe's shift to mainstream markets begs the question of whether there are benefits or risks associated with wearing this style of shoe. A lack of arch support, poor fit, and failure to use the heel-strap properly or at all raises concerns of whether Crocs® are detrimental to walking mechanics and lower-extremity health [4]. Despite growing popularity for their comfort and practicality, their biomechanical impact on gait and lower extremity mechanics has not been examined fully. The purpose of this study was to examine the impact of heel-strap use on walking performance and lower-body joint mechanics. Knowing the impact strapless shoes have on walking [5], it was hypothesized that participants would display faster completion times during gait assessments and would display differences in the sagittal plane joint kinematics while walking in Crocs® with the heel-strap, in comparison to walking in the shoe with the heel-strap or barefoot.

**Methods:** Thirty-one healthy adults participated in this randomized within-subjects design. Participants completed a total of nine walking trials at a fast self-selected pace (three trials for each shoe condition). They walked barefoot for the control (CON) condition, in the Crocs® with no heel strap for the comfort-mode (CM) condition, and with the heel-strap for the sports-mode (SM) condition. Seven inertial measurement units (120Hz) tracked participants and sagittal lower-body kinematics were computed using known segmental parameter information. A repeated measures analysis of variance (ANOVA) with one within-subject factor of three levels (i.e., CON, SM, and CM) was used to identify the potential effect of shoe condition on walking completion time and lower-body gait kinematics.

**Results & Discussion:** Significant differences were observed for walking velocity and completion times with the SM condition yielding increased velocity and faster walking completion times compared to the CM and CON conditions (Fig. 1). Significant differences were observed in the sagittal hip and knee kinematics in the SM and CM conditions compared to the CON condition, but at the ankle joint, there was a significant difference observed between the SM and CM conditions reinforcing the importance of heel-support and shoe fit on gait performance (Table 1).

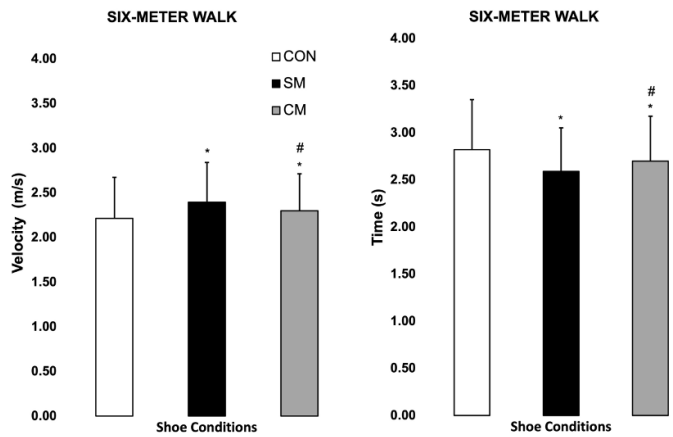


Fig. 1. Mean ± standard deviation values for the six-meter walking velocity and completion times for the control (CON), sports-mode (SM), and CM (casual-mode) shoe configurations. *Significantly different from CON. #Significantly different from CM.

Table 1 Ankle Angles (mean ± sd)

| Variables | CON | CM | SM | F | p |
|---|---|---|---|---|---|
| DF during stance (°) | 13.18±3.84 | 16.06±4.09* | 14.15+3.45# | 13.71 | <0.001 |
| DF during swing (°) | 6.65±2.90 | 9.94±2.81* | 10.09±2.71* | 24.12 | <0.001 |
| DF during foot strike (°) | -0.03±3.59 | 5.05±3.26* | 5.59±2.79* | 48.43 | <0.001 |
| PF during foot release (°) | -30.98±7.97 | -21.92±7.25* | -24.93±6.58*# | 37.14 | <0.001 |
| ROM in stance (°) | 46.44±8.15 | 39.23±6.51* | 40.02±5.86* | 20.41 | <0.001 |
| ROM in swing (°) | 42.16±7.95 | 38.53±7.21* | 40.8±6.73# | 17.31 | <0.001 |

*Significantly different from CON. #Significantly different from CM.

**Significance:** Our study findings indicate that adopting a strapped option like the Crocs® can have a positive influence on joint kinematics and walking performance. This study could be used to develop user guidelines, product modifications, and footwear recommendations that could aid in minimizing the potential for long-term foot issues associated with wearing Crocs®.

**References:** [1] Vaidya et al., (2021). *Ergonomics for Improved Productivity,* Proceedings of HWWE 2017 (pp. 699-703).
[2] Gangami, D.C., (2009). *New Expanded Gait Assessment, 1*(8).
[3] Shakoor et al., (2010). *Arthritis Care Research, 62*(7), 917-923.
[4] Morris et al., (2017). *Journal of Human Sport and Exercise, 4*(12), 1220-1229.
[5] Chard et al., (2013). *Journal of Foot and Ankle Research*, *6*(8), 1-8.

# EVALUATION OF PEDESTRIAN OVERTURN RISK ASSOCIATED WITH RAILING INTERACTION

*Robert T. Bove, Shady Elmasry, Dhara Amin, Rachael Aber, Elizabeth Rapp van Roden, Bruce Miller
Exponent, Inc., Philadelphia, PA
*Corresponding author's email: rbove@exponent.com

**Introduction:** Published biomechanical data regarding pedestrian interactions with and falls over railings are largely limited to qualitative test data collected by Fattal, et al. (1976) as part of an investigation of railing protection.[1] Current regulations and building codes (railing heights of 36 inches or greater for residential buildings and of 42 inches or greater for commercial buildings) are based in part on this research.[2] These railing heights were stipulated based on the Fattal study's binary qualitative analysis of whether a 95$^{th}$ percentile male anthropomorphic test device (ATD) fell over railings set at four different heights with two different approach speeds. At railing heights of 40 inches or higher, the ATD did not overturn. It was also noted by the authors that when the height of the ATD's center of gravity (CG) was below the railing height, overturns did not occur; however, tests were also performed with the CG above the top of the railing in which overturns did not occur. Fattal, et al., postulated that ATD overturn was dependent upon the height of the hip joint, and that railings above the hip joint limit upper body rotation about the upper railing surface. No quantitative analysis was performed to investigate this potential relationship, nor to evaluate the effect of the impact speed (limited to 3.3 mph in the study). This analysis was also limited to railing interactions for a 95$^{th}$ percentile male ATD at two approach speeds with the maximum speed limited to 3-1/3 mph. Therefore, the objective of this study was to better evaluate the effects of CG height, hip joint height, and approach speed on the risk of overturn for a pedestrian interacting with a railing.

**Methods:** Evaluations of several pedestrian-to-railing interaction configurations were conducted using a gravity-driven sled rail that accelerated ATDs into an adjustable instrumented railing at slow, medium, and fast speeds at a range of common walking speeds (Fig. 1). The railing was composed of a horizontal cylindrical steel bar (2 inches in diameter) spanning two gusseted, vertical steel posts affixed to a slotted tested bed. A Hybrid III 5th percentile female ATD (H3-5F) and a Hybrid III 50th percentile male ATD (H3-50M) were used as the pedestrian surrogates. The ATDs were equipped with pedestrian pelvises. For each test, the ATD was positioned standing upright on the sled, suspended by a cable release system. The timing of the release was regulated by the continued ATD forward movement relative to the sled in response to the sled deceleration prior to ATD impact with the railing. A speed trap at the end of the sled track measured speed immediately prior to the ATD interacting with the railing. Forty-three tests (24 with the H3-50M, 19 with the H3-5F) were conducted at railing heights ranging from 25 inches to 42 inches and speeds ranging from 2.0 to 4.6 mph. To evaluate the relationship between hip height and the risk of overturn, we fit a generalized linear model with a logit link function and binomial family (logistic regression) to the overturn data using the number of inches the hip height was above the railing as a predictor

**Figure 1.** Image showing ATD overturning after being propelled into the railing by the gravity-driven sled.

**Results & Discussion:** Overturns for the H3-5F and H3-50M occurred at all three speed ranges, but only occurred when the hip height and CG of the ATDs were above the railing. Instances of overturn occurred with hip heights ranging from 3 to 7 inches above the railing (7 inches above the railing was the maximum relative height tested). Instances of no overturn occurred with hip heights ranging from 12 inches below the railing to 6 inches above the railing. We found evidence at the 0.05 level to adopt a overturn risk model that includes the hip height above the railing (LRT p-value=6.791e-5) over a null (intercept-only model). The risk curve and data are shown in Figure 2. Other than the limited Fattal study, no other studies have been identified that establish a "critical" railing height. The current study expands on the Fattal study by using different ATD sizes, a wider range of relative railing heights, and a wider range of approach speeds, as well as capturing more quantitative data on overturn kinematics.

**Significance:** Statistical analysis indicates the significance of railing height relative to hip height in predicting pedestrian overturn on a railing, and the data provide a tool for evaluation of railing structures in commercial and residential walkways.

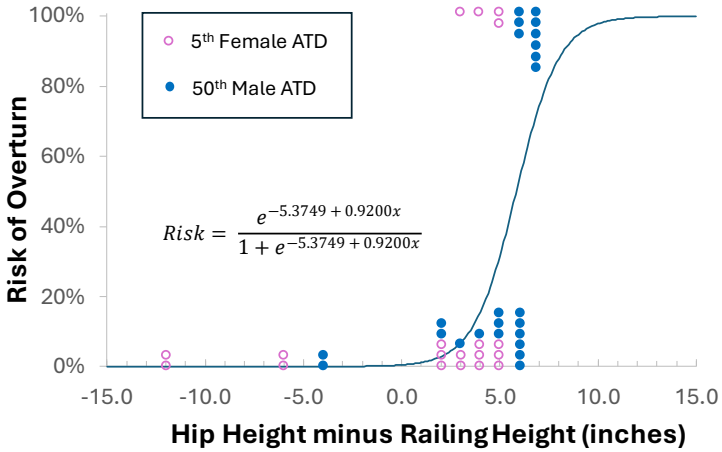


**Figure 2**. Plot showing the instances of overturn (top) and no overturn (bottom) at the varying hip heights relative to the railing height (hip height minus railing height) with the associated risk curve.

**References**: 1. Fattal, et al. NBSIR 76-1139 (1976); 2. International Building Code (2024)

# IMPACT DIRECTION AND BRAIN INJURY MECHANISMS IN SPORTS: A FINITE ELEMENT ANALYSIS OF GOLF BALL HEAD IMPACTS

Hossein Bahreinizad[1], *Suman K. Chowdhury[1]
[1]Department of Industrial and Systems Engineering, University of Florida, Gainesville, Florida, United States
*Corresponding author's email: sk.chowdhury@ufl.edu

**Introduction:** Traumatic brain injury (TBI) is a leading cause of death and disability, with approximately 190 TBI-related deaths occurring daily in the United States [1]. Due to the severe nature of TBI, it is crucial to understand its underlying mechanisms to develop effective protective strategies and treatment approaches. One of the most powerful tools for investigating TBI mechanisms is the finite element (FE) method. Although prior research has explored the effects of impact direction during falls [2], limited studies have examined the role of impact direction and location in sports-related head injuries. In particular, the effects of a golf ball impact to the head have not been investigated. This study aims to analyse how the direction of impact influence TBI mechanisms when a golf ball strikes the head, providing critical insights into sports-related brain injuries.

**Methods:** We used a validated, MRI-derived head-neck finite element model to study the effects of impact direction on TBI mechanisms during a golf ball strike. This model includes detailed anatomical structures such as the scalp, skull, cerebrospinal fluid (CSF), brain, dura mater, pia mater, cervical vertebrae, intervertebral discs, 14 ligaments, and 42 neck muscles. The simulation involved a golf ball impact with a velocity of 35 m/s at three different locations: frontal, side, and top. To assess the severity of injury, the maximum principal strain (MPS) was calculated in the frontal, parietal, temporal, and occipital lobes. Additionally, the head's centre of gravity (COG) acceleration was measured to determine the overall effect of the impact on head dynamics.

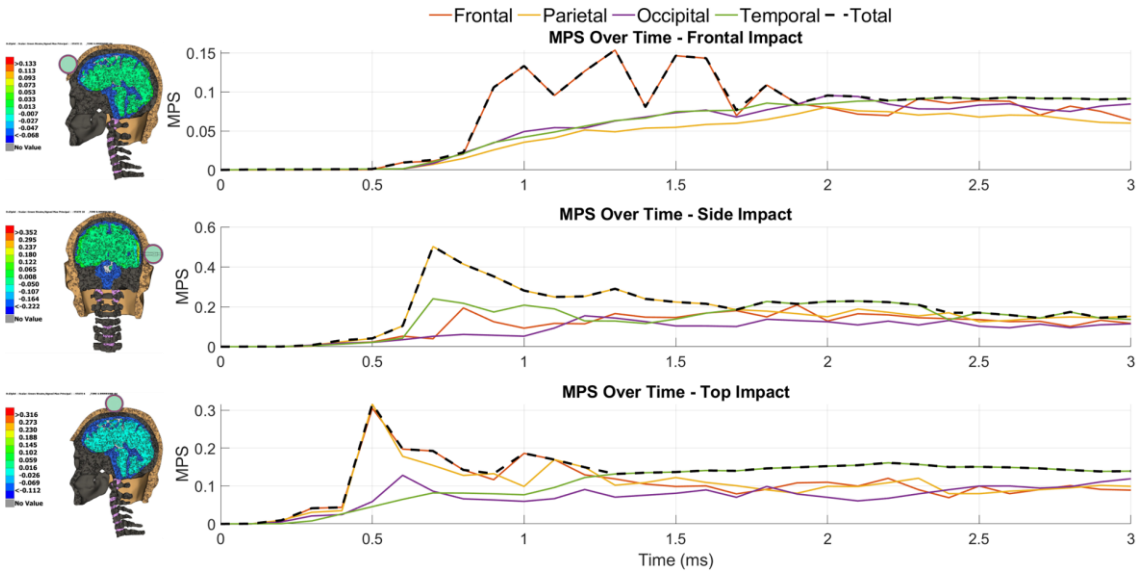


**Figure 1:** Time history of Maximum Principal Strain (MPS) for different brain regions (Frontal, Parietal, Occipital, and Temporal) and total MPS under three impact conditions: Frontal, Side, and Top. The dashed black line represents the total MPS in each case.

**Results & Discussion:** The severity and pattern of brain injury varied with impact direction and location. In the frontal impact, the maximum MPS was about 15%, below the injury threshold [3, 4]. Strain was initially highest in the frontal region, then shifted to the occipital and temporal regions (Fig. 1), showing a coup-contrecoup effect. The top impact resulted in a maximum MPS over 30%, indicating possible axonal and vascular injuries. The highest strain occurred in the frontal lobe but at a different location than in the frontal impact, later migrating to the temporal region (Fig. 1). Despite higher strain, head COG acceleration was similar to the frontal impact. The side impact caused the most severe injuries, with maximum MPS exceeding 50%, suggesting a high risk of axonal and vascular damage. The highest strain was first in the parietal lobe, then moved to the temporal region (Fig. 1), remaining above the injury threshold. Despite greater tissue damage, head COG acceleration was comparable to the frontal impact, highlighting the role of modelling accuracy in injury severity. Skull and CSF thickness influenced strain distribution. In the frontal region, the skull and CSF were about 10 mm and 9 mm thick, helping absorb impact forces. In contrast, the side impact region had a thinner skull (5 mm) and CSF layer (4 mm), contributing to higher strain. The skull thickness in the top impact location was similar to the frontal region (10 mm), but the thinner CSF layer (7 mm) led to increased strain and injury risk.

**Significance:** This study highlights how impact direction affects TBI severity in sports. Our findings can improve protective gear design, such as helmets, and guide clinical assessments and prevention strategies. Understanding the role of impact direction in injury risk helps identify high-risk scenarios and develop better safety measures for athletes.

**Acknowledgments:** This work was supported, in part, by the National Science Foundation (Award # 223910) and the Department of Homeland Security (Award # 70RSAT21CB0000023).

**References:** [1] https://wonder.cdc.gov/mcd.html (accessed February 2025); [2] Post et al. (2015), *Neurosurgery* 76(1); [3] Bain et al. (2000), *J. Biomech. Eng.* 122(6); [3] Monson et al. (2003), *J. Biomech. Eng.* 125(2).

# GROUND REACTION FORCE DISCREPANCIES BETWEEN FORCE PLATES AND FOOT INSOLES: IMPLICATIONS FOR IN FIELD MONITORING

Leutrim Mehmeti[1,2], Kaitlyn Buell[3,4], Felicia Davenport[1,5], Therese Parr[1,4], Charles Weisenbach[3], Jazmin Cruz[1,5], *Peter Le[1]
[1]711th Human Performance Wing (HPW), Air Force Research Laboratory (AFRL)
[2]Reef Systems, [3]Naval Medical Research Unit-Dayton, [4]Leidos, [5]Innovative Element, [6]Oak Ridge Institute for Science and Education
*Corresponding author's email: peter.le.3@us.af.mil

**Introduction:** Reports of low back pain (LBP) among test parachutists have prompted the Air Force Research Lab to investigate the effects of landings on low back loading. Assessing the forces transmitted through the body during landings requires ground reaction force (GRF) data, traditionally obtained using force plates (FP). However, force plates are impractical for field studies, requiring portable solutions. Pressure insoles (PI) provide a feasible alternative for collecting GRF data, akin to inertial measurement unit (IMU) sensors [1]. GRF data are critical for performing musculoskeletal (MSK) simulations to estimate lumbar loading metrics [2-3]. This study builds on previous work utilizing Tekscan insoles to drive MSK simulations and evaluate lumbar loading in military settings. Here, we assess whether GRFs from PI provide reliable inputs for wearable-driven, in-field MSK simulations and their utility during high-impact tasks. To address this, the objective of this work was to evaluate the GRF data discrepancies between FP and PI during dynamic, high-impact movements, with the goal of determining the viability of PI for in-field applications.

**Methods:** The data presented in this abstract is preliminary pilot data from an approved IRB study. PI data were collected from in-shoe pressure sensors (F-Scan, Tekscan™, Inc., Norwood, MA) sampling at 500 Hz. FP data were collected using Bertec force platforms (Bertec Inc, Columbus, OH) sampling at 1000 Hz. Our subject performed 4 repetitions of a drop landing task from a 60 cm platform under two weight conditions: bodyweight (BW) and with the addition of a 7.5 kg vest. Vertical GRFs (vGRF) from FP data were downsampled to 500 Hz to match PI data. Then for both systems, the stance phase was defined from the initial contact, identified as the first value exceeding 20 N, to 250 frames post-contact. The coefficient of determination ($R^2$) and Root Mean Square Error (RMSE) were computed to assess how well the PI data agreed with the FP data.

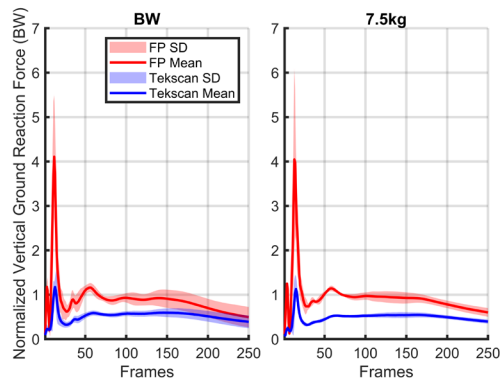


**Figure 1:** Right foot mean (SD) participants' waveforms for vGRF for the drop landing task.

**Results & Discussion:** The comparison of vGRFs between FP and PI revealed moderate agreement, with coefficients of determination ($R^2$) of 0.52 for the bodyweight condition and 0.50 for the 7.5 kg condition (Table 1). The RMSE between the two systems was 0.54 ± 0.08 BW and 0.60 ± 0.05 BW for the respective conditions, indicating higher discrepancies when additional load was applied. The moderate $R^2$ values suggest that PI data effectively capture the overall trends and timing of vGRF changes throughout the stance phase. The force plate data consistently exhibited higher initial peak vGRFs compared to the PI data, particularly within the first 50 frames after initial contact (Figure 1). This underestimation was more pronounced under the 7.5 kg condition, reflecting the limited ability of PI to capture high-impact forces accurately. However, this discrepancy can be attributed to the higher resolution and sensitivity of FPs, which allow for precise detection of high forces during dynamic movements. During the sustained loading phase, where forces are generally ≤ 1 BW, PI data reliably tracked submaximal force patterns. This suggests that PI are more accurate at capturing lower force magnitudes but face limitations in capturing high-impact landing forces [4]. Future work could explore integrating scaling factors into ML models to correct for this underestimation. While PI are limited in capturing accurate peak forces, they can provide valuable input for continuous monitoring of force profiles and overall loading patterns, making them suitable for wearable-driven applications.

**Table 1:** Summary of RMSE and $R^2$ values for vGRF under bodyweight (BW) and 7.5 kg conditions.

| Measure/Conditions | BW | 7.5 KG |
|---|---|---|
| RMSE (BW) | 0.54 ± 0.08 | 0.60 ± 0.05 |
| $R^2$ | 0.52 | 0.5 |

**Significance:** Our results indicate that PI are valuable for comparing tasks or conditions where relative load patterns are of more interest than force magnitudes. However, clinicians should apply caution when using PI data alone to classify patient risk levels due to underestimations of high-impact forces. Future work integrating PI with complementary sensors like IMUs may enhance ML models, improving GRF predictions and enabling in-field biomechanical assessments.

**Acknowledgments:** The views expressed in this abstract reflect the results of research conducted by the authors and do not necessarily reflect the official policy or position of the Department of the Air Force, Department of the Navy, Department of Defense, nor the U.S. Government. The data used in this abstract was not collected under an IRB protocol. Distribution Statement A: Approved for Public Release, Unlimited distribution. AFRL-2025-0798, Cleared 12 FEB 2025.

**References:** [1] Zago et al. (2021), *Front. Bioeng. Biotechnol.* 638793; [2] Ajay et al. (2018), *PloS Comput Biol.* 14(7); [3] Uhlrich et al. (2023), *L Biomech.* 111623; [4] Cudejko, T et al. (2023), *Sci Rep.* 14946.

# Assessing the Upper Limb Kinematics of a Novel Wheelchair Design for Participants with Spinal Cord Injury: A Pilot Study

John M. Looft[1,2*], Alexandria Richardson[1], Vibha Mavanji[1], Brogan Comstock[1], Amber Wacek[1], Myrriah Laine Dyreson[1], Gaura Saini[2], Paula Ludwig[2], Andrew Hansen[1,2]
[1]U.S. Department of Veterans Affairs, Minneapolis, MN
[2]University of Minnesota - Twin Cities, Minneapolis, MN
*Corresponding author's email: john.looft@va.gov

**Introduction:** Manual wheelchair users, including those with spinal cord injury, are at greater risk for developing upper-extremity injuries [1]. Previous work has suggested a more forward axle placement is correlated with improved wheelchair biomechanics with an ideal hub-shoulder-angle between -10° and -2.5° [2]. Our team has developed a novel experimental wheelchair with chain-driven anterior pushrims and posterior drive wheels, which allows for forward pushrim placement without sacrificing stability.

The objectives of this pilot study were to 1) compare the upper-limb kinematic and overall performance differences between the experimental wheelchair and a standard TiLite ZRA wheelchair on both hard flooring and carpet; 2) gather stakeholder feedback regarding the experimental wheelchair's design features. The primary hypothesis was that shoulder abduction, extension, and external rotation would be significantly reduced throughout the push phase in the experimental wheelchair. Secondarily, we hypothesized that elbow extension and wrist kinematics would exhibit no significant differences between wheelchairs. Our exploratory hypothesis was that performance outcome metrics, including (a) stroke time; (b) distance per push; (c) speed; (d) percentage of the hand rim utilized per stroke, would not be significantly different between the experimental and standard wheelchairs.

**Methods:** Ten Veterans with spinal cord injury (n =10 male, 50.3 ± 17.3 y.o.) completed data collection. Motion capture data for two subjects was excluded due to poor quality, resulting in a smaller sample size for kinematic analysis (n = 8). Participants completed testing in both a standard TiLite ZRA wheelchair (TiLite, Permobil, Timra, Sweden) and an experimental wheelchair featuring chain-driven anterior pushrims (Figure 1).

**Figure 1:** The experimental wheelchairs were fit with 24" Natural-Fit LT hand rims (Three Rivers Holdings LLC, Mesa, AZ).

Motion capture data was collected at 120 Hz and all testing was completed in the Minneapolis VA Health Care System's (MVAHCS) Motion Analysis Laboratory. Reflective markers were placed on anatomical landmarks of the trunk, upper extremities, and wheelchair. The medial and lateral epicondyles along with the radial and ulnar styloid were digitized with the digitizing pointer. Participants tested both the standard and experimental wheelchairs on hard flooring and carpet during steady-state propulsion. Upper limb kinematics were captured along with the percentage of the pushrim utilized per stroke. Participants then completed a 6-minute push test within the MVAHCS where stroke time, distance per push, and speed were measured. Finally, a short interview was conducted to gain Veteran feedback on the wheelchair design and usability. Comments were aggregated into domains and categorized into positive or negative comments.

**Results & Discussion:** ANOVA was used to determine the effects of wheelchair type and flooring type on the minimum, median, and maximum joint angles throughout the push phase for the following joint angles: (a) Shoulder flexion/extension; (b) Shoulder internal/external rotation; (c) Shoulder abduction/adduction; (d) Elbow flexion/extension; (e) Wrist flexion/extension; (f) Wrist radial/ulnar deviation, and; (g) Wrist pronation/supination. The effect of wheelchair type within floor type was examined using a pairwise paired t-test. Shoulder flexion/extension exhibited a significant difference between wheelchair types on both hard (minimum angle: $p = .018$, maximum angle: $p = 0.014$) and carpeted flooring (minimum angle: $p < .001$, maximum angle: $p = 0.01$). This may have a protective effect that could reduce risk of upper limb injury. Wrist flexion/extension also yielded significant differences between wheelchair types for the median joint angle on both hard ($p = 0.001$) and carpeted ($p < 0.001$) flooring. Veterans may have altered their propulsion pattern to avoid projections on the pushrim spokes, which was mentioned by 60% ($n = 6$) of Veterans as an issue. All other tested kinematic variables did not have a significant effect of wheelchair type or floor type at the specified joint angles.

The standard wheelchair performed significantly better ($p < 0.05$) than the experimental wheelchair for distance per push, stroke time, and speed outcome metrics as assessed by a Wilcoxon-signed rank test or paired samples t-test (dependent on parametricity of data). Veterans ($n = 8$) reported that the standard wheelchair was easier to propel, travel in a straight line, turn/stop, and coast; However, a few Veterans ($n = 2$) preferred the experimental wheelchair for long-distance propulsion. This contradicts our exploratory hypothesis described above and may be due to energy loss with the chain-driven system. There was no significant difference in the percentage of the pushrim utilized between the standard and experimental wheelchairs ($p = 0.173$), indicating that participants may propel with similar arcs regardless of anterior positioning. Veterans suggested that the experimental wheelchair may perform better if geared appropriately for rugged terrain, long-distance propulsion, and inclines.

**Significance:** Promising differences in shoulder flexion/extension suggest this design may reduce risk of shoulder pain or injury during propulsion. Future work will improve the pushrim user interface and explore multiple gearing options to maximize efficiency.

**Acknowledgments:** Thank you to the Frank J. & Eleanor A. Maslowski Charitable Trust for funding this work. We would also like to thank Patricia McCracken and Abigail Froechtenigt for their contributions towards this project.

**References:** [1] Finley & Rodgers (2007), *Archives of Physical Medicine and Rehabilitation* 88(12); [2] Slowik & Neptune (2013), *Clinical Biomechanics* 28(4).

# AUTOMATED RECOGNITION OF USER INTENT FOR DISHWASHER USE VIA MOTION CAPTURE ANALYSIS

Taehyung Kim[1], Kanghyeon Lee[1], Gwanseob Shin[1], Yoonhee Jeong[2]
[1]Department of Biomedical Engineering, Ulsan National Institute of Science and Technology, Ulsan, South Korea
[2]HS R&D Center, LG Electronics
*Corresponding author's email: skanrkdgus@unist.ac.kr

**Introduction:** With the rapid advancement of automation technology, its integration into everyday life is becoming increasingly prevalent [1]. One such application is the automation of household appliances, including dishwashers, which aim to enhance user convenience and efficiency. However, existing solutions primarily rely on conditional automation methods, where the door opens only when users perform specific actions, such as pressing a button or making a deliberate motion [2]. These methods still require user intervention, limiting the full potential of automation. In this study, we hypothesized that approach patterns differ depending on whether the user intends to operate the dishwasher, enabling the development of an algorithm for automatic intent recognition. Using a camera-marker system, we analyzed approach patterns by categorizing user scenarios based on dishwasher usage. Our findings revealed a distinct spatial pattern in foot trajectory, which we leveraged to design an algorithm capable of distinguishing user intent.

**Methods:** Five healthy adults (Male = 3, Female = 2; 23.2±1.8 years) participated in this study. To investigate approach motion in relation to dishwasher usage intent, we constructed a realistic kitchen environment and employed an OptiTrack motion capture system with a 100 Hz sampling rate. Markers were attached to the dishwasher and key body regions (hand, knee, foot, and ankle) that could be detected by dishwasher sensors (Fig. 1). Eight distinct user scenarios were established, and two representative kitchen layouts (Straight-line, L-shaped) commonly found in Korea were tested (Fig. 1), resulting in a total of 16 recorded approach sequences. The kitchen counter height was set to 850 mm, following standard kitchen dimensions, to ensure a realistic experimental setup [3]. Motion data were captured using seven cameras and 12 markers, providing comprehensive tracking of user movements.

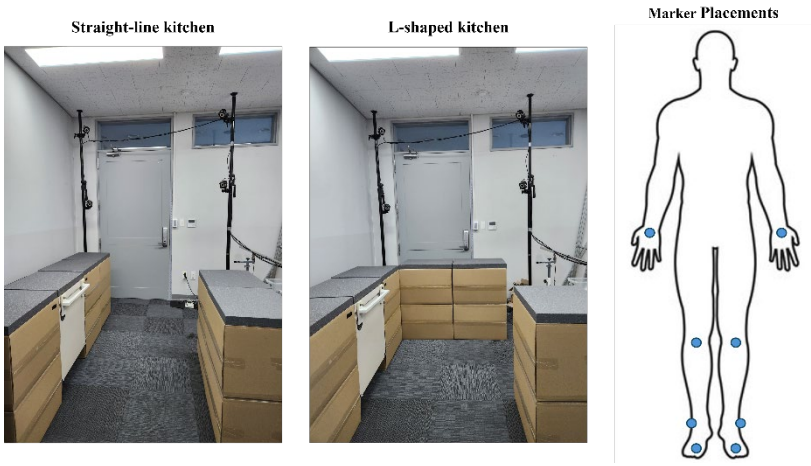


**Figure 1.** Experimental kitchen 2 layouts (Straight-line kitchen, L-shaped kitchen) and marker placements

**Results & Discussion:** Analysis revealed a consistent spatial zone that participants' feet did not enter when engaging with the dishwasher (Fig. 2A). This specific area was observed only in scenarios where the dishwasher was actively used, irrespective of the direction of approach (frontal, lateral, or diagonal). The consistency of this pattern across multiple trials suggests that users unconsciously maintain a predictable spatial boundary when operating the appliance. This phenomenon may be attributed to ergonomic factors, such as the natural positioning of the body to facilitate efficient interaction with the dishwasher, as well as a subconscious effort to avoid potential obstacles. By integrating foot placement patterns with hand motion data, we developed an algorithm capable of distinguishing dishwasher usage intent based on approach behavior.

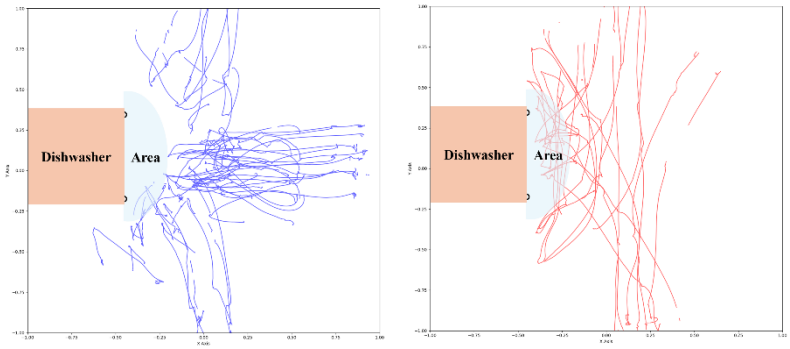


**Figure 2.** Foot trajectory in use (A) and non-use scenarios (B)

**Significance:** This study demonstrates a novel approach to achieving fully automated intent recognition in home appliances, moving beyond traditional conditional automation methods. Our findings suggest that user intent can be inferred from approach motion patterns, presenting significant implications for the development of intelligent home appliances. The methodology introduced in this study could be extended to other automated systems, such as smart doors or kitchen appliances, to create a more seamless and intuitive user experience in various contexts. Future work will focus on refining the algorithm through additional data collection and exploring AI-based comparative analyses to enhance accuracy.

**References:** [1] Nishida, D., et al. (2014). Development of intelligent automatic door system. *2014 IEEE International Conference on Robotics and Automation (ICRA)*, [2] Ahn, J., & Lim, D. (2021). Interactive automatic refrigerator door for emotional satisfaction. In *Advances in Usability, User Experience, Wearable and Assistive Technology* (Vol. 275), [3] Korea Housing Furniture Cooperative. (2022). SPS-KHFC 001-0438:2022 – Standard for household kitchen sinks. Korea Housing Furniture Cooperative

# COMPARISON OF LUMBAR LOADS DURING INITIAL GROUND IMPACT OF MILITARY PARACHUTE JUMPING TASKS

Jazmin Cruz*[1,2], Felicia Davenport[1,2], and Peter Le[1]
[1]711th Human Performance Wing (711HPW), Air Force Research Laboratory (AFRL), WPAFB, OH 45433
[2]Oak Ridge Institute for Science and Education (ORISE)
*Corresponding author's email: peter.le.3@us.af.mil

**Introduction:** Parachute jumping is essential for military operations but carries a high risk of injury, especially during the landing phase [1]. Two common parachute jump methods are static line (SL) and military freefall (MFF). The SL method requires a parachute landing fall (PLF) and the MFF method requires a running landing. According to the literature, the PLF generates large impact forces on the body [2]. As reported by military parachutists, low back injuries are among the most common [3]. Monitoring the biomechanics of parachutists during training is essential for injury prevention and personnel retention. Wearable sensors enable researchers to capture the kinematics and kinetics of parachutists in-field, allowing for the estimation of joint loading through musculoskeletal (MSK) modeling. We can assess injury risk by comparing our estimations to values reported in the literature [4] and validate our findings by comparing them to real-world parachutist injury data. The objective of this work is to quantify compressive lumbar loads and assess the risk of injury across three commonly used parachute jump profiles using in-field wearable data.

**Methods:** Five military-aged male test parachutists (93.28 kg ± 8.04 kg) participated in this study, performing up to six repetitions of three common parachute jump profiles (Fig. 1A): SL (MC-6), tactical MFF (RA-1), and nontactical MFF (Sabre). Whole-body kinematics and kinetics (foot forces) of the parachutists were recorded using a 15-sensor Inertial Measurement Unit (IMU) system (MVN Link, Movella™, Inc., Henderson, NV) and plantar pressure in-soles (F-Scan, Tekscan™, Inc., Norwood, MA), respectively (Fig. 1B). The in-field data collected by the wearables were used to drive a rigid-body MSK model (OpenSim 4.3, SimTK) to estimate lumbar loads via joint reaction analysis. Lumbar loads at ground impact were extracted, averaged, and compared to the NIOSH compression risk threshold of 3400 N for each jump profile [4].

**Results & Discussion:** The L5/S1 compression forces at ground impact for all jump profiles did not exceed the risk threshold of 3400 N (Fig 1C). Compression forces were lowest for nontactical MFF (1840.5 N ± 488.9 N, n =13), followed by SL (2085.3 N ± 825.0 N; n = 5), and highest for tactical MFF (2093.5 N ± 680.6 N, n = 4).

These results imply that each jump profile may not pose a risk of acute low back injury, but that nontactical MFF pose the least risk among the profiles investigated. This can be explained by the increased manoeuvrability that comes with using the nontactical parachute, which allows experienced parachutists to have precise control over their landings. However, it was unexpected that SL and tactical MFF produced similar compression values, given their differences in parachute manoeuvrability. Further research with larger sample sizes may reveal the expected differences in compression values between SL and tactical MFF, given the latter's superior manoeuvrability.

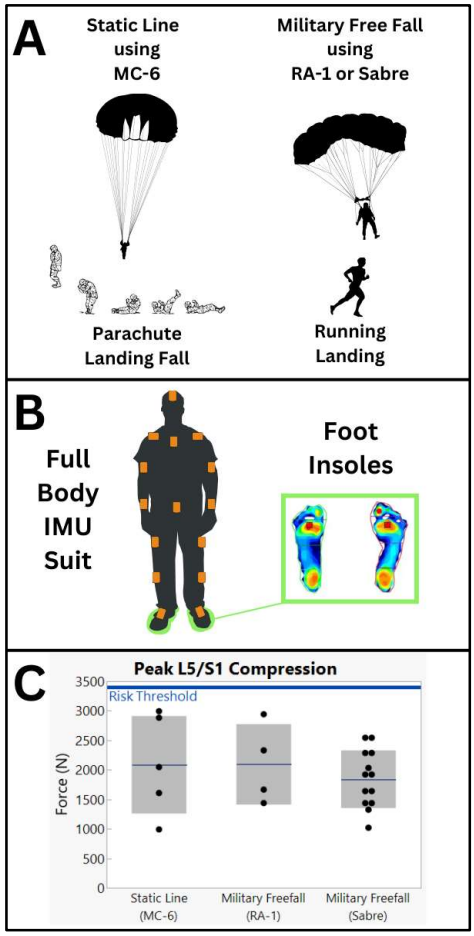


**Figure 1: (A)** Parachute jump profiles and their respective equipment and landing style [2]; **(B)** Instrumentation used on parachute jumpers (Tekscan™); **(C)** Peak L5/S1 Compression Force across jump profiles. Error band is representative of 1 SD from the mean.

**Significance:** This study provides valuable insights that can help guide injury prevention strategies for parachutists, such as monitoring lumbar load and setting limits on the number or type of jumps per day. By incorporating external loads, such as rucks, backpacks, and tandem barrels, and developing methods to assess across-body loading during the entire PLF, future research will further enhance our understanding of the physical demands of parachuting and inform safer jump practices.

**Disclaimer:** The views expressed in this abstract reflect the results of research conducted by the authors and do not necessarily reflect the official policy or position of the Department of the Air Force, Department of Defense, nor the U.S. Government. This research was supported in part by appointments to the Oak Ridge Institute for Science and Education. The study protocol was approved by the Institutional Review Board (IRB) at the Air Force Research Laboratory (AFRL). Unless otherwise noted, imagery in this document is property of the U.S. Air Force or Canva. Distribution Statement A: Approved for Public Release, Unlimited distribution. AFRL-2025-0801, Cleared 12 FEB 2025

**References:** [1] Bricknell and Craig (1999), *Occup. Med.* 49(1); [2] Steele et al. (2015), *Stud. Mechanobiol. Tissue Eng. Biomater.* 19; [3] Knapik et al. (2011), *Aviat. Space Environ. Med.*, 82(8); [4] NIOSH (1981), *Tech Report* 81-122

# IMPACT OF BACK-SUPPORT EXOSKELETONS ON TRUNK MUSCLE COACTIVATION DURING LIFTING

Rahul Narasimhan Raghuraman, *Divya Srinivasan
Department of Industrial Engineering, Clemson University, SC, USA 29634
*Corresponding author's email: sriniv5@clemson.edu

**Introduction:** Muscle coactivation is a key neuromuscular strategy for maintaining spinal stability during manual material handling. In lifting tasks, the coordinated activation of trunk flexors and extensors enhances spinal stiffness, reducing instability risk [1]. However, decrease in stiffness of agonist (i.e., trunk extensor) muscles due to factors such as fatigue or restrictive equipment can prompt increased antagonistic coactivation to restore stability. This compensatory response may lead to excessive coactivation and spinal compression, leading to increased risk of injury [2]. To mitigate musculoskeletal disorders (MSD) often linked to repetitive lifting, exoskeletons are being rapidly being deployed to provide external load support and reduce low-back strain, as evidenced by decreased trunk extensor muscle activity. However, it is currently unknown how external assistance from exoskeletons affect trunk neuromuscular control. Although some studies have begun to show that exoskeleton designs and mechanisms can significantly influence trunk stability and lumbar-pelvic coordination [3], the effects of exoskeleton-use on trunk muscle coactivation is yet to be understood. In this study, we examined how two different back-support exoskeleton designs (EXO) influence trunk muscle coactivation during lifting tasks. We expected to see significant differences in co-activation with EXO use, with further differences observed between the two design types.

**Methods:** A gender-balanced sample of fourteen adults (18-35 years) with no MSDs in the past 12 months were recruited. This study was approved by the University Institutional Review Board, participants provided written informed consent in accordance with the Declaration of Helsinki. Two EXOs that represented significantly different designs (Apex: light, textile based, passive vs. Apogee: heavy, rigid, powered) were evaluated. Three experimental conditions of control (i.e., no EXO), Apex 2 (HeroWear, USA), and Apogee (German Bionics, Germany) were tested; participants chose their preferred EXO assistance (low, medium, high) during a brief familiarization (~5 minutes). They performed symmetric sagittal lifting tasks from fixed ankle and knee heights to waist height with a 14 kg load, completing four consecutive lifts at each height. Inertial Measurement Unit (IMU) sensors (MTw Awinda, B.V., Netherlands) captured trunk kinematics, while surface electromyography (EMG) sensors (Noraxon, AZ, USA) were placed bilaterally on trunk extensors (thoracic and lumbar erector spinae) and flexors (rectus abdominis and external oblique) normalized to individual maximum voluntary contractions (MVC). Standard guidelines were followed for skin preparation, sensor placement, MVC tests, and data processing [4,5]. Coactivation ratio (CoAR) was calculated as [SUM Flexors average nEMG / (SUM Extensors + Flexors average nEMG)] * 100, with nEMG activity averaged across four repetitive lifts [6]. Each lift was time-normalized based on the median lifting time of all participants. CoAR was computed at 0%, 25%, 50%, 75%, and 100% of the lift. A 2-way ANOVA) was used to analyze the effects of EXO (3 levels) and biological sex (2 levels) separated by 'lifting %' and 'height'. Significant effects were further analyzed with post-hoc (Bernoulli) pairwise comparisons. Parametric assumptions were verified, and significance was set at $p<0.05$.

**Results & Discussion:** In the Control condition, CoAR ranged from ~35% for ankle-to-waist up to ~40% for knee-to-waist lifts. EXO use caused significant differences in CoAR, Apex showed a consistent reduction of ~36% across all lifting percentages and heights for both males and females ($p<0.01$), while Apogee had a more variable effect. Using Apogee led to a consistent increase in CoAR for females especially for ankle-to-waist lift. Fig. 1 summarizes CoAR findings for ankle-to-waist lifting. Overall, both EXOs showed reductions in trunk extensors and flexor nEMG. However, specifically in terms of flexor nEMG (as %MVC) reduction, Apogee was more beneficial to males (~30%) compared to females (~20%) for ankle-to-waist. These differences in response to the Apogee between males and females could be due to a few different factors: notably, males consistently preferred higher levels of assistive support from the device than females. Additionally, the significant weight of the device (Apogee: 7.3 kg) may have contributed to the higher CoAR in females, as the device weight was a greater percent of their upper body masses as compared to males. Thus, females may have needed to exhibit higher levels of coactivation to manage the higher relative mass of the exoskeleton on their torso (by increasing spinal stiffness), compared to males. We did not directly measure spinal stiffness in this study, and future work would need to also consider additional factors such as load levels, trunk extension velocity to understand differences in injury risk between males and females [7, 8].

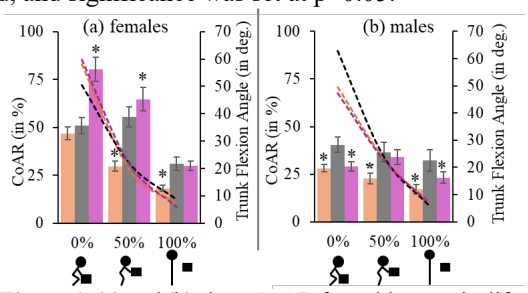


**Figure 1.** (a) and (b) show CoAR for ankle to waist lifts (0–100%) for females and males with overlayed dotted lines representing trunk flexion angle. EXO conditions: Apex (orange), Control (gray), Apogee (purple). Significant effects are marked with *.

**Significance:** Maintaining optimal spinal stability without the need for excessive coactivation is a requirement to keep injury risks lower in the long-term, especially when performing repetitive tasks like lifting. There has been little examination in the literature on what the long-term consequences of exoskeletons could be, to spinal health and injury risk. In this context, it is encouraging to note that coactivations of trunk muscles are not increased by the passive EXO examined in this study. Further work will have to understand whether device weight of powered exoskeletons cause significant differences in trunk neuromuscular control between men and women.

**Acknowledgments:** This work was funded by grants from Boeing Research & Technology and South Carolina Research Authority.

**References:** [1] *Spine*, 12(10), 1035-1040; [2] *Human factors*, *46*(1), 81-91; [3] *Journal of Biomechanics, 176, 112348*; [4] *Journal of Biomechanics, 35*(4), 543–548; [5] *Journal of Orthopaedic Research*, *26*(12), 1591-1597; [6] *Journal of Occupational Rehabilitation*, *7*, 121-138; [7] *Spine*, *20*(8), 913-919; [8] *Journal of Biomechanics*, *34*(9), 1117-1123

# The Relationship between an Individual's Height and the Movement Strategies Implemented to Perform Manual Patient-Handling Tasks

Regina Vicente, Elsa Brillinger, and Dr. Brooke Odle
Hope College, Department of Engineering, Holland, MI, USA
Email: regina.vicente@hope.edu

**Introduction:** Nurses are specifically at risk of low back pain and injury, which has been associated with the performance of daily tasks involving repositioning and handling patients in awkward postures [1]. We recently conducted a second proof of concept study to understand multi-joint coordination of the trunk, hips, and knees during the performance of several patient-handling tasks. While interpreting that data, we noted a difference in performance of shorter subjects versus taller subjects. In this study, we present a secondary analysis of that data that explores the relationship of the movement strategies selected during tasks (based on trunk, hip, and knee joint coordination) and subject height. We hypothesized that the movement strategy elicited by shorter subjects would entail more trunk engagement, while the strategy of taller subjects would entail more engagement of the lower limbs.

The long-term goal of our work is to develop effective training interventions for nursing students and personnel. Thus, we expect the preliminary findings will provide additional insight on whether the height of the nurse needs to be considered when developing training interventions and recommendations.

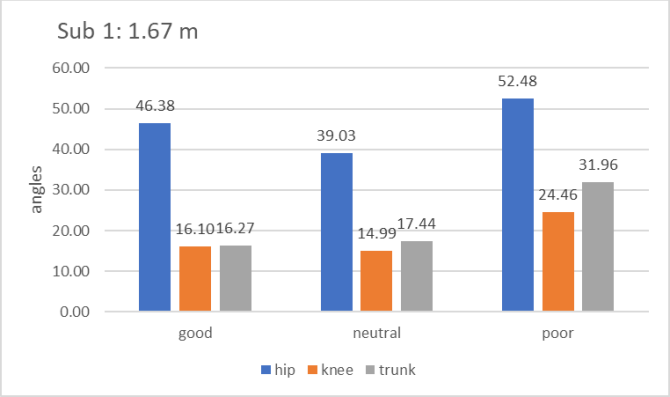


**Figure 1:** Short subject joint angle averages.

**Methods:** In the proof of concept study, seven volunteers (all female) that were between 19 and 24 years of age and had heights ranging between 1.6 and 1.88 m were recruited for participation. The subjects were all nursing students, who had already completed their clinicals training. All subjects signed informed consent forms approved by the Hope College Human Subjects Review Board.

Four iPhone XRs were synchronized and utilized OpenCap to collect and process kinematic data [2]. Subjects completed the following tasks: (1) repositioning a patient in bed using a sliding sheet, (2) turning a patient to one side, (3) sitting a patient up, (4) lifting patient's leg upwards, and (5) turning a patient on one side and placing a sling under the patient while another assistant holds the patient in that position. All tasks were performed on a height adjustable treatment table. In a given trial, each task was repeated twice at either hip height (good posture), mid-thigh height (neutral posture), or knee height (poor posture). The posture classifications are based on work by Freitag and colleagues [3], who investigated the relationship between bed height and tasks requiring forward bending. Manikins (Ruth Lee, Oxford, UK) served as patients and manikins of three different weights were used: 44 lb, 66 lb, 110 lb. One trial consisted of three repetitions of a task at a given table height. Two trials were collected for each task and table height. The order of tasks, table heights, and manikin weights were randomized to minimize fatigue.

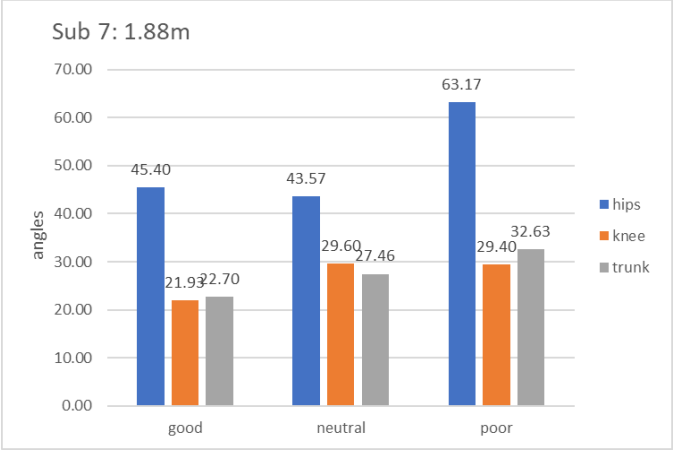


**Figure 2**: Tall subject join angle averages.

Kinematic data were filtered using a second-order Butterworth filter with a 12 Hz cut-off. A custom MATLAB (The Mathworks, Natick, MA) script was used to select peaks in trunk, hip, and knee flexion angles during each repetition in each trial across each task and posture type. The average peak of each angle, across all tasks for each posture type, was computed for each subject.

**Results & Discussion:** Preliminary analyses indicate that both tall and short subjects demonstrated comparable performance in patient handling tasks, evenly distributing their effort between their knee and trunk joints (figure 1 & 2). A notable difference between this study and the previous proof of concept is the training of participants. In this second study with nursing students as participants, it was possible to note their formal training and clinical experience demonstrating a better body mechanics which may explain the more expected distribution of effort of angles among joints. Data Analysis is still ongoing for three additional subjects, and results may vary further as data is processed.

**Significance:** These findings suggest that exposure and training play a significant role in performance. Nursing students showed a better usage body mechanics, in comparison to the previous participants who had no experience and relied on movement patterns. While these findings conflict with our takeaway from our previous study, we can now think how these finding may be helpful in developing future interventions for lay caregivers (those who care for family members and have no formal training). Again, this is a small sample size for both studies, so future work would need to explore the tasks with larger cohorts of non-nursing and nursing students.

**Acknowledgments:** This work was funded by the Restore Center and the Provost's Office at Hope College. The Restore Center is funded by the National Institutes of Health through grant P2CHD101913.

**References:** [1] Hoy, D. et al. Ann. Rheum. Dis. 2014, 73, 968–974.[2] Uhlrich, S. et al. 2022. biorxiv https://doi.org/10.1101/2022.07.07.499061 [3] Freitag, S, et al. *The Annals of Occupational Hygiene.* 2013.. https://doi.org/10.1093/annhyg/met071

# EVALUATING OPTIMIZATION CRITERIA IN THE ANYBODY MODELING SYSTEM FOR ESTIMATING MUSCLE ACTIVITY DURING LIFTING WITH AND WITHOUT A BACK-SUPPORT EXOSKELETON

Mohamad Behjati Ashtiani[1], Lingyu Li[1], Sunwook Kim[1], *Maury A. Nussbaum[1]
[1]Department of Industrial and Systems Engineering, Virginia Tech, Blacksburg, VA, USA
*Corresponding author's email: nussbaum@vt.edu

**Introduction:** Occupational back-support exoskeletons (BSEs) help reduce physical demands and the risk of work-related musculoskeletal disorders by reducing physical demands [1], [2]. Although BSEs decrease back muscle activity [3], [4], assessing muscle activity using surface electromyography (sEMG) is limited by electrode placement constraints, often restricting analysis to a few trunk muscles over short durations. Musculoskeletal modeling tools, such as the AnyBody Modeling System™ (AMS), offer an alternative by estimating muscle activity through inverse dynamics and static optimization. Common AMS optimization criteria include minimizing squared or cubic muscle stress and the min/max criterion [5]. Previous studies have evaluated these criteria within spine models [6], [7], yet they focused on relatively simple tasks (e.g., static or symmetric). To our knowledge, no study has compared model-based estimates from the AMS with measured muscle activity during dynamic lifting, particularly with BSE use. In the current study, we thus aimed to assess AMS estimates of muscle activation with accessible muscle activity levels measured via sEMG during symmetric and asymmetric dynamic lifting, both with and without a BSE. Given that BSEs can alter muscle coordination patterns [8], we hypothesized that the effectiveness of optimization criteria would vary depending on the condition (BSE vs. without BSE).

**Methods:** We used data from a previously published study [4], wherein 18 participants (9 males, 9 females) performed repetitive lifting/lowering across nine trials involving three *Task Conditions* (Ground_Sym, Knee_Sym, Knee_Asy) and three *Interventions* (suitX backX™ AC, Laevo™ V2.5, and no BSE). Whole-body kinematics were measures along with bilateral sEMG from the thoracic erector spinae, iliocostalis lumborum, rectus abdominis, and external oblique. Using the generic GaitFullBody model in AMS, we estimated muscle activation levels through inverse dynamics analysis by minimizing: 1) $\sum stress^2$; 2) $\sum stress^3$; and 3) muscle fatigue (min/max). We have provided detailed information about simulation workflows and BSE modelling in the AMS (Fig. 1) in a separate report [9]. We completed simulations (18 participants × 9 trials × 40 cycles × 2 movement phases [lifting/lowering]) in AMS for each optimization criterion. Model estimates were evaluated using pattern similarity and error magnitude between model-estimated and measured muscle activation within each task repetition, by calculating the Maximum Normalized Cross-Correlation coefficient (MNCC) and the root-mean-square error (RMSE) for each optimization criterion, respectively. Repeated-measures ANOVA was used to examine the effects of *Task Condition, Intervention, Movement Phase, Muscle Recruitment Criterion,* and biological *Sex* on MNCC and RMSE across the four back muscle groups. Estimated abdominal muscle activities were quite low, so were not analyzed further here.

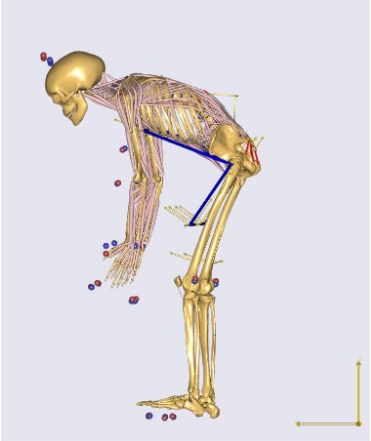

**Figure 1:** Illustrations of a virtual BSE representation in the AnyBody Modeling System (AMS).

**Results & Discussion:** MNCC and RMSE values using all Muscle Recruitment Criteria were comparable to previous studies [10],[11], demonstrating excellent similarity (mean MNCC >0.80) and relatively small errors (mean RMSE <0.20). Using $\sum stress^2$ generally outperformed both $\sum stress^3$ and min/max, yielding higher MNCC (0.92–0.94) and lower RMSE (0.13–0.15) across conditions, though differences were not always significant across conditions. Earlier results also suggested that $\sum stress^2$ might be the preferred criterion [6],[7]. Regardless of muscle recruitment criteria, tasks with more extremely trunk postures here had lower MNCC and higher RMSE, likely due to the simplified muscle model in AMS, which does not account for passive muscle forces in muscle activity estimation. This result suggests that caution is needed when interpreting muscle activity estimates in extreme postures. There was not a significant *Intervention × Muscle Recruitment Criterion* effect on RMSE, but this effect was significant for MNCC across all muscle groups. However, the best-performing criterion did not differ between Intervention levels, suggesting that the optimal muscle recruitment strategy may not change between BSE and no BSE conditions, potentially contradicting our hypothesis. For all Muscle Recruitment Criterion levels, muscle activity estimations generally had larger MNCC and smaller RMSE for NoBSE vs. BSE conditions, though differences were not always significant. This difference is likely due to simplified assumptions we used in modeling the human-BSE interface in AMS, such as applying an interaction force to a static single point on the chest. Future studies may require more detailed BSE-human co-simulation modeling to improve muscle activity estimation accuracy during BSE use.

**Significance:** Our results may help enhance BSE evaluation by assessing AMS-estimated muscle activity during dynamic lifting. Specifically, our findings could help to refine optimization strategies for musculoskeletal modeling, improving reliability in ergonomic and clinical applications. Overall, our results support simulation-based assessments of human-exoskeleton interactions.

**Acknowledgments:** This study was supported by Grant # 2128926 from the National Science Foundation (NSF).

**References:** [1] de Looze et al., 2016, *Ergonomics* 59(5); [2] Nussbaum et al., 2019, *IIE Trans Occup* 7(3-4); [3] Alemi et al., 2020, *Hum Factors* 62(3); [4] Madinei et al., 2020 *Appl Ergon* 88,103156; [5] Damsgard et al., 2001, *IDETC/CIE* V. 80272; [6] Arjmand et al., 2006, *Med Eng Phys* 28(6); [7] Wang et al., 2022, *Med Eng Phys*, 110, 103916; [8] Tan et al., 2019, *Front Hum Neurosci*, 13, 142; [9] Behjati Ashtiani et al., 2025, *SSRN* 5142080; [10] Alemi et al., 2023, *Ann Biomed Eng* 52(2); [11] Yan et al., 2024, *J Biomech* 176:112322;

# ANALYSIS OF THE EFFECTS OF HELMET INERTICAL PROPERTIES ON CERVICAL SPINE LOADING

Gustavo M. Paulon[1], Suman K. Chowdhury[1*]
[1]Department of Industrial and Systems Engineering, University of Florida, Gainesville, Florida, United States
*Corresponding author's email: sk.chowdhury@ufl.edu

**Introduction:** Many prior studies reported that the repetitive usage of heavyweight, imbalanced helmets during occupational tasks is associated with the development of neck muscle strain and pain [1, 2]. The usage of such helmets can increase the cervical intervertebral joint forces due to their inertial properties—mass, center of mass (COM), and moment of inertia (MOI)—and the cumulative exposure over time of such forces over time can lead to degenerative conditions on the neck passive tissues and strain of neck muscles. The injury mechanics of the cervical spine depends on many factors, such as head-neck posture, load type, and load frequency. For example, an in-vitro study showed that the application of a compressive force of 300 N on the lumbar spine resulted on an intervertebral disc height loss of 0.1 mm [3], and another study found that extending the ligaments for 50 minutes in a flexion posture increased the instability of the spine by 85% [4]. Therefore, the objective of this study was to assess the effects of firefighter helmet inertial properties on the cervical compressive and shear joint forces (C1-C2, C2-C3, C3-C4, C4-C5, C5-C6, C6-C7, and C7-T1). We hypothesized that the helmet COM location significantly induces increased cervical joint reaction forces (JRFs) alongside the helmet weight. We considered two different designs that are commonly used by firefighters: 1) a high-profile (far superior COM from C0-C1) US style helmet, and 2) a European (EU) helmet, characterized by its low-profile (COM closer to C0-C1 joint).

**Methods:** We analysed motion capture and force plate data from 10 male (90.6 ± 19.1 kg; height: 1.77 ± 0.066 m; BMI: 28.8 ± 2.85 kg/m2; Age: 38.2 ± 7.97 years) and 10 female (67.4 ± 8.28 kg; height: 1.67 ± 0.055 m; BMI: 24.2 ± 2.85 kg/m2; Age: 31.2 ± 8.62 years) firefighters. Participants performed head-neck flexion-extension movement during 3s and static flexion and extension exertions for 5s with three different helmet conditions, no helmet (NH), US helmet (1.77 kg; COM: 0.002 (anterior), 0.152 (superior), -0.006 (left) m), and European (EU) helmet (2.02 kg; COM:0.019 (anterior), 0.094 (superior), -0.008 (left) m) in a random order [5]. We used OpenSim MASI model [6] to build subject- and helmet-specific models and estimate cervical JRFs from individual helmet and task conditions (Fig. 1). To test our results, we implemented a randomized block Analysis of Variance (ANOVA) at a 95% confidence interval ($\alpha$=0.05) to study the effects of *helmet type* and *sex* on the inferior-superior (IS) compressive, anteroposterior (AP) shear, and mediolateral (ML) shear forces on cervical JRFs.

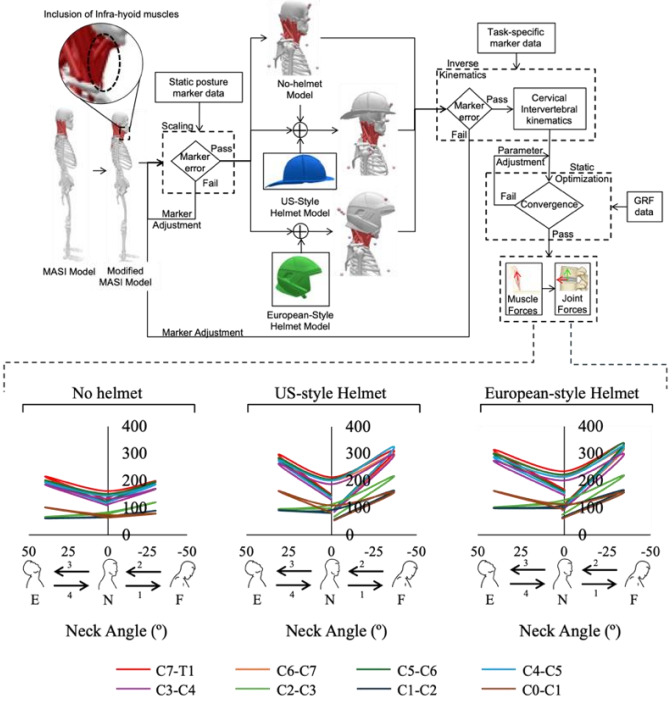


**Figure 1**: Graphical representation of the methodology used to calculate the joint reaction forces (top) and compressive forces magnitude with respect to head-neck flexion-extension angles (bottom).

**Results & Discussion:** Helmets significantly increased IS forces in static neck flexion ($p<0.001$; US: 61.6%; EU: 54.0%) and extension positions ($p<0.003$; US: 48.7%; EU: 52.1%) and during dynamic neck FE movement ($p<0.041$; US: 53.9%; EU: 44.6%) across all joints except for C7-T1 joint (Fig. 1). US helmet condition showed the highest AP shear forces during static flexion ($p<0.008$; 85.0% for NH and 3.70% for EU helmet) and FE movement ($p>0.049$; 58.3% for NH and 10.3% for EU helmet). Similarly, the ML forces were also found to be greater ($p>0.05$) for the US helmet across all joints in static neck flexion position (458% for NH and 305% for EU helmet) and dynamic FE movement (19.0% for NH and -20.1% for EU helmet). In contrast, during static extension, both helmets demonstrated lower AP forces (C7-T1, C3-C4, and C1-C2) and ML forces (C6-C7 and C5-C3 joints). The reduced neck extension angle with helmet use decreased the moment arm [5], lowering gravitational demand across cervical joints. Despite being 250g lighter, the US helmet's higher COM (5.8 cm above the EU helmet) increased MOI by 10% at C0-C1, leading to higher compressive and shear forces. These results highlighted the importance of designing a low-profile helmet with COM closer to the C0-C1 joint to reduce the likelihood of injuries and degenerative conditions in the cervical spine

**Significance:** The findings of this study revealed that helmets with a COM location closer to the C0-C1 joint (i.e., low-profile design) could decrease unhealthy cervical spinal joint loading significantly and, consequently, decrease the likelihood of developing any degenerative condition in the cervical spine. This study only evaluated head-neck FE movements, and the influence of the different helmet inertial properties should be assessed in both head-neck lateral bending and axial rotation.

**Acknowledgments:** We acknowledge the Department of Homeland Security & Technology (70RSAT21CB0000023) for the support.

**References:** [1] Mathys et al. (2012), *JOB* 45(14); [2] Barrett et al. (2022), *Human Fact.*; [3] Adams et al. (2000), *Spine* 25(13); [4] Solomonow et al. (1999), *Spine* 24(23); [5] Paulon et al. (2024), *JOB* p112364; [6] Cazzola et al. (2017), *PloS one* 12(1).

# BIOMECHANICAL ANALYSIS OF THE SHOULDER UNDERGOING INDUSTRY RELEVANT TASKS

Carlo Canezo[1*], Dustin Crouch[2], Greg Sawicki[1],
[1]Physiology of Wearable Robots Lab, School of Mechanical Engineering, Georgia Tech, Atlanta, Georgia
[2]Upper Limb Assist Lab, University of Tennessee, Knoxville, Tennessee
*Corresponding author's email: ccanezo3@gatech.edu

**Introduction:** Upper-body wearable devices such as exoskeletons have the potential to reduce injuries for industry workers completing highly repetitive or high load tasks. The challenge lies in developing effective control schemes over a set of diverse tasks while accounting for the physical interaction between the human and the device [1]. Unlike lower-body wearable devices where a design developmental framework has been established based on lower body biomechanics for common cyclic tasks such as walking or running [2], the upper body regime lacks a formal "roadmap" tailored to guide device designs. This is principally because upper-body tasks are high DOF, unstructured and non-cyclical. – all features that pose challenges for computing inverse dynamics. Our research aims to fill this gap by compiling data from real-world upper body tasks in a highly instrumented lab setting to drive computational models and calculate upper body joint-level outcome measures that can be used to identify injury "hotspots". In this study, we test the following hypothesis with a focus on the shoulder joint: a) increased interaction loads will lead to an increase in joint level biomechanical demand* that is exacerbated by b) increased proximity to the workspace extremes where demand* is measured via joint moments, powers, work, and impulse.

**Methods:** Our setup involved replicating a shelf stacking task across the upper body workspace for one arm. This was done by a 2x three level shelf setup (Fig.1). The participant (N=1) performed a static holding task at a specified workspace region by moving a weighted object to and from a specified home position in front of subject. Three interaction loads were used: Low (0.2kg), Medium (1.82kg), and High (3.75kg). Three task locations were chosen that involved moving the load closer to the "extreme" parts of the workspace, defined as needing greater than 90 degrees of the shoulder elevation angle, for a single arm. These were location A (close sagittal), location B (extreme sagittal), and location C (extreme frontal). Motion capture data were used to compute inverse kinematics and inverse dynamics in OpenSim while accounting for the added mass of the interaction loads with a specific focus on the shoulder joint [4]. We calculated shoulder elevator joint moment, joint power, and joint impulse and joint work to assess task demand and compare them across load and workspace region.

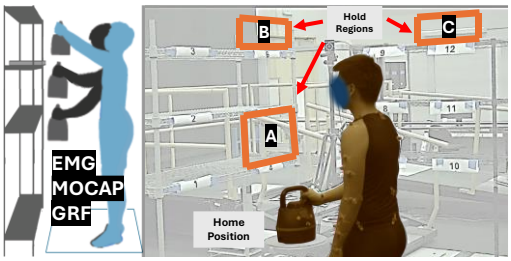


Figure 1: Experimental Workspace Setup for Upper body Tasks. Three locations are shown: A: Non-extreme Workspace, B: Extreme Workspace Sagittal Plane, C: Extreme Workspace Frontal Plane

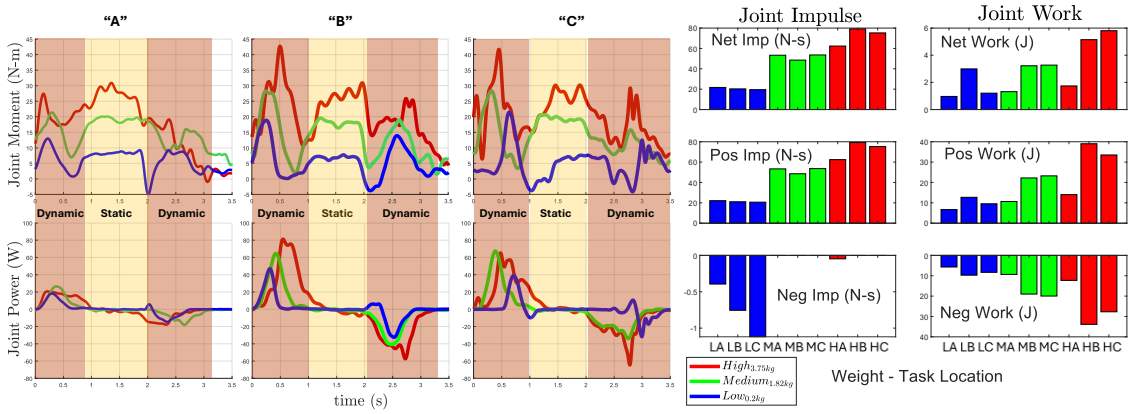


Figure 2: Shoulder mechanical demand for various weights and workspace locations. Dark shaded regions indicate dynamic motion, and light shaded region indicates when the interaction load is held statically.

**Results & Discussion:** As expected, within a given workspace location (A, B, or C), when interaction load increased (blue, green, red), the joint moment, net joint work and net joint impulse also increased (Fig. 2). Joint power output was more variable, and increased with load only for tasks at the workspace extremes. Within a given interaction load, joint moment, joint power, and net joint work all increased as the movement task approached the workspace extreme (A to B to C), while net joint impulse remained invariant across the workspace. Interestingly, adding asymmetry by layering sagittal + frontal ROM demands had little effect on mechanical demand. Overall, in line with biomechanical intuition, our data set identified key 'hotspots' in the acceleration and braking phases of the motion (dynamic phases) that were more pronounced with higher interaction loads (Fig 2 – dark shaded).

**Significance:** Key significance of this study is the application of computational biomechanics to understand upper-body joint-level mechanical demands across a range of industry relevant tasks. Data can now be analyzed to determine shoulder elevator joint torque vs angle curves than can be directly translated to upper body wearable device actuator design specifications. These data can also be used as 'ground truth' to train data-driven machine learning models that may be deployed for exoskeleton control [4].

**Acknowledgments:** This work is supported by NSF under Grant Award Number 2202862.

**References:** [1] Crouch et al. (2020), *J. App Biomech.* 36(2); [2] Nuckols et al. (2020), *PLOS ONE* 15(8); [3] Saul et al (2015), *Comp. Methods in Biomech & BioEng* 18(13) [4] Molinaro et al. (2024) *Nature* 635(8038).

# THE INFLUENCE OF SEX AND INDIVIDUAL VARIATION ON CONTRIBUTIONS TO TORSO LATERAL BENDING

*Jordan T. Sturdy, Anne K. Silverman
Department of Mechanical Engineering, Colorado School of Mines, Golden CO
*Corresponding author's email: sturdy@mines.edu

**Introduction:** Intervertebral force estimates via musculoskeletal modeling are sensitive to orientation definitions of vertebral bodies [1,2]. To mitigate errors, musculoskeletal models incorporate spinal rhythms, or prescribed contributions from individual vertebral bodies to overall torso motion [3]. However, this approach does not account for variation between individuals, demographic groups, injured populations, or across movement tasks that may require altered muscle control. Yet the relative sagittal rotations between lumbar regions has task dependence [4], and the regional contributions to trunk flexion during sit-to-stand depend on sex [5]. Lateral bending is useful for classifying people with low back pain by movement characteristics and lumbar contributions to the total bending range differ between clinical sub-groups [6]. Individual variation of regional coordination throughout the spine during a variety of movements among healthy participants may hinder the clinical relevance of averaged motion patterns [7]. However, many studies omit the thoracic region or include a single lumbar region, which makes extension to whole-body modeling difficult. The purpose of this study was to characterize the contributions of the lower lumbar, upper lumbar, and thoracic spine regions to total torso range-of-motion (ROM) during lateral bending in healthy, young participants. In addition, we evaluated sex-based differences and defined intracohort variation in the total torso ROM and the motion of different spine regions.

**Methods:** Kinematic data were collected using Qualysis Track Manager from 10 male (age: 27.9±5.3y, height: 1.76±.04m, body mass: 76.1±12.2kg) and 10 female (24.7±4.6y, 1.66±.06m, 60.3±10.5kg) participants without low back pain who performed their self-selected maximum torso lateral bending to each side three times. Reflective markers were placed bilaterally on the anterior and posterior iliac spines, on the L4, L1, and T6 spinous processes, with additional markers placed bilaterally to L5, L3, and T9. These markers were used to define pelvis, L4-L5, L1-L3 and T6-T9 segments using Visual3D, and relative angles between L4-L5 and pelvis (lower lumbar), L1-L3 and L4-L5 (upper lumbar), and T6-T9 and L1-L3 (thoracic) were calculated. The average lower lumbar, upper lumbar, and thoracic peak-to-peak ranges in the frontal plane of the three bending cycles was calculated for each participant. Total torso range-of-motion (ROM) was obtained by adding the angles from each joint together, and the relative contributions of each segment were calculated as a percentage of the torso ROM. One-factor ANOVA evaluated sex-based differences in absolute angles of lower lumbar, upper lumbar, thoracic, and torso ROM and relative % contributions from lower lumbar, upper lumbar, and thoracic to the total torso ROM.

**Results & Discussion:** Female participants achieved ~13 degrees greater torso ROM than male participants (Figure 1, ***p*=.035**). This corresponded with ~9 degrees greater upper lumbar range in female compared with male participants (***p*<.001**). However, when expressed as a percentage of the torso ROM there were no differences (Figure 1). An established lumbar rhythm used in musculoskeletal modeling [3] was compared to our results by combining the relative contributions from regions corresponding to the segments in our study (Figure 1). While our averaged results agree well with the existing rhythm, substantial individual variation in the ranges of regional contributions (lower lumbar 5-27%; upper lumbar 16-46%; thoracic 41-71%) suggest that averaging may obscure different underlying trends in spinal rhythm. For example, data from one F participant falls below the 5$^{th}$ percentile for upper lumbar but above the 95$^{th}$ percentile for thoracic. Omitting this participant resulted in different upper lumbar contributions between M and F participants (***p*=.007**) and eliminated the difference in torso ROM.

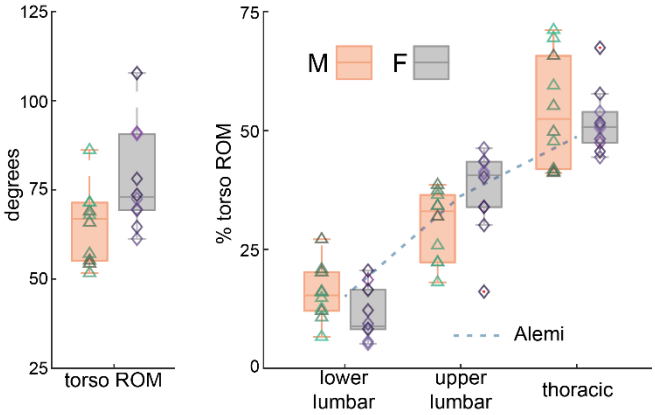


**Figure 1**: Total torso range of motion (left) and regional contributions (right). Male/Female groups shown with orange/grey box and whiskers, with green triangles/purple diamonds for individuals. Spinal rhythm from Alemi [3] shown for comparison.

**Significance:** These results do not strongly suggest that sex-based spinal rhythms are needed for modeling studies generalizing to healthy populations. However, an expanded data set may support such a recommendation as the upper lumbar % contribution was strongly influenced by one female participant. The variation in relative contributions between participants of greater than 22% difference for all torso regions may suggest two things. First, that an individualized modeling approach incorporating multiple spinal regions may improve accuracy of simulated muscle and joint contact forces. Second, that there may be specific trends for participant sub-groups characterized by something other than sex, such as stiffness or flexibility in specific spinal regions. Further investigation using musculoskeletal modeling with personalized spinal rhythms may reveal unique spinal joint contact force distributions that are important for understanding the mechanistic development and management of low back pain.

**Acknowledgments:** NSF BII: Integrative Movement Sciences Institute, award #2319710; Anna Corman, Ava Watson, Mike Miller

**References:** [1] D. Ignasiak, et. al., (2016) J. Biomech. 49. [2] A.G. Bruno, et.al., (2017) J. Orthop. Res. 35. [3] M.M. Alemi, et al., (2021) Front. Bioeng. Biotechnol. 9. [4] T. Mitchell, et. al., (2008) BMC Musculoskelet. Disord. 9. [5] S. Parkinson, et. al., (2013), Man. Ther. 18. [6] S.P. Gombatto, et. al., (20017) Phys. Ther. 87. [7] A. Leardini, et. al., (2011) Clin. Biomech. 26.

# THE MECHANICAL LOADING OF THE SPINE DURING PATIENT TRANSFER FROM BED TO WHEELCHAIR IN PHYSICAL THERAPISTS

Seyoung Lee[1], Kitaek Lim[1], Junwoo Park[1], Soyeon Yoon[1], Sungmin Chun[1], Donggeon Kim[1], Woochol Joseph Choi[1*]
[1]Injury Prevention and Biomechanics Laboratory, Dept of Physical Therapy, Yonsei University, South Korea
*Corresponding author's email: wcjchoi@yonsei.ac.kr

**Introduction:** Lower back pain is common in healthcare providers, and frequent loading of the spine during transfers are considered a cause [1]. We have estimated clinicians' physical stress at the intervertebral disc between L5 and S1 during patient transfers from bed to wheelchair, in order to examine how it was affected by circumstances of transfers.

**Methods:** Eight physical therapists (4 males, 4 females) transferred a patient from bed to wheelchair. Trials were acquired with two transfer method (manual and lift-assisted), two bed heights (10 cm and 30 cm below the anterior superior iliac spine (ASIS)), and two patient body weights (70 kg and 75 kg). During the trials, kinematics of the upper body was recorded with reflective markers placed on the wrist, elbow, shoulder, C7, L5, ASIS, and posterior superior iliac spine through eight motion capture cameras (Vero v2.2, VICON, Oxford, UK). During trials, the patient's feet remained in contact with a force plate (OR6-7-2000, AMTI, Waltham, MA, USA), allowing us to monitor actual patient body weight that subjects handled.

An outcome variable included a peak compressive force at L5/S1, which computed using static equilibrium equations (i.e., ΣF = 0; ΣM = 0) (Figure 1a). The centre of gravity of body segments and joint centers were acquired from anthropometric data [2], and calculated based on a 6-segment model [3], respectively.

Repeated measures ANOVA was used to test if the peak compressive force was associated with transfer method (2 levels), bed height (2 levels), and patient weight (2 levels) at a significance level of alpha = 0.05.

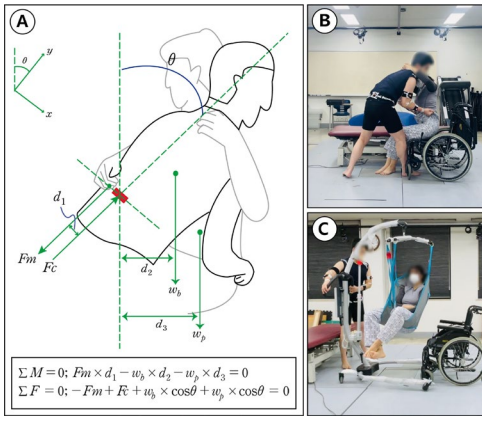


**Figure 1:** Patient Transfer from bed to wheelchair. (a) A free body diagram showing forces acting on the body segments during transfers (b) manually and (c) using a mechanical lift. Image courtesy of Lee at al.[4].

**Results & Discussion:** The peak compressive force ranged from 1,515 N to 8,231 N, suggesting that some patient transfers involved dangerous moments where the compressive force exceeded the NIOSH safety criterion (3,400 N). Our ANOVA suggested that the peak compressive force was associated with transfer method ($F = 226.3$, $p < 0.0005$) and patient weight ($F = 20.1$, $p < 0.005$), but not with bed height ($F = 2.4$, $p = 0.16$) (Figure 2). The peak compressive force was 68% lower in the lift-assisted transfer compared to the manual transfer (2213 [SD = 468] N vs. 6835 [SD = 798] N).

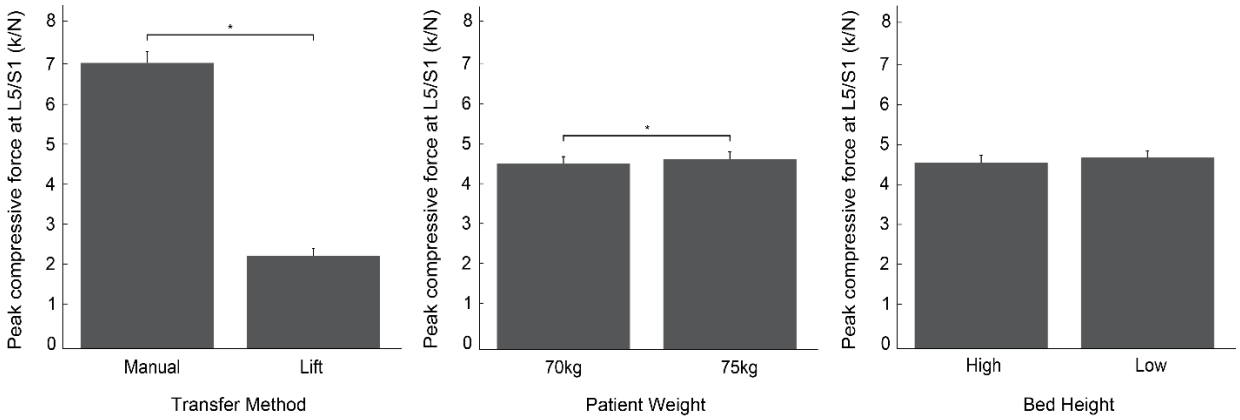


**Figure 2:** Effects of patient transfer on the peak compressive force. The peak compressive force was affected by transfer method and patient weight, but not by bed height. *p < 0.05.

**Significance:** When clinicians transferred a patient from bed to wheelchair, mechanical loading exceeding the NIOSH safety criterion was applied to a disc at L5/S1. This confirms that clinicians are at a greater risk for lower back pain/injuries. However, the risk could be mitigated with use of a mechanical lift.

**Acknowledgments:** This research was supported, in part, by the Transitional Research Program for Care Robots funded by the Ministry of Health & Welfare, Republic of Korea (HK21C0008) and by "Regional Innovation Strategy (RIS)" through the National Research Foundation of Korea (NRF) funded by the Ministry of Education (MOE) (2022RIS-005).

**References:** [1] Waters T.R. (2007), *The American journal of nursing.* [2] Winter (2009), *Biomechanics and Motor Control of Human Movement.* [3] Vaughan (1992), *Dynamics Of Human Gait.* [4] Lee et al. (2024), *Journal of Applied Biomechanics.*

**A Case Study Analysis of Ground Condition on Ladder Setup Angle and Climbing Friction**

Carson A Davis, Cole D Ward, Erika M Pliner
Department of Mechanical Engineering, University of Utah, Salt Lake City, USA
Email: *erika.pliner@utah.edu

**Introduction:** Falls are the leading cause of death in construction and every year falls from ladders make up nearly a third of those deaths [1]. This alarming statistic underscores a critical global challenge in occupational safety, particularly in an industry that forms the backbone of infrastructure development worldwide. While extensive research has established that an optimal ladder setup angle of 75.5° minimizes base movement and slip risk [2-4], there remains a significant gap on the influence of ground condition on worker decision-making of ladder setup and the associated ladder slip risk. Sloped surfaces can alter friction under the ladder feet and contribute to instability, yet common construction surfaces — such as dirt, gravel, stone pavers, and decking materials — effects on setup angle accuracy and slip risk remain unknown. Given that 23% of straight ladder accidents were due to the ladder sliding from its position [5], a deeper understanding of ground condition is critical to improving safety practices. This study aims to quantify the effect of ground surface conditions on ladder setup accuracy and climbing frictional requirements under the ladder feet.

**Methods:** A residential construction worker from the Salt Lake City Area was recruited to perform a common work task. The work task consisted of setting up a ladder, ascending the ladder to an elevated platform, hammering a support beam to an adjacent heightened frame, and descending the ladder. Task instruction focused the worker's attention to optimal performance for a level support beam, resulting in a more naturalistic ladder setup. The support beam task served to distract the participant from the study objectives, reducing bias and providing sufficient rest between climbs and capture of ladder climbing. The participant completed the ladder setup and associated work task across various ground surface conditions, including stone pavers and Trex deck on both flat and angled surfaces. Ladder angle was captured from reflective markers on the ladder and a 17-camera motion capture system. Kinetics were captured below the ladder feet from four force plates beneath the ground surface condition at 1200 Hz. To quantify the frictional requirements of the ladder feet with each ground condition during ladder climbing, the required coefficient of friction (RCOF) was quantified from the ratio of horizontal to normal force during ladder climbing [6]. RCOF was extracted when the normal force exceeded a 150 N threshold, as prior research has shown that the peak RCOF typically occurs when at least 25% of body weight is exerted during ladder climbing [6], ensuring that the selected data accurately reflects relevant slipping conditions. Both the mean and peak RCOF were extracted from this window during ladder climbing for each ground surface condition. Ladder climbing was defined as the time from foot contact with the ladder to foot lift-off on the last step. Below we present a case study of the RCOF for a residential construction worker across ground surface conditions during ascending climbs. Kinematic data will be processed to reveal worker decision-making ladder setup angle.

**Results & Discussion:** The results suggest that surface material and angle influence RCOF values, which are critical for assessing slip risk. The Stone Paver - Angled condition exhibited the highest global mean RCOF (0.500) and peak RCOF (0.510). In contrast, the Trex Deck - Angled condition had a significantly lower global mean RCOF (0.157) and peak RCOF (0.340). Interestingly, a flat surface condition for Trex Deck did not appear to greatly change the global mean RCOF (0.199) or peak RCOF (0.379), while a flat condition for the Stone Paver appears to lower the global mean RCOF (0.176) and peak RCOF (0.420) a substantial to moderate amount, respectively (Fig. 1). These observations suggest that the material properties of the surfaces may be influencing the frictional performance differently by angle. Stone paver performance reduces at steeper ground angles. In contrast, Trex deck material appears to perform similarly if not better at angled than flat ground surfaces.

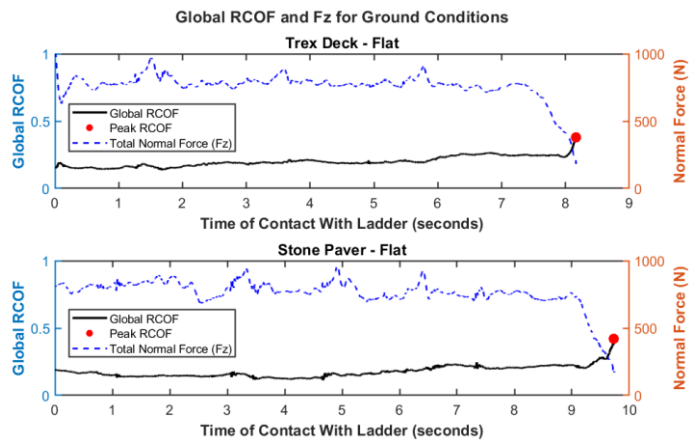


*Figure 1: Global RCOF and total normal force for Trex Deck and Stone Pavers in flat condition.*

**Significance:** These findings suggest that surface material properties play a significant role in frictional performance, especially when considering different angles. Stone pavers have greater frictional requirements at an angle, suggesting this material to increase ladder slip risk in unlevel working conditions. Conversely, the Trex deck showed more consistent RCOF across flat and angled conditions. Since many work environments include both surface types, maintaining lower frictional climbing requirements is crucial for reducing fall risk. Safety interventions, such as improved ladder shoe tread design or altering the material below the ladder feet could help mitigate slip potential, particularly on angled stone paver surfaces.

**Acknowledgements:** Job-Site Safety Institute, Little Giant Ladder Systems, Undergraduate Research Opportunity Program.

**References:** [1] Occupational Safety and Health Administration (2015), *Fall Prevention Training Guide: A Lesson Plan for Employers*; [2] C. C. Chang et al. (2005), Safety Science 43 (7); [3] W. R. Chang et al. (2005), Ergonomics 48 (9); [4] W. R. Chang et al. (2016), Ergonomics 59 (8); [5] S. Tsipouras et al. (2001), Medical Journal of Australia, 174 (10); [6] E. R. Martin et al. (2020), Journal of Biomechanics (99).

# Ladder Foot Friction Across Ground Conditions

Cole D Ward[1], Carson A Davis [1], Kurt E Beschorner[2], Erika M Pliner[1*]
[1]Department of Mechanical Engineering, University of Utah, Salt Lake City, UT, USA
[2]Department of Bioengineering, University of Pittsburgh, Pittsburg, PA, USA
Email: *erika.pliner@utah.edu

**Introduction:** Ladders accounted for over 22,700 workplace injuries and 161 fatalities in the US in 2020 [1]. A primary cause of these injuries is a ladder fall due to insufficient friction between the ladder feet and the ground. While previous work has examined the required coefficient of friction (RCOF) of the ladder feet-ground interface across varying ladder inclinations and ladder heights [2], there is a lack of knowledge on the friction available between ladder feet and diverse ground conditions. If the RCOF exceeds the available coefficient of friction (ACOF), a slip is likely to occur [3], causing the ladder and user to be at risk of falling. Ladders are used in diverse environments, yet no study has extensively evaluated the effects of ground condition on the ladder foot ACOF. To give greater context to the risk of ladder slip research (i.e. RCOF), there is a need to quantify the ACOF between the ladder feet and real-world ground conditions. This study addresses this gap by analyzing the influence of surface type (stone pavers, trex decking, and vinyl flooring) and weather conditions (dry and muddy) on the ladder foot ACOF. Understanding the frictional interactions between ladder feet and common ladder ground conditions is critical for improving ladder stability and worker safety. We hypothesized that the highest ACOF will be observed on stone pavers under dry conditions, while the lowest will be observed on vinyl flooring under muddy conditions. We also hypothesized that all muddy surfaces would have decreased ACOF compared to the dry conditions.

**Methods:** A 512 N load, simulating the vertical loading during ladder climbing of 60-70% of body weight [4], was applied to a ladder foot. A horizontal force (friction force) was applied to a ladder foot utilizing a frictionless string-pulley system. The pulley system was in line with a force sensor (Mark-10, Copiague, NY) to capture the applied frictional force. Three surface types - stone pavers, trex decking, and vinyl flooring - were tested under dry and muddy conditions. Mud was standardized using a 1:3 ratio of sodium bentonite to water, and 3.56 N of mud was applied to each surface type for muddy conditions. Ten trials were collected with a new ladder foot for each ground condition (surface type and weather condition). The force required to initiate ladder foot movement was recorded as the static friction force (F), and the ACOF was calculated as $ACOF = F/mg$ . To test our hypotheses, a repeated measures two-way ANOVA was performed with surface type and weather condition as the independent variables and ACOF as the dependent variable. If the interaction was found to be significant, Least Significant Difference post-hoc tests were performed between groups.

**Results & Discussion:** The ACOF was found to vary between 0.328 and 0.896 across surface types and weather conditions (Fig. 1). A two-way ANOVA revealed significant effects of ground conditions ($F_{2, 68} = 130$, $p < 0.001$), weather conditions ($F_{1, 68} = 246$ , $p < 0.001$) and their interaction ($F_{1, 68} = 10.4$ , $p < 0.001$) on ACOF. Under dry conditions, stone pavers had significantly higher ACOF than both vinyl ($p < 0.001$) and trex decking ($p < 0.001$), while vinyl and trex decking showed no significant difference ($p = 0.322$). In muddy conditions, ACOF differed significantly across all surfaces ($p < 0.001$), with stone pavers maintaining the highest values. Comparing dry to muddy conditions, ACOF dropped significantly for vinyl (-0.296, $p < 0.001$), stone pavers (-0.299, $p < 0.001$), and trex decking (-0.138, $p < 0.001$). The reduction in friction across all surfaces when exposed to mud indicates increased slip risk, particularly on vinyl flooring. Stone pavers provided the highest friction in both dry and muddy conditions, while trex decking and vinyl flooring pose greater ladder shoe slip risk. This work gives greater context to the RCOF of ladder climbing that has reported maximum values between 0.285 and 0.376 [3].

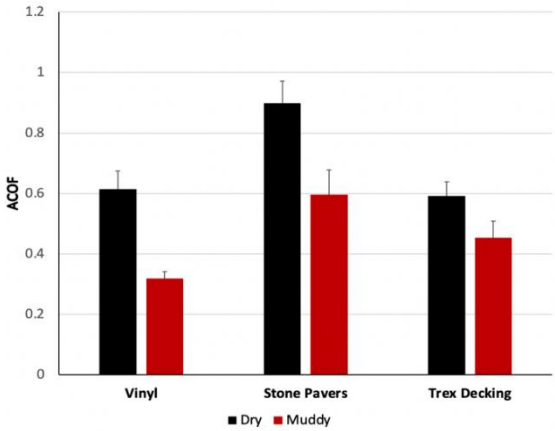


Figure 1: The average available coefficient of friction (ACOF) across vinyl flooring, stone pavers, and trex decking in dry (black) and muddy (red) conditions.

**Significance:** This study provides valuable insight for ladder safety. Context on the impact of ground condition on ladder foot friction can inform worksite safety guidelines, ladder design improvements, and slip prevention strategies. Such knowledge can advance the development of ladder foot materials for improved ACOF in adverse conditions to further injury prevention in occupational settings.

**Acknowledgements:** This research is supported by the Job-Site Safety Institute and Little Giant Ladder Systems.

**References**: [1] BLS (2022), The Economics Daily; [2] Chang et al. (2005), *Safety Science* 43; [3] Burnfield & Powers (2006), *Ergonomics* 49(10); [4] Bloswick & Chaffin (1990), *Int J Ind Ergonomics* 6.

# ARM SWING, TRUNK ROTATION, AND FREE MOMENT DURING RUNNING

Naomi Fay[1], Joseph M. Mahoney[2], Amanda Mueller[1], Abby Miller[1], Teresa B. Reed[3], Allison R. Altman-Singles[1,3*]
[1] Kinesiology, Penn State Berks College, Reading PA 19610
[2] Mechanical Engineering, Alvernia University, Reading PA 19601
[3] Mechanical Engineering, Penn State Berks College, Reading PA 19610
[*]Corresponding author's email: ara5093@psu.edu

**Introduction:** While running is a popular form of physical activity, 19-79% of runners are injured yearly [1]. While many factors cause overuse injuries, one mechanical factor is the torsional moment under the foot during stance phase, or free moment (FM). High FM characteristics are linked to bone stress overuse injuries in runners [2].

Research identified moderately increased FM characteristics when running with the arms across the chest [3], while running with two hands on a stroller significantly increased FM characteristics [4]. Taken together, there is a need to better understand the role of upper body rotation and arm swing on the FM. It is possible that increased FM is a compensation mechanism for the lack of rotation in the upper body when running with a stroller. The purpose of this study is to examine the effect of limiting arm swing and trunk rotation on FM characteristics. It is expected that limiting trunk rotation will result in the highest increase in FM, followed by limiting arm swing alone.

**Methods:** Healthy runners were recruited to run across an 18 m force plate (Bertec, Columbus, OH) instrumented runway during three conditions: running normally (control), running with arms down for no arm swing (NAS), and running with arms out to limit both arm swing and trunk rotation (NTR). Five trials were collected per condition.

Force and moment data were sampled at 2000 Hz and trimmed to stance phase. FM was calculated based on previously validated methods [2]. FM adduction (FMADD), FM at peak braking force (FMBRAK), absolute maximum FM ($|FM|_{max}$), and FM impulse (FMIMP) were extracted using custom MATLAB (Mathworks, Natick, MA) code. Median values for each subject in each condition were compared within subjects using bootstrapped, paired t-tests to assess statistical significance. Holm Bonferroni correction was used to correct the *p*-values for multiple comparisons.

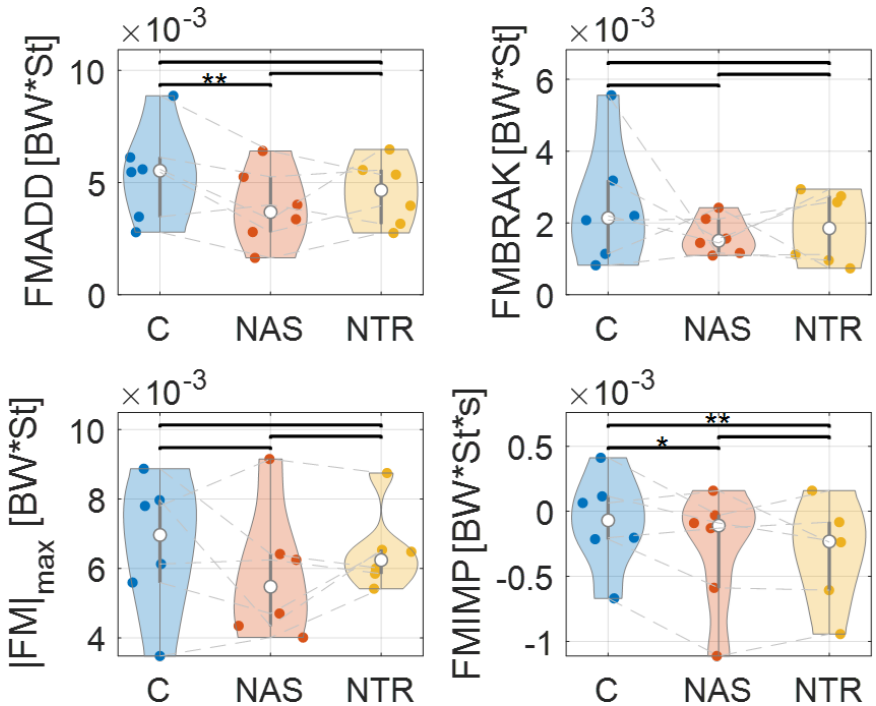


**Figure 1:** Violin plots of free-moment metrics. One star indicates $p < 0.05$, two stars indicate $p < 0.01$, three stars indicate $p < 0.001$.

**Results & Discussion:** Six runners (21±3 years, 1.64±0.05m, 62±7kg, 1 male, 5 female) completed all trials. FMADD significantly decreased 33% with no arm swing ($p<0.05$), but there was no difference for no trunk rotation. FMBRAK and $FM|_{max}$ were not different for any condition. FMIMP decreased 318% with no arm swing and 183% with no trunk rotation ($p<0.05$) (Figure 1).

Many of the FM parameters appear to have decreased when upper body rotation was limited. However, this only reached statistical significance for FMADD with no arm swing, and both rotation-restricted conditions for the FMIMP. These results may reveal additional differences when additional subjects are added. Contrary to our hypothesis that FM would be increased when rotation was restricted, FM parameters were mostly reduced. This indicates that FM may not be compensating for loss of rotation in the upper body. This suggests that reduced rotation may actually *reduce* FM parameters and, thus, decrease overuse injuries [2].

In the case of stroller running, these findings may indicate that the increased FM [4] is due to other factors, such as a need to control the direction of the stroller, or in response to the increased weight of the stroller. Future studies should continue to parse out the factors contributing to increased FM, as this is a potential risk factor for running overuse injuries [2].

**Significance:** The study highlights the complex interplay between upper body movements and lower limb mechanics during running and the potential implications for overuse injury risk. Coaches and clinicians could benefit from a better understanding of the need for upper body torsion to protect against lower extremity injury.

**References:** [1] Van Gent et al. (2007) *Br J Sports Med* 41; [2] Milner (2006) *J BioMech* 39; [3] Miller et al., (2009) *J Biomech Eng* 131; [4] Mahoney (2024), *ASB, Madison, WI*.

# VARIATION OF LUMBAR ROTATION DURING ASYMMETRIC PATIENT HANDLING TASKS

Elsa Brillinger*, Regina Vicente, and Dr. Brooke Odle
Hope College, Holland, MI, USA
Email: elsa.brillinger@hope.edu

**Introduction:** Musculoskeletal injury to the lower lumbar vertebrae is among high prevalence in nursing personnel. Many patient handling tasks (PHT) require nurses and other caregivers to lift and reposition patients of a variety of weights in varying postures, causing low back pain in nurses to range from 50-80% globally [1]. Currently, lumbar rotation during PHT is not widely studied. This work specifically investigated lumbar rotation in asymmetric PHT tasks- tasks where the arms or shoulders are used to reach different parts of a patient, causing the trunk to rotate. Previously conducted tests with college-age students have shown the existence of lumbar rotation during specific PHT, but the relationship between lumbar rotation, hospital table height, and patient weight is not yet known for nursing personnel. This study aims to assess the relationship between lumbar rotation, hospital bed height, and patient weight for currently enrolled nursing students during PHT.

**Methods:** A pilot study was conducted with 7 able-bodied nursing students enrolled at Hope College, all female between the ages of 18 and 22. Three PHT were analyzed: sliding a patient toward the head of the bed using a sling (2slide), lifting a patient's leg up to vertical (leg-lift), and sitting a patient up in bed (situp). To ensure consistency within and across participants, manikins were used for data collection. To assess how lumbar rotation during PHT changes based on patient weight and hospital bed height, all three tasks were completed with three different manikin weights (44lb, 66lb, 110lb) at three different table heights (knee, mid-thigh, and hip height). The table heights were kept consistent across all participants. The table heights are 34.5in for hip height, 28in for mid-thigh height, and 24.5in for knee height. OpenCap was used to record kinematic data. OpenCap is an open-source platform used to capture movement dynamics through video capture from at least two IOS supported devices [2]. Four iPhones set to collect data at 60 Hz were mounted on tripods to record movement. For each trial, three repetitions were completed of the selected task. Each task was completed two times with each table height and manikin weight.

Kinematic data collected via OpenCap were filtered using a 4$^{th}$ order Butterworth filter with a cutoff frequency of 12 Hz. The peaks of each repetition were manually selected. When selecting peaks, both the positive most and negative most peaks were selected to indicate rotation to the left or right, where rotation to the left is positive and rotation to the right is negative. Rotation in the positive and negative directions were assessed separately as each task requires differing amounts of rotation in each direction.

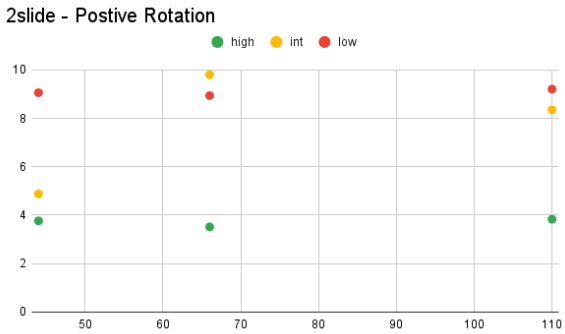


**Figure 1:** Lumbar rotation averages in the positive direction for the 2slide task.

**Results & Discussion:** Due to glitches in the data, some trials and repetitions were discarded. In all trials, there was no correlation between lumbar rotation, hospital bed height, or manikin weight in the positive or negative directions. However, in both the 2slide and leg-lift tasks, more trunk rotation was observed in the positive direction, giving insight into how both tasks are performed. Figures 1 and 2 show the resulting angles for the 2slide at each table height for each manikin. When completing the 2slide task, the manikin was moved to the head of the bed, then back to its original position. Because the same movement occurs on the right and left side of the body, the positive and negative rotation angles should be similar. However, for several data points, the rotation in the positive direction is about two times higher than the rotation in the negative direction. Analysis is ongoing with future analyses including comparing trunk flexion with lumbar rotation.

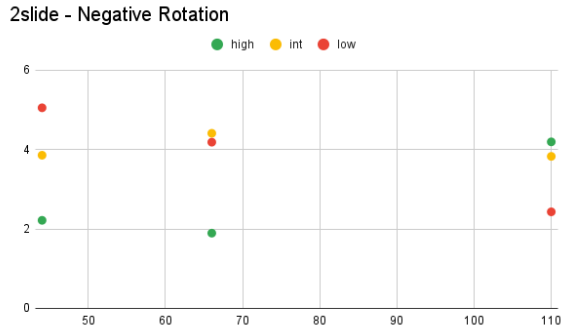


**Figure 2:** Lumbar rotation averages in the negative direction for the 2slide task.

**Significance:** Although current data does not show a correlation between lumbar rotation, manikin weight, and hospital bed height for asymmetric PHT, this data set gives insight into how PHT are completed. Understanding how each PHT is completed and the mechanics of movement utilized may have implications for injury mitigation approaches to train nursing students and re-train nurses in the workforce.

**Acknowledgments:** This work was supported by funding from the RESTORE Center and Clare Boothe Luce Program. The Restore Center is funded by the National Institutes of Health through grant P2CHD101913.

**References:**

[1] Budhrani-Shani, P, et al. National Library of Medicine. 2016.
[2] Uhlrich, S. et al. 2022. biorxiv https://doi.org/10.1101/2022.07.07.499061

# EVALUATING CONTAMINATION RISK DURING MEDICAL GOWN DOFFING USING MOVEMENT ANALYSIS: A PRELIMINARY STUDY

Jinfeng Li and Li-Shan Chou*
Department of Kinesiology, Iowa State University, Ames, IA, USA
*Corresponding author's email: chou@iastate.edu

**Introduction:** Medical gowns are commonly used in healthcare settings to protect staff from healthcare-associated infections [1]. Various doffing methods could lead to different contamination risks for healthcare workers [2]. Traditional motion capture systems often face challenges from garment interference, which can compromise the kinematic analysis of the doffing process. Furthermore, quantitative research is scarce investigating the contamination risk associated with finger contact during gown doffing. This study investigates the use of IMUs for detailed kinematic analysis during the doffing process and simulates the relative positions of fingers and the gown. The goal is to provide reliable quantitative data that could inform future medical protective clothing design and decrease the probability of infection during doffing for healthcare providers.

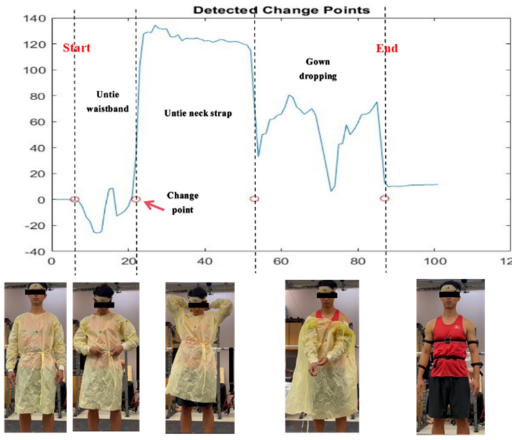


**Figure 1:** Temporal classification of doffing

**Methods:** One healthy young adult wearing a polypropylene isolation gown participated in the study. Kinematic data of the upper limbs during gown doffing were collected using five IMU sensors (SageMotion, USA) placed strategically: one on the xiphoid process, two on the upper arms' exteriors, and two on the forearms' exteriors. The IMU system was calibrated in the static standard anatomical position. Using SageMotion's customized app, joint angles for both shoulders and elbows were calculated with a 4th-order Butterworth low-pass filter set to 15 Hz. A twelve-camera motion analysis system (Qualisys AB, Sweden) also recorded the gown's contour and the fingers' trajectories. Ten markers were attached to the gown to delineate its boundaries at the shoulders, chest, back, waist, and hemline, while three markers were placed on each hand, specifically on the thumb, index, and little finger. To reduce noise and smooth the data, a 12 Hz 4th-order Butterworth low-pass filter was applied to the marker data. A customized Matlab program identified key doffing events by employing the root mean square (RMS) method to detect changes in the IMU signal. At every instant, the gown's contour was constructed using a cuboid model based on the ten gown markers. Distances between the fingers and constructed gown contour were calculated during the doffing process.

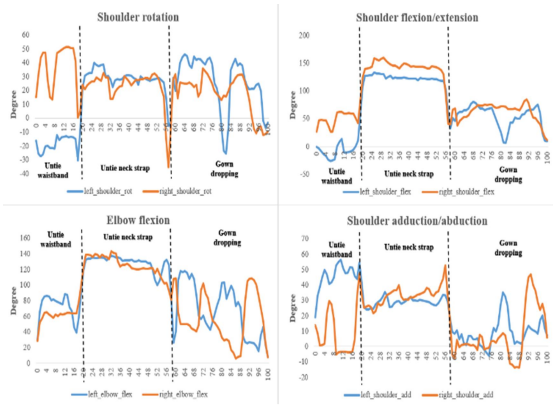


**Figure 2:** RoM of shoulders and elbows

**Results & Discussion:** Based on the change point detection results, the doffing process of medical gowns can be divided into three primary phases: untying the waistband, untying the neck strap, and gown dropping. By correlating these stages with video recordings, the true sequence of doffing medical gowns is accurately reflected (Fig. 1). Analysis of upper limb kinematic data from IMUs, alongside video comparisons, confirms that the IMU-driven motion model effectively captures the complex movements of the upper limbs during doffing. In the phase of untying the neck strap, characterized by symmetrical movements of both upper limbs, there is a notable consistency in the range of motion for bilateral shoulder and elbow joints. Conversely, during phases marked by asymmetrical bilateral movements, such as untying the waistband and gown dropping, the IMU measurements precisely delineate the distinct kinematic attributes of each upper limb (Fig. 2). The distance between the fingers and the gown could be used to describe the contamination risk. When the fingers touch or enter the boundary of the simulated gown contour, the distance is shown as zero (Fig. 3). From the results, it is observed that the fingers were closer to the gown during the early stages of untying the waist and neck straps. Due to garment interference data for the gown-dropping phase were lacking. However, this study followed the CDC-recommended sequence for doffing, where in the gown-dropping phase, the hands only contact the inside of the gown (non-contaminated area); thus, the contamination risk should be very low.

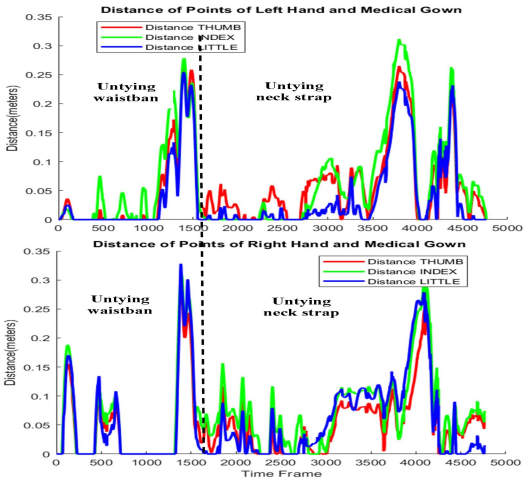


**Figure 3:** Distance of fingers and gown

**Significance:** This study highlights the feasibility of using IMUs to analyze the kinematics of gown doffing, combined with markers to track finger trajectories. By detailing the kinematic changes during different doffing phases, the research offers insights into potential contamination risks, especially during critical phases such as untying the waistband and neck strap. Further analyzing the distance between fingers and gowns, such as the difference in total contact time between fingers and gowns during doffing differently designed gowns, may build a bridge between medical gown design and infection control in the future.

**References:** [1] Chughtai, et al. (2018). *Am J Infect Control*, 46 (12). [2] Gurses, et al. (2019) *Infect Control Hosp Epidemiol*, 40 (2).

# SHOULDER EXOSKELETON EMG AND USABILITY ASSESSMENT AT A CONSTRUCTION WORKSITE

*Jason Gillette[1], Joshua Riesenberg[2], and Madeline Jenkins[1]
[1]Iowa State University, Ames, IA; [2]Scottish Rite for Children, Frisco, TX
*Corresponding author's email: gillette@iastate.edu

**Introduction:** Shoulder injuries result in days away from work at a rate of 6.3/10,000 for construction workers compared to 6.1/10,000 for all other industries [1]. Similarly, shoulder injuries represent 6.1% of all injuries for construction workers compared to 5.4% for all other industries. Within construction, the highest rate of shoulder injuries occurs for building and carpentry finishing contractors at 10.9/10,000. Previous research provided evidence that shoulder exoskeletons could potentially reduce injury risk in manufacturing jobs that require elevated arm tasks [2,3]. However, there is limited evidence that shoulder exoskeletons are a practical intervention in construction. The purpose of this study was to test a shoulder exoskeleton at a construction worksite. We hypothesized that anterior deltoid muscle activity and shoulder perceived exertion would be reduced when using the shoulder exoskeleton since it is designed to provide shoulder flexor support. However, we were unsure how construction workers would rate the usability of a shoulder exoskeleton.

**Methods:** Twenty-two workers (1 female, 21 males; age 33 ± 8 yr, height 1.73 ± 0.07 m, mass 90 ± 22 kg) at a database warehouse construction worksite participated in the shoulder exoskeleton assessment. Each worker was fitted with a Levitate Airframe Flex, which passively generates arm support during shoulder flexion. Participants completed approximately ten minutes of the same construction tasks with and without the shoulder exoskeleton. Most of the construction tasks involved overhead installation of wiring, conduit, and cable trays from a scissor lift. Muscle activity was measured for the dominant anterior deltoid, medial deltoid, upper trapezius, latissimus dorsi, and dominant/nondominant erector spinae using surface electromyography (EMG). Maximum voluntary isometric contractions (MVC) were collected and used to normalize EMG amplitudes. Participants rated perceived exertion for their shoulders, elbows, and low back and completed an exoskeleton usability survey. Median and peak (95$^{th}$ percentile) values were determined for EMG amplitudes.

**Results & Discussion:** Anterior deltoid median and peak (-1.9, -5.0 %MVC), medial deltoid median and peak (-1.2, -2.8 %MVC), upper trapezius median and peak (-2.3, -5.0 %MVC), and erector spinae peak (-7.1 %MVC) EMG amplitudes were significantly reduced with the shoulder exoskeleton (Figure 1).

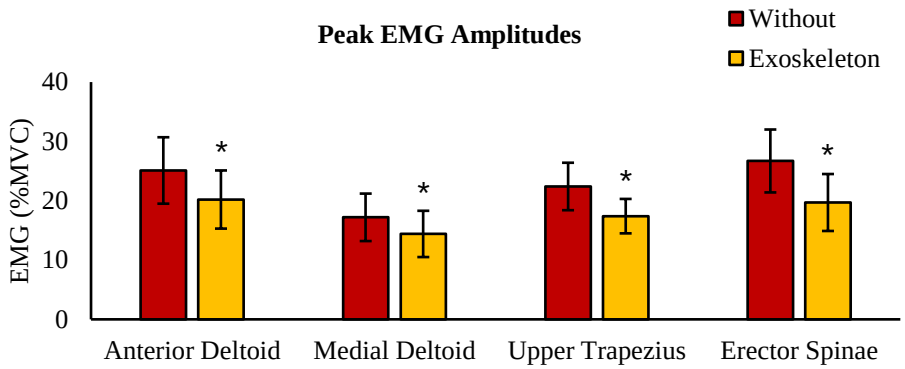


**Figure 1:** Peak muscle activity with and without a shoulder exoskeleton. Average values with 95% confidence intervals. * Indicates significant reductions ($p < 0.05$).

There was not a significant main effect of shoulder exoskeleton on perceived exertion. Participants were less confident when completing their job tasks (-0.68/5), felt their job tasks were harder to complete (+0.55/5), and rated their performance lower (-0.91/5) when wearing the shoulder exoskeleton. When asked 'Rate the level of anxiety you would feel about using an exoskeleton around co-workers', 17/22 rated 'Not Anxious', 4/22 rated mid-scale, and 1/22 rated 'Anxious'. When asked 'Rate how useful an exoskeleton was in performing your job tasks', 8/22 rated 'Useful', 7/22 rated mid-scale, and 7/22 rated 'Not Useful'. When asked 'Rate your overall satisfaction with using an exoskeleton', 9/22 rated 'Satisfied', 7/22 rated mid-scale, and 6/22 rated 'Dissatisfied'.

Our hypothesis that anterior deltoid muscle activity would decrease with the shoulder exoskeleton was supported by significant reductions in median and peak EMG amplitudes. In addition, muscle activity was significantly reduced in the medial deltoid, upper trapezius, and erector spinae. Our second hypothesis that participants would perceive reduced shoulder exertion with the shoulder exoskeleton was not supported with a statistically significant reduction. On a participant level, 12/22 perceived a reduction, 6/22 were neutral, and 4/22 perceived an increase in shoulder exertion with the shoulder exoskeleton. Shoulder exoskeleton usability ranged from a negative rating for effect on job performance to slightly positive in overall satisfaction to positive in using around co-workers.

**Significance:** This study provides evidence that an exoskeleton can reduce shoulder muscle activity for construction tasks and even provide benefits in the back, possibly due to improved posture. However, muscle activity reductions were not perceived by all workers and overall ratings were negative for several usability factors, potentially due to confined spaces in scissor lifts. It was encouraging that workers were comfortable wearing an exoskeleton around co-workers. The next steps are further analyzing differences between construction tasks with positive and negative results, simulating construction tasks in a controlled lab environment, and testing both back and shoulder exoskeletons for observed construction jobs that included both below waist and above shoulder tasks.

**Acknowledgments:** We would like to thank the National Safety Council MSD Solutions Lab Research to Solutions grant program for funding this study and to Levitate Technologies for donating the shoulder exoskeleton.

**References:** [1] U.S. Bureau of Labor Statistics (2023); [2] Gillette et al. (2019), *IIE TOEHF* 7(3-4); [3] Gillette et al. (2022), *Wearable Technol* (3)

# LUMBAR SHEAR LOADS OF ADLS/LIFTING TASKS AND REAR-END COLLISIONS

*Kevin Adanty[1], Jordan Ogbu Felix[1], Clyde Westrom[1], Keya Zambare[1], John Adam Caraan[1], Sean D. Shimada[1]
[1]Biomechanical Consultants
*Corresponding author's email: kevin@motionsandforces.com

**Introduction:** When evaluating an injury claim, legal specialists often consider whether the forces generated in a rear-end vehicle collision are sufficient to cause low back injuries. When faced with this consideration, a common method involves comparing the lumbar compressive loads from the collision to those typically experienced during non-injurious activities of daily living (ADLs) or common lifting tasks [1]. These ADLs or lifting tasks may include tasks such as push-pulling a trash can to squatting and lifting objects from the ground. However, the authors postulate two key limitations to this method. First, occupants in rear-end collisions are subjected to transverse loads [1], leading to a shear mechanism acting on the lumbar spine's vertebrae and soft tissues. Second, the duration of the peak force or loading rate on an occupant's lumbar spine in a collision may differ significantly from those experienced during ADLs or lifting tasks. This preliminary study aimed to quantify the differences in peak lumbar shear loads and loading durations between ADLs or lifting tasks and those experienced by occupants in rear-end collisions. The secondary aim of this study was to develop a linear regression model to estimate peak lumbar shear loads based on peak vehicle acceleration ($a_V$) during a rear-end collision.

**Methods:** The literature was reviewed to identify studies that measured peak posterior lumbar shear forces during non-injurious ADLs and common lifting tasks. These findings were compared with data from studies that reported peak lumbar shear loads between the T12 and S1 vertebral regions from belted anthropomorphic test devices (ATDs) or volunteers subjected to rear-end sled or crash tests. A linear regression was generated using jamovi statistical software to approximate peak lumbar shear loads based on $a_V$ [2].

**Results & Discussion:** The studies reviewed for ADLs/common lifting tasks included push-pull tasks and lifting items from the ground [3–7]. Items lifted from the ground included crates, pencils, boxes, and throw bags. Sled or crash tests primarily involved ATDs [1], with one study including human volunteers [8]. The range of peak lumbar shear forces observed in rear-end collisions overlapped with those reported during non-injurious ADLs or lifting tasks (Figure 1). Only two studies in the reviewed literature documented the peak loading duration of the lifting tasks (0.9 to 4.91 s) [6,7]. In contrast, the duration of peak lumbar forces during rear-end collisions was shorter than 250 ms. Indeed, like compression forces in the lumbar spine [1], it appears that the shear forces of non-injurious ADLs, lifting tasks, and rear-end collisions are consistent. However, the combination of high-magnitude forces and short durations in rear-end collisions increases the likelihood of microstructural damage, such as ligament and muscle tissue disruption [9]. This is consistent with the viscoelastic nature of biological tissue, which becomes more susceptible to injury as strain or loading rates increase. Future studies should implement paired experimental designs to allow statistical comparisons of peak lumbar loads between ADLs, lifting tasks, and simulated sled tests.

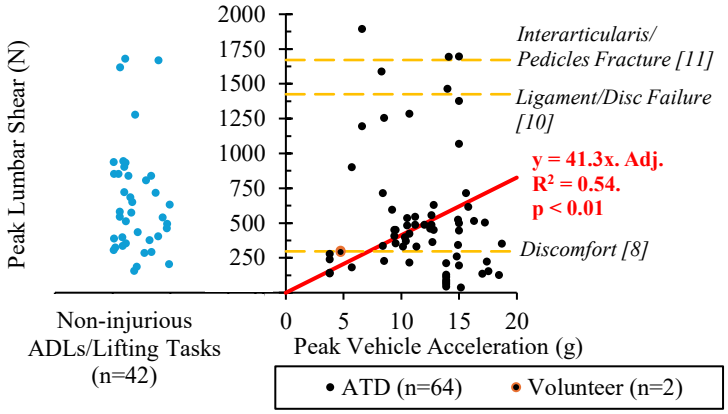


**Figure 1:** Linear regression of lumbar shear loads vs. $a_V$ coupled with lumbar shear loads in ADLs/ lifting tasks. Forces where lumbar injuries were reported are marked yellow dashes [8,10,11].

A linear regression analysis predicted peak lumbar shear loads based on $a_V$ (Figure 1), and the relationship was statistically significant ($p<0.01$). Depicted in Figure 1 are lumbar-related injuries at corresponding shear loads during sled testing with human volunteers or isolated vertebrae mechanical testing [8,10,11]. Reports of spinal instability and ligament failure were associated with shear forces exceeding 1.43 kN [10], whereas volunteers reported "discomfort" 24-hours post-sled-tests at shear loads at approximately 300 N [8].

**Significance:** This preliminary study showed that lumbar shear loads overlapped between non-injurious ADLs/lifting tasks and rear-end collisions. This finding aligns with the results of Kashdan et al., who reported a similar overlap in peak compression loads [1]. However, this overlap does not provide sufficient grounds for biomechanists to speculate whether an injury occurred in a collision. Unlike ADLs, the peak forces in a collision are applied over a short duration (<250 ms), which may induce pain-related symptoms not typically observed in longer-duration tasks [1]. The regression model presented in this study can serve as a tool for biomechanical and safety experts to estimate the shear loads experienced by an occupant during a rear-end collision.

**References:** [1] Kashdan, A. et al. (2023). SAE, 2023-01–0647. [2] The jamovi project (2024). jamovi (Version 2.6). [3] Beaucage-Gauvreau, E. et al. (2020). J. Biomech., 100: 109584. [4] Beaucage-Gauvreau, E. et al. (2019). Comput. Methods Biomech. Biomed. Engin., 22: 451–464. [5] Beaucage-Gauvreau, E. et al. (2021). Eur Spine J, 30: 1035–1042. [6] De Looze, M. et al. (1995). Ergonomics, 38: 1993–2006. [7] Laursen, B. and Schibye, B. (2002). Applied Ergonomics, 33: 167–174. [8] Fewster, K.M. (2020). Exploring Low to Moderate Velocity Motor Vehicle Rear Impacts as a Viable Injury Mechanism in the Lumbar Spine. [9] Fast, A. et al. (2002). American Journal of Physical Medicine & Rehabilitation, 81: 645–650. [10] Begeman, P. et al. (1994). SAE, 942205. [11] Cyron, B. et al. (1976). J Bone Joint Surg Br, 58-B: 462–466.

# FIREFIGHTER'S TURNOUT GEAR LIMITATIONS ON MOBILITY: A SCOPING REVIEW

Kuanting Chen*, Jennifer M. Yentes
Department of Kinesiology and Sport Management, Texas A&M University, College Station, TX
*Corresponding author's email: Kuanting.Chen@tamu.edu

**Introduction:** Turnout gear provides firefighters with strong protection against hazards on the fireground. However, the thick multi-layer material can impede firefighters' mobility and range of motion (ROM). Currently, there is a lack of synthesized knowledge regarding the impact of turnout gear on firefighters' mobility and ROM. Therefore, this scoping review aimed to (1) examine the breadth of existing literature on movement limitations associated with turnout gear, (2) evaluate the impact of turnout gear on firefighter's mobility and ROM, (3) identify the methodologies used to study turnout gear, and (4) determine the extent to which female firefighters are represented in this body of research.

**Methods:** Following the Preferred Reporting Items for Scoping Reviews (PRISMA-ScR), five databases (MEDLINE, Academic Search Ultimate, CINAHL, Embase, and SPORTDiscus) were searched using key search terms related to "firefighter turnout gear", "mobility", "range of motion", and "task". Studies were screened against the following eligibility criteria: (1) conducted in the United States or Canada, (2) subjects included career structural firefighters, (3) interventions included more than a single piece of gear, and (4) reported movement-related outcome variables.

**Results & Discussion:** A total of 703 records were identified, and 15 articles met the inclusion criteria, including 12 intervention studies, one survey study, one in-depth interview study, and one mixed-method study. Although 11 of these studies included female subjects, they represented only 11.3% of the total sample in the intervention studies. Turnout gear was evaluated during various activities (Table 1). In general, turnout gear reduced both upper- and lower-body ROM in static ROM testing and decreased walking speed, step length, and ROM during walking. It also impaired firefighters' ability to maintain dynamic balance and respond to external perturbations. However, some studies suggested that turnout gear might improve performance on certain job-related tasks and static postural balance by providing task-specific protections and triggering conditional reflexes (i.e., wearing turnout gear simulates urgent conditions). Female firefighters expressed lower satisfaction with the fit and functionality of turnout gear and experienced different regions of ROM limitation compared to their male counterparts. In addition, firefighters who did not engage in regular physical training demonstrated greater degree of impairment when wearing turnout gear during dynamic balance tasks.

**Table 1.** Characteristics of included articles.

| Author, Year | Sample (M/F) | % Female | Experimental Variables and Activities |
|---|---|---|---|
| Sobeih, T.M., et al., 2006 | 15 / 1 | 6.25% | COP variables during Static standing & Reaching |
| Coca, A., et al., 2008 | 5 / 3* | 37.50% | SJ ROM, Reaching performance, & Time to complete job-specific tasks |
| Coca, A., et al., 2010 | 5 / 3* | 37.50% | SJ ROM, Reaching performance, & Time to complete job-specific tasks |
| Park, K., et al., 2011 | 44 / 0 | 0% | Spatiotemporal gait variables during Walking & Obstacle negotiation |
| Kong, P.W., et al., 2012 | 23 / 0 | 0% | Functional balance during walking on a balance beam |
| Park, H., et al., 2014 | 8 / 4 | 33.33% | ROM of hip, knee, ankle, foot during overground walking |
| Park, H. & Hahn, K., 2014 | 202 / 314 | 60.85% | Survey on perceived fit in specific areas of turnout gear between genders |
| Park, H., et al., 2015 | 8 / 4 | 33.33% | COP & spatiotemporal variables during overground walking |
| Ciesielska-Wróbel, I., et al., 2017 | 10 / 0 | 0% | SJ ROM of elbow & shoulder; ROM of hip, knee, and trunk in squats |
| Brown, M.N., et al., 2019 | 20 / 1 | 4.76% | Static balance; Single leg perturbation, & Limits of stability |
| Colburn, D., et al., 2019 | 16 / 4* | 20.00% | Sensory organization test & Static postural perturbation |
| Games, K.E., et al., 2019 | 40 / 0 | 0% | Dynamic balance – Y Balance Test |
| McQuerry, M., 2020 | 10 / 6 | 37.50% | ROM of elbow, shoulder, hip, knee, and trunk during SJ movement |
| McKinney, E., et al., 2021 | 0 / 35 | 100% | Interviews about the perception of turnout gear |
| Wnag, S., et al., 2021 | US: 112 / 13 | 10.40% | Survey on perceived mobility and associated injury risks |

Note: Studies with non-firefighter subjects are marked with * in the Sample column. ROM – Range of motion; SJ - Single joint; COP-Center of Pressure

**Significance:** There is a consensus across the literature that wearing turnout gear affects firefighters' static ROM, walking, and dynamic balance, although its impact on performance during job-related tasks remains unclear. Current evidence suggests that female firefighters face unique challenges regarding gear fit and function, but there is limited understanding of the factors affecting their performance. Future studies should focus on the impact of gear during firefighting tasks and how various factors contribute to the variability in firefighter's mobility and ROM.

**Acknowledgments:** We would like to thank Margaret Foster and Kyle Holland from Medical Sciences Library, Texas A&M University for assisting with the literature search.

# VALIDATION OF AN ULTRASOUND-EMBEDDED SHOE FOR MEASURING PLANTAR TISSUE PROPERTIES

*Nicholas R. Ozanich[1,3], Scott Telfer[1,2,3], Ellen Li[3], William R. Ledoux[2,3]
Departments of [1]Mechanical Engineering and [2]Orthopaedics & Sports Medicine, University of Washington
[3]Center for Limb Loss and MoBility (CLiMB), VA Puget Sound Health Care System
*Corresponding author's email: ozanich@uw.edu

**Introduction:** Over 38 million people, or about 11.6% of the US population, live with diabetes mellitus [1], a condition that can lead to complications such as neuropathy and ulceration. Currently, clinical comorbidities and plantar pressure measurements are commonly used to assess ulceration risk [2,3]. While structural deformity is known to increase ulcer risk [2,4] and it has been hypothesized that changes in tissue structure can lead to ulcer formation [5,6], direct evidence studying in vivo dynamic imaging of the plantar soft tissue under loading conditions typical of gait has remained elusive.

Our laboratory has developed an ultrasound-embedded shoe, known as the Ultrashoe, to investigate the in vivo dynamic properties of the plantar soft tissue during gait [7]. The Ultrashoe houses an ultrasound probe (Humanscan, Gyeonggi-Do, South Korea) in series with four miniature load cells (Honeywell, Charlotte, NC) that measure tissue deformation and force at the heel or the second metatarsal head (MTH). Prior to human subject testing, a validation protocol is underway. The aims of this process are threefold: first, to determine the optimal speed of sound (SoS) for ultrasound imaging of the heel and second MTH by comparing distances measured in ultrasound images with those obtained from computed tomography (CT) scans; second, to validate the load cell readings in their housing against measurements from an Instron E3000 (Norwood, MA); and third, to synchronize and assess the accuracy of the measured deformation and force by comparing data from the Ultrashoe with that obtained from an Instron E3000 in series with cadaveric foot samples.

**Methods:** The first aim was executed by securing cadaveric feet (n=3) to the Ultrashoe and positioning it inside a LineUp cone-beam, weightbearing CT scanner (CurveBeam, Hatfield, PA). Ultrasound images and CT scans of various foot angles and amount of tibial loading (i.e., conditions, n=42) were captured at both the heel or the second MTH. Imaging was performed using multiple assumed SoS (1480, 1540, 1600, and 1660 m/s) for each position, for total of 168 scans (42 conditions x 4 SoS). Since the SoS varies between different tissues, and the heel pad and second MTH contains skin, fat, and muscle, this inquiry was undertaken to determine the optimal SoS for accurate ultrasound distance calculations. The CT scans were segmented using MIMICS (Materialise, Leuven, Belgium), and distances were calculated in Python with the vedo library [8] to compute the perpendicular distance from the probe surface to the bone, along the midline of the probe. The second aim focuses on validating the load cell readings against known forces and displacements measured by an Instron E3000. Load cells will be placed in the designated housing locations within the Ultrashoe, and known forces will be applied. This testing is designed to assess several factors: the accuracy of the force readings, the load cells' ability to reliably capture distributed forces, and their performance across a range of loading frequencies typical of gait. The third aim integrates the ultrasound sensor into the Ultrashoe to evaluate its performance alongside the load cells in collecting dynamic tissue deformation and force in a cadaveric foot. This enables the comparison between the force and displacement applied from the Instron and measured from the Ultrashoe sensors. We will assess different ramp and cyclic loading patterns applied to the tibia, controlling the orientation of the tibia and the line of applied force to be directly through the sensors.

**Results & Discussion:** For the first aim, assuming a speed of sound (SoS) of 1660 m/s yielded, on average, the lowest error for tissue measurements at the heel (0.211 mm difference) and the second MTH (0.285 mm difference) (Figure 1). This finding suggests that using a SoS of 1660 m/s may improve accuracy when utilizing ultrasound for imaging plantar tissue, rather than relying on the commonly assumed value for tissue of 1540 m/s [9]. However, it is important to note that these tests were conducted on cadaveric tissue, which may differ from in vivo tissue. The second aim is currently going through data collection and the third aim will be completely subsequently.

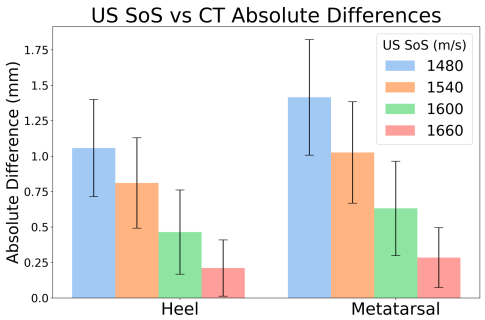


**Figure 1:** Comparison of absolute distances computed from different ultrasound (US) speed-of-sound (SoS) assumptions versus distances measured from computed tomography (CT) scans.

**Significance:** Ultrasound is an attractive modality for biomechanical assessments due to its affordability, portability, and versatility compared to other imaging methods. Its ability to capture dynamic images makes it particularly well-suited for investigating biological tissues, which are inherently viscoelastic. Successfully translating the Ultrashoe into a deployable research tool would enable the collection of in vivo data of the plantar soft tissue during gait, offering valuable insights into tissue behavior under physiological loading conditions. This capability would be a useful tool in biomechanics research and facilitate further inquiries into the effects of diabetes (as well as other diseases and injuries) on the plantar soft tissue.

**Acknowledgments:** This study was partially funded by NIAMS grant R21 AR072216; Tony Huynh and John Slevin also contributed.

**References:** [1] CDC (2023), National Diabetes Statistics Report; [2] Bus et al. (2020), Diabetes/Metabolism Research and Reviews 36:1-18; [3] Ledoux et al. (2013), J Diabetes Complications 27:621-626; [4] Reiber et al. (1992), Ann Intern Med 117:97-105; [5] Delbridge et al. (1985), Br J Surg 72:1-6; [6] Gefen (2003), Med Eng Phys 25:491-499; [7] T. C. Huynh, ProQuest Diss. Theses 2020; [8] M. Musy *et al.*, *"vedo, a python module for scientific analysis and visualization of 3D objects and point clouds"*; [9] Shin et al. (2010), J Ultrasound Med Biol 36:623-636.

# Potential Mechanical Biomarker for Chronic Lower Back Pain Using 3D-Ultrasound Strain Tensor Imaging

Zhiyu Sheng[1], Maryam Satarpour, John M. Cormack, Yu-hsuan Chao, Emily Landis-Walkenhorst,
Allison C. Bean, Ryan P. Nussbaum, Jiantao Pu, Ajay D. Wasan, *Kang Kim
[1]Department of Medicine, University of Pittsburgh, PA 15261, USA
*Corresponding author's email: kangkim@pitt.edu

**Introduction:** Chronic myofascial pain (MP) is a well-known significant public health problem and often appears in the lower back. In current clinics, lack of reliable quantitative diagnostic tools and poor understanding of the underlying mechanisms make it challenging to achieve a complete objective diagnosis of lower back pain (LBP). Therefore, this study aims to develop a quantitative surrogate mechanical biomarker of LBP from local muscular tissue deformations acquired by ultrasound imaging. A hypothesis investigated by a previous study [1] suggests that reduced shear motion in the thoracolumbar fascia (TF) during back flexion, indicating tissue stiffening, can quantify LBP. According to this, we designed a controlled lower back flexion protocol and implemented the recently advanced three-dimensional (3D) ultrasound imaging to quantitatively analyze myofascial motions. We reconstructed 3D strain tensors that indicate myofascial deformations and compared the results between LBP and control (healthy-normal, HNL) subjects.

**Methods:** Experiments were performed on 5 LBP and 5 HNL human participants and was approved by the Institutional Review Board. As shown in Fig. 1A, the participants lay prone on a motorized table that produced a back flexion at the hip of 12 degrees, which was confirmed by co-located inertial measurement units (IMU) measurements. We used a row (R) column (C) addressed array (RCA, Vermon RC6gV, 6 MHz) connected to a Vantage 256 system to acquire a 3D ultrasound images series at a volume rate of 100 Hz to record the myofascial motions. The imaging sites included left and right sides of the back that were 2 cm lateral to the midline at L2-L3 over the multifidus muscle. As illustrated by Fig. 1B and 1C, a 3D normalized cross-correlation based speckle tracking was used to compute the displacement vector field in the processing window that contains the TF area. The vector field was input to a differentiation filter to generate deformation gradient tensors, followed by computation of the $E_{xz}$ component of Green-Lagrange strain tensors to represent the shear motion inside TF, which is presented in Fig. 1E.

**Results & Discussion:** The displacement and velocity image in Fig. 1C and 1D showed a clear motion pattern of the myofascial tissue and demonstrated the feasibility of our approach to use 3D ultrasound imaging to quantify myofascial tissue motions. The observation of the tensor component, $E_{xz}$, compared between LBP and HNL groups suggested a decreased negative strain in TF for the LBP group. Fig. 1F illustrated the distributions of the mean and median of $E_{xz}$ for all the groups with t-tests that reported the p-value = 0.096 (mean) and p-value = 0.17 (median). The capability of diagnosing LBP from HNL using the mean and median was assessed by the ROC curves that reported the AUC = 0.72 (mean) and AUC = 0.65 (median). While the statistical significance (p-value < 0.05) was not shown in the 10-participant preliminary data, the observed pattern and trend is still considered promising and suggests a continued investigation on the on-going full cohort (n=130) of participants.

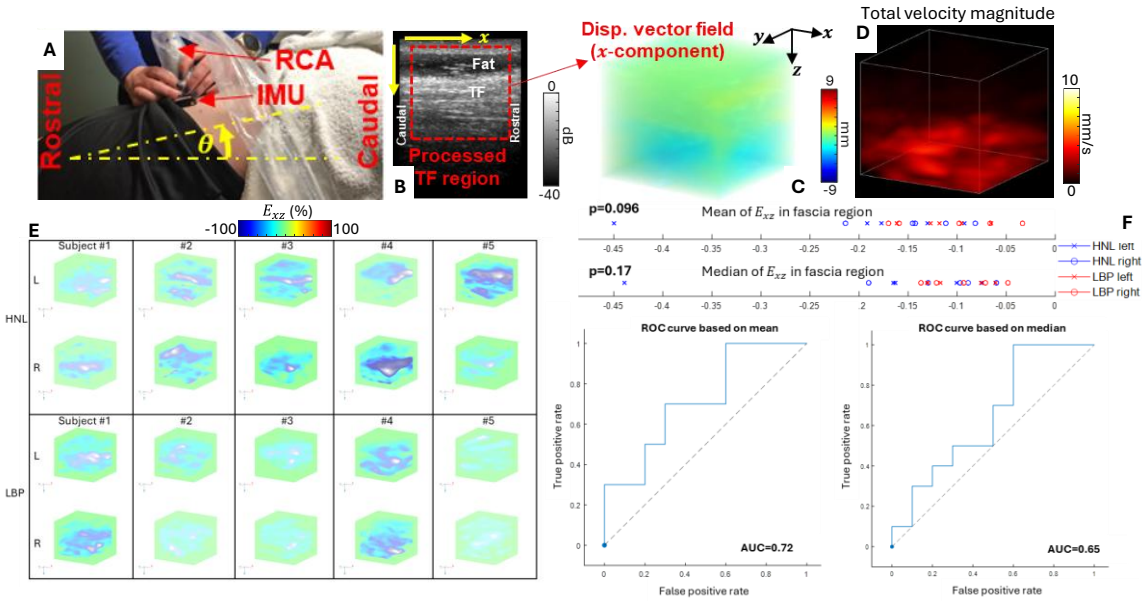


**Figure 1:** Experiment protocol, 3D ultrasound image acquisition and processing, and statistical analysis for comparing myofascial tissue motions among LBP and HNL groups.

**Significance:** The preliminary results demonstrate the feasibility of LBP assessment using 3D ultrasound strain tensor imaging. The study is promising to develop a novel quantitative mechanical biomarker for objective LBP diagnosis.

**Acknowledgments:** Funding: NIH Heal Initiative R61AT012282. Computation: University of Pittsburgh Center for Research Computing. Data storage: ACCESS program supported by NSF grants #2138259, #2138286, #2138307, #2137603, and #2138296.

**References:** [1] Langevin, Helene M., et al., BMC Musculoskelet. Disord. 12, 203 (2011).

# A reliable tool to characterize Achilles subtendon behavior within the tendon cross section

Kathryn S. Strand[1], Todd J. Hullfish[1], Maggie M. Wagner[1], Josh R. Baxter[1]
[1]University of Pennsylvania, Philadelphia, PA
strandk@seas.upenn.edu

**Introduction:** The Achilles tendon (AT) consists of three distinct fascicle bundles called subtendons, each corresponding to a head of the triceps surae muscles: the lateral gastrocnemius (LG), medial gastrocnemius (MG) and soleus. In a healthy AT, these subtendons deform relative to each other – often described as subtendon 'sliding' [1], [2]. In contrast, injured tendons exhibit more uniform deformation, suggesting a link between reduced sliding and plantar flexor function [3]. However, current techniques to safely and reliably evaluate subtendon behavior in vivo are lacking. Ultrasound is a widely available and effective modality for imaging the AT, and recent work has applied it in conjunction with neuromuscular electrical stimulation (NMES) to activate individual triceps surae muscles and monitor the corresponding displaced regions within the AT to identify separate subtendons [2], [3], [4]. Using these methodologies, the objective of this study was to evaluate the repeatability of an automated point-tracking tool to identify individual Achilles subtendon behavior. We hypothesized that this tool reliably (ICC>0.67) identifies localized regions of tendon displacement in healthy subjects across separate testing sessions and that this tool would be sensitive to changes in ankle joint position.

**Methods:** Eight healthy participants (4M, 4F) provided written informed consent to participate in this IRB approved study. Briefly, participants lay prone with their leg fully extended. We acquired ultrasound videos in the transverse plane using a 21 MHz linear ultrasound probe (L6-24, GE LOGIQ) positioned 3 cm proximal to the medial malleolus. Simultaneously, we delivered 1s pulse trains (30 Hz, 400 µs pulse width) through hydrogel electrode pairs placed over the MG and LG muscle bellies until movement in the AT was visible via the ultrasound video [3], [4]. We performed this testing with the ankle in neutral and 20° plantar flexion at the same stimulation amplitude. This protocol caused negligible plantar flexor torques (mean: 0.662 Nm), demonstrating safety for future use in clinical populations. We then repeated this protocol on a separate day to test repeatability. We processed experimental data using custom scripts (MATLAB, R2024a). We manually selected the tendon cross-sectional area as the tracking region of interest (ROI) and used a Kanade-Lucas-Tomasi point tracking algorithm to identify the displacement of 900 corner point eigenvalues within this ROI. Next, we performed k-means clustering (k=3 clusters, based on 3 known subtendons) of the points based on the trajectory angle at each frame which consistently produced two dominant clusters on the medial and lateral portions of the tendon cross section (**Fig. 1**). We then calculated the centroids and areas formed by these point clusters and calculated Intraclass Correlation (ICC) coefficients using a two-way random-effects model to establish inter-session measurement reliability. Lastly, we compared cumulative point displacement between ankle positions using paired t-tests. Significance levels were set to p<0.05.

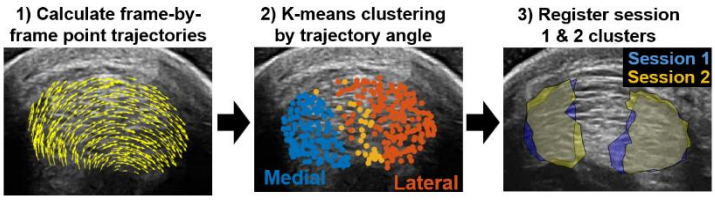


**Figure 1.** Point tracking and k-means clustering workflow to evaluate inter-session reliability

**Results & Discussion:** This tool demonstrated high reliability (ICC>0.95) in identifying cluster locations with the ankle in neutral under nominal load and unloaded plantar flexion (**Table 1**). While the cluster locations within the tendon cross section were consistent across sessions, cluster areas had lower repeatability in both ankle positions, ranging from 0.274-0.743 during GL stimulations and 0.381-0.694 during GM stimulations. The decreased ICC values for cluster areas likely reflect differential subtendon load sharing responses between sessions. During both GL and GM stimulations, the AT exhibited significantly greater displacements of both the medial and lateral clusters in 20° plantar flexion compared to a neutral position (p<0.0001) (**Fig. 2**). The larger displacements detected in plantar flexion agree with prior findings [2] and are likely due to decreased tension within the tendon.

**Significance:** This work provides new guidelines to reliably quantify Achilles subtendon function while ensuring reliable and safe patient evaluations. Future applications of this method can elucidate changes in subtendon behavior in different AT pathologies including rupture and tendinopathy. This reliable tool may also be used longitudinally to monitor tendon healing, providing valuable insight into the efficacy of certain rehabilitation protocols in restoring native AT structure and function.

**References:** [1] Clark et al. (2018) PeerJ. [2] Lehr et al. (2021) J. Exp. Biol. [3] Khair et al. (2022) J. Appl. Physiol. [4] Klaiber et al. (2023) Clin. Biomech.

**Acknowledgements:** This work was supported by NIH/NIAMS P50AR080581.

**Table 1.** ICC values for areas and locations (relative to the AT centroid) during GL and GM stimulations in neutral and plantar flexion.

| Intra-class Correlation Coefficients (ICC) | Lateral Gastroc Stimulation | | Medial Gastroc Stimulation | |
|---|---|---|---|---|
| Outcome Measure | Neutral | Planter Flexion | Neutral | Plantar Flexion |
| Lateral cluster area | 0.743 | 0.472 | 0.694 | 0.502 |
| Medial cluster area | 0.274 | 0.535 | 0.381 | 0.575 |
| Lateral cluster medial/lateral position | 0.986 | 0.963 | 0.995 | 0.986 |
| Lateral cluster anterior/posterior position | 0.995 | 0.983 | 0.981 | 0.987 |
| Medial cluster medial/lateral position | 0.990 | 0.992 | 0.997 | 0.998 |
| Medial cluster anterior/posterior position | 0.980 | 0.957 | 0.988 | 0.989 |

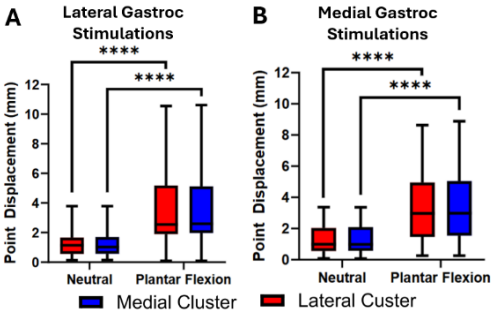


**Figure 2.** Mean total displacement of point clusters during A) LG stimulations and B) MG stimulations in neural and plantar flexion. ****p<0.0001.

# HANDHELD ULTRASOUND MEASUREMENT OF ACHILLES TENDON THICKNESS: INTRA- AND INTER-RATER RELIABILITY AT SINGLE LOCATION AND ORIENTATION

*Kendall Mulvaney, PA-C[1], Julia Dunn, PhD,[1], Julio Serrano Samayoa, MS[1], Michelle Sabick, PhD[1]
[1]Department of Mechanical and Materials Engineering, Ritchie School of Engineering and Computer Science, University of Denver, Denver, CO *kendall.mulvaney@du.edu

**Introduction:** Achilles tendon (AT) thickness is a key diagnostic criterion for tendinopathy, reflecting physiological changes in response to loading and strain [1]. Musculoskeletal ultrasonography (MSUS) provides an accessible and affordable alternative to MRI for evaluating AT in various settings [1]. However, MSUS results are subject to variability in image acquisition and thickness measurement from the image, as these are typically manual steps. Recent systematic reviews highlight the variety in methodology, impacting the ability to directly compare results among studies of reliability [2,3]. Optimal reliability can be achieved with one experienced operator, a standardized transducer location/orientation, and by averaging two to three measurements [2,3]. However, in both research and clinical settings there is often a need to have more than one person completing MSUS evaluations. The primary aim of this study was to assess the inter- and intra-rater reliability of handheld MSUS to measure AT thickness. Specifically, the study aimed to determine if there is a significant difference in inter-rater reliability for AT thickness measurement from images obtained by an examiner with clinical experience versus one without clinical experience; and to evaluate whether there is high intra-rater reliability for AT thickness measurement, regardless of the examiner experience for image acquisition.

**Methods:** Fourteen healthy participants were recruited with a median age of 27 years (21-59 range). For each participant, the left and right AT were imaged in the standardized prone positioning with 90º ankle flexion. A Butterfly IQ+ (Butterfly Network Inc, Burlington, MA, USA) handheld MSUS probe was used to obtain 2 repeated images on each tendon by both examiners. The probe was placed at midlength, defined as 3cm proximal to calcaneal edge and oriented longitudinal to the tendon fibers (Fig 1). Examiner A had clinical MSUS experience and B did not, although both underwent the same AT-specific training for the equipment used prior to data collection. Anteroposterior (AP) thickness was measured independently by each examiner on all images collected using an open-source software (ImageJ, National Institutes of Health, USA). Data processing included mean, standard deviation (SD), intra- and inter-rater intra-class correlation coefficient (ICC), standard error of measurement (SEM), and minimal detectable change (MDC) with significance set at $p<0.05$.

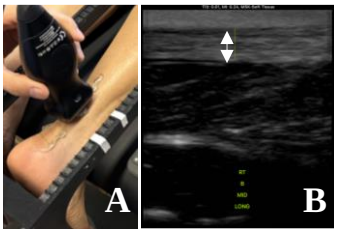


**Figure 1.** Midlength longitudinal: probe setup (A) and resulting MSUS image (B).

**Results & Discussion:** All ICC values were above the acceptable threshold of 0.70 for both inter- and intra-rater reliability [2,3]. In all images, inter-rater ICC values were above the acceptable level of 0.70, regardless of who acquired the images (Table 1). These results indicate that the experience level of the person performing the image acquisition and the person making the measurements from the images do not have to match, so images can be obtained from a clinic, and a trained researcher can process them. This allows for integration of clinical and research teams, further emphasizing the relevance of a standardized approach to AT thickness measurement.

All standard error of measurement (SEM) values were below 0.25 mm (<6%). The small error is consistent with previous studies (Table 1) [2,3]. The minimal detectable change (MDC) values were all below 0.70 mm, which is similar to the magnitudes of the standard deviations, indicating the high reliability of the protocol regardless of clinical experience. Inter-rater SEM and MDC were similar for all images. Examiner B intra-rater absolute reliability values suggest clinical experience is not necessary. There were significant differences in AT thickness measured from the two examiners for both AB images and B images, but not in those obtained by the examiner with experience ($p<0.05$).

**Table 1:** Descriptive statistics, relative and absolute reliability.

| **Images** | **Images Collected by A** | | **Images Collected by B** | | **Images Collected by Both** | | | |
|---|---|---|---|---|---|---|---|---|
| **Reliability** | **Inter-Rater A vs B** | | **Inter-Rater A vs B** | | **Intra-Rater A** | | **Intra-Rater B** | |
| | **Right AT** | **Left AT** | **Right AT** | **Left AT** | **Right AT** | **Left AT** | **Right AT** | **Left AT** |
| **ICC (95% CI)** | 0.92 (0.79-0.97) | 0.72 (0.46-0.89) | 0.74 (0.48-0.89) | 0.88 (0.70-0.96) | 0.80 (0.65-0.90) | 0.76 (0.60-0.87) | 0.82 (0.68-0.91) | 0.85 (0.73-0.93) |
| **Mean Thickness, mm (SD)** | 4.14 (0.49) | 4.53 (0.42) | 4.33 (0.43) | 4.54 (0.63) | 4.13 (0.51) | 4.39 (0.50) | 4.09 (0.50) | 4.47 (0.56) |
| **SEM, mm (SEM%)** | 0.14 (3.38%) | 0.22 (4.86%) | 0.22 (5.08%) | 0.22 (4.85%) | 0.23 (5.56%) | 0.24 (5.46%) | 0.21 (5.13%) | 0.21 (4.69%) |
| **MDC, mm** | 0.38 | 0.62 | 0.61 | 0.61 | 0.63 | 0.67 | 0.58 | 0.59 |

**Significance:** This study adds to the current literature that supports the use of MSUS for measuring AT thickness, even for researchers without previous clinical experience. This is important because it allows for the use of this measurement tool in various settings by a wide range of operators including clinicians, researchers and other members of a multidisciplinary team. Longitudinal assessments of AT health benefit from a consistent and reliable process of image acquisition and thickness measurement in the advancements of diagnosis and treatment of AT pathology.

**References:** [1] Johannsen et al (2016), *J Clin Ultrasound* 44(8); [2] McAuliffe et al. (2017), *Phys Ther Sport 26*; [3] Thoirs et al (2018), *Ultrasound Med Biol* 44(12); [4] Leung et al (2008), *J Clin Ultrasound* 36(1).

# CARPAL TUNNEL AREA MEASUREMENT USING ULTRASOUND IMAGING

[1]Mary N. Henderson, [1]David Jordan, [1,2,3]Zong-Ming Li
[1]Hand Research Laboratory, Department of Orthopaedic Surgery, University of Arizona, Tucson, Arizona; [2]Department of Biomedical Engineering, University of Arizona, Tucson, Arizona; [3]University of Arizona Arthritis Center, Tucson, Arizona
Email: lizongming@arizona.edu

**Introduction:** The carpal tunnel is formed by the carpal bones and transverse carpal ligament. Symptoms of carpal tunnel syndrome develop from compression of the median nerve, which can be attributable to carpal tunnel morphology. Various medical imaging techniques such as computerized tomography (CT) and magnetic resonance imaging (MRI) are non-invasive methods of viewing the components of the tunnel in vivo. However, disadvantages of using CT include difficulty visualizing soft tissues and radiation exposure, and the high costs associated with MRI make these methods suboptimal for routine clinical use [1-3]. Alternatively, ultrasound imaging is widely accessible in clinics, is less expensive, and provides images quicker compared to CT and MRI imaging modalities. While the concept of using ultrasound to view carpal tunnel area has been explored in research, difficulty visualizing deeper structures of the tunnel remain limitations of this imaging modality [4]. This study examines the use of ultrasound imaging to visualize and calculate the distal carpal tunnel area in a quick, reliable and inexpensive manner. The purpose of this study was to develop an algorithm that estimates the carpal tunnel area from ultrasound images, validated by MRI.

**Methods:** Three fresh frozen female cadaver hands were used for evaluations in this study (Age = 60.0 ± 6.928 years, BMI = 20.3 ± 4.041 kg/m$^2$). Each specimen was placed supine in a custom splint, with the palm, wrist and fingers secured in a neutral posture. Ultrasound gel was applied to the volar aspect of the wrist. An ultrasound probe was positioned on the wrist to image the distal carpal tunnel in the transverse direction. Images were taken to visualize the ridge of trapezium (TR), hook of hamate (HH), volar surface of capitate (CP) and the thenar muscles (Figure 1a). A 7-Tesla MRI machine with an 84 mm-diameter coil was used to image each specimen. A set of coronal images were taken to visualize the orientation of the hamate and trapezium. A scanning plane perpendicular to the cross-section was applied and an MRI image was taken. A single slice of the MRI scan containing the HH and TR was selected for analysis (Figure 1b). A local coordinate-system was established on both the MRI and ultrasound image with the origin set at the most radial-volar point of the HH. The x-axis was defined as the line from the origin to the most ulnar-volar point of the ridge of trapezium, and the y-axis was defined as perpendicular to the x-axis. A custom MATLAB program was used to manually trace the carpal tunnel boundary on the MRI images (Figure 1c). Seven unique points were manually chosen as landmarks on the MRI images: (1) the most radial-volar aspect of the hamate, H1, (2) the most ulnar-volar aspect of the ridge of trapezium, TRP, (3) the thenar muscle ulnar attachment point to the transverse carpal ligament, TUP, (4) the most volar aspect of the capitate, CPP, (5) the most ulnar point of the inner surface of the hamate, H2, (6) the midpoint, H3, between the H2 and H1, and (7) the most dorsal point of the inner surface of the hamate, H4. The minimum difference and corresponding translation vector from each landmark to the tunnel boundary was calculated and decomposed into x and y components. This was completed for specimens 1 and 2. On the ultrasound image of specimen 3, landmarks 1-4 were identified and translated using the average translation vectors from specimens 1 and 2. The x and y components of H2, H3 and H4 were normalized based on the length between H1 and TRP from specimens 1 and 2, and the averaged x and y components were used to estimate the positions on specimen 3. The estimated tunnel boundary was predicted onto the ultrasound image, aligned with the translated points. The carpal tunnel area was calculated on the ultrasound image with a spline fitted through the estimated tunnel points (Figure 1d). The carpal tunnel area calculated on the ultrasound image was compared to the area calculated in the MRI image from specimen 3.

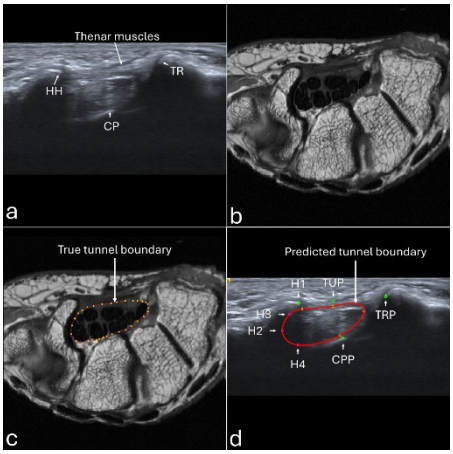


**Figure 1** a) Cross-sectional ultrasound image of distal carpal tunnel showing the HH, TUP, CP and thenar muscles. b) Cross-sectional MRI image of distal carpal tunnel. c) Cross-sectional MRI image showing the true carpal tunnel boundary d) Cross-sectional ultrasound image showing landmarks 1-4 (green), translated landmarks (yellow), estimated H2, H3 and H4 (magenta), and predicted carpal tunnel boundary (red).

**Results & Discussion:** The predicted carpal tunnel area in the ultrasound was 108.58 mm$^2$. The measured carpal tunnel area in the MRI was 111.19 mm$^2$. The difference between the predicted ultrasound area and the MRI area was 2.61 mm$^2$, corresponding to a 2.34% error. The difference between our algorithm-derived estimated tunnel area and the MRI validation showed a low error rate indicating its efficacy in estimating the carpal tunnel area utilizing a low-risk ultrasound imaging method. One study that estimated the tunnel showed minor differences between ultrasound measured area compared to anatomical area and showed larger average area measurements [4]. In this study, smaller specimens were chosen in order to fit inside the coil of MRI machine. This algorithm is a first step in estimating the carpal tunnel boundary and area based solely on an ultrasound image. Continued development of the model will include increasing the number of predicted points and using a larger sample size to strengthen the model and its applicability toward in-vivo studies.

**Significance:** This ultrasound imaging method serves as a low risk and inexpensive method of estimating the carpal tunnel shape and area which is valuable in characterizing and monitoring changes in morphological properties of the carpal tunnel.

**References:** [1] Merhar et al. (1986), Skeletal Radiol 15(7); [2] Mogk and Keir (2007), J Biomech 40(10); [3] Gabra and Li (2013), J Wrist Surg 2(102); [4] Kamolz et al. (2001), Surg Radiol Anat 23(2).

**Measurements of post-operative subsidence after trapeziectomy may be inaccurate when using standard posteroanterior and lateral radiographs**

Sanah Handu[1], Cortez L. Brown[1], Edward Godbold[1], Tom Gale[1], Zino Kuhn[1], Maria Munsch[1], John Fowler[1], William Anderst[1]
[1]Department of Orthopaedic Surgery, University of Pittsburgh Medical Center
SAH215@pitt.edu

**Introduction:** Thumb carpometacarpal (CMC) joint osteoarthritis (OA) is a prevalent disease that affects nearly 20% to 35% of patients over the age of 55 years.[1] Trapeziectomy is a common surgical intervention for patients afflicted with OA who experience increasing thumb pain, instability, and weakness. In addition to trapeziectomy, surgeons perform ligament reconstruction and tendon interposition (LRTI) or suture-only suspension arthroplasty (SSA) to prevent the thumb metacarpal from collapsing onto the scaphoid.[4] Surgeons assess the arthroplasty construct by measuring the amount of metacarpal subsidence on radiographic images collected in standard posteroanterior (PA) and lateral views.[2] However, these clinical measures of subsidence have not been validated, and a standard procedure is needed to improve rigor and reproducibility.[3,4] We hypothesize that standard true PA and lateral views are not sufficient to accurately measure subsidence. The long term goal of the study is to identify the optimal imaging configuration for estimating dynamic three-dimensional (3D) thumb CMC subsidence on two-dimensional (2D) radiographs.

**Methods:** Written informed consent was obtained for this IRB-approved study. CT scans of each participant's post-operative hand and wrist were segmented to create three-dimensional (3D), subject-specific bone models (Figure 1). PA and lateral view radiographs of the hand and wrist were digitally reconstructed, and the radiographs were used to depict the hand supinated and pronated in 5° and 15° increments from the PA and lateral views, respectively. Two orthopaedic surgery residents independently measured each increment using ImageJ to manually measure the shortest trapezial gap distance from the distal articular surface of the scaphoid to the proximal articular surface of the first metacarpal using clinical standards[4] when possible. The average of these measurements was compared against the known minimal trapezial gap distance, which was calculated from the 3D model.

***Figure 1.*** *2D generated PA and Lateral radiographs, post-trapeziectomy, with PA trapezial space highlighted in the white box and trapezial measurement is represented by white line.*

**Results and discussion:** Minimum trapezial distance data from 5 participants from this ongoing study have been analyzed (4 female; 62.4±6.3 years). The value of Cohen's kappa ranged from 0.429 to 0.745, indicating moderate to substantial agreement in the inter-rater measurements, however the average absolute difference between the raters was only 0.2±0.2mm. When analyzing the PA views, the measurements made at 5° pronation and 10° pronation had the smallest average absolute difference from the actual value (0.6±0.5mm and 0.6±0.4mm, respectively; Figure 2 left). However, the measurements at the neutral PA view were the third most accurate of the PA views, with an absolute difference from the actual value of 0.7±0.4mm, which is a negligible variance from the measurements at 5° and 10°. In the lateral view, the measurements made at 60° pronation had the smallest average absolute difference from actual (0.8± 0.7mm; Figure 2 right). The views from 30° supination to 30° pronation (including the neutral view) were the least accurate of all the radiograph views, each with an average absolute difference ≥ 2.3±1.4mm, and in the lateral views, measurements consistently underestimated the gap space. Further, there was no view (PA or lateral) for which all subjects yielded accurate measurements.

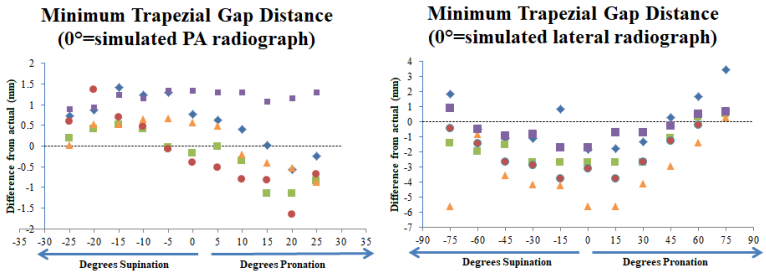


***Figure 2.*** *Minimum trapezial space measured at 5° increments of supination or pronation from the PA (Left) and at 15° from the lateral position (Right). Each color represents a different subject, and zero on the vertical axis indicate true 3D values.*

**Significance:** These preliminary findings suggest post-trapeziectomy measurements made of the hand at 5° and 10° pronation from neutral PA, or at neutral PA itself, appear most accurate; lateral views are poor for determining true subsidence. Determining the accuracy of clinical measurements of trapezial space made on 2D radiographs is important for proper post-operative assessment.

**Acknowledgment**: This work is supported by the National Institutes of Health under the award number R21AR081556.

**References**: [1] Van Heest et al., *JAAOS*, 2008; [2] Meyers et al. *PRS* 2023; [3] Miller et al., *J Hand Microsurg*, 2018; [4] Bhat et al., *J Hand Surg Am*, 2003

# A PRELIMINARY STUDY ON THE VALIDITY AND RELIABILITY OF FREEHAND 3D ULTRASOUND FOR GLUTEUS MEDIUS MUSCLE VOLUME QUANTIFICATION IN HEALTHY YOUNG ADULTS

Ali Karimi Azandariani[1], Megan Gordon[1], Irene Kaiser[1], Oluwagbemiga DadeMatthews[1], Ali Mirjalili[2], Guillaume Spielmann[1], *Hyun Kyung Kim[1]
[1]School of Kinesiology, Louisiana State University, Baton Rouge
[2]Anatomy and Medical Imaging, University of Auckland, Auckland
*Corresponding author's email: hkkim@lsu.edu

**Introduction:** Freehand 3-D ultrasound system (3DUS) is a reliable method for muscle volume quantification [1]. However, the acquisition and segmentation process can be challenging for large, convergent muscles, such as the gluteus medius (GMed). As a key hip stabilizer, the GMed has a width greater than the transducer's field of view, necessitating the use of a multiple-sweep 3DUS technique to capture the entire muscle. While magnetic resonance imaging (MRI) is often considered the gold standard for *in vivo* muscle volume measurements [2], its high cost, lack of portability, and contraindications for certain individuals limit its use. In contrast, freehand 3DUS offers a viable alternative that addresses these challenges. This study aims to validate the use of 3DUS for quantifying GMed volume with the multiple-sweep technique. It was hypothesized that freehand 3DUS, using multiple-sweep techniques, would demonstrate good reliability and validity.

**Methods:** Five healthy individuals (3 females and 2 males, age 21.8 ± 1.9, height 175.4 ± 7.8m, weight 69.2 ± 14.7kg) participated in this study. To measure GMed muscle volume on each side of hip, we used both 3DUS and MRI (T1 3D LAVA-FLEX, High resolution with Fat, Water, In/Out Phase). A computer-based B-mode ultrasound machine (MicrUs, TELEMED, Lithuania) with a linear transducer (field of view: 64 mm, depth: 60 mm, 8 MHz) was used to acquire ultrasound data via Stradwin software (v6.03, University of Cambridge, UK). To reconstruct a 3D model of the scanned muscle, the ultrasound machine was synchronized with four OptiTrack motion capture cameras (v2.3.6, Motive, US) to track the transducer's position using four markers placed on top of it. Participants were instructed to lie on their side with their to-be-scanned hip flexed to approximately 45 degrees, while keeping their knees stacked on top of each other. Multiple-sweep technique were applied to each side of the hip, with each scan comprising three proximal-to-distal sweeps to capture the GMed. For all analysis, the data from 10 limb scans were included. Bland-Altman analysis was utilized to assess agreement between MRI and 3DUS measurements. Inter-processor reliability was tested by having two different processors segmenting the GMed on 3DUS data and intra-processor reliability by one of the processors segmenting the GMed on the same data after two months. To assess inter- and intra-processor reliability of 3DUS segmentation, we calculated the Intraclass Correlation Coefficient (ICC) with 95% confidence intervals (CI). Additionally, the coefficient of variation (CV%) was calculated to evaluate variability relative to the mean.

**Results & Discussion:** The Bland-Altman analysis (Fig 1) demonstrates that the differences fall between the limits of agreement indicating a strong agreement between 3DUS and MRI. While the result for processor 1 underestimates the muscle volume against MRI, that of processor 2 shows a better agreement. All ICCs for inter- and intra-processor reliability of 3DUS in assessing GMed muscle volume were above 0.99, with CV% of 1.96 and 2.06, respectively, indicating minimal variability. The absolute difference between processors' segmentation were 5.61± 3.43ml and 5.44±3.69ml (Table 1), indicating good reproducibility of 3DUS segmentation across two different processors and over time. These findings align with previous studies introducing 3DUS as a viable means of muscle volume quantification [1,3]. Given the small sample size of this study, further validation on a wider population would provide stronger insights on reliability of 3DUS for GMed volume measurement.

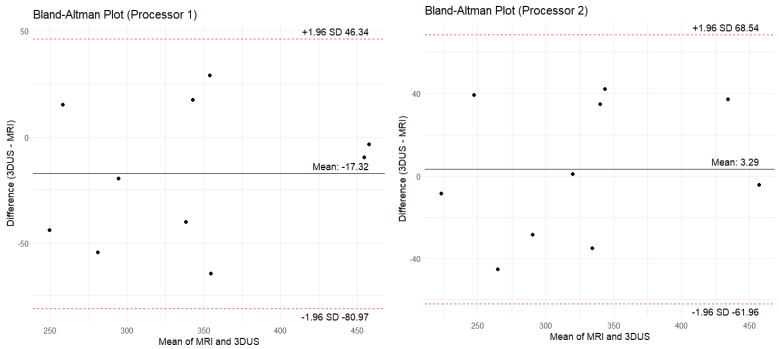


***Figure 1***. Bland-Altman plots comparing 3DUS and MRI muscle volume measurements for Processor 1 (left) and Processor 2 (right). The black line represents the mean difference, while the dashed red lines indicate the limits of agreement (±1.96 SD).

**Table 1:** GMed volume measurement for inter- and intra-processor reliability

| Inter-processor reliability | | | | Intra-processor reliability | | | |
|---|---|---|---|---|---|---|---|
| Seg1 (ml) | Seg2 (ml) | Absolute difference (%) | ICC | Seg1 (ml) | Seg2 (ml) | Absolute difference (%) | ICC |
| 329.84± 78 | 327.72± 78.49 | 5.61± 3.43 | 0.997 | 329.84± 78 | 302± 52.98 | 5.44± 3.69 | 0.992 |

**Significance:** This study suggests preliminary evidence on feasibility of 3DUS and multiple sweeps technique for GMed volume measurement by demonstrating high inter- and intra-processor reliability and a strong agreement with MRI. The validation of 3DUS for volume measurement of convergent muscles such as GMed would suggest a cost-effective, portable, and more practical means of muscle volume measurement for research and clinical practice.

**Acknowledgments:** The authors would like to thank all participants and the MRI technician at Pennington Biomedical Research Center. This study was partially funded by the State of Louisiana through GS and the Board of Regents (RCS).

**References:** [1] Bell, M., et al. (2022), *Ultrasound Med, Biol* 48(3): p. 565-574; [2] Arbeille, P., et al. (2009), *Ultrasound Med Biol*, 35(7): p. 1092–1097. [3] Umehara, J., et al. (2022) *Ultrasound Med, Biol.* 48(9): p. 1966-1976.

# MUSCLE ARCHITECTURE ANALYSIS OF AGONIST/ANTAGONIST PAIRS SHOW DIFFERENCES IN CEREBRAL PALSY COMPARED TO TYPICALLY DEVELOPING ADOLESCENTS

*Zhenhao Liu[1,2], Geoffrey Handsfield[1,2]
[1]MOBIOS Lab, Department of Orthopaedics, University of North Carolina at Chapel Hill, USA
[2]Lampe Joint Department of Biomedical Engineering, University of North Carolina at Chapel Hill and NC State University, USA
*Corresponding author's email: zhenhliu@unc.edu

**Introduction:** Cerebral palsy (CP) is characterized by abnormal neuromuscular development, which affects limb muscles and leads to pathological gait patterns and activity limitations. These impairments occur alongside altered muscle architecture, which may include abnormal muscle fiber orientation, fascicle length, physiological cross-sectional area (PCSA), and volume. Understanding muscle architectural differences in CP will abet our understanding of the condition and inform interventions such as physiotherapy and surgery to improve functional outcomes. This study aimed to investigate differences in muscle architecture between adolescents with CP and typically developing (TD) peers in an agonist/antagonist pair in the lower limb, to offer insight into altered growth patterns or biomechanical adaptations during development [1]. Reconstructing muscle architecture in vivo is challenging, but diffusion tensor imaging (DTI) offers insights into both muscle fiber architecture and muscle quality. Therefore, we evaluated the medial gastrocnemius (MG) and tibialis anterior (TA) as a muscle pair in CP and TD cohorts. We hypothesized that (1) muscle fiber orientation is disrupted in the MG and TA of individuals with CP, and (2) muscle length, PCSA, and volume are smaller in CP compared to TD.

**Methods:** Imaging data from 7 adolescents with CP (4M/3F) and 9 TD (5M/4F) controls from a previous study were used [2]. All participants provided informed assent, and parents/guardians gave consent. The University of Auckland Human Participant Ethics Committee approved the study. Two MRI sequences were acquired: a sagittal T1VIBE sequence for anatomical muscle data and an echo-planar DTI sequence of the same region. Both MG and TA were segmented in resampled T1VIBE datasets to create masks for DTI analysis. Muscle fiber tractography was performed in DSI Studio, and muscle architecture was calculated using custom Python code, following previous methods [3]. Muscle length, fascicle length, PCSA and volume were normalized by body size. Diffusion scalar measurements were computed using DIPY's TensorModel function. Independent t-tests were conducted for all measurements to assess intergroup differences. Levene's test was used to evaluate variance homogeneity within each group.

**Results & Discussion:** Pennation angles were significantly larger in the CP cohort compared to TD at the distal aponeurosis of the MG (27.770 ± 3.971˚ CP vs. 23.339 ± 3.835˚ TD, $p = 0.043$), while no significant differences were observed at the proximal aponeurosis of the MG or at either aponeurosis of the TA (Fig. 1a&1b). DTI scalars were assessed; apparent diffusion coefficient (ADC) was higher in CP than TD for MG ($(0.231 \pm 0.043) \times 10^{-3}$ mm²/s vs. $(0.182 \pm 0.038) \times 10^{-3}$ mm²/s), $p = 0.035$), but no significant difference was observed in TA. Fractional anisotropy (FA) was similar across groups both in MG and TA. The increased ADC in CP suggests greater water diffusivity, while the preserved FA indicates that, despite this increased diffusivity, the overall structural integrity and fiber alignment remain relatively intact. Normalized muscle length was shorter in CP than in TD for the MG (0.110 ± 0.015 vs. 0.132 ± 0.016, $p = 0.012$), whereas no significant differences were observed in the TA. Normalized muscle volume was significantly smaller in the CP cohort compared to TD for the TA (0.007 ± 0.001 $cm^3/m \cdot kg$ vs. 0.011 ± 0.001 $cm^3/m \cdot kg$, $p<0.001$), as was PCSA (0.416 ± 0.074 $cm^2/kg$ vs. 0.658 ± 0.107 $cm^2/kg$, $p<0.001$). Similarly, the MG exhibited significantly smaller normalized muscle volume (0.012 ± 0.005 $cm^3/m \cdot kg$ vs. 0.020 ± 0.007 $cm^3/m \cdot kg$, $p=0.026$) and PCSA (0.525 ± 0.232 $cm^2/kg$ vs. 0.874 ± 0.315 $cm^2/kg$, $p=0.029$) in the CP group (Fig. 1c&1d). These reductions in muscle size align with prior studies, indicating impaired growth in CP. Additionally, lower Z-scores in CP for both the TA (-2.274 ± 0.726) and MG (-1.172 ± 0.794) further support the observed reductions in muscle volume and PCSA.

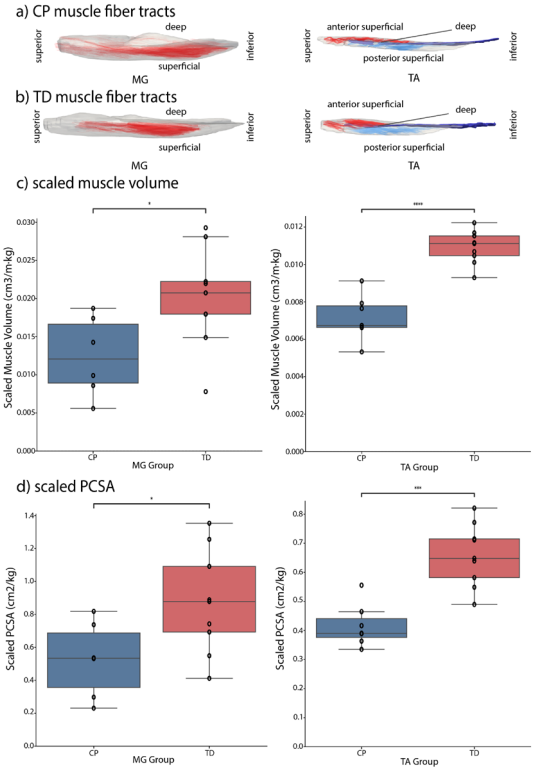


**Figure 1:** a & b: MG and TA muscle fiber in the CP and TD; c: Scaled muscle volume difference between CP and TD in MG and TA; d: Scaled PCSA difference between CP and TD in MG and TA.

**Significance:** This study highlights localized muscle architecture alterations in CP compared to TD. Muscle volumes and PCSAs showed comparable reductions in both muscles, whereas muscle length, DTI scalars, and pennation angles showed differing results between muscles. The use of DTI as a muscle microstructure assessment tool offers potential for tracking disease progression and refining treatment approaches. Assessment of agonist/antagonist pairs offers future potential for understanding CP progression.

**Acknowledgments:** We thank the Wishbone Trust, Maanya Bhutani, Adarsh Dandamudi, Chetan Daswani, and Kyle Royster for their assistance.

**References:** [1] Handsfield et al. (2022), *BMC Musc Disorder*, 23(1): 233; [2] Sahrmann et al. (2019), *PLoSOne*, 14(2): e0205944; [3] Bolsterlee et al. (2019) *J Biomech*, 86: 71-7

# Assessment of Calcaneal Morphological Differences of Pediatric Flatfoot via Statistical Shape Modeling

*Nick Slavik[1], Renae Lapins[2], Amanda T. Whitaker[3,4], Amy L. Lenz[2,5], *Karen M. Kruger[1,6]
[1]Joint Department of Biomedical Engineering, Marquette University and Medical College of Wisconsin, Milwaukee, WI, [2]Department of Biomedical Engineering, University of Utah, Salt Lake City, UT, [3]Department of Orthopaedic Surgery, University of California Davis, Sacramento, CA, [4]Shriners Children's Northern California, Sacramento, CA, [5]Department of Mechanical Engineering, University of Utah, Salt Lake City, UT, [6]Motion Analysis Center, Shriners Children's, Chicago, IL.
*Corresponding author's email: nslavik@mcw.edu

**Introduction:** Pediatric flatfoot (pes planovalgus) has a reported estimated prevalence of 44% and is among the highest prevalence for disorders affecting children and adolescents [1,2]. As these children develop, unresolved structural differences can lead to pain and dysfunction [3]. Early detection of morphological differences in pediatric bone development is critical to inform physicians and surgeons for corrective interventions prior to the onset of pain or maladaptive gait. Limited use of 3D imaging in pediatrics has restricted our understanding of bone morphology changes however, the increased use of clinical weightbearing computed tomography (WBCT) has potential to address these limitations. Given that loading impacts bone growth, the goal of this work was to compare foot and ankle bone morphology of children with diagnosed flatfoot to an asymptomatic population.

**Methods:** This IRB approved, retrospective study included two distinct participant groups: a control group (n=19, dominant limb) of adults without foot pathology and a flatfoot group (n=6 individuals, 10 feet) consisting of pediatric individuals (average age=12.2 years, range=10.0-15.8 years) who underwent clinical WBCT for treatment of flatfoot deformity at either the University of Utah or Shriners Children's Northern California. Initial calcaneal bone segmentations were semi-automatically generated using BoneLogic v2.1.4 (Disior, www.disior.com). Alignment of WBCT images and 3D segment origin transformations were performed with 3D Slicer v5.8.0 (Slicer, www.slicer.org); left calcanei were mirrored across the sagittal midline axis to remove laterality as a mode of variation. Initial bony segmentations were refined and verified using Mimics 25.0 (Materialise, www.materialise.com). The calcanei segmentations were utilized to create single domain statistical shape model (SSM) using ShapeWorks v6.5.1 (SCI Institute, www.sciinstitute.github.io/ShapeWorks). Segments were aligned in space and Procrustes analysis was used to remove orientation and size as modes of variation. Principal component analysis (PCA) was conducted to identify modes of largest variation. PCA component scores were exported, and parallel analysis was used to determine significant PCA modes. Hotelling's T-squared test with false discovery corrections utilized to identify regions of morphological differences; significance $\alpha \leq 0.05$. Surface distance differences of significant PCA modes visualized using CloudCompare v.2.14 (www.danielgm.net).

**Results & Discussion:** Hotelling's $T^2$-test comparisons of the control and flatfoot groups are shown in Fig. 1. Areas of significant morphological differences are indicated in red. Parallel analysis identified 5 significant modes of variation with 95% of the cumulative variance explained in the first 16 modes. The first mode explained 37.0% of overall variance; with 12.7%, 10.2%, 6.2%, and 5.5% of variance explained from the second, third, fourth, and fifth modes, respectively. After correcting for multiple comparisons, only the first PCA mode was significant when comparing PCA component scores, (p=0.0010, Student's $T^2$-test with Holm-Sidak correction). As shown in Fig. 2, this mode shows large variation at the subtalar joint between the control and flatfoot populations, Specifically, larger variation among the pediatric flatfoot group with trends towards larger more pronounced anterior processes, as well depressed posterior facets. Further, Mode 1 indicates a large variation in size and shape of the body of the calcaneus; possibly indicating maladaptive loading resulting in different morphologies around muscle insertions during bone development.

**Significance:** These preliminary findings show promising results in quantifying morphological differences in the bones of pediatric flatfeet. Providing key insights into maldevelopment of the foot and ankle leading to earlier clinical interventions and improved health outcomes for pediatric patients into adolescence and adulthood. Future work analyzing more bones of the foot and ankle as well as the corresponding 3D alignment will further increase our understanding of these morphological differences among this patient population.

**References:** [1] Pfeiffer et al. (2006), *Pediatrics* 118(2); [2] Sadeghi-Demneh et al. (2018), *Foot* (Edinb); [3] Bresnahan et al. (2020) *Front Pediatr.* 8(19).

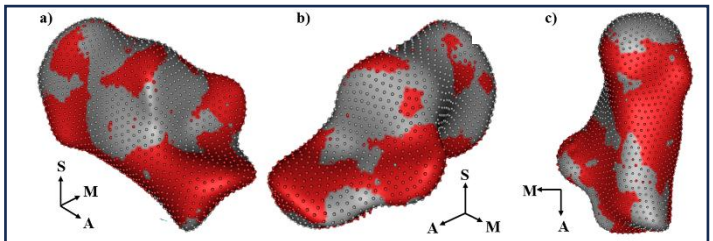


**Figure 1:** Dorso-lateral (left), medial-lateral (center), and inferior (right) views of mean mesh from SSM. Areas of significance from Hotelling's T2-test indicated in red ($\alpha < 0.05$).

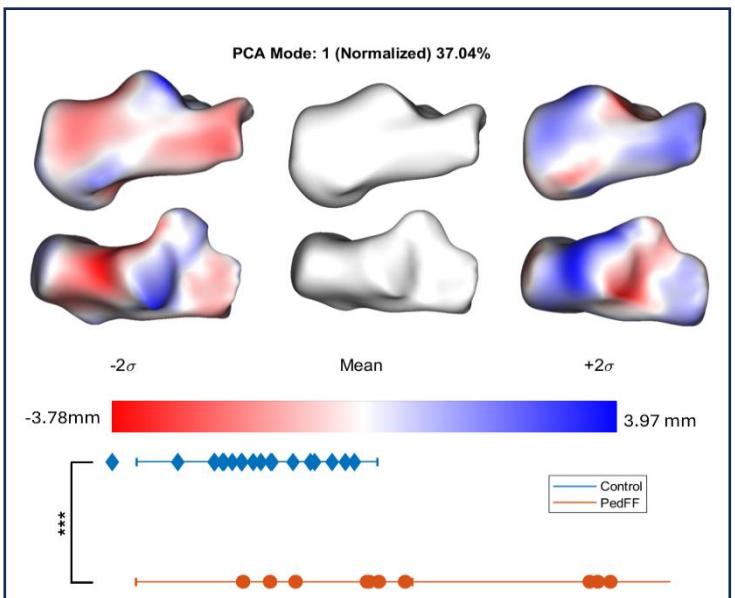


**Figure 2:** Lateral (top) and superior (bottom) views of first PCA mode with two standard deviations below the mean (left), mean mesh (center), and two standard deviations above the mean (right). Blue and red coloration indicate smaller and larger regions from mean mesh, respectively. ***: p-value = 0.0010

# REPEATABILITY OF HOUNSFIELD UNIT MEASUREMENT IN BONE FROM WEIGHT BEARING CT

Tyce C. Marquez,[*1] Anup Pant,[1] Tadiwa Waungana,[2] Sarah Manske,[2] Joshua E. Johnson,[1] Donald D. Anderson[1,2]
[1]University of Iowa, Iowa City, IA and [2]University of Calgary, Calgary, Canada
tyce-marquez@uiowa.edu

**Introduction:** The introduction of low-dose weight bearing CT (WBCT) has enabled cost-effective 3D imaging of joints under functional loading conditions with promise to advance diagnosis and treatment. Compared to plain radiography and conventional multi-detector CT (MDCT), WBCT reduces radiation dose and imaging time in the foot and ankle to provide better value [1]. Additionally, WBCT delivers comparable bone position angle measurements and maps of 3D joint space width compared to MDCT [2]. Although less well studied to date, WBCT can also provide information about the density of the peri-articular bone [3]. As WBCT studies continue to expand, there is an inherent need for image acquisition standardization across research sites to ensure measurement reliability [4]. The objective of this study was to evaluate the repeatability of gray scale value (Hounsfield unit, or HU) measurement in bone, indicative of X-ray attenuation, from WBCT at a single research site.

**Methods:** A radiographic knee phantom (Erler Zimmer, Germany) was used to assess the repeatability of WBCT HU measurement in bone. The phantom consists of a cadaveric distal femur, patella, and proximal tibia embedded in plastic (Fig. 1). WBCT scans were acquired at four separate timepoints using a CurveBeam HiRise scanner (CurveBeam AI, Hatfield PA) with the following acquisition parameters: 130 kV, 6.5 mA, 0.3 mm isotropic voxel size, and a 435x435x200 mm FOV. The phantom was placed in the center of the scanner for all image acquisitions. The first two scans (WBCT1 and WBCT2) were obtained consecutively without moving the phantom, while the latter two scans were performed 7 days (WBCT3) and 49 days (WBCT4) later, respectively. All WBCT data were registered to the first scan, used as reference. A region of interest (ROI) including peri-articular cortical and cancellous bone was selected for HU value comparisons using linear regression and Bland-Altman analysis.

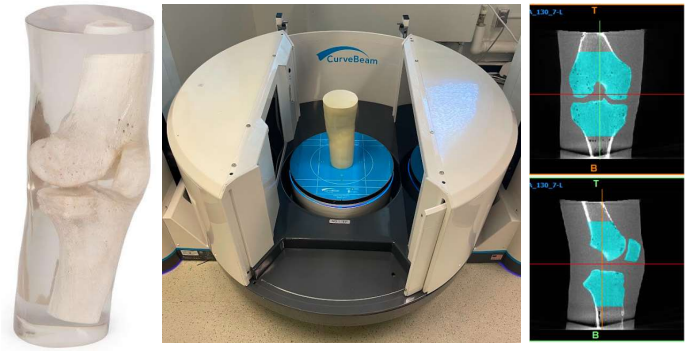


**Figure 1**. (left) Knee phantom with bones embedded in plastic, (middle) phantom centered in WBCT scanner, (right) ROI for analysis highlighted in cyan, including cortical and cancellous bone.

**Results & Discussion:** The HU values measured in bone across different timepoints demonstrated strong linear relationships (Fig. 2). All HU comparisons exhibited $R^2$>0.89 (range 0.89-0.94 (Table 1)). Not surprisingly, the highest agreement was observed in consecutive scans without repositioning the phantom (WBCT2 – WBCT1). This comparison also showed the smallest mean difference (-1.01 HU) in Bland-Altman analysis. The largest mean difference was 22.10 HU for WBCT3 – WBCT1 comparison. The WBCT3 – WBCT1 comparison showed the worst $R^2$ value and largest mean difference, however the third and fourth scans showed similar differences relative to the reference scan (WBCT1). Prior research has reported larger bone mineral density measurement errors in WBCT imaging (up to 15.3%) than MDCT (up to 5.6%) [5]. However, strong correlations were found between bone mineral density measured *in vivo* using WBCT and MDCT. Factors affecting WBCT reliability include patient positioning, unilateral vs. bilateral scanning protocols, techniques to reduce beam hardening, bone density calibration, and overall scanner parameter consistency [4]. These factors will need to be addressed and re-established to provide reliable data to support clinical WBCT use.

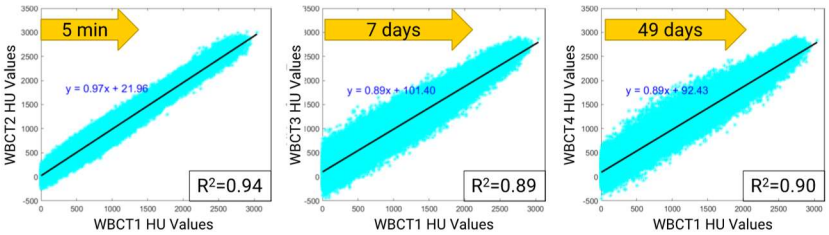


**Figure 2**. Comparisons of HU values from the different scans at different time points.

**Table 1**. Hounsfield unit repeatability comparison $R^2$ and Bland-Altman mean difference values.

| Comparison | $R^2$ | Bland-Altman Mean Difference |
|---|---|---|
| WBCT2 – WBCT1 | 0.94 | -1.01 |
| WBCT3 – WBCT1 | 0.89 | 22.10 |
| WBCT4 – WBCT1 | 0.90 | 14.60 |

**Significance:** Establishing the repeatability of bone HU value measurements is essential for standardizing WBCT acquisition protocols. This study provides an initial evaluation at a single site and will inform a future multi-center study investigating HU value variability across different WBCT scanners.

**Acknowledgments:** No specific funding was received for this research.

**References:** [1] Richter M, et al. (2020). Foot Ankle Surg 26(5):518-22. [2] Richter M, et al. (2014). Foot Ankle Surg 20(3):201-7. [3] Tazegul TE, et al. (2022). Foot Ankle Orthop 7(3):24730114221116805. [4] Brinch S, et al. (2023). Skeletal Radiol 52(6):133-40. [5] Waungana TH, et al. (2024). J Clin Densitom 27(3):101504.

# KINEMATICS OF THE PRE-OPERATIVE DYSPLASTIC HIP

Connor Luck*, Edward Godbold, Camille Johnson, Ashley Disantis, Craig Mauro, Michael McClincy, William Anderst

Department of Orthopaedic Surgery, University of Pittsburgh, Pittsburgh PA, USA

*Corresponding Author's email: luckcl@upmc.edu

**Introduction:** Acetabular dysplasia (AD) is a disorder that occurs when the acetabulum (hip socket) is abnormally shallow and doesn't provide sufficient coverage of the femoral head, causing instability of the hip joint. Over time, this instability causes damage to the labrum and cartilage, which can cause pain and lead to early hip osteoarthritis [1]. Periacetabular osteotomy (PAO) is the gold standard surgical procedure to treat symptomatic AD [2]. During the PAO procedure, the surgeon cuts the pelvis around the hip socket and repositions the acetabulum to properly cover the femoral head. Although hip joint kinematics during activities of daily living have been investigated in asymptomatic young adults [3, 4], the kinematics of the pre- and post-operative dysplastic hip remain elusive. Single-plane radiography indicates femoral head translation is greater in the dysplastic hip than in healthy hips during a stepping in place activity [5]. However, to our knowledge, 6-DOF kinematic variables during common weightbearing activities have not been evaluated in the pre-operative dysplastic hip. The present study is an interim analysis of an ongoing study comparing hip kinematics prior to and after PAO to hip kinematics in a healthy asymptomatic cohort.

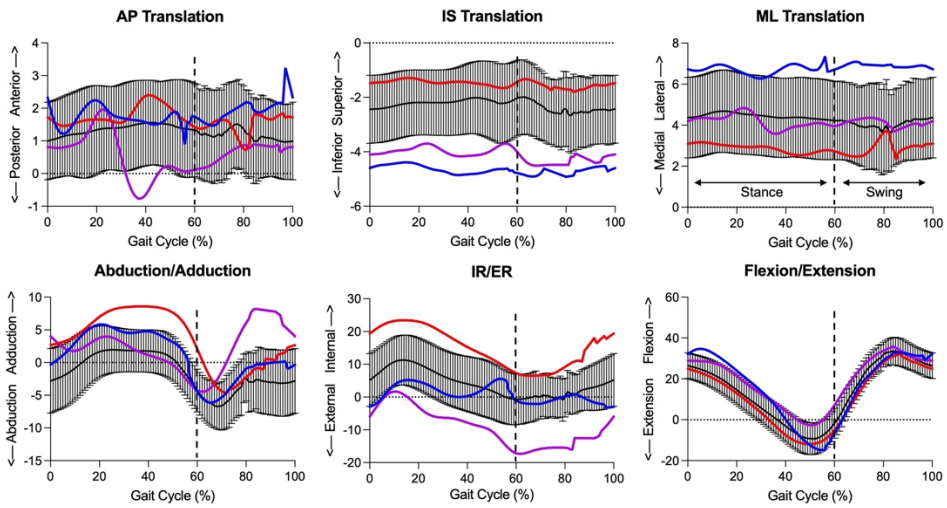


***Figure 1.*** *Average six degree-of-freedom kinematic waveforms for pre-operative dysplastic hips (solid colored lines) during gait across up to three walking trials. Black solid waveforms represent average kinematics from the asymptomatic hip cohort, with error bars depicting +/- 1 standard deviation. Dashed vertical line denotes toe-off.*

**Methods:** Thus far, three patients scheduled to undergo a PAO to surgically correct AD consented to be included in this IRB-approved study. Synchronized biplane radiographic images were collected pre-operatively at 50 images/sec for 1 second during treadmill walking at a self-selected speed (3 trials per hip). Computed tomography (CT) scans were manually segmented to create subject-specific bone models of the femur and hemi-pelvis for each hip. These models were then matched to the biplane radiographs by a validated volumetric model-based tracking technique to determine bone motion with submillimeter accuracy (bias: 0.2°, 0.2mm; precision 0.8°, 0.3mm) [6]. Anatomic coordinate systems were placed in each femur and hemi-pelvis [7], mirrored to the contralateral side, and co-registered to produce identical coordinate systems for each hip. A dataset of healthy control participants was used as a reference for this analysis. That dataset was comprised of 24 asymptomatic adults (13F, 11M; age 21.9±2.2 years; BMI 21.5±5.0 kg*m$^2$) who also performed treadmill walking within the dynamic biplane radiographic system [4].

**Results & Discussion:** Across the three dysplastic hips during gait, abduction/adduction ranged from –4.1° to 7.7°; internal/external rotation (IR/ER) from –6.5° to 11.9°; flexion/extension from –9.9° to 33.8°; anterior-posterior (AP) translation from 0.2mm to 3.4mm; inferior-superior (IS) translation from –4.0mm to –2.3mm; and medial-lateral (ML) translation from 3.3mm to 5.4mm [Figure 1]. For most of the gait cycle, each of the 3 patient's continuous kinematic waveforms fell within or close to the mean ±1 SD range previously seen in a healthy, asymptomatic cohort [4; Figure 1]. The absolute rotational side-to-side differences (SSD) between pre-operative surgical side and contralateral side was 6.8°±2.5° (IR/ER); 5.5°±2.4° (abduction/adduction); and 2.3°±1.5° (flexion/extension). The absolute translational SSD seen within these participants were 1.8mm±0.6mm (AP translation); 1.1±0.3mm (IS translation) and 2.7mm±0.3mm (ML translation). The SSD in translation within these hips are higher than what is seen in normal hips (≤0.6±0.5mm) [4] and provides insight into the relative translational instability of the femoral head within the dysplastic hip compared to the contralateral hip during daily activities. These interim results do not appear to indicate large differences in the kinematic waveforms of pre-operative, dysplastic hips compared to the asymptomatic individuals, however the SSD in translation appear to be 2 to 4 times larger than seen in healthy controls.

**Significance:** Insight into the in vivo kinematics of the dysplastic hip during weightbearing activities is necessary for identifying differences between the surgical and contralateral hips within PAO patients, and for quantifying the effects of symptomatic hip morphologies during activities of daily living in comparison with healthy hips. Our results expand upon previous studies of asymptomatic, healthy hips by providing reference values for the kinematics of dysplastic hips scheduled for PAO.

**References:** [1] Murphy et al. (1995), *J Bone Joint Surg Am* 77(7). [2] Holleyman et al. (2020), *J Bone Joint Surg Am* 102(15). [3] Ruh et al. (2022), *Clin Orthop Relat Res* 480(6). [4] Johnson et al. (2022), *J Biomech* 143. [5] Sato et al. (2017), *Clin Biomech* 46. [6] Martin et al. (2011), *J Arthroplasty 26(1).* [7] Wu et al. (2002), *J Biomech* 35(4).

# KNEE BONE ALIGNMENT IS PREDICTIVE OF NON-OPERATIVE OUTCOMES IN PATELLAR INSTABILITY

*Marissa Lee Sinopoli[1,2†], Anthony Gatti[2†], Christian Wright[2], Anna Bartsch[3], Matthew Veerkamp[5], Robert Boutin[2], Douglas Mintz[6], Kathleen Emery[5], Beth Shubin Stein[6], Shital Parikh[5], Kevin Shea[2], Akshay Chaudhari[2], The JUPITER Study Group, Seth Sherman[2], and Scott Delp[2]

[1]Harvey Mudd College, [2]Stanford University, [3]University Hospital Basel, [4]Stanford Medicine, [5]Cincinnati Children's Hospital Medical Center, [6]Hospital for Special Surgery

[†]Co-first authors *Corresponding author's email: msinopoli@hmc.edu

**Introduction:** Patellar instability can be treated non-operatively or operatively, and outcomes vary. Accurate, early prediction of patient responses to treatment is needed to personalize interventions, reduce recurrent instability, and improve outcomes [1]. Anatomic shape and alignment affect internal joint biomechanics and thus injury risk and recovery. Traditional methods that quantify anatomy and inform treatment planning rely on 2D imaging measures [2] and thus do not leverage 3D information contained in magnetic resonance images (MRIs). The purpose of this research was to compare how 3D bony alignment in the knee and 3D bone shape associate with one-year patient-reported outcomes in patients who received non-operative treatment for patellar instability.

**Methods:** This was a retrospective analysis of data from 244 patients with patellar instability and 26 controls with anterior cruciate ligament injury. We quantitatively characterized knee anatomy by first segmenting the femurs, patellae, and tibias from MRIs and then developing a statistical knee model. The statistical knee model quantifies 3D knee bone alignment (rotations and translations of the patella and tibia relative to the femur) and shape (variations in bone curvature). We developed several scores of patellar instability that projected each knee onto the line that separated the mean of the control cohort and the mean of the subset of the patellar instability cohort with multiple instability episodes. The three separate scores were developed based on 1) 2D imaging measures, 2) 3D bone alignment, and 3) 3D bone shape. Higher scores are associated with more severe patellar instability.

A subset ($n$ = 21) of patellar instability patients received non-operative treatment and reported one-year outcomes. Outcomes included the Kujala Anterior Knee Pain Scale (Kujala) [3], which reflects symptoms and functional limitations, and the Banff Patellofemoral Instability Instrument 2.0 (BPII 2.0) [4], which reflects quality of life. Higher scores are associated with positive outcomes. We computed correlations between the anatomical scores we developed and these outcomes. After evaluating these correlations, we conducted a subset analysis to create a 3D Patellar instability Anatomical Severity Score (3D-PASS) to best correlate with outcomes.

**Results & Discussion:** Individual factor correlations with one-year non-operative outcomes are reported in Table 1. Three-dimensional bone alignment was moderately correlated with non-operative outcomes. Worse outcomes were associated with greater patellar tilt, height, and lateral displacement; greater external rotation of the tibia relative to the femur; and more knee valgus. Each of these differences is associated with more lateral force on the patella or less constraint of the patella in the trochlear groove and thus theoretically contribute to instability. The scores based on traditional 2D imaging measures alone and 3D bone shape features alone were not associated with non-operative outcomes. This 3D analysis demonstrates that traditional measures are insufficient in predicting treatment outcomes, and 3D knee bone alignment is more informative than 3D knee bone shape in predicting treatment outcomes.

A subset analysis of the 3D bone alignment features revealed that a final score, the 3D Patellar instability Anatomical Severity Score (3D-PASS), was strongly correlated ($|r| > 0.68$, $p = 0.001$) with non-operative outcomes (Figure 1).

**Table 1.** Anatomical score correlations with one-year non-operative outcomes in patients with patellar instability. Statistically significant correlations are bolded. (Kujala = Kujala Anterior Knee Pain Scale, BPII = Banff Patellar Instability Instrument 2.0; * $p < 0.05$, ** $p < 0.01$, *** $p < 0.001$)

| score | Kujala ($n$ = 20) | | BPII 2.0 ($n$ = 20) | |
|---|---|---|---|---|
| | ***r*** | ***p*** | ***r*** | ***p*** |
| 2D imaging measures | -0.07 | 0.786 | -0.21 | 0.408 |
| 3D bone alignment | **-0.48** | *** 0.033** | **-0.58** | **** 0.008** |
| 3D bone shape | -0.20 | 0.399 | -0.08 | 0.723 |
| 3D-PASS | **-0.70** | ***** 0.001** | **-0.68** | **** 0.001** |

**Figure 1.** The 3D Patellar instability Anatomical Severity Score (3D-PASS) was strongly correlated with one-year non-operative outcomes in patients with patellar instability. Gray lines represent lines of best fit. (Kujala = Kujala Anterior Knee Pain Scale, BPII = Banff Patellar Instability Instrument 2.0)

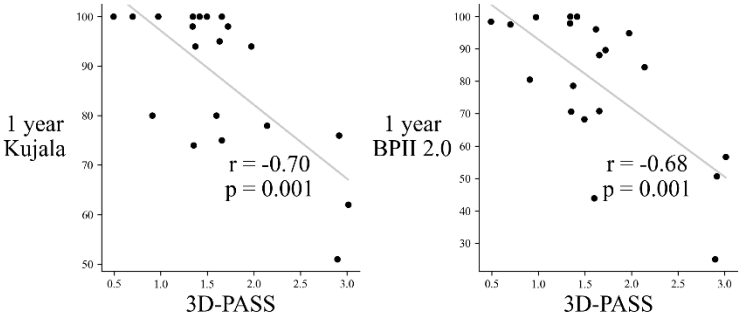


**Significance:** This novel metric of patellar instability, 3D-PASS, leverages 3D information in MRIs and is associated with patient-reported outcomes, which historically have not been predictable. 3D-PASS demonstrates the potential of an automated anatomical score that can inform patient-specific treatment decisions related to patellar instability.

**Acknowledgments:** Funding: AAOSM, AANA, CIHR, CONMED, NIH (P41EB027060, R01 AR077604, R01 EB002524, R01 AR079431), POSNA, Stanford Data Science, Stanford University, University of Cincinnati, Wu Tsai Human Performance Alliance.

**References:** [1] Dixit et al. (2017), DOI: 10.1097/JSA.0000000000000149; [2] Dejour et al. (1994), DOI: 10.1007/BF01552649; [3] Kujala et al. (1993), DOI: 10.1016/S0749-8063(05)80366-4; [4] Hiemstra et al. (2013), DOI: 10.1177/0363546513487981

# USING VIRTUAL MECHANICAL TESTING TO PROBE MECHANICAL STRAIN IN BONE FRACTURE HEALING

*Maham Tanveer[1], Alireza Ariyanfar[1], Peter Schwarzenberg[2], Peter Varga[2], Hannah L. Dailey[1]
[1]Lehigh University, Bethlehem, PA; [2]AO Research Institute Davos, Switzerland
*Corresponding author's email: hlr3@lehigh.edu

**Introduction:** Mechanoregulation plays a crucial role in bone fracture healing. Evidence from large animal and clinical studies show the significant impact of mechanical conditions at the fracture site on callus growth. During secondary healing, callus formation restores bone stability and causes reduced interfragmentary motion (strain) at the fracture site. Computational models of mechanoregulation in bone healing have been used to predict tissue differentiation under different strain conditions, but the rules for how strain directs the course of tissue formation have never been explicitly calibrated using in vivo imaging. To address this need, we used virtual mechanical testing with image-based finite element models to probe strain and colocalized this data with formation of mineralized tissue seen in longitudinal *in vivo* imaging. We hypothesized that the tissue formation limits, particularly for distortional strain, are higher than have been previously assumed in mechanoregulatory models of bone repair.

**Methods:** Healing of seven adult female Swiss alpine sheep (3.6 ± 0.8 years old; 69.5 ± 6.2 kg) with midshaft tibial osteotomies of variable size (0.6-10mm) was monitored using CT scans of limbs at multiple time points: 0, 4, 8, 12, 16 and 39 weeks. Each animal was treated with either a titanium or stainless-steel medial locking compression plate as reported in a previous study [2]. Immediate post-operative bone-implant scenario was created using 4-week scans. Quadratic tetrahedral elements (tet-10) were used to mesh the models with a maximum element edge length of 2 mm in bone and 0.85 mm in the strain visualization region around the fracture gap. Subject-specific elementwise material properties were assigned to the bone using a previously validated equation [1] and homogenous material properties were assigned to the plates ($E_{SS}$ = 183.6 GPa and $E_{Ti}$ = 104.6 GPa, $\nu$ = 0.35) and strain visualization region ($E$ = 0.5 MPa, $\nu$ = 0.45). Finite element modeling was performed in ANSYS Workbench Mechanical. Boundary conditions consisted of a representative immediate post-operative axial load of 600 N (~0.9BW) and a roller and pinned support at the proximal and distal joint centers respectively [3].

A three-channel point cloud of strain visualization zone (SVZ) containing bone mineral density (BMD), hydrostatic strain ($\varepsilon_{hydro}$), and distortional strain ($\varepsilon_{dist}$) were obtained using previously established methods [2]. Binary images of callus and cortical bone were then created from their corresponding point clouds. A distance transform filter from the scipy Python library was used to create an image representing the distance of each voxel to the closest cortical wall. Bone formation was defined with voxels in the tissue above the BMD threshold of 665 mgHA/cm$^3$, while soft callus was defined as voxels with BMD less than or equal to the threshold. A 2D density map for each combination of strain type and tissue change was obtained. The feature map concisely expressed the frequency of tissue change as a function of strain value and distance to cortical bone.

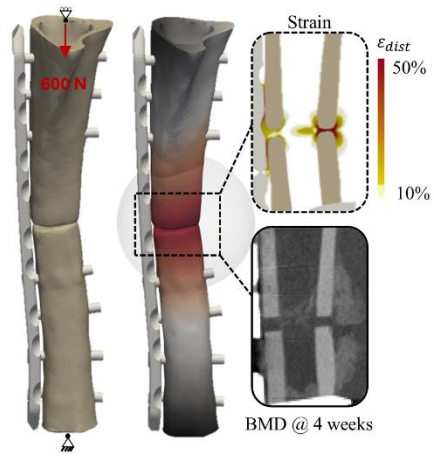


**Figure 1:** Interfragmentary strains were calculated in subject-specific finite element models representing each animal and mapped to downstream mineral density (BMD) in longitudinal *in vivo* CT scans.

**Results & Discussion:** Consistent with our previous results, high distortional and compressive hydrostatic strains were observed within the osteotomy (Fig. 1). Peak strains increased with decreasing osteotomy sizes and averaged 131% ± 69.0% for distortional and 13.1% ± 11.0% for compressive hydrostatic strain. The 2D feature map revealed the interaction between strain and distance from bone on the ability to form soft callus and woven bone at 4 weeks (Fig. 2). Woven bone formation voxels were concentrated in regions closest to the bone with a wide range of distortional strains and a stricter range of hydrostatic strain. Soft callus voxels showed a similar trend closest to the bone, with a wider range of distances away from the bone for a set strain range. These results show bone formation is tolerant to distortional strains which are not only high but also very variable, as compared to hydrostatic strains. They also corroborate the observation that cortical bone may serve as a source of mineral for new bone formation [4].

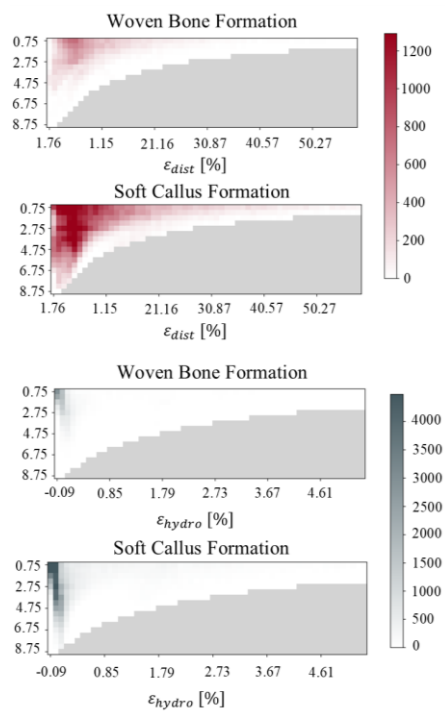


**Figure 2:** Feature maps reveal the limiting conditions for woven bone and soft callus formation as a function of distance cortical bone and $\varepsilon_{dist}$ (red) or $\varepsilon_{hydro}$ (blue) strains.

**Significance:** Mechanoregulation models depend on strain values to model accurate and robust bone fracture healing. This study provides groundwork for image-based calibration of the strain limits and rate constants used in mechanoregulatory models.

**Acknowledgments:** NIH award number R21AR081435.

**References:** [1] Inglis, B et al. (2022), *Comp Meth Biomech Biomed Eng*. 26(12); [2] Windolf et al. (2022), *Medicina*. 58(7), 858; [3] Tanveer, M et al. (2025), *Bone Joint Res*. 14(1); [4] Ariyanfar, A et al. (2024), *CMBBE: Imaging & Vis*. 12(1)

# QUANTITATIVE MRI EVALUATION OF THE MENISCUS WITH AND WITHOUT APPLIED LOAD IN PATIENTS 1-2 YEARS FOLLOWING ACL RECONSTRUCTION WITH MENISCAL SURGERY

Divya Pradip Roy, Sadegh Khodabandeloo, John C. Ramsdell, Bruce D. Beynnon, Mathew J. Faila, Jiming Zhang, Matthew Geeslin, Mickey I. Krug, Michael DeSarno, and Niccolo M. Fiorentino
Department of Electrical & Biomedical Engineering, University of Vermont, USA
email: divya-pradip.roy@uvm.edu

**Introduction:** Anterior cruciate ligament (ACL) injury is often accompanied by meniscus injuries, as studies have reported that ~40% of ACL injured individuals suffer concomitant meniscal tears [1]. As the menisci are important for transmitting contact stress across the tibiofemoral joint, surgeons repair and/or resect portion(s) of the injured meniscus during ACL reconstruction (ACLR+M), with the goal to improve the overall knee function [2]. Patients who undergo concomitant meniscal surgery with ACL reconstruction are at increased risk of developing post traumatic osteoarthritis (PTOA) in the long term [3,4]. Studying subjects early after ACLR+M surgery is important for understanding the healing response of the meniscus and how it responds to load. Measuring how normal and repaired/resected menisci respond to load will contribute to the understanding of PTOA development. Therefore, the purpose of this study was to evaluate the response of menisci in ACLR+M patients with and without applied load using quantitative magnetic resonance imaging (qMRI) 1-2 years after surgery.

**Methods:** Twelve subjects were recruited for this study 1-2 years after ACL reconstruction with a meniscal repair and/or partial meniscectomy. All subjects reported having an uninjured, healthy contralateral limb, and this was confirmed by a musculoskeletal radiologist's reading of the contralateral knee's MRI. A custom developed device was used to apply a compressive load (50% bodyweight) to the plantar aspect of the subject's foot while the knee was imaged with a 3T MRI scanner and 16-channel transmit/receive radiofrequency coil. T1rho relaxation times were measured from the posterior horn of the medial and lateral meniscus by averaging relaxation time values from five sagittal slices centered at 20% and 80% of the medial-lateral width of the tibial plateau. T1rho relaxation times were calculated with the subject's limb loaded and unloaded for the ACLR+M and uninjured sides (**Figure 1**). Two medial and one lateral meniscal compartments from the surgical sides were not included in the analysis due to signal artifacts.

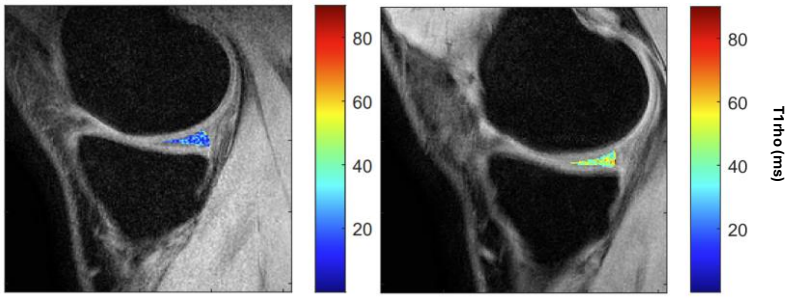


**Figure 1:** Example T1rho relaxation times from a loaded uninjured (left) and repaired (right) posterior horn of the medial meniscus from the same patient

**Results and Discussion:** The lateral menisci of the ACLR+M knees demonstrated significant increase with load compared to unloaded conditions ($p=0.003$), while the change was not statistically significant in the uninjured knees. The medial menisci of the ACLR+M knees showed a significant increase of T1rho relaxation times compared to the uninjured side ($p=0.02$). These results suggest that there are structural alterations and compromised load distribution capability 1-2 years after the index trauma and reconstruction in the surgical knee, as increased T1rho relaxation time is associated with decreased water and/or proteoglycan concentration in soft tissues. The majority of subjects in this study (9 out of 12) suffered an isolated medial meniscus injury that was repaired surgically, but still there was significant increase in T1rho in that compartment compared to the uninjured side, indicating compositional change. Additionally, the lateral meniscus of the surgical side showed significant increase in T1rho in response to applied load, which indicates its reduced capability to transmit contact stress during physiological loading of 50% body weight. Future work will assess the longitudinal changes in T1rho values 2-3 years after surgery (one year after the timepoint reported herein).

**Significance:** Alterations in the structural integrity of patients' meniscus in the surgical limb are present 1-2 years after surgery, even though they go through meniscal repair and/or resection of the damaged meniscal tissue. Due to the higher risk of ACLR+M patients developing PTOA compared to isolated ACLR patients, studying the differences at the early stages after surgery is crucial as it holds significance for potential future clinical interventions. Understanding the surgically repaired and/or resected meniscus' response to load provides insights into the mechanism of PTOA development in patients who have undergone ACLR and meniscal surgery.

**Acknowledgments:** Rebecca Choquette for coordination of the study, and Melissa Cuke for regulatory. NIAMS R21AR077371.
**References:**[1] Kilcoyne et al. (2012), Orthopedics 35(3); [2] Rodriguez et al. (2022), Arthroscopy 38(3); [3] Want et al. (2020), Arthritis Res Ther 22(57); [4] Altahawi et al. (2022), Am J Sports Med 50(4).

# IN VIVO CERVICAL SPINE KINEMATICS IN NECK PAIN AND GENERALIZED JOINT HYPERMOBILITY

*Rebecca Abbott[1*], Maxwell Carlson[2], Maxwell Carlson[2], Bryan Peralta Garces[2], May-Ling Li[2], Lacy Richter[2], Yaqoub Yusuf[2], Alan Mangen[2], Arin M. Ellingson[2]

[1]University of Colorado Anschutz Medical Campus, [2]University of Minnesota Twin Cities

*Corresponding author's email: rebecca.abbott@cuanschutz.edu

**Introduction:** Generalized Joint Hypermobility (GJH), excessive joint range of motion (ROM) throughout the body, is present in approximately 30% of young women and is associated with a nearly 2-fold increased prevalence of chronic neck pain [1]. Joint pain in those GJH is thought to be related to joint instability, but dynamic instability is yet to be directly measured. Typical diagnostic techniques are limited to static 2-D acquisitions, such as sagittal end-range flexion-extension x-rays. The objective of this work was to quantify and compare *in vivo* dynamic intervertebral neck kinematics within the functional ROM of women with neck pain, with and without GJH.

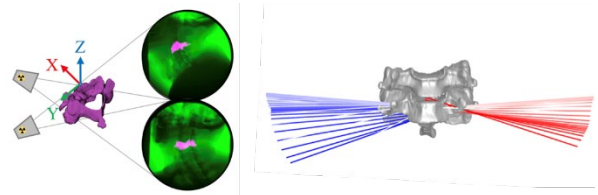


*Figure 1. Methods. Left: Biplane Videoradiography with DRRs to resolve 3-D intervertebral kinematics. Right: Instantaneous helical axes representing flexion-extension of C5-C6.*

**Methods:** After IRB approval and informed consent, 13 female participants were enrolled. Group 1: healthy controls (CTRL, n=6, age 31.5 +/- 6.1, Beighton Score (BS) 0.7 +/- 0.5), Group 2: neck pain (NP, n=4, age 36.8 +/- 11.5, BS 0.0 +/- 0.0), and Group 3: neck pain and GJH (NP-H, n=3, age 33.0 +/- 14.2, BS 7.0 +/- 0.0). Participants performed 3 trials each of 3 motions: axial rotation, flexion-extension, and lateral bending. Global kinematics (head-to-torso) were captured using optical motion capture (Vicon) and segmental kinematics (C4-C7) via biplane videoradiography using a CT-based digitally reconstructed radiograph (DRR) optimization approach [2,3], (**Fig. 1**). A Butterworth filter was applied (4th order, 3 Hz). Global and segmental angles and instantaneous helical axes (IHA) were analyzed within the functional neck ROM (neutral +/- 7-10 deg) [4]. Outcomes included the percent contribution of each joint to global neck kinematics within the functional ROM, IHA coupling computed from the primary component of the IHA vector (1=no coupling and 0=no motion about the primary axis), and IHA variability measured from the standard deviation of the primary IHA axis component as a measure of dynamic joint instability.

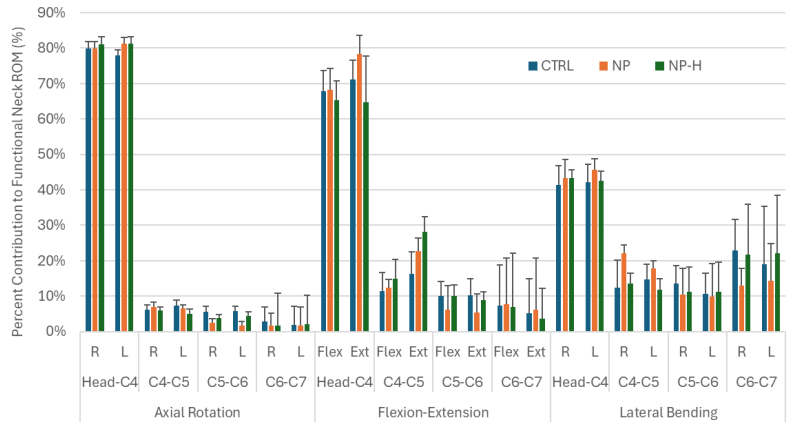


*Figure 2. Percent contribution of each segment to functional neck ROM: (segmental angle change) / (head-to-torso angle change) * 100.*

**Results & Discussion:** The segmental percent contributions are reported in **Fig, 2** and the summary statistics for IHA coupling and variability are in **Table 1**. The preliminary analysis indicates that a large proportion of cervical motion near neutral (functional ROM) occurs at the upper cervical spine in all groups, particularly in axial rotation (~80%) and flexion-extension (~65%). IHA coupling between ipsilateral axial rotation and lateral bending was identified in all groups. A consistent pattern of between group differences in IHA coupling or variability was not identified. Additional work is underway including additional recruitment and analysis to increase sample size, compare multiple phases (across the full ROM), and determine trial and level differences within and between groups.

**Significance:** Preliminary results demonstrate the feasibility of computing measures of dynamic neck stability and the contribution of individual cervical joints throughout functional neck ROM, not just at end-range, as is the status quo. Direct quantification of intervertebral kinematics in a larger cohort will provide valuable insights on the role of dynamic joint stability in GJH and neck pain.

**Acknowledgments:** Funding was provided by NIH/NICHD R03 HD09771 and NIH/NIAMS F32AR082276. Thank you to Dr. Craig Kage and Dr. Jonathan Sembrano for their contributions.

**References:** [1] Russek, L. Clin Rheum. 2016 [2] Kage C, PloS One, 2020 [3] Anderst, W. Spine, 2014 [4] Bible, J. Clin Spine 2010

*Table 1. Instantaneous Helical Axis Coupling and Variability. All values are unitless: mean (standard deviation).*

| | | Right AR | | Left AR | | Extension | | Flexion | | Right Lateral Bending | | Left Lateral Bending | |
|---|---|---|---|---|---|---|---|---|---|---|---|---|---|
| | | IHA Coupling | IHA Variability | IHA Coupling | IHA Variability | IHA Coupling | IHA Variability | IHA Coupling | IHA Variability | IHA Coupling | IHA Variability | IHA Coupling | IHA Variability |
| Head-Torso | CTRL | -0.99 ( 0.02) | 0.003 (0.003) | 0.99 (0.01) | 0.003 (0.003) | -0.99 (0.002) | 0.001 (0.001) | 0.99 (0.005) | 0.002 (0.003) | 0.96 (0.03) | 0.013 (0.009) | -0.98 (0.02) | 0.007 (0.005) |
| | NP | -0.99 (0.01) | 0.003 (0.002) | 0.99 (0.01) | 0.002 (0.002) | -0.99 (0.004) | 0.002 (0.002) | 0.99 (0.004) | 0.003 (0.002) | 0.96 (0.02) | 0.009 (0.005) | -0.95 (0.03) | 0.009 (0.007) |
| | NP-H | -0.96 (0.05) | 0.004 (0.004) | 0.96 (0.04) | 0.004 (0.003) | -0.99 (0.002) | 0.001 (0.001) | 0.99 (0.002) | 0.001 (0.001) | 0.92 (0.06) | 0.013 (0.008) | -0.92 (0.06) | 0.024 (0.016) |
| Head-C4 | CTRL | -0.99 (0.01) | 0.005 (0.004) | 0.98 (0.01) | 0.007 (0.004) | -0.99 (0.005) | 0.005 (0.005) | 0.99 (0.004) | 0.004 (0.003) | 0.84 (0.10) | 0.050 (0.033) | -0.81 (0.14) | 0.040 (0.026) |
| | NP | -0.98 (0.02) | 0.009 (0.009) | 0.90 (0.01) | 0.005 (0.003) | -0.99 (0.006) | 0.004 (0.005) | 0.99 (0.005) | 0.003 (0.002) | 0.87 (0.10) | 0.040 (0.020) | -0.84 (0.14) | 0.033 (0.012) |
| | NP-H | -0.94 (0.07) | 0.005 (0.004) | 0.94 (0.07) | 0.007 (0.004) | -0.99 (0.004) | 0.004 (0.003) | 0.99 (0.004) | 0.004 (0.001) | 0.93 (0.02) | 0.036 (0.025) | -0.93 (0.05) | 0.024 (0.012) |
| C4-C5 | CTRL | -0.63 (0.10) | 0.054 (0.040) | 0.67 (0.05) | 0.040 (0.028) | -0.95 (0.06) | 0.037 (0.049) | 0.95 (0.10) | 0.070 (0.157) | 0.67 (0.13) | 0.135 (0.105) | -0.74 (0.06) | 0.091 (0.119) |
| | NP | -0.68 (0.09) | 0.070 (0.056) | 0.68 (0.10) | 0.050 (0.028) | -0.96 (0.03) | 0.021 (0.016) | 0.98 (0.01) | 0.013 (0.012) | 0.72 (0.05) | 0.052 (0.024) | -0.69 (0.05) | 0.066 (0.035) |
| | NP-H | -0.70 (0.12) | 0.056 (0.054) | 0.61 (0.18) | 0.068 (0.031) | -0.97 (0.03) | 0.019 (0.021) | 0.99 (0.01) | 0.004 (0.003) | 0.76 (0.13) | 0.051 (0.047) | -0.71 (0.11) | 0.072 (0.032) |
| C5-C6 | CTRL | -0.64 (0.13) | 0.062 (0.040) | 0.74 (0.10) | 0.056 (0.055) | -0.87 (0.23) | 0.140 (0.276) | 0.85 (0.25) | 0.100 (0.140) | 0.68 (0.26) | 0.095 (0.098) | -0.76 (0.16) | 0.080 (0.110) |
| | NP | -0.53 (0.18) | 0.127 (0.084) | 0.43 (0.16) | 0.127 (0.084) | -0.86 (0.12) | 0.138 (0.125) | 0.73 (0.34) | 0.197 (0.234) | 0.76 (0.09) | 0.099 (0.061) | -0.80 (0.14) | 0.076 (0.080) |
| | NP-H | -0.60 (0.14) | 0.070 (0.030) | 0.67 (0.09) | 0.072 (0.066) | -0.92 (0.14) | 0.065 (0.130) | 0.79 (0.30) | 0.203 (0.296) | 0.76 (0.13) | 0.059 (0.077) | -0.74 (0.08) | 0.038 (0.016) |
| C6-C7 | CTRL | -0.42 (0.19) | 0.128 (0.115) | 0.42 (0.19) | 0.133 (0.153) | -0.79 (0.27) | 0.199 (0.262) | 0.72 (0.26) | 0.221 (0.224) | 0.90 (0.05) | 0.034 (0.033) | -0.87 (0.07) | 0.039 (0.029) |
| | NP | -0.55 (0.29) | 0.180 (0.142) | 0.45 (0.32) | 0.158 (0.073) | -0.85 (0.19) | 0.137 (0.229) | 0.15 (0.80) | 0.202 (0.234) | 0.80 (0.12) | 0.077 (0.069) | -0.78 (0.10) | 0.104 (0.122) |
| | NP-H | -0.41 (0.23) | 0.124 (0.068) | 0.42 (0.21) | 0.088 (0.083) | -0.95 (0.04) | 0.040 (0.031) | 0.61 (0.53) | 0.236 (0.303) | 0.88 (0.06) | 0.024 (0.009) | -0.85 (0.10) | 0.045 (0.046) |

# 3D MUSCLE-TENDON ANATOMY IN HEALTHY AND SURGICALLY REPAIRED BICEPS BRACHII

*Jorie D. Budzikowski[1,2], Samuel D. Gillespie[1,2], Ilana E. Deutsch[1,2], Stephen Gryzlo, MD[1], Wendy M. Murray[1,2]
[1]Northwestern University, Chicago, IL, USA
[2]Shirley Ryan AbilityLab, Chicago, IL, USA
*Email: JorieBudzikowski2024@u.northwestern.edu

**Introduction:** Anatomical studies describing the proximal tendon of the long head of the biceps (LHBT), used in the development and description of surgical technique to repair injury, are currently limited to cadavers (e.g., [1-2]). *In vivo* assessments in both non-operated limbs and surgical populations would be valuable for surgical planning as well as quantifying outcomes. For example, SLAP (superior labrum anterior-posterior) injuries can be repaired using: (i) SLAP repair, which reattaches the torn LHBT to its native origin, (ii) tenotomy, which releases the LHBT to adhere in the bicipital groove via scar tissue, and (iii) tenodesis, which resects and reattaches the LHBT to the humerus [3]. While each procedure provides pain relief, the decision of which procedure to perform has been described as "controversial" [4]. There is assumed to be variation in the amount of tendon retraction in tenotomy repairs; variability also exists in a surgeon's choice of reattachment site for tenodesis repairs (i.e., supra-pectoral, sub-pectoral). Here, we use magnetic resonance imaging (MRI) to reconstruct the 3D anatomy of the biceps brachii muscle-tendon complex among participants with different surgeries.

**Methods:** To date, 4 participants with unilateral labrum/LHBT surgical repair ($\mu$=4.3 ± 2.5 years post-op) have been enrolled. MR images of both the surgically repaired and contralateral arms were acquired using a Siemens Magnetom 1.5T scanner. Turbo spin echo, T2-weighted sequences of the LHBT were acquired in the axial, sagittal and coronal planes. Axial images of the muscle belly were acquired using a 3D, gradient echo, T1-weighted sequence [5]. Participants were lying supine; the lower arm was splinted using an orthosis to minimize movement. Images were segmented and 3D reconstructions generated in Horos (v3.3.6).

**Results & Discussion:** 3D reconstructions of the biceps muscle-tendon complex in the surgical and contralateral, non-operated limbs demonstrate the large distal shift in tendon attachment site introduced by tenotomy and tenodesis (Fig. 1). The muscle-tendon junction (MTJ) of the long head of the biceps for these two repair techniques was also shifted distally. The MTJs were highly consistent among each of the 4 contralateral limbs, located distal to the humeral head by a distance ~19% of the length of the humerus. The MTJ was shifted ~20% more distal than this average location for the tenotomies, compared to ~5% more distal for the tenodesis. In contrast, the muscle-tendon junction in the SLAP repair was shifted proximally; the 5% proximal shift relative to the paired, contralateral limb also exceeded 2 standard deviations from the average location on the non-operated limbs. Intra-articular tendon length ranged from 2.5 to 4.2 cm in SLAP repair and contralateral non-surgical limbs. These measures were slightly longer than cadaveric descriptions [1], perhaps due to differences in participant size or external shoulder rotation between studies. Interlimb differences in muscle volume were not consistent in our initial cohort. Analysis of the biceps cross-sectional area (CSA) at mid-humerus suggests the short head maintained CSA consistent with the contralateral limb in all surgical repairs. In contrast, the long head exhibited a drastic decrease in CSA (~75%) relative to the contralateral non-surgical limb following tenotomy while SLAP repair and tenodesis demonstrated small increases (10% and 8%, respectively). The more distally located muscle-tendon junction and decreased cross-sectional area in tenotomy are consistent with the type of muscle adaptations thought to result from under-tensioning. While smaller, the changes observed following SLAP repair highlight the possibility that surgical re-attachment may slightly over-tension the long head of the biceps, inducing adaptation as well.

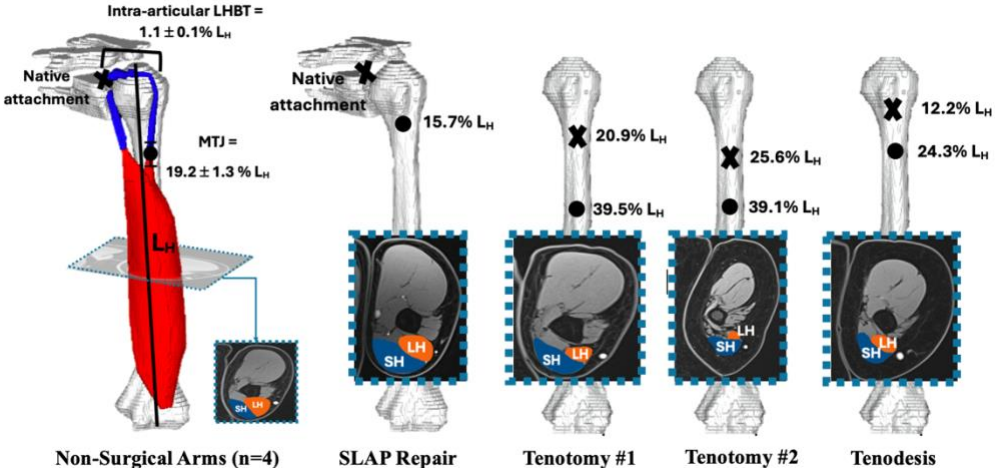


**Figure 1:** 3D reconstruction of biceps brachii: average native geometry of 4 non-surgical, contralateral (left) vs individual surgically repaired arms. Tendon attachment site (**X**), MTJ location (•), and short and long head contribution to CSA at mid-humerus (normalized to humerus length, $L_H$) are indicated.

**Significance:** Our initial results provide the first *in vivo* quantitative anatomical assessments of biceps brachii following SLAP lesion repair, and suggest different surgical techniques induce measurably different, chronic structural adaptations. These whole muscle scale adaptations were also correlated with adaptation at the fascicle scale, measured in a parallel study. Coordinating measures of muscle-tendon adaptation across scales with measures of isometric and isokinetic strength has the potential to inform surgical decision-making.

**Acknowledgments:** We thank the ASB Grant in Aid, ISB MDG, NU Alumnae Association, and NIH (T32EB025766) for support.

**References:** [1] Denard et al., "Anatomy of the biceps tendon", *Arthroscopy*, 2012. [2] Hussain et al., "Longitudinal anatomy of the long head", *Knee Surgery, Sports*, 2015. [3] Karataglis et al., *J. of Bone and Joint Surgery*, (2012). [4] Civan, et al., *J. of Orthop Surg (Hong Kong)* (2021). [5] Adkins, et al., *PNAS* (2021).

# QUANTITATIVE MEASURES OF BONE MARROW EDEMA TO ASSESS BONE STRESS INJURY RECOVERY

*Rachel Shalit[1], Olivia L Bruce[1], Kathryn J. Stevens[1], Yael Vainberg[1], Abigail McIntyre[2], Emily Kraus[2], Feliks Kogan[1]
[1]Department of Radiology, Stanford University School of Medicine, Stanford, USA
[2]Department of Orthopaedic Surgery, Stanford School of Medicine, Stanford, USA
*Corresponding author's email: rsh2001@stanford.edu

**Introduction:** Bone stress injuries (BSI) are overuse injuries that commonly occur in athletes due to an accumulation of microdamage associated with repetitive stress [1]. MRI is the diagnostic standard for BSI; the Fredericson grading scale is used to semi-quantitatively assess severity [2] but is semi-quantitative and coarse, with variance between reader assessments. There are currently no standard, objective measures used to assess recovery or readiness to return to sport. It is important to address this gap because BSI's have the highest recurrence rate of injuries in running sports [3]. Quantitative MRI measures of bone marrow edema present at the BSI over time may be useful as an indicator of injury acuteness or recovery. In this exploratory work, we deploy iterative decomposition of water and fat with echo asymmetry and least squares estimation (IDEAL) methods, which have previously been shown to accurately evaluate inflammatory edema [4], to quantitatively study bone marrow edema in BSI patients.

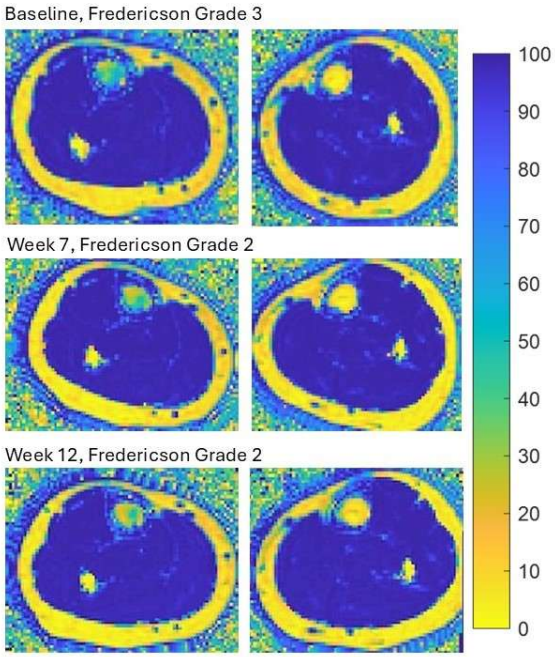


**Figure 1:** Edema fraction (%) data for a patient with BSI over 12 weeks of recovery. Left: Edema fraction maps (axial slices) showing greater edema fraction in the injured leg (left) when compared to the same slice at the contralateral leg (right).

**Methods:** Thirteen patients with suspected tibial BSI were recruited for scanning at baseline, 6 weeks, and 12 weeks. MRI scanning was performed on a 3T system using a flexible coil-array around each leg. The imaging protocol included a 2D STIR Fast-Spin-Echo scan in the axial and coronal plane and an axial 3D IDEAL IQ scan. The tibial bone marrow was automatically segmented from the fat IDEAL images. Mean edema fraction, defined as the water proton signal divided by the total (water and fat) proton signal, was calculated for each slice. Maximum slice-averaged edema fraction (EF) was determined for the BSI limb. For intrasubject reference and to study potential bilateral BSI effects, the EF in the contralateral limb was recorded at the same slice as the BSI. Edema size, intended to evaluate the spatial extent of the BSI, was then calculated as the number of contiguous voxels with edema fraction values greater than 15% around the BSI and if relevant on the contralateral side. Lastly, a clinical radiologist graded BSI severity in each scan [2]. EF and edema size were compared between the injured and contralateral legs, across timepoints, and with BSI grade.

**Results & Discussion:** Ten patients completed at least one follow-up and five patients completed two follow-ups. Seven of the visits across six patients were excluded from analysis due to fat-water swap. In patients with a BSI who completed all visits, EF decreased from baseline scan to 12-weeks (Figure 1). Edema size also decreased over time. Patients with a grade ≥ 2 BSI had larger EF and edema size in the injured leg when compared to the contralateral leg. Most patients with grade ≥ 2 BSI showed larger EF (11.6-64.8% vs. 5.6-16.1%) and edema size (12-491 voxels vs. 0-38 voxels) when compared to patients with grade 1 or no BSI. However, the ranges within grade 2 and 3 were large and overlapped.

**Significance:** The results of this pilot analysis suggest that the maximum EF and edema size measures presented here may indeed be feasible and useful measures to quantitatively assess BSI recovery. While anecdotal, there were several interesting findings with this approach. In general, both maximum EF and edema size were greater in patients and limbs with BSI grade ≥2. However, the large degree of variation in edema magnitude and spatial extent was observed within these semi-quantitative grades. Quantitative evaluation may offer a more standardized and robust method to characterize patients and changes over time. In subjects presenting with BSI grade 2 or greater who were scanned at multiple time points, there was constant decrease in both max EF and edema size. Of note, this decrease was observed with and without decreased BSI Fredericson grade and the slope of this recovery varied between subjects. In one case, a patient showed only slightly elevated edema fraction and size measures but was assigned a grade 2. This patient illustrated a large, diffuse area of increased signal in T2 images and returned to activity within two weeks of the baseline scan, suggesting that their BSI grade may have been a misdiagnosis. Additionally, the difference in maximum EF and size values between the injured and contralateral leg, and the large range of values observed within grades, indicate that this could be a useful quantitative measure to improve BSI severity grading during diagnosis. Future work will assess EF measures in a larger cohort of patients with a one-year follow-up period to evaluate clinical utility.

**Acknowledgments:** This work received research support from GE Healthcare and the Wu Tsai Human Performance Alliance.

**References:** [1] Hoenig et al. (2008), *Nat Rev Dis Primers* 8(1):26; [2] Fredericson et al. (1995), *Am J Sport Med.* 23(4):472-481 [3] George et al. (2024) Sports Med 54:2247-2265. [4] Bray et al. (2018), *Br J Radiol.* 90:20170344.

# KNEE JOINT ADAPTATIONS ASSOCIATED WITH PATELLA FEMORAL PAIN SYNDROME IN COLLEGIATE WOMEN VOLLEYBALL ATHLETES ACROSS A COMPETITIVE SEASON

* Erica L. King[1,2,3], Charlotte M. Lim[2], Morgan A. Lamarre[1,3], Lauren N. Distad[3], Abhishek Aher[1], Angela Miller[4], Margaret T. Jones[2,3,5], Parag V. Chitnis[1,3]

[1]Department of Bioengineering, George Mason University, Fairfax VA

[2] Patriot Performance Laboratory, George Mason University, Fairfax VA

[3] Center for Advancing Systems Science and Bioengineering Innovation, George Mason University, Fairfax VA

[4]Research Methods and Educational Psychology, George Mason University, Fairfax, VA

[5] Sport, Recreation, and Tourism Management, George Mason University, Fairfax, VA

*Corresponding author's email: eking20@gmu.edu

**Introduction:** Patellofemoral Pain Syndrome (PFPS) is prevalent in high-impact sports and is associated with altered patellofemoral joint kinematics, which increase joint stress and pain [1]. The Victorian Institute of Sport Assessment-Patella (VISA-P) is a measure to assess PFPS severity, often supplemented with MRI to evaluate structural adaptations in the patellofemoral joint [2]. Biomechanical factors, like patellar alignment, patellar height (Insall-Salvati (IS) Ratio), trochlear morphology (sulcus angle (SA)), and patellar tendon thickness (PTT), influence patellar tracking and tendon load, thereby contributing to PFPS risk. Increased athlete workload can exacerbate PFPS symptoms, highlighting the need to understand how biomechanical adaptations, including structural changes and neuromuscular performance (via countermovement jump (CMJ) metrics), interact with workload variables like total jump count (JC) and elevated landings (EL) [3]. This study investigates the relationship between biomechanical factors, PFPS, and workload over the course of a competitive season.

**Methods:** Seven NCAA Division I women volleyball (VB) athletes (mean ± SD; age: 19.59 ± 1.50 yrs, height: 177.52 ± 4.47 cm, weight: 77.86 ± 6.53 kg, % body fat: 30.03 ± 4.05) underwent pre- and post-season (12 weeks) MRI scans of the dominant knee. MRI measures included Insall-Salvati (IS) Ratio, sulcus angle (SA), and patellar tendon thickness (PTT) at proximal (Prox), mid (Mid), and distal (Dis) sites. Neuromuscular performance was assessed via CMJ testing, metrics included jump height (JH), reactive strength index modified (RSImod), and peak power (PP). Weekly ultrasound (US) imaging tracked PTT changes at Prox, Mid, and Dis sites. Athlete workload was monitored using an inertial measurement unit (IMU) worn during training and games, quantifying jump count (JC) and elevated landings (EL). Weekly workload (WL) was calculated from total jumps (TJ) and ELs. Statistical analyses included Pearson correlations to assess relationships among MRI-derived measures, PTT, VISA-P scores, JC, EL, and NP. MANOVA was used to examine timepoint effects (pre- vs. post-season), followed by ANOVAs for individual biomechanical and workload-related metrics. Hierarchical linear modeling (HLM) analyzed the impact of WL on US-PTT, accounting for individual VB positions (Libero = 1, Middle Blocker = 1, Outside Hitter = 2, Right Side Hitter = 1, Setter = 2). HLM interaction terms assessed whether PPT changes over time (week) varied by position. Statistical significance was set at $p < 0.05$.

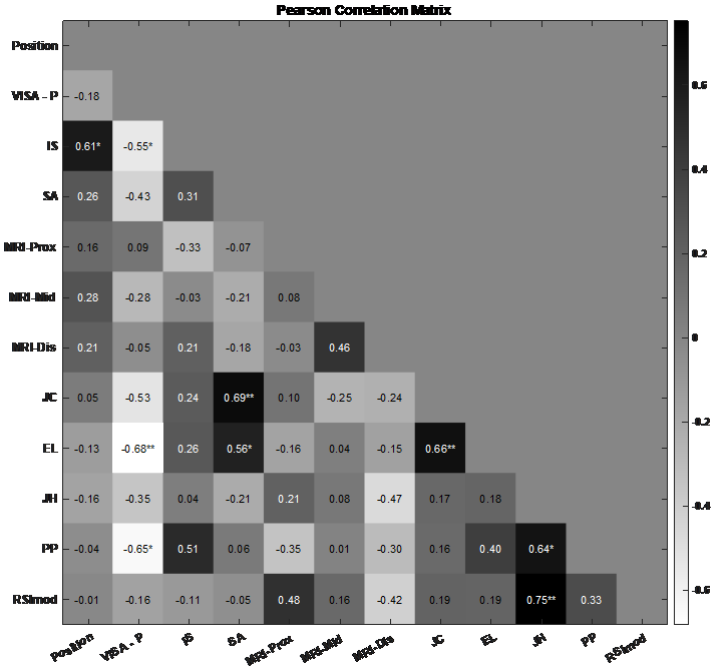


**Figure 1.** MRI Measures (Insall-Salvati (IS) Ratio and suclus angle (SA)), VISA-P, patellar tendon thickness measures by MRI at proximal (MRI-Prox), mid (MRI-Mid), and distal (MRI-Dis) sites. at the season total jump count (JC), season total number of elevated landings (EL), CMJ jump height (JH), CMJ Reactive Strength Index Modified (RSImod), CMJ Peak Power (PP), and VB position. Significance denoted as *p>0.05, **p>0.01

**Results & Discussion:** Pearson correlation analysis revealed relationships ($p < 0.05$) between VISA-P, PP, EL, and IS, while SA correlated with JC and EL, indicating its role in joint stability (Fig 1). VB position was related to IS ($p < 0.05$). MANOVA showed timepoint differences ($p < 0.05$), with ANOVAs revealing SA was influenced by time, suggesting structural adaptations. HLM modelling found US-PPT: Prox was affected by VB position ($p < 0.05$), weekly TJ ($p < 0.001$), and ELs ($p < 0.001$), while US-PPT: Mid ($p < 0.001$) and US-PPT: Dis ($p < 0.05$) were position-dependent. Week × position interactions showed position-specific PPT adaptations, with S ($p = 0.021$) exhibiting an initial increase before plateauing, possibly indicating an adaptive response. VB positions of MB ($p = 0.286$) and L ($p = 0.715$) trended toward tendon adaptations based on jump count. Results highlight the need for athlete load monitoring and position-specific load management to optimize tendon health.

**Significance:** Understanding how workload impacts patellar tendon structure and PFPS symptoms is essential for reducing injuries. Assessing biomechanical factors like PPT and workload helps identify and mitigate early dysfunction.

**Acknowledgments:** Effort sponsored by the Government under Other Transactions Number W81XWH-15-9-0001

**References:** [1] Smith, et al. (2018) *PLOS ONE* 13; [2] Loose et al. (2023) *J.Per Med.* 13; [3] Kraszewski, et al. (2024) *Orthop J Sports Med* 12

# STEPPING INTO MOTHERHOOD: PLANTAR FASCIA STIFFNESS AND ARCH HEIGHT DURING PREGNANCY

*Lauren R. Williams[1], Dustin Bruening[1]
[1]Brigham Young University
*Corresponding author's email: laur5252@byu.edu

**Introduction:** More than half of pregnant women report pain in their hip, knees, and feet during and after pregnancy [1]. These physical repercussions are a consequence of rapid physiological and anatomical changes, primarily increased body mass (17% on average [2]), and elevated hormone levels that affect tissue properties. In particular, relaxin activates collagenase which degrades the composition of collagen in tendons and ligaments [3], increasing joint laxity. While this laxity is beneficial for fetal delivery, it has secondary effects on peripheral joints, predisposing pregnant women to musculoskeletal injury [4].

Interventions designed to increase comfort and prevent injury during pregnancy often target the foot via footwear or orthotics [5]; however, a better understanding of the interplay between body mass and joint laxity in the foot may aid these efforts. One study that tracked medial longitudinal arch (MLA) changes across pregnancy [6] found a small drop in height that may be due to both increased body mass and increased foot laxity. Recent advances in shear wave ultrasound technology now allow for the quantification of tissue stiffness [7], which may help isolate laxity-based changes. The purpose of this study, therefore, was to investigate foot tissue characteristics across pregnancy. Specifically, we focused on the plantar fascia (PF), which is one of the main passive restraints of the MLA, measuring its stiffness, thickness, and length, along with MLA height for comparison. We hypothesized that PF stiffness and thickness would decrease across pregnancy comcomitant with decreased MLA height and increased PF length.

**Methods:** Fifteen primigravida women visited the laboratory four times during and after their pregnancy: TR1: before 13 weeks (first trimester), TR2: between 25 and 27 weeks (second trimester), TR3: between 35 and 37 weeks (third trimester), and PP: 8 to 10 weeks postpartum. During each visit, the stiffness of the PF was measured using shear wave elastography at approximately one cm distal to its insertion on the calcaneus (GE Logiq S8, GE, Healthcare, 0L and 6-15 ML MHz probes). Length and thickness of the PF at its insertion on the calcaneus were measured using B-mode. Participants laid on their side with a pillow between their knees and their ankle joint at a natural resting position. Following ultrasound measurements, anthropometric measurements were taken, and arch height was measured using the Arch Height Index Measurement System [9]. Within-subject repeated measures ANOVAs were performed for all metrics ($\alpha$=0.05).

**Results & Discussion:** Body mass increased, on average, by 10.5 kg (15.7%) between TR1 and TR3 ($p < 0.001$). PF thickness ($p = 0.58$) and length ($p = 0.14$) did not change across pregnancy. PF stiffness approached significance ($p = 0.053$), with an average decrease of 11.9% between TR1 and TR3. MLA height during static standing was significantly different between conditions ($p = 0.017$). However, rather than dropping with pregnancy as hypothesized, MLA height while standing increased by an average of 3.84% between TR1 and TR3. In studies looking at MLA deformation in response to wearing a weighted vest, they found no change in MLA height when 10% of body mass was added, but the MLA did drop with 20% added body mass [10]. Given that the mass gained in the current study was less than 20%, this may explain the difference between our findings. Another possible explanation for an increase in MLA height may stem from active MLA support. The muscles that cross the MLA have been shown to increase their activation during loading of the foot, attenuating MLA drop and even raising the MLA at high loads [8]. This suggests that despite a decrease in stiffness of the tissues that passively support the MLA, active components become activated to overcome this laxity.

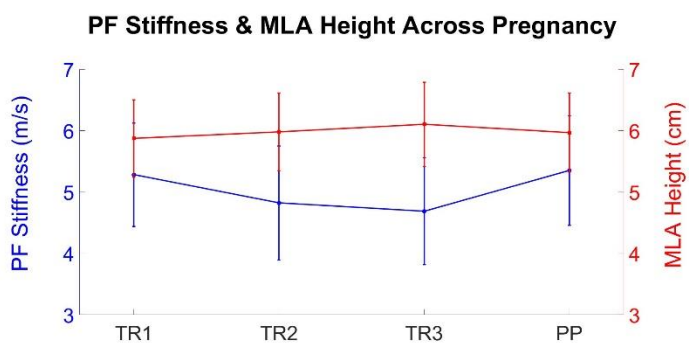


*Figure 1. PF Stiffness and MLA height during and after pregnancy*

**Significance:** PF stiffness decreased between TR1 and TR3 and the height of the MLA increased, possibly suggesting that intrinsic foot muscles become more activated to compensate for increased laxity. This compensation may explain some of the pain and fatigue women experience in their feet during pregnancy.

**Acknowledgments:** This material is based upon work supported by the National Science Foundation Graduate Research Fellowship Program under Grant No. 1840996

**References:** [1] Vullo et al. (1996), *J Fam Pract* 43(1), [2] Vico Pardo et al. (2018), *Women and Birth 31(2)*, [3] Dehghan et al. (2014), *Scand J Med Sci Sports* 24(4), [4] Chu et al. (2019), *PM&R* 11(2), [5] Bin (2022), *J Univ Med & Dental* 12(3), [6] Ramachandra et al. (2017), *Foot Ankle Spec* 10(6) [7] Romer et al. (2022), J Ultrasound Med 41(12), [8] Kelly et al. (2014), *J of Royal Soc Int* 11(93), [9] Butler et al. (2008), *J Am Podiatr Med Assoc.* 98(4), [10] Cen et al. (2020) *PeerJ* 21(8)

# USING DIGITAL IMAGE CORRELATION WITH A TENSILE TEST TO MEASURE STRAIN PROPERTIES OF THE INTERSPINOUS LIGAMENT

Isaac K. Kumi[1], Abed Khosrojerdi[1], Ahmadreza Ravangard[1], Oleksandr G. Kravchenko[1], Sebastian Y. Bawab[1], *Stacie I. Ringleb[1]
[1]Department of Mechanical and Aerospace Engineering, Old Dominion University, Norfolk, VA
*Corresponding author's email: sringleb@odu.edu

**Introduction:** Material properties of spinal ligaments used in biomechanical models are frequently obtained from literature that was published over 50 years ago. Human cadavers are difficult to test due to expense, and availability, and often the bones are not strong enough when collecting bone-ligament-bone samples [1]. Porcine ligaments have similar properties to human specimens [1] and can be obtained from younger specimens, thus increasing the integrity of the bone-ligament-bone samples. Measuring strain is challenging in small ligament samples because the displacement measurement in a materials testing machine isn't accurate enough and sensors are often too large to place on the ligaments. Digital Image Correlation (DIC) measures displacement and strain [2]. Studies using DIC in spine ligaments examined the strain in multi-vertebra spine segments [3,4] or isolated vertebra [2] focusing on a spinal range of motion, not the strain in individual ligaments. The purpose of this study was to determine if porcine spine ligament strain can be measured in a single ligament complex using DIC.

**Methods:** The spines of two adult pigs were extracted, and three vertebral pairs from the lumbar region (L1-L2, L3-L4, L5-L6) were dissected. Four bone-ligament-bone (BLB) Interspinous-Supraspinous ligament (ISL-SSL) complex samples were isolated for this study (length: 15.37±2.82 mm, width: 19.26±5.58 mm, thickness: 2.35±0.69 mm). The bony ends were embedded in a two-part epoxy using a 3D-printed clamshell-popsicle potting design. The potted specimens were secured in a fixation apparatus compatible with a 10ST tensile testing machine (Tinius-Olsen, Horsham, PA). Before static loading to failure at a rate of 0.01 mm/s, all ligaments underwent preconditioning, cyclic, stress relaxation, and creep. To prepare the specimens for strain data collection, each sample was coated with a matte white base layer and a black stochastic speckle pattern (Fig. 1a). The Digital image correlation (DIC) was used to measure the strain during testing by picking up the average strain of the speckled pattern on the surface of the ligament samples. The strain data were obtained until failure of the ligament after which processing was done using the GOM correlate software.

**Results & Discussion:** The strain-time analysis revealed segment-dependent strain responses in ISL-SSL ligament complex. The L1-L2 ISL-SSL ligament complex exhibited the highest strain (~32%), while the L5-L6 complex showed the least (~10%), with the L3-L4 ligaments displaying intermediate values (15–18%) (Fig. 1b-e). All segments demonstrated a rapid initial strain increase followed by a plateau, characteristic of the ligament's viscoelastic behavior. These differences may be due to the variations in the load-bearing capacity and structural properties of the different lumbar segments. As the lumbar spine progresses toward the sacrum, the vertebra increases in size due to the growing need for support down the spine [5]; hence an enhanced resistance to deformation may be likely as seen in the L5-L6 ISL-SSL ligament complex (Fig. 2). Future work can investigate additional ligaments and ligament complexes under different loading types and rates to obtain a complete viscoelastic material property set for lumbar spine ligaments.

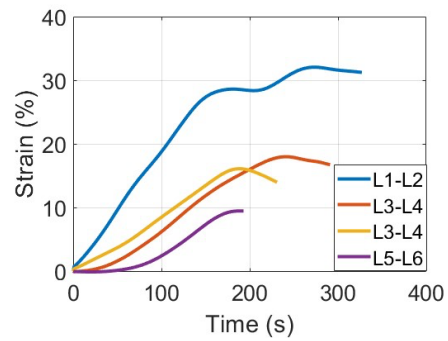


**Figure 2:** Strain response of ISL-SSL complex with time at different segments of the lumbar spine

**Significance:** The findings from this study can enhance spine modeling by providing empirical data towards the attainment of the viscoelastic material properties of different lumbar ligaments. Incorporating segment-specific viscoelastic properties of lumbar ligaments into computational models may help improve the accuracy of finite element (FE) simulations and improve our overall understanding of spine biomechanics.

**References:** [1] Busscher, I. et al. (2010), *Spine 35*(2), E35-E42; [2] Palanca, M. et al. (2015), *J Mechanics in Med & Bio 15*(02), 1540004.; [3] Kelly, B. P. et al. (2022), *J Biomechanics*, *135*, 111025.; [4] Palanca, M. et al. (2018), *Med engineering & physics 52*, 76-83. [5] Waxenbaum, J. A. et al. (2017).

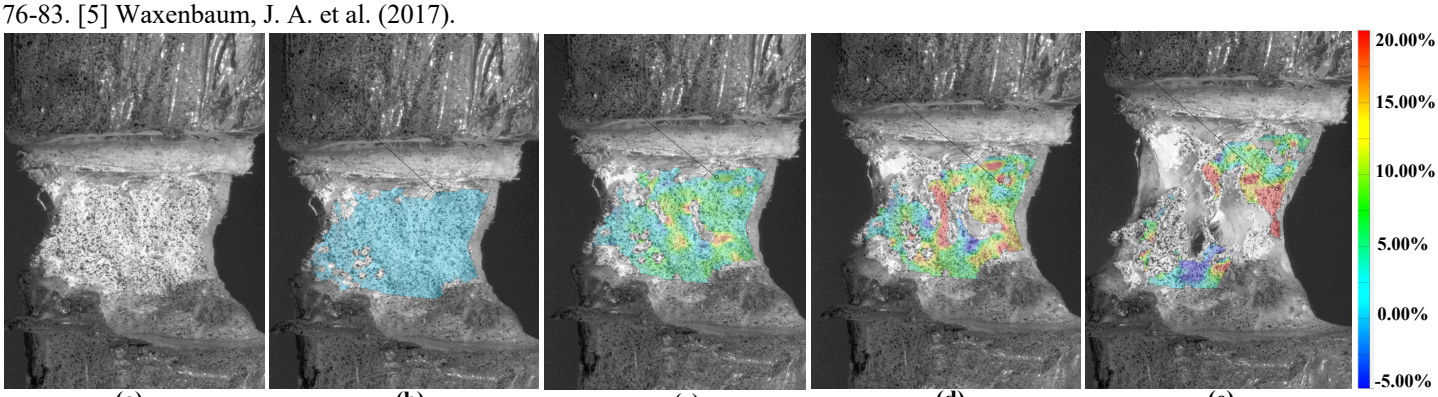


**Figure 1:** a) Ligament with speckle pattern and percent strain for L3-L4 with (b) No load, (c) after 80 seconds of load, (d) after yield point, and (e) after failure

**Annulus piston excitation minimizes tissue compression artifact in focused shear wave transient elastography**

*Yu-hsuan Chao[1,2], Kang Kim[1,2,3,4], John M Cormack[2,3,4]
[1]Department of Bioengineering, University of Pittsburgh, Pittsburgh PA, USA
[2]Pittsburgh Liver Research Center, University of Pittsburgh, Pittsburgh PA, USA
[3]Department of Medicine, University of Pittsburgh, Pittsburgh PA, USA
[4]Vascular Medicine Institute, University of Pittsburgh, Pittsburgh PA, USA
*Corresponding author's email: yuc125@pitt.edu

**Introduction:** Liver tissue stiffness measurement (LSM) with transient elastography (TE) is a popular method for fibrosis screening in the clinic. Current clinical devices for TE utilize vibration of a small, flat piston at the skin surface to generate shear waves for LSM. Shear waves generated by the small, flat piston source spread in all directions from the source, diverging from the LSM region. Thus, TE is prone to relatively high failure rates and unreliability, especially in patients with obesity.

Our group developed the focused shear wave elastography (fSWE), which employs vibration of a larger-diameter, concave shaped piston at the surface to generate shear waves that converge towards the LSM region, thereby increasing the signal amplitude available for tissue stiffness estimation [1].

Initial testing of fSWE in human subjects showed that the larger piston used in fSWE, while increasing the shear wave amplitude as desired, also increased the tissue compression artifact that accompanies piston motion. In certain subjects, the large tissue compression artifact introduced significant reverberation that masked the propagating shear wave of interest. Because the majority of shear wave generation occurs at the piston edge, we propose an annulus piston design to reduce the tissue compression artifact while retaining focused shear wave amplitude.

**Methods:** This study investigated tissue compression and focused shear wave generation from both full and annular concave pistons through numerical simulations and benchtop experiments using homogeneous tissue-mimicking gelatin phantoms. Numerical simulations were performed using a Helmholtz decomposition-based approach [2] at the acoustic source to calculate compression and shear wave amplitudes generated by annular pistons with varying ring thicknesses. For benchtop validation, waves were generated in tissue-mimicking gelatin phantoms via vibrations of (1) a full concave piston (50 mm diameter, 40 mm radius of curvature) and (2) a concentric annular concave piston (inner and outer diameters of 42 mm and 50 mm, 40 mm curvature). Compression and shear wave fields were recorded using high-frame-rate ultrasound imaging.

**Results & Discussion:** Simulations demonstrate qualitatively that the compressional signal amplitude decreases while the focused shear wave amplitude is maintained as the concave annular piston ring becomes thinner (Fig. 1A). Benchtop experiments in tissue-mimicking gelatin phantoms demonstrate that the annulus piston yields negligible compression signal (Fig. 1C) compared to the whole piston of the same outer diameter and curvature (Fig. 1B), while shear wave focusing remains effective.

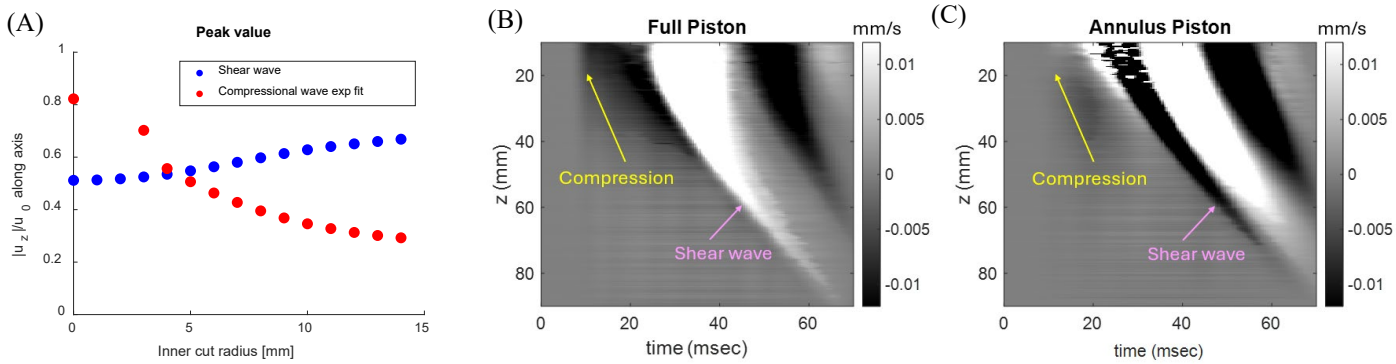


**Figure 1:** (A) Simulated peak wave displacement amplitude of shear wave (blue) and compressional wave (red) normalized by piston amplitude $u_0$ versus inner cut radius (outer radius is 25 mm). (B) and (C): Measured wave fields from vibration of full piston and annulus piston, respectively. Depth coordinate $z$ is oriented along the focused shear wave beam axis. Color scale is gelatin particle velocity (mm/s) measured by ultrasound imaging. In (B) and (C), yellow arrows indicate tissue compression, while pink arrows indicate the focused shear waves.

**Significance:** Accurate and robust measurement of liver mechanical properties is critical for diagnosing and staging diseases such as fibrosis and cirrhosis. Our novel fSWE technology can overcome the limitations of traditional TE technology in patients with obesity by increasing shear wave amplitude in deeper livers, but initial testing revealed increased imaging artifacts due to tissue compression.

This work addresses the limitation by demonstrating reduction of tissue compression artifacts using annular piston geometries, both in silico and on the benchtop, thereby improving shear wave visibility. Increasing the signal-to-noise ratio of shear waves in fSWE by optimizing the source design enables more robust LSM, especially in patients with obesity, thus reducing reliance on invasive biopsy and contributing to a needle-free future for liver disease assessment.

**Acknowledgments:** This work was supported by NIH grant nos. P30DK120531, R61AT012282, and R01HL152023, and by the University of Pittsburgh PhD Program.

**References:** [1] Cormack et al. (2024), *IEEE Trans. Biomed. Engr.* **71**(2); [2] Archer et al. (2023), *J. Acoust. Soc. Am.* **153**(3).

**Investigating upper trapezius muscle quality in people with or without chronic shoulder pain**

Chun-Kai Tang, PT, MSc[1], *Yi-Fen Shih, PT, PhD[1]

[1]*Department of Physical Therapy and Assistive Technology, National Yang Ming Chiao Tung University*

*Corresponding author's email: yfshih@nycu.edu.tw

**Introduction:** The upper trapezius (UT) plays a key role in maintaining proper scapulohumeral rhythm and is associated with the development of chronic shoulder pain (CSP). The echo intensity (EI) of the musculoskeletal ultrasound has been used to assess muscle quality, with a higher EI indicating a higher proportion of intramuscular adipose and fibrous tissue in the muscle, and a poorer muscle quality.[1] However, no previous study has measured upper trapezius muscle quality using EI. The purpose of this investigation is to assess and compare the EI of the UT between individuals with and without CSP. We hypothesize that the EI of the affected shoulder would be higher than that of the unaffected side and of the healthy controls.

**Methods:** Ten participants with CSP (six males, 1.69±0.08m, 62.6±5.37kg) and ten healthy controls (HC, six males, 1.69±0.08m, 62.6±8.04kg) were recruited. The inclusion criteria for the CSP group were (1) 18-50 years old, (2) unilateral and non-traumatic shoulder pain, (3) pain duration longer than 3 months, (4) pain intensity more than VAS=2 during movement, (5) presence 3 of 5 positive pain provocation tests: Hawkins-Kennedy test, Jobe test, Neer's test Painful Arc, and Resistance Test against External Rotation. The inclusion criteria of the HC group were (1) 18-50 years old; (2) no shoulder pain at rest or during daily activities; (3) negative pain provocation tests above and Spurling's neck compression test. Konica Minolta ultrasound (Sonimage MX1) was used to capture the image of the UT. The frequency was set at 11.0 MHz, gain at 40 dB, dynamic range at 85, and depth at 4 cm. The middle of the probe was placed in sagittal on the middle of the C7 and acromion. MATLAB® was used to calculate the echo intensity and subcutaneous fat thickness. The corrected factor (*cf*) for subcutaneous fat thickness was also calculated and would be applied if there were significant differences in subcutaneous fat between groups.

$$cf = -148.46 \times (1cm) + 183.65 = 35.19.$$

The paired t-test was used to compare the EI within the group, and the independent T-test was used to calculate the between-group differences. We also assessed the difference in subcutaneous fat thickness within and between groups.

**Results & Discussion:** There was no significant difference in the baseline characteristics and subcutaneous fat thickness between groups. Therefore, no corrected factor was used to normalize the EI. The average EI of the affected and unaffected sides of the CSP group was 93.53±5.12 and 92.51±6.77 Au, respectively. The average EI of the dominant and non-dominant sides of the HC group are 87.16±7.59 and 88.06±9.37 Au. The independent t-test revealed that there was a significantly higher EI in the affected side of the CSP group compared to the matched side of the HC group (p=0.041, mean difference=-6.37, ES=0.98). No significant differences were found between the unaffected and matched sides and within groups.

This study is the first to investigate the EI of the UT muscle and compare it between the CSP group and HC. Our results suggested that people with CSP had poorer UT muscle quality. Whether changes of muscle quality link to changes in UT muscle performance and shoulder kinematics, pain, and dysfunction require further studies to clarify. However, muscle quality did not seem to differ between the affected and unaffected sides. This may be due to compensatory loading on the unaffected side and the presence of neck pain in some CSP patients. Future research may consider subgrouping the patients with the presence of neck pain to minimize the influence. Although we did not find significant differences in subcutaneous fat thickness, correction factors should still be applied in future studies.

**Significance:** Echo intensity of the ultrasound imaging is an efficient method to qualify the muscle quality of the UT. Poorer UT muscle quality was observed in people with chronic shoulder pain.

**Acknowledgments:** We acknowledge Professor Chia-Feng Lu for his generous suggestions for image analysis. This study is partly funded by the National Science and Technology Council of Taiwan.

**References:**

1. Stock, M.S. and B.J. Thompson, *Echo intensity as an indicator of skeletal muscle quality: applications, methodology, and future directions.* Eur J Appl Physiol, 2021. **121**(2): p. 369-380.

# SUPRASPINATUS MUSCLE MORPHOLOGY AND ARCHITECTURE ASSESSMENT AFTER ROTATOR CUFF TEAR AND SURGICAL REPAIR USING DIXON AND DIFFUSION TENSOR IMAGING METHODS

*Raquel Miera[1], Kathryn T. Rex[1], Lilla Caton[1], April D. Armstrong[2], Thomas Neuberger[1,3], Meghan E, Vidt[1,4]
[1]Department of Biomedical Engineering, Pennsylvania State University, University Park, PA, USA
[2]Department of Orthopaedics and Rehabilitation, Penn State College of Medicine, Hersey, PA, USA
[3] Huck Institutes of the Life Sciences, Pennsylvania State University, University Park, PA, USA
[4]Department of Physical Medicine & Rehabilitation, Penn State College of Medicine, Hersey, PA, USA
*Corresponding author's email: rfm5887@psu.edu

**Introduction:** Rotator cuff tears (RCT) are a common musculoskeletal disorder that affect nearly 4.5 million people in the US every year [1]. Surgical repair is a common treatment for RCT, yet 10-48% of individuals experience a re-tear [2]. Prior research has shown fatty infiltration (FI) increases after RCT, but little is known how FI affects muscle architecture. This study aimed to quantify the change in muscle architecture and composition after RCT and surgical rotator cuff repair (RCR). Diffusion Tensor Imaging (DTI) and Dixon magnetic resonance imaging (MRI) methods were used to evaluate the fractional anisotropy (FA) and FI, in the supraspinatus muscle to determine how muscle diffusion changed with presence of FI. It was hypothesized that as time increased post-RCT and RCR that fat percentage would increase while FA values decreased as FI altered the muscle composition and architecture of the supraspinatus muscle.

**Methods:** Eighteen New Zealand White rabbits (7M/12F) were evaluated (IACUC #201800257). Animals were randomly assigned to a study time point, ranging from 2- to 16-weeks. Fourteen animals underwent RCT injury surgery on a randomly selected side, where the supraspinatus tendon was severed using sharp dissection [3]. Two RCT injury animals also underwent RCR surgery 8 weeks after injury surgery. Four animals underwent a sham injury surgery and two also underwent sham repair 8 weeks after sham injury surgery; animals that had a RCR or sham repair had a final time point 8-weeks after the repair surgery. Animals were euthanized at the assigned time point, and the affected forelimb was harvested for scanning. All samples underwent a Dixon scan and 16 also had a DTI scan after the Dixon scan. DTI and Dixon scans were conducted on a 7T MRI scanner (Bruker BioSpec 70/30 Avance III HD, Bruker, Ettlingen Germany). After scanning, DTI data was processed by motion correcting images using automatic image registration, followed by a manual segmentation of the supraspinatus muscle using MRI studio software [4]. MRtrix software was then used to calculate a diffusion tensor and create a FA map to assess the directionality of water in the muscle tissue [5]. FA was reported as an index ranging from 0 (anisotropic diffusion) to 1 (fully isotropic diffusion). Dixon scans were processed by first manually segmenting the supraspinatus using Avizo Software (Thermo Fisher Scientific, 2021). Muscle and fat volumes were calculated for the segmented muscle using a custom MATLAB script, then percentage of fat within the muscle volume was calculated. Formal statistics were not conducted due to small sample size, but qualitative assessments on the data were performed.

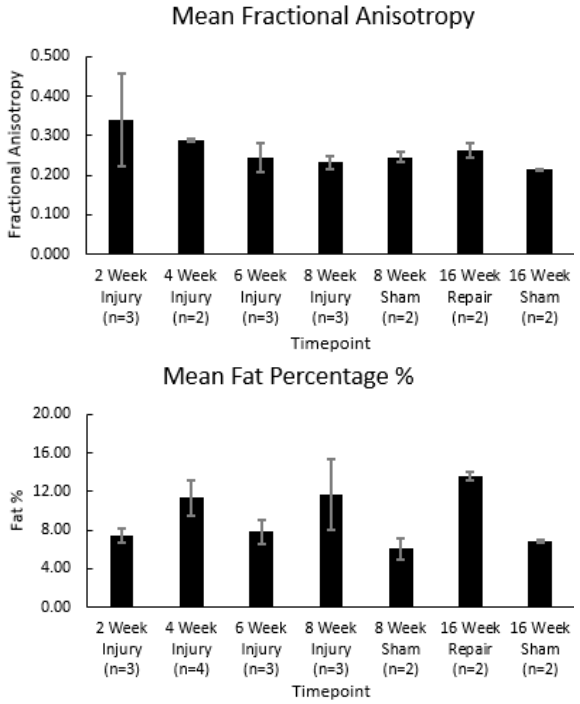


**Figure 1:** Mean FA and mean fat percentage of supraspinatus muscle.

**Results & Discussion:** As time post-injury increased, FA values decreased from an average of 0.34 (2-week) to 0.23 (8-week). For FA, values did not increase after RCR, but sham injury and repair resulted in lower values compared to 2-week injury values (Figure 1). While fat percentage increased from 7.38% (2-week) to 11.67% (8-week), fat percent continued to increase after RCR; fat percent remained relatively stable with sham samples (Figure 1). The decrease in FA values over time suggests an increase in diffusion directions within the muscle, indicating a change in muscle architecture as fat infiltrates the supraspinatus muscle and water is unable to smoothly diffuse along the muscle fibers. The Dixon results correspond to this change in FA, as fat percentage continues to increase with time after RCT and RCR, altering the muscle composition of the supraspinatus.

**Significance:** MRI scans of muscle using Dixon and DTI methods suggests a change in muscle architecture and morphology in the supraspinatus muscle after RCT, that does not improve after RCR. These results help provide a better understanding of the relationship between muscle architecture and composition after RCT and RCR. Ongoing work continues to expand these results in a larger sample size and examine the relationship of these findings to muscle function to inform treatment and repair for RCT.

**Acknowledgments:** NIH RO1AR079999; William Dearnaley; Penn State Animal Resource Program.

**References:** [1] Rahman et al. (2017). J Biomech Eng. November, 139(11): 110801; [2] Zhao et al. (2021). JSES, 30(11), 2660-2670; [3] Rubino et al. (2008) Arthroscopy, 24(8), 936–940; [4] Jiang et al. (2006). Comput. Methods Programs Biomed., 81(2):106–116; [5] Tournier et al. (2019). NeuroImage, 202:116137.

# COMPARING OBSERVED ACHILLES TENDON CHARACTERISTICS ACROSS SPORTS

Camille L. Nguyen[1]*, Joshua K. Sponbeck[2], Martina Uvacsek[3], Dora Molnar[3], A. Wayne Johnson[1]
[1]Brigham Young University, Provo, UT, US
*Corresponding author's email: nguyenca@byu.edu

**Introduction**: The Achilles tendon (AT) is the strongest and largest tendon in the human body and a commonly injured tendon in the athletic population that occurs due to repeated exposure to excessive strain which damages the tendon microscopically and finally macroscopical [1]. This macroscopic injury leads to increased medical costs, increased time out of sport, increased recurrence later in life, and many other complications [2, 3]. Certain sports, including women's gymnastics, men's and women's basketball (BBall), and distance running, report higher rates of Achilles tendinopathy, though the differences in AT characteristics among these populations are not well understood [2,4]. Conversely, aquatic based athletes such as swimmers and water polo (WP) players rarely report heel pain, nor are Achilles tendinopathies commonly diagnosed in aquatic sports but may be at risk of underloading the AT and may present with less organized tendon structure via ultrasound. A complicating factor of tendinopathy is the relationship between pain and structure; many individuals reporting pain have no observed structural tendon disorganization while others with significant structural disorganization report no pain. It is often these individuals that suffer traumatic rupture of the AT. Therefore, the aim of this study was to compare AT characteristics in male BBall players, runners, and WP players to determine what differences are present between these groups of different loading rates and magnitudes. It was hypothesized that BBall players and runners would exhibit similar tendon characteristics because both sports experience land-based loading; while WP players would exhibit different tendon characteristics (smaller tendon cross-sectional area and thickness) compared to the other sports because these athletes experience water-based loading after accounting for age and weight.

**Methods**: This study used data from 87 healthy adult males: 33 runners, 40 WP players, 14 BBall players. Runners had an average 5k time of 17.7±2.39 min and ran 22.8±15.7 mi/wk. Elite WP players, rostered on a national-level club team in Budapest, practiced in an all-deep pool 10.36±2.45 hrs/wk and participated in sport led land-based exercises 3.09±1.32 hrs/wk. BBall players were rostered on a male NCAA Division 1 team and participated in organized sport over 20 hrs/wk. All images were collected on a General Electric LogicE or Fortis ultrasound using a GE 8-18i-D or GE 9-12L transducer. Participants were imaged before any type of exercise was completed. A cross-sectional area (CSA) and thickness image were captured of the left and right AT. Images were processed using local internal GE software or from DICOM files on OsiriX. Tendons were stacked and averaged for each participant to account for possible confounding results in differences between left and right tendons during data analysis. A mixed-model ANOVA in R compared AT CSA and thickness across groups accounting for age and mass.

**Results & Discussion**: Significance was found for both CSA and thickness. A Tukey post-hoc test revealed significant differences in AT CSA average between WP and BBall ($p<.0001$) and runners and BBall ($p<0.000001$), with WP and runners trending toward significance ($p=0.087$) (Fig. 1). There was significant difference in AT thickness between WP and BBall ($p=0.022$), but not between WP and runners ($p=0.230$) and runners and BBall ($p=0.190$) (Fig. 1). Even after accounting for mass and age, BBall players tendons had significantly larger CSA averages than WP players and runners. This could be due to the higher forces experiences by BBall players when cutting, changing direction, and vertical jumping often while WP players and runners rarely experience those types of forces. BBall players also have a thicker AT than WP players. BBall players frequently experience high loading forces through jumping and running on hard-wood courts while WP players typically experience lower sport-induced force in water. Runners experience high frequency and higher total volume of loading through the AT across multiple running surfaces (e.g. concrete, asphalt, dirt, grass, track). Our hypothesis that BBall players and runners would have similar tendon characteristics was not supported, likely due to loading differences. Our finding that WP players and runners had similar tendons does not support our second hypothesis. There are likely other factors that need to be considered when assessing tendon characteristics across sports such as tendon shape, echo intensity, presence of blood flow, and stiffness.

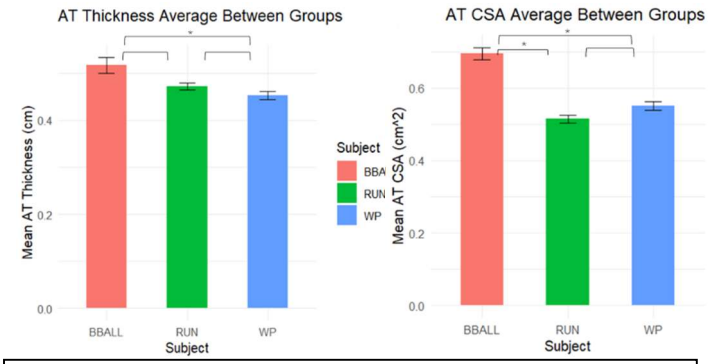


*Figure 1*. Graph representing the relationship between group mean CSA and thickness.

**Significance**: Sport-specific difference was observed in AT size and thickness. These differences are likely due to sport-specific requirements in type, amount, intensity, and total volume of loading. Additional tendon characteristics are needed to further understand the observed tendon differences across various sports. The combination of these characteristics will better inform clinicians, coaches, and athletes on how to mitigate and rehabilitate Achilles tendinopathies.

**Acknowledgements**: Many thanks to the diligent contributions from the Hungarian University of Sport Science.

**References**: [1] Leung and Griffith. (2008) *J Clinical Ultrasound* 36(1); [2] Chan et al. (2020), *Int Ortho* 44(3); [3] Hartman et al. (2024), *J Foot Ankle Surg* 63(5); [4] Nielsen et al. (2013), *Int J Sports Phys Ther.* 8(2).

# PREDICTING HEAD INJURY CRITERION IN REAL-WORLD REAR-END VEHICLE COLLISIONS

*Clyde Westrom[1], Kevin Adanty[1], Sean D. Shimada[1]
[1]Biomechanical Consultants
*cwwestrom@alumni.ucdavis.edu

**Introduction:** Peak head acceleration and 15 ms Head Injury Criterion ($HIC_{15}$) are common metrics biomechanists and safety engineers assess to determine the risk of injury to an occupant during a motor vehicle collision. However, their use has been limited to test environments, where head accelerations can be obtained from instrumented Anthropomorphic Test Devices (ATDs) in controlled laboratory settings. In real-world environments, pulse functions have been commonly used for estimating the acceleration-time history of a vehicle [1], but have been used less frequently for modeling head acceleration. Prior literature has calculated waveforms or head injury metrics by machine learning, but methodologies require extensive information about vehicle kinematics and other pre-crash characteristics [2,3]. Pulse functions are advantageous in being easily scalable by a peak value and a pulse width and have been shown to match kinematics in a crash adequately [4]. Previous work has used pulse functions to predict $HIC_{15}$ in the context of frontal impacts but not for occupants in rear impacts [5]. Head restraint interaction and rebound kinematics may make $HIC_{15}$ predictions based on frontal crash characteristics unreliable. This study developed a method to estimate $HIC_{15}$ in rear-end vehicle crashes using only the occupant's peak head acceleration and head impact duration by using a duration ratio to scale the pulse width for these pulse functions. This work will help safety experts and engineers improve injury evaluations, particularly analyses involving $HIC_{15}$ in real-world crashes.

**Methods:** Kinematic data from rear-end impacts in the Insurance Institute for Highway Safety (IIHS) TechData database was collected and filtered for valid data. All crash tests included a single BioRID IIg ATD occupant with a three-point belt. Resultant head acceleration channels were calculated from filtered individual head acceleration component channels. These tests were separated into two datasets for 'training' and 'testing' duration ratios. Duration ratios were scaling factors obtained from the 'training' phase that would scale a pulse function's duration to represent $HIC_{15}$ accurately. In the 'training' phase, rectangular, triangular, quadratic, half-sine, and haversine pulse functions were modeled on each test's peak head acceleration and impact duration based on data in the 'training' dataset. Next, the pulse duration of each pulse function was iteratively scaled until the $HIC_{15}$ value calculated from each pulse function was equal to the $HIC_{15}$ value calculated from the occupant's filtered head acceleration-time curve to obtain a ratio. Ratios obtained from each crash test in the 'training' dataset were averaged for each pulse function to obtain a duration ratio for each pulse function. Duration ratios were evaluated similarly in the 'testing' dataset, calculating the error in $HIC_{15}$ from the duration-scaled pulse function and the occupant's filtered head-acceleration-time curve.

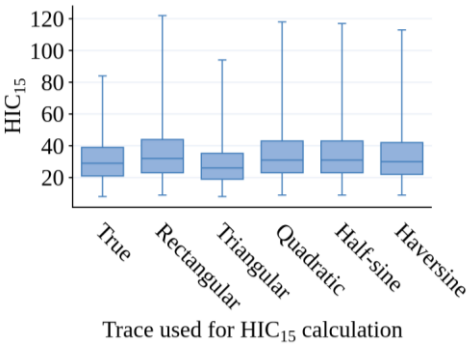


**Figure 1:** HIC15 calculated from the head acceleration traces in the 'testing' dataset and their corresponding modeled pulse functions.

| Pulse Function | Duration Ratio | Percent Error |
|---|---|---|
| Rectangular | 0.1767 | 11.85% |
| Triangular | 2.2502 | -9.58% |
| Quadratic | 0.5480 | 9.30% |
| Half-sine | 0.6077 | 8.70% |
| Haversine | 0.8273 | 5.80% |

**Table 1:** Duration ratios calculated from the 'training' dataset and mean percent error when used to calculate $HIC_{15}$ on the 'testing' dataset.

**Results & Discussion:** 617 rear-impact IIHS tests were used in the present analysis. The 'training' dataset had 308 occupants, while the 'testing' dataset had 309. The 'training' dataset had an average peak head acceleration of 21.96 g, while the 'testing' dataset's average was 21.88 g. Impact durations were also similar, with values of 92.45 ms and 93.51 ms, respectively. A one-way repeated measures ANOVA with a post-hoc test revealed statistically significant differences between duration ratios for all pulse functions ($F(1.15,353.68)=1636.07$, $p<0.001$). This indicates that each pulse function's shape and corresponding area are important in representing head injury potential, particularly shown by the rectangular pulse function's small duration ratio and the triangular pulse function's high duration ratio (Table 1). The haversine pulse function has a duration ratio near 1.00 and a low percentage error, suggesting that it is most representative of $HIC_{15}$ with a minor adjustment to its duration.

Another one-way repeated measures ANOVA with post-hoc test revealed statistically significant differences between every pulse function's predicted $HIC_{15}$ and each test's true $HIC_{15}$ value ($F(1.51, 466.02)=446.11$, $p<0.001$). It is important to note that these crash tests all present very low $HIC_{15}$ values (true values ranging from 8-84) and may not adequately represent the potential for injury in higher-speed vehicle impacts. Despite significant differences (Figure 1) and the percent errors above 5% (Table 1), a difference of 11.85% for the rectangular pulse function equates to a mean difference of less than 4.

**Significance:** This study provides a method to predict $HIC_{15}$ in real-world crashes with parameters similar to rear IIHS tests. Rectangular, triangular, quadratic, half-sine, and haversine pulse functions all demonstrated the ability to make accurate predictions, however, a haversine pulse function is the most ideal equation form to represent a crash pulse with the lowest percentage error and may be a desirable choice for experts in injury biomechanics.

**References:** [1] Höschele et al. (2022). SAE Int. J. Trans. Safety, 10: 185–210. [2] Bracali and Baldanzini (2022). Sensors, 22: 5592. [3] Hasija and Takhounts (2020). SAE Technical Paper, 2019-22–0016. [4] Varat and Husher (2003). 18th International Technical Conference on the Enhanced Safety of Vehicles, 9. [5] Westrom et al. (2025). SAE Technical Paper, 2025-01–8709.

# PRELIMINARY IMPACT TESTING OF AN OVINE MODEL TO VALIDATE A BIOMECHANICAL TEST METHOD FOR CADAVERIC STUDIES

*Madysn Cardinal[1], Abbie Underwood[1], John Desjardins[1], Gregory Batt[2]
[1]Department of Bioengineering, Clemson, SC 29634
[2]Department of Food, Nutrition, and Packaging Science, Clemson University, Clemson, SC 29634
*Corresponding author's email: mcardin@clemson.edu

**Introduction:** Concussions are common in a variety of settings, with almost 3.8 million concussions annually in American sports[1]. Concussions are the most common form of mild traumatic brain injury (mTBI), caused by direct or indirect head impacts that can lead to neurological impairment and severe long-term diseases[1] [2] [3]. Repeated exposure increases the risk of disability or death, often due to overlooked or misdiagnosed injuries[3]. Understanding the mechanisms of injury could allow for prevention and accurate diagnosis. Despite their prevalence, concussion mechanisms and kinematics remain unknown but are largely attributed to brain tissue deformation [2]. Head impacts result in linear and rotational motion, but the brain is most sensitive to rotational movement, with studies showing that higher rotational velocities and accelerations are associated with concussive injuries[4] [5]. Even still, the exact relationship between kinetic motion and brain injury remains uncertain[6]. Many impact studies make use of the Hybrid III model, which consists of a solid vinyl head form with internal sensors to detect head accelerations. However, this model severely lacks anatomical accuracy due to the lack of a brain component, which must be independently considered to quantify concussions.[7] Because concussions stem from brain mechanics and deformation, post-mortem human surrogates (PMHS) allow impact tests to account for brain tissue mechanics[7]. During PMHS testing, artificial fluids are perfused to mimic living brain conditions, often with the specimen inverted to improve perfusion[6] [8] [9]. Ovine specimens, or sheep, serve as a cadaver alternative due to their relative anatomical similarity and availability. Specifically, sheep have very similar head and neck anatomy and similar skin, tissue, and bone textures, while also excellent models for human circulatory interactions[10] [11]. This study explores the application of cadaveric ovine specimens in preliminary biomechanical impact testing.

**Figure 1:** Max Resultant Angular Velocity.

**Methods:** As previously mentioned, impacting cadaveric specimens in the inverted orientation aids in the perfusion of fluids and preserves fidelity. A fixture was fully designed, assembled, and evaluated to enable the testing of an inverted specimen. The fixture was designed around an industry-standard pneumatic linear impactor, allowing upright and inverted impact comparisons. A Cadex Linear Impact Testing Machine (CADEX Inc., Quebec, Canada) was used to impact the ovine specimen with an instrumented mouthguard (Diversified Technical Systems, Inc., Seal Beach, CA) fixed onto the specimen to measure head kinematics. The test method consists of ten bare-head impacts at 5.0 m/s at six different locations per the Helmet Test Protocol. Data was then analyzed using MATLAB, with maximum resultant angular velocity, linear acceleration, and rotational acceleration being the metrics evaluated.

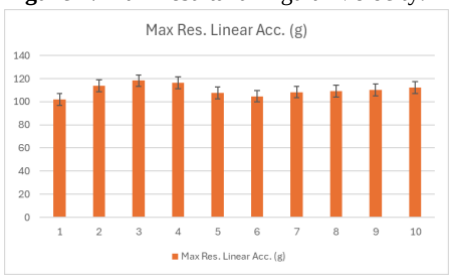


**Figure 2:** Max Resultant Linear Acceleration.

**Results & Discussion:** One ovine specimen has been tested at the side impact location, with additional testing planned at all locations in the coming months. Figures 1, 2, and 3 display the maximum resultant angular velocity, linear acceleration, and rotational acceleration from 5.0 m/s bare head impacts, respectively. The data remained consistent throughout testing, supporting the validation of specimen preparation and the test method for future cadaveric impact studies. This consistency suggests that the methodology is repeatable and effective, allowing for the refinement of testing protocols and measurement techniques before transitioning to cadaveric studies, where variability is higher, and specimen availability is limited.

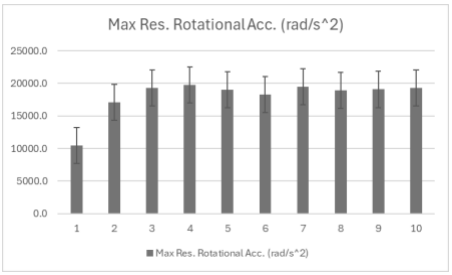


**Figure 3:** Max Resultant Rotational Acceleration.

**Significance:** PMHS testing remains essential for studying human brain injuries, but availability, cost, and specimen variability limit its feasibility in early-stage research. Using ovine models enables researchers to refine test methods and establish baseline data before transitioning to human cadavers. This approach enhances the reliability of impact testing, ultimately contributing to more accurate injury modelling.

**Acknowledgments:** Thanks to the Clemson Department of Bioengineering and the Clemson Department of Food, Nutrition, and Packaging Science for support of this study and the Robert Brooks Sports Science Institute for research funding.

**References:** [1] Hallock et al. (2023). *Neurol Clin Pract*; 13. [2] Graham et al. (2014). *National Academies Press*. [3] Tator. (2013). *CMAJ Canadian Medical Association Journal*; 185: 975–979. [5] Kleiven. (2013). *Front Bioeng Biotechnol*; 1. [6] Kimpara. (2012). *Ann Biomed Eng*; 40: 114–126. [7] Hardy et al. (2007). [8] Gabler et al. (2022). *Ann Biomed Eng*; 50: 1356–1371. [9] King et al. (2011). *Clinical Anatomy*; 24: 294–308. [10] Alshareef et al. (2018). *J Neurotrauma*; 35: 780–789. [11] Fermi et al. (2022). *Int. J. Environ. Res. Public Health*; 19, 3657. [12] DiVincenti et al. (2014). *J American Association for Laboratory Animal Science*; 53: 439-448.

# HIGH G-FORCES IN UNINTENTIONAL IMPROPER INFANT HANDLING: IMPLICATIONS FOR SHAKEN BABY SYNDROME

Lila T. Wayman[1], Kathryn L. Havens[2], *Jonathan S. Lee-Confer[1]
[1]SensorLab, Department of Physical Therapy, University of Arizona
[2]Division of Biokinesiology and Physical Therapy and Department of Biomedical Engineering, University of Southern California
*Corresponding author's email: leeconfer@arizona.edu

**Introduction:** Abusive head trauma, commonly referred to as Shaken Baby Syndrome (SBS), is diagnosed in approximately 33 per 100,000 infants annually in the United States [1]. Traditional diagnostic criteria for SBS include hemorrhages within the cranium and ocular regions which are commonly determined to come from an infant being shaken [2]. While intentional shaking is widely recognized as a cause of these injuries, the potential for similar forces resulting from improper or accidental non-recommended handling of infants has not been fully explored. This study aimed to quantify head accelerations in a model infant simulating improper handling and compare to those during maximum effort shaking.

**Case Facts:** An 8-month-old female infant born 34-week prematurely was brought to a local hospital in Texas after a distressed father called 911 and stated his baby became non-responsive and stopped breathing. The infant was 64.0cm in length and 8.62 kg in weight. The infant was diagnosed with COVID-19, panlobar pneumonia, and retinal and subarachnoid hemorrhages. The father denied any abuse but explained that he placed the child on a table with the head unsupported as he held the phone while talking to 911.

**Methods**: To simulate this case, a realistic silicone infant model (55.88 cm and 5.08 kg) was equipped with an inertial measurement unit (IMU) around the head at eye level to quantify head accelerations under two conditions: (1) placing the infant model on a table with the head unsupported (Table placement) and (2) manually shaking the model at maximum effort for five seconds (Maximal effort shaking). This was performed by two participants for five trials while holding the model by the torso. For Table placement, the peak head acceleration (anteroposterior) was identified as the first positive peak after the infant's impact with the table (Fig 1) and was averaged from the 5 trials. The peak head accelerations (anteroposterior) during the maximum effort shaking trials were extracted, rectified, and the highest 5 peak accelerations during the 5 second shake were selected and averaged. A paired t-test was used to determine differences in head acceleration between tasks ($\alpha < 0.05$).

| Condition | Mean Peak Head Acceleration (mg) | Standard Deviation (mg) | Range of Head Acceleration (mg) | p-value |
|---|---|---|---|---|
| Table Placement | +31,000 | +6,500 | +19,000 - +43,000 | $p < 0.0001$ |
| Maximum Effort Shaking | +11,000 | +1,900 | -16,000 - +10,000 | |

Table 1. Peak head accelerations (mg) observed when placing the infant model on the table with the head unsupported and when shaking the infant model with maximum effort.

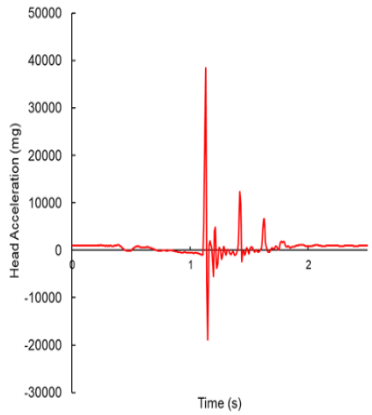


Figure 1. An example trace of the infant model's head acceleration during unsupported impact with the table.

**Results & Discussion:** Peak head acceleration during table placement of the infant model with the head unsupported was 181% higher than full force shaking (Table 1; $p < 0.0001$). No significant differences between participants were identified for either task ( $p = 0.89$), suggesting the tasks were performed similarly. The peak head acceleration from placing an infant model on the table exceeds the 29.3 G-forces experienced in an 18-mph car crash and exceeds the 5.2 G-forces head accelerations recorded in a 5-mph bumper car collision [3]. This study shows that improper handling of infants can result in high G-forces to the head, potentially causing injuries similar to SBS.

**Significance:** These findings are significant because they challenge the assumptions about the forces required to cause injuries associated with SBS. The study demonstrates that common improper handling scenarios, such as placing an infant on a surface without supporting the head, can generate head accelerations exceeding those from maximum effort shaking and even surpass forces experienced in vehicular collisions. This raises important questions about the potential for misdiagnosis of SBS and highlights the need for a more comprehensive understanding of accidental head trauma in infants. These insights could have critical implications for forensic investigations, child protection cases, and medical guidelines regarding infant handling and injury assessment, such as the case presented here.

**References:** [1] Shanahan et al. (2013), *Pediatrics* e1546-e1553; [2] Lopes et al. (2013), *J Pediatr.* 89; [3] Pfister et al. (2009), *J. Foren Med Path* 30;

# KINEMATIC RESPONSE TO WARNED AND UNWARNED PERTURBATIONS IN RUNNING HUMANS

*Alicia M. Boynton[1], Nathaniel G. Luttmer[2], Takara E. Truong[2], Mark A. Minor[2], David R. Carrier[1]
[1]University of Utah (School of Biological Sciences)
[2]University of Utah (Department of Mechanical Engineering)
*Corresponding author's email: aboynton@madonna.edu

**Introduction:** It is well documented that athletes, especially those participating in contact sports, experience an alarming amount of traumatic brain injuries [1,2]. An accumulation of minor traumatic brain injuries may contribute to an increased likelihood of developing neurodegenerative disorders [3,4]. When head acceleration was monitored during youth contact sports, the largest levels of acceleration were observed following blind-sided collisions in which players were not aware, nor able to prepare for the imminent impacts [5,6]. Awareness prior to impacts allows athletes to muscularly brace themselves prior to impact which may provide a level of stabilization that is absent when blind-sided [7,8]. Muscles of the core, including cervical muscles, are active during locomotion to provide stabilization to the head and body and could be recruited to a greater extent to increase core stabilization [9].

Warnings of imminent perturbations to the head are associated with increased activation of cervical muscles [7,8]. Importantly, the muscular bracing that occurred in warned trials significantly decreased angular acceleration of the head following lateral perturbations [8]. Our previous research suggests that when people are aware of an incoming perturbation, core musculature increases activity preemptively compared to the muscle activity seen during unwarned perturbations [10]. In this study we aimed to compare the kinematics of the head and body following unwarned and warned perturbations in running subjects. We hypothesized that participants display lower displacement, increased stiffness between body segments, and decreased acceleration in warned versus unwarned trials.

**Methods:** Fourteen male participants (20-35 years of age, height 1.83 ± 0.06m, body mass 77 ± 11 kg) with prior experience playing contact sports and no current musculoskeletal injuries were recruited for this study. Perturbations were applied to subjects running at 3 $ms^{-1}$ on a large treadmill through a system of 3 motor-controlled tethers [11]. The tethers were attached to a climbing harness which allowed for perturbations to be applied near the participants' center of mass. Perturbations were set to a level of 30% of participant body weight. By utilizing a full body marker set, a motion tracking algorithm, and seven infrared Vicon Bonita cameras (Vicon Inc., Oxford, UK) with Nexus software we captured kinematic data at 200 Hz. A combined visual and auditory warning was given 0.5 s prior to impact in all warned trials [12]. Perturbation forces pulled the participant in four directions: forward, backward, left or right in a random manner. The phase of the locomotor cycle (flight phase or stance phase) in which perturbations occurred were also randomized during all trials. Kinematic data analysis was performed using Visual 3D software (C-Motion©, Germantown, MD, USA).

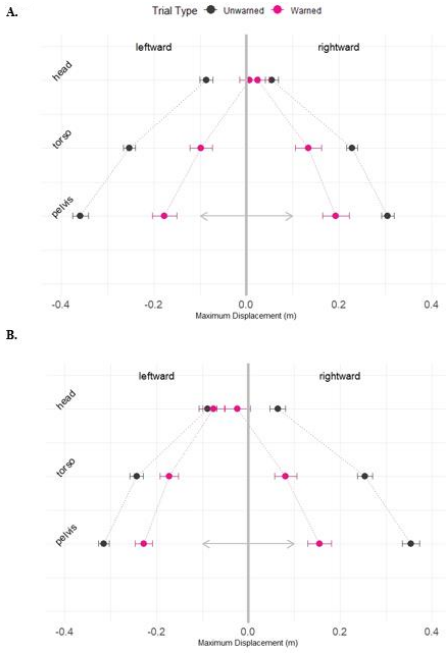


**Figure 1:** Maximum linear displacement (m) of the head, torso, and pelvis segments during the locomotor cycle following leftward and rightward perturbations given at right foot toe-off (A) and right foot stance (B). Values are the mean displacement during unwarned trials (black) and warned trials (pink) with standard error bars. The grey arrows indicate the direction segments were pulled away from the original center position.

**Results & Discussion:** The perturbations applied in this study were sufficient to destabilize running participants. The maximum linear displacement (m) of the pelvis, torso, and head segments following lateral perturbations can be found in Figure 1. The maximum displacement of the pelvis segment was significantly greater in the warned condition than in unwarned trials following perturbations in each of the directions. The relative angle between the pelvis, torso, and the head following perturbations was often reduced in the warned condition compared to unwarned. Our results suggest that when athletes are aware of an incoming impact they are better able to maintain their position (displacement), posture (relative body angles), and may undergo lesser angular accelerations compared to participants who were blind-sided by incoming perturbations.

**Significance:** Our data suggests that athletes who are aware of incoming perturbations may display decreased displacement and acceleration which could lead to a lower incidence of collision induced sports injuries, especially during contact sports.

**Acknowledgments:** Research was supported by the National Science Foundation under grant #1622741.

**References:** [1] Duma et al. (2005) *Clinical Journal of Sports Medicine*, 15(1), 3-8; [2] Mihalik et al. (2007) *Neurosurgery*, 61(6), 1229-1235; [3] McKee et al. (2009) *Neuropathology & Experimental Neurology*, 68(7), 709-735; [4] Mez et al. (2017) *JAMA*, 318(4), 360-370; [5] Mihalik et al. (2010) *Pediatrics*, 125(6): 1394-1401; [6] Lincoln et al. (2013) *American Orthopaedic Society for Sports Medicine*, 41(4); [7] Eckner et al. (2014) *American Journal of Sports Medicine*, 42(3), 566-576; [8] Homayounpour et al. (2021) *Journal of Biomechanics*, 128(9); [9] Boynton & Carrier, (2022) *Integrative Organismal Biology*, 4(1); [10] Boynton et al. (2023) *Human Movement Science*, 89:103096; [11] Luttmer et al. (2020) *IEEE International Conference on Robotics and Automation (ICRA)*, 9135-9142; [12] Luttmer et al. (2022) *arXiv preprint arXiv:2207.13835*

# A MULTIVARIABLE MODEL OF PEAK LOWER SPINE ACCELERATION DURING NEAR-SIDE LATERAL IMPACTS

*John Adam Caraan[1], Clyde Westrom[1], Kevin Adanty[1], Sean D. Shimada[1]
[1]Biomechanical Consultants
*jadam.caraan@gmail.com

**Introduction:** An occupant's kinematic response and subsequent injury potential during a vehicular impact are largely influenced by their seating position [1]. Side impacts are categorized as either near-side or far-side, with near-side occupants seated at the side of impact, and far-side occupants seated opposite to the side of impact. Belted near-side occupants are generally considered to be at higher risk for injury due to likely head contact with adjacent interior structures. Additionally, occupants may experience symptoms of soft tissue damage to their lower spine which increase with increasing impact severity [1-3]. Impact severity can be assessed through analysis of either a vehicle's peak acceleration or a change in velocity (ΔV). Despite the focus that near-side impacts have received in literature, there is a lack of research regarding the kinematic response, specifically acceleration, of a near-side occupant's lower spine during a side impact. While injury assessments of the lower spine and back are typically conducted utilizing forces and moments [2], lower spine accelerations offer an alternative insight into the low back response during side impacts.

The aim of this study was to develop a multivariable model to predict peak lateral thoracolumbar acceleration from peak lateral vehicle acceleration and lateral vehicle ΔV. This model would assist forensic biomechanists and safety experts in obtaining lower spine kinematics when presented with crash dynamics.

**Methods:** Occupant lateral lower spine and vehicle data from near-side impacts were collated from the National Highway Traffic Safety Administration (NHTSA) crash tests [4]. Data were limited to a principal direction of force of 270° ± 15°, and to occupants wearing a 3-point seatbelt. All impact tests in the data set utilized anthropomorphic test devices (ATDs) seated in the left front seat or left rear seat. All lower spine data from the ATDs were measured from their T12 vertebrae, which is generally considered as the thoracolumbar region. A multivariable regression was created in SPSS to model peak lower spine acceleration ($a_{spine}$) as a linear function of peak lateral vehicle acceleration ($a_v$) and lateral vehicle ΔV. The regression was set with a 0-intercept based on the assumption of a motionless lower spine at 0 g of vehicle acceleration and 0 km/h ΔV. Regression coefficients were evaluated for statistical significance using an alpha level of 0.05. The multivariable model's performance was evaluated by its adjusted $R^2$ value. A plot was created for the multivariable model using web-based plotting software [5].

**Results and Discussion:** Five hundred sixty-one near-side impacts were collected from NHTSA for analysis. Figure 1 exhibits a positive regression for $a_{spine}$, $a_v$, and lateral vehicle ΔV, during near-side impacts (N = 561, Adj. $R^2$ = 0.898). The regression analysis indicated that both $a_v$ and lateral vehicle ΔV were significant predictors ($p < 0.001$) of $a_{spine}$. The data set was limited to a range of 9.85-74.76 g for $a_v$, and 12.63-59.63 km/h for ΔV, suggesting a wide application of the model when given both variables. In this study, the data displayed a strong fit to the multi-variable model as indicated by the goodness-of-fit (Adj. $R^2$ = 0.898). The vehicle ΔV coefficient was reported to be approximately threefold that of the vehicle acceleration which suggests that vehicle ΔV has a greater influence on lower spine acceleration.

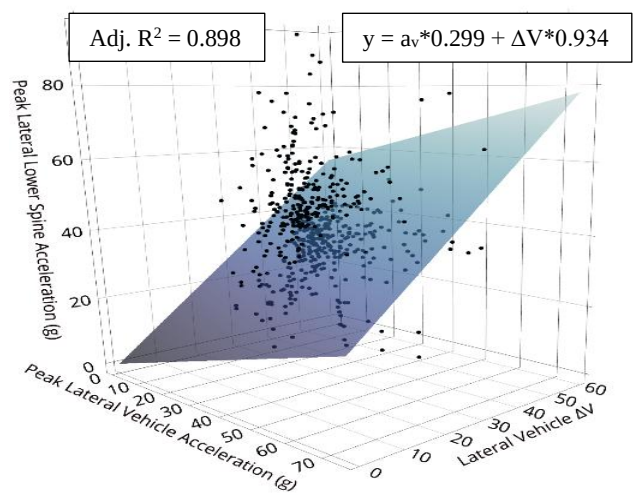


**Figure 1:** $a_{spine}$ in near-side impacts.

Prior literature on near-side impacts that include the lower spine response either report insufficient data [1] or do not report lower spine accelerations [2-3]. The current study addresses these limitations by collecting crash test reports, allowing for near-side data to be analyzed. These crash tests, however, utilized ATDs that lack the muscular resistance to vehicle impact observed in volunteer subjects [1], potentially leading to differing kinematic responses between the two occupant types.

The data analyzed for the current model were measured in the thoracolumbar region, at the T12 vertebra, whereas previous models of low back kinematics have primarily focused on the lumbar spine [6, 7]. However, the lower thoracic spine transitions structurally to that of the lumbar spine [8], therefore, a similarity in motion between T12 and the upper lumbar spine can be postulated.

**Significance:** This multivariable model will enable forensic biomechanists to predict an occupant's lateral lower spine acceleration based on a vehicle's acceleration and change in velocity during near-side impacts. This study provides insight into the potential risk of lower spine injuries across a range of impact severities. While the model's broad spectrum of impact severities concerning $a_v$ and lateral vehicle ΔV is insightful, its limitation to ATD data should be noted. Future investigations should incorporate post-mortem human subjects to observe the effects of near-side impacts on human structures and the injuries they may sustain.

**References:** [1] Furbish (2019), *WCX 2019*; [2] Toney-Bolger et al. (2020), *WCX 2020*; [3] Fugger (2002). *SAE 2002*; [4] NHTSA Database; [5] Plotly Chart Studio; [6] Caraan (2024) *CSB 2024*; [7] Westrom (2024) *ASB 2024*; [8] White (1990) *ISBN: 0397507208*

# A KINEMATIC COMPARISON OF LUMBAR SPINE AND PELVIC ACCELERATION IN IIHS REAR-END SLED TESTS

*Keya Zambare[1], John Adam Caraan[1], Clyde Westrom[1], Kevin Adanty[1], Sean D. Shimada[1]
[1]Biomechanical Consultants
*kszambare@ucdavis.edu

**Introduction:** Occupant kinematics during motor vehicle impacts are frequently studied to determine injury risk. During rear-end impacts, it is known that an occupant's rearward motion is restrained to an extent by the seatback [1], [2], [3], intuitively influencing an occupant's lumbar and pelvic acceleration. A close coupling between the lumbar and vehicle acceleration has been reported [4], while the pelvic acceleration has been previously reported to be higher [3]. Despite several studies exploring occupant lumbar and pelvic kinematics during motor vehicle collisions, there remains a dearth of research concerning the relationship between these two adjacent regions. In some cases, the pelvic and lumbar accelerations have been used interchangeably [5], further contributing to a decrease in understanding of how the two regions behave during rear-end impacts.

Therefore, the objective of this study was to compare the longitudinal accelerations between the vehicle, lumbar spine, and pelvis during rear-end sled tests. This information will provide a further understanding of occupant responses during rear-end impacts, which may aid biomechanical experts in assessing injury risks.

**Methods:** Rear-end impact sled tests were sourced from the Insurance Institute of Highway Safety (IIHS) TechData database. Tests were filtered to select for rear-end impact tests that measured peak longitudinal lumbar spine, pelvic, and vehicle acceleration. All crash tests utilizing a single BioRID IIg anthropomorphic test device (ATD) seated in the driver's seat with a 3-point belt were included in the analysis. Lumbar spine and pelvic accelerations were collected from the same ATD in each test. The three accelerations were assessed for significant differences with a one-way repeated measures ANOVA with a Greenhouse-Geisser correction ($\alpha$=0.05) using jamovi statistical software. Post hoc comparisons were conducted with a Bonferroni adjustment. Mean peak accelerations and 95% confidence interval error bars were plotted for each of the three accelerations. Peak lumbar spine and pelvic accelerations were also each normalized by peak vehicle acceleration.

**Results & Discussion:** Seven-hundred sixteen rear-end sled tests were identified and collected for data analysis. The data set ranged from vehicle accelerations of 9.47 g to 10.71 g. Figure 1 displays mean values and 95% confidence intervals for vehicle (10.06 ± 0.05 g), lumbar spine (8.36 ± 0.13 g), and pelvic (11.21 ± 0.20 g) accelerations. The conducted ANOVA resulted in significant differences between the three accelerations, ($F(1.80, 1288.15) = 641$, $p < 0.001$). The post hoc test with Bonferroni adjustment revealed significantly different peak accelerations between all three variables ($p<0.001$). The normalized lumbar spine acceleration (0.83 ± 0.19) was found to be lower than the corresponding normalized pelvic acceleration (1.11 ± 0.22).

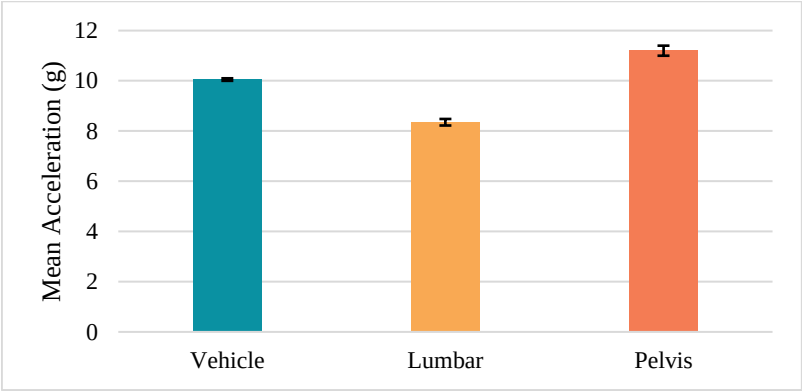


**Figure 1:** Average peak acceleration and 95% confidence interval errors for vehicle, lumbar, and pelvic acceleration (g).

Westrom et al. (2024) found a nearly proportional relationship (linear regression coefficient 1.05) between lumbar spine and vehicle acceleration [4], however, the present study found a significantly lower ratio between these variables (0.83 ± 0.19). This finding may be due to differences in tested vehicle acceleration ranges, as well as occupant types used in each study (human volunteers vs. ATDs). Notably, the present study indicates that pelvic acceleration is indeed greater than vehicle acceleration, consistent with findings reported in prior studies [3], [5].

While lumbar spine and pelvic acceleration were previously assumed to be comparable [5], these findings indicate that the two regions should be analyzed with distinction in future work. A likely reason for the difference in acceleration response between the two regions is the anatomical placement of the BioRID II ATD instrumentation, with accelerometers positioned at L1 and the sacrum, respectively [6]. Different lumbar responses may be observed in the lower regions (L5-S1), so it would be prudent to investigate the entire region in future studies.

**Significance:** This study contributes to present research characterizing lumbar spine, pelvic, and vehicle acceleration in rear-end impacts. Significant differences between lumbar spine and pelvic acceleration indicate that they cannot be considered representative of one another and necessitate individual consideration in low-speed rear-impact testing. Future work should compare lumbar spine and pelvic acceleration across a broader range of vehicle accelerations and various seat types.

**References:** [1] Welcher and Szabo (2001), Accid Anal Prev 33(3):289-304. [2] Szabo et al. (1994), SAE Technical Paper 940532. [3] Parenteau et al. (2022), SAE Int. J. Adv. & Curr. Prac. in Mobility 4(6):2147-2158. [4] Westrom et al. (2024), "Predicting Occupant Peak Lumbar Acceleration in Low-Speed Rear-End Impacts", *ASB 2024*. [5] McCleery et al. (2022), Accid Anal Prev 174:106761. [6] Humanetics (2025), BioRID-II Product Information.

# HEAD CONTACT POINTS AND ACCELERATION DURING VEHICLE COLLISIONS BY IMPACT ANGLE

*Jordan Ogbu Felix[1], Kevin Adanty[1], Sean Shimada[1]
[1]Biomechanical Consultants
*jogbufelix@outlook.com

**Introduction:** Head injury is a common cause of death during motor vehicle accidents [1]. Literature has discussed head biomechanics during vehicle impacts from different impact angles [3] and injuries that frequently occur when the head impacts the vehicle's interior structures [2]. There is also a focus on the resulting head injuries or injury severity when contacting interior structures from different impact angle ranges. [4,5]. However, head acceleration has seldom been assessed when comparing the effect of head contact to different interior structures, despite being an important metric for evaluating head injury risk [6]. Understanding the key head contact points and head accelerations can help biomechanists and safety engineers determine which interior structures may carry a higher potential for head injury during motor vehicle accidents. The study has two main objectives: (1) identify the contact points where an occupant's head impacts during three types of vehicle collisions—frontal, near-side lateral, and near-side oblique; and (2) analyze the peak head acceleration across these impact types to assess any statistical differences. The findings from the analysis can provide valuable insights for optimizing vehicles safety design and reducing head injury risk.

**Methods:** Crash test data was extracted from the National Highway Traffic Safety Administration (NHTSA) Vehicle Crash Test Database. Only sedans, hatchbacks, coupes, and SUVs were included. Occupants were restricted to 50th percentile male anthropomorphic test devices (ATD) positioned in the driver's seat. Peak resultant head acceleration from each crash was normalized by peak resultant vehicle acceleration to account for varying vehicle accelerations during crash testing. The first contact region of the head against interior structures was identified along with the vehicle's angle of impact. Crashes were separated by impact angle into frontal impacts between -15° and 15°, oblique impacts between -30° and -60°, and near-side impacts between -75° and -90°. The peak head accelerations between the impact angles were assessed for significant differences with one-way ANOVA. A post hoc power analysis was conducted to determine if the study had enough power to detect an effect.

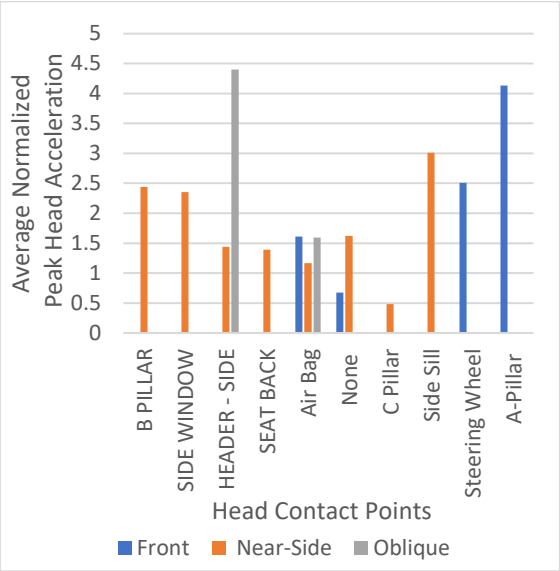


**Figure1:** Average Normalized Average Head Accelerations for head contact points.

**Results & Discussion:** Nine hundred and thirty-three crashes were collected from NHTSA consisting of frontal (n =130), oblique (n=6) and near-side lateral (n=797) impacts. In frontal collisions, the main head contact areas were the airbag and steering wheel, with one scenario involving contact with the A-pillar. Contact with the A-Pillar had the highest normalized head acceleration at 4.13 (Figure 1). For oblique impacts, the highest normalized peak acceleration was 4.40 due to head contact with the side header. In near-side lateral impacts, common head impact locations were the airbag, side header, side window, and B-pillar. The side-sill had the highest average normalized head acceleration of 3.01 (Figure 1). The normalized average peak head accelerations for the frontal, oblique, and near side impacts were 1.45, 2.06, and 1.26, respectively. The ANOVA resulted in no significant differences between the normalized peak head accelerations from frontal, near-side lateral, and oblique impacts ($F(2, 13) = 3.13$, $p = 0.078$, power=0.69).

Our current results suggest that head acceleration did not vary significantly across these different impact angles. The highest average peak acceleration occurred in oblique impacts, indicating that oblique impacts may pose a greater risk of head injuries. However, given the low power of the data, the current analysis would benefit from larger sample size, specifically for oblique impacts which had a few samples. Scenarios where the head struck the airbag yielded lower impact head accelerations than impacts with other interior locations for all impact angles. The B-pillar is a common contact point within side impacts, and given its high head acceleration, and appears to have a high potential for head injury which is consistent with current literature [4,5].

**Significance:** Our findings confirm that peak head acceleration from each contact point differs by impact type. Impact to the A-pillar in frontal impacts, side sill in oblique impacts, and side header in near-side lateral impacts were the contact points with the highest normalized average acceleration. Our findings can contribute to vehicle design research by identifying critical contact locations that should be focused on to reduce forces exerted on an occupant's head. The results provide useful information on head contact points and peak head accelerations in different impact types. Future considerations for our analysis would involve increasing the sample size to detect a true difference in head accelerations between the different impact angles.

**References:**[1] Augenstein, J. et al. (2000). SAE Technical Paper, 2000-01–0634. [2] Schmitt, K.-U. et al. (2019). Trauma Biomechanics: An Introduction to Injury Biomechanics; Springer Nature Switzerland AG. [3] Mackay, M. (1994). Injury, 25: 615–621. [4] Tanczos, R.L. and Shimada, S.D. (2021). Traffic Inj. Prev., S56–S61. [5] Yoganandan, N. et al. (2010). Accid. Anal. Prev., 42: 1370–1378. [7] Jeffs, S.B. et al. (2023). Accid. Anal. Prev., 193: 107303.

# ANKLE AND FOOT BIOMECHNICS DURING PREGNANCY USING MARKERLESS MOTION CAPTURE

Michelle Meyers[1], Afua Nkansah-Andoh[1], Devyn Russo[1], Ke Song, Ph.D.[1], Celeste Durnwald, M.D.[2], Casey Humbyrd, M.D., M.B.E.[1], Josh Baxter, Ph.D.[1]

[1]Department of Orthopaedic Surgery and [2]Department of Obstetrics and Gynecology, University of Pennsylvania, Philadelphia, PA

*Corresponding author's email: meyersm9@seas.upenn.edu

**Introduction:** Musculoskeletal pain is a universal symptom of pregnancy and contributes to increased anxiety and lower quality of life, which can increase perinatal complications [1]. Specifically, 30% of pregnant individuals report experiencing foot/ankle pain [2,3]. Additionally, falls during pregnancy is a huge clinical problem in which 27% of pregnant individuals fall. This population undergoes significant changes during pregnancy including increased body mass, postural adjustment, and circulating hormones that may contribute to musculoskeletal pain and increased risk of falls [4,5,6]. However, movement biomechanics during pregnancy is chronically understudied, and high throughput testing is critical to identify early predictors of pregnancy related pain, disability, and falls. Markerless motion capture is a new technique that allows for participants to wear street clothes and avoid marker placement, therefore, reducing the experimental burden of study participants [7]. The overall goal of this study was to use markerless motion capture to compare ankle kinematics, ankle kinetics, and foot center of pressure displacement path of third trimester pregnant and non-pregnant control participants to identify compensatory ankle and foot mechanisms during gait due to pregnancy. We hypothesized that markerless motion capture will detect differences in ankle and foot biomechanics between the two cohorts.

**Methods:** We recruited a cohort of third trimester pregnant participants (n = 37, gestational week = 35.4 ± 1.4 weeks, age = 33.4 ± 4.7 years) and a cohort of non-pregnant female control participants (n = 19, age = 27.6 ± 3.5 years) with IRB approval and written informed consent. Participants performed six walking trials at their self-selected normal walking speed over a 6-meter distance. We used a high-definition 8-camera markerless motion capture system (Optitrack) to quantify gait biomechanics as we previously described [8]. Specifically, we used commercially available markerless motion capture (Theia 3D) and biomechanical analysis (Visual3D) software to compute lower extremity sagittal inverse kinematics and inverse dynamics for each gait cycle. We used a statistical parametric mapping two-sample t-test (Spmd1, $\alpha = 0.05$) to evaluate ankle kinematics, kinetics, and foot center of pressure displacement.

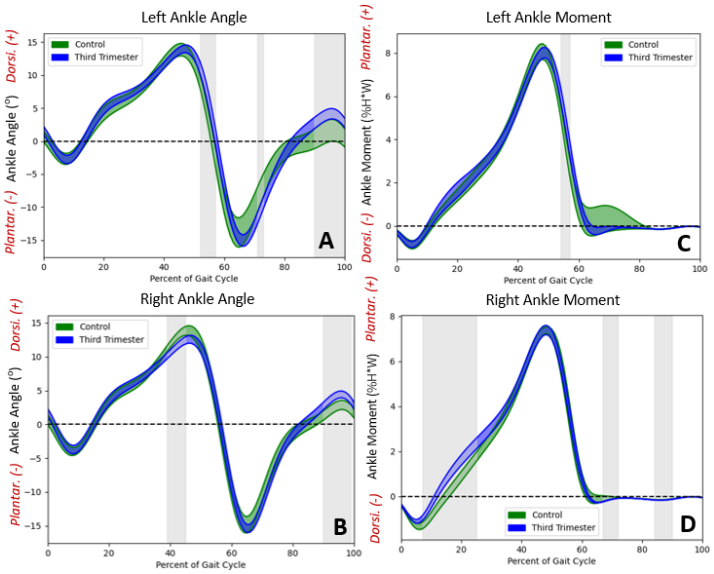


Figure 1. Ankle kinematics of the left (A) and right (B) foot. Ankle kinetics of the left (C) and right (D) foot. **Grey shading represents significant differences between the two cohort**

**Results & Discussion:** We found significant side differences between pregnant participants left and right foot ankle kinematics (43-54%, $p = 0.01$) and kinetics (47-60%, $p < 0.001$, 82-86%, $p = 0.02$, 94-95%, $p = 0.04$), presenting asymmetries in gait that may contribute to increased risk of falls. Additionally, we observed that ankle kinematics differed across the gait cycle (left: 52-57%, $p = 0.04$, 71-73%, $p = 0.04$, 90-100%, $p = 0.02$; right: 30-45%, $p = 0.03$, 90-99%, $p = 0.01$, Figure 1). Increased ankle dorsiflexion during gait aligns with reports from the chronic ankle instability population that shows this compensatory maneuver is utilized to increase stability in the ankle joint [9]. Increased production of the reproductive hormone relaxin and increased mass likely contribute to instability in the ankle joint, therefore causing this compensatory maneuver to occur during pregnancy. Additionally, pregnant individuals experienced increased right ankle plantarflexion moment during midstance (7-25%, $p < 0.001$, Figure 1), likely to support mass distribution and ankle instability while walking. We also found significant differences in left and right foot late stance medial-lateral center of pressure displacement (left: 92-98%, $p = 0.2$; right: 93-100%, 0.04, Figure 2). Throughout the stance phase of gait, we observed a medial shift in medial-lateral foot center of pressure displacement in the third trimester pregnant cohort. These results are potentially caused by the fall of the longitudinal arch of the foot which contributes to pain and discomfort while walking.

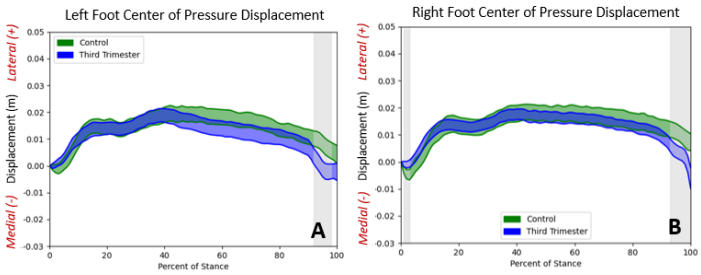


Figure 2. Left (A) and right (B) foot medial lateral center of pressure displacement through stance. **Grey shading represents significant differences between the two cohort**

**Significance:** Markerless motion capture allows us to sample larger patient cohorts by lowering the experimental burden imposed on this population, ultimately increasing our knowledge regarding compensatory gait strategies of the ankle and foot during pregnancy. This opens the door for preventative treatments and specialized musculoskeletal care for pregnant individuals to circumvent pain and falls during everyday actions such as walking.

**Acknowledgments:** We would like to thank the Ruth Jackson Orthopaedic Society (RJOS) and the American Orthopaedic Foot & Ankle Society (AOFAS) for their funding in this project.

**References:** [1] Vignato+2021; [2] Kesikburun+2018; [3] Vullo+1996; [4] Anselmo+2017; [5] Ftizgerald+2015; [6] Kristiansson+1996; [7] Keller+2022; [8] Song+2023; [9] Son+2017.

# FRONTAL PLANE JERK COST AND FLUCTUATION ANALYSIS FOR INDIVIDUALS WITH ACL RECONSTRUCTION AND OSTEOARTHRITIS

Nicholas L. Hunt[1*] and Tyler N. Brown[1]
[1]Boise State University, Boise, ID, USA
*Corresponding author's email: nichunt@u.boisestate.edu

**Introduction:** Following ACL injury and subsequent reconstruction (ACL-R), altered neuromuscular function and control may accelerate knee osteoarthritis (OA) development [1]. Assessing knee jerk, or the third time derivative of knee joint angle, following joint injury and disease may provide valuable insight into underlying gait neuromuscular control and joint loading that may contribute to long-term degenerative joint disease. Jerk cost and fluctuation analysis in both the time and frequency domain may effectively assess smoothness of knee joint motion and provide a biomechanical measure of dynamic neuromuscular control at the joint. We hypothesize that individuals with ACL reconstruction (ACL-R) and radiographic knee OA will exhibit "jerkier" knee motion with increased fluctuations in the frontal plane compared to healthy age-matched controls particularly during early stance loading of the joint.

**Methods:** Four cohorts (1: 14 ACL-R, 2: 14 young adult controls, 3: 9 radiographic knee OA and 4: 9 older adult controls) had knee biomechanics quantified during a 10-meter self-selected walk. During each walk, synchronous 3D marker trajectories and GRF data were collected using ten high-speed optical cameras and a single force platform. Marker and GRF data were lowpass filtered (12 Hz, 4$^{th}$ order Butterworth), and processed in Visual3D to obtain knee joint biomechanics.

Using filtered marker data, frontal plane jerk was calculated as the third time derivative of knee abduction-adduction angle from 0% to 100% of stance phase, while jerk cost was determined as the area under the logarithmically transformed jerk-time curve according to [2]. Then, peak, minimum, and range (peak minus min) of frontal plane jerk during stance as well as jerk cost during weight acceptance (initial contact to peak knee flexion angle) and full stance phase (0% to 100%) were quantified.

For fluctuation analysis, the jerk-time curve was submitted to a fast-Fourier transform to obtain the signal power spectral density (PSD). From the obtained PSD, mean, median, and peak power frequency (PPF) as well as total power of the signal were calculated. Specifically, mean frequency is the weighted average frequency of the signal, median frequency splits the area under the PSD curve into two equal parts, PPF was determined as the frequency with the highest power, and total power is the area under the PSD curve. Magnitude of fluctuations were calculated as the coefficient of variance (CV, $\partial/\mu$) of the jerk-time curve.

Jerk measures from the time and frequency domain were submitted to a one-way ANOVA to assess cohort (ACL-R, OA, and age-matched controls) differences.

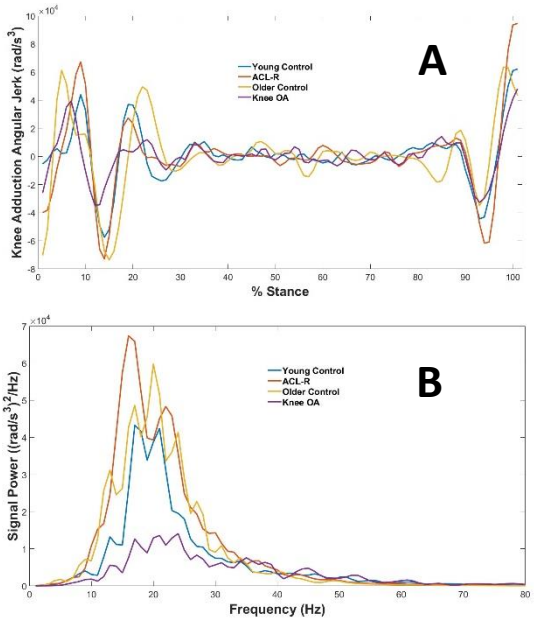


**Figure 1:** (**A**) Mean jerk-time curve and (**B**) mean power spectral density by cohort.

**Results & Discussion:** In partial agreeance with our hypothesis, we found significant cohort differences for time and frequency domain jerk measures. Specifically in the time domain, the ACLR and OA cohorts exhibited greater minimum and peak jerk than the older adult controls (all: $p<0.006$). The OA cohort exhibited significantly greater peak jerk compared to the young adult controls ($p=0.037$), while the ACLR cohort also exhibited significantly smaller jerk range than the young adult controls ($p=0.004$). Greater peak and minimum jerk in the clinical cohorts may indicate jerkier knee motion with more abrupt changes in knee positioning than they older adult controls. Further, the ACLR and OA cohorts exhibited significantly larger full stance jerk cost than the older adult controls ($p=0.003$ and $p=0.001$, respectively) while the OA cohort exhibited significantly greater weight-acceptance jerk cost than the older adult controls ($p=0.013$) indicative of less smooth knee motion particularly during early stance as the knee joint is loaded.

In the frequency domain, the ACLR and OA cohorts exhibited significantly smaller mean frequency than the young and older adult controls (all: $p<0.039$), and significantly smaller median frequency than the older adult controls ($p=0.004$ and $p=0.010$, respectively). Although the reduction in fluctuation frequency in the jerk waveform suggest the ACLR and OA cohorts restrict gait to stabilize the joint and protect from further injury, future research is necessary to understand the relationship between fluctuation content and neuromuscular control during gait.

**Significance:** These results provide valuable insight on neuromuscular control in individuals with ACL-R and OA during walking. Individuals with ACL-R and OA may exhibit harmful "jerkier" knee biomechanics and concurrently restrict frontal plane knee motion to protect the joint from further injury. Altered frontal plane jerk, particular during weight acceptance, may indicate altered neuromuscular control and contribute to cartilage loading that elicits knee OA development or progression. Thus, clinicians need to include rehabilitation that targets smoothness of knee motion to facilitate better neuromuscular control in ACL-R and OA populations.

**Acknowledgments:** NIH NIA (R15AG059655) and NIH NIGMS (2U54GM104944, P20GM109095, P20GM148321) supported this work.

**References:** [1] Tayfur et al. (2021), *Sports Medicine* 51. [2] Krammer et al. (2018), *Gait & Posture* 84.

# SIDE-STEPPING DOES NOT INCREASE INTACT KNEE MOMENTS IN BONE-ANCHORED PROSTHESES USERS COMPARED TO STRAIGHT-LINE WALKING

*Maliheh Fakhar[1], Jenna K Burnett[2], John R Pope[1], Gauri A. Desai[1], Ross H Miller[1], Jae Kun Shim[1]
[1]University of Maryland, School of Public Health, Kinesiology Department
[2]University of Utah, College of Health, Department of Health and Kinesiology
*Corresponding author's email: mfakhar@umd.edu

**Introduction:** The prevalence of intact knee osteoarthritis (OA) is greater among individuals with unilateral lower limb loss than the general population [1], potentially due to heavy reliance on the intact limb during walking [2]. Bone-anchored prostheses (BAP) have emerged as an alternative to traditional socket-suspended prosthetics [3], notably, decreasing intact-limb joint loading during walking [4]. However, the biomechanical risk factors associated with knee OA, such as knee adduction (KAM) and flexion moments (KFM) [5,6], remain understudied in transfemoral BAP users, particularly during functional movements beyond straight-line walking. For instance, side-stepping is frequently performed to avoid collisions in public environments [7] and may impose unique mechanical demands on the knee. As side-stepping involves lateral movement of both the leg and the center of mass, its muscle activation pattern differs from that of straight-line walking, potentially resulting in distinct joint loading. Since knee OA develops due to cumulative mechanical loads on cartilage [8], it is critical to assess the contribution of side-stepping to OA development. This study aimed to examine differences in intact limb KAM and KFM between side-stepping and straight-line walking in transfemoral BAP users. Given that side-stepping involves lateral in addition to sagittal-plane motion, we hypothesized that KAM would be greater during side-stepping than preferred walking, while KFM would remain comparable between the two movements.

**Methods:** Eight transfemoral BAP individuals (3*F*; 46±7.98*yrs;* 1.70±0.12*m*; 68.11±17.91*kg*) performed straight-line walking and walking with a sidestep on force plates at preferred speed while motion capture and ground reaction force data were recorded. Walking speed and sidestep width were not prescribed to replicate the natural execution of the task in daily activities. Averaged intact limb KAM and KFM waveforms, calculated through validated inverse dynamic pipelines in Visual3D (HAS Motion, CA), then normalized to body weight, height, and stance time, were compared between side-stepping and straight-line walking using 1D paired statistical nonparametric mapping ($\alpha = 0.05$) with a Bonferroni correction applied.

**Results & Discussion:** Intact limb KAM and KFM (Figure 1) did not differ between straight-line walking and side-stepping during the stance phase, partially supporting our hypothesis. This null finding may be explained by low functional demands of the side-stepping task and could have differed if a higher walking speed or a wider step width had been prescribed. It is noteworthy that the average center-of-mass velocities were not different between conditions (p = 0.38). These findings suggest that while side-stepping may contribute to knee OA in BAP users, its risks are not greater than those associated with straight-line walking at a preferred speed.

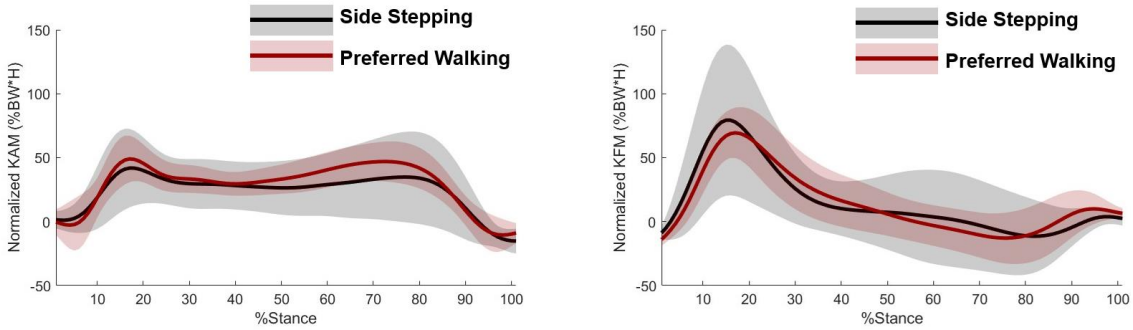


**Figure 1:** Statistical nonparametric mapping of KAM and KFM during preferred walking and walking with a sidestep; results do not show any differences during stance at significance level $\alpha = 0.05$ with Bonferroni correction.

**Significance:** Side-stepping may impose knee joint loads similar to straight-line walking, resulting in similar contributions to knee OA risk from both straight-line walking and side-stepping. Investigating the cumulative impact of various daily activities beyond walking is crucial for understanding their relative contribution to OA development and progression.

**Acknowledgments:** This study was supported by the CDMPR award number W81XWH-21-1-0423.

**References:**

[1] Struyf et al. (2009), *Arch. Phys. Med. Rehabil.*, *90*(3). [2] Nolan & Lees (2000), *Prosthet. Orthot. Int*, *24*(2).
[3] Hagberg et al. (2008), *Psychoprosthetics.* Springer London. [4] Vandenberg et al. (2023), *J. Biomech.*, *155*.
[5] Amin et al. (2004), *Arthritis Care Res.*, *51*(3). [6] Chehab et al. (2014), *Osteoarthritis Cartilage*, *22*(11).
[7] Boulo et al. (2025), *Exp. Brain Res.*, *243*(2) [8] Felson, D. T. (2013). *Osteoarthr Cartil.*, *21*(1).

# LONG-TERM STRENGTH DEFICITS POST-ACLR IMPACT HIGHER-DEMAND TASK PERFORMANCE

*Camille C. Johnson, Tereza Janatová, Meredith K. Owen, Brian Noehren[1]
[1]Biomoton Lab, Department of Physical Therapy, University of Kentucky, Lexington, KY, USA
*Corresponding author's email: Camille.Johnson@uky.edu

**Introduction:** Restoring normal knee movement and quadriceps strength is fundamental to post-operative management following an anterior cruciate ligament reconstruction (ACLR). While short-term gait impairments are well-known [1,2], there is a lack of robust literature characterizing the resolution of strength and movement impairments over longer follow-up. Furthermore, it remains unknown how strength deficits between the involved and non-involved limb affect biomechanics during tasks with increasing levels of quadriceps involvement. The goal of this study was to quantify long-term strength and biomechanical deficits during activities with different levels of demand in individuals >2 years post-ACLR. We hypothesized that between-limb biomechanical differences exist for higher-demand tasks (run, jump), but not lower-demand tasks (walk). Our secondary aim was to determine if strength asymmetries correlate with biomechanical asymmetries. We hypothesized that greater strength asymmetry is correlated to greater biomechanical asymmetry.

**Methods:** Thirty-six adults (24 F, age: 25.9±8.4 years, height: 1.71±0.11 m, weight: 76.51±14.58 kg, BMI: 26.04±3.32 kg/m$^2$) consented to participate in this IRB-approved study. Participants were 6±4 years post-ACLR (range: 2-21 years). Fifty-two reflective markers were placed on the trunk and lower extremities (27 anatomical landmarks, 25 tracking markers) and sagittal plane knee kinematics were collected at 200 Hz using a 13-camera motion capture system (Motion Analysis Corp, CA). Vertical ground reaction forces were simultaneously collected at 2000 Hz from two force plates within the instrumented treadmill (Bertec Corp., OH). All participants performed a static calibration, followed by four dynamic tasks. For the treadmill tasks, participants walked and ran (walk: 1.5 m/s, run: 3.0 m/s) for 10 seconds. Five strides per limb were extracted. Each participant then completed four double-leg countermovement jumps (DL CMJ) and four single-leg countermovement jumps (SL CMJ) on each limb. Knee extensor strength was assessed via four maximum voluntary isometric contractions per limb (90° flexion, 5 second hold, sampling frequency: 100 Hz) (Biodex Medical Systems, NY).

All data were filtered using a 4$^{th}$ order Butterworth low-pass filter with activity-specific cutoff frequencies. Sagittal plane knee flexion excursion, knee extension moment, and knee joint power were computed in Visual 3D and averaged across all trials for each task for each participant. Internal knee extension moment and power were normalized to participant height * mass. Peak knee extensor torque and rate of torque development (RTD) from each trial were averaged per participant. Data were assessed for normality using a Shapiro-Wilk test and either paired t-tests or Wilcoxon signed rank tests assessed between-limb differences in strength and biomechanics. Absolute side-to-side differences (SSD) were calculated. Spearman's correlation assessed relationships between SSD in strength and SSD in biomechanical variables with significant between-limb differences. Significance was set at p<0.05 for all tests.

**Results & Discussion**: The involved limb had 0.19 Nm/kg lower peak extensor torque and 1.10 Nm/(kg*s) slower RTD than the non-involved limb. Between-limb biomechanical differences were found during all four activities (Table 1). There were no significant relationships between SSD in strength and SSD in walk or run biomechanics. During SL CMJ, SSD in RTD correlated with SSDs in extensor moment (CON: p=0.04, r=0.357) and power generation (CON: p=0.004, r=-0.486). SSD in peak extensor torque correlated with SSD in power absorption (LAND: p=0.03, r=0.364). During DL CMJ, SSD in peak extensor torque correlated with SSDs in extensor moment (CON: p=0.04, r=0.356) and power generation (CON: p=0.01, r=0.433).

**Table 1:** Absolute mean differences (± SD) in knee biomechanics between involved (INV) and non-involved (NON) limbs. Jumps phases are concentric (CON) or landing (LAND). ***** indicates p<0.05.

| | *Walk* | *Run* | *SL CMJ* | | *DL CMJ* | |
|---|---|---|---|---|---|---|
| | | | *CON* | *LAND* | *CON* | *LAND* |
| *Knee Excursion (°)* | 1.6±2.6 ***p=0.001** INV<NON | 2.2±3.2 ***p<0.001** INV<NON | 1.6±8.6 p=0.27 | 3.9±6.5 ***p=0.001** INV<NON | 2.6±4.5 ***p=0.002** INV<NON | 2.1±4.0 ***p=0.005** INV<NON |
| *Knee Extensor Moment (N*m/(kg*m))* | 0.02±0.11 p=0.23 | 0.09±0.15 ***p=0.002** INV<NON | 0.05±0.13 ***p=0.03** INV<NON | 0.08±0.23 p=0.06 | 0.08±0.11 ***p<0.001** INV<NON | 0.13±0.24 ***p=0.002** INV<NON |
| *Power Absorption (W/(kg*m))* | 0.11±0.31 ***p=0.03** INV<NON | 0.76±1.21 ***p=0.001** INV<NON | 0.27±0.71 p=0.05 | 1.36±2.28 ***p=0.001** INV<NON | 0.01±0.52 p=0.94 | 1.26±2.24 ***p<0.001** INV<NON |
| *Power Generation (W/(kg*m))* | 0.16±0.32 ***p<0.001** INV<NON | 0.21±0.57 p=0.05 | 0.32±0.79 ***p=0.03** INV<NON | 0.04±0.17 p=0.05 | 0.07±0.85 ***p<0.001** INV<NON | 0.09±0.31 p=0.07 |

Contrary to our first hypothesis, our results demonstrate that long-term deficits in strength, gait, and jump biomechanics exist post-ACLR. If left unaddressed, these impairments may alter joint loading and contribute to eventual cartilage injury in the overloaded limb [3,4]. However, residual quadriceps strength asymmetry does not impact walk or run asymmetry. Targeting neuromuscular control to restore gait symmetry post-ACLR may be more effective than quadriceps strengthening long-term. Confirming our second hypothesis, greater strength asymmetry was related to greater moment and power asymmetries during jumps. This suggests targeted interventions to equalize quadriceps strength may prevent unequal joint loading during higher-demand activities, facilitating improved function.

**Significance:** Post-ACLR deficits in strength and function do not resolve at long-term follow-up. Asymmetries in quadriceps strength may increase loading asymmetries during higher-demand tasks such as countermovement jumps, increasing re-injury risk. Rehabilitation practices should focus on minimizing between-limb differences early in the recovery process.

**References:** [1] Arhos et al., *AJSM*, 2020, 49(2). [2] Knurr et al., *AJSM*, 2023, 51(12). [3] Erhart-Hledik et al., *JOR*, 2018, 36(5). [4] Erhart-Hledik et al., *JOR*, 2019, 37(7).

**Gait differences between fallers and non-fallers in people with knee osteoarthritis**

Joy O. Itodo, Steven A. Garcia, Oiza Peters, Paige Perry, Ogundoyin Ogundiran, Kharma C. Foucher
Biomechanics and Clinical Outcomes Laboratory, University of Illinois, Chicago
jitodo2@uic.edu

**Introduction:** People with knee osteoarthritis (OA) fall more frequently and at younger ages than people without knee OA[1]. Knee OA may heighten risk factors for walking-related falls, such as joint instability. People with knee OA walk with characteristic abnormalities in gait mechanics, such as lower speeds, higher knee adduction moments (KAM), and lower knee flexion moments (KFM). It is not known whether these abnormalities are further amplified in people with knee OA who experience falls. Gait mechanics associated with falls have been more widely studied in healthy older adults. These studies have linked falls to temporal-spatial characteristics such as shorter step lengths [2] and slower walking speeds[3]. Still, it is not known whether these same gait characteristics also differ in fallers and non-fallers with knee OA.

The purpose of this study was to specifically compare the biomechanical gait characteristics of fallers and non-fallers in people with knee OA. Understanding these differences may help identify key biomechanical gait factors associated with fall risk in people with knee OA and inform targeted interventions to improve stability and prevent falls. We hypothesized people with knee OA who report a fall in the past year exhibit alterations in temporal-spatial, kinematic, and kinetic variables compared to those without a history of falls.

**Methods:** We categorized 34 people with knee OA (Female = 20, age = 56 ± 9 years, height = 1.7 ± 0.1 m, mass = 100.5 ± 21.9 kg) into fallers and non-fallers based on the question: "Have you experienced a fall in the past 12 months?" Walking trials were conducted on an instrumented split-belt treadmill at each participant's preferred speed. Temporal-spatial parameters included step length, step width, cadence, and kinetic and kinematic metrics, including the first and second peak external KAM (KAM1, KAM2) during the stance phase, external KFM from the first half of the stance phase, and sagittal plane knee ROM during the gait cycle. These variables were selected because of either their association with knee OA or falls in older adults. Kinetic variables were normalized with the product of mass (kg) and height (m). The average from 10 clean steps was used for further analyses. Statistical analyses were conducted using SPSS v29. We used independent t-tests to compare fallers and non-fallers with knee OA ($\alpha = 0.05$). We also estimated effect sizes using Cohen's d, because of the small sample size (low: 0 - 0.2, moderate: 0.3 – 0.7, high: ≥ 0.8).

**Results & Discussion:** Ten participants (29%) were categorized as fallers. Fallers had a significantly lower body mass (85.86 ± 17.38kg) than non-fallers (106.64 ± 20.91kg; $p = 0.009$). Age, height, and the proportion of women were similar between groups ($p \geq 0.073$). Most temporal-spatial variables were not statistically different at the 0.05 level between groups (Table 1). However, cadence was 11% higher in fallers with a moderate effect size despite walking speeds that were not statistically significantly different (albeit a moderate effect size). Step width was lower in fallers, with a moderate effect size as well. There were no statistically significant differences between fallers and non-fallers in kinematic or kinetic variables. KAM2 was slightly lower in fallers with a moderate effect size, but the small difference is unlikely to be clinically meaningful.

The hypothesis of differences in gait variables between groups was partially supported. The most notable finding was that fallers walked at similar speeds but with higher cadence than non-fallers. This is in line with a previous study that reported that a fast cadence increases the risks of falls in older adults over the age of 75 [4]. Contrary to our hypothesis, none of the selected kinematic and kinetic variables typically associated with knee OA differed between fallers and non-fallers. Together, these results may suggest that the gait factors that predispose people with knee OA to falls are not different from those that predispose older adults to falls, although they may appear at earlier ages in people with knee OA. More work is needed to determine whether gait differences in cadence and other biomechanical metrics are a consequence of knee OA or a contributing factor to falls in people with knee OA.

**Significance:** There is a need for gait retraining programs to optimize step patterns to reduce fall risk in people with knee OA, informed by studies such as this one comparing gait in fallers and non-fallers with knee OA. As a first step, we investigated select variables associated with knee OA and/or falls in older adults, and the study showed that cadence may be a potential target variable for further investigation.

**Table 1.Comparison of Gait Variables Between Fallers (n=10) and Non-Fallers (n=24) with Knee Osteoarthritis.**

| | Walking Speed(m/s) | Step Length(m) | Cadence (steps/min) | Step Width(m) | KAM1 (Nm/kg*m) | KAM2 (Nm/kg*m) | KFM (Nm/kg*m) | Knee Sagittal Plane ROM(°) |
|---|---|---|---|---|---|---|---|---|
| **Fallers** | 0.59 ± 0.23 | 0.36 ± 0.11 | 99.15 ± 16.49 | 0.16 ± 0.04 | 0.54 ± 0.26 | 0.48 ± 0.29 | 0.43 ± 0.20 | 45.99 ± 10.04 |
| **Non-Fallers** | 0.46 ± 0.31 | 0.34 ± 0.09 | 88.71 ± 12.11 | 0.19 ± 0.05 | 0.52 ± 0.26 | 0.49 ± 0.26 | 0.38 ± 0.25 | 47.35 ± 12.30 |
| **P-value** | 0.163 | 0.533 | 0.048† | 0.067 | 0.934 | 0.443 | 0.530 | 0.760 |
| **Cohen's d** | 0.476 | -0.237 | -0.774 | 0.713 | 0.034 | 0.368 | -0.239 | -0.116 |

**Acknowledgments:** Pilot funding through UL1TR002003

**References:** [1] Wilfong et al., 2023, Arthritis Care Res; [2] Kwon et al., 2018 Technol Health Care [3] Auvinet et al., 2003, Journal of Aging and Physical Activity. [4] Shimada *et al.*, 2010, J Phys Ther Sci.

**Comparison of ankle kinematics between inertial measurement units and 3D optical motion capture system in various walking conditions**

Jongsu Kim[1], Lingchao Xie[1], *Sanghyun Cho[1]
[1] Surface Electromyography Laboratory, Department of Physical Therapy, College of Health Science, Yonsei University
*Corresponding author's email: fastcloud@yonsei.ac.kr

**Introduction:** Ankle kinematics is crucial in gait analysis, offering valuable insights for clinical rehabilitation, injury prevention, and biomechanical assessment. [1] In this regard, 3D optical motion capture system (OMCS) is widely recognized as the gold standard for the precise measurement of ankle kinematics. However, its practical use is limited due to high cost, excessive markers, complex data processing, and difficulty in using outside the laboratory. Due to these limitations, inertial measurement units (IMUs) have proposed as an alternative to OMCS. [2] While IMUs offer advantages to some of the limitations of OMCS, research on ankle kinematics using IMUs has been predominantly focused on the sagittal plane and limited to level walking in controlled laboratory environments. Such a unidirectional approach may disrupt the accurate biomechanical interpretation of common ankle problems in daily activities. [3] Thus, a comprehensive 3-plane motion analysis is essential to ensure more accurate interpretation, and incorporating various environments is necessary to expand the applicability of sensors in real-life conditions. To this end, this study aims to evaluate and determine the reliability and validity of ankle kinematics from IMUs in all planes of motion under diverse conditions by comparing with OMCS.

**Methods:** Twelve healthy young participants (6 males and 6 females) were recruited, and the sample size was determined using power 1d analysis. [4] Marker setup and sensor placement followed the reference studies. [1, 2] Participants walked on a level floor, an inward tilt wedge, and an outward tilt wedge. Each participant completed 10 walking trials for each condition. Kinematics of ankle joint were recorded by OMCS (Vicon Motion Systems, Oxford, UK) and IMUs (Ultium Motion, Noraxon, AZ, USA). Gait events were detected by gyroscopes in an electromyography (EMG) sensor (Ultium EMG, Noraxon, AZ, USA).

IMUs data were processed using MR software, and gait events were detected through EMG data. Data from the OMCS were processed using Vicon Nexus software, and gait events were detected through synchronization with IMU data. The Institute of Rizzoli foot model (IOR foot model) was used to process raw data from Vicon Nexus software and calculate ankle kinematics using Python. [1] Paired t-test using Statistical Parametric Mapping (SPM), which allows for a more detailed comparison and analysis of continuous data, was performed using Python to evaluate the validity of IMUs by comparing with the OMCS. [5] Intraclass correlation coefficient (ICC) (1,1) model was used to assess the reliability of IMUs in all three planes under each condition. [3]

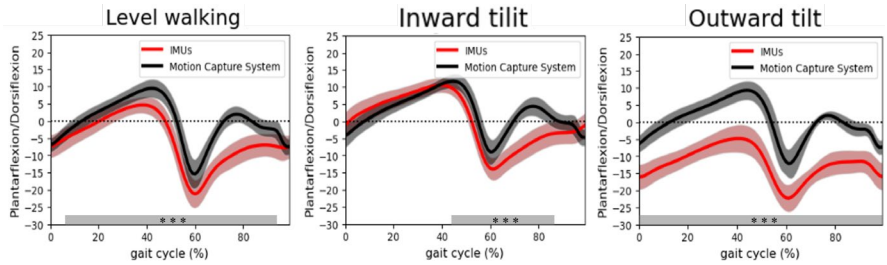


**Figure 1:** Comparison of ankle angle between IMUs and OMCS in sagittal plane at each condition. The gray bar indicates sections with statistically significant differences, and *** denotes $p < 0.001$

| ICC (95% Confidence Interval) | | Plane | | |
|---|---|---|---|---|
| | | Sagittal | Transverse | Frontal |
| Condition | Level walking | 0.982 (0.977-0.987) | 0.976 (0.968-0.982) | 0.973 0.965-0.980) |
| | Inward tilt | 0.986 (0.987-0.990) | 0.961 (0.949-0.972) | 0.954 (0.940-0.966) |
| | Outward tilit | 0.953 (0.938-0.965) | 0.933 (0.912-0.951) | 0.958 (0.945-0.969) |

**Table 1:** ICC of IMUs across all three planes under each condition, with 95% Confidence Intervals (CI).

**Results & Discussion:** The ankle kinematics in all three planes during level walking measured by OMCS and IMUs were consistent with the previous studies (Fig. 1). [1,6] When walking on an inward tilt, IMUs demonstrated higher push-off values in the sagittal and transverse planes but lower values during early and terminal swing in the frontal plane. On the other hand, outward tilt resulted in consistently higher sagittal-plane values without notable dorsiflexion, and higher measurements in the frontal and transverse planes during the stance and late swing phases, compared to the motion capture system ($p < 0.001$). These differences in ankle kinematics can be attributed to the fundamental differences in coordinate system framework. OMCS utilizes a marker-based coordinate system, allowing for immediate updates in marker positions in response to environmental changes, whereas IMUs rely on relative sensor data, which tends to preserve existing motion patterns despite external perturbations. This reliance on relative sensor data likely contributed to the high reliability (ICC > 0.75) observed in IMU measurements by minimizing the impact of external variations on movement. Following the same calibration process and performing the same task under identical conditions is expected to maintain a high level of consistency.

**Significance:** When comparing ankle kinematics with OMCS, significant results were observed primarily during level walking. Accordingly, when analyzing each plane using IMUs alone, it is possible to compare multiple participants within the same condition across various environments and to conduct pre-post comparisons within individuals. This suggests that IMUs can be effectively utilized in clinical studies to derive meaningful results

**References:** For example: [1] Leardini, A., et al. (2007), *Gait & posture*, *25*(3) 453-462; [2] Park, et al. (2021), *Sensors*, *21*(11), 3667; [3] Poitras, et al. (2019), *Sensors*, *19*(7), 1555; [4] Pataky, T. C. (2017), *PeerJ Computer Science*, *3*, e125; [5] Pataky, T. C. (2010), *Journal of biomechanics*, *43*(10), 1976-1982; [6] Bauer, L., et al. (2024), *BMC Musculoskeletal Disorders*, *25*(1), 606.

# EFFECT OF TREADMILL TRAINING ON JOINT KINEMATICS IN INFANTS WITH DOWN SYNDROME

* Yeon-Joo Kang[1], Robert Zeid [1], Alexandre dos Santos Kotarski[1], Amy Talboy [2], Seyda Ozcaliskan[1], Jianhua Wu[1]
[1]Georgia State University, [2]Emory University
*Corresponding author's email: ykang@student.gsu.edu

**Introduction:** Down syndrome (DS) is a genetic condition characterized by development delays compared to typically developing infants. Studies have shown that treadmill intervention can promote an earlier walking onset and improve walking pattern in infants with DS [1]. Previous research has shown that infants with DS who underwent the higher-intensity treadmill training displayed more advanced timing and magnitude of peak joint angles than those in the low-intensity training group [2]. However, it remains unclear to what degree joint kinematic patterns differ over the entire gait cycles between those with and without treadmill training. This study aimed to examine the effect of treadmill training on joint kinematics in infants with DS. We hypothesized that infants with DS who received the treadmill training (i.e., the experimental group) would demonstrate more advanced joint kinematic patterns, specifically in terms of timing, than those who did not receive the training (i.e., the control group) although both groups would show improvements.

**Methods:** Eleven infants with DS (6 in the experimental group and 5 in the control group) participated in a gait assessment at T1 and T2 (about 2 months and 8 months after walking onset, respectively). For the experimental group, the parents administered the treadmill intervention in their homes for 8 min/day, 5 days/week, with a belt speed starting at 0.1 m/s and increasing over time until the infants walked three steps independently. On average, it took about 10 months to complete the treadmill training for the experimental group. We used a 9-camera Vicon motion capture system and the Vicon lower-body model to collect the gait data when the infant walked barefoot over a 6-m walkway in our lab. The marker data were processed using the Vicon Nexus software and sagittal plane hip, knee and ankle joint angles were calculated via Vicon plug-in gait model. Peak flexion and extension angles for the hip, knee, and ankle joints were identified and the range of motion (ROM) for each joint was determined as the difference between peak flexion and extension. Two-way (2 group × 2 time) mixed ANOVA was conducted on peak joint angle, ROM and the timing of peak angles. For all statistical processes, R package 'afex' and 'emmeans' were used. A significance level was set as alpha = 0.05.

**Table 1**
Mean (SD) of peak joint angles (in degree) and timing of the peak joint angles and toe-off (in % gait cycle) and statistical results.

| | Training | | Control | | 2 Group X 2 Time | Experimental (T2) vs Control (T1) |
|---|---|---|---|---|---|---|
| | T1 | T2 | T1 | T2 | | |
| Peak hip flexion angle | 35.8 (6.2) | 44.6 (11.7) | 31.2 (3.8) | 42.3 (7.8) | $F(1,9) = 7.43$, $P = 0.023$ | |
| Peak hip extension timing | 44.8 (5.2) | 49.2 (2.5) | 43.6 (4.3) | 49.6 (3.7) | $F(1,9) = 6.92$, $P = 0.027$ | $t(9) = 2.44$, $P = 0.037$ |
| Peak knee extension timing | 60.8 (14.2) | 58.6 (8.1) | 64.5 (13.1) | 61.4 (22.7) | $F(1,9) = 30.36$, $P < 0.001$ | $t(9) = 2.53$, $P = 0.032$ |
| Peak ankle dorsiflexion timing | 44.3 (7.1) | 56.4 (11.6) | 46.6 (9.9) | 57.0 (10.8) | $F(1,9) = 5.71$, $P = 0.041$ | |
| Toe-off | 64.9 (6.98) | 57.1 (4.07) | 66.7 (6.24) | 56.9 (6.89) | $F(1,9) = 22.5$, $P < 0.001$ | $t(9) = 2.92$, $P = 0.015$ |

**Results & Discussion:** Both groups increased peak hip flexion angle and peak hip extension timing, ankle peak dorsiflexion timing, and knee peak extension timing from T1 to T2 (Table 1). However, no group difference has found in either timing or the magnitude of the peak joint angles. For the chronological age, the experimental group at T2 (M=26.3 months) was close to the control group at T1(M=26.6 months). Our secondary analysis was conducted between the two groups at this age via t-tests and revealed that the experimental group walked with greater peak hip extension timing and peak knee extension timing than the control group (Table 1). Our hypotheses were partly supported that both groups increased peak hip flexion angle, which allows efficient forward limb progression and clearance of the foot off the ground, and the experimental group increased peak hip and knee extension timing towards toe off compared to the control group when the data was analyzed based on chronicle age.

Our previous analysis found increased swing duration in both groups (Table 1). Peak ankle dorsiflexion timing closer to toe-off indicated that they could not utilize the ankle joint to transfer mechanical energy to swing the leg, which implies that they did not use the ankle joint to swing the leg and propel the body forward. Instead, increased timing of peak hip and knee extension towards toe-off indicates that they relied on hip and knee joints to compensate for less developed ankle function. Since this was a preliminary analysis for part of our study, the sample size may not have been sufficient to account for variability among subjects, potentially limiting our ability to detect differences between groups.

**Significance:** This study demonstrated that the treadmill training benefits infants with DS as the experimental group at T2 showed comparable or advanced joint kinematic patterns to that of control group at T1 when both groups were at the similar age. These findings indicate that treadmill training enhances walking development in infants with DS by accelerating their progress and leading to more refined gait patterns.

**Acknowledgments:** We thank NIH (R21HD105879) for funding and all the participants and their parents for their participation.
**References:** [1] Ulrich DA et al. (2001), *Pediatrics.2001;108(5).* [2] Wu J et al. (2010), *Phys Ther* 90(9).

# PROSTHESIS ATTACHMENT TYPE DOES NOT AFFECT THE GROUND REACTION FORCE AND LEG ALIGNMENT NOR THE METABOLIC COST OF WALKING IN TRANSFEMORAL AMPUTEES.

*Gauri A. Desai[1], Maliheh Fakhar[1], Chioma Ezeajughi [1], John R. Pope[1], Jae Kun Shim[1,2], Ross H. Miller[1,2]
[1]Department of Kinesiology, University of Maryland College Park, College Park, MD, USA
[2]Neuroscience and Cognitive Science Program, University of Maryland College Park, College Park, MD, USA
*Corresponding author's email: gdesai@umd.edu

**Introduction:** Oxygen consumption is ~28% greater in socket-suspended prosthesis (SO) users than bone-anchored prosthesis (BAP) users with above-knee (i.e., transfemoral) limb loss [1]. The abutment of a bone-anchored prosthesis is secured directly to the residual bone through osseointegration, eliminating the need for a socket and its related challenges [2] including rotations and translations of the residual limb that typically occur inside the socket [3], incurring an energetic cost [4]. Socket-related motion may influence the alignment of the prosthetic leg with the three-dimensional ground reaction force (GRF) vector generated during walking. Aligning the three-dimensional GRF vector with the leg during able-bodied gait is a proposed energy-saving mechanism as it reduces external joint moments and the muscle forces required to counteract them [5]. The compliance of the limb-socket interface may cause SO users to walk with the three-dimensional GRFs less aligned to their prosthetic leg, leading to bigger external joint moments that reflect a higher metabolic cost of walking than BAP users. Therefore, we aimed to examine the difference in GRF-prosthetic leg alignment between SO and BAP users and identify if this difference was reflected in their metabolic cost of walking. Since BAP users exhibit a lower metabolic cost of walking [1] and do not use a socket which likely alters GRF-prosthetic leg alignment, we hypothesized that the leg and GRF vectors would be more closely aligned for BAP than SO users which will reflect a lower metabolic cost of walking for BAP users.

**Methods:** High-functioning (Medicare K-level ≥3) BAP (n = 8) and SO (n = 11) users with transfemoral limb loss, aged 18-65, were recruited 18+ months post-surgery. Subjects walked overground at 1.0 m/s while we captured three-dimensional GRFs and retroreflective marker positions at the greater trochanter and lateral malleoli during five stance phases (foot-strike to toe-off). The alignment of the three-dimensional GRF vector with the prosthetic leg was calculated as the difference in the ground reaction force and leg axis angles [6]. The leg axis was defined as a three-dimensional vector between the greater trochanter and lateral malleoli markers. The ground reaction force angle and leg axis angle were defined relative to the global coordinate system's vertical. Alignment between the GRF and leg was the difference between the GRF and leg axis angles at the time of peak propulsive anterior-posterior GRF as it is tied to metabolic cost [6]. Oxygen uptake and carbon dioxide output were measured during ten minutes of treadmill walking at 1.0 m/s, and metabolic cost was calculated over the last three minutes of steady-state walking. Alignment and metabolic cost were compared between groups using independent samples t-tests or Wilcoxon rank-sum tests ($\alpha \leq 0.05$) for normally and non-normally distributed data, respectively.

**Results & Discussion:** The GRF-prosthetic leg axis alignment did not differ between groups (p-value = 0.82, Cohen's d = 0.05; Fig 1), with an exploration of the intact leg revealing similar findings (p = 0.20, d = 0.85), nor did metabolic cost (p = 0.60, d = 0.24; Fig 1). Therefore, we reject our primary hypothesis. Our findings suggest that high-functioning transfemoral amputees with BAP align their GRFs with their prosthetic leg similarly to those with SO and its related motions, reflecting a comparable metabolic cost of walking. However, the relationship between GRF-leg axis alignment and metabolic cost may differ by prosthetic attachment type; During able-bodied running, oxygen cost decreases with an improvement in GRF-leg axis alignment [6]. Our exploratory analysis revealed the metabolic cost of walking was not significantly correlated to GRF-prosthetic leg axis alignment in either group (BAP: p = 0.29, spearman's rho = -0.42; SO: p = 0.17, rho = -0.44). Thus, in addition to comparable GRF-leg axis alignment magnitudes and metabolic cost, the relationship between these variables is also not significantly different between SO and BAP users. Collectively, our findings suggest that the effect of GRF-leg axis alignment on the metabolic cost of walking among transfemoral amputees may not depend greatly on the prosthetic attachment type they are prescribed.

**Significance:** BAP users in our study were socket users pre-surgery with poor functional outcomes. The comparable metabolic cost and GRF-leg axis alignment between SO and BAP groups suggests a revision into a BAP can give such individuals mobility and function similar to the very high-functioning individuals with sockets we tested.

**Acknowledgments:** This work was funded by the Department of Defense's Congressionally Directed Medical 538 Research Program (HT9425-23-1-0103 to R.H.M).

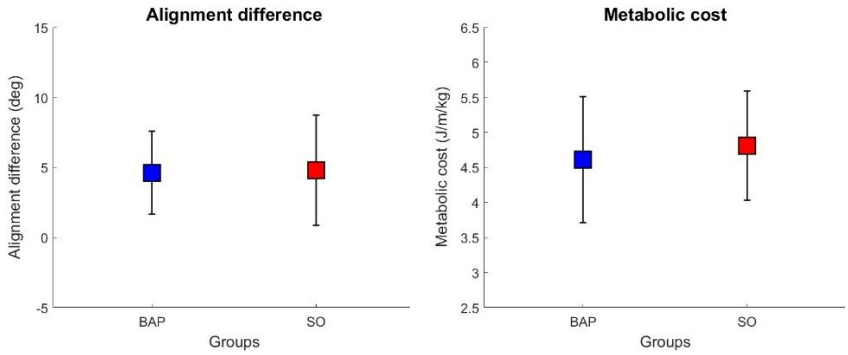


**Figure 1.** [Left] The difference in alignment between the ground reaction force angle and the leg axis angle for the bone-anchored prosthesis (BAP) and socket-suspended prosthesis (SO) users; [Right] Metabolic cost for each group.

**References:** [1] Kooiman et al. (2023), *Gait & Posture* 103:12-18; [2] Frölke et al. (2017), *Der Unfallchirurg 120(4)*; [3] Gale et al (2020), *J Biomech* 112, 110050; [4] Miller et al (2024), *PeerJ* 12, e16756; [5] Alexander (1991), *J Exp Bio* 160(1); [6] Moore et al (2016), *Scand J Med Sci Sports* 26(7).

# BONE-ANCHORED LIMB USE REDUCES HIP POWER AND WORK DURING SWING LIMB ADVANCEMENT

*James B. Tracy[1], Brecca M. M. Gaffney[1], Peter B. Thomsen-Freitas[1], Mohamed E. Awad[1], Danielle H. Melton[1], Cory L. Christiansen[1], Jason W. Stoneback[1]

[1]University of Colorado Anschutz Medical Campus, Aurora, Colorado, USA *Corresponding author's email: james.tracy@cuanschutz.edu

**Introduction:** Swing limb advancement after a transfemoral amputation relies primarily on the muscular actions at the hip to propel and position the prosthetic limb for stepping **[1]**. Using a simple relationship between input values (e.g., hip joint powers and work) and output values (e.g., step characteristics), we can gain insight into the effectiveness of the movement. Implantation of a bone-anchored limb (BAL) provides a direct connection between the residual limb and the prosthetic componentry distinct from that of a socket-type prosthesis **[2]**. Understanding how BAL use alters swing limb advancement will optimize walking rehabilitation and interventions specific to their altered demands. The purpose of this investigation was to compare swing limb advancement hip work and power and the step characteristics for individuals with unilateral transfemoral amputation before and one year after BAL implantation. We hypothesized that using a BAL would result in reduced hip power and work (i.e., inputs) during swing limb advancement without compromising step characteristics (i.e., outputs) compared to prior socket prosthesis use.

**Methods:** Twenty individuals who underwent unilateral transfemoral BAL implantation completed the same walking protocol prior to (i.e., using their socket prosthesis) and one year after BAL implantation, which included whole-body motion capture (Vicon) and in-ground force plates. Five representative trials of walking at self-selected speeds were used from each session to determine sagittal and frontal plane peak hip power, hip work, stride length, and stride width. We assessed positive hip power and work during swing generation (i.e., contralateral foot strike to mid-swing) and negative hip power and work during swing termination (i.e., mid-swing to ipsilateral foot strike) with all values scaled to body mass. We adjusted the prosthetic inertial properties by reducing the shank mass to one-third the intact limb shank mass and relocating the shank center of mass distal to the knee joint center by 25% of the shank length **[3]**. Dependent on Kolmogorov-Smirnov tests of normality, measures were compared between time points using paired t-tests with Cohen's *d* effect sizes and a Hedges' correction for small samples or Wilcoxon Signed-Rank tests with *r* effect sizes.

**Results & Discussion:** For the amputated limb, we observed no changes in hip power or work during swing generation, smaller peak negative hip powers and smaller negative hip work during swing termination, no difference in stride length, and a narrowing of stride width with BAL use compared to prior socket-type prosthesis use (Table 1).

No differences in the amputated limb hip peak power or work during swing generation with BAL use suggests that the more direct connection of the prosthetic components to the residual limb did not increase the contribution of the amputated side hip to swing limb advancement. Decreased sagittal and frontal plane amputated limb peak hip power and hip work during swing termination suggests decreased active control of the swing limb in preparation for foot strike with BAL use. Decreased active control of the hip may be the result of improved sensory perception (i.e., osseoperception) of the amputated limb with BAL implantation **[4]** leading to subtle adjustments to the swing limb during the entirety of swing limb advancement of the amputated limb. Decreasing stride width is associated with improved balance confidence, decreased fall risk, and reduced metabolic cost of walking **[5-6]**, which agrees with previous research showing improvement in these measures with BAL use **[7-8]**. The reduced hip power and work occurred with no shortening of stride lengths and a narrowing of stride width, which we interpret as an improvement in swing limb advancement effectiveness with BAL use.

**Significance:** Swing limb advancement is crucial to effective and safe ambulation. BAL users demonstrated improved swing limb advancement effectiveness which may contribute to increased independence, functional capacity, and overall quality of life.

**Table 1 – Results for amputated limb hip energetics and step characteristics.**

| Measure | Plane | Swing Phase | Socket Mean (SD) | BAL Mean (SD) | P-Value | Effect Size *d* | Effect Size *r* |
|---|---|---|---|---|---|---|---|
| Peak Hip Power (Watts/kilogram) | Sagittal | Generation | 0.913 (0.583) | 1.073 (0.606) | 0.24 | 0.26 (small) | |
| | | Termination | -0.175 (0.112) | -0.128 (0.056) | **0.05* | | 0.43 (medium) |
| | Frontal | Generation | 0.063 (0.056) | 0.088 (0.050) | 0.20 | 0.28 (small) | |
| | | Termination | -0.032 (0.030) | -0.016 (0.014) | **0.03* | | 0.50 (large) |
| Hip Work (Joules/kilogram) | Sagittal | Generation | 0.084 (0.050) | 0.096 (0.038) | 0.18 | 0.30 (small) | |
| | | Termination | -0.010 (0.007) | -0.006 (0.003) | **0.02* | | 0.53 (large) |
| | Frontal | Generation | 0.005 (0.004) | 0.005 (0.005) | 0.53 | 0.14 | |
| | | Termination | -0.002 (0.003) | -0.001 (0.001) | **0.02* | | 0.54 (large) |
| Stride Length (m) | Sagittal | | 1.24 (0.18) | 1.24 (0.11) | 0.91 | 0.02 | |
| Stride Width (m) | Frontal | | 0.17 (0.06) | 0.15 (0.06) | **<0.01* | 0.89 (large) | |

**Acknowledgments/References:** The Bone-Anchored Limb Research Group and the NIH (K01AR080776, R03HD111012, and UL1TR002535) funded this work. **[1]** Czerniecki (1996), *Arch Phys Med Reh* 77(3); **[2]** Brånemark (2001), *Rehab Res Dev* 38(2); **[3]** Hood (2020), *Sci Data* 7(1); **[4]** Häggström (2013), *Rehab Res Dev* 50(10); **[5]** Maki (1997), *Am Ger Soc* 45(3); **[6]** Donelan (2001), *Pro Roy Soc Lndn* 268(1480); **[7]** Gaffney (2023), *Gait Post* 100; **[8]** Van de Meent (2013), *Arch Phys Med Rehab* 97(11)

# TOWARDS A GREATER UNDERSTANDING OF BARRIERS TO OUTDOOR MOBILITY TO INFORM LOWER LIMB PROSTHETICS RESEARCH AND DESIGN

*Jenny A Kent[1], Szu-Ping Lee[1]
[1]Department of Physical Therapy, University of Nevada, Las Vegas
*Corresponding author's email: jenny.kent@unlv.edu

**Introduction:** In recent years, increased attention in the engineering and biomechanics communities has been directed towards analyzing and improving the mobility of lower limb prosthesis users (LLPUs) in non-level environments. It is well known that there are mobility barriers for LLPUs that lead to a restrictive fear of falling [1] and reduced quality of life [2], but also that the population is extremely heterogeneous with respect to health and function. The lack of an in-depth understanding of individual mobility limitations and apprehensions in outdoor environments, alongside potential inter-individual variation, may hinder progress towards the reduction of barriers to participation. As a first step in developing this understanding, the aim of this study was to gain further insights into prosthetic mobility in outdoor contexts through the lived experiences of LLPUs, via the research question "*To what extent do different walking surfaces and scenarios affect the mobility of lower limb prosthesis users, and why?*"

**Methods:** Procedures were approved by the University of Nevada Las Vegas Biomedical Institutional Review Board. Ambulatory lower limb prosthesis users (n = 8; 5M, 3F; 31-73yrs; level: 2 transtibial, 5 transfemoral, 1 hip disarticulation; 7 unilateral, 1 bilateral) with a range of functional abilities were recruited from the local community by purposive sampling. Participants attended an in-person semi-structured one-on-one interview. Images of outdoor walking scenarios (paved sidewalk, asphalt parking lot, outdoor café, grassy park, rocky path, snowy/icy field, and sandy beach; Fig. 1) were ranked by difficulty by participants, and used to prompt further discussion related to barriers and challenges, walking aids, falls, and sufficiency of prosthetic devices and rehabilitation. Interviews were transcribed verbatim, then coded and analysed in Atlas.ti (Atlas.ti GmbH) using the methods of inductive content analysis. Final coding was agreed by the two primary authors. Clarification and confirmation of interpretation was sought in follow-up interviews.

**Figure 1:** Two of seven walking scenario images: paved sidewalk (above); rocky path (below).

**Results & Discussion:** Despite cohort heterogeneity in prosthetic experience, health status and functional ability, ranking of the outdoor walking contexts and subsequent reasoning was often consistent; with rocky, snowy and sandy scenarios scored as more/most difficult, and parking lot, sidewalk and café as easier/easiest. Identified factors were extrinsic (e.g. surface quality, obstacles, climate) and intrinsic (e.g. anthropometric, experiential, motivational). The extent to which extrinsic factors presented barriers varied widely across participants, from them preventing participation in activities to posing "no problem". Surface unevenness and motility were challenging due to prosthesis limitations that had a destabilizing effect on walking and balance, and/or diminished walking efficiency. Rocks, given the combination of unevenness and potential motility, were noted specifically as a hazard. Sand was reported to be a challenging surface by all participants, due to inadequate foot function, poor grip and/or submersion of the foot, alongside ingress into the prosthetic componentry. Walking aids were pronounced to perform poorly in non-level and compliant environments; walkers became unstable, and crutches hindered ascent, wore out and became embedded. The hot outdoor climate caused components to heat up, and sweating that affected prosthesis suspension.

Familiarity played a role in the perception of each scenario and subsequent levels of confidence. Previous successes and failures influenced enthusiasm for walking in each context. Corroborating previous research [1], a fear of falling was described as prohibitive, and also to induce body tension that inhibited motion. For two individuals, experiencing structural failure of their prosthesis reduced their confidence outdoors. Conversely, high motivation appeared to override fears and reluctance. For example, two individuals were willing to cross a sandy beach to get to the water, and two described enjoyment embracing the challenge of rocky and hilly environments. Notably, only one individual described having received prosthetic gait training that targeted outdoor surfaces.

**Significance:** Findings from this small heterogeneous cohort of ambulatory LLPUs highlight important considerations for scientists and engineers seeking to further understand and improve mobility in LLPUs. From a design perspective, responses point towards a need for enhanced prosthesis durability, and walking aids that permit use on non-level surfaces, alongside the design of components, control mechanisms and prosthetic systems with a wide range of environments and scenarios in mind. Further research into the effects of surfaces on prosthetic gait and balance is warranted to assist in device and rehabilitation strategy development. Researchers seeking to further understand real world mobility should acknowledge that heterogeneity amongst LLPUs may be exacerbated on non-level surfaces, and that prior experience and motivation may play a large part in performance on non-level walking tasks. Further, as laboratory-based experiments frequently require LLPUs to travel to unfamiliar sites and *the unknown* can prohibit participation, providing prospective participants with pertinent information to reduce concerns may assist with study recruitment.

**Acknowledgments:** This work was supported by a University of Nevada Las Vegas Faculty Opportunity Award.

**References:** [1] Miller, WC. Arch Phys Med Rehabil. 82:1238-44, 2001. [2] Nugent, K et al. Int J Rehabil Res. 45:253-59, 2022.

# GAIT DIFFERENCES IN CHILDREN WITH DOWN SYNDROME WITH AND WITHOUT SUPRAMALLEOLAR ORTHOSIS

*Robert Zeid II[1*], Alexandre Dos Santos Kotarski[1], Yeon-Joo Kang[1], Jianhua Wu[1]
[1]Georgia State University, Department of Kinesiology and Health,
*Corresponding author's email: rzeid1@gsu.edu

**Introduction:** Individuals with Down syndrome (DS) have motor development delays due to muscle hypotonia, joint laxity, and underdeveloped balance and coordination [1]. These impairments lead to biomechanical deficits in stabilizing lower extremity joints, resulting in inefficient movements and compensatory strategies like wider step width, longer double support time, and increased co-contraction [2]. Supramalleolar orthoses (SMOs) are commonly used to provide ankle support and improve balance and gait biomechanics in children with DS [3]. However, there is limited research on the biomechanical impact of SMOs in this population, and no studies have compared gait patterns between children with DS who use SMOs and those who do not.

This study compares spatiotemporal gait parameters in children aged 2-6 years old who either use or do not use SMOs for daily walking. Specifically, we compare barefoot walking to walking with support (shoes only for the non-SMO group and shoes with SMOs for the SMO group). We hypothesize that both groups will show similar gait patterns barefoot, but the SMO group will show significant improvements in gait parameters with external support.

**Methods:** Preliminary results included 10 infants with DS (9M/1F). Subjects were allocated to the SMO group if they use SMOs over 50% of the day. The subjects arrived at our biomechanics lab for a one-time visit. We used a 9-camera Vicon® 3D motion capture system to record the walking trials. A 16-marker Vicon plug-in lower-body model was used to collect data at a sampling rate of 100 Hz. The children walked at their preferred speeds along a 6-meter walkway in two conditions: barefoot and with external support. At least five trials were collected for each condition. Vicon® Nexus was used to process the walking trials, and a custom MATLAB® program was used to analyze the spatiotemporal parameters including walking speed, cadence, stride time, step time, and double support duration. A two-way (2 group x 2 condition) mixed ANOVA was used for statistical analysis, with a statistical significance set at an $\alpha=0.05$.

**Results & Discussion:** Preliminary results included five children in the SMO group (29.11±3.93 months) and five in the non-SMO group (34.32±6.43 months). In the non-SMO group, the Opposite Foot Off phase was significantly lower in the barefoot condition (8.23±0.60) compared to support (10.29±0.70, $p = 0.036$). Similarly, in the SMO group, Opposite Foot Off was significantly reduced in the barefoot condition (8.12±0.53) compared to support (12.54±1.01, $p = 0.002$). The Foot Off phase in the SMO group was also significantly lower barefoot (57.60±4.93) compared to support (63.17±5.26, $p = 0.002$). Double Support was reduced in the SMO group barefoot (0.122±0.015) versus support (0.191±0.017, $p = 0.004$), while no significant difference was observed in the non-SMO group. No significant differences were found for other gait parameters. Both groups showed later push-offs and increased double support times with support. Table 1 highlights statistically significant gait parameters in the between group comparisons in each condition.

These results indicate that the non-SMO group tend to exhibit a more dynamic and efficient gait pattern, characterized by higher cadence, faster speeds, and reduced temporal durations, particularly in the barefoot condition. In contrast, the SMO group displayed a more cautious gait that may represent compensatory strategies, such as slower cadence, reduced speed, and prolonged temporal phases, to enhance stability. It is unclear whether SMOs are beneficial in improving overground walking compared to shoes alone. Continued subject recruitment may help further explain the effects of SMOs vs. shoes during overground walking.

**Table 1**: Between-group comparisons of SMO versus Non-SMO groups. Mean±SD and significance.

| Measure | Condition | Non-SMO (Mean ± SD) | SMO (Mean ± SD) | p-value |
|---|---|---|---|---|
| **Cadence** | Barefoot | 197.80 ± 7.37 steps/min | 166.15 ± 8.62 steps/min | 0.007 |
| | Support | 188.90 ± 8.01 steps/min | 167.37 ± 9.12 steps/min | 0.080 |
| **Walking Speed** | Barefoot | 0.936 ± 0.053 m/s | 0.759 ± 0.062 m/s | 0.032 |
| | Support | 0.972 ± 0.057 m/s | 0.828 ± 0.065 m/s | 0.100 |
| **Stride Time** | Barefoot | 0.630 ± 0.029 s | 0.745 ± 0.034 s | 0.007 |
| | Support | 0.658 ± 0.032 s | 0.769 ± 0.036 s | 0.025 |
| **Step Time** | Barefoot | 0.311 ± 0.015 s | 0.371 ± 0.018 s | 0.012 |
| **Opposite Foot Off** | Barefoot | 8.23 ± 0.60 | 10.29 ± 0.70 | 0.036 |
| | Support | 9.51 ± 0.89 | 12.54 ± 1.01 | 0.002 |
| **Double Support** | Barefoot | 0.087 ± 0.052 s | 0.122 ± 0.059 s | 0.080 |
| | Support | 0.122 ± 0.015 s | 0.191 ± 0.017 s | 0.004 |
| **Step Width** | Barefoot | 0.152 ± 0.008 m | 0.174 ± 0.009 m | 0.075 |

**Significance:** Though SMOs may help with standing balance by supporting the ankle in the frontal plane, the stiffness of the orthotic may impede gait efficiency during overground walking. Further studies to assess more complex gait tasks, such as obstacle crossing, would be beneficial to understand the benefits of SMO use.

**Acknowledgments:** We thank all of the participants and their parents for their participation.
**References:** [1] Jain et al. (2022), *Clin Exp Pediatr* 65(3); [2] Zago et al. (2020), *J Phys Ther Sci* 32(4), [3] Martin (2004), *Dev Med Child Neurol* 46(6).

# INERTIAL MEASUREMENT UNITS TO PREDICT PROSTHETIC PROPULSION AND POWER

*Thomas Madden[1], Corey Pew[1]
[1]Department of Mechanical & Industrial Engineering, Montana State University, Bozeman, MT
*Corresponding author's email: thomasmadden4@montana.edu

**Introduction:** Prostheses aim to restore walking ability for individuals with lower limb loss. However, individuals walking with passive prostheses show deficits in propulsive force ($F_P$; anterior ground reaction force) and walking speed as well as higher metabolic cost relative to able-bodied individuals [1,2]. $F_P$ directly relates to walking speed [3], which is important for mobility and function. In addition, increasing prosthetic ankle-foot power decreases the biological work done by the residual limb [4]. Therefore, increasing prosthetic leg $F_P$ and ankle-foot power represent important targets for rehabilitative outcomes and interventions. While these measurements currently require expensive and space prohibitive force plates and motion capture systems, wearable inertial measurement units (IMUs) measuring acceleration and angular velocity may provide a more accessible alternative to estimate $F_P$ and ankle-foot power. However, this approach has not been investigated for individuals with lower limb loss. Therefore, the purpose of this study was to evaluate the accuracy of IMU-based predictions of peak prosthetic leg $F_P$ and ankle-foot power during walking. Based on equations of motion and relationships observed in healthy young and old adults [5,6], we hypothesized that accelerations, angular velocities, and angles derived from body-worn IMUs can be used to accurately predict peak prosthetic leg $F_P$ and ankle-foot power.

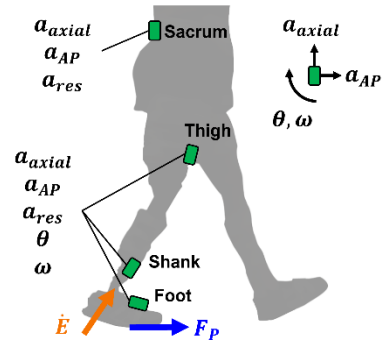


**Fig 1:** Predictor variables for peak $F_P$ and ankle-foot power ($\dot{E}$): peak axial ($a_{axial}$), anterior-posterior ($a_{AP}$), and resultant ($a_{res}$) accelerations, pitch angle ($\theta$), and angular velocities ($\omega$).

**Methods:** Four below-knee prosthesis users (2F/2M, 19-60 y, 56-120 kg, 164-188 cm) walked overground at three speeds (self-selected, 15% slower, 15% faster) while IMUs on the sacrum, thigh, shank, and foot (Fig. 1) recorded acceleration and angular velocity (148Hz) with synchronous motion capture (250Hz) and force plate data (1000Hz). Peak $F_P$ was taken from the anterior ground reaction force data, normalized by body weight (BW). Ankle-foot power, normalized by body mass, was calculated from motion capture and force plate data via unified deformable segment analysis [7]. Peak accelerations, segment angular velocities, and angles (estimated via sensor fusion [8]) near toe-off (0-250ms from time of peak $F_P$, which consistently identified peaks near toe-off across participants and speeds) were extracted from IMU data. This set of discrete variables (Fig. 1), along with each participant's mass and height, was used to predict peak $F_P$ and ankle-foot power using regularized regression [9] with leave-one-out cross-validation by participant, yielding prediction errors that would be expected for a new individual. Accuracy was evaluated as the mean absolute error relative to force plate/motion capture-based estimates. To compare sensor locations, regularized regression models were also evaluated for each specific location.

**Results & Discussion:** The full set of IMUs predicted peak $F_P$ with 0.002 BW (1.2%) accuracy. Models specific to distally placed sensors (closer to the foot-ground interaction) achieved greater accuracy than those using more proximally placed sensors (Fig. 2). Models predicting ankle-foot power failed to find coefficients that improved accuracy vs. the intercept alone, resulting in large error (0.38 W/kg, 46%). This could be due to insufficient training data (2 participants/set). Using data from all participants in each training set, the model predicted peak ankle-foot power with 6.6% accuracy, suggesting high sensitivity to participants. In partial support of our hypothesis, the most accurate models predicted peak $F_P$ with errors below intra-individual variation (5%) [10], providing evidence that IMUs can be used to detect clinically relevant changes in prosthetic $F_P$. Further, the model specific to the foot IMU yielded similar errors to the model using the full set, presenting a minimal burden alternative to estimate prosthetic $F_P$.

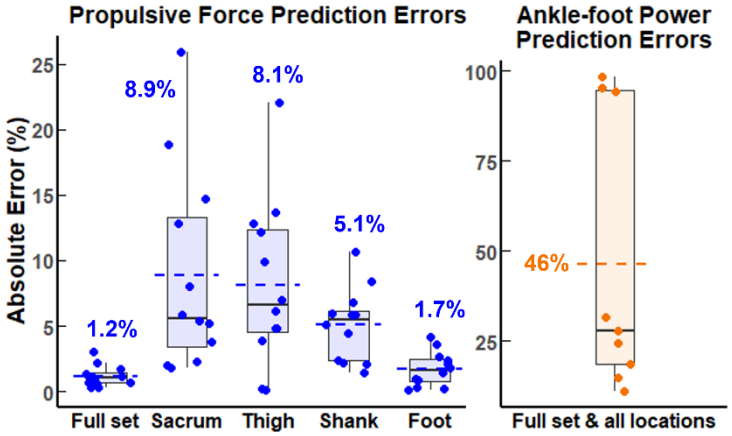


**Fig 2:** Absolute error boxplots for the full IMU set and specific locations (all equal for ankle-foot power). Dashed lines and values represent means. Ankle-foot power (right) was analyzed for only three participants.

**Significance:** These results suggest IMUs can be used to accurately predict peak prosthetic $F_P$. This will allow clinicians to assess changes in $F_P$ using small, inexpensive sensors, enhancing their abilities to implement and evaluate rehabilitative interventions for individuals with lower limb loss. Further work with larger datasets will help evaluate IMU-based predictions of ankle-foot power.

**Acknowledgments:** Supported by the NIGMS (P20GM103474) and NCATS (5TL1TR002318-08) of the NIH. The content is solely the responsibility of the authors and does not necessarily represent the official views of the NIH. Mojtaba Mohasel helped collect data.

**References:** [1] Carse et al. (2020), *Gait Posture* 75(1); [2] Silverman et al. (2008), *Gait Posture* 28(4); [3] Campanini et al. (2009), *Gait Posture* 30(2); [4] Segal et al. (2012), *Hum Mov Sci* 31(4) ; [5] Hsiao et al., *Hum Mov Sci* 39(1) ; [6] Pieper et al. (2020), *J Biomech* 98(1); [7] Takahashi et al. (2012), *J Biomech* 45(1); [8] Madgwick et al. (2011), *IEEE Int Conf Rehabil Robot* ; [9] Tibshirani (1996), *J R Statist Soc* 58(1) [10] Svoboda et al. (2012), *Prosthet Orthot Int* 36(2).

# PROPULSION CHANGES INDUCED BY DYNAMIC TREADMILL WALKING POST-STROKE

Brooke L. Hall[1], Caitlin L. Banks[1,2], Ryan T. Roemmich[1,2]*
[1] Center for Movement Studies, Kennedy Krieger Institute, Baltimore, MD, 21205
[2] Department of Physical Medicine and Rehabilitation, Johns Hopkins University School of Medicine, Baltimore, MD, 21205
*Corresponding author's email: rroemmi1@jhmi.edu

**Introduction**: Over half of ambulatory persons with stroke walk with gait asymmetry [1,2]. Many current methods of rehabilitation that aim to improve gait symmetry require specialized equipment that is not accessible in most clinics [3,4]. Recently, our lab developed a dynamic treadmill controller that can simulate a treadmill environment similar to split-belt walking with a conventional treadmill by selectively changing the speed within a gait cycle [5]. Dynamic treadmill walking can drive selective changes in clinically relevant gait parameters like peak propulsion. Here, we sought to understand how dynamic treadmill walking can induce gait changes in persons with stroke who exhibit gait asymmetry. We were particularly interested in propulsion asymmetry changes, as paretic propulsion deficits are common following stroke [6]. Our hypothesis was that dynamic treadmill walking would improve propulsion asymmetry in persons post-stroke who exhibited baseline propulsion asymmetry.

**Methods**: Nine people with stroke (7 M, 2 F, age: 62 ± 12 years) walked on an instrumented treadmill at speeds ranging from 0.2m/s-1.45m/s. These speeds were determined with participant's self-selected and fastest comfortable speeds. They were then exposed to dynamic treadmill walking, which changes between a fast and slow treadmill speed for 50% of the gait cycle, respectively. Each participant completed two trials where a metronome was used to target paretic leg stepping at different timings relative to the treadmill belt speed changes. We collected kinematic data using an eight-camera motion capture system (Vicon Motion Systems, Centennial, CO; 100 Hz) and ground reaction forces from independent force plates embedded in the belts of our instrumented treadmill (1000 Hz).

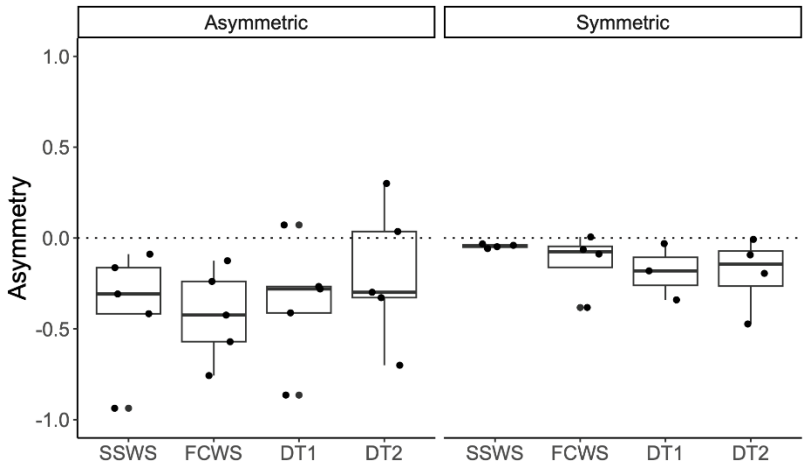


Figure 1: Propulsion asymmetry values for persons with stroke with asymmetric (left) and symmetric (right) propulsion values at baseline. Individual participants are shown as scatter points. The horizontal dotted line at y=0.0 indicates symmetry, while negative values indicate greater non-paretic than paretic propulsion values.

**Results:** Four participants were deemed symmetric at baseline and five asymmetric. Despite the fact that dynamic treadmill walking induces asymmetry in symmetric gait [5], we chose to assess individuals from both groups to gain perspective on changes that could be induced post-stroke. We performed a two-way mixed ANOVA comparing propulsion asymmetry between trials (self-selected walking speed, fastest comfortable walking speed, and the two dynamic treadmill walking trials) and within group (symmetric or asymmetric at baseline). This analysis revealed that propulsion asymmetry did not significantly differ between trials or within the groups (See Fig 1; all $p<0.05$).

**Discussion:** Overall, propulsion asymmetry was not significantly different between dynamic treadmill walking and baseline walking in this small sample of individuals post-stroke. Given the heterogeneity of our sample, a larger sample will be needed to determine whether dynamic treadmill walking can restore propulsion symmetry. Future work involves persons with stroke doing dynamic treadmill walking repeatedly over the course of an eight-week span, with an aim of investigating if long-term exposure to this novel environment can induce changes to propulsion asymmetry over time.

**Significance:** This work is significant because we are investigating if dynamic treadmill walking can be individualized in effectively restoring gait symmetry in persons post-stroke. Propulsion deficits, particularly on the paretic side, can increase fall risk [7] and metabolic cost [7]. The ability to selectively restore propulsion symmetry without the need for specialized equipment gives potential for the eventual clinical application of dynamic treadmill walking.

**Acknowledgements:** This work was supported by an American Heart Association Career Development Award #935556 (RTR). Brooke Hall is supported by a Research Supplement to Promote Diversity in Health-Related Research (#3R21HD110686-02S1, PI RTR). Caitlin Banks is supported by an American Heart Association Postdoctoral Fellowship (25POST1366391). Previously, CLB was supported by a training grant from the Eunice Kennedy Shriver National Institute of Child Health and Human Development (#5T32HD007414-29, PI Bastian). BLH and CLB implemented data science and visualization training in this work from the ReproRehab program (NIH NICHD/NCMRR R25HD105583, PI Liew).

**References:** [1] Patterson KK, et al. (2008), *Arch Phys Med Rehabil* 89(2); [2] Patterson KK, et al. (2010), *Gait Posture* 31(2); [3] Reisman D et al. (2010), *Neurorehabilitation Neural Repair J* 27(5); [4] Maceira-Elvira P, et al. (2019), *J Neuroengineering Rehabil* 16(1); [5] Browne MG et al. (2023), *PLOS ONE* 18(10); [6] Awad LN et al. (2020), *J Neuroengineering Rehabil* 17(1); [7] Weerdesteyn V, et al. (2008), *J Rehabil Res Dev* 45(8)

**Adaptive split-belt treadmill may improve propulsion symmetry in people with chronic stroke**

*Rucha Kulkarni[1], Jill S. Higginson[1,2]
[1]Dept. of Biomedical Engineering, University of Delaware, Newark, DE, USA
[2]Dept. of Mechanical Engineering, University of Delaware, Newark, DE, USA
*Corresponding author's email: rnk@udel.edu

**Introduction:** Around 800,000 people in the United States suffer from a stroke annually [1]. Stroke can lead to weakened muscles on the affected (paretic) side of the body, leading to decreased propulsion (push-off) on the paretic side during walking [2]. This asymmetry in propulsion can lead to slower walking speeds and poor walking function. Although paretic propulsion is highly correlated to walking speed, post-stroke training typically focuses on improving walking speeds [3]. Treadmill training is often used in post-stroke rehabilitation but shows mixed effectiveness due to fixed speeds which limits healthy gait variability [4]. Split-belt treadmills and adaptive treadmills (ATMs) have shown to target paretic limb function and allow for healthy gait variability respectively, but also show mixed effectiveness [3,5]. We believe that targeting paretic propulsion may provide a beneficial paradigm to improve walking function in people with chronic stroke (PwCS). Therefore, we developed an adaptive split-belt treadmill (sATM) that can be preferentially weighted to encourage increased unilateral propulsion. The purpose of this study was to determine the effect of increased unilateral weighting of propulsion on a sATM compared to no preferential weighting and a tied-belt ATM [3] on propulsion symmetry. We hypothesized that propulsion would be more symmetric in PwCS with an increase in paretic propulsion weighting. We further hypothesized that propulsion would be less symmetric in healthy adults with an increase in paretic propulsion weighting.

**Methods:** Sixteen participants (N=8 PwCS, N=8 healthy adults) performed a series of five trials on an adaptive split-belt treadmill (sATM). The sATM controller updates the speed of each belt independently at each step based on the propulsion of the respective limb and position on the treadmill using a custom-written MATLAB code. The control equation is thus defined as: $v_{i+1} = v_i + \gamma v_{PI} - \frac{\gamma}{25} v_i + \beta v_{COM}$ where $v_i$ is the current speed, $v_{PI}$ is the intermediate velocity due to propulsion, $v_{COM}$ is the intermediate velocity due to the position of the center of mass, $\gamma$ is the propulsion gain, and $\beta$ is the position gain. Participants performed five walking trials – one on a tied-belt ATM (Tied) where the belt speeds were always equal [3], and four on the sATM where the propulsion gain on the paretic side was varied in random order such that $\frac{\gamma_{paretic}}{\gamma_{non-paretic}}$ = 1, 1.25, 1.5, 1.75 (Normal, Low, Medium, High). Healthy participants were assigned a paretic side randomly (N=4 right, N=4 left). Participants were asked to maintain similar belt speeds while walking comfortably and safely. For each condition, they were given up to 5 minutes to reach a comfortable walking speed. Force data were collected and processed using a custom MATLAB code. The outcome measures were peak anterior ground reaction force (AGRF) asymmetry and AGRF impulse asymmetry.

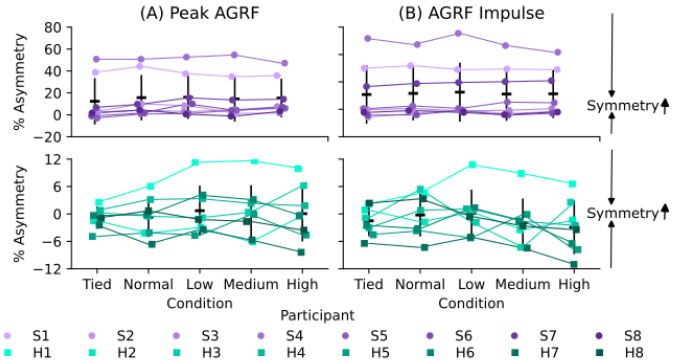


**Figure 1:** (A) Peak AGRF Asymmetry (B) AGRF Impulse Asymmetry. Percent asymmetry was calculated as $\frac{(Nonparetic-Paretic)}{(Nonparetic+Paretic)} * 100$. Purple markers represent PwCS, green represent healthy participants. Black lines represent the mean and std deviation plot. Zero asymmetry indicates perfect symmetry.

**Results & Discussion:** Peak AGRF asymmetry and AGRF impulse asymmetry were compared between all five conditions (Fig 1). Asymmetry values closer to zero indicate an increase in propulsion symmetry. Seven PwCS were more symmetric in at least one condition with preferential weighting compared to Normal, while five were more symmetric compared to the Tied condition. All healthy participants were less symmetric in at least one condition compared to Normal. Two PwCS who did not increase propulsion symmetry compared to Tied are within a healthy gait symmetry range [6] for all conditions (±7.8% for peak AGRF, ±9.2 for AGRF impulse) and the changes in symmetry are similar to the healthy participants. Lower symmetry in the Normal compared to the Tied condition may represent baseline overground asymmetry. Therefore, changes in asymmetry with increased paretic propulsion weighting compared to the Normal condition may represent changes in asymmetry relative to baseline symmetry. The preliminary results support our hypotheses – increasing paretic propulsion weighting encourages symmetric propulsion in PwCS and asymmetric propulsion in healthy adults. These findings demonstrate that PwCS can volitionally improve propulsion symmetry on an sATM compared to their baseline symmetry on the sATM or a tied-belt ATM.

**Significance:** Stroke is a leading cause of disability and can lead to decreased walking speeds [1]. Targeting paretic propulsion using an adaptive split-belt treadmill could improve gait symmetry and function. This preliminary study demonstrates that PwCS may volitionally increase propulsion symmetry on an sATM compared to baseline. An sATM could improve rehabilitation techniques and paradigms for post-stroke gait training interventions.

**Acknowledgments:** The study was funded by the NIH (# HD111071). We thank Tamara Wright, PT for her help in data collection.

**References:** [1] Tsao et al. (2023), *Circulation* 147; [2] Awad et al. (2020), *J. Neuroeng. Rehabil.* 17; [3] Pariser et al. (2022), *J. Biomech.* 133 [4] Gelaw et al. (2019), *Glob. Epidemiol.* 1, [5] Reisman et al. (2009), *Neurorehabil Neural Repair.* 23(7) [6] Herzog et al. (1989), *Med Sci Sports Exerc.* 21(1)

# ENERGETICS OF WALKING WITH WITHIN-STRIDE CHANGES IN TREADMILL SPEED POST-STROKE

*Caitlin L. Banks[1,2], Brooke L. Hall[2], Ryan T. Roemmich[1,2]
[1]Center for Movement Studies, Kennedy Krieger Institute
[2]Department of Physical Medicine and Rehabilitation, Johns Hopkins University School of Medicine
*Corresponding author's email: cbanks32@jhmi.edu

**Introduction:** More than 5.6 million Americans are living with mobility impairment as the result of a stroke [1]. One of the more common manifestations of mobility impairment is an asymmetric walking pattern [2]. While there are existing approaches to decrease asymmetry in the literature, many require expensive equipment that is not feasible for clinical translation [3]. Our lab recently developed a novel approach to modify gait symmetry called 'dynamic treadmill walking' where we change the speed of a single-belt treadmill within a single step, creating a split-belt-like asymmetry pattern [4]. Recently, we have begun to study the metabolic demands associated with this novel walking pattern. We found that young adults required more metabolic power for dynamic treadmill walking than walking at the average speed of the paradigm but less than the faster speed. Here, we studied the metabolic demand of dynamic treadmill walking in individuals post-stroke, a target population for this new gait training approach. We hypothesized that metabolic power will 1) be similar between dynamic treadmill walking and conventional treadmill walking, and 2) depend on the walking speeds of each participant.

**Methods:** To date, eight individuals with chronic (>6 months post infarct), hemiparetic stroke performed dynamic treadmill walking while undergoing metabolic analysis (8M/2F, age 61±13 years, median lower extremity Fugl-Meyer motor score 26 (range 20-34)). Individuals walked at their fastest comfortable treadmill speed during a prior visit. Speeds for this experiment were set at 50% (Slow), 75% (Intermediate), and 100% (Fast) of fastest comfortable treadmill speed (0.9±0.4m/s). We also assessed walking at each participant's overground comfortable walking speed (0.7±0.3m/s). Two trials of dynamic treadmill walking were performed with the belts spending 50% of a gait cycle at the Slow speed and 50% at the Fast speed, with right heel-strikes paced by a metronome. We also assessed Fast speed normal walking following dynamic treadmill walking. Participants wore a mask connected to a Parvomedics TrueOne 2400 metabolic system that sampled breath-by-breath oxygen consumption and carbon dioxide production. We calculated net metabolic power using the standard equations derived by Brockway [5]. Repeated measures ANOVA were conducted to determine how the net metabolic power varied across trials, followed by Dunnett's post-hoc tests for significant main effects.

**Results & Discussion:** Figure 1 shows net metabolic power across individuals (grey lines) and as a group (mean±standard error) by Condition. Repeated measures ANOVA revealed a main effect of Condition ($F(6,42)=2.94$, $p<0.01$). However, a Dunnett's post-hoc test using the intermediate speed as a control did not reveal significant pairwise differences (all $p>0.05$). Since participants walked at individualized speeds, we conducted a second repeated measures ANOVA that controlled for treadmill speed (using the intermediate baseline speed for dynamic treadmill conditions). This analysis showed a significant effect of Speed ($F(1,41)=14.76$, $p<0.01$) but no significant effect of Condition ($F(6,41)=0.77$, $p=0.60$). This indicated that the differences in net metabolic power observed were driven by treadmill speed.

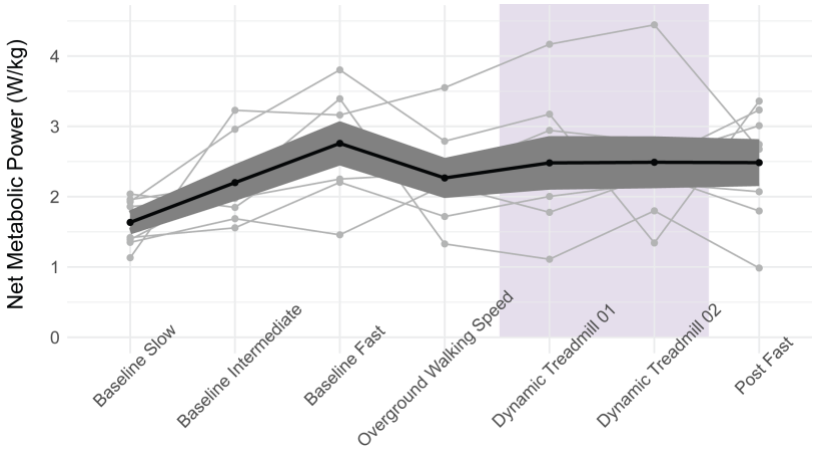


**Figure 1:** Net metabolic power scales with walking speed across normal walking and dynamic treadmill walking in individuals post-stroke. Each individual is represented by a thin grey line, group average is black, and group standard error of the mean in grey ribbon. Dynamic treadmill walking conditions are shaded purple.

Metabolic power is known to increase with walking speed in persons with and without stroke [6,7]. This pattern of behavior in dynamic treadmill walking also agrees with our previous findings in healthy young adults. While data collection is ongoing, these results provide an early indicator that dynamic treadmill walking does not provide additional challenge from a metabolic perspective in persons with stroke beyond that associated with fast walking.

**Significance:** Dynamic treadmill walking does not impart a greater metabolic demand than normal walking at matched speeds in persons with chronic stroke. This approach could serve as a potential strategy to improve gait symmetry in individuals with neurologic disease, and we are in the process of assessing responses of individuals post-stroke to repeated exposure to dynamic treadmill walking. This would present an exciting step forward in creating clinically translatable, individual-specific, rehabilitation tools.

**Acknowledgments:** This work was supported by AHA grants #25POST1366391 (CLB) and #935556 (RTR), NIH grant T32HD007414-29 (CLB previous trainee, PI Bastian), and NIH grant 3R21HD110686-02S1 (BLH trainee, PI RTR).

**References:** [1] Martin et al. (2024), *Circulation* 149(8). [2] Wall and Turnbull (1986), *Arch Phys Med Rehabil* 67(8). [3] Reisman et al (2013), *Neurorehabil Neural Repair* 27(5). [4] Browne et al. (2023), *PLoS ONE* 18(10). [5] Brockway (1987) 41(6). [6] Pimentel et al. (2022), *Front Sports Act Living* 4. [7] Brouwer et al. (2009) *Clin Biomech* 24(9).

# WALK, STUMBLE, RECOVER FASTER, AND PREVENT LONG-TERM EFFECTS WITH PINK NOISE

Marilena Kalaitzi Manifrenti[1], Nick Stergiou[1,2], Aaron D. Likens[1]
[1]Department of Biomechanics, University of Nebraska at Omaha, Omaha, NE, USA
[2]Department of Physical Education and Sport Science, Aristotle University, Thessaloniki, Greece

*Corresponding author's email: mkalaitzimanifrent@unomaha.edu

**Introduction:** Although extensive research has been conducted on gait perturbations, most of those studies focus on short-term responses, analyzing only ±3 strides before and after a perturbation [1,2]. Thus, we aimed to investigate longer-term consequences (20 minutes) of a mechanical perturbation. Using Interrupted Time Series Analysis (ITSA), a statistical method that evaluates the impact of an intervention by comparing trends in the data before and after its implementation, we examined both the immediate impact of a perturbation and the long-term recovery trends in gait variability [3]. Existing literature indicates that when the temporal structure of gait variability exhibits pink noise in its inter-stride intervals, the walking stability is restored faster than in other forms of noise [4]. Therefore, we hypothesized that participants pacing to pink noise cueing would recover significantly faster to pre-perturbation gait dynamics than other cueing conditions such as white noise, which are associated with older or pathological gait and linked to slower stability restoration [4,5]. Such other cueing conditions would remain affected by the perturbation longer than those pacing to pink noise.

**Methods:** 30 healthy young adults (age:19-30), performed 2 walking trials on a split-belt treadmill: (1) A 25-minute Baseline (not-reported), (2) A 45-minute Condition, during which participants paced to 1 of 4 variability temporally structured cues: Isochronous, Pink Noise, White Noise, and Control (no cues). At minute 25, the treadmill belt of the non-dominant leg was arrested, introducing an unexpected perturbation. The stride interval time-series were calculated from the gait kinematics captured by the Vicon Nexus system (100Hz). We computed the Hurst exponent, H, in 14 windows of 167 seconds each, which quantifies gait variability based on the temporal correlations of stride-intervals. We performed ITSA to understand if there were linear or quadratic trends in how H changed throughout the trial (Fig.1A,B). A linear mixed model was used to account for individual differences in Hurst exponent trajectories.

**Results & Discussion:** Pink noise, though seemingly affected by the perturbation (the significant drop at window 8, b:1.42, t(406)=5.712, p<0.001), exhibited the fastest recovery to pre-perturbation dynamics with a quadratic trend (b=-0.123, CL= (-0.172, -0.075)). Control followed similar significant trends (immediate impact: b: 0.817, t(406)=3.28, p=0.001; long-term recovery quadratic trend: b=-0.062, CL= (-0.111, -0.014)). Conversely, white noise, despite appearing less affected at first (b:0.838, t(406)=3.22, p=0.001), had no linear or quadratic recovery trend during the post-perturbation window (linear: b:0.0114, CL=(-0.227,0.456)| quadratic: b:-0.04, CL=(-0.09,0.006)), therefore failed to completely recover indicating a lasting perturbation effect. Isochronous remained unresponsive, showing lack of adaptability to varying situations. Our results extend prior findings, where those pacing with pink noise restored stability 3.3 seconds faster after a perturbation [4].

**Significance:** The significance of our work is twofold: (1) We extended the current literature's knowledge about how perturbations affect gait beyond the conventional 3-stride window, to 20 minutes following the event, (2) we introduced ITSA as a new method in the biomechanics gait perturbation literature.

**Acknowledgments:** The Center for Research in Human Movement Variability and the NIH [P20GM109090, P20GM152301].

A

| | | | | | | | | | | | | | | | |
|---|---|---|---|---|---|---|---|---|---|---|---|---|---|---|---|
| Window | 0 | 1 | 2 | 3 | 4 | 5 | 6 | 7 | 8 | 9 | 10 | 11 | 12 | 13 | 14 |
| Window² | 0 | 1 | 4 | 9 | 16 | 25 | 36 | 49 | 64 | 81 | 100 | 121 | 144 | 169 | 196 |
| PPW | 0 | 0 | 0 | 0 | 0 | 0 | 0 | 0 | 0 | 1 | 2 | 3 | 4 | 5 | 6 |
| PPW² | 0 | 0 | 0 | 0 | 0 | 0 | 0 | 0 | 0 | 1 | 4 | 9 | 16 | 25 | 36 |
| Perturbation | 0 | 0 | 0 | 0 | 0 | 0 | 0 | 0 | 1 | 1 | 1 | 1 | 1 | 1 | 1 |

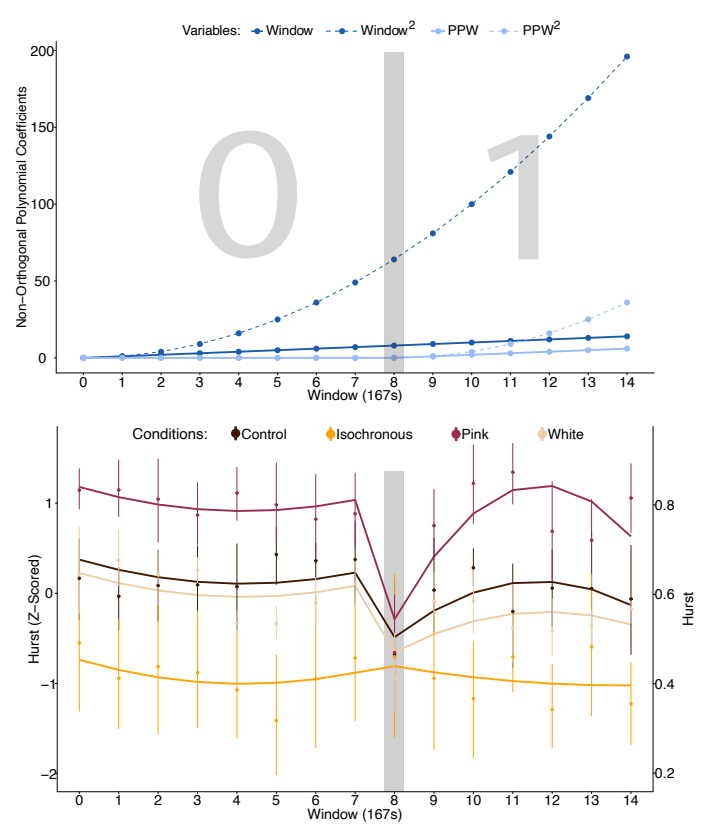


**Figure 1.** ITSA. (A) Five continuous vectors were generated: the Perturbation dummy vector (0: pre-perturbation, 1: during/post-perturbation) assessed the immediate impact, while Window (linear trend), Window² (quadratic trend), PPW (post-perturbation linear trend), and PPW² (post-perturbation quadratic trend) captured the long-term recovery rate. (B) A visual depiction of the vectors generated in panel A. Window on the x-axis demonstrates time. (C) The vectors were used as predictors in an LME model to analyze differences in H across groups. Thin vertical lines represent confidence limits. The grey shaded area marks the perturbation window which aligns across all panels.

**References:** [1] Eng et al. *Exp. Brain Res.* **102**(2), 339-349, 1994, [2] Roeles et al. *Med. Biol. Eng. Comput.* **56**(12), 2325-2335, 2018, [3] Lopez Bernal et al. *Int. J. Epidemiol.* **46**(1), 348-355, 2016, [4] Ravi et al. *J. Exp. Biol.* **224**(5), jeb237073, 2021, [5] Stergiou and Decker. *Hum. Mov. Sci.* **30**(5), 869-888, 2011

# COMPARISON OF THREE-DIMENSIONAL TRUNK AND UPPER EXTREMITY JOINT KINEMATICS DURING WHEELCHAIR PROPULSION USING MARKER- AND MARKERLESS-BASED MOTION ANALYSIS

Jungsun Moon[1], Matthew M. Hanks[1,2,3]*
[1]Department of Health and Kinesiology, University of Illinois Urbana-Champaign, Urbana, IL, USA
[2]Beckman Institute for Advanced Science and Technology, University of Illinois Urbana-Champaign, Urbana, IL, USA
[3]Disability Resources and Educational Services, University of Illinois Urbana-Champaign, Urbana, IL, USA
*Corresponding author's email: hanksm@illinois.edu

**Introduction:** Manual wheelchair users rely on their upper extremities to perform activities of daily living, including manual wheelchair mobility, which is believed to often result in shoulder pain [1]. Previous studies have sought to identify biomechanical predictors of shoulder pain during wheelchair propulsion using gold standard marker-based motion analysis [2-3]. However, some limitations of marker-based motion analysis, such as the need for the removal of clothing to affix markers and issues with palpation, marker placement, skin artifact, and marker occlusion [4-5], may limit the ease of use of optical motion analysis in clinical assessments and rehabilitative decision making with manual wheelchair users. Markerless-based motion analysis is an emerging technology capable of quantifying joint biomechanics without many drawbacks of marker-based motion analysis [6]; however, to our knowledge, its utility with manual wheelchair users remains understudied. Therefore, the purpose of this study was to compare three-dimensional (3-D) trunk and upper extremity joint kinematics during wheelchair propulsion using marker- and markerless-based biomechanical models.

**Methods:** Fifteen manual wheelchair users (7 males / 8 females, age: 22.5 ± 4.2 years, duration of wheelchair use: 11.61 ± 5.9 years) participated in this prospective, cross-sectional study. Participants were affixed with thirty-four passive, reflective markers on select trunk and bilateral upper extremity anatomical landmarks. Participants propelled their personal manual wheelchair on a stationary roller at a self-selected speed while 3-D marker trajectory and video data were collected simultaneously using twelve Qualisys Miqus hybrid cameras. Six infrared cameras collected 3-D marker trajectories at a sampling rate of 120Hz, and six video cameras collected 2-D video at a sampling rate of 60Hz. Marker trajectory data were analyzed and 3-D joint kinematics and joint centers were computed in Visual 3D using a custom upper extremity biomechanical model. Video data were processed in Theia3D and 3-D joint kinematics and joint centers were computed in Visual 3D using the Theia3D biomechanical model. ZXY and XYZ Cardan rotation sequences (sagittal-frontal-transverse) were used to compute joint kinematics with the marker- and markerless-based models, respectively. Ten, time-normalized manual wheelchair propulsion cycles (0-100%) were collected for each participant and analyzed using each model. Data were then averaged across all participants. Pearson correlation was used to describe the association and average root mean square differences (RMSD) were used to describe the agreement between the two models.

**Results & Discussion:** The correlation of joint angles and joint center positions between the models varied from weak (r = 0.19) to very strong (r = 0.99) depending on the joint and plane of motion. Trunk angles were strongly correlated in the sagittal and transverse planes (r ≥ 0.93) and weakly correlated in the frontal plane (r = 0.26) with good agreement in all planes (largest RMSD = 7.1°). Shoulder joint angles were strongly correlated in all planes (r ≥ 0.90; **Fig 1)** with good agreement in the sagittal and frontal planes (RMSD = 8.7°) but poor agreement in the transverse plane (largest RMSD = 36.6°). Elbow joint angles were strongly correlated with good agreement in the sagittal plane (r = 0.99; largest RMSD = 12.3°) and moderately correlated with poor agreement in the transverse plane (r ≥ -0.64; largest RMSD = 36.2°). Wrist joint angles were strongly correlated with moderate agreement in the sagittal and frontal planes (r ≥ 0.97; largest RMSD = 17.7°). Trunk joint center positions were strongly correlated in the anterior-posterior direction (r = 0.99) and weakly correlated in the medial-lateral and superior-inferior directions (r ≤ 0.22). Left shoulder joint center positions were weakly and moderately correlated in the anterior-posterior (r = 0.34) and medial-lateral directions (r = 0.65), respectively, and strongly correlated in the superior-inferior direction (r = 0.99). The right shoulder joint, bilateral elbow joint, and bilateral wrist joint centers were strongly correlated in all directions (r ≥ 0.78). Strong agreement in joint centers were observed for all joints in all directions (largest RMSD = 2.4cm). Our findings of strong agreement for all upper extremity joint centers yet poor agreement in transverse plane motion is consistent with previous research [6-8] and suggest that markerless-based motion analysis is comparable to marker-based motion analysis with wheelchair propulsion but with some differences in select joints and planes.

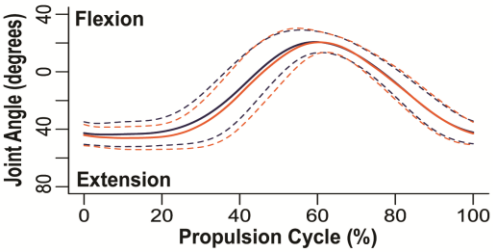


**Figure 1.** Average (bold) ± 1 standard deviation (dashed) shoulder joint motion during manual wheelchair propulsion using marker- (blue) and markerless-based (orange) biomechanical models.

**Significance:** Our analyses revealed similarities in 3-D trunk and upper extremity kinematics during manual wheelchair propulsion between marker- and markerless-based motion analysis. Due to its non-invasive nature and ease of use, markerless motion analysis may be a reliable alternative for the clinical assessment and rehabilitation of manual wheelchair users, though more research is warranted.

**Acknowledgments:** This work was supported by the University of Illinois Urbana-Champaign College of Applied Health Sciences Center on Health, Aging, and Disability.

**References:** [1] Morrow et al. (2010), *J Electromyogr Kinesiol* 20(1); [2] Briley et al. (2020), *J Biomech* 113; [3] Jayaraman et al. (2014), *PloS One* 9(3); [4] Della Croce et al. (2005), *Gait Posture* 21(2); [5] Chenier et al. (2023), *J Biomech* 156; [6] Kanko et al. (2021), *J Biomech* 127; [7] Lahkar et al. (2022), *Front Sports Act Living* 4; [8] Hansen et al. (2024), *Biomed.Eng.Adv* 7

# USE OF HAPTIC FEEDBACK TO INCREASE PLANTARFLEXION AND PROPULSION

*Margo C. Donlin[1]
[1]Bucknell University Department of Mechanical Engineering
*Corresponding author's email: mcd033@bucknell.edu

**Introduction:** Forward propulsion is commonly impaired in stroke survivors secondary to impaired motor control and spasticity. Clinicians and researchers have developed many rehabilitation technologies, but not all stroke survivors experience clinically meaningful improvements in propulsion following rehabilitation. Functional electrical stimulation, visual or auditory feedback, and fast treadmill walking are commonly used rehabilitation techniques that all show mixed results [1]. Haptic or vibration feedback has been used successfully to improve step length in individuals with Parkinson's Disease [2], but has not yet been used to promote increased propulsion in either healthy or post-stroke individuals.

The purpose of this work was to compare plantarflexion (PF) angle and anterior ground reaction force (AGRF) during overground walking between subjects' normal walking and when subjects were given haptic feedback to promote increases in PF. Because the plantarflexor muscles are a main contributor to forward propulsion [3], it was hypothesized that haptic feedback would increase PF angle and therefore increase propulsion.

**Methods:** Five healthy adults (1 M, 4 F; 30 ± 10 years; 1.66 ± 0.11 m; 71.98 ± 18.76 kg) completed five overground walking trials at their comfortable walking speed with simultaneous data collection in the SageMotion IMU system (100 Hz; Kalispell, MT, USA) and force plates (1000 Hz; AMTI, Watertown, MA, USA). IMUs were placed on the posterior pelvis, lateral thighs, lateral shanks, and dorsal feet of one leg, which was randomized between subjects. Code and additional information about the IMU-based joint angle calculation and haptic feedback delivery is available on the SageMotion open app center. During the baseline trial, subjects were instructed to walk at their comfortable pace in a loop around the lab, ensuring that they passed over the force plates once per loop. Peak PF angle was calculated for each stride and averaged together to obtain each subjects' typical PF angle. During the feedback trial, subjects were instructed to follow the same walking path at their comfortable speed, and were given haptic feedback when their PF angle exceeded a 10% increase over their typical PF angle. This 10% increase was selected in order to exceed the minimal detectable change for kinematic variables [4] and present the same level of difficulty for all subjects. Following the walking trials, force plate data were filtered with a fourth-order low-pass Butterworth filter (30 Hz), then segmented into gait cycles, which were averaged together for each subject. Peak (maximum) PF angle and AGRF were compared between the baseline and feedback trials using a paired t-test ($\alpha = 0.05$).

**Results & Discussion:** Peak PF angle increased by 7.76 ± 11.10° with haptic feedback, although not statistically significantly ($p = 0.19$). Four out of the five subjects increased their PF angle, with three increasing by more than 10°, suggesting that haptic feedback may be successful at increasing PF angle. Increases in PF angle may help subjects generate increases in forward propulsion due to changes in posture and ankle moment [3]. Additionally, these increases in PF demonstrate that individuals were able to interpret haptic feedback and alter their gait biomechanics accordingly, which is promising for future gait rehabilitation technologies.

Anterior ground reaction force was also not statistically significantly different between baseline and feedback conditions (Figure 1), but on average peak AGRF increased by 2% bodyweight (BW, $p = 0.30$) with three subjects increasing (+5% BW) and two subjects decreasing (-2% BW). Of the four subjects who increased their PF, three of them increased their forward propulsion, suggesting that increases in PF are related to increases in propulsion. It is possible that the subject who decreased forward propulsion but increased PF angle may have decreased walking speed, since speed was not tracked in this study but is known to be strongly related to propulsion [3]. When data from more subjects are added to these results, we may be able to demonstrate that haptic feedback to increase PF angle may be an effective mechanism to promote clinically meaningful increases in forward propulsion.

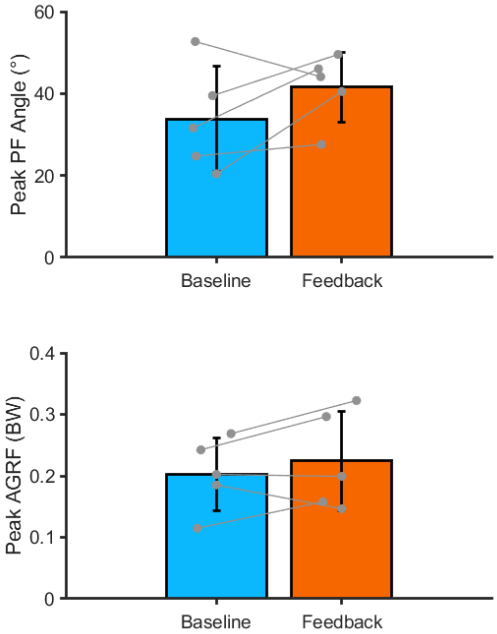


Figure 1: Mean ± one standard deviation PF angle (top) and AGRF (bottom) for the baseline trial (blue) and feedback trial (orange). Individual subject data points are gray with connecting lines between trials. There were no statistically significant differences between baseline and feedback trials for PF or AGRF, although both increased on average.

**Significance:** In rehabilitation applications, encouraging increases in propulsion may be difficult for subjects to contextualize. However, by delivering feedback based on an easily understandable joint angle, we may be able to induce meaningful increases in forward propulsion, suggesting that haptic feedback may be a valuable rehabilitation tool.

**Acknowledgments:** The authors would like to thank the employees of SageMotion for their technical support.

**References:** [1] Langhorne et al. (2009), *Lancet Neurol* 8; [2] Thompson et al. (2017), *Gait Posture* 58; [3] Awad et al. (2020), *J Neuroeng Rehabil* 17(1); [4] Kesar et al. (2011), *Gait Posture* 33(2).

# KNEE-JOINT LOADING DURING GAIT OF TKA PATIENTS 2 MONTHS AFTER SURGERY: A PRELIMINARY STUDY

Alejandro Ovispo-Martinez[1], Walt Menke[1], Tsung-Lin Lu[1], Katie Stevens[2], Harold Cates[2], Songning Zhang[1.]
[1]Biomechanics and Sports Medicine Laboratory, The University of Tennessee Knoxville, Knoxville, TN
[2] Tennessee Orthopaedic Alliance, Knoxville, TN, USA
Email: aovispom@vols.utk.edu

**Introduction:** Research on total knee replacement (TKA) populations has shown deficits in knee joint loading, range of motion, and altered gait patterns in their replaced limbs compared to the non-replaced and healthy control limbs even after more than a year of recovery. (1-4) It is not clear if this deficit is more severe in the early stage of recovery. Therefore, the purpose of this study was to analyze the variables associated with knee joint loading during level walking in TKA patients two months after TKA surgery. We hypothesize that the replaced limb in these patients will demonstrate a deficit in knee joint loading shown by decreased knee extension moments, reduced knee flexion range of motion, and decreased ground reaction forces as previously reported in this population.

**Methods:** Four TKA patients (Age: 65 ± 7.14 years, Height: 1.73 ± 0.16 m, Weight: 106.06 ± 21.65 kg, Gait Speed: 0.82 ± 0.08 m/s) were recruited from a local physical therapy clinic, all 1-2 months post-TKA surgery. They completed five trials of level walking at a self-selected speed. Three-dimensional (3D) kinematic and ground reaction force (GRF) data were captured using a 13-camera system (240Hz, Vicon) and two force platforms (1200Hz, AMTI) in Vicon Nexus software. 3D kinematics and joint moments were computed in Visual 3D (Version 6.1) during the gait cycle. The variables of interest included peak knee extensor moment, knee flexion range of motion (ROM), and peak vertical GRFs in both replaced and non-replaced limbs. A one-way repeated measures ANOVA ($p < .05$) was used to compare differences between limb variables.

**Results & Discussion:** There were no statistically significant differences in peak GFRs, peak knee flexion angles, knee flexion ROM, or peak knee extensor moments. (**Table 1**). During the loading response phase, the peak knee flexion angle for the replaced limb was -11.58° ± 7.29°, and for the non-replaced limb was -13.67° ± 5.40°. The knee flexion ROM was -5.38° ± 3.17° in the replaced limb compared to the non-replaced limb with -9.76° ± 4.39, suggesting a slightly stiffer knee joint for the replaced limb. The peak ground reaction force during the loading response phase was 1.27 N/kg ± 0.35 in the replaced limb and in the non-replaced limb was 1.21 N/kg ± 0.42. During push-off**,** the peak GRF in the replaced limb was 1.29 N/kg ± 0.36 and 1.20 N/kg ± 0.35) for the non-replaced limb. The peak knee extensor moment was 0.23 ± 0.05 Nm/kg in the replaced limb and 0.36 ± 0.28 Nm/kg for the non-replaced limb. aligning with previous studies that found TKA patients tend to offload the operated limb. While these findings did not reach statistical significance due to the small sample size, they partially support previous research suggesting that TKA patients alter knee joint mechanics to reduce loading on the replaced limb. These preliminary results provide further insight into post-TKA gait adaptations and support the need for a larger study with more participants to detect potential significant differences.

**Table 1.** Peak GRF (N/kg), sagittal knee joint kinematic (°) and extension moment (Nm/kg) variables of their replaced and non-replaced limbs for TKA patients (Mean ± Std).

| | Replaced | Non-Replaced | P-value | Partial eta squared |
|---|---|---|---|---|
| Peak LR GRF | 1.27 ± 0.35 | 1.21 ± 0.42 | 0.654 | 0.076 |
| Peak PO GRF | 1.29 ± 0.36 | 1.20 ± 0.35 | 0.461 | 0.192 |
| Peak LR KF | -11.58 ± 7.29 | -13.67 ± 5.40 | 0.41 | 0.23 |
| LR KF ROM | -5.38 ± 3.17 | -9.76 ± 4.39 | 0.071 | 0.72 |
| Peak KEM | 0.23 ± 0.05 | 0.36 ± 0.28 | 0.353 | 0.286 |
| *LR - Loading response, PO - Push off, KF -Knee Flexion, KEM - Knee Extension Moment | | | | |

**Significance:** This study provides valuable preliminary insights into early-stage gait adaptations in individuals following total knee arthroplasty. While no statistically significant differences were observed, analyzing movement patterns as early as two months post-surgery remains crucial for understanding post-TKA gait mechanics. Prior research suggests that TKA patients may develop movement asymmetries, which could influence rehabilitation strategies and long-term joint health. By examining gait characteristics at this early stage, this study highlights the importance of continued investigation into post-TKA biomechanics. Future research with larger sample sizes will be essential to determine whether meaningful differences exist and to guide evidence-based rehabilitation strategies that optimize functional recovery and joint loading symmetry in TKA patients.

**Acknowledgments:** This research was funded through donations through the International Society of Biomechanics Matching Dissertation Grant for 2024 in conjunction with funds from the KRSS Department at the University of Tennessee, Knoxville.

**References: 1.** Valenzuela KA et al. (2021) **2.** Wen C et al. (2019) **3.** Joshi H et al. (2024) **4.** Marino G et al. (2024)

# GAIT PHASE AND SLOPES AFFECT JOINTS' CONTRIBUTIONS TO STABILITY, NOT ORBITAL STABILITY

Chae Lynne Kim[1], Jungho Lee[1], Jooeun Ahn[1, 2] *
[1]Department of Physical Education, Seoul National University, South Korea
[2]Institute of Sport Science, Seoul National University, South Korea
*Corresponding author's email: ahnjooeun@snu.ac.kr

**Introduction:** Theoretically, the maximal (max) Floquet multiplier (FM), which is frequently used as an index of gait orbital stability, is time- and phase-independent in a strictly autonomous periodic system. Human gait, however, is not always purely periodic nor autonomous when exposed to various real-life circumstances. Past studies have observed how people manage to maintain an orbitally stable gait despite the destabilizing characteristics [1], and how humans respond differently to perturbations given at different gait phases [2]. However, we still lack knowledge of mechanisms accountable for stability of human locomotion in various environments and phases. Such mechanisms may vary throughout the gait cycle and walking conditions. Understanding how specific joints contribute to gait stabilization depending on gait phase and environment is crucial in identifying the most adequate joints and effective phases for stabilizing interventions or exoskeletal aid. Among diverse gait environments, we paid attention to slopes which not only abound in our daily life but also affect the joint power and muscle forces, posture, and strategy of gait [3-6]. By investigating the max FM and its corresponding eigenvector at multiple gait events under multiple slope conditions, we aim to scrutinize the stabilizing mechanisms in human walking.

**Methods:** Ten young and healthy adults (age: 21.4 ± 2.2 yrs, height: 1.77 ± 0.05 m, mass: 75.3 ± 5.4 kg) participated in the study. Each participant walked a total of 15 trials, consisting of 3 repetitions across 5 randomized slope levels (-12°, -6°, 0°, 6°, and 12°). In each trial, participants walked on a treadmill at 80% of their preferred walking speed for 5 minutes. Kinematic data were processed to form a 12-dimensional state vector consisting of lower-limb joint angles. For each slope condition, we analyzed the max FMs and the components of the corresponding eigenvector at four Poincaré sections, the bilateral heel strikes and toe offs, respectively.

**Results & Discussion:** We conducted a one-way repeated measure ANOVA within each slope condition to compare the max FMs and its eigenvector components across the Poincaré sections. As shown in Fig. 1, the max FM values are consistent across all Poincaré sections in all slope levels. This suggests that healthy individuals maintain a consistent level of orbital stability throughout the gait cycle even in various slope severities. In contrast, the eigenvector components in both legs show significant changes in their magnitude across the Poincaré sections (Fig. 2). The discrepancies between gait events are especially salient in the 6° and -6° slopes where an interchanging pattern between the right and left knees is observed throughout the gait cycle. In the 6° slope, the right knee's sagittal eigenvector component shows higher magnitudes in the right heel strikes and left toe offs, whereas the left knee's sagittal eigenvector component shows higher magnitudes in the left heel strikes and right toe offs. The exact opposite pattern is observed in the -6° slope.

**Significance:** Our findings suggest that healthy humans maintain a consistent level of orbital stability regardless of gait phase or slope gradient but adopt phase- and slope-dependent strategies with interchanging joint contributions to stabilization to achieve that consistent stability level. The obtained results can provide a basis for identifying critical phase and joints associated with an increased risk of falls during slope walking, and thus improving rehabilitation strategies and gait-stabilizing devices.

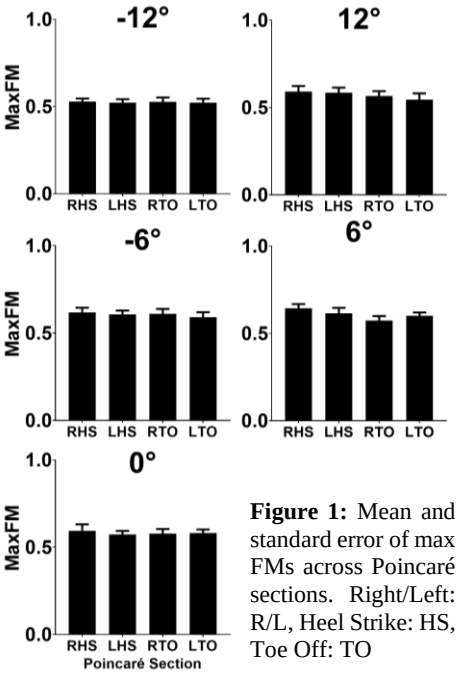


**Figure 1:** Mean and standard error of max FMs across Poincaré sections. Right/Left: R/L, Heel Strike: HS, Toe Off: TO

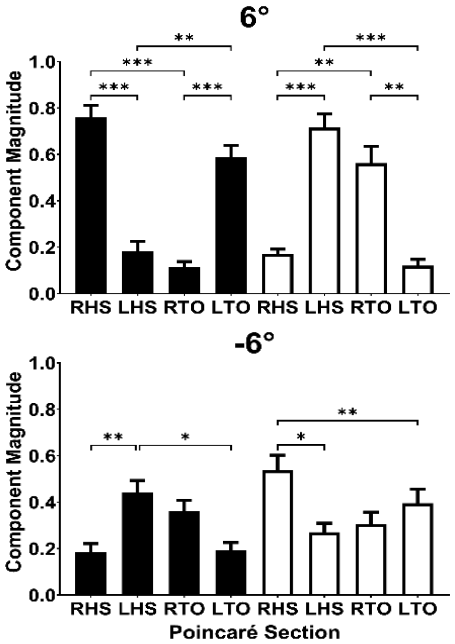


**Figure 2:** Mean and standard error of the right(filled) and left(unfilled) knee's sagittal eigenvector component magnitudes at each Poincaré section in 6° and -6°slopes. (*p < .05, ** p < .01, *** p < .001)

**Acknowledgments:** This work was supported in part by the Korea Health Technology R&D Project through the Korea Health Industry Development Institute (KHIDI) funded by the Ministry of Health & Welfare (No. HK23C0071), Industrial Technology Innovation Program (No. 20007058, Development of safe and comfortable human augmentation hybrid robot suit) funded by the Ministry of Trade, Industry & Energy (MOTIE, Korea), and the National Research Foundation of Korea (NRF) grants funded by the Korean Government (MSIT) (No. RS-2023-00208052).

**References:** [1] Dingwell et al. (2007), J Biomechanical Engineering 129(4); [2] Dietz et al. (2004), Experimental Brain Research 158(3); [3] Lay et al. (2006), J Biomechanics 39(9); [4] Nuckols et al. (2020), PLOS ONE 15(8); [5] Lay et al. (2007), J Biomechanics 40(6); [6] Leroux et al. (2002), Gait & Posture 15(1).

# THE ASSOCIATION BETWEEN CENTER OF MASS VARIABILITY AND DYNAMIC KNEE JOINT STIFFNESS IN PEOPLE WITH KNEE OSTEOARTHRITIS

*Ogundoyin J. Ogundiran[1], Steven A. Garcia[1], Joy Itodo[1], Oiza Peters[1], Paige Perry[1], Kharma C. Foucher[1]
[1]The University of Illinois at Chicago, Chicago, IL
*Corresponding author's email: oogund4@uic.edu

**Introduction:** People with knee OA are also known to be at higher than normal risk for falls [1]. This may be due to abnormal gait patterns associated with the disease, but, the specific aspects of gait that can predispose people with knee OA to balance impairments are unknown. Stiff knee gait is a common gait alteration observed in people with knee OA. A study by Dixon and colleagues demonstrated that people with knee OA walked with higher dynamic knee joint stiffness, but the clinical significance of higher stiffness by this measure was not clear [2]. We presume that walking with a stiffer knee may impact the control of the body center of mass (COM) movement, a factor in stability and balance during gait. This may ultimately increase the risk of experiencing a fall. Therefore, this study aimed to characterize the influence of joint level stiffness has on fall status, stability and balance measured through COM motions, and clinical symptoms. Understanding these associations can provide better understanding of mechanisms underlying abnormal gait in people with knee OA and their implications. This study hypothesized that in people with knee OA: 1) Self-reported fallers have lesser whole-body COM trajectory variability and higher dynamic knee stiffness during gait and 2) lower whole-body COM trajectory variability is associated with both higher dynamic knee stiffness during gait and more self-reported measures of stiffness and dysfunction.

**Methods:** This secondary analysis included 34 people with knee OA (aged 56 years ± 8, BMI 34.76 kg/m$^2$ ± 7). Fall status was determined by each participant's answer to the question: "Have you experienced a fall in the past 12 months?" Ten participants were classified as fallers. Participants completed the Knee Injury and Osteoarthritis Outcome Score (KOOS). The KOOS pain, symptoms, and ADL function subscales were used in the analysis. Notably, the KOOS symptom subscale includes questions regarding perceived joint stiffness. Gait biomechanics were assessed on an instrumented split-belt treadmill, using standard methods, as participants walked at a self-selected speed. Ten clean, consecutive steps were selected for analysis for each participant. For each step, whole-body COM was calculated in Visual3D. The coefficient of variation (SD/Mean x 100) of the displacement of the whole-body COM vertical trajectory was used to characterize COM variability. Knee dynamic joint stiffness was calculated as the change in the sagittal plane knee moment divided by the sagittal plane knee angle during early stance and midstance for both the affected and unaffected limbs. The mean value across the ten steps was utilized in the analysis**.** MATLAB Version R2024a, and SPSS Version 29.0.1 were used for data processing and statistical analysis. Pearson's correlation and independent t-test analyses were used for hypothesis testing ($\alpha$=0.05).

**Results & Discussion:** There were no differences between fallers and non-fallers in COM variability trajectory (effect size d=-0.333, p=0.407) or dynamic knee stiffness at early stance (effect size d=0.157, p=0.685) or midstance (effect size d=.309, p=.421). COM variability trajectory was not associated with dynamic knee stiffness of either the affected limb (early: p=0.073, midstance: p=0.973), or the unaffected limb (early: p=0.467, midstance: p=.661). However, greater COM variability was associated with higher KOOS pain, symptom and ADL function subscales (Fig. 1).

The purpose of this study was to explore the influence of dynamic knee joint stiffness on whole-body COM trajectory variability, and associations with falls and symptoms in people with knee OA. Contrary to the hypothesis neither dynamic knee stiffness nor COM variability differed in people who reported falls, compared to those who did not. Dynamic knee stiffness was not associated with COM variability, but greater COM trajectory variability was associated with less pain, less severe symptoms, including perceived stiffness, and better function. This suggests that walking with more COM variability is desirable and reflects better overall disease status, whether it is associated with fall risk or not.

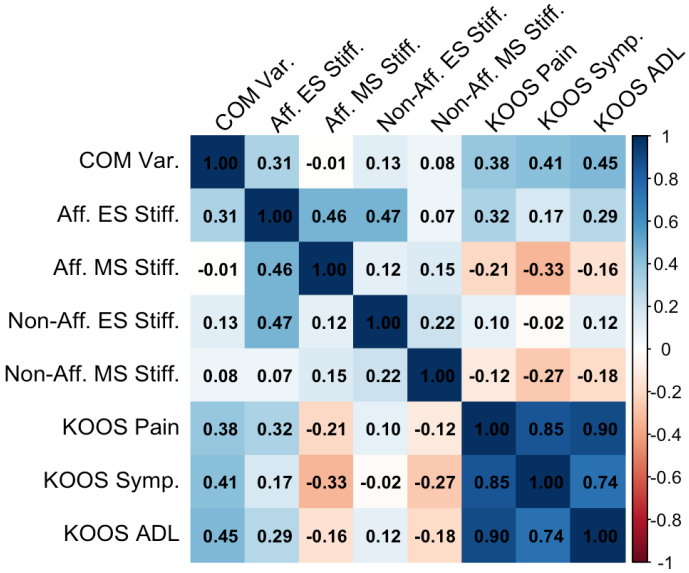


*Figure 1: Correlation Matrix of COM, DJS, and KOOS Subscales*

**Significance:** Falls are a significant obstacle for people with knee OA. For this reason, more foundational biomechanical studies are needed to better understand how abnormal gait due to knee OA influences global measures of balance and stability. Dynamic knee joint stiffness and whole-body COM trajectory variability did not play a role in fall status in these participants, but COM trajectory variability was positively correlated with clinical disease severity. Future studies can investigate other metrics of COM, such as excursion or velocity, and the contribution of individual lower limb segment COMs to better understand how they may influence balance and stability in people with knee OA.

**Acknowledgments:** Pilot grant funding from UL1TR002003

**References:** [1] Wilfong et al. (2023) Arthritis Care Res, 75:2336-44. [2] Dixon et al. (2010) Arthritis Care Res, 62: 38–44.

# RUNNING HABITS AND INJURY PATTERNS IN PARENTS USING RUNNING STROLLERS

Grace Kim[1], Andrew Friesen[2], Allison R. Altman-Singles[2,3]*
[1]Biology, [2]Kinesiology, [3]Mechanical Engineering, Penn State Berks, Reading, PA
*Corresponding author's email: ara5093@psu.edu

**Introduction:** Running is a widely accessible form of exercise that provides significant physical and mental health benefits [1]. However, when runners become parents, they may modify their exercise routines to accommodate childcare responsibilities. Running with a stroller is a common adaptation that allows parents to maintain their running habits while caring for their children [2].

The literature suggests that running with a stroller encourages a more flexed trunk, hip, knee, and ankle, and a shorter stride length [2,3]. Thus far, preliminary work suggests that ground reaction forces and impact loading are reduced [4], which may be indicative of reduced injury rates [5]. However, no research exists which tracks the injuries and injury rates of stroller runners.

The purpose of this study was to begin to characterize the running habits and distribution of injuries of runners when running with a stroller. It was expected that stroller runners would sustain a similar distribution of injuries to the general running population but may run less mileage when running with a stroller.

**Methods:** An online survey was distributed to parents who run and have young children. Participants must have been a parent for a minimum of 5 years. Parents who continued to run after having their child(ren) were separated into two groups, one who resumed running with a running stroller, and the other who did not use a running stroller. The survey collected self-reported demographic data, average weekly running volume with and without a stroller, and history of running-related injuries. Participants were asked about the types and locations of injuries sustained. Descriptive and inferential statistical analyses were conducted to examine differences in running volume and injury prevalence between stroller and non-stroller runners.

**Results & Discussion:** Fifty-seven runners completed the survey (37±5 years, 48 female, 9 male, age of first child 29±4; 2.1±0.7 number of children). Two did not resume running after becoming a parent, so 55 were included in the analysis. 44 chose to run with a stroller (stroller), while 11 did not (control). In the stroller group, 81% were injury free during this time, while 19% sustained running injuries. In the small control group, no specific injuries were reported. The types of injuries reported in the stroller group consisted of 4 cases of plantar fasciitis, 2 cases of shin pain, 2 cases of iliotibial band syndrome, 2 cases of hamstring pain, 1 metatarsalgia, and 1 calf strain.

Weekly mileage was highly variable between participants, but early evidence shows that the majority of stroller runner occurred between 12-36 months (Figure 1). In addition, it appears that runners who ran with strollers had a higher net mileage than those who did not during the early years of their children's lives. Interestingly, runners continued to use strollers until their child(ren) were between 6-10 years of age.

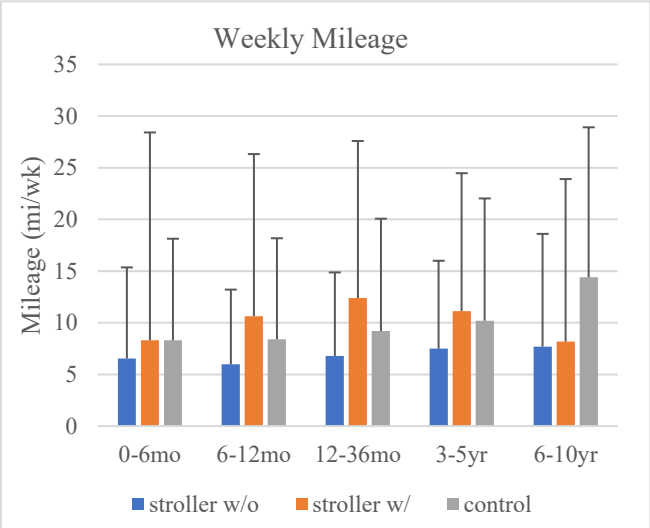


**Figure 1.** Weekly mileage in early parenthood when the child is 0 months old through 10 years old for those running with strollers (mileage without strollers – blue, mileage with strollers – orange), and those who do not run with strollers (control – gray). Error bars indicate standard deviation.

Despite the lack of injuries reported in the control group, evidence suggests that between 19-79% of typical runners are injured each year [6]. The control group in this study may have reduced their mileage, such that injury rates were virtually zero to accommodate for their childcare responsibilities in this phase of life, partially accounting for the 0% injury rates reported. In contrast, stroller runners were injured at a rate of 19%, which is on the lower end of the typical range. This in addition to the mileage, suggests that stroller running may help runners resume typical running habits in this early stage of their child(ren)'s life.

The distribution of injuries is similar to typical epidemiological reports, however, there may be a higher incidence rate of plantar fasciitis, potentially due to the reduced stride length and flexed limb posture that has been noted with stroller running. Despite several injuries reported, it is important to note that stroller runners rated their experience running with strollers at 7.8±2.4 out of 10, indicating an enjoyable experience. Future studies should focus on what motivates runners to choose to run with or without a stroller, to better guide recommendations to athletes, coaches, and clinicians.

**Significance:** While the results of this study are preliminary, it is the first to show relatively low injury rates in stroller runners, coupled with high mileage and high levels of enjoyment with the activity, suggesting that running with a stroller can be relatively safe, effective, and fun.

**Acknowledgments:** The authors of this study would like to thank Miguel Masa for his contributions to this work.

**References:** [1] Markotić et al. (2020), *Psychiatr Danub* 32 (Suppl 2) [2] O'Sullivan et al. (2016), *Gait Posture* 43; [3] Alcantera et al. (2017), *PlosONE 12(7)*; [4] Mahoney et al. (2022), *NACOB, Ottawa, CA*; [5] Davis et al. (2016), *Br J Sports Med* 50; [6] Van Gent et al. (2007) *Br J Sports Med* 41.

# INFLUENCE OF BALLET TECHNIQUE JUMP STYLE ON LOWER BODY MECHANICS

Hailey L. Wrona[1*], Glenna Clifton[2], Kathleen Bieryla[3], Shawn D. Russell[1,4]
[1]Departmant of Mechanical and Aerospace Engineering, University of Virginia, USA
[2] Department of Biology, University of Portland, USA
[3] Department of Mechanical and Biomedical Engineering, University of Portland, USA
[4] Department of Orthopaedic Surgery, University of Virginia, USA
*Corresponding author's email: hlw6br@virginia.edu

**Introduction:** Ballet is a demanding performing art that involves speed, agility, and endurance while requiring the ballet dancer to maintain precision, poise, and elegance of movement. Between 30% and 50% of time-loss injuries in ballet are caused by jumping movements [1]. The high magnitude of injuries related to performing jumps may be a result of the position in which the ballet dancer takes off and lands in. In the methods of Vaganova, the ballet dancer is taught that a jump should start and end from a plié [2,3], where the ballet dancer's hips are externally rotated with their knees in flexion and heels on the floor. In order to reach the plie position during the landing movement, the ballet dancers articulate through their feet in a toe-ball-heel sequence [2]. However, if they train in the method of Balanchine, also known as the American method, ballet dancers are encouraged to not land with their heels on the ground and instead to stay forwards on their toes [3]. Previous research studies have investigated biomechanical changes in rearfoot and forefoot jump landings in other disciplines like basketball [4] and volleyball [5], however, to the best of the authors' knowledge, the influence of different landing techniques in ballet dancers has not been investigated. Therefore, this study aimed to investigate the differences in lower body joint mechanics of ballet dancers in different ballet style landing modes.

**Methods:** A total of 15 pre-professional ballet dancers (men: n=2, age:18 y, height:1.69 ± 0.02 m, mass:61.2 ± 3.9 kg; women: n=13; age:16.8 ± 2.8 y, height:1.65 ± 0.07 m, mass:56.6 ± 8.1 kg) volunteered to engage in the research study. The single data collection was set up in one of the ballet institution's practice studios. An instrumented Bertec force plate was covered with a marley floor material to mirror the surrounding surface conditions and Optitrak cameras were used with the Rizzoli marker set to capture three-dimensional motion analysis. Participants completed three sets of 16 jumps for each landing condition with their right foot on the force plate. Subject-specific lower body models were scaled, and inverse kinematics and dynamics were performed in OpenSim. The jump cycles were time-normalized from the highest center of mass (COM) location of flight to the subsequent highest COM location to ensure the landing kinematics and kinetics were featured in the center.

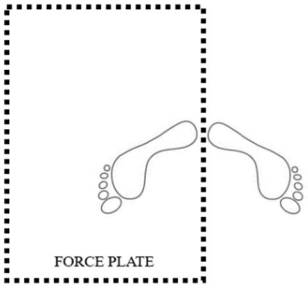


**Figure 1.** Jump position relative to the force plate

**Results & Discussion:** Peak vertical ground reaction forces (vGRF) were different between the two landing conditions. The Balanchine method, heels lifted, resulted in a peak vGRF 11.4% greater than the Vagaonava method, heels dropped. Additionally, the Balanchine method vGRF demonstrated a more rapid increase in force, pointing to a faster loading rate on the ball of the foot during the initial phase of the landing. Compared to the Vaganova method, the greater flexion was observed at the hip, knee, and ankle in the sagittal plane in the Balanchine method. Peak hip adduction and flexion, ankle dorsiflexion and inversion, and knee flexion moments were higher during the Balanchine landing style, as well. Finally, for any given jump in the Balanchine method, the dancer spent less time on the ground resulting in a left phase shift in the joint angle and moment curves.

**Significance:** The current study shows that there is a biomechanical difference between the landing strategies of two prominent ballet styles: Balanchine and Vaganova. The joint kinematics and kinetics for the Balanchine method tended to be greater in magnitude compared to the Vaganova method. A better understanding of how the different ballet styles landing mechanism's influence joint kinematics and kinetics is key to the advancement of injury prevention strategies and improving dancer safety in future research.

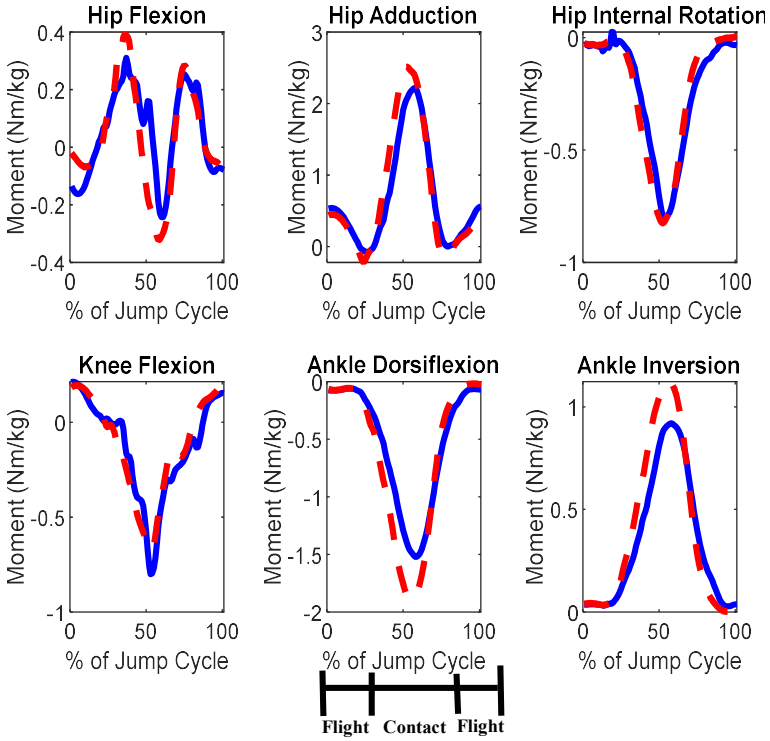


**Figure 2.** Normalized mean joint moments for the hip, knee, and ankle plotted across the time-normalized jumping cycle. **Balanchine** (Solid Blue) and **Vaganova** (Dashed Red) shown on the figure above.

**References:** [1] Mattiussi et al. (2021), *Br J Sports Med* 55(15); [2] Harwood et al. (2018), *Phys Ther Sport*; [3] Morris. (2022), *Research in Dance Education* 25(1); [4] Wang et al. (2023), *Am J Transl Res* 15(9); [5] Garcia et al. (2022), *BMC Sports Sci Med Rehabil* 14(1).

# Stress Fractures of Metatarsals in an Adolescent Cross-Country RUNNER – case study

Mika Ndikumana[1], Megan Gordon, Ali Karimi Azandariani[1], Julio Benjamin Morales, *Hyun Kyung Kim[1]
[1]School of Kinesiology, Louisiana State University, Baton Rouge
*Corresponding author's email: hkkim@lsu.edu

**Introduction:** Stress fractures cause major issues, particularly for athletes, as they interfere with training and competition and can result in extended periods of athlete absence, so prevention measures are essential. Due to the ongoing development of their musculoskeletal system, adolescents who participate in sports are more vulnerable to stress fractures. Between 1.54% and 10% of all injuries suffered by adolescent athletes are stress fractures, which are particularly common in cross-country runners [1, 2]. Long-distance running requires a lot of training, which can be too much for teenagers whose bones may not be ready for the prolonged, repetitive nature of the sport. Recently, we rarely recruited an adolescent runner who had experienced stress fractures in the second metatarsal of his left foot on four separate occasions over the past year. This case report aimed to examine the biomechanical characteristics associated with metatarsal stress fractures in young cross-country athletes, with the goal of identifying any biomechanics elements that might have contributed to these recurring stress injuries. It was hypothesized that the previously injured leg would exhibit differences in lower limb joint kinematics and plantar pressure patterns compared to the uninjured leg.

**Methods:** This study evaluated a 16-year-old male cross-country athlete (1.71m, 53kg, 18.1kg/m$^2$) who had experienced stress fractures in the second metatarsal of his left foot on four separate occasions over the past year. At the time of enrollment, he had fully healed. To identify potential biomechanical abnormalities, we assessed his lower limb biomechanics while running at his natural speed using an eight-camera motion capture system (Qualisys AB, Sweden), wearable intelligent wireless insoles (XSENSOR Technology Corporation, Calgary, Canada), and a split-belt treadmill with force plates (Bertec Corp, Columbus, OH). Key anatomical landmarks such as the pelvis, femoral epicondyles, malleoli, lateral thigh and shank, calcaneus, and metatarsal heads were marked with 36 reflective markers. Before starting the data collection, he was allowed to familiarize himself with running on a treadmill with the 1.8mm thick insoles placed in his shoes for about 1-2 minutes, as well as to determine his natural jogging speed (1.94m/s). We randomly selected three steps for each leg, averaging the results for further analysis. To calculate joint angles, torque (Nm/kg), and power (W/kg), Visual3D software (HAS-Motion, Ontario, Canada) was used. Peak plantar pressure was obtained using XSENSOR's Clinical Foot & Gait software and analyzed across 11 plantar regions: T1 (hallux), T2-5 (toes 2-5), M1-M5 (metatarsal heads 1-5), MM/LM (medial/lateral midfoot), and MH/LH (medial/lateral heel). Peak values during the stance phase for all measures were obtained and compared between previously injured and uninjured legs using a two-tailed paired t-test.

**Results & Discussion:** The findings revealed significant differences in ankle dorsiflexion and hip rotation angles between the previously injured (left) and uninjured (right) legs. The left hip showed a significantly (10.82±1.71° vs. 3.84±1.1°, $p$=0.003) less internal rotation at the heel strike than the right. During the terminal stance, the left leg displayed notably greater ankle flexion than the right (21.08±0.78° vs. 27.11±1.59°, $p$=0.03), which could point to asymmetries in movement coordination. Also, the peak plantar pressure under M4 ($p=0.01$) was significantly greater in left foot compared to the right foot, while the pressure under T2-5 ($p$=0.03) and M1 ($p$=0.009) was significantly lower in the left foot than in right foot. The findings indicate a noteworthy functional disparity between the right and left legs. The reduced internal rotation seen in the left leg during heel strike could reflect variations in joint movement or muscle activation between the two sides. Additionally, the increased ankle flexion in the left leg during the terminal stance may suggest that the left leg is compensating for biomechanical shortcomings during running. A more laterally directed plantar pressure during propulsion can potentially cause torque modification in the lower limb during gait, altering load attenuation [3]. These asymmetries could have consequences for understanding the risk of injuries or for creating strategies to enhance gait symmetry. Overall, these findings expand on existing knowledge of limb disparities in human movement and offer insights into how particular joint angles can impact overall walking efficiency.

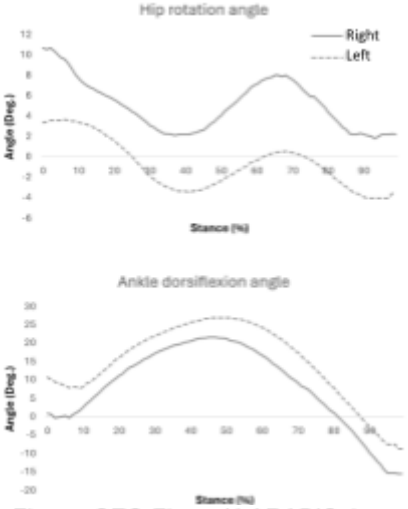


*Figure SEQ Figure * ARABIC 1.* A comparison of the angles of hip rotation and ankle dorsiflexion between the right (non-injured) and left (injured) legs while running.

**Significance:** This research highlights important biomechanical discrepancies in lower limb movement patterns during running, particularly between the previously injured and uninjured legs. While long-term monitoring of these discrepancies in lower limb biomechanics is required to confirm their effects, these variations could lead to uneven stress on the feet and potentially contribute to the recurrence of metatarsal stress fractures. This study could inform tailored rehabilitation programs, especially in adolescent distance runners who might be particularly susceptible to overuse injuries.

**Acknowledgments:** The authors would like to thank the participant. There were no sources of funding in relation to this case report.

**References:** [1] Marshall, A.N., et al., (2020), *J Athl Train*. 55(12); [2] Changstrom, B.G., et al., (2015). *Am J Sports Med*, 43(1); [3] Aliberti S,., et al., (2011) Clinics. 66(3).

# KINEMATIC DIFFERENCES EXIST AT THE HIP BUT NOT THE KNEE BETWEEN STANDARDIZED AND NORMALIZED RUNNING SPEEDS IN HEALTHY FEMALE AND MALE RUNNERS

*Eric Foch[1], Richard A. Brindle[2], Kevin R. Ford[3]
[1]Department of Health Sciences, Central Washington University, Ellensburg, WA, United States
[2]Shaw Sports Turf, Shaw Industries Group, Inc., Dalton, GA, United States
[3]Department of Physical Therapy, High Point University, High Point, NC, United States
*Corresponding author's email: eric.foch@cwu.edu

**Introduction:** Biomechanists investigating sex differences in runners' gait must decide whether to 'standardize' the protocol's running speed or to 'normalize' speed to participant's preferred pace. Controlling for running speed eliminates the potential effects that the covariate speed has on the biomechanical dependent variables, for example, peak joint angles. However, relatively small differences in running speeds, for example, 3.5 m•s$^{-1}$ [1] compared to 4.0 m•s$^{-1}$ [2] result in quite drastic pace differences over a typical training distance (7:40 min•mile$^{-1}$ versus 6:42 min•mile$^{-1}$). Depending on participants' comfort with the 'standardized' running speed, two different conditions could be collected, thus, affecting the results. Complicating the interpretation of kinematics are the small mean differences in peak joint angles reported between healthy female and male runners in the literature. For example, sex differences in sagittal and frontal plane hip and knee angles range from ~2 to 3.5 degrees [3]. If running speed was 'normalized', this may provide a clearer understanding of any reported differences between healthy female and male runners. Therefore, the purpose of this investigation was to determine whether kinematic differences existed between female and male runners at a 'standardized' and self-selected 'normalized' running speed. Due to physiological differences between sexes, we hypothesized that male runners 'normalized' pace would be faster than female runners' pace. Sex differences in 'normalized' running speeds would affect peak hip and knee joint angles differently between sexes for the two running conditions.

**Methods:** All procedures were approved by the University's Internal Review Board. A secondary analysis was performed on an existing data set investigating running biomechanics in collegiate cross-country runners from a single team (females (n = 8): 19 ±1 years, 54.7 ±4.5 kg, 1.68 ±0.08 m; males (n = 8, 19 ±1 years, 65.9 ±5.4 kg, 1.76 ±0.05 m). Three-dimensional gait analysis was performed during instrumented treadmill running at a 'standardized' 3.5 m•s$^{-1}$ and self-selected 'normalized' paces. Marker trajectories were collected for 30 trials within each condition ('normalized' followed by 'standardized'). Joint angles were computed via joint coordinate systems. Sagittal and frontal plane hip and knee peak angles were extracted during stance and averaged across participants' 30 trials. To determine any interaction between sex and running speed, separate two-way (group-by-condition) mixed-model analysis of variance (ANOVA) were performed with condition as the repeated measure. Post hoc independents t-tests compared joint angles between sex for each condition. Alpha was set at 0.05 for all tests.

**Results & Discussion:** There were significant group-by-condition interactions for peak hip flexion and hip adduction angles (Table 1). Hip flexion and adduction increased between the 'normalized' and 'standardized' conditions in female runners but remained unchanged in males. The 'normalized' running speed was a faster average pace for males (3.66 ±0.05 m/s) compared to female runners (3.17 ±0.04 m/s). However, only peak hip adduction angle was greater in female runners compared to male runners for the two conditions. At the knee, no interactions or sex differences were found.

Greater hip adduction angles exhibited in healthy female runners compared to males is consistent with the running literature regardless of whether running speed was 'normalized' or 'standardized' [1-5]. Only female runners increased hip flexion with increased speed is contrary to the literature where a greater peak hip flexion angle was observed in males running at a 'normalized' speed [4]. At the knee, no interaction suggests that female and male runners responded similarly to changes in speed. However, there are mixed results in the reporting of a higher peak knee abduction angle in female runners compared to males regardless of speed being 'normalized' [1-3,5].

**Significance:** Beyond peak hip adduction angle, there is a consistent lack of agreement in the reporting of sex differences in hip and knee kinematics in the running literature. Biomechanists examining sex differences in runners' kinematics may need to reconsider a 'standardized' speed protocol. Faster running increased the biomechanical demands at the hip in female runners more than males. Greater hip flexion was required to accommodate for the faster speed. Thus, a 'normalized' speed may be a better approach to ensure all runners are experiencing similar biomechanical demands for data collection.

**Table 1:** Hip and knee joint angles in female (F) and male (M) running during the two different speed conditions (mean (sd))

| | Two-way Repeated Measures ANOVA | | | | Independent t-test | |
|---|---|---|---|---|---|---|
| | | Condition | | Inter-Action Effect (*P*) | Condition | Between Sex Difference (*P*) |
| | Sex | Normalized | Standardized | | | |
| Hip flexion angle (°) | F | 25.0 (3.7) | 27.3 (2.6) | 0.007 | Normalized | 0.963 |
| | M | 24.9 (5.0) | 25.1 (5.0) | | Standardized | 0.289 |
| Hip adduction angle (°) | F | 15.6 (3.4) | 16.6 (3.8) | 0.002 | Normalized | 0.047 |
| | M | 12.7 (1.8) | 12.0 (1.9) | | Standardized | 0.009 |
| Knee flexion angle (°) | F | 39.5 (4.8) | 40.4 (2.9) | 0.333 | Normalized | 0.537 |
| | M | 40.8 (3.8) | 40.9 (3.9) | | Standardized | 0.794 |
| Knee adduction angle (°) | F | 1.8 (2.4) | 1.9 (2.4) | 0.475 | Normalized | 0.061 |
| | M | -0.8 (2.7) | -0.6 (2.8) | | Standardized | 0.074 |

**References:** [1] Willson et al. (2012) *Clin Biomech* 27; [2] Almonroeder & Benson. (2017). *J Sport Sci* 35; [3] Xie et al. (2022), *Front Physiol* 13; [4] Vannatta & Kernozek. (2021) *Sport Biomech* 20; [5] Ferber et al. (2003). *Clin Biomech* 18.

# ACTIVITY-INDUCED CHANGES IN PAIN AND GAIT IN ADULTS WITH AND WITHOUT KNEE OA

*Julien A. Mihy[1], Mayumi Wagatsuma[1], Katie A. Butera[1], Elisa S. Arch[1], Stephen M. Cain[2], Jocelyn F. Hafer[1]
[1]Biomechanics and Movement Sciences, University of Delaware [2]Chemical and Biomedical Engineering, West Virginia University
*Corresponding author's email: mihyj@udel.edu

**Introduction:** Pain with movement, or movement-evoked pain, is common in adults with knee osteoarthritis (OA), but the effect of this pain on gait is not well understood. A few studies have measured changes in pain and gait in response to activity; however, these studies analyzed timed intervals during continuous walking on a treadmill or measured overground gait mechanics before and after a treadmill walk that was intended to induce pain [1,2]. Further, these protocols required 20-45 minutes of continuous walking which may not represent behavior in the real-world as only 13-40% of adults with knee OA meet the minimum guidelines for moderate to vigorous physical activity [3]. Additionally, not all participants with knee OA had changes in pain in response to these walking protocols. In contrast, stairs are a common activity of daily living that are often painful even in relatively short bouts and in early stages of knee OA. Thus, bouts of stair ascent/descent may serve as a more ecologically relevant pain-inducing protocol to study changes in gait and pain. Further, multiple bouts of activity may influence gait mechanics independently of pain, therefore it is important to also examine how adults with knee OA respond to bouts of stair activity compared to their healthy counterparts. Therefore, the purpose of this study was to determine how pain and gait change in response to multiple bouts of stair activity in those with and without knee osteoarthritis.

**Methods:** 22 participants, 4 with self-reported physician-diagnosed knee OA that met clinical American College of Rheumatology criteria (3 female, 64.3±3.8 years) and 18 asymptomatic adults (9 female, 60.9±3.9 years) participated in this study. Four IMUs (Opal v2, APDM/Clario, Philadelphia, PA) were placed on the sacrum, thigh, shank, and foot of the right (healthy) or most symptomatic (OA) leg. Each participant completed four overground walks (each ~20m), one walk before and after each of two bouts of ascending and descending stairs (each bout is 2 flights=50 stairs) with a rest between walks 2 and 3 (Figure 1). Participants were asked to report their pain on a scale of 0-10 (0=no pain, 10=worst imaginable) during each of the four walks. Bouts of walking and gait events were identified via the motion or frequency of shank or foot data [4]. Spatiotemporal variables were calculated via a ZUPT approach [5]. Segment angular velocities about functionally oriented mediolateral axes were integrated to estimate segment excursions [6]. Joint ranges of motion (ROM) were then calculated as the difference in adjacent segment excursions. The outcome variables of interest were the post- minus pre-stair bout difference in pain, stride velocity, stride length, and hip, knee, and ankle joint ROM. The differences in response to stairs were compared between groups and stair bouts via a 2x2 mixed model ANOVA ($\alpha$=0.05). To determine whether pain affected bout or group comparisons, pain was used as a covariate for all gait kinematics tests.

**Results & Discussion:** Significant differences were only found at the knee and ankle. There was a greater decrease in knee ROM in response to bout repetition in the knee OA group compared to the healthy group (OA=-1.9±0.7°, healthy=-0.3±0.5°, p=0.028) (Figure 1). There was also a greater increase in ankle ROM following the second bout of stairs compared to the first (bout1=0.2±1.3°, bout2=0.9±1.1°, p=0.014). Pain had an influence on the effect of bout repetition on ankle ROM (p=0.033). These findings indicate both groups had different changes in ankle ROM in response to the second bout of stair activity compared to the first, and pain had a significant effect on the response.

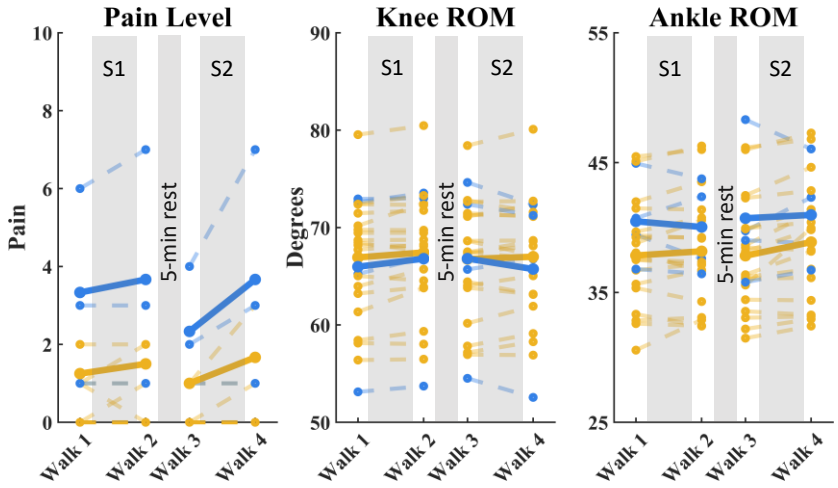


**Figure 1**. Changes in pain and gait in response to stair activity (S1&S2). Yellow lines = healthy adults & blue = adults with knee OA. Solid lines = group averages.

The change in pain during walking following a bout of stair activity ranged from -1 to +3 with half of the knee OA participants experiencing an increase in pain. The OA participant with the greatest overall pain and increase in pain had decreases in all joint excursion ROMs while the other OA participant that experienced increased pain had decreases in hip and ankle ROM but increases in knee ROM following the second bout of stairs. The two OA participants that had no change in pain increased their ankle ROM while decreasing their knee ROM following bouts of activity. Although the changes in ankle ROM were small (0-2.6 degrees), these findings replicate previous findings indicating there may be a relationship between changes in pain and an individual's ability to increase their reliance on their ankle mechanics to offload the symptomatic knee [2].

**Significance:** This project provides new insight into how gait mechanics and pain of individuals with and without knee OA respond to multiple bouts of stair activity. These findings reveal that 1) alternating multiple bouts of stairs and short overground walking can induce changes in gait and pain similar to longer treadmill bouts and 2) the ankle may be a target of interest for decreasing the likelihood of pain in response to bouts of activity in those with knee OA.

**Acknowledgments:** This work was supported by a University of Delaware KAAP Dissertation Grant.

**References:** [1] Farrokhi et al. 2017 *Gait Posture*; [2] Boyer & Hafer. 2019 *BMC Musculoskelet Disord.*; [3] Wallis et al. 2013 *Osteoarthr Cartil*; [4] Baroudi L et al. 2022 *Gait Posture*; [5] Rebula JR et al. 2013 *Gait Posture*; [6] Mihy JA et al. 2022 *medRxiv*

# WALKING KINEMATICS DURING TREADMILL, OVERGROUND, AND OUTDOOR WALKING

Jingjing Sun[1#], Diego Samson[1#], Chang Liu[1*]
[1]Department of Kinesiology and Nutrition, University of Illinois Chicago, USA
[*]Corresponding author's email: cliu67@uic.edu; [#]Equal contribution

**Introduction:** The ability to walk outdoors is essential for engaging in daily activities, maintaining independence, and improving quality of life [1]. Most studies have focused on understanding walking kinematics in the controlled laboratory setting due to technical limitations to capturing walking kinematics without a marker-based optical motion capture system. However, laboratory settings do not reflect the complexity of the real-world environment and heightened fall risks, such as turns, curbs, or uneven surfaces. Development with inertial measurement units (IMU) and force-instrumented insoles have allowed us to perform a comprehensive analysis of gait kinematics outside the laboratory [2] [3]. Prior research has shown that gait temporal parameters differ between walking on outdoor sidewalks and on the treadmill [4]. However, there is a lack of comparison in joint kinematics, which may be influenced by environmental requirements. Here, healthy young adults walk on the treadmill, overground, and outdoor environment. We hypothesize that, at the same walking speed, participants will have a higher cadence, shorter double support time, and longer swing time when walking outdoors compared to overground and treadmill and greater peak joint angle in the sagittal plane as the outdoor environment being more complex, with curbs and turns.

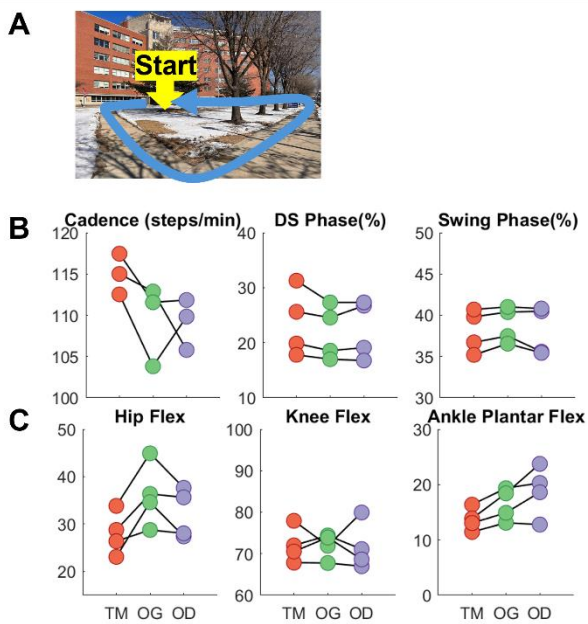


Fig.1: (A) Outdoor loop on the sidewalk. (B) Gait temporal parameters during treadmill walking, overground, and outdoor walking (n = 4). DS: Double support. (C) Peak hip flexion, knee flexion, and ankle plantar flexion (deg) during treadmill walking, overground, and outdoor walking. TM: Treadmill, OG: Overground, OD: Outdoor.

**Methods:** This is an ongoing project. Four young adults so far completed an in-lab treadmill trial, 10m overground and 10 laps of outdoor (161 meters/lap) walking. The outdoor surface was the flat concrete sidewalk with curves, three ~90° turns, and approximately 2-3 curb steps (Fig. 1A). We placed inertial measurement units (IMUs, Noraxon Ultium Motion Sensors, 200 Hz) on eight locations (thorax, pelvis, R/L thigh, R/L shank, and R/L feet) and insole force sensors (Noraxon, 500 Hz) in the participant's shoes. All data was collected using MyoResearch4. Participants first walked on the treadmill at 1.2 m/s for two minutes and then walked in a straight path at a controlled speed of ~1.2 m/s as overground trials. Outdoor trials consisted of ten laps, each lap lasting approximately 134 seconds, at a controlled speed of 1.2 m/s. We analyzed the middle 6-meter portion of the overground walking to obtain steady-state gait cycles and middle outdoor laps. We used MATLAB to compute temporal gait parameters (cadence, double support time/step time, swing time/stride time) and peak lower extremity joint angles in the sagittal plane (knee flexion/extension, hip flexion/extension, foot flexion/extension) for each condition and each participant. We will perform a one-way ANOVA to test if the walking environment changes gait kinematics.

**Results & Discussion:** Qualitatively, when walking speed was controlled, participants reduced their cadence when walking overground and outdoors compared to walking on the treadmill, which is contrary to our hypothesis (Fig. 1B). Participants also slightly reduced the double support phase (%) when walking overground and in the outdoor environment. For joint angles, peak hip flexion angle became greater during both overground and outdoor environments compared to treadmill walking (Fig. 1C). Peak ankle plantar flexion was the greatest during outdoor walking. These results suggest that greater hip flexion and ankle plantar flexion are needed to adjust for more complex walking environments with different surfaces and turns.

**Significance:** These findings suggest that walking kinematics, including both gait temporal parameters and joint kinematics, differ when walking in different environments after controlling for walking speed. This indicates that in-lab gait does not fully represent real-world gait behavior. Our next step is to investigate whether aging and neurological injuries (e.g., stroke) will have a greater effect on walking kinematics when walking outdoors.

**Reference:** [1] Mirelman et al. (2018), Handb Clin Neurol 159. [2] Mazzà et al. (2021), BMJ Open 11(12). [3] Tahir et al. (2020), Sensors (Basel) 20(4). [4] Wagatsuma et al. (2024), Gait Posture 113.

# LEVRAGING INERTIAL MEASUREMENT UNITS FOR QUANTIFYING VARIABILITY IN OUTDOOR WALKING

Ruchika Iqbal[1], Jeffery Haddar[1], *Satyajit Ambike[1]
[1]Department of Health and Kinesiology, Purdue University, West Lafayette, IN
Corresponding author's email: sambike@purdue.edu

**Introduction:** Controlled laboratory experiments are essential to identify fundamental principles of human movement control, but they do not capture how people move in complex outdoor environments [1]. To fill this gap, researchers now deploy wearable sensors to study natural human locomotion in free-living environments. Inertial Measurement Units (IMUs) have emerged as particularly valuable tools, offering continuous monitoring that can establish normative movement patterns and may also detect deviations from the norms.

IMUs provide good characterization of temporal gait features, capturing both average stride times and their natural variations. Their ability to measure spatial features like step lengths, however, remains limited to average estimates [2]. This is a bigger challenge when people walk on uneven terrain or have pathological gait, where traditional assumptions like pendular stance motion [3] may not apply. In outdoor environments, therefore, where distance measurements are less reliable, IMU analyses typically focus on temporal variables.

To address this issue, we propose analyzing net accelerations from ankle-mounted triaxial IMUs using a spatio-temporal index (STI). This metric was originally developed for speech science to quantify orofacial movement patterns and their pathological deviations [4]. We employ STI to capture stride-to-stride variability in walking patterns. We hypothesize that STI values will reflect walking surface characteristics: lower values on flat versus sloped surfaces, and lower values on concrete versus grass. Grass surfaces, with their inherent variations in level, softness, and texture, should produce more variable gait patterns and correspondingly higher STI values.

**Methods:** Eight young adults (5 men, 24±4.8 yrs) walked at their comfortable speed on a lightly populated outdoor path. No participant had to adjust their gait to avoid other pedestrians. The path included various surfaces: concrete sidewalks (flat: elevation = 0.4°, 300m, uphill and downhill: elevation 4°, 165m each way), grass surfaces (flat: elevation 0°, 170m, uphill and downhill: elevation 6.4°, 125m each way), and a concrete staircase (elevation 22.9°, 30m). Participants completed walking on each surface before proceeding to the next. Participants took about 45 minutes to complete the experiment, which included 16.4±1.9 minutes of walking time to traverse the 1 km route.

Two IMUs (Mbientlab) were attached near the lateral malleolus of each shank. The IMUs sampled 3D linear acceleration in their local inertial frame at 100 Hz. After filtering, the net acceleration was computed and parsed into strides. Strides data were time and amplitude normalized and pooled across legs. The STI was calculated by summing the across-stride standard deviations computed over two consecutive time point pairs [4] separately for each surface (Fig. 1A, 1B).

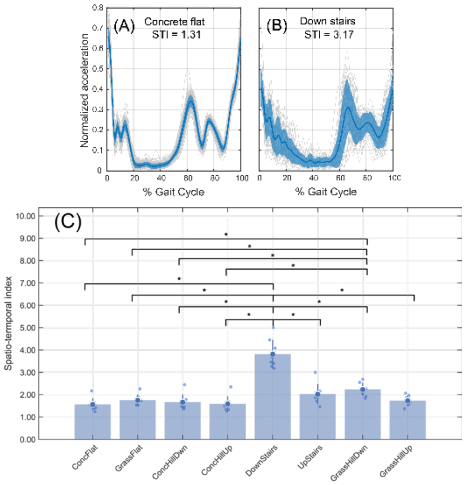


*Figure 1. Examples of STI computation (A) and (B). Mean and SD of STI for all surfaces (C).*

**Results & Discussion:** A one-way ANCOVA, controlling for walking speed, revealed a significant effect of surface on STI ($F_{(7,55)} = 43.31$, $p < .001$, partial $\eta^2 = .85$; Fig. 1C), while speed showed no significant influence ($p = .098$). Contrary to our hypothesis, surface type (concrete vs. grass) had minimal impact during flat and uphill walking. However, grass downhill walking showed elevated STI compared to all concrete surfaces (mean differences: 1.14-1.61, $p < .05$), partially supporting our prediction of higher variability on grass surfaces. The most striking finding was that descending stairs elicited significantly higher STI values compared to all other tasks (mean differences: 3.98-5.58, all $p < .001$). These results suggest that task difficulty, rather than surface characteristics, primarily influences movement variability. While elevated STI on grass downhill likely reflects motor adaptations to uncertain surface properties, the highest STI during stair descent – which presents an uneven by highly regular surface – suggests that task-specific biomechanical demands may override surface-related effects on movement variability.

**Significance:** STI can be computed for any periodic signal; indeed, it is computed for orofacial displacements in the speech sciences. We chose to analyze accelerations instead to avoid two well-known drift issues in IMU analysis: integrating accelerations to obtain spatial gait measures and integrating orientation information to transform accelerations into anatomical planes. These simplifications discard meaningful biomechanical information, yet the index was able to distinguish between types of gait and surfaces even in homogeneous healthy young participants. Furthermore, by combining STI with stride timing and acceleration magnitudes, we can obtain information about the regularity and intensity of natural walking performance. Finally, using these indices in conjunction with the knowledge of the environment, we can interpret the STI values as healthy adaptability or pathology.

Our long-term goal is to use IMUs to assess real-world mobility in various populations. Therefore, we endeavoured to our keep our analyses simple and interpretable, thereby improving their chances for clinical adoption. Clinicians could use our method to track how patients move in their communities, providing objective measures of the real-world efficacy of their protocols.

**Acknowledgment:** Ruchika Iqbal is supported by the Ross Graduate Fellowship awarded by Purdue University.

**References:** [1] Hillel et al. (2019), *Eur Rev Aging Phys Act* 16(6); [2] Din et al., (2016) *IEEE J. Biomed Health Inf* 20(3); [3] Zijlstra and Hof (2003) *Gait & Pos* 18; [4] Smith et al., (1995) *Exp Brain Res* 104.

# VALIDATION OF A SINGLE MASK TYPE IMU FOR RUNNING GAIT ANALYSIS

Yoojin Choi[1], Hyunji Kim[1], Kibeom Lee[2], Jaeyoun Choi[3], Jaehoon Kim[4], Jinmo Kim[2], Jooeun Ahn[1,5]*
[1]Department of Physical Education, Seoul National University, Seoul, Korea, [2]Neumafit Corporation, Seoul, Korea, [3]Department of Mechanical Engineering, MIT, MA, USA, [4]Department of Mechanical and Process Engineering, ETH Zurich, Zurich, Switzerland, [5]Institute of Sport Science, Seoul National University, Seoul, Korea
*Corresponding author's email: ahnjooeun@snu.ac.kr

**Introduction:** The COVID-19 pandemic has accelerated the emergence of devices that integrate assessment of physiological variables [1] and motion [2]. The smart mask, which combines respiratory monitoring with motion sensing using inertial measurement units (IMUs), is a representative example. However, no study to date has validated the reliability of mask type IMUs in assessing running kinematics. To fill this research gap, we aim to check the validity of such an IMU in estimating basic running kinematics. Given that a head-mounted IMU has demonstrated reliability in gait analysis [3], we hypothesize that a mask type IMU can be used to estimate basic temporal parameters and the vertical oscillation.

**Methods:** We estimated contact time, flight time, cadence, and the vertical oscillation using a mask type IMU, the prototype of PACER (Neumafit, South Korea), and compared the obtained values with those estimated using an instrumented treadmill (Bertec, USA) and a motion capture system (Qualisys, Sweden). Eighteen young and healthy adult males (age: 25.9± 3.7 y, height: 1.77 ± 0.07 m, mass: 77 ± 11.4 kg) ran on a treadmill at 10 km/h under three cadence conditions: their preferred cadence, preferred cadence -10%, and preferred cadence +10%, guided by a metronome. Each participant completed the three trials of 1-minute running with a randomized order. The raw accelerometer data was transformed using a composite rotation matrix derived from aerospace-standard Euler angles. A one-dimensional Kalman filter was applied to smooth vertical acceleration data, modeling the system as a random walk process and assuming gradual acceleration changes. The initial state was set as the mean of the first five time-series values to ensure a stable starting point. In the prediction step, the previous state estimate was used while incorporating process variance to account for system uncertainty. During the update step, the Kalman gain adjusted the predicted state based on the difference between observed and predicted values.

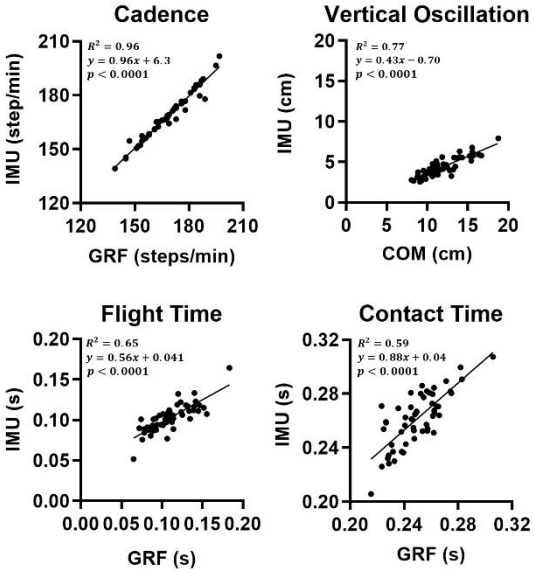


**Figure 1 :** Correlations between mask type IMU and GRF-derived running metrics.

**Results & Discussion:** The IMU-derived cadence exhibited a strong correlation with the cadence measured using the instrumented treadmill ($R^2$=0.96) and a small negative bias (−0.052 step/min). Vertical oscillation also showed a high correlation ($R^2$ = 0.87) though it was consistently underestimated (-7.5 cm). Moderate correlations were observed for flight time ($R^2$ = 0.65) and contact time ($R^2$ = 0.59) with the biases of -0.0071 s and 0.012 s, respectively. Our findings indicate that a mask type IMU can estimate the some basic kinematics of running with reasonable accuracy. The strong correlation in cadence is consistent with the result from a previous study on head-mounted sensors [3].

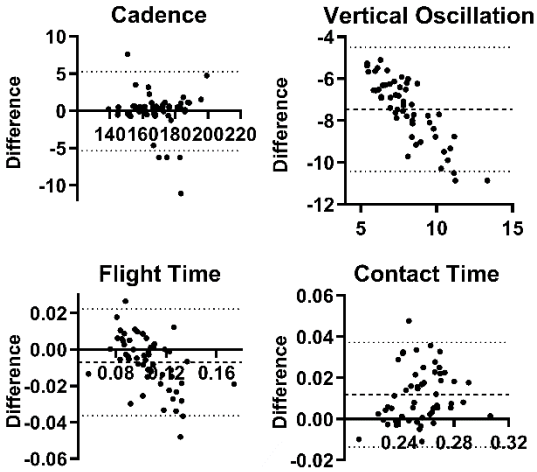


**Figure 2 :** Bland-Altman analysis. The sets of dotted horizontal lines represent the 95% limits of agreement (difference ± 1.96×standard deviation), and the dashed lines in the middle show the biases.

**Significance:** The compact integration of respiratory measurements with running kinematics acquisition, which can be achieved by sensing motion with a mask type IMU, is expected to offer more comprehensive and convenient evaluations of running. This study provides the first validation of a mask type IMU for running gait assessment. The observed accuracy in measuring the cadence particularly indicates that the mask type sensor can serve as a non-intrusive alternative to shank- or foot-mounted devices at least for measuring the running cadence. Machine learning technology may enhance the accuracy, and future research may explore the validity of mask type IMUs in estimating additional biomechanical parameters like step asymmetry and stiffness to expand the utility of such devices.

**Acknowledgments:** This work was supported in part by Industrial Technology Innovation Program (No. 20007058, Development of safe and comfortable human augmentation hybrid robot suit) funded by the Ministry of Trade, Industry & Energy (MOTIE, Korea), and the National Research Foundation of Korea (NRF) grants funded by the Korean Government (MSIT) (No. RS-2023-00208052).

**References:** [1] Heng et al. (2024), *Science 385(6712)*; [2] NeumaFit (2024), Retrieved from https://neumafit.co.kr/pages/why-pacer
[3] Hwang et al. (2018), *IEEE Trans. Consum. Electron.* 64(2)

# UNEVENLY ADDED MASS DECREASES PEAK HIP FLEXION AND INCREASES HIP EXTENSION IN NON-PREGNANT WOMEN DURING OVER GROUND WALKING

*Mathew Sunil Varre[1], Grace Watson[2], Janet Zhang-Lea[1]
[1]Department of Human Physiology, University of Oregon
[2] College of Arts and Sciences, Gonzaga University, Spokane, WA
* Email: varre@uoregon.edu

**Introduction:** Women with a normal weight BMI can gain 25-35 lbs during pregnancy, which increases the demand on the lower limb musculature during walking [1]. Previous biomechanical studies analyzed changes in walking kinematics during pregnancy and have reported reduced peak hip extension during stance phase and shorter stride length in pregnant women during the second and third trimesters, as well as compared to non-pregnant women [2-4]. These changes may be due to multiple factors such as increased anterior pelvic tilt, added mass, and hormonal variations and associated musculoskeletal adaptations. One study examined the effect of 100% anteriorly added mass on gait in non-pregnant women, and found reduced hip extension during stance phase and a shorter stride length with added mass increasing from 0 lbs to 20 lbs [5], which was consistent with previous studies in pregnant women. However, pregnancy-related weight gain is unlikely to be solely distributed in the anterior region, and previous studies focused on changes in walking kinematics across the gait cycle, but not within a specific phase during walking. In this study, we further investigated the effect of unevenly distributed mass on lower limb kinematics in non-pregnant women during over ground walking, distributing 60% of the added mass to the anterior and 40% to the posterior region. We hypothesized that walking with unevenly added mass would increase peak hip and knee flexion, and decrease hip and knee extension during stance phase of walking in non-pregnant women.

**Methods:** Five healthy non-pregnant women (Age: 29±4 years old; Height: 1.7±0.1 m; Mass: 64±9 kg) walked with a pregnancy sac (0.28 lbs) at their self-selected speed (1.22±0.05 m/s). They walked under four conditions, including one no-mass (NM) condition with pregnancy sac only, and 3 mass conditions with 10, 20, and 30 lbs added mass to simulate weight gain during different stages of pregnancy. When adding mass, 60% of the mass was placed anteriorly, and 40% posteriorly to the sac. The participants performed at least five walking trials within 10% variation of their self-selected speed per mass condition, and the sequence of testing condition was randomized. We collected kinematic data at 100 Hz (Motion Analysis Corp, USA), and processed the data using Visual 3-D (HAS-Motion, CA) to obtain joint kinematics in sagittal plane for at least 3 strides per leg per condition. We analyzed the stance phase variables for all three joints including peak hip flexion during the 1st double limb support phase (DLS), peak hip extension, peak knee flexion during DLS, peak knee extension during single limb support phase, peak ankle plantar flexion (PF) during DLS, peak ankle dorsiflexion (DF), and joint range of motion (ROM) for hip, knee, and ankle joints across a gait cycle. We normalized added mass to the participant's body mass in percentage, and used a linear mixed effect model to estimate the effect of percentage of added mass on the variables.

**Results & Discussion:** Linear mixed effect model analysis of the kinematic data revealed a 5.5° reduction in peak hip flexion during DLS ($p=0.004$), a 6.1° increase in peak hip extension ($p=0.002$), and 13.9° increase in hip ROM ($p=0.008$) with every 10% added mass. Knee joint kinematics variables did not change significantly with added mass ($p=0.59$-$0.94$). Ankle peak PF in DLS increased by 6.7° ($p=0.04$) with every 10% added mass, but there was no significant difference in peak ankle DF angle or ankle ROM as added mass increased ($p=0.42$-$0.71$).

We rejected our hypothesis as our results indicated that compared to walking with no added mass, non-pregnant women presented a less flexed and more extended hip joint when walking with 10-30 lbs of added mass. These findings did not align with those reported in pregnant women. One possible reason is that the participants in the study experienced immediate weight gain during data collection, whereas pregnant women experience a gradual weight gain over a longer period. Furthermore, unlike pregnant women, non-pregnant women do not experience large hormonal variations that lead to musculoskeletal adaptations such as increased laxity in joints and tendons, and increased pelvic tilt [1]. Our results also contradicted the previous findings for non-pregnant women with 100% anteriorly added mass [5], which could be a result of a different weight distribution used in this study (60% vs. 40%). Given our limited knowledge of weight distribution and geometrical changes in a pregnant human body, it remains unclear what type of weight distribution can most accurately reflect the weight gain experienced by pregnant women. This preliminary study findings highlight the need for a more comprehensive understanding of the weight distribution and development of a model specific for pregnant women to understand the effect of added mass on their walking kinematics.

**Significance:** The findings of this pilot study will enhance our understanding of biomechanical adaptions of gait during pregnancy, specifically related to weight gain, independent of the physiological changes associated with pregnancy. Gaining insights into these changes could be useful in understanding the demand from lower limb muscles, reducing the risk of musculoskeletal issues, such as lower back pain and knee pain, and prevent pregnancy-related falls.

**Acknowledgments:** The authors acknowledge contributions from Rhiana Bretl, and the support from Dr. Mike Hahn's research team at the University of Oregon, with special thanks to Rachel Robinson.

**References:** [1] Conder et al. (2019), *J. funct. morphol kinesiol. 4*(72); [2] Branco et al. (2013), *J. Pregnancy*; [3] Mei et al. (2018), *Sci. Rep.* 8; [4] Catena et al. (2020), *Gait & Pos* 80; [5] Ogamba et al. (2016), *J. Apl.Biomech* 32.

# BODY SIZE, GAIT MECHANICS AND MAXIMAL RUNNING SPEEDS

Gouresh Powar*, Peter Weyand
Locomotor Performance Lab, Kinesiology Department, Texas Christian University, 2012 W Berry St, Fort Worth, TX 76110
Email: g.m.powar@tcu.edu

**Introduction:** The world's fastest sprint runners excel at a highly specific mechanical task. While task specificity might be expected to favor a single body size phenotype, available data indicate otherwise [1]. World-class performers in the 100-meter event have been as short as 1.65, and as tall as 1.96 meters with body masses ranging 66 kg - 96 kg. The explanation for the body size heterogeneity observed is not known at present. The available race performance data suggests that height is beneficial for maximal sprinting velocities, but may impair acceleration performance [2]. Here, we posed a basic question about maximal running velocities and body size for human runners: do the maximal speeds of the swiftest human runners vary as a function of height? We opted to compare the maximal speeds of different sprinters using the Froude number (Fr). The Froude number is a dimensionless metric that quantifies speeds that are equivalent for runners who differ in body size [3].

$$Fr = \frac{u^2}{gL}$$

If maximal sprint velocities are achieved with dynamically similar sprint running gait mechanics, then different-sized sprinters should have the same Froude number at their respective maximum velocities [3]. This expectation, if correct, predicts that taller sprinters should have slightly faster velocities in absolute terms, but the same relative velocities, or Froude numbers, when height and leg length are taken into account.

**Methods:** We acquired running performance and body size data for 37 national and international calibre sprinters at their maximum instantaneous velocities (i.e. ≤ 2.0 seconds) on a level treadmill [4, 5, 6, 7] or during overground sprinting [8, 9, 10]. Maximal running velocities were determined from treadmill speed in the laboratory and high-speed motion capture techniques overground. The minimum speed required for inclusion was 10.5 m/s. Body size and gait parameters analyzed were: height (L), body mass ($M_b$), leg length ($L_o$), and maximal sprint velocity ($V_{max}$). Leg lengths were measured from the hip axis of rotation to the ground for the laboratory subjects, and assumed to be 0.55 height for the overground subjects. Scaling functions for $V_{max}$ and Fr with respect to body length were determined.

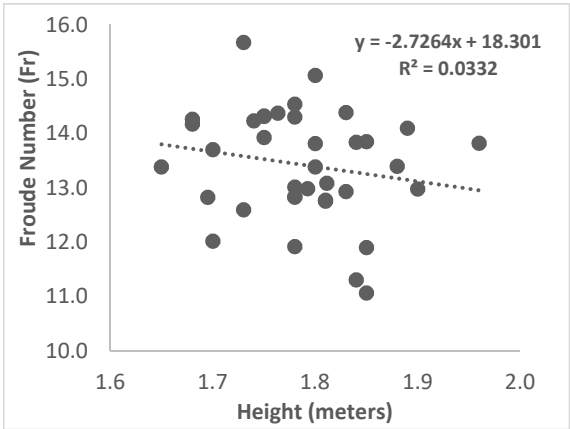


**Figure 1:** Relationship between Froude Number (Fr) and Height (meters) with linear trendline and equation. ($R^2$ = 0.03), (p = 0.28).

**Results & Discussion:** The observed mean ± standard deviation and ranges for the variables are as follows: $M_b$: mean ± SD = 77.2 ± 6.1 kg (range: min= 66.0 kg, max= 91.0 kg); L: mean ± SD = 1.788 ± 0.068 m (range: min= 1.65 m, max= 1.96 m); $L_o$: mean ± SD = 0.979 ± 0.039 m (range: min= 0.901 m, max= 1.078 m); $V_{max}$: mean ± SD = 11.341 ± 0.432 $ms^{-1}$ (range: min= 10.5 $ms^{-1}$, max= 12.1 $ms^{-1}$); Fr: mean ± SD = 13.43 ± 1.00 (range: min= 11.07, max= 15.67); Predicted $V_{max}$ using the constant mean Froude number observed for this population (Fr=13.43): mean ± SD = 11.35 ± 0.22 $ms^{-1}$ (range: min= 10.89 $ms^{-1}$, max= 11.91 $ms^{-1}$). Our analysis did not identify a relationship between height and Froude number among our group of elite male sprinters. The best-fit relationship indicated a slightly negative trend indicating taller runners may attain slightly lesser Froude numbers when running at their maximal sprint speeds.

**Significance:** Our findings indicate that height is not significantly related to maximal sprinting speeds of elite male sprinters when limb lengths are taken into account, and leave open the possibility that sprinters of different body sizes may run in dynamically similar gait mechanics.

**References:** [1] Weyand, P. G., & Davis, J. A. (2005). *J of experimental biology*, 208 (Pt. 14), 2625–263; [2] McClelland, E. L., & Weyand, P. G. (2022). *J of applied physiology (Bethesda, Md.: 1985)*, *133*(4), 876–885. [3] Alexander, R. et al. (1976). *Nature, 261*, 129–130. [4] Clark, K. P., & Weyand, P. G. (2014). J *of applied physiology (Bethesda, Md.: 1985)*, *117*(6), 604–615. [5] Weyand, P. G. et al. (2000). J *of applied physiology (Bethesda, Md.: 1985)*, *89*(5), 1991–1999. [6] Weyand, P. G. et al. (2009) J *of applied physiology (Bethesda, Md.: 1985)*, *107*(3), 903–91. [7] Weyand, P. G. et al. (2010J *of applied physiology (Bethesda, Md.: 1985)*, *108*(4), 950–961. [8] Moravec, P., et al. (1988). New Studies in Athletics, 3, 61–96. [9] Udofa, Andrew et al. (2017) *ISBS Proceedings Archive*: Vol. 35: Iss. 1, Article 120. [10] Mann, R., & Murphy, A. (2015). The Mechanics of Sprinting and Hurdling. Create Space Independent Publishing Platform.

# THE INFLUENCE OF SPEED ON STAIR ASCENT FUNCTIONAL DEMAND IS JOINT DEPENDENT

*Abigail K. Salvadore, Sarah A. Roelker
Department of Kinesiology, University of Massachusetts, Amherst, MA
*Corresponding author's email: asalvadore@umass.edu

**Introduction:** Older adults list stairs as one of the most challenging activities of daily living [1], yet negotiate, on average, the same number of flights each day as younger adults [2]. However, the challenge can become so great that stairs become a barrier to navigating the community, diminishing independence and quality of life [3]. Functional demand (FD) quantifies the difficulty of a locomotor task as the percentage of maximal strength used during a task [4] and is calculated as the ratio of the net joint moment (NJM) used during the task to the maximal voluntary torque that can be produced given the instantaneous joint angular velocity [5]. Regardless of age, FD is higher during stair ascent than stair descent [6-8].

The speed at which a locomotor task is performed influences FD, and the literature suggests age, speed, and FD may have a complex relationship. For example, in walking, *faster* walking speed is associated with higher FD at all three joints [5,9]. However, older adults often ascend stairs *slower* than younger adults [1], yet FD at peak NJM is higher for older adults at the knee [7-8]. One study reported no age-related differences in FD at the ankle during stair ascent [7], and the influence of age on FD of the hip extensors during stair ascent has not been reported. Thus, there is a need to differentiate between the contribution of speed and other age-related differences (e.g., strength) to differences in the FD of stair ascent between older and younger adults at all lower extremity joints. As an initial step to identify the factors contributing to the difficulty of stair ascent, the purpose of this study was to identify the effect of speed on FD of the hip, knee, and ankle extensors during stair ascent in younger adults. Due to the higher FD observed at faster walking speeds [5,9], we hypothesized faster stair ascent speed would require higher FD at all joints. Furthermore, while FD is typically calculated at the peak NJM, the peak FD (i.e., the most demanding instant of the task) may not correspond to the peak NJM. Thus, we also investigated differences in FD at peak NJM compared to peak FD, and the impact of speed on these differences.

**Methods:** Six participants (3M/3F, 26.7±4.5y, 1.7±0.1m, 70.3±14.7kg) performed 9 stair ascent trials, three each at self-selected (SS), fast, and slow speeds. Thresholds were set such that the fast (slow) speed was at least 15% faster (slower) than the SS pace. Isometric and isokinetic strength was assessed on a Biodex dynamometer at the hip (±60°/s, ±150°/s), knee (±90°/s, ±240°/s), and ankle (±60°/s, ±120°/s). Peak torque at each velocity was used to generate a torque-velocity curve for each participant and joint. For the hip, knee, and ankle extensors, FD at time *i* of the stair ascent stance phase was calculated as the NJM at time *i* divided by the torque from the torque-velocity curve, given the joint velocity at time *i* (Eq 1). For each joint, differences in peak FD between speeds were assessed with a RMANOVA. Pairwise differences were identified by t-tests with Bonferroni correction. For each speed and joint, paired t-tests assessed differences in 1) timing of peak FD and peak NJM, and 2) magnitude of peak FD and FD at the time of peak NJM. All $\alpha = 0.05$.

$$\text{Functional Demand (i)} = \frac{\text{Net joint moment (i)}}{\text{Torque (velocity (i)}} \quad \text{(Eq. 1)}$$

**Results & Discussion:** Average stair ascent speeds were SS: 0.47±0.04m/s, slow: 0.26±0.07m/s, fast: 0.73±0.14m/s. Peak ankle FD was significantly lower at a slow speed compared to the SS ($p < 0.001$) and fast ($p = 0.006$) speeds (Fig. 1A). Thus, slower stair ascent reduces FD on the ankle extensors, but faster ascent does not increase FD above that of SS speed. Peak FD occurred significantly later than peak NJM at the ankle at slow (mean difference ($\mu_d$): 4.6% of stance, $p = 0.007$) and SS ($\mu_d$: 2.1% of stance, $p = 0.008$) speeds and at the knee for fast ($\mu_d$: 4.8% of stance, $p = 0.04$) and SS ($\mu_d$: 0.8% of stance, $p = 0.02$) speeds. The FD at peak NJM was significantly lower than peak FD for the ankle at fast ($\mu_d$: 0.29, 16% difference, $p = 0.004$), slow ($\mu_d$: 0.36, 28% difference, $p = 0.002$) and SS speeds ($\mu_d$: 0.33, 18% difference, $p = 0.04$) (Fig. 1B).

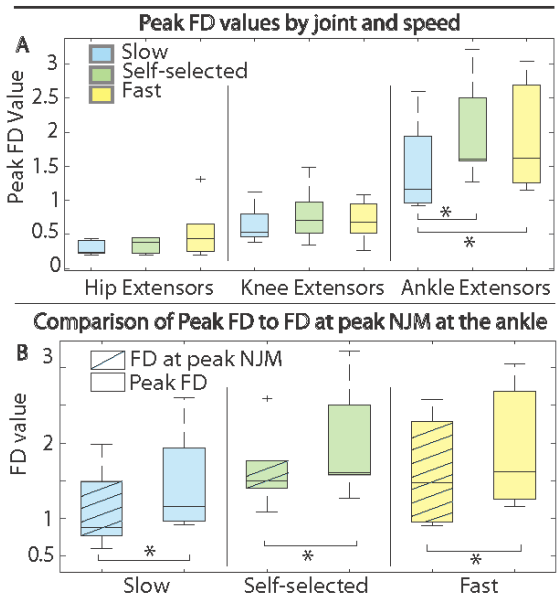


**Figure 1.** Peak FD values A) by joint and speed, and B) Compared to FD at peak NJM at the ankle. + denotes outliers. * denotes significant pairwise differences.

**Significance:** Stair ascent speed influenced FD values in younger adults, but only at the ankle. These results suggest speed alone may not explain age differences in functional demand on stairs and should be further investigated. Still, given that ascending stairs slower reduces FD at the ankle, slower stair ascent speeds in older adults may be a strategy to compensate for age-related reductions in plantarflexion function [10]. However, this hypothesis needs to be confirmed in an older adult cohort. Methodologically, while the difference in timing between peak FD and peak NJM is less than 5% of the stance phase, calculating FD at the peak NJM may inaccurately represent the peak demands of stair ascent by underestimating peak FD at the ankle.

**Acknowledgments:** Funding support: Edith Robinson Fellowship, University of Massachusetts Graduate School (AKS).

**References:** [1] Novak, 2011. *Gait Posture*. [2] Startzell, 2000. *J Am Ger Soc.* [3] Tiedemann, 2007. *J Geron.* [4] Holmes, 2022. *Gait Posture*. [5] Hafer, 2020. *J App Biomech.* [6] Reeves, 2008. *J Electro Kin.* [7] Reeves, 2009. *J Electro Kin.* [8] Hortobagyi, 2003. *J Geron.* [9] Spinoso, 2019. *J Aging Phys.* [10] Sloot, 2021. *Gait Posture*.

# STEP LENGTH AFFECTS METATARSOPHALANGEAL JOINT MOMENTS DURING FOREFOOT ROCKER PHASE OF WALKING

*Harsh H Buddhadev[1], Emily M. Lovekin[2]
[1]Department of Kinesiology, Sam Houston State University, Huntsville, TX
[2]Seattle Children's Hospital, Seattle, WA
*Corresponding author's email: hhb005@shsu.edu

**Introduction:** Walking is a vital activity of daily living required for functional independence, and therefore, it is important to maintain walking abilities especially in older adults and those with disabilities. Walking slowly and taking shorter steps are common strategies adopted by these individuals to reduce the demands on the lower extremity joints and muscles. Specifically, reduction in step length and walking speed are accomplished by reductions in push-off action during the late stance phase of walking, when the foot pivots forward (dorsiflexes) about the metatarsophalangeal (MTP) joint as the heel rises (i.e., forefoot rocker phase). This dorsiflexion at the MTP joint tightens the plantar fascia that wraps around the metatarsal heads thereby elevating and stabilizing the longitudinal arch and aiding in the push-off action via windlass mechanism. The stiffening of the MTP joint to aid push-off action is also facilitated via force production by plantar intrinsic muscles [1]. Several studies that used multisegmented foot models indicated that walking speed affects sagittal plane MTP joint kinematics and kinetics during the forefoot rocker phase [2, 3]. A recent study [4] showed that walking at different step lengths at the same speed also affects MTP joint kinematics. No research has examined how MTP net joint moments are affected when walking at different step lengths at the same speed. Examination of MTP joint moment during the forefoot rocker phase could provide insights on modulation of push-off effort at this joint associated with different step lengths. The purpose of our study was to investigate the effects of different step lengths at the same speed on peak MTP joint moments during the forefoot rocker phase of walking. We hypothesize peak MTP joint moments are greater for longer compared to shorter step lengths when walking at the same speed.

**Methods:** Twelve young healthy adults (6 females and 6 males; 22.9 ± 2.5 yrs; 168.2 ± 9.4 cm; 70.6 ± 17.1 kg) completed 5 overground walking trials at their preferred speed over a 12-m walkway. From those trials, the participants' average preferred walking speed, preferred step length (PSL), and step rate were calculated. Next the participants completed 5 overground walking trials within ±3% of the preferred speed that was determined previously under 3 step length conditions in a random order. Step length conditions were based on previous studies [4, 5] and consisted of PSL and PSL shortened and lengthened by 10% of leg length [LL] (PSL ± 10%LL). To implement the step length conditions, floor tapes were placed at distances corresponding to the calculated step length along the 12-m walkway. A metronome corresponding to the calculated step rate was used to help participants maintain the appropriate step rate. Marker positions of the combined Oxford foot and conventional gait model were captured at 100 Hz and ground reaction forces and moments from a force plate embedded in the middle of the walkway were synchronously captured at 1000 Hz. Sagittal plane MTP joint moments over the forefoot rocker phase were computed using an inverse dynamics approach using methods outlined previously [6, 7]. Peak moments in the sagittal plane were identified over the forefoot rocker phase and then normalized to the participants' body weight [BW]. Peak MTP dorsiflexion angle was also identified over the forefoot rocker phase. One-way repeated measure ANOVAs were used to examine the effects of step length on peak MTP dorsiflexion angle and plantar flexor moment. For significant main effect of step length, post-hoc analyses were performed with t-tests.

**Results & Discussion:** The step length conditions were successfully administered as demonstrated by speed, step length, and step rate data presented in Table 1. Throughout the forefoot rocker phase, MTP joint was going through dorsiflexion motion and the internal moments at the joint were plantar flexor. Sagittal plane MTP joint angle and moment profiles from the current study were consistent in shape and magnitude compared to previous research [8, 9]. Significant main effects of step length were observed for peak plantar flexor moment ($p<0.001$; $\eta_p^2=0.582$) and dorsiflexion angle ($p=0.001$; $\eta_p^2=0.495$). Both these variables increased systematically (PSL-10%LL < PSL < PSL+10%LL) with step length. These systematic increases in peak MTP moment may suggest an increase stiffening of the plantar fascia and an increase in contractile force generated by the plantar intrinsic muscles to systematically produce a more forceful push-off with increase in step length.

**Table 1.** Experimental variables associated with the forefoot rocker

| | PSL-10%LL | PSL | PSL+10%LL |
|---|---|---|---|
| Speed ($m \cdot s^{-1}$) | 1.30 ± 0.16 | 1.29 ± 0.16 | 1.31 ± 0.16 |
| Step length (m) | 0.60 ± 0.08 | 0.69 ± 0.07 | 0.78 ± 0.07 |
| Step rate (step/min) | 130 ± 12 | 113 ± 6 | 101 ± 6 |
| Peak MTP dorsiflexion angle (°) * | 46.7 ± 9.4 | 48.9 ± 11.1 | 51.2 ± 11.8 |
| Peak sagittal MTP moment (Nm/BW) * | 0.026 ± 0.008 | 0.032 ± 0.011 | 0.038 ± 0.013 |

Data presented as mean ± 1 standard deviation. * Statistically significant step length main effect (p<0.05

**Significance:** Examination of the MTP joint motion and moments during the forefoot rocker phase can provide insights into the modulation of push-off effort during walking. Taking longer steps at the same walking speed necessitate larger moments in the sagittal plane at the MTP joint.

**References:** [1] Farris et al. (2019), PNAS 116(5); [2] Tulchin et al. (2009), *J Appl Biomech* 25(4); [3] Eerdekens et al. (2019), *Gait Posture* 68(2019); [4] Lovekin et al. (2024), *J Biomech* 168(2024); [5] Buddhadev et al. (2020), *Hum Mov Sci* 71(2020); [6] Day & Hahn (2019), *J Biomech* 86(2019); [7] Nigro & Arch (2022), *J Appl Biomech* 38(5); [8] Bruening et al. (2012), *Gait Posture* 35 (2012); [9] Saraswat et al. (2014), *Gait Posture* 39 (2014).

# REVIEWING MEASURES OF METABOLIC RATE ACROSS WALKING SPEEDS AND ESTIMATING THE COST OF PREGNANT WALKING ACROSS GESTATION

*Elizabeth M. Bell[1], Jenna K. Burnett[2], Samantha J. Snyder[3]
[1]School of Health Professions, Department of Kinesiology, Towson University, Towson, MD, USA.
[2]College of Health, Department of Health and Kinesiology, University of Utah, Salt Lake City, Utah, USA.
[3]Department of Kinesiology, University of Maryland, College Park, MD, USA.
*Corresponding author's email: ebell@towson.edu

**Introduction:** To maintain health while prioritizing safety during pregnancy, many medical professionals recommend walking for physical activity and exercise. Pregnancy individuals experience increases in mass and physiological changes which progressively change walking biomechanics [1] and may increase the metabolic cost of walking, defined as metabolic energy expended per unit distance traveled. Most studies which have investigated the cost of walking in pregnant individuals have focused on comparing metabolic rate (kcal/min) across time points within the individual (e.g., between trimesters and postpartum). Still, between-study results are difficult to compare due to differences in the units in which it was expressed ae tendency to scale metabolic rate by current weight. Since energy expenditure is influenced by walking speed it's difficult to understand between group or longitudinal differences in metabolic rate. Examining available metabolic rate data across studies and walking speeds and using available results to estimate the metabolic cost of walking may help provide an understanding of how comfortable walking speed may change as pregnancy progresses and if aspects beyond walking speed and mass gain may contribute to changes in energy expenditure.

**Methods:** A systematic review search protocol was created to identify manuscripts reporting energy expenditure of pregnant individuals while walking and registered (Prospero#183127). A comprehensive search was performed in EBSCO Medline, ProQuest, PubMed, and Web of Science databases. Results were limited to human subjects and peer-reviewed articles in English. Studies which presented energy expenditure of pregnant walking using indirect calorimetry or oxygen analyzers were included. Group mean data were extracted for each study group: height (m), mass (kg), walking speed (in or converted to m/s), gestation time (in weeks or by trimester), and number of subjects (n), gross metabolic rate (in or converted to kcal/min). If rates were scaled to mass, then rates were estimated by multiplying the scaled value by group mass. When metabolic rates were not directly presented gross oxygen consumption and respiratory quotient data were used to compute mean carbon dioxide production of each group and metabolic rate, was computed via Brockway's formula [2] with Weir's method of protein correction [3]. An estimate of the group mean (SD) metabolic cost of transport was reported or estimated for each study. If normalized rates were not published walking cost estimation required scaling metabolic rates in kcal/min by individual (if available) or average group mass and dividing by average walking speed.

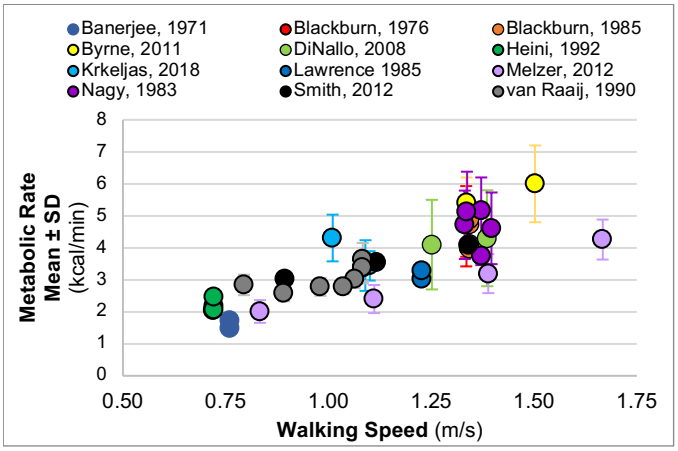


**Figure 1:** Metabolic Rate (kcal/min) between identified studies.

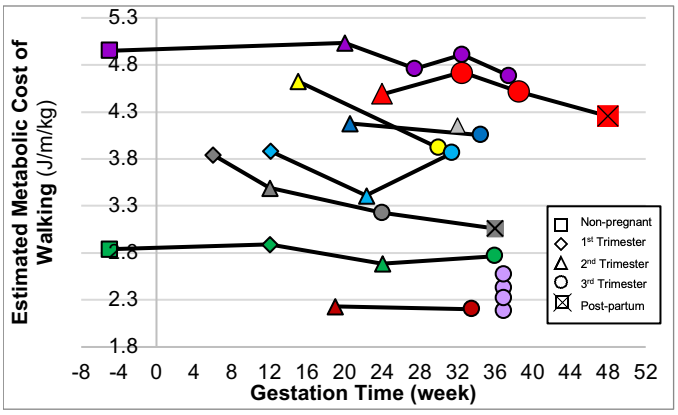


**Figure 2:** Estimated Metabolic Cost (J/kg/m) from each identified study over gestational time. The squares, diamonds, triangles, circles and crossed squares represent trimester or postpartum designation from each study. Group means are plotted at average gestational week reported.

**Results & Discussion:** Initially, 335 titles were identified, and abstracts were reviewed. 52 full-text manuscripts were screened, leaving 15 potentially suitable articles. Three did not assess pregnant participants, and two reported metabolic cost in kcal/min without group mass, excluding them from cost estimates. Metabolic rate increased with walking speed. Within-study trends in metabolic cost over gestation were inconsistent, but a within-subject analysis in the third trimester (Melzer, 2012) indicated greater increased cost at faster speeds, which may suggest walking strategy may be more expensive. Still, it is unclear if some available data are gross or net metabolic cost or if collection methods differ systematically. Most results are limited to group means, hindering transformation into similar units or correct scaling to individual mass or walking speed, making cost estimation the only option which allows for limited interpretation.

**Significance:** An impressive amount of data regarding the energy expenditure of walking in pregnancy have been compiled over the last 50+ years but it is not possible to correctly transform all available data into the same units. A more comprehensive, longitudinal evaluation of pregnant energy expenditure across multiple speeds is necessary to understand if progressive changes in gait mechanics, possibly apparent at faster walking speeds, influence the metabolic cost of walking and may also reduce self-selected optimal speeds.

**References:** [1] Forczek et al. (2019) Gait & Posture [2] Brockway (1987) Clinical Nutrition [3] Weir (1949) J. Physiol.

# 3D KINEMATICS OF UNEVEN-TERRAIN GAIT USING A MULTI-SEGMENT FOOT MODEL

*Tayler Hoekstra[1], Lisa MacFadden[2]
[1]Dordt University, Department of Engineering, 700 7th St NE, Sioux Center, IA 51250
[2]University of South Dakota, Department of Biomedical Engineering, 4801 N Career Ave, Sioux Falls, SD 57107
*Corresponding author's email: tayler.hoekstra@coyotes.usd.edu

**Introduction:** Kinematic analysis of gait has commonly been conducted using a rigid model for the foot. In recent years, there has been a shift to increase the complexity of this model to a multi-segment foot model (MSFM), of which there are a few[1,2]. Given the increased use and research into these models, their application continues to increase. As of yet, there has been little done to see how these MSFM might more deeply inform researchers into the unique compensations and movements of the foot during uneven terrain ambulation. The following research aimed to utilize the Rizzoli MSFM to describe the angular kinematics of the different foot segments defined by the model in all planes of motion and test whether angle calculations across one full gait cycle would differ significantly when quantifying the angles of ankle between the two models.

**Methods:** 6 healthy, barefooted individuals were outfitted with reflective markers according to the Rizzoli markerset and tasked with walking across an even-ground (i.e. flat) walkway for a total of 6 trials[3]. The walkway was then outfitted with square grid that had a random layout of 24 rectangular portions each of differing height mimicking a previously defined uneven terrain[4]. These squares were laid out at random on top of the even terrain and could be switched around between ambulation trials. A minimum of 6 trials were collected for each subject over the uneven terrain. Motion was recorded using a 10-camera circle of OptiTrack motion capture cameras and were analysed in Visual3D to compare differences in ankle angle kinematics (i.e. rigid foot model vs MSFM) between the even and uneven terrain trials. Kinematics of the other segments were also quantified and compared between even and uneven terrain gait. Statistical parametric mapping was used when comparing angle cures between model types and between terrain types[5].

**Results & Discussion:** When comparing differences in foot model type, significant differences were observed in all 6 subjects for almost all three dimensions, with only 2 subjects showing no significant differences between models for Inversion-Eversion curves. As for comparison of terrain type within the different joints of the Rizzoli MSFM, there were very few significant differences found between even and uneven terrain ambulation, with only occasional significant differences found between curves, but never more than 3 of the 6 subjects showing significant differences between the curves.

Regarding the significant differences seen between foot models, this study provides strong support for the continued development and use of MSFMs in biomechanics research, especially when analysing complex motions such as uneven terrain ambulation. Miscalculations in ankle joint kinematics (and furthermore, likely also moments and power) are likely to occur without a sufficient model to accurately define the ankle joint.

There is interest in the lack of significance between even and uneven ambulation trials within the sub-joints of the Rizzoli MSFM. One contributing factor may be the use of SPM. When utilizing SPM, the main benefit is that of analysing the curve as a whole as opposed to cherry-picking points of interest. However, SPM relies on Random Field Theory, which takes the overall curvature of the data into account. Given the high variability of uneven terrain ambulation, SPM analysis may not determine significant differences between trials where visual differences in the data may seem to occur. Future studies may look at higher effects of data smoothing on results or isolating specific planes of rotation of the foot that could then be applied to more general uneven terrain ambulation.

**Significance:** Those working the field of biomechanics well understand how the choice of model affects the results that can be quantified within a particular study. The choice to use a MSFM for analysing the complexities of uneven terrain ambulation can be clearly shown to affect the results of kinematic quantification. The choice of SPM statistical analysis also provides interesting insight given where differences between curves might be found as opposed to simply selection of points of interest to analyse for differences between curves. Furthermore, this research might begin to form a repository of kinematic data for describing the complex motion of uneven terrain based on a more descriptive model of the foot.

**Acknowledgments:** No outside funding was provided for the support of this research.

**References:**

1. Bruening, D. A., Cooney, K. M. & Buczek, F. L. Analysis of a kinetic multi-segment foot model. Part I: Model repeatability and kinematic validity. *Gait Posture* **35**, 529–534 (2012).
2. Seo, S. G. *et al.* Repeatability of a multi-segment foot model with a 15-marker set in healthy adults. *J. Foot Ankle Res.* **7**, 24 (2014).
3. Leardini, A. *et al.* Rear-foot, mid-foot and fore-foot motion during the stance phase of gait. *Gait Posture* **25**, 453–462 (2007).
4. Voloshina, A. S., Kuo, A. D., Daley, M. A. & Ferris, D. P. Biomechanics and energetics of walking on uneven terrain. *J. Exp. Biol.* jeb.081711 (2013) doi:10.1242/jeb.081711.
5. Pataky, T. C. Generalized n-dimensional biomechanical field analysis using statistical parametric mapping. *J. Biomech.* **43**, 1976–1982 (2010).

# EFFECT OF WALKING SPEED ON JOINT ANGLES DURING TREADMILL WALKING WITH RHYTHMIC AUDITORY STIMULATION AT PREFERRED CADENCE

*Haneol Kim[1], Matthew Beerse[2], Jianhua Wu[3]
[1]University of Wisconsin-La Crosse
[2]University of Dayton, [3]Georgia State University
*Corresponding author's email: hkim2@uwlax.edu

**Introduction:** Locomotion such as walking is essential for human daily activities and enables one's mobility and independence [1]. Walking is a complex process regulated by the human locomotor control system, in which the central nervous system coordinates various forms of human movement in response to task and environmental demands [2]. Walking speed is a key factor of biomechanical patterns and influences joint kinematics and kinetics. Increasing walking speed is often associated with greater ranges of motion at the hip, knee, and ankle joints, along with an increase in stride length and cadence [3]. In contrast, rhythmic auditory stimulation (RAS) sets an external temporal constraint and has been shown to affect gait parameters and improve pathological gait in clinical populations. However, limited research has yet explored how RAS interacts with walking speed in children. Therefore, this study aimed to investigate the effect of walking speed on joint angles during treadmill walking when RAS is set to one's preferred cadence.

**Methods:** Twenty healthy young adults aged 18-35 years and 20 typically developing children aged 7-11 years participated in this study. A 9-camera Vicon motion capture system with the Vicon Plug-in Gait lower body model was used to collect the kinematic data. All participants completed a 5-min walking trial at three treadmill speeds: 100TS denoting the preferred treadmill speed, and 75TS and 125TS representing 75% and 125% of preferred treadmill speed, respectively. Participants walked at the three speeds with the RAS frequency set to their preferred cadence. Joint kinematic variables included peak hip extension and flexion, peak knee extension and flexion, and peak ankle plantarflexion and dorsiflexion angles over the entire gait cycle. Two-way (2 Group × 3 Speed) mixed ANOVAs were conducted on peak joint angles at a significant level of α=0.05. Post-hoc pairwise comparisons with Bonferroni adjustments were completed when necessary.

**Results & Discussion:** Peak hip extension increased with treadmill speed for both children and adults (Fig. 1). There was a speed main effect ($p$<0.001), increasing from 75TS to 100TS to 125TS. Both children and adults increased peak hip flexion with treadmill speed ($p$=0.002), increasing from 75TS to 125TS. Also, children showed a greater peak knee extension than adults across the speeds with a group main effect ($p$=0.021). Both children and adults increased peak knee flexion with treadmill speed ($p$<0.001), increasing from 75TS to 100TS to 125TS. In addition, children and adults increased peak ankle plantarflexion with treadmill speed and adults increased it to a greater degree than children. A group by speed interaction was found in peak ankle plantarflexion ($p$=0.016). Both children and adults decreased peak ankle dorsiflexion with treadmill speed ($p$<0.001), increasing from 75TS to 100TS and 125TS. Children showed greater peak ankle dorsiflexion than adults across speed conditions ($p$=0.005).

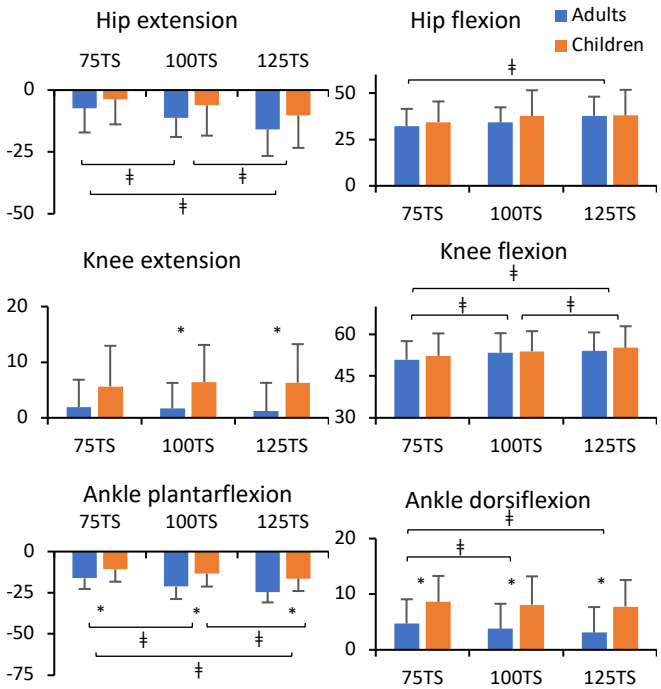


**Figure 1:** Mean and standard deviation of kinematic joint angles (in degrees) for peak hip extension and flexion, knee extension and flexion, and ankle plantarflexion and dorsiflexion. Symbol * indicates a group effect between adults and children; the symbol ǂ indicates a speed effect between 75TS, 100TS, and 125TS.

**Significance:** To increase walking speed under the same cadence, both children and adults significantly modified their joint kinematics by increasing peak joint flexion and extension angles and consequentially increase step length, which is consistent with previous research findings on kinematic variables when cadence was not constrained. While both groups exhibited similar biomechanical modifications in response to the task constraints, adults increased peak ankle plantarflexion to a greater degree but decreased peak ankle dorsiflexion compared to children. Differences between children and adults suggest that the refinement of gait development, including joint kinematics, continues into adolescence. These findings suggest that manipulation of treadmill speed while constraining RAS may empower healthy individuals and possibly those with disabilities to improve their joint range of motion and elicit better exercise or rehabilitation outcomes.

**Acknowledgments:** We are grateful to all the participants for volunteering their participation. This study was partially supported by the Georgia State University Provost's Dissertation Fellowship program.

**References:** [1] Roberts et al. (2017), *Phys. Ther. Rehabil.* 4(6); [2] Bastian. (2008), *Curr Opin Neurol.* 21(6); [3] Stansfield et al. (2001), *J. Pediatr. Orthop.*21(3).

# LONG-TERM TREND ANALYSIS OF SPATIOTEMPORAL MEASURES IN SELF-PACED TREADMILL WALKING.

Hong Min[1], Jangwhan Ahn[1], Jungho Lee[1], Jeongin Moon[1], Hyeonyong Lee[1], Jooeun Ahn[1, 2] *
[1]Department of Physical Education, Seoul National University, South Korea
[2]Institute of Sport Science, Seoul National University, South Korea
*Corresponding author's email: ahnjooeun@snu.ac.kr

**Introduction:** The self-paced treadmill (SPT) has been developed to allow wider ranges of gait speed variability, and thus enabling more natural gait than the conventional fixed-speed treadmill (FST). A previous study reported that the treadmill speed in SPT walking converges within a short time [1]. Another study reported that the mean of spatiotemporal variables in SPT walking are close to those of overground gait [2]. However, there is a lack of research on how the spatiotemporal variables in SPT walking converges to those in overground walking. We aim to fill this research gap by analyzing the long-term trends of spatiotemporal variables in SPT walking.

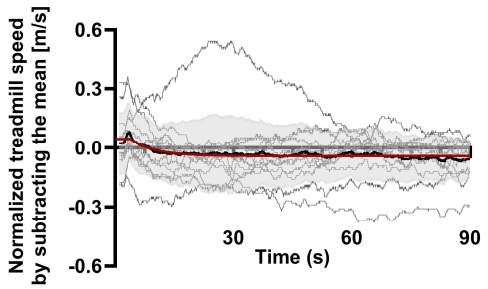


**Figure 1:** Normalized treadmill speed of the SPT. Normalization was performed by subtracting each participant's mean in overground walking. The black solid line and shaded areas indicate the mean and standard deviation of SPT speed. The red solid line represents the curve fitting line. Gray lines indicate each participant's speed profile.

**Methods:** We investigated spatiotemporal parameters including stride length and stride time. Twelve healthy young males (age: 23.3 ± 2.7 years; height: 174 ± 2.2 cm; weight: 71.7 ± 6.1 kg) participated in the study. Kinematic data were recorded using a motion capture suit (MVN Link, USA) equipped with 17 inertial measurement units. During session 1, all participants walked overground on a 1 km straight path at a self-selected speed. In Session 2, participants completed 5-minute adaptation trials on both the FST and SPT, and 12-minute trials in the FST and SPT in a random order. We analyzed the long-term changes using 600 strides in each of the three conditions. To account for individual trends, the average values during overground walking were subtracted from the values during treadmill walking for normalization for each participant.

**Results & Discussion**: Participants' mean speed in SPT plateaued at around 30 seconds (Fig. 1). As a sanity check, we analysed whether the stride length and time show any linear trend in overground walking. Analyses with general linear models concluded no linear trend in both variables ($p = 0.89$ for stride length and $p = 0.62$ for stride time, Fig. 2A). A post-hoc analysis of the linear mixed model showed that mean stride length in FST walking was significantly greater than that in SPT walking ($p < 0.001$), and mean stride time in SPT walking was greater than that in FST ($p < 0.001$) (Fig. 2B). The stride length ($p < 0.001$) and stride time ($p < 0.001$) significantly increased in SPT walking as stride number increased. In contrast, only stride time increased in FST walking ($p < 0.001$). Thus, we found that speed of SPT walking converges to that of overground walking quickly, whereas stride length and time do not.

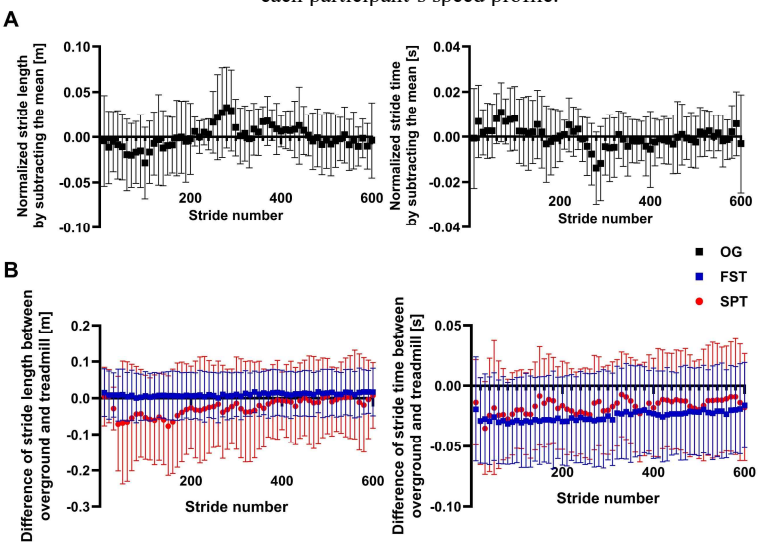


**Figure 2:** (A) Normalized stride length and stride time in overground walking, obtained by subtracting each participant's mean value. Each point represents the mean of 10 consecutive strides, with error bars indicating the standard deviation. (B) Differences in stride length and stride time between the overground mean and the two treadmill walking conditions. Each point represents the mean of 10 consecutive strides, with error bars indicating the standard deviation. Red circles indicate SPT walking and blue squares represent FST walking.

**Significance:** Previous studies analysed the mean values of spatiotemporal variables in self-paced treadmill walking [2, 3]. However, they did not analyze long-term trends in these variables under the SPT condition. Our results show that walking in an SPT leads to a long-term increase in stride length and stride time compared to overground walking, which contrasts with the rapid convergence of the SPT speed. This challenges the notion that the SPT enables fast adaptation.

**Acknowledgments:** This work was supported in part by the Korea Health Technology R&D Project through the Korea Health Industry Development Institute (KHIDI) funded by the Ministry of Health & Welfare (No. HK23C0071), Industrial Technology Innovation Program (No. 20007058, Development of safe and comfortable human augmentation hybrid robot suit) funded by the Ministry of Trade, Industry & Energy (MOTIE, Korea), and the National Research Foundation of Korea (NRF) grants funded by the Korean Government (MSIT) (No. RS-2023-00208052).

**References:** [1] Song et al. (2020), *J. NeuroEng. Rehabil., 17*; [2] Holmes et al. (2021), *J. Appl. Biomech*., 37(3); [3] Wiens et al. (2019), *J. Biomech., 83*

# GREATER TOE FLEXOR STRENGTH ASSOCIATES WITH LESSER SOLEUS ACTIVATION DURING WALKING

**Ross E. Smith**[1], Aubrey Gray[1], Howard Kashefsky[2], Kota Z. Takahashi[3], Jason R. Franz[1]
[1]Lampe Joint Department of Biomedical Engineering, UNC Chapel Hill and NC State University, Chapel Hill, NC, USA
[2]Divison of Vascular Surgery, University of North Carolina Medical Center, Chapel Hill, NC, USA
[3]Department of Health and Kinesiology, University of Utah, Salt Lake City, UT, USA
Email: rsmit@email.unc.edu

**Introduction:** The human foot is believed to be a key component enabling our adoption of upright gait, which is markedly more metabolically efficient than bipedal gait of other plantigrade apes [1]. While much research has focused on how distinct bony anatomical adaptations of human feet affect walking economy, recent evidence indicates that the toe flexor muscles play an important role in absorbing, returning, and generating energy during walking [2] and thereby may facilitate effective propulsion. For instance, active contributions from the plantar intrinsic muscles – many of which are toe flexors – stiffen the forefoot during push-off, which optimize leverage and kinetic output from the ankle joint [3]. Increasing forefoot stiffness via carbon fiber shoe inserts has been shown to increase plantarflexor (PF) leverage while decreasing whole-body metabolic cost during fast walking [4]. Thus, adequately strong toe flexors may provide relatively higher forefoot stiffness, enabling a more efficient transfer of PF force output (i.e. more strut-like foot) with lesser requisite PF excitation during push-off. Furthermore, stronger toe flexors may enable lesser relative toe flexor muscle excitations. However, these relations have to be empirically established. We sought to quantify the associations between toe flexor strength and excitation of ankle PF (lateral gastrocnemius [LG] and soleus [SOL]) and toe flexor (flexor digitorum brevis [FDB]) muscles during gait propulsion in young, healthy adults. We hypothesized that those with greater toe flexion torque ($T_{MTP}$) would have reduced root-mean-squared muscle excitation for the LG, SOL, and FDB muscles during stance when walking at 1.2 m/s. Such a finding would implicate the importance of toe flexor strength in facilitating metabolically efficient propulsion during walking, which may inform rehabilitation interventions and assistive device implementation in individuals with elevated metabolic walking costs.

**Methods:** 19 young adults (26.4 ± 5 yrs, 76.3 ± 13.7 kg) participated. Toe flexor strength was measured as peak MTP torque obtained from maximal voluntary isometric toe flexion contractions using a custom dynamometer with the ankle at 20° plantarflexion and the MTP joint at 60° extension. This position represents the highest $T_{MTP}$ values for 17 of 19 participants over a range of other ankle and metatarsophalangeal (MTP) joint orientations tested and emulates the common positions of these joints during push-off. Participants completed one-minute treadmill walking trials on an instrumented treadmill at 1.2 m/s while we collected surface electromyography (EMG) from the LG and SOL and fine-wire EMG from the FDB. EMG data was sampled at 1000 Hz, DC offsets were removed, bandpass filtering was applied at 20–450 Hz for surface and 20–800 Hz for fine-wire using a zero-lag, 4th-order Butterworth filter, then the signal was rectified and low-pass filtered at 10 Hz to complete a linear envelope for each signal. Each signal was normalized to its maximum value over the entire walking trial. EMG data are reported here as the average root-mean-square of each signal calculated using a 100 ms moving window with 50% overlap over 10 stance phases, with heel strike and toe-off events obtained from ground reaction force data (>50 N, <50N, respectively). Individual Pearson correlations were performed to assess the relation between $T_{MTP}$ and SOL, LG, and FDB EMG.

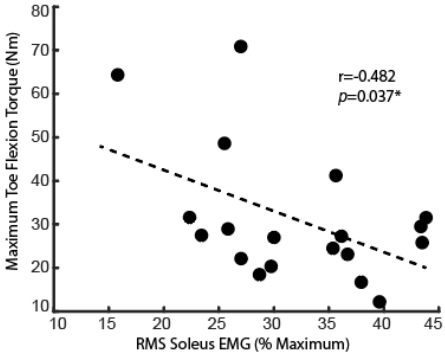


**Figure 1.** Maximum toe flexion torque versus root mean squared (RMS) soleus electromyography (EMG) normalized to maximum value during walking. * denotes significant correlations, $p$=0.05.

**Results & Discussion:** $T_{MTP}$ was not associated with the biarticular LG or FDB EMG (r=-0.08; $p$=0.74; r=0.06; $p$=0.98). However, larger $T_{MTP}$ was significantly correlated with lesser uniarticular SOL EMG (r=-0.482; $p$=0.03) (Fig. 1). Specifically, every 10 Nm increase in $T_{MTP}$ decreased relative SOL EMG by ~9%. Our coauthors previously found that carbon fiber insoles designed to enhance forefoot stiffness increased the ankle's external moment arm, which was accompanied by reduced whole-body metabolic costs [2]. Together, our findings indicate stronger toe flexors may allow reduction in relative PF activation via increases in forefoot stiffness. Such reductions could enable reductions in walking metabolic cost and/or walking fatigue accumulation. Future studies should examine: 1) the association between toe flexor weakness and reductions in propulsive power and 2) the latter's association with increased walking metabolic cost in older adults.

**Significance:** Our findings further expand the field's growing appreciation for and understanding of the importance of toe flexor strength in facilitating effective and efficient gait propulsion. Our findings may have implications for rehabilitation programs and assistive device designs seeking to improve quality of life and independence in individuals with elevated metabolic walking costs.

**Acknowledgments:** This study was supported by a grant from the NIH (R01AR081287).

**References:** [1] Rubenson et al. (2007), *J Exp Biol* 210(20); [2] Smith et al. (2021), *J Exp Biol* 224(13); [3] Farris et al. (2019), *PNAS* 116(5); [4] Ray et al. (2020), *Sci Rep* 6(1).

# ALTERED KINEMATICS AND MUSCLE SYNERGIES DURING GAIT IN PERSONS WITH MULTIPLE SCLEROSIS

*Qiang Guo, Haya Alharthi, Nessa Sontag, *Fan Gao
Department of Kinesiology and Health Promotion, University of Kentucky, Lexington, KY, USA
*Corresponding author's email: qgu225@uky.edu, fan.gao@uky.edu

**Introduction:** Multiple sclerosis (MS) is a chronic neurological disease often associated with gait impairments that adversely affect quality of life. During gait, individuals must coordinate multiple muscles while simultaneously processing sensory information, Neuromotor deficits commonly impact the lower limbs leading to gait abnormalities. Muscle synergy analysis provides a holistic evaluation of grouped muscle activities and quantifies the effectiveness of motor coordination in both healthy and neurological populations. The purpose of this study was to investigate the kinematics and muscle synergies during gait in individuals with MS compared to health controls (CON).

**Methods:** A total of 10 individuals with MS and 14 healthy control participants were included in this study. Each participant completed 20 successful walking trials at their self-selected speed. A total of 36 reflective markers were attached to each participant's lower extremity and 16 EMG electrodes were placed on eight target muscles bilaterally. Kinematics, kinetics and muscle activity were collected using a three-dimensional motion capture system, three force platforms and surface EMG at sampling rates of 250 Hz, 1000 Hz and 1000 Hz respectively.

Muscle synergies were calculated using non-negative matrix factorization (NMF), a linear decomposition technique according to equation $M = W \cdot C + e$ (where M is a linear combination of muscle weighting components W and activation signals C, and e is the residual error matrix). Synergy extraction was performed using a previously developed MATLAB toolbox, with each extraction repeated 50 times. The variance accounted for (VAF) was calculated for each possible number of synergies. The number of muscle synergies required to achieve >90% overall VAF and >75% VAF for each muscle was determined.[1]

An independent samples t-test was employed to compare the demographic, spatiotemporal, kinematic and synergy metrics including number of synergies (Nsyn), total variance accounted for by one single synergy (tVAF1) and muscle weightings between these two groups.

**Results & Discussion:** The major findings of this study demonstrate that individuals with MS showed significantly increased stance time (0.78±0.10s / 0.70±0.05s, P=0.03), double limb support duration(0.34±0.07s / 0.28±0.03s, P=0.01) and stance phase as a percentage of the gait cycle (64.86±2.86% / 62.83±0.98%, P=0.02) compared to CON. Additionally, MS participants showed significantly decreased swing phase as a percentage of the gait cycle (35.12±2.52% / 37.11±0.98%, P=0.01) and decreased right hip range of motion (ROM) (36.59±3.15° / 39.39±2.62°, P=0.03) compared to CON.

Muscle synergy analysis revealed a significantly reduced number of synergies (Nsyn) in MS patients compared to CON for the left gait cycle (P=0.03), but not for the right gait cycle(P=0.07). Three muscle synergies were sufficient for both sides of MS to meet the criteria of tVAF>90%, whereas four muscle synergies were required for both sides of CON. The total variance accounted for by one single synergy (tVAF1) was significantly higher in MS compared to CON (Right gait, 73.86% ± 9.74% / 61.51% ± 6.23%, P=0.003; Left gait, 71.77% ± 9.45% / 61.98% ± 7.95%, P=0.034). For direct comparison of muscle synergy weightings and activation signals, a four-synergy solution was created. In synergy weighting W1(SOL+LGS), which primarily involved the SOL as an ankle plantarflexor and LGS as a knee flexor during the forward propulsive phase, MS participants showed significantly lower SOL contribution (P=0.01) and higher LGS contribution (P=0.01) than CON.

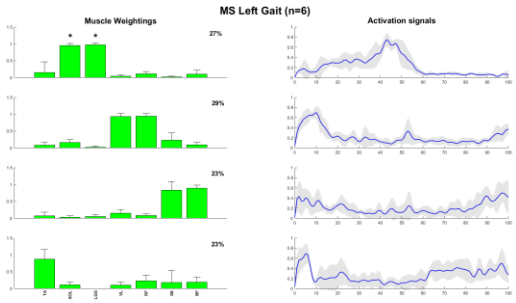


**Fig. 1:** Average muscle weightings and activation signals for a four-synergy solution in MS for left gait cycles. Significant differences(P<.05) between groups for muscle weighting W1 were marked with an asterisk (*)

This study examined kinematics and muscle synergies differences during gait in individuals with MS compared to CON group. The findings suggest that MS patients overall adopted a compensatory strategy characterized by prolonged stance time, increased double limb support duration, and decreased right hip ROM. These altered biomechanical characteristics, along with a reduced Nsyn and a higher tVAF1 suggested a simplified neuromuscular control strategy in MS.

**Significance:** Muscle synergies analysis can provide valuable clinical insights into the motor deficits associated with neurological disorders such as Multiple Sclerosis. A reduction in synergy complexity and number often indicates impaired muscle coordination. Identifying dysfunctional muscle synergies and their contribution to gait deficits could help develop more targeted and effective rehabilitation interventions aimed at improving motor function in individuals with MS.

**Acknowledgments:** This work was supported by the National Center for Research Resources and the National Center for Advancing Translational Sciences, National Institutes of Health, through Grant UL1TR001998. The content is solely the responsibility of the authors and does not necessarily represent the official views of the NIH.

**References:** [1] Chvatal and Ting (2013), *Front. Comput. Neurosci*. 48(7).

# POSITIVE RELATIONSHIP BETWEEN MOTOR AND PERCEPTUAL ADAPTATION DURING SPLIT-BELT WALKING

*Marcela Gonzalez-Rubio[1], Amber R. Costello[1], Pablo A. Iturralde[2], Gelsy Torres-Oviedo[1]
[1]Department of Bioengineering, University of Pittsburgh, Pittsburgh, PA, USA
[2]Engineering Department, Universidad Católica del Uruguay, Montevideo, Uruguay
*Corresponding author's email: mag356@pitt.edu

**Introduction:** The human motor system adapts our actions to counteract changes in the environment (e.g., walking on different terrains) or our bodies (e.g., growth). Motor control relies on sensory information to achieve motor adaptation by comparing the expected and actual sensory consequences of movements [1]. While the adaptation of motor output is well-documented [2,3], less is known about sensory adaptation and its relationship to motor output adaptation in walking. Previous studies have assessed sensory adaptation through active perception tasks [4], where participants reported perceived speed differences between their legs.

We hypothesized that baseline perceptual sensitivity to leg speed differences determines the extent of motor adaptation, a phenomenon observed in other modalities like speech, where the magnitude of adaptation is positively correlated with perceptual sensitivity [5]. Additionally, we hypothesized that perceptual adaptation during split-belt walking (i.e., one leg moves faster than the other) would correlate positively with motor adaptation, similar to observations made in reaching studies [6].

**Methods:** Perception of leg speed differences was assessed in young adults (n=8, 21±2 years old, 6 females) under a baseline (Base: 0m/s speed difference) and adaptation (Adapt: 0.5m/s speed difference) walking condition. Participants completed two-alternative forced choice tasks to indicate which leg felt slower, with stimuli ($\Delta V = V_R - V_L$) ranging between 0.05 and 0.45 m/s. Each stimulus was repeated at least 10 times, and visual or auditory sensory cures were minimized using a drape and headphones with white noise.

Data was analyzed by modeling the probability of a "*left*" choice as a logistic function for each participant: $p(response = left) = (1 + e^{-\mu_j})^{-1}$; where $\mu_j = \beta_{0j} + \beta_{1j}\Delta V$ for the baseline and adaptation epochs. In the expression $\mu_j$, $j$ refers to each individual participant and $\Delta V$ refers to the stimulus size (Fig 1A). Perceptual sensitivity ($JND_{Base}$; Fig 1B) and perceptual adaptation ($\Delta PSE$; Fig 1C) were computed using the regression coefficients per individual ($\beta_{0j}$ and $\beta_{1j}$). Perceptual adaptation was calculated as the change in perceptual bias during split-belt adaptation relative to baseline ($\Delta PSE = PSE_{Adapt} - PSE_{Base}$; Fig 1A). Motor adaptation was quantified by the extent of adaptation (AdaptExtent) which characterizes how well participants counteracted the split-belt perturbation [7]. Hypotheses were tested using one-tailed Spearman correlation at a 0.05 significance level.

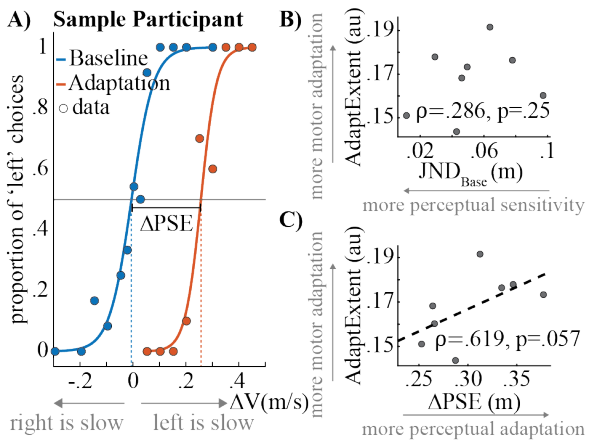


**Figure 1: A)** Overall proportion of 'left' choices by stimuli for a sample participant. Solid lines show the psychometric function for Base (blue) and Adapt (orange) epochs. Dotted lines indicate the PSE for each epoch. **B)** $JND_{Base}$ (perceptual sensitivity) vs. extent of adaptation (motor adaptation) where each dot is an individual participant. **C)** $\Delta PSE$ (perceptual adaptation) vs. extent of adaptation (motor adaptation). Dotted line indicates trending correlation.

**Results & Discussion:** We preliminarily found that the extent of motor adaptation is not related to baseline perceptual sensitivity for each individual (Fig 1B) but is associated with perceptual adaptation during split-belt walking (Fig 1C). Specifically, the extent of motor adaptation showed no significant association with individuals' baseline perceptual sensitivity ($JND_{Base}$ Fig 1B; $\rho = 0.286, p = 0.25$), but it was correlated with perceptual adaptation (a trending positive correlation, Fig 1C; $\rho = 0.619, p = 0.057$), which has also been reported in other motor tasks [6,8].

Data collection is ongoing; however, our preliminary results suggest that perceptual changes during locomotor adaptation reflect adjustments in how the nervous system predicts the sensory outcomes of motor commands. Therefore, perceptual changes can serve as a proxy for how the nervous system updates its internal representation of walking during split-belt walking. Although we did not see an association between baseline perceptual sensitivity and the extent of motor adaptation, we interpret our preliminary results under the assumption that motor adaptation is driven by prediction errors rather than solely by sensory information [1].

**Significance:** This study explores the relationship between sensory and motor adaptation during split-belt walking, focusing on whether perception of leg speed differences reflects updates in the brain's walking model. Understanding these mechanisms could reveal the signals driving locomotor adaptation and guide locomotor training.

**Acknowledgments:** This work was supported by NSF Career Award 1847891 and NIH R90DA0603040.

**References:** [1] Shadmehr and Mussa-Ivaldi (2012). *MIT Press*; [2] Torres-Oviedo et al. (2011), *Prog Brain Res* 191; [3] Dzewaltowski et al. (2021), *Neurorehabil Neural Repair* 35(7). [4] Hoogkamer et al. (2015) *J Neurophysiol* 114(3); [5] Trudeau-Fisette et al. (2024), *PLoS One* 19(8); [6] Salomonczyk et al. (2013), *Exp Brain Res.* 228(3); [7] Sombric et al. (2017), *Front Aging Neurosci*; [8] Ostry et al. (2010), *J Neurosci* 30(15)

# GOING DARK: BLINDFOLDED HYPOGRAVITY ADAPTATION DIFFERENTIALLY AFFECTS MOTOR AND COGNITIVE TASKS

Chase G. Rock, Lynn Kim, and Young-Hui Chang
Comparative Neuromechanics Laboratory, School of Biological Sciences, Georgia Institute of Technology, Atlanta, GA
*Corresponding author's email: crock@gatech.edu

**Introduction:** Sensorimotor adaptation is a complex process arising from the assessment of various sensory signals to adjust motor output. The sensory systems largely responsible for motor learning and adaptation are the visual and proprioceptive systems[1,2]. For example, when learning to move at a new gravity level, the visual flow moves with less vertical acceleration (visual) and with a reduced force requirement (proprioceptive), leading to an adaptive biomechanical response[3]. In previous work, we have shown that motor and cognitive tasks appear to share an internal model of gravity as they both experience aftereffects following exposure to jumping in hypogravity[4]. Yet, we do not know the relative contributions of different sensory modalities to the adaptation of these different action systems. By removing the influence of vision during adaptation, we can begin to unravel the influence of different sensory modalities to hypogravity adaptation. If vision is required, then we would expect no gravity-related aftereffects following blindfolded adaptation. Conversely, if the various other sensory modalities (including proprioception) are sufficient for adaptation, then we expect gravity-related aftereffects to persist.

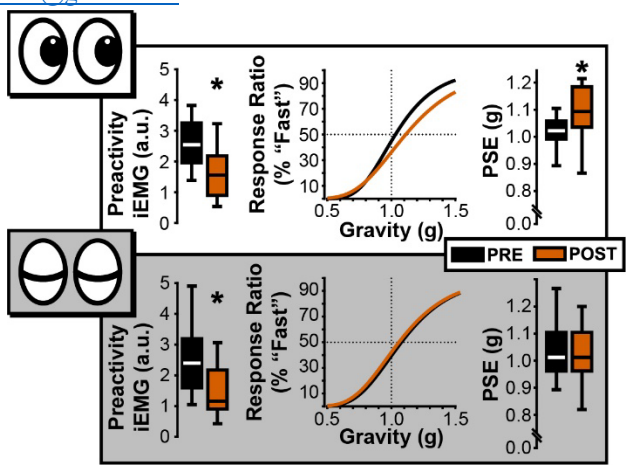


**Figure 1:** Aftereffects were observed in muscle preactivation in both vision conditions, but the cognitive aftereffect was only present when vision was available during adaptation. PSE: Point of Subjective Equality; * $p < .05$

**Methods:** All participants provided informed consent according to the protocol approved by the Georgia Tech IRB (H19325). Participants ($n$ = 15) each wore a blindfold while they performed vertically targeted jumps before (PRE), during, and after (POST) exposure to simulated hypogravity. Realtime audio cues were provided to inform participants of their relative vertical position as well as the result of each attempt to jump to the target. Hypogravity was simulated using a combination of constant-force springs mounted above the participant and attached to a customized rock-climbing harness[3,4]. Before and after jumping in simulated hypogravity, participants were shown a virtual scene of a ball suspended in the air. The ball fell to the ground with various accelerations, ranging from 50-150% Earth's gravity. Participants then indicated whether the ball appeared to fall 'fast' or 'slow'. Each gravity level was seen multiple times in random order, enabling us to construct psychometric curves for each participant and estimate the gravity level that they were equally likely to perceive as 'fast' or as 'slow' (Point of Subjective Equality, PSE). In addition to biomechanical analyses, neuromuscular aftereffects were investigated in the preactivity of the plantarflexor muscles in preparation for landing[3]. Cognitive aftereffects were investigated by assessing the change in the point of subjective equality. For additional context, results are also presented from a previous experiment[4] without a blindfold (Fig. 1, top; $n$ = 10).

**Results & Discussion:** Jumping in simulated hypogravity led to neuromuscular aftereffects regardless of the presence or absence of vision. Muscle preactivation was reduced following jumping in simulated hypogravity while wearing (Fig. 1, bottom; $p < .001$) and when not wearing a blindfold (Fig. 1, top; $p = .004$), indicating an expectation of reduced force and/or a delayed landing time. When vision was available, as in previous iterations of this paradigm, visual feedback was likely employed to facilitate accurate movement and adaptation, though the effect of vision could not be disentangled from that of other sensory modalities. When vision was removed in the present study, changes in muscle preactivation may be attributed to the other sensory systems, likely proprioceptive and vestibular.

In contrast to the neuromuscular results, vision appears to be required for gravity-related aftereffects to manifest in the cognitive task. While the motor and cognitive systems are often linked, this result points to a dissociation between the two. One explanation is that visual information can follow two different neural streams in the brain, one which prioritizes action and a second which prioritizes perception[5]. When vision was available, the action-focused stream could be updated during adaptation and share information with the perception-focused stream leading to an aftereffect in the cognitive task (Fig. 1, top; $p = .022$). When vision was not available, the action-focused stream had no opportunity to adapt, thereby preventing new gravity-related information from affecting the perception-focused stream, resulting in no aftereffect in the cognitive task (Fig. 1, bottom; $p = .571$).

**Significance:** The results of the current study are important first steps for differentiating the effects of vision and other sensory modalities on motor adaptation; more specifically, their effect on the motor, perceptual, and cognitive aspects of adaptation. By leveraging principles from cognitive neuroscience and psychology, paired with biomechanical analyses, we are gaining a more holistic view of sensorimotor adaptation in general and more specifically to the adaptations occurring in microgravity.

**Acknowledgments:** This material is based upon work supported by the NSF GRFP (DGE-1650044). Any opinions, findings, and conclusions or recommendations expressed herein are those of the authors and do not necessarily reflect the views of the NSF.

**References:** [1] Harris, C. S. *Science* (1963). [2] Tsay, J. S. *et al. J. Neurophys* (2021). [3] Rock, C. G. *et al. Front. Physiol.* (2024). [4] Rock, C. G. & Chang, Y.-H. in *ASB* (Madison, WI, 2024). [5] Creem-Regehr, S. H. & Kunz, B. R. *WIREs Cogn Sci* (2010).

# SIMILARITY ACROSS WALKING CONTEXTS IMPROVES THE GENERALIZATION OF MOTOR ADAPTED PATTERNS

*Adwoa Awuah, Dulce Mariscal Olivares[2], Krista Fjeld[3], Gelsy Torres-Oviedo[1,4]
[1]Department of Bioengineering, University of Pittsburgh
*ada157@pitt.edu

**Introduction:** Humans can carry over learned patterns from one situation to another, a concept known as generalization. For example, swimming patterns developed in an indoor pool can be applied to an outdoor pool or even the ocean, despite differing dynamics. Rehabilitation heavily relies on this concept as motor corrections made with training devices must generalize to movements without them (e.g. overground walking). However, device-induced training, such as split-belt treadmill walking, where different speeds are introduced to each leg, has shown limited generalization to walking without the device.[1] This limitation may be attributed to sensory and motor differences between split-belt treadmill and overground walking, including variations in visual flow (static on the treadmill vs. dynamic overground) [2], walking speeds (fixed on the treadmill vs. self-regulated overground)[3], step initiation (externally triggered on the treadmill vs. self-initiated overground). This raised the question of how contextual similarity between adaptation, where patterns are learned, and post-adaptation, where patterns are tested, affects generalization. To address this, we assessed generalization under distinct contextual similarity conditions. We hypothesized that greater contextual similarity between adaptation and post-adaptation conditions would facilitate the generalization of adapted patterns from the training (e.g., with a split-belt treadmill) to the testing environments (eg., overground), as sensory and motor demands would be more consistent between the two environments.

**Methods:** To test this hypothesis, we adapted thirty young adults on the split-belt treadmill (i.e., low contextual similarity group; n=10), a pair of motorized shoes (i.e., high contextual similarity group; n=10), which can induce the same adaptation as the split-belt treadmill while walking overground[4], and wearing a pair of the motorized shoes on the split-belt treadmill(i.e., very low contextual similarity group; n=10). Following adaptation, we further divided the groups to test the generalization of adapted locomotor patterns (i.e., aftereffects from first 5 strides post-adaptation) under two conditions: tested with the training device (i.e., treadmill, motorized shoes, or motorized shoes on the treadmill) or without the training device(overground). We anticipated observing an interaction effect such that contextual similarity would regulate the reduction in aftereffects, with greater reduction when tested without the device than with the device.

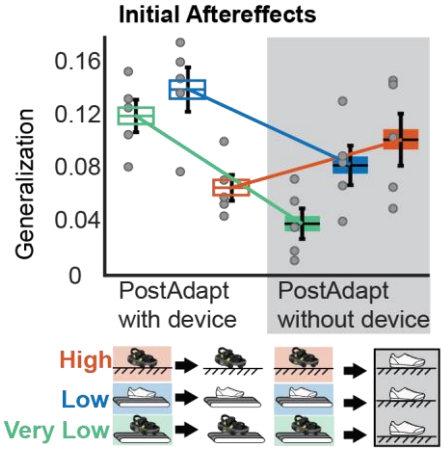


**Figure 1:** Mean aftereffect values for each group when assessed with the device (empty rectangles; white background) or without the device (filled rectangles; grey background). Colored lines represent the direction of the interaction effect between groups tested under different post-adaptation conditions.

**Results & Discussion:** Our findings revealed a significant interaction between contextual similarity and testing conditions ($p<0.001$). Participants in the low and very low contextual similarity groups (Figure 1: Blue and Green lines) exhibited reduced aftereffects when tested overground without the training device (Figure 1: grey background) compared to when tested with the training device (Figure 1: white background). These results corroborate previous reports indicating that adaptations induced by split-belt treadmill training often do not fully generalize to overground walking.[1] Conversely, the high contextual similarity group demonstrated consistent aftereffects across both testing conditions (Figure 1: Orange line), supporting our hypothesis that contextual similarity facilitates the generalization of adapted motor patterns. These findings suggest that the sensory and motor demands of walking with motorized shoes closely resemble those of overground walking, thereby enhancing the transfer of learned patterns to overground walking.

**Significance:** A key challenge in rehabilitation is ensuring that corrected patterns in the clinical or laboratory setting transfer to real-life scenarios. Our findings highlight contextual similarity as a critical factor in enhancing generalization, offering a potential strategy to improve locomotor rehabilitation. Traditional laboratory-based training often results in limited carryover of learned motor patterns to natural environments. However, by designing rehabilitation protocols that closely mimic real-world conditions, particularly overground walking, we can improve training effectiveness and facilitate greater transfer of corrected patterns under controlled settings to daily life.

**Acknowledgments:** This work was funded by the National Science Foundation Career Award (NSF 2419849)

**References:** [1] Reisman, D. S.; Wityk, R.; Silver, K.; Bastian, A. J. Neurorehabilitation and neural repair272 2009, 23, 735–744; [2] Torres-Oviedo, G.; Bastian, A. J. Journal of Neuroscience 2010, 30, 17015–17022.275 [3] Dingwell, J.; Cusumano, J. P.; Cavanagh, P.; Sternad, D. J. Biomech. Eng. 2001, 123, 27–32.278 [4] Aucie, Y.; Zhang, X.; Sargent, R.; Torres-Oviedo, G. Frontiers in neuroscience 2020, 14, 174.286

# IN ESTIMATING PARETIC PROPULSION, TRAILING LIMB ANGLE MAY BE LESS THAN THE SUM OF ITS PARTS

*Austin L. Mituniewicz[1], Jonathan Stallrich[2], Helen Huang[1], Michael D. Lewek[1, 3]
[1]Lampe Joint Department of Biomedical Engineering, University of North Carolina at Chapel Hill and North Carolina State University
[2] Department of Statistics, North Carolina State University
3 Division of Physical Therapy, Department of Health Sciences, University of North Carolina at Chapel Hill
*Corresponding author's email: amituniewicz@unc.edu

**Introduction:** The propulsive deficits present in many people recovering from stroke correlate to slower walking speeds [1], and limit the ability of people to participate in their communities [1]. To address reductions in paretic propulsion, some researchers have attempted to train for increased paretic trailing limb angles (TLA) (Figure 1a) during gait [1,2]. The trailing limb angle is intended to represent the anterior component of the ground reaction force (GRF), and is composed of three segments (thigh, shank, and foot). It remains unknown *how* the thigh, shank, and foot segment contributions to a given TLA will affect propulsion. Hence, this work 1) investigates TLA's underlying segmental composition and 2) examines the independent effect of these contributions on propulsion in people post-stroke.

**Methods:** Eleven people recovering from stroke with chronic hemiparesis walked at a variety of speeds on a split-belt instrumented treadmill, while motion capture and (GRF) data were recorded as part of a study investigating intrinsically generated trips (no steps that became trips were included). Thigh, shank, and foot segmental angles relative to the vertical were computed in Visual3D. TLA was defined as the angle between the vertical and a line from the greater trochanter to the fifth metatarsal [3] (Figure 1a). Both segmental angles and TLA were defined to be counter-clockwise positive; such that more inclined thigh, shank, and trailing limb angles would be more negative. Kinematic and AP GRF data were then extracted from the moment of paretic side peak anterior-posterior GRF ($AP_{Pk}$) for each paretic gait cycle. To address our study purpose, we sought to simplify the known non-linear structure of our variables by modelling TLA using a multivariate linear regression of segmental angles. We then created two additional regression models to estimate $AP_{Pk}$, one using only TLA and the other using the constituent segmental angles.

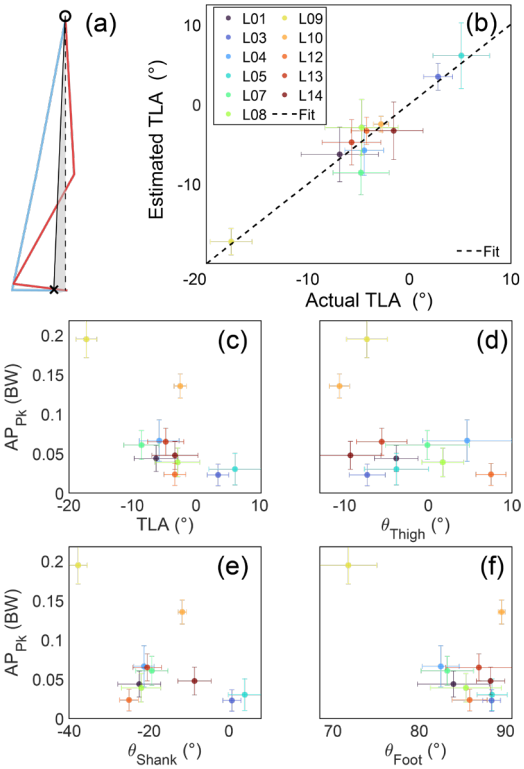


Figure 1: (a) A diagram of two hypothetical segment angle combinations in blue and red that would result in equivalent TLAs, depicted in grey. (b) Estimated vs. actual TLA's as determined by the multivariate linear regression of segment angles. Participant data averages and standard deviations are shown using different color markers and error bars, respectively. (c-f) Participant averages and standard deviations of the trailing limb, thigh, shank, foot, and angles plotted against their respective $AP_{Pk}$.

**Results & Discussion:** All segmental contribution terms in the multivariate linear regression of TLA were statistically significant ($p<0.0001$, $R^2=0.925$) (Figure 1b), with the shank angle emerging as the dominant term (standardized coefficients – thigh: 0.257; shank: 0.721; foot: 0.271). Despite its statistical significance ($p<0.0001$, $R^2=0.373$), modelling $AP_{Pk}$ with only TLA struggled to capture interparticipant variability (i.e. different $AP_{Pk}$, similar TLA) (Figure 1c). However, decomposing TLA into individual segment angles provided a much better fit ($p<0.0001$, $R^2=0.630$) (Figure 1d-f). Interestingly, when estimating $AP_{Pk}$, the thigh was the most influential factor in the multivariate model (standardized coefficients – thigh: -0.628; shank: -0.351; foot: -0.222). Although the thigh angle does not appear to correlate as well with $AP_{Pk}$, it also did not covary with shank and foot angles. These findings agree well with those from Lewek and Sawicki, who also reported a relatively low $R^2$ using TLA, computed as we did here, to model $AP_{Pk}$ in people recovering from stoke [3]. Additionally, they also found that hip extension angle, similar to our thigh angle, did not relate well to $AP_{Pk}$ on its own. In that work, they suggested that TLA can be used as a surrogate for $AP_{Pk}$. Indeed, Liu et al. went on to cue increased TLA using visual-feedback in young people without impairment, finding that participants both increased $AP_{Pk}$ from baseline and produced similar $AP_{Pk}$ compared to an AP GRF visual-feedback condition [2]. They also reported significant differences in TLA between these two feedback conditions, but not ankle moment, another measure strongly linked to $AP_{Pk}$ [4]. This result supports our findings, hinting that propulsion may not only be affected by TLA magnitude, but also *how* it is composed through its segmental orientation.

**Significance:** The results of this work have several implications. 1) Certain combinations of segment angles may generate greater propulsive forces. 2) The independence of the thigh angle from other variables and its overall importance to multivariate regression of $AP_{Pk}$ suggests it may be a useful target on its own or when training TLA. 3) Conventional methods to compute TLA require marker data and potentially force plates [3], limiting its translation outside of a gait lab. Not only does our segmental angle approach estimate $AP_{Pk}$ more accurately than these methods, but it also could be implemented in clinical rehabilitation settings with relative ease using an inertial measurement unit placed on the paretic thigh, shank, and foot segments [5].

**Acklnowledgements:** NSF Graduate Research Fellowship, NIH Grant # R21 HD098570

**References**

[1] Awad et al. (2020), *JNER* 17(1)
[2] Liu et al. (2020), *Gait and Posture* 83;
[3] Lewek and Sawicki (2019), *Clin. Biomech.* 67
[4] Hsiao et al. (2015), *Human Mov. Sci.* 39
[5] Revi et al. (2020), *JNER* 17(82)

# A finite element-based mesh morphing technique for subject specific human head modeling

Anu Tripathi[1*], Anastasia Tzoumaka[1*], Rika Carlsen[1]
[1] School of Engineering, Mathematics and Science, Robert Morris University, Moon Township, PA, USA
*Corresponding author's email: tripathia@rmu.edu, tzoumaka@rmu.edu

**Introduction**: Human digital twins (HDTs) are essential for assessing injury risks in high-impact environments such as the military, car crashes, and contact sports [1]. Given the complexity of the human body, finite element (FE) models of the head are typically developed and validated independently before being integrated with whole-body models to form a complete HDT. This integration requires precise alignment at the material interfaces to ensure biomechanical fidelity. However, traditional mesh morphing techniques commonly used to adapt FE head models to individual anatomies, often introduce excessive element distortion, imperfect interfaces, and require extensive manual corrections [2]. To address these limitations, we developed a mesh morphing technique, in which a displacement field is applied within the finite element framework. This approach enforces mechanical constraints on local deformations–including equilibrium, kinematics, and material stiffness–ultimately controlling element distortions. We compare our new method with an existing SyN registration-based method, which lacks these constraints on local deformations and often results in excessive element distortion.

**Methods:** We demonstrate our morphing method on the GHBMC50 skull and facial topology model with three distinct bones (outer table, diploe and inner table), to fit onto a highly detailed human brain model based on magnetic resonance imaging (MRI) data called the RMU brain (Fig. 1). The RMU brain model represents an 18 years old female and incorporates all essential anatomical features, namely gray matter, white matter, the cerebellum, the cerebrum, cerebrospinal fluid (CSF), and the dura mater. We first scale the skull uniformly to ensure that the brain model fits properly within the cranial cavity without any overlaps. The brain model retains its original size; therefore, we assign a rigid body constraint to it. We then perform two steps using the explicit solver in Abaqus finite element software to shrink the skull and achieve a proper fit with the RMU brain. In the first step, we apply a negative temperature differential to shrink the cranial cavity. After this step, minor gaps remain between the cranial cavity and the brain, which need to be resolved. In the second step, we apply negative pressure to the inner surface of the cranial cavity, allowing any remaining gaps to close completely (Fig 1.).

**Results & Discussion:** A detailed human facial skull model was successfully morphed and integrated with a detailed high-fidelity finite element (FE) brain model to create a new high-fidelity head model. The mesh quality of the morphed skull model, from the SyN registration and the FEA-based technique, was assessed using the scaled Jacobian of all elements. The scaled Jacobian is a mesh quality metric that measures element distortion by evaluating the ratio of the actual Jacobian determinant to the ideal element's Jacobian, scaled by the reference element's shape and size. It ranges from 0 to 1, where 1 indicates a perfectly shaped element, and values closer to 0 signify highly distorted elements. Preliminary results acquired on a slightly different model showed that the SyN registration mesh morphing method severely distorted the mesh, leading to approximately 10 times more failed elements with a scaled Jacobian below 0.1 (1,124 elements) and approximately 25 times more failed elements with an aspect ratio above 20 (680 elements). In contrast, the new morphing approach did not significantly increase the number of distorted elements compared to the original mesh, resulting in only 126 elements with a scaled Jacobian below 0.1 and 25 elements with an aspect ratio above 20. The FEA-based morphed model is currently being validated using existing kinematic data from drop test experiments and compared against previously obtained FE results from the RMU head model.

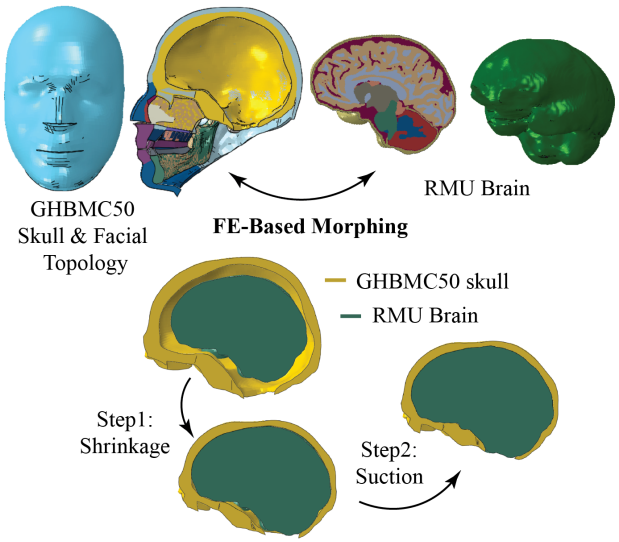


**Figure 1:** FE-based mesh morphing technique where the two steps of skull shrinkage and suction are shown.

**Significance:** The new mesh morphing technique dramatically reduces the distorted elements in the morphed model, which in turn significantly reduces the manual interventions and time to correct these elements in the morphed model. This FEA-based morphing technique will facilitate a fast and accurate generation of subject-specific models, enhancing our understanding and reliable prediction of injury risks in various scenarios

**Acknowledgments:** This research was funded by the U.S. Office of Naval Research (ONR) under award number N00014-24-1-2415 and PANTHER award number N00014-24-1-2118 through Dr. Timothy Bentley.

**References:** [1] Tianze Sun et al. (2023)., *Bioengineeirng 10(6)*, [2] Marek Bucki et al. (2010)., *Medical Image Analysis 14* 303–317

# VALIDITY OF MARKERLESS MOTION CAPTURE FOR ASSESSING OSTEOARTHRITIC KNEE BIOMECHANICS

*Ke Song[1], Carla R. Scanzello[1,2], Joshua F. Baker[1,2], Josh R. Baxter[1,2]
[1]University of Pennsylvania, Philadelphia, PA; [2]Corporal Michael J. Crescenz VA Medical Center, Philadelphia, PA
*Corresponding author's email: ke.song@pennmedicine.upenn.edu

**Introduction:** Knee osteoarthritis (OA) severely limits the performance of daily mobility tasks like walking and sit-to-stand [1]. Active individuals like military veterans are especially at risk for knee OA and related movement deficiencies [2]. Motion analysis is a standard for assessing musculoskeletal function in knee OA. It is well established that mechanical biomarkers like knee adduction moment (KAM) and valgus-varus angles are altered in knees with OA [3,4]. However, marker-based motion capture has lower accuracy and repeatability in knee off-sagittal axes, which reduces its reliability for assessing 3D knee mechanics [5,6]. The tediousness of marker-based analysis also limits its usability in clinical applications [5–7]. Markerless motion capture may overcome these practical barriers and improve data consistency [7]. A recent study used a markerless motion capture system to assess gait in knee OA patients and found high repeatability [8], but its comparative accuracy to marker-based estimate of biomarkers like KAM was not reported. Our prior study found a markerless system to have comparable accuracy to marker-based in lower extremity joint angles and moments [9], but our analysis at the knee was limited to the sagittal plane. Our current goal was to compare 3D knee kinematics and kinetics between marker-based and markerless motion capture during gait and sit-to-stand in knee OA patients. We hypothesized that markerless estimates of knee angles and moments would match marker-based estimates in the sagittal plane, while differences would be larger in the frontal and transverse planes.

**Methods:** In this IRB-approved study, we enrolled 6 male military veterans diagnosed with painful knee OA (Age: 68.7±4.7 y/o, BMI: 26.9±5.5 kg/m$^2$). They walked 2+ passes across an 8m walkway, then performed 30 seconds of sit-to-stand-to-sit at a self-selected pace. We recorded their movements using 12 marker-based cameras, 8 markerless video cameras (both at 100Hz), and 3 force plates embedded under the walkway (1000Hz). We used a marker-based link-segment model [10] and markerless deep learning motion tracker (Theia3D) [7,9] to concurrently calculate 3D kinematics (angle) and kinetics (moment) in their most painful knee affected by OA: flexion-extension (sagittal), valgus-varus (frontal), and internal-external rotation (transverse). We computed Pearson correlation ($r$) and root-mean-square difference (*RMSD*) between markerless and marker-based estimates of each angle and moment during gait and sit-to-stand. We averaged each $r$ and *RMSD* across 6 patients to determine an overall between-system agreement ($r$) and magnitude difference (*RMSD*). We defined $r \geq 0.7$ as a strong correlation [11], and *RMSD* ≤7.5° in joint angles and ≤1% body Height×Weight in joint moments as small differences.

**Results:** Markerless estimates highly matched marker-based in knee flexion angle ($r$: gait 0.96, sit-to-stand >0.99, **Fig. 1A**) and extension moment ($r$: gait 0.90, sit-to-stand 0.99, **Fig. 1B**). *RMSD* were small in sagittal angle (~7°) and moment (≤0.7%H×W). Correlations were weaker in both valgus-varus ($r$: gait 0.22, sit-to-stand 0.46, **Fig. 1B**) and transverse rotation angle ($r$: gait 0.08, sit-to-stand 0.68, **Fig. 1C**). *RMSD* were small in valgus-varus (3.4–5.7°) but larger in transverse rotation (up to 13.8°) with obvious offsets for both trials. Despite the kinematic mismatches, agreement remained strong in the frontal (i.e. KAM; $r$: gait 0.97, sit-to-stand 0.84, **Fig. 1E**) and transverse moment ($r$: gait 0.95, sit-to-stand 0.93, **Fig. 1F**), albeit markerless estimated a lower frontal moment at start of stand-up and end of sit-down (**Fig. 1E**). *RMSD* were small for all off-sagittal moments (≤0.27%H×W).

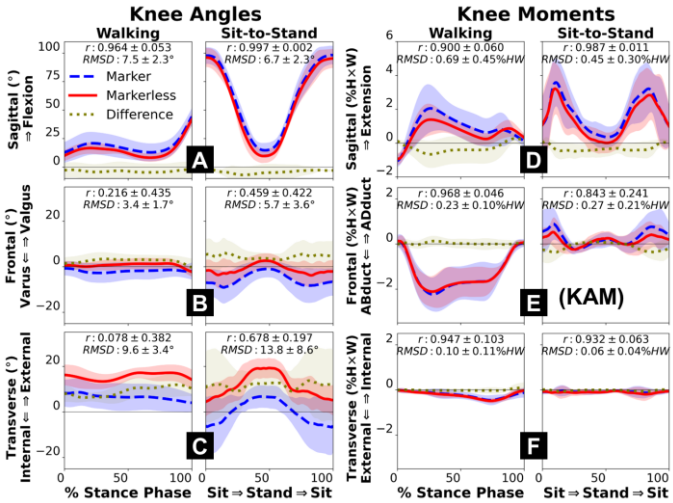


**Figure 1:** Knee sagittal, frontal, transverse angles **(A–C)** and moments **(D–F)** from marker-based (blue) versus markerless motion capture (red).

**Discussion:** Markerless estimates of the knee biomechanics strongly agreed with marker-based in sagittal plane angle/moment as well as frontal/transverse-plane moments. Strong agreements and low errors in the knee flexion-extension plane confirm past studies and support the validity of markerless motion capture in assessing sagittal knee biomechanics in OA patients [8,9]. Mismatches in frontal/transverse kinematics could be related to marker-based skin artifacts [5] and marker placement uncertainties [6]. Despite this, we found the marker-based and markerless systems to assess 3D knee kinetics like KAM with comparable accuracy, possibly because knee and ankle moments during sit-to-stand and the stance of gait are mainly driven by the ground contact force instead of the low dynamics of body inertia [12].

**Significance:** Markerless motion capture reduces the practical burden of marker-based experiments and will simplify the workflow of clinical movement analysis. We found markerless motion capture to maintain high fidelity in assessing sagittal knee biomechanics and the KAM, a frontal-plane mechanical biomarker strongly associated with knee dysfunction in OA [3]. The research community should verify and validate markerless motion capture specific to patient populations to support its usability in large-scale clinical applications.

**Acknowledgments:** US Department of Veterans Affairs I50RX004845; National Institutes of Health NIAMS R01AR078898 and P50AR080581. We thank Sarah Wetzel for patient enrollment, and Max Zewel and Jennifer Agli for data collection and processing.

**References:** [1] Bellamy+ *J Rheumatol* 1988. [2] Dominick+ *J Rheumatol* 2006. [3] Sharma+ *Arthritis Rheum* 1998. [4] Sharma+ *JAMA* 2001. [5] Leardini+ *Gait Posture* 2005. [6] Della Croce+ *Gait Posture* 2005. [7] Kanko+ *J Biomech* 2021. [8] Outerleys+ *J Biomech* 2024. [9] Song+ *J Biomech* 2022. [10] Slater+ *BMC Musculoskelet* 2018. [11] Schober+ *Anesth Analg* 2018. [12] Hullfish+ *J Biomech* 2021.

# PROSTHETIC PYLON EMULATOR FOR CONTROLLING STIFFNESSES UNDER GAIT LOADING

*Chelsea J. Haddy[1], Emma R. Caringella[1], Carl S. Curran[2], Joshua M. Caputo[2], Trevor D. Kingsbury[3], Matthew J. Major[4,5], Kota Z. Takahashi[1]
[1]University of Utah, Salt Lake City, UT, [2]Humotech, Pittsburgh, PA, [3]Naval Medical Center San Diego, San Diego, CA, [4]Northwestern University, Chicago, IL, [5]Jesse Brown VA Medical Center, Chicago, IL
*Corresponding author's email: chelsea.haddy@utah.edu

**Introduction:** Individuals with lower-limb amputation are at an increased risk of musculoskeletal disorders [1], possibly due to overcompensation in their sound limb [2] or due to inadequate attenuation of impact loads on the prosthetic limb [3]. Prosthetic shock-absorbing pylons (SAPs) have been shown to reduce work done on the sound limb [4] and reduce impact forces on the prosthetic limb [5]. However, these SAP resultant benefits are affected by material properties, such as stiffness [4]. Considering the implications of SAP stiffness on gait performance [4], there is a critical need for systematic evaluation of SAP properties and end-user outcomes. One valuable tool may be prosthetic emulator technology [6-8], which, using a cable-driven actuator, can simulate an extensive range of SAP mechanical properties (e.g., stiffness, damping). Expanding prosthetic emulator technology to include pylons will enable systematic gait studies of SAPs. Thus, the purpose of this study is to 1) design a new pylon emulator (PE) and 2) perform preliminary testing to evaluate the PE's capacity to vary stiffness under gait loading.

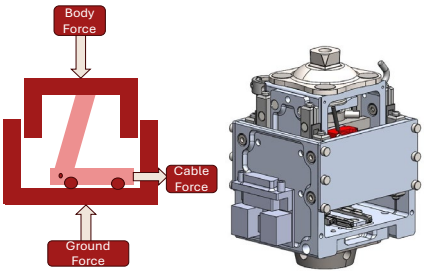


**Figure 1:** Diagram (left) of the inner carriage of the pylon emulator (right). The body force and the ground force compress the pylon, while the cable force from the actuator extends the pylon.

**Methods:** The PE's design consists of an upper and lower portion connected by frictionless square bearings [9] (Humotech, Pittsburgh, PA, Fig. 1). A cable from the actuator is connected to a rolling carriage on the lower portion of the pylon. A hinge joint connects the carriage to the upper portion to resist compression from opposing ground reaction force and body weight. As loading is applied during the stance phase of gait, an inline load cell returns axial load measurements to the controller [9]. The actuator releases the cable, allowing displacement proportional to the applied force. A string potentiometer returns the displacement to complete the feedback loop to the controller for real-time adjustments to control the pylon stiffness during the gait loading and unloading phase. To perform preliminary testing of the PE, we set the PE's control parameters to achieve two desired stiffnesses (167 kN/m and 125 kN/m) to emulate a passive SAP [10]. We also set the PE as an idealized spring with zero net work (i.e., 100% energy return). This study, considered development work and not human testing subjects, had one healthy participant walk on a level treadmill at 0.8 m/s for 2 minutes using the PE with a bent knee adapter. The force and displacements from each gait cycle and condition were recorded for comparison to the desired stiffness.

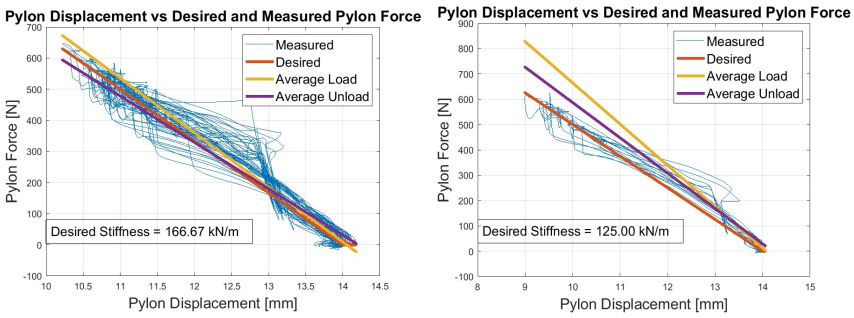


**Figure 1:** Pylon Displacement [mm] vs Pylon Force [N] for a desired stiffness of 167 kN/m (left) and 125 kN/m (right). The desired slope is the input stiffness (red line), while the average load (yellow line) and unload (purple line) is the actual stiffness of the gait testing during loading and unloading, respectively.

**Results & Discussion:** The average measured stiffness was 175.5 ± 13.3 kN/m for the desired stiffness of 167 kN/m (Fig.2 left) and 163.0 ± 26.4 kN/m for the desired stiffness of 125 kN/m (Fig. 2 right). As a result, there was a percent error of 5.1 ± 0.4 % for the desired stiffness of 167 kN/m and 30.4 ± 4.9 % for the desired stiffness of 125 kN/m. The more compliant spring had a greater percent error in spring stiffness, which may be explained by the propagated gain error (overcompensation in displacement for a change in force) that occurs when greater displacements are needed for a smaller change in force inputs. Although 100% energy return conditions were implemented, the percent energy return was 89.6 ± 22.0% for the desired stiffness of 167 kN/m and 94.6 ± 240.6% for the desired stiffness of 125 kN/m. Both stiffness conditions resulted in energy loss, likely from the controller gains underdamped tuning and Coulomb damping. The controllers' proportional and damping gain is being further tuned to improve accuracy in achieving a desired stiffness and energy return.

**Significance:** This proof of concept study will lay the foundation for further studies on a PE with several stiffness cases, power loss or return, and various participants with leg amputations. Validation of the performance of the PE will open doors for clinical use and allow prosthetists to effectively prescribe SAPs to patients based on their individual needs to reduce the risk of musculoskeletal disorders.

**Acknowledgments:** Funding was provided by the DoD and Prosthetics Outcomes Research Program (award #W81XWH2120007)

**References:** [1] Burke et al. (1978), *Ann Rheum Dis* 37(3); [2] Nolan et al. (2000), *Prosthet Orthot Int* 24(2); [3] Breakey et al. (1976), *Orthot Prosthet* 30(3); [4] Maun et al. (2021), *J Neuroeng Rehabil* 18(1); [5] Gard et al. (2003), *J Rehabil Res Dev* 40(2); [6] Caputo et al. (2015), *IEEE Int Conf Robot Autom* 2015; [7] Caputo et al. (2014), *J Biomech Eng* 136(3); [8] Caputo et al. (2022), *J Prosthet Orthot* 34(4); [9] Chen et al. (2024), *US Prov Patent App* 63/557,515.

# EVALUATING MARKERLESS MOTION CAPTURE IN CHILDREN WITH CEREBRAL PALSY WEARING GROUND REACTION ANKLE-FOOT ORTHOSES

*Riley Horn, John Collins, Heather Waters, Christine Amacker, Martins Amaechi, Rachel Thompson, Patrick Curran, Henry Chambers
Motion Analysis Laboratory, Rady Children's Hospital, San Diego, CA; *Corresponding author's email: rhorn@rchsd.org

**Introduction:** Three-dimensional motion capture is a valuable tool for informing clinical decision-making for ambulatory children with cerebral palsy (CP) [1]. Children with CP are often prescribed ankle-foot orthoses (AFOs) to manage their gait pattern and it is vital to capture the effects of orthoses on gait parameters [2]. While marker-based motion capture is the current standard, limitations include longer collection time, soft tissue artifact, and variable accuracy of marker placement. Markerless motion capture eliminates the need for marker placement, but the efficacy of the markerless algorithms for evaluating gait in AFOs is unknown [3, 4]. Thus, we compare kinematic data collected from marker-based and markerless systems in children with CP wearing ground reaction AFOs.

**Methods:** Individuals with CP undergoing routine gait analysis while wearing ground reaction AFOs were included for this study. Six patients (11 limbs in AFOs) were included (11.2 +/- 4.7 years; 5 male, 1 female). Retroreflective markers were placed using the CAST full body six degrees of freedom marker set. At the shank and foot, markers were placed on the shoe or orthosis aiming to best represent the underlying anatomy. Participants performed several gait trials along a 10-meter path at self-selected speeds. Strides from three selected trials were averaged for each limb. Kinematic data were collected simultaneously using a 10-camera marker-based Arqus system and a 10-camera markerless Miqus system (Qualisys, Goteborg, Sweden). The markerless data were processed using Theia3D software (v2024.1.19, Theia Markerless Inc.). Data were processed in Visual3D (C-Motion Inc.) and normalized to the gait cycle at 101 data points. Statistical parametric mapping (SPM1D, Python version 0.4.18; spm1D.org) was used for paired samples t-tests ($\alpha = 0.05$) to compare differences in joint angles across the gait cycle.

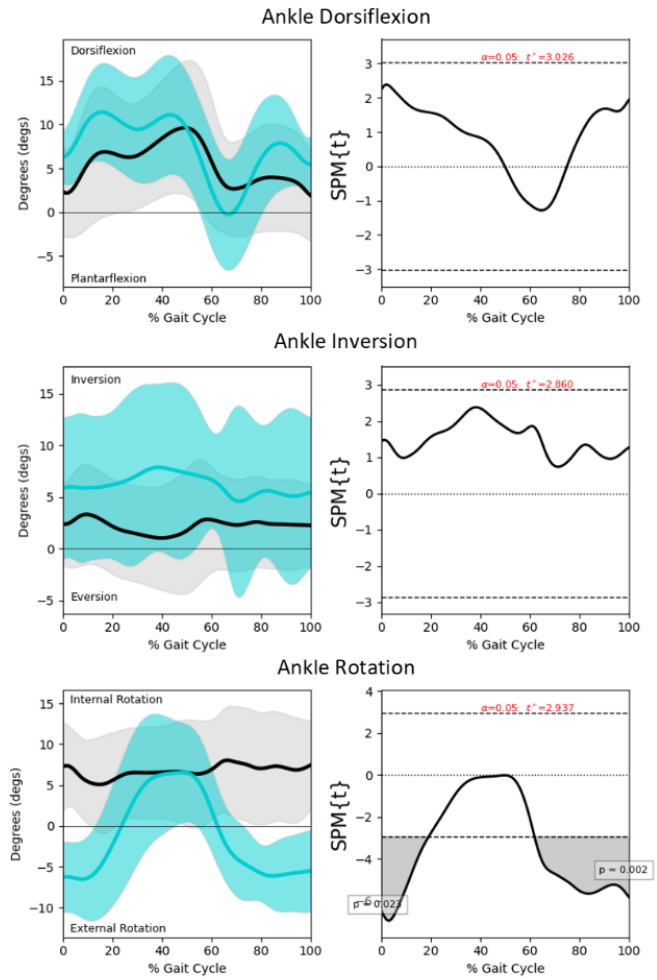


**Figure 1**. Comparison of average joint angles ± 1 standard deviation across the gait cycle for marker-based (black) and markerless (blue). SPM analyses (right) display the critical threshold (t*, dotted lines) for significant differences.

**Results & Discussion:** There were no significant differences in ankle kinematics in the sagittal or frontal plane between the markerless and marker-based data (Figure 1). Markerless motion capture displayed significantly more external ankle rotation during initial contact through midstance ($p = 0.023$) and mid-to-terminal swing ($p = 0.002$) compared to marker-based motion capture. It is clinically important to capture the effects of orthoses on gait parameters and this study demonstrates notable differences in output between marker-based and markerless systems. Markerless and marker-based kinematics were similar for ankle dorsiflexion and ankle inversion, which may be promising for use in the sagittal and frontal planes. Ground reaction AFOs are prescribed in part to restrict movement in the frontal and transverse planes. However, markerless motion capture observed more external ankle rotation in this study, which does not match clinical expectations [5]. The markerless system may be creating an inappropriate representation as it attempts to fit the data to its model of a typically developing adult. Markerless motion capture presents the potential for effective clinical gait analysis, although it is not yet an equivalent substitute for marker-based systems for patients wearing ankle-foot orthoses. To better understand how markerless motion capture is characterizing gait while wearing AFOs, further investigation assessing patient-specific differences is needed.

**Significance:** Markerless motion capture allows for efficient gait analysis for children with CP. Characterizing the ability of markerless motion capture to detect kinematic gait patterns in children with CP wearing orthoses in comparison with marker-based motion capture is a requisite step toward validating this technology for widespread clinical use.

**References:** [1] Wishaupt, K. et al. (2024) Scientific Reports; [2] Ricardo, D. et al. (2021) Children; [3] Wren, T. et al. (2023) Gait & Posture; [4] Kanko, R. M. et al. (2024) Journal of Applied Biomechanics; [5] Balaban, B. et al. (2007) Disability and Rehabilitation.

# BIOMECHANICAL SIMULATION OF 55 YOGA POSES REVEALS THAT THE YOGA POSES ARE MORE DIVERSE KINEMATICALLY THAN KINETICALLY

*Sriram Sekaripuram Muralidhar[1,2], Manoj Srinivasan[1]
[1]Mechanical and Aerospace Engineering, The Ohio State University, Columbus OH 43201
[2]Division of Biokinesiology and Physical Therapy, University of Southern California, Los Angeles CA 90033
*Corresponding author's email: srirammu@usc.edu

**Introduction:** Yoga involves holding a static (approximately isometric) pose against gravity. Yoga has physical, mental and cardio-metabolic health benefits, as suggested by many studies [1]. Despite such potential benefits and despite hundreds of millions of practitioners in the world, we still lack a deep biomechanical understanding of individual poses. Previous works that studied the physical impacts of individual poses are limited to a few poses or body parts due to time-consuming experimental measurements [2]. Predictive computational models generalizable to any pose can help address these limitations. However previous computational models work for only two segment contact poses and used unphysical assumptions [3]. Here, we create a new dataset involving 55 sagittal plane yoga poses, create a unified computational model for the simulation of such yoga poses (Fig 1A), and compute the joint angles and joint torques from the data and the model for all these poses. The computed joint angles demonstrate that the yoga poses are maximally expressive kinematically, while there is some redundancy in the joint torques.

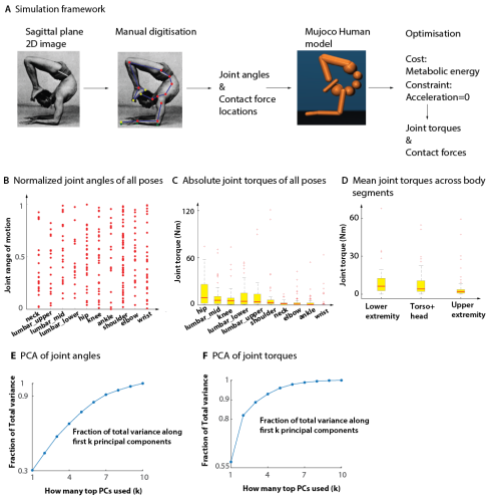


**Figure 1:** A) Simulation framework, B) Normalized Joint angles. C) Abs value of joint torques. D) Joint torques averaged across body parts. E) PCA joint angles. F) PCA of joint torques

**Methods:** We digitized images of 55 yoga poses that are symmetric about the sagittal plane from the book *Light on Yoga* [4], which is considered a modern foundational classic in the practice of yoga. Previous image datasets were either not exhaustive or had inconsistencies with pose descriptions. Using a custom MATLAB code, we extracted x-y coordinates of the joint centres, body segment extremes, and body segment contacts with the ground and between each other. Performing inverse kinematics resulted in a dataset consisting of joint angles and contact locations for the 55 yoga poses. We developed a 2D human model in sagittal plane consisting of 10 joints and 11 rigid segments, modified from a humanoid model in MuJoCo inventory [5], implementing a custom contact formulation. We hypothesise that humans perform these postures in an energy optimal or effort-minimal way. So, we frame this as a constrained optimisation problem with metabolic energy as the cost and static equilibrium as the constraint. We expressed metabolic cost as a function of joint torque based on an empirically based metabolic cost model (Metabolic energy $\propto \tau^{1.64}$) developed in our recent work [6]. The total metabolic cost is a sum over all 10 joints: $\sum_{i=1}^{10} a_i \, {\tau_i}^{1.64}$. We estimated joint torques and contact forces by minimizing this cost subject to the equilibrium constraints, solving the static indeterminacy. We analysed the resulting torques and joint angles across the 55 poses with respect to their diversity and comparing them with maximal physiological joint torques and angles.

**Results & Discussion:** Comparing the joint angles estimated for the 55 poses to the known joint ranges of motion (Fig 1B), we found that the 55 poses make use of essentially the entire range of motion of all the joints. Further, performing principal component analysis on the joint angle data (Fig 1E) revealed that the yoga poses did not admit a significant dimensionality reduction, with variance increasing gradually with number of principal components considered – this suggests that yoga poses are kinematically diverse.

Our predictive optimisations converged within few seconds for all the poses, with optimality and constraint violations less than 10^-4. From the model-predicted joint torques across all the poses, on average, we find yoga poses requires the highest torques from the hip joint followed by lumbar and knee; the least joint torques are required of the wrist joint across all the poses (Fig. 1C). When these joint torques are analyzed as groups across all poses, on average, lower extremity joints are required to produce the highest torques, followed by the torso-head and the upper extremity (Fig 1D). Perhaps this is natural, given that these lower limb joints usually carry much of the body weight – this dominance of lower limb torques was also reflected in a principal component analysis, revealing that three principal components capture 90% of the variance, making it less kinetically diverse (Fig 1F).

Our simulations have certain intentional simplifications, which can be relaxed in future work: 1) limited to 2D poses, 2) ignoring passive forces due to muscles or ligaments stretching, as we assume rigid body dynamics, 3) neglecting contact forces between body segments, which may impact joint torque predictions, and finally, 4) a joint-torque-based model that cannot predict muscle forces.

**Significance:** We have developed a simulation framework, whose predictions could be tested quantitatively in future work via careful experiments. Understanding the biomechanics of a large variety of yoga poses may allow us eventually to design yoga based physical therapies and test the impact of these poses on different movement disorders or injuries.

**Acknowledgements:** This work was supported by NIH-R01GM135923 and NSF SCH grant 2014506.

**References:** [1] Chu et al. (2016), Euro jour prev card; Reinbolt et al. (2005), *J Biomech* 38(3); [2] Salem et al. (2013), *J Evidence-based Comp and Alt Med*. [3] Omkar et al, (2011), J Bodywork and Movmt Thera. [4] B. K. S. Iyengar. (1979), Light on yoga. [5] Tassa et al, (2012), IEEE/RSJ. [6] Muralidhar et al. (2025). arXiv preprint arXiv:2501.00723.

# Manual vs Auto Labeling with and without a Functional Static

Alex Phan, Shawn Roberts, MS, Tishya Wren, PhD
Children's Hospital Los Angeles, Los Angeles CA; University of Southern California, Los Angeles CA
Email: aphan@chla.usc.edu

**Introduction:** Motion capture technology (MCT) provides critical insights into human movement by tracking markers affixed to the body, supporting treatment programs in sports medicine and clinical rehabilitation through detailed gait analysis [1,2]. To meet the growing demand for enhanced precision and speed in biomechanical data collection, recent advancements—such as markerless MCT—have been developed to streamline data processing [1,3]. However, despite these improvements the relative accuracy of manual labeling (ML) versus auto-labeling (AL) with and without the incorporation of a functional static trial has not been investigated in gait analysis, particularly when using Vicon Nexus. The purpose of our study was to compare the labeling accuracy and speed of ML to AL in Vicon Nexus in pediatric athletes during gait analysis.

**Methods:** Ten female athletes (median age 15.5 years, SD 1.2) that had undergone anterior cruciate engagement reconstruction (median: 10.4 months, SD 4.1) completed multiple walking trials, and marker data from those trials were collected using a 10-camera motion-capture system (Nexus2, Vicon, Oxford, UK) to develop 3D models for biomechanics assessments. Marker data for each athlete was processed until there were 10 strides in Vicon Nexus utilizing three methods: ML, auto-labeling with a functional static (ALF), and auto-labeling without a functional static (ALWF). Range of motion trial guidelines, outlined by Vicon Nexus were followed to create a functional static. A stride was defined as a full gait cycle, from initial foot contact to the subsequent contact with the same foot, with minimal marker occlusion and stable movement. Trial processing began by trimming the trial at the first step of a stride until no viable strides were left in the trial. Labeling—manually or with the auto-labeling pipeline in Vicon Nexus—was then performed once per trial on one frame near the beginning of the trial where all the markers were visible after trimming. For each trial the labeling time for each method was recorded. ML was collected with a stopwatch and for both AL methods the system-logs of when the AL pipeline started and ended were utilized to calculate processing time. Post-processing, the trials were reviewed on a frame-by-frame basis to identify incorrect markers. An incorrect marker was defined as any marker that (a) became unlabeled during a gap, (b) was switched with another marker, or (c) was not labeled at all. The number of errors was summed for each method to calculate an overall error count and was repeated for each patient. The aggregate accuracy and time were calculated across all trials for each method. The labeling accuracy and speed were compared across methods using repeated measures ANOVA with post-hoc Bonferroni corrected pairwise tests. Cohen's d was used to examine the effect size of pairwise comparisons for labeling accuracy.

**Results & Discussion:** There were no significant differences in labeling accuracy between the three methods ($F=1.304$, $p = 0.296$, Error rates (Total labeled incorrectly/Total frames x Markers): ML = 0.31%, ALF = 0.08%, ALWF = 0.21%) although effect size suggested that both auto labeling methods were moderately more accurate than manual labeling (ALF to ML: $d = -0.602$, ALWF to ML: $d = -0.619$) and ALF was slightly more accurate than ALWF ($d = 0.383$). There was a significant difference in labeling speeds ($F=1187.51$, $p < 0.001$), with both auto labeling methods being significantly quicker than manual labeling (ALF and ALWF to ML: $p < 0.0167$, Total labeling times (s): ML = 1693.30s, ALF = 134.38s, ALWF = 144.48s). This did not account for the time needed to create a functional static trial for ALF which increases overall processing time 5-10 minutes (depending on patient, technician, and a computer's trial processing capabilities).

**Significance:** The results suggest that AL both with and without a functional static may be slightly more reliable than ML. AL, especially when augmented with a functional static trial, may benefit from modest time savings for labeling marker-based motion capture data for large-scale projects and more complex dynamic trial data processing but those time savings are likely to be negated due to function static creation times when data processing is done for small-scale or single session data collection. Despite AL reliability and time savings, it is important to review marker labels for potential errors after auto labeling as all methods produced at least a small percentage of errors.

**References:** [1] Das, K et. al *Sci Rep* **13**, 22880 (2023), https://doi.org/10.1038/s41598-023-49360-2 [2] Mündermann, et al J *NeuroEngineering Rehabil* **3**, 6 (2006). https://doi.org/10.1186/1743-0003-3-6 ; [3] Ghorbani, S et al (2019). https://doi.org/10.1007/978-3-030-22514-8_14

# VALIDATION OF A MULTI-SEGMENT FOOT MODEL USING WEIGHT-BEARING CT

*Matheus M. Vilela[1,2], Pedro Benevides[1,2], Lucas Pallone[1,2], Leonardo Metsavaht [1,2], Gustavo Leporace [1,2], Jonathan A. Gustafson [1,2]
[1] Instituto Brasil de Tecnologias da Saúde, Brazil
[2] Department of Orthopedic Surgery, Rush University Medical Center, Chicago, IL, USA.
*Corresponding author's email: matheus_vilela@rush.edu

**Introduction:** Foot biomechanics is essential for understanding human movement, particularly in injury prevention, rehabilitation, and performance optimization. The intricate anatomy of the foot makes motion analysis challenging, especially in real-world, weight-bearing conditions where soft tissue deformations and complex interactions occur. Multi-segment foot models, such as the Ghent Foot Model[1], provide a promising approach to track the motion of individual foot segments using skin markers. However, these models have yet to be fully validated under weight-bearing conditions that closely simulate everyday activities and soft tissue displacements. This study aims to evaluate the ability of the Ghent multi-segment foot model to accurately capture movement between bones in three planes by comparing its results to those obtained from weight-bearing computed tomography (WBCT) scans of cadaver feet. We hypothesized that the multi-segment model, when applied in weight-bearing conditions, could offer a reliable method for capturing foot segment motion, potentially providing a more accurate representation of bone movement.

**Methods:** Ten below-knee fresh-frozen cadaveric specimens were used in this study (6 males and 4 females; mean age = 68 years [range= 59–92]). None of the specimens had gross deformity of the forefoot or any radiographic evidence of degenerative changes that could limit motion in our testing. A custom jig was developed to test the specimens under six different foot positions (neutral, eversion, inversion, dorsiflexion, plantarflexion, and hallux extension) under axial load of 20kg. Superficial markers were placed on the feet according to the Ghent Foot Model[1] to track segmental motion[2]. WBCT scans were performed to capture three-dimensional (3D) images of the bones and markers at each position (Fig. 1). Three dimensional models[3] of both the bones and skin markers were created for each specimen from the segmented images (Fig. 2). Distance measurements (Fig.3) were made between the markers and the underlying bones.

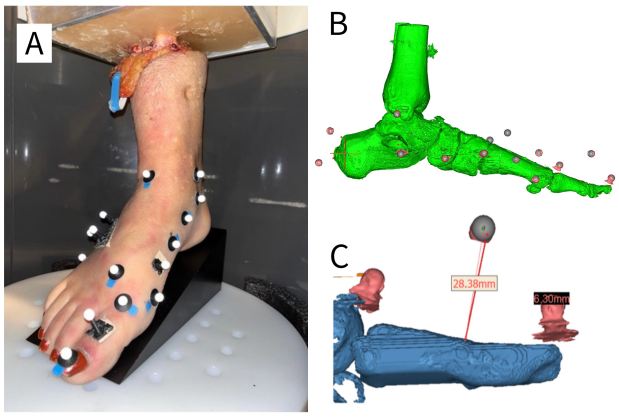


**Figure 1:** a) Specimen with markers, positioned in ankle plantarflexion in WBCT equipment; b) 3D models created with WBCT images, after bone and marker segmentations; c) Measurement of the distance marker-bone

| Reference | Segment | Mean (mm) | Lowest (mm) | Highest (mm) |
|---|---|---|---|---|
| Med Malleolus | Leg/Ankle | 15.9 | 14.7 | 17.5 |
| Lat Malleolus | Leg/Ankle | 20.3 | 19.7 | 21.1 |
| Calcaneus Sup | Hindfoot | 16.6 | 15.5 | 18.7 |
| Calcaneus Inf | Hindfoot | 17.8 | 16.8 | 18.4 |
| Sust Tali | Hindfoot | 28.4 | 27.6 | 29.3 |
| Tub Peronei | Hindfoot | 28.7 | 25.7 | 30.4 |
| Navicular | Midfoot | 21.4 | 20.6 | 22.2 |
| Cuboid | Midfoot | 23.3 | 22.2 | 24.3 |
| 1st Mtt Base | Med Forefoot | 22.0 | 20.8 | 23.5 |
| 1st Mtt Shaft | Med Forefoot | 23.8 | 23.6 | 24.5 |
| 1st Mtt Head | Med Forefoot | 13.4 | 12.4 | 14.2 |
| 1st Mtt Head (Lat) | Med Forefoot | 17.2 | 15.3 | 23.1 |
| 5 th Mtt Base | Lat Forefoot | 14.1 | 12.5 | 16.1 |
| 5 th Mtt Head | Lat Forefoot | 13.3 | 12.5 | 14.9 |
| Hal Prox Phallanx | Hallux | 12.0 | 11.2 | 14.4 |
| Hal Interphallanx | Hallux | 28.8 | 26.9 | 30.1 |
| Hal Tip (toenail) | Hallux | 9.5 | 7.7 | 10.2 |

**Table 1:** Summarized results of one specimen: mean distance marker-bone reference and range of variation.

**Results & Discussion:** We present preliminary data from one specimen as image processing and segmentation are ongoing. The average distance between skin-based marker placement and underlying bone centroids was 19.2mm. Across the tested loading positions, the marker with the smallest deviation from the bone centroid was the diaphysis of the first metatarsal (Table 1). This could be explained by the direct placement of the marker on the skin with minimal subcutaneous tissue and reduced soft tissue mobilization, thus minimizing soft tissue artifact (STA)[5]. The greatest deviation was from the first metatarsal head lateral marker. This could be explained by the position of the marker relative to the soft tissues and the range of motion of the hallux during dorsiflexion raising an hypothesis of the presence of STA related to this marker. Further analysis of the remaining collected samples is necessary to generalize these conclusions.

**Significance:** This study aimed to validate the Ghent multi-segment foot model by comparing its measurements with those obtained from weight-bearing computed tomography scans of cadaveric feet. The data to be generated will demonstrate the model's accuracy in different foot positions, providing a better understanding of its ability to capture the complex biomechanics of the foot. If successful, this model could significantly improve the accuracy of foot motion analysis in both clinical and research settings, especially for conditions related to foot pathology, injury prevention, and performance optimization.

**Acknowledgments:** Support from the Rush-IBTS Research Fellowship Program is appreciated.

**References:** [1] De Mits S et al. (2012), *J Orthop Res* 30; [2] Conconi M et al. (2021) *J Foot Ankle Res* 14; [3] de Carvalho KAM et al. (2022) *Foot Ankle Orthop* 7;[4] Leardini A et al. (2021) *J Biomech* 125; [5] Leardini A et al. (2005) *Gait Posture* 21.

# ESTIMATION OF THE HIP JOINT CENTER IN 3 MONTH OLD HUMANS

Abigail R. Brittain[1], John Collins[1,2], Michael D. Harris[3], Christine L. Farnsworth[2], Vidyadhar V. Upasani[2] and Erin M. Mannen[1]
[1]Boise State University, Boise, ID [2]Rady Children's Hospital - San Diego, San Diego, CA [3]Washington University School of Medicine, St Louis, MO
abbybrittain@boisestate.edu

**Introduction:** The challenges of estimating the human hip joint center (HJC) based on the location of bony anatomical landmarks have been well documented. In an effort to standardize the methodology used in human biomechanics research, the International Society of Biomechanics (ISB) recommends defining the HJC based on inter ASIS distance (dASIS) as described by Bell et al.[1] However, previous investigations have shown that the Bell methods are incapable of accurately and sufficiently predicting the location of the infant HJC[2]. Using the Bell equations, HJC estimation error for infants was found to be between 4-15mm; with 96% of estimations falling outside the femoral head entirely. The notable differences in pelvis and femur morphology, including absolute size, and the rapid development of the hip joint during infancy contribute to the need for an infant-specific methodology for estimating the HJC. The current study aims to develop a regression equation capable of predicting the infant HJC based on anatomical landmarks.

**Methods:** Hip and pelvis Magnetic Resonance Images (MRI, 1.5 Tesla) were identified under an approved IRB protocol at a pediatric hospital and health center. Six subjects (3 male, 3 female) aged 3 months old received MRIs for conditions unrelated to the hip joint and there were no known musculoskeletal pathologies. Coronal images (2mm thickness) were segmented and processed in Amira (Thermo Fisher Scientific, Waltham, MA, USA). Specifically, bilateral femoral heads, anterior superior iliac spine (ASIS), and posterior superior iliac spine (PSIS) were identified. After smoothing the boundary interfaces of each anatomical part, the center of mass (CoM) of each femoral head, ASIS, and PSIS were identified. The CoM of each femoral head was assumed to be the true HJC. Following the identification of each CoM, all coordinates were translated to the pelvic coordinate system, defined as the mid-point between ASISs with the X-axis pointing to the right ASIS, the Z-axis pointed anteriorly and bisecting the PSISs, and the Y-axis orthogonal to the other two axes. Three scaling factors were calculated for each participant: dASIS, dPSIS (distance between the right and left PSIS), and pelvic depth (PD; distance between the mid-ASIS and mid-PSIS). The distance between the HJC and origin of the pelvis coordinate system was calculated as a percentage of each scaling factor and then averaged to generate predictive equations. Four subjects (2 male, 2 female) were used to "train" the predictive equations, which were the applied to the remaining two subjects, and errors were calculated.

**Table 1:** Location of the hip joint center.

| Translation | Equation |
|---|---|
| *X (Lateral)* | dPSIS * 0.820 |
| *Y (Inferior)* | dASIS * 0.336 |
| *Z (Posteriorly)* | PD * 0.105 |

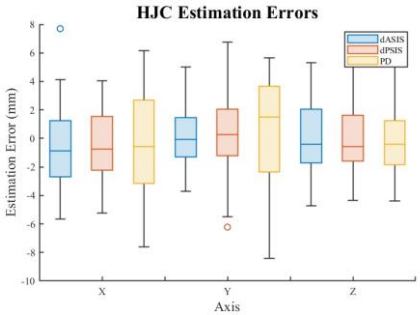


**Figure 1:** HJC Estimation Errors

**Results & Discussion:** From 4 scans of 3-month old heathy infants, the HJC is most accurately estimated as 82% of dPSIS laterally, 33.6% of dASIS inferiorly, and 10.5% of PD posteriorly from the origin of the pelvic coordinate system. Each scaling factor was chosen based on previous research showing dPSIS, dASIS, and PD were best at predicting the location of the HJC in the along the X, Y, and Z components, respectively (Figure 1).[3] Using these translations, the estimated HJC had an average 3-dimentional error of 3.0 ± 0.59 mm. The current study employs the same approach as used by Bell[1] to establish regression equations describing the infant HJC, with two notable modifications. First, instead of describing the HJC as a translation from the ASIS, the current study describes the HJC as a translation from the pelvic coordinate system. Secondly, we utilized three different scaling factors were utilized: dASIS, dPSIS, and PD. Notably, our current predictive equation relies on the accuracy and placement of four markers, rather than two as with the Bell equations[1]. These methods should be further explored to understand sensitivity errors in ASIS and PSIS locations. Although the errors we found are smaller than errors found when applying the Bell equations to infant hips, a larger sample size will build upon the current results. Additionally, and unsurprisingly, we found that by training our equations on only 3-month olds, we could more accurately predict the location of the hip joint center for 3-month olds. This further supports the necessity for age specific formulas or the inclusion of an age factor in predictive equations. A sex factor is likely not necessary due to limited sex dimorphisms in the infant skeleton. Future investigation will be needed to further validate the current equations across a larger dataset.

**Significance:** Currently there is not an accurate method to estimate the infant HJC based on anatomical pelvic landmarks. By limiting a training data set to only 3 months olds, we were able to estimate the infant hip joint center to ~3.0 mm of error.

**Acknowledgments:** National Institutes of Health IDeA INBRE and COBRE Programs, International Hip Dysplasia Institute, and NIH Grants No. P20GM103408, P20GM109095, and P20GM148321

**References:** The format of the reference list can be brief and does not have strict requirements but must include the minimum information needed for readers to unambiguously determine the reference. For example: [1] Reinbolt et al. (2005), *J Biomech* 38(3); [2] Finley et al. (2013), *J Physiol* 591(4). [3] Brittain et al. (2025) ORS Annual Mtg

# A NOVEL APPROACH TO UNCOVERING GOVERNING EQUATIONS OF SPORTS MOVEMENT

Seung Kyeom Kim[1], Tyler Wiles[1] & Aaron D. Likens[1]
[1]Department of Biomechanics, University of Nebraska at Omaha, Omaha, NE
*Corresponding author's email: seungkyeomkim@unomaha.edu

**Introduction:** The trajectory of a projectile launched by a trebuchet can be accurately predicted by understanding the sequential transfer of force through the trebuchet's components. By modeling the trebuchet's mechanics, one can determine not only the projectile's trajectory, but also its velocity and force applied to the trebuchet. Similarly, in baseball pitching, force is generated in the lower body, transferred through the kinetic chain, and ultimately transferred to the throwing arm to launch the baseball up to 105 miles per hour. The coordination of the legs, trunk, and throwing arm dictate mechanical efficiency, ball velocity, and accuracy. Efficient force transfer enhances ball velocity and mechanical efficiency, whereas disruption in force transfer may lead to poor performance and increased injury risk. This underscores the importance of investigating the underlying kinetics necessary for strong and safe mechanics [1,2]. In this study, we apply symbolic regression to derive accurate yet interpretable mathematical expressions that describe the joint moment interactions during pitching, providing a powerful tool for learning the biomechanical principles governing throwing from the mound.

**Methods:** Baseball pitching joint moment data of 100 participants were extracted from OpenBiomechanics dataset [3]. Joint moment data were sampled at 360Hz. Total joint moments time series were computed for the rear leg (ankle, knee, hip), lead leg (ankle, knee, hip), and throwing arm shoulder. The first and second derivatives of total joint moment time series were computed via numerical differentiation. The time series data starting from the planting of the lead foot to ball release were time normalized to 101 datapoints. The average total joint moment and its first and second derivatives of total joint moment time series were computed for each participant. Then, 10 participants were randomly sampled. Symbolic regression was performed for 10 minutes per participant to derive candidate models. The second derivative of total shoulder joint moment was set as the outcome variable, and all the lower limb joint moments were set as the predictor variables. The best model for each participant was selected among the candidate models according to Pareto fronts, balancing complexity—quantified as the total number of variables and operators in a model—and accuracy, quantified via randomized dependence coefficients (RDC). RDC values closer to 1 indicate strong dependence between two data, whereas values closer to 0 suggest little to no dependence. The selected models were fit to individual trials using ordinary least squares regression to evaluate their performance, and their predictive performance was assessed by computing RDCs between the actual and predicted second derivative of the shoulder joint moment time series.

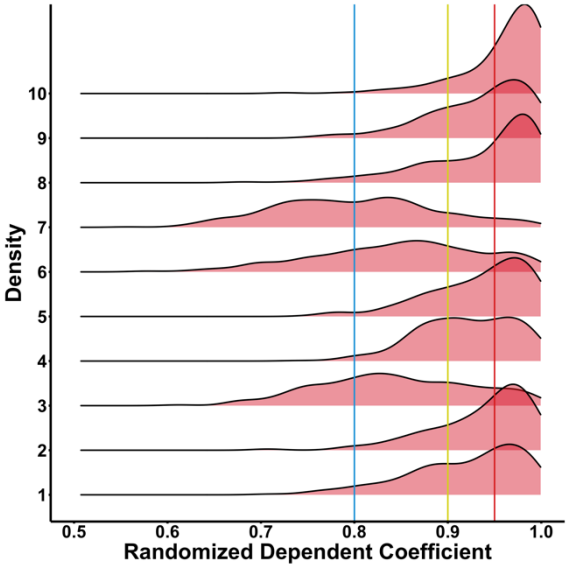


Figure 1. Density Plots of Randomized Dependent Coefficients between Actual and Predicted Data. Blue, yellow, and red vertical lines indicate randomized dependent coefficients of 0.8, 0.9, and 0.95 respectively. The y-axis indicates the indices of the randomly sampled participants.

**Results & Discussion:** The complexity of the selected models ranged from 3 to 13, while their accuracy, measured by RDC, ranged from 0.866 to 0.998. These results indicate that the best models selected for each participant were both simple and accurate. The set of predictor variables included in the best models varied, representing variability among each individual's kinetics. Despite inter-individual differences, the RDC values between the actual and predicted second derivative of the shoulder joint moment time series ranged from 0.558 to 1.000. A total of 87.239% of predicted time series achieved RDC values above 0.8, 59.303% exceeded 0.9, and 38.358% surpassed 0.95, demonstrating strong predictive accuracy (Figure 1). These high RDC values highlight that the best models selected for the ten randomly sampled participants were not only capturing inter-individual variability among athletes, but also accurately predicting the majority of the trials included in the dataset. These findings suggest a combination of common and unique patterns underlying joint moment coordination during baseball pitching. Overall, this study demonstrates that symbolic regression can effectively capture both common and individual-specific coordination in baseball pitching, providing interpretable models balancing accuracy and complexity.

**Significance:** By balancing model complexity and accuracy, our approach provides a novel modelling technique to quantify and understand the kinetics governing baseball pitching. The ability to extract equations of motion reveals both shared and unique coordination patterns among pitchers. This study lays the groundwork for personalized biomechanical modelling that could enhance athlete-specific training protocols and injury prevention strategies. Furthermore, the application of symbolic regression could be extended beyond baseball pitching to other movements, such as hitting, jumping, or cutting maneuvers in various sports.

**Acknowledgments:** Center for Research in Human Movement Variability at the University of Nebraska at Omaha, the University of Nebraska Collaboration Initiative, the NSF award 212491, the NIH awards P20GM109090 and P20GM152301

**References**: [1] Chu et al. (2016), PM&R, 8(3). [2] Seroyer et al. (2010), *Sports Health*, 2(2); [3] https://github.com/drivelineresearch/openbiomechanics

# GUIDELINES FOR PARAMETER SELECTION FOR CROSS RECURRENCE QUANTIFICATION ANALYSIS

Seung Kyeom Kim[1], Tyler Wiles[1], Nick Stergiou[1,2] & Aaron D. Likens[1]
[1]Department of Biomechanics, University of Nebraska at Omaha, Omaha, NE
[2]Department Physical Education and Sport Science, Aristotle University of Thessaloniki, Greece
*Corresponding author's email: seungkyeomkim@unomaha.edu

**Introduction:** Cross Recurrence Quantification Analysis (CRQA), a bivariate extension of RQA, is an increasingly used method in human movement science for visually and quantitatively capturing the coordination between two systems' behavior in a shared phase space [1-3]. Cross recurrence, the tendency of two systems to revisit regions of a shared phase space, forms the foundation of CRQA and offers valuable insights into the coordination dynamics. CRQA is particularly powerful for studying human movement coordination, as it quantifies variability, distinguishes between clinical groups, and accounts for the nonlinear complexity of real-world movement [1-3]. However, the reliability of CRQA depends heavily on parameter selection. Specifically, recurrence threshold (i.e., radius) plays a critical role. A radius that is too small may result in insufficient cross recurrences, whereas too large of a radius may result in spurious cross recurrences, both leading to meaningless CRQA metrics [4]. This study aims to establish guidelines for selecting an appropriate range of radii by systematically performing a parameter sweep on the radius.

**Methods:** 35 young adults, 36 middle adults, and 41 older adults each performed 18 trials of 4 minutes overground walking. Whole-body kinematics were collected via inertial measurement units at 200Hz [5]. For each trial, CRQA was performed on the bilateral thigh angle time series. Optimal time delays and embedding dimensions were first computed separately for the right and left thigh angle time series and then averaged. Based on the average time delay and embedding dimension, the right and left thigh angle time series were embedded into a shared phase space. Then, we computed cross recurrences using radii from 1% to 100% of the maximum distance among points in phase space, with 1% increments. The following CRQA metrics were calculated: % recurrence, % determinism, mean diagonal line length, maximum diagonal line length, entropy of the diagonal line length distribution, % laminarity, mean vertical line length, maximum vertical line length, entropy of the vertical line length distribution, entropy of weighted recurrence. Minimal line lengths that define diagonal and vertical lines were set to 60% of the average stride interval for each trial.

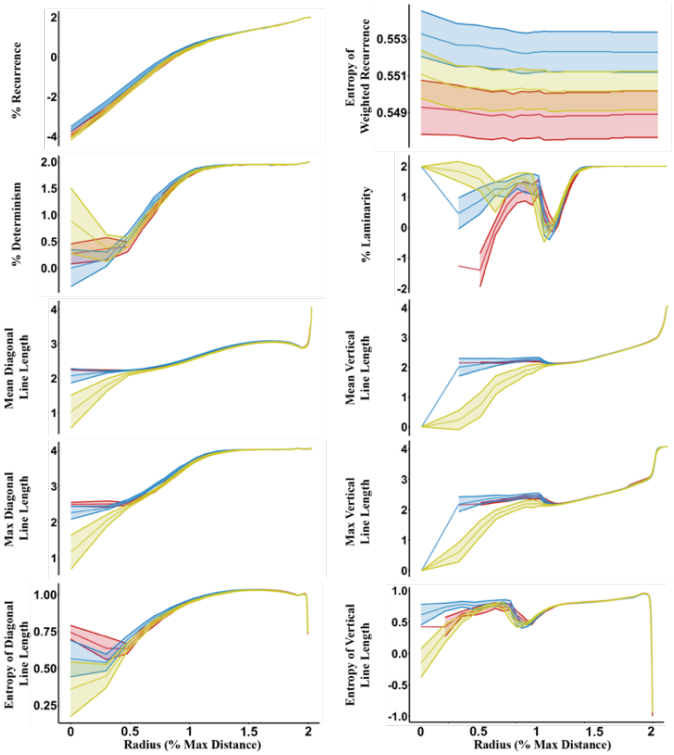


Figure 1. RQA Metrics Across Different Radii. All plots are on a double logarithmic scale. Red, blue, and yellow lines and shaded areas indicate means and 95% confidence intervals from young, middle, and older adults, respectively.

**Results & Discussion:** Webber and Zbilut (2005) suggested that 1) the radius should fall within the linear scaling region of the double logarithmic plot relating % recurrence and radius, 2) % recurrence should be relatively low (e.g., 0.1% to 2.0%), and 3) the radius may coincide with the first minimum in the double logarithmic plot between % determinism and radius [6]. Our results show that radii from $10^{0.602} \approx 4\%$ to $10^{0.903} = 8\%$ of the maximum distance among points in the phase space 1) fell within the linear scaling region of the double logarithmic plot between % recurrence and radius, 2) returned relatively low % recurrence from 0.1% to 2%, and 3) coincided with the first inflection point in the double logarithmic plot between % determinism and radius. Thus, when minimal line lengths are set to 60% of the average stride interval, radii from 4% to 8% of the maximum distance among points in phase space may be optimal for capturing meaningful variability while differentiating between populations. Further studies should investigate how different minimal line lengths influence the optimal range of radii, ultimately leading to a more complete prescription on RQA parameter selection.

**Significance:** This study establishes rigorous guidelines for selecting an appropriate recurrence threshold in Recurrence Quantification Analysis, ensuring the reliability of the analysis. Systematically identifying an optimal range of radii reduces the risk of misleading conclusions due to improper parameter selection. These findings contribute to standardizing RQA methodologies in biomechanics, enabling more robust and meaningful analyses of human movement dynamics across different populations and studies.

**Acknowledgments:** Center for Research in Human Movement Variability at the University of Nebraska at Omaha, the University of Nebraska Collaboration Initiative, the NSF award 212491, the NIH awards P20GM109090 and P20GM152301

**References:** [1] Richardson et al. (2007), *Biological Cybernetics* 96(1); [2] Sado et al. (2022), *Frontiers in Physiology* 13; [3] Stephenson et al. (2009), *Gait & Posture* 29(1); [4] Marwan (2011), International Journal of Bifurcation and Chaos 21(4); [5] Wiles et al. (2025), *Nature Scientific Data;* [6] Webber et al. (2005) *Tutorials in Contemporary Nonlinear Methods for the Behavioral Sciences.*

# VALIDATION OF OPENCAP DURING THE TRIANGLE COMPLETION TEST

*Ying Fang[1], Rachel Ludwig[1], Sabnam Hajari[1], Janet Helminski[1]
[1]Department of Physical Therapy, College of Health Professions, Rosalind Franklin University
*Corresponding author's email: ying.fang@rosalindfranklin.edu

**Introduction:** Spatial navigation and orientation integrates multimodal input, such as visual, vestibular, and proprioceptive input, to create a mental map of the surrounding environment. Spatial navigation becomes challenging with age, cognitive impairment, and vestibular dysfunction [1]. The triangle completion test is a clinical test of spatial navigation. A person wearing a blindfold and nose cancelling headset is guided along the first two legs of a triangle and is then given a sensory cue to turn and return to the starting position without sensory guidance (Fig. 1A). The end point error between the start and end position is calculated. An increase in end point error has been associated with vestibular dysfunction and Alzheimer's Disease [2-3]. OpenCap is ideal for clinical use because it is an open-source movement analysis platform that uses accessible equipment (iPad or iPhone) and is easy to set up [4]. However, OpenCap has only been validated for linear movement such as straight walking [5]. It is not known if it can accurately capture a complex movement such as walking with a series of turns. The purpose of this study is to determine the validity of OpenCap to measure end point error (distance error and angle error) of the triangle completion test. We hypothesize that OpenCap would result in "good to excellent" measurements of distance and angle errors.

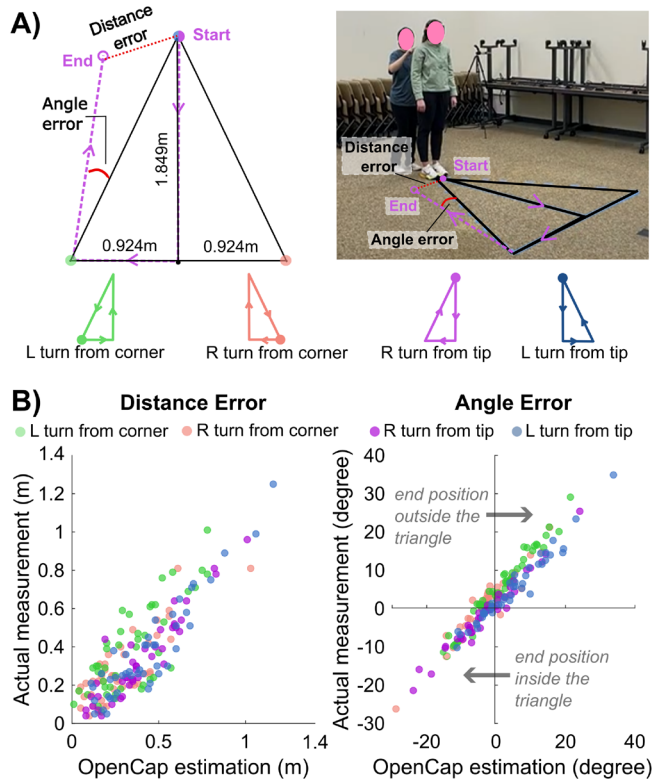


**Figure 1:** A) Experimental setup for the triangle completion test that involves 4 types of turns. B) Distance error and angle error from the digital image (gold standard) and OpenCap.

**Methods:** 16 healthy participants (10 females, age: 26.8 ± 8.3 years, mass: 76.5 ± 17.3 kg, height: 1.69 ± 0.1 m) completed 3 sets of the TCT. Each set included 4 paths involving either left or right turns (Fig. 1A). For each path, the participant's "start" and "end" positions were recorded – markers placed on the ground marking the midpoint between the left and right medial malleoli. A digital image was taken of the location of the markers and a white board as a reference. Each trial was also captured through the OpenCap platform using two iPads. The "gold standard" of displacement and angle error were calculated in Inkscape based on the digital image. OpenCap was used to obtain the same measurements based on the model's pelvis segment location at start and end of the trial. Outcomes calculated from the two methods were compared using intraclass correlation coefficient (ICC) in SPSS.

**Results & Discussion:** OpenCap did not compile 8% (16 out of 192) of collected trials. The average distance error was 0.34 ± 0.23 m and 0.37 ± 0.22 m based on the picture and OpenCap; the average angle error was 6.78 ± 6.25° and 7.07 ± 7.64° based on the picture and OpenCap. The two methods showed general agreement in distance and angle errors, and the slight differences (0.10 ± 0.08 m for distance error and 3.12 ± 2.02° for angle error) could be attributed to the two different methods used midpoint between the medial malleoli versus pelvis's center of mass.

When comparing OpenCap measurement to the "gold standard", the ICC was 0.923 for distance error and 0.98 for angle error. ICC values greater than 0.9 indicate excellent reliability, indicating that OpenCap is a valid tool to assess the outcome of the triangle completion test. A previous study reported that the average translation error by OpenCap is 0.12 m during walking [4], which is similar to our distance error (0.10 ± 0.08 m). This suggests that the performance of OpenCap would not be compromised by nonlinear movements such as turning. One limitation of OpenCap is its limited capability to identify two people in the same capture. In this project, OpenCap had difficulty distinguishing the participant and the guide. This is relevant to clinical practice because sometimes a spotter is required to walk along a patient to ensure safety.

**Significance:** OpenCap is a robust tool to capture a person's linear and nonlinear movement in space, making it suitable to assess spatial navigation and analyze movement that involves turning. Considering that the tool is also low cost and easy to use, it has potential to be used in the clinic to assist with evaluation of gait through markerless motion analysis.

**Acknowledgments:** We thank Monica Ramirez, Nia Alfaro, Matthew Muldoon, Djurdjina Jovanovic, Hannah Buscher, and Jennifer Molini for collecting the data.

**References:** [1] McLaren et al. (2022), *Front Hum Neurosci* 16; [2] Adamo et al. (2012), *Front Aging Neurosci* 4; [3] Anson et al. (2019), *Clin Neurophysiol* 130(11); [4] Uhlrich et al. (2023), *PLoS Comput Biol* 19(10); [5] Horsak et al. (2024), *J Biomech* 175.

# WEARABLE DELIVERY OF MECHANICAL STIMULUS TO IMPROVE TENDON HEALING

Andy K. Smith[1], Tomonobu Ishigaki[2], Karin Grävare Silbernagel[1], *Stephanie G. Cone[1]
[1]University of Delaware, Newark, DE, USA
[2]Niigata University of Health and Welfare, Niigata City, Japan
*Corresponding author's email: sgcone@udel.edu

**Introduction:** Achilles tendinopathy is a painful condition which affects 6% of the global population during their lifetime [1]. While gold-standard treatment – exercise therapy – improves patient symptoms overall, this treatment alone typically fails to recover patient function and pain to pre-tendinopathy levels. Supplemental treatments such as Shockwave therapy are used to enhance tendon healing by providing mechanical stimulation directly in the affected tendon, but Shockwave therapy is acutely painful and variable patient tolerance can limit the utility of this treatment [2]. Instead of using a very high magnitude mechanical stimulus in static postures (as in Shockwave therapy) our group aims to use a wearable tapping device with improved comfort, lower magnitude mechanical impulses, a longer duration of treatment, and superimposed stimulus with dynamic loading to deliver comparable therapeutic stimulus to the Achilles tendon. As an initial investigation in this line of research, Doppler imaging was used to quantify downstream tissue movement in the Achilles tendon during both Shockwave therapy and the use of our novel tapping stimulator. Here we aimed to demonstrate a wearable mechanical stimulator as an improved method for delivering mechanical stimulus to the Achilles tendon during functional tasks and hypothesized that our tapping device would be 1) as effective at providing mechanical stimulation spatially throughout the Achilles tendon and 2) it would provide a more consistent temporal stimulus compared to Shockwave pulses.

**Methods:** Three healthy young adults (3F/0M, 29±4yrs) were enlisted in this pilot study in the University of Delaware Muscle and Tendon Performance Lab. Doppler ultrasound imaging (GE Logiq e; Gain 5.0, 10Hz) was used to measure tissue movement over 5s periods in the left Achilles tendon during the delivery of both Shockwave and tapping treatments. A commercial probe holder (Usono) was used to secure the ultrasound probe over the tendon during dynamic tasks. First, a custom-built wearable tapping device consisting of a voice coil actuator (100hz square wave pulses, 3% duty cycle) was secured distally over the Achilles tendon near the calcaneal insertion. Each participant completed the following series of tasks while the tapping device was activated: static prone, static standing, single leg balance, single leg heel raises, step-ups, and walking. Next, the tapping device was removed, and radial Shockwave therapy was applied just proximal to the calcaneal insertion (DJO Global; 1.0 bar, 14Hz) while Doppler images were collected. Settings for the Doppler imaging were fixed across trials to highlight only the tissue movement from the mechanical stimulus, while eliminating sensitivity to voluntary movements. Cine-ultrasound images were collected in triplicate for each condition. Q analysis was used to identify the minimum and maximum ratios of moving to non-moving pixels within the region of interest during the 5s capture duration. The region of interest was selected by placing an ellipse in the central area of the tendon (Fig. 1). One-way ANOVA was used to assess for differences between conditions ($\alpha = 0.05$).

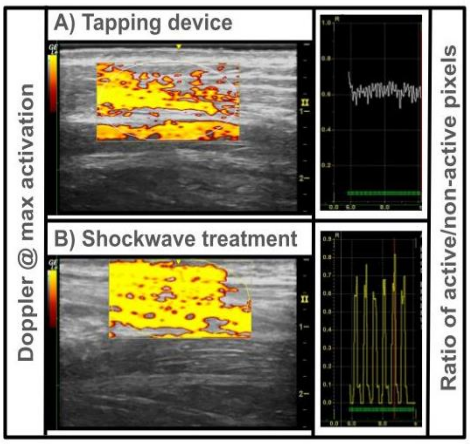


**Figure 1:** Doppler images indicate tissue movement throughout the Achilles tendon in response to both wearable tapping stimulus (A) and Shockwave (B) in a static, prone position.

**Results & Discussion:** The findings from this study support the hypothesis that our tapping device provides a more temporally consistent stimulus compared to that of shockwave therapy. While both prone tapping and Shockwave conditions demonstrated similar maximal areas of stimulus (max ratio: tap: 0.68±0.17, SW: 0.75±0.05, $p=0.250$), prone tapping and shockwave therapy differed in ranges of activation (max ratio – min ratio: tap: 0.14±0.03, SW: 0.75±0.05, $p<0.001$). Shockwave exhibits distinct still periods between impacts, while prone tapping maintained consistent tissue movement. This difference highlights the potential of continual mechanical stimulus from the tapper even in an unloaded prone position to rival the impact of Shockwave therapy. The tapper also shows promise during active conditions. Only the single leg balance activated less area in the tendon (max ratio: 0.36±0.16) compared to prone tapping ($p=0.038$), while all other functional tasks met or were close to the activation area in prone tapping ($p>0.103$). Interestingly, the active conditions demonstrated more temporal variability in tissue movement compared to the prone tapping, indicating that varied loading (and as such effective stiffness) can modulate the local stimulus from our tapping device. Overall, these findings are encouraging for future clinical applications as we have identified a wearable approach to elicit continual tissue stimulus during standard therapeutic tasks without discomfort, suggesting a potential alternative to Shockwave therapy.

**Significance:** Supplemental mechanical stimulation treatments have great potential to enhance outcomes in the clinical treatment of tendinopathies, but contemporary options are limited by in-clinic access, additional time burdens, and patient tolerance for painful treatment approaches. This study illustrates the efficacy of a comfortable, wearable device that could be used during regular exercise therapy bouts or activities of daily living to provide beneficial mechanical stimulus throughout rehabilitation. This approach has the potential to improve both treatment accessibility and overall return of function to patients affected by painful musculoskeletal conditions such as Achilles tendinopathy.

**References:** [1] Kujala et al. (2005), *Clin J Sport Med* 15(3); [2] Auersperg et al. (2020), *EFFORT Open rev* 5(10).

# INFLUENCE OF SITE ON PRE/POST CLINICAL PERFORMANCE AND PATIENT-REPORTED OUTCOME CHANGES OBSERVED WITHIN INTERVENTION GROUP IN A MULTISITE RANDOMIZED CLINICAL TRIAL

Adam G F Smith, Aaron J Krych, Nathan D Schilaty, Yi, Wei, Kim D Barber Foss, April L McPherson, Gregory D Myer, *Nathaniel A Bates[1]

[1]The Ohio State University Wexner Medical Center, Columbus, OH, USA

*Corresponding author's email: nathaniel.bates@osumc.edu

**Introduction:** Multisite investigational trials are advantageous as they offer flexibility in recruitment across a broader population than single-site studies. Expanded populations permit large-scale investigations of conditions with limited incidence such as ACL injury and ACL reconstruction (ACLR) recovery. However, multisite collaborations also introduce concerns related to consistency of protocol application and subsequent outcomes between institutions. The objective of this study was to examine how change in clinical performance from interventional training protocols varied between sites in a multisite trial. It was hypothesized that between-site measurements for clinical performance and patient-reported outcomes (PROs) would show consistency within each intervention group.

**Methods:** 91 subjects between two primary institutions of a four-site randomized clinical trial were analyzed in the subgroup. Study participants were age 13-30 years, with history of active sport participation, and cleared to return to sport after completing ACLR rehabilitation. Study participants were randomly assigned to a protocol group (STAN – standard of care, a 6-week period with no additional intervention; HOME – a 6-week structured running program; TNMT – a 6-week progressive targeted neuromuscular training regimen [1]). Clinical performance for strength (isokinetic knee flexion/extension at 180°/sec and 300°/sec), single leg hop distance (single, triple, triple crossover, 6 meter timed), as well as standardized PROs (Marx, Tegner, IKDC, KOOS, SKE, KOS questionnaires) were assessed. Changes in selected clinical outcomes (delta between pre and post intervention) were calculated for each study participant along with effect size. ANOVA was used to assess change in biomechanical measurements between institutions within group as well as to assess effect sizes between group.

**Results & Discussion:** Mean effect size of between site differences in selected biomechanical deltas between pre and post intervention was 0..31 (0.30) within STAN, 0.28 (0.30) within HOME, and 0.37 (0.27) within TNMT ($p = 0.70$). The STAN, HOME, and TNMT groups had 30, 31, and 30 study participants complete the clinical performance variables and 14, 22, and 22 complete the PRO surveys, respectively (Table 1). Only 2 of 39 variables assessed approached significance (TNMT isokinetic flexion @ 180°/sec $p = 0.05$; STAN single leg hop, $p = 0.07$)

Clinical performance and PRO metrics did not express significant differences between sites, nor were there differences in effect size between groups. Therefore, in multisite trials with targeted training interventions, it is reasonable to assume congruence across sites in terms of clinical variable outcomes within intervention groups. Conversely, for biomechanical outcomes, inter-site differences were observed in the STAN and HOME groups, but not TNMT [2]. Work continues to establish which clinical metrics best represent the complex biomechanical factors directly associated with increased injury risk in athletes. Future investigation should look to establish correlation and inconsistencies between the responsiveness of clinical and biomechanical factors following targeted interventions.

**Significance:** Congruence in was observed in responsiveness of clinical factors and PROs to specific interventions between institutions. The effect was consistent across all intervention groups. Further research is necessary to elucidate the relationship between clinical performance, biomechanical performance, and patient perception of function.

**Acknowledgments:** NIH NIAMS R01-055563; Florida Department of State Center for Neuromusculoskeletal Research.

**References:** [1] Di Stasi et al. (2013), *JOSPT* 43(11). [2] Yi et al. (2025) Am Society Biomech (abstract).

| | STAN | | | | HOME | | | | TNMT | | | |
|---|---|---|---|---|---|---|---|---|---|---|---|---|
| **PROs** | **Site1 (N=6)** | **Site2 (N=8)** | **p-value** | **Effect Size** | **Site1 (N=14)** | **Site2 (N=6)** | **p-value** | **Effect Size** | **Site1 (N=11)** | **Site2 (N=10)** | **p-value** | **Effect Size** |
| **Marx** | -0.7 (2.3) | 2.3 (3.5) | 0.10 | 1.01 | -2.4 (3.6) | 0.5 (0.8) | 0.07 | 1.11 | 0.5 (5.6) | -1.4 (1.6) | 0.32 | 0.46 |
| **Tegner** | 11.4 (14.6) | 4.1 (14.7) | 0.37 | 0.50 | -1.9 (11.7) | -4.2 (7.6) | 0.66 | 0.23 | 3.6 (21.2) | -0.7 (14.0) | 0.58 | 0.20 |
| **IKDC** | 5.0 (6.8) | 6.0 (4.5) | 0.73 | 0.17 | -1.3 (6.1) | 0.2 (15.3) | 0.75 | 0.13 | 4.1 (6.3) | 9.2 (6.9) | 0.09 | 0.77 |
| **SKE** | 4.6 (6.3) | 5.0 (4.6) | 0.90 | 0.07 | -1.5 (5.7) | -1.5 (9.5) | 0.99 | 0.01 | 3.5 (5.3) | 7.2 (6.8) | 0.18 | 0.61 |
| **KOOS** | 5.4 (6.0) | 4.9 (5.8) | 0.88 | 0.09 | -0.4 (5.4) | -2.1 (12.0) | 0.66 | 0.18 | -0.3 (7.9) | 6.4 (8.2) | 0.08 | 0.83 |
| **Clinical Measures** | **Site1 (N=21)** | **Site2 (N=9)** | **p-value** | **Effect Size** | **Site1 (N=25)** | **Site2 (N=6)** | **p-value** | **Effect Size** | **Site1 (N=17)** | **Site2 (N=13)** | **p-value** | **Effect Size** |
| **Isokinetic Flex 180 (Nm)** | 1.3 (10.6) | 0.3 (9.7) | 0.74 | 0.10 | -0.2 (12.8) | 0.1 (7.3) | 0.94 | 0.03 | 0.6 (11.1) | 5.6 (6.1) | 0.05 | 0.56 |
| **Isokinetic Flex 300 (Nm)** | 0.8 (11.9) | 0.7 (7.4) | 0.98 | 0.01 | -0.5 (11.6) | 1.9 (5.9) | 0.50 | 0.26 | 0.3 (9.7) | 3.2 (4.9) | 0.17 | 0.38 |
| **Isokinetic Ext 180 (Nm)** | 2.9 (10.3) | -0.5 (18.4) | 0.37 | 0.23 | 7.1 (13.7) | -0.2 (20.9) | 0.14 | 0.41 | 10.9 (12.6) | 11.0 (12.6) | 0.95 | 0.01 |
| **Isokinetic Ext 300 (Nm)** | 4.0 (8.2) | 6.9 (12.9) | 0.30 | 0.27 | 4.5 (11.3) | -2.1 (15.4) | 0.10 | 0.49 | 6.1 (15.5) | 6.6 (8.3) | 0.88 | 0.04 |
| **Single Hop (cm)** | 11.9 (19.8) | 1.5 (12.9) | 0.07 | 0.62 | -6.8 (17.8) | -5.5 (11.9) | 0.82 | 0.09 | -2.6 (34.1) | 0.7 (13.5) | 0.64 | 0.13 |
| **Triple Hop (cm)** | 2.5 (52.7) | 16.1 (31.8) | 0.37 | 0.31 | -12.7 (60.1) | -2.9 (42.0) | 0.60 | 0.19 | 16.5 (44.2) | 4.3 (39.2) | 0.27 | 0.29 |
| **Crossover Hop (cm)** | 12.3 (44.0) | 13.1 (32.6) | 0.95 | 0.02 | -4.4 (55.2) | -4.1 (49.6) | 0.98 | 0.01 | 38.5 (40.6) | 21.6 (40.3) | 0.12 | 0.42 |
| **6-meter Hop (cm)** | -0.17 (0.55) | 0.10 (0.13) | 0.67 | 0.68 | -0.01 (0.32) | -0.14 (0.26) | 0.24 | 0.45 | -0.14 (0.29) | -0.10 (0.27) | 0.60 | 0.14 |

**Table 1:** Mean change between pre- and post-assessments of PROs, clinical strength, hop testing performance at each site separated by intervention group. A lack of significance between sites was observed across all groups which speaks positively to the consistency of clinical measures regardless of location.

# INFLUENCE OF SITE ON PRE / POST BIOMECHANICAL CHANGES OBSERVED WITHIN INTERVENTION GROUP IN A MULTISITE RANDOMIZED CLINICAL TRIAL

Yi Wei, Aaron J Krych, Nathan D Schilaty, Adam G F Smith, Kim D Barber Foss, April L McPherson, Christopher DiCesare, Andrew Schille, Gregory D Myer, *Nathaniel A Bates[1],
[1]The Ohio State University Wexner Medical Center, Columbus, OH, USA
*Corresponding author's email: nathaniel.bates@osumc.edu

**Introduction:** Collaboration between multiple institutions allows for larger scale longitudinal studies to examine the effects of an intervention such as targeted neuromuscular training (TNMT) on biomechanics following a relatively uncommon outcome such as ACL reconstruction (ACLR). However, data consistency between institutions is required to validate inter-institution merging of results for statistical analysis. Due to the highly experienced nature of each investigative team as well as uniformity in dynamic task execution, it was hypothesized that between-site measurements would show consistency within each intervention group.

**Methods:** 77 subjects between two primary institutions of a four-site randomized clinical trial were analysed in the subgroup. All study participants were 13-30 years old, with history of active sport participation, and cleared to return to sport after completing ACLR rehabilitation at the time of enrolment. Study participants were randomly assigned to a protocol group (STAN – standard of care, a 6-week period with no additional intervention; HOME – a 6-week structured running program; TNMT – a 6-week progressive targeted neuromuscular training regimen [1]). Biomechanical performance was assessed for each study participant during a drop vertical jump (DVJ) task off a 31 cm box via marker-based motion capture (Qualisys or Motion Analysis Corp) with a 55-marker modified Hellen-Hayes model. Kinetic (Nm) and kinematic (°) measurements at the hip and knee were calculated in Visual3D. The DVJ task was selected based on prior studies supporting multi-institution reliability in healthy athletes [2]. Changes in selected biomechanical outcomes (delta between pre and post intervention) were calculated for each study participant along with effect size. ANOVA was used to assess change in biomechanical measurements between institutions within group as well as to assess effect sizes between group.

**Results & Discussion:** Mean effect size of between site differences in selected biomechanical deltas between pre and post intervention was 0.38 (0.23) within STAN, 0.47 (0.23) within HOME, and 0.24 (0.17) within TNMT ($p = 0.04$). The STAN, HOME, and TNMT groups had 23, 27, and 27 study participants complete the intervention, respectively (Table 1). 3 of 12 biomechanical deltas expressed significance within the STAN group; while 3 of 12 deltas expressed significance within the HOME group (Table 1). No significance was identified for deltas between institutions within the TNMT group ($p \geq 0.09$).

The STAN and HOME groups did not involve intervention tasks targeted towards biomechanical improvement. Accordingly, institutional differences in deltas in the STAN and HOME group are likely attributable to natural biologic variability (as between-site single-plane correlations range from 0.67-0.98) [2] and external activities/training, which were not restricted. STAN differences were in the sagittal plane, which is critical to force attenuation on landing, while HOME differences were in the frontal and transverse plane, which are critical to risk identification. Consistency in the TNMT group demonstrates that biomechanical response to targeted training can be expected to be more consistent between institutions than control or sham groups that have reduced guidance on implementation.

**Significance:** A general congruence was observed in responsiveness to specific interventions between institutions; however, the most consistent effect was noted in the TNMT group. Further research is needed to elucidate underlying causes of variable responses observed in non-targeted interventions groups between institutions utilized in multi-site RCT designs.

**Acknowledgments:** NIH NIAMS R01-055563; Florida Department of State Center for Neuromusculoskeletal Research.

**References:** [1] Di Stasi et al. (2013), *JOSPT* 43(11). [2] DiCesare et al. (2015), *TOJSM* 3(12).

| Kinetics (Nm) | STAN | | | | HOME | | | | TNMT | | | |
|---|---|---|---|---|---|---|---|---|---|---|---|---|
| | SITE1 (N=16) | SITE2 (N=7) | p-value | Effect Size | SITE1 (N=21) | SITE2 (N=6) | p-value | Effect Size | SITE1 (N=16) | SITE2 (N=11) | p-value | Effect Size |
| Hip Flexion | 0 (18) | 43 (97) | 0.02* | 0.62 | -2 (21) | -15 (32) | 0.11 | 0.63 | -4 (21) | -19 (56) | 0.18 | 0.36 |
| Hip Adduction | 3 (23) | 12 (21) | 0.18 | 0.41 | 3 (21) | 0 (22) | 0.75 | 0.14 | -6 (12) | -16 (37) | 0.16 | 0.36 |
| Hip Internal | -3 (12) | 5 (20) | 0.12 | 0.49 | 0 (9) | -11 (14) | <0.01* | 0.94 | -4 (11) | -8 (15) | 0.27 | 0.30 |
| Knee Flexion | 3 (13) | 20 (41) | 0.04* | 0.56 | -1 (15) | -14 (47) | 0.12 | 0.37 | 1 (14) | 2 (29) | 0.87 | 0.04 |
| Knee Abduction | -1 (9) | 2 (24) | 0.60 | 0.17 | 2 (13) | 13 (20) | 0.03* | 0.65 | 0 (11) | 1 (17) | 0.64 | 0.07 |
| Knee Internal | 0 (7) | 2 (8) | 0.47 | 0.27 | 1 (10) | 6 (14) | 0.18 | 0.41 | 1 (6) | 0 (11) | 0.65 | 0.11 |
| **Kinematics (°)** | **STAN** | | | | **HOME** | | | | **TNMT** | | | |
| | SITE1 (N=16) | SITE2 (N=7) | p-value | Effect Size | SITE1 (N=21) | SITE2 (N=6) | p-value | | SITE1 (N=16) | SITE2 (N=11) | p-value | Effect Size |
| Hip Flexion | 0 (15) | -5 (14) | 0.32 | 0.35 | 1 (9) | 4 (10) | 0.32 | 0.32 | 1 (10) | -2 (6) | 0.20 | 0.36 |
| Hip Adduction | 0 (4) | 1 (3) | 0.35 | 0.28 | 0 (4) | -2 (4) | 0.27 | 0.50 | -2 (4) | -2 (3) | 0.89 | 0.03 |
| Hip Internal | -2 (5) | 0 (5) | 0.37 | 0.40 | -1 (7) | -3 (4) | 0.35 | 0.35 | -2 (7) | 1 (5) | 0.17 | 0.49 |
| Knee Flexion | 2 (4) | -5 (11) | <0.01* | 0.85 | -1 (6) | -3 (6) | 0.28 | 0.33 | 2 (7) | 0 (7) | 0.31 | 0.29 |
| Knee Abduction | 0 (4) | 0 (6) | 0.92 | 0.05 | 0 (4) | 3 (4) | 0.04* | 0.75 | -1 (4) | -1 (6) | 0.82 | 0.04 |
| Knee Internal | 0 (3) | 0 (5) | 0.82 | 0.06 | -1 (4) | -2 (4) | 0.44 | 0.25 | 1 (5) | 3 (4) | 0.09 | 0.44 |

**Table 1:** Means (Standard Deviation) of change in Kinetic (Nm) and Kinematic measurements (°) pre- and post-intervention separated by protocol group as well as institution site. Significant differences were found between institutions in the STAN group for hip and knee flexion in the STAN group, as well as knee abduction in the HOME group.

# QUANTIFYING THE RELATIONSHIP BETWEEN INFANT BODY POSITION AND BREATHING: A PILOT STUDY

*Holly Olvera[1], Autumn Ost[1], Ryan Tam[1], Abby Britain[1], Chris Wilson[1], John Carroll[2], Brandi Whitaker[2], Megan Koster[1], Camille Stover[1], Andrew Bossert[1], Clare Fitzpatrick[1], Erin Mannen[1]
[1]Boise State University, Boise, ID; [2]Arkansas Children's Research Institute, Little Rock, AR.
*Corresponding author's email: hollyolvera@u.boisestate.edu

**Introduction:** In the U.S., infants spend an average of 5.7 hours (0-16 hours) per day in seated products like car seats, bouncers, rockers, and swings [1,2]. Excessive time spent in these products can be potentially dangerous for development and safety of infants. Because of these product's unique design features, infants may be forced into higher head-neck flexion and a slouched trunk position, increasing their risk of suffocation. Previous research is limited to studying the impact of body position on breathing in adults with fully developed respiratory systems and preterm or ventilated sedated infants with developing respiratory systems. These studies highlight the influence of trunk flexion and hip flexion on breathing abilities for adults [3,4], reduced airflow in preterm infants with neck hyperextension and flexion at 45° [5], and show no association between chest wall displacement and efficacy of gas exchange in ventilated sedated infants [6]. However, no research has explored these respiratory outcomes in relation to head-neck and trunk posture in healthy non-sedated infants. Therefore, the purpose of the overall study is to evaluate how thoracic expansion, muscle activity, and breathing metrics change in various supine body positions common in commercially available infant products compared to a flat surface. For this abstract, we explore thoracic expansion and breathing rate of our pilot subject, demonstrating the efficacy of our methods.

**Methods:** One healthy full-term male infant (8 weeks; 59.5 cm; 4.59 kg) participated in this IRB-approved study. The infant laid supine on a flat control condition, followed by two different device configurations: 15° and 45° head-neck flexion (**Figure 1**). An 8-camera motion capture system collected positional data of 23 reflective markers, each trial lasted for at least 2 minutes of calm breathing, up to 10 minutes. A strategic grid of the reflective markers was placed around the infant's torso from their armpits to their pelvis (**Figure 1A**). Thoracic expansion was calculated in 3D using a custom MATLAB code (**Figure 1E**). Breathing rate was measured using a Capnostream 35 (Medtronic, Minneapolis, MN). Paired t-tests ($p<0.05$) were used to compare the 15° and 45° head-neck flexion conditions to the control condition.

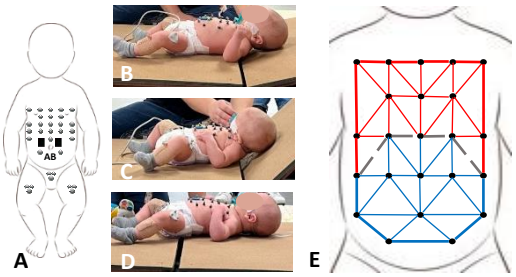


**Figure 1:** (A) Marker and EMG placement, (B) 15° head-neck flexion, (C) 45° head-neck flexion, (D) flat supine control, (E) two thoracic regions of interest for calculation (red: chest, blue: abdomen).

**Results & Discussion:** Decreased total thoracic expansion was found in both of the 15° and 45° head-neck flexion conditions compared to the flat condition (**Table 1**). This finding indicates the limited ability of the infant to expand their torso at increased angles in order to breathe. If we assume that the third dimension does not change, then the volumetric expansion for this infant is approximately 39,000 $mm^3$, or 39 ml on a flat surface. Infants take in a volume of air equal to 6-8 ml/kg of their body weight, considered normal tidal volume. This infant's normal range is between 27-37 ml, therefore magnifying our finding that the 45° head-neck flexion position is limiting their breathing abilities to only 13 ml. We also found that the contribution of chest expansion decreased and contribution of abdominal expansion increased from flat to 15° and 45°. Previous research has shown that inclined seated products require infants to use significantly more abdominal strength to maintain their position compared to lying on a flat surface [7]. A significant increase in breathing rate was also found in both of the 15° (72 bpm) and 45° (87 bpm) conditions compared to the flat condition (68 bpm) ($p = 0.0001$). The increased breathing rate and decreased total thoracic expansion at 15° and 45° head-neck flexion suggests greater effort for normal breathing when infants are forced into these postures and positions. Our future work will include collecting longitudinal data from several infants at three different time points (1-2 mo., 3-4 mo., 5-6 mo.), in three additional device configurations (15° and 45° thoracic flexion and 90° head-to-pelvis), with surface electromyography recording the cervical paraspinal and abdominal muscles, and new breathing metrics ($SpO_2$, heart rate, and $EtCO_2$).

**Table 1:** Total and compartmental surface area changes of the chest (CH) and abdomen (AB) and percent contribution of the CH and AB to the total.

| **Condition** | Total ($mm^2$) | CH ($mm^2$) | AB ($mm^2$) | CH (%) | AB (%) |
|---|---|---|---|---|---|
| Flat | 39,210 | 30,630 | 8,580 | 78.1 | 21.9 |
| 15° H-N | 28,690 | 20,660 | 8,030 | 72.0 | 28.0 |
| 45° H-N | 13,470 | 7,680 | 5,790 | 57.0 | 43.0 |

**Significance:** No prior research has explored the relationships between head-neck posture, thoracic expansion, and respiration in healthy non-sedated infants. Our novel approach to understanding this connection serves as the basis for future work aimed at recognizing suffocation risk factors associated with infant products.

**Acknowledgments:** This research is supported by the NICHD, NIH Grant No. 1R01HD113921.

**References:** [1] Little et al. (2019), *Inf Beh & Dev*; [2] Callahan et al. (1997), *Arc Peds & Ado Med*; [3] Lee et al. (2010), *Resp Physiol & Neur*; [4] Lin et al. (2006), *Arc of Phys Med and Rehab*; [5] Reiterer et al. (1994), *Peds Pulm*; [6] Zannin et al. (2019), *J Appl Physiol*; [7] Wang et al. (2020), *J Biomech*

# EFFECTS OF SLIP VELOCITY AND DURATION ON FALL INCIDENCE: EVIDENCE FROM UNEXPECTED SLIP PERTURBATIONS INDUCED BY A SPLIT-BELT TREADMILL

Chihyeong Lee[1], *Jooeun Ahn[1, 2], and *Beom-Chan Lee[2, 3]
[1]Department of Physical Education, Seoul National University, South Korea
[2]Institute of Sport Science, Seoul National University, South Korea
[3]Department of Health and Human Performance, University of Houston, USA
*Co-corresponding authors' email: ahnjooeun@snu.ac.kr and blee24@central.uh.edu

**Introduction:** Falls are primary causes of severe injuries across all age groups, predominantly resulting from slips [1]. While numerous studies have examined the body's responses to gait perturbations (e.g., slips and trips) induced by split-belt treadmills (see [2] for review), the identification of key control parameters, such as perturbation speed and duration, for effectively delivering gait perturbations remains insufficiently explored. The likelihood of a fall or successful fall recovery is highly dependent on these parameters as perturbations with greater speed and longer duration may exceed an individual's capacity to generate sufficient corrective responses, thereby increasing the risk of a fall. Therefore, this study aims to examine the effects of different slipping velocities and durations on fall incidence using a split-belt treadmill.

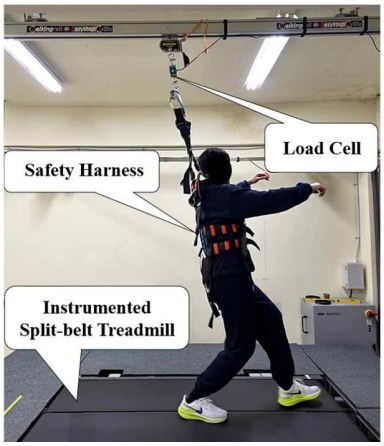


**Figure 1.** The customized fall-inducing system and an example of a participant experiencing a slip perturbation.

**Methods:** The customized fall-inducing system, which incorporated an instrumented split-belt treadmill equipped with two force plates (Bertec Corporation, OH, USA), delivered slip perturbations, as illustrated in Fig. 1. It induced slip perturbations by suddenly increasing belt speed in the forward direction, thereby causing a backward loss of balance [3]. Falls were identified when the loading force, measured via a load cell positioned between a safety harness and a stationary walking rail, exceeded 30% of the participant's body weight [4]. Sixteen healthy adults (8 males; age: 23.4 ± 2.5 years; height: 170.8 ± 6.8 cm; mass: 66.4 ± 10.5 kg) participated in this study. Before the experiment, each participant's preferred walking speed (PWS) was measured while walking on the split-belt treadmill. Participants then completed 10 trials, consisting of 8 perturbation trials, with slip perturbations applied at two velocities (0.5×PWS and 1×PWS), two durations (300 ms and 500 ms), and on both the left and right foot. Two trials without perturbations were also included to minimize potential learning effects. All trials were assigned in a random order, and slip perturbations were randomly applied between the 26th and 50th step while participants walked at their PWS.

**Table 1.** The number of falls, fall rates and statistical analyses for the two velocities and durations.

| | | Non-Falls (n) | Falls (n) | Fall Rate (%) | Effect | DF | Pearson chi-square | P-value | Cramér's V |
|---|---|---|---|---|---|---|---|---|---|
| Velocity | 0.5×PWS | 53 | 11 | 17.2 | 300 ms vs. 500 ms | 1 | 0.988 | 0.320 | 0.124 |
| | 1×PWS | 21 | 43 | 67.2 | | 1 | 0.638 | 0.424 | 0.100 |
| Duration | 300 ms | 40 | 24 | 37.5 | 0.5×PWS vs. 1×PWS | 1 | 17.067 | < .001 | 0.516 |
| | 500 ms | 34 | 30 | 46.9 | | 1 | 16.063 | < .001 | 0.501 |

**Results & Discussion:** Table 1 reports the statistical analysis of fall rates in response to slip velocity and duration. The main effect of slip velocity (i.e., 0.5×PWS vs. 1×PWS) on fall rates was significant for both slip durations ($p < .001$ for both). However, the main effect of slip duration (i.e., 300 ms vs. 500 ms) was not statistically significant at either slip velocity. Cramér's V values for the main effect of slip velocity exceeded 0.3, indicating a large effect size. Pairwise chi-square analyses revealed that Cramér's V values for slip velocity were higher at 300 ms than at 500 ms, but a Z-test indicated that this difference was not statistically significant ($Z = 0.085$, $p = 0.932$). These findings demonstrate that slip velocity significantly influences fall likelihood, whereas slip duration (300 ms vs. 500 ms) does not exhibit a comparable effect. This study provides valuable insights for researchers and clinicians by identifying slip velocity as a primary determinant of fall intensity when inducing controlled perturbations using a split-belt treadmill.

**Significance:** By refining current methodologies for perturbation-based balance assessments, this study establishes a structured methodology for investigating reactive balance responses. Our findings can contribute to optimizing fall prevention strategies and rehabilitation interventions for enhancing balance recovery and reducing fall risk in controlled settings utilizing split-belt treadmills.

**Acknowledgements:** Research was supported in part by Brain Pool Program (RS-2024-00446461) and ERC (No. RS-2023-00208052) grants funded by the Ministry of Science and ICT through the National Research Foundation of Korea, and the Korea Health Technology R&D Project through the Korea Health Industry Development Institute (KHIDI) funded by the Ministry of Health & Welfare (No. HK23C0071).

**References:** [1] Talbot et al. (2005), *BMC Public Health*, 5(86); [2] Chodkowska et al. (2025), *Appl Sci*, 14(21); [3] Lee et al. (2019), *IEEE Trans Neural Syst Rehabil Eng*, 27(7); [4] Yang et al. (2011), *J of Biomech,* 44(12)

# IMPLICATIONS OF TIME NORMALIZATION DURING BILATERAL LANDINGS IN PATIENTS WITH ACLR COMPARED TO HEALTHY CONTROLS

*Sam Weiss[1], Thomas Ollendick[1], Sara Arena[1], Kevin Ford[2], Joe Hart [3], Robin M. Queen[1]
[1]Virginia Tech, Blacksburg, VA, [2]High Point University, High Point, NC, [3]University of North Caroline, Chapel Hill, NC, USA
*Corresponding author's email: samweiss24@vt.edu

**Introduction:** Normalization procedures are used to scale or standardize datasets to perform analyses. These practices have been tested to ensure that data is not skewed and minimize inaccurate results primarily in healthy populations. For example, during bilateral landings, healthy participants are assumed to land with both feet at the same time. However, in patients who have ACL reconstruction (ACLR) landing mechanics are altered [1] with an average difference of seven milliseconds between each foot's initial ground contact [2]. Normalizing time to percent stance, the most common time normalization method, removes the time differences between each foot's initial ground contact during a bilateral landing. In this method both limbs' initial contact begins when the foot contacts the ground and is set at 0% and then take off is defined as 100% of the stance phase for each limb independently. The second method of interest is a time independent method that measures from the initial ground contact of either foot to the final take-off of either foot [3]. No prior studies have investigated the impact of normalization methods during a bilateral landing on ACLR data and the interpretation of results. The purpose of this study was to determine if there were differences in load symmetry when using percent stance phase and time independent normalization methods in healthy controls and patients with ACLR.

**Methods:** This study included 17 healthy controls (8M (20.3 ± 1.4yrs), 9F (24.1 ± 4.6yrs)) and 17 patients with ACLR (8M (18.6 ± 2.2yrs), 9F (17.7 ± 2.2yrs)). The normal force, normalized to body mass, was collected and processed at 100Hz using an in-shoe sensor, loadsol® (novel Electronics, Inc), during three stop-jump trials. The first bilateral landing in the stop-jump task was used for analysis. The two normalization methods, shown in Fig. 1 (time independent(A), percent stance(B)), were applied to the data. A cubic spline interpolation was used in the percent stance normalization to obtain an equal number of datapoints between lower limbs, and then normalized from 0-100% of stance. The time independent method was defined from the initial contact of either foot to the final take-off of either foot and is reported in seconds instead of percentage of the stance phase. Bilateral peak impact force (PIF), loading rate (LR), impulse, time to peak, and stance time were determined for each trial. PIF and LR, was determined for each limb independently and dependently. Meaning at each limbs' peak, shown by the black circle in Fig. 1, PIF and LR were determined independent of time, and at the NSx (D) and Sx (ND) limb's peak, shown by the corresponding dotted lines. Symmetry was calculated for each outcome of interest using the normalized symmetry index (NSI) [4]. A linear mixed effects model ($\alpha$=0.05) was used to determine statistical differences between the symmetry metrics with participant as the random effect while age, sex, group (ACL, Control) and normalization method were used as fixed effects using JMP software (SAS Institute Inc.).

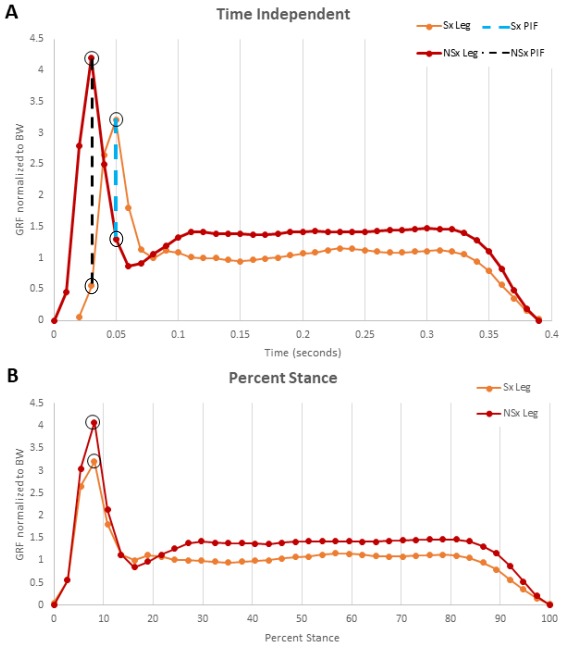


*Figure 1:* Representative patient with ACLR force curve showing time independent (A) and percent stance(B) normalization.

**Results & Discussion:** Significant differences were found between groups across all metrics ($p \leq 0.01$). Patients with ACLR continuously had higher average asymmetry. Main effects of age and sex were not significant. A Group*Method interaction in time to peak symmetry ($p = 0.012$) indicated group differences only in time independent method ($p = 0.032$). Normalization method was different for overall PIF ($p<0.001$), NSx(D) PIF ($p = 0.013$), NSx(D) LR ($p = 0.037$), and impulse ($p<0.001$). Therefore, normalizing SJ landing to percent stance alters symmetry outcomes for some metrics. In both NSx(D) PIF and NSx(D) LR, average symmetry between limbs was 39.7% and 36.1% when percent stance normalization was used and 48.4% and 40.8% for the time-independent method. This indicates percent stance normalization results in improved symmetry in both groups. With common return-to-sport (RTS) and rehabilitation criteria based on symmetry [5], if this method was used, it could result in patients with ACLR being released to RTS or daily activities earlier than if the time independent method was used, which could increase reinjury risk. These results demonstrate the impact of normalization methods on outcomes and how these choices could differentially impact clinical populations.

**Significance:** This work provides evidence that common practices and techniques developed using healthy controls may not be translatable to clinical populations. Future studies involving clinical populations should consider how normalization practices could influence results and interpretation.

**Acknowledgments:** We thank the ACL Consortium for their help with patient referral and recruitment. Support for this study was provided by a grant from the National Institute of Health: R01 AR078811-03.

**References:** [1] Goerger, BM et al. (2015), *British J Sport Med*; [2] Ford, KR et al. (2016), *Clin Biomech*; [3] Paterno, MV et al. (2010), *Am J Sports Med*; [4] Queen, RM et al. (2020), *J Biomech*; [5] Barber SD et al. (1990), *Clin Orthop Relat Res*;

**Enhancing gait retraining with musical feedback: speed, cadence, and biomechanical changes**

*Luisa Cedin[1], Camilla Antognini[1], Christopher Ferrigno[2], Christopher Knowlton[1], Markus Wimmer[1]
[1]Department of Orthopedic Surgery, Rush University Medical Center, Chicago, IL
[2]Department of Anatomy and Cell Biology, Rush University Medical Center, Chicago, IL
*Corresponding author's email: luisa_cedin@rush.edu

**Introduction:** Auditory feedback has gained recognition for improving motor learning in gait rehabilitation, enabling real-time sensory cues without restricting movement. [1] On the other hand, music has been shown to influence gait dynamics, offering a promising approach to modifying spatiotemporal patterns in rehabilitation settings. [2,3]. Recently, our own group has started to experiment with musical feedback [4], which offers an opportunity to combine both. While slowing down during gait retraining is expected for stability, the effects of musical feedback on walking adaptation remain unclear. [5] Therefore, our goal was to investigate how musical feedback tempo (normal or fast) influences walking speed and post-training velocity. Further, we aimed to investigate if the tempo influenced the amount of biomechanical change with the gait retraining. We hypothesized that speed would adjust to tempo, would slow while practicing a new walking pattern, and that biomechanical changes would be greater at a slower tempo.

**Methods:** Healthy subjects were recruited and underwent informed consent. Prior to testing, they were given two playlists, each containing 22 popular songs. The first playlist featured songs with tempos between 80-100 bpm; the second contained songs ranging from 101-120 bpm. Subjects selected three songs from each one and were asked to walk in a figure-8 shape for a total of 10 min at a self-selected pace. After baseline, slow-tempo songs were played for 2 min, followed by an additional 2-minute period of fast-tempo songs. Next, instructions on the musical feedback were provided, and 10 minutes of training was performed. For the training, subjects chose to listen to either slow- or fast-tempo songs. To provide musical feedback, the center of pressure (COP) was captured in real-time at 100 Hz from a wireless 16-sensor pressure insole (Insole3, Moticon ReGo AG). The insoles transmitted data to OpenGo smartphone app, then to the Moticon OpenGo desktop software, and finally to Max 8 (Cycling '74). A 25% decrease from baseline in average peak lateral COP was used as the threshold to provide the feedback. When COP exceeded this threshold, a low-pass filter was applied, muffling the sound. Subjects were instructed to avoid muffling the sound while maintaining a natural-feeling gait. Spatiotemporal parameters collected from the insoles were compared across conditions using repeated measures ANOVA with Bonferroni correction for multiple comparisons. Parameters from baseline and after-training trials were compared using paired t-tests ($p < 0.05$).

**Results & Discussion:** A total of 11 men and 9 women (29 ± 5 years old, 75.9 ± 10.5 Kg, 1.73 ± 0.07 m) participated. Slow-tempo music significantly increased walking speed but had no effect on cadence or stride length (Table 1). Subjects also walked faster at the fast-tempo songs with further adaptations to cadence and stride length. So, interestingly music made subjects walk faster, but contrary to our hypothesis, no significant differences were found between tempos. When the musical feedback was introduced at training, all participants medialized their COP. The peak percentage difference in the gait line ranged from -2.3% to -19% (-9.38% ± 4.09). While musical feedback significantly altered gait biomechanics, no change was observed in speed, cadence, and stride length, refuting our second hypothesis. To analyze the influence of tempo during training, subjects were divided into two groups according to music-tempo choice: slow and fast-tempo (14/20). Music tempo did not seem to affect spatiotemporal parameters (Fig. 1), also negating our hypothesis. Further analysis of COP shifting between groups did not show any differences (slow: -10.21% ± 4.12; fast: -9.02 ± 4.18). Music exerted a stimulating effect, potentially counteracting the expected slowdown when adapting to a new walking pattern. This suggests that musical feedback may help patients maintain cadence while modifying gait biomechanics. Limitations include a young, healthy sample, a short training period, controlled lab conditions, and a fixed playlist order. Further, no qualitative data on the music were collected, though most participants were familiar with and enjoyed the songs. In conclusion, participants increased their speed with music, regardless of the tempo. Subjects successfully adjusted their gait line using musical feedback cues without reducing cadence or speed. This highlights the potential of musical feedback as a tool for orthopedic clinical conditions involving gait asymmetries and movement impairments.

**Table 1.** Spatiotemporal parameters across all conditions

| | No Music | Slow Tempo | Fast Tempo | Training |
|---|---|---|---|---|
| Speed (m/s) | 1.17 ± 0.18 | 1.25 ± 0.18** | 1.27 ± 0.18*** | 1.23 ± 0.15 |
| Cadence (strides/min) | 51.61 ± 4.03 | 51.98 ± 4.13 | 52.86 ± 3.70** | 52.72 ± 3.60 |
| Stride Length (m) | 1.37 ± 0.14 | 1.41 ± 0.15 | 1.44 ± 0.17* | 1.40 ± 0.13 |

*Comparison with baseline (5min) * $p<0.05$, ** $p<0.01$, *** $p<0.001$*

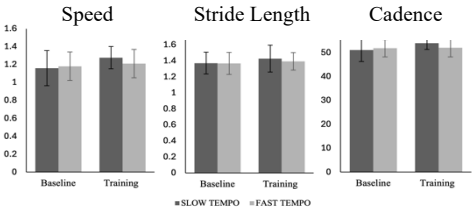


**Figure 1.** Spatiotemporal parameters at baseline and training for slow and fast tempo groups.

**Significance:** Musical feedback modified gait patterns without slowing walking speed. This is important for rehabilitation, where new biomechanical patterns often cause movement slowdowns. It may serve as a reinforcement tool to support gait retraining while maintaining the walking pace.

**Acknowledgments:** Supported by Grant T32AR 073157 from the NIAMS.

**References:** [1] Wall et al. (2024) Sensor 24(1), [2] Leman et al. (2013) Plos One 8(7), [3] Buhmann et al. (2016) Plos One 11(5), [4] Cedin et al. (2025) Healthcare 13(2), [5] Hak et al. (2013) Journal of Biomechanics 46.

# VALIDITY OF OPENCAP TO IDENTIFY MARKER LOCATIONS ON THE LOWER LIMB

Madison K. Arno[1], Louis A. DiBerardino III[1]
[1]Department of Mechanical Engineering, Ohio Northern University, Ada, OH, USA
Email: l-diberardino@onu.edu

**Introduction:** Markerless motion capture provides an accessible, cost-effective, and efficient alternative for assessing biomechanics. In contrast to the traditional method of a marker-based system, which limits the user to a laboratory, costs thousands of dollars, and can take days to process the data, markerless systems can broaden accessibility to those previously constrained by the high cost and equipment requirements of marker-based technologies, while simplifying the data processing pipeline. However, most markerless motion capture systems are still undergoing validation before widespread use.

OpenCap (Stanford, USA), a smartphone-based motion capture system, utilizes iOS devices, tripods, and a printed checkerboard to collect and process data in just 10 minutes [1]. While previous research has primarily focused on joint angle and relative motion validation using OpenCap, this study aims to assess the system's accuracy in identifying lower-limb marker locations during motions commonly assessed in lower-limb biomechanics studies. Given the prior validation of joint angles, we hypothesize that OpenCap will demonstrate similar accuracy for marker placement [2][3].

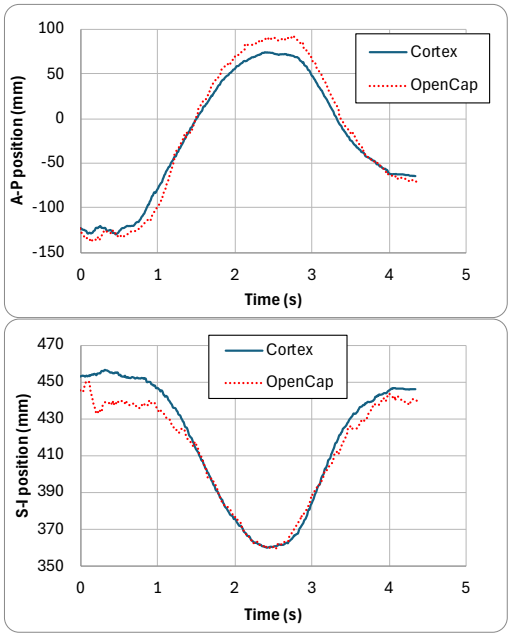


**Figure 1:** Marker locations of the right lateral knee marker in the anterior-posterior (top) and superior-inferior (bottom) direction during a squat.

**Methods:** After IRB approval, data were captured simultaneously using a three-dimensional motion capture system (Cortex, Motion Analysis) and OpenCap. The Cortex system, consisting of six Osprey cameras, surrounded the capture volume, while OpenCap employed six iPhones arranged in an arch anterior to the subject. Retroreflective markers were placed on both medial and lateral sides of the subject's knee and ankle to track position using the Cortex system. The subject performed a squat and a walk task. To align the systems' reference frames, both coordinate system origins were aligned, accounting for the height offset in the superior-inferior direction caused by OpenCap's checkerboard calibration process. The subject stomped their foot to synchronize the capture times of the two systems. The captured tracking data were then linearly interpolated to match sample times, plotted for comparison, and RMS error was computed (MATLAB, MathWorks).

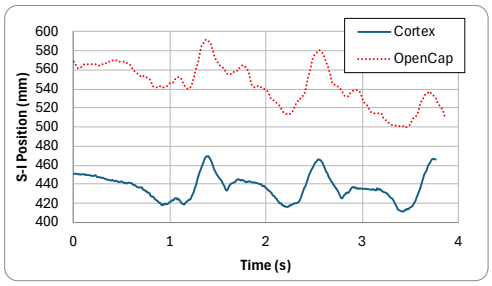


**Figure 2:** Marker locations of the right lateral knee marker in the superior-inferior direction during a walking trial.

**Results & Discussion:** Visual comparisons of marker tracking during the squat showed that the data from both systems were similar, with consistent overall shapes (Fig. 1). RMS error was between 7-12 mm for the three axes of motion, which falls within the normal errors seen in marker-based motion capture [4]. Overall features of the position data plots were similar for the walking trial. However, there was a large vertical offset (~115 mm) in lateral knee marker position, and it seems that the OpenCap data were slightly skewed. RMS errors were much larger, at 30-50 mm in the transverse plane, and 110 mm in the superior-inferior direction (reduced to 18 mm if the data are manually shifted down).

Due to the depth of the capture volume needed to perform the walking trial, OpenCap misinterpreted the floor as being slanted upward, causing the skewed data. However, this may not explain the large vertical position offset. The next step in this study is to construct a more accurate method of aligning the OpenCap checkerboard with the Cortex L frame, which could have also led to issues with the current data. In either case, anecdotally it seems that if raw position data is needed, OpenCap is more than well suited for "stationary" tasks near its origin but may not be suitable for tasks such as gait without further data corrections.

**Significance:** This study explored the potential of OpenCap as an affordable, efficient, and accessible alternative to traditional marker-based systems in biomechanics research and clinical practice. Accurate marker placement is essential for obtaining reliable data that reflects true joint movements. Inaccurate marker placement can lead to poor modeling of body mechanics, making it difficult to identify abnormalities in motion. By validating OpenCap's ability to accurately place joint markers, this study opens opportunities for researchers in low-resource settings. The ability to quickly collect and process biomechanical data with minimal equipment enables large-scale studies and provides patients or athletes with an opportunity to monitor joint movements remotely, either at home or in outpatient settings.

**References:**

[1] Ulrich et al. (2023), *PLoS Comput Biol* 19(10), [2] Horsak et al. (2023), *J Biomech* 159, [3] Turner et al. (2024), *J Biomech* 171, [4] Slater et al. (2018), *BMC Musculoskelet Disord* 19

# OFFSET FEET INDUCE GREATER PLANTARFLEXOR MUSCLE FORCES DURING RISING IN SIT-TO-WALK

Michael F. Miller[1*], Eline van der Kruk[2], Anne K. Silverman[1]
[1]Department of Mechanical Engineering, Colorado School of Mines
[2]Department of Biomechanical Engineering, Delft University of Technology
email: *mfmiller@mines.edu

**Introduction:** The sit-to-walk (STW) transition is a critical and frequent movement that requires coordination from several individual ankle muscles. Injuries and aging can introduce movement compensations, such as rising with one foot offset posteriorly; however, the effect that initial foot placement has on ankle muscle forces during STW is not well understood. Results from experimental STW studies have shown that rising from an offset position required greater plantarflexion moments and reduced muscle excitation compared to a symmetric foot position [1]. However, to understand how initial position in STW affects underlying muscle mechanics, musculoskeletal simulations are needed to quantify the force and length changes of the plantarflexor muscles. Therefore, we quantified the effects of initial foot position on peak plantarflexor muscle force production during the rising portion of STW. We expected greater force and tendon displacement when rising from the posteriorly offset foot position.

**Methods:** Handgrip strength (HGS) was measured using a handheld dynamometer [2] from five healthy younger (2M/3F, 24.6±3.8 yrs, 749.5±188.6 N, 1.78±0.07 m) adults. Full body motion (200 Hz), ground reaction forces (GRFs) (2000 Hz) and surface electrometry (2000 Hz) were collected to develop and validate STW simulations of self-paced STW from two initial foot positions: (1) a *symmetric* position with feet shoulder-width apart and knees and hips at 90°, (2) an anterior/posterior (A/P) offset position, with the dominant limb offset backward 2/3 the dominant foot length. A generic model containing 37 degrees of freedom and 80 hill-type musculotendon actuators [3] was scaled to each participant in OpenSim 4.5 [4, opensim.stanford.edu] by adjusting the segment sizes, masses, and lower limb muscle maximum isometric force by comparing measured HGS to the predicted HGS from the participants used to define the generic model [5]. Inverse kinematics solutions were determined for three trials/per participant with a global optimization algorithm and a residual reduction algorithm was performed to improve dynamic consistency between these solutions and the measured GRFs [6]. Muscle recruitment solutions driving the STW motion were determined for each participant model and initial foot placement using Computed Muscle Control [7]. The simulated muscle excitations when initiating STW from both foot positions were compared to 4$^{th}$ order Butterworth bandpass filtered (20-500 Hz), full-wave rectified surface electromyography signals from the medial gastrocnemius (MGAS), lateral gastrocnemius (LGAS), and SOL. Simulated excitations and processed EMG signals were both lowpass filtered and the root mean square difference between the two linear envelope curves was calculated. A muscle analysis was performed to evaluate passive, active, and total force contributions. Differences in the peak passive, active, and the total muscle force between initial foot placements for the MGAS, LGAS, and SOL were compared during the rising phase using a paired t-test ($\alpha$= 0.05).

**Results & Discussion:** All participants were right limb dominant, which was also the posterior stepping limb in the A/P offset position. Average residual forces and moments from the simulations were low and met established guidelines [8], and the muscle recruitment solution agreed with EMG signals. The A/P offset position had greater peak stepping limb SOL active ($p=0.006$), passive ($p=0.025$), and total muscle force ($p=0.008$) compared to the symmetric position (Figure). The A/P offset SOL had 71.7% greater active force, 25.9% passive force, and 51.2% total muscle force compared to the symmetric position. Greater muscle forces were also found for the MGAS ($p<0.001$ for all forces) and the LGAS (passive: $p=0.021$, $p<0.001$ active and total force). Greater active force production from the stepping limb SOL, MGAS, and LGAS contribute to greater experimental GRFs and ankle plantarflexion moments when rising from the A/P offset position [1]. Greater active force on the stepping limb, despite a reduction in excitation, may be due to a greater initial muscle length, facilitating operating lengths closer to optimal fiber length and thus producing larger dynamic forces during rising [9]. A SOL fiber length greater than the optimal fiber length also results in greater passive forces compared to the symmetric position. Future work will analyze older adult participants to assess age effects on muscle mechanics.

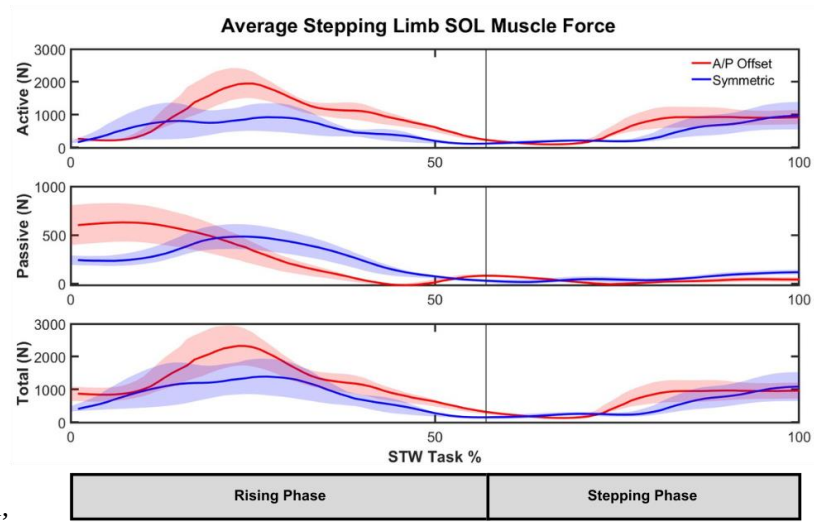


**Figure:** Active, passive, and total SOL muscle force signals for the stepping limb for sit-to-walk from a symmetric and offset position. Note the smaller y-axis range for passive force.

**Significance:** Rising with a limb posteriorly offset increased active and passive plantarflexor muscle force generation with lower muscle excitation, due to greater initial muscle length in the offset position.

**References:** [1] Miller *et al*, *J Biomech.*, vol. 177, 2024. [2] Mathiowetz, *et al.*, *J. Hand Surg.*, vol. 9. 1984. [3] Lai, *et al.*, *Ann Biomed Eng.*, vol. 45, 2017. [4] Seth *et al.*, *PLoS Comput. Biol.*, vol 14, 2018. [5] Handsfield, *et al.*, *J. Biomech.*, vol. 47, 2014. [6] Delp, *et al.*, *IEE Trans. Biomed. Eng.*, vol. 54, 2007. [7] Thelen *et al.*, *J Biomech.*, vol. 36, 2003. [8] Hicks *et al.*, *J Biomech Eng.*, vol 137, 2015. [9] Herzog, *et al.*, *J Appl Physiol*, vol. 126, 2019.

# ON BRACING THE NECK MUSCLES FOR A HEAD PERTURBATION: EXPERIMENTAL AND ANALYTICAL STUDY

*Hogene Kim PhD[1], Yumeng Wang MS[2], Anita Vasavada PhD, James A. Ashton-Miller PhD[1], James T Eckner M.D.[3]
Departments of [1]Mechanical Engineering, [2]Statistics, [3]Physical Medicine & Rehabilitation, University of Michigan, Ann Arbor, MI
*Corresponding author's email: hogenek@umich.edu

**Introduction:** Concussions remain a significant concern, with 14.3% of high school students experiencing at least one in the past year, and soccer players accounting for over 10% of cases [1]. Neck muscles contribute to head stability, yet their role in reducing concussion risk remains unclear. While some studies suggest that stronger and larger neck muscles can counteract head accelerations, others question whether increased co-activation meaningfully reduces impact forces. This study examines how bracing neck muscles affects peak head accelerations, a key factor in concussion risk. Unlike prior research that primarily focused on stiffness, this work also considers the role of muscular viscous resistance during impacts. To achieve this, the study employed a subject-specific, one-muscle equivalent head-neck mass-spring-damper model to estimate neck stiffness and damping in flexion, extension, lateral flexion and axial torsion.

**Methods:** Forty-three high school soccer players (16 female) participated in laboratory head impulsive perturbation tests. A 1 kg weight drop, applied after a random delay, induced head perturbations in four directions: flexion (FLX), extension (EXT), lateral flexion (LAT), and horizontal rotation (ROT). Forces and head kinematics were recorded at 500 Hz. A one-muscle-equivalent second-order mass-spring-damper model was employed to estimate subject-specific neck stiffness (K) and damping (B) coefficients to analyze the response. These values were derived using analytical calculations based on the recorded perturbation data. The K and B values were then compared across different perturbation directions and were determined using each participant's average peak head angular acceleration, velocity, and displacement during the head perturbation experiments.

$$J_{Head-neck}\frac{d^2\theta}{dt^2} = F_{ext}(t)\cdot L_{neck} - F_m \cdot d_m$$

$$where\ F_m = B_m\frac{d\theta}{dt} + K_m\theta \quad K_m = \frac{F_{ext}\cdot L_{neck}}{\theta_{peak}}$$

$$B_m = \frac{F_{ext}\cdot L_{neck} - J\cdot\ddot{\theta}_{Peak} - K\cdot\theta_{peak}}{\dot{\theta}_{peak}}$$

θ: angular displacement (x~θ)
$B_m$: damping coefficient of single neck muscle-equivalent
$K_m$: spring constant of single neck muscle-equivalent
$d_m$: lever arm distance from C7 to single neck muscle-equivalent
$F_{ext}(t)$: external force $F_{ext}$ applied to the system
$L_{neck}$: distance from the midpoint of C7-T1 to C1

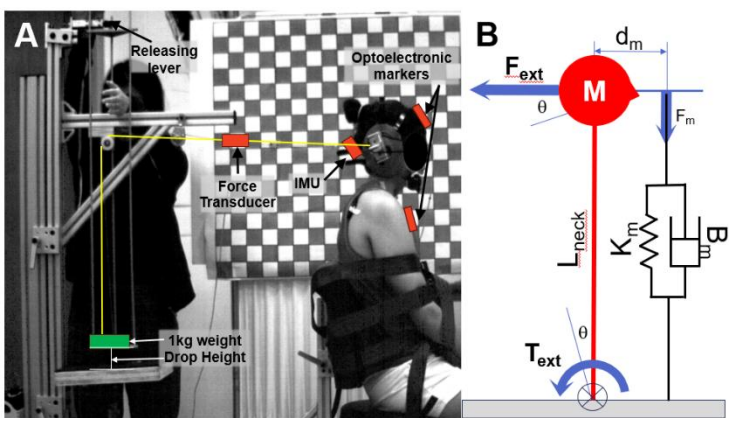


**Figure 2**: (A) Head impulsive perturbation test setup; (B) Example of one neck muscle equivalent second-order mass-damper-spring model for extension perturbation.

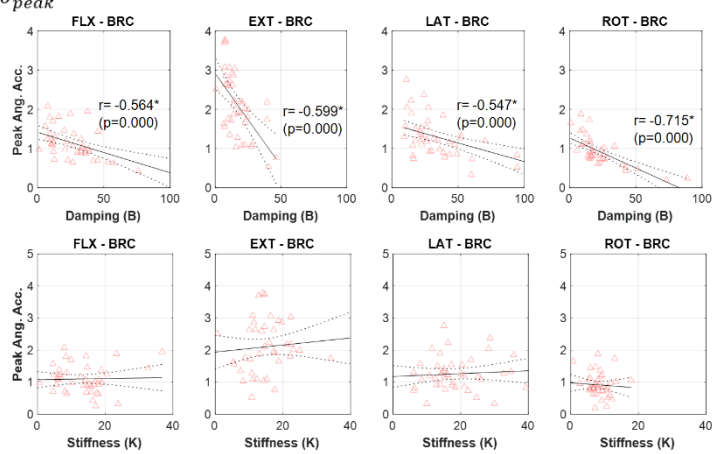


**Figure 1**: Relationships between stiffness & damping coefficients and peak head angular acceleration in response to 1 Kgf sudden perturbation by direction.

**Results & Discussion:** Bracing was effective because it had a significantly negative and strong linear correlation with peak angular acceleration in all directions—FLX (r=-0.684), EXT (r=-0.765), LAT (r=-0.721), and ROT (r=-0.699) ($p < 0.0001$). These findings align with the natural instinct to brace neck muscles in preparation for impact, potentially serving as a protective mechanism against head injuries during gameplay. No significant relationship was found between peak head angular acceleration and values of K (Fig. 2). But a negative linear correlation between peak angular acceleration and neck damping properties was observed across all four directions, suggesting that increased neck muscle damping reduces head acceleration during impact. Notably, in Figure 2, neck EXT exhibited a much steeper slope (in units of head angular acceleration divided by stiffness in Nm/rad)(-0.1015) compared to FLX (-0.0232), LAT (-0.0285), and ROT (-0.0149) with greater average peak acceleration (in rad/s$^2$) of (6.47), compared to FLX (3.38), LAT (3.99), and ROT (2.76); this indicates less protective in this direction. The average braced neck muscle stiffnesses, K, in all four directions (FLX (13.1 Nm/rad), EXT (14.9 Nm/rad), LAT (18.4 (Nm/rad) and ROT (8.0 Nm/rad) may be compared to those for a 7-segment cervical spine without muscles (FLX (3.5 Nm/rad), EXT (5.9 Nm/rad), LAT (5.5 Nm/rad), and ROT (9.4 Nm/rad) showing braced muscles can stiffen the ligamentous cervical spine by up to 3.7 times.

**Significance:** Bracing neck muscles was beneficial in reducing peak head angular acceleration. The damping coefficients in the head-neck one-muscle-equivalent model varied significantly with the direction of loading; the least muscular protection was afforded in head extension, meaning this may be the direction the brain is most exposed to accelerational damage.

**Acknowledgments:** This study was supported by a grant from the National Institutes of Health (Grant # NIH: R01HD093733)

**References:** [1] Sarmiento K, et al. (2023), *Am J Sports Med* 51(2), [2] Stewart WF et al. (2017) *Neurology* 88(9) [3] Moroney S, et al. (1988) *J Biom* 21(9)

# THE EFFECTS OF PSYCHOSOCIAL STRESS ON SURFACE ELECTROMYOGRAPHY SIGNALS OF THE LOWER LEG DURING ISOMETRIC CONTRACTIONS

*Sierra Eady[1], Ivan Nail-Ulloa[1], Michael Zabala[1]
[1]Department of Mechanical Engineering, Auburn University, Auburn, AL, USA
*Corresponding author's email: sje0011@auburn.edu

**Introduction:** Wearable assistive robotic devices (WARDs) are electromechanical devices, such as exoskeletons or prosthetics, designed to aid in activities of daily living (ADLs) for individuals with movement disabilities. Despite the potential benefits, WARDs are not widely accepted outside of controlled environments. Reasons for rejection include safety concerns, unmet expectations, practicality, and social acceptance [1,2]. Surface electromyography (sEMG) has been proposed as a solution to improve the human-robot interaction in WARDs by predicting motion, reducing errors, and improving efficiency. Studies show that incorporating sEMG can enhance motion recognition and prediction accuracy in both upper and lower limbs [3,4,5]. However, challenges remain when WARDs are used in real-world settings, such as interacting with objects or terrains they were not trained for [3].

Studies on psychosocial stress in people who may benefit from a WARD have identified social acceptance as one cause of stress while using the device [6,7]. Psychosocial stress has been linked to several short-term and long-term physiological effects [8], so it is reasonable to assume it may affect muscle function and thus muscle signal. Some studies have suggested that psychosocial stress may play a role in the etiology of musculoskeletal disorders [9]. While research on how psychosocial stress affects lower-body muscle signals is limited, it is possible that psychosocial stress could alter sEMG signals, impacting the performance of WARDs that rely on this signal input. Thus, it was hypothesized that psychosocial stress would have a measurable effect on sEMG mean amplitude and mean frequency.

**Methods:** Thirteen healthy participants (3 men, 10 women; age: 22.4 ± 2.9 years; weight: 65.2 ± 14.2 kg; height: 164.8 ± 9.5 cm) with no recent lower limb injuries were recruited. The protocol was approved by the Auburn University IRB (23-619 MR 2312) prior to data collection. The study involved three phases: pre-stress fatigue testing, a stress-inducing protocol, and post-stress fatigue testing. The sEMG signals from the tibialis anterior (TA) and gastrocnemius medialis (GM) were recorded during isometric dorsiflexion and plantarflexion. In Phase 1 (pre-stress fatigue testing), participants performed 3 MVCs followed by 3 fatigue trials where they attempted to maintain a contraction level of 60% MVC until they could not achieve 60% MVC for at least 3 seconds. This was done for the TA and the GM. In Phase 2, psychosocial stress was induced using the Trier Social Stress Test (TSST) [10], which involved public speaking and mental arithmetic tasks. In Phase 3 (post-stress fatigue testing), all actions from Phase 1 were repeated. Data were processed in MATLAB, and mean amplitude and mean frequency were analyzed for changes between pre- and post-stress conditions. Statistical analysis involved paired Wilcoxon signed-rank tests and equivalence testing using the two one-sided t-tests (TOST) method [11].

**Results & Discussion:** No significant differences in mean amplitude or mean frequency were found between pre-stress and post-stress trials for either the TA or GM. As seen in Figure 1, the mean amplitude of the GM (pre-stress: 28.7% MVC; post-stress: 27.9% MVC) was lower for all trials compared with that of the TA (pre-stress: 43.1% MVC; post-stress: 42.5% MVC). The opposite was true for the mean frequency, with the mean frequency of the GM (pre-stress: 266.9 Hz; post-stress: 268.3 Hz) being higher for all trials compared with that of the TA (pre-stress: 131.8 Hz; post-stress: 133.3 Hz). All TA comparisons of mean amplitude and mean frequency were found to be equivalent according to the TOST method. For the GM, the mean amplitude and mean frequency comparisons during Trial 1 were each found to be equivalent, as well as the mean amplitude comparison during Trial 3. As a result, the hypotheses that induced psychosocial stress would have a measurable effect on sEMG mean amplitude and mean frequency were rejected for both muscles. The rejection of the hypotheses suggests that for the TA and GM during isometric movements, psychosocial stress has a negligible effect on the mean amplitude and mean frequency.

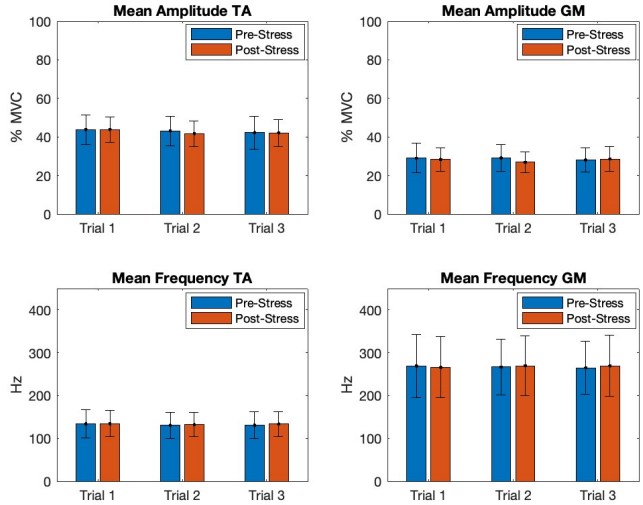


**Figure 1:** Comparison of mean amplitude and mean frequency for both the TA and GM before and after the TSST.

**Significance:** Previously, the effects of psychosocial stress on muscle activation had mostly been studied in the upper body and mostly from an ergonomics perspective. This study on how psychosocial stress affects the mean amplitude and mean frequency of sEMG signals is the first of its kind and introduces the topic to the field of WARDs. With the levels of psychosocial stress experienced by people who may use WARDs and with the number of WARDs utilizing sEMG in their control system, it is essential to understand if psychosocial stress impacts muscle function.

**References:** [1] Pinelli et al. (2024), *Disabil Rehabil Assist Technol* 19(6); [2] Ang et al. (2023), *Sensors* 23(6); [3] Martinez-Hernandez et al. (2021), *Sensors* 21(20); [4] Meng et al. (2021), *Sensors* 21(18); [5] Kawase et al. (2020), *Sensors and Materials* 32(3); [6] Kristjansdottir et al. (2020), *Hand Therapy* 33(4); [7] Arabian et al. (2016), *IEEE Glob Hum Technol Conf*; [8] Chrousos et al. (2009), *Nat Rev Endocrinol* 5(7); [9] Lundberg et al. (1994), *Behavioral Medicine* 1(4); [10] Allen et al. (2017), *Neurobiol Stress* 6; [11] Lakens, Daniel (2017), *Social Psychol Personal Sci* 8(4).

# THE EFFECTS OF SADDLE HEIGHT ON THE KNEE JOINT DURING CYCLING

Fangbo Bing[1], Tony Lin-Wei Chen[1,2], Yan Wang[1,2], *Ming Zhang[1,2]
[1]Department of Biomedical Engineering, Faculty of Engineering, The Hong Kong Polytechnic University, Hong Kong, China
[2]Research Institute for Sports and Technology, The Hong Kong Polytechnic University, Hong Kong, China
*Corresponding author's email: ming.zhang@polyu.edu.hk

**Introduction:** Cycling is growing in popularity because of its enjoyment and health benefits, while the relevant injuries are likewise becoming more common. The knee joint is one of the most affected body parts by overuse injuries [1], which are always caused by improper bike fitting. There is disagreement among scientists and athletes/coaches over the optimal bike configuration, particularly concerning saddle height. Previous studies demonstrated that saddle height is associated with motion angles and moments of the knee joint [2]. However, the reason behind the alterations in these kinetics and kinematics and the connections to knee pain are unclear. Here we related the variations in knee joint forces to the muscle forces of knee flexors and extensors and explored the knee stress with high stress indicating potential knee pain under different saddle heights. We found that the muscle forces of rectus femoris (RF), vastus lateralis (VL), vastus medialis (VM), and gastrocnemius (GAS) decreased as the saddle height increased, which contributed to the decline of knee joint forces, especially in the directions of medial-lateral and anterior-posterior. Furthermore, the stress and strain of knee cartilage and menisci were also reduced. The results indicated that lower saddle heights increase loads on lower-limb muscles and knee joint. Therefore, a higher saddle setting within the physiological range can help mitigate the risks of overuse injuries. We anticipate that this study could offer evidence-based and practical recommendations for cyclists and coaches for injury prevention.

**Methods:** Twenty-five subjects participated in cycling tests with saddle heights of 95%, 100%, and 105% of the greater trochanter height (GTH) and a constant cadence and workload. Trajectories of markers attached to subjects were acquired by a motion capture system. Pedal reaction forces (PRFs) and torques were recorded by force sensors on the pedals. These parameters were input into musculoskeletal (MSK) multibody dynamic simulation in Anybody to calculate knee joint forces and around muscle forces under different saddle heights.

A finite element (FE) model of the knee joint was established based on MRI. The calculated muscle forces were the force loads and joint angles were the displacement constraints in FE analysis. The flexion and extension motion of the knee joint was dynamically simulated during the crank angle from 90° to 180°. The stress and strain of knee cartilages and meniscus were compared under various saddle heights.

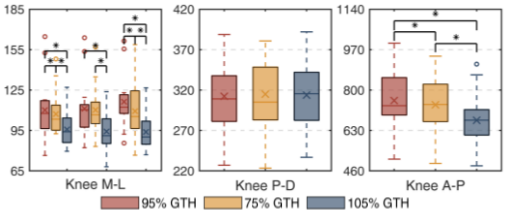


**Figure 1:** Mean of knee joint forces.

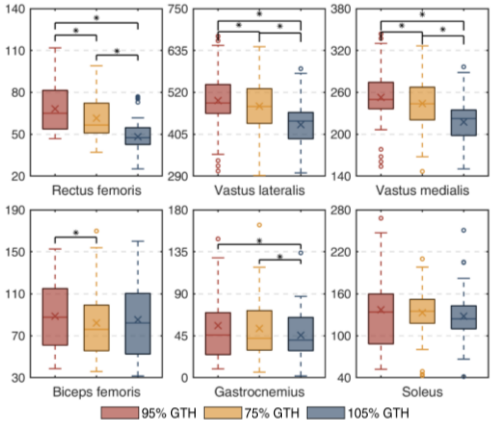


**Figure 2:** Mean of muscle forces.

**Results & Discussion:** The knee joint forces in medial-lateral (M-L) and anterior-posterior (A-P) directions decreased as the saddle height increased, contributing to the reduced resultant knee joint force (Fig.1). Raising the saddle height generally decreases lower-limb joint angulation then leading to lower forces in the shear planes [4]. The more extended knee position aligns its force vectors more closely with the pedal force direction and shifts more load to proximal-distal (P-D) direction. These resulted in P-D knee joint force not decreasing as much as the other two components. The muscle forces of RF, VL, VM, and GAS declined with each 5% increase in saddle height, while no significant change was found in soleus muscle force (Fig.2). BF and GAS are knee flexors. RF, VL, and VM are synergistic knee extensors. Their reduced muscle forces might be due to the less power demanded for propulsive. An elevated saddle height also can shift the working range of muscles closer to their optimal length, thereby lowering their activations [3]. Additionally, the reduction in muscle forces is one of the reasons for the decreased knee joint force.

The maximum and mean stress of femoral cartilage, tibial cartilage, and meniscus reduced when the saddle height increased, except for the maximum stress of meniscus caused by stress concentration (Table 1). Articular cartilage and meniscus wear are common causes of knee pain in riders. The stress distribution can provide information about the location of possible pain. The results indicate from a microscopic level that a higher saddle height is beneficial to relieving knee stress. Despite this, excessively high saddle heights may cause biomechanical inefficiencies and discomfort. A height of 100%-103% GTH would be an ideal selection that ensures efficient muscle activation, lowers joint contact force, and minimizes joint stress, which could reduce the risk of overuse injuries.

**Table 1:** Stress (MPa) of cartilages and meniscus.

| | Conditions | Maximum | Mean |
|---|---|---|---|
| Femoral cartilage | 95% GTH | 11.64 | 0.21 |
| | 100% GTH | 9.20 | 0.14 |
| | 105% GTH | 5.30 | 0.08 |
| Tibial cartilage | 95% GTH | 12.03 | 0.29 |
| | 100% GTH | 7.72 | 0.16 |
| | 105% GTH | 3.82 | 0.07 |
| Meniscus | 95% GTH | 9.16 | 1.64 |
| | 100% GTH | 9.55 | 1.42 |
| | 105% GTH | 8.58 | 1.05 |

**Significance:** This study methodically investigated the effect of saddle height on lower limb biomechanics. The calculated muscle force and tissue stress explain the variations in knee joint forces well. The findings indicate that higher saddle heights within the physiological range could alleviate knee joint stress to prevent overuse injuries. Cyclists and coaches can benefit from the recommendations on selecting an appropriate saddle height.

**References:** [1] Wanich et al. (2007), J Am Acad Orthop Surg 15(12); [2] Bini et al. (2022), J Sport Sci 40(4); [3] Ichinose, Y. (1997), Cells Tissues Organs 159(2); [4] Bini et al. (2011), Sports Med 41.

# USING CONTINUOUS RELATIVE PHASE TO ASSESS GROUND REACTION FORCE COORDINATION IN SINGLE LEG COUNTERMOVEMENT JUMPS

*Jeromy Miramontes[1], Megan Ward[1,2], Jay H. Patel[1,2]
[1]Prisma Health, Columbia, SC.
[2]The University of South Carolina, Columbia, SC.
*Corresponding author's email: miramontesjd@gmail.com

**Introduction:** Continuous Relative Phase (CRP) is a qualitative higher-order measure of coordination used to display the relationship between two or more quantitative measures in human movement (Emmerik, 1999). Dynamics Systems Theory utilizes CRP as a measure of relative inter- and intra-limb synergy in dynamic human movement. The countermovement jump (CMJ) is a dynamic coordinated total body athletic movement that has applications in a majority of professional sports. This study builds upon prior research assessing bilateral CMJ ground reaction force comparisons [1]. The single-leg countermovement jump (SLCMJ) has been used as an RTP benchmark movement specifically meeting a >90% limb synergy with strength and jump performance [2]. The goal of the SLCMJ is to reveal an athletes' ability to optimally and efficiently generate force using their entire kinetic chain to jump as high as possible while maintaining sufficient unilateral stability. While performing a unilateral lower body movement, force vector application becomes critical due to any deviation off the intended direction potentially leads to energy leakage throughout the movement. Due the added difficulty of SLCMJ vs bilateral CMJ and the biomechanics of the foot, there may be greater relative coordination synergy with the right vertical ground reaction force (RVGRF) and medial-lateral ground reaction force (MLGRF). The purpose of this study was to measure the level of in-phase (IP) and out-of-phase (OP) coordination between the RVGRF and RMLGRF and LVGRF and LMLGRF of a SLCMJ and estimated jump height performance among professional soccer players.

**Methods:** Thirty-six professional soccer players (mean (SD) age 20.78±1.67yrs, mean (SD) height 176.82±8.97cm, mean (SD) weight 73.98±10.10kg) were included in this pilot study. Manual muscle tests were conducted prior to jumping protocol to establish strength measures of the lower extremities. Once completed, athletes were shown how to perform the series of jumps with clear instructions to wait prior to each movement. Athletes stood on two triaxial AMTI Force and Motion force plates**.** First, athletes performed three bilateral CMJs, making sure to land with each foot back to the original force plate from which they took off. Next, they performed two right single-leg (RSL) CMJs, and two left single-leg (LSL) CMJs, landing on their respective force plate. Participants were instructed to pause prior to each jump and to hold the landing if possible. Univariate linear regression models examined relationships between left unilateral total VGRF vs left unilateral total MLGRF RMS CRP and jump height; and right unilateral total VGRF vs right unilateral total MLGRF RMS CRP and jump height.

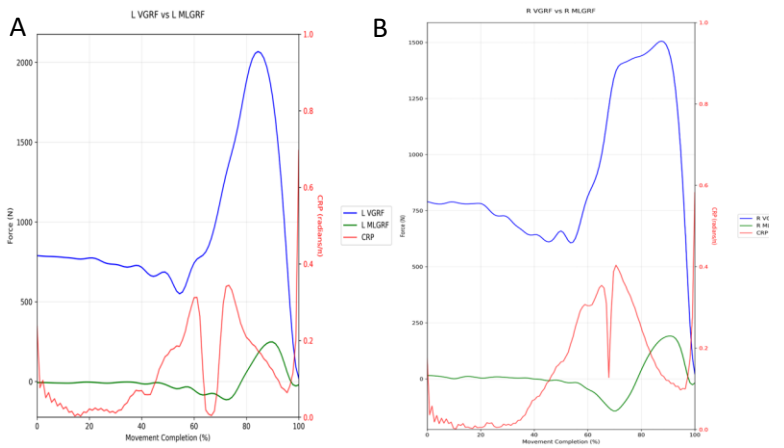


**Figure 1:** Panels A and B show Force (N) (left) and CRP (radians) (right). Panel A shows the LVGRF vs LMLGRF. Panel B shows RVGRF vs RMLGRF. Both panels are referencing single jumps and their corresponding CRP.

**Results & Discussion:** The RMS CRP of the LSL VGRF vs LSL MLGRF RMS CRP was not predictive of jump height ($R^2$=-1.62), suggesting a non-linear relationship between the two variables. The mean RMS CRP of the RSL VGRF vs RSL MLGRF RMS CRP was not predictive of jump height ($R^2$=-3.20), suggesting a non-linear relationship between the two variables. Both variable comparisons showed a non-linear relationship with jump height performance. This result is in line with our previous pilot study results in which there was a non-linear relationship between total VGRF vs total MLGRF RMS CRP and jump height prediction in bilateral CMJ. Figure 1 is an example of data collected and presented in order to show the relationship between the compared variables.

**Significance:** Our pilot study shows that CRP alone does not predict SLCMJ performance. To our knowledge this is the first study to use CRP to quantify ground reaction forces for the SLCMJ in professional soccer players. The study explores the idea of ground reaction forces and their relative coordination in sport performance. Does ground reaction force coordination better relate to jump performance when looking at specific planer rotations rather than vertical displacement? Future research should begin to look at variables that are specific to rotations of the ankle joint like anterior-posterior vs medial lateral.

**References:**

[1] Miramontes et al. [Poster presentation], SEACSM, 2025, Greenville, SC
[2] O'Malley et al. (2018), J of Athletic Training 53(7);687-695

# MOTOR UNIT RECRUITMENT VARIABILITY DURING STATIONARY CYCLING

*Alexander Wiggins, Robert Creath*
*Lebanon Valley College, Department of Exercise Science*
*Corresponding author's email:* creath@lvc.edu

Introduction: The Size Principle predicts the orderly recruitment of motor neurons (MUs) for increased isometric muscular efforts with a shift to larger MUs for greater efforts. Attempts to characterize dynamic muscle contractions have produced less coherent results. DeLuca et al [1] observed that motor unit substitution occurs during prolonged contractions, allowing fatigued motor units to be replaced by fresh ones to sustain force output. Following this, DeLuca et al [2] rescinded these previous findings. Subsequent experimental efforts showed that motor units undergo rotation during sustained isometric contractions, allowing for delayed fatigue and prolonged force production [3,4]. To date, a comprehensive model of MU recruitment remains elusive.

The goal of this experiment was to characterize dynamic MU recruitment using frequency-domain methods to see if the observable frequency content of similar muscle contractions was the same for a task that emphasized consistent, repeatable performance characteristics. In this experiment, participants rode a stationary exercise bike for 8.5 minutes at constant RPMs and effort for two experimental conditions: 1) 60 RPMs; and 2) 80 RPMs. We expected that the frequency analyses would yield similar spectra for pedal pushes (PPs) of similar power, and that the average frequency spectrums will resemble the frequency spectra observed for individual PPs.

The hypotheses are 1) the frequency distribution of the MUs would follow the Size Principle producing distributions that reflected the frequency composition needed to ride at constant cadence and effort; and 2) the average frequency spectrums for the entire 8.5-minute trial would show a shift to higher frequencies reflecting the different MUs needed to pedal at 80 RPMs compared to the 60 RPM condition.

Methods: Fifteen healthy participants (ages 22-25; 7 males, 8 females) completed two 8.5-minute cycling trials at 60 and 80 RPM while maintaining a constant pedal effort. Electromyography (EMG) electrodes (Delsys, Natick, MA) were placed on the vastus lateralis to measure muscle activation patterns. Force-sensing pedals (Favero Assioma, Italy) captured peak pedal force for each PP. FFTs were calculated using MATLAB (Mathworks, Natick, MA) on the EMG signal for individual PPs using Welch's method. Frequency spectra were averaged across 475 PPs for each trial. Pearson correlations were calculated between the frequency spectra for all pairwise combinations of PPs for each trial. Normalized average frequency distributions were compared between 60 and 80 RPM conditions. Correlation distributions were compared using the Wilcoxon non-parametric test for significant at alpha = 0.05.

Results & Discussion: Pearson correlations calculated between (PPs) showed significant variation between PPs. The majority of correlation values varied between 0.3 and 0.9 with no correlations close to the expected value of 1 for similar frequency spectra. The expectation was that frequency spectra would be similar between PPs of similar cadence and effort. The high degree of variation between PPs suggests that the recruitment sequence showed random variation between PPs.

Individual PPs exhibited unique MU recruitment patterns, suggesting deviation from strict Size Principle adherence. Although PP-to-PP variability suggests a flexible recruitment mechanism that appears as a random frequency distribution, when averaged across the entire trial period (n=475), the frequency distributions fell within a finite range. A comparison of average frequency distributions showed that some subjects demonstrated similar MU recruitment distributions between the 60 and 80 RPM conditions while others showed shifts in the distributions between the conditions. The expected result was that the frequency distribution for the 80 RPM condition would show a shift to a higher frequency range owing to the higher firing rate of larger MUs needed to achieve increased pedal effort when compared to the 60 RPM condition. Our results support the idea that MU recruitment is not strictly deterministic, rather it exhibits elements of flexibility, aligning with [4] Bawa's (2009) concept of motor unit rotation. The variability seen in MU selection between PPs suggests subtle adjustments in recruitment occur even when external conditions remain constant

Significance: This study contributes to an evolving understanding of MU recruitment, emphasizing its variability and task-dependent modulation rather than a strictly hierarchical activation pattern, i.e., the Size Principle. Future research should explore the interactions between fatigue, cadence, and neuromuscular control to refine training and rehabilitation strategies for optimizing motor function.

References: [1] Westgaard & De Luca (1999), J Neurophysiol 82(1). [2] Adam & De Luca (2003), J Neurophysiol 90(5). [3] Bawa et al. (2006), J Neurophysiol 96(3). [4] Bawa et al. C. (2009). *J Neurophysiol*, 96(3)

# MAXIMUM VOLUNTARY CONTRACTION MUSCLE ACTIVITY IN INDIVIDUALS WITH ACUTE TRANSTIBIAL AMPUTATION

*Mai-Ly Thompson[1], Nicole Stafford[1], Daniel P. Ferris[1]
[1]University of Florida J. Crayton Pruitt Family Department of Biomedical Engineering
*Corresponding author's email: mthompson2@ufl.edu

**Introduction:** Myoelectric control of lower limb bionic prostheses allows a user to volitionally alter the dynamics of the prosthesis based on residual limb electromyography (EMG). After amputation, neuromuscular plasticity leads to high interindividual variability of residual limb muscle activation. Individuals with transtibial amputations can learn to adapt muscle activity patterns to control a myoelectric prosthesis, but it usually requires guided training or visual feedback to see significant biomechanical benefits [1-3]. The goal of this study was to quantify the time course of muscle recruitment ability after amputation surgery, as neuromuscular plasticity affects myoelectric control training and rehabilitation [1, 4]. We collected maximal voluntary contraction of residual and intact lower limb muscles in indvidiuals soon after transtibial amputation to determine if surgery leads to changes in maximal recruitment ability.

**Methods:** We recorded surface electromyography of residual and intact *tibialis anterior* (TA) and *medial gastrocnemius* (GAS) of three individuals with unilateral transtibial amputation within a month of their amputation surgery. The participants performed three maximum voluntary contractions (3 seconds) of ankle flexion and extension with the intact leg and imagined ankle flexion and extension with the residual limb. We placed EMG electrodes using ultrasound imaging and manual palpation. Participants received verbal encouragement and visual feedback of muscle activity. We recorded EMG using a Raspberry Pi and two 1.3 mm Neuroline Surface Electrodes (Ambu, Columbia, MD, USA) paired with a Coapt amplifier (Coapt, LLC Chicago, IL, USA) sampled at 500 Hz. To keep electrode positioning consistent across visits, we measured the electrode locations based off of boney landmarks of the knee. We measured muscle signals across two visits post-surgery, which primarily occurred during their inpatient hospital or rehabilitation stay. We calculated the peak one second (RMS) from a running average RMS of the EMG after it was high pass filtered at 20 Hz with a second order Butterworth filter and full wave rectified. We normalized RMS values to the first visit intact limb RMS for each muscle. We used this to compare the muscle activation of the TA and GAS during the maximum volume contractions between the intact and residual limbs and across days.

**Results & Discussion:** The subjects had lower tibialis anterior activation in the residual limb than the intact limb on average (Figure 1; dashed line lower than solid line). Subjects A and C had identical RMS values for both the residual and intact limbs on the first visit (7 days and 5 days post-surgery, respectively). However, both subjects had a 200% increase in RMS on the intact side and no change on the residual side at 43 and 19 days after surgery, respectively. Subject B had a higher RMS for the residual limb 10 days after surgery, but both the intact and residual limbs had only 50% peak RMS 26 days after surgery.

There was not much difference in gastrocnemius activation between residual and intact limbs (note similar best fit lines). Both Subjects A and B had either the same peak RMS on both sides or a lower peak RMS on the residual limb at both post-surgery visits. Subject A had a lower RMS for the residual limb 10 days after surgery. Subject C, however, had slightly higher RMS for the residual limb a both post-surgery visits, with the bilateral difference decreasing at the second visit.

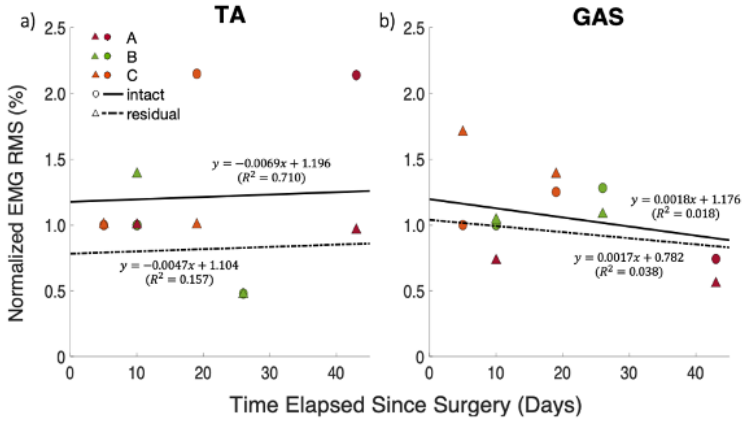


**Figure 1:** Normalized EMG RMS is plotted against the Time Elapsed Since Surgery across subjects for both the intact and residual limbs. We normalized the RMS values to the first visit intact limb RMS for each muscle. Each marker is an individual RMS. Solid lines indicate a model fit for the intact limb measures across subjects and dashed lines indicate a model fit for the residual limb measures across subjects. a) Residual and intact TA b) Residual and intact GAS.

There was large interindividual variability in our participants' data. We were limited to three subjects for our pilot data, and additional recruitment might provide greater confidence in the results.

**Significance:** Prior studies on muscle recruitment after transtibial amputation suggest high interindividual variability in the ability to recruit residual limb muscles, with some individuals unable to volitionally recruit muscles [1, 2]. Understanding how amputation affects muscle recruitment immediately post-surgery provides information about the time course of the neuromuscular plasticity related to muscle inhibition. A better quantitative understanding of maximal volitional recruitment of residual limb muscles may also aid in designing better myoelectric controllers and training paradigms for bionic prostheses.

**Acknowledgments:** We thank the participants for their contributions to the study. Funded by the Adenbaum Foundation.

**References:** [1] Fleming et al. (2021), *J Neural Eng* 18(4); [2] Huang, S. et al. (2012), *J Neuro Eng Rehabil* 9(55); [3] Alcaide-Aguirre et al (2013), *J Rehabil Research and Dev* 50(5); [4] Rubin et al (2024) J. *Neural Eng.* 21(1).

# EXPLORING NONLINEAR MUSCLE NETWORKS DURING YOGA POSTURES AND FUNCTIONAL TASKS

*Gaurav Seth[1,a], Soniya Kadam[1,a], Rory O'Keeffe[a], S. Farokh Atashzar, Smita Rao[1]
[1]NYU Steinhardt School of Culture, Education, and Human Development, New York
[a] Contribute equally to this study
*Corresponding author's email: gs3823@nyu.edu

**Introduction:** Surface electromyography (sEMG) and muscle network analysis provide valuable insights into neuromuscular coordination. In previous studies, we quantified nonlinear muscle network metrics such as degree, weighted clustering coefficient (WCC), and global efficiency (GE), established their reliability during activities of daily living (ADL) tasks, and their sensitivity to motor impairments and fatigue [1,2]. Investigation into network metrics and their reliability across a broader range of tasks, particularly those used in integrative medicine such as yoga, are lacking. Expanding reliability analysis across a broader range of static and dynamic tasks is essential for evaluating the consistency of these metrics and their potential applications in rehabilitation and performance training. Beyond reliability, understanding task-dependent variations in muscle network metrics is crucial. This study examines both trial-by-trial reliability and the effect of task on muscle network metrics across functional tasks and yoga postures.

**Methods:** Fifteen asymptomatic adults (6 females, 9 males; 23.52 ± 2.31 years; BMI: 25.98 ± 4.41 kg/m²) participated. sEMG data were recorded bilaterally from gluteus medius, gluteus maximus, rectus femoris, vastus lateralis, vastus medialis, semitendinosus, biceps femoris, and gastrocnemius during five yoga postures (Chair, One-Leg Balance, Warrior I, Warrior II, Prayer Squat) and four functional tasks (walking, sit-to-stand, step-up, step-down). Motion capture and force plate data segmented epochs, isolating the static hold in yoga, stance phase in walking, and sit-to-stand into separate phases. Nonlinear muscle network metrics (mean degree, mean WCC, and GE) were computed based on O'Keeffe et al. (2023) [3]. Figure 1A shows a representative muscle network. A Friedman test assessed task effects, with Wilcoxon signed-rank tests (Bonferroni $\alpha = 0.05/9$) for post hoc comparisons with walking as a referent condition. Kendall's W measured post hoc effect size [4]. ICC(3,*k*) was computed using a two-way mixed model with absolute agreement [5].

**Table 1:** ICC(3,*k*) values for mean degree, mean WCC, and GE across tasks. Higher values indicate stronger trial-by-trial reliability.

| Tasks | Degree | WCC | GE |
|---|---|---|---|
| Prayer pose | 0.861 | 0.934 | 0.879 |
| Chair pose | 0.918 | 0.927 | 0.922 |
| Warrior 1 | 0.879 | 0.95 | 0.877 |
| Warrior 2 | 0.802 | 0.915 | 0.793 |
| One-Leg Balance | 0 | 0.551 | 0 |
| Sit to Stand | 0.735 | 0.662 | 0.728 |
| Walk | 0.953 | 0.906 | 0.949 |
| Step-down | 0.886 | 0.631 | 0.892 |
| Step-up | 0.907 | 0.633 | 0.925 |
| Stand to Sit | 0.853 | 0.821 | 0.851 |

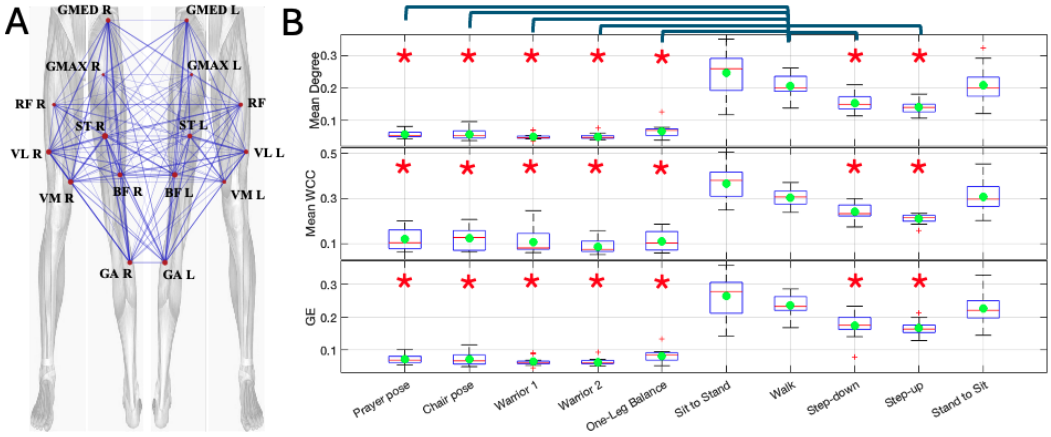


**Figure 1:** (A) Representative Muscle network (n=1, walking) where line width represents the Spearman power correlation between nodes, and circle size reflects the node's degree. (B) Box plots of network metrics across different tasks. Significant between-tasks comparisons are indicated with *

**Results & Discussion:** Trial-by-trial reliability is presented in Table 1. Based on ICC classification (0–0.4 = poor, 0.4–0.75 = moderate, >0.75 = good) [5,6,7], mean degree showed good reliability in 8/10 tasks, moderate in 1, and poor in 1. Mean WCC had good reliability in 6/10 tasks and moderate in 4/10. GE was good in 8/10 tasks, moderate in 1, and poor in 1. Walking demonstrated the highest reliability across all metrics, while yoga postures largely exhibited good reliability, supporting their use in neuromuscular studies. A significant task effect was found for mean degree, mean WCC, and GE ($p < .001$). Post hoc results (Figure 1B) indicate that all yoga postures, step-up, and step-down significantly differed from walking ($p < .005$). Yoga postures exhibited lower mean degree, mean WCC, and GE values, indicating reduced intermuscular connectivity requirements compared to functional tasks. Kendall's W was 1 for mean degree, mean WCC, and GE across all yoga postures, confirming a strong task effect. These findings suggest that yoga postures engage fewer muscle connections, whereas functional tasks, particularly walking and Sit-to-Stand, require greater neuromuscular coordination.

**Significance:** Trial-by-trial reliability and task effects offer insights into neuromuscular coordination in walking, ADLs, and yoga poses. Most tasks demonstrated good reliability, supporting their relevance for motor function assessment. Yoga poses required less muscle connectivity than functional tasks, highlighting their potential as controlled rehabilitation exercises.

**Acknowledgements:** SR was supported by NIH NIGMS R25GM154372, NIAMS R01AR079182, NCATS UL1TR001445 and the Georgeny High Priority Award from the Foundation for Physical Therapy Research.

**References:** [1] O'Keeffe et al. (2022), Sci Rep 12(1); [2] O'Keeffe et al. (2023), IEEE J Biomed Health Inform 27(4); [3] O'Keeffe et al. (2023), IEEE Trans Neural Syst Rehabil Eng 31; [4] Tomczak & Tomczak (2014), Effect Size Overview; [5] Portney & Watkins (2009), Foundations of Clinical Research, Ch. 26; [6] Khoddami et al. (2017), J Voice 31(3); [7] Fleiss (2011), Wiley & Sons.

# Sex-Based Differences in Glenohumeral Joint Function in Individuals with a Symptomatic Isolated Supraspinatus Tear after a 12-Week Personalized Exercise Therapy to 5 Years

Lidya Canturk[1], Luke T. Mattar[3], Jumpei Inoue[3] Adam J. Popchak[2,3], William J. Anderst[3,1], Volker Musahl[3,1], James J. Irrgang[2,3], Richard E. Debski[1,3]

[1]Departments of Bioengineering, [2]Physical Therapy, [3]Orthopaedic Surgery,
University of Pittsburgh, Pittsburgh, PA, USA
Email of Corresponding Author: lic232@pitt.edu

**Introduction:** Exercise therapy has shown favorable outcomes in in vivo glenohumeral kinematics and arthrokinematics, including increased glenohumeral internal rotation and decreased contact path length, immediately following therapy for the treatment of rotator cuff tears in males and females[1,2]. Healthy females are reported to have greater glenohumeral elevation and internal rotation than males when reaching behind the back[3]. Determining if sex-based differences in glenohumeral joint function are present in individuals with symptomatic rotator cuff tears are important for better personalized treatment outcomes. The objective of this study was to determine if there are sex-based differences in in vivo glenohumeral kinematics and arthrokinematics at baseline, immediately- and five-year after a personalized exercise therapy program for individuals with symptomatic isolated supraspinatus tendon tear.

**Methods:** 27 females (60.3 ±6.7 years) and 31 males (58.5 ±10.2 years) provided IRB-approved written informed consent before the completion of any research procedure. All the individuals participated in a prospective longitudinal observational study who underwent a 12-week personalized exercise therapy program for the treatment of a symptomatic isolated supraspinatus tear[2,4]. Using a previously validated model-based tracking method (accuracy of ± 0.4 mm and ± 0.5°)[5], glenohumeral subchondral bone kinematics and arthrokinematics were quantified while subjects sat on a chair and reached behind their back[2] at baseline, immediately-after (12-weeks), and 5-year after exercise therapy. To primarily focus on the internal rotation of humerus while reaching behind the back, we analyzed the second portion of the motion, where the subjects' arm crossed the midline of their torso and then stopped on their backs. The outcome parameters were maximum internal rotation and contact path length. The maximum internal rotation is calculated as the change in internal rotation during the motion, where the starting frame is normalized to 0 internal rotation. For each data frame, a 3D distance map was calculated between the humeral head and glenoid surfaces. Contact path length was determined as the total distance the contact center traveled on the glenoid while reaching behind the back[6]. Due to differences in bony morphology, contact path length was normalized to the width and height of the glenoid of each subject. The KS test was used to assess normality, and a 2-way ANOVA was used to determine differences between time points and sexes for the outcome parameters. Log-transformation (base-10) was applied to contact path length, as it was non-parametric. Significance was set to $p<0.05$ for all analyses.

**Results & Discussion:** For maximum internal rotation, the effect of time was significant ($p=0.029$), however, the effect of sex and the sex and time interaction were not significant ($p>0.05$). Specifically, females had increased maximum internal rotation immediately after exercise therapy (12 weeks) compared to baseline ($p=0.011$) (Fig 1). Higher maximum internal rotation in females was also reported in a healthy cohort[3]. This could indicate that females improved joint function more than males immediately-after exercise therapy but did not maintain it at 5-years. For contact path length, the effect of sex was significant ($p<0.001$), however, the effect of time and the sex and time interaction were not significant ($p>0.05$). Females had smaller contact path length than males at baseline ($p=0.008$), immediately-after ($p=0.011$), and 5-years ($p=0.021$) after a personalized 12-week exercise therapy program (Fig 1). A smaller contact path length indicates that the intact rotator cuff muscles may better control displacement of the humeral head on the glenoid. Therefore, females might have better joint function and muscle control than males before and after exercise therapy when reaching behind the back. The onset and size of the supraspinatus tear in this cohort might account for the reported sex-based differences. Additionally, subjects may utilize different strategies to reach behind their backs, which may affect contact path length. Future directions for this study are to investigate tear onset and size and to compare our findings to a healthy control group to assess if these sex-based differences in arthrokinematics are consistent within a healthy cohort.

**Significance:** Females with symptomatic isolated supraspinatus tears have better glenohumeral joint function compared to males when reaching behind the back.

**Acknowledgments:**
Support from the National Institutes of Health grant 5R01AR069503 is gratefully acknowledged.

**References:** 1) Baumer et al. *Orthop J Sports Med* 2016 2) Mattar LT et al. *J Clin Biomech* 2024 3) Kolz et al. *J. Biomech* 2022 4) Mattar LT et al. *J Biomech* 2023 5) Bey MJ et al. *J Biomech Eng*. 2006 6) Bey et al. *EUROSIP J Adv Signal Process* 2010

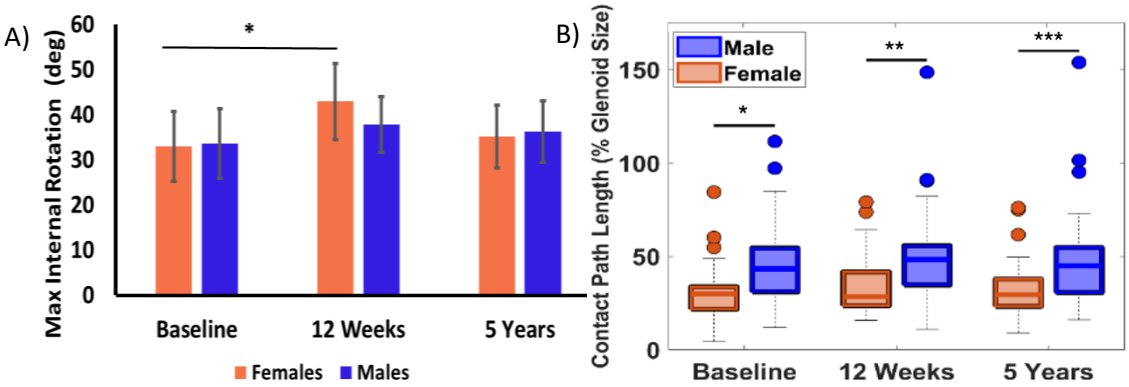


Figure 1: A) Maximum internal rotation and B) contact path length recorded at baseline and immediately- (12 weeks), and long-after and (5 years) personalized exercise therapy. (*Box midline → median, box → 25-75th percentile of data, whiskers → 0-100 percentile, and circles represent outliers)*

# KNEE MUSCLE COACTIVATION DURING YOGA AND ACTIVITIES OF DAILY LIVING

*Soniya Kadam, Rory O'Keeffe, Riva Karia, S. Farokh Atashzar, Smita Rao
[1]Department of Physical Therapy, NYU Steinhardt School of Culture, Education, and Human Development
*Corresponding author's email: sk9984@nyu.edu

**Introduction:** Muscle coactivation between the quadriceps and hamstrings plays a crucial role in joint stability, neuromuscular control, and injury prevention, particularly during functional movements.[1] While Activities of Daily Living (ADLs) require dynamic coordination between these muscle groups, yoga postures introduce unique biomechanical demands that may alter coactivation patterns. Understanding how knee muscle coactivation differs between ADLs and yoga can provide insights into rehabilitation, injury prevention, and performance optimization. This study aims to analyze quadriceps-hamstrings coactivation during key ADLs and yoga poses using surface electromyographic (sEMG) assessments. We hypothesize that muscle coactivation will be higher in yoga poses as compared to ADLs.

**Methods:** Fifteen adults (ages 18-50 years and BMI 18.5-35 kg/m²) performed nine tasks including ADLs [Walking, Sit-to-Stand (STS), Step Up (SU), Step Down (SD)[4] ] and yoga poses like Chair, One-Leg Balance (OLB), Warrior I, Warrior II, Prayer Squat.[5,6] Kinematic data were captured synchronized with two force plates. sEMG signals from the Rectus Femoris (RF), Vastus Medialis (VM), Medial Hamstrings (MH), and Lateral Hamstrings (LH) of the dominant leg were recorded at 2040 Hz (Trigno Avanti, Delsys, MA), band-pass filtered (20-400 Hz), and smoothed with a 150-ms window (Visual 3D, HAS Motion, Canada) software. Maximum voluntary isometric contractions (MIVCs) of the quadriceps and hamstrings on the dominant leg were recorded using a dynamometer (Biodex Medical Systems, Inc., Shirley, NY, USA). For walking and ADLs, muscle activation over a minimum of three trials was normalized over the stance phase. For yoga poses, muscle activation during a static 3-second hold was evaluated. Additionally, the duration of each task was measured in seconds from initiation of task to end. Co-contraction index (CCI) was the chief dependent variable.[5] Muscle co-activation was computed by first normalizing the RMS amplitude to MVIC. Then the normalized data was used, where for each sample $i$, $\text{lowerEMG}_i$ and $\text{higherEMG}_i$ represent the lower and higher RMS amplitudes, respectively, and dividing by 100 averages the ratio across the normalized interval.[5] The effect of the task was assessed with a linear regression model, Bonferroni adjusted pairwise comparisons were used to assess statistical significance between walking and other tasks. A Generalized Linear Model (GLM) was conducted to assess the effect of Time and Tasks on CCI. Model fit indices confirmed appropriate model specification (Deviance/df =0.042, AIC = -31.696)

**Results:** A linear regression model shows the statistically significant effect of tasks on CCI, after adjusting for time as a covariate ($F=59.559$, $p<0.001$). Bonferroni adjusted post-hoc comparisons indicate that CCI during walking is lower than Step Up.

***Table 1: Mean±SD of CCI during ADLs and Yoga * indicates statistically significant pairwise comparison***

| Sr.No. | Tasks | Mean±SD of CCI |
|---|---|---|
| 1 | Walk | 0.60±0.46 |
| 2 | Step Up | 0.99±0.26 * |
| 3 | Step Down | 0.65±0.23 |
| 4 | STS (Concentric) | 0.25±0.21 |
| 5 | STS (Eccentric) | 0.16±0.06 |
| 6 | Chair | 0.17±0.11 |
| 7 | OLB | 0.29±0.32 |
| 8 | Prayer | 0.17±0.09 |
| 9 | Warrior-I | 0.19±0.12 |
| 10 | Warrior-II | 0.19±0.12 |

**Discussion:** We evaluated CCI (Quadriceps: Hamstrings) during ADLs and Yoga. The findings indicate that muscle co-activation varies across functional tasks, with higher co-activation observed during biomechanically demanding activities such as Step-Up (Table.1). Our results align with those of Smith et. al. (2019), who observed that muscle co-activation peaked during stair ascent, suggesting that this increased co-activation in stair negotiation may serve as a strategy to enhance joint stability.[5] Our findings revealed that the CCI ranged from 0.17 to 0.29 during yoga poses, which is consistent with muscle coactivation values reported for yoga poses which involves squats and lunges by Longpre et. al. (2015).[6]

**Significance:** These findings highlight the task and time-dependent modulation of muscle co-activation, with implications for rehabilitation strategies aimed at optimizing neuromuscular control and reducing excessive joint loading in individuals with knee osteoarthritis or other musculoskeletal conditions.

**Acknowledgement:** SR was supported by NIH NIGMS R25GM154372, NIAMS R01AR079182, NCATS UL1TR001445 and the Georgeny High Priority Award from the Foundation for Physical Therapy Research.

**References:**[1] Davidson et.al. *J of Electromyography and Kinesology*. 2013;23(6), [2] Kelley et.al. *J. Bodywork and Movement Therapies*,2018;23(2), [3] Liu et.al. *Int. J. of Environ and Public health*, 2021,18(6), [4] Marshall et al. *Experimental gerontology*;2020;136, [5] Smith et. al. *Arthritis Care & Research*, 2019, 71(5), [6] Longpre et al. *Clinical Biomechanics*, 2015;30(8).

# Energy Absorption Analysis Reveals Persistent Knee Deficits Underestimated by Isokinetic Testing during Return-to-Sport Following ACL Reconstruction

Andrew Parker, MD[1], Samuel Imbus, PT, DPT, SCS[1]; Lin Wei, MS, PhD[1]
[1]Texas Health Sports Medicine Allen, 1110 Raintree Cir, Allen, TX, 75013, USA
Email: LinWei@texashealth.org

**Introduction:** Restoration of symmetrical quadriceps strength and functional performance is critical for reducing re-injury rate when returning athletes to sport after anterior cruciate ligament (ACL) reconstruction surgery [1,2,3]. Traditional assessments, such as isokinetic testing of knee extension strength, are often used to measure limb strength symmetry. However, these conventional measures may not fully capture dynamic functional deficits, particularly those related to the ability of the lower limb joints to absorb impact forces during athletic activities [4]. Previous studies have introduced the concept of energy absorption contribution (EAC) as a means to evaluate how athletes utilize their hip, knee, and ankle joints to dissipate forces [5]. This approach provides insight into joint-specific loading strategies that conventional isokinetic tests might overlook. In fact, recent research indicates that individuals post-ACL reconstruction can exhibit significantly lower knee EAC compared to healthy controls, suggesting altered joint loading strategies despite near-normal isokinetic performance [6]. The purpose of this study was to evaluate the relationship between isokinetic knee extension limb symmetry values, and EAC symmetry measurements obtained during a double limb squat (DLS), single limb squat (SLS), double limb jump-landing (JL) and single limb forward hop (HOP).

**Methods:** All individuals underwent ACL reconstruction surgery and were tested at time of return to sport. Participants were considered eligible for this study if they were between the ages of 13 and 25 years and participated in a level 1 (e.g. basketball, football or soccer) or level 2 sport (e.g. softball, baseball). Participants were excluded if they had chondral defects (≥1 cm²), grade II or III injury of the medial collateral ligament, lateral collateral ligament, posterior collateral ligament injuries, and simultaneous fracture with ACL tear. Participants met criteria performed during isokinetic knee testing at 60°/s. EAC was calculated during the descent phase of all tasks by integrating the negative portion of the net power. The EAC percentage for each joint was expressed as a percentage of the total energy absorption across the hip, knee, and ankle. The knee EAC deficit was calculated by determining the difference between the uninvolved and involved limb's values and then expressing it as a percentage of the uninvolved limb's value. Similarly, the isokinetic deficit was derived by subtracting the involved limb's peak knee extension torque from that of the uninvolved limb and expressing the result relative to the uninvolved limb's torque.

**Results and Discussion:** Thirty-four participants were included in the correlation analysis. Results revealed a medium but statistically significant association between the isokinetic knee extension deficit and the knee EAC during the HOP task (Pearson's $r = 0.33$, $p = 0.06$), whereas no significant correlation was observed during the DLS (Pearson's $r = 0.12$, $p = 0.49$), SLS (Pearson's $r = 0.11$, $p = 0.54$), and JL (Pearson's $r = 0.09$, $p = 0.61$). These findings suggest that isokinetic testing results may be more predictive of performance on the HOP task compared to the other tasks.

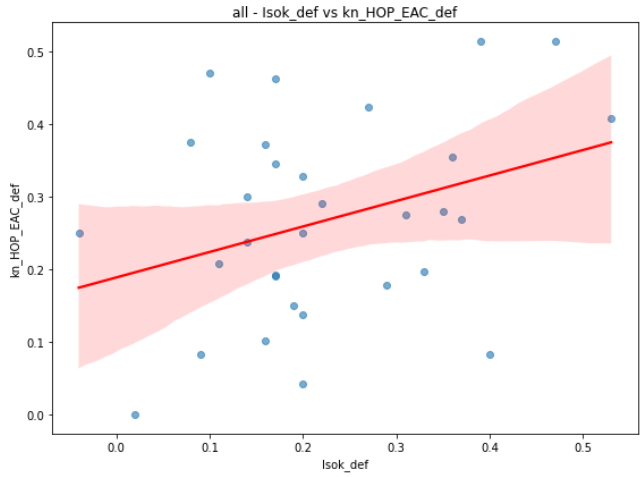


**Figure 1:** correlation between the isokinetic knee extension torque deficit (Deficit_Isok, x-axis) and the knee EAC deficit during the HOP (Deficit_EAC_HOP, y-axis). The medium and statistically significant positive correlation (Pearson's $r = 0.33$, $p = 0.06$, $n = 34$) suggests that as the isokinetic deficit increases, the deficit in knee EAC also tends to increase. The red line indicates the linear regression trend, and the shaded area represents the 95% confidence interval.

**Significance:** This study emphasizes the value of incorporating dynamic functional assessments into return-to-sport protocols following ACL reconstruction. While traditional isokinetic testing provides important information on quadriceps strength symmetry, our findings indicate that it may not fully capture dynamic deficits in energy absorption. In particular, the moderate association observed between isokinetic deficits and energy absorption during the HOP task suggests that such dynamic measures may offer additional insight into functional performance. These results support the use of tasks like the HOP, alongside conventional assessments, to better identify residual deficits and tailor rehabilitation strategies, ultimately helping to reduce re-injury risk.

**References** [1] Shi H et al. (2024) *Sports Health*. [2] Grindem H et al. *Br J Sports Med.* [3] Kyritsis et al. *Br J Sports Med.* [4] Wellsandt et al. *J Orthop Sports Phys Ther*. [5] Malafronte J et al. (2021) *Physical Therapy in Sport* [6] Kovacs T et al. (2022) *Journal of Sport Rehabilitation*.

# THE ROLE OF NEUROMUSCULAR CONTROL AND ELECTROMYOGRAPHIC PROPERTIES IN MAXIMUM VOLUNTARY CONTRACTION OF THE MUSCLE AFTER BRACHIAL PLEXUS INJURY

Sandesh G. Bhat, PhD[1], Zheng Wang, PhD[1], Alexander Y. Shin, MD[1], Richard L. Lieber, PhD[2], Kenton R. Kaufman, PhD, PE[1]*
[1]Department of Orthopedic Surgery, Mayo Clinic, Rochester, MN; [2]Shirley Ryan AbilityLab, Chicago, IL
*Corresponding author's email: Kaufman.Kenton@mayo.edu

**Introduction:** The path to recovery from a brachial plexus injury (BPI) poses significant challenges, that may involve intricate surgeries. In the most severe cases, a gracilis free functioning muscle transfer surgery (FFMT) is required to restore elbow flexion [1]. The FFMT utilizes a donor nerve to reinnervate the muscle. Previous studies performed on the physiological characteristics of the gracilis muscle [2, 3], and gracilis-powered elbow flexion [4, 5] revealed a large difference between the muscle's predicted maximum force ($F_{max}$) and the actual maximum force generated by the patient during voluntary contractions ($F_{MVC}$). The reason for such a large difference is unknown. Clinically, it is recognized that the recovery of $F_{MVC}$ is patient specific, with no relation to time post-surgery. As per our previous study, the neuromuscular control in the reconstructed elbow flexor is diminished compared to a healthy elbow flexor [4]. The electromyographic characteristics are also expected to differ by the amount of recovery in the participant's elbow flexor. Hence, the goal of the current study was to explore potential causes for the difference between $F_{max}$ and $F_{MVC}$. We hypothesized that the difference between these two measured forces could be explained by a decrease in neuromuscular control and the electromyographic properties.

**Methods**: Data were collected from 7 participants (age: 34 ± 12 years (±SD); BMI: 27.6 ± 7.7 kg.m$^{-2}$) under guidelines set by Mayo Clinic's IRB. All participants sustained a BPI prior to the study and were treated with FFMT to restore elbow flexion. The gracilis was reinnervated using the spinal accessory nerve. Physiological assessment of the gracilis muscle was performed during FFMT surgery [2, 3]. The predicted maximum muscle force $F_{max} = (F_{L-T} + F_P) * PCSA * \sigma$ was calculated from the $F_{L\text{-}T}$ = normalized muscle active length-tension relationship, $F_P$ = normalized muscle passive tension relationship, PCSA = physiological cross-sectional area of the transferred gracilis muscle, and σ = specific tension of the gracilis muscle [6]. Isometric elbow flexion torque ($\tau$) along with surface electromyography (sEMG) during a maximum voluntary contraction (MVC) was collected from the participant's affected arm at an average 23 ± 10 months post-surgery. After FFMT, the transferred gracilis was the only muscle creating elbow torque. The amount of force generated by the gracilis during MVC was calculated as $F_{MVC} = \frac{\tau}{l}$, where $l$ was the moment arm for the distal attachment of the gracilis during the FFMT and $\tau$ were measured elbow torque [7]. Measures of neuromuscular control (contraction latency ($t_{latency}$) and hold time ($t_{hold}$)) were collected [4]. Low $t_{latency}$ and high $t_{hold}$ correspond with good neuromuscular control [4]. Mean power frequency (MPF) was determined from the sEMG collected during the MVC. The value for $\Delta F$ was calculated as $\Delta F = F_{max} - F_{MVC}$. which describes the difference between the gracilis muscle's predicted maximum force and amount of actual force generated during an MVC. A multiple linear regression model was used to study the relationship between $\Delta F$ and MPF, $t_{latency}$, and $t_{hold}$. The interaction between $t_{latency}$ and $t_{hold}$ ($t_{latency} * t_{hold}$) was also considered as a variable.

**Results & Discussion**: $\Delta F$ increased significantly with a decrease in $t_{latency}$ (p = 0.028, Fig 1 (a)), $t_{hold}$ (p = 0.032, Fig 1 (b)), and MPF (p = 0.029, Fig 1 (c)) (overall model adjusted $R^2$ = 0.89; p = 0.07). The $t_{latency} * t_{hold}$ variable was not significantly related to $\Delta F$ (p = 0.516). The study's observations show that the participants with a higher MPF (higher proportion of type II fibers) and higher $t_{hold}$ (better neuromuscular control) were able to produce $F_{MVC}$ closer to their predicted maximum. In human muscles, a high MPF is associated with an increased proportion of type II fibers in the muscle [8]. Animal model studies have shown that in a donor reinnervated muscle, type II fibers are the first to be innervated [9]. To our knowledge, such a study has not been performed in humans. Neuromuscular control's effect on $\Delta F$ is also not completely understood. The role of neuromuscular control, MPF, and muscle fiber reinnervation on voluntary force generation in the gracilis muscle following a FFMT should be explored further.

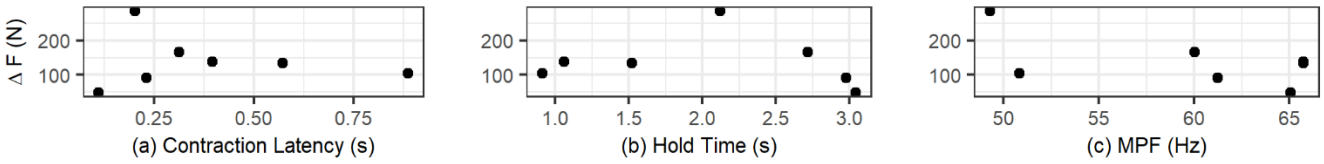


Figure 1. Linear negative relationship between $\Delta F$ and (a) contraction latency, (b) hold time, and (c) mean power frequency (MPF).

**Significance:** This pilot study demonstrates that neuromuscular control as well the physiological property of a muscle contribute to the discrepancy between its predicted and voluntary maximum force. Further research on these factors could inform surgical and rehabilitation strategies to restore neuromuscular control may improve functional strength in the reconstructed muscle.

**Acknowledgement**: The study was supported by the U.S. Department of Veterans Affairs (RX-002462-01-A1)

**References**: [1] Noland et al. (2019), JAAOS (27:19). [2] Persad et al. (2022), Sci Reports (12:1). [3] Persad et al. (2021), J Exp Bio (224-17). [4] Bhat et al. (2023), Clin Biomech (104). [5] Bhat et al. (2023), J Ortho Research (41:9). [6] Binder-Markey et al. (2023), J Physiol (601:10). [7] Persad et al. (2023), J Hand Surgery. [8] Gerdle et al. (1991), Acta Physiol Scandinavica (142:2). [9] Dum et al. (1985), J Neurophsiol (54:4).

# ELETROMYOGRAPHIC ANALYSES OF SHOULDERS POST- LATARJET PROCEDURE

*Renato Miyadahira[1,2], Joao Bonadiman [2], Vitor La Banca, Talissa Generoso[1], Felipe Gonzalez[1,2], Matheus Vilela [1,2], Grant Garrigues[1], Greg Nicholson[1], Jonathan Gustafson[1]
[1]Rush University Medical Center, Chicago, IL. USA
[2]Instituto Brasil de Tecnologia da Saúde – IBTS, Brazil
*Corresponding author's email: renato_miyadahira@rush.edu

**Introduction:** The Latarjet procedure is a common surgery for treating shoulder instability, but can lead to complications with reported rates ranging from 15% to 30%[1]. While most complications are associated with the technical aspects of the procedure and its non-anatomical modifications, such as fractures, infections, or implant loosening, the Latarjet procedure tends to induce scapular dyskinesis—maltracking of the scapula relative to the humerus[1,2]. One approach to evaluating scapular dyskinesis is the use of electromyography (EMG) to assess the complex interactions of shoulder muscle activation[3,4] The objective of this study was to assess the role of the external rotator muscles—infraspinatus and teres minor—as well as the posterior deltoid muscle in Latejet patients as compared to healthy individuals to overhead movement tasks. We hypothesized that Latarjet surgery would alter muscle activation during overhead movement tasks as compared to healthy controls.

**Methods:** Twenty adults (15 male vs 5 female) were invited to our cross-sectional study. We recruited ten patients who were at least 6 months post-op following a Latarjet procedure and ten healthy control participants. We measured muscle activation using electromyography (EMG, Noraxon U.S.A, Inc, AZ) from the infraspinatus, teres minor and posterior deltoid muscles. Electrode placement followed SENIAM guidelines and data were collected at 1500 hz[4].

Muscle activation was evaluated during the following functional tasks: bilateral shoulder arm elevation in the scapular plane (scaption) and external rotation with the shoulder at 90° abduction under weighted (3lb (1.4kg) dumbbells) and unweighted conditions. A metronome (2 second intervals) was used to control the rhythm up to 8 repetitions of upward and downward motions for each task. EMG data were processed using standard bandpass filters and RMS (100ms window) processing techniques. All EMG data were normalized to maximal activation throughout the entire visit. Normalized mean and maximal EMG activation were calculated for each subject across the tasks and a Mann-Whitney Test was performed to assess differences between the Latarjet and Control groups ($p<0,05$).

**Results & Discussion:** No statistical differences were found between the control group and the Latarjet group ($p < 0.05$) in terms of mean and maximum activation values during rotation movements, even in weighted testing. However, during scaption, a significa nt difference in infraspinatus activation was observed in the ascending phase (non-weighted: $p = 0.0058$; weighted: $p = 0.0266$) as well as in the descending phase (non-weighted: $p = 0.0311$; weighted: $p = 0.0087$) (Table 1). These findings are supported by a study conducted by Degot et al.[5], who confirmed the absence of abnormal scapular movements and scapulothoracic kinematics following the Latarjet procedure. Similarly, Sella et al.[3] reported no scapular dyskinesis, albeit with some alterations in the ascending and descending phases of scaption, while Ernstbrunner et al.[2] found hypertrophy of the subscapularis muscle without an increase in fatty infiltration. In our study, we evaluated the role of the external rotators; however, it is possible that other muscle groups could be coordinating in a different patter following Latarjet, and future work should conduct a comprehensive evaluation of the synergy-related changes in activations across the shoulder.

Table 1: Comparison in weighted tests

| Comparison | Mean | | | | | | Max | | | | | |
|---|---|---|---|---|---|---|---|---|---|---|---|---|
| | Post Delt | p | Infraspinat | p | Teres minc | p | Post Delt | p | Infraspinat | p | Teres minc | p |
| Rotation | -0.00446 | 1 | 0.07697 | 0.1824 | -0.00484 | 0.8589 | 0.2003 | 0.1309 | 0.1412 | 0.1113 | -0.0031 | 0.9674 |
| Scaption Ascending | 0.00905 | 0.8383 | 0.10422 | 0.0266 | 0.05927 | 0.1088 | 0.07355 | 0.6965 | 0.16548 | 0.1728 | 0.1473 | 0.237 |
| Scaption Descending | 0.0187 | 0.8241 | 0.128 | 0.0087 | 0.0675 | 0.0367 | 0.0693 | 0.7618 | 0.268 | **0.0434** | 0.179 | 0.0676 |

Post Delt: Posterior Deltoid Muscle

**Significance:** The Latarjet does not induce altered muscle activations in the shoulder. Other reasons for scapular dyskinesis in patients following Latarjet may be attributed to other components and should be investigated in the future.

**Acknowledgments:** This project was founded by Instituto Brasil de Tecnologia da Saúde e Lemann Foundation.

**References:** [1] Lavaill M.et al.(2023), J Biomech 155(6)111639; [2] Ernstbrunner L et al. (2019), Am J Sports Med. 47(13):3057-3064; [3] Sella GDV et al. (2022) Acta Ortop Bras. 23;30(3):e245237 [4] Boettcher CE et al.(2008), Journal of orthopaedic research. 26(12):1591-1597; [5] Degot M et al. (2025), J Shoulder Elbow Surg.34(1):e22-e34.

**Failure properties of muscle-tendon units under passive tension at different strain rates**

Adrina Iachini[1], Benjamin Wheatley[1]
[1]Department of Mechanical Engineering, Bucknell University, Lewisburg, PA
*Corresponding author's email: b.wheatley@bucknell.edu

**Introduction:** While skeletal muscle tissue generates contractile force to move the skeletal system, the passive properties of muscle tissue play key roles in force transmission and proper muscle function *in vivo*. Many musculoskeletal diseases are closely tied to changes in passive muscle properties; therefore, passive properties are of great scientific and clinical importance [1]. However, there is a paucity of information on the passive properties of muscle tissue. For example, there lacks a clear understanding of failure properties of passive muscle tissue, despite the high prevalence of injuries that are associated with damage to a muscle-tendon unit. Material properties of biological soft tissues such as tensile stiffness and ultimate tensile strength are typically acquired via tensile testing. Thus, the goal of this work was to perform pull-to-failure tensile tests on passively stretched whole muscle-tendon units at different strain rates, and to determine A) the approximate location and method of material failure, and B) the difference in ultimate tensile strength and toughness between muscle-tendon units subject to fast and slow strain rates. These data can then be used to develop more accurate, 3D computational models of muscle tissue for predicting and preventing muscle injuries and impairments.

**Methods:** The extensor digitorum longus muscle-tendon unit from both limbs of fifteen (n=15) New Zealand or California rabbits were isolated via post-mortem dissection. No live animal handling was performed by any the researchers involved in this study. Samples were loaded into a custom planar biaxial materials testing system (ADMET, Inc.) for tensile testing. First, a stress relaxation protocol was employed where samples are stretched 10% $sec^{-1}$ to 10% engineering strain and held under stress relaxation for 100 seconds. Then, samples were pulled to failure (Figure 1A) at one of two strain rates – either 10% $sec^{-1}$ or 0.1% $sec^{-1}$. Tissue strain during stress relaxation testing was measured using 2D digital image correlation with a graphite speckle pattern (Correlated Solutions, Inc.) and using engineering strain during pull to failure testing. A tangent modulus was fit to stress-strain data during initial loading and a power law relaxation equation was fit to stress-time data during stress relaxation. Ultimate tensile strength and toughness were calculated from pull-to-failure stress-strain curves as the maximum and area under the curve, respectively.

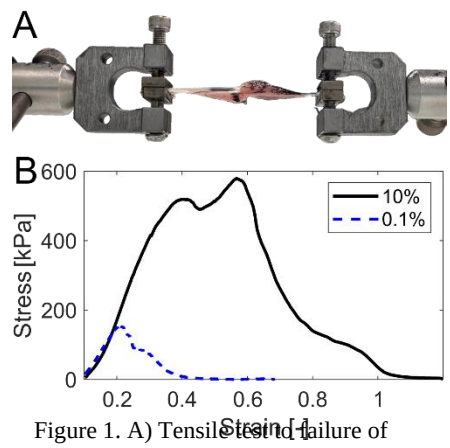


Figure 1. A) Tensile test to failure of whole muscle-tendon unit. B) Representative stress-strain plots for pull-to-failure tests between fast (black curve) and slow (dashed blue curve) samples from the left and right EDL muscles of the same animal.

**Results & Discussion:** Muscle tendon unit samples failed in the mid-substance (muscle tissue region), and not in the tendinous or aponeurotic regions (Figure 1A). These qualitative data provide important insight into muscle-tendon unit failure mechanisms and locations, as tendon ruptures, myotendinous damage, and aponeurosis damage can occur *in vivo*. The average tangent modulus (2.84 MPa, Table 1) is higher than many other studies of muscle tissue alone (~0.1 – 0.5 MPa), which is likely due to the contributions of the tendon and aponeurosis in the samples tested here [3]. When comparing the failure properties between strain rates, the faster strain rate (10% $sec^{-1}$) was found to exhibit a higher ultimate tensile strength ($p = 0.0036$) and a higher toughness ($p<0.001$) (Figure 1B, Table 1). These results contract our original hypothesis, and suggest that fast versus slow strain rates enact differences in microstructural deformations that could lead to differences in failure properties. Further microstructural studies are needed, however. Future work to develop damage models of muscle, aponeurosis, and tendon tissues could help to predict and prevent musculoskeletal injuries, and the data presented here could be used for model calibration and validation.

**Table 1.** Mean and standard deviation values for the tangent modulus, relaxation rate, ultimate tensile strength, and toughness of extensor digitorum longus muscles subject to tensile testing. P-values are provided for statistical evaluation of the significance of differences between strain rate during pull-to-failure tests.

| | **Tangent Modulus [MPa]** | **Relaxation Rate [$sec^{-1}$]** | **Ultimate Tensile Strength [MPa]** | **Toughness [kPa-mm/mm]** |
|---|---|---|---|---|
| **Fast – 10% $sec^{1}$** | 2.84 (3.26) | -4.55 (1.39) | 0.676 (0.171) | 0.350 (0.110) |
| **Slow – 0.1% $sec^{-1}$** | | | 0.385 (0.305) | 0.172 (0.136) |
| **p-value** | - | - | 0.0036* | < 0.001* |

**Significance:** The passive properties of muscle tissue can dictate proper muscle function *in vivo*. This study presents novel data on the failure properties of muscle-tendon units under different strain rates, which can be used to better understand muscle injuries and to develop more advanced computational models for injury prediction and prevention.

**Acknowledgments:** This work is supported by the National Science Foundation under Grants No. 2301653 and 1828082.

**References:** [1] Lieber. (2019), *J App Phys*; [2] Best. (1997), *Clin Sports Med* 16(3).; [3] Grega. (2020), *JMBBM* 110.

# BIOMECHANICS OF AN OPTIMIZED SPRINT START TESTING THREE DISTANCES FROM THE START LINE

M. Patton, Kurt M. DeGoede*
School of Engineering and Computer Science, Elizabethtown College
*Corresponding author's email: degoedek@etown.edu

**Introduction:** Sprinting in track and field requires extraordinary precision, where mere milliseconds can determine victories. This sensitivity to timing highlights the importance of optimizing every component of an athlete's technique, particularly in the setup and execution of the block start. Previous research has thoroughly explored numerous aspects of the block start, focusing on elements such as torso angle in the set position, the forces generated at different foot pedal angles, and the impact of varying block pedal angles [1]. Studies suggest that many athletes position their feet closer together than is optimal, potentially limiting their starting performance [1, 2, 3]. Findings indicate that the most effective block spacing occurs when the distance between an athlete's feet is approximately 45% of their leg length. However, most existing studies assume a standard two-foot distance between the front block pedal and the starting line, overlooking the potential effects of varying front block placements [1, 2]. This gap in the literature calls for a closer examination of how adjustments to the front block position influence the overall sprint start. Investigating these adjustments could provide insights that enhance starting performance, offering athletes and coaches actionable guidance on positioning the blocks for optimal results. It is hypothesized there is no statistically significant difference in the velocity of athletes when track starting blocks are set at 45%, 57.5%, and 70% of the athletes' leg length away from the starting line, with a consistent spacing of 45% of the leg length between the blocks. However, placing the blocks closer to the starting line results in a further second-step distance.

**Methods:** Eight participants (n=8) were recruited from the Elizabethtown College track team. Participants began by completing a 400-meter jog followed by a set of dynamic stretches over 20 meters to ensure proper warmup. Following this, each participant's leg length, height, and weight were recorded. They then completed six block starts in a randomized order, with the front block positioned at distances of 45%, 57.5%, and 70% of their leg length from the starting line. The spacing between the front and rear blocks was maintained at 45% of the participant's leg length, a setup identified as optimal in previous studies [1, 2]. Participants were given a six-minute rest period between each start to minimize fatigue. All starts were captured using OpenCap motion capture technology. Data from the starts were processed using OpenSim to generate inverse kinematics analyses. These reports were then analyzed in Python to identify significant differences in performance metrics. The primary metrics evaluated were Normalized Velocity (V at second foot strike / (100m / 100m PR time)), Normalized Distance (distance from start line to second foot strike / leg length), and Normalized Time (time to second foot strike / 100m PR time) [3]. Statistical analyses were conducted to determine significant differences in performance outcomes between block setups.

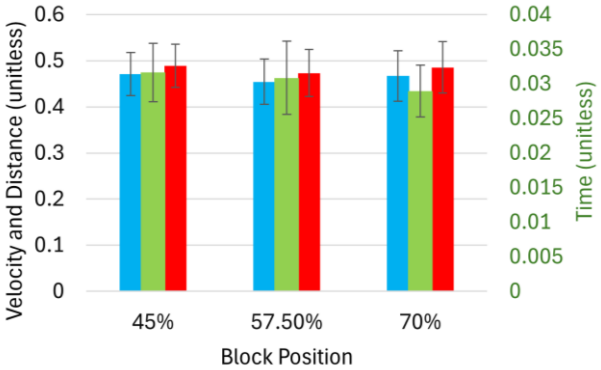


**Figure 1**: The x-axis represents three different block positions 45%, 57.50%, and 70%. The left y-axis corresponds to Blue: Normalized Velocity, Red: Normalized Distance, and Green: Normalized Time.

**Results & Discussion:** Results indicate no statistically significant differences in maximum velocities between the tested block lengths based on a one-factor ANOVA (F-value: 0.208, $p = 0.814$), suggesting that adjusting block positioning forward or back does not have a significant effect on sprint start performance (Figure 1). This finding implies that athletes may not experience a measurable advantage solely from modifying block distance. While no statistical effects were found, delta time data showed a slight trend, with Group 3 (farthest back) exhibiting the shortest mean delta time (2.9% of 100m PR) compared to Group 1 (3.2% of 100m PR) and Group 2 (3.1% of 100m PR), a difference of as much as 0.03 seconds Though small, such variations could hold practical significance in high-level competition where reaction and transition efficiency are crucial. However, the lack of a clear effect across all measured metrics suggests that block positioning alone may not be a decisive factor in start performance. Additionally, a key limitation of this study is the absence of training adaptation, as differences could emerge if athletes were given time to practice and optimize their starts with a specific block setting.

**Significance:** These results suggest athletes should choose block positions based on comfort, as no setup showed a clear advantage. While the 75% distance group had slightly shorter delta times, this did not translate into significant differences in velocity or distance covered. Prior data supports maintaining 45% leg length between blocks, but athletes should place them comfortably from the line for optimal performance [1,2,3]. Given the lack of a clear benefit, familiarity may be more important than adherence to a specific position.

**Acknowledgments:** Elizabethtown College SCARP program

**References:** [1] Cavedon et al. (2019), PLoS ONE 14(3): e0213979; [2] Chen et al. (2016), J Mech Med Biol 16(7): 1650099; [3] Valamatos et al. (2022), Int J Environ Res Public Health 19(7): 4074.

# BETWEEN-JOINT COORDINATION STRATEGY DOES NOT CHANGE AFTER A TOTAL KNEE ARTHROPLASTY

*Kathryn S. Blessinger[1], Jennifer A. Perry[1], Reese A. Lloyd[1], Laura C. Schmitt[1], Ajit M.W. Chaudhari[1], Robert A. Siston[1]
[1]The Ohio State University, Columbus, OH
*Corresponding author's email: blessinger.1@osu.edu

**Introduction:** Individuals receiving a total knee arthroplasty (TKA) for treatment of severe knee osteoarthritis (KOA) often experience continued postoperative functional limitations and altered kinematics and kinetics during activities of daily living, like the sit-to-stand task [1,2]. Previous work has suggested that motor control strategy is associated with a range of postoperative outcomes after a TKA [3]. One way to characterize motor control is by investigating the relative coordination patterns between pairs of joints [4]. Investigating these joint coordination patterns will allow for a better understanding of how changes in motor control may influence changes in task performance following a TKA. However, it remains unclear whether between-joint coordination strategies change after a TKA and how coordination strategies demonstrated before and after a TKA differ from those demonstrated by healthy, older adults. We hypothesized that individuals with KOA would demonstrate differences in the joint coordination patterns used to perform a common daily task, compared to the same individuals after receiving a TKA and compared to healthy controls. Additionally, we hypothesized that after receiving a TKA, patients would still demonstrate differences in joint coordination patterns when compared to healthy controls.

**Methods:** Seven individuals with medial compartment KOA who were scheduled to undergo a primary posterior-stabilizing TKA, a subset of the data presented previously [3,5], along with 7 healthy, older adults that served as a control group (HC) were included in this retrospective analysis. Individuals undergoing a TKA were tested before and 6-months after surgery. Three-dimensional whole-body kinematics were captured while participants performed at least four chair rises. One representative chair rise was analyzed for each participant. OpenSim [6] was used to compute joint kinematics [7], and a vector coding technique was used to compute the sagittal plane coupling angles between two linked joints for the trunk and involved limb (or a randomly assigned limb for HC) joint angle pairings (hip-lumbar, knee-hip, and ankle-knee) during each sit-to-stand cycle [4]. Coupling angles were classified as in-phase-distal-dominant (IPDD), in-phase-proximal dominant (IPPD), anti-phase-distal-dominant (APDD), and anti-phase-proximal dominant (APPD) [4]. The percentage of time spent in each coordination pattern classification [4] was examined in the following comparisons: KOA-HC, TKA-HC, and KOA-TKA. Wilcoxon rank sum testing was used to compare the KOA/TKA timepoints to healthy controls (HC), and Wilcoxon signed rank testing was used to compare paired data (KOA-TKA), where all $\alpha = 0.05$ (with Bonferroni correction).

**Results & Discussion:** Following TKA, there were no statistically significant postoperative changes in the time spent in each coordination pattern classification during sit-to-stand (KOA-TKA comparison). However, the knee-hip coupling angle motion was dominated by the knee for a greater percentage of the sit-to-stand task at each timepoint (KOA and TKA), compared to HC (IPDD knee-hip, all $p \leq 0.0157$, Fig 1). While not statistically significant, at each timepoint (KOA and TKA), the ankle-knee coupling angle motion was also dominated by the knee for a greater percentage of the sit-to-stand task, compared to HC (IPPD ankle-knee, Fig 1). These results suggest that both before and after a TKA, individuals are spending more time moving their knee through the necessary range of motion during sit-to-stand, compared to HC.

**Significance:** A lack of postoperative change in motor control strategy following a TKA, as supported by our findings, may be a factor contributing to the continued functional limitations often observed following a TKA. Future work is warranted to further understand joint coordination strategies during functional tasks after TKA, in order to improve outcomes following TKA.

**Acknowledgments:** The authors thank Megan Hughes, Rachel Hall, Sarah Roelker, Elena Caruthers, Greg Freisinger, and Jacqueline Devine for assisting with data collection and our funding source: NIH R01AR056700.

**References:** [1] Sonoo et al. (2019), *J Biomech* 96; [2] Wang et al. (2019), *J Arthroplasty* 34(10); [3] Koehn et al. (2022), *PLOS ONE* 17(4); [4] Needham et al. (2020), *The Foot*; [5] Freisinger et al. (2017), *J Orthop Res* 35(8); [6] Delp et al. (2007), *IEEE Trans Biomed Eng* 54(11); [7] Blessinger et al. (2024) *Proc ORS.*

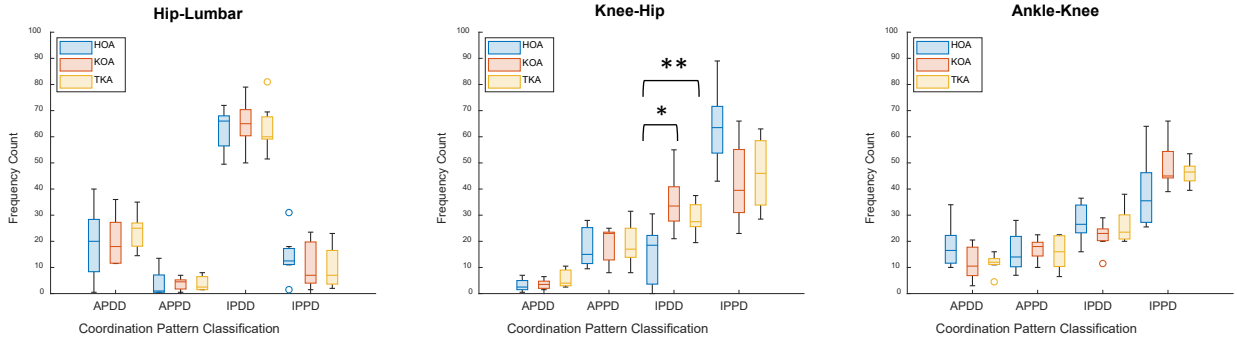


**Figure 1:** Coordination patterns during sit-to-stand demonstrated by individuals with KOA, the same individuals following a TKA, and by HC. *Significant difference between KOA and HC. **Significant difference between TKA and HC.

# FEEDBACK PARAMETERS FOR A CLOSED-LOOP MULTIPLE-INPUT MULTIPLE-OUTPUT MODEL OF THE UPPER LIMB

Ian Syndergaard[1], Dario Farina[3], *Steven Charles[1,2]
[1]Mechanical Engineering and [2]Neuroscience, Brigham Young University
[3]Bioengineering, Imperial College London
*Corresponding author's email: skcharles@byu.edu

**Introduction:** Many computational models of the upper limb have been used to study mechanisms of motor control, motor learning, and movement disorders. Although simple linear models have provided much insight, higher-fidelity models are able to capture additional phenomena and provide additional understanding. Two types of higher-fidelity models are closed-loop models and multiple-input multiple-output (MIMO) models. While both closed-loop and MIMO linear models of the upper limb exist, there are—to our knowledge—no published linear models of the entire upper limb that are both closed-loop *and* MIMO. Such a model would be valuable in simulating the effect of afferent feedback on general upper-limb movements. The primary difficulty in creating such a model is choosing appropriate feedback parameters, as no collection of feedback parameter values for the whole upper limb has been measured or reported in the literature. The purpose of this work is to 1) present a method for developing MIMO models of short-loop afferent feedback and 2) offer estimates of average feedback parameter values and ranges based on the currently available literature.

**Methods:** We combined measurements of feedback-related parameters available in 26 prior studies with known properties of system stability and behavior, resulting in estimated feedback gains and delays for a linear model of the upper limb with inputs into the 13 major superficial muscles and outputs to the 7 main joint degrees of freedom. This model includes homonymous feedback mediated by Golgi tendon organs (GTO), heteronymous feedback mediated by muscle spindles, and both afferent and efferent delays.

GTO-mediated feedback was modeled as pure force feedback. More specifically, expanding previous work by van der Helm et al, we modeled the neural feedback signal as $\nu \boldsymbol{C}^{-1}\boldsymbol{f}$, where $\boldsymbol{f}$ is the vector of muscle forces, $\boldsymbol{C}$ is the matrix of muscle strengths and $\nu$ is a proportionality constant. Spindle-mediated feedback was modeled as proportional+derivative feedback, with gains derived from prior reflex studies using either EMG averaging or peristimulus time histogram methods. In both methods, a *source muscle* (or nerve innervating the source muscle) was stimulated (electrically or mechanically), and changes in the activity of a *target muscle* were observed. The two method generated measures with different units; to compare values between different methods, groups of comparable values were scaled such that the sum of squared differences between methods was minimized. These values were gathered in a muscle spindle feedback matrix whose true scaling is not known, so we performed a stability analysis on a closed-loop version of the MIMO model proposed in [2] to identify an upper limit for the scaling of the feedback matrix. Afferent and efferent delays were also extracted from prior studies and compiled into coherent estimates.

As a partial validation of muscle-spindle feedback gains, we compared the sign of the estimated gains to known differences in excess central delay between excitatory and inhibitory connections. Finally, as a partial validation of delay times, we compared estimated delay times to measured innervation lengths.

**Results and Discussion:** Based on past studies, we were able to estimate homonymous GTO-mediated feedback gains for all 13 muscles, homonymous/heteronymous spindle-mediated feedback gains for 70 of the $13^2$=169 muscle pairs (Fig. 1), and both afferent and efferent delays for all 13 muscles. For positive perturbations in muscle length, agonist muscle pairs generally exhibited positive (faciliatory) spindle-mediated feedback, whereas antagonist muscle pairs generally exhibited negative (inhibitory) spindle-mediated feedback. The absolute value of the feedback gains tended to increase from proximal to distal.

The partial validation of spindle-mediated feedback gains proved correct in all 39 muscle pairs for which we had both estimated a feedback gain and found a measured excess central delay value in the literature. In the comparison of estimated delay times to measured innervation lengths, we found a strong correlation for efferent delays (R=0.88) and a moderate correlation for afferent delays (R=0.65), providing further partial validation of estimated delay times.

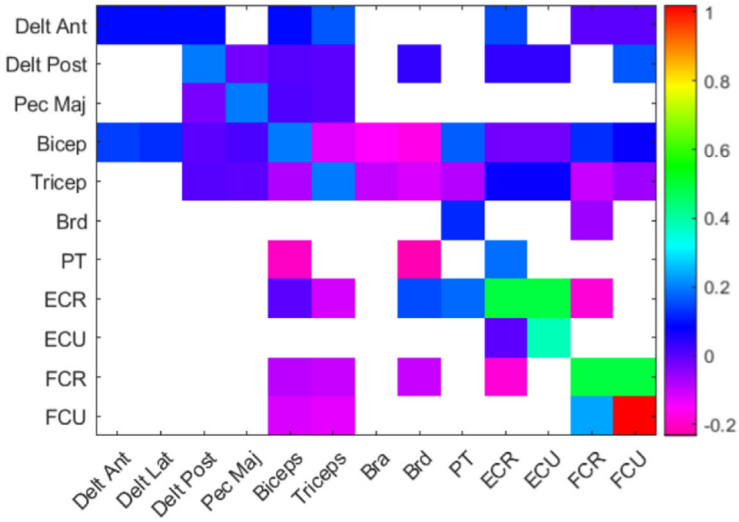


**Figure 1:** Spindle-mediated feedback gain values.

**Significance:** The feedback parameter values and ranges presented here can be used to develop closed-loop MIMO models of the neuromusculoskeletal system of the upper limb.

**Acknowledgments:** This research was funded in part by NIH NINDS R15 NS087447-02 and NSF 1806056 grants.

**References:** [1] van der Helm et al. (2000), *Biomechanics and Neural Control of Movement. Winters and Crago. New York, NY, Springer: 164-174*; [2] Corie et al. (2019), *J Biomech Eng-T ASME 141(8):17.*

# APPROACH TO RISING FROM A CHAIR DOES NOT CHANGE FOLLOWING TOTAL KNEE ARTHROPLASTY

*Kathryn S. Blessinger[1], Reese A. Lloyd[1], Laura C. Schmitt[1], Ajit M.W. Chaudhari[1], Robert A. Siston[1]
[1]The Ohio State University, Columbus, OH
*Corresponding author's email: blessinger.1@osu.edu

**Introduction:** Individuals receiving a total knee arthroplasty (TKA) for treatment of knee osteoarthritis (KOA) often experience continued postoperative functional limitations, quadriceps muscle weakness, and altered kinematics and kinetics during activities of daily living, like the sit-to-stand (STS) task [1-3]. Musculoskeletal simulations can be used to characterize the underlying "muscle function" used during dynamic tasks by quantifying individual muscle forces and their ability to accelerate the center of mass during a task [4,5]. It is well-established how kinematics can affect the potential of a muscle to accelerate the center of mass to meet the demands of the task, e.g., to accelerate the center of mass vertically and slow its forward progression during STS [5]. However, it remains unclear how patients' kinematic approach to rising from a chair affects their muscles' ability to accelerate the center of mass and whether there are postoperative changes in the way patients are approaching the task of rising from a chair following a TKA that could explain the persistent postoperative functional limitations. We hypothesized that individuals with KOA would demonstrate differences in the kinematics and muscle function during STS, compared to the same individuals after receiving a TKA, and compared to healthy controls. Additionally, we hypothesized that after receiving a TKA, patients would still demonstrate differences compared to healthy controls in their kinematics and muscle function during STS.

**Methods:** Seven individuals with medial compartment KOA who were scheduled to undergo a primary posterior-stabilizing TKA, a subset of the data presented previously [6-8], along with a baseline of 7 healthy, older adults that served as a control group (HC) were included in this retrospective analysis. Individuals undergoing a TKA were tested before and 6 months after surgery. Three-dimensional kinematic and kinetic data were collected while participants performed at least four chair rises [7]. One representative chair rise was analyzed for each participant. Musculoskeletal simulations of each representative STS cycle were conducted in OpenSim [4,6], where we computed individual sagittal plane muscle potentials to contribute to vertical and horizontal acceleration of the center of mass [5,9]. Kinematic and muscle potential waveforms were compared between timepoints (KOA-TKA) and between populations (KOA-HC and TKA-HC) using statistical parametric mapping [10] (SPM1d) for paired t-testing (between timepoints) or 2-sample t-testing (between populations). All $\alpha = 0.05$ (with Bonferroni correction). At each timepoint (KOA and TKA), muscle potentials were further categorized based on their magnitude relative to HC and whether this relative magnitude was mechanically advantageous or disadvantageous to meeting task demands for rising from a chair as defined by Caruthers et al. [9].

**Results & Discussion:** There were no statistically significant differences between timepoints (pre- versus post-TKA) in the STS kinematics or muscle potentials to contribute to center of mass accelerations. Both before and after TKA, individuals demonstrated significantly more dorsiflexion and more knee flexion, compared to HC (all $p \leq 0.011$). For muscle potential comparisons, both before and after TKA, individuals demonstrated significantly smaller gluteus maximus potentials in the vertical direction, compared to HC (all $p \leq 0.014$). There were no other significant differences in kinematics or muscle potentials between populations. While not statistically significant, there were additional qualitative differences between the KOA-TKA and HC groups in their muscle potentials, particularly within the third phase of the STS cycle [9] (Table 1). At each timepoint, the KOA-TKA groups trended towards smaller magnitudes of quadriceps potentials in both the vertical and horizontal directions (Table 1). Since the quadriceps contribute to accelerating the center of mass upward and slowing its forward progression during STS [9], the smaller magnitudes of quadriceps potentials observed both before and after TKA, relative to the HC group, suggest that patients receiving a TKA are not positioning their bodies in a way that is suited for meeting the demands of the task.

**Table 1:** Magnitudes of muscle potentials observed during Phase 3 of STS, for KOA and TKA timepoints, relative to those observed in HC. Green: matching task demand; Red: countering task demand [9]; +: larger magnitude compared to HC, -: smaller magnitude compared to HC.

| Muscle | Direction | Phase 3 |
|---|---|---|
| HIP EXT (GMax) | Horizontal | - |
| | Vertical | - |
| HIP FLEX (Iliacus & Psoas) | Horizontal | - |
| | Vertical | - |
| QUAD (RecFem & Vasti) | Horizontal | - |
| | Vertical | - |
| HAM (BiFem) | Horizontal | - |
| | Vertical | + |
| HAM (Semimem & Semiten) | Horizontal | + |
| | Vertical | - |
| PLANTARFLEX (GasMed, GasLat, & Soleus) | Horizontal | + |
| | Vertical | - |
| DORSIFLEX (TibAnt) | Horizontal | + |
| | Vertical | - |

**Significance:** A lack of a postoperative change in patients' approach to rise from a chair, as supported by our findings, may be a factor contributing to the continued functional limitations often observed following a TKA. Our findings suggest a need for teaching a new approach to rise from a chair in a manner that allows patients to capitalize on available muscle strength to better meet the task demands and improve task performance following TKA.

**Acknowledgments:** The authors thank Megan Hughes, Rachel Hall, Sarah Roelker, Elena Caruthers, Greg Freisinger, and Jacqueline Devine for assisting with data collection and our funding source: NIH R01AR056700.

**References:** [1] Sonoo et al. (2019), *J Biomech* 96; [2] Wang et al. (2019), *J Arthroplasty* 34(10); [3] Silva et al. (2003), *J Arthroplasty* 18(5); [4] Delp et al. (2007), *IEEE Trans Biomed Eng* 54(11); [5] Roelker et al. (2022), *PLOS ONE* 17(3); [6] Blessinger et al. (2024) *Proc ORS*; [7] Freisinger et al. (2017), *J Orthop Res* 35(8); [8] Koehn et al. (2022), *PLOS ONE* 17(4); [9] Caruthers et al. *J Appl Biomech* 32(5); [10] Pataky et al. (2016), *J Biomech* 49(9).

# TRANSTIBIAL BONE-ANCHORED LIMBS AFFECT SOUND LIMB KNEE CARTILAGE CONTACT PRESSURE

Mitchell A. Ekdahl[1*], Cory L. Christiansen[2], Jason W. Stoneback[2], Brecca M.M. Gaffney[1,2]
[1]University of Colorado Denver, [2]University of Colorado Anschutz Medical Campus
*Corresponding author's email: mitchell.ekdahl@ucdenver.edu

**Introduction:** People with unilateral transtibial amputation (TTA) are nearly 18 times more likely to develop knee osteoarthritis (OA) in the sound limb than individuals without amputation [1]. This increased risk is largely attributed to increased loading of the sound limb due to required compensatory movement patterns [2]. These altered biomechanics will contribute to chronically altered intra-articular cartilage pressure, an established etiological factor of OA [3]. Bone-anchored limbs (BALs) are a promising alternative to traditional socket prostheses that are mounted directly to the residual bone [4]. Early work has shown that BAL use does not change sound limb knee joint loading during walking compared to socket prostheses [5]. While joint loading is a common measure used to estimate OA risk, it is not always sensitive to altered intra-articular cartilage mechanics. Thus, the effects of BAL use on knee OA etiology in individuals with TTA remain unknown. The purpose of this study was to compare estimated knee cartilage contact pressure during walking in individuals with TTA before and after BAL implantation.

**Methods:** Overground walking motion capture data was collected from five adults with unilateral TTA (2F/3M; 52.2±16.3y; BMI: 29.5±3.9; time since amputation: 5.0±2.4y) at two timepoints: ~2 days prior to BAL implantation (in socket prosthesis) and one year following BAL implantation. Knee contact models for each participant were created in OpenSim using a previously developed musculoskeletal model with an integrated elastic foundation model for cartilage contact estimation [6, 7]. Muscle forces and segmental kinematics were estimated using the concurrent optimization of muscle activations and kinematics (COMAK) tool, and tibiofemoral joint cartilage contact pressures were calculated using the joint articular mechanics tool (Fig. 1a) [8]. Contact area and mean pressure in the medial and lateral tibiofemoral compartments were compared before (in socket prosthesis) and after BAL implantation at the first and second peaks of total tibiofemoral contact force during stance using Cohen's *d* effect sizes for paired samples (large effect: $d \geq 0.8$).

**Results & Discussion:** Cartilage contact area and mean contact pressure during walking was altered following BAL implantation (Fig. 1b). Lateral compartment contact area was reduced at the first peak of tibiofemoral pressure following BAL implantation (193.2±24.0 $mm^2$ (pre) vs. 154.9±26.1 $mm^2$ (post), $d$=2.23)), and medial compartment contact area was increased at the second peak (336.2±72.4 $mm^2$ (pre) vs 358.5±66.5 $mm^2$ (post), $d$=0.97). Mean cartilage contact pressure was decreased in the lateral compartment at both the first (4.3±0.3 MPa (pre) vs. 3.1±0.4 MPa (post), $d$=2.04) and second (5.8±0.6 MPa (pre) vs. 5.2±1.2 MPa (post), $d$=0.83) peaks of tibiofemoral pressure and increased in the medial compartment at the second peak of tibiofemoral pressure after BAL implantation (5.8±1.6 MPa (pre) vs. 6.3±1.3 MPa (post), $d$=1.11).

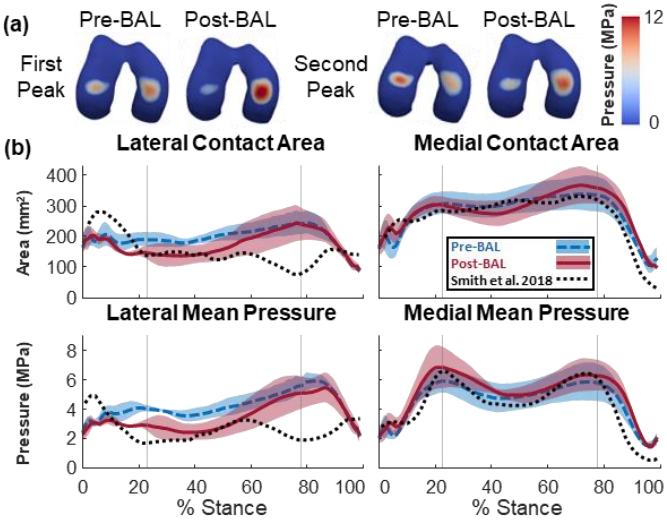


**Figure 1. a)** Representative pressure map of tibiofemoral cartilage contact pressure at each peak of contact force before and after BAL implantation. **b)** Contact area and mean contact pressure before (blue, dashed) and after (red, solid) BAL implantation in the medial and lateral compartments of the knee. Previously published values from an individual without limb-loss (black, dotted) using the same model are included for comparison [6]. Vertical gray lines indicate the approximate timing of the first and second peaks of tibiofemoral contact force.

Our results indicate that intra-articular cartilage mechanics in the sound limb knee are altered by BAL use. Mean pressure is reduced in the lateral compartment of the knee and increased in the medial compartment of the knee following BAL implantation, which suggests a shift to a more asymmetric loading pattern between the two compartments. This is further supported by the reduction in lateral compartment contact area observed in early stance. People without amputation load the medial compartment of the knee more than the lateral compartment [9], so the more asymmetric distribution of pressure between compartments following BAL implantation could represent a more normalized loading pattern. The increased peak medial compartment mean pressure after BAL implantation is more like an individual without limb-loss (Fig. 1b), so the medial compartment may be underloaded when using a socket prosthesis in this cohort. However, sound limb knee OA is more prevalent in the medial compartment than the lateral compartment, which is often attributed to the relatively higher experienced loads [10]. These results indicate that BAL use changes how tibiofemoral cartilage contact pressure is distributed during walking, but further investigation is needed to determine if these altered intra-articular mechanics have pathologic effects on the etiology of sound limb knee OA.

**Significance:** These results provide new insights into how transtibial BALs alter sound limb knee intra-articular cartilage mechanics during walking, which can be used to understand how BAL use modulates risk of OA development and progression in this population.

**Funding:** University of Colorado Bone-Anchored Limb Research Group and the National Institutes of Health (K01AR080776).

**References:** [1] Struyf (2009), *Arch Phys Med Rehab*; [2] Jaegers (1995), *Arch Phys Med Rehab*; [3] Guilak (2011), *Best Pr Res Clin Rheum* [4] Brånemark (2014), *Bone Joint*; [5] Vinson (2024), *J Biomech*; [6] Lenhart (2015), *Ann Biomed Eng*; [7] Smith (2018), *Comp Met Biomech Biomed Eng*; [8] Brandon (2018), *Handbook Hum Mot*; [9] Ahlbäck (1968), *Act Radiol Diag*; [10] Melzer (2001), *J Rheum*

# THE INFLUENCE OF PAIN CLASSIFICATION METHODS IN UNDERSTANDING THUMB JOINT LOADING IN WOMEN WITH CARPOMETACARPAL OSTEOARTHITIS

*Alexis R. Benoit[1], Tamara Ordonez Diaz[1], Yenisel Cruz-Almeida[2], Jennifer A. Nichols[1]
[1]J. Crayton Pruitt Department of Biomedical Engineering, University of Florida, Gainesville, FL
[2]Department of Community Dentistry and Behavioral Science, University of Florida, Gainesville, FL
*Corresponding author's email: abenoit1@ufl.edu

**Introduction:** Pain is the primary reason individuals with osteoarthritis (OA) seek clinical treatment [1]. However, pain can be measured in multiple ways. Clinical pain, as measured by patient-reported outcome measures, like the Australian Canadian Hand Osteoarthritis Index (AUSCAN), reflects persistent pain experienced over time, while movement-evoked pain (MEP) reflects pain that occurs during physical activity. Regardless of pain classification type, individuals with joint pain often modify their movement to avoid discomfort, which can lead to altered joint loading. In this study, we analyzed external thumb-tip forces and internal joint forces in women with carpometacarpal (CMC) OA during cylindrical grasp based on clinical pain and MEP groups. Cylindrical grasp was chosen as it mimics real-life scenarios requiring dynamic thumb stability and force production. We hypothesized that when compared to individuals with pain, individuals with no pain would (i) produce higher external thumb-tip forces and (ii) exhibit higher internal joint forces.

**Methods:** Thirty-one women with CMC OA were recruited for this IRB-approved study (IRB#201900693). To date, 17 participants (age: 61.6 ± 12.9 years) have been analyzed. External thumb-tip forces were recorded at 3,000 Hz using a multi-axis force sensor (ATI Mini40). Simultaneously, motion capture data was collected at 100 Hz with a 12-camera Vicon system using a custom hand marker set, with at least 3 markers on each thumb segment [2]. Each participant performed cylindrical grasp with their thumb on the force sensor for two tasks [maximal (100% effort) and submaximal (50% effort)] with three trials per task. The second trial from each task was analyzed. Participants reported their MEP based on a 101-point Visual Analog Scale (VAS) before, during, and after each trial. Two cohorts were defined: one by clinical pain and one by MEP. Clinical pain groups were determined by average AUSCAN pain score: clinical pain (AUSCAN ≥1, n = 8) vs. no clinical pain (AUSCAN <1, n = 9). MEP groups were determined by subtracting before-trial VAS scores from during-trial scores: MEP (MEP change >0, n = 12) vs. no MEP (MEP change = 0, n = 5). Internal joint forces were calculated at the interphalangeal (IP), metacarpophalangeal (MCP), and CMC thumb joints using OpenSim. Unpaired t-tests were performed in GraphPad to compare force magnitudes across pain groups.

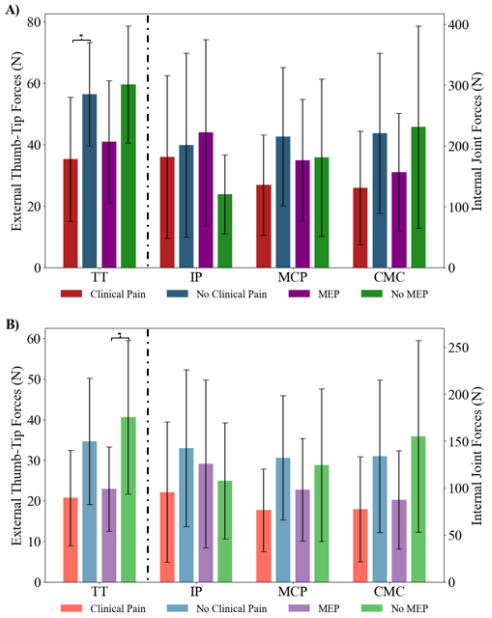


**Figure 1:** Dual y-axis bar plots depicting external thumb-tip forces (left y-axis, N) and internal joint forces (right y-axis, N) for (A) maximal cylindrical grasp and (B) submaximal cylindrical grasp. The dotted line separates data associated with the left and right y-axes. Data are presented as average force magnitude ± standard deviation. Asterisks (*) indicate statistically significant differences ($p < 0.05$). TT = Thumb-Tip, IP = Interphalangeal, MCP = Metacarpophalangeal, CMC = Carpometacarpal.

**Results & Discussion:** Findings were consistent across pain cohorts, indicating no clear advantage of using one pain metric over the other when evaluating thumb forces in CMC OA. The no pain groups produced greater external thumb-tip forces than the pain groups during both maximal [difference: 21.1 N (clinical), 18.6 N (MEP)] and submaximal [difference: 13.9 N (clinical), 17.7 N (MEP)] effort. Significant differences in external thumb-tip forces were observed between clinical pain groups during maximal effort (Fig. 1A) and MEP groups during submaximal effort (Fig. 1B). Internal joint forces were generally higher in the no pain groups, except at the IP joint, where the MEP group exhibited internal forces that were 101.3 N and 18.2 N higher than the no MEP group during maximal and submaximal effort, respectively. Trends in internal joint forces were consistent across both effort levels (Fig. 1), suggesting that a single effort level may be sufficient to assess pain-related effects on force production and joint loading.

Daily tasks can require up to 34.8 N of external thumb-tip force [3], which is comparable to the average force generated by our clinical pain group (35.2 N) during maximal effort. Since maximal effort is the highest force an individual can voluntarily produce, having to exert near-maximal force for routine tasks may lead to compensatory movements or task avoidance in CMC OA. A limitation of this study is the lack of direct reference values to validate our internal joint forces, as these data do not exist for the thumb. However, our findings indicate that internal thumb joint forces are lower than those reported for large joints (e.g., shoulder forces reach 1309 N, 5.7 times our highest average internal force) [4]. Study limitations also include an uneven distribution of participants across cohorts. Future work will expand the sample size, examine force directionality, and analyze individual muscle contributions to joint loading.

**Significance:** This study is a step toward understanding how different pain experiences influence biomechanical outcomes, such as joint loading. Understanding how clinical pain versus MEP influence force production in CMC OA can inform function preserving treatments.

**Acknowledgments:** Funding from National Institutes of Health (R01 AR078817, KL2 TR001429, F31 AG074645).

**References:** [1] Parker et al. (2008), *J Hand Surg* 33(10); [2] Ordonez Diaz et al. (2024), *J Orthop Res* 42(8); [3] Riddle et al. (2020), *J Hand Ther* 33(2); [4] OrthoLoad (2024), OrthoLoad Database, Available at: https://orthoload.com/.

# RIGID BODY MODELING OUTCOMES USING OSTEOGENESIS IMPERFECTA SPECIFIC GEOMETRY

*Maeve M. McDonald[1,2], Christina R. Garman[2], Rachel L. Lenhart[1], Jessica M. Fritz[1,2]
[1] Medical College of Wisconsin, Milwaukee, WI
[2]Marquette University, Milwaukee, WI
*Corresponding author's email: mmmcdonald@mcw.edu

**Introduction:** Osteogenesis imperfecta (OI) is a genetic bone disorder affecting the structural formation of type I collagen [1]. There are several types of OI, with type I being the mildest and most prevalent. Type I is characterized by bone weakness and mild bowing of the long bones, such as the femur, resulting from insufficient type I collagen production. In addition to altered bone properties, individuals with OI have decreased muscle and tendon mass as well as decreased force generation, resulting in increased fatigue and weakness [2]. While individuals with OI type I can ambulate, the altered muscle and bone properties increase fracture risk and negatively affect gait. Compared to healthy controls, individuals with OI showed diminished walking speed, reduced overall ankle ROM during stance, and reduced peak hip and knee extension [3]. Rigid body modeling is an important tool for creating patient specific assessments using gait analysis data and bone geometry obtained via imaging [4]. The goal of this study was to investigate the effect of using OI-specific femur geometry on kinematics during walking compared to healthy default femur geometry provided by rigid body modeling software. We hypothesize that simulated scale error, inverse kinematic error, and joint moments will be greater for OI-specific femur geometry during overground walking.

**Methods:** Deidentified motion analysis data was used from a previously conducted, IRB-approved study. Motion analysis data consisted of self-selected walking trials from nine OI type I subjects and nine healthy controls. Femur geometry for OpenSim modeling was obtained using a mesh file created from x-ray imaging of an OI type I patient with 5 mm of lateral bowing. The OI femur mesh was imported to nmsBuilder software and surface registration of anatomical landmarks using an iterative closest point technique was used to properly orient the OI femur with the default femur for use within the full rigid body model. Joint trajectories and torques were then generated in OpenSim using the scaling, inverse kinematics, and inverse dynamics tools for each subject with default femur geometry and reprocessed with OI type I femur geometry. Differences in rigid body model outputs using healthy and OI-specific femur geometry were compared across the gait cycle using a paired t-test with a significance set at $p < 0.05$.

**Results & Discussion:** Scaling error, kinematic error, and inverse dynamic outputs of the hip, knee, and ankle were included in this study. All scaling errors exhibited statistically significant differences when comparing femur geometry for OI walking. Significant differences were seen in total squared error and maximum Root Mean Square (RMS) error for the entirety of the gait cycle for OI walking data (Figures 1A & 1B). Maximum marker error was also significantly different at different points during stance and swing in control and OI walking (Fig 1C). Preliminary inverse dynamic outputs comparing model geometries showed differences in joint moments at the hip, knee, and ankle in the sagittal plane during the stance phase. Further analysis is needed to statistically assess differences in inverse dynamic output.

These results suggest that bone geometry plays a role in determining gait kinematics. Higher marker errors in OI walking data indicate less agreement between experimental markers and simulated model markers. Preliminary data indicates that further model refinement for OI walking data could reduce error and provide more accurate kinematic and dynamic output. Continued analyses include incorporation of kinetic data for the comparison of muscle forces and joint contact forces to verify the impact of geometry during rigid body modeling.

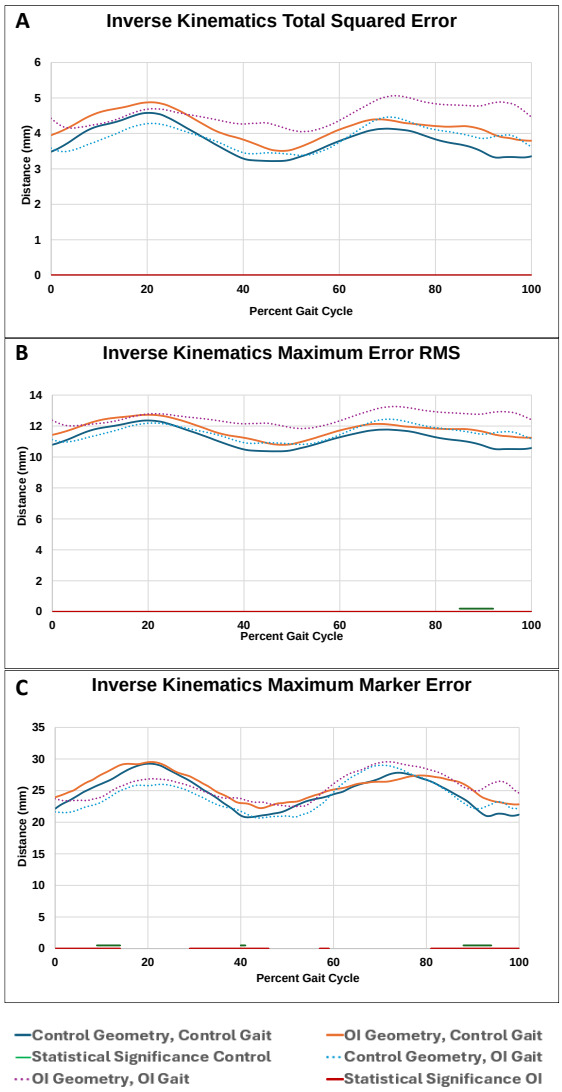


**Figure 1 A-C:** Total squared marker error (A), Maximum error RMS (B), and Maximum Marker Error (C), when calculating inverse kinematics for OI walking. Red and green bars along the x-axis indicate statistically significant differences

**Significance:** This study provides evidence that OI-specific geometry is necessary for more accurate outputs using rigid body modeling for OI. Accurate kinematic and dynamic calculations are vital for modeling of additional parameters such as muscle forces, and joint reaction forces during ambulation, which can then be implemented in fracture risk models and can help guide rehabilitation approaches to reduce or prevent injury.

**References:** [1] S. Subramanian and V. K. Viswanathan, Osteogenesis Imperfecta (2022). [2] Etich, et al. (2020) Mol Cell Pediatr. [3] Graf et al. (2009) Journal of Orthopaedic Research. [4] Delp et al. (2007) IEEE Transactions on Biomedical Engineering

# SAGITTAL PLANE STIFFNESS EVALUATION OF A SURROGATE NECK DEVICE AND A COMPUTATIONAL MODEL

Anthony P. Marino[1*], Reed D. Gurchiek[1], Greg Batt[1], and John D. DesJardins[1]
[1]Department of Bioengineering, Clemson University, Clemson, SC 29631
*Corresponding author's email: amarin2@clemson.edu

**Introduction:** Anthropometric test devices (ATDs) are human surrogate models that have been used in a variety of industries, including automotive and aerospace, to represent the response of the human body in the context of compliance and safety testing [1,2]. More recently, head and neck ATDs have been incorporated in linear impactor tests for the evaluation of helmet performance during direct head impacts in sports, specifically American football [3,4]. The Hybrid III ATD is validated to be biofidelic in its response only during an automotive frontal crash scenario that induces an inertial force on the body leading to anteroposterior motion of the head and neck [5]. In American football, impacts are not isolated to one direction and in many cases occur directly to the head, which will elicit a much different response. Little work has been done to characterize the Hybrid III behavior during sports-specific impacts, leading to an increased potential for inaccurate laboratory testing data. Additionally, the testing of injurious head impacts on human subjects is unethical, so a direct comparison is not currently possible. To address this gap in the current research, computational models of the head and neck, such as the HYOID OpenSim model, have been developed that achieve a high level of biofidelity in impact scenarios [6]. This study seeks to provide a comparison of the stiffness behavior of the Hybrid III ATD with the HYOID model to assess the present differences in both laboratory and computational representations of the human neck. Due to the dynamic capacity of the neck musculature, we expect that the HYOID model will exhibit a greater stiffness in the sagittal plane when compared to the Hybrid III ATD. Results from this work will act as a baseline for future comparisons in every plane of motion to improve the biofidelity of surrogate models used in the laboratory testing of head protective equipment for American football.

**Methods:** The HYOID neck model (72 muscles, 30 degrees of freedom (DOFs), and was scaled to a 50th percentile male to match the Hybrid III ATD) was used in the computation experiments in this study [6]. Static optimization was performed to maximize muscle activations, and the optimization was subject to the constraint that no net moment resulted from the activation scheme, creating a 'stiff' neck assumption. MATLAB's "fmincon" function was used to execute the optimization. From a neutral position, the head/neck was displaced 1º in flexion/extension until reaching a max displacement of 20º. From the displaced position, the optimal activation scheme was applied to the model to return it to the starting position. Muscle forces responsible for returning the head and neck to neutral position were calculated using the Hill muscle model and a rigid tendon assumption for all muscles. Net moments were then calculated about the DOF of interest ('pitch2'). HYOID model data was compared to previously collected data on two Hybrid III neckforms from two different manufacturers (Humanetics (HUM) and Jasti). Moment vs. displacement plots were created for all datasets and a line was fit to the data curves to obtain stiffness (N·m/deg).

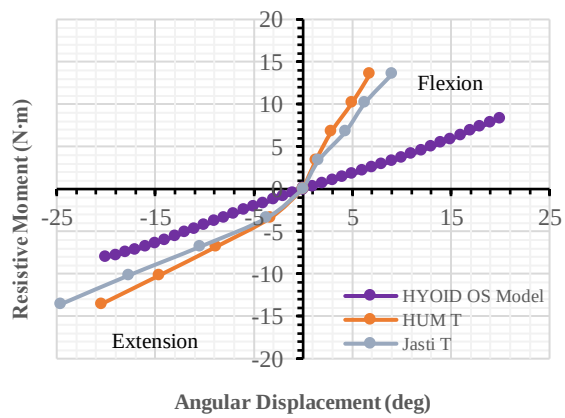


**Figure 1:** Resistive moments generated by neck musculature in HYOID model and ATD neck response across prescribed displacements in the sagittal plane (flexion/extension).

**Results & Discussion:** Resistive moment and angular displacement data for the HYOID model, HUM, and Jasti necks are shown in Fig. 1. In both flexion and extension, the HYOID model was less stiff than both ATDs. HYOID, HUM, and Jasti exhibited stiffness values of 0.415, 1.951, and 1.478 N·m/deg, respectively, in flexion and 0.413, 0.644, and 0.531 N·m/deg in extension. A symmetric response was observed in the HYOID model where the ATDs were stiffer in flexion than in extension. This is due to the design of the ATDs where more butyl rubber is present in the front half of the device, creating a greater resistive force when compressed in flexion. The behavior observed in the sagittal plane experiments contradicted the hypothesis: the active musculature during static tests does not result in stiffness values which are comparable to the Hybrid III. This result places emphasis on the need for further exploration in the response of the Hybrid III neckform as the extent of the disagreement between ATD and human body model in this study may allude to greater inaccuracies of the Hybrid III that are unnoticed when evaluating American football head impacts in a laboratory setting.

**Significance:** Without accurate laboratory testing methods and biofidelic equipment, researchers run the risk of basing protective gear (helmet) design assumptions on response data that does not truly characterize the risk imposed to the athlete in head impact scenarios. The results of this study will act as a benchmark for further studies that will seek to fully evaluate ATDs in all planes of motion that may be experienced in American football head impacts so that researchers can be sure that the data they collect in a laboratory setting is accurate in representing the human response, thus allow for the informed design of protective equipment that is more effective at reducing athlete injury risk.

**References:** [1] Albert et al. (2023), *Traffic Inj. Prev.* 24(sup 1); [2] Jones et al. (2019), *Traffic Inj. Prev.* 20(sup 1); [3] Viano et al. (2012), *Ann. of Biomed. Eng.* 40(1); [4] Bartsch et al. (2012), *Accid. Anal. Prev.* 48 [5] Foreman et al. (2011), *Proc. of 23rd Int Soc of Biomech Cong*; [6] Mortensen et al. (2018), *PLoS ONE* 13(6).

# WHAT DETERMINES WHETHER AN ANKLE SPRAIN OCCURS WHEN THE REAR FOOT LANDS ON AN IRREGULAR SURFACE? INSIGHTS FROM A FRONTAL PLANE DYNAMIC MODEL

*Andrea Kowalski[1], Hogene Kim[1], PhD and James A. Ashton-Miller[1], PhD
[1]Department of Mechanical Engineering, University of Michigan, Ann Arbor, MI
*Corresponding author's email: akowals@umich.edu

**Introduction:** Ankle inversion sprains are commonly responsible for lost playing time whether in running, court or field sports [1]. Apart from ankle muscle strengthening exercises, the most common prophylactic measures involve taping and bracing, neither of which offer reliable protection [2]. An inversion sprain is usually described as being due to "excessive ankle inversion and/or internal rotation" of the midfoot relative to the shank. While true, this explanation provides no information on the many biomechanical factors that interact to determine whether or not a sprain will actually occur. We examined the role of these factors when landing on a foreign body under the medial rear foot. In the frontal plane, the calcaneus would be forced into inversion by the ground reaction, R, acting about the subtalar joint, S. If we assume that the maximum permissible range of motion of the subtalar joint is 35° before a sprain occurs [3], we hypothesized that the risk of an ankle sprain varies with the magnitude, direction, and location of R; rearfoot foot/shoe mass; calcaneal height and width; shoe sole thickness and compliance; and the pre-activation state, strength, tensile stiffness and damping, and moment arm of a single evertor muscle-equivalent acting about S. Our objective was to study the sensitivity of the magnitude of subtalar joint rotation in the 100 ms following the rear foot landing on a foreign object to changes in these parameters using a simple planar, second-order, dynamic model (Fig 1).

$$J\frac{d^2\theta}{dt^2} = -B\frac{d\theta}{dt}d - K\theta d + R_H h + R_V r$$

**Methods:** For simplicity in this frontal plane model, we neglected the effect of forces in the transverse plane. We assumed that the calcaneus can rotate without friction about the subtalar joint. We lumped together calcaneal and rear shoe mass ($M_F$) and assumed its center of mass lies a distance, 2H/3, below the subtalar joint. The shape of the calcaneus was approximated to be an isosceles triangle with a height (H) and width (W). The shoe sole was assumed incompressible with a thickness, $H_S$, and adhered to the calcaneus. The foreign body was assumed to be located at a horizontal distance, W*, medial to the subtalar joint. The single evertor muscle-equivalent was assumed to act with lever arm, d, about the subtalar joint and have a tensile stiffness, K, and damping, B, proportional to the pre-activation state, a, of the muscle; its maximum isometric force was assumed to be $T_{iso}$, and its maximum force in an eccentric or lengthening contraction to be $2T_{iso}$. That state, a, could vary between 0.03 (resting) and 1.0 (fully activated). The end range of motion of the subtalar joint in eversion was assumed to be 34° after which a sprain would occur. The ground reaction force in a jump could vary from 1 to 4*BW [4], where body weight was assumed to be 82 kg and 69 kg for males and females, respectively. The ground reaction force was modeled as a Gaussian impulse having a peak at 100 ms. A female was assumed to have 33% less stiffness and damping than males [5]. A sensitivity analysis was performed by examining how varying each parameter by ±10% affected the change in peak subtalar angle.

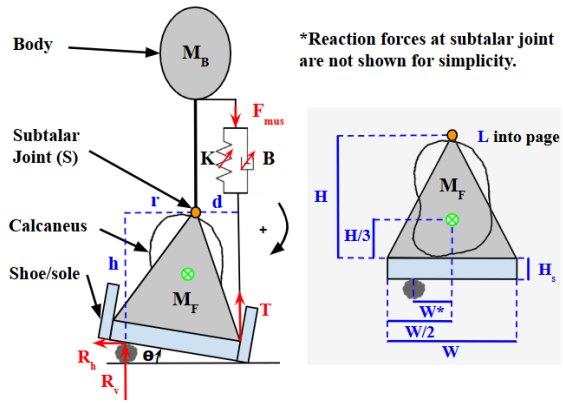


**Figure 1.** Planar model of the ankle and subtalar joint in the frontal plane.

**Results & Discussion:** Both males and females were most sensitive to changes in vertical ground reaction force, evertor tensile stiffness, and foot width, in order of sensitivity (Fig. 2). The magnitude of the vertical ground reaction force resulted in the largest subtalar angular displacement by more than twice most other parameters. Females were more sensitive than males to all tested parameters; the largest difference was in sensitivity to foot width (2.1 % greater resulting change in rotation).

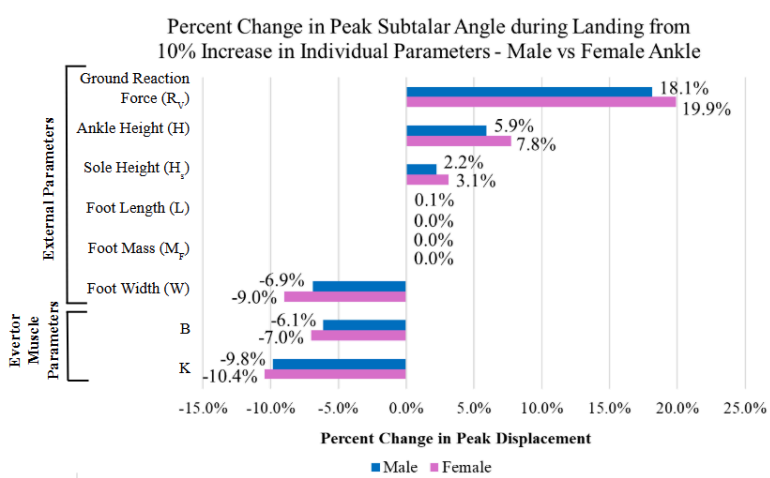


**Figure 2**. Sensitivity of peak subtalar angle change during a landing to changes in each individual parameter.

**Significance:** In trying to avoid an ankle sprain, some factors are modifiable (i.e., rear shoe sole thickness and width, muscle strength, choosing to land on a small stone versus a large stone, choosing to pre-activate evertor muscles maximally), while others are not (i.e., sex, size and shape of foot, body weight). The sex difference in evertor muscle ankle strength per unit body weight systematically places females at higher risk for ankle injuries.

**Acknowledgments:** Funding by the NIA Pepper Center Biomechanics Core P30 AG024824.

**References:** [1] Mack (1982), *Clin. Sports Med.*(1); [2] Ashton-Miller (1996), *Am J Sports Med* 24(6); [3] Stauffer (1977), *Clin Orthop Relat Res* 127 ; [4] Mcclay (1994), *J Appl Biomech* 10; [5] Ottaviani (1995 & 2001), *Am J Sports Med.*

# EFFECT OF KINEMATIC CONSTRAINTS AND BUSHING LOADS ON MODEL-PREDICTED CERVICAL SPINE JOINT LOADS

*Anita N. Vasavada[1], Jeffrey Reinbolt[2]
[1]Washington State University,[2]University of Tennessee Knoxville
*Corresponding author's email: vasavada@wsu.edu

**Introduction:** Musculoskeletal models are increasingly being used to evaluate loads in the spine. Two features often used in spine models are kinematic constraints and bushings. Kinematic constraints are incorporated to make the complex intervertebral kinematics tractable in models. This is usually accomplished in by constraining each intervertebral joint's motion to be a specified percentage of overall motion and is sometimes referred to as the "spinal rhythm." In OpenSim, the spinal rhythm is implemented using CoordinateCouplerConstraints. In effect, these constraints apply loads (forces and moments) to constrain the segmental kinematics. Bushings are also utilized in spine models to represent the rotational and translational stiffness of the passive elements of the spinal joint. Bushings may represent only the intervertebral disc, or the disc and ligaments together. Because kinematic constraints and bushings introduce additional loads in the model, we hypothesized that both kinematic constraints and bushings will affect the joint loads predicted in a cervical spine model.

**Methods:** An existing neck musculoskeletal model [1] was modified in OpenSim 4.3. Vertebral geometry was obtained from the Visible Human Male [2], and neutral posture was from an x-ray of a 50$^{th}$ percentile male. Kinematic constraints prescribed each intervertebral joint's motion as a percentage of overall head-trunk motion [3] using CoordinateCouplerConstraints. Bushings represented the intervertebral rotational joint stiffness of the disc and ligaments combined; these were defined as cubic polynomials, based on the meta-analysis of Zhang *et al.* [4].

Joint loads were calculated in OpenSim using the Static Optimization and Joint Reactions Analysis tools. Compressive and shear loads were calculated with the model in the neutral posture and in 20° flexion for four types of models: (1) With kinematic constraints and bushings (C/B); (2) With constraints but no bushings (C/NB); (3) Without constraints but with bushings (NC/B); (4) Without constraints or bushings (NC/NB).

**Results & Discussion:** Kinematic constraints and bushings affected joint loads at all cervical levels, although compressive loads were more affected than shear, and the effects were greater in flexed postures (Figure 1). In the neutral posture, bushings did not contribute to joint moments and therefore joint loads were unaffected (Figs. 1A and 1C). Including constraints in the neutral posture decreased compressive loads (Fig. 1A), but shear loads were affected differently in the upper, middle and lower cervical spine (Fig. 1C). Bushings and constraints interacted to affect joint loads in flexion. In 20° flexion, the presence of bushings decreased compressive loads when constraints were present but increased compressive loads when there were no constraints (Figs. 1B). Bushings affected shear loads differently in the upper and lower cervical region (Fig. 1D). Including constraints in 20° flexed postures usually decreased compressive loads when bushings were present and increased compressive loads when there were no bushings (Fig. 1B). Including constraints in 20° flexed postures usually increased absolute value of shear loads whether or not bushings were present (Fig. 1D).

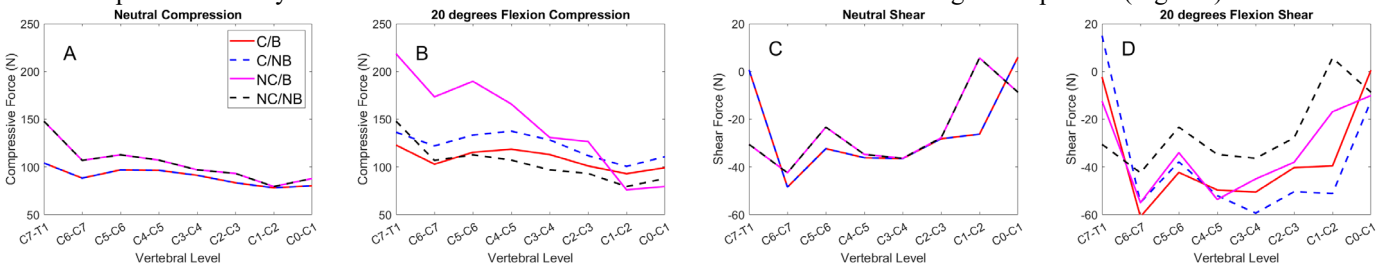


Figure 1: (A) Compressive loads in neutral posture. (B) Compressive loads in 20° flexion. (C) Shear loads in neutral posture. (D) Shear loads in 20° flexion. Positive shear is anterior on the upper segment and posterior on the lower segment. Note that scales are different for compression and shear.

Kinematic constraints are used in many spine models, but it is usually not acknowledged that these constraints are imposing loads to maintain a particular pose. Other options to define kinematics should be explored, such as optimizing the mechanical representation of anatomical elements to determine the amount of joint motion. Bushing loads in this model were averages from a meta-analysis; the magnitude of these moments needs to be compared to the net joint moment to understand the contributions of muscles. Moreover, these bushing definitions only included moment-rotation relationships and did not include force-displacement (additional compressive and shear forces) or damping properties, which may be important for dynamic simulations.

**Significance:** Spinal loads are important to know for injury prediction and prevention, designing spinal implants, or evaluating ergonomics or rehabilitation protocols. Users of musculoskeletal models need to be aware of how different model features, specifically kinematic constraints and bushings, affect the calculated joint loads.

**Acknowledgments:** Liying Zheng, Chandler Shannon, Steven Monda and Zane Duke. Funding from CFD Research Corporation.

**References:** [1] Vasavada *et al*. (1998), *Spine,* 23(4):412-422. [2] Spitzer *et al*. (1996), *J Amer Medical Informatics Assn* 3(2):118-130. [3] White and Panjabi, *Clinical Biomechanics of the Spine*, 1990. [4] Zhang *et al*. (2020), *J Biomech*, 100: 109579.

# SEQUENTIAL VS. SIMULTANEOUS PERSONALIZATION OF LOWER EXTRIMITY FUNCTIONAL AXES

*Robert M. Salati, Benjamin J. Fregly
Department of Mechanical Engineering, Rice University, Houston, Texas
*Corresponding author's email: rs200@rice.edu

**Introduction:** Patient-specific neuromusculoskeletal models to predict post-treatment walking function have shown great potential for treating movement disorders such as stroke, Parkinson's, or osteoarthritis [1]. A key step to predicting patient functional outcome is to create an accurate personalized kinematic model of the patient [2]. Researchers recently developed the Neuromusculoskeletal Modeling (NMSM) Pipeline [3]: a software toolset that facilitates model personalization and treatment optimization capabilities for OpenSim [4]. The NMSM Pipeline's Joint Model Personalization (JMP) tool personalizes joint functional axes to reduce inverse kinematics (IK) errors [2, 3]. JMP is a two-level optimization that solves IK on the inner level, and on the outer level, changes joint functional axis orientations and translations, scales bodies, and moves markers, to reduce IK errors. The tool has been shown to significantly reduce IK marker errors [2], but no studies have evaluated what the optimal problem formulation for JMP is. This study evaluates the effect of personalizing multiple joints inside one optimization versus personalizing one joint at a time in separate optimizations.

**Methods:** Experimental kinematic data were collected for one healthy subject. Functional joint trials were collected for the ankle, knee, and hip on both legs. For a functional trial, one joint is moved through its entire range of motion. Gait data were collected for the subject walking on a treadmill at his self-selected speed.
A scaled generic full body OpenSim model was created to match subject anthropometry. Preceding the JMP runs, knee adduction angles were personalized to best match static pose marker data. Next, JMP runs were set up to personalize the ankle and knee joint orientation parameters (Table 1), and to uniformly scale the pelvis. The JMP runs were organized in two different ways: sequential and simultaneous. In the sequential run, each joint was personalized independently of the other joints in 5 sequential tasks using their respective functional joint trials. The ankle (including subtalar) joints were personalized first, knee joints were personalized second, and hip joints (via pelvis scaling) were personalized last. For pelvis scaling, right and left functional hip trials were concatenated together to form a single file. In the simultaneous run, all joints were personalized together to capture the effect that changes in one joint will have on other joints. Each functional joint trial was concatenated together, and parameters were then personalized in a single optimization. Finally, both the sequential and simultaneous JMP runs were finished off with a task that personalized all previous parameters simultaneously using gait marker data.

**Table 1:** Joint axis orientation parameters personalized for each joint.

| Joint | Parent Frame | Child Frame |
|---|---|---|
| Knee | X Y | X Y |
| Ankle | X Y | - |
| Subtalar | Y | Y Z |

**Results & Discussion:** Model personalization quality was evaluated by running IK on both personalized models and the scaled generic model with marker data from a single gait cycle not used in the personalization (Figure 1). The simultaneous and sequential JMP runs produced 14% and 21% lower average RMS errors than the scaled generic model and improved the peak RMS errors by 33% and 36% respectively (Table 2). CPU time was measured on an AMD Ryzen 9 7950x 16-core processor and 32 GB of DDR5 5600MT/s RAM.
These results show that sequential JMP runs where one joint is personalized at a time give better results compared to personalizing all joints in the same optimization. The sequential JMP run produced a mean RMS error approximately 1 mm lower than the simultaneous run with significantly less CPU time.

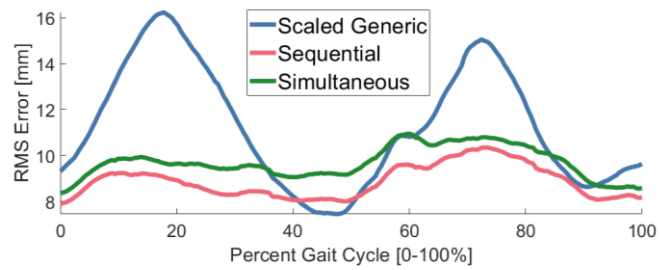


**Figure 1:** IK RMS errors throughout a sample gait cycle for the models created by simultaneous and sequential JMP runs, compared to a scaled generic model.

**Table 2:** RMS Errors and CPU time for sequential and simultaneous JMP Runs compared to a scaled generic model.

| Model | Mean RMS Error (mm) | Max RMS Error (mm) | CPU Time (Hours) |
|---|---|---|---|
| Scaled Generic | 11.3 | 16.2 | N/A |
| Simultaneous | 9.7 | 10.9 | 2.50 |
| Sequential | 8.9 | 10.3 | 0.55 |

**Significance:** This study explored some best practices for using the NMSM Pipeline's JMP tool. The results of this study suggest that the optimal way to use JMP is to sequentially personalize joints one at a time using functional joint trials. The requirements to run JMP include any OpenSim skeletal model, and marker data for relevant joints. Ideally, functional joint trials would be used to personalize each joint, but they are not required. Because of the significant reduction in IK error from JMP, there is potential for joint personalization to benefit any study where IK accuracy is important. Future validation work could include evaluation of JMP without functional joint trials, and evaluation of semi-simultaneous JMP runs in which multiple, but not all, joints are personalized at the same time.

**Acknowledgments:** This work was funded by the United States National Institutes of Health (NIH) grant R01EB030520. The NMSM Pipeline is available at https://simtk.org/projects/nmsm.

**References:** [1] Meyer 2016, *Front. Bioeng. Biotech.* [2] Reinbolt 2005, *J. Biomech*. [3] Hammond 2024, "NMSM Pipeline", *BioRxiv*. [4] Seth 2018 *PLoS Comput Biol*.

# AUTOMATIC FOOT-GROUND CONTACT MODEL PERSONALIZATION ROBUSTLY REDUCES FORCE PLATE POSITION ERRORS FOR MULTIPLE SUBJECTS

*Spencer T. Williams, Geng Li, Claire V. Hammond, Benjamin J. Fregly
Department of Mechanical Engineering, Rice University, Houston, Texas
*Corresponding author's email: stwilliams@rice.edu

**Introduction:** The optimization of treatments for movement impairments using personalized neuromusculoskeletal models requires the creation of models consistent with both rigid body dynamics and the available experimental data [1,2]. Automatically personalized foot-ground contact (FGC) models have been shown to improve the tracking of experimental data in dynamically consistent gait simulations [3]. However, simply tracking experimental kinematic and force data may make unsafe assumptions about sources of error. These "ground truth" data can be inconsistent if a force plate position is not known accurately within a lab coordinate system, resulting in incorrectly calculated center of pressure (CoP) locations; even CoP errors of less than a centimeter can cause errors of over 10% in downstream joint moment calculations [4]. This study evaluates the efficacy and reliability of a novel computational method to reduce force plate data errors by incorporating physics-based force plate position adjustments into an existing FGC model calibration process for two subjects [5].

**Methods:** The FGC calibration process used OpenSim [2] models of two subjects. The first (Subject 1) was a post-stroke subject walking on an instrumented treadmill at a self-selected speed of 0.8 m/s. The second (Subject 2) was a subject with a Type II pelvic sarcoma walking on a similar instrumented treadmill at a self-selected speed of 1.0 m/s. The two subjects' datasets were recorded at different labs with each location using its own equipment. Personalized FGC models were calibrated for both feet simultaneously for each subject using the Ground Contact Personalization (GCP) tool in the Neuromusculoskeletal Modeling Pipeline [5]. For each run, GCP placed a dense grid of contact elements, linear springs with nonlinear viscous damping and linear viscous friction, across the bottom of each foot, calibrating contact element parameters to reproduce experimental ground reactions by making minimal adjustments to experimental foot kinematics. This standard process was followed without modifications for Run 1, and variations on this process were performed for both subjects. For Run 2, the FGC model optimization was allowed to adjust freely the positions of the left and right force plates in the ground plane, effectively changing ground reaction moments (GRMs) by changing the point about which moments were calculated. Run 3 used the same settings as Run 2 except the experimental force plate data file was replaced with a file containing the adjusted plate positions from the Run 2 solution, thereby testing the solution robustness. Finally, Runs 4-11 were the same as Run 3 except in each case, errors of 1 cm were artificially introduced in various directions to initial force plate positions to test the consistency of the results from different initial guesses.

**Results & Discussion:** The personalized FGC models had lower tracking errors in every tracked quantity with adjusted force plate locations (Table 1). Frontal plane GRM errors were especially reduced, decreasing from 5.655 to 1.771 Nm on the right side for Subject 1 from Run 1 to Run 2. The reduced errors show that including force plate location adjustment in the model calibration process allows the optimization to more easily generate models more consistent with data. It is additionally significant that final force plate locations and tracking errors were highly consistent for both subjects across all runs adjusting force plate locations, Runs 2-11. This consistency shows that force plate location adjustments are robust to different initial values, indicating that the optimizations found actual solutions rather than taking advantage of the additional degrees of freedom in varied, indeterminate ways.

**Table 1:** RMS tracking errors in GCP Runs. Force plate position shifts for Runs 4-11 are reported relative to the new positions obtained in Run 2. Moments were calculated about midfoot superior markers projected onto the floor as within GCP [5]. Results are averaged for Runs 4-11.

| Run | Rotation (°) | Translation (mm) | Force (N) | Moment (Nm) | Right plate shift (mm) | Left plate shift (mm) | Runtime (min) |
|---|---|---|---|---|---|---|---|
| Sub 1, 1 | 1.196 | 7.075 | 7.523 | 2.932 | 0 | 0 | 23.99 |
| Sub 1, 2 | 0.636 | 5.334 | 5.204 | 1.139 | 19.213 | 23.430 | 11.66 |
| Sub 1, 3 | 0.632 | 5.212 | 5.238 | 1.141 | 0.242 | 0.226 | 9.63 |
| Sub 1, 4-11 | 0.632 | 5.261 | 5.218 | 1.140 | 0.216 | 0.197 | 11.37 |
| Sub 2, 1 | 0.888 | 6.589 | 12.126 | 2.509 | 0 | 0 | 25.81 |
| Sub 2, 2 | 0.611 | 5.871 | 7.494 | 1.593 | 21.780 | 20.319 | 23.51 |
| Sub 2, 3 | 0.611 | 5.851 | 7.491 | 1.593 | 0.033 | 0.027 | 25.33 |
| Sub 2, 4-11 | 0.610 | 5.836 | 7.510 | 1.595 | 0.052 | 0.059 | 21.06 |

**Significance:** These results indicate that adjusting force plate positions in FGC model calibrations produces adjusted ground reaction data more consistent with physics. A limitation of this study is that the actual location errors are unknown. Nonetheless, the consistency of these results supports further investigation of this approach.

**Acknowledgments:** This work was supported by grant 1842494 from the NSF and grant R01 EB030520 from the NIH.

**References:** [1] Meyer AJ et al. (2016). *Bioeng. Biotech*., 4. [2] Seth A et al. (2018). *PLos Comput. Biol*., 14(7). [3] Williams ST et al. (2024). *Proceed. Am. Soc. Biomech*. [4] McCaw ST and DeVita P (1995). *J. Biomech*., 28(8): 985-988. [5] Hammond CV et al. (2024). *bioRxiv*.

# DEVELOPMENT OF UPPER-LIMB MUSCLE ARCHITECTURE FOLLOWING BRACHIAL PLEXUS BIRTH INJURY

*Vivian M. Mota[1], Kyla B. Bosh[1,2], Marisa C. Boretti[1,2], Isabel Baillie[1], Christina Lasdin[1], Jacqueline H. Cole[1,2], Katherine R. Saul[1]
[1]North Carolina State University, Raleigh, NC, [2]University of North Carolina, Chapel Hill, NC
*Corresponding author's email: vmmota@ncsu.edu

**Introduction:** Brachial plexus birth injury (BPBI) is a nerve injury that occurs at birth due to extensive stretching of the neck and is the common pediatric neuromuscular injury with a prevalence of 1 in 1,000 live births [1]. Arm function impairment such as muscle paralysis, shoulder contracture, joint dislocation, and deformed scapular and humeral growth are all effects of BPBI [2-3]. Previous studies have examined altered muscle architecture for different injury locations, either nerve rupture (preganglionic injury) or nerve avulsion (postganglionic injury). At 8 weeks in a neonatal rat model, optimal muscle length and muscle mass were reduced after preganglionic injury compared to uninjured and postganglionic injury groups [4]. These earlier studies provided one timepoint at which muscle alterations are well established, but we do not yet know the timeline for initiation of altered muscle architecture. Clinically, there is little consensus on treatment and intervention timing. Our goal is to better understand the underlying muscle architecture (optimal muscle length, sarcomere length, and physiological cross-sectional area) at different developmental timepoints through musculoskeletal maturation as a foundation for evidence-based intervention timelines. We hypothesize that the postganglionic and disarticulation (altered limb loading without nerve injury) groups will initially exhibit lower muscle mass in the injured limb compared to the uninjured limb.

**Methods:** Four groups of Sprague Dawley pups underwent IACUC-approved surgeries 3-6 days post-birth. Two of the four groups underwent neurectomies at different locations relative to the dorsal root ganglion: the postganglionic group received a distal C5-C6 nerve root neurectomy, while the preganglionic group received a proximal C5-C6 nerve root neurectomy. The disarticulation group received amputation above the elbow to induce reduced limb usage [5], and the sham group underwent a sham surgery that kept the brachial plexus intact. Animals were separated for euthanasia at 2, 3, 4, 8, and 16 weeks (n=10 per timepoint and group). Ten muscles crossing the glenohumeral joint were dissected from injured and uninjured limbs, and muscle length and mass were measured. Muscle outcomes were compared between limbs (injured and uninjured) with Wilcoxon signed-rank tests and between surgical groups with Kruskal-Wallis plus Dunn's post hoc tests (GraphPad Prism 10, α=0.05).

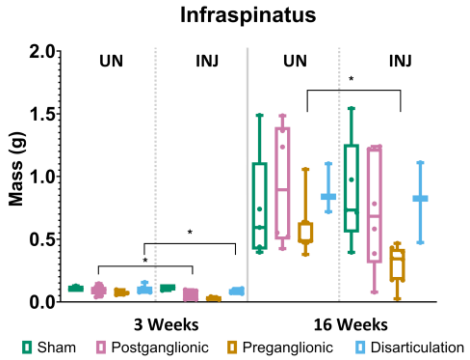


**Figure 1:** Infraspinatus muscle mass was lower in the injured vs. uninjured limb at 3 weeks for postganglionic and disarticulation groups (p=0.0195-0.0312) and at 16 weeks for the preganglionic group (p=0.0234).

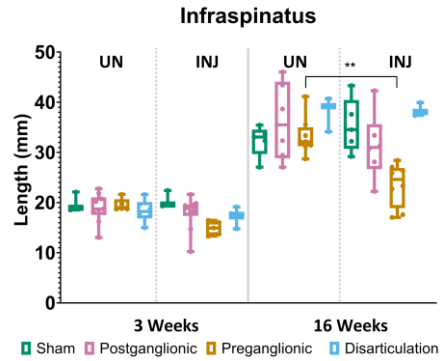


**Figure 2:** Infraspinatus muscle length was smaller in the injured vs. uninjured limb at 16 weeks for the preganglionic group (p=0.0078).

**Results & Discussion:** Preliminary analysis of sham, postganglionic, preganglionic, and disarticulation groups includes 3-week and 16-week time points (n=3-10). ***Muscle mass:*** Postganglionic and disarticulation group injured limbs had a lower muscle mass as compared to the contralateral uninjured limb at 3 weeks for the pectoralis, biceps long head, triceps, and infraspinatus (Fig.1) muscles (p=0.0020-0.0312). For the preganglionic group, significantly lower masses were detectable at 16 weeks for anterior deltoid, spinodeltoid, biceps short head, supraspinatus, infraspinatus (Fig.1), and triceps muscles (p=0.0032-0.0312). ***Muscle length:*** At 3 weeks, the postganglionic group injured limb had shorter muscle length for the biceps long head as compared to the uninjured limb (p=0.0312). The disarticulation group injured limb had shorter muscle length for the biceps short head and triceps compared to the uninjured limb (p=0.0312). At 16 weeks, the preganglionic group injured limb muscle length was decreased compared to the uninjured limb for the anterior deltoid, spinodeltoid, biceps short head, supraspinatus, infraspinatus (Fig.2), and triceps (p=0.0020-0.0405). Preliminary results suggest muscle architecture is altered in the postganglionic and disarticulation groups as early as 3 weeks, while alterations may occur later in the preganglionic group; however, analyses need to be completed for all subjects before conclusions can be drawn. Previous studies at 8 weeks showed similar reduced muscle mass in the injured limb for both postganglionic and preganglionic groups, while muscle length was decreased for only the preganglionic group [4]. Ongoing analysis of all timepoints will help us bridge the knowledge gap of muscle architecture development post-injury.

**Significance:** Understanding underlying muscle architectural development is critically needed to properly navigate patient rehabilitation following BPBI. Timing of changes to optimal length and muscle mass after injury will improve treatment planning.

**Acknowledgments:** NIH R01HD101406. We thank Dr. Kerry Danelson and Dr. Roger Cornwall for their surgical support and Brian Hua, Sidh Lad, and Monserrat Elizalde Martinez for help with tissue dissection and measurements.

**References:** [1] Defrancesco C (2019) *J Pediatr Ortho* 39:e134; [2] Hogendoorn S (2010) *J Bone Jt Surg Am* 92:935; ); [3]. Poyia T (2005) *J Pediatr Radiol* 35:402; [4] Dixit N (2020*) J Hand Surg Am* 46 (2) [5] Fawcett (2021) Dissertation, North Carolina State University https://www.lib.ncsu.edu/resolver/1840.20/39052

# Investigating the Influence of the Extrinsic Toe Flexors in Jumping

*Ben K Perrin, John H Challis
Biomechanics Laboratory, The Pennsylvania State University, University Park, PA 16802, USA
*Corresponding author's email: bkp5431@psu.edu

**Introduction:** The multiarticular extrinsic toe flexor's ability to transfer power between joints grants them unique utility in tasks involving proximal to distal activation sequences (e.g., jumping) [1]. These muscles, flexor hallucis longus (FHL) and flexor digitorum longus (FDL), are often overlooked due to their small size; having a physiological cross section area approximately seven times smaller and a plantar flexor moment arm that is approximately two times smaller than the triceps surae [2,3]. While we have previously investigated the behavior of the toe flexors, it is also important to consider their interaction with the other plantar flexors. To examine this, a musculoskeletal model was developed, and jumps were simulated with the knee and hip joints locked. Jumps were performed with varied force generating capabilities of the toe flexors and jump height and muscle energetics were compared between trials.

**Methods:** A musculoskeletal model was developed in OpenSim to perform forward dynamics, optimal control simulations of jumping with joints above the ankle locked and the goal of maximizing jump height [4]. The model's foot consisted of three segments (rearfoot, forefoot, and toes) joined by pin joints representing the midtarsal joint (rearfoot to forefoot) and metatarsophalangeal joint (forefoot to toes). Hill-type muscle models of the triceps surae (soleus and gastrocnemius) and extrinsic toe flexors (FHL and FDL) were used to actuate the model. Muscle parameters from previous studies were used [5,6]. A linear spring connecting the rearfoot to the toes was used to represent the plantar aponeurosis. Optimizations were run in SCONE, where three parameters per muscle (initial excitation level, final excitation level, and time of change in excitation) were varied in a piecewise, feedforward controller until jump height no longer increased [7]. Simulations were performed with varied toe flexor force generating capabilities (normal vs no force generating capabilities). Work produced by the plantar flexor muscles during the takeoff phase of the jump was compared between conditions. A brake-spring-motor index (BSM) was also calculated for each muscle to characterize their behavior during the takeoff phase [8]. This was calculated by dividing the net work of the muscle by the sum of the magnitudes of negative and positive work produced by the muscle. A BSM index close to zero indicates "spring-like" behavior of the muscle, while a BSM index close to one or negative one indicates "motor-like" or "brake-like" behavior, respectively.

**Results & Discussion:** The nominal model produced a jump height of 13.7 cm. In comparison, the model without toe flexors achieved a maximum jump height of 12.4 cm. Despite this, when the toe flexors were removed the triceps surae generated more work than it had during the default conditions (nominal model: 159.7 J; no toe flexor model: 166.4 J). Looking at the work done by the toe flexors (12.4 J) can explain how the nominal model was able to produce these higher jumps in spite of the diminished work done by the triceps surae. The toe flexors not only influenced the behavior of the other modeled muscles, but also produced 7.2% of the total work generated in the initial simulation condition (Figure 1). The BSM index of the gastrocnemius was consistent across the two conditions (0.90 for both), however the BSM index of the soleus decreased from 0.85 to 0.83 when removing the toe flexors, indicating the soleus' behavior being slightly more spring-like in those conditions.

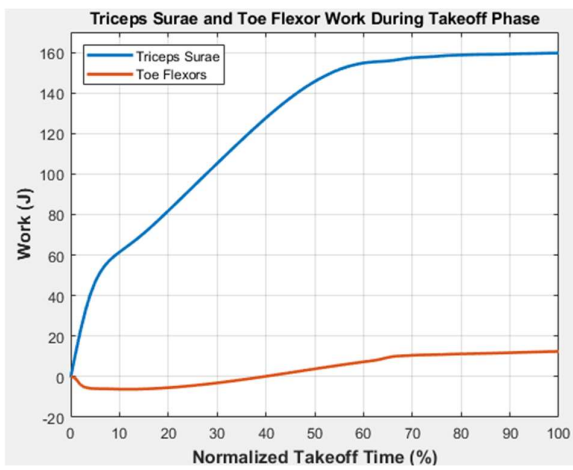


**Figure 1:** Triceps surae and extrinsic toe flexor work during the takeoff phase of jump.

**Significance:** These results suggest that despite their smaller size and smaller plantar flexor moment arm relative to the triceps surae, the extrinsic toe flexors have a significant role in jumping, and likely other proximal to distal activated forms of locomotion as well (i.e., walking or running). This not only indicates the importance of including the FHL and FDL muscles in musculoskeletal simulations but also raises the question of how changes in these muscles (e.g., weakening with age) may affect one's physical capabilities.

**References**

[1] Van Ingen Schenau (1989). *Hum Mov Sci.*, **8**(4): 301-337.
[2] Klein et al. (1996). *J Biomech,* **29**(1): 21-20.
[3] Wickiewicz et al. (1983). *Clin Orthop Relat Res.,* **22**(2): 275-283.
[4] Delp et al. (2007). *IEEE Trans Biomed Eng.,* **54**(11): 1940-50.
[5] Van Soest et al. (1993). *J Biomech.*, **26**(1): 1-8.
[6] Arnold et al. (2010). *Ann Biomed Eng.,* **38**(2): 269-279.
[7] Geijtenbeek (2019). *JOSS.,* **4**(38): 1421.
[8] Davis et al. (2023). *J Biomech., **151***: 111529.

# PREDICTION OF BONE INGROWTH INTO POROUS SWELLING BONE ANCHORS USING AN OSTEOCONNECTIVITY-BASED ADAPTIVE FRAMEWORK

*Amirreza Sadighi[1]*, Nolan Black[1], Mehrangiz Taheri[1], Moein Taghvaei[1], Sorin Siegler[1], Thomas P. Schaer[2], Ahmad R. Najafi[1]
[1] Department of Mechanical Engineering and Mechanics, Drexel University, Philadelphia, PA 19104, USA
[2] Department of Clinical Studies, New Bolton Center, University of Pennsylvania School of Veterinary Medicine, PA 19348, USA
*Corresponding author's email: as5547@drexel.edu

**Introduction:** This study aims to develop a finite element framework integrating bone ingrowth simulation with hygro-elastic swelling of porous co-polymeric bone anchors. The framework investigates how swelling-induced radial stresses influence bone ingrowth, fixation strength, and mechanical integrity of the swelling bone anchors and implants. It is hypothesized that a controlled swelling promotes favorable bone ingrowth, which could enhance anchor fixation as well as its mechanical integrity.

**Methods:** Finite Element Analysis (FEA) was used to simulate bone ingrowth. To do so, a strain-energy-density (SED) based bone ingrowth framework has been developed, which also incorporates an osteoconnectivity-based algorithm to ensure the sequential deposition of new bone [4]. The osteoconnectivity-based method has already been validated against experimental data, and the current framework has been verified against the available data and results. The swelling-induced radial stresses were applied as boundary conditions in FEA models with various pore geometries and sizes [5]. Parameters such as pore interconnectivity, pore size (average of 300, 450, and 600 µm), and ingrowth rates were analyzed. Additionally, analyses of mechanical integiruty and push-out were conducted to evaluate the influence of bone ingrowth on the added elastic response and fixation strength of these anchors pre and post-ingrowth.

**Results & Discussion:** The framework was initially verified against the results of the previously validated research [5]. Subsequently, it was applied to the swelling anchor FEM. Swelling generated radial stresses that stimulated bone ingrowth, enhancing mechanical integrity and fixation strength in all FEMs with different pore sizes and geometries. Smaller pore sizes (300 and 450 µm) seemed to stimulate faster and more extensive ingrowth compared to larger sizes (600 µm). Additionally, optimal pore interconnectivity facilitated deeper ingrowth. Moreover, it was revealed that the new bone formation into the porous region of bone anchors significantly increased the mechanical integrity of the bone anchors. Push-out simulations also exhibited the considerable impact of bone ingrowth on the added fixation.

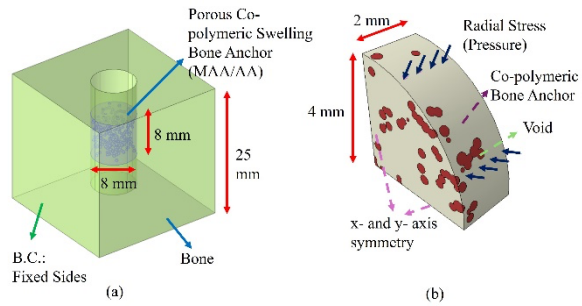


Figure 1. (a) The FEM of swelling bone anchor (to extract radial stresses at the interface), and (b) the quarter-slice FEM of porous bone anchor.

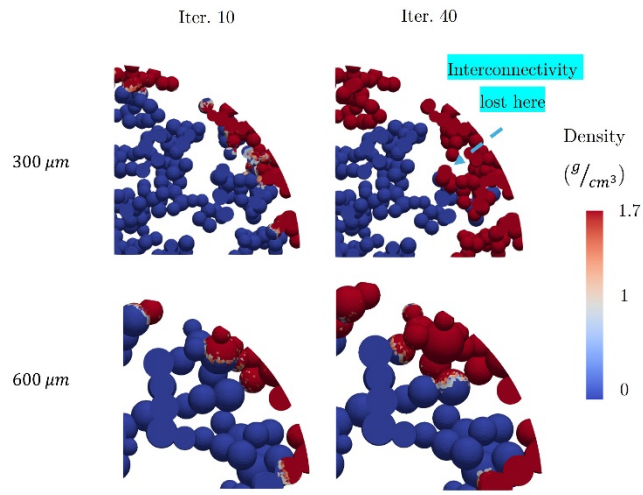


Figure 2. The side view of the void section with different average pore sizes (for conciseness, only the two sizes of 300 and 600 µm have been exhibited). The rate of bone ingrowth seemed to be slower for the big pore size. The interconnectivity of the pores played an important role in the progression of the bone ingrowth.

**Significance:** This work advances understanding of how swelling-induced mechanical stimuli drive bone remodeling and ingrowth. The results highlight the potential of porous co-polymeric bone anchors for providing osteoconductive properties and inducing bone ingrowth owing to the generated stresses at the bone-implant interface, suiting the applications requiring long-term stability and biocompatibility, such as orthopedic implants.

**Acknowledgments:** This project was financed through A. R. Najafi's faculty start-up funding from the MEM Department at Drexel University, and the Coulter-Drexel Translational Research Partnership Program. The work was performed at Drexel University in the Multiscale Computational Mechanics and Biomechanics (MCMB) Lab.

**References:** [1] Siegler et al. (2023) *J Biomed Mat Res Part B 111*(7). ; [2] Sadighi et al. (2023) *J mech beh of biom mat*, *143*.; [3] Weinans et al. (1992). *J of biomech*, *25*(12).; [4] Cheong et al. (2018) *Comp Meth in Biomech and Biomed Eng*, *21*(2).; [5] Cheong et al. (2018) *J mech beh of biom mat*, *87*, pp.230-239.

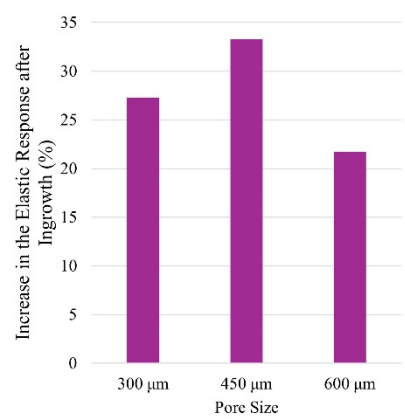


Figure 3. The increase in the elastic response due to the bone ingrowth for different pore sizes.

# FINITE ELEMENT ANALYSIS OF BONE REMODELING INDUCED BY SWELLING ANCHORS WITH HETEROGENEOUS PROPERTIES

*Amirreza Sadighi[1]*, Mehrangiz Taheri[1], Nolan Black[1], Jordan Stolle[1], Madeline Boyes[2], Sorin Siegler[1], Thomas P. Schaer[2], Ahmad R. Najafi[1]

[1] Department of Mechanical Engineering and Mechanics, Drexel University, Philadelphia, PA 19104, USA

[2] Department of Clinical Studies, New Bolton Center, University of Pennsylvania School of Veterinary Medicine, PA 19348, USA

*Corresponding author's email: as5547@drexel.edu

**Introduction:** This study evaluates how hygroscopic swelling of co-polymeric bone anchors induces bone remodeling and affects fixation strength [1]. In doing so, three different co-polymeric ratios of 80/20, 85/15, and 90/10 for Methyl Methacrylate and Acrylic Acid (MMA/AA) with distinct swelling ratios have been considered. Furthermore, for the FEM of the surrounding bone, heterogeneous trabecular bone properties have been obtained using the micro-CT of a vertebrae. It is hypothesized that a controlled swelling rate enhances mechanical stimulus, causing favorable bone remodeling without adverse resorption, further improving the fixation strength.

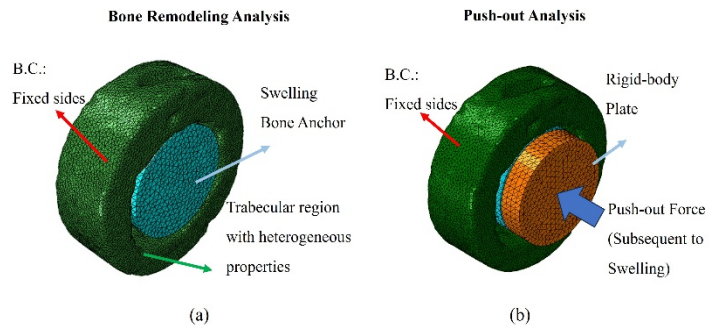


Fig. 1. The FEMs of: (a) Bone remodeling analysis, and (b) push-out analysis.

**Methods:** A hygro-elastic FEA framework simulated swelling-induced stresses, validated by experimental data [2]. Additionally, heterogeneous material properties derived from micro-CT data were integrated into the FEM. Furthermore, bone remodeling was captured using a strain energy density-based algorithm, examining three swelling ratios (MMA/AA compositions: 80/20, 85/15, and 90/10) [3, 4]. Subsequent to bone remodeling, push-out simulations were also conducted to evaluate the impact of bone remodeling on the fixation strength. FEMs of bone remodeling and push-out analyses can be checked in Fig. 1.

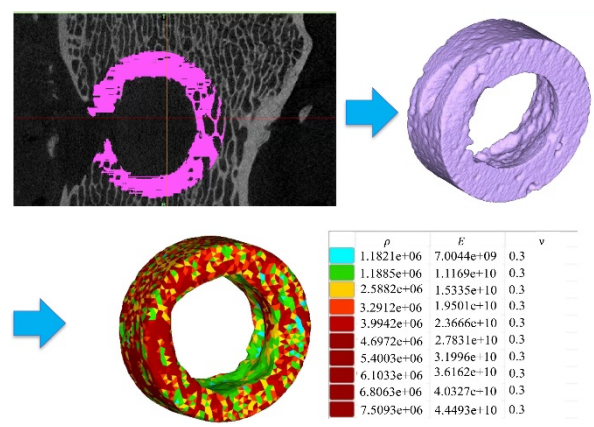


Figure 2. The generation of the trabecular bone FEM with heterogeneous material properties in Materialise Mimics software based on the HU in micro-CT.

**Results & Discussion:** The 85/15 composition optimized bone regeneration in the surrounding bone, increasing the average density at the interface by 43%. Excessive swelling ratios (80/20) were predicted to cause stress-induced resorption, while limited swelling (90/10) showed minimal densification. Furthermore, post-remodeling fixation strength increased by 23% compared to pre-remodeling.

**Significance:** This study highlights the biomechanical potential of swelling bone anchors with optimized compositions. Different co-polymeric ratios of MMA/AA could show distinct swelling ratios, which could significantly impact the magnitude of mechanical stimulus in the surrounding bone, and the associated bone remodeling. The findings contribute to the design of implants promoting favorable remodeling and long-term stability in orthopedic applications.

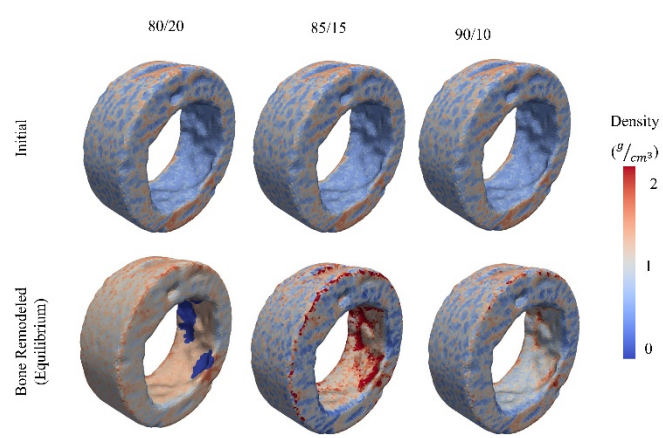


Figure 3. Bone remodeling in the trabecular region for the three co-polymeric ratios of swelling bone anchors. When the swelling was controlled within a specific limit (for the case of 85/15), favorable densification took place. However, the limited swelling ratio of 90/10 composition did not cause significant densification, and the excessive swelling ratio of 80/20 adversely resulted in overload resorption.

**Acknowledgments:** This project was financed through A. R. Najafi's faculty start-up funding from the MEM Department at Drexel University, and the Coulter-Drexel Translational Research Partnership Program. The work was performed at Drexel University in the Multiscale Computational Mechanics and Biomechanics (MCMB) Lab.

**References:** [1] Siegler et al. (2023) *J Biomed Mat Res Part B* *111*(7). ; [2] Sadighi et al. (2023) *J mech beh of biom mat*, *143*.; [3] Weinans et al. (1992). *J of biomech*, *25*(12).; [4] Li et al. (2007) *Dent mat*, *23*(9).

# ASSESSING THE INFLUENCE OF HIP DYSPLASIA SEVERITY ON FUNCTION, MOBILITY, AND PAIN

*Christina A. Bourantas, Madison M. Wissman, Molly C. Shepherd, Keith R. Lohse, John C. Clohisy, Michael D. Harris
Washington University School of Medicine in St. Louis, St. Louis, MO
*Corresponding author's email: bourantas@wustl.edu

**Introduction**: Developmental dysplasia of the hip (DDH) reduces hip stability and increases the risk for osteoarthritis [1,2]. Individuals with DDH have abnormal bony geometry and often altered biomechanics compared to controls [3]. Despite established relationships between abnormal bony geometry in DDH and the general adverse impact on hip joint mechanics, the variability in these effects based on disease severity remains understudied. Most studies of DDH joint mechanics average the data across individuals within a group, potentially masking important individual differences [4-6]. Examining the individual severity of bony deformity, rather than averaging across patients within a group, could provide more precise information about the links to abnormal joint mechanics, symptoms, and the risk for osteoarthritis. Assessments of patient-reported outcome measures (PROMs) and activity have become key metrics in evaluating patient perceptions of function, mobility, and pain. However, it is unknown how hip geometry impacts these patient perceptions and activity levels. Therefore, the objective of this study was to quantify the relationship between the severity of DDH geometric deformities, quantified by the lateral center edge angle (LCEA) and acetabular inclination (AI), and measures of patient-reported outcomes and activity. We hypothesized that individuals with smaller LCEAs and greater AI angles would report decreased mobility, decreased function, and increased pain.

**Methods:** PROMs and activity measures were collected from N=22 pre-surgical individuals with DDH after Institutional Review Board approval and informed consent. Steps per day were recorded for 7 consecutive days as individuals wore wrist-worn devices (Fitbit Inspire 3) at home. Once during those 7 days, participants completed PROMs including the International Hip Outcome Tool-12 (iHOT-12) and the National Institutes of Health Patient-Reported Outcome Measure Information System (PROMIS) Pain Interference, Mobility, and Physical Health surveys. Radiographic measurements of LCEA and AI were obtained to assess the severity of DDH. An unsupervised K-means clustering analysis was performed to categorize severity of DDH, based on LCEA and AI measurements. The elbow method, a clustering evaluation technique, was used to determine the optimal number of clusters within the data set (k=3) [7]. Linear regression analyses were then performed to investigate the relationship between average steps per day and PROM scores, considering the clusters to explore whether this relationship varied across different geometric profiles of DDH.

**Results & Discussion:** The K-means clustering analysis showed that individuals with greater LCEAs and lower AI angles were clustered, individuals with moderate angles of both measures were clustered together, and individuals with more severe measures (i.e. decreased LCEAs and greater AI angles) were clustered (Figure 1). The linear regression analyses revealed that average steps per day were significantly associated with PROMIS Mobility scores ($p=0.03$). Higher activity levels (i.e. higher average steps/day) were associated with better reports of mobility, particularly in less severe clusters (Figure 2). Thus, individuals with less severe DDH are able to maintain higher physical activity and mobility. Average steps per day were also significantly associated with PROMIS Pain Interference scores ($p<0.05$). Specifically, increased activity was associated with higher pain levels in the most severe cluster. This result is different than in the other clusters, suggesting that activity may exacerbate symptoms in severe cases of DDH. There was not a significant relationship between average steps per day and PROMIS Physical Health scores. However, higher activity levels and better reports of physical health trended together. Lastly, there was not a significant relationship between average steps per day and iHOT-12 scores. This result suggests that activity levels may not have a strong impact on hip-specific patient reported outcomes in this sample. Overall, these findings show the importance of considering severity of DDH when measuring and analyzing activity and patient-reported outcomes. Ongoing work involves recruiting more individuals with DDH and including three-dimensional measures of DDH severity.

**Significance:** This study highlights the importance of considering DDH severity when evaluating patient-reported outcomes and activity levels. Understanding and classifying severity of DDH can be useful for prognoses and prediction of functional changes over time.

**Acknowledgments:** Funding provided by the National Institute of Health T32HD007434 and R01AR081881.

**References:** [1] Wyles *Clin Orthop Relat Res* 2017. [2] Ganz *Clin Orthop Relat Res* 2008. [3] Harris *J Orthop Res* 2022. [4] Gaffney *Clin Biomech Bristol Avon* 2021. [5] Song *J Orthop Res Off Publ Orthop Res Soc* 2022. [6] Anable *Clin Biomech Bristol Avon* 2024. [7] Higgins *Comput Methods Biomech Biomed Engin* 2024.

**Figures:**

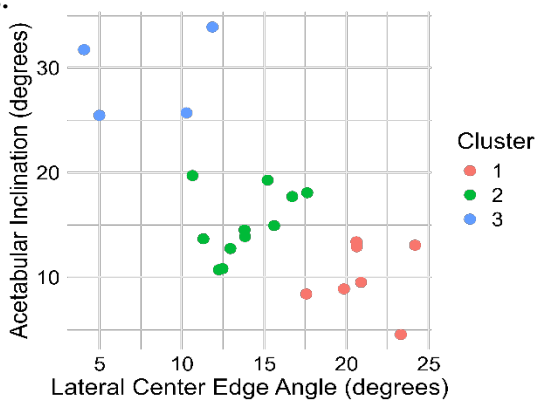


**Figure 1:** K-means cluster analysis (k=3) based on severity of DDH, categorized by LCEA and AI measurements.

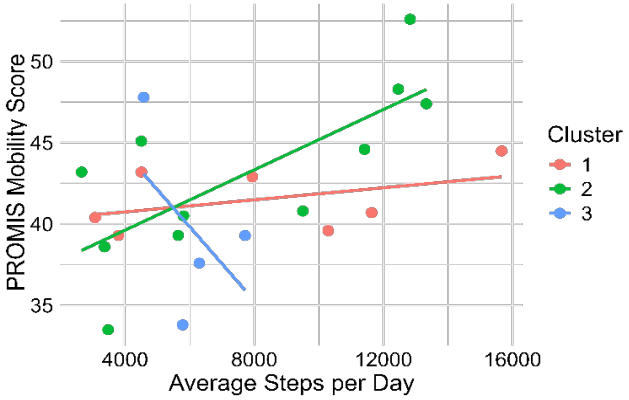


**Figure 2:** Plot of the relationship between average steps per day and PROMIS Mobility scores.

# DIFFERENCES IN YIELD STRESS AND STIFFNESS OF THE ILIOFEMORAL LIGAMENT ASSOCIATED WITH NORMAL AND HIGH BMI

Ana V. Figueroa*, Marc J. Brouillette, Victoria C. Tappa, Silvana Velasquez-Marin, Jacob M. Elkins, Jessica E. Goetz
University of Iowa, Iowa City, IA
anavictoria-figueroa@uiowa.edu

**Introduction:** In the year 2030, 572,000 Americans are predicted to receive a Total Hip Arthroplasty (THA), with about 40% of those patients being obese [1,2]. Current research has proven that excess adipose tissue due to obesity has potential to seed itself within the extra cellular matrix of some soft tissues resulting in disorganization of the fibers [3]. The presence of adipose tissue can also cause a systematic series of events that ultimately increases the cross-linking of fibers resulting in a change of material properties [4]. Mechanically altered soft tissue behavior may affect the ability of the tissue structure to stabilize the joint after a THA. Therefore, the goal of this study was to identify differences in iliofemoral ligament mechanical properties between normal and high BMI patients.

**Methods:** 17 partial iliofemoral ligament specimens, an average 4 cm in length, were harvested from consenting patients during an anterior approach THA surgery. BMIs ranged from 19.3 to 44.1. Harvested specimens were wrapped in saline-soaked gauze and stored at -20°F until testing. For testing, specimens were completely thawed in warm saline and secured in custom 3D-printed clamps with a standardized gage-length of 2 cm. Geometry of clamped specimens was captured using a 3D structured-light surface scan (Shining 3D) prior to mounting the specimen on an MTS actuator (MTS Inc. Eden Prairie, MN) to undergo uniaxial tensile testing. A 10 N preload was applied to tension the ligament, and a speckle pattern was painted on the ligament to enable surface strain measurement throughout the test using a digital image correlation (DIC) system (ARAMIS, GOM, Braunschweig, Germany). After patterning, specimens underwent preconditioning with 1.25% strain for 10 cycles at a rate of 0.5 mm/second and then specimens were tensioned until failure at a rate of 20 mm/min. Stress was calculated by dividing the applied force by the cross-sectional area obtained from the 3D surface scan and plotted against the DIC strain data (Fig. 1) to obtain stress-strain curves. A first-order Ogden strain-energy density (SED) function was fit to each curve up to 10% strain. The yield stress of the ligament was determined as the stress when visual separation of fibers occurred. Unpaired, t-tests with Welch's correction were used to determine the statistical significance ($p<0.05$) of differences in ligament mechanical behavior between the normal (BMI<30) and high (BMI≥30) BMI groups.

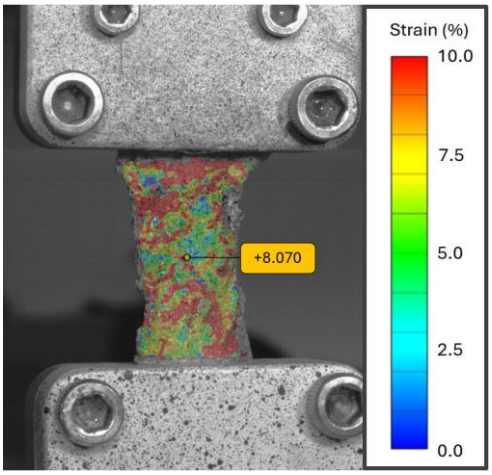


**Figure 1.** Digital image correlation analysis was conducted for each specimen to track the surface strain (%) of the sectioned iliofemoral ligament.

**Results & Discussion:** The average yield stress for the normal BMI group was 0.82 ± 0.33 MPa, while that for the high BMI group was slightly lower with an average of 0.70 ± 0.23 MPa (Fig. 2). This slight decrease was not significantly different ($p = 0.397$). The parameters μ and α were used to fit the SED function, where a larger μ indicates a stiffer material and $|\alpha|>1$ indicates a strain stiffening material [5]. The average μ in the normal and high BMI groups (Table 1) were 0.02 ± 0.03 and 0.05 ± 0.09, respectively. Although the high BMI group was stiffer, this difference was not significant ($p = 0.437$). The lack of significant differences could be a result from a limited sample size focused on those receiving an anterior approach THA with fewer individuals in higher BMI classes being eligible for that surgery.

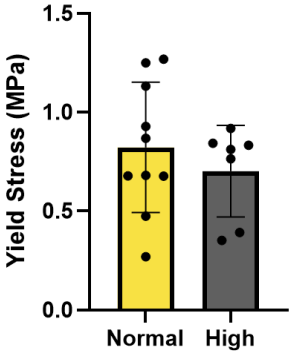


**Figure 2.** Tensile stress in the iliofemoral ligament immediately before failure.

**Table 1.** Best fit first-Order parameters to the iliofemoral stress-strain curves.

| # | 1 | 2 | 3 | 4 | 5 | 6 | 7 | 8 | 9 | 10 | 11 | 12 | 13 | 14 | 15 | 16 | 17 |
|---|---|---|---|---|---|---|---|---|---|---|---|---|---|---|---|---|---|
| **BMI** | 19.3 | 19.3 | 20.5 | 24.4 | 24.8 | 25.2 | 27.0 | 28.4 | 26.9 | 29.7 | 31.8 | 32.4 | 32.8 | 34.6 | 35.8 | 38.7 | 44.1 |
| **μ** | 0.002 | 0.022 | 0.004 | 0.007 | 0.013 | 0.082 | 0.004 | 0.062 | 0.007 | 0.005 | 0.002 | 0.033 | 0.003 | 0.253 | 0.018 | 0.028 | 0.011 |
| **α** | 1.923 | 1.204 | 1.947 | 1.687 | 0.665 | 1.031 | 1.672 | 0.712 | 1.653 | 2.013 | 1.699 | 0.974 | 1.68 | 0.584 | 1.331 | 1.244 | 1.386 |

**Significance:** THAs require transection of the hip capsule and ligaments. To better gauge post-operative risks, it would be beneficial to understand how hip ligament behaviour differs in normal and high BMI individuals. The results of this study indicate the hip capsule in obese individuals may behave stiffer but have lower yield than those with normal BMI, and future studies with larger group sizes and wider BMI ranges are warranted to understand implications for THA stability.

**Acknowledgments:** The authors would like to thank the University of Iowa for funding this study.

**References:** [1] Kurtz S., et. al., (2007) *J Bone Joint Surg Am.* 89(4) [2] Aggarwal, V. A., et. al., (2022) *Cureus*, 14(7) [3] Biancalana, A., et. al., (2012) *Micron*, 43(2–3). [4] Lee, J. M., et. al., (2019) *Journal of Applied Physiology*, 126(4). [5] Lohr MJ., et. al., (2022) *Phil. Trans. R. Soc. A*

# THREE-DIMENSIONAL PRINTED FEMORAL DIAPHYSES FOR FLEXURAL BIOMECHANICAL TESTING: PRINTER VARIABILITY AND VALIDATION

*Omar Manzur[1], Kishore Mysore Nagaraja[2], Blaine M Oldham[1], Richard Samade[1], Robert C Weinschenk[1], Wei Li[2]
[1]Department of Orthopaedic Surgery, The University of Texas Southwestern Medical Center
*Corresponding author's email: omar.manzur@utsouthwestern.edu

**Introduction:** The femur, the longest and strongest bone in the body, is essential for weight-bearing and locomotion. Understanding its mechanical properties is critical for improving orthopedic treatments, implant design, and surgical outcomes. Traditional biomechanical studies rely on cadaveric specimens and synthetic bone models, which present limitations such as biological variability, high costs, and supply chain delays. As a result, three-dimensional (3D) printing has emerged as a promising, cost-effective alternative. Polylactic acid (PLA), a biodegradable thermoplastic, has shown potential in replicating the flexural properties of human bone. However, the effects of different 3D printers and infill densities on biomechanical performance remain underexplored. This study aims to address these limitations by systematically investigating the effects of four different 3D printers on PLA femoral diaphysis models, each printed at two distinct infill densities (5% and 20%).

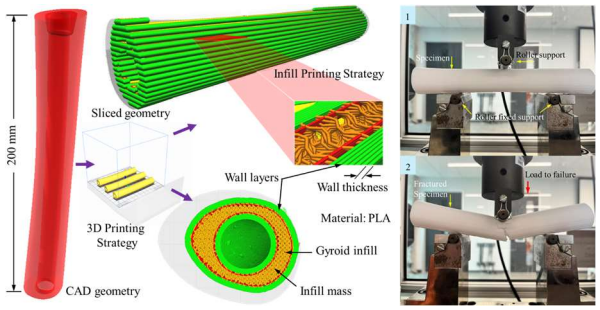


**Figure 1:** Representation of the computer-aided design of the diaphyseal section of the human. (1) Three-point bending test setup of the specimen supported without rotation degree of freedom prior to loading. (2) Specimen with fracture after loading.

**Methods:** Four different 3D printers (Prusa i3 MK3S+, Ultimaker 3, Flashforge Creator Pro 2, and Bambu Lab A1) were used to fabricate PLA femur diaphysis models at two distinct infill densities (5% and 20%), as per prior literature [1] (**Fig. 1**). Printing parameters, including nozzle temperature, print speed, and layer height, were standardized across all printers to ensure consistency. A gyroid infill pattern was selected to optimize structural stability. Flexural properties were assessed using a three-point bending test following ASTM F383-73 and F1264-03 standards. Each specimen, measuring 200 mm in length with a 20 mm diameter, was loaded at a strain rate of 0.025 mm/s until failure. Flexural modulus and strength were calculated from the resulting stress-strain curves. Standard deviation-based distributions were calculated to assess variability in mechanical performance. Additionally, a linear regression machine learning model was employed to analyze relationships between printing parameters and flexural properties, enabling predictive modeling of mechanical behavior.

**Results:** At 5% infill, Prusa, Ultimaker, Flash Forge, and Bambu printers yielded flexural moduli of 7.27 ± 0.21, 6.72 ± 0.18, 4.04 ± 0.08, and 4.21 ± 0.10 GPa, with flexural strengths of 177.3 ± 2.45, 181.3 ± 4.65, 174.2 ± 4.31, and 147.5 ± 3.02 MPa, respectively. At 20% infill, moduli were 18.4 ± 0.09, 12.4 ± 0.11, 10.7 ± 0.26, and 10.8 ± 0.15 GPa, while strengths were 844.0 ± 3.97, 550.9 ± 11.4, 550.9 ± 13.2, and 515.2 ± 6.04 MPa, respectively.

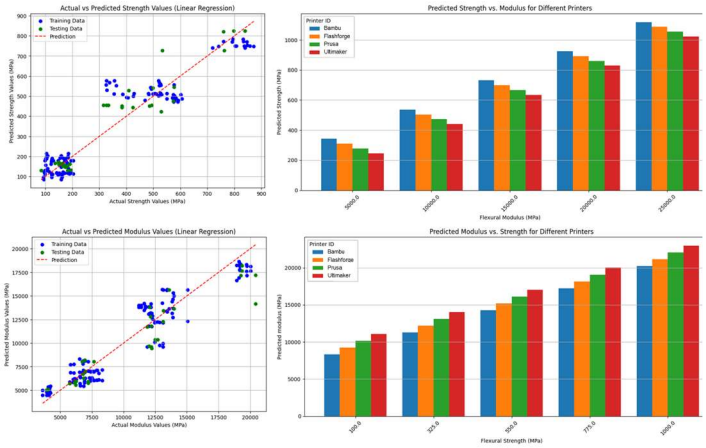


**Figure 2:** Linear regression machine learning model with a train-to-test ratio of 0.8 to 0.2 representing the relationship between flexural strength and modulus under the influence of infill density, printer type, and wall layers.

**Discussion:** This study demonstrates the influence of printer type, infill percentage, and wall layers on the mechanical properties of 3D-printed PLA femur models. Prusa achieved the highest flexural strength and modulus at 20% infill, indicating superior interlayer adhesion. In contrast, Bambu produced lower strengths, suggesting high-speed printing may reduce mechanical integrity. Ultimaker and Flashforge showed intermediate results, with Ultimaker displaying greater consistency. Linear regression analysis identified flexural modulus as the strongest predictor of flexural strength, followed by printer type, wall layers, and infill percentage (**Fig 2**). The model's R-squared values (0.78 for strength, 0.86 for modulus) confirmed a strong correlation between printing parameters and mechanical properties. Predictive models estimated an average modulus of 18.151 GPa, which aligns with literature regarding 3D femoral biomechanics emulating cadaveric values [1]. While results demonstrate inter-printer variability, each printer's average flexural moduli and strength fall within published cadaveric ranges, and the standard deviations demonstrate minimal intra-printer variability.

**Significance:** This study highlights how printer type, infill, and wall layers affect 3D-printed PLA femur mechanics. Linear regression enabled a predictive framework to optimize printing, enhancing biomechanical testing, surgical planning, and education. These findings reduce reliance on cadavers and costly models, making patient-specific, affordable 3D-printed bones more accessible.

**References:** [1] Weinschenk et al. (2024), *J Orthop Res* 42(12)

# CERVICAL HARD COLLAR IMMOBILIZATION: EVALUATING DYNAMIC INTERVERTEBRAL KINEMATICS

*M. Zino Kuhn[1], Clarissa LeVasseur[1,2], Adam Almoukamal[1], Aditya Padmanabhan[1], Eleanor Roberts[1], Rishabh Shetty[1], Andrew Sudar[1], William J. Anderst[1]

[1]Biodynamics Lab, [2]Bethel Musculoskeletal Research Center, Department of Orthopaedic Surgery, University of Pittsburgh, Pittsburgh, PA 15203

*Corresponding author's email: kuhnm4@upmc.edu

**Introduction:** Cervical spine injuries occur at a rate of nearly 25,000/yr in the United States, with the majority being treated nonoperatively in a hard collar orthosis [1,2]. Despite high injury incidence and therapeutic hard collar utilization, little is known about the dynamic intervertebral kinematics associated with hard collar immobilization [2-4]. We previously conducted a comprehensive evaluation of segmental cervical spine kinematics using validated dynamic biplane radiography (DBR) comparing motion restriction due to a soft collar, hard collar, and cervical thoracic orthosis (CTO) [4]. Results demonstrated limited efficacy of a soft collar and significant motion restriction with both a hard collar and CTO [4]. Given increased cost and complications associated with CTO, the aim of the present study is to focus on four different commercially available hard collar orthoses and compare dynamic segmental intervertebral kinematics associated with each. We hypothesized that all of the tested collars will decrease motion from the no collar condition, but there will be no differences between collars in intervertebral motion restriction.

**Methods:** Twenty healthy young adults (10M, 10F) without previous medical or surgical history involving their neck or spine provided written informed consent to participate in this IRB-approved prospective cohort study. All subjects completed a CT scan of their cervical spine and kinematic evaluation. Each subject completed five trials each of maximal neck flexion-extension (FE), axial rotation (AR), and lateral bending (LB) while seated within a DBR apparatus (four experimental conditions with different hard collars and a control condition with no collar). Condition order was randomized. All collars were fit to manufacturer recommendations by a licensed clinician. During each movement, synchronized biplane radiographs were collected at 30 frames per second for 3 seconds to capture a full range of motion (ROM) movement cycle. Bone tissue from the occiput and seven cervical vertebrae was segmented from the CT scan, and subject-specific 3D bone models were created. A validated, volumetric-based tracking technique was used to match the bone models to the biplane radiographs with submillimetre accuracy and six degree-of-freedom kinematics were calculated for each cervical spine motion segment using previously validated methods [5]. Repeated measures ANOVA with a post-hoc Bonferroni correction was used to identify differences in segmental kinematics between conditions. Significance was set at $p < 0.05$.

**Results & Discussion:** Eleven out of twenty participants (5M, 6F) with an average age of 26.1 ± 3.7 years and average BMI of 25.7 ± 3.1 kg/m$^2$ have been processed to date. All four collars restricted occiput-C7 motion in FE and AR movements (all $p < 0.001$) (Table 1). Only the Breg collar reduced occiput-C7 motion during LB (Table 1). The DonJoy collar significantly reduced occiput-C7 FE motion when compared to the Breg collar ($p = 0.026$). All collars reduced FE at each motion segment (all $p < 0.01$) (Fig. 1). All but the Breg collar reduced AR at C1-C2, a primary contributor to neck AR (all $p < 0.012$). The DonJoy collar reduced LB at each motion segment except C1-C2 (all $p < 0.03$) (Fig. 1).

Dynamic intervertebral kinematic data for all hard collars overall resembled that which was reported in our previous study comparing the efficacy of various cervical spine immobilization orthoses [4], however we now demonstrate nuanced kinematic differences between different commercially available hard collars. A notable limitation is that all participants had no neck pathology at time of testing.

**Table 1:** Average occiput-C7 motion across five experimental conditions during FE (top), AR (middle), and LB (bottom). Significant ROM reductions compared to no collar are indicated by an asterisk. All $p < 0.047$.

| | No collar | DonJoy | Aspen | Breg | Ossur |
|---|---|---|---|---|---|
| **FE** | 96.0±24.2° | **29.4±14.5°*** | **33.1±11.9°*** | **37.5±14.0°*** | **31.9±5.5°*** |
| **AR** | 128.4±22.5° | **61.4±38.2°*** | **68.3±32.6°*** | **69.7±34.2°*** | **63.1±29.1°*** |
| **LB** | 62.8±24.9° | 37.1±14.0° | 41.3±13.2° | **36.9±12.8°*** | 33.4±10.7° |

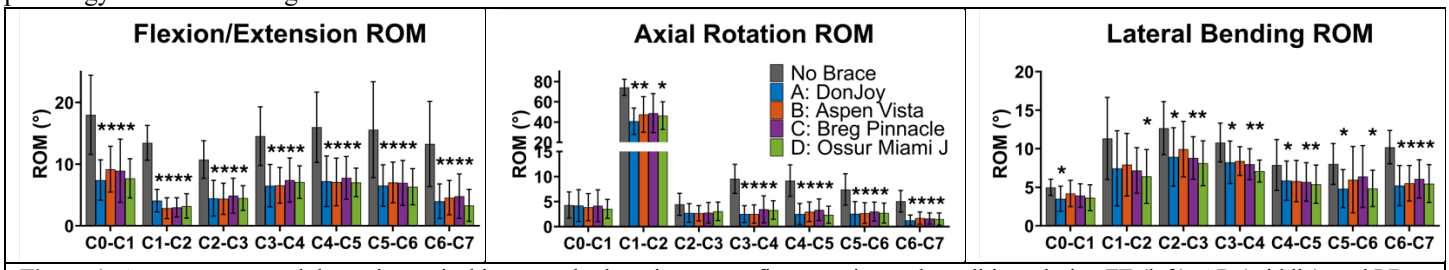


**Figure 1:** Average segmental dynamic cervical intervertebral motion across five experimental conditions during FE (left), AR (middle), and LB (right). Significant ROM reductions compared to no collar are indicated by an asterisk. All $p < 0.043$.

**Significance:** The results indicate that while hard collars do successfully restrict cervical ROM, FE and AR ROM restriction are more efficacious than LB ROM restriction. Differences between collars in their in intervertebral motion restriction primarily appear during lateral bending, however, those differences are relatively small and therefore may have limited clinical importance.

**Acknowledgments:** This study was sponsored by Enovis Corporation (Wilmington, Delaware, USA).

**References:** [1] US Consumer Product Safety Commission, NEISS (2018); [2] Agabegi et al. (2010), *JAAOS*; [3] Kim et al. (2020), *Hong Kong J Emerg Med;* [4] Oyekan et al. (2023), *Spine*; [5] Anderst et al. (2011), *Spine*.

# Are Favorable Patient-Reported Outcomes 3-Months after Anterior Cruciate Ligament Reconstruction Associated with Interlimb Loading Symmetry at 6-Months?

Abdulmajeed Alfayyadh[1], Jack R. Williams[2], Kelsey Neal[3], Ashutosh Khandha[4],
Kurt Manal[4], Lynn Snyder-Mackler[4], Thomas S. Buchanan[4]
[1]Jouf University, Al-Jowf, Saudi Arabia
[2]Northern Arizona University, Flagstaff AZ
[3]University of New Mexico School of Medicine, Albuquerque NM
[4]University of Delaware, Newark DE
Corresponding author's email: Abalfayyadh@ju.edu.sa

**Introduction:** Asymmetric interlimb loading 6-months after anterior cruciate ligament reconstruction (ACLR) is linked to long-term knee osteoarthritis (OA) development [1]. Identifying early indicators of asymmetric loading, often represented by peak medial compartment force (pMCF), may help inform rehabilitation strategies. Patient-reported outcome measures (PROMs), such as the Knee injury and Osteoarthritis Outcome Score (KOOS), Knee Outcome Survey – Activities of Daily Living (KOS-ADLS), ACL-Return to Sport after Injury (ACL-RSI), and Tampa Scale of Kinesiophobia (TSK), are often used to assess self-perceived function and psychological factors post-ACLR [2]. Several studies report the importance of PROMs [3, 4]; however, their relationship with interlimb pMCF asymmetry remains unclear. The purpose of this study was to examine whether PROMs three months post-ACLR predict interlimb pMCF asymmetry at six months. We hypothesized that better PROMs 3-months after ACLR would be associated with less interlimb pMCF asymmetry 6-months after surgery. Specifically, we hypothesized that KOOS, KOS-ADLS, and ACL-RSI scores (where higher scores are better) 3-months after surgery would be negatively associated with pMCF interlimb differences (ILDs) at 6-months, and TSK scores (where lower scores are better) would be positively associated pMCF ILDs.

**Methods:** 39 participants (19 men, age: 22 ± 6 years, BMI: 25.2 ± 3.7 kg/m$^2$) completed PROM assessments (KOOS [5 subscales: pain, symptoms, ADL function, sport and recreation function, and quality of life], KOS-ADLS, ACL-RSI, TSK) 3-months after unilateral ACLR. Six months post-surgery, these same participants underwent gait analysis at a self-selected speed. Kinematic, kinetic, and EMG data were collected bilaterally during overground walking and were analysed using Visual3D (C-Motion). Bilateral pMCFs were calculated using a validated EMG-based neuromusculoskeletal model [5] and were normalized to bodyweight (BW). The ILD of pMCFs for each participant was calculated by subtracting the value of the uninvolved limb from the involved limb. Pearson's correlation analyses ($\alpha = 0.05$) were used to assess associations between the PROMs and pMCF ILDs.

**Results & Discussion:** Our hypotheses were not supported. Surprisingly, significant positive correlations were observed between KOOS-ADLS ($r = 0.41$, $p = 0.01$, effect size = moderate), KOOS-Pain ($r = 0.36$, $p = 0.03$, effect size = moderate), and KOS-ADL ($r = 0.37$, $p = 0.02$, effect size = moderate) three months after surgery and pMCF ILDs at six months (**Table 1**). This suggests that better self-reported function and less pain at three months is associated with greater knee loading asymmetry (Involved limb is overloaded vs. uninvolved) at six months. Likewise, worse self-reported function and pain at three months was also associated with greater asymmetry (Involved limb is underloaded vs. uninvolved). While asymmetric knee loading 6-months post-ACLR is associated with knee OA development 5 years later [1], the findings of the current study indicate that both high and low PROM scores could be detrimental to long-term knee health. Identifying normative ranges for these measures may help guide clinicians and trainers in optimizing rehabilitation strategies. These findings emphasize the importance of considering both subjective and objective recovery metrics in post-ACLR rehabilitation, ensuring that treatment plans address both perceived function and biomechanical outcomes.

**Significance:** These findings suggest that early self-reported improvements in knee function and pain levels may not directly translate to optimal biomechanical recovery. Both high and low PROM scores early after ACLR may contribute to abnormal knee loading patterns, potentially compromising cartilage health. Future studies should explore the relationship between PROMs at three months and cartilage degeneration indicators, such as T2 relaxation time, at later stages to better understand their long-term implications.

**Table 1.** PROMs 3-months after ACLR vs. interlimb difference of pMCFs at 6-months after ACLR. (* = statistical significance.)

| Variable | | TSK | KOOS | | | | | ACL-RSI | KOS-ADLS | IKDC |
|---|---|---|---|---|---|---|---|---|---|---|
| | | | Symptom | Pain | ADL | Sports & Rec | Quality of life | | | |
| ILD of pMCF | *r* | 0.01 | 0.29 | 0.36* | 0.37* | 0.18 | 0.13 | 0.04 | 0.41* | 0.29 |
| | *p* | 0.93 | 0.07 | 0.03* | 0.02* | 0.27 | 0.43 | 0.79 | 0.01* | 0.08 |

**Acknowledgments:** NIH: R01-HD087459

**References:**

[1] Wellsandt E et al., (2016); [2] Randsborg P et al., (2022); [3] Palmieri-Smith RM et al., (2022); [4] Ithurburn MP et al., (2015); [5] Manal K et al., (2013).

# Improvement of Knee Adduction Moment and Function Following Six-Week Off-axis Stepping Training for Knee Osteoarthritis

Raziyeh Baghi[1], Wei Yin, Giovanni Oppizzi, *Li-Qun Zhang[1]
[1]University of Maryland Baltimore, Baltimore, United States
*Corresponding author's email: L-Zhang@som.umaryland.edu

**Introduction:** A key goal in rehabilitating medial knee osteoarthritis (KOA) is reducing peak knee adduction moment (KAM), which reflects medial compartment loading and cartilage damage progression (1). Gait modifications, such as altering foot progression angle (FPA)—the angle between the foot and forward motion—can lower pKAM. While prior studies used uniform FPA training, individualized FPA yielded better pKAM reductions (2, 3). Research has explored FPA adjustments from 25° toe-in to 30° toe-out, but testing multiple FPAs is time-consuming and may disrupt natural gait, limiting adherence. A solution is dynamically varying FPA within a toe-in/toe-out range during stepping, enabling individualized pKAM-FPA relationships to determine optimal FPA.

Neuromuscular control, essential for joint stability, is often impaired in KOA, particularly in the frontal plane, contributing to disease progression. Instability correlates with pain and functional decline. Bennell et al. found that a 12-week neuromuscular exercise program improved knee function and pain (4). Frontal plane gait perturbation training enhanced muscle activation, suggesting potential long-term benefits (5). A robotic elliptical system with perturbation and real-time knee moment estimation can optimize training by identifying subject-specific FPA for KAM reduction. This study examined a 6-week robot-guided off-axis stepping program using individualized FPA to reduce pKAM by at least 10% and improve frontal plane stability and function in medial KOA.

**Methods:** This study included eleven individuals with medial KOA. A specially designed elliptical trainer with multi-degree-of-freedom (DOF) controlled stepping was developed to assess knee moments during movement. The trainer's footplates were capable of rotating in the transverse plane and sliding in the frontal plane. The training program spanned six weeks, consisting of 18 training sessions and two evaluation sessions (pre- and post-evaluation). During the pre-evaluation, the optimal footplate position in the transverse plane—one that achieved at least a 10% reduction in pKAM—was identified and subsequently used in the training sessions to target pKAM reduction. Throughout the training, participants received real-time audiovisual feedback to help maintain proper mediolateral footplate positioning and lower limb alignment while stepping in free sliding mode. The pre- and post-evaluations included assessments of the Knee injury and Osteoarthritis Outcome Score (KOOS), timed-up-and-go (TUG) test, and a 30-second sit-to-stand (STS) test to measure the training program's effects on knee pain, quality of life (QOL), and motor function. The Wilcoxon signed-rank test was applied to compare scores between the pre- and post-evaluation sessions. Additionally, a paired sample t-test was conducted to analyze the impact of the six-week training program on various parameters, including stepping speed, sliding instability, maximum medial and lateral sliding distance, peak knee flexion moment (pKFM), pKAM, peak knee internal rotation (pKIRM), knee adduction moment impulse (ImpKAM) during stepping, STS, TUG, 20-meter walk test (20-MWT), four-square step test (FSST), spatiotemporal gait characteristics, and KOOS. Comparisons were made between baseline and post-training evaluations, as well as between baseline and follow-up assessments, with Bonferroni correction applied at a significance level of $p < 0.05$.

| | Baseline | Post-Training | Follow-Up |
|---|---|---|---|
| KAM (%BW*HT) | 2.40 ± 0.79 | 1.51 ± 0.69 * | 2.00 ± 1.05 |
| sliding stability (mm) | 10.91 ± 2.96 | 3.72 ± 3.27 * | 3.74 ± 5.29 * |
| Max lateral sliding (mm) | 32.99 ± 15.07 | 11.88 ± 12.63* | 8.89 ± 13.35* |
| Stepping speed (rpm) | 22.89 ± 12.55 | 34.49 ± 9.98* | 33.20 ± 8.30 |
| KOOS Symptoms | 61.31 (17.56) | 72.62 (14.23) * | 68.45 (21.95) |
| 20MWT (s) | 18.71 (2.51) | 16.47 (3.47) * | 16.94 (4.84) |
| STS (count) | 9.17 (3.06) | 10.16 (2.85) * | 9.75 (3.59) |
| Step Length: Right (cm) | 64.57 (8.00) | 67.18 (8.41) * | 66.03 (7.98) |
| Gait velocity (m/s) | 1.15 (0.24) | 1.22 (0.25) * | 1.14 (0.27) |

*Table 1. Primary outcome measures post-training and at follow-up. * p < 0.05.*

**Results & Discussion:** Study results are presented in Table 1. Significant differences were observed in normalized pKAM between pre- and post-evaluation ($p = 0.01$, $d = -1.63$), likely due to the individualized FPA, which reduced pKAM by at least 10%. These findings align with prior research showing toe-out and toe-in gait retraining reduces second and first pKAM, respectively, while improving pain and function (2,3). Sliding stability improved post-training ($p < 0.002$, $d = -1.83$) and was maintained at follow-up ($p = 0.038$, $d = -1.21$). Maximum lateral sliding distance significantly decreased post-training ($p = 0.022$, $d = -0.93$) and at follow-up ($p = 0.04$, $d = -1.19$). Stepping speed also increased post-training ($p = 0.026$, $d = 0.91$) and remained elevated at follow-up. These improvements likely resulted from the free sliding mode, which required active stability control, and real-time visual feedback, which reinforced proper movement patterns. The 6-week training enhanced KOOS symptoms subscale scores ($p = 0.036$, $d = 2.34$) and functional performance in 20-MWT ($p = 0.016$, $d = -1.47$) and STS ($p = 0.024$, $d = 1.35$). Walking velocity ($p = 0.018$, $d = 2.15$) and right step length ($p = 0.046$, $d = 1.61$) also improved. These functional and gait enhancements may be attributed to reduced KAM and better frontal plane stability, promoting a more efficient and stable gait.

**Significance:** These findings suggest that this novel training approach may be a promising non-invasive treatment option for managing medial KOA. The results contribute further to the growing body of evidence supporting targeted exercise interventions for individuals with KOA and provide a foundation for future research investigating the long-term effects and potential mechanisms underlying the observed improvements.

**Acknowledgments:** Funding/ financial support: NIDILRR 90REMM001. Authors have no conflict of interests.

**References:** [1] Sharma et al. (1998), *Arth & Rheum* 41(7); [2] Hunt et al. (2014), *Osteoarthritis & Cartilage* 22(7); [3] Shull et al. (2013), *J Biomech* 46(1). [4] Bennell et al. (2011) *Ann Rheum Dis* 70(10). [5] Rutherford et al. *Clin Biomech* (2022) 92(105574).

# PATELLOFEMORAL CONTACT FORCES DURING DIFFERENT TYPES OF WALKING IN ADULTS WITH AND WITHOUT KNEE OSTEOARTHRITIS

*Sharf M. Daradkeh[1,2], John D. Willson[3], Gretchen B. Salsich[1], Joshua J. Stefanik[4], Patrick Corrigan[1,2]
[1] Saint Louis University, [2] Cleveland Clinic, [3] East Carolina University, [4] Northeastern University
*Corresponding author's email: sharf.daradkeh@slu.edu

**Introduction:** Walking is recommended for reducing pain and physical disability in individuals with knee osteoarthritis (OA) [1]. However, certain types of walking may exacerbate symptoms and accelerate disease progression by exposing the joint to heightened contact forces [2]. With pain and pathology frequently occurring in the patellofemoral (PF) compartment [3], there is a need to understand how different real-world factors during walking influence PF contact forces. Gaining insights into PF loading patterns could assist with the prescription of walking for adults with knee OA as well as inform strategies for preventing PFOA. This study aimed to characterize PF contact forces across various types of walking in adults with and without knee OA, with a specific focus on walking speed and gradient.

**Methods:** 32 adults were enrolled, including 14 with unilateral symptomatic knee OA (9F; age = 60.6(8.6) years; body mass = 76.1(19.40) kg; height = 166.5(11.68) cm) and 20 without knee OA (14F; age = 59(8.1) years; body mass = 78(16.9) kg; height = 170.4(8.6) cm). Knee OA was clinically-defined based on the National Institute for Health and Care Excellence (NICE) criteria (≥ 45 years old, knee pain lasting > 3 months, knee pain ≥ 3/10 with walking, and knee stiffness lasting < 30 minutes). Each participant completed nine walking conditions on a force-instrumented split-belt treadmill (Bertec Inc., Columbus, OH) in a 6-camera, three-dimensional motion capture environment (Qualisys AB, Gotenberg, Sweden). Conditions were 2 minutes in duration, performed in a randomized order, and included level (0°), inclined (+4.8°), and declined (-4.8°) gradients at self-selected(ss), fast (ss+20%), and slow speeds (ss-20%). Ground reaction forces and marker coordinates were sampled (2160 and 180 Hz, respectively) during the second minute of each condition and reduced to 10 bilateral gait cycles. PF contact forces were estimated for each step using an inverse dynamics-informed musculoskeletal model [4]. After scaling the PF contact force signals to bodyweight (BW), we estimated cumulative PF load for 10 minutes of walking in each condition using average PF contact force impulse (BW*s/step) and cadence (steps/minute for a single limb). For analyses, conditions were ranked within each participant using cumulative PF load measures and mean-ranked within each group. This approach was used to facilitate a better understanding of how cumulative PF load may be incrementally increased or decreased during a walking program by manipulating speed and gradient. For visualization, heat maps were generated for each group based on the mean ranks. For analyses in the OA group, only data from the painful knee was used. In the non-OA group, data were averaged between limbs prior to ranking.

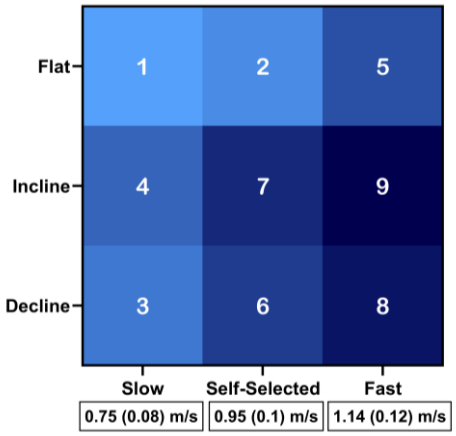


**Figure 1:** Mean-rankings of walking conditions (1-9) by cumulative PF load in the symptomatic limb of adults with knee OA.

**Results & Discussion:** In those with knee OA, average (SD) cumulative PF load for level walking at slow, self-selected, and fast speeds were 55.4 (23.2), 68.3 (31.9), and 69.4 (29.3) BW*s, respectively. Cumulative PF loads for inclined walking at slow, self-selected, and fast speeds were 74.2 (35.6), 84.2 (42.4), and 94.2 (46.3) BW*s, respectively. Lastly, cumulative PF loads for declined walking at slow, self-selected, and fast speeds were 70.1 (37.8), 75 (36), and 95.4 (44.7) BW*s, respectively. Group-level mean-rankings are shown in Figure 1. In general, cumulative PF loads seem to increase with faster walking speeds and follow the progression: Flat<Declined<Inclined.

In those without knee OA, average (SD) cumulative PF load for level walking at slow, self-selected, and fast speeds were 68.6 (24.8), 77.2 (25.6), and 90.3 (31.6) BW*s, respectively. Cumulative PF loads for inclined walking at slow, self-selected, and fast speeds were 94.7 (29.9), 105.5 (32.2), and 116.6 (37.5) BW*s, respectively. Cumulative PF loads for declined walking at slow, self-selected, and fast speeds were 83.15 (40.7), 95.7 (42.4), and 114.5 (43.7) BW*s, respectively. Group-level mean-rankings are shown in Figure 2. In general, the progression of cumulative PF load followed the same pattern as adults with knee OA. However, it should be noted that cumulative PF loads appear to be higher for all types of walking in adults without knee OA compared to adults with knee OA.

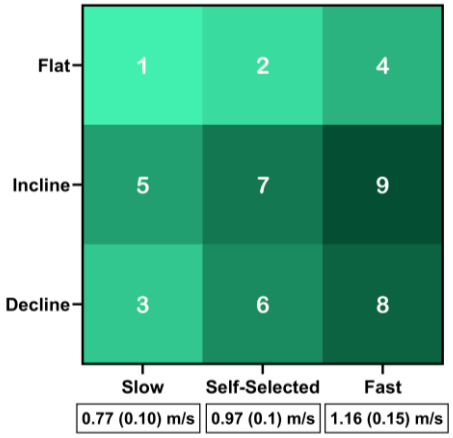


**Figure 2:** Mean-rankings of walking conditions (1-9) by cumulative PF load in adults without knee OA.

**Significance:** By identifying walking conditions that minimize PF compartment forces, this research could inform approaches to physical rehabilitation and OA prevention. This descriptive approach offers valuable insights to therapists for tailoring walking programs to accommodate joint loading limitations while maintaining physical activity.

**Acknowledgments:** Funding was provided by the Rheumatology Research Foundation and Academy of Orthopaedic Physical Therapy.

**References:** [1] White DK, et al. (2012), [2] Amiri P, et al. (2023), [3] Hart H, et al. (2017) [4] Willy RW, et al. (2016).

# WEIGHT-BEARING ASYMMETRY PATTERNS DURING SQUATTING AFTER FIBULAR FREE FLAP HARVEST

Adam Bunn[1,2*], Madeline Grosklos[1,2], Michelle Lockwood[3], Gaeryn Salverda[4],
Courtney Butowicz[5], Trevor Kingsbury[4], Marisa Pontillo[1,2]
[1]Extremity Trauma and Amputation Center of Excellence, San Diego, CA, USA
*Corresponding author's email: adam.c.bunn.civ@health.mil

**Introduction:** Fibular free flap (FFF) harvest is commonly used in reconstructive surgery, particularly following trauma or pathology. While surgeons primarily focus on recipient site outcomes, significant donor site morbidity can occur, potentially delaying recovery [1]. Previous studies have shown physical impairments from donor sites [2], but most research has focused on neurosensory outcomes rather than functional biomechanics. The lack of evidence-based post-operative paradigms leads to discrepancies in functional progressions, return to activity timelines, and rehabilitation resource utilization. This study aims to quantify weight-bearing asymmetry during squatting across three timepoints: one pre-operative and two post-operative. We hypothesized patients would initially demonstrate symmetrical weight distribution, followed by asymmetry away from the involved side post-operatively, with a subsequent return toward symmetry at follow-up.

**Methods:** Eleven patients undergoing FFF procedure (6 male/5 female, height:1.72±.36m, weight:76.0±14.9 kg,) completed comprehensive biomechanical assessments at a minimum two of the three time points: pre-operative (n=11), post-operative (upon clearance for ambulation without assistive devices) (n=11), and follow-up (n=8). Participants performed five consecutive bodyweight squats on two force decks (VALD Performance) during each visit. Asymmetry was calculated as the percentage difference between involved and uninvolved limbs for concentric mean force, eccentric mean force, and peak force and was averaged across all five squats. A repeated measures analysis of variance with a post-hoc Bonferroni correction was run for the 8 participants with three assessments to track the progression of squat performance across timepoints.

**Results & Discussion:** Post-operative assessments occurred at an average of 30.1 ± 13.5 days after pre-assessments, while follow-up evaluations were conducted at 126.2 ± 94.0 days after pre-operative assessment. Differences between assessments were observed for eccentric force, peak force, and squat depth ($p \leq .014$) (Figure 1). For eccentric mean force asymmetry, post-operative assessment asymmetry was significantly greater than both pre-op ($p=.010$) and follow-up ($p=.037$), but follow-up did not differ from pre-op. This shows that participants demonstrated a shift in weight distribution away from the involved limb from pre-operative to post-operative assessment, followed by a return toward the involved limb at follow-up. For peak force asymmetry, post-operative asymmetry was significantly greater than pre-operative asymmetry ($p=0.16$) but did not differ from asymmetry at follow-up. These findings suggest a protective mechanism where participants initially offloaded the surgical limb, then gradually increased loading as healing progressed. Although substantial functional recovery occurred by follow-up, asymmetry values remained biased toward the non-involved side, indicating subtle residual deficiencies persisted. These lingering asymmetries highlight the need for targeted interventions focused specifically on equalizing load distribution during functional activities, which may further optimize rehabilitation outcomes and potentially accelerate return to activity for individuals with lower extremity autologous graft procedures.

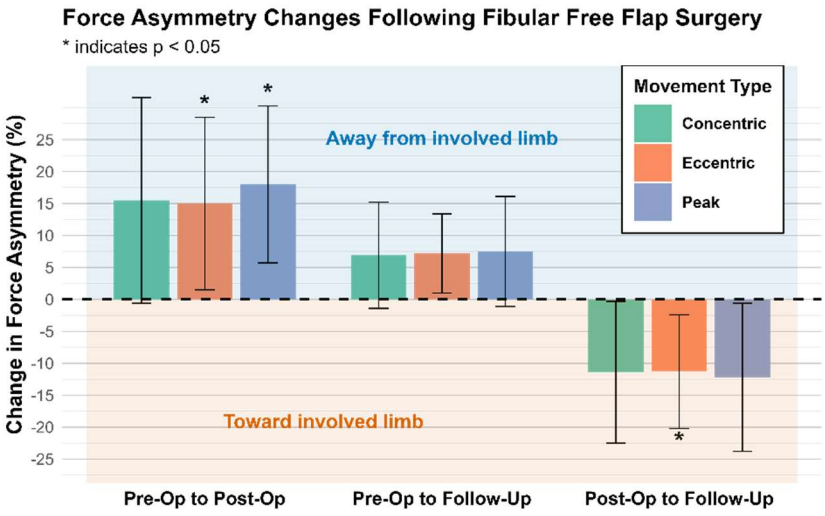


**Figure 1:** Squat Biomechanics following Fibular Free Flap Surgery (Mean ± SD). Note: Positive values for force asymmetry changes indicate a shift away from involved limb.

**Significance:** This study presents the first quantitative analysis of force distribution patterns during functional movements following FFF harvest. Our findings reveal a characteristic adaptation where patients redistribute weight away from the involved limb post-operatively and then progressively return toward more balanced loading during recovery. Understanding these biomechanical compensations provides critical insights for rehabilitation specialists designing interventions for all patients undergoing FFF procedures. Future research should investigate whether targeted interventions to normalize force distribution can mitigate long-term biomechanical compensations and improve functional outcomes.

**Acknowledgments:**The views expressed herein are those of the author(s) and do not reflect the official policy or position of the Naval Medical Center San Diego, the Defense Health Agency, the Department of Defense, or any agencies under the U.S. Government**.**

**References:** [1] Skoner J et al. (2003), *The Laryngoscope* 113; [2] Abo Sharkh et al. (2019), *J Oral Maxillofac. Surg.* 77.

# IN VIVO ASSESSMENT OF PATELLAR TENDON LOADING DURING BASAS SPANISH SQUATS WITH NEUROMUSCULAR ELECTRICAL STIMULATION

*Jack Felipe[1], Claudia Kacmarcik[2], João Luiz Quaglioti Durigan[3], Karin Grävare Silbernagel[2], Stephanie Cone[1]
[1]Department of Biomedical Engineering, University of Delaware, Newark, DE, USA
[2]Department of Physical Therapy, University of Delaware, Newark, DE, USA
[3]Universidade de Brasília, Laboratory of Muscle and Tendon Plasticity, Graduate Program in Rehabilitation Sciences, DF, Brazil
*Corresponding author's email: felipej@udel.edu

**Introduction:** Patellar tendinopathy is a painful condition affecting everyday functionality of the knee. The Basas Spanish squat with neuromuscular electrical stimulation (NMES) has been shown to decrease pain in individuals with patellar tendinopathy through mechanical strain of the tendon [1]. Experimental limitations have prevented measurement of the tension through the patellar tendon during Basas Spanish squats. Shear wave tensiometry is a technique that enables the direct measurement of soft tissue load [2]. This study aims to compare changes in patellar tendon loading during Basas Spanish squats with or without NMES superimposed. Due to the increased activation of the quadriceps, we hypothesize that Basas Spanish squats with NMES will yield the largest tendon load.

**Methods:** Twenty healthy adult participants (9M/11F) and five participants with patellar tendinopathy (4M/1F) were recruited for this study. The dominant or affected limb was fitted with two electrodes over the quadriceps motor points to deliver NMES [1] and a shear wave tensiometer was secured over the patellar tendon [2]. For the squat condition, participants performed 3 sets of 8 Basas Spanish [1] squats with a 5 second hold at 90º of knee flexion. For squat+NMES trials, the squat protocol was followed with the addition of NMES at 90º of knee flexion. Shear wave tensiometry was used to measure patellar tendon tension during each set of Basas Spanish squats. Following each set of squats, participants were asked to rate patellar tendon pain on a scale from 0 (no pain) to 10 (maximum pain imaginable). A mixed model in statistical parametric mapping (SPM) was used to identify differences in shear wave speed patterns between healthy and patellar tendinopathy participants as well as within participants during squat and squat+NMES conditions. A paired t-test was used to assess differences in perceived discomfort between the squat and squat+NMES conditions.

**Results & Discussion:** There was no main effect of group, condition, or interaction between the two on measured shear wave speeds. While there were no significant differences in loading patterns, there was an increase in healthy patellar tendon peak shear wave speed from the squat to squat+NMES condition (37.80 ± 27.8 to 43.14 ± 31.0 m/s). Whereas did not observe this trend in the patellar tendinopathy group from the squat to squat+NMES condition (58.47 ± 32.0 to 53.27 ± 31.1 m/s). A high degree of participant-specific differences in the biomechanical response to the stimulations was evident in some, but not all, participants. Loading patterns for a representative healthy participant (Fig. 1) show an individual response to added stimulation with increased shear wave speed in the squat+NMES condition. Our findings suggest that, in some healthy participants, Basas Spanish squats with superimposed NMES could increase patellar tendon tensile loading compared to without NMES. In the patellar tendinopathy group, we found no significant differences in patellar tendon load from the squat to squat+NMES condition, however we did find a trend in patellar tendon pain reduction from the squat to squat+NMES condition ($p = 0.05$), indicating that there is therapeutic benefit to Basas Spanish squats, even when there is no alteration to the mechanical strain in the patellar tendon. To better understand the population variability seen in this study, we can characterize strength and loading patterns using dynamometry and motion analysis. Future work will also use shear wave tensiometry to evaluate the Basas Spanish squat treatment longitudinally as both a short- and long-term treatment option.

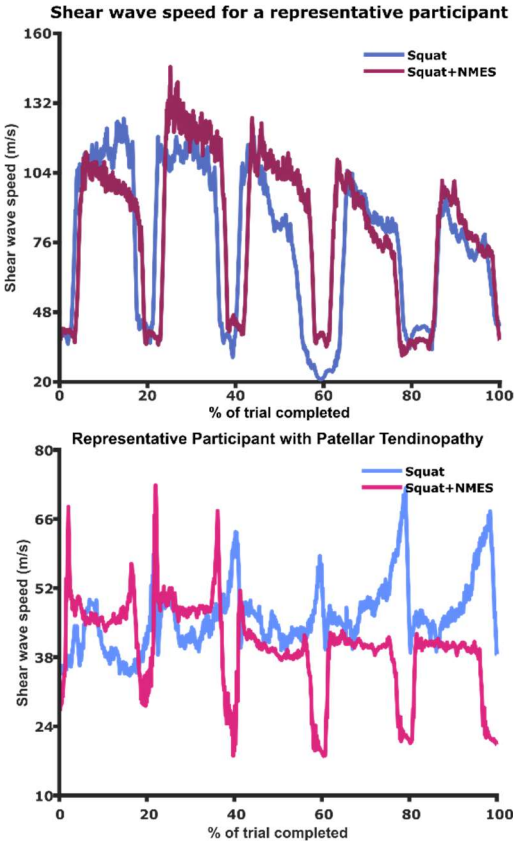


**Figure 1.** Shear wave speed patterns for a healthy representative participant (top) and a patellar tendinopathy participant (bottom) showing multiple repetitions of squat (blue) and squat+NMES (maroon or pink) tasks.

**Significance:** Patellar tendinopathy is a condition that causes pain and discomfort in athletic populations. This condition has prevented one-third of diagnosed athletes from returning to sports for more than 6 months and forced half of the diagnosed athletes to stop participating in sports at their prior level [3]. The Basas Spanish squat with superimposed NMES has been shown to increase the tendon strain and improve symptoms when used as treatment for patellar tendinopathy [1], however previous studies lacked the ability to directly observe the mechanical function of the patellar tendon. Implementation of shear wave tensiometry during Basas Spanish squats has allowed us to directly observe patellar tendon loading during these exercises.

**Acknowledgments:** This study was supported by a grant from NIH-NIGMS COBRE (P20GM139760).

**References:** [1] Basas et al. (2023). IJSPT. 18(6):1299-1307. [2] Martin et al. (2018). Nat Commun. 9:1592. [3] Peers et al. (2005). Sports Med. 35(1):71-87.

# PRE-INTERVENTION KINESIOPHOBIA AND SELF REPORTED KNEE FUNCTION DO NOT PREDICT POST-INTERVENTION LOAD SYMMETRY IMPROVEMENT AFTER TOTAL KNEE ARTHROPLASTY IN PATIENTS WHO RECEIVED PHYSICAL ACTIVITY AND SYMMETRY (PAS) AND CONTROL INTERVENTION

*Vaibhavi Rathod[1], Liubov Arbeeva[2], Carla Hill[3], Katie Huffman[2], Todd Schwartz[2], Kelli Allen[2,3], Robin Queen[1]
[1]Department of Biomedical Engineering and Mechanics, Virginia Tech, Blacksburg, VA; [2]Thurston Arthritis Research Center, University of North Carolina at Chapel Hill, [3]Department of Medicine, University of North Carolina at Chapel Hill
*Corresponding author's email: vrathod@vt.edu

**Introduction:** Kinesiophobia, or fear of movement due to pain, is common in individuals undergoing total knee arthroplasty (TKA) and is linked to persistent pain, delayed recovery, and reduced return to activity [1]. This psychological barrier often leads to movement avoidance, negatively impacting rehabilitation [2]. Self-reported knee function, assessed by the Knee Injury and Osteoarthritis Outcome Score (KOOS), is another key predictor of recovery, with lower preoperative scores associated with poorer outcomes [3]. While the role of kinesiophobia in long-term recovery is well-documented, its impact during early rehabilitation remains underexplored. Similarly, the predictive value of self-reported knee function on rehabilitation outcomes is not well understood. Therefore, the purpose of this study was to determine if kinesiophobia or self-reported knee function were associated with load symmetry improvement in patients receiving PAS intervention after TKA and in attention control group. We hypothesize that pre-intervention kinesiophobia or self-reported knee function will be associated with improvements in load symmetry.

**Methods:** This is secondary analysis of data from a randomized exploratory clinical trial (n = 60) [4]. Participants were enrolled 4–8 weeks after initiating post-TKA outpatient physical therapy (PT) and were randomized to either the PAS intervention or an attention control group, stratified by gender and presence of self-reported pain (≥3/10) in any lower extremity joint. The PAS intervention integrated physical activity counseling and balance exercises into routine PT and included two additional follow-up sessions (4 and 8 weeks post-PT) [4]. The attention control group received standard PT with equivalent follow-up sessions addressing general recovery benchmarks. Outcomes included objectively measured peak load symmetry during walking and self-reported outcomes that were assessed at baseline and 3 months later by blinded assessors. Limb load symmetry was assessed using a 3-sensor in-shoe load sensor (loadsol®, novel Electronics) during a 10m walking test (average of three trials). The Limb Symmetry Index (LSI) (|Surgical/Non-Surgical|*100) was calculated for each outcome measures of interest. The two main predictors of interest were the KOOS and the Tampa Scale of Kinesiophobia (TSK). Linear regressions were performed to explore the relationships between change in LSI from baseline at 3 months (post-intervention), with the TSK and KOOS pain score separately. The models were adjusted for baseline LSI, age, sex, gait speed, and treatment group.

**Results & Discussion:** A total of 32 patients (mean age: 68 ± 7 years, 13 females) completed the 3-month follow-up assessment. There were no associations between baseline TSK and improvements in peak impact force symmetry ($p = 0.875$), peak push-off force symmetry ($p = 0.742$) or peak impulse force symmetry ($p = 0.60$). Other variables, including baseline symmetry, age, sex, gait speed, did not show significant effects (all $p > 0.05$) in any of the models. While treatment type was significantly associated with peak impact force symmetry ($p=0.034$), the subgroup analysis did not yield statistically significant results. In addition, these analyses revealed that the KOOS pain score did not predict improvements in peak impact force symmetry ($p = 0.372$), peak push-off force symmetry ($p = 0.725$), or peak impulse force symmetry ($p = 0.609$). Contrary to our initial hypothesis, the findings of our study suggest that preintervention kinesiophobia and self-reported knee function scores do not predict improvements in peak force symmetry measures following the intervention in patients with TKA. One possible explanation for this outcome is that post-TKA load symmetry may be influenced more by biomechanical adaptations and movement pattern changes than by preexisting fear of movement or self-reported functional limitations [5]. While kinesiophobia and perceived knee function are known to influence movement patterns [6,7], their role in load symmetry improvements is limited. In our study, we found no association between kinesiophobia and self-reported knee function, suggesting that these factors may not be reliable indicators of load symmetry. Our findings align with those of Missman et al. (2025) [8], who also found no association between baseline patient reported outcome scores and rehabilitation outcomes post-TKA. Therefore, rehabilitation strategies should incorporate direct measures of load symmetry assessments rather than solely relying on patient-reported outcomes to assess progress. Considering these insights, it may be beneficial for clinicians to integrate objective biomechanical measurements in rehabilitation protocols for assessing patient progress and optimizing treatment strategies.

**Significance:** While self-reported kinesiophobia and knee function are relevant to rehabilitation, our study underscores the importance of a biomechanically focused approach to optimize load symmetry post-TKA.

**Acknowledgments:** This study was funded by the National Institute of Arthritis and Musculoskeletal and Skin Diseases (R21AR074149). We would like to acknowledge the contributions of physical therapists at in the UNC Healthcare System.

**References:** [1] Sullivan et al (2009) *Pain* 143 (1–2) [2] Aleksić et al (2024) *Geriatrics* 9(4) [3] Ware et al. (2018) *Am. J. Sports Med* 46 (4) [4] Queen et al (2024) *Osteoarthr. Cartil. Open* 6 (4) [5] Sackiriyas et al (2023) *Int. J. Sports Phys. Ther* 18(4) [6] de Oliveira Silva et al (2018) *Gait Posture* 66 (1) [7] Schmitt et al (2008) *Phys. Ther* 88(12*)* [8] Missmann et al (2025) *J. Rehabil. Med.*, vol. 57

# NO DIFFERENCES IN DROP VERTICAL JUMP BIOMECHANICS AT SEVEN YEARS WHEN LATERAL EXTRA-ARTICULAR TENODESIS IS ADDED TO ACL RECONSTRUCTION IN YOUNG ACTIVE PATIENTS: A SUB-ANALYSIS OF THE STABILITY RCT

*Richard E. Magony[1], Jane S. Thornton[2], Dianne M. Bryant[3], Alan M. J. Getgood[4], Derek N. Pamukoff[4]
[1]School of Kinesiology, Faculty of Health Sciences, Western University, London, ON
*Corresponding author's email: rmagony@uwo.ca

**Introduction:** Anterior cruciate ligament reconstruction (ACLR) often fails to restore knee stability with rotatory laxity and anterior translation persisting after surgery [1]. Augmentation with lateral extra-articular tenodesis (LET) has successfully reduced rates of graft failure and rotatory laxity at 2 years after ACLR [2]. However, reduction of anterolateral rotatory laxity caused by the addition of LET may have a negative impact on dynamic knee kinematics and functional performance during high impact tasks. Drop vertical jump (DVJ) tests are used to identify biomechanical asymmetries between limbs and assess individuals' risk of ACL re-injury after ACLR [3] [4]. In this study, we compared ACLR limb biomechanics between individuals with LET versus without LET at 7 years after surgery during a DVJ. We expected that ACLR limbs with LET would have lower peak knee abduction moment (KAbM) and greater peak knee flexion moment (KFM) and peak knee flexion angle (KFA) compared to those without LET, and that peak vertical ground reaction force (vGRF) and peak vertical loading rate (vLR) would not differ between groups.

**Methods:** 67 participants (58.2% female, 58.2% LET, 25.8 ± 2.9yo) were recruited for this study, representing a subset of patients from a single center in the Stability Study [5]. Participants performed DVJs at 7 years after ACLR (86.5 ± 3.9 mo) using a 12-camera 3D motion capture system, 21 retro reflective markers, and a 31-cm elevated box. Participants performed a static trial, 3 practice trials and 5 motion trials. Marker trajectories were tracked to collect kinematic data (Cortex 5, Santa Rosa, CA) and force plates measured vGRF and vLR. Marker position and force plate data were combined using Cortex software and exported for skeletal model construction (Visual 3D, Germantown, MD). External knee moments were calculated using inverse dynamics resolved in the tibial coordinate system and normalized to a product of bodyweight and height. vGRFs and vLRs were normalized to bodyweight. DVJ variables were compared between groups using independent t-tests and Mann-Whitney U-tests. Those with ipsilateral ACL re-injury, contralateral ACL injury, or meniscal injuries were excluded in sensitivity analyses.

**Results & Discussion:** There were no differences in any DVJ variables between those with LET versus without LET after unadjusted and sensitivity analyses (Table 1). These findings are consistent with the lack of differences in hop test results at 2 years after ACLR, suggesting that LET may not affect performance during jumping or landing tasks [6]. Therefore, the safety of returning to participation in high impact and dynamic activities after ACLR may not be influenced by the addition of LET. Future studies should consider investigating how LET may influence other long-term outcomes after ACLR such as pain, symptoms, function, and post-traumatic knee osteoarthritis.

**Significance:** LET addition does not influence DVJ biomechanics after ACLR and should not influence engagement in high impact and dynamic activities.

**Table 1** Differences in sex, BMI and DVJ variables between individuals with no LET vs. LET. Means and SDs are shown for parametric variables and medians and interquartile ranges for non-parametric variables.

| Variables | | | Primary Analyses | | Sensitivity Analyses |
|---|---|---|---|---|---|
| | No LET (n = 28) | LET (n = 39) | *P*-value | Effect Size | *P*-value |
| **Males** | 14 (50%) | 14 (35.9%) | 0.248 | Φ = -0.141 | 0.249 |
| **Females** | 14 (50%) | 25 (64.1%) | | | |
| **BMI (kg/m²)** | 25.5 (5.3) | 24.4 (8.1) | 0.446 | r = -0.093 | 0.810 |
| **Ipsilateral ACL re-tear** | 3 (10.7%) | 1 (2.6%) | 0.301 | Φ = -0.170 | N/A |
| **Contralateral ACL tear** | 4 (14.3%) | 6 (15.4%) | 1.000 | Φ = 0.015 | N/A |
| **Meniscal injury** | 8 (28.6%) | 9 (23.1%) | 0.610 | Φ = -0.062 | N/A |
| **Peak KAbM (BW×Ht)** | 0.029 (0.023) | 0.028 (0.012) | 0.949 | r = -0.008 | 0.650 |
| **Peak KFM (BW×Ht)** | 0.092 ± 0.016 | 0.090 ± 0.018 | 0.739 | d = 0.126 | 0.873 |
| **Peak KFA (°)** | -94.9 ± 13.7 | -95.2 ± 12.7 | 0.931 | d = 0.021 | 0.915 |
| **Peak vGRF (BW)** | 1.44 (0.43) | 1.37 (0.39) | 0.315 | r = -0.123 | 0.438 |
| **Peak vLR (BW)** | 107.4 (66.4) | 97.6 (61.9) | 0.263 | r = -0.137 | 0.769 |

**Acknowledgements:** This sub-study received funding support from the Lawson Internal Research Fund and Ontario Graduate Scholarship.

**References:** [1] Mohtadi & Chan (2019), *J Bone Joint Surg Am* 101(11); [2] Getgood et al. (2020), *Am J Sports Med* 48(2); [3] Kotsifaki et al. (2023), *Br J Sports Med* 57(20); [4] Gagnon et al. (2024), *J Biomech* 170; [5] Getgood et al. (2019), *BMC Musculoskelet Disord* 20(1); [6] Getgood et al. (2020), *Arthroscopy* 36(6).

# IMPACT OF GRAFT TYPE ON LOAD SYMMETRY AND PHYSICAL PERFORMANCE FOLLOWING ACL RECONSTRUCTION

*Vaibhavi Rathod[1], Pang Du[2], Laura Sands[3], Kevin Ford[4], Joseph Hart[5], Robin M. Queen[1]
[1]Department of Biomedical Engineering and Mechanics, Virginia Tech, Blacksburg, VA [2]Department of Statistics, Virginia Tech, Blacksburg, VA, [3]Center for Gerontology, Virginia Tech, Blacksburg VA, [4]Congdon School of Health Sciences, High Point University, High Point, NC [5]Department of Orthopaedic Surgery, University of North Carolina at Chapel Hill, NC
*Corresponding author's email: vrathod@vt.edu

**Introduction:** Anterior cruciate ligament reconstruction (ACLR) is a commonly performed surgical procedure to restore knee stability and function in individuals with ACL injuries [1,2]. The bone-patellar tendon-bone (BTB) autograft has been the gold standard for ACLR due to low failure rates, however, these patients have reported patellar fractures and persistent donor site pain [3]. Recently, the use of a quadriceps tendon (QT) autograft has gained popularity due to its favorable biomechanics, low morbidity, and ease of harvest [4]. While both graft types are considered effective, differences in graft characteristics such as healing potential, donor site morbidity, and mechanical properties may influence long-term functional recovery and the risk of re-injury [3]. A key consideration in ACLR rehabilitation is the restoration of load symmetry during functional tasks, as asymmetric loading during dynamic movements may contribute to higher injury risk [5]. However, the influence of graft type on biomechanical and performance outcomes is understudied. Therefore, the purpose of this study was to assess the influence of graft type (QT and BTB) on load symmetry and performance during landing and functional assessments. We hypothesized that QT grafts would yield better functional outcomes than BTB.

**Methods:** A total of 75 participants ((mean age: 19 ± 3 years), 28 female) who underwent primary ACLR using either QT or BTB autografts were recruited. To be eligible, participants had to 1) undergo primary ACLR with an autograft, 2) be between 14 and 25 years old, and 3) be returning to sport participation (sports exposure). Exclusion criteria included non-skeletal maturity, a history of multiple ACLR, tibial osteotomy during ACLR, allograft use, postoperative complications requiring additional surgery, hospitalization within the last 3 months for any reason other than ACLR and/or plans for future surgeries within the next 12 months. Participants completed functional tasks, including single-leg hop (SLH) (3 trials on each limb) and stop jump (3 trials), with an in-shoe load sensor (loadsol®, Novel Electronics) to assess load symmetry along with physical performance. Quadriceps strength was measured during 3 isometric tests using a handheld dynamometer (MicroFET®, Hoggan Scientific). Primary outcomes included peak impact force and loading rate symmetry during unilateral (SLH)) and bilateral (stop jump) landings, with secondary outcomes including isometric quadriceps strength and SLH distance symmetry. A t-test was conducted to compare age at surgery and time since surgery, while a chi-square test examined the association between graft type and sex assigned at birth. A linear mixed-effects model (LMEM) was used to evaluate the main effect of graft type ($\alpha = 0.05$) on each outcome, with age and sex as fixed effects and participant as the random effect.

**Results & Discussion:** The preliminary results of the main effect of graft type are summarized in Table 1. Sex assigned at birth significantly influenced unilateral landing biomechanics, with males showing improved peak impact force symmetry (Females = 113.1 (28.7), Males = 94.4 (18.2), p = 0.003) and loading rate symmetry (Females = 112.6 (33.9), Males = 93.9 (37.6), p= 0.03). Age did not have a significant impact on either outcome (p=0.702, p=0.219). No significant effects of age, or sex were observed on peak impact force (p= 0.566, 0.183) and loading rate symmetry (p= 0.935, 0.280) during bilateral landing. No significant effects of age (p=0.884), or sex (p=0.159) were observed on quadriceps strength symmetry. Additionally, no significant effects were found for sex (p=0.428) on SLH distance symmetry, age had a significant effect (p = 0.025), with older participants demonstrating better symmetry. Symmetry measures did not differ significantly between graft types (Table 1), indicating comparable outcomes. A post-hoc power analysis indicates that a minimum sample size of 256 is required to detect graft type differences in symmetry measures, at time of RTS clearance. Our quadriceps strength symmetry findings contrast with prior findings where quadriceps strength was lower in patients with QT grafts at seven months post-ACLR [6] and delayed quadriceps strength recovery and hop distance symmetry were reported in females with QT grafts [7]. These differences in outcomes could be due to the later testing time (greater than 8 months post-op) in the current cohort. Further research is needed to examine potential early post-op differences and assess whether these outcomes persist as patients progress through rehabilitation and return to sport (RTS). The reported sex differences may be due to variations in muscle strength, neuromuscular control, joint kinematics and hormonal changes [8], highlighting the need for sex-specific rehabilitation.

| Symmetry Measures | QT (n=25) | BTB (n=50) | p value |
|---|---|---|---|
| Participant Sex Assigned at Birth | 10F, 15M | 18F, 32M | 0.127 |
| Time Since Surgery (months) | 8.1 (1.9) | 9.5 (2.5) | 0.011 |
| Age at Surgery (years) | 19.2 (3.3) | 20.2 (2.8) | 0.222 |
| Peak impact force (unilateral)[1] | 103.6 (26.6) | 100.1 (23.1) | 0.799 |
| Loading rate (unilateral)[1] | 106.9 (34.6) | 97.9 (38.5) | 0.884 |
| Peak impact force (bilateral)[2] | 11.5 (25.6) | 11.5 (25.6) | 0.599 |
| Loading rate (bilateral)[2] | 15.0 (16.7) | 6.28 (27.3) | 0.134 |
| Quadriceps strength[1] | 85.3 (18.3) | 88.8 (22.1) | 0.521 |
| Single leg hop distance[1] | 88.5 (10.9) | 90.7 (10.5) | 0.328 |
| [1]Limb Symmetry Index (100 = perfect symmetry), [2]Normalized Symmetry Index (0 = perfect symmetry) | | | |

**Table 1**: Comparison of symmetry measures [Mean (SD)] between QT and BTB graft groups.

**Significance:** The choice of a BTB or QT graft may not affect functional and biomechanical outcomes at RTS.

**Acknowledgments:** Supported by NIH: R01AR078811-03

**References:** [1] Pereira et al (2021), *Knee Surg. Relat. Res* 33(7) [2] Yanke et al (2012) *Tech. Orthop* 27 (2) [3] Dai et al (2022) *Am. J. Sports Med* 50 (12) [4] Slone et al (2014) *Arthrosc. J.* 31(3) [5] Paterno et al (2010) *Am. J. Sports Med* 38 (10) [6] Holmgren et al (2024) *Am. J. Sports Med* 52 (1) [7] Ebert et al (2024) *Knee Surg. Sports Traumatol. Arthrosc* 32 (10) [8] Ito et al (2021) *J. Orthop. Res* 39 (5)

**Associations between PEDI-IKDC, hopping, and isokinetic torque in adolescents 6 to 12 months post-ACL reconstruction**

*Kalpaka Pradip[1], Chris Kuenze[2], Adam Weaver[3], ARROW Group, Caroline Lisee[1]
[1]Orthopedic Health in Motion Laboratory, University of Georgia, Athens, GA
Corresponding author's email: kp36839@uga.edu

**Introduction:** Anterior cruciate ligament (ACL) injuries are prevalent among adolescent athletes, often requiring surgical ACL reconstruction (ACLR) and extensive rehabilitation [1]. Persistent asymmetries in knee extension and flexion strength and hop performance can contribute to an increased risk of second ACL injury which is as high as 15% in adolescents post-ACLR [2]. Adolescents are not only more likely to engage in high-risk sports and activities that increase ACL injury risk, but they also exhibit distinct neuromuscular and developmental characteristics compared to adults, necessitating a focused approach to evaluating recovery post-ACLR [3]. The Pediatric International Knee Documentation Committee (PEDI-IKDC) questionnaire is a validated tool for assessing self-reported knee function in adolescent populations specifically [4]. This study aims to evaluate the relationship between self-reported knee function, as measured by the PEDI-IKDC—a tool specifically designed for adolescents—with objective measures of hop performance and isokinetic knee extension and flexion torque assessments in adolescents 6 to 12 months post-ACLR. Given the developmental differences between adolescents and adults, the PEDI-IKDC provides a more age-appropriate evaluation of knee function than adult-focused surveys. Due to previous research with the original IKDC in adults, we hypothesized that with higher Pedi-IKDC scores, we would see better performance.

**Methods:** This cross-sectional analysis of data from a multisite registry included adolescent patients (age ≤ 18) who underwent ACL reconstruction 6-12 months prior to data collection. Participants the PEDI-IKDC, hop tests for distance (i.e., single leg hop, triple hop, crossover hop [m]), and isokinetic knee extension and flexion torque testing at 60°/s (Nm) via the Biodex System. Isokinetic knee extension and flexion torque were normalized to bodyweight (i.e., Nm/kg). Limb symmetry indices (LSI) were calculated for hop and isokinetic torque testing by dividing the surgical limb by the non-surgical limb (%). Separate linear regression analyses were performed to assess associations of PEDI-IKDC scores with LSI hop performance as well as surgical limb and LSI knee extension and flexion torque while accounting for the influence of sex, time since surgery, age, and graft type. Alpha was set to 0.05.

| | $R^2$ | Unstandardized Beta [95% Confidence Interval] | P-Value |
|---|---|---|---|
| **Single Hop LSI** | 0.01 | -0.08[-0.23, 0.67] | 0.28 |
| **Triple Hop LSI** | 0.001 | 0.023[-0.11, 0.15] | 0.73 |
| **Crossover Hop LSI** | 0.001 | 0.03[-0.13, 0.18] | 0.71 |
| **LSI Isokinetic Knee Extension Torque** | 0.004 | 0.12[-0.16, 0.40] | 0.38 |
| **ACL Isokinetic Knee Extension Torque** | 0.01 | 0.006[-0.001, 0.013] | 0.09 |
| **LSI Isokinetic Knee Flexion Torque** | 0.002 | 0.068[-0.15, 0.28] | 0.53 |
| **ACL Isokinetic Knee Flexion Torque** | 0.006 | 0.068[-0.002, 0.007] | 0.53 |

Table 1: Associations of PEDI-IKDC scores with hop and isokinetic torque outcomes. P-value <0.05 indicates statistical significance.

**Results & Discussion:** A total of 194 participants were included in this study (age = 16.03±1.4 years, sex = Female (50.5%), Men (49.5%), Time Since Surgery = 7.7±1.8 months, Graft Type = Allograft (1.5%), Bone-patellar tendon bone (5.6%), Hamstring autograft (60.7%), Quadriceps Tendon Graft (32.1%)). After controlling for covariates, no significant associations were observed between PEDI-IKDC scores and functional outcomes, as indicated by non-significant p-values across all measures (p-value range: 0.09–0.73).. Additionally, regression analyses indicated minimal variance explained by the models across all functional outcome measures after controlling for covariates ($R^2$ range: 0.0002 - 0.01) (Table 1). Overall, our hypotheses were not supported suggesting a lack of association between self-reported knee function objectively measured with adolescent-focused surveys, muscle strength, and functional performance in adolescents post-ACLR. Our results differ from previous studies reporting statistically significant associations between self-reported knee function, muscle strength and functional performance in adults using the Adult IKDC and other surveys validated for adult populations. Other factors influencing recovery should be explored, as the low $R^2$ values suggest that the PEDI-IKDC may not adequately capture meaningful variations in muscular recovery or functional asymmetries. Additionally, the lack of significant associations between predictor variables and functional measures highlights potential limitations of using self-reported questionnaires as standalone metrics for recovery assessment.

**Significance:** These findings suggest that self-reported knee function, as measured by the PEDI-IKDC, may not fully capture the complexity of muscle strength and functional performance recovery in adolescents post-ACLR. While self-reported measures remain valuable in adults, adolescent recovery may be influenced by additional factors that warrant further investigation. Exploring alternative or supplementary assessment tools may provide a more comprehensive understanding of neuromuscular recovery and functional asymmetries in adolescent populations. Identifying these factors can help clinicians refine rehabilitation strategies to optimize functional outcomes and mitigate re-injury risk in adolescent athletes.

**Acknowledgments:** The authors would like to acknowledge all members of the ACL Reconstruction Rehabilitation Outcomes Workgroup (ARROW) for their contributions.

**References:** [1] Kocher et al. (2011), Am J Sports Med 39(5); [2] Saper et al. (2021), Arthros Sports Med Rehabil 3(3); [3] Dekker et al. (2017), Am J Sports Med 45(6) [4] Van der Velden et al. (2019), BMC Musculoskeletal Disord 20(1)

# The Accuracy of Manual Clinical Exams for Detecting Lumbar Spine Instability During Flexion/Extension

Caitlyn Johnson[1], Clarissa Levasseur[1,2], M. Zino Kuhn[1], Gina McKernan[3], Sara Piva[4], William J. Anderst[1]
[1]School of Medicine, Department of Orthopaedic Surgery, [2]Bethel Musculoskeletal Research Center, [3]Department of Physical Medicine and Rehabilitation, [4]Department of Physical Therapy, University of Pittsburgh, Pittsburgh, PA
caj136@pitt.edu

**Introduction:** Lumbar spine instability (LSI) is a notable subgroup of chronic low back pain (cLBP)[1,2]. Accurate identification of LSI can be beneficial for assigning patients to treatments that target LSI[3]. Flexion-extension (FE) radiographs are the gold-standard method to diagnose LSI via interpreting intervertebral anteroposterior (AP) translation[4]. Clinically, the lumbar segmental mobility/pain test (LSMPT) and the prone instability test (PIT) are validated to accurately identify patients who respond to stabilization exercises for LSI; however, these clinical tests have not been compared to radiographic instability[3,5]. This study aimed to determine whether the LSMPT and PIT are reasonable surrogates for dynamic LSI measured using radiography.

**Methods:** Participants were enrolled from a larger study of 1000 individuals that sought to identify biological, biomechanical, and behavioural characteristics of cLBP[6]. The LSMPT and PIT were administered by a licensed physical therapist. All participants received a computed tomography (CT) scan and were imaged at 20 images/second while standing and flexing forward within a biplane radiography system. Lumbar intervertebral translation and rotation during flexion was measured with sub-millimeter and sub-degree accuracy using validated software that matched 3D bone models, created from CT, to the biplane radiographs[7]. Intervertebral translation (slip) was measured as the distance between landmarks placed on the superior posterior and inferior posterior endplates of each 3D bone model[7], and slip was interpolated to every degree of intervertebral FE. Group averages and standard deviations (SD) were calculated for each lumbar motion segment at every 1° of intervertebral FE. The threshold for instability was AP slip greater than two SDs above the group average at any 1° increment of intervertebral FE (Figure 1). The sensitivity, specificity, positive likelihood ratio (LR+) and negative likelihood ratio (LR-) of the LSMPT and the PIT were calculated.

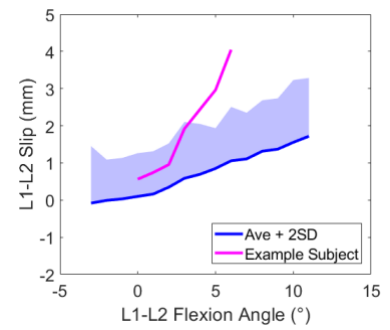


**Figure 1:** Example of a positive slip test. The subject's L1-L2 slip becomes greater than two SDs above the group average at 4° of flexion.

**Results & Discussion:** 125 individuals (72 females; age: 52.9±16.6 years; BMI: 25.7±3.6 kg/m$^2$) completed testing. 38 subjects translated above the two SD cut-off at any of the five motion segments (Table 1). LSI was least common at L5-S1 (7 subjects) and most common at L1-L2 and L4-L5 (12 subjects each). Sensitivity ranged from 0.08 to 0.50, specificity ranged from 0.48 to 0.83. The maximum LR+ was 1.56 and the minimum LR- was 0.77 (Table 2). Our results indicate a 30.4% prevalence of LSI in a cohort of 125 with cLBP. These results suggest the LSMPT and PIT are not sensitive or specific to dynamic LSI, leading to poor LR+ and LR-.

**Table 1:** Threshold for dynamic LSI (upper bound of mean+2SD) for each motion segment at 1° increments of intervertebral FE.

| Flexion Angle | -3° | -2° | -1° | Standing Neutral | 1° | 2° | 3° | 4° | 5° | 6° | 7° | 8° | 9° | 10° | 11° | 12° | 13° | 14° |
|---|---|---|---|---|---|---|---|---|---|---|---|---|---|---|---|---|---|---|
| L1-L2 (mm) | 1.5 | 1.1 | 1.1 | 1.3 | 1.3 | 1.5 | 2.1 | 2.1 | 1.9 | 2.5 | 2.4 | 2.7 | 2.7 | 3.2 | 3.3 | | | |
| L2-L3 (mm) | | | 2.0 | 1.5 | 1.3 | 1.5 | 1.7 | 2.0 | 2.1 | 2.3 | 2.5 | 2.4 | 2.5 | 2.8 | 3.0 | 3.5 | 3.9 | |
| L3-L4 (mm) | | | 1.1 | 1.1 | 1.1 | 1.6 | 1.5 | 1.6 | 1.8 | 2.0 | 2.1 | 2.5 | 2.5 | 2.7 | 2.9 | 3.0 | 3.3 | 3.5 |
| L4-L5 (mm) | | | 0.7 | 0.9 | 1.1 | 1.1 | 1.3 | 1.6 | 1.8 | 2.1 | 2.1 | 2.3 | 2.2 | 2.5 | 2.8 | 2.9 | 3.0 | 3.3 |
| L5-S1 (mm) | 1.9 | 2.1 | 1.7 | 3.0 | 2.0 | 2.1 | 2.0 | 1.9 | 1.5 | 1.8 | 1.2 | 1.4 | 1.5 | 1.7 | 1.9 | 2.1 | 2.5 | 3.0 |

**Table 2:** Sensitivity, specificity, LR+ and LR- (95% confidence intervals) for the PIT and LSMPT at each motion segment.

| Test | True + | True - | False + | False - | Total | Sensitivity | Specificity | LR+ | LR- |
|---|---|---|---|---|---|---|---|---|---|
| PIT | 15 | 65 | 22 | 23 | 125 | 0.39 (0.25-0.55) | 0.75 (0.65-0.83) | 1.56 (0.92-2.66) | 0.81 (0.61-1.08) |
| L1-L2 LSMPT | 1 | 89 | 18 | 11 | 119 | 0.08 (0.01-0.32) | 0.83 (0.75-0.89) | 0.50 (0.07-3.39) | 1.10 (0.91-1.33) |
| L2-L3 LSMPT | 2 | 83 | 26 | 8 | 119 | 0.20 (0.04-0.50) | 0.76 (0.68-0.84) | 0.84 (0.23-3.03) | 1.05 (0.78-1.46) |
| L3-L4 LSMPT | 4 | 72 | 38 | 4 | 119 | 0.50 (0.19-0.81) | 0.65 (0.56-0.73) | 1.42 (0.68-2.98) | 0.77 (0.38-1.56) |
| L4-L5 LSMPT | 4 | 48 | 49 | 7 | 119 | 0.42 (0.18-0.69) | 0.54 (0.45-0.64) | 0.91 (0.45-1.83) | 1.08 (0.65-1.79) |
| L5-S1 LSMPT | 1 | 54 | 58 | 6 | 119 | 0.14 (0.01-0.50) | 0.48 (0.39-0.57) | 0.28 (0.05-1.71) | 1.78 (1.24-2.54) |

**Significance:** The PIT and LSMPT alone may not be sufficient to accurately diagnose dynamic LSI in individuals with cLBP.

**Acknowledgment**: This research is supported by the NIH through the NIH HEAL Initiative under award number U19AR076725. The content is solely the responsibility of the authors and does not necessarily represent official views of NIH or its NIH HEAL Initiative.

**References:** [1] O'Sullivan (2000), *Man. Ther.;* [2] Fritz et al. (2005), *EurSpineJ*; [3] Fritz et al. (2005), *Arch Phys Med Rehabil*; [4] Majid & Fischgrund (2008), *JAAOS*; [5] Hicks et al. (2003), *Arch Phys Med Rehabil*; [6] Vo et al. (2023), *PMAEAP*; [7] Dombrowski et al. (2018), *EurSpineJ*; [8] Plante & Vance (1994), *LSHSS*.

# PRE-TREATMENT IMPAIRMENTS DEFINE ROTATOR CUFF TENDINOPATHY PHENOTYPES THAT RESPOND DIFFERENTLY TO EXERCISE REHABILITATION

Oscar Vila-Dieguez[1], Matt D Heindel[1], Chethan Reddy[1], Lori A Michener[1]
[1]University of Southern California, Los Angeles, California, USA
*Corresponding author's email: viladieg@usc.edu

**Introduction:** Every rotator cuff tendinopathy clinical practice guideline recommends resistance exercise for patients with rotator cuff tendinopathy.[1] Unfortunately, the number of people who do not respond to this intervention is high,[2,3] suggesting that mechanisms underlying how exercise works and who can benefit from exercise are warranted. Neuromuscular factors, tendon tissue, psychological factors, and pain sensitivity play a role in symptom severity in those with rotator cuff tendinopathy.[4–9] Baseline heterogeneity in these factors may predict patient prognosis, but subgroups within this population remain poorly defined. This study aimed to identify subgroups of patients with rotator cuff tendinopathy based on baseline deficits across multiple domains and to characterize their recovery trajectories during an 8-week resisted exercise intervention.

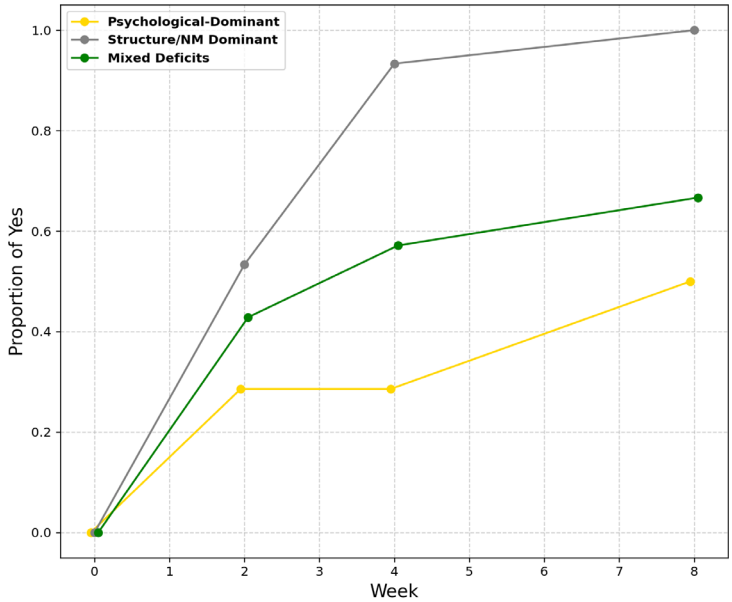


**Figure 1:** Predicted PASS trajectories for each patient cluster based on data at baseline and weeks 2, 4 and 8.

**Methods:** Sixty-five participants with rotator cuff tendinopathy underwent baseline assessments of tendon morphology, neuromuscular function, and psychological factors, followed by an 8-week standardized resisted exercise program. K-means clustering was used to identify patient subgroups. The recovery of 50 participants who completed the entire 8-week intervention was assessed using the Penn Shoulder Score (Penn), a 0-100 scale with 100 being no disability. Additionally, the Patient Acceptable Symptom State (PASS) was used for determining patient response to treatment. The PASS provides a simple yes/no evaluation of whether a patient's current condition would be acceptable if it were maintained long term. Linear mixed-effects and logistic regression models analyzed changes in Penn scores and PASS outcomes over time.

**Results & Discussion:** Three subgroups were identified: Structure/Neuromuscular-Dominant, Psychological-Dominant, and Mixed-Deficits. The Structure/Neuromuscular-Dominant cluster demonstrated the most significant improvements in Penn scores ($\beta = 8.75$, $p = 0.016$) and PASS outcomes by Week 8. The Psychological-Dominant cluster showed slower recovery trajectories, while the Mixed-Deficits cluster exhibited intermediate outcomes. Improvements in Penn scores exceeded the minimal clinically important difference (MCID) in all subgroups, though the rate and extent of recovery varied.

**Significance:** Distinct baseline deficits define recovery trajectories in rotator cuff tendinopathy. Tailoring interventions to patient subgroups—addressing psychological barriers or systemic health factors as needed—may enhance treatment outcomes. Future research should validate these findings in larger cohorts and explore biological mechanisms driving recovery.

**Acknowledgments:** American Society of Biomechanics, International Society of Biomechanics and Foundation For Physical Therapy Research

**References:** [1] Doiron-Cadrin, *Arch Phys Med Rehabil*.2020, [2] Babatunde *Ther Adv Musculost Dis*.2021, [3] Naunton, *Clin Rehab*.2020, [4] Porter, *Scand J Med Sci Sports*.2020, [5] McCreesh, *BMJ.* 2017, [6] Ginn, *J Electromyogr Kinesiol*.2022, [7] Worsley, *JSES.*.2013, [8] Farzad, *Rehab Res*.2021, [9] Coronado, JOSPT. 2011, [10] Leggin, JOSPT. 2009

# Are Affected Limb Joint Powers Associated with Physical Activity in People with Knee Osteoarthritis?

*Oiza Peters[1], Steven Garcia[1], Joy Itodo[1], Ogundoyin Ogundiran[1], Paige Perry[1], Kharma Foucher[1]
[1]Department of Kinesiology, University of Illinois, Chicago.
*opeter2@uic.edu

**Introduction:** Insufficient physical activity (PA) is reported among people living with knee osteoarthritis (OA) [1]. We have recently evaluated biomechanical factors that may influence PA in people with knee OA, including walking inefficiencies, gait speed, and peak sagittal plane joint moments [2,3,4]. While these biomechanical variables are associated with PA, joint power is essential for forward progress in walking and may, therefore, directly influence physical activity. In addition, interventions for knee OA aimed at improving PA have often focused mainly on the affected joint; however, the contributions of the ankle and hip are critical for propulsion. Further, the relative contributions of the hip, knee, and ankle to support during gait differ in people with knee OA compared to healthy controls [5,6]. A more specific understanding of how each joint contributes to biomechanical determinants of PA in people with knee OA could lead to more effective interventions. Therefore, this study aimed to investigate the influence of affected limb joint powers on PA levels in people with knee OA. We hypothesized that (i) hip, knee, and ankle joint powers are associated with subjective and objective PA measures, and (ii) ankle power is most strongly associated with PA.

**Methods:** We evaluated 25 people with knee OA (Sex= 16 Females, Age= 56±8 years, BMI= 33.2±5.9 kg/m$^2$) walking at self-selected speeds on an instrumented split-belt treadmill, using standard motion capture methods. We selected 10 consecutive clean steps for analysis and calculated sagittal plane peak positive joint powers of the hip, knee, and ankle during stance. Subjective PA was assessed using the UCLA activity scale. Scores range from 1 (wholly inactive) to 10 (regularly participate in impact sports). Objective PA was measured using ActiGraph activity monitors worn for at least one week after the gait evaluation. Average steps per day were extracted for analysis. Statistical analysis was conducted using SPSS Version 29. We used Spearman and Pearson correlations to quantify the association between joint powers and PA. Finally, we used multiple linear regression to evaluate the influence of each joint power on PA, controlling for sex. Standardized coefficients (β) and partial $R^2$ values indicated the relative strength of the association for each joint.

**Results & Discussion:** UCLA scores ranged from 2-10 ($\bar{x}$=5), while participants took an average of 9192.01± 2827.93 steps per day. Although no association was found between peak hip positive power and UCLA scores, greater peak knee positive power and peak ankle positive power were associated with higher levels of PA (Fig. 1). There were no significant associations between joint powers and steps per day (p = 0.508 to 0.987). In the regression model, joint powers explained 46% of the variance in UCLA scores (p=0.013). Peak knee positive power had the strongest influence in the model (β=1.100, p=0.038, Partial $R^2$ = 0.198). Peak ankle positive power (β=–0.378, p=0.542, Partial $R^2$ = 0.026) and peak hip positive power (β=–0.140, p=0.529, Partial $R^2$ = 0.020) did not significantly influence UCLA scores in this model. This was contrary to our second hypothesis. As expected, based on the bivariate correlations, the regression model had no combined association of joint powers on steps per day (p=0.241). As hypothesized, there was a positive association between the ankle and knee joint power and UCLA scores. However, contrary to our hypothesis, the knee, not the ankle, had the greatest statistical influence on PA. This aligns with common rehabilitative interventions focusing on the knee joint in this population but suggests that addressing any impairment in ankle function may also be beneficial.

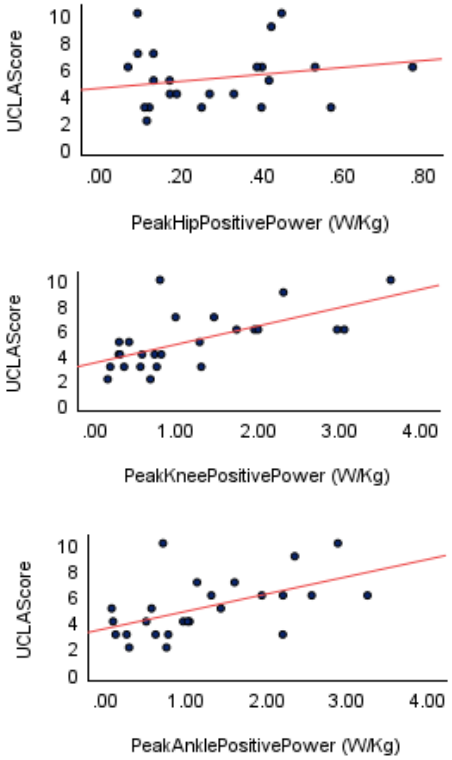


**Figure 1:** Higher peak knee (rho=0.508, p=0.010) and ankle (rho=0.428, p=0.033) positive powers were associated with higher PA levels. Peak hip (rho=0.079, p=0.706) positive power was not associated with PA levels.

**Significance:** There is a clinical need for more effective interventions to improve PA in people with knee OA based on their specific biomechanical adaptations. This study found a relationship between ankle and knee joint power and subjective PA levels, suggesting a need for multilevel joint rehabilitation.

**Acknowledgments:** R21AG052111 and Pilot funding through UL1TR002003.

**References:** [1] Hawker (2019), *Clin Ex Rheumatol* 37; [2] Foucher et al. (2021), *Clin Biomech*; [3] Aydemir et al. (2022), *J Orthop Res* 40(5); [4] Aydemir et al (2023), *J Orthop Res* 41(12); [5] Levinger et al. (2013), *J Arthro* 28(6); [6] McGibbon et al. (2002), *The J Rheum* 29(11).

# PROXIMAL FEMUR BONE STRENGTH IN PERSONS WITH SPINAL CORD INJURY: DEVELOPMENT OF A COMPUTATIONAL FRAMEWORK TO SIMULATE SIDEWAYS FALL FROM A WHEELCHAIR

Anmol S. Doss[1], William Kuo[1], Christopher M. Cirnigliaro[2], William A. Bauman[3], *Saikat Pal[1,2]
[1]New Jersey Institute of Technology, Newark, NJ, USA; [2]James J. Peters Veterans Affairs Medical Center, Bronx, NY, USA;
[3]Icahn School of Medicine at Mount Sinai, New York, NY, USA
Corresponding author's email: pal@njit.edu

**Introduction:** Persons with spinal cord injury (SCI) experience rapid and progressive bone loss below their injury lesion and are at a high risk of fragility fractures. Up to 70% of persons with SCI sustain a long-bone fracture over time [1]. The proximal femur accounts for ~10% of fragility fractures, but the mortality rates post proximal femur fractures are as high as 22% [2, 3]. Current clinical evaluation of bone strength relies on dual-energy absorptiometry (DXA) and peripheral quantitative computed tomography (CT) scans [4, 5], which do not account for bone geometry, mineral distribution, mechanical properties, and mode of loading [6, 7, 8]. Recent studies have reported that finite element (FE)-based metrics are better indicators of bone strength than DXA or CT-based metrics [6, 7, 8]. Sideways fall from a wheelchair is the most common cause of proximal femur fracture in persons with SCI [9]. As such, the **goal** of this study was to develop a non-invasive framework to simulate sideways fall and quantify two FE-based metrics of bone strength: compressive strength ($C_{ult}$) and compressive stiffness ($K_c$).

**Methods:** We recruited 14 (11M, 3F) participants with SCI (duration of injury 8.4±4.8 years) and 4 (3M, 1F) able-bodied (AB) participants between the ages of 24-62 years. Participants were informed on all aspects of the study and provided consent according to the policies of our IRB. Participants received a bilateral hip scan in a clinical CT scanner (Siemens Somatom, Fig. 1A). For each participant, the 3D CT images were used to create a solid mesh of the right proximal femur with 1.5 mm, linear tetrahedral elements (Figs. 1B-D). We extracted subject-specific variable bone material properties using calibration phantoms and established methods (Figs. 1E-H) [10, 11]. All bones were cut to 13 cm and aligned to 10° adduction and 15° internal rotation to simulate an unprotected fall to the side of the hip [12]. Boundary conditions were assigned to apply a compressive displacement to the femoral head until failure (Fig. 1I) [12]. The bottom 6 mm of the greater trochanter was fixed, the distal end was fixed in rotations and inferior-superior translation, and a linear displacement was applied vertically downwards on the top 6 mm of the femoral head [13]. The FE simulations were run in Abaqus/Explicit (SIMULIA, Providence, RI), and the reaction forces at the femoral head until failure were extracted (Fig. 1J-K). Compressive strength was the reaction force at failure, and compressive stiffness was the slope of the displacement-force curve from the first 0.3 mm displacement (Fig. 1K). The FE-based metrics of bone strength were best fit with a non-Gaussian, two-parameter Weibull model, with coefficients of determinations ($R^2$) ≥ 0.81 in both cases.

**Results & Discussion:** Compressive strength ($C_{ult}$) ranged from 3.08-9.86 kN and 8.02-14.00 kN/mm for the SCI and AB groups, respectively (Fig. 2A). Compressive stiffness ($K_c$) ranged from 2.70-9.85 kN/mm and 6.86-14.12 kN/mm for the SCI and AB groups, respectively (Fig. 2B).

**Significance:** The results from this study provide a foundation for statistical models fitting the distributions of FE-based metrics of bone strength, and confidence interval-based thresholds to predict fracture risk of the proximal femur in persons with SCI.

**Acknowledgments:** VA RR&D #1 I01 RX003561.

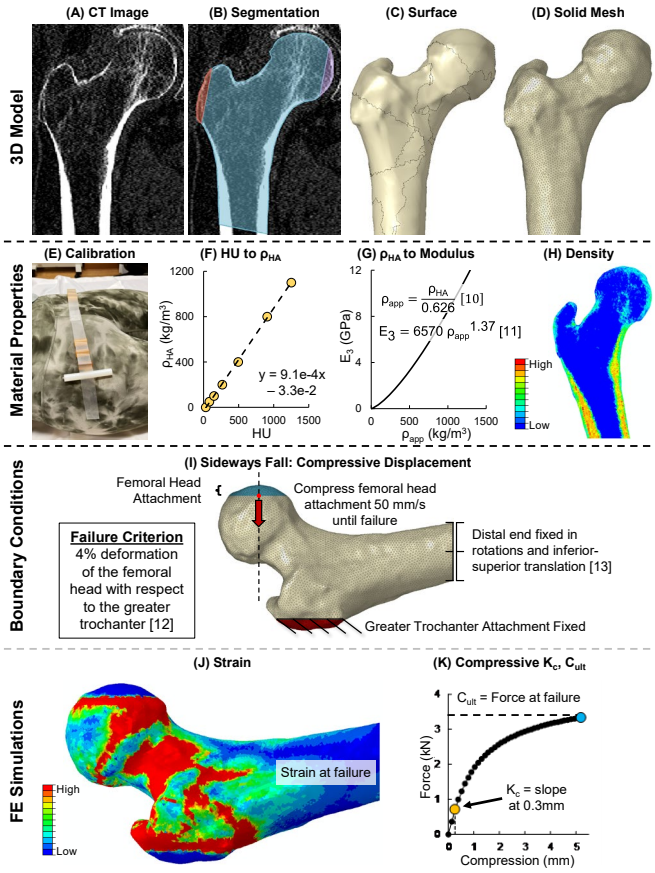


**Figure 1:** A framework to simulate sideways fall to quantify proximal femur strength using subject-specific FE modeling.

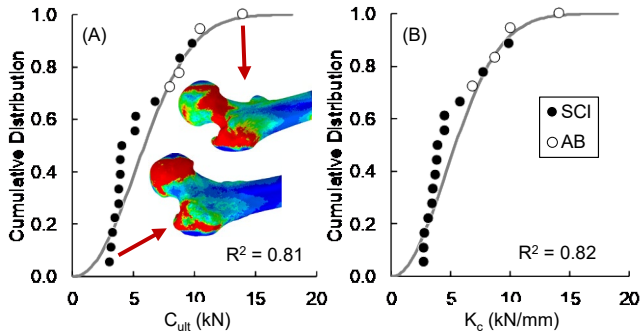


**Figure 2:** The distributions of (A) compressive strength $C_{ult}$ and (B) compressive stiffness $K_c$ from SCI and AB participants.

**References:** [1] Morse et al. 2009, *Am J Phys Med Rehab* 88(1); [2] Logan et al. 2008, *Arch Phys Med Rehab* 89(2); [3] Downey et al. 2019, *World J Orthop* 10(3); [4] Garland et al. 2004, *J Sp Cord Med* 27(3); [5] Eser et al. 2005, *Arch Phys Med Rehab* 86(3); [6] Edwards et al. 2013, *J Biomech* 46(10); [7] Edwards et al. 2014, *Osteop Int* 25(3); [8] Haider et al. 2021, *Ann Biomed Eng* 49(2); [9] Morse et al. 2009, *Osteop Int* 20(3); [10] Dalstra et al. 1993, *J Biomech* 26(4-5); [11] Rho et al. 1995, *Med Eng Phys* 17(5); [12] Keaveny et al. 2008, *J Bone Miner Res* 23(12); [13] Edwards et al. 2014, *J Bone Miner Res* 29(9).

# THE RELATIONSHIP BETWEEN FOOT POSTURE, DORSIFLEXION RANGE OF MOTION AND LOWER EXTREMITY BIOMECHANICS DURING A DROP-LANDING TASK

*Kendra Graham[1], Joshua T. Weinhandl[1]
[1]Department of Kinesiology, Recreation, and Sports Studies, The University of Tennessee, Knoxville, TN
*Corresponding author's email: kgraha29@vols.utk.edu

**Introduction:**

Knee injuries, including to the Anterior Cruciate Ligament (ACL), are commonly experienced by collegiate athletes and can include significant ramifications to acute and lasting health outcomes, warranting further investigation into possible mechanisms for knee injury in this population [1]. Restricted Dorsiflexion Range of Motion (DROM) is associated with increased knee valgus and frontal plane excursion, reduced knee and hip sagittal excursion, and increased peak vertical ground reaction force (vGRF) during landing [2]. When assessed in a weight-bearing position, DROM restriction is correlated to dynamic knee valgus during landing [3]. Restrictions in DROM are therefore linked to deleterious sagittal and frontal plane knee and hip kinematics during landing. However, previous research inconsistently concludes that excessive foot pronation is a risk factor for knee injury, and few studies have examined the relationship between foot posture, lower extremity kinematics and kinetics during landing [4,5]. Therefore, the purpose of this study was to investigate the relationship between foot posture, DROM, and drop-landing biomechanics. We hypothesized that foot posture and DROM would influence landing kinetics and kinematics at the knee, ankle, and hip.

**Methods:** Fifteen physically active participants with experience in sports requiring change of direction were included. The FPI-6 was used to assess static foot posture, with higher positive scores indicating a more pronated foot posture. The weight-bearing lunge test (WBLT) was used to assess maximal weight-bearing DROM. Sagittal and frontal plane kinematics and kinetics of the hip, knee, and ankle were assessed during three trials of a single leg drop-landing task on the dominant limb (preferred leg used to kick a ball) using motion analysis. While standing on their non-dominant limb, participants dropped off the box onto the force plate and performed a single-legged landing on their dominant limb. Kinematics were captured through an 8-camera 3D motion analysis system (Vicon Motion Systems, Denver, CO) at a sampling rate of 200 Hz. Kinetic data were captured synchronously using a force plate (Bertec Corp, Columbus OH) at a sampling rate of 1000 Hz. Box height for the drop-landing task was set to each participant's maximum vertical jump height. Pearson correlations (r) along with the coefficient of determination ($r^2$) were performed to examine the relationship between the FPI-6, DROM, and individual landing kinematic and kinetic variables. In cases where both FPI-6 and DROM significantly correlated to a biomechanical variable, backwards multivariate linear regression was used to model the relationship. Pearson correlations were interpreted as weak (0.10-0.40), moderate (0.41-0.69), or strong (>0.70).

**Results & Discussion:** FPI-6 scores displayed a significant negative correlation with knee abduction angle at initial contact (r=-0.59, p=0.021) and ankle sagittal plane excursion (r=-0.63, p=0.013), as well as a significant positive correlation with knee adduction moment (r=0.60 p=0.017) (Table 1). WBLT was significantly correlated with knee adduction moment (r=-0.59, p=0.020). The combination of FPI-6 and DROM accounted for 56% of the variance in knee adduction moment (r=0.75, p=0.008), indicating that those with a more pronated foot posture and decreased DROM had an increased adduction moment at the knee. Potentially, participants who demonstrated a more pronated static foot posture experienced lesser dynamic foot pronation during landing, limiting force attenuation capacities of the foot. These findings align with previous research suggesting restricted DROM may alter landing mechanics, increasing knee injury risk [3]. DROM and foot posture were not significantly correlated, suggesting they individually and uniquely interact with knee adduction moments during landing.

Table 1. Pearson correlation coefficients (r) between FPI, WBLT, and all landing kinematics and kinetics.

| | FPI | WBLT |
|---|---|---|
| Hip flexion angle at IC | 0.01 | 0.12 |
| Hip adduction angle at IC | 0.13 | 0.071 |
| Knee extension angle at IC | 0.11 | -0.08 |
| Knee abduction angle at IC | -0.59* | 0.19 |
| Ankle dorsiflexion angle at IC | 0.32 | -0.40 |
| Hip flexion total excursion | -0.26 | 0.07 |
| Hip adduction total excursion | 0.17 | 0.28 |
| Knee extension total excursion | 0.30 | -0.17 |
| Knee abduction total excursion | -0.23 | -0.01 |
| Ankle dorsiflexion total excursion | -0.63* | 0.468 |
| Ankle inversion total excursion | 0.05 | -0.001 |
| Hip extension moment | 0.06 | -0.12 |
| Hip extension moment | 0.06 | -0.12 |
| Hip abduction moment | -0.43 | 0.20 |
| Knee extension moment | -0.06 | -0.18 |
| Knee adduction moment | 0.60* | -0.59* |
| Ankle plantarflexion moment | 0.06 | -0.15 |
| Ankle eversion moment | -0.06 | 0.09 |

FPI= Foot Posture Index, WBLT= weight-bearing Lunge test, IC=initial contact
* Denotes significant Pearson correlation between variables (p>0.05).

**Significance:**
Lesser DROM and a pronated foot posture result in an elevated maximum knee adduction moment during drop landing, indicating an increase in valgus knee loading. Our findings suggest that DROM and foot pronation are important to evaluate and consider for knee injury prevention and rehabilitation in this population or to those who participate in landing tasks. Future research into the relationship between these factors is essential, as is the development for interventions addressing and preventing limitations in DROM and excessive foot pronation.

**References:** [1] Hootman et al. (2007), *J Athl Train*, 42(2):311-319; [2] Lima et al. (2018), *Phys Ther Sport*, 29:61-69; [3] Mason-Mackay et al. (2017), *J Sci Med Sport*, 20(5):451-458; [4] Neal et al. (2014), *J Foot Ankle Res* 7(1):55; [5] Tong & Kong (2013) *J Orthop Sports Phys Ther*, 43(10):700-714.

# IMPACT OF SPORTS SPECIALIZATION ON LOAD SYMMETRY DURING UNILATERAL AND BILATERAL LANDINGS AFTER ANTERIOR CRUCIATE LIGAMENT RECONSTRUCTION

*Renoa Choudhury[1], Joe Hart[2], Kevin Ford[3], Robin M. Queen[1]
[1]Department of Biomedical Engineering and Mechanics, Virginia Tech, [2]Department of Orthopaedics, University of North Carolina at Chapel Hill, NC, [3]Congdon School of Health Sciences, High Point University, High Point, NC
*Corresponding author's email: renoac@vt.edu@vt.edu

**Introduction:** The growing trend of early sports specialization contributes to approximately 4.5 million sports-related injuries each year among children and young adults [1]. Sports specialization is operationally defined as "intensive, year-round training in a single sport while excluding participation in others" [2]. According to the American Orthopedic Society for Sports Medicine, early specialization may elevate the risk of injuries and burnout, with no clear evidence indicating that it improves the chances of reaching elite-level performance [3]. Athletes who focus exclusively on one sport frequently experience repetitive stress on the same muscles and joints [1]. However, there is a knowledge gap regarding how sport specialization levels affect movement asymmetry following Anterior Cruciate Ligament Reconstruction (ACLR). Many patients exhibit movement asymmetry up to 24 months post-ACLR. Given the higher risk of ACL injuries among female athletes, there is also a need to understand whether the impact of sport specialization on loading asymmetry post-ACLR varies by sex. To address these knowledge gaps, this study examines how sports specialization affects loading symmetry during unilateral and bilateral landings in male and female athletes following ACLR. It was hypothesized that high-specialized athletes would show significantly greater loading asymmetry than low- and moderate-specialized athletes, irrespective of sex.

**Methods:** 70 athletes post-ACLR (age = 19.17± 3.10 years), who had a primary ACLR using an autograft and were cleared for return to sport by their treating orthopaedic surgeon, were enrolled. Participants performed three trials of single leg hop (SLH) for each limb and three trials of stop jump (SJ), while plantar loading data was collected using an in-shoe load sensor (loadsol®, novel Electronics). All load data were normalized to body mass, and the Limb Symmetry Index (LSI) was calculated for peak impact force (PIF) and loading rate (LR) for each trial of SLH, and SJ first landing. The level of sport specialization was determined by pre-surgery sports activity meeting the following criteria: i) having one main sport, ii) exclusion of other sports, and iii) more than eight months of training in their main sports annually [2]. Meeting all three of these criteria, participants were defined as high-specialization, meeting two criteria as medium-specialization, and meeting one or none as low-specialization. One-way ANOVA was performed to examine the group differences in age and time since surgery. A linear mixed-effects model was used to determine the main effects of sport specialization level (low, moderate, high) and sex (male, female) and their interaction on each LSI outcome ($\alpha$=0.05).

**Results & Discussion:** Among 70 athletes post-ACLR, 22.9% were high-specialized (n = 16; male: female = 9:7; height = 1.73 ± 0.10 m, mass = 74.6 ± 14.9 kg), 37.1% were medium-specialized (n = 26, male: female = 13:13; height = 1.73 ± 0.12 m, mass = 78.7 ± 20.3 kg) and 40% were low-specialized athletes (n = 28, male: female = 20:8; height = 1.74 ± 0.09 m, mass = 74.6 ± 15.5 kg). High-specialized athletes were significantly younger than low-specialized athletes (18.1 ± 3.17 years vs 20.3 ± 3.16 years, p=0.05) but not than medium-specialized athletes (18.7 ± 2.67 years, p=0.018). No significant group differences were found for the time since surgery. A significant interaction (p=0.03) was found for SLH PIF LSI, with no significant effect of age and time since surgery. Post-hoc comparison revealed that high-specialized female athletes had greater SLH PIF asymmetry (p<0.05) than low-specialized athletes, irrespective of sex (Figure 1). The SLH PIF asymmetry was similar between high- and medium-specialized females (p=0.096) but was different between high-specialized females and medium-specialized males (p=0.002). In high-specialized athletes, sex differences were observed for SLH PIF asymmetry (p=0.005). No significant interaction or main effects of sport specialization or sex were found for SLH LR LSI, SJ PIF LSI, and SJ LR LSI. Prior research found that females who specialized in a sport had an increased injury risk [3]. The observed sex differences in PIF asymmetry among high-specialized athletes suggest that female athletes may be more prone to asymmetrical loading patterns, possibly due to anatomical or neuromuscular factors that affect movement mechanics [4]. Also, the lack of significant differences between high- and medium-specialized females suggests that, beyond a certain threshold, increased specialization may not further impact loading asymmetry. Further research is needed to support these findings in larger cohorts of athletes post-ACLR.

**Significance:** Given the high re-injury rate in athletes returning to sport post-ACLR, it is essential to address the key risk factors for second ACL injuries. These findings highlight the impact of sport specialization and sex on lower limb asymmetry post-ACLR, which may contribute to injury risk in athletes and can inform rehabilitation strategies tailored to the specialization level. Also, it demonstrates the potential use of loadsol® in objectively quantifying loading symmetry in patients post-ACLR and establishes a baseline for future studies to study the role of sports specialization in post-ACL recovery.

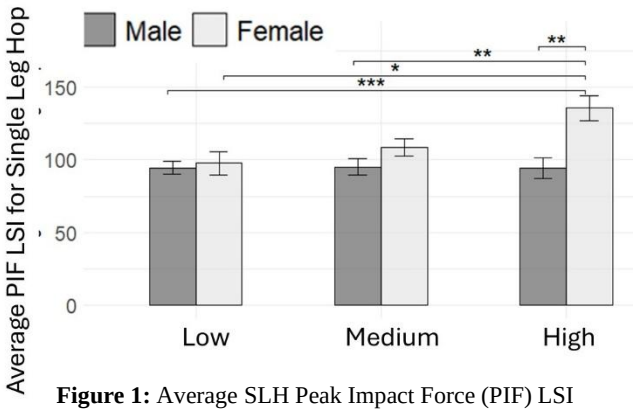


**Figure 1:** Average SLH Peak Impact Force (PIF) LSI between low-, medium and high-specialized athletes, *< 0.05, **< 0.01, ***<0.001

**Acknowledgments:** This study was supported by a grant from the National Institute of Health: R01 AR078811-03. We thank the ACL-CARE Consortium for their help in patient referral and recruitment.

**References:** [1] Fernandez et al. (2007), Acad Emerg Med, 14, [2] Jayanthi et al. (2015), Am J Sports Med 43(4), [3] Field et al. (2019), Orthopaedic Journal of Sports Medicine, 7(9), [4] Lin et al. (2018), PM&R, 10(10).

# SINGLE LEG CROSSOVER DROP PROVIDES DISTINCTIVE CLUSTER OF RISK FOR SECONDARY ACL INJURY

Jacob A. Connolly[1], Lauren A. Luginsland[1], Nathan D. Schilaty[1], Aaron J. Krych[2], Nathaniel A. Bates[3]
[1]Neurosurgery & Brain Repair, University of South Florida, Tampa FL
[2]Orthopedic Surgery, Mayo Clinic, Rochester, MN
[3]Orthopaedics, The Ohio State University, Columbus, OH
*Corresponding author's email: connolly45@usf.edu

**Introduction:** Anterior cruciate ligament (ACL) injuries remain a significant challenge in sports medicine, with a high likelihood of secondary injury following reconstruction (ACLR). Return-to-sport assessments often emphasize strength and neuromuscular testing but may fail to identify underlying biomechanical deficits that contribute to re-injury. The single-leg crossover drop landing is a dynamic movement that incorporates lateral motion to exacerbate lateral trunk bending, knee valgus, and increased external knee load—factors traditionally linked to a higher risk of ACL tear in subjects with poor neuromuscular control. Single-leg landings impose greater joint loads and altered movement patterns compared to double-leg landings [1]. Evaluating single-leg crossover drop landing mechanics offers valuable insight into neuromuscular control and lower limb asymmetries, providing a more comprehensive assessment of an athlete's readiness to return to play. Given the incidence of secondary ACL injuries [2], analyzing these dynamic movements could help identify key risk factors, enhancing clinical assessments and rehabilitation strategies.

**Methods:** 77 athletes post-ACLR surgery (43F:34M, Median age at surgery 16.7 [15.0, 18.9] yrs., median months from surgery to testing: 12.3 [11.0, 14.8], height: 171±7.2 cm, mass: 66.2 [61.0, 74.5] kg) successfully completed motion analysis evaluations as part of a multicenter clinical trial (Emory University, Cincinnati Children's, Mayo Clinic, The Ohio State University). Participants were instructed to balance on their non-injured leg atop a 31 cm box. They then dropped off the box, landing on their injured leg while swinging it across the front of their body during the descent. Data were collected using a modified Helen Hayes markerset (n=55). Motion capture and force data were recorded with the 14-40 camera system at sampling rates of 100-240 Hz and Bertec force plates at 1000-1200 Hz. Higher-rate data were downsampled to 100 Hz and 1000 Hz respectively. Post-processing was performed in Visual3D using a recursive, fourth-order, low-pass Butterworth filter with a 50 Hz cutoff frequency. Peak kinematic and kinetic variables for the involved limb's ankle, knee, and hip were then imported into *JMP 18 Pro* (Cary, NC). These discrete variables (n=228) were entered into a response screening process for predicting secondary injury and variables that met a Logworth ≥ 2.0 (n=7) were included in further analysis. A self-organizing map of three clusters was created. The three clusters were then compared to secondary ACL injury outcome with Chi-squared analysis (Fisher's Exact) and odds ratios were determined.

**Results & Discussion:** The overall Chi-square model was significant ($p$=0.009) and demonstrated cluster 3 > 2 > 1 relative to the probability of secondary ACL injury within each cluster. Cluster 3 (48% of population) had an odds ratio of 2.2 (1.1, 4.4) and 8.3 (1.1, 63.0) for secondary injury compared to Cluster 2 (41% of population) and Cluster 1 (11% of population), respectively. Cluster 2 had an odds ratio of 3.8 (0.5, 30.0) for secondary injury compared to Cluster 1.

| Variable | p-value | Logworth |
|---|---|---|
| Body Vertical Center of Gravity | 0.002 | 2.769 |
| Frontal Knee Angular Velocity | 0.002 | 2.611 |
| Hip Angle Flexion | 0.003 | 2.504 |
| Sagittal Hip Angular Velocity at Initial Contact | 0.003 | 2.458 |
| Vertical Hip Joint Center | 0.004 | 2.362 |
| Lateral Ankle Angular Velocity | 0.006 | 2.229 |
| Knee Angle Flexion | 0.007 | 2.181 |

**Table 1:** Seven kinetic/kinematic variables that predict secondary ACL injury in a 3-risk (low, medium, high) cluster classification.

**Significance:** The results demonstrate that clusters were successfully organized within an ACLR population based on seven prediction variables collected from motion capture biomechanics during a single leg crossover drop task. Secondly, these clusters exhibited low, medium, and high-risk potential for secondary ACL injury. These results demonstrate that motion analysis biomechanics at time of return to sport can be utilized to determine which athletes are at highest risk for secondary ACL injury following ACLR.

**Acknowledgments:** Funding provided by NIH (R01AT055563) and the Florida Department of State Center for Neuromusculoskeletal Research.

**References:**

[1] Xu et al., 2021. *Applied Sciences*, 11(1), 130
[2] Schilaty et al., 2017. *Am J Sports Med*, 45(7):1567-1573.

# Exploring the Effect of Propulsive Ground Reaction Biofeedback on Baseball Pitching Biomechanics

Dimitri Haan[1], Adam B. Rosen, PhD, ATC[2], Samuel J. Wilkins, PhD, ATC[2], & Brian A. Knarr, PhD[1]
[1]Department of Biomechanics, University of Nebraska Omaha, Omaha, NE USA
[2]School of Health & Kinesiology, University of Nebraska Omaha, NE USA
Email: dhaan@unomaha.edu

**Introduction:** The most widely used measurement of skill for baseball pitchers is the velocity of their fastball pitch. Increased fastball velocity gives batters less time to react to the pitch and gives baserunners less time to get to the next base. Thus, pitchers train to improve fastball velocity to increase effectiveness and overall skill. Ground reaction forces (GRF) have been found to show moderate significant correlations to velocity,[1] as well as significant increases in GRF measurements in high velocity pitchers.[2] Significantly higher pelvis velocity was also found in pitchers throwing at a higher velocity.[2] Previous literature shows that there are positive correlations and significant increases in GRF values in high velocity pitchers[2,3], but it provides no insight into how pitchers may increase their GRF. Biofeedback is defined as the technique that provides subjects with information about how their body is moving with the goal of mastering and maintaining motor skills.[3] Biofeedback has been used widely in biomechanics research, but its uses in sports have been limited comparitively.[3] While biofeedback shows positive results in decreasing knee injury risk in soccer athletes,[4] it has yet to be used in baseball pitching. Therefore, the purpose of this study was to provide baseball pitchers with ground reaction force biofeedback and assess variations in performance-related metrics, including peak ground reaction forces and maximum pelvis rotation. It was hypothesized that significant differences will be measured in GRF maximums in all directions, pelvis velocity maximums and in fastball velocity.

**Methods:** 40 healthy high school and college aged pitchers (age: 18.4 ± 2.66 years, height: 182.9 cm ± 14cm, mass: 83.3 ± 12.5kg) participated in this study. Prior to evaluation, subjects had 41 retroreflective markers placed on anatomical landmarks and then completed a self-selected warmup. Pitchers then threw fastballs in front of Qualisys Motion Capture cameras (Qualisys, Gothenburg, SWE) capturing at 320 Hz. Kinetic data was collected via force plates underneath the pitching mound at 1280 Hz (Bertec, Columbus OH, USA). During the pre-biofeedback condition, pitchers threw fastballs at their maximum comfortable intent, and the fastest 3 pitches were chosen for analysis. During the biofeedback condition, pitchers threw three pitches at maximum comfortable intent and were provided biofeedback between each pitch. The biofeedback information provided was a time series graph displaying the ground reaction force in the forward direction with a textbox displaying the maximum number. Between each pitch during the biofeedback section, pitchers were given external cues to increase the forward force by "driving into the mound" and "drive forward". Motion capture data was exported to Visual3D (HASMotion, Kingston OT, CA) where data was normalized to 101 data points and model-based computations were completed. GRF in all directions, axial pelvis velocity was measured between setup and release. Setup was automatically defined as the frame where the front toe marker exceeded 0.02 m/s, offset by -1 frame. Model-based computations were exported to a custom MATLAB script (MathWorks, Natick, MA, USA) for analysis. Maximum GRF and axial pelvis rotational velocity were extracted for each pitch and averaged for each pitcher. Paired samples t-tests were calculated in SPSS (SPSS Inc, Chicago, IL, USA) with the conditions of before and after receiving biofeedback. Significance was set at $\alpha=0.05$.

**Results and Discussion:** After receiving biofeedback pitchers were found to throw significantly slower ($p<0.001$) and achieved a significantly lower maximum pelvis velocity ($p<0.001$). No significant differences in maximum GRFx ($p=0.475$), GRFy ($p=0.605$), GRFz ($p=0.685$) or loading strategy ($p=0.948$) were measured. The hypothesis that significant differences would be measured in each of these variables was partially supported with velocity and maximum pelvis velocity being the hypotheses supported. These results indicate that pitchers who receive propulsive GRF biofeedback information during a practice session are more likely to throw at a significantly lower velocity immediately after receiving GRF information, likely due to a significantly lower maximum pelvis rotational velocity. It is hypothesized that biofeedback information and delivery of cues creates a dual task for athletes pulling attention away from their preferred mechanics, as dual tasking has been found to acutely decrease motor performance in athletes.[5] Further research will investigate if all forms of GRF biofeedback coincide with acute decreases in performance measurements, or if propulsive GRF biofeedback is unique.

| | Maximum GRFx (%BW) | Maximum GRFy (%BW) | Maximum GRFz (%BW) | Fastball Velocity (mph/kg) | Maximum Pelvis Velocity (°/s) |
|---|---|---|---|---|---|
| Pre-Biofeedback Mean | 5.93 ± 2.53 | 18.93 ± 10.29 | 130.8 ± 14.1 | 0.999 ± 0.13 | 684.9 ± 92.57 |
| Post-Biofeedback Mean | 5.75 ± 2.72 | 18.52 ± 9.77 | 130.4 ± 14.8 | 0.968 ± 0.13 | 654.7 ± 89.22 |
| p-values | 0.475 | 0.605 | 0.685 | < 0.001* | < 0.001* |

**Table 1** displays the average maximum GRFx, GRFy, GRFz, normalized fastball velocity (mph/kg) and maximum pelvis axial rotation velocity (°/s) for the conditions of before and after receiving biofeedback. *Significant differences ($\alpha<0.05$).

**Significance:** This research provides information into how coaches can provide information to their athletes, regardless of being in a lab setting. Based on the results of this research, pitching coaches should be advised to avoid delivering cues to pitchers to increase their forward force as the acute response is likely to be a decrease in force and decrease in velocity. Effects of chronic biofeedback training remain unknown at this time.

**References:** [1] Oyama S and Myers JB (2018) *J. Strength and Conditioning Research,* 5: 1324.; [2] Kageyama M et al. (2014) *J. Sports Science and Medicine* 4: 742-750.; [3] Zhang X et al. (2019) *Applied Sciences* 2: 226.; [4] Ford K et al. (2015) *J. Sports Rehabilitation* 2.; [5] Moreira et al. (2021) *IJ Environmental Research and Public Health* 4: 1732.

# KINEMATIC AND KINETIC DIFFERENCES IN TRUNK ROTATIONAL VELOCITY AND TRUNK TILT

Brandon Muczynski, Adam Rosen, Samuel Wilkins, Brian A. Knarr
email: bmuczynski@unomaha.edu

**Introduction:** Despite increased awareness and injury prevention programs, elbow injuries rates have disproportionally been on the rise. Age-related trends have been identified, with the largest increases in rates per 100,000 in 15- to 19- year and 20- to 24-year-old groups [1]. Pitching is a highly dynamic task involving a complex interplay of explosive movements and stabilization. The coordination of muscles, beginning with the legs and transferring up the pelvis and trunk, place high loads on the joints and structures of the upper extremity. The trunk kinematics and kinetics become an important factor in predicting ball velocity, as well as estimating elbow varus moments. Solomito et al. studied the effects of lateral trunk tilt in college pitchers and indicated that for every 10 degrees increase in lateral trunk tilt, ball speeds increased by 0.5 m/s, and elbow varus moments increased by 3.7 N·m [2]. A study by Cohen et al. found that increasing maximum trunk rotational velocity by 100°/s between foot contact and maximum shoulder external rotation could lead to a 0.70 m/s increase in ball velocity and up to a 2.9 N·m increase in elbow varus moment [3]. Prior research has shown that trunk tilt and trunk rotation affect ball velocity and are linked to increased elbow varus moments. While this relationship has been investigated extensively, the associations between trunk tilt and trunk rotational velocity during key moments of the pitching delivery are yet to be explored. Therefore, this study aims to investigate the relationship between lateral trunk tilt and trunk rotational velocity at foot contact (FC), maximum external rotation (MER), maximum elbow varus torque (MEV), and ball release (BR).

**Methods:** Forty-two collegiate pitchers (Age: 21.06 ± 1.31, Weight: 200.47 ± 28.23, Height: 72.92 ± 3.03) were extracted from the UNO biomechanics pitching database. Each pitcher completed a self-selected warm-up before 41 retroreflective full-body markers were placed on anatomical landmarks. Kinematic data was recorded using a 12-camera motion analysis system (Qualisys, Göteborg, Sweden). Trunk rotational velocity and lateral trunk tilt were extracted from Visual3D (C-Motion,Germantown,MD). Due to the transition of the lab to a new space, 11 subjects used were recorded in 300Hz while 31 were recorded at 320Hz. A Spearman correlation test was conducted to assess relationships between lateral trunk tilt and trunk rotational velocity at key moments of the pitching delivery. CLT (lateral trunk tilt) refers to the lateral tilt of the trunk toward the non-throwing side. Similarly, Thorax (trunk rotational velocity) denotes the rotational velocity of the trunk with the phase of the pitching motion indicated after the underscore (e.g., CLT_Max_El_Varus represents contralateral tilt at maximum elbow varus torque).

| Variable 1 | Variable 2 | Spearman's rho |
|---|---|---|
| CLT_Max_El_Varus | CLT_BR | 0.959 |
| Thorax_Max_El_Varus | Thorax_BR | 0.591 |
| CLT_Max_Sh_ER | Thorax_Vel_FC | 0.427 |
| CLT_Max_El_Varus | Thorax_Max_Sh_ER | 0.378 |
| CLT_BR | Thorax_Max_Sh_ER | 0.344 |
| CLT_Max_El_Varus | Thorax_BR | -0.316 |

**Table 1**: Spearman's rank correlation coefficients (ρ) between key trunk kinematic variables during pitching.

**Results & Discussion:** A strong positive correlation was observed between lateral trunk tilt at MEV and at BR ($\rho = 0.959$, $p < 0.001$), suggesting that pitchers who exhibit greater lateral trunk tilt at MER tend to have greater lateral trunk tilt at BR. Similarly, trunk rotational velocity at MEV and at BR demonstrated a moderate-to-strong positive correlation ($\rho = 0.591$, $p < 0.001$), suggesting that pitchers who generate greater thorax rotational velocity at MEV also tend to exhibit higher thorax rotational velocity at BR. This indicates a consistent rotational velocity pattern through the arm acceleration phase of the pitching motion. Moderate significant correlations were found between lateral trunk tilt at shoulder MER and trunk rotational velocity at FC ($\rho = 0.427$, $p = 0.005$), indicating that pitchers who exhibit greater trunk rotational velocity at FC also tend to achieve higher shoulder external rotation. Additionally, lateral trunk tilt at MEV and trunk rotational velocity at shoulder MER ($\rho = 0.378$, $p = 0.014$) and lateral trunk tilt at BR and trunk rotational velocity at shoulder MER ($\rho = 0.344$, $p = 0.026$) demonstrated positive correlations. This suggests that pitchers with greater lateral trunk tilt at key phases may also generate higher trunk rotational velocity, highlighting an interdependence between these kinematic factors during the pitching motion. A weak but significant negative correlation was observed between lateral trunk tilt at MEV and trunk rotational velocity at BR ($\rho = -0.316$, $p = 0.041$), indicating that pitchers who exhibit greater lateral trunk tilt at MEV tend to generate lower trunk rotational velocity at BR.

**Significance:** These findings emphasize the importance of trunk mechanics in pitching performance and injury risk. The strong correlation between lateral trunk tilt at MEV and BR suggests that pitchers who tilt more laterally at MEV also tend to maintain that tilt through BR, pointing to a consistent movement pattern. Similarly, the relationship between thorax rotational velocity at MEV and BR indicates that pitchers who generate more rotational speed earlier in the delivery tend to sustain it through release. Preliminary analysis from Cohen et al., found similar positive associations between maximum trunk rotational velocity and lateral trunk tilt at FC, MER, MEV, and BR [3]. These positive correlations support the idea that lateral trunk tilt and rotational velocity are biomechanically linked throughout the pitch, highlighting their interconnectedness and reinforcing their role in both ball velocity and joint loading. However, this study found a weak negative correlation between lateral trunk tilt and trunk rotational velocity at BR suggests that excessive lateral trunk tilt may come at the expense of maintaining rotational velocity late in the pitch, which could have implications for both performance and injury risk.

**Acknowledgments:** We would like to thank the Department of Biomechanics at the University of Nebraska at Omaha for providing research support and resources.

**References:** [1] Mahure et al. (2016), *Journal of Shoulder and Elbow Surgery* 25(6); [2] Solomito et al. (2015), *The American Journal of Sports Medicine*. 43(5) [3] Cohen et al. (2019), *The American Journal of Sports Medicine*. 47(12)

# Evaluating Fastball Biomechanical Responses to Cumulative Pitch Count: A Comparison of N-of-1 and Group Modeling Approaches

Garrett Fernandez,[1] Garrett S. Bullock,[1] Kristen F. Nicholson,[1]

1. Department of Orthopaedic Surgery & Rehabilitation, Wake Forest University School of Medicine, Winston-Salem, NC, USA

**Introduction:** Pitch count is a critical factor in both performance and injury risk among baseball pitchers. However, the individual biomechanical responses to increasing cumulative pitch loads remain poorly understood [1]. An N-of-1 design is a methodological approach that focuses on repeated, within-individual measurements, enabling the capture of personalized responses over time [2]. This approach is particularly valuable when high inter-individual variability is expected, as it reveals nuanced changes that may be masked in group-level analyses. This study employs observational N-of-1 methods to investigate the associations between rolling pitch count and key biomechanical outputs for fastballs, including maximum elbow varus torque, elbow angle at ball release, hip shoulder separation, shoulder rotation, lead knee flexion at release, shoulder abduction at release, and maximum shoulder distraction force, in collegiate pitchers during the 2024 season, with ongoing data collection into the 2025 season. It was hypothesized that models would identify varying key response variables highlighting the need for individualized analysis and the significance of N-of-1 analysis.

**Methods:** This study is a prospective cohort study approved by the University's Institutional Review Board, with participants being healthy D1 collegiate male baseball pitchers. The study investigates external load via rolling pitch count and internal load through daily HRV measurements (WHOOP). In-game biomechanics are captured using Kinatrax motion tracking. An N-of-1 time series framework employs mixed-effects regression, with least absolute shrinkage and selection operator (LASSO) identifying key predictors, including pitch count, travel, appearance intervals, and injury history. Generalized additive mixed models (GAMM) is then used to optimize interaction terms and smooth functions, while model selection relies on Akaike information criteria (AIC), Bayesian information criteria (BIC), root mean squared error (RMSE), and adjusted $R^2$, followed by bootstrapping for stability and predictive validation.

| Pitcher | Response Variable | N-1 RMSE | Group RMSE | N-1 $R^2$ | Group $R^2$ |
|---|---|---|---|---|---|
| **1** | Elbow Flexion (BR) | 2.452 | 2.449 | 0.182 | 0.789 |
| **2** | Shoulder Abduction (BR) | 2.038 | 2.721 | 0.454 | 0.846 |
| **3** | Shoulder Rotation (MER) | 1.567 | 3.418 | 0.589 | 0.773 |
| **4** | Elbow Flexion (BR) | 1.917 | 2.449 | 0.580 | 0.789 |
| **5** | Shoulder Rotation (MER) | 1.434 | 3.418 | 0.666 | 0.773 |
| **6** | Max Elbow Various Torque | 7.863 | 10.219 | 0.541 | 0.814 |
| **7** | Hip Shoulder Separation (FC) | 2.516 | 4.344 | 0.634 | 0.781 |
| **8** | Lead Knee Angle (BR) | 5.413 | 6.920 | 0261 | 0.841 |

**Table 1. N-of-1 vs. Group Model Performance for Pitching Biomechanics:** Summary of root mean squared error (RMSE) and adjusted $R^2$ values for each pitcher's N-of-1 and group models, based on the most predictive biomechanical response variable. Abbreviations: Ball Release (BR), Max External Rotation (MER), Foot Contact (FC).

**Results & Discussion:** When all model development was complete, each pitcher had 7 models developed, one for each biomechanical response variable. These models were then compared to a traditional group model that was nested by pitcher. When comparing the two modeling methods it was shown that on average the group model was better at representing the total variability with higher $R^2$ values shown on **table 1**. However, on average the AIC, BIC and RMSE was lower in the N-of-1 models, with RMSE being shown in **table 1**. When investigating the variable selection of the two models, the group model often utilized a majority of the initial predictor variables presented, while the N-of-1 models commonly used 3-4 initial predictors. Interpretation of these results reveals that the group model, through its inclusion of a broad set of predictors, robustly captures inter-pitcher variability across the cohort. In contrast, the N-of-1 models, by isolating the most statistically significant predictors for each individual, provide a more targeted assessment of the determinants underlying each pitcher's biomechanical behavior. Collectively, these findings suggest that while group models are effective in representing overall trends, the N-of-1 approach offers enhanced specificity in identifying the critical factors driving individual biomechanical differences.

**Significance:** This study advances the field of sports biomechanics by demonstrating that an N-of-1 analytical approach can uncover individualized associations between cumulative pitch load and biomechanical responses, insights that are often masked by traditional group-level analyses. By isolating the most critical predictors for each pitcher, these findings pave the way for personalized training and injury prevention strategies, offering a more precise risk assessment than conventional models. Moreover, the integration of individualized and group-level methodologies not only refines our understanding of pitching mechanics but also has the potential to inform clinical practices and broaden the application of personalized monitoring techniques in other high-variability sports and performance domains.

**References:** [1] Shanley et al. (2015), Phys Ther Sport 16(4):344–348 [2] Senarathne et al. (2020), Stat Med 39(29):4499–4518

# COMPARISON OF THREE LANDING TASKS AND THEIR ABILITY TO PREDICT LIKELIHOOD OF SECONDARY ACL INJURY

Lauren A. Luginsland[1], Jacob A. Connolly[1], Nathan D. Schilaty[1], Aaron J. Krych[2], Nathaniel A. Bates[3]
[1]Neurosurgery & Brain Repair, University of South Florida, Tampa FL
[2]Orthopedic Surgery, Mayo Clinic, Rochester, MN
[3]Orthopaedics, The Ohio State University, Columbus, OH
*Corresponding author's email: lluginsland@usf.edu

**Introduction:** Anterior cruciate ligament (ACL) injuries remain a significant concern in the field of sports medicine, particularly due to the elevated risk of re-injury following reconstruction (ACLR). While assessments for return-to-sport generally emphasize strength and neuromuscular evaluations, it is crucial to also take into account any underlying biomechanical impairments that may contribute to injury risk, particularly considering that nearly 80% of all ACL injuries are non-contact [1]. Three dynamic movements that are commonly used to evaluate return-to-play readiness and identify risk for reinjury include the drop vertical jump (DVJ), single-leg landing (SLL), and single-leg crossover drop (SCD). These drop landings increase lateral trunk bending, knee valgus, and increased external loads on the knee for individuals with poor neuromuscular control; these dynamics are traditionally associated with increased risk of ACL tear. Research indicates that single-leg landings result in higher joint loads and altered movement patterns compared to double-leg landings [2]. Specifically, vertical jump assessments are known to reveal neuromuscular deficits and biomechanical asymmetries in ACLR athletes even when symmetrical limb performance has been restored [2], [3]. The purpose of this study was to compare all three landing tasks and assess their ability to predict a secondary ACL injury. Given the high rates of secondary ACL injuries, predicting these injuries through specific dynamic movements may provide insight on key variables in clinical assessments and rehabilitation.

**Methods:** 77 athletes post-ACLR (43F:34M, Median age at surgery 16.7 [15.0, 18.9] yrs., median months from surgery to testing: 12.3 [11.0, 14.8], height: 171±7.2 cm, mass: 66.2 [61.0, 74.5] kg) completed motion analysis evaluations as part of a randomized, multicenter clinical trial (Emory University, Cincinnati Children's, Mayo Clinic, The Ohio State University). Participants were asked to stand on top of a 31 cm box. They were then asked to drop off of that box and land according to the instructed task, whether DVJ, SLL, or SCD. Data was captured with a modified Helen Hayes markerset (n=55). Motion capture and force data were collected using 14-40 cameras that sampled at 100-240 Hz and Bertec force plates that sampled at 1000-1200 Hz. Higher rate collections were down sampled to 100 Hz and 1000 Hz, respectively, and post-processed in *Visual3D* using a recursive, fourth-order, low-pass digital Butterworth filter with a cutoff frequency of 50 Hz. Discrete kinematics and kinetics of the ankle, knee, hip, and trunk were imported into *JMP 18 Pro* (Cary, NC). These variables (n=228; including *initial contact*, *maximums*, *minimums*, and *range of motion*) were entered into a Stepwise model with a Bayesian Inference Criterion stopping point. The resultant variables were entered into nominal regressions and variables narrowed down stepwise until 10 variables remained. These 10 variables were utilized for prediction of secondary ACL injury.

**Results & Discussion:** The DVJ regression had 10 included variables (Logworth ≥ 2.12). The DVJ model had an AUC of 0.85, specificity of 76%, and sensitivity of 80%. The SLL regression only resulted in 2 included variables (Logworth ≥ 3.57). The SLL model had an AUC of 0.69, specificity of 73%, and sensitivity of 61%. The SCD regression had 10 included variables (Logworth ≥ 2.45). The SCD model had an AUC of 0.90, with specificity of 79%, and sensitivity of 86%. Confusion matrices comparing the three models is observable in **Table 1**. The data demonstrates that the SCD may be a more effective assessment tool for predicting secondary ACL injuries in comparison to the DVJ and SLL tasks because of the higher positive prediction value, AUC, and specificity/sensitivity. This increased predictive capacity with the SCD model is likely derived from the frontal plane movements and subsequent loads during the SCD task. While the DVJ and SLL are known to elucidate frontal plane deviations in subjects with poor neuromuscular control, the SCD requires subjects to resist frontal plane motion as lateral movement is incorporated in the task.

| | 2nd Injury | Predicted Count | |
|---|---|---|---|
| DVJ | Actual Count | Yes | No |
| | Yes | 12 | 44 |
| | No | 5 | 397 |
| SLL | 2nd Injury | Predicted Count | |
| | Actual Count | Yes | No |
| | Yes | 4 | 50 |
| | No | 0 | 360 |
| SCD | 2nd Injury | Predicted Count | |
| | Actual Count | Yes | No |
| | Yes | 20 | 24 |
| | No | 8 | 247 |

**Table 1:** Confusion matrices of each model demonstrate the utility of prediction of second injury for each activity.

**Significance:** When assessing biomechanical risk factors for predicting risk of a secondary ACL injury, the SCD may be superior in comparison to the DVJ and SLL. These findings include important precautions and recommendations that particularly emphasize the need to consider the specific movements and tasks involved in the sports to which an ACLR athlete aims to return.

**Acknowledgments:** Funding provided by NIH (R01AT055563) and the Florida Department of State Center for Neuromusculoskeletal Research.

**References:** [1] Alsubaie et al., 2021. Medicine, 100, e24171. [2] Xu et al., 2021. *Applied Sciences*, 11(1), 130; [3] King et al., 2022. American J Sports Medicine, 47(5), 1175-1185; [4] Kotsifaki et al., 2022. *British J of Sports Medicine*. 56(9), 490-498.

# BCMJ VARIABLES MEAN POWER AND CONCENTRIC IMPULSE CORRELATE TO FASTBALL VELOCITY

Yasmine Jutt
Marshall University
yasmine.jutt@gmail.com

**Introduction:** Baseball pitchers at the professional level repetitively throw at velocities close to 100 miles per hour. To accomplish this impressive task, high power output is required, and it must be efficiently transferred from the legs up to the ball with precise timing [1]. Exploring how lower body power is transferred up the kinetic chain to result in high velocity fastballs is an active area of research [2]. Currently, scientists are trying to establish what variations of lower body power assessments demonstrate the kinetic transfer that occurs in pitchers. Ideally, the power assessment would correlate to fastball velocity. Having a testing battery that represents power transfer in pitchers would be a great way for scouts to help identify emerging talent. In addition, a desired test could also help sport scientists and coaches identify experienced pitchers whose power transfer needs improvement [3]. Lastly, evidence is emerging that efficient transfer of lower body power can decrease elbow varus torque [4], which is a key factor in ulnar collateral ligament injuries of the elbow. There is a need for a reputable power test in baseball pitchers, but currently there is no consensus on the best practice [3]. This study aimed to contribute evidence to the emerging foundation of power assessment tests in pitchers. The goal of this study was to examine the correlation of bilateral counter-movement jump (BCMJ) variables to fastball velocity. I hypothesized that mean overall power in the BCMJ would be correlated to fastball velocity based on the mean power during cycling representing anaerobic capacity [5;6]. This is because pitchers require excellent anaerobic capacity to maintain pitching velocity [5]. I also hypothesized that the modified reactive strength index (mRSI) would correlate with fastball velocity, since it is a measure that represents good coordination [3]. Good coordination is required for the BCMJ [3], and for efficient power transfer in pitching.

**Methods:** 19 male NCAA division 1 baseball pitchers were included in this study. Counter-movement jump data was collected using AMTI force plates on 2 occasions in September and November 2024. Pitching velocities were captured using TrackMan through a series of 9 scrimmages occurring between January and February 2025. Relative speed of each pitcher's fastballs were recorded and averaged. A repeated measure correlation statistical test was performed in Python where the average fastball velocity was paired with each trial of the BCMJ variable with a significance level of alpha = 0.05. The BCMJ variables were jump height, mean overall power, maximum overall power, eccentric impulse, concentric impulse, counter-movement depth, and mRSI.

**Results:** Mean overall power ($r = -0.49$) and concentric impulse ($r = -0.21$) were significantly correlated to fastball velocity. Jump height, maximum overall power, eccentric impulse, countermovement depth and mRSI were not significantly correlated to fastball velocity.

**Discussion:** My hypothesis was partially correct, since mean overall power was significantly correlated to fastball velocity, but mRSI had no meaningful effect. However, it should be noted that both mean overall power and concentric impulse were only weakly correlated, although statistically significant. It is possible that this result could differ if there were more BCMJ trials, or the data collection occasions took place in the same month instead of several months apart, which is a limitation of this study. In addition, the sample size of this study was small, and different results could occur with more pitchers sampled.

Maximum and mean overall power is consistent with the explanation provided by Donahue et al. (2018). The researchers describe that maximum overall power is a negligible point in the dataset for an exercise or skill, whereas mean overall power is more representative of the entire movement [5]. For example, to have a high mean pitching velocity, a pitcher must have a high anaerobic capacity to maintain the effort to keep a high mean [5]. Interestingly, the study by Donahue et al. (2018) conflicts with the results of this study since they found no significant relationships between any vertical jump variables and pitching velocity. One study did find that concentric impulse correlated to fastball velocity [7], which agrees with the present findings. However, this study also found a significant correlation with peak power and did not test mean overall power [7].

**Significance:** Overall, this study adds evidence that concentric impulse and mean overall power are weakly correlated to fastball velocity. Additional studies should investigate these two variables using the BCMJ with a larger sample size. Also, further research should evaluate concentric impulse in other jumps shown to be potentially more related to pitching power transfer, such as the unilateral lateral to medial jump (ULMJ) [3]. The ULMJ may be better for pitchers due to similarities of the jump to the side the pitcher throws from [8] so it would be interesting to see if concentric impulse and mean overall power are more strongly correlated in this variation.

**References:** [1] Fortenbaugh et al. (2009), *Sports Health* 1(4); [2] King et al. (2024), *J Strength Conditioning Research* 39(2); [3] Lis et al. (2024), *National Strength and Conditioning Association* 46(5); [4] Dowling et al. (2024), *Orthopaedic J Sports Medicine* 12(8); [5] Donahue et al. (2018), *J in Trainology* 7; [6] Zupan et al. (2009), *J Strength and Conditioning Research* 23(9); Sakurai et al. (2024), *National Strength and Conditioning Association* 38(7); [8] Lehman et al. (2013), *J Strength and Conditioning Research* 27(4).

# ANALYSIS OF PEAK HAMSTRING LENGTH DURING DECELERATIVE RUNNING

Andrew Polson[1], Ryan Culin[1], *Reed D. Gurchiek[1]
[1]Department of Bioengineering, Clemson University, Clemson, SC
*Corresponding author's email: rgurchi@clemson.edu

**Introduction:** Hamstring strains are the most prevalent time-loss injury in field-based sports [1] with high reinjury rates [2]. Previous research suggests injury risk is greater in high-speed running due to the large eccentric loads and long lengths required of the hamstrings during that task [3,4]. However, recent analyses [5,6] of in-game video found injuries often occur during accelerative and decelerative running. We recently demonstrated hamstrings stretch more and faster during accelerative running compared to speed-matched constant-speed running, but we did not consider deceleration [7]. While deceleration biomechanics have been characterized in some contexts, there has been no investigation of hamstring mechanics in particular and with an emphasis on hamstring injury mechanisms and risk. A better understanding of hamstring mechanics during deceleration could improve injury risk analysis, load monitoring, and preventive and rehabilitative efforts. Thus, the objective of this descriptive study was to quantify hamstring kinematics during decelerative running.

**Methods:** We recorded videos of 11 participants during maximal effort, decelerative running trials in an out-of-lab environment. Participants ran on artificial turf wearing their own cleats. They were instructed to run forward as fast as possible, come to a complete stop at a cone, and backpedal. They were encouraged to complete the task as quickly as possible, but we did not specify the point at which they must begin decelerating. Rather, they determined when to begin decelerating individually to facilitate a natural strategy to accomplish the task. Two trials were performed: one with the cone at 15 meters from the start of the sprint and one at 20 meters. They were given as much time as needed to familiarize themselves with the task and to rest to avoid fatigue. OpenCap [8] was used to automate recording, synchronization, and processing of the videos from two iPhone cameras (see [7] for a description of the camera setup). We used OpenSim and a three-dimensional musculoskeletal model to calculate the biceps femoris long head (BFLH) muscle-tendon unit (MTU) length and running speed (Fig. 1) [7]. MTU lengths were normalized by the length observed in an upright standing posture. The primary goal of this study was to describe the peak MTU length during decelerative running. Thus, for each running trial we calculated the greatest local maximum in MTU length (right or left leg) observed after the initiation of deceleration and before coming to a complete stop.

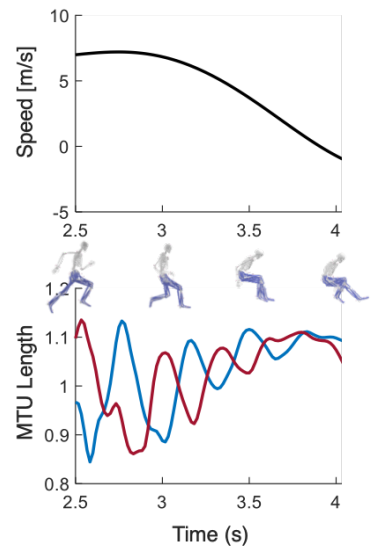


**Fig. 1.** Using OpenCap and OpenSim the running speed (top) and normalized BFLH MTU length (bottom) were calculated during deceleration, from which peak hamstring length was determined.

**Results & Discussion:** The median normalized peak MTU length was 1.08 and 1.09 for the 15 and 20 m trials, respectively (Fig. 2), which is comparable to that previously observed in top speed running [6,7]. We observed considerable range in peak MTU lengths (1.05-1.16 for 15 m, and 1.06-1.13 for 20 m) indicating athletes adopt a wide range of kinematic patterns in decelerative running. We included the 15 and 20 m trials in an attempt to quantify the effect of deceleration rate and expected greater deceleration magnitude in the 20 m trials. However, the average deceleration rates were slightly greater in the 15 m trials (median 4.7 vs. 4.1 m/s/s) which likely explains the statistically insignificant differences in peak MTU length between the two tasks. We considered the peak MTU length regardless of where in the deceleration phase it occurred. For most trials (68%), MTU length peaked early in the deceleration phase when running speed was still relatively high (>90% top speed) whereas for others, MTU length peaked closer to the end of the deceleration phase (<40% top speed). It may be that peak hamstring length for each step is relatively constant throughout the deceleration phase (Fig. 1). This should be explored in future work along with consideration of MTU lengthening velocity and load.

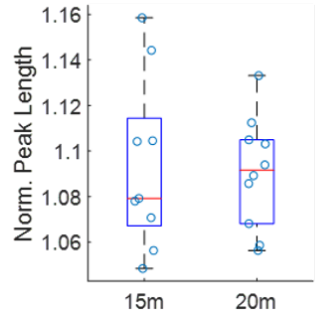


**Fig. 2.** Boxplot of peak hamstring length during deceleration for both 15 and 20-meter sprint distances. Lengths are normalized by the length during standing posture.

**Significance:** Our results highlight the wide range of kinematic patterns adopted during maximal effort decelerative running and the implications for peak hamstring length. While this is a preliminary analysis on a relatively small sample, it may indicate some kinematic patterns have lower injury risk. This motivates follow-up prospective research toward identifying features of decelerative running that could be used for movement screens.

**Acknowledgments:** This project was supported by the Clemson University Creative Inquiry Program and the SC TRIMH Center through the NIH/NIGMS P20GM121342.

**References:** [1] Visser et al. (2012), *Br J Sports Med* 46(2); [2] Maniar et al. (2023) *Br J Sports Med* 57(2); [3] Chumanov et al. (2007) *J Biomech* 40(16); [4] Thelen et al. (2005) *Med Sci Sports Exerc* 46(4); [5] Aiello et al. (2023) *J Sci Med Sport* 26(9); [6] Kerin et al. (2022) *Br J Sports Med* 56(11); [7] Gurchiek et al. (2025) *Med Sci Sports Exerc* 57(3); [8] Uhlrich et al. (2023) *PLOS Comput Biol* 19(10).

# SEX-SPECIFIC EFFECTS OF ECCENTRIC STRENGTH TRAINING ON LOWER-LIMB SPRINTING KINEMATICS

*Samantha M. Kahr[1], Jack A. Martin[2], Scott K. Crawford[1,2,3]
[1]Department of Biomedical Engineering, [2]Department of Orthopedics & Rehabilitation, [3]Department of Kinesiology
University of Wisconsin-Madison, Madison, WI, USA
*kahr2@wisc.edu

**Introduction:** The hamstring muscle group experiences large excursions, maximal eccentric loads, and high negative work during the swing phase of sprinting. As an athlete nears maximum speed, these features increase substantially and make the hamstrings susceptible to strain injury [1]. Though running biomechanics do not differ between individuals with and without a history of hamstring strain injury (HSI) [2], hip kinematics during maximal velocity sprinting have been related to higher incidence of in-sport HSI [3].

Eccentric (ECC) strength training programs have been suggested for reducing HSI risk. A particular multimodal intervention including ECC training increased peak hip flexion in terminal swing [4]. However, it is unclear whether this effect is consistent across males and females, who exhibit differences in both HSI incidence and kinematics [5, 6]. Recent evidence shows that males have a higher incidence of HSI compared to females [5] and that sex-specific differences in peak hip flexion exist during swing phase in high-speed running [6]. This exploratory study investigated how ECC strength training influences sex-specific kinematics during high-speed running.

**Methods:** Sprint testing was performed on 18 participants (7 females) before a progressive overload ECC resistance training program consisting of the Nordic hamstring exercise and Romanian deadlift (Base), after 6 weeks of intervention (Post), and following two weeks of detraining (DT) [7]. Each participant performed three maximal-effort 60 m sprint trials. Joint kinematics were collected with eight IMUs (Xsens Technologies) placed on the sternum, sacrum, and bilaterally on the thighs, legs, and feet.

Kinematic data from the fastest trial were analyzed in MATLAB. Strides at or above 95% of maximum speed based on the pelvis segment velocity were extracted for each participant, and joint angles were normalized to percent gait cycle and averaged across strides.

Each participant's peak hip flexion and knee extension angles during terminal swing (55-100% of gait cycle) were determined and compared across time (Base, Post, DT) and sex (M, F). Full factorial linear mixed effects models with fixed effects of time and sex and limb nested within a random effect of participant were used to investigate differences in peak hip flexion and knee extension angles during terminal swing. Data are presented as least square means [95% confidence intervals].

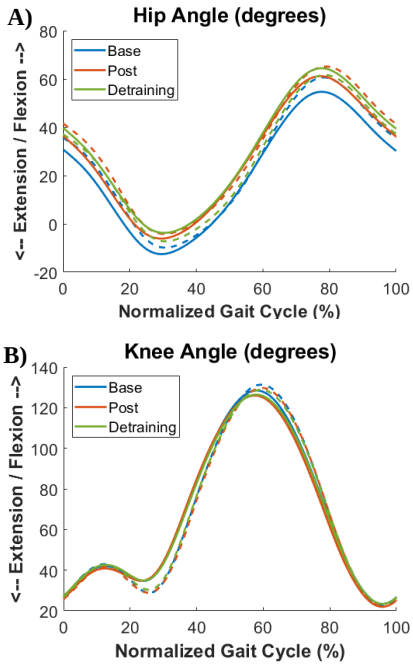


**Figure 1:** Average hip (A) and knee (B) angles across intervention timepoints. Males-Solid lines, Females-Dashed lines

**Results & Discussion:** A significant time by sex interaction for peak hip flexion (p=0.001) was observed (Figure 1A). *Post hoc* pairwise comparisons showed increases in hip flexion between Base-Post (3.5° [0.2, 6.9], p=0.03) and Base-DT (6.4° [3.0, 9.8], p<0.001) for males and between Base-Post (4.6° [0.4, 8.8], p=0.03) for females (Figure 1A). No differences were observed between Post-DT for males or females (p>0.13). Neither a significant interaction (p=0.71) nor significant effects of time (p=0.17) or sex (p=0.88) were observed for peak knee extension (Figure 1B).

Our findings indicate that ECC training may induce changes in hip kinematics during terminal swing of maximal sprinting. *Post hoc* analyses were performed to investigate the potential mechanism of increased hip flexion. Hip flexion was primarily related to 4.7° increase in anterior pelvic tilt from Base to Post (collapsed across sex) without concurrent changes in thigh orientation. The pelvis orientation did not change from Post-DT (p=0.99).

ECC training increases both ECC strength in a lengthened position and hamstring flexibility [8]. The increase in anterior pelvic tilt after the ECC training intervention is of the same magnitude observed between adolescents with and without hypermobility [9], suggesting increased hamstring flexibility may be a contributing factor to increased hip flexion. Low ECC strength, hamstring flexibility, increased hip flexion, and increased anterior pelvic tilt are linked to higher HSI risk [2, 10]. This suggests a complex relationship may exist between these factors and changes in running kinematics (i.e., anterior pelvic tilt). Future studies should measure changes in hamstring flexibility following ECC training to determine the relationship between ECC strength, flexibility, and running mechanics.

**Significance:** ECC training had a similar effect across sexes, leading to increased hip flexion in late swing via greater anterior pelvic tilt. These are each thought to be risk factors for HSI; thus, we must consider how other effects of ECC training may offset potential increases in risk related to kinematic changes and how this influences preventative training interventions and rehabilitation.

**Acknowledgments:** Funding provided by the Wisconsin Alumni Research Foundation and Clinical and Translational Science Award Program, through the NIH National Center for Advancing Translational Sciences, grant UL1TR002373 and KL2TR002374 (SKC).

**References:** [1] Chumanov et al. (2007), *J Biomech* 40(16); [2] Schuermans et al. (2017), *Gait Posture* 57; [3] Kenneally-Dabrowski et al. (2019), *J Biomech* 92; [4] Mendiguchia et al. (2022), *Int J Sports Physiol Perform* 17(3); [5] Hardaker et al. (2024), *Sports Med* 54(6); [6] Dahl et al. (2019), *Front Physiol* 10; [7] Crawford et al. (2023), *BMC Sports Sci Med Rehabil* 15(1); [8] Medeiros et al. (2021), *J Sport Rehabil* 30(3); [9] Garcia et al. (2022), *Gait Posture* 93; [10] Mizutani et al. (2023), *BMC Musculoskelet Diord* 24(1)

# PLANTARFLEXION/DORSIFLEXION IN BALLET SAUTÉS: A MULTI-SEGMENT FOOT ANALYSIS

*Kathleen A. Bieryla[1], Glenna Clifton[2]
[1]Department of Mechanical and Biomedical Engineering, University of Portland, Portland OR
[2]Department of Biology, University of Portland, Portland OR
*Corresponding author's email: bieryla@up.edu

**Introduction:** There are many different styles of ballet, including a traditional style where dancers land jumps with their heels down (HD) and Balanchine style where dancers land jumps with their heels slightly off the ground (HU). Ballet dancers complete a large number of jumps in a training session, averaging between 106 – 169 jumps, and this high repetition may lead to injury [1]. A jump completed often during training is the sauté which involves jumping and landing with both feet. Serval studies have examined the kinematics of jumps in ballet dancers, but none have examined differences in foot kinematics between the two styles of landing, HU and HD. Due to the complexity of the foot during sautés, it should not be modeled as a single segment. Few studies have used a multi-segment foot for dance studies with only one research group to our knowledge using it for ballet study [2]. It is hypothesized the hallux-metatarsal joint will have the largest plantarflexion/dorsiflexion excursion angle and will be larger in HD than HU due to the increased range of motion needed to complete a jump HD.

**Methods:** Fifteen dancers (aged 16.9 ± 2.5 years, training 11.1 ± 4.1 years) participated in the study. Informed consent was obtained and the study was approved by the university's IRB. Kinematic data was collected using a 10-camera system (OptiTrack, Corvallis, OR) from forty-four reflective markers placed on the participant's body. Each dancer performed a total of six trials, three HU and three HD with 15 sauté jumps in loose first position for each trial. A multi-segment foot model was used to calculate 3D kinematic measures [3, 4]. Right foot data from three segments: hallux-metatarsals, metatarsals-midfoot, midfoot-calcaneus is presented in this study with a focus on plantarflexion and dorsiflexion. Jump styles were compared using a one-way mixed model ANOVA with significance set at $p<0.05$.

**Results & Discussion:** Total plantarflexion/dorsiflexion excursion for the three segments only differed on average a maximum of 1.1° between HU and HD (Fig. 1). The largest excursion occurred at the hallux-metatarsals joint with HU being slightly larger than HD (41.8°± 8.7° HU, 41.0°± 7.4° HD, $p=0.005$). Although the total excursion difference between HU and HD was small, variability within subjects differed, with one subject having a difference of 7.1° between HU and HD. HU had a larger maximum dorsiflexion angle (31.2°± 5.8° HU, 27.4°± 5.3° HD, $p<0.001$) while HD had a larger maximum plantarflexion angle (10.6°± 8.2° HU, 13.6°± 8.0° HD, $p<0.001$) at the hallux-metatarsal joint. The pattern of a larger dorsiflexion angle in HU and larger plantarflexion angle at HD held true for all subjects. The total excursion at the hallux-metatarsal joint in this study is larger than total excursion in a prior study (32.1 ± 3.6°) [2]. A key difference between the two studies is the number of segments in the foot. The angle reported in the prior study was between the foot segment defined as a single segment from the calcaneus to the metatarsal heads [2]. Ballet has a high injury rate, particularly at the metatarsals including stress fractures and hallux rigidus [5] therefore breaking the foot into more than two segments can be crucial to understand the mechanics of the foot. The second largest excursion occurred at the midfoot-calcaneus joint (28.9°± 7.0° HU, 29.5°± 6.8° HD, $p<0.001$). HD had larger maximum dorsiflexion (12.9°± 3.2° HU, 13.0°± 3.2° HD, $p=0.100$) and maximum plantarflexion angles (15.9°± 6.1° HU, 16.5°± 5.9° HD, $p<0.001$) at the midfoot-calcaneus.

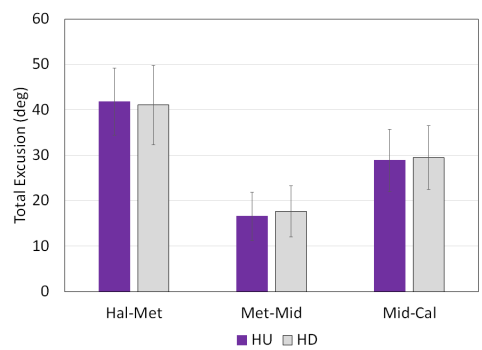


**Figure 1:** Total plantarflexion/dorsiflexion excursion for the hallux-metatarsal (hal-met), metatarsals-midfoot (met-mid), and midfoot-calcaneus (mid-cal). Error bars represent standard deviation.

Fourteen out of 15 dancers had no prior HU training. This may be one reason there was minimal difference between the two conditions. Obtaining data on dancers who have been trained in both HU and HD may show a difference between the styles. While training level of the dancers was collected, we were unable to determine if training level had an impact the kinematics of the foot due to the small sample of dancers in each level.

**Significance:** While this study shows there are minimal differences when averaging across subjects, there is variability between subjects in foot kinematics. This study is the first in the field to describe plantarflexion/dorsiflexion kinematics in a foot with more than two segments during sautés. Future work should use professional dancers in the field to determine if there are kinematic differences in HU and HD. Due to the large number of jumps that occur during training, understanding kinematic differences may lead to understanding injury mechanisms in this population.

**Acknowledgments:** Funding provided by Shiley Grant for Faculty Research and Development.

**References:** [1] Maloney et al. (2024), *Scand J Med Sci Sports* 34(1); [2] Jarivs et al. (2016) *J Sports Sci* 34(17); [3] Leardini et al. (2007) *Gait Posture* 25; [4] Portinaro et al. (2014) *J Foot Ankle Res* 7; [5] Kadel (2006) *Phys Med Rehabil Clin N Am* 17(4);

# INCREASING NEUROCOGNTIVE TASK COMPLEXITY IN A RUN TO CUT MANEUVER: UNDERSTANDING THE INFLUENCE ON KNEE BIOMECHANICS AND IMPLICATIONS FOR ANTERIOR CRUCIATE LIGAMENT INJURY

*Katherine Perille[1] Joshua T. Weinhandl[1]
[1]Department of Kinesiology, Recreation, and Sports Studies, The University of Tennessee, Knoxville, TN
*kperille@vols.utk.edu

**Introduction:** Non-contact anterior cruciate ligament (ACL) injuries are prominent in many sporting scenarios [1,2]. A survey done by Kaneko et al. (2017) found that 61% of ACL injuries are a result of non-contact mechanisms and 55% of those non-contact injuries occurred during a cutting movement. The running/cutting maneuver is a nearly unavoidable task in sports such as soccer. The dynamic uncontrollable environment of the soccer field is difficult for coaches, trainers, clinicians, and players to simulate. Increased research has presented the connection of neurocognitive "challenges" [3] and physical tasks. Current injury prevention programs often fail to create an environment that closely simulates in-game scenarios. While many return to play protocols include quick maneuver cutting and emphasize neuromuscular training throughout rehabilitation, integration of neurocognitive training is often overlooked [4]. The purpose of this study is to examine differences in lower limb biomechanics during reactive cutting in response to an increasingly complex visual stimulus. It is hypothesized that as task complexity increases, there will be an increase in peak knee abduction moment, decreased knee flexion at initial contact, increase knee abduction angle at initial contact, and increased maximum knee abduction angle.

**Methods:** The study involved seven recreationally active female participants (67.19 ± 10.92 kg, height 1.69 ± 0.06 m). 3D marker coordinates (200 Hz, Vicon) and ground reaction force data (GRF; 2000 Hz, AMTI) was collected while participants performed 20 successful unanticipated 45°±10° run to cut maneuvers in response to a visual stimulus. The visual stimulus included five arrows shown at once and participants were instructed to cut in the direction of the middle arrow (i.e., Flanker Task). When the arrows were congruent was considered the low cognitive demand conditions, while the high cognitive demand conditions include incongruent arrows with the center arrow facing opposite of the arrows flanking it. The four conditions were randomized using a custom LabView program (v2024, National Instruments Corporation). Timing gates were used to control participants' entrance and exit speeds at 3.5±.25 m/s, as well as trigger the visual stimulus 400-460 ms prior the force plate.

Knee kinematics and kinetics of the right and left leg were calculated using the 3D marker coordinate and GRF data. Visual3D was used to find peak knee abduction moment, knee flexion angle at initial contact, peak knee flexion angle, knee abduction angle at initial contact, and peak knee abduction angle. Separate 2×2 ANOVAs (limb × cutting condition) were run on the cutting conditions (low demand and high demand) for knee kinetics and kinematics. Significance for all tests was set as α=0.05.

**Results & Discussion:** There were no significant interactions in the frontal plane. However, in the sagittal plane, the main effect of cutting condition was significant for initial contact knee flexion ($p<0.005$, $d=0.49$) and peak knee flexion ($p<0.003$, $d=0.74$). Decreased knee flexion is typically a known risk factor for ACL injury; however, higher knee flexion during greater cognitive demand may be due to reduced neuromuscular control or slower movement pattern adjustments to protect the knee. For peak knee abduction moment (KAM) the interaction between demand and limb was trending towards significance ($p=0.072$). Specifically, during high demand conditions peak KAM was significantly greater on the right side compared to the left ($p=0.028$, $d=0.92$). Peak knee abduction angle for cutting condition was also trending towards significance ($p=0.08$, $d=0.16$).

Table 1. Effect of limb and cutting condition on mean (SD) of joint kinetics and kinematics. Positive joint angles represent knee extension and adduction. Positive moments represent an external knee abduction moment.

| | Low Demand | | High Demand | |
|---|---|---|---|---|
| | Right | Left | Right | Left |
| Peak KAM | 43.29 (11.13) | 34.02 (11.13) | 44.89 (22.58) | 28.79 (10.25) |
| Knee Abduction Angle @ Initial Contact | -7.47 (4.14) | -6.94 (5.35) | -8.53 (6.35) | -7.01 (6.03) |
| Peak Knee Abduction Angle | -14.38 (6.77) | -12.47 (5.52) | -15.8 (7.4) | -13.13 (6.77) |
| Knee Flexion Angle @ Initial Contact* | -36.34 (19.27) | -40.21 (9.29) | -45.72 (17.24) | -44.5 (13.68) |
| Peak Knee Flexion Angle* | -52.46 (7.65) | -55.09 (7.05) | -60.2 (12.8) | -60.06 (8.5) |

* Significant cutting condition main effect ($p<0.05$)

In tasks that require a higher cognitive demand, movement mechanics often change due to altered attention. Our preliminary results indicate there may be a difference between limbs in peak knee abduction moment, a known risk factor for ACL injury and knee valgus collapse, when there is an increase in task complexity that requires higher cognitive demand. When focus is divided, movement patterns may become less efficient, increasing ground reaction forces and knee abduction loading. Peak knee abduction angle is a known biomechanical risk factor for ACL injury, particularly in non-contact mechanisms. When the knee moves into deeper valgus, greater stress is placed on the ACL.

**Significance:** Due to the preliminary nature of this ongoing study, there is still more to learn regarding an increasingly complex neurocognitive task and the effects on lower body biomechanics. Understanding how increasing task complexity impacts lower body biomechanics can be useful for understanding and better preparing athletes for in game scenarios, specifically in return to play protocol.

**References:** [1] Fauno et al. (2006). *Int J Sports Med*, 27:75-9; [2] Kaneko et al. (2017), *Asian J of Sports Med*, 8(1); [3] Walker et al. (2021), *Phys Ther Sport*, 51:1-24 [4] Mass General Brigham *Rehabilitation Protocol*.

**Strategy to step on obstacle safely during cross-country race**

Emanuela H. Kang[1], Jan Karel Petric[2,3], *Sophia Ulman[2,3]
[1]Hockaday School, Dallas, Texas
[2] The University of Texas Southwestern Medical Center, Dallas, Texas
[3] Scottish Rite for Children, Frisco, Texas
*Corresponding author's email: Sophia.Ulman@tsrh.org

**Introduction:** Overuse injuries are a significant concern in high school athletics, particularly in endurance sports like cross-country running. Among high school cross-country runners, overuse injuries impact approximately 28-38% of athletes within a single season [1,2]. These injuries are commonly associated with repetitive stress and inadequate recovery [1,2], which are inherent to the sport due to high training volumes and intensities. The impact that overuse injuries have on an athlete is substantial, as they often require extensive medical rehabilitation and physical therapy that can last for months. To take preventive measures and minimize injury risk, this study aims to analyze the effects of three different positions of foot placement (medial, central, and lateral midfoot) on bone stress and soft tissue strain during obstacle interaction. The hypothesis is that central foot placement, specifically at the center of the plantar surface of the midfoot, provides the safest positioning and reduces the risk of injury when stepping on obstacles.

**Methods:** An in-silico model was developed to simulate a "stepping on obstacle" scenario, a common occurrence during cross-country running. For this study, a custom shoe and obstacle model was developed and integrated into an existing foot model, part of the validated [3] human body model, THUMS (Fig. 1). To simulate the running motion in a computationally efficient way, ground reaction force was applied to the foot by moving the obstacle upward to impact the foot from below, while the proximal ends of the tibia and fibula and the ground plate were fixed. The mean peak-to-peak vertical ground reaction force during the running cycle, three times of the body weight [4-6] at 3.15 $ms^{-1}$ speed, was applied on the impactor [4]. Since midfoot consistently experiences the highest impact during the running cycle [4], it served as the impact point in the simulation. Therefore, only medial, central, and lateral variations of midfoot placement were considered to evaluate tissue responses. Stress on bones and strain on soft tissues were recorded at every 1ms. Material properties in the model were assigned by using THUMS definition directly or based on literatures [3,4,7,8]. To represent diverse foot conditions, joint laxity (original, laxity 30%, and laxity 60%) and friction levels (0.2, 0.5, and 0.8 as friction coefficient) were used in each of the foot placement locations. This resulted in a total of 27 scenarios: three different foot placement locations x three joint laxity levels x three friction levels. To investigate the effects of foot placement on bone stress and soft tissue strain in the nine different joint laxity and friction level scenarios, one way ANOVA with post-hoc Tukey test was used. Statistical significance was set at 0.05.

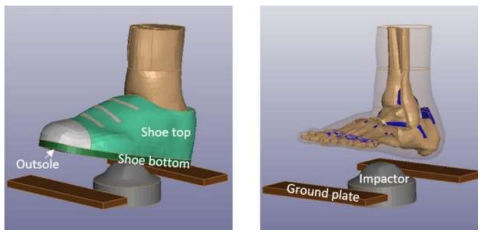


**Figure 1:** Schematic images of in-silico model setup mimicking the stepping on obstacle

**Results & Discussion:** In all 27 simulations, the peak bone stress was seen in the talus. The average of that bone stress increased from 73.0±8.7 MPa in the medial to 79.7±5.5 MPa in central and 84.9±3.2 MPa in lateral impact locations. This accounted for a 9% increase from medial to the central (p=0.0097) and 16% increase from medial to the lateral (p=0.0032) impacting locations. The significant difference in stress between the central and lateral case was also observed (p=0.031). The distribution of bone stress in the foot is demonstrated in Figure 2. Unlike the lateral case, the medial foot placement resulted in the dissipation of obstacle impact through the hallux and medial longitudinal arch, in addition to aligning the axis of impact to the axis of the ankle. The peak strain was predicted in the anterior tibiotalar ligament in all 27 simulations. Its average was the lowest in the medial condition (11.5±1.5%) and increased to 19.9±1.6% in lateral (p<0.001) and 20.2±2.0% (p<0.001) in central impact locations (Fig. 3).The results of this in-silico study demonstrate that bones and soft tissues experienced significantly lower peak stress and strain under the medial impact condition compared to central and lateral impacts, thus the hypothesis is rejected.

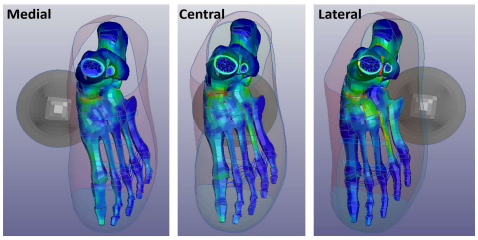


**Figure 2:** Stress distribution in the foot at three different impact locations with 60% of joint laxity condition and medium level of friction

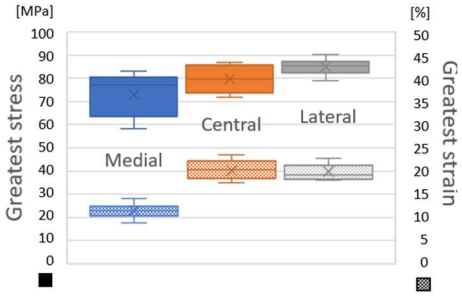


**Figure 3:** Greatest stress (left axis) and strain (right axis) in three different foot placements

**Significance:** When stepping on an obstacle, statistically significant reductions in bone stress and soft tissue strains are predicted in medial midfoot placement, compared to central or lateral midfoot placements. The evidence suggests that during endurance running, athletes should step on the obstacles with the medial side of their midfoot, to minimize bone stress and soft tissue strain in their feet. This strategy will help protect these athletes by decreasing chances of overuse injuries. A larger, clinical study is needed to support these claims in real-life scenarios.

**References:** [1] Marshall et al. (2020), *J Athl Train* 55(12); [2] Mikel et al. (2024), *J Orthop Sports Phys Ther* 54(2); [3] Kitagawa et al. (1998), *Stapp Car Crash J* 42; [4] Wong et al. (2020), *Front Bioeng Biotechnol* 8; [5] Weiss et al. (2018), *J Orthop* 36(12); [6] [8] Zec et al. (2010), *J Biomech Eng* 132; [7] Papagiannis et al. (2017), *Mater Sci Eng* 254; [8] Serra et al. (2019), *Polymers* 11(10).

**Comparison of joint contributions to total support moment during single-leg hopping between collegiate male athletes with neutral versus low arch heights**

*Brandi E. Decoux[1], Christopher M Wilburn[2], Wendi H. Weimar[2]
[1] Southeastern Louisiana University, Hammond, LA
[2]Auburn University, Auburn, AL
*Corresponding author's email: brandi.decoux@selu.edu

**Introduction:** The arch of the foot plays a key role in supporting the body and absorbing impact with the ground during various movements, especially athletic tasks. Previous research has shown that joint contributions during drop landings [1] and muscle activity during running [2] differ according to arch height. However, the role of lower extremity joints in supporting the body during vertically directed cyclical tasks like hopping in place are less understood. Hopping is a fundamental movement skill that involves a loading phase followed by quick propulsion. Its repetitive nature makes it a useful way to study how arch height affects lower body support strategies in experienced athletes. This study aimed to compare total support moment (TSM) characteristics between athletes with neutral arches and those with low arches during single-leg hopping.

**Methods:** Twenty-four male collegiate athletes (88.7 ± 11.7 kg; 1.84 ± 0.06 m) provided informed consent to participate in this IRB-approved study. All participants were healthy with no lower extremity musculoskeletal injuries within the previous six months and no history of foot or ankle surgery. Foot anthropometrics were measured using an arch height index measurement system device to compute arch height index (AHI) [3-4]. Participants with AHI values less than or equal to 0.31 were included in the low arch group while those with AHI values greater than 0.31 were included in the neutral arch group.

Kinematic and ground reaction force data were collected during three stationary single-leg hopping trials using an eight-camera motion capture system (100 Hz, Vicon Motion Systems Ltd., Oxford, UK) and a force platform (1000 Hz, AMTI, Watertown, Massachusetts), respectively. Participants performed ten consecutive hops on their dominant limb for each trial. Visual 3D software (C-Motion, Inc., Rockville, Maryland) was used to calculate ankle, knee, and hip extensor moments normalized to body mass, with the sum of these sagittal joint moments serving as the total support moment (TSM). Joint contributions of ankle, knee, and hip to the peak TSM and TSM impulse were computed and expressed as a percentage.

Data from the middle three hops of the three trials were averaged and then statistically analysed in SPSS. Mann-Whitney U tests were performed to evaluate whether peak TSM, TSM impulse, and individual joint contributions of the ankle, knee, and hip to peak TSM and TSM impulse differed between the neutral arch and low arch groups ($\alpha = .05$).

**Results & Discussion:** Descriptive statistics for variables related to peak TSM are summarized in Table 1 while descriptive statistics for variables related to TSM impulse are summarized in Table 2. The ankle's contribution to TSM impulse was significantly higher in the neutral arch group compared to the low arch group ($U = 29.5$, $p = .014$). No significant differences between groups were detected for any of the other variables analyzed.

**Table 1**. Mean ± standard deviation for all variables of interest related to peak total support moment (TSM).

| | Ankle contribution to peak TSM (%) | Knee contribution to peak TSM (%) | Hip contribution to peak TSM (%) | Peak TSM (Nm/kg) |
|---|---|---|---|---|
| Neutral Arch | 40.9 ± 11.8 | 28.0 ± 9.7 | 31.1 ± 16.9 | 6.86 ± 1.46 |
| Low Arch | 35.0 ± 9.0 | 32.3 ± 10.1 | 32.7 ± 12.0 | 6.57 ± 1.40 |

**Table 2**. Mean ± standard deviation for all variables of interest related to total support moment (TSM) impulse.

| | Ankle contribution to TSM impulse (%) | Knee contribution to TSM impulse (%) | Hip contribution to TSM impulse (%) | TSM impulse (Nm·s/kg) |
|---|---|---|---|---|
| Neutral Arch | 55.0 ± 9.4 | 23.7 ± 5.9 | 25.1 ± 13.6 | 1.23 ± 0.34 |
| Low Arch | 45.6 ± 5.9 | 26.4 ± 8.9 | 28.7 ± 10.8 | 1.30 ± 0.37 |

These findings suggest that athletes with neutral arches rely more on kinetic contributions at the ankle to support the body during single-leg hopping compared to those with low arches, suggesting that arch structure influences cumulative ankle joint loading strategies during cyclical movements. This differential ankle contribution to total support moment impulse may represent a compensatory mechanism where individuals with low arches redistribute loads to minimize stress on the medial longitudinal arch structures. Nonetheless, the overall similarity in TSM values between groups indicates that athletes achieve comparable functional outcomes through different joint mechanics. Future research should investigate whether these biomechanical differences translate to performance advantages or injury risk variations among athletes with different foot structures, particularly during sport-specific movements.

**Significance:**
The study provides insight into the role of foot arch height in shaping lower limb loading strategies during hopping, which may help guide sport-related training programs aimed at improving movement efficiency, performance, and injury prevention in athletes.

**References:** [1] Powell D et al., 2016. *Hum Mov Sci*. 49: 141-147. [2] Hajilou B et al., 2024. *Sci Rep*. 14: 25221. [3] Williams D & McClay I, 200. *Phys Ther*. 80: 864-871. [4] Butler R et al., 2008. *J Am Podiatr Med Assoc*. 98: 102-106.

# EFFECT OF COGNITIVE MOTOR INTERFERENCE ON LANDING AND JUMPING KINEMATICS FOLLOWING ANTERIOR CRUCIATE LIGAMENT RECONSTRUCTION

*Alexander M. Morgan[1], Jacob Petrus[1], Alek Johnson[1], Justin Blankenburg[2], Aaron Harris[1], Aaron Montgomery[1], Ryan Guggenheim[1], Harry Costlow[1], Bailey Hall[1], John Abt,[3] Jacob Calcei[4], James Voos[4], John Polousky[5], Melanie Morscher[5], Jennifer Kadlowec[1], Patrick S. Ledwidge[6]

[1]Baldwin Wallace University, Berea, OH; [2]Kent State University, Kent, OH; [3]Children's Health Andrews Institute for Orthopaedics & Sports Medicine, Plano, TX; [4]University Hospitals Department of Orthopaedic Surgery; [5]Akron Children's Hospital Department of Orthopaedics, Akron, OH; [6]Western Kentucky University, Bowling Green, KY

*Corresponding author's email: amorgan@bw.edu

**Introduction:** 24% of athletes < 25 years old who return to sport will suffer a secondary Anterior Cruciate Ligament (ACL) injury [1]. Altered hip and knee kinematics have been identified as risk factors for first and second ACL injury. Hip adduction post-ACL reconstruction (ACLR) has been reported to be 5-6° greater than matched controls [2]. In addition, athletes who suffer an ACL injury exhibit significantly lower peak knee flexion during landing [3]. Finally, female athletes who have experienced an ACL injury display 8.4° higher knee abduction angles at initial contact than controls [3]. Cognitive motor interference (CMi), which occurs during dual cognitive-motor tasking, amplifies these risk factors during landing and jumping tasks [4]. Limited literature exists on the effects of dual task activities on bilateral landing and cutting mechanics after ACLR. The purpose of this study was to examine the effects of a dual task bilateral drop jump (DJ) on knee flexion, knee abduction, and hip adduction during the landing phase between athletes post-ACLR and healthy controls. It was hypothesized that post-ACLR athletes would demonstrate poorer landing mechanics, specifically less knee flexion, greater knee abduction, and hip adduction, and that these measures would worsen during dual task conditions.

**Methods:** Participants included 14 post-ACLR athletes < 25 years old no more than 4 years post-surgery who had returned to sport and 14 age-, sport-, and BMI-matched controls. An eight-camera 3D motion capture system (OptiTrack PrimeX 13W; Motive 2.3.1) tracked 30-retroreflective markers placed on lower body anatomical landmarks. Participants dropped from a 12-inch plyometric box, landed bilaterally, and completed a secondary jump leftward, rightward, or upward as indicated by a visually presented arrow (E-Prime 3.0 PST). Participants completed DJs under two conditions: anticipated (single task) and unanticipated (dual task). The direction of the secondary jump was presented prior to the start of the trial for the anticipated condition, and 250 ms after the participant's foot left the box for the unanticipated condition [5]. Participants completed 15 randomized trials per condition (5 per direction). Peak knee flexion, peak knee abduction, and peak hip adduction values of the injured or matched limb were identified, and linear mixed-effects models were implemented in R's REML package to assess effects of group and condition on lower extremity kinematics.

**Results & Discussion:** Significant interactions between group and condition were identified for knee flexion ($p < .001$) and knee abduction ($p < .001$): angles increased from the anticipated to unanticipated condition for the ACLR group only (Fig. 1). Hip adduction was greater in unanticipated than anticipated condition for both groups ($p < .001$). These findings demonstrate that post-ACLR deficits in lower-extremity kinematics may be specific during dual-task landings. However, increased, rather than decreased, knee flexion in the unanticipated condition was unexpected. Participants may have increased time on the ground during the unanticipated condition via greater knee flexion due to the complexity of the task. Additionally, decreased variability for frontal plane kinematics post-ACLR may have been a strategy to repeat frontal plane movements while allowing for variability in the sagittal plane to comfortably complete a complex task. The opposite occurred for the control group, as they may have prioritized sagittal plane repeatability rather than frontal plane. Finally, it appeared that participants adopted a strategy to stabilize more at the hip than at the knee during a dual task, regardless of group. These strategies may explain the lack of a significant group by condition interaction at the hip.

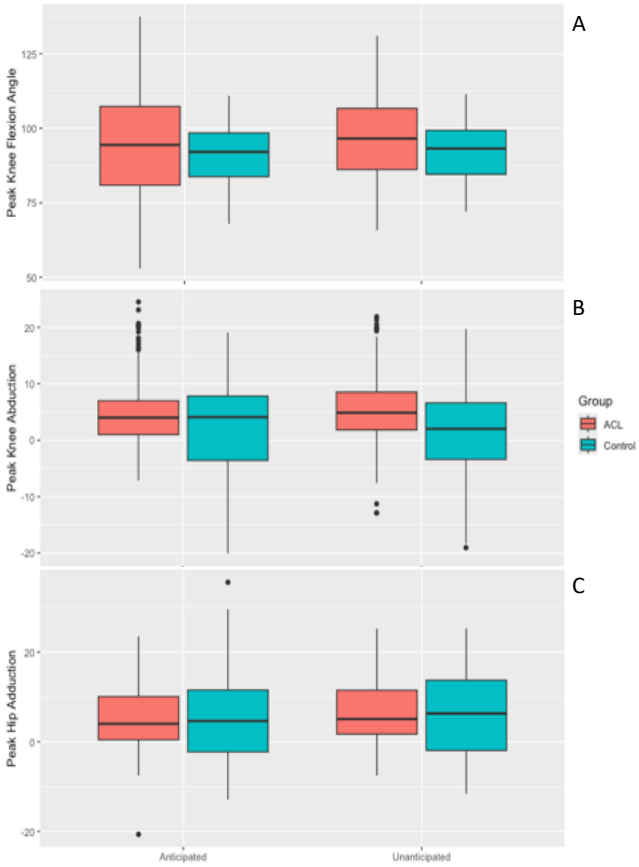


**Figure 1:** Differences in peak knee flexion (A), peak knee abduction (B), and peak hip adduction (C) by group and condition.

**Significance:** Complex dual tasks may elicit movement strategies prioritizing more knee flexion and less variable frontal plane movement post-ACLR. Future research following similar methodology should consider contact time when examining CMi during jumping and cutting activities and when designing ACL rehabilitation programs that implement dual task activities.

**References:** [1] Zacharias et al. (2021), *Am J Sports Med* 49(4); [2] Delahunt et al. (2012), *J Orthop Res* 30(1); [3] Hewett et al. (2005), *Am J Sports Med* 33(4); [4] Almonroeder et al. (2018), *J Orthop Sports Phys Ther* 48(5); [5] Herman & Barth (2016), *Am J Sports Med* 44(9)

# LOWER-BODY POWER GENERATION AND PITCHING VELOCITY: INSIGHTS FROM JOINT TORQUE POWER

Takato Ogasawara[1*], Adam B. Rosen[2], Samuel J. Wilkins[2], Brian A. Knarr[1]
[1]Department of Biomechanics, University of Nebraska at Omaha, Omaha, NE, USA
[2]School of Health and Kinesiology, University of Nebraska at Omaha, Omaha, NE, USA
*Corresponding author's email: togasawara@unomaha.edu

**Introduction:** Recent studies emphasize the role of the lower body in generating energy during pitching, particularly through the drive leg with coordinated movements at the lower extremity joints to maximize ball velocity (BV) [1]. A deficiency in lower body power generation can lead to compensatory shoulder power generation, increasing the risk of upper extremity injury. Ground reaction forces (GRF) are commonly analyzed to assess power generation mechanics. However, relying solely on GRF data may overlook the complex interactions involved in power generation during a pitch [1]. Previous research has leveraged joint torque power (JTP) analysis to investigate the power generation (concentric contractions) and absorption (eccentric contractions) occurring at each drive leg joint and has highlighted the characteristics of JTP [2,3]. While peak JTP at individual joints has been studied, its direct relationship with BV has not been fully established. Additionally, it remains unclear whether the distribution of JTP, relative to overall leg power, plays a significant role in pitching performance. This study aimed to examine the relationships between absolute and relative JTP peaks and BV, which could provide deeper insights into the most effective power generation strategies for optimizing pitching performance. It was hypothesized that the absolute JTP peak generation at the hip would demonstrate the strongest positive correlation with ball velocity.

**Methods:** Fifty-nine competitive baseball pitchers aged 11 to 24 (18.4±2.7 years, height=1.82±0.1m, mass=82.8±14.0kg) were extracted from the UNO Pitching Lab database. After a self-selected warm-up, pitchers performed 15 to 20 maximal-effort pitches from a mound and the average of the three fastest pitches was used for the analysis. High-speed motion capture (320 Hz), and ground reaction forces (1280 Hz) were recorded using 41 reflective markers and force plates. JTP at the drive leg ankle, knee and hip were calculated using the following formula.

$$JTP = T_p \cdot (\omega_d - \omega_p)$$

$T_p$ is the joint toque vector acting on a segment at the proximal joint $p$, and ω is the segmental angular velocity vector of a segment at proximal segment *s* and distal segment *d*. Positive JTP values indicate power generation (concentric contraction), while negative values represent power absorption (eccentric contraction). To assess absolute JTP (ABS), both peak power generation and absorption magnitudes at each joint were extracted from maximal knee height to stride foot contact. To evaluate relative JTP (REL), JTP at each joint was normalized to the total power generated by the drive leg, providing a measure of power distribution among the joints. Pearson correlation coefficients were calculated to assess the relationship between JTP peaks and BV, with significance set at $p < 0.05$.

**Results & Discussion:** The correlation analysis between JTP peaks and BV is presented in Table 1. For absolute JTP, power generation at the hip and knee showed the moderate positive correlations with BV, suggesting that greater power output at these joints is relevant to pitching performance. A similar trend was observed for power absorption, indicating that eccentric control at the knee and hip may aid in optimizing energy transfer and force transmission during the pitching motion. In contrast, neither power generation nor absorption at the ankle showed a significant correlation with BV, suggesting that ankle power may not play a primary role in velocity production. However, relative JTP distribution revealed a negative correlation between ankle JTP and BV, suggesting that a higher proportion of power generated at the ankle, relative to total leg power, is associated with lower BV. It indicates that excessive reliance on ankle power generation may be detrimental to pitching performance.

**Table 1:** Correlation between JTP peaks at each joint and ball velocity, $p < .05$ (*) and $p < .01$ (**). ABS: Absolute value, REL: Relative value

| | Generation | | Absorption | |
|---|---|---|---|---|
| | ABS | REL | ABS | REL |
| Ankle | .18 | **-.55**** | .13 | .15 |
| Knee | **.36**** | .19 | **.39**** | -.14 |
| Hip | **.39**** | .24 | **.32**** | .08 |

**Significance:** These findings suggest that maximizing absolute power at the hip and knee plays a crucial role in achieving higher BV. The significant positive correlations between absolute JTP at these joints and BV indicate that greater power generation at the proximal lower extremity contributes to velocity production. Additionally, power absorption at the knee and hip may play a crucial role in energy storage through eccentric muscle contraction, which contributes to momentum control and effective energy transfer. The lack of correlation between absolute ankle power and BV suggests that the ankle may play a lesser role in force generation for pitching. The previous research reported a greater amount of joint torques at hip and knee [4] and our results highlight the importance of developing hip and knee power to optimize lower-body mechanics and enhance pitching performance.

Although relative JTP did not identify a specific dominant joint for power generation, the results indicate that over-reliance on ankle power negatively affects BV. While this suggests that lowering the proportion of power generated at the ankle may be beneficial, it does not necessarily imply that all pitcher can be applied to a universally hip- or knee-dominant strategy. As variability in movement patterns and biomechanical adaptations has been observed across different performance levels [4], optimal power distribution may differ between athletes. Future research should explore different lower-body power generation strategies based on individual mechanics, strength levels, or pitching styles. This result provides valuable insights for training strategies aimed at optimizing lower-body power generation, improving pitching performance, and potentially reducing upper-extremity injury risk.

**References:** [1] Oyama and Myers (2018), *J of Strength & Con Research*, 32(5), [2] Pryhoda et al. (2022), *Front Sports Act Living* 4; [3] de Swart et al. (2022), *Sports Biomech*. [4] Kageyama et al. (2015), *J of Sports Sci & Med*

# ASSESSING INTERRELATIONSHIPS BETWEEN INDIVIDUAL HAMSTRING MUSCLE VOLUMES

Jack A. Martin[1,2*], Silvia S. Blemker[4], David A. Opar[5], and Bryan C. Heiderscheit[1,2,3]
University of Wisconsin-Madison [1]Badger Athletic Performance and Depts. of [2]Orthopedics & Rehabilitation and [3]Biomedical Engr.
[4]Springbok Analytics and University of Virginia Department of Biomedical Engineering
[5]Australian Catholic University SPRINT Research Center and School of Behavioral and Health Sciences
*Corresponding author's email: jamartin8@wisc.edu

**Introduction:** The risk for hamstring injury in athletes is multifactorial, and understanding risk factors is the first step towards implementing preventative strategies for at-risk individuals. The biceps femoris long head is at particularly high risk for injury during high-speed running, and it is likely that anatomical factors play a role in determining injury risk. The individual hamstring muscles are generally highly redundant, but relative force production between the muscles is affected by joint angles [1], and the individual muscles have distinct activation patterns during high speed running [2]. Hence, it is possible that the relative size and strength of individual hamstring muscles may affect injury risk during different activities. For instance, a relatively small biceps femoris long head may predispose an athlete to injury during the late swing phase in sprinting, even if total hamstring size is large. However, it is unknown whether there are large differences in the relative sizes of hamstring muscles across individuals. Thus, the purpose of this analysis is to assess relationships between the sizes of the four individual hamstring muscles: semimembranosus (SM), semitendinosus (ST), and biceps femoris long head (BFL) and short head (BFS).

**Methods:** This analysis uses data collected from 508 Division I collegiate football players (mean (SD) – mass: 103.1 (19.4) kg; height: 1.87 (0.07) m) as part of the HAMstring InjuRy (HAMIR) study [3]. MRI examinations of the lumbo-pelvic region and bilateral lower extremities were performed on players, and hamstring muscles were segmented using Springbok Analytics machine learning technology [4]. Muscle volumes were normalized to the height-mass product [5], and bilateral values were averaged. Coefficients of determination ($R^2$) were calculated between each pair of normalized hamstring muscle volumes and between the summed medial (SM, ST) and lateral (BFL, BFS) volumes.

**Results & Discussion:** Normalized volumes (mean (SD)) were 1.72 (0.30), 0.89 (0.18), 2.15 (0.38), and 2.01 (0.40) $mL \cdot kg^{-1} \cdot m^{-1}$ for the BFL, BFS, SM, and ST, respectively. Mean $R^2$ values ranged from 0.20 to 0.40 for comparisons between individual normalized muscle volumes (Fig. 1). All correlations were positive and significantly different from zero ($p < 0.001$).

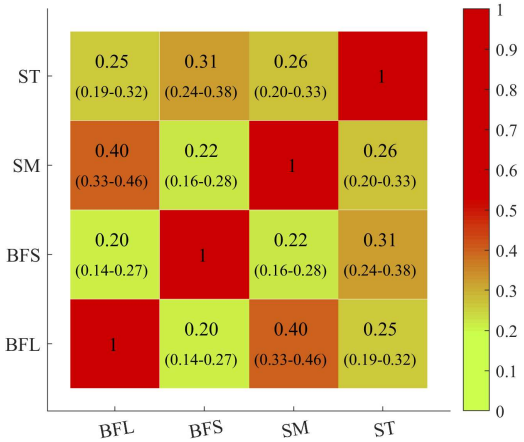


**Figure 1:** Coeff of determination ($R^2$) between each pair of normalized hamstring volumes: mean (95% CI).

The pairs of medial (SM, ST) and lateral (BFL, BFS) hamstring muscles had low $R^2$ values, indicating that these pairs of muscles may have a compensatory relationship, where relatively greater size in one may partially compensate for relatively smaller size in the other. This may be particularly important in rotation of the knee. This is in line with the relatively stronger relationship between the summed medial and summed lateral muscle volumes ($R^2 = 0.43$ (0.36-0.49)), which may indicate a need for balance between internal and external knee rotation contributions. The stronger relationships between individual muscles were observed between BFL and SM and between BFS and ST. This observation may relate to a need for balance between hip extension and knee flexion capacity. The former pair of muscles has origins and insertions that allow them to provide more even contributions at the two joints, whereas the latter pair are more biased towards knee flexion and hip extension, respectively.

Regardless of the biomechanical drivers for the relationships between muscle sizes, they were of only low to moderate strength overall, indicating that individual hamstring muscle sizes vary somewhat independently across individuals. Thus, measures of total hamstring size or strength may have limited value when considering injuries to individual hamstring muscles. This may explain why Nordic hamstring exercise (NHE) performance is not predictive of hamstring injury risk [6], even while inclusion of NHE in a training program has been shown to improve hamstring strength [7] and reduce hamstring injury risk [8]. It is possible that the size and strength of the specific injured muscle or the relationship between two or more muscles may have greater predictive power. Future work will assess the relationships between these and injury incidence.

**Significance:** This work examines the strength of relationships between individual hamstring muscle sizes. The findings indicate that the sizes of these muscles vary somewhat independently, which casts doubt on the use of global hamstring metrics in predicting injury risk in specific muscles, e.g., using NHE performance to predict injury to BFL during high speed running. Consequently, these findings motivate further study of muscle specific metrics in predicting hamstring injury.

**Acknowledgments:** The authors thank the NFL for their support of the work presented here. Neither had any role in this study or our decision to present the results. Drs. Blemker (Co-founder and Chief Science Officer) and Heiderscheit (advisory board member) declare potential competing interests related to this work due to their roles with Springbok Analytics.

**References:** [1] Beyer et al. (2019), *Int J Sports Phys Ther* 14; [2] Suskens et al. (2023), *Scand J Med Sci Sports* 33; [3] Heiderscheit et al. (2022), *BMC Sports Sci Med Rehabil* 14; [4] Ni et al. (2019), *J Med Imaging* 6; [5] Handsfield et al. (2014), *J Biomech* 47; [6] Opar et al. (2021), *Sports Med* 51; [7] Timmins et al. (2024), *Med Sci Sports Exerc* 56; [8] van Dyk et al. (2019), *Br J Sports Med* 47.

# DUAL-TASK COST OF SIT-TO-WALK IN OLDER ADULTS: PRELIMINARY RESULTS

Marvin Alvarez[1], Angeloh Stout[1], Kaye Mabbun[1], Stacy Nguyen[1], Pranav Ranganath[1], Macie Kauffman[1], *Gu Eon Kang[1]
[1]University of Texas at Dallas, Department of Bioengineering
*Corresponding author's email: gueon.kang2@utdallas.edu

**Introduction:** Sit-to-walk is a fundamental activity of daily living for people of all ages. It is not merely a sequential combination of sit-to-stand and subsequent gait initiation, but rather a cohesive, fluid transition between the two movements (Figure 1). Recent studies have examined various biomechanical characteristics of sit-to-walk, such as the total duration, phase durations, and the trajectories of the center of mass [1,2]. Notably, sit-to-walk hesitation, defined as a reduction in forward center-of-mass velocity during sit-to-walk, has emerged as a significant quantitative indicator of the fluidity of this movement [3]. Particularly, sit-to-walk hesitation may indicate age-related mobility decline. However, to date, studies have predominantly examined hesitation and other sit-to-walk variables under single-task conditions. This study aims to compare sit-to-walk hesitation between single-task and dual-task in healthy older adults and to contrast these findings with those from healthy young adults.

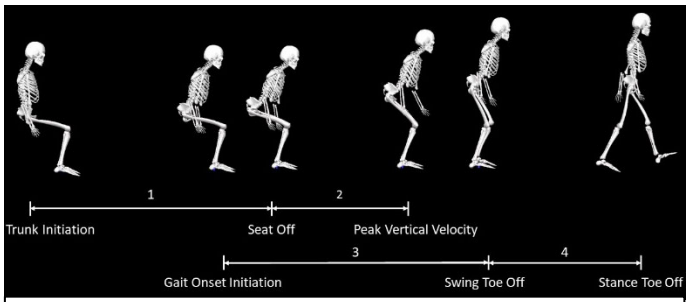

Figure 1. Biomechanical illustration of sit-to-walk.

**Methods:** We conducted a preliminary analysis for an ongoing study. We recruited 28 healthy young adults (11 females; mean age = 22.4 ± 5.2 years; mean body mass index = 23.9 ± 2.7 kg/m$^2$) and one healthy older adult (male; 75 years; body mass index = 26.8 kg/m$^2$). All participants were cognitively intact, as assessed by the Montreal Cognitive Assessment, and had no history of neurological disorder. To perform sit-to-walk, participants were asked to walk out from an armless chair in a single fluid motion under two conditions: without any concurrent task (single-task) and while performing a concurrent mathematical processing task (dual-task). Each condition was repeated three times. During sit-to-walk, we collected data from 74 reflective markers using a 16-camera motion capture system (Vicon, UK). Data analysis was performed using Visual3D (HAS Motion, Canada). We created a 15-segment biomechanical model and calculated trajectories of the center of mass. We measured sit-to-walk hesitation and the total duration of the sit-to-walk transition (Figure 2). Statistical analysis was performed to compare sit-to-walk hesitation and duration between single-task and dual-task conditions within health young adults using paired t-tests. Differences in these variables between young and older adults under both task conditions were assessed using unpaired t-tests.

**Results & Discussion:** In healthy young adults, sit-to-walk hesitation significantly increased from the single-task condition (30 ± 20%) to the dual-task condition (40 ± 20%) ($p < 0.05$). Similarly, sit-to-walk duration also significantly increased from single-task (1.8 ± 0.3 seconds) to dual-task (2.0 ± 0.4 seconds) in healthy young adults ($p < 0.05$). In the single healthy older adult, sit-to-walk hesitation increased from single-task (43 ± 5%) to dual-task (58 ± 8%), and sit-to-walk duration also increased from single-task (1.8 ± 0.1 seconds) to dual-task (2.0 ± 0.1 seconds). However, these changes were not statistically analyzed due to the small sample size.

One of the most interesting findings was the difference in sit-to-walk hesitation between the single older adult and the group of young adults. Notably, the older adult's hesitation during the single-task condition was greater than that observed in the young adults during the dual-task condition. This suggests that even in standard conditions, older adults may experience challenges that are exacerbated under dual-task demands typically observed in younger individuals. The increase in hesitation and duration from single-task to dual-task conditions in young adults indicates that dual-tasking imposes additional cognitive and physical demands, affecting completing sit-to-walk. This aligns with previous research documenting dual-task interference in motor tasks. For older adults, while the trend suggests a similar increase in hesitation and duration under dual-task conditions, the findings should be interpreted cautiously due to the small sample size. This underlines the need for future research with a larger cohort of older adults to validate these preliminary findings and to understand better how aging influences the ability to manage dual tasks during locomotion.

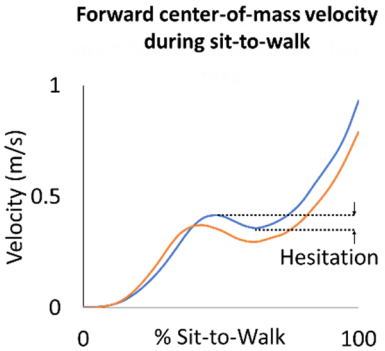

Figure 2. Forward Center-of-Mass Velocity Profile During Sit-to-Walk: This graph depicts the velocity profiles of healthy young adults performing the sit-to-walk transition under single-task (blue) and dual-task (orange) conditions. The sit-to-walk hesitation is quantified as the percentage drop in velocity relative to the initial peak.

**Significance:** This preliminary analysis forms part of an ongoing study. Although the current data did not show a significant difference between healthy young adults and the single healthy older adult, the observed trends suggest that additional data collection and analysis are necessary. Notably, the increase in sit-to-walk hesitation from single-task to dual-task scenarios in the older adult—referred to as the dual-task cost of sit-to-walk hesitation—was more pronounced than the dual-task cost typically reported for gait in existing literature. This finding underscores the need for further investigation into the biomechanics of sit-to-walk in older adults and possibly across lifespan, particularly how cognitive and physical demands influence their mobility.

**References:** [1] Kang and Gross (2015), *Hum Mov Sci*, 40, 341-351; [2] Kerr et al. (2004), *Clin Biomech* 19, 385-390; [3] van Del Kruk et al. (2021), *J Biomech*, 122, 110411.

# EFFECTS OF VISUAL COMPLEX CUES ON TEMPORAL STEPPING MECHANICS

Ruba Alraqibah[1*], Nooshin Seddighi[1], Peter C. Fino, PhD[1,2], Erika Pliner, PhD[1].
[1]University of Utah, Department of Mechanical Engineering, Salt Lake City, UT, USA
[2]University of Utah, Department of Health & Kinesiology , Salt Lake City, UT, USA
Email: *ruba.alraqibah@utah.edu

**Introduction:** Falls are the leading cause of injury, particularly among older adults, with one in four older adults experiencing a fall annually in the United States [1]. With an increasing aging population, fall-related injuries are expected to rise, placing a heavy burden on the healthcare system [2]. To address this issue, effective prevention strategies are essential. The risk of falls can be reduced through targeted interventions that focus on key risk factors such as balance, strength, and cognition [3]. Studies show that exercise interventions that incorporate step training can reduce falls in older adults by 50% [4]. However**,** the effectiveness of step training in reducing fall risk varies across individuals, likely due to differences in step training design parameters and age-related abilities [4]. Regardless of these factors, step training requires motor processes that challenge balance, but there is a lack of knowledge on how design parameters influence the balance demands. To design more effective step training interventions, we are investigating the effect of design parameters on stepping performance. Specifically, this study examines the effect of visual cue complexity on challenging the biomechanical stepping response. We hypothesized reaction and movement time would be slower with a greater visual cue complexity. This would suggest that our paradigm effectively challenges balance.

**Methods:** This preliminary study is intended to inform our approach to designing more effective fall prevention strategies. We plan to recruit 40 participants to address the broader objective of designing more effective fall prevention strategies. A sub-analysis will be conducted on 10 participants to confirm that the experimental protocol effectively challenges balance. Although statistical analyses have not yet been performed, we plan to employ paired t-tests once additional participants are enrolled. To date, two healthy younger adults were recruited to participate in our preliminary study and were asked to complete a total of six stepping trials. These trials consisted of three simple stepping and three complex stepping trials in a randomized order. Simple stepping trials comprised cues to step in one of six locations. Complex stepping trials comprised cues to step and inhibitory cues to not step in one of six locations. Center of Pressure (CoP) data were collected from four force plates at 1200 Hz, while stepping cues were controlled using E-Prime software to ensure millisecond-level accuracy in synchronizing cueing events with biomechanical data. Participants were instructed to follow the on-screen prompts, stepping or withholding steps when cues were presented. Temporal biomechanical metrics of stepping were analyzed from this pilot data. Specifically, we assessed reaction time (time from cue onset to foot lift-off) and movement time (time from foot lift-off to step response contact) for all accurate stepping responses. An accurate stepping response was classified as foot lift-off, followed by step response contact in the target location. Reaction time (RT) marked the initiation of movement. Movement time (MT) marked the duration of movement. The average reaction time and movement time were extracted for each trial and averaged across corresponding trials (simple and complex) for each participant. The standard deviation is reported across the trial average. Human research ethics approval (IRB_00183429) and informed consent were obtained.

**Results & Discussion:** Preliminary analyses of the pilot data suggest that increased cue complexity is associated with longer reaction times and slower movement times **(**Fig.1**)**. Complex cues increased reaction time by 88.3 ms (SD = 38.9 ms) and increased movement time by 77.1 ms (SD = 45.0 ms). These initial findings highlight a potential relationship between cue complexity and decision-making efficiency, suggesting that more complex visual cues may challenge participants' ability to respond quickly and accurately.

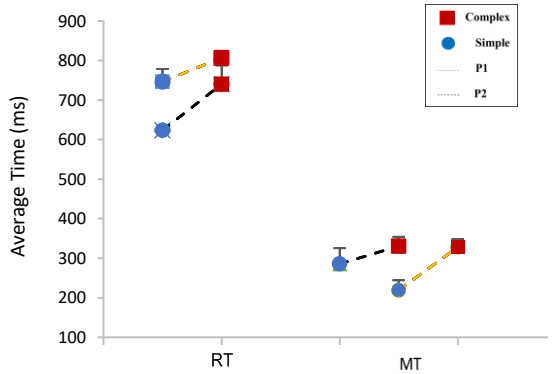


**Figure 1: Average reaction time and movement time during simple and complex trails across participants**

**Significance:** These preliminary results underscore the potential impact of cue complexity on balance and stepping performance. These pilot findings will allow us to verify that our methods challenge balance before proceeding to the target older adult population. A greater understanding of how design parameters affect step training will lead to improved administration of these interventions for age-friendly care and fall prevention.

**Acknowledgments:** This work is supported by the Center on Aging at the University of Utah.

**References:** [1] CDC (2021.), About older adult fall prevention. [2] Houry et al. (2016), *Am J Lifestyle Med.*10(1):74-77 [3] Lajoie & Gallagher (2004), *Arch Gerontol Geriatr*, 38(1), 11–26. [4] Pai et al. (2014), J Gerontol 69(12):1586–1594. *J. Gerontol.*

# EVALUATING OBSTACLE COURSE WALKING AS A FORM OF CLINICAL TESTING FOR GAIT METRICS

*Norah Stivala[1], Galen Holland[2], Michelle Harter[1], Ethan Hicks[1], Amanda Bicket[3], Mark S. Redfern[1], Rakié Cham[1,2]
[1]Department of Bioengineering, University of Pittsburgh [2]Department of Ophthalmology, University of Pittsburgh
[3]Dept. of Ophthalmology & Visual Sciences, University of Michigan *Corresponding author's email: nes127@pitt.edu

**Introduction:** A person's mobility underpins their independence and ability to maintain quality of life [1]. As people age, their mobility may decrease due to a multitude of chronic diseases and injuries they may be experiencing, including vision loss [1,2]. For these reasons, it is important to understand the environmental contexts of task performance to improve upon rehabilitation techniques [1]. Current assessments of a person's mobility typically include a flat surface, but this is not representative of the real-world environment [1]. Therefore, it is necessary to test mobility in an environment that is varied. Here we use a simple course to evaluate differences in obstacle avoidance between healthy younger adults, older adults, and those with glaucoma. Due to their vision loss, we hypothesized that glaucoma participants would have slower course completion times, longer step durations, lower harmonic ratios (HR), and increased postural instability when compared against both the older and younger adults.

**Methods:** 5 healthy, young adults (23 ± 5 years, 4F), 8 healthy, older adults (62 ± 7 years, 5F), and 5 people with glaucoma (68 ± 4 years, 4 F; visual field mean deviation better/worse eye: -6.6±5.4/-9.0±4.3 dB) participated in a single visit. During this visit, subjects walked an indoor obstacle course under well-lit (~500 lux) conditions. The participants all wore the same brand of shoes and walked at their normal speed in a counterclockwise direction while attempting to avoid 5 obstacles. Subjects began a step behind the first obstacle, a small 6-inch tall cone, and then stepped over a 5-inch tall shoebox, before avoiding 2 more cones and stepping over a final shoebox (Fig. 1). The 5 obstacles were each spaced about 2 to 3 steps apart. The subject repeated this loop 3 times. For analysis, the subjects wore APDM Opal inertial measurement units (IMUs, Clario, USA, 128 Hz) on the sternum, lumbar spine, and the feet. The data were separated into two categories: walking and obstacle steps. The Opal data was processed using Matlab (version 2023b, MathWorks, Inc., USA). A transformation matrix was derived to align the data with earth vertical. This was achieved by applying an NED Kalman Filter to the average values of the accelerometer, magnetometer, and gyroscope from quiet standing. After reorientation, the accelerometer data was filtered using a 3-Hz cut off, 4$^{th}$-order, low-pass Butterworth filter. The following outcome measures were calculated: step time, cadence, harmonic ratio (HR), the total time spent to complete the course, trunk sway, and path length [3]. Harmonic ratio was calculated in the vertical direction using the sternum sensor. Statistical analysis was done in JMP (version 17, JMP Statistical Discovery LLC). Student's t-test at an alpha value of 0.05 were performed to identify differences in the metrics listed above across the three groups.

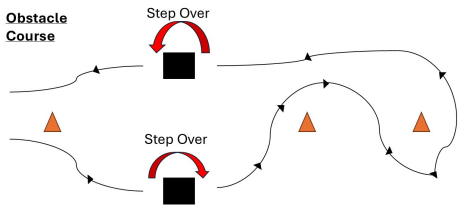


**Figure 1:** The obstacle course consisted of 5 obstacles (3 cones and 2 boxes). Participants walked 3 loops of the course.

**Results & Discussion:** Total course completion time was significantly different between glaucoma and older ($p=0.01$) and approached significance between glaucoma and younger ($p = 0.06$), with glaucoma participants having slower completion time and no significant difference between older and younger groups. The higher significance between older and glaucoma (compared to glaucoma and younger) was due to a larger spread in times of older adults, with several older participants achieving the fastest course completion times across all groups. The data collected during the walking phase yielded no significant difference between the groups regarding step duration, cadence, or harmonic ratio. This may be due to the small sample size and the obstacle course including mostly turns, which may cause these measures to be less sensitive compared to straight walking. In addition, the visual field loss of 4 out of the 5 glaucoma participants was superior, indicating they could likely still see floor-level obstacles in their periphery, so this task may not have posed a notable challenge for them. Trunk sway was also analyzed as an indicator of postural stability. Trunk sway RMS ($m/s^2$) was significantly lower in the mediolateral direction for those with glaucoma when compared against the younger controls ($p<0.01$) and older adults ($p<0.01$) with no difference between older and younger adults and one participant removed from each of the glaucoma and older groups with values 2 SD away from the mean. The glaucoma groups' lower values indicate they maintained a stiffer posture, potentially in an effort to increase stability while walking. Furthermore, the foot sensor path length and RMS were analyzed during the obstacle phase. Younger controls had a significantly larger path length in the vertical direction during second step over the obstacle when compared to the glaucoma group with a p-value of 0.01 ($p=0.07$ compared to older), and no difference between older and glaucoma. Similarly, younger controls also had a larger RMS in the vertical direction during the lagging step when compared to the other two groups with p-values of 0.001 and 0.01, suggesting greater clearance of the foot over the obstacle. This may indicate that the older and glaucoma groups experienced increased instability (i.e. unable to lift foot higher off the floor), which may in turn increase risk of trips and falls.

**Significance:** The obstacle course allows for a test that evaluates people in a more realistic environment compared to the 6-minute or 2-minute walk test. Typically, people do not only walk on a straight and flat surface during their everyday lives, so incorporating the obstacle course evaluates mobility level more completely. Additionally, results may change as lighting changes, and this effect will be explored in future studies. Our findings support the use of such a test to assess mobility in adults with glaucoma or older adults.

**Acknowledgments:** Hillman Foundation, Department of Ophthalmology, University of Pittsburgh

**References:** [1] Patla A.E. et al. (1999). *J. of Aging and Phys. Activity, 7*, 7-19. [2] Suri A. et al. (2021). *The journals of gerontology. Series A, Biological sciences and medical sciences*. [3] Kvist, A., Tinmark, F., Bezuidenhout, L., Reimeringer, M., Conradsson, D. M., & Franzén, E. (2024). *J. of Biomechanics*, *162*, 111907.

# THE EFFECTS OF REPETITIVE HEAD IMPACTS ON POSTURAL CONTROL IN MATURE ADULTS

*Caitlin A. Gallo[1], Christopher A. Knight[1], Jeremy R. Crenshaw[1], Tiphanie E. Raffegeau[2], Melissa N. Anderson[3], Thomas A. Buckley[1]
[1]University of Delaware, Newark DE; [2] George Mason University, Fairfax VA; [3]Ohio University, Athens OH
*Corresponding author's email: cagllo@udel.edu

**Introduction:** Repetitive head impacts (RHI) are common in contact sports and have been associated with neurocognitive decline.[1–5] However, the effects of RHI on postural control in mature adults remain unclear. Gait speed has been referred to as the "6th vital sign" due to its association with clinically meaningful changes in quality of life and its predictive value for later-life health outcomes, such as functional independence and community ambulation.[6,7] Gait initiation (GI) and dual-task (DT) gait tests can place increased demands on the postural control system and consistently distinguish neurologically impaired populations from healthy age-matched individuals.[8–10] Most RHI research focuses on cognitive deficits and a clear knowledge gap exists on postural control in mature adults (>50 y.o.). There appears to be a dose response whereby increased RHI may promote accelerated neurocognitive aging. Conversely, early life sports-related physical activity may mediate healthy aging but is an additional knowledge gap related to RHI.[11] Thus, the trade-off between RHI-related negative consequences compared to the benefits of physical activity on postural control in mature adults remains to be elucidated. Therefore, the purpose of this study was to identify the effects of RHI exposure on postural control in mature adults.

**Methods:** 21 adults (age: 57.6±6.9 years, height: 1.72±0.09 m, mass: 81.0±14.5 kg) were divided into three groups: 1) former contact/collision sport athletes who participated in High-Risk RHI Sports (HRS; N=6), 2) physically active former Non-Contact sport Athletes (NCA; N=11), and 3) former NON-contact athletes or non-athletes who are not physically active (NON; N=4). Single-task (ST) GI trials began with the participant standing on a force plate. A verbal cue was given to initiate gait and continue walking 5 meters at their self-selected speed. The DT condition required participants to walk while simultaneously responding verbally to an Auditory Stroop cognitive challenge. 5 trials of ST and DT were performed. Kinematic data were collected with a 12-camera whole-body motion capture system (Qualisys; 120 Hz), along with three adjacent force plates (AMTI Inc, Watertown, MA, USA).[12] Dependent variables included center of pressure (COP) displacements and velocities during the anticipatory postural adjustment (APA) phase of GI, peak COP-center of mass (COM) displacement, and initial step characteristics (i.e., length, width, and velocity). DT cost (DTC) was calculated as ((DT-ST)/ST) x 100 for each outcome, with negative values indicating worse performance. One-way ANOVAs were performed for each dependent variable to determine significant differences between groups. Effect sizes are reported as $\eta^2$ (small = 0.01 - <0.06; medium =0.06 - <0.14; large = 0.14).

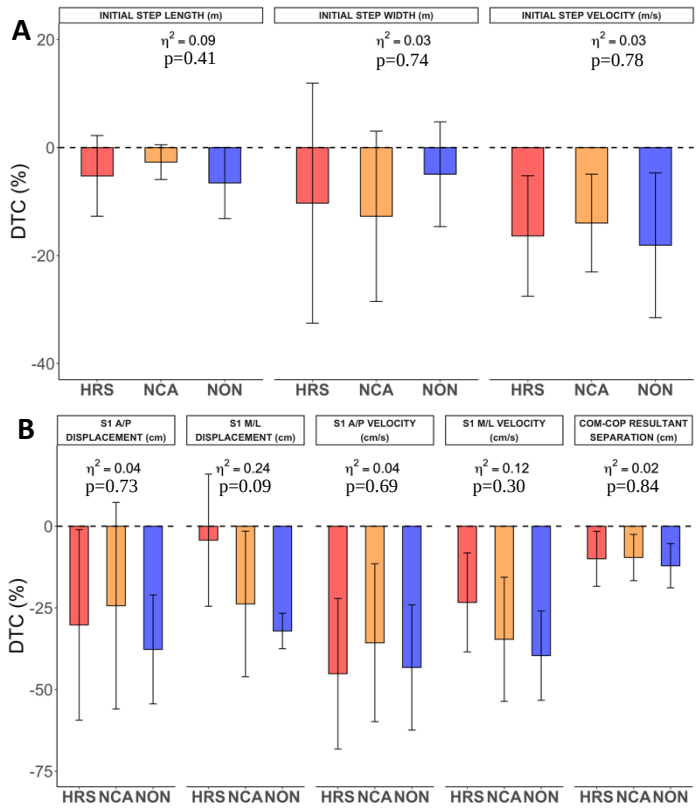


*Figure 1. HRS: former high-risk RHI sport atheltes, NCA: physically active former non-contact sport athletes, NON: physically inactive former non-contact/non-athletes. Panel A: DTC performance for GI initial step characteristics. A negative DTC reflects a greater reduction (worsening) in DT performance for step length and velocity. A positive DTC reflects a greater reduction (worsening) in DT performance for step width; Panel B: DTC performance for GI dependent variables. A negative DTC reflects a greater reduction (worsening) in DT performance.*

**Results & Discussion:** For GI initial step characteristics, there were small overall effect sizes ranging from $\eta^2$:0.03 – 0.9 with NON having the greatest (worst) DTC. (Figure 1, Panel A) GI APA phase showed mixed results. COM-COP displacement and A/P displacement had small overall effect sizes ($\eta^2$: 0.02 and 0.04) with NON having the greatest (worst) DTC (-12.1 and -37.7%). The M/L velocity and displacement had medium to large effect sizes ($\eta^2$: 0.12 and 0.24) with NON having the greatest (worst) DTC (-39.6 and -32.1%). (Figure 1, Panel B) Overall, those with lower physical activity levels exhibit the greatest decline in postural control under DT conditions. While small to medium effect sizes were observed, the preliminary findings suggest that higher levels of both current and early-life physical activity may mitigate postural control declines, potentially offsetting RHI-related effects in mature adults.

**Significance:** Understanding the long-term impact of RHI on postural control in aging populations is critical for developing targeted interventions to reduce fall risk and maintain functional independence. This study will contribute to identifying potential late-life manifestations of RHI exposure and inform strategies to promote healthy aging among former athletes.

**References:** [1] Bailes et al. (2013), *J Neurosurg* 119(5); [2] Mckee et al. (2016), *Neurosurg Clin N Am* 27(4); [3] Montinegro et al. (2017), *J Neurotrauma* 34(2); [4] Hunter et al. (2019), *J Physiol* 123; [5] Mez et al. (2020), *Ann Neurol* 87(1); [6] Fritz & Lusardi (2009) *J Geriatr Phys Ther* 32(2); [7] Middleton et al. (2014), *J Aging Phys Ther* 23(2); [8] Al-Yahya et al. (2011), *Neurosci Biobehav Rev* 35(3); [9] Halliday et al. (1998), *Gait Posture* 8(1); [10] Hass et al. (2008), *Clin Biomech* 23(6); [11] Sadaqa et al. (2023), *Front Public Health 11;* [12] Davis et al. 1991, *Hum Mov Sci* 10(5).

# WHAT CAN 400 MILES OF OVERGROUND WALKING TELL US ABOUT THE INDIVIDUALITY OF GAIT?

Tyler M. Wiles[1*], Seung Kyeom Kim[1], Nick Stergiou[1,2], Aaron D. Likens[1]
[1]Department of Biomechanics, University of Nebraska at Omaha
[2]Department of Physical Education & Sports Science, Aristotle University, Thessaloniki
*Corresponding author's email: tylerwiles@unomaha.edu

**Introduction:** Picture yourself in a crowded concert venue. You spot someone you think you recognize. At a distance, their facial features are obscured by the darkness and flashing stage lights, but the way they walk gives you a clue. You walk closer. Finally, you recognize what was once only the outline of your roommate who joined you for the concert. What makes it possible for you to recognize your friend from only a distant, shadowy figure? In this paper, we investigate what has been termed a *gaitprint*, a set of gait features observable when walking that uniquely identify someone, similar in fashion to a fingerprint [1]. In previous work, we showed that a curated set of biomechanically meaningful gait features could reliably identify a person with >98% accuracy [1]. Presently, we expand that work by asking: Can people be identified from a few seconds of walking using just a handful of gait features?

**Methods:** Twenty-five young (12 female, 24.5 ± 2.1 years old, 174.4 ± 7.2 cm tall, weighing 72.9 ± 15.7 kg), 31 middle (24 female, 46.5 ± 6.0 years old, 171.4 ± 8.2 cm tall, weighing 82.1 ± 15.1 kg), and 35 older adults (16 female, 64.3 ± 5.9 years old, 172.3 ± 9.1 cm tall, weighing 81.4 ± 15.6 kg) were sampled from the NONAN GaitPrint datasets [2-3]. Participants completed 18, four-minute overground walking bouts, evenly split into two days. Only participants that returned one week following their first session were used. Lower body kinematic data was collected using inertial measurement units recording at 200Hz from approximately 400 miles (n = 1,638 trials) walked at a preferred pace. Next, we calculated the 14 most important gait features (Fig. 1) for the entire four-minute duration, as well as for the final two minutes, one minute, 30 seconds, 15 seconds, and 5 seconds of data [1]. Then, a random forest, support vector machine, multilayer perceptron, and ADA Boost algorithm were initiated across a range of parameters while trained on a random 70% of the data (70/30), trials from day 1 (Day 1), or the first trial (Trial 1).

**Most important gait features for identification**
- Left Ankle Mean Peak Velo
- Right Ankle Mean Peak Flex
- Left Knee Mean Velo Peak
- Right Swing Time
- Left Ankle Mean Peak Flex
- Left Knee Mean ROM
- Single Support Time
- Right Ankle Mean Peak Ext
- Right Ankle Mean Peak Velo
- Right Stride Length
- Left Stride Length

**Least important gait features for identification**
- Right Hip Mean Peak Velo
- Right Knee Mean ROM
- Right % Stance

- **Velo:** Velocity
- **Flex:** Flexion
- **Ext:** Extension
- **ROM:** Range of Motion

Figure 1: Feature list.

**Results & Discussion:** We iterated through 1,296 support vector machines with differing parameters and achieved our best accuracy of 99.39% in identifying participants (Fig. 2). This accuracy was achieved twice when training our models on 70% of the data from one minute of walking—once with 13 features and once with 14 features. Surprisingly, identification accuracy did not consistently decrease with walking duration. Four minutes of walking was not always the most accurate, nor was five seconds always the least accurate. The range of maximum accuracies only spanned by 3.25% (70/30), 10.99% (Day 1), and 15.71% (Trial 1) (Fig. 2). This inconsistent trend suggests a small degree of stochasticity in either our data or models. We observed two expected trends: accuracy decreased as training size decreased (70/30 > Day 1 > Trial 1) and increased with the number of features (Fig. 3). Notably, we achieved 87.19% accuracy using only the five most important features (4-minutes). Remarkably, just seven features measured over five seconds were enough to achieve 80.28% accuracy, suggesting that unique gait characteristics emerge within roughly five strides using only a handful of features.

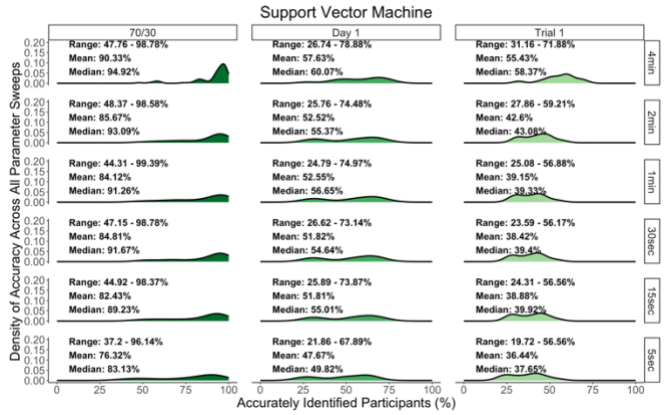


Figure 2: In total, 1,296 support vector machines attempting to identify our participants were run and each subplot contains 72 instances across all parameter sweeps.

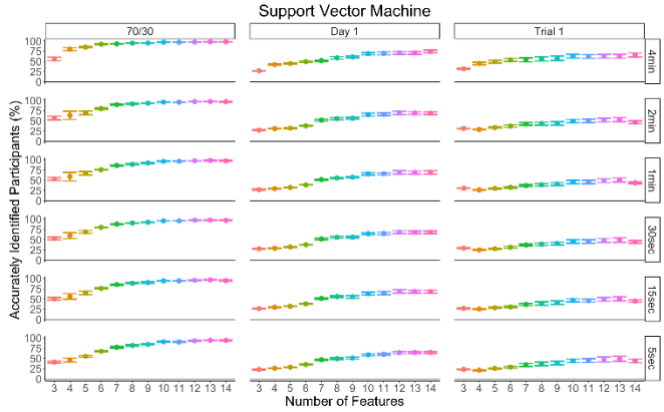


Figure 3: The same data as Figure 2 split by accuracy (mean ± one standard deviation) and feature number.

**Significance:** We supplement previous research by demonstrating the uniqueness of human walking, a person's gaitprint [1,4-5]. Our results also demonstrate that even brief walking durations and a limited set of gait features are sufficient to capture the unique signatures of an individual's movement. Furthermore, because unique movement can be characterized within only a few strides, the identification of clinical groups with mobility deficits becomes more feasible.

**Acknowledgements:** NSF 212491, NIH P20GM109090, P20GM152301, University of Nebraska Collaboration Initiative, the Center for Research in Human Movement Variability at the University of Nebraska at Omaha, NASA EPSCoR, IARPA.

**References:** [1] Wiles et al. (2024) *Comput. Struct. Biotechnol. J.* 281-291; [2] Wiles et al. (2023) *Sci. Data* 10; [3] Wiles et al. (2025) *Sci. Data* 12; [4] Horst et al. (2017) *PLOS ONE* 12; [5] Horst et al. (2016) *Gait Posture* 49.

**AI-Based Wearable Gait Analysis for Proactive Fall Risk Prediction**

* Nathaniel Im[1]
[1]Portsmouth Abbey School
*Corresponding author's email: Nathanielim1234@gmail.com

**Introduction:** Falls remain a major public health challenge, particularly among older adults, accounting for approximately 684,000 fatalities globally each year [1]. Current fall-prevention strategies often rely on reactive measures, which limit opportunities for timely clinical intervention. The recent proliferation of wearable sensor technology, combined with advances in deep learning, presents a promising avenue for proactive fall risk prediction. By continuously tracking subtle changes in gait patterns, these technologies have the potential to detect pre-fall indicators several weeks or months in advance, thereby enabling more effective preventive strategies.

**Methods:** A multi-sensor wearable system was developed to integrate inertial measurement units (IMUs) and pressure sensors placed at key anatomical locations, including the trunk, lower limbs, and specialized insoles. Data were collected at sampling rates exceeding 100 Hz, capturing tri-axial accelerations, angular velocities, and plantar pressure distributions. Sensor fusion and signal preprocessing algorithms were implemented to align and filter these data streams in real-time. The preprocessed signals were then fed into deep learning architectures—specifically temporal convolutional networks (TCNs) and long short-term memory (LSTM) recurrent neural networks—to analyze spatiotemporal gait features and predict fall risk. Publicly available fall-detection datasets were used for initial model training and cross-validation, ensuring a diverse range of gait characteristics. To assess generalizability, cross-dataset validation was performed, revealing a mean accuracy of 91% (±3%) and an area under the receiver operating characteristic (ROC) curve (AUC) of 0.92 (±0.02). A subsequent small-scale pilot study was then conducted with 20 older adult participants, each monitored over a two-week period using the proposed wearable system. Preliminary findings from this pilot study showed an 88% accuracy and an F1-score of 0.85, demonstrating the system's potential applicability in real-world conditions.

**Results & Discussion:** The IMUs and pressure insoles captured a continuous stream of biomechanical data, which were processed by an embedded microcontroller for noise reduction and normalization. A lightweight deep learning model performed on-device inference to classify fall risk. In offline tests using public datasets, the TCN-based model achieved 89% sensitivity and 93% specificity, surpassing the LSTM model by approximately 4%. This approach also showed a 30% reduction in false alarms compared to single-sensor systems. The preliminary findings indicate that integrating multiple sensor modalities and employing robust deep learning algorithms can significantly enhance fall risk prediction accuracy while minimizing false-positive alerts. Future research will explore expanded, long-term field trials with diverse populations to further validate model performance and generalizability. Additional efforts will focus on optimizing power consumption, user comfort, and cloud-based analytics, ultimately laying the groundwork for large-scale deployment and improved healthcare outcomes.

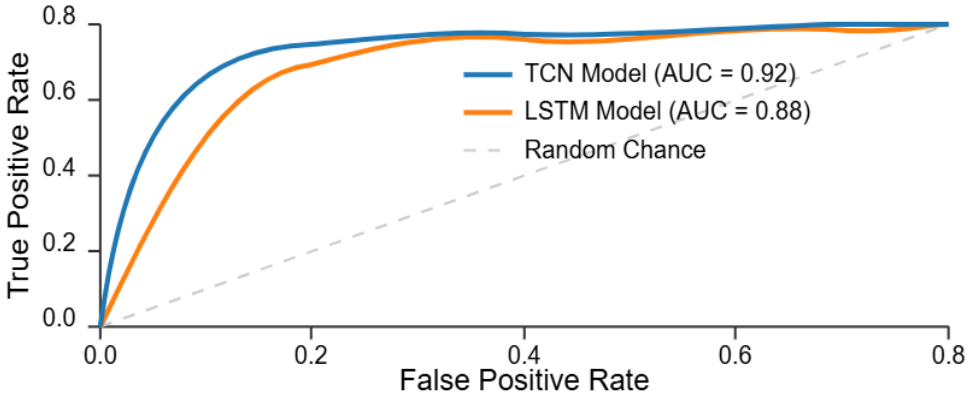


Figure 1. ROC curves comparing the performance of TCN and LSTM models for fall risk prediction. The TCN model demonstrates superior performance with an AUC of 0.92 compared to the LSTM model (AUC = 0.88). Both models significantly

**Significance:** The capacity to identify fall risk proactively through multi-sensor gait analysis has profound implications for clinical practice and public health. Early alerts enable healthcare providers and caregivers to implement targeted interventions—ranging from exercise regimens to medication reviews—well before a fall occurs. This capability extends the independence of older adults, improves their quality of life, and substantially reduces healthcare costs and resource utilization associated with fall-related injuries. Furthermore, by offering continuous, unobtrusive monitoring, the proposed system addresses patient compliance challenges commonly associated with periodic clinical assessments.

**References:** [1] WHO Global Report on Falls Prevention in Older Age (2023). [2] Igual, R., Medrano, C., & Plaza, I. (2015). *A comparison of public datasets for acceleration-based fall detection. Medical Engineering & Physics*, 37(9), 870–878. [3] Kim, J., Campbell, A.S., de Ávila, B.E.F., & Wang, J. (2019). *Wearable biosensors for healthcare monitoring. Nature Biotechnology*, 37, 389–406.

# INFLUENCE OF OBESITY ON WALKING STABILITY CONTROL IN OLDER ADULTS

*Nancy T. Nguyen[1], Carrie P. Earthman[1], Jocelyn F. Hafer[1], John J. Jeka[1], Noah J. Rosenblatt[2], Jeremy R. Crenshaw[1]
[1]University of Delaware, Newark, DE
*Corresponding author's email: nanguy@udel.edu

**Introduction:** About 40% of U.S. adults aged 65 and older are considered to have obesity, a condition linked to an increased risk of falls and worse walking balance performance [1]. These outcomes may reflect the combined effects of older age and obesity on the control of walking stability. Obesity is associated with increased frontal plane motion (i.e. poorer control) during walking. Such motion is actively controlled through mechanisms that include trailing-limb push-off and stepping-limb foot placement [2]. Individuals with obesity exhibit altered gait mechanics, including smaller relative vertical ground reaction forces (GRFs), wider step widths, and shorter swing phases [1,3]. These alterations may impact the contributions of push-off or foot-placement mechanisms. We hypothesized that, in older adults with a range of body sizes, increased non-muscular mass will correlate with smaller push-off contributions and larger foot-placement contributions to controlling lateral COM motion.

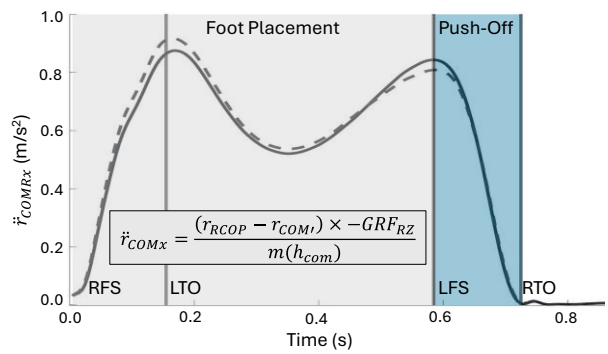


**Figure 1**. Example of frontal plane COM acceleration ($\ddot{r}_{COMRx}$) estimated from **force-plate** data (dashed) of the right-limb. The **foot-placement** contribution was evaluated from right foot strike (RFS) to left foot strike (LFS). The **push-off** contribution was evaluated from LFS to right toe off (RTO). $\boldsymbol{r}$ represents the lateral position of the **COP** or **COM'** (vertical COM projection on the treadmill surface). $\boldsymbol{GRF_{RZ}}$ represents the vertical ground reaction force, $\boldsymbol{m}$ is mass, and $\boldsymbol{h_{com}}$ is COM height. Positive accelerations are directed medially (i.e. to the participant's left). Marker-based analysis is shown by the solid line for comparison.

**Methods:** This is a preliminary analysis of three healthy older adults (ages 56-69 years; 2 females; BMI 23.8-33.3 kg/m$^2$). Participants completed a whole-body dual energy X-ray absorptiometry (DXA) scan (Horizon, Hologic Inc, USA) to measure relative fat-mass and appendicular lean soft tissue indexes (ALSTI). Muscle ultrasound imaging (Logiq E, GE Healthcare, Chicago, IL) was used to measure quadriceps muscle thickness. Muscle thickness was calculated as the ratio of the thickness of the rectus femoris and vastus intermedius to the total anterior midthigh thickness, serving as an indicator of the fat-to-muscle ratio in the thigh. Stability control was evaluated using an instrumented, split belt treadmill (Bertec, Columbus, OH) during a four minute walk at preferred speed. Given the potential limitations of marker-based motion capture in individuals with obesity, force plate data were used to calculate push-off and foot placement contributions (Figure 1). To calculate center of mass (COM) displacements, we first double integrated and high-pass filtered vertical and shear GRFs [4,5]. Vertical COM trajectory was obtained by adding this vertical displacement to COM height as determined with reaction board techniques. The mediolateral COM trajectory was obtained by low-pass filtering center of pressure (COP) and adding the GRF-derived mediolateral displacement [4,5]. Given the small sample size of this preliminary data, we subjectively evaluated the relationships between body composition and push-off/foot placement contributions.

**Results & Discussion:** A partial trend supported our hypotheses. Foot-placement contributions were larger with greater body size, while push-off contributions showed no clear trends (Table 1). We are recruiting more participants of various body sizes to better address our hypothesis. If our predicted relationships do not emerge, we will explore how individuals with obesity may compensate for lower relative vertical GRFs by placing steps wider relative to the COM, achieving similar push-off contributions as those without obesity.

**Significance:** The results of this study may inform hypotheses for how targeting walking mechanics (e.g. increasing push-off) or fat mass may improve walking stability control. Future work will evaluate how stability-control mechanisms are related to walking balance capacity and walking efficiency, potentially identifying pathways to improve walking stability and reduce fall risk in this population.

**Acknowledgments:** We thank Ahmed Alkaye and Megan Reading for their assistance with data collection for this study.

**References:** [1] Kim et al. (2022), *J Biomech* 144(111308); [2] Riemann et al. (2018), *Kines. Review* 7(1); [3] Browning (2012), *Curr. Obes. Rep.* 1(3); [4] Schepers et al. (2019), *TBME* 56(4); [5] Buurke et al. (2023), *J Biomech* 146(111415).

**Table 1: Preliminary Data**

| Subject | PWS* (m/s) | Relative Fat Mass (Body Fat %) | ALSTI* (kg/m$^2$) | Muscle Thickness (%length) | Foot Placement (m/s$^2$) | Push-Off (m/s$^2$) |
|---|---|---|---|---|---|---|
| **1** | 1.05 | 41.6 | 8.43 | 0.54 (0.004) | 0.80 (0.10) | 0.67 (0.08) |
| **2** | 0.70 | 39.6 | 6.35 | 0.74 (0.002) | 0.52 (0.09) | 0.23 (0.06) |
| **3** | 1.50 | 27.0 | 7.33 | 0.76 (0.002) | 0.48 (0.12) | 0.36 (0.09) |

*Preferred walking speed (PWS); Appendicular lean soft tissue index (ALSTI). Muscle thickness, foot placement, and push-off are shown as a mean (standard deviation).

# CORRELATIONS OF OBJECTIVE MEASURES OF GAIT WITH CLINICAL AND SUBJECTIVE MEASURES

*Chitra Banarjee[1,2], Patria Marcano Maldonado[2], Hwan Choi[3], Md Sanzid Bin Hossain[1], Rui Xie[2,4,5], Ladda Thiamwong[2,5]
[1]University of Central Florida (UCF) College of Medicine, [2]UCF College of Nursing, [3]UCF College of Engineering and Computer Science, [4]UCF College of Sciences,[5]Disability, Aging and Technology Cluster
*Corresponding author's email: chitra.banarjee@ucf.edu

**Introduction:** Falls are the leading cause of injury-related death for older adults, aged 60 years and older, one of the fastest growing demographics in the United States with limited care systems to address their many health concerns[1]. Falls have resulted in decreased quality of life, increased risk of chronic diseases, and limited physical and psychosocial functioning, adding to the burden of care in the United States healthcare system. Because falls often occur during movement, it is crucial to understand dynamic balance[2]. Available fall risk screening tools rely on subjective questionnaires or assessments of balance and mobility[3, 4] that separately focus on physical and cognitive functioning[5]. Commonly used in clinical settings is the Timed Up and Go (TUG), which is commonly assessed by the healthcare provider timing the duration of the test[5]. While some studies have explored instrumented TUG (iTUG), which utilizes wearable devices alongside the TUG, many of these studies solely focus on the physiological parameters of gait without considering subjective measures, such as fear of falling (FoF)[6]. Previous work by our team has demonstrated the Fall Risk Appraisal matrix (Figure 1), which evaluates perceived fall risk using FoF and physiological fall risk using static balance (SB)[7]. In this study, we focus on the relationship between objective measures of gait with clinical measures of static balance and FoF. By identifying how gait is linked to these measures, interventions can be more precisely targeted to address both physical and psychological factors.

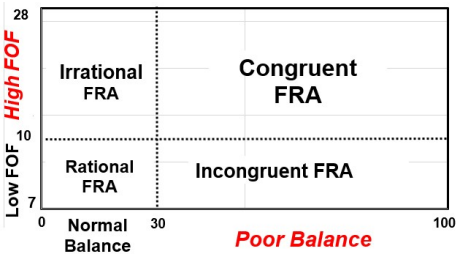


Figure 1. FRA Matrix

**Methods:** 12 older women ($M_{Age}$ = 74.23 ± 5.25 years) were included in the present study. Participants were instructed to complete the TUG test (standing up from a chair, walking 3 meters leading with preferred foot, returning in either direction, and sitting), scored by a human observer as the duration to complete the test. They then repeated the test 3 times using the pressure insoles (iTUG, XSENSOR Foot & Gait System, X4, Alberta, Canada). From the XSENSOR software, gait analyses were performed, and the following parameters were extracted: center of pressure (COP) velocity, single support phase (SSP) duration, and stride length and velocity. Duration of the iTUG was averaged across the trials. FoF was assessed using the Short Falls Efficacy Scale International and SB using the force plate embedded balance measurement system (BTracks Balance System, San Diego, CA). Statistical analyses were performed in R and involved Spearman correlations and paired t-tests.

**Results & Discussion:** Correlation analysis (Figure 2) revealed significant negative associations such that increased FoF was correlated with decreased COP velocity and SSP duration but not stride length or velocity. SB was not correlated with any of the objective measures. Additionally, correlations between the objective measures with the TUG score (as measured by the human observer), showed that the iTUG measures were related to the clinically relevant measure as used in functional practice. Finally, the duration of the iTUG test vs TUG test did not show statistically significant differences as determined by paired t-test, but wearing the insoles did increase the time to complete the test ($M_{iTUG}$ = 13.75 sec, $M_{TUG}$ = 11.72 sec, $p$ = 0.271). These results demonstrate that increased FoF likely reflects a more cautious and conservative gait strategy aimed at increasing stability and reducing fall risk. Lack of significant associations between the objective measures of dynamic balance with SB confirms that they are capturing different aspects of postural control. Further research should explore the comparative efficacy of the static and dynamic measures in predicting future falls, as well as considering both when conducting fall risk assessments.

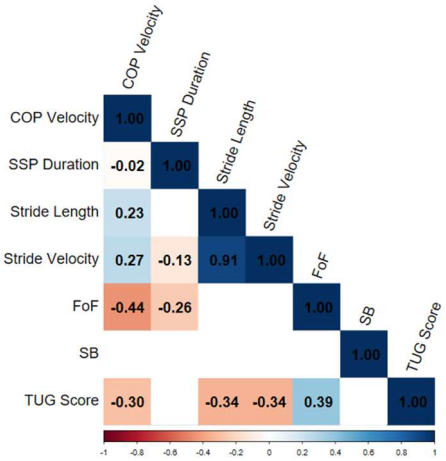


Figure 2. Correlation analyses of objective gait measures and clinical measures. Blank values indicate non-significant correlations.

**Significance:** Correlations between objective gait measures and subjective and clinical variables reveal the complexity of fall risk. The effects of FoF on gait is seen not through easily quantifiable measures such as stride length or velocity, but the more subtle variables of COP velocity and SSP duration. The results imply the future inclusion of objective gait metrics in fall risk assessments, alongside subjective measures such as FoF and clinical variables such as SB.

**Acknowledgments:** This work was supported by the NIMHD and NIH under grants R01MD018025, R01MD018025-02S2. We would like to thank our research assistants for data collection, and most of all, the older adults who participated in the study.

**References:** [1] R. Kakara, *Morbidity and Mortality Weekly Report.* 72, 2023. [2] N. Takeshima, et al., *Geriatrics & gerontology international,* 14(3), 2014. [3] D. K. Singh, et al, *Clinical interventions in aging,* 2015. [4] S. L. Whitney, et al, *Physical therapy,* 85(10), 2005. [5] O. Beauchet, et al, *The journal of nutrition, health & aging,* 15, 2011. [6] P. Ortega-Bastidas, et al, *Sensors,* 23(7), 2023. [7] L. Thiamwong, et al, *Clinical gerontologist,* 44(5), 2021.

# DIRECTIONAL STABILITY: A NEW PRESENTATION OF THE MARGIN OF STABILITY DURING WALKING

*Sydney Garrah[1], Amy Coyle[1], W. Scott Selbie[1], Richard Hugh Moulton[1]
[1]HAS-Motion Inc., Kingston, ON, Canada
*sydney.garrah@has-motion.ca

**Introduction:** Stability involves maintaining postural balance by keeping the body's projected center of mass within the Base of Support [1,2]. The Margin of Stability (MoS) quantifies stability during standing, but its interpretation during walking is debated. Traditionally, assessment relies on the MoS's sign to classify stable versus unstable posture with a larger positive MoS suggesting increased stability [2]. However, studies have shown that stable walking can reliably include negative MoS scores caused by the anterior-posterior (AP) direction, which complicates assessment [3]. Due to the MoS measure's traditionally binary nature, we believe a presentation incorporating the direction of instability will be more useful for assessing stability during gait. Here we assess the AP and medial-lateral (ML) MoS of 14 aging individuals, comparing the traditional measure with our new presentation.

**Methods:** We acquired treadmill walking data for 14 aging adults (7 male, 7 female, age 61.1 ± 5.5 years) at 7 different speeds using a publicly available dataset from Fukuchi et al. [4]. We determined the Base of Support (BoS) using a bounding box that encompassed the Heel, M1, and M5 markers, projected onto the treadmill surface in the direction of gravity. We computed the extrapolated Center of Mass (xCoM) by finding the position of the CoM projected onto the ground, plus its velocity times a factor $\sqrt{l/g}$, $l$ being leg length and $g$ the acceleration of gravity [3]. The MoS was measured as the distance between the xCoM and the nearest boundary of the BoS. Modeling, calculations, and processing were done in Visual3D and Sift (HAS-Motion Inc.). For the traditional MoS presentation, instances where the xCoM was inside the BoS were reported as positive MoS, while instances where it extended beyond the BoS were reported as negative MoS. In our modified presentation, xCoM extensions beyond the BoS in the anterior or right directions were noted as positive MoS, posterior or left extensions as negative MoS, and an xCoM inside the BoS was returned as 0.

**Results & Discussion:** We found that by modifying the MoS measure to reflect the direction of instability provided us with richer insight into the subjects' walking behavior and inherent stability patterns. In the new ML and AP MoS presentations illustrated in Fig. 1C and Fig. 1D, respectively, the average MoS across all 14 subjects reveals the inherent direction of instability during the single support phase. At any given moment, we can discern whether an individual is positioned behind, in front, inside, or to the left or right of their BoS. The single support phase of the gait cycle was selected to effectively demonstrate our new presentation, as there were no regions of "instability" during double support. Although the magnitude of the MoS remains consistent between interpretations during unstable periods of Fig. 1, the change in sign offers additional context to the reported value. The MoS measure indicates that we spend most of our walking time in an "unstable" state, which increases with faster walking speeds.

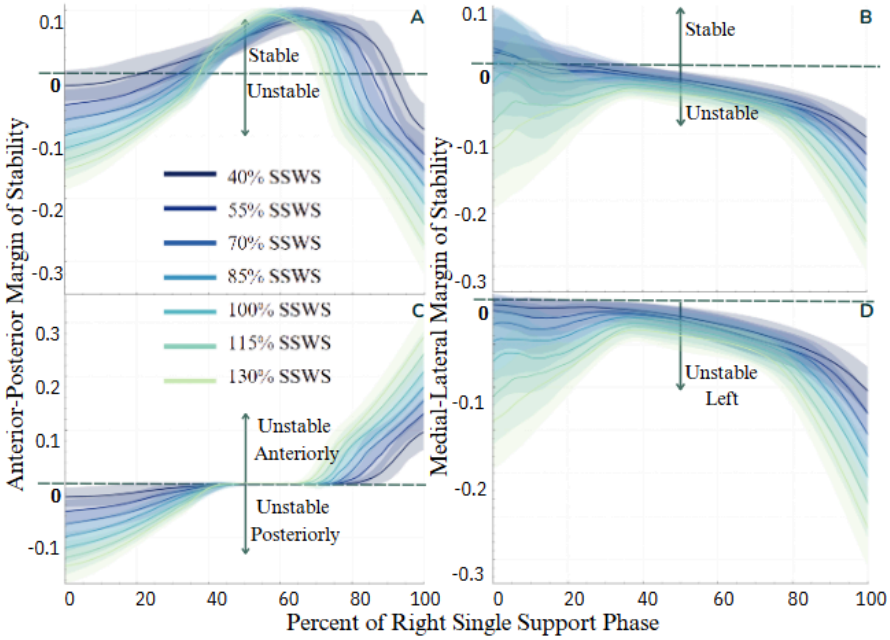


**Figure 1**: Average MoS during right foot single support phase of aging subjects at various percentages of self selected walking speed (SSWS), presented with original (A,C) and new (B,D) presentations of the MoS.

**Significance:** While we remain cautious about the MoS measure's applicability in dynamic scenarios, we believe that our presentation enhances its utility. By incorporating the directional component of our revised MoS presentation, we gain valuable insights into the directional stability patterns seen among aging individuals. This could pave the way for observing MoS patterns in other populations and lead to understanding how these patterns shift when individuals encounter genuine moments of instability.

**References:** [1] G. Meyer et. al. (2006), EURAPA 3(1):29-33; [2] Watson et. al. (2021), BMC Musculoskelet. Disord. 166; [3] Sangeux et. al. (2024), Sci. Rep. 14; [4] Fukuchi et. al. (2018), PeerJ 6:e4640.

# THE EFFECTS OF FOOT-ANKLE WORK ON MARGIN OF STABILITY DIFFER BY AGE AND WALKING SLOPE

*Paula S. Kramer[1], Aubrey J. Gray[2], Kota Z. Takahashi[1], Jason R. Franz[2], Peter C. Fino[1]
[1] Department of Health & Kinesiology, University of Utah
[2]Lampe Joint Dep. of Biomedical Engineering, UNC Chapel Hill & NC State University, Chapel Hill, NC, USA
*Corresponding author's email: paula.kramer@utah.edu

**Introduction:** Bipedal walking requires frontal plane balance control and forward propulsion on a step-by-step basis [1,2]. While frontal plane balance control can be accomplished by multiple mechanisms (e.g., foot placement, hip torque, ankle torque) [1], modulating foot and ankle work by changing push-off force can effectively regulate balance while also contributing to forward propulsion [3]. For example, increasing foot mechanical work throughout stance can influence stability on the subsequent step, as greater push-off force can create larger frontal-plane moments and greater mediolateral (ML) center of mass (CoM) velocities [3]. As such effects could be mitigated through complementary balance mechanisms, such as simultaneously adjusting step width or cadence [1], it remains unclear how changes in foot-ankle mechanical work associate with stability, or how this relationship may differ across age or different walking slopes that alter mechanical work and balance control [4]. For example, older adults have different balance control integrity and force production capacities than younger adults, which may change the relationship between foot-ankle mechanical work and stability [5,6]. Based on prior work [3], we expected foot-ankle mechanical work to be inversely associated with dynamic stability of the subsequent step, and that this relationship may by age and walking slope.

**Methods:** Eight participants (4 young adults (mean [range] age: 26 years [20–31 years]; 3F / 1M) and 4 older adults (mean [range] age: 64 years [61– 86 years]; 3F / 1M) walked barefoot on a split-belt instrumented treadmill (Bertec, Corp.) for six minutes at fixed speed (1.2 m/s) in three different slope conditions: level (0°), incline (5°), and decline (5°). Ground reaction forces and lower extremity kinematics were recorded at 1 kHz and 250 Hz, respectively, during the last two minutes of each trial utilizing a six-degrees-of-freedom marker set [7] in conjunction with a validated multi-segment foot model [8]. Raw data were smoothed using a 6 Hz (kinematic) or 15 Hz (kinetic) second-order dual-pass low-pass Butterworth filter. Positive foot-ankle phase work during stance was determined by integrating the positive power phase of foot-ankle mechanical power using the multi-segment foot model and a six-degrees-of-freedom ankle power analysis [9,10]. Stability was quantified using the medial-lateral Margin of Stability (MoS), calculated as the difference between the lateral calcaneus and the extrapolated center of mass at contralateral toe-off [11], where the CoM position was estimated using the pelvis. Linear mixed-effects regression models were fit for MoS for all steps, with fixed effects of stance phase foot-ankle positive mechanical work, age group, and the interaction between mechanical work and age. To account for the potential temporal relationship between positive foot-ankle phase work and stability, observations of MoS and foot-ankle work were matched based on the toe-off event (i.e., foot-ankle work for a right step was paired with the MoS of the subsequent left foot, extracted at toe-off of the right foot). Models included random intercepts for each subject. Separate models were fit for each slope conditions (decline, level, decline).

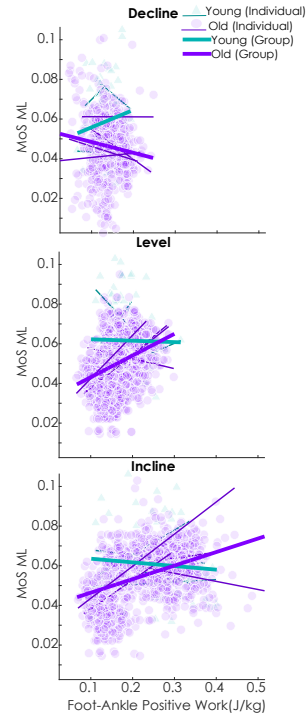


**Figure 1.** Scatter plots with regression lines for each subject (thin) and group (thick) showing the relationship between ankle-foot positive work (J/kg) and medial-lateral margin of stability (MoS ML). Available right and left steps varied by group (young = 16 steps, old = 30 steps).

**Results & Discussion:** Current data available for young adults did not exhibit an association between ankle-foot positive work and MoS of the subsequent step. The lack of association may indicate that younger adults use complementary balance control mechanisms (e.g., changes in step width and cadence) to regulate MoS. Conversely, older adults exhibited a positive relationship between foot-ankle work and MoS during inclined and level walking ($\beta$-*incline* = 0.07, $\beta$-*level* = 0.14, both $p < 0.001$), but they exhibited a negative association between foot-ankle work and MoS during decline walking ($\beta$-*decline* = -0.09, $p < 0.001$). Such results (Fig.1) suggest that older adults also use complementary balance control mechanisms, but they may overcompensate, relative to young adults, for changes in foot-ankle work during incline and level walking. The negative association observed in older adults during decline walking may be influenced by a redistribution of joint mechanical work [12] or differences in control of falling forward versus ML stability.

**Significance and Future:** Preliminary results suggest the association between positive stance-phase foot-ankle work and MoS differs between young and older adults and by walking slope. Future analyses will incorporate a larger participant sample and additional gait variables (step width and cadence), negative foot-ankle work, and work distribution to more thoroughly examine complementary balance control mechanisms.

**Acknowledgments:** We want to acknowledge Daniel Davis, Christopher Long, and Rohit Kundu and funding from NIAMS/NIH (R01AR081287, R01AR081287-03S1).

**References:** [1] Reimann et al. (2017), [2] Kreter & Fino (2024), *R. Soc. Open Sci,* 21; [3] Kim & Collins (2015), *J. of Neuro. and Rehab.12*; [4] Strutzenberger et al. (2022), *Gait & posture,* 91.[5] Browne & Franz (2018), *PloS one*, *13*; [6]Takahashi et al. (2022), *Biomech*, *2*(4); [7] Wilken et al. (2012), *Gait & Posture*, *35*(2); [8] Bruening et al. (2012), *Gait & posture*, *35*(4); [9] Takahashi et al. (2012), *J. Biomech.* 45; [10] Buczek et al. (1994), *J. Biomech.* 27(12). [11] Watson et al. (2021), BMC Musculoskelet Disord, 22(1); [12] Franz et al. (2012), *J. of Biomech.*, *45*(2).

# SENSOR-BASED TRACKING GAME TO ASSESS PROPRIOCEPTIVE DEFICITS IN OLDER ADULTS

Monica Hruzd[1], Kubra Akbas[2], Mohammad Hosseinalizadeh[1], *Nima Toosizadeh[12]
[1]Rutgers Department of Biomedical Engineering, School of Graduate Studies, Rutgers University, Newark, NJ 07107
[2]Department of Rehabilitation and Movement Science, School of Health Professions, Rutgers University, Newark NJ 07107
*Corresponding author's email: nima.toosizadeh@rutgers.edu

**Introduction:** This study examined the use of a Sensor-based Real-time Tracking-game (SRT) of a moving target on a screen to assess ankle proprioceptive performance. Proprioceptive performance relates to the perception of muscle and joint position, which can be compromised in older adults, leading to an increased risk of falling. The most common methods used for assessing proprioceptive performance are joint position sense, kinesthesia, and force sense. However, these methods have been argued to not be sensitive enough to capture minor deficits in proprioception, require customized platforms for assessment, and are influenced by the participant's attention level. Using SRT, by measuring the amplitude and directional accuracy during the tracking, we engage ankle proprioceptive function based on correction mechanism of tracking error through the open-loop reflexive responses and closed-loop adjustment within the central nervous system. The goal of the current study was to assess the validity of SRT for assessing proprioceptive performance. Our main hypotheses were: 1) SRT is sensitive to aging-related changes in proprioceptive performance; 2) alteration in proprioceptive performance due to outside stimulation (vibratory stimulation of muscles) would affect SRT outcomes; and 3) SRT is sensitive enough to detect differences in proprioceptive performance in the dominant vs. non-dominant side.

**Methods:** Participants included 19 young, healthy participants between the ages of 18 and 40 years (mean age=21.8±1.32, 55% female) and 10 older adults 65 years and older (age=73.6±7.73, 60% female). Exclusion criteria were disease-related motor deficits, vestibular or vision disorder, and dementia. Participants answered baseline questionnaires, including fear of falling, comorbidities, depression, pain in legs, muscle strength, ankle function and vestibular measurements and these were accounted as confounding variables. For SRT of the ankle joint, each participant sat on a chair and was strapped into the seat at the thigh to restrict movement to the ankle only. The game involves following a moving target on a screen for 30 seconds by rotating the ankle joint in the plantarflexion/dorsiflexion and abduction/adduction directions. A gyroscope was placed on the top of the intermediate cuneiform bone on the foot. The game involved three levels, each with a separate predetermined track. To disturb proprioceptive performance, vibratory stimulation was applied to tibialis anterior, peroneus longus, soleus, and gastrocnemius. Each level was done with different frequences of vibration: 0 Hz, 40 Hz, and 80 Hz (18 tests in total, nine each side, with randomized exposures). SRT outcomes included amplitude and directional accuracy. Amplitude accuracy was calculated as the straight-line distance (radius) between the tracking position and pre-defined track position. Directional accuracy was defined by determining percentage of time the participant kept the tracking circle within the "free zone" of the pre-defined track. The free zone was calculated using the shape and size of the tracker at every instant of time based on one standard deviation distance data from the young participants.

**Results & Discussion:** The results of repeated measures analysis with groups (young vs. old) as between-subject and vibration frequency, difficulty level, and foot side as within-subject variables suggest a significant effect of age ($p$<0.0001, effect size – ES=0.63) and vibration condition ($p$=0.03, ES=0.1) for amplitude accuracy (Figure 1). For directional accuracy, we observed a significant effect of age ($p$=0.001, ES=0.57), vibration frequency ($p$=0.02, ES=0.15), and foot side (p=0.008, ES=0.38) (Figure 1). As one ages, muscle spindle function declines due to the natural demyelination, which contributes to proprioceptive deficits. Further, by implementing vibration, muscle spindle sensing threshold alters, mimicking proprioceptive deficits. Current findings suggest that SRT is sensitive enough to detect subtle changes in proprioceptive performance due to aging, disturbance using vibration stimulation, and dominant side of testing.

**Figure 1:** Mean and standard errors for (a) amplitude accuracy and (b) directional accuracy, across groups and testing conditions.

**Significance:** Falls are the leading cause of traumatic injury in older adults with tripping being the most common cause. Evidence indicates that proprioception deficits are highly associated with poor balance recovery after tripping; however, a robust method for assessing age-related proprioceptive deficits is lacking. In the present study, we establish a novel Sensor-based Real-time Tracking-game to assess the ankle proprioceptive performance, requiring one motion sensor that can be available through a smartwatch.

**Acknowledgments:** I give acknowledgement to the facilities at Rutgers School of Professional Studies, as well as the University of Arizona students who gathered prior data.

**References:** [1] Asghari et al. (2024), *Heliyon* 10(4); [2] Espejo-Antúnez L et al. (2020), *Archives of physical medicine and rehabilitation* 101(10); [3] Sorensen K et al. (2002), *Experimental brain research* 143(1); [4] Toosizadeh N et al. (2018), *Biomedical engineering online* 17(51).

# TOTAL HIP ARTHROPLASTY AND STATIC POSTURAL BALANCE: A PRE- AND POST-OPERATIVE ANALYSIS

*Danielle E. Peters[1], Sheryl Bourgaize[1], Alyssa M. Tondat[1], Emiko Arshard[1], Marina Mourtzakis[1], Tina Mah[2], Matthew Snider[3], Paul Grosso[3], Brandon Girardi[3], Oliver Gauthier-Kwan[3], Stephanie Nemirov[3], Carla Girolametto[3], Kailyn Clarke[3], & Andrew C. Laing[1*]
[1]Department of Kinesiology and Health Sciences, University of Waterloo, Waterloo, ON, Canada. [2] Schlegel-UW Research Institute for Aging, Waterloo, ON, Canada. [3]Grand River Hospital, Kitchener, ON, Canada
*Corresponding author's email: actlaing@uwaterloo.ca

**Introduction:** Total hip arthroplasty (THA) is one of the most prominent and rapidly growing orthopedic surgeries worldwide, known for its high success rates, reproducibility, and cost-effectiveness for treating hip osteoarthritis (OA) [1,2,3]. Overall goals of THA include enhancing hip joint function, alleviating pain, enhancing mobility and stability, and improving quality of life [4,5]. However, problems with posture and balance have been reported post THA [6], and approximately 25% of patients fall within the first year [7]. The purpose of this study was to examine the effects of THA on static postural balance during stance. Due to the expected improvements in strength, proprioception, and neuromuscular control following rehabilitation, we hypothesized that metrics of underfoot center of pressure (CoP) would improve following THA. Due to pain and compensatory offloading, we hypothesized an asymmetry in weight distribution between limbs preoperatively, with a progressive increase in weight-bearing on the surgical limb post-surgery.

**Methods:** Ten participants (6 male/4 female, age: 66.2 ± 8.7, height: 1.73 ± 0.11 m, mass: 93.76 ±17.32 kg) with a scheduled THA were recruited from Grand River Hospital. Each participant completed visits to the laboratory at three time-points: within 1-week pre-THA, 6-weeks post-THA, and 6-months post-THA. Double-leg stance trials on two force platforms (AMTI; MA, USA) were conducted with both eyes and open closed. Force and moment data were used to compute net CoP and weight distribution between the surgical and non-surgical limbs. One-way repeated measures ANOVAs and post-hoc pairwise comparisons were conducted to assess the influence of surgical time-point on weight distribution and CoP metrics including root-mean-square amplitude (RMS), maximum amplitude, velocity, and total excursion in the mediolateral (ML) and anteroposterior (AP) planes.

**Results & Discussion:** *Weight Distribution.* Pre-THA, patients (on average) supported more weight on their non-surgical limb (Figure 1a). In the eyes closed stance condition, there was a significant shift to a more symmetrical weight distribution at 6-months post THA ($p = 0.015$). The same trend was observed with eyes open ($F = 2.63$, $p = 0.09$). *CoP Metrics.* There were no significant differences in the ML plane across time points for all metrics ($p > 0.05$). However, in the AP plane, there was an influence of time-point on RMS characterized by a significant decrease from pre-THA to 6-months post-THA ($p = 0.035$) (Figure 1b). A similar (but non-significant) trend was observed for maximum anterior amplitude ($p = 0.11$).

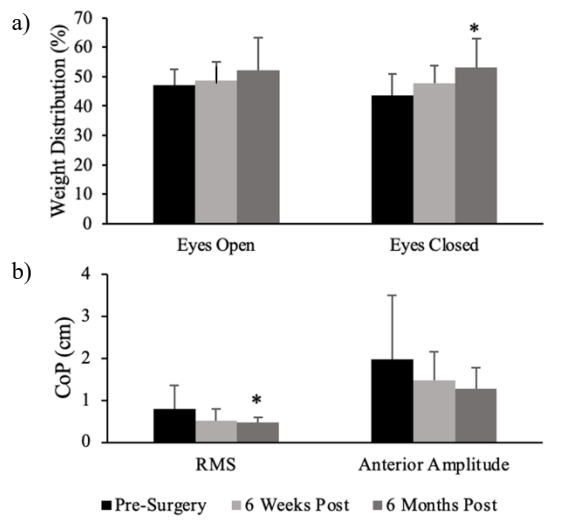


**Figure 1:** Influence of surgical timepoint on a) weight distribution across limbs, and (b) CoP RMS and amplitude during eyes open stance. * Indicates significant changes from pre-surgery values.

The shift towards a more symmetrical weight distribution post-THA may be due to pre-surgical asymmetries in muscle capacity and pain, and improved proprioception, muscle function, and confidence in using the surgical limb as rehabilitation progressed. Despite a global shift in ML balance (as evidenced by changes in weight distribution), it was interesting that no changes in COP metrics of ML balance control were observed. In contrast, the general post-surgical decreases in AP COP RMS and amplitude suggest improved control of forward/backward body motion – these changes are also potentially linked to progressively reduced pain and enhanced sensory pathways and muscle function post-surgery. Overall, these findings suggest that the process of THA and subsequent rehabilitation can lead to improvements in standing balance and stability. Additionally, the data suggests potential value in rehabilitation approaches that differentially challenge (and improve) balance control in the AP and ML directions following THA.

**Significance:** This study was novel in using objective, quantifiable metrics to characterize balance control in THA patients. The findings demonstrate that THA (and associated post-surgical changes) can lead to significant improvements in standing balance. The differences in outcomes across ML and AP planes, and the progressive enhancements noted for the 6-month vs. 6-week post-surgical time points, provide important insights to inform the focus and time-course of optimal rehabilitation programs.

**Acknowledgments:** This study was supported by Ontario Ministry of Health and was carried out in collaboration of Grand River Hospital (registry #: NCT05416463; THREB #: 2022-0747).

**References:** [1] Reinbolt et al. (2005), *J Biomech* 38(3); [2] Finley et al. (2013), *J Physiol* 591(4). [3] Varacaloo et al. (2018), *J. Orthop* 15(2). [4] Nantel et al. (2008), *Clin Biomech (Bristol)* 23(4). [5] Di Laura Frattura et al. (2022). *Diagnostics (Basel, Switzerland)* 12(3). [6] Lablanca et al. (2021). *BMC Musculoskelet. Disord*, 22(1). [7] Hunter et al. (2020). *AJPM&R*, 99(9).

# PERSONALIZED SONIFIED BIOFEEDBACK FOR OLDER ADULTS TO IMPROVE TURNING GAIT: A PILOT STUDY

*Zahava M Hirsch[1], Jun M Liu[1], Erin Kreis[1], Antonia Zaferiou[1]
[1]Stevens Institute of Technology, Department of Biomedical Engineering, Hoboken, NJ USA
*Corresponding author's email: zhirsch@stevens.edu

**Introduction:** Falls are a leading cause of injury in older adults [1] and falls during turns are 7.9 times more likely to result in a hip fracture [2], highlighting the need to focus on improving turning mechanics in older adults. Best practices for clinical therapy have been shown to be patient-specific [3]. Additionally, emerging research shows that sonified biofeedback with musical sounds, "music biofeedback," can improve biomechanics during gait training [4]. Music biofeedback can convey changes in biomechanical metric(s) of interest through precise changes in musical sounds. We completed a pilot study using personalized music biofeedback gait training during straight-line gait and pre-planned turning tasks. Our purpose was to determine the immediate effects of using music biofeedback to improve personalized gait metrics for older adults. We hypothesized that the biomechanical metric of interest will improve during music biofeedback training for both straight-line gait and pre-planned turns as compared to baseline.

**Methods:** Three older adult participants completed pre and training lab visits during which, they performed straight-line gait and pre-planned turning tasks. A physical therapist (PT) was present for all visits. Between the lab visits, we selected a metric the PT believed to be most beneficial for the participant that was within our current design capabilities. A music biofeedback design was created for each participant. Optical motion capture (250 fps; OptiTrack USA) and MATLAB were used to compute the metric of interest, and Max MSP was used to map the metric changes to produce changes in musical sounds. The training visit began with interactive familiarization. Participants demonstrated sufficient understanding by evoking requested music changes with self-selected body movements. Next, each participant performed eight to ten straight-line gait and pre-planned turning trials using the music biofeedback to train to improve the metric of interest. Participant one (f, 70 years) practiced increasing step length, defined as the antero-posterior distance from the back heel to the front heel. A personalized threshold was determined by the PT, and each time the participant's step length reached the threshold distance, a drumbeat sound would play (**Fig. 1A**). Participant two (f, 68 years) practiced increasing step width to avoid crossover steps, which narrows the base of support and may lead to a trip and fall. Step width was computed as the medial distance from the back toe and back medial heel to the front toe and front medial heel, the smallest of these four medial distances was used as step width. When the step width narrowed, the music pitch increased, and when a crossover occurred (i.e., step width was negative) the pitch increased dramatically (example video from different study). Participant three (f, 74 years) practiced improving posture angle, defined as the angle from the center of the pelvis to the vertex relative to vertical in the sagittal plane. As the posture angle increased, the pitch increased linearly. (Anatomic frames for all three metrics depended on the pelvis orientation.) During walking and turning training trials, each participant was asked to generate the desired sound (drum beat for the step length, and low pitch for the step width and posture angle). For participant three, six post training trials were performed without sound biofeedback to determine if changes learned during music biofeedback training were immediately retained without music biofeedback present. Statistical comparisons per participant used the Mann-Whitney U test to account for uneven number of trials and non-normality.

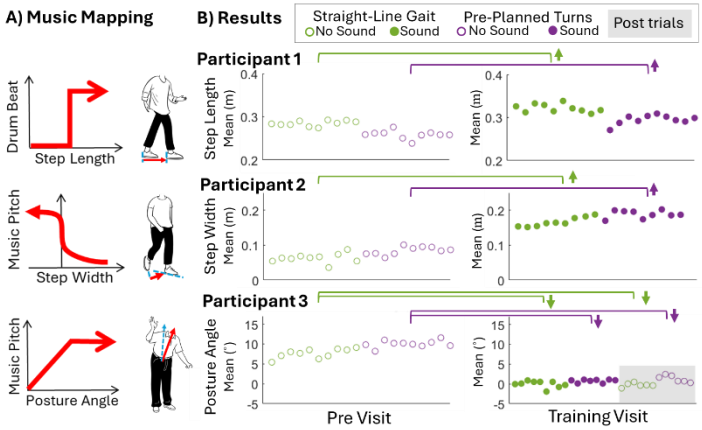


***Figure 1: A)** Music mapping designs. **B)** Pre and training visit mean gait metric data for all three participants. Bars indicate significance p<0.001.*

**Results & Discussion:** There were significant improvements in the metric of interest between the pre visit trials without music biofeedback and the training visit trials with music biofeedback for all three participants for both straight-line gait and pre-planned turns. Participant one's step length significantly increased, participant two's step width significantly increased, and participant three's posture angle significantly decreased during music biofeedback training (**Fig. 1B**). These results indicate that music biofeedback was understood and successfully utilized by these older adults. Furthermore, participant three significantly improved posture angle between the pre visit trials and the training visit post training trials. Additionally, for participant three, there was no significant difference between the training visit trials with music biofeedback and the post training trials without music biofeedback. This indicates that music biofeedback training was retained immediately post training. Overall, findings support music biofeedback as a promising tool to improve personalized gait metrics for older adults. We are encouraged as the work expands to more participants and as we formalize a decision tree for personalization. This complements our parallel efforts to train postural control longitudinally with retention tests and faded biofeedback.

**Significance:** This study evaluated the immediate effects of personalized music biofeedback gait training to improve biomechanical metrics in older adults during walking and turning. These results add to the existing literature showing that sonified biofeedback is an effective tool to improve gait metrics [4] but provides initial evidence of its utility to help older adults during turning gait.

**Acknowledgments:** National Science Foundation Award #1944207. Special thanks to the study participants and PTs.

**References:** [1] Moreland et al. (2020), *Morb. Mortal. Wkly Rep*. 69(27); [2] Cumming et al. (1994), *J. Am. Geriatr. Soc.* 42(7); [3] Deutsch et al. (2022), *Phys. Ther. & Rehab*. 102(3); [4] Zaferiou et al. (2025), *J. Neuroeng. Rehabil.* forthcoming.

# OBESITY INCREASES FALL RISK IN OLDER ADULTS FOLLOWING A STANDING-SLIP

Jiyun Ahn[1*], Diane' Brown[1], Sara Mahmoudzadeh Khalili[1], Caroline Simpkins[1], Feng Yang[1]
[1]Department of Kinesiology and Health, Georgia State University, Atlanta, GA, 30303, USA
[*]e-mail: jahn12@student.gsu.edu

**Introduction:** Falls in older adults are a global health concern [1]. Aging and obesity are independent fall risk factors. Obesity exacerbates the fall risk among older adults [2]. While the metabolic and physiological consequences of obesity have been widely examined, its impact on fall risk remains understudied. Several studies have reported a higher fall incidence among individuals with obesity compared to those without obesity [3-5]. However, those studies mostly relied on self-reported fall data collected from surveys and interviews, subject to recall bias and inaccuracy. In addition, the uncontrolled causes of falls could introduce further confounders. Given the rising prevalence of obesity and aging populations, it is imperative to investigate the effects of obesity on the risk of falls among older adults in a well-controlled environment. This study examined whether obesity increases fall risk among older adults following an unexpected and standardized standing-slip compared to lean individuals. It was hypothesized that older adults with obesity would exhibit a higher fall risk compared to their lean counterparts.

**Methods:** Thirty-seven older adults formed two groups based on body mass index (BMI): obese (BMI $\geq$ 30) and lean (BMI $\leq$ 25). Participants' basic demographic information along with their cognitive function (assessed by the Montreal Cognitive Assessment or MoCA [6]) were first measured. After a warm-up, participants completed the Timed Up and Go (TUG) and 5-Time Sit-to-Stand (5×STS) tests to assess dynamic balance and leg muscle power. They then walked on the ground at self-selected fast and normal speeds in a random order. Three walking trials were performed for each speed condition. Next, they wore a safety harness and stepped onto the Activestep treadmill (Simbex) to complete three standing trials followed by an unexpected standing-slip. Participants were informed that a slip may or may not occur. The slip intensity was set at a belt acceleration of 4 m/s$^2$, peak velocity of 1.2 m/s, and a slip distance of 0.36 m [7]. A loadcell connected to the harness recorded the force applied on the harness. Lastly, maximum voluntary isometric contraction (MVIC) was assessed using a dynamometer (Biodex, NY) for knee extension/flexion and ankle plantar/dorsiflexion. Slip outcome (fall or non-fall), the primary outcome, was defined as a fall when the peak loadcell force exceeded 30% of the participant's body weight. The secondary outcomes included normal and fast gait speeds, time to complete TUG and STS, and leg joint strengths. Gait speed was averaged from three trials per condition and normalized by body height. The lower limb muscle strength was normalized by body mass. $\chi^2$ tests compared slip outcomes and sex between groups (obese vs. lean). Independent *t*-tests were used for between-group comparisons of demographic information except for sex, gait speed, TUG and 5×STS performance, and MVIC metrics. Statistical analyses were done using SPSS 29.0 (IBM) with an α of 0.05.

**Table 1**. Comparisons of outcome measures between groups, presented as mean (standard deviation) and *p*-value. *bh*: body height.

| Measure | Obese | Lean | *p*-value |
|---|---|---|---|
| Age (years) | 63.31 (9.35) | 64.62 (9.21) | 0.290 |
| Sex (male/female) | 0/16 | 6/15 | 0.059 |
| Body mass (kg) | 92.3 (12.48) | 63.77 (9.60) | < 0.001 |
| Body height (m) | 1.62 (0.06) | 1.70 (0.11) | 0.06 |
| BMI (kg/m$^2$) | 34.96 (3.67) | 22.08 (2.57) | < 0.001 |
| Slip outcome (fallers/non-fallers) | 15/1 | 11/9 | < 0.001 |
| Fast gait speed (/*bh*) | 0.92 (0.12) | 1.11 (0.15) | < 0.001 |
| Normal gait speed (/*bh*) | 0.65 (0.09) | 0.78 (0.13) | < 0.001 |
| Timed Up-and-Go (s) | 10.63 (1.98) | 9.06 (1.68) | 0.014 |
| 5×Sit-to-Stand (s) | 12.04 (2.85) | 9.12 (1.94) | < 0.001 |
| Knee extensor (Nm/kg) | 1.09 (0.21) | 1.62 (0.50) | < 0.001 |
| Knee flexor (Nm/kg) | 0.75 (0.20) | 1.25 (0.38) | < 0.001 |
| Ankle plantarflexor (Nm/kg) | 0.63 (0.14) | 0.88 (0.30) | 0.006 |
| Ankle dorsiflexor (Nm/kg) | 0.24 (0.08) | 0.42 (0.11) | < 0.001 |
| Montreal Cognitive Assessment (/30) | 25.38 (2.53) | 27.86 (1.49) | < 0.001 |

**Results & Discussion:** Age, height, and sex distributions were comparable between groups (Table 1). The body mass and BMI were larger in the obese group than in the lean group. More participants in the obese group fell than in the lean group after the standing-slip. The obese group walked more slowly than their lean counterparts under both speed conditions. Individuals in the obese group took longer time to perform the TUG and 5×STS tests. The obese group exhibited lower knee and ankle strength in both directions. Additionally, the obese group demonstrated a poorer MoCA score than the lean group. The findings supported our hypothesis that obesity increases fall risk, as evidenced by the significantly higher fall rate in the obese group compared to the lean group. These findings align with previous studies that indicated the negative impacts of obesity on stability and balance control, increasing fall risk. In addition, obesity was associated with impaired sensorimotor (as reflected by the slower gait speed, poorer balance, smaller leg muscle power, and reduced lower limb strength) and cognitive (as indicated by the lower MoCA score) impairments relative to those without obesity. Our results suggest that obesity detrimentally affects the body's biomechanics, neuromuscular function, and cognition, finally contributing to elevating fall risk. More studies are needed to further identify the pathways through which obesity increases fall risk in older adults.

**Significance:** The findings from this study reinforce obesity as a significant fall risk factor, demonstrating its negative impact on cognition, functional capacity, and lower limb strength. Given the increasing prevalence of obesity among older adults, this study highlights the need for fall prevention strategies that consider both biomechanical, neuromuscular, and cognitive impairments associated with excessive body mass. Understanding how obesity influences fall risk can contribute to developing targeted interventions to reduce falls and improve the quality of life among individuals at high risk of falls.

**References:** [1] Stevens et al. (2006), *Inj Prev* 12(5); [2] Neri et al. (2020), *J Gerontol A Biol Sci Med Sci*, 75(5); [3] Fjeldstad et al. (2008), *Dyn Mad* 7; [4] Himes et al. (2012), *JAGS* 60(1); [5] Mitchell et al. (2014), *Aust N Z J Public Health* 38(1); [6] Nasreddine et al. (2005), *JAGS*. 53(4); [7] Ahn et al. (2024), *J Biomech* 164.

# EFFECTS OF PROLONGED WALKING ON TOE CLEARANCE AND STABILITY MARGINS IN OLDER ADULTS

*Nancy T. Nguyen[1], Fany Alvarado[1], Millissia A. Murro[1], Grace K. Kellaher[1], Mayumi Wagatsuma[1], Jocelyn F. Hafer[1], Jeremy R. Crenshaw[1]
[1]University of Delaware, Newark, DE
*Corresponding author's email: nanguy@udel.edu

**Introduction:** Falls are the leading cause of injury among older adults, with one in four experiencing a fall each year. Up to 53% of falls are due to a trip while walking [1]. The likelihood of or inability to recover from a trip may be exacerbated by fatigue in response to daily activity. Therefore, this study aimed to determine how two gait kinematics related to the risk of a trip-related fall, minimum toe clearance [2] and anterior stability margins [3,4], changed after a prolonged bout of walking in older adults. We hypothesized that, when using measures that account for within-participant variability (Figure 1), individuals would exhibit less toe clearance [2] and more unstable anterior margins [5] with prolonged walking.

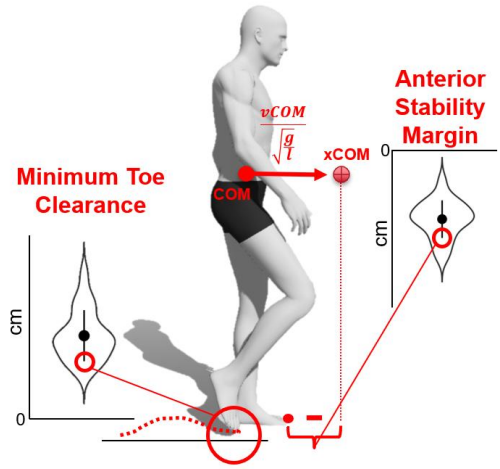


**Figure 1.** Conceptualization of walking-related mechanisms of minimum toe clearance and the anterior stability margin at that time point. The stability margin accounts for the center-of-mass position (COM) and velocity relative to the stance-limb toe. The crosshatched circle represents the extrapolated center of mass (xCOM), the horizontal arrow represents the scaled velocity (vCOM), the dashed vertical line represents the vertical projection of the xCOM, the red circle on the stance limb toe represents the defined base of support, and the red bracket represents a negative margin of stability value.

**Methods:** This is preliminary data of 4 healthy male older adults (Age: 65 (0.5) years; BMI: 25.5 (3.6) kg/m$^2$). Participants were equipped with a full-body marker set, the trajectories of which was recorded (Miqus, Qualisys) as participants walked on a treadmill at a preferred speed (average speed: 1.5 (0.2) m/s). The 34-minute treadmill walk included 1-minute challenge periods at minutes 7, 17, and 27, where the treadmill speed was increased by 50% and was designed to simulate variations in walking intensity/effort that could occur in real-world walking. We analyzed 4 minutes of data at the beginning and end of the walking protocol. We focused our analysis on minimum toe clearance and the anterior margin of stability at minimum toe clearance (Figure 1). For both outcome variables, the lower quartile was used for analysis to capture both central tendency and variability within our measures.

**Results & Discussion:** With prolonged walking, toe clearance was meaningfully reduced (≈ 3-4 mm) for some, but not all participants (Figure 2). There were no discernible trends in stability margins. Based on self-reported ratings of perceived exertion (RPE), these participants may not have been substantially fatigued with this prolonged walk (ΔRPE = 1 to 3). We are continuing this study to determine how our outcomes relate to *fatigability* (i.e. the susceptibility to transient decrements in muscle power) across participants, further characterizing fatigability through muscle strength output. Additionally, we will investigate how such variables and their changes with prolonged walking may differ in a matched group with knee osteoarthritis—a condition characterized by greater fatigability and an elevated fall risk.

**Significance:** Fatigability may be a modifiable target for fall-prevention interventions, and the variables presented here are candidates for how fatigability may influence the risk of a trip-related fall while walking. This study is the first to explore how prolonged walking may affect biomechanical mechanisms underlying such risk in older adults with and without knee osteoarthritis.

**Acknowledgments:** Work supported by NIGMS/NIH grant U54-GM104941

**References:** [1] Pavol et al. (2001), *J Gerontol A Biol Sci Med Sci* 56(7); [2] Nagano et al. (2014), *JNER* 11(155); [3] Hof et al. (2005), *J Biomech* 38(1); [4] Schulz (2017), *J Biomech* 55(107); [5] Kao et al. (2018), *PLoS One* 13(7).

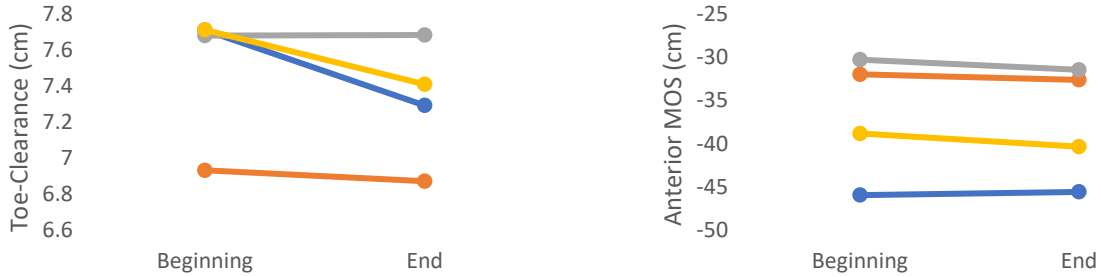


**Figure 2.** Preliminary data of the lower quartile of toe-clearance (left) and lower quartile of the anterior margin of stability at minimum toe clearance (right). Each participant is represented by a colored line. Data shows beginning and end of the 34-minute bout of walking on our measured outcomes.

# SUSTAINABILITY FRAMEWORK APPLIED TO BIOMECHANICS COURSE MODULES TO MOTIVATE OPPORTUNITES AND COLLABORATION

*Eric G. Meyer[1]
Biomedical Engineering, Lawrence Technological University, Southfield, MI, USA
*Corresponding author's email: emeyer@ltu.edu

**Introduction:** Global challenges, such as the United Nations Sustainable Development Goals (SDGs) can be inspiring for students by calling attention to important real-world problems that might lead to opportunities for widescale impact (https://sdgs.un.org/). Biomechanics courses typically use analysis of the individual to provide real world examples and don't consider how interconnections such as system/network effects, value tensions between stakeholders, empathetic design and strategic foresight can inspire engagement with a future that is larger than oneself [1]. While this approach may lead to the development of technical abilities and scientific knowledge, important learning opportunities, such as why concepts are important and multidisciplinary collaborations are missing [2]. Recent examples have applied sustainability frameworks to biomedical engineering and encouraged instructors to find ways to adapt the process to other pedagogical environments [3]. The aim was to develop course modules that promote opportunities for technological innovation, social transformation and value creation in biomechanical collaborations between engineers, researchers, designers, clinicians and trainers.

**Methods:** BME 3303 is a required 3-credit junior Biomedical Engineering that follows Physics and Statics prerequisite courses and covers topics including; static equilibrium, kinematics and kinetics of human movement, deformation, stress and strain, loading and biological tissue properties. The weekly schedule has been updated over the past 15+ years to include active learning modules and a design project that supplement the lectures, homework assignments and quiz/exam assessments [4]. Four additional projects were developed to relate with specific technical topics while expanding the scope to emphasize non-technical reflections and opportunities to create value for stakeholders. Detailed instructor guides for modules, project assignments and other resources that were developed, are shared with faculty through engineeringunleashed.com.

**Results & Discussion:** SDG #3 "Ensure healthy lives and promote well-being for all at all ages" was introduced to the students to help motivate the course. The sustainability-themed projects (Table 1) were completed by 18 students enrolled in one section of the course. The course online learning platform was used for discussion board posts to share reflections and additional materials.

| Lecture | Topic | In Class | Assignment |
|---|---|---|---|
| 1 | Biomechanics Introduction | Example video analysis | Students demonstrate a movement and describe one biomechanical principle. |
| 4 | Linear Kinematics | Inertial Measurement | Record a daily activity's motion at the center of gravity (COG) of the body. |
| 6 | Linear Kinetics | Grip Strength with dynamometer | Analyze the data set to compare with Perplexity.ai to create useful insights. |
| 10 | Angular Kinematics | Swing/hitting performance | Ideation, design selection, prototype testing and creating value for athletes/coaches. |
| 23 | Stability and Walking | Sit-to-Stand test (Figure 1) | Reflect on their performance, then expand the assessment to stakeholder groups. |

**Table 1:** Course technical topics, active learning modules and assignments.

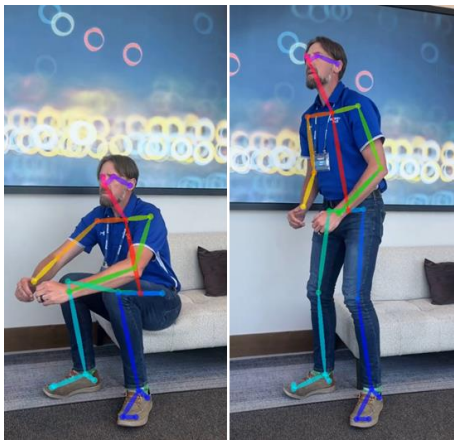

**Figure 1:** Example of using sit2stand.ai computer vision for biomechanical assessment of the functional movement.

Most students, despite their prior lack of knowledge of dynamics topics, were able to use the measurement and analysis techniques to quantify human movements. These hands-on activities, such as the inertial measurement sensors, hand dynamometer and video analysis were brought into the classroom to support lecture topics instead of completing them as typical laboratory activities. This allowed students to gain experience and perspective for aspects of human biomechanics, engineering design, innovation/entrepreneurial minded learning and sustainability goals. The intention was to support their professional vision and strategies for making informed decisions in engineering or other disciplines. While these projects were limited in duration and didn't "solve" the problems of sustainability for human health and well-being, this real-world theme supported student learning of the biomechanical concepts. Student feedback showed that they enjoyed the hands-on aspects of the modules and the open-ended, real world nature of the projects. The development of appropriate resources and materials was guided by inductive learning pedagogies and supported the course learning objectives.

**Significance:** This course supports the Lawrence Tech motto of "Theory & Practice" and is part of a curriculum sequence of courses to repeatedly expose students to the entrepreneurial mindset. The ultimate goal is to improve student experiences and skills for their senior capstone projects as well as their professional careers.

**Acknowledgments:** The authors acknowledge support from the Kern Entrepreneurship Education Network and the faculty development workshop "Unraveling the Value Tensions of Sustainability" (June, 2024) for expertise and guidance.

**References:** [1] Warren et al. (2010), *J Sustainability Ed 6*; [2] Hu et al. (2023), *Sustainability* 15(11); Tranquillo (2018), *ASEE Proc*; Meyer and Ulrey (2016), *ASEE Proc*; Boswell et al. (2023) *Digit Med* 6(32).

# MEASURED EFFECTS OF STACK HEIGHT, DROP, AND MIDSOLE HARDNESS ON GAIT: MINIMALIST SHOES INCREASE CADENCE, SINGLE LIMB SUPPORT, AND STANCE PHASE DURATION IN ADULTS OVER 50

*Keven Santamaría-Guzmán, Damaris C. Cifuentes, Kenneth D. Harrison, Brandon M. Peoples, Silvia E. Campos-Vargas, Bria R. Smith, Jaimie A. Roper
Locomotor and Movement Control Laboratory, Auburn University, Auburn, AL, U.S.A.
*Corresponding author's email: kgs0071@auburn.edu

**Introduction:** Falls in older adults, affecting one-third of those over 50 annually, constitute a major public health challenge with costs exceeding $50 billion[1]. While multiple fall risk factors exist, footwear characteristics represent one of the most readily modifiable interventions[2]. Walking stability fundamentally depends on the interaction between foot and footwear, yet the current understanding of how specific footwear features influence gait parameters remains limited[3]. Previous research has established general associations between footwear and fall risk but has not systematically investigated how individual characteristics such as stack height, drop, and midsole hardness affect spatiotemporal parameters during standardized walking assessments[4]. This knowledge gap is particularly critical given that footwear characteristics have been identified as potentially modifiable factors in fall risk among older adults[5]. Our study investigates how specific footwear characteristics (shoe mass, stack height, drop, heel-to-toebox width ratio, and midsole hardness) influence gait parameters in community-dwelling adults over 50 years old. Based on biomechanical principles suggesting differences in sensory feedback and cushioning between footwear designs, we hypothesized that temporal gait parameters would show temporospatial adaptations between minimalist and maximalist footwear conditions.

**Methods:** Sixty-nine healthy community-dwelling older adults (57 females, 12 males; age: 64±8 years, mass: 68.31±10.26 kg, height: 158.42±7.57 cm) participated. Individual footwear characterization included mass (g), stack height (average of heel and toebox heights, mm), heel-to-toe drop (difference between heel and toebox heights), midsole hardness (Shore A durometer), and width ratio (heel-to-toebox width) were assessed. The Instrumented Stand and Walk test protocol was performed[6]. Kinematic data were collected using six synchronized APDM Opal inertial sensors (128 Hz) positioned at the sternum, lumbar region, bilateral wrists, and feet. K-means cluster analysis was used to classify footwear into two groups. MANOVA with Wilks' lambda examined between-group differences in gait parameters.

**Results & Discussion:** Cluster analysis yielded two distinct footwear groups based on structural characteristics. Stack height ($F= 54.676$, $p < .001$), drop ($F= 50.645$, $p < .001$), midsole hardness ($F= 18.573$, $p < .001$), and shoe mass ($F= 9.642$, $p = .003$) differences divided the sample into a minimalist (n=39) and maximalist (n=30) footwear groups. MANOVA showed significant differences between footwear conditions (Wilks' $\lambda$=.000, $F=263.87$, $p<.0001$). Minimalist footwear exhibited higher cadence (129.55±9.41 vs 124.62±6.70 steps/min; $F= 5.901$, $p= .018$), longer single limb support (42.60±1.37 vs 41.86±1.03 %GCT; $F= 6.109$, $p= .016$), and extended stance phase (59.29±1.34 vs 58.10±1.06 %GCT; $F= 15.946$, $p< .001$) (Fig.1). These findings suggest reduced cushioning in minimalist footwear may lead to compensatory gait strategies. The increased cadence may represent a strategy to spend less time between steps to maintain stability, while the extended stance phase and longer single limb support time could indicate enhanced proprioceptive feedback from the foot due to reduced cushioning. This adaptation pattern suggests that minimalist footwear might promote more active control of stability during walking through enhanced ground contact and sensory feedback.

**Significance:** This study reveals how footwear characteristics influence temporal gait parameters in adults over 50. The combination of increased cadence, extended single limb support, and longer stance phase suggests minimalist footwear may promote more active walking stability control through enhanced ground contact and sensory feedback. Clinically, the observed acute changes (5 steps/minute higher cadence, 0.74% GCT longer single limb support, and 1.19% GCT extended stance phase with minimalist footwear) demonstrate how footwear directly moderates temporal walking aspects routinely assessed in mobility evaluations. Future studies should examine long-term effects of different footwear types on these parameters in older adults, particularly whether systematic footwear interventions can produce sustained changes in locomotor patterns. These findings provide evidence-based insights for optimizing footwear selection in aging populations.

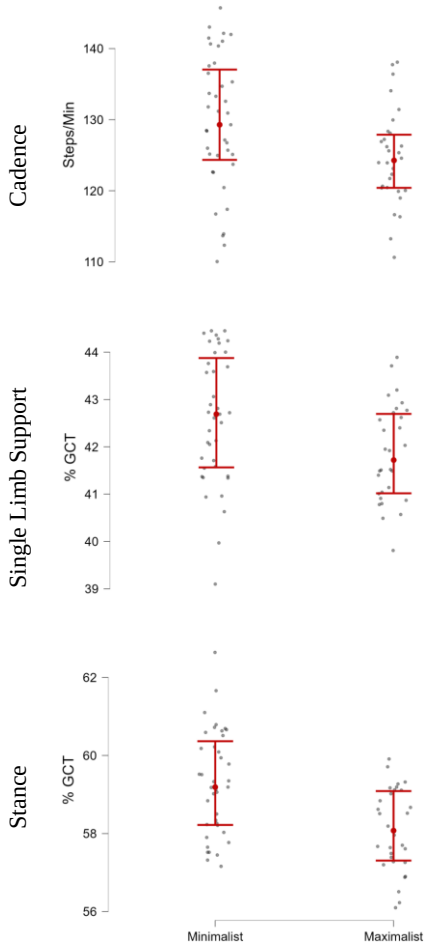


**Figure 1.** Gait kinematics distribution between minimalist and maximalist footwear.

**References:** [1] Florence et al. (2018), J Am Geriatr Soc, 66(4); [2] Kim & Hegazy (2024), Ann Geriatr Med Res; [3] Davis et al. (2019), Footwear Sci 11(1); [4] Menant, et al. (2008), J Reh Research & Develop, 46(8). [5] Cammen, et al. (2016), Ergonomics, 9(1); [6] Horak et al. (2023), GeroScience, 45(2).

# MOBILITY OUTCOMES IN OLDER ADULTS WITH AND WITHOUT CARBON FIBER INSOLE

Rohit R. Kundu[1*], Daniel J. Davis[1], Paul A. Estabrooks[1], Jason R. Franz[2], Kota Z. Takahashi[1]
[1]Department of Health & Kinesiology, University of Utah, Salt Lake City, UT
[2]Lampe Joint Department of Biomedical Engineering, UNC Chapel Hill & NC State University, Chapel Hill, NC
*Corresponding author's email: kundu.rohit@utah.edu

**Introduction:** Older adults choose to walk at slower speeds than younger adults [1], possibly due partly to reduced plantar flexor force output [2]. One potential intervention to enhance ankle plantar flexor force output is footwear stiffness modifications, such as using carbon fiber insoles (CFIs) [3]. In younger adults, CFI has been shown to enhance plantar flexor force output across a range of walking speeds [3]. If CFI increases plantar flexor force output in older adults, this may result in beneficial increases in walking speed. However, a recent study in older adults wearing CFIs showed no improvement in walking speed during a 6-minute walk test (6MWT) [4]. This may be because fatigue effects may mask initial benefits in walking speed during endurance tests like the 6MWT, so participants cannot maintain a given speed. As such, this study examined whether CFI could improve the acute walking speed of older adults, both comfortable and maximum, during short walking bouts. In addition to traditional biomechanics measures, perceived comfort, and usability will likely influence footwear adoption in older adults. As such, these variables must be carefully considered when developing and prescribing countermeasures to enhance mobility for older adults. This study integrates objective (comfortable and maximum walking speed) and subjective (perceived perceptions) measures to understand CFIs' potential benefits and limitations for older adults. We hypothesized that increased footwear stiffness would improve older adults' objective mobility outcomes and subjective perceptions.

**Methods:** To date, six healthy older adults (2M/4F, 65.9 ± 3.0 yrs, 164.8 ± 8.9 cm, 66.8 ± 11.8 kg) have participated. Participants completed three trials of comfortable and maximum walking along 20-m and 10-m walkways, respectively, each under three footwear conditions: 1) Control Shoe (S00), 2) Control Shoe + 1.6 mm CFI (S16), and 3) Control Shoe + 3.2 mm CFI (S32). The speed was measured using the Dashr-Blue laser module. These trials were conducted on two separate visits in a multi-visit study. Comfortable and maximum walking speed trials for one of these footwear conditions were completed during the first visit, and trials for the other two were completed during the second visit. The order among the three footwear conditions was randomized. Participants also responded to a nine-question survey adapted from an established framework assessing the perceived usefulness, ease of use, and overall impressions of the CFIs [5]. Participants rated their responses on a 7-point Likert scale (1= 'completely disagree'; 7= 'completely agree'). A one-way repeated measures ANOVA was conducted to investigate how footwear stiffness influences the average comfortable walking speed and maximum walking speed in older adults. Descriptive statistics were performed for each participant survey question for each footwear condition. For this abstract, we reported the responses to three questions for brevity (Table 1).

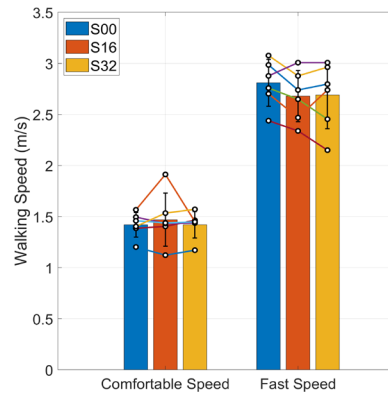


**Figure 1:** Comfortable and fast walking speed across three footwear conditions: 1) Control Shoe (S00), 2) Control Shoe + 1.6 mm CFI (S16), and 3) Control Shoe + 3.2 mm CFI (S32).

**Result & Discussion:** Footwear conditions did not significantly affect comfortable ($p = 0.502$) or maximum ($p = 0.203$) walking speeds (Figure 1). Four of six participants increased their comfortable walking speed in the S16 compared with the S00 condition. In contrast, in the S32 condition, only 2/6 participants exhibited a rise compared with the S00. In the S16 condition, only one participant had a higher maximum walking speed than the S00 condition, while in the S32 condition, 2/6 participants reported an elevation compared with S00. Participant perceptions of footwear conditions varied across key survey questions (Table 1). Comfort ratings diminished as stiffness increased, with the highest score attributed to S00 (5.6 ± 1.1) and the lowest to S32 (2.4 ± 1.1). Similarly, participants reported feeling they could walk faster in S00 (5.2 ± 1.1) compared with S16 (3.6 ± 0.9) and S32 (3.4 ± 2.3). Conversely, opinions regarding the difficulty of assessing the benefits of the footwear showed mixed trends, with S16 receiving the highest uncertainty rating (5.2 ± 1.3) and S32 the lowest (3.8 ± 2.3).

**Table 1:** Mean ± SD of participant's perception across three footwear conditions (1 = 'completely disagree'; 7 = 'completely agree').

| Survey Questions | S00 | S16 | S32 |
|---|---|---|---|
| I feel more comfortable walking in these shoes | 5.6 ± 1.14 | 3.8 ± 1.30 | 2.4 ± 1.14 |
| I feel like I can walk faster in these shoes | 5.2 ± 1.10 | 3.6 ± 0.89 | 3.4 ± 2.30 |
| It is hard to see if these shoes are helping | 4.8 ± 1.64 | 5.2 ± 1.30 | 3.8 ± 2.28 |

**Significance:** Preliminary findings indicate that increased stiffness may decrease perceived comfort and walking speed in older adults, impacting individuals' willingness to adopt the footwear intervention.

**Acknowledgments:** This work was supported by the NIH (R01AR081287), awarded to KZT and JRF, and NIH T32TR004394, awarded to DJD.

**References:** For example: [1] Himann et al. (1988), *Med & Sci Sport & Exer 20(2)*; [2] Delabastita et al. (2021), *J Med & Sci Sport 31(5)*; [3] Ray et al. (2020), *Sci Rep 10(1)*; [4] White et al. (2025), *J Appl Biomech Adv Onl Pub*; [5] Moore et al. (1991), *J Inf Syst Research 2(3)*.

# REDUCED TOE-OFF ANGLE USING AT-HOME FOOTWEAR: IMPLICATIONS FOR FALL RISK IN OLDER ADULTS

*Damaris C. Cifuentes[1], Keven Santamaría-Guzmán[1], Eduardo S. López[2], Silvia E. Campos-Vargas[1], Kenneth D. Harrison[1], Brandon M. Peoples[1], Bria R. Smith[1], Francisco Siles[2], Jaimie A. Roper [1]
[1]Locomotor and Movement Control Laboratory, Auburn University, Auburn, AL, U.S.A.
[2]Human Movement Science Research Center, University of Costa Rica, San Jose, C.R.C.
*Corresponding author's email: dcc0062@auburn.edu

**Introduction:** The growing aging population commonly experiences discrepancies in walking mechanics compared to younger populations [1,2]. This decline in proper gait function among this population comes with an increasing trend in fall-related injuries with majority of falls often occurring within or around a household setting in adults sixty-five years or older[3]. Fall-related injury prevention methods have identified footwear characteristics as a modifiable mechanism that can influence stability and balance during gait among older adults[4]. While the effect of footwear characteristics on gait within the older population has been addressed, gait variability under different footwear conditions, specifically in preferred footwear design used within a household setting (at-home footwear), in the aging population remains largely unexplored. Our study investigated the impact of footwear preference, specifically in most commonly worn athletic footwear and most commonly worn at-house footwear conditions, in gait during a standardized walking test in older adults to understand the effects of footwear conditions and preference within a population that experiences high rates of fall-related injuries. Based on the effect footwear conditions can have on gait, we hypothesized there to be variability in walking performance between all conditions with at-home footwear have the highest variability in gait parameters linked to reduced gait function.

**Methods:** Forty-two healthy older adults (33 females, 7 males, 2 prefer not to say; age: 67.71±9 years; height: 160.86±8.38cm; mass: 67.71±11.24kg) performed a 40-meter walk test under three different footwear conditions: barefoot, most commonly worn athletic footwear, and most commonly worn at-home footwear at self-selected and max speed. Six ADPM Opal inertial sensors were administered at the sternum, lumbar region, bilateral feet and wrists to quantify kinematic gait parameters. The following footwear characteristics for each footwear condition was measured: mass (g), heel height (mm), forefoot height (mm), heel external width (mm), toe box external width (mm), sole grip, heel hardness (Shore A Durometer) and forefoot hardness (Shore A Durometer). ANOVA was used to analyze differences between footwear conditions and gait parameters.

**Results & Discussion:** ANOVA revealed a significant decrease in toe-off angle when using most commonly worn at-home footwear (mass: 227.18±65.52g; heel height: 33.34±38.05mm; forefoot height: 20.97±23.81mm; heel external width: 77.37±10.67mm; toe box external width: 97.19±9.15mm; sole grip: 7.29±10.01; heel hardness: 41.36±14.70; forefoot hardness: 40.57±13.6) compared to barefoot and most commonly worn athletic footwear (mass: 226.86±65.63g; heel height: 33.30±38.06mm; forefoot height: 20.96±23.82mm; heel external width: 77.41±10.68mm; toe box external width: 97.06±9.16mm; sole grip: 7.32±10.00; heel hardness: 41.22±14.62; forefoot hardness: 40.42±13.56) during the 40-meter walk test at both self-selected and max speeds ($F= 4.408$, $p= 0.013$; $F= 2.080$, $p= 0.151$). This significant difference in toe-off angle between most commonly worn at-home footwear and both barefoot and most commonly worn athletic footwear ($t=2.620$ & $2.534$, $p<0.05$) was evident at both self-selected and max speeds (Fig.1). These findings suggest that at-home footwear preferences from an aging population may lead to a reduced ability to effectively push off during ankle propulsion and may promote limited leg joint mobility during gait. This gait readaptation reflected from this footwear condition may lead to irregularities in gait patterns, which may put older adults at an even higher risk of fall related injuries.

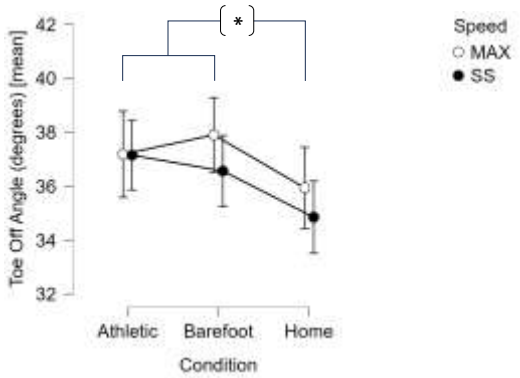


**Figure 1.** Mean toe-off angle (degrees) between barefoot, most worn athletic footwear, and most worn house footwear conditions at self-selected (SS) and max (MAX) speeds.

**Significance:** This study supports that at-home footwear choices and preference in style significantly affect a critical gait parameter in older adults. Footwear characteristics were similar across both at-home and athletic footwear conditions which indicates there may be a potential unmeasured footwear characteristic that is inducing this gait readaptation. The reduced toe-off angle observed with at-home footwear suggest compromised propulsive leg joint kinetics during walking; these alterations promote a shuffling gait pattern that may increase fall risk, particularly in household environments where majority of falls occur within this population. Given the underlying issues that arise due to age alone, these results reveal potential modifiable factors related to footwear that can guide our understanding to enhance and not limit mobility among older adults. These findings have direct implications for footwear recommendations by health professionals, suggesting that greater attention should be paid to at-home footwear selection to minimize fall risk and optimize gait mechanics in aging populations.

**References:** [1] Boyer et al. (2017), Exp Gerontology, 95, 63-70; [2] Franz J. R. (2016), Exerc and Sport Sci Rev, 44(4); [3] Gelbard et al. (2014), The Am J of Surgery, 208(2); [4] Rosen et al. (2013), J of Inj & Violence Res, 5(1).

# ARE ALTERED KNEE JOINT FORCES A CONTRAINDICATION FOR THE USE OF CARBON FIBER INSOLES TO ENHANCE WALKING PERFORMANCE IN OLDER ADULTS?

*Elizabeth Bjornsen[1], Aubrey J. Gray[1], Chase Aiken[2], W. Zachary Horton[3], Brian Pietrosimone[4], Kota Z. Takahashi[5], Jason R. Franz[1]
[1]Lampe Joint Department of Biomedical Engineering, University of North Carolina-Chapel Hill and North Carolina State University
[2]North Carolina School of Science and Mathematics
[3]Department of Statistics, University of California at Santa Cruz
[4]Department of Exercise and Sport Science, University of North Carolina at Chapel Hill
[5]Department of Health and Kinesiology, University of Utah
*Corresponding author's email: ebjornse@email.unc.edu

**Introduction:** 21% of older adults aged 65 and older report difficulty walking [1]. Decreases in the quality and quantity of walking are associated with higher rates of hospitalizations and greater healthcare costs [2-4]. Lesser ankle moment and power generation are hallmark signs of age-related declines in walking performance [5]; however, both are modifiable targets for intervention. Carbon fiber insoles may be a highly suitable option due to their low cost and potential to augment ankle moment in older adults [6]. However, footwear modifications seeking to enhance walking performance in aging may be contraindicated should they negatively affect other aspects of walking quality, such as knee joint loading – a factor associated with the onset and progression of knee osteoarthritis [7]. Therefore, the purpose of the study was to determine the magnitude of differences in model-predicted knee joint loading (i.e., medial and lateral tibiofemoral joint contact forces) in otherwise healthy older adults walking with three footwear conditions (i.e., standard walking shoes with and without 1.6- and 3.2-mm carbon fiber insoles). We test the null hypothesis that carbon fiber insoles would have no measurable effect on medial and lateral compartment joint loading.

**Methods:** Healthy older adults (65-85 yrs.) completed three, 2-minute walking trials (i.e., no insole, 1.6-mm, and 3.2-mm insole) on a dual-belt instrumented treadmill at self-selected overground walking speed. Marker trajectories and ground reaction forces were extracted from a single step occurring at the midpoint of the trial and used as inputs to a computational cost-optimization algorithm (i.e., Concurrent Optimization of Muscle Activation and Kinematics [COMAK]) to estimate medial and lateral tibiofemoral joint contact force magnitudes. A repeated-measures, functional linear model [8] compared within-subject joint contact force profile differences, vertical ground reaction forces (vGRF), and – as a determinant of medial vs. lateral force distribution - frontal plane knee angle between walking conditions throughout the stance phase (0-100%). We reported regions where the 95% confidence intervals did not include zero.

**Results and Discussion:** Fourteen individuals participated in the repeated measures experiment [25.8±3.3 kg/m$^2$, 57% female, 1.08±0.15 m/s, 70.4±4.2 yrs]. Compared to standardized footwear alone, neither the 1.6-mm nor 3.2-mm carbon fiber insole significantly altered knee joint contact forces (Fig.1), vGRF, or frontal plane knee joint angle. We thus could reject the null hypothesis. That said, we did find greater lateral compartment tibiofemoral joint contact force magnitudes for the 3.2-mm insole compared to the 1.6-mm insole, though these were isolated to a small portion of late stance (81-91%; +0.23 kN, $d$=1.53; Fig 1A). Qualitatively, it is possible that increased lateral compartment loading in the stiffest insoles and decreased lateral loading in the thinnest insole condition during late stance reflects opportunities for precision prescription to address multi-morbidities in aging. Indeed, older community members rarely only have walking difficulties or osteoarthritis. Future work with larger samples may seek to determine whether certain carbon fiber insole stiffnesses designed to enhance foot leverage and ankle joint moments during push-off can simultaneously elicit desirable changes in tibiofemoral joint loading.

**Significance:** Altered knee joint forces may not be a contraindication for the use of carbon fiber insoles to enhance walking performance in older adults.

**Acknowledgments:** Research was supported by the ASB Grant-In Aid award and the UNC Dissertation Completion Fellowship to AJG and NIH R01AR081287 to JRF/KZT.

**References:** [1] U.S. Census Bureau, 2022; [2] Cesari et al., 2005; [3] Falvey et al., 2019; [4] Studenski et al, 2011; [5] Pol et al., 2021; [6] White et al., [7] Andriacchi et al., 2004; [8] FunctionalMixedEffects.R, GitHub

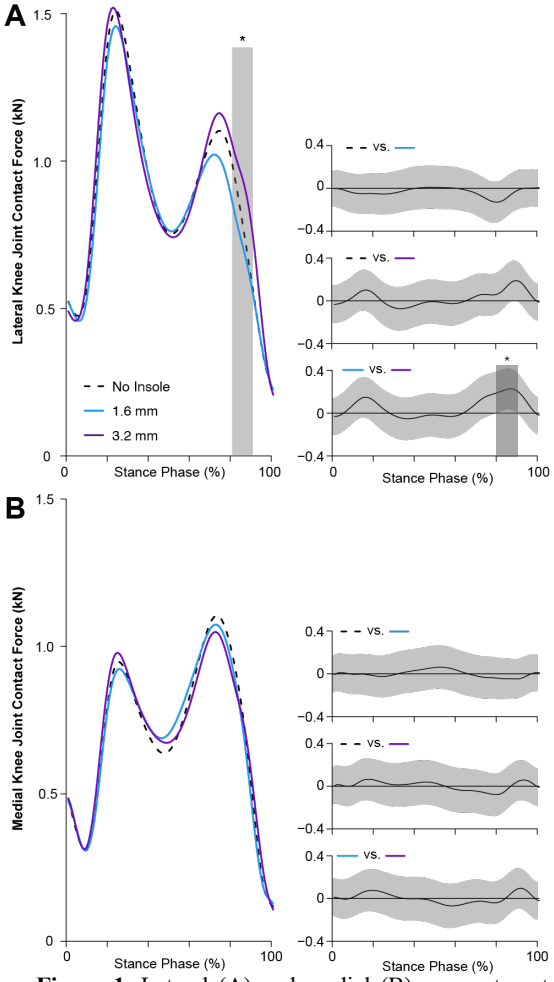


**Figure 1**. Lateral (A) and medial (B) compartment profiles for tibiofemoral joint contact force profiles are displayed across stance phase of gait (0-100%). Mean difference curves with accompanying 95% confidence intervals (grey) comparing each insole condition are shown at right. *Denotes statistically significant region.

# EFFICACY OF THERAPEUTIC SHOES IN REDUCING PLANTAR PRESSURE IN PATIENTS WITH FOOT PAIN

Krista Samreth[1], Karishma Sebastian, Elnaaz Eskandari, Sabrina Winkler, Javier La Fontaine, Luis Venegas, Hafizur Rahman[1,2,3]*
[1]School of Podiatric Medicine, University of Texas Rio Grande Valley
[2]College of Engineering and Computer Science, University of Texas Rio Grande Valley
[3]School of Medicine, University of Texas Rio Grande Valley
*Corresponding author's email: hafizur.rahman@utrgv.edu

**Introduction:** Approximately 600,000 people visit outpatient clinics due to their foot pain. With repetitive stress and excessive pressure, callus formation can occur and lead to ulceration. Patients with foot discomfort exhibit increased mechanical stress and strain on regions of the foot [1]. Previous studies demonstrated that individuals with foot pain generate higher peak plantar pressure under the foot compared to individuals without foot pain. To lessen peak plantar pressure in specific locations, custom-fit footwear options such as depth shoes, orthotic adjustments, and inserts can distribute pressure regions more evenly. This study evaluates the effects of OrthoFeet Hands-Free therapeutic shoes in reducing plantar pressure compared to patients' own regular footwear. We hypothesize that the degree of foot pain mitigates more with reduced peak plantar pressure in patients with foot pain after a 6-week intervention of wearing OrthoFeet HandsFree Therapeutic shoes compared to patients wearing their own shoes.

**Methods:** The local maximum plantar pressure was measured and analyzed for four patients (age: 76.8 ± 5.5 years; body mass index: 24.3 ± 5.4 kg/m$^2$). Experimental data was collected two times: i) before the intervention starts as *Pre*, and ii) after 6 weeks of intervention as *Post*. Patients participated in an in-shoe plantar pressure measurement test. PedarX insole sensors (Novel GmbH, Munich, Germany) were placed inside both shoes to measure in-shoe dynamic plantar pressure. For the experimental test, patients walked along a 10-meter walkway in a laboratory setting at a self-selected speed, ensuring that we collected at least 12 mid-gait steps per foot. For *Pre* condition, plantar pressure data was reported for both regular shoe and OrthoFeet shoe. For *Post* condition, the plantar pressure value was reported only for OrthoFeet shoes. The pressure values were reported for the forefoot, midfoot, and rearfoot regions for both feet, as all four of our patients had bilateral foot pain.

**Results & Discussion:** Patients had an initial maximum plantar pressure ranging from 86.85 kPa to 215.62 kPa on their left foot (forefoot, midfoot, and rearfoot) while walking using their normal sneakers (Table 1). Peak pressure was observed in the forefoot. The maximum plantar pressure for the right foot ranged from 98.78 kPa to 183.01 kPa for normal sneakers. Similar to the left foot, the peak plantar pressure also occurred in the forefoot region for the right foot (Table 1).

From the initial visit of using the OrthoFeet Hands-free therapeutic shoes (*Pre* condition), patients had maximum pressure ranging from 84.42 kPa to 217.90 kPa on their left foot, almost similar pressure distribution patterns to their regular sneakers (Table 1). However, for the right foot wearing the OrthoFeet Handsfree therapeutic shoes, although peak pressure slightly decreased in the midfoot region (normal: 98.78 kPa; OrthoFeet shoe *Pre*: 85.11 kPa), the peak pressure increased in a larger magnitude in the forefoot region (normal: 183.01 kPa; OrthoFeet shoe *Pre*: 223.99 kPa) (Table 1). This increment in plantar pressure could be the causes of the unfamiliar use and without adaptation of the new footwear, further providing the room for an intervention period.

After 6 weeks of using the OrthoFeet HandsFree therapeutic shoes, the peak plantar pressure was reduced for all three regions (forefoot, midfoot, rearfoot) for both feet compared to their pre OrthoFeet values and normal shoe values. For example, the peak pressure in the left foot following 6 weeks of intervention was 178.15 kPa in the forefoot region wearing OrthoFeet shoes, which was 215.62 kPa for normal shoes at baseline. Overall, our preliminary findings demonstrate an overall reduction in the forefoot, midfoot, and rearfoot maximum pressure for both feet, suggesting that patients had an overall decrease in general foot pain and patients had the potential and direct benefit from using OrthoFeet shoes that lower the peak plantar pressure.

Table 1: Peak plantar pressure in forefoot, midfoot, and rearfoot regions

| | **Right Foot** | | | **Left Foot** | | |
|---|---|---|---|---|---|---|
| | **Forefoot** | **Midfoot** | **Rearfoot** | **Forefoot** | **Midfoot** | **Rearfoot** |
| **Normal shoe (*Pre*)** | 183.01 ± 15.37 | 98.78 ± 25.75 | 115.67 ± 3.23 | 215.62 ± 82.19 | 86.85 ± 18.40 | 136.83 ± 11.91 |
| **OrthoFeet shoe (*Pre*)** | 223.99 ± 65.10 | 85.11 ± 27.22 | 107.40 ± 26.35 | 217.90 ± 135.18 | 84.42 ± 26.66 | 99.68 ± 14.16 |
| **OrthoFeet shoe (*Post*)** | 178.98 ± 68.26 | 85.95 ± 27.34 | 96.76 ± 12.08 | 178.15 ± 81.96 | 72.95 ± 25.64 | 99.42 ± 15.03 |

* Values are expressed as mean ± standard deviation. Pressure values are expressed in kPa.

**Significance:** Our findings suggest that patients with foot pain exhibited lesser stress and plantar pressure with the OrthoFeet HandsFree therapeutic shoes compared to their regular shoes after 6 weeks of intervention. Once patients were adjusted to the appropriate orthotic, results demonstrated decreased foot pain and plantar pressure in local regions. Based on this analysis, OrthoFeet HandsFree therapeutic shoes can improve and effectively lower pressure distribution in patients with general foot pain, reducing the possibility of ulcer formation. Preventing foot ulceration at an early stage with the use of orthotics and conservative management can lower the chances of infections and amputation rates.

**References:** [1] Karen MJ et al. (2010), *Journal of the American Geriatrics Society* 10.

# MDS-UPDRS SECTION III SCORE PREDICTION USING NEURAL NETWORK APPROACH WITH MOBILE PHONE APPLICATION DATA

Seonghyeon Hwang[1], Jeongsik Kim[1], Ryeongah Kim[1], Ryul Kim[2], *Kiwon Park[1]
[1]Dept. of Biomedical & Robotics Engineering, Incheon National University, Incheon, South Korea
[2]Dept. of Neurology, SMG-SNU Boramae Medical Center, Seoul National University College of Medicine, Seoul, South Korea
*Corresponding author's email: kiwon@inu.ac.kr

**Introduction:** Parkinson's disease (PD) is a neurological disorder characterized by symptoms such as tremors, bradykinesia, and freezing. PD is caused by a lack of dopamine neurons in the substantia nigra, and there is no cure yet, so it can only be slowed down with exercise and medication. The population of PD patients with these characteristics has more than doubled since 1990 due to aging and industrialization [1]. Currently, a medical professional usually diagnoses PD face-to-face using the MDS-UPDRS test. This method is time-consuming and requires a person to see a medical professional in person, which is limited in time and space, making it impossible to access medical services in some areas. Research is being conducted to solve these constraints and problems using electronic devices such as mobile phones as medical diagnostic devices. As one of these studies, this study aims to use a simple application to collect finger movement data of PD patients using a smartphone to predict the MDS-UPDRS III score, which indicates the motor symptoms of PD patients based on finger movements. Such a system would benefit people with or at risk of PD in underserved areas, such as developing countries and parts of the industrialized world, with poor access to healthcare.

**Methods:** The application was tested with 121 PD patients and 82 healthy controls, and only data from PD patients were used to predict the MDS-UPDRS III score. The tests included two types: a touch test and a drawing test. The touch test consisted of touching an area divided by the index and middle fingers for 15 seconds, and the drawing test involved tracing four shapes. The collected data was utilized to create a Long Short-Term Memory (LSTM) based predictor in time series data. In addition, noise injection-based data augmentation was used to augment the data in score bands (low and high) where the patient population was relatively sparse. For the validation step, k-fold cross-validation was used.

**Results & Discussion:** The accuracy of the MDS-UPDRS III Score predicted by the LSTM-based predictor trained with finger movement data was determined using the Mean Square Error (MSE). For MSE, the Training MSE at the last epoch showed a value of 0.75 and the Validation MSE 5.22. To visualize the predictor's performance, we plotted the actual MDS-UPDRS III Score against the predicted MDS-UPDRS III Score in a scatter plot (Figure 1). In Training, we can see that the training was sufficient except for one case. For Validation, we can see that it correctly predicts most of the participants but fails to predict some of them. This was the first fold in the k-fold validation; similar results were seen in other folds.

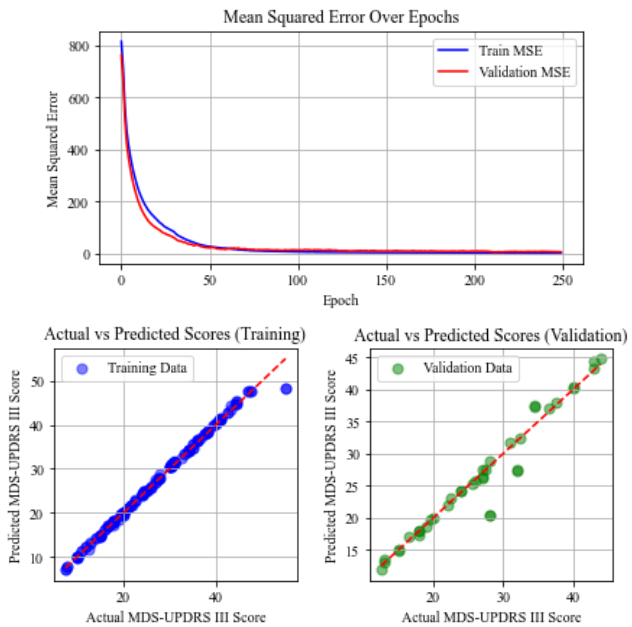


**Figure 1.** Mean Square Error and Training and Validation Scatterplot for LSTM-based Predictor

These results suggest that the LSTM-based predictor has the potential for a PD diagnostic tool. The predictor performed well enough compared to the accuracy of previous studies that predicted MDS-UPDRS III scores using gait data [2]. This suggests that a relatively simple mobile phone test can predict severity and support telehealth more straightforwardly than earlier studies. However, when the training/validation dataset changes, the performance of learning/prediction sometimes decreases, so it is necessary to improve models such as multivariate LSTM, transformer, etc., using various data to increase accuracy. In addition, there is a need for more accurate and diversified predictions with MDS-UPDRS I, II, and total score predictions.

**Significance:** The study suggests that it is possible to predict the severity of PD using a mobile phone. Severity prediction using mobile phones can effectively overcome the limitations of existing studies on gait (expensive equipment, need for specialists, ample space, inability to walk) and speech (inability to pronounce, only trained in a specific language). This means that telehealth services can be made widely available to people living in hard-to-reach places and those with difficulty walking and testing their speech. Further improvements, such as improved total score prediction and accuracy, could lead to better-performing teleassistance. It can also be used as a classification tool to distinguish PD patients from the general population, reducing the risk of misdiagnosis and enabling better quality medical support. This study demonstrates the potential for telehealth services based on predicting the severity of PD.

**Acknowledgments:** This research was funded by the National Research Foundation (NRF) grant funded by the Korea government (MSIT) (No. RS-2023-00222406).

**References:** [1] Luo et al. (2025), Front. Aging Neurosci. 16, 1498756.; [2] Rehman et al. (2021), EMBC 43rd Annu. Int. Conf., IEEE, 249-252.

# Concurrent assessment of markerless and marker-based motion capture for kinematics and kinetics during functional activities in knee osteoarthritis

Rhodora Therese Torres[1], Benjamin Senderling[1,2], Ehyun Kim[1], Michael Rose[1, 3], Tuhina Neogi[1], *Deepak Kumar[1]
[1]Boston University, Boston, MA, United States
[2]Drexel University, Philadelphia, PA, United States
[3]University of California Los Angeles, Los Angeles, CA, United States

*Corresponding author's email: kumard@bu.edu

**Introduction:** Knee osteoarthritis (OA) affects around 14 million people [1]. Altered knee mechanics during functional activities play a key role in the progression of knee OA [2]. Assessment of knee biomechanics is crucial for developing therapeutic strategies, but traditional marker-based (MB) motion capture systems have limitations for clinical use [3]. Markerless (ML) motion capture systems offer a potential solution [4-5], however rigorous comparisons with MB methods in people with knee OA are lacking. Our objective was to compare knee kinematics and kinetics during walking and sit-to-stand (STS) between MB and ML motion capture systems in people with knee OA.

**Methods:** We used data from participants enrolled in a clinical trial (NCT04243096). Data from a single time-point per participant was used. Participants performed several trials of walking at self-selected and fast paces and STS. MB and ML data were concurrently captured by synchronizing 12 infrared and 8 color video cameras (Qualisys, Sweden) at 250Hz and 50Hz, respectively. Video data were processed using an artificial intelligence-based pose estimation algorithm (Theia3D v2022.1.0.2309, Canada). Sagittal and frontal knee joint angles (in ˚) and moments (in %BW*ht) were derived from both MB and ML data for the stance phase of walking and ascent phase of STS tasks. We compared discrete kinematic and kinetic metrics between MB and ML systems using intraclass correlation coefficients (ICCs). We also calculated average root mean square difference (RMSD) between ML and MB for the time-normalized kinematic and kinetic waveforms. Only data from the index knee (more painful or randomly selected knee if equally painful) are presented.

**Results & Discussion:** Data from 22 participants (14 females, 8 males; age 63.7±7.6 years; BMI 28.2±4.7 kg/m2; Knee Injury and Osteoarthritis Outcome Score [KOOS] Pain 68.8±13.2, and Symptoms 66.9±13.6) were available. ICC are reported in Table 1 and RMSD in Figure 1. Our results revealed better agreement in terms of sagittal knee kinematics and frontal knee kinetics. Sagittal plane knee movements are larger, making them easier to capture accurately compared to the more subtle movements in the frontal plane. The poor agreement on some of the kinematic and kinetic parameters may have been rooted in the algorithm of the ML system, which were mostly trained in healthy individuals unable to fully capture the altered characteristics and biomechanics of patients with knee OA.

| | | SELF-SELECTED SPEED (1.5±0.2 m/s) | | FAST SPEED (1.9±0.2 m/s) | |
|---|---|---|---|---|---|
| | | Mean Diff. (95% CI) | ICC | Mean Diff. (95% CI) | ICC |
| Walking (W: $n = 22$; FW: $n = 18$) | Peak Flexion Angle | 2.4 (0.4, 4.3) | 0.57 | 2.7 (0.8, 4.7) | 0.71 |
| | Peak Adduction Angle | -3.4 (-4.3, -2.5) | 0.71 | -3.4 (-4.5, -2.3) | 0.74 |
| | Sagittal ROM | -0.8 (-2.0, 0.4) | 0.83 | -0.6 (-2.2, 0.9) | 0.78 |
| | Frontal ROM | 1.0 (-0.3, 2.3) | 0.04 | 0.5 (-0.7, 1.7) | 0.41 |
| | 1st Peak Flexion Moment | -0.7 (-1.0, -0.3) | 0.79 | -0.8 (-1.2, -0.5) | 0.85 |
| | 2nd Peak Flexion Moment | 1.2 (1.0, 1.4) | 0.22 | 1.0 (0.7, 1.3) | 0.50 |
| | 1st Peak Adduction Moment | -0.2 (-0.4, 0.0) | 0.94 | -0.2 (-0.5, 0.1) | 0.92 |
| | 2nd Peak Adduction Moment | -0.1 (-0.3, 0.1) | 0.88 | 0.1 (-0.1, 0.3) | 0.89 |
| | Flexion Moment Impulse | 0.1 (0.1, 0.2) | 0.63 | 0.1 (0.1, 0.2) | 0.81 |
| | Adduction Moment Impulse | -0.0 (-0.1, 0.0) | 0.95 | -0.0 (-0.1, 0.0) | 0.95 |
| STS ($n = 21$) | Sagittal ROM | 5.1 (3.2, 7.1) | 0.63 | | |
| | Frontal ROM | 2.1 (0.4, 3.9) | 0.07 | | |
| | Peak Flexion Moment | 0.4 (0.2, 0.6) | 0.79 | | |
| | Peak Adduction Moment | 0.2 (0.1, 0.2) | 0.68 | | |

**Table 1**. ICC between MB and ML metrics. Green = excellent (ICC >0.90), yellow = good (ICC 0.75-0.90), blue = moderate (ICC 0.5-0.75), red = poor (ICC < 0.5)

**Significance:** ML motion capture system holds significant potential for clinical and research applications in knee OA populations. While some differences in the estimations remain, ML system offer an efficient alternative for knee biomechanics analysis, with potential for further improvements.

**Acknowledgements:** We would like to acknowledge Brian Friscia, Michael Rose, Mary Gheller, and Kaveh Torabian for assisting with recruitment, data collection, and data processing. We also want to thank the participants for their time.

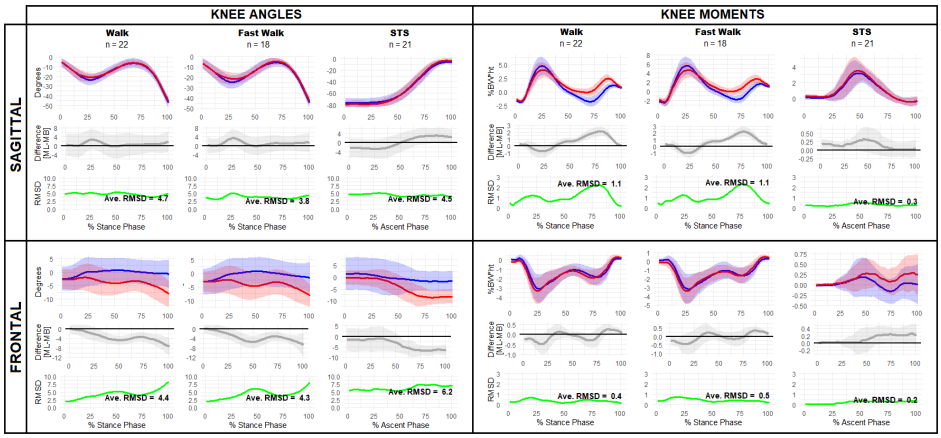


**Figure 1:** MB (red) and ML (blue) waveforms, difference (grey), and RMSD (green) and average RMSD inset.

**References:** [1] Allen et al. (2022), *Osteoarthritis Cartilage* 30(2); [2] Favre & Jolles. (2017), *EFORT Open Rev* 1(10); [3] McGinley et al. (2009), *Gait Posture* 29(3); [4] Carbajal-Mendez et al. (2024), *Osteoarthritis Cartilage* 32(1); [5] Wade et al. (2022). *PeerJ* 10

# PHYSICS-INFORMED STATISTICAL SHAPE MODEL FOR GEOMETRY PREDICTION OF NONUNION SCAPHOID FRACTURES

*Junjun Zhu[1], Weimin Zhu
[1]School of Mechatronic Engineering and Automation Shanghai University, China, 200444
*Corresponding author's email: junjunz@shu.edu.cn

**Introduction:** Scaphoid fractures are a common wrist injury. By providing biological and mechanical support, bone grafts help stimulate the healing process, improve union rates, and restore function. Given the high risk of nonunion and avascular necrosis in scaphoid fractures due to complex vascular and structural challenges, accurately predicting the original scaphoid geometry is essential for effective preoperative planning and treatment optimization. Current research gaps include limited predictive accuracy, lack of personalized treatment strategies, and insufficient understanding of biomechanical factors. In recent years, statistical shape modeling (SSM) has shown significant potential in various applications, including skeletal modeling[1]. Yet, none of these methods have thoroughly evaluated the biomechanical accuracy of its predicted shapes under physiological loads and taken the results into an algorithm. This study addresses these limitations by proposing the iterative kernel principal polynomial shape analysis-finite element (iKPPSA-FE) method, applying finite element (FE) analyses to scaphoids predicted by the iKPPSA model, and simulating varied loading conditions that reflect real-world fracture scenarios. We further utilized the FE simulation results as feedback in the calculation to minimize the difference between the prediction and intact scaphoid. We evaluated the biomechanical performance of iKPPSA-FE predicted scaphoids in comparison with their original forms across TF, PF, and IN types, hypothesizing that the predicted shapes would exhibit similar biomechanical characteristics to the intact scaphoid under these loading conditions.

**Methods:** The proposed approach incorporates the finite element analysis of the iKPPSA-predicted shape to further refine the prediction (Figure 1). Briefly, the iKPPSA scaphoid SSM model was trained with 65 intact scaphoid images and their corresponding defects models, another 9 image sets were used to verify the final model through finite element analysis against the original biomechanical model including typical defects (TF, PF, IN). A 1.6KN and a 4KN load was applied at referenced points along the distal scaphotrapeziotrapezoid (STT) joint, with fixed supports at anatomical sites [3]. Bayesian optimization is a probabilistic technique used to optimize complex and computationally expensive functions. Three fractured scaphoid defects were virtually created based on the Herbert classification. The location of the defects was determined based on reported literature. The material of the scaphoid bone is assumed to be homogeneous and linear-elastic with a Young's modulus of 10 GPa and a Poisson's ratio of 0.3. The study placed the force surfaces at different locations along the line: at the articular surface between the scaphoid bone and the trapezium bone, at the articular surface between the scaphoid bone and the trapezoid bone, and along the entire STT articular surface.

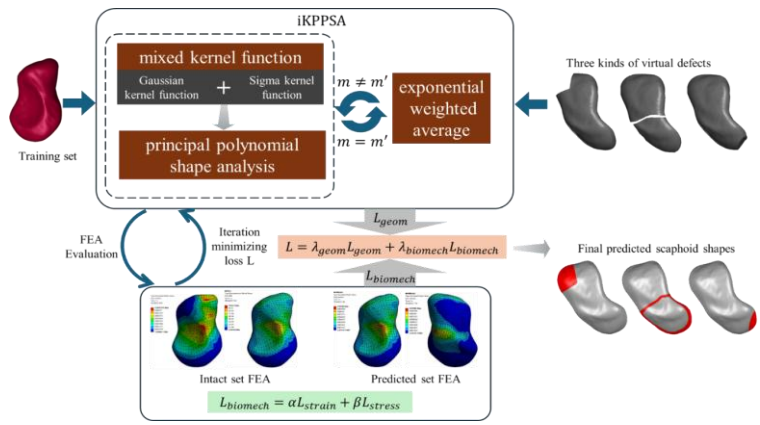


**Figure 1:** Flow chart of the proposed iKPPSA-based statistical shape model (m, the number of leading modes 153 used)

**Results & Discussion:** When the load was applied to the scaphoid-trapezoid surface under high-energy loading, it resulted in a 24.1% reduction in deformation relative to the intact scaphoid. It suggests that predicted shape using the iKPPSA-FE method could lead to less deformation under external loadings than intact scaphoid shape. When loading the entire STT surface, stress concentration occurred at the edge of the scaphoid fossa and the waist of the scaphoid bone. With the scaphoid-trapezium surface load, the predicted maximum stresses for Tubercle and Proximal fractures were higher than those of the intact bone. Conversely, in cases of ischemic necrosis, there was a 3.7% reduction in maximum stress. With the scaphoid-trapezoid surface load, the iKPPSA-FE method predicted lower maximum stresses under both loads. Notably, when the entire STT surface was considered, the intact scaphoid bone exhibited superior mechanical properties under ischemic necrosis conditions, with a 3.6% reduction in maximum stress.

When the load was applied at the scaphoid-trapezium surface, the primary strain occurred at the edge of the scaphoid fossa. In contrast, with a scaphoid-trapezoid load surface, the strain was mainly concentrated at the region where the ligament connects to the back of the scaphoid. When the entire STT surface was considered, the maximum strain remained at the upper edge of the scaphoid fossa, while the strain in the fossa itself was less pronounced. Findings indicate that while the intact scaphoid demonstrates elevated strain under scaphoid-trapezium loading, fractured models exhibit a reduced strain response, particularly under low load. However, under high load, PF exhibits a notable strain increase that exceeds that of the intact scaphoid, revealing potential vulnerabilities in mechanical stability.

**Significance:** The iKPPSA-FE method demonstrates reliable potential for simulating realistic scaphoid geometries and predicting strain outcomes, suggesting its utility in clinical decision-making and preoperative planning for scaphoid fracture management.

**References:** [1] Schumann et al. (2010), Med Eng Phys, 32(6); [2] Berger (2001) Hand Clin, 17(4).

# VALIDATION OF AI-DRIVEN MARKERLESS MOTION CAPTURE SYSTEM FOR SPATIOTEMPORAL GAIT ANALYSIS IN STROKE SURVIVORS

*Balsam J. Alammari[1], Brandon Schoenwether[2], Zachary Ripic[2], Neva Kirk-Sanchez[1], Eltoukhy, Moataz[2], Lauri Bishop[1]
[1]University of Miami Department of Physical Therapy, Coral Gables, FL, USA
[2]University of Miami Department of Kinesiology and Sport Sciences, Coral Gables, FL, USA
*Corresponding author's email: lauri.bishop@med.miami.edu

**Introduction:** Gait impairments often persist after rehabilitation from stroke. Valid assessment of post-stroke gait deficits is useful to design targeted interventions, monitor rehabilitation progress, and predict real-world walking recovery [1]. Conventional gait assessments, such as the 10-Meter Walk Test (10MWT) are frequently utilized in clinical settings. While technology-based gait analyses, like instrumented walkways and marker-based motion capture provide high-precision measures, their integration into clinical settings has been limited by the extensive training requirements and instrumentation costs systems. Alternatively, the utilization of AI-based markerless motion capture (AI-mocap) to identify key points in the human body [2] during gait analysis could provide an unconstrained option to heavily instrumented traditional gait analysis systems [3-5]. Yet, there is a lack of large-scale post-stroke research utilizing multi-view AI-mocap. If valid, AI-mocap could provide an accurate and streamlined clinical gait assessment.

The study aims to evaluate the concurrent validity of spatiotemporal gait parameters obtained from a multi-view three-dimensional (3D) AI-mocap, KinaTrax (KinaTrax Inc., Boca Raton, FL), compared to a gold-standard instrumented walkway (Protokinetics Zeno™ Walkway Gait Analysis System, Havertown, PA) in stroke survivors [6]. Due to the high validity established in populations of healthy adults and people with Parkinson's disease (PD) [3], we hypothesize that spatiotemporal gait parameters measured by AI-mocap and the instrumented walkway would have good to excellent agreement in individuals post-stroke.

**Methods:** Stroke survivors performed three trials of a 10MWT at a comfortable speed over the instrumented walkway with simultaneous recording via the AI-mocap. Spatiotemporal metrics (i.e., gait speed, cadence, double-limb support time (DLS), stride length, and step length of paretic and non-paretic limbs) were collected. Absolute agreement and relative consistency were determined by calculating an intraclass correlation coefficient (ICC (3,1), 95% CI). Bland-Altman plots estimated bias and Limits of Agreements (LoAs).

**Results:** Table 1 details the absolute agreement and relative consistencies using ICCs with respective 95% CI limits for each gait parameter. Bland-Altman bias and LoAs are also represented. The absolute agreement and relative consistency between the AI-mocap and the instrumented walkway were excellent for gait speed, cadence, and stride length parameters. DLS and step length of paretic and non-paretic limbs showed good agreement and consistency. AI-mocap underestimated all parameters ≤ 5%, save DLS. DLS was overestimated by 4.38% in the AI-mocap. LoAs were within acceptable bounds in all parameters except step length.

| Parameter | Absolute Agreement | Relative Consistency | Bland-Altman |
|---|---|---|---|
| | ICC (95% CI) | ICC (95% CI) | Bias [LoA] |
| **Gait Speed (m/s)** | 0.962 (0.905-0.983) | 0.970 (0.943-0.984) | 0.04 [-0.11,0.19] |
| **Cadence (steps/min)** | 0.905 (0.809-0.951) | 0.915 (0.843-0.955) | 2.21 [-8.50,12.10] |
| **DLS (sec)** | 0.860 (0.748-0.925) | 0.865 (0.755-0.927) | -0.02 [-0.15,0.12] |
| **Stride Length (m)** | 0.960 (0.924-0.979) | 0.959 (0.923-0.979) | 0.01 [-0.15,0.17] |
| **P-Step Length (m)** | 0.722 (0.526-0.845) | 0.732 (0.541- 0.851) | 0.02 [-0.03,0.07] |
| **NP-Step Length (m)** | 0.776 (0.612-0.877) | 0.782 (0.619-0.880) | 0.03 [-0.21,0.26] |

**Table 1.** Intraclass Correlation Coefficients (ICCs, 95% CI) of absolute agreements and relative consistencies, bias with Limits of Agreements [lower-upper bound] between AI-mocap and the instrumented walkway are represented. DLS: Double-Limb Support time.; P-Step Length: Paretic Step Length; NP-Step Length: Non-Paretic Step Length.

**Discussion:** Hypotheses were supported by study findings. Our findings of excellent agreement and relative consistency between AI-mocap and instrumented walkway are comparable with prior studies that used only single or dual cameras AI-mocap in stroke survivors [7]. Similarly, prior work also demonstrated lower agreement of the DLS and step length parameters [4,7]. It is plausible that the large gait variability in DLS and step length in stroke survivors contributes to the lower agreements. An overestimation of DLS was also noted in prior work [7], suggesting that virtual key point estimation by AI-mocap might not be ideal for individuals with large gait deficits. Nevertheless, all errors and/or bias in our sample were less than the minimally detectable change (MDC) [8]. Our findings are comparable to other multi-view 3D AI-mocap validation studies performed inside [3,5] and outside [4] the laboratory in non-stroke populations. Overall, our outcomes support the use of the 3D AI-mocap for post-stroke clinical gait analysis.

**Significance:** The use of a valid, 3D AI-mocap, is a time-efficient and user-friendly alternative to capture post-stroke gait metrics in a clinical setting. Furthermore, 3D AI-mocap may be equally valuable outside the clinic in a home and/or community setting, which could be transferable to develop interventions delivered directly in environments that are salient to individuals post-stroke.

**Acknowledgments:** There was no direct funding support for this project.

**References:** [1] Grau-Pell et al., (2019), *Top Stroke Rehabil* 26 (5); [2] Kidziński et al., (2020), *Nat Commun* 11(1); [3] Ripic et al., (2023), *Biomech* 155: 111645; [4] McGuirk et al., (2022), *Front Hum Neurosci 16*:867485; [5] Kanko et al., (2021) *J Biomech 122*, 110414; [6] Sanders et al., (2024), *Sensors (Basel)* 24(14); [7] Cimolin et al., (2022), *Sensors (Basel)* 22(3); [8] Geiger et al., (2019), *Hum Mov Sci* 64:101-107

**Concurrent Validity of a Markerless Motion Capture System for the Maximal Instep Soccer Kick**

Ivan Palomares-Gonzalez, Jacob Goodin, Brent Alvar, Arnel Aguinaldo
Point Loma Nazarene University, San Diego, CA, USA
Email: ipalomar0023@pointloma.edu

**Introduction:** Marker-based motion capture is considered the practical gold standard assessment of three-dimensional kinematic measurements [1]. *Theia3D (Theia Markerless, Kingston, ON)* is a markerless motion capture system that uses an algorithm built upon deep convolutional neural networks for feature recognition and trained on digital images of over 500,000 human movements [2]. With the introduction of this novel markerless technology, it is necessary to test the equivalence of this system to the practical gold standard using common dynamic movements, such as the instep soccer kick. The previous literature supports markerless motion capture in gait and a soccer kick [2,3]. Dynamic movements, like a maximal instep soccer kick, have yet to be investigated for criterion validity. Therefore, this study aims to examine the agreement between *Theia3D* and marker-based motion capture for kinematics of the lower body and trunk in the instep soccer kick.

**Methods:** Eight healthy division II soccer players were recruited (20.38 ± 1.18 years, 1.68 ± 0.06 m, 66.52 ± 7.75 kg, 15.63 ± 1.77 years of playing experience) to be assessed concurrently by a markerless and marker-based system during a maximal instep soccer kick. In a lab setting, each participant approached and kicked a soccer ball into a wall with the top of their foot. The joint range of motion data was analyzed in the sagittal plane for the ankle and the sagittal, frontal, and transverse plane for the knee, hip, pelvis, and torso. A concordance correlation coefficient, root mean square error (RMSE), and modified Bland Altman plots were used to analyze discrete metrics during right toe-off (RTO), ball contact (BC), and maximum hip flexion (MHF). Statistical parametric mapping (SPM) t-tests were used to analyze time series data from RTO to MHF of all joints assessed.

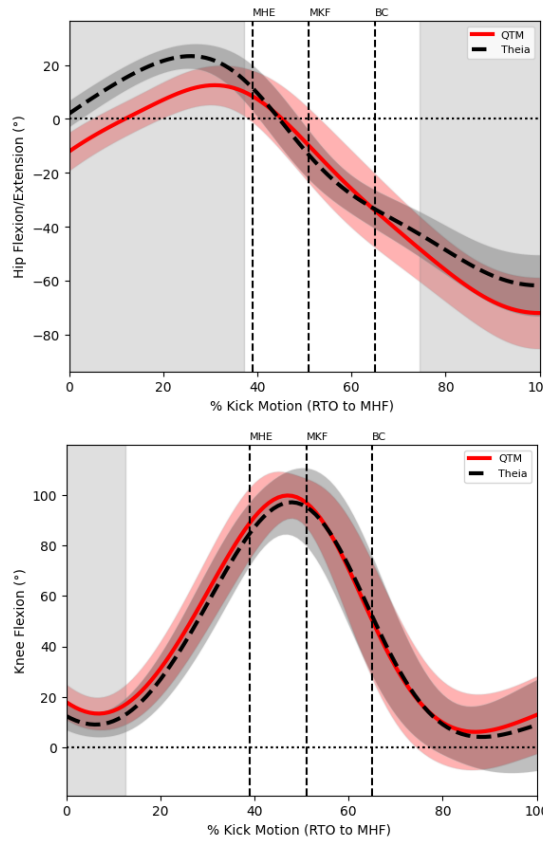


**Figure 1:** Statistical Parametric Mapping t-tests for the hip and knee in the sagittal plane with distinct events, maximum hip extension (MHE), maximum knee flexion (MKF), and ball contact (BC) with suprathreshold regions highlighted in gray.

**Results & Discussion:** This is the first study to compare a marker-based and markerless motion capture system for the instep soccer kick using both time series and discrete metric analyses. For discrete metric analysis, the hip (CCC = 0.608) and ankle (CCC = 0.608) had moderate agreement in the sagittal plane at BC and RTO, respectively. This is where they had the highest agreement compared to all other events and planes. There was excellent agreement during discrete metrics at the knee in the sagittal plane at BC and MHF (CCC = 0.881; 0.838), the pelvis in the transverse plane at RTO (CCC = 0.902), and the trunk in the frontal plane at BC (CCC = 0.876). Discrete metric RMSE ranged between 5.12° in the knee and 15.37° in the trunk for the sagittal plane, 3.66° in the trunk and 17.3° in the hip for the frontal plane, and from 4.25° in the pelvis to 19.26° in the knee for the transverse plane. An SPM t-test in the ankle showed a statistically significant difference between measures in the sagittal plane throughout the motion. SPM t-tests in the knee and hip showed the most significant agreement between measures in the sagittal plane, with the knee having significant differences for the first 15% of the kick and the hip having distinct differences for the first 35% and the last 25% of the kick (Figure 1). SPM t-tests in the trunk showed the best agreement in the frontal plane with a significant difference for the first 25% of the kick, and the pelvis in the transverse plane showed significant differences between 40 and 80 % of the kick.

**Significance:** Marker-based and markerless motion capture systems have inherent differences in how kinematics are derived. Therefore, perfect equivalence is not likely. Similar curvatures were found when comparing time series data with biases accounted for using RMSE at discrete points. Furthermore, discrete metric analysis found a moderate to excellent agreement in at least one plane of motion for each joint. Although markerless motion capture does not perfectly correlate with the practical gold standard in all joints and planes, the authors deemed it sufficiently accurate for dynamic sporting movements such as the instep soccer kick. Caution would be warranted if measures taken from a markerless system were to be compared to other motion capture methods. More analyses should be performed to assess the equivalence of these systems when considering ground force reactions, angular acceleration, and ball speed to add to the validity of markerless motion capture in the instep soccer kick and other dynamic movements.

**References:**

[1] *Ceseracciu, E, et al., (2014) PloS one, **9**(3)*
[2] *Kanko, R.M., et al., (2021), Journal of Biomechanics, **127***
[3] *Palucci-Vieira, L., et al., (2022), IJERPH, **19**(3)*

# WEARABLE IMU GROUND REACTION FORCE ESTIMATION VIA HYBRID GRU MODEL

Zakir Ullah[1], Zach Strout[2], Dong Wang[3], *Peter B. Shull[4]
[4]Peter B. Shull is with State Key Laboratory of Mechanical System and Vibration, Shanghai Jiao Tong University, Shanghai, China.
*Corresponding author's email: pshull@sjtu.edu.cn

**Introduction:** Accurate ground reaction force (GRF) estimation is crucial for gait analysis, rehabilitation, and athletic performance. Capturing bilateral GRFs in non-laboratory contexts remains challenging [1,2]. Can machine learning (ML) models reliably measure GRFs outside controlled environments using wearable inertial measurement units (IMUs)? Do simple, population mean–based baselines capture real-world variability and peak loading, or do advanced ML architectures provide a distinctly superior, subject-specific approach? To address these questions, we developed an ML framework integrating bidirectional gated recurrent units (GRUs) with low-rank bilinear fusion of accelerometer, gyroscope, and subject's height and weight as input parameters. This approach aims to deliver near-real-time GRF predictions, capturing temporal dependencies and individual biomechanical nuances in bilateral gait. We benchmarked the Hybrid GRU model against a population mean baseline to ensure improvements reflect meaningful biomechanical insights rather than statistical artifacts. By deploying this model on a commercially available wearable system, we aim to translate laboratory-based gait research into everyday settings for more precise, personalized analysis.

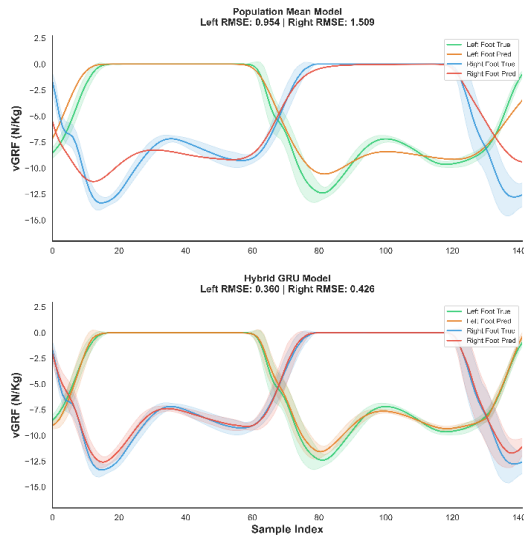


**Figure 1:** GRF Predictions: Population Mean vs Hybrid GRU Model

**Methods:** Seventeen healthy male subjects (age: 23.2 ± 1.1 years; height: 1.76 ± 0.06 m; weight: 67.3 ± 8.3 kg) walked on a treadmill at 1.16 ± 0.04 m/s with Bertec force plates, wearing five SageMotion IMUs on the pelvis, thighs, and feet. Trials included foot progression angle (baseline ± 15°), step width (baseline ± 0.054–0.070 m), and trunk sway (4°–12°) at self-selected speeds. GRF and IMU signals were recorded concurrently, with strides defined as the interval from heel strike to the next heel strike of the right foot, including a 0.2-second overlap for continuous GRF estimation. A hybrid bidirectional GRU captured temporal dynamics, predicting bilateral weight-normalized GRFs across three axes. Low-rank bilinear fusion combined accelerometer, gyroscope, and subject parameters (mass, height). Validation used a Leave-One-Subject-Out (LOSO) cross-validation protocol. The GRF data were resampled to a uniform stride length and averaged across subjects to compute a mean profile. Evaluation metrics included MSE, RMSE, and Pearson correlation. Comparative analysis against the subject-excluded population mean employed paired t-tests and Cohen's d using RMSE and Pearson correlation.

**Table 1:** Hybrid GRU Model vs Population Mean Model

| Model | Axis | Pearson Correlation (r) | RMSE (± SD) BW |
|---|---|---|---|
| Hybrid GRU Model | Mediolateral | 0.948 ± 0.015 | 0.214 ± 0.027 |
| | Anterior-Posterior | 0.975 ± 0.007 | 0.231 ± 0.041 |
| | Vertical | 0.994 ± 0.004 | 0.484 ± 0.074 |
| P. Mean Model | Mediolateral | 0.786 ± 0.038 | 0.329 ± 0.040 |
| | Anterior-Posterior | 0.823 ± 0.028 | 0.500 ± 0.054 |
| | Vertical | 0.842 ± 0.034 | 2.293 ± 0.221 |

**Results & Discussion:** While the population mean model approximates overall force trends (average r = 0.81), it fails to capture inter-individual variability and peak loading events critical to accurate gait assessment (Fig. 1). In contrast, the GRU-based model demonstrates superior predictive power across mediolateral, anterior-posterior, and vertical axes (Table 1). Paired t-tests revealed large effect sizes (Cohen's d = 3.7–10.6) and substantial RMSE reductions (0.113–1.843 BW; 95% CI: 0.097–1.945 BW; $p < 0.0001$), underscoring the model's subject-specific accuracy. The trained model, using the SageMotion wearable system, enables continuous GRF monitoring outside laboratory settings. This framework enables individualized feedback during gait tasks, with applications in rehabilitation and performance enhancement. However, the inclusion of only healthy male participants under treadmill conditions limits the model's generalizability. Future work should explore diverse populations and overground walking to extend its clinical and practical relevance. Despite these limitations, this study establishes the GRU-driven GRF estimation framework as a robust, data-driven tool for wearable gait analysis, enabling adaptive and patient- centered applications.

**Significance:** This study demonstrates that a hybrid bidirectional GRU model reliably predicts GRFs, using commercially available wearable systems. By enabling precise, subject-specific peak-force estimations, the framework advances out-of-lab gait analysis for rehabilitation and training. The rapid deployment of the developed app addresses critical challenges in translating ML methods to clinical and natural environments, supporting feedback-based gait retraining and rehabilitation. Additionally, the presented framework and dataset provide researchers with a foundation for extending GRF estimations to dynamic activities such as running or jumping, broadening its applications in diverse populations and real-world settings.

**Acknowledgments:** This study was funded by the National Natural Science Foundation of China (Grant W2441018). Peter B. Shull is a co-founder of SageMotion, and Zach Strout is affiliated with the company.

**References:** [1] Md Sanzid Bin Hossain et al. (2023), *IEEE Journal of Biomedical and Health Informatics* 38; [2] Tan Tian et al. (2024), *IEEE Transactions on Biomedical Engineering*.

# A REAL-TIME ALGORITHM FOR DETECTING GAIT EVENTS IN LOWER-LIMB PROSTHESIS USERS USING A MARKERLESS MOTION CAPTURE SYSTEM

Liang-Wei Huang[1], Mu-Hua Wang[1], Bo-Hung Chen[1], Kai-Han Su[2], Cheng-Hung Tsai[3], You-Yin Chen[1], *Hui-Ting Shih[2]
[1]National Yang Ming Chiao Tung University, Department of Biomedical Engineering, Taiwan
[2]National Yang Ming Chiao Tung University, Department of Physical Therapy and Assistive Technology, Taiwan
[3]III Software Technology Institute, Institute for Information Industry, Taiwan
*Corresponding author's email: huiting.shih@nycu.edu.tw

**Introduction:** Markerless motion capture systems greatly reduce the time required for data collection and processing, thereby enhancing the efficiency of motion analysis [1]. Additionally, real-time gait analysis enabled by the markerless motion capture system has the potential for immediate assessment and feedback [2,3]. People with amputation typically undergo a period of physical therapy to rehabilitate and adapt to their prosthetic devices. However, amputation-related rehabilitation requires significant time and resources, posing a substantial challenge for healthcare systems [4]. The markerless system with a real-time algorithm provides opportunities for this population's recovery. Precise gait analysis is based on the accurate detection of heel strike (HS) and toe-off (TO) [5]. Previous gait detection algorithms were designed for marker-based motion capture systems and post-processing circumstances [6]. Therefore, we propose a real-time algorithm for identifying gait events in lower-limb prosthetic users, offering improved accuracy compared to existing methods.

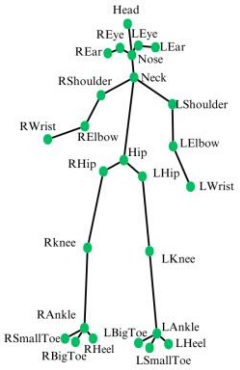


**Figure 1:** The definition of 26 key landmarks of the AI models.

$$V_{xy} = V_x \times V_y$$

$$\text{Threshold} = \frac{5 * peak\ value}{100}$$

$$\text{Slope} = \frac{2 * peak\ value}{100}$$

**Figure 2:** The formula of HS detection.

**Methods:** Four participants with unilateral lower limb amputation volunteered, including three with above-knee (AK) and one with below-knee (BK) amputations. They walked a 5-meter walkway three times at a self-selected pace surrounded by our markerless motion capture system. The system consisted of two RGB cameras (30 Hz) positioned 2.5 meters from the walkway's centerline to capture sagittal plane data. An AI model extracted 26 key landmarks per frame (Fig. 1), providing pixel-based coordinate information. All gait events were manually labeled through video annotation. We compared the HS and TO identified by previous and current methods against the manual labels and calculated the frame discrepancy.

The baseline algorithm [6] detects HS events using the local maximum of the x-coordinate difference between the pelvis and ankles, while TO events are based on the local minimum. A 4th-order low-pass filter (cutoff = 7 Hz) with a real-time window of 17 frames was applied. The coordinates of the ankles and hip were used. HS detection is based on the x and y coordinate differences of the heels to compute horizontal (Vx) and vertical (Vy) velocities, with Vxy = Vx × Vy. The peak Vxy of each gait cycle serves as a reference, and HS is detected when Vxy and its slope fall below dynamic thresholds (Fig. 2). TO detection follows the same process using small toes, identifying events when Vxy and its slope exceed set thresholds (Vxy > 5, slope > 2). A moving average filter (window = 4) reduces noise.

**Table 1.** The mean and standard deviation of frame error.

| | Non-Amputated Limb | | Amputated Limb | |
|---|---|---|---|---|
| BK 1 | HS | TO | HS | TO |
| Previous Method | 0.65±0.61 | 2.22±1.06 | 0.73±0.79 | 1.89±1.36 |
| Proposed Method | 0.65±0.70 | 0.67±0.77 | 0.93±0.88 | 0.67±0.91 |
| AK 1 | HS | TO | HS | TO |
| Previous Method | 0.44±0.53 | 1.92±0.79 | 1.75±0.75 | 1.00±1.15 |
| Proposed Method | 0.67±0.71 | 0.41±0.51 | 0.83±0.72 | 0.62±0.51 |
| AK 2 | HS | TO | HS | TO |
| Previous Method | 0.44±0.53 | 2.58±0.90 | 1.85±0.90 | 1.14±1.10 |
| Proposed Method | 0.89±0.33 | 0.25±0.45 | 1.46±1.20 | 0.43±0.65 |
| AK 3 | HS | TO | HS | TO |
| Previous Method | 0.88±0.64 | 2.43±1.51 | 1.00±0.82 | 2.56±1.59 |
| Proposed Method | 0.75±0.89 | 0.71±0.49 | 0.71±0.48 | 0.78±1.64 |

**Results & Discussion:** Experimental results (Table. 1) show that for the non-amputated limb, both our method and the previous method exhibited similar HS detection accuracy, while our method performed better in TO detection. For the amputated limb, our method consistently achieved higher accuracy in both HS and TO events. This improvement may stem from our approach, which considers both horizontal and vertical heel velocities (Vxy), capturing the moment when both approach near zero at HS. In contrast, the previous method relies on horizontal displacement between key points, which may be less reliable for abnormal gait patterns. The more accurate TO detection across both limbs suggests that TO is a more distinct event, while HS variability in the non-amputated limb may result from natural gait asymmetry. These findings highlight our method's potential for more robust gait event detection in amputee users, particularly in abnormal gait patterns.

**Significance:** The results of this study demonstrate that our real-time algorithm accurately detects gait events in prosthetic users, especially for amputated limbs. This enables precise gait training with markerless motion capture, supporting personalized rehabilitation while reducing costs.

**Acknowledgments:** Taiwan National Science and Technology Council grant 113-2221-E-A49 -015 -MY2 and 113-2321-B-A49 -016.

**References:** [1] Wade et al. (2022), PeerJ 10; [2] Vun et al. (2024), Gait & Posture 112(95-107); [3] Darter et al. (2011), Phys Ther 91(9); [4] Pasquina et al. (2015), AMA J Ethics 17(6); [5] Maqbool et al. (2017), IEEE Trans Neural Syst Rehabil Eng 25(9); [6] Vafadar et al. (2022), Gait & Posture 94(138-143).

**Utilizing Reinforcement Learning to Overcome the Challenge of Muscle Specific EMG Placements for Musculoskeletal Models**

Reilly Stafford[1*], Katherine R. Saul[1], Helen Huang[1]
[1]Department of Mechanical and Aerospace Engineering, North Carolina State University, Raleigh, NC, USA
*Email: reillystafford05@gmail.com

**Introduction:** Prosthesis control has seen two different approaches in recent years. One approach is machine learning based [1], which is powerful but is a complete black box. Another approach is model based [2-3], which has looked into utilizing electromyography (EMG)-driven musculoskeletal (MSK) models. The advantages of the latter approach include its robustness in estimating joint position [4] and its ability to unveil physiological information of the user's muscle properties. However, this approach has been challenged by the need of muscle-specific EMG recordings to drive the MSK model. Recording muscle-specific EMG signals using surface electrodes (sEMG) with minimum crosstalk can be difficult because of muscle overlap and their close proximity in the forearm [5]. Recording is more difficult on individuals with upper limb amputations who have a different muscle anatomy than an able-bodied (AB) person [6]. To overcome this challenge, this research aims to develop a novel algorithm based on reinforcement learning (RL) to predict specific muscle excitations from a ring of non-specific sEMGs to drive a MSK model for hand/wrist motion estimation and future upper limb prosthesis control.

**Methods:** Motion capture and EMG data were simultaneously collected for one AB participant performing 22 one-minute trials of wrist and metacarpophalangeal (MCP) flexion/extension. The subject provided written informed consent in accordance with North Carolina State University Institutional Review Board. EMG was acquired using a ring of 8 bipolar sEMGs around the forearm, and wrist and MCP angles were recorded using Vicon. The EMG electrodes were not aligned with specific muscles. During each trial, the participant was asked to move the joint(s) in a random pattern at varying speeds throughout the 60 seconds. After data collection, the 8 channels of EMG signal were enveloped and normalized by the maximum voluntary contraction. Trials were used for training, validation during training, and offline testing. The normalized EMG signals and joint angles informed a deep deterministic policy gradient RL algorithm that returned 4 predicted muscle actuator (flexor and extensor for each degree-of-freedom (DOF)) excitations. These excitations were used to drive the 2 DOF (wrist and MCP) MSK model. The RL agent reward tried to minimize the error between the estimated and experimentally measured angles for each joint. For one AB participant, the performance of the framework was evaluated offline with the testing data set by looking at the normalized root mean squared error (NRMSE) and the Pearson R value.

**Results & Discussion:** After performing hyperparameter tuning, the training lasted 30 episodes with a total training time of $12.90 \pm 0.26$ hours. Cross validation was done on 7 different configurations of data grouping. This resulted in a mean NRMSE of $0.11 \pm 0.01$ and R value of $0.69 \pm 0.03$. The NRMSE was comparable to a previous study ($0.15 \pm 0.04$) using similar methods [7]. The R values were a little lower than those found in the previous study ($0.88 \pm 0.07$) [7]. This is likely due to the training being stopped prematurely before convergence. Further testing will be done with allowing training to continue for more episodes and on more participants.

**Significance:** This work enables information to be gathered from specific muscles, without actually having to target that muscle through EMG placement. Implementing this will make it easier for EMG-driven MSM models to be used with amputees for control over their prosthesis. These methods can also be applied to work using EMG-driven MSK models for different purposes besides prosthetic control, and can help obtain signals from muscles that may usually be hard to capture.

**Acknowledgements:** This work was supported in part by the National Science Foundation (No. 2221479).

**References:** [1] Nuesslein et al. (2024), *IEEE RA-L* **9**(5); [2] Berman et al. (2024), *IEEE TNSRE* **32**; [3] Crouch et al. (2016), *J Biomech* **49**(16); [4] Pan et al. (2018), *IEEE TNSRE* **26**(7); [5] Farina et al. (2014), *IEEE TNSRE* **22**(4); [6] Wentink et al. (2013), *J NeuroEng and Rehab* **10**(87); [7] Berman et al. (2023), *IEEE TBME*, **70**(4).

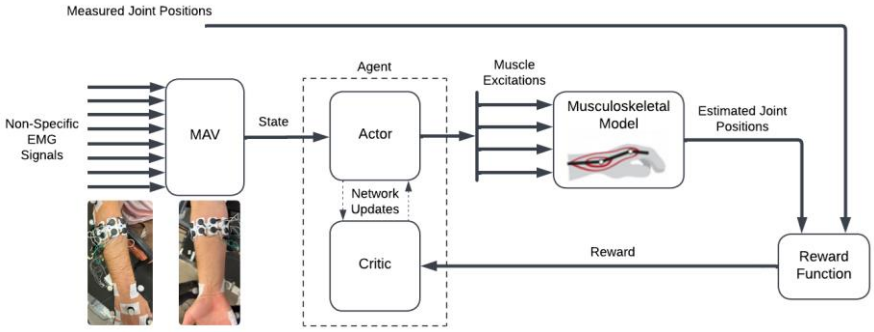


**Figure 1**: RL framework for going from a ring of 8 non-specific sEMGs to 4 predicted muscle actuator excitations, which are used to drive a 2 DOF MSK model for wrist and MCP flexion/extension

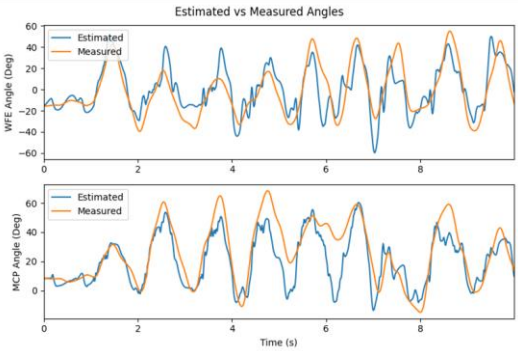


**Figure 2**: Estimated angles from RL predicted muscle actuator excitations versus experimentally measured angles for a window of testing data

# DYNAMIC MODE DECOMPOSITION IDENTIFIES DOMINANT MEDIAL COLLATORAL LIGAMENT STRAIN PATTERNS UNDER KNEE LOADINGS

*William G. Gamble[1], Michael DiNenna[1], Armin Runer[2,3], Anja Wackerle[2,3], Michael P. Smolinski[1], Mark C. Miller[1], Volker Musahl[3], Patrick J. Smolinski[1]

[1]Department of Mechanical Engineering and Material Science, University of Pittsburgh, Pittsburgh, PA, USA

[2]Department for Orthopaedic Sports Medicine, Klinikum rechts der Isar, Technical University of Munich, Munich, Germany

[3]Department of Orthopaedic Surgery, University of Pittsburgh, Pittsburgh, PA, USA

*wig14@pitt.edu

**Introduction:** Knowledge of ligament loading is fundamental to the understanding joint function, injury mechanisms and improving tissue reconstructions. Strain in the tissue, a measure of tissue loading, under different knee kinematics has been studied to determine medial collateral ligament (MCL) ligament function [1]-[4]. No studies have measured the strain distributions in the MCL under relevant and controlled knee loads. In this study the strain fields were measured in the MCL under valgus and external tibial torques using digital image correlation (DIC). Dynamic mode decomposition (DMD) was used to assess the predominant pattern of the strains for the loadings over all flexion angles.

**Methods:** Institutional approval (Corid 1186) was given to use a robotic system to measure the kinematics of nine (N=9) left, fresh frozen cadaveric knees. The kinematics of the non-dissected knees were measured under a 5 N-m external rotational (ER) and a 7 N-m valgus rotational (Val) tibial loads at 0, 15, 30, 45, 60, 75 and 90 degrees of flexion. The knees were then dissected to expose the MCL (sMCL), and the ligament was colored and speckled with ink. The kinematics of the non-dissected knee under loading was imposed on the dissected knee while recording a video of the MCL. From the video, digital image correlation (VIC3D, Correlated Solutions Inc.) was then used to track deformation and calculate the strains in the ligament. Strains from the specimens were converted to a common file format and any missing data was interpolated. Then the strain data from the specimens was averaged at each flexion angle for the different loads. Computational dynamic mode decomposition (DMD) was applied to the data to find the underlying common patterns (modes) of strain among all the flexion angles. The modes were calculated based on the representation of 95% of the energy of the data [5]. Note that the contour plots of the strain at each flexion angle are mapped to a single idealized geometry of the ligament at 0° of knee flexion.

**Results & Discussion:** Figure 1 shows the mean longitudinal (long axis of ligament) normal strain distribution as a function of flexion angle for ER load and DMD analysis yields a single mode for the loading.

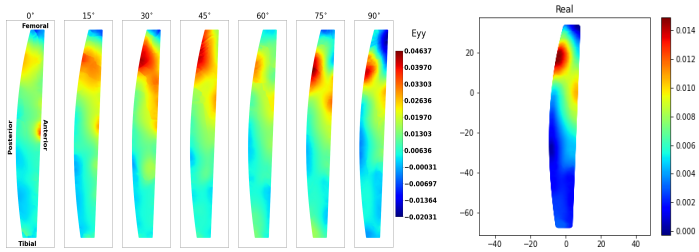


**Figure 1:** Mean experimental longitudinal strains in the sMCL by flexion angle (left) and DMD mode shape, 95% energy, (right) for external rotational torque.

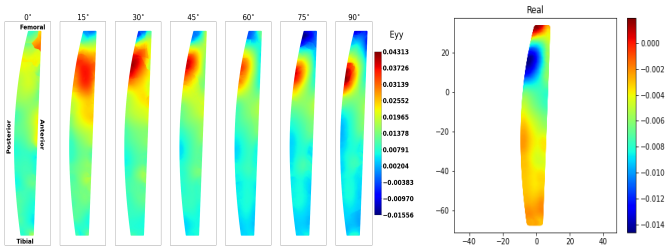


**Figure 2:** Mean experimental longitudinal strains in the sMCL by flexion angle (left) and DMD mode shape, 95% energy, (right) for valgus rotational moment.

Figure 2 shows the mean longitudinal strain contours as a function of flexion angle for the valgus load and gives single DMD mode for the loading.

DMD analysis resulted in one mode shape for each of the loadings based on representation of 95% of the energy. For external rotation, the peak strain was 0.046 at the posterior edge under the femoral insertion and for valgus loading the peak strain was 0.043 nearer the posterior femoral insertion. This is similar to other studies that found peak longitudinal strains near the femoral insertion.

**Significance:** The main finding of this study is that a single pattern was sufficient to describe longitudinal strain in the ligament at all flexion angles. This is true for both the valgus and external rotational moments. That is, the pattern of strain in the ligament induced by the loading was essentially the same at all flexion angles (0-90°) for each load. It is noted that the strain field was more complex at the femoral insertion (near the posterior oblique ligament) and become more uniform away from this region.

The main clinical finding of this study is that the longitudinal strain patterns in the sMCL due to internal or valgus loading do not change with knee flexion. This data will provide information on the function of the sMCL under different knee loadings at different flexion angles and provide benchmark data for evaluating sMCL reconstructions.

**References:** [1] Bates, *AJSM*, 2017, [2] Schilaty, *AJSM,* 2018, [3] Lujan, *AJSM*, 2007, [4] Lim, *KSSTA*, 2022, [5] Badoo, *Proc Royal Soc*, 2023

**Clustering IMU data of patients with spinal sagittal imbalance using machine learning**

Sadegh Madadi[1], Mostafa Rostami [*1], Hadi Farahani [2], Farshad Nikouee [3], Mohammad Samadian [4], Ram Haddas [5]
[1] Amirkabir University of Technology, Faculty of Biomedical Engineering, Tehran, Iran
[2] Shahid Beheshti University, Department of Computer and Data Sciences- Faculty of Mathematical Sciences, Tehran, Iran
[3] Iran University of Medical Sciences, Bone and Joint Reconstruction Research Center- Shafa Orthopedic Hospital, Tehran, Iran
[4] Shahid Beheshti University of Medical Sciences, Department of Neurosurgery, Tehran, Iran
[5] Texas Back Institute, University of Rochester Medical Center, NY, USA
*Corresponding author's email: rostami@aut.ac.ir

**Introduction:** The diagnosis and treatment of spinal pathologies require a comprehensive assessment by a healthcare professional, such as a physician, orthopedic surgeon, or neurologist. The latter is sometimes difficult to detect and can affect the vertebrae and change their mechanical properties, which may lead to deformation [1–3]. Patient's motions and gaits can now be measured with an IMU sensor without regard to physical space because of recent advancements in sensor technology [4], Gait assessment and study of movement disorders [5–7]. Most joint studies between ML methods and gait data obtained from IMU attempt to use algorithms to reduce a large set of primitive features to clinically relevant gait variables [8–9]. In this study, a hypothesis has been investigated using IMU to cluster the walking data of patients with the control group with the help of machine learning models.

**Research Question:** Can unsupervised clustering techniques effectively segment inertial measurement unit (IMU) data from patients with sagittal spine imbalance, and how do different clustering algorithms compare in terms of accuracy and interpretability?

**Methods:** Table 1 shows unsupervised learning models, including Agnes, Birch, Clara, Cure, and K-means. These unsupervised learning models have achieved an accuracy of more than 87%, and the cure model has achieved an accuracy of over 96% in all separate data. This emphasizes their potential suitability for the clustering of movement data from SSI patients and the detailed analysis of the dataset. Right Shank Data has the highest accuracy of all models.

**Results:** Table 1 shows the unsupervised learning models, including Agnes, Birch, Clara, Cure, and K-means. These unsupervised learning models were able to accurately predict more than 80% of postsurgical outcomes. This accuracy is obtained by comparing the outputs of unsupervised models with the clinical outputs and supervised models that have been calculated previously. The cure model has more accurate results compared to other models and can indicate the strength of this model for the data of SSI patients.

**Discussion:** The consistently high accuracy of data across all evaluated unsupervised learning models, including Agnes, Birch, Clara, Cure, and K-means, and the remarkably high 96% accuracy of the cure model across all input data, demonstrate its potential importance in clustering and Effective analysis of movement data obtained from SSI shows a positive clustering trend for data from SSI patients. Therefore, the CURE model offers promising ways to accurately analyze and generate insights in the monitoring and evaluation of SSI patient treatment. These results emphasize the importance of applying advanced unsupervised learning techniques for clustering and accurate interpretation of movement data, especially in the context of clinical applications such as SSI patient evaluation.

**. Table1. Output of clustering accuracy and class validation of gait data of SSI patients and control group**

| Dataset | Models | | | | |
|---|---|---|---|---|---|
| | Agnes | Birch | Clara | Cure | K-means |
| Pelvic | 96% | 96% | 96% | 99% | 96% |
| Left Thigh | 97% | 94% | 97% | 96% | 97% |
| Right Thigh | 98% | 80% | 84% | 99% | 97% |
| Left Shank | 97% | 94% | 94% | 99% | 97% |
| Right Shank | 99% | 99% | 99% | 99% | 99% |
| Left Foot | 98% | 99% | 99% | 98% | 98% |
| Right Foot | 87% | 90% | 88% | 97% | 91% |

**Reference**

1. Netter, F. H. (1974). Atlas of Human Anatomy. http://ci.nii.ac. Jp/ncid/BB15336618.
2. Panjabi, M. M., & White, A. A. (1980). Basic biomechanics of the spine. Neurosurgery, 7(1), 76–93.
3. Roaf, R. (1960). A STUDY OF THE MECHANICS OF SPINAL INJURIES. The Journal of Bone and Joint Surgery, 42-B(4), 810–823.
4. Prasanth, H., Caban, M., Keller, U., Courtine, G., Ijspeert, A. J., Vallery, H., & Von Zitzewitz, J. (2021b). Wearable SensorBased Real-Time GAIT Detection: A Systematic Review. Sensors, 21(8), 2727.
5. Mannini, A., Intille, S., Rosenberger, M. E., Sabatini, A., & Haskell, W. L. (2013). Activity recognition using a single accelerometer placed at the wrist or ankle. Medicine and Science in Sports and Exercise, 45(11), 2193–2203.
6. Bonomi, A. (2010). Physical activity recognition using a wearable accelerometer. In Philips Research (pp. 41–51).
7. Twomey, N., Diethe, T., Fafoutis, X., Elsts, A., McConville, R., Flach, P. A., & Craddock, I. (2018). A comprehensive study of activity recognition using accelerometers. Informatics (Basel), 5(2),
8. Hayashi, H., Toribatake, Y., Murakami, H., Yoneyama, T., Watanabe, T., & Tsuchiya, H. (2015). GAIT analysis using a support vector machine for lumbar spinal stenosis. Orthopedics, 38(11).
9. Galarraga, A. C. O., Vigneron, V., Dorizzi, B., Khouri, N., & Desailly, E. ´ (2017). Predicting postoperative gait in cerebral palsy. Gait & Posture, 52, 45–51.

**Using imu data and unsupervised learning to predict outcomes in spinal sagittal imbalance surgery**

Sadegh Madadi[1], Mostafa Rostami [*1], Hadi Farahani [2], Farshad Nikouee [3], Mohammad Samadian [4], Ram Haddas [5]
[1] Amirkabir University of Technology, Faculty of Biomedical Engineering, Tehran, Iran
[2] Shahid Beheshti University, Department of Computer and Data Sciences- Faculty of Mathematical Sciences, Tehran, Iran
[3] Iran University of Medical Sciences, Bone and Joint Reconstruction Research Center- Shafa Orthopedic Hospital, Tehran, Iran
[4] Shahid Beheshti University of Medical Sciences, Department of Neurosurgery, Tehran, Iran
[5] Texas Back Institute, University of Rochester Medical Center, NY, USA
*Corresponding author's email: rostami@aut.ac.ir

**Introduction:** A complex condition known as spinal sagittal imbalance (SSI) results in back pain, nerve involvement, and a markedly worsened quality of life for the patient. Although there are numerous causes of SSI, most of them lead to the spine bending forward [1-3].It's challenging to identify, classify, and diagnose any of these symptomatic diseases. Sensors are one of the devices that may measure walking and movements; walking has9 been evaluated using quantitative approaches [4–5]. IMU sensor technology enables the use of sensor devices to measure the movements of both healthy and patient groups without regard to spatial constraints [6].According to preoperative kinematics, physical examination, and postoperative surgical data, prior research used machine learning (ML) and postoperative lower limb kinematics to gather data that may be helpful for the patient as well as the examiner [7].

**Research Question:** Can unsupervised models predict outcomes after sagittal imbalance of the spine surgery?

**Methods:** The data for this study was obtained using a 9-axis IMU system with a MyoMotion sensor (Noraxon USA Inc., Scottsdale, USA) capable of recording movement patterns with a frequency of 100 Hz. There are 50 participants in the patient group, aged 58 ± 8.94, who have been diagnosed with SSI) and 50 participants in the control group, aged 41 ± 1.48, who have never had surgery or movement abnormalities. Every participant was able to move, did not take any neuropsychiatric medications, and had a healthy visual system. Additionally, for the patient group to be included in the study, the sagittal vertical axis (SVA) measurement needed to be greater than 5 cm

**Results:** Table 1 shows the unsupervised learning models, including Agnes, Birch, Clara, Cure, and K-means. These unsupervised learning models were able to accurately predict more than 80% of postsurgical outcomes. This accuracy is obtained by comparing the outputs of unsupervised models with the clinical outputs and supervised models that have been calculated previously. The cure model has more accurate results compared to other models and can indicate the strength of this model for the data of SSI patients.

**Discussion:** The evaluation of unsupervised learning models, such as Agnes, Birch, Clara, Cure, and K-means, against clinical outcomes demonstrates their remarkable accuracy in predicting postoperative outcomes, consistently exceeding 80%. The findings underscore the potential of these unsupervised methods for effectively clustering motion data from SSI patients and conducting in-depth analyses of post-surgery datasets. As such, integrating these models into clinical practice could offer valuable insights for optimizing patient care and surgical outcomes in the field of orthopaedics.

**Table 1: Output of clustering accuracy and class validation of gait data for post-surgery**

| Dataset | Models | | | | |
|---|---|---|---|---|---|
| | Agnes | Birch | Clara | Cure | K-means |
| Pelvic | 88% | 88% | 88% | 90% | 88% |
| Left Thigh | 80% | 80% | 80% | 80% | 80% |
| Right Thigh | 82% | 80% | 80% | 84% | 80% |
| Left Shank | 86% | 86% | 80% | 86% | 86% |
| Right Shank | 84% | 84% | 84% | 80%% | 84% |
| Left Foot | 80% | 80% | 80% | 86 | 80% |
| Right Foot | 80% | 80% | 80% | 86% | 80% |

**Reference**

1. Booth, K. C., Bridwell, K. H., Lenke, L. G., Baldus, C., & Blanke, K. (1999). Complications and predictive factors for the successful treatment of flatback deformity (Fixed sagittal imbalance). Spine, 24(16), 1712.
2. Casey, M. P., Asher, M. A., Jacobs, R. R., & Orrick, J. M. (1987). The effect of Harrington rod contouring on lumbar lordosis. Spine, 12(8), 750–753.
3. Farcy, J. C., & Schwab, F. J. (1997). Management of flatback and related kyphotic decompensation syndromes. Spine, 22 (20), 2452–2457.
4. MacWilliams, B. A., Rozumalski, A., Swanson, A. N., Wervey, R., Dykes, D. C., Novacheck, T. F., & Schwartz, M. H. (2014). Three-Dimensional lumbar 14 spine vertebral motion during running using indwelling bone pins. Spine, 39(26), E1560– E1565.
5. Yagi, M., Kaneko, S., Yato, Y., Asazuma, T., & Machida, M. (2016). Walking sagittal balance correction by pedicle subtraction osteotomy in adults with fxed sagittal imbalance. European Spine Journal, 25(8), 2488–2496.
6. Prasanth, H., Caban, M., Keller, U., Courtine, G., Ijspeert, A. J., Vallery, H., & Von Zitzewitz, J. (2021). Wearable Sensor-Based Real-Time GAIT Detection: A Systematic Review. Sensors, 21 (8), 2727.
7. Reches, T., Dagan, M., Herman, T., Gazit, E., Gouskova, N., Giladi, N., Manor, B., & Hausdorff, J. M. (2020). Using Wearable Sensors and ML to Automatically Detect Freezing of Gait during a FOG-Provoking Test. Sensors, 20(16), 4474.

# VIDEOS CAPTURE FUNCTIONAL STRENGTH DEFICITS FOLLOWING ACL RECONSTRUCTION

*Zhixiong Li[1], Chaeeun Lee[1], Kunwoo Lee[1], Evy Meinders[1], Andrew L Sprague[2], James J Irrgang[2], Volker Musahl[2], Eni Halilaj[1]
[1]Carnegie Mellon University, Pittsburgh, PA, USA [2]University of Pittsburgh, Pittsburgh, PA, USA
*Corresponding author's email: zhixionl@andrew.cmu.edu

**Introduction**: Video-based markerless motion tracking is demonstrating ever-improving accuracy in estimation of three-dimensional (3D) kinematics and kinetics [1-3], yet its clinical impact remains underexplored. The hope is that these passively collected biomechanical outcomes will replace time-consuming laboratory and clinical tools, possibly helping scale up gait analysis and guiding rehabilitation therapies toward a higher level of personalization than previously possible. Accordingly, the primary goal of this study was to determine if kinematic and kinetic inter-limb asymmetries derived from passively collected video data can act as a surrogate for clinical strength-test outcomes in patients following anterior cruciate ligament reconstruction (ACLR). A secondary goal was to provide insight into whether these video-based biomechanical outcomes match kinematic and kinetic outcomes estimated in a gait laboratory equipped with marker-based motion capture and force-plate systems.

**Methods:** Following approval from the Institutional Review Boards of the University of Pittsburgh and informed consent, we collected data from 20 participants (15F, 5M; mean age: 24.2±8.1 yrs) at three months post ACLR. In a clinical setting, each participant performed at least three repetitions of a lateral step-down exercise with each leg, while motion was captured with six RGB cameras (Sony RX0 II, Sony, Minato, Japan). We used OpenCap [2] with two of these cameras positioned at approximately 45° of each other to estimate kinematics and kinetics. OpenCap uses muscle-driven dynamic optimization to estimate kinetics without force-plate data. Derived outcomes were hip, knee, and ankle range-of-motion (ROM) and peak-moment asymmetry. Isometric strength tests were performed using an electromechanical dynamometer (Biodex Medical Inc., Shirley, NY) and a hand-held dynamometer (Lafayette Instrument, Lafayette, IN) to record peak knee flexion and extension torque, and peak hip abduction, extension, and external rotation force, respectively. To test the primary hypothesis that video data captures functional strength-test outcomes, we used canonical correlation analysis (CCA), finding a linear combination of video-based outcomes (Video Index) that was highly correlated with a linear combination of strength-test outcomes (Strength Index). We tested this relationship on left out data, using a leave-one-out pre-validation approach. Participants were also monitored in a gait laboratory using infrared and RGB cameras (OptiTrack, Corvallis, OR), along with force plates (Bertec, Columbus, OH). Marker-based motion capture and force-plate data were used to compute ground-truth kinematics and kinetics. To test the second hypothesis that video-based inter-limb asymmetries are accurate compared to ground-truth outcomes, we used a pairwise Wilcoxon signed-rank test.

**Results & Discussion:** CCA identified a Video Index and a Strength Index that were highly correlated ($r=0.85$, $p < 0.0001$) on left out data (Fig. 1A). Knee flexion ROM and peak-moment asymmetries, as well as hip kinematic and kinetic asymmetries in secondary degrees of freedom (i.e., ab/adduction and int./ext. rotation) were most affective of the Video Index (Fig. 1B). Interestingly, analogous strength-testing outcomes (i.e., knee flexion/extension and hip abduction and external rotation) were most affective of the Strength Index (Fig. 1B). Laboratory experiments confirmed that video-based motion capture detects inter-limb asymmetries with comparable sensitivity to marker-based motion capture across many degrees of freedom (Fig. 2). Hip ab/adduction ROM and peak-moment asymmetry, as well as peak hip external/internal rotation moment asymmetry were underestimated by video-based compared to ground truth analyses. Nevertheless, given the use of dynamic optimization, without force plate data, these accuracies are encouraging—giving rise to a set of outcomes that collectively represent strength-test performance exceptionally well (Fig, 1A). As markerless tracking continues to improve, entirely passive evaluation of patient recovery is an exciting direction, modernizing research and clinical practice.

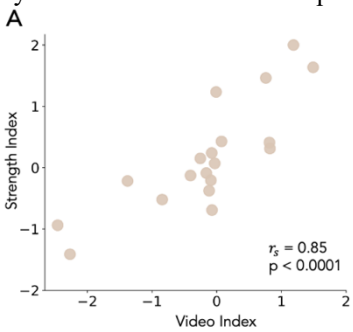


B

| Video Index | Loading | p-value |
|---|---|---|
| Knee flex/ext ROM | 1.00 | p < 0.0001 |
| Knee flex/ext moment | 0.91 | p < 0.0001 |
| Hip ab/add ROM | 0.74 | p = 0.0003 |
| Hip int/ext rotation moment | 0.57 | p = 0.0117 |
| Hip int/ext rotation ROM | -0.49 | p = 0.0328 |
| **Strength Index** | | |
| Hip abduction | 0.92 | p < 0.0001 |
| Knee extension | 0.87 | p < 0.0001 |
| Hip external rotation | 0.41 | p = 0.0016 |
| Knee flexion | 0.58 | p = 0.0087 |

**Figure 1: CCA Analysis.** (A) A Video Index is highly correlated with a Strength Index derived from traditional strength-testing clinical tools. (B) Knee flexion/extension and secondary degree of freedom in the hip are salient features capturing inter-limb asymmetries in each approach. Non-significant variables are not listed here.

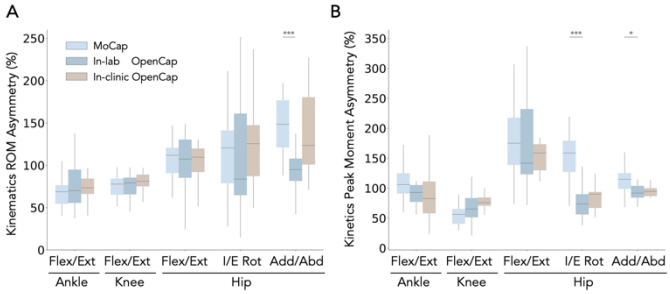


**Figure 2: Video-Based Outcome Accuracy.** (A) Kinematic and (B) kinetic outcomes from videos generally match the accuracy of laboratory tools, with few exceptions (*p<0.005; ***p<0.0001).

**Significance:** Current easy-to-use open-source tools for video-based analysis reliably capture clinically meaningful outcomes, offering the promise of more frequent patient status assessment at home or in high-volume clinics not equipped for frequent strength testing. Such assessments would make personalized rehabilitation more accessible than ever before and possibly improve long-term outcomes.

**Acknowledgements:** This project has been funded by the NIH (R01AR080310), Chan Zuckerberg Initiative, and NSF (CBET 2145473). We thank Bryan Galvin, Alec Howard, as well as Drs. Hughes, Rabuck, and Lesniak, for their support with recruitment.

**References:** [1] Shin et al., *IEEE TBME* 2023; [2] Ulrich et al., *PLOS Com Bio*, 2023; [3] Song et al., *J Biomech* 2023

# UPPER EXTREMITY VIRTUAL REALITY MOTION CAPTURE USING MACHINE LEARNING

*Skyler A. Barclay[1], Trent Brown[1], Tessa M. Hill[2], Allison L. Kinney[1], Timothy Reissman[1], Ann Smith[2], Megan E. Reissman[1]
[1]University of Dayton, Dayton, OH, USA
[2]Dayton Children's Hospital, Dayton, OH, USA
*Corresponding author's email: millers53@udayton.edu

**Introduction:** Virtual reality (VR) has become popular in biomechanical research due to its ability to present clear and customizable tasks, with a majority of metrics including spatiotemporal, visual, or pre- and post- VR intervention outcomes [1]. Camera based infrared (IR) motion capture has been typically included when collecting full kinematic data during such interventions. However, the high cost and lack of portability do not make it very feasible to clinics that may want adopt VR therapy. Vive trackers (HTC Cooperation, Taiwan) allow for integrated IMU wearables and VR therapy at a lower price and space capacity [2]. Prior human subject research is limited and has looked at positional error of the tracker rather than joint angle error with an exception that found a joint angle RMSE of ±6° and ±42° [2]. Due to the large error values in the prior research, our current VR motion capture system uses information from the IR motion capture to build the joint segment model. This approach allows us to find the error of the tracker itself, independent from any joint segment model discrepancies. Aim 1 for this study is to compare the tracking capabilities of our VR motion capture system to the industry standard of IR motion capture. Since aim 1 will require IR motion capture at every collection, aim 2 is to then output kinematics from the raw VR motion capture data using a Bidirectional Long-Short-Term-Memory (BLSTM) Machine Learning algorithm trained with joint kinematics calculated from the IR motion capture system and quantify the prediction error.

**Methods:** Healthy controls as well as people with a variety of movement impairments (spinal cord injury, post-traumatic brain injury, cerebral palsy, and multiple sclerosis) participated in this study (21 participants, overall, 29 data collections, 14 male and 7 female, aged 31.65±13.72 years). For all collections, IR and VR motion capture of the upper extremity was collected simultaneously at 240 Hz while participants played customized levels in a commercially available VR game, *Beat Saber* (Beat Games, Czech Republic). The participants were instructed to slice through the virtual blocks with a saber in the directed position and orientation with the correct arm. IR and VR data was collected in Nexus 2 (Vicon Industries, Hauppauge, NY) and Brekel Open VR respectively. Once the data was spatially and temporally aligned, Visual 3D (HAS-motion Inc., Ontario, CA) was used for all joint kinematic calculations. In Visual 3D, the IR joint segment model was defined using traditional techniques, while the VR joint segment model was defined by the IR markers and tracked using the VR markers. The average error between the VR and IR systems was calculated for the shoulder, elbow, and wrist joint kinematics. To determine if shoulder, elbow, and wrist joint kinematics can be predicted using raw VR motion capture data, from Brekel, a subject specific BLSTM algorithm was trained in Python (Python Software Foundation, Wilmington, DE) for 3 subjects on IR joint kinematics from the first visit with 100 lookback time steps in each direction and tested on the subjects' second visit data.

**Table 1:** Average Error (Mean ± Standard Deviation) for Each Joint Angle

| | Direct Measurement Error (VR-IR) | | BLSTM Prediction Error (Pred – Actual) | |
|---|---|---|---|---|
| **Average Error** | **Left** | **Right** | **Left** | **Right** |
| Elbow | 0.17°±6.0° | 0.12°±6.1° | -0.31°±6.9° | -0.21°±9.3° |
| Shoulder Elevation | 2.30°±4.3° | 1.49°±4.3° | 0.35°±3.9° | 0.29°±5.0° |
| Horizontal Abduction | -1.67°±7.4° | 0.47°±7.3° | -0.12°±6.9° | 0.13°±8.4° |
| Sagittal Wrist | -0.68°±7.6° | -0.05°±7.0° | -0.07°±11.6° | -0.13°±9.7° |
| Frontal Wrist | -2.32°±6.7° | -3.82°±6.6° | -0.04°±7.47° | 0.02°±7.1° |

**Results & Discussion:** For both aims, error values were found for left and right sides separately, due to the significant difference between sides. Error is also given as a raw value, this does not take into account the differing ranges of motion for a given joint. All direct measurement errors between the VR and IR skeletal models were within ±8° (Table 1). Frontal wrist angle had the largest error, most likely due the hand being tracked by the controller, instead of a tracker on the actual hand segment. BLSTM results found that all errors were within ±10° (Table 1), showing slightly larger results compared to the direct measurement error (VR-IR). Sagittal wrist had a slightly larger standard deviation for the left side, most likely due to the controller tracking the hand. The predicted BLSTM data followed very closely to the actual data (joint kinematics from IR skeletal model), with smoother curves compared to some of the higher frequency parts of the data. However, there was a bias error in some of the joints, so the average of each plot was subtracted to evaluate the accuracy of range of motion. The bias shift can be corrected in the future by collecting known joint angle poses (0°, 90°, 180°). Additional filtering and hyperparameter tuning, such as epochs and lookback values, is likely to decrease the standard deviation.

**Significance:** The VR and IR motion capture system comparisons showed that the Vive trackers can accurately track body segments. The BLSTM results were within a similar accuracy to the VR motion capture skeletal model but still have additional options that could decrease the error. This means one baseline IR capture could make it possible for clinics to predict upper extremity joint kinematics of a patient during these customizable *Beat Saber* therapy games, and possibly other motions, with only the VR equipment, Brekel, and Python. The diverse cohort allows these results to be translated into more clinical applications. Additionally, the use of VR therapy allows for individualized and fun therapies with quantitative results to track progress.

**Acknowledgments:** This material is based upon work supported by the National Science Foundation Graduate Research Fellowship under Grant No. 1946084. We acknowledge the funding support that was granted by the Chancellor of the Ohio Department of Higher Education from the Research Incentive Third Frontier Fund.

**References:** [1] Shahmoradi et al. (2021), J Bodyw Mov Ther 26; [2] Vox et al. (2021), Sensors 21(9)

**Video-based analysis for estimating knee impact angle during a fall using pose-estimation**

Reese P. Michaels, Yaejin Moon
Syracuse University
Corresponding author's email: yamoon@syr.edu

**Introduction:** Falls are a prevalent incident and a leading cause of accidental death among elderly individuals [1]. A practical method of reducing severe fall-related injuries is employing protective movement responses prior to impact [2,3]. Of particular interest is the extent to which a person flexes their knee during a fall (i.e., knee joint angle), a key component of protective responses [2-4]. However, the knee kinematics of falling have not been thoroughly investigated due to safety concerns associated with fall experiments and technological limitations, like marker occlusions during the fall. An alternate approach to evaluate fall biomechanics is to analyze video footage of falls [3] through the manual annotation of body landmarks in each frame [5], a process that is both time- and labor-intensive. To streamline the annotation process, the recent development of AI-based pose estimation models presents a promising tool to automatically detect and track the position of human body parts, allowing for efficient extractions of movement kinematics from video. Here, we evaluated the accuracy of the 3D pose tool *WHAM* in estimating the knee impact angle of video-captured older adult falls.

**Methods:** We analysed a secondary dataset containing 122 videos, recorded at 30Hz, of 13 older adults (10 male, age = 64.0 ± 5.9 years) falling sideways in an experimental setting [4]. In the original study, participants were instructed to fall naturally, later classified as "stick-like" and "knee block", and for select trials to employ a "tuck and roll" falling strategy (Fig. 1A) [4]. The video data was accompanied by synchronous motion capture (VICON) data, which served as the ground truth measurement. WHAM was applied to each video to spatiotemporally detect 2D key points of the hip, knee, and ankle for each leg, then reconstruct 3D global joint coordinates to align with the original video pixels [6]. Then, using the joint coordinates, a custom Python script calculated the knee flexion angle at impact with the ground for the impacted leg (i.e., leg on the falling side). To measure agreement between the gold standard measurement (truth value) and WHAM (estimated value), we assessed three validation metrics: 1) mean absolute error (i.e., MAE = |WHAM – Gold Standard|), 2) mean absolute percentage error (i.e., $\frac{Error}{Gold\ Standard\ Measure} \times 100\%$), and 3) bias (i.e., mean of error = WHAM – Gold Standard). Additionally, Pearson's correlation analyses were performed to determine associations between reference measurements and WHAM estimations for the knee impact angle. We also examined the discriminative validity of WHAM (i.e., ability to characterize differences in knee impact angle between fall strategies) by comparing its estimations to reference measurements via separate one-way ANOVAs with Bonferroni post-hoc tests (SPSS v27).

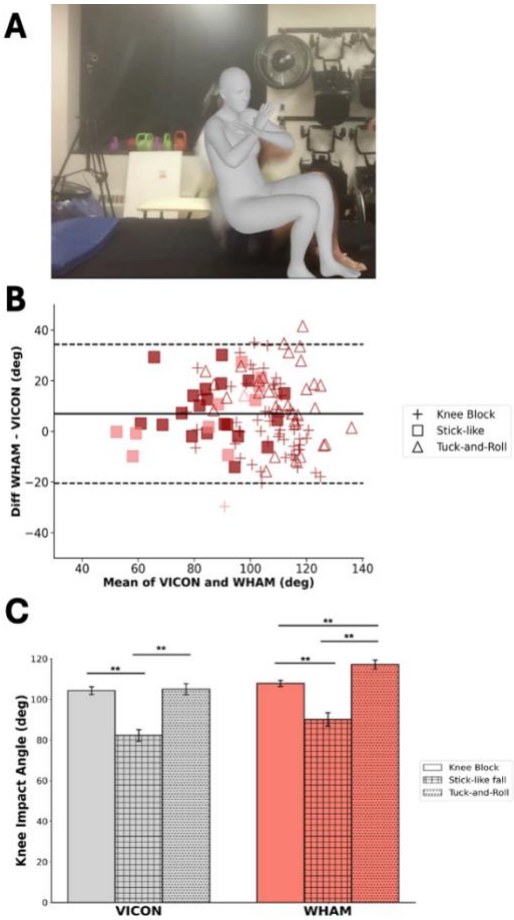


Figure 1. A) Example video frames overlaid with 3D joint reconstruction from WHAM showing a tuck and roll fall; B) a Bland-Altman plot of the knee impact angle of VICON (truth value) vs. WHAM (estimated); C) a bar plot comparing the mean knee impact angle of three fall strategies between VICON

**Results & Discussion:** Overall, the knee impact angle measured by WHAM had acceptable agreement with the reference standard (MAE: 12.43 ± 9.49°, 13.37 ± 11.44%) with minimum bias (6.95°, 8.41%; Fig. 1B). There was also a moderate correlation between the ground truth measurement and WHAM estimates of knee impact angle ($r=0.67$, $p<0.01$). WHAM accurately characterized the knee angle during stick-like falls, showing that the stick-like fall strategy resulted in significantly less knee flexion compared to the other two strategies (p's < 0.01). This observation was consistent with the reference measurements (p's < 0.01). However, WHAM overestimated the knee angle during the tuck-and-roll strategy. Specifically, WHAM indicated significantly greater knee flexion during the tuck-and-roll strategy compared to the knee block strategy ($p < 0.01$; Fig. 1C), whereas the reference measurements showed no significant difference in knee angle between the two strategies ($p = 1.00$).

**Significance:** This is the first study to apply a pose estimation model, WHAM, for estimating the knee kinematics of a fall. WHAM is capable of accurately estimating knee impact angle, a key factor in the protective movement response [2-4]. Further study is warranted to improve the discriminative capabilities of WHAM to accurately characterize movement profiles during descent, especially in cases of backward body rotation near impact. These results support the use of the 3D pose model for video-captured fall analysis, which will eventually enable the extraction of key biomechanical features from real-life fall videos.

**References:** [1] Centers for Disease Control and Prevention (2020); [2] Moon & Sosnoff (2017), *Arch Phys Med Rehabil*. 98(783-794); [3] Robinovitch et al. (2022), *Age and Ageing* 51(12); [4] Moon et al (2019), *J of Biomechanics* 83(291-297); [5] Choi et al. (2015), *J of Biomechanics* 48(911-920); [6] Shin et al (2024), *IEEE/CVF Conference* pp. (2070-2080).

# IDENTIFYING THE OPTIMAL NUMBER AND LOCATION OF IMU SENSORS TO CLASSIFY OLDER ADULTS AT HIGH RISK OF A FALL WHILE WALKING

Junwoo Park[1], Kitaek Lim[1], Seyoung Lee[1], Jongwon Choi[1], *Woochol Joseph Choi[1]
[1]Injury Prevention and Biomechanics Laboratory, Department of Physical Therapy, Yonsei University, South Korea
*Corresponding author's email: wcjchoi@yonsei.ac.kr

**Introduction:** IMU sensor data during gait have been used to determine fall risk in older adults [1]. However, no one suggested the optimal number and location of sensors to meet accuracy and practicality. We evaluated classification performance with IMU sensor data acquired from body segments while walking, in order to identify the best combinations of the number and location of sensors that maximize classifying performance on fall risk.

**Methods:** Ninety-three community-dwelling older adults (19 males, 74 females) participated. We measured participants' fall risk scores using a short-form physiological profile assessment (PPA). We then grouped them into "low risk" if a score was within the age-specific normal range or "high risk" if it was greater than the upper limit of the range (Figure 1) [2]. Then, we placed IMU sensors (Xsens Dot, Xsens Technologies, Enschede, The Netherlands) on the participants' head, waist, upper arms, lower arms, upper legs, and lower legs (a total of 10 sensors). They then walked straight 10 meters at a self-selected speed.

A total of 654 gait cycles (303 from high risk, 351 from low risk) were acquired across all subjects, and the mean and variance of linear acceleration and angular velocity of IMU sensor data were extracted from each gait cycle, to be used as input features. For machine learning, we identified features that were statistically different between high and low fall risk groups, using an independent t-test, and normalized them to a range of 0 to 1 [3]. To identify the optimal number and location of sensors, we evaluated the classification accuracy with support vector machine (SVM), decision tree (DT), and random forest (RF). All data analyses were conducted using a customized Matlab routine (Matlab R2024a, Mathworks, Natick, MA, USA).

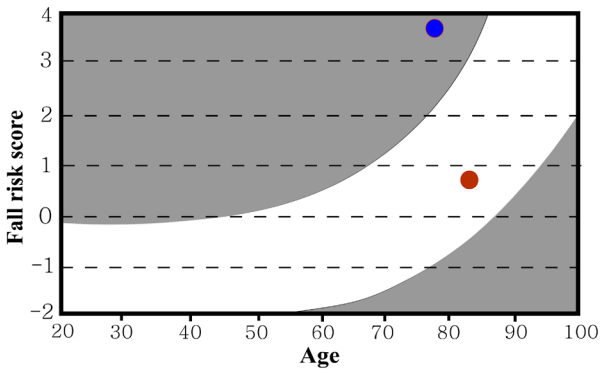


**Figure 1:** PPA scores along with the age-specific normal range (white band), which were used to determine participant's fall risk, high (blue dot) or low (red dot).

**Results & Discussion:** Among 93 older adults, 42 (6 males, 36 females) were classified as high risk, and 51 (13 males, 38 females) as low risk. With 10 sensors, the best-performing classifier was SVM (99.8% accuracy), followed by RF (99.1% accuracy) and DT (89% accuracy). With a single sensor, the accuracy varied from 62.5% (head) to 91.7% (right lower leg) for SVM, 61.9% (head) to 84% (left lower leg) for DT, and 63.8% (head) to 89.5% (left lower leg, left upper arm) for RF. With multiple sensors, the accuracy varied depending on how they combined: SVM (70.5% to 99.3%), DT (81.1% to 89%), and RF (90.9% to 98.7%). For a given number of sensors, the sensor combination that led to the highest accuracy has been provided in Table 1.

| # of sensors | Sensor Combination | Model | Accuracy (%) |
|---|---|---|---|
| 1 | LLL | SVM | 91.7 |
| 2 | LLL, RLL | RF | 96.0 |
| 3 | LUA, LUL, LLL | RF | 97.4 |
| 4 | RUA, LLL, RUL, RLL | RF | 98.3 |
| 5 | LUA, RUA, LUL, LLL, RLL | RF | 99.2 |
| 6 | LUA, LLA, RUA, LUL, LLL, RLL | RF | 99.1 |
| 7 | LUA, LLA, RUA, LLL, RUL, RLL, W | SVM | 99.2 |
| 8 | LUA, LLA, RUA, RLA, LLL, RUL, W, H | SVM | 99.5 |
| 9 | LUA, LLA, RUA, LUL, LLL, RUL, RLL, W, H | SVM | 99.7 |
| 10 | All sensors | SVM | 99.8 |

**Table 1:** Sensor combinations that led to the highest accuracy for a given number of sensors. LUA: Left upper arm, LLA: Left lower arm, RUA: Right upper arm, RLA: Right lower arm, LUL: Left upper leg, LLL: Left lower leg, RUL: Right upper leg, RLL: Right lower leg, W: Waist, H: Height.

**Significance:** We identified the optimal number and location of IMU sensors to classify fall risk in older adults while walking. For accuracy, we recommend using 10 sensors with SVM. For practicality, we recommend using a single sensor placed on the left lower leg with SVM.

**Acknowledgments:** This work was supported, in part, by the "Brain Korea 21 FOUR Project", the National Research Foundation of Korea (Award number: F21SH8303039) for Department of Physical Therapy in the Graduate School of Yonsei University, and by the "Regional Innovation Strategy (RIS)" through the National Research Foundation of Korea (NRF) funded by the Ministry of Education (MOE) (2022RIS-005).

**References:** [1] Nishiyama et al. (2024), *Clinical Biomechanics* 115; [2] Park et al. (2023), *Physical Therapy Korea 30:102-109*; [3] Hua et al. (2009), *Pattern Recognition* 42:409-424.

# REAL-WORLD EVALUATION OF A LABORATORY-BASED FALL DETECTOR FOR LOWER LIMB AMPUTEES

*Mojtaba Mohasel[1], Lindsey K. Molina[2], Richard R. Neptune[2], Shane R. Wurdeman[3], Corey A. Pew[1]
[1]Montana State University, Mechanical and Industrial Engineering, Bozeman, MT, USA
[2]Walker Department of Mechanical Engineering, The University of Texas at Austin, Austin, TX, USA
[3]Department of Clinical and Scientific Affairs, Hanger Clinic, Austin, TX, US
*Corresponding author's email: seyedmojtabamohasel@montana.edu

**Introduction:** Individuals with lower limb amputation (LLA) have a higher risk of falling compared to individuals without LLA, which presents a major health risk [1]. Clinicians use fall history as an indicator of future fall risk which can guide rehabilitation therapy and adjustment of prosthetic hardware [2]. Currently, fall history is recorded through surveys and self-reporting, but patient memory and recall over time is often inaccurate [3]. Quantitative fall detection methods are critically needed to provide objective information about patients' fall history for clinicians. Creating a fall detection system (FDS) for individuals with LLA faces several challenges including: 1) Collecting an appropriate volume of data from the amputee community for machine learning (ML) model training is time consuming, and 2) An FDS developed using data from laboratory-based, simulated falls may perform poorly in real-world settings. In an effort to develop a FDS for individuals with LLA, **the purpose of this study was to determine if 1) data from control participants could be utilized to develop an ML FDS suitable for individuals with LLA, and 2) an ML FDS model based on simulated falling in the laboratory is suitable for real-world settings?** We evaluate the following hypotheses:

*Hypothesis 1: An ML FDS trained on a majority control participants achieves similar fall detection for LLA and control individuals.*
*Hypothesis 2: Laboratory-based ML FDS exhibits a similar performance (F1-score) when evaluated in the lab and in the real world.*

**Methods:** Hypothesis 1 utilized data from 30 control (9 males, 21 females; age: 28 ± 9 years;) and 5 individuals with LLA (4 male, 1 female; age: 43 ± 14 years) for creating a lab-based fall detector. Inertial measurement unit (IMU) sensors (100 Hz) were placed proximally on the participants' upper shanks. Participants were instructed to perform several activities of daily living (ADL, walking, turning, sit/stand, stairs, running, turning) and simulated falls (forward, backward, lateral, and stumble). A 1D convolutional neural network (1D-CNN) was trained and optimized with an automated ML framework [4]. A binomial generalized linear mixed model was used to test for correct fall detection (Sensitivity) for LLA versus control individuals with p-value >0.05.

Hypothesis 2 utilized data from 20 individuals with LLA (11 males, 9 Females; age: 48 ±11 years) wearing an IMU sensor (10 Hz) placed on the upper part of the prosthesis (Fig. 1, left). Participants performed their routine daily activities for two consecutive days (~ 3 hours of data collected each day). The real-world data collection frequency differed from that of the laboratory. Therefore, we resampled the lab data and retrained the 1D-CNN lab model with the 10 Hz data. In addition, no falls occurred during real-world data collection. Consequently, we considered only ADL F1-scores to test Hypothesis 2. F1-scores from 20 participants in the real world were compared with F1-scores from 35 participants in the lab from the 1D-CNN model from the lab-based data. A Wilcoxon signed-rank test was used to test Hypothesis 2 with a p-value > 0.05.

**Results & Discussion:** Analysis for Hypothesis 1 found that the correct fall detection rate for the control group (Sensitivity = 0.84) was similar to that of the amputee group (Sensitivity = 0.70) (z=1.18, p-value =0.236). Therefore, control participants can be used to develop an ML-based FDS for individuals with LLA. **This highlights the potential of utilizing non-amputee data as a training resource to mitigate the challenge of limited data availability from the amputee population.**

The Wilcoxon signed-rank test for Hypothesis 2 indicated no difference between the F1 ADL score of the lab-based model and real-world model (Wilcoxon U Statistic = 392.50, P-value = 0.238). **This indicates that the model developed in the laboratory would perform similarly in real-world settings**. Despite the similarity in model performance for detecting ADL, the current laboratory-based model still generates false positive predictions, which would relate to annoying false alarms (Fig.1, right). The model is currently trained to emphasize detection of falling as it was deemed more important to not miss a falling event than to reduce false alarms. However, excessive false alarms may be annoying for users, causing them to abandon the system and reduce the clinical relevance of the FDS. Transfer learning offers a solution to the problem of inaccurate action detection. By leveraging knowledge from related tasks, the transfer learning framework solves new tasks and accounts for variations in data distributions between tasks [5]. Given these advantages, future work will explore the potential of transfer learning to improve FDS using real-world data. Specifically, we will update the laboratory-based model with the real-world data and compare the false alarm rate to the rate generated by the current FDS. A limitation of our study is the lack of real-world fall data, preventing a comprehensive evaluation of model performance during actual fall events. Future research should focus on collecting real-world fall instances to further enhance model robustness.

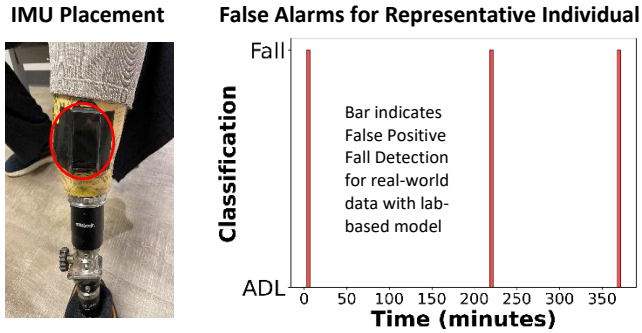


**Figure 1:** Left: Red circle example sensor placement on prosthesis. Right: Single participant false alarm example with false fall alarm events over a 6-hour time during real-world activities of daily living.

**Significance:** This study represents the first effort to validate a laboratory-based FDS in real-world scenarios for individuals with LLA. We found that data from control individuals can be used for FDS utilized for individuals with LLA. These findings will facilitate the creation of FDS for individuals with LLA in real-world settings.

**Acknowledgments:** Funding was provided by the CDMRP Grant W81XWH-20-1-0164.

**References:** 1) Miller et al, Arch Phys Med Rehabil, (82) 2001; 2) Tobaigy et al, PM&R, 2022; 3) Ganz et al, J Am Geriatr Soc, (53) 2005; 4) Mohasel et al, ASB, 2022; 5) Butt et al, Wireless Personal Commun, (126) 2022.

# PERIODIC AUTOENCODER FOR INJURY DESIGNATION USING MARKER POSITION

*Alex Dzewaltowski[1], and Christopher Connaboy[1]
[1] Scholl College of Podiatric Medicine, Rosalind Franklin University of Medicine & Science, North Chicago, Illinois, USA.
*Corresponding author's email: alex.dzewaltowski@rosalindfranklin.edu

**Introduction:** Identifying indicators of injury or pain can improve clinical decision making, direct people to seek care, and provide unbiased metrics to support access to care. Movement measurements are a rich source of complex information which can contain indicators of injury onset, pathology, and underlying mechanisms. Current tools and applications for identifying indicators of injury, mobility decrements, and disease vary widely, spanning assessments of kinematics, kinetics, the creation of composite scores, extraction of spectral components, and nonlinear analyses[1,2]. There is a wide variety of movement measurements and numeric analyses that can provide indicators of injury or disease. However, a centralized approach to identification of injury from movement data may be possible using tools derived from machine learning methods. While there are clear drawbacks from using machine learning tools due to 'black-box' interpretation, machine learning techniques may be well suited to extract potential indicators of injury that are consistent across designations. We analyzed an existing dataset with a compilation of a total *n*=1879 unique participants, without injury and with a wide variety of musculoskeletal injuries; with the preliminary intent of classifying participants as "injured" or "uninjured"[3]. We posited that there are 'healthy' movement behaviors which are representative across uninjured participants, the existence of which, would allow for a delineation between uninjured and injured participants regardless of their injury designation. Our machine learning approach adapts the periodic autoencoder described in Starke et al., (2022) [4].

**Methods:** The existing, publicly available dataset is composed of walking and running trials[3]. We extracted position data from seven retroreflective markers placed bilaterally on the thigh, shank, and foot segments as well as the pelvis. Marker data were originally recorded at 100Hz and filtered using a fourth order, low-pass Butterworth filter with 10Hz cutoff frequency. 396 subjects have only walking data, 112 have only running data, and 1290 have both running and walking data. Subject data ranges from 20s to 110s for walking or running.

The five most common injuries were Achilles tendonitis, iliotibial band syndrome, osteoarthritis, patellofemoral pain, and plantar fasciitis. However, 415 participants had an injury designation defined as either 'Other' or 'Pain'. For the training and testing of our periodic autoencoder, these individuals were included and labeled as 'Injured'.

A periodic autoencoder was used for dimensionality reduction and classification (Fig. 1). Training data included 763 participants' walking and 763 participants' running data. Test data included 1102 participants' walking and 1102 participant running data. Note: Participants may be represented in training and test data but the same participants' same locomotor data was not present in training and testing. Root-Mean-Square-Error was used to calculate the encoder-decoder loss and Cross Entropy was used to assess classification loss. The periodic autoencoder and linear classifier were trained simultaneously where their corresponding loss values were multiplied for backpropagation and ADAM optimization with learning rate of 1E-4.

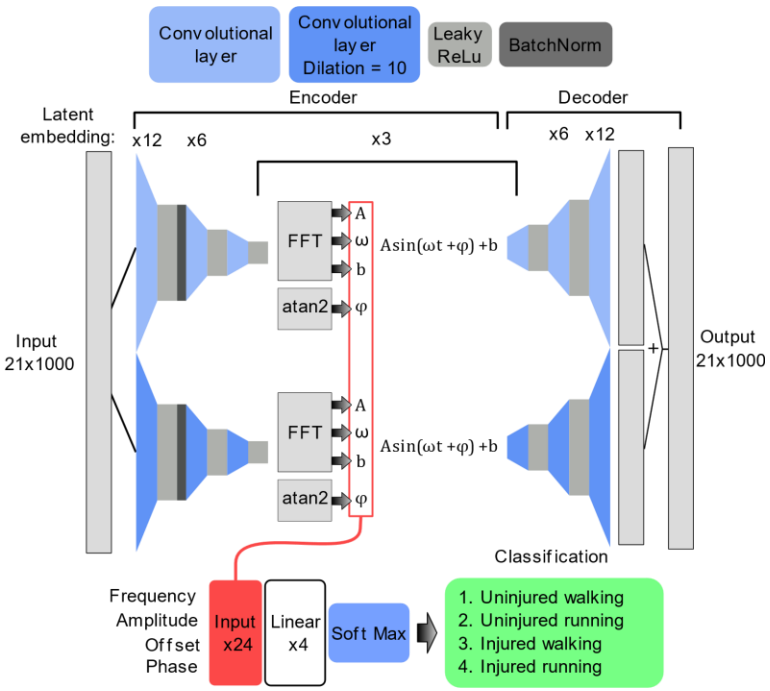


**Figure 1:** The encoder was composed of three convolutional layers with leaky rectified linear activation functions compressing 21 features (marker data) into a latent embedding of six features. From these latent features, representative spectral components (frequency, amplitude, offset, and phase) were extracted. The spectral components were used for linear classification of injury (uninjured vs injured) and gait (walking vs running) for 4 different classifications. For the decoder, the latent spectral components were first used to construct simplified, representative waveform for six features. The decoder then largely mirrored the encoder to reconstruct the original marker data (21 features).

**Results & Discussion:** The encoder portion of the periodic autoencoder reduced 10s marker data segments with 21 columns, effectively 42,000 individual data points, into a representation of 24 spectral components to be used for classification. Current, classification accuracy of training was 87.9% and test accuracy was 77.4%.

**Significance:** Short locomotor bouts of, at most, 110s with lower-limb segment position measurements may be sufficient to delineate between healthy and injured movement. The current machine learning implementation of a periodic autoencoder presents a promising tool for analyzing movement, with the potential to lead to analytical approaches that can detect early indicators of movement adaptations associated with the onset of an injury.

**Acknowledgments:** We would like to thank and acknowledge our funding sources, U.S. Air Force (AFWERX) #FA864922P1145

**References:** [1] Chalchat E., et al., (2022) *PLOS One* [2] Bonazza N. A., et al., (2016) *Amer J Sports Med* [3] Ferber R., et al., (2024), *Scientific Data*. [4] Starke S. et al., (2022), *ACM TOG*

**Machine learning-based sex-specific prediction of fatigue during running using inertial measurement unit sensors**

*Yiyang Chen[1,2], Oussama Jlassi[1], Jill Emmerzaal[1], Caroline Paquette[1,2], Julie N. Côté[1,2], Philippe C. Dixon[1]
[1]Department of Kinesiology and Physical Activity, McGill University, Montreal, Canada
[2]Jewish Rehabilitation Hospital Site of CISSS-Laval and Research Site of the Montreal Centre for Interdisciplinary Research in Rehabilitation, Laval, Canada
*Corresponding author's email: Yiyang.chen3@mail.mcgill.ca

**Introduction:** Biomechanical features are associated with running-induced fatigue, with some showing sex specificity [1]. Deep learning models have shown good classification accuracy for fatigue recognition during running using IMU sensors [2]; however, which biomechanical features can best predict running-induced fatigue and whether males and females show similar features in predicting fatigue is less clear. This study aimed to determine 1) which biomechanical and statistical features collected from IMU sensors can accurately predict running-induced fatigue and 2) if males and females show similar features. Due to the identified sex differences in hip and knee joint kinematics during running [3], we expected that males and females to exhibit different predictive features, with sex-specificity in hip and knee joints.

**Methods:** Thirty-two endurance trained runners (16 females; weekly running distance: females: 59 ± 26 km; males: 68 ± 30 km) performed a fatiguing running task until volitional exhaustion of 20 on a Borg CR20 scale. IMUs (APDM, Inc., Portland) were placed on the pelvis and the right thigh, shank, and foot. Statistical properties (e.g. min, max, skewness) of biomechanical (e.g. IMU orientations, joint angles of hip, knee, and ankle) features were calculated per gait cycle. Then, feature reduction was performed, retaining features that had low correlations (<0.8) and high variance (>0.1) across fatigue states. The preprocessed and reduced dataset was split into a training (80%) and test (20%) set using a subject-wise split. We trained binary XGBoost classifiers with 5-fold cross validation using a grid search method for hyperparameter tuning to predict fatigue conditions in a) males, b) females, and c) both sexes combined. Model performance was assessed on the test set using the F1-score. Feature importances were computed using the gain metric (average improvement in accuracy from a feature across all the trees in the model).

**Results & Discussion:** In males, the model achieved an F1-score of 86%. Results show that orientation data of the thigh sensor in the frontal plane best predicts fatigue (Fig. 1 top). In females, the model resulted in an F1-score of 61%. Results show that hip angle in the sagittal plane best predicts fatigue in females (Fig 1. bottom). For both sexes, performance was highest with an F1-score of 91%. The top feature to accurately predict fatigue is the skewness of pelvis sensor anteroposterior acceleration. Males and females exhibit different fatigue predictability performance and distinct fatigue-related feature importances. Predictive features differed by sex, with frontal plane thigh orientation for males and sagittal plane hip angles for females being most important. A 3rd, different predictor should be used to detect fatigue in a population of unknown/undetermined/non-binary sex, or to train a group regardless of their sex. Future research will investigate why fatigue was harder to predict in females compared to males.

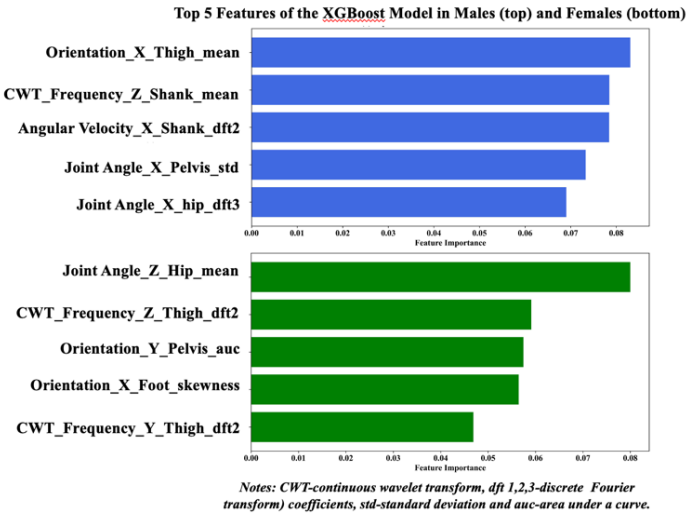


**Figure 1:** Top five features extracted from the XGBoost model to classify fatigue in males (top) and females (bottom).

**Significance:** Our results emphasize the importance of using sex-specific features in fatigue prediction in running. The identified predictors could be integrated into wearable technologies for personalized fatigue monitoring. This approach has the potential to enhance performance optimization and fatigue-related injury prevention strategies in endurance running by addressing individual fatigue patterns.

**Acknowledgments:** We would like to acknowledge colleagues who contributed to the data collection. This project was supported by a Sports Science Project Grant from the Sylvan Adams Sports Science Institute at McGill.

**References:**
[1] Lessi et al. (2017). *J Electromyogr Kinesiol*, 32: 9-14.
[2] Chang et al. (2023). *Front Bioeng Biotechnol*, 11.
[3] Xie et al. (2022). *Front Physiol*, 23.

# QUANTIFYING ARTIFICIAL TURF STIFFNESS USING WEARABLE SENSORS AND MACHINE LEARNING

*Jake Ruschkowski[1,2], Danielle Whittier[1,2], Reed Ferber[1,2], W. Brent Edwards[1,2], John W. Wannop[1,2]
[1]Human Performance Laboratory, Faculty of Kinesiology, University of Calgary, Alberta, CANADA; [2]Department of Biomedical Engineering, Schulich School of Engineering, University of Calgary, Alberta, CANADA
*Corresponding author's email: jake.ruschkowski1@ucalgary.ca

**Introduction:** Artificial turf surfaces are widely used in sports such as football, soccer, and rugby, offering advantages in durability and accessibility compared to natural grass. Maintaining optimal surface stiffness can be essential to athlete performance and injury prevention. Over time, turf stiffness changes due to environmental factors and athlete usage, necessitating frequent testing to ensure compliance with safety standards set by organizations such as FIFA and the NFL [1]. Traditional methods for assessing turf stiffness rely on mechanical devices such as the Advanced Artificial Athlete (AAA), which are costly, heavy, and require substantial time and labor to operate [2]. Wearable sensors, particularly inertial measurement units (IMUs) and pressure-sensing insoles, present a promising alternative for assessing turf stiffness. These sensors can provide real-time data on the interaction between an athlete and the playing surface, potentially offering a more efficient method of evaluating field conditions. By leveraging machine learning algorithms to analyze sensor data, this research aims to develop a system capable of predicting turf stiffness with high accuracy, reducing the need for cumbersome mechanical testing [2, 3].

**Methods:** The study recruited 50 recreational athletes (25 male, 25 female) to perform walking, running, and drop landing movements on five different artificial turf surfaces of varying stiffness levels (Table 1). The surfaces were constructed using materials supplied by FieldTurf (Tarkett, Montreal, QC, Canada) in a controlled lab environment, ranging from very low to very high stiffness, measured using a Clegg Impact Hammer, which collects peak deceleration upon impact ($G_{max}$), and an AAA device, which determines impact force reduction (FR) compared to concrete as a reference surface, to establish baseline mechanical properties [1,2]. During data collection, athletes wore identical shoes equipped with two types of sensors: IMUs (BlueTrident, Vicon) attached to the heel cup of both shoes to measure acceleration data at 1125 Hz and pressure-sensing insoles (XSENSOR) to record plantar pressure at 150 Hz. Machine learning models, including a feature-based model, support vector machine (SVM), and a signal-based model, convolutional neural network (CNN), were trained on the collected data to classify turf surfaces based on stiffness. Data was split into training (40 subjects) and testing (10 subjects) sets. A priori feature extraction focused on statistical and frequency domain biomechanical parameters such as peak accelerations, angular velocities, and pressure amplitude during gait and jump cycles for a total of 390 features [4, 5]. The CNN architecture utilized accelerometer and insole signals alone and consisted of four convolutional layers with ReLU activation functions, along with batch normalization, and dropout layers to prevent overfitting. The models were evaluated using stratified 5-fold cross-validation to ensure generalizability.

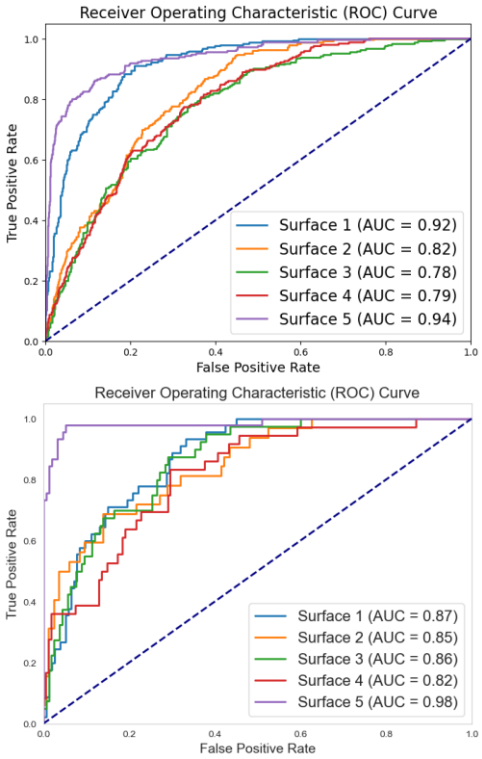


**Figure 1:** Receiver operating characteristic curves for the SVM (top) and CNN (bottom)

**Table 1:** Stiffness properties of constructed artificial turf surfaces.

| Surface | 1 | 2 | 3 | 4 | 5 |
|---|---|---|---|---|---|
| Clegg ($G_{max}$) | 121g | 100g | 75g | 53g | 30g |
| AAA (FR) | 42% | 53% | 62% | 73% | 82% |

**Results & Discussion:** Data processed from 50 participants included over 3,500 trials across walking, running, and drop landing movements. Analysis using the SVM and CNN classifiers showed promising results, with the models effectively ranking surface stiffness levels. Feature-based learning extracted temporal, frequency, and gait parameters from IMU and insole data, highlighting accelerations, estimated load and pressure as key distinguishing factors. The SVM achieved an average area under the curve (AUC) score of 0.85±0.03, indicating robust classification performance across trials (Figure 1, top). However, the model struggled with exact class assignment when distinguishing adjacent stiffness levels, especially between the surfaces with stiffness similar adjacent to the control. The CNN model demonstrated comparable performance to the SVM, AUC:0.87±0.04, but required longer training times (Figure 1, bottom). Both models performed well when classifying surfaces into three broad categories (soft, control, hard), suggesting that simplifying the classification task could improve accuracy.

**Significance:** The results indicate that wearable sensors show promise predicting artificial turf stiffness, with machine learning models providing valuable insights into biomechanical interactions with playing surfaces. Future work will focus on optimizing feature selection, refining model thresholds, and testing new model options in order to enhance accuracy and generalizability. This research can provide field managers and athletes with continuous feedback, improving field conditions, ultimately reducing injury risk, and enhancing performance.

**Acknowledgments:** FieldTurf supplied the artificial turf materials and partially funded this project.

**References:** [1] Jastifer et al. (2022). Int. Turfgrass Soc. Res. J., 14(1):352-363, [2] Fleming et al. (2020). Proceedings, 49:130.[3] Worsey et al. (2021). Sports Eng., 24(1). [4] Dixon et al. (2019). Gait Posture, 74:176-181. [5] Ng et al. (2022). Master's Thesis, Univ. of Nebraska. an

**Lightweight real-time human activity recognition approach using biomechanical features**

Ehsan Sharafian M.*, Colby Ellis, Babak Hejrati
Department of Mechanical Engineering, University of Maine, Orono, ME 04469
Corresponding author's email: ehsan.sharafian@maine.edu

**Introduction:** Human activity recognition (HAR) is a crucial component of health monitoring systems, playing a key role in assessing daily activity levels. However, one major challenge in developing such systems is the need for extensive datasets and the computational complexity associated with real-time implementation. Moreover, most existing HAR systems are tested on younger adults, neglecting the unique movement characteristics of older individuals. While deep learning techniques can yield high accuracy, they demand large amounts of data and complex computations complicating their real-time deployment. In contrast, leveraging physics-based features can achieve acceptable accuracy with lower computational cost. Cheng et al. [1] used the thigh angle as a feature to detect transitions between walking and stair negotiation, achieving 99.4% accuracy in a real-time application. Similarly, Bartlett et al. [2] employed an IMU on the thigh to detect stair negotiation and uphill/downhill walking in real-time with 98.4% accuracy, based on a phase variable technique. In this study, we develop a system for detecting dynamic activities, including walking, stair ascent, and stair descent, as well as static postures of standing and sitting, using selected biomechanical features. The model is trained on younger adults and tested on older adults, with deployment on a smartphone to facilitate home-based monitoring.

**Methods:** For training the model, we consider the biomechanical features of the lower limbs. Two IMUs stream data from the thigh and foot and the maximum and minimum angles of the foot and thigh for each movement cycle were extracted as features. An adaptive time windowing technique based on toe-off events was employed to segment the data. For offline training, machine learning methods including KNN, SVM, LDA, and NB were evaluated, and the best performing model was implemented in a real-time smartphone application. The model is initially trained on data from 10 healthy younger adults and subsequently validated on an independent set of 5 younger adults and 5 older adults. Figure 1 shows the location of IMUs and the selection of the features during stair ascending.

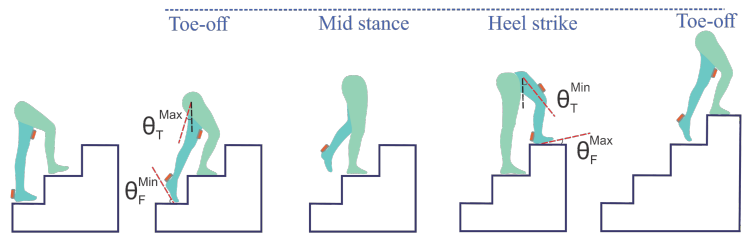


Figure 1 Stair ascending with toe-off moment as the criteria for time windowing segmentations with showing the location of the IMUs

**Results & Discussion:** Statistical analysis revealed significant differences in features across activities ($p < 0.001$), but no significant differences between younger and older adults, indicating that a model trained on younger adults can be effectively applied to healthy older adults. Offline evaluation showed that both KNN and SVM achieved 100% accuracy. The KNN classifier was then selected for real-time deployment reaching 99.6% accuracy for younger adults and 99.4% for older adults. Detailed accuracy for each activity as confusion matrices is presented in Figure 2.

**Significance:** Our model, based on a select set of thigh and foot biomechanical features, demonstrates that real-time HAR can be achieved with minimal computational cost and a limited dataset. Moreover, the model trained on younger adults generalizes well to older adults. Implementing the model on a smartphone paves the way for home-based health monitoring, providing a promising solution for daily activity recognition and improved health outcomes in aging populations.

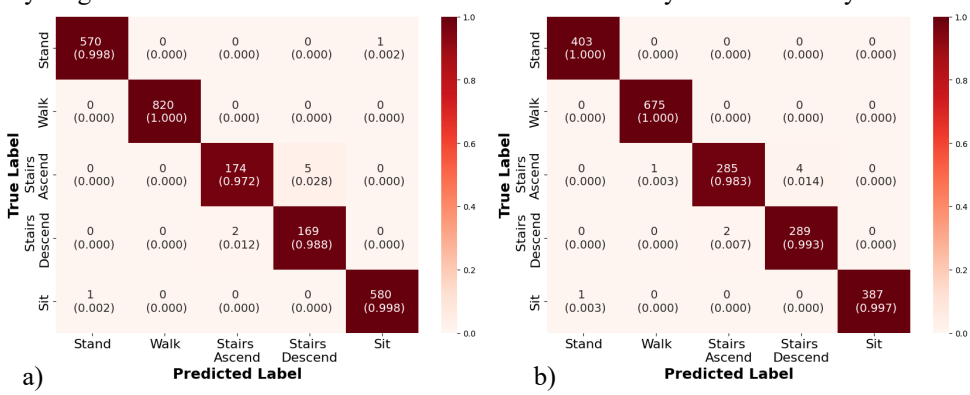


Figure 2 Confusion matrix with accuracy of activity detection based on the sample of data as the segmented window for a) younger adults' group, and b) older adults one.

**Acknowledgments:** This study is supported by the National Institute on Aging of the National Institutes of Health (NIH/NIA) under Award Number 1R15AG078865-01A1 as well as the National Science Foundation (NSF) under Grant 2145177

**References:**

[1]: Cheng, Shihao, "Real-time activity recognition with instantaneous characteristic features of thigh kinematics." IEEE Transactions on Neural Systems and Rehabilitation Engineering.

[2]: Bartlett, Harrison L.,"A phase variable approach for IMU-based locomotion activity recognition." IEEE transactions on biomedical engineering.

# PSEUDO-TARGETS AS A PRESELECTION METHOD FOR FEATURE ENGINEERING IN CONTINUOUS ACTIVITIES

*Louis J. Dankovich IV[1], Andrew Tweedell[1], Chloe Callahan-Flintoff[1], Richard Diego [2]
[1] US Army Research Laboratory, Aberdeen Proving Ground, MD [2] DCS Corp., Aberdeen Proving Ground, MD
*Corresponding author's email: louis.j.dankovich.ctr@army.mil

**Introduction:** Human Activity Recognition (HAR) relies on machine learning (ML) models to recognize the intent of human operators. ML is only as reliable as the features used to build it. Feature selection involves paring away uninformative and redundant features, and is a critical step in building learning models [1], [2]. Physical activities are generally continuous actions from start to finish, with definitive labels on end action of stages of action (e.g. pulling of a trigger during a shooting task). These labeled samples often represent a very small portion of the dataset, leading to highly imbalanced classification models. For example, in a target search and shooting task, the action of preparing, aligning, and trigger pull of a shooting action may account for 40% of the data, but labeled trigger pulls (TP) represent <1% of the data. While Label Spreading (LS) can generate more labeled samples, it requires knowledge of important features and time windows. These are often unknown a priori and uninformative features can significantly degrade model performance[3]. Using conventional feature selection methods and metrics on highly imbalanced data sets can result in failure of models to identify the activities for which limited data is available [3]. Here, we seek to improve the accuracy of feature selection for semi-supervised ML, during a search and shooting activity using a next-labeled-action pseudo-target (PT). We hypothesized that using PT for feature selection would improve performance of LS and better classify the shooting activities. We observed a decrease in misclassification of labeled samples by LS when using PT for label selection algorithm from 60% to 3%. Common methods for feature selection such as using Principle Component Analysis (PCA), correlations using individual class labels, and Boruta selection may fail to perform well in unsupervised tasks or obscure physical phenomena.[3], [4] PCA casts features to a lower dimensional space which can mask the importance of individual features in predicting physical phenomena. Our method preserves the relationship between individual features and physical phenomenon. Correlation with individual classes and Boruta often produce unreliable results in heavily imbalanced semi-supervised learning settings [3], [4]. By using PT and the assumption of continuous activities we can use correlation to preselect meaningful features which are then passed to Boruta to find the most important features. While our results focus on searching and shooting activities, we hope that PT will prove effective in LS and feature selection for HAR in any continuous physical activity.

**Methods:** 10 subjects performed a search and shoot task in a VR environment presented by an HTC Vive headset using an Airsoft rifle as a controller. Subjects and the rifle were outfitted with Inertial Motion Units (IMU) which recorded motions at 200Hz, eye data was tracked at 120 Hz using the *sranipal* library, while aim points and trigger pulls (TP) were tracked by an Unreal application at 60 Hz. A set of typical features from HAR research were generated over a variety of time windows [2]. PT based on time and distance to next shot were generated from the TP under the assumption that all blocks of samples for a given shot will end in a labelled TP. 5-Fold cross validation with 70/30 train test splits was used to compare the results of model pipelines. A hybrid constrained Boruta and LS model was used, with an equal proportion of randomly selected non-TP samples and TP labelled samples as a starting point [5]. Two ML pipelines were compared to test the usefulness of PT in selecting features: (1) $P_{All}$ used all available features for modelling, while (2) $P_{Select}$ used only the features which had the highest correlations to PT, and <0.5 correlation to each other.

**Results & Discussion:** After generating the selected time windows and engineered features, there were *2090* starting features, many of which were redundant or irrelevant. $P_{select}$ performed better, misclassifying on average $4\% \pm 2\%$ of TP while classifying 44%±1% samples in the shooting class. $P_{All}$ misclassified $60\% \pm 42\%$ of TP and still managed to significantly underrepresent the shooting class as $1\% \pm 1\%$ samples. While the $P_{All}$ model only spread shooting labels to a small percentage of samples, for 3 of the subjects they were very accurate in classifying TP with $1\% \pm 1\%$ misclassification while the other 7 misclassified TP samples $89\% \pm 33\%$ of the time.

**Significance:** This work demonstrated the use of PTs to enhance feature selection during HAR of a search and shooting task. The principle of continuous motions applies to activities ranging from gesture recognition to activity recognition to sporting activities, as do the challenges of poor labelling and lack of a priori knowledge of feature importance. By using PT to transform under-represented classes into continuous variables, significantly more data is made available to assign feature importance based on correlations. This results in significant enhancements of the results of LS and captures samples more accurately with minimal human intervention.

**Acknowledgments:** This study was funded by Oak Ridge National Laboratories (grant number W911NF-23-2-0205).

**References:**

[1] R. Dwivedi, A. Tiwari, N. Bharill, M. Ratnaparkhe, and A. Tiwari, "A taxonomy of unsupervised feature selection methods including their pros, cons, and challenges," *The Journal of Supercomputing*, vol. 80, pp. 1–29, Jul. 2024, doi: 10.1007/s11227-024-06368-3.
[2] A. Bulling, U. Blanke, and B. Schiele, "A tutorial on human activity recognition using body-worn inertial sensors," *ACM Comput. Surv.*, vol. 46, no. 3, p. 33:1-33:33, Jan. 2014, doi: 10.1145/2499621.
[3] J. E. van Engelen and H. H. Hoos, "A survey on semi-supervised learning," *Mach Learn*, vol. 109, no. 2, pp. 373–440, Feb. 2020, doi: 10.1007/s10994-019-05855-6.
[4] D. Cai, C. Zhang, and X. He, "Unsupervised feature selection for multi-cluster data," in *Proceedings of the 16th ACM SIGKDD international conference on Knowledge discovery and data mining*, Washington DC USA: ACM, Jul. 2010, pp. 333–342. doi: 10.1145/1835804.1835848.
[5] Dankovich IV, Louis, A. Tweedell, C. Calahan-Flintoff, and R. Diego, "On Target: Constant Activity Constrained Semi-Supervised Feature Selection for Marksmanship Activity Classification," *Human Computer Interfaces International Conference 2025*, Jun. 2025.

# EVALUATING STRIDE RATE AND GROUND TIME ACCURACY IN RUNNING USING MONOCULAR POSE ESTIMATION

*Luke VanKeersbilck, Iain Hunter
Brigham Young University, Provo, UT
*Corresponding author's email: l.vankeersbilck@gmail.com

**Introduction:** Markerless motion capture has exploded in the last ten years. It promises cost effective, convenient, and accessible motion capture technology but the accuracy of these techniques is still a major concern. One type of markerless motion capture is Monocular pose estimation which uses a single camera to attempt to reconstruct human motion using machine vision algorithms such as open pose, blazepose, mediapipe pose, and other custom methods. Much of the validation work on Monocular pose estimation has focused on the accuracy of joint center positions and sagittal plane joint angles. These algorithms have been validated for joint kinematics in both walking and running [1]. However, there has been less focus on their accuracy in detecting gait events, with some studies assessing event detection in walking but far fewer examining its reliability in running [2]. The purpose of this study was to evaluate the accuracy of Monocular pose estimation in identifying gait characteristics, specifically stride rate and ground time, by comparing it to measurements obtained from an instrumented treadmill.

**Methods:** Ten subjects (6 men, 4 women) ran at a self-selected speed (3.4 ± .21 m/s) on a treadmill while being filmed by a traditional 12 camera motion capture system (Qualysis and Visual 3D) and a single cell phone camera (iPhone SE 2020, Apple Corp) at 240 Hz for 30 seconds. The cell phone was placed 30° backward from completely sagittal. Forces were collected at 960 hz. MediaPipe Pose (MP) and Visual 3D were used to produce 3D positions of anatomical landmarks for the cell phone video and motion capture system respectively. Positions and forces were filtered using a Butterworth filter. Footstrike and toe off were established for the motion capture system using force thresholds. The footstrike for the machine learning approach used the minimum vertical position of the heel marker. Toe off was defined as peak knee extension. These definitions for footstrike and toe off were based on methods for estimating footstrike and toe off from marker-based kinematic data. Stride rate was calculated using the time between consecutive footstrikes and ground time was the time between footstike and toe off. A paired t-test was run on the mean stride rate and ground time for each method ($\alpha$=0.05). Bland Altman plots were also created to investigate the differences between the two methods.

**Results & Discussion:** Both stride rate and ground time were significantly different between the two methods. However, the mean difference between the two systems was very low for stride rate (-0.0027 steps/sec), representing a good estimation of stride rate. On the other hand, ground time was not estimated well and had larger mean differences (0.05 sec). Although these definitions for footsrtike and toe off have been validated and used in kinematic analysis using traditional marker-based motion capture they appear to not be sufficient when using single camera markerless motion capture. There appears to be too much variability to accurately estimate ground time, other methods may need to be developed to obtain accurate ground times using a single camera system.

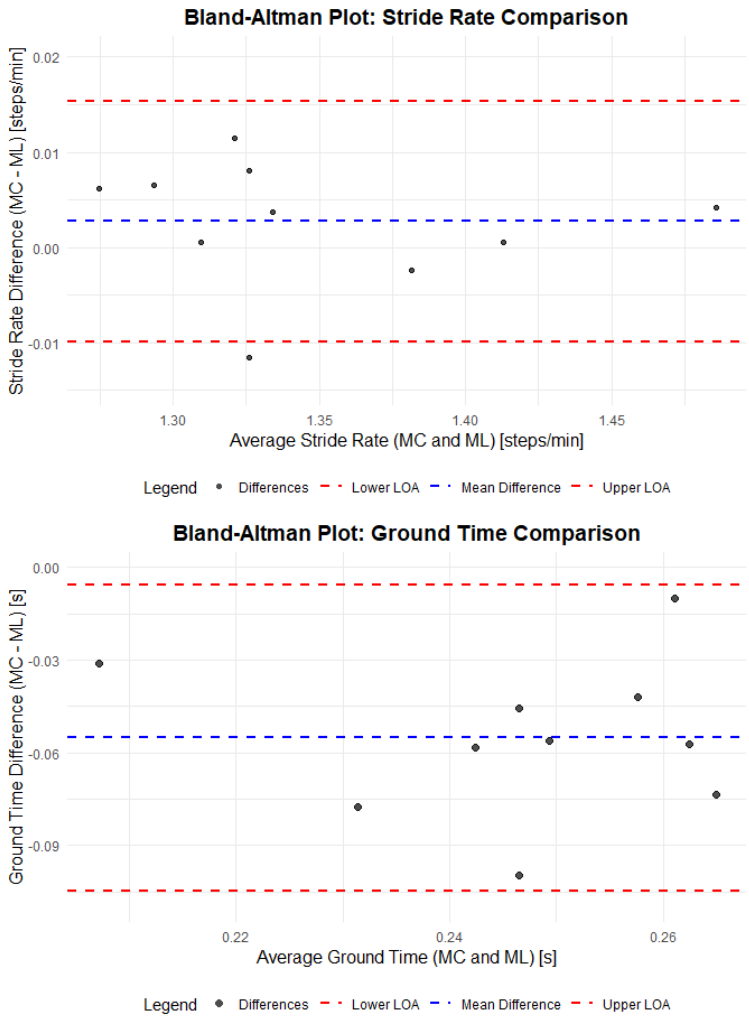


**Figure 1:** The Bland Altman plot for stride rate and ground time. The difference between motion capture (MC) and the machine learning Monocular pose estimation (ML). The blue line is the mean difference, and the red lines are the upper and lower LOA.

**Significance:** Ground time and strike rate are important parts of gait analysis, and the accuracy of these measures has not been well studied in running using Monocular pose estimation. These results inform the development of future solutions for markerless motion capture and the need for additional methods to estimate ground time.

**References:** [1] Ota et al. (2021), Gait Posture 85. [2] Wang et al. (2024), J Biomech 165. [3] Fellin et al. (2010), J Sci Med Sport 13(6).

# ARTIFICIAL INTELLIGENCE-BASED VIRTUAL SURVEILLANCE: FORECASTING BIOMECHANICAL WALL STRESS AND 3D SURFACE GEOMETRY OF ABDOMINAL AORTIC ANEURYSMS

Aakash K. Kottakota[1], Jason Y. Lee[1], Pete H. Gueldner[1], Nathan L. Liang[1-3], David A. Vorp[1-2, 4-11], Timothy K. Chung[1,8]
[1]Department of Bioengineering [2]Department of Surgery, [3]Division of Vascular Surgery, [4]McGowan Institute for Regenerative Medicine, 5Department of Chemical and Petroleum Engineering, [6]Department of Cardiothoracic Surgery, [7]Clinical & Translational Sciences Institute, [8]Department of Mechanical Engineering and Materials Science, [9]Center for Vascular Remodeling and Regeneration, USA [10]Magee Women's Research Institute, University of Pittsburgh, Pittsburgh, PA, USA [11]School of Medicine, University of Pittsburgh Medical Center, Pittsburgh, PA, USA
*Corresponding author's email: tkc12@pitt.edu

**Introduction:** Abdominal aortic aneurysms (AAAs) are a leading cause of mortality in the United States, ranking as the 13th leading cause of death [1]. The progressive ballooning of the abdominal aorta characterizes this life-threatening condition. The primary guideline for surgical intervention is based on the maximum diameter criterion, recommending surgery when the aneurysm reaches 5.5 cm in men and 5.0 cm in women. However, this approach is flawed, as studies have demonstrated that aneurysms can rupture below these thresholds in 5.6% of men and 11.5% of women [2], underscoring the urgent need for a more accurate predictive model of rupture risk. To address these limitations, our research group is developing an artificial intelligence model for virtual surveillance of AAAs, aiming to enhance clinical decision-making.

**Methods:** Data for this study was obtained from a clinical trial, the Non-Invasive Treatment of Abdominal Aortic Aneurysm Clinical Trial (NTA3CT), and transferred to the University of Pittsburgh under data use agreement #DUA00002636. The longitudinal data covered up to 24 months, collected every 6 months from the time of screening for small AAAs. This study presents a comprehensive workflow to predict the morphological evolution and wall stress distributions of abdominal aortic aneurysms (AAAs) over time using deep learning models. For the morphological model, longitudinal AAA scan data were processed into 3D point clouds with a custom MATLAB script. The point clouds included nodes with Cartesian coordinates (X, Y, Z) at various time points. The surface growth model leveraged a TensorFlow model built with Long Short-Term Memory (LSTM) layers to analyze spatiotemporal dynamics. Each node's displacement trajectory was used to train the model, enabling it to predict future node positions based on historical data. The dataset (n=4, two-week intervals over two years for each patient) was randomly divided into training, validation, and testing sets to ensure model robustness. Predicted node positions were organized into future point clouds, which were converted back into 3D surface meshes using MATLAB for visualizing anticipated aneurysm growth. Model accuracy was validated by comparing predicted geometries with ground truth using established morphological metrics and qualitative alignment analyses.

**Results & Discussion:** The findings show a strong alignment between predicted and actual aneurysm geometries and consistent stress distribution patterns in both models. Qualitative and quantitative analyses (**Figure 1 & Table 1**) assessed prediction accuracy and reliability. An overlay of the predicted and actual final geometries, as shown in **Figure 2**, reveals close visual alignment with an average displacement variation of 0.16 ± 0.39 mm per node, highlighting the machine learning-based morphological prediction model's effectiveness.

**Table 1: Summary of morphological features from ground truth and predicted surfaces.**

| | MEAN ± STANDARD DEVIATION | | P-VALUE |
|---|---|---|---|
| | *Ground Truth* | *Predicted* | |
| MAXIMUM DIAMETER (cm) | 4.71 ± 0.19 | 4.58 ± 0.09 | 0.23 |
| DISTAL NECK DIAMETER (cm) | 0.61 ± 0.29 | 0.68 ± 0.38 | 0.42 |
| PROXIMAL NECK DIAMETER (cm) | 1.68 ± 0.39 | 1.57 ± 0.27 | 0.38 |
| SAC HEIGHT (cm) | 6.46 ± 0.89 | 6.06 ± 0.89 | 0.34 |
| SAC LENGTH (cm) | 9.68 ± 0.56 | 10.07 ± 0.43 | 0.24 |
| NECK LENGTH (cm) | 0.52 ± 0.01 | 0.58 ± 0.09 | 0.24 |
| NECK HEIGHT (cm) | 4.79 ± 1.19 | 5.71 ± 1.56 | 0.27 |
| BULGE HEIGHT (cm) | 2.74 ± 0.90 | 3.25 ± 0.97 | 0.31 |
| BULGE LOCATION | 0.24 ± 0.07 | 0.28 ± 0.09 | 0.33 |
| MEAN WALL ASYMMETRY | 6.61 ± 0.48 | 7.09 ± 0.90 | 0.27 |
| MAX WALL ASYMETTERY | 10.77 ± 1.18 | 11.94 ± 1.82 | 0.25 |
| WALL TORTUOSITY | 1.08 ± 0.02 | 1.09 ± 0.01 | 0.45 |

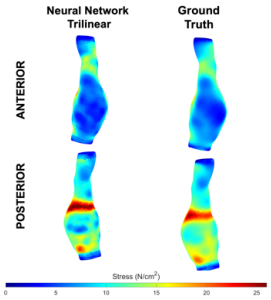


**Figure 1: Wall stress predictions using a trained neural network.**

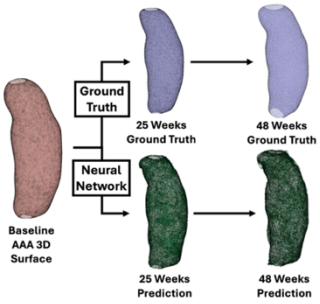


**Figure 2: Baseline AAA 3D input into a trained LSTM neural network to predict intermediate surface changes.**

**Significance:** Virtual surveillance using artificial intelligence would enable clinicians to better manage patients with AAA. Understanding the evolution of biomechanical and morphology provides a novel approach.

**Acknowledgments:** Pittsburgh Health Data Alliance, Institute for Precision Medicine University of Pittsburgh UPMC, NIH Grant no. HL156246, the University of Pittsburgh's Clinical and Translational Science Institute Pittsburgh Innovation Challenge, and Chancellor's Gap Fund, NVIDIA academic hardware grant award. This work was also supported by the NSF Graduate Research Fellowship Program under Grant No. 1747452 (PHG) and the American Heart Association Fellowship Grant No. 24PRE1195123 (PHG.). Any opinions, findings, and conclusions or recommendations expressed in this material are those of the author(s) and do not necessarily reflect the views of the NSF.

**References: [**1] Vorp, D.A., *J Biomech*, 40:1887-1902, 2007 [2] *Kontopodis, N., Front. Surg*. 3:1-6, 2016

# EFFECTS OF SLOPE GRADIENT ON THE CONTRIBUTION OF JOINTS TO DESTABILIZATION OF GAITS

Jungho Lee[1], Chae Lynne Kim[1], Jeongin Moon[1], Jooeun Ahn[1, 2]*
[1]Department of Physical Education, Seoul National University, South Korea
[2]Institute of Sport Science, Seoul National University, South Korea
*Corresponding author's email: ahnjooeun@snu.ac.kr

**Introduction:** Walking on inclined/declined surfaces is a daily activity that significantly increases demand on the locomotor system and raises the risk of falls, so maintaining a stable gait on slopes is a common challenge [1]. Walking on slopes requires different postures, muscle activity, and joint mechanics compared to level walking, and it is highly plausible that such difference results in different stabilizing mechanisms. Therefore, the slope gradient possibly changes not only the contribution of each joint to the power generation and absorption during locomotion but also the contribution of each joint to the overall orbital stability. However, no previous study investigated the effects of slope gradient on the relative contribution of each joint on the orbital stability. This lack is particularly noteworthy considering the recent spread of gait assisting devices that focus only on adding power to a specific joint whether the user walk on a level, declined, or inclined surface. Blind use of such device without understanding the effects of slopes on the role of each joint in destabilizing the gait might jeopardize gait stability, which should have higher priority than efficiency obtained by the assistance in power generation. We aim to contribute to resolving this issue by quantifying the orbital stability and the relative contribution of each joint to the orbital stability across various slope conditions.

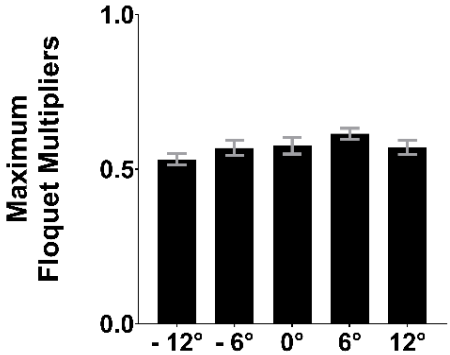


**Figure 1**: Mean and standard error of the max FM for all participants across slope conditions.

**Methods:** We investigated the maximum Floquet multiplier (max FM) and the components of the eigenvector corresponding to the max FM for walking on surfaces with five inclination angles. Thirteen young and healthy adult males (age: 21.4 ± 2.1 y, height: 1.77 ± 0.05 m, mass: 74 ± 5.6 kg) participated in the study. All participants walked on a treadmill (Bertec,USA) with the slope angles of -12°, -6°, 0°, 6° and 12° at a speed of 80% of their preferred walking speed [2, 3]. A total of 15 trials consisting of 3 repetitions of 5-minute trials for each slope condition were conducted in a randomized order. We analyzed kinematic data to construct a state vector containing 10-dimensional joint angles. The Poincaré section was anchored at the right heel strike.

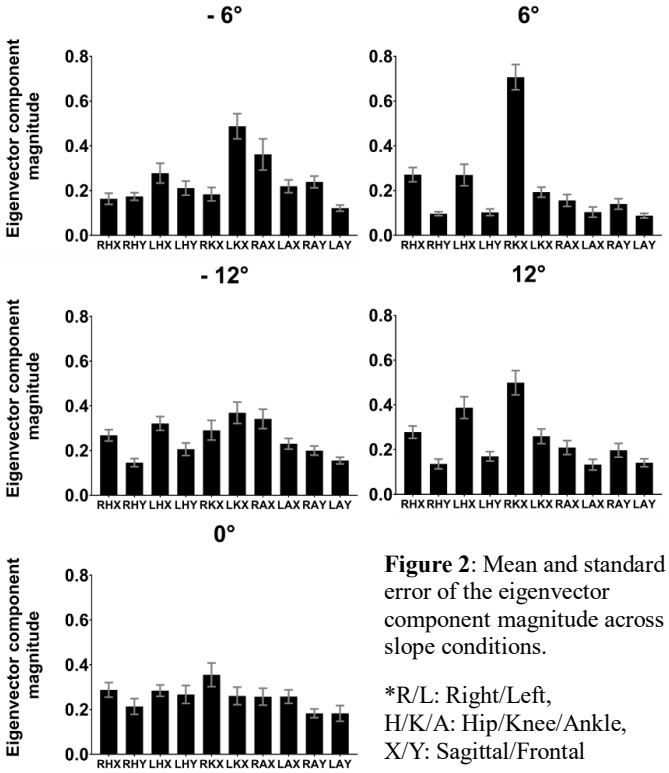


**Figure 2**: Mean and standard error of the eigenvector component magnitude across slope conditions.

*R/L: Right/Left, H/K/A: Hip/Knee/Ankle, X/Y: Sagittal/Frontal

**Results & Discussion:** A one-way repeated measure ANOVA revealed that there is no statistically significant difference in max FM between the slope conditions (Fig. 1). However, evaluation of the components of the 10-dimensional eigenvector corresponding to max FM revealed that the maximum eigenvector component appears in the leading leg's knee during uphill walking and in the trailing leg's knee during downhill walking (Fig. 2). The eigenvector corresponding to max FM indicates the direction of the perturbation that can make the gait most vulnerable to instability. Therefore, our results imply that the perturbation to the knee joint of the leading/trailing leg renders the highest risk of destabilizing the uphill/downhill walking.

**Significance:** A previous study analyzed gait stability of walking on slopes by assessing the margin of stability and maximum Lyapunov exponent [3], but it did not evaluate how each individual joint contributes to stability. Our results extend understanding of gait stability on inclined and declined surfaces by exploiting the multi-dimensional information obtained from the eigenvector corresponding to max FM. Our findings can also contribute to advancing assistive devices like exoskeletons and prosthetics; if possible, stabilizing the knee joints should be prioritized over stabilizing other joints for walking on slopes.

**Acknowledgments:** This work was supported in part by the Korea Health Technology R&D Project through the Korea Health Industry Development Institute (KHIDI) funded by the Ministry of Health & Welfare (No. HK23C0071), Industrial Strategic Technology (No. 20018157) and Industrial Technology Innovation Program (No. 20007058, Development of safe and comfortable human augmentation hybrid robot suit) funded by the Ministry of Trade, Industry & Energy (MOTIE, Korea), and the National Research Foundation of Korea (NRF) grants funded by the Korean Government (MSIT) (No. RS-2023-00208052).

**References:** [1] Alexander et al. (2017), Journal of Biomechanics, 61(5); [2] Alexander et al. (2016), Gait &Posture,45; [3] Vieira et al. (2017), Journal of biomechanics,54(6)

# STANDING BALANCE ENHANCEMENT WITH A PORTABLE BILATERAL HIP EXOSKELETON DURING HARD SURFACE PERTURBATION.

Johnnie T. Reed[1], Oluwasegun T. Akinniyi[1], Chang Liu[2], Qiang (Jason) Zhang[1]
[1]The University of Alabama, Department of Mechanical Engineering, Tuscaloosa, AL, USA

[2]University of Illinois Chicago, Department of Kinesiology and Nutrition, Chicago, IL 60612
Corresponding author's email: qiang.zhang@ua.edu

**Introduction:** The ability to recover balance during hard surface perturbation is critical for maintaining mobility and postural control. Perturbations, such as those induced by slips, often cause forward trunk flexion, requiring significant muscular effort to restore an upright posture. Trunk extension and stabilization to restore balance depend on the proper coordination of intrinsic muscle activation, hip joint torques, and ground reaction forces. Electromyographic (EMG) studies have demonstrated the critical role of trunk stabilizers such as the quadratus lumborum and iliocostalis muscles in maintaining postural control during various motor tasks, including recovery from forward flexion [1, 2]. Wearable exoskeletons offer a promising approach to enhance balance stability during recovery by providing external torque assistance to reduce musculoskeletal stress and improve biomechanical efficiency. We hypothesize that applying counterclockwise torque to the pelvic segment using a bilateral hip exoskeleton will improve standing balance after slip perturbations.

Here, we investigate the application of counterclockwise torque to the pelvic segment using a bilateral hip exoskeleton during slip perturbations when standing. In accordance with Newton's Third Law, the applied torque generates a counteracting normal force, reducing the biomechanical load on the trunk-hip system. This redistribution of mechanical load will facilitate trunk extension by reducing reliance on the erector spinae, quadratus lumborum, and abdominal muscles, thereby improving recovery dynamics. The potential of wearable exoskeletons to augment biomechanical recovery mechanisms is explored in the context of slip perturbations induced by sudden posteriorly directed surface translation, which allows for precise control of speed, acceleration, and timing [3, 4].

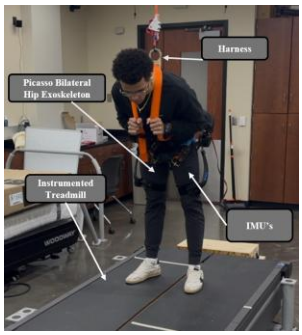


**Figure 1**. Experimental setup showing the instrumented treadmill for surface slip perturbation, hip exoskeleton and measurement sensors attached to participant.

**Methods:** Slip perturbations were induced on an instrumented treadmill (BertecCorp., Columbus, OH, USA) at a velocity of 0.50 m/s and an acceleration of 2.60 m/s² during standing to create controlled forward trunk flexion, causing a forward shift in the participants' center of mass (COM) beyond the acceptable range for postural stability. Participants were secured with a harness to prevent ground contact during instability. Each wore a bilateral hip exoskeleton equipped with inertial measurement units (IMUs) for control. The exoskeleton applied counterclockwise torque to the upper trunk-hip system during recovery to reduce biomechanical load on the trunk and hip extensors, facilitating trunk extension and postural stability.

Data collection involved four conditions: (1) no exoskeleton, where the participant wore only the harness; (2) passive exoskeleton, where the exoskeleton was worn with zero torque; and (3-4) two active states with low and high torque. The exoskeleton activation was timed relative to the treadmill perturbation: 0.5 seconds before, simultaneous with, or 0.5 seconds after.

We measured trunk and hip extensor activation using electromyography (EMG) (Delsys, Inc., Natick, MA, USA) to measure, ground reaction forces, trunk and hip kinematics via motion capture (Vicon, Location?) and exoskeleton torques. We quantified recovery time and mechanics by comparing EMG activation and kinematics across conditions with varying torque assistance and unassisted trials. The EMG analysis focused on key muscles such as the quadratus lumborum and iliocostalis, which are known to exhibit high activity during trunk extension and balance recovery [1, 2, 5].

**Results & Discussion** Current efforts are focused on refining the experimental protocol to ensure reliable data collection and analysis in future phases. We expect to find reduced activation of trunk extensor muscles, particularly the iliocostalis and quadratus lumborum, during assisted recovery, supporting the hypothesis of mechanical load redistribution [1, 2]. Initial observations suggest that the exoskeleton may enhance trunk extension, improve recovery trajectories, and reduce recovery times. These advancements support the exoskeleton's potential for rehabilitation and mobility aid, especially for those with balance or musculoskeletal impairments.

**Significance:** This study highlights the potential of wearable exoskeletons to enhance dynamic balance stability by augmenting biomechanical recovery strategies during perturbations. By reducing muscle activation and improving postural control, exoskeleton-assisted recovery could transform rehabilitation and mobility assistance technologies, particularly for individuals with impaired balance. Future research should explore optimizing adaptive control algorithms to expand the applicability of exoskeletons across diverse perturbation types and user needs. Additionally, the potential for long-term use in elderly populations and those recovering from injury presents exciting opportunities to improve functional mobility and accelerate rehabilitation outcomes.

**Acknowledgments:** The authors extend their gratitude to Yun Chen for his contributions to software development.

**References:** [1] Bankoff et al. (2000), Electromyogr Clin Neurophysiol, 40; [2] Bogduk et al. (2001), J Biomech, 38(3); [3] Finley & Bastian (2017), Neurorehab & Neur Rep, 31(2); [4] Lee et al. (2025), Sci Rep, 15 – Effects of perturbation intensities on backward slip-falls via split-belt treadmill; [5] Nakayama et al. (2006), J Phys Ther Sci, 18

# EFFECTS OF HIP EXOSKELETON ASSISTANCE ON GAIT STABILITY

Arash Mohammadzadeh Gonabadi[1,2*], Farahnaz Fallahtafti[2], Sara A. Myers[2,3], Judith Burnfield[1]
[1] Institute for Rehabilitation Science and Engineering, Madonna Rehabilitation Hospitals, Lincoln, NE, USA
[2] Department of Biomechanics, University of Nebraska at Omaha, Omaha, NE, USA
[3] Department of Surgery and Research Service, Nebraska-Western Iowa Veterans Affairs Medical Center, Omaha, NE, USA
*Corresponding author's email: agonabadi@madonna.org

**Introduction:** As individuals age, various factors contribute to reduced stability and an increased risk of falls, including visual impairments, joint instability, muscle weakness, and unreliable postural reflexes [1-2]. While traditional assistive devices have not fully addressed these challenges, advancements in exoskeleton technology offer the potential to improve stability and prevent falls. This study examined the effects of five distinct hip exoskeleton assistance timings and two torque magnitudes on gait stability, specifically focusing on the Margin of Stability (MoS) in the anterior-posterior (AP) and medial-lateral (ML) directions.

**Methods:** Ten healthy young adults (four males, six females; age: 27.6 ± 5.9 years, body mass: 65.3 ± 13.1 kg, height: 1.66 ± 0.08 m) participated in this study. The session began with a five-minute standing trial to measure resting metabolic rate, followed by a 20-minute warm-up with assisted exoskeleton conditions and gain-tuning adjustments. Participants wore a fall-arresting harness for safety, though no weight was supported. The testing protocol included 10 walking conditions performed at a fixed speed (1.2 m/s) with varying timing of assistance (21%, 28%, 35%, 42% and 49% of the gait cycle) and peak torque magnitudes (0.06 and 0.12 Nm/kg), and two reference conditions (Powered-Off and No-Exo). The protocol had three blocks with randomized conditions. Each block began and ended with a five-minute trial, while intermediate trials lasted two minutes. Participants rested for at least 10 minutes between blocks. All trials used a semi-rigid hip exoskeleton system to provide targeted assistance during specific gait phases [4]. Motion capture (VICON Vero, 2000 Hz) recorded kinematic data from 23 reflective markers. MoS (mean and standard deviation) were calculated for the AP and ML directions using the extrapolated center of mass (COM) and base of support following the method described in Fallahtafti et al. [3]. Statistical analyses included linear mixed-model ANOVA, followed by paired t-tests or Wilcoxon signed-rank tests, where applicable. The Holm–Sidak correction was applied for multiple comparisons ($\alpha = 0.05$) [4].

**Results & Discussion:** High exoskeleton torque assistance delivered during mid stance (28% stride) significantly increased MoS in the AP direction compared to the Powered Off condition ($p = 0.006$; Figure 1). Earlier (21% stride) and later (42% stride) torque assistance also evidenced a trend towards increased AP MoS compared to the Powered Off condition ($p < 0.1$). Greater movement of the extrapolated COM relative to the BoS suggests enhanced stability in the AP direction with torque assistance. In the ML direction, MoS improved even when the exoskeleton was powered off ($p = 0.03$) suggesting the exoskeleton's structure enhanced ML stability even in the passive state. Torque assistance delivered during terminal stance (35% and 42% stride) evidenced a trend towards increased MoS in the ML direction compared to the No Exoskeleton condition ($p < 0.1$). However, added weight, reduced hip mobility [5], and lower muscle effort [6] may have contributed to increased mean step width, potentially serving as a compensatory mechanism to prevent falls. Despite these improvements, step variability did not change significantly. Collectively, these findings suggest that the exoskeleton enhanced balance in both active and passive states. These findings highlight the potential for hip exoskeletons to improve MoS during walking. Future research should explore long-term adaptation and the clinical applicability of exoskeletons in populations at risk of falls.

**Significance:** Targeted hip exoskeleton assistance can improve gait stability, offering a promising strategy to reduce fall risk and enhance mobility in individuals with gait impairments.

**Acknowledgments:** This research was funded by the United States Department of Veterans Affairs through Merit Awards (I01RX000604, I01RX003266).

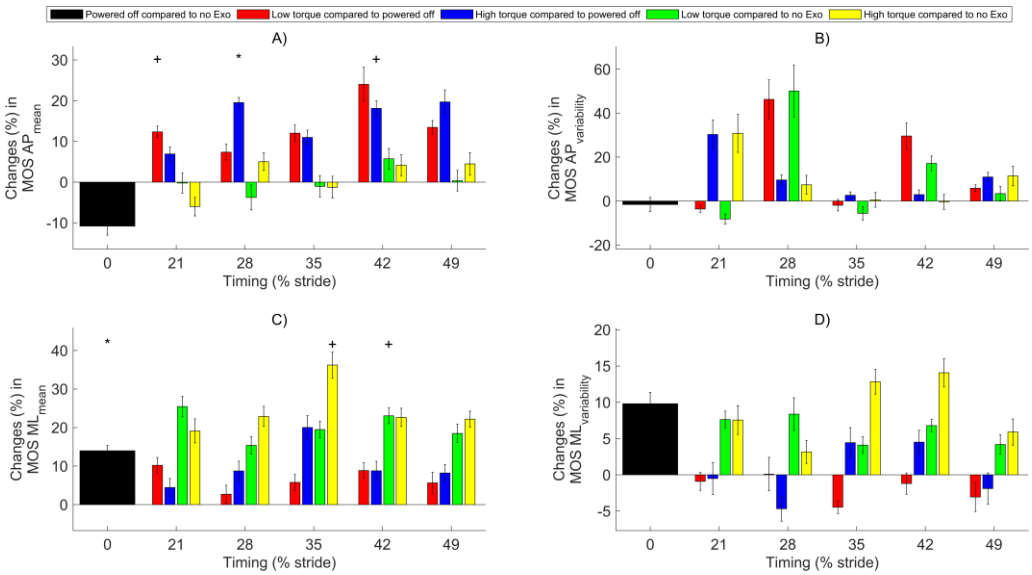


**Figure 1:** (A) MoS ML mean, (B) MoS ML variability, (C) MoS AP mean, and (D) MoS AP variability. Red and blue bars represent low and high torque-assisted conditions compared to Powered-Off. In contrast, green and yellow bars represent low and high torque-assisted conditions compared to No-Exo. Black bars represent the No-Exo condition. Asterisks (*) and plus signs (+) indicate significant differences ($p < 0.05$ and $p < 0.1$, respectively).

**References:**

[1] Wang et al., (2024). Aging Dis.
[2] Lanza et al. (2022). Arch Phys Med Rehabil; 103(8):1651-1662.
[3] Fallahtafti F, Gonabadi AM, Samson K, Yentes JM (2021). Biomechanics (Basel); 1(1):118-30.
[4] Mohammadzadeh Gonabadi A et al. (2024). Biomimetics; 9(4):211.
[5] Normand et al. (2023). J Biomech; 152:111552.
[6] Wu et al. (2015). Int J Adv Robot Syst; 12(3):18.

**The relationship between assistance torque and muscle activity during lifting with Back-Support Exoskeletons**

Amir Mehdi Shayan[1], Zeinab Kazemi[2], Divya Srinivasan[1,2]*
[1]Department of Bioengineering, Clemson University, Clemson, SC, USA.
[2]Department of Industrial Engineering, Clemson University, Clemson, SC, USA.
*Corresponding author's email: sriniv5@clemson.edu

**Introduction:** Active back-support exoskeletons offer varying levels of support to users, yet there are no standard guidelines for optimizing assistance to individual needs or task demands. Improper assistance can lead to over-reliance or inadequate support, potentially compromising user performance, comfort, and long-term musculoskeletal health [1]. Prior work exploring optimal assistance patterns in ankle exoskeletons has shown that the relationship between metabolic rate and peak assistance torque exhibited an asymptotic exponential function, with decreasing returns at higher levels of torque assistance [2]. It is unclear whether this relationship would also hold for back-support exoskeletons, and how higher torque support from an exoskeleton translates to muscle relief (instead of metabolic rate). This study examines whether muscle activity of the trunk extensor muscles changes systematically with increasing support levels from a powered back-exoskeleton during repetitive lifting tasks, and whether this trend is influenced by the load level. We used an active rigid exoskeleton called the Apogee (German Bionic Systems GmbH, Augsburg, Germany), with two electric torque generators aligned with the hip joints, for this study. We systematically adjusted the support settings of the device (EXO) in increments of 10%, from 20 to 80%, as users performed repetitive lifting tasks with loads adjusted to 10% and 20% of their respective body masses.

**Method:** Sixteen healthy participants (10 males aged 27.7 ± 8 years and 6 females aged 29.5 ± 8) lifted and lowered a box at 10% (low-load) and 20% (high-load) of their body mass @ 4 lifts per minute for 90 seconds, under 9 conditions: without EXO (control), while wearing the EXO but without any assistive support from the device, and while using the EXO at seven different levels of assistance ranging from 20 to 80%. The order of exposure of each participant to the different conditions was randomized. Inertial Measurement Unit (IMU) sensors (MTw Awinda, Xsens, B.V., Netherlands) were used to capture trunk kinematics, while surface electromyography (EMG) sensors (Ultium EMG system, Noraxon, AZ, USA) were placed bilaterally on trunk extensors (thoracic and lumbar erector spinae). EMG data were normalized to individual maximum voluntary contractions (MVC), as per standard guidelines for sensor placement, MVC tests, and data processing [3,4]. Peak thoracic (TES) and lumbar (LES) erector spinae muscle activities, and peak trunk flexion angle (pelvis-T8 segment) in the sagittal plane were extracted for the control condition, and at 20% (low), 40% (medium), and 80% (high) support levels of the EXO. Separate repeated measures ANOVAs were performed to assess the effects of support level on EMG and postural measures in low-load and high-load conditions, with significance at $p < 0.05$.

**Results and Discussion:** EXO had a significant main effect on the peak muscle activities of TES ($p = 0.046$ and 0.003 in low and high loads respectively) and LES ($p = 0.012$ and <0.0001 in low and high loads respectively). In the low load condition (left panel of Fig. 1), Tukey HSD post-hoc comparisons revealed that TES activity was significantly lower than control at the 40% support level (reduction of ~15%), and LES was significantly lower at 40% and 80% support levels (reduction of ~20%). In the high load condition (right panel of Fig. 1), TES activity was significantly lower than control at the 80% support level (reduction of ~25%), and LES was significantly lower at all support levels (reduction of ~25% at 20% and 40% support, and reduction of ~45% at 80% support). In all EXO conditions and all load levels, trunk flexion angle was significantly lower than in the control condition ($p$=0.002). Overall, while increasing torque assistance offered smaller returns in the low-load condition when going from medium to high level of assistance, when the load level was increased to 20% of body mass, there was substantially greater impact on muscle activity at the 80% assistance level. Trunk flexion angles were significantly lower across all support levels, indicating that using the powered exoskeleton promotes a more upright posture, potentially due to the weight of the device loading the back of the users. Future work is needed to examine whether inter-individual differences in muscle activity benefits can be explained by subject-specific modeling; and, whether subjective changes in perceived exertion and fatigue align with the objective EMG changes across varying assistance levels from the EXO.

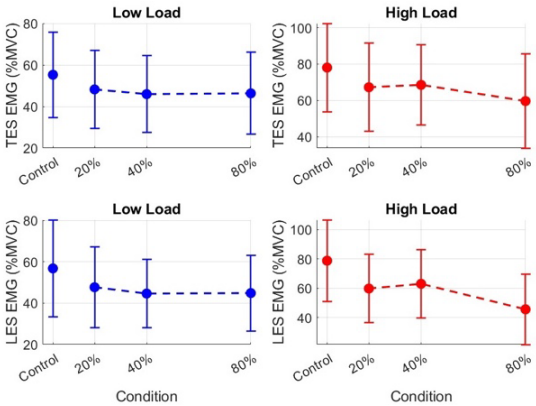


**Figure 1.** Peak thoracic (TES) and lumbar erector spinae (LES) EMG in control and EXO conditions of 20%, 40% and 80% torque assistance.

**Significance:** This study highlights that the relationship between exoskeleton assistance levels and objective biomechanical benefits is not linear and that it is modulated based on task demands. The findings emphasize the need for further understanding of whether individualized exoskeleton tuning to balance muscle relief may enhance long-term safety and usability of back-support exoskeletons.

**Acknowledgments:** This research was supported by NIOSH grant #T42OH008436.

**References:** [1] Hu et al. *Ergonomics*, 2025 1-13; [2] Miller et al. *JNER*, 2022 19(1)-46; [3] Wu et al. *JBiomech,* 2002 35(4):543-8; [4] Boettcher et al. *J Orth Res*, 2008 26(12).

# EVALUATION OF THE EFFECTS OF SPRING STIFFNESS IN KNEE AIDS ON THE KNEE JOINT LOADING

John Z. Wu[1]*, Kevin D. Moore[1], Liying Zheng[1], and Ting Xia[2]
[1]National Institute for Occupational Safety and Health, Morgantown, WV, USA.
[2]Department of Mechanical Engineering, Northern Illinois University, DeKalb, Illinois, USA. *Email: jwu@cdc.gov

**Introduction:** Osteoarthritis (OA) is a chronic disease that affects 32.5 million people in the US [1]. Occupational activities that require frequently performing high knee-flexion tasks are associated with a higher prevalence of knee OA compared to the average population [2,3,4]. Spring knee-aids have been used to protect the knee joints during dynamic high knee-flexion tasks. However, current commercially available knee aid products have not been thoroughly investigated or designed based on biomechanical principles. The current study aims to analyze knee joint biomechanics during deep squatting while wearing knee aids with different spring stiffness.

**Methods:** A knee aid is a hinge system consisting of a spiral spring and two flaps. Before being used in the simulations, the mechanical characteristics of the knee aids were tested and the spring constants of a representative pair of spring knee aids were determined. Based on our previous study [5], the normal tissue contact forces between the thighs and calves are modeled using a linear rotational spring. In the contact interactions, the thigh-calf and thigh/calf-knee-aid contact forces were considered as external forces applied onto the thighs and calves in the inverse dynamic analysis. Mechanically, the thigh-calf and knee-aid-thigh/calf contact forces form pairs of balanced forces that cancel each other out. An existing whole-body human model with detailed anatomical components of the knee (AnyBody Model version 7.2, Repository 2.0) was adopted and modified for the current study. The model contains the skeleton of the whole body; however, it only includes the muscles of the lower extremity. A total of 159 muscles in the lower extremity were included in the model. The effects of the mass and inertia properties of the upper extremity, trunk, neck, and head were included. The human model (80 kg weight and 1.70 m height) is approximately the average body measurements of North American men and women [6]. The knee flexion angles as a function of time were assumed to be a smooth cosine function with a peak around 150° and a period of 3 seconds. Four knee aid conditions were considered in the simulations: (1) without wearing knee aids, (2) wearing the regular spring knee aids, (3) wearing the knee aids with double spring stiffness, and (4) wearing the knee aids with four-times spring stiffness.

**Figure 1:** Commercially available spring knee aids (Left) and biomechanical model (Right).

**Results & Discussion:** The simulated effects of knee aids' use on the maximums of Quad forces, tibiofemoral (TF) contact ($TF_2$) and shear force ($TF_s$), patellofemoral (PF) contact ($PF_2$) and shear force ($PF_s$) are summarized in Fig. 2. The results show that the use of the regular knee aids (`1x') helped to reduce Quad forces, TF contact and shear forces, and PF contact and shear forces by 9%, 7%, 8%, and 7%, respectively. By increasing the spring stiffness, the force reduction in Quad, $TF_2$, $TF_s$, $PF_2$, and $PF_s$ reached as much as 33%, 23%, 33%, and 35%, respectively.

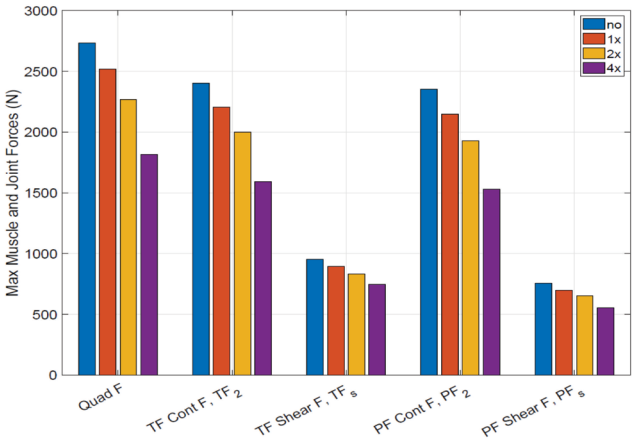


**Figure 2:** The maximal Quad muscle forces, and the normal contact and shear forces of the TF and PF joints for four different knee aids usage scenarios. "no", "1x", "2x", and "4x" imply without knee aids, with normal knee aids, with knee aids of two-times and four-times spring stiffness, respectively. The subscripts "s" and "2" in TF and PF indicate the shear and normal direction, respectively.

**Significance:** Our analysis indicated that wearing typical commercial knee aids during deep squatting helps reduce the quadriceps force, the PF and TF joint contact forces in the knee by about 7-8%; and the musculoskeletal loading reduction can be up to 33% by redesigning the knee aids to increase the spring stiffness by 1-3 times. Our results provided a biomechanical basis for improving the design of commercially available knee aids, which would help to reduce the risk of knee OA for workers who frequently perform high knee-flexion tasks.

**Disclaimers:** The findings and conclusions in this report are those of the authors and do not necessarily represent the official position of the National Institute for Occupational Safety and Health, Centers for Disease Control and Prevention. Mention of any company or product does not constitute an endorsement by the National Institute for Occupational Safety and Health, Centers for Disease Control and Prevention.

**References:** [1] Zhang et al. (2010) *Clin Geriatr Med* 26 (3) 355–69. [2] Coggon et al. (2000) *Arthritis Rheum* 43 (7) 1443–9. [3] Anderson et al. (1988) *Am J Epidemiol* 128 (1) 179–89. [4] Wang et al (2020) *Arthritis Care Res* 72(9)1213–1223. [5] Wu et al. (2024) *Proc of ASB-2024*. [6] Fryar et al. (2021) Anthropometric Reference Data for Children and Adults: United States, 2015-2018. Vital Health Stat 3. (36):1-44.

# ROBOTIC PNEUMATIC SHOES ELICIT ADAPTATIONS TO WEIGHT BEARING SYMMETRY DURING WALKING

*Mark Price[1,2], Sarah Szemethy[2], Wouter Hoogkamer[1], Meghan E. Huber[2]
[1]Department of Kinesiology, University of Massachusetts Amherst, USA
[2] Department of Mechanical & Industrial Engineering, University of Massachusetts Amherst, USA
*Corresponding author's email: mprice@umass.edu

**Introduction:** Stroke is a leading cause of long-term disability in the U.S., induces gait impairments in 80% of cases [1], many of which exhibit as gait asymmetries [2]. Split-belt treadmill training has demonstrated potential in correcting these asymmetries through asymmetry perturbations, but the effects do not extend to critical kinetic measures like paretic propulsion and weight bearing [2,3]. Surface stiffness perturbations have been proposed to elicit promising changes in weight bearing symmetry post-intervention via stiffness-controlled treadmills [4]. There is evidence, however, that adaptations to treadmill-based perturbations have limited transfer overground [5]. Furthermore, adjustable stiffness treadmills are not widely available, limiting the accessibility of interventions that use ground stiffness perturbations. Therefore, we developed variable stiffness robotic shoes to enable foot-ground stiffness perturbations during walking overground, on conventional treadmills, and out of the laboratory. The objective of this study is to quantify the adaptation effects from shoe-based stiffness perturbations on a treadmill to establish a comparative baseline against treadmill-based stiffness perturbation studies. We hypothesized that exposure to asymmetrical stiffness imposed by the robotic shoes results in asymmetrical vertical ground reaction forces (vGRF) after symmetrical stiffness is restored.

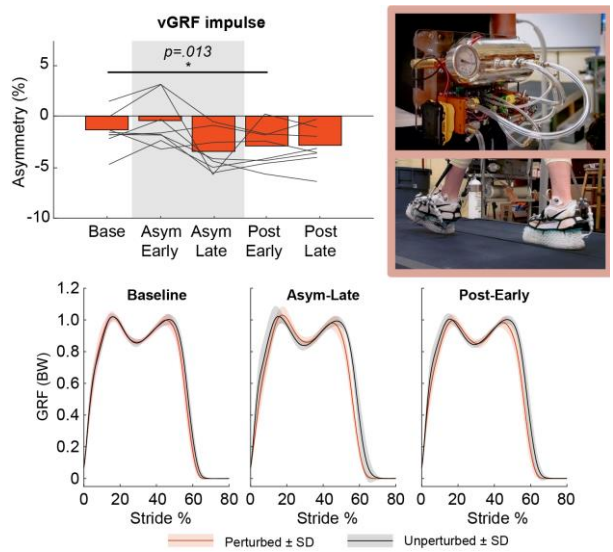


**Figure 1:** Top left: vGRF impulse asymmetry per condition. Individual participant values are overlaid on group means. Top right: Full wearable system including waist-mounted pneumatic control system and variable stiffness soles. Bottom: vGRF profiles averaged for 20 stride windows per highlighted condition.

**Methods:** Each pneumatic sole consists of a pair of soft 3D printed air pockets housed inside a flexible lattice (Fig 1a). A microcontroller-embedded wearable pneumatic system controls the stiffness of each shoe independently. A full-range stiffness change (~300 kN/m – 30 kN/m) takes ~4 seconds and is triggered remotely via RF keyfob by a bystanding operator.

Eight individuals with no musculoskeletal or neurological injuries completed one continuous 20 minute bout of walking on an instrumented dual-belt treadmill (Bertec, Columbus, OH, USA) with each belt traveling at 1.0 m/s. Participants walked for 5 minutes with both shoes set to maximum stiffness ("Baseline"), after which one shoe was decreased to minimum stiffness for another 10 minutes ("Asym"). The shoes then returned to symmetrically high stiffness for the final 5 minutes of walking ("Post"). We evaluated changes between sides by calculating the asymmetry ratio for each measure, defined as the difference between measures (M) recorded for the perturbed (P) and unperturbed limb (U) as a ratio of their sum: $(MP-MU)/(MP+MU)\times 100\%$. We calculated the average of this ratio over 20-stride windows at the end of the Baseline condition, the start and end of the Asym condition (Asym-Early and Asym-Late), and the start and end of the Post condition (Post-Early and Post-Late). We performed a repeated measures ANOVA to evaluate the effect of stiffness condition on vGRF symmetry during weight acceptance and push-off, vGRF impulse, and stance time. Paired t-tests were used to determine the presence of a post-intervention aftereffect (Baseline vs. Post-Early) for measures with a significant effect of condition.

**Results & Discussion:** Changing stiffness had a significant effect on vGRF impulse asymmetry ($p = .002$) and stance time asymmetry ($p=.013$). There was an aftereffect in vGRF impulse asymmetry (Mean difference: -1.69%, $p=.012$) and in stance time asymmetry (Mean difference: -0.55%, $p=.087$) toward the unperturbed side, though the stance time effect was not significant. The observation of an aftereffect in vGRF impulse asymmetry suggests that the intervention elicited a neuromotor adaptation in weight bearing symmetry during walking, as expected.

Unlike the effects seen from exposure to an adjustable stiffness treadmill, weight acceptance and push-off vGRF peaks were not significantly affected by changing stiffness, while impulse was significantly affected. It is possible that these differences are due to the high damping properties of the pneumatic shoes as opposed to the treadmill, which is underdamped [4]. Determining the effect of asymmetry perturbations with different mechanical impedance parameters will be an avenue of future work, as will studying overground stiffness perturbations using the novel footwear technology.

**Significance:** Changing the foot-ground interface stiffness during walking via pneumatic shoes elicits weight bearing asymmetry aftereffects in healthy participants. This result is promising toward eliciting weight bearing adaptations in individuals with neurological disorders, and eventually toward applying low-cost wearable technology to hemiparetic gait rehabilitation.

**Acknowledgments:** This work was supported by the NIH NIBIB under Grant 1R21EB033450.

**References:** [1] Duncan PW et al. (2005), *Stroke* 36; [2] Hendrickson J et al. (2014), *Gait Posture* 39; [3] Hoogkamer W (2017), *Exerc Sport Sci Rev* 45; [4] Price MA et al (2025), *T-MECH*; [5] Reisman DS et al. (2009), *Neurorehabil Neural Repair* 23.

# ROBOTIC ANKLE EXOSKELETON REDUCES ANKLE MUSCLE DEMAND DURING WALKING IN PERIPHERAL ARTERY DISEASE

Farahnaz Fallahtafti[1*], Zahra Salamifar[1], Iraklis Pipinos[2,3], Sara A. Myers[1,2]
[1] Department of Biomechanics, University of Nebraska at Omaha, Omaha, NE USA
[2] Department of Surgery and Research Service, Omaha Veterans' Affairs Medical Center, Omaha, NE USA
[3] Department of Surgery, University of Nebraska Medical Center, Omaha, NE USA
*Corresponding author's email: ffallahtafti@unomaha.edu

**Introduction:** Lower limb peripheral artery disease (PAD) is a cardiovascular condition caused by the narrowing or blockage of arteries supplying blood to the legs [1]. Claudication is the cramping pain experienced in the legs of individuals with PAD, triggered by physical exertion and alleviated by rest. Our research has highlighted a clear association between the walking limitations of claudicating patients and a deficit in the posterior calf muscles' ability to generate adequate ankle torque and power [2]. Previous work has also demonstrated the potential of wearable assistive devices to improve walking performance in patients with PAD [3]. A portable, robotic ankle exoskeleton (Biomotum, OR, US) (Figure 1) has been effective in increasing gait speed and efficiency during overground walking in children with cerebral palsy [4]. Therefore, this study aimed to determine the effect of this bilateral robotic ankle device on ankle joint biomechanics in patients with PAD. We hypothesized that the ankle exoskeleton would reduce muscle workload during push-off.

**Figure 1:** A patient with PAD wearing the exoskeleton footwear used in the study.

**Methods:** Nine patients with PAD (Age: 72.7±6.6 years, height: 1.76±0.05 m, and body mass: 90.01±13.9 kg) were evaluated while walking overground at their preferred speed across force plates embedded in the floor (AMTI, Watertown, MA, 1000 Hz; Figure 1). Participants wore form-fitting suits, and 33 retro-reflective markers were placed on specific anatomical landmarks on the subject's pelvis, thighs, shanks, and feet. Kinetics and kinematics data were recorded and combined to quantify ankle torques and powers during the stance period of the gait cycle. Participants walked under four conditions: 1) without the exoskeleton, 2) exoskeleton but zero torque, 3) exoskeleton with 0.2 Nm/kg torque (Low), and 4) exoskeleton with 0.3 Nm/kg (High), applied during plantar flexion to support push-off. Participants repeated five walking trials for each foot in which heel-strike and toe-off events were within the boundaries of the force plate. Dependent variables were peak discrete points from ankle angle, torque, and power curves. We used a one-way repeated measure ANOVA to test the effect of the condition on ankle joint biomechanics.

**Results & Discussion:** Peak dorsiflexion angle was reduced during both assisted walking conditions compared to walking without the exoskeleton and under the zero-torque condition, $F(3,24) = 16.26$, $p < 0.001$. We observed a significant decrease in peak ankle plantarflexor torque under assisted conditions relative to the zero-torque condition, $F(3,24) = 5.53$, $p = 0.005$ (Figure 2). The reduced plantar flexor torque during assisted conditions indicates that the assistance provided by the robotic device offloaded the demand from the calf muscles compared to zero torque condition. Ankle power absorption during the midstance phase of gait significantly varied across conditions, $F(3,24) = 16.43$, $p < 0.001$ (Figure 2). Under assisted conditions, the peak magnitude of ankle power absorption was lower than that observed without the exoskeleton or under the zero-torque condition. ~~A~~The reduction in ankle power absorption under assisted conditions indicates that the robotic device decreases the power needed for ankle movement during walking.

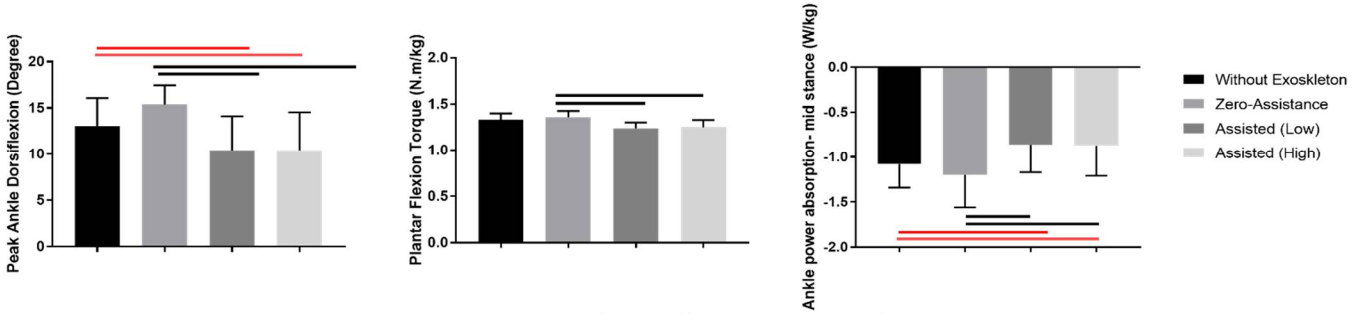


**Figure 2:** Ankle joint kinematic and kinetic data revealed significant differences among the four walking conditions: Black and red horizontal bars in the figure indicate significant differences of assisted conditions from no exo and zero torque conditions, respectively ($p < 0.05$).

**Significance:** The robotic ankle exoskeleton shifted ankle dynamics through the substitution paradigm. This can help patients with PAD expend less energy while walking, enabling them to walk further and with less pain.

**References:**

1. Criqui et al., (2021). *AHA.* CirC. 144(9)
2. Schieber et al., (2018). *J Vasc Surg.* 66(1), 178-186
3. Mays et al., (2019). *J Vasc Med.* 24(4), 324-331.
4. Orekhov et al., (2021). *J NeuroEngineering Rehabil*. 18; 163.:797147.

**Acknowledgments:** This research was funded by the United States Department of Veterans Affairs through AWARD (I01RX000604, I01RX003266).

# BIOMECHANICAL EVALUATION OF HIP PROTECTORS AND COMPLIANT FLOORING: A SYSTEMATIC REVIEW AND QUALITATIVE ANALYSIS

Kitaek Lim[1], Seyoung Lee[1], Junwoo Park[1], Woochol Joseph Choi[1]*
[1]Injury Prevention and Biomechanics Laboratory, Dept of Physical Therapy, Yonsei University, South Korea
*Corresponding author's email: wcjchoi@yonsei.ac.kr

**Introduction:** Falls are a leading cause of injuries among older adults, and hip protectors and compliant flooring have been developed to help address the fall-related injuries. While they are designed to reduce impact forces to lower injury risk (i.e., hip fracture), its clinical efficacy is contentious [1-2]. In this study, we systematically reviewed its effects on impact force attenuation during a fall. We also examined the relationship between the stiffness of the hip protectors and compliant flooring and its ability to attenuate impact forces.

**Methods:** A systematic review was conducted following the PRISMA guidelines. A comprehensive search strategy was applied using PUBMED, MEDLINE (ProQuest), EMBASE, Web of Science, and SportDiscus for articles published from 2014 to 2024. Studies reporting the biomechanical efficacy of hip protectors and flooring were included. Conference papers, abstract-only publications, dissertations, and articles unrelated to the study's aim were excluded. After initial screening, three researchers (KL, SL, and JP) independently reviewed the titles and abstracts to select articles meeting the inclusion criteria. To compare impact force attenuation, we calculated the average values of impact force in both padded (with a hip protector or compliant flooring) and unpadded conditions. For qualitative analysis, we determined percentage force attenuation (PFA) using average values provided in each paper, which defined as '(mean impact force in unpadded - mean impact force in padded) / mean impact force in unpadded * 100'. We also determined the stiffness ($k$) of hip protectors or compliant flooring, which calculated as follows: $k = \frac{F^2}{m*v^2}$, where $F$ = impact force in padded, $m$ = mass of a falling body, $v$ = impact velocity. Outcome variables included PFA and $k$. Mann-Whitney U test was used to test whether PFA differed between hip protector and compliant flooring. Spearman's correlation analysis was also used to examine the relationships between PFA and $k$, depending on protective strategies.

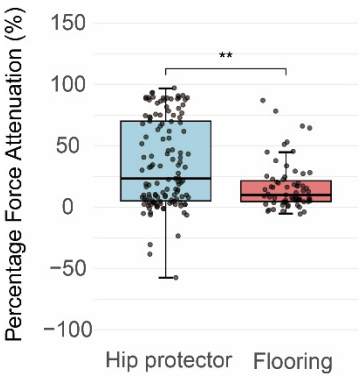


**Figure 1:** Biomechanical Efficacy of hip protector and compliant flooring in impact force attenuation during a fall

**Results & Discussion:** A total of 21 studies (14 on hip protectors, 7 on compliant flooring) met the inclusion criteria. For hip protector studies, experimental setups used to measure PFA included a drop tower (DT) (n = 7), inverted pendulum (IP) (n = 5), and pelvis release experiments with human subjects (PR) (n = 2). For compliant flooring studies, experimental setups included DT (n=2), IP (n = 2), PR (n = 2), and falling from standing height experiments with human subjects (n = 1). A total of 129 testing conditions were examined for hip protectors, including different drop heights and weights, impact velocities, brands and models (DT = 56, IP = 46, and PR = 27). Similarly, 67 conditions were examined for compliant flooring (DT = 16, IP = 24, PR = 24, and falling experiment = 3).

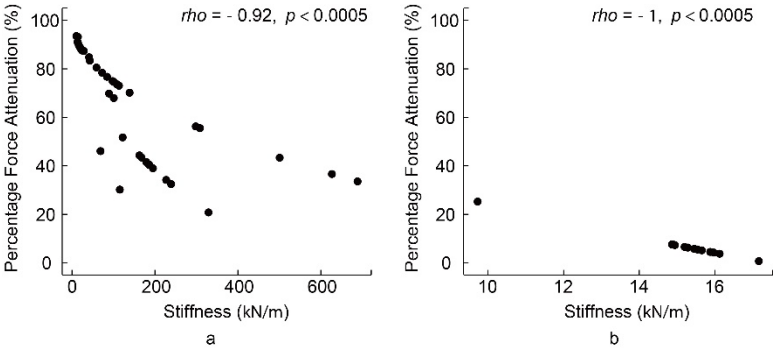


**Figure 2:** Correlation between the percentage force attenuation and the stiffness of hip protector (a), and compliant flooring (b).

Our descriptive statistics suggested that the median PFA was 23.3% (IQR: 5.2–70.2%) for hip protectors and 10.0% (IQR: 4.5–21.5%) for flooring (Figure 1). Mann-Whitney U test suggested that PFA differed between hip protector and compliant flooring ($W = 5508$, $p < 0.005$), and impact force attenuation was greater with hip protectors than compliant flooring.

Our correlation analyses showed that there were significant negative correlations between PFA and $k$ for hip protectors and compliant flooring (rho = -0.927, $p < 0.0005$; rho = -1, $p < 0.0005$; respectively).

**Significance:** Our results suggest that hip protectors exhibit greater force reduction compared to compliant flooring, indicating their superior ability to attenuate impact forces during falls. Additionally, the negative correlation between the stiffness and impact force attenuation capacity highlights the importance of structural or material properties of hip protectors and compliant flooring to improve clinical efficacy in reducing impact force.

**Acknowledgments:** This research was supported by Basic Science Research Program (RS-2023-00270689) and by the Brain Korea 21 FOUR Project", the Korean Research Foundation.

**References:** [1] Mackey et al. (2019), *PLoS Med* 16(6); [2] Robinovitch and Onyejekwe (2023), *J Am Med Dir Assoc* 24(7).

# CAN VIRTUAL NEUROMUSCULAR EXOSKELETON CONTROL PROVIDE SPEED-ADAPTIVE GAIT ASSISTANCE?

*Rish Rastogi[1], Max K. Shepherd[1,2], Seungmoon Song[1]
[1]Department of Mechanical & Industrial Engineering, College of Engineering, Northeastern University
[2] Department of Physical Therapy, Movement, & Rehabilitation Sciences, Bouvé College of Health Sciences, Northeastern University
*rastogi.ris@northeastern.edu

**Introduction:** Exoskeletons have the potential to improve mobility by providing assistive torque. For this potential to be realized, the timing of assistive torque from these devices must adapt to non-steady-state conditions. Promising advances have been made in task-agnostic control [1], however such controllers can be outperformed in steady-state motion contexts by optimized controllers. For example, human-in-the-loop optimized phase-based control of ankle exoskeletons can reduce metabolic cost of transport by as much as 39% [2]. Phase-based control often estimates gait phase based on prior stride durations and modulates plantarflexion torque accordingly during the stance phase of gait. While this gait phase estimation could be enhanced by a higher level controller [3], phase-based control can be ineffective or even dangerous during non-steady-state conditions such as abrupt speed changes (Fig. 1).

In this project, we propose virtual neuromuscular control (VNMC) as an alternative approach. We hypothesize that VNMC can adapt to sudden gait changes without high-level modulation. Rather than relying on predefined gait phases, VNMC takes ankle angle as input to generate human-like joint torque by emulating a musculoskeletal model that is activated by a reflex control model. This virtual torque is then scaled and commanded as the target assistance torque. VNMC is adapted from a reflex-based neuromechanical model that has demonstrated robust human-like walking in computer simulations [4]. Various versions of VNMC have been applied to steady-state walking [5], however, its effectiveness in abrupt changes during walking has not been evaluated. Thus, the objective of this study is to determine whether VNMC is more adaptive than phase-based control when users experience rapid speed changes while walking. To assess this, we will compare the two controllers' ability to modulate torque during speed transitions and the associated metabolic energy expenditure during these bouts.

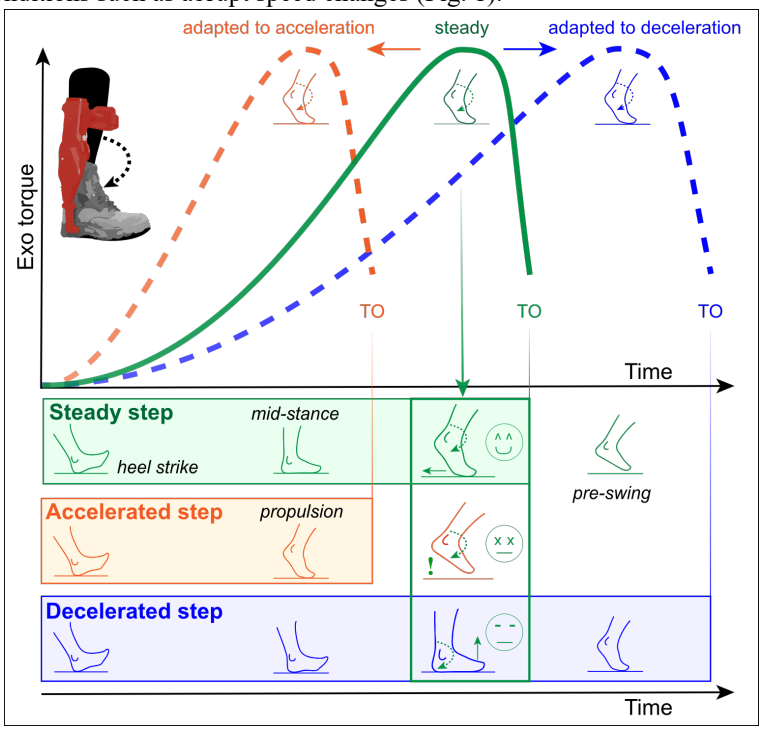


**Figure 1:** To be assistive, ankle exoskeleton torque needs to adapt appropriately during abrupt speed changes in gait. During an acceleration, step frequency drops. Thus, assistive torque should be delivered earlier in time to avoid unintended plantarflexion after toe-off (TO), which could trip the user. Conversely, during a deceleration step frequency rises, so assistive torque should be delivered later in time to match the propulsive phase of stance. We hypothesize that VNMC has the potential to shift torque timing suddenly and will thus outperform phase-based control in abrupt speed changes during walking.

**Methods:** Consenting healthy young adults will walk on an instrumented treadmill while wearing ankle exoskeletons (Dephy Exoboot, Dephy, Inc.) programmed with phase-based control, VNMC, or no assistance. In each condition, the treadmill will undergo 5 minutes of rapid speed changes where participants decelerate and accelerate from a moderate speed (1.25 m/s) to both a slower speed (0.75 m/s) and faster speed (1.75 m/s) at 1 m/s$^2$ acceleration. Participants will be able to see treadmill speed 2 seconds in advance to simulate real-world scenarios where they must quickly adjust their speed, such as crossing the street or avoiding collisions in a crowd.

We will primarily evaluate controller performance based on how well each control strategy adjusts its torque output in response to speed transitions and its effect on metabolic cost of transport. Specifically, we will assess how accurately commanded torque aligns with altered gait phase following a speed transition. Secondary measures will include joint kinematics and user preference.

**Initial Results:** Preliminary results (n=2) suggest that VNMC adapts to abrupt speed changes and delivers torque with appropriate timing whereas the phase-based controller struggles. During accelerations, the phase-based controller can induce up to 20% more peak plantarflexion (Fig. 1, steady torque profile applied to accelerated step) than VNMC due to a delay in commanded torque.

**Significance:** Findings from this study will inform the development of control strategies that enable exoskeletons to function effectively in dynamic environments, helping bridge the gap between controlled laboratory studies and real-world mobility applications. Such insights could contribute to the broader goal of making exoskeletons a practical mobility aid outside the lab.

**Acknowledgments:** This research is partially funded by the National Institutes of Health (R00AG065524).

**References:** [1] Molinaro et al. (2024), *Nature* 635; [2] Poggensee & Collins (2021), *Sci. Rob.* 6(58); [3] Shepherd et al. (2022), *IEEE Rob. & Automat. Lett.* 7(2); [4] Song & Geyer (2017), *Front. Comp. Neurosci.* 11; [5] Shafer et al. (2021), *Front. Bioeng. Biotech.* 9.

# JOINT POWER RESPONSES OF INDIVIDUALS POST-STROKE WALKING WITH A POWERED HIP EXOSKELETON WITH DIFFERENT LIMB ASSISTANCE STRATEGIES

*Kristen M. Stewart[1], Gregory S. Sawicki[2], Aaron J. Young[2], Richard R. Neptune[1]
[1]Walker Department of Mechanical Engineering, The University of Texas at Austin, Austin, TX
[2]Woodruff School of Mechanical Engineering, Georgia Institute of Technology, Atlanta, GA
*Corresponding author's email: kristen.stewart@utexas.edu

**Introduction:** Powered exoskeletons offer the potential to improve mobility for individuals post-stroke with hemiparetic gait. Typically, individuals post-stroke exhibit distal muscle weakness and pre-swing deficits [1], thus hip exoskeletons can be advantageous due to the proximity of the device mass relative to the body center-of-mass and the ability to do positive work on the leg to help initiate leg swing. However, there are various control parameters and assistance strategies that can be utilized. Typical exoskeleton devices vary control parameters such as timing and magnitude [e.g., 2], but few studies have investigated the impact of limb assistance on walking mechanics. While the paretic limb often exhibits less propulsion, shorter stance time and impaired distal muscle function [e.g., 3], there is an increased dependence on the nonparetic limb, which may adversely affect their gait. Recent work investigating hip exoskeleton assistance strategies in individuals post-stroke found that bilateral assistance increased self-selected walking speed overground [4]. However, it is unclear how lower-limb joints respond to different exoskeleton limb assistance strategies. Therefore, the purpose of this study was to determine how lower-limb joint power changes based on different limb assistance strategies for individuals post-stroke walking with a powered hip exoskeleton. We expected that net hip joint power with the exoskeleton would increase and subsequently knee and ankle joint power would decrease when the respective limb is assisted relative to no assistance.

**Methods:** Kinematic and kinetic data were previously collected from five individuals post-stroke (age: 52 ± 10 years; time after stroke: 5 ± 2 years; height: 173 ± 10 cm; mass: 75 ± 13 kg) [4]. Each subject walked at their self-selected speed on an instrumented treadmill wearing the Samsung GEMS hip exoskeleton (mass = 3.3 kg) with four different assistance conditions: unassisted (UN), paretic limb assistance (P), nonparetic limb assistance (NP) and bilateral assistance (PNP). The exoskeleton provided flexion and extension torque throughout the gait cycle with a maximum magnitude of 6 Nm. Hip, knee and ankle net joint powers including the exoskeleton power were calculated for the paretic and nonparetic limbs and normalized by body mass. Joint work was calculated by integrating joint power over the gait cycle.

**Results & Discussion:** For both the paretic and nonparetic limbs, positive hip work increased with ipsilateral limb and bilateral assistance relative to UN (Figs. 1A & 1B), which aligned with our expectation. Hip power increased in early stance (0-10% gait cycle) when the exoskeleton provided ipsilateral hip extension assistance as well as in late stance (45-65% gait cycle) when the exoskeleton provided ipsilateral hip flexion assistance (Figs. 1A & 1B), suggesting the exoskeleton acted to help accelerate the leg into swing. Negative paretic knee power decreased for all powered assistance strategies (Fig. 1A), which reflects less power absorption in late stance. Interestingly, ankle power increased in all powered assistance strategies relative to UN (Figs. 1A & 1B), suggesting an increase in propulsion [5]. Increasing paretic propulsive force is a key focus in rehabilitation to increase walking speed [6], which is consistent with our previous work demonstrating the exoskeleton with unilateral and bilateral assistance increased overground walking speed in these individuals [4]. Overall, both limbs responded similarly to exoskeleton assistance, with the most notable changes occurring with the ipsilateral and bilateral assistance strategies.

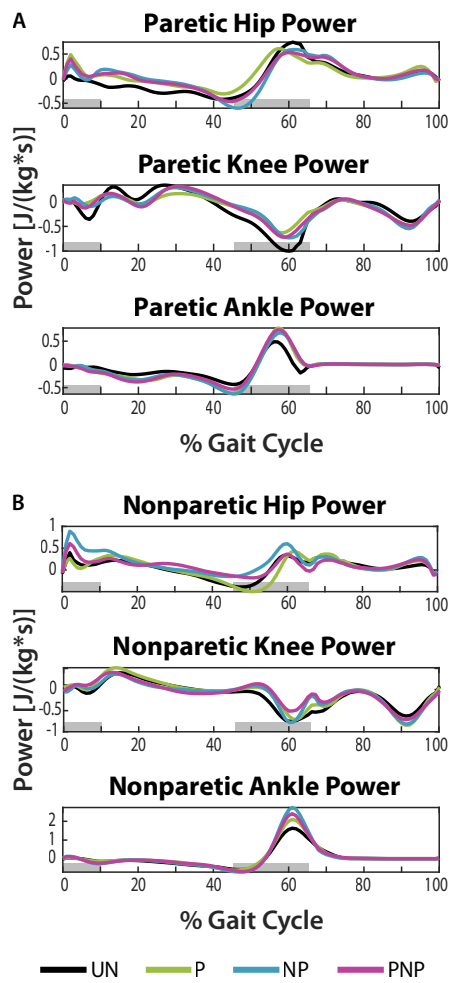


**Figure 1:** Net joint power at the hip, knee and ankle for the (A) paretic and (B) nonparetic limbs for all limb assistance strategies. Joint power is normalized by body mass and averaged across all subjects. Gray shaded regions represent ipsilateral limb exoskeleton assistance timing.

**Significance:** Understanding how individuals post-stroke respond to different limb assistance strategies can help inform clinicians on how to customize the assistance strategy to improve each individual's gait. Further, identifying the ideal limb assistance strategy will help provide the framework for the development of novel assistive devices and control strategies to further improve walking performance for individuals with mobility impairments.

**References:** [1] Peterson et al. (2010), *J Biomech* 43; [2] Galle et al. (2017), *J NeuroEngineering Rehabil* 14; [3] Hall et al. (2011), *Clin Biomech* 26(5); [4] Pan et al. (2023), *Ann Biomed Eng* 51(2); [5] Huang et al. (2015), *J Exp Biol* 218(22); [6] Bowden et al. (2006), *Stroke* 37(6).

# BIOMECHANICAL EFFECTS OF VARYING ASSISTANCE MAGNITUDE DURING LEVEL-GROUND AND RAMP-ASCENT LOCOMOTION USING A ROBOTIC HIP EXOSKELETON

*Jimin An[1], Eni Halilaj[1], Inseung Kang[1]
[1]Carnegie Mellon University, Pittsburgh, PA, USA
*Corresponding author's email: jimina@andrew.cmu.edu

**Introduction:** Instantaneous estimation of an individual's biological joint moment and mapping it into a torque command for exoskeleton control can enhance locomotor performance [1]. In contrast to earlier control strategies limited to steady-state locomotion, this method adapts to transitions among diverse locomotor tasks by adjusting exoskeleton assistance based on the estimated joint moments, without needing any extra modifications [2]. While the existing approach reliably estimates the user's moment, mapping that moment into exoskeleton torque remains simple, with linear scaling of magnitude and a uniform delay in assistance timing. Given the distinct biomechanical characteristics of different tasks, the static state-to-torque mapping function's suitability across varied tasks remains questionable. To address this gap, we investigated the impact of assistance magnitude on a user's biomechanical demands at different locomotion tasks by examining positive joint work and biological hip joint torque. We hypothesized that the optimal assistance magnitude for ramp ascent (RA) would be higher than that for level ground (LG) condition, given that increased slope naturally imposes greater physical demands [3], reflecting the need for a task-specific scaling factor.

**Methods:** One able-bodied male subject completed walking trials with a speed of 1.0m/s on 0° and +10° slopes while wearing a bilateral robotic hip exoskeleton (Fig. 1A). The exoskeleton utilized hip encoder data to estimate gait phase and subsequently apply a predefined assistance profile with variable magnitudes. This assistance profile was calibrated via pilot experiments to match the subject's biological hip joint moment, with peak torque magnitudes set at 12.5%, 11.25%, 10%, 8.75%, 7.5%, 6.25%, and 5% of their body weight (Fig. 1A). Data for each assistance condition, as well as a control trial without the exoskeleton (No-Exo), were collected during a 30-second trial on an instrumented treadmill, using a markerless motion capture system (Theia3D, Ontario, Canada). We evaluated the following primary outcomes: 1) positive hip joint work; 2) peak extension and flexion moment. To test the driving hypothesis, we used a one-way analysis of variance (ANOVA) with the significance level set to 0.05 and post-hoc pairwise comparisons with a Bonferroni correction on positive hip joint work to determine which assistance magnitude significantly differed from the No-Exo condition.

**Results & Discussion:** Positive hip joint work, measured at various assistance magnitudes, exhibited distinct trends between level ground and ramp ascent (Fig. 1B). For level ground, joint work increased with excessive assistance magnitudes. Compared to the No-Exo condition, joint work was significantly higher at 12.5%, 11.25%, 10% assistance levels, while lower at 5% assistance level ($p<0.0018$). This pattern aligns with a previous study that an optimal level of assistance exists and excessively high magnitudes may actually penalize user performance [4]. In contrast, during ramp ascent, increasing assistance magnitude led to a continuous decrease in joint work, with significant reduction at all conditions except 10% magnitude relative to the No-Exo ($p<0.0018$). This joint work analysis supports our hypothesis that ramp ascent requires higher assistance magnitudes to manage increased physical demands compared to level ground, suggesting that a fixed scaling factor is inadequate across tasks. Furthermore, the analysis of peak extension and flexion moments revealed that extension peaks consistently decreased while flexion peaks consistently increased across all conditions. The average percentage change in moment peaks for both level ground and ramp ascent show that the tested assistance magnitudes do not reduce the flexion peak, unlike the extension peak (Fig. 1C). This finding highlights the importance of incorporating a phase-adaptive component into the control mapping function. If assistance magnitude is not the primary factor in reducing the biological joint moment during the flexion phase, then varying the assistance timing may be more effective for enhancing user performance. Yet, the stark contrast between the flexion and extension phases still suggests that applying a constant delay to both phases would be inadequate.

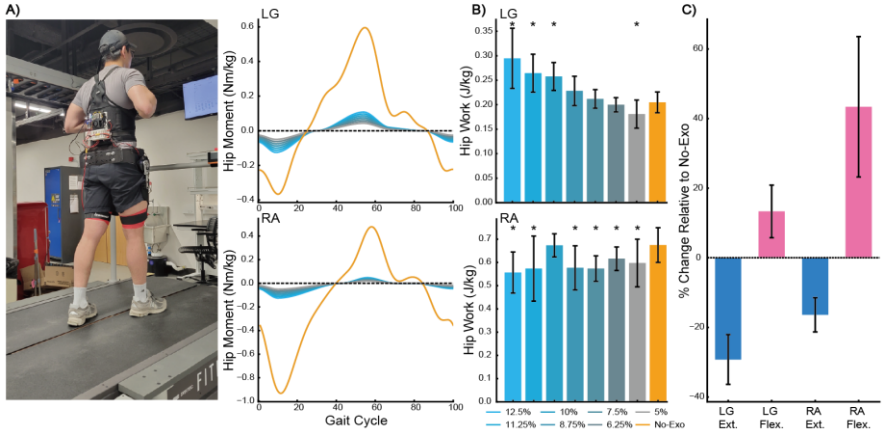


**Figure 1:** A) Subject with the bilateral robotic hip exoskeleton, assistance profiles with varying magnitude, and the subject's biological hip joint moment (orange) at level ground and ramp ascent. B) Average positive hip joint work for each magnitude level and No-Exo condition. * indicates a statistical difference from the No-Exo condition ($p<0.0018$). C) Average extension and flexion peak moment percentage changes normalized to No-Exo condition.

**Significance:** This study demonstrated that varying assistance magnitudes yield distinct benefits across locomotion modes and gait phases. This indicates that the current static state-to-torque mapping strategy is not effective in optimizing exoskeleton performance across locomotor tasks. A single uniform scaling approach may not account for the varying biomechanical demands across tasks. Future work should investigate the advantage of utilizing a task- and phase-adaptive state-to-torque mapping strategy.

**References:** [1] Molinaro et al. (2024), *Sci R obot*; [2] Molinaro et al. (2024), *Nature*; [3] K ang et al. (2002), *Eur J Appl Physiol*; [4] Shepertycky et al. (2023) *Plos one*

# TOWARDS SIMULATION-BASED EXOSKELETON CONTROL DESIGN AND OPTIMIZATION

Calder Robbins[1*], Chun Kwang, Tan[1], Seungmoon Song[1]
[1]Department of Mechanical and Industrial Engineering, Northeastern University, Boston, MA, USA
*Corresponding author's email: robbins.cal@northeastern.edu

**Introduction:** Developing effective exoskeleton control traditionally requires extensive human subject trials due to the variability of individual responses. Researchers have employed different forms of human-in-the-loop optimization [1,2] and data-driven control [3] to provide effective control to all users, but most approaches demand substantial experimental data, making optimization difficult. Phase-based feedforward ankle exoskeleton controllers have successfully reduced energy expenditure during walking, with previous studies demonstrating up to 40 ± 8% metabolic cost reduction [4]. This method, which parameterizes assistance torque through a spline with four tunable parameters for rise time, peak time, fall time, and peak torque, has been widely adopted. However, evaluating the effects of increasing or reducing spline parameters would require additional human subject experiments, limiting further optimization and investigation. Predictive neuromechanical simulations provide a scalable alternative by modeling natural gait patterns and optimizing control parameters in dynamic environments [5]. Recent advancements in imitation-based musculoskeletal simulations have enabled in-silico evaluation of exoskeleton controllers, reducing reliance on costly human trials [6]. However, the extent to which these simulations can reliably inform exoskeleton control requires further validation. Here, we leverage a MyoSuite-based simulation environment to systematically evaluate phase-based exoskeleton control strategies, determining whether the conventional four-parameter spline is near optimal or if alternative parameter structures offer greater benefits. This study contributes to the broader goal of designing and assessing exoskeleton controllers through simulation by analyzing the trade-offs between controller complexity and effort reduction.

**Methods:** Simulations were conducted using MyoSuite, a physics-based musculoskeletal simulation framework [7]. A reflex-based neuromechanical model with 22 muscles, 47 control parameters [5], and an ankle exoskeleton were implemented to evaluate exoskeleton control strategies during walking (Figure A). Assistance was applied at the ankle joint using a phase-based controller, with the torque profile defined using a piecewise cubic Hermite interpolating polynomial (PCHIP). Each PCHIP spline is specified by $n$ points, leading to $2 \times n$ parameters, corresponding to the time and magnitude of each point. The four-parameter phase-based spline controller served as the baseline. Eleven parameter configurations will be tested, comparing the baseline four-parameter spline to $n = 1$ through $n = 10$ point splines (Figure B). Optimization is performed using the Covariance Matrix Adaptation Evolution Strategy (CMA-ES), which simultaneously optimizes both musculoskeletal model parameters and exoskeleton control parameters. The primary cost function, *cost of transport*, was calculated as the sum of squared muscle activations normalized by distance travelled and the number of muscles. Each $n$-point spline condition will be evaluated over five independent trials to ensure robustness. Two additional baseline conditions will be included: one without an exoskeleton and another with the exoskeleton modelled but no active assistance.

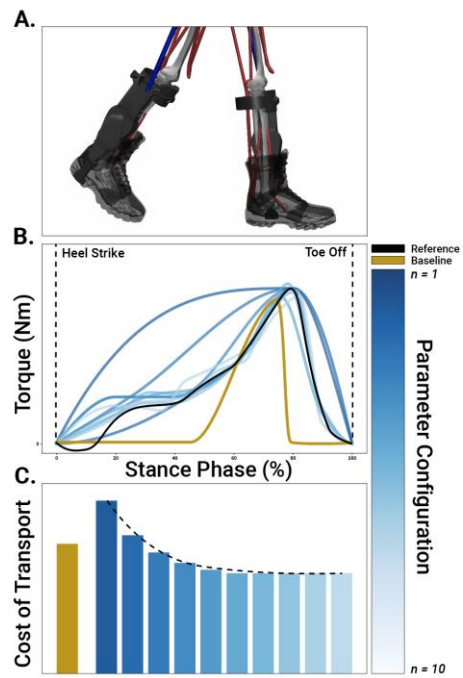


**Figure.** Neuromechanical model (A), possible spline configurations for each control parameter configuration, (B) and resulting effort cost (C). *Results presented are potential results.*

**Expected Results & Discussion:** Varying the number of spline parameters is expected to reveal a trade-off between complexity and effectiveness. While the baseline phase-based controller spline is widely used for its simplicity, it is unlikely to be optimal. Increasing control points should initially improve assistance by better shaping the torque, but these cost reductions are expected to plateau. Moving from three to four or six points may meaningfully reduce effort cost, but excessive parameterization (e.g., 10 points) is unlikely to provide further benefit, while adding unnecessary complexity (Figure C).

**Significance:** Our simulation results will reveal the potential benefits of adding more spline points, enabling us to make better-informed decisions about the relationship between control complexity and cost of transport. By utilizing predictive musculoskeletal simulations, we may reduce the need for extensive human subject testing while providing insights into the optimal balance between controller flexibility and practical implementation.

**Acknowledgments:** This research is funded by the National Institutes of Health (R00AG065524).

**References:** [1] J. Zhang *et al.*, *Science*, (2017). [2] Slade, P., Kochenderfer, M. J., Delp, S. L. & Collins, S. H., *Nature* (2022). [3] D. D. Molinaro, I. Kang, and A. J. Young, *Science robotics*, (2024). [4] Poggensee KL, Collins SH., *Science Robotics*, (2021)
[5] S. Song and H. Geyer, *The Journal of Physiology*, (2015). [6] S. Luo *et al.*, *Nature*, (2024). [7] Caggiano, V. *et al.*, *PMLR* (2023)

# OPTIMIZING LOWER-LIMB EXOSKELETON ASSISTANCE THROUGH SUBJECT-SPECIFIC PREDICTIVE GAIT SIMULATIONS: TORQUE PROFILES AND METABOLIC COST SAVINGS

Neethan Ratnakumar[1], *Xianlian Zhou[1]
[1]Department of Biomedical Engineering, New Jersey Institute of Technology, Newark, NJ 07102
*Corresponding author's email: alexzhou@njit.edu

**Introduction:** Lower limb exoskeletons have significantly improved gait assistance by reducing metabolic energy expenditure, muscle activations, and even increasing walking speeds [1]. These improvements hold great promise for enhancing mobility and quality of life. However, achieving personalized, optimal assistance remains a challenge. While human-in-the-loop (HIL) experiments [2] are commonly employed to determine effective torque profiles, this study investigates subject-specific predictive gait simulations for optimal assistance. We examine how variations in individual anthropometry affect metabolic cost reductions and assistive profiles, and whether generalized findings from generic simulations [3] hold true across diverse body types.

**Methods:** A 2D generic musculoskeletal (MSK) model with 10 degrees of freedom and 18 muscles was anthropometrically scaled to six able-bodied distinct individuals (4 males, 2 females; 1.75 ± 0.10 m, 72.4 ± 15.4 kg). Maximum isometric muscle forces ($F_{max}$) were scaled based on subject height ($H$) and weight ($M$):

$$F_{max} = F_{max}^{G} \times \frac{M}{M^{G}} \times \frac{R_{MSK}}{R_{MSK}^{G}} \times \frac{H^{G}}{H}$$

where superscript $G$ denotes generic model parameters, and $R_{MSK}$ is the muscle-to-body mass ratio [4]. Predictive simulations were first performed in OpenSim MOCO [5] to simulate unassisted gait with muscle control. The cost function included metabolic cost ($J_{MER}$), muscle effort ($J_{Effort}$), minimum joint acceleration ($J_{Joint}$), minimum center of mass acceleration ($J_{COM}$), and reference movement tracking ($J_{Track}$):

$$J_T = \int_{t=0}^{t_f} \left(w_1 J_{MER} + w_2 J_{COM} + w_3 J_{Joint} + w_4 J_{Effort} + w_5 J_{Track}\right) dt$$

We then co-optimized various combinations of idealized assistive torques (Hip, Knee, Ankle, Hip+Knee, Hip+Ankle, Knee+Ankle, Hip+Knee+Ankle) with muscles using the same cost functions (Fig. 1(A)). The maximum torque limits set for all joints are 100 $Nm$.

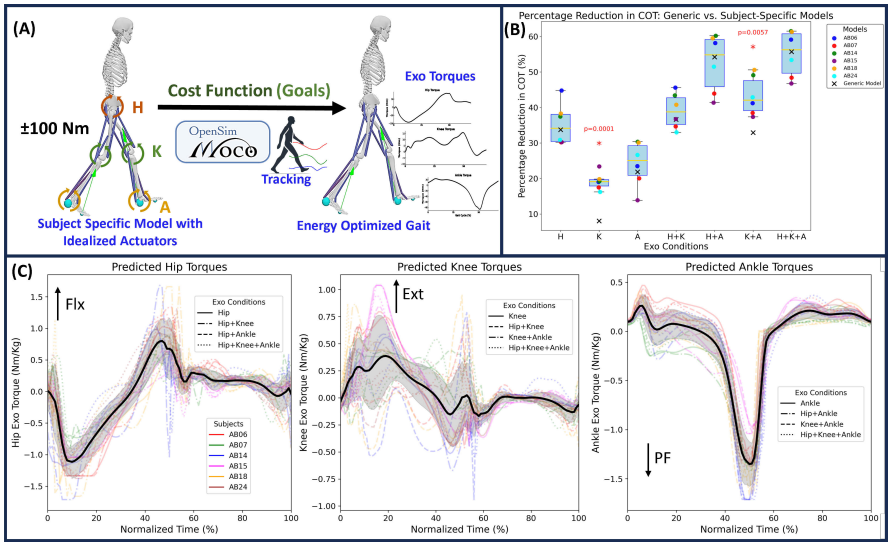


**Figure 1:** (A) Subject-specific models with idealized actuators are used in predictive simulations to obtain energy optimized gait and assistive torque profiles. (B) Predicted percentage CoT savings in comparison to the unassisted case. (C) Predicted assistive torques for all cases; dark black lines are the means across all conditions and all subjects.

**Results & Discussion:** All assistive cases reduced the CoT relative to unassisted baselines (Fig. 1(B)). Among single-joint configurations, the Hip was the most effective. For dual-joint setups, the Hip+Ankle combination provided the highest benefits, while adding knee assistance (Hip+Knee+Ankle) yielded the best overall performance; though only marginally better than Hip+Ankle. Subject-specific CoT reductions aligned with those observed in the generic model [3], except for the Knee ($p = 0.0001$) and Knee+Ankle ($p = 0.0057$), where subject-specific performance was superior. Comparing our results to emulator-based HIL studies such as [2], our Hip condition outperformed the Ankle condition; in contrast to [2], where ankle assistance achieved similar or slightly better CoT savings relative to the hip. Notably, only the Ankle condition in our study resulted in slightly lower savings than those corresponding reported in [2], while all other conditions showed marginally higher reductions. Although [2] used a no-torque baseline and our study a no-exoskeleton baseline, the comparisons remain analogous given our use of idealized actuators. The predicted torque profiles were mostly consistent across all six individuals for the hip and ankle joints (Fig. 1(C)), though more variability was observed in knee assistance; particularly in the Hip+Knee condition. Moreover, predicted hip, knee, and ankle torque patterns closely resemble biological moments. These idealized torque profiles could serve as an effective starting point for designing energy-efficient exoskeleton assistance.

**Significance:** Predictive simulations for exoskeleton control with subject-specific models enable rapid, cost-effective evaluation of control strategies without extensive prototyping and experimental testing. By using idealized, massless motors and setting a high torque limit, our simulations predict the maximum potential CoT savings and identify optimal assistance patterns, offering valuable insights for guiding design of optimized lower-limb exoskeleton assistance.

**Acknowledgments:** We thank Vinay Devulapalli and Niranjan Deepak for assisting with generic model simulations.

**References:** [1] Lakmazaheri et al. (2024), *JNER* 21(1); [2] Frank et al. (2021), *Wearbl Tech* 2(e16); [3] Ratnakumar et al. (2022), *Proc 7th Int DHM Symp* 7(1); [4] Wang et al. (2022), *Saf Health Wrk* 13(3); [5] Dembia et al. (2020), *PLOS Comp Biol* 16(12), e1008493.

# CHANGES IN PHYSIOLOGICAL BIOMARKERS DURING GAIT ADAPTATION TO HIP VS. ANKLE EXOSKELETONS

*Hansol X. Ryu[1,2], Dongho Park[1], Kennedy G. Kerr[1,2], Amro Alshareef[1], Hangyeol Song[1], Aaron Young[1], Gregory S. Sawicki[1]
[1]Georgia Institute of Technology, Atlanta, GA, USA
[2] Emory University, Atlanta, GA, USA
*Corresponding author's email: hansol.ryu@gatech.edu

**Introduction:** Humans adapt to changing locomotion environments, including interactions with wearable robots. While various factors such as metabolic rate and muscle activities change during gait adaptation, the relationships between these biomarkers remain to be explored. A previous study [1] reported different time scales in muscle activities, step frequency, and their variabilities, suggesting that initial exploration contributes to metabolic rate reduction over multiple days of testing with an ankle exoskeleton. Another study [2] observed adaptations in metabolic rate, muscle activities, and mechanical power utilization over 3 days of testing ankle exoskeleton.

These studies focused on ankle exoskeletons, but comparing adaptations to hip and ankle exoskeleton may allow us to better understand adaptation mechanism across joints. Notably, ankle muscles are connected to more compliant tendons than hip muscles, and compliant tendons may add complexity to responses from sensor organs like muscle spindle [3]. Thus, assistance primarily targeting ankle joint may be more challenging to adapt to, because sensory feedback plays a critical role in motor adaptation. We hypothesize that hip exoskeleton will have a bigger effect on adaptation than ankle exoskeleton across various physiological biomarkers.

**Methods:** One able-bodied subject with no known musculoskeletal conditions participated in the study, wearing either hip or ankle exoskeleton. The participant continuously walked at 1.25 m/s for 6 minutes without exoskeleton assistance, 30 minutes with assistance ("adaptation"), and 6 minutes without assistance ("de-adaptation"). We measured metabolic rate using indirect calorimetry, lower-body muscle activities using surface electromyography (EMG) sensors, and ground reaction force and moments using the instrumented split-belt treadmill. Vertical ground reaction forces were used to detect heel-strike and toe-offs of each foot, and step length was calculated from the belt speed, center of pressure trajectory and heel-strike and toe-off timings. Average EMG was computed by integrating filtered EMG signals over each stride and dividing by the stride duration. To model adaptation, we fitted a first order curve $y = a_1 e^{-t/\tau} + a_0$ to each biomarker $y$, where $t$ represents time, and coefficients $a_0$, $a_1$ and time constant $\tau$ were fitting variables.

The hip exoskeleton was custom-built [4] and generated about 10% of participant's hip torque during walking using on-line hip joint torque estimation [5]. Ankle exoskeleton (Dephy EB60 Exoboots, USA) generated torque using a spline approximation of the typical ankle torque based on a gait phase estimator, with the peak plantar-flexion torque set at 15Nm. Although controllers are different, spline-based and estimated-torque-based controllers are expected to produce similar assistance during normal steady-state walking.

**Results & Discussion:** We observed overall similar, but more pronounced gait adaptation patterns with a hip exoskeleton than with an ankle exoskeleton (Fig. 1). There was a rapid increase and decrease in step length variability ($\tau$=0.06 for hip, 0.21 for ankle) and at the onset of the assistance. Step lengths had longer time constants ($\tau$=1.50 for hip, 4.18 for ankle) than their variabilities, but were quicker than EMG and metabolic rate changes. Differences between hip and ankle exoskeletons were more evident in EMG patterns and metabolic rate. With hip exoskeleton, muscle activities and co-activation increased at the onset of adaptation and de-adaptation, then gradually decreased throughout the adaptation period at a slower rate ($\tau$=5.43 and 5.47). In contrast, there were less clear adaptation patterns in EMG using ankle exoskeleton. Metabolic rate changes followed a similar trend ($\tau$=4.36 for hip, 6.74 for ankle) to EMGs, with a more prominent adaptation pattern with hip exoskeleton even though we believe that ankle exoskeleton delivered a larger percentage of the joint torque.

These results are consistent with our hypothesis that adaptation patterns are more pronounced with the hip exoskeleton than ankle exoskeleton. Future work will include designing exoskeleton control policies that enable more rigorous comparisons.

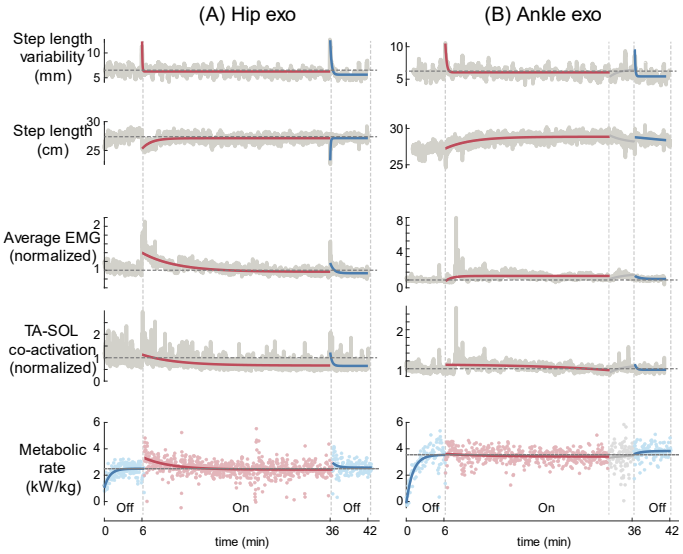


**Figure 1:** Changes in step length and variability, average EMG and soleus-tibialis anterior co-activation, and metabolic rate using either (A) hip or (B) ankle exoskeleton.

**Significance:** With growing interest in exoskeletons, it would be valuable to gain understandings on similarities and differences in gait adaptation to hip and ankle exoskeletons. This could help develop methods to predict and enhance motor adaptation while providing insights into broader motor adaptation mechanisms, focusing on sensorimotor interactions and human physiology.

**Acknowledgments:** This work was supported by NSF-BII 2319710.

**References:** [1] Abram, SJ., et al. (2022) *Curr. Biol.* [2] Sawicki GS, Ferris DP. (2008) *J. Exp. Biol.* [3] Abbott EM., et al. (2024) *Exp. Physiol.* [4] Park, D., et al. (2025) *IEEE TBME* (2025). [5] Molinaro DD, Kang I, Young AJ. (2024) *Sci. Robot.*

# METABOLIC DIFFERENCES IN GAIT ADAPTATION TO AN ANKLE VS. HIP EXOSKELETON

*Kennedy G. Kerr[1,2], Hansol X. Ryu[1,2], Dongho Park[1], Amro Alshareef[1], Hangyeol Song[1], Aaron J. Young[1], Gregory S. Sawicki[1]
[1] Georgia Institute of Technology, Atlanta, GA
[2] Emory University, Atlanta, GA
*Corresponding author's email: kgkerr@emory.edu

**Introduction:** Transient dynamics of adaptation to a powered exoskeleton reflect motor learning occurring over many minutes to hours, and the mechanism of this adaptation may be joint-specific [1, 2, 3]. While net metabolic cost reduction is similar when an assistive exoskeleton torque is provided at the ankle or hip with the same control paradigm [3], the mechanism of adaptation at a distal vs. proximal joint may differ, based both on musculotendon anatomy and individual user differences. For example, signaling from the sensory organs that drive motor learning (e.g., spindles) can be attenuated when there is significant tendon compliance in series with muscles [4]. Additionally, prior work has shown reduced metabolic cost and ongoing kinematic changes as participants become expert exoskeleton users over multiple training sessions [1, 2]. Understanding adaptation over a single walking bout may reveal additional insights about underlying structural and functional differences between the ankle and hip joints. Here, we preliminarily investigated within-participant metabolic differences between adaptation to an exoskeleton acting at the ankle compared to the hip. We predicted that adaptation would be observed in both conditions, where metabolic cost will peak and then decay following the onset and offset of exoskeleton assistance, in line with exoskeleton adaptation literature [1, 2]. We further hypothesized that this effect would be smaller at the ankle, where increased tendon compliance would attenuate sensory input from exoskeleton torque, slowing motor adaptation.

**Methods:** One able-bodied young adult walked on a treadmill at 1.25m/s with either an ankle or hip exoskeleton. Metabolic cost was collected using indirect calorimetry. One continuous trial consisted of 6 minutes of quiet standing, 6 minutes walking without assistance, 30 minutes walking with a torque applied at the hip or ankle, 6 minutes walking without assistance, and 6 minutes quiet standing (Fig. 1A). The ankle exoskeleton (Dephy EB60 Exoboots) delivered 15 Nm of peak plantarflexion torque using a spline-based optimized torque assistance profile controller [5], which we estimated to be similar to or greater than 10% of the participant's biological torque. A custom hip exoskeleton delivered 10% of biological hip flexion torque during swing phase using a deep learning real-time estimate of biological torque [6]. Metabolic power from each walking block was fit with a first-order exponential. We normalized metabolic cost to participant weight and reported the percent change in metabolic cost from steady-state walking. We defined steady-state as minutes 3-5 of the initial unassisted walking block. Early and late adaptation phases are the first and last 2 minutes of walking with the exoskeleton on, and post-adaptation is the first 2 minutes of the second unassisted walking block.

**Results & Discussion:** Metabolic power data showed a greater adaptation effect in the hip exoskeleton condition compared to the ankle, as shown by the larger spike in metabolic cost and smaller time constant at the onset and offset of exoskeleton assistance (Fig. 1B). The ankle condition did not show the expected increase in metabolic cost compared to baseline walking during early and post adaptation (Fig. 1C), suggesting less adaptation occurred. Less pronounced adaptation effects at the ankle compared to the hip may reflect underlying structural differences in the muscle-tendon unit. Sensory organs in ankle muscles may not as directly reflect changes to the joint due to the more compliant Achilles tendon, attenuating sensory signals driving motor adaptation. Limitations of this protocol include that the control algorithm and percentage of biological torque delivered differed between devices. Future work will use the same torque estimation controller on both joints and investigate whether the magnitude of exoskeleton torque influences adaptation rate and extent.

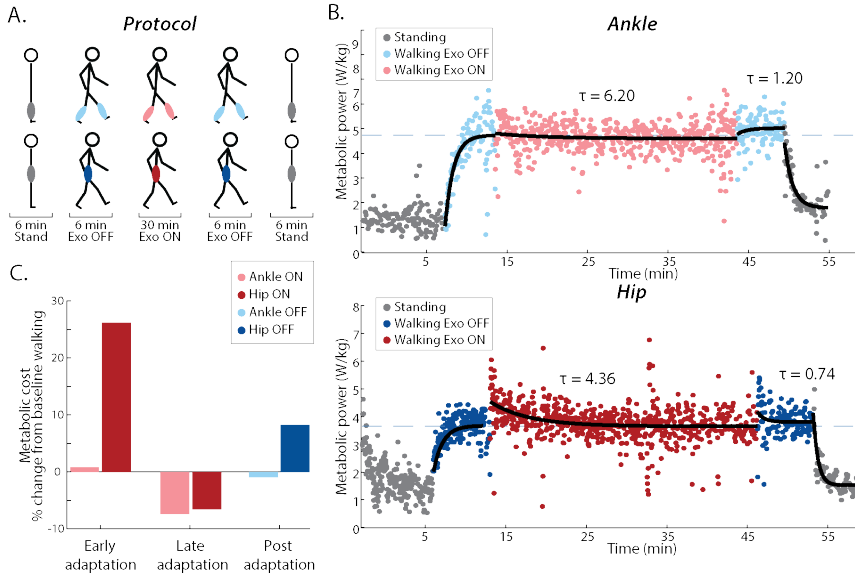


**Figure 1:** (A) Trial structure for an ankle (top) and hip (bottom) exoskeleton. (B) Breath by breath metabolic power during each adaptation trial. τ (in minutes) is the time constant of the adaptation and de-adaptation exponential fit. (C) Percent change of mean metabolic cost from steady state walking during early adaptation, late adaptation, and post-adaptation.

**Significance:** User adaptation to assistive exoskeletons can be a long process. Understanding mechanisms of adaptation at different joints and on shorter time scales may allow for more personalized and efficient exoskeleton selection.

**Acknowledgments:** This research was funded by NSF-BII 2319710 and NIH T32 EB025816

**References:** [1] Poggensee and Collins (2021), *Science Robotics* 6(58). [2] Sawicki and Ferris (2008), *J Exp Bio* 211(9). [3] Franks et al. (2021), *Wearable Technol* 2(16). [4] Abbott et al. (2024), *Exp Physiol* 109(1). [5] Zhang et al. (2017), *Science* 356(6344). [6] Molinaro et al. (2024), *Nature* 635(377-344).

# EFFECTS OF BODY WEIGHT SUPPORT ON CENTER OF MASS KINEMATICS DURING INFANT CRAWLING

Tristan McCarty[1], Leah Nguyen[2], Cole Galloway[3], Elena Kokkoni[1]*
[1]Dept. of Bioengineering, University of California, Riverside, Riverside, CA 92521, USA
[2]Dept. of Biology, University of California, Riverside, Riverside, CA 92521, USA
[3]Dept. of Physical Therapy, Baylor University, Waco, TX 76706, USA
*Corresponding author's email: elena.kokkoni@email.ucr.edu

**Introduction**: Crawling is the earliest form of independent locomotion, enabling humans to explore more distant surroundings for the first time. Certain diagnoses, such as Down Syndrome (DS) may affect crawling skill quality and performance [1]. Dynamic body-weight support (BWS) may enhance motor performance by modulating the gravitational load on the extremities during locomotion [2]. As the gravitational load varies, locomotion cycles and forward translation of the body are affected, which can be mechanically represented by shifts in the body's Center of Mass (CoM) [3]. Studies with adults using BWS during walking have demonstrated a reduced variation in CoM excursion, indicating greater stability and reduced energy cost [4]. Nevertheless, current knowledge regarding the effects of BWS on the CoM is predominantly limited to adult walking gait [3]. Therefore, the goal of this preliminary work was to explore changes in CoM motion from BWS use during crawling locomotion early in human life.

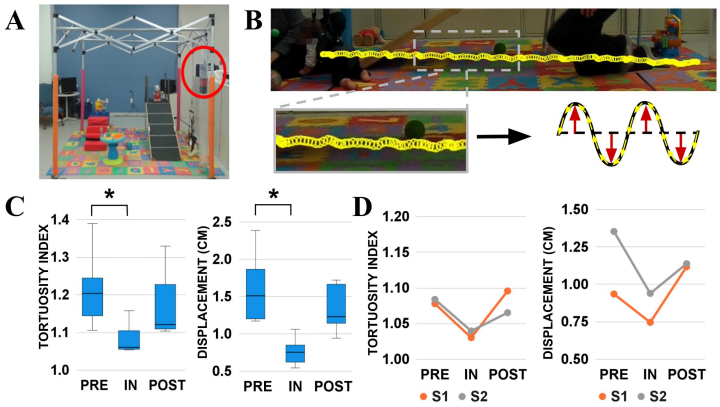


**Figure 1:** **(A)** The portable overground BWS system. **(B)** *IN* condition segment. Inset of CoM trajectory, used to calculate vertical oscillation (up and down movement, red arrows), CoM path length (length traveled by the CoM, yellow arrows), and tortuosity index (ratio of total path length and net displacement, dotted line). Tortuosity index and vertical oscillation for TD **(C)** and DS **(D)** infants.

**Methods**: Data from six typically developing (TD) infants ($M_{age}$ = 10.5 ± 1.2 months) and two infants diagnosed with DS ($M_{age}$ = 19.2 ± 0.8 months) were analyzed in this work. Infants participated in two lab sessions, during which they performed crawling trials under three experimental conditions: without assistance from the BWS device *(Pre)*; with BWS assistance (~20% of the infants' body weight) *(In)*; and again, without BWS assistance *(Post)*. A portable, commercially available BWS device was used (PUMA®, Enliten, LLC, Newark, DE). The device contains a counterweight pulley system connected to a soft wearable harness (My Early Steps™, Little Dundi, LLC) to manipulate the amount of assistance by providing constant vertical support. Video-recordings were used to identify crawling segments in which a minimum of three consecutive crawling cycles were performed without interruptions. A circular marker placed in the lumbar region of the infants' trunk (to approximate CoM) was digitized in each frame (DLTdv tool in MATLAB [6]) to obtain its x and y coordinates in the sagittal plane [7]. Crawling segments in which the marker was occluded for more than 30 consecutive frames or five percent of the total segment duration were excluded from analysis; shorter gaps in the trajectories were filled using the Modified Akima piecewise cubic Hermite interpolation. The following variables were computed: Path Length, Vertical Oscillation, and Tortuosity Index. Given the different group characteristics, Wilcoxon Signed-rank tests were conducted for the TD group, while an exploratory descriptive approach was followed for the DS group.

**Results & Discussion**: In TD infants, vertical CoM oscillation was less during *In* compared to *Pre* ($p$ = 0.028); however, CoM marker oscillation was not significantly different between *Pre* and *Post* ($p$ = 0.173) (Fig. 1). Smaller tortuosity index in the *Pre* condition compared to the *In* condition ($p$ = 0.028) was observed, but not between *Pre* and *Post*; ($p$ = 0.249). For the two infants with DS, vertical CoM oscillation seems to be less with BWS assistance ($M_{In}$ = 0.84, $SD_{In}$ = 0.14), compared to *Pre* ($M_{pre}$ = 1.14, $SD_{pre}$ = 0.30), and *Post* ($M_{Post}$ = 1.13, $SD_{Post}$ = 0.01). Similar patterns exist in the tortuosity index, BWS assistance results in a lower index ($M_{In}$ = 1.03, $SD_{In}$ = 0.006) compared to *Pre* ($M_{Pre}$ = 1.08, $SD_{Pre}$ = 0.004) and *Post* ($M_{Post}$ = 1.08, $SD_{Post}$ = 0.02) (Fig. 1). Both infants with DS seem to present similar CoM trajectory patterns (SDs reported above) whereas the TD infants display greater variability in vertical oscillation ($SD_{Pre}$ = 0.46, $SD_{In}$ = 0.18, $SD_{Post}$t = 0.31) and tortuosity index ($SD_{Pre}$ = 0.10, $SD_{In}$ = 0.04, $SD_{Post}$ = 0.09), which may be due to the fact that the sample of TD infants is larger leading to more inter-subject variability. Nevertheless, data from the infants with DS suggest a pattern of change in CoM trajectory across conditions, similarly to TD infants. Overall, the CoM motion paths from all infants were straighter when assisted by BWS. The reduced load provided by BWS assistance may result in less energy requirements to move their extremities, meaning the effort needed to maintain balance and propulsion may be lessened with the use of the BWS device [4]. Both populations seem to adapt rapidly to BWS assistance, but these adaptations may not be immediately retained when BWS is removed. A larger longitudinal study will define the BWS training exposure duration needed for transfer of effects.

**Significance**: Although the crawling patterns of TD infants have been studied, there is limited information on how BWS affects CoM motion in infants without and with motor challenges, such as DS. By reducing the gravitational load, training with BWS may help infants with DS move more efficiently, making crawling motion more stable and less effort-intensive. This information can be used to develop strategies for training programs that promote crawling locomotion in infants with mobility challenges.

**References**: [1] Malak et al. (2015) Med Sci Monit 21:1904; [2] Hagio et al. (2021) *Sci Rep* 11(1):14749; [3] Tesio et al. (2019) *Front Neurol*, 10:999; [4] Bannwart et al. (2020) *J Neuroeng Rehabil* 17:1-15; [5] Malloggi et al. (2019) *Int J Rehabil Res* 42(2):112-119; [6] Hedrick, (2008) *Bioinspir Biomim* 3(3):034001; [7] Napier et al. (2020) *J Biomech* 108:109886.

# QUANTIFYING NONLINEAR ANKLE QUASI-STIFFNESS BEHAVIOR DURING SLOPED WALKING

*Emma R. Caringella[1], Kota Z. Takahashi[1]
[1]Department of Health and Kinesiology, University of Utah, Salt Lake City, UT
*Corresponding author's email: emma.caringella@utah.edu

**Introduction:** An important functional property of the human ankle joint is natural ankle quasi-stiffness — a measure of the ankle's ability to control the joint rotational motion of the lower leg during stance phase of gait [1]. Natural ankle quasi-stiffness is used to inform the design of mobility devices such as prostheses, orthoses, and exoskeletons. Historically, linear or first-order regression models for natural ankle quasi-stiffness (slope of ankle moment vs ankle angle) have been used to understand ankle function [2]. These linear models are analogous to a rotational spring with constant stiffness [3] and are directly transferrable into passive mobility devices. However, linear models do not fully capture the stiffness progression of the human ankle as the joint dorsiflexes during a step (i.e. nonlinear stiffening behavior) [4]. Neglecting to model this nonlinear stiffness can have consequences such as rendering passive prostheses overly stiff in some phases of stance [5], which studies have predicted could lead to increased energy expenditure [6] and asymmetrical gait [7]. Recent studies have quantified quasi-stiffness using nonlinear models (second and third-order polynomial regressions) during level ground walking [8], but quasi-stiffness behavior on unlevel terrain, such as uphill and downhill walking, has not yet been studied. Improving the design of passive prostheses to account for different slopes will enable prosthesis users to ambulate with greater safety and independence. We hypothesize that across all sloped conditions, nonlinear regression models will better fit the data compared with linear regression models. If supported, these findings can be used to improve the design of passive prostheses, enabling individuals with lower-limb amputations to traverse terrain beyond a flat road.

**Methods:** Twelve healthy young adults (3F/9M, 25.5 ± 2.5 yrs, 75.0 ± 15.5 kg) participated in this study. Participants walked barefoot on an instrumented split-belt treadmill (Bertec Columbus OH, USA) for 5 minutes at 1.25 m/s in five slope conditions in randomized order: decline (-10°, -5°), level (0°), and incline (5°, 10°). The treadmill's sampling rate was 1000 Hz. A 14-camera motion capture system (Vicon, Oxford, UK) captured kinematic data from a six-degree-of-freedom marker set on the lower extremities at 100 Hz. Inverse dynamics were conducted using Visual 3D (C-Motion, Inc., USA) software. The ankle joint angle was defined as the motion of calcaneus relative to the shank, with the neutral position (ankle angle of 0°) defined as the plantar surface of the foot perpendicular to the shank. We filtered the raw data from marker trajectories and ground reaction forces using a second-order dual-pass low-pass Butterworth filter of 6 Hz for kinematic data and 25 Hz for kinetic data. Right ankle angles and ankle moments were analyzed with a custom MATLAB (R2024A, The MathWorks, USA) code. The stance phase of gait was extracted and further divided into the loading phase, defined as the onset of plantarflexion moment to the peak plantarflexion moment. Linear, quadratic, and cubic polynomial least-square best-fit regressions on net ankle moment vs. ankle angle were computed for the loading phase of each slope condition. Adjusted $R^2$ and RMSE were calculated for each regression.

**Results & Discussion:** A cubic regression model, compared to quadratic and linear models, best fit the loading phase curves for Decline -10° (adjusted $R^2$ = 0.975), Decline -5° (adjusted $R^2$ = 0.997), and Level 0° (adjusted $R^2$ = 0.998). A quadratic model best fit the Incline 5° condition, albeit with low goodness of fit (adjusted $R^2$ = 0.444) (Figure 1). These results partially support our hypothesis and indicate that the human ankle displays nonlinear stiffness on level and nonlevel slopes. However, the Incline 10° condition was insufficiently modeled by linear and nonlinear regressions (adjusted $R^2$ = 0.213 for all model types), and the overall slopes of the regressions notably violated the capabilities of a passive spring. During the later portions of the loading phase, the ankle begins plantarflexing while the plantarflexion moment is increasing, revealing that mechanical energy is injected into the ankle. Altogether, our results suggest that passive mobility devices (prostheses, orthoses, exoskeletons) could emulate key features of the natural ankle quasi-stiffness via nonlinear rotational springs. Still, for steeper slopes above a 5° incline, a powered device may be needed.

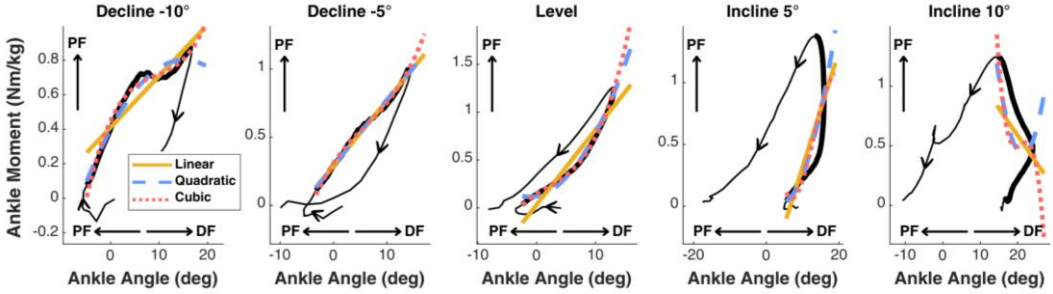


**Figure 1:** Ankle angle vs. net moment (normalized to body mass) curves for slope conditions: decline (-10°, -5°), level (0°), and incline (5°, 10°). Linear, quadratic, and cubic polynomial least-square best-fit regressions are displayed for the loading phase of each curve (PF = plantarflexion; DF = dorsiflexion).

**Significance:** Results from this study provide insight into the variation in ankle stiffness during walking on unlevel terrain. This knowledge is essential for improving the design of biologically inspired devices, including passive and powered prostheses.

**References:** [1] Nigro L. J Biomech Eng, 2022. [2] Shamaei, K. PLoS ONE 2013. [3] Hendrick E.A. J NeuroEng Rehabil 2019. [4] Nigro, L. Gait Posture. 2021. [5] Arch, Elisa S. Journal of Prosthetics and Orthotics [6] Quesada RE, Journal of Biomechanics, 2016. [7] Wang X. Mechanical Sciences, 2020. [8] Brockett, CL. Orthop Trauma. 2016.

**Characterizing the Dynamic Stiffness of Twisted and coiled artificial muscles for powered Ankle-Foot Orthoses**

*George S. Elias[1], Braeden C. Harrell[2], Kirsten M. Anderson[3],
Jason M. Wilken[3], Caterina Lamuta[1], & Deema Totah[1]
[1] Department of Mechanical Engineering, [2] Department of Biomedical Engineering, [3] Department of Physical Therapy and Rehabilitation Science, University of Iowa, Iowa City, IA
*Corresponding author's email: george-elias@uiowa.edu

**Introduction:** Ankle foot orthoses (AFOs) are devices designed to help manage abnormal neuromuscular function, like muscle weakness, by providing structural support around the ankle to assist in controlled movement. Passive AFOs may use mechanical elements like springs and dampers, but provide limited functional assistance and lack the ability to vary the amount of stiffness (i.e. support) provided to the user. Active AFOs, characterized by the addition of positive power about the ankle, offer the advantage of tunable assistive torque and variable stiffness, but this often comes at the expense of increased device weight and high power requirements. Twisted and coiled artificial muscles (TCAMs), a new smart material actuator containing both passive and active assistance within a singular component, balance the need for low-cost, lightweight and flexible actuation, with high force output and low power requirements [1]. TCAM contraction is driven by joule heating from electrical current induced by a voltage source. The heating causes radial expansion leading to controlled contraction. Prior dynamic testing of TCAM bundles showed their potential to replicate soleus muscle force output [2]. Further testing is needed to characterize their active and passive properties within an AFO context and under gait-relevant motion. Here, we present an experimental characterization of a TCAM actuation module within a powered AFO undergoing flexion through a gait cycle's range of motion.

**Methods:** A powered AFO (Fig. 1) was created out of a carbon fiber shell and a dual-action ankle joint (Nexgear Tango Ankle Joint, Ottobock). The powered AFO is actuated by 32 twisted and coiled artificial muscles (TCAMs) affixed to its posterior side, with the ability to generate a plantarflexor moment. A hall-effect sensor (AS5048B, ams-OSRAM) placed at the ankle joint measures flexion angle, while a single-axis loadcell (LCM300, Futek) in-line with the TCAMs measures the force they generate. The resulting force is a function of the applied voltage across the TCAMs and amount of pre-tension they are subjected to.

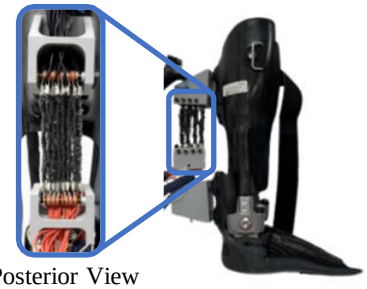


**Figure 1:** Powered AFO with TCAMs

To characterize the **dynamic**, **passive** properties of the TCAMs, the powered AFO was dorsiflexed from 0 to 13 degrees at 8 deg/s (equivalent to ~0.3 m/s walking speed) in an existing AFO testing apparatus [3]. The powered AFO was cycled 10 times at three different TCAM pre-tensions T0, T1, and T2, corresponding to low, medium and high tension, respectively. We calculated torque-angle profiles from the measured force and angle data. Testing was also done to measure force output of the **active** component in static flexion (10 degrees of dorsiflexion) when a 10 V step input is applied.

**Results & Discussion:** This preliminary testing shows that just by utilizing the **passive** properties of TCAMs (through pre-tensioning), we are able to achieve dynamic torque profiles reaching 12 - 20 Nm (figure 2). This corresponds to 10 - 20 % of biological ankle moment in an 85 kg healthy individual [4]. As for the **active** components, powering the TCAMs with 10 V step input increased force output by ~25%. By tuning the TCAMs' active and passive components, we can generate customized torque profiles that provide biomimetic supplemented stiffness and force profiles during gait. Future testing includes investigating the response time of the active component and its ability to provide real-time adaptive support during AFO deflection in the mid- to late-stance phase of gait.

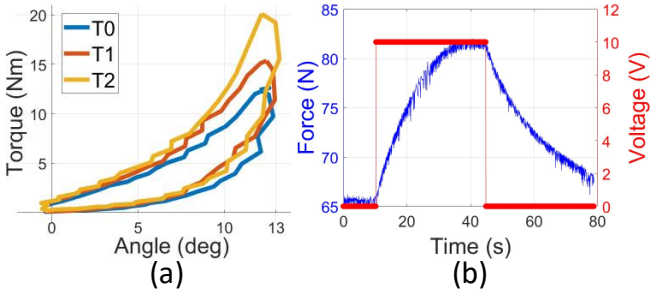


**Figure 2: (a)** Passive torque-angle curves demonstrating the effect of pretension on resistance to rotation. **(b)** Force output of TCAMs with a 10V step voltage input in static flexion.

**Significance:** The ability to characterize the active and passive components of smart, artificial muscles in gait applications presents transformative potential for assistive devices towards improved mobility and independence. These TCAMs have the potential to augment or compensate for muscle forces across various joints in a lightweight, low-cost, and high-power design.

**Acknowledgment:** Supported by start-up funds from the University of Iowa. Thank you to Jeffrey Palmer, CPO for AFO manufacturing.

**References:** [1] Lamuta et al., Smart Mater, 2018; [2] Kotak et al., Journal of Biomechanical Engineering, 2021; [3] Totah et al., Mechatronics, 2021; [4] Sharma et al., Gait and Posture, 2025

# EFFECTS OF ASYMMETRIC STIFFNESS WALKING ON JOINT KINEMATICS AND KINETICS

Leah Metsker[1*], Mark Price[2,3], Jenna Chiasson[2], Elena Schell[2], Jonaz Moreno Jaramillo[2], Meghan E. Huber[3], Wouter Hoogkamer[2]
[1] Department of Biomedical Engineering, University of Massachusetts Amherst
[2]Department of Kinesiology, University of Massachusetts Amherst
[3]Department of Mechanical and Industrial Engineering, University of Massachusetts Amherst
*Corresponding author's email: lmetsker@umass.edu

**Introduction:** Stroke, a leading cause of long-term disability, leaves about 80% of survivors with gait impairments and about 55% of chronic stroke survivors exhibit gait asymmetries [1]. Symptoms of post-stroke gait include decreased hip, knee, and ankle flexion and hip extension in the paretic limb [2]. Research shows increased paretic plantarflexion angle after dual-belt speed interventions in individuals' post-stroke, which improves post-stroke step length asymmetry [3]. However, this intervention does not improve weight bearing and propulsion symmetry during walking [4]. Prior work has shown that walking on an asymmetric stiffness dual-belt treadmill can evoke interlimb coordination pathways leading to aftereffects in vertical ground reaction forces (vGRFs) [5]. The objective of this study was to explore the effects of a single bout of asymmetric foot-ground stiffness walking on joint kinematics and kinetics in healthy participants. We expected that participants would adapt towards putting less weight on the low stiffness side (perturbed) but would require greater push-off on that side to initiate swing. We hypothesized that peak plantarflexion angle and moment during push-off on the low stiffness side increases, and the dorsiflexion angle during swing phase on the high stiffness side increases, immediately after the perturbation compared to baseline.

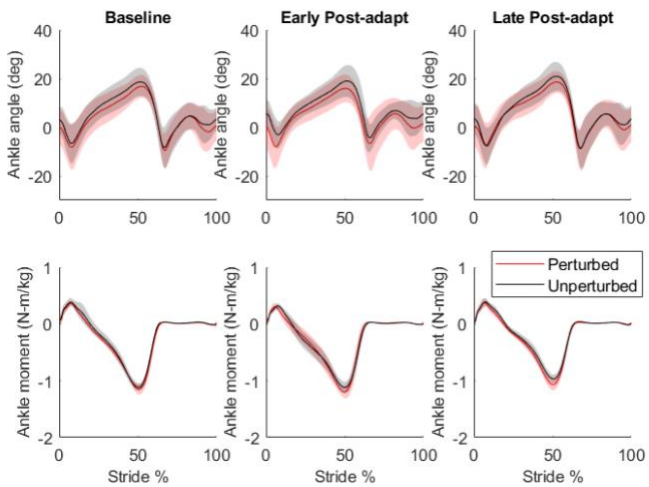


**Figure 1:** Ankle angles and moment averaged across five participants before, immediately after, and 5-minutes after the asymmetric stiffness perturbation. Shaded lines represent mean ± 1 SD.

**Methods:** Ten healthy individuals (age: 19-22; mass: 67 ± 6.78 kg) with no musculoskeletal or neurological injuries participated in this study. Participants completed a single session of 3 bouts of walking at 1.25 m/s. Participants completed a 5-minute baseline on an instrumented treadmill (Bertec, Columbus, OH, USA). Then, participants performed a 10-minute walking trial on a dual-belt adjustable stiffness treadmill (AdjuSST [6]) with the stiffness of the left belt lowered to 15 kN/m while the right belt remained rigid (300 kN/m). Walking kinematic aftereffects were assessed during a 5-minute trial on the instrumented treadmill. Kinematic data was analyzed from five participants using OpenSim. The changes in vGRF and joint moments between sides were evaluated by calculating the difference for each measure (M), defined as the difference between measures recorded for the perturbed (P) and unperturbed (U) limb divided by their sum: $(M_P-M_U)/(M_P+M_U)$. Changes in joint angle were evaluated simply as $(M_P-M_U)$ to avoid dividing by very small denominators. We calculated the average of this ratio over 10-stride windows at the end of the Baseline condition, and the start and end of the Post condition ("Early-Post" and "Late-Post"). We performed a repeated measures ANOVA to evaluate the effect of stiffness condition (Baseline, Post-Early, Post-Late) on vGRF during weight acceptance, mid-stance, and push-off, on peak plantarflexion angle and peak plantarflexion moment at push-off, and on dorsiflexion angle averaged across the swing phase. Planned comparisons in the form of paired t-tests on were used to evaluate our hypotheses for all asymmetry measures (Baseline vs. Post-Early).

**Results**: The ANOVA revealed significant effects of asymmetric stiffness walking on peak push-off vGRF ($p<0.001$), mid-stance GRF ($p<0.001$), and stance time ($p=0.005$). The effect of asymmetric stiffness condition on weight acceptance vGRF was not significant ($p=.065$). Planned comparisons revealed that peak push-off vGRF shifted toward the perturbed side ($p<0.001$), weight acceptance shifted toward the perturbed side ($p=0.037$), mid-stance vGRF shifted toward the unperturbed side ($p=.002$), and stance time increased on the unperturbed side relative to the perturbed side ($p=0.025$). The ANOVA did not reveal a significant effect of condition on ankle joint angle measures, contrary to our hypothesis. The ANOVA found an effect on peak plantarflexion moment ($p=.050$), although the planned comparison did not find a significant difference between Baseline and Early-Post ($p=0.12$). Because joint mechanics were measured with fewer participants than the ground reaction force measures, we will continue to analyze these measures in future work, with particular attention toward peak plantarflexion moment asymmetry.

**Significance**: These results show that changing foot-ground stiffness during walking can elicit changes in ground reaction force and joint moment symmetry after the perturbation, suggesting that neuromotor adaptation has occurred. The observed aftereffects in weight-bearing, and joint moment symmetry during walking is promising for the potential of this intervention and warrants further study to investigate if these changes occur in people after stroke, and if they persist with repeated training.

**References:** [1] Duncan, et al. (2005) *Stroke*, *36*(9); [2] Roelker et al. (2019) *Gait & Posture* 68(x); [3] Lauziere et al. (2014) *PubMed,* 46(9); [4] Reisman et al. (2013). *Neurorehabilitation and neural repair*, *27*(5); [5] Chambers & Artemiadis. (2023) *Frontiers in robotics and AI*, *9*(3); [6] Price, et al. (2024) *IEEE/ASME Trans Mechatron.*

# THE BENEFITS OF GAIT RETRAINING WITH VIBROTACTILE FEEDBACK OUTWEIGH HIGHER PERCEIVED MENTAL LOAD

*Vani Hiremath Sundaram[1], Nataliya Rokhmanova[1,2], Eni Halilaj[2], Katherine J. Kuchenbecker[1]
[1]Haptic Intelligence Department, Max Planck Institute for Intelligent Systems, Stuttgart, Germany
[2]Carnegie Mellon University, Pittsburgh, PA, USA
*Corresponding author's email: vsun@is.mpg.de

**Introduction:** Knee osteoarthritis (KOA) affects over 654 million adults aged 40 and older worldwide, with this statistic trending upwards [1]. Addressing factors that can exacerbate cartilage damage, like excessive knee joint loading [2], might help slow the progression of KOA. Training a patient to walk with a specific foot progression angle (FPA) has emerged as an intervention to reduce knee adduction moments [3], a surrogate measure of medial knee joint load [4]. Biofeedback methods that provide intuitive corrective cues at each incorrect step have been utilized to assist in this training; however, it is unclear whether the extra effort involved in implementing biofeedback is justified by learning outcomes. This research explores whether receiving vibrotactile biofeedback when training to perform a modified gait affects both retention of the new FPA and perceived cognitive workload. We expect that subjects who receive vibrotactile feedback will demonstrate a decreased error in both learning and retention, but higher workload compared to those who do not receive feedback. Additionally, we predict that providing more detailed information about the magnitude of the error through vibrotactile cues will amplify differences in error and workload.

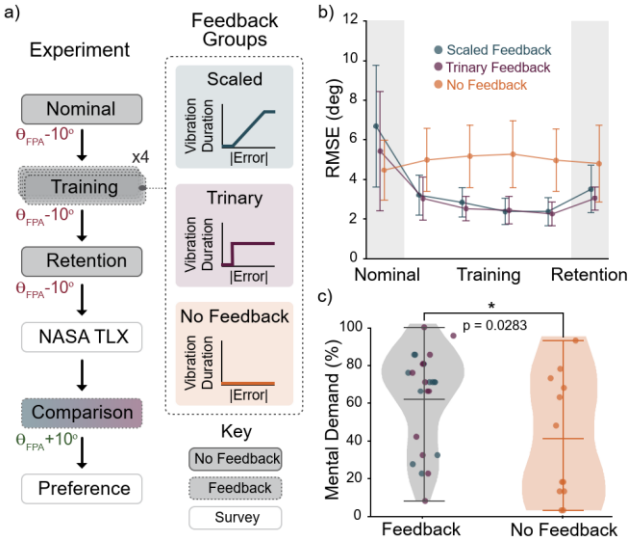


**Figure 1: (**a) ***Experimental Overview*** **–** Sequence of events when all participants walked without feedback, when the three groups trained with different feedback, and when all participants completed surveys. (b) ***Walking Performance*** **–** Average RMSE (±1 SD) during the nominal, training, and retention trials, comparing errors across the three feedback conditions. The Scaled Feedback group reduced their RMSE between the nominal and retention trials significantly more than the No Feedback group. (c) ***Cognitive Workload*** **–** Perceived mental demand (% agreement) was higher for participants receiving feedback vs. no feedback.

**Methods:** Thirty-six healthy adults (18F, 18M; mean age = 27 ± 5 years) participated in a 20-minute treadmill training session to adopt a 10° toe-in gait (Fig. 1a). The target FPA was set by subtracting 10° from their average baseline FPA, measured using a motion-capture system (Vero, Vicon) during a baseline walking trial. After a nominal trial attempting the modified gait without feedback, participants were randomly assigned to one of three feedback groups for four 5-minute training blocks (Fig. 1a). The Scaled Feedback (SF) group received corrective vibration feedback that scaled in duration with FPA error magnitude. The Trinary Feedback (TF) group received constant-duration vibration. Both feedback groups received feedback only when the FPA deviated more than 2° from the target FPA, with the vibrating actuator indicating the direction of the error (push feedback). The No Feedback (NF) group wore the haptic device but received no feedback. A retention trial followed the 20-minute training session, during which no feedback was given. Subjects then completed the NASA Task Load Index (TLX) [5] to assess perceived workload. Finally, they all performed a short 10° toe-out walking trial to compare the two feedback types and indicate their preference. One-way ANOVAs were used to compare the relative changes in RMSE across the groups during training and retention, with Tukey's HSD for post-hoc pairwise comparisons and $\alpha = 0.05$. Group differences in NASA TLX scores were evaluated using independent t-tests.

**Results & Discussion:** When comparing the relative change in RMSE from the nominal trial to the final training trial across groups (Fig. 1b), subjects in both the SF (–57.2 ± 18.4%) and TF (–50.5 ± 17.9%) groups significantly outperformed ($p < 0.0001$) those in the NF group (+19.5 ± 43.2%). In retention, the SF group maintained a significantly lower change in RMSE from the nominal trial compared to the NF group ($p = 0.0166$), while the TF group did not ($p = 0.0697$). Receiving either type of corrective haptic cues while learning the new gait increased the perceived mental demand compared to subjects who did not receive feedback ($p = 0.0283$) (Fig. 1c). There were no significant differences in relative training or retention error or overall NASA TLX scores between SF and TF. These results highlight that vibrotactile feedback significantly improves both gait training and short-term retention outcomes compared to training without feedback. Importantly, scaled feedback led to better retention than no feedback, suggesting that the added mental demand is justified to support lasting gait modifications. Interestingly, after the comparison trial, subjects across all three groups believed vibrotactile feedback, especially scaled feedback, enhanced learning. Despite similar performance outcomes between the two feedback groups, 32 out of 36 subjects chose scaled feedback as the best method for learning a new gait, with no votes for no feedback. This preference shows that users recognize the utility of vibrotactile feedback for gain retraining and appreciate more-informative cues.

**Significance:** This research shifts the discussion from whether biofeedback is useful to how to deliver it best, emphasizing user-centered preferences and associated cognitive demands. Our findings demonstrate that receiving vibrotactile biofeedback significantly improves both learning and short-term retention in gait retraining. Additionally, users perceived the benefits of vibrotactile guidance as outweighing its added cognitive demand and preferred vibrations scaled with error magnitude. Aligning feedback delivery with user preference could help untangle the relationship between training outcome, device usability, and satisfaction, with the hope of improving user compliance for at-home rehabilitation technologies, enabling patients to manage their conditions independently and effectively.

**References:** [1] Cui et al. (2020), *EClinicalMed.*, [2] Andriacchi et al. (2009) *J Bone Joint Surg. Am.* 1(91), [3] Uhlrich et al. (2022), *J Biomech* 144:111312, [4] Kutzner et al. (2013), *PLoS ONE.* 8(12), [5] Hart (2006), *P Human Factors Erg. Soc. Annu. Meet.* 50(9).

# HAPTIC CUEING MODULATES GAIT VARIABILITY AND IS MORE USER FRIENDLY THAN VISUAL CUES

Kolby J. Brink[1*], Mehrnoush Haghighatnejad[1], Tyler Wiles[1], Nikolaos Stergiou[1,2], and Aaron D. Likens[1]
[1]Department of Biomechanics, University of Nebraska at Omaha, Omaha, NE USA
[2]Department of Physical Education and Sport Science, Aristotle University of Thessaloniki, Thessaloniki, Greece
*Corresponding author's email: kolbybrink@unomaha.edu

**Introduction:** Gait variability provides insights into sensorimotor control, with healthy gait exhibiting a variability reflective of statistical pink noise[1]. Pink noise is a phenomenon that has been attributed to promoting stability and adaptability[2]. Aging and pathology shift gait variability toward white noise, increasing randomness and fall risk[3]. External cueing, such as visual and auditory stimuli, helps restore healthy variability[4,5] but has practical limitations—visual cues obstruct awareness, and auditory cues interfere with situational hearing. Haptic cueing offers a promising alternative by providing rhythmic vibrations without these drawbacks, though its impact on gait variability remains unexplored. This study tested whether haptic cueing effectively modulates gait variability, comparing it to visual cueing across three variability conditions: white noise, pink noise, and invariant (constant intervals).

**Methods:** Ten healthy young adults (Age = 26.70 ± 3.23 years, Height = 176.55 ± 12.48 cm, Mass = 71.93 ± 20.83 kg) participated in two randomized sessions comparing visual and haptic cueing modalities. During each session, participants first completed a 12-minute self-paced walk to establish baseline cadence, followed by three 12-minute walking trials synchronizing to either visual or haptic cues. Visual cues were delivered through non-prescription glasses with a mini-HDMI display showing an oscillating bar, while haptic cues were delivered via a C2 tactor worn on the left wrist. Both modalities delivered cues with three different statistical structures: white noise (no correlations), pink noise (strong long-range correlations), and invariant (perfect correlation). Participants wore nine inertial measurement units recording at 400 Hz on their lower limbs and trunk to capture kinematic data and heel strike times. Gait variability was assessed through the Detrended Fluctuation Analysis (DFA) scaling exponent, α, while synchronization was measured by the timing between heel strikes and metronome cues. A modified System Usability Scale (SUS) questionnaire evaluated both cueing methods.

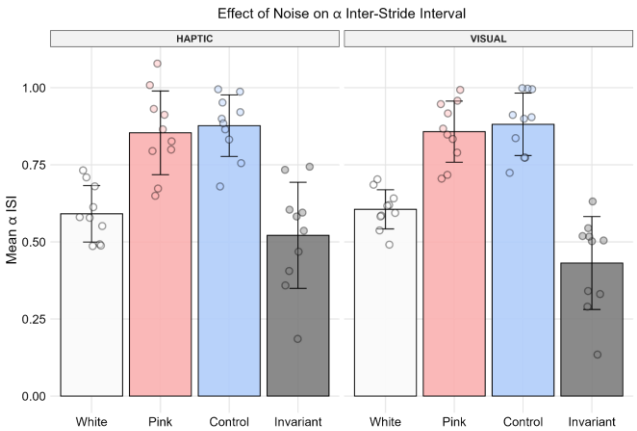


**Figure 1**: Bar graphs of mean α-ISI values across noise conditions for haptic and visual modalities. Error bars show standard deviations, with individual points as jittered circles.

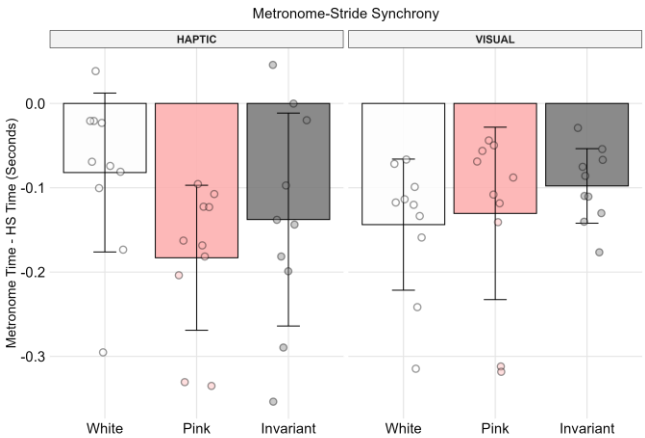


**Figure 2**: Density plots of asynchrony values across noise conditions. Curves represent time differences between heel strikes and stimulus occurrences. The dashed line at 0 indicates perfect synchrony, with negative values for early heel strikes and positive values for delayed strikes. Colors denote noise conditions.

**Results & Discussion:** Both visual and haptic cueing modulated gait variability, with no significant differences in α or asynchrony between modalities (Fig. 1). White noise and invariant conditions significantly reduced α-inter-stride-intervals (α-ISI) values compared to control (white noise: -1.34 ± 0.16 SDs, $p < 0.001$; invariant: -1.95 ± 0.16 SDs, $p < 0.001$, Fig. 1). Pink noise showed no significant difference from control. Averaging across noise and modality, participants anticipated cues by ~0.13 seconds [95% CI: 0.11, 0.15], and there were no statistical differences between noise types (Fig. 2).

Results from the SUS indicated that haptic feedback was perceived as less awkward (Wilcoxon signed-rank test, $w = 36$, $p = 0.01$), more confidence-inspiring ($w = 127.5$, $p = 0.02$), and more practical ($w = 134$, $p = 0.01$). Given that visual cueing often obstructs spatial awareness, haptic cueing presents an alternative that maintains environmental awareness, making it a more viable option for real-world gait rehabilitation and assistive technologies.

**Significance:** These findings support the viability of haptic cueing as an effective and user-preferred method for modulating gait variability. By offering comparable synchronization accuracy to visual cueing while enhancing usability, haptic feedback systems have the potential to be integrated into wearable technologies such as smartwatches and other assistive devices. This study contributes to the growing body of research advocating for haptic-based rehabilitation strategies, providing a foundation for future developments in fall prevention, gait rehabilitation, and adaptive locomotion training.

**Acknowledgments:** KB is supported by the NASA Nebraska Fellowship Award and UNO GRACA. TW is supported by the GRACA and the UN Collaborative Initiative (CI) grant. MH is supported by the GRACA and the UN CI grant. AL and NS are supported by awards from the NIH (P20GM109090, 1P20GM152301-01, and R01NS114282), the NSF (2124918), and the UN CI grant.

**References:** [1] Delignières D. et al. *J Appl Physl.* 2009; **106**, 1272–1279. [2] Stergiou, N. et al. *Hum Mov Sci* **30**, 869–888 (2011). [3] Hausdorff, J. M. et al. *Hum Mov Sci* **26**, 555–589 (2007). [4] Hunt, N. et al. *Sci Rep* **4**, 5879 (2014). [5] Raffalt, P. et al. *Neuro Let* **763**, 136193 (2021).

# ESTIMATING KNEE JOINT IMPEDANCE ACROSS VARYING WALKING SPEEDS FOR ADAPTIVE CONTINUOUS IMPEDANCE CONTROL IN POWERED KNEE PROSTHESES

*Woolim Hong[1], He (Helen) Huang[1]
[1]Lampe Joint Department of Biomedical Engineering, North Carolina State University, Raleigh, NC 27695
[1] Lampe Joint Department of Biomedical Engineering, University of North Carolina at Chapel Hill, Chapel Hill, NC 27514
*Corresponding author's email: whong3@ncsu.edu

**Introduction:** Lower-limb amputation represents a significant disability that affects individuals both physically and psychologically. It not only increases the risk of falls and injuries but also limits participation in daily activities and community engagement [1]. Over the years, powered prostheses have emerged as a promising solution to replicate natural gait across various ambulation tasks. Recently, continuous impedance control has gained attention for its ability to generate smooth, human-like movement in these devices [2, 3]. In our previous study, we introduced a tuning approach for continuous impedance control that adjusts the weights assigned to the principal components of continuous stiffness, damping, and equilibrium angle throughout the gait cycle [4]. However, the impact of varying walking speeds on continuous impedance and its adaptability remains under-explored. Therefore, the primary objective of this study is to examine how continuous knee impedances change with different walking speeds and to identify effective tuning strategies for powered knee prostheses under these conditions.

**Methods:** We proposed a continuous impedance control framework for a powered knee prosthesis that requires continuously varying stiffness, damping, and equilibrium angle throughout the gait cycle [4]. To estimate these continuous impedance functions for the knee joint, we formulated a convex optimization problem that fits the estimated joint torque—based on impedance control—to the human knee torque data from an open-source human walking dataset [5]. This dataset includes treadmill walking data from 22 able-bodied (AB) participants across various walking speeds ranging from 0.5 m/s to 2.1 m/s. For this study, we excluded data from two participants based on outlier criteria, defined as joint position, velocity, or torque trajectories deviating by more than ±2 standard deviations from the mean trajectory at any point in the gait cycle. We then categorized the remaining data into eight walking speed groups: SC1 (0.5–0.7 m/s), SC2 (0.7–0.9 m/s), SC3 (0.9–1.1 m/s), SC4 (1.1–1.3 m/s), SC5 (1.3–1.5 m/s), SC6 (1.5–1.7 m/s), SC7 (1.7–1.9 m/s), and SC8 (1.9–2.1 m/s). Given the hardware constraints of the powered prosthesis, we focused on walking speeds below 2.0 m/s (i.e., SC1–SC7). Using the proposed convex optimization approach, we estimated the continuous knee impedances for these seven walking speed groups to identify continuous knee impedances change with different walking speeds.

**Results & Discussion:** Figure 1 illustrates the estimated knee stiffness, damping, equilibrium angle, and generated torque within the impedance control framework, averaged from 20 AB participants. As walking speed increases, knee stiffness shows an increasing trend (see Fig. 1a). Meanwhile, damping exhibits a decreasing trend during the middle of the gait cycle and an increasing trend in the late swing phase (Fig. 1b). As shown in Fig. 1c, the equilibrium angle increases between 20–40% of the gait cycle, while remaining largely unchanged in other regions as walking speed increases. Additionally, the estimated knee joint torque increases proportionally with walking speed (Fig. 1d). The increase in knee equilibrium angle and stiffness between 20–40% of the gait cycle could be related to greater knee flexion during the weight acceptance and mid-stance transition, facilitating impact absorption as walking speed increases. These results demonstrate that knee joint impedances follow distinct trends based on walking speed, which can be modulated using the proposed tuning parameters from our previous study [4]. Future work will involve implementing these speed-adaptable continuous joint impedances in a walking experiment using the custom-built powered knee prosthesis.

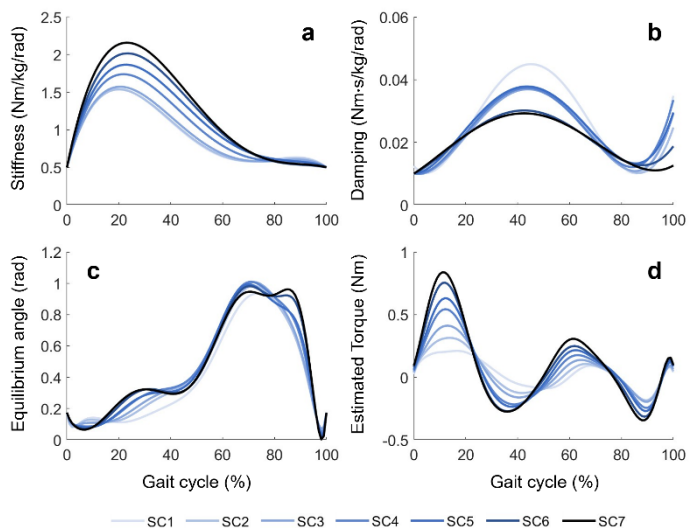


**Figure 1:** Estimated knee joint impedances and generated torque across different walking speed groups. (a) Stiffness, (b) Damping, (c) Equilibrium angle, and (d) Estimated torque using the computed joint impedances. Darker lines represent higher walking speed groups, highlighting variations in impedance properties throughout the gait cycle.

**Significance:** The significance of this study lies in identifying how continuous knee impedances change with different walking speeds. Using a convex optimization approach, it reveals distinct trends in stiffness, damping, and equilibrium angle, providing key insights for speed-adaptive control of powered knee prostheses. These findings emphasize the importance of adapting impedance control to enhance prosthetic performance across different walking speeds.

**Acknowledgments:** This work was supported by the National Science Foundation (NSF #2211739) and by the National Institute on Disability, Independent Living, and Rehabilitation Research (NIDILRR #90ARHF0004 and #90SFGE0050).

**References:** [1] Miller et al. (2001), Arch Phys Med Rehab 82(9); [2] Best et al. (2023), IEEE Trans Robotics; [3] Anil Kumar et al. (2021), ICRA, pp. 3219–3225; [4] Hong et al. (2023), ICORR, pp. 1-6; [5] Camargo et al. (2021), J Biomech.

# PAIRING LIMB ANGLE BIOFEEDBACK WITH AN ANKLE EXOSKELETON TO AUGMENT PROPULSION IN INDIVIDUALS WITH CHRONIC HEMIPARESIS

*Steven A. Thompson[1], Emily E. Foley[1], Sonia R. Wrobel[2], Jason R. Franz[1], Gregory S. Sawicki[3], Michael D. Lewek[1,2]
[1] Lampe Joint Dept. of Biomedical Engineering, UNC-Chapel Hill & NC State University, Chapel Hill, NC
[2] Division of Physical Therapy, Department of Health Sciences, UNC-Chapel Hill, Chapel Hill, NC
[3]George W. Woodruff School of Mechanical Engineering, Georgia Institute of Technology, Atlanta, GA
*Corresponding author's email: sathom22@ad.unc.edu

**Introduction:** Following stroke, paretic limb propulsion deficits may arise from a reduced ankle plantarflexor moment and/or trailing limb angle (TLA). Ankle exoskeletons (EXOs) can increase the plantarflexor moment although this has not reliably increased propulsion [1-2]. Instead, people post-stroke tend to reduce their TLA while walking with a powered ankle EXO such that a greater paretic plantarflexor moment does not translate to increased paretic propulsion [1-2]. In other studies without EXOs, people post-stroke have been cued to increase TLA with visual feedback to augment propulsion [3], suggesting that pairing visual feedback of TLA with an ankle EXO to augment plantarflexor moment may provide a method for conveying benefit to paretic limb propulsion. The purpose of this study was to assess the combined effect of a powered ankle EXO (to increase plantarflexion moment) and visual biofeedback (to increase TLA) on paretic propulsion and lower-limb joint kinetics in individuals with chronic hemiparesis following stroke. We hypothesized that: (1) increasing TLA with visual feedback would increase paretic propulsion independently from EXO assistance, and that (2) increasing the amount of EXO assistance would further increase paretic propulsion when feedback of TLA is provided. Based on pilot data from unimpaired individuals, we also hypothesized that (3) both total positive mechanical work performed by the paretic lower limb and the percentage of ankle contribution to total positive mechanical work would increase with the provision of both TLA and EXO assistance.

**Methods:** Thus far, 3 individuals following stroke (recruitment and data collection ongoing) walked on a dual-belt instrumented treadmill (Bertec) at their comfortable treadmill speed while wearing a powered ankle EXO (Biomotum). The EXO provided plantarflexor assistance to the paretic limb only. First, each participant's typical peak TLA was measured during a 30-s walking trial while wearing the EXO in a transparent mode. Then, using a block-randomized design, participants walked either without feedback, or with feedback of TLA using a target set at either the typical peak TLA or 5° greater than typical (noFB, baseline, baseline+5°, respectively). Within each feedback condition, participants walked with 3 magnitudes of peak plantarflexor assistance (0%, 15%, and 25% BW) in random order. Real-time paretic limb TLA and a peak TLA target were displayed on a TV monitor in front of the treadmill during feedback conditions. We collected 30 s of kinematic data with marker-based motion capture (Vicon) and ground reaction forces from the treadmill. Paretic propulsive impulse and the positive mechanical work performed by the paretic ankle, knee, and hip were calculated and compared across conditions. To address the study purpose, we removed any steps that did not fall within the ±1° target TLA range for feedback conditions. When necessary, we included the next closest steps to the target, provided these steps were not within the other target zone; to reach a minimum of 5 steps within the target zone.

**Results & Discussion:** Preliminary results suggest that people with stroke can increase paretic propulsion by increasing their TLA with and without EXO assistance (Fig. 1). These data suggest that feedback of baseline+5° peak TLA may augment propulsion, however, participants struggled to reach this target consistently (only 30±30% of steps). Participants may benefit from longer accommodation while walking with feedback to consistently increase TLA. Additionally, EXO assistance inconsistently altered paretic limb propulsion. For lower-limb joint kinetics, total positive mechanical work performed by the paretic limb increased by 0.1 J/kg when feedback of baseline was provided and 0.24 J/kg with feedback of baseline+5°. EXO assistance magnitude had variable effects on total work between participant and condition. The percentage of ankle contribution to total work increased by 5% and 7% with feedback of baseline and baseline+5°, respectively, but remain unchanged when walking without feedback. Surprisingly, data thus far does not suggest a clear relationship between EXO assistance and the percent of total positive mechanical work performed by the ankle.

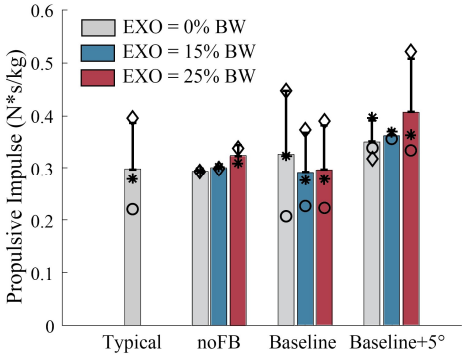


**Fig. 1:** Propulsive impulse for each TLA feedback target (group) and EXO assistance magnitude (color) condition.

**Significance:** As assistive devices continue to be developed for use in the daily lives of humans, it is important that people can gain the full potential of these devices. To achieve this, people's movements (rather than just the device itself) may need to be adjusted. Our preliminary results suggest that when walking at a fixed speed, the ankle EXO does not consistently increase limb propulsion. Providing biofeedback may be one approach to coordinating movement between the human and device, although longer accommodation to both feedback and the device itself may be necessary to ensure the best use of an ankle EXO for people with chronic stroke. This study emphasizes consideration for the person's control of movement in both design and implementation of assistive devices.

**Acknowledgments:** NIDILRR – RERC: REGE22000170: Assisting Stroke Survivors with Engineering Technology (ASSET). NSF 2306660: Improving Older Adults' Mobility and Gait Ability in Real-World Ambulation with a Smart Robotic Ankle-Foot Orthosis.

**References:** [1] McCain et al. (2019), *J Neuroeng Rehabil* 16(1):57. [2] Takahashi et al. (2015), *J Neuroeng Rehabil* 12:23. [3] Santucci et al. (2023), *J Neuroeng Rehabil* 20:37.

**Comparing the Transfer of Treadmill-Based and Overground-Based Exosuit Training toward Overground Gait**

Sangwon Shin, Pieter Van den Berghe, Mukul Mukherjee, Philippe Malcolm
Department of Biomechanics, University of Nebraska at Omaha, Omaha, NE, USA
Email: sangwonshin@unomaha.edu

**Introduction:** Gait rehabilitation plays a pivotal role in helping individuals with neurological conditions or mobility impairments regain functional independence. Numerous interventions, including split-belt treadmill training and exoskeleton-assisted walking, have been introduced to optimize locomotor recovery[1–3]. However, questions remain about how the walking surfaces in which these devices are used influence motor learning and the transfer to everyday movement. Treadmill walking is popular because it requires little space and is easy to supervise clinically[4]. However, overground walking more closely represents the variability of real-world locomotion[5]. In this study, we investigated the effects of a gait retraining exosuit used in both treadmill and overground contexts. We hypothesized that training on a surface consistent with the testing environment would lead to more pronounced aftereffects on step length symmetry.

**Methods:** Sixteen healthy adults were allocated to two groups matched for bodyweight and sex (Treadmill (TM) vs. Overground (OG)). The experiment consisted of three stages: Baseline, Adaptation, and Post-adaptation (Fig. 1A). Participants walked repeatedly via a 9 m overground walkway for 15 minutes in the Baseline. Then, all participants donned a chest part of the exosuit with retractor-springs that pulled the right thigh forward with 15% of body weight (*bw*) and the left thigh backward with 10% of *bw*. During the Adaptation stage, the OG group walked with the exosuit along the walkway for 15 minutes on the overground, while the TM group walked with the exosuit on a treadmill at their self-selected speed, also for 15 minutes. Upon completion of the Adaptation, the retractor cables were removed, and all participants were instructed to walk overground for the last 15 minutes without force from retractors. We defined the step length as the anterior-posterior distance between the leading foot coordinates and the trailing foot coordinates measured using motion capture. Gait symmetry based on the step length was quantified using the symmetry index (SI)[6], calculated as: $Symmetry\ Index\ (SI) = (Right\ step - Left\ step)/(0.5 \times (Right\ step + Left\ step)) \times 100$. We performed a mixed effect ANOVA (2 groups [TM and OG] × 3 time points [Late Baseline, Initial Adaptation, and Initial Post-Adaptation]) and post-hoc testing with multiple comparison correction.

**Results & Discussion:** We detected a group × timepoints interaction effect ($p$ = 0.013). The SI of each group was near-zero SI at the Baseline, indicating symmetrical walking. When exposed to walking with the exosuit, the OG group showed a significant increase in SI (i.e., more asymmetrical; 20%, $p$ < 0.001), while the TM group still maintained SI values near 0% ($p$ > 0.05). Post-Adaptation, both groups exhibited a rapid aftereffect in the opposite SI ($p$ < 0.05 for OG, $p$ < 0.01 for TM). Contrary to our hypothesis, this aftereffect did not differ between groups (12% for OG and 16% for TM, $p$ = 1). Both groups gradually returned toward symmetrical walking over 15 minutes (Fig. 1A). The TM group may have resisted applied forces more intensely to avoid falling off the treadmill while walking asymmetrically. Additionally, past gait adaptation studies suggested that sensorimotor constraints can independently affect walking mechanics (Adaptation) or neural mechanisms (Post-Adaptation)[7–9]. The treadmill's pre-set speed may also have restricted movement adjustments, as it could be slower than the participants' comfortable gait speed. Our findings suggest that continuous exosuit training induces asymmetry within 15 minutes in healthy individuals. Moreover, this exosuit could serve as an alternative to split-belt treadmills, as our results demonstrated similar adaptation trends from past studies using split-belt treadmills[1,10]. Based on these results, we propose that our device may have the potential to facilitate symmetrical recovery in clinical populations, such as stroke survivors, in the future.

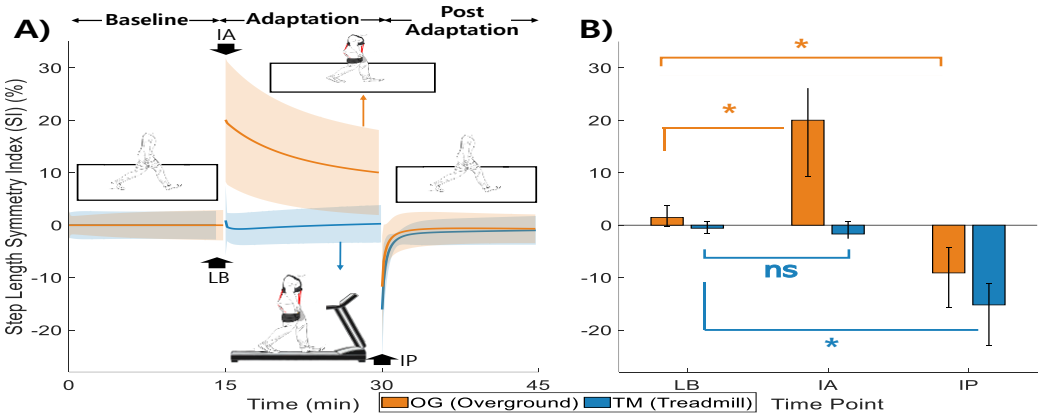


**Figure. 1. A)** Effects of Overground (OG, Orange) and Treadmill (TM, Blue) exosuit training on step length symmetry index**.** (Mean ± 1SD), **B)** Bar plot shows the pairwise comparisons between three key time points: Last Baseline (LB), Initial Adaptation (IA), and Initial Post-adaptation (IP). (*ns*: not significant, * $p$ <0.05). (Mean ± IQR)

**Significance:** This study shows that a soft, passive, hip exosuit can produce large aftereffects in step length symmetry after treadmill and overground walking. The finding of aftereffects across both treadmill and overground training broadens the applicability of our exosuit to any walking conditions. This could be useful to determine the rehabilitation environment in clinical populations that could benefit from interventions that alter symmetry, such as chronic stroke survivors.

**Acknowledgements:** NU GRACA; AHA 25PRE1378622; NIH P20GM109090 and P20GM152301; NSF 2203143, Philippe Malcolm is an inventor of WO2023192982A2

**References:** 1. Reisman et al. *NNR* (2009). 2. Betschart et al. *Physiother Theory Pract* (2018). 3. Awad et al. *Sci. Transl. Med.* (2017). 4. Lee et al. *J. Appl. Physio.* (2008). 5. Slade et al. *Nature* (2022). 6. Robinson et al. *J. Manip. Physiol. Ther.* (1987). 7. Sado et al. *Exp. Brain Res.* (2022). 8. Mukherjee et al. *Exp. Brain Res.* (2015). 9. Eikema et al. *Exp. Brain Res.* (2016). 10. Reisman et al. *Brain* (2007).

# DEVELOPMENT OF AN ACTIVE WHEELCHAIR SEAT CUSHION TO ADDRESS PRESSURE INJURIES

Evelyn A. Ochoa Arias [1], Diane V. Gonzalez[1], Natalie M. Taylor[1], Jason Robinson[1], Jooyoung Hong[1], Patricia Richards [1], J.J Guedet[2], Matthew S. Nieukirk[2], Emily E. Pisani[2], Mary J. Schopp[2], Britny H. Coyle[2], Christopher M. Zallek[2], Laura A. Rice[1], Joohyung Kim[1], Elizabeth T. Hsiao-Wecksler[1], Holly Golecki[1]

[1]University of Illinois Urbana-Champaign, Urbana, IL, [2]OSF HealthCare, Peoria, IL

*Corresponding author's email: eochoa20@illinois.edu

**Introduction:** Pressure injuries (PI) are a common clinical presentation of individuals with limited mobility and can lead to serious health issues. PIs occur when constant pressure slows blood flow, harms tissue, and raises the risk of infection [1]. While regular seat cushions can relieve pressure, the design depends on inactive materials and fixed designs that need frequent manual re-positioning by the individual or healthcare providers [2]. Assistive technology engineers have developed automated systems that monitor and adjust pressure on vulnerable areas using pressure mapping and modulation [3]. However, these solutions tend to be bulky, difficult to use, or uncomfortable, limiting their commercial adoption. We are addressing these challenges by developing an active seat cushion that employs custom pneumatic air bladders to continuously and adaptively redistribute pressure as proposed by previous work [4]. To establish design criteria using clinician input, we spoke with healthcare providers. They agreed on five key considerations (Fig. 1). When considering a simplified design, the key engineering approach is the fabrication parameters. To decrease the number of individual parts in the seat cushion, one possibility is to create a cushion consisting of connected bladder chambers. However, it is first necessary to understand the design parameters of pneumatic air bladders.

**Figure 1:** Action items for Design Considerations

**Methods:** This cushion design is based on soft robotic principles. Air bladders fabricated from heat-fused 2D polymer sheets have been identified for initial testing based on their lightweight and customizability for user-specific bladder designs [5]. Different bladder designs were explored to understand the effect of width on inflation height (Fig. 2). Air bladder prototypes were fabricated from heat-fused thermoplastic polyurethane (TPU) sheets using a CNC heat-sealing process, the same CNC as Sanchez et al. [6]. A finite difference simulation, governed by the Poisson equation, was used to model TPU deformation under internal pressure of 34.5 kPa, predicting inflation behavior. Experimental testing compared inflation height and chamber shape to simulation results.

**Results & Discussion:** Both the simulation and experiments were in good agreement for larger chamber widths (Figs. 2-3). They demonstrated that the model correctly predicted how TPU changed. Changes in seam width chamber size affected inflation height and pressure spread. These results drove changes in connected bladder chambers to boost cushion action and user ease.

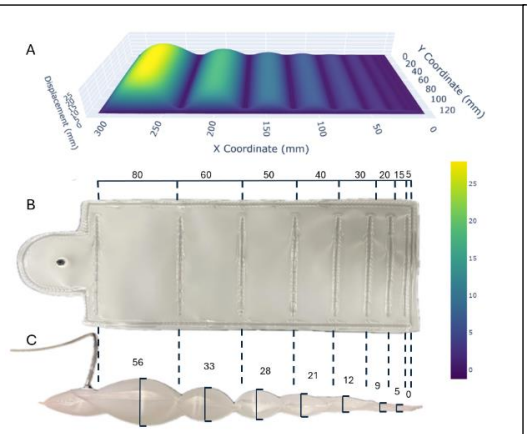


**Figure 2:** (a) 3D Simulation of TPU airbladder (mm) (b) CNC manufactured air bladder top view deflated (c) Side view: inflated with tube airflow inlet

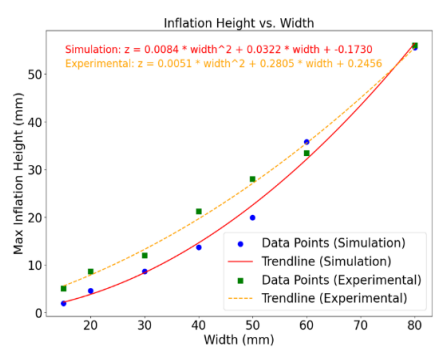


| Distance (mm) | 5 | 20 | 30 | 40 | 50 | 60 | 80 |
|---|---|---|---|---|---|---|---|
| % Error | 0.606 | 0.472 | 0.281 | 0.356 | 0.289 | 0.040 | 0.008 |

**Figure 3:** Plots of Experimental and Simulation Inflations vs Width distance

**Significance:** An active cushion design may provide a light, automatic way for pressure release and may reduce PI in wheelchair users. By combining simulation with quick prototyping, this method moves forward the design of custom, user-focused pressure-relief cushions, potentially leading to improved health outcomes and greater mobility

**Acknowledgments:** This project is supported by the Jump ARCHES program.

**References:** [1] Lyder & Ayello (2008), in Patient Saf Qual Handb., [2] Theaker et al. (2000), Anaesthesia 55(3), [3] Carrigan et al. (2019), Med Eng Phys 69, [4] Robinson et al. (2023), 2023 Des. Med Devices Conf., [5] Edward et al. (2022), IDETC-CIE 2022, [6] Sanchez et al. (2019), IEEE RoboSoft 2nd Conf.

# ACCURATE ASSESSMENT OF PASSIVE IMPAIRMENT COUPLING ACROSS FIVE DIGITS POST STROKE

Giovanni Oppizzi [1], Soh-Hyun Hur[2] , Dali Xu[2], Xiaoyan Li[1], Derek Kamper[3], Li-Qun Zhang[1,2*1]
[1] University of Maryland, College Park, MD, USA
[2] University of Maryland, Baltimore, MD, USA
[3] North Carolina State University, Raleigh, NC, USA
* Correspondence: zhangl@umd.edu

**Introduction:** Each year, in the United States alone, 800,000 strokes occur [1], making it the leading cause of adult disability in the country. 80% of patients exhibit hemiparesis to the contralateral upper limb, which in 50% of cases becomes a chronic condition [23]. Upper extremity impairment severely limits the independence of the 50-70% of stroke victims [3] . The arm and hand are the organs we use the most when interacting with the world around us. It is an incredibly complex mechanism, both from the mechanical and the control dynamics point of view. As of today, there's a lack of methods and devices capable of accurately measuring the multi-digit passive properties across the five digits. The absence of a comprehensive hand assessment robot is even more significant because of the high complexity of the organ. Five digits can each articulate in flexion, extension as well as abduction and adduction, adding up to a total of 27 degrees of freedom (DoF) [4]. While it's already extremely challenging and requires years of training for a human to assess the inter-joint properties of the arm, with its 7 DoF [5], it's evident that even the most skilled examiner cannot paint a complete picture for the multidigit hand sensory characterization. Hence, in this work, we introduce a new robotic device, the Hand of Hope modified (HoHm), with the intention of accurately assessing the multi-digit passive properties of the hand.

**Methods:** To asses the passive hand properties, the patient's hand is first attached to the most suitable HoHm size and side, by way of Velcro straps through the wrist, palm and digits. The digits are then brought to their neutral position, defined as 50% of the ROM of the linear actuators. Here the force offsets can be measured for all digits. The passive assessment protocol consists of five consecutive trials. In each of them, one digit at a time is moved five times at 5mm/s throughout the full ROM. The ROM of the HoHm is mechanically limited between 0 an 30mm of linear actuation, roughly equivalent to 0 and 45 degrees of MCP flexion and 0 and 60 degrees of Proximal Inter-Phalangeal (PIP) joint flexion. While one digit is being moved, the remaining four are kept locked, via a position control algorithm, at neutral position (i.e., 15mm). Force is simultaneously measure at all five digits. The relationship between each digit's motion and the induced forces, can be explained by a set of five Newton-Euler equations[6], which can be simplified by restricting the ROM and actuation velocity to reduce the effects of inertia and viscosity. The resulting system is expressed as:

$$\begin{bmatrix} F_1 \\ F_2 \\ F_3 \\ F_4 \\ F_5 \end{bmatrix} = \begin{bmatrix} K_{1,1} & K_{1,2} & K_{1,3} & K_{1,4} & K_{1,5} \\ K_{2,1} & K_{2,2} & K_{2,3} & K_{2,4} & K_{2,5} \\ K_{3,1} & K_{3,2} & K_{3,3} & K_{3,4} & K_{3,5} \\ K_{4,1} & K_{4,2} & K_{4,3} & K_{4,4} & K_{4,5} \\ K_{5,1} & K_{5,2} & K_{5,3} & K_{5,4} & K_{5,5} \end{bmatrix} \begin{bmatrix} \Delta X_1 \\ \Delta X_2 \\ \Delta X_3 \\ \Delta X_4 \\ \Delta X_5 \end{bmatrix}$$

$F_n$ are the forces generated at the digits, the $K_{n,n}$ matrix elements are the local and coupled stiffnesses and finally $\Delta X_n$ represents the digit displacement.

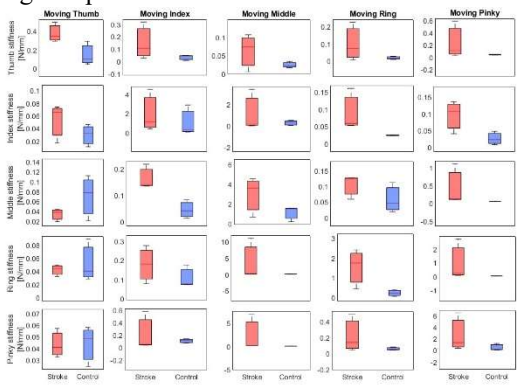


Figure 1 Showing the local and coupled stiffness values for stroke (red) and control (blue) group, in a 5-by-5 matrix, reflecting the K matrix.

**Results & Discussion:** Here we present the preliminary results on passive properties of the hand for three stroke survivors and three healthy subjects. Looking at the hand stiffness matrix in Figure 1, in particular at the diagonal elements, we can see a clear increase in local stiffness throughout all digits. This is expected, since a common effect of stroke is an increased muscle tone, in the form of spasticity, on the flexor muscle group.

The HoHm of course also enables us to look at the coupled stiffnesses. Here we can note an interesting pattern. First, looking at the thumb and index column, we can see that the absolute values of the coupled stiffness are low, throughout all digits. This could be explained by the fact that biomechanically speaking, the two first digits of our hand, the thumb and finger, serve an especially important role in fine motor tasks. As such, their anatomy is noticeably different from the other fingers, they in fact are actuated by independent muscle groups, (abductor pollicis brevis, flexor pollicis brevis, and opponens pollicis, for the thumb, and first dorsal interosseous muscle and the first palmar interosseous muscle for the index). For the last three fingers, the change in coupled stiffness between stroke and control subjects is profound. The last three fingers are primarily used to grab objects and are less important during fine motor tasks. For this reason, they actually share muscle groups, like the flexor digitorum superficialis (FDS). It therefore is clear that, if the FDS has spasticity, this would be observable among all the last three digits, even when not actuated.

**Significance:** Our work brings, quite literally, a new dimension to our understanding of the effects of stroke, enabling us to look at the coupled relationship between digits, which can better inform the development of future rehabilitation strategies. This type of study wouldn't be possible without a highly sophisticated device, the HoHm.

**References:** [1]Benjamin et al. (2017), *Circulation 135* (10). [2]Cramer et al. (1997), *Stroke 28* (12).[3]Doyle et al. (2010), *Cochrane Database of Systematic Reviews* .[4]Gao et al. (2021), *2021 IEEE International Symposium on Mixed and Augmented Reality Adjunct (ISMAR-Adjunct)* .[5]Kim et al. (2011), *Annual International Conference of the IEEE Engineering in Medicine and Biology Society. IEEE Engineering in Medicine and Biology Society. Annual International Conference 2011*.[6]Zhang et al. (2007), *2007 IEEE 10th International Conference on Rehabilitation Robotics*.

# ROBOTIC ANKLE EXOSKELETON ENHANCES GROUND REACTION FORCES IN PATIENTS WITH PERIPHERAL ARTERY DISEASE

* Zahra Salamifar[1], Farahnaz Fallahtafti[1], Jania Williams[1], Iraklis Pipinos[2,3], Sara A. Myers[1,2]
[1]Department of Biomechanics, University of Nebraska at Omaha, Omaha, NE, USA
[2]Department of Surgery and Research Service, Omaha Veterans Affairs Medical Center, Omaha, NE, USA
[3]Department of Surgery, University of Nebraska Medical Center, Omaha, NE, USA
*Corresponding author's email: ssalamifar@unomaha.edu

**Introduction:** Peripheral artery disease (PAD) occurs due to atherosclerotic blockage of the leg arteries. Intermittent claudication is the most common symptom in patients with PAD, which is pain during physical activity that is relieved with rest [1]. PAD impacts the gait patterns of patients even before claudication pain onset [2]. Previous studies indicated that compared to healthy controls, patients with PAD have lower anterior-posterior, lateral, and vertical peak ground reaction force (GRF) points but higher peak medial GRF [2,3]. Robotic exoskeletons improve GRFs in patients with spinal cord injuries and cerebral palsy to be more comparable to healthy individuals [4,5]. However, the effect of robotic exoskeletons on the GRFs of patients with PAD has not been studied. This study assessed the effect of a bilateral ankle robotic exoskeleton device on the GRFs during walking in patients with PAD. We hypothesized that walking with robotic exoskeletons would improve GRFs in patients with PAD to be more comparable to healthy individuals.

**Methods:** A robotic ankle exoskeleton (Biomotum, OR, US) was provided for patients with PAD to support ankle plantarflexion during push-off. Nine patients with PAD (Age: 72.7±6.6 years, height: 1.76±0.05 m, and body mass: 90.01±13.9 kg) were assessed while GRF in three directions was recorded. Subjects wore a form-fitting suit, and standard shoes were provided for each participant. Thirty-three retroreflective markers were attached to lower extremity anatomical landmarks. Participants walked with preferred walking speed over embedded force plates on the floor (AMTI, Watertown, MA, 1000 Hz). GRFs were recorded while patients walked under four conditions: C1: walking without an exoskeleton, C2: walking with an exoskeleton but zero torque, C3: walking with an exoskeleton with 0.2 N.m/kg assistive torque, C4: walking with an exoskeleton with 0.3 N.m/kg assistive torque [6]. The assistive torques were applied during plantar flexion to support push-off. During assisted conditions, a 0.05 N.m/kg torque was applied during the swing phase for smoother walking. One-way ANOVA ($p<0.05$) was conducted using SPSS (IBM SPSS Statistics 26) to compare the peak points in each GRF direction across the four walking conditions (Figure 1).

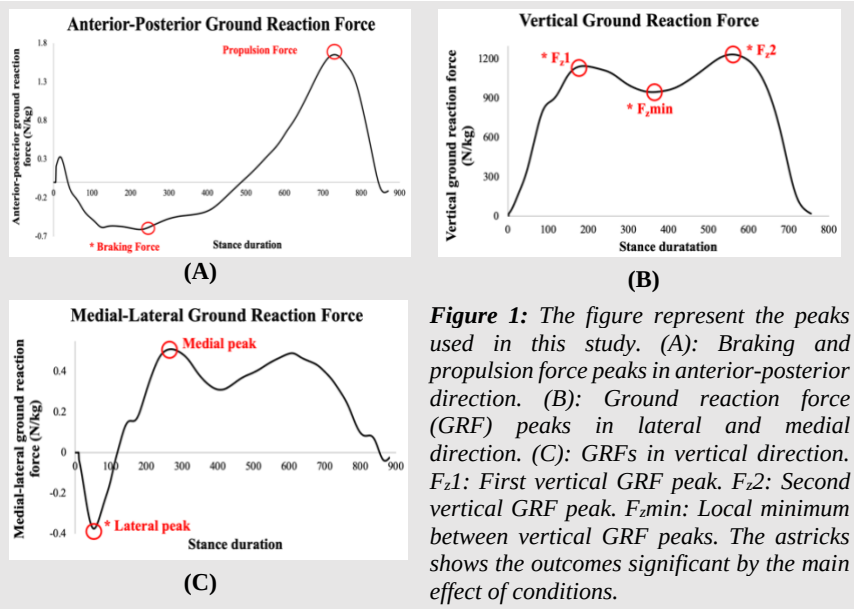


***Figure 1:*** *The figure represent the peaks used in this study. (A): Braking and propulsion force peaks in anterior-posterior direction. (B): Ground reaction force (GRF) peaks in lateral and medial direction. (C): GRFs in vertical direction. $F_z1$: First vertical GRF peak. $F_z2$: Second vertical GRF peak. $F_z$min: Local minimum between vertical GRF peaks. The astricks shows the outcomes significant by the main effect of conditions.*

**Results & Discussion: Anterior/posterior GRFs:** Compared to C2, C4 showed significantly reduced braking force ($p=0.02$). This aligns with a previous study that showed exoskeleton-assisted reduced braking forces compared to unassisted exoskeleton, possibly due to less demand on calf muscle [7]. No significant effect of the exoskeleton on the propulsion GRF was observed ($p=0.5$). **Medial-Lateral GRFs:** Compared to C1, walking with the exoskeleton in all three exoskeleton conditions (C2, C3, and C4) significantly reduced lateral GRFs ($p<0.01$). Potentially, the exoskeleton structure provided ankle stability by reducing foot drop [8]. However, the exoskeleton did not significantly affect medial GRFs ($p=0.6$), indicating the robotic exoskeleton had more effect on the lateral GRFs compared to medial GRFs. **Vertical GRFs:** Patients with PAD have lower vertical ground reaction force compared to healthy individuals. Compared to C1, C3 significantly increased the first vertical GRF peak ($p<0.01$). Compared to C1, walking with the exoskeleton in all three conditions (C2, C3, and C4) significantly increased the second vertical GRF peaks ($p<0.01$) and the local minimum between the first and second peaks ($p<0.01$). [2]. Therefore, using the robotic exoskeleton may increase vertical GRFs to be more comparable to healthy individuals [2].

**Significance:** A robotic ankle exoskeleton can assist walking in patients with PAD. The exoskeleton significantly reduced braking and lateral GRFs, potentially reducing demand on the calf muscles during walking. The exoskeleton also enabled patients with PAD to generate vertical GRFs more closely resembling healthy individuals. Future studies of how exoskeletons and other assistive walking devices impact gait kinetics are needed to understand the potential for assistive device interventions to help patients with PAD.

**Acknowledgments:** This study was supported by the United States Department of Veteran Affairs (I01RX000604, I01RX003266).

**References:** [1] Aday et al. (2022), *Circ Res* 128(12); [2] Fallahtafti et al. (2024), *Int J Cardiol* 407(1); [3] Bapat et al. (2023), *J Vasc Med* 28(1); [4] Fineberg DB et al. (2013), *J Spinal Cord Med* 36(4); [5] Wang et al. (2022), *Front. Neurorobotics* 15(1). [6] Orekhov et al. (2021), *J NeuroEng Rehabil* 18(1); [7] Chandran et al. (2022), *J PLoS One* 18(2). [8] Schmidt et al. (2011) *Foot Ankle Int* 32(1).

# HIGHER LEVELS OF ASSISTANCE FROM AN ANKLE EXOSKELETON DECREASE HEART RATE BUT INCREASE TIBIALIS ANTERIOR FATIGUE RATIO

Jania Williams [1]*, Jonathan Kirkland [1], Gabrielle Moser [1], Farahnaz Fallahtafti[1], Sara Myers [1,2]
[1]Department of Biomechanics, University of Nebraska at Omaha, Omaha, NE, USA
[2] Department of Surgery and VA Research Service, VA Nebraska-Western Iowa Health Care System, Omaha, NE 68105, USA
Email: janiawilliams@unomaha.edu
Presentation Preference: Oral Presentation

**Introduction:** Assistive exoskeletons have the potential to help individuals improve walking performance, quality of life, and physical activity levels by applying support that complements natural movements [1,2]. This research investigated the effects of a portable, robotic ankle exoskeleton on walking performance and exercise outcomes in healthy young individuals during a progressive treadmill test—a protocol commonly used to assess walking capacity. We hypothesized that higher levels of assistance would result in improved walking performance and enhanced exercise outcomes.

**Methods:** Five healthy young participants completed a progressive treadmill test protocol [3] at a self-selected speed while wearing a bilateral ankle exoskeleton. Subjects walked for ten minutes as the slope increased by 2% every 2 minutes, beginning at 0%. Four conditions were completed: 1) baseline with no exoskeleton, 2) exoskeleton with no assistance, 3) exoskeleton assistance of 0.2 Nm/kg, and 4) exoskeleton assistance of 0.3 Nm/kg, in a randomized order. Walking performance was assessed by muscle activity and fatigue ratio of the right limb (lateral gastrocnemius (LG), tibialis anterior (TA), and soleus (Sol) muscles). The fatigue ratio was calculated by dividing the average muscle activity for each muscle during the last five minutes by the first five minutes. A ratio of less than 1 means a decrease in muscle activity over time, indicating fatigue, while a ratio near or greater than 1 suggests that muscle activity was sustained or increased. Exercise outcomes included heart rate, blood pressure, and perceived rate of exertion (Borg Scale). A one-way repeated measure analysis of variance (ANOVA) was performed to determine differences across conditions ($\alpha<0.05$), and the least significant difference (LSD) post hoc tests were applied to significant findings for pairwise comparisons.

**Results & Discussion:** Significant effects for the tibialis anterior (TA) muscle fatigue occurred between conditions 1 and 2 (p=0.017), and conditions 2 and 4 (p=0.022) (Figure 1B). Higher levels of exoskeleton assistance reduced fatigue—reflected by a fatigue ratio equal to or greater than 1—and sustained muscle activity over time. The fatigue ratio from condition 2 differed from the highest assistance condition due to the additional mass of exoskeleton users must carry. During push-off and swing phases, exoskeleton assistance promotes dorsiflexion to prevent tripping while maintaining muscle activation during walking. A significant effect on heart rate occurred between all conditions except 1 and 3 (Figure 1A), suggesting that 0.2Nm/kg assistance does not overcome the exoskeleton's added mass to yield cardiovascular benefits. No significant differences emerged in blood pressure, Borg scale ratings, average muscle activity for any muscle (Figure 1C), or muscle fatigue for LG and Sol muscles. Thus, muscles targeted by exoskeleton assistance show minimal variations in muscle activity and fatigue across conditions. Furthermore, blood pressure and rate of perceived exertion were not strongly influenced by exoskeleton assistance. Given the healthy young population, future work in clinical populations may reveal differences in walking performance and exercise outcomes.

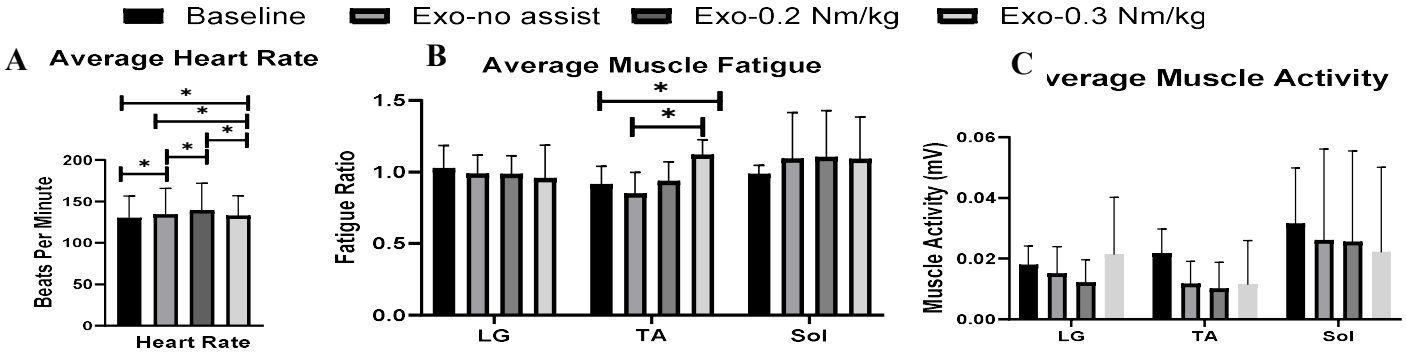


**Figure 1**.Average heart rate, muscle fatigue, and activity in all conditions. (A) Significant effects were observed for heart rate between all conditions except between conditions 1 and 3 (p=0.88). (Conditions: 1-2: p=0.007, 1-4:p=0.035, 2-3: p=0.038, 2-4: p=0.007, 3-4: p=0.0049) (B) A significant effect was observed for muscle fatigue of the TA between conditions 1 and 4 (p=0.017) and conditions 2 and. 4 (p=0.022). (C) No significant differences were observed for muscle activity. * Indicates significant differences.

**Significance:** These findings demonstrate that higher levels of assistance reduce cardiovascular strain while maintaining the muscle activity of the TA during physical activity. Therefore, increased assistance may reduce fatigue-related declines in the dorsiflexors.

**Acknowledgments:** Project funded by the Graduate Research and Creative Activity program at the University of Nebraska Omaha's Office of Creative Research.

**References:** [1] Collins, S, Nature, 522(7555), 212–215. (2025) [2] Mooney, L. M., J. Neuroeng. Rehabil. 11, 82. (2014) [3] Thurston, N*Trends Nur Health Care Res* (Vol. 2, pp. 1–17). (2024)

# HOW HOSPITAL ROOM DESIGN IMPACTS GAIT IN OLDER ADULTS

Nooshin Seddighi[1*], Oliver Rhodes[1], JunSeop Son[1], Rebecca Go[2], K. Bo Foreman[1], Ellen Taylor[3], Bob Wong[1], Peter C. Fino[1]
[1]The University of Utah, Salt Lake City, UT, USA
[2]Stevenson University, Owings Mills, MD, USA
[3]The Center for Health Design, Concord, USA
*Corresponding author's email: Nooshin.Seddighi@utah.edu

**Introduction:** Falls are significant and preventable healthcare concerns, impacting patient safety and contributing to increased healthcare costs, longer hospital stays, and reduced quality of life [1]. Environmental design is a critical yet often underestimated factor that significantly impacts fall risk among older adults [2]. The way a space is designed can either facilitate safe movement or introduce hazards that increase the risk of falls, particularly for older adults with slower gait speeds or mobility impairments [3]. For instance, narrow or cluttered hallways can force individuals to twist or step sideways, making it harder to maintain balance [3]. Prior work using augmented reality (AR) highlighted two areas that may impact patients' behaviors: the type of door and the room layout [4]. The goal of this study was to understand how different hospital room design features, specifically, room layout (headwall vs. footwall) and door type (sliding vs. swinging), affect older adults' walking trajectory and mobility.

**Methods:** We recruited 18 (10 male and 8 female) older adults who could walk independently. The participants had a mean age (SD) of 74.28 (4.14) years. Each participant completed standardized mobility assessments (not reported here) and a task that involved walking in a simulated hospital room. For the simulated hospital room task, participants were instructed to start in a seated position on a hospital bed, to stand up and walk to the bathroom door, walk into the bathroom, close the door, sit on the toilet, stand and walk to the sink, simulate washing their hands, walk back through the bathroom door and return to sitting on the bed. The simulated hospital room included two manipulated factors: 1) the room configuration (Headwall vs. Footwall), and 2) the door type (Sliding vs. Swinging), resulting in four unique room layouts (Figure 1) [4]. Participants completed four trials in each room; two trials were completed without additional requirements, and two trials were completed while the participant was attached to an intravenous (IV) pole. Room layouts were randomized by subject, and IV conditions were randomized within each room.

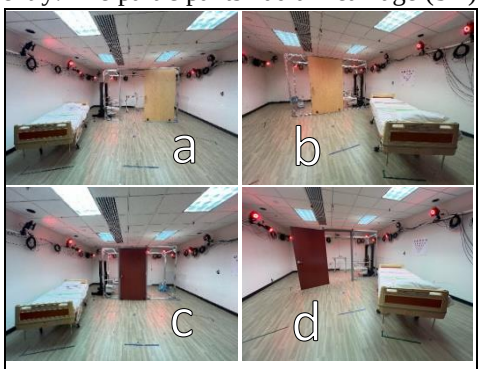


**Figure 1.** Different room layouts of the simulated hospital environment. a) Sliding Headwall, b) Sliding Footwall, c) Swinging Headwall, d) Swinging Footwall room

Kinematic data were collected for each trial using a full-body marker set and 20 motion capture cameras (Vicon MX20 and MX40). Path trajectory variables included total trial time, distance traveled (sideways, backward) while spatiotemporal gait variable includes pelvis speed turns. Small turns were defined as 10°–45° and large turns as >45°. The dataset was divided into IV and No-IV groups, which were analyzed independently. For each outcome variable, Linear Mixed-Effects Models (LMM) were applied with fixed effects included room configuration (headwall vs. footwall), door type (sliding vs. swinging), along with their interactions. Random intercepts for each participant were included in the model. Significant results were further examined using post hoc pairwise comparisons. Statistical significance was set at $\alpha = 0.05$. The study was approved by the University of Utah Institutional Review Board, and informed consent was obtained prior to participation.

**Results & Discussion:** At the time of this abstract, data from three participants had been analysed. Overall, the preliminary results indicated an interaction between IV pole, layout, and door type on participant's movement within hospital rooms. Participants completed the trial faster in headwall rooms ($\beta = -9.76$, SE = 1.98 seconds with IV; $\beta = -5.42$, SE = 1.38 seconds without IV) compared with footwall rooms. With the IV pole, participants had greater sideways movement in rooms with swinging doors compared with sliding doors ($\beta = 0.70$, SE = 0.29 m), and this effect was amplified when paired with a footwall layout ($\beta = 0.78$, SE = 0.27 m). Headwall rooms reduced backward motion ($\beta = -0.43$, SE = 0.20 m) and swinging doors also contributed to this reduction ($\beta = -0.59$, SE = 0.20 m) when walking with the IV pole. In absence of IV pole, trials times in rooms with swinging doors were faster than rooms with sliding doors ($\beta = -4.04$, SE = 1.38 seconds), swinging doors reduced sideways movements ($\beta = -0.63$, SE = 0.20 m), and headwall rooms further reduced lateral motion ($\beta = -0.78$, SE = 0.20 m). Small turns speed did not differ significantly by room layout or door type, regardless of IV pole presence. In contrast, for large turns speed, no significant effects were observed when an IV pole was present. However, in the absence of an IV pole, headwall rooms reduced large turns speed ($\beta = -7.25$, SE = 1.81 deg/s) compared to footwall rooms, and rooms with swinging doors showed a reduction ($\beta = -5.12$, SE = 1.81 deg/s) relative to sliding doors.

**Significance:** These findings highlight the impact of room configurations and ergonomic design factors on patient walking patterns. Future work will extend these outcomes to include balance and stability measures and include the full sample of participants.

**Acknowledgments:** Funding from AHRQ R18HS025606. We would like to express our heartfelt thanks to Christina Geisler, Mackenzie Alison Elliot, Zachary Olson, and Cecilia Monoli for their contributions in data collection and room construction.

**References:** [1] Callis, N., Appl. Nurs. Res., 2016, DOI: 10.1016/j.apnr.2015.05.007. [2] Pati, D., et al., J. Patient Saf., 2021, DOI: 10.1097/PTS.0000000000000339**.** [3] Novin, R.S., et al. *HERD*, 2021, https://doi.org/10.1177/1937586720959766. [4] Seddighi, N., et al. *HERD*, 2024, https://doi.org/10.1177/19375867241238434.

# HEAVY LIFTS, SMALL BODIES: THE INFLUENCE OF TASK AND WEIGHT IN INFANT LIFTING MECHANICS

*Safeer F Siddicky[1], Melvin Leon[2], Kathryn L. Havens[2,3]
[1]Department of Kinesiology and Health Education, The University of Texas at Austin, Austin, TX, USA; [2]Division of Biokinesiology and Physical Therapy and [3]Department of Biomedical Engineering, University of Southern California, Los Angeles, CA, USA
*Corresponding author's email: safeer.siddicky@austin.utexas.edu

**Introduction:** Infant caregiving requires frequent lifting, yet the biomechanical demands of these daily tasks remain underexplored. Our preliminary research on postpartum mothers has demonstrated task-related biomechanical differences when mothers lifted their infant from the floor, within a car seat from the floor and from a changing table [1]. Other research has highlighted that caregivers experience significant mechanical loads when carrying infants while walking, with postpartum individuals demonstrating altered movement patterns compared to nulliparous controls [2,3]. However, little is known about baseline biomechanics of infant lifting in nulliparous individuals. Understanding how lifting biomechanics varies across different caregiving contexts and infant weights is essential for identifying potential musculoskeletal risks and informing injury prevention strategies. Thus, we investigated the effect of infant lifting tasks and infant weight on trunk and lower extremity kinematics and kinetics in nulliparous individuals.

**Methods:** 7 healthy nulliparous women (Age: 29.8 ± 3.1 years; Height: 1.7 ± 0.1 m; Weight: 68.9 ±12.0 kg) participated in this study. Participants performed three semi-continuous lifting tasks (Fig. 1) using a newborn infant manikin (3.23 kg) and an infant manikin weighted to emulate a 3-month-old infant (6.17 kg). Three tasks were performed: lifting off the floor, lifting within a car seat from the floor, and lifting off a changing table. Reflective markers tracked 3D kinematics (150 Hz; Qualisys) and forces were collected with force platforms (1500 Hz; Bertec). Kinematic and kinetic data were processed in Visual3D (HAS-Motion) and MATLAB (The Mathworks). Descriptive statistics are presented.

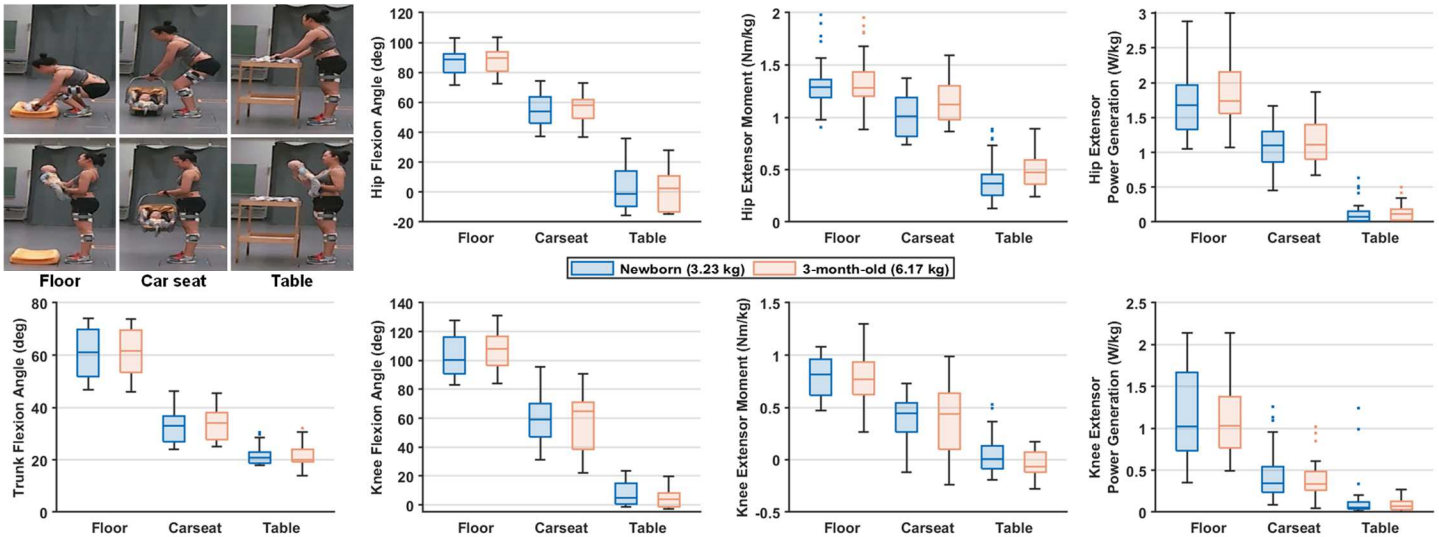


**Figure 1:** Lifting task photos, average peak sagittal kinematics of the trunk, hip, and knee, and average peak sagittal kinetics of the hip and knee.

**Results & Discussion:** The sagittal plane biomechanics of the hip, knee, and trunk play a crucial role in lifting tasks, and this study demonstrates that these are altered with caregiving task demand, consistent with previous research [1,4]. Lifting an infant from the floor required the greatest hip and knee flexion, extensor moments, and extensor power generation, while lifting from the changing table involved minimal hip and knee involvement, relying primarily on the trunk (Fig 1). Lifting an infant in a car seat introduced unique constraints due to the additional weight but the elevated handle height reduced trunk and lower extremity flexion compared to the floor task. Increasing infant weight variably affected joint moments and trunk flexion. Hip extensor moments notably increased, while knee extensor moments remained largely unchanged, consistent with Kim et al. [4].

These findings highlight the demands of caregiving lifting tasks and suggest biomechanical adaptations required as infants grow. As babies grow heavier and continue to be lifted by caregivers into their school-age years, the biomechanical differences observed with a modest 3 kg increase are likely to become even more pronounced when lifting larger loads, such as 10 kg or more. Future directions for this work include investigating trunk and lower extremity muscle activity for nulliparous women, asymmetries involved in each lifting task, and how lifting mechanics differ from postpartum mothers.

**Significance:** Investigating how lifting mechanics vary by task and infant weight in nulliparous individuals provides a critical comparison for understanding the effects of experience and musculoskeletal adaptations on movement patterns. This has broader implications for injury prevention, ergonomic interventions, and the development of guidelines to support safe lifting strategies for both new and experienced caregivers.

**References:** [1] Havens & Siddicky, *J Biomech* (In review), [2] Havens et al., *J Applied Biomech* 40(2), 2023, [3] Bagwell et al., *Gait & Posture* 81, 2020. [4] Kim et al., *Technol Heal Care* 30, 2022.

# LEG LENGTH AND WAIST-TO-HEIGHT RATIO ARE ASSOCIATED WITH FOOT PLACEMENT LOCATION WHILE CLIMBING DOWN A LADDER

*Sarah C. Griffin[1], Kurt E. Beschorner[1]
[1]University of Pittsburgh Bioengineering *Corresponding author's email: scg57@pitt.edu

**Introduction:** In the United States, ladders cause over 22,000 workplace accidents that result in days away from work and 170 deaths annually [1]. The effect of individual factors, such as height or obesity, on climbing mechanics and fall risk is not well understood despite other studies identifying individual factors like sex as contributors to fall risk [2]. To reduce the burden of ladder falls it is crucial that we work to understand how different individuals climb ladders.

Ladders are used by people of all ages, sexes, shapes, and sizes. Differences in strength, coordination, or body shape could influence the way a person is able to climb a ladder. It is unclear if individual factors, like leg length, age, obesity, or sex, influence the way that people climb ladders. If individual factors are associated with climbing strategy, some demographics may be at an increased risk of experiencing a fall and could benefit from specific training. Foot placement location is a key biomechanical factor that is associated with ladder fall risk [3]. There are two main risks with foot placement: 1) a person must place their foot far enough on the rung (i.e. rung far enough from the toes) to be stable and 2) climbers must be consistent in their foot placement so that they do not accidentally miss a rung or need to readjust after placing their foot. The purpose of this work is to determine if individual factors are associated with foot placement location and variability when climbing down a ladder. It was hypothesized that a shorter leg length would be associated with foot placement closer to the toes, because the leg is not long enough to allow a more anterior foot placement, and age would be associated with higher foot placement variability due to age related loss of motor control.

**Methods:** 76 healthy adults (41 F, 42.5 ± 12.7 years, 1.70 ± 0.09 m, 26.8 ± 4.3 kg/m$^2$) who regularly climb ladders were included in this study. A stratified recruitment ensured sufficient spread across the following individual factors: height, obesity, age, and sex. The ladder had round rungs and was oriented at 75º and 90º. Participants wore safety equipment and 79 reflective markers. Participants climbed down five rungs of the ladder at a comfortable but urgent pace as though they were trying to complete a task. Kinematic data was collected using optical motion tracking cameras (Vicon).

Foot placement was calculated on one rung as a percentage of foot length, where 0% indicates the rung center contacting the toe and 100% the heel. The mean and standard deviation of foot placement were calculated across three replicate trials to capture the location and consistency of foot placement. Two repeated measures mixed regression models were generated with the mean or standard deviation of foot placement as the dependent variable. Models included the following predictors: sex, age, leg length, waist-to-height ratio, and ladder angle.

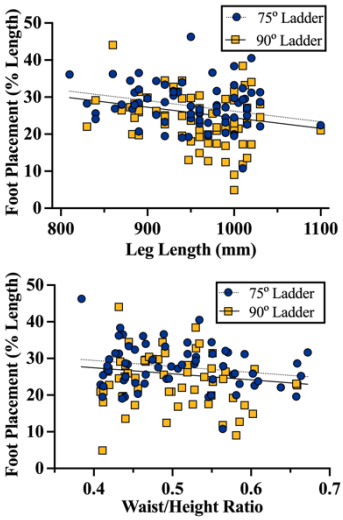


**Fig 1**: The association between foot position and leg length (top) or waist-to-height ratio (bottom). Ladder angles are indicated by colors and shapes

**Results & Discussion:** Leg length ($F_{1,62}$ = 6.99, p = 0.010), waist-to-height ratio ($F_{1,66}$ = 4.65, p = 0.035), and ladder angle ($F_{1,58}$ = 22.13, p < 0.001) were associated with the average foot placement (Fig. 1), but age ($F_{1,62}$ = 2.15, p = 0.148) and sex ($F_{1,62}$ = 0.40, p = 0.527) were not. According to parameter estimates, an increase of 10 cm in leg length, corresponds to a foot placement 3.4% of foot length closer to the toe. It was hypothesized that longer legs would allow someone to place their foot with the rung further from the toe and this would be favored because it decreases the ankle moment arm. The opposite effect was observed. Individuals with a longer leg length likely have a longer foot length. Because the foot position was calculated as a percent of foot length, a smaller foot position on a person with a longer foot could be the same raw distance from the toe as a larger foot position on a person with a shorter foot.

An increase of 0.1 in the waist-to-height ratio corresponded to a foot position 2.4% of foot length closer to the toe. This was unexpected as obesity was not hypothesized to have an association with the foot position. Individuals with a higher waist-to-height ratio may place their foot with the rung closer to the toes due to their body shape. Someone with a high waist circumference may not be able to bring their hips as close to the ladder, and thus may be unable to place their foot in the same location as someone without obesity.

None of the individual factors presented significant associations with the standard deviation of foot placement (age: $F_{1,60}$ = 0.26, p = 0.62, sex: $F_{1,60}$ =1.47, p = 0.23, leg length: $F_{1,60}$ = 0.65, p = 0.42, waist-to-height ratio: $F_{1,66}$ = 0.052, p = 0.82, ladder angle: $F_{65}$ = 2.0, p = 0.16). It was expected that increased age would be associated with higher foot placement variation due to the age-related loss of motor control that is associated with aging. Lack of significance indicates that increased age may not pose a risk for unsafe foot placement strategies while climbing down the ladder.

**Significance:** This work could have a direct impact on ladder safety training programs. People with longer legs or higher waist-to-height ratios may be at an elevated risk of experiencing a fall from a ladder due to their foot placement location. These individuals may benefit from training to place their foot further anterior on the rung while climbing down ladders to increase their safety.

**Acknowledgments:** This research was funded by NIOSH R01OH011799 and NSF GRFP 2139321.

**References:** [1] U.S. BLS (Data from 2019). 2023, Dpt of Labor. [2] Pliner et al. (2017), *Appl. Ergon. 60* 163-170. [3] Pliner et al. (2014), *Ergonomics (57)11*. 1739-1747.

# THE KINEMATICS AND KINETICS OF UNEXPECTED LADDER SLIP EVENTS

*Violet M. Williams[1], Sarah C. Griffin[1], Mark S. Redfern[1], Kurt E. Beschorner[1]
[1]Department of Bioengineering, University of Pittsburgh, Pittsburgh, PA, USA.
*Corresponding author's email: Violet.Williams@pitt.edu

**Introduction:** Ladder falls accounted for over 48,000 occupational injuries and 333 fatalities in the US between 2021-2022 [1,2]. Slips are a common initiating event in ladder falls, accounting for 14% of ladder falls [3]. To help prevent these falls from occurring, researchers need a method to evaluate the friction performance of ladder rungs, which has not yet been well developed.

Mechanical slip testing is used to measure the coefficient of friction (COF) between two surfaces, typically using standardized test conditions that ensure comparable results across different labs and studies. Ideally, these standards use biofidelic testing conditions that reproduce the dynamics of slip events such as slipping speed, shoe-floor angle, normal force, and contact time which have all been found to impact COF outcomes [4]. While these metrics have been categorized in level-walking, the under-shoe conditions of ladder slip events have yet to be characterized in the same way. The aim of this study was to quantify the biomechanical variables of unexpected slips during ladder climbing to inform biofidelic testing conditions for the mechanical slip-testing of ladder rungs.

**Methods:** This study utilized a custom instrumented ladder apparatus with 3 discrete rotation angles and interchangeable rungs. The 3rd rung of the ladder was rigidly attached to a force plate (AMTI) while motion tracking cameras (Vicon) collected time-synced kinematic data. Participants climbed a series of ladder configurations consisting of eight unique rung designs and three unique angles. Participants were instructed to climb with an urgent pace, stopping at the 5th rung of the ladder, before climbing back down the ladder. Prior to the participant's last climb, a liquid contaminant (90% glycerol + 10% water) was added to the 3rd rung. Participants completed a word puzzle task to distract them from the application of the contaminant to ensure the slip was unexpected. Some participants (n = 46) completed this task on the 5th rung of the ladder with the contaminant applied prior to their descent while the remaining participants (n = 42) complete this task on the ground facing away from the ladder prior to their ascent. To increase the slipping rate, the final 59 participants had plexiglass installed in front of the rung to limit toe clearance.

Slip trials were first categorized using a k-means cluster analysis where trials were grouped together using the variables of peak slipping speed and slip distance. Peak slipping speed was the maximum resultant velocity of the foot center during contact. Local minima, corresponding to start and end of slip, were required to exist before and after this maximum. Slip distance was the total displacement of the foot center between these local minima. Then, two reviewers observed videos from the slip trials (high slipping speed, high slip distance) to confirm which trials should be classified as slips. Slipping speed, normal force (perpendicular to sole), shear force (parallel to sole) , shoe-rung angle (angle between shoe and rung surface), transverse foot angle (medial-lateral rotation), and foot position (anterior-posterior & medial-lateral relative to the rung) were quantified during the start of slip and the time of peak slipping speed for each trial classified as a slip. Mean values and 95% confidence intervals were calculated for each of these metrics.

**Results & Discussion:** There were a total of eleven slip trials with nine forward slips and two backward slips. Due to the lack of backward slips, kinematic and kinetic averages only include the forward slips trials (Table 1).

**Table 1:** Slip kinematic and kinetic means and confidence intervals at the start of slip and the time of peak slipping speed.

| | ***Slip Start*** | | ***Peak Slipping Speed*** | |
|---|---|---|---|---|
| ***Metric*** | **Mean** | **95 % Confidence Interval** | **Mean** | **95% Confidence Interval** |
| ***Slipping Speed (m/s)*** | 0.05 | 0.02 - 0.07 | 0.34 | 0.28 - 0.41 |
| ***Shoe-Rung Angle (°)*** *(+ = dorsiflexion)* | 7.6 | 1.7 – 13.5 | 7.0 | 3.6 – 10.5 |
| ***Transverse Foot Angle (°)*** *(+ = toe out)* | 7.6 | 1.6 - 13.7 | 9.5 | 2.1 – 16.8 |
| ***Normal Force (% BW)*** | 38.3 | 11.6 – 65.0 | 58.6 | 39.7 – 77.4 |
| ***Shear Force (% BW)*** * | 7.1 | 0.01 – 0.10 | 13.2 | 6.7 – 19.8 |
| ***AP Foot Position (%)*** | 21.2 | 19.1 - 23.3 | 26.8 | 25.0 – 28.6 |
| ***ML Foot Position (%)*** | 55.2 | 47.2 – 63.2 | 55.5 | 47.6 – 63.4 |

* Values were log transformed to calculate the confidence interval

**Significance:** These slip kinematics and kinetics will help inform future mechanical slip-testing of ladder rungs through the creation of biofidelic standards. The difference in slipping speeds between the start of slip (0.05 m/s) and peak slipping speed (0.34 m/s) indicate the importance of both static and dynamic friction in testing. Thus, we recommend two mechanical slip tests for ladder rungs consisting of forward slips at 0.05 m/s and 0.34 m/s, a normal force of 400 ± 50 N, and a foot angle of 8° dorsiflexed.

**Acknowledgments:** The authors would like to acknowledge Richard Smith, Jenna Trout, and the undergraduate students who assisted with this work. This work was supported by NIOSH R01OH011799, NSF GRFP 2139321, and NCRR S10RR027102.

**References:** [1] U.S. BLS (2024), *Fatal Occupational Injuries,* U.S. DOL; [2] U.S. BLS (2024), *Nonatal Occupational Injuries,* U.S. DOL; [3] Cohen et al. (1991), J. Saf. Res. 22(1); [4] Iraqi et al. (2018), J. Biomech. 74;

# WEIGHT SHIFTS AS A MARKER OF DISCOMFORT DURING PROLONGED SITTING

*Krista Dronzek[1], Rutuja Kulkarni[2], April Chambers[1,3]
*Corresponding author's email: kjd83@pitt.edu
[1] Department of Bioengineering, University of Pittsburgh, Pittsburgh, PA

**Introduction:** For those who spend most of their time sitting, there is an increased risk for all-cause mortality, cardiovascular disease, cancer, and type 2 diabetes [1]. More than 80% of jobs in the United States involve mostly sedentary activities [2], and these employees spend 62% of their days sitting [3]. Because of this lack of movement, 60% of office workers complain about physical discomfort [4]. Sit stand desks have been implemented into the workplace to allow workers to complete the same task from a workstation with an adjustable seated or standing height and have the potential to decrease the issues associated with prolonged sitting [5]. To maximize the potential health benefits of sit stand desks, the optimal dosage of sitting to standing must be established. The long-term goal of this research is to determine the ratio of sitting to standing that provides the most comfort for office workers. The objective of this study is to determine the feasibility of using weight shifting as a marker of discomfort and fatigue during seated office work, and it is hypothesized that weight shifting during seated office work will be associated with self-reported discomfort and fatigue.

**Methods:** Seventeen healthy, middle-aged participants were screened and consented to participate in this study. Mean (SD) Demographics of participants were as follows: age=44.59 (4.52) years, height=172.24 (9.72) cm, mass=80.41 (20.54) kg. All study procedures were approved by the University of Pittsburgh Institutional Review Board. Participants participated in one 90-minute seated visit. The standard office chair was instrumented with a seated pressure pad (Vista Medical). Participant completed a computer task while their discomfort and fatigue were recorded every five minutes using a visual analogue scale (VAS). Additionally, whether they wanted to take a break and stand or continue to stay seated was also recorded. Center-of-pressure (COP) data was analysed to find the total number of weight shifts over the 90-minute interval [6].

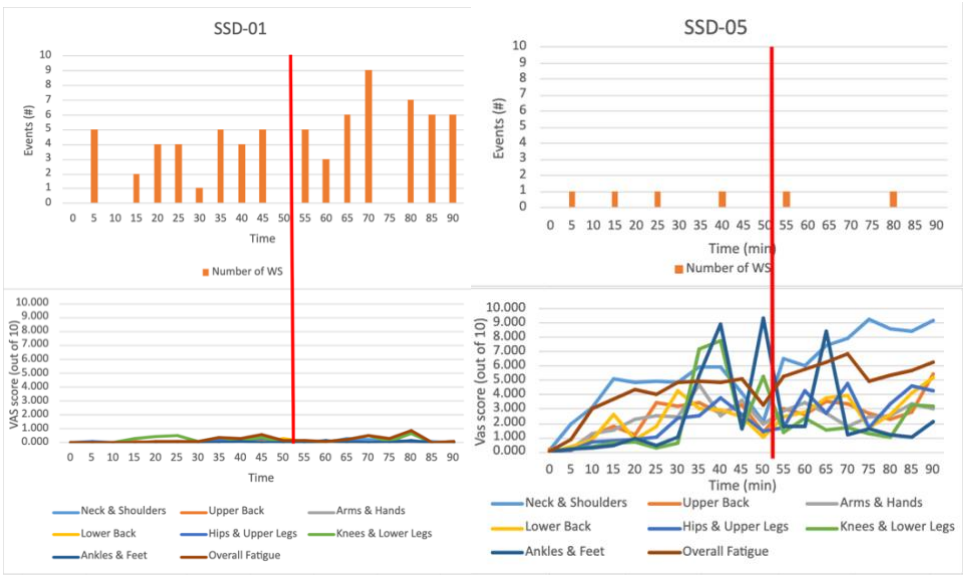


*Figure 1(a and b): Subject 01 and 05 weight shifts (top) and discomfort score on the visual analogue scale (bottom) over 90 minutes. The red line indicates a break taken. Graphs in AP direction*

**Results & Discussion:** In general, discomfort levels and number of weights tended to increase across time spent sitting. It was noted that participants had different shifting strategies. Participants who demonstrated a higher volume of weight shifts throughout their sitting reported less discomfort (Fig. 1a). Participants who did not have many weight shifts tended to have higher discomfort ratings (Fig. 1b). Only four participants requested a standing break. This occurred at an average time of 50 minutes with discomfort ratings tending to increase until a break was provided.

**Significance:** Weight shifting patterns during prolonged seated work appear to have potential to be an objective measure to inform personalized best practice of sit stand desk use. Different strategies point to the importance of personalized ratios of sitting to standing. Future research should consider weight shifting as a potential measure to inform sit stand desk dosage.

**Acknowledgments:** Funding provided by the Office of Ergonomics Research Committee.

**References:** [1] Biswas (2015), [2] Church (2011), [3] Jones (2019), [4] Agarwal (2018), [5] Karakolis (2014), [6] Rekant (2019)

# VALIDATION OF AN IMU AND PRESSURE INSOLE MOTION TRACKING SYSTEM ACROSS STOOP AND SQUAT LIFTING POSTURES

*Vicki Z. Wang[1], Rutuja Kulkarni[1], Alicia M. Koontz, PhD[1,2]
[1]Human Engineering Research Laboratories, Department of Veteran Affairs
[2]School of Medicine, University of Pittsburgh
*Corresponding author's email: vzw4@pitt.edu

**Introduction:** The usage of wearable inertial motion tracking (IMC) systems has been growing in biomechanics research, due to the benefits over traditional optokinetic motion capture (OMC) systems in flexibility of use [1]. Camera and force plate systems, while accurate, face issues such as camera line-of-sight, limited capture area, and an inability to test outside the lab. IMC systems utilize IMU sensors and pressure insoles to capture body movement and ground reaction forces, providing flexibility to obtain data in real-world environments. Considering their potential, evaluation of IMC accuracy across a variety of movements and settings is paramount. While there have been many studies evaluating their performance during gait and quiet standing [2], there are far fewer investigations into lifting. In this study, we compared the agreement between vertical ground reaction forces (vGRF) measured by an IMC system vs a traditional OMC system during stoop and squat lifting and found only moderate agreement. The insoles consistently overestimated the vGRFs, and correlation decreased as vGRF increased. These results indicate that caution should be exercised if directly comparing ground reaction forces between IMC and OMC systems.

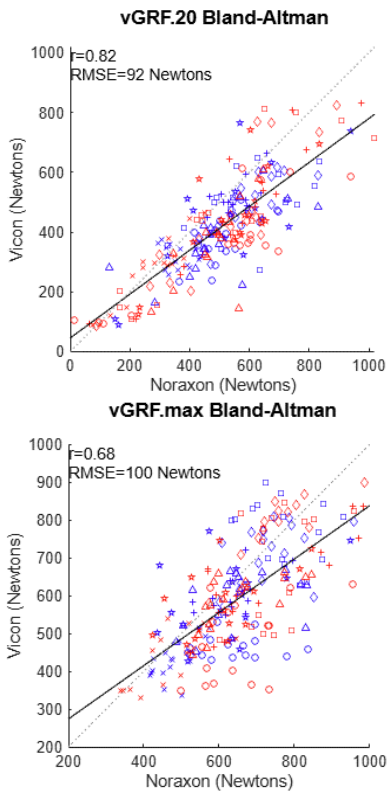


**Figure 1:** Correlation plots for $vGRF_{20}$ and $vGRF_p$ values across all subjects and trials. Datapoints from the squat condition are in blue, stoop in red.

**Methods:** 7 subjects completed 16 lifting trials each, with motion capture measured concurrently by an IMC system (Noraxon, Scottsdale AZ) and an OMC system (Vicon, Oxford, UK). Subjects lifted with feet set shoulder-width apart, and trials varied by posture (knee flexion dominant "squat" vs trunk flexion dominant "stoop") as well as differences in the starting position of the weight (directly in front or to the left/right), to evaluate robustness across a greater variety of movements. vGRFs were measured for each foot, along with knee flexion. Since maximum shear in the low back, highly clinically relevant in lifting, occurs at ~20% of the way through the lift cycle in both squat and stoop [3], this timepoint ($t_{20}$) was used for analysis, along with peak vGRFs that occurred during the trial overall. Peaks in knee flexion from IMC/OMC were individually interpreted to determine the lift cycle as according to each system. Bland-Altman plots, Pearson's correlation, and RMSE values are reported.

**Results & Discussion:** Linear regression of $vGRF_{20}$ and $vGRF_p$, Figure 1, shows the correlation between insole and force plate measurements, with r = 0.82, RMSE = 92N and r = 0.68, RMSE = 100N respectively. The cone shape of the scatter plots indicates that correlation decreases with higher vGRFs. Additionally, the majority of the line of best fit for both plots exists below the r = 1 line; i.e, the insoles overestimate vGRFs. This is confirmed in the Bland-Altman analysis; the insoles measured, on average, 88N (21.2%) higher than the force plates at the $vGRF_{20}$ timepoint, and peak vGRFs were higher by an average of 60N (10.1%). The limits of agreement were 200N and 210N respectively.

Another aspect of IMCs that must be considered is the impact of forces in the directions orthogonal to the insole, as IMCs do not measure horizontal ground reaction forces (hGRFs), even though they may contribute heavily to overall GRFs (especially in gait [4]). hGRFs measured by the OMC at $t_{20}$ showed an average value of 9.3% ± 6.4% (relative to $vGRF_{20}$) – given this, it would be up to the researcher to evaluate the postures, movements, and analysis to determine if the exclusion of hGRFs would significantly affect study results.

Previous studies have shown strong correlation between joint angles from OMCs and IMCs, especially in the lower body [5]. The addition of validated ground reaction forces in the IMC system would allow for reliable calculation of clinically relevant joint forces and moments. However, the results at hand suggest that current IMC technology has yet to reach significant enough corroboration with the gold standard OMC methods to validate direct comparisons of the vertical ground reaction forces, or calculations utilizing GRFs for this particular movement application. Yet, the correlation from each trial as time series data is relatively strong (r = 0.77 ±0.12) – this suggests that IMC systems could still be accurately used for relative comparisons. Additionally, if an in-lab validation of the IMC against a robust OMC can be performed, a model accurately relating the two could then be created to allow greater IMC accuracy in experiments thereafter, as demonstrated by Fong et al [6].

**Significance:** These results add to the growing body of knowledge surrounding the application of IMCs to biomechanics. Future research that requires the greater flexibility afforded by these systems can have greater insight as to exactly how the vGRF values they measure may differ from the OMC gold standard, and evaluate the impact of that difference on their results and conclusions.

**References:** [1] Hafer et al. (2023), *J Biomech 157(111714);* [2] Lee et al. (2022), *Sensors 22(7);* [3] von Arx et al. (2021)*;* [4] Nilsson et al. (1989), *Acta Physiol Scand 136(2);* [5] Poitras et al. (2019), *Sensors 19(7);* [7] Fong et al. (2008) *10.1016/j.jbiomech.2008.05.007*

# CENTER OF PRESSURE ANALYSIS OF PERCEPTION TO FALLING OBJECTS

Sophie A Pearson* and Erika M Pliner
Department of Mechanical Engineering, University of Utah, Salt Lake City, UT, USA
Email: *sophie.pearson@utah.edu

**Introduction:** Contact with objects and equipment is the third leading cause of work-related fatalities and the second leading cause of days away from work, restricted activity, or job transfer [1]. Attention and perceptual human errors are key contributors to these accidents [2], but there is a lack of knowledge characterizing human perception of hazardous objects and equipment. Understanding of human perception ability and limitations is necessary to guide safety interventions for object and equipment hazards. Analyzing biomechanical metrics provides a promising objective measure of workers' perception of hazards. Perception of a hazard can trigger a startle response [3]. Startle research has primarily focused on muscle response, but these responses often lead to postural adjustments [3]. Postural adjustments can be assessed biomechanically through body movements such as quick displacements (fidgets) in the center of pressure (CoP) [4,5]. Therefore, biomechanical data should be explored as a marker for worker hazard perception, such as falling objects. The objective of this analysis is to identify biomechanical metrics of postural adjustments to a startle event initiated from a falling hazard. This will provide valuable insights into which biomechanical metrics can aid in falling hazard interventions. We hypothesize that exposure to a falling object will result in larger fidget amplitudes and postural movement compared to no-hazard.

**Methods:** This work presents a case-study of a healthy younger adult participant to explore promising biomechanical metrics of falling hazard perception. Institutional Review Board (IRB) approval and informed consent was obtained prior to the study. The participant completed 32 randomized trials while standing in a comfortable position. Falling hazards can produce visual and auditory stimuli, thus, these trials consisted of being exposed to three different startle types (auditory, visual, or auditory-visual) with a control of no-startle. The stimuli comprised of a released object (i.e. falling object). The location and material of the falling object varied, producing either a visual, auditory or visual and auditory stimulus. The location and time of the visual and/or auditory stimulus was randomized between the left and right sides of the participant. CoP data was collected from two force plates at 1200 Hz. Body movements were characterized by CoP fidgets and movement. These metrics were calculated over a two second timeframe after object release. The resultant CoP distance (RD) was used to calculate fidgets. RD was calculated as the vector distance from the mean CoP to CoP location at that point in time. Fidgets were detected by extracting the absolute peak RD value with respect to the moving average RD across the two second timeframe [4]. The fidget width was estimated as the full width at half maximum and the amplitude threshold was set at two standard deviations from the mean of the moving time window of one second [4]. If a peak satisfied these conditions the amplitude was calculated. Postural movement was calculated from CoP path length and the mean RD. One-way ANOVAs were performed on biomechanical metrics with startle type as the independent variable. If startle type was found to be significant, a Tukey's HSD postdoc was performed to determine which startle types differed.

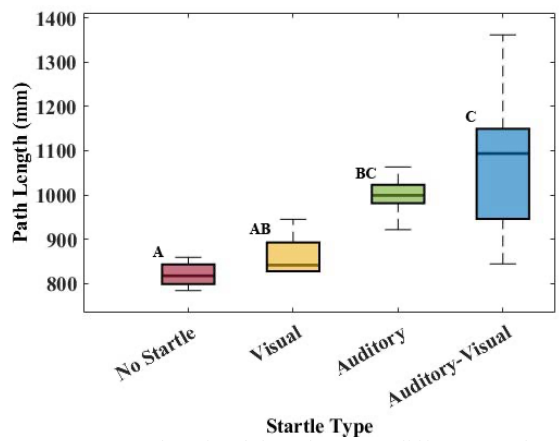


**Figure 1:** Box plot of path length among different startle types. Non-matching letters indicate conditions that are significantly different than one another.

**Results & Discussion:** This exploratory analysis found path length to vary across startle type ($F_{3,28} = 14.5$, $p < 0.001$), but no difference in fidget amplitude ($F_{3,28} = 0.653$, $p > 0.5$) and mean RD ($F_{3,28} = 1.12$, $p > 0.3$) across startle type. Thus, fidget amplitude and mean RD may not indicate hazard perception. This suggests small, fidgets relative to a falling object may be similar to natural postural adjustments. However, path length differed between the no-hazard condition and both the auditory ($p = 0.002$) and auditory-visual conditions ($p < 0.001$) (Fig. 1). These initial findings suggest total CoP displacement may be more reflective of startle-induced postural adjustments in response to auditory and auditory-visual startles.

**Significance:** These preliminary results will allow us to verify our methods to identify key biomechanical metrics prior to targeting manual labour workers. Future work will continue to investigate the relationship between postural adjustments and hazard perception to determine whether path length is a reliable indicator across different individuals. Identifying biomechanical metrics of hazard perception may inform the design of targeted workplace safety interventions, including PPE improvements and hazard alert systems.

**Acknowledgments:** This work is supported by the National Institute of Occupational Safety and Health of the National Institutes of Health under the ERC grant T420H008414.

**References:** [1] BLS, (2023) *Stats. Report;* [2] Hasanzadeh, S. et al. (2017) J. Construct. Eng. Mgmt. [3] Nonnekes, J. et al. (2015) Neurosci Biobehav Rev. [4] Duarte and Zatsiorsky (1999) Motor Control. [5] Prieto, TE. Et al. (1996) IEEE Trans Biomed Eng.

# AGE AND KNEE EXTENSION STRENGTH ARE ASSOCIATED WITH LADDER CLIMBING STRATEGY

*Luke A. Snyder[1], Sarah C. Griffin[1], Kurt E. Beschorner[1]
[1]University of Pittsburgh Department of Bioengineering *Corresponding author's email: las452@pitt.edu

**Introduction**: Ladders are a common but dangerous tool that are used by all ages in both occupational and non-occupational settings. Ladder use and its associated risk, however, differs across ages [1]. In contrast to walking, ladder climbing is a physically rigorous task that requires sufficient strength, coordination, and balance to enact cyclical quadrupedal motion. In particular, knee extension strength is crucial for ladder climbing, as the quadriceps are a primary mover in this task. Differences in strength across populations may pose the need for adaptations to ladder climbing [2]. Previous biomechanical work typically included small samples of healthy, young adults. Generally, these individuals step with one foot per rung while ascending and descending the ladder. As people age, strength, coordination, and balance tend to decrease. It is unclear how older adults or individuals with lower strength might adapt their climbing strategies to be different than young, healthy adults. One adaptive strategy could involve an individual using two feet per rung (double stepping) if they lack sufficient strength. This study aims to investigate how age and knee extension strength influence the likelihood of double stepping during ladder climbing. By exploring these correlations, we aim to establish a foundation for further research on safety and training interventions. We hypothesized that increased age and lower knee extension strength would be positively associated with using two feet per rung.

**Methods:** Eighty healthy adults (40 F, 43 ± 12.4 years, 1.71 ± 0.09 m, 27.2 ± 4.36 kg/m$^2$), recruited through a stratified design to achieve a range in age from 18 to 65 years, participated in the study. After being fitted with safety equipment, each participant completed three ladder climbing trials across up to 8 rung designs and 3 ladder angles. Participants encountered between 9 and 24 ladder configurations and were instructed to climb to the fifth rung of the ladder, pause for a moment and then descend to the ground. Participants were instructed to climb quickly, as though they were trying to complete a task. The use of two feet per rung during a particular trial was recorded and participants were categorized as double steppers if they performed a double step during at least one trial. Next, participants completed three five-second-long maximum voluntary contraction isometric strength trials on their knee extensor muscles using an isokinetic dynamometer (Biodex Medical Systems, Shirley, NY, USA, Computer Sports Medicine Inc., Stoughton, MA, USA). The single maximum value for each participant was selected and normalized to their body weight. Two univariate logistic regression models were generated with the occurrence of a double step as the dependent variable and either knee extension strength or age as the predictor.

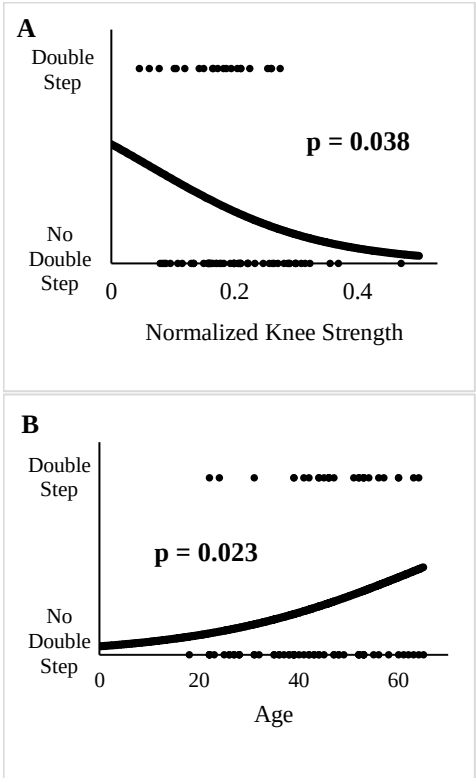


**Figure 1:** The relationship between double stepping and normalized knee strength (A) and age (B).

**Results & Discussion:** Both normalized knee extension strength ($\chi^2 = 4.29$, $p = 0.038$, Fig 1A) and age ($\chi^2 = 5.21$, $p = 0.023$, $p < 0.05$, Fig 1B) were significantly associated with double stepping. As hypothesized, lower knee strength and higher age were associated with increased likelihood of a double step outcome. The prediction model shows that people who are 60 years of age are 30% more likely to perform a double step than people who are 25 years of age. Similarly, people with a normalized knee strength of 0.1 are 30% more likely to double step than people with a normalized knee strength of 0.4. These findings suggest that double stepping may serve as a compensatory strategy for those with insufficient quadriceps strength or individuals experiencing age-related declines in coordination or balance. It can be speculated that this strategy increases safety while climbing because it reduces the amount of vertical distance that is needed to be travelled at one time and the amount of sequential time in single support. Further research is needed to confirm the motivation and safety implications of this strategy.

**Significance:** Results indicate that certain groups may employ different climbing strategies, potentially due to lacking physical characteristics to climb regularly. These changes in strategy may reflect a reduced ability to climb ladders safely and could be a biomarker for those who are at risk of a ladder-related injury. Strength training programs could be recommended to individuals at an increased risk of needing compensatory strategy. Future work should seek to determine if double stepping is a positive or negative compensatory strategy and if it should be recommended to individuals at an elevated risk of experiencing a fall.

**Acknowledgments:** This research was assisted by Violet Williams and Jenna Trout and was funded by NIOSH R01OH011799 and NSF GRFP 2139321.

**References:** [1] Pliner et al. (2024), J. *Geriatr*,, *9*(3), 61. [2] Bloswick, D. S., & Chaffin, D. B. (1990).. Int. J. Ind. Ergon, 6, 17–27.

**Effects of Ladder Rung Design on Available Coefficient of Friction During Forward and Lateral Slip Testing**

Jaspreet S. Chera[1*], Madison R. Flaugh[1*], Violet M. Williams[1], Richard W. Smith[1], Kurt E. Beschorner[1]
[1]University of Pittsburgh, Department of Bioengineering
*Corresponding authors' email: jsc89@pitt.edu, mrf98@pitt.edu

**Introduction:** Ladders were the primary source for 22,710 nonfatal and 161 fatal injuries in 2020 [1]. Slipping from ladders is responsible for 14% of falls [2], yet the causes of these slips during ladder climbing are not fully understood. The available coefficient of friction (ACOF) is a metric that quantifies the maximum amount of friction that can occur between two surfaces with higher ACOF values corresponding to a lower slip risk (level-walking) [3]. However, there is currently a gap in the literature regarding the effects of ladder rung design on ACOF. Mechanical slip testing is commonly used to determine ACOF by reproducing the under-shoe conditions of natural slip events (normal force, slipping speed, contact time, and shoe-floor angle). While mechanical slip testing has been used to determine ACOF for footwear and flooring in level walking conditions [4], testing for ladder rung configurations is not as well developed. Also, certain ladder activities such as roof-to-ladder transitions create a potential risk of lateral slips [5]. The aim of this study was to characterize how ACOF is impacted by rung surface texture, rung geometry, and slip directionality during ladder climbing to create slip prevention measures both forward and laterally.

**Methods:** This study utilized a mechanical slip testing device (STEPS device) to replicate dynamic slipping motions while measuring ACOF for ladder rungs. Two custom rung apparatuses were fabricated for forward and lateral testing. Seven ladder rungs were tested that varied in frictional claims (nonslip, no claim), shape (rectangular, circular), and size (small, large) (Figure 1). A men's size 9 Vans shoe was used across all trials. Standard testing values (velocity = 0.3 m/s, normal force = 500 N, 0º dorsiflexion), adopted from level-walking COF parameters [6,7], were used for forward slip testing where the fore foot part of the shoe slides forward perpendicular to rung. The rungs were uniformly coated with a contaminant (90% glycerol + 10% water) prior to each set of rung trials and reapplied as needed. For each rung, five trials were collected in which the force and speed were met for 50 ms. The same process and testing parameters were used for lateral slip testing where the fore foot was set to slide along the rung in the lateral direction. A two-way ANOVA was run to find significance in ladder rung, direction, or their interaction effect on ACOF outcomes. Tukey HD post hoc tests used to find significant differences between rungs.

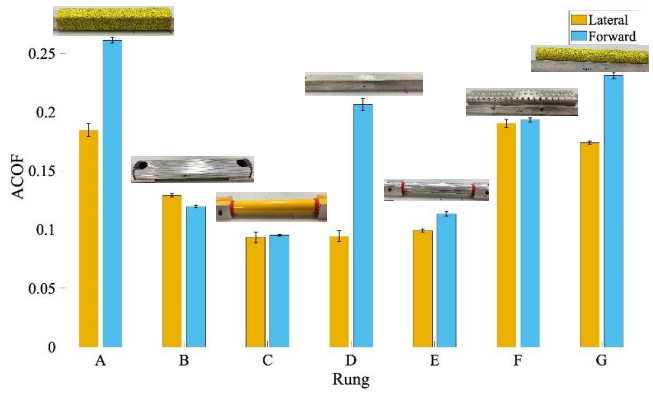


**Figure 1:** Average ACOF values for all rungs, both forward and laterally, represented by blue and orange bars, respectively.

**Results & Discussion:** ACOF values were significantly different for rung type ($F_{6,56}$=2551, p<0.001), direction ($F_{1,56}$=2336, p<0.001), and their interaction effect ($F_{6,56}$=530, p<0.001) (Figure 1). Post hoc testing indicated that most pairwise comparisons were significant for most groups. These significant differences revealed notable patterns across size, shape, and slip-resistance claim classification categories. For forward slips, smaller rungs (0.198) demonstrated higher ACOF values than larger rungs (0.142), suggesting that reduced rung size may decrease slip risk during climbing. Rectangular rungs (0.196) exhibited higher slip resistance than circular rungs (0.158), showing that rectangular rung design may also reduce slip risk. Rungs with a nonslip claim (0.228) had the highest ACOF values, likely due to designs featuring grit textures and perforations compared to the rungs with no claim (0.134) that had smooth surfaces or lateral ridges. Forward slip testing (0.174) resulted in higher ACOF values on average compared to the lateral slip testing average (0.138), suggesting that the current focus on preventing forward slips may leave users more vulnerable to lateral slips. This trend was particularly evident for Rung D, which had a high forward ACOF value (0.206) higher than lateral ACOF (0.094), possibly due to the corners providing resistance in the forward direction when the shoe was sliding across the corner but not when sliding in the direction of the edge. Additionally, lateral ridges did not provide any significant frictional benefits in either direction, suggesting that non-directional, non-slip features (grit or perforations) may be more beneficial for improving traction.

**Significance:** These findings provide quantitative evidence for how ladder rung design (size, shape, and frictional claims) affects ACOF in both forward and lateral directions, addressing a critical gap in ladder safety research. Rungs with multi-directional textured surfaces provided the highest ACOF, regardless of size and shape, suggesting that future ladder designs should focus on implementing these features in rung design to decrease slip risk.

**Acknowledgments:** The authors would like to thank Sarah Griffin, Jenna Trout, and the undergraduates who assisted with this work. This work was supported by NIOSH R01OH011799.

**References:** [1] U.S. BLS (2022), U.S. DOL; [2] Cohen et al. (1991), J. Saf. Res. 22(1); [3] Iraqi et al. (2018), Appl. Ergon 70; [4] Beschorner et al. (2023), Appl. Ergon 108; [5] Griffin et al. (2023), J Biomech 159; [6] ASTM F2913-19 (2024); [7] ISO 13287 (2019)

# VISUAL GAZE DURING LADDER CLIMBING: EFFECT OF CLIMBING DIRECTION

*Jared D. Kolarcik[1], Sarah C. Griffin[1], Rakié Cham[1,2], and Kurt E. Beschorner[1]
[1] University of Pittsburgh Department of Bioengineering; [2] University of Pittsburgh Department of Ophthalmology
*Corresponding author's email: jdk106@pitt.edu

**Introduction:** In the US, over 22,000 non-fatal and 161 fatal workplace accidents were caused by ladders in 2020 [1]. Ladder climbing is a complex activity requiring awareness of the location of fixed contact points (rungs) and coordination across all four limbs. Therefore, vison is likely a key contributor to safe ladder climbing but has not yet been examined in this task.

Gaze fixation analysis offers insight into how people map their surrounding environment and plan their movements. Previous work has found correlations between gaze fixations and movement metrics in tasks like stair climbing or level walking. For example, in stair climbing, visual focus typically stays within four steps of the current location, suggesting that visual information is used in planning upcoming steps [2]. Visual information may be especially relevant for ladder climbing given that foot placement location is a key variable influencing fall risk [3]. This study aims to categorize the visual information people collect during ladder climbing and determine differences in visual strategy between ascending and descending climbing phases. We hypothesize that individuals will show a greater focus on the limbs leading their climb (i.e. hands during ascent and feet during descent).

**Methods:** Twenty healthy participants (10M, 10F, 1.70 ± 0.09 m, 78.35 ± 17.8 kg, 36.4 ± 16.1 years) completed four climbing trials on an eight step A-frame ladder with flat rungs. Participants began each trial at the base of the ladder, climbed up to the fifth rung, paused momentarily, and climbed down to the ground. Eye tracking glasses (Tobii AB, Danderyd Municipality, Sweden) were used to monitor and record focal fixation points at a sampling rate of 50 Hz. Based on a preliminary analysis of common focal fixation locations, fixations were categorized into five categories: 1) rung that was being grasped next, "Next Hand"; 2) rung currently being grasped, "Current Hand"; 3) the ladder rail; 4) the rung that was being stepped to next, "Next Foot"; and 5) a rung currently supporting the foot, "Current Foot". The datapoints were separated by climbing phase (ascent and descent) and fixations were calculated as a percent of a participant's total number of fixations for ascent and descent. A mixed-model ANOVA test analyzed the effects of climbing phase, location, and their interaction on the percent of visual fixations in each group ($\alpha = 0.05$, JMP 16 Pro). Tukey HSD post-hoc tests examined pairwise comparisons and identified significant differences for the interaction effect to determine how visual strategy differs between ascent and descent.

**Results & Discussion:** Participants tend to look at their hands more than their feet ($F_{4,190} = 19.3$, $p < 0.001$) regardless of climbing direction. A significant interaction between phase and location ($F_{4,190} = 10.4$, $p < 0.001$) suggested differences in fixation strategy between ascending and descending a ladder (Fig. 1). Post-hoc analysis found more fixations for the Next Hand during ascent than descent ($t_{190} = 5.48$, $p < 0.001$), but fewer for the Current Foot during ascent than descent ($t_{190} = -3.77$, $p = 0.008$).

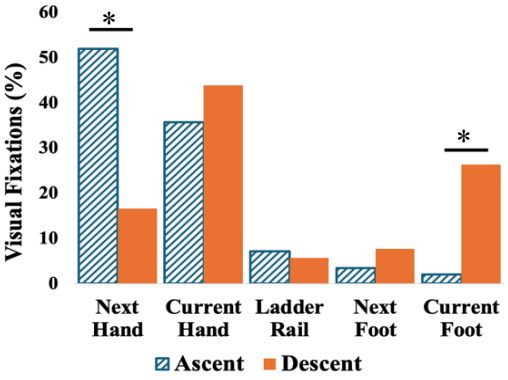


**Figure 1:** The visual fixation as a percent of all gazes across the five locations and two climbing phases. Significant differences across climbing direction are noted with an asterisk.

As hypothesized, people focus their vision on future grasping locations while ascending a ladder. Although a shift was observed during descent where participants spent a greater share of gazes on their feet, most of their gazes were still on their hands during descent. It is possible that participants build a mental map of rung positions and spacing in their mind during ascent and rely on that mental map to know where to place their feet during descent.

The prioritization of gazes on the hands over the feet may be due to their positions during ladder climbing. When climbing a ladder, the hands are often directly in front of the eyes and a person can look at these rungs with a neutral neck posture. However, gazing at the feet requires substantial head flexion and is often obstructed by the climber's body. Additionally, eye tracking glasses can have difficulty capturing the pupils when someone looks down, so some fixations may have been insufficiently counted during descent. A larger number of fixations in ascent than descent may support this claim. Despite the effort involved, participants altered their visual strategy during descent to include more foot fixations, indicating the importance of visual information to guide stepping during ladder descent.

**Significance:** These findings provide a basis for further vision studies involving ladder climbing. Differences in visual strategy may indicate a varying role of vision between ascent and descent. Participants may only have access to visual information leading their limb during ascent, which may contribute to misstep risk during descent. Future work could investigate the impact of assigned visual strategies on known fall risk factors (i.e. foot placement). This research could reveal optimal visual strategies which could be incorporated into training protocols, thus reducing injuries from ladder climbing accidents.

**Acknowledgements:** This research was funded by NIOSH R01OH011799 and NSF GRFP 2139321. Graduate student Violet M. Williams and lab manager Jenna M. Trout played instrumental roles in project development.

**References:** [1] U.S. BLS (Data from 2020). 2022, Dpt of Labor. [2] Miyasike-daSilva et al. (2011), *Exp. Brain Res.* **209**: 73-83. [3] Pliner et al. (2014), *Ergonomics*. **57**: 1739-1749.

# DEVELOPMENT OF A WALKING TECHNIQUE TO REDUCE BAREFOOT WALKING IMPACT

*Yunbeom Nam, Taehyung Kim, Kanghyeon Lee, Gwanseob Shin
Department of Biomedical Engineering, Ulsan National Institute of Science and Technology, Ulsan, South Korea
*Corresponding author's email: bbbeommm@unist.ac.kr

**Introduction:** Noise from barefoot indoor walking is a major social problem in Korea where 80% of population live in multi-story residential buildings. Footstep impact from upper-floor occupants is directly transmitted to lower floors, often causing legal disputes as well as sleep disturbances. In our recent study, walking slowly or landing with forefoot first has been associated with lower footstep impact during barefoot walking [1]. Such non-natural walking patterns may not be applicable to our daily life. The current study proposes a walking strategy to lower the footstep impact without altering landing patterns or sacrificing walking speed. It involves leaning the upper body backward, lifting the foot less during the swing phase, and maintaining normal walking speed. The effects of the quiet walking strategy on lowering footstep impact along with muscular loads on ankle flexors have been quantitatively evaluated.

**Methods:** Twenty healthy young adults (10F/10M, age: 26.1 ± 4.8 years, height: 167.8 ± 9.0 cm, weight: 66.3 ± 15.0 kg) participated in this within-subject experiment. They walked on a 10-meter walkway with an embedded pressure mat (FDM-1.5, Zebris Medical GmbH, Germany). Each participant performed 3-minute walking trials under two conditions at their self-selected speed: Normal Walking (NW) and Quiet Walking (QW). QW instructions included: 1) Leaning the upper body slightly backward to shift the center of mass posteriorly at initial contact, 2) keeping the foot clearance smaller than usual during the swing phase, 3) maintaining a walking speed similar to their normal indoor walking. Vertical ground reaction force (vGRF) and gait parameters were collected using the pressure mat. The vertical loading rate was calculated as the local maximum vGRF divided by impact time (time to peak force) (fig 1). Surface electromyography (EMG) signals were recorded at 2,000 Hz (Ultium EMG, Noraxon, USA) from the tibialis anterior and gastrocnemius lateralis muscles. The recorded sEMG signals were processed as follows: full-wave rectification, band-pass filtering (10–450 Hz), and the fourth-order Butterworth filter (6 Hz cut-off frequency) [2]. EMG signals of each muscle were normalized to the root mean square value of the linear envelope EMG in the NW trial to be presented in relative voluntary contraction (RVC) [3]. Differences in vertical loading rate, gait parameters, and EMG values between the two walking conditions were analyzed using paired t-tests.

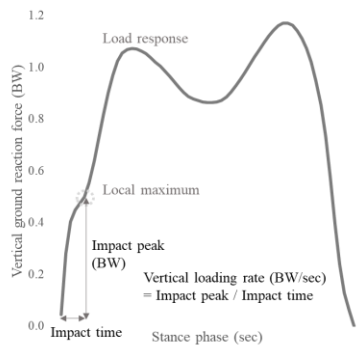


**Fig1.** A representative plot of the vertical ground reaction force during an NW trial, illustrating the definitions of footstep impact variables. BW: body weight.

**Results & Discussion:** Vertical loading rate decreased 29.0% in the QW condition, and the difference was statistically significant ($p<0.05$) (Table 1). The significantly longer impact time in QW indicates that the QW strategy helped participants distribute impact forces over a longer duration. Despite the instruction to walk as fast as in the NW condition, participants walked 9.2% slower in the QW condition. Keeping the foot clearance lower than NW might make them walk more cautiously with shorter step length. The significantly greater activity of the tibialis anterior in the QW condition implies that they might intentionally make larger dorsiflexion to avoid toe contact with the floor during the swing phase while maintaining the real foot height lower than that of NW. Data of this study suggest that the QW strategy could be an effective remedy against footstep noise problems when properly practiced and employed in our daily life.

| | NW | QW |
|---|---|---|
| Vertical loading rate (BW/sec) * | 11.98 (3.13) | 8.50 (2.58) |
| Impact peak (BW) | 0.38 (0.14) | 0.33 (0.10) |
| Impact time (sec) * | 0.030(0.01) | 0.037 (0.01) |
| Step length (m) * | 0.59 (7.23) | 0.56 (6.74) |
| Step time (sec) * | 0.56 (0.07) | 0.58 (0.07) |
| Velocity (m/s) * | 1.09 (0.75) | 0.99 (0.65) |
| Tibialis anterior (%RVC) * | 78.1 (4.09) | 91.3 (21.13) |
| Gastrocnemius lateralis (%RVC) | 66.9 (7.09) | 60.9 (18.06) |

* $p<.05$

**Table 1:** Footstep impact parameters, spatiotemporal gait parameters, and %RVC EMG amplitudes under NW and QW conditions.

**Significance:** This study provides insights into the biomechanics of QW and its potential to reduce barefoot footstep noise in residential buildings. Unlike common recommendations such as forefoot strike walking or slower walking, the QW of the current study aims to make effective and efficient indoor walking. The findings of this study indicate the positive effect of the QW in lowering the footstep impact with some side effects. The efficiency of the QW, including the walking speed and the muscular load, needs to be tested in future research with longer exposure or adaptation periods in real residential environments.

**Acknowledgments:** This work was supported by the Ulsan Metropolitan City, Korea.

**References:** [1] Yoon et al. (2025), *Ergonomics* 68, 112-119; [2] Ghazwan et al. (2017), *PLoS One* 12(4); [3] Burden et al. (2003), *Journal of Electromyography and Kinesiology* 13, 519-532

# COMPARING WHOLE BODY CENTER-OF-MASS KINEMATICS BETWEEN A SMARTPHONE-BASED SYSTEM AND TRADITIONAL MOTION CAPTURE

*Jian Zhang[1], Julie Ferrell-Olson[1], Andrew Sawers[1]
[1]University of Illinois Chicago, Department of Kinesiology and Nutrition
*Corresponding author's email: jzhan83@uic.edu

**Introduction:** Efficient and stable locomotion is essential to human movement. Center of mass (COM) kinematics, including position and velocity, are key to locomotor stability and efficiency. Accurate estimates of whole-body COM position and velocity are therefore paramount to studying stability and efficiency. Traditional motion capture (MoCap) systems are commonly used to analyze COM kinematics but are limited to controlled laboratory conditions. Smartphone-based motion capture systems, such as OpenCap [1] have recently been developed for quantifying human movement in various environments. While able to accurately estimate joint kinematics and kinetics [1], it is unknown if the same is true for whole-body COM kinematics. The aim of this study was to compare whole-body COM kinematics obtained from OpenCap and a MoCap system. Based on OpenCap's ability to accurately estimate joint kinematics, we hypothesized OpenCap would also accurately estimate whole-body COM position and velocity relative to traditional MoCap.

**Methods:** 10 adults (7 female, age: 22.6±2.9 yrs, body mass: 62.9±9.1 kg, height: 1.64±0.05 m) walked on a treadmill at their preferred speed (1.42±0.067 m/s). Ground truth kinematics were captured using an 8-camera optical motion capture system (Motion Analysis Corp., Santa Rosa, CA, USA) tracking a full-body marker set (53 markers) at 120Hz. Simultaneously, video was recorded with OpenCap's web application and two iPhones positioned 1.25m off the ground, 3.5m from the treadmill center, and 45° from the participants. MoCap marker trajectories and segment COM positions were processed and modelled in Visual 3D to match OpenCap's post-processing and anthropometricsWhole-body COM position was estimated as the weighted sum of the segment COM positions. Whole-body COM position and velocity trajectories were segmented into gait cycles, and time-normalized to 101 data points. Differences in medial-lateral and vertical COM kinematics were quantified using wavelet functional ANOVAs (wfANOVA) [2]. Timing and magnitude of significant differences in whole-body COM position and velocity across the gait cycle are reported between MoCap and OpenCap. Error magnitude was interpreted relative to published differences in COM kinematics between conditions or groups.

**Results & Discussion:** In support of our hypothesis, comparisons between OpenCap and MoCap revealed subtle but statistically significant differences in ML and vertical COM position and velocity across the gait cycle. OpenCap significantly overestimated vertical COM position from 4-43% of the gait cycle (max diff: 0.35cm at 28% GC, $p<0.05$) and underestimated it from 44-75% (max diff: 0.44cm at 50% GC, $p<0.05$) (Fig 1A). Critically, the largest difference (0.44cm) was smaller than the reported 1.0cm difference between lower limb amputees and controls [3], suggesting that OpenCap may detect differences in vertical COM position among different clinical populations. ML COM position was not significantly different between OpenCap and MoCap ($p\geq0.05$, Fig 1B). For velocity, OpenCap significantly underestimated the vertical component from 27-50% of the gait cycle (max diff: 4.8cm/s at 43% GC, $p<0.05$), and overestimated it from 50-82% (max diff: 2.8cm/s at 58% GC, $p<0.05$). The max difference in vertical COM velocity was smaller than that reported between level and incline walking surfaces (i.e., 8cm/s) [4], suggesting OpenCap may be able to detect differences in vertical COM velocity across terrains. Finally, OpenCap overestimated ML COM velocity from 23-43% of the gait cycle (max diff: 2.3cm/s at 32% GC, $p<0.05$) and underestimated it from 75-100% (max diff: 2.5cm/s at 86% GC, $p<0.05$) (Fig 1D). The max difference in ML COM velocity (2.5cm/s) was smaller than the difference between perturbed and unperturbed walking (7.0cm/s) [5], suggesting OpenCap may be suitable for detecting differences in COM velocity during more dynamic balance tasks.

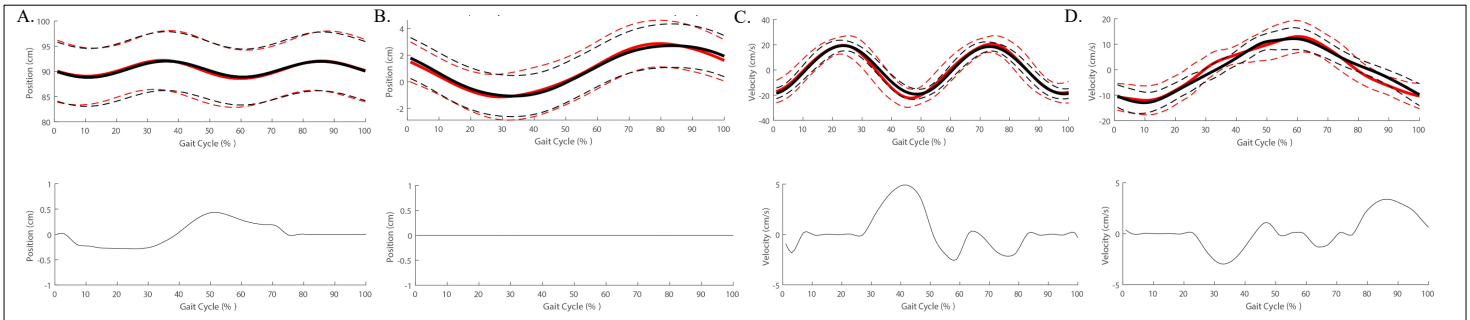


**Figure 1:** Mean ±1SD COM position (A: vertical, B: medial-lateral) and velocity (C: vertical, D: medial-lateral) trajectories (top row) and wfANOVA contrasts (bottom row) between OpenCap (red) and MoCap (black) over the gait cycle. wfANOVA contrast plots visualize the timing and magnitude of significant differences in COM dynamics between the two systems over the gait cycle.

**Significance:** This study shows that OpenCap is a cost-effective, accessible alternative to MoCap for tracking whole-body COM kinematics. Limitations include a small sample size, a single gait speed, minimal balance challenge, and the absence of clinical populations, who may use different COM control strategies. This study lays the initial work for large-scale balance studies in real-world environments that were previously constrained by the limitations of traditional motion capture systems.

**References:** [1] Uhlrich, et al. (2023) PLoS Comput Biol 10(19); [2] McKay, et al. (2013) J Neurophysiol 2(109); [3] Weinert-Aplin, et al. (2017) Gait Posture (51); [4] Hong, et al. (2018) Appl. Bionics Biomech. (2018); [5] Lee-Confer, et al. (2023) J. Biomech. (157).

# MEASUREMENT OF THRESHOLDS ON GAIT PARAMETERS: A PSYCHOPHYSICAL APPROACH USING VIRTUAL REALITY

Vimal Chander[1], Manivannan[1]
[1 2] Indian Institute of Technology Madras
am22d008@smail.iitm.ac.in[1], mani@smail.iitm.ac.in[2]

**Introduction:** Psychophysics investigates the relationship between physical stimuli and subjective perception. In this study, we explore how virtual reality (VR) alters gait parameters [1] by measuring the Just Noticeable Difference (JND) in knee range of motion. Grounded in the Weber–Fechner law [3], our work examines the detection of minimal perceptible changes during gait an approach that has broader implications for understanding sensorimotor integration.

**Methods:** Ten healthy participants performed tasks on a treadmill under both baseline and VR-modified conditions. Using a marker-less capture system (mediapipe) and an RGB camera [2], knee angles were recorded as subjects walked on slopes with various gradients (0, ±10, ±20, ±30, ±50, ±70, ±90).
The experiment employed the method of constant stimuli along with psychometric function analysis to determine the threshold level. In the VR environment, two conditions were tested: an upward (inclined) and a downward (declined) adjustment of the virtual scene.

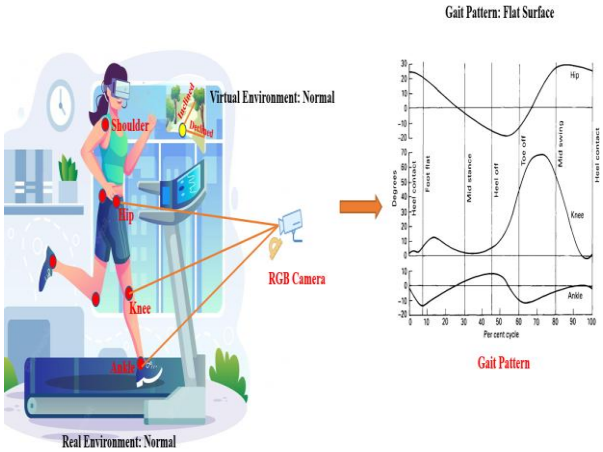


**Figure 1:** Setting up the VR to calculate JND by using treadmill

Changes in virtual environment through VR affecting the gait parameter in real environment for normal subject. Subject undergoes three tasks such as walking during VR-induced zero, inclined, and declined slopes. The following figure shows the result of baseline in real environment and baseline in virtual environment. In our study we follow the five principles of psychophysics SMAMT. Stimulus – Visual Stimulus, Method – Constant Stimulus, Analysis – Psychometric curvature, Measure – Gait Parameter (Knee angle), Task: Changing virtual environment (upward and downward). The JND has been measured in terms of percentage change of knee angle.

**Results & Discussion:** For the VR inclined task, psychometric analysis indicated that the absolute threshold (50% response) occurred at a 4° change in knee angle, with a higher threshold of 6° corresponding to a 75% response level. In contrast, for the VR declined condition, a 50% response was observed at –4°. These findings suggest that VR manipulations significantly affect perceptual thresholds in gait, underscoring the influence of visual inputs on motor control and sensory discrimination.

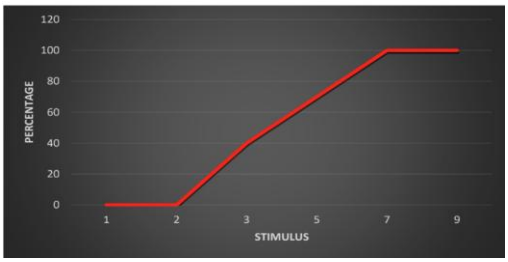


**Figure 2:** Task - VR inclined, Treadmill Baseline

**Significance:** This study demonstrates that VR-induced modifications in the visual environment can measurably alter gait parameters. By quantifying the JND in knee range of motion, the research provides insight into the dominance of visual cues over motor planning. The results have potential applications in designing rehabilitation protocols and developing VR-based interventions for improving gait and balance in clinical populations.

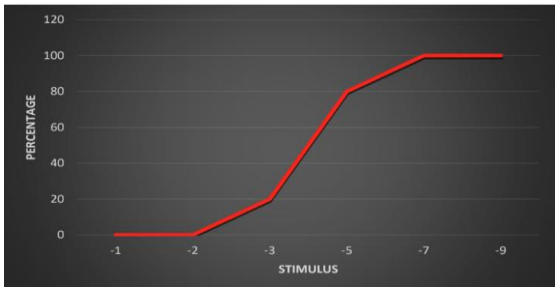


**Figure3:** Task - VR declined, Treadmill Baseline

**References:**

[1] Mahnan et al. (2020), Proceedings - Design of Medical Devices Conference.

[2] Ping et al. (2017) *Advanced Robotics*, *31*(1-2).
[3] Weir et al. (2007), *Theoretical Issues in Ergonomics Science*, *8*(3).

# STEPPING STONE WALKING ALTERS EARLY STANCE AND SWING PHASE SAGITTAL KNEE KINEMATICS

Brandon Peoples[1], Bella Helm[1], Grant Renfrow[1], Jacob Jerkins[1], Kenneth Harrison[1], Keven Santamaria-Guzman[1], & *Jaimie Roper[1]
[1]Auburn University, School of Kinesiology
*Corresponding author's email: bmp0049@auburn.edu

**Introduction:** Two important components of human locomotion when traversing complex and challenging terrains are weight acceptance and dynamic stability facilitated by sagittal knee extension and flexion [1]. Proper knee mechanics ensure effective weight distribution and balance, allowing precision when navigating obstacles or encountering varying surfaces[1]. For example, this functionality is paramount for movement efficiency and maintaining balance during hiking, climbing, and other outdoor activities where encountering uneven ground is inevitable[2]. Treadmill-based studies have provided valuable insights into kinematic patterns of the knee; however, these studies do not fully capture the rich complexity of real-world locomotor behaviors. Conversely, stepping-stone walking represents a unique paradigm combining precise foot placement, speed modulation, and dynamic balance control[3]. Despite its ecological relevance, the biomechanical demands of stepping stone navigation regarding sagittal knee joint kinematics remain limited, with many studies using overground projections or visual feedback[3]. This knowledge gap is relevant given the increasing development of lower-body assistive devices and bipedal robots. Therefore, the purpose of this study is to investigate sagittal knee kinematics during overground stepping-stone walking under different task constraints. We hypothesize that interlimb sagittal kinematics will slightly differ across all conditions due to leg dominance. Next, we hypothesize initial contact, early stance, and swing mechanics will differ across each condition due to speed changes based on evidence from overground walking research[4].

**Methods:** Twenty-five healthy young adults (aged 18-27) performed overground stepping stone walking while equipped with a 53-marker plug-in gait full-body marker set using Vicon marker-based motion capture. Sagittal knee angle and power data were analyzed across three conditions for each leg: baseline (self-selected walking speed), stop (full stop at each stone before progression), and fast (maximum safe crossing speed). All gait data was normalized to 100% of the gait cycle, heel strike to heel strike. A two-way repeated measures ANOVA using Statistical Parametric Mapping (SPM) in MATLAB using the spm1d package compared knee angles across sides (left, right) and conditions (baseline, stop, fast), examining both main effects and interactions throughout the gait cycle.

**Results & Discussion:** SPM analysis revealed significant main effects between side (left vs right) ($p < 0.001$) and condition ($p < 0.001$), with notable interaction effects ($p < 0.001$). Side differences were most pronounced during early stance (10-20% gait cycle) and late stance/pre-swing (70-80% gait cycle). Condition effects showed the strongest differences during early to mid-stance (0-40% gait cycle) and throughout the swing phase (60-90% gait cycle), with peak differences occurring at approximately 70% of the gait cycle. Significant side-by-condition interactions were observed during loading response (0-20%), mid-stance (40%), and terminal swing (90%), indicating the condition affected the leading each leg differently.

**Significance:** In our sample, sagittal knee kinematics during stepping-stone walking revealed significant differences between legs and across speed conditions during early stance and swing phases. These distinct patterns emerged when participants navigated physical stepping stones under varying task constraints, providing insights beyond traditional treadmill-based studies. The observed bilateral coordination strategies and speed-dependent adaptations demonstrate how humans modulate sagittal knee mechanics to maintain stability during stepping stone walking. This knowledge is crucial for engineers developing assistive devices and bipedal robots that must function effectively in real-world terrains, enabling the creation of mobility technologies that better replicate human adaptability across challenging environments.

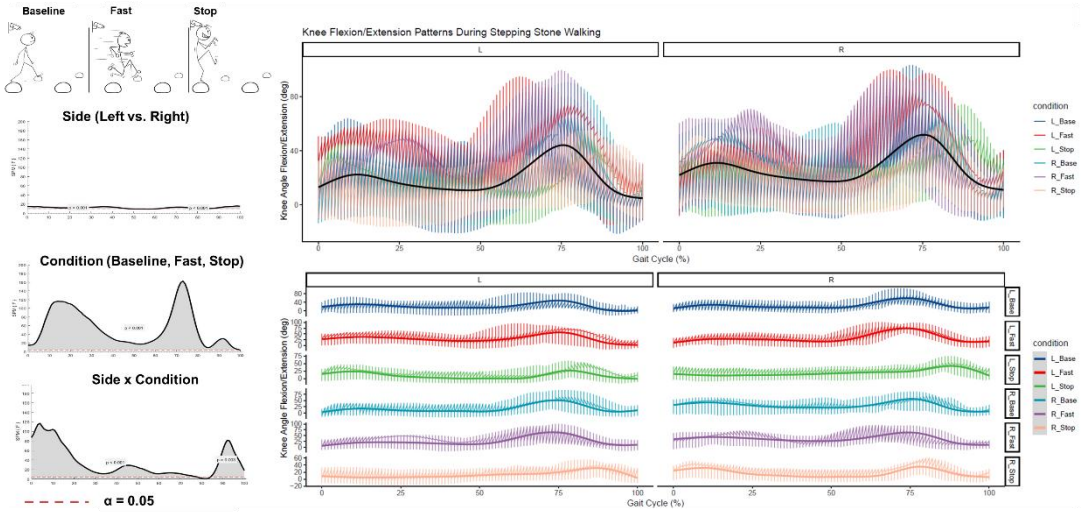


**Figure 1**: Statistical Parametric Mapping (SPM) analysis of knee flexion/extension patterns during stepping stone walking under different conditions (Baseline, Fast, Stop) and sides (Left vs. Right). The left panels show SPM results indicating main effects of Side (top), Condition (middle), and their interaction (bottom), with significance threshold $\alpha = 0.05$ shown by the dashed red line. The right panels display mean knee angle trajectories across the gait cycle for both left (L) and right (R) sides under each condition, with shaded areas representing standard deviations. Individual condition comparisons are vertically offset for clarity, showing distinct kinematic patterns across walking speeds and stopping conditions.

**References:** [1] Foster, Hudson, & Smith. (2020), *The Knee 27* (6); [2] Bottoni et al. (2014), *J Ergonomics* 4(2); [3] Zhang et al. (2020), *J Physiol* 598(10); [4] Fukuchi, Fukuchi, & Duarte, (2019), *Systematic Reviews* 153(8)

# VISUAL CONTEXT AFFECTS LATERAL BALANCE WHILE WALKING ON WINDING PATHS

Anna C. Render[1], Tarkeshwar Singh[1], Joseph P. Cusumano[2], Jonathan B. Dingwell[1*]
[1] Department of Kinesiology, Pennsylvania State University, University Park, PA, USA
[2] Department of Engineering Science & Mechanics, Pennsylvania State University, University Park, PA, USA
*Corresponding author's email: dingwell@psu.edu

**Introduction:** Effectively navigating real world environments necessitates delicately balancing stability and adaptability. Walking relies on a complex integration of sensory feedback, primarily from vision, to achieve this. This study examined how visual context affects task performance and lateral balance while walking on straight or winding paths in different visual contexts. We hypothesized that altering available visual information would modify task performance, but might or might not disrupt balance. This research extends previous studies of only path curvature [1] by systematically manipulating visual input, thereby elucidating the interplay between visual perception and mechanical demands in maintaining balance while walking.

**Methods:** Twenty-eight adults (16F/12M; age 26.2±4.2) walked on straight and winding 0.45m wide virtual paths [2] projected onto a 1.2m wide treadmill (Motek M-Gait). Each path was presented in high (HC) or low (LC) contrast color combinations, in each of two virtual environments: a dense forest (Rich) or open grassy plain (Sparse). Participants were instructed to "walk on the path" and to minimize steps off the path. Each participant completed two 3-minute trials per condition.

For each condition, we analyzed the first 250 steps of each trial. To quantify task performance, we computed the percentage of stepping errors, defined as steps landing outside the path's boundaries. To quantify lateral balance, we calculated the minimum mediolateral margin of stability ($MoS_L$) [2] at each step. Using mean ($\mu$) and standard deviation ($\sigma$) of $MoS_L$, we then computed lateral Probability of Instability ($PoI_L$) [3] to quantify participants' risk of taking unstable ($MoS_L < 0$) steps.

Dependent measures were compared using 2×2 (contrast × environment) ANOVA for each path (straight versus winding) separately.

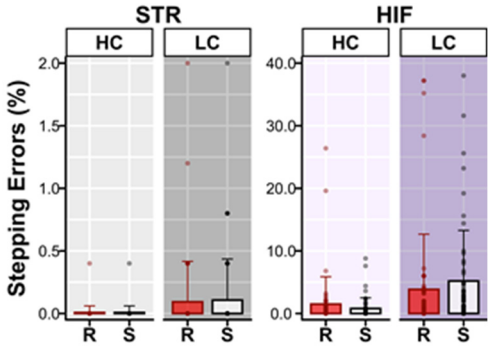


**Figure 1: Stepping Errors**. Results for straight (STR) and winding (HIF) paths, for high (HC) and low (LC) contrast, in Rich (R) and Sparse (S) environments. Note vertical scales are different.

**Results & Discussion:** On straight (STR) paths, stepping errors increased on LC versus HC paths ($p < 0.001$; Fig.1, left). On winding (HIF) paths, stepping errors were highest on LC paths in Sparse environments ($p < 0.006$; Fig. 1, right). Thus, overall, participants made more stepping errors when these paths were harder to see.

On STR paths, $\mu(MoS_L)$ did not change with visual context ($p \geq 0.109$), while $\sigma(MoS_L)$ decreased slightly on LC paths ($p = 0.031$). Together, these changes yielded no significant changes in $PoI_L$ ($p > 0.126$; Fig. 2, left). Thus, despite participants taking more steps off the LC STR paths (Fig. 1), this did not degrade their balance.

On HIF paths, participants exhibited smaller $\mu(MoS_L)$ on LC paths ($p < 0.001$), but no differences in their $\sigma(MoS_L)$ ($p \geq 0.314$). Together, however, participants exhibited increased $PoI_L$ both in Sparse environments ($p = 0.017$) and on LC paths ($p = 0.001$; Fig. 2, right). Thus, participants were more likely to need to correct unstable steps while walking in environments with fewer visual landmarks (Sparse) and/or reduced path visibility (LC).

We note that on winding (HIF) paths, participants exhibited both far more stepping errors (Fig. 1), and far greater likelihood of taking unstable steps (Fig. 2), than on straight (STR) paths. This was consistent with prior findings [1]. Here, the magnitudes of these differences between STR and HIF paths far exceeded the effects of the visual manipulations within each path.

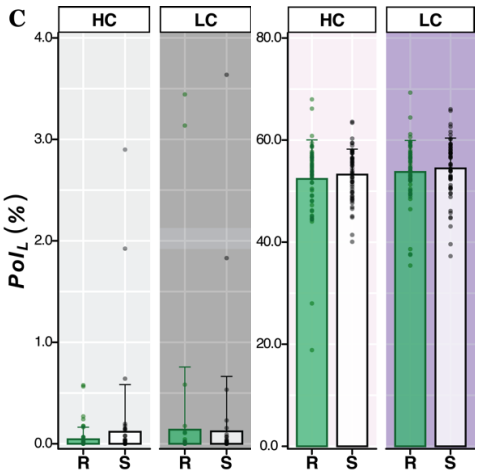


**Figure 2: Probability of Instability (PoI)**. Results for STR and HIF paths, high (HC) and low (LC) contrasts, in Rich (R) and Sparse (S) environments. Note vertical scales are different.

**Significance:** Stepping errors indicate failures in accurate foot placement. Conversely, $PoI_L$ reflects changes in balance control. Increased stepping errors without a corresponding rise in instability may suggest compensatory strategies. Here, on STR paths, participants were able to adequately compensate to maintain lateral balance, despite making additional stepping errors to do so. On the LC HIF paths, however, participants were less able to compensate and thus showed increased $PoI_L$, indicating that reduced visual information compromised overall balance control. That the effects of degraded visual information were more pronounced on winding paths, hindering both performance (Fig. 1) and balance maintenance (Fig. 2), indicates that these HIF paths challenged demands of both mechanical and sensory mechanisms underlying balance control.

**Acknowledgments:** NIH / NIA Grants # R01-AG049735 & R21-AG053470, and Sloan Foundation Grant # G-2020-14067.

**References:** [1] Render et al. (2024), *J Biomech* 176; [2] Hof (2005), *J Biomech* 38(1); [3] Kazanski et al. (2022), *J Biomech* 144.

# MEDIOLATERAL DYNAMIC POSTURAL STABILITY DURING STAIR ASCENTS IN INDIVIDUALS WITH A ROTATIONPLASTY ABOUT THE KNEE

*Kellen T. Krajewski[1,2], Amanda L. Vinson[3], Mia A. Lundin, Nathan Rogers[1,2], Susan Kanai[3], Lucas Moore[3], James J. Carollo[1,2,3], Steven W. Thorpe[1,2], Anne K. Silverman[4], Nathan J. Donaldson[1,2]
[1]Musculoskeletal Research Center, Pediatric Orthopedics, Children's Hospital Colorado, CO, USA
[2]Department of Orthopedics, University of Colorado School of Medicine, CO, USA
[3]Center for Gait and Movement Analysis, Children's Hospital Colorado, CO, USA
[4]Functional Biomechanics Laboratory, Department of Mechanical Engineering, Colorado School of Mines, CO, USA
*Corresponding author's email: Kellen.krajewski@cuanschutz.edu

**Introduction:** Type A rotationplasty is a limb-salvage surgery for osteosarcoma, infection, or trauma about the knee. The procedure transects the femur and tibia, with the latter rotated 180º and fused to the femur, repurposing the ankle joint as the new knee joint. The plantar flexors and dorsiflexors are then fused to the quadriceps and hamstrings respectively to achieve active 'knee' flexion and extension. Rotationplasty is recommended over other treatment options for patients who desire a more active lifestyle with no activity restrictions, yet, only the biomechanics of level walking has been examined. Ascending stairs is critical to functional independence and is a difficult task for amputees. Moreover, the use of prosthetics challenges dynamic postural stability, increasing the risk of falls even in younger more active cohorts. Therefore, the purpose was to examine dynamic mediolateral postural stability in individuals with rotationplasty while ascending stairs.

**Methods:** Nine male participants (15.7±5.1 years, 1.7±0.2 m, 60.0±25.6 kg) executed four trials of ascending stairs (15.24 cm tall, 24.13 cm deep with bilateral handrails) leading with each limb (surgically repaired limb (SL) & intact limb (IL)). Participants ascended at a self-selected velocity and were allowed to use the handrails if necessary. 3D kinematics were captured via 13 infrared cameras (120 Hz) utilizing a modified Helen-Hayes marker configuration consistent with the conventional gait model. Lateral margin of stability ($MoS_L$) was calculated using methods described by Render et al 2024[1]. Briefly, $MoS_L$ represents a linear distance in the mediolateral plane between the state of the pelvis (center of mass position and velocity) and the lateral edge of the support foot generating a time series of values from foot contact to toe off. From this single step time-series, the minimum value was extracted ($MOS_{Lmin}$) with positive values indicating the pelvis state within the base of support (BOS) during the entire step representing a 'stable step'. Negative values indicate the pelvis state traversed laterally beyond the lateral edge of the BOS where the probability of a fall increases during the step, thus representing an 'unstable step'. Mean ($\mu MOS_{Lmin}$) and standard deviation ($\sigma MOS_{Lmin}$) was calculated. Percentage of unstable steps (%US) was calculated for each limb separately. To examine the effect of leading limb and limb, 2x2 RMANOVA were conducted separately for $\mu MOS_{Lmin}$, $\sigma MOS_{Lmin}$, and %US. Alpha set $p \leq 0.05$.

**Results & Discussion:** See Table 1 for descriptive statistics. Two participants used one handrail while ascending (One ipsilateral and one contralateral to the SL), five participants used both handrails, and two never touched the handrails. For $\mu MOS_{Lmin}$, there was an interaction between leading limb and limb ($p<.001$). When stepping on the IL while the IL was leading, $\mu MOS_{Lmin}$ was less ($p=.003$) than when stepping on the IL while the SL was leading. For $\sigma MOS_{Lmin}$, there was an interaction between leading limb and limb ($p=.001$) with the IL having greater ($p=.009$) variability than the SL while the IL was leading, and the IL while the IL was leading having greater ($p=.042$) variability than the IL while the SL was leading. For %US, there was an interaction between leading limb and limb ($p<.001$) with the IL while it was leading having a lower percentage of unstable steps ($p=.010$) than the IL when SL was leading.

| Outcome | Leading Limb | Limb | |
|---|---|---|---|
| | | Intact | Surgical |
| Unstable Steps (%)† | Intact | 61.1±22.0 | 79.5±36.3 |
| | Surgical | 91.4±10.7* | 75.8±39.6 |
| $\mu MOS_{Lmin}$† | Intact | -25.2±58.3 | -83.1±84.5 |
| | Surgical | -78.8±39.8* | -59.9±105.0 |
| $\sigma MOS_{Lmin}$† | Intact | 96.8±35.4 | 36.1±12.8* |
| | Surgical | 51.8±21.8* | 46.2±23.0 |

**Table 1.** Lateral Stability Parameters (mean ± standard deviation); †=Significant interaction ($p \leq .05$) between leading limb and limb; *=Significant difference (Bonferroni adjusted $p \leq .05$) from intact limb while the intact limb is leading

**Significance:** Regardless of condition/limb, $\mu MOS_{Lmin}$ was negative indicating a less stable body position that increases the probability of a fall despite the use of handrails. This may be a consequence of the kinematic constraints of the SL requiring whole body compensation to advance the SL to the next step. Overreliance on the use of handrails could be problematic for individuals with rotationplasty if their hand slips or if the stairs lack adequate handrails (e.g. missing or weakly secured). %US was consistently high in the SL regardless of leading limb, however, when IL was trailing, IL executed the greatest %US (Table 1). The IL as a trailing limb is potentially less capable of compensating for greater postural deviation while stepping, thus, utilizing a SL leading strategy when ascending stairs could portend greater risk of falling in individuals with rotationplasty about the knee.

**Acknowledgments:** This project was funded by the CCTSI Co-Pilot Award

**References:**[1] Render AC et al. (2024), *J Biomech* 176: 112361.

**The Effect of Prosthetic Foot Stiffness on Stability and Balance Confidence During Walking in Lower Limb Prosthesis Users**

T Ho[1*], E Halsne[1], A Sawers[2], S Koehler-McNicholas[3], A Hansen[3], A Lloyd[3], J Cave[3], N Schaumann[3], C Carranza,[1] D Morgenroth[1]
[1]VA Puget Sound Health Care System, Seattle WA; [2]Department of Kinesiology, University of Illinois Chicago, Chicago, IL;
[3]Minneapolis VA Health Care System, Minneapolis, MN *Corresponding author's email: tyler.ho@va.gov

**Introduction:** Lower limb amputation results in a wide range of mobility limitations [1], primarily due to the loss of the biologic foot-ankle. Balance and stability deficits are a problem in this population, and falls are common [2], with more than half of people with amputation reporting at least one fall per year [3]. Lower balance confidence has also been shown to be associated with reduced community participation and lower perceived mobility [4]. The stiffness properties of prosthetic feet have been linked to effects on dynamic balance and perceived stability [5]. For example, prosthetic foot stiffness may affect center of mass (COM) dynamics and the base of support during prosthetic stance phase [6]. Previous research on the effects of stiffness has been limited to studies of experimental feet that have adjustable sagittal plane stiffness but may not reflect the properties of prosthetic feet used clinically. Previous comparisons of stiffness also assessed multiple conditions within one session, limiting the amount of time that prosthesis users had to accommodate to each prosthetic foot. The aim of this study was therefore, to assess the effects of commercially available prosthetic feet of varying stiffnesses on measures of gait stability and balance confidence among unilateral transtibial prosthesis users (TTPUs).

**Methods:** Five male unilateral TTPUs [mean(SD) age=61.6(11.6) years; height=180.2(3.4) cm, mass=103.1(3.9) kg, comfortable walking speed=0.9(0.2) m/s] have completed the study protocol thus far. Each participant was fitted with two commonly prescribed prosthetic feet of differing stiffness (i.e., AllPro (lower stiffness) and Vari-Flex (higher stiffness) [7]). Participants, masked to foot type, wore each foot at home and in their community for at least one week [8] in a randomized order before returning for gait assessment. Participants walked on a level treadmill at a self-selected walking speed for at least 30 seconds while kinematic data were recorded via a 16-camera motion capture system (Vicon Nexus 2.14). Walking speed was controlled within each participant across prosthetic feet. After each walking trial, participants were asked to rate, on a scale from 0-10, how confident they were that they could keep their balance while walking with that foot at a comfortable walking speed [9]. Kinematic data were imported to Visual3D and passed through a 4th-order Butterworth filter with a cut-off frequency of 6Hz. The minimum mediolateral margin of stability (MoS) is a commonly used outcome to assess dynamic stability in TTPUs [10] by measuring the relationship between the COM position and COM velocity relative to the base of support. MoS and step width were calculated during each step for the prosthetic and intact limbs. Due to the small sample size in these preliminary data, we calculated descriptive statistics (i.e., mean and SD) for each outcome. The median and interquartile range are depicted in Fig 1 to further illustrate the variation in the data.

**Results & Discussion:** Prosthetic limb minimum MoS decreased in the higher stiffness prosthetic foot condition [mean(SD)=12.2(1.6) cm] compared to the lower stiffness foot [12.9(1.8)cm], while step width did not differ between feet [higher stiffness: 17.2(3.1) cm and lower stiffness: 17.4(3.3) cm] (Fig 1). Participants also reported improved balance confidence while walking with the higher stiffness prosthetic foot [score of 9.3(1.0)] compared to the lower stiffness foot [8.5(1.7)]. These initial results support the previous findings in experimental feet, suggesting an association between improved prosthesis-side stability and balance confidence with increasing prosthetic foot stiffness properties. Given the lack of change in step width, the observable difference in MoS may be attributable to the COM dynamics changing in response to foot stiffness. Intact limb MoS [higher stiffness: 12.1(1.8) cm and lower stiffness: 12.0(1.8) cm] and step width [higher stiffness: 17.2(3.5) cm and lower stiffness: 17.3(3.5) cm] also did not differ between foot conditions either. While these results are preliminary due to the small sample size thus far, the findings contribute to our understanding of the effects of stiffness on stability during walking based on evaluating commonly prescribed prosthetic feet after participants have had extended accommodation periods with each foot and while they are masked to foot condition. Further, these results link participants' reported balance confidence to biomechanical measures of stability, which provides context for interpreting the MoS and step width results.

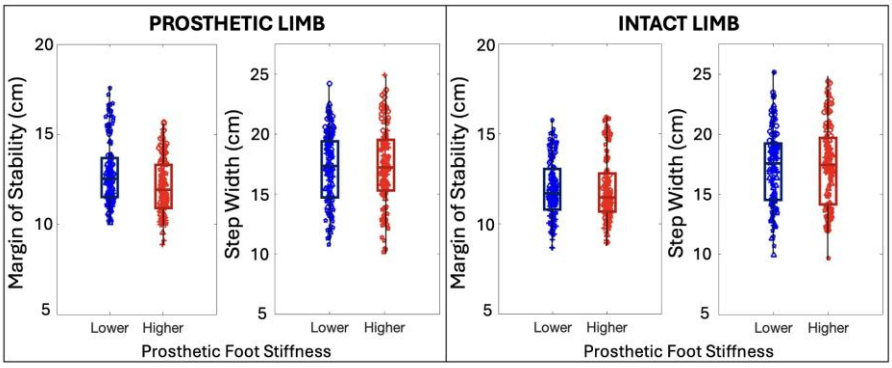


**Figure 1:** Median (IQR) MoS and step width across prosthetic foot stiffness conditions. Each data point represents a step and box plots are shown across all participants (n=5).

**Significance:** These findings highlight the importance of understanding how prosthetic stiffness properties affect stability and balance confidence. These results could guide prosthetic foot prescription and enhance our understanding of how TTPUs adapt their walking in response to foot stiffness, which may help improve stability and ultimately reduce falls in TTPUs.

**Acknowledgments:** This study was supported by the Department of Defense Congressionally Directed Medical Research Programs Orthotics and Prosthetics Outcomes Research Program under Award No. W81XWH-20-1-0291 (PI: Morgenroth).

**References:** [1] Czerniecki et al. (2012), [2] Kulkarni et al. (1996), [3] Kim et al. (2019), [4] Sions et al. (2018), [5] Major et al. (2016), [6] Zelik et al. (2011), [7] Ruxin et al. (2022), [8] Zhang et al. (2019), [9] Ruxin et al. (2024), [10] Gates et al. (2013)

**Effects of different cueing strategies on sit-to-walk in individuals with Parkinson's disease**

*Naghmeh Gheidi[1], Ying Fang, Thomas Kernozek
[1] Occupational Therapy Program, Health Professions Department, University of Wisconsin- La Crosse
*Corresponding author's email: ngheidi@uwlax.edu

**Introduction:** Parkinson's disease (PD) impacts gait, balance, and task transitions, such as sit-to-walk (STW), a critical movement requiring stability and coordination. Cueing involves temporal or spatial stimuli and has been shown to improve gait and sit-to-stand (STS) in individuals with PD where internal cues (e.g., singing) have been shown a greater impact than external cues (e.g., auditory, visual, tactile) [1, 2, 3]. However, the effects of internal versus external cues on STW remain unclear [4]. Our study examined the impact of different cueing modalities on STW biomechanics in individuals with PD compared to age-matched healthy controls. It was hypothesized that cueing would enhance STW by increasing center of mass (CoM) anterior-posterior (AP) velocity, first step length, and vertical ground reaction force (VGRF) asymmetry during STS phase of STW.

**Methods:** Eight volunteers > 60 yrs (mean age: 73 ± 6 yrs) participated in this study. The PD group (n=4, three men, height: 1.75 ± 0.51 m, mass: 87.3 ± 27.9 kg) had a mean Hoehn and Yahr score of 2.5, and the control group (n=4, three women, height: 1.7 ± 0.07 m, mass: 81.3 ± 16.9 kg) was age matched. Individuals with other neurological or physical conditions were excluded. Each were fitted with the same model of footwear and equipped with 54 markers for 3D motion capture. Participants completed five randomly ordered cueing conditions: (1) no cue (baseline), (2) auditory (98 BPM metronome), (3) visual (LED floor lights at 98 BPM), (4) tactile (vibrating wristwatch at 98 BPM), and (5) singing ("Row, Row, Row Your Boat" at 98 BPM). Participants performed STW each condition three times while kinematic (180 Hz, 15-camera motion capture) and kinetic (1800 Hz force platform) data were collected. We measured CoM AP velocity at gait initiation (GI), VGRF asymmetry, and step length. Due to the low number of participants, Cohen's d effect size was used to compare between cues and groups (PD/control).

**Results & Discussion:** CoM AP velocity at GI was slower in PD group compare to control (Cohen's d=1.5). Likely due to kinetic energy deficits and postural instability in people with PD [5, 6]. Cueing negatively impacted the COM AP velocity in PD. with visual cues having the greatest negative impact (Table 1). Controls also exhibited decreased CoM AP velocity with tactile cues having the greatest negative impact (Table 1). VGRF asymmetry between groups during STS was similar (Cohen's d=0.14) at the baseline. Auditory and tactile cues reduced asymmetry in PD group despite high standard deviation. Cues appeared to cause those with PD and some controls to split the task into STS and walk instead of a single continuous task (**Fig. 1**). Therefore, cueing may have diversified the strategies our PD cohort used to complete the STW task, as demonstrated in the high variability of VGRF asymmetry**.** First step length following STS was shorter in PD (Cohen's d=1.11). Compared to baseline, auditory cue increased step length in PD, and auditory and tactile cues reduced step length in control group. The internal cue of singing did not make the expected improvement [3]. This could be related to the level of difficulty in performing STW rather than just gait. This may be also explained by Constrained Action Hypothesis where the use of internal cues may disrupt the automaticity of coordination processes [4].

**Table 1:** Average ± standard deviation of center of mass (CoM) anteroposterior (AP) velocity at gait initiation, vertical ground reaction force (VGRF) asymmetry from sit to stand, and first step length of the Parkinson (PD) and control groups. * Different from baseline with medium effect, ** Different from baseline with large effect.

| | | Baseline (B) | Auditory (A) | Singing (S) | Tactile (T) | Visual (V) |
|---|---|---|---|---|---|---|
| COM AP (cm/s) | PD | 0.11±0.07 | 0.056±0.049 | 0.066±0.056 | 0.057±0.039 | 0.044±0.040 |
| | | Cohen's d | B vs. A=0.89** | B vs. S=0.7* | B vs. T=0.94** | B vs. V=1.16** |
| | Control | 0.20±0.05 | 0.18±0.09 | 0.20±0.12 | 0.10±0.09 | 0.17±0.05 |
| | | Cohen's d | B vs. A=0.27 | B vs. S:0 | B vs. T:1.3** | B vs. V:0.6* |
| VGRF Asymmetry (%) | PD | 45.39±24.85 | 24±32.63 | 43.6±28.39 | 28±33.66 | 54±24.45 |
| | | Cohen's d | B vs. A=0.74* | B vs. S=0.07 | B vs. T=0.59* | B vs. V=0.35 |
| | Control | 49.18±28.17 | 41.18±28.18 | 53.71±27.08 | 33.15±32.82 | 41.94±27.54 |
| | | Cohen's d | B vs. A=0.28 | B vs. S=0.14 | B vs. T=0.52* | B vs. V=0.26 |
| Step Length (m) | PD | 0.50±0.03 | 0.7±0.41 | 0.49±0.07 | 0.45±0.13 | 0.49±0.03 |
| | | Cohen's d | B vs. A=0.7* | B vs. S=0.2 | B vs. T=0.5 | B vs. V=0.3 |
| | Control | 0.56±0.07 | 0.52±0.04 | 0.53±0.12 | 0.56±0.06 | 0.43±0.23 |
| | | Cohen's d | B vs. A=0.7* | B vs. S=0.3 | B vs. T=0 | B vs. V=0.8** |

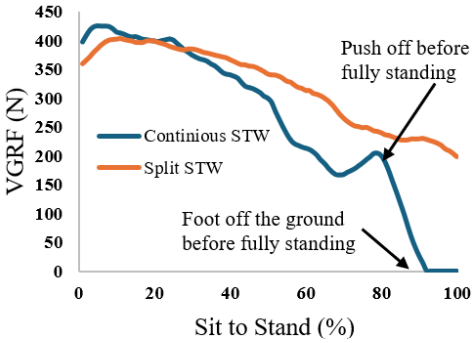


**Figure 1.** Vertical ground reaction force (VGRF) of the lead food during sit-to-stand showing two patterns. For a continuous sit-to-walk (STW), gait initiation starts before the person achieves full standing.

**Significance:** Despite the small sample size, we demonstrated that auditory cue improved STW performance in PD compared to other cues. STW is a complex task, and using simple external cue of audio may have helped our PD cohort to split the continuous task into simpler steps, which improved step length and symmetry. Future studies with larger sample size should test this theory.

**Acknowledgments:** A Research, service, and educational leadership mini grant was received. Many thanks to all graduate occupational therapy students for their assistance with data collection on this ongoing research project.

**References:** [1] Giorgi at al. (2024), *Appl. Sci* 14(11781); [2] Bhatt et al. (2012), *J Phys Ther* 93(4); [3] Harrison at al. (2018), Sci. Rep. (8) 15525 ; [4] Becker& Hung. (2020), *Hum. Mov. Sci.* 72; [5] Buckley et al. (2008), Movement Disorders 23(9); [6] Pelicioni et al. (2020), Clin Biomech 75.

# CHARACTERIZING CENTER OF MASS CONTROL DURING GAIT OF PERSONS WITH MOTOR INCOMPLETE SPINAL CORD INJURY: A STATISTICAL PARAMETRIC MAPPING ANALYSIS

*Oliver J. Daliet IV[1], Charles J. Creech[1,2], Edelle C. Field-Fote[1,2,3]
[1]Crawford Research Institute, Shepherd Center, Atlanta, Georgia, United States of America
[2]Program in Applied Physiology, Georgia Institute of Technology, School of Biological Sciences, Atlanta, Georgia
[3]Division of Physical Therapy, Department of Rehabilitation Medicine, Emory University School of Medicine, Atlanta, Georgia
*Corresponding author's email: Oliver.Daliet@shepherd.org

**Introduction:** Control of the center of mass (CoM) is an important characteristic of efficient and safe walking, requiring precise coordination of multiple joints in the lower extremities that contribute to appropriate accelerations of the CoM [1]. Following motor incomplete spinal cord injury (MISCI), the transmission of both afferent and efferent signals affecting CoM control can be altered due to damage to spinal tracts [2]. The resultant altered motor control can reduce functional mobility and increase risk of falls [3]. Despite its significant implications, control of CoM during overground walking is understudied within MISCI research. A key question that remains unanswered is how the use of assistive devices influences accelerations of the CoM during phases of gait.

The objective of this analysis was to compare mediolateral (ML) CoM accelerations in individuals with MISCI who use rolling walkers (RWs) versus those who do not use an assistive device (AD) during the stance phase of overground gait. We compared the ML CoM accelerations of both groups using statistical parametric mapping (SPM) to decompose the gait cycle to identify differences during specific phases of gait. We hypothesized ML CoM accelerations during specific sub-phases of stance phase would be significantly different between people with MISCI who do not use an AD and those who use a RW.

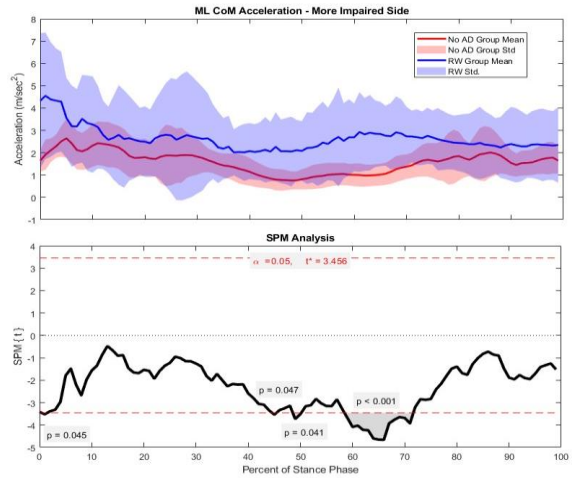


**Figure 1:** The average (solid line) and standard deviation (shaded region) of ML CoM acceleration of the more impaired limb in the no AD group (red) and the RW group (blue) are shown in the top plot. The statistical parametric map (SPM{t}) comparing each group is shown in the bottom plot. Regions of significant difference between the groups are identified when the curve (black) crosses the critical threshold |t*| (dashed red) and are depicted with gray shading.

**Methods:** Kinematic data were collected using an IMU system (Xsens MVN Biomech Awinda, Movella) during the 10-meter walk test (10MWT). Data from participants using a rolling walker (RW, n = 18) or no AD (n = 16) were included in this analysis. Participants completed 1-3 trials of the 10MWT. For each trial, a custom MATLAB code (MathWorks, Inc.) was used to identify gait events and time-normalize the data (0 - 100% of stance phase) using cubic spline interpolation. The magnitude of ML CoM accelerations was approximated from the sensor located at S1. This data were averaged for all steps during the middle 10 m of the 10MWT across all trials for each participant, bilaterally, and normalized to average gait speed to remove its effect on ML CoM acceleration. The more impaired and less impaired limbs were identified using lower extremity motor scores (LEMS). If the LEMS scores were equal, strong and weak limbs were self-identified by the participant. Using the SPM approach, a two-sample t-test was used to compare the magnitude of ML CoM accelerations of the more impaired limb between the RW group and the no AD group. Phases of the gait cycle with significant differences were identified between the two groups. All analyses were performed using the "spm1d" open-source package (version M.0.4.10) for MATLAB (https://spm1d.org/).

**Results & Discussion:** When comparing the magnitude of ML CoM accelerations of the more impaired limb between the RW group and the no AD group (Fig. 1), the SPM{t} curve exceeded the critical threshold (|t*| = 3.456) from 0-1%, 44-45%, 48-50% and 58-71% of stance phase. ML accelerations of the more impaired limb in the no AD group were significantly lower than that of the RW group in all regions ($p = 0.045$, 0.047, 0.041, and > 0.001, respectively). The largest of those regions occurs near the end of terminal stance, progressing into pre-swing. During this sub-phase of gait, the CoM is transitioning from being positioned over the current stance limb to the subsequent stance limb, requiring precise motor input with the goal of maintaining an appropriate CoM position within the base of support. This finding suggests that people with MISCI who use a RW have reduced ML control of their CoM, which is consistent with findings related to ML CoM control in people with stroke [4].

**Significance:** Previous literature has highlighted the importance of ML CoM control for safe functional mobility and balance in people with MISCI [5]. Highlighting sub-phases of the gait cycle where CoM control is altered could provide clinicians with granular information regarding deficits resulting in impaired overground walking, decreased balance, and reduced community participation.

**Acknowledgments:** The authors would like to acknowledge: S. Estes, N. Evans, and A. Zarkou for their contributions to data collection; the participants for volunteering their time; and Wings for Life (WFL-US-2/17 (S.E.)) and the National Institute on Disability, Independent Living, and Rehabilitation Research (NIDILRR; grant nos. 90SI5016 and 90SIMS0002 (E.F-F.)) for funding.

**References:** [1] Tramontano et al. (2024), *Sensors (Basel)* 24(8); [2] Abdolrezaee. (2019), *Front Neurol* 10: p. 282; [3] Wirz and van Hedel. (2018), *Handb Clin Neurol*, 159: p. 367-384; [4] Cicarello et al. (2023), *Clin Biomech* 107; [5] Dusane et al. (2023), *Front Neurol* 14.

# CENTER OF MASS CONTROL IS SIGNIFICANTLY IMPACTED BY INTRA-LIMB COORDINATION IN PEOPLE WITH MOTOR INCOMPLETE SPINAL CORD INJURY

*Charles J. Creech[1,2], Oliver J. Daliet IV[1], Edelle C. Field-Fote[1,2,3]
[1]Crawford Research Institute, Shepherd Center, Atlanta, Georgia, United States of America
[2]Program in Applied Physiology, Georgia Institute of Technology, School of Biological Sciences, Atlanta, Georgia
[3]Division of Physical Therapy, Department of Rehabilitation Medicine, Emory University School of Medicine, Atlanta, Georgia
*Corresponding author's email: cjcreech@gatech.edu

**Introduction:** In people with motor incomplete spinal cord injury (MISCI) who walk as their primary means of mobility, falls are common and most often occur during functional mobility, such as walking [1, 2]. During walking, balance is essential for functional and safe mobility. Accordingly, balance during functional mobility requires the integration of somatosensory, vestibular, and visual information [3]. In response to this information, the body must produce motor outputs to control its center of mass (CoM). To achieve safe, efficient walking, reciprocal lower extremity movements must be coordinated to produce symmetrical and low-amplitude movements of the body's center of gravity [4]. Precise coordination of multiple joints in the lower extremities contributes to appropriate accelerations of the CoM [5].

Following MISCI, the transmission of both afferent and efferent signals contributing to CoM control can be delayed or absent due to damage to spinal tracts [8]. The resultant altered motor control can reduce functional mobility and increase risk of falls [9]. Despite its significant implications, control of CoM during overground walking is understudied within MISCI research. Lower extremity kinematics are comprised of many components. In people with MISCI, two components that are likely to make meaningful contributions to accelerations of the CoM are intra-limb coordination and propulsion. This analysis assessed how mediolateral (ML) CoM control is influenced by lower extremity intra-limb coordination and by propulsion in people with MISCI. We hypothesized that both intra-limb correlation and propulsion would have a significant effect on the control of CoM acceleration.

**Methods:** Kinematic data were collected during the 10-meter walk test while participants utilized their usual assistive device (AD). A full-body IMU system (Xsens MVN Biomech Awinda, Movella) was used. CoM acceleration data was collected from the sensor at S1 as an approximation for the CoM. ML CoM acceleration was normalized to gait speed. Individual gait cycles were identified using a custom computer code developed in MATLAB (MathWorks Inc.). We analyzed intra-limb coordination (quantified as the angular coefficient of correspondence (ACC) [7]) and propulsion (using the trailing limb angle (TLA) as a surrogate [6]). ACC values were calculated for the hip-knee joints of the bilateral lower extremities. TLAs were calculated for each step in both lower extremities. A weighted multiple linear regression was utilized for this analysis with the normalized root mean square of ML CoM acceleration (nML-CoM) as the dependent variable. The independent variables included the ACC of the hip and knee (less-impaired ($ACC_L$) and more-impaired ($ACC_M$) limb) and the TLA (less-impaired ($TLA_L$) and more-impaired ($TLA_M$) limb).

**Results & Discussion:** The equation for the fitted regression model was: nML-CoM = 7.957 - 9.288($ACC_L$) + 1.444($ACC_M$) + 0.063($TLA_L$) + 0.006($TLA_M$). The overall regression model was statistically significant ($R^2 = 0.529$, $R^2_{Adjusted} = 0.485$, $F(4,43) = 12.063$, $p = < 0.001$). We found that $ACC_L$ significantly impacted nML-CoM ($t = -4.242$, $p < 0.001$). In contrast, $ACC_M$, $TLA_L$, and $TLA_M$ did not significantly impact nML-CoM ($ACC_M$: $t = 0.621$, $p = 0.538$; $TLA_L$: $t = 0.915$, $p = 0.365$; $TLA_M$: $t = 0.082$, $p = 0.935$).

The results partially support our hypothesis as only $ACC_L$ significantly affected CoM control. Intra-limb coordination is a cumulative output of both descending motor control originating in supraspinal centers as well as spinal reflexes. Both of these contributors to motor output are altered following MISCI. One interpretation of these results is people with MISCI may be reliant on their less-impaired limb to control their CoM, masking the deficits in their more-impaired limb. Consequently, people with bilateral impairment following MISCI may have less CoM control, while those with more asymmetrical involvement resulting in a "stronger" leg may have greater CoM control. Additionally, people with MISCI may be utilizing their ADs to control their CoM. Absence of influence of TLA could be indicative of less dependency on TLA for propulsion during gait in people with MISCI. As a result of this lower dependency, TLA may play a lesser role in control of the CoM than in other neurologic populations [10].

**Significance:** Intra-limb coordination is known to be responsive to training in people with MISCI [11]. Based on this analysis, focusing clinical treatment on improving the coordination of the hip-knee joint timing in people with MISCI could result in greater CoM control in people with MISCI. This is impactful as CoM control is known to play a significant role in safe and efficient functional mobility in people with MISCI [12]. Improvement in CoM control could result in improved balance, decreased risk of falls, and improved quality of life.

**Acknowledgments:** The authors would like to acknowledge: S. Estes, N. Evans, A. Zarkou, and A. Norfleet for their contributions to data collection; the participants for volunteering their time; Wings for Life: WFL-US-2/17 (S.E.) and the National Institute on Disability, Independent Living, and Rehabilitation Research (NIDILRR): 90SI5016 and 90SIMS0002 (E.F-F.) for funding.

**References:** [1] Khan et al. (2019), *Spinal Cord* 57(7); [2] Phonthee et al. (2013), *Spinal Cord* 51(5); [3] Horak (2006), *Age Ageing* 35(Suppl 2); [4] Waters and Mulroy (1999), *Gait Posture* 9(3); [5] Tramontano et al. (2024), *Sensors* 24(8); [6] Lewek and Sawicki (2019), *Clin Biomech* 67; [7] Sparrow et al. (1987), *J Mot Behav* 19(1); [8] Alizadeh et al. (2019), *Front Neurol* 10; [9] Wirtz and van Hedel (2018), *Handb Clin Neurol* 159; [10] Todaka et al (2024), *Hum Mov Sci* 93; [11] Field-Fote and Tepavac (2002), *Phys Ther* 82(7); [12] Dusane et al. (2023), *Front Neurol* 14

# GAIT PARAMETERS RELATED TO DYNAMIC BALANCE AND BILATERAL TEMPORAL COORDINATION IMPROVE WITH SLEEP EXTENSION, BUT ARE NOT AFFECTED BY MOTOR DUAL TASKING IN YOUNG ADULTS

*Bria R. Smith[1], Kenneth Harrison [1], Brandon M. Peoples [1], Meral N. Culver [1], Keven Santamaría-Guzmán [1], Silvia Campos-Vargas [1], Austin T. Robinson [2], Jaimie A. Roper [1]
Auburn University [1], Auburn AL
Indiana University[2]
*Corresponding author's email: bzs0144@auburn.edu

**Introduction:** It is recommended that young adults receive 7-9 hours of sleep each night [1]. However, many fail to meet recommended sleep dosages, which can have detrimental effects on multiple motor and cognitive processes [2,3]. There is an abundance of literature discussing the effects of sleep deprivation on cognitive and motor processes, but there is limited research considering the effects of sleep extension, especially in relation dynamic balance and motor control. We selected dynamic balance as our primary outcome measure because sleep deprivation impairs postural control by affecting vestibular function and proprioceptive integration [6]. This stability during movement can be objectively assessed through gait parameters such as double support time (DST), swing time, and gait asymmetry (GA) [4,5]. Swing time and gait asymmetry can also function as indicators of bilateral temporal coordination (BTC), which involves the coordination and control required to move each leg during the gait cycle. Based on existing literature focusing on the effects of sleep on motor control and balance, we hypothesized there would be a decrease in DST and GA with sleep extension. Additionally, we predicted an increase in DST and BTC between the single- and dual-tasking conditions.

**Methods:** Twenty-eight young adults (11M/17F; SD 23±2) who self-reported sleeping <7 hours per night were instructed to extend their sleep by one hour for two weeks. The Pittsburgh Sleep Quality Index (PSQI) was used to measure sleep duration in hours and global score on a scale of 0-21, with lower scores indicating worse sleep quality. Participants performed a 7-meter instrumented stand and walk (iSAW) and 2-minute walk (2MW) during a verbal fluency task to create a dual-tasking environment. Swing time and double support time were measured during single- and dual-tasking conditions using inertial movement units (IMU). Gait asymmetry was used as a predictor of BTC and calculated with the following equation: ln(swingtimeL/swingtimeR) [5]. DST and GA between single- and dual-tasking conditions, as well as before and after extending sleep, were compared using an analysis of covariance (ANCOVA).

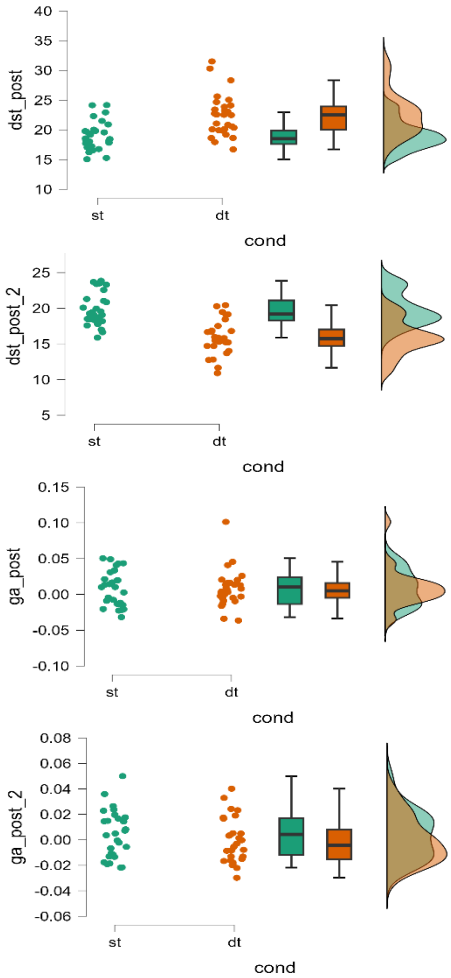


**Results & Discussion:** Participants reported increases in sleep duration (6.2±0.9 vs. 7.3±1.0 hours, p<.001) and lower PSQI scores (5.4±1.6 vs. 3.4±1.4, p<.001) after the sleep extension intervention. No significant differences in GA or DST were found across the single- or dual-tasking conditions. However, participants showed a decrease in GA for the iSAW (p<.001) and 2MW (p<.001) after sleep extension. An increase in DST during the iSAW (p<.001) and 2MW (p<.001) were also reflected in the data after sleep was extended. After sleep extension, participants demonstrated a significant decrease in GA during both the iSAW (p<.001) and 2MW (p<.001) tasks, alongside an increase in DST during the iSAW (p<.001) and 2MW (p<.001). The decreased GA indicates improved bilateral coordination, while increased DST suggests a more cautious gait pattern—indicating sleep extension influences different aspects of gait control through distinct mechanisms.

**Significance:** Our study addresses the effects of sleep extension on dynamic balance and bilateral coordination through analysis of key gait parameters. The findings reveal that extending sleep leads to improvements in bilateral coordination (as indicated by decreased gait asymmetry) while simultaneously resulting in increased double support time. This pattern suggests that sleep extension may influence different aspects of gait control through distinct mechanisms rather than producing uniform improvements across all parameters. While our hypothesis regarding decreased gait asymmetry was supported, the increased double support time contrasted with our expectations, highlighting the complex relationship between sleep and motor control. The absence of significant differences between single- and dual-tasking conditions further suggests that these sleep-related gait adaptations may be relatively consistent across varying cognitive demands. These insights contribute to the emerging research on sleep extension and have practical implications for sleep-deprived individuals and those with elevated fall risk. Future work will explore additional gait parameters and examine how sleep extension influences motor and cognitive performance across varied task environments.

**References:** [1] Watson et al. (2015), *Sleep* 38(6); [2] Umemura et al. (2022), *Front Neurosci* 16; [3] Paillard (2023), *Front Hum Neurosci* 17;[4] Gabell & Nayak (1984), *J Geront* 39(6); [5] Plotnik et al. (2020), *Sci Rep* 10(1238) ; [6] Plotnik et al. (2013), *Gait Posture*, 38(4).

# LOCOMOTOR ADAPTATIONS TO PREDICTABLE AND UNPREDICTABLE BALANCE PERTURBATIONS IN PEOPLE WITH CHRONIC STROKE

Ashley Maloney[1*], Shamali Dusane[2], Heather Henderson[2], Anna Shafer[3], Keith E. Gordon[2,3]
[1]Department of Biomedical Engineering, Northwestern University, [2]Physical Therapy and Human Movement Sciences, Northwestern University, [3]Research Service, Edward Hines Jr. VA Hospital
*Corresponding author's email: ashleymaloney2025@u.northwestern.edu

**Introduction:** Among people with chronic stroke (PwCS) poor balance significantly impairs walking[1] and is challenging to improve through physical therapy[2]. According to the motor learning principle of task-specific practice, improving a behavior requires practicing that specific behavior[3]. To this end, researchers are investigating whether applying balance-challenging external forces during gait training can enhance walking balance in PwCS. The ability of PwCS to predict the characteristics of these external may be a critical factor in the type of locomotor response they adapt. When the characteristics of balance-challenging external forces are unpredictable, people will likely adapt "cautious gait patterns" (shorter, wider steps) that generally improve the body's resistance to any perturbation. In contrast, when the characteristics of balance-challenging external forces are predictable, individuals may allow temporary reductions in gait stability, e.g., greater lateral center of mass (COM) excursions. Here, we explore how PwCS adapt to the application and removal of balance-challenging external forces during walking. We use a cable-driven robot to apply two different laterally-directed force fields to the pelvis during treadmill walking. The Random Perturbation Field applies unpredictable lateral forces of varying amplitude and direction (left or right). To the Random Perturbation Field, we hypothesize that PwCS will adopt a cautious gait pattern, characterized by shorter and wider steps, to minimize lateral COM excursions. The Movement Amplification Environment (MAE) applies predictable continuous forces proportional in magnitude and direction to the participant's real-time lateral velocity. To the MAE, we hypothesize that PwCS will not significantly alter their stepping response to the MAE, leading to greater lateral COM excursions.

**Methods:** Three ambulatory PwCS (66 ± 3 years) performed three blocks of treadmill walking trials at their preferred speed. During each block, participants completed 400 steps. The first 100 steps established a **Baseline** measure of walking without external forces. Next, an external force **Field** — either the MAE or Random Perturbations — was applied to the pelvis for 200 steps. Without stopping the treadmill, the force field was then removed, and participants walked for another 100 steps to assess **After-effects**. We collected 3D kinematic data using 19 reflective markers placed on the pelvis and lower limbs and a 12-camera motion capture system (Qualisys, Gothenburg Sweden). To evaluate participants' responses to both the application and removal of the force fields, we analyzed lateral COM excursion per stride, step length, and step width. These measures were taken from the last 20 steps of Baseline, the last 20 steps in the Field (Late Field), and the first 20 steps of the After-effects period.

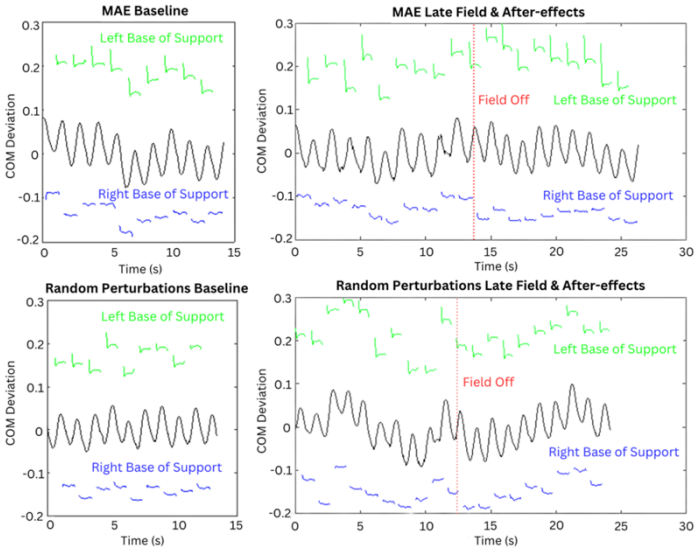


**Figure 1. Walking in MAE and Random Perturbations.** Lateral center of mass (COM) deviation and base of support across conditions. (Top) MAE condition during baseline, late field, and aftereffects. (Bottom) Random Perturbations condition during baseline, late field, and aftereffects. The vertical red dashed lines indicate force removal.

**Results & Discussion:** Participants exhibited distinct stepping characteristics and COM excursions in response to the two different balance-challenging force fields. In the Random Perturbation Field, participants adopted steps that were 10.3 ± 2.2% shorter and 16.9 ± 3.6% wider than Baseline. These changes resulted in a 20.2 ± 4.3% decrease in lateral COM excursion despite experiencing lateral perturbations. When the Random Perturbation Field was removed, participants continued to walk with steps that were 5.6 ± 1.7% shorter and 10.5 ± 2.9% wider than Baseline, and with a lateral COM excursion that was 8.5 ± 2.4% less than Baseline. In contrast, in the MAE field, participants' step width and length did not change from Baseline, 1.5 ± 0.7% and 1.4 ± 0.7%, respectively. As a result of not changing stepping characteristics, lateral COM excursion in the field was 5.8 ± 1.9% greater than Baseline. The removal of the MAE may have been perceived as balance-challenging to participants as they demonstrated steps that were 8.8 ± 2.0% shorter and 7.5 ± 2.0% wider than Baseline. During the MAE After-effects period, lateral COM excursion was 8.4 ± 2.2% less than Baseline.

**Significance:** Stroke is a leading cause of long-term disability, with many PwCS experiencing impaired balance and gait, which increases fall risk and limits physical activity. Understanding how PwCS adapt to balance-challenging forces can inform more effective rehabilitation strategies aimed at improving stability and adaptability. These findings suggest that PwCS adapt their gait patterns differently depending on if they can predict the characteristics of balance-challenging external forces. Future work is needed to determine if extended practice responding to either predictable or unpredictable forces will ultimately lead to improvements in walking balance.

**Acknowledgments:** Supported by the U.S. Department of Veterans Affairs, RR&D Service #1 I21 RX00488, and NSF Graduate Research Fellowship Program ID #2023357128.

**References:** 1)*Tyson et al. Physical Therapy*. 2006. 2) Zhang et al. *Frontiers in Neurology*. 2023. 3) Kleim & Jones. *Journal of Speech, Language, and Hearing Research*. 2008.

# TEST EQUIVALENCE ON DYNAMIC AND STATIC BALANCE SYSTEMS

*Kiara Barrett[1], Neha Kapoor[1], Megan Cotterman[1], Kristinn Heinrichs[1], Kamran Barin[1]
[1]Bertec Corporation, Columbus, OH
*Corresponding author's email: kiara.barrett@bertec.com

**Introduction:** Balance is the foundation of voluntary movement [1]. As such, it is imperative to quantitatively assess balance; this can be accomplished via the use of force plates and other instrumented balance devices. Computerized Dynamic Posturography (CDP) is the current gold standard in balance testing and offers a variety of options to assist clinicians in targeting balance deficiencies. Other static force plate options, like the Portable Essential (PE), are a more affordable alternative. While the static plate does not offer the Sensory Organization Test, the most extensive and targeted balance assessment, it does provide two commonly utilized measures of balance: the Limits of Stability (LOS) and Rhythmic Weight Shift (RWS) tests.
The LOS and RWS tests are frequently utilized by clinicians to assess voluntary postural control [2,3]. Improvements in endpoint and excursion metrics in the LOS have been linked to decreased risk of falls [3]. It is unknown whether the static system is equivalent to the gold standard dynamic system, and if the CDP visual environment has a significant influence on performance in these balance tests. The purpose of this study is to determine if the static plate is equivalent to the CDP for these two specific balance tests; we hypothesize the static system will show equivalence to the dynamic system.

**Methods:** This study is a part of a larger ongoing study assessing balance in healthy individuals. 20 healthy participants (27±5yrs, 1.75±.10m, 77.88±18.32kg) completed a single visit testing session lasting around 2.5 hours. They performed a series of balance tests including the RWS and LOS on Bertec's CDP and PE devices. In the RWS, participants shifted their weight side to side, then forward and backward, keeping pace with a visual cue. The LOS consists of shifting one's weight as far as possible and holding it, aiming for targets in 8 different directions. Order of test and device was randomized according to a Latin squares design to minimize a learning effect. Bland-Altman plots were generated in python to determine upper and lower equivalence bounds based on 2 standard deviations above and below the mean [4]. These bounds were then inputted into the Two One-Sided equivalence Tests (TOST) performed in Jamovi 2.6 statistical software with the TOSTER module to determine device equivalence [5]. The alpha level for all statistical tests was set at .05.

**Results & Discussion:** Equivalence bounds and results of the TOSTs are reported in Table 1.
The static and dynamic posturography systems were found to be statistically equal for five out of six variables analysed. These results show the static plate is an equivalent device to the CDP when performing the LOS and RWS tests.

Table 1. Two One-Sided Tests of Equivalence Results

| Test | Variable | T-test | Lower Bound | | Upper Bound | |
|---|---|---|---|---|---|---|
| | | p-value | Value | p-value | Value | p-value |
| LOS | Composite Endpoint | .691 | -13.03 | <.001 | 13.19 | <.001 |
| | Composite Excursion | .266 | -13.09 | <.001 | 11.47 | <.001 |
| RWS | F/B Composite DC | .642 | -5.27 | <.001 | 6.05 | <.001 |
| | F/B Composite MV | .214 | -0.91 | <.001 | 1.27 | <.001 |
| | L/R Composite DC | <.001 | -7.95 | <.001 | 2.78 | 0.624 |
| | L/R Composite MV | .199 | -1.21 | <.001 | 1.70 | <.001 |

LOS: Limits of Stability, RWS: Rhythmic Weight Shift, F/B: Forward/Backward, L/R: Left/Right, DC: Directional Control, MV: Movement Velocity

The results of this study support our hypothesis: the dynamic and static systems showed significant equivalence for metrics in the LOS and RWS assessments. The Bertec CDP includes a visually immersive dome, while the static plate software is displayed on a standard laptop screen. Equivalence between devices was shown despite the disparity in visual displays. This lends credence to the use of the static plate and laptop display; clinicians and health professionals can be confident in their RWS and LOS testing protocols using the more basic static plate.
It should be stated that the static system is a limited version of the dynamic posturography machine. Equivalence was shown for two specific tests (LOS and RWS); however, due to the moving plate and immersive visual field, the CDP provides a battery of balance testing, including the SOT, unavailable on the static plate. Dynamic balance tests provide a more in-depth analysis of the contribution of visual, somatosensory, and vestibular systems to balance; to obtain the most robust picture of a patient's balance, dynamic plate assessments should be included in regular clinical practice.

**Significance:** This study provides empirical evidence for the equivalence of static and dynamic balance systems when performing the RWS and LOS tests. These static balance tests are crucial for testing voluntary postural control [1] and should be incorporated into regular practice. Clinicians should feel comfortable using the static plate to complete these tests, although dynamic posturography is still recommended for more in-depth balance assessments.

**References:** [1] Huxham et al. (2001) *Aus J. Physio* 47(2) [2] Vervoort et al. (2013) *Parkinsons Dis.* 971480; [3] Faraldo-Garcia et al. (2016) *Acta Oto-Laryn* 136(11) [4] Lakens. (2017), *Soc Psych and Pers Sci* 8(4); [5] Giavarina. (2015), *Biochem Med* 25(2).

# ASSESSMENT OF RIFLE AND POSTURE SYNCHRONIZATION METRICS FOR DETECTING THREAT ENGAGEMENT READINESS POSTURES

*Leah R. Enders[1], Mike Nonte[2]
[1]U.S. Army DEVCOM Army Research Laboratory, Aberdeen Proving Ground, Maryland, United States of America
[2]DCS Corporation, Alexandria, Virginia, United States of America
*Corresponding author's email: leah.r.enders.civ@army.mil

**Introduction:** Operational data obtained through the passive sensing of behaviors can provide context and insight into how humans, both as individuals and teammates, navigate complex real-world environments. This information can guide development of algorithms/models and build more effective communication mechanisms between humans and intelligent systems (e.g. drones) and (military) commanders. Initially, we will develop models of soldier engagement and readiness using virtual reality (VR). Unsupervised learning methodology will identify regions of time containing consistent behaviors across subject labeled video data. To give context to these behaviors and to create a label-space to describe them, we can use a series of weapon/limb synchronization threshold metrics (TMs) to detect when a soldier is alerted to threats and assuming threat engagement readiness postures [1]. Segment-Rifle Linkage, L = $(mean(||\omega_{segment}||/||\omega_{rifle}||)$, where $\omega$ = angular velocities and a L ~1 implies joint movement, and Segment-Rifle Steadiness, S = $(1/RMS(||a_{segment}/_{rifle}||)$, where a = acceleration and greater S implies greater steadiness, have previously been used to assess differences between expert and novice marksmen in a dynamic shooting task of static targets [2]. It is unknown if these metrics can be adapted as TMs, to detect initiation response postures when a soldier may detect, mitigate/shoot, and confirm an unexpected threat or if TMs can detect differences in readiness of different threat types. Given general threat engagement postures [1], we expect (1) regardless of threat type, linkage TMs will occur soonest after threat attack, followed by Head-Rifle steadiness, then Head-Rifle Velocity synchronizations, and (2) overall time to initiate TMs will be longer when no pre-attack threat information is provided.

**Methods:** Subjects (N = 10, male) performed a surveillance task on a cityscape rooftop in VR (Meta Quest Pro). For the pilot study, subjects were not required to have tactical weapons training. Subjects walked freely and VR controllers were fixed into a simulated, weighted rifle (Fig. 1). Fifteen inertial measurement units (IMUs) were affixed to trunk, head, lower and upper body, with one additional IMU on the weapon. Over 23 trials, friendlies and threats appeared pseudo-randomly in surrounding building windows. Subjects were instructed to mitigate/shoot threats, not friendlies, as soon as possible. Included were two threat types, evenly: (1) Informed Threats- immediately prior to first threat shot, subjects were given an alert and the general threat location, and (2) Uninformed Threats- no location information/alerts were provided pre-attack.

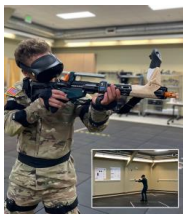

**Figure 1:** IMU(s) affixed to limbs, weapon

TMs were calculated from raw acceleration and angular velocity IMU data and included: Torso-Rifle Linkage and Head-Rifle Linkage (weapon raised, moving with torso/head); Head-Rifle Steadiness (rifle/head synchronized, rifle against head); and Head-Rifle Velocity Initial Sync and Head-Rifle Optimal Sync capturing when head/rifle angular velocities simultaneously dropped towards zero (weapon sighted, aligned, prepping to shoot) (Fig. 2, bottom). TM optimal/lowest time point was determined using a 0.5 second moving window algorithm, starting immediately after initial threat shot until threat death (MATLAB). An ANOVA accessed differences in initiation time points of TMs (with respect to first threat shot) and threat types. Threat Death included to understand time course.

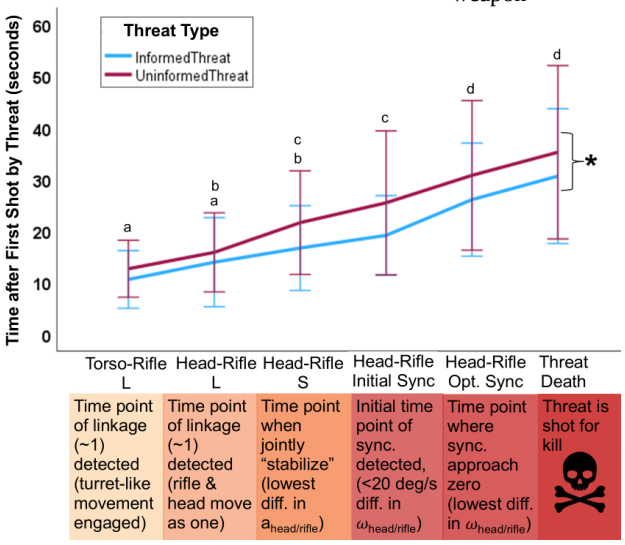


**Figure 2:** Mean ± SD initiation time after first shot by threat (y-axis) & TMs, described bottom (x-axis), were detected with differences between threat types. TMs with same letter not significantly different.

**Results & Discussion:** There was a significant main effect of Threat Type ($p$<.001) where the Mean Time after Threat's First Shot was significantly longer overall for the Uniformed Threats compared to the Informed Threats (Fig. 2). There was a main effect of TM ($p$<.001). Post-hoc analysis determined similarity in timing across Torso-Rifle and Head-Rifle Linkages, between Head-Rifle Steadiness and the Head-Rifle Synchronizations, and Head-Rifle Optimal Sync and Threat Death, indicating possible cooccurrence of these actions (and usefulness in predicting subsequent actions). Overall, TMs captured expected differences in Threat Type and followed the expected time course based on general threat engagement readiness postures [1].

**Significance:** These results demonstrated the potential of using TMs to detect important time points related to weapon/limb synchronization during the threat readiness response, helpful for us (and others) in labeling and validating our model work, especially in the absence of video labeling in future in-field testing. Future work will refine TM metrics and confirm how well TMs can be used to understand behaviours segmented by unsupervised learning methods. We will also determine how previous threat engagement and threat location impacts subsequent postures and explore how tactical weapons training impacts TMs.

**References:** [1] HQ, Department of the Army (2016) TC 3-22.9; [2] O'Donovan et. al., (2024) Applied Ergonomics 114.

# EFFECTS OF COLD-WATER IMMERSION ON SHIVERING MAGNITUDE AND POSTURAL STABILITY

*Amy B. Schwartz[1,2], Douglas M. Jones[1], Rebecca J. McClintock[1,2], Rebecca S. Weller[1,2], Tony C. Duong[1,2], Amy Silder[1]
[1]Naval Health Research Center, Warfighter Performance Department
[2]Leidos, Inc., Military and Veterans Health Solutions
*Corresponding author's email: amy.b.schwartz2.ctr@health.mil

**Introduction:** Accidental immersion in cold water can result in a substantial decrease in body temperature. Concomitant shivering can significantly impair fine motor control [1], muscular function [2], gait [3], and cognition [4]. During initial rewarming, core temperature continues to drop as peripheral vasodilation begins to rewarm the extremities [5]. For service members and first responders, these effects can impair operational performance, impede mission readiness, and impose additional safety risks for themselves and others. The impacts of cold are frequently researched with regards to dexterity and core temperature, but postural stability is also of importance to help understand the risks associated with the ability to move to safer conditions or remain operationally effective. In our study, we used acceleration to quantify the magnitude and frequency of thermal-induced shivering and explored the relationship between postural stability and skin temperature, core temperature, and shivering magnitude after a 10-minute cold water immersion and changes therein after 40-minutes of active rewarming. We hypothesized that lower core and foot temperature would be strongly correlated with increased shivering magnitude and impaired postural stability.

**Methods:** Active duty service members (28M/1F; 29±7 y; 175±11 cm; 86.9±12.5 kg) were immersed up to the neck in a near-frozen (water: 1.3º C; air: -4.2º C) outdoor pond for ten minutes as part of a standard training exercise. After immersion, participants immediately changed into dry clothes and began active rewarming, consisting of stair stepping in place for 40 minutes. Accelerations were recorded (60 Hz) from an IMU (Movella DOT, The Netherlands) secured to the skin on the pectoralis major. Skin temperatures were recorded (1 Hz) using iButtons (Whitewater, WI) secured immediately adjacent to the IMU, and on the shoulder, hand, thigh, and foot. Mean Skin Temperature (MST) was subsequently estimated from a weighted average of 50% chest, 34% thigh, and 14% shoulder temperatures. Core temperature was recorded (1 Hz) using VitalSense ingestible capsules (Bend, OR). Postural stability was evaluated with eyes open and hands on hips during three 60-second periods – indoor baseline, post-immersion after changing clothes, and after rewarming. All data were time-synchronized prior to analyses, and only the 1-minute periods during the postural stability tests were considered. Shivering frequency and magnitude were estimated by applying a 3-15 Hz Butterworth filter to the magnitude of the acceleration, then determining the time and magnitude between peaks in the signal. Postural stability outcomes of 95% confidence ellipse area and root-mean-square velocity were calculated after applying a 10 Hz lowpass filter to the center of pressure (COP) data. Hypothesis testing for shivering metrics were performed using paired t-tests, while analyses of variance and multiple comparisons using Dunnett's method were used for postural stability outcomes ($\alpha = 0.05$; MATLAB R2024b, Mathworks Inc., Natick, MA). The Pearson's coefficient was calculated to assess correlation between outcomes (*corrcoef*, MATLAB).

**Results & Discussion:** Mean shivering frequency fell within reported ranges [6] and remained constant, while average shivering magnitude decreased from post-immersion to post-rewarming. Although rewarming increased core temperature (post-immersion: 36.3±1.4 ºC; post-rewarming: 36.52±0.91 ºC) and improved postural stability, participants remained at a deficit compared to pre-immersion baseline, as anticipated. There was no significant relationship between shivering magnitude and MST, hand, or foot temperature, but lower post-immersion core temperatures correlated strongly with increased shivering magnitude ($r=-0.68$, $p=.002$) and correlated moderately with reduced post-immersion RMS velocity ($r=-0.58$, $p=.003$). There was also a strong correlation between decreased shivering magnitude after rewarming and relative recovery of core temperature ($r=-0.81$, $p<.001$) and postural stability (RMS: $r=0.91$, $p<.001$; Area: $r=0.74$, $p<.001$).

**Table 1:** Mean and standard deviation (SD) shivering and postural stability values from 1-miute baseline, post-immersion, and post-rewarming balance periods. * p<.001 relative to baseline. † p<.05 relative to baseline. ‡ p<.001 relative to post-immersion.

| Value | Baseline Mean (SD) | Post-Immersion Mean (SD) | Post-Rewarming Mean (SD) |
|---|---|---|---|
| Shivering Frequency (Hz) | --- | 8.36 (1.48) | 8.33 (1.99) |
| Shivering Magnitude ($m/s^2$) | --- | 2.85 (1.71) | 0.23 (0.16) ‡ |
| 95% Confidence Ellipse Area ($mm^2$) | 0.88 (0.43) | 19.62 (16.76) * | 4.02 (5.27) *‡ |
| RMS Velocity (mm/s) | 0.89 (0.25) | 7.51 (5.28) * | 1.87 (1.58) *‡ |

**Significance:** These data suggest that shivering-induced thermogenesis can have significant, detrimental effects on postural stability that may not resolve despite a near full recovery of core temperature. The inability to safely and effectively perform necessary operational tasks after an accidental cold-water immersion can jeopardize both individual and mission safety.

**References:** [1] Meigal et al. (1998), *Acta Phys Scand* 163(1); [2] Bell & Lehmann (1987), *Arch Phys Med Rehab* 68(8); [3] Eils et al. (2004), *Gait & Posture* 20(1); [4] Muller et al. (2012), *Ergonomics* 55(7); [5] Romet (1988), *J App Phys* 65(4); [6] Sessler et al. (1988), *Anesthesiology* 6(68).

# THE MISUSE OF BIOMECHANICAL EVIDENCE IN SHAKEN BABY CASES

Barbara Pfeffer Billauer JD MA (Biomechanics) PhD
The Institute of World Politics
Omniscience@starpower.net bpbillauer@iwp.edu

**Introduction:** In recent years, the medical diagnosis of *Shaken Baby Syndrome (SBS)* has come under attack. A small cadre of medical experts and biomechanics professionals claim that no scientific evidence exists to support the diagnosis, which is typically characterized by objective injuries, both internal and external, including subdural (brain) and retinal hemorrhage and encephalopathy caused by repeated shaking resulting in the brain banging against the skull (a *contre coup* lesion). Additional diagnostic signs and symptoms include irritability, difficulty staying awake, seizures, abnormal breathing, poor eating, bruises, vomiting and skull fracture. This position has been relied on by various courts to exonerate defendants. In one recent legal case, the medical diagnosis, itself, was rejected by the court on the grounds that it was not supported by the biomechanics community. The case was dismissed even before the particular (specific) evidence regarding the case was examined.

This research reviews biomechanical evidence introduced in legal proceedings to discern whether this position is valid from both a legal and scientific viewpoint. The two legal standards governing admission of scientific evidence are the *Daubert* standard [1], which requires scientific evidence to be reliable and relevant. (Validity is only mentioned in a footnote). Further, the *Daubert* standard requires that opinions of the experts must be tethered to the data obtained in experimentation.[2] Six state jurisdictions still use the older *Frye* standard [3], which turns on the consensus of the scientific community. That the biomechanics community (as represented by the American Biomechanics Society or similar organizations) has not taken a position by the courts is ignored by the courts. In jurisdictions where the *Frye* standard is used, the courts rely on opinions of a small cadre of individual biomechanics to substitute for "consensus" of the professional community. As for evaluation by the *Daubert* standard, thus far courts have not undertaken a didactic assessment of the evidence (likely because the prosecution has not raised it). This research seeks to fill that lacuna

**Methods:** This research evaluates the biomechanical/medical evidence adduced in *State of New Jersey v. Darryl Neives and Michael Cafelli [4],* leading to the courts rejecting the SBS diagnosis entirely. The evidence submitted by the defendants' biomechanics expert relies on six articles, plus amici briefs by legal organizations supporting defendants' rights. The studies relied on were evaluated for scientific reliability and validity and legal relevance. The studies are assessed for their relevance to human subjects (babies) typically diagnosed with the condition to determine whether the results and testimony based thereon are reliable, relevant and valid to assess the issue.

**Results & Discussion:**

| Author | Test subject | Legal Relevance to humans | Reliability | Scientific Validity |
|---|---|---|---|---|
| Prange et al (2003) | Average doll | None/ external force/ 1 shake | None | None |
| Jenny et. al. (2017) | doll | None/external force/1 shake | None | None |
| Finnie et al. (2010) | Lambs | 3/9 lambs died from SBS-like signs | None | Weak-some |
| Finnie et al. (2010) | Lambs | 7 lambs acute stress response | None | Weak- some |
| Van Ee ?? | Not reported | ?? Not published – none | None | None |
| Papetti et. al. (2019) | Review | Law Review Article - none | None | None |

The studies relied on via expert testimony (that evidence does not support the claim that repeated shaking causes SBS) requires a double extrapolation (since tests in babies have not (and ethically cannot) be done). The tests do not assess the biological/physiological effects of *repeated* shaking in humans – the premise to be tested. They merely calculate the *external* force generated by a single shake in a dummy or an animal (where 33% of the test subjects actually sustained injuries consistent with SBS). The results of the single thrust (measuring external force) are then compared to animal and adult force results, and mathematical extrapolation to babies is calculated. Test subjects are constructed to resemble "average" babies and subjected to a single shake, not duplicative of actual conditions (hence invalid) to determine effects of repeated shaking in a premature or vulnerable child. Since SBS involves internal injuries (via *contre coup* lesion) generated by a cascade of physiological responses e.g., hematological, immunological, and anatomical, these tests are irrelevant (i.e., scientifically invalid) to rule out the impact of repeated shaking in immature or vulnerable infants. Reliability is not calculated – as too few subjects were used. In the absence of shaking, no other explanation is offered to explain the injuries (and is not legally required).

**Significance:** This work demonstrates the uses – and misuses -- of biomechanics and the dangers when the science is taken beyond its limits. Until the recognized bioethics community takes a position either disavowing the diagnostic implications of these studies in human shaken baby cases or disavowing use of biomechanics when the matter involves a cascade of physiological responses, individual biomechanics will continue to sway courts. While lawyers representing defendants are thrilled, the child who has been severely damaged (or has died) is without redress.

**References: [1]** *Daubert v. Merrell Dow (1992), [2] Joiner v. General Electric, (1997) [3] Billauer, (2016.), State of New Jersey v. Darryl Neives, and Michael Cafelli (2023).*

**/keywor**d(s) Impact Biomechanics and Trauma; Pediatrics; Education and Outreach in Biomechanics

# A PRELIMINARY REVIEW OF INFANT CRANIUM DEVELOPMENT DURING THE FIRST SIX MONTHS OF LIFE

*Shameka Kimmel[1], Erin Mannen[1]
[1] Mechanical and Biomedical Engineering, Boise State University, Boise, Idaho
*shamekakimmel@u.boisestate.edu

**Introduction:**
Infant cranial development undergoes rapid changes during the first six months of life, influenced by genetic and environmental factors. Understanding these developmental patterns is essential for distinguishing between normal variation and pathological conditions. While previous studies have explored cranial growth, most have focused on abnormalities such as plagiocephaly and craniosynostosis, leaving a gap in knowledge regarding typical skull morphology. Here, we review existing literature on the three-dimensional (3D) evolution of the infant cranium between birth and six months. By identifying key growth patterns and methodological limitations in current research, we may establish the need for further longitudinal studies on healthy infants. These findings will contribute to the foundation for improved (1) clinical guidelines and interventions, and (2) inputs for computational models to further investigate infant biomechanics, ultimately promoting optimal cranial development and health in early childhood.

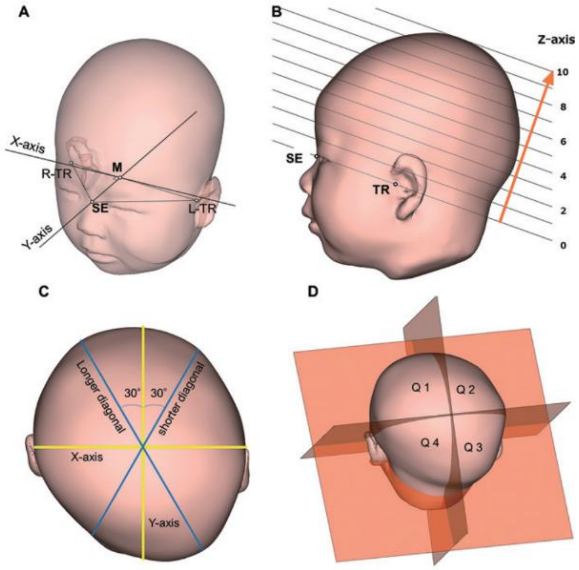


**Figure 1: This figure demonstrates methods of determining reference plane and axes of an infant cranium to track development [2].**

**Methods:**
A literature review involving an evaluation of existing literature was conducted to assess current literature on healthy infant cranial morphology between birth and six months. Using PubMed, we focused this initial search on studies employing advanced imaging techniques, particularly 3D stereophotogrammetry and computed tomography (CT), to document normal cranial shape evolution in healthy infants. The studies were evaluated for methodological rigor, sample composition, and the extent of their focus on healthy infants without cranial deformities. Data on cranial width, length, cephalic index, and volume changes were extracted and synthesized.

**Results & Discussion:**
The results of our literature review investigating cranial development yielded a total of 20 articles. Eighteen of these articles were excluded from further review due to focus on pathologic conditions, a focus on landmarks on the face instead of skull shape, and a focus on children >12 months. Two studies were included for further analysis: one analyzing normative cranial growth using 3D imaging from infancy through early childhood [1], and another establishing reference values for cranial morphology in one-month-old infants [2]. Infant cranial development follows a non-uniform growth pattern, with the most rapid changes occurring between three and six months [1]. While existing studies provide valuable baseline data, they highlight critical gaps in literature. Most studies on early cranial development focus on abnormalities, such as plagiocephaly and craniosynostosis, rather than natural shape variation [2]. Additionally, while 3D imaging methods provide more precise measurements than traditional 2D techniques, comprehensive longitudinal studies tracking typical skull development in healthy infants are scarce. Future research should aim to establish normative growth curves using larger, diverse cohorts and assess the long-term effects of environmental factors such as sleep position and caregiver handling. There are many gaps within this research such as diversity among a single region due to small sample sizes. This leads to lack of understanding across many regions [2]. Along with diversity gaps caused by small sample sizes, having overall understanding for age groups is difficult in this age range [1]. Expanding this knowledge base will contribute to more accurate clinical assessments and interventions for optimizing early cranial development. This initial review has motivated our ongoing systematic review on this same topic. Expanding the project to a systematic review is crucial for strengthening evidence, enhancing reliability, and broadening applicability. A thorough understanding of relevant studies will help fill identify knowledge gaps to motivate future studies.

**Significance:**
By providing a clearer picture of normal head shape progression, this research has the potential to (1) inform pediatric guidelines, enhance early diagnosis of cranial abnormalities, and improve recommendations for infant care practices, and (2) provide inputs for computational infant models.

**Acknowledgements:** This research is supported by the NICHD, NIH Grant No. 1R01HD113921.

**References:** 1. Meulstee et al. (2020), International Journal of Oral and Maxillofacial Surgery 49(6); 2. Miyabayashi et al. (2022), Neurologia medico-chirurgica 62(5).

# PILOT SUMMER RESEARCH PROGRAM: HIGH SCHOOL STUDENTS EXPLORE BIOMECHANICS AT UT DALLAS

*Gu Eon Kang[1], Macie Kauffman[1], Marvin Alvarez[1], Angeloh Stout[1], Kaye Mabbun[1], Tiffany Willoughby[2]
[1]University of Texas at Dallas (UT Dallas), Department of Bioengineering
[2]UT Dallas, Office of Research and Innovation
*Corresponding author's email: GuEon.Kang2@utdallas.edu

**Introduction:** There is an increasing demand for a science, technology, engineering, and mathematics (STEM) workforce in human motion research, driven by the booming fields of assistive rehabilitation technology and humanoid robotics [1]. Yet, there is a significant lack of educational opportunities in this area, particularly for students considering it as a future major in college. This gap hinders the development of a skilled and diverse workforce equipped to meet the challenges of the future. To address this need, the Neuromuscular and Musculoskeletal Biomechanics Laboratory (NMBL), directed by Dr. Gu Eon Kang, in the Department of Bioengineering at the University of Texas at Dallas (UT Dallas), has launched a pilot summer research program for local high schoolers. This initiative introduces talented STEM-focused high school students to the dynamic field of biomechanics and human motion research, offering them unique access to state-of-the-art facilities and hands-on experience in human motion research.

**Program Overview:** The pilot program, spanning five weeks, was developed in collaboration with Ms. Tiffany Willoughby, the Associate Director for UT Dallas Research Education Program Development and Outreach in the Office of Research and Innovation. We hosted 14 rising 10th to 12th graders from a local STEM-focused high school (Harmony School of Innovation – Dallas). The program kicked off with an introductory meeting where we provided a snapshot of NMBL's work in human motion research (Figure 1) and outlined the objectives and activities planned for the research program. Two teachers from the participating high school accompanied the students, enhancing the educational support and engagement during this session.

**Figure 1.** Introductory meeting between NMBL and Harmony School of Innovation-Dallas held on February 8, 2024.

**Specific Activities:** Before participating in summer, all students have undergone Collaborative Institutional Training Initiative (CITI) training for human subject research. For the five weeks, each Monday, students attend a 45-minute research presentation followed by a 45-minute lecture on biomechanics research methods (Figure 2A). From Tuesday to Friday, students engage in hands-on human movement research, divided into four groups of 3-4 due to space limitations. Each group attends sessions twice a week, either in the morning or afternoon, guided by PhD, master's, and undergraduate students. Students were involved in data collections for several UT Dallas Institutional Review Board (IRB) approved projects: "Thinking while Moving" (UTD-IRB-22-569), "Motion and Emotion" (UTD-IRB-22-579), "Biomechanics and Energetics of Load Carriage" (UTD-IRB-23-492), "Biomechanics of Unweighted Walking" (UTD-IRB-23-570), and "Baseball Biomechanics" (UTD-IRB-23-723) (Figure 2B). On July 29, we had a ceremony to recognize the students' participation in the summer program (Figure 2C).

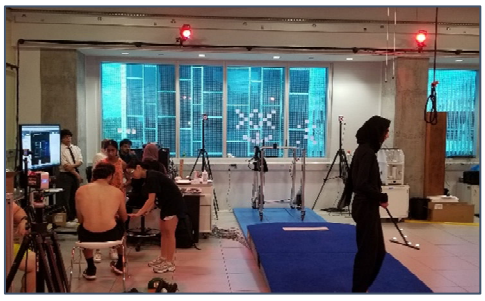

**Figure 2A (Left):** Students are participating on lectures biomechanics. **Figure 2B (Middle):** Students are assisting data collection for baseball biomechanics. The assist included calibrating motion capture cameras, anthropometric measurements, and attaching markers. **Figure 2C (Right):** On July 29, we had a ceremony to recognize Harmony students, and UT Dallas mentors.

**Implication:** At the conclusion of the pilot research program, we collected verbal feedback from the participating high school students. Overall, the responses were positive, with many students expressing that it was their first exposure to the field of human motion research and motion capture technology. On the mentors' side, experiences were mixed. A positive highlight was the opportunity to introduce students to human motion research, potentially nurturing future STEM talent. However, mentors also reported challenges, notably feeling overwhelmed by the number of students, which limited the depth and focus of interactions. In conclusion, while this pilot program marks just the beginning and there is substantial room for refinement to enhance its effectiveness and official status, it nonetheless represents a promising start.

**Acknowledgments:** We thank the high school students and teachers from the Harmony School

**References:** [1] Metcalf et al. (2013), *IEEE Trans Biomed Eng* 60(8).

# FRAMEWORK FOR DEVELOPMENT, EVALUATION, AND TRANSLATION OF BIOMECHANICS CURRICULUM

*Kayla Pariser[1,2], Amy Trauth[3,4], Margo Donlin[2,5], Laurie M. Dearolf[2], Amelia Lanier-Knarr[2], Jill Higginson[1,4], Jenni M. Buckley[12,4]
[1]University of Delaware, Institute for Engineering Driven Health| [2]The Perry Initiative | [3]American Institutes for Research
[4]University of Delaware, Dept of Mechanical Engineering | [5]Bucknell University, Dept of Mechanical Engineering
*Corresponding author's email: pariserk@udel.edu

**Introduction:** Musculoskeletal diseases impact more than one in three people in the United States, placing a heavy burden on the health care system [1]. Strengthening the STEM talent pipeline is a critical step towards solving grand challenges in musculoskeletal health, and early exposure to biomechanics in STEM curriculum can promote workforce development. Since the founding of National Biomechanics Day (NBD) in 2016, NBD has exposed over 42,000 high school students and teachers to biomechanics, increasing society awareness and interest in the field [2]. With the increased awareness and interest in biomechanics, there is a need for biomechanics curriculum that is friendly and approachable enough for teachers to incorporate into their own classroom throughout the school year. This abstract provides a framework for the development, evaluation, and translation of The Perry Initiative Orthopedics in Action® (OIA) hands-on biomechanics-themed curriculum for elementary, middle, high school, and college STEM classrooms.

**Methods:** The Perry Initiative is a nonprofit organization that hosts outreach programs targeting high school and medical students. There are 20,000+ alumni of these programs, many of whom have become surgeons and engineers [3]. OIA® stand-alone curriculum was developed in response to requests from teachers whose students attended the Perry Outreach Programs and wanted to bridge the gap between math, science, biomedical sciences, and engineering concepts. When developing OIA® curriculum the following design principles are followed: 1) flexibility to adapt to needs of students and teachers, 2) economical with as little consumable goods as possible, 3) incorporate real-world scenarios, and 4) align with national math and science standards [4]. Partnerships with the University of Delaware College of Education and Human Development and local STEM educators are essential to the curriculum development.

During the development process, each OIA® lesson undergoes pilot testing and formative evaluation from early adopter teachers through professional development workshops led by The Perry Initiative, national workshops for STEM educators such as the Project Lead the Way (PLTW) Summit, or testing in local STEM classrooms. During evaluation sessions, teachers are guided through the student exercise and then asked to provide feedback on their interest in the lesson, scaling of the lesson content for their students or course, adequacy of instructional materials, and likelihood they will adopt the lessons in their curriculum.

Curriculum translation is key to expanding the reach of OIA® lessons to more grade-levels, courses, in-person or online settings, and ultimately to more students. OIA® lessons have instructional material designed to map to different grade-levels and STEM disciplines (e.g. biology, engineering, physics, math), so teachers can choose the concepts that are appropriate for their students and courses. And with the ever-changing classroom environment, multiple OIA® lessons have been reworked to enable both in-person and online versions for teachers to more easily pivot between the two. Finally, academic partnerships with the University of Delaware, corporate partnerships such as with Sawbones, and a nonprofit partnership with PLTW have enabled increased reach by providing low-cost materials and increasing awareness of the available lessons.

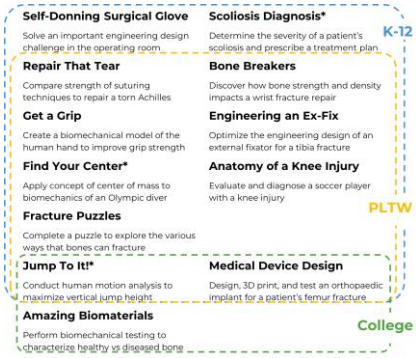


**Figure 1:** OIA® lessons currently available or in-progress, arranged by grade level and PLTW status. *Lessons with virtual options.

**Results & Discussion:** Currently there are twelve OIA® lessons available or in-progress. Nine of the lessons are designed for K-12 grades, three with college course options, three with virtual classroom options, and nine lessons are currently or in the works to be incorporated into PLTW engineering or biomedical sciences curriculum (Fig 1). Two of the lessons, Anatomy of a Knee Injury and Fracture Puzzles, have already been integrated into the PLTW Human Body Systems course and, through that partnership, now reach 165,000 high school students nationally in 1,700 schools.

Feedback from local STEM educators has been both largely positive and informative [5-6]. The Perry Initiative held an OIA® workshop at the PLTW 2024 Summit and received feedback from 100+ attendees. Comon themes from the feedback were that the teachers appreciated the interactive hands-on nature of the lessons as well as the real-world applications, and they want more lessons, especially lessons applicable to elementary and middle school grade levels. Additionally, teachers wanted to see modifications to the durable goods that correspond to the lessons. This feedback was then used to further engage our corporate partner Sawbones to brainstorm potential cost-effective changes to meet the needs of the educators.

**Significance:** To date OIA® lessons are currently being used in approximately 1,700 schools nationwide and counting. As the field of biomechanics continues to grow and gain interest at all educational levels, this framework for development, evaluation, and translation of biomechanics curriculum may guide other biomechanists in their curriculum outreach efforts. This outreach is crucial to empower workforce development in the field of biomechanics to solve grand challenges in musculoskeletal health.

**Acknowledgments:** Zimmer Biomet Foundation, Stryker Corporation, Sawbones, The Perry Initiative, NSF ART 2331440

**References:** [1] Nguyent et al. (2024), *Lancet Reg Health Am* 29; [2] DeVita. (2018), *J Biomech* 71; [3] Harbold et al. (2021), *Curr Rev Musculoskelet Med* 14; [4] NGSS Lead States (2013), *NAP*; [5] Pariser et al. (2022), *Proc of ASEE*; [6] Buckley et al. (2025), *Proc of ASEE*.

# BROADENING PARTICIPATION FOR BIOMECHANICS: IMPACT OF AN NSF-FUNDED TRAVEL AWARD

* Kurt Beschorner [1], Anna Bailes[1], Christopher Wilburn[2], Allison Altman Singles [3]
[1]Department of Bioengineering, University of Pittsburgh
[2]School of Kinesiology, Auburn University, [3] Kinesiology & Mechanical Engineering, Penn State Berks
*Corresponding author's email: beschorn@pitt.edu

**Introduction:** The American Society of Biomechanics (ASB) Annual Meeting creates an opportunity for students to learn technical skills, gain feedback when presenting their research, and develop critical network connections that can provide future collaborative or professional opportunities. However, attendance to the Annual Meeting also requires significant resources to cover travel to the meeting and the registration fee. This cost burden may be especially challenging for undergraduate students [1]. Furthermore, the size of the meeting and numerous options for programming may overwhelm first-time attendees. The benefits of attending a scientific conference have the potential to springboard a student's career with many student attendees reporting that scientific conferences can be a transformational space, especially for undergraduate students [2]. Therefore, addressing the barriers to attend a conference has the potential to create substantial individual career and societal value. The purpose of this study was to assess the impacts of a travel award funded by a new grant mechanism to support attendance at the ASB Annual Meeting through financial and professional support.

**Methods:** Twelve awardees were selected from more than 130 applicants. The awardees were selected based on a combination of financial need, broadening participation in the meeting, and potential for a positive impact on their career. Awardees received funding to support the cost of attending the meeting including travel, registration, and hotel. Awardees were expected to participate in one of two pre-meeting webinars and workshop on how to network. Participants could select between attending a webinar on how to create a presentation and poster or a webinar on how to plan attendance for the ASB Annual Meeting. The how-to-network workshop was held in person on the first day of the meeting. Also, awardees were given the opportunity to be matched with an experienced student attendee ("Conference Veterans") who would serve as a student mentor during the Annual Meeting. Awardees completed a pre-conference and post-conference survey. In the pre-conference survey, participants answered questions about their available funding and likelihood of attending the conference prior to having received the award. They were also asked to rate their skills (using a Likert Scale) in several areas including: networking, technical understanding of biomechanics, presenting research, planning goals for a conference, pursuing career opportunities, asking questions, and creating a plan for events to attend. The awardees rated these skills again during the post-award survey. In addition, the post-survey asked awardees to rate their overall satisfaction with the conference, rate the impact of the grant activities (webinar, workshop, and mentoring) on their conference experience, and to provide narrative feedback. Paired t-tests were used to analyze change in skills from the pre- and post-survey ($\alpha = 0.05$). Thematic analysis was applied to narrative responses. IRB review of the research activities was conducted, and the research was determined to be exempt under Category 4.

**Results & Discussion:** Awardees were all students (5 undergraduate and 7 graduate students) with 7 of 12 coming from non-research-intensive universities (i.e., not R1 based on Carnegie Classification). Eleven of 12 awardees were first-time attendees. Three participants were from states that were not well represented in the 2023 meeting and 5 met the criteria for being economically disadvantaged. Only 1 attendee had other funding to fully cover their expenses and 9 of 12 awardees had no other source of funding. Based on the participants assessment, significant improvements were observed for skills related to networking ($p = 0.025$), presenting research ($p = 0.042$), and pursuing career opportunities ($p = 0.039$), while other skills showed non-significant improvements (Fig. 1). The majority of awardees who attended the pre-conference grant activities rated that these events made an improvement on their ability to benefit from the conference. All participants rated being Extremely Satisfied with their conference experience. The narrative responses for suggestions for future years indicated that the awardees wished there were more opportunities for them to interact with other awardees.

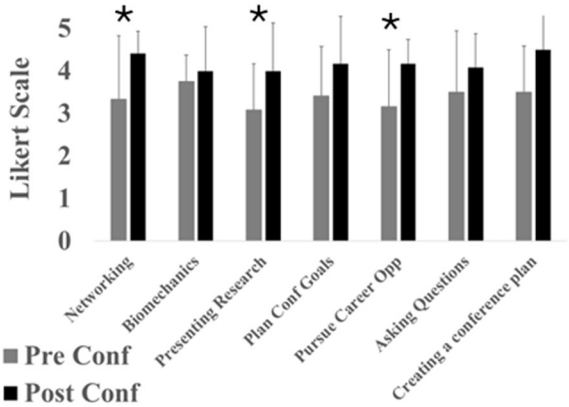


Fig. 1 Self-rating on skills in each area (5 = strongly agreed that they have necessary skills). Stars indicate significant effects.

This study characterized the benefits of financial and programming support for attending the ASB Annual Meeting. All awardees expressed high levels of satisfaction with the overall conference and with the grant activities. Awardees expressed improvements in skills for three areas- two of which were specifically targeted with grant activities (networking and how to present research). The awardees suggested more opportunities to meet with other awardees, which could be integrated into future implementations of this activity.

**Significance:** Overall, this study demonstrates the significant impact of funding support in increasing participation and professional development for first-time attendees and from groups who do not typically have the resources to attend the ASB Annual Meeting.

**Acknowledgments:** This research was supported the National Science Foundation (Grant 2421459).

**References:** [1] Caprio and Hackey (2014) *J Health Admin Ed* 31(3), 247-266; [2] Little (2020), *Educ Research* 62(2), 229-245.

**Empowerment in Motion: A Collaborative Mentoring Program for Underrepresented Scholars in Biomechanics**

*Edward Ofori[1], Jazmin Cruz[2], Elisa Romero Avila[3], Alyssa Vanderlinden[4], Jordan Barajas[1], Tiphanie Raffegeau[5]

[1]College of Health Solutions, Arizona State University, Phoenix, AZ, USA
[2]Air Force Research Laboratory, Wright-Patterson AFB, Riverside, OH, USA
[3]Rehabilitation and Prevention Engineering Department, RWTH Aachen University, Germany
[4]Department of Kinesiology, New Mexico State University, Las Cruces, NM, USA
[5]School of Kinesiology, George Mason University, Manassas, VA, USA
*Corresponding Author's Email: edward.ofori@asu.edu

**Introduction:** The lack of ethnoracial and gender diversity in STEM disciplines, including biomechanics, hampers the collective potential of scientific innovation [1]. To address these persistent disparities, the Black Biomechanists Association (BBA) in collaboration with Latinx in Biomechanix (LiB), and International Women in Biomechanics (IWB) launched the Empowerment in Motion Mentoring Program (EMMP). The mission of EMMP is to elevate and empower underrepresented scholars by providing pathways to opportunities in Biomechanics. Inspired by the "Coaches Corner" framework introduced at the 2024 annual meeting, EMMP integrates three key support roles—mentor, coach, and sponsor—to provide underrepresented scholars with comprehensive professional guidance [2]. Specifically, mentors focus on knowledge transfer and psychosocial support, coaches assist with skill refinement and goal attainment, and sponsors create advanced career opportunities. We hypothesized that a combined "multirole mentoring" approach would yield stronger professional identity, skill development, and community integration than traditional one-dimensional models.

**Methods**: In Fall 2024, the EMMP recruited participants from diverse academic and professional backgrounds. Each participant self-identified as either a mentor (faculty, industry professional, postdoc) or a mentee (undergraduate, graduate student, early-career researcher) Participants could also serve as both a mentor and a mentee. Mentor–mentee pairs were matched based on shared professional goals. Pairs committed to monthly check-ins, documented via a Google Form. Participants attended two online meetups (November 15 and March 15) and skill-focused workshops (April 2 and 4th). Initial feedback was gathered via a "Match Checkpoint" survey (n=35) until January 2025. Key metrics included communication frequency, perceived relationship quality, and satisfaction with the multirole mentoring structure.

Figure 1. Thematic Word Cloud. The word cloud indicates common themes such as resume discussions, career planning, and goal-setting.

**Results & Discussion:** Preliminary results indicated high engagement among active pairs, with over 70% of participants reporting at least one substantive meeting per month. Common discussion themes included résumé refinement, career planning, and shared goal setting (Figure 1). Pairs favoring video calls or text messaging reported stronger mentor–mentee bonds compared to those relying primarily on phone or email. This finding aligns with previous literature suggesting that multimodal communication fosters more trusting and productive mentoring relationships [1,2]. Qualitative feedback highlighted the value of exchanging research ideas, navigating academic culture, and discussing work–life balance. Early indicators suggest that the EMMP structure effectively supports meaningful mentorship for Biomechanics scholars.

**Significance:** By connecting underrepresented biomechanics scholars at all levels with experienced mentors, the EMMP promotes both individual career success and broader disciplinary inclusivity. Strengthening professional networks in this manner may have long-term benefits such as improved retention, expanded research collaborations, and heightened diversity in academic and industry positions in STEM. Facilitating career development and creating mentorship pipelines are key steps toward reducing disparities in biomechanics and allied fields [1,2].

**Acknowledgments**: We gratefully acknowledge the members of BBA, LiB, and IWB for their support and participation. We also thank all mentors and mentees for their commitment to advancing equity within the biomechanics community.

**References:** [1] Crisp, G., & Cruz, I. (2009). Mentoring college students: A critical review of the literature between 1990 and 2007. Research in Higher Education, 50(6), 525–545. [2] Pfund, C., House, S., Asquith, P., Spencer, K., Silet, K., & Sorkness, C. (2014). Training Mentors of Clinical and Translational Research Scholars: A Randomized Controlled Trial. Academic Medicine, 89(5), 774–782.

# UNDERGRADUATE EXPERIENTIAL LEARNING THROUGH BIOMECHANICS CURRICULUM DESIGN

Kayla Pariser[1,2], Amy Trauth[3,4], Amy Posch[5], Amelia Lanier-Knarr[2], Jill Higginson[1,4], Jenni M. Buckley[2,4]
[1]University of Delaware, Institute for Engineering Driven Health | [2]The Perry Initiative | [3]American Institutes for Research
[4]University of Delaware, Dept of Mechanical Engineering | [5]Sawbones - Pacific Research Labs
*Corresponding author's email: pariserk@udel.edu

**Introduction:** Multidisciplinary engineering capstone design projects have been shown to improve student confidence in their project management and teamwork skills [1]. Due to the interdisciplinary nature of biomechanics, biomechanics-themed projects are primed for this type of capstone course. Across the ASB community there are many examples of biomechanics design projects spun from non-profit, clinical, or industry partners [2-4], all of which result in a physical product for the client. While many engineering students will choose to pursue careers in industry following completion of their bachelor's degree, recently the percentage of graduate students in science, engineering, and health fields have increased [5], suggesting that undergraduate students may be interested in attaining experiences applying the design process outside of strictly standard industry product development. This abstract details a unique senior design experience sponsored by The Perry Initiative, where interdisciplinary engineering student teams at the University of Delaware (UD) were tasked to design and test biomechanics-themed curriculum for the collegiate or K-12 grade levels.

**Methods:** The mission of the Perry Initiative is to build the talent pipeline in the biomechanics sub-fields of engineering and orthopaedics through hands-on STEM curriculum [6]. In Fall 2024, The Perry Initiative sponsored two senior design projects in UD's Interdisciplinary Senior Engineering Design course: curriculum design of 1) a college level musculoskeletal tissue material characterization laboratory, and 2) a K-12 capstone project to design, 3D print, and test custom orthopaedic implants.

Students were instructed to follow the engineering design process to develop curriculum [7]. First, the students defined the problem by conducting background research into existing curriculum and by speaking with stakeholders. While The Perry Initiative was the project sponsor, both projects required the students to speak with multiple stakeholders: corporate partners Sawbones and Vernier to help build low-cost accessible materials for the lessons, nonprofit partner Project Lead the Way (PLTW) to gauge their interest in adopting the curriculum into their courses, and teachers that would potentially use the curriculum. Next, students generated conceptual designs based on their knowledge of engineering concepts like mechanical design and testing, knowledge of biomechanics concepts like bone health, and research into best teaching practices. The conceptual design phase was complex as teams created lessons to meet national science and math standards including the power points, instructional materials for teachers, and resources for the hands-on lesson components. Finally, students shared the prototyped lessons and conducted interviews with potential curriculum teachers.

**Results & Discussion:** Both project teams presented their curriculum at the Fall 2024 University of Delaware Engineering Design Celebration (Fig 1A), and the biomaterials lab curriculum was recently accepted for presentation at the American Society of Engineering Education 2025 conference [8].

In interviews, faculty interested in adopting the biomaterials lab course shared that lab content was well aligned with their bioengineering and biomechanics courses and commented that the lab logistics were affordable and feasible for use in their class labs. However, faculty requested that the design team reiterate on some of the labs to enable implementation in combined undergraduate and graduate lab courses and to refine surrogate models (Fig 1B) to better match biological tissue properties [8].

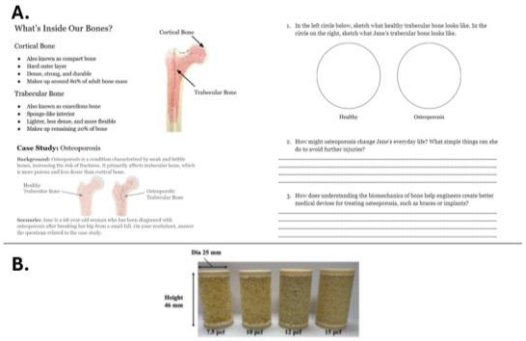


**Figure 1:** Example lesson material from the K-12 capstone medical device design course (A) and trabecular bone surrogate models for the college biomaterials laboratory (B).

The student team working on the K-12 capstone curriculum similarly received positive and informative feedback and is in conversation with PLTW to implement the lessons into their Medical Interventions course. In interviews with PLTW teachers, they said the content fully met the national science and math standards and would be compatible to pair with their current lessons. One teacher described the lessons as "very engaging" and another as "challenging but doable for students."

In addition to feedback on the curriculum from stakeholders, it is important to note that although the Interdisciplinary Senior Engineering Design course at UD is only one semester, both student teams have elected to return in the Spring 2025 semester to continue to perfect the lessons as an independent study course. This continued student interest may suggest that engineering students find value in experiential learning opportunities to apply the design process to biomechanics curriculum design.

**Significance:** Two student teams at the University of Delaware engaged in a unique engineering interdisciplinary design project to design biomechanics-themed curriculums. While both lesson plans are still in progress, the lessons have received overwhelming positive feedback from health science and engineering educators. Based on the early success of these projects, future work will seek to replicate this unique senior design experience to provide biomechanics and engineering students design of curriculum experience.

**Acknowledgments:** Engineering design conducted by 2024 Senior Engineering Team Members Aisley Bergdoll, Kyle Crawford, Nikos Demetriou, Laura Weinstein, Diana Lara-Ruiz, Ellie Stevens, Kylie Taylor, and Benjamin Yaroch; NSF ART 2331440

**References:** [1] Buckley et al. (2005), *ASEE Proc.*; [2] Shaw (2024), UDayton Magazine; [3] Haessler (2016), DU News; [4] Lauria (2022), UDaily; [5] NGSS Lead States (2013), NAP; [6] Harbold et al. (2021), Curr Rev Musculoskelet Med 14; [7] Buckley et al. (2017) *ASEE Proc.*; [8] Buckley et al. (2025) *ASEE Proc.*

# PRE-CONFERENCE ACTIVITIES FOR BIOMECHANICS TRAINEES: IMPACT OF NSF FUNDED PROGRAMMING

*Anna H. Bailes[1], Sarah Hemler[2], Kurt Beschorner[1]
[1]Bioengineering, University of Pittsburgh; [2]Unit of Therapeutic Patient Education, Faculty of Medicine, University of Geneva
*Corresponding author's email: anb254@pitt.edu

**Introduction:** Over 40% of members in the American Society of Biomechanics (ASB) are students. Student involvement in ASB is highly prioritized as part of the organization's culture. Dedication to student concerns is evidenced by the election of a student member to the Executive Board, who among other responsibilities, plans and executes student-related events at the Annual Meeting. Academic conferences such as the ASB Annual Meeting provide students with excellent opportunities for building networking connections and gaining feedback on their research. Capitalizing on conference opportunities requires specialized skills that new attendees often lack, including selecting and prioritizing conference activities, science communication, and networking. These required skills are sometimes described as a 'hidden curriculum,' professional and social norms that are not explicitly stated. The hidden curriculum can be elusive, especially for new conference attendees or those from diverse groups who have been previously excluded from science.[1] Previous studies have identified strategies that explicitly explain these professional and social norms to help students uncover the 'hidden curriculum.'[2] The purpose of this study was to evaluate the impact of using those strategies at the 2024 ASB Annual Meeting. Specifically, we implemented and measured the impact of three pre-conference activities developed to prepare students to 1) present their research, 2) navigate the Annual Meeting, and 3) develop a networking strategy.

**Methods:** Pre-conference programming consisted of three distinct events. A virtual webinar was held 2.5 weeks prior to the Annual Meeting, consisting of both instruction and reflection exercises intended to help students build skills in presenting their research. Next, a virtual Q&A panel was held 1.5 weeks prior to the Annual Meeting, which covered logistics of navigating the meeting. The final aspect of pre-conference programming included an on-site workshop the day prior to the Annual Meeting. The workshop focused on strategies for networking and opportunities to practice with peers through development of an 'elevator pitch.' After each pre-conference event, attendees were encouraged to complete a post-survey which included questions on satisfaction with the event (5-point Likert scale) and likeliness to implement new conference preparation strategies (3 response options: unlikely to implement changes, likely to implement small changes, likely to implement substantial changes). The Q&A panel post-survey also probed self-perceived conference preparedness before and after the panel. A McNemar-Bowker test was used to determine differences in reported preparedness before and after the panel. Surveys also included text options to provide feedback, which were assessed using informal thematic analysis. The study was approved as Exempt (Exemption #4) by the University of Pittsburgh Institutional Review Board.

**Results and Discussion:** Eighty-three participants attended the webinar, 25 attended the virtual Q&A panel, and approximately 50 attended the pre-conference workshop. The response rate for the post-survey was 57%, 68%, and ~48% for the webinar, panel, and workshop respectively. More than one-third of responders for each event identified themselves as being an ASB travel award recipient, suggesting that those who were prioritized for awards were especially likely to take advantage of these opportunities. The majority of responders reported that they were 'somewhat' to 'extremely' satisfied with pre-conference events and were likely to implement either 'small' or 'substantial' changes to their conference preparation based on learned techniques (Table 1). Attendee responses indicated that there was a significant increase ($\chi^2$=9.0, $p<0.01$) in attendees' perceived preparedness following the Q&A panel, with 100% indicating that they felt 'somewhat' or 'very well' prepared for the Annual Meeting at the conclusion of the panel. Based on open text responses, it appeared that attendees appreciated opportunities for skills practice (e.g., elevator pitches) and shared examples (e.g., good and bad posters). Several attendees included comments referencing their appreciation for techniques to reframe negative thinking surrounding networking and presenting. For example, they found it helpful to think about "serv[ing] the audience" rather than "try[ing] to survive…the presentation without messing up." As with any survey-based study, this study was limited by non-response bias and social desirability bias.

*Table 1: Results of survey data: number of participants with given response (% of responders with given response).*

| | Webinar (47 responders) | Panel (17 responders) | Workshop (24 responders) |
|---|---|---|---|
| Overall satisfaction | Extremely: 39 (83%)<br>Somewhat: 7 (15%)<br>Neither satisfied nor dissatisfied: 1 (2%) | Extremely: 12 (71%)<br>Somewhat: 5 (29%)<br>Neither satisfied nor dissatisfied: 0 | Extremely: 19 (79%)<br>Somewhat: 4 (17%)<br>Neither satisfied nor dissatisfied: 1 (4%) |
| Likeliness to implement changes | Substantial: 19 (40%)<br>Small: 25 (53%)<br>Unlikely: 3 (6%) | Substantial: 5 (29%)<br>Small: 10 (59%)<br>Unlikely: 2 (12%) | Substantial: 9 (38%)<br>Small: 14 (58%)<br>Unlikely: 1 (4%) |
| ASB award recipients | 17 (36%) | 6 (38%)* | 11 (46%) |

*n=16 responders

**Significance:** This study suggests that a series of pre-conference events were both engaging to trainees and enhanced their conference preparation, especially through opportunities for skill practice and thought reframing. Events such as these may help to build a more transparent culture in academic societies through explicit detailing of the 'hidden curriculum,' especially for newer attendees or students with minimal mentorship or institutional opportunities.

**Acknowledgments:** This research was supported the National Science Foundation (Grant 2421459).

**References:** [1] Caro-Diaz, et al., (2024), *J Natural Prod* 38(3); [2] Enders, et al., 2021, *J Clin and Trans Sci*

# WHY MENTOR UNDERGRADUATE RESEARCHERS IN BIOMECHANICS?

David A. Phillips[1*], Jacob W. Hinkel-Lipsker[2], Craig M. Goehler[3], Allison R. Altman-Singles[4], Michael V. Potter[5], Mukul C. Talaty[6], Brooke M. Odle[7], and Kimberly E. Bigelow[8]

[1]Oregon State University, Cascades; [2]California State University, Northridge; [3]University of Notre Dame; [4]Penn State Berks; [5]Francis Marion University; [6]Penn State Abington; [7]Hope College; [8]University of Dayton

*Corresponding author's email: david.phillips@osucascades.edu

**Introduction:** It has been established that involving undergraduates (UGs) in research is beneficial for students, faculty, and institutions alike [1]. Benefits to students consist of increased confidence, improved overall academic performance, and identifying career preferences [2]. Faculty benefit from undergraduate research due to its contribution to their teaching, scholarship, and self-satisfaction [3]. Institutions note a major benefit from undergraduate research is increased student and faculty engagement, along with increased student success and retention [1]. Previous work has evaluated these benefits in a broad range of undergraduate research topics [1,2]. However, little is known regarding the motivations of investigators to get involved in mentoring undergraduate research. In addition, biomechanics presents some unique opportunities and challenges in undergraduate research that warrant additional study into metrics of student achievement [3]. The purpose of this study was to assess a broad range of perspectives within the biomechanics field regarding the motivation to mentor undergraduate researchers and benchmarking methods for undergraduate researchers' achievements. A greater understanding of motivation and benchmarking methods may provide more clarity for aspiring undergraduate research mentors and institutions when structuring opportunities and measuring success in biomechanics.

**Methods:** Data on UG recruitment methods and engagement practices were collected via a survey distributed through various biomechanics community channels and completed online by individuals identifying as a primary investigator (PI) with UGs participating in their lab. From this larger survey, open-ended questions were used to probe PI's perspectives in motivations to perform mentorship of undergraduate research, goals/success criteria for undergraduate researchers, and intangible outcomes for undergraduate researchers. Nineteen PIs answered at least one of the open-end questions. Each author reviewed each qualitative response and identified if a theme was present in the response. The mean and standard deviation for the number of times each authors identified a theme were calculated and the spread of observations were visualized in box and whisker plots.

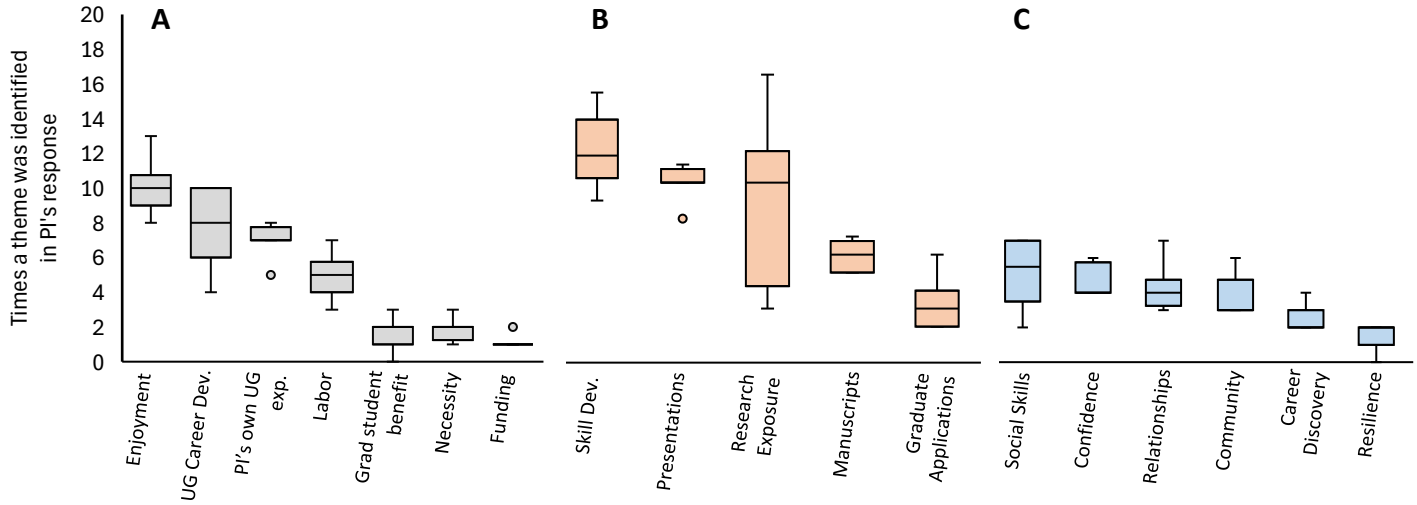


Figure 1: Number of times a theme was identified in a PI's response. **A** represents PIs' motivations for engaging UGs, **B** represents the subjective goals and success criteria for UGs, and **C** represents the intangible outcomes from participating in research. A larger spread of data represents less agreement between the authors.

**Results & Discussion:** PIs were primarily motivated to engage UGs from their own enjoyment of the process, to provide career development opportunities for UGs, and from their own UG research experience (Fig 1A). PIs specifically want UGs to develop new skills and provide opportunities to present their work (Fig 1B). Lastly, PIs identified social skills and relationships to be important intangible benefits of UGs participating in research (Fig 1C).

**Significance:** PIs that engage undergraduates primarily do so from intrinsic motivations (their own enjoyment and personal UG experience) and altruism – prioritizing skill and career development – over tangible outcomes which benefit the PI such as laboratory labor and manuscripts. This qualitative data implies a feedback loop where if a PI engaged in UG research, they may also then engage UGs in their own careers. It is therefore important that institutional policies support the inclusion of UGs in biomechanics research laboratories and provide PIs sufficient resources to support the future development of PIs in biomechanics research.

**References:** [1] Malachowski (2019), *Scholarship and Practice of Undergraduate Research* 3; [2] Haeger (2020), *SPUR* 3; [3] Altman-Singles (2023), *J Biomech 159*.

# INTEGRATING FTIDR-BASED PRESSURE MAPPING AND REAL-TIME VISUALIZATION IN FORCE DISTRIBUTION

Debadutta Subudhi [1], Vimal Chander [2], Manivannan[3]
[1 2 3] Indian Institute of Technology Madras
dev.subudhi49@gmail.com[1], am22d008@smail.iitm.ac.in [2], mani@smail.iitm.ac.in[3]

**Introduction:** This study introduces a novel force distribution plate based on frustrated total internal reflection (FTIR) [1, 2]. The medium through which light gets frustrated is generally made up of an rubber layer through which light gets frustrated by the applied force [3]. It employs the exponential decay of evanescent waves to measure force distribution [3]. The existing literature lacks sensitivity in lateral deformation. We employ an elastomeric composite, constituting Ecoflex 00-31 and processed bubbles embedded inside it for improving all-around sensitivity in normal and lateral direction of loading. The thinning of films in the bubble with loading causes destructive interference of light thereby changing it's intensity measured by the vision system. Therefore, the principle is coined as frustrated total internal destructive reflection (FTIDR). This approach enables real-time pressure mapping and visualization. This method addresses challenges in performance optimization in sports, clinical areas like gait analysis and physiological assessment.

The study is based on the hypothesis that integrating a bubble composite layer into an FTIDR-based pressure mapping system will significantly enhance its sensitivity and dynamic range. In particular, we propose that:

- Develop a real-time system utilizing **Frustrated Total Internal Destructive Reflection (FTIDR)** based sensing to detect and quantify force distributions, and translate pixel intensity variations into precise pressure mappings across a surface.

The transition from FTIR to FTIDR is driven by the need for improved sensitivity and dynamic range in force detection. Traditional FTIR measures changes in light intensity as an object disrupts total internal reflection, but its response can be limited when it comes to capturing subtle or dynamic force variations.

In this study, the following key parameters are measured:

- Light intensity changes, contact area, distribution of light intensity, Calibration Data (Force vs. Intensity), Force Resolution and Sensitivity

These measurements collectively enable the translation of optical signals into precise pressure maps, which are critical for both dynamic load analysis and applications in various fields such as space exploration, sports and clinical areas.

**Methods:** A multilayer optical assembly where a white-foam layer is combined with a bubble composite (clear elastomer embedded with 0.5 mm spherical bubbles) to allow large deformations near the foam. This design enhances the disruption of light, transitioning the system from FTIR to FTIDR.

Use of a collimator and camera to capture pixel-level light intensity variations. As force is applied, the deformation of the bubbles leads to changes in light scattering and interference patterns, which are recorded and analyzed.

Calibration of the system by correlating known forces with corresponding changes in light intensity. This calibration facilitates the quantitative conversion of optical signals into pressure values.

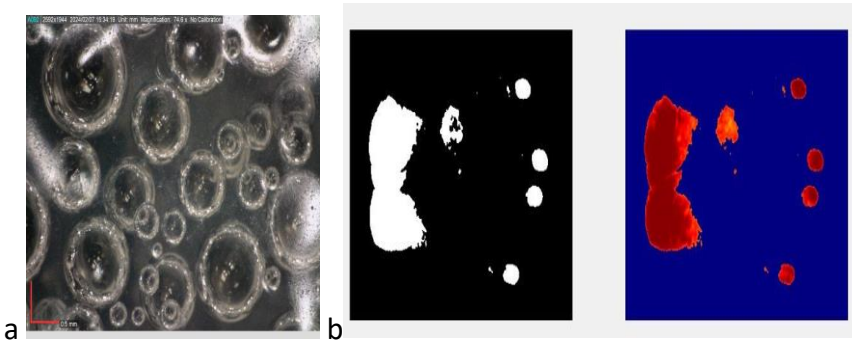


**Figure 2: a. Distribution bubbles in the elastomer b. Lateral glitches from FTIDR**

Application of mathematical models such as using the Laplacian of the intensity to extract detailed pressure distribution maps from the optical data.

$$p(x,y) = K \cdot \nabla^2 I(x,y)$$

This integrated approach not only heightens sensitivity during dynamic loading but also improves the spatial resolution of the force mapping, thereby overcoming limitations inherent in traditional FTIR techniques.

**Results & Discussion:** Our experiments focused on mapping foot pressure distribution using the FTIDR system. Tests with hand loads showed that the bubble composite layer dramatically enhances the sensitivity, enabling high-resolution pressure maps that clearly delineate pressure hotspots from fingertip and palm. The FTIDR approach is highly effective for detailed foot pressure mapping, offering significant improvements over conventional techniques.

**Significance:** The presented FTIDR-based sensing system offers a robust, real-time solution for pressure mapping in improving posture and injury prevention in sports and clinical area like gait lab. By providing detailed, quantifiable insights into force distributions, this method paves the way for advancements in both applied biomechanics and optical sensing technologies.

**References:**

[1] Zhu et al. (1986), *American Journal of Physics* 54.7. [2] Bland et al. (2005), *Journal of Optical Technology, 25(3)*. [3] Sharp et al. (2018), *Physical Review Applied* 10.3.

# DO STIFFER FOOT ARCHES IMPROVE TOP SPRINT SPEED?

*Kamen Wong [1], Hui Tang, Gautam Penna, & Owen N. Beck
[1]Department of Kinesiology and Health Education, The University of Texas at Austin, TX
*Corresponding author's email: kamenwong1@utexas.edu

**Introduction:** A sprinter's speed is the product of the step length and step frequency. To attain faster top speeds, sprinters primarily increase step length by generating greater vertical ground reaction forces (vGRF) relative to body weight (BW) [1]. A potential way to further improve lower-limb force production and augment top speed is to reduce lower-limb muscle shortening velocities during stance [3]. Slower muscle fiber contractions may be enacted by increasing foot stiffness, which shifts the center of pressure anteriorly and lengthens the ankle-to-ground reaction force moment arm during stance. This enhanced 'gear ratio' reduces plantar flexor muscle shortening velocity per unit mechanical power and increases force output per unit activation [4]. Here, we seek to determine whether stiffening the foot via socks that increase transverse arch curvature enhances top sprint speed. Increasing the curvature of the transverse arch stiffens the entire foot [5]. We hypothesized that wearing socks that stiffen feet will increase lower limb ground force production, increase step length, and improve top sprint speed.

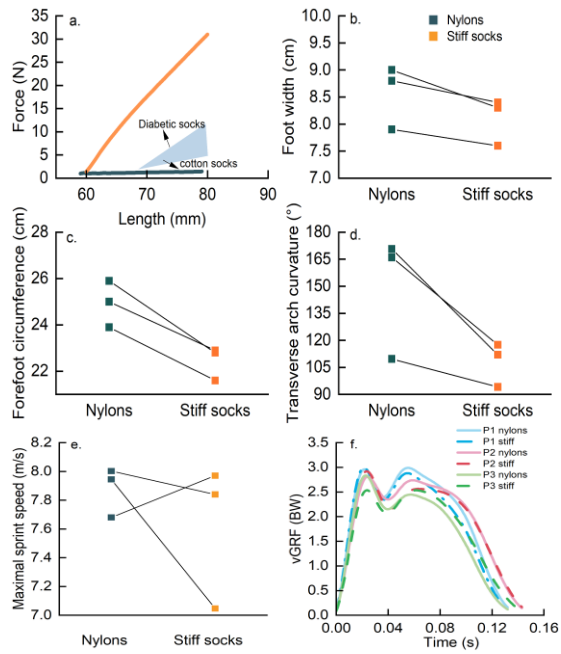


**Figure 1.** a) force–length profiles for 4 socks. b) Foot width, c) forefoot circumference, and d) transverse arch curvature for nylon and stiff socks. E) Top over-ground sprint speed of each participant (squares). f) vertical ground reaction force in units of body weight (BW) of each participant for each sock condition.

**Methods:** Three recreational athletes participated (mean ± SE: age: 22.7 ± 1.8 yrs; height 174.0 ± 3.8 cm; mass: 85.1 ± 5.1 kg). We tested their overground top speed and treadmill running biomechanics in two conditions: shod with nylon socks and shod with stiff socks—custom socks that increase user transverse arch curvature (Fig. 1). Participants wore standard shoes without arch support for all conditions (Converse, MA). Each participant performed two trials per condition (A: nylon, B: stiff) in a counterbalanced order (n=2 ABBA & n=1 BAAB). We performed mechanical testing on stiff socks, nylons, diabetic socks, and everyday cotton socks. Before sprint testing, we measured participant foot width, circumference, and transverse arch curvature for each condition. After a brief warm-up, participants sprinted 45 m in a corridor, while a sagittal plane camera recorded running speed between 38 - 42 m. Participants rested for ≥6 min between trials. Next, participants ran on the force-measuring treadmill for at least 20 steps at 3, 4, 5, 6, and 7 m/s. We computed ground reaction forces and stride kinematics during treadmill running in each condition.

**Results & Discussion:** Stiff socks modified foot and running mechanics. The stiff socks were the stiffest, followed by the diabetic, cotton, then nylon socks (Stiff: 1.46, Diabetic: 0.13, Cotton: 0.10, Nylons: 0.02 N/m) (Fig. 1). Compared to the nylons, stiff socks reduced user foot width by 4.1% ± 2.3% (mean ± SE), forefoot circumference by 10.0% ± 1.1%, and transverse arch curvature by 25.9 ± 6.1% (Fig. 1). One participant improved top sprint speed in stiff socks vs. nylons, but on average, top sprint speed in the stiff socks was slower than in the nylons (Nylons: 7.94 ± 0.1 vs. Stiff: 7.75 ± 0.3 m/s). Running in stiff socks reduced stance average vGRF across all submaximal speeds. Participants also exhibited greater step frequencies, aligning with the theory that faster sprint speeds are primarily driven by longer steps via greater vGRFs, rather than shorter, more frequent steps [1].

**Table 1.** Running biomechanics in nylons and stiff socks at 7 m/s.

| Athlete | Contact time (s) | | Step length (m) | | Step Frequency (Hz) | | $vGRF_{avg}$ ($vGRF_{avg}$ / BW) | | Duty Factor | | Leg Stiffness (kN/m) | |
|---|---|---|---|---|---|---|---|---|---|---|---|---|
| | Nylon | Stiff | Nylons | Stiff | Nylons | Stiff | Nylons | Stiff | Nylons | Stiff | Nylons | Stiff |
| P1 | 0.134 | 0.124 | 1.92 | 1.86 | 3.65 | 3.77 | 2.74 | 2.68 | 0.49 | 0.47 | 13.3 | 15.6 |
| P2 | 0.144 | 0.146 | 1.88 | 1.82 | 3.73 | 3.85 | 2.61 | 2.51 | 0.54 | 0.56 | 10.6 | 10.5 |
| P3 | 0.130 | 0.136 | 1.65 | 1.68 | 4.24 | 4.17 | 2.42 | 2.35 | 0.55 | 0.57 | 18.1 | 15.9 |

**Significance:** Stiffer shoes, such as through the inclusion of carbon fiber soles, increase top speed [6], suggesting that stiffening the transverse foot arch using our custom socks may have similar benefits. By examining whether foot stiffness enhances sprint speed, our study can help optimize athletic footwear design.

**Acknowledgements:** We thank 361° Ltd. for providing the stiff socks.

**References:** [1] Weyand et al. (2000), *J. Appl. Physiol. 89*(5), 1991–1999. [2] Miller et al. (2012), *J. Biomech. 45*(6), 1092–1097. [3] Hill (1997), *Proc. R. Soc. Lond. Ser. B. Biol. Sci.* 126(843): 136-195. [4] Ray & Takahashi (2020), *Sci. Rep. 10*(1), 8793. [5] Venkadesan et al. (2020), *Nat. 579*(7797), 97–100. [6] Robert et al. (2018), *J. Sports Sci. 6*(4).

# SEGMENTAL FOOT KINEMATICS ARE ALTERED IN INDIVIDUALS WITH DIABETES, EVEN WITHOUT DIABETIC NEUROPATHY

Roya Hoveizavi[1]*, Simon J. Fisher[2], Joshua C Joiner[3], Johnathan D. Martin[4], Fan Gao[4]
[1] Department of Kinesiology, California State University- Sacramento, Sacramento, CA
[2] Division of Endocrinology, Diabetes and Metabolism, Dept. of Internal Medicine, University of Kentucky, Lexington, KY
[3] Department of Orthopaedic Surgery and Sports Medicine, College of Medicine, University of Kentucky, Lexington, KY, USA,
[4] Department of Kinesiology and Health Promotion, University of Kentucky, Lexington, KY, USA
*Corresponding author's email: roya.hoveizavi@csus.edu

**Introduction:** Diabetes-related alterations in foot kinematics are increasingly recognized as significant contributors to compromised foot function, potentially precipitating complications such as elevated plantar pressure, ulceration and amputations. However, the extent of these changes in intrinsic foot mobility and their relationship to altered gait biomechanics in individuals with diabetes remains unclear. This study utilizes a comprehensive multi-segment foot and lower extremity model to examine gait kinematics and kinetics in individuals with diabetes without neuropathy (DM) and non-diabetic controls (CON).

**Methods:** Eleven individuals with type 2 diabetes mellitus (DM), without a history of diabetic neuropathy (53 ± 11 yrs.; 87 ± 16 kg; HbA1C, 7.37±1.80; duration of disease 75±79 months), and 13 non-diabetic controls (CON, 46 ± 16 yrs.; 76 ± 14 kg) were recruited. Gait analysis was conducted using a three-dimensional motion capture system and force platforms during 20 barefoot walking trials at a fixed speed (0.89–0.9 m/s). A four-segment foot model (hindfoot, midfoot, forefoot, and metatarsals) was implemented. Statistical parameter mapping (SPM1d) was applied to compare time-dependent kinematic and kinetic profiles throughout the entire gait cycle (GC).

**Results & Discussion:** As compared to the CON group, DM showed significantly decreased stride length (p=0.024), increased hip flexion (0-20% GC; p = 0.032 and 75-100% GC; p= 0.028), increased calcaneal eversion (0-45% GC; p=0.004, and 68-100% GC; p= 0.013), increased midtarsal dorsiflexion (15-25% GC; p= 0.042, and 35-82% GC; p=0.003), and increased tarsometatarsal plantarflexion (10-47% GC; p= 0.024). These findings, particularly the reduced step length and increased calcaneal eversion, indicate a shift toward a more conservative gait strategy, highlighting challenges in maintaining dynamic stability in individuals with diabetes. The presence of these alterations despite the absence of neuropathy suggests that factors, such as muscle-tendon stiffness or early neuromuscular changes associated with diabetes, may contribute to these gait adaptations. Early identification of these biomechanical changes could guide the development of targeted interventions to improve gait function and overall mobility in this population.

**Significance:** This study demonstrates altered multi-segment foot kinematics in individuals with diabetes before the onset of neuropathy, suggesting that gait impairments may arise in the early stages of diabetes. These findings indicate that factors beyond neuropathy may contribute to gait deterioration in those with diabetes. Recognizing these biomechanical changes early could inform targeted interventions to preserve foot function, enhance stability, and reduce the risk of complications such as ulceration or amputation.

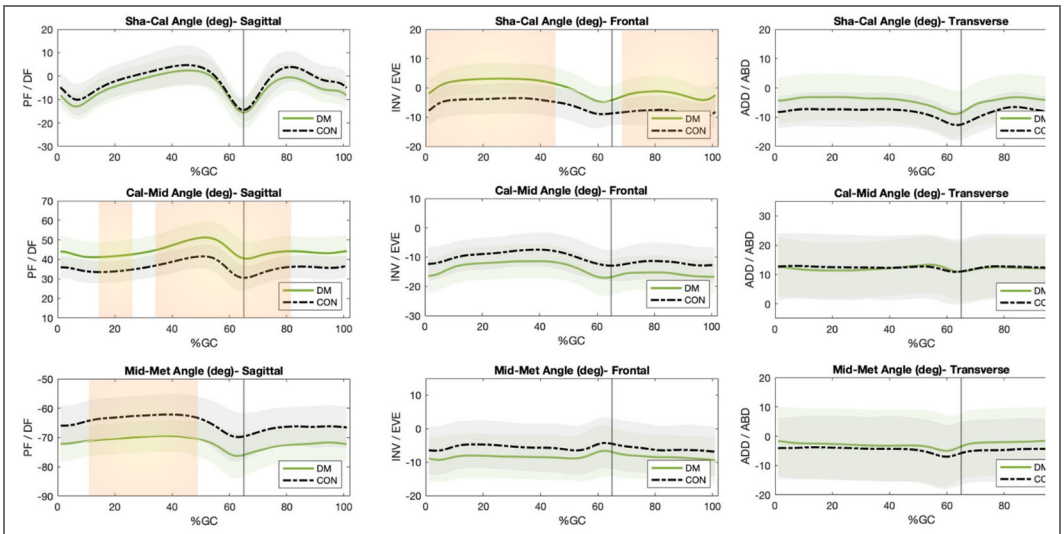


**Figure 1:** Foot angles (degrees) and the corresponding SPM1d results shown on the bottom of each foot kinematic graph. Results are shown as mean values shaded by the standard deviation for DM (solid line) and CON (dashed line). The highlighted region is significant at 0.05 level.

**Acknowledgments:** This work was supported by the teaching assistantship provided by the department of Kinesiology and Health Promotion at the University of Kentucky (to RH), in part by the National Institute of Diabetes and Digestive and Kidney Disease (R01DK118082 to S.J.F.), and the Barnstable Brown Diabetes Center and University of Kentucky Diabetes and Obesity Research Priority Area (to S.J.F).

**References:** [1] Sacco, I., et al., *Role of ankle mobility in foot rollover during gait in individuals with diabetic neuropathy.* Clinical Biomechanics, 2009. **24**(8): p. 687-692. [2] Rao, S.R., et al., *Increased passive ankle stiffness and reduced dorsiflexion range of motion in individuals with diabetes mellitus.* Foot & ankle international, 2006. **27**(8): p. 617-622. [3] Rao, S., C.L. Saltzman, and H.J. Yack, *Relationships between segmental foot mobility and plantar loading in individuals with and without diabetes and neuropathy.* Gait & posture, 2010. **31**(2): p. 251-255.

# WEARING SOCKS THAT STIFFEN FOOT ARCHES REDUCE THE METABOLIC COST OF WALKING

Hui Tang*& Owen N. Beck
Department of Kinesiology and Health Education, The University of Texas at Austin, TX
*Corresponding author's email: hui.tang@utexas.edu

**Introduction:** Humans have pronounced foot arches that are thought to facilitate walking [1]. Transverse tarsal and medial longitudinal arch mechanics interact, such that increasing transverse arch curvature stiffens the longitudinal arch [2]. Walking with stiffer foot arches better resist deformation, which in turn reduces net mechanical energy dissipation. As such, walking with stiffer feet requires less net mechanical work from metabolically active leg muscles [3]. Stiffer arches may also increase the ankle's gear ratio, increasing ankle muscle force production and reducing ankle muscle shortening velocity per unit mechanical power [3-4].

The goal of this study was to determine whether transverse tarsal foot arch curvature affects walking mechanics and metabolism. To accomplish our goal, we tested participants walking with and without custom 'stiff socks' that increase user transverse arch curvature. We hypothesized that walking in stiffer socks would reduce leg muscle activation and metabolic cost during walking compared to compliant 'Nylon' socks.

**Methods:** Twelve young adults participated (Avg ± SE: age: 28 ± 5 yrs; height: 1.76 ± 0.08 m; mass: 81.15 ± 12.8 kg). Each participant performed 5-min walking trials at 1.25 m/s on a force-instrumented split-belt treadmill in two conditions: shod with nylon socks 'nylons' and shod with 'stiff socks' that are tight about the user's transverse arch. Participants wore standard shoes without arch support for all conditions (Converse, MA). Each participant performed two trials per condition in a counterbalanced order (n=6 ABBA & n=6 BAAB). Prior to treadmill walking, we measured each participant's foot width and circumferences about the metatarsophalangeal joint with no load. During each walking trial, we collected motion capture, ground reaction force, electromyography (EMG), and metabolic data.

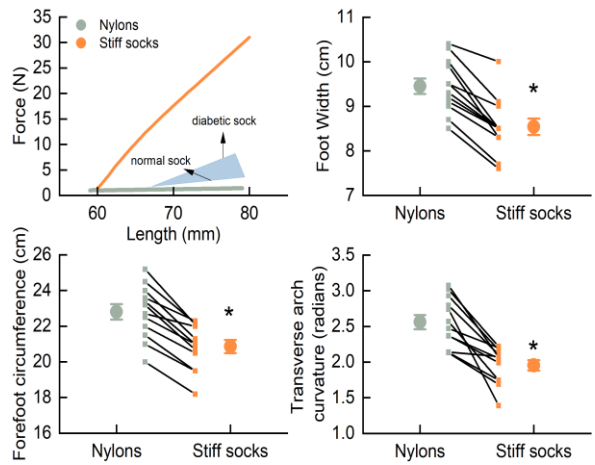


**Figure 1. Mechanical and foot stiffness in nylons and stiff socks.** a) Force-length profiles of four kinds of socks in tensile testing, where shaded triangle indicates diabetic and normal sock range. b-d), Avg ± SE and individual data of foot width, forefoot circumferences, and transverse arch curvature in nylons and stiff socks.

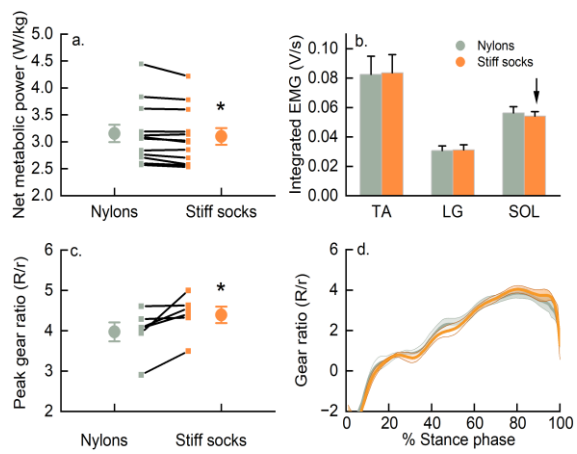


**Figure 2. Participant walking performance in nylons and stiff socks.** a) Avg ± SE and individual data of net metabolic power, b) average muscle activation rates of tibialis anterior, lateral gastrocnemius and soleus; c) Avg ± SE and individual data of peak ankle gear ratio; d) ensembled curve of gear ratio during walking stance phase.

**Results & Discussion:** Wearing stiff socks modified foot mechanics and reduced user whole-body metabolic cost during walking. Stiff socks reduced user foot width 9.6 ± 3.7% ($d = 2.42$, $p < 0.001$) and forefoot circumference by 8.5 ± 2.7% ($d = 2.84$, $p < 0.001$) compared to nylons. Stiff socks increased user transverse arch curvature 17.11 ± 7.03% ($d = 1.31$, $p < 0.001$) compared to nylons (Fig. 1). Ten out of 12 participants expended less net metabolic power in stiff socks than nylons, with a reduction of 1.95 ± 0.54% across all 12 participants ($d = 0.93$, $p = 0.008$) (Fig. 2). Biomechanically, both conditions had insignificant differences in the following ankle mechanics: moment (average: nylons: 0.64 ± 0.03 vs. stiff socks: 0.60 ± 0.04 Nm/kg; peak: nylons: 1.66 ± 0.07 vs. stiff socks: 1.62 ± 0.03 Nm/kg), peak mechanical power (nylons: 3.90 ± 0.37 vs. 3.71 ± 0.02 W/kg), peak angular velocity (nylons: -5.90 ± 0.25 vs. stiff socks: -5.72 ± 0.31 radian/s), and mechanical work rate (positive: nylons: 0.40 ± 0.04 vs. stiff socks: 0.41 ± 0.02 J/s/kg; negative: nylons: -0.55 ± 0.05 vs. stiff socks: -0.51 ± 0.08 J/s/kg). Notably, stiff socks increased the ankle's peak gear ratio compared to the nylon condition ($d = 1.10$, $p = 0.043$) (Fig. 2), without detectable differences in tibialis anterior, lateral gastrocnemius, or soleus muscle activation (Fig. 2). Overall, walking in socks that increase user transverse arch curvature reduced the metabolic cost of walking by ~2%, with minimal changes to ankle neuromechanics.

**Significance:** Socks that increase user transverse arch curvature facilitate walking. Thus, socks that accentuate the evolved mechanics of human feet may enable users walk using less effort in their daily lives.

**Acknowledgements:** We thank 361° Ltd. for providing the stiff socks.

**References:** [1] Welte et al. (2018) *J R Soc Interface* (145). [2] Venkadesan et al. (2020), *Nature*, 579(7797). [3] Takahashi et al. (2016), *Sci Rep.* (6). [4] Davis & Challis (2024), *Comput Methods Biomech Biomed Engin*. 1-12.

# DECREASED LOWER-LIMB MUSCLE ACTIVATION IN ADVANCED FOOTWEAR TECHNOLOGY

* Iain Hunter, Adam Wood, Luke VanKeersbilck
Brigham Young University, Provo, UT
*Corresponding author's email: iain_hunter@byu.edu

**Introduction:** Since the Nike Vaporfly 4% debuted in 2017 with its claims of improved running economy [1], running shoe innovation has surged, creating a category known as advanced footwear technology (AFT). World Athletics rules allow these shoes to have a curved carbon fiber plate, up to 40 mm of responsive foam, and a pronounced toe rocker. Such design elements have been linked to a 0.9–4% improvement in running economy [1,2,3] across speeds from 10 km/h to 18 km/hr, with elite marathoners shaving roughly 2% off race times [4].

One possible mechanism involves muscle energetics, where oxygen consumption is tied to motor unit recruitment. In elite runners, the triceps surae muscles contribute about 25% of total energy expenditure—rising to nearly 40% in less-trained athletes [5]. Thus, AFT shoes may improve running economy by reducing motor unit recruitment and muscle activation. This study compares muscle activation patterns between AFT and traditional racing flats, hypothesizing that decreased muscle activation underlies the lower energy cost of running.

**Methods:** Following a five-minute warmup, twenty-one men completed runs on an instrumented treadmill at 3.35 m/s and 4.46 m/s with force (1000 Hz) and EMG (2000 Hz) data being recorded for 30 s. Two shoe conditions were utilized, one in a control shoe (Saucony Type A) and another in AFT (Saucony Endorphin Pro3) across the two running speeds. The total of four conditions were completed in random order and replicated during the same data session.

The ground contact time, stride rate, peak force normalized to subject mass, and muscle activation were measured and averaged over 30 seconds. The two trials of each shoe and speed condition were averaged and included in linear models with shoe, speed, and subject as factors. Alpha was set at 0.05.

**Results & Discussion:** Peak force, ground contact time, and stride rate all changed significantly with running speed, but not by shoe condition. Only the gastrocnemius and soleus showed significant decreases in muscle activity during the EP condition. All muscles showed significant increases in activity during the faster running. With a large amount of oxygen uptake being connected with triceps surae activity, the decreased activity observed in this study could explain much of the metabolic savings associated with AFT footwear.

With triceps surae activity being smaller, there could be a need to provide some extra loading in that area when AFT shoes are worn regularly in training to avoid muscle and tendon atrophy. This may be added with strength training, hill running, or other modalities that provide an overload.

Runners should also consider whether AFT shoes should be used primarily for racing and not training while using more traditional shoes for training in order to maintain neuromuscular strength.

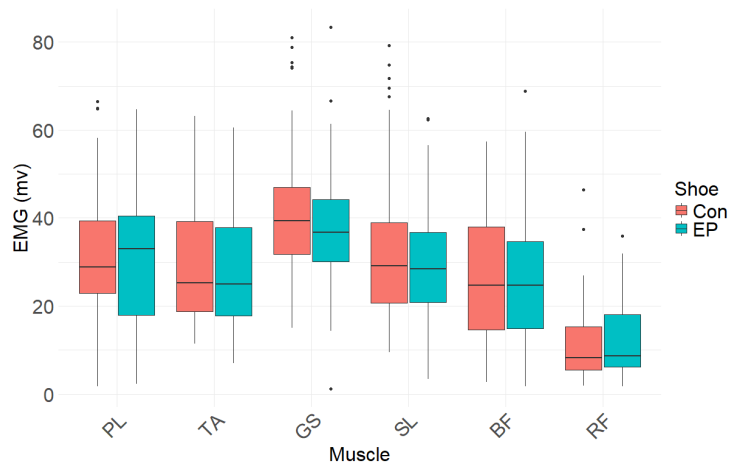


**Figure 1:** Muscle activity between shoe conditions. Peroneus longus (PL), tibialis anterior (TA), gastrocnemius (GS), soleus (SL), biceps femoris (BF), rectus femoris (RF). Significant differences observed for GS and SL.

**Significance:** The difference in muscle activity while wearing AFT shoes is through the triceps surae musculature. While future research will be needed to get at the reasons why this difference was observed, runners need to consider the training and racing implications of the decreases activity while running.

**Acknowledgments:** Thank you to Saucony Corp for providing the shoes for this study.

**References:** [1] Hoogkamer et al. (2018), *Sports Med* 48(4); [2] Hunter et al. (2019), *J Sports Sci* 37(20); [3] Joubert et al. (2023), *Int J Sports Physiol Perf* 18(2); [4] Senefeld et al. (2021) *J App Physiol* 130; [5] Fletcher et al. (2017), *Sec Exer Physiol* 8.

| Measure | Peak Force | Stride Rate | Ground Time | PL | TA | GS | SL | BF | RF |
|---|---|---|---|---|---|---|---|---|---|
| Percent Diff from Control | -0.83 | 0.3 | -0.35 | 1.3 | -0.98 | -6.21* | -8.22* | -0.09 | 4.76 |
| F and p values | -1.82, 0.202 | -0.71, 0.479 | 0.30, 0.767 | 0.338, 0.736 | -0.40, 0.687 | -2.42, 0.017 | -2.54, 0.012 | -0.03, 0.979 | 1.06, 0.291 |

**Table 1:** Differences between AFT and control shoes expressed in percentage form expressed relative to the control condition. *significantly different with alpha = 0.05.

# THE EFFECTS OF ADVANCED FOOTWEAR TECHNOLOGY ON THE METABOLIC COST AND BIOMECHANICS OF RUNNING IN SUB-ELITE AND ELITE DISTANCE RUNNERS

*Bradley J. Needles[1], Alena M. Grabowski[1]
[1]University of Colorado Boulder
*Corresponding author's email: Bradley.Needles@Colorado.edu

**Introduction:** Since the release of advanced footwear technology (AFT) track spikes, 800-m to 10,000-m race times for elite runners have improved by 0.9% compared to pre-AFT race times [1]. The midsole of AFT spikes typically has more compliant and resilient (lower hysteresis) foam, double the thickness, and an embedded rigid plate compared to traditional spikes [2]. Footwear midsole foams and surfaces can be described by their compliance, which is the reciprocal of stiffness, i.e. as compliance decreases, stiffness increases. Previous studies have found that runners wearing AFT shoes designed for road racing have a 4% lower metabolic cost when running at 14 to 18 km/hr (3.8 to 5 m/s) compared to traditional road racing footwear [3]. The metabolic cost of running at a given speed, typically reported as watts per kilogram of body weight (W/kg), is a key factor in race performance. A lower metabolic cost of running has been linked to improved race speeds [4] and, since AFT shoes contain the same midsole foams and construction techniques used in AFT spikes, it has been theorized that AFT spikes may reduce the metabolic cost of running and improve race performance. One possible reason for a reduced metabolic cost of running in athletes wearing AFT spikes is increased leg stiffness while running due to increased AFT spike midsole compliance. Increased leg stiffness at a given running speed could improve a runner's effective mechanical advantage, leading to reduced active muscle volume required by the lower limbs, and, in turn, reduce the metabolic cost of running [5]. Kerdok et al. found that a 12.5-fold reduction in treadmill surface stiffness resulted in a 29% increase in leg stiffness and 12% reduction in the metabolic cost of running [6]. Additionally, Kram and Taylor proposed that increasing contact time during running may reduce the metabolic cost of running at a given speed [7]. Hoogkamer et al. reported increased contact time for participants wearing AFT shoes compared to traditional road racing shoes while running at 14 to 18 km/hr (3.8 to 5 m/s) [3]. Based on the increased midsole foam compliance of AFT spikes and prior research, we hypothesized that sub-elite and elite runners wearing AFT spikes would experience reduced metabolic cost of running, increased leg stiffness, and increased contact time compared to wearing traditional spikes.

**Methods:** 16 (10 male and 6 female) sub-elite to elite runners completed two separate sessions of 8, 5-min running trials while wearing four shoe conditions: Nike ZoomX Dragonfly (NDF) and On Cloudspike 10,000 m (OCS) AFT spikes, Nike ZoomX VaporFly Next % 2 (NVN) AFT shoe, and Nike Zoom Victory 3 (NZV) traditional spike. During each trial, females and males ran at 15 and 17 km/hr, respectively, on a force measuring treadmill (Treadmetrix, Park City, UT) while breathing into an expired-gas analysis system (ParvoMedics TrueOne 2400, Sandy, UT). We measured ground reaction forces at 1000 Hz for two, 30 second periods per trial and metabolic rates throughout each 5-min trial. The footwear conditions for the trials were mirrored and randomized for each day so that each participant ran twice in each shoe condition during each session. We calculated the metabolic cost of running from minutes 3-5 using the Perronet equation [8] and leg stiffness using the spring-mass model [9]. Contact time was defined with a 20 N vertical ground reaction force threshold. Vertical footwear stiffness was determined by applying a compression force onto each shoe using a prosthetic foot with a cosmesis that was secured inside the shoe and attached to a materials testing machine (Instron 5982, Norwood, Massachusetts).

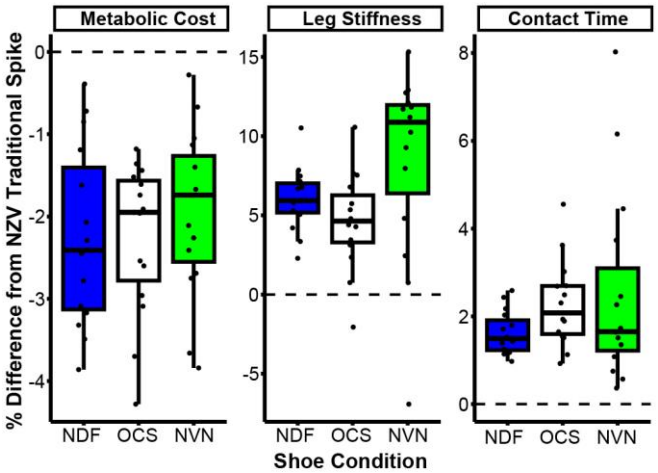


**Figure 1:** Percentage difference in the metabolic cost of running, leg stiffness, and contact time while runners wore the Nike ZoomX Dragonfly (NDF), On Cloudspike 10,000m (OCS), and Nike ZoomX Vaporfly Next % 2 (NVN) advanced footwear technology shoes compared to the Nike Zoom Victory 3 (NZV) traditional spike. The metabolic cost of running was significantly lower while leg stiffness and contact time were significantly higher for all AFT shoe conditions versus the traditional spike ($p < .05$). Dashed horizontal lines at 0 represent no change from the traditional spike.

**Results & Discussion:** We found that the metabolic cost of running while wearing the NDF, OCS, and NVN decreased by 2.3, 2.3, and 2.0%, respectively, compared to the NZV traditional spike ($p < .001$; Fig. 1A). A ~2% decrease in the metabolic cost of running is predicted to improve race speed by roughly 1.4% [4], which corresponds to 3 sec per mile while running at 6.7 m/s (4 min/mile). The decrease in the metabolic cost of running may have been due to increased leg stiffness and contact time. While wearing the NDF, OCS, and NVN AFT footwear, leg stiffness increased by 5.7, 4.4, and 8.0%, respectively, (Fig. 1B) and contact time increased by 1.5, 2.2, and 2.4%, respectively, compared to the NZV traditional spike ($p < .005$).

**Significance:** Runners wearing AFT spikes used on average 2.2% less metabolic energy to run at the same speed compared to traditional spikes. To maximize race performance, future generations of AFT spikes should consider midsole foams even more compliant than the midsole foams currently used in AFT spikes.

**References:** [1] Needles et al., *JAP*, 137(6), Dec. 2024 [2] Healey et al, *Sports Med*, 52(6), Jun. 2022 [3] Hoogkamer et al., *Sports Med*, 48(4), Apr. 2018 [4] Kipp et al., *Front Physiol*, 10, Feb. 2019 [5] Biewener et al., *JAP*, 97(6), Dec. 2004 [6] Kerdok et al. *JAP*, 92(2), Feb. 2002 [7] Kram et al., *Nature*, vol. 346, Jul. 1990 [8] Kipp et al., *Appl. Physiol. Nutr. Metab*., 43(6), Jun. 2018 [9] Farley et al., *J of Exp Bio*, 185(1), Dec. 1993

# How does Surface Stiffness and Frequency Affect Leg Stiffness and the Metabolic Cost of Hopping?

Luis Morata[1], Alena M. Grabowski[1,2]
[1]Applied Biomechanics Lab, University of Colorado Boulder, Boulder, CO, USA
[2]Department of Veterans Affairs Eastern Colorado Healthcare System, Denver, CO, USA
*Corresponding author's email: Luis.MorataMoreno@colorado.edu

**Introduction:** External passive-elastic devices such as footwear, compliant surfaces, and exoskeletons have significantly affected biomechanics and reduced metabolic cost for humans during bouncing gaits such as running and hopping. Previous studies found that leg stiffness ($k_{leg}$) changes to accommodate in-series stiffness[1], which affects metabolic cost, and thus performance, and that this relationship may depend on running speed[2] and hopping frequency. When humans hopped in place at 2Hz on surfaces with over a 1000-fold decrease in stiffness (35,000 kN/m to 26.1 kN/m), $k_{leg}$ increased 3-fold (17.8 kN/m to 53.3 kN/m)[3]. Similarly, Kerdok et al. (2002) found that when humans run on a treadmill at 3.7 m/s with a 12.5-fold lower surface stiffness ($k_{surf}$), $k_{leg}$ increased by 29%, and metabolic cost was ~12% lower compared to a stiff surface. These results suggest further reductions in in-series stiffness may reduce metabolic cost, but previous studies found that extremely compliant (>20 kN/m), compared to stiff surfaces (~35000 kN/m) increase metabolic cost through significant changes in leg mechanics during running[4] and hopping[5]. Moreover, recent research of running footwear found that greater foam compliance (reduced stiffness) improves running performance via reductions in metabolic cost; however, these improvements appear to be running speed and sex dependent[2] and may or may not be related with changes in $k_{leg}$. Thus, we determined how different in-series (surface) linear stiffness and frequency influence $k_{leg}$ and metabolic cost during double-legged stationary human hopping. We hypothesized that: 1) $k_{leg}$ would increase as $k_{surf}$ decreases so that the total stiffness of the system ($k_{tot}$; combined compliance of $k_{leg}$ and $k_{surf}$) would be invariant for different $k_{surf}$ at a given hopping frequency [3,6], and 2) there would be an interaction effect between $k_{surf}$ and hopping frequency on metabolic cost, such that the $k_{surf}$ that results in the lowest metabolic cost would be stiffer as hopping frequency increases.

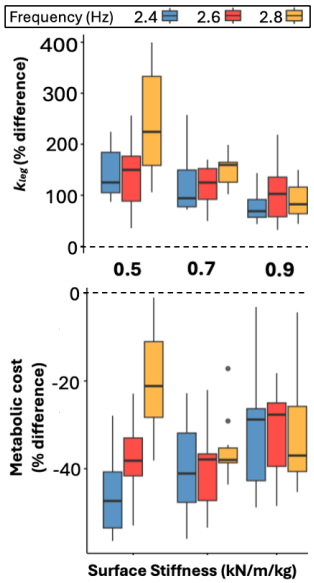


**Figure 1:** Box plot and whiskers showing the median (horizontal line) and interquartile range, and the minimum and maximum metabolic cost and leg stiffness ($k_{leg}$) as a percentage difference with respect the stiff surface of 13 subjects hopping on surfaces with different body-mass normalized linear stiffness at 2.4 Hz (blue), 2.6 Hz (red) and 2.8 Hz (orange).

**Methods:** 13 healthy adults (8 M, 5 W) aged 18–50 who engaged in moderate-vigorous aerobic exercise for ≥30 min per day and 3 days per week participated. Each subject completed 12, 5-min double-legged hopping trials over on two separate days. The trials were randomized and included hopping at three frequencies (2.4, 2.6, 2.8 Hz)[3] on a rigid force plate (~35000 kN/m) and three body mass normalized linear $k_{surf}$ (0.5, 0.7, 0.9 kN/m/kg). We controlled hopping frequency via an audible digital metronome and changed $k_{surf}$ using a custom platform mounted to the force plate. We measured and averaged metabolic power using indirect calorimetry (K5, Cosmed, Italy) from the last 2 min of each trial, and lower limb kinematics (Vicon Nexus, Oxford, UK; 200 Hz) and ground reaction forces (GRFs; AMTI, Watertown, MA, USA; 1000 Hz) for 30 s during min 3 and 4. We computed $k_{leg}$, and $k_{tot}$ from peak vertical GRF, pelvis displacement, and surface displacement during ground contact for each trial using a custom Matlab script[3,6] .Linear mixed models (LMMs; RStudio, Boston, MA, US; $\alpha = 0.05$) were employed to evaluate the effects of $k_{surf}$ and hopping frequency on dependent variables. Each LMM included $k_{surf}$, hopping frequency, and their interaction as fixed effects, with subjects as a random intercept. Significant effects were examined using post-hoc pairwise comparisons with Bonferroni corrections.

**Results & Discussion:** Our results support our first and second hypotheses. We found a significant main effect of $k_{surf}$ on metabolic cost ($p < 0.001$) and $k_{leg}$ ($p < 0.001$) (Fig. 1). Less stiff surfaces led to lower metabolic cost and increased $k_{leg}$ compared to the rigid surface. Hopping frequency also affected metabolic cost ($p < 0.001$) and $k_{leg}$ ($p < 0.001$) (Fig. 1). On average, for the same $k_{surf}$ faster versus slower frequencies led to increased metabolic cost and $k_{leg}$ compared to slower hopping frequencies. In addition, we found a significant interaction between $k_{surf}$ and hopping frequency for metabolic cost ($p < 0.001$) and $k_{leg}$ ($p < 0.001$) (Fig. 1). For the lease stiff $k_{surf}$, an increase in hopping frequency from 2.4 to 2.8 Hz resulted in a 25.3% increase in metabolic cost ($p < 0.001$). However, for the 0.9 kN/m/kg surface, an increase in hopping frequency from 2.4 to 2.8 Hz led to a 1.7% decrease in metabolic cost ($p = 0.014$). Overall, our findings suggest that compliant surfaces reduce metabolic cost more at slower hopping frequencies, while at faster frequencies, stiffer surfaces reduced metabolic cost more than compliant surfaces. In addition, $k_{leg}$ increases on compliant surfaces and this effect is greater at faster frequencies.

**Significance:** This study offers a novel, proof-of-concept approach using a controlled environment (hopping) to test the biomechanical mechanisms underlying metabolic cost reductions in bouncing gaits. Our results could provide a scientific basis to inform the design of future passive-elastic devices that act in-series with the leg, such as athletic footwear, prostheses, and compliant surfaces that could be tailored to improve performance, rehabilitation and/or injury risk reduction.

**References:** [1] Kerdok et al. (2002), *J Ap Physiol* 92(2); [2] Needles & Grabowski (2024), *J Ap Physiol* 137(6); [3] Ferris & Farley et al (1997), *J Ap Physiol* 82(1); [4] Lejeune et al. (1998), *J Exp Biol* 201(13); [5] Moritz & Farley (2003), *Proc R S Lond B Bio Sci* 270(1525); [6] Farley et al (1998), *J Ap Physiol* 85(3).

# BAREFOOT VERSUS FLIP-FLOP WALKING GROUND REACTION FORCES

*Emily Gerstle[1]
[1]Univerisity of Scranton, Leahy College of Health Sciences, Scranton PA
*Corresponding author's email: emily.gerstle@scranton.edu

**Introduction:** The use of flip-flops as footwear is estimated to have a market size of $32 billion by the year 2032 (Polaris Market Research), indicating use of flip-flops as daily footwear will continue to increase. Although flip-flops are a common footwear option, knowledge of how gait is impacted when wearing flip-flops is limited. The small number of studies examining walking gait ground reaction forces (GRF) in flip-flops compared to barefoot [1-3] have thus far focused on discreate points or predefined phases. Previous studies found walking in flip-flops increases the stance time [3], has a lower loading rate [1, 2], and lower initial vertical impact peaks [2]. Other variables examined, but with no differences found, include braking and propulsive peaks in the anterior-posterior (AP) direction.

Recently statistical parametric mapping (SPM) has been introduced as a way to examine timeseries data by comparing complete curves allowing sections difficult to define by an event come to light as potential regions of interest [4]. The purpose of this study was to examine differences in lower extremity GRFs (vertical and anterior-posterior) walking barefoot compared to walking in flipflops. Secondarily, the aim was to examine differences found using SPM in relation to the more traditionally found discrete points. It was anticipated the flip-flop trials would result in a longer stance time with potential differences in the weight acceptance region (lower loading rates and impact peaks).

**Methods:** Thus far five participants (1M/4F, 19.6 ± 1.1 years, 1.7 ± 0.04m, 79 ± 21.3kg) were asked to walk five trials at their self-selected comfortable pace while barefoot and in flip-flop sandals (Old Navy, LLC.). A successful trial had participants making complete contact with the right foot on an AMTI force plate (collecting at 1000Hz) embedded in the ground without altering their gait.

Force plate data was filtered at 15Hz with initial contact defined as 15N or greater. Stance time, two vertical GRF peaks, initial loading rate, posterior breaking peaks, and anterior propulsive peaks were calculated via a custom MATLAB script and tested via separate paired t-tests. Statistical Parametric Mapping (spm1d.org) t-tests were done on timeseries of vertical GRF and AP GRF.

**Results & Discussion:** Discrete data calculations are in Table 1. With the only significant differences in vertical loading rate and peak braking. Vertical GRF curves did not demonstrate any significant differences across the stance phase utilizing SPM. In the anterior-posterior direction the braking phase demonstrated a small region of difference (Figure 1), with flip-flop walking having a larger breaking force.

| | Barefoot | Flip-flop | p-value |
|---|---|---|---|
| Stance time (s) | 0.71(0.079) | 0.706 (0.06) | 0.35 |
| Peak 1 (N/BW) | 1.08 (0.098) | 1.11 (0.066) | 0.134 |
| Peak 2 (N/BW) | 1.18 (0.089) | 1.16 (0.068) | 0.29 |
| Loading rate (N/BW*s) | 5.55 (1.52) | 6.16 (1.07) | **0.038** |
| Braking peak (N/BW) | -0.15 (0.054) | -0.18 (0.049) | **<0.001** |
| Propulsive peak (N/BW) | 0.21 (0.055) | 0.20 (0.04) | 0.269 |

**Table 1:** Means (SD) of discrete data calculations.

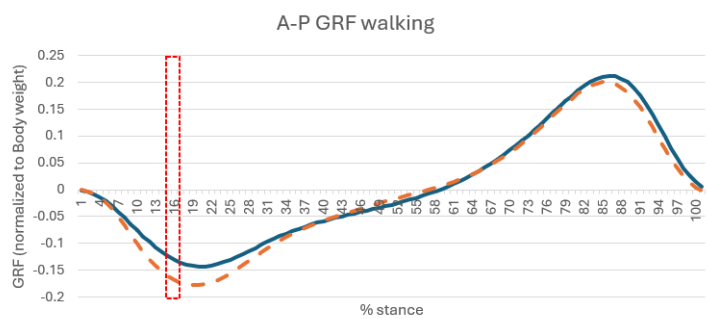


**Figure 1:** Anterior-posterior GRF curves of barefoot walking (blue line) and flip-flop walking (orange dashed line). Red dotted rectangle indicates region of significant difference (15-17% of stance) via SPM.

As anticipated, differences were found during initial weight acceptance; however, stance time was not significantly different between conditions. It is possible differences in stance time may be due to walking speed. The current study was self-selected speed while the previous study [3] had a set walking speed. The flip-flop loading rate here was found to be significantly greater, which conflicts with previous findings. It is possible the current study is limited by number of participants and/or the self-selected speeds may differ between studies.

Although propulsive peak was not significant, the braking peak was significantly greater in flip-flops. Further this was supported by the SPM results finding the region just before braking peak to be significantly greater in flip-flop walking. This may be due to the cushioning of the flip-flop sole allowing higher braking forces at a similar comfort level.

Regarding SPM, it is interesting to note the significant region of difference was close to but not at the peak of the braking phase. This supports the differences in breaking peak but refines the timing, demonstrating the greatest differences are occurring just before the peak. It is possible previous studies may have had differences in this region without braking peaks demonstrating significant differences.

**Significance:** This study adds to the knowledge of how walking in flip-flops differs from barefoot walking, however, more study is warranted before recommendations of flip-flops as footwear can be made. Furthermore, the results of this study suggest SPM could be a valuable addition in examining timeseries data, potentially demonstrating differences that may otherwise be masked by only examining discrete points.

**References:** [1] Price et al. (2014), *J Foot and Ankle Research* 7(1); [2] Wallace et al. (2018) *R Soc Open Sci* 5(3); [3] Zhang et al. (2013) *J Foot and Ankle Research* 6(1); [4] Pataky et al. (2016) *PeerJ* 4.

# SIMULATING EARLY STANCE FOOTWEAR-GROUND INTERACTION WITH AN INVERTED PENDULUM FOR SLIP RESISTANCE ASSESSMENT

Cédric Dessureault[1], Gaspard Diotalevi[2], Chantal Gauvin[3], François Martel[1], Nicolas Zabjesky[1], Cécile Smeesters[2], *Denis Rancourt[1]
[1]Department of Mechanical Engineering, Université de Sherbrooke, Sherbrooke (Qc), Canada
[2]Research Centre on Aging, CIUSSS de l'Estrie – CHUS, Sherbrooke (Qc), Canada
[3]Institut de recherche Robert-Sauvé en santé et en sécurité du travail, Montréal (Qc), Canada
*Corresponding author's email: denis.rancourt@usherbrooke.ca

**Introduction:** Current whole-footwear slip testing methods, such as those defined by ISO 13287 [1] and ASTM F2913 [2], rely on systems that do not fully replicate critical gait characteristics, including heel strike (HS) dynamics, variations in ground reaction forces (GRFs) during early stance, initiation of slip events, and the evolution of both contact surface area and pressure distribution at the shoe-ground interface. To address these limitations, a whole-footwear slip device was developed with the potential to better replicate walking conditions. The passive device is designed to approximate HS and early stance dynamics, along with the GRFs observed in humans, enabling realistic and repeatable footwear-ground interaction testing. This study evaluates the system's repeatability and its ability to cover parameter ranges commonly used in bipedal walking models.

**Apparatus and Methods:** The device consists of a stationary launch ramp, as well as a prismatic spring-loaded inverted pendulum (SLIP) with a damper and a shoe last. Both the ramp and the SLIP are adjustable to control initial conditions at HS and mechanical impedance properties of the inverted pendulum (Fig. 1A). Repeatability was assessed by conducting multiple launch trials on dry floor using the same initial parameter values and the same shoe. GRFs were measured with an AMTI force platform, while initial kinematic conditions were recorded using an OptiTrack system. The assessed parameter ranges included walking speed ($\dot{y}_{CoM}$), initial leg attack angle ($\theta_{in}$), pendulum length ($L_p$), leg stiffness ($k_l$), and damping ratio ($\xi_l$). Actual values from the literature were used as a comparison basis (Table 1).

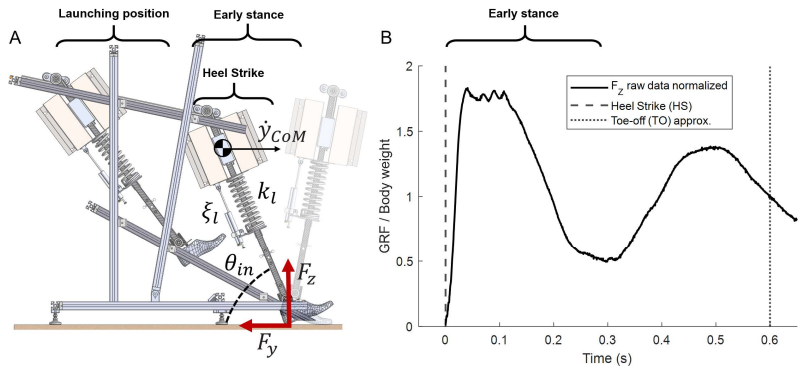


**Figure 1:** [A] Side view of the launch ramp and prismatic inverted pendulum, shown in the launching position, at heel strike and at the end of the trial illustrating the gravity-driven transition from launch to heel strike. [B] Typical normalized vertical GRF of a single trial for a given pendulum impedance.

**Table 1:** Device parameter ranges compared to the literature, and system repeatability.

| Study | $\dot{y}_{CoM}$ (m/s) | $\theta_{in}$ (°) | $L_p$ (m) | $k_l$ (kN/m) | $\xi_l$ (%) |
|---|---|---|---|---|---|
| Whittington, 2009 [3] | 1.07-1.59 | 62.5-66.5 | 1 | 21-24 | - |
| Kim & Park, 2011 [4] | 0.8-2.2 | - | - | 14-23 | 3-8 |
| Qin, 2013 [5] | 1.09-1.32 | 66–70 | 1 | 16-23 | 5-8 |
| Vega, 2022 [6] | 0.82-1.56 | 68-74 | 0.98-1.26 | 13-34 | 3-13 |
| **Our device range** | 0.75-1.75 | 60-75 | 0.96-1.07 | 13-28 | 6.3-9.6 |
| CV $\left(\frac{\sigma}{\mu}\right)$ for N= 10 trials | 0.37% | 0.11% | N/A | N/A | N/A |

**Results & Discussion:** Tests confirmed that the device exhibits significantly lower variability in initial conditions at HS compared to human data, with a coefficient of variation (CV) for walking speed being 0.37% for the device versus ~10% for humans [6]. The GRF measurements also demonstrated excellent repeatability, with a CV of less than 1%. Results also confirmed that the device can cover parameter ranges typically used in bipedal walking models (Table 1). Furthermore, results indicated that, even without specific tuning, the device generates typical M-shaped profiles of vertical GRFs, especially during heel strike and early stance (Fig. 1B). However, parasitic vibrations were observed at the first peak, originating from the system's structural vibrations. The next phase of this work will focus on reducing these vibrations and fine-tuning the device to replicate human GRFs and gait dynamics. These results confirm the potential of the device as a reliable platform for evaluating footwear-ground interaction.

**Significance:** This study shows the potential of an inverted pendulum to simulate footwear-ground interactions, providing repeatable behavior and the ability to tune its impedance properties and heel strike kinematics to human-like values. Once structural vibrations are sufficiently reduced, the system could be used to test footwear on different slippery surfaces, allowing for multidimensional load interaction, sole deformation and naturally unconstrained slip scenarios at heel strike and during early stance.

**Acknowledgments:** The Natural Sciences and Engineering Research Council of Canada (NSERC, ALLRP 570347-21) for their financial support. Ludovic Tremblay for his assistance with the manufacturing and assembly of the device.

**References:** [1] ISO 13287:2019. *Personal protective equipment: Footwear: Test method for slip resistance*. [2] ASTM F2913-24. *Standard Test Method for Measuring the Coefficient of Friction for Evaluation of Slip Performance of Footwear and Test Surfaces/Flooring Using a Whole Shoe Tester*. [3] Whittington et al. (2009), *J Biomech Eng* 131(1); [4] Kim & Park. (2011), *J Biomech* 44(7); [5] Qin et al. (2013), *J of Sound and Vib* 332(4); [6] Vega et al. (2022), *Mec Sys and Signal Pro* 167

# UNDER-SHOE BIOMECHANICAL CONDITIONS DURING ROOFING WALKING: IMPLICATIONS FOR FRICTION TESTING

*Richard Smith[1], Kurt E. Beschorner[1]
[1]University of Pittsburgh, Department of Bioengineering
*Corresponding author's email: rws72@pitt.edu

**Introduction:** Compared to the average worker, roofing workers have a roughly six times higher risk for fatal occupational injuries, with falls accounting for 75% of these cases [1]. Friction performance between shoes and flooring materials has been shown to be a significant predictor of slip risk [2] and high friction is especially important on roofing surfaces given the added risk from inclined surfaces [3]. Most shoe-floor friction testing methods have been developed for early stance slips during level walking, and therefore may not be applicable to conditions on a sloped roof. This work aims to compare underfoot conditions during sloped and level walking to assess the applicability of one testing method, the NFSI B101.7 standard, to roofing conditions. The results may motivate the development of a specialized roofing friction test methods.

**Methods:** Five healthy adults (5M, 1.78±0.05 m, 84.6±6.1 kg) completed walking trials on a custom-built adjustable angled platform. Participants completed 24 trials on flat ground, 24 cross-slope trials, 12 up-slope trials, and 12 down-slope trials, at two roof angles (14, and 27 degrees) for a total of 120 trials. Motion capture and force plate data was collected. The required coefficient of friction (RCOF), a measure of a task's friction demands [2], was extracted and peak values were identified. Cross slope steps typically had RCOF peaks during both early and late stance, while down and up slope steps only had a peak during early and late stance, respectively. Because slip events typically occur between heel contact and the peak RCOF, under-shoe biomechanical metrics were characterized at either of these times. Sliding speed and shoe-floor angle were only characterized at foot contact (for early stance RCOF peaks) or foot off (for late stance RCOF) since these parameters were typically 0 at the time of RCOF. Normal force was characterized only at RCOF since it was 0 at foot contact and foot off.

A repeated measures ANOVA and Tukey post hoc analyses were performed to compare outcomes across different step types.

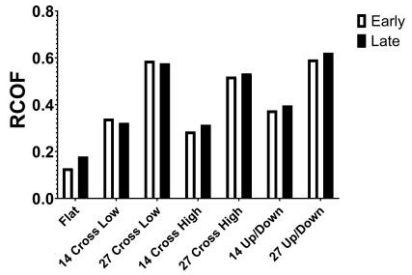


Figure 1: Average peak RCOF values for early and late stance conditions.

**Results & Discussion:** Early and late peak RCOF values scaled with the slope and was somewhat higher for up/down slope than cross-slope (Fig. 1). Late peak RCOF values were very similar to early peak values, suggesting that late and early stance have similar slip risks. This provides motivation for the development of a late stance slip testing procedure.

Under-shoe conditions varied across slope condition but not consistently across the slope conditions (Figure 2). During down slope walking, slower sliding speeds and higher shoe-floor angles were observed. During cross-slope walking, faster sliding speed was observed at heel contact. Cross-slope walking led to lower shoe-floor angle and higher sliding speeds but just for the upslope shoe. The impact of sloped walking on under-shoe biomechanical parameters was highly context-dependent and was not consistent across up slope, down slope, or cross-slope walking. Unless tests were created specifically for each of these conditions, this study does not provide robust evidence for modifying testing parameters universally for all roof walking conditions. Future work should investigate roofing conditions with a larger sample size and slipping data to further examine these differences.

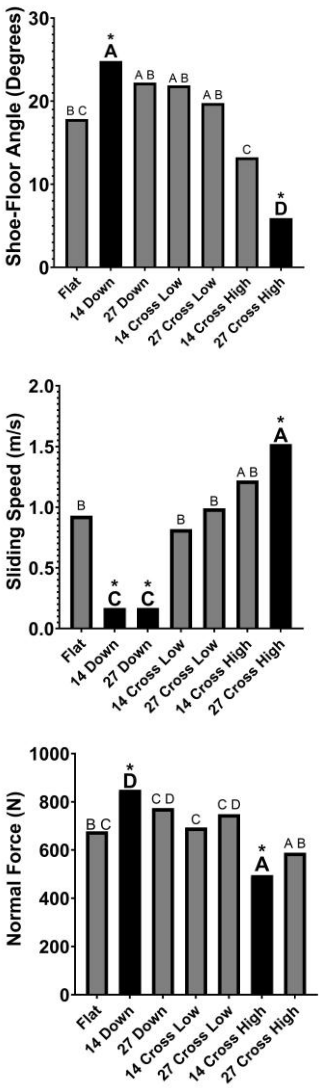


Figure 2: Average values in different conditions for sagittal shoe-floor angle at heel contact, sliding speed at heel contact, and normal force at peak RCOF. Tukey Pairwise comparison groups are indicated by letters, and groups significantly different from flat are darkened and bold.

**Significance:** These results provide motivation to develop a late stance slip test method (toe slipping) given the high RCOF values that were observed. The effect of slope on under-shoe conditions varied across the direction of walking and consistent changes were not observed. Thus, this study does not provide robust evidence for modifying the early-stance friction testing method when considering roofing materials.

**Acknowledgments:** Robert Carey, John Wu. This research was funded by NIOSH contract #75D30123P16637

**References:** [1] Ruser, J. W. (1995), *Report* **891**: 18-22. [2] Beschorner et al. (2016), *Gait & Posture* **48**: 256-260. [3] Hanson et al. (1999), *Ergonomics* **42(12)**: 1619-1633

# FlyBand® ExoBoots Allow for Increased Ankle Range of Motion During Walking Compared to Conventional Boots

Moser, G[1,2], Williams, J[1,2], Rasmussen, C.M.[1,2,3], Fallahtafti, F. [1,2], Eriks, K[4], Cotton, T[4], Roser, M.C.[1,2,4], Myers, S.A.[1,2]
[1] Dept. of Biomechanics, University of Nebraska-Omaha, Omaha, NE USA
[2]Research Service, Omaha Veterans' Affairs Medical Center, Omaha, NE USA
[3] Dept. of Exercise Science & Pre-Health Professions, Creighton University, Omaha, NE USA
[4]Results Group LLC dba Motive Labs, Glastonbury, CT USA
Email: gabriellemoser@unomaha.edu

**Introduction:** Lateral ankle sprains (LAS) are the most common musculoskeletal injury (MSKI) among soldiers [1]. Current standard of care for LAS are ankle braces, however service member adherence is low. FlyBand® ExoBoots were designed with adjustable carbon fiber cartridges to enable customizable lateral stability while allowing for more natural ankle motion during gait. We hypothesize that for healthy individuals in flat over-ground walking, FlyBand ExoBoots will allow for greater ankle range of motion in both the mediolateral and anteroposterior planes compared to conventional military boots and braces.

**Methods:** Ten healthy service-aged adults participated in this study and completed walking trials under six different boot-ankle brace conditions. Each condition was a unique combination of a military boot (either Conventional or FlyBand) and a bracing level (Low, Mid, or High). Participants were instructed to walk along a 15-meter flat walkway at a self-selected pace. Kinematic data for gait were measured using a 17-camera motion capture system (Motion Analysis Corp, Santa Rosa, CA; 100 Hz). Each subject was fitted with a sleeveless, formfitting bodysuit, and 33 retro-reflective markers were placed on specific anatomical landmarks on the subject's pelvis, thighs, shanks, and feet [2]. A two-way repeated-measures ANOVA with statistical parametric mapping (SPM) was conducted to analyze the main effects of boot type, bracing level, and their interactions.

**Results & Discussion**: FlyBand ExoBoots had a significant main effect for inversion/eversion angle (0-2% and 17-25% of gait cycle, $p=0.024$ and $p<0.001$, respectively) and ankle moment (20-25%, $p<0.001$). More inversion at heel strike (0-2%) was observed while wearing the FlyBand boots and more eversion angle and moment during mid stance phase (17-25%) was also observed in the FlyBand boots (Figure 1A). Boot and bracing interactions were observed for plantar/dorsiflexion angle (94-100% of gait cycle) and ankle moment (10% of gait cycle). For ankle moment, no interaction ($p = 0.30$) or bracing effect ($p = 0.48$) was found, but a boot type effect ($p = 0.034$) revealed greater peak eversion moments and smaller peak inversion moments at high bracing levels. Ankle power showed no significant effects ($p > 0.05$). A boot and brace interaction was observed in knee flexion/extension angle at 2-7% and 9-10% of the gait cycle ($p = 0.017$, $p = 0.043$), indicating early stance variations based on bracing condition (Figure 1B). No significant effects were observed at the hip joint ($p>0.05$).

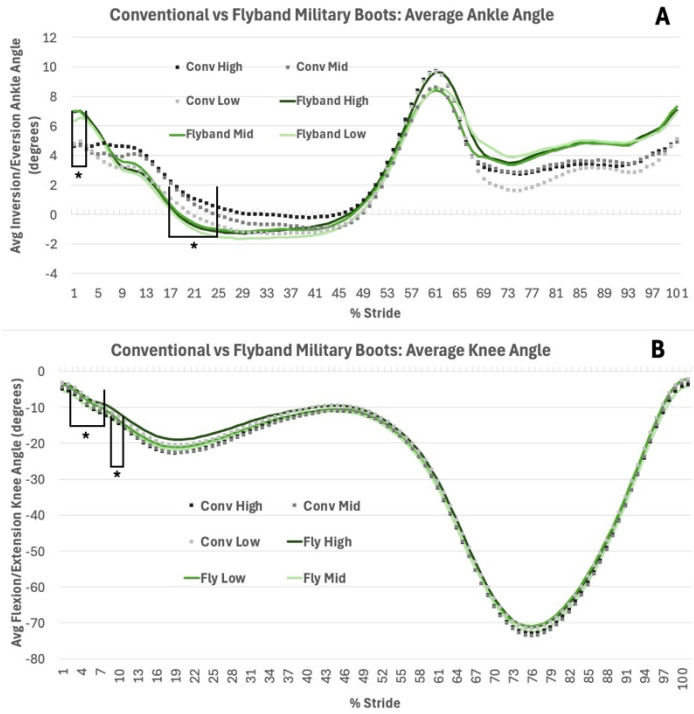


**Figure 1:** (A) FlyBand® ExoBoots significantly altered ankle inversion/eversion at 0-2% and 17-25% of the gait cycle, enhancing mediolateral stability. (B) A boot type × bracing level interaction in knee flexion/extension at 2-7% and 9-10% suggests potential biomechanical adaptations. Flyband boots provide comparable ankle support without compromising anteroposterior motion.

**Significance:** Findings demonstrate that FlyBand ExoBoots allow for more ankle inversion at early-stance and more ankle eversion during mid-stance phase, which suggests a more natural range of motion compared to conventional boots with braces. Knee mechanics in the Flyband boot at higher bracing levels led to less knee flexion during heel strike due to greater plantarflexion range of motion in the ankle; this finding suggests that FlyBand also allows for increase plantarflexion range of motion. Future research should investigate the impact Flyband Exoboots and various bracing levels in Service members with chronic ankle instability and for walking tasks across uneven surfaces.

**Acknowledgements**: This research was supported by a Defense Health Agency SBIR Phase II reward. The authors would like to thank Yassine Mahamane Iro, Zahra Salamifar, Joe Neihart, and Nataliya Rokhmanova, PhD for their contributions to this project.

**References:** [1] Def. Ctrs. Public Health. (2020). *2020 HEALTH FORCE REP.*; [2] Fallahtafti, F., et. al. (2024). *Int. J. Cardiol.* 407.

This material is based upon work supported by the DoD SBIR Program/U.S. Army Medical Research and Development Command (USAMRDC)/Congressionally Directed Medical Research Programs (CDMRP) under Contract No. W81XWH-22-C-0103. Any opinions, findings and conclusions or recommendations expressed in this material are those of the author(s) and do not necessarily reflect the views of the DoD SBIR Program/USAMRDC/CDMRP or the U.S. Army Medical Research Acquisition Activity (USAMRAA).

# Medial Longitudinal Arch Stability Assessment During Midstance: Influence of Diabetic Peripheral Neuropathy

*Jessi K. Martin-Liddy[1,2], Georgeanne Botek[1], Ahmet Erdemir[1], Brian L. Davis[2]
[1]Cleveland Clinic Foundation Cleveland, OH
[2]Cleveland State University Cleveland, OH
*Corresponding author's email: j.k.martin42@vikes.csuohio.edu

**Introduction:** Diabetic Peripheral Neuropathy (DPN) is a debilitating condition stemming from damage to peripheral nervous system neurons. It is prevalent in both Type 1 and Type 2 diabetic patients and results in impaired communication between body extremities and the central nervous system. As a result, DPN leads to altered proprioception, diminished neuromuscular control, and gait abnormalities. Additionally, improper pressure forces cause further complications such as tissue ischemia and microangiopathy within the foot leading to further diabetic complications such as diabetic foot ulcers, and Charcot neuropathic sarco-osteoarthropathy (CNSOA).

Our study aims to utilize differences in step-to-step pressure distribution values as a means to quantify foot arch stability in DPN individuals. We hypothesize that increased variability in pressure distribution reflects compromised foot function during midstance. By capturing dynamic changes in arch health, which traditional imaging techniques cannot visualize, this approach provides a new understanding of arch degradation. Recognizing that dynamic arch stability often diminishes before static stability, our proposed method could serve as an early indicator of compromised foot structures in DPN patients, which could lead to improved methods of monitoring diabetic foot complications and earlier intervention.

**Methods:** Forty-eight participants (aged 45-84) were categorized into three groups: non-diabetic, non-neuropathic; diabetic, and diabetic neuropathic. Neuropathy severity was stratified based on the Michigan Neuropathy Screening Instrument (MNSI) score. Peak pressure data were collected using the Novel Pedar-x insole system and analyzed with MATLAB. The statistical analysis was conducted in R. Within MATLAB, 10 subsequent steps were extracted. To address any potential experimental variability within the analysis, both the x- and y- axes were standardized. The pressure variability was measured via an integration of the area measurements between two sequential steps (steps 1 to 2, 2 to 3, etc.). The statistical analysis included a Kruskal-Wallis test to quantify differences in the integrated area (variability) and raw MNSI score between the 3 groups. Post hoc testing (Dunn Test) was conducted to further investigate group differences.

**Results & Discussion:** As the MNSI score increases from non-neuropathic (MNSI Score of 0 – 3.0) to neuropathic (MNSI score of 3.5 – 20), the step-to-step variability increases. (Figure 1) The Kruskal Wallis Test illustrated a statistically significant difference in the integrated area (pressure variability) between at least one of the groups ($p < 0.001$). Further post hoc testing with a Dunn Test revealed statistically significant variability differences between healthy controls and diabetic controls ($p < 0.001$), healthy controls and diabetic neuropathic individuals ($p < 0.001$), as well as diabetic controls and diabetic neuropathic individuals ($p = 0.03$).

Therefore, the peak pressure trajectory variability within the midfoot illustrated that the presence of diabetic peripheral neuropathy inherently degrades the dynamic arch loading ability to appropriately and consistently transfer loads within the midfoot before the static loading ability is impacted. Additionally, the progressive development of DPN has a proportional relationship with the progressive degradation of the dynamic loading abilities of the medial longitudinal arch (MLA) of the midfoot. These results concur with the trends presented by Pierre-Jermone, *et al.*[1]

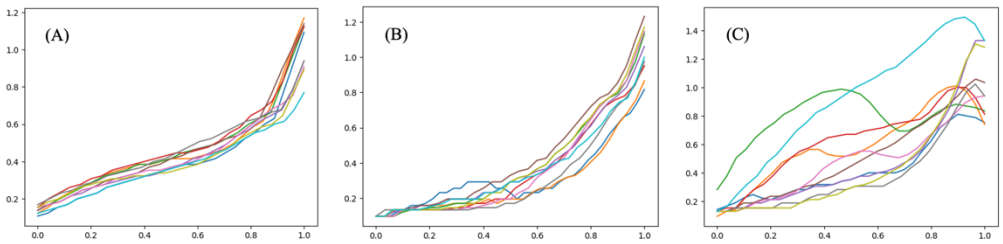


**Figure 1:** *Illustration of 10 Step-to-Step Peak Pressure Distributions for (A) Healthy, (B) Diabetic, and (C) Neuropathic Groups During Midstance. The x-axis is standardized time (start to end of midstance). The y-axis is standardized pressure to remove the influence of patient weight on pressure measurement variability. The x-axis is standardized midstance duration.*

**Significance:** To date, there has been no identifiable and non-invasive metric to quantify the loss or degradation of the dynamic arch loading ability of the midfoot arch. The ability to understand the multifaceted nature of the dysregulation of the midfoot arch system could aid in the discriminatory ability to track detrimental changes to MLA health and integrity. This knowledge could thus be applied to furthering investigations into the development and manifestation of the early-stage CNSOA condition within the midfoot. Specifically, the clinical utility of the MNSI as a non-invasive tool to monitor progressive changes in midfoot loading in DPN patients. Early detection of dynamic arch instability, preceding static changes, could enhance monitoring and early intervention for diabetic foot complications.

**Acknowledgments:** This work is supported by the T-32 NIH Training Grant: 5 -T32 - HL150389 – 03.

**References:** [1] Claude Pierre-Jerome. *The Essentials of Charcot Neuroarthropathy*. Elsevier; 2022. doi:10.1016/C2021-0-02165-9

# THE EFFECT OF ANKLE & HALLUX POSITIONING ON HALLUX FORCE PRODUCTION: A CASE STUDY OF FLEXOR HALLUCIS LONGUS

Mickelle A. MacCabe[1], Logan Smith[2], Andrew Westwood[3], Wayne Johnson[4], Dustin Bruening[5]
Brigham Young University
Department of Exercise Sciences: Foot & Ankle Research Group
Mamaccabe03@gmail.com

**Introduction:** Dynamic activities like walking involve movements at the foot and ankle joints. During the late-stance phase, the extended hallux (big toe) flexes to propel the body forward, initiating the swing phase of gait. Key muscles involved in this process include the Flexor Hallucis Longus (FHL) and Flexor Hallucis Brevis (FHB). Historic models of foot movement treat the foot as a rigid lever, but exploring intrinsic muscles of the foot can provide a more accurate model, enhancing our understanding of movement energetics [1] and muscle-tendon dynamics [2]. This study investigates how ankle and hallux positioning affect isometric hallux flexion force by using a custom-designed force-measuring device (FMD) (*see Fig. 1*). Based on the anatomy of the FHL, we hypothesize FHL length changes will influence hallux force production. We also investigated correlations between force differences, arch height, and BMI.

**Methods:** Eighteen healthy adult volunteers participated in this study, with written consent. Demographic information including arch height index (AHI – sitting), was collected prior to testing. Participants were assigned randomized orders of the 4 testing positions: ankle neutral (90°) – hallux neutral (0°) (ANHN), ankle neutral (0°) – hallux extended (30°) (ANHE), ankle plantarflexed (45°) - hallux neutral (0°) (APHN), and ankle plantarflexed (45°) – hallux extended (30°) (APHE) *(see Fig. 1)*. After assuming position for the right leg, participants performed a maximal isometric flexion of the hallux for 3 seconds, resting for 1 minute between trials – this was then repeated for each position. Representative 1 second plateaus were analyzed from the force data. Repeated measures ANOVA, Holms-pair wise comparisons, and correlations were then performed.

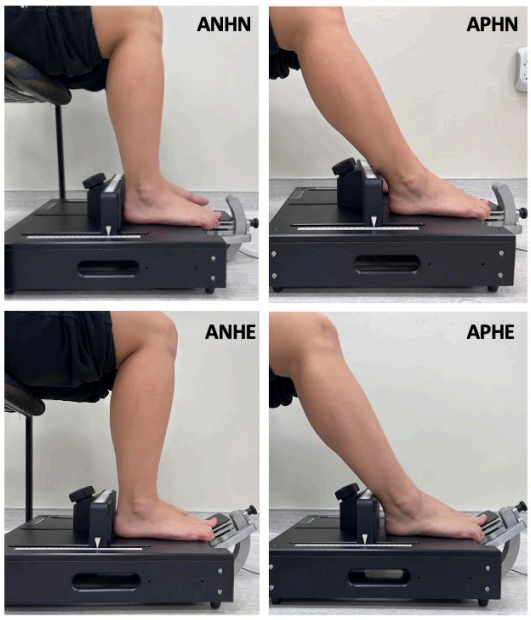


**Figure 1:** *The novel FMD consists of a small force plate for the hallux and adjustable positions. For testing, participants sat in a chair, flexed 90° at the knee, and assumed the associated positions for the ankle and hallux.*

**Results & Discussion:** There was a significant main effect for position ($p<0.001$) with a large effect size ($\omega^2 = 0.223$). The ANHE condition produced the greatest force (17.6 ± 7.3 N); pairwise, this was significantly greater than the force in all other conditions except APHE. In the ANHE condition, the FHL was at its most lengthened. Conversely, the APHN condition produced the least force (8.2 ± 4.2 N), which was pairwise significantly less than all other conditions. Here, the FHL was at its most shortened. ANHN and APHE resulted in similar force production (13.4 ± 6.3 N and 14.0 ± 6.3 N, respectively) *(see Fig. 2)*. In both conditions one joint was altered, resulting in somewhat similar FHL lengths (although FHB is longer in APHE). The difference between ANHE and APHN was not significantly correlated with seated AHI ($p=0.230$, $r=-0.30$) or BMI ($p=0.156$, $r=0.35$).

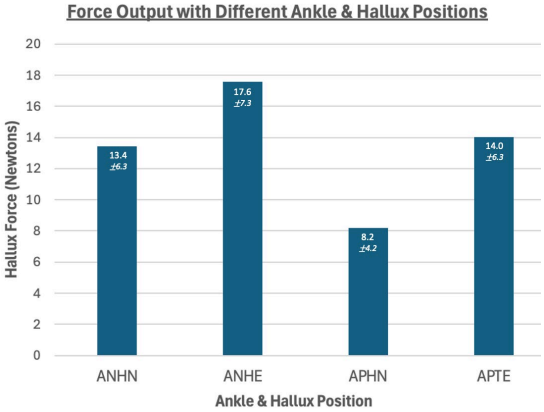


**Figure 2:** *The average mean force productions across the 3 trials and 18 individuals for this study. The standard deviation of those values is depicted below the mean.*

**Significance:** Our results validate previous studies,[3] while also introducing a novel methodology to measure force production in varying positions. In plantarflexed positions, FHL shortens, reducing its effectiveness due to less optimal positioning of cross-fibers in sarcomeres. In hallux extended positions, FHL lengthens, increasing its effectiveness with more optimal positioning of cross fibers, regardless of ankle position. It also appears likely the FHL contributed much more to hallux force than the FHB. We hope this information will ultimately influence applications in footwear design. Additionally, these insights offer practical knowledge for optimizing hallux flexion exercises and advancing rehabilitation strategies for foot deformities.

**References:** [1] Bruening et al. (2011), *Gait & Posture* 35(4), 535-540; Farris et al. (2019) [2] Proceedings of the National Academy of Sciences, 116(5), 1645-1650. [3] Kusagawa et al. (2024) Acta of Bioengineering and Biomechanics 26(3), 35-33

# Effects of minimal footwear on foot intrinsic and extrinsic muscles size in people with plantar fasciitis: A randomized control trial

Halime E. Gulle[1*], Jennifer Bergeron[2], Sarah Ridge[2], Irene S. Davis[1]
[1]School of Physical Therapy and Rehabilitation Science, University of South Florida, FL, USA
[2] College of Education, Nursing and Health Professions, University of Hartford, USA

**Introduction:** Plantar fasciitis (PF), a common painful foot condition, is often treated with inserts and supportive shoes to unload the plantar fascia. However, this can lead to muscle atrophy and high recurrence rates. An alternate approach to this problem is to employ minimal shoes to strengthen foot muscles, reducing plantar fascia strain and improving PF. Therefore, the purpose of this study is to compare changes in intrinsic foot muscle size between individuals with PF randomized to a minimal shoe (MS) and those in a conventional shoe (CON) group with an additional supportive insole. We hypothesized that those in the MS group would exhibit increases in foot muscle size while those in the CON group would exhibit reductions in foot muscle size.

**Methods:** This is an ongoing clinical trial aimed at individuals between 40-70 yrs with PT. To date, 24 (of 120) individuals have completed the 6-month follow-up. These individuals (22F/2M, 52.33 ± 7.70 yrs) were randomized into the MS group (n=12) and the CON group (n=12). At baseline, the cross-sectional areas (CSA) of 4 intrinsic and 3 extrinsic muscles were determined following the digitization of these images by a blinded assessor. These included Abductor Hallucis Brevis (ABD), Flexor Digitorum Brevis (FDM), Quadratus Plantae (QP), Abductor Digiti Minimi (ADM), Tibialis Posterior(TP), Flexor Hallucis Longus (FHL), Flexor Digitorum Longus (FDL). Participants then completed a transition, gradually increasing their time in their prescribed shoes, such that they were wearing their footwear for 80% of their daily step count. The ultrasound assessment was repeated at the 6-month follow-up. The CSAs of all muscles were compared between the MS and CON groups at baseline, and at the 6-month follow-up. Due to the preliminary nature of these data, means (sd) and % changes are presented.

**Results & Discussion:** The results thus far indicate that participants in the minimal shoe group generally experienced increases in muscle CSA over time. As can be seen in the table below, there was a 1-37% increase in the size of these muscles. The largest increases were seen in the FDL and ADM muscles. These results are consistent with all studies of the effect of habitual use of minimal footwear on foot muscle size (1) In contrast, the conventional shoe group generally exhibited a reduction in muscle CSA, with decreases ranging between 1 and 20 %. Similarly, the largest decreases were seen in the FDL and ADM muscles. This is in agreement with a recent study demonstrating that adding support to the foot leads to a 10-17% reduction in intrinsic muscle foot size (2). These results will be further examined statistically, with a larger sample as the study proceeds.

**Significance:** These changes in muscle size due to footwear have been documented in healthy individuals, but not in individuals with PF. This study highlights the promising benefits of minimal shoes in enhancing foot strength in this patient population. This is highly significant as PF is associated with weak feet (3). Therefore, use of minimal footwear may be an effective rehabilitation strategy for individuals with plantar fasciitis and other foot related pathologies.

| | MINIMAL SHOES | | | CONVENTIONAL SHOES | | |
|---|---|---|---|---|---|---|
| | Baseline | 6 Months Follow-Up | Change (%) | Baseline | 6 Months Follow-Up | Change (%) |
| Abductor hallucis brevis | 1.83±0.46 | 2.09±0.44 | +14 | 1.92±0.26 | 1.68±0.42 | -13 |
| Flexor digitorum Brevis | 1.56±0.21 | 1.63±0.17 | +4 | 1.59±0.22 | 1.57±0.26 | -1 |
| Quadratus Plantae | 1.12±0.25 | 1.13±0.23 | +1 | 1.07±0.34 | 0.99±0.24 | -8 |
| Abductor Digiti Minimi | 0.65±0.19 | 0.77±0.18 | +18 | 0.81±0.43 | 0.67±0.29 | -20 |
| Tibialis Posterior | 3.63±0.90 | 3.80±1.16 | +4 | 3.38±0.63 | 3.00±0.64 | -12 |
| Flexor Hallucis Longus | 2.37±0.68 | 2.56±0.44 | +8 | 2.51±0.72 | 2.40±0.74 | -04 |
| Flexor Digitorum Longus | 1.16±0.47 | 1.60±1.77 | +37 | 1.20±0.26 | 1.04±0.42 | -15 |

**References**

1. Xu, J., S.A. Saliba, and A.H. Jaffri, *The effects of minimalist shoes on plantar intrinsic foot muscle size and strength: a systematic review.* International journal of sports medicine, 2023. **44**(05): p. 320-328.
2. Protopapas K, Perry SD. The effect of a 12-week custom foot orthotic intervention on muscle size and muscle activity of the intrinsic foot muscle of young adults during gait termination. Clinical Biomechanics. 2020;78:105063
3. Cheung RTH, Sze LKY, Mok NW, Ng GYF. Intrinsic foot muscle volume in experienced runners with and without chronic plantar fasciitis. *J Sci Med Sport*. 2016, 9(9):713-5

This work was supported by the National Institute for Aging of the NIH under award number R01AG071646.

# EFFECTS OF BAREFOOT VS SHOD CONDITIONS ON CONVENTIONAL AND SUMO DEADLIFT TECHINQUES

*Paige M. Agnew[1], Kevin A. Valenzuela[3], Zachary A. Sievert[2], Hunter J. Bennett[1]
[1]Old Dominion University
[2]University of Cincinnati
[3]California State University, Long Beach
*Corresponding author's email: pagne002@odu.edu

**Introduction:** The deadlift is a commonly programmed strength training exercise for athletes and general population to activate the posterior chain musculature to move resistance from the floor up the body through extension of the lower extremity joints [1]. There are two common deadlift techniques, conventional and sumo, which involve different ranges of motion and emphasize different musculature [1-2]. In addition to technique, lifters may also elect to exercise barefoot in lieu of shod to elicit increased power [3], rate of force development [2], reduced work and center of pressure excursion [2,4] and increase stability [1]. Despite possible improvements in performance, it remains unknown how barefoot lifting impacts joint-specific loading profiles and how foot condition interacts with deadlift technique. The purpose of this study is to compare the effects of shod/barefoot sumo and conventional deadlifts on frontal and sagittal plane joint moments.

**Methods:**
This study included 8 males and 7 female (n = 15) participants that performed the sumo or conventional deadlift at least 2 days per week for >6 months. On day 1, each participant's 1-repetition maximum (1RM) for each deadlift variation was collected using NSCA guidelines, with a 10-minute rest period between. On a subsequent day, marker trajectory (Qualisys Oqus 200; 240 Hz) of the pelvis and lower extremities while simultaneous ground reaction forces (Bertec FP4060, 1200Hz) were recorded while participants performed 3 deadlift repetitions at 70% 1RM for each variation under barefoot and shod conditions. Five minutes of rest were provided between each set. Marker and force data were low pass filtered at 5Hz. A 6-degree of freedom inverse dynamics model was created for each participant to estimate sagittal and frontal plane hip, knee, and ankle joint moments (Fig. 1) which were time normalized from the start of the deadlift until the participant reached a standing posture. 2 (barefoot/shod) x 2 (conventional/sumo) repeated measures ANOVA were performed using Statistical parametric mapping (SPM; spm1d.org) to test each of the 6 variables. Alpha level was set at 0.01. Timings (% lift) and mean differences (Nm) are reported when significant suprathreshold clusters were found.

**Results & Discussion:** There were no deadlift variation (conventional/sumo) x foot (shod/barefoot) interactions for any variables. However, there were significant deadlift variation main effects for all joints and planes. Hip flexion (0-42% lift, mean 20.9Nm), ankle plantarflexion (0-54% lift, 26.79Nm), and ankle inversion (3-55% lift, 12.22Nm) were greater during conventional deadlifts. Hip abduction (17-32% lift, 20.5Nm; 65-100% lift, 30.25Nm), knee extension (11-49% lift, 38.81Nm; 84-100%, 15.94Nm), and knee abduction (0-61%, 27.51Nm; 80-100%, 17.19Nm) moments were larger for sumo deadlifts.

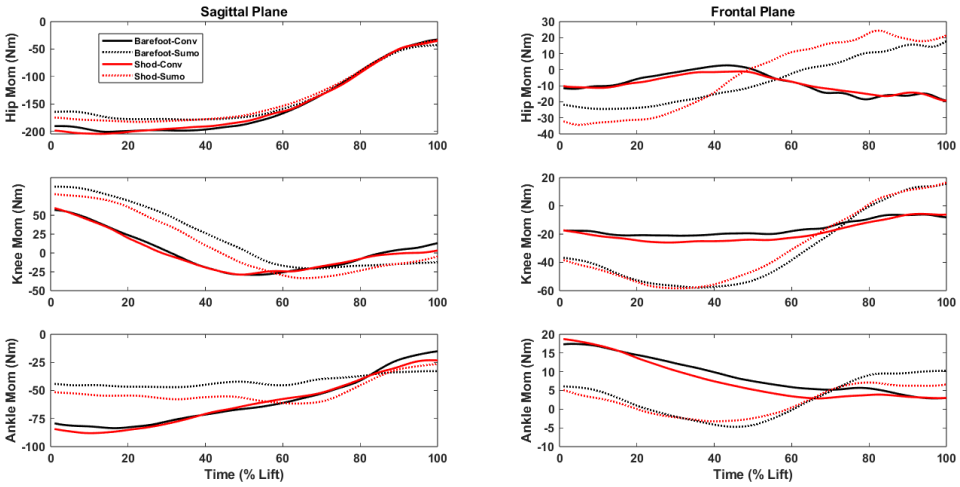


**Figure 1:** Ensemble hip, knee, and ankle sagittal and frontal plane moments for conventional (solid lines) and sumo (dashed lines) deadlifts barefoot (black) and shod (red).

Despite the advantages of barefoot lifting on barbell performance [1,3-4], we were not able to detect any impact on joint-level dynamics. Our results contradict many of those reported in Escamilla [1]; contrary to [1], we found knee extensor and flexor moments for both sumo and conventional deadlifts and ankle moments were always plantarflexion. Differences between studies are likely attributed to recent improvements in technology and our inclusion of only non-competitive, but trained males and females. The significantly greater hip and knee abduction moments found during sumo deadlifts may be controversial for lifters with preexisting knee stability issues or injuries [2]. Increased knee abduction moments could be used to enhance frontal plane mechanics and improve strength for the abductors, but may also exacerbate preexisting conditions (i.e., frontal plane knee malalignment). Additionally, conventional deadlifting may be more beneficial to increase muscle engagement from the hip extensors, ankle plantarflexors, and invertors [2].

**Significance:** The findings of this study, in conjunction with the current literature, illustrate that no discernible (dis)advantages exist at the joint level for barefoot lifting; thus, barbell improvements appear to come with little added cost. However, programming conventional or sumo technique requires much consideration based on their quite variable loading profiles.

**References:** [1] Hammer et al., 2018, *J Str Cond Res* ; [2] Escamilla et al 2000, *Med Sci Sports Exerc*; [3] Shorter et al. 2011, ISBS ; [4] Valenzuela et al., 2021, *Sports*

# EFFECTS OF MIDSOLE CUSHIONING AND OUTSOLE TRACTION ON ANKLE KINEMATICS DURING DOWNHILL TRAIL RUNNING

*Kathy E. Reyes[1], Anna Bennes[2], Amy Farley[2], Kelsey Goertzen[2], Austinn S. Rossetti[2], Loren Bruce Trottmann[2], J.J. Hannigan[2]

[1]Program in Kinesiology, Oregon State University, Corvallis, OR USA

[2]Program in Physical Therapy, Oregon State University-Cascades, Bend, OR USA

*Email: Reyeskat@oregonstate.edu

**Introduction:** Footwear companies incorporate features into trail running shoes that differ from road shoes, such as outsole traction lugs, to enhance the performance of trail runners and reduce the risk of injury. However, despite these incorporated features, trail runners still experience a significantly high risk of injury, with reports indicating up to 61.2 injuries per 1000 hours of running [1]. While trail running, runners encounter uneven surfaces and downhill conditions, which can lead to variation in foot-strike pattern [2], increasing the variability in ankle kinematics.

Maximal shoes, characterized by higher midsole stack height, were originally introduced by footwear companies to cater to the comfort needs of long-distance ultra runners who often run on trail surfaces. With the growing popularity of trail running and the high risk of ankle injury [3], the purpose of this study was to determine, in trail runners, the effects of midsole stack height (maximal vs traditional shoes) and the effects of outsole traction (no traction vs. high traction) on ankle kinematics while running downhill. Based on previous research, we hypothesized that peak ankle dorsiflexion and peak ankle eversion would be greater in maximal versus traditional shoes [4] and that peak dorsiflexion would increase in traditional shoes with no traction lugs compared to those with high outsole traction during downhill running.

**Methods:** Four experienced trail runners, aged 18 to 45, with at least three years of running experience, running a minimum of 15 miles per week, including at least one day or five miles on a trail, have participated in this study to date. Participants completed a 10-minute outdoor warm-up at a self-selected pace. They then performed five successful downhill trials per shoe condition at a comfortable pace, wearing Altra Olympus 6 (heel stack: 33 mm, forefoot stack: 33 mm) maximal shoes with high traction; Altra Lone Peak 8 (heel stack: 25 mm, forefoot stack: 25 mm) traditional shoes with high traction; and Altra Lone Peak traditional shoes with no traction lugs (Figure 1). Trials within ±5% of the established pace were considered successful.

**Figure 1:** From left to right, the men's traditional, traditional with no traction lugs, and maximal shoes used in this study (size 9.0).

Ten Sony RX0 II (Sony Corporation, Minato, Japan) cameras were synchronized using the Sony Camera Control Box and arranged along the downhill slope to collect data at 120 Hz. Video data were processed using Theia3D (Theia Markerless Inc., Kingston, ON, Canada), and ankle kinematics (initial contact angle, peak angle, joint excursion, and toe-off angle) of the dominant limb were calculated using Visual3D (HAS-Motion, Kingston, ON, Canada) in the frontal and sagittal planes. Biomechanical variables were compared between footwear conditions using repeated measures ANOVA ($\alpha = 0.05$). Bonferroni-corrected paired t-tests were used to identify specific differences between shoes.

**Results & Discussion:** Dorsiflexion at initial contact (Max: -17.92±6.64, No Lug: -21.87±7.94, Trad: -20.34±9.59, $p$=0.13), peak dorsiflexion (Max: 8.20±2.16, No Lug: 8.10±1.36, Trad: 7.14±1.61, $p$=1.00), dorsiflexion excursion (Max: 26.13±5.12, No Lug: 29.97±6.68, Trad: 27.48±9.02, $p$=0.35), inversion initial contact (Max: 2.65±2.97, No Lug: 2.40±3.45, Trad: 0.95±2.22, $p$=1.00), peak eversion (Max: -1.76±4.02, No Lug: -0.70±3.02, Trad: -1.50±2.77, $p$=1.00), eversion excursion (Max: 4.40±3.69, No Lug: 3.10±3.75, Trad: 2.45±1.03, $p$=0.37), showed no significant differences between shoe conditions at the ankle.

There were no significant differences in ankle joint kinematics between footwear conditions during downhill trail running, rejecting our hypothesis regarding both cushioning and traction. This could imply that footwear modifications targeting cushioning and traction may have a limited effect on ankle kinematics during downhill trail running. However, the study is ongoing, and future data collection may provide further insights.

**Significance:** This research examines how trail running footwear midsole cushioning and outsole traction affect ankle kinematics on downhill terrain, addressing a gap in the literature. With trail running participation increasing over the past decade, the impact of footwear on ankle kinematics and injury risk remains unclear. Identifying differences in ankle kinematics and footwear-traction interactions may help reduce ankle injuries, guide footwear selection, and support long-term running longevity.

**Acknowledgments:** I would like to thank the American Society of Biomechanics for awarding me the Grant-in-Aid and Dylan K. Schmidt for their assistance with data collection.

**References:** [1] Horvais, N., & Giandolini, M. (2013). *Footwear Sci*, *5*(sup1), S26–S27; [2] Viljoen et al., (2022), *Phys Therapy in Sport*, *56*, 60–75. [3] Hamill et al., (2022). *Footwear Sci*, *14*(2), 113–121. [4] Hannigan & Pollard, *J Sci Med Sport*. (2020), *23*(1), 15–19

# CREATING BIOFIDELIC REARFOOT AND FOREFOOT COMPRESSION TESTS TO QUANTIFY MECHANICAL BEHAVIOR OF RUNNING FOOTWEAR CUSHIONING

Rebekah R. Pallone*, Aymeric Feyfant, Bryan Conrad, Evan M. Day
Brooks Sports Inc.
*Corresponding author's email: rebekah.pallone@brooksrunning.com

**Introduction:** The mechanical properties of running footwear cushioning affect runner experience, especially beneath the rearfoot (RF) and the forefoot (FF) as these regions experience high forces during landing and push-off. To our knowledge, standards for quantifying RF and FF cushion properties beyond impact testing do not currently exist. While the ASTM F1976 5J impact test is the current industry standard for quantifying footwear cushion properties associated with decelerating a runner's effective mass in the first 35ms of stance, RF and FF loading cannot be described as "impact" [1]. Thus, force-controlled compression tests informed by running data may be more appropriate. While previous studies have explored force-compression tests in running footwear [2,3], the use of vertical ground reaction force (vGRF) data alone does not allow for isolation of the regional RF and FF pressures that contribute to the overall force magnitude. The purpose of this work was to develop data-informed force-compression tests using plantar pressure and vGRF data.

**Methods:** Plantar pressure data were collected from 14 recreational runners (8/6 M9/W8.5 US shoe size; 10 RF strikers) using an instrumented insole within the right shoe (200 Hz, Pedar, Novel). Runners performed 1-minute treadmill-running trials across 18 conditions consisting of 3 speeds (10, 12, 14 kph) in 6 shoe models of varying midsole materials, stack heights, and geometries. Ten steps from the end of each trial were analyzed. Contact time ($t_c$) was averaged across all steps, conditions, and runners, and pressure data were then splined to 101 data points. Data from RF strikers only (n=10) were utilized for RF analysis. The FF region was defined by 21 insole cells beneath the ball of the foot, and the RF region was defined by 20 insole cells beneath the heel (Fig. 1b). Pressure data from each region were converted to force using regional areas (Fig. 1a). Time to peak RF and FF force were defined as percentages of stance ($t_{peak,RF/FF}$), and the percentage of RF and FF force ($f_{peak,RF/FF}$) with respect to total-foot force were defined at their respective peak times. Regional force profiles, $t_{peak,RF/FF}$, and $f_{peak,RF/FF}$ were averaged across all steps, conditions, and runners. Regional force profiles were also normalized to peak for later scaling.

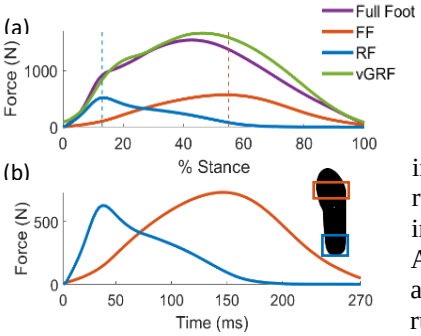


**Figure 1.** (a) RF, FF, and full-foot forces. Vertical lines represent timing of peak RF and FF forces. (b) RF and FF compression test waveforms.

To provide a more robust dataset beyond the 14 runners and 6 shoes from our pressure insole dataset, we utilized vGRF data from the past 3 years of Brooks product testing (~300 runners, Brooks and competitor footwear). vGRF data were collected at 2000 Hz from a Bertec instrumented treadmill at 12 kph (Fig. 1a) and normalized to bodyweight and shoe plantar area. Approximate peak RF and FF forces were calculated as $f_{peak,RF/FF} \times \text{vGRF}(t_{peak,RF/FF})$, averaged across all runners, and scaled to the bodyweight and regional foot areas of an average 700 N, M9 runner. RF and FF regional force profiles were time-scaled to $t_c$ and magnitude-scaled to peak RF and FF forces, respectively, and were prescribed to a linear dynamic test apparatus (ElectorPuls E3000, Instron) to define the RF and FF compression tests. A hemispherical tup was implemented for the RF test to represent the regional heel geometry, and a custom tup with an anatomic cross-rocker was implemented for the FF test to represent the regional forefoot geometry.

**Results & Discussion:** Average contact time, $t_c$, was 270 ms, average peak RF force was 630 N, and average peak FF force was 730 N (Fig. 1b). These force magnitudes are lower than previously published work (1000-2000 N) [1-3], as the current work isolated regional forces in the RF and FF (Fig. 1b) where we hypothesize runners will feel the cushion the most. Fig. 2 represents the force-displacement outputs from the RF and FF compression tests on 3 example shoes.

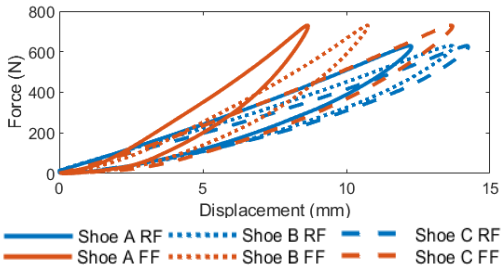


**Figure 2.** Force-displacement output curves from the rearfoot (RF) and forefoot (FF) compression tests for 3 example shoes.

One advantage to this force-driven method over a standard 5J energy-driven impact test is that it allows us to examine differences in midsole energy storage and return. RF/FF energy storage values from the example shoes in Fig. 2 are different from the current standard 5J impact test (Shoe A: 3.9/2.7 J; Shoe B 4.3/3.3J; Shoe C 4.4/4.7 J), lending greater insight into the benefit to the runner [4].

A key contribution of this work is that it may serve as a framework for the development of future biofidelic tests aimed to understand the mechanical properties of footwear under specific loading conditions (e.g. walking, different shoe sizes, elite athlete product). Additionally, while footwear is often designed with specific heel-toe offsets, mechanical differences in the RF and FF of a shoe can result in different dynamic offsets under load, leading to an undesired running experience. This work will help inform footwear design with a more comprehensive understanding of the mechanical behaviour of running footwear than the 5J impact test alone. Future work will correlate mechanical cushioning properties to runner perception to further improve shoe design.

**Significance:** This work presents a framework for creating biofidelic mechanical testing methods to quantify the cushioning behaviour of specific regions of running footwear. This work may inform running footwear design to achieve specific cushioning properties.

**Ref:** [1] Shorten & Mientjes. (2011), *Footwear Sci*, 3(1); [2] Dorschky et al. (2019), *Comput Methods Biomech Biomed Engin*, 22(8). [3] Hoogkamer et al. (2017), *Sports Med*, 48(4). [4] Worobets et al. (2014), *Footwear Sci*, 6(3).

**Vagus nerve stimulation paired with lower limb rehabilitation improves walking after chronic spinal cord injury: a pilot study**

*Spencer Dunbar[1,2], Emmanuel Adehunoluwa[1,3], Joe Epperson[1,2], Rhys Switzer[1,3], Robert Rennaker[1,3], Michael Kilgard[1,3], Seth Hays[1,2]

[1]Texas Biomedical Device Center, University of Texas at Dallas,

[2]Erik Jonsson School of Engineering and Computer Science, University of Texas at Dallas,

[3]School of Behavioral and Brain Sciences, University of Texas at Dallas

*sms180017@utdallas.edu

**Introduction:** Spinal cord injury (SCI) is a debilitating injury that affects 300,000 people in the United States alone, with 17,500 new cases occurring each year [1]. Among those with spinal cord injury, the ability to walk is often reported as one of the highest priorities for recovery [2]. Vagus nerve stimulation (VNS) has been approved by the United States Food and Drug Administration as an adjuvant treatment to be paired with upper limb physical therapy in some neurodegenerative disorders, such as stroke, and is currently being investigated as a treatment for spinal cord injury (NCT04288245).

Due to the significant improvements that have been observed in upper limb rehabilitation paired with VNS, we expected to see functional changes in the lower limbs when VNS was administered during lower limb therapy. This treatment is administered by pairing bursts of VNS with specific rehabilitative training, resulting in reinforcement learning through increased release of neuromodulators such as norepinephrine, acetylcholine, and serotonin. In the current study, VNS was paired with multiple exercises targeting the lower limb muscles activated in regular gait, as well as different walking variations such as backwards, sideways, and normal gait.

**Methods:** An algorithm was developed to stimulate the vagus nerve coinciding with the desired motion. This algorithm used an inertial measurement unit (IMU) on the midthigh to track the motion of the more impaired limb. This allowed us to track acceleration and changes in hip and knee angle for the subject so that stimulation could be paired temporally, as well as give us the ability to individualize treatment or exercises specific to participants. Additional IMUs were placed on the ankles to collect spatiotemporal gait parameters intermittently throughout the course of therapy.

Three participants were recruited that had previously received a vagus nerve stimulator implant as part of a prior study. These participants were required be ambulatory with a gait impairment. All participants completed 24 lower limb therapy sessions, each consisting of walking exercises as well as conditioning exercises for lower limbs. Participants underwent clinical assessments during enrollment, after 12 therapy sessions, and following their 24th therapy session. Clinical assessments included 6-minute walk test, 10-meter walk test, lower extremity motor score, Berg Balance Score, Timed Up and Go, and Walking Index for Spinal Cord Injury II.

In this study we aimed to examine the safety and feasibility of paired VNS with lower limb rehabilitation. Secondarily, we examined functional improvements like gait speed, timed distance, and gait quality using the aforementioned clinical measures.

**Results & Discussion:** No serious device related adverse events were reported in this study, indicating the potential safety of VNS paired with lower limb rehabilitation. All participants met and exceeded the minimally clinically identifiable difference(MCID) in both the 6-minute walk test (MCID = 45.8m) and 10-meter walk test (MCID = .13 m/s) [3]. In addition to substantial improvements in clinical assessments, participants also exhibited improvements in spatiotemporal gait parameters including increases in stride length, cadence, and speed over the course of therapy. These improvements in spatiotemporal gait parameters drew participants closer to the normative values for age and sex-matched healthy individuals [4].

The results from this study indicate the potential for VNS paired with lower limb rehabilitation for chronic incomplete spinal cord injury as a treatment to continue to make functional improvements. This also exhibits the need for a future randomized controlled trial to further investigate the effects of VNS paired with lower limb rehabilitation.

**Significance**: This study, as well as previous studies, demonstrates the potential for VNS paired with physical therapy in chronic SCI. Improvements in motor function could significantly improve the quality of life for participants. This study also provides information for power analysis for a future larger study to validate the results seen in this preliminary study.

**Acknowledgments**: This work was supported by the National Institute of Health UG3 NS131971. Research was performed at the University of Texas at Dallas. We would like to thank Christi Stevens for consultation and overview of the physical therapy. We would also like to thank Lazslo Demko, Armin Curt, and the rest of the ZurichMove team for their collaboration. We would like to thank Sukhran Chandrasekar and Noor Amous for assistance in data collection and entry. We would like to thank Holle Gallaway for technical support and expertise with study software and hardware. Additionally, we thank Alvaro Carrera for coordinating the clinical trials.

**References**: [1] National Spinal Cord Injury Statistical Center. (2012). The journal of spinal cord medicine, 35(4), 197–198.; [2] Anderson et al. (2004), Journal of Neurotrama 21(10); [3] Lam et al. (2007) Spinal Cord 46; [4] Rossler et al. (2024) Gait & Posture 109;

# SHORT WALKING TRIALS PRODUCE RELIABLE HURST EXPONENTS

Vasileios Mylonas[1*], Seung Kyeom Kim[1], Tyler M. Wiles[1], Nick Stergiou[1,2] & Aaron D. Likens[1]
[1]Department of Biomechanics and Center for Research in Human Movement Variability, University of Nebraska at Omaha, US
[2] Department of Physical Education and Sport Science, Aristotle University of Thessaloniki, GR
*Corresponding author's email: vmylonas@unomaha.edu

**Introduction:** Numerous experiments underscore the importance of nonlinear analyses to evaluate gait variability in understanding pathology [1]. These analytical approaches offer insights into the temporal structure of stride-to-stride fluctuations during walking. This structure is usually quantified through the Hurst exponent using Detrended Fluctuation Analysis (DFA). DFA is limited, however, as it requires long time series (≥ 512 points) [2,3] and produces weak-moderate reliability across trials [4-7]. These constraints pose challenges for clinical use, especially for groups who may be unable to sustain prolonged walking trials [3]. Another method, the Hurst-Kolmogorov (HK) algorithm delivers accurate estimations of the Hurst exponent with as few as 65 data points [2, 8]. However, its reliability has yet to be systematically evaluated. The present study evaluates the reliability of Hurst estimates in stride-to-stride intervals during preferred overground walking using the HK algorithm.

**Methods:** Walking data from 112 subjects from the NONAN GaitPrint dataset were used [9, 10]. Full body kinematic data was collected using inertial measurement units (200Hz). Participants completed 18 trials, each lasting 4 minutes (3 trials × 3 blocks × 2 days). Reliability was assessed using the Intraclass Correlation Coefficient (ICC) computed using the *psych* library in R. A two-way mixed effects ICC with consistency was used for all comparisons [11]. ICCs were calculated between all 18 trials (ICC (3,1)) and between days. ICCs between days were calculated for all 9 trials (9 trials in each day; ICC (3, k)), for each block (3 trials in each day; ICC (3, k)), and for each trial (1 trial in each day; ICC (3, 1)). The Hurst exponent of the right stride-to-stride interval time series was estimated using the HK algorithm ($H_{HKP}$). ICCs were calculated for Hurst exponents using time series containing the last 50, 100, 150 strides, and the entire stride interval time series for each trial (219.92 ± 17.51 strides).

**Results & Discussion:** Our results suggest poor to moderate reliability when using all 18 trials (Table 1). Excellent reliability was found when comparing the 9 trials between days with ≥ 100 strides (Table 1). The reliability of trials across days was found to be poor to moderate (Figure 1A). Finally, the reliability of blocks across days was good even for 50 strides (Figure 1B). Like DFA, the Hurst exponent calculated using the $H_{HKP}$ describes poor to moderate reliability across all 18 trials and improves with longer time series. Our findings further indicate that calculating Hurst exponents from 9 trials displays good to excellent reliability between days. Moreover, a block of trials (three 4-minute trials) also exhibits good to excellent reliability for trials with ≥ 100 strides. In contrast, lower levels of reliability are reported for a single trial between days. Previous work showed that $H_{HKP}$ is accurate with 64 strides [2]; our results show that three 4-minute trials are the minimum to yield reliable results. The narrower confidence intervals for the block-by-block (0.62-0.92) analysis compared to trial-by-trial (0.19-0.78) further support this claim (Figure 1).

**Table 1.** All cells contain ICC values [95% Confidence Intervals] based on the number of strides and comparison.

| Comparison | ICC Formula | 50 Strides | 100 Strides | 150 Strides | Individual Strides |
|---|---|---|---|---|---|
| Among all 18 trials | ICC (3, 1) | 0.45 [0.38,0.54] | 0.56 [0.49,0.64] | 0.63 [0.56,0.70] | 0.66 [0.60,0.73] |
| Between days for all 9 trials | ICC (3, k) | 0.88 [0.82,0.92] | 0.90 [0.85,0.93] | 0.92 [0.88,0.94] | 0.91 [0.87,0.94] |

**Significance:** For healthy adults**,** we presented evidence that three 4-minute trials yield good to excellent reliability for $H_{HKP}$. Shorter assessment protocols, including three 4-minute walking trials, are feasible for those with declined mobility, addressing the challenges associated with longer evaluations and the limitations of using the DFA algorithm. Future studies are needed to investigate the reliability of the Hurst exponent in walking of pathological groups to provide more extensive clinical recommendations.

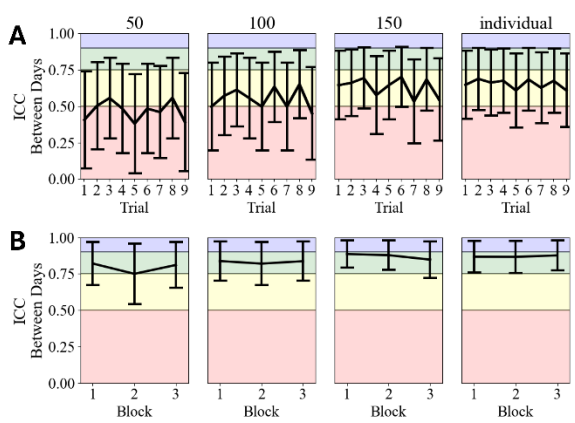


*Figure 1. Intraclass Correlation Coefficient for Hurst exponents for the* ***between day reliability of each trial*** *(A) and the* ***between day reliability of each block*** *(B). Error bars represent the 95% Confidence Intervals. The shaded red, yellow, green, and blue areas represent poor (< 0.5), moderate (0.5–0.75), good (0.75–0.9) and excellent (> 0.9) reliability, respectively.*

**Acknowledgments:** NSF: 212491, NIH: P20GM109090, P20GM152301, and the Nebraska Collaboration Initiative.

**References:** [1] Stergiou & Decker (2011) *Hum. Mov. Sci.*, 30(869–888). [2] Likens et al. (2023) *arXiv*. [3] Marmelat & Meidinger (2019) *Gait Posture*, 70(229–234). [4] Pierrynowski et al. (2005) *Gait Posture*, 22(46–50) [5] Choi et al. (2015) *J. Biomech.*, 48(1336–1339) [6] Slattery et al. (2024) *Gait Posture*, 114(257–262). [7] Raffalt et al. (2018) *J. Biomech. Eng.*, 140(124501). [8] Tyralis & Koutsoyiannis (2011) *Stoch. Environ. Res. Risk Assess.*, 25(21–33). [9] Wiles et al. (2023) *Sci. Data*, 10(867). [10] Wiles et al. (2025) *Sci. Data*, 12(143). [11] Shrout & Fleiss (1979). *Psychol. Rev.*, 86(2)

Effect of hip joint center location on lower extremity angles and moments during running

*Madeline Grosklos[1], Adam Bunn[1], Marisa Pontillo[1]
[1]Extremity Trauma and Amputation Center of Excellence, San Diego, CA, USA
*Corresponding author's email: grosklos.2@osu.edu

**Introduction:** Accurate measurement and quantitative analysis of human movement is imperative for assessing clinical conditions, optimizing recovery from injury, and enhancing athletic performance. Musculoskeletal models used to describe such movement can vary greatly. For example, hip joints centers (HJCs) can be defined using anatomical landmarks (AHJC) or functional movement trials (FHJC). While FHJCs are often preferred [1], they require more time and effort and may not be obtainable in all situations. Additionally, existing published data contains results from models using varied HJC methods, which are continuously referenced and used to generate new hypotheses. The purpose of this study was to quantify the differences in lower extremity angles and moments during running between models that differed only in the determination of HJCs (anatomical versus functional) and to evaluate whether these differences exceed clinically meaningful thresholds based on standard measurement error for modern 3D motion capture systems [2].

**Methods:** In this secondary analysis of a dataset for run retraining in U.S. service members with lower extremity pain, 72 individuals (144 limbs treated as individual observations) with unilateral or bilateral knee pain were included (47 male, age:31.8±7.7 years, BMI:26.3±4.1 kg/m$^2$). Participants underwent 3D motion capture of running (120Hz) at a self-selected pace on an instrumented treadmill (1200Hz). Prior to running trials, participants performed the STAR-ARC movement [3], used to calculate the functional HJC in Visual3D (v2024.10.1) (Gillette algorithm [4]). The two models applied to each participant in Visual3D had sex-specific inertial parameters and were identical aside from the hip joint center and pelvis kinetics. The anatomical model had a CODA pelvis and the associated AHJCs [5] whereas the custom model applied FHJCs and a custom FHJC-pelvis segment for use in kinetic calculations. Kinematics for both models used the CODA pelvis to maintain physiological pelvic tilt. Relevant sagittal and frontal plane hip and knee kinetics and kinematics were averaged over one 20-second running trial. Peak value differences were calculated at the index of the AHJC model peaks to maintain consistent timing between compared values. Least Absolute Shrinkage and Selection Operator (LASSO) regression was performed with 10-fold cross-validation to identify significant relationships between HJC position differences in all three planes and differences in peak hip/knee angles and moments for each observation (limb) in R (v4.4.1, package glmnet).

**Results & Discussion:** The FHJCs were, on average, 2.29cm more inferior (range: -6.75, 3.30), 0.88cm more anterior (range: -3.70, 5.22) and 0.48cm more lateral (range: -2.35, 3.75) than AHJCs (negative = inferior, posterior, and medial). LASSO revealed strong, plane-specific relationships between HJC displacement and kinematic outcomes ($R^2$ = 0.91-0.95) (Table 1). Compared to AHJC, a 1 cm posterior displacement of the FHJC was strongly associated with increased peak hip flexion (+1.29°) and knee flexion (+1.27°) and decreased peak hip extension (-1.31°) and knee extension (-1.27°). The largest difference between HJCs in the anterior-posterior axis was 5.22cm, indicating that HJC choice could account for a change in peak hip and knee flexion angles of over 6.5°. Conversely, a 1 cm lateral displacement was associated with increased peak hip adduction (+1.29°) and knee abduction (+1.18°) and decreased hip abduction (-1.26°) and knee adduction (-1.17°). The greatest lateral difference in HJCs estimated 4.43° more knee abduction, which is 22% of this cohorts' average range of motion for the knee in the frontal plane (19.75°). Predictions for hip and knee adduction and knee flexion moment were moderately strong ($R^2$=0.81–0.88). The largest effect for kinetics was hip adduction moment; a 1cm lateral displacement of the HJC was associated with a 0.19Nm/kg or 12% increase. Displacements in the superior-inferior axis showed smaller effects across all variables, and predictions for hip flexion and extension moments were less robust (Table 1).

| AHJC-FHJC | Hip Kinematics | | | | Knee Kinematics | | | | Hip Kinetics | | | Knee Kinetics | |
|---|---|---|---|---|---|---|---|---|---|---|---|---|---|
| | Flex | Ext | Add | Abd | Flex | Ext | Add | Abd | Flex | Ext | Add | Flex | Add |
| $R^2$ | 0.946 | 0.950 | 0.937 | 0.950 | 0.944 | 0.944 | 0.911 | 0.923 | 0.378 | 0.234 | 0.884 | 0.829 | 0.812 |
| λ | 0.0193 | 7.75E-03 | 0.0162 | 4.88E-03 | 0.0307 | 0.0336 | 4.62E-03 | 4.62E-03 | 2.90E-04 | 0.0121 | 6.40E-04 | 3.00E-05 | 1.20E-04 |
| HJC_x | -0.0400 | -0.0780 | -1.29 | -1.26 | -0.0200 | -8.00E-03 | -1.17 | -1.18 | 0.0120 | 0 | -0.189 | 8.00E-03 | -0.0290 |
| HJC_y | -1.29 | -1.31 | 0 | -0.0570 | -1.27 | -1.27 | -0.0880 | -0.0720 | -0.0670 | -0.0210 | 0.0120 | 1.00E-03 | -3.00E-03 |
| HJC_z | 0.0930 | 0.0910 | 0.0690 | 0.0530 | 0.0620 | 0.0540 | 0.0550 | 0.0440 | 0.0330 | 0 | 0.0310 | -1.00E-03 | 3.00E-03 |
| MAE | 0.294 | 0.289 | 0.268 | 0.235 | 0.302 | 0.308 | 0.305 | 0.281 | 0.108 | 0.0480 | 0.0530 | 3.00E-03 | 0.0110 |

**Table 1:** LASSO regression results. Flex=flexion; Ext=extension; Add=adduction; Abd=abduction; MAE=mean absolute error

**Significance:** Changes in sagittal plane kinematics caused by HJC location exceed the 5° threshold typically accepted as measurement error for marker-based motion capture systems [2]. Further, changes in frontal plane angles and moments reached 22% and 45% of average peak values, respectively. These results indicate that HJC methodology alone can have impacts on running data that may change clinical interpretation of movement patterns. This is important to consider when comparing results across studies, where HJC methods may be only one of multiple data collection and processing differences.

**Acknowledgments:** The views expressed are those of the author(s) and do not reflect the policy or position of any agencies under the U.S. Government. This project was supported by an appointment to the Research Participation Program for the Sponsor administered by Oak Ridge Institute for Science and Education through an agreement between the U.S. Department of Energy and the Agency.

**References:** [1] Kainz et al. (2015), *Clin Biomech* 30; [2] McGinley et al. (2009) *Gait&Post* 29(3); [3] Camomilla et al. *J Biomech* 39(6); [4] Schwartz & Rozumalski (2005) *J Biomech* 38(1); [5] HAS-Motion Documentation. Coda Pelvis. wiki.has-motion.com.

# A NOVEL ALGORITHM ESTIMATING RATES OF DIVERGENCE REVEALS AGE-RELATED GAIT DYNAMICS

Seung Kyeom Kim[1], Tyler Wiles[1], Nick Stergiou[1,2] & Aaron D. Likens[1]
[1]Department of Biomechanics, University of Nebraska at Omaha, Omaha, NE
[2]Department Physical Education and Sport Science, Aristotle University of Thessaloniki, Greece
*Corresponding author's email: seungkyeomkim@unomaha.edu

**Introduction:** When we speak about mathematically chaotic systems, we mean those that produce complex, unpredictable behavior despite being highly deterministic. On the same realm, chaotic biological behaviors, including repetitive human movements like walking and running, are depicted as quasi-periodic patterns that appear similar in each cycle but are never truly identical. A key metric to quantify chaos is the largest Lyapunov exponent ($\lambda$) [1, 2, 3], which measures the rate at which nearby trajectories in a system's phase space diverge over time. A positive $\lambda$ indicates divergence and mathematical instability, while a negative $\lambda$ signifies convergence and mathematical stability. In an n-dimensional system (i.e., a system with n-state variables), n $\lambda$s can be estimated, each representing the system's behavior on each principal axis of motion. Chaotic behavior involves a spectrum of positive and negative $\lambda$s. However, most existing algorithms mainly focus on the largest Lyapunov exponent, $\lambda_1$, limiting our understanding of movement. This study introduces a novel algorithm that quantifies divergence rates across all principal axes and applies this approach to human overground walking.

**Methods:** 35 young adults, 44 middle adults, and 41 older adults each performed 18 overground walking trials lasting 4 minutes. Whole-body kinematics were collected via inertial measurement units at 200Hz [4]. For each walking trial, the thigh segment angle time series was differentiated to obtain the thigh segment angular velocity and acceleration time series. Then, 3-dimensional phase spaces were reconstructed by using thigh segment angle, angular velocity, and acceleration as the axes. Next, 10,000 datapoints were randomly sampled for each walking trial. For each datapoint, 100 nearest neighbors in the phase space were identified based on Euclidean distance, and these neighbors were tracked forward for 1,000 timepoints. At each timepoint, eigenvalue decomposition was performed on the covariance matrix of the 100 nearest neighbors to obtain the eigenvalues on their principal axes. For each trial, 3 eigenvalue time series, each of length 1,000, were generated for all sampled datapoints. Each eigenvalue time series was then averaged across the 10,000 data points at each time point and log transformed. Lastly, the slope from the start of each log transformed time series to its first peak were computed to quantify the rate of divergence. Three rates of divergence ($\lambda_1$, $\lambda_2$, and $\lambda_3$) were estimated per walking trial. A multivariate multilevel model was used to examine the effect of age group on each rate of divergence.

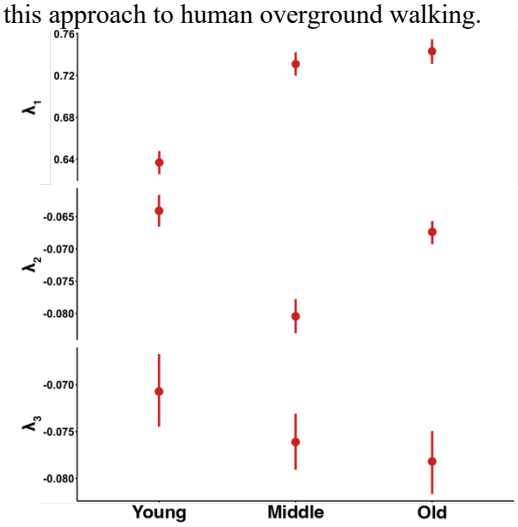


**Figure 1.** Rates of Divergence Across Groups. Red dots indicate mean values. Red vertical lines indicate 95% confidence intervals.

**Results & Discussion:** Across all walking trials, $\lambda_1$ ranged between 0.138 and 1.097, $\lambda_2$ ranged between -0.380 and -0.014, and $\lambda_3$ ranged between -0.377 and -0.015. These ranges indicate the divergent behavior of walking on the first principal axis and the convergent behaviors of walking on the second and third principal axes of the nearest neighbors. That is, thigh dynamics is indeed chaotic, ensuring both flexibility and stability. The multivariate multilevel model revealed a significant main effect of age group on $\lambda_1$ and $\lambda_2$ (Figure 1). To investigate the main effect of age group, we performed pairwise comparisons among age groups. With respect to the main effect of age group on $\lambda_1$, young adults had significantly lower $\lambda_1$ compared to middle and older adults (95% credible interval: [-0.153 -0.045], [-0.161 -0.051]) (Figure 1 top). Regarding the main effect of age group on $\lambda_2$, middle adults had significantly lower $\lambda_2$ compared to young and older adults (95% credible interval: [-0.027 -0.006], [-0.021 -0.002]) (Figure 1 middle). In general, the differences in $\lambda_1$ and $\lambda_2$ among age groups suggest that there may be an interplay between the rate of divergence and convergence in their gait dynamics across the lifespan. An optimal balance between divergence ($\lambda_1$) and convergence ($\lambda_2$, $\lambda_3$) may allow both adaptability and stability during walking, which would be the case in young adults. Disruption of this equilibrium due to excessive divergence ($\lambda_1$) may imply instability, leading to greater demand in compensatory convergence ($\lambda_2$, $\lambda_3$) as shown in middle adults. In older adults, however, divergence increased, whereas convergence decreased, potentially reflecting impaired motor function. By capturing divergent and convergent behaviors across all principal axes, the new algorithm provides a more holistic view of how gait evolves with age.

**Significance:** This study introduces a novel algorithm that quantifies rates of divergence across all principal axes of the nearest neighbors. Our algorithm enables researchers to capture both the divergent and convergent properties of movement dynamics, offering a more nuanced view of chaotic behavior in human movement. This study revealed age-related differences in $\lambda$s, providing new insights into how gait dynamics may be altered with aging. Our findings not only advance theoretical understanding of gait as a high dimensional dynamical system but also have practical implications for rehabilitation optimizing gait stability and mobility among aging populations.

**Acknowledgments:** This work was supported by the Center for Research in Human Movement Variability at the University of Nebraska at Omaha, the University of Nebraska Collaboration Initiative, the NSF award 212491, the NIH awards P20GM109090, R01NS114282, and P20GM152301

**References:** [1] Wolf et al. (1985), *Physica D: Nonlinear Phenomena* 16(3); [2] Rosenstein et al. (1993), *Physica D: Nonlinear Phenomena* 65(1-2); [3] Mehdizadeh et al. (2019), *Journal of Biomechanics* 85; [4] Wiles et al. (2025), *Nature Scientific Data.*

# REVISITING HOF'S INVERTED PENDULUM WALKING MODEL FROM A STATE SPACE PERSPECTIVE

*J. P. Cusumano[1], W. Corvino[1], N. S. Patil[1,2], and J. B. Dingwell[2]
[1]Department of Engineering Science & Mechanics; [2]Department of Kinesiology
Pennsylvania State University, University Park, PA, USA
*jpc3@psu.edu

**Introduction:** The margin of stability (MoS) is widely used in experimental gait analysis to characterize dynamic stability. However, its interpretation remains a topic of scientific debate, primarily because normally walking humans routinely take steps with negative MoS without experiencing falls or other adverse consequences [1].

In developing the MoS [2,3], Hof et al. used a simple walking model, or *template* [4,5]: a single degree-of-freedom (DOF) inverted pendulum (IP) [3]. However, while this describes within-step dynamics in the sagittal or frontal planes separately, it does not capture the motion of the human center of mass (CoM) while walking in two dimensions. This contributes to ambiguities in the interpretation of MoS and hinders the model's wider application, particularly to the study of step-to-step dynamics.

Here, we reexamine Hof's model and argue that it can be better formulated as a *spherical* inverted pendulum (SIP) with a *moving base*, giving it a 5-dimensional (5D) state space comprised of 2 positions, 2 velocities, and time, which enters through the prescribed CoP (Fig. 1). This state space structure is obscured by the original focus on the planar IP model [2,3]. We describe the general form of a 4D stepping (Poincaré) map defined at step transitions, which relates sequences of steps to continuous-time motions of the CoM. Analysis of the map's stability properties leads to an improved understanding of the IP template and, in turn, the MoS.

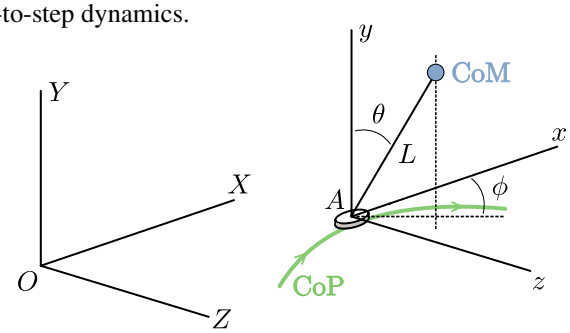


**Figure 1:** Inertial $\{X, Y, Z\}$ and body-fixed $\{x, y, z\}$ reference frames for spherical inverted pendulum (SIP) with origins at $O$ and $A$, respectively: $O$ is fixed, $A$ moves with center of pressure (CoP; green curve in horizontal plane).

**Methods:** We derived the SIP model from mechanical first principles for an arbitrary time-dependent CoP. For small deviations from the vertical, the model is well-approximated by uncoupled linear IP models in the sagittal and frontal planes, as in [3]. However, we also identify the coupling between sagittal and frontal planes for CoM excursions beyond the linear limit.

Using the uncoupled linearized IP models in $z$ and $x$ (Fig. 1), with constant CoP within each step and a "constant offset" regulation scheme, as in [3], we obtained the 4D stepping map in analytical form. The unique fixed point of the map was found, yielding an expression for the model's steady gait and conditions for its local stability, both as a function of system parameters.

We thereafter focused on lateral stepping, which was simulated numerically starting from each initial condition in a fine grid of the lateral walker's state space (Fig. 2). Each simulation was run until it either reached the stable gait or was stopped because it required a crossover step or a step width exceeding a prescribed maximum, here set to $0.8L$.

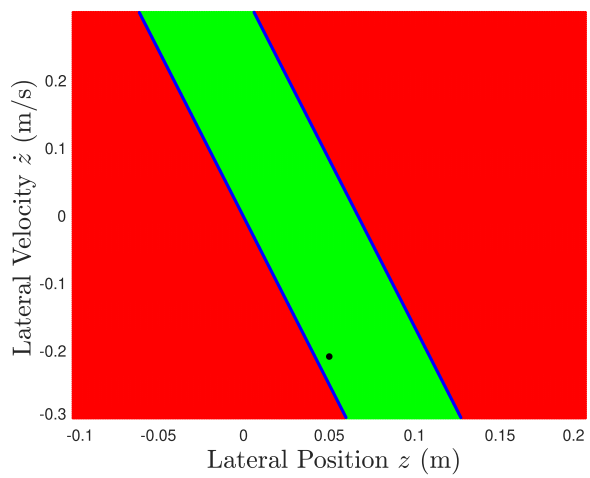


**Figure 2:** Typical numerical result showing the *recovery basin* (green region) obtained with the lateral stepping map derived from Hof et al.'s IP model with constant offset regulation [3]: starting from states in the recovery basin, the walker can return to the stable gait (black dot); starting from states in the red region, the walker cannot recover with steps satisfying biomechanical constraints. Numerical basin boundaries match analytical expressions (dark blue lines).

**Results & Discussion:** The numerical results identified the *recovery basin*, shown in Fig. 2: starting from states *within* the basin (green region) the walker can take viable steps [5] that return to the stable gait (black dot); states *outside* the basin (red region) lead to steps that violate the model's biomechanical constraints. The boundaries of the recovery basin were also found analytically (dark blue lines): they correspond to constant MoS values, in general not equal to zero, determined by regulator parameters. Recovery basins thus suggest that, rather than determining stability per se, the MoS defines a state space boundary or *threshold* [1] beyond which a walker needs to change regulation schemes and/or recruit DOF outside of a given template to keep taking viable steps.

**Significance:** The SIP (Fig. 1) clarifies the state space structure of Hof's original IP model [3] and facilitates its generalization, while enabling the unambiguous determination of steady gaits and their local stability. This state-space approach opens the door to further experimental applications of this class of template, with the aim of relating the continuous-time dynamics of the CoM and the discrete-time dynamics of stepping under various hypothesized stepping regulation strategies, including those involving modulations to the CoP.

**Acknowledgments:** This work was partially funded by NIH/NIA Grant #R01-AG049735 and a Penn State Erickson Discovery Grant.

**References:** [1] Kazanski et al. (2024) *Gait & Post.*; [2] Hof et al. (2005) *J. Biomech.*; [3] Hof (2008) *Hum. Mov. Sci.*; [4] Full & Koditschek (1999) *J. Exp. Biol.*; [5] Patil et al. (2024) *Interface*.

# 5-TIMES SIT TO STAND PERFORMANCE IN UNILATERAL TRANSTIBIAL PROSTHESIS USERS SHOULD BE SCALED TO BODY SIZE

*Alyssa McIntosh[1], Brian J. Hafner[2], Andrew Sawers[1]
[1]University of Illinois Chicago, [2]University of Washington
*Corresponding author's email: amcint23@uic.edu

**Introduction:** The Five-Times Sit-to-Stand (5xStS) test is a widely used measure of lower-limb strength in research and clinical settings [1]. However, traditional 5xStS scoring does not account for anthropometric differences, which may influence performance and confound interpretation, particularly in populations with mobility impairments such as lower limb prosthesis (LLP) users [2]. Body size - the product of mass and height - has been shown to confound and alter the interpretation of isometric measures of hip strength in LLP users [3]. Despite the frequency with which timed sit-to-stand tests are used to assess lower-limb strength, whether they are also susceptible to the confounding effects of body size is unknown. The primary objective of this study was to determine if body size had a confounding effect on 5xStS performance in unilateral transtibial prosthesis users (TTPU), and whether any confounding effect altered interpretation of 5xStS performance. A secondary objective was to determine the suitability of the 5xStS test as designed (i.e., without upper body assistance) for TTPUs.

**Methods:** 191 unilateral TTPUs were recruited for the study. Participants performed the 5xStS as able (e.g. with or without upper body assistance). Chi-squared tests were run to identify characteristics (e.g., sex, K-level, and etiology) of TTPUs who did and did not require upper body assistance to perform the 5xStS test. An independent samples t-test was conducted to compare the age, time since amputation, and average grip strength between the assist and no assist groups. Allometric scaling [2,4] was used to determine the extent to which 5xStS performance was associated with, and therefore needed to be adjusted for the influence of body size. Following allometric scaling, several inferential analyses were conducted to determine if the interpretation of 5xStS performance was altered by scaling performance to body size. First, independent sample t-tests were run to determine if 5xStS performance between sexes (M vs. F), mobility levels (K3 vs. K4), and amputation etiology (traumatic vs. dysvascular) were affected by scaling.

**Results & Discussion:** 191 unilateral TTPUs completed the 5xStS test (134 males; age: 51±15.7 years; body mass: 87.8±21.3kg; height: 1.7±0.09m; time since amputation: 14 years; dysvascular etiology: 33). 89 (47%) of the participants were able to perform the 5xStS test as designed (i.e. with no upper body assistance) (60 males; mean age: 46±15.7 years; time since amputation: 14yrs ± 14.1 years; dysvascular etiology: 8). TTPUs who required upper body assistance to perform the 5xStS test were significantly older and had lower grip strength than those that did not (age: assist group=55±4.6 years, no assist group=45±15.7 years, $p<0.001$), (grip strength: assist group=33.3N, no assist group: 38.2N, $p=0.002$). Time since amputation had no effect on the use of assistance (14±15 years; $p=0.972$). Our results suggest that when administered as designed (i.e., no upper body assist), the 5xStS test appears best suited to younger TTPUs (i.e.,≤ 55 years old). Modifications to the design and administration of the 5xStS test may be required to increase its appropriateness as a measure of lower limb strength or power among TTPUs (e.g., modified squat test) [5]. Allometric scaling revealed that the 95% confidence interval for the slope of log-transformed 5xStS times and log-transformed body size included neither 0 nor 1 (slope=0.221 [0.027, 0.415]), indicating a non-linear association between the 5xStS times and body size. Upon scaling 5xStS times to body size (i.e., scaled 5xStS = unscaled 5xStS / body size$^{slope}$) the 95% confidence interval for the slope of the log-transformed scaled 5xStS time and log-transformed body size included 0 (slope=0.080 [-0.056, 0.216]), indicating a slope that was not significantly different from 0 (i.e, no association between scaled 5xStS performance and body size). These results suggest that allometric scaling can successfully identify and remove the confounding effect of body size on 5xStS performance in TTPU. Prior to scaling, 5xStS times were significantly longer in moderate (K3) than high activity (K4) TTPUs (K3: 11.5±2.5; K4: 10.3±2.7, $p=0.041$). After scaling 5xStS times to body size those differences in 5xStS times between K3 and K4 TTPUs were no longer significant ($p=0.072$). From this we conclude that body size confounds the effects of mobility on 5xStS performance (i.e., lower limb strength) among TTPUs. In contrast, 5xStS times were significantly different based on amputation etiology prior to ($p=0.030$) and after scaling ($p=0.047$), suggesting that body size does not confound the effect of amputation etiology on 5xStS performance.

**Significance:** In the absence of considering the need to scale 5xStS performance to body size in TTPUs, performance may be misinterpreted. Our results emphasize the importance of scaling functional assessments for anthropometric variability to improve accuracy in evaluating strength and mobility in LLP users and other clinical populations [6]. When administered as designed, timed sit-to-stand tests may have limited application among TTPU. In light of the significant role played by hip strength in determining LLP users' balance and mobility [7], clinically feasible and physically achievable performance tests of lower limb strength are needed.

**References:** [1] Alcazar et al. (2018). *Exp. Gerontol*, 112:38–43. [2] Jaric, S. (2003). *ESSR*, 31(1):8–12. [3] Sawers and Fatone (2022). *Clin Biomech*, 57. [4] Nevill et al. (1992). *Eur J Appl Physiol Occup Physiol*, 65(2):110–7. [5] Tapanya et al., (2024). *Ann Geriatr Med Res*, 28(2): 209-18. [6] Pua et al. (2006). *Phys Ther*, 86(9):1263-70. [7] Sawers and Fatone (2025). *PM R*, 17(2):147-58.

# TIMING IS EVERYTHING: THE EFFECT OF MEASUREMENT TIMING ON THE VALIDITY OF TRAILING LIMB ANGLE IN GAIT ANALYSIS

Sally Kenworthy PhD, CPO[1,2], Stacey Gorniak PhD, FAHA[1]
[1]University of Houston, Department of Health and Human Performance, Center for Neuromotor and Biomechanics Research
[2]Baylor College of Medicine, School of Health Professions, Orthotics and Prosthetics
Sally.Kenworthy@bcm.edu

**Introduction:** Propulsion is a key component of efficient human gait [1, 2] and is often impaired after neurological injury, such as stroke [3]. Propulsion is commonly defined as the anterior component of the ground reaction force (AGRF). Impaired propulsion negatively affects step length asymmetry, 6-minute walking distance, and walking speed [4, 5, 6]. Despite its clinical relevance, propulsion is difficult to measure without access to force plates. Trailing limb angle (TLA), which reflects limb position at push-off, has emerged as a valid and accessible proxy for AGRF parameters [4, 5, 6] and is a useful biofeedback target in gait rehabilitation [7]. However, inconsistent measurement approaches hinder clinical translation. Studies have calculated TLA at different times in the gait cycle, including toe-off, terminal stance, and double support. This study aimed to describe the timing of peak propulsion timing in older, unimpaired adults and compare the different approaches to TLA measurement. Given the dynamic model of human walking [2], we hypothesized that peak propulsion would occur before contralateral heel strike (HS) and that there would be significant differences in TLA measurements among the different approaches.

**Methods:** This observational cross-sectional study was approved by the University of Houston Institutional Review Board (STUDY00002095). Older, unimpaired adults between 50 and 65 years of age were recruited for this study. A 16-camera VICON motion capture system was used to collect 3D positions of reflective markers using the VICON Plug-In-Gait-Model with the Oxford Foot Model extension. Participants walked for 3 1-minute trials at their self-selected walking speed (SSWS) on a Bertec instrumented split-belt treadmill. Propulsion was defined as peak AGRF normalized to body weight. Peak AGRF timing, ipsilateral toe-off (TO), and contralateral HS were expressed as a percentage of the total gait cycle. HS and TO identification thresholds were set at 30N. TLA was defined at the angle between the laboratory's vertical axis and the vector connecting the greater trochanter and a distal landmark on the 5$^{th}$ metatarsal head (TLA5M) or lateral malleolus (TLALM). Paired t-tests and ANOVA were calculated to compare timing events and TLA measurement approaches with significance level set at $p$ <.05.

**Results & Discussion:** Nineteen older unimpaired adults (mean age [SD]: 56.42 [4.14]) completed the study. In support of our hypothesis and the dynamic model of walking, the results of this study showed that peak AGRF occurs (47.50%) statistically significantly earlier than contralateral HS (49.99%, $p$ <.001) in unimpaired gait (Figure 1). Peak AGRF occurred significantly earlier than ipsilateral TO, indicating that peak propulsion occurs during single support, rather than the double support phase. Therefore, TLA measured during double support may not be valid alternative measure of peak propulsion. Notably, TLALM peaked on average 1.27% before ipsilateral TO and TLA5M peaked on average .50% after, aligning closely with TO timing. This proximity may partially explain the frequent use of this measurement approach in the literature. However, our results suggest that TLA measurements at ipsilateral TO do not represent peak propulsion but rather the peak value of TLA. This critical distinction is emphasized by directly comparing the result of each measurement approach. Peak TLA5M (22.77° [3.03]) and TLALM (27.88° [2.31]) were statistically significantly larger than TLA measured at the time of peak propulsion (16.08° [1.77], and 23.69° [1.75] respectively, $p$ <.001).

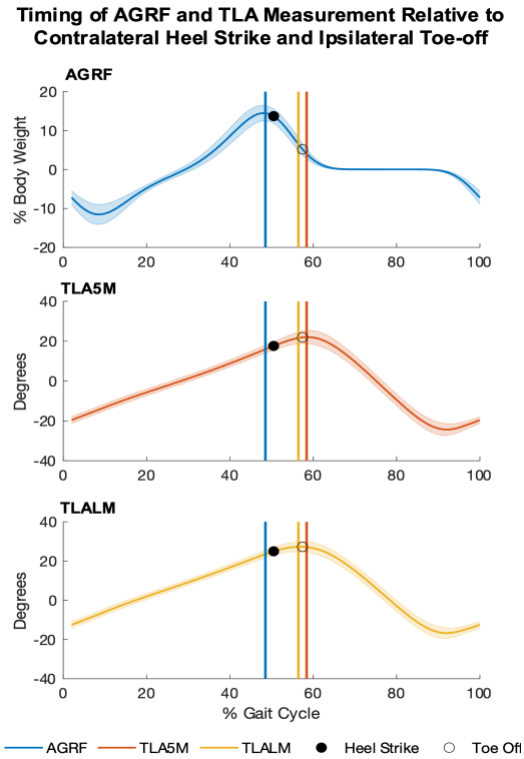


**Figure 1:** Sample mean (solid lines) and SD (shaded area) of AGRF, TLA5M, and TLALM. Vertical lines represent the timing of the peak value of each color coded respective variable.

**Significance:** TLA could offer a clinically accessible, point-of-care assessment for propulsion in impaired populations and has recently been used as a biofeedback measure in gait training. However, our study highlights that the timing of TLA calculations is crucial. We found that peak TLA does not necessarily coincide with peak AGRF, challenging the assumption that they can be used interchangeably. This discovery lays a stronger foundation for future research to optimize the timing of TLA calculations in the assessment of pathological gait, when timing of key gait events is likely altered.

**Acknowledgments:** We would like to acknowledge Leah Karels and Abigail Clement for their assistance with data collection for this study.

**References:** [1] Donelan et al. (2002), *J Exp Biol.* 205; [2] Kuo & Donelan (2010), *Phys Ther.* 90; [3] Roelker et al. (2019) *Gait Posture* 68; [4] Balasubramanian et al. (2007), *Arhc Phys Med Rehabil.* 88; [5] Bowden et al. (2006), *Stroke.* 37; [6] Awad et al. (2015) *Neurorehab and Repair*, 29; [7] Liu et al. (2021), *Gait Posture*. 83;

# CAN THE OPENCAP MARKERLESS MOTION CAPTURE FRAMEWORK DETECT LOWER EXTREMITY KINEMATIC CHANGES DURING A FATIGUING RUN

Sean P. Doherty[1], Alan R. Needle[1, 2], Robert J. Kowalsky[1], Herman van Werkhoven[1]*
[1]Department of Public Health and Exercise Science, Appalachian State University, Boone, NC, USA
[2]Department of Rehabilitation Sciences, Appalachian State University, Boone, NC, USA
*Corresponding author's email: vanwerkhovenh@appstate.edu

**Introduction:** During endurance running, biomechanical changes in running form can be detrimental to performance and can increase the risk of injury. A traditional "gold standard" method to study these changes, 3D passive reflective marker-based motion capture systems, presents several barriers to use including financial cost, space, and accessibility limitations. The OpenCap markerless motion capture framework utilizes an open-source algorithm to compute and process kinematics and dynamics of human movement [1]. With two or more smartphones and an internet connection, OpenCap provides a more accessible alternative method for motion capture. This validation study investigated the ability of the OpenCap framework to detect kinematic changes at the hip, knee, and ankle due to a fatiguing run when compared to a marker-based motion capture system. Previous literature reported a kinematic root mean square error of 5.8 ± 1.8° for OpenCap during walking gait, potentially above the expected joint angle changes seen during fatigued running (<2°) [2, 3]. Due to this, it was hypothesized 1) that the lower extremity kinematics measured by OpenCap would significantly differ from those measured with a marker-based motion capture system, and 2) that OpenCap would not be able to detect lower extremity joint angle changes caused by fatigue.

**Methods:** Thirteen participants completed a fatiguing treadmill run. Participants began running at a self-selected "easy" effort pace before gradually speeding up in two-minute intervals until reaching a "somewhat hard" effort (RPE ≥ 13). Participants maintained the pace until reaching a "very hard" effort (RPE ≥ 17, predicted HR ≥ 90% $HR_{MAX}$), at which point the run concluded. At 2-minute intervals OpenCap recorded data (120 Hz) from two smartphones mounted at 45° to the left and right in front of the treadmill. Concurrently, a marker-based motion capture system (Vicon) was used to record data (120 Hz) from nine cameras tracking marker clusters placed on the participant. Marker-based kinematic data was processed in Visual3D. Joint angle *vs*. time data for both systems were used to calculate the range of joint motion throughout each stride ($ROM_{STRIDE}$ = $Angle_{MAX}$ - $Angle_{MIN}$). $ROM_{STRIDE}$ values were averaged across 5 synchronized strides from participants' first and final intervals. $ROM_{STRIDE}$ values detected by each system (Vicon, OpenCap) over time (Pre-fatigue, Post-fatigue) were analyzed using a 2x2 repeated measures ANOVA at each joint (hip, knee, and ankle).

**Results & Discussion:** Hip results showed that OpenCap was able to detect differences due to fatigue: $ROM_{STRIDE}$ values were higher post- *vs*. pre-fatigue. However, a system-by-time interaction effect indicated a difference between the two systems' $ROM_{STRIDE}$ results pre-fatigue ($F(1,10) = 7{,}127$, $p_{BONF} = 0.024$) (Fig. 1A). At the knee, there was a main effect of time ($F(1,10) = 32.822$, $p < 0.001$), indicating significant changes in knee $ROM_{STRIDE}$ due to fatigue, but no significant difference between the two systems (Fig. 1B). At the ankle, there was also a main effect of time ($F(1,10) = 47.670$, $p < 0.001$), showing changes in ankle $ROM_{STRIDE}$ due to fatigue, but no significant difference between the two systems (Fig. 1C).

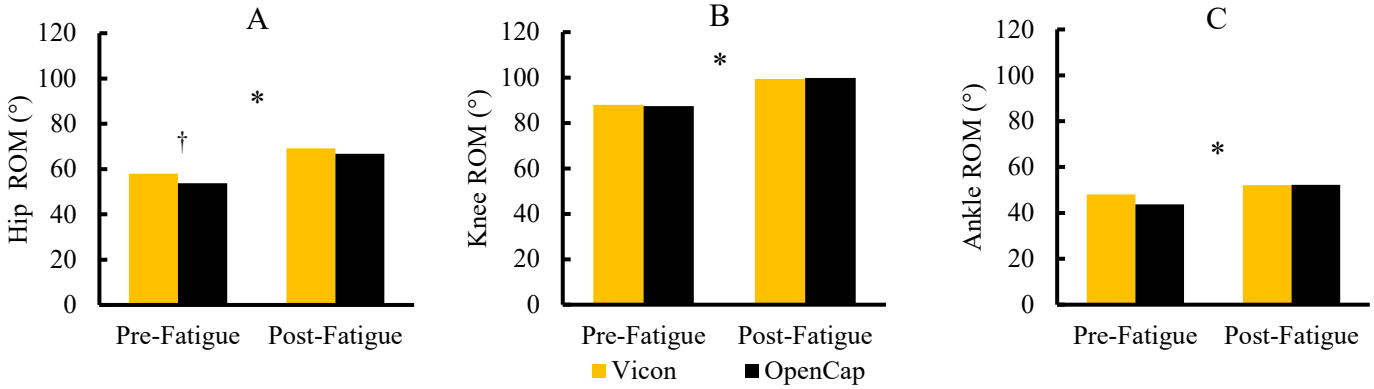


**Figure 1:** Joint ROM Pre- and Post-fatigue as measured using Vicon (yellow) and OpenCap (black). † - significant differences between systems. * - significant differences pre-/post-fatigue

**Significance:** Contrary to our hypotheses, the findings of this study shows the potential use of the OpenCap framework as a viable alternative to marker-based motion capture when studying running gait. Specifically, at the knee and ankle joint OpenCap was able to detect joint range of motion changes due to fatigue without any differences between the markerless and marker-based systems. Improvements to the framework's algorithm continue to be made, which may lead to better capabilities at the hip. The setup using just two smartphones offers OpenCap as a more affordable and portable method of motion capture, making motion capture more accessible to athletes, coaches, clinicians, and patients.

**Acknowledgments:** This research was partially funded by an Appalachian State University Office of Student Research Grant.

**References:** [1] Uhlrich et al. (2023). *PLoS Comp Bio.* 19(10); [2] Horsak et al. (2023). *J Biomech.* 159; [3] Dierks et al. (2010). *J Biomech. 43.*

# IMPACT OF ACHILLES TENDON MOMENT ARM ON FOOT GEARING

*Alexander Gioia[1], Daniel Schmitt[2], Robin M. Queen[1]
[1]Virginia Tech, Blacksburg VA
[2]Duke University, Durham NC
*Corresponding author's email: agioia@vt.edu

**Introduction:** The foot and ankle form a complex unit that propels the body by generating high force and power. Measurements of foot gear ratios -- defined as the resultant ground reaction force (rGRF) gear (*R*) divided by the Achilles tendon moment arm ($AT_{ma}$) gear (*r*) (Figure 1) -- have provided profound insight into ankle torque generation and performance optimization during walking and running [1-3]. Gear ratios can vary during movement shifting between low and high gears by enhancing muscle stretch in early stance and power in later portions of stance [1-3]. Investigations of walking and running foot gearing show that the gear ratio is highly dependent on the rGRF gear given its larger variance than the $AT_{ma}$ gear [1,4]. However, no studies have investigated the effect of the small changes in $AT_{ma}$ length on gear ratio. If it is possible to use a constant value for the $AT_{ma}$ gear or to determine the $AT_{ma}$ through modeling [5,6], it will allow for the determination of gear ratios from a wider range of data conditions, especially in cases where Achilles tendon markers haven't or can't be placed. The purpose of this study was to determine if there are differences in gear ratio when the $AT_{ma}$ gear was treated as time-varying (measured throughout stance) or simply as a constant (taken at midstance) or predicted values from equations presented in Sheehan [5], and Rasske et al. [6] during walking and running. Our null hypothesis was that no differences in gear ratio would exist between any of the methods during walking and running.

**Methods:** 20 young adults (9 M, 11 F) were recruited. 3D motion capture (Qualisys, 240Hz) and force plate based kinetic (AMTI, 1200Hz) data were collected. Participants completed three tasks: walking at a regular (1.35 m/s) and fast (1.6 m/s) speed and running at 3.2 m/s. Timing gates (Brower) were used to measure and maintain gait speed. Gear ratios were determined as the rGRF gear divided by the $AT_{ma}$ gear and were calculated using four methods throughout stance: (1) a time-varying $AT_{ma}$ determined using marker position, (2) constant $AT_{ma}$ (value taken at 50% stance), and predictions based on equation for $AT_{ma}$ from (3) Sheehan [5] and (4) Rasske et al. [6]. Sheehan defined $AT_{ma}$ as a function of ankle angle using an ankle loading device with magnetic resonance imaging (MRI) [5]. Rasske et al. defined $AT_{ma}$ as a function of ankle angle and stance during walking (1.25 m/s) using ultrasound radiofrequency. A one-way repeated measures ANOVA in statistical parametric mapping (SPM) was used to assess differences in gear ratio between the four methods for each task independently. Post-hoc paired t-test in SPM were used for pairwise comparisons if the ANOVA indicated statistical differences during the movement.

**Results & Discussion:** Gear ratios with a constant $AT_{ma}$ gear, compared to the measured time-varying $AT_{ma}$, were significantly higher in regular walking during 7-11% ($p=0.031$) and 90-97% ($p=0.012$) of the stance phase, in fast walking during 23-33% ($p=0.001$) and 85-99% ($p<0.001$) of the stance phase, and in running during 87-100% ($p<0.001$) of the stance phase. These results highlight the role that the $AT_{ma}$ plays in gear ratio during both the early and late phases of stance [1-3] and the need for a time-varying $AT_{ma}$ when calculating the gear ratio. If a time-varying $AT_{ma}$ was not collected, predictions from equations from Sheehan [5], which defines $AT_{ma}$ as a function of ankle angle, and Rasske et al. [6], which defines $AT_{ma}$ as a function of ankle angle and the percentage of the stance phase during walking, could be used to estimate the time-varying $AT_{ma}$. Gear ratios calculated using the approach of Sheehan $AT_{ma}$, when compared to measured $AT_{ma}$, are significantly higher in regular walking during 71-87% ($p=0.001$) of the stance phase, in fast walking during 72-85% ($p=0.003$) and 98-100% ($p=0.043$) of the stance phase, and in running during 33-81% ($p<0.001$) of the stance phase. Gear ratios calculated using the equations from Rasske et al. to estimate $AT_{ma}$, when compared to measured $AT_{ma}$, were not different for any of the tasks. Given the rGRF is the same between calculations, a higher gear ratio is the result of a smaller $AT_{ma}$ which would require more load through the Achilles tendon to produce the same moment than a larger $AT_{ma}$ would in the same scenario and would result in less stretch of the Achilles tendon during early stance, which may not be favourable for performance [1-4].

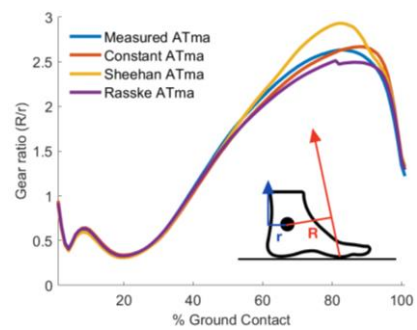


**Figure 1:** Gear ratios during regular walking with the measured $AT_{ma}$ (blue), constant $AT_{ma}$ (red), Sheehan $AT_{ma}$ (yellow), Rasske $AT_{ma}$ (purple).

**Significance:** A time-varying $AT_{ma}$ accurately determines gear ratio during the early and late phases of walking and running. If the $AT_{ma}$ is not collected through the placement of an Achilles tendon marker at the time of initial data collection, predictions using the equations from Rasske et al. are effective in estimating $AT_{ma}$ and calculating gear ratios. These findings demonstrate the impact that the $AT_{ma}$ gear has on gear ratios and the interpretation of the efficiency and performance of the foot and ankle complex.

**References:** [1] Carrier et al. (1994), *Science*; [2] Zeininger et al. (2024), *Front. Earth Sci.*; [3] Karaminidis and Arampatzis (2006), *Gait and Posture*; [4] Braunstein et al. (2010), *J. Biomech*; [5] Sheehan (2011), *J. Biomech.*; [6] Rasske et al. (2017), *Comput Methods Biomech Biomed Eng*

# ESTIMATING LOWER EXTREMITY JOINT KINETICS USING 1D OR 2D GROUND REACTION FORCES

Christina Kyriacou[1], Robin M. Queen[2], *Cherice Hill[1]
[1] University of Rochester, Biomedical Engineering, [2] Virginia Tech, Biomedical Engineering and Mechanics
*Corresponding author's email: cherice.hill@rochester.edu

**Introduction:** Lower extremity joint moments and powers are crucial to consider when characterizing normative and pathologic gait. For example, greater peak knee adduction moment is associated with knee osteoarthritis progression [1], cumulative hip adduction moment predicts hip osteoarthritis progression [2], and leg power during gait shifts from ankle to hip with aging [3]. Estimation of joint kinetics is typically done through inverse dynamics using 3D motion capture and 3D force plate data. However, 3D force plates are expensive and often only available in motion analysis labs, thereby preventing 'real-world' or community-based data collection. Alternatives such as pressure and force insoles and 2D portable force plates are cost-effective and portable but only measure or estimate 1D or 2D force as opposed to the 3D force used in inverse dynamics calculations. The purpose of this study was to evaluate the feasibility of estimating lower extremity sagittal and frontal plane joint kinetics during walking using only 1D or 2D force data and 3D motion capture data.

**Methods:** This study involved secondary analysis of a dataset (n=90) previously collected as part of an institutional review board approved study where 3D motion capture and 3D force plate data were recorded during set-speed walking (1.35m/s). Sagittal and frontal plane ankle, knee, and hip moment and power were calculated and exported from Visual 3D using (1) 3D force data (3D), (2) vertical force data only (V), (3) medial-lateral and vertical force data only (ML+V), and (4) anterior-posterior and vertical force data only (AP+V); excluded force plate components were set to 0. Peak (maximum and minimum) kinetic values were extracted in MATLAB for each participant. Linear regression models were fit to predict the kinetic peaks calculated using 3D force data from the kinetic peaks calculated in the V, ML+V, and AP+V conditions; $R^2$ values and correlations (r) from the resulting regression models were determined. Intra-class correlation coefficients (ICCs) were also calculated to assess agreement between predicted and calculated (3D) kinetic peaks.

**Results & Discussion:** Figure 1 shows example kinetic curves for one participant. Some curves were similar across conditions while others varied substantially. The AP+V condition aligned closely with the 3D gold standard across most variables while the V and ML+V conditions showed marked differences in multiple measures. Although agreement in curve shape varied, the magnitudes of the predicted peaks were highly correlated (r=0.85-1, p<0.01). Despite curve shape differences between conditions, predicted kinetic peaks in V, ML+V, and AP+V conditions strongly agree with kinetic peaks calculated using the 3D gold standard method. The predicted peaks explained 73-100% of the variability in the calculated peaks ($R^2$ = 0.73-1), and the ICC values indicate good to excellent agreement between predicted and calculated peaks (Table 1, ICC = 0.79-1); sagittal and frontal plane ankle moment for the V and ML+V condition showed good agreement while all other variables and conditions showed excellent agreement. These results support the feasibility of using 1D or 2D force data from in-shoe insoles or 2D portable force plates that are time synchronized with 3D motion capture to estimate sagittal and frontal plane joint kinetics outside of the lab. It should be noted, however, that this study analyzed force plate data collected at 1920 Hz. The limited sampling frequencies available with portable systems (i.e., 150-200 Hz for in-shoe sensors) could pose additional challenges for kinetic prediction; future studies will further investigate the validity of these alternatives.

| | | Moment | | | Power | | |
|---|---|---|---|---|---|---|---|
| | | V | ML+V | AP+V | V | ML+V | AP+V |
| Ankle | DF | 0.85 | 0.79 | 0.98 | 0.95 | 0.90 | 0.96 |
| | PF | 0.96 | 0.93 | 0.96 | 0.94 | 0.93 | 1.00 |
| | EV | 0.99 | 0.99 | 0.99 | 0.96 | 0.94 | 0.98 |
| | IN | 0.83 | 0.93 | 0.93 | 0.92 | 0.96 | 0.96 |
| Knee | EX | 0.95 | 0.94 | 0.99 | 1.00 | 1.00 | 1.00 |
| | FL | 0.96 | 0.95 | 1.00 | 1.00 | 1.00 | 1.00 |
| | AD | 1.00 | 1.00 | 1.00 | 1.00 | 1.00 | 1.00 |
| | AB | 1.00 | 1.00 | 1.00 | 1.00 | 1.00 | 1.00 |
| Hip | FL | 0.95 | 0.91 | 0.97 | 0.92 | 0.91 | 0.96 |
| | EX | 0.94 | 0.92 | 0.98 | 0.94 | 0.93 | 0.99 |
| | AD | 1.00 | 1.00 | 1.00 | 1.00 | 1.00 | 1.00 |
| | AB | 1.00 | 1.00 | 1.00 | 1.00 | 1.00 | 1.00 |

**Table 1:** ICCs showing good (yellow) or excellent (green) agreement between predicted and calculated kinetics.

**Significance:** This study provides insight regarding the use of more accessible and cost-effective alternatives to estimate key biomechanical metrics related to injury and disease risk in various clinical and/or athletic populations. These results suggest that estimation of joint kinetics is not out of reach for research or community facilities that do not have access to 3D force plates.

**Acknowledgments:** Funding provided by the Gilliam Fellowship (HHMI) and VT ISCE for dataset collection.

**References:** [1] D'Souza et al. (2022), *OAC*, 381-394. [2] Tateuchi et al. (2017), *OAC*, 1291-1298. [3] Cofré et al. (2011), *Gait Posture*, 484-489.

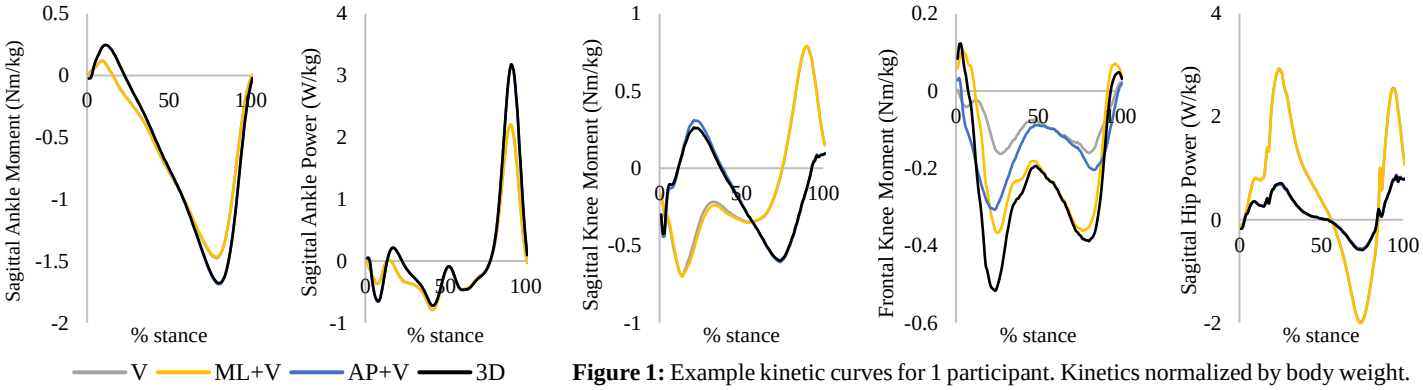


**Figure 1:** Example kinetic curves for 1 participant. Kinetics normalized by body weight.

# VALIDATION OF XSENSOR IN-SHOE PRESSURE INSOLES

Chelsea Maynard[1], Sakura Herron[1], Dennis Nimoh[1], Christina Kyriacou[1], *Cherice Hill[1]
[1] University of Rochester, Biomedical Engineering
*Corresponding author's email: cherice.hill@rochester.edu

**Introduction:** Gait is essential to everyday life and health. The study of biomechanics as well as the associated data is becoming more prominently used to inform injury and disease prevention and optimize clinical care and athletic performance [1]. As the use of this data grows, ensuring its broad accessibility becomes increasingly important. Movement kinetics are commonly captured by force plates within gait lab settings, but multiple in-shoe pressure and force insoles, each with their own advantages and limitations, have been developed to enable measurement of kinetics in 'real world' settings outside of gait labs [2]. One such insole system is the XSENSOR Intelligent Insoles, which were developed recently to enable kinetic movement analysis with high resolution in an accessible and affordable way. These insoles tout advantages over other similar systems such as improved pressure resolution, but the XSENSOR system's force estimations have not yet been fully validated in dynamic and realistic use scenarios. The purpose of this study was to assess the accuracy of the XSENSOR Intelligent Insoles in capturing loading kinetics compared to force plates.

**Methods:** 26 participants (9 male, 17 female) completed walking, jogging, and drop vertical jump tasks across or on a force plate walkway while wearing shoes containing the XSENSOR Intelligent Insoles. Walking and jogging trials were completed at the participant's self-selected speed. During the drop vertical jump trials, participants were instructed to complete a maximum height jump after their initial landing from a block. Participants completed 5 trials of each motion task. Individual steps were isolated from both the force plate and insole data for pairwise comparison. Peak vertical ground reaction force (pvGRF), vertical ground reaction force impulse (Imp), and stance time (ST) were calculated from the force plate and insole data for each step. Outcome measures calculated from force plate and insole data were compared using $R^2$ and intraclass correlation coefficients (ICCs) to evaluate agreement between the methods.

**Results & Discussion:** Figure 1 presents an example of vertical ground reaction force data from the force plates (solid line) and the XSENSOR insoles (dashed line) during the following movement tasks: walking, jogging, and drop vertical jump. The XSENSOR insole data mirrors the force plate data, especially for drop-vertical jump, although the magnitudes are consistently lower. Walking and jogging also show high consistency, with some deviations seen with jogging; overall, similarity in curve shape is displayed across pairwise comparisons. All outcome measures showed strong associations ($R^2$ = 0.84–0.99) and agreement (ICC = 0.87–0.98) across methods, supporting the potential use of XSENSOR insoles for field-based ground reaction force assessments. There are, however, noteworthy limitations of the XSENSOR insoles. The limited sampling frequency (150Hz) and dependence on Bluetooth connectivity may present challenges for insole utilization in certain contexts. Additionally, continued contact between the foot and insole during the swing phase of gait makes gait event identification less straightforward than when using a force plate, which may affect other measures of interest more than those assessed in this study. Despite these limitations, the described results suggest that the XSENSOR insoles provide a reliable estimation of vertical GRF across different movement tasks. By validating the accuracy of the insoles across different movements—walking, jogging, and drop vertical jumps—this study supports their use for monitoring biomechanical performance, injury prevention, and clinical assessments outside of laboratory conditions.

**Significance:** The significance of this study lies in its potential to enhance the practical application and accessibility of ground reaction force measurements across movement and balance tasks. Force plates are often described as the gold standard for measuring ground reaction forces, but they are expensive, require a highly controlled lab environment, and have limited real-world applications. Findings of this study demonstrate that XSENSOR Intelligent Insoles provide a high-resolution alternative, making kinetic assessment more feasible outside of the lab in field-based settings such as sports medicine, injury rehabilitation and gait analysis.

**References:** [1] Yeadon et al. (2023), *J Biomech.* [2] Heuvelmans et al. (2022), *J Sports Biomechanics*

| | pvGRF | Imp | ST |
|---|---|---|---|
| **Walk** | | | |
| $R^2$ | 0.90 | 0.93 | 0.92 |
| ICC | 0.93 | 0.96 | 0.95 |
| **Jog** | | | |
| $R^2$ | 0.92 | 0.84 | 0.94 |
| ICC | 0.92 | 0.91 | 0.96 |
| **Drop-Vertical Jump** | | | |
| $R^2$ | 0.97 | 0.94 | 0.98 |
| ICC | 0.87 | 0.97 | 0.99 |

*Table 1: Comparison of outcome measures from force plate and XSENSOR insole data. Excellent (green), good (yellow) consistency.*

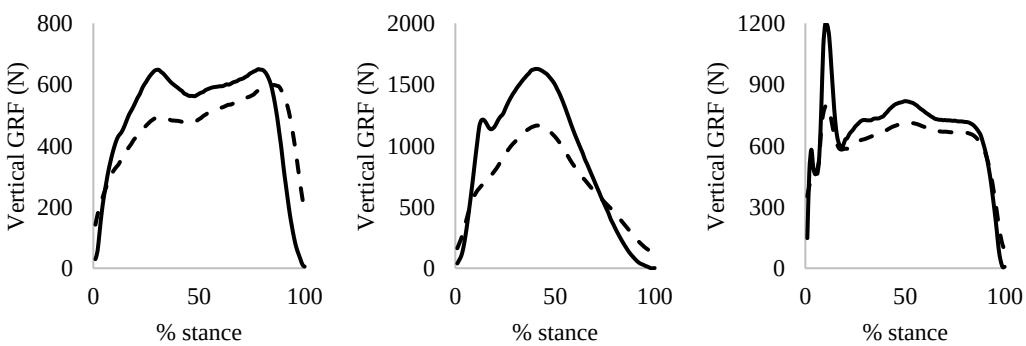


*Figure 1: Example vertical ground reaction force (GRF) data from the force plates (solid) and XSENSOR insoles (dashed) during walking (left), jogging (center), and a drop vertical jump*

# Metabolic Efficiency for Different Gear Ratios on a Novel Manual Wheelchair

*Madeline A. Czeck[1], Henry L. Wyneken[1], Laura K. Hogan[1], Andrew H. Hansen[1,2], John M. Looft[1,2]
[1]Minneapolis VA Health Care Systems, Department of Veterans Affairs, Minneapolis, MN
[2] University of Minnesota – Twin Cities, Minneapolis, MN
*Corresponding author's email: madeline.czeck2@va.gov

**Introduction:** Manual wheelchairs have a coupled pushrim and drive wheel positioned posterior to the user's center of mass for stability. This posterior pushrim positioning places the user's shoulders in an awkward position during propulsion. More anterior pushrim positioning has been shown to improve wheelchair biomechanics [1]. However, a more anteriorly placed axle may compromise stability of current manual wheelchairs.

Our group has designed a chain drive manual wheelchair where the pushrims are located anteriorly and the drive wheel posteriorly (Fig. 1). This design aims to increase stability for wheelchair users while improving shoulder kinematics during propulsion [2, 3]. While the novel wheelchair design may improve propulsion biomechanics, wheelchair users face obstacles carrying out daily tasks, including propulsion over different terrains (e.g., carpet, ramps/inclines, etc.).

Previous studies have reported an increased metabolic cost to propel over various surfaces, especially carpet [4]. Geared manual wheelchairs have been developed. However, the pushrim and drive wheel placement remain unchanged from typical manual wheelchairs. Also, with these systems the user needs to stop their momentum to switch gears. Therefore, our research group has expanded our novel manual wheelchair to include three gear ratio options – low (2:3), medium (1:1), and high (3:2).

**Figure 1:** Chain drive experimental manual wheelchair with anterior pushrims and posterior drive wheel.

The purpose of this study was to explore the effect of different gearing options on Veteran wheelchair user steady-state propulsion efficiency. We hypothesize Veterans will be more efficient in moving the wheelchair during the Six-Minute Push Test (6MPT) on hard level terrain when using higher gear ratios compared with lower gear ratios.

**Methods:** Nine Veterans with spinal cord injuries or disorders completed four 6MPTs on a hard floor surface using different gear ratios – personal chair, low, medium, and high. Veterans were included in the study if they used a manual wheelchair daily, over 18 years old, and had a body size appropriate to fit within the wheelchairs (16" and 18" seat widths). Total distance and number of dominant arm push strokes were measured for the entire six minutes. Borg Rate of Perceive Exertion (RPE) and Borg CR10 scores for upper limb pain were recorded prior to the start of the test and upon completion of the test. During each 6MPT, oxygen uptake and carbon dioxide production were measured using a COSMED K5 portable metabolic measurement system. To assess efficiency, we divided the total distance travelled in kilometers (km) by the total kilocalorie (kCal) used over the 6MPT and adjusted for participant weight (kilogram). Higher (km*kg)/kCal suggests higher efficiency, similar to miles per gallon in a car. Cost of transport was assessed and is the amount of energy it takes to move the body over a set distance (kCal/(km*kg)). A lower cost of transport is indicative of higher efficiency. We used a linear mixed model accounting for speed, number of dominant arm push strokes, the interaction between speed and number of push strokes, trial number, and participant to compare outcomes between the different geared ratio wheelchairs.

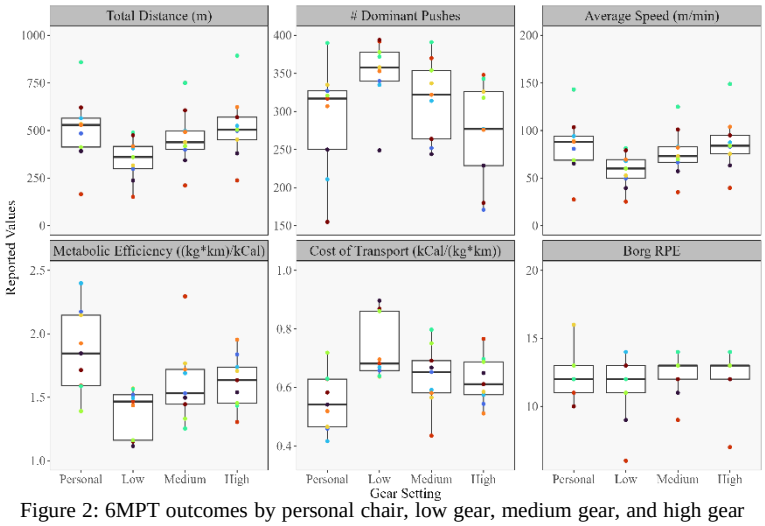


Figure 2: 6MPT outcomes by personal chair, low gear, medium gear, and high gear for each subject. Each subject is represented by a different color dot. From left to right, top row: Total distance, Number of Dominant Arm Push Strokes, Average Speed. From left to right, bottom row: Metabolic Efficiency, Cost of Transport.
**Results are trending in the direction we hypothesized; data collection continues*

**Results & Discussion:** Our preliminary results indicate that Veterans using the medium ($t = 2.616$) or high ($t = 1.481$) gear wheelchair had higher metabolic efficiency and lower cost of transport when compared to the low gear wheelchair (Fig. 2). These results indicate gear ratio may not only impact metabolic efficiency of propulsion but may also impact push strokes and total distance covered.

**Significance:** Increasing propulsion efficiency may decrease the effort to complete certain activities. Thus, different gear ratios may have the ability to impact the way wheelchair users engage with their environment.

**Acknowledgments:** This project was funded by the U.S. Department of Veterans Affairs RRDT MERIT 5I01RX003664.

**References:** [1] Boninger et al. (2000), *Arch Phys Med Rehabil* 81; [2] Lindenberg et al. (2014), *RESNA Annual Conference*; [3] Fairhurst et al. (2016), *J Med Devices* 10(3); [4] Wolfe et al. (1977), *Phys Therapy* 57(9).

# ASYMMETRY IN SPATIOTEMPORAL CHARACTERISTICS IN RUNNERS WITH KNEE PAIN IS ASSOCIATED WITH PERCEIVED GLOBAL FUNCTION

Marisa Pontillo[1], Madeline Grosklos[1], Adam Bunn[1]
*Corresponding author's email: marisunta.l.pontillo.civ@health.mil
[1]Extremity Trauma and Amputation Center of Excellence, Defense Health Agency, San Diego, CA

**Introduction:** Spatiotemporal variables (e.g., stride length, stance time) are often used to quantify running performance. While it is postulated that gait asymmetries during running may generate differences in mechanical stress exposure and injury risk, some level of asymmetry is considered 'normal' and there is no consensus as what level of symmetry should be deemed normal, nor is there evidence suggested a particular level of asymmetry could predispose runners to future injury [1]. The purpose of this study was to determine if global self-reported function could be predicted from pain, fear avoidance, and spatiotemporal variables in runners with knee pain, using stance time and stride length symmetry. Due to the ability of symmetry scores to detect small discrepancies in metrics, we hypothesized that stride length and stance time symmetry would contribute to the variance seen in self-reported function. We also hypothesize that both pain and fear of movement (i.e., kinesiophobia) would be related to function in runners with knee pain.

**Methods:** 51 active-duty service members with unilateral knee pain underwent 3D motion capture (120 Hz) of running at a self-selected speed on an instrumented treadmill (1200 Hz). Spatiotemporal data (stance time and stride length) were averaged over one 20-second trial period and symmetry was calculated (involved/ uninvolved*100). Peak pain with running was assessed via the numeric pain rating scale (NPRS). Demographic data was recorded, and patient reported outcomes included the Tampa Scale of Kinesiophobia (TSK) and the Single Assessment Numeric Evaluation (SANE). SANE is a patient rating from 0-100, where participants rate their current illness score in relation to their pre-injury baseline. Commonality analyses determine the unique, common, and total (unique+common) contribution of demographics, TSK, NPRS, stride length and stance time to SANE variance by decomposing the total $R^2$ of the regression model into the percent of variation attributable to each variable and each pair of variables, called a commonality coefficient. Commonality coefficients can be further divided into positive and negative, where the positive effect is the expansion of explained variation attributable to the addition of the variable and the negative effect is the suppression of explained variation of the other variables in the model when said variable is introduced. Variables contributing at least 1% of unique variance to SANE score were included in the regression model. Linear regression determined if NPRS, TSK, and stride length could predict SANE score. All analyses were performed with R (version 4.4.1, yhat package).

**Results & Discussion:** This cohort included 51 service members (35 male; age=32.18±8.17 years; body mass index= 25.94±3.97 m/kg$^2$). Average SANE score was 61.63±16.50; TSK= 37.00±6.09; NPRS=4.24±2.08; stride length symmetry= 99.99±0.06%. TSK, NPRS, and stride length were able to predict SANE, adjusted $R^2$=0.18, P<0.01. TSK was the only independent predictor, P=0.02. Although TSK, stride length symmetry, and NPRS only each contributed 1-11% of the unique variance to SANE score, all 3 variables also contributed shared variance, explaining 33% of the variance in SANE scores. Additionally, TSK, NPRS, and stride length explained over 60% of the explained variance. Commonality coefficients and unique contribution to total explained variance are reported in Table 1.

**Table 1**: Contribution of Peak Running Pain, Kinesiophobia, and Stride Length Symmetry to SANE Score.

| | Commonality Coefficients | | | Unique Proportion of Total Explained Variance |
|---|---|---|---|---|
| | Unique | Common | Total | |
| Pain | 0.01 | 0.08 | 0.10 | 5.36% |
| TSK | 0.11 | 0.08 | 0.19 | 46.62% |
| Stride Length Symmetry | 0.02 | 0.02 | 0.04 | 10.48% |

**Significance:** When predictor variables are considered independently, kinesiophobia was the strongest predictor of self-reported function. This is not surprising, as the average TSK score indicated a high level of kinesiophobia [2]. Stride length contributed the second highest amount of explained variance, indicating that offloading strategies and altered running mechanics may be present and influence function independently of the magnitude of peak running pain. These results also indicate that asymmetry in spatiotemporal variables in running may be more sensitive than absolute variables, particularly considering that average symmetry was close to 100%. Regardless, pain is an important factor when considering the predictors of overall self-reported function in runners, who experienced moderate levels of peak pain while running. The relationship between pain and function is greatly strengthened when combined with other predictor variables due to their additive effects.

**Acknowledgments:** The views expressed are those of the author(s) and do not reflect the policy or position of any agencies under the U.S. Government.

**References:** [1] Malisoux et al (2024), *BMJ Open Sport Exerc Med* 10; [2] Pontillo et al (2023), *Musculoskelet Sci Prac* 65.

# ANALYSES OF GROUND REACTION FORCE WAVEFORMS REVEAL PROLONGED PERIODS OF ALTERED INTACT LIMB LOADING AMONG PERSONS WITH UNILATERAL TRANSFEMORAL LIMB LOSS

Steven D. Voinier[1-3*], Claire Kettula[1-4], Julian C. Acasio[2,3], Brad D. Hendershot[2,3,5]
[1]Oak Ridge Institute for Science and Education; [2]Walter Reed National Military Medical Center; [3]Extremity Trauma & Amputation Center of Excellence; [4]University of Maryland; [5]Uniformed Services University of the Health Sciences
*Corresponding author's email: steven.d.voinier.ctr@health.mil

**Introduction:** Individuals with vs. without unilateral lower limb loss are at increased risk for early onset osteoarthritis (OA) in the contralateral ("intact") knee, thought to be mechanically driven by repeated exposures to altered loading. However, most biomechanical investigations correlate OA risk after limb loss with discrete features of a particular loading outcome during walking, such as peak vertical ground reaction force (VGRF) [1, 2]. Given cartilage responds to time-varying (and multi-dimensional) load [3], discrete and uniaxial parameters may not fully represent the mechanical load on the knee. Analyses of full loading waveforms during walking after limb loss are scarce [4, 5] and, moreover, generally ignore the anteroposterior (APGRF) and mediolateral (MLGRF) GRF components (despite their contributions to OA development after ACL reconstruction [6]). Thus, the purpose of this study was to compare VGRF, APGRF, and MLGRF waveforms of the intact limb among individuals with unilateral transfemoral limb loss (TFL) vs. uninjured controls (CTR). We hypothesized TFL vs. CTR would exhibit prolonged regions of larger loading across all components of GRF.

**Methods:** Bilateral GRF data were sampled (1200Hz) from 11 individuals with TFL (mean±standard deviation age=39.0±6.9yr, time since amputation=13.5±10.8yr) and 11 uninjured CTR (age=31.1±9.8yr) walking overground at speeds ranging from 0.93m/s to 1.77m/s. Bodyweight-normalized GRF waveforms during intact (TFL) and right (CTR) limb stance were statistically compared with separate generalized linear models (for each GRF component) leveraging 1-dimensional statistical parametric mapping (SPM; $p<0.01$ to account for non-sphericity in the generalized linear models), while controlling for walking speed (to account for the influences of speed on GRF magnitude). For regions of stance with between-cohort differences, the mean percent difference in estimated marginal means (TFL vs. CTR) of each waveform are reported to quantify the corresponding magnitude of loading.

**Results & Discussion:** Considering VGRF (Fig. 1A), TFL vs. CTR exhibited a 21% larger vertical load following heel strike, consistent with previously reported larger VGRF loading rates [1, 2]. However, this SPM analysis did not detect a difference in VGRF at first peak, contradicting previous studies [1, 2] and even identified a region in mid-stance with 10% smaller vertical loads. Considering APGRF (Fig. 1B), TFL vs. CTR exhibited 22-29% larger braking and propulsive forces, also consistent with previous studies [5] but prolonged over >15% of stance, implicating extended anterior-posterior shear forces that can shift the stress patterns within the knee. Considering MLGRF (Fig. 1C), TFL vs. CTR exhibited 11-13% larger medial-lateral force in early and late stance, consistent with previous research [5], but did not have an elongated region at midstance, contradicting previous work.

**Significance:** Regardless of walking speed, TFL vs. CTR exhibited 8-29% larger magnitudes across all GRF components, for prolonged regions of the waveforms and thus supporting our hypothesis. Prolonged regions of loading, concurrently in multiple planes, may uniquely shift loading patterns to relatively unconditioned locations within the knee [7] and likely implicate degenerative risk through the cumulative load paradigm [8], as peak loads may not solely predict OA development [9]. Future work will further leverage these GRF waveforms alongside knee motions as inputs to a materials testing simulation framework to facilitate more direct quantification of knee stress profiles toward maximizing joint health after limb loss.

**Acknowledgments:** This research was supported in part via an interagency agreement between the DoE and the DoD (contract number DESC0014664). The views expressed herein are those of the authors and do not necessarily reflect the official policy of the USUHS, DHA, DoD, nor the US Government.

**References:** [1] R.H. Miller *et al.*, *PeerJ*, 2017. [2] A.L. Pruziner *et al.*, *Clin. Relat. Res.*, 2014. [3] J. Bleuel *et al.*, *PLoS One*, 2015. [4] G. Hisano *et al.*, *J. Biomech.*, 2021. [5] D.P. Soares *et al.*, *Prosthet. Orthot. Int.*, 2016. [6] E. Bjornsen *et al.*, *Arth & Rheum*, 2024. [7] A. Heijink *et al.*, *Knee Surg Sport. Traumatol Arthrosc*, 2012. [8] M.R. Maly, *Current Opinion in Rheumatology*. 2008. [9] R.H. Miller, *Exerc. Sport Sci. Rev.*, 2017.

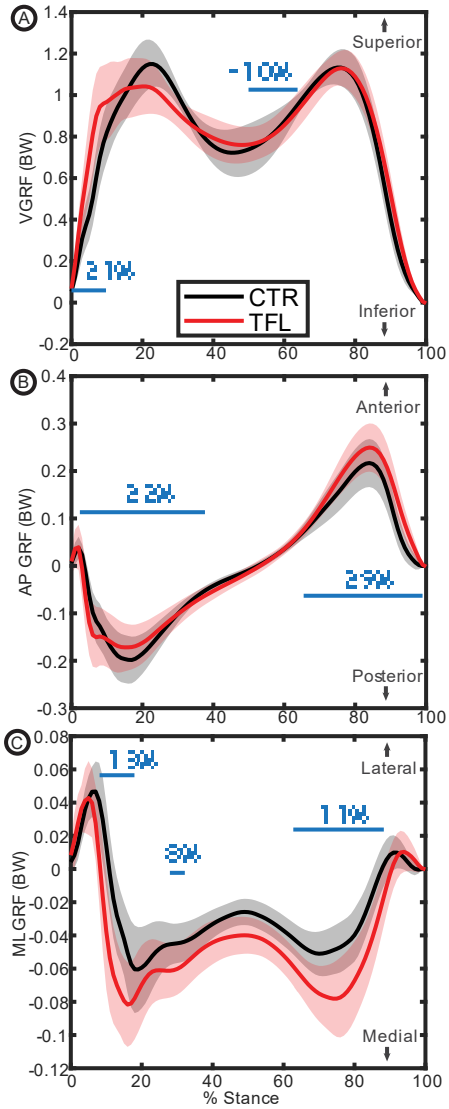


**Figure 1:** Ensemble averaged A) VGRF, B) APGRF, and C) MLGRF waveforms by persons with transfemoral limb loss (TFL) and uninjured controls (CTR). Horizontal blue bars signify significant between-group differences, with the accompanying percentages representing the mean percent difference of TFL vs. CTR (positive percentage = larger magnitude).

# INFLUENCE OF SPEED ON CONTINUOUS INTER-LIMB GAIT COORDINATION AND STABILITY IN VETERANS AND SERVICE MEMBERS WITH TRANSTIBIAL LIMB LOSS

**Alexis Sidiropoulos, PhD[1], David Herlihy, BS[1,2], Jason Maikos, PhD[1]**
[1]Department of Veteran Affairs New York Harbor Healthcare System, New York, NY, USA
Narrows Institute of Biomedical Research and Education, Inc., Brooklyn, NY, USA
[*]Corresponding author's email: alexis.sidiropoulos@va.gov

**Introduction:** Continuous inter-limb coordination and stability represent different aspects of walking [1] and may be impacted differently by speed. This information could directly influence rehabilitation prescription for Veterans and Service Members (SMs) with lower limb loss, as these individuals experience slower gait speeds [2] and lower levels of coordination and stability [3] compared with intact individuals. Though continuous measures provide superior sensitivity over traditional spatiotemporal measures [4], little is known about the impact of walking speed on these measures with the most commonly prescribed ankle-foot device types (i.e., Energy Storing and Returning (ESR), articulating ESR (ART), and powered ESR (PWR)). Coordination and stability are important measures of mobility for individuals with limb loss, as they represent potential targets to improve whole-body dynamics. This study aimed to identify the influence of gait speed on continuous coordination and stability using three different prosthetic ankle-foot device types. We hypothesized that individuals with transtibial limb loss (TLL) will experience greater coordination, but less stability at faster speeds.

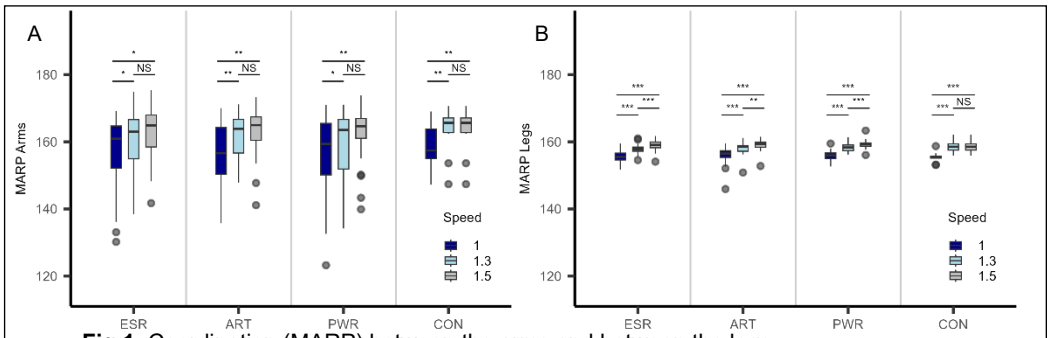


**Fig 1.** Coordination (MARP) between the arms and between the legs

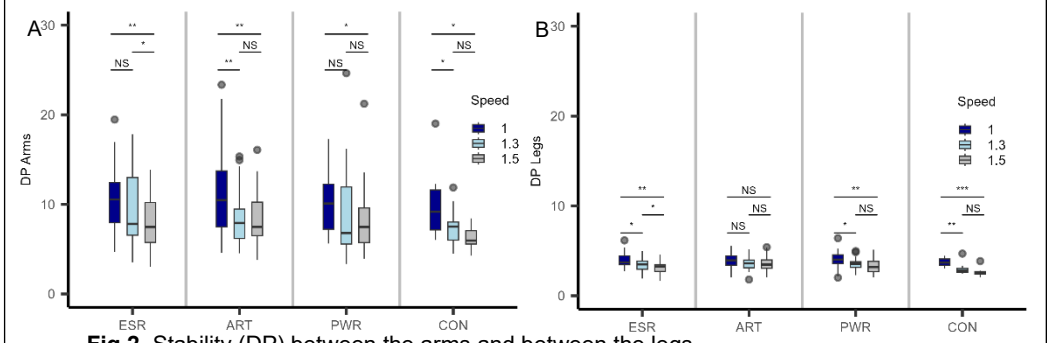


**Fig 2.** Stability (DP) between the arms and between the legs

**Methods:** Twenty-six individuals with unilateral TLL were fit and evaluated with ESR, ART, and PWR devices. Participants separately acclimated to each device for 1 week, followed by biomechanical gait analysis. Ten intact individuals comprised a control group. All participants walked at slow (1.0 m/s), moderate (1.3 m/s), and fast (1.5 m/s) speeds across a 10-meter instrumented walkway until at least 15 steps per foot were recorded. Relative Phase (RP) analysis calculated continuous measures of coordination, Mean Absolute Relative Phase (MARP), and stability, Deviation Phase (DP), between upper and between lower limbs. Low MARP indicates an in-phase relationship, while high MARP indicates an anti-phase relationship. Low DP indicates a stable organization of the neuromuscular system. Linear mixed effect models compared MARP and DP between speeds. Pairwise comparisons used estimated marginal means. Significance was set at $p<0.05$.

**Results and Discussion:** Improvements in both coordination (Fig. 1A,B) and stability (Fig. 2A,B) were associated with increasing walking speed. This relationship was true for individuals with and without TLL. Importantly, most improvements were associated with speed that increased from slow to fast, indicating that larger changes in gait speed via appropriate rehabilitation may result in the greatest gains in gait pattern coordination and stability. However, no differences between device types were observed, indicating that none of the devices pose an advantage of better coordinated and more stable gait patterns for individuals with TLL. It may be beneficial to examine the relationship between the upper and lower extremities to identify potential benefits of one device for these continuous measures. This study highlights the sensitivity of RP analysis to identify changes in coordination and stability with speed, in addition to the notion that speed is a large contributor to both continuous coordination and stability of the gait pattern of individuals with TLL.

**Significance:** The improvements in coordination and stability associated with increased speed among Veteran and SMs with TLL across different types of prosthetic ankle-foot devices can help support development of rehabilitation programs using the most appropriate walking speed to improve coordination and stability. These findings can directly influence prescription guidelines to optimize healthcare for all Veterans and SMs with TLL, helping them to live high quality, active lives.

**Acknowledgments:** This study was funded by DoD OPORP (W81XWH2-1-0409). We thank Dr. Timothy Moore for his contributions.

**References:** [1] Krasovsky et al. (2014), *Gait & Posture,* 39(1); [2] Batten et al. (2019), *P&O international,* 43(2); [3] Donker et al. (2002), *Acta Psychologica,* 110(2-3); [4] Haddad et al. (2010), *J App Biomech*, 26(1).

# DYNAMIC PLANTAR PRESSURE CHARACTERISTICS OF CMT PATIENTS COMPARED TO HEALTHY CONTROLS

Tyce C. Marquez*, Lauren Crowe, Bopha Chrea, Jason Wilken, Donald D. Anderson
University of Iowa, Iowa City, IA
tyce-marquez@uiowa.edu

**Introduction**: Charcot-Marie-Tooth (CMT) disease is the most common form of inherited peripheral neuropathy, affecting approximately 1 in 2,500 people in the United States [1]. Progressive distal muscle weakness and imbalance often result in cavovarus foot deformity [2], which contributes to poor gait mechanics, abnormal plantar pressure distributions, and an increased risk of falls – ultimately reducing quality of life [3]. In CMT patients, abnormal plantar pressure patterns in the rearfoot and forefoot have been significantly linked to foot pain [4] and associated with altered gait kinematics [5]. The aim of this study was to evaluate regional dynamic plantar pressure patterns throughout the stance phase of gait in CMT patients compared to healthy controls.

**Methods**: Twenty-five CMT patients (44.0±18.6 years, 15M/10F) and eighteen healthy controls (44.5±17.3 years, 9M/9F) each completed three walking trials per foot across a plantar sensor platform (Novel EMED, Munich, Germany) [6]. The foot was divided into five regions based on foot length and the long plantar angle [7]. The rearfoot (31% of foot length), midfoot (19%), and forefoot (50%) were initially separated, and then the midfoot and forefoot were further divided into medial and lateral regions. To evaluate loading at different periods over the stance phase of gait, the foot was divided into two regions, lateral and medial, based upon the long plantar angle. Pressure-time integral (PTI) and peak pressures were recorded for both CMT patients and healthy controls.

**Results & Discussion**: CMT patients exhibited higher peak pressures in the lateral foot regions compared to healthy controls (Table 1). The largest absolute differences were observed in the lateral forefoot, followed by the lateral midfoot. Throughout the stance phase of gait, CMT patients demonstrated a greater lateral-medial peak pressure loading ratio, whereas healthy controls exhibited a reduced loading ratio (Fig. 1). The lateral-medial loading disparity was most evident during midstance. Cavus foot and forefoot adduction have been linked to increased risk of fifth metatarsal fractures, particularly in zones two and three [8]. The increased lateral forefoot loading observed in CMT patients may contribute to this injury risk. Additionally, CMT patients exhibited greater PTI across all foot regions compared to healthy controls, potentially influenced by factors such as walking speed, BMI, or sample variability. PTI and peak pressure differences will continue to be evaluated as enrolment of both CMT patients and healthy controls continues.

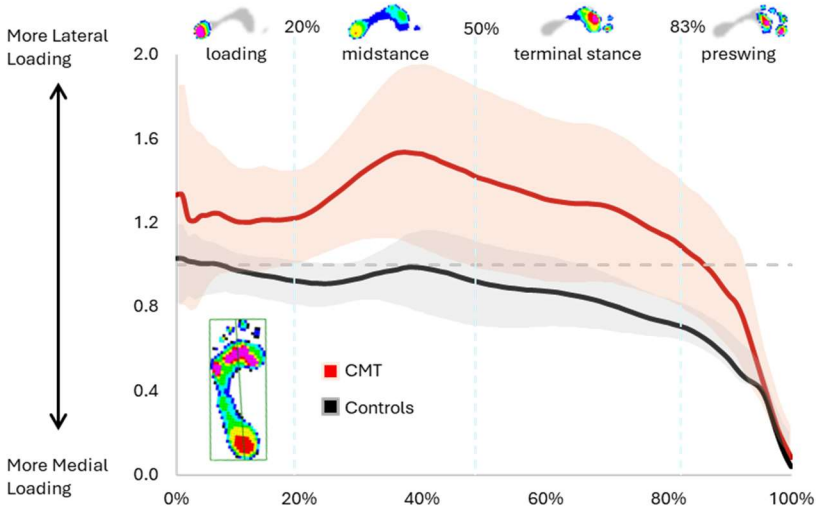


**Figure 1**: Lateral/Medial Peak Pressure Ratio Throughout the Stance Phase of Gait for CMT Patients and Healthy Controls.

**Significance**: Increased lateral foot loading observed in CMT patients may put them at higher risk of fifth metatarsal fractures. In addressing cavus foot deformity with surgical intervention, reducing lateral loading, primarily in the forefoot, should be considered to reduce fracture risk. Understanding these differences may inform surgical interventions and efforts to mitigate fracture risk in the CMT population.

**Acknowledgments:** This research is supported by startup funding provided to Dr. Bopha Chrea by the University of Iowa Department of Orthopedics and Rehabilitation.

**References:** [1] Laura M., et al. Muslce Nerve. (2018), 57(2):225-259. [2] HH, T. *Peroneal Type Progressive Muscular Atrophy*. 1886. [3] Burns, J., et al. Neurology. (2010), 75(8):726-31. [4] Burns J., et al. Clin Biomech. (2005), 20:877-882. [5] Giacomozzi, C., et al. J of Biomech. (2014), 47:2654-2659. [6] MidPoil, T.G., et al. J Am Podiatr Med Assoc. (1999), 89(10):495-501. [7] Lin, T., et al. Neuro Disorders. (2019), 29:427-436. [8] Jones, C.P. Clin Sports Med. (2020), 793:799.

**Table 1**: Pressure-Time Integral (PTI) and Peak Pressure Values (Average±Standard Deviations) for the Five Foot Regions.

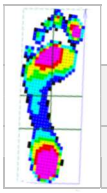

| | | Rearfoot | Midfoot - *Medial* | Midfoot - *Lateral* | Forefoot - *Medial* | Forefoot - *Lateral* |
|---|---|---|---|---|---|---|
| CMT | PTI (kPa*s) | 149.8±83.6 | 10.8±16.7 | 92.4±133.5 | 253.6±140.3 | 349.6±233.7 |
| | Peak Pressure (kPa) | 374.0±105.7 | 27.6±33.0 | 203.4±284.9 | 656.4±284.5 | 743.9±383.3 |
| Control | PTI (kPa*s) | 84.4±19.4 | 7.4±7.8 | 27.9±14.8 | 204.9±74.7 | 176.8±68.5 |
| | Peak Pressure (kPa) | 399.1±101.8 | 40.1±36.4 | 99.6±45.8 | 696.6±174.2 | 552.3±165.7 |

# RELATIONSHIP BETWEEN ALTERING GAIT SPEED AND COGNITIVE ABILITIES IN CHILDREN WITH AUTISM

Alyssa O. Vanderlinden[1]*, Meagan R. Kendall[2], Rhonda Manning[3], Jeffrey D. Eggleston[4]
[1]Department of Kinesiology, New Mexico State University, Las Cruces, NM, USA
*Corresponding author's email: avander@nmsu.edu

**Introduction:** Autism Spectrum Disorder (ASD) affects 1 in 36 children in the United States, and is primarily considered a behavioral disorder [1]. However, emerging evidence suggests ASD may also manifest as a movement disorder, with children exhibiting significant motor impairments, including deficits in locomotor skills, compared to their neurotypical (NT) peers [2]. Beyond behavioral symptoms and motor deficits, cognitive impairments are also prevalent in children with ASD [3]. Research indicates that children with ASD perform worse on cognitive tasks than NT controls, with approximately one-third exhibiting multiple cognitive impairments [3]. Specifically, deficits in executive function, perception, and attention have been identified as key cognitive challenges in ASD [4]. Prior studies have explored the link between cognitive function and gait adaptability, suggesting that increased cognitive resources are required to walk faster than one's preferred speed to maintain balance and respond to environmental changes [5], and slower fast-walking speeds have been associated with overall cognitive decline [6]. Research in older adults has found that cognitive impairments are linked to a diminished ability to increase walking speed [5]. Furthermore, kinematic differences have been observed in children with ASD when modifying gait speed [7]. Therefore, the purpose of the current study is to investigate the relationship between cognitive abilities and walking speed in children with ASD, compared to NT children. It is hypothesized that children with ASD will exhibit lower cognitive abilities than their NT peers and that this will be associated with slower walking speeds and a lower walking speed reserve.

**Methods:** 14 children **(**12 males, 11.64±2.13 years, 1.55±0.15 m, 54.40±20.16 kg) with a clinical diagnosis of ASD and 13 NT children (11 males, 11.23±2.05 years, 1.54±0.13 m, 55.98±25.27 kg) participated in the current study. Cognitive function was assessed using the NIH Toolbox Cognitive Battery (Pattern Comparison Processing Speed Test, Flanker Inhibitory Control and Attention Test, and Dimensional Change Card Sort Test). Participants then walked overground at 3 speeds (preferred, slow, and fast) in a randomized order for 12 trials per speed. Kinematic data were collected using a 10-camera three-dimensional motion capture system (200 Hz; Vicon Motion Systems, Oxford, UK). Data were smoothed using a low-pass Butterworth filter (6 Hz), and then imported to Visual3D (C-Motion, Inc., Germantown, MD, USA) for analysis. Descriptive statistics were calculated for gait velocities in each condition. Walking speed reserve (WSR) was calculated as the difference between fast and preferred speed [5]. Descriptive statistics were calculated for each group's computed cognitive assessment score. Independent t-tests and Mann-Whitney U tests ($\alpha$=0.05) compared group differences in cognitive scores and WSR. Repeated measures ANOVA ($\alpha$=0.05) assessed group and condition effects on gait velocity. Pearson's correlation (r) examined associations between cognitive scores and gait velocity ($p<0.05$).

| | ASD (n=14) | NT (n=13) |
|---|---|---|
| **Pattern Comparison Processing Speed Test** | | |
| Computed Score * | 46.64 ± 13.01 | 59.23 ± 11.85 |
| **Flanker Inhibitory Control and Attention Test** | | |
| Computed Score * | 6.60 ± 1.15 | 8.01 ± 0.37 |
| **Dimensional Change Card Sort Test** | | |
| Computed Score * | 6.40 ± 1.23 | 7.60 ± 0.52 |

**Table 1:** Mean (±SD) for each cognitive assessment. (*) indicates a statistically significant ($p<0.05$) difference between groups.

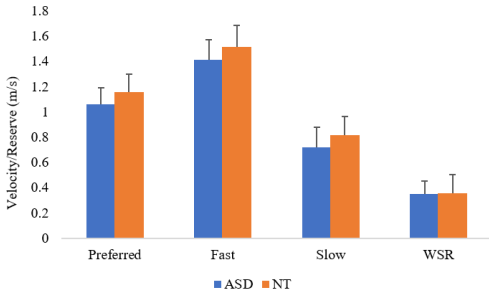


**Figure 1:** Mean (+SD) for velocities during the preferred, fast, and slow conditions and walking speed reserve for each group. (*) indicates a statistically significant ($p<0.05$) difference between groups. (WSR: Walking Speed Reserve)

**Results & Discussion:** Participants with ASD scored lower on the Pattern Comparison Processing Speed Test ($t(25)=-2.62$, $p=0.01$), Flanker Inhibitory Control and Attention Test ($U=19.00$, $p< 0.001$), and Dimensional Change Card Sort Test ($t(25)=-3.28$, $p=0.002$) **(Table 1)**. Children with ASD presented with reduced cognitive abilities in the areas of attention, processing speed, and executive function, consistent with previous literature [4]. A main effect of speed was found for gait velocity ($F_{(2,50)}=276.11$, $p<0.001$, $\eta^2=0.92$), but no significant participant group effect ($F_{(1,25)}=4.22$, $p=0.06$, $\eta^2= 0.14$) or participant group × speed interaction ($F_{(2,50)}=0.002$, $p=0.99$, $\eta^2=0.001$). WSR did not differ between groups ($t(25)=-0.08$, $p=0.94$) **(Figure 1)**, and no significant correlations were found between gait velocity and cognitive scores. These findings contrast with previous research suggesting cognitive impairments negatively impact gait [5,6]. The lack of associations may indicate that children with ASD do not rely on cognitive abilities to adjust gait speed, or the task of changing speed was not complex enough to reveal this relationship. Additionally, similar walking velocities and WSR between groups suggest participants with ASD can mechanically alter gait speed like NT peers. This could be advantageous for children with ASD, as decreased cognitive abilities may not impact daily locomotion.

**Significance:** Understanding the role of cognitive abilities in locomotion for children with ASD is crucial, as motor impairments are a common symptom of the disorder. Expanding normative gait data and identifying key areas for intervention can enhance movement therapies. Despite evidence that children with ASD experience motor deficits, participation in physical therapy remains low. This highlights the need for more targeted physical therapy programs and better-informed clinical approaches to improve movement therapy and promote physical activity in this population.

**References:** [1] Maenner (2023), *MMWR.Srvllnce Summ*., 72; [2] Green et al., (2009). *Dvlpmntl Med & Ch Neuro*, 51(4); [3] Brunsdon, et al. (2015), *Jrl Ch Psycho & Psychi*, 56(8); [4] Kas et al. (2014). *Psychphrm*, 231(6); [5] Callisaya, et al. (2017), *Grosci*, 39(2); [6] Deshpande et al. (2009), *Age & Aging*, 38(5); [7] Olivas et al. (2022). *Clncl Bmch*, 100

# STIFFNESS AND DEFLECTION OF CUSTOM-FIT, 3D-PRINTED ANKLE-FOOT ORTHOSES DURING WALKING AND THE INFLUENCE OF ANTHROPOMETRIC VARIABILITY

*Jacquelyn Brokamp[1], Ryan Pollard[1], Iván Nail-Ulloa[1], Michael Zabala[1,2]
[1]Department of Mechanical Engineering, Auburn University, Auburn, AL, USA, [2]XO Armor Technologies, Inc., Auburn, AL, USA
* jrb0209@auburn.edu

**Introduction:** Ankle-foot orthoses (AFOs) assist individuals with musculoskeletal and neurological disorders by improving gait parameters such as step length, gait speed, and swing-phase dorsiflexion [1]. They are commonly used to manage equinus deformity, characterized by excessive plantarflexion in conditions like cerebral palsy, muscular dystrophy, and post-stroke impairments [2]. Although traditional custom fabrication methods yield improved gait outcomes, the manufacturing process is laborious and takes several weeks for the patient to receive their device [3]. Additive manufacturing (AM) offers a faster, cost-efficient alternative, but the mechanical strength and fatigue properties of 3D-printed AFOs during ambulation are insufficiently characterized in the literature [4]. Benchtop testing and computational methods are commonly used to evaluate AFO mechanical properties; however, predicting the behavior of AM parts remains challenging due to their anisotropic material properties and variable print parameters. Additionally, many studies overlook ankle quasi-stiffness, which influences AFO mechanical stress throughout gait [5]. While prior research has examined AFO strut stiffness [6], the overall quasi-stiffness of the AFO-ankle complex, incorporating both active and passive ankle contributions, has yet to be explored. Therefore, this study aims to understand how both the AFO-ankle complex quasi-stiffness and participant-specific anthropometric measures (height and body mass) affect AFO deflection throughout the gait cycle to inform future benchtop testing of 3D-printed, custom-fit AFOs. We hypothesized that (1) AFOs increase ankle quasi-stiffness, (2) quasi-stiffness increases with anthropometric measures, (3) larger anthropometric measures result in greater AFO deflection, and (4) greater AFO-ankle complex quasi-stiffness reduces peak AFO deflection.

**Methods:** Nine unimpaired individuals (4 male, 5 female; age: 27.9 ± 13.2 years; height: 169.4 ± 15.3 cm; body mass: 85.9 ± 29.4 kg) participated. Inclusion criteria required participants' height and body mass to fall within the 25th percentile or below, 50th percentile ± 12.5%, or 75th percentile and above for their biological sex, based on CDC data [7]. The study was approved by the Auburn University Institutional Review Board (no. 23-476 MR 2310), and all participants provided written informed consent. The study occurred over two sessions. On the first day, height and body mass were recorded, and one leg was randomly selected to be 3D scanned using XO Armor® 3D-scanning technology. The AFO was then modeled and 3D-printed using fused deposition modeling with proprietary PLA material. On the second day, after confirming AFO fit, gait analyses were conducted under AFO and no-AFO conditions, focusing on three subphases of stance: controlled plantarflexion (CPF), controlled dorsiflexion (CDF), and powered plantarflexion (PPF). Kinematic and kinetic data were collected using a Vicon motion capture system and two AMTI force plates (2000 lb. capacity). Sagittal plane ankle and AFO-ankle complex kinematics and kinetics were extracted using Visual3D. Quasi-stiffness ($k_{AFO,subphase}$) was determined from the ankle moment-angle relationship during stance subphases [5]. AFO deflection was calculated from AFO-ankle complex angles. Statistical analyses included paired t-tests and Pearson correlations to assess the effects of anthropometrics and quasi-stiffness on AFO deflection ($\alpha = 0.05$).

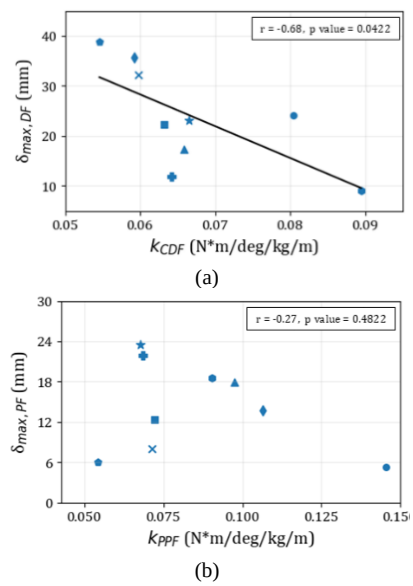


**Figure 1:** Pearson correlation coefficients ($r$) describing the linear relationship between (a) $k_{AFO,CDF}$ and $\delta_{DF,max}$, (b) $k_{AFO,CDF}$ and $\delta_{PF,max}$. Shapes represent individual subjects.

**Results & Discussion:** AFO intervention significantly increased AFO-ankle complex quasi-stiffness ($k_{AFO,subphase}$) compared to the no-AFO condition in all stance subphases ($p \leq 0.0031$, d = 1.43–2.01), confirming that AFOs increase ankle quasi-stiffness. Body height and mass positively correlated with stiffness during multiple phases of gait ($k_{AFO,subphase}$, r = 0.67–0.94), supporting the hypothesis that larger body sizes increase quasi-stiffness, potentially due to AFO size. However, an exception was that no correlation was found between height and $k_{AFO,CPF}$. AFO deflection in dorsiflexion ($\delta_{DF,max}$) was positively correlated with height and body mass ($p \leq 0.0101$), but no relationship was found with plantarflexion ($\delta_{PF,max}$). Additionally, $k_{AFO,CDF}$ showed a significant inverse correlation with $\delta_{DF,max}$ (r = -0.68, $p < 0.05$), suggesting that higher AFO quasi-stiffness during CDF reduces deflection (Fig. 1a). No significant relationship was found between $k_{AFO,PPF}$ and $\delta_{PF,max}$ (Fig. 1b), indicating that plantarflexion deflection may be more influenced by muscle-tendon dynamics than AFO mechanical properties or anthropometric measures.

**Significance:** This study highlights the influence of quasi-stiffness and anthropometric measures on AFO deflection, emphasizing the need for patient-specific considerations in AFO design and testing. Findings demonstrate that quasi-stiffness during CDF significantly impacts AFO deflection, providing a key parameter for improving benchtop fatigue testing. These results suggest that integrating user-specific mechanics can enhance AFO fatigue life predictions and optimize clinical prescriptions.

**Acknowledgments:** We would like to thank the Advanced Medical Technology Initiative (G00016390), in partnership with Madigan Army Medical Center and the US Army xTech Program ((Direct to Phase II SBIR: A234-P010 W51701-24-C-0078) for funding this study. **References:** [1] Aboutorabi et al. (2017) *Ann. Phys. Rehabil. Med* 60(6); [2] Wren et al. (2004) *J Biomech* 37(9); [3] Silva et al. (2022) J Bioeng 9(6); [4] Wojciechowski et al. (2019) *J Foot Ankle Res* 12(1); [5] Safaeepour et al. (2014) *Biomed Eng Online* 13(19); [6] Khaing et al. (2021) *BMEiCON 2021;* [7] Fryar et al. (2021) *NCHS.*

**Effect of serial casting on idiopathic toe walking**

***Martins E. Amaechi[1]**, John D. Collins[1], Christine Amacker[1], Heather Waters[1], Riley Horn[1], Rachel M. Thompson[1], Patrick Curran[1]
[1]Motion Analysis Laboratory, Rady Children's Hospital, San Diego, CA, USA
*Email: mamaechi@rchsd.org

**Introduction:** About 2% of typically developing children ambulate with a persistent toe walking gait pattern referred to as idiopathic toe walking (ITW) [1]. This gait pattern deviation from typically developed children can result in contractures, fatiguability, poor balance and social stigmatization [2], [3]. Serial casting is a common non-operative modality used to treat ITW though its long term-effects are unknown [1]. The aim of this study is to quantify changes in gait kinematics in ITW following serial ankle dorsiflexion stretch casting pre and at least six months following casting. We hypothesize that serial casting treatment will improve the passive and dynamic dorsiflexion range of motion during gait after six months due to prior reported improvements in dorsiflexion after serial casting [2].

**Methods:** Six ITW participants (2 females, age = 8.3 ± 1.2 years, height = 1.3 ± 0.1 m, and mass = 31.3 ± 7.8 kg) presenting with equinus contracture were included as a subset of a larger cohort if they: (1) underwent bilateral course of care for serial casting for 3 to 4 weeks; (2) had no neurologic diagnosis; (3) had not received neurotoxin injection within 4 months, and (4) participated in 3D motion analysis (3DMA) on the day of first casting and at least 6 months post cast removal. Five age matched control were used for comparison of 3DMA kinematics. Serial casting was performed by experienced neuromuscular clinicians, with weekly cast changes until 10 degree of passive dorsiflexion was achieved. Participants were classified based on ITW severity as mild (presence of first ankle rocker), moderate (presence of early third ankle rocker), and severe (predominant first ankle moment) [4]. 3DMA was performed using 10 marker-based cameras (Qualisys, Goteborg, Sweden) and four force plates (AMTI, Watertown, MA) collecting at 120 Hz and 1200Hz respectively while walking barefoot. Data processing was done in Visual3D (C-motion, Rockville, MD, USA) and maximum dynamic dorsiflexion (DDF) range of motion throughout the gait cycle was derived. Passive dorsiflexion (PDF) range of motion was obtained pre and post casting. Differences in pre-post serial casting was determined for PDF and DDF using Student's t-tests. Differences in the ITW severity and control was determined using one-way ANOVA and Kruskal-Wallis test ($\alpha<0.05$).

**Results & Discussion:** Our study shows participants had increased PDF post-casting (1.5±6.2°) compared to pre-casting (-10.7±5.4°) ($p=0.0002$) (Fig. 1) confirming our hypothesis. Contrary to our hypothesis, 3DMA showed no significant differences in DDF following serial casting treatment (-1.9±4.5°) compared to pre-cast (-2.2±8.0°) ($p=0.9$). However, 3DMA showed differences in DDF between ITW severity groups and control before casting between the groups ($p<0.005$). Post-hoc analysis showed that control (5.1±2.3°) had greater DDF compared to moderate ITW (-4.6±6.7°) ($p=0.006$), and severe ITW (-7.5±4.1°) ($p<0.005$) but not mild (6.5±3.6) ($p=0.76$). We also found mild ITW participants had greater DDF compared to moderate ($p=0.008$) and severe ($p<0.005$) ITW participants. After serial casting, the severe ITW participants (-2.41±2.1°) had lesser DDF (-5.14±2.3°) compared to the control group ($p=0.01$). Our results suggest that serial casting, on average, does increase passive dorsiflexion range of motion. However, it may not improve dynamic dorsiflexion (throughout gait) in ITW. Differences seen between control and severe ITW following casting suggests recurrence of contracture after 6 months of serial casting in severe ITW. As such, serial casting may serve as a temporizing treatment modality for certain ITW severity groups. Future studies are necessary to determine which patients may benefit from serial casting. Furthermore, investigating the kinetics and quasi-stiffness property may highlight differences in the groups. Serial casting could help increase passive dorsiflexion in ITW however, its effect on dynamic dorsiflexion ranges of motion may vary dependent on the severity of ITW.

| | PDF | DDF | MILD (°) | MODERATE (°) | SEVERE (°) |
|---|---|---|---|---|---|
| Pre-Casting | -10.7 ± 5.4 | -2.2 ± 8.0 | 6.5 ± 3.6 | -4.6 ± 6.7 | -7.5±4.1 |
| Post-Casting | 1.5 ±6.2 | -1.9 ± 45 | 4.5 ± 4.5 | -3.83 ± 3.1 | -2.04 ± 1.01 |

**Figure 1:** A figure showing the mean maximum passive dorsiflexion (PDF), and dynamic dorsiflexion (DDF) during gait across all participants. The maximum dynamic dorsiflexion of the mild, moderate and severe ITW groups is also presented. All measurements in degrees.

**Significance:** The significance of this study lies in its contribution to understanding the potential role of serial casting in managing ITW. This study offers valuable insights into the effectiveness of this non operative treatment. While the study suggests that serial casting improves passive dorsiflexion, it also highlighted that its impact on dynamic gait patterns, especially in more severe cases may be limited. These findings question the assumption that serial casting uniformly improves all ITW classifications and suggests that its effectiveness may vary depending on severity of ITW. Ultimately this research could inform treatment protocols, providing clinicians with more evidence-based tools for managing ITW and improving patient outcomes.

**References:** [1] Ruzbarsky et al. (2016), *Curr. Opin. Pediatr* 28(1); [2] Van Bemmel et al. (2014), *Musculoskelet. Surg.* 98(2). [3] Chu et al. (2023), *Physiother. Theory Pract.*, 39(11). [4] Alvarez et al. (2007). *Gait Posture* 26(3).

# TREADMILL OSCILLATION WALKING ENHANCES PARETIC LIMB LOADING IN INDIVIDUALS POST-STROKE

Jason Tsai[1]*, Keng-Hung Shen PhD., M.D.[2], Hao-Yuan Hsiao PhD.[1]
[1]Department of Kinesiology and Health Education, University of Texas at Austin, [2] Department of Neuroscience, Washington University School of Medicine, St. Louis
email: jasontsai17@utexas.edu

**Introduction:** Stroke survivors with hemiparesis commonly struggle with limb loading and weight transfer to the paretic leg[1]. Deficits in paretic limb loading ability contribute to balance instability and are associated with risk of falling in individuals post-stroke[2]. Thus, restoring limb loading and weight transfer ability is an important goal for rehabilitation[3]. Knee extension and hip abduction torque production are key elements of weight transfer[4]. Abnormalities in knee extension and hip abduction torque production coupling[5] and deficits in isolated knee and hip joint torque generation[6] have been identified after stroke. An potential approach to trigger hip and knee muscle activities is to apply lateral walking surface translation[7]. The purpose of this study was to determine the immediate effects of treadmill oscillation walking on hip abductor and knee extensor muscle activation and limb loading compared to walking with no oscillation. We hypothesize that participants will show corresponding increases in peak vertical ground reaction force (vGRF) production, peak hip abductor and knee extensor torque and muscle activity, and decreased weight transfer time during treadmill oscillation walking, reflecting enhancement of weight transfer ability through increased hip and knee muscle contribution.

**Methods:** Fifteen participants with chronic stroke (age: 59±12 yrs.; 8 male; 9 left paretic) walked at baseline self-selected speed with and without lateral sinusoidal treadmill oscillation. The oscillation magnitude was 1-cm and the frequency was tailored to the individual's stride frequency during baseline walking to minimize potential gait disruption. We used a 10-camera motion capture system (Vicon-USA, Denver, CO), an instrumented split belt treadmill (Motek), and a surface electromyography (EMG) system (Delsys) to record kinematic, kinetic, and muscle activity data. We analyzed single leg stance time, vertical ground reaction force, weight transfer time, gluteus medius and vastus lateralis EMG activation, and joint torques. Paired t-tests were used to compare differences with and without oscillation. Data processing was performed in MATLAB and calculations were performed in Visual 3D.

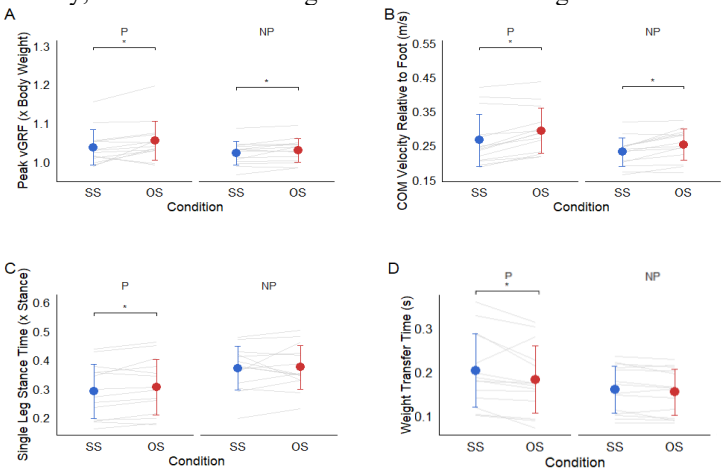


***Figure 1**: Group mean (±SD) changes in key gait parameters across conditions without oscillation (SS) and with oscillation (OS) for the paretic (P) and non-paretic (NP) limbs.*

**Results & Discussion:** Compared to walking without oscillation, participants walked with increased vGRF on both paretic and nonparetic sides. This was accompanied by decreased weight transfer time towards the paretic side and increased paretic single leg stance time (Fig.1). Additionally, greater COM velocity and larger COM displacement towards the paretic side were observed during walking with treadmill oscillation. These findings suggest that treadmill oscillation walking facilitates increased paretic limb loading and more rapid weight transfer, both essential for functional gait recovery post-stroke. In addition, stepwise linear regression revealed that the changes in paretic peak vGRF were predicted by changes in paretic peak hip torque (Fig.2), with an additional contribution from changes in paretic gluteus medius peak EMG activity. This underscores the role of hip musculature in actively supporting limb loading. Together, these results support the potential of oscillatory treadmill walking as a rehabilitation strategy to improve paretic limb loading and weight transfer function in individuals post-stroke.

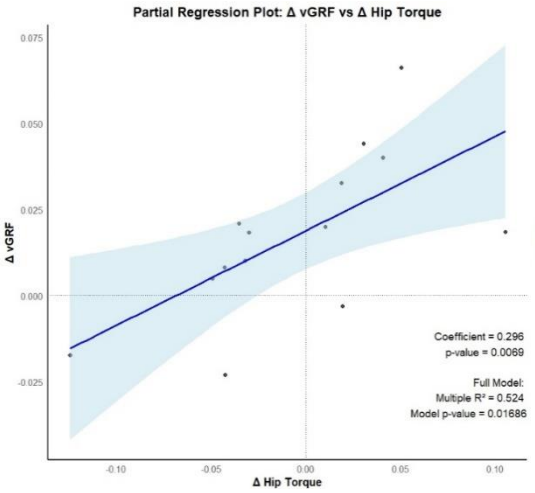


***Figure 1**: Relationship between changes in paretic peak vertical ground reaction force (vGRF). Changes in paretic peak hip torque (p = 0.007) was a significant predictor of changes in vGRF.*

**Significance:** Small magnitude treadmill oscillation walking may be an effective mechanism-based intervention to improve limb loading in stroke survivors. These findings indicate that controlled mediolateral oscillation can facilitate functional adaptations in gait, which may enhance balance stability in stroke survivors. These immediate benefits could potentially be implemented in long-term training protocols to improve gait speed, functional mobility, and walking independence. Emphasizing limb loading in rehabilitation may also drive improvements in functional balance and gait may reduce the risk of falling and improve quality of life for stroke survivors.

**Acknowledgments:** Support provided by NIH R21HD107461. We thank Dr. Robert Lee from St. David's Rehabilitation Hospital for providing clinical oversight of this project.

**References:** [1] Dettmann et al., 1987. Am. J. Phys. Med. 66:77-90; [2] Cheng et al., 2001. Arch. Phys. Med. Rehabil. 82:1650-1654; [3] Winstein et al., 1989. Arch. Phys. Med. Rehabil. 70:755-762; [4] Aruin et al., 2012. Top. Stroke Rehabil. 19:556-563; [5] Cruz TH, Dhaher YY. 2008. Stroke. 39:139-147; [6] Cruz et al., 2009. J. Biomech. 42:1673-1677; [7] Henry et al., 1998. IEEE Trans. Rehabil. Eng. 6:32-42.

# THE EFFECT OF WEAKNESS ON SPATIOTEMPORAL ASYMMETRY IN PREDICTIVE WALKING SIMULATIONS

Nicholas L. Yaple[1*], Anne E. Martin[1]
[1]Mechanical Engineering, Penn State, University Park, PA, USA
*Corresponding author's email: nxy5047@psu.edu

**Introduction:** People post-stroke often have chronic impairments such as hemiparesis, defined as weakness or reduced mobility in one half of the body [1]. Consequently, they walk with slower preferred speeds, asymmetric gait, and increased metabolic cost [2]. However, the underlying factors causing the asymmetry are not well understood. Since it is difficult to perform physical experimental studies on how people with post-stroke hemiparesis self-select their gait, simulations are often used. However, few predictive simulations have been leveraged for hemiparetic gait. Using a 2D predictive walking model [3], this abstract investigates how spatiotemporal asymmetry and energetic cost changes with joint-level unilateral weakness.

**Methods:** Predictive walking simulations were generated with a sagittal, six-link, lower body biped with each leg consisting of a thigh, shank, and circular foot [3] (Fig. 1). The joints were actuated with ideal actuators. A simulated gait was two alternating steps, with each step consisting of a double and single support phase. The gait was found by minimizing the weighted sum of the squared active joint torques [4]. Weakness was implemented in one leg by limiting the active joint torque in the affected knee, ankle, and hip: $u_{j,lim} = (1-w)\max(|u_{j,act}|)$ where $u_{j,lim}$ is the maximum allowable joint torque, $w$ is the percent weakness, and $u_{j,act}$ is the maximum active joint torque without weakness. Using a model with a leg length of 0.9 m and a mass of 87 kg, slow (0.8 m/s) and normal (1.2 m/s) speed gaits with weaknesses up to 50% (or up to the highest weakness achievable were generated. Energetic cost (EC) was quantified using the objective function. Step length asymmetry (SLA) and step time asymmetry (STA) were quantified using $Asym = \frac{X_N - X_A}{X_N + X_A} \times 100\%$ where $Asym$ is the asymmetry measure, $X$ is the relevant metric, and $N$ and $A$ indicate the normal and affected sides, respectively. When the normal step was greater than the affected step, asymmetry was positive. Linear fits between the metrics and weakness were found, along with the coefficient of determination.

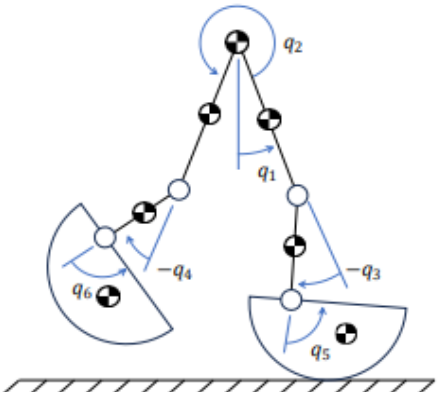


**Figure 1:** A diagram of the six-link planar biped. One hip joint ($q_2$) and both ankle and knee joints ($q_3$ through $q_6$) were actuated with ideal actuators.

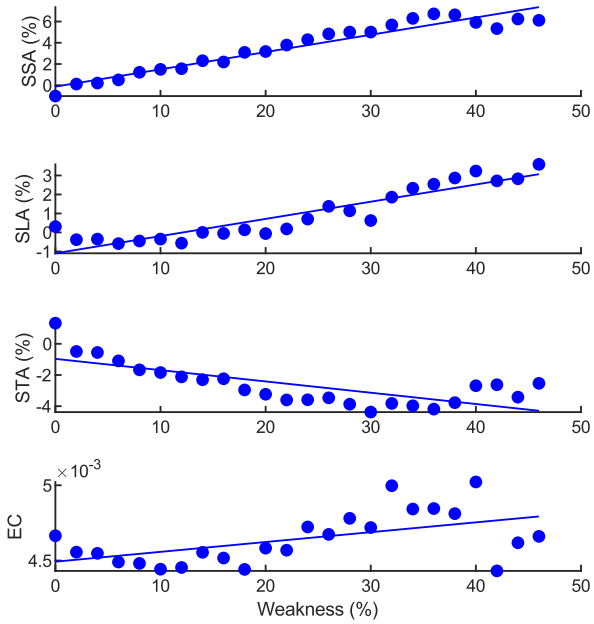


**Figure 2:** SSA (top), SLA (second), STA (third), and EC (bottom) as weakness varied up to 46% for the slow speed. Results were similar for the normal speed. The asymmetry magnitude and energetic cost increased with weakness, but not as much as observed in experimental studies.

**Results & Discussion:** The maximum weakness achieved for the slow and normal speed gaits were 46% and 42%, respectively. Without weakness, the gait was slightly asymmetric (Fig. 2). This indicated that slight asymmetry in a gait can be energetically beneficial and supports previous observations of asymmetry in healthy gait [5]. At both slow and normal speeds, the change in step asymmetries and energetic cost with weakness were generally similar. As expected, step speed asymmetry (SSA) increased approximately linearly with weakness ($R^2$>0.9), with the unaffected leg taking a faster step. The speed was faster because it took a longer step in a shorter time. Step length asymmetry increased with weakness ($R^2$>0.6 for the slow speed and 0.1 for the normal speed). Step time asymmetry (STA) also increased with weakness ($R^2$>0.5) but appeared to plateau at higher weaknesses. Overall, asymmetries were small (<10%), meaning only slight adaptations were necessary to accommodate weakness. Increasing weakness slightly increased the energetic cost, but does not increase to expected values in a hemiparetic gait [7]. Overall, this agrees with similar work showing that weakness can increase gait asymmetry [6], but weakness alone was not capable of reproducing experimentally observed asymmetry or energetic cost in hemiparetic gait [2].

**Significance:** These results suggest that additional factors beyond weakness significantly contribute to gait asymmetry. This supports previous research in rehabilitation that restoring strength does not completely restore gait symmetry [7].

**Acknowledgments:** This work was supported by NSF award 1943561.

**References:** [1] Bourbonnais & Noven (1989) *Am. J. Occup. Ther.* 43(5); [2] Padmanabhan et al. (2020) *J. NeuroEngineering Rehabil.*17(105); [3] Martin & Schmiedeler (2014) *J. of Biomech.* 47(6); [4] Arnold et al. (2010) *Ann. Biomed. Eng.* 38(2); [5] Lathrop-Lambach et al. (2014) *Gait Posture* 20(4); [6] Nguyen et al. (2020) *J. NeuroEngineering Rehabil.*17(119); [7] Wist et al. (2016) *Physical Rehabil. Medicine* 114(124); [7] Kramer et al. (2016) *Archives of Physical Medicine and Rehabil.* 97(4).

# DYNAMIC MOTOR CONTROL DURING WALKING CAN BE ACUTELY MODULATED THROUGH MANIPULATIONS IN ENVIRONMENT AND SPEED IN CHILDREN WITH CEREBRAL PALSY

*Stephanie N. Mace[1], Joseph W. Harrington[1], Vivek Dutt[2], Brian A. Knarr[1], David C. Kingston[1]
[1]Department of Biomechanics, University of Nebraska Omaha, Omaha, NE, 68182
[2]Department of Orthopaedic Surgery, University of Nebraska Medical Center, Omaha, NE, 68105
*Corresponding author's email: smace@unomaha.edu

**Introduction:** Children with cerebral palsy (CP) suffer a brain injury that affects their dynamic motor control [1-3], or one's ability to voluntarily activate muscle groups in a selected pattern without obligatory contractions of other muscles [5]. Prior literature investigating overground and treadmill walking in children with CP shows reduced muscular synergies [1-5] compared to typically developing (TD) children, indicating simplified neuromuscular control. Additional work investigating the effect of surgical interventions on muscle synergies in CP has indicated minimal changes post-operatively [2]. Therefore, there is a need to identify interventions that challenge motor control in children with CP. The dynamic motor control index during walking (walk-DMC) can be used to quantify dynamic motor complexity by combining clinical and control values into a single metric, where values below 100 (TD baseline) indicate simplified neuromuscular complexity [1-3]. Despite previous investigations in CP indicating reduced walk-DMC during overground and treadmill gait, a knowledge gap remains for walk-DMC modulation in varying environments and walking speeds [6]. Therefore, the primary aim of this study was to assess how neuromuscular control is acutely affected for the more-affected limb across different walking environments and speeds in children with CP. We hypothesized that walk-DMC will be lower in the aquatic environment due to body weight offloaded. We also hypothesized that fast speeds would increase, and slow speeds would decrease walk-DMC as reported in prior literature [1]. Finally, we hypothesized that slow walking in an aquatic environment would result in the lowest walk-DMC due to buoyancy and hydrodynamic drag.

**Methods:** Eight children with CP (5 males; age: 12.62 ± 3.99 years; height: 1.52 ± 0.20 m; weight: 54.55 ± 30.83 kg) and fifteen TD children (7 males; age: 11.33 ± 4.27 years; height: 1.46 ± 0.18 m; weight: 44.20 ± 16.80 kg) performed walking trials in three environments: conventional treadmill (DRY; Precor TRM 835 V2, Precor, Woodinville, WA, USA), overground (OG), and aquatic treadmill (WET; 300 Series, HydroWorx, Middletown, PA, USA). For DRY and WET environments, participants completed 3-minute trials. In the OG environment, they walked a 10-meter pathway at least three times for each speed. Walking speeds (slow, normal, fast) were randomized within each environment. Waterproof wireless surface electromyography (EMG) equipment (Mini Infinity Waterproof, Cometa, Milan, IT) was placed bilaterally on the tibialis anterior, medial gastrocnemius, rectus femoris, and semitendinosus and sampled at 2000 Hz, bandpass filtered at 10 Hz with a 4th order Butterworth filter [1,2,7]. EMG data were then normalized by the absolute peak of the entire walking trial for each muscle separately, with amplitude ranging from 0 to 1 [1,2]. EMG data was segmented and normalized to 101 data points prior to concatenating five consecutive strides, or the maximal number of available strides for each condition [7]. Non-negative matrix factorization was used to determine synergy weights and activations [1,2,7]. The variance accounted for in the first synergy was then determined (Figure 1a) to calculate walk-DMC (Figure 1b) [2].

a) $$\mathrm{VAF} = 1 - \frac{\|\mathrm{EMG} - (\mathrm{W} * \mathrm{C})\|^2}{\|\mathrm{EMG}\|^2}$$

b) $$\mathrm{WalkDMC} = 100 + 10 * \left[\frac{\mathrm{VAF}_{1\ \mathrm{TD_Ave}} - \mathrm{VAF}_{1\ \mathrm{CP}}}{\mathrm{VAF}_{1\ \mathrm{TD_SD}}}\right]$$

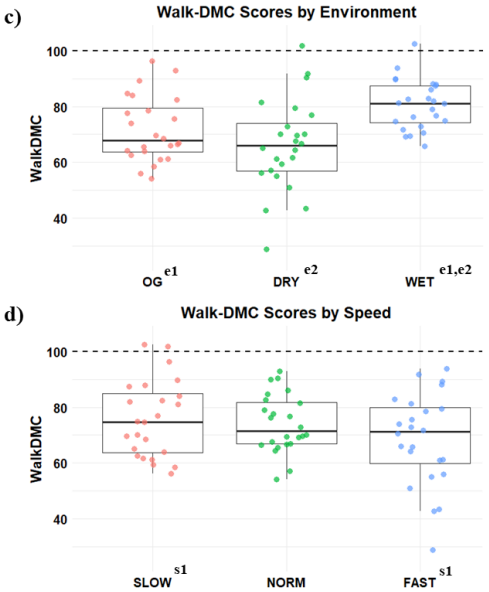


**Figure 1.** a) Equation for determining the variance accounted for across synergies with the original signal (EMG) and the reconstructed signal (W*C); b) Equation for calculating walk-DMC; c) *Results of the main effect of environment for OG (red), DRY (green), and WET (blue) environments; d) *Results of the main effect of speed for slow (red), normal (green), and fast (blue) speeds. *Shared superscripts indicate pairwise differences ($p < 0.05$).

**Results & Discussion:** A linear mixed effects analysis was used to evaluate walk-DMC across three levels of environment and walking speed for the more-affected limb. A main effect of environment was significant ($p < 0.001$, $\eta p^2 = 0.38$, Figure 1c), indicating a large effect of environment on walk-DMC. It was observed that the WET environment had a significantly higher walk-DMC when compared to the OG environment (estimate = 8.96, $p = 0.002$) and the DRY environment (estimate = 14.62, $p < 0.001$). A main effect of speed was also observed ($p = 0.014$, $\eta p^2 = 0.14$, Figure 1d), indicating a large effect of speed on walk-DMC. It was observed that walk-DMC increased during slow walking speeds when compared to fast walking speeds (estimate = 7.23, $p = 0.015$). Our findings suggest that the WET environment and slow walking speeds acutely evoked an increase in neuromuscular complexity for the more-affected limb.

**Significance:** These findings offer new perspectives on optimizing walking rehabilitation by accounting for the interplay between task demands and motor function. However, future studies should investigate repeated exposures to novel gait rehabilitation environments, particularly in a WET environment at slow and fast walking speeds.

**References:** [1] Steele et al. (2015), *Dev Med Child Neuro* 57(12); [2] Shuman et al. (2019), *J Neuro Eng Rehab* 16(1); [3] Schwartz et al. (2016), *Dev Med Child Neuro* 58(11); [4] Fowler et al. (2010), *Dev Med Child Neuro* 52(3); [5] Tang et al. (2015), *J Neural Eng.* 12(4); [6] Novak et al. (2020), *Curr Neurol Neurosci Rep.* 20(2); [7] Oliveira et al. (2014), *Front Hum Neurosci.* 8.

# ELUCIDATING THE ROLES OF MOTOR FUNCTION AND COGNITIVE SWITCHING IN LOCOMOTOR SWITCHING AFTER STROKE

*Nathan W. Brantly[1,2], Dulce M. Mariscal Olivares[1,2], Jiwon Choi[1,2], Andrea Weinstein[3], Helmet T. Karim[1,3], Gelsy Torres-Oviedo[1,2]
[1]Department of Bioengineering, University of Pittsburgh
[2]Center for the Neural Basis of Cognition, Pittsburgh, PA
[3]Department of Psychiatry, University of Pittsburgh
*Corresponding author's email: nwbrantly@pitt.edu

**Introduction:** Locomotor switching is the ability to shift walking patterns in response to shifts between familiar environments (e.g., widening stance when transitioning from walking on a dry to a slippery surface). Failure to switch walking patterns to best suit the current context may increase the likelihood of a fall. The neural mechanisms underlying locomotor switching are unknown. Sombric et al. found a correlation between locomotor switching and the ability to switch between tasks cognitively (i.e., cognitive switching) in older adults suggesting cognitive switching brain resources may support locomotor switching[1]. Stroke survivors can have deficits in paretic leg motor function, which can cause walking impairments, including slow and unstable gait[2-5] and locomotor switching deficits[6]. However, the relationship between locomotor switching and cognitive switching and motor function post-stroke is unknown. We hypothesized that participants with better cognitive switching after a stroke would exhibit better locomotor switching due to shared neural resources underlying these behaviors. Similarly, we hypothesized that participants with better motor function after a stroke would also exhibit better locomotor switching due to the necessity of a high-functioning motor apparatus for locomotor switching.

**Methods:** To measure locomotor switching, we adapted 16 participants who have had a stroke (6 female, mean age 57.9 years +/- 13.0 years SD, one extreme outlier measurement was omitted from analysis) to split-belt treadmill walking for 900 strides (2:1 belt-speed ratio, +/- 33% of 85% of the 6-Minute Walk Test speed) before having those participants shift to walking overground. We characterized locomotor switching performance as the initial aftereffects, which is a measure of how perturbed the gait is, averaged over the first five strides of post-adaptation overground walking. We measured locomotor aftereffects in both the muscle activity (i.e., the magnitude of the EMG activity across all 28 muscles, 14 each leg) and kinematics (i.e., step length asymmetry). Previous studies suggest muscle activity measures may be more sensitive to deficits in locomotor adaptation than kinematic measures, which is why we have chosen it as our primary outcome measure[7]. Cognitive switching was assessed using the Trail Making Test (parts A and B)[8]. We measured motor function using the lower extremity Fugl-Meyer Assessment motor function score[9]. We tested the following associations: locomotor switching with motor function and locomotor switching with cognitive switching.

**Results & Discussion:** We are actively collecting data toward our target N = 43 participants with stroke to detect a moderate effect size, and we have evaluated preliminary associations (Fig. 1). We found a $\rho = -0.004$ for the Spearman rank order correlation between the muscle activity measure of locomotor switching and cognitive switching (Fig. 1B, df = 13, 95% CI = [-0.572,0.605]). We found a $\rho = -0.366$ for the correlation between the muscle activity measure of locomotor switching and motor function (Fig. 1A, df = 13, 95% CI = [-0.796,0.286]). Our preliminary results suggest distinct neural substrates for locomotor and cognitive switching rather than shared brain resources. Our results have implications for the role of the function of the motor apparatus and cognitive switching resources in locomotor switching ability, which could inform rehabilitation strategies for stroke survivors with gait impairments.

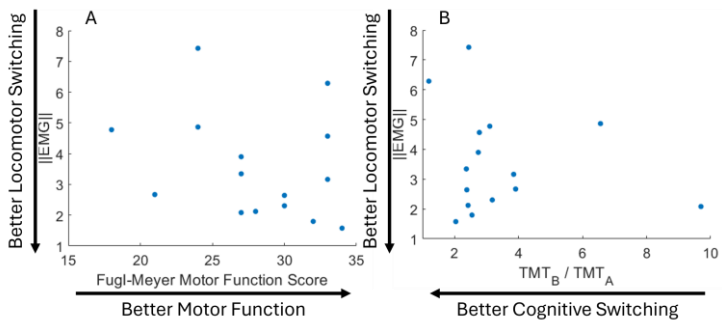


**Figure 1:** A) Association between the magnitude of the muscle activity measure of locomotor switching and the Fugl-Meyer motor function score (34 is maximum score). B) Association between the same locomotor switching measure and the Trail Making Test ratio (Part B / Part A) as a measure of cognitive switching.

**Significance:** The ability to switch between established walking patterns in response to changes in the environment may be important for mobility and community ambulation, which are important for independence and quality of life. It is critical to understand the role of motor function and cognitive switching in locomotor switching to develop effective gait rehabilitation strategies for individuals with mobility impairments, including those due to stroke. Further, our muscle activity characterization of locomotor switching in participants who have had a stroke represents a novel contribution to the scientific study of motor adaptation in this population.

**Acknowledgments:** We would like to thank Prachi Mital for assistance with data entry. We are grateful to the Western Pennsylvania Patient Registry for participants referrals and all stroke survivors who volunteered for our study. Nathan W. Brantly is supported by the NIH Bioengineering in Psychiatry T32. We are grateful to Aaron Batista and Darcy Reisman for their helpful input in this study.

**References:** [1] Sombric, Torres-Oviedo (2021), *Front. Aging Neurosci.*; [2] Olney et al. (1994), *Phys. Ther.*; [3] Roth et al. (1997), *Am. J. Phys. Med. Rehabil.*; [4] Patterson et al. (2008), *Arch. Phys. Med. Rehabil.*; [5] Lewek et al. (2014), *J. Appl. Biomech.*; [6] Reisman et al. (2009), *Neurorehabil. Neural Repair*; [7] Iturralde, Torres-Oviedo (2019), *eNeuro*; [8] Bowie, Harvey (2006), *Nat. Protoc.*; [9] Fugl-Meyer et al. (1975), *Scand. J. Rehab. Med.*

# EFFECTS OF ERROR FUNCTION SELECTION AND NORMALIZED FIBER LENGTH RANGE IN NUMERICAL ESTIMATION OF TENDON SLACK LENGTH

*Hudson Burke[1], Xiao Hu[1,2], Shawn Russell[1,2,3]
University of Virginia, [1]Department of Mechanical and Aerospace Engineering, [2]Biomedical Engineering, [3]Orthopaedic Surgery
*Corresponding author's email: hpb7kr@virginia.edu

**Introduction:** In musculoskeletal models incorporating Hill-type muscles, parameters must be specified to determine the forces generated by the musculotendon unit. One of the most influential parameters is tendon slack length. Tendon slack length is originally posited as a representation of the length at which the tendon begins to produce a restorative force and has been estimated in various ways throughout literature. This value cannot simply be measured directly as tendons often parallel the fibers of the muscle. One of the more popular human models used especially for lower limb gait modeling from Rajagopal [4] estimates tendon slack length based on the fiber length at a specific joint configuration. Manal [2] proposed an optimization technique to minimize the error between tendon slack lengths estimated at a range of muscle lengths using the active and passive force-length curves for the muscle along with the tendon force-length curve. We extend this technique to analyze the effect that normalized fiber length range and different error functions have on the estimated tendon slack lengths in an effort to inform a robust methodology for numerically tuning tendon slack length in new musculoskeletal models.

**Methods:** This methodology follows the same concept proposed in Manal [2] in that it utilizes equations derived from Zajac [4] to calculate tendon slack length from measured muscle parameters and interpolated force values. The optimization differs by using Sequential Least SQuares Programming (SLSQP) instead of Generalized Reduced Gradient (GRG) as an algorithm for optimization because of its availability and popularity in Python. Furthermore, the active and passive fiber and tendon force length curves were taken from the Millard [3] muscle as seen in Fig. 1 instead of Zajac's curves [4], and lengths were chosen from the whole range of motion of the muscles instead of a short and long length within ten percent of the minimum and maximum flexion angles and averaging the two for a third middle length. The tendon slack lengths were estimated for the lateral gastrocnemius (gaslat), long head of the biceps femoris (bflh), and the soleus to demonstrate application across muscles of differing architectures in terms of tendon to fiber ratio. In addition to the sum of squared differences between each element originally used by Manal [2], three additional error functions were utilized: the standard deviation, the variance, and the sum of squared differences between each element and the mean. and iterate through all of the degrees of freedom to get a minimum of 100 musculotendon lengths for each muscle. Then, SLSQP minimization from the scipy optimization library in Python is utilized to minimize the error function of the calculated tendon slack lengths at each musculotendon length. This was performed using a full range of normalized fiber lengths to capture the main force-producing part of the fiber force-length curve, using estimates of the operating range of each muscle during gait as reported by Arnold [1], and using only the ascending portion of the curve as done in Manal [2].

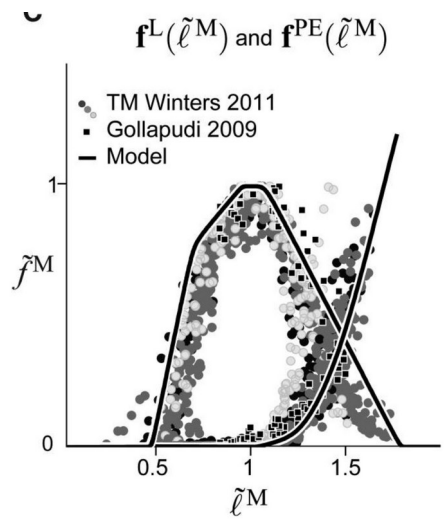


**Figure 1**: Millard fiber force-length curves [3].

**Results & Discussion:** The mean tendon slack lengths across error functions for each normalized fiber range are summarized in Table 1. The chosen error function did not make a large difference in the calculated mean tendon slack lengths nor variances except for utilizing variance as the error function for the bicep femoris short head which resulted in a tendon slack length standard deviation 20-100 times greater than the other methods. More investigation will be required to determine the root of this difference. A much more influential value is the range of normalized fiber length. The different ranges produced different tendon slack lengths with no clear correlation between the muscles. This demonstrates the importance of using an appropriate normalized fiber length operating range when estimating tendon slack length. Likely, muscles will have to be tuned individually for a specific range of motion and normalized fiber length operating range to best characterize the force being generated by muscles for specific motions. Using time-series dynamic experimental data would also allow for the use of the Millard [3] force-velocity curves in the optimization that cannot be used when optimizing parameters at static positions.

| | Rajagopal | Manal | Arnold | Full Range |
|---|---|---|---|---|
| **gaslat** | 0.374 | 0.37595 | 0.359575 | 0.3537375 |
| **bflh** | 0.3325 | 0.367045 | 0.346725 | 0.3366175 |
| **soleus** | 0.28135 | 0.296895 | 0.2791725 | 0.2805275 |

**Table 1**: Tendon slack lengths from normalized fiber length ranges.

**Significance:** This paper presents data from numerical estimation of tendon slack lengths across different error functions and normalized fiber length ranges. It reveals the need for careful choice of normalized fiber length ranges when performing numerical optimization of tendon slack lengths.

**References:** [1] Arnold et al. (2011), *Philos Trans R Soc Lond B Biol Sci*; [2] Manal et al. (2004), *J Appl Biomech*; [3] Millard et al. (2013), *J Biomech Eng*; [4] Rajagopal et al. (2016), *IEEE Trans Biomed Eng*; [5] Zajac (1989), *Crit Rev Biomed Eng*

# A MATHEMATICAL MODEL OF HOPPING WITH STOPPING CONTROLLED BY MUSCLE DAMPING INSTANTANEOUS CHANGE: BIOLOGICAL IMPLICATIONS AND LIMITATIONS

*Alessandro Maria Selvitella[1], Kathleen Lois Foster[2]
[1]Department of Mathematical Sciences, Purdue University Fort Wayne | eScience Institute, University of Washington
[2]Department of Biology, Ball State University
*Corresponding author's email: aselvite@pfw.edu

**Introduction:** Animal life is strictly linked to the capability of animals to move, which is necessary for survival. To understand gait patterns, researchers develop mathematical models, ranging from high-dimensional, which prefer accuracy, to low-dimensional, which focus on biological interpretability [1,2]. Reductionist models concentrate on the essential dynamics, most often of the center of mass, and describe motion through a system of ordinary differential equations (ODEs). This reduction is not trivial because it is hard to encompass the key biological features in a handful of variables and because these reductions must include latent variables, which do not have direct biological correspondence [3]. This is the case when hopping, jumping, and running are represented by a spring-mass damped oscillator during stance (and ballistic motion during flight), since there, the stiffness and muscle damping constants are quantities summarizing heterogeneous contributions. Nevertheless, these reductionist models succeed in describing and give approximate representations of important biological parameters and tend to fit kinematics and kinetic data accurately. However, often these models aim at describing only the periodic motion of a perpetual gait and neglect the starting and stopping phases. This is also the case for 1-dimensional models describing hopping on the spot. The goal of this abstract is to start filling this gap and introduce a new model of hopping with stopping controlled by an instantaneous change in the damping of the muscle.

**Methods:** We consider a point mass $m$ $(kg)$ that moves straight in the vertical direction. The motion is driven by a (hybrid) linear second order ODE, linking the mass acceleration $y''$ $(m/s^2)$ with the velocity $y'$ $(m/s)$ and the height $y$ $(m)$ of the mass. The elastic force, with spring constant $k$ $(N/m)$ and compression given by $l - y$ ($l$ equals both the leg length and the height at touch down and take off), and the muscle damping force, proportional to the velocity of the mass with damping constant $b$ $(kg/s)$, act only during contact phases, while the force of gravity with constant $g$ $(m/s^2)$ acts during both the flight and the stance phases. The stopping stance is triggered by an instantaneous increase in the muscle damping constant at the beginning of the stance phase.

**Results & Discussion:** Our model treats the stopping phase as happening at a different time scale $T \sim b$, where $m/b^2$ is infinitesimal. Due to this, the dynamics in the stopping phase is essentially described by a first order ODE. Although parameters such as $b$ vary discontinuously, the height, velocity, and acceleration of the mass remain continuous, as observed in human or animal hopping. As depicted in Fig. 1, the stopping phase relaxes the body mass to a height that is lower than the leg length. This limitation is present in the current version of the model, but can be easily overcome by introducing a recovery phase, in which damping decreases again or where the stiffness compensates for the increased damping. Solutions of this model can be written explicitly, even if the system is hybrid (continuous plus discrete) because all the phases are described by linear ODEs. Analyzing this model qualitatively, one finds that stopping is only possible when the squared pendulum velocity $g/l$ is smaller than the squared spring velocity $k/m$. The current model has not been validated using animal data yet (e.g. human or kangaroo) and this will be done in future work.

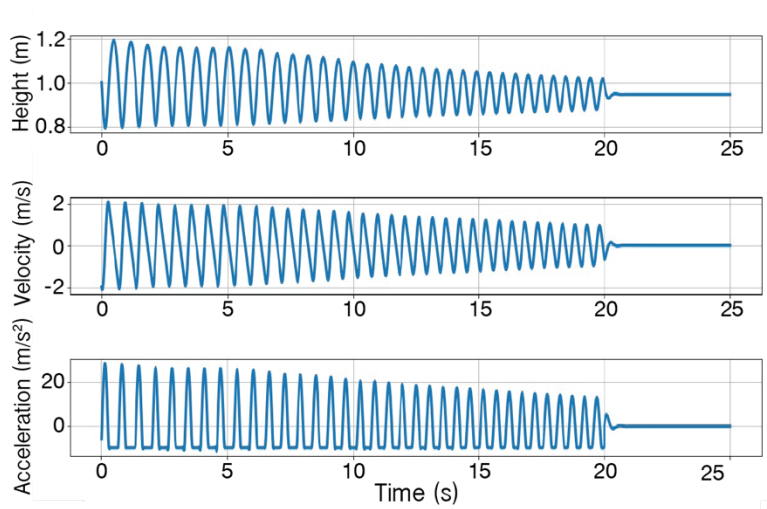


Figure 1: Simulation of mass height, velocity, and acceleration using our hopping with stopping model. Here m=80 kg, l=1 m, k=15,000 N/m and b=10 kg/s (stance) or b=1000 kg/s (stopping). The movement starts at a height of 1 m, with initial velocity of -2 m/s.

**Significance:** If not the first, our model is one of the few that accounts for stopping, as it introduces a terminal stride that concludes the periodic motion with relaxation towards an equilibrium position. This model is interesting beyond hopping because the idea of introducing a stopping phase can be extended to walking, running, and multipedal motions and might be part of a controller for jumping or running robots. Successful stopping is an important part of rehabilitation following knee or ankle surgery and so extensions of this model can be implemented to verify progress in muscle recovery.

**Acknowledgments:** AMS and KLF are supported by the collaborative NSF Awards #2152789 and #2152792 on *RUI: Collaborative Research: DMS/NIGMS 1: The mathematical laws of morphology and biomechanics through ontogeny*.

**References:** [1] Selvitella and Foster. (2022), *Integr Comp Biol*, **62** (5); [2] Selvitella and Foster. (2024), *J Theor Biol*, **595**; [3] Selvitella and Foster. (2023), *R Soc Open Sci*, **10**.

# INDIVIDUAL MUSCLE CONTRIBUTIONS TO ANKLE QUASI-STIFFNESS DURING HEALTHY WALKING

*Stephanie L. Molitor[1] and Richard R. Neptune[1]
[1]Walker Department of Mechanical Engineering, The University of Texas at Austin, Austin, TX
*Corresponding author's email: stephanie.molitor@utexas.edu

**Introduction:** Maintaining sufficient ankle joint stiffness is critical for walking performance, as it affects essential biomechanical functions of walking such as maintaining balance [1] and providing body support and propulsion [2]. Furthermore, ankle stiffness is modulated throughout the gait cycle and for different walking conditions [3]. Although the overall importance of ankle stiffness has been documented, it is not yet clear how specific muscles modulate ankle stiffness throughout the gait cycle. For dynamic tasks such as walking, quasi-stiffness is often used to quantify joint stiffness as it accounts for passive soft tissue stiffness as well as active muscle force generation [4]. Quasi-stiffness is defined as the slope of the joint moment-angle curve during discrete phases of the gait cycle. Therefore, identifying the primary muscle contributors to each of the net joint moment and angle can elucidate how muscles are coordinated to modulate ankle quasi-stiffness. The objective of this study was to identify individual muscle contributions to sagittal-plane ankle quasi-stiffness during walking using musculoskeletal modeling and simulation. While we expected the primary contributors to ankle quasi-stiffness would be the ankle dorsiflexors/plantarflexors as they cross the joint and directly impact the net ankle moment, we also expected distant muscles to contribute to quasi-stiffness by modulating the ankle joint angle through dynamic coupling [5].

**Methods:** Musculoskeletal models and simulations of 15 healthy young adults (8 female; age: 25 ± 4 years; height: 169 ± 13 cm; mass: 69 ± 12 kg) were developed in OpenSim 4.4 [6], using previously collected walking data [7]. Individual muscle contributions to sagittal-plane ankle moments [8] and angles [9] were determined within discrete phases of the gait cycle (Dorsiflexion phase: ~12-35% gait cycle, Dual-Flexion phase: ~35-51%, Plantarflexion phase: ~51-65%) [10]. Moments were normalized by participant height and body weight. Angles were converted to radians. Muscles were combined into groups with similar anatomical functions, and individual muscle moment and angle contributions were summed, respectively, within functional groups. Muscle groups were rank-ordered for their group-averaged contribution to the net joint moment and angle components of quasi-stiffness for each phase of the gait cycle.

**Results & Discussion:** As expected, the ankle plantarflexors (soleus: SOL, gastrocnemius: GAS, peroneus: PER) and dorsiflexors (tibialis anterior: TA) were the primary contributors to both the net ankle moment and ankle angle during all three phases (Fig. 1). However, muscles that cross the hip joint including the gluteus medius (GMED), vasti (VAS), gluteus maximus (GMAX) and iliopsoas (IL) were also notable contributors to the ankle angle during various phases (Fig. 1). The contributions of these distant muscles to the ankle angle, and ultimately ankle quasi-stiffness, highlight the effects of dynamic coupling, through which muscles can accelerate joints they do not span [5].

**Significance:** Results from this study emphasize the importance of considering the role of distant muscles when designing rehabilitation programs and assistive devices to restore or replicate ankle function. Furthermore, these results establish a framework for future studies to investigate muscle contributions to quasi-stiffness at other joints and how contributions change for individuals with altered neuromotor control and stiffness deficits.

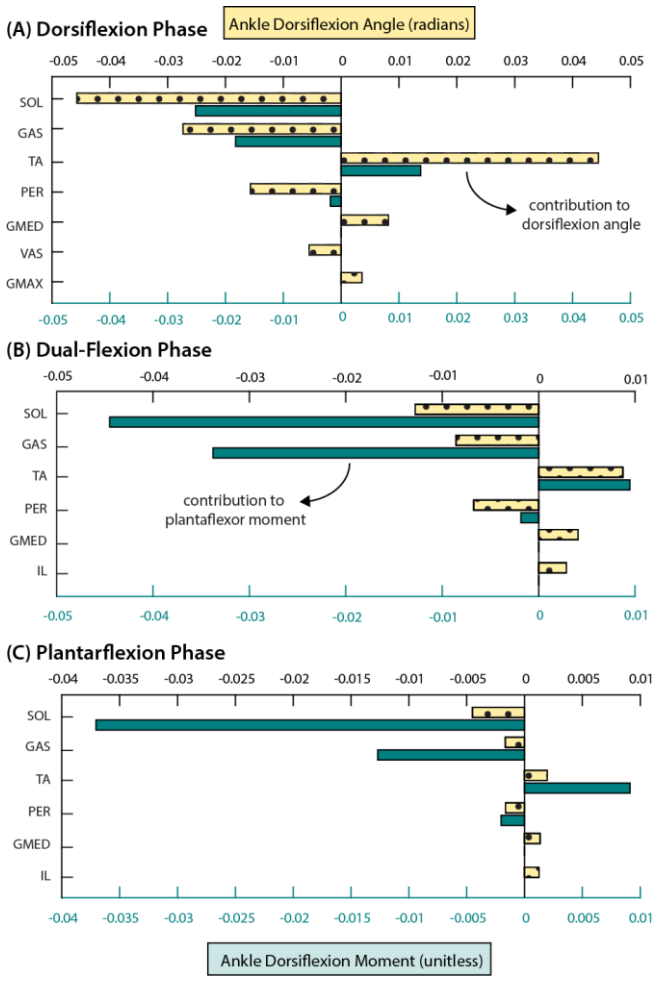


**Figure 1:** Primary muscle contributors to sagittal-plane ankle angle and moment during the Dorsiflexion (A), Dual-Flexion (B), and Plantarflexion (C) phases. Dotted and solid bars represent contributions to the ankle angle and moment, respectively. Positive values indicate dorsiflexion angles and moments, negative values indicate plantarflexion angles and moments.

**Acknowledgments:** This work was funded in part by the NSF GRFP.

**References:** [1] Shell et al. (2017), *Clin Biomech 49*; [2] Fey et al. (2013), *J Biomech 46*(4); [3] Frigo et al. (1996), *JEK 6*(3); [4] Davis & DeLuca (1996), *Gait Posture 4*(3); [5] Zajac et al. (2002), *Gait Posture 16*(3); [6] Delp et al. (2007), *TMBE 54*(11); [7] Molina et al. (2023), *J Biomech 157*; [8] Kipp et al. (2022), *JSCR 36*(2); [9] Anderson et al. (2004), *J Biomech* 37(5); [10] Molitor & Neptune (2024), *J Biomech 162*.

Step time and length asymmetry increase tibiofemoral joint contact peak forces and impulses via predictive simulation.

Ryan D. Wedge[1*] and Russell T. Johnson[2]
[1]Department of Physical Therapy, East Carolina University
[2]Department of Physical Medicine and Rehabilitation, Northwestern University
*Corresponding author's email: wedger19@ecu.edu

**Introduction:** Gait asymmetry is observed across many clinical populations, such as people with unilateral lower limb amputation [1] and people post-stroke [2]. These populations often have musculoskeletal pain and an increased incidence of knee osteoarthritis [3,4]. Rehabilitation interventions frequently target restoring symmetric gait for these individuals, intending to reduce joint loads and the reliance on the unaffected limb. However, inducing spatiotemporal gait asymmetries in healthy young adults has not been associated with increased knee joint reaction force or loading rates [5]. Therefore, whether the gait asymmetries may increase osteoarthritis development risk is unclear. Modeling and simulation allow us to isolate the effects of spatiotemporal gait asymmetries on knee contact forces without potential confounding factors of gait acclimation or neuromuscular impairment. Here, we aimed to determine if bilateral tibiofemoral joint loading is greater when walking with asymmetric step lengths and times compared to symmetric gait via predictive simulations using a sagittal-plane musculoskeletal model. We hypothesized that asymmetric gait would increase joint contact forces. A comprehensive understanding of the relationships between gait asymmetry and joint loading is crucial to developing personalized rehabilitation interventions to improve mobility and reduce the risk of secondary musculoskeletal complications.

**Methods:** We used a musculoskeletal model with 12 degrees-of-freedom and 28 (14 per limb) Hill-type muscles based on the *DeGrooteFregley2016Muscle*. We used OpenSim Moco [6] to generate optimal control simulations of walking with different step length and step time asymmetries (-10, -5, 0 +5, and +10% asymmetry targets). Each optimization minimized a weighted objective function with the following three terms: 1) the sum of the integrated muscle excitations cubed, and the difference between the target and the achieved 2) step time and 3) step length asymmetry [5]. Our outcome measures were right and left limb tibiofemoral joint contact 1) peak forces and 2) impulses. We computed local vertical joint reaction forces using the OpenSim Joint Reaction Analysis and multiplied average force by stance time to calculate impulse.

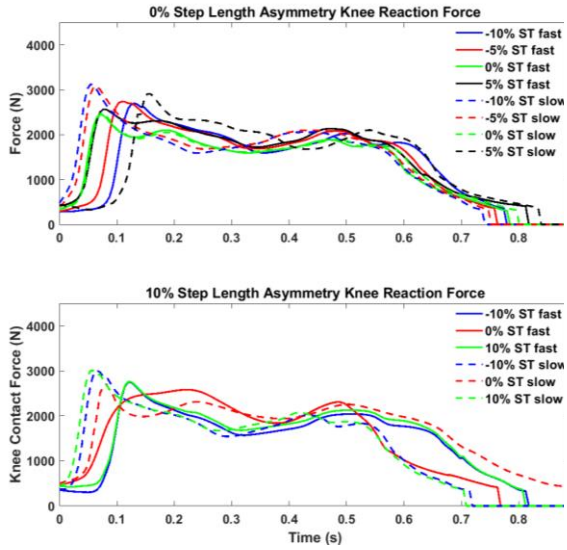


**Figure 1:** Knee reaction force for 0% step length asymmetry (top) and 10% step length asymmetry (bottom) for fast (solid) and slow (dashed) legs across step time asymmetries. Generally, the slow limb had greater forces.

**Results & Discussion:** Both step length and step time asymmetries resulted in greater tibiofemoral joint peak forces and impulses for both limbs across all combinations compared to symmetric step timing and lengths, except for the slow limb impulse for the -10% step time (slow limb = greater step time) with 10% step length asymmetry (Fig 1; Table 1). Both limbs had increased forces with asymmetric gait, yet the slow limb had larger force and impulse increases than the fast limb across combinations except for the two isolated conditions (Table 1). The step time asymmetries had a greater effect on forces and impulses than the step length asymmetries, with a range of 115-657 N and 128-241 N increases, respectively. There are no comparisons in the literature for prosthesis users or people post-stroke, but when comparing people who are overweight to those with class 1 and 2 obesity, there is a 361 N and 582 N difference in knee joint contact force, respectively [7]. In our study, some asymmetries led to increases beyond those clinically significant differences in knee joint contact forces seen in people with different levels of obesity. These relationships may not hold with people who have anatomical asymmetries, such as unilateral prosthesis users, since joint forces depend on the device and anatomical makeup.

**Significance:** Step time and length asymmetries led to greater tibiofemoral peak contact forces and impulses, with step time asymmetries having a greater effect. The magnitude of change may be clinically significant and indicates further emphasis on restoring spatiotemporal gait symmetry in clinical populations.

**Acknowledgements:** This research was supported in part through the computational resources and staff contributions provided for the Quest high performance computing facility at Northwestern University.

**Table 1:** Differences in knee joint peak contact forces and impulses from baseline symmetry across step length (SL) and step time (ST) asymmetries (Asym).

| | | Peak (N) | | Impulse (N·s) | |
|---|---|---|---|---|---|
| ST Asym | SL Asym | Fast | Slow | Fast | Slow |
| -10 % | 0 % | +243 | +657 | +37 | +51 |
| | 10 % | +298 | +536 | +91 | -11 |
| -5 % | 0% | +288 | +609 | +59 | +76 |
| 0 % | 0% | Baseline | | | |
| | 10 % | +129 | +241 | +122 | +332 |
| 5 % | 0 % | +115 | +442 | +143 | +87 |
| 10 % | 10 % | +309 | +539 | +150 | +16 |

**References:** [1] Sanderson & Martin (1997) *Gait & Posture* 6(2); [2] Finley & Bastian (2017) *NNR* 31(2); [3] Waters et al., (1976) *J Bone Jt Surg* (58); [4] Fournier et al., (2021) *Stroke* 52(10); [5] Johnson et al. (2022) *PLOS CB* 18(9); [6] Dembia et al. (2020) *PLOS CB* 16(12); [7] Messier et al., (2014) *Osteoarthritis Cartilage* 22(7).

# COMPREHENSIVE ANALYSIS OF NEUROMECHANICAL CONTROL MODELS OF HUMAN WALKING IN PHYSICS-BASED SIMULATIONS

*Vincent Ton[1], Seungmoon Song[1]
[1]Northeastern University, Department of Mechanical and Industrial Engineering
*Corresponding author's email: ton.v@northeastern.edu

**Introduction:** Neuromechanical simulations, which integrate a control model driving a musculoskeletal model within a physics engine to produce motion, hold great promise in creating digital twins of human movement. However, accurately modeling human locomotion control remains a significant challenge, as the underlying motor control mechanisms are not yet fully understood. Various motor control models have been proposed to study human locomotion, but they have been implemented in different simulation environments, with differing musculoskeletal properties, and varying parameter tuning criteria. These inconsistencies make biological and biomechanical comparisons between each proposed control models challenging.

**Methods:** We implemented previously proposed neural control models, each representing a different motor control hypothesis, within the same neuromechanical simulation framework. Specifically, we implemented a fully reflex-based control model [1], a muscle synergy-based control model [2], a central pattern generator with reflexes control model (CPG-reflex) [3], and a CPG with reflexes and synergies control model (CPG-reflex-synergy) [4]. We evaluated these models in two key areas: 1) the ability to produce human-like walking, and 2) the capability for each model to generate a variety of gait patterns. To assess human-like walking, we optimized the model to fit reference human gait kinematics at 1.2 m/s, testing its ability to reproduce human-like movement. Deviation from the reference kinematics is scored by R, the cross correlation dissimilarity coefficient accumulated over all joints. Additionally, we optimized the model to walk with minimal muscle effort, examining whether human-like walking naturally emerges from this principle. We then examined the models' capability to walk across different speeds and slopes, assessing the range of locomotor conditions it could handle.

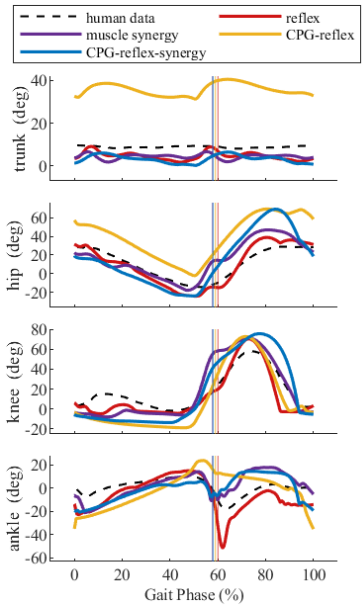


**Figure 1:** Kinematic gait analysis of simulated gait at 1.2 m/s. Trunk, hip, knee, and ankle joint kinematics are compared to experimentally collected data. The vertical line marks the toe-off phase in the gait cycle.

**Results & Discussion:** Each neural control model generated gait patterns comparable to human gait (Fig. 1). The pure reflex model produced the most human-like walking, with an R of 0.4 compared to human data. The CPG-reflex-synergy model also exhibited human-like kinematics with R of 0.8. Excessive hip flexion and delayed peak knee flexion was observed during swing phase, likely due to the control model's CPG and synergies. The muscle synergy model deviated from human kinematics (R=0.9) mostly at toe-off, displaying peak flexion at the hip and knee joints likely due to the constraints on the timing and shape of muscle synergy activations. The CPG-reflex model produced the least human-like kinematics (R=1.1). The large deviation from trunk and ankle joint is likely due to the unique pattern from the CPG neural oscillator dynamics.

The capability of the model was evaluated by assessing each model's ability to maintain stable gait across various speeds and terrain slopes (Fig. 2). Preliminary results indicate that the reflex model exhibits the most robust walking performance across different speeds and terrain slopes. In contrast, the CPG-reflex-synergy and muscle synergy models are constrained by the structure of the pulses the models use to produce the baseline activation patterns, limiting the velocity ranges achieved. Additionally, the high number of parameters required for optimization in the CPG-reflex-synergy model makes it challenging to achieve the desired locomotion behavior. Lastly, the muscle synergy and CPG-reflex models lack sensory feedback mechanisms for muscle synergy pulses and CPG modulation, respectively, which may hinder the ability to achieve stable locomotion across varying speeds and terrain.

Optimization across different slopes is ongoing (results expected before the conference date). Additional gait analysis data (i.e. joint dynamics, ground reaction forces, and muscle activations), will also be available.

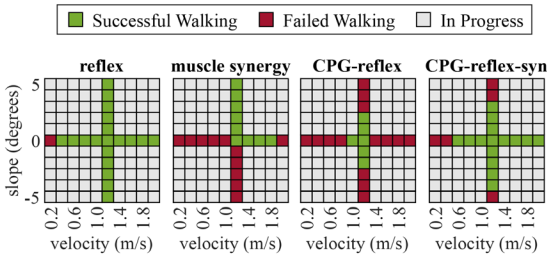


**Figure 2:** Simulated walking performance evaluated across target velocities (0.2–2.0 m/s) and terrain slopes (-5° to 5°). Success was defined as achieving six consecutive steady steps. Full results across all velocity and slope ranges are in progress and expected by the conference date.

**Significance:** To our knowledge, this is the first study to evaluate and compare various neuromechanical control models and their ability to generate different locomotion behaviors within a unified simulation framework. This approach is crucial for advancing our understanding and modeling of human motor control. Preliminary findings indicate that the pure reflex model outperforms the other models in both aspects. Although more rigorous analysis still needs to be conducted, this raises questions about the role of other control mechanisms, such as CPGs and muscle synergies, which are widely accepted as crucial for locomotion control.

**Acknowledgments:** This research is funded by the National Institutes of Health (R00AG065524).

**References:** [1] Song & Geyer (2015), *J Physiol* 593(16); [2] Aoi et al. (2019), *Sci Rep* 9; [3] Ogihara & Yamazaki (2001), *Biol Cybern* 84(1); [4] Di Russo et al. (2023), *J Neural Eng* 20(6).

# TIBIOFEMORAL CONTACT LOADS ACROSS WALKING, KNEELING, AND JUMPING TASKS WITH AND WITHOUT COGNITIVE CHALLENGES

Scott M. Monfort[1*], Devon Doud[1], Corey Pew[1], David J. Saxby[2], David F. Graham[1,2,3]
[1] Montana State University, MT, USA; [2] Griffith University, Gold Coast, AUS; [3] Children's Health Queensland, Brisbane, AUS
*Corresponding author's email: scott.monfort@montana.edu

**Introduction:** Manual laborers have elevated risk of knee osteoarthritis (OA) compared to the general population [1]. A contributing factor may be the movements (e.g., kneeling or squatting) common to manual labor which involve deep knee flexion and may result in larger knee contact forces than in walking [2] in addition to tasks performed in cognitively challenging scenarios. Characterizing knee contact loads across diverse movements and in the presence of relevant cognitive challenges is necessary to understand and address factors that elevate OA risk in this population. The purpose of this study was to examine tibiofemoral contact forces during walking, kneel-to-stand, and jump landing during single- and dual-task conditions. In addition to a goal of describing the contact loads during these tasks, we hypothesized that adding a cognitive challenge would result in increased contact force.

**Methods:** Participants (n=24, 3f/21m; 25.6±5.4 years, 1.77±0.09m; 73.4±11.1 kg) were manual laborers and/or physically active adults without prior lower body surgery or lower body injury in the past three years. Participants completed three movement tasks: walking at a self-selected pace (WALK), standing from a deep kneeling position (KNEEL), and a jump landing (JUMP), each with a cognitive challenge (COG) and without (BASE). The cognitive challenge for each task was as follows: WALK was performed with a visual Stroop task, KNEEL was performed with a Go-/No Go reactive stimulus used to initiate the movement, and JUMP was performed with a rapid decision-making challenge where secondary jump directions were displayed to participants ~250 ms prior to ground contact. Markers (250 Hz) and ground reaction forces (1000 Hz) were recorded for each movement. Electromyography (EMG) data (1000 Hz) were collected for 8 muscles on the dominant limb (gluteus maximus, gluteus medius, rectus femoris, vastus lateralis, semimembranosus, bicep femoris, tibialis anterior, and medial head of gastrocnemius). Calibrated EMG-informed neuromusculoskeletal modelling was used to estimate tibiofemoral contact loads (normalized to bodyweights, BW) following a previously reported modelling workflow [4,5]. Analysis focused on the stance phase of the self-reported dominant limb. Stance phase for KNEEL was defined as the instant the contralateral knee left the ground until just before the contralateral foot contacted the ground. Peak tibiofemoral contact loads (medial condyle, lateral condyle, and total) during the stance phase were primary outcomes. Statistical analysis consisted of mixed effects models with Participant as a random factor and Task (WALK, KNEEL, JUMP), Condition (BASE/COG), and Task*Condition as fixed factors.

**Results & Discussion:** There was a main effect of Task for medial, lateral, and total tibiofemoral contact forces (all $p<0.005$). JUMP produced the largest medial (3.0±0.5 BW), lateral (5.0±1.4 BW), and total (7.5±1.9 BW) contact forces. Contact forces during KNEEL were higher than WALK for total (4.8±0.9 BW vs. 3.7±0.7 BW) and lateral condyle (2.8±0.7 BW vs. 1.5±0.4 BW); however, medial condyle contact forces were higher for WALK (2.4±0.4 BW) than KNEEL (2.2±0.4 BW).

There were no significant Task*Condition interactions, although the interaction for the medial condyle trended towards significance ($p=0.069$) (**Fig. 1A**). The trend may be driven by the cognitive challenge eliciting *decreased* peak medial contact loading during the cognitive task during WALK ($p = 0.019$), which was explained by a 0.11 m/sec decrease in walking speed during COG relative to BASE. No statistical differences in peak forces between BASE and COG were detected for KNEEL or JUMP. Interestingly, differences between BASE and COG may exist throughout the stance phase rather than isolating to peak contact loads, as indicated by an exploratory statistical parametric mapping analysis that indicated *increased* medial contact loads for COG relative to BASE for a portion of the KNEEL stance phase (**Fig. 1B**). Furthermore, WALK contact loads poorly correlated to contact loads during KNEEL and JUMP (Spearman $\rho = 0.1\pm0.2$), although KNEEL and JUMP maintained moderate rank-order consistency (Spearman $\rho = 0.7\pm0.1$). Strong rank-order correlations existed between BASE and COG conditions within a given task (Spearman $\rho = 0.8\pm0.1$).

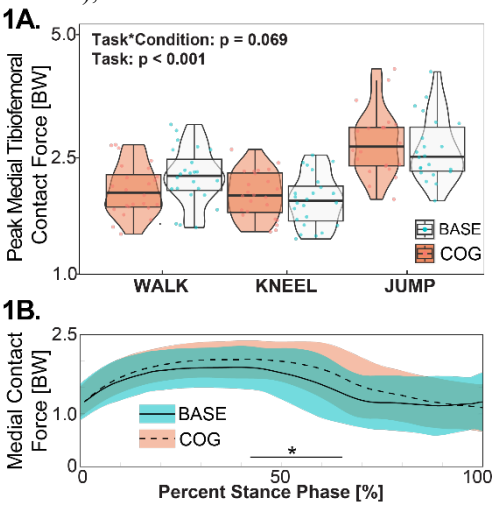


**Fig 1: A)** Peak medial tibiofemoral contact forces across movement tasks and conditions. **B)** Medial tibiofemoral contact forces throughout KNEEL, with * indicating region where BASE and COG are different.

**Significance**: Total knee contact loads ranged from 3.7-7.5 BW across three tasks that reflect a range of movements potentially encountered during manual labor. External stimuli that mimic distracting and reactive demands experienced in real-world tasks elicited a trend towards task-specific responses in medial tibiofemoral contact loads. The lack of rank-order consistency between contact loads during walking with contact loads during more dynamic tasks motivates the need to sample a representative range of motor tasks and situational demands for the population of interest to reflect real-world contact loads and study their relation to knee OA.

**Acknowledgments:** Funding was provided by the Montana State University (MSU) Center for American Indian and Rural Health Equity and MSU Office of the Vice President for Research.

**References:** [1] Andersen et al. (2012), *Occup Environ Med* 69; [2] Pollard et al. (2011), *J Applied Biomech* 27(3); [3] Hillel et al. (2019), *Eur Rev Aging Phys Act* 16; [4] Pizzolato et al. (2015), *J Biomech* 48(14); [5] Saxby et al. (2016), *J Biomech* 49.

**Comparing torsional gait kinematics between marker-based and markerless motion capture**

Benjamin B. Wheatley[1]*, Allyson K. Clarke[2], Kailey M. Granger[1], Mark A. Seeley[3]
[1]Department of Mechanical Engineering, Bucknell University, [2]Department of Mechanical Engineering, University of Washington, [3]Department of Orthopaedic Surgery, Geisinger Medical Center
*Corresponding author's email: b.wheatley@bucknell.edu

**Introduction:** Torsional malalignment syndrome (TMS) is characterized by excessive axial rotation of the femur and tibia, and often results in joint pain and impaired gait [1]. Due to patient variability, bone remodeling with age, and a lack of clarity in long term disease progression, it is not clear which patients should be treated with highly invasive operative methods versus less invasive non-operative methods such as physical therapy and shoe orthoses. Traditional marker-based motion analysis can be used to estimate gait biomechanics, which is useful for treatment decisions (surgery, PT, etc.). While marker-based motion capture is the gold standard for gait analysis, a single gait session typically requires highly trained expertise, expensive equipment, and multiple hours of clinician and patient time. Markerless motion analysis techniques, such as OpenCap, leverage smartphone video data for motion analysis, enabling a cheaper, faster, and easier to use method for clinical gait analysis [2]. However, it remains unclear if markerless motion can accurately capture gait kinematics under excessive torsional conditions, and the extent to which it can measure changes in gait dynamics due to interventions such as a shoe insert orthoses. Therefore, the goal of this study was to compare gait kinematics between marker-based VICON and markerless OpenCap systems for different torsional gait patterns and different shoe insert orthoses.

**Methods:** Seven participants (5F, 2M ages 18-22) were recruited for the study, which was IRB approved at Bucknell University (IRB #2324-118). Forty-eight markers were placed on the lower and upper extremities of each subject and subjects were instructed to walk with three gait profiles: 1) their natural gait, 2) a target of 45° toe-in gait, and 3) a target of 45° toe-out gait with four different insole conditions: baseline (no additional inserts), a lateral wedge, a medial wedge, and a heel lift. OpenCap and VICON motion capture were recorded simultaneously, and both motion analysis methods were analyzed in OpenSim to generate gait kinematics. VICON kinematics were generated by inverse kinematics in OpenSim. OpenCap kinematics were obtained by running optimal control simulations with OpenSim Moco to track virtual marker positions from the OpenCap video recordings. Statistical parametric mapping was used to perform T-tests to determine regions of significant difference between systems for each joint angle.

**Results & Discussion:** Marker-based (VICON) and markerless (OpenCap) motion analysis methods provided similar kinematics across all three gait profiles (natural, toe-in, and toe-out), especially for hip and knee kinematics (Figure 1). However, ankle and subtalar angles showed statistical differences between measurement techniques, especially for toe-in and toe-out gait patterns, suggesting these measures are less accurate under markerless motion capture (Figure 1). Strong agreement between hip rotation angles between measurement techniques suggests markerless motion capture could reliably estimate hip rotation angles for patients with excessive femoral torsion. No major differences in kinematic patterns were observed for any of the insole conditions, although further analyses are needed to determine the extent to which markerless motion capture and optimal control musculoskeletal modelling may be able to characterize differences in foot-ground contact mechanics from insoles or orthoses. Future work to validate gait dynamics and joint loads between marker-based and markerless motion analysis methods in a clinical population would be a major benefit to the field.

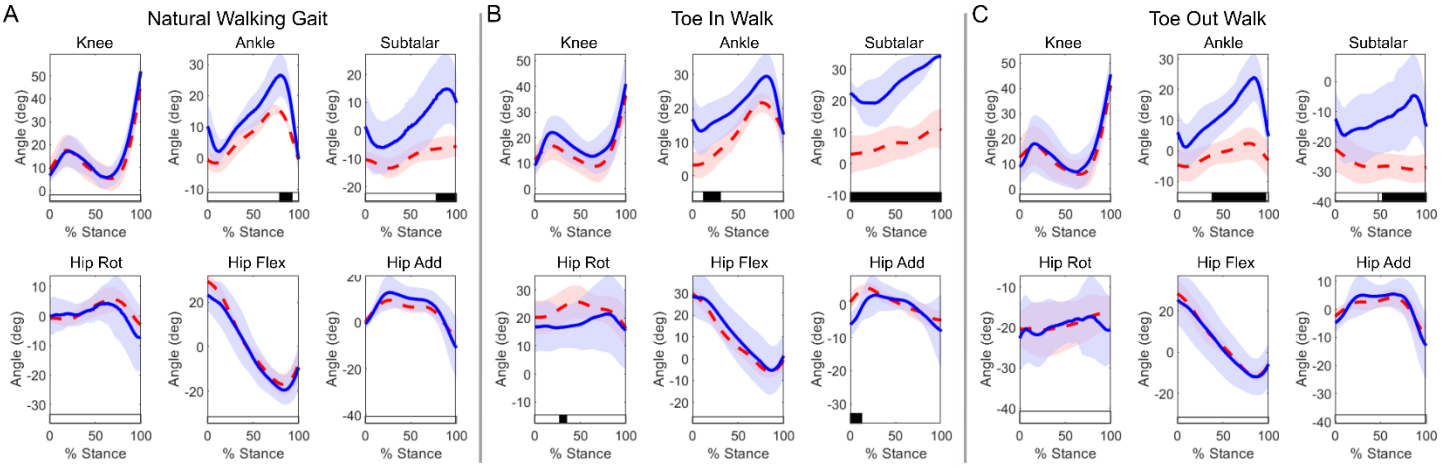


**Figure 1.** Joint kinematics produced by marker-based motion capture (VICON, blue solid curves with standard deviation) and markerless motion capture (OpenCap, red dashed curves with standard deviation) under A) natural walking gait, B) targeted 45° toe-in gait, and C) targeted 45° toe-out gait. Solid black bars below each graph indicate statistically significant differences.

**Significance:** Our results suggest markerless motion analysis can be used to evaluate differences in hip and knee kinematics due to torsional gait profiles. Using a low-cost, quick, and accurate gait analysis tool such as OpenCap to assess kinematics may assist clinicians in treatment decisions for individuals with TMS, though future work to validate gait kinetics remains.

**References:** [1] Holbert et al, (2023). *SN comp clin med*, 5(112); [2] Uhlrich et al, (2023). OpenCap. *PLOS Comp Biol*

# IMPACT OF AGE OF INJURY ONSET ON PEAK NORMALIZED ROTATOR CUFF MUSCLE FORCES AND GLENOHUMERAL JOINT CONTACT FORCES DURING MANUAL WHEELCHAIR PROPULSION

*Zhao H.[1], Cho, Y.[1], Cordes, C.M.[2], Schnorenberg, A.J.[2] , Slavens, B.A.[2] Peterson, C.L.[1]
[1]Virginia Commonwealth University, [2]University of Wisconsin-Milwaukee
*Corresponding author's email: zhaohs@vcu.edu

**Introduction:** Paraplegia, paralysis affecting the lower extremities, is commonly caused by spinal cord injury and disorders (SCI/D) such as multiple sclerosis and spina bifida. Paraplegia due to SCI/D is the leading cause of manual wheelchair (MWC) usage with approximately 302,000 individuals living with SCI/D within the United States [1]. MWC users with SCI/D have reported high incidence of shoulder pain along with nearly all MWC users exhibiting some form of shoulder pathology [2]. Among MWC users with SCI/D, age of SCI/D onset is of particular interest due to adults with pediatric-onset SCI/D reporting lower incidences of shoulder pain (48%) when compared to adults with adult-onset SCI/D (84%) despite having more years of wheelchair usage [2]. Furthermore, only 15% of adults with adult-onset SCI/D reported having shoulder pain prior to wheelchair usage [3]. Thus, age of SCI/D onset may be an important factor in the development of shoulder pain. Shoulder muscle and joint forces during wheelchair propulsion presumably contribute to the development of shoulder pain and pathology [4]. Rotator cuff muscles forces are of interest with pathologies commonly found in the MWC population relating to the rotator cuff muscles [4]. Quantitative research investigating the relationships among the biomechanics of MWC propulsion, shoulder pain and pathology, and age of SCI/D onset are needed to improve rehabilitation towards reducing pain in MWC users. Based on the greater occurrence of shoulder pain in individuals with adult-onset SCI/D, we expect that peak normalized rotator cuff muscle forces and glenohumeral joint contact forces will be greater in these individuals relative to adults with pediatric-onset SCI/D. The goal of our work is to elucidate the effect of age of SCI/D onset on rotator cuff muscle forces and glenohumeral joint contact forces during wheelchair propulsion.

**Methods:** 82 MWC users were recruited by our collaborators at UWM and participated. This preliminary analysis includes 13 participants who were divided into one of three subgroups: children (age = 15.2 ± 2.2 years), adults with pediatric-onset SCI/D (age = 34.2 ± 15.3 years), and adults with adult-onset SCI/D (age = 27.6 ± 3.4 years) with a planned total of 36 (12 in each subgroup). For each participant, maximum voluntary isometric contractions (MVIC), anthropometric measures, marker-based motion capture, handrim forces, and EMG were recorded. Participants were instrumented with nine wireless surface EMG electrodes and then performed MVICs to measure maximum isometric joint moments in five different shoulder joint postures and two elbow joint postures. Marker trajectories, handrim forces, and EMG data were recorded as described by Schnorenberg et al., (2014) as participants propelled a MWC at self-selected speeds [1]. A scapulothoracic shoulder model [5] was adapted to include forearm and wrist muscles from Saul et al. [6]. Musculoskeletal model scaling, inverse kinematics, a residual reduction algorithm, computed muscle control, and joint reaction analysis were performed using OpenSim to generate simulations that emulated the experimental kinematics and kinetics. Additionally, the models were scaled to represent each participant's individual strength by calculating the ratio between the experimental MVIC moment and the simulated MVIC moment as described by Cho et al., (2023) [7]. Individual muscle forces and activations including the rotator cuff muscles along with glenohumeral joint contact forces were extracted from these simulations.

**Results & Discussion:** Peak normalized rotator cuff muscle forces over the propulsion cycle for 13 participants averaged by subgroup are presented in Table 1. EMG onset and offset timings aligned well with simulated muscle activations for most muscles.

Preliminary analysis supports our hypothesis with results showing that adults with adult-onset SCI/D have the highest peak normalized force. The forces we estimated are higher relative to other studies investigating patients with paraplegia [4]. Possible explanations could be related to our musculoskeletal model allowing for independent scapula movement and more accurate muscle representations resulting in increased usage of shoulder muscles [4-6].

| | Peak Normalized Muscle Force (%) | | |
|---|---|---|---|
| **Muscle** | Children (n=5) | Adults with pediatric-onset SCI/D (n=6) | Adults with adult-onset SCI/D (n=2) |
| **Infraspinatus_I** | 41.1 ± 23 | 26.3 ± 25 | 53.1 ± 26 |
| **Infraspinatus_S** | 29.0 ± 15 | 32.5 ± 21 | 60.2 ± 33 |
| **Teres Minor** | 17.9 ± 13 | 4.5 ± 2 | 45.5 ± 27 |
| **Subscapularis_S** | 28.6 ± 4 | 49.9 ± 14 | 58.3 ± 30 |
| **Subscapularis_M** | 11.9 ± 4 | 14.1 ± 16 | 62.3 ± 24 |
| **Subscapularis_I** | 43.5 ± 30 | 39.8 ± 31 | 73.2 ± 22 |
| **Supraspinatus_P** | 19.5 ± 1 | 21.6 ± 1 | 48.7 ± 33 |
| **Supraspinatus_A** | 28.7 ± 4 | 24.6 ± 3 | 56.3 ± 25 |

**Table 1**: Average normalized peak rotator cuff forces from cohorts. I = Inferior, S = Superior, M = Medial, P = Posterior, A = Anterior

**Significance:** Preliminary analysis provides evidence that increased mechanical loading during wheelchair propulsion in adults with adult-onset SCI/D relative to children and adults with pediatric-onset SCI/D, may contribute to their increased incidence of shoulder pain. This would suggest a need to further investigate wheelchair propulsion techniques and combinatorial approaches to reduce mechanical loading. Identifying relationships between rotator cuff muscle forces and glenohumeral joint contact forces during wheelchair propulsion with age of SCI/D onset and shoulder pain and pathology will ultimately provide rationale for rehabilitation approaches that reduce shoulder demand after SCI/D.

**Acknowledgments:** Funding from the Eunice Kennedy Shriver National Institute of Child Health and Human Development (NICHD) of the National Institutes of Health (award number R01HD098698).

**References:** [1] Schnorenberg, A. J., et al., *J. Biomech*. 2014 47(1); [2] Brose, S. W., et al., *Arch Phys Med Rehabil* 2008 89(11); [3] Slowick, J. S., et al., *Clin Biomech* 2016 33; [4] Walford, S. L., et al., *J Biomech* 2024 146(4); [5] Seth, A., et al., *PLOS ONE* 2016 11(1); [6] Saul K, et al. *Comput Methods Biomech Biomed Engin*. 2015 18(13); [7] Cho Y., et al., 2023 [*Master's thesis, VCU*]

# ANKLE BIOMECHANICS IS COMPROMISED IN PATIENT WITH FOREFOOT AMPUTATION: A CASE STUDY

Anthony Melgar[1], Karishma Sebastian, Dumitru Caruntu, Javier La Fontaine, Luis Venegas, Hafizur Rahman[2,3,4]*
[1]Department of Biomedical Engineering, University of Texas Rio Grande Valley
[1]School of Podiatric Medicine, University of Texas Rio Grande Valley
[2]College of Engineering and Computer Science, University of Texas Rio Grande Valley
[3]School of Medicine, University of Texas Rio Grande Valley
*Corresponding author's email: hafizur.rahman@utrgv.edu

**Introduction:** Forefoot amputation is a surgical procedure that requires the disarticulation of both the interphalangeal and metatarsophalangeal joints. Unfortunately, the Rio Grande Valley (RGV) has a high rate of patients who either suffer or are expected to receive this type of surgical procedure. According to the state health agency, the RGV's diabetic amputation rate was 50% higher than the state average in 2015 [1]. The aim of this case study was to understand how the ankle biomechanics alters during walking with patients who have received a transmetatarsal amputation (TMA). We hypothesized that the patients with TMA have a limited range of motion at the ankle joint.

**Methods:** For this abstract, we included the results of a single patient (age: 61 years, height: 173 cm, weight: 69 kg) who underwent TMA surgery. The patient participated in a walking test to determine the lower extremity biomechanics, as explained in the previously published article [2]. Before the walking test, 27 retro-reflective markers were placed on specific anatomical locations on each of the participant's lower extremity utilizing the marker systems of Vaughan [3] and Nigg [4]. For the overground trials, participants walked at a self-selected pace across a 10-meter pathway containing a force platform that is set level with the floor. Lower extremity 3-dimensional kinematics and kinetics data were recorded using a 16 high-speed infrared camera system (60 Hz, Motion Analysis Corporation, Rohnert Park, CA) and force platforms (600 Hz, AMTI, Watertown, MA). The kinematics data at the ankle and knee joints was extracted and expressed as % of the stance phase.

**Results & Discussion:** For the ankle joint motion, the ipsilateral limb had a peak plantar flexion angle of 17° during the heel strike, whereas the contralateral limb peak plantar flexion angle was 14° at the heel strike (Fig. 1). The peak dorsiflexion angle from mid-stance to late stance was 4° in the contralateral limb. However, the ankle position was still somewhat dorsiflexed for the ipsilateral limb, without proper plantarflexion motion during the push-off phase. In summary, the ankle range of motion (ROM) for the ipsilateral limb was only 10°, whereas the ROM for the contralateral limb was 18° (Fig. 1).

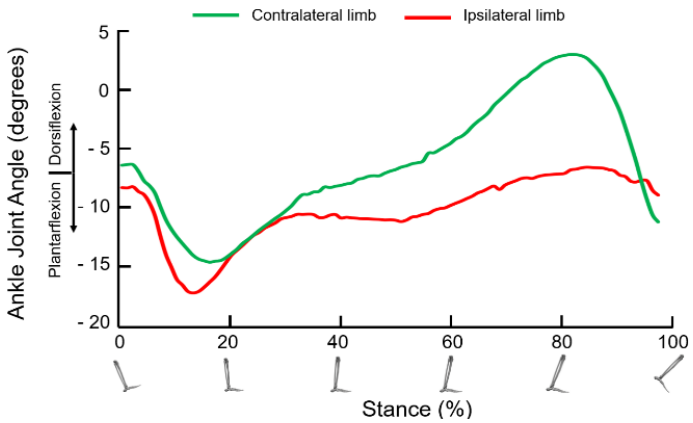


**Figure 1:** Ankle joint angle kinematics for both the contralateral limb and ipsilateral limb.

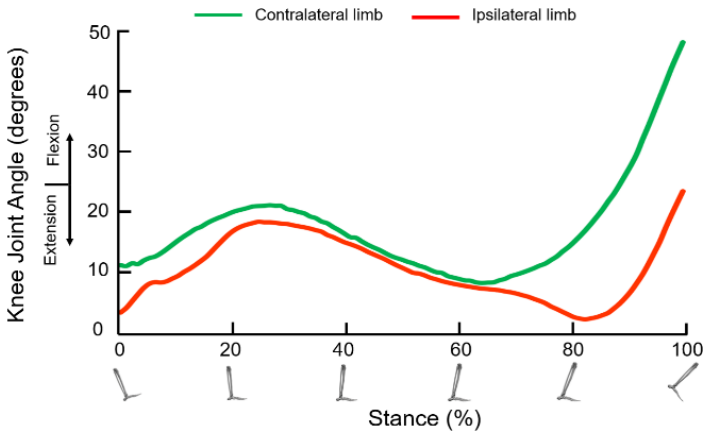


**Figure 2:** Knee joint angle kinematics for both the contralateral limb and ipsilateral limb.

Similar to ankle joint motion, knee joint motion was also compromised in the ipsilateral limb. Although the peak flexion ankle during early stance was similar for both limbs (contralateral limb: 21°, ipsilateral: 18°), the most notable difference was observed during the flexion at the push-off phase (Fig. 2). The contralateral limb had a peak flexion angle of 48°, whereas ipsilateral limb had only 23° knee flexion (Fig. 2). The results show that both knee and ankle biomechanics was compromised in ipsilateral limb compared to contralateral limb, suggesting that our hypothesis was correct.

**Significance:** Our findings suggest that there was compensation in the knee joint angle kinematics data and ankle joint kinematics data for the TMA patient. Understanding the physiological changes occurring in these patients will help create patient-specific orthotics to alleviate any discomfort. This study also contributes to a better understanding the rehabilitation process, whether creating a new or modifying any existing method. For future studies, focusing on individual muscle forces during the given motion of an amputated patient will generate innovative comprehension of the overall biomechanical changes that occur within the patient.

**References:** [1] Novack S et al. (2021) *Life and Limb*, The Texas Observer; [2] Rahman H et al. (2024), *JBJS Annals of Physical and Rehabilitation Medicine* 67(1); [3] Vaughan CL. (1999), *Dynamics of human gait*; [4] Nigg BM et al. (1993), *J Biomech* 26(8).

# DEVELOPMENT OF THE ENDOVASCULAR ORIFICE DETECTOR: A NOVEL DEVICE FOR ANTEGRADE IN-SITU FENESTRATION OF OFF-THE-SHELF ENDOGRAFTS

*Cyrus Darvish[1], Mohammad Eslami[9], David Vorp[1-8], Timothy Chung[1,5]
[1]Department of Bioengineering, [2]Department of Mechanical Engineering and Material Science, [3]McGowan Institute for Regenerative Medicine, [4]Department of Surgery, [5]Clinical and Translational Sciences Institute, [6]Department of Cardiothoracic Surgery, [7]Department of Chemical and Petroleum Engineering, [8]Magee Women's Research Institute, University of Pittsburgh, Pittsburgh, PA, USA, [9]Division of Vascular and Endovascular Surgery, Charleston Area Medical Center, Charleston, WV, USA
*Corresponding author's email: cjd121@pitt.edu

**Introduction:** An abdominal aortic aneurysm (AAA) is the irreversible local dilation of the aorta below the diaphragm, which can lead to life-threatening rupture [1]. Endovascular repair (EVAR) has become the more popular treatment due to its lower perioperative mortality, lower recovery times, and lower blood loss when compared to open aortic repair [2]. Complex aneurysms extend superiorly into key branching arteries and remain a challenge to treat because there is little room to seal and anchor an endovascular graft properly [3]. While there are viable methods for treating complex aneurysms, such as fenestrated custom-made devices (CMDs) and physician-modified endovascular grafts (PMEGs), these methods are not readily available in all centers due to the long manufacturing times of CMDs and lack of investigational device exemptions for PMEGs [4]. In-situ fenestration (ISF) has emerged as a safe, effective, and durable method for repairing complex aneurysms that have the potential to reduce costs and time to surgery; however, there are difficulties in identifying the orifice of the target arteries for fenestration [5]. The proposed design for the EOrD utilizes fiber optics to transmit a light source placed endovascularly into the target visceral artery. Due to fiber optics' ability to transmit light long distances, we expect that they can serve as a method for detecting the orifice of a visceral artery in conjunction with a light source emitted from a target artery.

**Methods:** The study first investigated the attenuation of infrared and white wavelengths of light when transmitting through endograft material and blood using fiber optics as the transmission method. A novel endovascular orifice detector prototype was designed and created using a steerable catheter and fiber optic strands. A custom MATLAB code was constructed to act as a graphical interface that the end user, a vascular surgeon, could follow for accurate localization of the target artery orifice. The prototype was deployed in a human cadaveric torso to evaluate its ability to detect the orifice of a visceral artery and fenestrate accurately alongside a Philips Excimer Laser system. A fully pulsatile aortic flow loop was created and validated with an ideal geometry anatomically accurate compliant AAA phantom for future surgical simulation studies.

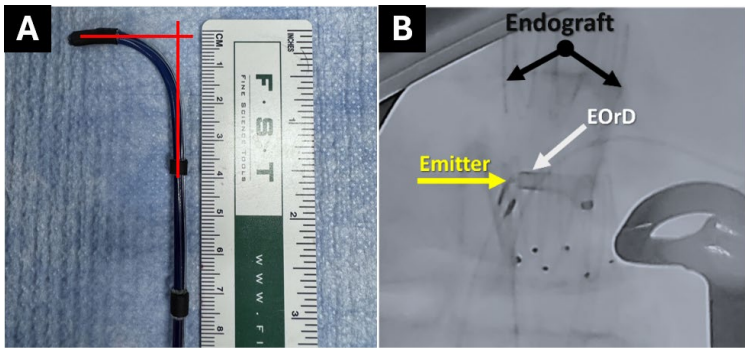


**Figure 1: A)** The prototype EOrD device created from a steerable sheath with five fiber optic strands constrained radially. **B)** Moment the EOrD located an IR emitter placed into a renal artery of a cadaveric torso.

**Results & Discussion:** Both the infrared and white light wavelengths penetrated the endograft material while submerged in blood, with signals transmitted through the fiber optics up to 8 mm from the light source. This data reveals that infrared and white light are wavelengths of light that can potentially be used to detect target visceral arteries through endograft material and that fiber optics can be a helpful transmission modality. A prototype steerable EOrD device was successfully created with five fiber optic cables constrained radially around a steerable catheter using heat shrinks (**Figure 1A**). One successful fenestration was made in a human cadaveric torso, using the EOrD prototype and MATLAB graphical interface in tandem with fluoroscopic guidance (**Figure 1B**). A second test was attempted, but the cadaver was heavily occluded due to calcification. An ideal AAA phantom was successfully molded with anatomically accurate dimensions. It was placed in a pulsatile flow loop, and the flow loop was validated with physiologic pressures and flow rates of 80 to 120 mmHg and 2.47 L/min, respectively. The successful creation and validation of a pulsatile flow loop for surgical simulation allows for a controlled environment for testing the device. The cadaveric tests were costly, and complications with calcification led us to generate a surgical simulation bench for testing at this level of development. Future work will include operating on the in-vitro test bench, creating patient-specific AAA phantom models for testing, and, once the device is optimized, resuming cadaveric studies.

**Significance:** The findings from this investigation highlight the potential for the EOrD to visualize the orifice of an artery in situ using fiber optics. The proposed technology is meant to expand the current indications of use for endovascular repair of complex AAAs. The potential for an endovascular device to create fenestrations in off-the-shelf endovascular grafts can allow for a minimally invasive approach to treating patients who are ineligible for EVAR due to constraints surrounding their anatomy.

**Acknowledgments:** We would like to thank the National Institutes of Health HL157646 for funding this work.

**References:** [1] Sakalihasan et al. (2005), *The Lancet* 365(9470): 1577-1589; [2] Drury et al. (2005), *J. Brit Surg* 92(8): 937-946; [3] Marone et al. (2020), *Ann Vasc Surg* 62: 173-182; [4] Ricotta II et al. (2012), *J. Vasc Surg* 56(6): 1535-1542; [5] Glorion et al. (2016), *Eur J. Vasc Endovasc Surg* 52: 787–800.

# DOES WALKING EFFICIENCY INCREASE AFTER SELF-EXPLORATION OF WALKING WITH A PASSIVE DYNAMIC ANKLE-FOOT ORTHOSIS FOR INDIVIDUALS POST-STROKE? A PILOT STUDY

*Shay R. Pinhey[*1,2], Darcy S. Reisman[1,3], Elisa S. Arch[1,2]
[1]Biomechanics and Movement Science Interdisciplinary Program, [2]Department of Kinesiology and Applied Physiology, [3]Department of Physical Therapy, University of Delaware, Newark, DE
*Corresponding author's email: spinhey@udel.edu

**Introduction:** Stroke is one of the primary causes of long-term disability and often results in inefficient gait, limiting community ambulation [1-3], which can have a negative impact on overall health and well-being [1,4]. To help address inefficiencies, passive dynamic ankle-foot orthoses (PD-AFOs) are often prescribed after a stroke. PD-AFOs are designed to help control rotation of the tibia during midstance and store and return energy to assist with push-off [5,6]. PD-AFOs have been shown to improve ankle mechanics and walking energetics for some individuals who have had a stroke, however effects were mixed with some showing improved mechanics and energetics while others showed little to no change [6-8]. Thus, it is clear that not all individuals are capitalizing on the energetic benefits that a PD-AFO offers. In order to increase the number of individuals capitalizing on the energetic benefits of the PD-AFO, we first need to better understand what factors affect walking with this device, such as device acclimation.

Acclimating to a new assistive device is important to elicit the optimal benefits of the device. Currently, there is no standardized way of acclimating a user to a PD-AFO. Previous literature has shown that self-exploration protocols, which consist of guided gait alterations such as changing step length or step frequency, help healthy individuals converge on their energy optimized walking pattern [9,10]. Our prior work has shown that, for individuals post-stroke, the PD-AFO induces biomechanical and energetic changes throughout the lower-extremity system and that these changes vary from person to person [11]. There is currently no evidence to drive exploration of a single variable of walking as multiple walking adaptations and multiple joints may contribute to improving walking energetics for individuals post-stroke. A self-exploration protocol gives individuals the freedom to explore the device and harnesses the individualized nature of PD-AFO responses that were seen previously. This study, therefore, evaluated self-exploration as a method of device acclimation for individuals post-stroke wearing a PD-AFO. The goal of this work is to provide insights into the viability of self-exploration as a strategy to ultimately improve walking outcomes for post-stroke PD-AFO users. To evaluate the effects of self-exploration on walking energetics, this study used a metric of walking efficiency, defined as the ratio of walking speed to mechanical cost of walking. We hypothesized that walking efficiency would increase after self-exploration with the PD-AFO.

**Methods:** 3 participants (Age: 63 ± 15 yrs, Time since stroke: 3.9 ± 0.2 yrs, Height: 170 ± 15 m, Mass: 98 ± 38 kg) with chronic stroke were enrolled in this study so far. First, participants were fit to a PD-AFO in lab, then their preferred PD-AFO walking speed was determined via a 10 meter walk test. Participants then walked on an instrumented treadmill (Bertec, USA) while full body motion capture data was collected (Qualisys, USA) to measure baseline walking efficiency. Next, participants underwent a self-exploration protocol. Prior to exploration, the function of the PD-AFO was explained and walking alterations such as increasing speed, taking even steps, and loading the PD-AFO were described as suggestions of what to try during the explorative walking portion. Participants then walked over ground while wearing the PD-AFO for three rounds of 5 minutes of walking: 1 minute of comfortable walking, 3 minutes of exploration, and 1 minute of return to comfortable walking. Rest was provided between walking bouts. At the end of the exploration protocol, participants' new self-selected walking speed was determined, and then data on the instrumented treadmill was again collected to measure post-exploration walking efficiency. All data was processed in Visual 3D (HAS Motion, CA).

**Results & Discussion:** Table 1 shows walking efficiency before and after self-exploration for each participant. Notably, 2 of the 3 participants improved their walking efficiency after exploration. For these two participants, their speed did not change after exploration, therefore their increased walking efficiency post-exploration was a result of a reduced cost of walking. These results demonstrate that self-exploration with a PD-AFO can be done successfully and may improve walking efficiency with a PD-AFO for individuals post-stroke. Data from additional participants will strengthen conclusions.

**Table 1:** Walking efficiency before and after self-exploration with a PD-AFO

| Participant Number | Walking Efficiency [(m/s)/(j/kg/m)] | |
|---|---|---|
| | Before Exploration | After Exploration |
| 1 | 0.466 | 0.471 |
| 2 | 0.442 | 0.471 |
| 3 | 0.387 | 0.371 |

**Significance:** The knowledge gained from continued collection of data for this study will build a foundational understanding of the efficacy of self-exploration as a PD-AFO acclimation strategy. Ultimately, improving our understanding of how to increase the likelihood that individuals elicit the energetic benefits of a PD-AFO will likely enable individuals post-stroke to improve their walking efficiency. Long term, improved walking efficiency will lead to increased community ambulation and quality of life for individuals with chronic stroke.

**Acknowledgments:** This work was supported by the University of Delaware Kinesiology and Applied Physiology Dissertation Grant and the USAMRAA Orthotics & Prosthetics Outcomes Research Program (Award No. HT94252310106).

**References:** [1] Chen et al. (2005), *Gait Posture*. 22(1); [2] Detrembleur et al. (2003), *Gait Posture*.18(2); [3] Tsao et al. (2023), *Circulation*. 147(8); [4] Physical Activity Guidelines for Americans. (2022), *CDC*; [5] Arch et al. (2016) *Prosthet Orthot Int*. 40(5); [6] Arch and Reisman (2016), *J Prosthetics and Orthotics* 28(2); [7] Koller et al. (2021), *Prosthet Orthot Int*. 45(4); [8] Skigen et al. (2024), *J NeuroEngineering Rehabil*. 21(1); [9] Selinger et al. (2019), *J Exp Biol*. jeb.198234; [10] Selinger et al. (2015), *Curr Biol*. 25(18); [11] Skigen et al. (2024), *J Biomech*. 177:112414.

# DEVELOPMENT AND SPECIFICATIONS OF PLANTAR CUTANEOUS VIBRATION STIMULATION THERAPY DEVICE

*Shaye M. Tiell[1], Brian L. Davis[1]
[1]Center for Human Machine Systems, Washkewicz College of Engineering, Cleveland State University, Cleveland, OH, USA
*Corresponding author's email: s.tiell@vikes.csuohio.edu

**Introduction:** Parkinson's disease (PD) is one of the most prevalent neurodegenerative diseases worldwide [1]. Parkinsonian symptoms are primarily due to a lack of dopamine, resulting in atypical neural synchronization within the basal ganglia [2]. Due to the high risks associated with pharmaceutical and surgical interventions [2-6], non-invasive alternatives, such as vibration therapy (VT), offer considerable benefits with minimal risks.

**Methods:** *Vibrotactile Stimulation*: First discovered in the 19th century by Charcot, vibrotactile stimulation as a form of VT is used to disrupt the characteristic, abnormal neural rhythms of PD, thus targeting the underlying cause of symptom manifestation [2,7,8]. VT has been applied in various forms, including whole-body (WBV), physioacoustic (PAV), and locally applied (LAV). Despite promising initial results, VT remains an adjunct therapy and is not yet widely accessible. Further studies are needed to refine its long-term use for PD patients. This non-invasive device aims to explore VT's potential through an accessible insole.

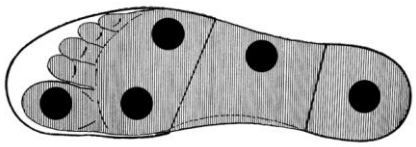

**Figure 1:** The figure above shows the right insole with five (5) vibrotactile actuators under the great toe, lateral arch, medial metatarsals, lateral metatarsals, and heel. Actuators target FA mechanoreceptor dense areas for optimal VT delivery and therapeutic effects.

*Plantar Cutaneous Receptors*: LAV targets areas with dense mechanoreceptors to desynchronize abnormal neural oscillations [2]. Plantar cutaneous feedback involves fast-adapting (FA) mechanoreceptors, with FAI and FAII afferents sensitive to dynamic stimulation like vibration. FAI afferents are most dense in the toes and lateral arch, while FAII afferents are concentrated in the great toe and middle metatarsals [2,9,10]. Vibratory stimulation in the 30–60 Hz range for FAI and 100–300 Hz for FAII is optimal [2,11]. Studies show vibration improves balance across various populations [12,13], and PD does not significantly affect plantar receptor sensitivity [14], making plantar cutaneous vibratory stimulation a viable therapy.

*Device Design and Specifications*: The insole delivers targeted VT via vibration motors embedded in cushioned layers, with battery-powered actuators operating at a frequency of 150 Hz and an amplitude of 0.1 mm. The strategic placement ensures effective therapy while maintaining comfort (Figure 1). The choice of a lower operating frequency depends on the imposed load (Figure 2). The insole is designed to fit seamlessly into most footwear, combining functionality, ease of use, and accessibility.

**Discussion:** This device utilizes an insole with five actuators delivering vibratory stimulation at parameters specific to targeting FAII afferents in key plantar regions to improve motor function, balance, and gait in PD patients [10,12]. The insole offers a non-invasive, portable, and discreet therapy option, with a localized design that ensures effective stimulation without discomfort. Enhancing sensory input and potentially mitigating dopamine loss and abnormal neural synchronization [2,8], VT complements current long-term treatments and may serve as an alternative to surgical interventions like DBS. However, further research is needed to validate the device's long-term effects, clinical efficacy, and potential in combination with other rehabilitation methods.

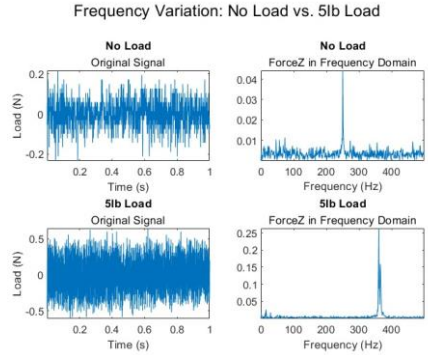


**Figure 2:** The figure above shows static compression testing of a vibrating insole was conducted using a 5lb load to simulate stance weight under the hallux, while a 250 Hz vibration motor was activated.

**Significance:** Vibrotactile stimulation delivered through a wearable insole as a non-invasive alternative to traditional treatments for individuals with Parkinson's disease builds on the established therapeutic benefits of VT for individuals with PD. Given the growing prevalence of PD worldwide, the development of low-risk, easily accessible therapies, such as the proposed VT insole, could play an important role in improving the quality of life for patients, especially as part of a comprehensive approach. Future studies and refinements of the design could pave the way for a widely adopted, non-invasive, and cost-effective intervention to assist individuals with PD in maintaining mobility and independence.

**Acknowledgments:** The work presented in this paper was supported by the National Science Foundation (NSF) Graduate Research Fellowship Program (GRFP) under Award No. 2239682. Any opinions, findings and conclusions or recommendations expressed in this publication are those of the authors and do not necessarily reflect the views of the National Science Foundation.

**References:** [1] Balestrino & Schapira (2020), *Eur J Neurol* 27(1); [2] Tass (2017), *Cureus*; [3] Koschel et al. (2022), *J Neural Transm* 129 (9); [4] Hariz & Blomstedt (2022), *J Intern Med* 292(5); [5] Halli-Tierney et al (2020), *Am Fam Physician* 102(11); [6] Haas et al (2006), *NeuroRehab* 21(1); [7] Mosabbir et al (2020), *Healthcare* 8(2); [8] Pfeifer et al (2021), *Front Physiol* 12; [9] Viseux et al (2019), *Neurophyiol Clinique* 49(3); [10] Inglis et al (2002), *AEMB* 508; [11] Strzalkowski et al (2018), *J Neurophysiol* 120(3); [12] Priplata et al (2003), *The Lancet* 362 (9390); [13] Alfuth (2017), *Gait Posture* 51; [14] McKeown et al (2016), *Neurosci Lett* 629

# USE OF OPENCAP TO ASSESS KINETIC VALUES FOR SINGLE LEG VERTICAL JUMP TASKS: A PILOT STUDY

*Sophia Stemler[1], Fatemeh Aflatounian[1], Alexandra Lynch[1], David F. Graham[2], Scott M. Monfort[1]
[1]Montana State University, Bozeman, Montana, USA, [2] Children's Health Queensland, Brisbane, Australia
*Corresponding author's email: sophia.stemler@student.montana.edu

**Introduction:** Anterior cruciate ligament (ACL) tears are a common athletic injury and are associated with a high risk of reinjury even after return to sport (RTS) protocols [1]. The single leg vertical jump (SLVJ) test has been proposed as a valuable component in RTS protocols, as it accentuates knee imbalances in movement often developed to compensate for an ACL-injured limb [2]. Measuring and tracking changes in joint kinetics, such as the knee extensor moment (KEM), provide quantifiable standards to identify athletes at risk of reinjury during RTS testing [2]. However, estimating joint-level kinetics typically requires costly and time-consuming motion capture that is impractical for use in most clinical settings. OpenCap is a markerless motion capture method that enables estimation of kinematic variables using two or more iOS devices, also providing the possibility to extend an analysis to estimate kinetic variables using additional musculoskeletal simulation (i.e., OpenSim Moco [3]). The joint kinematics from OpenCap align well with kinematics measured using optical motion capture systems (MoCap) [3]; however, the agreement between kinetic variables estimated from OpenCap when compared to MoCap is less understood. Addressing this gap could provide clinicians with a reliable, low-cost tool to aid in assessment of patient recovery following an ACL injury. The purpose of this pilot study was to evaluate the agreement between KEM from an OpenCap and OpenSim Moco workflow compared to KEM from marker-based motion capture with force plates. Given the reported agreement in kinematics [3], we hypothesize there will be a significant correlation in KEM.

**Methods:** Eight healthy athletes (4F/4M, 19.8±2.3 yrs; 1.66±0.18 m; 67.8±11.0 kg; Tegner: 7.5±1.3; Marx: 10.6±3.6) completed 6 SLVJ trials on each leg using previously reported methods [4]. All trials were concurrently recorded with OpenCap and a marker-based motion capture system (10 cameras, Motion Analysis Corp, 5 force plates, OPT464508-2K; AMTI). The MoCap data was processed using an inverse kinematics model in Visual 3D. The OpenCap processing pipeline 'example_kinetics.py' was used to import kinematics generated in OpenCap, augment the OpenSim model with contact spheres on the stance limb, and run an OpenSim Moco torque-driven simulation. OpenCap data were separated into propulsion (0.4s prior to takeoff until takeoff) and landing (initial takeoff to peak knee flexion) rather than simulating both phases in the same trial, as this improved speed and convergence of the simulations [2]. Peak KEM (pKEM) values were determined for propulsion and landing, normalized by height and weight, and averaged for limb. This yielded left and right limb data points in both phases for each participant. Spearman correlations were found in MATLAB, with a bootstrap confidence interval (CI) calculated to determine the range of correlation strength across the small sample size of the pilot study.

**Results & Discussion:** Neither propulsion (*r = -0.44, CI: [-0.87, 0.38], p = 0.12)* nor landing (*r = 0.48, CI: [-0.22,0.85], p = 0.09)* phases were found to have a significant correlation between OpenCap and MoCap pKEM values (**Figure 1**). These data show a gap in estimating KEM during SLVJ from OpenSim Moco, as they did not track with estimates from marker-based motion capture. The added challenge of calculating kinetic variables without force data is likely a major reason for the limited correlations. However, kinetics could have also been affected by kinematic errors such as differences in the modeling system between the two methods, underrepresentation of SLVJ in the OpenCap algorithm, and compounding error from poor agreement of ankle kinematics, reported in previous studies [5]. Furthermore, it is important to note that ~14% of the trials did not yield kinetic values due to the simulations not converging or other errors in Moco. Also, one participant had outlier pKEM values which were eliminated. These inconsistencies could indicate suboptimal experimental setups that would have also altered the kinetic variables being extracted. A need exists to further refine the OpenSim Moco workflow to enable more robust kinetic estimates from OpenCap data. Future work includes expanding the sample size beyond the pilot group, capturing SLVJ trials with different camera orientation for cleaner motion capture, and revisiting the foot-ground contact model.

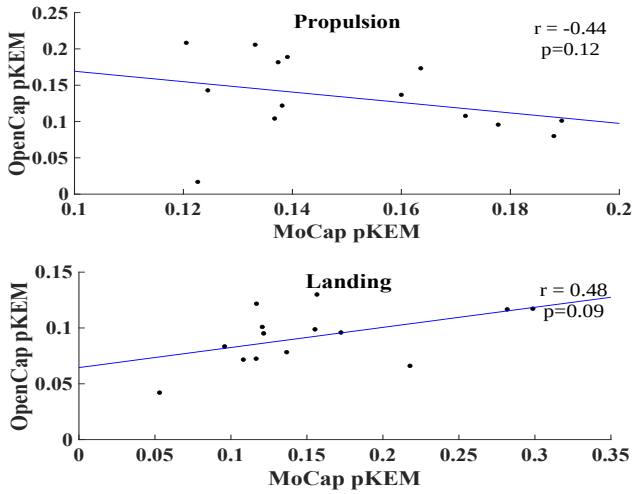


**Figure 1.** Correlations between estimates of peak Knee Extension Moment (pKEM), normalized to body weight and height, from an OpenCap + OpenSim Moco workflow versus MoCap workflow for the propulsion and landing phase of a SLVJ.

**Significance:** The accessibility and ease of use of OpenCap has substantial potential for clinical applications. Where an optical motion capture setup requires significant investment, an OpenCap data collection could easily occur in a medical center to evaluate post-surgical outcomes and RTS readiness. This pilot study revealed challenges with estimating KEM from SLVJ via an OpenCap and OpenSim Moco workflow. The findings motivate the need for further work to improve consistency of KEM estimates with estimates from marker-based motion capture, particularly to produce values tolerable for clinical settings.

**Acknowledgements:** This research was supported by the NIH award R03HD101093.

**References:** [1] Webster et al. (2019), *Sports Med* 49(6); [2] Kotsifaki et al. (2022), *Br J Sports Med* 56(9); [3] Uhlrich et al. (2023) *PLoS Comput Biol* ***19***(10); [4] Farraye et al. (2023) *J Sport Rehabil* 32(7); [5]Horsak et al. (2023) *J Biomech* 159

# The Acute Effects of Transcranial Direct Current Stimulation on Sports Performance

Jesse Yun[1], Kelly J. Jantzen[1], David N. Suprak[1], Leanne G. Robbins[1], Ella N. Wyrick[1], Alexa P. Nooney[1] and Jun G. San Juan[1]
[1]Western Washington University
yunj3@wwu.edu

**Introduction:** Transcranial direct current stimulation (tDCS) is a non-invasive brain stimulation method that has gained popularity due to its ease of application compared to other brain stimulation approaches like transcranial magnetic stimulation. The precise mechanism by which tDCS alters function in the primary motor cortex is not fully understood. However, it has been postulated that the primary mechanism for the effects on human movement is an increase in intracellular calcium concentration, decreasing the resting membrane potential, and increasing corticomotor excitability [1,2,3]. Thus, although an influx of intracellular calcium from tDCS is insufficient to elicit movement alone, it can lower the threshold for generating actions [2,3], potentially increasing force production and lowering central fatigue. However, the effect of anodal motor cortex tDCS on muscle force output is unclear, as the studies in this area have produced mixed results. Therefore, the purpose of this study is to evaluate the effects of tDCS on the performance of lower body power output, time to exhaustion, and maximal strength output. Based on these potential mechanisms, it is hypothesized that tDCS applied over the motor cortex representation of the lower limbs will improve performance measures of vertical jump height, time to exhaustion (TTE), and maximal strength of the knee extensors.

**Methods:** Twenty-eight healthy participants (age = 22.03 ± 2.23 years; height = 170.36 ± 8.31 cm; mass = 75.67 ± 14.84 kg) were included in this study. The Halo Sport was used to apply tDCS. Participants were randomly assigned to one of three tDCS conditions, which included anodal stimulation of the leg area with the cathode placed over the hand area of the motor cortex (leg group), anodal stimulation of the dominant hand area with the cathode placed over the non-dominant hand area of the motor cortex (hand group), and a sham condition. The stimulations lasted 21 minutes: A 30-second ramp-up at the beginning, 20 minutes of stimulation, and a 30-second ramp-down period. The sham stimulation intervention included a 30-second ramp-up period, after which stimulation was terminated for the remainder of the 21 minutes. The headset was placed on the participant's head, and the headphone band was placed across the midpoint between the external occipital protuberance and the upper root of the nose bridge. Effects of tDCS were evaluated by comparing performance from three pre-stimulation trials to three post-stimulation trials. Isometric maximal voluntary contraction torque of knee extension was measured in three trials utilizing the Biodex System 4 isokinetic dynamometer, each for 20 seconds with a 30-second rest interval between trials. The Biodex was also used to measure TTE of the knee extensors as the time from peak torque to a 30% decrease. The impulse-momentum equation was used to calculate vertical jump height from the vertical ground reaction forces measured from an AMTI force plate collected at 1000 Hz.

| Stimulation Group | Vertical Jump Height (m) | | Peak Knee Extensor Torque (Nm) | | Time to Exhaustion (s) | |
|---|---|---|---|---|---|---|
| | Pre | Post | Pre | Post | Pre | Post |
| Hand | 0.42 ± 0.08 | 0.40 ± 0.07 | 315.79 ± 82.20 | 310.91 ± 72.66 | 18.52 ± 1.41 | 16.77 ± 2.03* |
| Sham | 0.33 ± 0.14 | 0.32 ± 0.11 | 230.88 ± 43.36 | 217.36 ± 39.74 | 16.64 ± 2.17 | 16.04 ± 2.45 |
| Leg | 0.39 ± 0.09 | 0.38 ± 0.10 | 240.46 ± 50.75 | 239.91 ± 51.47 | 18.9 ± 1.18 | 17.91 ± 1.31* |

**Table 1**. Pre- and post-stimulation measurements of hand, sham, and leg stimulations. Values are presented as mean ± SD. *Significance ($p < 0.016$)

**Results & Discussion:** The hypothesis was not supported. There was no group by time interaction of tDCS on vertical jump height ($F[2, 25] = 0.916$, $p = 0.413$, $\eta = 0.068$). The findings of the current study were not consistent with previous studies of the effects of tDCS on jump height. This inconsistency could be attributed to the anode and cathode placement of the Halo Sport. Previous studies used an extracephalic stimulation pattern, with cathodes placed on regions that are not on the motor cortex, whereas the Halo Sport used a cephalic stimulation pattern, placing the anode and cathode on the motor cortex. There was no group by time interaction of tDCS on peak knee extensor torque ($F[2, 25] = 0.694$, $p = 0.509$, $\eta = 0.053$). The result of the maximal strength output of the current study was inconsistent with previous studies measuring peak knee extensor torque. In the current study, pre- and post-tDCS measurements of maximal strength output were completed in one session. In contrast, previous studies measured pre- and post-tDCS measurements in two different sessions to combat the onset of fatigue, resulting in a significant increase in maximal strength output of the knee extensors. There was a group by time interaction of tDCS on knee extensor TTE ($F[2, 25] = 0.4738$, $p = 0.018$, $\eta = 0.275$). Paired t-tests using a Bonferroni corrected alpha of 0.016 showed a significant main effect of time for both hand ($p = 0.002$) and leg ($p < 0.001$) groups. No prior literature measured TTE as a decrease from peak isometric torque. Other studies measured TTE as repetitions at submaximal force output as maximal repetitions of submaximal contractions showed a significant effect on TTE when the anode is placed over the targeted underlying motor cortex. Based on the current study, it is feasible to speculate that tDCS modulation of neuronal excitability will increase the endurance of maximal contractions.

**Significance:** The current study provides individuals with information that a cephalic tDCS pattern does not improve vertical jump height or maximal force output. The current study provides data to prove tDCS manipulates TTE of maximal strength output.

**References:** [1] Purpura & McMurty (1964), *J. Neurophysiol. 28*(1); [2] Christie et al. (2011), *Nat. Neurosci 14*(1); [3] Vasu & Kaphzan (2022), *Brain Stimulation, 15*(1).

# CADAVERIC VALIDATION OF AN EXTRA-ARTICULAR IMPLANT TO PREVENT ACL INJURY

Ophelie Herve[1], Sean Thomas[1,2], Thomas J. Kremen[2], David R. McAllister[2], *Tyler R. Clites[1,2]
[1]Department of Mechanical and Aerospace Engineering, University of California Los Angeles
[2]Department of Orthopaedic Surgery, David Geffen School of Medicine, University of California Los Angeles
*Corresponding author's email: clites@ucla.edu

**Introduction:** Traumatic injury to the anterior cruciate ligament (ACL) has become a public health epidemic, especially among young athletes, with at least 400,000 documented ACL injuries per year in the United States [1]. Short-term consequences of ACL injury include pain, joint instability, temporary disability, absence from work or sports, and the financial burdens of treatment and rehabilitation. Even in cases of successful reconstruction, ACL-injured knees develop osteoarthritis at a rate of 60% and are seven times more likely to need a knee replacement. Prevention is crucial, but current preventative measures such as training programs and bracing are controversial and have not been shown to decrease the risk of ACL injury. External bracing is particularly challenging, because the compliance of soft tissue makes it impossible to restrict injury-inducing motions without severely limiting knee motion. We here present an extra-articular implanted knee brace to reduce ACL injury risk by inhibiting motions that endanger the ACL, without impeding normal knee motions or functions. The implant is a non-extensible extra-articular synthetic ligament that anchors to the femur and tibia, and is tensioned such that it *only* creates resistance to offload the ACL during potential injury scenarios (Fig 1A).

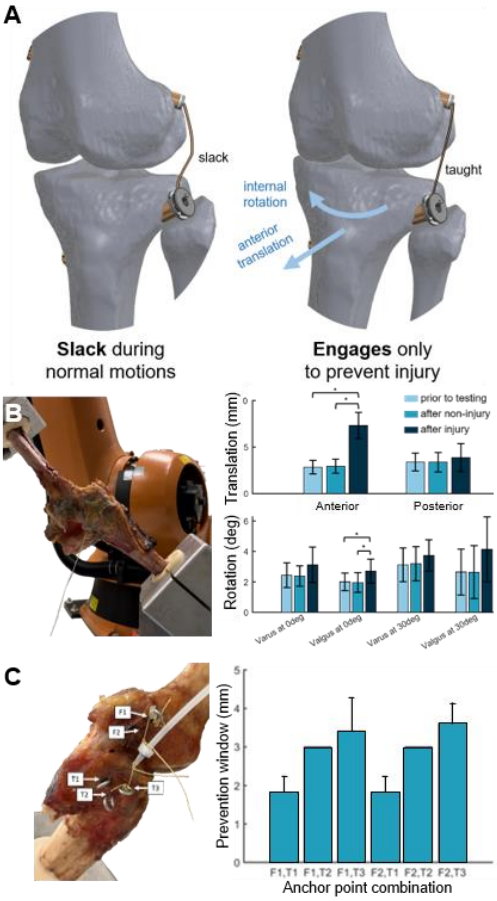


**Figure 1: (**A) Implanted knee brace concept. (B) Validation of the robotic pipeline (adapted from [5]). (C) Prevention window for selected combinations of potential anchor points.

**Methods:** Cadaveric knee specimens (32-66 years of age) were dissected to expose the ACL, and the femur and tibia were potted in polymethyl methacrylate (PMMA). Key anatomical landmarks were digitized to identify consistent specimen-specific tibial and femoral coordinate frames. Each knee was then fixed to a 6-DOF robotic manipulator (KR210; KUKA Robotics), which was programmed to recreate clinical tests of knee stability, active non-injurious motions (walking, running, and drop jump) [2], [3], and published motions known to induce ACL injury [4]. We also used the robotic system to assess combinations of potential anchor points for the implanted knee brace. A non-extensible cable with a simple ratcheting mechanism (easily lengthened but not shortened) was installed between one point on the femur and one point on the tibia. Each knee specimen was moved through several cycles of the non-injurious motions, such that the ratcheting cable measured the longest instantaneous distance between the two anchor points across all three motions. We then reset the cable length, moved the knee through the injury motion until the point where ACL injury had previously occurred, and measured the length of the cable at the point of injury. The difference between the length at injury and the length during healthy motions was deemed the "Prevention Window" which serves as an indicator of how effectively a cable between that combination of points could prevent injury. One combination of points was selected for further analysis, a cable was applied between those points, and the specimens were moved through healthy and injury motions until the cable engaged, all while reaction forces were measured.

**Results & Discussion:** Kinematics for walking, running, and drop jump were successfully enforced on the robotic platform, with an average RMS error below 0.05 mm in translation and 0.005 deg in rotation with respect to the published kinematic trajectories. Robot-simulated clinical stability tests showed that the structural integrity of the knee ligaments was not compromised during non-injurious motions, but showed clinical signs of ACL injury following the injury motion (Fig 1B). Six combinations of anchor points were successfully tested across several gait activities, and several combinations were identified with positive Prevention Windows (Fig. 1C). The prototype cable between the selected points did not engage during non-injurious motions, but did engage to offload the ACL prior to rupture. These results provide evidence that there exist combinations of extra-articular anchor points that would allow the cable to engage only when the ACL is at risk of injury, and otherwise remain slack.

**Significance:** We validated a robotic pipeline capable of reproducing both active non-injurious and injury-inducing knee motions. We used this pipeline to identify potential anchor points for an implanted knee brace that only constrains knee motions that endanger the ACL. Such an implant would help avoid the downstream effects of ACL injury, including instability, pain, and separation from sports.

**Acknowledgments:** This work was supported through in-kind cadaver donations from MTF Biologics, Inc.

**References:** [1] Englander et al. (2019). *Am. J. Sports Med.* 47(13); [2] Nishida (2022). *J. Orthop. Res.* 40(1); [3] Li et al. (2009). *J. Orthop. Surg. Res.* 4(1); [4] DeMorat et al. (2004). *Am. J. Sports Med.* 32(2); [5] Herve et al. (2025). *Ann. Biom. Eng.* 25(5).

Raiyan Talukder[1*], Veronica Stuckey[1]
[1]Texas A&M School of Engineering Medicine
email: *talukderraiyan@tamu.edu

**Title: An Anatomy-Inspired Transvaginal Drug Delivery Device For Women's Health**

**Introduction:** The vagina is primarily studied as a reproductive organ, and it has recently been a focus for improved drug delivery. Transvaginal drug delivery is an effective route to administer medication because it has minimal enzymatic activity, ideal mucosal surface area, and can bypass the first-pass effect [1]. This phenomenon, coined as "the uterine first pass effect" is particularly advantageous for local and direct administration of medication to the female reproductive organs [1]. The current applicators are injection molded, hard, cylindrical plastic syringes with blunted ends which can be incredibly uncomfortable for older patients, the main population utilizing vaginal creams [2,3]. As such, there is a need for an easy-to-use applicator that conforms to the anatomy of the vaginal canal for the administration of various drugs to increase patient comfort and compliance.

**Methods** We used computer aided design and published survey results to design a transvaginal applicator. Our proposed design is rounded at the distal end, providing easier insertion and more comfort. The overall design is curved, and the material is flexible, allowing for better compliance with the vaginal anatomy. The patent canal is dose calibrated so that patients can apply the appropriate amount of their medication. The proximal tip has a standard luer lock so that it is compatible with estradiol ointment tubes.

**Results & Discussion** Our current iteration can be 3D printed with flexible material. A mold is currently being processed for silicone molding (Fig. 1). It successfully delivered water (1 centipoise viscosity) and honey (10,000 centipoise) to mimic the delivery of a gamut of drug or ointment viscosities. Validation studies will be conducted to determine the willingness to use our design compared to the current applicator.

Women's health is starkly understudied and underfunded [4]. Recent advancements in drug delivery systems have targeted the vaginal canal for better bioavailability and reduced systemic effects [1]. However, the delivery system for these drugs remains a significant pain point for users which reduced patient compliance or inadequate dosing [2]. We have an improved design for a vaginal applicator that is inspired by the vaginal anatomy to promote patient comfort and compliance while retaining manufacturability and compatibility with standard ointment tubes and syringes. Future directions include manufacture testing and determining if more viscous medications are compatible to ultimately mass manufacture an improved vaginal applicator that maximizes patient comfort without reducing drug delivery efficacy.

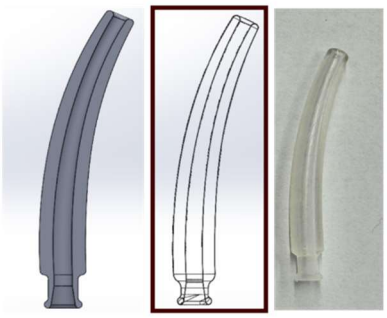

**Figure 1:** Initial sketches of a proof of concept for our transvaginal delivery system. Shown is the beveled slope that is based on measurements of the vaginal canal anatomy and patency for use with various creams and ointments. Current iterations are being streamlined for manufacturability via rapid silicone injection molding and user surveys on willingness to use.

**Significance:** The local administration of certain drugs, like clotrimazole or estradiol, can reduce systemic symptoms and their risk of cancer [5]. The current vaginal applicator market is around $5 billion with a 5.6% compound annual growth rate [6-7]. Despite the advancements in vaginal drugs, current transvaginal applicator systems are not anatomically friendly and lead to reduced patient compliance due to discomfort and difficulty of use [5,8]. An easy-to-use applicator that conforms to the anatomy of the vaginal canal for the administration of various drugs will ultimately increase patient comfort and compliance to improve women's health.

**References:** [1] Hussain et al. (2005) *Journal of Controlled Release* 103(2); [2] Bakke et al. (2001) *Scientific Reports;* [3] Archer. (2004) *OBG Management*; [4] Women's health research lacks funding – these charts show how. https://www.nature.com/immersive/d41586-023-01475-2/index.html; [5] Comini et al. (2023) *JCO.* 41(16); [6] Persistence Market Research. Vaginal Applicators Market worth will reach US$ 7.4 Billion by 2030; [7] Vaginal Applicator Market. https://www.futuremarketinsights.com/reports/vaginal-applicators-market; [8] *Vaginal Estrogen for Post-Menopausal Women*. https://www.youtube.com/watch?v=gc24lLNfoLc

# EFFECT OF MATERIAL ON CARDIOVASCULAR STENT MECHANICAL PERFORMANCE

*Lucinda Duncan[1], Josiah Owusu-Danquah, PhD[1]
[1]Cleveland State University, Cleveland, Ohio, Center for Human-Machine Systems
*l.r.duncan@vikes.csuohio.edu

**Introduction:** Coronary artery disease impacts a significant portion of the global population. Treatment advancements for atherosclerotic and stenotic arteries have progressed from balloon angioplasty to drug-eluting stents. However, complications with stents remain. Restenosis is the re-narrowing of a blood vessel that has been previously treated with a stent. High force interactions between implant and tissue can cause injury to the endothelial layer of the arterial wall. This is a known trigger for the cascade of events leading to restenosis, which can serve as a metric in the assessment of stent design performance. The way a stent interacts with surrounding tissue is dependent on the endovascular insertion technique. This insertion is furthermore related to the material of the mesh. To optimize the entire intervention process, we must first address the stent itself.

Elastic recoil and flexibility are critical properties of cardiovascular stents, ensuring proper function and minimizing complications [1]. A low elastic recoil rate is ideal, as it helps keep the artery open, while excessive recoil can lead to restenosis or poor embedding. Flexibility is essential for navigating and deploying stents in complex and curved structures of arterial systems. Since recoil requires stiffness and flexibility requires pliability, these properties are inherently a tradeoff, raising the question of the optimal balance for treating diseased arteries.

Both properties are influenced by material and geometry. This study examines the role of materials in identifying ideal stent properties. Three materials were analyzed: bare metal (stainless steel), polymer (poly-ether-ether-ketone), and shape memory alloy (Nitinol). These materials differ in mechanical properties and insertion techniques – balloon-expanded for non-shape memory materials and self-expanding for shape memory.

**Methods:** Finite element analysis via Abaqus CAE was performed to assess the specified parameters of three stents with the same geometry but differing materials.

Elastic recoil was defined as a percentage: $\frac{d_{expanded}-d_{recoiled}}{d_{expanded}} \times 100$, where $d$ refers to the diameter of the stent [2]. A four-point bending test was performed to test flexibility. Flexibility was quantified as the inverse of bending stiffness, calculated as: $\frac{\frac{P\times L}{3}\times L_{stent}}{2\times\alpha}$, where $P$ is the force applied, $L$ is the length from the end of the load bar to the point of loading, $L_{stent}$ is the length of the stent, and $\alpha$ is the angle of the loading point from horizontal when displaced [3] (Figure 1). Nitinol's superelastic behavior enables it to achieve near-complete recovery with minimal elastic recoil. However, because its operational mechanism differs from that of balloon-expanded stents, we did not include its values in our elastic recoil comparison.

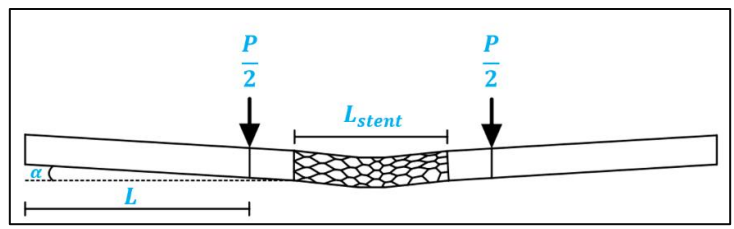


*Figure 1. Four-point bending test schematic. The load bars on either side of the stent were assigned as nondeformable.*

**Results & Discussion:** Each computational test revealed insight into the mechanical performance of each material. All results from the previous described tests are summarized in Table 1.

*Table 1. Elastic Recoil and Flexibility Test Results*

| Material | Elastic Recoil (%) | Bending Stiffness ($N\times mm^2$) | Flexibility ($1/N\times mm^2$) |
|---|---|---|---|
| 316L-SS | 8.26 | 2883.88 | 0.0003 |
| PEEK | 9.25 | 54.08 | 0.0185 |
| Nitinol | X | 959.75 | 0.0010 |

Stainless steel exhibited a lower elastic recoil than PEEK. This suggests that metals are more suitable for maintaining long-term lumen patency in stenosed arteries. In contrast, PEEK offers greater flexibility, making it ideal for use in curved or tortuous vessels and for navigating complex cardiovascular anatomy. Nitinol falls between these two extremes in terms of flexibility. Our results indicate that it provides greater flexibility than stainless steel, and we anticipate its elastic recoil to be nearly 0%. Future studies will incorporate shape-memory materials modeled in a manner comparable to balloon-expanded stents. Unlike metals and polymers, where lumen patency is restored during deformation, these materials will achieve lumen restoration through shape recovery.

**Significance:** A deeper understanding of stent biomechanics will enable the development of interventions that increase compliance while reducing restenosis rates. Optimizing cardiovascular stents has the potential to improve long-term patient outcomes, minimize surgical burden or reintervention requirements, and advance cardiovascular care. Pairing this study with future studies directed towards stent geometries and arterial interactions can lead to novel designs and enhance patient-specific intervention strategies.

**Acknowledgments:** This work is supported by the T32 NIH Training Grant: 5-T32-HL150389-03

**References:** [1] Watson et al. (2017), *OpenHeart* 4(2); [2] Okereke et al. (2021), *Mechanics of Materials, 163*; [3] Mori et al. (2005), *Annals of biomedical engineering, 33*

# GENDER REPRESENTATION OF SUBJECTS OVER FIVE DECADES OF THE JOURNAL OF BIOMECHANICS

*John H Challis, Axelle M Wasiak
Biomechanics Laboratory, The Pennsylvania State University, University Park, USA
*Corresponding author's email: jhc10@psu.edu

**Introduction:** Historically biomedical studies have been predominantly conducted using male subjects, which either assumes no biological differences between men and women or ignores those differences [1]. The National Institutes of Health have clear policies on the justification of the sexes in their funded studies, but females are still underrepresented in medical and biomedical research and sex/gender are poorly reported [2]. The purpose of this study was to quantify the historical inclusion of female subjects in studies published in the Journal of Biomechanics.

**Methods:** All research articles published in the Journal of Biomechanics for one year of each decade (1970, 1980, 1990, 2000, 2010, and 2020) were analysed; the Journal of Biomechanics was first published in 1968. Two trained assessors independently determined if each study had subjects, and if so the number of subjects, and the gender distribution of the subjects. If the two assessors differed in their evaluations both revisited the publication to resolve any discrepancies. It is acknowledged that the terms sex and gender have different meanings even though they are often used interchangeably [3], in this study the term gender is adopted as in the reviewed studies it generally not clear what criteria were used to describe their subjects.

**Results & Discussion:** A total of 1492 publications were reviewed, of which 658 were experimental studies with subjects. There has been improvement in the frequency with which studies provide information on the number of subjects (Table 1). There has been a large improvement in the frequency with which studies provide gender distribution for their subjects.

**Table 1:** The reporting of the number of subjects and gender of subjects for studies published in the Journal of Biomechanics over the last fifty years.

| **Year** | **1970** | **1980** | **1990** | **2000** | **2010** | **2020** |
|---|---|---|---|---|---|---|
| ***Number of Subjects Not Specified*** | 36.4% | 20% | 20% | 17.5% | 7.7% | 2.7% |
| ***Gender of Subjects Not Specified*** | 71.4% | 40% | 37.5% | 27% | 21.3% | 11.6% |

Across the decades the distribution of subjects by gender has changed (Figure 1). There has been growth in the number of female participants in experimental studies, but it has not yet reached equality. These results mirror those for ASB conference abstracts [4].

The trends reported in this study are encouraging but opportunities to promote further improvement should be explored, this should include requiring all studies report the gender distribution of their subjects. In addition, when a study focusses on one gender only the authors should provide a justification for their study design.

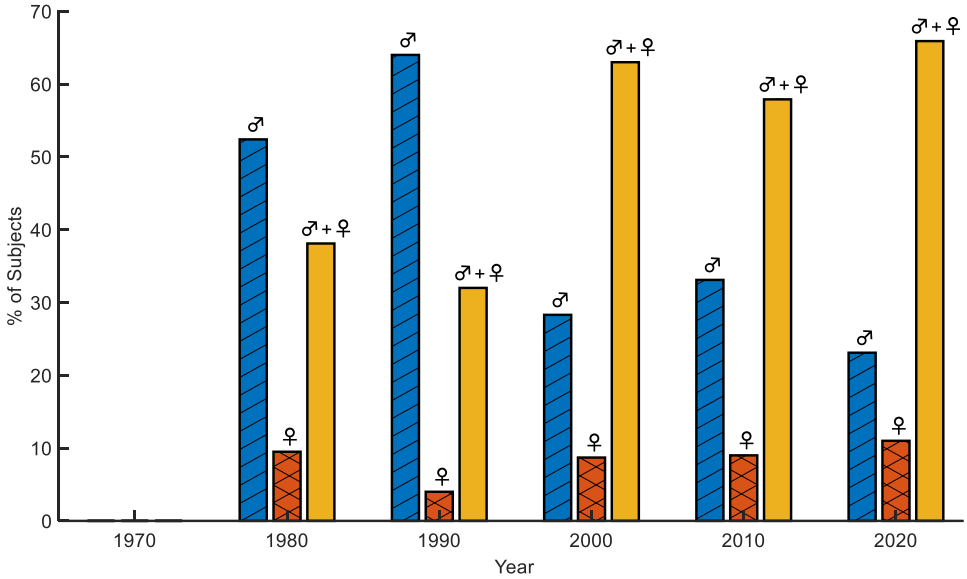


**Figure 1:** The reporting of subject gender in for studies published in the Journal of Biomechanics over the last fifty years. Note in 1970 there was insufficient reported data.

**Significance:** This study provides information on both the reporting of subject gender in studies published in the Journal of Biomechanics in a 50 year period, and also reports the distribution of subjects in studies by gender. These results provide important benchmarks, and provide areas for improvement. Suggestions are provided for improvements in both the reporting of gender and recruitment of subjects for biomechanical studies.

**References**

[1] Beery, A. K., & Zucker, I. (2011). *Neurosci Biobehav Rev.*, **35**(3), 565-572.
[2] Merone, L., et al. (2022). *Women's Health Rep.*, **3**(1), 49-59.
[3] Pryzgoda, J., & Chrisler, J. C. (2000). *Sex Roles*, **43**, 553-569.
[4] Bach, S., et al. (2015). *PLoS One*, **10**(3), e0118797.

# VALIDATION OF KINEMATIC AND SPATIOTEMPORAL PARAMETERS OF TREADMILL STEPPING IN INFANTS WITH DOWN SYNDROME: A COMPARISON OF OPENPOSE AND NORAXON MYOVIDEO

*Matthew Beerse[1], Alexandre dos Santos Kotarski[2], Amy Talboy[3], Seyda Oscaliskan[2], Jianhua Wu[2]
[1] University of Dayton, Dayton, OH, USA; [2] Georgia State University, Atlanta, GA, USA; [3]Emory University, Atlanta, GA, USA.
*Corresponding author's email: mbeerse1@udayton.edu

**Introduction:** Marker-based motion capture has widely been considered as the gold standard for motion analysis of human movement. However, it can be a challenge when applied to special populations such as infants with Down syndrome (DS) due to their skin sensitivity to marker attachment and lack of cooperation. Further, the time scale to assess motor development using marker-based motion capture systems has been limited due to logistical challenges of collecting data in a laboratory setting. Advances in computer vision has allowed the development of open-source markerless-based software to analyze human movement, such as OpenPose [1], which can alleviate these challenges. It is possible for caretakers to collect video data at an infant's home, at a high frequency, without specialized markers or knowledge of marker placement. The automatic registration of body landmarks with computer vision facilitates the processing and analysis of these potential big datasets. We aimed to conduct a validation assessment of hip, knee, and ankle joint angles, as well as step length from Noraxon MyoVideo and OpenPose for bodyweight-supported treadmill stepping in infants with DS. We hypothesized that OpenPose will produce similar joint kinematics and step length values as Noraxon MyoVideo.

**Methods:** The participants were taken from a wider, comprehensive study to evaluate the effect of early motor interventions in infants with DS. Our analysis included 9 infants with DS aged 11.8±2.6 months at entry into the study. Researchers visited each infant once a month to collect treadmill stepping data. The data collected from the last visit before the infant's walking onset were used here. For the marker-based analysis, reflective markers were placed on the right hip, knee, ankle, and foot. A Noraxon Ninox 125 camera was used to record a 3-minute trial from the infant's right side and the Noraxon MyoResearch 3 software was used to process the video data. The same video was imported to OpenPose, which registered 25 body landmarks. Landmark trajectories were gap-filled using a spline filter and then filtered using a 2$^{nd}$ order one-dimensional median filter [2]. The right hip, knee, ankle, heel, and small toe landmarks were used to estimate hip, knee, and ankle joint angles. Strides were visually coded. Step length was calculated as the difference of ankle position at toe-off and initial contact for each stride. To convert pixels to centimeters, a known distance of 10 cm was used to calibrate the space. Peak hip, knee, and ankle extension and flexion positions were identified for each stride and averaged across the trial. Bland-Altman plots were constructed to compare the similarity of outcome variables between OpenPose and Noraxon. A positive mean difference indicates OpenPose, on average, overestimated outcomes compared to Noraxon.

**Results & Discussion:** OpenPose underestimated step length by 2.05 cm, with limits of agreement (LOA) of -11.94 and 7.84 cm. Peak hip angles showed mean differences of 1.64 degrees (LOA: -40.84, 44.11) for extension and -0.42 degrees (LOA: -23.94, 23.11) for flexion. Peak knee angles displayed mean differences of 3.46 degrees (LOA: -47.14, 54.06) for flexion and 15.78 degrees (LOA: -5.81 and 37.37) for extension. Peak ankle angles demonstrated mean differences of 6.66 degrees (LOA: -12.07, 23.38) for extension and -14.32 degrees (LOA: -34.68, 6.04) for flexion. The mean differences <7 degrees found for hip and knee joint angles, as well as peak ankle extension, aligned with validation analyses of other markerless motion capture systems, such as OpenCap [3]. These results indicate that OpenPose is consistent with marker-based video analysis, but the wide LOA suggest that individual trials might differ greatly. Noraxon registered hyperextension positions for peak knee extension resulting in the large positive mean difference. Higher mean differences for peak ankle angles indicate infant foot segment identification might be challenging for OpenPose.

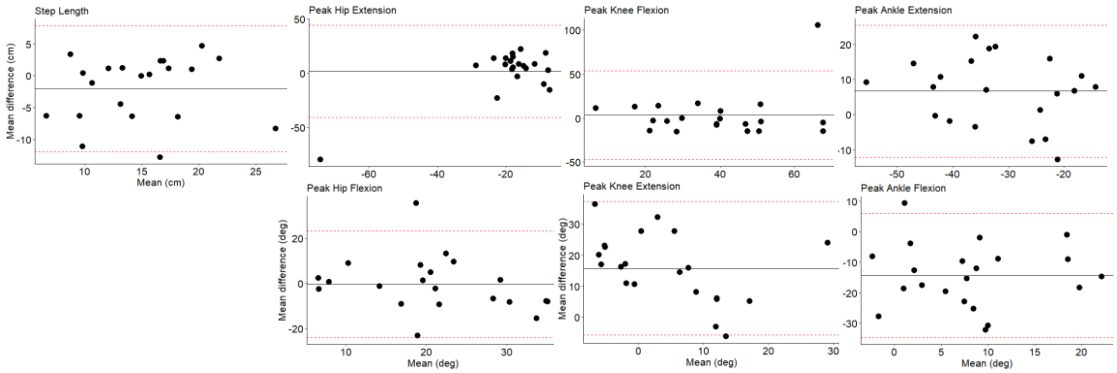


**Figure 1:** Bland-Altman plots of step length and peak hip, knee, and ankle angles. Solid black line represents mean difference. Dashed red lines indicate limits of agreement.

**Significance:** Markerless software for the analysis of human movement has the potential to expand motor development research by enabling caregivers to collect video data of their infant in a home setting at a higher frequency than what is generally feasible in a laboratory-based system. Our study presents encouraging validation results for OpenPose to assess both joint kinematic outcome variables and step length for treadmill stepping in infants with DS.

**Acknowledgments:** We are grateful for the participants and their families. This study was funded by NIH R21HD105879.

**References:** [1] Cao et al. (2018) *IEEE TPAMI* 43(1); Ossmy & Adolph (2020) *Curr Bio* 30(23); Turner et al. (2024) *Jour of Biomech* 171.

# COMPARISON OF FINITE ELEMENT ANALYSIS WITH DIGITAL IMAGE CORRELATION FOR ESTIMATING LINER STRAINS IN TWO TRANSTIBIAL SOCKET DESIGNS

Mohammadreza Freidouny[1], Carson Squibb[1], Masaki Hada[1], Abbie Bailey[1], Brian Kaluf[2], Trevor Johnson[3], Michael K. Philen[1], Michael L. Madigan[1*]

[1]Virginia Tech, Blacksburg, Virginia, USA. [2]Ottobock, USA [3]Virginia Prosthetics & Orthotics, Christiansburg, VA, USA

* Corresponding author email: mlm@vt.edu

**Introduction:** Poor fit of prosthetic sockets can lead to discomfort and skin issues [1]. Measuring strains and stresses of the residual limb at the socket interface can help evaluate socket fit and improve its design [2]. Finite element analysis (FEA) has been widely used to estimate such strains and stresses [3]. However, FEA estimates can benefit from validation with empirical measurements. Digital image correlation (DIC) is a powerful optical method that can be used to obtain such empirical measurements. The goal of this study was to compare FEA estimates of strain on a prosthetic liner to DIC measurements with total surface bearing (TSB) and patellar tendon-bearing (PTB) sockets.

**Methods:** One male subject (46 years, 85 kg) with a left transtibial amputation was recruited for this study. The subject donned a speckled liner and a clear prosthetic socket and was asked to stand on his residual limb. The clear socket allowed the DIC system to track the liner speckles and measure the liner strain on the anterior side when the limb was being loaded (Figure 1). The field of view available for DIC measurements was rather limited due to a sock worn proximally and a rigid wrap distally (Figure 1). An FEA model of the subject's residual limb with both socket designs was developed to estimate liner surface strains. FEA estimates of liner strain were compared with DIC measures.

**Figure 1:** Anterior (left) and lateral (right) view of the residual limb donned with a speckled liner and a clear socket. The dashed red rectangle on the anterior side represents the area where DIC measured liner strains.

**Results & Discussion:** FEA estimates of liner strain showed some level of quantitative agreement with DIC measures (Figure 2). More specifically, both FEA and DIC showed higher tensile strain values around the tibial tuberosity when using both sockets. For the TSB socket, both methods estimated peak tensile strain values of approximately 0.08. For the PTB socket, both methods estimated peak tensile strain values of approximately 0.12. These findings align with previous research [4] which reported higher contact pressure in the proximal anterior region with the PTB socket compared to the TSB socket.

**Significance:** This study demonstrates an approach for validating FEA strain estimates in prosthetic liners using DIC. By implementing two widely used socket designs, TSB and PTB, this study demonstrated the potential of the developed FEA model and DIC system to distinguish strain differences between these designs. Subsequently, the validated FEA model maybe be useful to evaluate fit and user comfort across different socket designs.

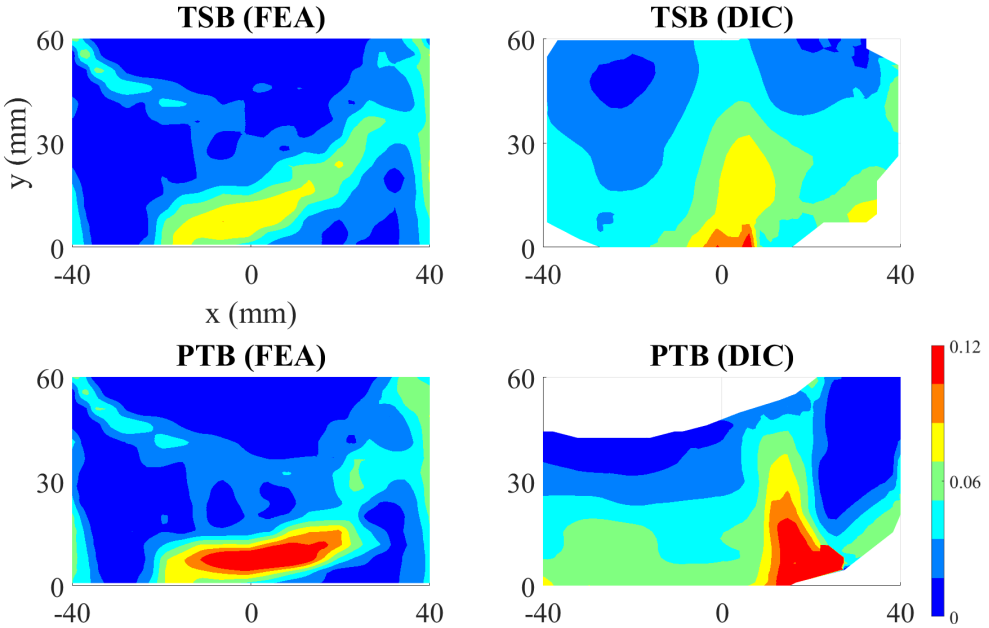


**Figure 2:** Comparison of FEA and DIC estimates of maximum principal (tensile) strain on the liner surface when using a TSB and PTB socket.

**Acknowledgments:** This work was supported by U.S. Army Medical Research and Development Command under award number: W81XWH- 21-1-0220

**References:** [1] Turner et al. (2020), *Arch Rehabil Res Clin Transl*; [2] Silver-Thorn. (1996), *JRRD*; [3] Dickinson et al. (2017), *Med Eng Phys*; [4] Gholizadeh et al. (2016), *Prosth & Orth Int*.

# Real-Time Spatial Filtering Methods of High-Density sEMG for Lower Limb Prosthetic Control Signals

Joseph R. Redmond*, Corey A. Pew
Department of Mechanical and Industrial Engineering, Montana State University, Bozeman, MT
*joesph.redmond@msu.montana.edu

**Introduction:** Active prostheses incorporate surface electromyography (sEMG) sensors as an intuitive control interface for users, enabling a higher quality of life for individuals with limb loss [1]. Standard bipolar sensors (SDsEMG, Fig 1, Left) read myoelectric signals indicating muscle activity through the voltage difference of on-skin electrodes, noninvasively leveraging the body's built-in control for prosthesis actuation. However, electrical noise from skin impedance, motion of the skin relative to the muscle, and sensor displacement are common for sEMG, reducing robustness [1]. Lower limb prostheses (LLP) require reliable control signals, as any error can risk fall and injury [2], limiting commercial integration for LLP control. High-Density (HDsEMG) sensors (Fig. 1, Right) include an array of electrodes. The increased data density allows for spatial filtering and selectivity of electrodes with lower noise artifacts when producing a single quantification of muscle activation [3]. This study aims to determine how real-time spatial filtering of HDsEMG signals may enhance signal quality in application to prosthetic control. We hypothesize that real-time evaluation, selection, and compositing of electrodes from a HDsEMG sensor array, will produce higher Signal-to-Noise Ratio (SNR) compared to SDsEMG.

*Fig 2- Left: SDsEMG and Right: HDsEMG Sensors*

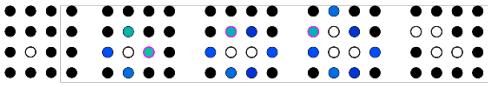

*Fig 1 – Neighborhood Search Clustering Model using Signal Quality Metric*

**Methods:** ***Data Collection:*** 8 non-amputee participants were included in this study (5M, 3 F, 19-41 yrs.). Delsys SDsEMG sensors and 16 channel HDsEMG sensors measured four superficial knee extensor and flexor muscles (Vastus Lateralis, Rectus Femoris, Semitendinosus, Biceps Femoris) on the dominant limb. Sensors were placed optimally on the muscle belly, and distally 1cm to simulate noise from sensor displacement during prostheses pistoning. Participants were recorded in overground, straight walking at a self-selected speed. ***Composite Algorithms:*** Signal quality was defined using a SNR with a signal band of 20 – 350Hz [4]. Five algorithms were developed to select HDsEMG signals for compositing: 1) Summation of 16 Electrodes (Cmp16), 2) Highest Quality Electrode (Bst1), 3) 4 Highest Quality Electrodes (Bst4), 4) Highest Quality 2x2 Spatial Filter (Sqr4) [3], and 5) Cluster of 4 Electrodes (Nbr4) selected using a neighbor search, with a starting electrode chosen by a weighted regional average of the quality metric (Fig 2). Signal selection algorithms were assessed over a 300ms rolling window and selected electrodes were updated at 20Hz rate [5]. ***Quality Analysis:*** Trials were separated into gait cycles by dominant limb heel-strike. Gait Cycle signal quality was quantified using a mean SNR (mSNR) of the rolling window. mSNR was averaged across all trials for each algorithm. A Wilcoxon Rank Sum test with a null hypothesis of an equal median was used to mSNR between HDsEMG composites and SDsEMG.

**Results & Discussion:** When optimally placed, SDsEMG averaged 5.96dB mSNR over a 300ms rolling window of a walking gait cycle (Fig. 3). Compared to the SDsEMG, HDsEMG Cmp16 showed -18% mSNR difference (p=0.01), as the composite included electrodes on a sensor field larger than the optimal sensor placement, including the use of poor-quality signals. Bst1 improved mSNR by +35% (p=0.02), showcasing adaptive signal selection from a sensor field can provide a higher quality signal. For the 4-channel signals, Sqr4 showed the lowest improvement (+15%, p=0.64), given the rigid structure of a 2x2 square does not account for strongest signal zones around the edge of the sensor field. Bst4 had the highest 4-channel improvement in mSNR (+20%, p=0.29), as it did not account for relative electrode locations in selection. Nbr4 (+17%, p=0.48) allows the selection of electrodes in any contiguous shape (Fig. 2). While Nbr4 trended towards a lower mSNR than Bst4, the constraint of a clustered selection mitigates the risk of crosstalk on a large sensor field. When displaced 1cm distally to introduce noise, SDsEMG showed a -13% difference in mSNR relative to an optimally placed sensor (-0.82dB, p=0.17). Bst1 only showed an -8% difference relative to an optimally place sensor (-0.65dB, p=0.65). This moderate trend suggests that HDsEMG may counteract noise due to sensor placement, motion of the skin, or movement of the muscle under the skin.

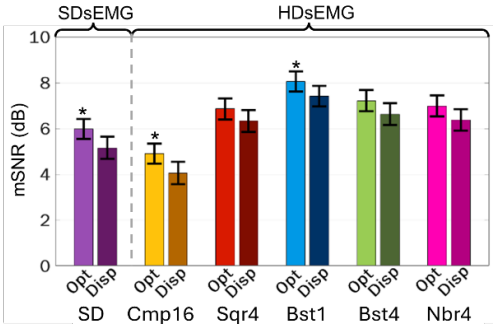


*Fig 3 – Average mSNR of 300ms rolling window in walking gait cycle by sensor configuration, both Optimally placed (Opt, n=82) and Displaced distally 1cm (Disp, n=91)*

mSNR quantifies signal quality in the manner of application to a real-time control system, however, the metric is shape-dependent with respect to the signal over a gait cycle and should only be considered comparatively within this study. Further analysis is needed to normalize mSNR values, as well as consideration of root-mean-square power (RMS) of composite signals to evaluate signal strength in addition to quality. **HDsEMG compositing methods using spatial filtering showed improvements in mSNR over SDsEMG.**

**Significance:** An improved mSNR suggests higher quality data obtained, which may allow real-time integration of intuitive sEMG control into LLP. Future work will evaluate if higher quality HDsEMG composite signals show a stronger correlation to real-time knee mechanics, and whether motion artifacts influencing selected signal location on the sensor array are indicative of changes to muscle position and can inform joint kinematics.

**Acknowledgements:** Support from the NIGMS, NIH under grant number U54 GM104944.

**References:** [1] Gehlhar et al. (2023) Annual Reviews in Control (55); [2] Ahkami et al. (2022) IEEE TMRB (5-3); [3] Barbero et al. (2012) Springer-Verlag; [4] Fraser et al. (2014) IEEE TIM (63-12); [5] Fleming et al. (2021) Journal of Neural Eng. (18-4);

# DELTACUFF: A NOVEL DEVICE TO MEASURE VENOUS COMPLIANCE FROM ACOUSTIC SIGNALS

*John A. S. Buttles[b], Jason Y. Lee[i], Cyrus J. Darvish[a], Pete Gueldner[a], Rabih Chaer[d,e], David A. Vorp, Ph.D.[a-h,j], Timothy K. Chung, Ph.D.[a,h]

[a]Department of Bioengineering, [b]Department of Mechanical Engineering and Materials Science, [c]McGowan Institute for Regenerative Medicine, [d]Department of Surgery, [e]Division of Vascular Surgery, [f]Department of Chemical and Petroleum Engineering, [g]Department of Cardiothoracic Surgery, [h]Clinical and Translational Sciences Institute, [i]Department of Computer Science, [j]Magee Women's Research Institute, University of Pittsburgh, Pittsburgh, PA

*Corresponding author's email: jab558@pitt.edu

**Introduction:** Deep vein thrombosis (DVT) is the third most common vascular disease, affecting roughly 900,000 Americans annually, and is responsible for over 100,000 fatalities each year [1, 2]. Among individuals aged 65 and older, the annual incidence of DVT increases to 10 per 1,000 people. Black communities experience disproportionately high rates of DVT, while pregnant women are five times more likely to develop the condition [1, 3]. In addition to DVT, nearly 50% of all cases progress to post-thrombotic syndrome (PTS), which results in a lower quality of life and higher cost burden [4, 5]. Currently, there exists no reliable gold standard for diagnosing those who will transition to PTS [6]. DeltaCuff represents a significant step forward in predicting DVT and PTS at early stages of the clinical timeline. By capturing acoustic signals from the thigh and incorporating post-processing algorithms, the proposed technology not only has the potential to enhance diagnostic accuracy but also to alleviate the healthcare and economic burdens associated with DVT and PTS. Identifying at-risk patients early will lead to interventions such as aggressive compression therapy or thrombolytic treatment can be deployed to mitigate progression to PTS, ultimately improving patient outcomes and quality of life [7]. DeltaCuff exemplifies a novel tool for predictive medicine that improves not only the patient's outcome, but the clinician's efficiency.

**Methods:** DeltaCuff consists of four Arduino Nano microcontrollers, nine piezoelectric sensors, two pumps, one solenoid valve, one 5 V pressure transducer, one pressure cuff, and one 3D printed structure to house all components as shown in **Figure 1**. The piezoelectric sensors are arrayed along the pressure cuff and contact the bare leg, measuring the change in pressure while the pressure cuff is pressurized to 10 kPa and then depressurized. Using the analog input pins on the Arduino Nano, changes in voltage from the sensors are recorded and then sent over the universal serial bus to a local computer. The voltages are then stored and plotted in real-time on the computer using Python. Once the Python application finished, the voltages from each sensor are exported as a comma-separated values file for post processing with MATLAB as shown in **Figure 2**.

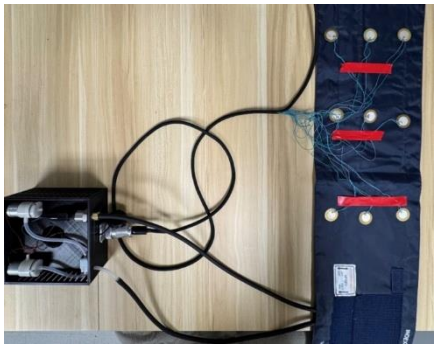

**Figure 1:** DeltaCuff fully assembled. PCB and electrical components housed on the left. Pressure cuff and piezoelectric array on the right. Tubing and wires run in between.

**Results & Discussion:** We developed a prototype of DeltaCuff that records acoustic signals while simultaneously pressurizing an off-the-shelf blood pressure cuff. Voltages from the nine piezoelectric sensors demonstrated consistent, repeatable waveform patterns during the pressurization and depressurization cycles. The device's ability to process and store data efficiently with any modern computer demonstrates its potential for hassle-free deployment in clinical environments. Real-time visualization and data exportation via Python reduced latency, enhancing the accuracy of the device for clinical assessments. These findings suggest the potential of the device to assess venous compliance and detect differences indicative of pathological states such as DVT or PTS; however, DeltaCuff's functionality was verified on healthy veins instead of diseased counterparts.

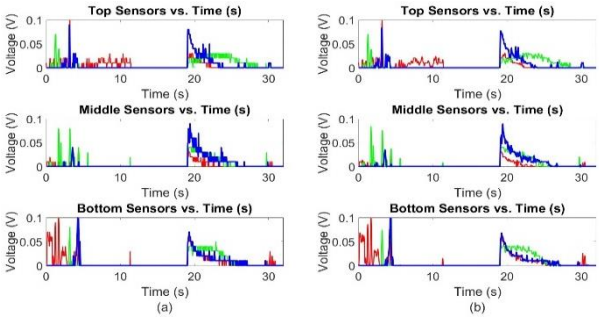


**Figure 2: (a)** MATLAB plot of voltages exported from Python script. **(b)** A 3rd degree polynomial Savitzky-Golay filter was applied to the voltages. Top sensors refer to those furthest away from the enclosure in Fig. 1.

**Significance:** DeltaCuff holds significant potential to revolutionize the diagnosis and management of DVT and PTS. By identifying at-risk patients earlier, DeltaCuff enables pre-emptive interventions such as compression therapy or thrombolytic treatments, which could mitigate progression to PTS, reduce healthcare costs, and improve patient outcomes. Successful validation of the acoustic signals will justify the existence of a new, necessary tool in predictive medicine.

**Acknowledgments:** The pilot study funding was provided by the Center for Medical Innovation Swanson School of Engineering at the University of Pittsburgh Award 347-2024.

**References:** [1] "Data and Statistics on Venous Thromboembolism." Centers for Disease Control and Prevention. https://www.cdc.gov/blood-clots/data-research/facts-stats/index.html (accessed 2025); [2] Y. Freund, F. Cohen-Aubart, and B. Bloom, *JAMA*, vol. 328, 2022, doi: 10.1001/jama.2022.16815; [3] K. McLendon, A. Goyal, and M. Attia, "Deep Venous Thrombosis Risk Factors," in *StatPearls*. Treasure Island (FL), 2024; [4] A. Rabinovich and S. R. Kahn, *J Thromb Haemost*, vol. 15, 2017, doi: 10.1111/jth.13569; [5] A. A. Ashrani and J. A. Heit, *J Thromb Thrombolysis*, vol. 28, 2009, doi: 10.1007/s11239-009-0309-3; [6] S. R. Kahn *et al.*, *J Thromb Haemost*, vol. 7, 2009, doi: 10.1111/j.1538-7836.2009.03294.x; [7] R. S. Chitsike *et al.*, *J Thromb Haemost*, vol. 10, 2012, doi: 10.1111/j.1538-7836.2012.04872.x

# VALIDITY OF MOVEO EXPLORER™ FOR LOWER EXTREMITY JOINT ANGLE APPROXIMATIONS DURING GAIT

*Olivia R. Greene[1], Douglas N. Martini[1]
[1]Movement Neuroscience Laboratory, University of Massachusetts Amherst, Department of Kinesiology
*Corresponding author's email: oliviagreene@umass.edu

**Introduction:** Many clinical decisions for physical rehabilitation are often made by comparing patient joint angles to those of healthy controls. Optical motion capture, the gold standard in kinematic gait analysis, requires prohibitive cost and expertise that many clinical settings cannot afford. Comparatively, inertial measurement units (IMUs; wearable sensors incorporating tri-axial accelerometers, gyroscopes, and magnetometers), offer an affordable, portable, user-friendly system for gait analysis, and hence are increasingly used in clinical settings. To be implemented with confidence by both clinicians and researchers, IMUs and their operating systems must be validated against gold standards. Moveo Explorer™ (APDM Inc., a Clario Company) is a commercially available IMU system that was validated against an instrumented walkway and optical motion capture for some postural sway and spatiotemporal gait parameters only [1-5]. The Moveo Explorer™ system also produces kinematic gait variables, though these parameters have not been validated for joint angle approximations during gait. Given that clinical decisions for treatment are often made by comparing patient joint angles to healthy control subjects [6], as well as the rise in adoption of commercial IMU systems by clinicians [7], there is an urgent need to validate the joint angle approximations provided by the Moveo Explorer system.

The purpose of this study is to determine the validity of a commercially available wearable sensor system (Moveo Explorer ™) for measures of joint angle approximations during gait in young adults. We aim to identify whether joint angle approximations measured by this system demonstrate sufficient agreement with those recorded by an optical motion capture system.

**Methods:** Five young adults (target n = 40) were fitted with 85 reflective motion capture (Qualisys, Inc.) markers to form a modified full body, validated marker set [8-10]. The markers were bilaterally affixed to anatomical landmarks on both feet and legs, hips, lower/upper back, chest, both shoulders, arms, and wrists (*Fig. 1)*. Participants were then fitted with 12 IMUs (Opal 2, APDM Inc.) that were mounted on both feet and legs, lower back, chest, both arms, and wrists (*Fig 1)*. Once the marker and sensor setups were complete, participants completed one 5-minute treadmill walk trial. The treadmill belt was set to a self-selected speed. Optical motion capture cameras recorded movement of each participant's body segments during the trial. Data recordings from the trial were used to calculate joint angle approximations and served as the reference against which equivalent measures from IMUs were compared.

**Figure 1:** Motion capture marker set and IMU placement.

The motion capture data was analyzed by first identifying all markers in Qualisys Track Manager (Qualisys, Inc.) and then imported to Visual 3D (C-Motion, Inc.) to calculate joint angle approximations. From Moveo Explorer™, joint angle approximations were automatically calculated and readily available for export. Mean peak hip, knee, and ankle joint angles approximations, in all 3 planes, from each system were compared using mean difference and intraclass correlations (ICC). ICC reliability estimates were calculated using SPSS statistical package version 29 (SPSS Inc.) based on a mean-rating (k = 2), absolute agreement, 2-way mixed-effects model [11].

**Results & Discussion:** The mean differences in peak hip joint angles were: 0.38° and 2.65° for flexion and extension; 0.2° and 4.09° for adduction and abduction; 3.31° and 1.20° for internal and external rotation respectively. The mean differences for peak knee joint angle were: 1.64° and 3.49° for flexion and extension; 8.26° and 21.77° for varus and valgus; 10.11° and 1.29° for internal and external rotation respectively. Lastly, for peak ankle joint angles the mean differences were: 10.74° and 8.49° for dorsi- and plantar flexion; 6.57° and 6.51° for eversion and inversion; 4.76° and 9.40° for adduction and abduction respectively. Measurement system performance consistency ranged from good to excellent. Mean peak hip and knee joint angles were both classified as excellent, with an ICC reliability estimates of 0.946 and 0.953, respectively. Meak peak ankle joint angles were classified as good, with an ICC reliability estimates of 0.838. Although our preliminary results show that our intraclass correlations between measurement systems is good to excellent, we acknowledge that these results will be more robust with the enrollment of more participants.

Previous reports found a maximum difference of only 6° between the IMU system and motion capture system during short bouts of walking at prescribed speeds, jumping jacks, and jump turns [12].We expect that our results will be similar, if not more accurate, since we are testing participant-specific walking speeds over a longer walking duration and are utilizing a much more robust optical motion capture marker set. Critically, we also expanded validity observations by assessing knee and ankle joint approximations.

**Significance:** The results of this study are relevant to the field of gait analysis and physical rehabilitation. Validating Moveo Explorer™ as an accurate measurement of joint angle approximations will enhance the reliability of IMU gait assessments. This allows clinicians and researchers to confidently use these sensors, affording great accessibility to objective gait analysis and assessment in clinical settings. Ultimately, clinicians will be able to make informed treatment decisions that have deeper relevance for the patient's real-world environmental demands.

**References:** [1] Hou et al., 2021; [2] Mancini et al., (2016); [3] Morris et al., 2019; [4] Schmitz-Hübsch et al., 2016; [5] Tack & Choi, 2017; [6] Romkes & Bracht-Schweizer, 2017; [7] Picerno et al., 202; [8] Bennetti, 1998; [9] Wu et al., 2002; [10] Wu et al., 2005; [11] Koo & Li, 2016; [12] Horenstein, 2019.

# A NONINVASIVE DEVICE FOR THE QUANTITATIVE CHARACTERIZATION OF MELANOMA *IN SITU*

Stephanie Anyanwu,[1*] Ethan Chang,[1*] Ella Holtermann,[1*] Sharanya Parvathaneni,[1*] *Sabahat Rahman,[1*] Smriti Srikanth,[1*]
Tina Tian,[1*] Brendon Young,[1*] Vito Rebecca, PhD,[2] Luo Gu, PhD,[3] Elizabeth Logsdon, PhD[1]
[1] Department of Biomedical Engineering (BME), Johns Hopkins University; [*]Indicates equal contribution
*Corresponding author's email: srahma22@jh.edu

**Introduction:** Melanoma is a form of skin cancer that presents as pigmented lesions and will affect over 100,000 Americans in 2025 [1]. Suspicious moles are typically visually examined by dermatologists to determine whether they should be biopsied for histological analysis [2]. For every 27.8 skin biopsies taken, only one results in a positive diagnosis [3], highlighting the low specificity of the screening process and the financial burden for patients/insurers. This can be attributed to the gold standard in dermatologists' screenings, which relies on dermoscopy and is overly dependent on visual attributes. Hence, dermatologists require an objective metric to increase the specificity of their screening process and reduce the number of unnecessary skin biopsies.

Interestingly, there is a well-elucidated relationship between skin cancer and tissue stiffness, which could offer a numerical property by which to assess potential malignant lesions [4]. However, the mechanical properties of skin are not factored into the melanoma screening process because there is a lack of established quantitative characteristics describing these properties, specifically for melanoma lesions [5]. Existing methods for measuring soft tissue mechanical properties include indentation-based methods like atomic force microscopy (AFM), imaging-based methods, and others. These approaches are insufficient for the *in situ* characterization of skin, as they are *ex vivo*, invasive, and/or lack the resolution necessary for skin. Here is proposed a microindentation-based device for the noninvasive mechanical characterization of melanoma *in situ*, which can be leveraged to objectively assess skin lesions.

**Methods:** The current proof-of-concept prototype consists of a load cell mounted on an actuator, as well as a probe with a spherical tip (⌀ = 1 mm) attached to the force-sensing region of the load cell. The device tip is positioned flush with the patient's skin. The device begins collecting force data when the user presses a button, and the tip indents by 0.5 mm (Fig. 1). From the force readout, elastic modulus can be calculated using Hertz Contact Theory, a mathematical model for representing forces applied during interactions between spherical surfaces [6].

To validate the accuracy and reliability of the device, preliminary data was obtained from performing indentation trials on four polymers with comparable elasticity to skin using a benchtop setup. A commercial tensile tester, Mark-10, was used as a control for all measurements.

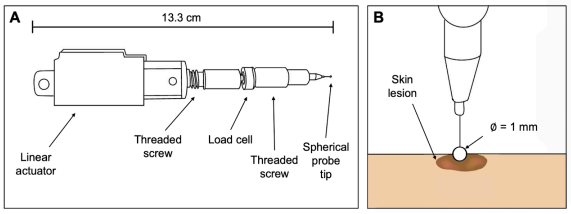


**Figure 1:** Assembled device. (A) Device components. (B) Close-up view of probe tip scale relative to skin lesion.

**Results & Discussion:** The device demonstrated the capacity to reliably differentiate between homogeneous polymers of varying stiffnesses, as well as reproduce the measurements of the Mark-10 with moderate precision (Fig. 2). The differences in elastic moduli between materials produced by the microindenter were found to be statistically significant ($p<0.001$), confirming its capability to distinguish relative stiffnesses of the polymers. Differences in calculated elastic moduli between the device and the Mark-10 were not significantly different on the Ecoflex 00-50 polymer, indicating the device's optimal working range of around 90 kPa. These initial tests enabled the development of a robust testing setup to ensure device readings were consistent across trials and comparable to a control.

Subsequent testing on galline and murine samples will be performed to demonstrate the device's ability to characterize elastic moduli of heterogeneous tissues. Tests on mice injected with human melanoma cells will confirm the ability to distinguish between melanoma lesions and healthy tissue, motivating the use of elastic modulus for characterizing cancerous skin lesions.

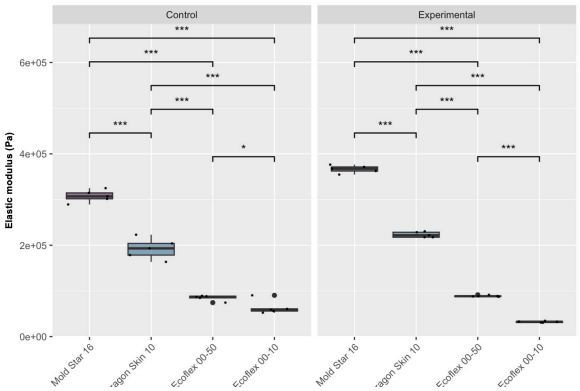


**Figure 2:** All raw data were processed to obtain elastic moduli of all polymers. One-way ANOVA was performed ($p<0.05$) comparing all polymers within control and experimental groups; all differences within groups were found to be statistically significant. Significance bars indicate results of unpaired two-tailed t-tests within each group (*: $p<0.05$, **:$p<0.01$, ***:$p<0.001$).

**Significance:** This proof-of-concept introduces a tool for dermatologists to apply in skin cancer screenings, which can increase confidence in decision-making for taking biopsies and reducing the number of unnecessary ones. Further adaptations of the device in research settings may also enable quantifying elastic modulus for other *in situ* applications where tissue mechanics play a role.

**Acknowledgements:** Johns Hopkins BME Undergraduate Design Team Program. Design Team Teaching Assistants: Aditi Sriram, Natasha Mody.

**References:** [1] American Cancer Society, Key Statistics for Melanoma Skin Cancer; [2] Garbe et al. (2019), *Eur J Cancer.* 2020;126:141-158; [3] Matsumoto et al. (2018), *J Am Acad Dermatol.* 2018;78(4):701-709.e1; [4] Park et al. (2023), *Front Bioeng Biotechnol.* 2023;11:1162880; [5] Ng. (2023), Oral communication; [6] Kontomaris et al. (2020), *Mater Res Express.* 2020;7(3).

**Investigating Impact of Varying Fidelity in Human Head Models on Blast-Induced Traumatic Brain Injury**

Manik Bansal[1], and Rika Wright Carlsen[1]
[1] Injury Biomechanics Laboratory, Department of Engineering, Robert Morris University, Moon Township, PA-15108.
*Corresponding author's email: bansal@rmu.edu

**Introduction:** Blast-induced traumatic brain injury (bTBI) is the most common and concerning injury for military personnel operating handheld weapon systems. Traumatic brain injury (TBI) can involve diffused microscopic injuries at the cellular level which are invisible to non-invasive standard imaging methods like computer tomography (CT) and magnetic resonance imaging (MRI). A recent post-mortem study [1] indicates the occurrence of chronic traumatic encephalopathy (CTE) is low for bTBI compared to impact TBI, suggesting that the mechanism of injury is different for bTBI. The exact mechanism of primary neuronal injury in brain tissue resulting from blast wave interactions remains unclear. Additionally, the accuracy of predicting potential blast-induced neuronal injury mechanisms, driven by shear strain and intracranial pressure, depends on various geometric [2] and material fidelities [3] incorporated into the human head model. This study aims to examine variations in the biomechanical response of cortical brain tissue under blast exposure by evaluating different geometric and material fidelities, including: 1) folded (gyrencephalic) versus smooth (lissencephalic) brain structures, 2) presence versus absence of the human facial bone structure, 3) sub-arachnoid space with and without trabeculae beams, and 4) cortical white matter material modeling without and with anisotropy, incorporating axonal orientation.

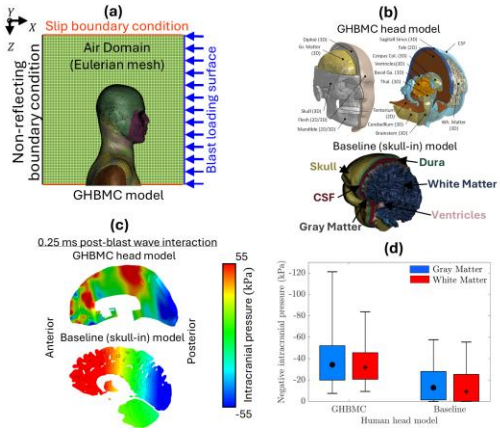


**Figure 1:** (a) Boundary conditions for simulation planar frontal blast exposure, (b) Anatomical details of GHBMC and baseline head model, (c) Spatial distribution of intracranial pressure in the sagittal section of cortical tissue for both models at 0.25 ms post-blast wave interaction and (d) Candlestick plot depicting the range of the elemental maximum negative intracranial pressure in cortical tissue (gray and white matter) for both models, where the wicks represent the 97.5th and 2.5th percentiles, and the box spans the interquartile range.

**Methods:** In this study, the baseline head model with cortical folds was developed using MRI (T1-MPRAGE and T2-weighted sequences) scans of a healthy 18-year-old female. The brain is segmented using FREESURFER, and the model is meshed with all-hexahedral elements using CUBIT. The anatomical details of baseline model are shown in Figure 1b. Building on the baseline model, three additional models were developed: Model A (Baseline + facial bone structure), Model B (Model A + subarachnoid space with trabecular beams), and Model C (Model B + anisotropic properties based on axonal orientation). The facial bone structure was mapped from the GHBMC-M50-Pv5.3.4 model [4]. The subarachnoid space was defined by a pia layer and randomly distributed 1D beam elements between the dura and pia mater, with cerebrospinal fluid (CSF) simulated using smoothed particle hydrodynamics (SPH). Axonal tracts (elemental orientation and fractional anisotropy) from diffusion tensor imaging (DTI) scans were incorporated into the Holzapfel–Gasser–Ogden (HGO) model to represent anisotropic behavior of white matter. We implemented the Prescribed Inflow-Arbitrary Eulerian-Lagrangian (PIF-ALE) approach using LS-Dyna to model planar blast wave interaction with the human head model. The PIF-ALE approach models the ideal Friedlander waveform with the positive overpressure duration. The implementation details of PIF-ALE are available in [5]. In brief, the blast wave was simulated by defining a temporal curve for volume change, temperature variation, and particle velocity at the inflow surface of the air domain surrounding the head model, while a non-reflecting boundary condition was applied to the opposite surface, as illustrated in Figure 1a. The Lagrangian mesh is kept constraint free. A penalty-based approach was used in LS-dyna to model the interaction between blast wave (Eulerian air mesh) and head model (Lagrangian mesh).

**Results & Discussion:** In our preliminary study, we simulated the interaction of a planar frontal blast wave (8 psi and 2 ms) with two models: one with cortical folds (baseline model) and the other without folds (GHBMC model). The tissue material properties were the same in both models. For gray matter (Figure 1d), the 50th percentile maximum negative intracranial pressure (MNICP) in the GHBMC model (-35 kPa) is at least three times higher than in the baseline model, while the 97.5th percentile MNICP (121 kPa) is at least twice as high. In contrast, the median MNICP for white matter is 10% lower in the GHBMC model and 28% lower in the baseline model compared to gray matter. Although the results reveal a significant difference in predicted MNICP values, a direct comparison between the two models remains challenging due to substantial anatomical differences. As the next step, we will rerun the baseline model with smoothed cortical folds, along with Models A to C, to enable a more accurate comparison.

**Significance:** This study will enhance the understanding of blast-induced biomechanical responses in brain tissue. By integrating key fidelities into the computational model, it will help develop more effective protective strategies and improve injury risk assessment tools for military personnel safety.

**Acknowledgments:** This material is based upon research supported by the U.S. Office of Naval Research under PANTHER award number N00014-24-1-2200 and N00014-22-1-2828 through Dr. Timothy Bentley.

**References:** [1] Shively et al. (2016), *Lancet Neurol* 15(9); [2] Subramaniam et al. (2021) *Front Bioeng Biotechnol* 9; [3] Duckworth et al. (2021), *Int J Numer Meth Biomed Eng* 37(4); [4] Sutar and Ganpule (2022), *J Biomech Eng*, 144(5); [5]Yu and Ghajari (2019), *Int J Numer Meth Biomed Eng* 35(12).

# NOVEL EXOSKELETAL SYSTEM FOR REDUCED TIBIAL LOAD DURING WALKING

*Ciera A. Price[1,2], Robert L. McGrath[1,2], Sarah Pesquera[2,3], Julia Gambill,[1,2], Wayne Board[1,2], W. Brett Johnson[2,3], W. Lee Childers[2,3]
[1]The Henry M. Jackson Foundation for the Advancement of Military Medicine, Inc., Bethesda, MD [2]Center for the Intrepid, Brooke Army Medical Center, JBSA Fort Sam Houston, TX [3]Extremity Trauma and Amputation Center of Excellence, USA
*Corresponding author's email: ciera.a.price2.ctr@health.mil

**Introduction:** Bone stress injuries (BSIs) are prevalent amongst athletes and military recruits due to repetitive, high-intensity training. The tibia is the most common site of BSIs, with an incidence rate of 23.6% [1]. Conventional management requires anywhere from four to eighteen weeks of rest and activity modification, leading to high attrition rates and reduced Military readiness [2]. Therefore, a solution to improve trainee retention following tibial BSI is critical. The Intrepid Dynamic Exoskeleton Orthosis (IDEO), a custom-fabricated ankle-foot orthosis designed for limb salvage, has been shown to reduce tibial strain in a validated robotic surrogate model previously developed by our team [3]. Building on the clinical success of the IDEO, our team has now developed a novel, size-adjustable exoskeletal system aimed at reducing tibial load and expediting a return to activity for injured Service members. The objective of this study is to pilot the exoskeleton on healthy Service members and assess its ability to reduce tibial load *in vivo.*

**Methods:** Two active-duty Service members (1 female, age 31 yrs, height 165.1 cm, mass 67.8 kg; 1 male, age 34 yrs, mass 161.5 cm, weight 77.3 kg) without history of tibia fracture participated in this protocol. The study was approved by the San Antonio Institutional Review Board in compliance with all applicable Federal regulations governing the protection of human subjects, and written informed consent was obtained.

Participants wore standard-issue combat boots with pressure insoles against the plantar surface of the foot. Participants completed up to eight trials of overground walking at their self-selected speed in three device conditions in a randomized order: 1) baseline (no device), 2) the exoskeleton, and 3) a tall Controlled Ankle Motion (CAM) boot. All devices were fit to the left limb by a Certified Orthotist. Kinetic and kinematic data were recorded using a 32-camera motion capture system and 5 embedded force plates. Total plantar force and center of pressure were derived from the pressure insoles. Ankle angle was derived from motion capture and synchronized with plantar force data from the pressure insoles according to heel strike and toe off events. These data were input into a simplified quasi-static ankle model [4] to estimate distal tibial load (normalized to body weight) during stance. A linear mixed-effects model with a fixed effect of condition (baseline, exoskeleton, CAM boot), a random effect of subject (1, 2), and a within subject correlation structure was utilized to compare peak tibial loads across device conditions for each participant.

**Results & Discussion:** The mean reductions in peak tibial load from the exoskeleton condition compared to the baseline condition were 41% and 23% for participants 1 and 2, respectively (Figure 1). Mean peak tibial load was 3.9, 2.2, and 1.1 times body weight (BW) for participant 1 in the baseline, exoskeleton, and CAM boot conditions, respectively. Mean peak tibial load for participant 2 was 3.0, 2.2, and 1.6 BW in the baseline, exoskeleton, and CAM boot conditions, respectively. Both the exoskeleton ($p < 0.001$) and CAM boot ($p < 0.001$) demonstrated statistically significant reductions in peak tibial load relative to baseline. The novel exoskeleton unloaded the tibia *in vivo*, which is consistent with the IDEO's performance during robotic surrogate testing at the distal, middle, and proximal tibia. However, the quasi-static ankle model used for data analysis is limited to calculating distal axial load and cannot account for the bending moment observed in the robotic surrogate model [3].

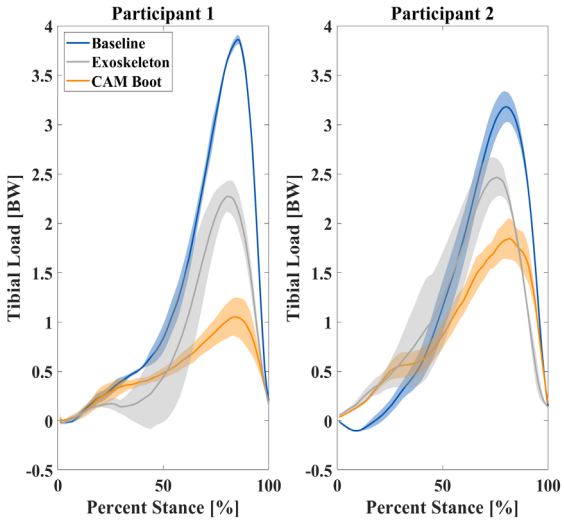


**Figure 1:** Calculated mean and standard deviation of distal tibial load during stance for two participants during overground walking at self-selected speed.

**Significance:** BSI management typically requires weeks of recovery with axillary crutches or pneumatic bracing (e.g., CAM boots) to reduce weight bearing [5]. This standard of care disrupts training and may lead to trainees separating from the armed services. Preliminary results suggest that the novel exoskeleton reduces distal tibial load compared to no device during overground walking. While the CAM boot also reduces tibial load during walking, it cannot support dynamic tasks like running. The novel exoskeleton may improve care by promoting healing through unloading and enabling continued physical activity. Future work will test the novel exoskeleton on additional participants with expanded device conditions, increased speeds, and task variation.

**Acknowledgments & Disclaimer:** This work was funded by the Department of Defense Peer Reviewed Orthopedic Research Program, award number W81XWH2120013. The views expressed in this abstract are those of the authors and do not necessarily reflect the official policy or position of the Henry M. Jackson Foundation for the Advancement of Military Medicine, Inc., the Defense Health Agency, Department of Defense, nor the U.S. Government.

**References:** [1] Patel et al. (2011), *Am Fam Physician* 83(1); [2] Claassen et al. (2014), *MSMR* 21(9); [3] McGrath et al. (2024), *Bioengineering* 11(5); [4] Matijevich et al. (2020), *Hum Mov Sci* 74; [5] Jacobs et al. (2014), *Cl Sprt Med* 33(4).

**Prosthetic Socket Type and User Satisfaction Significantly Impact Walking Performance: A Pilot Study**

Silvia E. Campos-Vargas*1, Brandon M. Peoples1, Kenneth Harrison[1], Jaimie A. Roper
Auburn University[1], Auburn, AL, U.S.A.
Corresponding author email: szc0259@auburn.edu

**Introduction**: Veterans with limb prostheses often wish to return to military service. Military organizations use the Comprehensive High-Level Activity Mobility Predictor (CHAMP) to evaluate service members with lower-limb loss who want to remain in duty [1]. However, little is known about how CHAMP scores relate to common gait assessments such as the 5 sit-to-stand test (5XTSST), Time up and go (TUG), and 6-minute walking test (6MW). Additionally, how prosthetic type and user satisfaction affect these assessments remains unclear. This study examines the relationship between CHAMP scores, prosthetic features, and performance on the 5XTSST, TUG, and 6MW tests. We hypothesize that higher CHAMP scores correlate with better assessment results and that prosthetic features significantly impact performance.

**Methods:** Seven healthy young adults with unilateral amputation below the knee (7M; age: 32±10 years). The reasons for amputation were Combat Blasts, Gunshot Wounds, Accidents, Cancer, and Motor Vehicle Accidents. All participants were treated at the Walter Reed National Military Medical Center. Participants performed the walking tasks with the device they wore most often. We conducted three Linear Regression models, using the 5XTSST, TUG, and 6MW tests as response variables to identify the relation between the Comprehensive High-Level Activity Mobility Predictor (CHAMP) and the prosthetic features as it is the socket type they use and the level of satisfaction with the weight and comfort of the prosthesis. Estimated marginal means were calculated to get the contrast. We also conducted Pearson's correlation to determine the correlation between the CHAMP and the walking tasks.

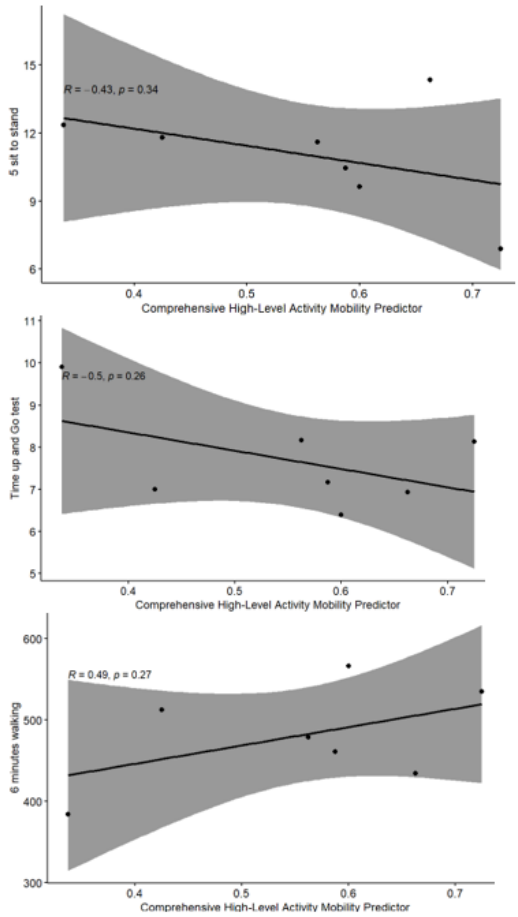


**Figure 1.** Pearson's correlation between CHAMP and 5XTSST, TUG, and 6MW testes

**Results & Discussion:** Results revealed significant effects of prosthetic comfort and socket type on the 5XTSST test ($p<0.01$). Higher comfort satisfaction correlated with faster completion times, and participants using locking socket systems completed the test 4.68 seconds faster than those with suction sockets. Similarly, for the TUG test, higher satisfaction with prosthetic comfort and weight significantly improved performance ($p<0.01$). No significant effects were found for the 6MW test. Contrary to expectations, CHAMP scores did not correlate significantly with any gait assessment (Figure 1). Our findings suggest that prosthetic satisfaction and socket type significantly influence gait performance. A larger sample size may be needed to detect potential correlations between CHAMP scores and gait assessments.

**Significance:** This pilot study demonstrates that prosthetic socket type and user satisfaction significantly impact functional mobility in individuals with lower-limb amputation. While prosthetic design advancements remain important, our findings highlight the critical role of patient-reported satisfaction with comfort and weight in optimizing performance during everyday activities such as sitting, standing, and walking. The absence of correlation between CHAMP scores and standard gait assessments suggests these tools may evaluate different aspects of mobility. Future research with larger sample sizes should further explore these relationships to better inform clinical decision-making for veterans seeking to return to military service. These findings may help clinicians optimize prosthetic prescription and rehabilitation strategies to improve functional outcomes.

**Reference:** [1] Gailey, R.S., et al (2022), Clinical Rehabilitation 26(5)

# A SINGLE-SUBJECT COMPARISON OF PROSTHETIC FOOT PUSH-OFF POWER AND WORK BEFORE AND AFTER TRANSFEMORAL OSSEOINTEGRATION USING PASSIVE AND POWERED PROSTHETIC FEET

*K.F. Ash[1,2], P.R. Golyski[2,3], J.T. Maikos[4], B.D. Hendershot[2,3,5]
[1]Henry M. Jackson Foundation for the Advancement of Military Medicine, Inc., Bethesda, MD; [2]Walter Reed National Military Medical Center, Bethesda, MD; [3]Extremity Trauma & Amputation Center of Excellence, Falls Church, VA, [4]Veterans Affairs New York Harbor Healthcare System, New York, NY; [5]Uniformed Services University of the Health Sciences, Bethesda, MD
*Corresponding author's email: kiichi.f.ash.ctr@health.mil

**Introduction:** For individuals with lower limb loss who are challenged with traditional prosthetic sockets, osseointegration (OI) can greatly improve prosthesis use, mobility, and quality of life [1-2]. Mechanically, direct skeletal attachment of a prosthesis dramatically alters the transmission of force and energy through a prosthetic limb while walking [3]; despite clear implications on the human-device interaction, studies comparing prosthetic componentry after OI are lacking [4]. The purpose of this case study was therefore to evaluate prosthetic foot mechanical energetics in a person with unilateral transfemoral amputation (UTFA), before OI (using a powered ankle-foot prosthesis) and 12-months after OI (using both a powered and passive ankle-foot prosthesis). Based on the rationale that more rigid coupling between the prosthesis and skeleton amplifies force sensation/control, we hypothesized the participant would exhibit (1) larger peak prosthetic foot push-off powers and work using powered vs. passive foot, and (2) larger peak prosthetic foot push-off power and work with the powered foot after vs. before OI.

**Methods:** A male service member with UTFA (~40y of age, >15y since amputation) completed a full-body gait evaluation at two controlled velocities (1.0m/s and 1.3m/s), before and 12-months after OI. Pre-OI data was collected wearing a powered (POW) foot; post-OI data was collected wearing a passive energy storing and returning (ESR) and POW foot on separate days. The same prosthetic (microprocessor) knee was used for all evaluations. After OI, the POW foot was initially fit and tuned throughout several in-clinic visits before ultimately taking home for ~2 weeks. Six degree-of-freedom prosthetic ankle-foot power was calculated using OpenSim (v4.4) and custom MATLAB (2022b) scripts, and integrated by time during the push-off phase to calculate push-off work [5].

**Results & Discussion:** Across both walking speeds, peak prosthesis push-off power and work were respectively 38-102% and 150-300% larger with the POW vs. ESR prosthetic foot, supporting the first hypothesis. After OI, peak prosthesis push-off power for the ESR foot was within 0.5 W/kg of ESR push-off among individuals with unilateral transtibial amputation [6], and peak push-off power for the POW foot was within 0.3 W/kg of ankle push-off of uninjured individuals at similar walking speeds [5]. Push-off power was 10-15% larger after OI, and push-off work was 17% smaller (at 1.0m/s) and 33% larger (at 1.3m/s) after OI; thus, partially supporting the second hypothesis.

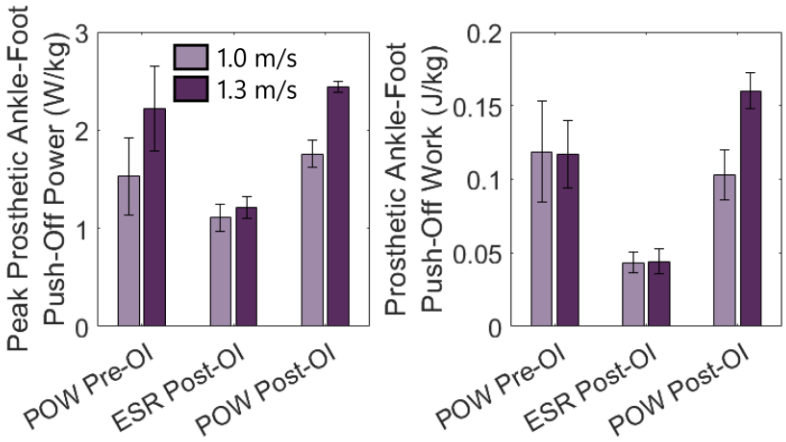


**Figure 1:** Prosthetic push-off power (left) and work (right) pre- and post-OI, by walking speed and prosthetic foot.

**Significance:** We investigated biomechanical outcomes, specifically prosthetic push-off power and work, in the first reported instance of an individual with UTFA using a POW prosthetic foot before and 12-months after OI. Beyond demonstrating the feasibility of powered prostheses in combination with OI, this analysis suggests a speed-dependent relationship such that peak push-off power and work are improved at faster walking speeds with the POW prosthetic foot after vs. before OI. Although this participant was an experienced POW prosthetic foot user before OI (~8yr), future efforts should explore longer acclimation times (i.e., >2weeks) or time since OI (i.e., >12months). Considering the more rigid coupling between the prosthesis and skeleton, additional fine tuning of prosthesis settings and task-specific training may further optimize biomechanical outcomes after OI, particularly when using advanced prosthetic components within unique patient populations like young service members with traumatic lower limb loss.

**Acknowledgments:** This work was supported by DoD Award W81XWH-17-1-0568. The authors acknowledge the Limb Optimization and Osseointegration Program. The views expressed herein are those of the authors and do not reflect the views of Henry M. Jackson Foundation for the Advancement of Military Medicine, Inc., USUHS, DHA, DoD, VA, nor the U.S. Government.

**References: [1]** Hagberg K, Brånemark R (2009) *J Rehabil Res Dev* **[2]** Van de Meent H et al. (2013) *Arch Phys Med Rehabil* **[3]** Blumentritt S et al. (2023) *Clin Biomech* **[4]** Frossard L et al. (2021) *Clin Biomech* **[5]** Takahashi K et al. (2012) *J Biomech* **[6]** Müller R et al. (2019) *Plos ONE*

# GENDER DISPARITIES IN ACL INJURY RISK

*Veronica Venezia[1], Alex Wiggins[1], Blair Shaffer[1], Cayce Onks[2], Jennifer Nyland[2],
Terrence Murphy[2], Ram Narayanan[3], Robert Creath[1]
[1]Lebanon Valley College
[2]Penn State Health, [3]Penn State Engineering
*Corresponding author's email: vvenezia44@gmail.com

**Introduction:** Anterior cruciate ligament (ACL) injuries affect approximately 250,000 individuals annually in the U.S., with females experiencing a 2–8 times higher risk of primary injury compared to males [1],[2]. Reinjury rates remain high, particularly among individuals who have undergone ACL reconstruction, with some reporting reinjury rates as high as 20% [1]. While much of the research has focused on valgus collapse (see Figure 1) as a primary risk factor for ACL injuries [3],[4], other biomechanical, neuromuscular, and structural factors may also contribute to ACL injury risk, particularly in females [5]. Ford [4] calculated total valgus knee motion as the difference between knee distance before initial contact and the minimum knee distance during the stance phase, reflecting the range of inward knee motion. This study expanded on this concept for calculating the range of inward motion by performing a similar assessment for inter-knee velocity throughout the entire landing cycle. Multiple factors contribute to ACL injuries and help explain why some people are at higher risk. This exploratory study aims to expand the understanding of ACL injury risks by expanding upon known risks to gain a deeper understanding of gender-specific risk factors, recognizing that males and females experience distinct injury mechanisms.

**Methods:** A total of 102 subjects (55 females, 47 males; 18 with prior ACL reconstruction) completed controlled drop box jumps (DBJs) while motion capture and ground reaction forces (GRFs) data was recorded. Kinematic data was collected using an 8-camera motion capture system (240 Hz; Moton Analysis Corp, Rohnert Park, CA), and GRFs were measured using two AMTI force plates (240 Hz; AMTI Inc. Watertown, MA). Data was processed in Visual3D (HAS-Motion, Kingston, Ont.) and MATLAB (Mathworks, Natick, MA) with calculations for inter-knee velocity, landing impact force, and hip moment asymmetry. Independent t-tests assessing gender differences in these variables was performed in Excel (Microsoft Corp., Redmond, WA).

**Results & Discussion:** Females exhibited significantly greater inward inter-knee velocity at landing impact compared to male ACL subjects ($p=0.034$) and male controls ($p<0.001$), as well as during the drop period compared to male controls ($p<0.001$), indicating increased knee instability and valgus collapse risk [3],[4]. However, male controls demonstrated greater outward movement pre-impact compared to female controls ($p<0.001$), suggesting males use a stabilization strategy that may reduce valgus collapse but does not eliminate ACL injury risk. Unlike previous studies that focused on valgus collapse at impact [3], this study captured inter-knee motion pre- and post-landing impact.

Males with ACL injuries were the only group with statistically significant differences seen between legs for ground reaction landing impact force ($p=0.023$). This imbalance indicates uneven distribution of landing forces, which can place excessive strain on the healthier leg, potentially increasing the risk of reinjury [1],[6]. Prior studies linked peak GRFs to ACL injury risk [2],[3], but this study highlights post-injury force distribution asymmetries, emphasizing their role in reinjury risk.

Females with ACL injuries exhibited greater hip ($p = 0.038$) moment asymmetries, consistent with prior findings linking joint asymmetry to increased ACL strain and inefficient load distribution [6],[7]. This points to a reliance on hip strength to stabilize the knee when force control is compromised. While this strategy may temporarily aid stability, it places additional stress on the hips and knees, potentially increasing ACL vulnerability.

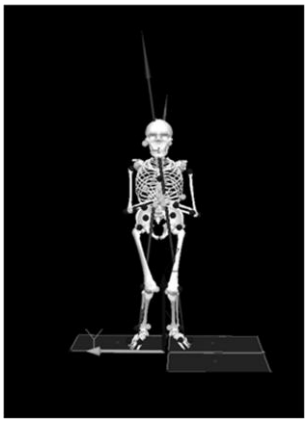

**Figure 1:** This figure represents an exemplar female subject demonstrating valgus collapse at impact.

**Significance:** This study expands upon the understanding of ACL injury risk by identifying distinct biomechanical factors contributing to injury risk. The results suggest that females experience greater knee instability due to increased inward inter-knee velocity which may increase susceptibility to valgus collapse. In contrast, males without prior ACL injuries exhibited outward knee movement before landing which may serve as a protective mechanism but does not eliminate overall risk. Among individuals with prior ACL injuries, males displayed uneven landing force distribution, which could place excessive strain on the uninjured leg and increase reinjury risk. Additionally, females with ACL injuries demonstrated hip moment asymmetries, suggesting a compensatory strategy that may inadvertently increase stress on the ACL. This study offers a new perspective of gender differences in ACL injury by evaluating inter-knee velocity, force distribution asymmetries, and joint moment imbalances during pre- and post-landing impact.

**Acknowledgments:** This Project is Supported by U.S. Army Medical Research Award No. W81XWH2210684

**References:** [1] Paterno et al. (2010), *J Sports Med*; [2] Boden et al. (2010), *J American Ortho Surgeons*;[3] Hewett et al. (2005), *J Sports Med*; [4] Ford et al. (2003), *Med & Science in Sports & Exercise*; [5] Mohamed et al. (2012), *African Health Sciences*; [6] Schmitt et al. (2012), *J Ortho & Sports PT*; [7] Yu et al. (2006), *Clinical Biomech*.

# ASYMMETRICAL LIMB LOADING DURING SIT-TO-STAND FOLLOWING ACL RECONSTRUCTION

Blair R. Shaffer[1], V Venezia[1], A Wiggins[1], C Onks[2], T Murphy[2], J Nyland[2], R Narayanan[3], *R Creath[1]
[1]Lewis Human Performance Lab, Lebanon Valley College, Annville, PA
[2]Penn State Health, The Pennsylvania State College of Medicine, Hershey, PA
[3]Penn State Engineering, The Pennsylvania State University, State College, PA
* creath@lvc.edu

**Introduction:** Anterior cruciate ligament (ACL) ruptures are very common, with approximately 100,000 ACL reconstruction (ACLR) procedures annually in the United States [1]. Known asymmetries following ACLR can present up to 2.5 years after surgery [2], which extends past the typical return-to-sport clearance, contributing to the 20% rate of secondary ACL injury [1]. Interlimb disparities in vertical ground reaction forces (vGRF), knee extension moments, and knee power have been documented after ACLR, where the surgical limb is underloaded compared to the non-surgical contralateral limb. Post-rehabilitation limb bias during sit-to-stand (STS) has not been studied to the extent of more dynamic tasks such as jumping. The STS movement is integral to daily living, as healthy individuals rise from a seated position approximately 60+ times per day [3]. The purpose of this study is to quantify post-rehabilitation asymmetries that persist past the typical period for medical clearance. Ground reaction forces, joint extension moments and power during STS within the ACLR group were compared to healthy controls across the hip and knee. The expected outcome was that observable asymmetries persist in post-rehabilitation ACLR patients.

**Methods:** Forty-five adult participants (17 ACLR; 23.6 ± 5.1 yrs) performed STS from a stool with 90 degrees of knee flexion from a seated position. Five STS trials were recorded for each subject. Variables were calculated using mean values across 5 trials. Kinematic data were collected via an 8-camera motion capture system at 240 Hz (Motion Analysis, Rohnert Park, CA). Kinetic data were collected with two force plates at 240 Hz (AMTI, Watertown, MA). Joint moments and power for the hips and knees were estimated along the joint flexion-extension axis via inverse dynamics using Visual3D (HAS-Motion, Kingston, ON). Peak moments, power, and vGRF were calculated in MATAB (MathWorks, Natick, MA). Joint moments depicted hip and knee extension. Joint power represented the concentric contraction about the hip and knee joint. Asymmetry indices (AI) were calculated using a method derived from Jordan et al. [4]. A 5-variable MANOVA was conducted to depict group differences. Individual post hoc differences were identified using ANOVAs. All statistical tests were evaluated using the R Studio (The R Foundation, Indianapolis, IN) at the alpha = 0.05 level of significance.

**Results & Discussion:** Individuals demonstrated significantly greater interlimb asymmetries after completion of ACLR rehabilitation compared to healthy controls. The MANOVA calculated on AIs for vGRF, joint extension moments, and joint concentric power of the hips and knees showed a significant group effect ($p = 0.008$) between ACLR and control subjects.

Interlimb asymmetries following ACLR for vGRF, knee extension moments, and knee power persist past medical clearance. ACLR subjects on average demonstrated an increased utilization of their non-surgical limb relative to their ACLR limb. Post-hoc ANOVAs identified significantly larger ACLR AIs for vGRF ($p = 0.002$), knee extension moment ($p < 0.001$), and knee power ($p < 0.001$) compared to controls. Interlimb asymmetries observed at the hip joint were not significantly different for extension moments ($p = 0.277$) or power ($p = 0.597$) between the ACLR and control groups.

Underloading of the ACLR limb may serve as a protective measure early in rehabilitation, becoming a learned compensatory pattern as the patient returns to normal activity levels. Increased usage of the contralateral limb can elicit additional strain and result in an increased risk for additional ACL injuries to the non-surgical leg. Knee power asymmetries indicate a velocity-dependent mechanism of underloading bias towards the contralateral knee. Similar degrees of symmetry for hip moments and power between groups suggest similar functional levels regardless of rehabilitation intervention, consistent with previous findings [2]. Asymmetries in STS following ACLR have been linked to knee underloading during a range of daily activities [5], leading to chronic underuse of the surgical leg.

**Significance:** The findings from this study suggest current methods of rehabilitation provide incomplete return to full knee function following ACLR. Chronic underloading of the ACLR limb during STS may lead to an increased risk for secondary ACL injury. Interlimb power disparities denote a velocity-dependent mechanism that is not addressed via typical rehabilitation. Understanding compensatory patterns that individuals develop post-ACLR is critical to reducing reinjury risk.

**Acknowledgments:** This project was sponsored by U.S. Army Medical Research Award No. W81XWH2210684.

**References:** [1] Renner et al. (2018), *J Orthop Res* 36(7); [2] Butler et al. (2016), *Clin J Sport Med* 26(5); [3] Li et al. (2021), *Medicine* 100(22); [4] Jordan et al. (2015), *Scand J Med Sci Sports* 25; [5] Chan & Sigward (2022), *J Orthop Res* 40.

**Changes in kinetic and kinematic countermovement jump performance in response to 6-week mountain military training**

*Lily J Rosenblum[1], Bobby G Rawls[1], Ayden McCarthy[2, 3], Evan D Feigel[1], Kelly H Mroz[1], Todd J Stefl[1], Mita Lovalekar[1], Kristen Koltun[1], Brian Martin[1], Kai Pihlainen[4], Tommi Ojanen[5,6], Tim L A Doyle[2, 3], Bradley C Nindl[1]

[1]University of Pittsburgh, Neuromuscular Research Laboratory/ Warrior Human Performance Research Center, Pittsburgh, PA
[2]Faculty of Medicine, Health, and Human Science, Macquarie University, Sydney, Australia
[3]Biomechanics, Physical Performance, and Exercise Research Group, Department of Health, Medicine, and Human Science, Macquarie University, Sydney, Australia
[4]Defence Command, Finnish Defence Forces, Helsinki, Finland
[5]Finnish Defence Research Agency, Finnish Defence Forces, Riihimäki, Finland
[6]Faculty of Sport and Health Sciences, University of Jyväskylä, Jyväsklä, Finland
*Corresponding author's email: ljr56@pitt.edu

**Introduction:** The United States Marine Corps Mountain Warfare Training Center (MCMWTC) is a high-altitude training environment for advanced tactical training. A six-week course is conducted at the MCMWTC to build skills in leading tactical operations in mountainous environments for active-duty military personnel. Countermovement jump (CMJ) performance can decline due to neuromuscular fatigue [1,2, 3] from military training. The aim of this study was to assess CMJ performance change in response to six-week MCMWTC training.

**Methods:** CMJs were performed at weeks one, four, and six of the MCMWTC course. CMJs were recorded on dual force plates (1000Hz) with a single-camera markerless motion capture system (30 Hz). CMJ measures of interest included: jump height (m); contraction time (s); reactive strength index-modified (m/s); relative eccentric peak force (N/kg); relative concentric peak force (N/kg); relative peak power (W/kg); countermovement depth (cm); and takeoff peak knee and hip flexion (°). The participants were instructed to "jump as high and fast as possible." Friedman tests were conducted to assess changes in CMJ kinetic and kinematic performance outcomes during the six-week course ($\alpha$=0.05).

**Results and Discussion:** Sixteen male military personnel completed the 6-week course (age: 27.5 (5.0) y; height: 177.6 (7.2) cm; weight: 188.3 (20.7) kg). Relative peak power decreased progressively between the measurements. Contraction time increased from week one to week four, but then fell below the baseline at week six. Reactive strength index-modified reduced from week one to week four, but then increased from week four to week six. Relative eccentric peak force showed similar patterns of change (reduced from week one to week four, and then increased from week four to week six). No other measures significantly changed over the duration of the course. These results show that kinetic measures are more sensitive than kinematics during arduous military training.

Table 1: Countermovement jump kinetic and kinematic outcomes during the six-week Marine Corps Mountain Warfare Training Center course (n = 16)

| | Dependent variable | Week 1 | Week 4 | Week 6 | *p*-value |
|---|---|---|---|---|---|
| Kinetic | Jump height (cm) | 31.7 (3.7) | 30.5 (.056) | 29.0 (.049) | 0.250 |
| | Relative peak power (W/kg) | 47.7 (5.3) | 45.4 (5.5)* | 43.8 (4.8)*^ | **0.005** |
| | Contraction time (ms) | 834.3 (171.5) | 894.3 (142.2)* | 837.3 (136.1)* | **0.026** |
| | Reactive strength index-modified (m/s) | 0.40 (0.1) | 0.35 (0.1)* | 0.36 (0.1)^ | **0.017** |
| | Relative eccentric peak force (N/kg) | 21.9 (3.6) | 20.9 (3.2)* | 22.8 (3.3)^ | **<0.001** |
| | Relative concentric peak force (N/kg) | 23.3 (3.6) | 22.6 (2.7) | 23.6 (3.7) | 0.202 |
| | Countermovement Depth (cm) | -31.8 (6.5) | -33.9 (5.6) | -33.6 (8.0) | 0.141 |
| Kinematic | Left knee flexion (°) | 94.7 (10.9) | 98.5 (9.5) | 91.3 (19.1) | 0.368 |
| | Right knee flexion (°) | 91.5 (8.4) | 98.5 (10.3) | 90.4 (18.9) | 0.601 |
| | Left hip flexion (°) | 95.1 (11.2) | 99.5 (10.1) | 92.5 (22.0) | 0.187 |
| | Right hip flexion (°) | 94.7 (10.6) | 100.2 (8.9) | 92.3 (23.0) | 0.601 |

Data in table are mean (standard deviation)
*Significantly different from week 1; ^Significantly different from week 4

**Significance:** We expect that participants in military courses would see a decrement in performance over time. Those who did not experience negative changes due to the course may be more physically fit and adapted to performing in arduous military training than those who experienced changes. During serial monitoring of a military course, movement strategies associated with fatigue may only be apparent in kinetic and not kinematic changes for trained military personnel. Further inspection of key takeoff and landing variables is needed for an in-depth neuromuscular profile.

**Acknowledgements:** This work was funded by the Office of Naval Research (N-00014-22-1-2769 and N-00014-23-1-2795).

**References:** [1] Pihlainen et al. (2018), *J Strength Cond Res* 32(4); [2] Welsh et al. (2008), *Int J Sports Med.* 29(1); [3] Murray et al. (2025), *Sports Med Open 11*(1)

# OPTIMAL LOCATION OF A SINGLE ACCELEROMETER FOR CHARACTERIZATION OF CENTER OF PRESSURE

*Kate Curran[1], **Paige Barta[1], James Peterson[1], Christopher Aliperti[1], Josiah Steckenrider[1], Rebecca Zifchock[1]
[1]Department of Civil and Mechanical Engineering, The United States Military Academy
*katecurrann@gmail.com, **paigekbarta@gmail.com

**Introduction:** Postural control consists of the actions humans take in adjusting their center of pressure (COP) to keep their center of mass (COM) balanced. Analyzing one's postural control can serve a variety of purposes, including the diagnosis of traumatic brain injury, musculoskeletal injury, and fatigue [1]. Force plates have long been used to measure COP and its oscillations over a period of time to characterize postural control. However, while force plates are practical for a lab environment, they are not as portable for real-world environments such as athletic fields or combat situations. Using accelerometers to characterize COP has shown promise as a way to identify impairments in a field environment. However, while previous research has started to examine optimal locations to place the accelerometers [2], it is unclear whether there is a single best location that can characterize postural control. Therefore, the purpose of this study is to understand whether there is a single body location to place an accelerometer from which calculated COP data parameters are most closely correlated to those from a force plate. It was hypothesized that a location closest to the COM would be most highly correlated.

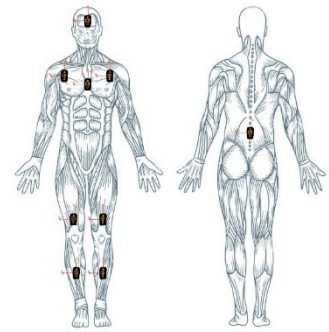

**Figure 1:** Diagram of accelerometer placement on body

**Methods:** Accelerometers (I Measure U; Vicon) were placed in nine locations that represent the head, trunk, and legs and secured with medical tape (Fig. 1). Eight total trials were conducted per subject, four each on two surfaces: a bare force plate and a foam surface placed on top of the force plate. The four trials were in different positions: feet apart, feet together, right foot only, and left foot only. These were intended to represent a range of destabilizing conditions. For each trial, data were collected simultaneously from the accelerometers and force plate while the participant stood in the desired position and looked straight ahead at an eye-level target for 15 seconds. COP in the medial-lateral (ML) and anterior-posterior (AP) directions was calculated throughout each trial for the force plate using the forces and moments and each accelerometer using methods discussed in [3]. In order to characterize postural control, two discrete variables, range and mean velocity, were calculated for both the AP and ML directions. The range is the maximum spread of the COP, while the mean velocity is the average rate at which the subject's COP changed over time. As shown in Fig. 2, the time trace for the force plate and accelerometers are similar shapes over the course of the trial, but the force plate values tend to be much smaller, as seen in previous research [3]. Therefore, the discrete variables from the two methods (force plate and accelerometer) were compared using Pearson correlations, and the value of the correlations were compared among the sensor locations to identify the optimal location.

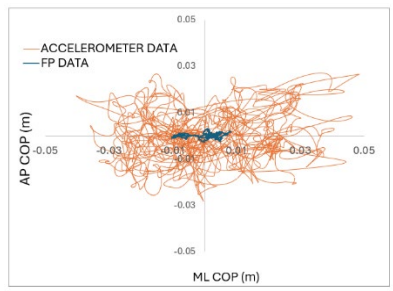


**Figure 2:** Center of pressure path over time for a single accelerometer and the force plate

**Results & Discussion:** To date, data have been collected from three subjects. The results show that the correlations were highest for the head overall ($R_{average} = 0.78$), and lowest for the sternum ($R_{average} = 0.59$, Fig. 3). It is interesting to note that the correlations in the ML direction tended to be lower and less consistent than those in the AP direction. It is important to point out that this study was conducted in a highly controlled environment where the subjects were instructed to maintain a neutral head and spine position for the duration of data collection. Given that the head is most likely to move with outside distractions, it is possible that the next-highest correlation (left shin) could be the best accelerometer to predict a person's COP. However, these results are preliminary and include data for only three participants. It is likely that the findings will be strengthened with the planned inclusion of more participants.

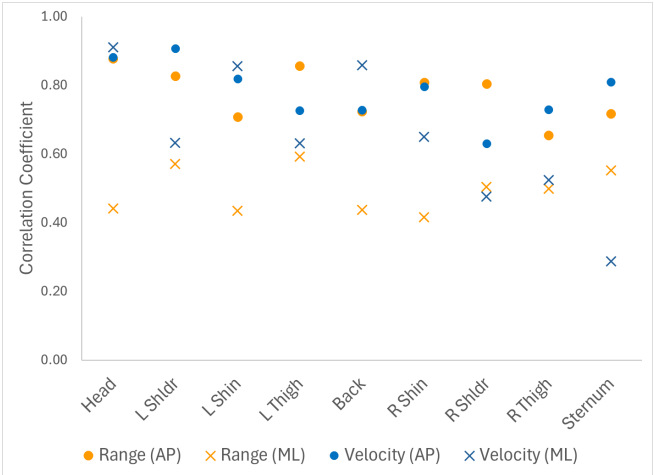


**Figure 3:** Correlation coefficients for each accelerometer, highest to lowest average correlation from left to right

**Significance:** The use of a single inexpensive accelerometer, in lieu of a force plate, to characterize postural control could improve injury tracking in athletic and military populations. While the current conclusions are limited, it appears that there are several locations on the body that could serve as a single attachment point for an accelerometer to estimate COP-derived metrics to characterize postural control.

**References:** [1] Appeadu et al. (2023), StatPearls ; [2] Foulger et al. (2025), PLOS One ; [3] Mayagoitia et al. (2002), Gait & Posture

# MECHANISMS OF MOTOR SEGMENTATION IN PARKINSON'S DISEASE

*Rebecca J. Daniels, Christopher A. Knight
Kinesiology and Applied Physiology, University of Delaware, Newark DE
*Corresponding author's email: rdaniels@udel.edu

**Introduction:** In people with Parkinson's disease (PwPD), the surface electromyogram (EMG) recorded during rapid contractions provides information about the disease state that is distinct from normal aging [1,2]. More EMG bursts are required to complete a rapid contraction and the initial EMG amplitude and duration are reduced [1,2,3]. Such EMG characteristics have been used to assess the mechanisms of Parkinson's disease (PD) symptoms [1], the effects of medication [2] or exercise treatment [3], and distinguish PwPD from healthy adults [1,2]. Though informative, EMG is more complex than the recording of isometric muscle force, due to the need for additional instrumentation, expertise, and time. Meanwhile, PD-related abnormalities in isometric force production include prolonged contraction times, reduced rates of force development (RFD) and a greater number of zero crossings in the second derivative of force (motor segmentation) [4]. These dependent measures are reliable in PwPD [4] and faster and easier to obtain than EMG-based measures, making isometric force recordings a practical, less costly, and informative method to test for disease-specific impairments in the field or clinical environments. However, less is known about the direct relationships between EMG burst measures and those that quantify motor segmentation. Therefore, our purpose was to quantify relationships between EMG and force measures obtained during rapid isometric contractions. We hypothesized that there would be significant relationships between EMG and force measures because disruptions in neuromuscular excitation are the mechanistic basis for the disruptions in motor output.

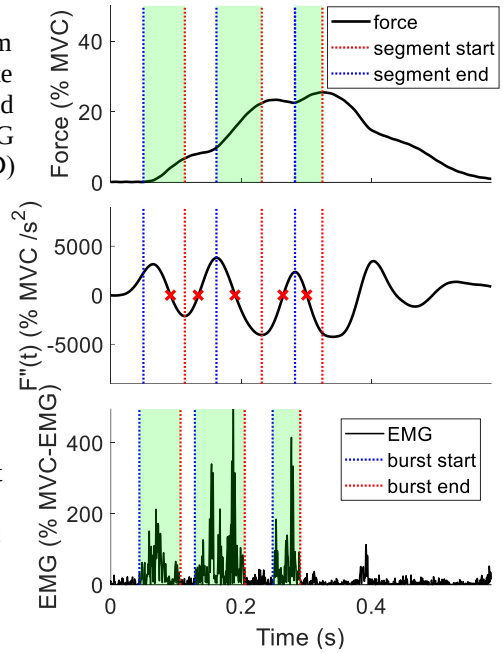


**Figure 1:** Segment durations were calculated from peaks and troughs between zero crossings in the second derivative of force (middle panel) for each force pulse (top panel) while burst durations were calculated for each EMG burst (bottom panel) prior to peak force.

**Methods:** Thirteen PwPD (aged 70.0±5.7 years, diagnosed 6.0±4.5 years, Hoehn and Yahr stage=2.0±0.7) produced rapid isometric finger abduction force pulses to 40% of their maximal voluntary contraction (MVC) force while bipolar EMG was measured from the first dorsal interosseous. EMG was demeaned, bandpass filtered between 10-500 Hz using a 4$^{th}$ order Butterworth filter and rectified. EMG was normalized to the root mean square amplitude computed over a 0.5s window prior to peak force during the MVC. EMG bursts were defined as EMG that remained above 10% MVC-EMG for at least 10 ms. Dependent measures included the first burst duration, amplitude, and integral, the duration of the first silent period between the first two bursts, and the number of bursts prior to peak RFD, peak force, and force relaxation while accounting for electromechanical delay. Force onset and relaxation were determined by a +/- 20% MVC/s RFD threshold and confirmed by a trained investigator. The first and second time-derivatives of force were calculated using a moving slope function with an overlapping 50 ms window. The number of force segments were calculated according to Howard et al [4] between force onset and peak force (Fig. 1). Additional dependent measures from force recordings included the duration of the first segment and the first plateau region between segments, peak RFD within the first segment, and the number of zero crossings in RFD. Pearson and Spearman correlations were used to quantify relationships between median force and EMG variables for normally distributed and non-normally distributed data, respectively.

**Results & Discussion:** Peak RFD during the first segment was significantly related to amplitude ($r=0.65$, $p=0.017$), duration ($r=0.59$, $p=0.033$), and the integral ($\rho=0.59$, $p=0.049$) of the first EMG burst. The first segment duration related to the first EMG burst duration ($r=0.59$, $p=0.033$) and the first force plateau duration related to the first EMG silent period ($\rho=0.72$, $p=0.009$). The number of bursts to peak force related to the number of force segments up to peak force ($\rho=0.78$ $p=0.002$). The number of zero crossings in the first derivative of force related to the number of EMG bursts ($\rho=0.92$, $p<0.001$). The number of EMG bursts prior to peak RFD related to peak RFD ($\rho=-0.67$, $p=0.013$). Relationships between EMG and force measures were moderate to strong, with the strongest relationships occurring between the number of segments and the number of EMG bursts across different force landmarks.

**Significance:** Dependent measures from rapid isometric force recordings in PwPD are reliable, easy to obtain, and distinguish PwPD from healthy aging [4]. The present findings demonstrate that these measures also have moderate to strong relationships with disease-related abnormalities in EMG. These factors support the force-based measures of motor segmentation as being linked to specific physiological mechanisms. Furthermore, that these measures are non-invasive, inexpensive, reliable, sensitive, quantifiable and objective, suggests that they may address a need in clinical research while other biomarkers are developed.

**Acknowledgments:** This research was funded by Shake It Off Inc., West Chester, PA, Delaware Curative Workshop Inc., Greenville, DE, and the University of Delaware Graduate College through the Doctoral Fellowship for Excellence.

**References:** [1] Hallett & Khoshbin. (1980), *Brain* 103(2); [2] Vaillancourt et al. (2006), *Mov Disord* 21(1); [3] David et al. (2016), *J Neurophysiol* 116 (5). [4] Howard et al. (2022), *Exp Brain Res* 240(7-8).

# INFLUENCE OF BODYWEIGHT SUPPORT ON MOTOR CONTROL IN CHILDREN WITH CEREBRAL PALSY

*Allyson K. Clarke[1], Andrew Ries[2], J Maxwell Donelan[3], Michael H. Schwartz[2], Katherine M. Steele[1]
[1]Department of Mechanical Engineering, University of Washington, Seattle, WA
[2]James R. Gage Center for Gait & Motion Analysis, Gillette Children's, St. Paul, MN
[3]Department of Biomedical Physiology and Kinesiology, Simon Fraser University, Burnaby, British Columbia, Canada
*Corresponding author's email: akc02@uw.edu

**Introduction:** Children with cerebral palsy (CP) have greater co-contraction and recruit fewer synergies during dynamic tasks, which has often been interpreted as a sign of simplified motor control [1, 2]. Prior research has hypothesized that this simplified control is the result of altered supraspinal input, but biomechanical constraints can also alter motor control. For example, flexion-extension synergies are common in hemiparetic stroke survivors and limit reaching, but their impacts can be reduced if the arm is supported, reducing deltoid activation [3]. For individuals with CP, a resistive ankle exoskeleton increased synergy complexity, suggesting motor control may be altered with devices that provide assistance or support [4]. While prior studies suggest that synergies during gait remain relatively stable in CP after treatment, whether biomechanical constraints like bodyweight support (BWS) alter motor control remains unknown [5]. The purpose of this study was to investigate how muscle activity and synergies change with bodyweight support during gait for children with CP and non-disabled (ND) peers.

**Methods:** We recruited 15 children with CP (ages 8-17, 12M, 3F) and 9 ND peers (ages 9-16, 5M, 4F) for motion analysis at Gillette Children's (St Paul, MN). Electromyography (EMG) sensors were placed bilaterally on the gastrocnemius (GAS), soleus (SOL), anterior tibialis (AT), medial hamstring (MH) vastus lateralis (VL), gluteus medius (GMED), and gluteus maximus (GMAX). Participants completed 5-minute walking trials on an instrumented treadmill at a fixed speed, while constant vertical support was applied to the pelvis at four levels of bodyweight support (1, 20, 40, 60% bodyweight) by a mechatronic system (Humotech). Order of support was randomized. EMG data were filtered, rectified, and normalized to the 95th percentile of maximum excitation across all trials for each participant. A low pass filter was used to obtain a linear envelope of the EMG signal. To measure changes in activations for each muscle, area under the curve (AUC) was averaged across all gait cycles. Percent AUC change was calculated as the relative difference between baseline (1% BWS) and each experimental condition (20, 40, 60% BWS). Nonnegative matrix factorization (NNMF) was used to calculate synergies (W) and their activations (C) such that $muscle\ activations = W * C + error$ [2, 5]. The total variance accounted for by $n$ synergies (tVAFn) is inversely related to muscle synergy complexity, such that a larger tVAFn indicates reduced motor control complexity. The tVAFn was calculated by comparing the reconstructed muscle activations from NNMF to the EMG data. An ANOVA was used to evaluate differences between support levels, with a Holm-Šídák test to correct for multiple comparisons.

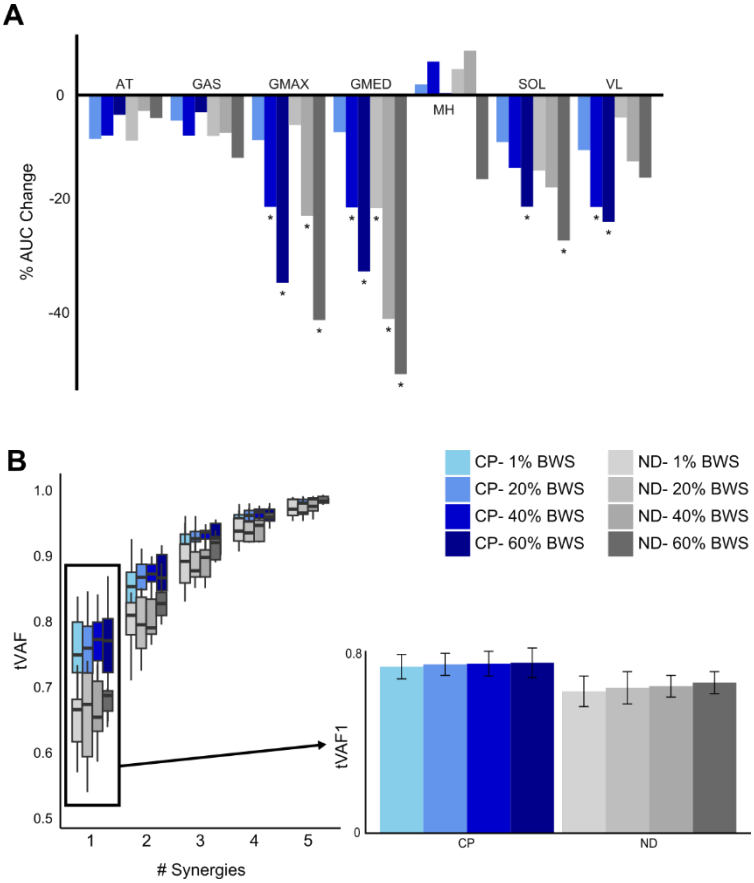


**Figure 1. A)** Changes in muscle activations for CP and ND participants walking with added support (20, 40, 60% bodyweight) compared to baseline (1% bodyweight). * indicates muscles and support levels with significant differences from baseline ($p < 0.05$). **B)** Total variance accounted for by n synergies, with n ranging from 1-5. Error bars represent ± one standard deviation.

**Results & Discussion:** As bodyweight support increased, participants decreased GMED, GMAX, SOL, and VL activity (Figure 1A). No significant changes were observed in the GAS, AT, or MH activity. Bodyweight support did not impact tVAFn for either group. Across all levels of support, tVAFn remained constant ($p > 0.05$, Figure 1B). Consistent with prior studies, average $tVAF_1$ for the CP group was higher than ND peers, indicating a simplified control strategy (CP $tVAF_1$: $0.76 \pm 0.06$, ND $tVAF_1$: $0.66 \pm 0.06$, $p = 0.006$) [2, 5]. Despite reduced activity of key support muscles like the GMAX and VL, our results show that bodyweight support did not impact synergies for children with CP.

**Significance:** Changes in muscle activity and synergies with altered biomechanical constraints can help us understand how common assistive technology may influence motor control in individuals with CP. The results of this study suggest that altered bodyweight support does not change motor control complexity for individuals with CP, despite significant changes in key support muscles. Thus, interventions like gait training or exoskeletons that reduce the load on supportive muscle groups may not alter motor control in CP.

**Acknowledgments:** This work was supported by R21HD104112 and R01NS091056.

**References:** [1] Bekius et al. (2020), *Front Physiol* 11(632); [2] Steele et al. (2015), *Dev Med Child Neurol* 57(12); [3] Dewald et al. (2001) *Top Stroke Rehabil* 8(1); [4] Conner et al. (2021) *J Biomech* 126(110601); [5] Shuman et al. (2019) *J Neuroeng Rehabil* 16(1)

# MECHANISMS OF SPLIT BELT TREADMILL ADAPTATION IN CHILDREN WITH CEREBRAL PALSY

*Mackenzie N. Pitts[1], Alyssa Spomer[2], Andrew Ries[2,3], Michael H. Schwartz[2,3], Katherine M. Steele[1]
[1]Department of Mechanical Engineering, University of Washington, Seattle, WA
[2]Center for Gait & Motion Analysis, Gillette Children's, St. Paul, MN
[3]Department of Orthopedic Surgery, University of Minnesota, Minneapolis, MN
*Corresponding author's email: mnp0020@uw.edu

**Introduction:** Children with cerebral palsy (CP) experience motor impairments that impact walking and often undergo rehabilitation to induce changes in walking function [1]. Split belt treadmill locomotion – in which gait asymmetry is induced by driving treadmill belts at different speeds – provides a method to analyze how an individual adapts their gait in response to repeated perturbation and may serve as a viable rehabilitation in CP [2]. Similar to other populations with motor impairments, children with CP are able to increase their step length on the fast belt to achieve step length symmetry [3]. However, there are many ways to adapt to fast belt perturbations: an individual may increase hip and knee extension, or ankle power [4]. The strategy chosen by an individual may reflect their gait pattern, motor control, or other factors. Understanding the mechanics by which individuals modulate their step length is valuable for evaluating gait adaptation in CP and optimizing split belt treadmill training as a therapeutic intervention. The purpose of this study was to quantify lower limb kinematics and kinetics in children with CP relative to typically developing (TD) peers during split belt treadmill walking.

**Methods:** Six children with diplegic CP (age: 9-13 years; GMFCS: I-II) and four TD children (9-14 years) completed a split belt treadmill protocol which included the following: one minute each at self-selected, fast, and self-selected tied belt speeds; six minutes of split belt walking; and a two-minute washout. TD participants' nondominant limb and CP participants' more affected limb was subjected to the fast belt, which operated at a speed of 1.65-1.8 times the self-selected speed (slow belt). Lower limb kinematics (modified Vicon Plug-In Gait marker set; 120 Hz) and kinetics (Bertec; 2160 Hz) were collected continuously during walking. Marker trajectories were used to derive hip, knee, and ankle angles and powers using the Plug-In Gait pipeline with functional hip and knee axes, then segmented by stride. Step length, peak hip extension, peak knee extension, and peak ankle power were computed for each cycle on the fast belt limb. The change in each variable from early to late adaptation was calculated as the difference between the average value across the first 20 cycles and the last 20 cycles of split belt walking, respectively.

**Results & Discussion:** Both cohorts increased step length on the fast belt (Figure 1A), however, they appeared to use different strategies to achieve this goal. Step length increased by an average of 4.3 [Range: -1.3, 11.5] cm for CP and 5.4 [2.4, 8.8] cm for TD. TD peers increased ankle power by 0.59 [0.32, 1.07] W/kg, whereas CP individuals did not adjust peak ankle power (Figure 1B); the latter aligns with prior observations in transtibial amputees [5]. Interestingly, the CP group increased both hip extension (2.9° [-1.2, 9.2°]) and knee extension (1.4° [-0.8, 5.4°], while the TD group only increased knee extension (2.1° [0.2, 5.5°]). This suggests that individuals with limited plantarflexion strength, as is common in CP, rely on more proximal strategies to modulate step length. Increased extension in both joints contrast previous findings of children with CP undergoing a 6-minute tied belt paradigm [6], indicating that a split belt protocol may be more useful for extending joints.

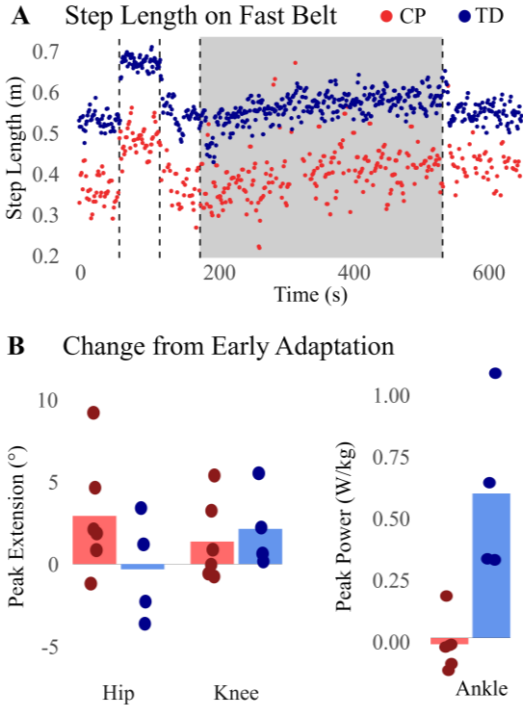


**Figure 1:** (**A**) Step length per cycle across the training protocol on the fast belt for representative CP (red) and TD (blue) subjects. Vertical lines indicate changes in belt speed, and the shaded region shows the split belt period. (**B**) Change from early to late adaptation in peak hip extension, peak knee extension, and peak ankle power. Points show individual participants, and bars represent the average change across each population.

**Significance:** Split belt treadmill adaptation induces changes in step length in children with CP, and repeated exposure to a split belt paradigm supports motor learning [3]. Our results show that children with CP adapt their step length using strategies different from TD peers. Since gait patterns largely contribute to metabolic power [7], our findings indicate a need to target specific biomechanical measures to optimize gait training during split belt walking. Specifically, modulating ankle power is more efficient than the hip [8], so addressing the discrepancy in peak ankle power produced between groups may ensure gait training is metabolically efficient for children with CP.

**Acknowledgments:** Funding for this research was provided by R01NS091056. We also thank Jennifer Nelson, Rocio Riveros-Charry, Mahamed Abdulahi, and Marissa Esterley for their assistance in collecting data.

**References:** [1] Booth et al. (2018), *Dev Med Child Neurol* 60(9); [2] Roemmich et al. (2019), *Neurorehabil Neural Repair* 33(8); [3] Mawase et al. (2016), *Front. Hum. Neurosci.* 10; [4] Fukuchi et al. (2019), *Syst. Rev. 8(1)*; [5] Selgrade et al. (2017), *J. Biomech.* 53; [6] Parent et al. (2016), *Clin. Biomech.* 34; [7] Gill (2023), *PLoS ONE* 18(5); [8] Kuo (2002), *J Biomech. Eng.* 124(1).

# KINEMATIC AND SPATIOTEMPORAL PARAMETERS OF INFANTS WITH DOWN SYNDROME AFTER TREADMILL TRAINING

*Alexandre dos Santos Kotarski[1], Matthew Beerse[2], Robert Zeid[1], Amy Talboy[3], Seyda Oscaliskan[1], Jianhua Wu[1]
[1]Georgia State University, Atlanta, GA, USA; [2]University of Dayton, Dayton, OH, USA; [3]Emory University, Atlanta, GA, USA.
*Corresponding author's email: adossantoskotarski1@student.gsu.edu

**Introduction:** Down syndrome (DS) is a genetic disorder associated with several brain deficits and delayed psychomotor development [1]. Infants with DS generally take twice the time to achieve independent walking and even a longer time to develop walking skills compared to typically developing (TD) infants. Early motor intervention has shown to advance walking onset in both TD infants and those with DS and enhance their developmental and educational gains [2]. Early treadmill training appears to be an effective method to advance walking onset and improve gait pattern in infants with DS [3, 4]. While these results are promising, the progression of stepping pattern, particularly the biomechanics of bodyweight-supported stepping, is unknown over the course of the training. This study aimed to register the developmental profile of treadmill stepping in infants with DS during the bodyweight-supported treadmill training. We hypothesized that infants with DS will improve joint kinematics such as peak hip, knee and ankle flexion/extension angles and joint angular velocities as well as spatiotemporal variables (such as step length, and stance and swing time).

**Methods:** Preliminary results included 13 infants with DS (9M/4F, 11.2±2.5 months at entry into the study). A pediatric treadmill was provided to the infant, and the parents were instructed to conduct the training at their home for 8 min/day, 5 days/week, with a belt speed of 0.1 m/s initially and increasing it gradually to 0.25 m/s at an incremental of 0.05 m/s when the infant could take 30 or more steps at the current speed. We visited each infant once a month to collect the treadmill stepping data. A Noraxon® Ninox 125 camera was used to record a 3-minute trial from the infant's right side. Reflective markers were placed on the right hip (greater trochanter), knee, ankle, and foot (the 2$^{nd}$ metatarsal head). The Noraxon MyoResearch-3 software was used to process the video data. Here we report results from three timepoints, T1 (the first visit), T3 (the last visit before the infant's walking onset), and T2 (roughly the midpoint between T1 and T3). Peak joint flexion/extension angles and spatiotemporal variables were calculated using a custom MATLAB® program. A one-way (Time) repeated measures ANOVA was conducted using RStudio software. A significance level was set at alpha=0.05.

**Results & Discussion:** While peak hip flexion and extension angles did not change substantially from T1 to T3, peak knee and ankle angles showed an upward trend (Table 1). Peak knee flexion increased from 38.91° at T1 to 46.71° at T3. Peak knee extension reduced from -2.61° at T1 to -0.52° at T3. Peak ankle dorsiflexion decreased from 20.40° at T1 to 13.40° at T3. Peak ankle plantarflexion decreased from 35.41° at T1 to 28.75° at T3. Average hip angular velocity increased from 38.37°/s at T1 to 52.13°/s at T3 ($p$ = 0.001). Average knee angular velocity increased from 48.82°/s at T1 to 55.77°/s at T2 and then to 73.47°/s at T3 ($p<0.01$). Average ankle angular velocity increased from 58.18 °/s at T1 to 62.98 at T3. In addition, stance time decreased from 1.60 seconds at T1 to 1.19 seconds at T3 (p=0.01). Swing time decreased from 0.81 seconds at T1 to 0.70 seconds at T2, and then to 0.52 seconds at T3 (p=0.01). Step length increased from 139.40 mm at T1 to 168.11 mm at T2 and 167.39 mm at T3.

These results demonstrate that early treadmill intervention produced positive changes in the kinematic and spatiotemporal variables of treadmill stepping in infants with DS, by demonstrating a longer step length, a reduced stance and swing time, and a higher joint angular velocity over the course of the treadmill training. This enabled the infant to learn to use their ankle plantarflexion more efficiently during the push-off and ankle dorsiflexion during the swing phases. The enhanced stepping pattern helped increase stepping frequency and consequently the total volume of stepping practice. Improvements in spatial parameters are closely linked to changes in lower-limb kinematics [5], thus, indicating a dynamic interaction between movement kinematics and spatiotemporal gait characteristics as infants adapt to treadmill training. Early treadmill intervention may help improve trunk and leg muscle strength, increase joint range of motion, and facilitate the development of postural control, which may contribute to advanced walking onset and better walking patterns.

Table 1: Mean of the kinematic variables.

| *Visit* | *Peak Hip Flexion (°)* | *Peak Hip Extension (°)* | *Peak Knee Flexion (°)* | *Peak Knee Extension (°)* | *Peak Ankle Dorsiflexion (°)* | *Peak Ankle Plantarflexion (°)* |
|---|---|---|---|---|---|---|
| *T1* | 22.22 | -16.47 | 38.91 | -2.61 | 20.40 | -35.41 |
| *T2* | 22.21 | -17.62 | 41.33 | 0.63 | 17.00 | -31.03 |
| *T3* | 23.70 | -16.52 | 46.71 | -0.52 | 13.40 | -28.75 |

**Significance:** Understanding the biomechanical mechanisms of early intervention in infants with DS is crucial for improving the design of the treadmill intervention and enhancing motor skills and development in this population. Treadmill training has shown to be effective in eliciting bodyweight-supported alternating stepping and learning to regulate the spatiotemporal and kinematic patterns of stepping in infants with DS over the course of training. These results support the addition of early treadmill training in rehabilitation protocols for infants with DS and provide an opportunity for clinicians and researchers in the field to expand their rehabilitation tools while working with this population. Follow-up studies are warranted to test these predictions and provide further evidence on the effectiveness of treadmill intervention in infants with DS.

**Acknowledgments:** We thank NIH (R21HD105879) for funding and all the participants and their parents for their participation.

**References:** Malak R, et al (2015), *Med Sci Monit*, 21; [2] Ulrich B, et al (1995), *Phys Ther,* 75(1); [3] Ulrich D, et al (2008), *Phys Ther,* 88(1); [4] Wu J, et al (2007), *Dev Med Child Neurol*, 49(11); Campos D et al (2022), *Gait Posture*, 96.

# THE IMPACT OF NEUROMOTOR CONTROL DIFFERENCES ON UPPER LIMB BIOMECHANICS IN INDIVIDUALS WITH RHEUMATOID ARTHRITIS

Kaitlyn A. Wojciechowski[1], Yousef H. Qadumi[1], Nikole Galman[1], Madison Weeks[1], Julianna Ethridge[1], Georgia Parnell[1], * Dr. Nicholas P. Murray[1]
[1]Department of Kinesiology, East Carolina University, Greenville, NC, USA
*Corresponding author's email: murrayni@ecu.edu

**Introduction:** Rheumatoid arthritis (RA) is an autoimmune disorder, leading to chronic systemic inflammation of the synovial joints [1]. RA is the most common inflammatory joint disease, affecting 0.1 - 2.0% of the population worldwide, and is 3x more common in women than men [2,3,4]. As a systemic disease, RA presents pain, stiffness, and swelling of the joints, among other symptoms, which can lead to permanent joint damage, limited range of motion (ROM), chronic pain, cognitive deficits, and depression, all of which greatly reduce quality of life (QOL) and increase mortality [3]. Rheumatoid arthritis can affect any joint in the body; however, it is most prevalent in the upper extremities, specifically, the small, distal joints of the hands [5,6]. This disparity results in a decline in hand and pinch grip strength, endurance, and dexterity [4,5], all of which are essential for upper extremity functioning [4]. In addition to physical deficits, the prevalence of cognitive dysfunction in RA has been well documented with a prevalence rate between 30-70% [8]. For those suffering with RA, loss of physical function paired with an increase in cognitive dysfunction greatly impacts their ability to perform activities of daily living and maintain functional independence. Currently, much of the research on RA focuses on treating the disease pharmacologically or by using assistive devices to compensate for decreased hand dexterity. By developing an understanding of how individuals with RA approach activities of daily living (ADLs) both physically and cognitively, we may better tailor therapeutic treatments to their conditions, preventing further joint damage, reducing cognitive fatigue, and improving their quality of life. Therefore, the purpose of this study was to quantify both changes in movement patterns caused by RA as well as changes in cognitive burden.

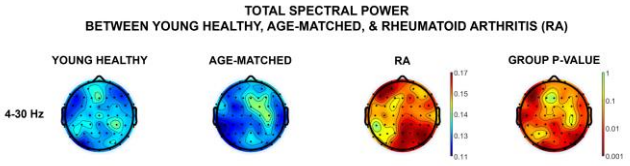


**Methods:** Ten healthy young adults with a mean age of 20.9 years, ten individuals with RA with a mean age of 61.82 years, and 10 healthy, age-matched controls with a mean age of 58.83 years were recruited for this study. Participants were fitted with a 64-electrode Neuroscan EEG cap, which was used to analyze neuromotor processes and cognitive workload during two marble tasks: large marble movement and small marble movement. Participants were also outfitted with twenty-five motion capture pearl markers. All participants completed eight trials each (four using either hand) of two tasks manipulating fifteen marbles with tweezers. A Biopac pressure transducer was used to mark the start and end of each trial. Using tweezers, participants reached across their body, selecting one marble (either large or small depending on condition) from the cup, and then transporting it to the empty cup above their resting hand. Vicon Nexus software was used to capture shoulder and elbow joint displacement using Vicon's Upper Limb Model. Visual 3D was used to calculate the participant's shoulder and elbow joint angle displacement. EEG data was processed and analyzed using EEGLAB. To test the hypotheses, we completed a 3 (Group) x 2 (Marble) x 2 (Arm) RMANOVA.

**Results**: More than 50% of the individuals in the RA group reported a lack of participation in ADLs such as feeding, grooming, and dressing due to moderate to severe upper extremity pain daily. Overall, findings demonstrated significant differences in mean event-related changes in spectral power within the beta frequency band (12-30 Hz) between young adults, aged-matched controls, and RA groups, especially for Beta band frequency within the frontal and posterior parietal regions ($p < 0.01$). Follow-up revealed significant differences between RA patients and young adults and age-matched controls ($p < 0.05$) representing increased neural activity across all spectral power bands. There was no significant main effect due to marble size (small marble vs. large marble) in spectral power, however, significant main effects of marble size were observed on both elbow and shoulder displacement ($p < 0.05$).

**Discussion**: Our findings suggest that individuals with RA demonstrate significantly more cognitive burden than both young, healthy individuals and similarly aged individuals when completing a hand dexterity task, potentially altering upper limb biomechanics. While all groups yielded higher displacement when doing the small marble task in comparison to the large marble task, our findings insinuate that individuals with RA apply more cognitive effort to achieve an equal outcome. Future research should further investigate the relationship between cognitive load and altered upper limb movement patterns in individuals with RA.

**Significance**: Understanding the relationship between physical functioning and cognitive burden in individuals with RA may prove useful in guiding therapeutic treatments.

**References: [1]** Gue et al. (2018), *Bone research* 6(15); [2] Almutairi et al. (2021), *Rheumatology international* 41(5); [3] Gikaro et al. (2022), *BMC Musculoskeletal Disorders* 23(1); [4] Freeman (2018, October 27), *Rheumatoid Arthritis;* [5] Gur Kabul et al. (2022*), International Journal of Rheumatic Diseases* 25*;* [6] Freeman (2018, October), *Rheumatoid Arthritis;* [7] Said et al. (2019), *Immunopharmacology and Immunotoxicology* 41(6)

# A Comparison of Different Surgical Approaches for Anterior Distal Femoral Hemiepiphysiodesis on Sagittal Knee Kinematics

*Jessica L. Stockhausen, MS[1,2]; Kellen T. Krajewski, PhD[1,2]; Amanda L. Vinson, MS[3]; Lucas Moore, MS[3]; Scott Miller, MS[2]; James J. Carollo, PhD, PE[2,3]; Mariano Garay, MD[2]; Radomir Dimovski, MD[2]; Jason Rhodes, MD[1,2,3]; Sayan De, MD[1,2,3]

[1]Department of Orthopedics, University of Colorado School of Medicine, Aurora, CO
[2]Musculoskeletal Research Center, Department of Orthopedics, Children's Hospital Colorado, Aurora, CO
[3]Center for Gait and Movement Analysis (CGMA), Children's Hospital Colorado, Aurora, CO
*Corresponding author's email: Jessica.Stockhausen@cuanschutz.edu

**Introduction:** Knee flexion contractures (KFC) are prevalent in children with cerebral palsy, which results in limited knee extension during gait impairing the ability to ambulate independently. Anterior Distal Femoral Hemiepiphysiodesis (ADFH) surgery is an effective corrective procedure[1]. ADFH entails inserting two screws through the anterior third of the distal femoral physis, typically inserted superior to the physis (antegrade), however, the screws must transect muscle, tissue and circumnavigate major blood vessels, impeding insertion parallel to the long axis of the femur. Our surgeons have developed a novel technique approaching inferior to the physis (retrograde) with limited tissue transection and a 'flatter' surface for screw insertion[2]. It is unknown how retrograde ADFH impacts sagittal knee kinematics during stance phase of gait. Therefore, the purpose was to compare ADFH approaches by examining knee kinematics in the sagittal plane during stance phase pre- and post-surgery.

**Methods:** Eleven patients (19 knees) who underwent ADFH (5 antegrade, 8 knees; 6 retrograde, 11 knees) had a gait analysis preoperatively and 4 months to 4 years post-operation. Kinematic and kinetic data was collected via 13 infrared cameras (Vicon, Oxford, UK) sampling at 120 Hz and 10 force plates (Bertec, OH, USA) sampling at 2160 Hz; utilizing a modified Helen-Hayes marker-set consistent with the conventional gait model. Sagittal knee angles at heel-strike (HS), mid-stance (MS), toe-off (TO), and peak knee extension were extracted for all steps of the surgically repaired knee. Time to peak knee extension was obtained and calculated as a percentage of stance phase. Sagittal knee excursion was calculated for stance phase to represent that active range of motion (ROM). To examine the effects of time and surgical approach a mixed factor 2x2 RMANOVA was conducted separately for each discrete knee angle, time to peak knee extension, and knee excursion. Alpha set to $p \leq 0.05$.

**Results & Discussion:** See Table 1. for sagittal knee kinematics. A main effect of time was observed for HS ($p=0.025$), MS ($p=0.012$), peak knee extension ($p=0.004$), and knee excursion ($p=0.003$) with all increasing knee extension and ROM from pre- to post-surgery. Differences were found between approach for knee excursion ($p<0.001$); however, this difference was observed at pre ADFH and both approaches increased (13.0° for antegrade and 7.8° for retrograde). Additionally, there were no effects of time or approach on TO or time to peak knee extension. Increases in sagittal knee angles at HS and MS, peak knee extension and knee excursion during walking demonstrate there is a similar improvement in functional outcomes for both insertion approaches. Future research should examine gait following retrograde ADFH with a larger, adequately powered sample to confirm results observed here. Additionally, long-term (i.e., ≥5 years) gait analyses should be conducted to determine if improvements in gait are sustained as the individual grows.

| Approach | Time | HS (°)* | MS (°)* | TO (°) | Peak Extension (°)* | Excursion (°) | Time to Peak (%) |
|---|---|---|---|---|---|---|---|
| Antegrade (n=8) | Pre | 41.9 ± 12.7 | 42.5 ± 12.6 | 56.5 ± 12.4 | 39.3 ± 11.6 | 49.0 ± 17.0 | 39.6 ± 34.2 |
| | Post | 29.0 ± 6.75 | 31.2 ± 6.56 | 45.0 ± 14.9 | 23.7 ± 6.85 | 62 ± 29.8 | 42.4 ± 37.0 |
| Retrograde (n=11) | Pre | 42.2 ± 9.91 | 35.4 ± 7.85 | 45.7 ± 14.3 | 33.9 ± 8.33 | 19.9 ± 6.0 | 54.5 ± 18.5 |
| | Post | 42.6 ± 13.5 | 38.4 ± 15.6 | 48.4 ± 6.07 | 31.2 ± 15.9 | 27.7 ± 10.1 | 52.4 ± 12.1 |

**Table 1. Sagittal Knee Outcomes.** *= *a main effect of time ($p<0.05$). Differences were found between surgical approach for knee excursion*.

**Significance:** Both approaches increased sagittal knee angles at HS and MS, knee excursion, and peak knee extension angles, demonstrating that retrograde improves sagittal knee kinematics similar to the established antegrade approach. An increase of knee extension angle at mid-stance could make it easier for the patient to advance the contralateral limb, thereby reducing hip/pelvis compensation and increasing stride length. Increases in knee extension could assist in changing from a "crouch gait" type pattern, characterized by continuous hip flexion and knee flexion throughout the gait cycle, to a more upright gait pattern, decreasing metabolic demand of walking when the patient is able to passively support themselves with greater knee extension.

**References:**

1. Al Badi, H., et al., *Distal Femur Anterior Hemiepiphysiodesis for Fixed Knee Flexion Deformity in Neuromuscular Patients: A Systematic Review.* JBJS Rev, 2023. **11**(6).
2. Krajewski, K.T., et al., *Retrograde Insertion Approach for Anterior Distal Femoral Hemiepiphysiodesis Procedure: A Case Report.* JBJS Case Connect, 2024. **14**(3).

# AQUATIC TREADMILL DECREASES LOWER-LIMB JOINT COORDINATION VARIABILITY OF CEREBRAL PALSY AND TYPICALLY DEVELOPING CHILDREN

*Oluwaseye P. Odanye[1], Joseph W. Harrington[1], David C. Kingston[1], Brian A. Knarr[1]
[1]Department of Biomechanics, University of Nebraska at Omaha, NE, USA
*Corresponding author's email: oodanye@unomaha.edu

**Introduction:** Cerebral palsy (CP) is a non-progressive motor impairment that causes posture and movement disorders that could appear as paresis of muscles, spasticity, and a lack of selective motor control [1]. These issues cause gait deviations in limb movements with inconsistent inter-joint and inter-segmental coordination [2]. Evidence exists of gait alterations that limit the community ambulating tendencies of affected children [1], making rehabilitation interventions necessary to improve walking. Aquatic treadmill (AT) walking is an intervention that improves mobility and functional gait parameters of children with CP [3]. AT utilizes the intrinsic characteristics of water to offer partial body weight support for performance of more functional activities with less exertion than in dry conditions [4]. While some studies have shown evidence of how exercise-based aquatic interventions improve the functional outcomes of children with CP [5], evidence documenting the impact of AT on walking is scarce. Continuous Relative Phase (CRP) could be used to investigate how AT walking impacts lower-limb joint coordination of children with CP in speed-varied conditions. CRP analysis has quantified the joint coordination of children with CP while they walked overground, using Mean Absolute Relative Phase (MARP) and Deviation Phase (DP) values [6]. MARP defines the in-phase/out-of-phase coupling relationships of joint pairs, so that a value of 0° means the joints are completely 'in-phase' while 180° means they are 'out-of-phase', and the DP quantifies the inter-joint coordination variability for joint pairs [6]. CRP has been used to show the kinematic strategies of CP children during daily live gait challenges, like walking on uneven surfaces [6]. In this study, CRP outcomes were compared for CP and typically developing (TD) children, while walking at different treadmill speeds in wet and dry conditions. We hypothesized that the CP group would have a more out-of-phase coordination pattern at a wet-decreased treadmill speed when compared to other conditions, as the AT has been shown to improve their walking [3].

**Methods:** Eight CP (4:4 M:F, age; 12.4 ± 3.6 yrs) and 15 TD (7:8 M:F, age; 11.3 ± 4.1 yrs) children were recruited [7]. Each participant walked on a wet and dry treadmill at fast (125%) and slow (75%) speeds relative to their predetermined normal speed for each environment. Joint angle data were collected using waterproof inertia measurement units (IMU) (Wave Track Waterproof IMU, Cometa, Milan, Italy). CRP analysis used Lamb and Stöckl's approach [8] to derive the MARP and DP of the ankle-knee (AK) and hip-knee (HK) joint pairs. Statistical analysis used a multilevel model with an analysis of variance to determine how walking speed (fast and slow), environment (wet and dry), and group (CP and TD) impacted the MARP and DP of the participants' joint pairs at the stance and swing gait phases with $\alpha = 0.05$.

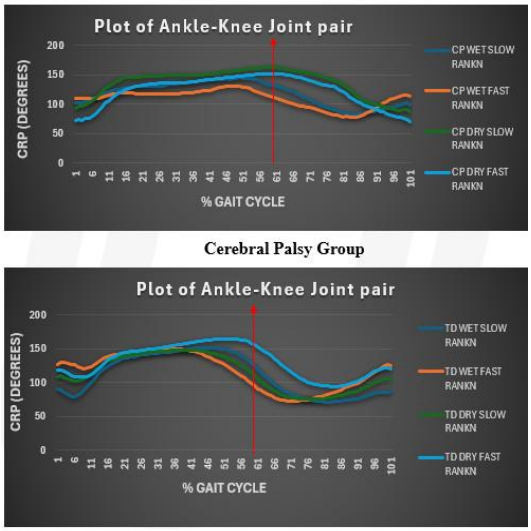


**Figure 1:** Time series of the MARP for the ankle-knee joint pair. The image shows the mean absolute relative phase of the CP and TD groups at stance and swing. The time series values are normalized to a 100% gait cycle.

**Results & Discussion:** The MARP of the AK joint pair in swing showed a fixed effect of environment ($p < 0.001$) and group ($p = 0.013$) conditions. A pairwise comparison showed that the MARP was 20.2% higher in the dry (114.6°) compared to the wet (91.5°) environment ($t$ (5.57), $p < 0.0001$) implying more in-phase coordination on the AT. In addition, MARP was 10.40% ($t$ (2.49), $p < 0.015$) higher in the CP (108.7°) compared to the TD (97.4°) group (Figure 1), suggesting CP children had more out-of-phase coordination compared to TD children, irrespective of speed and environment. For the HK joint pair, there was a fixed effect of group in stance ($p < 0.001$), with pairwise comparison showing more in-phase coordination of CP children (52.3°) compared to TD (67.3°), while the swing phase had a fixed effect of environment ($p = 0.0002$) and group ($p < 0.0001$). Pairwise comparison showed the CP (57.4°) children had more in-phase coordination than the TD (76.1°) ($p < 0.001$), and more in-phase coordination at the dry (72.0°) than the wet (61.5°) walking environment ($t$ (-6.11), $p < 0.001$). These results demonstrate that the AT may decrease gait variability in children with CP by increasing in-phase joint coordination, this is reinforced by the observed lower DP values in the wet than dry environments for the KH pair in stance ($t$ (2.41), $p = 0.018$) and in swing ($t$ (6.49), $p < 0.0001$).

**Significance:** This study demonstrates the potential of AT to reduce joint coordination variability in children with CP. We speculate that this is due to a more challenging walking environment created by the intrinsic properties of water. A less variable gait for children with CP may aid motor learning for improved walking outcomes following AT walking. For this study, shared joint segments were analyzed as joint pairs and gait events were defined using standard biomechanical gait features which are limitations that could affect the interpretations. Future work will improve understanding of the intervention for a more structured use in rehabilitation programs.

**References:** [1] Phoithitook et al. (2023), *Int J Environ Res Pub Health* 20, 1854; [2] Carollo et al. (2018), *Clin Biomech (Bristol, Avon)*, 59, 40–46; [3] Hill et al. (2015), *The FASEB J.* 29, 983.10; [4] Badawy, W.M. (2019), *Med. J. Cairo Uni.* Vol. 84, 1–8; [5] Ballaz et al. (2011), *Disability & Rehab* 33, 1616–1624; [6] Dussault-Picard et al. (2023), *Sci Rep*, 13, 21779; [7] Harrington et al. (2023), *J. of EMG and Kinesiology*, 68, 102737; [8] Rosenbaum et al. (2006), *NeoReviews*, 7, e569–e574.

# INTRODUCING NOCICEPTIVE BIOFEEDBACK: USING DISCOMFORT TO CONDITION SAFER WALKING MECHANICS

*Alex C. Dzewaltowski[1], Ryan Crews[1], Charles Layne[2], and Christopher Connaboy[1]
[1] Scholl College of Podiatric Medicine, Rosalind Franklin University of Medicine & Science, North Chicago, Illinois, USA.
2 Department of Health and Human Performance, University of Houston, Houston Texas, USA
*Corresponding author's email: alex.dzewaltowski@rosalindfranklin.edu

**Introduction:** Patients with diabetic peripheral neuropathy (DPN) regularly develop diabetic foot ulcers (DFU) or wounds on the plantar surface. Patients adopt an irregular walking strategy due to the neuropathic loss of peripheral sensation. The irregular walking leads to increased mechanical stresses serving as primary rationale for the development of DFUs. Patients are provided off-loading therapeutic footwear to reduce these mechanical stresses which effectively reduce risk for ulceration. However, patient adherence to their footwear is poor, with rates as low as 28%[1]. When not worn, off-loading therapeutic footwear is immediately ineffective defining a need for strategies that continue to mitigate ulceration risk in the absence of adherence.

Patients with DPN have lost their protective pain sensation, regularly referred to as the "gift of pain"[1]. The loss of pain sensation is ultimately a root cause for developing a DFU. Therefore, to prevent DFU development, it may be beneficial replace the lost sensation and provide discomfort during walking. Here, we provided low-level discomfort in the form of electrical stimulation when participants stepped with elevated plantar pressure (i.e., nociceptive biofeedback). Biofeedback has been shown to change movement behavior in a variety of patient populations[2]. Moreover, nociceptive sensation, by evolutionary imperative, directionally motivates short-term and long-term behavior away from harm[3]. Therefore, nociceptive biofeedback may present a strong potential to persistently modify movement behavior, especially, for patients with DPN who have a lack of protective pain sensation. To evaluate the efficacy of nociceptive biofeedback, we compared its effectiveness to innocuous (e.g., vibration) biofeedback during a single session walking protocol in four healthy, young adults. We hypothesized that nociceptive biofeedback will lead to greater, more rapid reductions in peak zonal plantar pressure than innocuous biofeedback.

**Methods:** Participants walked on a treadmill for 5min as a baseline, 5min with innocuous biofeedback tied to heel pressure, 5min with nociceptive biofeedback tied to forefoot pressure, 5min with innocuous biofeedback tied to heel pressure, and 5min with nociceptive biofeedback tied to forefoot pressure. Treadmill speed was set to 1.25ms$^{-1}$. A stimulator unit capable of applying a vibratory stimulus or an uncomfortable electrical stimulus was placed on each upper shank. The level of discomfort from nociceptive biofeedback was set to a level that corresponded to a participant Visual Analog Scale score of 1 or 2 prior to the treadmill walking protocol.

The threshold triggering feedback was set to the mean peak zonal pressure (heel or forefoot) from the last two-minutes of baseline walking. A stimulus was provided immediately following every set of three steps completed by the same leg which had a mean pressure above the participant's baseline threshold. Pressure measurements were recorded using Pedar-X insoles (Novel, Munich, Germany) at 100Hz. We identified peak zonal pressure from each step and calculated the mean peak zonal pressure for each minute of treadmill walking. Findings are presented as a percent change relative to the baseline threshold.

**Results & Discussion:** Note: the biofeedback conditions were not randomized and in addition to the small sample size, are not sufficient for statistical comparison. Nociceptive biofeedback led to greater reductions in zonal peak plantar pressure than innocuous biofeedback during the second 5min exposure by 10%. Percentage changes across participants varied widely with average 5min section standard deviations of 35%.

**Significance:** Nociceptive biofeedback for modification of movement behaviour may address gaps in patient with DPN's adherence to off-loading therapeutic footwear.

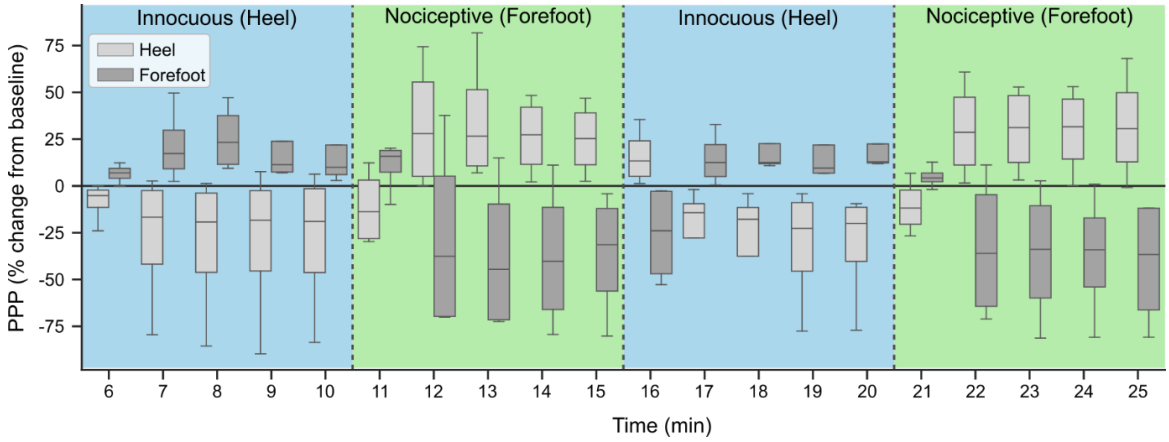


**Figure 1:** Four participants walked for 25min with minutes 1-5 being baseline and for minutes 6-25, participants received biofeedback. Peak plantar pressure (PPP) per zone were averaged for each participant for each minute and normalized relative to their mean across baseline. Box plot edges represent interquartile range and centerline represents the median change in PPP across the five participants. Participants received innocuous biofeedback tied to peak pressure at the heel during minutes 6-10 and 16-20. Participants received nociceptive biofeedback tied to peak pressure at the forefoot during minutes 11-15 and 21-25. Participants greatly reduced zonal plantar pressure based on the biofeedback provided.

**Acknowledgments:** We would like to thank Maria Contreras-Ramos, Jenna LaRue, JoAnn Micah Sedoriosa, and Nahir Negron Fernandez for assistance with protocol formulation and data collection.

**References:** [1] Armstrong, D. G., et al., (2017), *N. Engl. J. Med.* [2] Martini, E.,et al., (2021) *IEEE Trans. Neural Syst. Rehab. Eng.* [3] Seymour, B., et al., (2005) *Nat Neurosci*

# MUSCLE SYNERGY ANALYSIS DURING GRASPING TASKS IN INDIVIDUALS WITH CEREBRAL PALSY: A FRAMEWORK FOR TELEREHABILITATION

Hyunji Kim[1], Chae Lynne Kim[1], Yoojin Choi[1], *Jooeun Ahn[1,2]
[1]Department of Physical Education, Seoul National University, Seoul, Korea
[2]Institute of Sport Science, Seoul National University, Seoul, Korea
*Corresponding author's email: ahnjooeun@snu.ac.kr

**Introduction:** Spastic cerebral palsy (CP) is characterized by increased muscle tone and movement limitations that significantly impact grasping ability in activities of daily living. Traditional rehabilitation for spastic CP emphasizes functional adaptation and targeted movement therapy [1]. To facilitate adoption of rehabilitation systems including exoskeletons and telerehabilitation platforms, kinematic analysis-based feedback has been investigated [2]. However, these approaches often lack insights into the compensatory mechanisms and motor control patterns that are particularly crucial for understanding movement strategies in spastic CP. Muscle synergy analysis has emerged as a promising complementary framework as it has been increasingly utilized as a potential biomarker for assessing motor function and impairment during reaching and grasping tasks [3]. The number of muscle synergies required to reconstruct original muscle activation patterns serves as an indicator of neuromuscular complexity, with fewer synergies suggesting simpler control strategies. Previous studies have shown that stroke and spinal cord injury populations typically employ simpler neuromuscular control strategies compared to non-disabled individuals. However, in CP, such patterns have only been investigated during reaching, not grasping tasks. This study aims to analyze muscle synergy patterns during various grasping tasks in adults with spastic CP across different manual levels and task types. We seek to provide insights into movement quality and motor control strategies, ultimately enabling more effective personalized remote therapy approaches.

**Methods:** Six adults with spastic CP (**Table 1**) were classified according to the manual ability classification system (MACS levels I-III) and performed grasping tasks with 14 objects related with activities of daily living (ADL). Data collection included three smartphone cameras (iPhone 13, Apple Inc., USA), an 18-camera motion capture system (Optitrack Prime 13, Natural Point Inc., USA), and a wireless EMG system (Trigno, Delsys Inc., USA). Participants executed natural reaching, grasping, and manipulation movements with objects positioned on a desk (80 cm height, 15-20 cm distance). Surface EMG signals were recorded from 12 muscles of the dominant upper limb. EMG signals were processed using band-pass (20-500 Hz) and low-pass (10 Hz) filtering to obtain linear envelopes. After normalization to the maximum value of each muscle per participant, a non-negative matrix factorization algorithm was applied to the EMG matrix to extract muscle synergies, with a 90% variability accounted for (VAF) threshold determining the minimum number of synergies required. The Jonckheere-Terpstra test was used to assess trends in synergy numbers across MACS levels.

**Table 1. Participant demographics**

| Sub | Sex | Age (yrs) | TCP | Dominant side | MACS |
|---|---|---|---|---|---|
| 1 | M | 37 | SD | L | I |
| 2 | M | 29 | SD | R | I |
| 3 | F | 33 | SD | R | II |
| 4 | M | 47 | SD | R | II |
| 5 | M | 57 | SQ | R | III |
| 6 | M | 53 | SD | L | III |

TCP: type of CP. MACS: the manual ability classification system. High MACS scale means bad manual dysfunction. SD: spastic diplegia; SQ: spastic quadriplegia.

**Results & Discussion:** Fourteen objects were classified into four grasp types for analysis: power palm, power pad, precision pad, and precision side [4]. The number of muscle synergies showed a significantly decreasing trend with increasing MACS level (**Fig. 1**; MACS I: 2.93±1.10, II: 2.50±0.86, III: 2.14±0.83, $p < 0.01$). This trend was observed in most grasp types (power pad, precision pad, and precision side), but power palm grasps showed no consistent pattern. Similar to previous studies of motor impairments, our analysis captured trends in neuromuscular complexity related to functional ability levels although this pattern was not consistent across all grasp types [3]. Our preliminary analysis focused on muscle synergy complexity of the grasp phase. Future investigation will include analysis of synergy structure and temporal coefficients, along with examining movement sequence (reach, grasp, manipulation, and release).

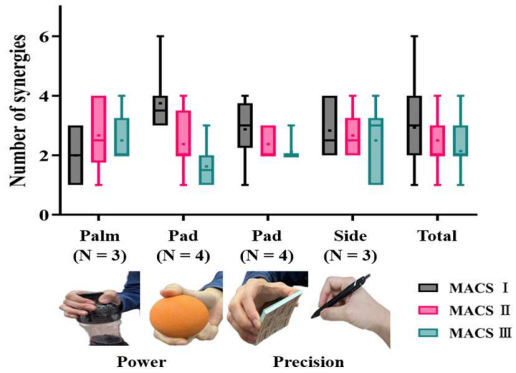


**Figure 1: Comparison of muscle synergy complexity across different grasp types in adults with spastic CP.** The median (central line), mean ('+' symbol), first and third quartiles (lower and upper box boundaries), and minimum and maximum values (lower and upper whiskers) of the number of synergies are shown

**Significance:** This comprehensive analysis of muscle synergy patterns could provide quantitative indices for motor control strategies during ADL grasping tasks in individuals with CP, potentially enhancing the assessment and personalization of telerehabilitation interventions. Notably, while muscle synergy analysis has been limited in CP studies, this approach has not been previously applied to investigate grasping movements in this population.

**Acknowledgments:** This study was supported in part by the Korea Creative Content Agency, funded by the Ministry of Culture, Sports and Tourism (RS-2024-00396700).

**References:** [1] Hoare et al. (2019), *Cochrane Database Syst Rev* 4; [2] Luciani et al. (2024), *arXiv.2412.06596*; [3] Zhao et al. (2023) *Heliyon* 9(5); [4] Feix et al. (2016) *IEEE Transactions on Human-Machine Systems* 46(1).

# ANALYSIS OF MOVEMENT QUALITY OUTCOME MEASURES FOR QUANTIFYING SYMPTOMS OF FUNCTIONAL MOVEMENT DISORDER

*Garrett Weidig[1], Alysha DeMay, OTRL[2], Olivia Risko, DPT[2], *Tamara Reid Bush, PhD[1]
[1]Department of Mechanical Engineering, Michigan State University, East Lansing, MI, 48824
[2]The Recovery Project, Lansing, MI, 48911
*Corresponding author's email: weidigga@msu.edu, reidtama@egr.msu.edu

**Introduction:** Functional Movement Disorder (FMD) is a debilitating disorder that is associated with involuntary, erratic movements such as tremors and jerks, particularly for the upper extremity [1]. FMD largely affects females (roughly 75% of cases), takes a long time to successfully diagnose (between 4-6.5 years) and treatments result in nearly $1 billion worth of U.S. healthcare costs annually [1]. Studies have shown that intensive treatment and therapy results in "more controlled" movements. However, "more controlled" is typically documented through self-reporting questionnaires and there is no proven approach to determine improvements in movement for FMD patients [2]. Thus, there is a need to quantify movement quality so that changes can be identified. The goal of this work was to evaluate five possible approaches for quantifying changes in movement quality for FMD patients. Ideally, the best movement quality approach will be able to differentiate between different movement symptoms (e.g., intermittent jerk from a constant tremor).

**Methods:** Five geometric curves were created to represent different FMD movements, such as arhythmic jerks and varying degrees of tremor (Fig. 1). These geometries were printed on paper and put on a table in front of participants. 20 healthy participants (11F, mean age 40 years (S.D. 22 years)) were recruited for this study (IRB #00008658) and instructed to trace geometries with their right hand, just above the printed paper. Additionally, four FMD participants with ranging symptoms were recruited to complete a simulated drinking task. A six-camera motion capture system (Qualisys, Gothenburg Sweden) was used to obtain position data from the right index finger. Five movement quality approaches were calculated, comparing: Spectral Arc Length Method (SPARC), Log Dimensionless Jerk (LDLJ), number of peak velocities per meter (NoP), normalized summed centripetal acceleration (SCA), and velocity peak frequency (PF) [3].

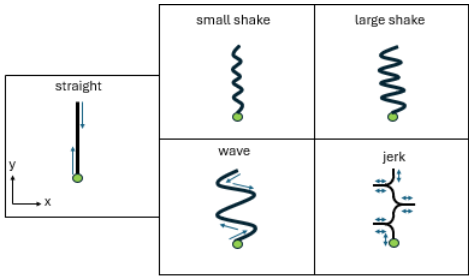


**Figure 1:** Geometric curves. Movements were completed by following the curve; in the jerk geometry, participants were instructed to jerk outward when approaching horizontal lines.

For the healthy data, the first question was: "Could an approach differentiate between geometries"? To answer this, multiple comparison tests were run for each approach between two geometries (significant $p$ values were <0.05). The next question was: "Can a combination of approaches better differentiate between geometries"? Finally, the five movement quality approaches were applied to the FMD data to determine if the trends discovered in the geometric curve portion yielded similar results when applied to FMD movements.

**Results & Discussion:** The results from the multiple comparison tests indicated which approaches differentiated between geometries. The SCA approach indicated the straight geometry had the highest movement quality (i.e., nothing that resembled a jerk or tremor), the wave and small shake had similar values with moderate levels of quality, and jerk and large shake had the lowest quality (highest value) (Fig. 2a). Still, SCA alone was not able to differentiate between all geometries. Interestingly, SPARC, which has been regarded as the most successful approach when applied to groups that have tremors, which tend to be small/subtle (e.g, Parkinsons), was not able to differentiate between some of the rhythmic geometries, such as the wave and the small shake (Fig. 2b). Because of this, approaches were paired. The most successful pairing in differentiating geometries was the pairing of LDLJ vs SCA. These results were further investigated with FMD participants.

When the four FMD movements were analyzed, the best differentiation of movements occurred by pairing PF with either LDLJ or SCA. This change is not entirely surprising, as PF allows the symptom frequency to be calculated and both LDLJ and SCA can be too sensitive to the length of the test (i.e., trial time). In the future, pairing LDLJ or SCA with PF has strong potential to be used to quantify the changes in movement quality associated with FMD treatment or progression.

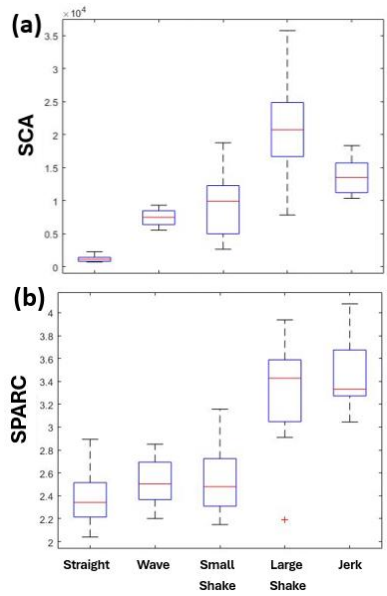


**Figure 2:** Geometry output values from SCA (a) and SPARC (b), which are both unitless.

**Significance:** Persons with FMD can have wide-ranging movement symptoms that have not been quantified. Through this study, it was discovered that combinations with LDLJ, SCA, and PF were able to differentiate between movement types which will make it possible to quantify and monitor FMD movements. Also, although this study used a motion capture setup, it may be possible to gather these data through wearable devices with accelerometers in the future, which would make at home or everyday monitoring possible.

**References:** [1] Lidstone et al. (2017), *J Neurol Neurosurg Psychiatry* 93(6); [2] Czarnecki et al. (2012), *J Neurol* 262(3); [3] Balasubramanian et al. (2012), *IEEE Trans Biomed Eng* 59(8).

**Driving Task Conditions Change the Predictability and Persistence of Steering Behaviour**

*Narges Shakerian[1], Jorge Zuniga[1], Aaron Likens[1]
[1]Division of Biomechanics and Research Development, Department of Biomechanics and Center for Research in Human Movement Variability, University of Nebraska at Omaha, Omaha, Nebraska, USA
*Corresponding author's email: nshakerian@unomaha.edu

**Introduction:** Steering variability, a critical aspect of driving behavior, is the continuous adjustment to maintain control while driving a vehicle [1]. Steering variability is not random but follows structured patterns shaped by sensorimotor coordination, highlighting the interplay between perception and action for the purpose of vehicle control. Beyond the magnitude of steering variability (standard deviation), changes in steering angle over time may reveal how drivers maintain vehicle control. Two key characteristics of steering variability are predictability, or how well future adjustments can be anticipated from past adjustments, and persistence, which describes whether adjustments have trends, be they positive (persistence) or negative (anti-persistence). However, little is known about how these properties change under different driving conditions. This study aimed to examine how steering variability changes with task demands.

**Methods:** Thirty healthy participants (15 females, 15 males) between 19- 36 years old (26.9 ± 3.38 years) completed 12 three-minute driving tasks in a simulated environment with manipulation of speed (slow, fast), steering wheel condition (compatibility, i.e., mirror-reversed steering), and track direction (straight, left, right) [2]. Steering wheel angle data was analyzed using two nonlinear metrics: Detrended Fluctuation Analysis (DFA) and Sample Entropy (SampEn) to assess persistence and predictability in steering, respectively. Linear mixed-effects models determined whether those measures depended on a combination of direction, speed, and compatibility. Standardized coefficients quantified effect sizes.

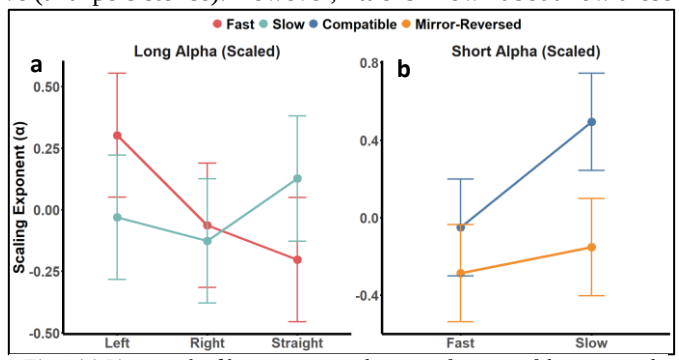


*Fig 1.(a) Line graph of long-range α values as a function of direction and speed. (b) Line graph of short-range α values as a function of direction and steering wheel condition. Error bars indicate 95% confidence intervals.*

**Results & Discussion:** Results revealed that DFA short-range scaling exponents (α) were significantly affected by steering wheel condition ($F(1,318.14)=25.76$, $p<0.001$, $\eta_p^2=0.22$) and speed ($F(1,318.03)=15.26$, $p<0.001$, $\eta_p^2=0.60$), with an interaction between these factors ($F(1,318.03)=5.61$, $p=0.018$). Simple effect analysis indicated that mirror-reversed steering led to more erratic steering corrections, particularly at slower speeds ($t(318.03) = 5.26$, $p<0.001$, $d = 0.64$). Long-range scaling exponents (α) were significantly influenced by the interaction between direction and steering wheel condition ($F(2,318.14)=3.59$, $p=0.029$, $\eta_p^2=0.78$), and direction and speed ($F(2,318.14)=3.45$, $p=0.033$, $\eta_p^2=0.77$). Simple effect analysis showed that mirror-reversed steering resulted in significantly higher long-range α values in leftward turns ($t(318.14) = 2.34$, $p = 0.02$, $d = 0.38$), but no significant differences were found for rightward turns or straight-line driving ($t(318.14) = 0.83$, $p = 0.41$, $d = 0.12$) (Fig 1). SampEn analysis indicated significant effects of direction ($F(2,318.01) = 23.46$, $p < 0.001$, $\eta^2 = 0.072$) and steering wheel condition ($F(1,318.02) = 32.36$, $p < 0.001$, $\eta^2 = 0.092$), along with an interaction of these two factors ($F(2,318.01) = 5.96$, $p = 0.003$, $\eta^2 = 0.027$) (Figure 2). Simple effect analysis indicated that in mirror-reversed conditions, steering adjustments during right turns were significantly more unpredictable than in left turns ($t(318.01) = 2.62$, $p = 0.025$, $d = 0.42$) and straight-line driving ($t(318.01) = 3.24$, $p = 0.0038$ $d = 0.51$). Similarly, left turns in mirror-reversed conditions were significantly less predictable than in other directions ($t(318.01) = 5.85$, $p < 0.001$, $d = 0.92$). Under compatible steering conditions, right turns were significantly more predictable than left turns ($t(318.01) = 2.21$, $p = 0.071$, $d = 0.35$) and straight-line driving ($t(318.01) = 4.95$, $p < 0.001$, $d = 0.79$) (Fig 2). These findings highlight how the temporal structure of steering behavior adapts to environmental factors, with variations in predictability and persistence shaping individual driving patterns. Specifically, immediate steering control is primarily influenced by task constraints such as steering wheel condition and speed, whereas longer-term adaptations depend more on road geometry and directional context.

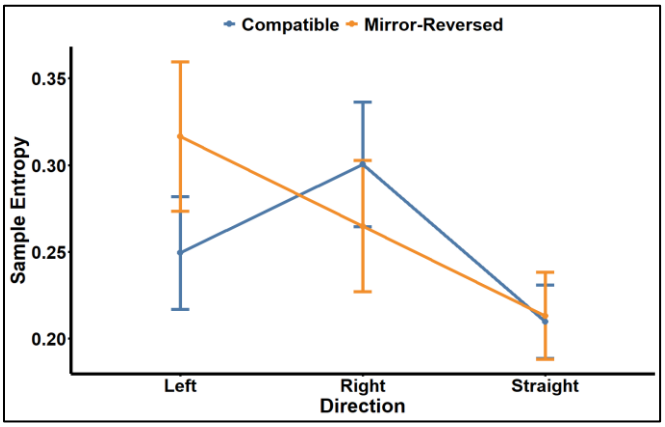


*Fig 2. Line graph of Sample Entropy (SampEn) as a function of direction and compatibility condition. Error bars indicate 95% confidence intervals.*

**Significance:** This study reveals how movement variability in steering control adapts to changes in speed, direction, and steering wheel condition, offering new insights into short- and long-range motor control adjustments. These findings have broad implications, from enhancing vehicle assistive systems and autonomous driving algorithms to informing rehabilitation strategies for individuals with neuromotor impairments. By bridging the gap between motor control, human factors, and clinical applications, these insights can also contribute to driver training programs to improve control precision in challenging conditions, ultimately enhancing road safety.

**Acknowledgments:** This project was supported by NSF EPSCoR funding resources.

**References:** [1] Kolekar et al. (2018), *IEE transactions on Human Machine System 48*(3; [2] Likens et al. (2015), *Experimental Brain Research* 233(10).

# INTRALIMB CONTROL DURING REACHING BEHAVIORS IN INFANTS WITH DOWN SYNDROME

*Matthew Beerse[1], Robert Zeid[2], Amy Talboy[3], Seyda Ozcaliskan[4], Jianhua Wu[2]
[1]Department of Health and Sport Science, University of Dayton
*Corresponding author's email: mbeerse1@udayton.edu

**Introduction:** Reaching motor development is often delayed by two months in infants with Down syndrome (DS), which negatively impacts their social and cognitive development [1]. The use of "sticky mittens" to encourage reaching behaviors has advanced reaching development in typically developing infants [2]. However, this intervention has not been systematically implemented for infants with DS. This study aimed to assess reaching motor control in infants with DS who received the "sticky mittens" training. We implemented an uncontrolled manifold (UCM) analysis to evaluate the capacity to operationalize segmental variability to stabilize reaching trajectory. Further, we employed computer vision software OpenPose to conduct markerless motion analysis [3]. We hypothesized that infants with DS might show an increased capacity to stabilize wrist position by employing trunk, shoulder, and elbow variability post-training.

**Methods:** Eleven infants with DS (8.36±1.6 months at entry) completed a 2-month long "sticky mittens" intervention. Parents administered training for 8 minutes/day, 5 days/week at their home. During training, toys were presented at an arm-length distance. Video data was collected at 60 Hz at three time points: pre-training, post-training, and 5-months thereafter. During data collection, researchers held toys in front of the infant, who did not wear sticky mittens. Video captured right side sagittal plane motion and OpenPose automatically registered body landmarks from the video data. Landmark trajectories were down-sampled to 30 Hz and filtered using a 2$^{nd}$ order one-dimensional median filter [3]. Landmark data quality of the mid-hip, neck, right shoulder, right elbow, and right wrist were visually inspected and corrected using MATLAB code [4]. The trunk segment was defined with the mid-hip and neck markers, upper arm segment with the shoulder and elbow markers, and forearm segment with the elbow and wrist markers. Trunk segment angle relative to the vertical and shoulder and elbow joint angles were calculated and time normalized to 101 points across each reach.

A geometric model relating the trunk, shoulder, and elbow angles to wrist position in the sagittal plane was constructed. A traditional UCM analysis was then performed on each 1% of the reach using the reference configuration of the average posture across reaching behaviors. Goal-equivalent (GEV) and non-goal equivalent variances (NGEV) were determined and the index of motor abundance (IMA) estimated. To assess stabilization, two-tailed one sample t-tests were conducted on time normalized IMA using statistical parametric mapping (SPM). IMA significantly greater than 0 indicated stabilization. In addition, we assessed how GEV and NGEV changed across time points using one-way (time) ANOVAs with repeated measures. A significance level was set as α=0.05.

**Results & Discussion:** Pre-training, infants with DS stabilized wrist trajectory at the mid-point and end of the reach (Fig. 1d). Post-training, stabilization occurred for the second half of the reach (Fig. 1e) but disappeared 5-months thereafter (Fig. 1f). Infants with DS were better able to maintain a consistent wrist trajectory by exploiting trunk, shoulder, and elbow angle variability post training, which helped contact the toy. The disappearance of stabilization was unexpected at 5-months post training. Consistent wrist trajectory might no longer be a task goal of the neuromotor system. Or shift in reaching strategy might have occurred, such as increased elbow motion [5], which could destabilize performance.

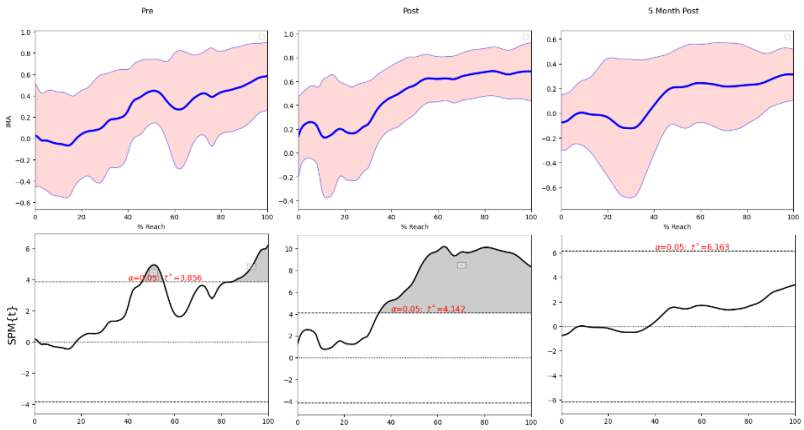


**Figure 1:** Mean IMA across 100% of the reach for pre-training (a), post-training (b), and 5-months thereafter (c) in the first row. Two-tailed one sample t-tests using SPM (d-f) in the second row. Shaded regions indicate different from zero.

A clear trend of GEV decreasing from post-training to 5-months thereafter (d=1.06) and NGEV decreasing from pre-training to post-training (d=0.77) was consistent with previous motor learning research, where initially errors decreased (NGEV) followed by a reduction of solutions (GEV) [6]. The reduction of GEV at 5-months post training suggests infants with DS refined their reaching behavior by exploiting preferred solutions. The capacity to reduce the solution space is encouraging as previous research found increased GEV in the DS population, likely to compensate their increased movement variability [7].

**Significance:** Our findings present encouraging results for the "sticky mittens" training as an early physical intervention to advance reaching development in infants with DS. Moreover, computer vision software, i.e., OpenPose, has the potential to expand motor development research, as it facilitates high frequency in-home data collection. Lastly, this study employed a UCM framework to establish how reaching coordination develops with practice and age, suggesting that infants with DS are capable of prioritizing error reduction followed by exploitation of preferred solutions with continued practice.

**Acknowledgments:** We are grateful for the participants and their families. This study was funded by NIH R21HD105879.

**References:** [1] Ejiri & Masataka (2001) *Dev Sci* 4(1); [2] Libertus et al. (2016) *Dev Sci* 19(6); [3] Ossmy & Adolph (2020), *Curr Bio* 30(23); [4] Stenum et al. (2021) *PLOS Comp Bio* 17(4); [5] Berthier & Keen (2006) *Exp Brain Res* 169(4); [6] Wu & Latash (2014) *Ex Sport Sci Rev* 42(1); [7] Black et al. (2007) *Exp Brain Res* 184(4).

# MOTOR DEVELOPMENT OF ARM REACHING COORDINATION IN INFANTS WITH DOWN SYNDROME

Robert Zeid II[1*], Jackelyne Perez[1], Amy Talboy[2], Seyda Ozcaliskan[1], Jianhua Wu[1]
[1]Georgia State University, Department of Kinesiology and Health, [2]Emory University
*Corresponding author's email: rzeid1@gsu.edu

**Introduction:** Cognitive, visual, and proprioceptive inputs influence an infant's arm reaching strategy. The shoulder and elbow joints coordinate together to move the hand closer to the object, while the distal trunk muscles become more involved during the reach as the infant ages [1]. In children with Down syndrome (DS), muscle hypotonia and delayed brain development lead to developmental delay of motor skills such as arm reaching, thus reducing the opportunities of environmental exploration. "Sticky mittens" training provides opportunities for practicing arm reaching and enhancing object exploration strategies [2]. Vector coding is a biomechanical tool for quantifying inter-joint coupling angles throughout a movement: in-phase (same direction) and anti-phase (opposite direction). This analysis sheds light on whether the proximal or the distal joint is dominant and leads the movement [3, 4].

The preliminary results reported here are part of a comprehensive, longitudinal study which assesses motor, cognitive, and language development in infants with DS who all receive an early treadmill intervention: one half received the "sticky mittens" training (i.e., GMFM group) and the other half did not receive the mittens training (i.e., GM group). We aim to understand the coordination of the trunk, shoulder, and elbow during arm reaching between the two groups. We hypothesize that the GMFM group will display a more anti-phase, distal dominant coordination pattern and a higher trunk range-of-motion (ROM) than the GM group.

**Methods:** Our preliminary results included 11 infants with DS (6M/5F). We visited the infant's home once a month to record reaching and grasping a set of toys presented at the infant's arm length. Reflective markers were placed on the infant's right iliac crest, shoulder, elbow, and wrist. A 60 Hz camera was used to record arm reaching from the infant's right side. Noraxon ® MyoResearch 3 software was used to process the trials. A custom MATLAB® program was used to calculate the trunk, shoulder, and elbow angles. Trunk angle was defined from the hip and shoulder marker with respect to the vertical line. The shoulder angle was defined from the hip, shoulder, and elbow markers. Elbow joint angle was defined by the shoulder, elbow, and wrist markers. Kinematic variables included trunk, shoulder, and elbow ROM from two time points: T2 (at the conclusion of the mittens training for the GMFM group; GM mean age = 12.6 months; GMFM mean age =11 months) and T3 (about 6 months thereafter). The coupling angle was calculated between the shoulder and elbow joints to define the coordination pattern using vector coding analysis. A coupling angle of 135º-180º indicates an anti-phase, proximal dominant coordination and a coupling angle of 90º-135º indicates an anti-phase, distal dominant coordination. A two-way (2 group x 2 time) mixed ANOVA was conducted for joint kinematics and coupling angles. A significance level was set as alpha=0.05.

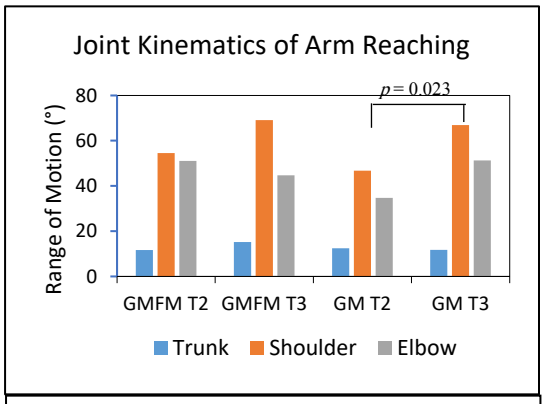


Figure 1: Mean values of trunk, shoulder, and elbow ROM for both groups across time points.

**Results & Discussion:** Trunk ROM remained similar for the GM group over time. However, the GMFM group slightly increased trunk ROM from 11.66º±2.27 at T2 to 15.20º±1.67 at T3. Shoulder ROM increased in the GM group across time points (46.73º±8.43 at T2 to 66.87º±6.21 at T3, $p$=0.023), whereas the GMFM group showed an increasing but non-significant trend (54.52º±9.24 at T2 to 69.05º±6.81 at T3). The GM group exhibited a trend for significance in increasing the elbow ROM (34.67º±5.74 at T2 to 51.24º±7.32 at T3, $p$=0.051), while no significant change was detected in the GMFM group. The coupling angles between the shoulder and elbow slightly decreased in the GMFM group (145.70°±19.67 at T2 to 141.21°±18.84 at T3), remaining in an anti-phase, proximal dominant coordination pattern. The GM group revealed a larger decrease in the coupling angle (150.70°±21.82 at T2 to 136.85°±27.63 at T3), remaining anti-phase, proximal dominant but transitioning closer towards an anti-phase, distal dominant coordination pattern.

Preliminary results demonstrated that from about 12 months to 18 months, the GMFM group generally produced a greater ROM of the shoulder and elbow joints than the GM group. Also, the GMFM group showed a consistent reliance on trunk and shoulder mobility than elbow mobility during reaching, while the GM group relied less on trunk mobility and an increased reliance on distal motion. It seemed that the mittens training did not change the developmental trajectory of joint coordination during arm reaching in infants with DS although the GMFM group was about 1-2 months younger than the GM group. Because arm reaching is a multi-planar movement, one limitation is that the use of 2D motion analysis to capture sagittal plane kinematics may not reveal possible movement in the third plane (such as circumduction). Additionally, there is no comparison of arm reaching kinematics and coordination between the DS subjects and typically developing infants. Such comparisons will help understand the unique features of segment control and joint coordination during arm reaching in children with DS.

**Significance:** The "sticky mittens" training may increase joint ROM and the variability of arm reaching in infants with DS. Studying the biomechanics of arm reaching would help rehabilitation practitioners understand trunk mobility and joint coordination and aid in the development of rehabilitation protocols to train infants' arm reaching in different positions and strategies.

**Acknowledgments:** We thank NIH (R21HD105879) for funding and all the participants and their parents for their participation.
**References:** [1] Lieke et al. (2012), *Exp Brain* Res 220; [2] Needham et al. (2002), *Infant Behavior & Development* 25; [3] Needham et al. (2020), *The Foot* 44; [4] Celestino et al. (2019), *Human Movement Science* 68.

# REINFORCEMENT LEARNING AS A TOOL FOR LOWER LIMB MOTOR TRAINING: INSIGHTS AND OUTCOMES

*Stephanie B. Hernández Hernández[1], Peter G. Adamczyk[1],
[1]Department of Mechanical Engineering, University of Wisconsin - Madison
*Email: peter.adamczyk@wisc.edu

**Introduction:** Understanding motor control principles can contribute to the development of targeted rehabilitation therapies that enhance essential daily activities. While most motor control research has primarily focused on the upper limb[1-2], investigating how motor control functions in the lower limbs could inform rehabilitation strategies for walking, standing, balance, and other leg and foot movements, particularly for individuals recovering from neural injury. Therefore, our goal is to explore and better understand the dynamics of motor learning in the lower limbs.

NOTTABIKE, a custom haptic leg robot, was designed to train and test new motor control tasks through novel haptic environments [3]. In this study, we examine how individuals learn a new motor skill with their legs by learning how to reach to an obscured target while only receiving success/failure feedback (reinforcement learning). We hypothesize that participants will improve target accuracy over the progression of multiple trials, with reduced error and stopping angles closer to the target. Motor exploration should decrease as accuracy improves, with more exploration being higher after failure when compared to proceeding success feedback.

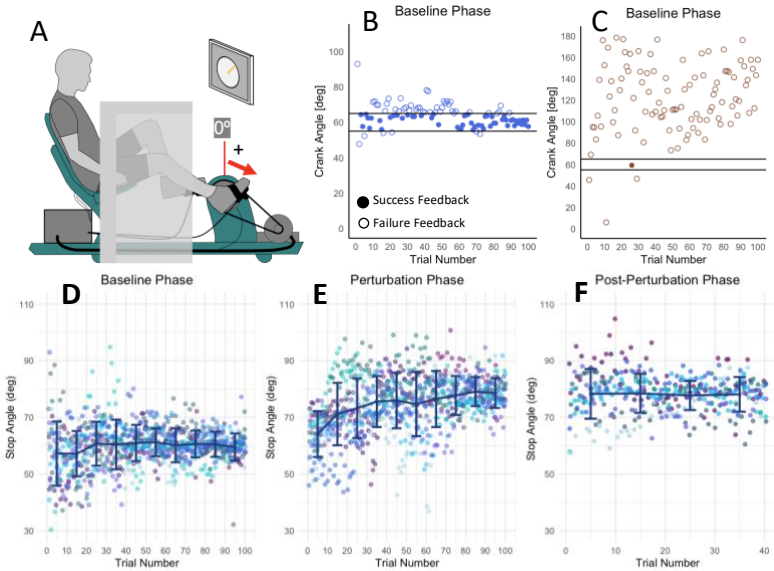


**Figure 1:** (A) NOTTABIKE Diagram and experimental set up. For all blocks participants had their legs covered. Baseline phase stopping angle example data for a (B) learner and a (C) partial learner. (D) Stopping angle data for all participants in the learners group for all the three phases.

**Methods:** Sixteen healthy young adults (9 F, 25 ± 4, right-side dominant) participated in this study. Participants performed a leg-reaching task targeting a position on the pedal in a zero-torque environment using NOTTABIKE (Fig 1A). Accuracy feedback (success/failure) was provided via visual and auditory cues. The study included three phases done on the same day. Baseline (Base) consisted of 100 trials where participants learned to reach a target at 60° with a fixed accuracy window of 60°±5° . Perturbation (Pert), had 100 trials and the physical target was shifted to 80° while the visual cues remained at 60°, creating a visual-proprioceptive conflict. This phase used a moving accuracy window based on the average crank angle of the previous 10 trials. The goal was to gradually narrow the target range to ensure participants moved from the to the learned 60° target to the shifted one. Post-Perturbation (Post) consisted of 40 trials where feedback was withheld to assess retention. Data analysis focused on stopping angle, change in reach angle, and absolute error.

**Results & Discussion:** Participants were categorized as learners or partial learners based on their Base performance. Fig. 1B shows a participant who successfully learned the target using binary feedback, while Fig. 1C shows a participant who did not. Even though not everyone successfully learned in Base, both groups learned the shifted target, as the moving accuracy window gradually guided them toward success. For the learners groups, during Base (Fig 1D), participants became consistent in reaching within the 60° window after ~60 trials. In Pert (Fig 1E), they gradually shifted their movements toward the 80° target with the help of the moving accuracy window and continued reaching the shifted target during Post (Fig 1F), even without feedback. This shows that participants were able to adapt to the new target using only reinforcement feedback. We also quantified learning rate, which was faster in Pert compared to Base, likely due to the moving accuracy window assisting participants in reaching the shifted target. Motor exploration varied across phases. During Base, more exploration occurred after failure feedback, supporting the idea that failure prompts participants to adjust their movements. Exploration was higher early in Base and reduced later, as participants fine-tuned their movements. However, in Pert, exploration did not significantly change over time, as the moving window guided participants toward the shifted target, leading to less exploratory behavior. This suggests that task design, such as using a fixed or moving window, impacts the level of motor exploration. Despite less exploration in Pert, accuracy improved significantly in both phases, confirming that participants learned to reach the target over time. These findings underscore the role of feedback in motor learning and highlight the importance of task design for promoting exploration and improving performance, particularly in rehabilitation contexts.

**Significance:** This study showed that participants could learn to reach a target with only binary success/failure feedback, and better results were achieved using a moving accuracy window. While motor exploration decreased in Base, no clear pattern emerged in Pert, highlighting the need for further research. These findings underscore the potential of reinforcement learning in enhancing motor skill recovery and acquisition, with potential applications to rehabilitation for individuals with motor impairments.

**Acknowledgments:** NSF grants (CMMI-1830516, HRD-1612530), and UW-Madison OVCRGE with funding from WARF.

**References:** [1] Latash+ 1996 Dis & Reh; [2] Leech+ 2022 PT; [3] Dawson-Elli 2022 PhD Diss., UW-Madison.

# ASSESSING KNEE PROPRIOCEPTION DEFICITS IN INDIVIDUALS WITH A HISTORY OF A KNEE INJURY

*Huaqing Liang[1], Cameron Ferguson[1], Sydney McComas[1], Bre Gahm[1], Melanie Lambert[2], Steven Leigh[3]
[1]School of Physical Therapy, Marshall University, Huntington, WV
[2]College of Nursing and Health Sciences, University of Colorado, Colorado Springs, CO
[3]School of Health and Movement Sciences, Marshall University, Huntington, WV
*Corresponding author's email: liangh@marshall.edu

**Introduction:** Following a knee injury, there is a significant decline in proprioception, which can cause increased instability of the knee, increased susceptibility of re-injury, and early development of arthritic joint changes [1]. Proprioception training is included in rehabilitation programs [2], yet whether proprioception deficits linger in individuals with old knee injuries is unknown. The most common measurement tool for knee proprioception in clinical settings is the assessment of joint position sense (JPS), where blinded individuals actively move their knees to reproduce a target angle [3]. However, this assessment fails to replicate the actual use of the proprioception system in motion and does not examine the contribution of proprioception to movement coordination. There is a need to develop a functional assessment to evaluate knee proprioception and coordination. The purposes of this study were: 1) assessing whether knee proprioception deficits linger after a knee injury, and 2) evaluating whether a novel action-perception task was sensitive to detect such deficits.

**Methods:** Participants included eight young adults (2M/6F, aged 24.8±1.1 years) with a history of knee injury at least one year prior, and termination of physical therapy no less than 6 months ago. The leg with a history of knee injury was coded as the involved side, and the other leg coded uninvolved side. During the data collection session, we assessed the proprioception of the bilateral knees with JPS test using two methods: an isokinetic dynamometer and a hand-held goniometer at 20 and 50 degrees. We tested each angle with each method 3 times for each leg, and we calculated the mean absolute error.

We also asked the participants to perform a functional action-perception task to quantify their knee function during movement. The action-perception task included having the participant tap an 18-inch obstacle placed in front of them with the toe of the involved leg, close their eyes, move one step laterally, and tap the obstacle 10 times while keeping their eyes closed. The same task was repeated for the contralateral limb. We used seven Noraxon IMUs to record the movement and obtain the joint angle time series data for analysis. For the last 10 repetitions, we plotted a knee-hip angle-angle graph (Fig. 1), calculated the polar coordinate angle of the angle-angle graph, and normalized each repetition to 100% of the movement cycle. To calculate the spread of the polar coordinate angles of the 10 repetitions, we calculated the difference between the max and min polar coordinate angles at every 5% interval, and defined the average value as the dispersion index (DI). A larger DI value represents more dispersion and more dissimilar movements, a smaller DI value represents less dispersion and more similar movements across 10 repetitions.

We conducted dependent t-tests for the JPS errors and DI values between the involved side and the uninvolved side. We used an alpha value of 0.05.

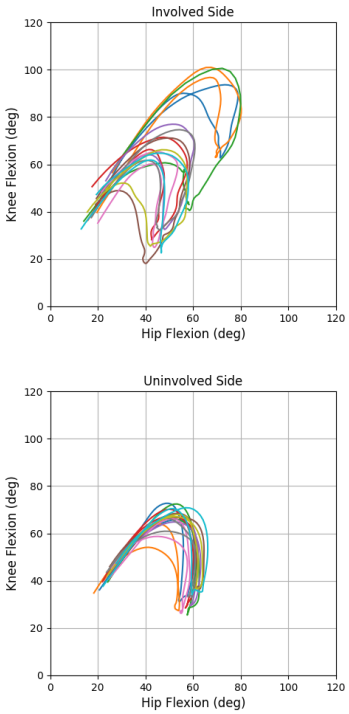


**Figure 1:** The bilateral angle-angle graphs of the last ten repetitions of the action-perception task of a representative participant.

**Results & Discussion:** The involved side displayed a higher DI than the uninvolved side (0.20 vs. 0.15, p=0.04), indicating less consistency in hip-knee joint coordination during functional movements in the leg with a history of knee injury. Our results also suggest that this novel action-perception task is a sensitive task to detect knee proprioception deficits. We presented the knee-hip angle-angle graphs of both sides of a representative participant in Figure 1.

There were no differences between the involved and the uninvolved sides in JPS errors (Table 1). Even though it was not the original purpose of this study, we noticed that the JPS errors measured by a hand-held goniometer might not provide an accurate reading similar to the more objective isokinetic dynamometer, with the difference between the two measurement methods larger at the smaller angle tested. We plan to investigate these data further in the future.

**Table 1. Means ± SD of the JPS errors using two methods at two different targeted angles**

| JPS errors (degrees) | IsoK at 20° | Goni at 20° | IsoK at 50° | Goni at 50° |
|---|---|---|---|---|
| Involved side | 9.0 ± 6.3 | 4.2 ± 1.7 | 4.2 ± 3.2 | 6.3 ± 4.5 |
| Uninvolved side | 4.6 ± 3.3 | 3.5 ± 2.1 | 4.0 ± 1.6 | 6.9 ± 3.3 |

JPS: joint position sense; IsoK: measured with an isokinetic dynamometer; Goni: measure with a hand-held goniometer

**Significance:** For individuals with a knee injury history, there might be remaining deficits in knee proprioception years after the injury, despite completion of a full rehabilitation program. Our results indicate that JPS test commonly used in the clinical settings may not be accurate or sensitive to detect the remaining deficits. Our novel action-perception task can detect knee-hip coordination deficits during dynamic movements, and has the potential to be used in the clinical settings as a functional proprioceptive assessment tool during rehabilitation programs following knee injuries.

**References :** [1] Relph et al. (2014) *Physiotherapy.* 100(3):187-95; [2] Jeong et al. (2019), *J Athl Train.* 54(4):418-428; [3] Smith et al. (2012) Knee. 20(3):162-9.

# AN INVESTIGATION INTO NEUROCOGNITIVE CHANGES IN HIGH SCHOOL-AGED SPORTS SHOOTERS FOLLOWING EXPOSURE TO RECOIL

Suzanne M. Konz[1], Caleb S. McComas[1], & Steve Leigh[1]
1Marshall University, Huntington WV, USA
*Corresponding author's email:* konz@marshall.edu

**Introduction:** Sport-shooting at the high school level is rapidly growing, with participation increasing by 28% since 2001 [1,2]. High school shooters can fire more than 300 rounds in a day, leading to cumulative head acceleration from firearm recoil. Prior research indicates that repeated low-level head accelerations can contribute to neurocognitive decline [3]. The mechanical force of recoil generates oscillatory movement in the brain, potentially impacting cognitive function over time. This study aimed to determine the cognitive effects of sport shooting and identify a potential round limit. We hypothesized that cumulative recoil-based head acceleration would increase in a cubic form, that post-shooting cognitive scores would be lower than pre-shooting scores, and that body mass would influence recoil transmission.

**Methods:** Fifteen male high school sport shooters (96.50±2.98 kg, 1.80±0.07 m, 29.76±3.92 kg/m²) participated in this study. Data collection occurred at a local gun club using a Mossberg 835® 12-gauge shotgun and Estate® 2 3/4 inch shells with 7 1/2 shot BBs. Vicon Blue Trident IMUs (500 Hz) were affixed to the mastoid process and firearm stock to capture recoil-based head accelerations. The sensors provided real-time measurements of head kinematics, allowing for analysis of directional accelerations. Cognitive testing (Human Benchmark visual sequence memory) was conducted pre- and post-shooting. Participants fired one round of 25 shots before post-test cognitive assessment. T-tests compared cognitive scores pre- and post-shooting, and a general linear model (GLM) was used to determine acceleration patterns. Additional analyses explored correlations between body mass and acceleration absorption.

**Results & Discussion:** The results revealed that participants experienced an average of 0.23 ± 0.04 g per shot, accumulating 5.78 ± 1.59 g over 8.18 ± 0.89 sec. Contrary to the hypothesis that cumulative acceleration would follow a cubic function, the results demonstrated a linear accumulation pattern. This suggests that the progressive impact of recoil-based head acceleration remains steady rather than exponentially increasing. Body mass played a significant role in dampening recoil transmission, with heavier participants experiencing lower acceleration levels. These findings align with prior research indicating that mass composition—particularly the ratio of muscle to fat—affects recoil absorption efficiency [4].

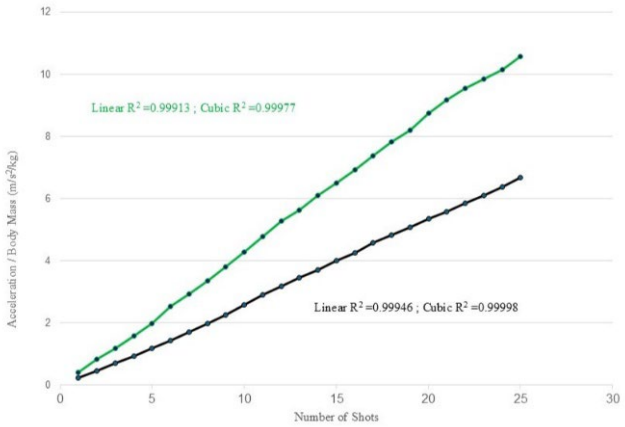


Figure 1. Graphic regression function representation of cumulative acceleration related to body mass of the gun (green) and head (black).

Cognitive testing pre- and post-shooting revealed significant decrements in cognitive performance, with scores declining from 14.93 to 13.27 ($t = 6.168$, $p < .001$). Participants reported symptoms such as headaches, temporary visual disturbances, and dizziness, aligning with previously documented concussion-like symptoms in non-contact brain injuries [5,6]. This supports the assertion that repeated sub-concussive impacts, even at low magnitudes, can have measurable neurocognitive effects [5].

A limitation of this study was the variability in shooting experience among participants, which may have influenced recoil mitigation through positioning and firearm handling. Despite the limitation, our findings highlight the potential risks of accumulated head acceleration in high school sport shooters. Given that no standardized round limit exists [7], future investigations should explore individualized shot thresholds based on body mass and recoil absorption characteristics. Given the link between repetitive low-level impacts and chronic traumatic encephalopathy [5], further research is needed to determine if exposure guidelines are necessary to mitigate long-term neurological consequences.

**Significance:** This study provides novel insights into the neurocognitive effects of firearm recoil in high school-aged shooters. The findings suggest that even low-level head accelerations may contribute to cognitive decline over time, warranting further investigation into round limits and safety guidelines. Given that sport shooting is becoming increasingly popular among youth athletes, understanding the long-term neurological implications is crucial for injury prevention and policy development. Further studies should investigate how different firearm types and shooting frequencies affect neurocognitive function over extended periods. The implementation of standardized concussion-like symptom assessments for sport shooters may offer valuable preventive strategies. With the rapid growth of sport shooting, research on cumulative impacts is critical for athlete health and policy development. Future studies should explore long-term effects and potential intervention strategies, such as optimized recoil-dampening techniques and equipment modifications.

**References:**[1] Duda et al. (2017) 11(2). [2] Gregory, S. (2019), *Time*, March 7. [3] Burns, B. (2012), US Army Research Laboratory. [4] NSCA Rulebook. (2024). [5] Daneshvar et al. (2023), *Nature Communications* 14(1). [6] Sarmiento et al. (2021), Am J Sports Med 49(8). [7] Waltzman et al. (2021), *Sports Health* 13(5).

# Does Increased Cognitive Load Further Effect Lower-Extremity Landing Mechanics During Unanticipated Change of Direction Tasks?

Nikolaj Freschlin[1*], Kevin Valenzuela[1], Scott Ducharme[1] & Samuel Zeff[1]
[1]Department of Kinesiology, California State University, Long Beach, California, USA
*Corresponding author's email: nikolaj.freschlin01@student.csulb.edu

**Introduction:** Multi-directional sport requires rapid adjustments to a continuously evolving environment, where athletes must identify, process, and react to ever changing stimuli while also remembering critical information relevant to performance outcomes. Anterior Cruciate Ligament (ACL) screenings attempt to recreate sport-specific environments, where cues to change, direction are reduced to a single arrow or light [1, 2, 3]. However, the ecologic validity of such paradigms has been questioned [4], as this reductionist approach may neglect the additional cognitive demands, which have been shown to influence ACL injury risk factors [5]. While reducing available planning time, through unanticipated change of direction tasks increases ACL risk factors, further increasing visual discriminatory complexity may further challenge athletes while improving ecologic validity. Therefore, the purpose of this study was to determine the effects of increasing cognitive load, through discriminatory complexity, on ACL injury risk factors during unanticipated change of direction tasks. The incongruent flanker task (Fig 1C), which previously has been shown to influence ACL injury risk factors compared to planned conditions [6], was compared to a standard arrow task (Fig 1A) to determine whether more complex unanticipated stimuli further affect lower extremity biomechanics during change of direction (CoD) tasks. We hypothesized that the incongruent flanker task condition will result in increased peak vertical ground reaction force (vGRF), frontal plane knee valgus angle and moment, and increased sagittal plane knee extension from initial contact to 70ms post landing compared to the standard arrow condition.

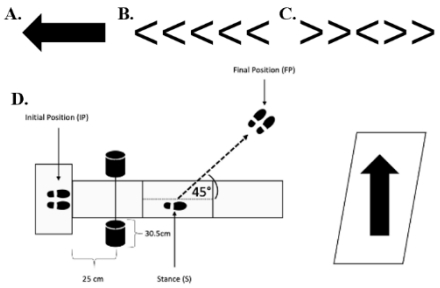


**Fig 1**: A. Standard arrow, B. congruent flanker, and C. incongruent flanker visual cues to change direction to left. D. Athletes jumped over a hurdle, landed unilaterally and cut towards the direction the visual cue.

**Methods:** 9 Division 1 athletes (Age: 19.82±1.67) completed a of series anticipated and unanticipated jumping tasks in response to both standard arrow, congruent, and incongruent flanker tasks to the left and right (Figure 1), though only the unanticipated standard arrow and incongruent flanker tasks were analysed in the present study (2 tasks total). Athletes were instructed to jump bilaterally from their initial starting position, land unilaterally and immediately follow the prompt to change direction at a 45° angle as far as possible. Data was collected until each participant completed 3 valid trials in each condition. Images appeared on the screen at the apex of the initial jump, triggered when the vGRF fell below 20 N. 3D marker-based motion capture (Qualisys) was synchronized with force platforms to quantify vGRF, frontal plane knee valgus angle and moment, and sagittal plane knee extension. The peaks were taken from initial contact to 70ms post landing. Differences in Peak vGRF, frontal plane knee angle and moments, and knee extension angles were analyzed via paired t-tests between unanticipated standard arrow and incongruent flanker conditions ($\alpha = 0.05$). Cohen's *d* effect sizes are presented.

**Results & Discussion:** The type of visual cue did not significantly influence ACL injury risk factors during unanticipated change of direction tasks. Peak vGRF (Arrow: 4.05±0.62 N/kg; Flanker: 4.05±0.62 N/kg, $p$=0.845, $d$=0.03), frontal plane knee angles (Arrow: 3.84±4.62°; Flanker: 2.72±6.11°, p=0.329, $d$=-0.21), frontal plane knee moments (Arrow: 0.59±0.44 Nm; Flanker: 0.60±0.44 Nm, $p$=0.947, $d$=0.03) or sagittal plane knee flexion angle (Arrow: 11.18±3.65°; Flanker: 13.35±5.12°, $p$=0.122, $d$=0.49) did not differ. While limited by a small sample size, the present results suggest increasing visual task complexity does not influence ACL injury risk factors during unanticipated tasks. While increasing cognitive load during planned conditions can increase ACL risk factors [5], adding an additional cognitive challenge while reducing planning time appears to have a negligible effect. These findings imply reducing planning time may be sufficient to screen for ACL injury risk factors.

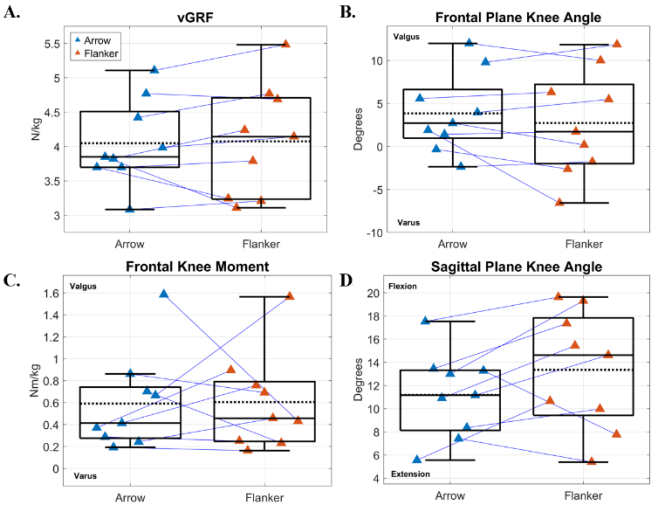


**Fig 2:** Boxplots and scatter plots for peak A. vGRF, frontal plane knee B. angles and C. moments and D. sagittal plane knee angles for each visual cue.

**Significance:** A standard unanticipated arrow task may be sufficient to screen for biomechanical risk factors associated with ACL injury, suggesting that increasing visual discriminatory task complexity may not be necessary.

**References:** [1] Almonroeder et al. (2018), *J Orthop Sports Phys Ther* 48(5); [2] Herman et al. (2016), *Am J Sports Med* 44(9); [3] Shibata et al. (2018), *Phys Ther Res* 21(2); [4] Bolt et al. (2024), *Sports Biomech* 23(10); [5] Hughes & Dai (2023), *Sports Biomech* 22(1); [6] Saadat et al. (2023), *Sports Biomech*

# EFFECTS OF SHOT DISTANCE AND ACCURACY ON INTER- AND INTRA-LIMB COORDINATION PATTERNS IN BASKETBALL THROWS

*Zhichen Feng[1], Yu Song[2], Issac Mason[1], Michale Torres[1] Qin Zhu[1]
[1]University of Wyoming, Laramie, WY
[2]University of Kansas, Lawrence, KS
*Corresponding author's email: qzhu1@uwyo.edu

**Introduction:** Effective basketball shooting is essential for team success [1]. Although free throws can account for a significant portion of a team's points (up to 69% [2]), the strategic importance of three-point shots continues to grow. Achieving a swish shot requires precise control of ball release, which depends on coordinated movement between the upper and lower limbs. While prior research has examined release parameters like height, velocity, and angle [3-4], the underlying inter- and intra-limb coordination patterns crucial for optimal shooting performance remain poorly understood. The current study used pre-release kinematic data to examine how shot distance and accuracy affect inter- and intra-limb coordination patterns in basketball, aiming to better understand the movement adaptations supporting accurate shooting.

**Methods:** Thirty-four recreational basketball players each completed a one-hour session wearing spandex shorts, a shirt, and athletic shoes. Reflective markers were placed on the shooting-side wrist, elbow, shoulder, hip, knee, ankle, and toe, with additional tape on the pinky finger. Participants performed free-throw and three-point shots in a randomized order, aiming for 10 swish and 10 missed shots per location. All trials were recorded using a GoPro 9 camera mounted on a tripod positioned 7 meters away from and perpendicular to the shooting plane. Joint positions were tracked in MaxTRAQ from initial movement to ball release. MATLAB processed the tracked joint positions to recover the time series of angular displacements and velocities of wrist, elbow, knee, and ankle, which were then used to compute continuous relative phase (CRP) for the joint couplings both within and between limbs. Statistical Parametric Mapping (SPM) and a two-way repeated measures ANOVA were used to examine the effects of shot distance and accuracy, as well as their interaction.

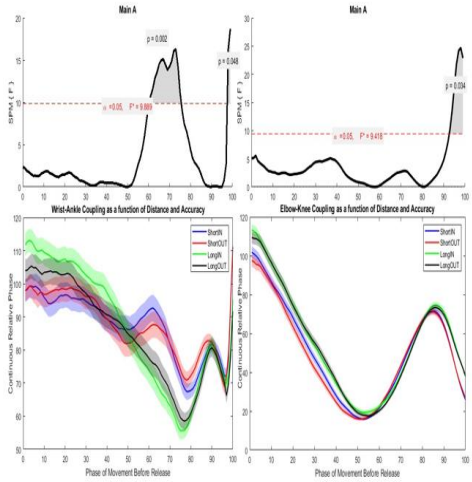


**Figure 1 Wrist-Ankle & Elbow-Knee CRP coupling**

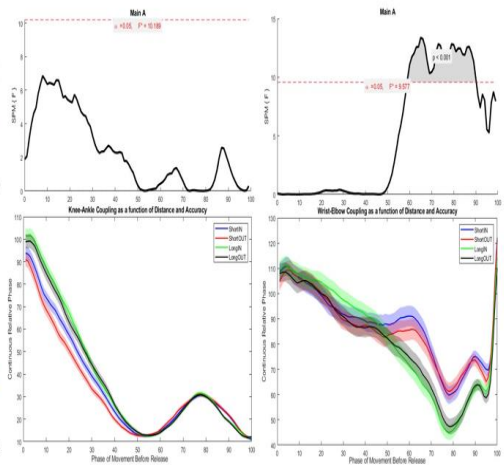


**Figure 2 Knee-Ankle & Wrist-Elbow CRP coupling**

**Results & Discussion:** We examined inter-limb coordination (Figure 1) by focusing on distal (wrist-ankle) and proximal (elbow-knee) couplings, and intra-limb coordination (Figure 2) by assessing wrist-elbow and knee-ankle couplings within upper and lower limbs. All joint couplings exhibited double phase shifts in the second half (50% beyond) of movement duration, suggesting the necessary control adjustments prior to release. However, the adjustments for the wrist-related couplings occurred later (at 75%) than those for the knee-related couplings (at 55%). SPM analysis showed a significant effect of shooting distance on wrist-ankle coupling between 60–75% ($F_{1,33} = 9.889$, $p = 0.002$) and wrist-elbow coupling between 60–90% ($F_{1,33} = 9.577$, $p < 0.001$), indicating the greater synchronization among wrist, elbow, and ankle in long-distance shots. For the knee-related couplings, a significant distance effect was found only in elbow-knee coupling ($F_{1,33} = 9.418$, $p = 0.034$) during the final phase (90–100%), indicating the greater synchronization in proximal coupling for short-distance shots. The observation aligns with the studies conducted by Kudo et al [5], which have shown that variations in inter-limb coordination significantly influence throwing performance. Moreover, expert athletes rely on stable coordination patterns to adapt to varying task demands [6], supporting our findings that distinct joint coupling patterns in different shooting conditions. These findings suggest that athletes use compensatory strategies to maintain shot accuracy despite coordination changes. Future research should examine how release parameters and coordination variability affect shooting performance.

**Significance:** Understanding how the upper and lower limbs coordinate in basketball is crucial for optimizing shooting technique and improving accuracy. The current study showed that inter- and intra-limb coordination patterns exhibited a pronounced shift toward in-phase synchronization during the pre-release phase. While coordination involving the wrist was significantly influenced by shot distance during the late pre-release phase, shot accuracy had no discernible effect.

**References:** [1] Button et al. (2003), *QRES* 74(3); [2] Navarro et al. (2009), *RPD/JSP* 18(3); [3] Hore et al. (1995), *Exp.Brain Res* 103; [4] Hamill et al. (1999), *Clin Biomech* 14(5); [5] Kudo et al. (2000), *J.Mot.Behav* 32(4); [6] Davids et al. (2003), *Sports Med* 33, 245-260.

# WHEN INTER-LIMB COORDINATION GETS CHALLENGING, VARIABILITY DRIVES TRANSITIONS

Marilena Kalaitzi Manifrenti[1], Nick Stergiou[1,2], Aaron D. Likens[1]
[1]Department of Biomechanics, University of Nebraska at Omaha, Omaha, NE, USA
[2]Department of Physical Education and Sport Science, Aristotle University, Thessaloniki, Greece

*Corresponding author's email: mkalaitzimanifrent@unomaha.edu

**Introduction:** Stirring a pot of pasta with one hand while rhythmically shaking a saltshaker with the other, is no simple task—1 spoon rotation for every 3 salt bursts equate to a difference in angular velocity between the two limbs. The different velocities form what is known as a multifrequency ratio, i.e., 1:3. If you were to keep adding salt and stirring, then the current mathematical model for multifrequency coordination predicts that your hands would eventually transition and perform a more stable, lower-level ratio, such as 1:1 [1,2; Fig.1]. However, if you stirred and salted very slowly, you would be more likely to sustain your initial 1:3 ratio [1]. Nevertheless, these predictions by the current model do not account for the inherent variability present in human movement. Specifically, the movement time-series of young healthy adults are temporally structured to exhibit variability that has the form of pink noise, which allows them to be adaptable in the face of unstable coordinative conditions [3,4,5]. Therefore, we hypothesized that when participants paced any ratio to pink noise cues, they should be more likely to transition to more stable, lower-level, ratios than when paced with other types of noise.

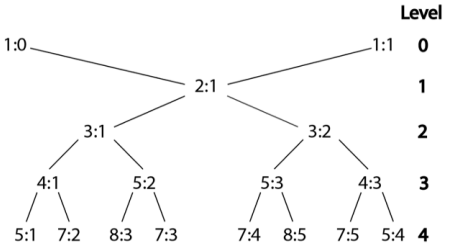


***Figure 1. Farey Tree.*** Lowers levels (e.g. 0-1) are considered more stable and 'easier' to perform than higher levels (e.g. 3-4), based on predictions made by the two-frequency resonance map model: $\theta_{n+1} = \theta_n + \Omega + \frac{K}{2\pi} sin(2\pi\vartheta_n)$

**Methods:** 34 participants performed a bimanual multifrequency wrist flexion/extension task, pacing their dominant hand to regular (Isochronous) and irregular (White, Pink, Brown noise) auditory cueing, while their nondominant hand was guided through a ratio template shown in a TV in front of them. Participants produced three intended ratios (1:2, 1:3, 1:4) at slow and fast speeds. Each unique combination was tested twice for a total of 48 trials, lasting 1 minute each. From the captured tapping trajectories (240Hz; PhaseSpace Inc.), the frequency ratio between the two hands was evaluated on a cycle-by-cycle basis. A generalized linear mixed-effects (LME) model with a binomial error distribution was used to evaluate the proportion of correct cycles (as in the performed cycle-by-cycle ratio matching the intended ratio) for a given intended ratio, while accounting for speed, noise effects and individual differences.

**Results & Discussion:** Across all noises, the probability of stably performing ratios 1:2, 1:3, and 1:4 when going slow was 100%, 99%, and 97% more likely than when tapping fast ($p<0.00001$; for all), respectively. However, speed also influenced ratio stability order, such that accuracy followed 1:2 ≥ 1:3 ≥ 1:4 when tapping slow, but reversed order when tapping fast, 1:2 <1:3 < 1:4. Lastly, while there were no noise differences when tapping slow, accuracy when tapping fast was moderated by noise type, and trends differed based on intended ratio. Accuracy measures, however, are global summaries that say nothing about cycle-by-cycle dynamics. Therefore, we applied a Markov model to find transition probabilities (TPs; the probability performing a certain ration at time, *t*, given performing the same or another ratio at time *t*-1), which characterized the systematic tendencies of participants towards specific (un)intended ratios. While the LME suggested no apparent accuracy differences across noise types at the 1:3 ratio during slow speeds for example, the TPs revealed differences in both the number of available ratios and the frequency of transitions (Fig.2). When participants taped to Pink or Brown noise, their coordination was strongly attracted to the intended ratio, and deviations were limited to fewer alternative ratios compared to White or Isochronous taping. The prevalence of numerous ratios in the latter two conditions suggested incoherent cycle-by-cycle coordination patterns.

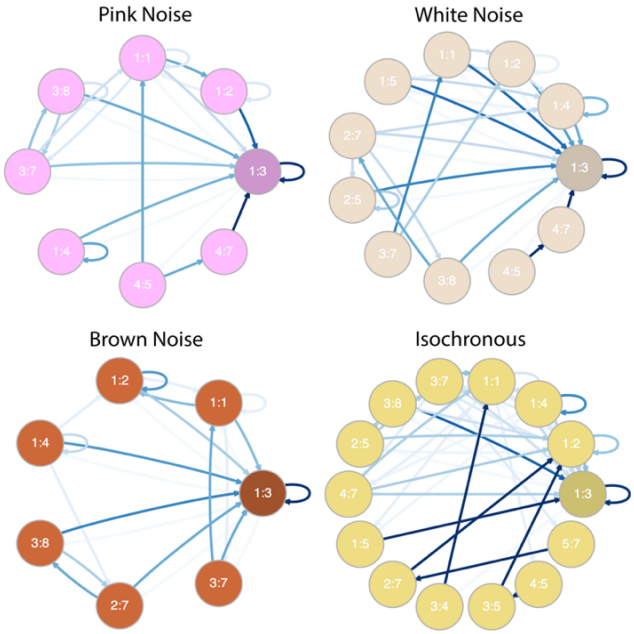


***Figure 2. Markov Chain Network Plots for Performed Ratio 1:3 at Slow Speed.*** *Arrows show transition direction of a given ratio to another. Bolder arrows indicate higher transition probability.*

**Significance:** Our findings revealed that the temporal structure of movement variability is a key determinant of multifrequency inter-limb coordination stability, directly challenging current models. This underscores the need to refine frameworks to integrate variability-driven transitions for a more accurate understanding of coordinated movement.

**Acknowledgments:** The Center for Research in Human Movement Variability and the NIH [P20GM109090, P20GM152301].

**References:** [1] Peper et al. *J. Exp. Psychol*. **21**(5), 1117-1138, 1995, [2] Hardy and Wright. *Oxford University Press*. 1960, [3] Stergiou and Decker. *Hum. Mov. Sci.* **30**(5), 869-888, 2011, [4] Ravi et al. *J. Exp. Biol*. **224**(5), jeb237073, 2021, [5] Brink et al. *Proc. Natl. Acad. Sci. U.S.A.* **121**(31), e2400687121, 2024.

# VISUAL OFFSET OF ONE HAND IN VIRTUAL REALITY DOES NOT ALTER LIMB SYMMETRY DURING SHOULDER FLEXION

Taylor J Wilson*, Motoki Sakurai, Andy Karduna
University of Oregon, Eugene, Oregon, US
*Corresponding author's email: twilson8@uoregon.edu

**Introduction:** The brain integrates sensory information like vision and proprioception to determine agreeability between two or more senses. For instance, when grabbing a coffee cup, we visually see the distance and fullness of the cup before reaching for it. We estimate the weight based on vision and previous experiences and compare this to the weight of the actual cup through proprioception. If sensory information from one stimuli is more variable, the system will shift the sensory reliance towards the least variable stimuli [1].

With recent technological advancements, virtual reality (VR) has been used to investigate and alter our sensory reliance. Researchers can change the environment, and thus the visual stimuli, to measure sensory reliance and reweighting. In fact, previous studies have looked at altering vision in VR with a visual offset (i.e., the arm could be at 90º shoulder flexion in real life, but shown at 100º in VR) [1]. Interestingly, even when an explicit offset in vision is given, the weighting of vision still influences the weighting of other sensory stimuli and cannot be completely ignored [2]. Although previous studies have investigated the effect of visual offsets on task performance, these studies have only looked at visual offsets applied unilaterally to the dominant arm [1, 2], as well as only performed static (stationary target) joint position sense tests [1, 2, 3]. We are unsure if these results would hold true (reliance on incorrect visual stimuli) during a dynamic (moving task) and if the visual presentation matters on the right versus left side. Thus, altering visual stimuli in VR during a dynamic bilateral task could aid in understanding the scaling of sensory reliance. Subjects were hypothesized to be less symmetrical when a visual offset is present, with no differences in symmetry when presented with the right or left hand.

**Methods:** Twenty-four healthy subjects (Sex: 13 Females/11 Males, Age: 20.8 ± 3.5 years (mean ± 1 std), Height: 171.2 ± 10.4 cm, and Mass: 70.8 ± 15.3 kg) were included and completed the informed consent approved by the University of Oregon Institutional Review Board. Participants were excluded if they had experienced chronic upper body pain in the past three weeks, upper limb injury in the past year, history of neurological disorder(s), or uncorrected impaired vision.

An HTC VIVE VR headset with over-the-ear headphones was placed on the subject's head and HTC VIVE wrist trackers were secured to the subject's wrist. A three-dimensional visual environment (white walls and floor) with the subject's wrist position (black sphere) was presented. Subjects were seated and required to keep limb symmetry from 40º to 100º shoulder flexion, while raising both arms. All participants performed shoulder flexion 10 times per condition, which consisted of accurate vision of the left or right hand only (AVL or AVR, respectively) and offset vision of the left or right hand only (OVL or OVR, respectively), where the hand was offset by +8º of shoulder flexion angle. For example, in OVR, the subject would only see their right arm at 88º in VR, while their right arm would be at 80º in the real world. A statistical parametric mapping (SPM) analysis test was used to compare the limb asymmetry (LA) difference, defined as LA during OVL minus LA during AVL at each shoulder flexion angle (this considers subject variability/baseline error during AV), to zero. An SPM analysis was also run for the limb asymmetry difference on the right side (LA Difference OVR – LA Difference AVR at each shoulder flexion angle).

**Results & Discussion:** SPM analysis found no differences in LA difference left (Fig. 1) or LA difference right (not shown) when compared against zero, indicating that offset vision of one limb in virtual reality does not influence limb symmetry during a shoulder flexion arm raising task when provided vision of one side. However, since vision was only provided to one side, this may not have been enough stimuli (compared to both arms) to rely on offset visual cues. Secondly, subjects were instructed to face forward the entire time, thus only allowing a field of view between 70º to 110º. Therefore, proprioception may have been relied upon initially but then continued to be relied upon primarily. Further, participant's arm raising velocity was not constrained.

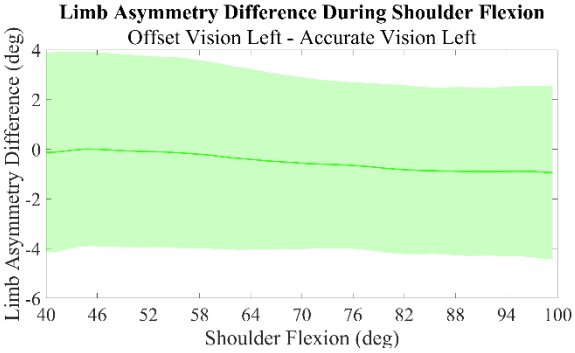


**Figure 1.** Left limb asymmetry difference during 40º to 100º shoulder flexion (mean ± 1 std).

**Significance:** Our results do not align with previous work of unilateral static tasks, which found visual offsets affecting joint position sense accuracy [1], but could be due to the experimental design differences from the unilateral test described above. Our next research question will address how we can utilize visual offsets during intermanual transfer of tasks, or the phenomenon of training one hand leading to better performance of the untrained hand [4]. In those who have suffered a stroke or hemiplegic cerebral palsy for example, poorer motor control has been seen on the affected side. Recent studies have shown that seeing your left hand [4] or both hands [5] in VR while performing a right-handed task improves intermanual transfer to the unused left hand, thus we would like to investigate if this phenomenon is more pronounced when given a visual offset in both healthy and unhealthy adults.

**Acknowledgments:** A huge thank you to the undergraduates in our lab for helping with data collection and recruitment: Hanna Lindstrom, Kaylin Kisor, Noa Neser, and Ella Brauer.

**References:** [1] Spitzley & Karduna (2022), *J Mot Behav* 54(1); [2] Morehead et al. (2017), *J Cogn Neurosci* 29(6); [3] King et al. (2013), *J Mot Behav* 45(6); [4] Ossmy & Mukamel (2016), *Cell Rep* 17(11); [5] Xiao et al. (2020), *IEEE Conference on VR*.

# From Disruption to Enhancement: The Impact of Noise on Haptic Perception

Alli Grunkemeyer[1], Aaron D. Likens[1]
[1]Department of Biomechanics, University of Nebraska at Omaha, Omaha, NE USA
*Corresponding author's email: agrunkemeyer@unomaha.edu

**Introduction:** Dynamic touch refers to the ability to perceive object properties, such as weight and length, through movement-based interactions. This process is mediated by the forces and torques exerted during wielding, allowing individuals to extract meaningful information from an object's inertial properties [1]. Stochastic resonance (SR), a phenomenon in which the introduction of subthreshold noise enhances sensory signal detection, has been widely studied in perceptual and motor control domains [2,3]. Prior research has demonstrated that SR can improve proprioceptive accuracy and postural stability, yet its effects on haptic perception during object manipulation remain unclear [2,3]. Previous studies suggest that the properties of noise, such as its alignment with the movement patterns, may significantly affect perceptual accuracy [3]. In this study, we examine how subthreshold vibrotactile noise influences perceptual judgments of object properties, specifically focusing on how the coherence between the noise and the wielding movements impacts accuracy. Using varying object masses and analyzing the 3D Euclidean distance time series of wielding movements, we aim to identify the optimal noise conditions that enhance haptic perception.

**Methods:** Ten healthy adults (3 males and 7 females) (age 26 ± 2.97 years) were seated for the duration of the trial with a haptic device fastened to their wielding arm, as seen in **Figure 1**. Subthreshold stimuli were introduced via a haptic device with different types of colored noise, stochastic signals that varied power spectral slope. Subjects wielded an occluded object with varying masses. There were four different mass stimuli being presented (in terms of added mass: 0, 50, 100, and 150 g). Subjects rated the heaviness of the object in relation to a standard object by marking their perceived heaviness on a scale presented at the end of each trial. These responses were used to calculate perceptual accuracy.

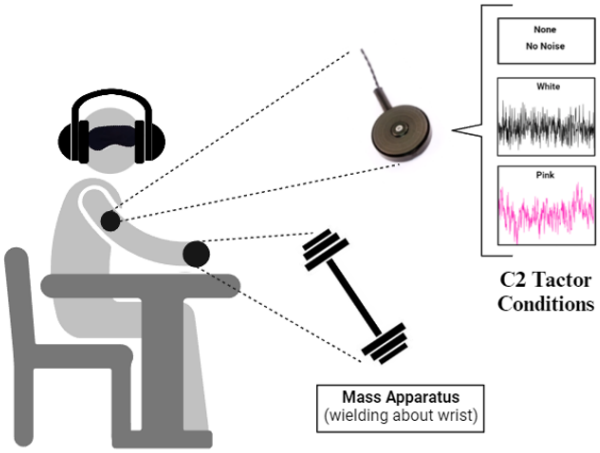


**Figure 1.** Experimental set up. Active markers (PhaseSpace Inc.) were placed on the participants' wielding hand, forearm, upper arm, and the apparatus.

For statistical analysis, we fit a series of Tweedie-Generalized linear mixed effect (LME) models with percent error as the outcome variable and fixed effects of noise, mass, movement dynamics (*d*), mean coherence, and their interactions. Subsequent models were compared by likelihood ratio tests for model improvement. Movement dynamics, quantified by the fractional integration parameter (*d*) was calculated using ARFIMA modeling, which measures long-range dependence in the time series, with higher *d* values indicating stronger long-term correlations. Mean coherence was computed through spectral analysis, measuring the linear relationship between the noise signal and the corresponding 3D distance time series across frequencies, with a value of 1 indicating near-identical signals and 0 indicating no relationship. These metrics were used to assess how noise coherence with movement influenced perceptual accuracy.

**Results & Discussion:** With *d* as the response variable, the best-fitting model included all four terms, [$\chi^2(6) = 13.5963$, $p = 0.03449$]. A simple slope analysis revealed that the relationship between mean coherence and *d* was moderated by both mass and noise type. Specifically, as mean coherence and mass increased, *d* decreased under pink noise, but increased under white noise (*Estimate = -3.537, p = .0325*). With percent error (PE) as the response variable, the optimal model included three terms, [$\chi^2(2) = 8.7615$, $p = 0.01252$]. A simple slope analysis indicated that PE increased with mean coherence in the presence of pink noise, but decreased with white noise (*Estimate = 679, p = .0314*). These results suggest that noise type plays a crucial role in modulating both long-range correlations in the wielding movements and perceptual accuracy, with pink noise degrading perceptual performance as mean coherence increases and white noise enhancing it.

**Significance:** Our results indicate that pink noise disrupts sensory processing by introducing structured low-frequency components that align with natural movement patterns, causing confusion in movement perception. As the coherence between the noise and movement increases, this interference intensifies, reducing long-range correlations (*d*) and increasing percent error (PE). In contrast, white noise, with its random spectral distribution, does not interfere with long-range correlations, allowing participants to maintain perceptual accuracy. As coherence between white noise and movement increases, participants' ability to judge the relationship between the two improves, leading to lower percent error. This suggests that structured noise (pink noise) destabilizes the sensory system and reduces perceptual stability, while random noise (white noise) does not cause the same disruption and may even enhance perceptual accuracy. Future work should explore the impact of various noise types on sensory processing by examining a wider range of noise conditions and movement tasks, further clarifying the mechanisms behind perceptual accuracy and long-range correlations.

**Acknowledgments:** This research was supported by an UNO GRACA, and NASA Nebraska Space Grant FY23 Fellowship to AG.

**References:**

[1] Streit et al. Psychonomic Bulletin & Review, 14(5): 1001-1006, 2007.
[2] Hoskins et al., Journal of Surgical Endoscopy, 30: 4214-4219, 2016.
[3] Yamagata et al. Journal of Neuroscience Letters, 842: 138008, 2024.

# NEURAL-CARDIAC COUPLING ACROSS VARIOUS PSYCHOPHYSIOLOGICAL STATES

Maxine He[1], Jonathan Cerna[1], Hamzah Jamal[2], Jiaqi Zhao[3], Simon Yu[2], Elizabeth T. Hsiao-Wecksler[1,4,5], Manuel E. Hernandez[1,3,5]
[1]Neuroscience Program, [2]Electrical & Computer Engineering, [3]Computer Science, [4]Mechanical Sciences & Engineering, [5]Biomedical and Translational Sciences, University of Illinois Urbana-Champaign, Urbana, IL
*Corresponding author's email: mhernand@illinois.edu

**Introduction:** The relationship between brain activity and cardiac function represents a significant aspect of human psychophysiology of how the central autonomic network interacts with cardiovascular function through sympathetic and parasympathetic pathways [1]. Electroencephalography (EEG) frequency bands and heart rate variability (HRV) metrics provide complementary windows into central nervous system activity and autonomic regulation, offering potential insights into how specific brain oscillations relate to cardiac control. Despite growing interest in neural-cardiac coupling, most studies have examined these connections in isolated contexts rather than comparing patterns across diverse conditions. Understanding how brain-heart coupling differs between conditions—such as seated state versus dual-task walking cognitive tasks, physiological versus psychological stressors, and anxious versus meditative states—could reveal distinct mechanisms of psychophysiological adaptation. This study addressed these gaps by examining brain-heart coupling across five distinct conditions: relaxation through video guided mindfulness practice, Cold Pressor Test (CPT, physical stress), Trier Social Stress Test (TSST, psychological stress), seated Stroop Task (cognitive challenge), and walking Stroop Task (combined cognitive-physical challenge while walking on a treadmill). By analyzing correlations between EEG frequency bands and HRV measures, we aimed to characterize condition-specific patterns of neural-autonomic interaction during stationary and movement-based tasks.

**Methods:** Simultaneous 64-channel EEG (Brain Vision ActiChamp, North Carolina, USA) system and ECG from a Hexoskin (Carré Technologies, Montreal, Canada) smart wearable shirt were recorded in 40 young adults during each condition. EEG raw signals were processed by filtering and independent component analysis to remove movement artifacts, and power spectral density across 5 frequency bands (delta, theta, alpha, beta, gamma) were calculated in 26 electrodes that represent frontal, central, parietal, occipital regions. Heart rate variability (HRV) was extracted from raw ECG signals using Kubios Scientific Software, including time domain features like mean heart rate (HR) and mean R-peak to R-peak intervals, and frequency domain measures like high frequency (HF) power, low frequency (LF) power, and their ratio (LF/HF). Neural-cardiac coupling was assessed using Pearson's correlation coefficients between EEG and HRV features.

**Results & Discussion:** Correlation analysis revealed condition-specific patterns of brain-heart coupling across different frequency bands. The relaxation condition demonstrated moderate associations between gamma ($r = 0.396$, $p = 0.011$) and beta ($r = 0.344$, $p = 0.029$) activity in frontoparietal (FC4, Pz) regions and heart rate standard deviation (std_HR) and HF power, respectively. CPT also exhibited moderate correlations ($r = 0.48$, $p = 0.01$) between gamma activity in occipito-parietal regions and LF/HF ratio. The TSST condition showed prefrontal (Fz) delta and beta band correlations with mean HR (delta: $r = 0.38$, $p = 0.016$; beta: $r = 0.33$, $p = 0.038$). The seated Stroop task revealed weaker correlations, primarily involving gamma activity in frontocentral (FC3) and parietal regions (P5, CP4) with mean HR ($r = 0.38$, $p = 0.018$) and LF/HF ratio (P5: $r = 0.366$, $p = 0.020$; CP4: $r = 0.331$, $p = 0.037$). In contrast, the walking Stroop condition produced the strongest correlations in our study, with central EEG activity (Cz) showing robust associations with HRV measures ($r = 0.813$ for theta-Cz and std_HR, $p < 0.0001$; $r = 0.818$ for delta-Cz and HF power, $p < 0.0001$; $r = 0.804$ for gamma-Cz and std_HR, $p < 0.0001$).

Our findings suggest distinct patterns of brain-heart coupling that vary across experimental conditions, suggesting task-specific neurophysiological mechanisms in autonomic regulation. During relaxation, we observed correlations between frontoparietal gamma/beta activity and std_HR, supporting findings by [2] on meditation-induced changes in autonomic function. The CPT, a well-established physiological stressor, showed widespread correlations across occipital and frontal regions, predominantly in gamma and beta bands. These results align with the findings by [3], who reported increased high-frequency EEG synchronization with cardiac signals during pain processing, corresponding to the bottom-top regulation from peripheral to the brain. The TSST condition revealed prefrontal correlations, particularly between delta activity at Fz and LF power, which aligns with the work demonstrating prefrontal involvement in stress-related cardiovascular regulation [4]. The seated Stroop task showed weaker correlations, primarily involving gamma activity in frontocentral and parietal regions with mean heart rate and LF/HF ratio. The involvement of multiple frequency bands at central and frontal regions during walking likely reflects the motor planning and execution and cognitive load under the dual tasking condition [5]. The difference in correlation strength between seated and walking conditions (average $r = 0.33$ for seated vs. 0.47 for walking) suggests that physical movement and cognitive load may amplifies brain-heart coupling during cognitive challenge.

Across all conditions, our findings reveal various patterns of neural-cardiac coupling strength, with dual-task walking Stroop test showing the strongest correlations, followed by physical stressors (CPT), psychological stressors (TSST), meditation, and finally cognitive challenge (seated Stroop) alone. Our findings suggests that the degree of neural-cardiac coupling may reflect the overall demand for integrated whole-body responses, with more complex and demanding tasks requiring tighter coordination between central neural activity and peripheral autonomic function.

**Significance:** Our findings reveal that brain-heart coupling is enhanced during walking compared to seated conditions, with central sensorimotor cortex (Cz) showing the strongest correlations with HRV during dual-task performance (walking Stroop). The neural-cardiac signatures identified across conditions provide potential biomarkers for detecting specific psychological and physiological states using wearable monitoring technology.

**Acknowledgments:** Funding via Jump ARCHES program at University of Illinois Urbana-Champaign.

**References:** [1] Thayer and Lane. 2009. Neurosci and Biobehav Rev. [2] Tang et al. 2015. Nature Revies Neuroscience. [3] Catrambone et al., 2024. Hum Brain Mapp. [4] Gianaros and Wager. 2015. Curr. Dir. Psychol. Sci. [5] Beurskens et al., 2016. Neuroplast.

# EFFECTS OF FATIGABILITY ON MOVEMENT VARIABILITY USING WEARABLE TECHNOLOGY

*Carla Pérez-Chirinos[1], Vinyet Solé[1], Víctor Toro-Román[1], Víctor Illera[1], Sara González-Millán[1], Lluís Albesa[1], Gerard Moras[1], Sara Ledesma[1], Oriol Teruel[1], Felipe de Jesús Alviso[1], Doyin Ogundiran[2], Bruno Fernández-Valdés[1]

[1]Department of Health Sciences, Research Group in Technology Applied to High Performance and Health (TAARS), TecnoCampus, Universitat Pompeu Fabra, Mataró, Barcelona, Spain
[2]Department of Kinesiology and Nutrition, University of Illinois at Chicago, 1919 W. Taylor St., 650 AHSB, Chicago, IL 60612, USA

*Corresponding author's email: cperezchirinosb@tecnocampus.cat

**Introduction:** Fatigability, defined as the progressive increase in fatigue during activity, is a multifactorial process that significantly alters human movement across various tasks, [1]. Among the methods used to examine the level of fatigue in humans is movement variability (MV) [2], which refers to the natural variations or fluctuations that occur in motor behavior during the repetitive execution of an action [3]. Analyzing these variations can provide valuable insights into how fatigue influences motor control. Nonlinear techniques (NLTs), such as entropy measures, are mathematical methods designed to capture temporal variations in motor output behavior [3]. These tools offer greater sensitivity than traditional linear measures, potentially enhancing fatigue detection [3]. A key concept in this framework is the "loss of complexity" theory, which suggests that fatigue leads to a reduction in the complexity of motor output, reflecting a diminished ability of the neuromuscular system to adapt to perturbations [3,4]. This loss of adaptability has been linked to impaired motor control, aging, and increased injury risk [3]. In this study, we aim to investigate the effects of fatigability on MV using wearable technology (inertial measurement units, IMUs). Specifically, we employ entropy as a NLT to analyze MV, as it allows us to assess motor output in response to fatigue. We hypothesize that contrary to findings predominantly observed in isometric contractions, dynamic fatiguing contractions induce an increase in entropy, possibly reflecting a compensatory adaptation of the neuromuscular system to maintain movement efficiency despite fatigue.

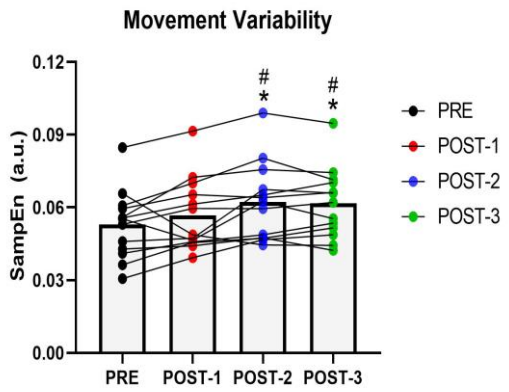


**Figure 1:** Movement variability (MV) during 30-seconds maximum-intensity set of half squats. * $p < 0.05$ vs. PRE; # $p < 0.05$ vs. POST-1 (One-factor ANOVA with Hommel post hoc statistical test).

**Methods:** Thirteen healthy young participants (23.5 ± 2.8 years; 67.8 ± 9.7 kg; 1.71 ± 0.05 m) were recruited for this study. The experimental protocol consisted of two key phases: **(1) fatigue induction** through three repeated exhaustive Wingate tests and **(2) MV assessment** via a body-weight half-squat task performed before (PRE) and immediately after each Wingate test (POST-1, POST-2, POST-3). Each Wingate test (30 seconds all-out) was conducted with an individualized workload, calculated as 5.76 J/rev/kg × body weight (kg) [5], while cadence and torque were monitored. MV during squatting was analysed using IMUs (WIMU, Realtrack Systems, Spain), placed at the pelvis. For the calculation of MV through Sample entropy (SampEn), the raw acceleration signal in the three axes was extracted from the system-specific software. SampEn calculation was performed using dedicated routines programmed in Matlab.

**Results & Discussion:** The results indicate that fatigue significantly affects MV. IMU data showed an increase in movement pattern variability following fatigue, with significant differences observed between **Pre vs. Post 2** ($p = 0.030$), **Pre vs. Post 3** ($p = 0.045$), **Post 1 vs. Post 2** ($p=0.041$), and **Post 1 vs. Post 3** ($p=0.037$) (Fig. 1). Our study suggests that dynamic contractions elicit a different neuromuscular response, potentially reflecting an adaptive strategy to sustain performance under fatigue. Similar to findings by Cortes et al. [4], where fatigue-induced variability changes were task-dependent, our data indicate that MV cannot be universally characterized as a decline but rather as a shift in complexity. In the presence of fatigue, the neuromuscular system rapidly searches for a new movement solution to preserve task performance. This is evidenced by increased MV after fatiguing. Further analysis is required to quantify these changes more precisely.

**Significance:** These findings may provide insights into fatigue-related alterations in motor control and contribute to the development of strategies for optimizing athletic performance and reducing injury risk. Additionally, wearable IMU technology offers a practical and non-invasive method for assessing MV in real-world scenarios.

**Acknowledgments:** We thank all participants for their involvement in the study and acknowledge the support from the Research Group Technology Applied to High Performance and Health (TAARS).

**References:**

[1] Enoka, R. M., & Duchateau, J. (2008). *The Journal of physiology*, 586(1), 11-23.
[2] Stergiou, N. (2004). *Champaign: Human Kinetics*.
[3] García-Aguilar, F., et al. (2022). *Frontiers in Physiology*, 13, 1074652.
[4] Cortes, N., Onate, J., & Morrison, S. (2014). *Gait Posture*, 39(3), 888–893.
[5] Bar-Or O. (1987). *Sports Medicine*, 4(6), 381-394.

# NEURAL AND ATTENTIONAL CORRELATES OF TASK-SWITCHING PERFORMANCE

Alexandra C. Lynch*, Fatemeh Aflatounian, Keith A. Hutchison, Scott M. Monfort
Montana State University, Bozeman, MT, USA
*Corresponding author's email: alexandra.lynch@montana.edu

**Introduction:** The ability to adaptively switch between tasks underpins decision making and goal-directed behavior. In sport, athletes are continuously faced with scenarios where attention must be directed toward multiple stimuli. As focus rapidly switches between tasks, performance on each task declines to a unique extent for each individual. Attention control (AC) plays a role in task-switching where performance decrements are linked to executive control and switch costs. These costs arise as individuals are required to reconfigure new tasks sets and inhibit the previous task. Consequently, task-switching events result in slower reaction times and increased errors compared to non-task-switching conditions [1]. Executive (dys)function during task-switching can be quantified and monitored through functional neuroimaging, typically in the dorsolateral prefrontal cortex (DLPFC) [2,3]. Strengthening our understanding of cognitive and neural correlates of sport-relevant task-switching could provide deeper insight into individual factors that differentiate high vs. low performers. The understanding of these factors may help develop injury risk screening and/or intervention tools to improve performance. Therefore, the purpose of this study was to assess performance in task-switching involving whole body movement through attention control scores and neural activation. We hypothesize higher attention control scores will be associated with decreased reaction time and decreased neural activation in the DLPFC, and decreased reaction time will be associated with decreased neural activation during a novel, sport-like, task-switching paradigm, following a neural efficiency framework.

**Methods:** 18 healthy controls participated in this study (20.5±1.6 years, 9 females, 1.75±0.08m, 77.2±12.8kg, 7.9±0.5 Tegner, 13.3±1.9 Marx). AC was assessed through the Stroop Squared, Flanker Squared, and Simon Squared tests with weighted scores loaded onto a latent variable (weights: 0.66, 0.72, 0.76, respectively) [4]. Task-switching performance was measured through a novel sport-like paradigm where reaction time and accuracy were emphasized. Participants were asked to shift their weight to either foot in response to a visual stimulus shown on either side of a screen (away from a defender, towards a ball). This paradigm was repeated for 5 blocks of 16 randomized pictures (randomized 1 or 2 second picture delay). Performance was assessed by averaging reaction time (RT) to a correct decision (away from defender, towards ball), across all trials. DLPFC activation (BA46 and BA9) was monitored during the task-switching paradigm using functional near-infrared spectroscopy (fNIRS; 8-source, 7-detectors, 8-short separation channels, NIRSport2). A 30-second baseline period was collected prior to each block of pictures. fNIRS data analysis followed previous methods[5]. Optical density time series were processed by applying temporal derivative distribution repair and a lowpass 0.5 Hz cutoff filter prior to applying the modified Beer-Lambert law. T-statistic values calculated through an autoregressive, iteratively reweighted least squares regression model were used to characterize subject-specific neural activation. Pearson correlations (Spearman if not normally distributed) assessed correlations between neural activation (i.e., T-values), RTs, and AC scores.

**Results & Discussion:** A negative, albeit non-significant, relationship was found between RT and DLPFC activation (BA46 rho = -0.33, p = 0.187; BA9 rho = -0.30, p = 0.221). No other correlations were found between dependent variables (Fig. 1A). Post-hoc bootstrap analysis (1000 resamples with replacement) for RT correlations (BA46 [-0.681, 0.093] and BA9 [-0.653, 0.1]) indicated a clustering of moderate-strength correlation coefficients (Fig. 1B), albeit with large variance for the current small sample size. Although not reaching statistical significance and needing additional data to verify, the data are more aligned with increased DLPFC activation associating with improved performance (i.e., faster reaction times) rather than a neural efficiency relationship (i.e., less activation to perform the same task) for this challenging task. Inverse relationships between DLPFC activation and motor performance in dual-task scenarios has previously been reported during walking [6], along with the potential for task-specific relationships with cognitive and/or motor performance and neural activation. Although individuals were instructed to equally focus on reaction time and correct decisions, differences in interpretation of the task goals could influence neural activation patterns and ultimately dissociate AC scores from task performance. AC performance appears to be a strong predictor of various cognitive processes and cognitive multitasking; however, its ability to serve as a correlate for cognitive-motor function appears limited in this task-switching paradigm.

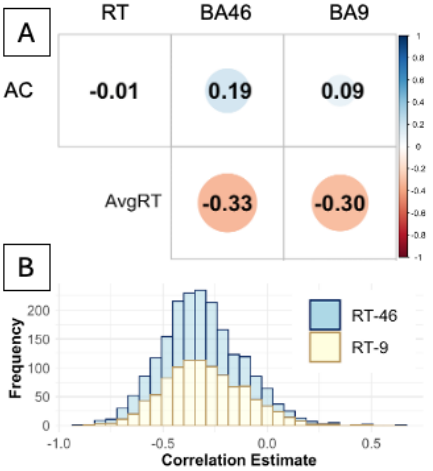


*Figure 1: A) Correlations between neural activation (BA46/BA9), RT, and AC performance. B) Frequency of correlation estimates between RT-BA46 and RT-BA9 from bootstrap analysis.*

**Significance:** Weak-to-moderate strength correlations between DLPFC activation and task-switching performance may become clearer upon increasing statistical power with a larger sample size. This relationship would provide a neural correlate of sport-relevant task that could augment screening and training efforts, injury prevention, and performance optimization. The lack of relationship between performance and attention control outcomes may indicate a variable strategy towards the novel, task-switching task.

**Acknowledgements:** Funding via MSU VPREDGE Research Expansion Fund.

**References:** [1] Kiesel et al. (2010). Psych. Bul. [2] Krawczyk. (2002). Neurosci. Biobehav. Rev. [3] Hyafil et al. (2009). J. Neurosci. [4] Burgoyne. (2023). J. Exp. Psychol. Gen. [5] Reed et al. (2022). Hum. Mov. [6] Mirelman et al. (2014). J. Neuroeng & Rehab.

# The Effect of Emotion on Kinematics of Choreographed Dance Movements

*Katherine M. Elder[1], M. Melissa Gross[1]
[1]Department of Movement Science, School of Kinesiology, University of Michigan, Ann Arbor, MI
*kmelder@umich.edu

**Introduction**: Emotion expressed during ordinary movements like gait and sit to stand can be recognized by others and affects the movement kinematics [1,2]. Gait speed increases and body posture is more flexed with sadness and gait speed decreases and body posture is more upright with high-arousal emotions (i.e., joy and anger) compared to neutral [1]. Similarly, emotion can be recognized in novel movements without a functional goal, e.g., choreographed dance movements performed for emotionally expressive or aesthetic purposes [3]. Much less is known about the effect of emotion on the kinematics of choreographed movements, however, due to limitations in the choreographed movement itself or the biomechanical variables analyzed. For example, in a study of an arm gesture comprising shoulder adduction from vertical to horizontal position with free movement of elbow and wrist joints, investigators found that maximum linear velocity and acceleration of the fingertips were significantly greater for anger than for sadness [4]; further, the authors suggested that full-body measures may better distinguish emotions quantitatively. The purpose of this study was to further investigate the effect of emotional expression on the kinematics of choreographed movements.

**Methods**: After providing consent, two dancers with professional dance experience were outfitted with a full-body set of 61 motion capture markers. Each dancer was asked to create four short, neutral movement phrases using their: (1) full body while staying in place, (2) upper body only, (3) lower body only, and (4) full body while translating. They were then asked to perform three trials of each phrase while expressing each of four emotions: neutral, sadness, anger, and joy. Trials were recorded using an 18-camera motion capture system. Kinematics were calculated using Visual 3D. Movement phrase events were identified for each joint and were described by onset time, amplitude and duration. Significant differences were detected using ANOVA and post hoc comparisons ($p<.05$). The effect of emotion on the one movement phrase (full body while staying in one place) is reported here for one dancer.

**Results & Discussion**: As observed by others for functional tasks, emotion significantly affected movement time ($p<.01$). The movement phrase took longer to complete when expressing sadness (8.0±2.3s) than for anger (6.2±0.5s, $p<.01$), joy (6.4 ±0.5s, $p<.01$) and neutral (6.3±0.3s, $p<.01$) trials. Movement events were defined for each joint as the interval between adjacent minima. The eight movement events identified for shoulder abduction are shown in Fig. 1. The relative durations of the movement events were similar among emotions, differing from neutral (0.8±2.5%), suggesting that emotion affects total phrase time but not the relative duration of events within the phrase. In contrast, emotion affected the peak magnitude of shoulder movement compared to neutral. For example, at at event 1, abduction angle increased for anger (116%) and sadness (12%), but decreased for joy (22%), and at event 3, abduction angle increased with anger (91%), joy (15%) and sadness (61%). The time that peak joint motion occurred also changed with emotion. With sadness, shoulder abduction occurred 2.0% and 3.7% earlier for events 1 and 5, respectively, but 3.3% later for event 8 compared to neutral. With joy, peak shoulder abduction occurred 2.7%, 4.0% and 2.0% later for events 2, 3, and 7, respectively. In contrast, the time of peak abduction with anger changed little across events (range 0.3-1.0%).

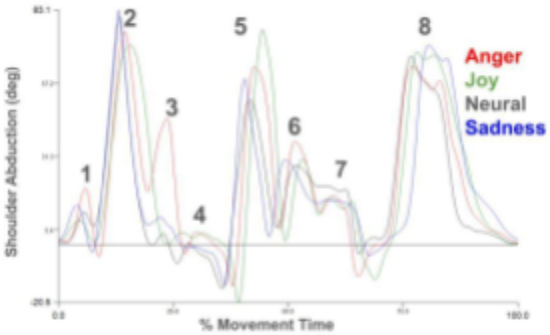


**Figure 1**. Left shoulder abduction angle during the full-body movement phrase. Numbers indicate movement events.

Four movement events were identified for hip flexion during the movement phrase. Like for the shoulder, the relative durations of the movement events were similar to neutral for anger and sadness (0.7±3.5), but changed with joy by as much as 5%. Peak amplitude also increased with emotion at the hip. For example, at event 1, flexion increased 11, 6 and 15% with anger, sadness and joy, respectively, and at event 3, flexion increased 14 and 8% with anger and sadness, respectively, but decreased 4% with joy. The time of peak hip flexion also changed with emotion. The time that flexion peaked changed most for event 1, occurring 10, 28 and 10% earlier with anger, sadness and joy, respectively.

Our results suggest that both upper and lower extremity joint motions are affected by emotion, including magnitude and timing of events within a full-body choreographed movement. The relative timing of events within phrases was less affected by emotion in more complex choreographed movement sequences than investigated in previous studies.

**Significance:** Research in emotional expression in novel movements provides insight into the role of body language in communication. Understanding how emotion affects biomechanics of novel body movements also contributes to robotics development and virtual rendering of human movement.

**Acknowledgments:** We thank W Zhou, A Kramer, and AJ Santalone Levin for their assistance with data analysis. This research was supported by a University of Michigan Rackham Graduate Student Research Grant.

**References:** [1] Gross et al. (2012) *Hum Mov Sci* 31:202; [2] Kang & Gross (2015) *Hum Move Sci* 40:341; [3] Smith & Cross (2023), *Psych Res* 87:484; [4] Sawada et al. (2003) *Percep Mot Skill* 97:697.

# THE IMPACT OF FATIGUE ON LANDING STABILITY IN FEMALE COLLEGIATE BASKETBALL ATHLETES

Authors: Suzanne M. Konz[1], Brandi Anders[2]
[1]Marshall University, School of Health & Movement Sciences, Huntington, WV; [2]Marshall University Sports Medicine Department, Huntington, WV
Corresponding Author Email:konz@marsdhall.edu

**Introduction:** Fatigue impairs movement mechanics and elevates lower-limb injury risk in basketball [1,2]. High-intensity movements like jumping and landing exacerbate fatigue and diminish neuromuscular control [3,4]. This negatively impacts jump performance, shock absorption, and postural stability, increasing injury risk [5,6]. This study examines the relationship between fatigue, landing force, and postural stability in female collegiate basketball players. We hypothesize that increased task duration (a proxy for fatigue) will correlate with decreased postural stability, increased time to stabilization, and altered landing force. We also investigate the influence of biomechanical asymmetry (Right-to-Left Impulse Ratio and COP asymmetry) on jump height and takeoff velocity, hypothesizing that greater asymmetry will be associated with reduced jump performance and increased landing instability under fatigue.

**Methods:** Data was collected over two sessions. Fifteen female collegiate basketball players performed trials of doulbe and single-leg takeoff and landing on a force plate. Calculated metrics included maximum landing force (BW), shock absorption time (s), dynamic postural stability index (DPSI), and time to stabilization (TTS) in anterior-posterior (AP) and medial-lateral (ML) directions. Biomechanical asymmetry was assessed using right-to-left impulse ratio (R2LI) and center of pressure (COP) asymmetry measures in both anterior-posterior and medial-lateral directions. These were compared to jump height, takeoff velocity, and stability indices to determine their impact on performance. Fatigue was quantified using task duration and shock absorption time. Pearson correlations assessed relationships between fatigue indicators and landing stability measures. A comparative analysis examined differences between November and December data.

**Results & Discussion: Results & Discussion:** Task time showed a moderate positive correlation with maximum landing force ($r = 0.262$, $p = 0.054$), suggesting fatigued athletes experienced higher impact forces [1]. Increased impact may elevate the risk of lower-limb injuries [2]. Task time also correlated negatively with postural stability (DPSI) ($r = -0.329$, $p = 0.014$), indicating less controlled landings and compromised stability [1,2]. Right-to-Left Max Force Ratio was significantly correlated with lower jump height ($r = -0.512$, $p < 0.001$) and takeoff velocity ($r = -0.550$, $p < 0.001$), indicating that athletes with greater asymmetry generated less vertical force. Additionally, Right Leg COP Range negatively correlated with jump performance, suggesting potential stability deficits in asymmetric athletes. Shock absorption time was significantly correlated with TTS-AP ($r = 0.542$, $p < 0.001$) and TTS-ML ($r = 0.326$, $p = 0.015$), demonstrating that athletes who took longer to absorb impact required more time to regain balance post-landing [3]. This delay in stabilization may negatively affect an athlete's ability to react to dynamic game situations, potentially leading to compensatory movements and increased risk of non-contact injuries [2,3]. Our findings align with previous research showing that fatigue-induced impairments in neuromuscular control contribute to altered landing kinematics, making athletes more vulnerable to ACL and ankle injuries [2,3]., suggesting instability is systemic rather than movement-specific. This highlights the importance of monitoring fatigue-related changes over time.

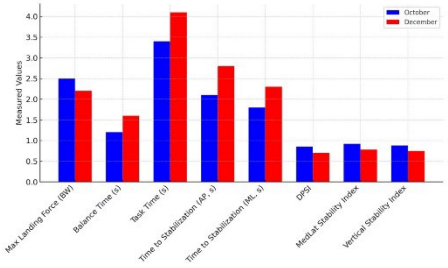

Table 1. Landing Stability Metrics Comparison

Comparing sessions, Max Landing Force significantly decreased from November to December ($p = 0.035$), while Balance Time and Task Time significantly increased ($p < 0.0001$), indicating greater instability and fatigue accumulation. Time to Stabilization (AP & ML) also increased ($p < 0.001$), suggesting prolonged balance recovery. DPSI, MedLat Stability Index, and Vertical Stability Index significantly decreased ($p < 0.0001$), reinforcing declines in postural stability. These findings align with research demonstrating that basketball-specific fatigue impairs neuromuscular control and landing biomechanics [3,4].

Fatigue significantly impacts postural stability and injury risk. While fatigue negatively affected landing stability, our findings also demonstrate biomechanical asymmetry's role in limiting jump performance and increasing instability, suggesting that fatigue alone does not dictate injury risk. Pre-existing asymmetry may compound performance declines under fatigue. Training programs should incorporate fatigue-resistance drills and neuromuscular re-education [5]. Real-time monitoring of task duration and landing mechanics can inform tailored recovery and workload management [1,2].

**Significance:** This study highlights the importance of addressing biomechanical asymmetry and managing fatigue in basketball training and injury prevention. Strength and conditioning programs should include neuromuscular training and recovery strategies to prevent fatigue-induced declines in landing stability [5]. Coaches and sports scientists should monitor task duration and landing mechanics to optimize workloads and minimize injury risk [1].

**References:** [1] Dehnavi et el. (2013), [2] Lin et el. (2022), [3] Shaabani et el. (2022), [4] Pappas, E., & Carpes, F. P. (2012), [5] Zhang, S., & Li, L. (2013).

# METATARSAL STRAINS DURING PASSIVE FOOT MOTION AND WINDLASS MECHANISM ENGAGEMENT

*Julia M. Nicolescu[1], Anthony H. Le[2], Andrew C. Peterson[2], Amy Lenz[2], Karen L. Troy[1]
[1]Dept. of Biomedical Engineering, Worcester Polytechnic Institute, Worcester, MA *jnicolescu@wpi.edu
[2]Depts. Of Biomedical Engineering and Orthopaedics, University of Utah, Salt Lake City, UT

**Introduction:** There are no clinical interventions to prevent bone stress injuries (BSI) even though they account for up to 20% of injuries reported to sports medicine centers [1]. The metatarsals (MTs) account for 38% of BSIs in collegiate athletes [2] and 58% in military recruits [3]. BSIs result from an accumulation of microdamage that arises from repetitive bone strain. There is benefit in understanding how weightbearing and motion influence MT strain so we can identify modifiable biomechanical risk factors to reduce risk of BSI. Cadaveric studies have been used to measure MT strains during loading [4,5]. Here, we tested cadaveric specimens on a robotic actuator to measure strains of MTs 2-4 during passive motion of the foot. We also used our novel setup to engage the windlass mechanism. Given the greater frequency of BSI in MT2 and its longer anatomical shape, we expected to observe the greatest strains in MT2. We also expected to observe increased strains in MTs 2-4 when the windlass mechanism was engaged due to increased arch height.

**Methods:** Three fresh-frozen lower leg and foot cadaveric specimens (3 males, 49 $\pm$ 14 years old) with no history of foot and ankle injury or surgery underwent the following experimental protocol. Specimens were fixed at the proximal tibia in a 6-axis industrial robotic actuator (M-20iA, FANUC America). The actuator was used to apply 25% body weight and move the ankle/foot through its envelope of passive motion via prescribed tibial dorsal/plantar flexion, external/internal rotation, and varus/valgus alignment motion. Stacked strain gage rosettes were adhered to the dorsal surface of MTs 2-4 at the midshaft location (Vishay #031WWA, 250 Hz) (Figure 1). The windlass mechanism was engaged by placing a 45° wedge beneath the phalanges. All data were collected continuously during motion trials. Strain gage data were processed to calculate maximum and minimum principal strains of each MT (Figure 2).

**Results & Discussion:** Strains in MTs 2-4 were highest in dorsiflexion and tibial varus alignment. The effect of the windlass mechanism on strain was both MT and motion specific. MT2 had the greatest principal strains during dorsi/plantar flexion for both neutral and windlass conditions, but not during other motions. MT2 strains increased with the windlass mechanism during all motions. MT3 strains increased with the windlass mechanism during dorsi/plantarflexion and during external rotation but decreased during internal rotation and varus/valgus alignment. In contrast, MT4 strains decreased during dorsiflexion, external rotation, and tibial varus alignment. This suggests that the windlass mechanism has more impact medially than laterally. Additionally, both conditions suggest that tibial varus alignment affects metatarsal strains more than valgus alignment. This may be explained by the notion that tibial varus alignment causes foot pronation and arch flattening while valgus does not. MT3 and MT4 strains during varus alignment decreased under the windlass condition, which suggests that the windlass mechanism may limit the arch flattening that occurs during varus alignment. For all MTs, plantarflexion caused less MT strain than dorsiflexion. Overall, both of our hypotheses were partially supported by the results.

**Significance:** This study informs our understanding of the transmission of loads within the foot, which is currently unknown. The current results and continued work help explain some of the known risk factors for metatarsal BSI. This work can directly inform the biomechanical assessment and direction of athletes to mitigate metatarsal strain, and in turn reduce the risk of metatarsal BSI.

**Figure 1:** Experimental setup of robotic actuator and specimen.

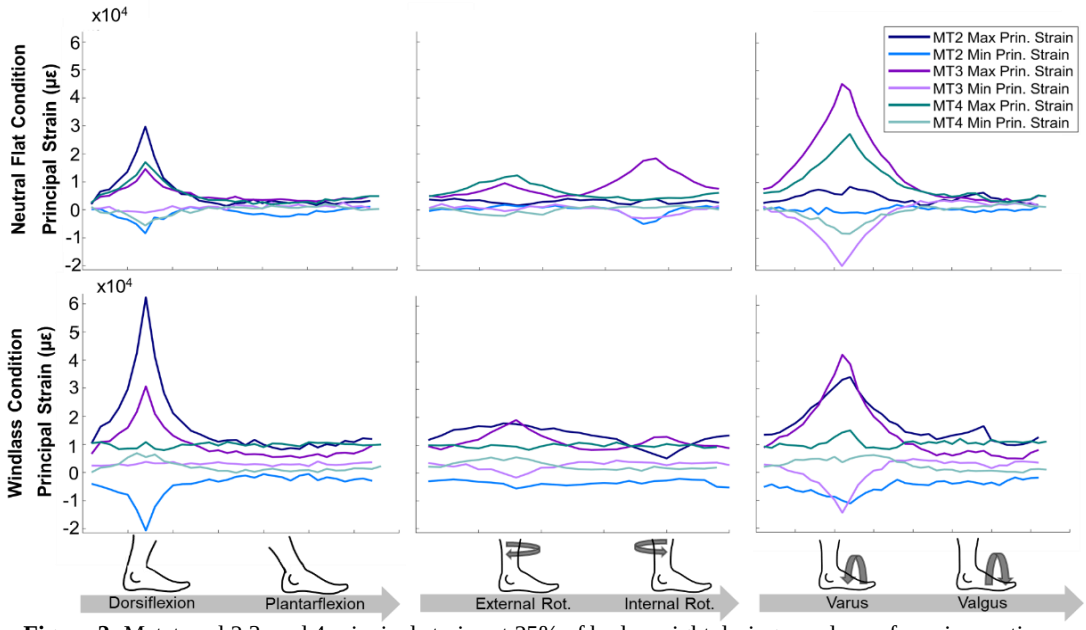


**Figure 2:** Metatarsal 2,3, and 4 principal strains at 25% of body weight during envelope of passive motion.

**Acknowledgements:** This work was partially supported by the ASB Research Travel Grant (to KLT).

**References:** [1] Fredericson et al. (2006), *Topics in MRI* 17(5); [2] Rizzone et al. (2017), *J Athl Train* 41(8); [3] Cosman et al. (2013), *Bone* 55(2); [4] Donahue et al. (1999), *J Bone Joint Surg* 81(9); [5] Sharkey et al. (1995), *J Bone Joint Surg* 77(7).

**Effect of hop distance on single-leg hop landing kinematics in healthy persons**

*John D. Holtgrewe[1], Crystal J. Murray[1], Dominique A. Barnes[1], Janine Molino[1], Braden C. Fleming[1], Jillian E. Beveridge[1]
[1]Brown University and Rhode Island Hospital, Providence, RI
*Corresponding author's email: john_holtgrewe@brown.edu

**Introduction:** Differences in knee joint mechanics may be a contributing factor to the elevated risk of posttraumatic osteoarthritis (PTOA) after anterior cruciate ligament (ACL) injury and surgery.[1] Our previous work (Study 1) using biplane videoradiography (BVR) has shown that for the same knee flexion angle during a single-leg hop landing, ACL reconstructed (ACLR) patients at 10-15 year follow-up (NCT00434837) land with their tibia anteriorly translated by up to 9.5 mm compared to uninjured controls.[2] Our current work (Study 2) continues to investigate this topic and its potential relevance to neuromuscular function and patient outcomes as an ancillary study to the BEAR-MOON randomized clinical trial (NCT03776162).[3] For both studies, subjects performed a 1-leg hop for distance activity that involves taking off and landing on the same leg; the activity was chosen because of its regular use as an ACL rehabilitation milestone to gauge dynamic strength, neuromuscular control, and return to sport readiness.[4] In Study 1, participants were asked to "stick the landing" but could take a step to regain balance if needed. In Study 2, participants were instructed to hold their balance for up to 30 seconds after landing. To evaluate the robustness of our methodology against variation in hop distance, we sought to quantify the difference in hop distance between studies, assess the strength of the correlation between hop distance and our primary kinematic outcome - peak anterior tibial translation - and quantify the degree of cross-study variability in the relationship between peak tibial translation and flexion angle. We hypothesized that Study 2 participants would experience less anterior tibial translation during the loading phase of a shorter hop.

**Methods:** **Subjects.** Data from 25 subjects with healthy knees were analyzed. Eleven subjects (5 F, 6 M, average age 38.2 ± 7.6 yrs) were part of the long term ACLR study cohort (Study 1). Fourteen subjects (9 F, 5 M, 29.7 ± 9.7 yrs) were recruited for the ongoing BEAR-MOON ancillary study (Study 2). An index limb was randomly assigned to each subject in both cohorts. All procedures were reviewed and approved by our Institutional IRB. **Hop activity.** Study 1 participants were instructed to stick the landing while Study 2 participants were instructed to hold their balance for 30s upon landing. To ensure hop activity reproducibly, hop distance was reduced to 65% of their average maximum hop distance during kinematic recording. **Kinematic recording.** Hop landings of the index limb were recorded using BVR at 250 Hz with a source-to-image distance of ~185 cm and a separation angle of ~55°. Ground reaction forces were recorded simultaneously at 3000 Hz using a force plate (Kistler) and used to temporally align kinematic data. **Kinematic reconstruction.** Computed tomography (CT) scans were taken of each subject's knees to build subject-specific bone models needed for model-based tracking using Slicer-Autoscoper (https://www.slicer.org/, accessed April 2024), and to construct anatomical coordinate systems as reported previously.[6] Six-degree-of freedom hop landing kinematics were reconstructed from ground contact to 0.2s afterwards. Peak anterior tibial translation and the flexion angle at that peak value were the primary kinematic outcomes. **Statistical analysis.** An unpaired t-test was used to test for differences in hop distance between studies. Linear regression analyses assessed the correlation between hop distance and peak anterior position and between hop distance and flexion angle. Differences in the slopes and intercepts of the relationship between peak anterior tibial position and flexion angle were analyzed using a 2-way analysis of covariance (ANCOVA). All analyses were conducted in Prism version 10.2.3 (GraphPad). Differences were considered significant if $P < 0.05$.

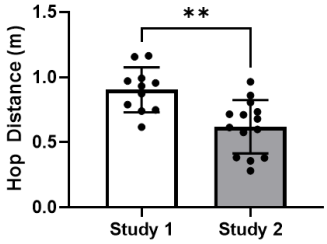


*Figure 1. Average hop distance (±SD)*

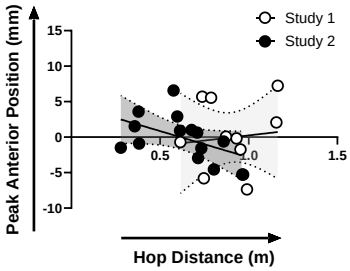


*Figure 2. Peak anterior position plotted against hop distance.*

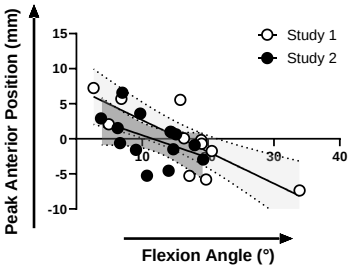


*Figure 3. Peak anterior tibial translation during single leg hop landing plotted against flexion angle.*

**Results & Discussion:** Hop distances were significantly shorter in Study 2 by 0.28±0.08m ($p=0.0012$) (Fig 1), but were not correlated with anterior tibial translation (Fig 2). There were no significant differences in regression model slopes (-0.45mm/degree vs. -0.32mm/degree, $p=0.53$) or intercepts (3.7mm vs. 7.2mm, $p=0.17$) in Fig 3. Our hypothesis that a shorter hop distance would correspond with less anterior tibial translation was not supported, but the trend of greater anterior tibial translation as a function of flexion angle for Study 1 in Fig 3 suggests that the analyses could benefit from a larger sample size. The difference in hop distance between the two studies was unexpected and points to the importance of subject instruction.[7]

**Significance:** Even a small change in how the same 1-leg hop activity is implemented may have an effect on kinematic outcomes with more conservative hop landing strategies resulting in reduced anterior tibial translation.

**Acknowledgements:** NIH NIAMS (K99/R00-AR069004, R01-AR083168, R01-AR047910, R01-AR074973, R01-AR078924); NIGMS (P30-GM122732, P20-GM139664); and the Lucy Lippitt Endowment.

**References:** 1. Beveridge, J.E. et al. JOR, 2014. 2. Beveridge, JE. et al. Trans ORS, 2023. 3. Spindler, K.P. et al. OJSM, 2022. 4. Davies, G.J. et al. Curr Rev MM, 2017. 6. Miranda, D.L. et al. J Biomech Eng 7. Nishida, K. et al. JOR, 2021.

# SIDE-TO-SIDE DIFFERENCES IN ARTHROKINEMATICS AT 1-2 YEARS POST ACLR+M CORRELATE WITH LONGITUDINAL CHANGES IN ARTICULAR CARTILAGE T1RHO RELAXATION TIMES ONE YEAR LATER

*Sadegh Khodabandeloo[1], John Ramsdell, Bruce Beynnon, Mathew Failla, Mathew Geeslin, Michael DeSarno, Niccolo Fiorentino[1]
[1]Department of Mechanical Engineering, University of Vermont, USA
email: sadegh.khodabandeloo@uvm.edu

**Introduction:** Post-traumatic osteoarthritis (PTOA) is common after anterior cruciate ligament reconstruction (ACLR), with a higher risk in ACLR combined with meniscus surgery (ACLR+M) cases, affecting 50–80% of patients 10–20 years post-surgery [1]. The degenerative pathway to OA is not completely understood. However, abnormal joint arthrokinematics – the relative position of the articulating surfaces during movement – have been implicated as one of the driving factors of cartilage degeneration post-ACLR [2], We propose that short-term abnormalities in joint arthrokinematics drive longitudinal changes in the composition of cartilage. This study aimed to test the hypothesis that early post-surgical asymmetrical arthrokinematics correlate with longitudinal cartilage composition changes, which are early signs of PTOA. Therefore, the objectives of this study were to quantify: 1- side-to-side difference of arthrokinematics at two timepoints (1-2 years and 2-3 years post-ACLR+M), 2- side-to-side differences in cartilage T1rho relaxation times at the same timepoints, and 3- the correlation between side-to-side differences in arthrokinematics at the earlier timepoint (1-2 years post-ACLR+ M) with the longitudinal changes in articular cartilage T1rho relaxation times from 1-2 to 2-3 years post-surgery.

**Methods:** Twelve patients were recruited 1–2 years after ACL reconstruction with concomitant meniscal repair and/or partial meniscectomy, and 10 returned for a second visit 2–3 years post-surgery. All patients reported having an uninjured, normal contralateral limb, which was confirmed by a radiologist assessment of an MR scan. Each participant performed two dynamic activities, walking and jogging, three times for both surgical and uninjured knees. These tasks were chosen for determining the 3-dimensional arthrokinematics of common daily activities. Patient-specific tissue models from MRI, and a validated MBT method [3], were used to measure the side-to-side (surgical vs contralateral) differences of the overlapping area of tibial and femoral cartilage (contact overlap) and the weighted centroid of contact area between the cartilage surfaces (**Figure 1**, left). For both timepoints, results were reported at 6 and 3 percent of the gait cycle for walk and jog, respectively, because these were the portion of the gait cycle at which the highest number of trials were included across all the subjects. For qMRI, T1rho relaxion times were measured at the regions of tibial and femoral cartilage that were in contact in the medial and lateral compartments (**Figure 1**, right).

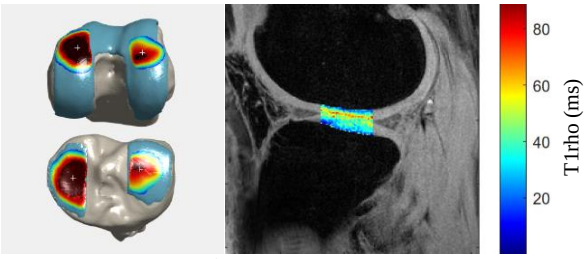


**Figure 1:** An example of the contact overlap (dark red area) and the weighted centroid of contact area (white markers) between two cartilage surfaces (left). An example of T1rho relaxion times on the region of articular cartilage-cartilage contact (right).

**Results & Discussion:** Compared to the contralateral knee, the ACLR+M knee showed increased anterior tibial translation during walking (2.4 mm, P=0.01; 2.6 mm, P=0.01) and jogging (1.9 mm, P=0.01; 2.1 mm, P=0.01) at 1–2 and 2–3 years post-surgery, respectively. No significant change was found in side-to-side osteokinematics differences between timepoints. A posterior shift in the medial compartment's contact centroid occurred during walking at 1–2 years (1.6 mm, P=0.008) and 2–3 years (2.9 mm, P=0.002), with a trend toward increased side-to-side difference over time (1.7 mm, P=0.06). Increased lateral tibial translation was observed during both activities at both timepoints. Medial compartment contact overlap rose at 1–2 years (16%, P=0.01) and trended higher at 2–3 years (10%, P=0.06), with no significant change between timepoints. T1rho relaxation times increased in ACLR+M femoral compartments at 1–2 years (medial: 5.1 ms, P=0.03; lateral: 4.9 ms, P=0.02), but only the medial tibial compartment trended higher at 2–3 years (4.7 ms, P=0.07). Side-to-side T1rho differences increased significantly in the lateral tibial compartment (4.3 ms, P=0.05) and trended in the medial (4.3 ms, P=0.09) from 1–2 to 2–3 years. A trend toward a positive correlation linked anteroposterior (AP) contact centroid differences during walking at 1–2 years with longitudinal T1rho changes in the lateral tibial compartment (R=0.62, P=0.058), and a negative correlation with the lateral femoral compartment (R=-0.62, P=0.057). No correlations were found between jogging arthrokinematics and T1rho relaxation times. In ACLR+M knees, increased anterior and lateral tibial translation, along with a posterior shift in the contact centroid at both timepoints—further emphasized at 2–3 years than 1–2 years—suggests that surgery and rehabilitation do not fully restore tibial positioning during ambulation, possibly due to permanent elongation of the ACL graft during healing and return to preinjury activities [4]. Lastly, the correlation between side-to-side arthrokinematics differences at 1–2 years and longitudinal T1rho relaxation time changes suggests that arthrokinematics may drive early PTOA onset, as elevated T1rho times are linked to PTOA post-ACLR [5].

**Significance:** Given that not all ACLR+M patients develop PTOA, identifying early arthrokinematics abnormalities and their correlation with longitudinal T1rho relaxation time changes in high-risk individuals is critical for understanding PTOA initiation. This study is the first to link altered arthrokinematics with cartilage composition changes in ACLR+M patients 1–3 years post-surgery, suggesting these factors may drive early degeneration. These insights highlight the potential for early targeted interventions, such as optimized rehabilitation or altered surgical procedures, to mitigate long-term joint damage in this vulnerable population.

**Acknowledgments and References:** Rebecca Choquette for coordination of the study. NIAMS R21AR077371. [1] Lohmander et al. (2007), J Sports Med 35(10); [2] Chaudhari et al. (2008), MSSE 40(2). [3] Ramsdell et al. (2023), Med Eng Phys 114. [4] Beynnon et al. (2011) AJSM 39(12) [5] Casula et al. (2017) J Mag Res Imag 46(3).

# SINGLE-LEG CROSSOVER DROP ACCURATELY PREDICTS LIKELIHOOD OF SECONDARY ACL INJURY

Nathan D. Schilaty[1], Jacob A. Connolly[1], Lauren A. Luginsland[1], Aaron J. Krych[2], Nathaniel A. Bates[3]
[1]Neurosurgery & Brain Repair, University of South Florida, Tampa FL
[2]Orthopedic Surgery, Mayo Clinic, Rochester, MN
[3]Orthopaedics, The Ohio State University, Columbus, OH
*Corresponding author's email: nschilaty@usf.edu

**Introduction:** Anterior cruciate ligament (ACL) injuries continue to pose a substantial challenge in sports medicine, with a high risk of secondary injury post-reconstruction (ACLR). While return-to-sport assessments often focus on strength and neuromuscular testing, they may overlook underlying biomechanical deficits that contribute to re-injury. The single-leg crossover drop (SCD) landing is a dynamic movement that emphasizes lateral trunk bending, knee valgus, and increased external load on the knee, each of which are traditionally associated with the increased risk of ACL tear. Research indicates that single-leg landings result in higher joint loads and altered movement patterns compared to double-leg landings [1]. Specifically, vertical jump assessments are known to reveal neuromuscular deficits and biomechanical asymmetries in ACLR athletes even when symmetrical limb performance have been restored [2], [3]. Assessing SCD landing mechanics provides valuable insight into neuromuscular control and lower extremity differences, offering a more comprehensive evaluation of athlete readiness to return-to-play. Given the high rates of second ACL injuries,[4] predicting these injuries through specific dynamic movements could allow focus on key variables in clinical assessments and rehabilitation.

**Methods:** 77 athletes post-ACLR (43F:34M, Median age at surgery 16.7 [15.0, 18.9] yrs., median months from surgery to testing: 12.3 [11.0, 14.8], height: 171±7.2 cm, mass: 66.2 [61.0, 74.5] kg) completed motion analysis evaluations as part of a multicenter, randomized clinical trial (Emory University, Cincinnati Children's, Mayo Clinic, The Ohio State University). Participants were asked to balance on a limb on top of a 31 cm box; they then were asked to drop off that box and land on their opposite limb after swinging it across the front of their body during the drop. Data was captured with a modified Helen Hayes markerset (n=55). Motion capture and force data were collected using 14-40 cameras that sampled at 100-240 Hz and Bertec force plates that sampled at 1000-1200 Hz. Higher rate collections were down sampled to 100 Hz and 1000 Hz, respectively, and post-processed in *Visual3D* using a recursive, fourth-order, low-pass digital Butterworth filter with a cutoff frequency of 50 Hz. Discrete kinematics and kinetics of the ankle, knee, hip, and trunk were imported into *JMP 18 Pro* for analysis. These variables (n=228; including *initial contact*, *maximums*, *minimums*, and *range of motion*) were entered into a stepwise model with a Bayesian Inference Criterion stopping point. The variables were then input into a nominal regression model and further eliminated in a stepwise manner until 10 variables remained for secondary ACL injury prediction.

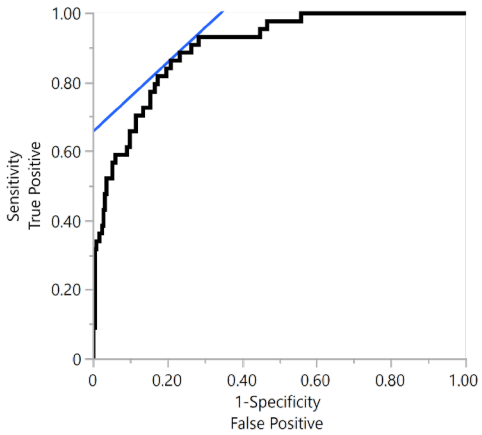


**Figure 1:** SCD Nominal Regression model for secondary ACL prediction based on 10 discrete kinetic/kinematic input variables.

**Results & Discussion:** The 10-variable SCD nominal regression model ($p<0.001$) is summarized in **Table 1**. The area under the curve (AUC) was 0.90, with a specificity of 79% and a sensitivity of 86% (**Fig. 1**). The positive prediction rate was 46% and the negative prediction rate was 97%. The original model included 17 variables and presented a greater AUC of 0.96, with a specificity of 85% and sensitivity of 93%. With the 17-variable model, the positive prediction rate increased to 73% with no further improvement in the negative prediction rate. Overall, the 10-variable SCD model had an 'excellent' prediction for secondary ACL injury. Negative prediction rate was better than positive prediction rate.

**Significance:** The variables that predicted secondary injury included vertical position of the hip, knee, and ankle; frontal plane knee moment; trunk angle at initial contact; and various ankle kinematics. These variables demonstrate that a subset of patients with history of ACL injury require enhanced control of the ankle, knee, and hip to reduce their increased relative risk for secondary ACL injury.

| Variable | *p*-value | Logworth |
|---|---|---|
| Hip Joint Center Min. Vertical Position | <0.001 | 8.104 |
| Flex/Ext Trunk Angle at IC | <0.001 | 6.876 |
| Ankle Max. Inversion Angle | <0.001 | 6.487 |
| Knee Joint Center Vertical Position at IC | <0.001 | 6.101 |
| Ankle Joint Center Vertical Displacement | <0.001 | 4.922 |
| Hip Max. Internal Rotation Angle | <0.001 | 4.376 |
| Ankle Max. Inversion Angular Velocity | <0.001 | 4.237 |
| Abduction/Adduction Knee Moment at IC | <0.001 | 3.367 |
| Ankle Int/Ext Rotation ROM | 0.001 | 2.999 |
| Ankle Angular Velocity at IC | 0.004 | 2.435 |

**Table 1:** Ten kinetic/kinematic variables that predict secondary ACL injury. IC = initial contact; ROM = range of motion.

**Acknowledgments:** Funding provided by NIH (R01AT055563) and the Florida Department of State Center for Neuromusculoskeletal Research.

**References:** [1] Xu et al., 2021. *Applied Sciences*, 11(1), 130; [2] King et al., 2022. American J Sports Medicine, 47(5), 1175-1185; [3] Kotsifaki et al., 2022. British J of Sports Medicine. 56(9), 490-498; [4] Schilaty et al., 2017. *Am J Sports Med,* 45(7):1567-1573.

# INFLUENCE OF WEIGHT AND SIZE ON ELBOW VARUS TORQUE IN BASEBALL PITCHING

*Jonathan S. Slowik, Kyle D. Planchard, James R. Andrews, Glenn S. Fleisig
American Sports Medicine Institute, Birmingham, AL, USA
*jons@asmi.org

**Introduction:** Injury to the ulnar collateral ligament (UCL) of the elbow is related to the high varus torque requirements placed upon the ligament in order to counteract the valgus loads generated during the throwing motion [1,2]. Various risk factors for UCL injury have been identified with recent work highlighting characteristics related to the pitcher's anthropometric characteristics [e.g., 3]. A recent in-vitro study measured UCL failure torque in a sample of 20 cadaveric right arms from relatively young (33 ± 6 years) male donors and found no significant correlations with bodyweight or height [4]. The purpose of the present study was to evaluate the relationships between elbow varus torque requirements and anthropometric characteristics (height, weight, and upper extremity segment lengths) in adult baseball pitchers, as higher load without higher UCL strength would likely result in increased injury risk. We hypothesized that increased anthropometric measurements would correlate with increased torque.

**Methods:** We performed a retrospective analysis of 627 healthy adult (465 professional, 162 collegiate) baseball pitchers. Height, weight, and biomechanical data had previously been collected, and elbow varus torque had been calculated via standard inverse dynamics techniques [e.g., 5,6]. Body-mass index (BMI) was calculated as weight divided by height-squared. Weight x height was also calculated because elbow varus torque is often normalized by this value in pitching biomechanics studies. The relationship of each of these variables with varus torque was first assessed using a Pearson's correlation test. Then, a stepwise multivariate regression analysis was performed to determine how well a combination of parameters could explain the variance in varus torque. The stepwise criteria to enter was set at $p \leq 0.05$, while the criteria to remove was set at $p > 0.10$.

**Results & Discussion:** Varus torque mean±SD was 94.8±17.0 Nm. There were strong correlations with weight and weight x height; a moderate correlation with BMI; and weak correlations with forearm length, height, and upper arm length (Table 1). The multivariate regression (Table 2) resulted in a model (Table 3) that passed all multicollinearity checks and statistically significantly predicted varus torque: $F(3,623)=126.3$, $p<0.001$, adjusted $R^2=0.375$. Weight appears to have the strongest contribution to varus torque, explaining 35% of the variance on its own. To help explain the sign difference for upper arm length between the two analyses, post hoc testing including velocity-related parameters was performed. Those results suggested that upper arm length may not directly influence varus torque, but that pitchers with lower forearm-to-upper-arm length ratios may more efficiently produce ball velocity (i.e., higher velocity per unit torque). This further highlights the influence of anthropometric and inertial properties on elbow varus torque in pitching.

**Table 1:** Correlation of continuous parameters with elbow varus torque (Nm), in decreasing strength order. *denotes statistical significance ($p<0.05$). Strong correlations ($0.7>R\geq0.5$) in bold text; moderate correlations ($0.5>R\geq0.3$) in italicized text; and weak ($R<0.3$) in plain text.

| Parameter | Mean ±SD | p-value | Pearson's R |
|---|---|---|---|
| Weight (N) | 917 ±99 | <0.001* | **0.593** |
| Weight x Height (Nm) | 1734 ±219 | <0.001* | **0.580** |
| BMI (kg/m$^2$) | 26.3 ±2.5 | <0.001* | *0.475* |
| Forearm Length (cm) | 26.9 ±1.7 | <0.001* | 0.290 |
| Height (m) | 1.89 ±0.06 | <0.001* | 0.288 |
| Upper arm length (cm) | 34.5 ±2.3 | 0.015* | 0.097 |

**Table 2:** Regression model step summary.

| Step | Entered parameter | R | $R^2$ | Change in $R^2$ | Adjusted $R^2$ | Standard error of the estimate |
|---|---|---|---|---|---|---|
| 1 | Weight | 0.593 | 0.351 | 0.351 | 0.350 | 13.73 |
| 2 | Forearm length | 0.601 | 0.361 | 0.010 | 0.359 | 13.63 |
| 3 | Upper arm length | 0.615 | 0.378 | 0.017 | 0.375 | 13.46 |

**Table 3:** Final regression model details. *denotes statistical significance ($p<0.05$). Available for selection, but not selected by the model: Weight*Height, BMI, Height

| | Unstandardized coefficients | | Standardized coefficients β | t-statistic | p-value |
|---|---|---|---|---|---|
| Parameter | B | Standard error | | | |
| Constant | −2.906 | 10.098 | --- | −.288 | 0.774 |
| Weight (N) | 0.100 | 0.006 | 0.584 | 17.143 | <0.001* |
| Forearm length (cm) | 1.622 | 0.365 | 0.159 | 4.441 | <0.001* |
| Upper arm length (cm) | −1.095 | 0.265 | −0.146 | −4.124 | <0.001* |

**Significance:** When considered with previous literature [3,4], these results suggest that larger pitchers – in particular, heavier pitchers – may be at greater risk of UCL injury. In addition, this study highlights the strong influence of the inertial properties of the arm, especially more distal segments (e.g., the forearm vs. the upper arm). The effect of increased muscle mass on these properties should be considered when recommending strength training of the forearm [e.g., 7].

**References:** [1] Anz et al. (2010), *AJSM* 38(7); [2] Van Trigt et al. (2021), *Intl Biomech* 8(1); [3] Chalmers et al. (2016), AJSM 44(8); [4] Beason et al. (2025), *OJSM* 13(2); [5] Escamilla et al. (2018), *J Appl Biomech* 34(5); [6] Slowik et al. (2019) *J Athl Train* 54(3); [7] Fukunaga et al (2023), *IJSPT* 18(1).

# HOW DO ACHILLES TENDON CROSS-SECTIONAL AREAS DIFFER BETWEEN MALES AND FEMALES WHEN ACCOUNTING FOR MUSCLE VOLUME AND SUBJECT ANTHROPOMETRY?

Remy Brettell[1], Emily McCain[1], *Silvia Blemker[1]
[1]Department of Biomedical Engineering, University of Virginia, Charlottesville, VA
*Corresponding author's email: rbrettell3@gmail.com

**Introduction:** The Achilles tendon is the most ruptured lower limb tendon in humans [1]. Its structure develops differently based on many subject-specific parameters such as height, mass, physical activity, and prior injury [2][3]. Differences in development or current activity level can lead to higher susceptibility for Achilles tendon injury, which most commonly occurs in the free Achilles tendon 2-6 cm above the calcaneal insertion. Achilles tendon ruptures are more common in males, despite having larger Achilles tendon cross-sectional areas [4]. Further, the geometry of the free tendon, particularly its thickness and cross-sectional area (CSA), has been shown to impact injury incidence [5]. However, there is little literature accounting for the influence of sex-specific factors such as body size. Identifying correlations unique to males and females may uncover key morphological differences contributing to rupture risk in males or reducing risk in females. **Therefore, this study will investigate the impacts of sex, height, mass, tibia length, foot length, and triceps surae muscle (TS) volume on average minimum Achilles tendon CSA**. *Hypothesis*: Due to sex differences in subject anthropometry, we expect significant differences in the male and female relationships of average minimum Achilles tendon CSA with height, mass, tibia length, foot length, and TS volume.

**Methods:** 60 healthy subjects (30M/30F) laid supine during a two-point Dixon sequence with field of view: 280 mm x 450 mm, slice thickness: 5 mm, and in plane spatial resolution: 1.1 mm x 1.1 mm, 3T MRI scanner (Trio, Siemens, Munich Germany) to identify muscle, tendon, and bone boundaries. This scan allowed for volume calculations of muscle through a deep convolution neural network-based segmentation method [6], and manual vetting (Springbok Analytics, Charlottesville, VA). Achilles tendons (from calcaneal insertion to the most distal region of the scan above the soleus insertion) were segmented manually in 3D Slicer. The segmentation files were exported into MATLAB (MathWorks, Natick, MA) and resliced at each axial slice to measure tendon CSA. CSAs between 2-4 cm above the calcaneal insertion, or 2 cm up to the soleus insertion if the free tendon was not 4 cm long, were averaged to capture the tendon's minimum CSA then plotted against subject height, mass, tibia length, foot length, and TS volume. Linear regressions were fitted to the male and female data, with $R^2$ values for each sex represented with a subscript "M" or "F" respectively. Significance of sex differences in average CSAs were determined using a paired t-test. Significance of the fit lines and the difference between their slopes was determined using Pearson correlation ($\alpha < 0.05$) and Fisher's Z-test respectively. Paired t-tests were also used to identify differences between male and female average CSAs when normalized by each significantly correlated subject anthropometry.

**Results & Discussion:** The average CSAs for males and females were significantly different (0.68 $cm^2$ vs. 0.53 $cm^2$, $p < 0.0001$) (**Fig. 1A**). Both male and female average CSAs correlated significantly ($p < 0.05$) with subject height ($R^2_M = 0.20$, $R^2_F = 0.24$), tibia length ($R^2_M = 0.21$, $R^2_F = 0.20$), and TS volume ($R^2_M = 0.26$, $R^2_F = 0.37$). Females had a significant correlation with subject mass ($R^2_F = 0.19$), but males had no significant correlation. Meanwhile, neither sex had significant correlations with their foot lengths. When both sexes were aggregated, there were significant correlations with overall foot length ($R^2 = 0.55$) and overall subject mass ($R^2 = 0.55$), agreeing with prior literature looking at combined male and female correlations [7]. Across all variables, none had significant differences between male and female fit line slopes. When normalized by the subject anthropometry, males showed significantly larger ratios than females between their average CSAs and either height or tibia length (**Fig. 1B-C**). Females had a slightly higher ratio when normalized by TS volume, but this was not significant ($p = 0.19$) (**Fig. 1D**). Further work investigating other physiologically relevant parameters is required.

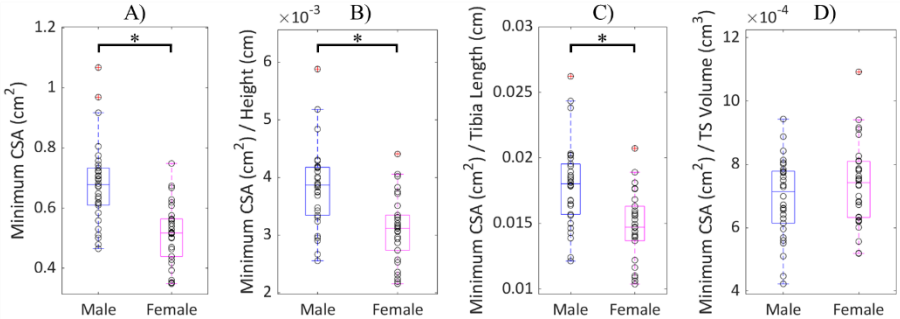


**Figure 1:** Average minimum Achilles tendon CSAs (Minimum CSA) for males and females normalized by A) none, B) subject height, C) tibia length, D) triceps surae (TS) volume. *two-tailed p value < 0.05 with the paired t-test.

**Significance:** Males have larger average minimum Achilles tendon CSAs, even when accounting for parameters subject height and tibia length. No parameters identified significantly higher ratios in females either to explain lower rupture rates, though the ratio between CSA and volume were similar between male and female subjects. Future work should investigate other muscle and non-morphological factors such as fiber length, pennation angle, and tendon stiffness that may better highlight differences in rupture risk relative to sex.

**Acknowledgements:** Research funded by NIH Grant #R01AR078396.

**References:** [1] Shamrock et al. (2024), *StatPearls* [2] Deng et al. (2021), *Life (Basel)* [3] Hullfish et al. (2018), *J Appl Physiol* [4] Vosseller et al. (2013), *Foot Ankle Int* [5] Intziegianni et al. (2017), *Sports Med Int Open*, [6] Ni et al. (2019), *J Med Imaging* [7] Gonzalez et al. (2020), *J Foot Ankle Surg*

# KINEMATICS IN PITCHERS WHO LATER SUSTAIN UCL TEAR VS THOSE WHO DO NOT: SPM ANALYSIS

*Jessica K. Geiger[1,2], Blake W. Jones[1], Kristen F. Nicholson[2]
[1]Wake Forest School of Medicine, [2]Department of Orthopaedic Surgery & Rehabilitation, Wake Forest School of Medicine
*Corresponding author's email: blwjones@wakehealth.edu

**Introduction:** The overarm throwing motion is one of the fastest human movements, generating elbow valgus stress that can exceed the ulnar collateral ligament's (UCL) tensile strength [1]. With pitchers throwing harder and more frequently, UCL injuries are rising [2]. Pitch velocity, workload, and pitch type contribute to injury risk, but pitching mechanics also play a crucial role [3]. Certain mechanical patterns—such as early trunk rotation, increased shoulder external rotation, and decreased elbow flexion—elevate valgus stress [4] and are assumed to increase injury risk. Prior studies have compared biomechanics in pitchers with and without prior UCL injuries [5], but no research has analyzed pre-injury motion capture data to identify time series kinematic differences via statistical parametric mapping (SPM) that may predispose pitchers to UCL tears.

This study aims to identify biomechanical factors common to pitchers who later tear their UCL to elucidate which athletes may be at greater risk of UCL injury. We hypothesized that there will be a significant kinematic difference between pitchers who later sustain a UCL injury and those who remain healthy.

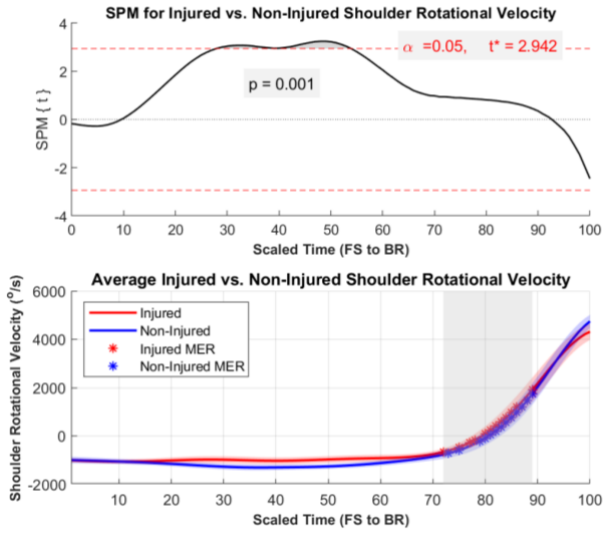


**Figure 1**: Shoulder rotational velocity: SPM and Time-Series

**Methods:** Retrospective pitching motion capture data from 8 players who sustained UCL ruptures at a time after their data was collected were analyzed. These data were categorized into the injury group. Retrospective pitching motion capture data from 8 players who remained healthy following their data collection were playing level, handedness, and starter/reliver matched to the injury group. The data from these eight pitchers formed the non-injury group. Time-series kinematic data from each player's three fastballs were extracted. Using MATLAB, data were trimmed from foot strike (FS) to ball release (BR), key events were identified, and data were interpolated to 101 normalized time points. Kinematic time series data were analyzed via two-tailed T-tests ($\alpha = 0.05$) using SPM, with additional event-specific T-Tests at maximums, FS, maximum shoulder external rotation (MER), and BR.

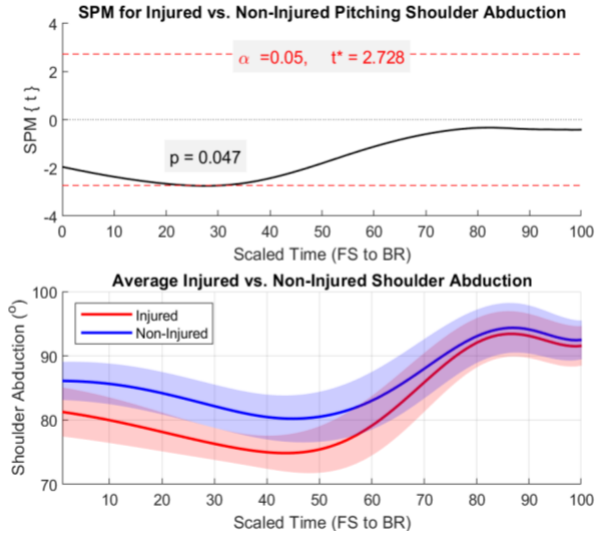


**Figure 2**: Shoulder abduction angle: SPM and Time-Series

**Results & Discussion:** SPM analysis revealed significant differences between pitchers who later sustained elbow injuries and those who remained healthy in shoulder rotational velocity ($p$=0.001) and shoulder abduction angle ($p$=0.047). Significant differences were found in maximum lead leg ground reaction force (GRF) ($p$=0.011), trunk lateral tilt at foot strike ($p$=0.039), trunk rotation at ball release ($p$=0.049), and maximum pitching shoulder velocity ($p$=0.022).

Pitchers who later sustained an elbow injury exhibited slower rotational velocity during the external rotation/layback portion of the pitching sequence (25% to 55%) and peak velocity (4994 vs. 5355°/s) (Figure 1). Additionally, pitchers who later sustained injury have lower abduction angles between FS and MER (Figure 2). Lower shoulder abduction and decreased maximum shoulder rotation velocity have previously been associated with UCL injury risk [7]. Proper sequencing through the kinetic chain is critical for efficient energy transfer. Ideally, the trunk remains over the pelvis with 0° lateral tilt at FS, but pitchers who later sustained injury averaged 4.76° (vs.-1.57°), indicating poor alignment. Additionally, trunk rotation should stop when facing home plate (0°), yet pitchers who sustained injury continued rotating at BR (3.38° vs. -2.27°), disrupting momentum transfer. Proper lead knee extension and higher braking GRF facilitate force transfer for high-velocity pitching. Pitchers who sustained injury had higher GRF (2.42 %BW vs. 2.06 %BW), which is typically associated with greater ball velocity. However, when this force is not effectively converted into upper-extremity mechanics, compensatory movements may increase joint stress, elevating injury risk.

**Significance:** This study identifies key biomechanical differences in pitchers who later suffered UCL ruptures vs those who did not, particularly in shoulder kinematics via SPM, trunk mechanics at FS and BR, and peak lead leg force absorption. Understanding these risk factors may inform injury prevention strategies and mechanical adjustments to reduce UCL stress in overhead athletes.

**References:** [1] Werner et al. (2001), *Am J Sports Med*, *29*(3); [2] Mahure et al. (2016), *J Shoulder Elbow Surg 25*(6); [3] Labott et al. (2023), *Arthroscopy* 39(8); [4] Aguinaldo & Chambers (2009), *Am J Sports Med*, 37(10); [5] Hamer et al. (2021), *Orthop J Sports Med*, 9(3); [6] Manzi et al. (2022), *Shoulder & Elbow*, 14(1)

# IN-VIVO JOINT DYNAMICS CONSERVE THE ACUTE COMPRESSION AND RECOVERY RESPONSE OF CARTILAGE IN CADAVERIC JOINTS

Tejus Surendran[1], *Axel C. Moore[1]
[1] Biomedical Engineering, Carnegie Mellon University, Pittsburgh, PA, USA
*Corresponding author's email: axelm@andrew.cmu.edu

**Introduction:** Articular cartilage supports joint loads and enables low-friction interfacial sliding through poroelastic fluid pressure [1]. However, during prolonged loading fluid is expelled from the cartilage and results in reduced pressure, and increased tissue deformation and friction. Restoring poroelastic pressure, hydration, and deformation is critical for maintaining cartilage function.

Cartilage recovery in vivo has been observed under two conditions. The first is joint unloading, which was demonstrated by Eckstein et al. in subjects who remained supine after an initial loading task [2]. The second is joint activity, which was demonstrated by Kust et al. in subjects who performed a brief walk after an initial loading task [3]. While recovery during static joint unloading is well-explained by poroelastic theory, recovery during walking and other dynamic tasks is more complex due to cyclic loading, contact exposure, and cartilage sliding, all of which affect fluid and solute transport.

To investigate these factors, we aim to develop a cadaveric joint model that preserves in vivo dynamics. We **hypothesize** that replicating in vivo joint kinematics and kinetics in a cadaveric model will conserve the native cartilage deformation patterns. To validate this ex vivo model we will mirror our previous in vivo protocol (30 minutes of standing, 10 minutes of walking, 30 minutes of standing, and 50 minutes supine [3]) and compare the deformation response. A valid ex vivo model will enable a systematic investigation of gait speed, body mass, and activity duration, providing insights to the mechanics that drive cartilage recovery.

**Methods:** Specimens and Setup: Three adolescent female Duroc pig stifle joints were obtained from a local butcher. All major musculature and soft tissue were removed except for the collateral ligaments, cruciate ligaments, and menisci. The femoral and tibial shafts were then potted in polymethyl-methacrylate and mounted on a multi-axis robotic test frame comprising a KUKA KR160 serial arm robot, two ATI FT44208 six-axis load cells, and an OptiTrack Prime X13 motion capture system. These components were integrated via SimVITRO software to enable precise six-axis control of joint kinematics and kinetics. Task Sequence: A custom protocol was developed to replicate the tasks from our previous in vivo study [3]. Before the task sequence began, a reference state was established by simulating 5 min of standing at -521 N along the superior/inferior (SI) axis, followed by 560 walking cycles. The axial force was then reduced to -50 N with all other axes kinematically locked. Once the target load was reached, the joint position along the SI axis was recorded ($SI_{Ref}$). Next, a 30 min standing period was simulated by locking all axes except the SI axis, which was loaded to -521 N. Deformation was measured every 100 s. A 10 min walking period was then simulated using a scaled version of the ASTM F3141 gait profile. Deformation was recorded every 100 s. A second 30 min standing period followed, after which we simulated 50 min of lying supine by holding the SI load at -50 N and continuously recording deformation. Data Analysis: Cartilage deformation ($\delta$) was quantified by measuring joint translation along the SI-axis: $\delta = SI_{Task} - SI_{Ref}$, where $SI_{Ref}$ and each subsequent measure ($SI_{Task}$) were quantified at the same joint position and load.

**Results & Discussion:** Simulated standing caused progressive cartilage deformation eventually reaching an average of -1.3 mm (compressive deformation) during the first standing phase (**Fig 1**). During simulated walking, the cartilage recovered an average of 0.9 mm (70% recovery). At the start of the second standing phase there was a residual deformation of -0.3 mm. After 30 min of simulated standing this deformation reached an average of -1.5 mm. During the supine period, the cartilage experienced progressive recovery, regaining 0.9 mm (64% recovery) over 50 minutes.

These task-time-dependent changes in cartilage deformation are consistent with existing in vivo and ex vivo literature [2–4,]. Moreover, the observed nonlinear deformation and recovery profiles align with cartilage's poro-viscoelastic characteristics [1,4,7]. Although all specimens followed similar trends (**Fig 1**), variations in deformation magnitude were observed and may be linked to differences in cartilage thickness, material properties, and joint geometry.

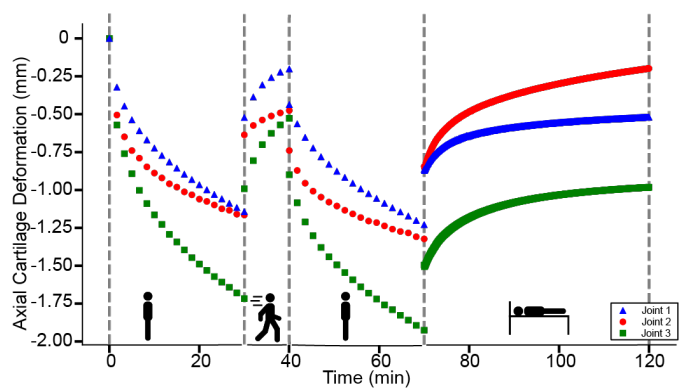


**Figure 1:** Task- and time-dependent cartilage deformation for three joints (coded by color and shape). Breaks in the x-axis at 30, 40, and 70 min indicate pauses in the experiment for data writing.

**Significance:** Our findings demonstrate that simulated standing causes time-dependent compressive deformation, while simulated walking and lying supine provide time-dependent recovery. These results are consistent with recent in vivo [2–3] and ex vivo [5,6] studies, laying the groundwork for future investigations that will assess the role of different physiological parameters.

**References:** [1] Ateshian GA. J Biomech. 2009 Jun 19;42(9):1163-76.; [2] Eckstein, F. Anat Embryol 200, 419–424 (1999).; [3] Kust SJ. Osteoarthritis Cartilage Open. 2024;6(4):100526.; [4] McCutchen CW. Wear. 1962;5(1):1-17.; [5] Moore AC. Osteoarthritis Cartilage. 2017 Jan;25(1):99-107.; [6] Herberhold C. J Biomech. 1999 Dec;32(12):1287-95.; [7] Mow, V. C. ASME. J Biomech Eng. February 1980; 102(1): 73–84.

# THREE-DIMENSIONAL PRINTED FEMORAL CANCELLOUS BONE MODELS FOR BIOMECHANICAL TESTING

*Omar Manzur[1], Kishore M. Nagaraja[2], Richard Samade[1], Wei Li[2], Robert Weinschenk[1]
[1]Department of Orthopaedic Surgery, University of Texas Southwestern Medical Center
*Corresponding author's email: omar.manzur@utsouthwestern.edu

**Introduction:** The femur, as the primary load-bearing bone of the lower limb, is essential for maintaining posture, mobility, and joint function. Conditions compromising its biomechanical integrity, such as fractures, tumors, and osteoarthritis, often necessitate surgical intervention supported by rigorous biomechanical testing to ensure procedural safety and efficacy. Traditional biomechanical studies frequently rely on cadaveric specimens, which present challenges including high costs, limited availability, and inter-specimen variability [1]. In response, three-dimensional (3D) printed models have emerged as a promising, cost-effective alternative for simulating bone mechanics. However, cancellous bone's heterogeneous anisotropic trabecular structure plays a complex role in fracture pathology. Efforts to replicate this structure through 3D printing have explored various composite materials that are expensive, inaccessible, require impractical manufacturing requirements, and exhibit biomechanical limitations [2]. We hypothesize that 3D printed polylactic acid (PLA) cancellous bone models printed using an affordable fused deposition modeling (FDM) process would exhibit similar compressive properties as cadaveric cancellous bone, measured by compressive modulus (GPa) and compressive strength (MPa).

**Methods:** PLA cancellous bone models were fabricated using an Ultimaker S5 FDM printer. Printing parameters included a 0.2 mm layer height, 0.4 mm nozzle, 60 mm/s speed, and gyroid infill. Models were printed in two batches. In the initial batch, rectangular prisms measuring 50.8 mm x 50.8 mm x 25.4 mm were printed with infill densities ranging from 5% to 60% in 5% increments. This range was selected to evaluate the relationship between infill percentage and mechanical properties. Uniaxial compression testing was performed according to ASTM F1839-08 and ASTM C273/C273M standards (**Fig 1**).

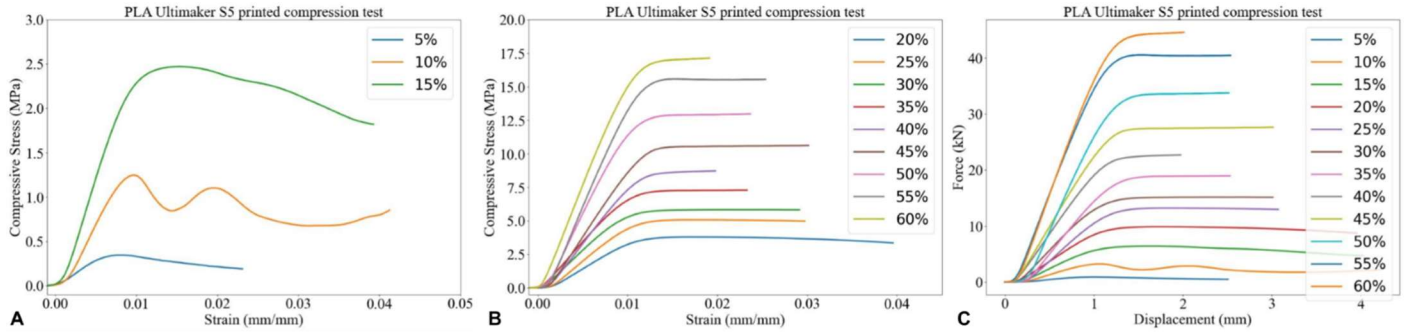


**Figure 1:** (A) PLA cancellous prisms stress-strain curve from 5%-15% infill percentages. (B) PLA cancellous prisms stress-strain curve from 20%-60% infill percentages. (C) PLA cancellous prisms force displacement curve from 5%-60% infill percentages.

Linear regression analysis of these results was compared to published cadaveric data, which identified a compressive modulus and strength of 0.441 GPa ± 0.271 and 6.8 MPa ± 4.8, respectively [3]. This comparison identified an infill density of 22.5% as the closest match to published cadaveric cancellous bone data, predicting a compressive modulus of 0.488 GPa and a compressive strength of 4.13 MPa. In the second batch, 10 prisms were printed and underwent the same testing procedures, with mechanical properties compared to cadaveric data using Welch's t-test with an alpha of 0.05.

**Results:** The compressive properties of 10 PLA cancellous prisms printed at 22.5% infill were analyzed. The average compressive modulus was 0.486 GPa (SD 0.013, CV 2.67%), while the average compressive strength measured 4.03 MPa (SD 0.419, CV 10.4%). These results closely aligned with theoretical predictions of 0.488 GPa and 4.13 MPa, respectively. Comparative analysis with published cadaveric data of proximal femur cancellous bone (0.441 ± 0.271 GPa; 6.8 ± 4.8 MPa) demonstrated no statistically significant differences in compressive modulus ($p = 0.5699$) or compressive strength ($p = 0.1013$).

**Discussion:** 3D-printed PLA cancellous bone models exhibit compressive modulus and strength values that closely match those reported in prior cadaveric literature, which is consistent with the study's hypothesis that cost-effective 3D-printed models can replicate key biomechanical properties. Additionally, the low coefficients of variation observed in the PLA models, compared to the higher variability reported in cadaveric samples, suggest that 3D printing may offer more consistency for standardized biomechanical testing.

**Significance:** These findings are significant to the field of orthopedic biomechanics, as they offer a scalable, standardized, and accessible solution for biomechanical research without the logistical, ethical, and financial constraints associated with cadaveric bone. Beyond orthopedics, the methodology used in this study could be adapted to model cancellous bone structures in other anatomical regions, facilitating broader biomechanical investigations across disciplines. The enhanced consistency and reduced variability of these models may improve the reliability of experimental results, advancing preclinical testing of orthopedic implants and surgical techniques. Clinically, these models have the potential to aid in resident training and preoperative planning by providing realistic representations of cancellous bone behavior under load.

**References:** [1] Yammine K. (2019), *Clinical Anatomy* 33(5); [2] Tyler et al. (2016), *Adv Drug Delivery Rev* 107: 163-175. [3] Keaveny et al. (2001), *Annu Rev Biomed Eng* 3: 307-333.

# ULTRASONIC TRACKING OF ULNAR NERVE MORPHOLOGY: METHODS

*Mark Carl Miller[1], Sruthi T Venjamuri[1], Benjamin Moyer[1]
[1]University of Pittsburgh
*Corresponding author's email: mcmllr@pitt.edu

**Introduction:** The non-zero complication rate of surgical intervention for ulnar neuropathy justifies research into the nerve's physiological environment and the implications of surgery. Previous research has examined compression and strain in the nerve and it is known that the blood supply can have an effect on nerve function. In its course from the shoulder to the hand, the nerve fibers must change their orientation and even location due to movements arm movements. The amount of the change, the direction of the change and ability of the nerve to accommodate the changes may be expected to all contribute to a nerve's ability to perform its tasks. One means to quantify the importance of the orientation and location of the nerve is to obtain better mechanical measurements of the physiological environment of populations with and without ulnar neuropathy and then compare quantitative measurements of nerve orientation. The quantification of the nerve's orientation can also be applied to patients before and after surgery. To this end, we seek to mathematically describe the path of the nerve provide numerical values of the nerve's bends and twists along it path.

**Methods:** A six degree of freedom robot was fabricated and the measurement capabilities of the end effector were determined, showing an accuracy of 0.5mm. After construction of a special adapter for the robot arm's end effector, the robot held an ultrasound sensor (Logiq e GE portable with a 12L-RS linear array probe) firmly fixed to the last link in both position and orientation. The robotic arm operator held the sensor and manipulated the arm freely while the ultrasound unit recorded the two dimensional images obtained by the sensor (Figure 1).

An analog/digital converter (NI USB-6001 DAQ, National Instruments, Austin TX), concurrently recorded the position of the robot arm. The operator placed the manipulator on the forearm of a subject with no upper extremity pathologies, identified the ulnar nerve and tracked the nerve from 10 cm distal to the elbow to 5 cm proximal to the elbow. After recording the two-dimensional US images of the nerve tracking, the operator identifies the location of the nerve in each image and software in the US unit permitted measurement of the nerve's location in the image.

The nerve location as measured in each image was then added to the end effector's position and orientation as recorded by the robot arm. After digital filtering, the path was plotted for visual inspection (Figure 2); custom software fit a cubic spline to the path and computed the radius of curvature (bending) and torsion (twisting) at each point along the nerve's traverse of the elbow.

The accuracy of the system was further tested to establish the viability of the technique. Acrylic plastic sections of known curvature were place in thin plastic sheeting tubes filled with water. The edges of the acrylic were recorded with the US system. The know curvature were calculated and proved to be within better than 1% of the known values.

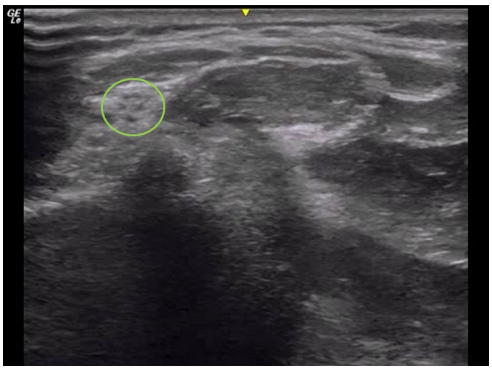

Figure 1: A typical sonogram of the nerve
Note the fascicles..

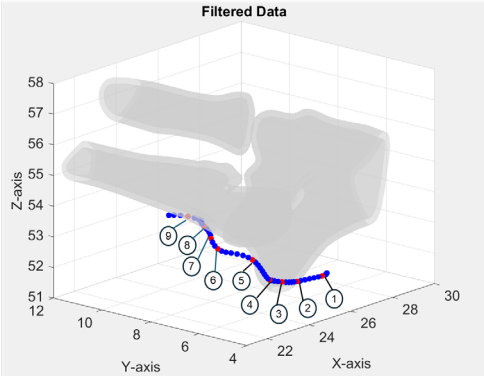


Figure 2: The path of the ulnar nerve with locations for documented measurements.

**Results & Discussion:** The radii of curvature varied from 0.36 to 64.6 and the torsion from -5.6 to 22.9 (Table 1). The smallest radius of curvature (the greatest bend) occurred immediately distal to the cubital tunnel at the joint line and the largest torsion (i.e., one measure of the amount that the nerve twists) occurred after the arcade of Struthers. Negative torsion indicated a reversal in the direction of twisting.

Ultrasound successfully tracked the ulnar nerve and the measurements produced the bending and twist in the nerve. A greater density of tracked points could improve the curvature and torsion calculations and MRI imaging could improve the fidelity of the tracking itself. The system can readily be applied in clinical comparisons of normal and neuropathy subjects.

**Table 1: Radii of Curvature and Torsion at Selected Points**

| Location in Figure 2 | Description | Radius of Curvature [cm] | Torsion |
|---|---|---|---|
| 1 | Upper arm | 64.58 | 22.94 |
| 2 | Middle of upper arm | 2.98 | 5.29 |
| 3 | Medial Epicondyle | 4.15 | 3.94 |
| 4 | Cubital Tunnel I | 0.68 | -5.57 |
| 5 | Cubital Tunnel II | 1.74 | 0.94 |
| 6 | Joint line at elbow | 0.36 | 1.83 |
| 7 | Into forearm muscles | 0.41 | 1.52 |
| 8 | A sharp turn in forearm | 0.10 | 4.79 |
| 9 | End of curve | 1.67 | 0.17 |

# THE IMPACT OF LAMINOTOMY WIDTH ON SPINAL STRESS DISTRIBUTION DURING FLEXION: A FINITE ELEMENT STUDY

Isaac K. Kumi[1], Sennay Ghenbot[2], Courtney Butowicz[2], AJ Pisano[2], Sebastian Bawab[1], *Stacie I. Ringleb[1]
[1]Department of Mechanical and Aerospace Engineering, Old Dominion University, Norfolk, VA, USA
[2]Defense Health Agency, Walter Reed National Military Medical Center, Bethesda, MD, USA
*Corresponding author's email: sringleb@odu.edu

**Introduction:** Laminotomy is a surgical procedure used to relieve pressure on the lumbar spinal nerves caused by compressive conditions such as spinal stenosis and disc herniation. The procedure involves the removal of portions of the posterior spinal elements, which can affect the overall stability of the spine. Though clinically effective, the width of bone that can be safely removed without compromising the biomechanical integrity of the spine remains poorly defined. Understanding how different laminotomy widths affect stress distribution, particularly under typical spinal motions can inform surgical decisions and improve patient outcomes.
This study used a finite element model to investigate how different laminotomy widths influence stress distribution at some locations in the Pars interarticularis (PI) and superior lamina using an L4-L5 functional unit of the lumbar spine. By simulating incremental motion angles in flexion and comparing them to an intact spinal model, we aim to provide insights into how bone resection affects spinal biomechanics.

**Methods:** A finite element (FE) functional unit model was obtained from SimTK [1]. The model incorporated vertebral, disc, and ligament properties from existing literature [2,3] and was subjected to a pure moment of 7.5Nm to simulate flexion. The laminotomy procedure involved removing part of the lamina of the L4 spinous process as well as the ligamentum flavum. Also, a small portion of the top of the L5 spinous process was removed to match the access route used to clear the ligamentum flavum. Three laminotomy width sizes 4,8 and 12 units were analyzed for stress variations in the PI from 1-5 degrees of flexion in four locations (Fig 1).

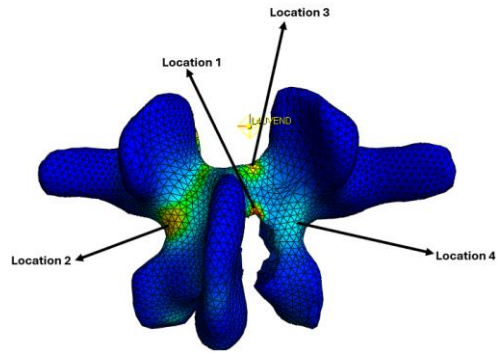


**Figure 1:** Model showing the four locations analyzed in the study.

**Results & Discussion:** Stress increased between intact and all laminotomy conditions. Notably, the largest increase in stress in Location 1 occurred in the laminotomy condition with the largest width (Fig 2a). This may indicate a higher risk of stress fractures when more bone is removed. At the contralateral PI (Location 2), stress rose with both motion and laminotomy width compared to the intact model, with largest width showing the highest stress at higher motion angles (Fig. 2b). This suggests that wider widths in laminotomies may cause asymmetric load redistribution and shift to the contralateral side to maintain equilibrium. The stress at Location 3 increased as the width of the laminotomy increased (Fig. 2c), indicating a correlation between laminotomy width size and stress concentration in this area. An immediate stress reduction near the facet joints occurred in location 4, with no change between sizes of laminotomy. Thus, removing posterior elements offloads stress from the facet-adjacent region, while shifting stress to the contralateral side and the area around the cut. In summary, wider laminotomy widths increased stress at multiple locations during flexion, including the contralateral side of the vertebra. Thus, in addition to the risk of stress fractures near the site of the laminotomy, there could be the potential for longer term degeneration of the vertebra. Understanding the impact of bone resection on stress in additional loading conditions such as extension, lateral bending, and axial rotation may assist surgeons in surgical decision making for the laminotomy procedure.

**Significance:** This study highlights how important it is to carefully consider the width of a laminotomy on the stress on the entire vertebra. Bone resection has an impact on both increasing and decreasing loads in various areas of the vertebra. This wholistic approach may help surgeons understand the risk of fractures in the PI and other loading that may cause long term degeneration in other areas of the vertebra. Further investigation should include the adjacent vertebra as well as loading of the intervertebral discs.

**References:** [1] Finley et al. (2018), Comp. Method in Biom. 21(6); [2] Naserkhaki et al. (2018), J Biomech 70; [3] Rohlmann et al. (2016), J Biomech 39.

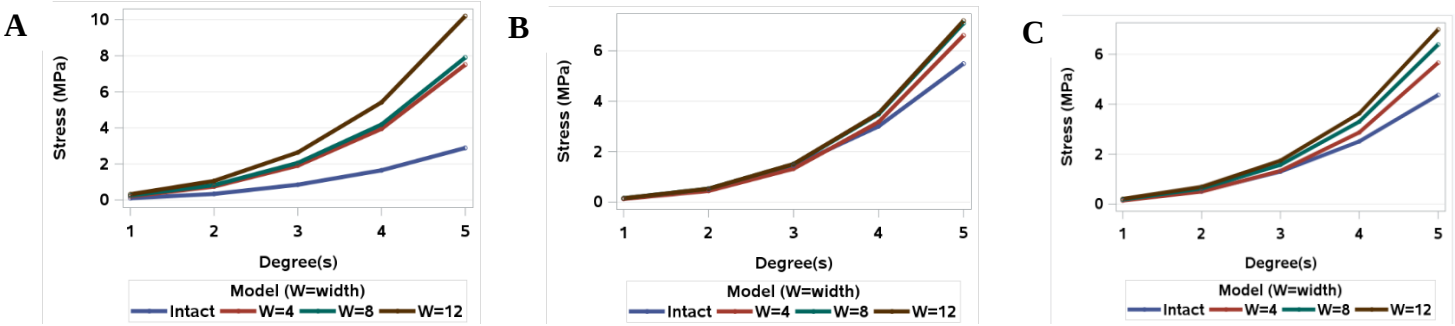


**Figure 2**: Stress Distribution at Pars Interarticularis at the area adjacent the cut (A), the contralateral Pars Interarticularis (B) and bone around the superior lamina (C) during Flexion at Increasing Motion Angles for all 3 different widths and intact model.

# BONE MINERAL DENSITY OF VERTEBRAL BODY IS SIGNIFICANTLY LOWER THAN THAT OF POSTERIOR ELEMENTS IN LUMBAR VERTEBRAE OF CHRONIC LOW BACK PAIN PATIENTS

*C. James Kim[1,3], Clarissa M. LeVasseur[1,2], Richard Wawrose[1], Michael Spitnale[1], William Donaldson[1], Joon Lee[1,2], Gwendolyn Sowa[4], Gina McKernan[4], William Anderst[1]

[1]Biodynamics Laboratory, Department of Orthopedic Surgery [2]Bethel Musculoskeletal Research Center, [3]School of Medicine, [4]Department of Physical Medicine and Rehabilitation, University of Pittsburgh, Pittsburgh, PA

*Corresponding author's email: chk163@pitt.edu

**Introduction:** Chronic low back pain (cLBP) patients experience higher incidences of osteopenia and osteoporosis compared to age-matched subjects in the general population[1]. Therefore, vertebral fracture risk assessment through accurate bone mineral density (BMD) measurements is crucial in these patients. The current gold-standard method of BMD measurement in the lumbar spine, the anterior-posterior dual-energy X-ray absorptiometry (AP-DEXA) scan, measures BMD of the total vertebra and does not consider the non-uniform distribution of bone mineral density (BMD) between anatomic regions[2-4]. Prior studies have shown BMD differences between anterior and posterior structures[2-4] as well as within the vertebral body[7,8]. The BMD measurements in these studies, however, were made *ex vivo*[2,8], in young healthy subjects[3], or using DEXA scans[3,4] whose accuracy may be influenced by soft tissue density variations. In this study, we measured BMD in cLBP patients using quantitative CT to provide a more accurate BMD measurement of lumbar vertebrae. We hypothesized BMD would be higher in posterior compared to anterior structures, and as a secondary analysis, we assessed the effects of age and sex on region-specific BMD measurements.

**Methods:** Participants with cLBP (defined as LBP >3 months with pain existing >50% of the time in the last six months) provided written, informed consent to participate in this IRB-approved study. High-resolution CT scans of the lumbar spine (L1-L5) were collected from 40 subjects (average age 53 years; range 18-82 years; 20F, 20M). Lumbar vertebrae were separated into the vertebral body and posterior elements by defining a plane at the intersection of the anterior region of the pedicle and the vertebral body in the 3D view as seen from a transverse top-down view. Small edits based on sagittal plane views were made to the initial plane to ensure the entire pedicle was separated from the vertebral body. Once the vertebral body was separated from the posterior elements, endplates were separated by defining a plane using points placed on the border between high and low intensity pixels on the sagittal view in both the anterior and posterior sections of the vertebral body. The plane was then translated up or down to ensure all high intensity values were included in the endplate definition. A 5 sample $K_2HPO_4$ and $H_2O$ equivalent density phantom, 18 inches long, was included with each patient-specific CT scan (Mindways Software, Inc). This calibration phantom was used to convert Hounsfield Units (HU) into bone mineral density (BMD) for this analysis. Friedrich's test with Dunn's correction was used to compare the BMD between regions at each lumbar level. Regression analysis using a generalized linear model was performed to evaluate the effects of age (<60 vs. ≥60) and sex (M vs. F) on BMD. Analyses were performed in R-studio or Prism (v.10.4.1)

**Results & Discussion:** At L1, L2, L3, and L4, the BMD of the posterior elements was significantly higher than each of the anterior structures. At L5, the BMD of the posterior elements was higher than the vertebral body and superior endplate (EP) but not inferior EP. When averaged across all lumbar vertebrae, the BMD of posterior elements was higher than the average BMD of each anterior structure (Figure 1). Age ≥60 was significantly correlated with lower BMD in the vertebral body ($\beta$ = -59.9, 95% CI:[-90.9, -28.8], $p < 0.001$), inferior EP ($\beta$ = -74.6, 95% CI:[-114.4, -34.4], $p < 0.001$), and posterior elements ($\beta$ = -99.2, 95% CI:[-155.2, -43.2], $p = 0.001$) but not the superior EP ($\beta$ = -30.8, 95% CI:[-64.9, 3.4], $p = 0.09$). Sex differences were not significant (Table 1). These findings are consistent with studies showing significant contribution of posterior elements to the total BMD of lumbar vertebrae *ex-vivo*[2] and in younger individuals[3]. Though a sex-specific difference in posterior element BMD were found in young healthy subjects[3], it was not shown in this cohort of cLBP patients.

**Significance:** These results suggest a need to perform an isolated BMD measurement of individual structures when assessing for vertebral fracture risk or the risk of pedicle screw loosening during posterior lumbar fusion.

**Acknowledgments:** This research is supported by the National Institutes of Health (NIH) through the NIH HEAL Initiative under award number U19AR076725. The content is solely the responsibility of the authors and does not represent the official views of the NIH or its NIH HEAL Initiative.

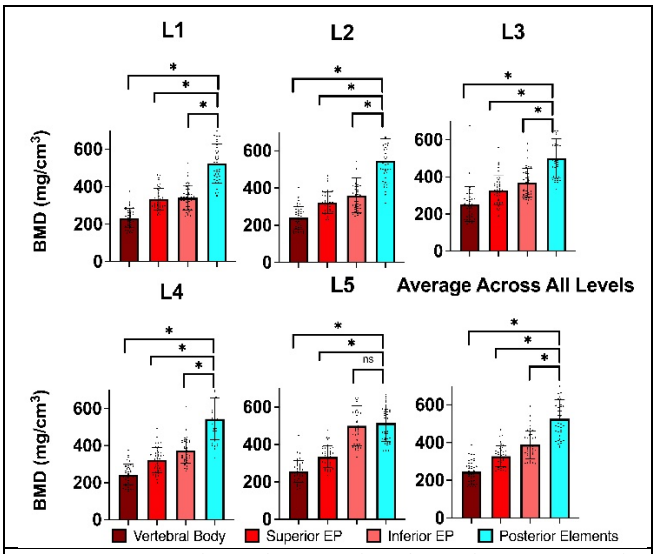


**Figure 1.** Comparison of Bone Mineral Density By Anatomic Region at Each Vertebral Level

**Table 1.** Average Bone Mineral Density of Each Anatomic Region Across All Vertebral Levels by Age and Sex (Values expressed as Mean (95% CI); All units are mg/cm$^3$)

| | Vertebral Body | Superior Endplate | Inferior Endplate | Posterior Elements |
|---|---|---|---|---|
| **<60** | 275.1 (250.6, 299.6) | 343.1 (316.5, 369.7) | 428.8 (391.1, 460.6) | 575.2 (529.0, 621.5) |
| **≥60** | 215.2 (193.6, 236.9) | 312.3 (296.7, 355.4) | 351.2 (327.8, 374.6) | 476.0 (439.2, 512.7) |
| **F** | 243.5 (211.4, 275.5) | 327.0 (297.9, 356.1) | 386.1 (347.7, 424.4) | 529.8 (477.9, 581.8) |
| **M** | 246.8 (225.5, 268.1) | 328.4 (304.9, 352.0) | 390.9 (360.5, 421.4) | 521.3 (477.5, 565.1) |

**References:** [1] Gaber et al. (2002), *Clin Rehabil*; [2] Hohn et al. (2017), *Global Spine J;* [3] Lee et al. (2009) *J Bone Miner Res.*; [4] Shin et al. (2023) *Front Endocrinol (Lausanne);* Bassani et al. (2024), *Orthop. Trauma: Curr. Concepts Best Pract.*; Chen et al. (2024), *Front. Endocrinol. (Lausanne)*; [7] Ortiz et al. (2011) *AJNR Am J Neuroradiol.*; [8] Zhao et al. (2008) *Bone*.

**The centrode changes with vertebral level in patients with chronic low back pain**

*Clarissa LeVasseur[1,2], Tom Gale[1], Sabreen Megherhi[1], Gina McKernan[3], Richard Warwose[1], Michael Spitnale[1], William Donaldson[1], Joon Y Lee[1,2], William J. Anderst[1]
[1]Biodynamics Lab, [2]Bethel Musculoskeletal Research Center, [3]Department of Physical Medicine and Rehabilitation, University of Pittsburgh
*Corresponding author's email: cll100@pitt.edu

**Introduction:** Identifying the optimal treatment for low back pain on a patient-specific basis is an important and unresolved challenge in medicine. Tailoring interventions according to patient movement characteristics may improve clinical outcomes. Conventional movement analysis of the spine focuses on overall body movement, however, the underlying intervertebral kinematics remain unclear. Intervertebral range of motion (ROM) is typically measured on static radiographs to evaluate segmental kinematics, but ROM only describes the quantity of motion rather than the quality of motion (i.e. how the motion occurs) [1]. The path of the instantaneous center of rotation between adjacent vertebrae (*i.e.,* the centrode) has been proposed to evaluate motion quality [2]. Therefore, the aim of this study was to evaluate the intervertebral centrode during lumbar flexion/extension in people with cLBP. Based on similar analysis of cervical spine kinematics[3], we hypothesized that the centrode would be located more superior in each successive caudal motion segment and that the centrode would move less in the anterior-posterior direction in each successive caudal motion segment.

**Methods:** Three hundred participants were recruited from a larger study of individuals with cLBP [4]. Participants performed three trials of flexion/extension while synchronized biplane radiographs of the lumbar spine were captured at 20 images per second over the 3 second duration of each movement trial (85kV, 320mA, 4ms pulse width). Bone tissues of L1 through the sacrum were segmented from CT scans (0.4x0.4x0.625mm) and used to create subject-specific 3D bone models. Vertebral motions were tracked in the biplane radiographs using a validated process that matched digitally reconstructed radiographs created from the CT-based bones to the biplane radiographs with an accuracy of better than 1mm in translation and 1° in rotation [5]. The helical axis of motion (HAM) was then calculated using the finite helical axis method [6]. The intersection of the HAM and the sagittal plane of the inferior vertebra was then calculated at every 1° increment of intervertebral flexion/extension to determine the centrode of each motion segment [6]. One-way repeated measures ANOVA was used to identify vertebral level differences in the average superior-inferior (SI) location of the centrode and in the average change in centrode anterior-posterior (AP) location with every degree of flexion, with the Bonferroni correction applied to account for multiple comparisons. Significance was set at $p < 0.05$ for all tests.

**Results & Discussion:** Data from 125 individuals (72 females, age: 52.9±16.6 years, BMI: 25.7±3.6 kg/m$^2$) of the 300 collected have been processed and included in this analysis. During flexion/extension, the centrode is in the posterior/superior quadrant of the inferior vertebrae and it moves anteriorly with increasing flexion (Figure 1). Average centrode SI location at L4-L5 was more superior than at L1-L2, L2-L3, and L3-L4 (all $p<0.034$), while the average centrode SI location at L5-S1 was more superior compared to all other motion segments (all $p < 0.001$). No level-dependent differences in the change in centrode AP location with flexion were found ($p = 0.061$). These results are similar to those previously reported for healthy individuals during a lifting task [6]. A study limitation is the lack of centrode data from healthy, age-matched controls to provide context for this group of individuals with cLBP.

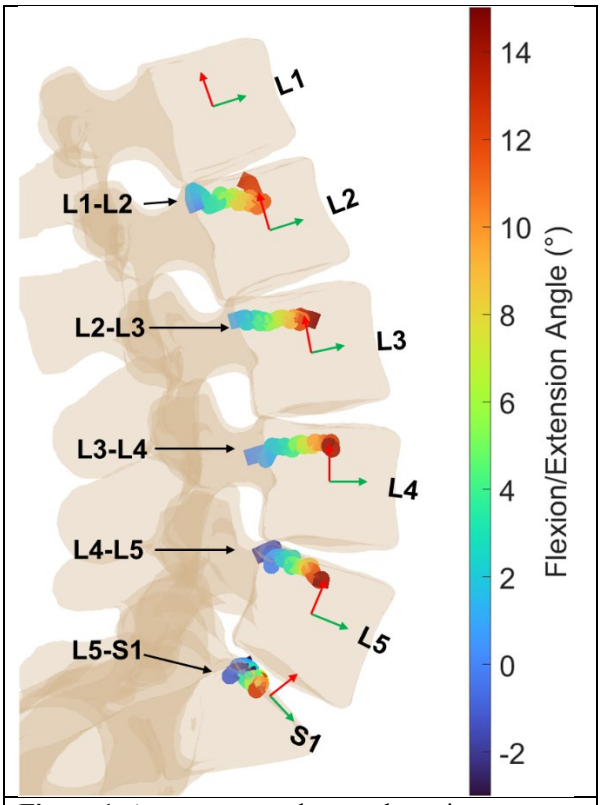


**Figure 1.** Average centrode at each motion segment during flexion/extension. Dark blue indicates intervertebral extension while dark red indicates high intervertebral flexion.

**Significance:** Knowledge of centrode kinematics may be used to improve lumbar disc replacement design to replicate the moving center of rotation and level-dependent differences in the centrode during flexion/extension.

**Acknowledgments:** This research is supported by the National Institutes of Health (NIH) through the NIH HEAL Initiative under award number U19AR076725. The content is solely the responsibility of the authors and does not represent the official views of the NIH or its NIH HEAL Initiative. The would like to acknowledge Joseph Shoemaker, Caroline Pellegrini, Cate Gray, and Patrick Smith for their contributions to this data.

**References:** [1] Bogduk et al. (2000) *Clin Biomech.* [2] Bogduk et al. (1995) *Proc Inst Mech Eng H*. [3], Anderst et al (2013) *Spine*. [4] Vo et al. (2023), *PainMed*. [5] Dombrowski et al. (2018). *EurSpineJ*. [6] Aiyangar et al. (2017) *JBiomech*.

# CONTRIBUTIONS OF CARPAL MOTION TO THUMB MOTION ARE COMPLEX AND TASK DEPENDENT

Joseph J. Crisco*, Amy M. Morton, Douglas C. Moore
Department of Orthopaedics, Warren Alpert Medical School of Brown University, Providence, RI
*Corresponding author's email: joseph_crisco@brown.edu

**Introduction:** Thumb carpometacarpal (CMC) osteoarthritis is highly prevalent with aging, especially in women. To assess progression, and efficacy of treatments and therapies, thumb range of motion (ROM) is an important metric. However, thumb motion - herein equivalent to measuring motion of the first metacarpal (MC1) with respect to the radius (i.e., Rad-MC1) is complex because it includes three joints: the radius-scaphoid joint (Rad-Sca), the scaphoid-trapezium joint (Sca-Tpm) and the trapezium-MC1 joint (Tpm-MC1), also referred to as the first CMC joint) (**Fig. 1**). The contributors of these three carpal joints to thumb motion has not been previously investigated. Thus, the aim of this study was to exam carpal bone motions in this thumb carpal pillar and to determine if these contributions vary with the thumb tasks performed.

**Methods:** Computed Tomography (CT) volumes from 46 healthy subjects (24F, 22M) were analysed using advanced 3D image-based tracking algorithms to compute Rad-MC1, Rad-Sca, Sca-Tpm, Tpm-MC1 motion from a neutral thumb position to 10 discrete thumb poses: four with the thumb at maximum active ROM tasks (extension, flexion, abduction, and adduction), and six while performing functional unloaded and loaded tasks: jar lid twisting ("jar"), lateral key pinch ("key"), and grasping ("grasp"). The CT scans were acquired as part of a longitudinal study of CMC biomechanical changes in early osteoarthritis (NIH R01 AR059185). Each bone was segmented in the neutral position, then registered to its location in each subsequent task using established image-based tracking algorithms. The motions were described using the rotation angle computed from helical axis of motion (HAM) parameters and then reduced to the percentage of Rad-MC1. Differences in motion contributions by task were assessed with a repeated-measures two-way ANOVA and a Tukey's multiple comparisons test.

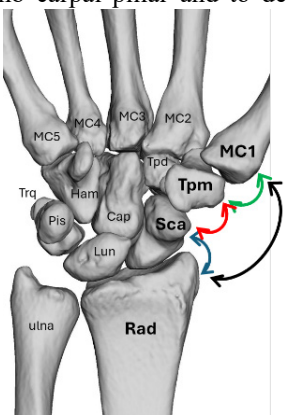


**Figure 1.** Diagrammatic representation of the relative joint motions that were analyzed. Rad-MC1 (*black*) motion occurs through a carpal pillar of three joints: Rad-Sca (*blue*), Sca-Tpm (*red*), and Tpm-MC1 (*green*).

**Results & Discussion:** Most notable was that the thumb carpal pillar joint rotations summed to more than Rad-MC1 rotation itself across all tasks, by at least 50% and in some poses by approximately 100% (**Fig. 2**). In other words, the total rotations across these carpal joints were greater than that of thumb rotation, and for jar lid twisting (Jar), for example, the rotations summed to nearly twice that of thumb motion. The analysis was limited to the HAM rotation; thus the directions of the rotations were not considered. It is possible, and likely given our findings, that when the thumb (Rad-MC1) flexed, for example, the scaphoid-trapezium (Sca-Tpm) could have extended or rotated in another direction.

The contributions of the three joints in the thumb carpal pillar (Rad-Sca, Sca-Tpm, Tpm-MC1) varied by task (**Fig. 2**). For example, in thumb extension the Tpm-MC1 rotation was greater than both Sca-Tpm and Rad-Sca rotations, which were not different from each other. In thumb flexion, each joint rotated different amounts, with the magnitude of rotations increasing from proximal to distal. The greatest rotations at the Rad-Sca joint occurred in Grasp-Loaded and Jar and notably these rotations were nearly 100% of thumb rotation (Rad-MC1). The greatest contributions in a single task (98%) occurred at the Tpm-MC1 joint in abduction. Across all tasks, the contributions were the least from the Sca-Tpm joint (37%) and greatest from the Tpm-MC1 joint (76%). The mechanism behind the various contributions is not known, but it is clear they are complex and vary by task. We would note that the Rad-Sca, Sca-Tpm, Tpm-MC1 kinematic calculations are based upon static 3D CT imaging and that they would be impossible to determine using skin-based technologies that measure thumb motion, such as goniometers and optical motion capture systems.

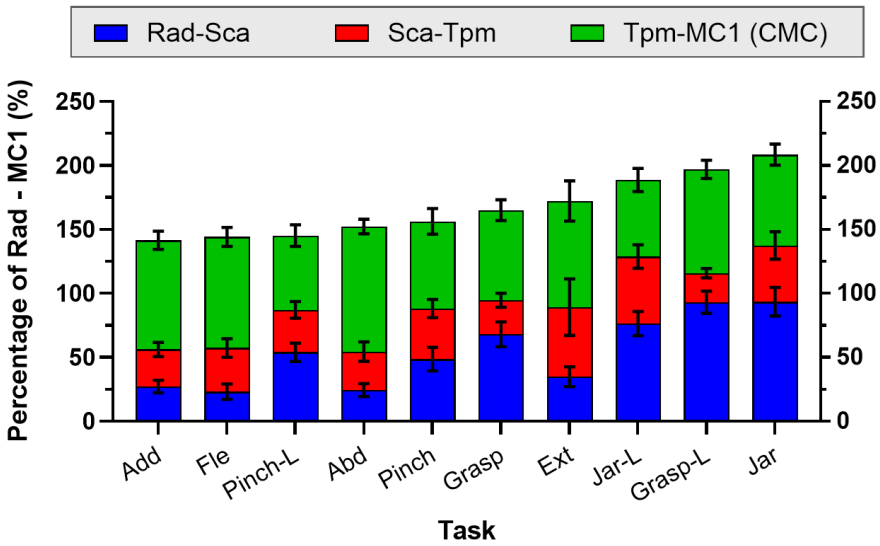


**Figure 2.** The contributions (mean and 95% CI) of the three thumb carpal pillar joints (radius-scaphoid (Rad-Sca), scaphoid-trapezium (Sca-Tpm), and trapezium-first metacarpal (Tpm-MC1)) to overall thumb motion (radius-first metacarpal (Rad-MC1)) varied for each thumb task (Abd – abduction, Add – adduction, Ext – extension, Fle – flexion, Grasp and Grasp-Loaded, Jar and Jar-Loaded, and Pinch and Pinch-Loaded.

**Significance:** Painless thumb function is critical for activities of daily living. When pathologies such as CMC OA develop there are numerous treatments, many of which have limited evidence of efficacy. Rigorous measurements of thumb carpal pillar kinematics are essential for assessing disease progression, treatment and therapies. It is important to appreciate that that thumb motion (Rad-MC1) cannot be used to infer function at any of the three joints that make up the carpal pillar of the thumb.

**Acknowledgments:** This research was supported by NIAMS of NIH under Award Number AR059185. The content is solely the responsibility of the authors and does not necessarily represent the official views of the National Institutes of Health.

# BILATERAL FRONTAL-PLANE KNEE JOINT MOMENTS DURING DIFFERENT TYPES OF WALKING IN ADULTS WITH UNILATERAL KNEE OSTEOARTHRITIS

*Samantha K. Price[1,2], Joshua J. Stefanik[3], Cara L. Lewis[4], Irene S. Davis[5], Patrick Corrigan[1,2]
[1]Saint Louis University, [2]Cleveland Clinic, [3]Northeastern University, [4]Boston University, [5]University of South Florida
*Corresponding author's email: prices16@ccf.org

**Introduction:** Osteoarthritis (OA) is a leading cause of disability that is particularly prevalent in the knee joint [1]. For many adults, knee OA begins as a unilateral disease, with pain and structural disease in only one knee. Yet, 90% of individuals with unilateral knee OA develop bilateral knee OA within 10 years [2]. Biomechanical measures, such as external knee adduction moments (KAM), have been associated with knee OA progression [3-4]. Yet, current studies that evaluate KAM in adults with knee OA typically only describe loading in the most painful limb during flat walking [5], limiting our understanding of biomechanical mechanisms involved in contralateral knee OA development. Expanding current research efforts by evaluating knee joint kinetics in adults with unilateral knee OA during different types of walking could enhance our understanding of unilateral-to-bilateral knee OA progression and assist with identifying potential rehabilitation approaches that prevent contralateral knee OA development. The purpose of this study was to compare frontal-plane knee joint moments between limbs during flat, inclined, and declined walking at self-selected, slow, and fast speeds in adults with unilateral knee OA. We hypothesized that more difficult walking conditions (e.g., faster speed and gradient) would result in higher KAM in the contralateral knee compared to the OA knee.

**Methods:** Adults with clinically defined symptomatic unilateral knee OA were recruited and enrolled. Inclusion was based on the National Institute for Heath and Care Excellence (NICE) criteria (≥ 45 years, knee pain lasting >3 months, knee pain ≥ 3/10 with walking, and knee stiffness lasting <30 minutes in one knee). Participants completed nine 2-minute walking conditions on a force-instrumented split-belt treadmill (Bertec Inc., Columbus, OH, USA) in a 3D motion analysis environment (Qualisys AB; Gotenburg, Sweden). The gradient of the treadmill was set to flat (0°), inclined (+4.8°), and declined (-4.8°). At each gradient, three speeds were collected: self-selected (ss), slow (ss-20%), and fast (ss+20%). Ground reaction forces and kinematic data were sampled (2160 and 180 Hz, respectively) in the second minute of each condition. Frontal-plane knee joint moments were calculated for 10 gait cycles and normalized to body mass and height. For statistical analysis, average frontal-plane knee moment curves were compared between limbs for each of the nine walking conditions using statistical parametric mapping (SPM(F)) paired t-tests.

**Results & Discussion:** 22 adults were included (13 F; age=60(7) years; height=170(10) cm; body mass=82(21) kg) Average(SD) ss walking speed was 0.91(0.1) m/s. Median(IQR) pain with walking, on an 11-point scale, was 2(2) for all self-selected conditions, slow decline, and fast flat walking, 1(2) during slow incline and slow flat walking, 2(3) during fast incline walking, and 3(2) during fast decline walking. Average frontal-plane knee joint moments between the painful and nonpainful limbs for all nine types of walking are shown in Figure 1. SPM(F) analyses indicated there were no significant differences between limbs in any of the nine walking conditions.

While there were no significant differences in these preliminary analyses, adults with unilateral knee OA may load their painful knee more than their nonpainful knee during decline walking, regardless of speed. In all other walking conditions adults with unilateral knee OA may load their nonpainful knee more than their painful knee. Variability in the painful limb and underpowered analyses could explain the lack of significant differences between limbs.

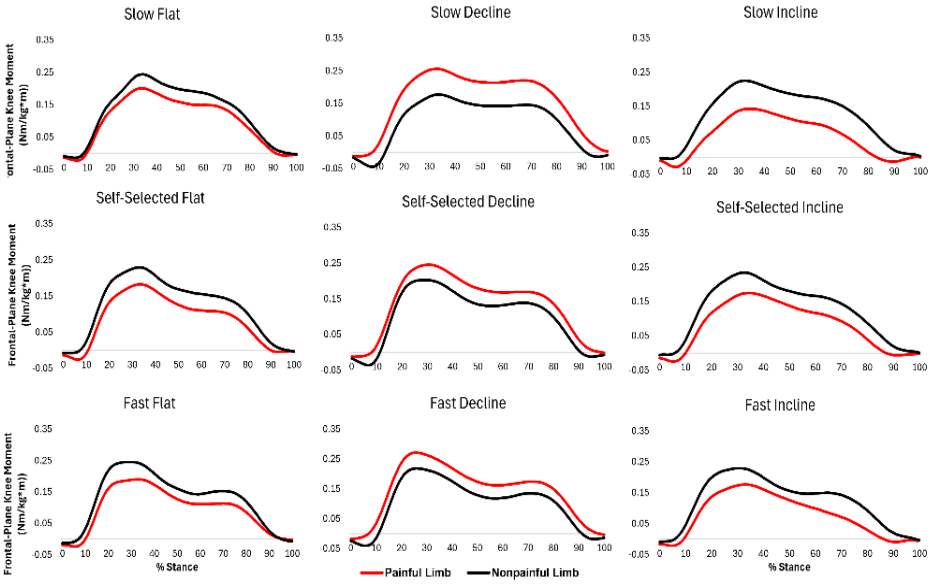


**Figure 1:** Average frontal-plane knee joint loading in the painful and nonpainful limbs during all nine walking conditions

**Significance:** There were no differences in frontal-plane knee moments between the painful and nonpainful limbs in adults with clinically defined unilateral knee OA. Further research is needed to understand unilateral-to-bilateral knee OA progression.

**Acknowledgments:** Funding was provided by Rheumatology Research Foundation and Academy of Orthopaedic Physical Therapy

**References:** [1] Bannuru et al. (2019); [2] Jones et al. (2013); [3] Chehab et al. (2014); [4] Miyazaki et al. (2002); [5] D'Souza et al. (2021)

# BIOMECHANICAL COMPARISON OF THREE PLATE AND SCREW SYSTEMS FOR THE TREATMENT OF DISTAL FIBULAR COMMINUTED FRACTURES

*Matheus M. Vilela[1, 2], Arthur P. G. Santos[1], Andre L. A. Pizzolatti[1], Felipe F. Gonzalez[2], Renato Miyadahira [2], Carlos R. M. Roesler[1]
[1]Biomechanical Engineering Laboratory of the Federal University of Santa Catarina, Florianópolis, SC, Brazil
[2]Department of Orthopaedics, Rush University Medical Center, Chicago, IL, USA
*Corresponding author's email: matheus_vilela@rush.edu

**Introduction:** Fractures of the ankle are common injuries reported as 10.2% of all bone injuries[1]. Surgical treatment, including open reduction and internal fixation is often required for unstable fractures. The technique of bridge plating can be used for comminuted fractures, where the implant serves as an extramedullary support, fixing the main fragments while leaving the fracture zone undisturbed[2]. This study aims to investigate and compare the mechanical stability provided by different plating techniques in comminuted Weber B fibula fractures (transsyndesmotic).

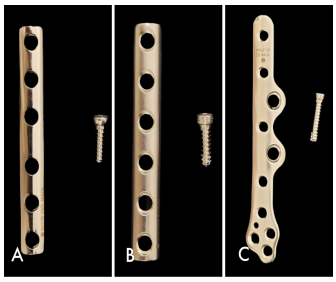


**Figure 1:** a) one-third tubular plate (OTP); b) locking one-third tubular plate (LOTP); c) locking distal fibula plate (LDFP).

**Methods:** Thirty fourth-generation composite fibulas were randomly divided into three groups, with each group receiving a different type of stainless-steel bone plates (Fig.1): a six-hole one-third tubular plate (OTP), a six-hole locking one-third tubular plates (LOTP) and a locking distal fibula plates (LDFP). Comminuted Weber B fractures were simulated by creating a 3.5 mm gap between fragments. Each group underwent stiffness testing for torsion, axial compression, and lateral bending (Fig. 2). For destructive testing, each group was subdivided into two subgroups of five constructs, one for torsion and the other for lateral bending. Torsional and axial stiffness were measured using a universal testing machine (Zwick/Roell model Z2.5 TN; Ulm, Germany). Axial stiffness was measured by applying a preload at 1 mm/min until 5 N, followed by loading at 0.02 mm/min until 30 N. Torsional stiffness was assessed with a preload at 5 degrees/min until 0.02 N·m, followed by loading at 10 degrees/min until 0.4 N·m. Lateral bending stiffness was evaluated using a servo-electric universal testing machine (Shimadzu AGS-X 100 kN, Kyoto, Japan) with a 1 kN load cell. A preload at 1 mm/min was applied until 2 N, followed by loading up to 20 N. Destructive tests for maximum strength were performed using the same setup as the stiffness tests. For maximum torsional strength, a preload of 5 degrees/min was applied to 0.02 N·m, followed by a load of 15 degrees/min until failure while maintaining an axial load of 30 N. Maximum lateral bending strength was assessed by applying a displacement at 1 mm/min until 2 N, then increasing the load at 10 mm/min until failure. Data analysis included assessing homogeneity of variances with the qualitative graphical q-q method and Levene's test. A one-way ANOVA was used to evaluate the effects of plate type on stiffness and strength measurements, with Tukey's test for pairwise comparisons. For data with heterogeneous variances, logarithmic transformation or the nonparametric Kruskal-Wallis test was applied. Statistical significance was set at alpha = 0.05.

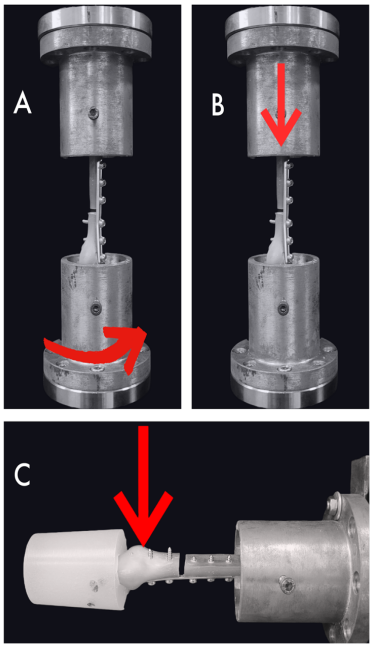


**Figure 2:** Representation of testing loads: a) torsional; b) axial; c) lateral bending

**Results & Discussion:** Torsional stiffness ($p < 0.001$) and lateral bending stiffness ($p < 0.001$) were significantly higher for the locking one-third tubular plate (LOTP) system compared to both the locking distal fibula plate (LDFP) and one-third tubular plate (OTP) systems. However, no significant differences were observed in axial stiffness ($p = 0.08$) across the three groups. In terms of maximum force, the LOTP system demonstrated greater resistance in both lateral bending and torsional tests. It was significantly higher than the LDFP system for lateral bending ($p < 0.01$) and showed higher torsional resistance than the OTP system ($p < 0.001$). The LDFP system, while superior to the OTP system, did not outperform the LOTP in either maximum force measurement. Results indicate that locking plates, particularly the LOTP system, provide superior mechanical stability compared to OTP. This is consistent with previous studies that have demonstrated the advantages of locking plates in preventing screw loosening and enhancing fracture stability. However, while the LDFP showed improved maximum load resistance, it did not exhibit significantly better fracture protection during peak loading when compared to the OTP.

**Significance:** These results can offer valuable insights into the most effective treatment strategies for comminuted Weber B fibula fractures. Ultimately, this study could help refine surgical practices and improve the management of ankle fractures, particularly in patients with complex fracture patterns or additional risk factors.

**Acknowledgments:** We would like to thank Hexagon Brasil and the Biomechanical Engineering Laboratory of the Federal University of Santa Catarina (Brazil) and all the collaborators who supported this work.

**References:** [1] Paul Tornetta III, et al. (2025) Rockwood and Green's fractures in adults, Ed.10th; [2] Stefan Rammelt, et al. (2020) Manual of Fracture Management—Foot and Ankle

# SINGLE-BUNDLE MCL RECONSTRUCTION WITH ANATOMIC SINGLE-BUNDLE ACL RECONSTRUCTION DOES NOT RESTORE KNEE KINEMATICS

*Weimin Zhu[1] Junjun Zhu, Patrick Smolinski
[1]Shenzhen 2nd People's Hospital (The First Affiliated Hospital of Shenzhen University), Guangdong, China
*Corresponding author's email: szhzwm@email.szu.edu.cn

**Introduction:** The medial collateral ligament (MCL) complex is one of the most common injured ligamentous structures of the knee [1]. It has been reported to occur in between 20 to 38% of all ACL injury cases [2]. The MCL complex includes three structures: the superficial MCL (sMCL), the deep MCL (dMCL) and the posterior oblique ligament (POL) [3]. Different MCL reconstruction techniques have been developed for combined ACL and severe MCL injuries. However, a cadaver knee biomechanics study with different MCL reconstruction techniques has not been performed. It is not known whether the anatomical reconstruction of both the sMCL and POL is required, if changing the POL graft attachment point has an effect on the biomechanical outcome, or if a single bundle sMCL is sufficient to restore intact knee kinematics. Thus, the purpose of this study was to compare knee kinetics and kinematics following single-bundle anatomic ACL reconstruction and either single-bundle sMCL reconstruction, double-bundle anatomical MCL reconstruction or modified triangular reconstruction of the sMCL and POL in a cadaveric model. It has been hypothesized that the double-bundle anatomical MCL reconstruction and the modified triangular MCL reconstruction would yield better rotational stability compared to single bundle sMCL reconstructions in the setting of single-bundle anatomic ACL reconstruction.

**Methods:** Ten fresh-frozen cadaveric knees (Age 41 ± 15.4 years) were used and exclusions included ligamentous laxity, osteochondral lesions greater than grade 2 and previous surgery. All specimens were tested with four different loading conditions: (1) an 89 N anterior tibial (AT) load, (2) a 7 N-m valgus (VAL) load, (3) a 5 N-m tibial internal rotation (IR) load and (4) a 5 N-m tibial external rotation (ER) load at full extension (FE), 15°, 30°, 45°, 60° and 90° of knee flexion. Six different knee states were compared in this study: (1) intact knee, (2) single bundle (SB) ACL reconstruction with intact MCL complex (ACLR) (3) single bundle (SB) sMCL reconstructed with single-bundle (SB) ACL reconstruction, (4) anatomical double-bundle (DB) MCL reconstruction with (SB) ACL reconstruction; (5) modified triangular MCL reconstruction with (SB) ACL reconstruction and (6) deficient ACL and MCL complex. Three reconstruction states were tested in a randomized order.

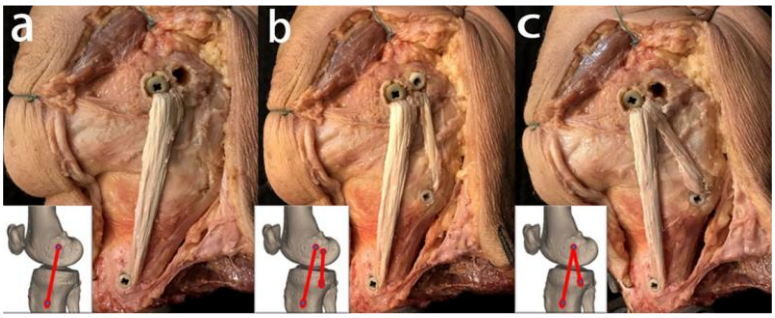


**Figure 1: a** Single-bundle (SB) sMCL reconstruction, **b** anatomic double-bundle (DB) MCL reconstruction, and **c** modified triangular MCL reconstruction

**Results & Discussion:** Removing the ACL and MCL complex significantly increased the anterior tibial translation (ATT) at all knee flexion angles (full extension, 15°, 30°, 45°, 60°, and 90°) . When compared to the intact knee, all three MCL reconstructions with SB ACL reconstructed knees were able to restore intact knee kinematics, significantly decreasing the ATT after reconstruction (Figure 2). The most important finding of this study was that modified triangular and double-bundle MCL reconstructions best restored the kinematics to that of the intact MCL in the setting of single-bundle ACL reconstruction. Our study found that an anatomic ACL reconstruction with SB MCL reconstruction was able to restore anterior tibial translation and internal rotation to intact knee values but failed to restore most of the internal and valgus rotatory stability. Anatomical DB MCL reconstruction (with SB ACL reconstruction) was slightly better in restoring the kinematics and in-situ force of intact knee than the modified triangular MCL reconstruction (with SB ACL reconstruction). Clinically, the modified triangular MCL reconstruction may be more practical, because it is less invasive, has fewer tunnels and is technically simpler.

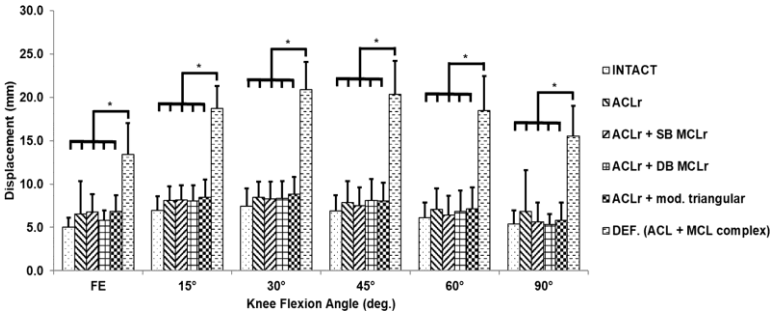


**Figure 2:** Anterior tibial translation under an 89 N anterior tibial load (*p < 0.05)

**Significance:** With combined ACL and severe sMCL injury, single- bundle MCL with single-bundle ACL reconstruction does not restore knee kinematics. Clinically, the modified triangular reconstruction may be a better option, since it can restore nearly normal knee kinematics and is less invasive.

**References:** [1] Elliott et al. (2015) Orthopedics 38; [2] Zaffagnini et al. (2011) J Bone Joint Surg Br 93; [3] Fetto et al. (1978) Clin Orthop Relat Res 132.

# MECHANICAL COMPETENCE OF BONE FROM PERSONS WITH SPINAL CORD INJURY: DEVELOPMENT OF A NON-INVASIVE FRAMEWORK TO QUANTIFY TORSIONAL AND COMPRESSIVE STIFFNESS AND STRENGTH

William Kuo[1], Anmol S. Doss[1], Albin F. Mullan[1], Christopher M. Cirnigliaro[2], William A. Bauman[3], *Saikat Pal[1,2]
[1]New Jersey Institute of Technology, Newark, NJ, USA; [2]James J. Peters Veterans Affairs Medical Center, Bronx, NY, USA;
[3]Icahn School of Medicine at Mount Sinai, New York, NY, USA
Corresponding author's email: pal@njit.edu

**Introduction:** Persons with spinal cord injury (SCI) experience rapid and progressive sublesional bone loss and are at high risk of fragility fractures. Over 80% of these fractures occur in the lower extremities, with the most common site being the knee region (distal femur and proximal tibia) [1]. Clinical evaluation of bone strength currently includes radiography-based metrics from dual-energy x-ray absorptiometry (DXA) and peripheral quantitative computed tomography (pQCT) scans [2, 3]. However, several recent studies have described that radiographic measurements alone are insufficient to evaluate the mechanical competence of bone, which depends on parameters like geometry, mineral distribution, material properties, and mode of loading [4, 5, 6]. The complex interactions among these parameters can be captured by finite element (FE) methods. Prior studies have reported that the FE-based metrics are better indicators of bone strength than DXA- and CT-based metrics [4, 5, 6]. As such, the **goal** of this study was to develop a non-invasive framework to quantify four FE-based metrics of bone strength: torsional stiffness ($K_t$), torsional strength ($T_{ult}$), compressive stiffness ($K_c$), and compressive strength ($C_{ult}$) from persons with SCI and able-bodied (AB) control participants.

**Methods:** We recruited 19 (14M, 5F) participants with SCI (duration of injury 8.6±6.7 years) and 4 (3M, 1F) AB participants. Participants were informed on all aspects of the study and provided IRB consent. All participants were between 24-62 years of age, and there were no statistical differences in age or body mass index between SCI and AB participants. We computed the four FE-based metrics of bone strength from 37 SCI and 8 AB proximal tibias (Fig. 1). Bilateral knees from each participant were scanned in a clinical CT scanner (Siemens Somatom, Fig. 1A). The 3D CT images were used to create a solid mesh using 1.5 mm, linear tetrahedral elements (Figs. 1B-D). We extracted subject-specific variable bone material properties using calibration phantoms and established methods (Figs. 1E-H) [7, 8]. We reoriented each model to align the long axis of the bone in the inferior-superior direction and cut the bone to 13 cm [9]. Boundary conditions were assigned to apply torsional (Fig. 1I) and compressive (Fig. 1J) displacements in increments until failure [4, 5]. The FE simulations were run in Abaqus/Explicit (SIMULIA, Providence, RI), and custom Python scripts were used to extract the reaction torque and force values until failure (Fig. 1K-N). The FE-based metrics of bone strength were best fit with a non-Gaussian, two-parameter Weibull model, with coefficients of determinations ($R^2$) ≥ 0.92 in all cases.

**Results & Discussion:** Torsional stiffness ($K_t$) ranged from 7.9-53.2 Nm/deg and 28.6-77.2 Nm/deg for the SCI and AB groups, respectively (Fig. 2A). Torsional strength ($T_{ult}$) ranged from 21.9-160.6 Nm and 131.3-286.4 Nm for the SCI and AB groups, respectively (Fig. 2B). Compressive stiffness ($K_c$) ranged from 0.9-15.1 kN/mm and 12.3-22.4 kN/mm for the SCI and AB groups, respectively (Fig. 2C). Compressive strength ($C_{ult}$) ranged from 1.4-18.9 kN and 12.3-28.0 kN for the SCI and AB groups, respectively (Fig. 2D).

**Significance:** The results from this study provide a foundation for statistical models fitting the distributions of FE-based metrics of bone strength, and confidence interval-based thresholds to predict fracture risk in persons with SCI and other osteoporotic populations.

**Acknowledgments:** VA RR&D #1 I01 RX003561.

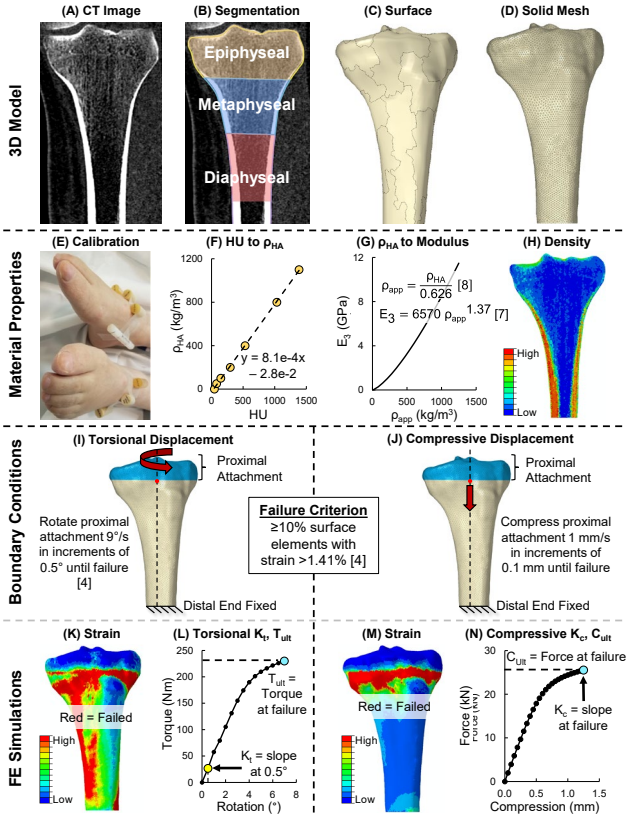


**Figure 1:** A non-invasive framework to quantify bone strength using clinical CT scans and subject-specific FE simulations.

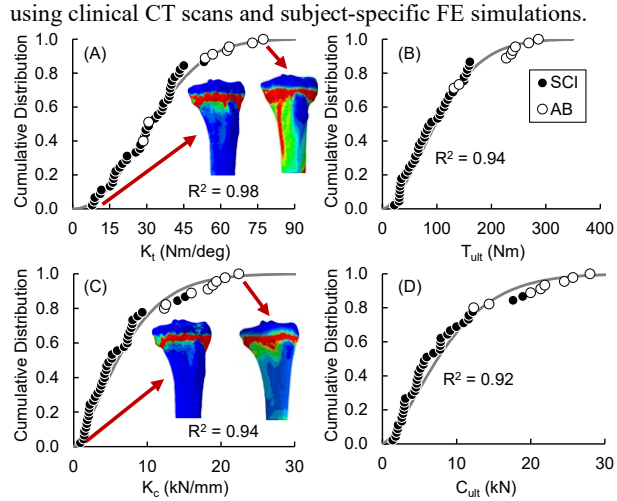


**Figure 2:** The distributions of (A) torsional stiffness $K_t$, (B) torsional strength $T_{ult}$, (C) compressive stiffness $K_c$, and (D) compressive strength $C_{ult}$ from SCI and AB participants.

**References:** [1] Grassner et al. 2018, J. Spinal Cord Med. 41(6); [2] Garland et al. 2004, J. Spinal Cord Med. 27(3); [3] Eser et al. 2005, Arch. Phys. Med. Rehabil. 86(3); [4] Edwards et al. 2013, J. Biomech. 46(10); [5] Edwards et al. 2014, Osteoporos. Int. 25(3); [6] Haider et al. 2021, Ann. Biomed. Eng. 49(2); [7] Rho et al. 1995, Med. Eng. l'hys. 17(5); [8] Dalstra et al. 1993, J. Biomech. 26(4-5); [9] Crack et al. (2024), JBMR Plus. 8(7).

# EFFECT OF PAIN RELIEF ON TIBIOFEMORAL CONTACT FORCES DURING DIFFERENT TYPES OF WALKING IN ADULTS WITH KNEE OSTEOARTHRITIS

*Patrick Corrigan[1,2], David T. Felson[3], Tuhina Neogi[3], Cara L. Lewis[3], Irene S. Davis[4], Samantha K. Price[1,2], Sharf Daradkeh[1,2], Jamil Neme[2], John D. Willson[5], Joshua J. Stefanik[6]
[1]Cleveland Clinic, [2]Saint Louis University, [3]Boston University, [4]University of South Florida,
[5]East Carolina University, [6]Northeastern University
*Corresponding author's email: corrigd4@ccf.org

**Introduction:** Knee osteoarthritis (KOA) is a leading cause of chronic pain and disability [1]. Evidence-based guidelines highly recommend exercise as a first-line strategy for managing pain and preventing functional decline [2,3]. Walking continues to be the most common form of exercise for adults with KOA [4]. However, individuals with KOA often receive other pain-relieving treatments alongside exercise (e.g., injections, medications). Since increased knee joint forces while walking are associated with the development and progression of KOA, there is a critical need to understand how pain-relieving treatments influence joint loading. The purpose of this study was to determine if pain relief leads to immediate changes in tibiofemoral (TF) contact forces during different types of walking in adults with KOA. Our overall hypothesis was that decreasing knee pain would result in immediate increases in TF contact forces.

**Methods:** Adults with clinically-defined unilateral, symptomatic KOA were recruited and enrolled. Each participant completed two visits separated by approximately one week. The first visit included a biomechanical walking assessment while participants experienced their typical knee pain. During this assessment, participants completed nine different types of walking on a force-instrumented split-belt treadmill (Bertec Inc., Columbus, OH) in a three-dimensional motion capture environment (Qualisys AB, Götenberg, Sweden). The nine types of walking included flat (0°), uphill (+4.8°), and downhill (-4.8°) gradients at self-selected (ss), fast (ss+20%), and slow (ss-20%) speeds. Conditions were two minutes in duration to avoid fatigue and performed in a random order. The second visit was identical to the first, including gait speeds, except participants received a pain-relieving ultrasound-guided intraarticular knee injection (10 mL of 1% lidocaine hydrochloride) immediately before repeating the biomechanical walking assessment. Using force and marker data from each walking condition at both visits, TF contact forces were estimated using a validated inverse dynamics-informed musculoskeletal model [5]. Statistical parametric mapping was used to compare TF contact force signals between the two visits (painful vs little-to-no pain) for each type of walking. All analyses were performed after scaling TF contact force signal magnitudes to bodyweight (BW) and signal durations to stance time.

**Table 1. Median (IQR) Knee Pain**

| | Visit 1 | Visit 2 |
|---|---|---|
| Slow flat | 1.5 (2) | 0(1) |
| Slow uphill | 1.5(1.3) | 0(1) |
| Slow downhill | 2(2) | 1(2) |
| Self-selected flat | 1.5(3) | 0(1) |
| Self-selected uphill | 2(2) | 1(1) |
| Self-selected downhill | 2(2) | 0(1.3) |
| Fast flat | 1(2) | 1(2) |
| Fast uphill | 2(3) | 1(2) |
| Fast downhill | 2.5(2) | 1(1.5) |

**Results & Discussion:** Twenty-five participants completed both visits (16 female; mean(SD) age: 62(8) y; height: 169(11) cm; mass: 81(20) kg). On a 0-100 scale, mean(SD) knee pain in the past week at the first visit was 37(18). Knee pain severity during the different walking conditions are shown in Table 1, with fast downhill walking eliciting the most pain. As expected, knee pain was successfully reduced at the second visit even though overall pain severities were quite low. Mean(SD) self-selected gait speed during the gait assessment was 0.93(0.10) m/s, which resulted in slow and fast conditions being performed at 0.75(0.10) m/s and 1.12 (0.10) m/s, respectively. When comparing the TF contact force signals between visits for each walking condition, we found no significant differences (see Figure). These findings suggest that relieving pain in those with unilateral symptomatic KOA does not immediately affect TF contact forces when walking at different gradients and speeds.

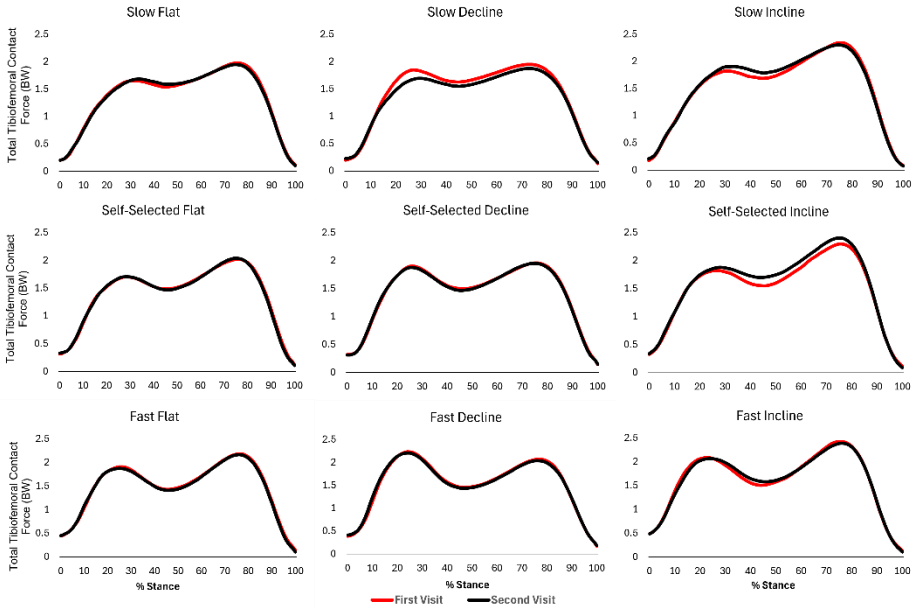


**Figure 1.** Tibiofemoral contact forces for each type of walking

**Significance:** While it is uncertain if these results are generalizable to other pain-relieving treatments, our data suggest that reducing knee pain does not immediately change knee joint kinetics.

**Acknowledgments:** Funding from the Rheumatology Research Foundation and Academy of Orthopaedic Physical Therapy.

**References:** [1] Lawrence et al. (2008), *Arthritis Rheum* 58(1); [2] Bannuru et al. (2019), *Osteo Cart* 27(11); [3] Kolasinski et al. (2020), *Arthritis Rheum* 72(2); [4] Dai et al. (2015), *J of phys act & health* 12 Suppl 1; [5] Devita et al. (2001), *J. Appl Biomech* 17(4).

# DECIPHERING THE "ART" IN MODELING AND SIMULATION OF THE KNEE JOINT: BENCHMARKING

Maryam Nazem[1], Thor E. Andreassen[1], Nancy Kim[2], Kate Moyle[2], Jason P. Halloran[3], Casey A. Myers[1], Snehal Chokhandre[4], Thor F. Besier[3], Carl W. Imhauser[5], Kevin B. Shelburne[1], Ahmet Erdemir[4], *Peter J. Laz[1]
[1]University of Denver, Denver, CO [2]Auckland Bioengineering Institute, Auckland, New Zealand
[3]Washington State University, Spokane, WA [4]Cleveland Clinic, Cleveland, OH [5]Hospital for Special Surgery, New York, NY
*Corresponding author's email: peter.laz@du.edu

**Introduction:** Given the strong ties to data sharing and the responsible use of resources, reproducibility of modeling & simulation practice is of paramount importance in science. Computational models in orthopaedics provide insight into healthy and injured joint mechanics and can inform clinical decision-making. The KneeHub project investigated the impact of modeler's decision and the "art" in simulation and modeling; five teams developed and calibrated knee models using the same experimental data sources [1-3]. Model benchmarking evaluates the predictive ability of a model under conditions that were not considered in the model development and calibration process. Accordingly, the objective of the current study was to evaluate the accuracy of predictions of knee-specific joint biomechanics for benchmark scenarios of simulating an ACL tear and combined loading, while also considering the impact of modeler decision-making. All data and results for the KneeHub project are publicly available on the SimTK website [4].

**Methods:** Leveraging open datasets, teams developed models for two knees (Natural Knee Dataset (DU02) and Open Knee (OKS003)), primarily using imaging data [2]. Models were then calibrated to reproduce experimental laxity testing in various degrees of freedom and at multiple flexion angles by tuning ligament properties and reference strain [3]. Experimental data were earmarked for use in model benchmarking and thereby were not used in calibration.

For the DU02 knee, the model benchmarking cases involved removal of the anterior cruciate ligament (ACL) and evaluation of the knee for three laxity tests: anterior-posterior (AP), internal-external (IE), and varus-valgus (VV) at two flexion angles (15º and 55º), and passive flexion (0º to 120º). For the OKS003 knee, a loading condition that combined IE and VV applied moments at four distinct flexion angles (0º, 30º, 60º, 90º) was utilized. Kinematics for the tibiofemoral joint simulation were compared with the experiment, and RMS errors were calculated to evaluate each model and condition. To facilitate comparisons, all model predictions were transformed into the coordinate system of the experiment. RMS errors between the model predictions and experiment were computed for each test with standard deviations capturing variability of predictive accuracy among teams.

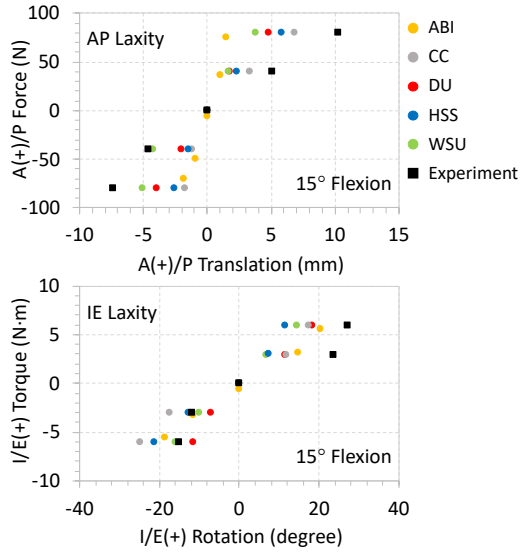


**Figure 1:** Benchmark laxity curves (no ACL) comparing simulations for the 5 teams with DU02 experimental data.

**Table 1:** RMS errors (mean and standard deviation) comparing kinematic predictions to experiment for all teams. Shaded cells correspond to loaded degrees of freedom.

| Model | Test | AP (mm) | IE (deg) | VV (deg) |
|---|---|---|---|---|
| Natural Knee (DU02) No ACL | AP Laxity | 6.59 ± 2.39 | 13.53 ± 12.85 | 3.74 ± 1.96 |
| | IE Laxity | 4.69 ± 2.98 | 8.76 ± 4.18 | 3.34 ± 1.70 |
| | VV Laxity | 4.98 ± 3.37 | 8.81 ± 7.41 | 5.31 ± 3.35 |
| | Passive flexion | 6.12 ± 5.30 | 7.39 ± 5.83 | 3.97 ± 1.86 |
| Open Knee (OKS003) | Combined Loading | 1.61 ± 0.78 | 7.29 ± 3.77 | 1.71 ± 0.92 |

**Results & Discussion:** Benchmarking conditions were designed to challenge models beyond the calibration conditions and in clinically relevant ways—such as by removing a key structure (e.g., ACL) or applying combined loading to simulate a pivot shift exam. As such, benchmarking evaluated whether the relative contributions of the structures of the knee were adequately represented to capture knee biomechanics accurately. In general, the models reasonably predicted the overall trends in kinematics and kinetics; however, the comparisons showed differences with the experiment and between teams (Figure 1). In the DU02 knee (no ACL), RMS errors for the laxity tests were larger than for passive flexion (Table 1), likely due to the larger applied forces/moments. The calibrated models were observed to be stiffer, underpredicting the laxity of the experiment. In the OKS003 knee (intact) under combined IE and VV loading, the model for one team experienced numerical instability, while the model for another team failed to converge at the 90° flexion angle. These data points were excluded in the calculation of the errors. The RMS errors in IE rotation were larger than in VV, even though the applied VV torque (10 N·m) was twice as high as the IE torque (5 N·m); while not directly loaded, results for AP translation showed the smallest errors. Across both knees and all tests, IE rotation showed the largest errors, which may have been influenced by modeler-specific decisions related to the representation and properties of the soft tissue structures. Teams employed distinct calibration strategies—some focused on isolating structures in a particular activity, while others tuned multiple structures across multiple degrees of freedom and flexion angles. As researchers often extend models beyond the conditions used to calibrate them, quantifying model accuracy and limitations with benchmarking represents an important step toward reproducibility and improving confidence in modeling in our community.

**Significance:** The benchmarking phase evaluated the accuracy of calibrated models under previously-unseen conditions: simulating an ACL tear and combined loading. By enhancing model reproducibility and documenting model decision-making, the open source KneeHub project supports the broader adoption of computational knee biomechanics in research and clinical applications.

**Acknowledgments:** NIH-NIBIB R01EB024573

**References:** [1] Erdemir et al., *J Biomech Eng* 141, 2019. [2] Rooks et al., *J Biomech Eng* 143, 2021, [3] Andreassen et al., *J Biomech Eng* 145, 2024. [4] https://simtk.org/projects/kneehub.

# RELATIONSHIP BETWEEN KOOS JR AND PHYSICAL PERFORMANCE MEASURES: ASSESSING CHANGES IN FUNCTION FOLLOWING TOTAL KNEE ARTHROPLASTY

Youngjae Lee*, Garret Burks, Devon R. Pekas, Peter J. Apel, Benjamin R. Coobs
Department of Orthopaedic Surgery, Institute for Orthopaedics & Neurosciences, Carilion Clinic, Roanoke, Virginia, United States
*Corresponding author's email: ylee1@carilionclinic.org

**Introduction:** The knee injury and osteoarthritis outcome score for joint replacement (KOOS JR) is a commonly used patient reported outcome measure (PROM) that aims to assess knee health related to stiffness, pain, and function before and after primary total knee arthroplasty (pTKA) [1, 2]. Despite its widespread use, to our knowledge, no studies have investigated how KOOS JR relates to other measures of function such as objective physical performance measures (PPMs) among pTKA patients. Understanding this relationship is important as prior studies have concluded that PROMs may over- or under-estimate the acute functional decline and recovery trajectories due to discrepancies between how patients perceive their function and how it is objectively measured [3, 4]. Moreover, the proposed use of a patient-acceptable symptom state (PASS) for KOOS JR presents an opportunity to determine differences in PPMs among pTKA patients who did or did not achieve the PASS threshold in KOOS JR and further investigate any discrepancy in what patients perceive when compared to their measured physical abilities. The goal of our study was to investigate the relationship between KOOS JR and PPMs among pTKA patients. We hypothesized (H1) KOOS JR would show no or weak correlation with PPMs and (H2) patients' PPMs would not differ regardless of whether they achieved the KOOS JR PASS threshold.

**Methods:** This is a secondary analysis of a prospective pTKA study that investigated return to function and recovery timelines [5]. Data were collected on 156 patients (94 F and 62 M; mean ± SD age = 67.7 ± 8.1 years; BMI = 32.5 ± 5.2 kg/m$^2$) across three post-operative visits at 2-week, 6-week, and 12-week where both KOOS JR and PPMs were obtained. The PPMs included chair rise (sit-to-stand repetitions in 30 sec), step up (step-up-and-down repetitions in 30 sec), and seated 3-dot heel touch (inverted-triangle-vertices touches with surgical leg's heel in 15 sec). A Spearman's rank correlation coefficient was used to characterize the relationship between KOOS JR and PPMs. Patients were grouped by whether or not they achieved a PASS of 71 in KOOS JR [6] at each post-operative visit, and the group differences in PPMs were determined using a non-parametric Wilcoxon rank sum test or chi-square test, where appropriate.

**Results & Discussion:** KOOS JR showed no correlation with the three PPMs and patient demographics, except with the step up measure that showed weak correlation at the 2-week post-operative visit (Table 1). None of the PPMs or patient demographics differed between pTKA patients who did or did not achieve the KOOS JR PASS threshold of 71 (Table 1). These results supported our hypotheses and suggested that KOOS JR may not accurately capture patient's physical abilities and that other objective measures may be required to characterize post-pTKA functional recovery status. The dependency on patient's perception and disproportionate focus of the KOOS JR on pain (i.e., four of the seven question items are related to pain) may explain this finding.

Table 1. Summary of the results, with a significance level of 0.05. Bold indicates statistical significance. BMI = body mass index.

| | H1: Spearman's rank correlation coefficient (*p*-value) vs. KOOS JR | | | H2: Did KOOS JR achieve PASS? No vs. Yes Median [interquartile range] or percentage (*p*-value) | | |
|---|---|---|---|---|---|---|
| | 2-week | 6-week | 12-week | 2-week | 6-week | 12-week |
| Chair rise (rep) | -0.01 (0.921) | 0.09 (0.403) | 0.22 (0.304) | 9.0 [4.0] vs. 8.0 [3.0] (0.785) | 12.0 [4.0] vs. 13.0 [5.0] (0.198) | 12.0 [3.5] vs. 13.5 [5.8] (0.331) |
| Step up (rep) | 0.19 (**0.049**) | 0.18 (0.072) | 0.13 (0.534) | 0.0 [6.0] vs. 0.0 [0.5] (0.382) | 9.5 [10.0] vs. 11.0 [7.8] (0.163) | 10.5 [6.0] vs. 12.0 [3.8] (0.576) |
| Seated 3-dot heel touch (rep) | 0.03 (0.754) | 0.04 (0.692) | 0.10 (0.649) | 31.0 [17.5] vs. 25.0 [11.5] (0.287) | 36.5 [18.0] vs. 34.5 [8.0] (0.600) | 33.0 [9.5] vs. 39.5 [9.5] (0.151) |
| Age (years) | 0.13 (0.161) | 0.16 (0.093) | 0.10 (0.525) | 69.0 [11.0] vs. 71.0 [12.0] (0.630) | 68.0 [14.0] vs. 69.0 [7.0] (0.223) | 70.0 [12.0] vs. 67.0 [10.0] (0.948) |
| BMI (kg/m$^2$) | <0.01 (0.962) | -0.02 (0.865) | -0.07 (0.649) | 32.7 [8.8] vs. 33.1 [10.4] (0.422) | 32.9 [9.7] vs. 33.1 [6.7] (0.832) | 34.2 [11.0] vs. 33.0 [5.2] (0.938) |
| Sex (%Female) | - | - | - | 64.3% vs.47.1% (0.281) | 61.9% vs. 57.6% (0.825) | 65.5% vs. 57.1% (0.845) |

**Significance:** While KOOS JR is a widely used metric, our study showed that it alone may be a limited measure of post-pTKA physical abilities. KOOS JR and PPMs synergistically complement each other and may allow surgeons to better understand post-pTKA recovery trajectories and changes in function after surgery.

**Acknowledgments:** Research reported here was supported by the Carilion Clinic Research Acceleration Program Grant. The content is solely the responsibility of the authors and does not necessarily represent the official views of Carilion Clinic.

**References:** [1] Ramkumar et al. (2015), *Bone Joint Res* 4(7); [2] Lyman et al. (2016), *Clin Ortho Relat Res* 474(6); [3] Mizner et al. (2011), *J Arthro* 26(5); [4] Luna et al. (2017), *Bone Joint J* 99(9); [5] Pekas et al. *JBJS* (accepted; in press); [6] Dekhne et al. (2024), *Clin Ortho Relat Res* 482(4).

# BIOMECHANICAL STRENGTH OF STATIC SPACERS USED IN TWO-STAGE REVISION KNEE ARTHROPLASTY

*Maxwell Y. Sakyi[1], Taylor J. Den Hartog[1], Nicole A. Watson[1], Jessica E. Goetz[1,2], Jacob M. Elkins[1,2]
[1]Department of Orthopaedics and Rehabilitation, University of Iowa, Iowa City, IA, USA
[2]Department of Biomedical Engineering, University of Iowa, Iowa City, IA, USA
*Corresponding author's email: maxwell-sakyi@uiowa.edu

**Introduction:** Periprosthetic joint infection (PJI) is a devastating complication following Total Knee Arthroplasty (TKA) with an overall reported incidence of 0.5-2.0% [1-2]. Two-stage revision TKA remains the gold standard treatment for PJI [3]. This process typically involves first explanting the prothesis and implanting an antibiotic-laden mobile or static bone cement spacer, followed by a second surgery to replace the spacer with revision total knee components. Static spacers are necessary in unstable, chronically infected TKAs which result in significant bone loss, large soft tissue wounds and collateral ligament insufficiency, [4-5] in patients unable/unwilling to follow weightbearing restrictions, and in significantly comorbid patients unable to undergo a second surgery for revision arthroplasty. However there has been no consensus on mechanically optimal spacer construct, and this information would be particularly helpful for patients with spacers used as definitive treatment. The goal of this study was to biomechanically evaluate different static spacer constructs to determine which static spacer construct provided the highest failure force, minimum displacement under cyclic loading, and had minimal comminution when failure occurred.

**Methods:** Sixteen femur-tibia constructs made with cortical strength Sawbones models were divided into four static spacer groups with n=4 each: Rush Rod reinforced cement dowels, external fixator (ex-fix) rods, retrograde/anterograde intramedullary (IM) femoral nails, and Merete intramedullary diaphyseal segmental fixation nail. A servo-hydraulic mechanical testing machine (MTS) was used to subject each construct to 10 cycles of incrementally increasing offset torsion/bending cyclic loading (50-100N, 100-200N, 200-300N, and in increments of 100N until failure) at a rate of 0.25 Hz, with a preload of 50N at a 2N/s rate prior to each cycle (Fig 1). Force and displacement data were collected simultaneously at 100Hz. Concurrently, a 3D digital image correlation system (ARAMIS) was employed to capture local Sawbones deformations and displacements at 40Hz during the biomechanical testing. Failure load was defined as a sudden deviation in the measured force curves. Other parameters assessed included the displacement and velocity of femur and puck regions of interest, as well as distinct landmark points on these sections prior to and at the moment of fracture. Differences in forces, displacement, and mechanical work between the different constructs were compared using a Kruskal-Willis test with Dunn's multiple comparisons (GraphPad Prism, v10.4.1).

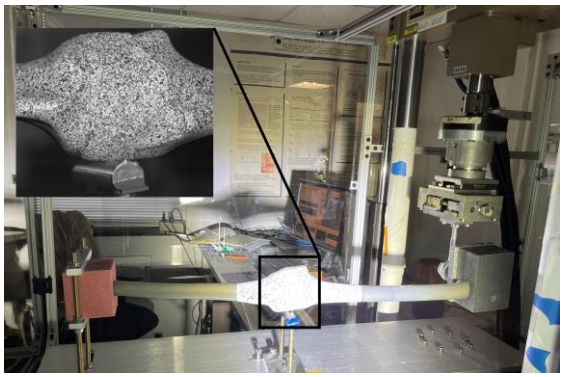

**Figure 1:** Tibia/femur construct mounted in MTS for combined offset torsion/bending testing. The inset shows the pattern sprayed on the space and Sawbones for tracking displacement and surface strain.

**Results & Discussion:** Fractures were generally an oblique distal femur fracture originating near the puck-femur interface distally and medially and exiting superior and lateral near the supracondylar region. The Merete constructs were significantly stronger than the IM nail constructs (p=0.029) and could withstand higher loads than the ex-fix and Rush Rod constructs (Fig 2). Merete constructs also had the largest work to failure, although this was not significantly greater than the other constructs. It was observed that the Merete, IM nail and ex-fix constructs had simple transverse fractures whiles the Rush Rod constructs had erratic/comminuted fractures.

When selecting a static spacer design for clinical use, both the strength and the stability of the construct should be considered. Our data suggest a static spacer with a Merete nail can provide maximum strength, although failure load was similar across constructs. Rush Rod constructs have very unpredictable fracture patterns that may be harder to repair if needed, and thus more caution should be exercised in its applications.

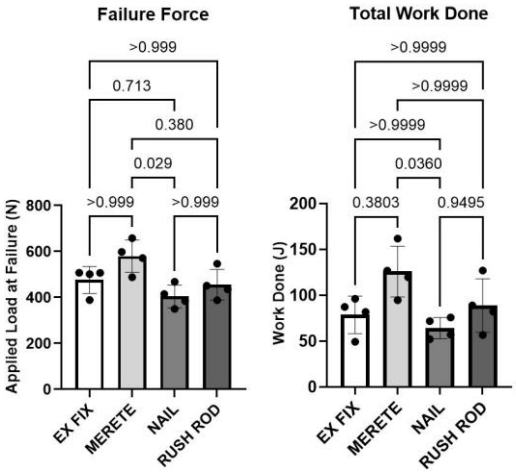


**Figure 2:** Failure force (left) and total work (right) for each static spacer construct through all cyclic loading up to fracture.

**Significance:** PJI is a devastating complication that can be compounded by patients with significant comorbidities and those that have failed prior two-stage exchange who may not be candidates for TKA reimplantation. These individuals require a destination spacer which is not intended to be removed. The Merete nail offers maximum mechanical strength, which can potentially decrease risk of spacer/implant fracture necessitating repeat operative and/or hospital stays.

**Acknowledgments:** The authors would like to thank the University of Iowa for funding this work.

**References:** [1] Philips et al. (2006), *J. Bone Jt Surg Br* 88(7); [2] Nickinson et al. (2012), *The Knee* 19(1); [3] Lichstein et al. (2016), *CORR* 474(1); [4] Nahhas et al. (2020), *J. Bone Jt Surg Am* 102(9); [5] Haddad et al. (2000), *J. Bone Jt Surg Br* 82.

# Effect Of Hip Symptom Duration on Total Support Moment During Unilateral Squat in Individuals with Hip-Related Pain

Holly Stanze[1*], Bethany J Wilcox[2], Anthony A. Mangino[3], Kate N Jochimsen[4,5], Michael A Samaan[1]
[1] *Dept. of Kinesiology & Health Promotion, University of Kentucky*
*Corresponding author's email: hmst263@uky.edu

**Introduction**: Hip joint-related pain (HRP) is a term used to describe non-arthritic, intra-articular hip conditions with and without bony deformities[1]. In the HRP population, long symptom duration is defined as hip pain persisting at least 24 to 36 months [2]. Individuals with HRP exhibit altered lower limb mechanics compared to asymptomatic controls [3, 4] and higher fear of movement [5] (kinesiophobia). Yet, differences in movement patterns, kinesiophobia, and hip pain during movement between individuals with short- and long-term HRP are poorly understood. Understanding the potential connections between hip-related symptom duration, lower limb mechanics, kinesiophobia, and hip pain during movement may allow for more efficient referrals to rehabilitation clinicians.

Alterations in hip joint mechanics are more pronounced during a single limb squat (SLS), compared to a bilateral squat task, in individuals with femoroacetabular impingement syndrome (FAIS) [4], the most common HRP condition. Individuals with HRP also exhibit lower limb muscle dysfunction [6], yet eccentric and concentric muscle function required to stabilize the lower limb during dynamic activity is not well understood. The total support moment (TSM) is a measure of the total lower limb extensor torque needed to maintain lower limb support and is sensitive enough to detect alterations in hip mechanics during a sit-to-stand task in individuals with FAIS [7]. The TSM may be beneficial in assessing eccentric and concentric muscle function needed to support the lower extremity in individuals with HRP. Therefore, the purpose of this study was to analyze whether self-reported hip pain during an SLS task, kinesiophobia, and TSM-related parameters during the eccentric and concentric phases of an SLS task differ based on hip symptom duration in individuals with HRP.

**Methods**: Involved limb hip, knee, and ankle sagittal plane moments during the SLS were obtained for 25 subjects with HRP. Subjects reported hip pain during the SLS using a verbal Numeric Pain Rating Scale (0 – 10), and kinesiophobia was assessed using the Tampa Scale for Kinesiophobia (TSK-11). Subjects were divided into two groups based on the median duration (36 months) of hip pain. The whole-body vertical center of gravity position was used to denote the start and end of the SLS. The SLS was divided into the eccentric (0 – 50%) and concentric (51 – 100%) phases after time normalizing to 101 points (0-100%). The summation of the average hip extensor, knee extensor and ankle plantarflexor moments during the eccentric and concentric phases of the SLS were used to calculate the TSM. Hip, knee and ankle joint moment percent contributions to the TSM were also calculated. Between-group differences in age, sex distribution, body mass index (BMI), TSM-related outcomes, TSK-11 scores, and hip pain during the SLS were assessed using independent-samples t-tests and Mann-Whitney U tests, as appropriate, with significance set at the 0.05 level. Cohen's d effect sizes were used to determine the magnitude of between-group differences.

**Table 1:** Group-Related Outcomes

| | Short Duration (N=14) | Long Duration (N=11) | P-Value | Effect Size |
|---|---|---|---|---|
| **Eccentric Phase** | | | | |
| **TSM (Nm/kg)** | 1.77 ± 0.2 | 1.67 ± 0.5 | 0.50 | 0.28 |
| **Hip Extensor Moment (Nm/kg)** | 0.60 ± 0.2 | 0.40 ± 0.2 | 0.03* | 0.94 |
| **% Hip Contribution** | 32.9 ± 8.7 | 21.9 ± 7.5 | <0.01* | 1.28 |
| **% Knee Contribution** | 36.2 ± 10.0 | 43.6 ± 8.1 | 0.06 | 0.77 |
| **Concentric Phase** | | | | |
| **TSM (Nm/kg)** | 2.18 ± 0.3 | 2.01 ± 0.6 | 0.38 | 0.37 |
| **Hip Extensor Moment (Nm/kg)** | 0.82 ± 0.3 | 0.55 ± 0.2 | 0.02* | 0.98 |
| **% Hip Contribution** | 36.3 ± 8.7 | 26.3 ± 6.2 | <0.01* | 1.25 |

**Results & Discussion**: There were no differences ($p$>0.05) in age, participant sex, BMI, or TSK-11 scores between the short (N=14) and long (N=11) symptom duration groups. The longer symptom duration group exhibited lower average hip extensor moments during the eccentric and concentric phases of the SLS (Table 1). Despite a similar TSM, the longer symptom duration group exhibited a lower hip joint contribution and a slightly higher knee joint contribution to the TSM. The longer symptom duration group also reported significantly higher hip pain than the short symptom duration group during the SLS (Long: 3.5[1 – 6], Short: 2[0 – 7], p=0.03). Conclusions cannot be drawn on the relationship between kinesiophobia and lower-limb mechanics as both groups exhibited high fear of movement (Long: 18.5[14 - 34], Short: 20[15 - 40], p=0.131)

**Significance**: Individuals with longer hip symptom duration exhibit similar levels of kinesiophobia compared to individuals with shorter hip symptom duration, yet significantly worse hip pain and lower hip extensor moments during the SLS task. Our results suggest that alterations in lower-limb mechanics are associated with more severe HRP. However, given the study design, we cannot determine if altered mechanics lead to increased hip pain or are a compensation for increased hip pain. Either way, the results suggest a need to intervene early after the onset of HRP in order to prevent detrimental alterations in lower-extremity mechanics, which may perpetuate chronic hip symptoms and negatively affect long-term joint health. Further study is required to determine the association between kinesiophobia and movement patterns in individuals with HRP.

**Acknowledgements**: NIH (K23-AT011922, K01-AG073698), American College of Sports Medicine, Mid-Atlantic Regional Chapter (MARC) Early-Stage Investigator Award, West Virginia University Research and Scholarship Advancement Grant

**References:** [1] Weir, A., et al. (2015), *J Sports Med* 49(12); [2] Kahlenberg, C.A., et al., (2014), *Orthop J Sports Med* 2(3); [3] Bagwell, J.J., et al., (2016), *Clin Biomech* 31; [4] Malloy, P., et al., (2019), *JOSPT* 49(12); [5] Jochimsen, K.N. et al., (2021), *J Athl Train* 56(10); [6] Harris-Hayes, M., et al., (2020), *JOSPT* 50(5); [7] Samaan, M.A., et al., (2017), *PM R* 9(6);

# EVALUATION OF CLAVICLE MORPHOLOGY USING STATISTICAL SHAPE MODELING

Lydia M. Nicholson[1], Erin C.S. Lee[2], Michael J. Rainbow[2], Benjamin M. Zmistowski[3], *Rebekah L. Lawrence[1,3]
[1]Program in Physical Therapy, Washington University School of Medicine; St. Louis, MO, USA
[2]Department of Mechanical and Materials Engineering, Queen's University; Kingston, ON, Canada
[3]Department of Orthopaedic Surgery, Washington University School of Medicine; St. Louis, MO, USA
*Corresponding author's email: r.lawrence@wustl.edu

**Introduction:** The clavicle is one of the three bones in the shoulder girdle and serves as the only rigid attachment between the arm and thorax. There appears to be wide variability across individuals in clavicle shape, and it remains unclear how this variability impacts shoulder girdle function. For example, the clavicle's sigmoid shape may increase the scapula's arc of movement while minimizing proximal displacement at the sternoclavicular joint. To understand the relationship between clavicle shape and function, metrics of shape are required. Previous studies that have used scalar metrics to describe simple curvatures [1,2]. However, this approach may be subjective and limited to 2D descriptions. By contrast, a statistical shape model (SSM) can identify primary modes of variation within 3D morphology. Thus, the purpose of this project was to develop a SSM to comprehensively quantify 3D clavicular morphology.

**Methods:** Our model included 54 clavicles which were segmented from CT scans of the dominant shoulder in asymptomatic individuals (55±4 years, 61% female, 89% right). Left clavicles were reflected to resemble right clavicles. ShapeWorks, an open-sourced shape modelling software, was used to optimize the placement of 1,024 correspondence particles placed on each surface using a gradient descent energy function [3]. Model development included steps for mesh grooming (to reduce the number of vertices and rigidly align all clavicles), Procrustes registration (to remove variation due to overall scale, translation, and rotation), and model optimization (to optimize particle spacing and correspondence). We performed iterative parameter tuning using specificity, compactness, generalization, and maximum reconstruction error metrics to inform model selection. Once selected, we determined the number of principal components (PCs) to interpret by identifying the elbow of a scree plot of explained variance. Finally, we used these PCs to qualitatively identify our sample's relevant independent variations in clavicle morphology.

**Results & Discussion:** Our final SSM had 53 modes of variance, and the fifth PC was determined to be the elbow of the curve for explained variance. This indicates that PCs 1-5 were the strongest contributors to variance (Figure). Additionally, the final model demonstrated strong specificity, compactness, and generalization metrics, with the fifth PC achieving metrics of 1.1 mm, 76% of cumulative explained variance, and 1.1 mm, respectively. Each clavicle could be reconstructed within a 2.0 mm surface-to-surface distance of its original groomed mesh, further suggesting excellent performance by the SSM. Maximum errors were generally located on the sternoclavicular and acromioclavicular joint surfaces, likely high variation in articular morphology between individuals.

The first PC represents 30% of the variance and seems to primarily represent the inferior bend of the lateral aspect of the clavicle in the frontal plane. PC 2 accounts for 22% of variance, and it appears to represent the thickness of the medial and lateral ends. Explaining 14% of the variation, PC 3 seems to represent the overall thickness of the clavicle. PC 4 accounts for 6% of the variance and appears to describe the tradeoff between thickness in the medial and lateral ends (i.e. as the medial end thickens, the lateral end becomes thinner and vice-versa). Finally, PC 5 seems to represent the intensity of the sigmoid shape in the transverse plane, and it explains 4% of the variation.

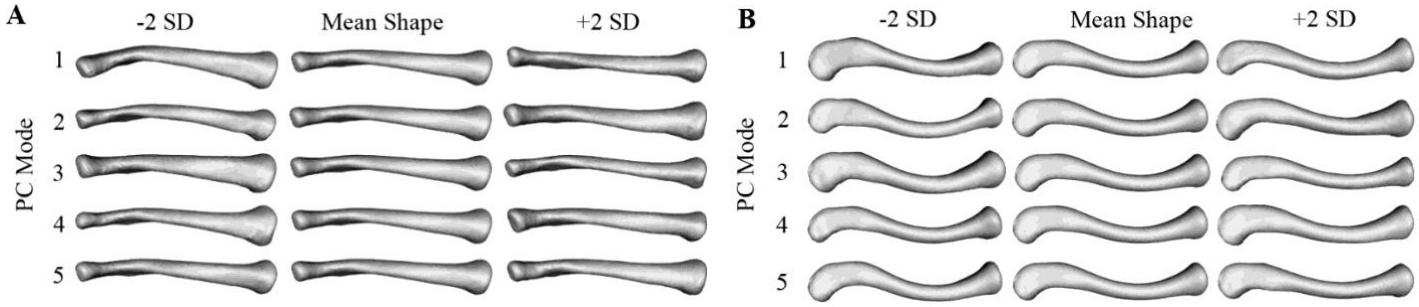


**Figure**: The first 5 PCs of the SSM model from the frontal plane (A) and transverse plane (B). This accounts for 76% of the explained variance of the sample, with modes 1-5 representing 30%, 22%, 14%, 6%, and 4% of the variation respectively.

**Significance:** Overall, there appears to be substantial variability in clavicle shape across individuals. Although it remains unclear the degree to which clavicle shape impacts shoulder girdle function, the coupling relationship between the clavicle and scapula may be influenced. For example, the degree to which the scapula upward rotates may be impacted by the clavicle's sigmoid shape, which may explain some of the movement variability we often see in clinical populations [4]. This hypothesis will be explored in future work.

**Acknowledgments:** This work was funded by the National Institutes of Health under award number K99/R00-AR075876.

**References:** [1] Bachoura et al., *J Shoulder Elbow Surg*, 2013;22(1). [2] Aira et al., *J Orthop Res*, 2017;35(10). [3] Cates et al., *Inf Process Med Imaging*, 20. [4] Lawrence et al., *J Orthop Sports Phys Ther*, 2014;44(9).

# BONE-ANCHORED TRANSFEMORAL PROSTHETIC USERS SHOULD CARRY SIDE LOADS ON THE INTACT SIDE TO REDUCE KNEE ADDUCTION MOMENT

*John R. Pope[1], Jenna K. Burnett[1,2], Ross H. Miller[1], Jae Kun Shim[1]
[1]University of Maryland, College Park, MD, U.S.A,
[2]University of Utah, Salt Lake City, UT, U.S.A,
*Corresponding author's email: jpope84@umd.edu

**Introduction:** Transfemoral prosthetic users (TFPU) with socket prostheses face a higher risk of osteoarthritis (OA) in the intact knee then able-bodied persons [1]. Osseointegrated (bone-anchored) implants offer an alternative to socketed suspension, but their effect on knee loading during activities of daily living remains unclear. Load carriage alters gait biomechanics, raises metabolic costs, and increases fall risk for both amputees and able-bodied individuals alike [2-4]. Side load carriage is a practical option that frees one hand but challenges lateral balance—potentially worsening gait mechanics. TFPU tend to exhibit increased lateral trunk bending over the stance leg, a stabilizing mechanism that positions center of mass over base of support to aid in stability[5,6]. During intact limb stance this consequently reduces external knee adduction moments (linked to OA risk). Carrying a side load adds difficulty for TFPU and may affect loads at the knee. The **Purpose** of this study is to distinguish the effects of lateral load carriage side on knee adduction moment and adduction moment impulse in bone-anchored TFPU. **Hypothesis**: Previous work has shown that load carriage position effects joint kinetics, therefore we expect bone-anchored TFPU to show smaller intact knee adduction moment (KAM) and adduction moment impulse (KAMp) carrying a side load on the intact limb side compared to the prosthetic limb side and unloaded walking [3]. We expect this to occur because carrying the load on the intact side will encourage a shift of the TFPU center of mass lateral to knee center, effectively reducing medial knee joint load. Understanding how lateral load carriage side effects movement of TFPU is important to preserve intact limb health and functional independence.

**Methods**: 7 bone-anchored TFPU (49 ± 11 yrs, 1.74 ± 0.16 m, 74.80 +- 20.9 kg) carried an intact limb side load (IL) and a prosthetic limb side load (PL) at 15% of body mass (kg) across a 15-meter instrumented platform. Outcome variables were peak knee adduction moment (KAM) and knee adduction moment impulse (KAMp) and were scaled by total bodyweight (including prosthesis) and height (%BW*Ht). Two-tailed matched-pair t-test was conducted to compare outcome variables between IL and PL carriage conditions and against a no-load (NL) control. Statistical significance was set at $\alpha = 0.05$ and adjusted to $\alpha$ **(0.05/3)**. A strong effect size was defined as Cohen's d > 0.8.

**Results & Discussion**: Pairwise comparisons of coronal plane peak KAM in the intact limb showed lower KAM in the IL condition compared to PL and NL conditions ($p > 0.016$; Figure 1A), with a strong negative effect size. KAMp was smaller in the IL condition compared to NL ($p < 0.016$) and PL ($p < 0.016$; Figure 1B), also showing a strong negative effect size between IL and both NL and PL conditions. Findings partially supported our hypothesis:

- **Intact Load**: IL side carriage produced smaller peak intact KAM compared to both PL and NL but findings were not significant. However, significantly smaller KAMp during IL carriage compared to both PL and NL carriage may indicate that IL carriage produces biomechanics that reduce cumulative knee loading without magnifying peak moments.
- **Prosthetic Load:** PL side carriage likely resulted in a greater KAM and KAMp because the laterally placed load (opposite the stance limb) exceeds the intact limbs ability to maintain stability. PL side carry did not result in significantly greater KAM or KAMp compared to NL walking, suggesting that for TFPU with greater gait instability during prosthetic limb stance, carrying a lateral load opposite the intact limb does not significantly increase acute knee joint loading and may be a viable load transport strategy without worsening intact limb stress.

Figure 1.

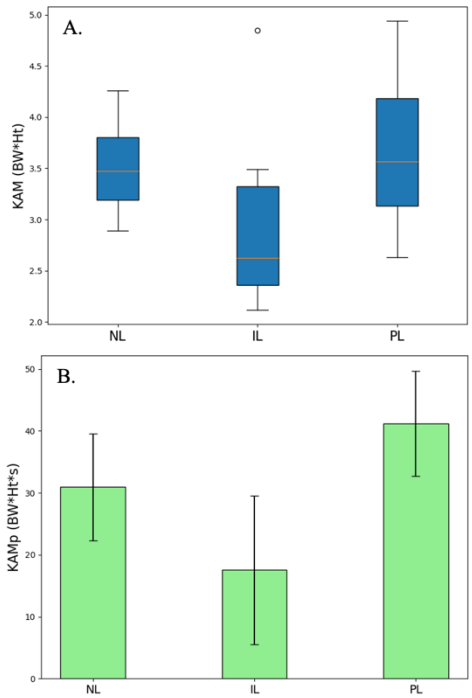


**Figure 1A:** Comparison of mean intact limb peak knee adduction moments during load conditions.
**Figure 1B:** Comparison of mean intact limb knee adduction moment impulse during load carriage conditions. All data is averaged over a full gait cycle and scaled to %BW*Ht.

**Significance:** TFPU face a higher OA risk in the intact limb due to increased loading and overuse during activities of daily living. It is recommended that TFPU should carry a side load on the intact limb side to reduce KAM. Load carry tasks are challenging for TFPU and warrant consideration as a rehabilitation tool to dynamically improve strength without measurable increasing acute intact limb KAM.

**Acknowledgments:** Data collection for this study was supported by the CDMPR award number W81XWH-21-1-0423.

**References:** [1] Wedge RD et al. (2022), *Clin Biomech* ***94,*** 105-632. [2] Butowicza et al. *(2020), Clin Biomech* ***71****, 160-166*. [3] Ardianuari S et al. (2024), *J Biomech* **177**. [4] Nolan et al. (2000), *O&P Int* **24**, 117-125 . [5] Hendershot et al. (2014), *Clin Biomech* **29,** 235–242. [6] Carse et al. (2020), Post &Gait **75**, 98-104

# VALIDATION OF A SENSOR FOR MONITORING LOAD IN LOWER LIMB PROSTHESIS

Theophilus Annan[1*], Amit Chaudhari[3], Sagar Doshi[2,3,4], Erik Thostenson[2,3,4], Jill Higginson[1,2]
[1]Dept. of Biomedical Engineering, University of Delaware
[2]Dept. of Mechanical Engineering, University of Delaware
[3]Center for Composite Materials, University of Delaware
[4]Dept. of Materials Science and Engineering, University of Delaware
*Corresponding author's email: tannan@udel.edu

**Introduction:** Patients with unilateral lower limb amputation often exhibit asymmetric interlimb gait patterns and deviations from normal gait in spatiotemporal and ground reaction force parameters [1]. Over time, the asymmetries between the intact and prosthetic limbs and excessive loading on the intact limb may result in secondary physical issues, such as joint and bone degeneration or lower back pain. Individuals with lower limb amputation are reported to be at a greater risk of developing osteoarthritis (OA) in the knee or hip of the intact limb than non-amputees [2]. Approaches to minimize gait deviations and improve the quality of life for lower extremity amputees include prescribing appropriate prosthetic components and providing physical therapy for gait training [3]. The conventional rehabilitation process helps patients progress from strength training to gait training, with a focus on weight bearing and coordination. Despite advancements made in quantitative biomechanical analysis tools, clinicians continue to use qualitative assessments in part due to high-cost equipment, complex protocols, diverse training, and varying biomechanics experience and knowledge [4]. **The objective of this study is to validate the repeatability of a wearable sensor to monitor prosthetic limb load.** Obtaining out-of-lab feedback has the potential to guide and assess the performance of prosthetic limb usage [4].

**Method:** We have developed a portable novel fabric-based pressure sensor [5] that can potentially monitor limb loads during activities both inside and outside laboratory settings. We conducted quasi-static loading and unloading of the sensor using a screw-driven load frame (Instron 5985). The sensor was subjected to forces ranging from 50N to 1600N at a displacement rate of 0.5mm/min. Five independent tests were performed, each consisting of 10 consecutive loading and unloading cycles. Loading of the sensor leads to a decrease in resistance, whereas unloading increases the resistance of the sensor. We compared the sensor's repeatability within and between tests for a selected force range within 10N intervals. To test the repeatability of the sensor within tests, we compared the resistance change (%) for both loading and unloading trials of all the tests independently for the selected force range. To test the sensor's repeatability between tests, we compared the loading and unloading resistance change (%) for the selected force range in all 10 trials for each test.

**Results and Discussion:** The sensor showed consistent repeatability for both loading and unloading cycles within tests (Fig. 1). When the resistance changes by 1% - increasing during unloading or decreasing during loading - the sensor detects distinct ranges of force values. This is observed both within (Fig. 2) and between tests (Fig. 3). The sensor's resistance change (%) within the selected force range demonstrates its potential for threshold detection, particularly for force ranges where the corresponding resistance changes differ by at least 1%.

**Significance:** This could be used to detect 25%, 50%, 75%, and 100% of total body weight during weight monitoring training for amputees. Additionally, it can be used to monitor limb loads during activities of daily living, thereby preventing the risk of developing OA in the intact limb. Monitoring changes in load distribution can offer valuable insights into an amputee's activities and enable personalized rehabilitation recommendations following amputation.

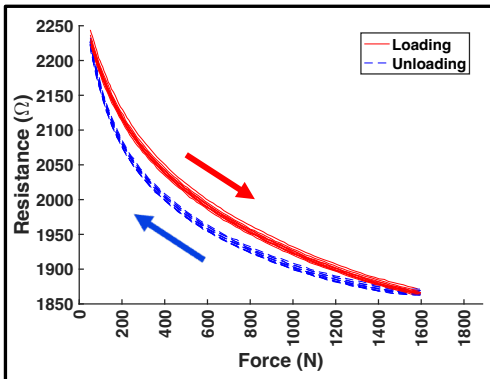


**Figure 1:** Loading and unloading response for ten consecutive cycles

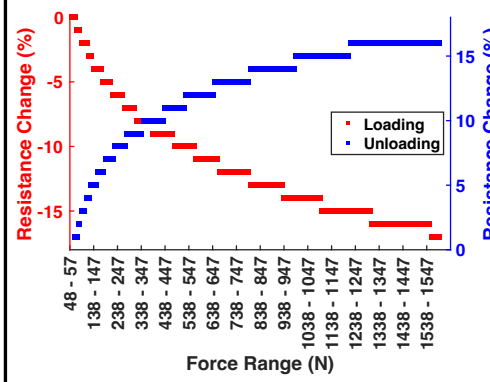


**Figure 2:** A 1% change in resistance detects different force range values within tests.

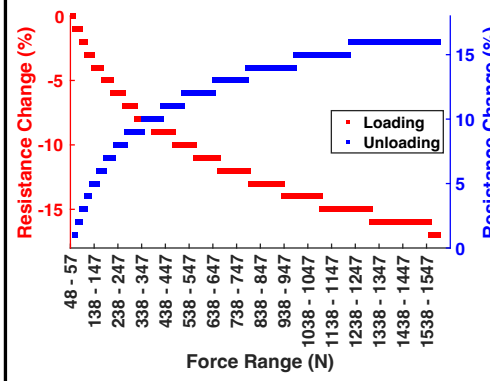


**Figure 3:** A 1% change in resistance detects different force range values between tests.

**Acknowledgments:** This work is supported by the Delaware Bioscience Center for Advanced Technology, NSF ART Award: 2331440 and NSF PFI-TT Award: 2329838.

**References:** [1] Nolan et al. (2023), [2] Struyf et al. (2009), Norvell et al. (2005), [3] Highsmith et al. (2016), [4] Hulleck et al. (2022), [5] Doshi et al. (2018).

# BONE ANCHORED TRANSFEMORAL PROSTHESIS USERS DO NOT SHOW INTERLIMB WALKING SYMMETRY ACROSS DIFFERENT TERRAINS

*Chioma M. Ezeajughi[1], Gauri A. Desai[1], Maliheh Fakhar[1], John Pope[1], Ross H. Miller[1], Jae Kun Shim[1]
[1]University of Maryland, College Park, MD, USA
*Corresponding author's email: cezeaju@terpmail.umd.edu

**Introduction**: Individuals with lower limb loss use prosthetic devices to enhance mobility and improve quality of life. Bone-anchored prosthesis (BAP) represents an innovative fixation method to improve inter-limb loading symmetry [1]. Gait asymmetry, where the intact limb experiences greater loading than the prosthetic limb, can contribute to secondary joint injuries over time. Joint loading imbalance may be further exacerbated when walking on different terrains [2]. Previous research indicates that unilateral transfemoral amputees with socket fixation respond differently to level ground floor terrain types leading to significant changes in the peak plantar pressure between the intact and prosthetic limb [2]. However, the effect of varying terrain stiffness on limb loading symmetry in unilateral transfemoral BAP users remains unknown. Given that these individuals frequently navigate diverse terrains in daily walking activities, understanding how limb loading symmetry varies with terrain stiffness is important. This study investigates the effects of walking on grass, carpet, and hard floor on interlimb walking asymmetry in unilateral transfemoral BAP users, assessed at the whole-limb level using ground reaction forces (GRFs). We hypothesize interlimb walking symmetry on hard floors, with loading on the intact limb comparable to that on the prosthetic limb. In contrast, we expect more asymmetry on carpet and grass, with loading on the intact limb higher than the prosthetic limb. The rationale for this hypothesis stems from material stiffness testing, which showed that carpet is the least stiff surface, followed by grass, with hard flooring being the most rigid. A less stiff surface may reduce the prosthetic limb's ability to generate efficient GRF, leading to compensation with the intact limb.

**Methods**: Eight unilateral transfemoral BAP users were included in the analysis (Age = 51.1 ± 10.09 yrs, height = 1.7 ± 0.15m, body mass = 67.67 ± 21.76 kg). The amputees walked at a self-selected speed on grass (average walking speed = 0.61m/s), carpet (average walking speed = 0.59m/s), and hard floor (average walking speed = 0.59m/s) on a 15m level walkway. Kistler force plates were utilized to measure the GRF for the intact and prosthetic limbs. The interlimb asymmetry for the vertical, anteroposterior (AP), and mediolateral (ML) GRFs was calculated for each percentile of the stance [3]. Statistical Parametric Mapping with a 1-way ANOVA and two sample T-tests were used to analyze statistical differences ($\alpha = 0.05$).

**Results & Discussion**: The interlimb asymmetry revealed a statistically significant difference in vertical, AP, and ML GRFs across the terrains. For vertical GRFs, the participants had similar asymmetry in the whole stance with the timing of the maximum peaks different in grass Figure 1-A. In the AP direction, GRFs were significantly different in the early stance and also in the late stance as shown in Figure-B. In the ML direction, significant differences were also observed in the early and late stances, as shown in Figure 1-C. Post-hoc test revealed a significantly greater difference in grass, followed by carpet and hard floor. We hypothesized that transfemoral BAP would lead to more symmetrical limb loading on hard floor and asymmetry on grass and carpet; however, our findings partially supported the hypothesis. The results suggest that BAP users still rely on the intact limb across different terrains.

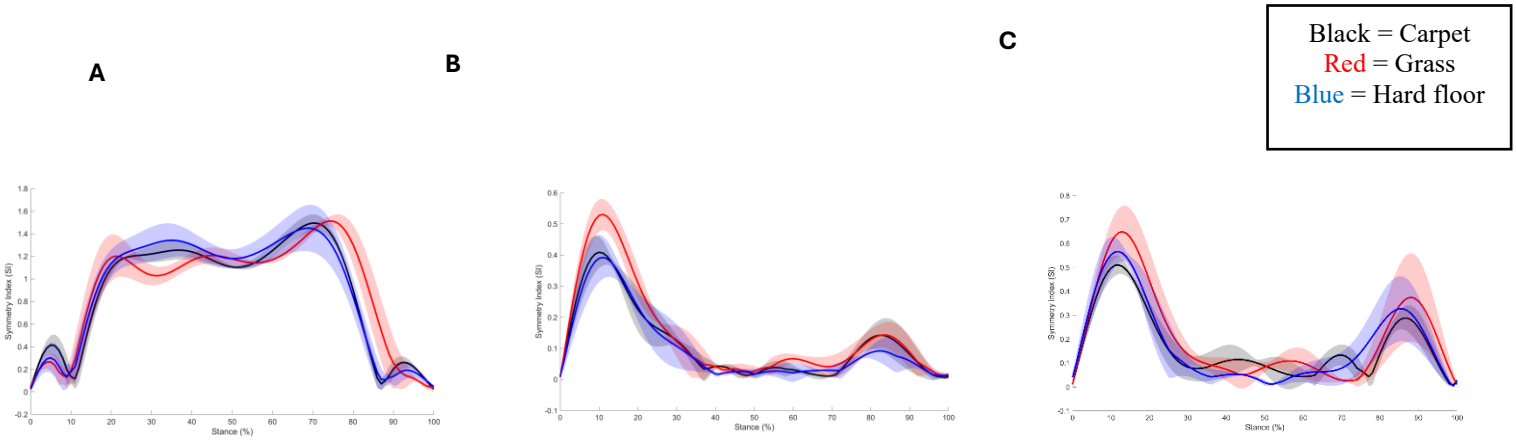


Figure 1: The effect of interlimb asymmetry (**red** = Grass, **blue** = Hard floor, black = Carpet) on **A** vertical, **B** AP, and **C** ML GRFs.

**Significance**: Our findings suggest that despite the benefits of transfemoral BAP use, users still rely on the intact limb across different terrains. This reliance may increase on compliant terrains, as the prosthetic limb may not fully support the balance demands, leading to greater compensation with the intact limb.

**References**: [1] Brånemark et al. (2001) J. Rehabil 38 : 175-181. [2] Choi et al. (2024) J. Biomech 170: 112177. [3] Winiarski et al. (2021) *Gait Posture*, vol. 90: 9–15

# DOES MOVEMENT ASYMMETRY GENERALIZE ACROSS TASKS IN UNINJURED ATHLETES?

*Sydney Savage[1], Allyson Richardson[1], Olivia Cunningham[1], Andrew Polson[1], Reed D. Gurchiek[1]
[1]Department of Bioengineering, Clemson University
*Corresponding author's email: savage7@clemson.edu

**Introduction:** Gait asymmetry is often quantified for evaluating rehabilitation progress following lower-limb injuries which seeks to normalize and restore function [1]. This is often due to a lack of pre-injury data in which case the contralateral, uninjured limb is used as a reference. However, studies have shown that asymmetries exist even in able-bodied individuals [2,3], and this limits the utility of gait asymmetry as a biomarker of recovery. While some research has quantified gait asymmetry in healthy individuals, few have investigated if movement asymmetries generalize across tasks. Moreover, most quantify asymmetry in terms of metrics not readily provided by scalable technologies like markerless motion capture or wearable sensors (e.g., ground reaction force, joint moment). These technologies allow collecting large amounts of movement data toward characterizing gait asymmetry in uninjured populations. A better understanding of movement asymmetry in basic functional tasks would improve interpretation of gait asymmetry in clinical contexts. To this end, we aimed to characterize gait asymmetry in uninjured, collegiate athletes with OpenCap [4] and to determine if movement asymmetry generalizes across tasks. To investigate task generalization, we used body-weight squats because it is common for functional assessment [5,6], is categorically different than gait (stationary vs. locomotive), and OpenCap has been validated for characterizing kinematics during squatting motion. We hypothesized there would be a relationship between kinematic gait and squat asymmetries.

**Methods:** We recruited 119 subjects (53 female, aged 18-27 years) to participate in this study. Videos of 3 10-meter walking trials and body-weight squats were recorded using OpenCap on two iPhones. Walking trials were performed at a self-selected, normal speed, and the squatting trials were standardized using a metronome set to 90 beats per minute (such that the athlete reached the bottom position with thighs parallel to the ground in 1.33 seconds and stood up in 1.33 seconds) with arms extended. Joint angles during the movements were calculated automatically in OpenCap using OpenSim's inverse kinematics tool. All videos were visually inspected for quality reconstructions and an athlete was removed from the analysis if the kinematic reconstruction failed for any trial or if they reported a lower limb injury within 6 months prior to testing. Asymmetry was assessed using two metrics per task based on measurements describing each leg independently. For squats, we calculated the peak knee flexion angle (SA1) and pelvis lateral position relative to the right or left foot (SA2) in the bottom position. For gait, we calculated the duty factor (stance time divided by stride time, (GA1) and peak knee flexion angle during stance (GA2). Gait asymmetry was calculated as the percentage of the left leg value relative to the right leg value (sometimes called a limb symmetry index). Pearson's correlation coefficient was used to quantify the strength of the relationships between each of the gait and squat asymmetry metrics.

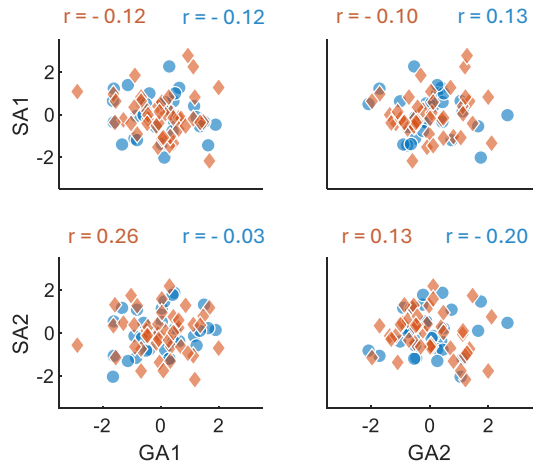


**Fig. 1.** Scatter plots between squat asymmetry (SA1 and SA2, y-axes) and gait asymmetry (GA1 and GA2, x-axes) for females (blue circles) and males (red diamonds). The Pearson correlation coefficient (r) is displayed in each of the plots with the left showing correlation for women and the right for men. Data were transformed using z-scores for graphical depiction of the relationships.

**Results & Discussion:** In both male and female athletes, movement asymmetry was most evident in SA2. The average value was 1.08 for both sexes indicating an asymmetry wherein the pelvis was 8% closer to the left leg at the lowest point in the body-weight squat. While this may be expected to result in differences in knee angle at the same instant in squatting, we observed little variation and there was on average no asymmetry in this measure (average value of SA1 was 1.00 for both sexes). Furthermore, there was no correlation between any gait and squat asymmetry measures (Fig. 1). This was contrary to our hypothesis and suggests asymmetries observed in one task do not necessarily translate to others. Our findings could be limited by task and metric selection. For example, our analysis considered only temporal and kinematic variables and tasks with relatively low effort (far below requiring maximal capacity). The generalization of movement asymmetry across tasks may manifest more strongly in kinetic variables and/or in tasks requiring maximal effort (e.g., counter movement jump or sprinting). Nonetheless, our results provide a reference against which post-injury asymmetry measures can be compared.

**Significance:** These findings provide important context for interpreting movement asymmetry during rehabilitation. That movement asymmetries do not generalize across tasks motivates using multi-task movement assessment as observed asymmetries may be causally independent.

**Acknowledgments:** This work was supported by the Clemson University Creative Inquiry program, the Clemson University Dept. of Bioengineering, and SC-TRIMH (NIH: P20GM121342).

**References:** [1] Gurchiek et al. (2019) *Sci Rep* 9; [2] Sadeghi et al. (2000). *Gait & Posture*, *12*(1); [3] Lambach et al. (2015). *Gait Posture,* 40(4); [4] Turner et al. (2024) *J of Biomech, 171;* [5] Johnson et al. (2022) *J of Biomech*, *143;* [6] Cook et al. (2006) *N Am J Sports Phys Ther* 1(2)

**An early increase in early rate of force development predicts a positive response to exercise for rotator cuff tendinopathy.**

*Daniel C McPherson[1], Oscar Vila Dieguez[1], Matthew D Heindel[1], Lori A Michener[1]
[1]Division of Biokinesiology and Physical Therapy, University of Southern California, Los Angeles, CA
*Corresponding author's email: dcmcpher@usc.edu

**Introduction:** Rotator cuff (RC) tendinopathy is a common musculoskeletal condition causing shoulder disability. Unfortunately, outcomes are highly variable, with up to 40-50% experiencing recurrent or chronic pain.[1,2] Resistance training is a recommended exercise intervention for RC tendinopathy with the intention to provide mechanical load to facilitate tendon remodeling.[3] However, resistance exercise clinical trials show inconsistent changes regarding peak force (PF) and its relationship with shoulder disability.[4,5] Defining neuromuscular performance using PF only may not be sufficient, as it only captures the maximal force exerted.[6] Alternatively, rate of force development (RFD) depicts the speed at which the force is exerted, which may be more relevant for daily function.[7] Whether baseline and early changes in neuromuscular variables can predict the response to resistance exercise is unknown. Improved understanding of the relationship between RFD and peak force with changes in shoulder disability could enhance clinical practice and provide therapeutic targets for more specified resistance exercise. Here, we characterize the relationship between changes in external rotation (ER) RFD and PF and changes in shoulder disability. We hypothesize that ER RFD metrics will be related to improved shoulder disability after a resistance exercise intervention, while ER PF metrics will not.

**Methods:** Participants (n=40, 12 female, 26 male, 1 transgender, 1 non-binary; age=30.8±10.3) were clinically diagnosed with RC tendinopathy and screened with ultrasound imaging to rule out full thickness RC tendon tears.[8] All participants underwent an 8-week standardized progressive resistance exercise protocol.[9] Measures were taken at baseline, 2-weeks, and 8-weeks. Shoulder disability outcomes were measured with the Penn Shoulder Score (PENN). Maximum isometric strength during ER was measured with a load cell at 1000Hz over 2 trials. PF was the maximum force produced. RFD was calculated as the change in force over time for epochs of 0-50ms, 50-100ms, and 100-200ms. Two linear regression models were run for each force variable; one for 0 to 2 weeks and one for 0 to 8 weeks as the predictors. Change in PENN weeks 0 to 8 was the outcome for all models. Baseline PENN, baseline RFD, and body weight were included as covariates in all models.

**Figure 1:** The relationship between the changes in ER RFD <100 ms from baseline to 2 weeks and changes in PENN score from baseline to 8 weeks.

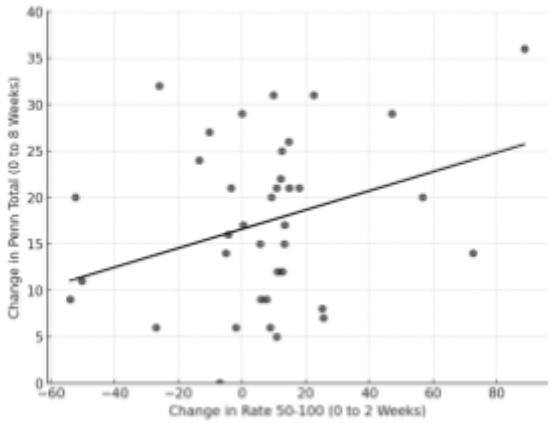


**Results & Discussion:** Changes from 0-2 weeks in ER RFD 0-50ms explained 23% of the variance in PENN changes from baseline to 8 weeks, and baseline PENN ($\beta$=-0.55, p=0.00) and ER RFD 0-50ms ($\beta$=0.18, p=0.03) were significant predictors. The model for changes at 2 weeks in ER RFD 50-100ms explained 28% of the variance in PENN changes from baseline to 8 weeks, and baseline PENN ($\beta$=-0.5, p=0.00) and ER RFD 50-100ms ($\beta$=0.11, p=0.04). The lone predictor in 0 to 8-week models was baseline PENN. None of the RFD predictors were significant from 0-8 weeks. RFD 100-200 and PF models were insignificant for 0 to 2 weeks or 0 to 8 weeks. Baseline PENN and changes in early RFD (<100ms) within the first 2 weeks of resistance training predict long-term patient-reported shoulder disability. Those who exhibit an increase in early RFD (<100ms) early in the course of care (within the first 2 weeks of exercise) are more likely to demonstrate significant improvements in shoulder disability in 8 weeks.

**Significance:** Identifying therapeutic intervention targets can enhance clinical decision-making efficiency for rehabilitation practitioners. Our findings suggest clinicians should consider using ER RFD <100ms, over ER peak force and ER RFD 100-200, to assess response to resistance exercise. Early change in ER RFD <100ms (0-2 weeks) may serve as a prognostic indicator for successful response to resistance exercise at 8 weeks. These results agree with prior studies that claim PF demonstrates little to no relationship with clinical improvement in shoulder disability. Future research is needed to investigate the impact of refining the resistance exercise program to enhance RFD on muscle performance and clinical outcomes.

**Acknowledgments:** Funding: NIH-NIAMS, Foundations for Physical Therapy Research, and Charles and Mary Bauer Foundation. The authors wish to acknowledge the participants who spent their time on this clinical trial.

**References:** [1] Leong et al. (2019), *J Rehabil Med*; [2] Hopman et al. (2013), *University of New South Wales*; [3] Desmeules et al. (2025), *JOSPT*; [4] Clausen MB et al. (2021), *Am J Sports Med*; [5] Hopewell S et al. (2021), *Health Technol Assess*; [6] Chen et al. (2021), *Strength. J Sport Rehabil*; [7] Turpeinen et al. (2020), *Scand J Med Sci Sports*; [8] Michener et al. (2009), *Arch Phys Med Rehabil*. [9] Mintken et al, (2016), *J Orthop Sports Phys Ther*

# CORRELATIONS OF RANGE-OF-MOTION AND FUNCTIONAL MOVEMENT ASSESSMENTS TO BASEBALL PITCHING BIOMECHANICS

*Jonathan S. Slowik[1], Claudia Leonardi[2], Linus I. Igbokwe[1], and Glenn S. Fleisig[1]
[1]American Sports Medicine Institute, Birmingham, AL, USA
[2]Louisiana State University Health Sciences Center, New Orleans, LA, USA
*jons@asmi.org

**Introduction:** Baseball pitching is a complex athletic movement that requires both strength and flexibility [1]. Previous studies utilizing goniometer/inclinometer-based measurements of passive ranges-of-motion (ROM) have demonstrated that ROM deficits adversely affect injury risk in baseball pitchers [2,3]. Technological advances may enable quicker, more objective ROM measurements [4]. The purpose of this study was to evaluate the relationships between biomechanical parameters measured during pitching to passive ROM measurements and functional movement assessment measures. In particular, we were interested in external rotation (ER) and internal rotation (IR) of the dominant/throwing shoulder, trunk axial rotation to the dominant side, as well as biomechanical measurements related to the strength of each leg. We hypothesized that there would be positive correlations for all variable combinations within each category (see Table 1).

**Methods:** This study analyzed data collected from 59 healthy baseball pitchers (43 high school, 12 collegiate, and 4 professional). Prior to warming up to pitch, passive ROM measurements of shoulder ER and IR were taken using an inclinometer and methods previously described [2,3,7]. The pitcher then underwent a functional movement assessment using a nine-camera marker-less motion capture system (DARI Motion Inc., Overland Park, KS, USA), including bilateral measurements of maximum ER, maximum IR, maximum trunk axial rotation (trunk separation, shoulders relative to hips), and single-leg jump height [5]. Pitching biomechanics were then assessed using a 12-camera marker-based motion capture system (Motion Analysis Corporation, Rohnert Park, CA, USA) [6]. Biomechanical pitching parameters included maximum values of ER, IR, and trunk separation; the amount the front knee extended between the instants of front foot contact and ball release; and stride length (expressed as a percentage of height), which is generated in part by rear leg push-off. The linear associations between all possible pairs of variables in each category were assessed using the Pearson correlation coefficient ($\alpha$=0.05).

**Results & Discussion:** Significant correlations were found for three of the five categories of parameters (Table 1). All three maximum shoulder ER parameters were significantly correlated with each other. Maximum shoulder IR during pitching was correlated with the passive ROM value, but neither of their comparison to the functional movement measure reached statistical significance (p=0.12-0.13). This unexpected lack of significance may be due to differences in scapular movement during the functional movement (for the passive measurement, the coracoid process was held stationary [2,3,7]; while it is possible that the higher abduction and horizontal abduction during pitching may similarly constrain the scapula). There was no relationship found between pitching and functional movement values of trunk separation (p=0.62), which was surprising. While the positioning of the legs was different between pitching and the functional movement, we still expected to find a relationship. Perhaps there are competing objectives during pitching that prevent some pitchers from utilizing their maximum achievable separation. Front knee extension during pitching had a statistically significant, positive correlation with the same side's single leg jump height (p=0.02), which supports our belief that many pitchers who lack knee extension may not have the strength required to do so. Finally, we could not find significance between stride length and rear leg jump height (p=0.15). This was less surprising, as we already believed that optimal pitching biomechanics may not include maximization of this parameter.

**Table 1:** Correlations between pitching, passive ROM and functional movement. Significant correlations (p<0.05) are show in **bold**.

| Category | Parameter (mean ± standard deviation) | | | Pearson's R correlation (p-value) | | |
|---|---|---|---|---|---|---|
| | Pitching Biomechanics | Passive ROM with inclinometer | Functional Movement | Pitching vs. Passive | Pitching vs. Functional | Passive vs. Functional |
| Shoulder ER | External rotation (162.8±11.3°) | External rotation (114.3±10.1°) | External rotation (98.2±13.4°) | **0.577 (<0.001)** | **0.401 (0.002)** | **0.571 (<0.001)** |
| Shoulder IR | Internal rotation (−5.0±10.0°) | Internal rotation (47.9±10.6°) | Internal rotation (67.7±15.5°) | **0.342 (0.008)** | 0.200 (0.128) | 0.205 (0.120) |
| Trunk separation | Trunk separation (52.1±10.7°) | | Trunk axial rotation to the dominant side (34.9±7.6°) | | 0.071 (0.619) | |
| Front leg | Front knee extension (6.1±9.7°) | | Non-dominant leg jump height (21.9±3.5 %height) | | **0.297 (0.022)** | |
| Rear leg | Stride length (81.6±4.6 % height) | | Dominant leg jump height (20.6±3.4 %height) | | 0.192 (0.145) | |

**Significance:** Functional movement assessment measures and passive ROMs showed relationships with pitching biomechanics, demonstrating usefulness as part of evaluations of baseball pitchers. Some functional movements could be refined to better reproduce joint constraints during baseball pitching and/or isolate individual joint movements (e.g., constrain the scapula). Furthermore, these results suggest that during pitching, optimal values for some key biomechanical parameters may not be the pitcher's maximal achievable values.

**References:** [1] Amin et al. (2015), *JAAOS* 23(12); [2] Wilk et al. (2014), *AJSM* 42(9); [3] Wilk et al. (2015), *AJSM* 43(10); [4] Aleksic (2023) *SEEMEDJ* 7(1); [5] Phillipp et al. (2024), *Front Sports Act Living* 6; [6] Escamilla et al. (2018), *J Appl Biomech* 34(5); [7] Wilk et al. (2009), *Sports Health* 1(2).

# WHEELCHAIR PROPULSION MUSCLE ACTIVATION STRATIFIED BY AGE OF SPINAL CORD INJURY ONSET

*Anna Hazzard[1], Whitney Harmon[1], Alyssa Schnorenberg[2], Brooke Slavens[2], Carrie Peterson[1]
[1]Dept. of Biomedical Engineering, Virginia Commonwealth University
[2]Dept. of Mechanical Engineering, University of Wisconsin-Milwaukee
*Corresponding author's email: hazzardaj@vcu.edu

**Introduction:** Manual wheelchair (MWC) propulsion imposes significant mechanical demands on the shoulders, contributing to a high prevalence of pain and injury among individuals with spinal cord injury and disease (SCI/D) [1]. Differences in propulsion biomechanics between pediatric-onset and adult-onset SCI users suggest that motor control strategies influence injury risk [2]. Electromyography (EMG) provides a useful tool for quantifying muscle activation patterns during propulsion, yet its application in pediatric MWC users remains limited [3]. This study examines EMG characteristics across pediatric, pediatric-onset adult, and adult-onset adult MWC users. We hypothesize that pediatric-onset users will exhibit distinct EMG profiles and reduced shoulder pain relative to adult-onset users, reflecting differences in movement variability and neuromuscular adaptation [4].

**Methods:** Participants were divided into groups according to their current age, and the age at which they sustained their SCI: children (ages 7–17; n = 5; 2 females, 3 males; mean age = 15.19 years), adults with pediatric onset (injury occurring before age 18; n = 6; 3 females, 3 males; mean age = 34.27 years), and adults with adult onset (n = 2; 2 males; mean age = 27.61 years). Nine surface EMG electrodes were placed on the biceps brachii (BB), long head of triceps brachii (TB), sternocostal head of the pectoralis major (PM), and the anterior, medial, and posterior heads of the deltoid (AD, MD, PD), as well as the upper trapezius (UT), latissimus dorsi (LD), and infraspinatus (IS). Participants performed MVICs relative to each aforementioned muscle while seated in a Biodex System 3 or BTE PrimusRS. Each participant performed at least three MVIC trials, with a 3-5 second contraction. EMG was recorded during propulsion at self-selected speed. Handrim kinetics (SmartWheel) were used to identify individual cycles. Custom code was used to identify the peak EMG value for each muscle during MVIC, followed by calculating the RMS within a 10 ms window around the peak. Similarly, for each propulsion trial, the peak value was determined for each muscle during the push and recovery phases within the identified cycle frames, and a 10 ms RMS was computed around the peak. The RMS values were averaged across all trials for presentation in Table 1.

**Results & Discussion:** Preliminary analysis of peak EMG amplitude (%MVIC) across propulsion cycles varied across the three groups for the AD, MD, PD, BB, PM, and IS. Pediatric-onset users exhibited the highest average activation during propulsion for the AD, MD, BB, and IS (Table 1). In contrast, the adult-onset users demonstrated the lowest average muscle activation for the BB, PM, and IS. Notably, the pediatric group showed the highest activation for the PM, suggesting differences in propulsion strategies and muscle development. Both adult groups demonstrated increased reliance on the anterior and middle deltoid, consistent with prior research [5].

Table 1. Peak EMG amplitude during wheelchair propulsion; reported as %MVIC. *--- indicated unavailable data.

| Subject | Pediatric | | | | | Pediatric Onset | | | | | | Adult Onset | |
|---|---|---|---|---|---|---|---|---|---|---|---|---|---|
| **Muscle** | **1** | **2** | **3** | **4** | **5** | **6** | **7** | **8** | **9** | **10** | **11** | **12** | **13** |
| **AD** | 8.05 | 57.42 | 15.63 | 26.22 | 18.40 | 15.31 | 36.05 | 10.15 | 13.62 | 84.55 | 53.89 | 22.42 | 29.10 |
| **MD** | 15.77 | 41.15 | 9.95 | 23.33 | 14.26 | 13.32 | 44.95 | 37.52 | 36.82 | 71.96 | 30.88 | 26.17 | 24.85 |
| **PD** | 20.67 | 28.90 | 40.32 | 23.01 | 6.37 | 8.90 | — | 36.20 | 24.81 | 31.41 | 7.95 | 56.08 | 47.77 |
| **BB** | 22.75 | — | 9.50 | 58.59 | 19.99 | 14.54 | 32.11 | 9.68 | 10.27 | 64.51 | 62.95 | 15.88 | 11.27 |
| **PM** | 61.51 | 71.14 | 34.79 | 23.06 | 23.68 | 16.61 | 78.04 | 17.46 | 15.79 | 48.73 | 47.85 | 23.15 | 18.02 |
| **IS** | 31.29 | 44.64 | 15.97 | 20.63 | 30.13 | — | 52.09 | 38.01 | 25.56 | 76.71 | 55.97 | 19.61 | 18.07 |

**Significance:** Shoulder pain and injury interfere with mobility and independence in individuals with SCI/D. This study examines EMG patterns across different age groups to identify biomechanical differences influencing shoulder health. Findings of our ongoing work will inform age-specific rehabilitation strategies to enhance mobility and reduce long-term musculoskeletal complications.

**Acknowledgments:** Supported by NICHD R01HD098698.

**References:** [1] Slavens, B. A., et al. (2019). *Medical Engineering & Physics*, *70*, 1–8; [2] Slavens, B. A et al. (2015). *Biotechnology*, *3*; [3] Louis, N., & Gorce, P. (2010). *Clinical Biomechanics*, *25*(9), 879–885; [4] Schnorenberg, A. J., et al. (2014). *Journal of Biomechanics*, *47*(1), 269–276 [5] Souza, A. L., et al. (2005). *The Journal of Spinal Cord Medicine*, 28(1), 26–32.

# EFFECTS OF MOVING OBJECTS ON INFANT REACHING KINEMATICS

Ipsita Sahin, Melanie Barahona, Elena Kokkoni*
Dept. of Bioengineering, University of California, Riverside, Riverside, CA 92521, USA
*Corresponding author's email: elena.kokkoni@ucr.edu

**Introduction**: Reaching actions may be influenced by moving objects being reached for. Prior studies in a controlled lab environment have assessed infant reaching with an object moving along the transverse plane [1-3]. These studies focused on changes observed in handedness, success rate of reaching, motor strategies for ipsilateral and contralateral reaching, but not reaching kinematics. Our work examined changes in infant reaching kinematics as objects are moving along the sagittal plane (moving towards the body of the infant). In addition, the data presented here were extracted from infants reaching for objects in natural environments, mirroring natural object presentation from an ecological perspective, to understand the adaptive mechanisms of early motor control. The findings from this work will contribute to a better understanding of the adaptive nature of infant reaching in response to dynamically moving objects, which can also inform the design of controllers in wearable devices to assist infant reaching [4].

**Methods**: A total of 48 reaching segments from 15 infants ($M_{age}$ = 7.29±1.50 months) were examined. The segments were extracted from 18 publicly available videos showing infants sitting and reaching for objects across everyday natural settings, such as homes and clinics. Inclusion criteria for segment extraction were: (i) the full arm (including shoulder, elbow, wrist, hand, and metacarpophalangeal joints) is visible throughout the reaching segment, (ii) targeted object is moving towards the infant and is visible throughout the reaching segment, (iii) the camera remains stable throughout the reaching segment. Out of the 48 reaching segments, the object was presented at the midline of the infant's body 24 times, whereas the object was presented at the right and left of the infant's body for 16 and eight times respectively. The objects were categorized based on their average motion speed into three groups: slow-moving (less than 40 cm/s), medium-speed (40–60 cm/s), and fast-moving (above 60 cm/s). The wrist joint of the infant and the moving object were tracked to obtain their position (2D coordinates) in each frame (using Kinovea and DLTdv8a in MATLAB [5]). Movement Units ($MU_R$ and $MU_O$) and Average Speed ($S_{avg_R}$ and $S_{avg_O}$) were computed for both the wrist and object, as well as the time to achieve peak velocity, expressed as a percentage of total reaching duration. To examine the relation between $MU_R$ and $MU_O$, the non-parametric Spearman correlation analysis was performed (violation of normality was confirmed using the Kolmogorov-Smirnov test). We hypothesized that the $MU_R$ and $MU_O$ would be positively correlated. To evaluate changes in Average Speed of the infant's wrist across the different categories of object speed, the Kruskal-Wallis H test was performed. We hypothesized that the infant's wrist speed would be affected by the different types of object speed. Statistical analysis was performed in SPSS v.30.

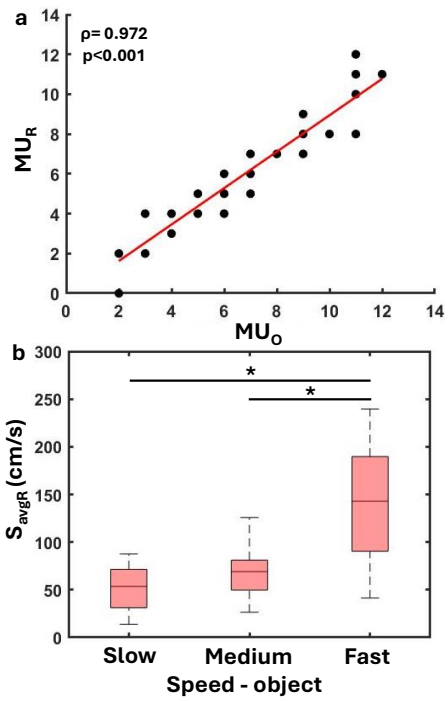


**Figure 1:** **(a)** The Spearman correlation plot between $MU_R$ and $MU_O$ *(the red line indicates the fitted line)*; and **(b)** Boxplots of the average speed of the infant's reach, showing significant differences owing to the different speed of objects.

**Results & Discussion**: The reaching duration was on average 0.76±0.38 seconds. A strong and significant positive correlation between $MU_R$ and $MU_O$ (Spearman's $\rho = 0.972$, $p < 0.001$) was observed (Fig. 1a). On average, the peak speed was achieved at 56.15±23.56% and 56.28±26.06% of the total duration of the reaching action and the object's motion, respectively. In almost 77% of the actions (37 out of the 48 reaches), the infant adjusted their peak speed to match the peak speed of the object. Taking these findings together suggests a coupling between the infant's reaching motion and the object's motion. In addition, there was an effect of the different types of object speed on the Average Speed of the infant's wrist motion ($\chi^2(2) = 20.036$, $p < 0.001$), as also depicted in Fig. 1b. Post-hoc tests demonstrated that the infant's wrist moved significantly faster when fast-moving objects were presented to them compared to those moving at slow ($p < 0.001$) and medium $p = 0.004$) speed. No significant difference was found in the Average Speed of the infant's wrist motion when reaching for slow-moving and medium-speed moving objects ($p = 0.784$).

**Significance**: The results from this work highlight the adaptive nature of humans to adjust their reaching actions to moving objects presented in the real world from a very young age. Our findings not only support that object motion affects reaching kinematics, but they also reveal a crucial positive coupling, suggesting that infants actively integrate object motion into their motor planning. This information can also be used in the development of wearable assistive devices for infant populations with or at risk of upper extremity motor impairments [4]. Object motion information can be used to determine objectives for the motion controllers of the wearable devices to similarly guide the hand to the object [6].

**References**: [1] von Hofsten et al. (1979). *J Exp Child Psychol* 28:158-173; [2] Fagard et al. (2009). *Infant Behav Dev* 32:137-146; [3] von Hofsten (1980). *J Exp Child Psychol* 30:369-382 [4] Kokkoni et al. (2020). *J Eng Sci Med Diagn Ther* 3:021109-021117; [5] Hedrick (2008). *Bioinspir Biomim* 3:34001-34008; [6] Mucchiani et al. (2023). *IEEE IROS*, 559-566.

# DO 3D PRINTED AFOS PROVIDE BENEFITS VS. OFF-THE-SHELF ONES FOR STROKE INPATIENTS?

Sarah N. McGuckin[1], *Mukul C. Talaty[1,2]
[1]Penn State Abington, Division of Science & Engineering, Abington, PA USA
[2]Gait & Motion Analysis Lab, Jefferson-Moss-Magee Rehab, Elkins Park, PA USA
*Corresponding author's email: mxt103@psu.edu

**Introduction:** Ankle foot orthoses (AFOs) are often used during gait training in inpatient rehabilitation. Insurance driven limitations in length of stay require use of non-custom off-the-shelf (OTS) AFOs. Use of OTS AFOs can burden therapist to properly fit the brace and the possibility of sequelae (skin breakdown and pain) due to improper fit and sub-optimal walking recovery due to improper AFO function. 3D printed (3DP) braces are less expensive, can be custom fitted and produced quickly and may address these issues. This study's provides pilot data on feasibility of providing and benefits of the use of 3DP braces during the inpatient rehabilitation stay.

**Methods:** Patients were recruited from an impatient rehabilitation facility and provided informed consent for this IRB approved study. In Phase I, patients were recruited into the OTS arm of the study. In Phase II, patients received the 3DP braces (ongoing). Study braces came from one of three places: 1) the OTS braces were obtained from a cache of "extra" braces, 2) some 3DP braces were provided by a commercial outfit using polypropylene (PP) created via an SLS process on an HP Multijet fusion machine and 3) some 3DP braces were fabricated in-house using PP using either FDM or FGM methods. Brace models were created from leg scans using various software packages. Gait training was done during therapy by PTs with either OTS or 3DP AFOs. Patients received the standard of care which was 3 hours of daily therapy – split as needed between PT, OT and speech (5 times a week). Skin integrity, general and limb pain and modifications made to the brace were logged pre and post each therapy session. Efficiency and satisfaction surveys were completed by the therapists. Data analysis was done by the study team medical residents and an undergraduate student.

**Results & Discussion:** The OTS arm of the study satisfied enrollment target (30) with 26 providing usable data. The 3DP arm of the study is still enrolling subjects with a current N of 13. Length of stays were similar (16 for OTS vs. 15.1 for 3DP). To date, the 3DP braces have been printed by a commercial outfit and it has taken 8.4 days (N = 13) for the 3DP brace to arrive leaving just under 5 days of use before discharge. Therapist used OTS braces until 3DP study braces were available. Two of the subjects never wore their study brace as they were discharged or received their definitive custom AFOs by the time the study brace arrived. Two subjects had medical complications necessitating return to acute care and were not able to complete the study course.

The onset for pain was 1.2 days and the onset for skin complications was 1 day for the 3DP group (Table 1). This was *after having worn an OTS brace for 8.4 days* as that was time to receive the 3DP brace – so overall these times were comparable once this was factored in. The rate of occurrence of skin issues was comparable between OTS and 3DP. The general pain did seem to occurr at a lower rate and severity in the 3DP group than in the OTS. Rate of limb pain was similar though scores did seem to be lower. Statistical analysis comparing groups have not yet been performed due to group size imbalance and the confound of Phase II using both OTS and 3DP braces, but analyses are planned.

**Table 1:** Occurrence and timing of skin issues, general and limb pain for OTS and 3DP cohorts.

| Category of Event | | Skin Issues | General Pain | Limb Pain |
|---|---|---|---|---|
| Phase I (OTS, N=26) | #Occurrences (%) | Ns = 12 (42%) | NGP = 16 (62%) | NLP = 15 (46%) |
| | (Pre. / Post) (% Chg.) | 1.9 / 2.7 (42%) | 1.7 / 2.4 (41%) | 0.7 / 1.5 (114%) |
| | Timing | Onset, 9.5 days | Onset, 8.1 days | |
| Phase II (3DP, N=13) | #Occurrences (%) | Ns = 7 (54%) | NGP = 1 (8%) | NLP = 5 (39%) |
| | Pre / Post (% Chg.) | 0.27 / 0.46 (67%) | 0.02 / 0.02 (0%) | 0.02 /0.13 (760%) |
| | Timing | Onset, 1 day | Onset, 1.2 days | |

The average satisfaction rating of PTs with using the 3DP AFO was 7.3 out of 10, and 7.0 out of 10 for orthosis optimization efficiency. Of the subgroup using the 3DP AFO for three or more sessions, 50% (n=6) never developed pain or skin changes; the other 50% developed skin changes after 1 session, all of which were superficial and temporary. The 3DP AFOs were durable and did not cause any severe injury. Of the 26 patients using *only* OTS AFOs, 46% developed orthosis related limb pain, 62% developed general pain and 42% had orthosis related skin changes. For the Phase I group, the onset of skin complications was 9.5 days, and the onset of pain was 8.1 days (Table 1). Phase I skin and pain rates initially seemed high, suggesting reduction may be possible with better fitting AFOs. Due to use of OTS braces until 3DP braces were ready, comparisons of skin and pain issues are not straightforward. Long delivery time for 3DP braces has clouded our understanding of the benefits of 3DP AFOs. In addition, the 3DP braces tended to be very stiff likely affecting both comfort and performance. It will be interesting to assess if custom 3DP AFOs can improve *functional* outcomes and the overall care for inpatients.

**Significance:** This work demonstrates that providing 3DP braces to inpatients is feasible though challenging. With a large team of partially rotating therapist providing care and residents involved with consenting and compiling data – there were many staff changes. This is not to mention the inherent challenges with inpatients themselves. Going forward, printing braces in house will reduce or eliminate use OTS and simplify interpretation. 3D printing has gained widespread use but underutilized in the inpatient rehabilitation clinical setting. Trials like this one demonstrate feasibility and larger trials may also show improved patient outcomes.

# GAIT ADAPTATION AND QUALITY OF LIFE OUTCOMES IN TRANSTIBIAL AMPUTEES USING THE MERCER UNIVERSAL PROSTHESIS (MUP®) IN 1-YEAR STUDY

Trung T. Le[1,2*], Craig T. McMahan[2], Ha V. Vo[2], Scott C. E. Brandon[1]
[1] School of Engineering, University of Guelph, Ontario, Canada
[2] School of Engineering, Mercer University, Georgia, USA
*Corresponding author's email: tle20@uoguelph.ca

**Introduction:** In the clinical fitting of transtibial prostheses, achieving gait symmetry between the prosthetic and intact limbs typically requires dynamic socket alignment (DA). This tuning process is time-consuming, costly, and demands expertise in prosthetic fitting. Despite efforts to optimize DA for transtibial gait symmetry, studies on socket DA within the clinically accepted 10° tolerances have not demonstrated significant gait changes[1]. If DA can be avoided, the cost of prosthetic fitting will be significantly reduced; this will reduce costs and improve access to prosthetic care, particularly in developing countries. The Mercer Universal Prosthesis (MUP) (US Patent #8870968) was designed to incorporate a standardized "neutral" socket alignment and has been effective in streamlining the transtibial fitting process while reducing prosthetic healthcare costs. Since 2009, it has benefited over 19,000 amputees in underserved regions of Vietnam and Cambodia. Initial findings[3] suggest that, immediately after fitting experienced prosthesis users with an MUP, prosthetic limb joint mobility (i.e. knee and hip range of motion, ROM) is enhanced versus gait when using their baseline, DA-fitted conventional prosthesis (CVP). However, prosthetic users require extended periods to adjust to a new prosthesis; literature suggests that gait adaptation should be assessed over at least 10 weeks to 3 months post-fitting[3]. Therefore, this study aims to assess the use of the MUP transtibial prosthetic over a one-year period to (i) examine longitudinal gait adaptation and (ii) evaluate quality-of-life outcomes. It is hypothesized that participants using the MUP device will exhibit progressive improvements in gait symmetry, demonstrating adaptation to the prosthesis and ultimately enhancing their overall quality of life.

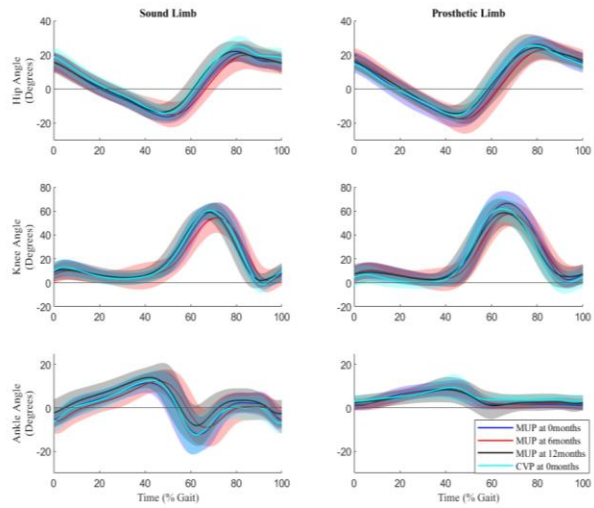


**Figure 1**: Sagittal joint angles of the MUP (at 0,6 and 12 months) and CVP reported at 0 months[2]

**Methods:** 20 experienced transtibial amputees (19 male, 1 female; age 60 ± 7 years) wearing CVP were fitted with the MUP at 0 months and participated in this study. Outcome assessments were conducted at three time points: baseline (0 months), 6 months, and 12 months. Data collection included (i) clinical gait analysis and (ii) quality-of-life assessment using the SF-36 medical survey. Gait analysis was performed using the Ultium® Portable Lab (Noraxon Inc., USA), incorporating lower-limb IMU motion sensors (200 Hz) and surface EMG sensors (2000 Hz). At three designated timepoints, temporal/spatial gait, kinematics, and surface EMG data were collected for each subject. Peak values and ROM were evaluated for the sagittal joint angles (i.e. hip, knee and ankle), and gait symmetry index (GSI)[2] was computed for temporal/spatial and kinematics outcomes. Since maximum voluntary contractions were not collected, raw EMGs of knee flexor (biceps femoris) and knee extensor (rectus femoris) were filtered and enveloped (Noraxon Inc, USA), interpolated to 101 points representing 0-100% of the gait cycle, and magnitude-normalized to the maximum during each recorded trial. Cumulative muscle effort was as the integral of the muscle contraction throughout gait. A two-factor repeated measures ANOVA (with within-subject's factors: limb and time) was used for statistical analysis ($p<0.05$). Post hoc analyses conducted using a Bonferroni – Holm.

**Results & Discussion:** At baseline (0 months), all participants accepted the MUP device, and they reported using it for more than 10 hours per day throughout the study. Temporal and spatial gait outcomes showed no significant changes over time with MUP use. However, kinematic outcomes revealed a significant interaction between limb*time for hip flexion (**$p = 0.04$**), knee flexion (**$p = 0.042$**), and ankle plantarflexion (**$p = 0.037$**). Post-hoc analysis revealed a significant reduction in hip and knee flexion from 0 to 6 months, followed by an increase at 12 months, contributing to improved gait symmetry. The GSI (temporal, spatial, and kinematic parameters) remained statistically unchanged from 0 to 12 months. Additionally, at the end of one-year, joint ROM (hip and knee) in the MUP group was comparable to kinematic outcomes reported for conventional prosthetic (CVP)[3] (Figure 1). Muscle effort initially showed asymmetry between limbs immediately after MUP fitting (0 months), but this difference was no longer observed at 12 months. Medical assessments using the SF-36 survey showed significant improvements in general health **($p < 0.001$),** health change **($p < 0.001$),** and pain reduction **($p = 0.005$)**. However, energy fatigue outcomes remained unchanged **($p = 0.211$)**.

**Significance:** Significant gains in general health, pain reduction, and perceived well-being highlight the MUP's enhancing quality of life. The low-cost MUP with standard 'neutral' alignment device also promotes long-term gait adaptation.

**Acknowledgments:** This study was funded by the Mercer On Mission Office.

**References:** [1] Jonkergouw, N et al. (2016). PLoS ONE, 11(12). [2] Herzog,W et al. (1988). Medicine and Science in Sport and Exercise 21(1). [3] Le, T. et al (2025). Preprints https://doi.org/10.20944/preprints202502.0708.v1.

# Design of a Concussion Recovery Device

*Daniela Scagnetti[1], Jeffry Fuhrmann[2], Sydney Robinson[2], Amber Drvodelic[2], Eric G. Meyer*[2]*
[1] Mechanical Engineering, Lawrence Technological University, Southfield, MI, USA
[2] Biomedical Engineering, Lawrence Technological University, Southfield, MI, USA
*Corresponding author's email: emeyer@ltu.edu

**Introduction:** According to the NCBI, 12% of young athletes experience a concussion in their sports career, yet the indicators for safe return to play remain unclear and uncharted [1]. Currently, athletic trainers rely on simple assessments, such as symptom checklists, the Balance Error Scoring System (BESS), vestibular ocular motor screening (VOMS), and the Standardized Assessment of Concussion (SAC) within the Sport Concussion Assessment Tool 5 (SCAT5) [2]. These evaluations often require multiple tools to perform and rely heavily on athletes' self-reported symptoms, which may be subjective or inconsistent. For athletes, this process is often frustrating, as there are no clear milestones between "injured" and "cleared" and for trainers, it is hard to select which symptoms to use as the best indicators as to whether or not an athlete can safely return to play. To address these limitations for both athlete and clinician, we propose the Concussion Recovery Device (CRD), which objectively measures reaction time, balance, and grip strength – three of the key factors affected by concussions [3]. Unlike traditional symptom checklists, our device provides quantifiable recovery metrics, allowing athletes, trainers, and healthcare providers to track progress more accurately and help to visualize the recovery process. With consistent use of this device, users can observe trends that reflect recovery improvement over time. This device aims to offer an accessible and reliable method for monitoring concussion recovery, reducing dependence on subject self-assessments.

**Methods:** Expert interviews were conducted with physical therapists and sports trainers to understand what indicators the target audience would need in order to make a device in this field effective. Three main ideas were created from a brainstorming session by the group, and a selection criteria matrix determined that a recovery tracking device would be the most impactful design. The form factor of the device was iterated from a game-controller wheel into the current design, to ensure maximum useability and effectiveness. There are three functional user assessments for the complete recovery monitoring: grip strength, reaction time, and a balance test.

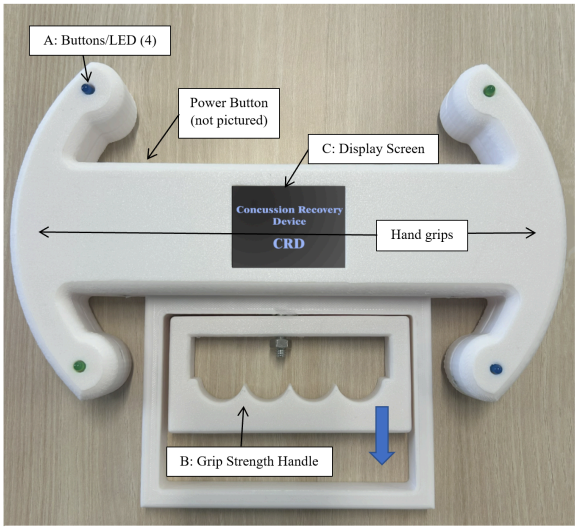

Figure 1: CRD current design, as of February 2025

**Results & Discussion:** The screen is used to display instructions to the user on how to execute each assessment and show results as the user goes through each test. The external components used in this device, shown in Figure 1, are as follows: four LEDs and buttons (A), grip strength handle (B), and a 2.4'' display screen (C). The electrical and internal components housed within the 3D printed casing of the device consists of: Adafruit M0 Wifi board, 9V battery, load cell, and a BNO055 inertial measurement unit (IMU) that includes 3D accelerometers, gyroscopes, and orientation sensors. A more thorough description of the equipment used for each assessment can be found in Table 1. At the end of the combined assessment, the device will provide the user with a score which can be used to track recovery progress.

Table 1: Assessment Tests and Required Equipment

| Grip Strength Test | Balance Test | Reaction Time Test |
|---|---|---|
| - Load cell and amplifier<br>- Handle (applied load) | - Gyroscope (rotational change)<br>- Accelerometer (magnitude of movement) | - Arcade style button and LED<br>- PCB board to interconnect lights |

In order to calibrate this device, each assessment will be run side-by-side with a predicate device of similar functionality. The load cell will be calibrated with known weight amounts. The balance test will be compared to phyphox, a smartphone gyroscope/acceleration app for validation. The reaction time will be compared to a slow motion video showing the time elapsed between stimuli and response. The printed housing will also undergo multiple strength and endurance tests.

**Significance:** Ultimately, the goal is that it will help prevent long-term brain damage by providing precise, data-driven insights to guide return-to-play decisions. Making informed return-to-play decisions after a concussion is both challenging and critical. Relying solely on introspective symptom tracking is often unreliable and difficult to track. Objective measurements of balance, grip strength, and reaction time can provide individuals and healthcare providers with valuable data to assess and save recovery progress. Ensuring proper recovery before resuming physical activity is essential to prevent long-term neurological damage.

**Acknowledgements:** We would like to thank Dr. Hao Jiang, Nathan Strnad and John Peponis for their support throughout this project.

**References:** [1] Tsushima, William et al. 2018 *Arch Clin Neuropsychol* (34(1):60–69); [2] Danielli, Ethan et al. 2023 *Front Neurol* (14:1136367); [3] Howell, David et al. *Phys Ther Sport* 2021 (52:132-139);

# The learning effects on lower limb kinetics during single-leg forward and backward hopping

Yu Gu[1], Wanyan Su[1], Nawfal Malik[1], Thanh Nguyen[1], Anne Jordan[1], *Yu Song[1]
[1]Biomechanics Laboratory, Department of Health, Sport & Exercise Sciences, University of Kansas, Lawrence, Kansas
*Corresponding author's email: yusong@ku.edu

**Introduction:** Single-leg forward hopping for distance is the most popular task to evaluate knee function in patients following anterior cruciate ligament (ACL) injuries. However, a similar forward hopping distance cannot ensure that knee function is fully restored in the involved leg [1]. This is likely due to inconsistent task execution in clinical settings and compensatory movements at the hip and/or ankle joints. On the one hand, inconsistent practice trials were employed in clinics, which may mislead the data interpretation and comparisons. On the other hand, single-leg backward hopping for distance has been suggested to be more appropriate for assessing knee function, as it places greater knee demands compared to forward hopping [2]. Therefore, this study aimed to quantify the learning effects on lower limb (hip, knee, and ankle) mechanics during single-leg forward and backward hopping.

**Methods:** Forty-five injury-free participants (age: 21.0 ± 0.7 years old, height: 1.7 ± 0.1 m, body mass: 68.9 ± 11.9 kg) performed 10 single-leg forward and backward hops on one leg while motion and force data were collected [2]. Hopping performance, peak power, and work of hip, knee, and ankle joints during jumping were calculated for each trial. To quantify learning effects, the 10 trials for each hopping direction were grouped as one practice trial, Block 1 (average of trials 2-4), Block 2 (average of trials 5-7), and Block 3 (average of trials 8-10). Such arrangements were based on previous studies, which commonly reported an average of three trials with a single practice at the beginning of the testing [3]. Two-by-three repeated-measures ANOVAs were applied to all dependent variables.

**Results & Discussion:** For the learning effect (Table 1), hopping performance and peak hip power significantly increased across three Blocks, with the greatest hip work observed in Block 3, regardless of hopping direction. No significant differences were found in peak knee power and knee work across all Blocks for both hopping directions. Although hopping performance increased, knee measurements (peak knee power and knee work) remained consistent. As such, the increased performance might be achieved through greater hip power and work rather than greater knee involvement. For the hopping directions (Table 1), single-leg backward hopping demonstrated smaller hopping distance, smaller peak power and work of hip and ankle joints, but greater peak knee power and work compared to forward hopping, regardless of Blocks. The results were consistent with a previous study [2], which showed that single-leg backward hopping requires greater knee demands compared to forward hopping.

**Significance:** Single-leg backward hopping imposes greater knee demands than forward hopping, suggesting its potential as a more appropriate task to assess knee function in patients following ACL injury. Additionally, one practice trial might be appropriate when using performance to evaluate knee function during single-leg forward and backward hopping. Future studies need to investigate the relationships between hopping performance and knee metrics in patients following ACL injuries to extend the current findings to the clinical population.

**References:** [1] Cristiani R et al. (2022), Knee Surg Sports Traumatol Arthrosc 30(5); [2] Song, Y. et al. (2024), J Sport Health Sci.14,100976; [3] Read P et al. (2021), Br J Sports Med. 55(1).

**Table 1:** Mean ± Standard deviation of dependent variables during single-leg forward and backward hopping.

| | | Single-leg Forward Hopping | Single-leg Backward Hopping |
|---|---|---|---|
| Performance (m) | Block 1 | 1.17 ± 0.28 $^{c*}$ | 0.77 ± 0.16 $^{c*}$ |
| | Block 2 | 1.22 ± 0.28 $^{b*}$ | 0.81 ± 0.17 $^{b*}$ |
| | Block 3 | 1.26 ± 0.29 $^{a*}$ | 0.83 ± 0.19 $^{a*}$ |
| Peak Hip Power (W/(BW*BH)) | Block 1 | 0.855 ± 0.194 $^{c*}$ | 0.359 ± 0.143 $^{c*}$ |
| | Block 2 | 0.887 ± 0.206 $^{b*}$ | 0.360 ± 0.147 $^{b*}$ |
| | Block 3 | 0.904 ± 0.210 $^{a*}$ | 0.377 ± 0.152 $^{a*}$ |
| Peak Knee Power (W/(BW*BH)) | Block 1 | 0.294 ± 0.110 $^{*}$ | 0.563 ± 0.177 $^{*}$ |
| | Block 2 | 0.288 ± 0.109 $^{*}$ | 0.574 ± 0.166 $^{*}$ |
| | Block 3 | 0.294 ± 0.118 $^{*}$ | 0.569 ± 0.177 $^{*}$ |
| Peak Ankle Power (W/(BW*BH)) | Block 1 | 0.933 ± 0.177 $^{*}$ | 0.460 ± 0.114 $^{a*}$ |
| | Block 2 | 0.924 ± 0.170 $^{*}$ | 0.436 ± 0.110 $^{b*}$ |
| | Block 3 | 0.938 ± 0.169 $^{*}$ | 0.424 ± 0.101 $^{b*}$ |
| Hip Work (J/(BW*BH)) | Block 1 | 0.110 ± 0.035 $^{b*}$ | 0.046 ± 0.023 $^{b*}$ |
| | Block 2 | 0.112 ± 0.034 $^{b*}$ | 0.044 ± 0.024 $^{b*}$ |
| | Block 3 | 0.115 ± 0.034 $^{a*}$ | 0.047 ± 0.025 $^{a*}$ |
| Knee Work (J/(BW*BH)) | Block 1 | 0.020 ± 0.011 $^{*}$ | 0.045 ± 0.019 $^{*}$ |
| | Block 2 | 0.020 ± 0.011 $^{*}$ | 0.047 ± 0.020 $^{*}$ |
| | Block 3 | 0.020 ± 0.012 $^{*}$ | 0.047 ± 0.021 $^{*}$ |
| Ankle Work (J/(BW*BH)) | Block 1 | 0.071 ± 0.013 $^{*}$ | 0.047 ± 0.009 $^{a*}$ |
| | Block 2 | 0.071 ± 0.013 $^{*}$ | 0.045 ± 0.009 $^{b*}$ |
| | Block 3 | 0.072 ± 0.013 $^{*}$ | 0.045 ± 0.008 $^{b*}$ |

Notes: BW: body weight, BH: body height. a, b, and c, significantly different among the blocks: a is the greatest, b is the second greatest, and c is the least. * significant difference between forward and backward hopping.

# KNEE STRENGTH ASYMMETRY DOES NOT EXPLAIN GAIT ASYMMETRY IN UNINJURED FEMALE ATHLETES

Allyson M. Richardson[1], Sydney Savage[1], Andrew Polson[1], Olivia Cunningham[1], Amanda Taylor[2], *Reed Gurchiek[1]
[1]Department of Bioengineering, Clemson University; [2]Athletics Department, Clemson University
*Corresponding author's email: rgurchi@clemson.edu

**Introduction:** Lower-limb gait asymmetry is a key factor in assessing movement during rehabilitation following anterior cruciate ligament reconstruction surgery (ACLR). In this clinical context, gait asymmetry is thought to contribute to the development and progression of post-traumatic osteoarthritis [1]. Gait asymmetry can manifest early post-surgery [2] and thus effective early-stage rehabilitation is critical [3]. However, a poor understanding of the source of the gait asymmetry limits intervention efforts because the underlying cause is unknown. Several factors could contribute to post-ACLR gait asymmetry including pain, kinesiophobia, compromised proprioception, limited range of motion, and/or weakness [4]. It is difficult to control for any one of these factors experimentally using a sample of athletes with authentic injuries. However, strength asymmetry is observed in uninjured athletes for whom the effects of the other injury-specific factors would be non-existent or negligible. Therefore, the purpose of this study was to quantify the relationship between knee extension strength asymmetry and gait asymmetry in a sample of uninjured athletes. Knee extension torque during normal walking on level ground requires much less than the maximal effort of the relevant knee musculature [5]. Thus, we hypothesized there would be no relationship between strength asymmetry and gait asymmetry.

**Methods:** We recorded videos of 29 female collegiate lacrosse athletes during a movement assessment using two iPhones. Data for an athlete were included only if they reported no history of lower limb injuries within the 8 months prior to testing. They were instructed to walk normally along a straight, 10-meter path over level ground for 3 trials. OpenCap [6] was used to automate video recording, synchronization, and processing from which joint angles were calculated. We visually assessed all videos to verify a quality reconstruction. An athlete's data was included only if every video passed our data quality check. For each leg, we calculated duty factor (stance time divided by stride time) and the peak knee flexion angle during stance phase. Limb symmetry index (LSI) was then quantified for each gait variable separately, calculated as the ratio between the left leg measure and the same right leg measure. We used the LSI formula to quantify knee extensor strength asymmetry wherein strength was determined separately for each leg via hand-held dynamometry. Strength assessments were administered by a trained professional (team athletic trainer) on a different day than the gait assessment (separated by at most two months).

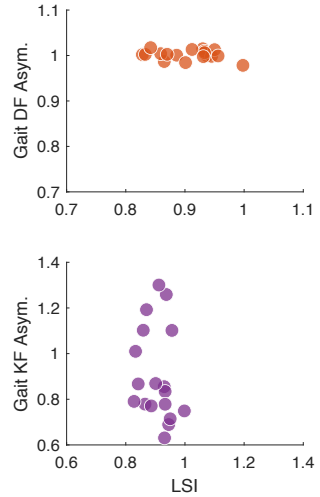


**Fig. 1.** We found no correlation between strength asymmetry (x-axis) with either of the considered gait asymmetry metrics (top: duty factor; bottom: peak knee angle in stance).

**Results & Discussion:** Data from 18 athletes met the criteria for analysis. Despite a considerable range in strength asymmetry (0.8 to 1.0), we observed no significant correlation between strength asymmetry and either duty factor ($r = -0.22$, $p = 0.38$) or knee flexion angle ($r = -0.18$, $p = 0.49$) asymmetry (Fig. 1). For duty factor, this was due in part to a relatively small range in the data across our sample. While duty factor asymmetry has been shown sensitive to rehabilitation progress [2], our results suggest this is not due to strength asymmetry. In contrast, the range in asymmetry based on peak knee flexion angle during stance was much larger (0.63-1.30). Nonetheless, strength asymmetry explained only 3% of that variability. These results are consistent with our hypothesis which was based on the rationale that knee extensor torques observed in normal walking require much less than the maximal capacity of the relevant musculature [5]. These conclusions are further supported given our sample (no lower limb history within the 6 months prior to testing) which we pursued to control for other ACLR-related phenomena that potentially contribute to gait asymmetry. However, the strength asymmetry in our sample may not reflect that observed post-ACLR for which considerable quadriceps atrophy is consistently reported [7]. There is likely a threshold strength asymmetry below which gait would be affected, and while an injured sample may better approximate that threshold, it becomes more difficult to control for other injury-related confounders (e.g., pain and kinesiophobia). Predictive simulation may provide novel insight for elucidating this relationship further [8]. Our study focused primarily on temporal and kinematic asymmetry metrics that can be measured with scalable technologies that facilitate practical use in clinical settings. However, there may be kinetic measures that are related with strength asymmetry. Furthermore, while we focused on female athletes for whom ACL injuries are more common, there may be an effect of sex. These limitations should be explored in future work.

**Significance:** Our results suggest hesitancy in attributing gait asymmetry to knee extensor strength asymmetry. Further research is necessary to confirm this in an ACLR population toward a means for identifying the underlying cause. This could provide new directions for improving early-stage rehabilitation following ACLR toward normalizing gait and delaying the onset and rate of progression of post-traumatic osteoarthritis.

**Acknowledgements:** This work was supported by the Clemson University Creative Inquiry program, the Clemson University Dept. of Bioengineering, and SC-TRIMH (NIH: P20GM121342).

**References:** [1] Butler et al. (2009), *Br J Sports Med* 43; [2] Gurchiek et al. (2019) *Sci Rep* 9; [3] Buckthorpe et al. (2024) 54; [4] Gokeler et al. (2015) *Int J Sports Phys Ther* 8(4); [5] Arnold et al. (2013) *J Exp Biol* 216(11); [6] Uhlrich et al. (2023) *PLOS Comput Biol* 19(10); [7] White et al. (2024) *J Orthop Res* 42(11); [8] Ong et al. (2019) *PLOS Comput Biol* 15(10)

**Reaction Time as a Predictor of Cognitive Function in Collegiate Athletes with Concussion History**

Amin Mohammadi[1], Reza Pousti[1], Eric Schussler[1], Tom Campbell[1]*
[1]Ellmer College of Health Sciences, Macon & Joan Brock Virginia Health Sciences at Old Dominion University
*Corresponding author's email: trcampbe@odu.edu

**Introduction:** Concussions are a prevalent concern in athletics, particularly among collegiate athletes, due to their potential for long-term cognitive impairments. Sport-related concussions can lead to deficits in executive function, psychomotor speed, memory, and reaction time, which may persist beyond the acute recovery phase [1]. While many athletes return to play after symptom resolution, research suggests neurocognitive deficits may linger, affecting overall cognitive performance [2]. Reaction time is particularly relevant in assessing post-concussion recovery, as slowed reaction times have been associated with altered brain function and prolonged cognitive dysfunction [3]. Additionally, impairments in executive function and psychomotor speed are known to impact decision-making and motor coordination, both critical components of athletic performance. Despite the widespread implementation of neurocognitive testing in concussion management, there is a need for further research on how these deficits manifest in collegiate athletes with a history of concussion [4].

This study aims to examine the relationships between reaction time, executive function, psychomotor speed, and memory in NCAA Division I athletes with a history of concussion. Understanding these associations may help refine post-concussion assessments and inform return-to-play decisions.

**Methods:** 112 college-aged athletes (M: F = 72:40) from a NCAA Division I institution with a self-reported history of concussion were included in this cross-sectional study. Reaction Time Composite (RT-Comp), executive function, and psychomotor speed were assessed using Concussion Vital Signs (CNS Vital Signs LLC), a computerized neurocognitive assessment. Immediate memory and delayed recall were evaluated as part of the Sport Concussion Office Assessment Tool – 6th edition (SCOAT-6) [5]. Correlations were analyzed using Pearson's correlation to assess the strength of associations. A priori p-value was set at $p < .05$.

**Results & Discussion:** RT-Comp demonstrated significant negative correlations with executive function ($r = -0.430$, CI [-0.572, -0.265], $p < 0.001$), indicating that slower reaction times were associated with reduced cognitive flexibility and decision-making abilities. A similar negative correlation was observed with psychomotor speed ($r = -0.355$, CI [-0.508, -0.184], $p < 0.001$), suggesting impairments in motor response efficiency. Additionally, slower RT was associated with lower scores in immediate memory ($r = -0.307$, CI [-0.469, -0.127], $p = 0.001$) and delayed recall ($r = -0.233$, CI [-0.403, -0.043], $p = 0.013$), highlighting potential long-term cognitive consequences of concussion.

The results of this study indicate that reaction time impairments in collegiate athletes with a history of concussion are significantly associated with deficits in executive function, psychomotor speed, and memory. These findings are consistent with previous literature that has demonstrated persistent neurocognitive deficits in concussed athletes, even after symptom resolution [1]. The significant negative correlations observed between reaction time and executive function suggest that slower cognitive processing may contribute to diminished decision-making abilities, which could affect athletic performance and daily cognitive tasks. The association between reaction time and psychomotor speed further supports the notion that concussions can impact motor coordination and response efficiency. Previous studies have found that reaction time impairments can persist for weeks after concussion, and in some cases, these deficits are linked to altered brain network connectivity [3]. The observed correlations between slower reaction times and memory impairments in both immediate and delayed recall suggest that concussions may have lingering effects on information processing and retention. These results align with studies indicating that concussed athletes demonstrate prolonged deficits in verbal and visual memory [2].

**Significance:** This study underscores the importance of comprehensive neurocognitive assessments in concussion management, highlighting persistent deficits in reaction time, executive function, and memory among collegiate athletes. These impairments may increase the risk of re-injury and hinder cognitive performance, even after athletes appear symptom-free.

Findings support the need for long-term monitoring and individualized rehabilitation strategies to ensure a full cognitive recovery before returning to activity. Refining post-concussion protocols based on neurocognitive testing can enhance player safety, minimize recurrence risk, and improve long-term outcomes in student-athletes.

**Acknowledgements:** We would like to thank Josh Lawton, Gabriel Rankin, Isaac Avis, Braden Footer, Aubrey Thames, Joee Crocker, Tiera Washington, and Kyla Formey for their valuable contributions to this study.

**References:**

**1.** Fazio, V., et al., NeuroRehabilitation, 2007. **22 3**: p. 207-216.
**2**. Covassin, T., D. Stearne, and R. Elbin, Journal of athletic training, 2008. **43 2**: p. 119-124.
**3**. Churchill, N., et al., Brain Imaging and Behavior, 2020. **15**: p. 1508-1517.
**4**. Asken, B., et al., Journal of athletic training, 2017. **52 1**: p. 51-57.
**5**. *Sport Concussion Assessment Tool 6 (SCAT6).* British Journal of Sports Medicine, 2023. **57**(11): p. 622.

# A SYSTEMATIC REVIEW AND META-ANALYSIS ON THE USE OF REAL-TIME BIOFEEDBACK ON INDIVIDUALS FOLLOWING ANTERIOR CRUCIATE LIGAMENT RECONSTRUCTION

*Carly M. Rauch[1], Anthony S. Kulas, PhD, ATC[1], John D. Willson, PhD, PT[2]
[1]Department of Kinesiology, East Carolina University, Greenville, NC, USA
[2]Department of Physical Therapy, East Carolina University, Greenville, NC, USA
*Corresponding author's email: rauchc24@students.ecu.edu

**Introduction:** The anterior cruciate ligament (ACL) is the most frequently injured ligament in the knee, affecting more than 200,000 individuals annually within the United States [1]. Injury to the ACL is detrimental, as it plays a crucial role in the function, support, and stability of the knee joint. Following both an ACL injury and ACL reconstruction (ACLR) surgery, individuals experience altered knee function with differences in joint kinematics, quadriceps and hamstrings muscle strength, proprioception, and neuromuscular control [2]. Real-time biofeedback of movement, posture, or forces during physical activities represents an emerging rehabilitation option to address common post-surgical deficits. However, variability in the real-time biofeedback treatment effects exists in current literature. Thus, the purpose of this study was to determine the effectiveness of real-time biofeedback on knee biomechanical outcomes and ground reaction forces. Specifically, we aim to perform a meta-analysis on current studies evaluating the effects real-time biofeedback on relevant lower extremity biomechanics to draw conclusions on how this emerging technology may affect ACLR rehabilitation outcomes.

**Methods:** A comprehensive search of electronic databases (PubMed, MEDLINE, EMBASE, SCOPUS, Web of Science) in the past 20 years was conducted using relevant keywords related to ACLR and real-time biofeedback. Studies were included if they were randomized controlled trials (RCTs) comparing the impact of real-time biofeedback with no feedback on biomechanical outcomes following ACLR. For outcomes with sufficient data to perform meta-analysis intervention effects were extracted from each study and used to calculate standardized mean differences. Summary (pooled) intervention effect estimates (mean differences (MD) were calculated as weighted averages of the intervention effects estimated from the individual studies using Revman 5 software. This search resulted in four RCTs that met the pre-established criteria. From these four RCTs, the outcomes with the highest frequencies were knee flexion angle (KFA), knee flexion excursion (KFE), peak knee extensor moment (pKEM), and vertical ground reaction forces (vGRF). When looking at the randomized control trials, [4] utilized auditory feedback to elicit changes in the participants' walking cadence, [5] utilized visual and tactile feedback during bilateral squats, [6] utilized visual feedback during the first 50% of stance phase during gait, and [7] elicited changes in pKEM during walking using visual biofeedback.

**Results & Discussion:** Figure 1 shows the results of the meta-analyses for each outcome variable. Overall, only treatment effects associated with biofeedback were greater than control conditions for pKEM (SMD = 0.84 [0.30, 1.37], Z=3.06). KFE showed no significant difference (SMD = -0.36, [-0.74, 0.03], Z=1.82). KFA showed no significant difference (SMD = -0.47 [-1.74, 0.81], Z=0.72). Lastly, there was no significant difference for vGRF (SMD = 0.83 [0.91, 2.57], Z=0.94). Heterogeneity across studies was evident for KFA, vGRF, and pKEM analyses based on Chi-square statistics and $I^2$ ranged from 0.6-0.96 for these variables. The observed differences in the SMD effect sizes suggest that real-time biofeedback had varying impacts across the analyzed parameters.

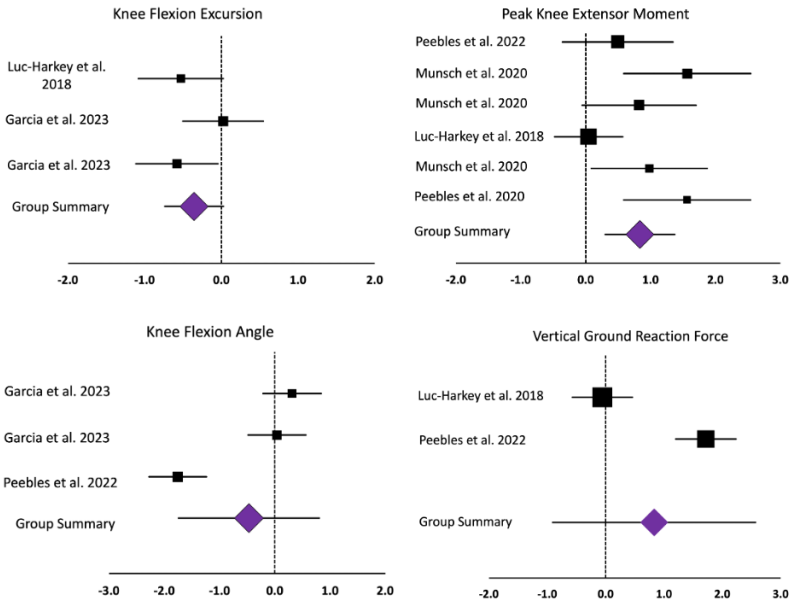


**Figure 1.** Forests plots of knee flexion excursion, peak knee extensor moment, peak knee flexion angle, vertical ground reaction forces with lines representing the 95% confidence interval, squares indicating sample SMD, and diamonds representing the group SMD.

**Significance:** The findings from this systematic review and meta-analysis are beneficial in providing researchers and practitioners with suggestions to what parameters should be primarily focused on and can be altered more influentially through biofeedback in rehabilitation programs following ACLR. These findings aid in developing potential applications of real-time biofeedback in aiding the rehabilitation of individuals following ACLR as well as minimizing the risk of re-injury. From this review, it is important to note that increased pKEM was the most affected by visual biofeedback. Given the persistent quadriceps deficits ACLR patients usually demonstrate, this finding illustrates the unique capabilities of visual biofeedback in the rehabilitation process. However, despite its increased popularity, relatively few studies report biomechanical treatment effects of biofeedback relative to conventional rehabilitation for individuals following ACLR, indicating the need for future research to expand this small evidence base.

**References:** [1] Mushal et al. (2019), *New England Journal of Medicine* 380(24); [2] Lanier et al. (2021), *J Orthop Res.*; [3] Giggins et al. (2013), *J Neuroengineering and Rehabilitation*; [4] Garcia et al. (2023), *Sports Health* 16(3): 420-428; [5] Peebles et al. (2022), *Phys. Ther Sport* 57:78-88; [6] Luc-Harkey et al., *J Biomechanics* 76:94-102; [7] Munsch et al. (2020), *PeerJ*

# COMPARISON OF TIBIAL ACCELERATIONS DURING THE SINGLE LEG HOP TEST IN ACL-RECONSTRUCED, UNINJURED AND CONTROL LIMBS

*Haley B Hartman, Justin J Payette, Corrie Mancinelli, Edward B McDonough, Derik Geist, Jean L McCrory
School of Medicine, West Virginia University, Morgantown, WV
*Corresponding author's email: hbh0003@mix.wvu.edu

**Introduction:** Anterior cruciate ligament (ACL) injuries are among the most common traumatic knee injuries, with over 400,000 ACL reconstructions performed annually in the United States[1]. These injuries predominantly occur in non-contact scenarios, such as cutting or landing, and are prevalent among athletes[2]. ACL reconstruction is associated with post-operative muscle weakness, functional instability, and an increased risk of re-injury to the reconstructed ACL graft or the contralateral ACL[3]. Prior to clearance to play, athletes often complete a return to sport (RTS) test battery that evaluates muscle strength, lower limb function, and psychological readiness[3]. The most commonly used criterion in current RTS assessment for clearance to play is a limb symmetry index (LSI) of >90% in both the strength assessment and distance hopped in the functional hop tests protocol[3]. However, using the distance hopped as the outcome measure may underestimate performance deficits in lower limb function and stability, resulting in a greater risk of re-injury[4]. Linear accelerations are commonly used to assess and quantify human movement[5]. New wearable devices such as the inertial measurement unit (IMU) may provide illustrative data on lower limb "stability" via 3D linear accelerations during landing. The purpose of this study was to evaluate the use of IMU technologies in detecting differences to knee stability in ACL-reconstructed athletes between the ACL reconstructed and uninjured limbs during ACL return to sport assessment and an uninjured control group. A secondary purpose was to examine the relationship between the selected acceleration variables and the distances hopped. We hypothesized that due to compensatory landing strategies post-ACL reconstruction, the ACLR limbs would have higher longitudinal, mediolateral, and shear tibial accelerations than the uninvolved limb during single-leg hop tasks. However, we did not expect to see a difference in these outcome variables between the uninvolved limbs and the controls. By quantifying tibial accelerations, this study aims to address limitations in current RTS criteria and improve the assessment of lower limb stability and function in individuals recovering from ACL reconstruction.

**Methods:** Participants were recruited during their ACL RTS assessment at WVU (16F/14M, ages: 20.5±6.7years, mass: 76.4±15.8 kg, height: 1.74±.08 m, time since surgery: 8.0±2.6 months). Healthy controls were recruited from our campus (7F/9M, ages: 22.6±2.1years, mass: 70.9±11.7kg, height: 1.74±.09m). IMUs were secured to the proximal tibias with tape and coban wrap to collect acceleration data during single-leg single hop tests with two successful trials. Vertical peak acceleration, mediolateral acceleration, and resultant shear acceleration were calculated in MATLAB. ANOVAs were used to compare between limbs (ACLR involved, ACLR uninvolved, and the dominant limb of healthy controls; $p<0.05$). Our dependent variables were vertical acceleration, mediolateral acceleration, shear acceleration, and distance hopped. Tukey post-hoc tests were run if appropriate. Regression analyses were performed on each acceleration variable vs the distance hopped ($p<0.05$).

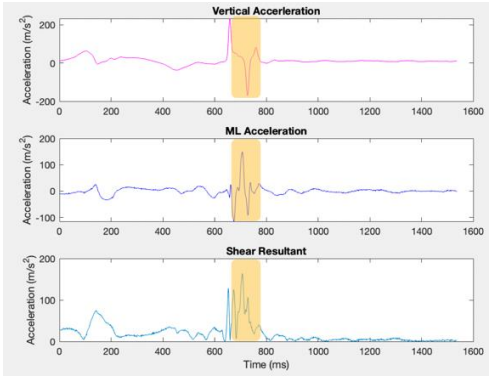


**Figure 1:** Typical acceleration patterns during the single-leg single hop tests when performed by healthy individuals. Top- longitudinal acceleration, middle- mediolateral acceleration, bottom- shear (horizontal plane) acceleration.

**Results & Discussion:** IMUs acceleration data were not significantly different between lower limbs. There were no significant differences in vertical ($p=.818$), mediolateral ($p=.710$). or shear ($p=.649$) accelerations when comparing the involved and uninvolved limbs of ACLR patients, and control limb from healthy individuals. This suggests that these IMU-derived acceleration variables may lack the ability to detect subtle deficits in lower limb stability following ACL reconstruction. However, Controls hopped significantly further than ACLR subjects (156.09±29.4cm), with no differences between injured (128.04±36.0cm) and uninjured limbs (137.62±30.3cm) ($p<.001$). This shows that while acceleration measures did not differentiate between groups, this functional performance test, which is measured by the distance hopped, still reflects bilateral deficits post-ACL reconstruction. There was a positive correlation between distance hopped and all the acceleration measures (vertical $R=0.317$, ML $R=0.314$, shear $R=0.356$, all p-values were $<.001$). This suggests that the distance hopped influences the three acceleration variables more than the deficits present during rehabilitation following ACL reconstruction. These findings highlight the complexity of assessing lower limb function post-ACL reconstruction. While IMUs provide valuable data, alternative measures may be needed to assess lower limb deficits following ACL reconstruction.

**Significance:** Despite undergoing surgery and extensive rehabilitation protocols following ACL reconstruction, the risk of reinjury remains as high as 40%[6]. Clinically accepted outcome measures such as LSI, based on distance hopped, may overestimate rehabilitation status and overlook crucial deficits in lower extremity function and stability. A more comprehensive strategy to evaluate lower limb function following ACL repair is needed. Future research is needed on the use of IMUs to assess lower limb accelerations during other functional assessments to determine if they provide insight into biomechanical stability and functional recovery.

**References:** [1]Murray(2021), OrthopRes 39(9); [2]Kaeding et al.(2017), ClinSportsMed 36(1); [3]Rivera-Brown et al.(2022)PMR 14(5); [4]Unverzagt et al.(2021)Int J SportsPhysTher16(4); [5]Dyer et al.(2024)SciRep [6]Wilk et al.(2023)Int J SportsPhysTher 18(1)

# EFFECTS OF NEGATIVE PRESSURE OF FOUR-CUP CUPPING THERAPY ON HEMODYNAMIC RESPONSES OF THE GASTROCNEMIUS

Mansoureh Samadi a , Liwan Huang a , Pu-Chun Mo a , Manuel Hernandez a,b,
Isabella Yu-Ju Hung c , Yih-Kuen Jan a,
a Department of Health and Kinesiology, University of Illinois at Urbana-Champaign, Urbana, IL, USA
b Department of Biomedical and Translational Sciences, University of Illinois at Urbana-Champaign,
Corresponding author's email: msamadi2@illinois.edu

**Introduction:**
Cupping therapy, a form of alternative medicine, is growing in popularity, yet the scientific understanding of its physiological effects remains limited. Specifically, the impact of multi-cup cupping therapy on muscle oxygenation has not been well explored. Previous research has demonstrated the efficacy of single-cup cupping therapy, but it remains unclear whether similar benefits are observed when multiple cups are used, and whether a lower negative pressure can achieve similar vasodilatory effects to higher pressures. The hypothesis driving this study is that four-cup cupping therapy at −225 mmHg would elicit the same hemodynamic response as −300 mmHg, but with a lower pressure applied over a larger treatment area.

**Methods:**
This study employed a repeated measures design to evaluate the hemodynamic responses to four-cup cupping therapy at three different pressure levels: −75, −225, and −300 mmHg. Twelve healthy adults participated, and muscle oxygenation was measured using near-infrared spectroscopy (NIRS) on the gastrocnemius muscle. The main outcomes included oxyhemoglobin, deoxyhemoglobin, blood volume, and oxygenation levels, measured at several locations on the muscle. Statistical analysis involved two-way ANOVA with repeated measures to assess the interaction between pressure levels and locations of measurement.

**Results & Discussion:**
The results revealed significant effects of both pressure levels and anatomical location on muscle oxygenation. At −300 mmHg, the highest increase in oxyhemoglobin, deoxyhemoglobin, blood volume, and oxygenation was observed. The −225 mmHg pressure produced similar but less pronounced effects, while −75 mmHg showed minimal changes. These findings confirm that a higher negative pressure is more effective at improving muscle oxygenation and facilitating metabolic waste removal. The results also suggest that the effectiveness of cupping therapy is influenced by the pressure applied as well as the location of the cups on the body. The study extends previous research on single-cup cupping therapy and demonstrates the potential of optimizing protocols for musculoskeletal rehabilitation.

**Significance:**
The study provides valuable insight into how multi-cup cupping therapy could be used for musculoskeletal rehabilitation. It suggests that using lower pressures with multiple cups may be as effective as higher pressures, which could make cupping therapy a more practical option for certain applications. By improving muscle oxygenation and reducing metabolic waste, cupping therapy may be beneficial for athletic recovery, pain management, and muscle function enhancement. This research paves the way for refining cupping protocols and potentially increasing their clinical relevance.

**Acknowledgments:**
The authors thank all participants for their involvement in the study. No external funding was received for this research.

**References:**

1. Samadi M., et al. (2025), "Effects of negative pressure of four-cup cupping therapy on hemodynamic responses of the gastrocnemius." *Journal of Bodywork & Movement Therapies*, 42, 446-451.
2. Al-Bedah, A. M., et al. (2019), "The medical perspective of cupping therapy: effects and mechanisms of action." *J. Tradit. Complement. Med.*, 9, 90-97.
3. Wang, X., et al. (2020), "Effect of pressures and durations of cupping therapy on skin blood flow responses." *Front. Bioeng. Biotechnol.*, 8, 608509.
4. Lowe, D.T. (2017), "Cupping therapy: an analysis of the effects of suction on skin and the possible influence on human health." *Compl. Ther. Clin. Pract.*, 29, 162-168.

# A CASE-SERIES DESCRIPTION OF DAILY ARM MOVEMENT AND PATHOLOGY PROGRESSION IN MANUAL WHEELCHAIR USERS WITH SPINAL CORD INJURY

*Hannah Houde[1], Omid Jahanian[2], Kathy Pinnock Branford[3], Meegan VanStraten[2], Stephen Cain[3], Melissa Morrow[1]
The University of Texas Medical Branch at Galveston, Galveston, TX[1]; Mayo Clinic, Rochester, MN[2], West Virginia University, Morgantown, WV[3]
*Corresponding authors' emails: hrhoude@utmb.edu and memorrow@utmb.edu

**Introduction:** Manual wheelchair (MWC) users with spinal cord injury (SCI) face an increased risk of shoulder pathology compared to able-bodied individuals. This increased risk stems from their reliance on upper extremities for mobility and daily activities, leading to overuse and accelerated development of shoulder issues beyond natural aging. Through a longitudinal case series, this research investigates daily arm movement and changes in shoulder pathology among MWC users with SCI over time. The study aims to provide insights into the progression of shoulder pathology.

**Methods:** Under Mayo Clinic IRB approval, participants had bilateral shoulder MRIs at baseline and after a 5 or 8year follow-up period. This case series focuses on the dominant supraspinatus tendon. A musculoskeletal radiologist evaluated and graded the progression or stability of rotator cuff tendon pathology over time. During a free-living environment data collection, eight inertial measurement units (IMU, Axivity-AX6; range: ±16 g, ±2000 deg/s; sampling frequency: 100 Hz) were worn for 7 days. IMUs secured to the arms, trunk, and MWC provided data to quantify periods of activity and rest, as well as mobility (i.e. propulsion) and non-mobility. Daily computations included the cumulative duration of active and resting bouts, along with a novel shoulder exposure score (SES). The SES, inspired by the Rapid Upper Limb Assessment (RULA), is calculated daily using duration, repetition, and arm posture scores during active arm movement periods; a higher SES indicates an elevated risk for shoulder-related injuries. These metrics were determined separately for mobility and non-mobility movements. Cumulative active and resting periods were determined by summating periods across 7 days. Descriptive statistics were used to determine means and standard deviations for SES metrics across the 7 days.

**Results & Discussion:** Data from three cases of individuals with SCI with varying degrees of supraspinatus pathology are presented (Table 1). Case 1, a 30-year-old male with a T4 level of injury, showed development from an unaffected supraspinatus at baseline to mild tendinopathy at the 8-year follow-up, suggesting a stability over time since mild tendinopathy is common in able-bodied 30-year-olds. Case 2, a 30-year-old male with a C7 injury, had a partial low-grade tear to mild tendinopathy at the 5-year mark, which suggests improvement at 5-year follow-up. Case 3, a 51-year-old male with C6-7 injury and mild tendinopathy at baseline progressed to full-thickness tear at the 5-year follow-up, representing the most significant change in pathology among the three cases.

While no minimal clinically important difference is known for the SES, it is noted that Case 2, who did not experience tendon pathology worsening, had a relatively lower mobility SES (~38% lower) than Case 1 or 3 (Table 1). The non-mobility SES scores did not show much variation. The dominant total 7-day active periods vary from 22.8 hours (Case 3) to 27.8 hours (Case 1), while rest periods range from 57 hours (Case 1) to 83.9 hours (Case 3). Case 3, the oldest participant with supraspinatus full-thickness tear, had the lowest cumulative active period and the highest cumulative rest period. Case 2 (C7 SCI) uses a power wheelchair for transportation to work and a MWC while at work, which contributes to lower Mobility SES and higher cumulative rest periods.

**Table 1**. MRI pathology and arm movement metrics from the free-living environment for the dominant arm. **Age** = age at the time of follow-up MRI, **SES**= Shoulder exposure score, **LOI** = Level of spinal cord injury, **F/U**= Follow-up

| **Case (C) #, F/U MRI Age, Sex, LOI** | **Supraspinatus Pathology - Baseline** | **Supraspinatus Pathology – F/U** | **Time between F/U MRI & Sensor Collection** | **Mobility SES** (unitless, mean ± SD) | **Non-mobility SES** (unitless, mean ± SD) | **Cumulative Active Period over 7-days** | **Cumulative Rest Period over 7-days** |
|---|---|---|---|---|---|---|---|
| **C1**, 30y M, T4 | Unaffected | **YEAR 8** Mild tendinopathy | **1 day** | 639 ± 219 | 2683 ± 782 | 27.8hrs | 57.7hrs |
| **C2**, 30y M, C7 | Partial low-grade tear | **YEAR 5** Mild tendinopathy | **1 day** | 380 ± 78 | 2590 ± 643 | 24.9hrs | 69.5hrs |
| **C3**, 49y M, C6-7 | Mild tendinopathy | **YEAR 5** Full-thickness tear | **1 year & 9 days** | 603 ± 325 | 2397 ± 921 | 22.8hrs | 83.9hrs |

**Significance:** The combination of imaging data with IMU measures of arm use provides a more comprehensive picture than either method alone. The longitudinal design captures changes over extended periods (5-8 years), which is particularly valuable for understanding how shoulder pathologies change. Future research should consider adding metrics such as levels of physical activity, weight (BMI), comorbidities, wheelchair specifics (e.g., weight or wheel size), occupation, transportation, or community environment characteristics to provide more context about contributors to rotator cuff pathology changes.

**Acknowledgments**: Funding was provided by NIH/NICHD R01 HD084423-08

**References**: [1] Jahanian, O., et al. (2022), *J Spinal Cord Med 45(4);* [2] Goodwin BM., et al. (2021), *Sensors (Basel) 21(4).*

# PRE-OPERATIVE FUNCTION IS NOT RELATED TO VENTRAL HERNIA WIDTH

*Ajit M.W. Chaudhari[1], Peter Edwards[1], Kiana Shannon[1], Savannah Renshaw[1], Elanna K. Arhos[2], Lai Wei[1], Benjamin Poulose[1], Stephanie Di Stasi[1]
[1]Ohio State University Wexner Medical Center, Columbus OH; [2]Northwestern University, Chicago, IL
*Corresponding author's email: chaudhari.2@osu.edu

**Introduction:** Ventral hernia repairs (VHR) are one of the most common surgeries performed in the United States [1], and patients typically live with the hernia for an extended period of time before making the decision to undergo repair. Since a hernia is defined by a tear or hole in the abdominal wall musculature, functional consequences can be expected that may be associated with hernia severity. However, this relationship remains unknown due to a lack of performance-based objective data on functional measures in this population. Therefore, the purpose of this study was to test our hypothesis that associations would exist between hernia severity, as measured by intra-operative transverse hernia width, and objective functional measures including the five times sit-to-stand (5xSTS), timed-up-and-go (TUG), and quiet unstable sitting test (QUeST).

**Methods:** Participants were involved as part of an ongoing randomized controlled trial (NCT05142618) designed to test the efficacy of post-operative physical therapy (PT). Enrolled participants were between 18-70, diagnosed with a ventral hernia, and scheduled for elective VHR. Participants were excluded if they had a transverse hernia width <2cm, have a movement disorder, use assistive devices, or had current PT. Participants included in this analysis were at the pre-operative timepoint and had not yet received surgery or randomization to PT. The 5xSTS was assessed as the time taken to stand up and sit down from a standard height chair five times. TUG was assessed as the time taken to stand up, walk forward to a mark 3m away, turn around and return to a seated position. The QUeST is an assessment of abdominal core function using postural sway while seated on an unstable surface, eyes closed, with a cognitive dual task, where 0 represents normal and <0 represents lower core stability [2]. Due to non-normal distributions of all variables, Spearman's rank correlation analyses were used to identify univariate associations between hernia width and the three functional measures.

**Results & Discussion:** 111 participants with complete data were included in the analysis (50.1±10.2y, 43F/68M). None of the three functional measures were associated with hernia width (all $p>0.05$, Table 1). As can be seen from Figure 1, each of the functional measures was highly variable, including individuals with function within normal limits as well as individuals with significant disability. Moreover, a large fraction of the participants had relatively small hernias, with 58 (52%) having a hernia width of 4cm or less, and many of these participants had function as poor or worse than those with the largest hernias that would require extensive reconstruction of the abdominal musculature to close the hernia. It is also important to note that no apparent associations between core stability (QUeST) and either TUG or 5xSTS were observed (Figure 1), in spite of the fact that the core musculature is primarily affected by hernia. TUG and 5xSTS were significantly associated with one another ($\rho=0.63$, $p<0.0001$), which suggests that an in-depth examination comparing the biomechanics of 5xSTS and TUG in this population compared to healthy individuals could yield insights into the source(s) of their functional limitations.

**Significance:** The lack of a significant association between transverse width (a surrogate for hernia severity) and function suggests that other factors than size alone, e.g. symptom duration, pain severity, or co-morbid conditions, may play a more dominant role in determining functional outcomes or the decision to seek VHR. More work may be needed to identify a measure that more fully captures the severity of ventral hernia.

**Acknowledgements:** This study is supported by the National Institute of Diabetes, Digestive and Kidney Diseases (R01-DK131207).

**References:** [1] Poulose et al. (2012) *Hernia* 16(2); [2] Chaudhari et. al (2022), *Clin Biomech* 93.

| | Association with Transverse Width (Spearman's ρ, p-value) |
|---|---|
| 5xSTS | ρ=0.12, p=0.19 |
| TUG | ρ=0.13, p=0.16 |
| QUeST | ρ=-0.04, p=0.67 |

Table 1. None of the 3 pre-operative functional measures were associated with transverse hernia width.

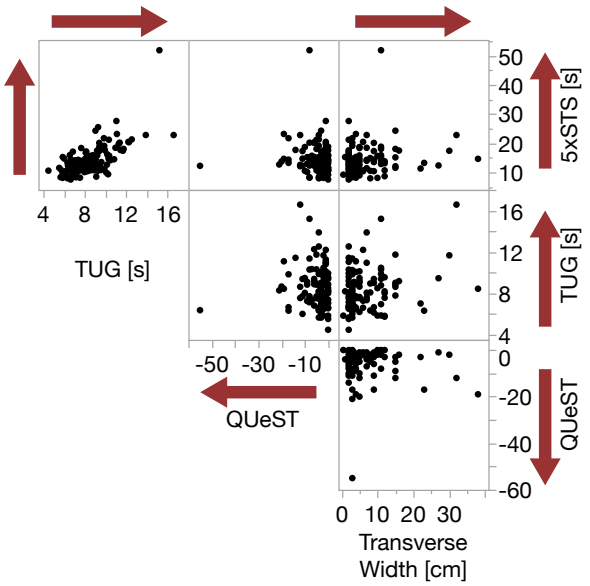


Figure 1. Associations between transverse hernia width, 5xSTS, TUG, and QUeST. Arrows indicate direction of poorer performance or greater hernia severity. Only 5xSTS and TUG were significantly associated with each other (top left).

# VIRTUAL-REALITY TRAINING TO PROMOTE IMPAIRED ARM USE IN FUNCTIONAL ACTIVITIES

Mada Alghamdi[1,2], Hien Nguyen[1,2], Massimo Tschantret[3], Ha Tang Ngo[1,2], and *Sang Wook Lee[1,2]
[1]Catholic University of America
[2]National Rehabilitation Hospital
[3]Pfizer Inc
*Corresponding author's email: leesw@cua.edu

**Introduction:** Learned nonuse is a behavioral phenomenon frequently found among stroke survivors, wherein they avoid using their more-impaired arm and compensate with their less-impaired arm, resulting in diminished motor performance and increased reliance on the healthy arm [1]. During physical and/or occupational therapies that many stroke survivors receive after discharge, compensatory strategies to use their less-affected arm are often encouraged [2], while behavioral modification of learned nonuse is rarely targeted. In a recent study [3], we found that decision-making of arm use is altered following stroke, as their arm choice becomes significantly more sensitive to the effort required, and that the use of more-impaired arm can be encouraged by 'virtually' increasing its range of motion in virtual reality (VR) environment. While previous studies encouraged arm use by virtual amplification of its range-of-motion (ROM) in VR-based games [4], arm use in the context of functional activities, which typically require concurrent use of the hand (e.g., reach and grasp), were not targeted. The objective of this study was to develop and evaluate the efficacy of a novel virtual reality (VR) environment that promotes arm and hand use in functional daily activities via lowering efforts.

**Methods:** Twelve chronic stroke survivors (age = 53.1 ± 14.1 yrs; 5 females), were recruited from MedStar National Rehabilitation Hospital for a 6-week at-home training. The protocol was approved by the MedStar Institutional Review Board (IRB), and the written consent was obtained from all participants. Four mini games were developed using Unity (Unity Software Inc., CA), which are designed to encourage stroke survivors to use their more-impaired arm in functional tasks in a choice paradigm. During these games, movements of more-impaired arm (ROM) and hand (aperture) were amplified to encourage its use. In Game 1 (gift box), participants grasped objects randomly placed on the table and put them in a basket (Fig. 1A). In Game 2 (serving), participants picked up the food requested by virtual characters on their left or right sides and give it to them (Fig. 1B). In Game 3 (eating) participants picked up the food from the food trays on the table and ate (by bringing it to their mouth) as much as they could (Fig. 1C). Finally, in Game 4 (balloon popping), they popped the balloons that rose from random spots on the ground before they flew away (Fig. 1D). Each of the four games lasts for about one minute, and players are required to engage in any of the four games for a minimum of 30 minutes daily as indicated by the timer. The game features a scoring system that tracks both daily scores and personal bests to motivate players to surpass their highest achievements in each game. The ROM amplification gain was initially set to 1.8 and was reduced every other week to increase the training intensity.

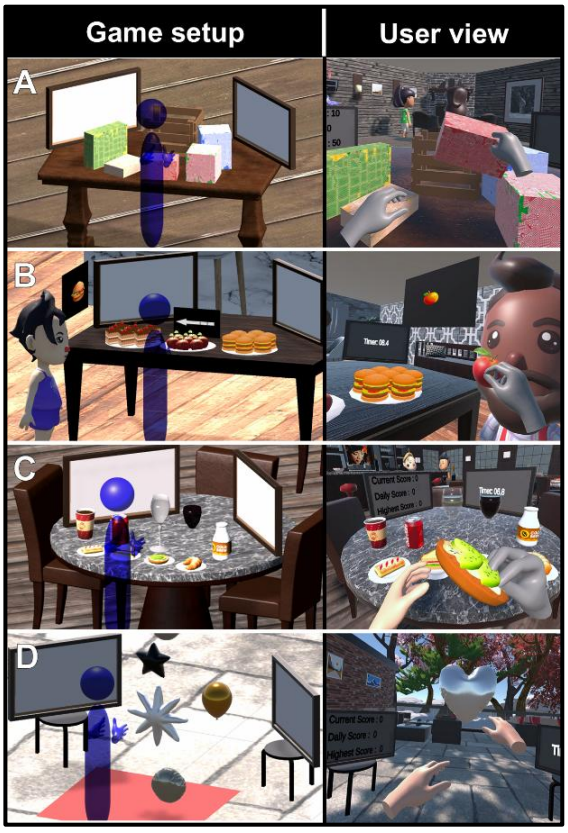


**Figure 1: (A)** Captured screenshots of the Game 1 (gift box). **(B)** Captured screenshots of the Game 2 (serving). **(C)** Captured screenshots of the Game 3 (eating). **(D)** Captured screenshots of the Game 4 (balloon popping).

**Results & Discussion:** Two of the twelve patients have withdrawn during the study due to personal reasons. Based on their actual play time at home, the participants were classified into two groups, 2 compliant (>75% of required play time) and 8 non-compliant subjects. The compliant subjects showed a significantly greater improvements; a 7 point (23.7%) increase in their Fugl-Meyer Assessment (FMA; 29.5 ± 6.4 to 36.5 ± 12.0) and 1.5 point (16.7%) increase in their Action Research Arm Test (ARAT; 9.0 ± 4.2 to 10.5 ± 2.1) were observed in the compliant group, while the noncompliant group showed a smaller degree of increase in FMA (36.0 ± 7.3 to 36.9 ± 7.8) and a decrease in ARAT (17.0 ± 8.4 to 15.5 ± 8.2), which underscores the importance of compliance in home training. The results indicate that the VR training protocol via visual feedback modulation may have encouraged stroke survivors to use their more-impaired arms, which led to the observed improvements. The current game appears to be more effective in improving upper limb motor impairment (FMA) than in restoring its function (ARAT).

**Significance:** The proposed VR-based therapy could reverse learned non-use by increasing engagement, reducing perceived effort, and providing real-time feedback to encourage the use of the more-impaired arm.

**Acknowledgments:** This work was supported by National Institute on Disability, Independent Living, and Rehabilitation Research (90REGE0004; 90REMM0001).

**References:** [1] Taub et al. (2006) Eura Medicophys 42: 241-55; [2] Dobkin (2004), Lancet Neurol 3: 528-36; [3] Nguyen et al. (2023), Neurorehabil Neural Repair 37: 183–193. [4] Ballester et al. (2015), J Neuroeng Rehabil 12: 1–11.

# HANDGRIP STRENGTH PREDICTS SHOULDER FUNCTION BEFORE AND AFTER MASTECTOMY AND BREAST RECONSTRUCTION SURGERY IN BREAST CANCER PATIENTS

*Layla Lynch[1], Susann Wolfram[2], David B. Lipps[1]
[1]School of Kinesiology, University of Michigan, Ann Arbor, MI, USA
[2]Department of Sport, Exercise and Rehabilitation, Northumbria University, Newcastle, UK
*Corresponding author's email: lclynch@umich.edu

**Introduction:** Breast cancer is highly prevalent among women in the United States, with a 5-year survival rate of over 90% [1]. Many breast cancer patients undergo mastectomy to remove the entire breast tissue followed by breast reconstruction to restore the breast mound. Post-mastectomy breast reconstruction improves patient-reported outcomes such as quality of life and psychological health [2,3]. However, a mastectomy surgery can leave patients with greater post-operative shoulder morbidity (e.g., lymphedema, reduced range of motion, and pain) [4], which is amplified by post-mastectomy breast reconstruction [5,6]. Additionally, breast cancer patients, undergoing more complex surgeries face the risk of developing rotator cuff pathology [7]. Post-operative shoulder function can be measured in various ways, from subjective questionnaires to laboratory-based biomechanical assessments. Handgrip strength offers clinicians quick, easy, non-invasive, objective insights into upper extremity health. Handgrip strength is linked to shoulder function in healthy individuals [8] and predicts shoulder function in post-operative rotator cuff tear patients [9]. This is likely due to shared neural pathways coordinating the synergistic activity between forearm flexors and shoulder stabilizers [10]. This study investigated the link between handgrip strength and shoulder function in breast cancer patients undergoing mastectomy with breast reconstruction. We hypothesized handgrip strength would predict shoulder strength before breast cancer surgery but not after surgery.

**Methods:** 26 females diagnosed with a primary breast cancer diagnosis (mean ± SD, age: 50.0 ± 11.1, height: 164.2 cm ± 6.6, weight: 80.5 ± 21.9 kg) enrolled in the study and provided written consent. Testing was performed before their mastectomy and breast reconstruction surgery and ~1 year post-surgery. Handgrip strength was measured using a hand dynamometer (Lafayette Instruments) on the affected arm (if participants had bilateral surgery, the dominant limb was utilized). The maximum value of three attempts was recorded. Isometric shoulder torque was measured by securing the affected limb inside a rigid cast attached to a computer-controlled rotary motor with the affected shoulder placed at 90° abduction, 0° flexion, and 0° humeral rotation. The motor rotation axis was aligned with the center of rotation of the glenohumeral joint, and a six-degree-of-freedom load cell (JR3 Inc., Woodland, CA) was used for shoulder torque calculations. Participants generated maximal shoulder torques in the positive and negative directions of each measurement plane for five seconds. The maximum torque of two attempts was recorded. Univariate regression analysis for the six torque directions examined the relationship between handgrip strength and shoulder torque, both before and after breast cancer treatment.

**Results & Discussion:** Handgrip strength exhibited statistically significant relationships with all shoulder torque directions before surgery (all $p < 0.047$) (Fig. 1). Postoperatively, handgrip strength exhibited statistically significant relationships with most shoulder torque outcomes ($p < 0.021$) (Fig. 1) except abduction or flexion.

Our findings agreed in part with our hypothesis. Pre-operatively, handgrip strength is predictive of shoulder torque and can be used to assess baseline shoulder function; while post-operatively, handgrip strength only predicted shoulder strength for adduction, internal rotation, external rotation, and extension. For these specific torque directions, mastectomy and breast reconstruction surgeries did not influence the shared neural pathway responsible for coordinating synergistic forearm flexor and shoulder stabilizer activity. A limitation of our study is that various breast reconstruction procedures were included, but due to the limited sample size, we did not investigate differences between surgical procedures. Future research should consider whether rehabilitation training after surgery can improve shoulder function for patients with lower grip strength.

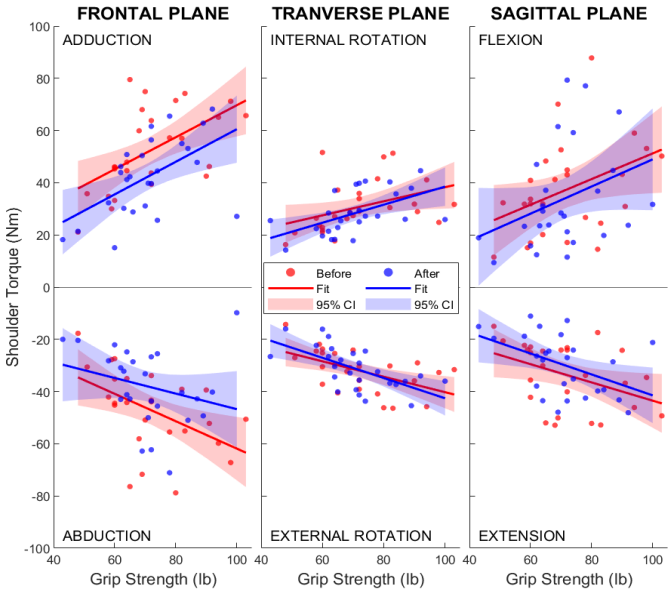


**Figure 1:** Scatter plots of shoulder torque versus handgrip strength, with regression lines and 95% confidence intervals, measured before (red) and after surgery (blue) across three planes of motion in both positive and negative directions.

**Significance:** This study provides new insights into the predictive ability of handgrip strength on pre- and post-operative shoulder function in women undergoing breast cancer surgery. Handgrip strength is an accessible, non-invasive assessment tool that can aid the clinical assessment of shoulder function and recovery, enhancing rehabilitation strategies for women after breast cancer treatment.

**Acknowledgments:** American Cancer Society RSG2001601CCE

**References:** [1] Giaquinto et al. (2024), *CA Cancer J Clin*. 74(6); [2] Panchal et al. (2017), *Plast Reconstr Surg.* 140(5S); [3] Howard-McNatt, M. M. (2013), *Breast Cancer (Dove Med Press)*; [4] Nesvold et al. (2008), *Acta Oncol.* 47(5); [5] Leonardis et al. (2019), *J Orthop Res.* 37(7); [6] Leonardis et al. (2019), *Breast Cancer Res Treat.* 173(2); [7] Lang et al. (2022), *Ann Med.* 54(1); [8] Horsley et al. (2016), *Shoulder Elbow*. 8(2); [9] Liu et al. (2024), *J Orthop Surg Res.* 19(1); [10] AlAnazi et al. (2022), *Biomed Res Int.* (1)

# EVALUATING RANGES OF MOTION OF VR REHABILITATION FOR INDIVIDUALS WITH SCI

*Andrew Hill[1], Rebekah Revadelo, Skyler Barclay, Trent Brown, Allison Kinney, Timothy Reissman, Megan E. Reissman
[1]University of Dayton, Dayton, Ohio, USA
*Corresponding author's email: hilla32@udayton.edu

**Introduction:** Virtual reality (VR) is increasingly being explored as a tool for rehabilitation, providing immersive and engaging environments that encourage movement [1]. Among VR-based rehabilitation approaches, rhythm-based games such as *Beat Saber* require dynamic upper limb movements, making them promising tools for improving motor function in individuals with spinal cord injuries (SCI) [2]. Previous studies have demonstrated that interactive VR exercises can enhance range of motion (ROM) and motor control, but the specific movement patterns and gameplay conditions that yield the greatest ROM improvements remain unclear [2]. Here, we analyze how different movement conditions designed as custom *Beat Saber* levels affect shoulder, elbow, and wrist ROM in individuals with SCI. We hypothesized that Paired movements will result in the highest range of motion (ROM) due to the need for larger, consecutive complementary motions, while Fast movements will produce the lowest ROM as participants prioritize speed over full movement execution.

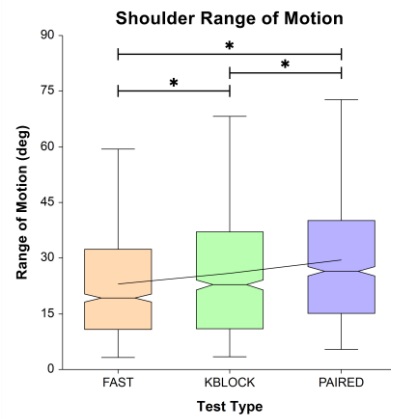


**Figure 1:** This box plot demonstrates the shoulder ROMs from Fast to K-Block to Paired movement criterion. Each with P < 0.0001 in relation one another.

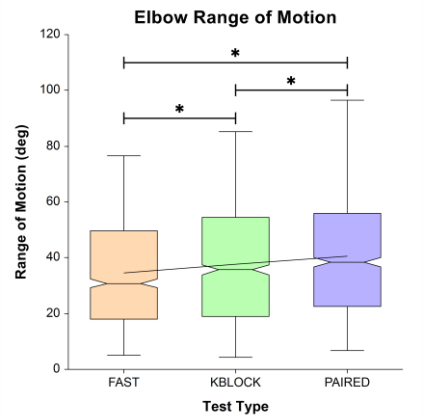


**Figure 2:** This box plot demonstrates the elbow ROMs from Fast to K-Block to Paired movement criterion. Each with P < 0.003 in relation one another.

**Metho**ds: A cohort with a history of spinal cord injury (n=7, 5 males, 30.37±15.86 years, 4 C level injuries, 3 T level injuries, 12.44±8.18 years since injury) engaged in a *Beat Saber* session while their upper limb kinematics were tracked using IR motion capture (10 Vicon Vero cameras). Using both IR motion capture and VR technologies, participants played custom-designed levels in *Beat Saber*, specifically created for this study. Levels were also personalized based on a prior day's testing to include the 30 movement tasks that resulted in the highest net kinematic range for that individual, reduced from 90 possible tasks. For this subset, three versions were tested. Fast, emphasizes quick instinctual movements; K-Block uses each participant's optimal movements from an initial baseline session; and Paired, which compounds two contrasting movements, such as an upward cut following a downward cut. These levels incorporated different movement patterns, including mirrored, opposing, and unilateral motions. ROM measurements for the shoulder (abduction/adduction), elbow (flexion/extension), and wrist (sagittal and frontal plane movements) were recorded for each movement task. Repeated measures ANOVA was performed (NCSS v.2024) on each joint with a factor of trial type and Tukey-Kramer pairwise comparisons with significance set to $P < 0.05$.

**Results & Discussion:** Significant differences due to trial type were observed in the shoulder, and elbow ROM. When significant differences occurred, the same trend occurred with Fast having the lowest ROM, then K-Block, and Paired having the highest ROM. For the shoulder vertical abduction/adduction mean angles were 23.4°, 26.1°, and 29.7° respectively with significant differences between each pairing (Fig. 1). For the elbow flexion/extension ROM mean angles were 35.6°, 38.8°, and 41.4° respectively, again with significant differences between each pairing (Fig 2). Overall, the shoulder and elbow ROM results agree with our hypothesis. The K-Block movements were designed to be the best movements for a given player personalized based on a prior day's testing. The Paired movements result in larger motions compared to K-Block likely since there are two consecutive complimentary motions which require a larger movement pattern to accomplish and engage sweeping behaviors. In the Fast trial, participants reduced their larger joints (shoulder and elbow ROM) as expected but did not increase their Wrist ROM as hypothesized. This suggests that they found alternate kinematic methods to accomplish the tasks which were not reflected in the ROM metrics.

**Significance:** Our study showed that the style of task presentation is able to further exaggerate kinematic behaviours in an SCI cohort even when the movement tasks included reflect tasks that previously elicited maximum ROM for the individual. Suggesting that personalized designs can be effective in enhancing kinematic expression. Also, understanding how VR-based rehabilitation protocols can help individuals with SCI has the potential to make therapy more engaging and effective. The results of this study show that Paired movements may be effective in rehabilitation focused on expanding the ROM for individuals with SCI. While the Fast trial type tended to reduce ROM movements this style may be appropriate if rehabilitation goals were performance training or fine-tuned motions. *Beat Saber* particularly may serve as a customizable and motivational tool for encouraging targeted and controlled limb movement patterns that enhance functional recovery.

**Acknowledgments:** We acknowledge the funding support that was granted by the Chancellor of the Ohio Department of Higher Education from the Research Incentive Third Frontier Fund.

**References:** [1] Barclay et al. (2024), J *Sensors*, 24 (1) [2] Montoya et al. (2022), *J Sensors*, 22 (7)

# EFFECTS OF HEIGHT ON WEIGHT BEARING LUNGE TEST EVALUATION

*Harsh Buddhadev[1], Kierra M. Anstee[1], Emme T. Loman[1]
[1]Department of Kinesiology, Sam Houston State University, Huntsville, TX
email: * hhb005@shsu.edu

**Introduction:** Plantar flexor (PF) flexibility is crucial for daily activities and athletic performance and is often assessed using the weight-bearing lunge test (WBLT). This test measures distance from the big toe to the wall to indirectly assess dorsiflexion (DF) range of motion at the ankle joint. The cut-off values for adequate PF flexibility are 9 cm on the WBLT [1] and 35° DF angle at the ankle joint [1]. Restricted DF range has been linked to altered gait mechanics and reduced sports performance [2, 3]. While the WBLT is commonly used in both athletic and clinical settings, its traditional distance-based measurement for evaluation [1] presents a potential bias due to variations in individual height. This method could disproportionately favor taller individuals, as they may achieve a greater distance to the wall with a lesser DF angle compared to shorter individuals. This effect of height on WBLT could lead to misclassification of PF flexibility, potentially impacting injury risk assessment, rehabilitation protocols, and return-to-play decisions. The purpose of the study was to examine the difference in WBLT performance between taller and shorter adults as they performed the WBLT test to maximum, criterion distance of 9 cm, and criterion angle of 35° DF. We hypothesize that 1) taller adults would achieve the 9 cm criterion WBLT distance with lesser DF angle than shorter adults, 2) to achieve the criterion 35° DF during WBLT, taller adults would have greater distance to the wall than shorter adults, and 3) for maximum WBLT, there will be no difference in DF angle between the taller and shorter adults, however, the distance to wall will be greater for tall compared to short adults.

**Methods:** Thirty-one adults participated, and they were assigned to tall (*n*=18, 8 females, 10 males, 21±2 yrs, 1.80±0.08 m, 200±57 lbs) and short groups (*n*=13, 8 females, 5 males, 20±2 yrs, 1.55±0.09 m, 137±32 lbs) based on their height. In a single session, participants completed 3 trials of the 3 test conditions in a random order. Tests conditions were 1) WBLT performed to criterion of 9 cm distance where DF angle was measured, 2) WBLT performed to criterion 35° DF angle while the distance was measured, and 3) maximum WBLT where distance and DF angle were measured. To perform WBLT, participants stood with their feet in a tandem position with their dominant leg forward and hands placed on the wall in front of them. Then they performed a forward lunge with their dominant leg (as the shank dorsiflexed at the ankle joint) attempting to touch the wall with their knee while maintaining heel contact with the ground. The maximum distance between the big toe and the wall where a participant could touch their knee to the wall while maintaining heel ground contact was determined and measured using a soft tape measure. While the participants maintained this forward lunge position, DF angle was measured by placing the gold standard Lafayette Instruments' Range of Motion Inclinometer [4] on the midpoint of the shin of the participant's dominant leg. Ankle DF angle was measured as the extent of forward rotation of the shin that occurred during the forward lunge with respect to the vertical shin position in standing. Prior to the analysis, the data were averaged across trials for each condition. Independent samples t-test were used to determine group differences across the test conditions.

**Results & Discussion:** The data supported our hypotheses that WBLT performance disproportionately favours taller adults. Taller adults were able to achieve the criterion distance of 9 cm on WBLT with lesser DF angle compared to shorter adults (Table 1). Also, when asked to perform WBLT to the criterion 35° DF angle, taller adults produced that angle with much greater distance to wall than the shorter group. For the maximum WBLT, there was no significant difference between the groups for the ankle DF angle. However, distance to wall for the maximum WBLT was greater for taller compared to shorter adults. An interesting finding was that although taller adults had lesser ankle DF angle compared to shorter adults for the 9 cm criterion WBLT distance, their mean angle (37.8°) was still slightly greater than the cut-off value for adequate ankle DF of 35°. On the other hand, the mean DF angle for shorter adults (41.6°) was substantially larger than the cut-off value of 35° for the 9 cm criterion WBLT distance. Using the cut-off value of 9 cm distance on WBLT to make decision about adequate PF flexibility, may be appropriate for taller but not for shorter adults. Shorter adults may have adequate PF flexibility with 35° of weight bearing ankle DF but they may fail to achieve the cut-off value of 9 cm on the WBLT.

**Table 1.** Demographics and WBLT performance differences between groups

| | Tall (*n*=18) | Short (*n*=13) | *p* value |
|---|---|---|---|
| Height (m)* | 1.80 ± 0.08 | 1.55 ± 0.09 | <0.001 |
| Dorsiflexion (DF) angle (°) for criterion 9 cm WBL* | 37.8 ± 2.3 | 41.6 ± 3.3 | <0.001 |
| Distance to wall (cm) for criterion 35° DF* | 7.0 ± 1.1 | 4.6 ± 1.2 | <0.001 |
| Distance to wall (cm) * for max WBLT | 11.6 ± 2.9 | 9.2 ± 2.6 | 0.011 |
| DF angle (°) for max WBLT | 42.2 ± 5.4 | 43.9 ± 5.6 | 0.194 |

Data are mean ± 1 standard deviation. * Statistically significant (p<0.05)

**Significance:** The data from our study show that evaluation of PF flexibility based on the 9 cm cut-off distance for the WBLT is susceptible to errors based on the individual's height. Clinicians and researchers who use the WBLT could avoid errors in PF flexibility assessment by using 35° DF angle cut-off value over the criterion value of 9 cm distance to wall for evaluation purposes.

**Acknowledgments:** This study was funded by the College of Health Sciences BRIDGE program at Sam Houston State University.

**References:** [1] Clanton et al. (2012), *Sports Phys Ther* 4 (6). [2] Rao et al. (2024), *Front Neurol* 14 (1269061); [3] Yun & Kim (2016), *J Phys Ther Sc*i 28(8); [4] Konor et al. (2012), *Int J Sports Phys Ther* 7(3).

# EFFECTIVENESS OF BICYCLE, MOTORCYCLE, AND SKATEBOARD HELMETS IN REDUCING RISK OF CONCUSSION AND SKULL FRACTURE ACROSS VARIOUS IMPACT LOCATIONS AND VELOCITIES

*Bruce Miller[1], Shady Elmasry[1],Sarah Sharpe[1], Leigh Allin[1], Zdravko Salipur[2]
[1]Exponent, Inc., [2]Brillouin Consulting
*Corresponding author's email: Bmiller@exponent.com

**Introduction:** Head injury is among the most serious injuries sustained during recreational activities including cycling, motorcycling, and skateboarding [1-5]. Helmet use is associated with a significant reduction in head and brain trauma. While standards have been developed to ensure a baseline protective performance in commercially available helmets, individual helmets often exceed the performance requirements. The objective of this study was to quantify head kinematics and evaluate the risk of concussion and skull fracture for typical helmets used in bicycling, motorcycling, and skateboarding when subjected to realistic fall heights at various orientations onto an asphalt surface.

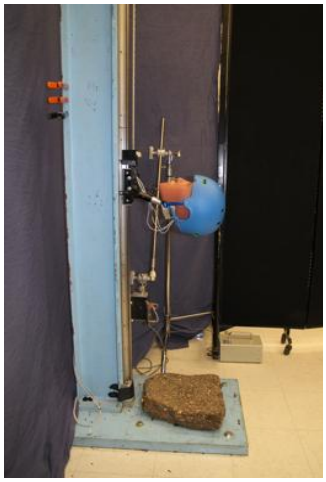

**Figure 1:** Skateboard helmet drop test on asphalt.

**Methods:** A Hybrid III 50th-percentile headform was mounted to a support assembly and attached to a monorail drop test system (Fig. 1). Drop tests onto asphalt were conducted for four types of helmets: (1) CPSC certified bicycle helmets, (2) DOT certified motorcycle full-face helmets, (3) DOT certified motorcycle half helmets, and (4) CPSC certified skateboard helmets. Impact locations included parietal, lateral, posterolateral, occipital, and vertex. Drop heights were 4 or 6 feet. A new helmet was used for each test trial. Head linear acceleration was measured using a triaxial accelerometer and the impact velocity was measured 40 mm or less from the asphalt impact surface using a laser line break speed trap. Head acceleration data were processed per SAE J211 standards [6]. Head Injury Criteria ($HIC_{15}$) was computed using head linear acceleration. Injury risks for concussion and skull fracture were calculated based on published risk curves [7-8].

**Results & Discussion:** Impact speeds ranged from 9.5 to 13.1 mph, peak linear accelerations were measured between 86.9 and 169.5 g, and $HIC_{15}$ were calculated between 297 and 1015 (Table 1). The risk of concussion was between 0.5% and 24% across all helmets. For bicycle, full-face motorcycle, and skateboard helmets, the greatest calculated risks of concussion (24%, 24%, and 19%, respectively) were produced by lateral impacts; for motorcycle half helmets, the greatest risk of concussion (7%) was produced by a frontal impact (Fig. 2). The risk of skull fracture was less than 3% across all helmets. All tested helmets substantially outperformed acceleration requirements for the relevant standards for their intended usage based on a drop from a similar height. This performance was observed in orientations across the helmet surface. Additionally, the recorded head accelerations were associated with a low-risk of concussion and skull fracture with impact velocities up to and exceeding free-fall drops from a standing height (or seated height on a motorcycle or bicycle).

**Table 1**: Drop tests impact locations, impact speed, headform peak linear acceleration, and $HIC_{15}$

| Helmet Type | Impact Location | Impact Speed (mph) | Peak Linear Acceleration | $HIC_{15}$ |
|---|---|---|---|---|
| Bicycle | Parietal | 10.1 | 105.2 | 427 |
| Bicycle | Parietal | 12.9 | 167.8 | 966 |
| Bicycle | Lateral | 10.6 | 169.4 | 568 |
| Bicycle | Lateral | 10.6 | 112.2 | 432 |
| Bicycle | Lateral | 12.9 | 160.7 | 811 |
| Bicycle | Posterolateral | 10.6 | 89.1 | 331 |
| Bicycle | Posterolateral | 13.0 | 114.3 | 628 |
| Motorcycle Full-Face | Frontal | 12.8 | 91.0 | 638 |
| Motorcycle Full-Face | Lateral | 13.1 | 169.5 | 775 |
| Motorcycle Full-Face | Parietal | 12.8 | 145.3 | 971 |
| Motorcycle Full-Face | Occipital | 11.7 | 108.4 | 512 |
| Motorcycle Full-Face | Vertex | 9.7 | 123.2 | 539 |
| Motorcycle Full-Face | Vertex | 11.8 | 144.1 | 760 |
| Motorcycle Half | Vertex | 11.8 | 126.9 | 704 |
| Motorcycle Half | Vertex | 9.6 | 86.9 | 297 |
| Motorcycle Half | Frontal | 12.9 | 141.2 | 841 |
| Motorcycle Half | Frontal | 12.8 | 126.8 | 740 |
| Motorcycle Half | Lateral | 13.1 | 118.6 | 565 |
| Motorcycle Half | Parietal | 13.0 | 133.9 | 746 |
| Motorcycle Half | Occipital | 12.9 | 111.7 | 576 |
| Skateboard | Frontal | 10.4 | 118.8 | 468 |
| Skateboard | Frontal | 12.8 | 160.4 | 828 |
| Skateboard | Lateral | 13.1 | 164.0 | 859 |
| Skateboard | Parietal | 12.9 | 159.7 | 1015 |
| Skateboard | Occipital | 9.5 | 128.7 | 539 |
| Skateboard | Occipital | 11.6 | 137.7 | 615 |

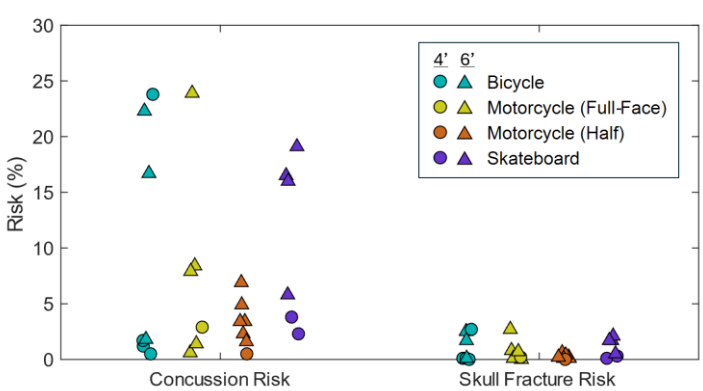


**Figure 2**: Risk of concussion and skull fracture for all tested helmets at 4-foot (circles) and 6-foot (triagles) drop heights

**Significance:** The findings of this study further corroborate and contribute to the collective scientific literature and data demonstrating the efficacy of helmets in reducing head injury risk when properly used, and encourage continued and increased awareness in promoting helmet usage in cycling, motorcycling, and recreational activities.

**References:** [1] Eilert-Petersson et al. (1997), *Accid Anal Prev* 29(3); [2] Persaud et al. (2012) *CMAJ* 184(17); [3] Lin et al. (2009) *Accid Anal Prev* 41(4); [4] Lustenberger et al. (2010) *J Trauma* 69(4); [5] Tominga et al. (2015) *Brain Inj* 29(9); [6] SAE J211-1 (2014); [7] Rowson et al. (2011) *Ann Biomed Eng* 39(8); [8] Mertz et al. (2016) *Stapp Car Crash J* 60.

# DEVELOPMENT OF A METHOD TO SIMULATE SPORTS-RELATED IMPACTS KNOWN TO CAUSE COMMOTIO CORDIS FOR THE EVALUATION OF FOOTBALL CHEST PROTECTIVE EQUIPMENT

*Bianca J. Henline[1], Anthony P. Marino[1], Erin Meinecke[1], Zachary Dolan[1], Gregory Batt*[1], John D. DesJardins*[1]
[1]Clemson University, Clemson, SC
*Corresponding author's email: gbatt@clemson.edu

**Introduction:** Commotio cordis (CC) refers to ventricular fibrillation induced by a blunt, non-penetrating impact to the chest in the absence of structural damage to the heart or surrounding tissues [1]. The US Commotio Cordis Registry in Minneapolis confirmed only 200 instances worldwide [2]. Although CC incidents are infrequent, their severity should not be disregarded. Unfortunately, the most common outcome of CC is sudden death, with young athletes being most at risk due to their chest wall compliance [1]. Non-sports related activities such as automotive accidents, child horseplay, or violent attacks have been associated with CC, however 75% of CC cases have occurred during sports related impacts [3]. Athletes participating in sports involving hard projectiles, such as lacrosse, baseball, and ice hockey, are at higher risk for experiencing a CC event. However, it would be remiss to suggest that sports not involving projectiles are without risk. Researchers have shown that 3% of high school and collegiate football fatalities are attributed to CC [3]. Currently, there is only one method used to evaluate the performance of sports chest protective equipment. The National Operating Committee on Standards for Athletic Equipment (NOCSAE) introduced the ND200 standard that uses an instrumented thoracic surrogate to certify baseball and lacrosse chest protectors based on peak force values across the cardiac silhouette [4]. In this study, researchers developed a novel method using a pneumatic linear impactor and a thoracic surrogate equipped with advanced technology to simulate football impacts known to cause CC. This method was then employed to quantify the effect of these impacts on various combinations of two types of football shoulder pads and two different padded undershirts. Injury metrics relating to CC, including impactor forces, rib deflections, and viscous criterion (VC) values, were used to assess the chest protectors' effectiveness in reducing CC risk. Due to inconsistencies in implementation and the exclusion of relevant injury metrics of the ND200 standard, we hypothesize that football chest protectors to not be effective in preventing CC.

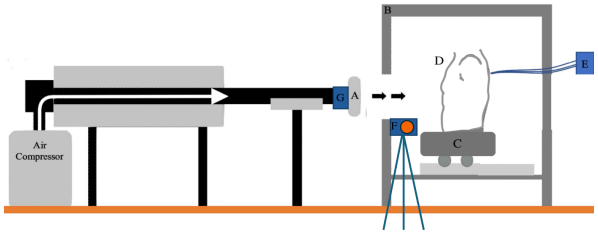


**Figure 1:** Cadex pneumatic linear impactor experimental setup with A) impactor arm, B) protector cage C) cliding table, D) thoracic surrogate, E) RibEye system, F) high-speed camera, and G) accelerometer.

**Methods:** In this study, a Cadex pneumatic linear impactor was used along with a Hybrid III Upper Torso Assembly (Humanetics, Farmington Hills, MI) (Fig. 1) to evaluate the impact performance of seven different protector combinations consisting of two types of football shoulder pads, two different padded undershirts, and bare chest impact conditions. The impacting speeds of 5.5 m/s and 7.4 m/s were chosen based on published literature on football impacts [5]. Additionally, the two impact locations were identified from literature on vulnerable locations for CC [2]. Four testing sequences were developed from the two impact velocities and the two chest impact locations, with each protector combination subjected to four impacts per testing sequence. A total of 112 impacts were conducted during this investigation. An Olympus i-SPEED 3 high-speed camera captured each impact, and video analysis using Tracker software was used to determine the magnitude and rate of external chest displacement to calculate VC values.

**Results & Discussion:** The maximum VC values calculated from the high-speed video analysis are shown in Fig. 2. A maximum VC value of 1.2 has been associated with a 25% risk of CC [6]. For the 7.4 m/s impacts, all protector combinations exceeded this threshold. In contrast, regarding the 5.5 m/s impacts, only the bare chest condition exceeded this threshold. No statistical significance was observed between the two impact locations. Since the 7.4 m/s impacts represent the average speed of a football tackle [5], the results suggest that these football chest protectors fail to provide sufficient protection against CC events.

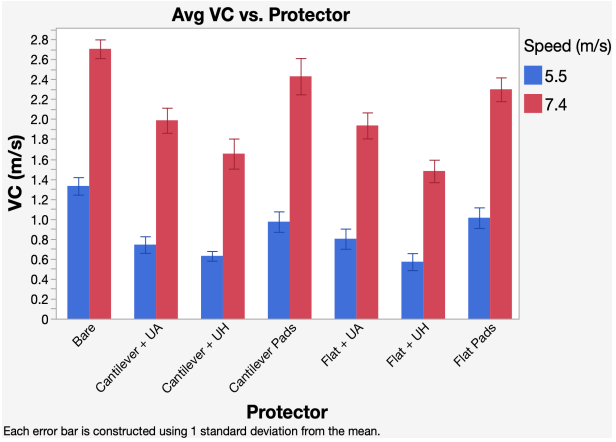


**Figure 2:** Average maximum VC values for each protector combination at 5.5 m/s and 7.4 m/s impact velocities.

**Significance:** Ultimately, this study emphasizes the need for an effective method to evaluate chest protective equipment in reducing CC incidence among football athletes. These results suggest that modifying football chest protective gear is pivotal in reducing CC occurrence in football athletes.

**Acknowledgments:** Thanks to the Clemson College of Engineering, Computing, and Applied Science, the Clemson College of Food, Nutrition, and Packaging Science, and the Robert H. Brooks Spors Science Institute for funding. Thanks to the United States Army Aeromedical Research Laboratory for equipment support.

**References:** [1] Tainter et al. (2023), *Commotio Cordis*; [2] Dickey et al. (2013), *J Biomech* 144(5); [3] Menezes et al. (2017), *Med, Sci, Law* 146-151; [4] NOCSAE. (2022); [5] Viano et. al. (2011), *J Ann. Biomed. Eng. 40(1); [6] Bir (2000).*

# STRIDE LEG GROUND REACTION FORCE IMPULSE AND ITS EFFECT ON STRIDE HIP POWER IMPULSE IN BASEBALL PITCHERS

*Brandon Doehne[1], Takato Ogasawara[1], Adam B. Rosen[2], Sam Wilkins[2], Brian A. Knarr[1]
[1]Department of Biomechanics, University of Nebraska at Omaha, Omaha, Nebraska, USA
[2]School of Health and Kinesiology, University of Nebraska at Omaha, Omaha, Nebraska, USA
*Corresponding author's email: bdoehne@unomaha.edu

**Introduction:** Previous literature has investigated the purpose of stride leg ground reaction force (GRF) impulse within the pitching delivery [1], and its role in energy flow [2] and ball velocity [3]. Additionally, previous research has investigated how power is absorbed and then generated by the stride hip, which can be used to predict ball velocity [3]. Another study has speculated that stride leg GRF impulse is considered a more informative variable than stride leg peak force due to its inclusion of the force-time relationship [2]. The purpose of this study was to investigate the effects of the stride leg GRF impulse on the power by the stride hip during the pitching delivery. We hypothesize that pitchers with greater stride leg anterior/posterior (AP) and vertical impulses will also have greater total and positive power impulse values. We also hypothesize that an increase in a pitcher's total and positive power impulses will also have greater ball velocities.

**Methods:** Thirty-nine baseball pitchers aged 15 to 24 were extracted from the UNO Pitching Lab Database registry. Each pitcher followed their habitual warmup before pitching 15 to 20 maximal intent pitches from a mound. The three fastest pitches of each pitcher were used for analysis. The pitcher's mechanics were captured by 21 high-speed cameras (320 Hz) with 41 reflective markers. The pitching mound captured each pitcher's GRFs (1280 Hz). Stride foot contact event was created using a uniform force threshold and then modified by up to two frames to ensure the alignment of the center of pressure of the footstrike. The stride leg impulse was calculated as the integral of GRF produced from stride foot contact to ball release for AP and vertical components. Power was found using a joint torque power analysis (JTP), calculated by dot products of the proximal and distal joint angular velocities and joint torques. Total power is the summation of the power absorbed and generated while a negative JTP represented power that was being absorbed and a positive JTP represented power being generated. The impulse of the JTP was found to indicate the total, generated, and absorbed from stride foot contact to ball release. Spearman rank correlation coefficients ($p<0.05$) were calculated to assess the relationship between stride leg impulse components and JTP impulse at the stride hip.

**Results & Discussion:** Our analysis (Table 1) found that pitchers with a greater stride leg vertical impulse have greater power generation at the stride hip. Initially, the stride hip absorbs power as the stride leg lands with up to three times the pitcher's mass in force GRF force, then the stride hip generates force to reduce linear momentum of the pitcher's center of mass. Power that is being generated has been defined as a concentric movement of supporting musculature while power being absorbed has been defined as an eccentric movement [5]. We speculate that the increase in stride leg vertical impulse creates more force and energy that is redirected into the stride leg due to the equal and opposite normal force the ground imposes on the stride leg. The additional force and energy are then transferred up the kinetic chain to the stride hip creating a greater supply for power to be countered and generated. We also found there are weak correlations between ball velocity and total power impulse, and ball velocity and power generation impulse at the stride hip. A previous study indicated that segmental power increases as it moves up the kinetic chain due to larger supporting muscles, at the superior joints, which generate greater power rather than a summation of energy between joints [4]. Following this approach, we speculate that the increase in power, both total and generated, at the stride hip reduces the linear momentum of the pitcher's center of mass, allowing the torso to rotate on a stabilized base of support to create more power [4], resulting in greater ball velocities.

**Table 1.** Correlations among impulse, ball velocity, and joint torque power variables.

| Correlation | Rho - value | p - value |
|---|---|---|
| AP Impulse and JTP Absorption Impulse | -0.1535 | 0.3772 |
| AP Impulse and JTP Generation Impulse | -0.1527 | 0.3656 |
| AP Impulse and JTP Total Impulse | -0.1918 | 0.2544 |
| Ball Velocity and JTP Absorption Impulse | 0.3067 | 0.0688 |
| Ball Velocity and JTP Generation Impulse * | 0.3413 | 0.0360 |
| Ball Velocity and JTP Total Impulse * | 0.3898 | 0.0156 |
| Vertical Impulse and JTP Absorption Impulse | -0.0080 | 0.9636 |
| Vertical Impulse and JTP Generation Impulse ** | 0.4271 | 0.0080 |
| Vertical Impulse and JTP Total Impulse | 0.2522 | 0.1264 |

Table 1 denotes a significant weak and moderate correlation with a (*) and (**) respectfully.

**Significance:** These results are significant because it reinforces the relationship between stride hip power and ball velocity, which has previously been found [3], as well as signifying the importance of vertical GRF impulse as a contributing factor to greater stride hip power generation impulse. Vertical GRF impulse should be a metric of importance when coaching a pitcher through stride leg mechanics in order to reduce the pitcher's linear momentum, resulting in the torso to generate more power to create greater ball velocities. Future research should investigate stride leg ground interactions to see if there is an optimal stride leg landing position or mechanism that produces more power in the stride leg.

**References:** [1] Liu et al. (2022), Sports Biomech. 1-16, [2] Howenstein et al. (2020), Journal of Biomechanics, 108, July. [3] Aguinaldo & Nicholson. (2021), ISBS 39, [4] Pryhoda & Sabick. (2022), Front Sports Act Living. 2022 Sep 21. [5] Robertson & Winter. (1980), Journal of Biomechanics, 13(10), 845-854.

# THE IMPACT OF TRUNK, HUMERAL, AND WRIST VELOCITIES DURING THROWING ON MEDIOLATERAL TRANSLATION OF THE NON-THROWING SHOULDER

Diego Ferreira, Jeff Barfield*
Lander University, Greenwood, SC
*Corresponding author's email: jbarfield@lander.edu

**Introduction:** Overhand throwing is a complex motion that combines linear movement with high angular velocities. Researchers have attributed the idea of efficient throwing motion to proper segmental sequencing and energy flow occurring within the kinetic chain. [1,2,3] Murata demonstrated a relationship between minimal motion of the non-throwing shoulder with improved ball velocity and attributed minimal motion of the non-throwing shoulder to a higher skilled group of baseball pitchers.[4] Further studies on glove arm kinematics have concluded the need for an active glove-arm in both baseball and softball pitchers.[5,6] Minimizing non-throwing shoulder motion may enhance trunk rotation and throwing efficiency, but the specific relationship between the non-throwing shoulder, trunk, and throwing arm mechanics has not been fully explored.

Therefore, the purpose of this study was to investigate the impact of peak trunk and humeral internal rotational velocities, and peak wrist linear velocity occurring during the throwing motion on non-throwing shoulder translation in the mediolateral direction. We hypothesized that increased trunk rotational and humeral internal rotational velocities would have an inverse relationship with mediolateral translation of the non-throwing shoulder whereas wrist linear velocity would show minimal correlation.

**Methods:** Ten collegiate softball players (20.73±1.79 years; 1.69±0.04 m; 74.15±7.68 kg) performed five trials of the overhand throw. Kinematic data were collected at 240 Hz using an electromagnetic tracking system. Peak trunk rotational velocity, throwing arm humeral internal rotation velocity, and linear wrist velocity occurring during the throwing motion were calculated using the MotionMonitor software (Innovative Sports Training). Non-throwing shoulder mediolateral translation was calculated over the whole throwing motion in reference to the world axis. Correlation analyses were conducted between the mediolateral translation variable and (1) peak trunk rotation velocity, (2) peak humeral internal rotation velocity, and (3) linear wrist velocity. Additionally, a within-subject regression analyses with mediolateral translation set as the dependent variable was used to test the hypothesis. Only the middle three trials were analysed to account for the Hawthorne effect.

**Results & Discussion:** The results from this study indicate that there is a moderate near statistical correlation between the shoulder medial/lateral translation (1) peak trunk rotational velocity and (2) peak wrist velocity, and a weak correlation with peak humeral internal rotation (Table 1). The regression model examining mediolateral translation as the dependent variable demonstrated no significant effect of velocities as a predictor ($F(5) = 1.15$, $p = 0.369$).

**Table 1**: Means and standard deviation of kinematic variables and statistical results.

| Variable | Mean (SD) | Statistical Results |
|---|---|---|
| Shoulder Mediolateral Translation (m) | 0.3554 (0.0486) | |
| Peak Trunk Rotational Velocity (°/s) | 339.03 (179.24) | r= -0.579, p= 0.0794 |
| Peak Humeral Internal Rotation Velocity (°/s) | 4752.74 (828.36) | r= -0.263, p= 0.4622 |
| Peak Linear Wrist Velocity (m/s) | 12.8 (0.99) | r= -0.628, p= 0.0517 |

*Note: Peak velocity for the trunk, humerus, and wrist were obtained from the foot contact to the ball release time frame. For statistical analysis, the correlation values are measured in comparison with the shoulder mediolateral translation variable. Significance level was set at $\alpha = 0.05$.*

The preliminary results of this study indicate that shoulder mediolateral translation of the non-throwing arm during overhand throwing may have a moderate relationship with peak trunk rotational and linear wrist velocity among a group of college softball players, though the effects did not reach statistical significance. Increased mediolateral translation during an overhand throw may be associated with reduced wrist velocity at release, however a larger sample size is needed to detect subtle effects. Future studies should consider the complex relationship between the non-throwing shoulder, trunk, and humeral kinematics and the resulting effect on loading placed on the throwing shoulder, elbow, or lower extremities.

**Significance:** These findings suggest increased non-throwing shoulder mediolateral translation during the overhand throw may be associated with reduced peak trunk rotational and linear wrist velocity, potentially impacting performance. However, weak correlation with humeral internal rotation velocity and the non-significant regression model indicate mediolateral translation of the non-throwing shoulder alone is not a strong indicator of velocity-based mechanics. These results highlight the need for further research on the interaction between non-throwing shoulder stability, trunk rotation, and wrist velocity to optimize performance and reduce injury risk.

**Acknowledgments:** No financial support was received for this project.

**References:** [1] Manzi et al. (2024). *The American Journal of Sports Medicine*, *52*(11); [2] Manzi et al. (2021). *The American Journal of Sports Medicine*, *49*(12); [3] Owens et al. (2024). *Orthopaedic Journal of Sports Medicine*, *12*(11); [4] Murata, A. (2001). *Journal of biomechanics*, *34*(12); [5] Barfield et al. (2018). *Orthopaedic Journal of Sports Medicine*, *6*(7); [6] Barfield et al. (2019). *International Journal of Sports Medicine*, *40*(03).

**EFFECTS OF SEX-DIFFERENCES AND SPORT CLASSIFICATION ON WHEELCHAIR BASKETBALL SPRINT PERFORMANCE**

*Hannah Houde[1], Melissa Morrow[1], Jiefei Wang [1], Christopher Wilburn[2], Wendi Weimar[2], Jerad Kosek[3], Bahman Adlou[2], John Grace[2]
The University of Texas Medical Branch at Galveston, Galveston, TX[1], Auburn University, Auburn, AL[2], University of Evansville, Evansville IN[3]
*Corresponding author's email: hrhoude@utmb.edu

**Introduction:** Wheelchair basketball is a popular and highly competitive sport with a classification system meant to ensure fair and competitive play. Athletes receive a score from 1.0 (disability significantly impacts mobility) to 4.5 (minimal impairment) based on functional capacity during gameplay. While differences across classification levels have been explored, there is limited data on the trunk and upper body kinematics across classification levels during sport-specific tasks and sex differences. The purpose of this study was to analyze the effects of sex, sport classification, and trunk displacement in the frontal and sagittal plane on sprint performance during a change of direction (COD) task.

**Methods:** Collegiate wheelchair basketball athletes from the National Wheelchair Basketball Association with ≥6 months of experience and no upper extremity/trunk injuries were recruited. The wheelchair basketball classification of each participant was determined by certified classifiers. Xsens inertial measurement unit sensors were placed bilaterally (shoulders, upper/lower arms, hands) and singularly (head, T12, pelvis, wheelchair back). Athletes performed a 5-10-5 (COD) drill three times with 30-second rest intervals while wearing a Jawku timing watch, which provided an auditory cue to regulate the start of each trial. The drill required pivoting from the center position, sprinting 5m, pivoting 180°, sprinting 10m, pivoting 180° again, and returning 5m to start. Kinematic analysis focused on the 1st (initiation), 3rd (transition), and 5th (maintenance) pushes during the straight-line portion following pivots. Data processing used MVN Analyze and Visual3D software to calculate the sagittal and frontal plane angular trunk displacement. Statistical analysis (SPSS version 27) included one-way ANOVAs comparing sprint performance times (s) across classification (1-4.5), sex (M/F), and experience levels (years playing collegiate wheelchair basketball. Simple (SLR) and multiple linear regression (MLR) were used to identify trunk kinematic predictors of sprint performance time (s) while adjusting for the other covariates. All analysis is done separately for male and female.

**Results & Discussion:** 53 collegiate wheelchair basketball athletes (35 males, 18 females) across the full range of wheelchair basketball classification groups (1-4.5, Figure 1) were included in the analysis. Sex significantly affected COD sprint performance ($F(1,52) = 6.538$, $p = .01$), with females demonstrating faster times (8.92±0.61s) than males (9.61±1.04s). No significant differences were found between classification groups ($F(7,52) = 0.916$, $p = 0.503$), though Class 2 athletes achieved the fastest times (8.8±1.06s) while Class 1 (9.83±1.36s) and Class 4 (9.71±0.74s) athletes were slowest. Athletes with 3-6 years of experience tended to perform faster (8.5-9.2s) than those with 6 months to 2.5 years (9.2-10s), though this difference was not statistically significant.

For male athletes, trunk displacement in the frontal plane demonstrated significant relationships with sprint performance. The SLR revealed the 1st push, increased trunk lean was associated with faster sprint times, with statistical analysis revealing a moderate correlation ($R = .384$, $R^2 = .148$, $p = .023$), as well as years of experience in playing collegiate wheelchair basketball ($R = .376$, $R^2 = .141$, $p = .026$). MLR identified two critical trunk movement predictors: frontal trunk displacement during the 1st push (more to less trunk lean), and 3rd push (less to more trunk lean), which collectively significantly predicted improved sprint performance. For female athletes, no statistical significance was found. However, the SLR revealed two variables approaching statistical significance in the SLR model: sagittal trunk displacement during the 1st push (trunk extension to flexion, $p = .065$) and frontal trunk displacement during the 3rd push (less to more trunk lean, $p = 0.73$). However, the smaller sample size limited statistical power, suggesting potential need for further investigation into biomechanical differences between male and female wheelchair basketball athletes.

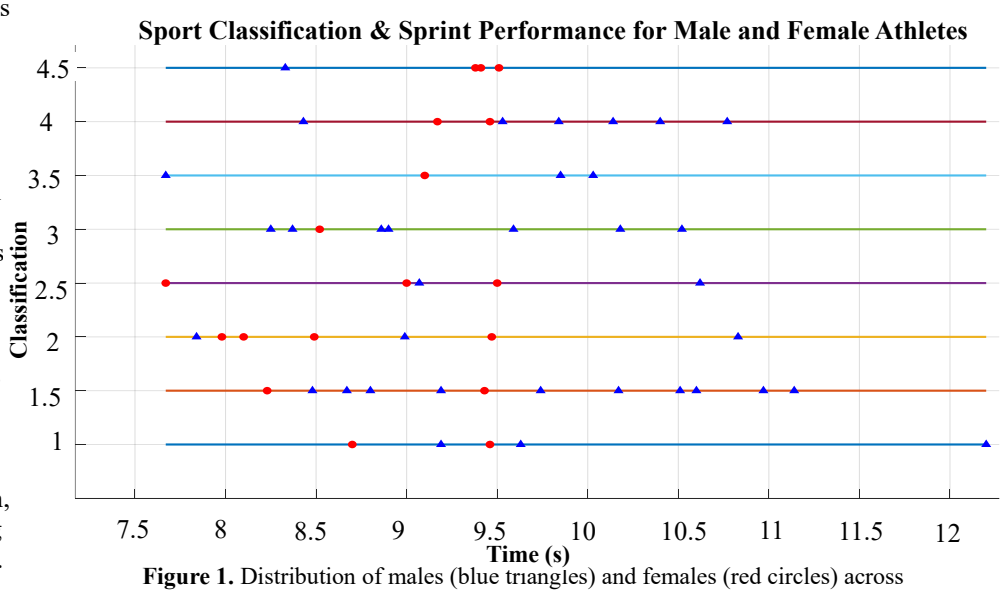


**Figure 1.** Distribution of males (blue triangles) and females (red circles) across classification scores and sprint performance time (s).

**Significance:** Overall, this study highlights the importance of sex-specific assessments in wheelchair basketball, given the observed differences in trunk movement strategies between male and female athletes. The finding that classification level was not a significant predictor of sprint performance suggests a more intricate relationship between classification, biomechanics, and overall athletic performance, warranting further investigation.

**References:** [1] Bergamini, E., et al. (2015). *BioMed Rsch Intl*, (1). [2] Iturricastillo, A., et al. (2023). *Intl J of Spt Phys & Perf*, *19*(2).

# EFFECTS OF STANCE FOOT MECHANICS ON GROUND REACTION FORCE, BALL SPEED, AND STRIDE KINEMATICS IN AMATEUR BASEBALL PITCHERS

*Sakiko Oyama[1], Brian Stephens[1]
[1]University of Texas at San Antonio (UTSA), Department of Kinesiology
email: Sakiko.oyama@utsa.edu

**Introduction:** Ball speed is one of the key predictors of success in baseball pitchers. While various factors have been demonstrated to contribute to ball speed, no study has examined how the stance foot mechanics, such as the center of pressure (COP) location and the timing when the heel lifts from the ground, affect the pitching biomechanics. Therefore, there is no consensus among the expert coaches regarding how the pitchers should balance on the stance foot during the push-off. Peak ground reaction force (GRF) at the time of peak anterior force strongly correlates with hand velocity [1]. Also, the horizontal impulse produced during the stride is associated with greater transfer of energy into the pelvis, trunk, and arm. [2] Thus, identifying the stance foot mechanics that lead to greater GRF production can provide evidence-based recommendations to the coaches and athletes. Furthermore, stance foot mechanics can influence the stride leg and pelvis kinematics during the stride phase, which has been linked to joint loading during pitching.[3] The purpose of the study was to investigate the effects of anterior-posterior COP location and timing of heel lift of the stance leg on ground reaction force (GRF), ball speed, and stride kinematics in high school and collegiate baseball pitchers. We hypothesized that more posteriorly located COP at the time of maximum anterior force and later occurrence of heel lift would be correlated with greater ground reaction force, ball speed, longer stride, and more closed pelvis orientation at the lead foot contact.

**Methods:** Fifty-two pitchers pitched from an indoor pitching mound. A three-dimensional motion capture system (600Hz) and two force plates (1200Hz) embedded in the mound, and a radar gun were used to collect the data. A pitching rubber was secured onto the force plate using double sided tape. Reflective markers were placed on the anatomical landmarks, including anterior-superior iliac spines, posterior superior iliac spines, medial and lateral knees, medial and lateral malleoli, heels, and the tip of the shoes. The marker on the tip of the stance foot was removed after the calibration, and the toe tip was defined as the virtual marker in the foot coordinate system defined by the medial malleolus, lateral malleolus, and heel marker. The filtered marker coordinates were used to calculate 1) the COP location along a vector extending from the heel to the virtual toe marker, 2) the timing of heel lift (>0.02m), 3) stride foot mechanics (i.e., length, width, and foot progression angle), and 4) pelvis axial rotation angle in the global coordinate system. The COM location was expressed as the %foot length from the heel (0% = heel, 100% =toe). The timing of heel lift was expressed as a percentage of the stride phase duration, from maximal knee height to lead foot contact. The GRF was normalized to body weight. The three fastest pitches were used for analysis. The relationship among COP location at peak anterior force, timing of heel lift, stride length and width, foot progression angle, pelvis orientation at lead foot contact, peak anterior GRF, and resultant GRF at peak anterior force were examined using the Pearson correlation coefficients ($\alpha<.05$).

**Results & Discussion:** The COP at peak anterior force was, on average, located 82.7±5.3% foot length from the heel, and the heel started lifting off the ground 85.9%±8.1% into the stride phase. The earlier timing of heel lift was correlated with more anteriorly located COP at peak anterior force ($r=.565$, $p<.001$, Figure 1) and a more open pelvis orientation at lead foot contact ($r=-.456$, $p=.001$, Figure 2). However, the COP location or timing of heel lift was not correlated with peak GRF magnitudes, ball speed, or stride leg kinematics.

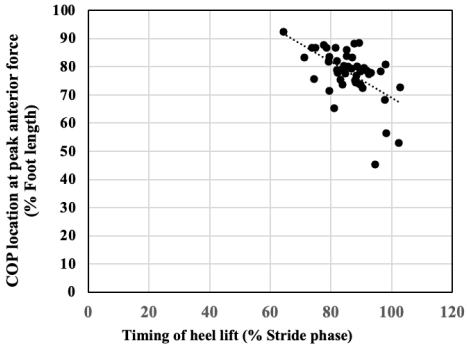


**Figure 1:** Correlation between timing of heel lift and COP location at peak anterior force.

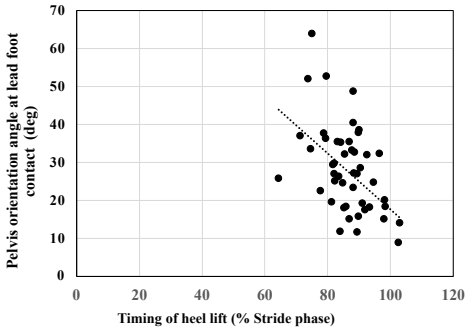


**Figure 2:** Correlation between timing of heel lift and pelvis orientation at lead foot contact.

**Significance:**
Pitchers who kept the heel down longer during the stride tended to produce peak anterior force through the heel and demonstrated more closed pelvis orientation at the lead foot contact. The pelvis orientation at stride foot contact has been associated with shoulder and elbow joint moments.[3] The relationship between the timing of heel lift, COP location at peak anterior force, and pelvis orientation at lead foot contact suggests that COP location during the stride may be incorporated as a potential instructional strategy to modify the timing of pelvis rotation in amateur pitchers. The COP location and the timing of heel lift we not linked to the peak GRF magnitudes or the stride foot mechanics.

**Acknowledgement:** This manuscript is based on the data collected in a project funded by the National Athletic Trainer's Association Research and Education Foundation.

**References:** [1] McWilliams (1998), *Am J Sports 26(1):66-71*; [2] Howenstein (2020), *J Biomech Jul 17:108:109909*, [3] Wight (2004) Sports Biomech 3(1):67-83

# USING MARKERLESS MOTION CAPTURE TO EXAMINE SHOULDER JOINT KINEMATICS DURING THE BENCH PRESS EXERCISE IN COMPETITIVE POWERLIFTERS

*Jodi G. Motlagh[1], David B. Lipps[1]
[1]School of Kinesiology, University of Michigan
*Corresponding author's email: jmotlagh@umich.edu

**Introduction:** The barbell bench press is a foundational exercise in competitive powerlifting, primarily used to train the chest, shoulders and back of the arms [1]. Between 18-46% of reported injuries in sub-elite and elite powerlifters were attributed to the bench press [2]. In the past two decades, participation in competitive powerlifting has increased by 1,067% in males and 2,529% in females. While injury incidence appears similar between male and female powerlifters, females report higher injury rates in the neck and thoracic region [3]. Factors such as using a wider grip width, high exercise dose, repetitive strain, and altered proprioception following an injury increase the risk of bench press injury [4-6]. Despite these findings, sex differences in joint kinematics during multiple-repetition sets are largely understudied. Several studies utilized marker-based motion capture, currently considered the "gold standard" technology, to measure shoulder kinematics during the bench press [7-9]. However, reflective markers on the back side of the body are not captured due to participant positioning during the bench press [10]. Given this limitation, markerless motion capture may be better suited for comprehensive motion analysis during the bench press exercise. Therefore, this study aimed to use markerless motion capture technology to examine differences in shoulder joint kinematics throughout the completion of a standardized bench press protocol. We examined the hypotheses that (i) shoulder joint range of motion would increase in both intra-set and inter-set measures and (ii) shoulder joint range of motion would be exaggerated in female lifters compared to male lifters.

**Methods:** Nineteen competitive powerlifters (8 M, 11 F; mean (SD) age: 23.5(4.8); height: 169.8(10.5) cm; weight: 81.2(16.9) kg; Shoulder Pain and Disability Index (SPADI) score: 1.3(3.1)) were enrolled in this study and provided written informed consent. All participants completed a uniform dynamic warmup and self-reported their bench press one-repetition maximum (1RM). Participants performed three sets of eight repetitions at a load equivalent to 74% of their 1RM. A 16-camera Qualisys system with hybrid video cameras captured full-body movements of the participant during the three sets of bench press. Theia3D was used to create a digital skeleton of the participant from the video data. Visual3D was then used to calculate shoulder joint angles throughout the exercise (XZY rotation sequence where X = humeral rotation, Y= elevation, and Z = plane of elevation). To determine the range of motion from joint angle measurements, the minima was subtracted from the maxima for both the first and second-to-last repetitions. Repeated measures ANOVA was used to examine how fatigue (both intra- and inter-set, assessed as within-subjects repeated measures) affects our outcome measure, shoulder joint range of motion. Biological sex was used as a between-subjects factor.

**Results & Discussion:** While there were no significant inter-set changes in shoulder joint range of motion (all $p>0.144$), a main effect of repetition was observed between the first and second-to-last repetition in a bench press set. These results were consistent in humeral rotation ($p = 0.002$), elevation ($p < 0.001$), and plane of elevation ($p < 0.001$) movement patterns (**Figure 1**). Additionally, biological sex had a significant main effect on shoulder joint range of motion. Females had greater range of motion than males during the bench press in humeral rotation ($p = 0.011$) and elevation ($p = 0.036$) but not plane of elevation ($p = 0.518$).

Our findings agreed in part with our hypotheses. While a fatiguing bench press protocol did not result in inter-set changes in shoulder joint range of motion, intra-set increases were exhibited across the three planes of movement. When looking at humeral rotation and elevation specifically, females displayed a greater range of motion than males. This raises some concerns with bench press injury incidence in both male and female powerlifters, as intra-set movement patterns alter shoulder kinematics during the bench press. Special consideration may also be needed for female lifters, who may be at greater risk of injury when nearing end-ranges of the shoulder joint.

**Significance:** This study provides novel biomechanical insights into how markerless motion capture may be a promising alternative to traditional marker-based technology when observing shoulder joint kinematics throughout a bench press protocol. Addressing changes in shoulder joint range of motion between males and females during a fatiguing bench press protocol will allow for a greater understanding of training modifications that may benefit long-term injury prevention.

**Acknowledgments:** University of Michigan Rackham Graduate Student Research Grant

**References:** [1] Algra B. (1982), *Strength Cond J.* 4(5); [2] Bengtsson et al. (2018), *BMJ Open Sport Exerc Med.* 4(1); [3] Strömback et al. (2018), *Ortho J Sports Med.* 6(5); [4] Fees et al. (1998), *Am J Sports Med.* 26(5); [5] Green and Comfort (2007), *Strength Cond J.* 29(5); [6] Reeves et al. (1998), *Phys Sportsmed* . 26(3); [7] Mausehund and Krosshaug (2023), *J Strength Cond Res.* 37(1); [8] Mausehund et al. (2022), *J Strength Cond Res*. 36(10); [9] Noteboom et al. (2024), *Front Physiol.* 15; [10] Motlagh and Lipps (2024), *J Strength Cond Res.* 38(12).

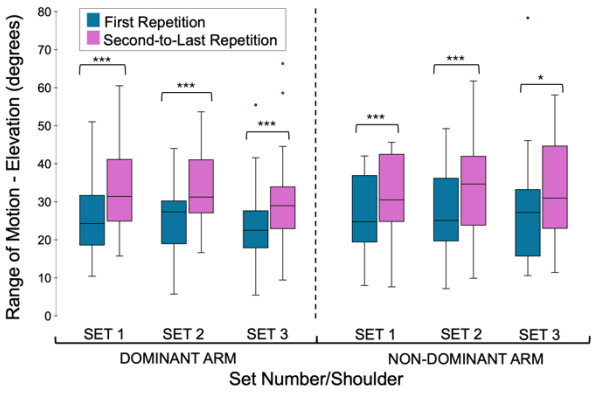


**Figure 1:** Box plots of shoulder joint range of motion in elevation. The first and second-to-last repetition across three sets of bench press are examined, in addition to the differences between dominant and non-dominant arms. A significant main effect of repetition ($p < 0.001$) is indicated using (***).

# UPPER EXTREMITY KINEMATIC SYNERGIES IN BASEBALL PITCHING: INSIGHTS FROM THE OPENBIOMECHANICS PROJECT

*Arjun Parmar[1], Derek Dewig[2], Albert Cohen[3], Garett Bullock[4], Anthony Gatti[5], Matt Harkey[1]
[1]Department of Kinesiology, Michigan State University, East Lansing, MI, USA
*Corresponding author's email: parmarar@msu.edu

**Introduction:** Kinematic analysis of baseball pitching is fundamental to improving performance, with multijoint coordination playing a crucial role in generating pitch velocity. Traditional baseball biomechanical analyses have focused on discrete values, such as peak elbow flexion angle, which may overlook how upper extremity joints interact throughout the pitching motion. Functional data analysis and its extension, multivariate functional principal component analysis (MV-fPCA) may identify kinematic synergies across multiple joints, thus describing upper extremity joint coordination during pitching. The purpose of this study was to identify kinematic synergies underlying arm motion during pitching and the relationship of these kinematic synergies with ball velocity. Due to the interdependence between upper extremity joints during pitching, we expect MV-fPCA to reveal a limited number of synergies that explain most kinematic variance, with specific synergies associating with pitch velocity.

**Methods:** Eighty-seven male pitchers (age: 21.3±2.2 years, height: 1.9±0.1 m, mass: 90.5±10.0 kg) were extracted from the OpenBiomechanics Project dataset [1], each with three to five recorded pitches. Upper extremity kinematics during fastball pitches were recorded utilizing an instrumented mound (1080 Hz, Bertec), and optical motion capture (360 Hz, OptiTrack). Additionally, ball velocity was measured with a radar gun (Stalker). Kinematic waveforms of the shoulder, elbow, and wrist were time-normalized to 1001 points and segmented into four phases: stride (75.4%), cocking (16.8%), acceleration (3.4%), and deceleration (4.4%) using piecewise linear length normalization. MV-fPCA, using a univariate PCA basis for each joint waveform, identified functional principal components (fPCs), each describing a single kinematic synergy. Five-fold cross-validation assessed the descriptive accuracy of MV-fPCA. In each fold, the test data (20%) were reconstructed using the MV-fPCA model trained on the remaining data (80%), retaining only fPCs that explained ≥90% of the variance. The root mean squared error (RMSE) was then calculated between the original and reconstructed waveforms for each joint component. We then applied MV-fPCA to the full dataset. Participant fPC scores, for the retained fPCs, and ball velocities were averaged across trials. A linear regression was fit between fPC scores and ball velocity.

**Results & Discussion:** The average RMSE was 7.75° across the 5 folds of the cross-validation. All folds of the cross-validation and the MV-fPCA fit to the full data set required 16 fPCs to explain ≥90% of the kinematic variance. The 16 identified synergies explained 50.8% of ball velocity variance ($p < 0.01$). Two synergies were significantly related to ball velocity: synergy #14 ($p = 0.04$, $\beta = 0.91$) and synergy #16 ($p = 0.03$, $\beta = 0.94$). While these synergies account for only 2.7% of the total kinematic variance (1.6% and 1.1%, respectively), their association with ball velocity suggests that small variations in arm kinematics have a meaningful impact on pitch speed. Figure 1 illustrates the kinematic synergies that were significantly related to ball velocity. Each joint angle curve is three standard deviations from its mean (zero-line), and represents higher ball velocity, for that respective fPC. For example, during early stride, fPC 14 indicates that faster pitches have less wrist extension than average, while fPC 16 shows that faster pitches have greater wrist extension. Synergy #14 (fig 1a.) largely describes shoulder and wrist joint angle variation. During the pitch the shoulder is less horizontally adducted and less adducted. However, the shoulder is more internally rotated during stride and more externally rotated for the reminder of the pitch. Synergy #16 (fig 1b.) captures amplified cocking motion during the cocking phase with increased wrist extension, elbow flexion, shoulder horizontal abduction, and shoulder external rotation are all associated with higher ball velocity. Importantly, both synergies share common features associated with higher ball velocity. At maximal external rotation (fig 1. transition 2), both synergies describe greater external shoulder rotation, elbow flexion, and pronation compared to the mean waveforms. Additionally, reduced shoulder adduction during the second half of the pitch is observed. Finally, greater elbow pronation during the acceleration and deceleration phases suggests its role in both generating ball velocity and arm deceleration after ball release associated with high-velocity pitching. Notably, the synergies linked to ball velocity also involve more extreme joint angles, which may increase injury risk. This includes injuries like superior labrum anterior-posterior lesions and ulnar collateral ligament sprains, both common in baseball pitchers.

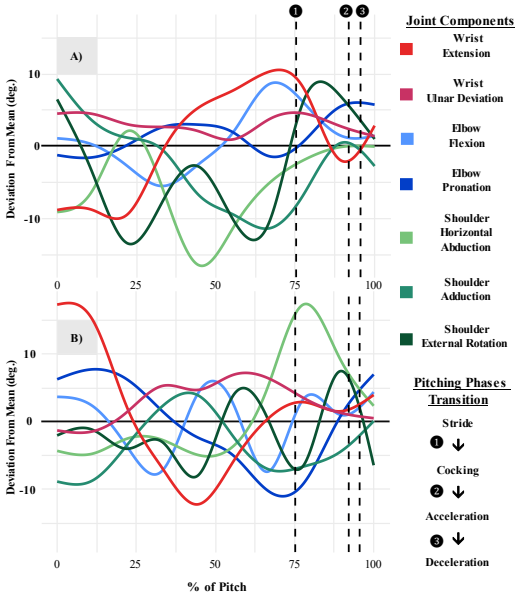


**Figure 1:** Joint angle deviation from the mean function for synergies #14 (A) and #16 (B). Curves reflect fPC scores three standard deviation from the mean. The horizontal reflects the mean waveform.

**Significance:** This study enhances the understanding of pitching arm kinematics by identifying joint angle synergies related to ball velocity. These synergies may inform targeted training to optimize pitching joint coordination for velocity. MV-fPCA may be applied to decompose other complex movements and may be well suited for the clustering and classification of multijoint movements.

**References:** [1] Wasserberger et al. (2022), *The OpenBiomechanics Project*

# COMPARISON BETWEEN BASEBALL AND SOFTBALL CATCHERS' THROWING-ARM KINEMATICS

*Ryan M. Zappa[1], Anthony W. Fava[1], Billy Lozowski[1], Gretchen D. Oliver[1]
[1]Sports Medicine and Movement Laboratory, Auburn University, Auburn, Alabama
*Corresponding author's email: rmz0004@auburn.edu

**Introduction:** While the literature on baseball pitching is extensive, research on catchers is sparse. Moreover, baseball (BB) and softball (SB) catchers are frequently combined into a single group for analysis. This combined analysis has been done in past work since catchers in both sports share key responsibilities, like receiving a pitch, quickly getting into an upright position, and rapidly delivering an accurate throw to a base [1,2]. Using this grouped approach, researchers have reported descriptive kinematic and electromyographic data on catchers performing kneeling and pop-up throw-downs [3,4,5].

One of these aforementioned studies compared kinematics of the pelvis and trunk between the sports [5]. Using a discrete analysis, Plummer and Oliver found differences in pelvis and trunk kinematics between BB and SB catchers at two time points: maximum shoulder external rotation and maximum shoulder internal rotation. Despite differences observed at these time points, no research has assessed whether kinematic differences would extend to the throwing arm itself. Considering factors that shape the movements (e.g., ball size, field dimensions, biological sex, etc.), along with the key kinematic differences at the pelvis and trunk that help transfer force from the lower extremity to the throwing arm via the kinetic chain [6], it is reasonable to hypothesize that differences may exist between the two sports concerning the kinematics of the throwing arm. Therefore, this study compared BB and SB catchers' arm kinematics when throwing to second base.

**Methods:** Kinematic data were collected between 100 and 240Hz for 20 catchers, 10 BB (1.84 ± 0.08m, 81.92 ± 14.12kg, 16 ± 2y) and 10 SB (1.66 ± 0.07m, 70.47 ± 10.64kg, 17 ± 2y), using an electromagnetic motion capture system. Participants completed three maximal intensity pop-up throws to a target simulating a throw to second base (BB: 27.4m, SB: 25.6m). Local coordinate systems and the appropriate rotation sequences for each segment were defined by ISB recommendations [7]. Data were then filtered using a fourth-order Butterworth filter (13.4Hz) [8] before being exported at 100Hz. Exported data were interpolated to 101 data points between front-foot contact (0%) and maximal shoulder internal rotation (100%). Statistical parametric mapping (SPM) independent-samples t-tests ($\alpha$ = .05) were performed in Python (Version 3.12.4) to compare throwing-arm kinematics between BB and SB catchers using the spm1d package [9].

**Results & Discussion:** Significant differences were observed across all kinematics assessed (Figure 1). BB catchers displayed greater shoulder external rotation angles between 23.4 and 53.4% of the throwing cycle compared to SB catchers ($p < .001$). Shoulder elevation ($p < .001$) and shoulder plane of elevation ($p < .001$) also showed significant differences from 0-95.9% and 0-100% of the throw, respectively**;** with SB catchers displaying greater values in both. Elbow flexion angle was different at two time periods. SB catchers displayed greater flexion from 0-13.3% and BB catchers showed a greater flexion angle from 99.3-100% of the throw ($p$ = .008). These results build on previous work where BB and SB catchers exhibited differences in pelvis and trunk kinematics [5]. Differences might be attributed to a plethora of potential factors, such as ball size, throw distance, sex differences, and overhead pitching mechanics translating into the BB catcher's throwing mechanics. Moreover, our findings suggest that, although the positions are the same ostensibly, considering them separately may be more pragmatic when coaching technique and conducting research on this population.

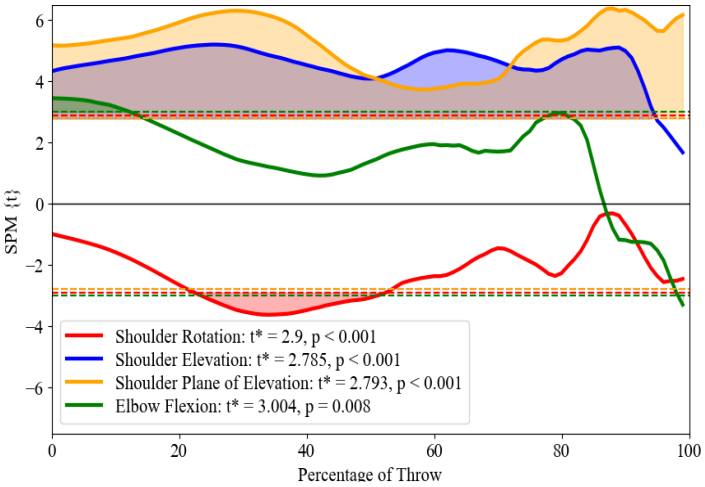


**Figure 1**: Results of SPM independent samples t-test (0-100%).

**Significance:** While the same position is being investigated, previously reported differences in pelvis and trunk kinematics [5] and differences in throwing-arm kinematics observed here indicate that performance strategies and injury prevention may be specific for each sport. This approach agrees with Fleisig et al. [10] and may encourage sports biomechanists to consider the constraints of the task before deeming that different populations will have similar mechanics.

**References:** [1] Oliver GD et al. (2015), *Sports* 3(3); [2] Lund et al. (2014), *Sport J* (1); [3] Plummer H, Oliver GD. (2013) *J Sports Sci.* 31(10); [4] Plummer H, Oliver GD. (2016), *J Electromyogr Kinesiol.* (29); [5] Plummer H, Oliver GD. (2014), *J Strength Cond Res.* 28(1); [6] Ellenbecker et al. (2020), *Curr Rev Musculoskelet Med.* 13(2); [7] Wu G et al. (2005), *J. Biomech* 38(5); [8] Fleisig et al. (1996), *J. Appl. Biomech.* 12(2); [9] Pataky TC. (2012), *Comput. Methods Biomech. Biomed. Engin.* 15(3); [10] Fleisig et al. (2011), *J. Orthop. Sports Phys. Ther.* 41(5)

# THE EFFECT OF A GAME-LIKE BASKETBALL CUTTING TASK ON LATERAL KNEE ACCELERATION

*Aaron Harris[1], Mason Kiesel[1], Kelly Carver[1], Kalyn Rich[1], Alexander M. Morgan[1]
[1]Baldwin Wallace University, Berea, OH
*Corresponding author's email: aharris21@bw.edu

**Introduction:** Non-contact Anterior Cruciate Ligament (ACL) tears account for 70% of all ACL injuries [1]. Athletes who suffer ACL tears are six times more likely to suffer another ACL tear within two years [2], and those below the age of 25 are even more likely to suffer a second ACL injury [3]. ACL injuries often occur when decelerating due to the over activation of the quadriceps and lack of activation of the hamstrings [4]. Athletes exhibit greater initial contact knee abduction angles, knee abduction moments, anterior tibial shear force, and lateral ground reaction forces when completing unanticipated cutting maneuvers that involve significant deceleration, and each has been related to increased risk for ACL injury [4,5,6]. Measuring each of these risk factors may require costly equipment, while inertial measurement units (IMUs) measuring acceleration serve as a less expensive option. Lateral accelerations measured from the tibia have displayed moderate positive correlations with knee moments and stiffness [7]. Female athletes display significantly higher knee valgus angles when making a 45-degree cut when compared to men, and both sexes display significantly higher knee valgus angles when making a 90-degree cut when compared to their angles from the 45-degree cut [8]. Additionally, attending to visual cues while cutting has shown negative impacts on biomechanical risk factors for ACL injury, such as knee valgus angle [9,10]. Finally, basketball players are at higher risk for ACL injury due to the dynamic movement inherent in the sport [6], and are more likely to suffer an ACL injury if they heavily rely on driving to the basket when compared to players who rely more on long distance shooting [11].

While previous studies have evaluated knee kinematics at varying cutting angles for basketball players, there is no literature investigating the difference between a 110-degree cut and other lateral or diagonal cuts. Additionally, there is a lack of research regarding the effect of unanticipated cuts dictated by an audio cue on lateral knee accelerations in basketball players. As such, this study aims to determine if there is a significant difference in lateral knee accelerations when dribbling a basketball, performing an unanticipated cut at either 45, 90, or 110 degrees as dictated by an unanticipated audio cue, and then shooting a basketball. It is hypothesized that lateral knee acceleration will be greatest when performing the 110-degree cut when compared to the 45-degree and 90-degree cut, with the 90-degree cut condition eliciting greater lateral accelerations compared to the 45-degree cut.

**Methods:** Eligible participants were basketball athletes who currently or previously participated in organized basketball activities (high school, collegiate, recreational) twice weekly and were between the ages of 18 and 25. Participants were excluded if they had previous ACL injury, lower limb surgery, or lower limb injury in the past 6 months. Participants were guided through a basketball task in which they approached the free throw line on a basketball court from half-court at a speed of 2-3 m/s. Participants were required to dribble with their dominant hand and once they reached the free-throw line, then cut off the ipsilateral limb toward a specific angle in the contralateral direction. An audio cue was played 3.6 m before reaching the free-throw line to direct the participant toward the correct cutting angle. In a randomized order, participants were directed to cut in one of three directions associated with a color (45 [blue], 90 [yellow], and 110 [white] degrees). A total of 15 correct trials were collected, 5 at each angle. Lateral acceleration values at the instant of the cut were obtained with an Shimmer3 Inertial Measurement Unit (IMU) (Dublin, Ireland) attached to the tibial tuberosity of the cutting limb. Lateral acceleration values were then analyzed to determine peak lateral acceleration during the cutting maneuver. Preliminary descriptive analyses were performed using IBM SPSS Statistics (Chicago, IL).

**Results & Discussion:** Five participants were collected as a part of this pilot study to assess feasibility. Means and standard error of lateral accelerations for each of the three cutting angles are presented in box plot form in Figure 1. Data suggests that it is feasible to obtain lateral accelerations from various cutting angles while dribbling, responding to a randomized audio cue, and shooting. Further data is necessary to assess differences in lateral accelerations between cutting angles.

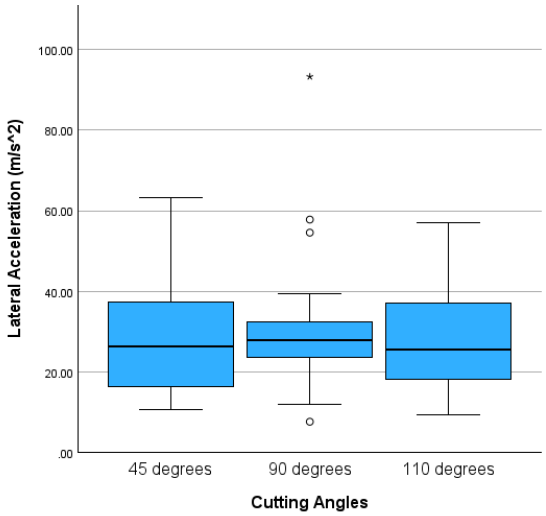


**Figure 1.** Box plot of lateral acceleration ($m/s^2$) for three different cutting angles. Solid black lines indicate mean acceleration. Vertical black lines indicate standard error.

**Significance:** This study is relevant due to the high incidence of ACL injury in cutting sports like basketball. This pilot study serves to display the feasibility of examining the effect of a dual-task protocol requiring a response to an audio cue on lateral knee acceleration values, thereby filling a gap in the literature.

**References:** [1] McNair et al. (1990), *N Z Med. J* 103(901); [2] Paterno et al. (2014), *Am J Sports Med.* 42(7); [3] Wiggins et al. (2016), *Am J Sports Med.* 44(7); [4] Shimokochi et al. (2008); *J Athl Train* 43(4); [5] Peel et al. (2019), *J Appl Biomech* 35(2); [6] Zhu et al. (2024); *Sensors (Basel)* 24(14); [7] Jones st al. (2022), *Sensors (Basel*) 22(23); [8] Sigward et al. (2016), *Clin J Sports Med.* 25(6).; [9] Heidarnia et al. (2022), *J Biomech* 133(1); [10] Monfort et al. (2019), *Am J Sports Med.* 47(6); [11] Schultz et al. (2021), *Orthop J Sports Med.* 9(11).

# IMPACT360 COLLAR FOR HEAD IMPACT RISK ASSESSMENT

Chloe Carpenter, Alaina Smythe, Taylor Huschke, Hannah Dean, Dr. Eric Meyer
Department of Biomedical Engineering, Lawrence Technological University, Southfield, MI
ccarpent1@ltu.edu

**Introduction:** Concussions and head injuries are a pressing concern in contact sports, where these injuries are most common [1]. These types of injuries typically go underreported due to subjective assessment methods and external pressures on athletes to perform, which can lead to long term detrimental effects. The Impact360 collar addresses this issue by providing a real-time, data centered solution for head impact detection without hindering athletic performance. This neck worn device integrates accelerometers and gyroscopes positioned at cervical vertebrae 2 and 5 to monitor motion and acceleration [2]. This specific placement allows accurate detection of linear and rotational events that can be linked to a head impact [3]. Existing solutions like mouthguards or helmet systems are sport-specific, bulky, and can produce unreliable or inconsistent results to measure impacts or injury potentials. The Impact360 collar overcomes these limitations with a lightweight, ergonomic design that would encourage athletes in all sports to participate in protecting their own health.

**Methods:** The design process for the Impact360 collar involved extensive brainstorming, iterative prototyping, and material evaluation. Early prototypes involved multi-sensor and pressure fit designs that were inspired by the form factor of existing athletic wear that users had rated highly in comfort. The initial design focused specifically on accelerometer placement on the sides of the neck. This placement was proven to be ineffective in collecting accurate data, resulting in further refinement to provide better emphasis on accuracy and functionality. The design details depicted in Figure 1 include IMU sensors on the C2 and C5 vertebrae to more accurately measure sensor data [2]. 3D printing was used to test different hardware placements and determine the specifics of a comfortable neck worn device. Prototypes revealed challenges in material comfort and limited flexibility, resulting in adjustments to better focus on the overall form factor and material selection.

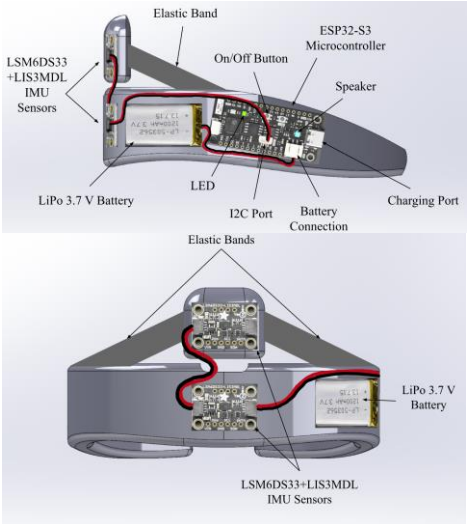


**Figure 1:** Design details, placement of the sensors on C2 and C5, as well as the electronics and hardware included in the back and on the side of the collar. Components include; Arduino feather board, charging port, LED, and switch.

**Results & Discussion:** Testing has demonstrated the Impact360 collar's ability to perform risk assessment analyses for head impacts and accurately track linear and rotational velocity thresholds [3]. The final Impact360 design features a flexible, comfortable collar that is able to securely house IMU sensors while allowing for free athletic movement. Device placement and fit is displayed in Figure 2. Data verification processes confirmed sensor placement and the ability to collect meaningful data, ensuring the differentiation between routine athletic motion like running, walking, or stopping abruptly from potentially harmful impacts. Projected results include reliable real-time impact detection and risk assessment, along with significantly low error rates in the differentiation between movements. Once the form factor and layout were confirmed with 3D printed prototypes, a silicone elastomer with high cross linking was selected for the material. This allows the collar to be both flexible and durable in the production of our final functional device. Further protocols include material testing, calibration utilizing motion capture systems, and human trials to validate preset thresholds as well as data measurements and calculations within the code. These test methods help to improve the user experience and credibility of device detections. Conclusive results to this testing would address critical shortcomings in existing solutions that are limited due to discomfort or lack of protective equipment like helmets or additional padding in sports like soccer or women's lacrosse [1]. The Impact360 device is expected to provide actionable insights into head impact risks, empowering trainers and coaches to make informed decisions on athlete safety.

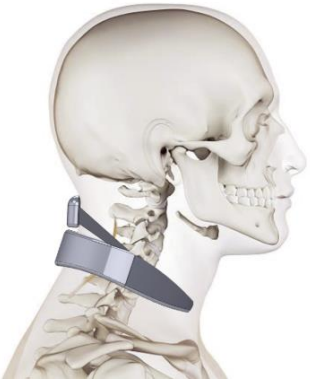

**Figure 2:** Impact360 device layout worn on the neck. Alignment with C2 and C5 vertebrae along with the final design.

**Significance:** The Impact360 device represents an advancement in head impact monitoring and risk assessment, emphasizing a user-centered, athlete first design. By providing real-time, reliable data on head impacts, the device addresses a critical need in athletic health and objective sports injury monitoring [1]. The lightweight and ergonomic form factor promotes widespread usage across various sports and athletic events, encouraging a proactive role in injury prevention. The collar's innovative integration of IMU sensors and real-time data collection has the potential to provide a lasting impact on head injury management, reducing the risk of underreporting errors and mitigating long-term cognitive risks [3]. The Impact360 collar exemplifies the future of wearable technology in athlete health and safety.

**Acknowledgments:** We thank Lawrence Technological University for supporting this project. We would also like to thank Dr. Eric Meyer, and Professor John Peponis for their support and guidance.

**References:** [1] O'Connor et al. (2017), J Athl Train 52(3); [2] Smotrova et al. (2021), Eur Spine J 30(12); [3] Zhang et al. (2004), J Biomech Eng 126(2).

# The effects of acute plantarflexor stretching on ankle biomechanics during pickleball maneuvers

*Thomas B. Young[1], Lauren E. Kalchbrenner[1], Taylor Q. Mink[1], Alexis J. Allen[1], Rachel L. Tatarski[1], Songning Zhang[1]
[1]The University of Tennessee, Knoxville, TN, U.S.A
*Corresponding author's email: tyoung34@vols.utk.edu

**Introduction:** Pickleball is the fastest growing sport in America and is often described as a combination of tennis, badminton, and table tennis.[1] However, with the rise in participation, there has also been an increase in injuries. A recent article highlighted the incidence of injury has increased 6.5-fold from 2019 to 2023 with the most common injury to be Achilles Tendon Ruptures.[2] Little is known about pickleball-specific movements and their effects on the lower extremity injury risk. Therefore, it is pertinent to investigate the biomechanical characteristics of the ankle joint during high loading movements as there has been an increase in ankle injuries and Achilles tendon ruptures. A well-known method to mitigate susceptible muscle tendon injuries is to implement a stretching regiment and could be a potential method to reduce injury risk. The purpose of this study was to investigate effects of acute static stretching on ankle biomechanics during pickleball-style movements with the long-term goal of developing a stretching protocol to reduce Achilles Tendon injuries. We hypothesized that 1) static ankle stretching will increase ankle dorsiflexion range of motion during cutting tasks; 2) ankle angular velocity will increase after stretching during cutting tasks; 3) internal ankle moment will not be different after stretching; and 4) ankle power will not be different after stretching.

Ankle Non Significant Variables

| Condition | Variable | Baseline | Acute Stretching | p-value |
|---|---|---|---|---|
| Backstep | Peak Plantarflexion Moment | -1.283 | -1.289 | 0.914 |
| | Minimum Ankle Power | -3.677 | -4.064 | 0.134 |
| Right Forward Take-off | Peak Plantarflexion Moment | -0.598 | -0.575 | 0.476 |
| | Minimum Ankle Power | NA | NA | NA |
| Left Forward Take-off | Peak Plantarflexion Moment | -0.555 | -0.572 | 0.652 |
| | Minimum Ankle Power | NA | NA | NA |
| Right Forward Landing | Peak Plantarflexion Moment | -1.081 | -1.024 | 0.087 |
| | Minimum Ankle Power | -2.999 | -2.926 | 0.340 |
| Left Forward Landing | Peak Plantarflexion Moment | -0.989 | -1.027 | 0.219 |
| | Minimum Ankle Power | -2.856 | -2.570 | 0.389 |

**Table 1:** Variables of interest that were not significant across all conditions with alpha = 0.05. NA values are represented as these events were not selected due to the participant starting on the force plate.

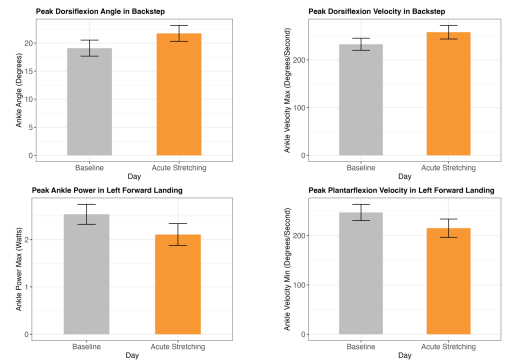


**Figure 1:** Graphs showing statistical significance with an alpha level of 0.05.

**Methods:** Twenty-nine participants between the ages of 18-80 were recruited for this within subjects design to achieve an effect size of 0.5, power of 0.8, and alpha level of 0.05. Participants completed two separate days of testing. The experimental protocol was an 8-minute stretching session targeting the gastrocnemius and soleus muscles of each leg. The volume of stretches performed was 4 sets of holding the stretch for 30 seconds with the participant standing with each leg on a 30-degree incline board alternating between the knee extended and flexed position. AMTI force platforms recorded at 2000 Hz, and Vicon 3D motion analysis 12-camera infrared system recorded at 200 Hz were used for data collection for 5 pickleball specific conditions. Condition 1, backstep, was defined as a single step backwards onto the force plate the subjects dominate leg to complete an overhead motion. Conditions 2, right forward take-off, and 3, left forward take-off, were defined with the participant leaving the force plate the with the right/left foot respectively to complete a groundstroke 1.5 meters from the plate. Conditions 4, right forward landing, and 5, left forward landing, were defined by the participant starting 1.5 meters behind the force plate to hit a ground stroke while landing on the force plate with the right / left foot respectively. Visual 3D (C-Motion, Inc. Germantown, MD, USA) was used to compute the 3D kinematic and kinetic variables listed in Table 1 and Figure 1. ANOVAs were used to detect differences between dependent variables. Peak variables were determined using a customized computer program (VisualBasic).

**Results & Discussion:** Several critical events were captured from 5 common maneuvres in pickleball executed in the sagittal plane. We expected to see a significant increase in maximum ankle dorsiflexion across all the conditions, but this was only found in the backstep condition (Figure 1). Stepping backwards can be dangerous in any sport for any age, so this is good to see the stretching intervention worked for this dynamic movement. This finding also suggests that the effect of static stretching on ankle dorsiflexion may be specific to certain movement contexts or task demands. We can further quantify this increase in dynamic range of motion with the increase in ankle velocity as seen in Figure 1. Table 1 shows peak plantarflexion moment and minimum ankle power exhibited no significant change as hypothesised across all conditions. Performance was maintained following the stretching intervention, indicating that stretching did not have a detrimental effect. Ankle power maximum remained stable across all conditions with the exception of left forward landing. Again, this pickleball maneuver involved the subject running toward the plate to hit a groundstroke while landing on the force plate with the left foot. Unexpectedly, we saw a decrease in power which may be attributed to the decrease in velocity (Figure 1). These findings highlight the complex and potentially condition-specific effects of static stretching on lower extremity biomechanics during cutting maneuvers. The study is still ongoing where we plan to separate young adults vs old adults in the final analysis.

**Significance:** The results of this study helped us determine that an acute static stretching session can increase ankle dorsiflexion maximum during specific pickleball movements. Understanding these injury mechanisms can highlight the importance of further researching pickleball maneuvers as the sport is expected to exponentially increase. This information can help provide guidance and education of injury prevention for novice players. This study is novel as it is the first to our knowledge to look at pickleball ankle movements to evaluate the risk of lower limb lower limb injuries.

**Acknowledgments:** This study was funded by the Graduate Student Research Award through The University of Tennessee

**References:** [1] Heo J et al. (2023), *Int J Aging Hum Dev*; [2] Kingston et al. (2024), *Foot Ankle Int* 45(11).

# MECHANICAL WORK AS A MEASURE OF EFFICIENCY IN ATHLETES PERFORMING CHANGE OF DIRECTION DRILLS

*Hailey Wrona[1] and Shawn Russell[1,2]
[1]Departmant of Mechanical and Aerospace Engineering, University of Virginia, USA
[2] Department of Orthopaedic Surgery, University of Virginia, USA
*Corresponding author's email: hlw6br@virginia.edu

**Introduction:** Performance in athletics can be evaluated using physiological, psychological, biochemical, and subjective assessments. When looking to quantify the physical aspects of performance, practitioners often measure speed, power, strength, and endurance variables [1]. Although these physical variables provide insight into the strength or speed of an athlete, they do not indicate the efficiency of the athlete during the measured movement. Through calculating mechanical work, the summation of the torque of every joint multiplied by the angle changes at each matching joint [2], efficiency at the whole-body can be assessed. The purpose of this study was to use mechanical work calculations as a measure of efficiency in athletic motions and examine the relationship between mechanical work calculations and level of play.

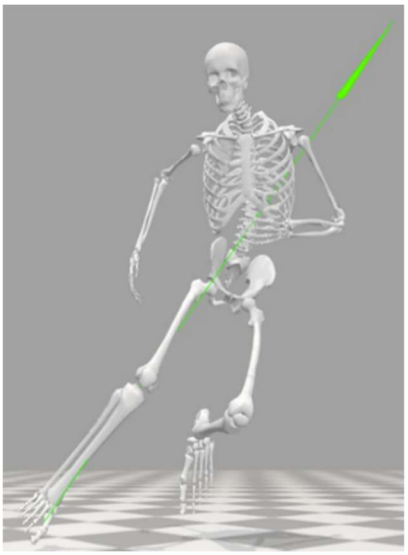

**Figure 1.** V-Cut motion shown on OpenSim Model.

**Methods:** Three subjects of different competitive level statuses performed a cutting drill three times that involved one 90 degrees cut on the outside foot (Fig.1). The subjects used their right foot for their outside footstep in all trials. All trial motion data was collected with a three-dimensional motion analysis camera system, and ground reaction force data was recorded at the feet using nine in-ground force plates. An updated OpenSim model that allows for high hip flexion and improved thoracic motion was used as the base model and scaled subjected specific models were created. Inverse kinematics and inverse dynamics were collected in OpenSim as well. Measured joint angles and torques were then used to perform joint and whole body-mechanical work calculations in MATLAB.

**Results & Discussion:** The results from the mechanical work calculations during the outside cutting motion highlight similarities and differences between the different athlete levels in the subject population. The mechanical work performed for the professional and retired professional athlete were found to be closely aligned, and both demonstrated values within one standard deviation of each other. In contrast, a larger separation was observed between the collegiate level athlete and the two professional level athletes. The collegiate level athlete displayed the highest proportion of upper body work during the cutting motion highlighting potential difference in overall movement strategy when executing the cutting motion.

| Player Level | Mechanical Work | | |
|---|---|---|---|
| | Total (J/kg) | Upper-Body (J/kg) | Lower-Body (J/kg) |
| **Collegiate (s=1)** | 5.57 ± 0.44 | 0.225 ± 0.05 | 2.55 ± 0.22 |
| **Professional (s=1)** | 6.02 ± 0.45 | 0.189 ± 0.04 | 3.07 ± 0.21 |
| **Retired (s=1)** | 6.16 ± 0.35 | 0.177 ± 0.04 | 3.19 ± 0.29 |

**Table 1.** Mechanical Work during stance of the V-Cut motion (Mean ± SD).

**Significance:** The current study shows that skill level and time spent in the sport may influence mechanical efficiency. Additionally, the findings highlight that further investigation is required into joint level mechanical work to break down these differences at the joint level to better understand how athletic experience and skill level contribute to mechanical work and movement efficiency during high-intensity movements like cutting.

**References:** [1] James et al. (2024), *Front Sports Act Living* 6; [2] Russell et al. (2012), *J Biomech* 46(4).

# EFFECTS OF ATTENTIONAL FOCUS ON GROUND REACTION FORCE AND JUMP LENGTH IN THE LONG JUMP

*Brian P. Selgrade[1], Paige Moroney
[1]Department of Sports Medicine & Human Performance, Westfield State University
*Corresponding author's email: bselgrade@westfield.ma.edu

**Introduction:** Previous studies have found that external attentional focus results in better athletic performance than internal attentional focus [1,2]. Internal focus may hamper performance by shifting focus away from the environment in which the task is performed or by causing conscious control to interfere with more automatic control processes [1]. In hopping, leg force and length appear to be goals of motor control more than individual joint angles [3], which are often at the center of internal focus instructions. Thus, external focus on a parameter such as force in the long jump could take attention away from the environmental context of the task (maximizing jump length) without interfering with automatic control processes. However, prior studies of attentional focus in standing long jump used an external focus on jump length [2], so the way an external focus on ground reaction force affects performance during standing long jump is unknown. Therefore, the purpose of this study was to examine how attentional focus on force production and jump distance affect performance in the standing broad jump, which is often used to measure athletes' power. Due to its interference with automatic motor control processes, we hypothesis that an internal focus on joint extension will yield shorter jump distance & lower ground reaction force compared to a control condition, an external focus on jump length, & an external focus on force applied to the ground.

**Methods:** Twelve NCAA Division III athletes (age = 19.6, 8 male), all experienced long and/or triple jumpers, gave informed consent and participated in the study. These athletes regularly performed standing long jumps in track & field team practice. No prior study has examined attentional focus in trained long jumpers.

Subjects performed 5 practice jumps, then completed a total of 16 jumps, 4 per condition, with 2-minute rests between trials. Subjects jumped from a force plate, which measured ground reaction force (GRF) of each jump. We measured jump length from the subject's back foot at landing & calculated sagittal plane angle of ground reaction force (force angle) at peak GRF. Condition order was randomized.

Subjects were instructed to jump as far as possible for the control condition, to jump as far past the start line as possible for the external performance focus condition, to push off as forcefully as possible for the external kinetic focus condition, & to extend their knees as fast as possible for the internal focus condition. We analyzed jump length with a one-way, repeated measures ANOVA & post hoc t-tests (parametric data) & Friedman & post hoc Wilcoxon signed rank tests (vertical GRF, which was not normally distributed).

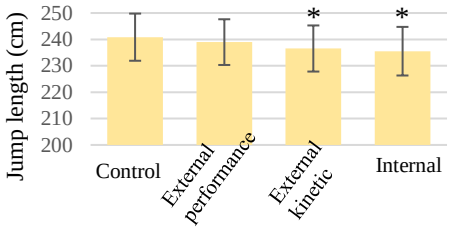


**Figure 1:** Effect of focus of control on standing long jump length. * denotes significant difference from the control trial

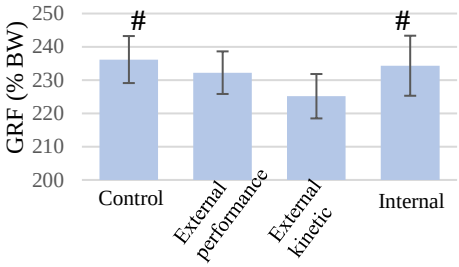


**Figure 2:** Effect of focus of control on result and GRF during standing long jump. # denotes significant difference from external kinetic focus

**Results & Discussion:** Repeated measures ANOVAs revealed significant main effects of condition on jump length (p=0.017) and resultant GRF. The main effect for force angle did not reach significance (p=0.090). External kinetic focus (p=0.022) and internal focus (p=0.039) both caused shorter jump lengths than the control condition (Figure 1). External kinetic focus caused significantly lower peak vertical (p=0.015), anterior-posterior (p=0.04) and resultant (p=0.008) GRF than the control condition, and significantly lower vertical GRF than internal focus (p=0.041; Figure 2). These results partially support our hypothesis; we expected internal focus to cause shorter jumps than the control condition by interfering with automatic control, and our results are consistent with that hypothesis. However, external kinetic focus also caused shorter jump length, contrary to our hypothesis. This suggests that attentional focus hurts performance when an instruction takes attention away from the performance of the task, not just when one is instructed to focus on a single joint. This result is consistent with the idea that taking focus away from the task & environment in which it is performed hurts performance.

The most surprising result, was that external kinetic focus condition, in which participants were instructed to push off the ground forcefully, produced significantly lower GRF than two of the other conditions. GRF correlates with jump length [4, 5], and, presumably, subjects who are accustomed to jumping for maximum lengths would naturally produce high GRFs to achieve such lengths without being instructed to do so. It seems that the instruction to push off forcefully interfered with the automatic motor control of jumping that produces high forces naturally. This raises the question of whether less experienced long jumpers would be affected by external kinetic focus instructions in the same way, which should be investigated further. The current results indicate that, for non-force tasks, a conscious focus on force hurts performance at least as much as consciously focusing on a rapidly extending a specific joint.

**Significance:** The results of this study bolster the view that coaches' instructions during completion should be simple and focused on performing the task, rather than details of technique such as force applied or extension of specific joints. The surprising GRF results also suggest the need for larger studies of how focus of attention affects GRF during jumping.

**Acknowledgments:** We thank all of the athletes who participated in this study. This research was not funded.

**References:** [1] Wulf & Prinz, *Psych Bull Rev* 8:648-60;2001 [2] Wu et al. *J Strength Cond Res* 26:1226-31; 2012 [3] Yen et al. *Exp Brain Res* 190:439-51; 2009 [4] Harry, et al. J Appl Biomech 37:400-7; 2021 [5] Ramos, et al. J Appl Biomech 35:52-60;2019.

**Stiff competition: assessing the relationship between mechanical properties and athlete perception of sports surfaces**

*Rachel L Hybart[1], Carter Terry[1], Rosemarie Figueroa Jacinto[1], Jessica Zendler[1]
[1]Rimkus, Houston, TX
*Corresponding author's email: Rachel.hybart@rimkus.com

**Introduction:** While playing surface is commonly believed to have an important role on player injury and performance, there is minimal knowledge in hard-court sports on how the mechanical properties of the hardwood court correlate to player biomechanics and perception of the surface, or in turn, injury risk and performance. Current test standards were developed over 50 years ago and generally have been applied to all playing surfaces (e.g., ASTM F2772-11). Yet the testing tools, such as the Advanced Artificial Athlete (AAA) and FieldTester (FT), and associated outputs [force reduction (FR), vertical deformation (VD)] have been primarily researched and developed for natural and artificial turf [1,2]. Thus the purpose of this study was to assess the extent to which: 1) the impact response to a standard surface testing method (FT) was consistent with an athlete impact on the court, 2) standard measures (FR, VD) predict athlete perception of the court, and 3) novel metrics related to the vibration response of the floor provide a better predictor of athlete perception of the floor.

**Methods:** Seven different hardwood court samples were assessed along with a level concrete slab, natural grass, and an asphalt surface as comparative sports surfaces. We recruited recreational athletes to perform two representative movements (countermovement jump, a drop landing from 1 foot; five trials per movement) on each surface. Additionally, we conducted standard impact testing (FR, VD) per ASTM F2772-11 using the FieldTester (Deltec, Netherlands). Inertial measurement units (IMUs, ENDAQ, USA) were placed at 3 and 6 feet away from the impact location and recorded data for all human and FT trials. IMU data were recorded at 4000 Hz and filtered at 240 Hz with a second-order Butterworth filter. Following the completion of all jumping trials, athletes were asked to rank the court surfaces based on their perception of the stiffness from least stiff (1) to most stiff (7).

**Results & Discussion:** Three athletes have been tested to date with additional athletes enrolled. Fig 1 presents exemplar data from a 176-lb male participant. The impact response characteristics are similar for the FieldTester and human drop for grass but diverge substantially for the hardwood court and asphalt surface. When examining the vibration response, significantly higher peak accelerations are seen for the hardwood courts than for the other surfaces, even though the hardwood court represents an intermediate value for FR and VD. Considering athlete perception, traditional measures FR and VD were strongly inversely correlated (R2 = 0.76 and R2 = 0.74) with athlete perception of the hardwood court samples, with courts with higher FR and VD rated as more stiff. Peak acceleration results indicate an even stronger inverse correlation (R2= 0.83) with athlete perception, with a higher peak acceleration corresponding to a higher perceived stiffness. However, when considering the vibration response, natural frequency of the floor was a positive predictor of athlete perception (R2= 0.62) with higher natural frequency occurring on less stiff floors. It is worth noting that the athlete grouped the courts (3,6,7 and 1,2,4,5) by the type of supports the court had underneath. The 3 courts ranked as the least stiff did not have additional supports, but the 4 more stiff courts had plastic feet beneath the wooden structure.

**Significance:** Mechanical testing methods developed and researched on grass surfaces produce substantially different results on hardwood courts, indicating that work must be done to better characterize the mechanical properties of wood courts and to identify properties that connect to athlete biomechanics and human factors (e.g., perception). The next step in this research is to assess the relationship between the vibration response, player perception, biomechanical measures, and sports performance metrics.

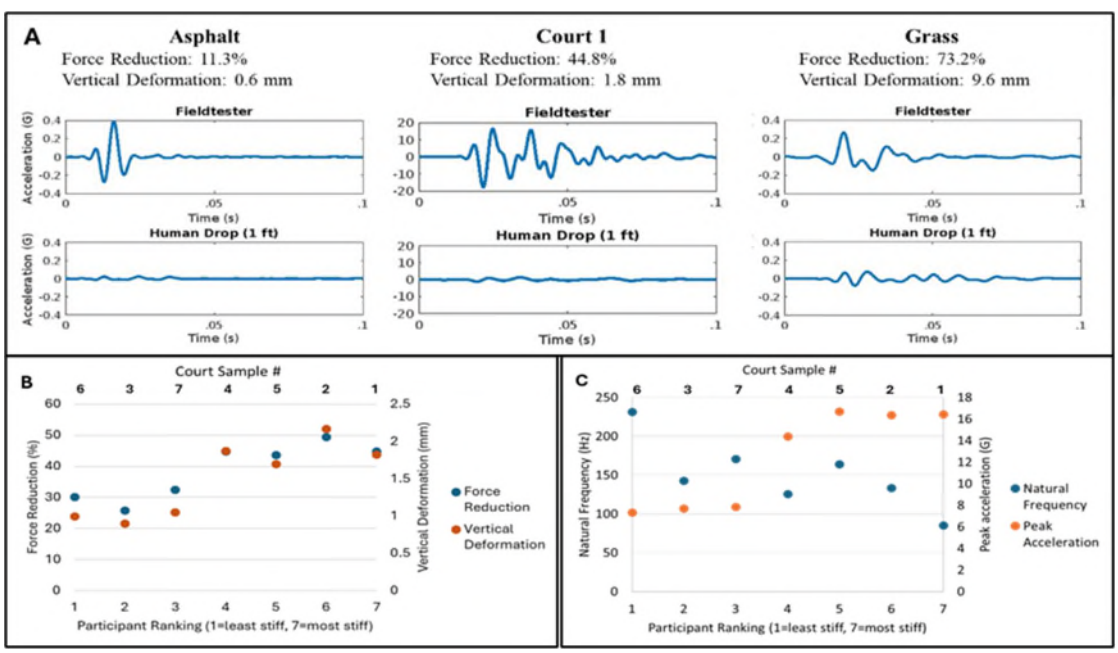


Figure 1. A. Example accelerations on 3 different surfaces during a FieldTester and human drop. B. The relationship between participant perception of stiffness and the force reduction (%) and vertical deformation (mm) of the 7 different courts. C. The relationship between participant perception of stiffness and the Natural frequency (Hz) and Peak Acceleration (G) of the 7 different courts.

**References:**

[1] Colino, et al. (2017), *Polymer Testing* 62; [2] Fleming, et al. (2020), *Proceedings* 49

# SEX PERFORMANCE DIFFERENCES IN VERTICAL AND HORIZONTAL JUMPING

*Emily L. McClelland & Peter G. Weyand
Locomotor Performance Laboratory, Texas Christian University, Fort Worth, TX 76109
*Corresponding author's email: e.l.mcclelland@tcu.edu

**Introduction:** Between-sex differences in athletic performance are larger and more variable for jumping than running. For example, sex differences in jumping events regularly exceed those in running events by two-fold or more and are consistently greater for vertical vs. horizontal jumps. Because jumping performance is directly influenced by the ground forces jumpers can apply, the proportion of the body's mass comprised of skeletal muscle likely influences jumping capabilities.

Existing data identify the smallest sex differences for horizontal Olympic-style run-in jumps (long and triple jumps) ranging from 15-18%, moderately larger differences for the high jump (~ 20%), and the largest differences for jumps initiated from a standstill such as the vertical countermovement jump (25-50%).

Here we hypothesize that sex differences in jumping performance vary in accordance with the relative requirement of the jump for vertical motion. We expect this due to: 1) the mechanical requirement to overcome gravity for vertical ($F_{z\text{-net}} = F_{z\text{-total}} - mg$), but not horizontal, motion, and 2) females having relatively less muscle and muscular force available to offset gravity and elevate the body's mass.

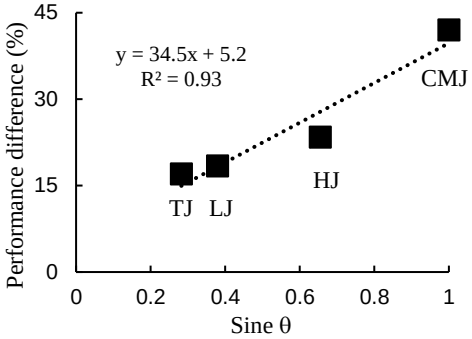


**Figure 1**: Mean sex differences in performance as a function of the vertical component of the take-off angle of each type of jump, TJ, LJ, HJ, and CMJ.

**Methods:** We tested this hypothesis using available or acquired data from four types of jumps differing in their relative requirements for horizontal vs. vertical motion: triple jump (TJ), long jump (LJ), high jump (HJ), and countermovement jump (CMJ). Male and female performance data were compiled from World Athletics lists (2003-2018) for the three Olympic jumps (n=40 per sex) and acquired from male and female collegiate athletes (n=19 per sex) for the CMJ.

Force and time data for CMJs were acquired from a Bertec force plate system. Take-off velocity ($V_{TO}$) was determined using the impulse-momentum relationship. CMJ height (JH) was then determined from $V_{TO}$ ($JH = V_{TO}^2/2g$). The vertical component of the take-off angle of each type of jump was acquired from World Athletics Biomechanical reports for TJ, LJ, and HJ [1,2] and assumed to be 90º for the CMJ.

Percent sex differences were calculated for each of the four jump types. Simple regression was utilized to analyze the relationship between the sex difference in performance and the sine of the take-off angles (sine θ) for the respective jump types. Sex differences in total ($F_{z\text{-total}}$) and net ($F_{z\text{-net}}$) vertical forces, were determined for the original CMJ data.

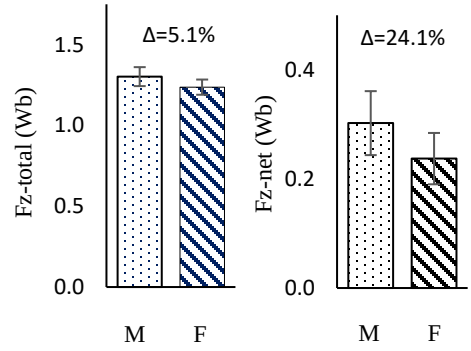


**Figure 2**: Mean normalized total (a) and net (b) vertical ground reaction force for the collegiate athletes CMJ in units of the body's weight.

**Results & Discussion:** Sex differences in performance spanned almost a two-and-a-half-fold range from the most horizontally oriented (TJ=17%) to the most vertically oriented (CMJ=42.1%) jump type. Per our hypothesis, nearly all variance in sex performance difference was accounted for by the vertical requirement of the motion (sine θ, Fig. 1).

Because male athletes are relatively more muscular than female athletes [3], we expected our male subjects to apply greater mass-specific ground forces and jump higher. The CMJ males in our dataset, on average, had absolute $F_{z\text{-total}}$ (F/kg) values that were 5.1% greater and $F_{z\text{-net}}$ (F/kg) values that were 24.1% greater than females (Fig. 2). Additionally, due to small sex differences in time of force application males had 21.3% greater $V_{TO}$ values.

Because gravitational forces continue to oppose vertical, but not horizontal, bodily motion after a jumper leaves the ground, vertical distances (i.e. jump heights) are a function of the vertical take-off velocity squared ($Height = V_{TO\text{-}z}^2/2g; \propto V^2$). In contrast, horizontal jump distances are the product of horizontal take-off velocity and aerial time ($Distance = V_{TO\text{-}y} \bullet t_{air}; \propto V^1$). In this regard, take-off velocity differences are amplified when athletes jump for height, but not when they jump for distance - thereby explaining the greater sex performance differences observed for more vertically oriented jumps as illustrated in Figure 1.

**Significance:** Although sex-specific force/mass capabilities of male and female jumping athletes differ by relatively constant margins, sex performance differences in jumping performance do not. Rather they vary over a broad range and do so in direct accordance with the relative requirement for vertical motion. Understanding the biological and mechanical basis of sex performance differences has immediate relevance for population norms, do athletes first training applications, and policies for athletic in numerous court and field sports.

**Acknowledgments:** This work would not have been possible without the support for data acquisition and subject recruitment from Sunil Prajapati and Emily Baird as well as the participation of our subjects.

**References:** [1] Hay , 1992, *J Sports Sciences,* 10: 4. [2] World Athletics biomechanical reports: Triple jump (2009, 2017, 2018, Long Jump (1997, 2007, 2018) High jump (1997, 2017, 2018) [3] Prior et al., 2001, *j Applied Physiology.* 90: 1523-153.

# DO MEASURES OF ATTENTION CONTROL PREDICT DECISION-MAKING PERFORMANCE ON A REACTIVE JUMP LANDING TASK?

*Fatemeh Aflatounian, Keith A. Hutchison, and Scott M. Monfort
[1]Montana State University, Bozeman, Montana, USA
*Corresponding author's email: fatemehaflatounian@montana.edu

**Introduction:**
Non-contact anterior cruciate ligament (ACL) injuries are often attributed to motor coordination errors, highlighting a critical link between cognitive function and movement [1-3]. Dual-task screening integrates cognitive challenges with physical tasks to better evaluate biomechanical risk factors [4]. During unanticipated dual-task protocols, participants typically have some fraction of trials where they fail to react correctly to the cognitive tasks or otherwise successfully complete the jump landing. These 'failed' trials may indicate poor neuromuscular control and increased re-injury risk [5]. Giesche et. al. [6] found that more standing errors during unplanned single-leg landings correlated to better cognitive flexibility, working memory and short-term memory; and poor decision-making (more unanticipated landing errors) resulted from deficits in cognitive flexibility, working memory and short-term memory. Moreover, attentional errors can reduce temporospatial awareness of a player's movement direction, potentially impairing motor control and increasing the risk of ACL injury [7]. Further understanding the relationships between cognitive function (e.g., attentional control and reaction time) and decision-making errors during dynamic sport movements may elucidate novel injury risk reduction opportunities. Therefore, we examined the relationship between frequency of failed decision making during unanticipated jump-landing tasks and cognitive performance in athletes. We hypothesized that worse performance on reaction time and attention control tests would be associated with having more failed trials during unanticipated conditions.

**Methods:** 15 healthy athletes (7F/8M, 24.0±4.1 yrs; 1.74±0.09 m; 70.1±10.3 kg; Tegner: 6.5±0.9; Marx: 9.7 ±3.2) completed cognitive tasks and the drop jumping task under anticipated and unanticipated conditions. A 3-task test battery was used to characterize participants' attentional control [8], and a computerized complex reaction time task was used characterize reaction time. Then, participants performed a jump landing from a 30 cm box, followed by landing on their left leg, right leg, or double-leg and then immediately jumping straight up as high as possible. Unanticipated conditions included a simple cognitive task (**Simple**) of landing on the limb towards an image on one side of the screen, and a complex cognitive task (**Complex**) of landing on the limb towards the picture of the basketball or away from a picture of a simulated opponent. Failed trials were defined as trials where participants reacted incorrectly to the cue and landed on the wrong leg(s). The percentage of number of failed trials were calculated for both simple and multiple cognitive tasks in unanticipated conditions. Pearson correlations tested for cognitive variables and percentage of failed trials from unanticipated drop jumping tasks (**Simple** and **Complex**), with a bootstrapping procedure used to generate confidence intervals for the coefficients.

**Results & Discussion:** No significant correlations were detected for any of the cognitive tasks and percentage of the failed trials ($p$ >0.05, **Figure 1**). Our preliminary data indicate these variables are likely not correlated, suggesting that despite the robust role of attention control as a cornerstone of cognitive performance including for cognitive multitasking [9], it is less clearly related to decision-making success in a dynamic jumping task. More robust measures of visual-spatial processing speed and/or working memory may provide alternate cognitive processes that remain promising for their associations with cognitive-motor function, including during jumping/cutting tasks [1, 10]. Additionally, the extent to which cognition-biomechanics relationships vary by situations is not clearly understood. It is noteworthy that data collection is ongoing for this study, highlighting the preliminary nature of the findings reported here.

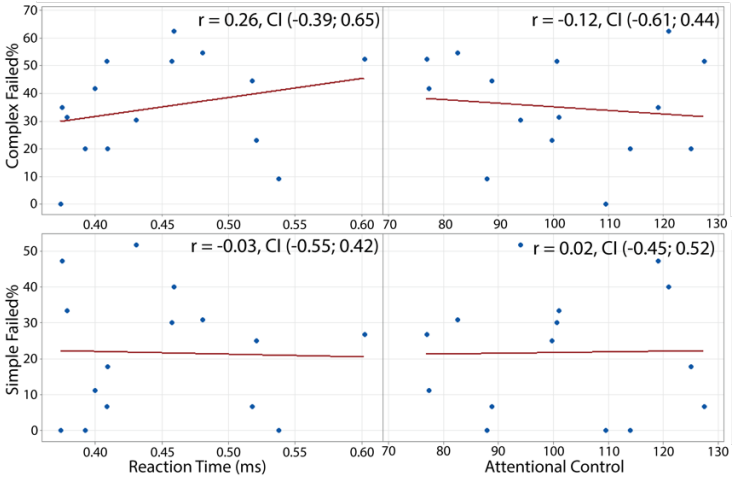


**Figure 1:** Scatterplots of cognitive function scores and failed percentages; CI: Confidence Intervals

**Significance:** This study examines the relationship between cognitive performance and movement errors in unanticipated jump-landing tasks, considering failed trials as potential indicators of neuromuscular control deficits. The lack of significant correlations suggests that attentional control alone may not predict an athlete's decision-making accuracy during dynamic movements. These preliminary findings highlight the need for further research to confirm these findings, as data collection is ongoing.

**Acknowledgments:** This research was supported by the MSU NACOE TEER grant. We would also like to thank Luke Juergensen, Max Johnsen and Sophie Stemler for their help.

**References:** [1] Monfort et al. (2019) *Am J Sports Med* 47(6), [2] Grooms et al. (2022) *PLoS One* 17(8), [3] Miko et al. (2021) *J Sci Med Sport* 24(2), [4] Wiggins et al. (2016) *Am J Sports Med* 44(7) [5] Wikstrom et al. (2021) *J Med Sci Sorts* 18(1), [6] Giesche et al. (2020) *J Sci Med Sport* 23(1), [7] Gokeler et. al. (2024) *J Athl Train* 59(3), [8] Burgoyne et. al. (2023) *J Exp Psychol Gen* 152(8), [9] Burgoyne et al. (2020) *Current Directions in Psychological Science* 29(6), [10] Herman et. al. (2016) *Am J Sports Med* 44(9)

# BIOMECHANICAL CONSEQUENCES OF UNBALANCED JUMP LANDINGS

*Fatemeh Aflatounian, James N. Becker, Corey Pew, Keith A. Hutchison, and Scott M. Monfort
Montana State University, Bozeman, Montana, USA
*Corresponding author's email: fatemehaflatounian@montana.edu

**Introduction:** Over 120,000 anterior cruciate ligament **(**ACL) injuries occur annually in the U.S., a majority from noncontact mechanisms [1,2]. Jump-landing tasks, like the drop vertical jump, assess neuromuscular control but often fail to replicate real-world, unanticipated movements requiring rapid decisions and divided attention. During protocols that introduce directional cues to elicit rapid decision-making demands, participants typically have some fraction of trials where they fail to successfully land (e.g. landing on the incorrect limb or direction, unable to keep their balance). These unsuccessful movements are frequently removed from research data sets; however, removing trials with large-scale task failure may mask potentially relevant findings, as these scenarios may more completely encompass athletes' actions in real-life environments. Failed trials may indicate poor neuromuscular control and increased re-injury risk [5]. Therefore, the purpose of this study was to explore the relationship between unbalanced trials and knee motion outcomes related to ACL injury during different levels of cognitive challenges, aiming to improve risk assessment tools by simulating real-world athletic demands. We hypothesized knee motion related to primary ACL injury (e.g., peak knee flexion angle (pKFA), peak knee abduction angle (pKAbA), and peak knee abduction moment (pKAbM)) would be exacerbated during unbalanced trials during the more challenging cognitive tasks compared to successful trials.

**Methods:** 13 healthy athletes (7F/6M, 23.4±3.3 yrs; 1.73±0.10 m; 69.6±10.9 kg; Tegner: 6.5±0.9; Marx: 10 ±3.2) completed a drop jumping task under anticipated and unanticipated (i.e., cue presented just before landing) conditions. Kinematics and ground reaction force data were collected as participants performed a jump landing from a 30 cm box, followed by landing on left, or right leg, or double-leg landing following by jump up as high as possible. We captured these movements using markerless motion capture system (10 cameras, Qualisys, Theia3D, 6 force plates, OPT464508-2K; AMTI). Conditions included: Baseline (**Baseline,** anticipated direction, no cognitive task), Simple cognitive task (**Simple,** landing on the limb towards an image on one side of the screen), Complex cognitive task (**Complex,** landing on the limb towards a picture of a basketball or away from a picture of a simulated opponent, displayed on one side of a screen). Unbalanced trials were defined as trials where participants reacted correctly to the cue (correct landing decision) but were unable to keep their balance for 2 seconds. Dependent variables were peak values of knee flexion angle (pKFA), knee abduction angle (pKAbA), and external knee abduction moment (pKAbM) normalized to body weight (BW) and height (HT) within the first 100 ms following initial contact for the single-leg landings on the dominant limb [6]. Mixed effect statistical models tested for Condition*Success interactions as well as differences between unbalanced and successful trials.

**Results & Discussion:** No significant Condition*Success interactions were detected. Significant differences between unbalanced and successful trials were observed for pKAbM ($p$=0.012). Post-hoc analysis indicated higher values of pKAbM, associated with riskier knee mechanics, for the unbalanced trials (5.3±2.1% BW-HT) compared to successful trials (4.8±1.7% BW-HT, **Figure 1**). Condition differences were observed for pKAbA ($p$ = 0.003) and pKAbM ($p$ = 0.007), with post-hoc analysis displaying increase in (riskier) knee mechanics for cognitive-challenging conditions compared to baseline, specifically between Complex and Baseline for pKAbM (Complex: 5.5±2.0% BW-HT and Baseline: 4.2±1.3% BW-HT, **Figure 1**) and between Simple and Baseline for pKAbA (Simple: -3.05±3.25° and Baseline: -2.27±2.45°). Our preliminary data show differences for unbalanced compared to successful trials, which supports value in considering a broader scope of task performance when studying on ACL injury in future studies. Also, condition differences between cognitive challenges and baseline movements further highlight the effects of cognitive challenges on influencing biomechanics during jumping tasks, which may better reflect performance during real-world sport performance. It is noteworthy that data collection is ongoing for this study, highlighting the preliminary nature of the findings reported here.

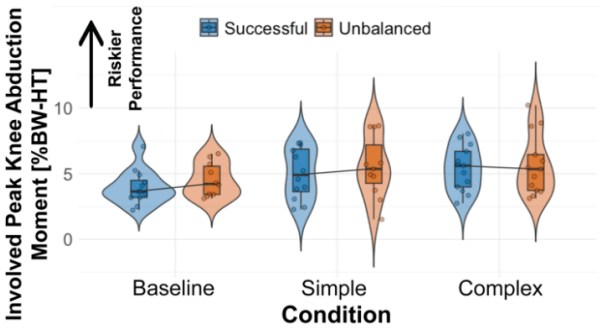


**Figure 1:** Violin plots of successful and unbalanced trials during different conditions for pKAbM [%BW-HT]

**Significance:** This study highlights the value of considering unbalanced jump-landing trials for ACL injury research, as they may reflect real-world scenarios where athletes struggle to maintain stability. The findings suggest that unbalanced trials exhibit riskier knee mechanics than the successful trials, particularly in pKAbM, emphasizing the need to reconsider how biomechanical screening accounts for jump landings when studying primary ACL injury risk. Additionally, the study underscores the impact of cognitive challenges on knee mechanics, reinforcing the value of incorporating decision-making tasks in ACL injury prevention training. However, further research is needed to confirm these preliminary findings, as data collection is ongoing.

**Acknowledgments:** This research was supported by the MSU NACOE TEER grant. We would also like to thank Luke Juergensen, Max Johnsen and Sophie Stemler for their help in collecting data.

**References:** [1] Kaeding et. al. (2017) *Clin Sorts Med* 36(1), [2] Chia et. al. (2022) *Sports Med* 52, [3] Fischer et al. (2021) *J Applied Biomech* 37(4), [4] Gokeler et al. (2021) *BMJ Open Sport Excer Med* 7(2), [5] Wikstrom et al. (2021) *J Med Sci Sorts* 18(1), [6] Krosshaug et. al. (2007) *Am J Sports Med* 35(3)

# No Impact of Biceps Femoris Activation on Drop Jump Landing Mechanics

David Phillips[1*], Bethany Burr
[1]Program in Kinesiology, College of Health, Oregon State University, Cascades, Bend OR
*David.phillips@osucascades.edu

**Introduction:** The drop vertical jump (DVJ) maneuver is a stress movement that is used to evaluate individuals for potential lower extremity injury risk [1]. Biomechanical variables believed to be predictive of lower extremity injury are measured across three, five, and sometimes up to 10 trials. Kinematic and kinetic variables show good intersession reliability for these trial ranges [2]. While participants demonstrate consistent kinematic and kinetic patterns, the underlying neuromuscular coordination appears less reliable. Coordinated contraction of the hamstring is important for both athletic performance and possibly ACL injury risk [3]. Since the contraction behavior of the muscle is less consistent compared to kinematics and kinetics, the current standard for number of measured trials may be insufficient to understand the hamstring's role in landing mechanics. The purpose of this study is to examine differences in landing kinematics and kinetics based on hamstring activation during initial contact, 0-100ms across 30 trials. We hypothesized that lower hamstring (measured from the biceps femoris) activation during initial contact will be associated with biomechanical factors associated with injury risk: decreased peak joint flexion and excursion angles, increased knee valgus, increased knee abduction moments, higher peak vertical ground reaction forces (vGRF), and higher vGRF loading rates.

**Methods:** 25 participants (12F, 13M) completed 30 trials of a standard DVJ protocol. The DVJ protocol has a participant jump a forward distance of 50% of their height from a 30 cm high box onto force plates and then immediately execute a maximum vertical jump and land back with feet on the force plates. During the DVJ, participant kinematics were recorded using a 10-camera motion capture system (Qualisys), with retroreflective markers placed on anatomical landmarks and clusters on lower extremity segments at 200 Hz. Two in-ground AMTI force plates measured ground reaction forces at 1000 Hz for each limb separately. Lasty, nine wireless electromyographic (EMG) sensors were placed on the right side to record muscle activity at 2000 Hz from the medial and lateral gastrocnemius, tibialis anterior, semitendinosus, biceps femoris, vastus medialis, rectus femoris, gluteus medius, and gluteus maximus. All data were synchronously sampled through QTM software then exported to Visual 3D for processing and analysis. Prior to normalization, smoothed EMG data (30 ms sliding window) from each trial were carefully screened for large amplitude artifacts. Following EMG screening, EMG data were normalized to the maximum value measured across the 30 trials for each muscle. The integrated EMG (iEMG) for the biceps femoris over the first 100 ms of contact were used to identify the five trials with the highest and the five trials with the lowest biceps femoris activation at contact. The ensemble average of biceps femoris activation, peak angle of ankle, knee, and hip flexion; ankle, knee, and hip sagittal excursion; peak knee valgus angle; peak ankle, knee, and hip extension moment; and peak knee abduction moment were compared using paired *t*-tests ($\alpha = 0.01$). In the case of a significant results, a correlation between the biceps femoris activation with the variable is calculated across all recorded trials.

**Results & Discussion:** There was a significant difference in biceps femoris activation between trials identified with a low activation and high hamstring activation, $p < 0.001$, Cohen's $d = 12.3$. No significant differences were found between high hamstring and low hamstring activation trials across the kinematic and kinetic variables, $p > 0.01$ in all variables (biceps femoris activation and peak knee flexion angle presented in Fig. 1). Despite what would be classified much greater than a large effect size, biceps femoris activation during initial contact had a minimal effect on standard biomechanical measures of DVJ performance. Observable kinematics and measurable kinetics therefore provide limited information about the underlying neuromuscular coordination pattern of the biceps femoris muscle. Given the hypothesized importance of the hamstring muscle group in unloading the ACL during landing, it may be a shortcoming of the DVJ, often scored only qualitatively, to identify individuals at high risk of an ACL tear. Participants in this study were able to generate similar kinematic and kinetic outcomes despite significant differences in their hamstring behaviour during initial contact.

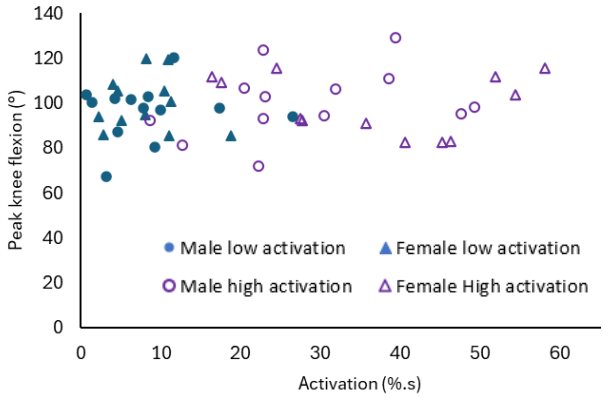


Figure 1: Low and high biceps femoris activation and peak knee flexion

**Significance:** Kinematics and kinetics from a DVJ protocol cannot discriminate between landings with high biceps femoris activation during initial contact with low biceps femoris action during initial contact. Observable, safe landing mechanics may not be indicative of low loading on the ACL or low injury risk.

**References:** [1] Padua et al., (2015), *J. Athl. Train,* 50(6); [2] Malfait et al., (2014), *Med Sci Sports Exerc,* 46(4); [2] Nasseri et al., (2021), *Med Sci Sports Exerc,* 52(6).

# ANGULAR AND LINEAR IMPULSE AS KEY PERFORMANCE INDICATORS FOR COLLEGIATE GOLFERS

*Cameron Jensen[1], Sam Wilkins[2], Adam B. Rosen[2], Brian Knarr[1]
[1]Department of Biomechanics, University of Nebraska at Omaha, Omaha, Nebraska, USA
[2]School of Health and Kinesiology, University of Nebraska at Omaha, Omaha, Nebraska, USA
*Corresponding author's email: cameronjensen@unomaha.edu

**Introduction:** Ground reaction forces (GRFs) are useful in understanding the biomechanics of a golf swing as higher peak GRFs are associated with better golf performances, specifically higher clubhead speeds (CHS) [1]. However, peak GRFs alone may not fully capture the forces in a golf swing. Impulse, which measures force over time, provides a more comprehensive assessment of force and momentum and is strongly correlated with athletic movements such as jumping, sprinting, and change of direction tasks [2]. While extensively studied in linear movements, impulse's role in rotational movements is less clear. Both linear and angular impulse are crucial for balance regulation in the golf swing. Skilled golfers adjust these impulses for stability and swing adaptation [3]. Research links higher impulse in jump and isometric strength tests to improved golf performance, particularly CHS [4], [5]. However, no studies have directly investigated the relationship between impulse produced during the golf swing and CHS. This study aims to determine how linear and angular impulse during the swing relate to clubhead speed. Given golf's rotational nature and the link between impulse and performance in other sports, it is hypothesized that higher angular impulse and lower linear impulse will correlate with greater CHS.

**Methods:** As part of a larger protocol, 9 right-handed female collegiate golfers (age: 20 ± 0.9 yrs; height: 167.6 ± 4.6 cm; mass: 64.1 ± 5.4 kg, handicap: 8.2 ± 2.3) completed three driver swings while standing on two force plates in a controlled indoor environment. Linear impulse was calculated by integrating the force-time curves (X, Y, and Z) from takeaway, defined as the first observable movement of the club away from the ball to impact. Angular impulse was calculated by integrating the moment-time curves over the same period. Impulse values were normalized by body weight. CHS was collected using a golf launch monitor. Pearson correlation tests assessed the relationships between the average impulse values and average clubhead speed, with statistical significance set at $p < 0.05$.

**Results & Discussion:** A moderate significant negative relationship was found between back foot horizontal angular impulse and CHS (R = -0.674, p = 0.046, Fig. 1A), with larger negative values associated with higher CHS and larger positive values associated with lower CHS. This suggests that the back foot plays a critical role in coiling the body into the backswing, where greater clockwise rotational torque can improve CHS by generating more rotational impulse. A moderate significant negative relationship was found between total frontal angular impulse and CHS (R = -0.648, p = 0.049, Fig. 1B), with higher frontal angular impulse associated with lower CHS. High frontal impulse suggests that energy is directed toward lateral bending or tilting rather than rotating. This relationship indicates that minimizing excessive lateral bending may be helpful in improving CHS. Total linear impulse in the X-direction (toward the target) also showed a moderate significant negative relationship with CHS (R = -0.629, p = 0.050, Fig. 1C), with higher impulse values associated with lower CHS. Applying excessive force toward the target may disrupt rotational mechanics and limit power generation, so optimizing force distribution for rotational acceleration over linear force enhances CHS and performance.

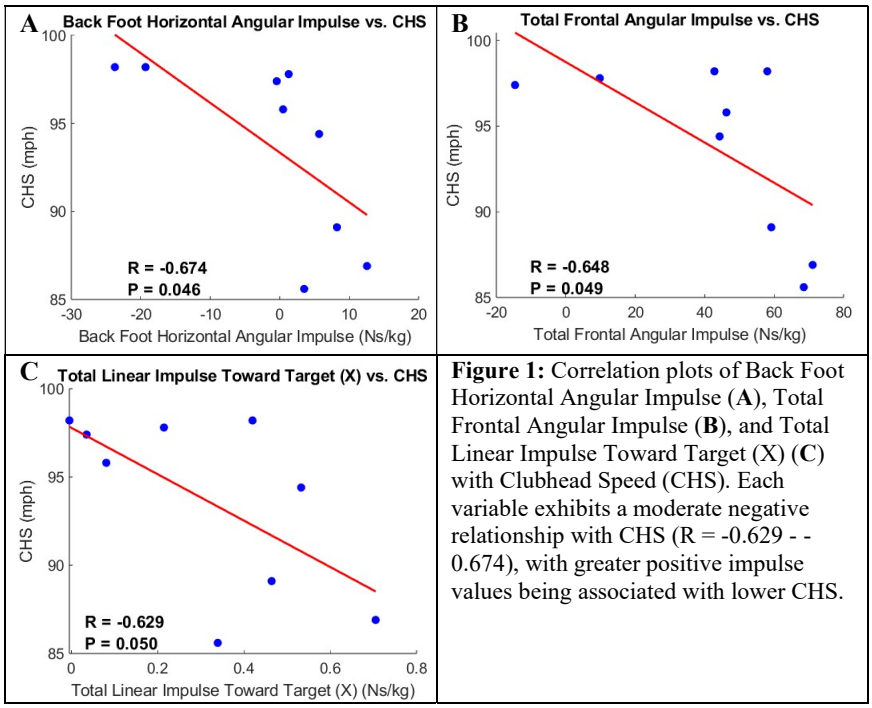


**Figure 1:** Correlation plots of Back Foot Horizontal Angular Impulse (**A**), Total Frontal Angular Impulse (**B**), and Total Linear Impulse Toward Target (X) (**C**) with Clubhead Speed (CHS). Each variable exhibits a moderate negative relationship with CHS (R = -0.629 - -0.674), with greater positive impulse values being associated with lower CHS.

**Significance:** As golf is a rotational sport, optimal performance relies on applying force over time in a way that maximizes rotational efficiency about the golfer's vertical axis, rather than forces that cause excessive tilting, bending, or lateral shifting [6]. Golfers should focus on applying sustained force through the back foot to effectively coil into the backswing, while minimizing forces that contribute to unnecessary lateral movement or bending. By optimizing force application, golfers may improve energy transfer and increase clubhead speed, thereby improving overall performance.

**Acknowledgments:** Funding was supported by the GRACA Grant [Grant number 50210]. Equipment was supported by the Center of Research in Human Movement Variability of the University of Nebraska at Omaha and the NIH [Grant number P20GM109090].

**References:** [1] Han et al. (2019), *Sports Biomech* 18(2); [2] Knudson (2009), *J Strength Cond Res* 23(6); [3] Peterson et al. (2016), *J Appl Biomech*.; [4] Wells et al. (2018), *J Sports Sci* 36(16); [5] Leary et al. (2012), *J Strength Cond Res* 26(10); [6] Rose et al. (2024) *TPI Certification Level 1.*

# ISOMETRIC MID-THIGH PULL PERFORMANCE IS RELATED TO BAT SPEED

*Neha Kapoor[1], Kiara Barrett[1]
[1]Bertec Corporation, Columbus, OH
*Corresponding author's email: neha.kapoor@bertec.com

**Introduction:** Enhancing muscular strength is essential to improving sport performance as it directly influences power. Strength training enhances the muscle's ability to produce maximal force and improves the nervous system's ability to recruit muscle fibers quickly, leading to powerful, explosive movements. Strength assessments such as the isometric mid-thigh pull (IMTP) have been widely studied for their correlation with sports performance: IMTP peak force (PF) has been strongly correlated with competition performance for weightlifters [1]; in golfers the rate of force development (RFD) and force at 150ms ($F_{150}$) in the IMTP were correlated with maximal club head speed [2]. Similarly, research has explored the correlation and predictive value of IMTP metrics in baseball players, with findings suggesting moderate to strong correlations between IMTP kinetic variables and offensive performance [3]. However, no study has specifically examined the relationship between IMTP kinetic variables and bat speed. This study aims to expand on existing research by analyzing the correlation between IMTP metrics and bat speed in collegiate baseball hitters, providing further insight into how isometric force production relates to batting statistics. We hypothesize IMTP metrics will be significantly correlated with bat speed.

**Methods:** Batting and performance data from 73 collegiate hitters (88.43±10.14 kg) during regular training sessions at Driveline were retrospectively analysed via the opensource OpenBiomechanics dataset [4]. Batters were categorized into three different bat speed (BS) groups: Low (<65 mph), Moderate (65-70 mph), and High (>70 mph). At-bats were performed on Bertec's triaxial force plates in a batting cage at Driveline Baseball's facility. The IMTP was performed with players pulling a stationary bar upwards as hard as possible while standing on force plates. Peak vertical force (PF), RFD, $F_{150}$, and forces at 100ms ($F_{100}$) and 200ms ($F_{200}$), were evaluated for their relationship to BS. Net PF was normalized by bodyweight; RFD was calculated from 0 to 200ms. Normality was assessed via Shapiro-Wilk's test, and Welch's ANOVA with Games Howell post-hoc tests were conducted to determine metric associations with BS groups. The alpha level for all statistical analyses was set at .05.

**Results & Discussion:** Only $F_{150}$, $F_{200}$, and RFD were normally distributed across all BS groups ($p > .05$). IMTP metric results by BS group can be found in Figure 1. Welch's ANOVA testing revealed a main effect of group ($p<.001$). Post-hoc analyses revealed players in the High BS group had significantly higher PF than the Moderate ($p<.001$) and Low ($p<.001$) groups, with the Moderate group having significantly higher PF than the Low group ($p<.001$). For $F_{150}$, $F_{200}$, and RFD, the Low BS group was significantly lower than the Moderate ($p<.05$) and High ($p<.05$) BS groups, with no difference between High and Moderate groups ($p>.05$). For $F_{100}$, the High BS group displayed significantly higher forces compared to the Low BS group ($p<.05$), with no differences between the Low and Moderate ($p=1.31$) or the High and Moderate ($p=.512$) groups. As hypothesized, these findings suggest that higher BS is associated with greater PF production in the IMTP, highlighting the importance of maximal strength in optimizing bat speed. The significant difference between the Low and High BS groups for $F_{100}$ may indicate that the ability to generate force rapidly within the first 100ms yields higher BS; however, the lack of significance between Low and Moderate groups suggests early force production alone is not sufficient to reach moderate bat speeds. Furthermore, the lack of differences in $F_{150}$, $F_{200}$, and RFD between Moderate and High BS groups suggests that once a sufficient level of force production is reached, additional increases may not necessarily translate to further improvements in bat speed.

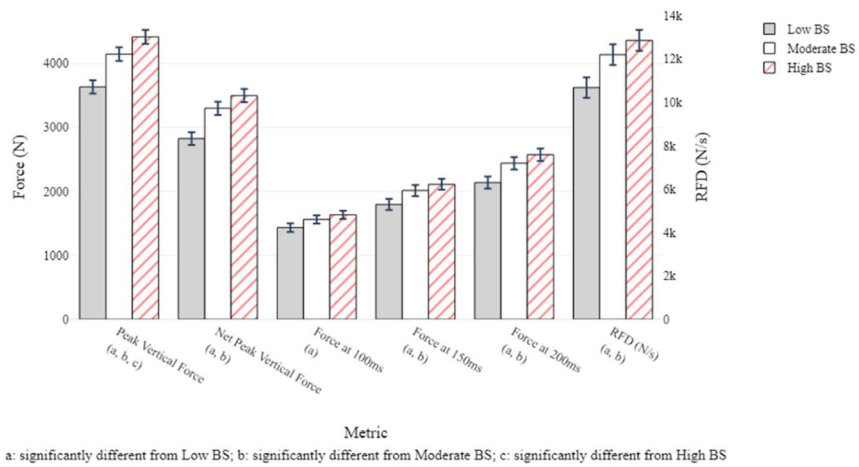


**Figure 1**: IMTP Metrics for Low, Moderate, and High BS Groups

**Significance:** This study provides valuable insights into the relationship between force production and bat speed. The IMTP's lower and upper-body engagement provides an excellent measure of explosive force application, critical for batting performance. These findings reinforce the role of strength and power training, particularly targeting PF and RFD, to optimize batting performance. Baseball professionals should consider integrating such training to enhance BS.

**Acknowledgments:** Joeseph Marsh at Driveline Baseball.

**References:**[1] Beckham et al. (2013), *J Sports Med Phys Fitness* 5; [2] Leary et al. (2012), *J Stren. Cond. Res.* 26(10); [3] Bailey et al. (2013), *10.13140/2.1.1227.6162*; [4] Wasserberger et al. (2022), The OpenBiomechanics Project.

# HOW DO GYMNASTS WITH CHRONIC ANKLE INSTABILITY RESPOND TO STRESSFUL EXERCISE?

*Divya Bhaskaran, PhD[1], Oliva Tobin[2], Laurel Raymond[3]
[1]Hamline University,
*Corresponding author's email: dbhaskaran01@hamline.edu

**Introduction:** Women Gymnasts perform the vault, balance beam, floor exercise and uneven bars. These events require balance, strength, flexibility and adaptability to quickly maneuver complex movement patterns. Ankle sprains are the top diagnosed injury for gymnasts [1]. Previous research has found correlation between fatigue and acute ankle sprains. Fatigue has proven to have effects on the functionality of the proprioceptive system [2]. Even with current rehabilitation protocol and treatments, acute ankle sprains have a high recurrence rate, which is highly associated with the development of chronic ankle instability (CAI) [3]. Through previous research it has been discovered that 70% of gymnastics with previous ankle sprains have developed CAI [4]. Additionally, CAI has shown to lead to deficits in ankle strength [5]. This study will aim to assess the effects of fatigue on the ankles of gymnasts with varying levels of chronic ankle instability. The objective of this study is to assess how gymnasts with varying levels of chronic ankle instability react to stressful exercise. Our hypothesis is that gymnasts with lower CAI scores, when fatigued will behave more efficiently than those with higher CAI scores.

**Methods:** Fifteen female Division III gymnasts ages (18-22) participated in the study, approved by the IRB at Hamline University. Cumberland Ankle Instability Tool was self-reported and used to report on CAI [6]. Muscle activation of the medial gastrocnemius (MG), peroneal longus (PL) and Tibialis anterior (TA) is measured using a Delsys Electromyography unit. After the EMG sensors are placed on both legs, the participants perform baseline activities Here is the list of activities performed atop a force plate: (1) Single leg hops for both legs, (2) Land from a box with a height of 46 inches with both feet. (3) Single leg stance on both legs for 2 minutes. Postural sway/ balance is measured by the area of the ellipse that encloses the Center of Pressure (COP) movement/path with 95% confidence interval will be measured (95%COP) using a Bertec force plate. Participants then engage in multiple rounds of an ankle fatiguing protocol "Fig. 1" adapted by a previous study [7]. The participants will be asked to continue through this cycle until they hit fatigue. Fatigue is classified as 1) having a 50% increase from their fastest time to complete the course, 2) repeated inability to clear the 10 cm barriers on the bilateral hops, or 3) becoming unwilling to continue the course. Following the fatigue protocol the participants will be asked to repeat the pre-fatigue activities. The data was statistically analyzed using R Studio, paired t-tests and Pearson correlation tests were conducted to illuminate the effects of fatigue.

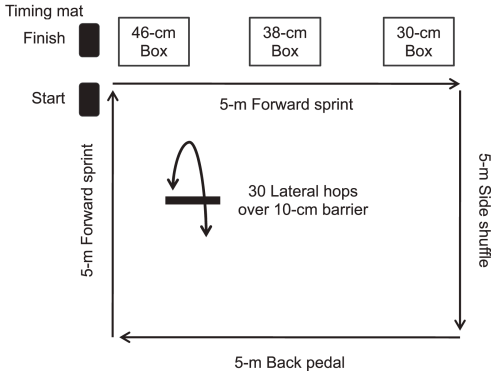


**Figure 1:** Ankle fatigue protocol

**Results & Discussion:** Muscle activation was normalized to their maximum voluntary contractions (MVC) while analysing data. Single leg hopping (Fig 2) and Drop landing (Fig 3) from 46cm box demonstrated significantly lesser activation of all three muscles in both legs post fatiguing exercise. These demonstrate that the fatigue protocol successfully fatigued the muscles. COP 95 was significantly higher post fatigue on the left leg (Pre= 946.89± 402.92 $mm^2$, Post = 1383.33±892.48 $mm^2$). The data was consistent with previous studies that also observed increases in postural sway and reduction in muscle activation after fatigue [8]. There was a low but significant correlation between CAI scores and muscle activity was only seen in the Left Peroneal longus muscle pre-fatigue (R=0.23). This indicates that participants with higher CAI had higher PL activation. No significant relationship was found between other variables and CAI, this could be due to the low number of participants.

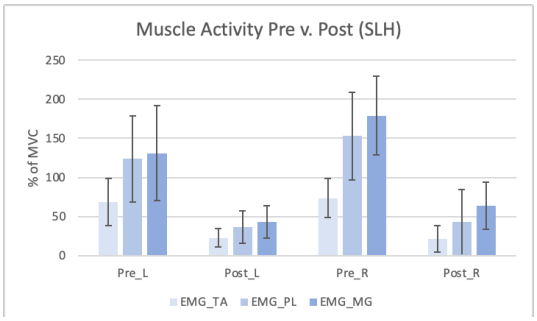


**Figure 2:** Muscle activation of TA, PL and MG during the Single Leg Hopping pre and post

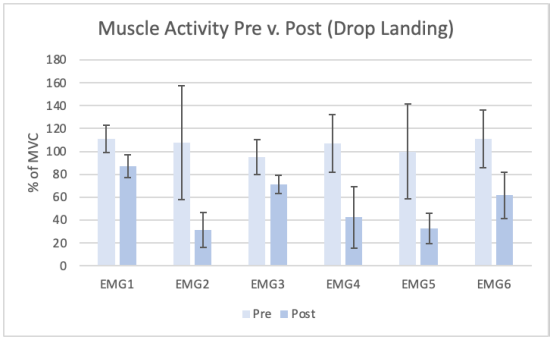


**Figure 3:** Muscle activation of TA, PL and MG while drop landing from 46cm box, Where EMG 1,2 and 3 are the left TA, PL and MG, while 4,5,6 and the same muscles on the right side pre and post exercise.

**Significance:** This study demonstrated that participants with higher CAI score had higher activation of the peroneal longus muscle. These findings confirm that gymnasts with a history of CAI perform differently as their peroneal longus muscle is not completely recovered. Findings from this study can help inform and design gymnast-specific ankle rehabilitation protocols to prevent recurrent ankle sprains and improve ankle instability.

**Acknowledgments:** Thanks to Hamline's Summer Collaborative Undergraduate Research for funding this study.

**References:** [1] Albright et al. (2022), Sports Health 15(3); [2] Forestier et al. (2022), Med Sci Sports Exerc; [3]Herzog et al. (2019), J Athl Train; [4] Zhang et al. (2022), J Clin Med 11(24); [5] Liu et al. (2024), *Motor Control*, *28*(4); [6] Hiller et al. (2006), Arch Phys Med & Rehab; [7] Webster et al.(2016), Journ of Athl Train 51(8); [8] Da Silva et al. (2022), Frontiers in Physiology 13

# The Effects of Different Land Widths on Lower Extremity Joint Work During Bilateral Drop Landings

Lauren A. Crawford, Kaileigh E. Estler, Jake A. Melaro, & Joshua T. Weinhandl
Department of Kinesiology, Recreation, and Sports Studies, The University of Tennessee, Knoxville Tn
LCrawf21@uthsc.edu

**Introduction:** Excessive knee joint loading increases the risk of ligament injury. To mitigate this joint load, soft landing techniques may be employed. These techniques incorporate greater ranges of hip and knee flexion, which allow energy to dissipate more evenly across the lower extremities over time [1,2,3]. Norcross et al., [4], refers to joint work as the joint biomechanics and muscle actions occurring during landing including net joint moments, eccentric muscle actions, and work performed by the extensor muscles of the ankle, knee, and hip.

During landing, the hip and knee joints exhibit greater power [5] and are primary contributors to energy absorption and stability [1,6,7]. Yeow et al. [5] observed that a greater peak external hip adduction moment was associated with a higher peak ground reaction force. However, no differences in joint power were noted between the hip and knee joints [5], suggesting a frontal plane hip-dominant landing strategy may reduce knee and ankle joint demands, lowering ACL injury risk. Interfoot width distance (IFD) is a crucial factor in hip-dominant landing strategies. Various stance widths have been shown to affect hip and knee joint kinematics and kinetics [8,9,10].

Having greater insight into IFD magnitudes may prove to be important for ACL injury risk mechanics during landing. To date, no studies have investigated the effect of altered landing foot width on lower extremity kinetics. Therefore, the purpose of this study was to examine the effects of modifying IFD during bilateral drop lands on hip, knee, and ankle work. Based on previous literature, we hypothesized that increasing IFD would increase the total work at the hip and knee joints.

**Methods:** Participants of this study were fourteen recreationally active males (80.0±8.2 kg, 1.78±6.9 m) and fourteen females (62.4±8.5 kg, 1.65±7.8 m) aged 18-25 years. 3D kinematics and kinetics were collected while participants performed double-leg drop landings from a trapeze bar for IFD landing conditions: Narrow, Preferred, and Wide. The overhead trapeze bar was set so that their feet were at a height equivalent with 90% of their average maximum countermovement jump height. IFD stance conditions were defined as 100% (Preferred), 50% (Narrow), and 150% (Wide) of the average stance width measured from the countermovement jumps. Five trials per condition were completed via a counterbalance design. Only the dominant kicking leg was analyzed for this study.

**Results & Discussion:** A significant IFD by sex interaction was reported for hip work (p=0.005, $\eta_\rho^2$=0.187) and ankle work (p=0.015, $\eta_\rho^2$=0.150). Compared to females, greater magnitudes of negative hip work were generated by males at Narrow (p=0.015, d=0.95), Preferred (p=0.021, d=0.90), and Wide (p=0.005, d=1.13). In the male group, greater eccentric work was observed as IFD increased from Narrow to Preferred (p=0.034, d=0.10) and Wide (p<0.001, d=0.35), and from Preferred to Wide (p<0.001, d=0.23). Males displayed reduced ankle eccentric work during Preferred (p=0.007, d=0.33) and Wide (p=0.003, d=0.42) compared to Narrow. In the females' group, eccentric work decreased from Narrow to Wide (p=0.023, d=0.37). No significant interactions were reported for knee work, however, there was a significant main effect of IFD, showing a linear relationship (p<0.001, $\eta_\rho^2$=0.246). A significant sex main effect was reported (p<0.001), as males generated greater eccentric knee work for all conditions compared to females (p<0.001). Overall, there was a noted significant increase in the eccentric work at both the hip and the knee joints during Wide landings and an observed increase in hip work that is essential for maintaining whole-body balance, relative to the altered center of gravity.

**Table 1:** Effect of sex and interfoot width distance on Mean (SD) of joint work (J/kg) during stance.

| | Narrow | | Preferred | | Wide | |
|---|---|---|---|---|---|---|
| **Joint Work** | Female | Male | Female | Male | Female | Male |
| **Hip Work*[a]** | -0.44 (0.32) | -0.91 (0.59) | -0.49 (0.32) | -0.97 (0.66) | -0.52 (0.35) | -1.1 (0.67) |
| **Knee Work*#** | -0.78 (0.32) | -1.39 (0.47) | -0.82 (0.31) | -1.4 (0.45) | -0.90 (0.35) | -1.5 (0.45) |
| **Ankle Work‡[ab]** | -0.44 (0.17) | -0.51 (0.20) | -0.47 (0.16) | -0.43 (0.24) | -0.40 (0.16) | -0.43 (0.17) |

‡ Significant sex×IFD interaction (p<0.05); * Significant IFD main effect (p<0.05); # Significant sex main effect (p<0.05); a Significant IFD main effect for males (p<0.05); b Significant IFD main effect for females (p<0.05)

**Significance:** This study sought to explore how modifying interfoot width landing distance could alter lower extremity biomechanics that contribute to ACL injury mechanisms. Data suggests that a wider stance may enhance hip stability & increase valgus demands at the knee. These findings provide valuable insights into the influence of stance width and joint work during landings; however, limitations were present. Participants performed landings using their natural landing style and variations in trunk positioning likely influenced lower extremity biomechanics.

**References:** [1] Larwa et al. (2021), *J Environ Res Public Health* 18(7) [2] Pollard et al. (2010), *Clin Biomechanics* 25 [3] Tamura et al. (2021) *Int J Environ Res Public Health* 18 [4] Nocross et al. (2013), *J Athl Train.* 48(6) [5] Yeow et al. (2009), *J of biomechanics* 42 [6] Coventry et al. (2006), Clin Biomech (Bristol, Avon) 21 [7] Kellis and Kouvelioti (2009), *J Electromyogr Kinesiol* 19 [8] Escamilla et al. (2001) *Med Sci Sports Exerc.*33 [9] Lahti et al. (2019), *Scand J Med Sci Sports*.29 [10] Lorenzetti et al. (2018), *BMC Sports Sci Med Rehabil*.10

# RELATIONSHIP BETWEEN COLLEGIATE GYMNAST ACHILLES TENDON ANATOMY AND JUMP PERFORMANCE

Grace Cordova[1], Julia A. Dunn[1], Michelle Sabick[1*]
[1]Center for Orthopaedic Biomechanics, University of Denver, Denver, CO, USA
*Corresponding author's email: michelle.sabick@du.edu

**Introduction:** Female collegiate gymnasts experience Achilles tendon (AT) injuries at the highest rate among college athletes, particularly during the takeoff phase of floor routine jumps [1]. Due to the unilateral nature of these ruptures, it is important to explore potential asymmetries in AT function and anatomy. This study aims to deepen the understanding of the relationship between AT performance during jump tests and anatomical changes over the course of the competitive season. Jump test metrics were selected for their relevance to Achilles tendon function and performance. Specifically, peak vertical ground reaction forces have been shown to reflect the load on the tendon [2]. Eccentric mean force and eccentric peak force indicate dynamic strength and the efficiency of the stretch-shortening cycle [3]. Rate of force development (RFD) and ground contact time (GCT) were chosen as potential indicators of AT stiffness and explosive strength deficits associated with tendinopathy [4, 5]. Our hypothesis was that increased asymmetry in jump performance would result in increased AT thickness asymmetry in collegiate gymnasts, and that reported perceived pain would strengthen this relationship.

**Methods:** Fifteen female collegiate gymnasts from the University of Denver gymnastics team participated in the study. During the 2023-24 season, athletes completed weekly AT ultrasounds, subjective pain surveys, countermovement jumps (CMJ) and drop jumps (DJ). The ultrasounds were performed with the probe in line with AT, at the midlength of the tendon and. Athletes reported current pain in each AT on a scale from 0-10, where 0 is no pain. The jump tests were performed as a part of existing strength and conditioning protocols and athletes were instructed to jump with maximal effort. Ground reaction force data were collected using two VALD ForceDecks at 1000 Hz, then normalized by bodyweight. For each metric, the Normalized Symmetry Index (NSI) was calculated for each trial and averaged [6]. Pre-season NSI was set as the baseline for each athlete. Normalized change from the baseline for each jump metric were compared to changes in AT NSI throughout the season. Linear regression models were produced to determine whether increases in jump metric asymmetry were predictive of increases in AT thickness. Athletes were assigned a pain status of 1 if they had reported AT pain in either the left or right tendon at any point during the season and a pain status of 0 if no pain was reported. The models were repeated to include pain as an interaction term to determine the effect that pain might have on the model. Significance was set at $p<0.05$.

**Results & Discussion:** Excluding perceived pain as an interaction, with changes in AT thickness asymmetry. However, when perceived pain was included, five jump metrics had statistically significant linear relationships with changes in AT thickness asymmetry (Table 1). Therefore, accounting for perceived pain may improve our ability to predict changes in the AT thickness asymmetry, as opposed to jump metrics alone. Of these five metrics, four were derived from DJ tests, while only one came from CMJ tests. However, it is challenging to make clear conclusions, because more DJ tests were conducted than CMJ tests, which may affect the statistical outcomes. This disparity is a limitation in the study and a result of athlete training and competition schedules. Despite higher p-values among DJ metrics, the CMJ metrics yielded higher R-squared values, indicating that future work may benefit from prioritizing CMJ over DJ. As changes in concentric RFD symmetry increased, changes in AT thickness symmetry decreased. This relationship is the inverse of what was expected, however, it is unclear if the model is predictive of injury because there were no recorded AT injuries through the season.

**Table 1:** Results of linear regression models with and without pain only concentric RFD had a statistically significant linear relationship as an interaction term for each jump metric. *p<0.05

| Jump Metric | Without Pain Interaction Term | | With Pain Interaction Term | |
|---|---|---|---|---|
| | $R^2$ | P-Value | $R^2$ | P-Value |
| Concentric RFD (CMJ) | .34 | 0.014* | .48 | 0.034* |
| Eccentric Mean Force (CMJ) | .01 | 0.623 | .45 | 0.718 |
| Eccentric Peak Force (CMJ) | .11 | 0.118 | .17 | 0.282 |
| Take-Off Peak Force (CMJ) | .03 | 0.460 | .04 | 0.837 |
| Eccentric Braking RFD (CMJ) | .00 | 0.755 | .03 | 0.887 |
| Drop Landing RFD (DJ) | .00 | 0.901 | .08 | 0.030* |
| Landing RFD (DJ) | .00 | 0.985 | .07 | 0.040* |
| Peak Drive Off Force (DJ) | .00 | 0.682 | .06 | 0.060 |
| Peak Drop Landing Force (DJ) | .00 | 0.590 | .08 | 0.020* |
| GCT (DJ) | .00 | 0.322 | .07 | 0.049* |

**Significance:** Including subjective pain in predictive models to assess the relationship between changes in asymmetries in jump test performance and AT anatomy strengthened the statistical significance and predictive capability of the model. Of the tests conducted, metrics deriving from CMJ may produce more valuable indicators for assessing AT anatomical asymmetries, particularly concentric RFD. Future studies should explore these relationships across multiple seasons and teams.

**Acknowledgments:** This research was supported in part by the Praxis program at Smith College which provided funding for the student author.

**References:** [1] Bonanno, et al. (2021), *Sports Health* 14(3);[2] Koshino, et al. (2023), *Scand J Med Sci Sports* 34(1);[3] Debenham, et al. (2016), *J Sci Med Sport* 19(1);[4] McAuliffe, Sean. (2019), *J Athl Train* 54(8);[5] Abdelsattar et al. (2018), *J Sports Sci Med* 17(2);[6] Queen, et al. (2020) *J Biomech* 99

# THE EFFECTS OF PRACTICE DRILL INTENSITIES ON CUMULATIVE HEAD IMPACT EXPOSURE IN NCAA DIVISION I COLLEGE FOOTBALL PLAYERS

*Christopher J. Otwell[1], Steven Leigh[1], Suzanne Konz[1]
[1]Department of Biomechanics, School of Health and Movement Science, Marshall University
*Corresponding author's email: otwell3@marshall.edu

**Introduction:** Concussions are one of the most common injuries in collegiate-level football. It is also known that there is a relationship between cumulative head impact exposure (HIE) and the risk of concussion [1]. Furthermore, collegiate football players are known to experience upwards of 66.9% of HIE during practices in any given season [2]. For the purposes of this study, head impact exposure is defined as a multi-factorial term that includes the frequency, magnitude, and head impact criterion score (hic) of each registered head impact by a given athlete. When examining the HIE in college football practices, important variables to consider are drill type, drill intensity, and player positions. Since practice drill types can vary drastically due to every coach having their own practice philosophy, it can be more realistic to analyze HIE across practice drill intensities, which are more generalizable to different teams. According to USA Football, the levels of intensity in football practices (ranked from lowest to highest) are air, bags, control, thud, and live. The frequency of impacts at the high school level increases significantly as drill intensity increases, while also demonstrating position-specific frequency differences [3]. There are position-specific differences in impact frequency between drill types in college football practices, showing that offensive linemen sustain the highest rate of impact compared to other groups at the college level [4]. However, there is no evidence examining HIE based on drill intensity at the collegiate level.

Therefore, the purpose of this study is to determine if there is a relationship between cumulative HIE and prescribed drill intensities in NCAA Division I football practices, while also examining for position-specific differences. Based on previous research, we hypothesized that HIE would significantly increase as drill intensity progressed from 'air' to 'live'. Additionally, we hypothesized that position groups such as offensive line (OL), defensive live (DL), tight ends (TE), and linebackers (LB) would have significantly higher HIE than other position groups such as quarterbacks (QB), running backs (RB), wide receivers (WR), and defensive backs (DB).

**Methods:** A total of 40 players from a single NCAA Division I football program (21.5±1.4years, 186.6±6.2cm, 105.5±25.6kg) were included in this study due to being a football player, within the 2-deep depth chart; and not having a current or recent musculoskeletal injury in the previous 6 months. Players were divided into position groups based on their reported position on the roster (OL, n=7; D, n=7; TE, n=2; LB, n=3; QB, n=2; RB, n=1; WR, n=8; DB, n=10). To collect head impact exposure data, each subject had a head impact sensor (CUE™ Sports Sensor, Athlete Intelligence, Kirkland, WA) specifically assigned to them and installed in the upper right section of their helmet shell before practice each day which was removed upon completion of every practice to charge and store data. These sensors collected peak linear acceleration (PLA) (g), peak rotational acceleration (PRA) (rad/s$^2$), time of impact, and head impact criterion (HIC) score. Differences of HIE frequencies for both position and intensity were analyzed through Chi-squared tests with post-hoc analysis. Differences between positions and kinematic variables were analyzed through multiple 2-way ANOVA tests with post-hoc analysis. All statistical analyses were performed using SPSS software (Version 28, SPSS, Inc., IMB Inc., Chicago, IL).

**Results & Discussion:** Data analysis on HIE frequency across drill intensities shows significant differences between all intensities ($\chi^2$=306.274, p<0.001) in ascending order (p<0.005) which is consistent with our first hypothesis. These differences reflect similar results demonstrated in previous research at lower levels of play [3]. Analysis of HIE frequency at the positional level showed significant differences between groups ($\chi^2$=996.578, p<0.001). A post-hoc analysis included 36 different possible combinations of position comparisons, of which only 5 were not significantly different (OL-TE, OL-WR, DL-DB, QB-RB, WR-DB) which partially contradicts our 2nd hypothesis since OL did not differ in HIE from WR and DL did not differ from DB. With kinematic variables, PLA displayed no main effect of position or intensity (p>0.05), PRA displayed a main effect of position (p=0.028) in which post-hoc analysis showed that OL were 13.8rad/s$^2$ greater than DB on average (p=0.001), and HIC score analysis showed no main effect of position or intensity, which is not consistent with our hypotheses. The similarities in frequency between OL and WR may be explained by the vast number of 'live' drills prescribed, giving more opportunities for WR to sustain more impacts, and the same can be said to explain the similarities between DL and DB. The OL group displaying significantly higher PRA than DB can be explained by general understanding of football positions. Typically, OL must remain stationary or move backwards to overcome full speed impacts from DL or LB which can result in elevated PRA while DB typically match the speed and direction of WR, thus absorbing less force and creating less PRA.

**Significance:** Overall, the results of this study indicate that at the college level, there is a higher cumulative HIE as prescribed practice intensities increase while there is little change in kinematic variables across position with no change across intensity. These findings may suggest that adjusting practice structures to reduce high-intensity drill exposure, especially for high-risk positional groups, may help mitigate cumulative HIE and reduce concussion risk.

**References:** [1] Chandran et al. (2021), *J Ath Train* 56(7); [2] McCrea et al. (2021), *JAMA Neurol* 78(3); [3] Kercher et al. (2020), *PloS One* 15(8); [4] Asken et al. (2019), *Ann Biomed Eng* 47(10)

# EFFECT OF A SINGLE-SEASON NECK STRENGTHENING PROGRAM ON NECK FLEXION ANGLES AND HEAD ACCELERATION MAGNITUDES IN YOUTH SOCCER HEADING

*Samantha DeAngelo[1], Carly McPherson[1], Carly Smith[1], James Harrison[2], Nathan Edwards[1], Enora Le Flao[1], Nick Shoaf[1], Jaclyn Caccese[1]

1. The Ohio State University, Columbus OH
2. Liverpool John Moores University, Liverpool UK

*Corresponding Author's Email: Samantha.deangelo@osumc.edu

**Introduction:** Injury risk reduction is an important aspect of athlete safety in contact sports, such as soccer, where purposeful heading is a common action. Heading exposes athletes to repetitive head impacts (RHIs), which have been linked to neurocognitive impairments in several studies.[1], [2], [3] Additionally, higher head acceleration during RHIs is associated with a higher risk of brain injury.[4] The potential for neurocognitive impairments following RHIs has driven interest in modifiable risk factors, such as neck strength and activation, to reduce head acceleration during heading.[5] Stronger neck musculature has been associated with lower head acceleration during soccer headings,[6] likely due to better head-neck-torso alignment, increasing effective mass, which helps offset the force of the ball upon impact.[4] Youth and female soccer athletes typically exhibit lower neck strength [7] and experience higher head acceleration during purposeful heading compared to males.[4] Therefore, this study aimed to determine whether a neck strengthening and activation program would reduce head acceleration during purposeful soccer heading. We hypothesized that the intervention would result in lower head accelerations and decreased neck flexion angles due to better head-neck alignment during heading.

**Methods:** Athletes from one female youth soccer program were invited to participate. Participants were fit with a boil-and-bite Impact Monitoring Mouthguard (Prevent Biometrics, Edina, MN) to record peak linear acceleration (PLA) and peak rotational velocity (PRV) during a purposeful heading paradigm. At baseline, each athlete completed five headers from a 5-meter distance, with balls thrown by a research team member simulating a throw-in. Head and neck biomechanics were captured using an 8-camera markerless motion capture system (OptiTrack, Corvallis, OR) and processed with Theia3D (Kingston, Ontario), and Visual3D, (Kingston, Ontario). Neck flexion was calculated as the angle between the head and neck at the moment of impact. Following the baseline assessment, athletes completed a neck strengthening and activation intervention, including the FIFA 11+ (Level 1) warm-up with an additional 2 minutes of neck strengthening and activation exercises, twice per week for 14 weeks. After the intervention, participants completed the same soccer heading paradigm. Paired t-tests were used to examine changes in PLA, PRV, and neck flexion angle from pre-season to post-season. Pearson correlations were used to examine the association between changes in PLA/PRV and changes in neck flexion angle from pre- to post-season.

**Results:** Seven athletes (14.5±.6 years, 161±6 cm, 52±9 kg) were included in this analysis. From pre- to post-season, there were significant differences in the neck flexion angle (Pre:18.812±7.326; Post:30.141±12.701, t=-3.367, p=.015, Cohen's d=-1.273) and PLA (Pre:12.003±.769; Post:10.025±1.437, t=3.818, p=.009, Cohen's d=1.443), but not PRV (Pre:4.135±.936; Post:5.248±1.590, t=-1.467, p=.193, Cohen's d=-.555). There was no correlation between the change in neck flexion angle and change in PLA (r=.388, p=.390) or PRV (r=.002, p=.996).

**Discussion:** Results partially support the hypothesis that a season-long neck strengthening and activation program would result in lower head acceleration and reduced neck flexion angles during purposeful heading. Although PLA decreased, neck flexion angles unexpectedly increased from pre- to post-season. A possible explanation for the increase in neck flexion angles is change in heading technique. Post-season, athletes may have used a more aggressive heading style, moving into the ball rather than passively waiting for it, which could result in greater forward motion of the head at impact. Though there was no statistically significant correlation between neck flexion angle and PLA, we observed a medium effect size, suggesting that our study may have been underpowered to detect this effect. These findings suggest that a structured neck strengthening and activation program may help reduce PLA during heading.

**Significance:** More investigation needs to be done to investigate the effects of an isometric neck strengthening program on neck flexion angles and head acceleration values in a larger sample size and with a control group. Given that a neck strengthening program can be designed to require minimal time and equipment, it represents a feasible and practical intervention for reducing head acceleration during purposeful heading. Implementing such programs may be an effective strategy to reduce RHI exposure in youth female soccer players.

**Acknowledgments:** This work was supported through The Ohio State University Chronic Brain Injury Program.

**References:** **[1]**C. F. Levitch *et al.*, Feb. 2018, doi: 10.1017/S1355617717000790., **[2]**M. R. Zhang, S. D. Red, A. H. Lin, S. S. Patel, and A. B. Sereno, Feb. 2013, doi: 10.1371/journal.pone.0057364., **[3]**A. M. Spiotta, A. J. Bartsch, and E. C. Benzel, Jan. 2012, doi: 10.1227/NEU.0b013e31823021b2., **[4]**J. B. Caccese and T. W. Kaminski, Nov. 2016, doi: 10.1007/s40279-016-0544-7., **[5]**K. Peek, J. M. Elliott, and R. Orr, May 2020, doi: 10.1016/j.jsams.2019.11.004., **[6]**J. B. Caccese *et al.*, Oct. 2018, doi: 10.1080/14763141.2017.1360385., **[7]**E. Catenaccio *et al.*, Sep. 2017, doi: 10.1016/j.pmrj.2017.01.005.

# CAN STRIDE LENGTH BE ACCURATELY CALCULATED USING DATA FROM A SHANK-WORN INERTIAL SENSOR?

Spencer N. Miller[1*], Julien A. Mihy[2], Mayumi Wagatsuma[2], Jocelyn F. Hafer[2], Stephen M. Cain[1]
[1]West Virginia University, Morgantown, WV, and [2]University of Delaware, Newark, DE
[*]Corresponding author's email: sm00170@mix.wvu.edu

**Introduction:** Gait analysis is a common technique used to study the movements of a person during walking to identify anomalies in biomechanics [1]. While in-lab gait analysis is the most common approach, real-world gait analysis has become more popular as sensor technology and algorithms improve. A foot-mounted inertial sensor can enable highly-accurate calculations of spatiotemporal metrics using the zero-velocity update approach, which utilizes the fact that the velocity of the foot is approximately zero when the foot is on the ground [2,6]. However, a foot sensor is easily moved or removed throughout the day resulting in inconsistent results during data processing [3]. To combat this issue, single-sensor-based approaches were developed that use sensor data from the shank [4]. Here, we extend the approach of Li et al, which assumes the shank has a velocity of zero during midstance, by implementing a zero velocity update method similar to a foot mounted zero velocity update (ZUPT) algorithm [5,6].

**Methods:** Using data from our IRB-approved study, we analyzed data from nine participants, five with symptoms matching ACR clinical criteria for medial compartment knee osteoarthritis (OA) and four healthy controls. Participants wore a total of five IMUs (APDM Opal; linear acceleration ±160m/s$^2$, angular velocity ±2000deg/s, sampling frequency 120Hz) for three consecutive days: one each on the sacrum, dominant or affected thigh, dominant or affected shank, right foot, and left foot of the subject. We calculated stride length from the dominant or affected foot-mounted sensor data using a ZUPT algorithm [6]. Then, using data from the dominant or affected shank sensor, we calculated stride length using a modified approach of Li et al. [5], applying a ZUPT algorithm to the shank IMU data. Using the angular velocity from the shank sensor, midstance was identified by selecting the angular velocity closest to zero between initial and final foot contact. These midstance points were then used as the zero-velocity point when applying the ZUPT algorithm [6]. The calculation of stride length from the shank was completed using the same process as the stride length from the foot. Shank-calculated stride lengths were compared to foot-calculated stride lengths, which we consider the gold standard for real world gait analysis. This comparison was done using a Bland-Altman plot with 95% confidence intervals to evaluate the accuracy of the algorithm.

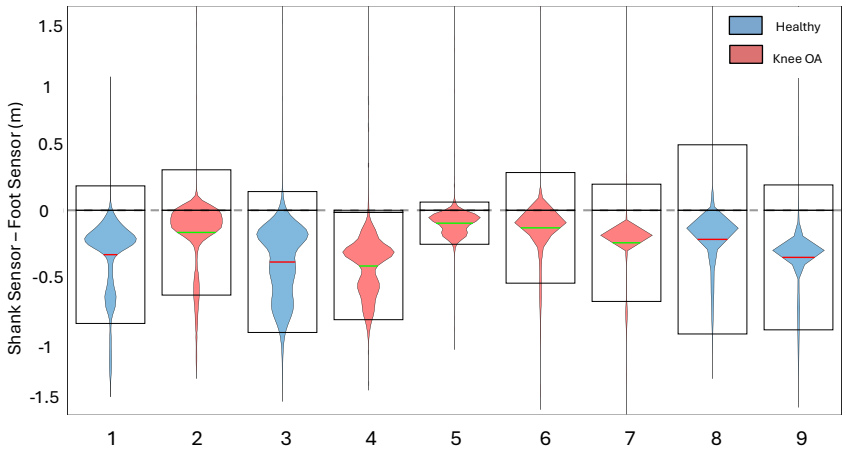


**Figure 1:** Violin plot with mean and limits of agreement for the difference between stride lengths calculated from the foot and shank sensor.

**Results and Discussion:** Fig 1 shows a violin plot of the results for each participant with the blue showing the healthy controls and the red showing those with knee OA. The limits of agreement for shank- vs foot-calculated stride length are larger than anticipated with the average for those with knee OA being 0.131 to -0.609 meters and 0.261 to -0.934 meters for the healthy participants. Ideally, limits of agreement would be within ±0.1 meters as this allows researchers to accurately detect clinically meaningful gait changes [7]. The results also show a consistent underestimation of stride length when applying the ZUPT algorithm to the shank sensor. This is likely due to the assumption that the shank IMU is at zero velocity at midstance. It is possible that due to the angular velocity of the shank and placement of the IMU, the velocity of the shank sensor will not reach zero. Future work to implement correction for this underestimation could improve a shank-based approach, enabling accurate calculations of stride parameters possible from a more easily worn shank sensor.

**Significance:** The single sensor shank approach for calculating stride parameters is an important step towards enabling real-world gait analysis without inconvenient foot sensors. However, before implementing the algorithm, the accuracy of the method must be improved and evaluated against a trusted method (i.e., foot sensor based ZUPT) in an uncontrolled (non-laboratory) environment.

**Acknowledgments:** This work was supported by a grant from the National Institute on Aging (R21AG076989) from NIH.

**References:** [1] Michael W. Whittle (2014) *Gait Analysis: An Introduction* [2] Anwary et al. (2018) *Sensors* [3] Young et al. (2022) *Sports Science, Technology and Engineering.* [4] Liu (2009) *Measurement* [5] Li et al. (2010) *Journal of Biomechanics* [6] Rebula et al. (2013) *Gait Posture* [7] Bohannon, R., & Glenney, S. (2014) *Journal of Evaluation in Clinical Practice*

# A FRAMEWORK FOR LONGITUDINAL REMOTE PATIENT MONITORING STUDIES WITH PRESSURE-SENSING INSOLES

*Katherine M. Rodzak[1], Cameron A. Nurse[1], Peter Volgyesi[1], Meredith K. Owen[2], Tereza Janatova[2], Brian Noehren[2], Karl E. Zelik[1]
[1]Vanderbilt University, Nashville, TN, [2]University of Kentucky, Lexington, KY
*Corresponding author's email: katherine.rodzak@vanderbilt.edu

**Introduction:** Many researchers are excited about the possibility of using wearable sensors to study human movement biomechanics "in the wild" and to perform remote, longitudinal data collections. However, a sensor being wearable is only one small aspect of designing a successful remote monitoring study, and few researchers actually conduct these studies, particularly those that involve wearable force or pressure sensing. These are daunting studies given the current state of sensor technology, the need for drastically different study designs vs. in lab, and a myriad of challenges associated with remote and prolonged data collection. The purpose of this Abstract is to share the study framework we developed to use pressure insoles to conduct a 1-year remote monitoring study of patients after a tibia shaft fracture and surgical fixation. Tibia shaft fractures are a common lower extremity trauma [1], where surgical fixation involves an intramedullary nail being inserted into the bone. Following definitive fixation of a tibia shaft fracture, little is known about how people load their bone. What is known is that patient recovery 1 year following surgery is poor and inconsistent, with 65% of patients reporting an inability to perform pre-injury leisure activities and 47% still not able to fully return to work [2, 3]. One of the few factors found to be associated with better recovery is bearing enough weight on the injured limb to stimulate bone remodeling pathways [4]. However, there is currently no ability to monitor patients, or their bone loading, when they are not in the clinic. Previous lab research found that data from wearable pressure insoles and an IMU could be used to estimate tibial bone force [5]. Now, the challenge is figuring out how to operationalize this wearable sensing capability and to design a study to collect weeks or months of tibial force data without disrupting a patient's daily life. If successful, this would provide first-of-its-kind data on tibia bone load and recovery after surgery.

**Methods:** Designing the study was an iterative, multi-month process. At a high-level, it involved two main steps that had to be done in parallel: (1) Identifying and vetting sensor hardware and software systems that would enable reliable, practical, remote data collection and estimation of tibial bone force, and (2) Designing the remote monitoring study, from patient recruitment and data privacy protocols to compliance monitoring, logistics, and data analysis workflows. We created extensive technical requirements and user (patient) needs for both steps. We evaluated over a dozen pressure insoles, downselected to 4 systems, then quantified how many of those systems met each of our technical and user requirements. In the process, we met with numerous wearable sensor manufacturers and did a deep dive into their capabilities, limitations, and trade-offs. We did pilot tests on various systems and obtained input from other researchers and subject matter experts.

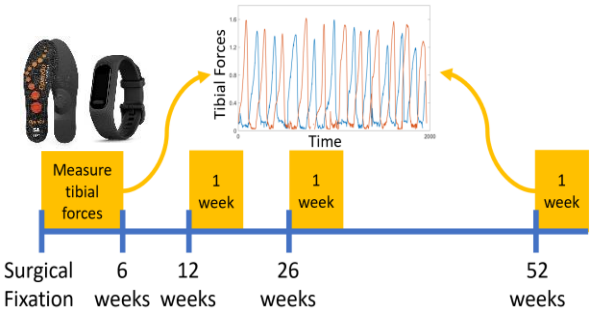


**Figure 1:** Study design: using pressure insoles and a fitness tracker in combination with machine learning algorithms, we aim to monitor tibial forces experienced at home during the first 6 weeks after surgical fixation, and for one week at 12, 26, and 52 weeks post-surgery.

**Results & Discussion:** Of the downselected insoles, we found that 3 (of 4) quantified and stored the center of pressure and total force data that we needed, 3 stored time stamped data, all 4 met our minimum sampling frequency of 20 Hz, 2 had multi-day battery life and storage capacity, 2 had on-board data storage (which was desirable to minimize risk of data loss), and 2 provided access to raw data. None of the insole systems met all the ideal requirements and user needs, but we identified the Moticon OpenGo insoles as the best fit for our study. These insoles met most requirements and in our initial tests allowed for 3-4 days of continuous data collection (without recharging, at 25 Hz with insensitive sleep setting). We worked closely with Moticon to develop our study protocol based on the capabilities and limitations of their system. We hired them to modify their phone app to enhance our ability to monitor compliance and to help simplify patient interactions and study logistics. We settled on a 52-week protocol that would involve 8 total weeks of full-day remote data collection per patient (Fig. 1). We realized that we would need a suite of wearable sensors and software (not insoles alone) to conduct this study and ensure reliable data collection and transmission. We incorporated an independent remote phone access app (AirDroid) to enhance the remote monitoring capabilities of the study team. Since patients do not wear insoles (or shoes) during every waking moment, we also give them a wrist-worn Garmin fitness tracker. We will use Labfront software to export minute-by-minute fitness tracker data and use it with a previously developed machine learning algorithm to estimate tibial force and fill in gaps when the insoles are not worn [6]. To minimize the burden on patients and limit their interaction with the sensors or phone apps, we developed a bespoke logistical protocol whereby multiple pressure insoles are used per patient, and these are periodically mailed back and forth by the study team and patient. Patient enrollment has begun and this study is ongoing.

**Significance:** The study framework we developed will enable the first large-scale, longitudinal monitoring of tibial force in patients in daily life post-surgery. This work could lead to new insights on how to optimize rehabilitation programs, or quantitative biomarkers that help identify patients early on who are on track vs. at risk for poor recovery after tibial shaft fracture surgery. Finally, the study framework and considerations presented here may be beneficial to other researchers seeking to perform remote monitoring studies.

**Acknowledgments:** This work was supported by NIAMS R01AR080708. **References:** [1] Antonova (2013), *BMC Musculoskelet Disord* [2] Gross (2016), *Journal of Orthopaedic Trauma* [3] Ferguson (2008) *Injury*), [4] Findakli (2021), *Clin Orthop Relat Res* [5] Matijevich (2020), *Human Movement Science* [6] Nurse (2025), *Sensors.*

# ROTATIONAL VARIABILITY DURING AN ANXIETY-INDUCTION TASK IN CHILDREN WITH MENTAL HEALTH DIAGNOSES

Jenna G. Cohen[1*], Guido Mascia, Bryn C. Loftness, Ellen W. McGinnis, Ryan S. McGinnis
[1]Biomedical Engineering, University of Vermont
*jenna.g.cohen@uvm.edu

**Introduction:** More than one in five children have a mental health diagnosis, including ADHD, anxiety, and depression [1], [2]. Since children cannot reliably report on their symptoms, current screening relies on parents who often underreport due to symptoms being unobservable [1]. When stressed, children with ADHD and internalizing diagnoses (anxiety, depression) exhibit distinct bio-behavioral responses as compared to children without these diagnoses [3]. In this analysis, we consider children's range in angular velocity of their torso as a bio-behavioral measure of stress reactivity during a standardized laboratory stress induction task. Prior work has demonstrated child orientation and/or movement in response to stressful stimuli differs by mental health diagnosis [3], therefore, we hypothesize that children's rotational variability would differentiate amongst children by diagnosis type.

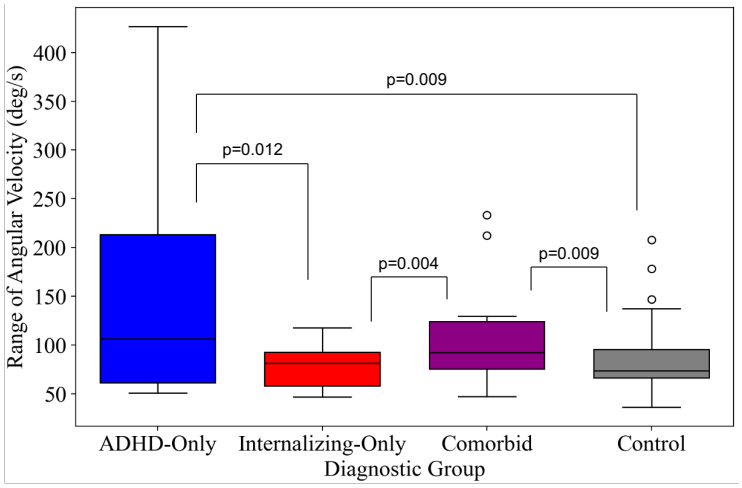


**Figure 1:** Mean and standard error of range in angular velocity of the sacrum during an anxiety-induction task.

**Methods:** We present sacrum gyroscope data from children ages 4-8 (N=91, 42% female) with and without mental health diagnoses captured during a task designed to induce fear and anxiety [2]. During the 30-second task, the child was led by an administrator into an unfamiliar, darkened clinic room toward an unknown object hidden underneath a blanket. For consistency, the first 5 seconds of data were excluded due to protocol variability. From 5 to 19 seconds the child was led into the room slowly, from 19 to 25 seconds the child was gestured to pause in front of the unknown object while a beeping sounded to induce a sense of urgency, and at 25 seconds the blanket was removed revealing an empty box. Child mental health diagnoses were determined via a gold-standard semi-structured interview (KSADS-PL). We consider range in angular velocity, derived from the sacrum BioStamp® recording gyroscope data, to analyze rotational variability across the following diagnostic groups: ADHD-Only (ADHD, no internalizing diagnosis, n=9), Internalizing-Only (anxiety and/or depression, no ADHD, n=23), Comorbid (ADHD and at least one internalizing diagnosis, n=11), and Control (no ADHD, no internalizing diagnosis, n=48). One-way ANOVAs were performed to examine movement by diagnostic groups across the task.

**Results & Discussion:** The ADHD-Only and Comorbid groups had a significantly greater range of angular velocity of their sacrum as compared to the Internalizing-Only (p=0.012, p=0.004) and Control (p=0.009, p=0.009) groups (Fig. 1). This suggests that children with ADHD, regardless of a comorbid internalizing diagnosis, have greater variation in the speed at which they are turning their torso towards and away from the potential threat throughout the entire anxiety-induction task. This could be because children with ADHD have higher overall activity levels [4], while children with internalizing diagnosis are typically behaviorally inhibited [5]. This is the first study that was able to differentiate ADHD in only 25 seconds of data, likely as behaviors are exaggerated in response to stress, however, future studies should investigate unstructured motion data using the same brief period to examine the salience of stress response in using motion to detect child mental health disorders. It is notable that children with ADHD did not differ in movement regardless of comorbid internalizing diagnoses, despite typically exhibiting more impairment. Future studies should incorporate other metrics such as heartrate and voice data during anxiety-inducing tasks to examine whether children with internalizing diagnoses (comorbid or alone) can be further differentiated.

**Significance:** During a 30-second anxiety-inducing task, the range in angular velocity, interpreted as rotational variability, provides a potential objective biomarker of ADHD in young children.

**Acknowledgments:** Research supported by the US National Institutes of Health (MH123031) and the US National Science Foundation (2046440).

**References:** [1] K. B. Madsen et al. (2018), *Eur Child Adolesc Psychiatry*; [2] B. C. Loftness et al. (2023), *IEEE JBHI*; [3] L. S. Wakschlag et al. (2005), *Clin Child Fam Psychol Rev* 8(3); [4] F. De Crescenzo et al. (2016), *Sleep Medicine Reviews;* [5] American Psychiatric Association (2013), *Diagnostic and Statistical Manual of Mental Diagnosis.*

# CALIBRATION OF WEARABLE KNEE SLEEVE SENSORS FOR KNEE FLEXION ANGLE MEASUREMENT

*Rosalind C. Bendell[1], Amit Chaudhari[3], Sagar M. Doshi[3,1], Erik T. Thostenson[1,4,3], Jill S. Higginson[1, 2]
[1]Department of Mechanical Engineering, University of Delaware, Newark, DE
[2]Department of Biomedical Engineering, University of Delaware, Newark, DE
[3]Center for Composite Materials, University of Delaware, Newark, DE
[4]Department of Materials Science & Engineering, University of Delaware, Newark, DE
*Corresponding author's email: rbendell@udel.edu

**Introduction:** Anterior Cruciate Ligament (ACL) injury is one of the most common and damaging knee injuries, with over 200,000 ACL injuries occurring annually in the US alone [1] [2]. ACL injuries are often sustained during non-contact cutting, pivoting, landing, or sudden deceleration during sports participation by young, active populations [2]-[6]. After ACL injury, ACL reconstruction (ACLR) is customary and often required to return stability to the knee joint and allow the individual to resume activities of daily living and for athletes to return to sports [4] [7] [8].

Wearable sensors have the potential to help prevent injury, monitor rehabilitation efforts and disease progression, and quantify activity levels regardless of the environment. Our collaborators have developed a novel sensor integrated into a wearable compression knee sleeve – the Smart Sleeve – to provide feedback during exercise or rehabilitation [9]. The flexible, novel sensors are created by depositing a carbon nanocomposite coating on stretchable textiles. The electrical resistance of the sensor changes when the sensor is elongated [9].

The objective of our study is to assess repeatability and calibrate the Smart Sleeve with joint angles during movement. Due to the ultra-sensitivity of the Smart Sleeve, we hypothesize that the Smart Sleeve will accurately and repeatably detect knee flexion angles with sensor changes in resistance.

**Methods:** In this preliminary study, a single participant performed five seated leg extensions with knee flexion angles from 0 to 90 degrees while wearing the Smart Sleeve. The knee sleeve was positioned over the knee such that the sensor was over the anterior knee and anatomically centred along the medial-lateral and cranial-caudal knee axes.

The sensor was connected to a custom data acquisition system with an Arduino Uno R3, an analogue-to-digital converter, and a microSD card to store data [10]. A voltage dividing circuit within the data acquisition system was used to measure the change in sensor resistance with elongation, in units of Ohms, with a sampling rate of 20 Hz [10].

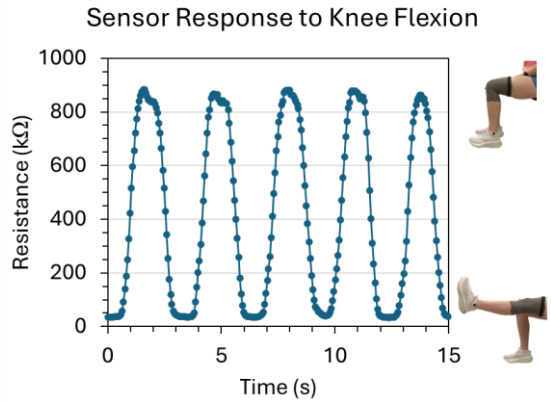


**Figure 1:** Sensor resistance (kΩ) measured by the Smart Sleeve over time (s) during five seated leg extensions with knee flexion angles from 0 to 90 degrees.

**Results & Discussion:** The integrated sensor was unstretched when the participant's leg was straight at 0 degrees, resulting in a resistance of approximately 34.5 kΩ. The peak values, measured at a knee flexion angle of 90 degrees, were 874 ± 8.5 kΩ. An increase in knee flexion angle caused an increase in electrical resistance of the (Fig. 1).

Preliminary work suggests a consistent relationship between Smart Sleeve resistance and knee flexion angles. Future work will demonstrate repeatability and accuracy in resistance readings of identical exercises. Then, a linear regression will be used to calibrate the change in sensor resistance with knee flexion angle, reported in degrees. To improve data quality, we will create a more securely fitting compressive sleeve and collect a larger sample using motion capture for comparison with the knee sleeve across a range of dynamic activities.

**Significance:** In addition to ACL injury prevention and rehabilitation, the Smart Sleeve will have broader applications for all knee injuries. While the numbers for ACL injuries are already staggering, knee joint monitoring with the Smart Sleeve could positively impact nearly 4 million Americans every year with improved rehabilitation outcomes – increased patient strength and flexibility – and faster return to activities of daily living, hence improved quality of life [11].

**Acknowledgments:** Funding provided by NSF PFI-TT 2329838, NSF ART Award 233144, and the Helwig Fellowship in Mechanical Engineering (Bendell).

**References:** [1] Sherman, S.L., et al., J ISAKOS. 2021, 6(6):322-328. [2] Kiapour, A.M. and Murray, M.M., Bone Joint Res. 2014, 3(2):20-31. [3] Peterson, J.R. and Krabak, B.J., Phys. Med. Rehabil. Clin. N. Am. 2014, 25(4):813-828. [4] Neal, K.A., 2023. [5] Clayton, R.A.E. and Court-Brown, C.M., Injury. 2008, 39(12):1338-1344. [6] Yu, B. and Garrett, W.E., Br. J. Sports Med. 2007, 41:47-51. [7] Stasi, S.L., et al. Am J Sports Med. 2013, 41(6):1310-1318. [8] Unverzagt, C., et al., Int J Sports Phys Ther. 2021, 16(4):1169-1177. [9] Doshi, S.M., et al., J. Mater. Chem. C. 2022, 10(5):1617-1624. [10] Burch, K. et al., Wearable Technol. 2023, 4(8). [11] Feng, J.E., et al., J Multidis Health. 2018, 25(11):63-73.

# BIOMECHANICAL ANALYSIS OF THE FIELD HOCKEY SWEEP SKILL

*Hillary J. Cox[1], Rachel V. Vitali[1]
[1]University of Iowa, Iowa City, IA, USA
*email: hillary-cox@uiowa.edu

## Introduction

In the sport of field hockey, players train to successfully execute a variety of technical skills that directly impact their ability to assist the team towards winning games. For example, players will often 'sweep' the ball forward for another player to touch into the goal during an offensive penalty corner play. Better executed sweeps lead to more goal scoring, therefore increasing a team's probability of winning. Various technical skills have been studied, such as the drag flick and hit skills, that focus on short, sharp body movements. For the drag flick skill, it was found that a wide stance, rapid flicking action of wrists, trunk rotation, and sequential movement of pelvis, upper trunk, and stick lead to superior performance [1] [2]. For the hit (also known as a drive) skill, it was found that the separate but coordinated (i.e., out of phase) movements of joints and limbs leads to a more powerful hit, as opposed to stiff limbs and joints that move as a single unit [3]. These findings are often applied during coaching instruction to other skills like the field hockey sweeps, but there is currently no evidence that these findings translate to other technical skills like the sweep skill that is relatively understudied. In fact, only one study explored how joint angles and loads differed for a variety of ball placements, with a special emphasis on injury prevention [4]. This study aims to contribute to sports research by better quantifying superior performance during a sweep skill.

**Methods:** A sample of 8 female participants with experience performing the field hockey sweep skill were recruited for this study. All study activities were approved by the University of Iowa Institutional Review Board and participants gave informed consent. Participants performed the data collection using a field hockey stick of their choosing. Participant height, age, nationality, team membership, and sweep experience was collected. The participants were instructed to simulate a penalty corner where they 'sweep for a tip' (i.e. to another player) positioned at a marked location 7 yards in front of the goal mouth. Each ball was still when hit from slightly outside of the sixteen-yard-circle edge. Nine inertial measurement units (IMUs) were attached to the participants' left hand, left forearm, left upper arm, sacrum, sternum, left foot, left shin, left thigh, and stick grip. These sensors measure triaxial angular velocity, acceleration, and magnetic field, which are fused to provide 3-dimensional orientation estimates. Three ground markers indicating foot placements in front of, in line with, and behind the ball were included to study the effects of foot placement on sweep skill performance. Each participant chose the distance between their front foot and the ball, while the alignment of the foot and ball was determined by the researcher. Each participant performed a sweep up to 24 times, eliminating sweeps where the foot is off the mark. Each sweep was categorized based on bounciness and accuracy. The ball speed was determined from synchronized video data.

**Results & Discussion:** The preliminary data analysis focused on the stick grip sensor to better understand the pitch and roll of the field hockey stick during the sweep skill. Figure 1 shows the average and standard deviation for the pitch during the sweep movement for two representative participants, with blue shaded areas representing the standard deviation at each time point. The linear acceleration peak denoted the point of impact between the stick and the ball (vertical red line in Fig. 1&2). Figure 2 shows the roll for the same two representative participants. Across all participants, the stick movement is very consistent (i.e., small deviations from the average) just before impact. In other words, each participant followed the same unique movement pattern. The pitch and roll profiles are useful in identifying trends in the sweep movements. For example, the roll profiles show that participants snap their wrists from an open position to a closed position as the stick is approaching the impact with the ball. This insight is new to the field hockey research literature and would not have been possible without a sensor attached to the field hockey stick. Future work will continue to analyze the data collected by the other IMUs to better understand the effects of hip angle, knee angle, and foot placement on sweep performance in addition to the stick pitch and roll.

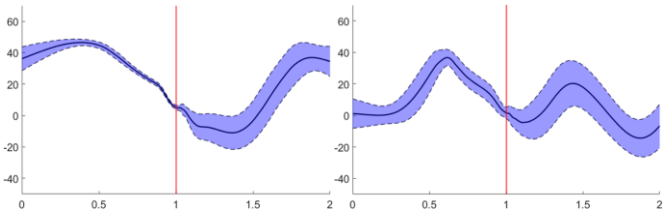


**Figure 1:** Pitch in degrees of the field hockey stick over the two second duration of a sweep for two representative participants

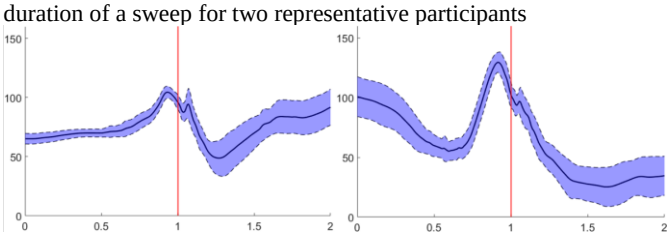


**Figure 2:** Roll in degrees of the field hockey stick over the two second duration of a sweep for two representative participants

**Significance:** This study aims to further knowledge about the sport of field hockey to increase the level of skill present in the game. By conducting research about field hockey, awareness of and attention to the sport will likely increase. The information gained from this study may also provide information to assist in the possible future study of injury risk prevention through a greater understanding of the movements made by players during skill execution.

**Acknowledgments:** This material is based upon work supported by start-up funds from the University of Iowa.

**References:** [1] De Subijana et al. (2010), *Sports Biomechanics*, 9(2); [2] Ibrahim et al. (2017), *Sports Biomechanics*, 16(1); [3] Brétigny et al. (2008), *Journal of Applied Biomechanics*, 24(3); [4] Aikman et al. (2019), *BMJ Open Sport & Exercise Medicine*, 5, e000582;

# RELATIONSHIP BETWEEN DIFFERENT BOUT LENGTH DEFINITIONS AND REAL-WORLD GAIT KINEMATICS

*Mayumi Wagatsuma[1], Julien Mihy[1], Spencer N. Miller[2], Stephen M. Cain[2], Jocelyn F. Hafer[1]
[1] Kinesiology & Applied Physiology, University of Delaware, [2] Chemical and Biomedical Engineering, West Virginia University
*Corresponding author's email: mayumiw@udel.edu

**Introduction:** In real-world gait studies, data are often processed or analyzed within bouts (akin to trials in a lab) but the way in which a bout is defined may affect study results. Real-world gait allows for walking bouts that vary in time, step count, or walking distance. Research groups often define bouts and bout length differently, such as by using bouts of a similar distance to an in-lab walkway, or including bouts based on a minimum number of steps [1, 2]. We have shown that gait kinematics differ based on bout duration (sec) in supervised walking outside of the lab [3] and others have similarly shown that longer walking bouts typically result in faster walking speeds and longer stride lengths compared to shorter walking bouts in the real world [2]. Whether bout length definitions besides duration similarly correlate with gait kinematics is unknown. Therefore, the purpose of this study was to examine the relationship between different bout length definitions (duration, stride number, and distance) and real-world gait kinematics.

**Methods:** Twenty-nine participants (51.3±18.1 yrs) wore five inertial measurement units (IMUs) [Opal v2, APDM, Clario] on the sacrum, thigh, shank, and both feet for three days of real-world activity. Walking bouts were identified based on the correlation of the oscillation of the thigh and foot sensors. Bouts were defined as at least five consecutive strides with inter-stride times of no longer than 60-seconds. Gait events were identified from raw acceleration and angular velocity from foot sensors using a continuous wavelet procedure. A zero-velocity update algorithm was used to calculate stride length and walking speed [4]. Medial-lateral axes for the thigh, shank, and foot were defined using a functional sensor-to-segment orientation method [5]. The stride-by-stride integral of angular velocity for each segment was used to estimate segment angular excursion [6]. Steady-state strides (coefficient of variance between strides for both stride length and stride speed less than 0.07 and a change in direction no greater than 40.1°) were selected for analysis. Walking speed, stride length, and knee and ankle range of motion (ROM) were averaged within each bout. Bouts were then defined based on duration (sec), number of strides, and distance (m; sum of all stride lengths). Pearson correlation coefficients were used to examine the relationship between gait variables and bout length for each definition ($\alpha$=0.05).

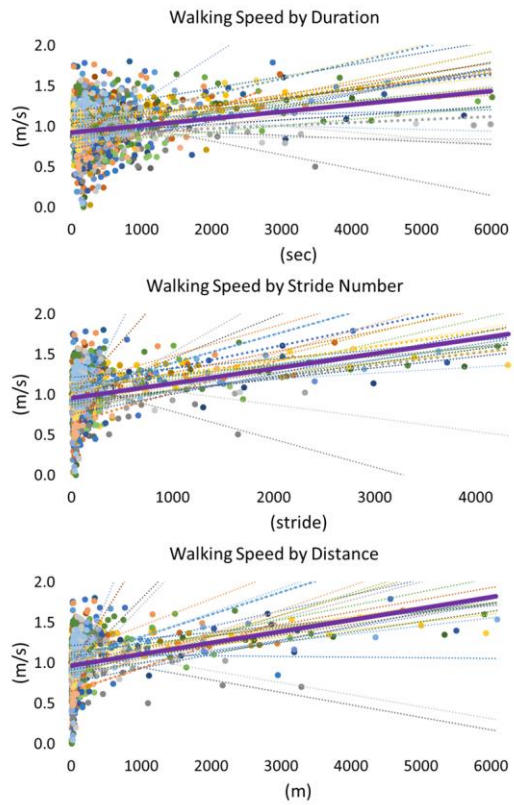


**Figure 1:** Scatterplots for significant relationships between gait variables and bout length definition (duration, stride number, and distance). Purple solid lines represent trendlines for all participants. Colored dots and lines represent each participant.

**Results & Discussion:** A total of 1770 walking bouts were collected from all participants. Across all bouts, the average duration was 431.7±647.7 sec (range 19.2-6012.1 sec), the average stride number was 165±393 strides (range 4-4318 strides), and the average distance was 190.0±541.2 m (range 3.3-6091.7 m). Walking speed had significant but weak positive correlations with duration ($p$<0.001, r=0.204), stride number ($p$<0.001, r=0.268), and distance ($p$<0.001, r=0.281) [Fig 1]. Stride length showed similar trends as walking speed ($p$<0.001, r=0.191; $p$<0.001, r=0.244; $p$<0.001, r=0.264). Additionally, knee ROM showed significant but weak positive correlations with stride number ($p$<0.05, r=0.054) and distance ($p$<0.05, r=0.68) but no correlation with duration ($p$>0.05). In addition, ankle ROM didn't show any significant correlation with any bout length definition ($p$>0.05). These results showed that longer bout lengths, whether defined by duration, number of strides, or distance travelled, are associated with faster walking speed and longer stride length, which is consistent with a previous real-world study [2]. This finding emphasizes the need for researchers to assess and report what types of bout lengths were included in analyses as different average bout lengths between groups or studies may influence the interpretation of results. Further, our findings suggest that bout length in distance travelled may be a stronger correlate of real-world gait kinematics compared to bout length in duration of time. Thus, if researchers must choose a single way in which to characterize real-world walking bouts, we suggest reporting bout length in distance.

**Significance:** Real-world gait variables differ by bout length regardless of definition (duration, stride number, or distance). It is essential to report the bout definition and bout length selection and should be considered when working with real-world gait data.

**Acknowledgments:** This work was supported by a grant from the National Institute on Aging (R21AG076989) from NIH.

**References:** [1] Carcreff et al. (2020), *Sci. Rep* 10(1); [2] Rehman et al. (2022), *Front. Aging Nuerosci* 14 808518; [3] Wagatsuma et al. (2024), *Gait Posture* 113; [4] Rebula et al. (2013) *Gait Posture* 38 974-980; [5] Mihy et al. (2022), *medRxiv* 11.29.2228289; [6] Hafer et al, *J Biomech*, 2020; 99 109567.

# VALIDATION OF A NOVEL WEARABLE SENSOR IN THE FREE-LIVING ENVIRONMENT

*Sydney M Lundell M.S.[1], Kenton R Kaufman PhD PE[1]
Mayo Clinic Motion Analysis Laboratory, Rochester, MN
*Corresponding author's email: lundell.sydney.edu

**Introduction:** Wearable devices are growing in popularity as a tool to (a) monitor individual physical activity and (b) manage population health needs [1-4]. Movement and activity-which are directly corelated to overall physical, cardiovascular, and mental health-are the primary focus of most wearable health monitors [5]. The advantage of these sensors is their ability to quantify changes in activity more accurately than patient journals, as well as to incentivize users to increase their daily step count.[6]. However, the accuracy of these devices is commonly determined in a controlled laboratory environment during straight walking tasks which is not representative of the real-world environment [7]. The goal of this study was to validate a novel wearable sensor in the real-world environment by quantifying the wear time sensitivity and specificity, step counts during walking bouts, and accuracy of total steps per day.

**Methods:** A total of 32 participants, aged 28±6 years, were recruited through word of mouth and institutional advertisement. The study was approved by the Mayo Clinic Institutional Review Board (#23-009687). All participants provided informed consent either in person or via email. Of the initial cohort, two subjects were excluded due to sensor failure, and three were removed for not completing data collection. Each participant wore five sensors: one Actigraph on the waist and two sensors (Actigraph and OPOS1) on each ankle. The Actigraph sensors were secured using adjustable Velcro straps, while the OPOS1 sensors were worn with elasticized material near the Actigraph devices. Participants were instructed to wear the sensors for 2 days, removing them before bed or when they might be exposed to water.

The OPOS1 sensor, which was the focus of this study, uses a low-power Inertial Measurement Unit (IMU) mode to track step count using separate settings for threshold, debounce time, and debounce steps. Optimization of these settings was completed prior to collections [8]. Data was collected over 48 hours in either 10-minute bins, 1-minute bins, or 10-second bins depending on sensor configuration. Concurrently, Actigraph sensors collected continuous raw acceleration data at 50Hz. The raw data was processed using MATLAB to calculate step count, activity levels, and cadence, while being synchronized to match the OPOS1 binning intervals [9].

To evaluate wear time, the OPOS1 sensor reported time in 10-minute intervals, marking a bin as worn if any movement occurred within it. True wear time was validated using the ActiGraph normalized acceleration readings, where values exceeding 1.1 g indicated genuine sensor use. Step count accuracy was assessed using Bland-Altman plots to determine bias and the limits of agreement (LOA). Continuous walking bouts were identified based on the assumption of 100 steps/minute adjusted. Finally, total daily step counts were calculated. An ANOVA was used to examine the effect of different sampling frequencies on measurement accuracy.

**Results & Discussion:** When compared to the Actigraph, the OPOS sensor reported on average a sensitivity of 0.93 and specificity of 0.98 for wear time. Accuracy increased as walking bouts became smaller (Table 1). This was anticipated since of 60% of walking bouts are less than 30 seconds [7]. The error in total step count per day was approximately 15% and did not vary with collection rate. Total steps per day error is independent of the bin duration but inversely related to the magnitude of steps per day ($p = 0.014$). Wearable step counting devices are heavily impacted by the location of the device and complex gait tasks [9]. Step counting sensor located at the ankle (where the OPOS sensor was located) are considered the most accurate for step counting suggesting error comes from initiating and stopping gait multiple times [10]. Due to the minimum debounce steps required to detected steps as walking bouts, smaller groups of steps (< 7) were excluded, causing increased undercounting in bins larger than the walking bout. Concluding that while the OPOS sensor readings are corelated to the reference Actigraph sensor, the OPOS sensors tended to under count steps no matter the bin size or walking bout with an average error of 15% for total steps per day. This can be improved by decreasing the minimum debounce step setting.

**Significance:** This study provided the accuracy of a new wearable sensor outside of a laboratory environment in a healthy population. The accuracy reported is more representative of activities of daily living than typically collected in a laboratory environment.

Table 1: Biases and Limits of Agreement for all collection rates during both non-continuous and continuous walking bouts alongside the total step per day error.

| | Non- Continuous walking bouts | | Continuous walking bouts | | Total Steps per day |
|---|---|---|---|---|---|
| **Collection Bins** | Bias (Steps) | LOA | Bias (Steps) | LOA | Percent Error |
| **10 Minutes** | -25 | (96, -140) | -120 | (160, -400) | 15.8% |
| **1 Minute** | -3 | (26, -31) | -10 | (8, -28) | 16.1% |
| **10 Seconds** | -4.9 | (3.7, -3.8) | -4.9 | (27, -38) | 13.4% |

**Acknowledgments:** Partial funding for this study provided by the Mayo Clinic Graduate School and OPOS1.

**References:** [1] Cooper,D.M. et. Al. JB JS, 2022. 7(2), [2] Ghosh,A et al., Micromachines (Basel), 2022. 14(1), [3] Adans-Dester et al., NPJ Digit Med, 2020. 3 [4] Stavropoulos, T.G., et al., Sensors, 2020. 20(10)., [5] Strain,t et al., Lancet Glob Health, 2024. 12(8)., [6] Wang J B, et al. Telemed J E Health. 2015 Oct; 21(10) [7] Orendurff et al., J Rehabil Res Dev. 2008;45(7), [8] Lundell et al., *Bioengineering* **2024**, *11*(6). [9] Fortune et al., Med. Eng. & Phy. 2014, 36(6) [10] Düking P et al., Front. Digit. Health 2024; 6(1). [11] Nakagata T, et al., BMC Sports Science, Medicine, and Rehabilitation 2024;16(156).

Muscle oxygenation during an isometric wall squat to fatigue using near-infrared spectroscopy

*Katherine Wells[1], April Chambers[1,2], Zachary Wilson[1]
[1]Department of Health and Human Development, University of Pittsburgh, Pittsburgh, PA
[2]Department of Bioengineering, University of Pittsburgh, Pittsburgh, PA
*Corresponding author's email: kjw139@pitt.edu

**Introduction:** Near infrared spectroscopy (NIRS) is a non-invasive tool that uses light to measure and monitor tissue oxygenation status [1]. NIRS can be applied to both clinical and non-clinical settings. Clinical use has been to assess microvascular function in patients with cardiometabolic diseases as well as muscular atrophy and disease, and peripheral artery disease [2]. For non-clinical populations, NIRS devices allow for measuring oxygen delivery versus consumption in the muscle it is applied to, given that the muscle does not have restricted blood flow [2]. NIRS has the potential to describe muscle oxygenation response to exercise, providing an understanding of the underlying physiology. This study utilizes NIRS in a non-clinical setting to assess muscle oxygenation of the vastus lateralis before, during, and after an isometric wall squat to fatigue. Post exercise, blood flow exceeds normal perfusion to the tissue called "post-exercise hyperemia." This idea suggests that following non-ischemic (non-vessel occluding) exercise, there is a subsequent increase in flood blow. The intensity of the exercise plays a role in the amount of hyperemia seen, and a subject is taken to fatigue, an increase in blood flow and muscle oxygenation is expected [3]. Wearable NIRS devices allows for portable, non-invasive muscle oxygen saturation readings and Moxy monitors have shown reliability in muscle oxygenation measurements [4][5]. In this study we expect to see muscle oxygenation levels drop during a wall squat to fatigue, followed by an increase above baseline muscle oxygenation response during recovery.

**Methods:** Healthy young adults were recruited for participation in this study. Moxy Monitors were placed on the main muscle belly of the vastus lateralis of the subjects' dominant leg. Subjects completed a 10-minute warm up according to American College of Sports Medicine guidelines, while wearing the device confirming comfort and achievement of full range of motion. After completion of the warm up, the subjects sat down and a 30 second seated baseline of muscle oxygenation levels was recorded. After 30 seconds, the subjects moved to designated wall. At the 45 second mark, subjects lowered into a wall squat with knees, hips, and ankles at 90º of flexion. Subjects held wall squat until failure. Once achieved, subject stood up and walked around to allow reperfusion of muscle. After 2 minutes of standing with movement, the subject sat down for the remainder of the recovery recording. For 15 minutes post wall squat termination, the monitor captured the recovery phase.

**Results & Discussion:** A typical subject is provided in Figure 1. The average baseline muscle oxygenation ($SmO_2$) level recorded was 62.3%. During the wall squat, $SmO_2$ levels dropped to the lowest value of 0.4%, with an increase to 22.7% at point of failure. This increase is likely due to the subject starting to plantarflex the foot to alleviate demand on the quadriceps muscle group. After cuing to maintain full foot contact, $SmO_2$ dropped again. An inability to maintain this position was seen and the test was concluded. During the 15-minute recovery period, the $SmO_2$ levels reached an average level of 78.7%. The average baseline $SmO_2$ level was achieved during recovery after 1 minute and 8 seconds. Oxygen is being consumed by the muscle, as shown by the decrease in $SmO_2$, but blood flow continues to the muscle. Our data shows that following an isometric exercise to fatigue, muscle oxygenation levels increase above baseline levels. This is due to post-exercise hyperemia and the fitness level of the subject. The subject's $SmO_2$ levels increased after the test was terminated and the increase above baseline occurred 68 seconds later. This quick increase shows low levels of post-exercise oxygen consumption (EPOC) indicating that the subject was able to begin recovery and stop oxygen consumption quickly, indicating a high fitness level.

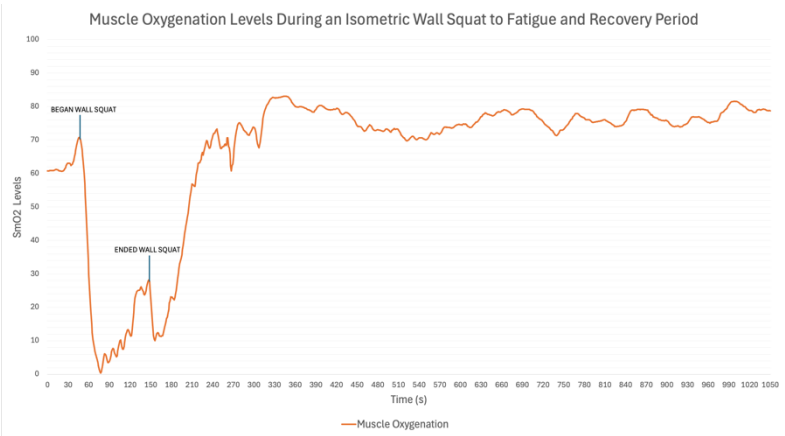


**Figure 1:** Muscle oxygenation before, during, and after wall squat to fatigue for a typical subject. Beginning and end of wall squat are highlighted on the graph. Recovery period beginning and end are also highlighted. After 2 minutes of standing recovery, the subject sat down, as shown on the graph.

**Significance:** The utilization of wearable NIRS technology during exercise and the expected outcome observed continues to expand the application and use of these devices. This study describes the muscle oxygenation in the vastus lateralis in response to a wall squat to fatigue. It demonstrates the ability of wearable NIRS to be used in non-clinical settings, allowing for the expansion of current research in understanding muscle health and performance. This technology could also benefit the educational space in providing information on underlying muscle physiology during various activities.

**References:** [1] Barstow. (2019. *Journal of Applied Physiology, 126*(5), 1360–1376. [2] Jones et al. (2016). *Artery Research, 16*, 25–33. [3] Osada, et al (2003) *Journal of Physiological Anthropology, 22*(6), 299–309. [4] Feldmann, et al (2019). *Journal of Biomedical Optics, 24*(11). [5] Crum et al (2017). *European Journal of Sport Science, 17*(8).

# DOES SENSOR POSITION AFFECT SPATIOTEMPORAL VARIABLES CALCULATED FROM IMUS ON THE FOOT?

*Grace V. Chesley, Mayumi Wagatsuma, Julien A. Mihy, Jocelyn F. Hafer
Department of Kinesiology & Applied Physiology, University of Delaware
*Corresponding author's email: gracevchesley@gmail.com

**Introduction:** Inertial measurement units (IMUs) enable the measurement of spatiotemporal gait parameters outside the lab. IMUs placed on the feet are often used to calculate spatiotemporal variables and the position of sensors may need to vary due to shoewear or medical devices. Previous research has shown there to be a difference in IMU vs. motion capture calculated stride length between sensors placed on the heel, instep, lateral and medial foot, insole, and in a midsole cavity [1]. Other research using similar sensor placements found that a sensor embedded within a cavity in a shoe's midsole was the best location for reconstructing foot trajectories and stride length during running [2]. While previous studies have compared spatiotemporal gait parameters between motion capture and multiple foot IMU locations, to our knowledge, there have been no studies that compare spatiotemporal variables between the different IMU locations. Therefore, the purpose of this study was to determine if there is a difference in stride length, stride velocity, stride height, or change in stride direction measured by IMUs on the dorsum of the foot, lateral instep, and heel.

**Methods:** Ten healthy young adults (28.1±3.4 years) walked ten times on a 10-meter walkway at their self-selected comfortable walking speed while wearing 3 IMUs (Opal v2, APDM, Clario) on their right foot. Sensors were placed on the dorsum, lateral instep, and heel of participants' own shoes. Foot trajectories (i.e., linear velocity and displacements) were calculated for each sensor using a zero-velocity update algorithm [3]. Gait events were identified to segment data into strides. Outcome variables were stride velocity, stride length, stride height, and change in stride direction. Four strides of steady-state data were included per participant. Outcome variables were compared between sensor locations using repeated measures ANOVAs with a significance level of $p<0.05$. We also compared outcomes between sensors on a participant-specific level by calculating root mean square differences (RMSD) between sensors on the dorsum and lateral instep, dorsum and heel, and lateral instep and heel.

**Results & Discussion:** There was a significant difference in stride velocity and stride length between sensors ($p<0.001$). Pairwise comparisons indicated that stride length and stride velocity were greater for the lateral instep sensor compared to the sensors on the dorsum ($p<0.001$ for length and velocity) and heel ($p<0.01$ for length and velocity) [Fig 1]. Individual participant RMSDs between sensor locations were <0.09 m for stride length, <0.08 m/s for stride velocity, <0.08 m for stride height, and <5° for stride direction for all but one participant. Overall, results indicate that different IMU locations on the outside of a shoe provide similar spatiotemporal outcomes.

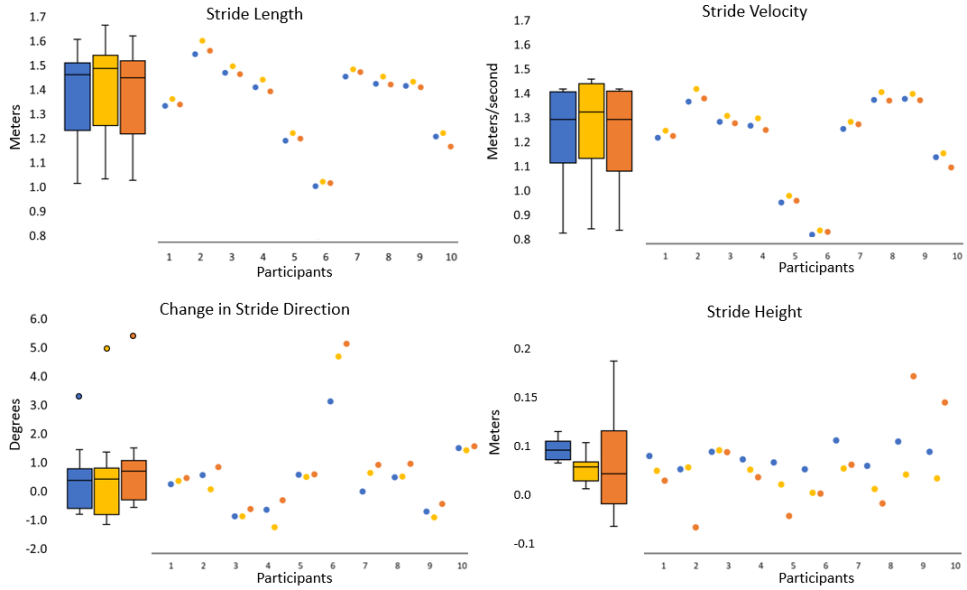


**Figure 1**. Individual and group data for stride velocity, stride length, change in stride direction, and stride height. Box plots represent group data. Dots represent individual participant data. Colors denote IMU location: blue=dorsum, yellow=lateral instep, orange=heel.

**Significance:** This study addresses whether spatiotemporal gait parameters differ when measured by IMUs placed at different locations on the outside of a shoe. For the tested locations, which avoided locations where the shoe deforms or where sensors may rub against the ankle, our results indicate that IMU placement does not significantly affect outcomes. Flexibility in the location of IMUs on the foot may make it easier to measure spatiotemporal variables in clinical populations or across different performance settings.

**References:** [1] Kurderle, et al. (2022). *PLoSONE*. [2] Zrenner, et al. (2020). *Sensors*. [3] Rebula et al. (2013). *Gait & Posture.*

# CHARACTERIZING KINEMATIC PATTERNS OF DAILY ARM USE OF MANUAL WHEELCHAIR USERS WITH CLUSTER ANALYSIS

Kathy Pinnock Branford[1]*, Meegan G. Van Straaten[2], Omid Jahanian[2], Hannah Houde[3] Melissa M. B. Morrow[3], and Stephen M. Cain[1]
[1]West Virginia University, Morgantown, WV, [2]Mayo Clinic, Rochester, MN and [3]Univ. of Texas Medical Branch, Galveston, TX
*kp0107@mix.wvu.edu, stephen.cain@mail.wvu.edu

**Introduction:** Shoulder pain and pathology is associated with overuse of the shoulder joint from the performance of repetitive and weight-bearing tasks necessary for manual wheelchair (MWC) users [1]. Current research on MWC users with SCI lacks insight into real-world movement patterns [2-4]. This study aims to address these gaps by analyzing movement data at a higher resolution by using kinematic features extracted from inertial measurement (IMU) data to quantify variations in arm use and clusters of daily activities. The cluster analysis approach allows for objective identification of natural groupings in movement patterns, providing insights into functional arm use that might be missed by traditional assessments or broader activity categories.

**Methods:** We used five IMUs (Axivity-AX6; range: ±16 g, ±2000 deg/s; sampling frequency: 100 Hz) placed on each wrist, upper arm, and chest. Data was collected from an SCI participant (Female, age range: 40-49 years, SCI level: Mid (T1-T8), time since injury: 8 years, employment status: part-time, computer work) over seven consecutive days during unsupervised real-world daily activities. Additionally, one supervised data collection session (IMUs and video) was conducted at the participant's home to provide pseudo-validation and to examine how these supervised home activities would compare to or cluster within the patterns identified in the unsupervised data collection. We defined Arm Movement Bouts (AMBs) as continuous periods of arm activity separated by at least 5 seconds of inactivity. From these bouts, 16 biomechanical features (*e.g., segment velocities and angles*) were calculated from IMU data.

Data from one day (wear time: 15 hours) was analyzed using K-means clustering to classify AMBs into clusters, where the optimal number of clusters was determined using the elbow method [5]. The resulting cluster centroids (mean values) were used to classify AMBs for the remaining 6 days of the unsupervised data collection and for the supervised data collection. Each new AMB was classified by calculating its Euclidean distance to all centroids and assigning it to the nearest one, ensuring consistent classification across all days of data collection.

**Results and Discussion:** The cluster analysis used these features: mean angular velocity magnitude, percent movement time (forearm-only, whole-arm, bilateral), mean upper arm elevation angle, mean thorax angle, mean wrist height, and wrist height variance. Four distinct clusters emerged from this analysis (Fig 1), with upper arm elevation angles remaining relatively consistent across all clusters (34-42 deg). The supervised data collection provided both face and criterion validity for clusters 1 and 2, while activities classified into clusters 3 and 4 were not observed during the supervised data collection session.

Further examination of cluster composition revealed activity patterns aligned with the participant's known routines. The participant works remotely doing computer work, evident in real-world data (Cluster 2) but absent from the supervised collection. In the real-world data, time spent in each cluster varies between days (Fig. 1). This variability highlights potential patterns or trends in the participant's daily routine and provides insight into the unique characteristics of their activities and the factors influencing their behavior.

| Cluster | Characteristics |
|---|---|
| 1 | high-speed movements (*e.g.*, household chores) |
| 2 | low-speed movements (*e.g.*, desk work) |
| 3 | thorax angle measurements (*e.g.*, lying or reclining) |
| 4 | bilateral movements (*e.g.*, propulsion). |

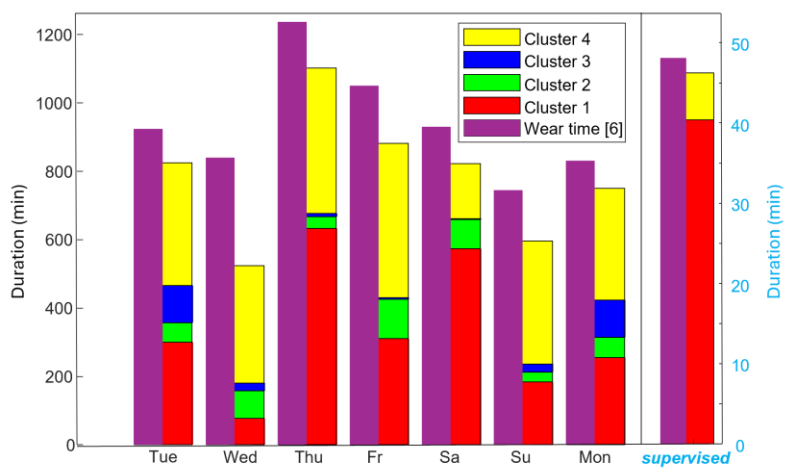


**Figure 1.** Cumulative duration spent on clusters across days. Each cluster is represented by a different color cluster 1(red), cluster 2(green) and cluster 3 (blue) cluster 4 (yellow). The left y-axis represents the cumulative duration for the unsupervised data collection, while the right y-axis represents supervised duration

**Significance:** This analysis provides unique insight into the upper extremity demands of MWC users by classifying arm movement bouts. The findings suggest that differences between days can be identified by examining the duration spent in each cluster, offering a new method for interpreting large amounts of data in a meaningful way. In addition, our analysis suggests that it could be beneficial to modify supervised data collections so that the structure of activities more closely resembles daily life.

**Acknowledgments**: NIH Eunice Kennedy Shriver National Institute of Child Health and Human Development (R01HD084423)

**References:** [1] Soslowsky et al (2002) Annals of Biomed Eng, 30 (8), [2] Jahanian, O., et al. (2022), J Spinal Cord Med 45(4); [3] Goodwin BM., et al. (2021), Sensors (Basel) 21(4). [4] Amrein, S., et al. (2023). Sensors, 23(3). [5] Umargono, E., et al. (2020) ISSTEC. van Hees VT ., et al. (2011), PLOS ONE 6 (7)

# *Thank you to our Sponsors*

AMTI
FORCE AND MOTION

BIOEX
CONSULTING
EXCELLENCE · EXPERIENCE · EXPERTISE

**THE** BIOMECHANICS
**INITIATIVE**

MAYO
CLINIC

novel

University of Pittsburgh | Swanson School of Engineering Bioengineering